SAE TRANSACTIONS

1959

Digitized by the Internet Archive
in 2023

https://archive.org/details/sae-transactions_1959_67

SAE TRANSACTIONS

TL
1
S6
vol. 67

Society of Automotive Engineers, Inc.
485 Lexington Avenue New York 17, New York

Leonard Raymond
President

John A. C. Warner
Secretary and General Manager

B. B. Bachman
Treasurer

E. D. Allen
Editor

Kathleen Napier
Assistant Editor

All articles appearing in SAE Transactions are indexed by Engineering Index, Inc.

Copyright 1959, Society of Automotive Engineers, Inc.

Price: $3 to members, $7 to public and college libraries and U. S. Government Agencies, $10 to nonmembers. Foreign: $3 to members, $8 to public and college libraries, $11 to nonmembers.

Photolithographed reproductions are available of any article published in SAE Transactions. Prices, on quantities of 100 copies or more, varying with number of pages and illustrations, can be obtained upon request from SAE Special Publications Department, 485 Lexington Avenue, New York 17, N. Y.

Contents

The Comprex Diesel Supercharger—Max Berchtold 5

Riding on Air—Hulki Aldikacti, Edward W. Anderson, and Robert D. Harrison 15

How Performance Factors Affect Transmission Design—E. A. Richards 26

Some Observations on the Aging of Low-Carbon Sheet Steel—E. R. Morgan 34

Research in Magnetohydrodynamics—William McIlroy 39

An Investigation of the Control of Tire Thump by Tire Shape—Guy J. Sanders 44

Simulating Road Shake in the Laboratory—K. P. Pettibone 51

The Effect of Engine Mounting on Car Shake—L. M. Morrish 54

Routes of Crankcase Oil Loss—J. S. Coon and D. E. Loeffler 59

New Industrial Tools Utilizing Phosphors—C. W. Wallhausen 71

Vehicle Suspensions Using Coil Springs—M. C. Turkish 74

Possibilities and Problems of Some High Energy Fuels for Aircraft—Walter T. Olson 82

Chrysler Corporation's New V-8 Engine—R. S. Rarey and E. G. Moeller 95

Engineering the "W" Engine, Chevrolet's 348-cu-in. V-8—J. T. Rausch, H. H. Kehrl, and D. H. McPherson 103

A New Look at High Compression Engines—D. F. Caris and E. E. Nelson 112

New Combustion Problems—Starting and Stopping Modern Engines—V. F. Massa 125

Thudding in High Compression Ratio Engines—W. E. Morris and D. C. Fariss 134

Rumble—A Deposit Effect at High Compression Ratios—A. E. Felt, J. A. Warren, and C. A. Hall 138

Knock-Knock: Spark Knock, Wild Ping, or Rumble?—R. H. Perry, Jr., and H. V. Lowther 145

Knock, Rumble, and Ping—H. F. Hostetler and W. R. Tuuri 152

Engine Pounding—Its Causes and Control—J. L. Bame and R. G. Tuell 158

Investigating Rumble in Single-Cylinder Engines—J. A. Robison, M. D. Behrens, and R. G. Mosher 169

If You Squeeze Them, Must They Scream?—W. M. Wiese 175

Pyroceram—W. W. Shaver and S. D. Stookey 184

Ion Rocket Engine Development—Donald L. Eschner 187

A Progress Report—Dry-Type Air Cleaners on Farm Tractors—J. C. Siemens and J. A. Weber 191

Now—Practical "Double Dry" Filtration with Donaclone—H. M. Turner and D. K. Anderson 197

Vol. 67, 1959

Limited Slip Differentials—R. P. Lewis and L. J. O'Brien 203
How a Diesel Engine Rates Itself—W. J. McCulla 213
Pneumatic Power Control Systems for Trucks, Trailers, Buses—Stephen Johnson, Jr. 221
The Ion Rocket Engine—R. H. Boden 227
Automobile Head-On Collisions—Series II—D. M. Severy, J. H. Mathewson, and A. W. Siegel 238
"Delrin" Acetal Resin—A New Engineering Material—H. H. Goodman and J. D. Young 265
Single-Cylinder Engine Fuel Research—A. W. Pope, Jr. 271
Supercharging in the Free-Piston Cycle—H. G. Spier 281
Optimization Study, Missile Auxiliary Power Systems (as viewed by the equipment supplier)—E. I. Brown and R . W. McJones .. 289
Aluminum Engines—Design for Modern Fabrication—J. M. Smith and R. M. Smith 295
Steering and Traction Characteristics of Rubber-Tired and Crawler Vehicles—W. J. Adams, Jr. 312
The Potential of Unconventional Powerplants for Vehicle Propulsion—Peter Kyropoulos 319
Some Thoughts on Optimum Combinations of Wings and Vertical Thrust Generators in VTOL Aircraft—W. Z. Stepniewski 326
Iron-Aluminum Base Alloys—Cheap Stainlesses of the Future?—Blake King, J. J. Mueller, N. N. Ida, and F. G. Tate 335
The Economics of High-Octane Gasolines—F. W. Kavanagh, J. R. MacGregor, R. L. Pohl, and M. B. Lawler 343
Priming Aids for Cold Starting Diesel Engines—J. J. DeCarolis, W. E. Meyer, and P. W. Espenschade 351
The Teracruzer—A High Mobility Vehicle—G. D. Simonds 365
Ford Free-Piston Engine Development—Paul Klotsch 373
Recent Developments Make Engineering Specifications More Realistic—Dorian Shainin 379
Selection of Optimum Modes of Control for Aircraft Engines—A. J. Sobey 383
Engagement Characteristics of Wet-Type Clutches—L. P. Ludwig 391
An Evaluation of Aftercooling in Turbocharged Diesel Engine Performance—J. E. Mitchell 401
The Buick Flight Pitch Dynaflow—Forest McFarland and Charles S. Chapman 414
The Behavior of Radiation-Resistant ANP Turbine Lubricants—J. M. Clark, Jr., and G. C. Lawrason 424
Status of the SAE S-12 Approach to Vibration Isolation of Aircraft Electronic Equipment—Fred Mintz 434

continued

Contents, continued

Metallurgical Developments in Brake Drums—V. A. Crosby 441

Diesel Engines for Use in Light Delivery Vehicle and Taxi Service —J. S. Bright 449

Indoor Climatic Testing of Automotive Engine Cooling and Air-Conditioning Systems—C. V. Hawk and J. W. Godfrey .. 456

Theory and Instrumentation of Inertial Navigation Systems— J. Statsinger 463

The Advantages of the New SAE Standard for Involute Splines from a Design Standpoint—L. N. DeVos 469

Practical Design Suggestions for Users of Brazed Honeycomb Sandwich—F. F. Rechlin 472

Thermal Loading and Wall Temperature as Functions of Performance of Turbocharged Compression-Ignition Engines— E. T. Vincent and N. A. Henein 478

The Design of Planetary Gear Trains—Oliver K. Kelley 495

What's New in Brake Linings—N. H. McCuen 509

Some Aspects of the Operation of Utility Engines—E. C. Paige and H. T. Mueller 516

Development of the Suppressor and Thrust Brake for the DC-8 Airplane—L. R. Jordan and C. M. Auble 524

Digital Computer Analysis and Interpretation of Turbocharged Diesel Engine Performance—H. A. Cook 532

New Fluoroester Lubricants for High-Temperature Applications— E. C. Ballard and E. E. Sommers 545

Muffler Corrosion—Its Cause and Control—R. A. Heath 553

Exhaust Systems, Fundamentals and Design Considerations— L. E. Muller 559

The Use of Bench Wear Tests in Materials Development— G. H. Robinson, R. F. Thomson, and F. J. Webbere 569

Aluminum Die-Cast Cylinder Blocks in Outboard Motors— W. C. Conover and R. C. Nelson 580

Strength and Thermal Limitations of Materials for Airframe Components—J. C. Ekvall 590

GM Diesel's Additional Engines—New Vees and In-Lines— K. L. Hulsing and C. E. Ervin 596

Radioactive Tracers Cast New Light on Fuel Distribution— D. E. Cooper, R. L. Courtney, and C. A. Hall 619

Automatic Transmission Testing—H. H. Kehrl, M. R. Marsh, and R. A. Gallant 640

Some Recent Experiments on the Friction, Wear, and Deformation of Solids—F. P. Bowden 650

Design Problems of Very High Speed Flight—K. E. Van Every 659

Index 669

THE COMPREX DIESEL SUPERCHARGER

Max Berchtold, I-T-E Circuit Breaker Co.

This paper was presented at the SAE Summer Meeting, Atlantic City, June 12, 1958.

THE Comprex is one of the recent developments aimed toward improvement of the turbocharger. The device seems to be most adaptable to small-sized diesel engines where high turbocharger efficiency is hard to achieve.

In the Comprex, the theory of nonsteady flow permits an accurate analysis of a cycle in order to optimize such parameters as air- and gas-intake temperatures, air intake and discharge pressures, air and gas mass flows, porting arrangements, rotor size and speed.

Experiments thus far indicate that the Comprex is capable of delivering high-density air over a wide range of engine speed and permits immediate load changes without lag and smoke.

PIONEERED by Dr. Moss in this country and by Dr. Alfred Buchi in Switzerland in the 1920's, the turbocharging of diesel engines today has gained tremendous ground. It has been introduced successfully in small traction engines where the requirements, operational conditions, size, and price are most challenging. The Comprex[1] essentially fulfills the same task as the turbocharger; however, it uses entirely different phenomena to perform this function. Work performed during the past five years has shown that the Comprex has several advantages over the turbocharger.

History

A direct transmission of energy from one gas to another has been considered by many inventors for the past 50 years. A British patent issued in 1913 describes a device which resembles the Comprex very closely. Many similar devices proposed in the following years were not reduced to practice until 1940 when Claude Seippel of the Brown Boveri Co., in an effort to develop the Lebre principle for a heat pump, recognized the fact that compression and expansion waves could be utilized for the efficient transmission of the energy of an expanding gas to another gas to be compressed. In this device the gases are in direct contact; there is no physical separation such as pistons, compressors, or turbines.

The first machine was built to serve as the high-pressure stage for a gas turbine set. It showed great promise but Brown Boveri, being fully engaged in the development of large capacity gas turbine powerplants, was unable to make the concentrated effort to solve all the problems of this entirely novel device.

In the United States, Johann Wydler built a rotating valve which utilized the exhaust gas energy to precompress the air charge of a reciprocating engine directly. The device, even though it produced considerable boost pressures, was not commercially exploited. In England, Kadenacy used pressure waves in tuned exhaust pipes which resulted in a considerable increase of power output. The gain, however, is limited to a narrow engine speed range.

Working at the National Advisory Committee for

[1] "Comprex" is a trademark of I-T-E Circuit Breaker Co.

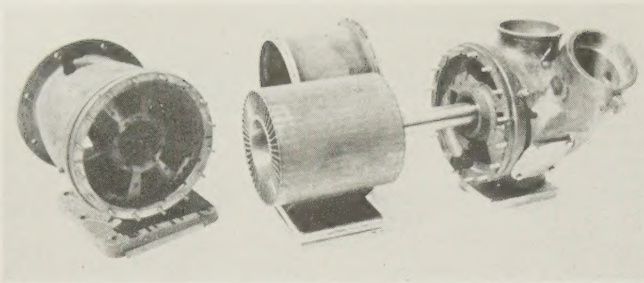

Fig. 1 — Comprex components

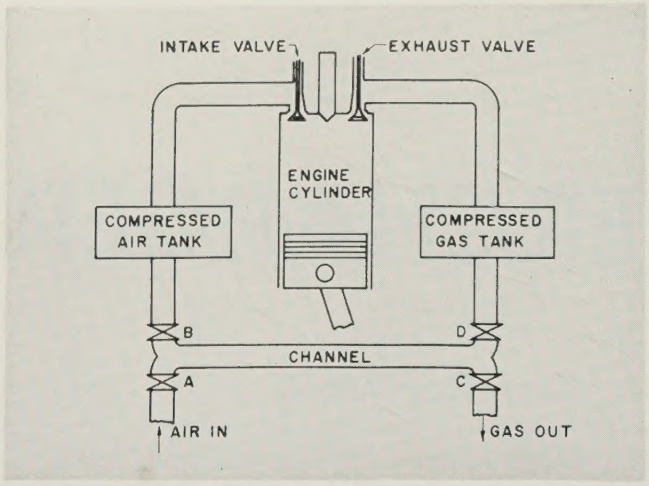

Fig. 2 — Single-channel model

Aeronautics in Langley Field, Va., and later at Cornell University, Prof. A. R. Kantrowitz designed and built a small unit fully utilizing compression and expansion waves. His efforts were directed toward high pressure ratios; however, mechanical difficulties also hindered his progress.

In Germany, the Heinkel-Hirth Co. had built a small powerplant designed to deliver shaft power, but it was not designed for the proper utilization of nonsteady flow. The low efficiency and the small power output of this machine discouraged further development of it.

In a joint effort sponsored by the Bureau of Aeronautics and the I-T-E Circuit Breaker Co. with Prof. Kantrowitz as a consultant, a small test unit in the 20-hp size class was built to gather the test data necessary to establish a correlation between measured performance and theory. The design started in 1949 and by 1951 encouraging results had been accumulated. As part of an application study sponsored by the U. S. Navy Bureau of Ships, the principle appeared particularly promising for the supercharging of 2-stroke diesel engines. As a result, a private research and development program was initiated by my company in 1953.

The first tests were run in September, 1954. Many problems remained to reduce this device to practice. After several mechanical improvements the machine was tested with a diesel engine. A cooperative program with the Caterpillar Tractor Co. was started in August, 1955. As a result, a smaller Comprex prototype was designed incorporating the experience gained. Tests at I-T-E continued and endurance

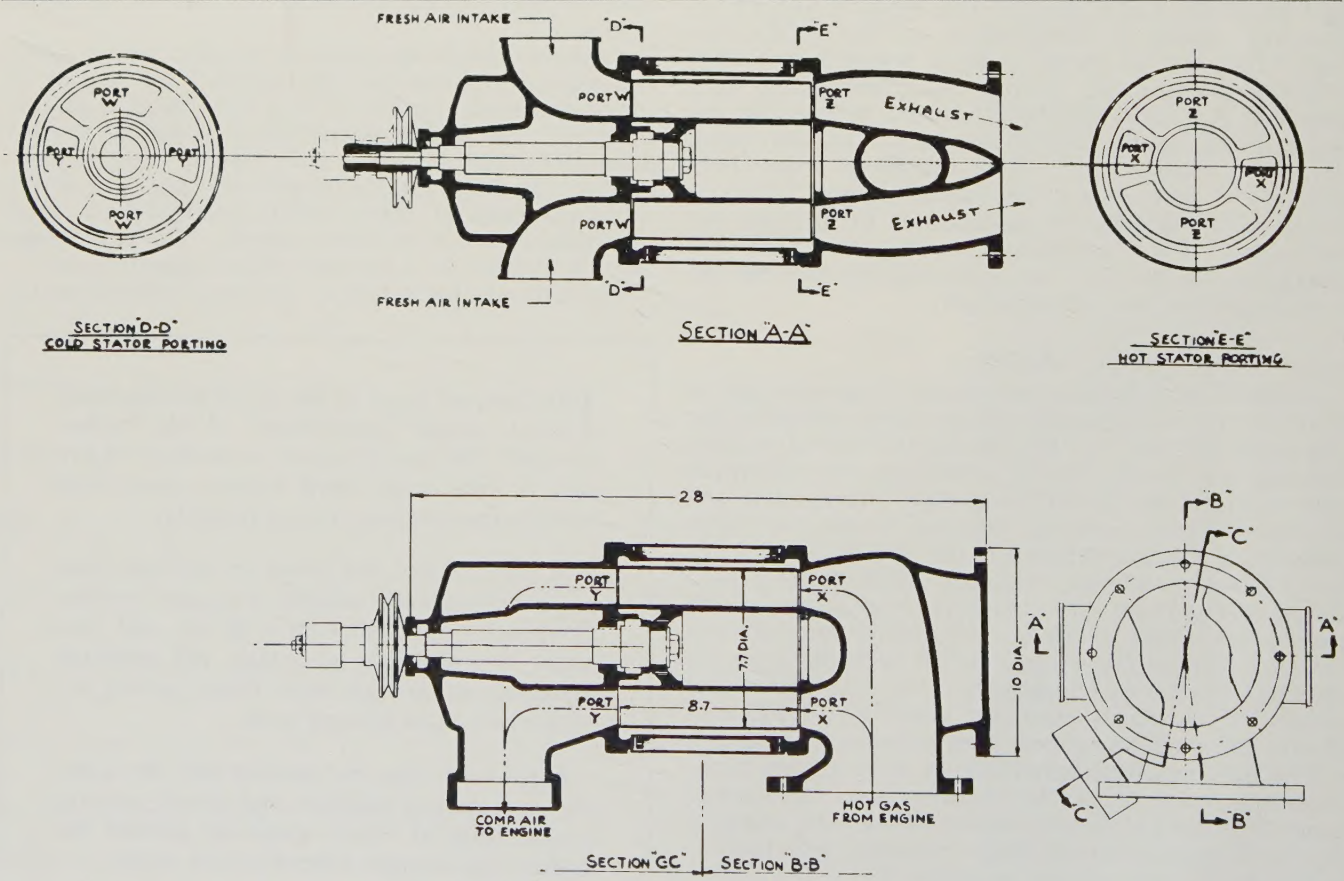

Fig. 3 — Comprex supercharger cross-section

time of many hundreds of hours at various extreme conditions was accumulated. Dynamometer tests were completed early in 1957 and vehicle tests in the field have been in progress since.

The following performance characteristics have been established:

1. The Comprex can deliver high air density over a wide engine speed range.
2. The Comprex permits immediate load changes without lag and smoke.
3. The Comprex is a simple, rugged, low-speed device.

Principle of Operation

The Comprex has one rotating element in which both compression and expansion takes place. The four components of the machine are shown in Fig. 1. The expanding gas acts directly, that is, in physical contact, on the air to be compressed. This action occurs within the straight passages of the rotor. The rotation serves only as a means of connecting each channel with the desired port at the desired time.

A few commonly known facts of nonsteady flow will help in understanding the principle of the Comprex. The effect of an explosion some distance away is felt not by the physical contact with the explosives but by the change of air pressure in the surrounding area, which is called a shock wave. It is also known that the passing wave has in its wake a deep vacuum which causes in many instances even more serious damage. This part is called an expansion wave. Thus, the energy of the explosive charge is transmitted through the air, until its energy is finally dissipated.

In the Comprex consecutive compression and expansion waves traverse the channels and thereby transmit energy from one gas to another. In the design of reciprocating engine manifolds considerable experimental efforts have been made to utilize pressure waves. In the Comprex, the theory of nonsteady flow permits an accurate analysis of a cycle in order to optimize such parameters as air- and gas-intake temperatures, air-intake and discharge pressure, air and gas mass flows, porting arrangements, rotor size, and speed. It is due to this method that progress was made in this field.[2]

The actual operation can best be explained by following one of the rotor channels through a complete cycle. As a single channel of the rotor passes by a stator port, it is opened and closed. This is equivalent to a pipe with valves A, B, C, and D as shown in Fig. 2. Valves A and B are located on one side of the channel and control the airflow; valves C and D on the other side of the channel control the exhaust gases. Valves B and D control the high-pressure portion of the cycle whereas valves A and C connect the pipe to ambient pressures.

We begin the cycle at a time when the channel contains air at rest and at ambient pressure; all valves are closed. First we open valve D and the hot gas which is at a pressure greater than ambient enters the channel and pushes the air in the channel ahead. A pressure front is created which travels at approximately the speed of sound through the channel; and the front of the hot gas, which we call the interface, travels slower and lags behind the shock front or wave front. Wherever the shock front passes, the air pressure rises and the gas starts to move. We now open valve B to receive the arriving compressed air, and close it again before the hot gas interface arrives. Valve D was closed earlier, resulting in an expansion wave which emanated at valve D. This expansion wave travels at approximately the speed of sound, and wherever this wave passes the pressure drops and the flow stops.

In this first phase we have replaced the air by hot gas. Energy originally contained in the hot gas has been passed on to the air. When we open valve C the gas in the tube is still above ambient pressure. Therefore, a second expansion wave is generated, this time accelerating the hot gas and resulting in outflow of this hot gas into the exhaust port. When this expansion wave reaches valve A the entire hot gas column, which is now at ambient pressure, is in motion, and by opening valve A fresh air is drawn in. We keep both valves C and A open until the head of the fresh air reaches valve C and we have fully scavenged the channel.

We can now close valve A since the air column has a forward motion toward valve C. A third expansion wave is created which lowers the pressure in the tube slightly below ambient pressure. When the entire air column in the channel has come to rest, valve C is closed and the cycle starts over again. The creation of the vacuum by closing valve A before valve C is advantageous for the supercharger, inasmuch as the gases, after the opening of valve D, enter the channel at higher speed due to a higher pressure differential. This arrangement also has the advantage that some pressure drop through an air cleaner in the intake and a pressure drop in the exhaust can be tolerated.

In the actual Comprex, the valve timing is accomplished by the motion of the rotor between two stator plates which have ports so arranged as to control conditions for a cycle. There are many (for instance, 35) passages in the rotor, all of which participate simultaneously in different phases of the cycle. The multitude of channels results in a continuous flow of compressed air through the compressed-air discharge port. Fig. 3 shows different sections through the unit. The rotor has straight axial passages. The two stators show the porting arrangement. For symmetry, each stator has two sets of ports. This means two complete cycles are made as a rotor channel makes a full revolution. Fig. 4A shows an unwrapped picture of the rotor. The pressure and flow conditions, the position of the wave fronts and interfaces are shown during each phase of the cycle. Fig. 4B shows the same diagram in simplified form. In reality, the cycle deviates from these idealized conditions inasmuch as the wave fronts and interfaces are not well-defined owing to the gradual opening and closing of the channels, mixing at the interface, and the theoretical divergence of expansion fronts.

The effects of mixing are undesirable and can be eliminated by slight overscavenging during the low-pressure gas-air exchange phase, and by a slight underscavenging during the high-pressure air-gas exchange phase.

The fact that the same rotor is in contact with both the cold air and the hot gas results in some heating of the air and cooling of the gases. This effect, even though small, is undesirable for best diesel performance. However, it has the advantage

[2] "Nonsteady Aerodynamics of Comprex Supercharger," by H. U. Burri. Paper presented at ASME Gas Turbine Power Conference, Washington, D. C., March, 1958.

that the metal temperature of the rotor remains substantially below the gas temperature, and plain steel has proved a suitable metal for rotor construction.

The Comprex, being essentially a valve which does not produce shaft power, has to be driven to overcome bearing friction and windage losses, and to add angular momentum to the air entering the channels. By proper choice of the flow angles, the required drive power can be reduced to less than 15% of the engine output.

It appears from this description that the Comprex operates only at a single design point. Experience, however, has proved quite the contrary; the device operates over a wide range of pressure, mass flow, and rotor speed.

1. For example, if the pressure of the incoming exhaust gas decreases, the flow velocities decrease and, as a result, the gas and air mass flows become smaller. The speeds of the waves do not change substantially. The desired speed of the rotor remains, therefore, essentially constant. Fig. 5, which represents a wave diagram for reduced pressure, shows that in this case a portion of the air remains in the rotor acting as a piston.

2. If the compressed-air mass flow is reduced at constant exhaust gas pressure, a second compression wave is generated at the opening edge of the pickup port. Fig. 6 represents a cycle with such a receiving shock wave. As a result of this wave, the flow velocity in the pickup port decreases and the pressure increases. This results in higher exhaust velocities for the low-pressure gas and a stronger suction on the fresh air.

3. If the speed of the rotor is changed, the timing of the waves deviates from the optimum condition. However, since the channels do not open or close instantaneously there is a certain time latitude for the waves to arrive. This means the speed can be varied within ± 10% with only a small loss in performance.

The Comprex, as any other compressor, has its own behavior. A performance map can be established by means of a simple test setup (Figs. 7 and 8) where the compressed air is heated, throttled, and discharged as hot gas into the Comprex. The parameters are the air-intake conditions (pressure and temperature), the gas-intake conditions, the mass flows (air and gas flow must be equal for a supercharger application), the air-discharge temperature, the Comprex rpm, the energy efficiency (combined component efficiency), the equivalent compression efficiency, the pressure loss through the intake and exhaust ducts, and mufflers.

The test stand performance map (Fig. 9) is adapted for correlation with a 4-stroke engine. The common ordinate for all curves is the air-discharge pressure given as pressure ratio as well as in in. of

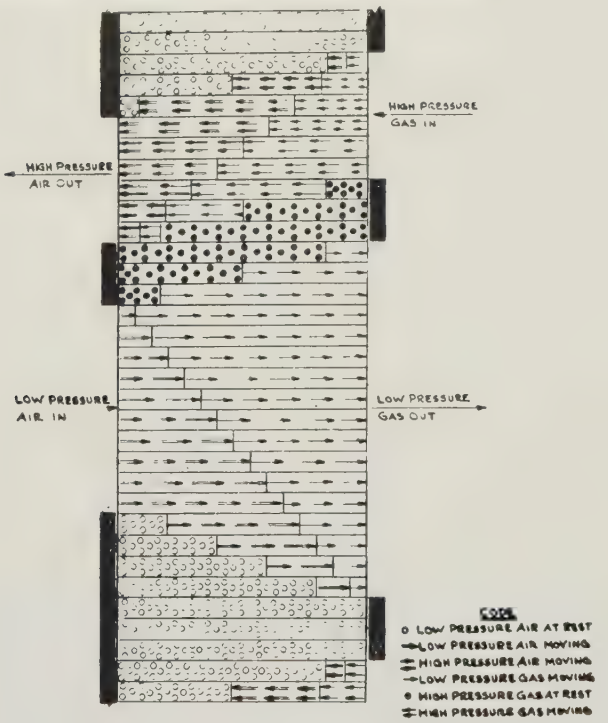

Fig. 4A — Comprex supercharger wave flow diagram

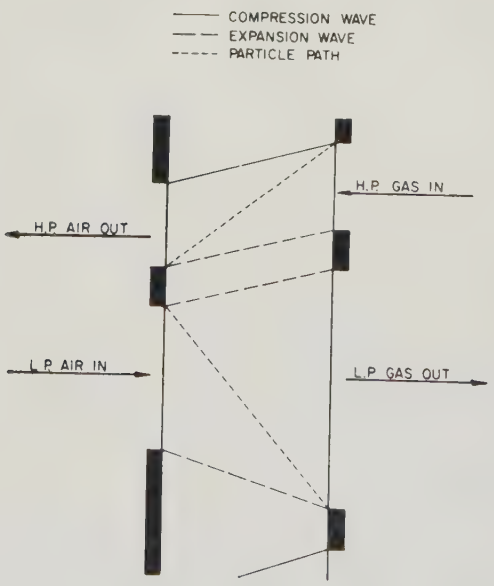

Fig. 4B — Simplified wave flow diagram

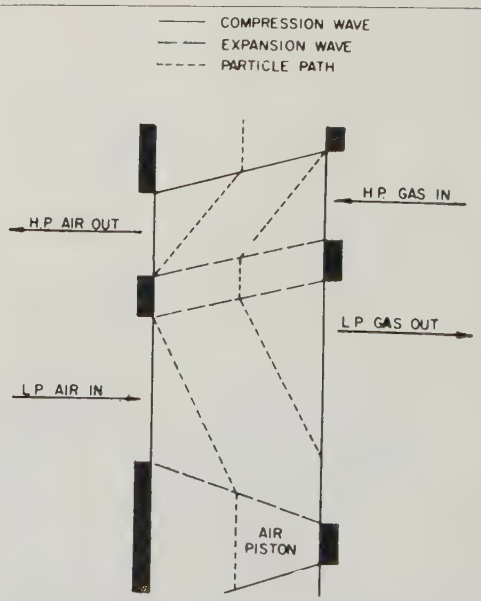

Fig. 5 — Simplified wave flow diagram, operation at reduced pressure ratio

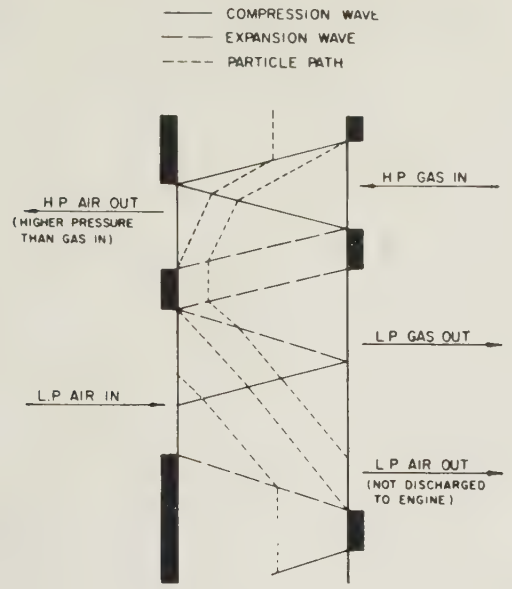

Fig. 6 — Simplified wave flow diagram, operation with receiving shock for reduced output flow

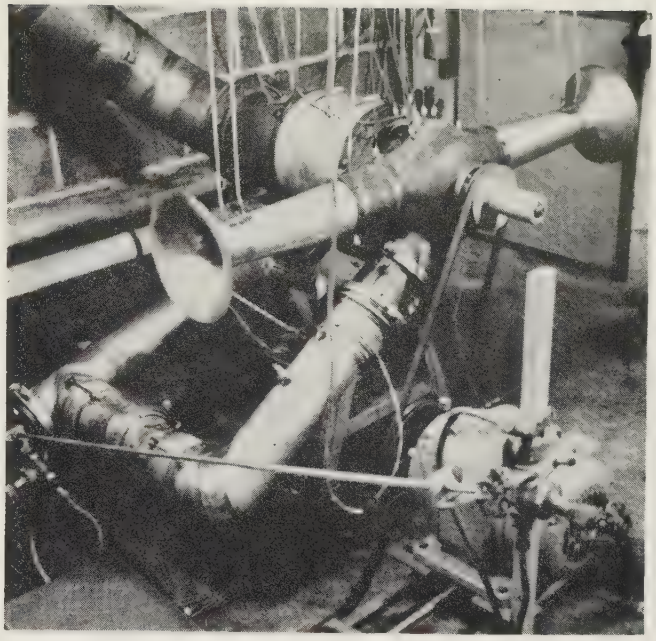

Fig. 8 — Test stand

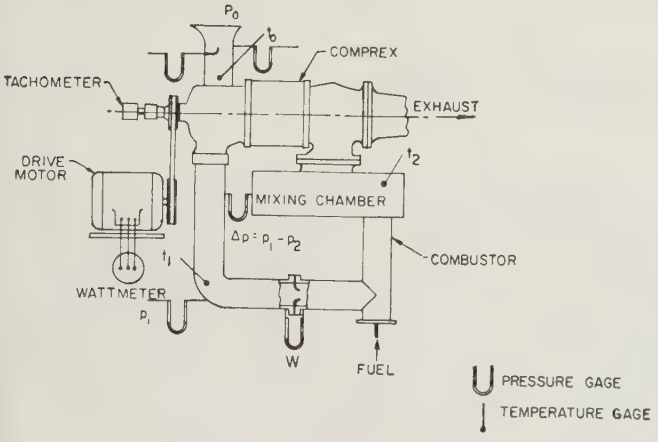

Fig. 7 — Test arrangement

Hg based on 30 in. of Hg ambient pressure. The family of curves on top gives the exhaust gas temperature for constant discharge volume, which is equivalent to constant engine rpm.

The relationship between reciprocating engine speed and Comprex discharge volume flow is:

$$n = \frac{Q}{\eta_v b^2 \frac{\pi}{4} \frac{sZ}{2}} = \frac{Q}{\text{constant}} = \frac{W}{\rho \text{constant}} \qquad (1)$$

where:

Q = Air volume at Comprex discharge, cu ft per sec
W = Airflow, lb per sec
ρ = Weight density at Comprex discharge, lb per cu ft
n = Diesel engine revolutions per sec
b = Bore, ft
s = Stroke, ft
η_v = Volumetric efficiency
Z = Number of cylinders

The constant discharge volume curves are given in cu ft per sec. The quantities given pertain to the

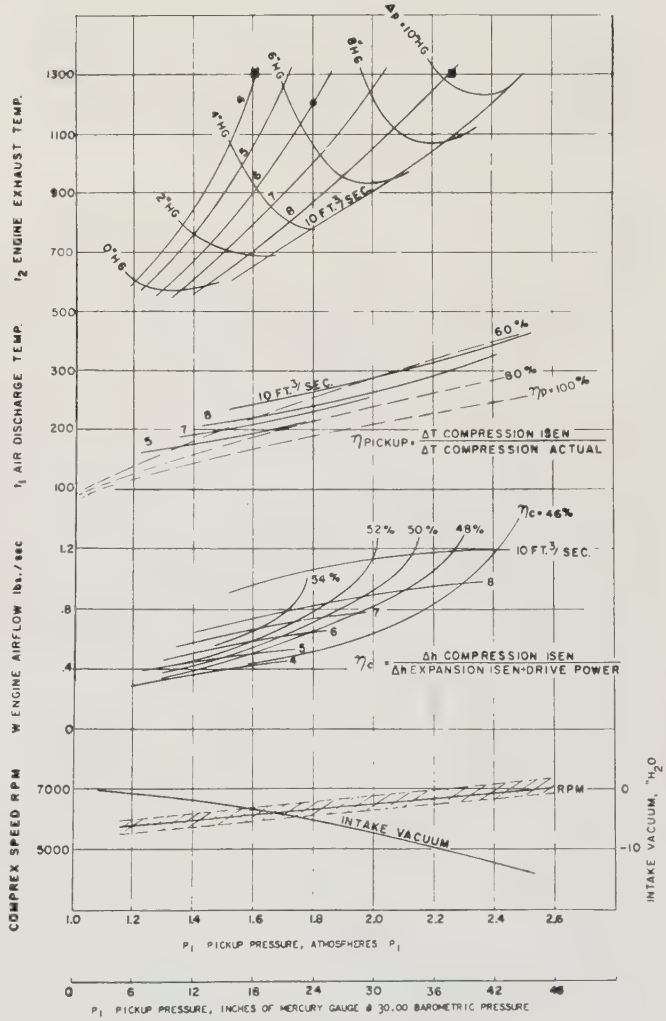

Fig. 9 — Comprex supercharger performance map corrected to 90 F and 30 in. of Hg, correlated to 4-stroke diesel cycle characteristics where volume flow (cfs) corresponds to constant rpm curves with constant volumetric efficiency

particular unit tested; the dimensions are given in Fig. 3. The chart can be generalized for relative sizes and corrected thermodynamic conditions.

The family of curves showing constant pressure drop as the parameter is of interest since this pressure differential acting on the piston allows a partial power recovery.

The air discharge temperature curves for constant engine rpm do not reveal the compression efficiency since the temperature rise is partly due to mixing and heat exchange. However, this temperature is important to the engine inasmuch as it determines the air density and, therefore, affects the admitted airflow. Furthermore, it affects the thermal loading of the engine. For this reason equivalent constant efficiency lines are included in this plot. The equivalent compression efficiency is as high as 85%.

The decrease of equivalent compression efficiency at high output volume is due to the hot gas mixture from the interface entering the pickup port, thus raising the air temperature. At low output pressures the equivalent efficiency decreases owing to insufficient energy to scavenge the gas. As a result, some of the hot gas remains in the rotor. This gas is recycled and eventually some of it is discharged with the compressed air.

The mass flow curves in the next lower group also show the combined efficiency. This efficiency can be compared directly with the products of compressor and turbine efficiency, and mechanical efficiency of a turbosupercharger.

The definition of the combined Comprex efficiency is

$$\eta_c = \frac{\Delta h_c}{\Delta h_T + E} \qquad (2)$$

where:

Δh_c = Isentropic enthalpy change between air intake and discharge pressure, Btu per sec
Δh_T = Isentropic enthalpy change between gas intake and discharge pressure, Btu per sec
E = Shaft power required, Btu per sec

This efficiency is computed from the measured exhaust gas temperature, air-intake temperature and pressure ratios, and the shaft power.

The Comprex rpm at which the data is taken as well as the intake vacuum caused by the intake metering system are given in the map (Fig. 9). All plotted points were taken at the optimum rpm. Fig. 10 shows the effect of speed variation at a typical point of the performance map. The gas temperature was maintained constant during speed variation, resulting in a pressure decrease on either side of the optimum condition. The change in the compressed air output, as well as the reduction in combined efficiency, are shown in Fig. 10. The broad speed range eliminates the need for accurate speed control.

The major losses of the Comprex occur as leakage of compressed air and gas at the high-pressure ports. It is essential to establish a design permitting operation at the smallest possible clearances between rotor and stators at all operating conditions, as well as during all transients. The kinetic energy of the exhaust gas leaving the rotor represents another loss. Further losses are due to incomplete conversion of the compressed air discharge velocity into pressure in the pickup diffuser. The drive power

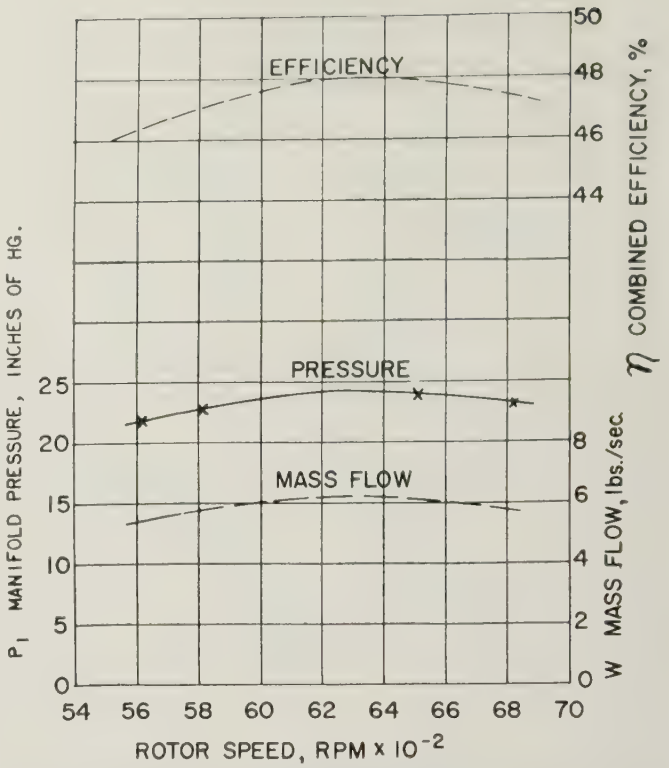

Fig. 10 — Comprex speed versus air manifold pressure, mass flow, and combined efficiency with 1205 F engine exhaust temperature and constant orifice

necessary to overcome windage and bearing friction represents an additional loss. A further braking effect is due to the air essentially entering axially into the rotor, thus exerting a negative angular momentum on the blades. By slightly bending the blades near the exhaust end of the rotor, the drive power requirement can be reduced and some of the exhaust gas kinetic energy can be utilized which otherwise would be lost.

Design Description

The sections in Fig. 3 show the principal dimensions as well as the arrangement of the essential components. In the present design, the rotor is supported by a cantilever shaft by means of two sleeve bearings which are located in the cold stator housing. This eliminates the need for bearing cooling and the need for precision alignment of the two stators. The thin wall hub of the rotor has straight axial dovetail grooves into which the blades are inserted. The hub has a heavier section near the cold end to provide for attachment of the shaft. Identical dovetail joints are used between the blades and the shroud. During operation, the rotor assumes an approximately linear temperature distribution along the axis; the original cylindrical shape of the hub becomes slightly conical. It is, therefore, essential that the hot end is free to expand. The blades and shroud, being made of light-gage stock, follow temperature changes faster than the hub during transient operating conditions. Therefore, a structure flexible to thermal expansion is necessary. The shroud is made in several segments with overlapping joints for sealing. The blades which are secured radially by means of the dovetail joint are free to expand in the axial direc-

tion, since the blades are held axially in a groove at only one point approximately in the center plane. The shroud segments are secured axially to the blades in the same plane. This rotor construction has proved itself to be free from thermal distortion. The design lends itself to simple production methods.

The cold stator houses the two bearings; the larger bearing near the rotor face also acting as a thrust bearing. There are two separate air-intake passages. The compressed air pickup ports lead to a scroll collector which has a single compressed air discharge duct. Commercial gray iron or aluminum can be used.

The hot stator, which has essentially the same porting and ducting requirements as the cold stator, is considerably simpler since there are no bearings on this side. The hot stator is designed to be bolted directly to the exhaust manifold. This method of utilizing the exhaust manifold as a support of the Comprex eliminates the need for pressurized hot expansion joints. The cold stator, and hence the rotor, is carried by means of a tubular structure between the stators. This housing is made of relatively light-gage steel. It is insulated on the outside in order to follow changes in rotor temperature without delay, thus maintaining proper hot stator-rotor clearance.

Comprex as 4-Stroke Diesel Engine Supercharger

The proper matching of the Comprex supercharger to the diesel engine is of great importance to obtain the most desirable engine characteristic. There are several considerations such as torque characteristics, response requirements, altitude and climatic conditions, which must be met.

The naturally aspirated diesel engine can fulfill the extreme operating requirements expected from the medium-size traction engines. Supercharging is an effective means of increasing the horsepower output. It is, however, essential that no sacrifice has to be made with respect to torque characteristic, rapid load response, or fuel consumption. The Comprex supercharger is capable of satisfying the airflow requirement over a wide engine speed range. This means the density of the air delivered to the engine is essentially independent of the mass flow; it is only a function of the engine exhaust temperature. The Comprex supercharged engine can produce a high torque at low engine speed with nearly the same air/fuel ratio as it does at high engine speed. This will result in a considerable gain in fuel consumption at maximum torque and reduced engine speed. The fuel consumption curves shown in papers by Reiners, et al., would, therefore, remain about constant over the full engine operating range.[3,4] The recommendations made by Miller and Ucko gain more significance in connection with supercharged vehicle engines, since it is now possible to operate the engines at high torque and low speed with a substantial gain in fuel economy.[5,6]

The Comprex size is laid out so that the engine performance points fall in the desirable performance range of the Comprex performance map (Fig. 9). If it is desirable to obtain a high torque over a 2/1 engine speed range the performance points marked in Fig. 9 at the 8 cu ft per sec and the 4 cu ft per sec output volume line should furnish possibly a constant air density for this mass flow range. The delivered air density variation for this engine operating range and the variation of the combined Comprex efficiency are shown in Fig. 11. The measured performance map of a Caterpillar engine with a Comprex supercharger is shown in Fig. 12. The operating speed range is between 400 and 1200 rpm; the Comprex is driven from the engine by means of a variable speed drive which maintains an approximately constant Comprex speed over the operating speed range of the engine. The graph gives torque expressed in bmep versus engine speed with lines of constant exhaust gas temperature and air manifold pressure as parameters. The specific fuel consumption for a constant 1300 F engine exhaust temperature is shown in Fig 11.

The measured performance map of the Caterpillar engine with a standard "V" belt drive to the Comprex (fixed ratio drive) is shown in Fig. 13. The engine speed range over which maximum bmep has been obtained is reduced in comparison to the maximum bmep range of Fig. 12. The engine speed for optimum timing of the Comprex is determined by the belt drive ratio and the relative setting of the cold and hot stator. As the engine speed deviates, the Comprex efficiency falls off due to increasing

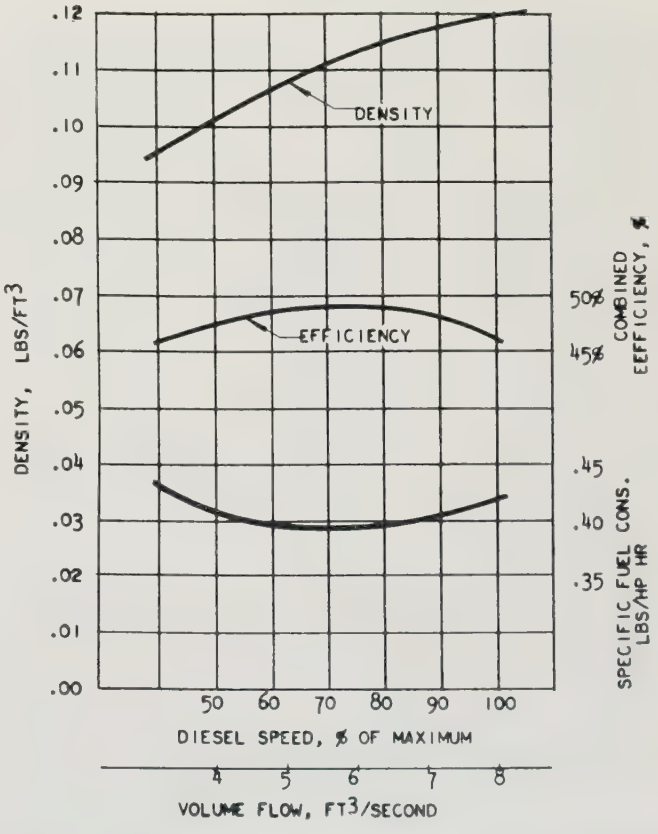

Fig. 11 — Intake manifold density, combined efficiency, and fuel consumption for constant engine exhaust temperature versus diesel engine speed

[3] "Turbocharging High-Speed, High-Output Diesel Engines," by N. M. Reiners and W. E. Wollenweber. Paper presented at SAE Annual Meeting, Detroit, Jan. 9–13, 1956.

[4] "Cummins Turbocharged Engine," by N. M. Reiners and W. D. Schwab. Paper presented at SAE National Transportation Meeting, Cleveland, Nov. 4–6, 1957.

[5] "Factors Affecting Fuel Economy (MPG)," by J. C. Miller. Paper presented at SAE Summer Meeting, Atlantic City, June 2–7, 1957.

[6] "The Future of the Diesel Engine in Commercial Vehicles," by Bernard Ucko. Paper presented at SAE Summer Meeting, Atlantic City, June 2–7, 1957.

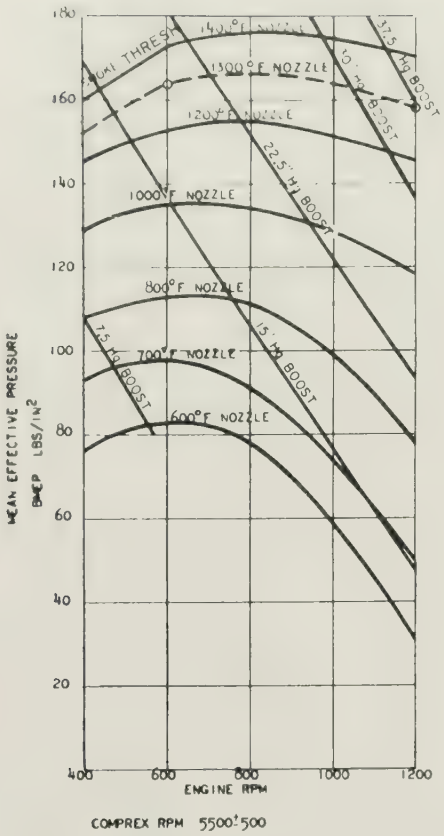

Fig. 12 — Engine performance constant Comprex speed, variable belt ratio, constant stator setting

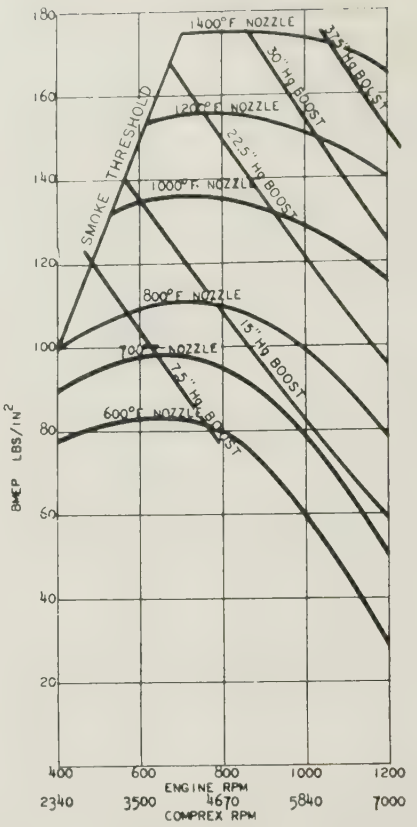

Fig. 13 — Engine performance variable Comprex speed, constant belt ratio, constant stator setting

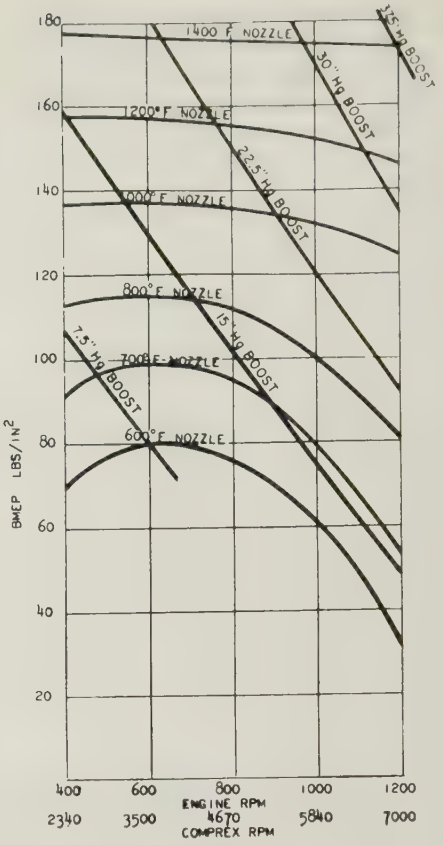

Fig. 14 — Engine performance variable Comprex speed, constant belt ratio, variable stator setting

mistiming. This results in a drop of the delivered air density and, therefore, a drop of the available air for combustion. By changing the drive ratio and the stator setting, the maximum bmep curve can be affected.

There are many engine applications where a compromise in the torque curve in favor of a simple mechanical drive is preferable. The envelope of all curves with different stator settings in combination with a fixed ratio drive represents a desirable engine speed torque curve. Mechanical means to take advantage of this characteristic have been designed. This arrangement, which permits constant Comprex efficiencies over a large engine speed range in conjunction with a simple belt drive, consists of an adjustable plate between the face of the cold stator and the rotor. The plate is automatically positioned as a function of Comprex speed in order to establish proper wave timing at all engine operating speeds. The engine performance characteristic with the automatically timed Comprex is shown in Fig. 14. The Comprex, operating at higher speed with the proper stator setting (and, therefore, the best wave timing), is capable of furnishing more air flow than it would at lower speed with the respective stator setting. Since this characteristic matches the requirement of the engine, the Comprex with adjustable stator plate allows ideal airflow matching the two components. This makes it possible to choose the size of the Comprex so that the pressure difference between the air manifold and the exhaust manifold stays within desirable limits over a wide engine speed range. This not only permits good scavenging of the diesel engine; it also provides for effective scavenging of the Comprex, resulting in lower air manifold temperatures. In comparing Figs. 12 and 14, it can be seen that the air manifold pressure for 1400 F exhaust temperature between 400 and 1200 rpm changes from 14 to 40 in. of Hg in Fig. 12, and from 19 to 37.5 in. of Hg in Fig. 14. The smoke threshold shown in Figs. 11 and 12 is not reached in Fig. 14. This indicates the performance superiority of the Comprex with variable stator plate, since the air density is more nearly constant over the full engine speed range.

The Comprex with the automatically positioned stator plate has a characteristic similar to the turbocharger with variable turbine nozzles. In the Comprex, because the control elements are on the air side, there should be no difficulties due to seizing and distortions. A simple hydraulic actuator which operates the plate as a function of engine speed has been built, and the initial tests have given satisfactory performance. Only extended field tests can prove the practical feasibility of this control feature.

There are several additional operational problems peculiar to the Comprex supercharger. Even though the combined efficiency is high at low-pressure operation, the minimum required exhaust gas temperature for proper Comprex operation is higher than the available engine exhaust gas temperature during low load and idling operation. This means the Comprex is unable to furnish the airflow required by the engine. As a result, the airbox pressure falls below the exhaust manifold pressure and, consequently, the Comprex is no longer properly scavenged. The

recirculation thus induced is undesirable since it leads to carbon deposits in the intake manifold. This difficulty is overcome with an automatically operated butterfly valve between the Comprex and the engine which maintains the air pressure of the Comprex discharge at a pressure equal to the exhaust manifold pressure. This throttling valve can be operated directly by a membrane on which the airbox pressure acts on one side and the exhaust gas pressure on the other. The butterfly valve so controlled will prevent exhaust gas and soot from reaching the air manifold.

Engine starting offers another difficulty as the Comprex is running too slow for proper wave timing because the cranking speed is only about one-tenth of full engine speed. The same butterfly throttle valve which is required for low-load operation enables starting since no exhaust gas is admitted to the engine as long as the butterfly valve is closed. A spring in the membrane actuator holds the butterfly closed as long as Δp remains zero. An alternate air intake becomes necessary. A check valve which opens when the air box pressure falls below ambient pressure will serve this purpose and facilitate starting. Fig. 15 shows a schematic picture of the control elements necessary for starting and low-load operation.

The Comprex dimensions lend themselves to a compact installation on the exhaust manifold inasmuch as the Comprex drive pulley falls into the engine auxiliary drive plane so that it is quite easy to arrange a belt drive from an existing fan generator or idler shaft. The required power to drive the Comprex is 1.2% of the engine shaft power output. In cases where the belt drive is undesired, a hydraulic drive can be used in conjunction with a constant volume control flow valve. For narrow engine speed range using torque between 100% and 60% engine speed, the fixed ratio drive is most suitable. In the case of a flat or rising torque curve between 100% and 40% engine speed, the Comprex with fixed ratio drive and the automatically positioned stator plate offers the most desirable torque characteristics.

The Comprex can be scaled up or down and the efficiency is practically independent of scale. This makes the Comprex particularly advantageous in the small engine sizes where it becomes increasingly difficult to obtain high turbocharger efficiency.

Summary

The Comprex has the advantage of:
Simplicity and ruggedness.
Low-speed operation, low sensitivity to unbalance.
Rapid load response.
Wide range of operation.
No danger of overspeed.
No watercooling.
Engine oil lubrication.
Large flow passages, no danger of clogging.

The disadvantages are:
The necessity of a drive.
The necessity of a control system for low load idling and starting.

The Comprex will increase the power output for today's high-duty vehicles. The rising torque with drop in engine speed will reduce the frequency of gear shifting. At moderate output the engine speed is reduced, and the lower engine friction at optimum air/fuel ratio will give improved economy. In addition, the immediate load response of the engine permits full utilization of the vehicle.

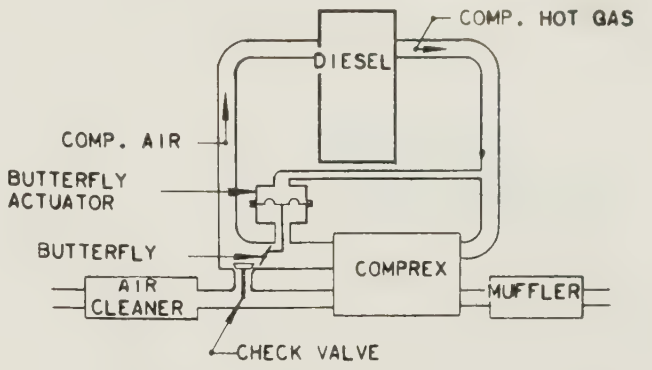

Fig. 15 — Comprex control arrangements

Conclusions

The results of the work accomplished indicate a definite place for the Comprex supercharger on the 4-stroke diesel engine. The performance results adapted to 2-stroke engines without scavenging blower are very promising. Preliminary tests now running at our laboratories indicate that this system has many features desirable for spark-ignited engines.

Additional References

1. "An Improved Compressor Air Pump," by Hans Burghard. British Patent No. 19421, issued 1913.
2. "Process of and Apparatus for Performing Conversion of Mechanical and Thermal Energy," by A. F. Lebre. U. S. Patent No. 2045152, issued June, 1936.
3. *Mechanical Engineering,* Vol. 69, 1947: "Recent Development of Gas Turbines," by Adolph Myer.
4. "Engine Supercharger," by Johann T. Wydler. U. S. Patent No. 2264126, issued November, 1941.
5. *The Oil Engine,* November, 1934: "The Kadenacy System," by Kadenacy. Also in *Engineering,* October, 1945.

DISCUSSION

Finds Heating of Air Charge To Be Undesirable

— James F. Blose
U. S. Naval Engineering Experiment Station

THE author and his co-workers are to be congratulated on the development of an ingenious and novel type of supercharger which should be less costly to build than competitive types and will certainly require less use of materials which would be in critically short supply in case of war. It is interesting to note that units of this type are also undergoing development in Great Britain as evidenced by recent articles in a British trade journal, *The Oil Engine and Gas Turbine.*

The author states that, since the same rotor is in contact with both the cold air and hot gas, heating of the air and cooling of the gases occurs. This is an advantage in that it permits the use of plain steel in the rotor construc-

tion. However, heating of the air charge is undesirable for two reasons: (1) it increases fuel consumption at all power outputs and (2) it reduces the maximum power that can be obtained from the engine. The curves in Fig. 9 show that, at a pickup pressure of two atmospheres, an air discharge temperature of 270–290 F will be obtained. We recorded temperatures of 225–230 F at this pressure during tests on a 2-stroke engine using a turbocharger. It seems desirable that the Comprex should be used with an aftercooler.

The upper curves on Fig. 9 also seem to indicate that no boost pressure is obtained at engine exhaust temperatures below 570–600 F. This appears to be a somewhat high temperature, especially for possible use on a 2-stroke engine which requires scavenge air at low as well as high power outputs. Is there any prospect of improving performance of this unit at lower exhaust gas temperatures?

The author is requested to discuss whether the Comprex has a surge condition similar to that existing in centrifugal compressors.

Comments and Questions About Comprex Supercharger

— Kurt A. Beier
Schwitzer Corp.

MY COMMENTS on this paper can be enumerated as follows:

1. Rapid response. Low rotor inertia and proper engine matching can result in turbocharge response rates permitting no power lag and performance of the vehicle essentially the same as Roots blown engines.
2. Broad operating range. Latest tests of the 4-in. turbo show a usable engine speed range down to 45% of maximum engine speed. Engines should not be lugged down below about 60% of maximum for good engine life.
3. A control device is necessary with Comprex to bypass it at low loads, idling and starting. This is not needed with the turbocharger. The controls necessary with the Comprex must function a large portion of the time on a vehicle in traffic and must be foolproof, or the engine will stall.
4. The size of Comprex appears larger and heavier than a comparable turbocharger.
5. The effect of heating of the intake air charge by heat transfer from the exhaust pulse offsets the density increase of supercharging air.
6. The Comprex supercharger should suffer from density loss at high altitude. The turbocharger can compensate for altitude operation.
7. Turbocharger appears to lend itself to simpler and easier installation.

I have several questions to ask the author:

1. What is the effect of exhaust back pressure and intake restriction on the performance of the engine supercharged by the Comprex?
2. What is the noise level of the Comprex and what are the silencing problems?
3. What are effects on rotor and housing parts of the Comprex from shock waves and thermal cycles?

Author's Closure To Discussion

MR. BLOSE points out the important problems of the Comprex as a 2-stroke engine supercharger. The higher air manifold temperature appears as a disadvantage as long as the density of the fresh charge at the beginning of the next compression stroke is reduced. It is possible to lower the compressed air temperature by better matching of the Comprex to the engine. The reported tests represent the first attempt of 2-stroke operation. It has been recognized that the full potential of the system lies in the capability of the Comprex for scavenging and supercharging the 2-stroke engine without the need of a separate displacement blower. This can be accomplished with the proper exhaust and intake pipes between the Comprex and the engine. At the full-load point, this arrangement will provide a higher pressure differential between the air box and the exhaust manifold, resulting in a more effective scavenging. The system will also improve the next point raised in the discussion. The Comprex is capable of utilizing the blowdown energy to compress air. Sufficient pressure is available at low load and idling to scavenge the engine. An aftercooler would be of interest in the case of high-pressure supercharging.

The Comprex is independent of any surge line as it exists on turbocompressors. The reason for this lies in the basic difference of its operating principle. The flow instabilities due to flow separation do not exist in the Comprex, where compression occurs instantly as the compression wave passes through the air.

Mr. Beier has pointed out the results of his efforts to improve the response and operating range of turbosuperchargers. The wide engine speed range which Mr. Beier reports has probably been accomplished on an engine with large valve overlap. Recently, turbochargers with control elements at the hot end have been introduced to improve the operating range. The control element used on the Comprex for idling operation rather than wide speed range is considerably simpler and is placed at the cold end. The size and the weight of the new Comprex model compares well with turbochargers of equal capacity. The installation of a Comprex which has a smaller diameter, even if it is somewhat longer, should be easier to install than the turbocharger. To answer Mr. Beier's specific questions, it can be said that the desirable low-pressure drop air cleaners and mufflers used on turbocharged engines can be used on Comprex-charged engines. If the total pressure drop exceeds 3 in. of Hg, the scavenging of the Comprex suffers, resulting in an increase of the air manifold temperature due to recirculation of exhaust gas.

The noise level comparison of a turbocharged truck and a Comprex-charged truck with standard intake air cleaner and exhaust muffler is identical. To the ear, a high pitch (3500 cps) noise is distinctly audible but can be reduced by the proper tuning of the muffler.

ORAL DISCUSSION

— Reported by W. J. Pelizzoni
Mack Trucks, Inc.

Dr.-Ing. Alfred J. Buchi, Swiss Institute of Technology: I think that the Comprex will be good for the gas turbine. The original gas turbine work, of course, led to the development of the turbocharger. The results obtained by the author are very good.

Edgar Rose, Kiekhaefer Aeromarine Motors, Inc.: What change in engine exhaust pressure did the Comprex cause? If of any magnitude, did it have any effect on exhaust valve life?

Mr. Berchtold: Engines with Comprex had same back pressure as the turbocharged engines. There was no valve problem.

W. J. Pelizzoni: What are the possibilities of a radial flow machine instead of axial flow?

Mr. Berchtold: This is being studied and has some possibilities. However, nothing has been built this way.

He'muth Braendel, Wilkening Mfg. Co.: What are relative costs as compared to the turbocharger?

Mr. Berchtold: I believe that the price in equal production quantities would be competitive to the turbocharger. The reduction in fuel consumption and maintenance costs would also be attractive.

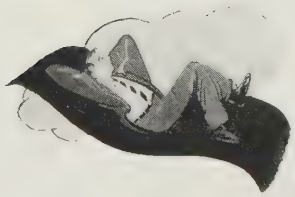

RIDING ON AIR

Hulki Aldikacti, Pontiac Motor Division, General Motors Corp.
Edward W. Anderson, Cadillac Motor Car Division, General Motors Corp
Robert D. Harrison, Edsel Division, Ford Motor Co.

This paper was presented at a Junior Panel Meeting of the SAE Detroit Section, Nov. 25, 1957.

THIS symposium describes in detail the air-suspension systems available on the 1958 models of the Pontiac, Cadillac, and Edsel.

The Pontiac is a modified closed cycle system, comprising an air compressor, air tank, height control valves, and air springs. The Cadillac system employs leveling valves, compressor, high-pressure check valve, high-pressure storage tank, and flow control orifices. The Edsel design is made up of the air supply, control, and spring systems, which incorporate a compressor, reserve air tank, leveling valves, and air springs.

Air suspension is not a new idea in springing automobiles, but the recent trend toward lower cars has renewed interest in the potentials of the method.

Ever-Level Air Ride

by Hulki Aldikacti

ONE of the major trends in automobile design has been to build lower cars without sacrificing the ride, handling, or comfort of the passenger. Ride and comfort basically require low-rate springs, but weight variation causes excessive suspension deflection. This affects handling because of geometry change and affects ride from loss of jounce. Therefore, the lower car trend and softer springs require height compensation. Also, soft springs have low energy storage so rate buildup is necessary. This is quite difficult to do with a mechanical spring, although many different schemes have been designed and used.

Normally, a car is designed to be level at a 3- to 5-passenger load and as most of the passenger load is taken by the rear axle, the car may ride with rear end high. When the springs take some set, the fully loaded car may ride with front end high. This is very undesirable from the driver's point of view, and at night headlamp aiming can be affected. Also, we are reaching the rate limit of the low rates we can attain from coil springs without overstressing the spring in the space available.

Knowing what is desired in a car spring, required

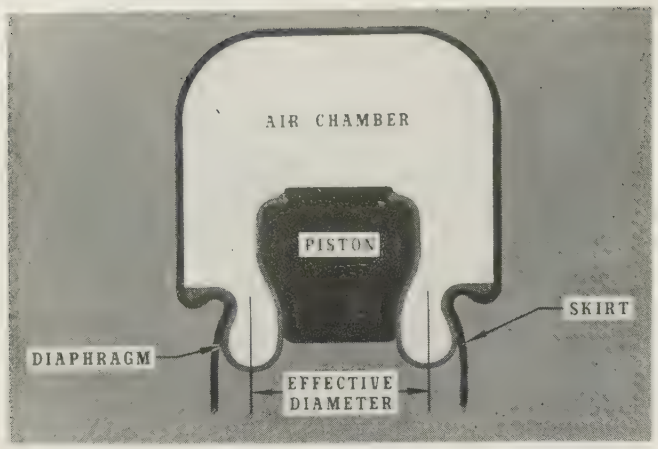

Fig. 1 — Basic air spring

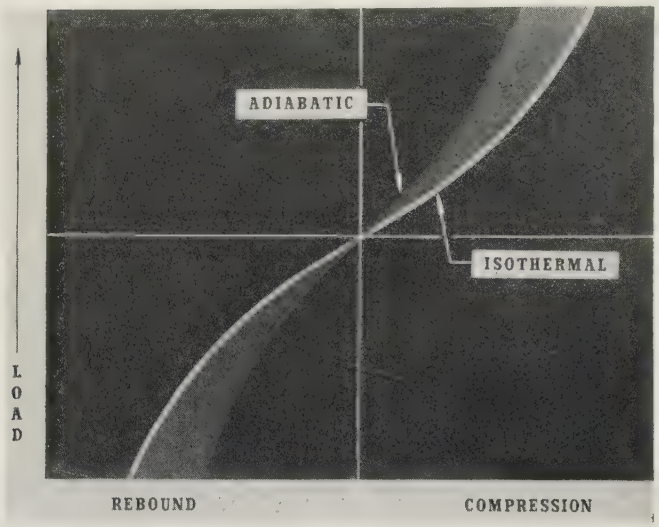

Fig. 2 — Load deflection curve

characteristics may be summarized as follows:

1. Should be designed into the same space as the present coil spring.
2. Any desired spring load deflection characteristics must be attained.
3. Should be adjusted for any height position under any loading condition.

Design of Air Spring

Reference to an air spring (Fig. 1) shows a basic air spring which consists of:

1. Air can which contains a volume of air.
2. A diaphragm or bellows which is basically a rolling seal.

3–4. Piston and skirt. Together they define the contour for the diaphragm to roll between.

In designing an air spring we have three main parameters which may be used to specify a spring for a given load and a required load deflection curve. These are: volume, pressure, and effective area.

Load carried by a spring may be defined as a product of the pressure and the effective area, that is:

$$F = P_g A$$

but:

$$P_g = P_a - 14.7$$

and:

$$P_a = \frac{P_o V_o^N}{V^N}$$

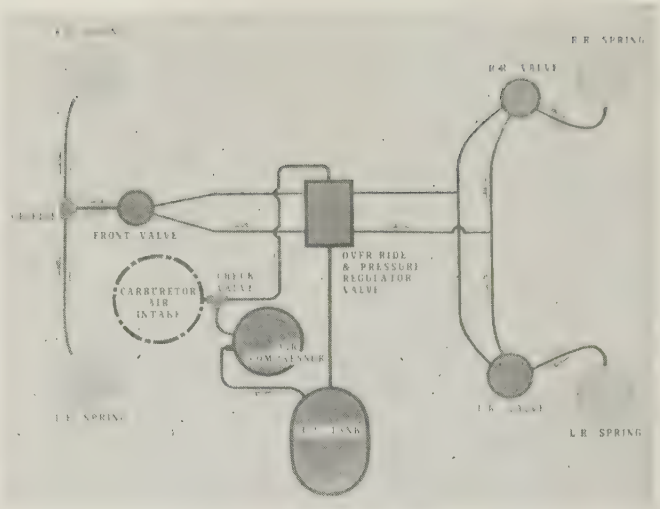

Fig. 3 — Pontiac's air-spring system

then:

$$F = \left[\frac{P_o V_o^N}{V^N} - 14.7\right] A \qquad (1)$$

where:

F = Load carried, lb
P_g = Gage pressure, psi
P_a = Absolute pressure, psia
V = Volume, cu in.
N = Gas constant
A = Effective area, sq in.

Subscript o refers to static position

Rate is the slope of the load deflection curve. Therefore, when the equation for load is differentiated with respect to displacement, the rate equation becomes:

$$\frac{df}{dx} = R = \left[\frac{P_o V_o^N}{V^N} - 14.7\right]\frac{da}{dx} - \frac{N P_o V_o^N A^2}{V^{(N+1)}} \qquad (2)$$

Since the gas constant N is 1.4 for adiabatic conditions and 1 for isothermal conditions, the spring will have two different load deflection characteristics that form the limits to the band within which the spring will operate (Fig. 2).

At the static point $F = P_g A$:

$$\text{Adiabatic Rate} = P_g \frac{dA}{dx} - \frac{1.4\,(P_g + 14.7)\,A^2}{V} \qquad (3)$$

$$\text{Isothermal Rate} = P_g \frac{dA}{dx} - \frac{(P_g + 14.7)\,A^2}{V} \qquad (4)$$

The parameters in the above relationships are F, P_g, A, V, $\frac{dA}{dx}$, R_a, R_i. Whenever four of them are assigned, the other three may be calculated. As shown above, when the pressure is increased, the area and the volume will decrease for a given load and rate.

After the basic spring effective areas have been determined, a piston, skirt, and diaphragm combination must be designed. This may be done by layout but this is a very time-consuming and tedious task. However, if high-speed computing equipment is available, the job may be done quickly and cheaply with the added advantage that a number of parameters may be changed and the desired spring may be chosen from a large selection. For example, on the 704 IBM computer, we recently designed six

springs for various rates and pressure in a total computing time of 4 min.

Air-Spring System

The basic components of the system are:

1. Air compressor — to supply the spring with compressed air.
2. Air tank — to store a reserve of high pressure air.
3. Height control valve — to admit or exhaust air from the spring.
4. Air spring.

Fig. 3 shows the schematic layout of the four springs and 3-wheel valve system configuration which is the typical 1958 Pontiac installation. This is a modified closed-cycle system; that is, the gas medium (air) is obtained from the atmosphere, compressed, and used in the system while exhaust of the springs is released to the atmosphere and/or to the intake of the compressor so that only the make-up air is obtained from the atmosphere. The system would lose air if it were exhausted when the engine was not running.

The front two springs are interconnected with an orifice, so one valve admits and exhausts for the two front springs at the same time. Each rear spring is controlled by an individual wheel valve.

Following the circuit, starting from the atmosphere, air is compressed with an air pump and stored in the high-pressure tank. The tank is connected to a pressure regulator valve. This valve outlet leads to the front height control valve and both of the rear height control valves; these valves are connected to the springs and their exhaust line runs back to the pressure regulator valve again. In turn, the pressure regulator valve leads to a junction block, which exhausts the air to the atmosphere and/or to the compressor intake. This junction block is located in the carburetor air cleaner which behaves as a silencer and air cleaner for the system at the same time (Fig. 4).

Compressor — The compressor (Fig. 5) is a single-stage twin-cylinder, 90-deg V-type assembly, having a displacement of 5 cu in. per revolution and a terminal pressure of 250 psi. It is a self-contained unit receiving its lubrication from a reservoir mounted on the rear. The compressor is driven by the same pulley as the power steering pump if the car is so equipped and mounted on the engine. The compressor uses the engine air cleaner for intake air.

High-Pressure Air Tank — The high-pressure tank is mounted on the front sheet metal next to the radiator (Fig. 6). The air inlet and outlet is mounted

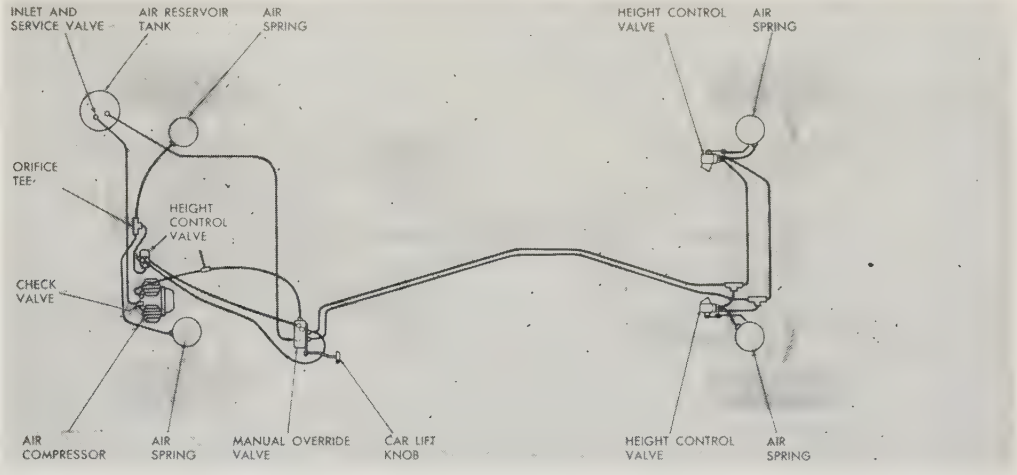

Fig. 4 — Layout of Pontiac system

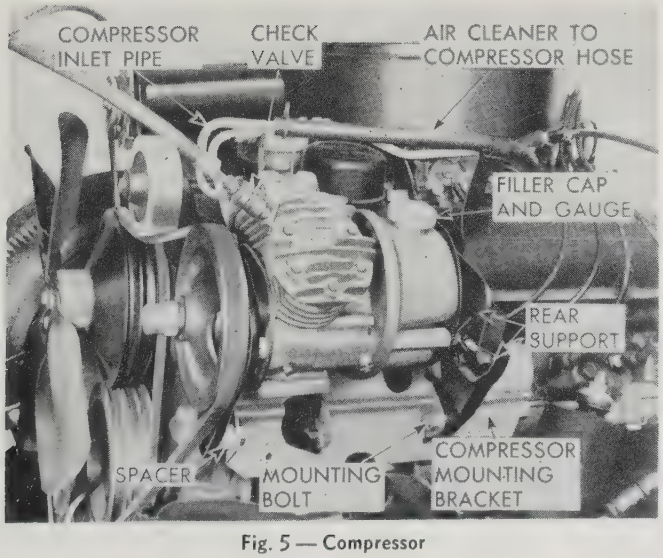

Fig. 5 — Compressor

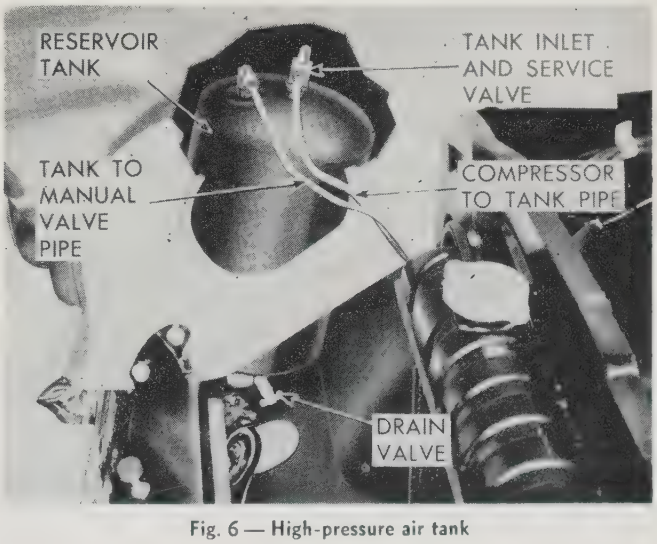

Fig. 6 — High-pressure air tank

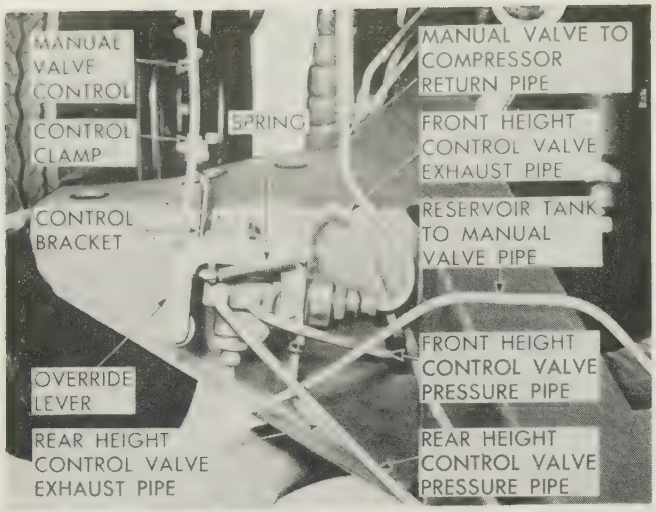

Fig. 7 — Pressure regulator and override valve

near the top of the tank and the drain plug is at the bottom. The tank has a displacement of 550 cu in. and is designed and tested for a 1200-psi burst pressure.

Pressure Regulator and Override Valve — The pressure regulator and override valve combination unit is located on the frame under the firewall (Fig. 7). It is a simple spring-loaded pressure regulator which regulates the high-pressure tank supply air pressure for the height-control valve to 125 psi. This valve is manually controlled by cable connection to a knob on the dash. This permits the driver to override the control system by switching the high-pressure side to the exhaust line. This will lift the car to the rebound bumpers. This feature has been tried and proved to be very useful in such instances as going over ditches and through fields or over the obstacles higher than the ground clearance would normally allow, as well as adding stability for jacking. The regulator valve has a 0.030-in. orifice at the exhaust side which restricts the exhaust of the springs.

Height Control Valve — There are only three valves employed, since three points determine a plane. Any more reference points could cause an unstable condition. All valves are mounted solidly to the frame. At the front, the valve is connected to the roll bar and at the rear they are connected to the rear suspension lower control arms. (See Fig. 8.)

Each valve body contains two Schraeder valves which are operated by an arm. The valve body is normally at the same pressure as the spring and is connected to the spring with a ball check restricted fitting. The intake valve from the reservoir is a push-type valve and also a check valve in series which prevents leakage of air from the spring to the high-pressure tank in the event the pressure in the high-pressure tank drops below the spring pressure. The exhaust valve is a pull-type valve and normally is sealed by the pressure in the valve body. The arm is provided with an adjustable dead band between intake and exhaust which regulates the sensitivity of the valve.

Air Springs — All four springs are basically the same except for the front and rear piston contour. The volumes are different for different arm ratios

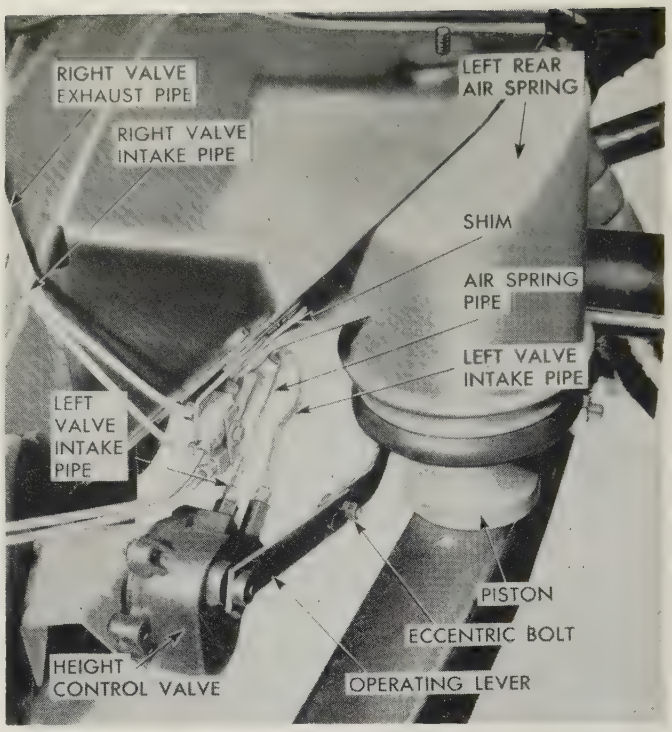

Fig. 8 — Height-control valve

and different wheel rates and loads. (See Fig. 9.)

Methods of Height Correction — When the system is installed on the car, the valve arms are adjusted to keep the car at designed position regardless of the load and its distribution in the car. For example, assuming three rear-seat passengers and a driver enter the vehicle, immediately rear and front suspension go into jounce. In the rear, the valve arms are connected to the lower control arms of the rear suspension so that they are displaced. This arm motion opens the valve to let air from the reservoir (high-pressure tank) via the pressure regulator to the spring. The quantity of air in the spring is increased and the car automatically rises. Since the valve arm is connected to the lower control arm, the arm is moved in the direction which cuts off the air. Just before the predetermined design height is reached, the air is cut off thus leveling the car. The same thing takes place in the front except both front springs are controlled by the same valve which senses the position through stabilizer bar. The right and left front springs are interconnected through an orifice, the purpose of the orifice being to prevent air transfer from one side to the other during the car roll.

Development of Air-Spring System in Pontiac Cars — Pontiac Motor Divison spent about three years in the design and development of the air-spring system. During this period more than 400,000 miles have been covered by the car equipped with air springs. This mileage includes Belgian Blocks, General Motors Proving Ground Road Test Schedules, cross-country, high altitude, and city driving under all climatic conditions. As many as five other basic control systems and combinations were evaluated before this system was finally selected, including:

1. Lockout system — which corrected the height and altitude of the car statically and locked out the

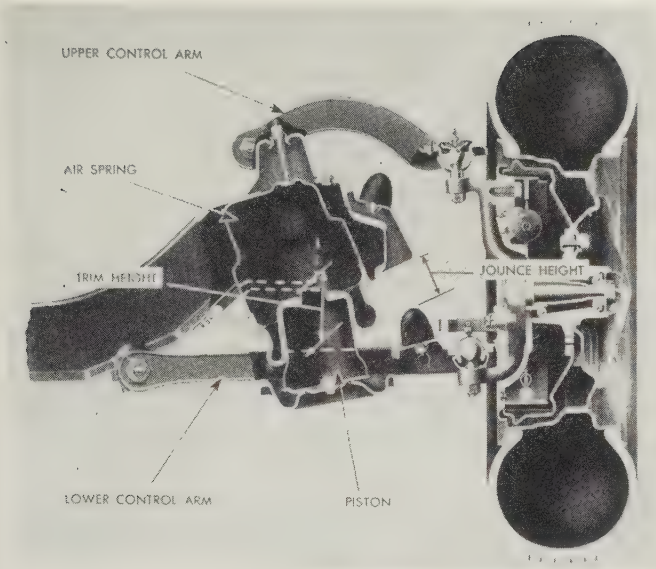

Fig. 9 — Air springs

springs dynamically. This was rejected because the temperature buildup under dynamic conditions were sufficient to pump the car up against the rebound bumpers.

2. Cross-connection — this connected the exhaust and intake of the front springs simultaneously and prevented the air transfer between the front springs during roll. This system required a double valve at the front; the performance was not sufficiently improved to justify it.

3. Blocker valve system — a flow sensitive system. The exhaust and intake valves are energized by the pressure in the lines. It did not have any transfer during roll either, but was relatively complex.

4. Close-cycle system — this system did not use air from the atmosphere and the pump. Therefore, to run continuously in order to complete the cycle it needed an added low-pressure tank in the system.

5. Open-cycle system — which exhausted the air to the atmosphere and the pump continuously made up the loss from the atmosphere. This required a larger capacity pump.

The air-spring cars are designed for lower wheel rates; and for lower rates considerably less friction can be tolerated in the suspension, since the decrement per cycle for coulomb damping is inversely proportional to the spring rate of the system. The magnitude of friction in the standard Pontiac car suspension is satisfactory for coil springs; however, for the lower rate air spring suspension, rubber bushings on the control arms are specified. The rubber bushings, of course, add some rate to the system but it has been compensated for by the design rate of the air spring.

In summary, it can be seen that the air spring as used by Pontiac meets all three of the design objectives we specified initially. By choosing the proper pressures and rates we can hold the volume required in the space available for the coil spring. The rates may be varied in any manner desired, and the car can be held at a given design position regardless of the load.

1958 Cadillac Air Suspension

by E. W. Anderson

It has long been the aim of automotive engineers to reduce the spring rates and suspension frequencies to provide a smoother and softer ride for the passenger. Around 1910 a great majority of the automotive manufacturers were using longitudinal semielliptical springs coupled with one-piece axles front and rear. The spring rates were high and the static deflections were in the range of 3–5 in. front and rear. (Static deflection = sprung weight ÷ wheel rate.) The front rates were high for steering purposes and the rear rates had to be approximately the same for overall balance. This combination of rates served its purpose but left a great deal to be desired by the passenger as he was bounced down the street by his car. In the years that followed, it was found that if the static deflection of the front suspension was higher than the rear it would give the car better fore and aft pitch balance, but this was not practical with the solid axle. In the early 1930's, the independent front suspension was adopted and this permitted higher static deflections of the front suspension without affecting the steering characteristics. By 1935 the static deflection of the front suspension had increased to 9 in. while the rear remained at about 8 in. This produced a better pitch balance and reduced the ride frequencies. The next 20 years brought many suspension refinements but only a slight change in ride frequencies. Styling, horsepower, and space limitations more or less closed the door on further reduction in the rates of conventional springs. Therefore, it was apparent that an entirely new concept for springing the car was required. Ideally, the new suspension would provide low spring rates to produce a low-frequency ride. Furthermore, it would provide a constant-frequency ride and a constant standing height independent of passenger or trunk load. The suspension selected by Cadillac as an option to the conventional springs was air suspension. Since the rate of the air spring increases with air pressure and air pressure increases with load, the air suspension has ideal rate-versus-load characteristics to provide a constant frequency ride at any load.

Air springs when used on the 1958 Cadillac give spring rates and ride frequencies that are lower than the 1958 model with coil springs:

	Effective Static Deflection, in.		Ride Frequencies, cpm	
	Front	Rear	Front	Rear
1958 Steel	12	9	60	70
1958 Air	23	14½	43.5	60.0

The lower ride frequencies give a pleasingly slow-moving flat ride which is noticeably less fatiguing to the passengers than that obtained with the more conventional frequencies.

New problems were created when air springs with approximately 50% less rate were used on the car. The past practice has been to design the steel spring suspensions with the fact in mind that the car will be at one height for curb load and successively lower as one to five passengers are loaded in the car. If the same analogy was used to design the suspension with 50% lower rate air springs, the dif-

ference between curb height and five-passenger height would be twice the band of the higher rate steel springs and would not be practical from the suspension ride travel standpoint. Furthermore, the large change in car altitude from curb to load conditions would detract from the car's styling lines. To overcome this characteristic of large static deflections during loading, it was necessary to design a system that would detect any change in load, and automatically correct the suspension to the optimum design height. We shall refer to this as an "automatic leveling system."

The automatic leveling system's primary purpose is to maintain a constant car height. Furthermore, it must provide foolproof leveling action and at a uniform flow rate. To achieve these results, the following components are used in the Cadillac automatic leveling system: three leveling valves, compressor, high-pressure check valve, high-pressure storage tank, pressure regulator, air lines, and flow control orifices. (See Fig. 10.)

Number of Leveling Valves — Some of you have probably been wondering why the Cadillac leveling system has three leveling valves instead of four. Before this is explained, let us state a hypothetical case. Suppose you had to perform a delicate job that required a steady table. You have the choice of two tables — one has three legs and the other four. A drawback is that each table has one leg that is longer than the others. You would choose the table with three legs because it will be stable and not rock, even though one leg is longer than the other two. If a weight was placed on the centroid of each table, each leg of the three-legged table would carry one-third the total load, whereas, the total load on the four-legged table would be carried by the long leg and the diagonally opposite leg. Imagine, now, a leveling system with four valves, one at each wheel. If each valve was set perfectly and had a zero free center, the system would operate effectively, just as a table with four equal-length legs will be steady on a level floor. Now suppose that, because of production variation, one of the front leveling valves causes the car to be high at that corner. Now a condition exists where most of the weight of the car is distributed between the high corner and the diagonally opposite corner, as the four-legged wobbly table.

This condition on a car would cause many undesirable characteristics such as: erratic braking due to unequal tire-to-ground loads, poor handling, and undesirable ride with a tendency to waddle on a diagonal axis. These undesirable characteristics are prevented by the Cadillac system of three leveling valves — one in the front and two in the rear (one at each air spring). If any one of the three valves is slightly out of adjustment, the weight is still distributed equally on all three points, as on the three-legged table.

In a three-valve system the single valve controls the vertical level only at its location, while the other two valves control the lateral level of the entire car as well as the vertical level at each location. Two leveling valves were placed in the rear of the suspension due to the weight distribution characteristics of the passenger and trunk loads.

Type of Leveling Valve — The leveling valve that controls car height is a simple device that has an intake valve and an exhaust valve of the tire-valve type that will transfer air either to or from the spring when actuated. The free travel between these valves and the valve arm linkage ratio determines the static leveling sensitivity of the suspension. The free travel is held to a minimum in the leveling valves and a $\pm \frac{1}{4}$ in. leveling sensitivity results. Dynamic operation of the leveling valve increases the sensitivity to about $\pm \frac{1}{8}$ in. due to averaging in the free-travel band. The leveling valves are frame mounted and are connected to the suspension arms in the rear, and to the center of the stabilizer bar in the front, by links which translate body or wheel motion. The front valve is actu-

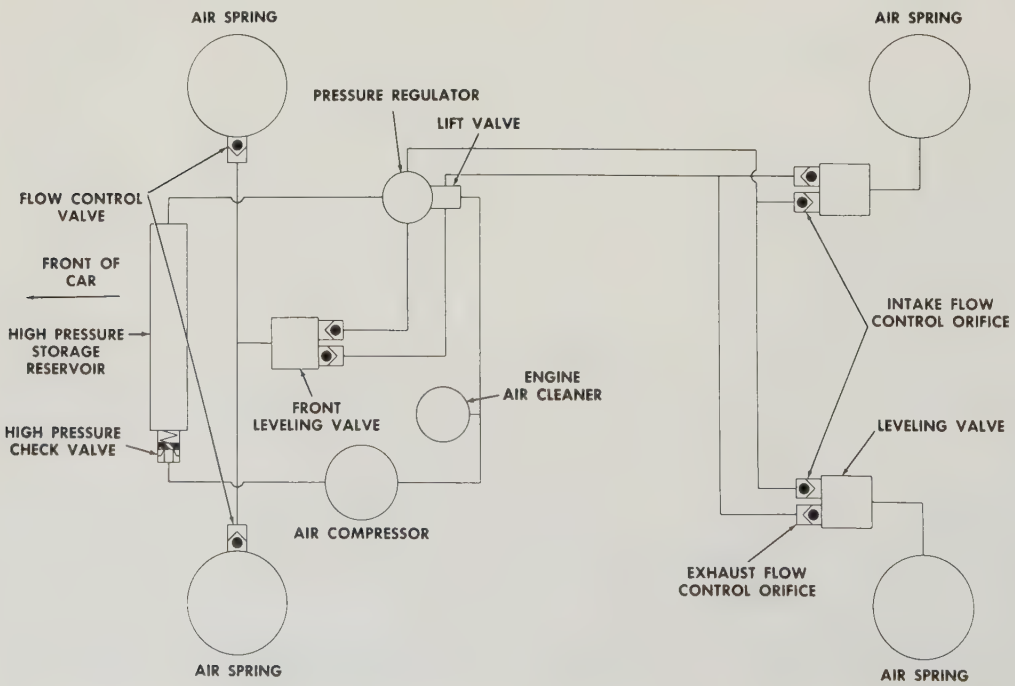

Fig. 10 — Cadillac's leveling system

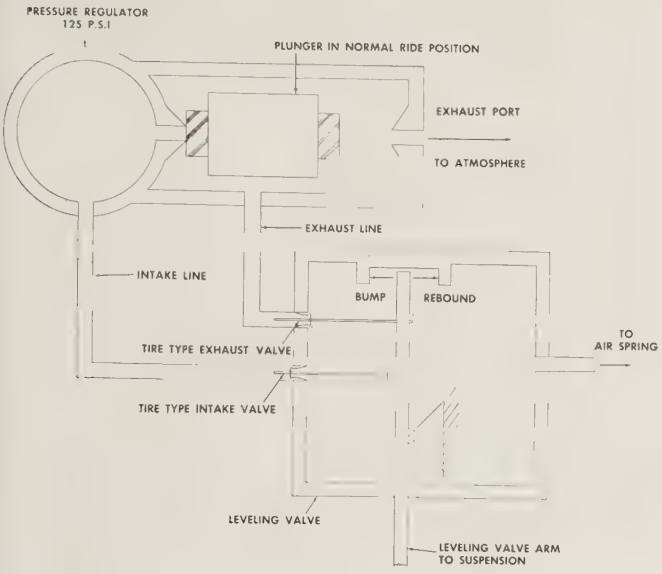

Fig. 11 — Lift valve of Cadillac system

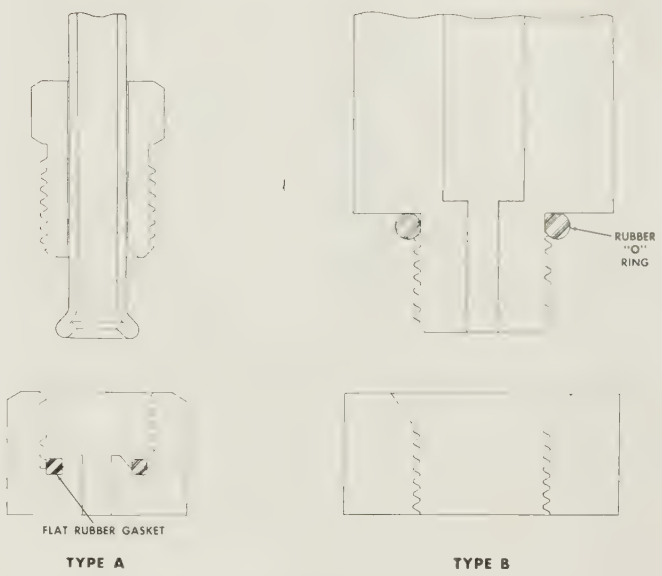

Fig. 12 — Air line fittings of Cadillac

ated in vertical ride motion only and remains closed when the two front wheels are moving in opposite directions, vertically, as experienced in body roll during cornering.

Air Compressor — The belt-driven compressor supplies all the air for the suspension. At engine idle the air delivery is 0.65 cfm of free air at 125 psi and at an absolute intake pressure of 14 psia. Under the same conditions but at a higher engine speed, the maximum delivery is 2.3 cfm with a horsepower consumption of 1.4 hp. The maximum pressure in the air reservoir is 300 psi. This is determined by the compression ratio of the compressor, that is, the volume of air compressed from bottom dead center to top dead center in the relationship of $P_1V_1/T_1 = P_2V_2/T_2$ determines the maximum pressure the compressor will deliver. The delivery and pressure decrease at lower intake pressures, as experienced at high altitudes. However, the compressor will supply all the demands of the leveling system at altitudes up to 14,000 ft.

Flow Control — The flow control orifices have a very important function in the dynamic operation of the leveling system. They are necessary to control the airflow rate during handling, braking, acceleration, and passenger load changes. A pressure regulator set at 125 psi is incorporated in the system to give consistent results during the above conditions. The desired leveling characteristics during handling are controlled by: (1) the intake and exhaust flow control orifices at each leveling valve, (2) the stabilizer bar connection of the front leveling valve, (3) the flow control orifices placed at each front spring. During a turn the system will operate in the following manner: the intake flow control orifice at one rear valve will allow a slight intake of air. The opposite rear valve will allow a slight exhausting of air. The front leveling valve is inactive due to its position at the center of the stabilizer bar (zero angular rotation) and the flow control orifices at each front spring prevent a high transfer of air between the springs during the turn. The resultant level of the car after the turn is within the design limits. Therefore, only a slight leveling action takes place during turns and this does not detract from the car's good handling characteristics.

The orifices at each leveling valve prevent adverse leveling during braking and acceleration. They also control the leveling time during load changes. This action is subtle, taking 30 sec to correct for a 5-passenger load change.

High-Pressure Reservoir — The high-pressure tank is a reservoir that stores a supply of air for suspension operation when the compressor is not running. It has a manual drain valve that can be used if oil or water vapors should accumulate. The reservoir has a capacity of 300 cu in. and provides a reserve of high-pressure air more than sufficient to level the car from curb to full load without additional air from the compressor.

Lift Valve — The lift valve incorporated in the leveling system is a manually operated valve that can be actuated by the driver anytime he desires added road clearance. This feature is desirable when such conditions as flooded streets, snow drifts, deeply rutted country roads, or a steep driveway, where added ramp or departure angles would make added ground clearance a valuable asset.

The lift action is achieved by diverting regulated 125 psi air into the leveling valve exhaust line system after sealing off the common exhaust port to the atmosphere. (See Fig. 11.) The double-ended plunger in the lift valve performs the diverting and sealing operations. As the air is diverted into the exhaust lines the pressure builds up, lifting the exhaust tire-type valve in each leveling valve off its seat, and allowing the air to pass directly into the spring. The addition of air in each spring raises the car to give the added road clearance.

The lift action is also utilized during the shipment of the cars. The cars are driven on the haul-away or railroad cars at design height and tie-down chains are placed loosely on the frame. The lift valve is then actuated, raising the car and tightening the chains.

Air Lines and Fittings — From the conception of the Cadillac air suspension idea, it was realized that

the leveling system would have to be 100% leak free. To achieve this, two distinct types of fittings are used (Fig. 12). Type A has a flat rubber gasket in the female fitting and is used in conjunction with the SAE standard double-flare tube and nut. All tubing in the leveling system has this type of fitting and seat. Type B, with the rubber "O" ring gasket on the male thread is used on fittings at the air-spring reservoirs and the high-pressure storage tank. By using rubber to seal against leaks, the fittings need to be torqued only to 5 ft-lb to prevent them from vibrating loose. This feature is desirable from the manufacturing and service standpoint. The "O" ring principle is also incorporated in the design of the leveling valves and air springs to effectively seal against leaks.

The 3/16 in. OD tubing used throughout the leveling system is made of copper to avoid any possibility of rust forming and entering the leveling components.

Conclusion

The air springs on the 1958 Cadillac give a new and better ride and the automatic leveling system provides the control that makes this possible.

The Edsel Air Suspension

by Robert D. Harrison

Very soft springing for passenger cars has long been recognized as a giant step towards providing the American public with the ultimate "floating on a cloud" type of ride. To design or manufacture conventional steel springs with very soft springing is not at all difficult. Every manufacturer has experimentally tested such a vehicle with low-rate springs and knows that under certain specific road and load conditions the vehicle is significantly superior to the conventional sprung car. This same vehicle, however, when unloaded looks ridiculously high and when fully loaded practically rides on the compression bumpers. Handling and road stability suffer because of excessive body roll and special costly provisions must be made to incorporate the longer, larger steel springs necessary to obtain the lower rates.

Moreover, since steel springs are essentially constant rate devices, very soft springing presents difficult problems in providing adequate cushioning at the jounce and rebound stops. Passenger-car suspensions to date, then, have consistently been a compromise in order to have a degree of softness yet retain acceptable handling characteristics, rough road control, and styling car height appearance.

For these reasons air as a spring medium was investigated. The air suspension in its simplest form is no more than a rubber ball full of air placed so that the passenger or load is isolated from the unsprung mass or the rolling wheels. The container of air or air spring as we know it today was recognized as a suspension device many years ago. In fact, on Jan. 3, 1905, a patent was issued to a Mr. H. E. Irwin to cover his design of a heavy rubber enclosed volume of air that separated the bed of a wagon from the spoked wheel axle. Air suspension as a concept is quite old. But the refinements and provisions necessary for its satisfactory operation as applied to a high-speed passenger car are quite new.

The Edsel air system (Fig. 13) was designed to overcome the shortcomings of low-rate conventional steel-spring suspensions and yet to retain the proved acceptable handling qualities of standard rate suspensions. The air spring provides a soft pitch free ride, a small but worthwhile reduction in harshness and road noise, and yet displays a phenomenal ability to absorb the severest road conditions encountered anywhere. These benefits are accomplished by an automatic leveling system,

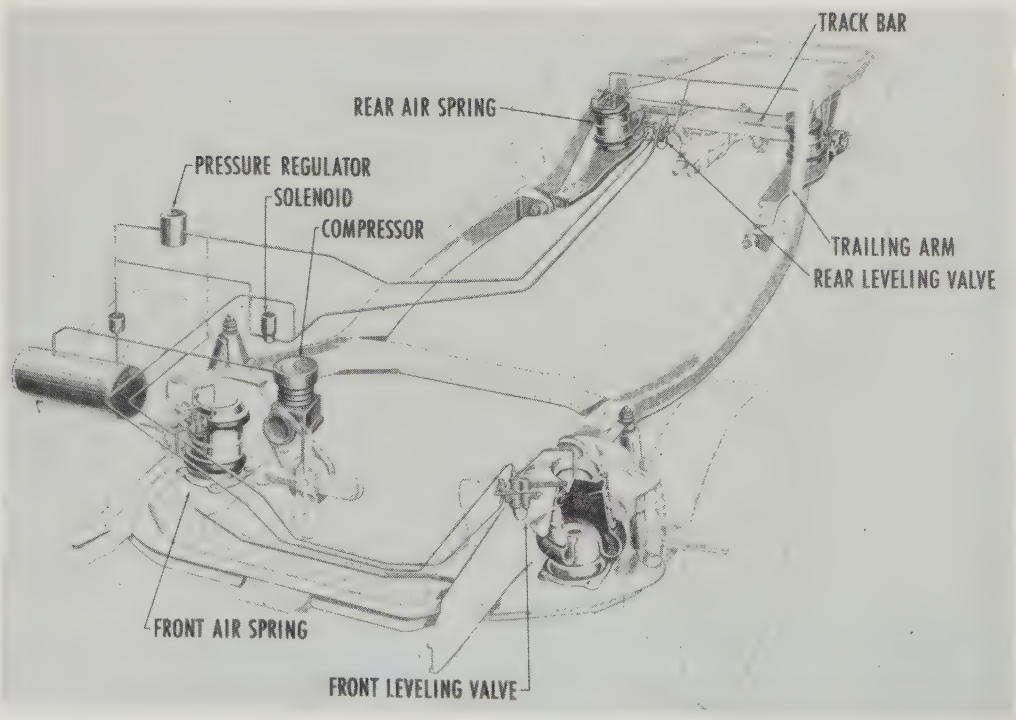

Fig. 13 — Edsel's air-suspension system

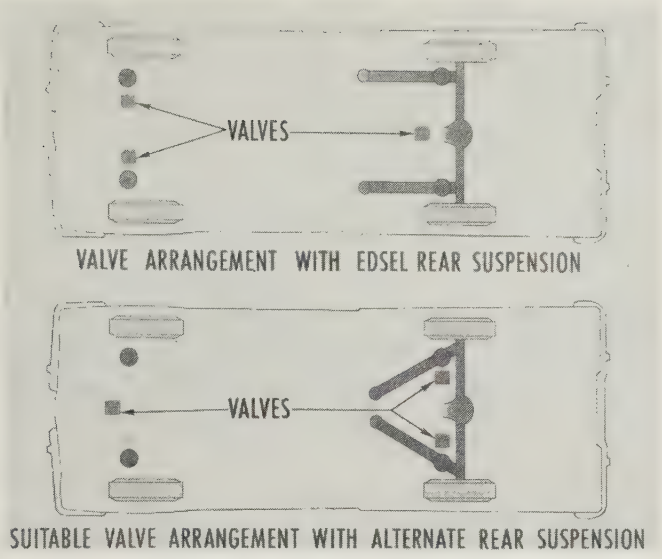

Fig. 14 — Leveling valve arrangement

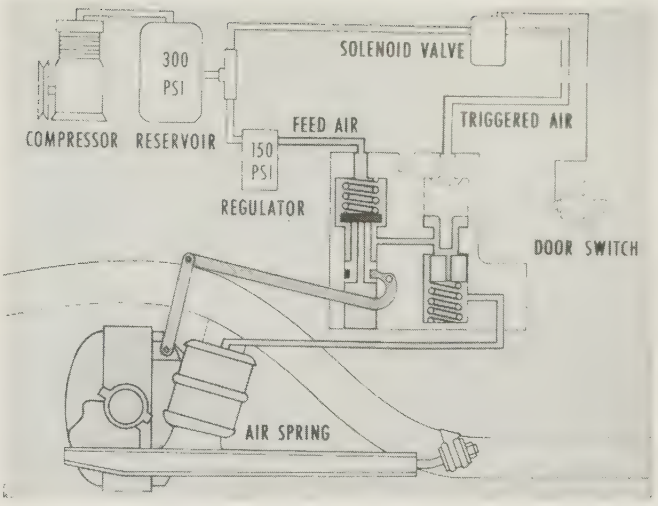

Fig. 15 — Leveling operation (slow)

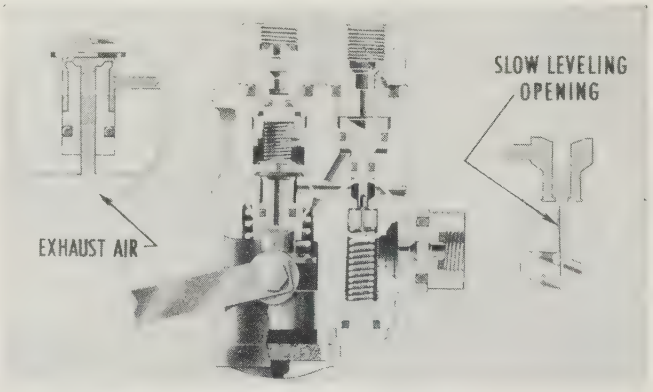

Fig. 16 — Leveling valve, slow-leveling operation

ultra-soft normal springing, and a smooth rate buildup pattern in jounce and rebound. The Edsel air suspension in its assembled form is composed of three major systems which are interconnected by copper and nylon air lines. These systems are: air supply system, control system, and spring system.

Air Supply System

The air supply system consists of two items, a compressor and a reserve air tank. The specially developed compressor is a single-cylinder unit, engine mounted, belt driven at approximately engine speed, and lubricated by engine oil. The compressor has a maximum power requirement of about 1 bhp with a balance pressure of approximately 300 psi. Compressed air is delivered through a flexible hose and a check valve to the tank which is mounted in the right fender just aft of the headlamp. The 400-cu-in. displacement tank at 300 psi provides enough air for three complete fill-and-exhaust cycles of the four air springs. The tank also includes a manual drain valve at its lowest point for removal of any accumulated moisture.

Control System

Of all the components that compose the control system, the most important are the leveling valves. As its name implies, the function of the leveling valve is to maintain the vehicle at the correct car height regardless of the passenger load or road condition. There are three valves in the system to establish a relative platform between the sprung and the unsprung mass (Fig. 14). Two of the valves are located at the front while one valve is located at the rear. This arrangement was selected for two reasons: more accurate leveling and better handling. The reason for the improved leveling is rather obscure except for perhaps the visual attitude of the car to the driver. The effect on handling, however, is quite apparent. The Edsel rear suspension geometry provides sufficient roll control so that little roll resistance is required from the rear air springs. Air is permitted to flow freely between the springs. It may be pointed out that if a different rear suspension arrangement were employed (bottom of Fig. 14) it is entirely possible that the car would require the dual-valve location at the rear suspension. The use of two valves at either the front or rear separates the two springs pneumatically and, therefore, utilizes their roll couple effect.

Each of the three leveling valves is mounted on the chassis frame with an actuating lever linked to the unsprung mass. This means that the leveling valve, with a small null range, is in constant operation and, therefore, continually refills and exhausts air from the springs during any normal jounce or rebound movement. This continual action of the valves is known as the slow-leveling system and is in operation whether the car is driven or in the parked position. Incorporated in the same valve assembly, there is also a fast-leveling circuit that functions only when a door is opened. The valve design brings about a dual or "slow-fast" continuous height control system. The reasons for this design will become apparent.

The leveling valve operation is fairly straightforward when it is known that the fast-leveling fill-and-exhaust cycles differ from the slow cycles only in the respect that air flows around an orifice rather than through it.

Air for the slow-leveling system is obtained from the reservoir at 300 psi through a regulator valve at 150 psi (Fig. 15). As the valve control arm is rotated, a cam attached to the arm causes the plunger

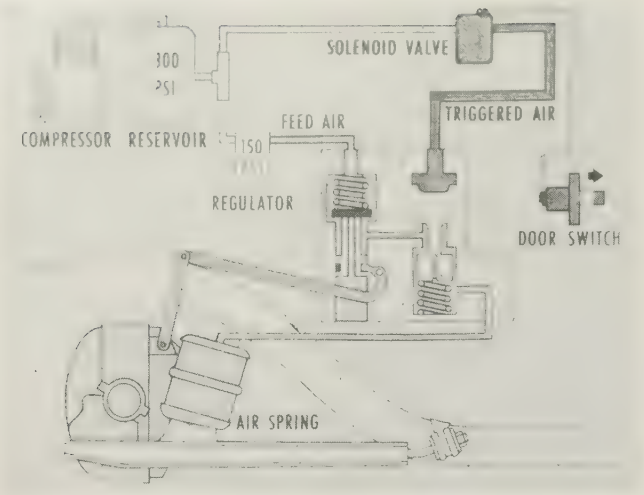

Fig. 17 — Leveling operation (fast)

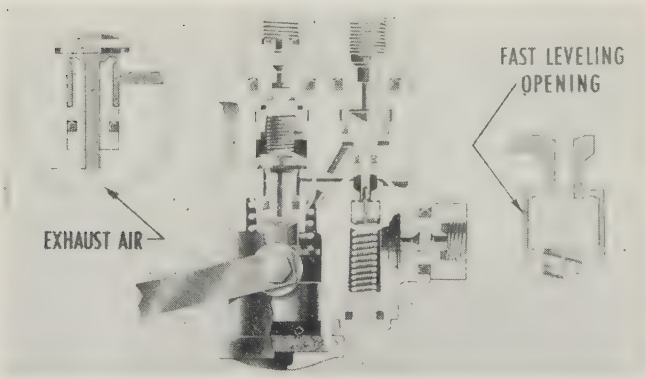

Fig. 18 — Leveling valve, fast-leveling operation

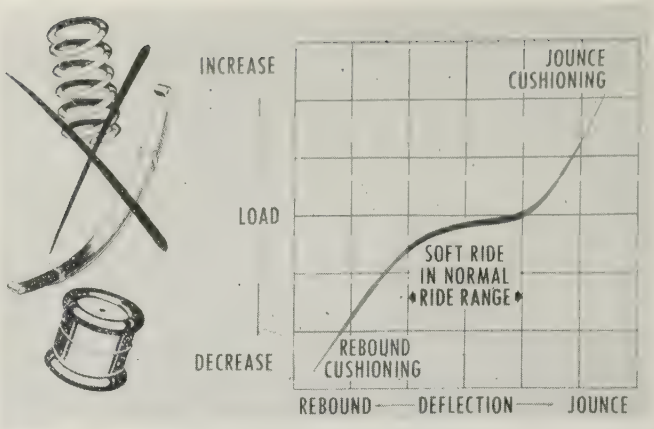

Fig. 19 — Air-spring characteristics

Fig. 20 — Load characteristics, static versus dynamic

to move up if the car is too low, down if it is too high. An upward movement of the plunger lifts the seal disc off its seat, admitting air at 150 psi to the valve passage. The air passes slowly through the restricted orifice to the appropriate air spring or springs (Fig. 16). Similarly, if the car is too high, the plunger moves downward away from the seal disc and exhausts air from the spring via the orifice and passage and then through the vertical hole in the middle of the plunger to the atmosphere. The size of the orifice is small enough to prevent rapid leveling whenever the vehicle is in a roll, climbing, or braking attitude. It might be of interest to note that the hole is comparatively large because of a simple self-cleaning device. A wire pin that is allowed to float has been passed through the hole, thus preventing clogging of the orifice in the event that foreign material reaches the valve assembly.

The slow-leveling system would eventually level the vehicle for all load and road conditions. With this system, however, it would be somewhat disconcerting for the average customer to find he must wait a relatively long period of time before his car could clear the driveway ramp after three or four passengers have entered. To overcome this difficulty a fast-leveling circuit has been provided in the same valve assembly (Fig. 17). Air is supplied at 300 psi directly to the valve by nylon lines through a solenoid valve which is electrically operated when a door is opened. The high-pressure air triggers the fast-leveling plunger which unseats the nylon piston through which the slow-leveling orifice passes (Fig. 18). The unseated piston thus allows air from the regulator valve to flow comparatively unrestricted through the valve passage to raise the car if required and similarly allows free passage of air if exhausting is called for by the leveling valve.

Reference has been made of a pressure regulator valve in the line from the reservoir to the leveling valve at 150 psi. This valve serves the specific function of maintaining an approximate balance between the system-to-spring and the spring-to-atmosphere differential pressure. The balance is primarily required for rough road operation where the leveling valves are working continually. If, for example, the system were operated at 300 psi reservoir pressure, there would be an 80 psi differential to exhaust the rear springs and a 220 psi differential to fill them. On a long stretch of rough road, far more air would be admitted during jounce motions than could be exhausted during rebound motions. The car would soon be riding hard against the rebound stops in spite of the highly restricted passages in the leveling valves.

Since the leveling valves are in continuous operation, a provision was included to prevent extreme leveling action when not desirable. This condition might occur when jacking for a flat tire or when the car is parked with one wheel in the rebound position. To solve this problem, T-check

valves were inserted between the springs and the leveling valves to prevent the springs from exhausting below a set minimum pressure.

Air-Spring System

The load deflection curves of any suspension can describe the basic ride characteristics of a vehicle rather completely. The curve with the characteristics as indicated (Fig. 19) is a typical load deflection diagram of the Edsel air suspension. The flat slope in the middle portion of the curve indicates exceptionally soft ride movements in the normal ride range. With larger wheel movements the slope of the curve becomes gradually steeper both in the rebound and jounce position. This smooth transition of the curve from the normal to the extreme wheel positions indicates excellent rough road cushioning.

The use of air as a spring medium, however, presents a major problem because air is inherently a variable element. That is, the exponential value of N in the gas formula $PV^N = K$ varies from the limits $N = 1$ to $N = 1.4$, depending upon the rate of compression or expansion of the air. The slope of the curve thus changes depending upon the value of N. For the value of $N = 1$, (that is, the static load deflection curve) the Edsel has a suspension rate of approximately 20 lb per in. (Fig. 20). The static wheel rate is highly important for it must be sufficiently positive to provide good stability when accelerating or when approaching and emerging from curves. The static rate also portrays the car's response to load changes or, in effect, its leveling behavior.

The corresponding dynamic load deflection curve for the same spring is also shown (Fig. 20). This curve was obtained electronically while the spring was being deflected at approximately sprung mass resonant frequency. It is seen that the dynamic rate is four times that of the static rate at 80 lb per in. Although the dynamic rates are considerably higher than the static rates, they provide bounce and pitch frequencies in the neighborhood of 50 and 55 cpm respectively on the Edsel cars. These frequencies are sufficiently low for the attainment of excellent riding qualities.

This points out one of the major pitfalls in the development of low-volume air springs. In an effort to reduce dynamic rates it is all too easy to arrive at a negative rate at the normal riding height. Among other antics that result, a vehicle with a negative wheel rate is likely to cycle slowly between full jounce and full rebound while standing at the curb.

The air-spring design (Fig. 21) is composed of four basic parts; rubber air cell, retainer band or girdle, piston or pedestal, and upper seat. The rear air springs, in addition, include clamps at both upper and lower seals to prevent unseating if the shock absorbers are disconnected while the car is on a hoist.

It is evident that as the piston travels up and down within the cell, its effective area varies considerably. The character of this area variation depends basically upon the slope of the pedestal. Since area is a factor in the rate equation, the shape of the load deflection curves can be controlled by pedestal design. It was this feature that primarily solved the problem of obtaining the smooth jounce and rebound cushioning previously shown in the dynamic curve.

In the enclosed cell type of spring with rolling lobes, rate buildup in rebound is inherent. As full rebound is approached, the spring straightens out. This decreases the lobe and, consequently the effective area while the pressure is also decreasing because of increasing volume. To provide the low normal ride rates, the pedestal is modified by giving it an inward slope. This changes the area-pressure combination to a low ride rate at normal riding heights. An outward slope at the lower portion of the pedestal decreases the effective area and provides the jounce rate buildup. Other factors may be varied to a limited extent for the final tailoring including cord modulus, rubber compounding and thickness, and the molded shape of the air cell.

The rear suspension of the Edsel car is a trailing arm type (Fig. 22). The forward end of the arm is attached to the frame by large spike end rubber bushings similar to those found in shock absorber ends. This design permits rather large axial but only small radial deflections which greatly reduces rear-end harshness without affecting rear-end steering. The rear end of the trailing arms are attached to the axle by a pair of transverse rubber bushings spaced some 5 in. apart. This arrangement ties the axle and trailing arms together in such a way that they constitute a roll stabilizing unit. The axle housing acts as a torsion member.

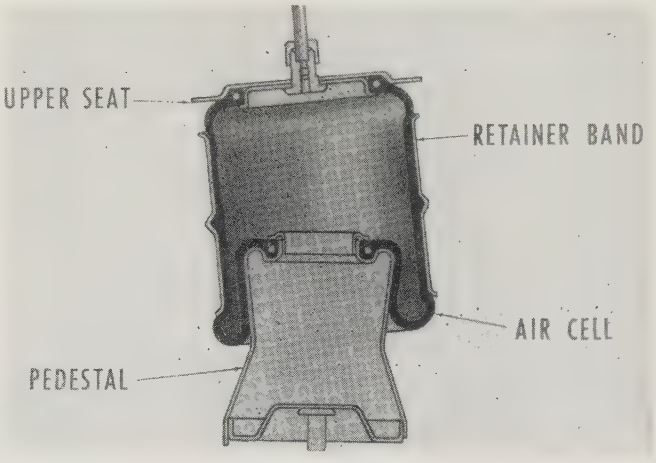

Fig. 21 — Air spring

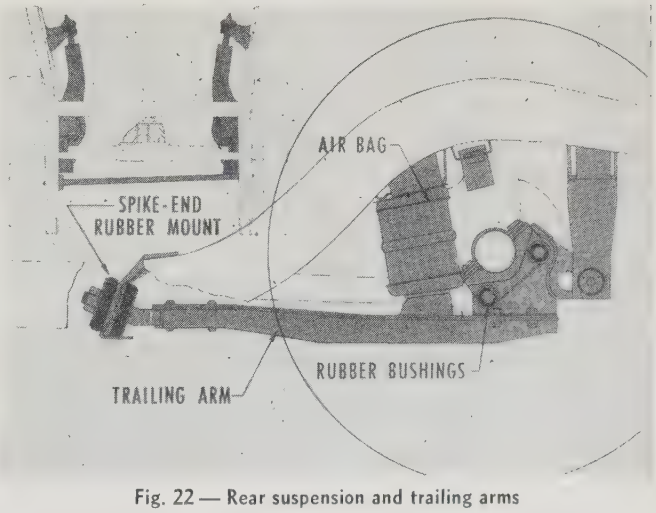

Fig. 22 — Rear suspension and trailing arms

How Performance Factors Affect Transmission Design

E. A. Richards, Rockford Clutch Division, Borg-Warner Corp.

This paper was presented at the Earthmoving Industry Conference of the SAE Central Illinois Section, Peoria, April 16, 1958.

THE overall design problem of the transmission engineer is to effect a distribution of power from a given source to a load requirement. While the most desirable distribution is affected by particular work cycle requirements and their relationship to the mechanism being used, there has always been a drive toward the development of a general purpose mechanism to make this distribution as even and as high as possible over an acceptable speed range. The infinitely variable transmission, of course, has served as the ideal for such a mechanism since the beginning and has always ranked high as subject for speculative thought. To date its technical and economic problems have prevented its widespread use.

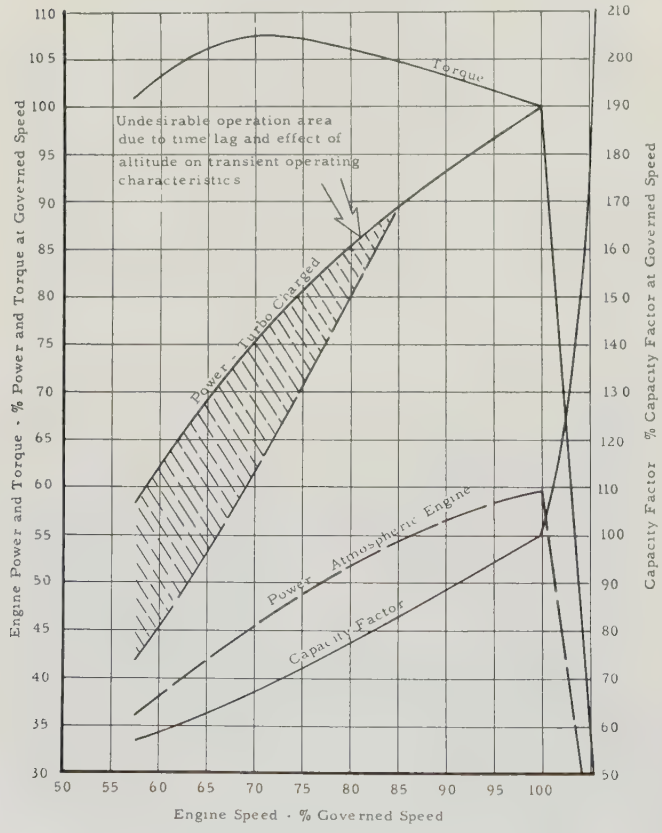

Fig. 1 — Dimensionless engine performance factors

Two acceptable approaches to the problem have been made to date. The first was, of course, through the mechanical gearbox and the second through the torque converter. This paper will touch upon some of the factors from each of these approaches. It will also deal in a general way with some of the evolving characteristics of present-day diesel engines, since these are currently the most widely used power source for heavy-duty equipment.

The general subject of the use of torque converters as a component in the drive system for heavy-duty vehicles has received considerable technical treatment. In general, its performance advantages can be summed up briefly. The converter is a very good means for establishing a condition where the powerplant is allowed to develop close to its maximum horsepower continuously. The converter transmits this power to the load but also consumes a portion of it in the process. Under conditions where the amount it consumes is less than the amount it allows the engine power to increase, the resulting power at the load is greater with a torque converter drive, and so more work is accomplished if at a sacrifice in fuel consumption.

This advantage is most predominant where the rate of change in load is great and under conditions where ratio changes in a mechanical drive are either difficult to manage or are time consuming. Such conditions predominate in vehicles where the kinetic energy content of the load is low with respect to its rolling resistance. There is considerable experience to indicate that the lower third of the operating speed range of an off-highway hauler encounters these conditions almost continuously.

It is also recognized that as the ratio of kinetic energy to rolling resistance increases, the mechanical drive improves with respect to the torque con-

verter drive. There is a point where the mechanical drive will equal the torque converter drive and also a point at which it will accomplish more work.

However, these points are also dependent on a number of variables which to date have not been sufficiently measured and analyzed to provide a basis for predictable performance comparisons. It can be accepted then that the torque converter performance advantages will be most prominent in low speed ranges and the advantages in mechanical drives will be most prominent in the high speed ranges. The balance of this situation would be shifted to some degree if the ability to power shift were to be applied to the mechanical drive. Its tendency would be to move the breakeven point in performance toward a lower ratio of kinetic energy to rolling resistance.

Recognition of the above situation has in the past suggested that a mechanism which would utilize a converter at low speeds and a mechanical drive at higher speeds would represent an effective combination. Transmission arrangements to date combine torque converter drive with mechanical drives by means of a lockup clutch in the converter. However, both the lockups and the converter ranges are alternately spaced throughout the operating speed range. In this respect, they vary to some degree with the pattern suggested by the inherent advantages of the two types of drives.

Powerplant

For this paper a hypothetical engine has been selected. It is of the high-speed turbocharged type now widely used in construction equipment.

The coordinates selected to describe its characteristics are dimensionless and should provide the reader with general performance characteristics which are quantitive without the introduction of gross error, and which can be interpreted rather easily for illustrative purposes.

Fig. 1 shows this hypothetical unit both as an atmospheric induction engine and as a turbocharged engine. It is evident that there is a very considerable increase in maximum horsepower resulting from the turbocharger. This power increase can be achieved with a decrease in bsfc.

Considerable latitude exists in the matching of the turbocharger with the engine to achieve desirable engine characteristics. One of the important factors involved in the choice of this match is the speed range over which the engine is required to deliver its power at full throttle. In general, the allowable increase in power is greater as the speed range over which the engine must operate is narrowed. This results in an interrelationship involving the transmission, the engine, and the vehicle.

Aside from the steady state characteristics as described by the performance curve, dynamic conditions involved in starting and in operational transients are present. Again, narrowing of the operational speed range of the engine increases the turbocharger power-gain possibilities.

The curve shown illustrates, in principle, the effect of turbocharging and its influence on desirable operating speed range of the engine. This is shown only to indicate its influence on the selection and arrangement of transmission components.

The engine capacity factor curve is shown with the torque and power curves. The capacity factor (used in calculating the combined effects of engine and torque converter characteristics) is made dimensionless by relating its value over the speed range to its value at maximum power, which is in this case also at governed speed.

Torque Converter

This discussion will be limited to the characteristics obtained by a single-stage multielement torque converter of the rotating housing type.

Quite a variety of characteristics can be obtained by manipulating the blading in torque converters of this type. In general, they range from low stall ratio converters with capacity factors which increase with speed ratio, to high stall torque ratio converters with factors which vary little from stall up to the point of maximum efficiency.

Fig. 2A illustrates the low torque ratio type unit. It is plotted on the conventional dimensionless coordinates used for describing converter characteris-

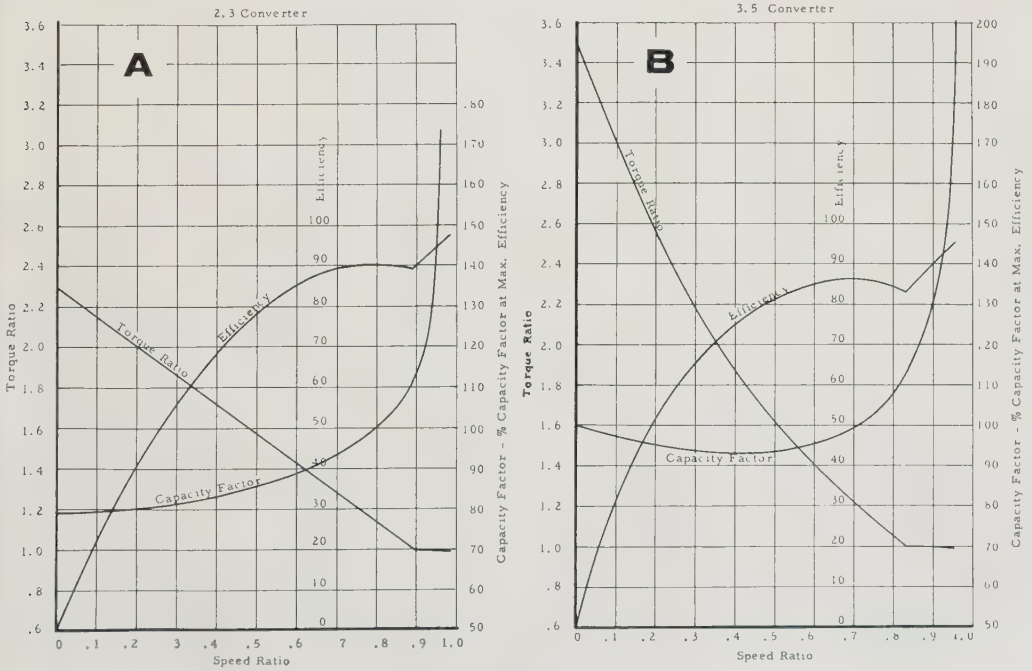

Fig. 2 — Torque converter performance characteristics

tics. The capacity factor is made dimensionless by expressing it as a ratio of the capacity factor $\left(K = \frac{N}{T^{0.5}}\right)$ at any speed ratio to the capacity factor at the point of maximum efficiency. It can be noted that the capacity factor at stall is 79.3% of the capacity factor at 0.8 speed ratio, which is the point of maximum efficiency.

Fig. 2B illustrates the high torque ratio type unit. It is characterized by a higher torque ratio at stall and a maximum efficiency that is somewhat lower and occurs at a lower speed ratio. The capacity factor becomes numerically lower as speed ratio increases up to 0.3 speed ratio and then rises until at a maximum efficiency it is numerically equal to its value at stall. As in the 2.3 converter, the capacity factor is expressed as a percentage of the capacity factor at the point of maximum efficiency. The fact that it is 100% at stall is coincidental with the blading design.

Figs. 3A and 3B show the combined effect of engine and converter characteristics on an output power basis. The power curves shown are made up of a family, each of which is expressed in terms of the percentage of power developed by the engine at the point of maximum converter efficiency. As a family, this plot illustrates the effect of the capacity of the torque converter to absorb power and the relative capacity of the engine to produce it. The curves shown represent different sized converters with similar blading and ascend in size as the power developed at the maximum efficiency point is reduced.

It can be seen that a match which favors the lower speed ranges sacrifices power availability in the higher speed ranges.

A lockup clutch is conventionally interposed to make available the desirable low-speed characteristics without making the resulting sacrifice in the higher speeds.

The effect of the capacity factor of the converter is also indicated in the corresponding family of engine speed curves. It is apparent that the capacity characteristics and the size of the converter will have much to do with the amount of turbocharging that can be applied to the engine without encountering undesirable results.

The general effect of the match can best be expressed by relating the average power availability over a speed ratio range such as would be imposed by adjacent ratios in a gearbox between the converter turbine and the load.

Figs. 4A and 4B show the effect of both the match and the size of the ratio steps on the average power availability, and the effect of the engine alone.

For an engine where maximum power is at governed speed, the highest average power available is achieved where the engine develops its maximum power at the maximum efficiency point of the torque converter.

It should be mentioned that there are two basic ways of handling the engine-converter match. One method is to use geometrically similar blading and vary the size of the converter; and the other is to maintain a constant size and to vary the capacity through blading changes. The first method preserves the performance character and the latter preserves the space relationships of the unit. Combinations of the two can also be used. In general, the converters having a uniform capacity over a wide speed ratio range tend to be slightly larger in diameter for a given engine than do those with rising speed curves. This brings up an interesting point with regard to increasing engine power through turbocharging. If converter capacities are increased within a given size range by means of blading changes, the general effect is to change the capacity curve from the flat type to one with a rising characteristic. Such a change imposes a wide operating speed range on the engine if the converter

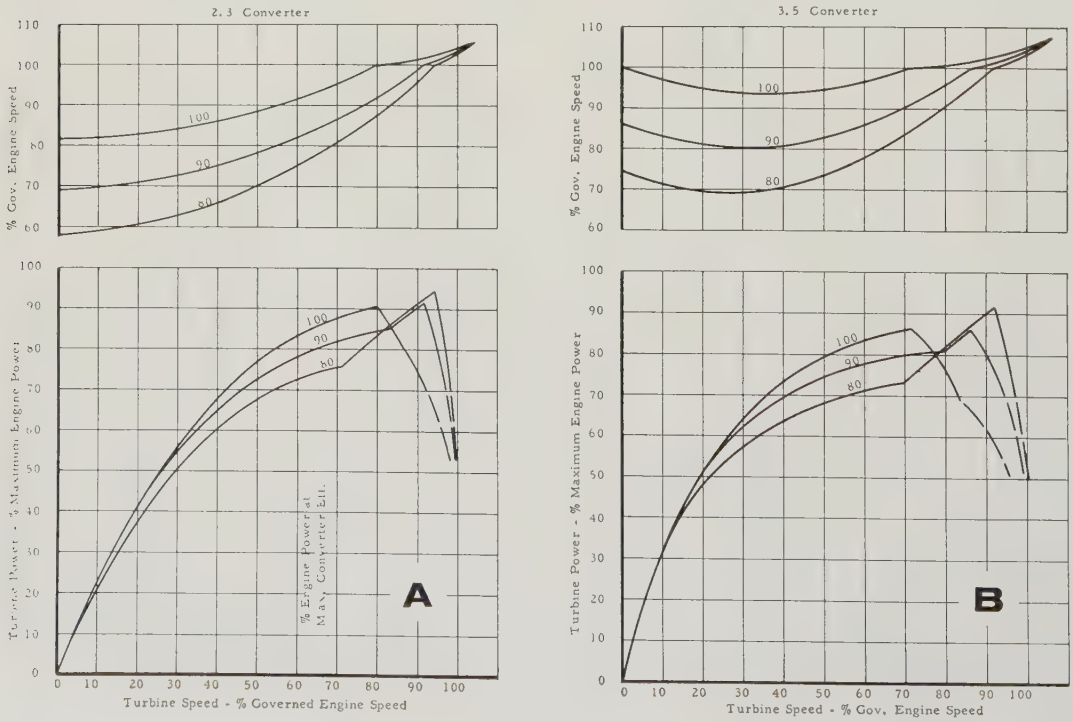

Fig. 3 — Effect of converter size on combined performance

capacity is to be maintained at the maximum efficiency point. Since the general effect of turbocharging is to narrow the operating speed range of the engine, the two processes are inherently opposed. If carried far enough they can become incompatible.

It should be pointed out that converters for general use cannot be made available in an infinite number of sizes and that an optimum match is thus a coincidence.

A nominal spacing of converter sizes results in about 1.2 ratio steps between capacity factors for adjoining sizes of converters. Thus, all matches will fall between these two capacities. The match which occurs midway between the extremes will be used for the remainder of the plots.

Figs. 5A and 5B show a comparison of these nominal plots between the low and high stall ratio units on both an output torque and output power basis. Since both plots are expressions of the same basic data, the output power curves will be used to illustrate power availability and the output torque curves will be used to illustrate starting characteristics. It can be seen that the nominal match on the low-ratio type with the rising capacity factor will result in an operating range which is likely to prejudice the behavior of a heavily charged engine. In this respect, the converter with the more uniform capacity characteristics, though larger in size, can be considered more desirable for widespread application.

Two-Speed Drive

An interesting performance result accrues from providing a shiftable ratio between the engine and torque converter. Interposing a ratio between the

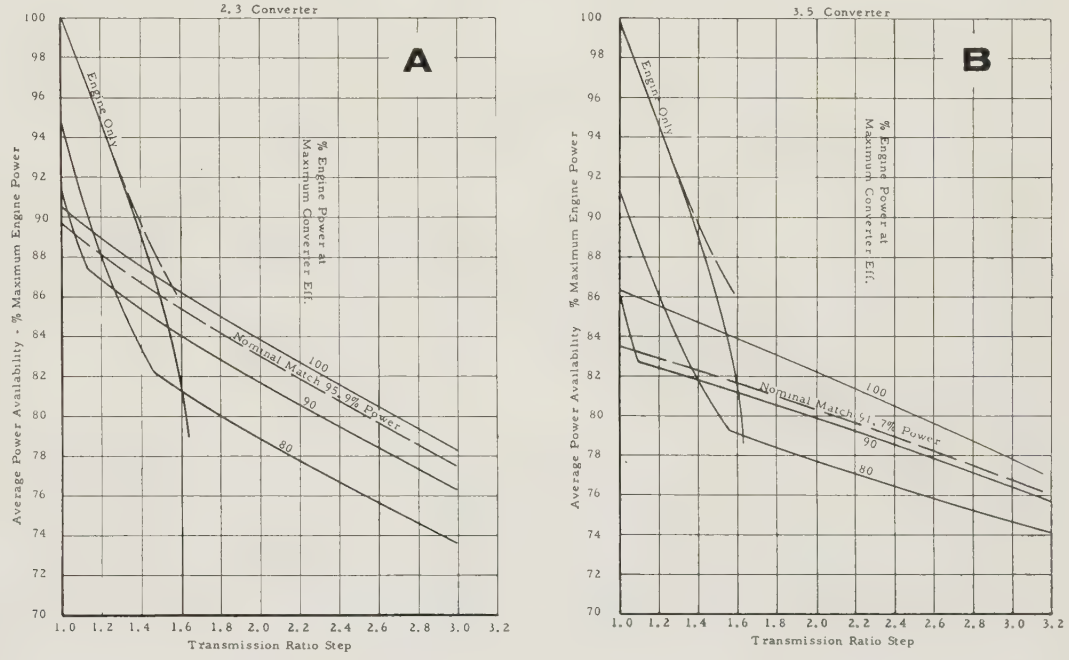

Fig. 4 — Effect of converter match on power availability

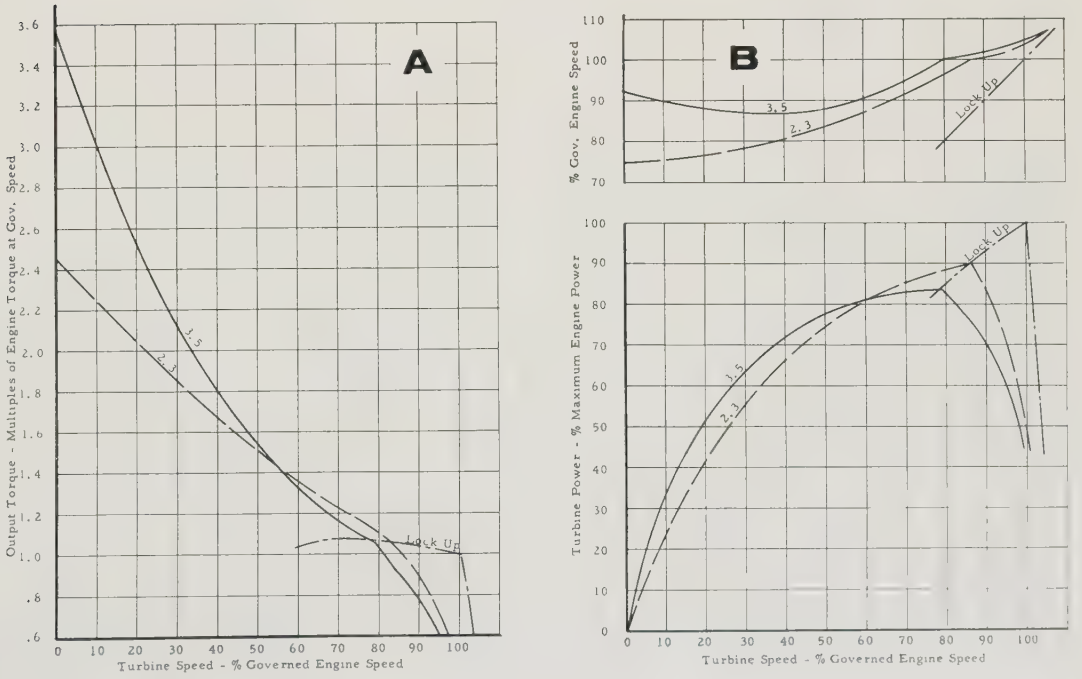

Fig. 5 — Comparison of converter output torque performance

engine and the converter affects the capacity factor of the converter at the engine in proportion to the 1.5 power of the ratio. Thus, a shiftable ratio results in two matches between the engine and the converter with the simultaneous effect of a ratio change in the drive train. This provides a match which favors low speeds at the low-speed end of the operating range as well as a match which favors high speeds at the high-speed end of the range.

Figs. 6A and 6B show the effect of such a ratio on the power curve of an engine-converter combination. It is interesting to note that if the shift occurs at the point where the power curves intersect, the impeller and turbine speeds are the same after the shift as they were prior to the shift. This produces the highly desirable effect of a power shift which involves no detectable feel. The resulting power curve spans considerably more speed ratio than can be accomplished by a single match. Among the applications of this arrangement is its use as a splitter for the gearing used after the torque converter.

Figs. 7A and 7B illustrate on a comparative basis these three arrangements.

Effect of Transmission Ratios

It is informative to consider the effect on relative vehicle performance of introducing ratios between the engine-converter combination and the load.

The starting characteristics of the vehicle result from the combined effects of the torque ratio characteristics of the converter and the ratio coverage of the transmission.

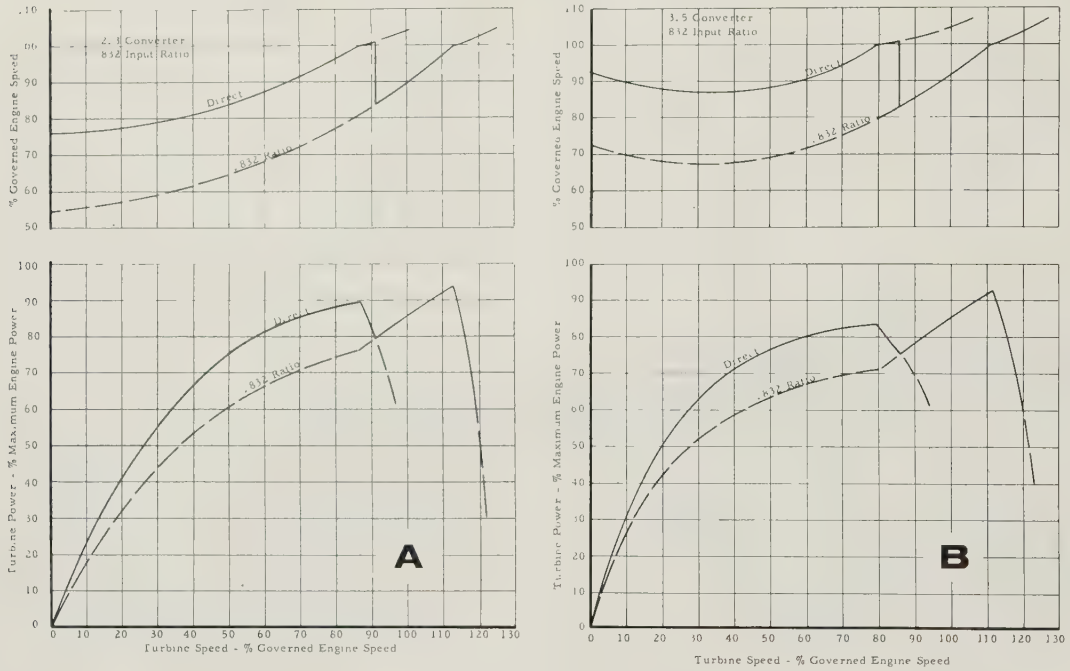

Fig. 6 — Effect of 2-speed drive on converter performance

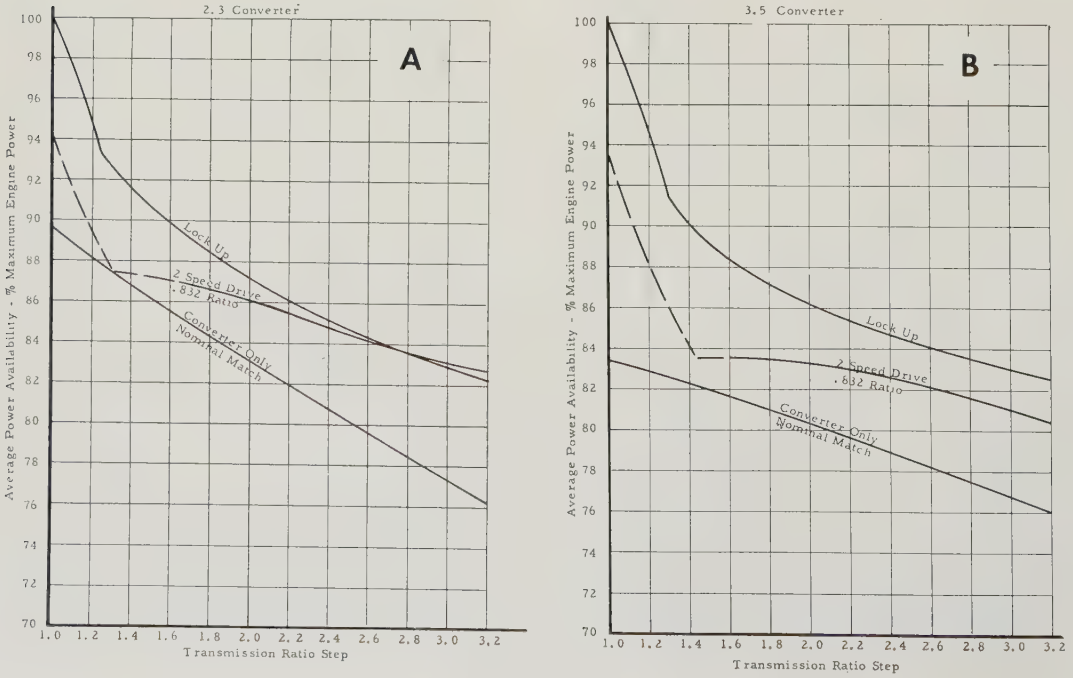

Fig. 7 — Effect of converter arrangement on power availability

An expression of these characteristics can be made dimensionless by relating them to the engine torque and the overall ratio of the driveline in high gear.

Figs. 8A and 8B show how the torque ratio of the converter combines with the ratio coverage of the transmission to give the starting characteristics in low gear.

In general, the choice in spacing of ratios is dependent upon the constraints imposed by the transmission gearing arrangement. Compound arrangements force repetition of ratio steps and ordinarily result in geometric spacing. Full parallel systems offer possibilities of variation of this pattern, although constraints are still present where gears are common in the parallel paths.

Fig. 9 shows how the various arrangements influence the average available power over the speed range. The average power is determined by the area under the power curve. The average power availability curve is drawn through the average points for each of the ratios. The starting characteristics for a range of ratio coverages is also shown.

It is evident that the area under the curve is increased significantly by the addition of a lockup clutch. However, in practice this area gain is not always realized because with automatic lockup the driver often waits until he is perceptibly lower in power in the converter range before he downshifts. Quite often this will bring him into the next lower gear at a speed below which the automatic lockup will engage the clutch. It is quite possible that use of lockup to lock up shifts will encourage the operator to make use of the full performance in down shifting as well as upshifting.

Gearbox

The most effective use of the torque converter to date has been in combination with a hydraulically shifted gearbox. It is desirable to make these shifts

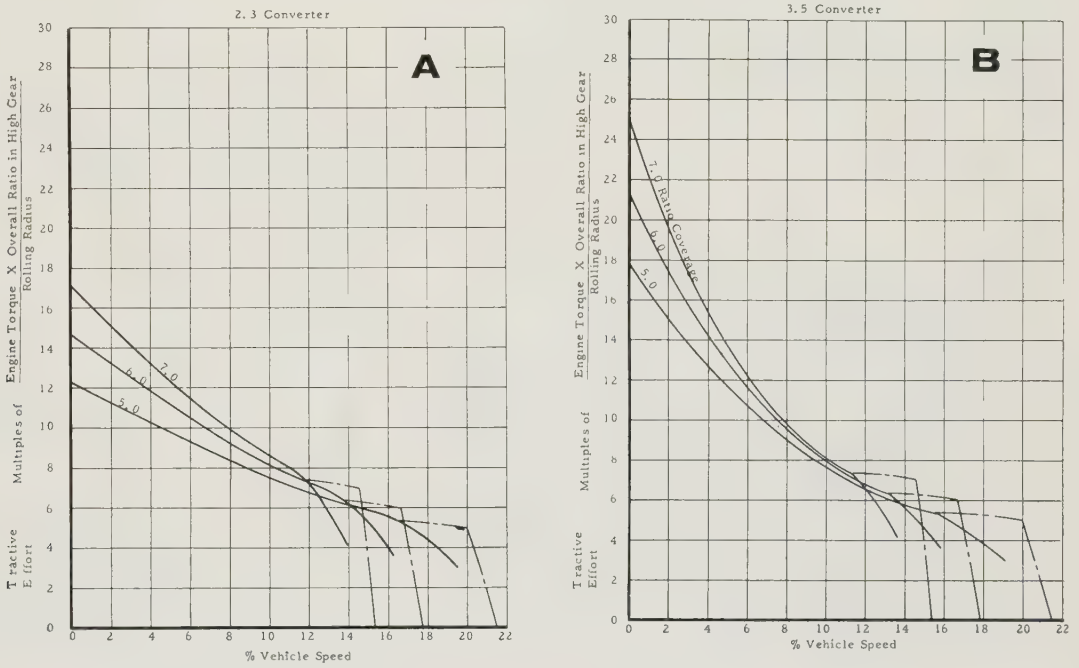

Fig. 8 — Effect of ratio coverage on tractive effort for starting

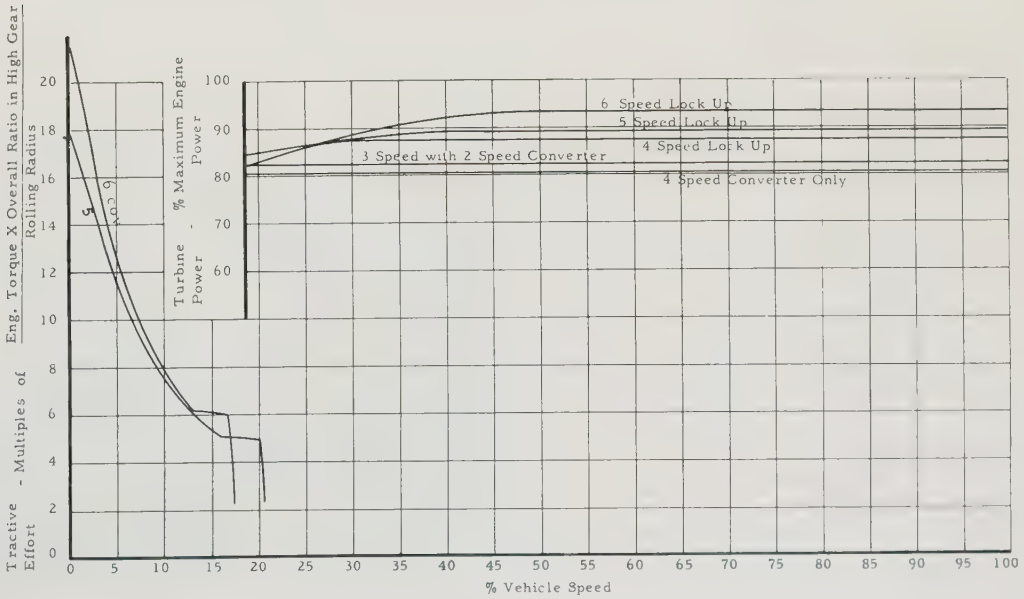

Fig. 9 — Effect of transmission configuration on performance factors

without a reduction in engine power and to accomplish this with output torque transients which do not prejudice the life of the driveline components.

Two general types of gearing are usable in achieving a power-shifting device. Reaction members on epicyclic gearing can be selectively grounded to the case through hydraulic or air clutches. Rotating clutches can be used to enforce selective torque paths through constant mesh countershaft gearing.

Multiple-disc hydraulically operated clutches have led all other means in providing control of the torque path selection and have been developed to the point where they provide a durable means for making the selection without the reduction of engine power.

Of the many factors involved, the selection of epicyclic gearing is influenced by the fact that the clutches for reaction members are stationary with respect to the transmission case which facilitates the handling of the apply oil in the case of hydraulic clutches.

Rotating clutches must have either bearings in the apply system or rotating oil cavities. The rotating cavity produces a centrifugal effect on the oil, resulting in forces which vary with the square of the rotating speed and are additive to the apply pressure. These forces are often accepted while the clutch is applied and are removed by bleeding the cavity when the clutch is disengaged. Also, the rotating cavity must be fed through its associated shaft, which may impose some limitations on the size of the oil passages.

Such a rotating clutch is involved in the epicyclic gear train where a direct drive is provided.

Fig. 10 shows the cross-section of a clutch which has been designed specifically for power-shift use. The clutch is designed to provide two selectable ratios in such a manner that the centrifugal effects on the oil in the rotating cavities act in opposite directions, thus effecting a cancellation.

Provision is also made to effect an oil transfer from one cavity to the other during the piston displacement. This results in an 80% reduction in oil flow during the apply cycle. The same mechanism used to accomplish the transfer function provides a means for controlling the rate of buildup of the apply forces.

Integral with the supporting shaft is a reaction member which separates the two rotating cavities. The apply mechanism consists of a closed-end slideable cylinder encompassing the reaction member.

Concentric with the cylinder and its supporting shaft is an auxiliary piston cavity having a displaced volume approximating one-fifth of the total displaced volume of the clutch. Three one-way passages exist through the reaction member in each direction from one cavity to the other. Introduction of oil into the auxiliary piston produces a force equal to one-fifth of the apply force which moves the cylinder toward the apply position and produces the oil transfer from the unapplied cavity through the reaction member to the cavity being applied. When the normal running clearance has been taken up, oil flow through the bleed hole between the auxiliary cavity and the main apply cavity causes the pressure to rise in the apply cavity, producing the force to apply the clutch pack. Sufficient elasticity exists in the members involved in the apply force path to allow accurate control of the rate of pressure rise in the apply cavity.

A wide variety of gearing arrangements are possible with these components. Typical possibilities are: 8-speed forward, 4-speed reverse unit with an automatic splitter ahead of the converter (Fig. 11); 4-speed forward, 4-speed reverse box with identical ratios in both directions for use with 4-wheel drive vehicles (Fig. 12).

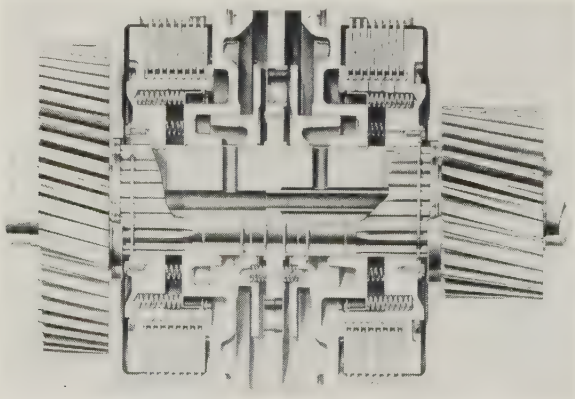

Fig. 10 — Double-acting clutch

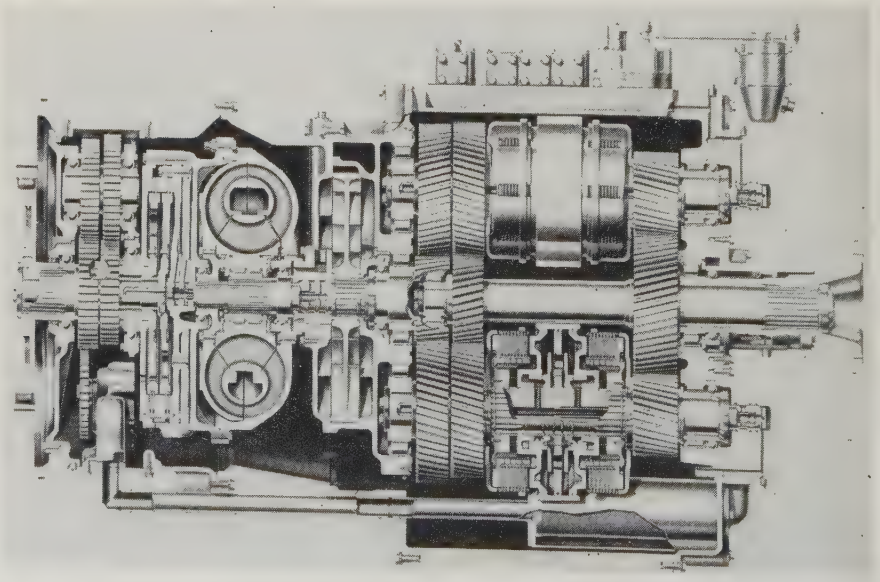

Fig. 11 — Gearing arrangement, series 1400, 8-speed forward, 4-speed reverse

APPENDIX

Converter Matching and Sizing Equations

N = Impeller speed, rpm
Ne = Engine speed, rpm
T = Impeller torque, lb-ft
Te = Engine Torque, lb-ft
D = Converter diameter, in. (at torus OD)
n = Converter speed ratio = $\frac{\text{Turbine rpm}}{\text{Impeller rpm}}$
t = Converter torque ratio = $\frac{\text{Turbine torque}}{\text{Impeller torque}}$
r = Geared ratio = $\frac{\text{Engine rpm}}{\text{Impeller rpm}}$
K = Capacity factor = $\frac{n}{T^{0.5}}$
(converter), plotted versus n (engine), plotted versus Ne
HP = Converter impeller power, horsepower
E = Converter efficiency = $\frac{\text{Turbine hp}}{\text{Impeller hp}}$

Converter Characteristics

The following assumptions are reasonably true:

E (Converter efficiency) and t (Converter torque ratio) remain constant for a torus, blading configuration, and speed ratio at all diameters and at all input speeds.

K (Converter capacity factor) remains constant for a torus, blading configuration, and speed ratio at all input speeds.

For a torus, blading configuration, and speed ratio: T is proportional to D^5

Therefore: $$\frac{T_1}{T_2} = \frac{D^5{}_1}{D^5{}_2} = \left(\frac{D_1}{D_2}\right)^5 \quad (1)$$

$$T_1 = T_2\left(\frac{D_1}{D_2}\right)^5 \quad (2)$$

and: $$D_1 = D_2\left(\frac{T_1}{T_2}\right)^{0.2} \quad (3)$$

For a torus, blading configuration, and speed ratio: T is proportional to N^2

Therefore: $$\frac{T_1}{T_2} = \frac{N^2{}_1}{N^2{}_2} = \left(\frac{N_1}{N_2}\right)^2 \quad (4)$$

$$T_1 = T_2\left(\frac{N_1}{N_2}\right)^2 \quad (5)$$

and: $$N_1 = N_2\left(\frac{T_1}{T_2}\right)^{0.5} \quad (6)$$

Since HP is proportional to NT, and T is proportional to N^2, then HP is proportional to N^3. Thus:

$$\frac{HP_1}{HP_2} = \frac{N^3{}_1}{N^3{}_2} = \left(\frac{N_1}{N_2}\right)^3 \quad (7)$$

and: $$HP_1 = HP_2\left(\frac{N_1}{N_2}\right)^3 \quad (8)$$

Relationship of K to D for a torus, blade configuration, and speed ratio:

Since $K = \frac{N}{T^{0.5}}$ when N is constant and K is proportional to $\frac{1}{T^{0.5}}$,

therefore: $$\frac{K_1}{K_2} = \frac{T^{0.5}{}_2}{T^{0.5}{}_1} = \left(\frac{T_2}{T_1}\right)^{0.5} \quad (9)$$

$$K_1 = K_2\left(\frac{T_2}{T_1}\right)^{0.5} \quad (10)$$

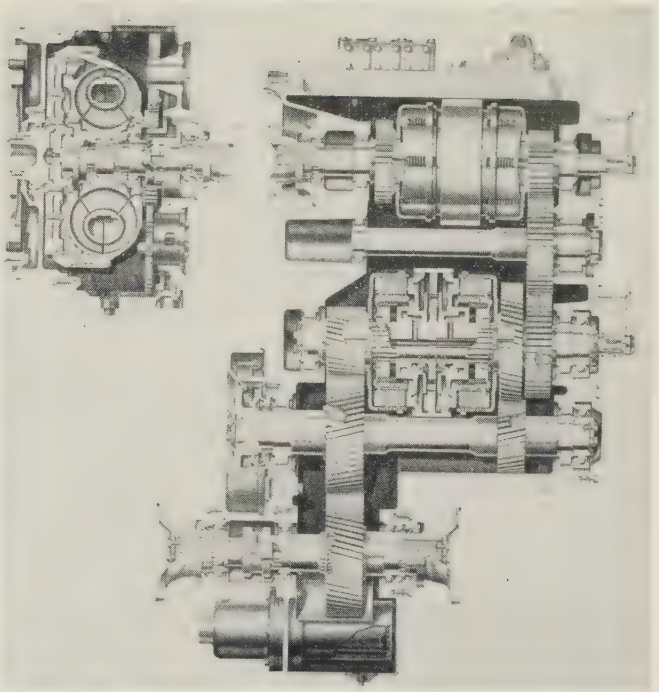

Fig. 12 — Gearing arrangement, series 1200, 4-speed forward, 4-speed reverse

Since: $\frac{T_2}{T_1} = \left(\frac{D_2}{D_1}\right)^5$, then:

$$K_1 = K_2\left[\left(\frac{D_2}{D_1}\right)^5\right]^{0.5} \quad (11) \qquad K_1 = K_2\left(\frac{D_2}{D_1}\right)^{2.5} \quad (12)$$

To determine K of the converter at the engine when driven through a gear set of ratio r:

Since for the converter: $K = \frac{N}{T^{0.5}}$

and for the engine: $Ke = \frac{Ne}{Te^{0.5}}$

and $Ne = N(r)$, $Te = \frac{T}{r}$

Then: $$Ke = \frac{Nr}{\left(\frac{T}{r}\right)^{0.5}} = \frac{Nr^{1.5}}{T^{0.5}} \quad (13)$$

Substituting K for $\frac{N}{T^{0.5}}$ in the above equation:

$$Ke = K\,r^{1.5} \quad (14)$$

To determine the performance characteristic of an engine-converter, match at a given converter speed ratio:

An engine and converter are in equilibrium when

$$K = Ke$$

1. Obtain the K factor of the converter at the speed ratio desired.
2. Find the engine speed at which the Ke (engine K factor) is identical.
3. Input conditions of speed, torque, and horsepower can be determined by

$$T = \frac{N^2}{K} \quad (15) \qquad \text{HP} = \frac{N^3}{K^2} \quad (16)$$

4. Converter output conditions can be determined by:

Output torque = $t \times$ input torque
Output rpm = $n \times$ input rpm
Output hp = $E \times$ input hp

THIS paper outlines a comprehensive theory for the yielding and aging of low-carbon steel, explaining the occurrence of aging and the significance of the observed stages of aging.

Aging is a problem in steelworking because it causes the yield point—which was removed in processing by the steelmaker—to return, with an accompanying loss of ductility. This in turn causes stretcher strains to appear during forming operations.

Some AGING of

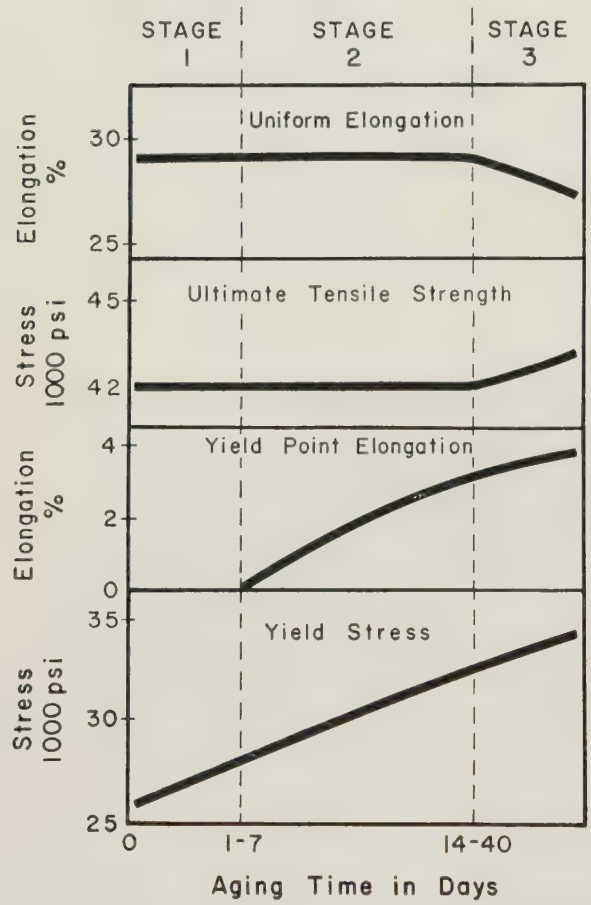

Fig. 1—Changes in tensile properties of temper-rolled rimmed steel

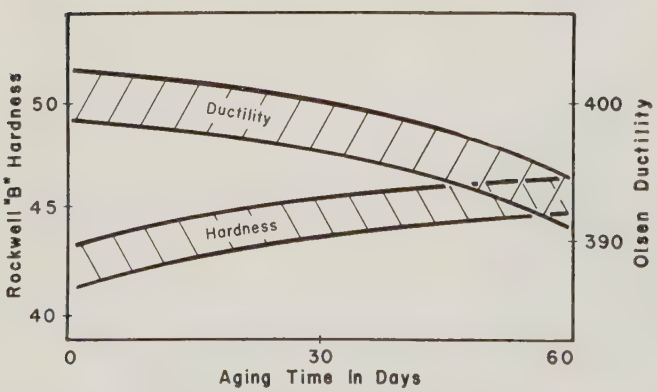

Fig. 2—Changes in hardness and ductility of temper-rolled rimmed steel

A PRIME property requirement of sheet steel to be used for automobile pressings is that it should not possess a yield point, since a yield point would lead to stretcher strains during the forming operation. In order to remove the yield point, the steelmaker resorts to light cold-working, usually temper rolling, before shipment. This is fine except that in the period between temper rolling and use by the customer, many steels age, the yield point returns, and there is sometimes a serious loss of ductility. The rates at which these changes occur in temper-rolled, rimmed steel can be observed by means of tension tests (Fig. 1).

During the first stage of aging, the only observable change is the increase in yield stress which, in practice, leads to buckling and bad shape in drawn parts. At a later stage, the yield point returns, and stretcher strains can be observed. Finally, in the last stage of aging, there is an increase in strength and loss of ductility which is often the cause of tearing during pressing operations. While the increase in yield strength and the yield point can be suppressed by roller leveling before pressing, the lost ductility cannot be restored.

In practice, Rb hardness and Olsen ductility are used as a measure of drawing quality but, as will be seen in Fig. 2, these tests do not lead to a clear observation of the same stages of aging. Apparently, the changes are gradual and because the measurements obtained are not usually precise, it is difficult to follow the progress of aging by this means. Moreover, when high hardness and low ductility are observed in a given batch of steel after storage, it does not necessarily imply that aging has taken place. High hardness and low ductility can be observed in unaged steel which has been taken from segregated portions of an ingot or has been improperly processed.

Even though tension test results can be a sensitive measure of the degree of aging in steel, such tests give variable results when applied to different batches of steel which have been subjected to ap-

Observations on the

LOW-CARBON SHEET STEEL

E. R. Morgan, Jones & Laughlin Steel Corp.

This paper was presented at the SAE National Passenger-Car, Body, and Materials Meeting, Detroit, March 5, 1958

parently identical processing and have similar analyses. This fact, although confusing at first glance, has led to the development of a comprehensive theory of aging which can explain not only why aging occurs and the significance of the observed stages of aging, but also why the observed rate of aging varies from one batch of steel to another.

There have long been adequate economic incentives to justify the development of nonaging steel, but efficient control of strain aging is difficult unless a complete understanding of the mechanism of yielding and aging can be developed. It is the object of this paper to outline a comprehensive theory of yielding and aging and to explain what difficulties have been encountered in applying this theory to the control of aging in commercial steels.

Basic Theory of Strain Aging

Because strain aging leads in the early stages to an increase in yield stress and to a return of the yield point, it is logical to expect that the mechanism of aging is related to the phenomenon of yielding.

Yielding is the result of localized plastic flow (Fig. 3). The Lüder's band or stretcher strain which forms initially will involve a localized strain of perhaps 5–6%, whereas the average strain over a 2-in. gage length may be only a small fraction of 1%. As the total strain is increased, the increase in strain may be the result of growth of the original stretcher strain, which formed at a stress concentration, or to the formation of new stretcher strains. This type of plastic behavior may be sharply contrasted with that of copper and many other metals where macroscopically homogeneous plastic flow begins at minute strains.

Plastic deformation in all metals is known to occur via the movement of linear lattice defects called "dislocations." In annealed copper, many dislocations can be moved by the application of low stresses. According to the Cottrell theory of the yield point, the dislocations in annealed low-carbon steel are locked in place by atmospheres of carbon and nitrogen atoms and thereby prevented from moving at low stress levels. When larger stresses are applied, some dislocations break free in the region of stress concentrations and, once they have broken free, they can move more easily, rapidly increase in number and also transmit plastic deformation from grain to grain in avalanche fashion until it has traversed the entire cross-section of the sheet. This theory provides a ready explana-

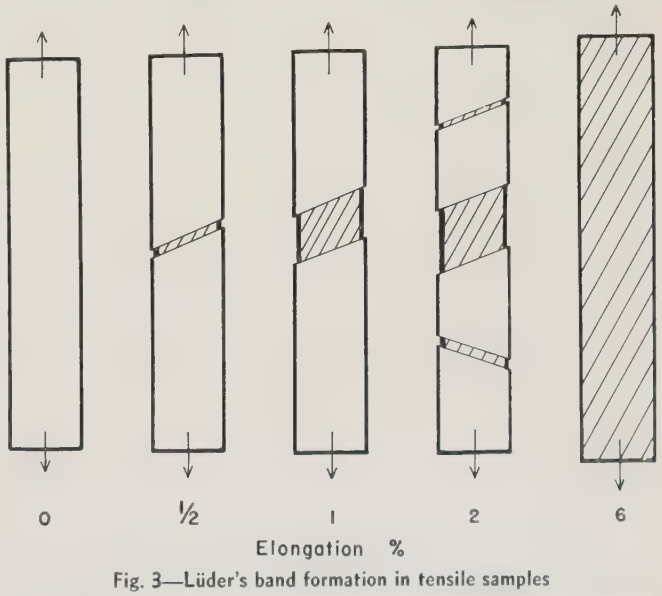

Fig. 3—Lüder's band formation in tensile samples

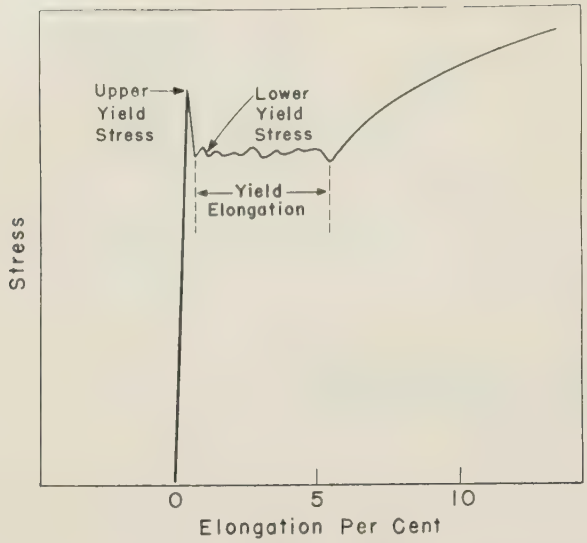

Fig. 4—Typical yield point in annealed low-carbon steel

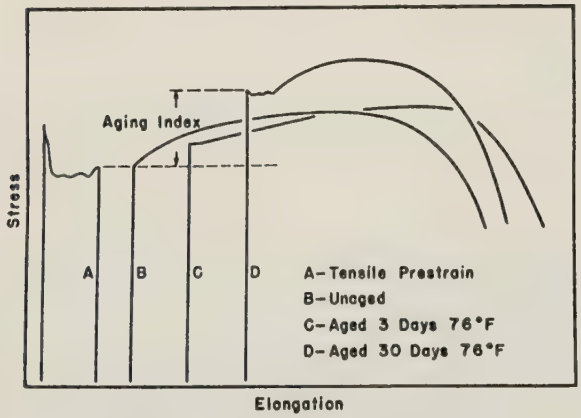

Fig. 5—Tension test curves for rimmed low-carbon steel, tensile prestrained and aged as shown

tion for the yield point (Fig. 4). The stress level must be raised to the upper yield stress in order to free dislocations and initiate yielding, but plastic flow will then continue at a lower stress level, the lower yield stress. When the whole of the sample gage length has been plastically deformed by the growth of the Lüder's bands, the total elongation will be equal to the yield elongation. Beyond that point, plastic flow will be homogeneous and yielding will have been eliminated. This is the manner in which cold-working can remove the yield point.

As the cold-worked sample is aged, there is a migration of free carbon and nitrogen atoms through the lattice, and many of the migrating atoms again become bound at free dislocations and produce a locking force which results in the reappearance of the yield point. This theory of strain aging can readily account for the early changes in properties like the return of the yield point but cannot account for the loss in ductility which is known to occur during a later stage of aging.

Stages of Strain Aging

In order for dislocation locking by the Cottrell mechanism to take place during aging, it is merely necessary for one or two carbon or nitrogen atoms in each plane to arrive at each dislocation. Experimental work has shown that the equivalent of 15 to 50 solute atoms per dislocation per plane go

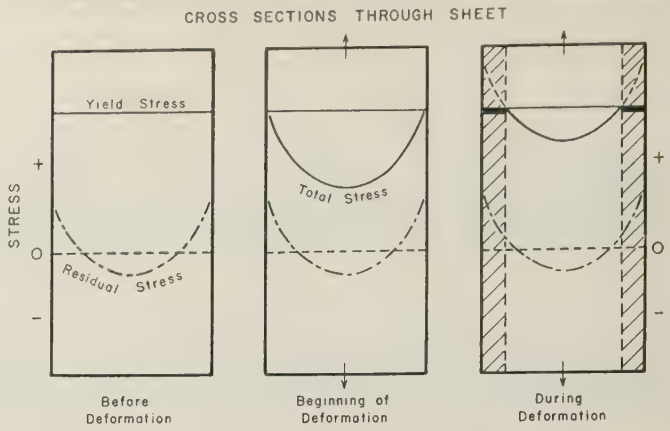

Fig. 6—Effect of residual stresses on deformation characteristics of temper-rolled low-carbon sheet

out of solution during normal strain aging. From the kinetics of such measurements, it can be concluded that the carbon and nitrogen atoms not only form locking atmospheres at dislocations during aging but also form minute precipitates at suitable dislocation sites. When the dislocations are subsequently torn away from their atmospheres, the precipitate particles will give rise to excessive localized work hardening and will thus reduce the ductility of the steel. The magnitude of the effect will depend on the number of dislocations present and the size of the precipitate particles. This is why loss of ductility during aging appears at a late stage of aging and becomes more serious as the amount of prior cold-work and the time of aging increase.

From this model, it may be deduced that if the number of carbon and nitrogen atoms which are free to migrate can be restricted so as to prevent formation of precipitate particles, then it may be possible to restrict aging to a return of the yield point without loss of ductility. This phenomenon has been observed in the laboratory.

Combining the Cottrell theory with that of precipitation during strain aging results in a theory which can explain both the occurrence of aging and the observation of different stages of aging. In order to complete the picture, it is also necessary to explain why the observed rates of aging can vary from batch to batch of rimmed steel.

Observed Rate of Aging

If a sample of rimmed steel which has been prestrained in pure tension is aged at room temperature for 2–3 days, there will be a noticeable change in the yield stress (Fig. 5). This rapid aging is entirely consistent with the Cottrell theory as outlined. A temper-rolled, rimmed steel should always strain age because it can be demonstrated that such steels contain relatively large amounts of carbon plus nitrogen which can migrate to free dislocations.

In practice, however, when press performance is the criterion by which aging is measured, this rapid aging is not always observed in rimmed steel. For example, most rimmed steels do not exhibit stretcher strains during pressing even 2 weeks after temper rolling.

The answer to this apparent anomaly lies in the nature of yielding of low-carbon steel. A yield

point is only observed when localized[1] plastic deformation passes through the entire cross-section of the sheet. If, in some way, the plastic deformation is prevented from becoming localized, there will not be an observable yield point.

When residual stresses of the type shown in Fig. 6 are present in a tensile sample, the yield point will be masked. During tensile loading, the effective stress will be the sum of the residual and applied stresses. As loading begins, the total stress in the surface regions will reach the upper yield stress and these areas can begin to deform plastically. There will be no localized deformation, however, because the outer regions are integral with and are constrained by the inner regions which are still deforming elastically. As loading continues, the homogeneous plastic deformation will move progressively towards the center, so that localized plastic flow can at no time run through the cross-section from surface to surface.

Residual stress patterns of the type illustrated in Fig. 6 are typical of those found in the rolling direction in temper-rolled sheet. The residual stresses in the transverse direction will be different and, in consequence, the degree of masking of the yield point will differ in the rolling and transverse directions, whereas the changes in tensile strength and loss of ductility will be the same in each direction. Apart from the described macrostresses, there will also be microstresses between grains which will affect the progress of plastic deformation and thus be of importance during yielding.

One of the problems associated with this theory of masking of the yield point by residual macrostresses is that the yield point can return during aging and yet it is known that the residual stress pattern is not destroyed by aging, and also that elastic stresses of this magnitude do not affect the rate of migration of carbon and nitrogen.

A study of the distribution of plastic deformation throughout the thickness of the sheet during light temper rolling has shown that more homogeneous deformation exists in the surface regions (Fig. 7). Although it is difficult to understand why this particular distribution of plastic deformation occurs, the fact that it does occur may be why aging can often nullify the masking effect of residual stresses.

Those regions which were deformed plastically will undergo an increase in yield strength which can be as much as 9000 psi in rimmed steel. At the same time, the regions which were only deformed elastically should not exhibit an increase in yield strength during aging. As shown in Fig. 8, although the yield strength would be constant throughout the thickness of the sheet before aging, it should be greater in the surface regions after aging. The exact distribution of aged yield strength would depend upon the distribution of plastic deformation during temper rolling.

If the patterns of aged yield strength and residual elastic stresses are of the same shape, it is possible that aging will effectively result in the reduction of the masking effect. As shown in Fig. 9, the final result will depend upon the relative magnitudes of the residual stresses, and the increase in yield strength during aging. When the actual yield strength becomes approximately constant during

[1] The term "localized" refers to restriction of plastic deformation within a narrow region in the longitudinal direction.

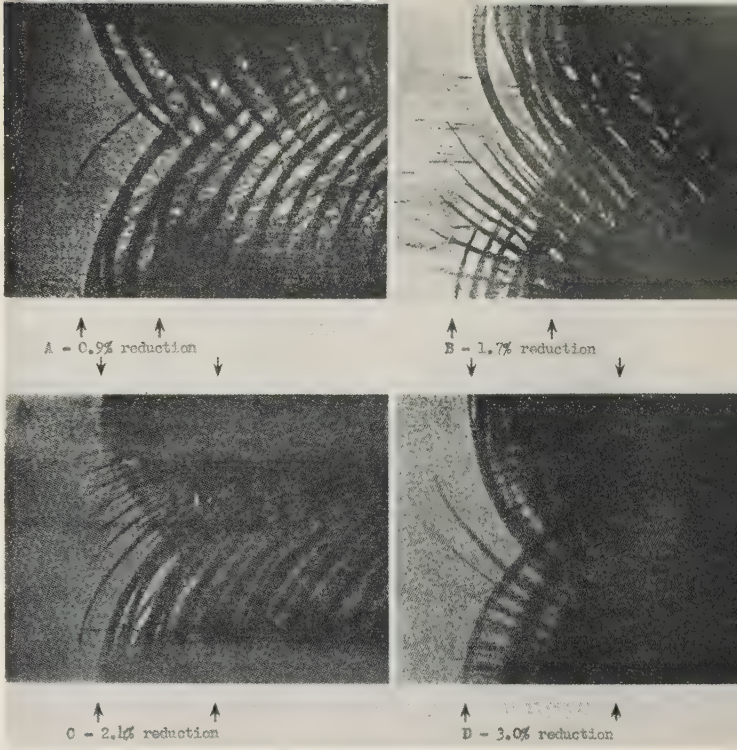

Fig. 7—Lightly rolled and etched low-carbon steel (after Hundy)

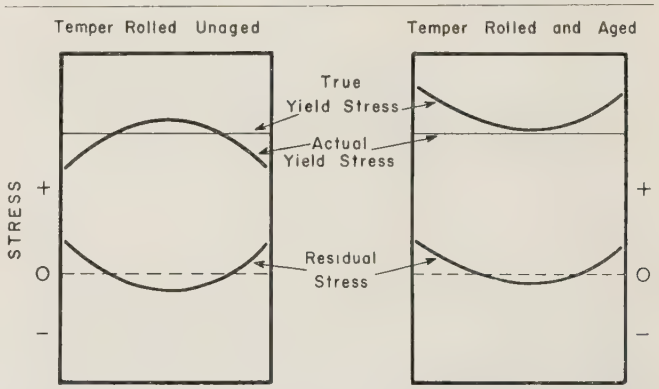

Fig. 8—Effect of aging on actual yield strength of temper-rolled rimmed steel (actual yield strength = true yield strength – residual stress)

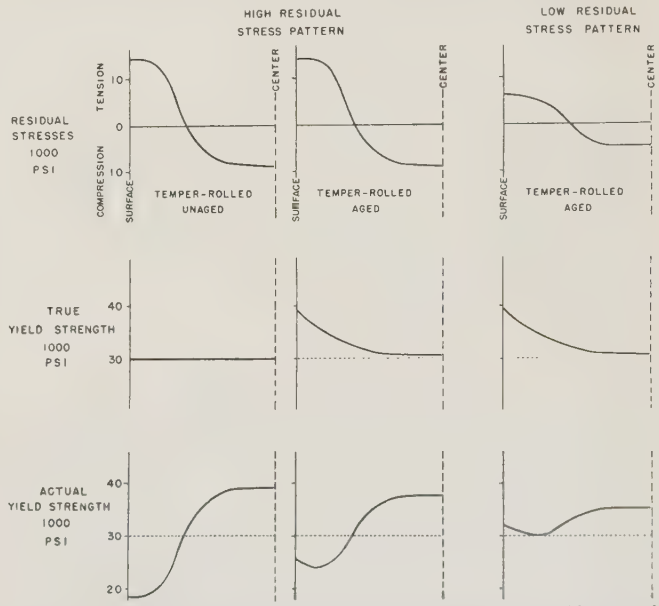

Fig. 9—Relationship between actual yield strength and true yield strength in temper-rolled and aged rimmed low-carbon sheet steel (actual yield strength = true yield strength – residual stress)

aging, it will be possible for the yield point to reappear. It is apparent that on the basis of this hypothesis, high residual stresses would be more effective as a masking agent than would low residual stresses. This deduction is entirely consistent with practical observations.

Practical Control of Aging

If the process of strain aging results from the migration of carbon and nitrogen atoms as suggested by Cottrell, it would seem logical to conclude that aging might be controlled by: (1) the rate of migration, (2) the time available for migration, and (3) the amounts of carbon and nitrogen which are free to migrate.

The rate of migration of carbon and nitrogen could be decreased by decreasing the storage temperature, but the cost of refrigerating stocks of deep-drawing steels would be exorbitant.

Strain aging normally cannot be controlled by controlling the time of aging because in practice, temper rolling is applied before shipping, and the aging period is determined by shipping and inventory times. If the customer received "as-annealed" coils and temper-rolled or roller-leved them to eliminate the yield point immediately before use, the problem of strain aging would disappear. In the absence of such action, the steelmaker must attempt to control aging by controlling the amounts of carbon and nitrogen in solution in steel and must also temper roll immediately before shipping.

The amount of carbon in solution can be so efficiently reduced by careful box-annealing that carbon is no longer a significant contributor to strain aging. In contrast, nitrogen is always a problem because of the difficulty in precipitating sufficient nitrogen during processing. With all present steelmaking processes, the amount of nitrogen remaining in solution in box-annealed, rimmed steel is sufficient to result in significant aging within a short storage period.

Nitrogen can be effectively removed from solution by alloying with a strong nitride-forming element. When aluminum, titanium, zirconium, or niobium are used for this purpose, they produce a killed steel which, by virtue of its poor yield, is relatively expensive. There are two elements which will combine strongly with nitrogen yet need not result in a killed steel; these elements are vanadium and boron. Unfortunately, both of these elements have disadvantages. Vanadium-treated steel must be very carefully processed in order to guarantee nonaging properties and boron has a moderately strong affinity for dissolved oxygen in the steel and leads to steelmaking problems.

Present State of Control Aging

From what has been previously described, it may be concluded that two distinctly different types of aging control processes may be used. The first of these would consist of chemical control whereby the amount of nitrogen in solution would be adjusted by means of alloying additions, whereas the second type of control would consist of masking the yield point by means of mechanical working. Chemical control, if efficiently applied, can completely eliminate all aging effects, whereas mechanical control can mask only the yield point effects and cannot control loss of ductility. For deep-drawn parts where ductility was important, it would be necessary to apply chemical control; but in shallow-drawn parts where only surface finish is wanted, the use of mechanical control alone might be sufficient.

Within the chemical control classification, attempts are being made to improve the surface of aluminum-killed steels, which are presently the generally available source of nonaging steel. One approach to this problem is to pour a partially killed steel into a mold which contains a suspended bar of aluminum. The aluminum melts readily and kills the steel, but there is less tendency for it to produce surface defects. An alternative approach is to push a bar of aluminum into the middle of a mold which has just been filled with rimming steel; this too results in improved surface quality.

The use of vanadium has been stimulated by the realization that it can be used more efficiently by means of mold additions. Studies of the aging characteristics of vanadium-treated steels have shown that carefully controlled annealing can produce a nonaging steel.

Boron additions have been successful in producing rimmed and capped nonaging steels, but the affinity of boron for oxygen means that special addition techniques must be used. Boron has also been used to produce nonaging semi-killed steels. In this case, the problem is chiefly that of controlling the oxygen content of the steel so as to obtain a good ingot structure. A rapid oxygen analysis test has been developed for this purpose, but progress has been retarded by lack of a good oxygen-sampling procedure.

Vanadium- and boron-treated nonaging steels have been and are being used on a limited scale but require further development. Even when these elements are not completely successful in eliminating aging, they may so restrict the degree of aging that loss of ductility does not occur during prolonged storage, even though the yield point reappears.

This degree of control would be sufficient if such steelmaking practices can be combined with mechanical control developed to the point where prolonged aging did not restore the yield point. Now that it has been established that masking of the yield point is most effective in those steels which possess high residual stress patterns, it has been possible to plan detailed examination of the mechanical factors which give rise to such patterns.

It has already been determined that such factors as roll size, roll roughness, and sheet grain size are of importance. Many other commercial factors such as the effect of initial shape and the amount of tension during temper rolling have not been adequately examined. The experimental work on commercial rolling mills is now being undertaken.

Now that it has been demonstrated that all of the effects of aging can be eliminated by combined chemical and mechanical control without the necessity for complete control by either, there are good prospects that new nonaging steels can be produced in the future.

Although this review of the status of present developments necessarily does not include all of the advances made by all steelmakers, it should be obvious that the steel industry has progressed towards the solution of a problem which has long plagued the users of low-carbon sheet steel.

Research in Magnetohydrodynamics

William McIlroy, Republic Aviation Corp.

This paper was presented at the SAE National Aeronautic Meeting, New York, April 8, 1958.

THIS paper presents in simple terms some of the fundamental ideas underlying the study of the relatively new field of magnetohydrodynamics. The basic theory is discussed in terms of the familiar dynamo principle. Several of its applications are described, including instruments such as the induction flowmeter and the electromagnetic pump. The important pinch process is briefly treated.

Finally, a short nonmathematical discussion of investigations made at Republic Aviation Corp. concerning the future potential of the theory is presented. Such items as reduction of aerodynamic heating at the nose of a re-entry missile, the possibilities of a plasma engine for flight into outer space, and the regeneration of electricity from the fluid are considered.

AS ITS name implies, magnetohydrodynamics is concerned with the flow of a conducting fluid in the presence of magnetic and electric fields. The fluid may be a liquid metal such as mercury, sodium potassium, and the like, or a gas at elevated temperatures such as occur behind the bow shock of a high hypersonic missile.

Although the name magnetohydrodynamics (or hydromagnetics, as it is sometimes called) is a formidable one, the basic principle is relatively simple. It is none other than the familiar dynamo theory, except that we are considering a gas with a comparatively low value of electrical conductivity rather than a solid conductor of high conductivity. There is a coupling between the electrical properties of the fluid and its mechanics; and the motion can no longer be described by the familiar equations of hydrodynamics alone, but only in conjunction with the equations of electromagnetic theory as formulated by Maxwell. The resulting set of differential equations for the magnetic, electric, and velocity fields, and their boundary conditions, become quite involved. Few solutions exist at the present time and only some of the simpler one- and two-dimensional problems have lent themselves to analytic solutions.

Prior to a few years ago, magnetohydrodynamics was principally the concern of the astro- and the geo-physicist. With it the geophysicist was able to advance a theory for the earth's magnetism, and the astrophysicist to develop theories explaining such cosmic phenomena as sunspots, magnetic stars, solar corona, magnetic storms, and the auroras.

Today the field of magnetohydrodynamics opens up a seemingly endless stream of bright possibilities. One that has proved extremely important has been the recent widely publicized application of the so-called "pinch effect" to the confinement of a plasma

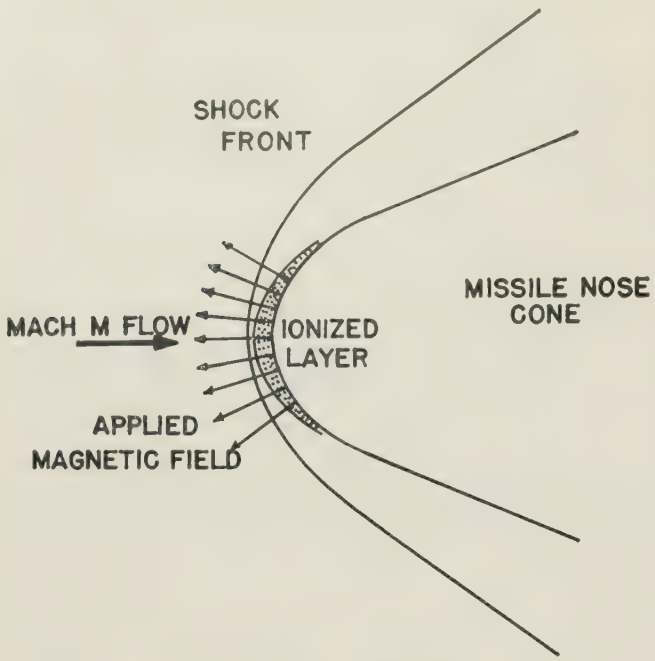

Fig. 1 — Nose cone configuration

in a fusion reactor. This will ultimately lead to the harnessing of nuclear power for peaceful purposes.

Ionization

A plasma is a gaseous mixture (usually defined as electrically neutral) containing negatively charged particles (electrons) and positively charged particles (ions). Ionization in a gas takes place when the energy level is raised to a point where, due to the violent collisions of the atoms and molecules, the orbital electrons around the atom nuclei are so agitated that they can jump from their ground states to higher levels, and finally are shed, one by one, from the outer orbits to leave positively charged ions. By virtue of this, the gas now has free electrons and ions and is capable of being influenced by external magnetic and electric fields. The electrical conductivity depends upon the number of electrons and ions in the gas, as well as their velocities, which in turn are directly related to the gas temperature.

There are a number of methods for obtaining ionization in a gas:

1. On application of a sufficiently high voltage between two electrodes, the gas is excited and ionized to produce an electrical discharge. When a high radio frequency is used, the ionization can be produced at much lower voltages. The process can be further accelerated by employing a light source directed at the cathode.

2. If the gas is on the verge of ionizing, particle emitters could possibly be used to accelerate the process. However, a few rough calculations indicated that a prohibitive amount of plutonium, radium, or other radioactive sources would be necessary to produce any marked increase. In addition, such amounts of radioactive material would present a definite health hazard.

3. Ionization is produced when the gas is heated to extremely high temperatures. This occurs naturally when the air ahead of a high hypersonic missile is rapidly decelerated through the bow shock wave that forms ahead of the body (Fig. 1). At a Mach number around 18, the air is reasonably ionized. In fact, high radio frequency transmission through the blanket of ionized gas formed around the nose of the missile becomes extremely difficult.

4. Ionization results from seeding the hot gas with an alkali metal, such as sodium or potassium which has a low ionization potential. Not only is this readily ionized, but it will behave as a catalyst to accelerate the ionization of the gas itself.

In Fig. 2 the electrical conductivity of air is plotted against the temperature behind the bow shock and the Mach number of the flow ahead of the shock. These results were obtained by Lin.[1] It is interesting to note that the value of 0.25 mhos/cm, occurring around Mach number 12, is simply the conductivity of a concentrated solution of salt in water.

If the degree of ionization is insufficient at a given Mach number, it is possible that some of the methods outlined above could be developed to increase the supply of electrons and ions.

The Basic Theory

It is probably most advantageous at this point to refresh ourselves on the operating principle of the dynamo.

When a conducting wire is thrust through a magnetic field, strength H, with a velocity V whose direction is perpendicular to the wire and is inclined to the direction of the H field at an angle ϕ, an electric field (E ind) is induced in the wire (Fig. 3).

The value of the induced E field is equal to the product of the permeability of the medium, μ, the strength of the magnetic field H, and the component of the velocity normal to the H lines ($V \sin \phi$); that is, $E_{ind} = \mu HV \sin \phi$. A current of density J equal to σE_{ind} will flow in the conductor, where σ is the conductivity of the wire.

As the wire is pushed through the magnetic field, it experiences a resisting force F per unit volume of the wire. This force acts in a direction perpendicular to both the H field and the E field, and equals μJH or $\sigma\mu^2H^2V \sin \phi$. It should be noted that this force is influenced only by the component of the velocity normal to the magnetic lines of force. There is no interaction between H and the velocity component $V \cos \phi$ since they both lie in the same direction. This resisting force per unit volume is termed the "ponderomotive force."

Let us turn our attention from the solid conductor to the case of a plasma. The plasma, as mentioned above, contains free ions and electrons, so that when an electric field is impressed on the gas a current will begin to flow. This is the case of the neon light, for instance, once the gas has been broken down by a high voltage source. The ionized gas behaves exactly like a conductor, when considered on a macroscopic scale; when it flows across a magnetic field a current is induced, and a force tending to slow down the motion of the gas is experienced. The above equations for the solid conductor still apply. This is the fundamental idea behind the magnetohydrodynamic interaction, and it

[1] "Electrical Conductivity of Thermally Ionized Air Produced in Shock Tube," by S. C. Lin. AVCO Research Laboratory, Research Report 5, February, 1957.

is simply an application of dynamo theory to conducting gases rather than to solid conductors.

This ponderomotive force must now be introduced into the hydrodynamic momentum equations as an additional body force, representing the coupling effect of the flow and the magnetic field.

In addition to the modification of the flow field, the flow interacts with the H field and can modify it substantially. We have seen that an electric field is induced normal to the magnetic field H. The induced currents set up their own magnetic fields which modify the original pattern. This modified H field in turn perturbs the modified flow field, and the process continues until equilibrium is attained.

Induction Flowmeter and Electromagnetic Pump

The induction or magnetic flowmeter is a very simple application of the dynamo principle just described. This instrument measures the rate of flow of high-temperature liquid metals. One of its advantages is that the measuring apparatus is entirely outside of the pipe and, therefore, the maintenance problem is minimized.

A transverse magnetic field is established by a permanent magnet, and the liquid metal flows across it. As we established above, an electric field is set up across the tube perpendicular to the flow direction. By having two electrodes situated to pick up the induced current, a measurable potential difference proportional to the flow rate is measured. An integrating device could be installed to record the total mass flow over a given period of time.

The sensitivity of the flowmeter is affected by the velocity profile in the pipe, and this must be accounted for in the theory. Another important restriction is that the pipe dimensions should be such that the flow remains laminar.

The electromagnetic pump is another application of the theory. Whereas in the flowmeter we had a moving fluid and a fixed H field inducing an electric field normal to both the H and V directions, in this case we have a fluid at rest, an applied H field, and an applied E field. In other words, we now have the equivalent of an electric motor, whereas previously we had an electric dynamo action. On account of the coupling of the H and E fields, there results a pressure gradient equal to the ponderomotive force F. This pressure provides the pumping action. To obtain appreciable working pressures the conductivity of the fluid must be reasonably high.

Pinch Process

It will be interesting to include a few remarks on another phase of the interaction of an ionized gas

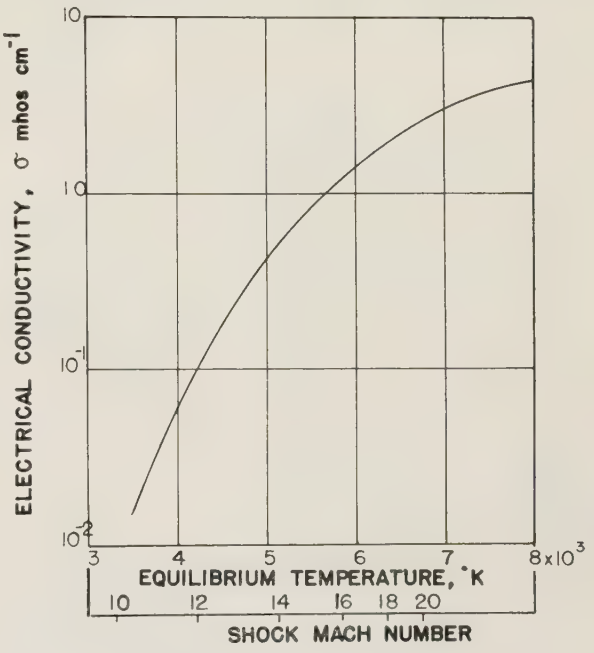

Fig. 2 — Electrical conductivity of air

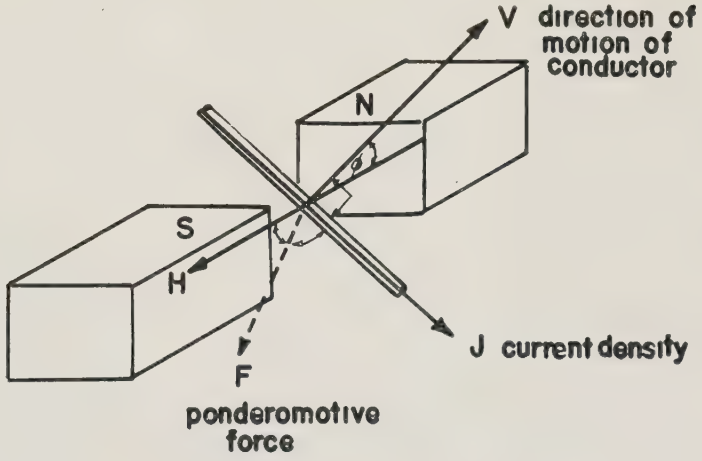

Fig. 3 — Dynamo principle

ϕ = Inclination of V to the magnetic field H

$J = \sigma \mu V H \sin \phi$

$F = \sigma \mu^2 H^2 V \sin \phi$

and a magnetic field. Consider a tube containing a low pressure gas (Fig. 4). If an electric field is applied across the two ends of the tube a current, initially confined to a thin skin at the outer diameter, will flow through the gas. This current gives rise to a magnetic field encircling the gas; and due to the pressure it exerts, the magnetic field squeezes the tube of gas so that its diameter contracts until there is equilibrium between the internal and magnetic pressures. In this way the temperature of the gas is further increased, but the important fact is that the hot gases are no longer in contact with the wall. The magnetic field acts somewhat like a furnace liner in the tube, preventing the gas particles from contacting the wall. One of the difficulties is that the plasma column can become unstable due to very small kinks. It may buckle like a structural column or it may form a neck along its length. Stabilization can be achieved by:

1. Applying a longitudinal magnetic field inside the plasma and along its axis, which provides it with a "backbone."

2. Using the outer walls of the tube as the return path for the current. On the onset of instability, the rapidly deflecting plasma will drive the magnetic field across the conducting walls. Currents are induced in the conductor interacting with the magnetic field to produce a stabilizing force on the plasma.

By controlling the instability of a plasma, the pinch can be maintained for much longer periods. Recently reported results indicate that the British, with stabilization, have succeeded in raising a deuterium plasma to "temperatures" of 2,000,000 to 5,000,000 C; while maintaining the pinch for a period of 0.002–0.005 sec. Previously the maximum "temperatures" achieved were of the order of 1,000,000 C with times of the order of 1 microsec.

These "temperatures" refer to the directed kinetic energy of the electrons, and not the random energy of the molecules. They are defined as

$$(m_e v^2_e/3k) \qquad (1)$$

where:

m_e = Electron mass
v_e = Electron velocity
k = Boltzmann constant

The "temperature" of the ions will be different, since they have higher masses and lower velocities. In a successful fusion reaction, power will have to be generated in pulses lasting several seconds each.

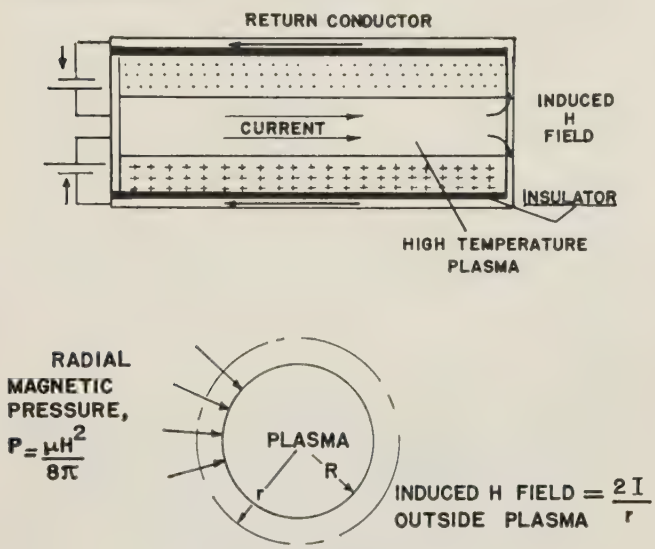

Fig. 4 — Pinch process

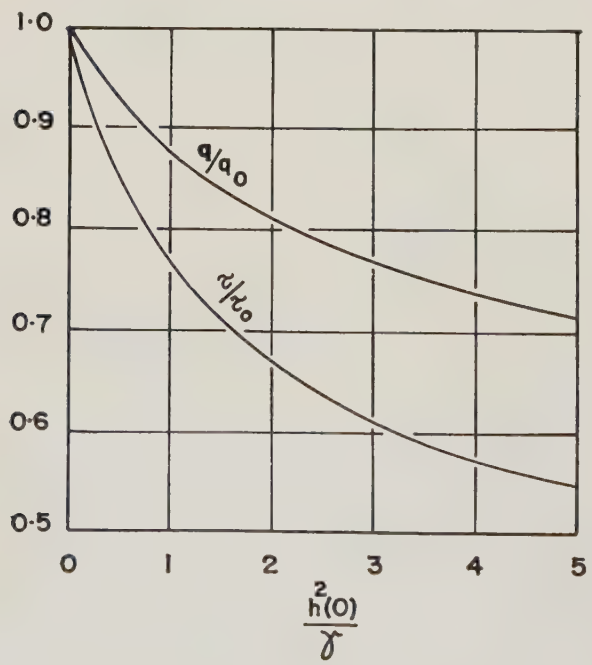

Fig. 5 — Reduction in shear and heat transfer

Aerodynamic Applications

It was previously noted that behind the bow shock ahead of a re-entry missile traveling at Mach numbers of the order of 18, there is a cap of ionized air around the nose. It is well-known that the aerodynamic heating which takes place in this vicinity has presented a serious problem. The question arose, in the light of the fundamental ideas on magnetohydrodynamics, whether a magnetic field could be applied at the nose to interact with this ionized region and possibly produce a reduction in the heating. At Republic we carried out a mathematical analysis of a simplified model[2,3] and the results were most encouraging. They indicated that even with low values of conductivity σ of about 2.5 mhos/cm (corresponding to a Mach number of about 18), a reduction of the order of 28% in the heating rate and 45% in the skin friction might be expected with a magnetic field of 23,000 gauss. In Fig. 5 the ratios q/q_o and τ/τ_o are plotted against the interaction parameter $h^2(0)/\gamma$. This parameter is simply related to the product of the conductivity σ and the square of the applied H field for a given density and velocity behind the shock. q_o and τ_o are the heating rate and surface shear stress respectively before application of the magnetic field.

The interaction may be explained in nonmathematical terms as follows: On approaching the stagnation point, the flow divides symmetrically on

[2] "Incompressible Two-Dimensional Stagnation Point Flow of Electrically Conducting Viscous Fluid in Presence of Magnetic Field," by J. L. Neuringer and W. McIlroy. Republic Aviation Report, June 12, 1957. Also *Journal* of Aeronautical Sciences, Vol. 25, March, 1958, pp. 194–198.

[3] "Hydromagnetic Effects on Stagnation Point Heat Transfer," by J. L. Neuringer and W. McIlroy. Republic Aviation Report, Nov. 26, 1957.

either side of a zero streamline, and the velocity vector has two components u and v, along and normal to the surface. At the wall, since the fluid is viscous and the surface nonporous, these velocities are both zero. The magnetic field is applied normal to the surface and is assumed to be of constant strength H_o. As we have seen, the magnetic field interacts only with the component of the velocity parallel to the surface, that is, u. An electric field is set up and a current flows normal to both the H lines and the u direction. A ponderomotive force, $\sigma\mu^2 u H_o^2$ per unit volume, acts in the opposite direction to the velocity u, and, consequently, tends to slow down the motion. Since the velocity u in a region close to the wall varies from zero at the wall to the inviscid flow velocity away from the wall (Fig. 6) due to the viscosity of the gas, the retarding force must also vary from zero at the wall to a uniform value in the inviscid flow. The interaction has two effects:

1. It reduces the velocities in the outside inviscid flow field (Fig. 6). On this account the detachment distance between the shock and the body surface is increased.
2. The velocity profile in the viscous region close to the body surface is modified. The actual thickness of the "boundary layer" is seen to increase with increasing H_o.

The *dimensionless* velocity profiles approach more and more the shape associated with a turbulent boundary layer when the applied magnetic field is increased. This would lead one to believe that the magnetic field has the added effects of increasing the stability of the flow and delaying separation.

The analysis also indicates that both effects are equally important where shear is concerned. For heat transfer, however, the reduction is due mainly to the first, modifications in the dimensionless profile being relatively unimportant.

These results are, of course, theoretical and require experimental verification. At Republic, an experimental program has been put into effect to carry out such an investigation, and results should be forthcoming in the very near future.

Future Research

In the section on basic theory it was demonstrated that circulating currents are present in the moving plasma due to the hydromagnetic interaction. The possibility arises of collecting this current and using it to partially regenerate the magnetic field described above. If this can be accomplished the weight of electrical equipment should be greatly reduced.

Another phase of our investigations at Republic is the development of a plasma engine, in which small amounts of plasma are ejected at extremely high velocities. At the Naval Research Labs, for example, plasmas have been driven magnetically at speeds equivalent to Mach numbers in excess of 200.[4] This type of engine seems to offer exceptional possibilities for flight in outer space. The drag at such altitudes is practically negligible and very little thrust is required to overcome it, either to maintain constant speed or to accelerate. In our opinion, this method is more favorable than the ion propulsion, which has been receiving much publicity. This opinion was voiced also by Bostick at the Astronautical Society meeting.[5]

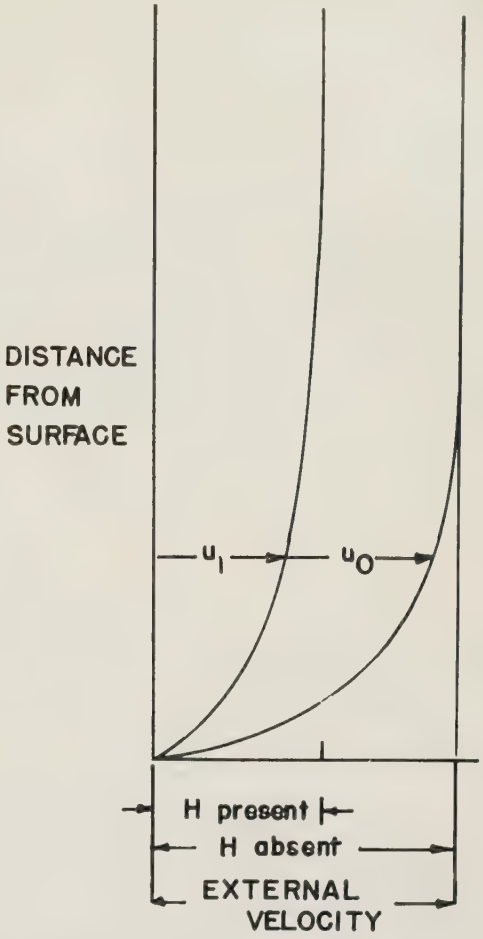

Fig. 6 — Effect of H field on the velocity profile

A number of basically aerodynamic studies would be very useful. It may be possible to generate lift and effect some method of control at extremely high altitudes. Delaying the onset of transition of a boundary layer from laminar to turbulent flow, and preventing separation of flow at corners, and the like, would be extremely important contributions to the design of ultra high-speed aerodynamic vehicles.

The pinch effect may find much the same application in rocket engines as it has found in the fusion reactor. It may then be possible to have engines working at temperatures far in excess of the limiting values for the metals being used in their construction. This would lead to the development of engines with very high efficiencies.

Conclusion

In the light of current investigations, magnetohydrodynamics seems to be a promising new field with unlimited interesting possibilities for research and development, both theoretically and experimentally. In its applications it may prove to be one of the most important phases of the space age.

[4] "Magnetohydrodynamics." Ed. by R. Landshoff. Pub. by Stanford University Press, 1957.
[5] "Plasma Motors," by W. S. Bostick. Paper presented at Annual Meeting, American Astronautical Society, January, 1958.

An Investigation

Control of Tire Thump by

Guy J. Sanders, Armour Research Foundation of Illinois Institute of Technology

This paper was presented at the SAE National Passenger-Car, Body, and Materials Meeting, Detroit, March 4, 1957.

WITH the advent of low-pressure tires and the success of car noise reduction efforts by automotive engineers, tire thump has become a more noticeable problem. This paper discusses some recent research in this area.*

A tire's susceptibility to thump can be predicted from the difference frequency between diametrical and circular modes of vibration. The author describes the testing and procedure uses to find the source of thump.

The way to minimize thump is to shape and construct the tire so that it does not permit coincidence of two natural frequencies with two revolution rate harmonics in the 20-35 mph speed range.

TIRE thump is a low-pitched noise repeated periodically once per tire revolution or about six times a sec at 30 mph. The frequency of the noise is about 40 cps. This noise is present at many car speeds; however, it is often hidden by other car noises at speeds above 35 mph. It has become audible in postwar cars for two reasons. First, the automobile industry has spent a considerable amount of time and effort reducing the more objectionable noises in passenger cars. This art of noise reduction has reached such an advanced state in the industry that low-level noises such as tire thump are now audible.

The second reason for the appearance of tire thump is the advent of low-pressure tires (26 lb). These tires have certain dynamic characteristics which make possible the production of loud tire thump in the 25–35 mph speed range, where it is

* This work was done at the Armour Research Foundation under the sponsorship of the Goodyear Tire & Rubber Co.

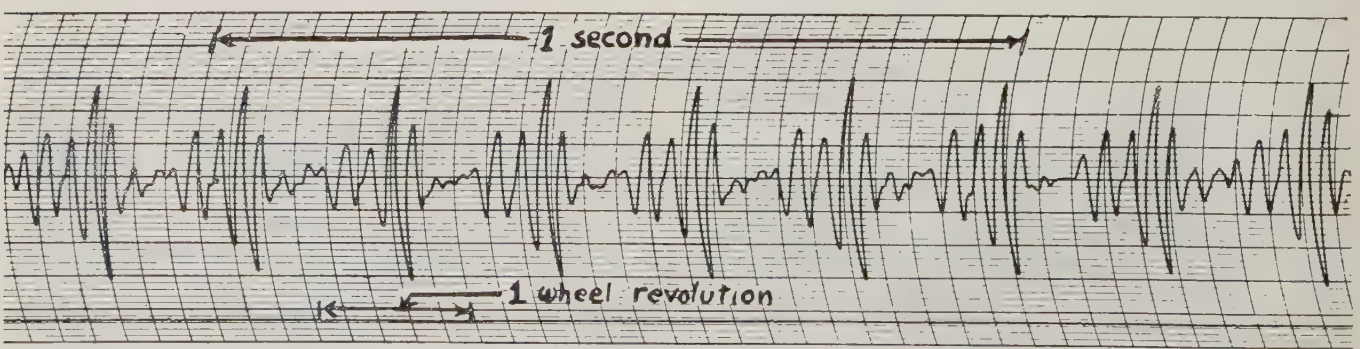

Fig. 2 — Recording of sound in back seat of automobile on test stand showing thump from double bead block tire on front left wheel. The event marks, resulting from closing of wheel switch once per revolution, make it possible to correlate thump with tire position

of the

Tire Shape

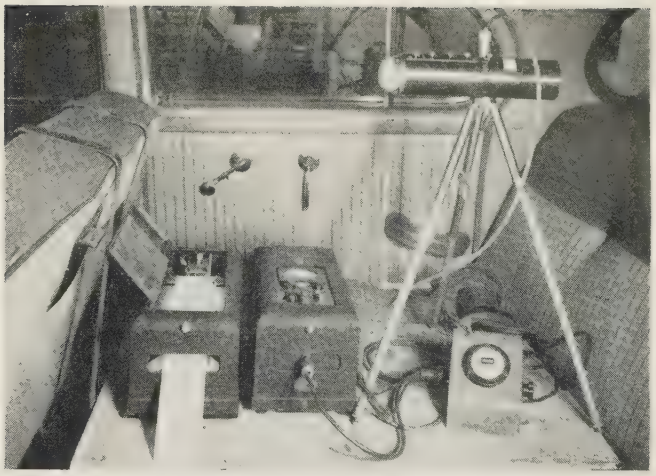

Fig. 1 — Sound level meter on tripod, amplifier, and recording oscillograph set up in rear seat of automobile for thump measurements

readily heard. Fortunately, the new 14-in. rim, 22-lb tire will be slightly less susceptible to thump in this speed range and will present a little less of a problem to the automotive industry.

This paper will describe some of the facts that have been discovered about the production of tire thump and thereby point the way that work can progress toward the reduction of this nuisance.

Instrumentation Techniques

Many techniques have been used to measure and rate tire thump. Most of these have been described previously by others; therefore, only the method found most useful by Armour Research Foundation will be discussed. Early measurements revealed that the primary concern was with frequencies between 30 and 50 cps; for sound measurements in the car a microphone and pre-amplifier system which cuts off quite sharply below 30 cps was used to eliminate low-frequency noise. The signal from this system was fed into an amplifier and direct writing recorder which cuts off near 60 cps. This system produces a very good picture of the thump noise rejecting most of the other sounds which might make thump analysis difficult. Pictures of the instrumentation and a sample of the thump record it produces are shown in Figs. 1 and 2.

Records similar to this can also be made from the output of a vibration pickup mounted on the axle or brake backup plate of the wheel with a thumping tire. For this system a filter is needed to cut off the frequencies below 30 cps.

With the addition of a timing switch which closes once each wheel revolution when the same spot on the tire tread is at the ground, the location on the tire which corresponds with the start of the thump impulse can be found. For this purpose a d-c voltage was applied in series with the switch and with one channel of the same recorder on which the vibration of the thumping tire was recorded as shown in Fig. 3.

It can be seen from this graph that the angular displacement between the switch closing point and the start of the tire vibration can be measured. This then is the same angle from the point on the tire that is in contact with the ground when the thump vibration starts. By this method it is possible to locate the point on the tire which causes thump.

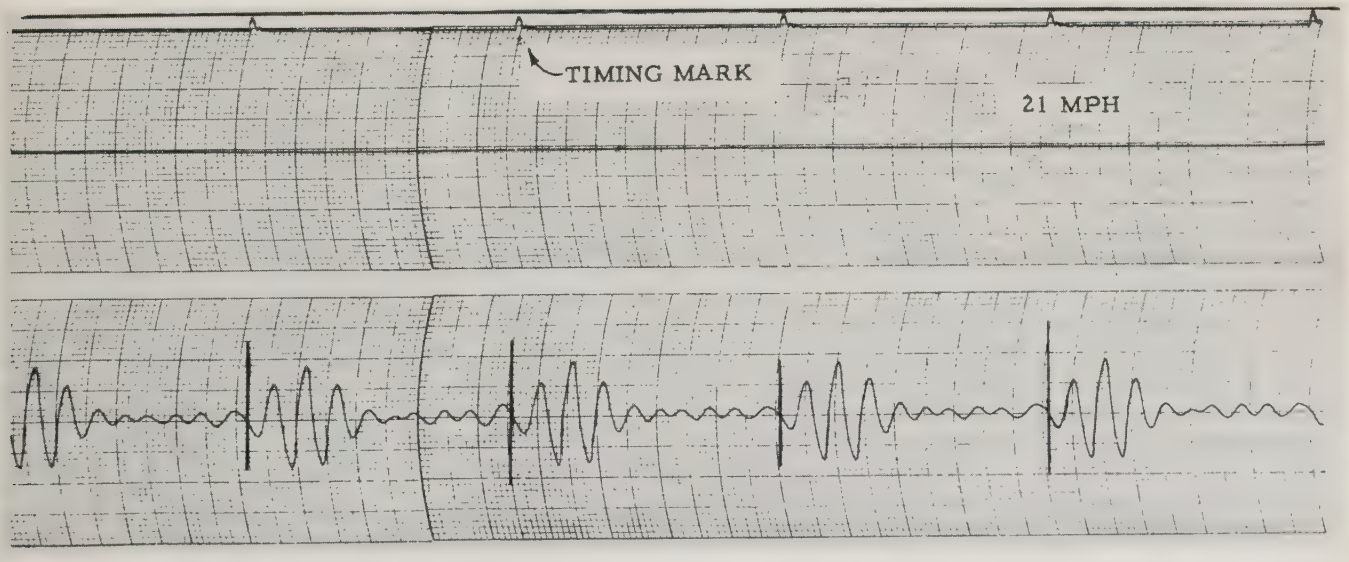

Fig. 3 — Vibration of thumping tire

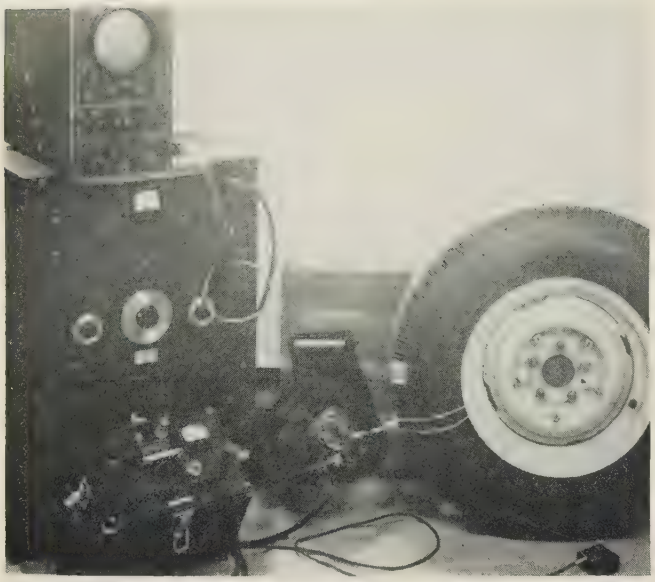

Fig. 4 — Equipment for measuring tire resonant modes of vibration involved in tire thump

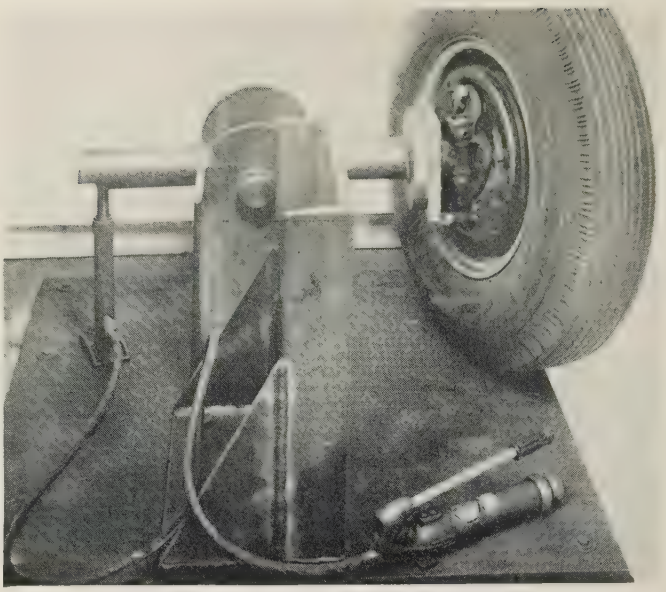

Fig. 5 — Static rig for studying tire thump frequencies

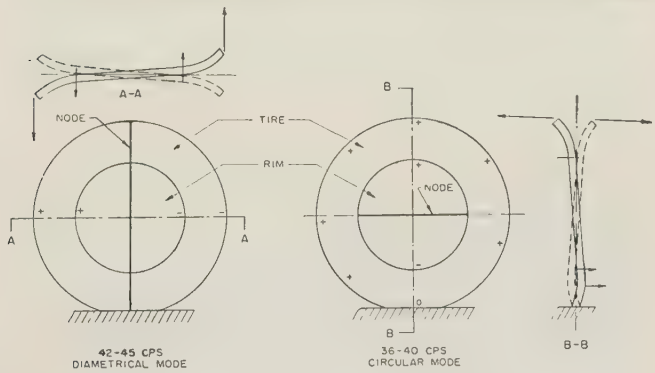

Fig. 6 — Tire vibration modes causing thump

With this recording system, it is possible to determine how thump varies with speed, how it varies with different size and location of exciting discontinuities and also what frequencies are involved.

Why a Tire Thumps

As can be seen from Fig. 3, in the simplest case of thump there is just one modulated wave per wheel revolution always starting at the same point in the wheel revolution. The modulated wave has a frequency of about 40 cps.

In order to find out why thump was always around 40 cps, it was first necessary to find the source of the thump. An intensive study of the entire car showed that the thump vibration could be found all over the body frame and suspension system when there was a thumping tire on one wheel. However, the strongest thump vibration was always found nearest the wheel with the thumping tire. It was, therefore, decided to construct a rig so that the vibrations of a tire wheel could be studied separately. A tire and wheel were driven by an electromagnetic exciter to find the predominant tire resonances. The instrumentation for this procedure is shown in Fig. 4 and the wheel mounting in Fig. 5.

Two modes of vibration of the tire are of importance in thump. These modes are shown in Fig. 6. In the first, called the circular mode, the tire moves sideways with respect to its rim as if it were trying to dismount itself first off one side and then off the other. The amplitude of this motion is maximum at the top of the tire and minimum at the ground and all parts move in phase. In this mode the rim has a horizontal node. The natural frequency of this circular mode on the front wheel of the 1954 Dodge Meadowbrooks used during this investigation under normal conditions of load, tire pressure, and the rest, is about 38 cps.

The second, or diametrical, mode involved has a natural frequency of about 44 cps under normal conditions of load and tire pressure on the front wheel of the test cars. In this mode of vibration the tire and wheel bend and pivot about a vertical axis through the center of the tire and wheel in a manner similar to the motion of the wheel and tire if the steering wheel were turned left and then right at a rate of 44 times per sec.

The frequency of these modes of vibration can also be determined by impacting the tire and wheel while mounted on the rig (Fig. 5). While on this rig the tire was compressed by loading the hydraulic jack simulating the mounting of a front wheel. The axle height was lowered 1 in. from the free condition to simulate the loaded condition of the tire on the front wheel of a car. Under this condition, striking the edge of the tread at the top of the tire in a sideways direction makes the tire vibrate predominantly in the circular mode. A vibration pickup mounted at the top of the rim and measuring motion in a sideways direction produces a signal which when recorded gives a pure decay pattern of the circular mode vibration of the tire and rim. To record the decay pattern of the diametrical mode of vibration the pickup must be placed on the back side of the rim 90 deg from the top of the tire, and in such a direction as to measure sideways motion of the rim. Striking the tire in such a manner as to excite only the diametrical mode of the tire is quite difficult; however, it can be done by hitting the edge of the tread 90 deg from the top of the tire in a direction 45 deg between radial and sideways. From the decay patterns of the two modes, the frequencies and the sharpness of the resonances can be meas-

ured. A sample of these records is shown in Fig. 7. The lowest record shows the beats produced when both vibration modes are excited as in tire thump.

The natural frequencies cannot be determined more accurately than about ±0.5 cps because the frequencies depend on many factors including air pressure, load, contact area between tire and ground, wheel bearing adjustment, temperature of tire, and many others. The frequencies were found to shift from day to day in response to the effects of the above mentioned variables. The tire resonances are quite sharp. When the tire is struck a sideways blow it rings for quite a number of cycles before dying out. A measure of this factor is called the Q of the resonance. The Q of these resonances in the tire has a value of between 15 and 30. This may be computed from the formula $Q = \frac{8.7}{D}$, where D is the rate of decay in db per cycle as found from a record such as Fig. 7.

It can be readily seen that the frequencies of these two resonances are about 6 cps apart. It is well-known in vibration theory that, if two resonances are harmonics of an exciting force and are only a few cycles apart, and the exciting force has a frequency equal to the difference in the frequency of the two resonances, there can be a beat produced such as was shown in previous thump records. This is exactly what happens in thump. The exciting discontinuity produces an impact force which, similar to a note on a musical instrument, contains the fundamental frequency and quite a few harmonics of this frequency. For example: when the car tire is rotating at 30 mph, a once per revolution discontinuity will excite 6, 12, 18, 24, 30, 36, 42, 48 . . . cps vibrations. In our case the sixth and seventh harmonics of the force frequency coincide with the resonances of the tire and produce a beat at the difference frequency. Whenever any two harmonics of the exciting force coincide with the two resonances a loud thump will be produced. Under any condition other than double coincidence, the thump level will be lower and less audible.

Fig. 8 is a graph which has been made to show why the test car used in these studies has the worst thump speeds at 27 and 32 mph. This curve has

SIDEWAYS ACCELERATION ON TOP OF RIM

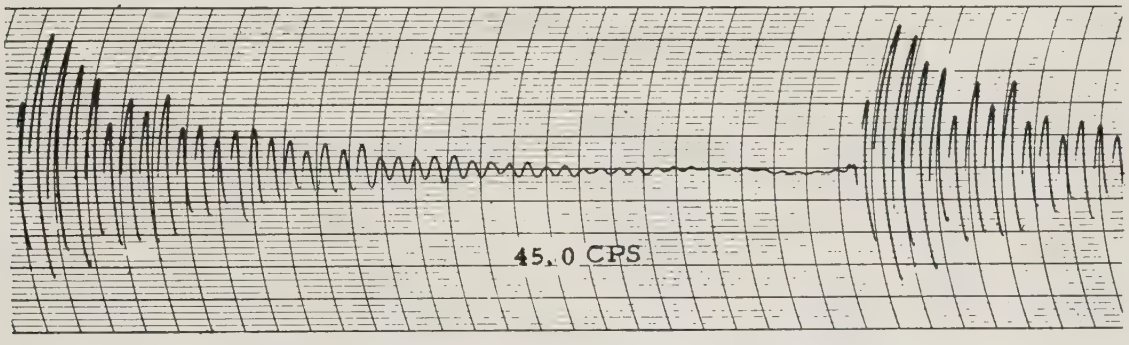

SIDEWAYS ACCELERATION ON SIDE OF RIM

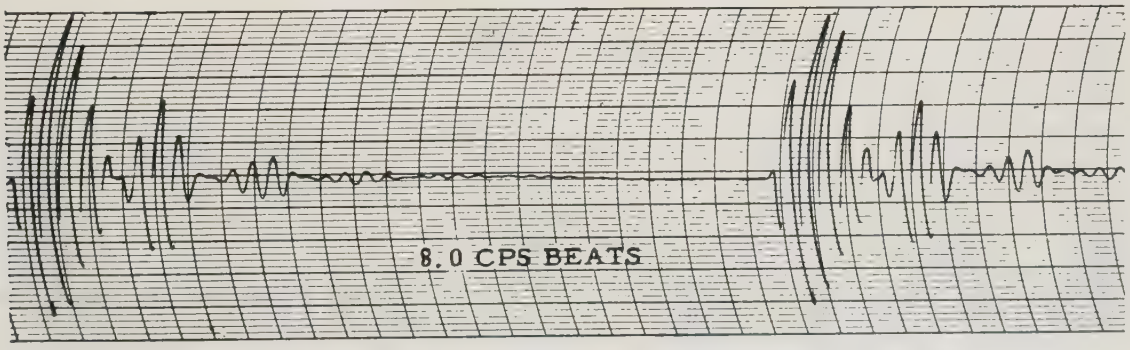

SIDEWAYS ACCELERATION 45° FROM TOP OF RIM

Fig. 7 — Natural frequencies and beats excited by sideways impact on tire, 26-psi tire pressure, normal tire load, tire mounted on test rig

car speed in mph as its ordinate and frequency as its abscissa. There are plotted a series of diagonal lines. The most nearly vertical of these shows the revolution rate in cps of a 7.10-15 tire and wheel. The second most nearly vertical line plots the second harmonic or twice the revolution ratio, and so forth. In this figure if vertical bands are plotted including the ½ power points of amplitude compared to peak resonant amplitude at each of the tire resonant frequencies, a visual observance of the curve will show speeds of maximum thump. As was shown previously, whenever two harmonics of the thump exciting force coincide at the same car speed with the two tire resonances loud thump will result. To use this statement it is necessary only to go vertically down the page in the area of the two tire resonance bands and find the speeds at which any two harmonics coincide with the two tire resonances. In this case coincidence is 16, 19, 22, 24, 27, 32, and 37 mph with the bands at 27 and 32 mph being by far the most pronounced.

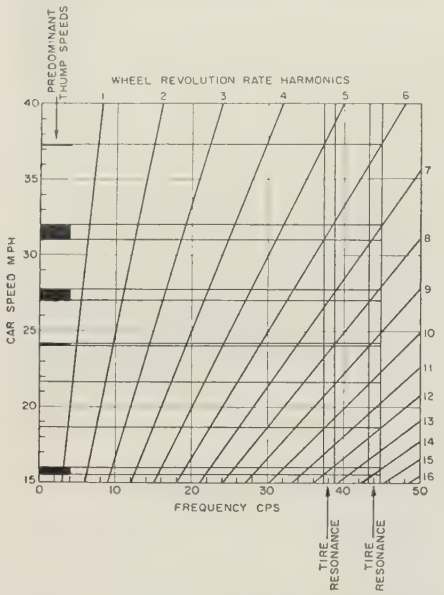

Fig. 8 — Pedominant thump speeds for left front wheel of test car

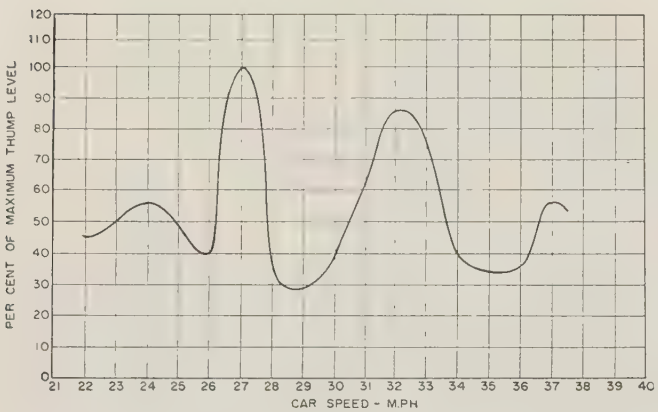

Fig. 9 — Variation of thump level of double bead block tire with speed

How to Reduce Tire Thump

The theory of why a tire thumps the most at certain specific car speeds is easily substantiated by plotting thump level in the car against car speeds. This has been done for a 7.10-15 tire and wheel in Fig. 9. As can be seen the maximum thump speeds predicted from Fig. 8 agree very well with the thump speeds found in Fig. 9. Similar curves were drawn for several different size tires which had different resonant frequencies, and close agreement found.

A close analysis of curves like Fig. 8 show why high-pressure tires (28 lb of air) did not produce much thump. Fig. 10 is the plot using the natural frequencies of a 600-16 tire used just after World War II. The natural frequencies of these tires are 38 cps for the circular mode and 42 cps for the diametrical mode. These frequencies are only about 4 cps apart. As shown in the figure, there are no predominant thump speeds above 23 mph except a marginal case at 26.5 mph.

A similar procedure for a 7.5-14 tire which has natural frequencies of 35.4 cps for the circular mode and 43.7 cps for the diametrical gives the predominant thump speeds shown in Fig. 11. There will also be a higher thump speed at about 42 mph.

Three other factors come to bear on the thump problem. The first is other car noises (or masking noises). At speeds above 35 mph engine noise, wind noise, and others become so loud that they hide some thump noise and make it less objectionable.

Second, the thump exciting force, which should

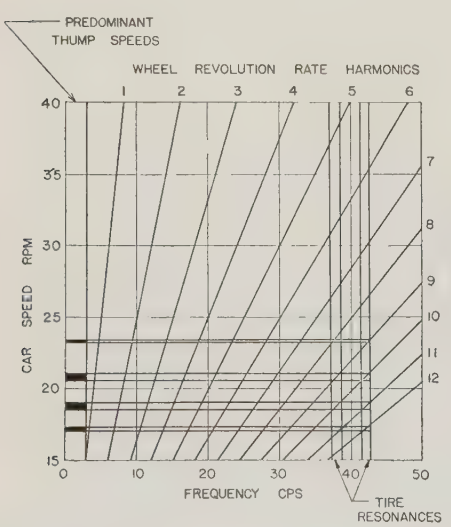

Fig. 10 — Predominant thump speeds for tire resonant frequencies 4 cps apart

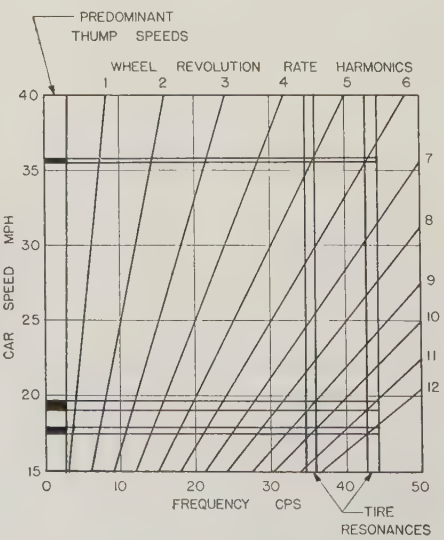

Fig. 11 — Predominant thump speeds of 7.5-14 tire on 1954 Dodge

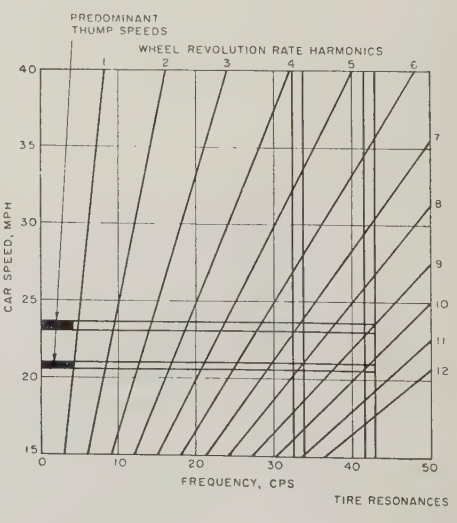

Fig. 12 — Predominant thump speeds for tire resonant frequencies 9 cps apart

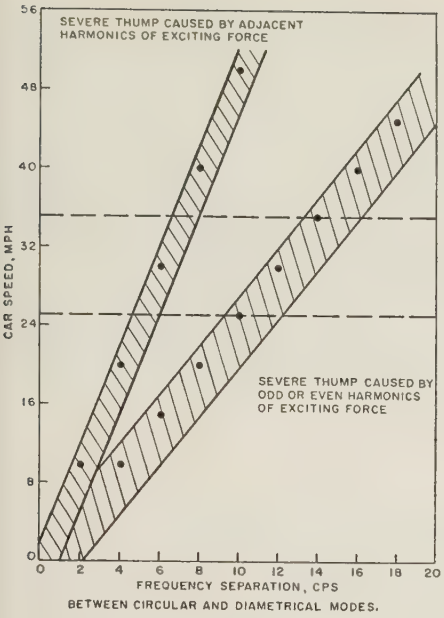

Fig. 13 — Predominant thump speed variation for various tire resonant frequency separations

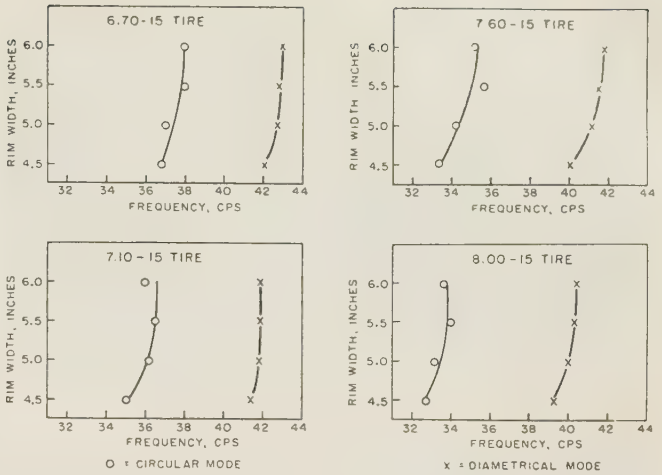

Fig. 14 — Natural frequencies of 15-in. tires on static test rig, 24 lb of air, 1-in. tire deflection

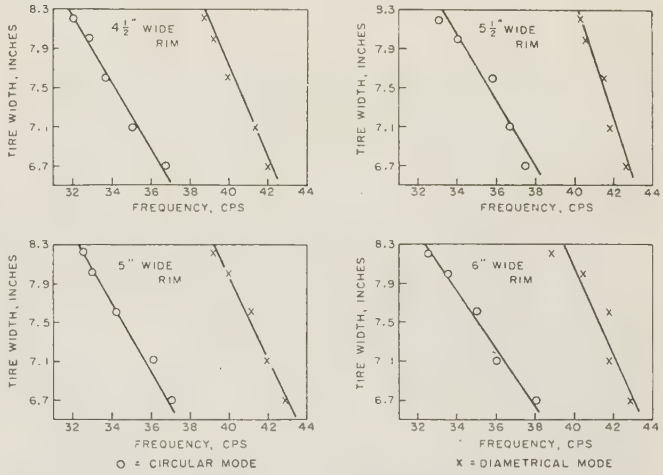

Fig. 15 — Natural frequencies of 15-in. tires on static test rig, 24 lb of air, 1-in. tire deflection

be proportional to angular acceleration or to the square of the tire revolution rate, becomes very small at speeds below about 20 mph and, therefore, produces very little thump. The force is expected to be only a little over half as large at 20 mph as it is at 30 mph. These factors limit the major objectionable thump range to speeds from 20 to 35 mph.

The third factor influencing thump is a dynamic characteristic of the beat phenomenon. In order for two frequencies to beat together and produce a modulated pattern the difference frequency must be small in comparison to the two base frequencies. Otherwise, the addition of the two frequencies will produce very irregular looking pattern which when heard would not seem like a modulated tone such as thump but a disorganized noise such as tire roughness. In the 30–50 cps frequency range of interest in thump study, the frequency separation above which a disorganized pattern is produced is about 10 cps.

Knowing these facts, it is possible to predict what types of tires are susceptible to thump and what type are not. First, tires which have a difference frequency of less than 4 cps between the diametrical and circular modes of vibration will thump only below 23 mph where the relatively small exciting force will not produce much thump. This is shown graphically in Fig. 10. Tires which have a difference frequency of between 4 and 7–8 cps can produce easily audible thump between 20 and 35 mph as shown in Fig. 8. Those which have a difference frequency of from 8–10 cps will produce thump below 23 and a little above 35 mph but somewhat less between 23 and 35 mph (Fig. 12). Below 20 mph the exciting force is reasonably small and above 35 mph the masking noise is large enough to reduce the effect of the thump noise. Above 10 cps the frequency separation is large enough to make the sound or vibration waves add in a relatively disorganized fashion which will sound more like roughness than thump. Most of these factors are plotted on Fig. 13, which shows graphically what the acceptable tire natural frequency ranges are from a thump standpoint. If the difference between natural frequencies of the circular and diametrical modes are plotted on this curve the primary thump speeds will be those for which the two natural frequencies are in the upper shaded region with a little less thump when they are in the lower shaded region. At those speeds where the natural frequencies are in the clear region between the two shaded areas thump produced by the tire will be reduced.

Using the above described technique, the natural frequencies and Q's of 6.70, 7.10, 7.60, 8.00, and 8.20 tires were measured on $4\frac{1}{2} \times 15$, 5×15, $5\frac{1}{2} \times 15$, and 6×15 in. rims. From these data the curves of Figs. 14 and 15 were drawn. From the curves on Fig. 14 it can be seen that for a given size tire the frequencies of both modes of vibration increase as rim width is increased. It can also be seen that the difference between the two frequencies changes very little. Fig. 15 shows that for a given rim width the frequency of the two modes decreased as tire size is increased; however, again the difference between the two frequencies changes very little.

Conclusions

The criteria then for minimum thump is to have a shape and construction which does not permit the coincidence of the two natural frequencies with two revolution rate harmonics in the 20–35 mph range. This was substantially accomplished in 6.00-16 tires and is partially accomplished in most new 14 in.

tires. These considerations of critical thump speeds hold in general for all cars. If there are body panels which have a sharply tuned resonance very close to these frequencies, however, the thump level will be amplified; thus explaining the difference between different models. Within a particular model one of the largest variables is the isolation properties of the body mounts. A slight lack of trueness in either the body or the frame can upset the designed mount attenuation. Overtightening the mounts may either reduce or increase the level, depending on what the mount resonant frequency is compared with the tire natural frequencies.

DISCUSSION

Describes Tire Thump Tests At Cornell Laboratory

— **Hugo S. Radt**
Cornell Aeronautical Laboratory

THE investigation of the thump phenomenon described by Mr. Sanders represents the "research" approach to the problem and embodies careful experiments correlated with theoretical concepts. His approach is the only one which will lead to a final determination of the method for elimination of thump.

A similar investigation, also sponsored by the Goodyear Tire and Rubber Co., is being conducted at the Cornell Aeronautical Laboratory to determine the mechanism and means of curing thump. A 1957 Dodge was instrumented to measure and record sound and vibration in the passenger compartment and three perpendicular motions of the right front wheel. This car was then driven over a smooth road using natural bad thumping tires. Due to the presence of road roughness occurring in the same frequency range as thump, the recordings did not show the repetitive nature of Fig. 2. For this reason, the records were analyzed to determine the content only at frequencies equal to multiples of the wheel frequency or harmonics of the wheel frequency. The content at these harmonics was then averaged over many wheel revolutions to eliminate the effects of road roughness. At this point, it was found that the thump sound in the passenger compartment contained frequencies at many different harmonics of wheel rate, rather than having a predominant pair of harmonics.

In order to provide an understanding of how these harmonics add together to produce the thump sound, a specialized instrument was constructed. This instrument, called a harmonic generator, is capable of providing electrical signals with variable phases and amplitudes at a fundamental frequency and at each of nine other harmonics. Adjustment of the fundamental frequency allows exact matching of the wheel frequency. This harmonic generator was connected to a suitable speaker system and the resulting sounds were subjected to a series of listening tests.

From the listening tests it was found that the character and intensity of thump could be accurately simulated in the laboratory using the harmonic content from the actual road tests. It was also discovered that the first three harmonics could be neglected because, for thump speeds, they are below the range of audibility. Finally, recordings were made of the sound from road tests, including only the fourth through the tenth harmonics. These records have the same appearance as Fig. 2 but contain more than a pair of harmonics. Hence, it was concluded that the thump sound is not a beating between two harmonics of wheel frequency, but a variation in the amplitude of a more complicated wave. The intensity of thump, then, depends on the relative magnitude of the variations in amplitude. Similar results were obtained for measurements of wheel motions. Again, more than a pair of harmonics were significant.

If we consider the tire vibrations to be transmitted directly through the wheel suspension to the passenger compartment, we would expect to find two predominant frequencies in the sound measurements. These frequencies would be equal to the two resonances mentioned by Mr. Sanders. However, additional frequencies or harmonics were found in the sound measurements and were large enough to be important. How can the appearance of these additional harmonics be explained? Three possible reasons are given. First, consider a bad thumping tire with irregularities distributed in some fashion around the circumference. As these irregularities pass through the contact region, forces are generated within the tire. These forces, in turn, excite the natural modes of vibration. Although there may be two major tire vibration modes, there also may exist other minor modes. Now, provided the exciting force is sufficiently great at frequencies corresponding to the minor modes, they too may be excited. Thus, vibrations might occur at frequencies other than those of the two major tire modes. Second, resonances of the wheel suspension system, in each of three directions, may amplify the vibrations induced in the tire at frequencies other than the two main natural frequencies. Finally, the sound in the passenger compartment is affected by the resonance characteristics of the many body panels and by the acoustic characteristics of the enclosed chamber. In the thump frequency range, the response of sound to wheel motions at various frequencies shows numerous peaks and valleys. Each of these may amplify or attenuate vibrations coming from the tire at frequencies off the two main resonant frequencies described in the paper.

In view of these considerations, it is not unusual that content at more than two harmonic frequencies appears in the sound and wheel motions. Further research on the vibration characteristics of the rolling tire-wheel combination should determine whether consideration of several harmonics, rather than a single pair, is required to understand and to eliminate thump.

ORAL DISCUSSION

Reported by G. M. Vanator, General Motors Corp.

L. A. Nedley, General Motors Corp.: What effect does tire pressure have on the principal tire mode frequencies? In Figs. 11 and 12 there are speeds indicated where the beats are not due to adjacent harmonics but are separated by two orders. Does this sound like two thumps per wheel revolution or one?

Mr. Sanders: Insofar as the two primary tire resonances are concerned, an increase in tire pressure increases the frequency of both modes. The diametrical mode, however, increases in frequency more rapidly than the circular mode; hence, the frequency separation increases. Above 50 psi there is not much thump left. Except for intensity, the sound does not change a great deal with tire pressure.

As for beats produced by frequencies that are separated by two orders of wheel speed, the resulting thump generally sounds like one thump per wheel revolution but, under certain circumstances, can sound like two thumps per wheel revolution.

M. E. Weldy, General Motors Corp.: Were tests made comparing rim sections? 550 K and 550 L rims have different flange heights, which might have an effect on thump.

Mr. Sanders: We did not make tests of this nature. However, we did stiffen a rim by welding a 1-in. square section ring to the inside. This had no appreciable effect on thump.

D. C. Apps, General Motors Corp.: The author's data predicts a lessening of the thump problem with the advent of 14-in. tires. Do the tire companies have sufficient data to confirm or deny this?

Dr. W. H. Hulswit, U. S. Rubber Co.: Our experiences do not show a definite trend. On the 1957 Chevrolet, 14-in. tires did not make a change in thump; however, I think that the 1957 Chevrolet was somewhat more sensitive to thump than the 1956 model. I am not certain what the effect of tire size change has been with the other GMC cars.

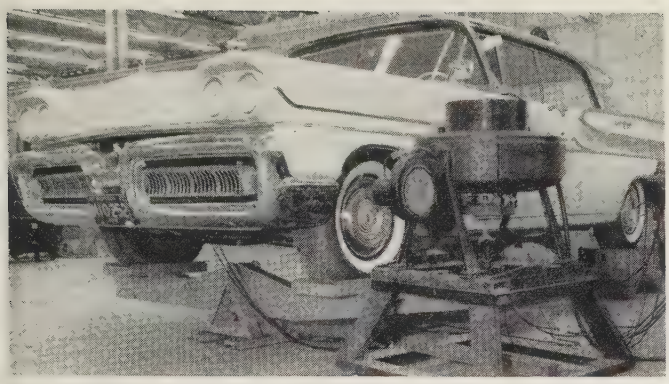

Fig. 1 — Torsional vibration setup

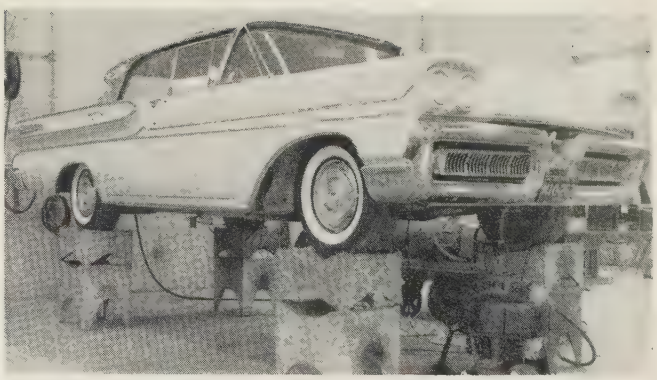

Fig. 2 — Bending vibration setup

Simulating Road Shake in the Laboratory

K. P. Pettibone, Ford Motor Co.

This paper was presented at the SAE National Passenger-Car, Body, and Materials Meeting, Detroit, March 4, 1958.

BEFORE investigating car shake in the laboratory, shake measurements and observations are made on the road. The observations indicate the areas of objectionable shake which will be carefully investigated during the laboratory testing, and the measurements determine the mode or manner in which the car shakes. To effect a cure in the laboratory, the correct mode must be reproduced. The measurements also indicate the frequencies of shake occurring on the road and the frequencies of vibration of the front and rear wheels, the source of the exciting forces. With this information, the critical road shake can be reproduced in the laboratory for study under controlled conditions.

To obtain the mode of shake that occurs on the road, velocity pickups are located at certain key points on the car:

1. Right front fender (vertical).
2. Left front fender (vertical).
3. Frame or body just aft of the midpoint both right and left (vertical).
4. Steering wheel (vertical and lateral).
5. Front seat frame (vertical and lateral).
6. Front and rear wheels (vertical).

Oscillograph recordings of a signal proportional to amplitude (velocity integrated) with a time base are made on typical shake roads. A study of the oscillograms indicates whether the fenders vibrate primarily in phase for a symmetrical or bending mode of shake or 180 deg out of phase for a torsional mode of motion. Since torsional shake of the front-end sheet metal may be accompanied by either a bending or torsional shake of the center of the car, the phase relationships of the pickups at that location are also noted. The frequencies of the maximum amplitudes of vibration determined on the road are investigated for possible resonant conditions during the laboratory test. Also, the wheel frequencies obtained from the oscillograms indicate the ranges outside of which it is desirable to have structural natural frequencies occur.

In the laboratory, the predominant or objectionable mode of shake may be reproduced in several ways. One method is the use of large rotating drums that not only support either the front or rear wheels but actuate wheel motion by surface irregularities. This method is particularly good for studying suspension or driveline action. However, since the structure was of primary concern, a way of exciting the shake was developed that permitted close observation and amplitude measurements along the length of the vehicle, and that used available laboratory equipment. For *torsional shake,* the front or rear wheels of the car are supported on and excited by a transverse beam pivoted at the longitudinal centerline of the car. The wheels at the end of the vehicle opposite the "shake rig" are supported on wheel blocks. To excite the vibration, an electromagnetic vibrator is attached to the transverse beam outboard of the vehicle (Fig. 1). The force applied to the beam by the vibrator is monitored by a load transducer and a direct-inking oscillograph. After an arbitrary force is selected that can be maintained through the range of shake frequencies, about 10–20 cps, the natural frequencies of the various modes of torsional shake may be obtained. This is accomplished by applying the constant maximum exciting force and measuring the shake amplitudes at the locations checked on the road at ½ cps increments of frequency. The frequency at which the

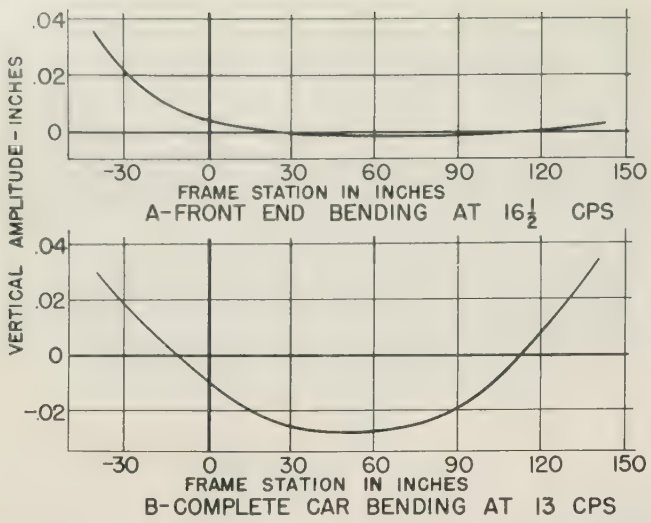

Fig. 3 — Bending at different frequencies

amplitudes of shake are a maximum is considered to be the natural frequency for that mode. One of the two most predominant modes of torsional shake is recognized as front-end torsion and is identified by maximum shake amplitudes about 180 deg out of phase for the front fenders. At this time the center and rear of the car are relatively quiet. The second common mode, identified as complete car torsion, occurs when the motion of the front end of the car is 180 deg out of phase with the rear and the relative movement between the front and rear is a maximum.

Symmetrical or *bending shake* is produced by supporting the vehicle on wheel stands and locating the vibrator centrally at the front, center, or rear of the chassis (Fig. 2). A constant maximum force is applied to the frame at one of the above locations by an electromagnetic vibrator. Amplitudes at the various locations on the car are measured at ½ cps increments of frequency through the shake range. In the same manner as for torsion, the natural frequency of the various bending modes is indicated by maximum shake amplitudes. One of the two most common modes is the primary mode of complete car bending indicated by maximum center of the car vertical shake amplitudes and accompanied by a peak in the amplitudes of the front and rear ends of the car (Fig. 3B). The other is that of front-end shake. During this mode, the center of the car is relatively quiet. The deflection of the structure for this mode of shake is shown in Fig. 3A.

To determine the natural frequency of front-end shake, characterized by maximum vertical amplitudes of the front-end sheet metal, the exciting force should be applied at the front end of the vehicle. The natural frequency for the center of the car vertical shake may be obtained with the exciting force applied at the front, rear, or center of the car.

The amplitude versus frequency response curves for the front-end sheet metal and front seat frame of a typical car are shown in Fig. 4. The first peak in the amplitude curve for the sheet metal corresponds with the peak for the front seat frame and indicates the natural frequency of the mode of complete car shake shown in Fig. 3B. The second peak in the sheet metal curve which is missing from the seat frame curve indicates the natural frequency of the front-end bending mode (Fig. 3A).

In attacking vibration problems, the most desirable solution is the elimination or isolation of the exciting forces. Since automobile shake is generally excited by the suspension system which is in turn excited by irregularities in the road surface, this would mean providing smoother roadways or changing the isolation characteristics of suspensions. In the future, improved roads and suspension systems may eliminate the problem of car shake, but for the present, a more practical means must be pursued. The frequently used method of capping the frame or reinforcing the structure may reduce shake in proportion to the increased rigidity, which for economic reasons usually is small, provided that the part of the structure doing the actual deflecting is reinforced. A more positive method of reducing shake makes use of the principle that an exciting force which occurs at the natural frequency of a vibrating system may produce amplitudes 10 times those occurring for the same force three cycles away from natural frequency (Fig. 5). This method (known as "detuning") is possible because the suspension systems tend to transmit sustained forced vibrations for a limited range of frequencies. The natural frequencies of the various modes of vibration of the structure may then be detuned as far as possible from the frequencies of the suspension movement occurring on the road. For example, a convertible car having excessive shake on the road was found to have a natural frequency for the torsional mode in the laboratory of 12.5 cps. This was not only the frequency of structural shake occurring on the road but also the frequency of the front suspension. A 58% reduction in the car's torsional rigidity lowered its natural frequency from 12.5 to 8.5 cps. Detuning the natural frequency of the structure from the frequency of the suspension movement on the road resulted in about a 20% reduction in shake amplitudes determined on the highway (laterally at the instrument panel and vertically at the front fenders). When practical, increasing rigidity to move the natural frequency of the structure above road frequencies may be more desirable.

Along with detuning, isolation by the removal of or increased flexibility of certain body mounts may also reduce shake. Finally, after detuning and isolation have been explored, there remains the possibility of absorbing the exciting forces. Generally, this last method should be considered only as a last resort since it is frequently accompanied by difficulties.

To indicate how an actual shake problem may be investigated in the laboratory, it will be assumed that a vehicle has objectionable front-end sheet metal shake. First, the mode and frequency of the front-end shake are determined on the road along with the frequency of wheel movement. Then the car is brought into the laboratory and the structure is vibrated in the mode and at the frequency of shake occurring on the road. At this time, the masses vibrating (front-end sheet metal, engine, and front end of the frame) are noted as well as the part of the structure acting as the "spring" with the idea of detuning in mind. In finding the "spring" the shake amplitudes of the fenders, hood, radiator support, frame cross members, and side rails are checked. If the front-end sheet metal shake is

greater than that of the frame side rails, the possibility exists of changing the rigidity of the offending part of the structure between the frame and fenders, such as the hood lock plate. Should the sheet metal and frame be in phase and have the same amplitude, the amplitudes of the side rails and sheet metal are obtained along the structure and plotted to determine the area acting as the "spring."

The natural frequency of the particular mode involved is obtained and compared with the frequency of the shake occurring on the road and the suspension frequencies. Generally, if objectionable shake occurs on the road, the natural frequency found in the laboratory either corresponds exactly or is very close to the frequency occurring on the road. Therefore, knowing the vibrating masses and the "spring," the principle that natural frequency varies directly with the square root of the spring rate or stiffness of the deflecting structure and inversely with the square root of the mass is explored. Since the engine represents a large percentage of the vibrating masses, varying its mounts is investigated in an effort to detune the natural frequency of front-end shake. By using mounts with a high vertical rate, the engine mass may be made to move with the frame or by using low rate mounts, the engine may be isolated from the frame or actually made to move out of phase with the frame. The high vertical rate then increases the effective vibrating mass, whereas the low rate reduces the effective mass. Substantial changes in natural frequency and front-end sheet metal shake have been produced by changes in engine mounts (Fig. 5). Engine mounts having different rates are installed to determine the lowest vertical rate resulting in the desired change in natural frequency. Other characteristics such as noise and harshness are affected by the engine mounts so that a compromise is generally necessary. Since mounts having high vertical rates usually result in the least front-end shake, an evaluation as to how high the rate may be without the sound and harshness becoming objectionable should be made.

If sufficient detuning and shake reduction is not accomplished completely with engine mount changes, the survey of the structure is made to determine an area of possible local weakness. With the car vibrating at the frequency of road shake, amplitude measurements are taken along the structure at 10-in. stations and the deflection curve is plotted similar to the usual static deflection curves. (see Fig. 3.) Assuming the natural frequency of the front-end shake was found to be higher than the frequency of the disturbing road shake, the area indicating a weakness can be reinforced further both to detune the frequencies and to quiet the shake due to the increased rigidity. If, however, the natural frequency of the structure is below that of the shake on the road, reinforcing the structure tends to make the two frequencies coincide and in spite of the increase in rigidity, the shake amplitudes may tend to increase.

It is interesting to note that some cars have natural frequencies of both torsion and bending in the frequency range of wheel movement on the road. In most of these instances, the torsional mode occurred more frequently on the road. Comparing two cars, one was reported to have objectionable center-of-car lateral shake and the other was considered quite acceptable. The acceptable car had the natural frequency of torsion above the range of wheel frequencies and the objectionable car had its natural frequency of torsion directly in the range. Both cars, however, had the natural frequency of bending in the range of wheel frequencies. In other words, the torsional mode may be excited more frequently on the road, probably as a result of road irregularities being unsymmetrical for the right and left wheels. Detuning the natural frequency of torsional shake from the suspension frequencies may be more important than detuning the bending frequencies.

In conclusion, the procedure proposed for investigating shake problems in the laboratory may be summarized as follows:

1. Determine the mode and frequency of the objectionable shake on the road and the frequency of front and rear wheel movement.
2. Reproduce the same mode of shake in the laboratory and determine its natural frequency.
3. Note the principal masses of the vehicle that are vibrating and determine the part of the structure which, by its distortion, is acting as the "spring" of the vibrating system.
4. Vary first the effective mass (make changes in engine mounts) and then change the "spring" rate to detune the natural frequency of the structure as far as possible from the wheel frequencies.
5. Try isolation and absorption if necessary.

After completion of the above program, the reduction in car shake — although indicated by the laboratory measurements — should be evaluated by observation ratings and amplitude measurements made on the road.

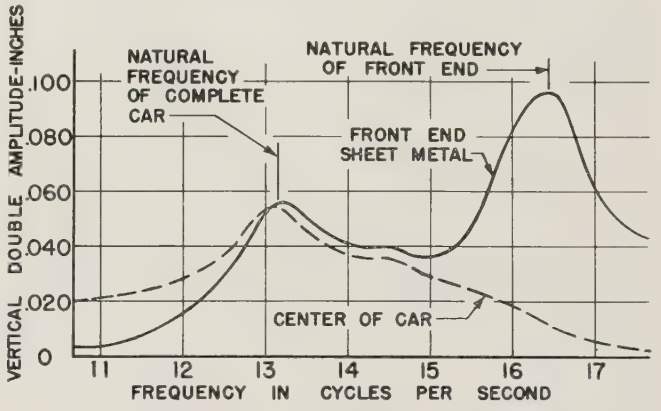

Fig. 4 — Natural frequencies indicated for bending excitation

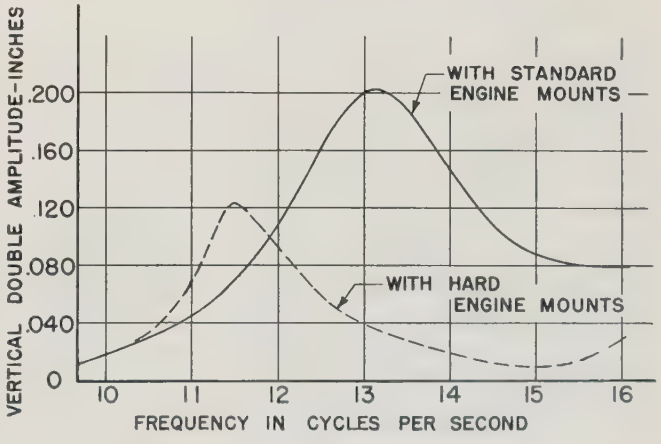

Fig. 5 — Front-end shake with different engine mounts

The Effect of Engine Mounting on

L. M. Morrish, Buick Motor Division, General Motors Corp.

This paper was presented at the SAE National Passenger-Car, Body, and Materials Meeting, Detroit, March 4, 1958.

JOHNNY, bouncing down the road in his 1928 Maxwell, is not interested in car shake. Farmer Pete, using his well-loaded but poorly lubricated pickup truck for a Sunday jaunt across the country, recognizes the problem but considers it normal. The modern automotive engineer is very interested in this subject and cannot consider shake as normal, or even as a necessary evil. Today's car, with its greater power, larger tires, longer wheelbase, heavier weight, and softer ride presents a challenge to any engineer interested in dynamics. The effect of engine mounts on car shake could be considered as nil if mounting engineers were allowed to stiffen the mounting of all of the other components, disregarding the adverse effect this would have on their other functions. The frame engineer, for one, could likewise solve some of his problems by changing engine mounts without regard to their primary function.

ENGINE mountings exercise considerable control on car shake, provided other major shake-affecting components are designed within a reasonable limit from optimum. Although they have very little effect on the overall static strength of a car, it is possible to make changes in the car's behavior by controlling the frequencies of the powerplant and the damping of its mounts.

The author discusses methods of reproducing shake in the laboratory: the stroking machines used to determine dynamic rates and hysteresis of spring members and the Buick mount testing machine for determination of dynamic rate and efficiency of mounts. He also mentions the effects of tuning and damping.

Engine mountings do exercise considerable control on car shake, provided that the other major shake-affecting components have been designed within a reasonable limit from the optimum. No mounting change can appreciably correct a poorly designed and weak frame structure; no mounting change will prevent wheel hop.

Knowledge of the role played by all major car components on car shake can save many hours of cut-and-try road work. Because the powerplant represents a large spring-suspended mass, it is only natural that we take a close look at its effects upon shake early in our study.

We have available some tools for shake test work:

1. Nature provides us with meters in the seat of our pants which, by reading the effects of our natural balance and motion mechanisms, can be very useful. This natural meter can function very well with certain limitations: it is very poorly calibrated; it has no permanent recording devices and thus has a very poor memory; it is influenced by external fields which may be psychological or physiological in nature. Because this meter is the final "go, no-go" gage of public approval, we must use it; but we may well leave it as a final check against other more efficient methods.

2. All automotive engineers are familiar with shake roads as shown in Fig. 1—roads which may display many types of random or repetitive patterns, but roads on which the shake-causing characteristics

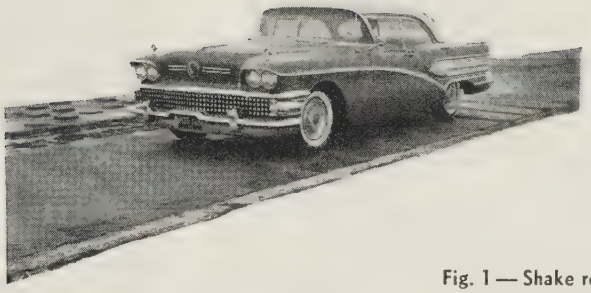

Fig. 1 — Shake road

Car Shake

will be maintained for long periods of time. These roads, combined with either human or mechanical measuring devices, can be of great help. Again, this tool can best be used for checking other tools and for a final check on results obtained by other means having fewer variables present.

3. The shake rolls or bump rig (Fig. 2) can help to remove some of the road variables by bringing the shake test into the laboratory. Again the human shake meter will work, but it can now be combined more effectively with another meter of nature, the human eyes. Visual observation of many portions of the car, especially with the help of strobe lights, can be effective. This second human meter has all the shortcomings of the one mentioned earlier. But now we can more effectively use man-made measuring and recording devices. The complexity of these recorded results indicates that further simplification might be desirable.

4. So we turn to artificial methods for producing resonant conditions of car units. Two examples, a mechanical and a magnetic, are shown in Fig. 3. Shakers installed on the frame (Fig. 4) can reveal basic facts and shakers installed on the powerplant (Fig. 5) or on other large members can supplement these facts. Stroking machines can determine dynamic rate and hysteresis of spring members. Fig. 6 shows the Buick mount testing machine which is an invaluable tool for determination of dynamic rate and efficiency of all types of mounts and which can also provide effective life comparisons by the application of a constant deflection or constant energy stroke.

5. Another effective tool which recently has been added to our list is the complex computor, such as the Buick IBM 705.

Testing

All car shake testing requires that knowledge of the overall problem be available. This paper cannot cover all facets of shake testing; therefore, the discussion will be limited principally to shaker-imposed vibrations in the laboratory. Only frame-

Fig. 2 — Bump rig

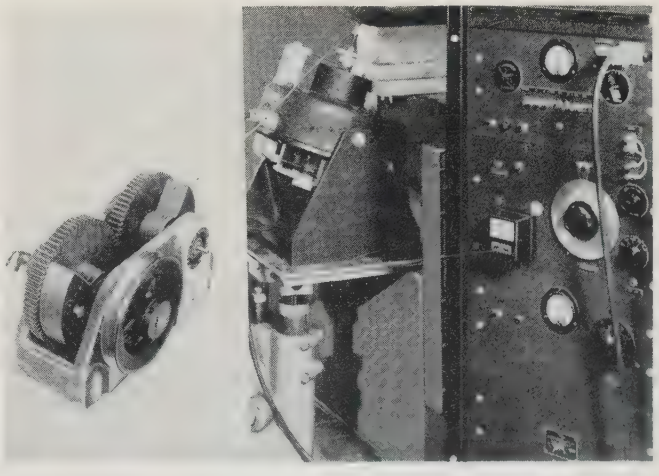

Fig. 3 — Mechanical and magnetic shakers

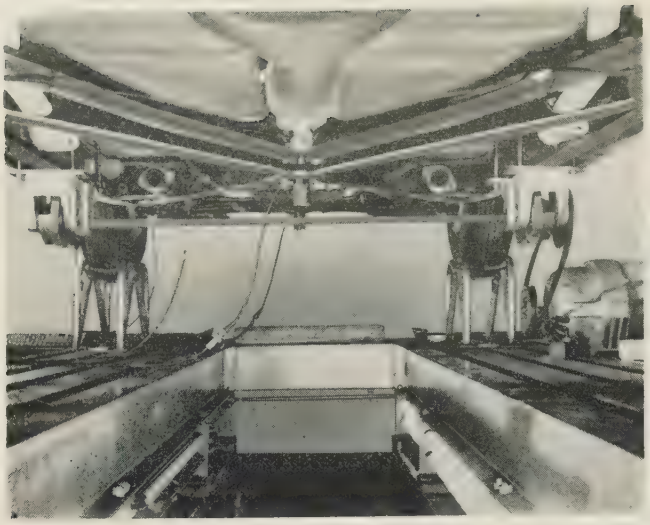

Fig. 4 — Mechanical shakers on frame

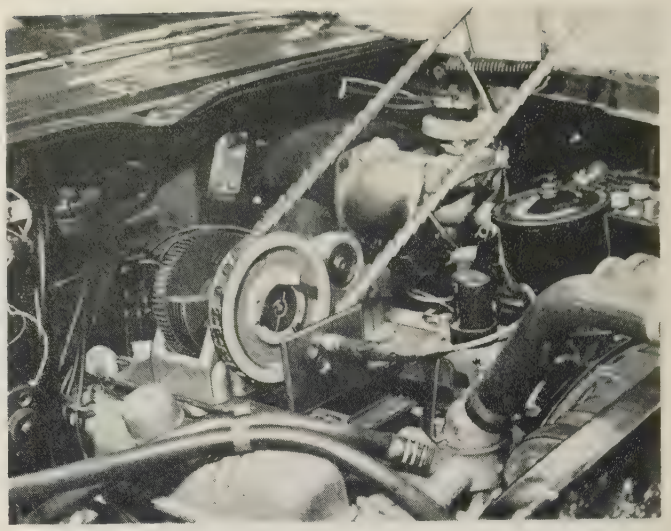

Fig. 5 — Mechanical shakers on powerplant

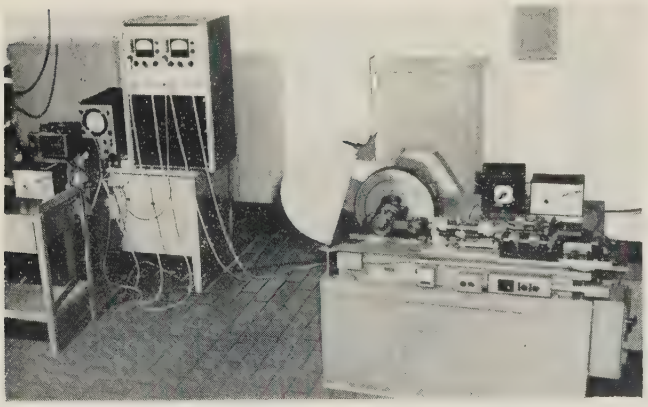

Fig. 6 — Dynamic mount testing machine

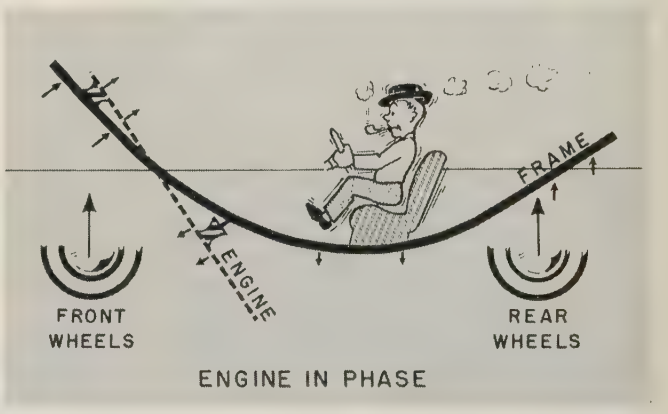

Fig. 7 — Relative frame beaming amplitudes at frame natural frequency, poorly tuned mounts

body beam bending in the vertical plane and engine vertical or pitch modes will be considered.

Engine mounts have an important primary function, as evidenced by their name. First, they must mount or support the engine under all load conditions. An implied and very important consideration is that they also support the engine with minimum transmission of noise and vibration into the frame. If nothing else is considered, it becomes immediately apparent that the softest mounts which are economically feasible would be ideal. Most modern mounting systems have spring rates which are materially reduced from past years. Reduction of spring rates means reduction of resonant frequencies. Such a reduction can tend to remove the mass effects of the powerplant from the mass of the frame-body, thus the frame-body shake frequencies can be expected to raise while the powerplant resonant frequencies lower. Proper control of these factors can pay dividends.

Motor mounts have been shown to have very little effect on the overall static strength of a car but, by controlling the frequencies of the powerplant and the damping of its mounts, appreciable changes can be made in the behavior of the automobile due to the influence of the dynamic stiffness and mass of the powerplant. Fig. 7 shows the little man shaking down the road while sitting in a car that has much wheel hop, a weak frame, and poorly tuned or located engine mounts. You will note that the rear of the engine appears to be moving further than does the frame. Also, Fig. 8 shows that the phase relationship is such that no help can be expected from the powerplant acting as a dynamic absorber, except for that energy absorbed by viscous action of hysteresis of the mounts. Fig. 9 shows this same little man in his new car which has been designed to reduce shake. The bounce amplitude of the little man is considerably reduced; also, the powerplant motion relative to the frame has changed. This standard frame has been graphed to show no particular local weakness and, while it may not be ideally stiff, bending is relatively uniform.

No motor mount corrections can be expected to replace the need for proper structural design. A check of Fig. 10 will show that the powerplant may now have the proper phase relationship to indicate that it is working as an oversize dynamic absorber. This requires that the mounting system be tuned so that a correct phase relationship will exist at peak shake frequencies as the passenger knows them. A plot of the frame displacement curves will also indicate this (Fig. 11). For many years we have attempted to make better use of the fact that the phase relationship between moving units of the car can be a most important factor for determination of resonance. It has only been in recent years that tools have been made available which allow us

to determine quickly and easily accurate phase relationships. Fig. 12 shows a powerplant and frame displacement recording with enlarged sections taken at specific points of interest. These enlarged sections can be one way to determine phase relationships. Other accurate methods are now in use which do the same thing.

The well-known Frahm dynamic absorber, which the powerplant now appears to simulate, can be replaced by an equivalent mass attached to the main system so that the equivalent mass is positive for slow disturbing frequencies, is infinitely large for excitation at the absorber resonant frequency, and is negative for high-frequency excitation. This absorber acts like an infinite mass for the frequency to which it is tuned, thus enforcing a *node* at the point of its application. For other frequencies, it acts like a mass which is not infinitely large and thus does not particularly affect the situation. The absorber can be made to work to advantage by the introduction of a certain amount of damping in its spring. The addition of damping results in some interesting effects. There can be no damping energy dissipated without motion. When the damping force is zero, no work is done by the absorber and, hence, the amplitude of the resonant system is infinite. When the damping force is infinite, the two masses are locked to each other so that their relative displacement is zero; and again, no work is done. Somewhere between a zero and an infinite damping, there is a value for which the product of the damping force and displacement becomes a maximum and the resonant amplitude will be small. No attempt will be made here to show how this optimum damping range can be achieved, inasmuch as this procedure is a full presentation by itself.

Damping is advantageous in the region where the ratio of the impressed frequency to the resonant frequency approaches one; but for all values where the mounting can be expected to reduce transmission (of noise and vibration in this case of comparison), the presence of damping makes transmissibility worse. (See Fig. 13.) Luckily, this bad effect of damping is not great, so that a desired mount efficiency may have a reasonable tolerance spread

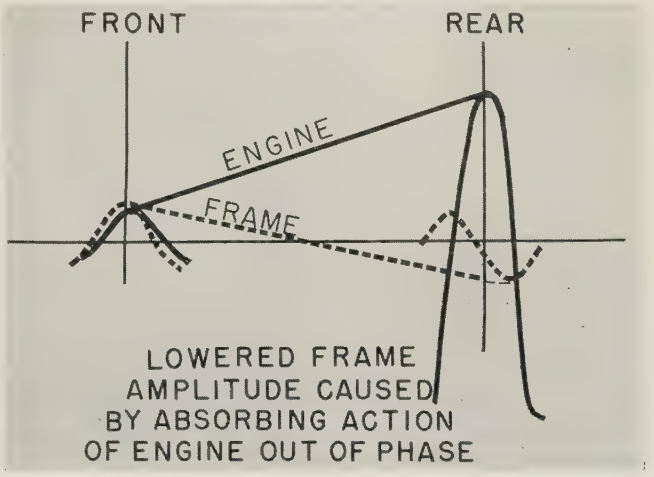

Fig. 10 — Instantaneous displacement curves, showing rear mount working and engine absorbing

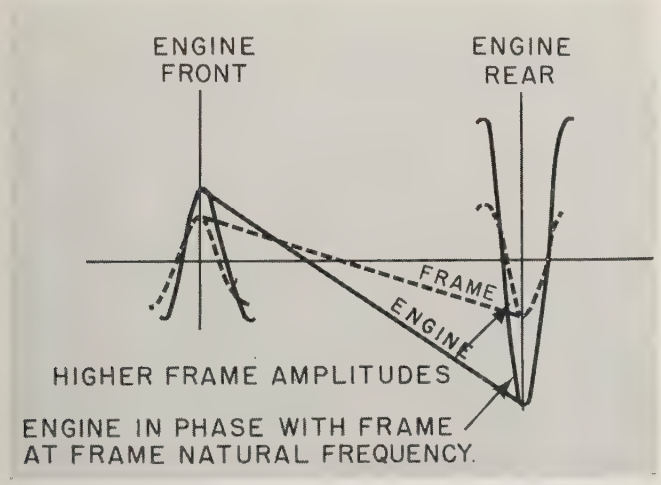

Fig. 8 — Relationship of poorly tuned engine mounts

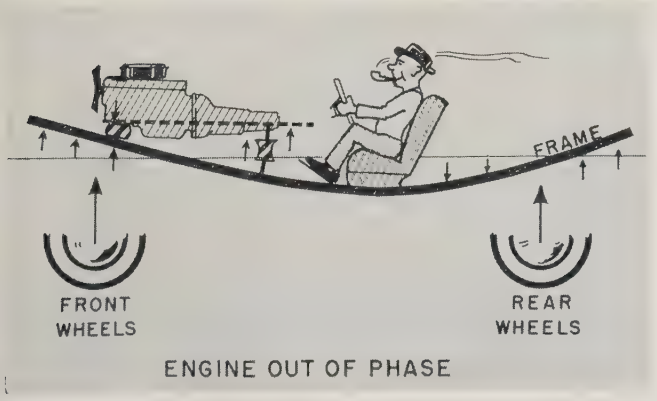

Fig. 9 — Relative frame beaming amplitudes at frame natural frequency, properly tuned mounts

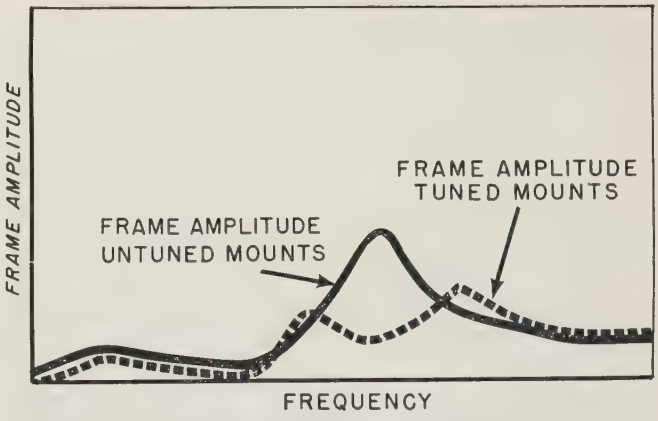

Fig. 11 — Damping action of tuned engine mounts

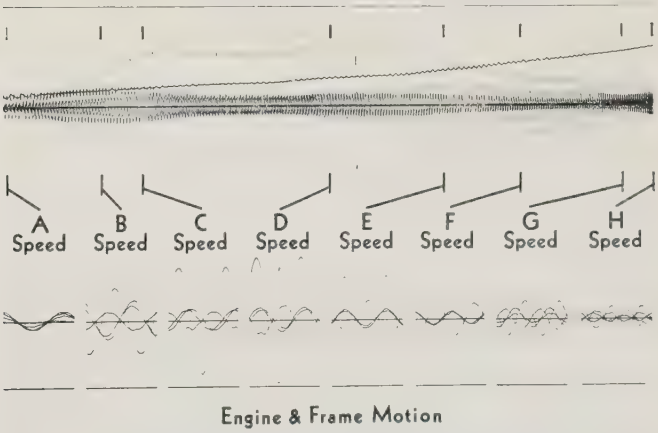

Fig. 12 — Comparative frame and engine motion from which phase relationship can be determined

to satisfy the manufacturing needs and to maintain optimum damping within the operating temperature variations.

Of course, it is not the general intention to design mounts which will be required to operate continuously in an engine speed range where resonance can occur because, as can be seen, noise and vibration problems could be severe. But most modern automobiles do have engine mounting systems which resonate in some mode adjacent to peak shake frequency ranges. Therefore, serious consideration must be given to the effects of tuning and damping. If the natural frequency of the powerplant mounting is far below that of the impressed forces, the powerplant ceases to move and, as a result, will proceed down the road in a straight line regardless of the shake imposed on the frame end of the mounts. This, of course, can result in the absorption of energy by low-efficiency mounts; but can also result in a very low-frequency jack-rabbit effect of the powerplant oscillations when low-frequency disturbances are imposed. Such a soft mounting would show large static deflections due to engine weight, and might require extra room due to engine roll caused by torque reaction. Suspension frequencies would introduce new problems.

It could be shown that, ideally, the absolute motions of the sprung and unsprung masses (powerplant and frame in this case) should be damped independently. The practice of damping the relative motions between these units is a compromise. The efficiency and the dynamic rate are controlled in Buick mounts; durometer hardness and static spring rate are rarely mentioned.

Most automotive design engineers cannot foresee the day that their management will approve the use of independent dampers representing up to 10% of the weight of each sprung mass, so that these masses (body, frame, powerplant, suspension systems, and the like) can be damped by units which have no other function.

Another important consideration which affects both the tuning and the damping of the mounting system is the relative mechanical impedance of the attaching parts. When using a shaker which applies a harmonic force of which the frequency can be gradually changed, if we measure the force as well as the motion amplitude and the phase angle for each frequency, we can then show the mechanical impedance. This can be very important when large masses, such as automotive powerplants, are designed to be spring-suspended from relatively light foundations, such as the automotive frame. Actually, all the considerations mentioned regarding the function of the mounts on shake can ultimately be considered as a function of mechanical impedance and impedance ratios. The dynamic spring rate of the rubber mounts must be appreciably lower than the attaching members so that a favorable impedance ratio can be noted — this requires that such units as cross members be made relatively stiff so that maximum mount benefits will be gained.

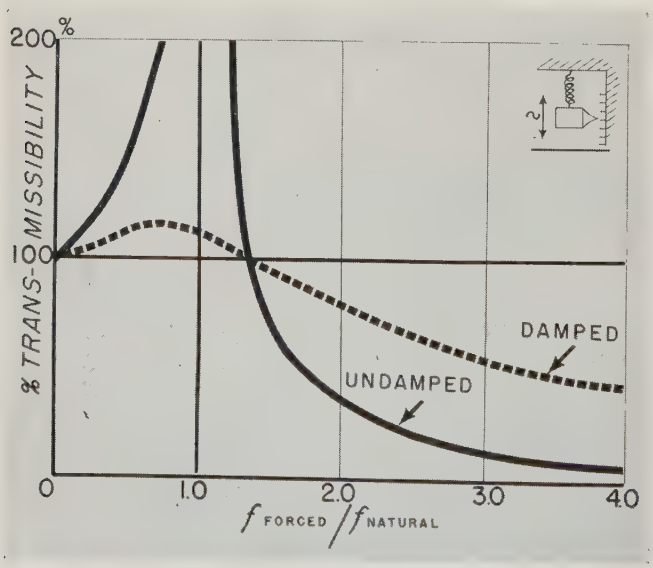

Fig. 13 — Typical transmissibility curve

While many valid conclusions can be drawn from this type of work, it would be wrong to suggest here that this simplified example is complete to the point where we could now release drawings for production and sit back until a new problem is presented. Nothing is further from the truth. Only partial effects of two modes of engine motion have been considered, no discussion has been presented regarding the important effects of wheel hop, sheet metal shake, or many other controlling spring-mass factors. The effects of forces imposed by the particular type of drive must be considered; the benefits of proper mount location, as indicated by the present trend toward the center-of-percussion positions, are important. It can be readily seen why so many shake investigations are still recorded principally by that meter in the seat of our pants.

Summary

The function of engine mountings on car shake can be summarized to be twofold:

1. Because of their ability to control the resonant shake frequencies of the power plant to a great extent, and because of their ability to control the resonant shake frequencies of the frame-body to some lesser extent, an engine mounting system can be tuned for optimum shake results. Generally, such tuning will force the necessity for a recheck of the noise and vibration results, after which time a compromise may be in order. Changes in mount spring rate, changes in mount location on the engine and frame, and changes in mount positioning relative to the rubber shear and compression planes are effective methods for providing changes in tuning. The last two methods are used when resonant frequency changes are desired in one mode only.

2. Internal damping (or hysteresis) in the mounts can be effective for energy absorption, but must be controlled so that noise and vibration transmission is not appreciably worsened.

Acknowledgment

Sincere thanks are extended to Elmer Green and Al West for their help in preparing the test material, and to George Fetzer for his electronic computer calculations which have effectively verified our test results.

References

1. "Mechanical Vibrations," by J. P. Den Hartog. Fourth edition. Pub. by McGraw-Hill Book Co., Inc., New York, 1956.

2. "Walls of Jericho," by L. E. Muller. Paper presented at SAE National Passenger Car and Production Meeting, March 3–5, 1948.

ROUTES OF CRANKCASE OIL LOSS

J. S. Coon and D. E. Loeffler, Shell Oil Co.

This paper was presented at the SAE Summer Meeting, Atlantic City, June 10, 1958.

THIS paper presents the results of oil consumption tests in laboratory engines equipped with external sumps, providing separate cylinder and overhead valve lubrication systems. These results show that from one-third to two-thirds of the oil consumed by the engine was lost by way of the valve assembly.

It was also found that, although viscosity is the most important oil property affecting consumption, over one-third of the reduction in consumption in going from a typical SAE 10 to a typical SAE 30 oil is due to the decrease in the volatility of the blend. The results are interpreted in terms of oil-loss mechanisms governed by oil viscosity and volatility. The application of the results to the formulation of multigrade oils is demonstrated.

THE control of oil consumption in automotive engines is one of the most challenging and interesting problems facing industry today. It is an important part of the more general problem of achieving the proper compromise between performance and operating economy of automobiles.

In this paper the routes by which oil is lost from an engine will be briefly discussed. This discussion will lead naturally to a consideration of the factors affecting oil consumption, and of their effect on oil loss by the routes previously outlined. In this section considerable data will be presented, some of it obtained by the use of a divided engine. The major factors affecting consumption will be related to consumption by a simple equation resulting from statistical treatment of the data, and will be used as the basis for a discussion of the mechanism of oil consumption. Finally, the mechanism will be used to examine the very complex question of the optimum formulation of multigrade oils.

Routes of Oil Consumption

For the sake of completeness it may be well to review the paths by which oil may be consumed in engine operation. These paths fall into two general categories:[1]

1. External — leakage past gaskets, seals, or bearings, or loss through the breather.
2. Internal — loss by way of: valve assembly, piston-cylinder assembly.

Dilution of the oil by fuel is a "negative" oil consumption to which careful consideration must be given, particularly in field studies of oil consumption rates. Certainly, it cannot be denied that leakage *can* provide the major path by which oil is lost from an engine. With these potentially major oil consumption paths corrected for or presumed absent, the remaining routes are the internal paths via the piston-cylinder and the valve assemblies. The absolute consumption rate, the ratio of consumption past the rings and valves, and the effect of operating conditions and oil properties on these quantities, are the major subjects of this paper.

The first section of the paper will deal with fac-

[1] "Some Factors Affecting Oil Consumption," by H. W. Lowther. Paper presented at SAE National Fuels and Lubricants Meeting, Tulsa, November, 1956.

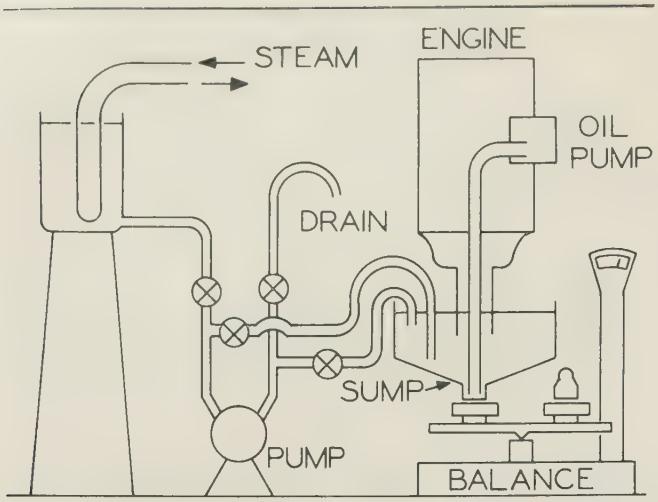

Fig. 1 — Schematic diagram of oil consumption apparatus

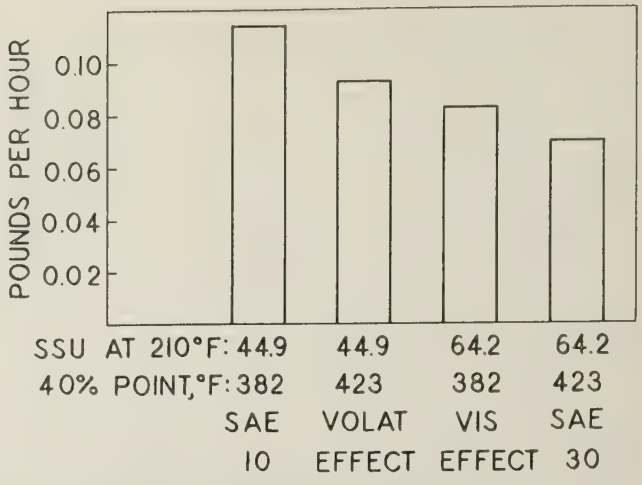

Fig. 2 — Effects of oil volatility and viscosity on oil consumption

tors affecting total internal consumption, using results from an engine with a single lubrication system. In the second section the routes of oil consumption will be separated using results from an engine with a separate overhead lubrication system.

Test Method

Description of Method — To measure the relative importance of the overhead and cylinder routes, a separate lubrication system for the overhead valves was built. For the determination of the overall consumption of the engine, the normal overhead lubrication system was retained and a modification of the method of Stewart and Risk was used.[2] A block diagram of this test arrangement is shown in Fig. 1. The main point of interest in this diagram is the external sump which was mounted on a platform balance below the engine. In this way the weight of oil in the sump was determined hourly to the nearest 0.01 lb. Oil changes between tests were made without stopping the engine, using at least two complete flushes of new test oil before adding the new oil charge. With this procedure carry-over of old oil into the next test could be neglected. Whenever the weight of test oil fell more than 3 lb below its initial value an additional quart of fresh oil was added to the sump. Thus, the oil level was never allowed to fall below 70% of the initial charge.

Each test engine was operated many hundreds of hours and was reconditioned in part or wholly during this time. Thus, the engines were operated over a range of mechanical conditions similar to that of vehicles on the road. Although during each reconditioning period the consumption level remained fairly constant, reconditioning sometimes brought about a change in this level.[1] To overcome this change in oil consumption level, a reference oil of SAE 10 grade was run every third test. Most of the results in this paper are reported as oil consumption relative to this reference oil or oil mileage as a percentage of a reference SAE 30 oil.

Corrections — Where necessary, correction for oil leakage was made by collecting oil in tared rags. The amount of oil lost by leakage was then subtracted from the total oil consumption. No measurement was made of loss by way of the crankcase breather.

At relatively low consumption rates, dilution of the oil by fuel became significant. To correct for fuel dilution, a determination of the amount of light ends was made on the initial and final oil samples by steam distillation using ASTM Method D-322-55T.

With these two factors removed from consideration the reported results represent oil consumption by internal routes only, that is, by way of the valves and the piston-cylinder assembly.

Repeatability — The repeatability of the oil consumption results was calculated by standard statistical methods. It was found that the standard deviation for a single test varied from 7.0 to 22.8% of the test value, depending upon the design of the engine used and accordingly upon the absolute level of consumption. Since smaller differences than these are of importance in the studies, each test at low consumption rates was run at least three times. Thus, in the worst case the standard deviation of the reported results is $22.8\%/\sqrt{3}$, or 13.% of the reference oil consumption. At higher consumption rates the standard deviation of results is of the order of 5% of the reference oil consumption.

Effects of Oil Viscosity and Volatility

In the present work the relative importance of oil viscosity and volatility was determined by measuring the consumption rates of 21 different oils representing a wide range of both viscosity and volatility. Oil volatility was found to be a major factor, and its effect on consumption as well as the effect of viscosity, were quantitatively assessed by statistical methods. The viscosity of the test oils ranged from 38 to 116 SSU at 210 F, while the volatility

---

[2] SAE *Journal*, Vol. 33, October, 1933, p. 42: paragraph in meetings story about paper by J. P. Stewart and T. H. Risk.

[3] MVI — Medium viscosity index.
HVI — High viscosity index.

[4] SAE *Quarterly* Transactions, Vol. 4, July, 1950, pp. 410–421: "Performance of High V.I. Motor Oils," by C. L. Fleming, Jr., B. W. Geddes, N. V. Hakala, and C. A. Weisel.

[5] *Industrial Engineering Chemistry*, Vol. 45, October, 1953, pp. 2336–2346: "Friction and Consumption Characteristics of Motor Oils," by D. Frazer, A. R. Klingel, and R. C. Tupa.

[6] "Lubricant Factors Affecting Passenger Car Oil Consumption," by J. K. Patterson and R. C. Gregor. Paper presented at SAE National Fuels and Lubricants Meeting, Cleveland, November, 1957.

[7] Ch. 12 of "Methods of Correlation Analyses," by M. Ezekiel. Pub. by John Wiley and Sons, Inc., New York, 1941.

[8] Ch. 10 of "Industrial Experimentation," by K. A. Brownlee. Pub. by Chemical Publishing Co., Inc., Brooklyn, 1947.

extremes were those of a blend consisting chiefly of mineral seal oil and of an oil containing principally bright stock. Two methods were used to vary the volatility and viscosity independently. These were (1) choice of either MVI or HVI base stocks,[3] which have different volatilities for the same viscosity; and (2) the addition of polymeric additives, which produce a large thickening effect with very little change in volatility. The oil consumption rates were measured under the high-speed, road-load conditions listed in Table 1, and the properties of the 21 test oils with their corresponding consumption rates are given in Table 2.

The major problem in correlating the consumption data with the viscosity and volatility values is the choice of the best definition for these variables. The viscosity may be measured at any temperature, and some workers[4,5] indicated that 300 F is the best choice. In the present program viscosities both at 210F and at 300F of both new and used oils were considered.

Various definitions for volatility suggest themselves such as (1) flash point, (2) the temperature at which a certain fraction is distilled in a standard vacuum distillation, (3) the fraction distilled when a certain temperature is reached in a vacuum distillation, or (4) the fraction volatilized in a molecular still or in a flash distillation under certain conditions of temperature and pressure. In this program the first three definitions were considered; however, the fourth while a nonstandardized procedure has some theoretical advantages because it is a nonequilibrium procedure which might resemble the evaporation phenomena on cylinder walls.

The dependent variable, oil consumption, can also be directly expressed in pounds per hour or as oil mileage, that is, miles per quart. Some workers[5,6] have found the best correlation is obtained by using the logarithm of the consumption. All of these possibilities have been considered in this work.

The combination of variables which gives the best linear correlation was found by standard methods of correlation analysis.[7] For the V-8 overhead-valve engine, the following combination gave the best fit:

Per cent oil mileage (basis SAE 30 = 100) = $-161 + 1.45 \times$ (used oil viscosity, SSU at 210 F) $+ 0.43 \times$ (20% distillation temperature at 1 mm of Hg, F). (1)

Table 2 also contains the 210 F viscosity of the *new* oils and the *40%* distillation temperature because the correlation between these parameters and oil mileage is nearly as good as the best, shown above. The above equation is the best of those studied, however, and for this correlation an analysis of variance by the method of Brownlee[8] has been made. This analysis shows that in the correlation equation shown above, both the viscosity and the volatility terms are significant with greater than 99.9% confidence.

Aside from the obvious use of this equation to predict the consumption properties of new oil blends, the coefficients of the viscosity and volatility terms are a measure of the relative importance of these oil properties in determining consumption rates. In this engine a change of 3.4F in the 20% distillation temperature is equivalent to a viscosity change of one SSU at 210 F.

To reduce these numbers to familiar terms, the separate effects of viscosity and volatility upon consumption have been calculated for a change from a typical SAE 10 to an SAE 30 oil using the above equation. These values have been converted into consumption rates in pounds per hour using the average value of 0.08 lb per hr for the SAE 10 reference oil. The results are shown in Fig. 2. It is seen that over one-third of the reduction in consumption in going from an SAE 10 to an SAE 30 is due

Table 1 — Conditions of Oil Consumption Measurement Tests

Engine	1	2
Year of manufacture	1951	1954
Number Cylinders	6	V-8
Bore, inches	3.437	4.000
Stroke, inches	4.50	3.20
Type of head	L-head	overhead valve
Test Conditions		
Speed, rpm	3000	
Load, bhp	30	
Jacket outlet temperature, F	160	
Oil temperature, F	205	
Test duration, hr	15	20

Table 2 — Properties of Test Oils and Consumption Data

Engine: 1954, V-8, overhead valve Test Conditions: Standard

Oil	V.I. Improver, %w	Viscosity, SSU at 210 F		Volatility		V.I.	Consumption, % (SAE 10 = 100)	Mileage, % (SAE 30 = 100)
		New	Used	20% Point, F	40% Point, F			
Commercial SAE 10 HVI	0	45.4	45.4	382	399	100	100	69
Commercial SAE 30 HVI	0	64.2	57.7	423	455	87	69	100
Commercial SAE 10W-30	5	58.9	52.4	387	399	136	87	79
75 SSU at 210 F HVI	0	76.7	69.5	449	493	91	59	117
80 SSU at 100 F HVI + Polymer X	8	57.4	51.9	311	339	159	167	41
320 SSU at 100 F HVI	0	53.5	51.6	433	460	95	71	97
100 SSU at 210 F HVI	0	95.5	82.3	474	552	88	46	150
70 SSU at 210 F MVI	0	71.2	64.0	457	497	60	47	147
100 SSU at 100 F MVI	0	38.9	38.9	341	351	42	197	35
250 SSU at 100 F MVI	0	50.1	49.2	428	443	94	68	101
Wide Range MVI[a]	0	38.3	41.2	276	300	62	270	26
Wide Range HVI[b] + Polymer X	8	52.6	51.6	293	320	162	244	28
100 SSU at 100 F HVI + Polymer Y	10	62.4	56.8	376	388	156	67	103
700 SSU at 100 F HVI + Polymer Y	8	116.5	88.2	440	482	121	43	160
100 SSU at 100 F MVI + Polymer Y	10	60.4	58.7	335	345	152	104	66
400 SSU at 100 F MVI	0	53.2	50.0	411	433	55	89	78
400 SSU at 100 F MVI + Polymer Y	6	77.9	63.2	410	436	111	49	141
80 SSU at 210 F MVI	0	81.0	51.2	501	529	63	57	121
80 SSU at 210 F HVI	0	37.9	38.7	357	376	89	151	46
550 SSU at 100 F MVI + Polymer X	5.5	92.6	75.4	421	449	110	60	115
100 SSU at 100 F HVI + Polymer Z	10	67.1	51.2	369	380	160	109	63

[a] 75% 60 SSU at 100 F MVI + 25% 80 SSU at 210 F MVI.
[b] 87% 60 SSU at 100 F MVI + 13% 80 SSU at 210 F MVI.

Table 3 — Comparison of Consumption-Volatility Correlations

Viscosity of all oils was about 63 SSU at 210 F

Author	Engine	Per Cent Mileage Decrease Caused by 50 F Reduction in 40% Point of Oil[a]
Davis, Best	1933, 6-cyl	15[b]
Overcash, Hart, McClure	L-head, 6-cyl	20
Present	L-head, 6-cyl	13
Present	Overhead valve, V-8	19

[a] Mileage is expressed as per cent relative to reference SAE 30 grade oil. The 40% point is the 40% distillation temperature in F at a pressure of 1 mm of Hg.

[b] For this work a change in the 5% point, rather than the 40% point, was used.

Table 4 — Comparison of Consumption-Viscosity Correlations

Author	Test Engine	Per Cent Mileage Decrease Caused by Change from 65 to 55 SSU at 210 F
Patterson, Gregor	Mixed field[a]	31
Lowther	Mixed field[a]	35
Overcash, Hart, McClure	L-head, 6-cyl[b]	21
Present	L-head, 6-cyl	16
Present	Overhead valve, V-8	15

[a] Distillation properties of test oils not reported.

[b] Test oils had constant mole fraction of highly volatile component to minimize volatility differences among oils.

Table 5 — Effects of Speed and Load on Oil Consumption

Engine: 1954, V-8, overhead valve
Oil: SAE 10 reference oil

Speed, rpm	Load		Manifold Vacuum, in. of Hg	Oil Temperature, F	Relative Oil Consumption, %[a]
	psi	bhp			
3000	44	52	15.5	205	90
2500	44	43	16.1	195	35
1500	44	26	16.0	180	8
3000	25	30	18.9	200	100
3000	25	30	—	190	84
2500	25	25	18.9	195	39
1500	25	15	18.3	175	5
3000	0	0	23.0	190	122
2500	0	0	23.5	175	82
2000	0	0	22.8	175	27
1500	0	0	22.4	165	1

[a] Expressed as the percentage of the consumption of the same oil at 3000 rpm and 30 bhp.

Table 6 — Operating Conditions for Overhead Oil Consumption Tests

Engine: 1954, V-8, overhead valve

Speed, rpm	Load		Average Oil Temperature, F	Manifold Vacuum, in. of Hg
	Bmep, psi	bhp		
1500	0	0	169	17.8
2250	0	0	185	19.0
2250	25	23	190	16.2
2250	44	39	202	12.0
3000	0	0	202	19.2
3000	25	30	211	15.0

to the rise in the 20% distillation temperature alone. The remainder is attributable to the change in viscosity alone. The significance of this volatility effect in the formulation of multigrade oils will be discussed in a later section.

It is of interest to compare the consumption-viscosity-volatility relationships found in this work with published results. Overcash, Hart, and McClure[9] have recently measured the consumption of a series of oils of different volatilities in a 6-cyl L-head engine at 3150 rpm and 60 bhp. All oils were of SAE 30 grade blended to a constant viscosity at 350 F using neutral and residual stocks. In the much earlier work of Davis and Best[10] a 1933 Chevrolet engine was run at several speeds, also using SAE 30 grade oils of various volatilities. For comparison with the present work, the results of these published studies were converted to similar units and appropriate graphical correlations were obtained. Table 3 shows the results of this comparison. The oils used by Davis and Best had a viscosity at 63 ± 1 SSU at 210 F, while those used by Overcash, Hart, and McClure had viscosities ranging from 58 to 63 SSU at 210 F. The values in this table represent the dependence of consumption on volatility at a fixed viscosity, and the agreement among these values is excellent considering the variety of test methods and engine involved.

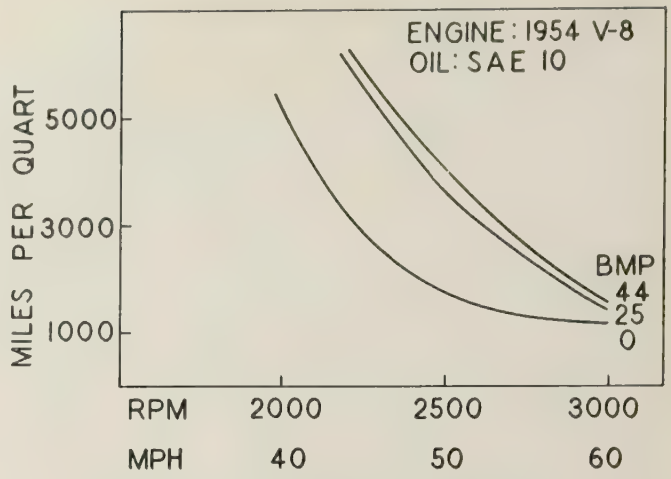

Fig. 3 — Effects of speed and load on oil mileage

It should be noted that in the case of the results of Davis and Best, the volatility is expressed in terms of the 5% rather than the 40% distillation temperature at 1 mm of Hg, since satisfactory correlation could not be obtained using the 40% distillation temperature. As pointed out in the discussion following their paper, this is caused by the short duration of only 3 hr for each test, so that in the case of maximum consumption only 7% of the oil charge was consumed. Under these conditions the most volatile components influenced the consumption disproportionately. In the work reported here, up to 30% of the initial charge was used before oil was added to the sump, and it is reasonable that the best correlation was with a point further along the distillation curve. Since the range of consumption before adding oil in these tests was more representative of consumer practice, it is believed that the resulting correlations may be more practical.

These considerations suggest that consumption rate varies with time, being initially higher while the most volatile components are being removed. In most cases this effect would be so small as to be obscured, but in the present work changes in the consumption rate with time were actually observed using blends of two oils having widely separated volatilities.

A comparison of the present viscosity coefficient of oil consumption with published values can also be made. In this case the comparison is more difficult because volatility data on oils described in the literature are usually not available. Frequently all of the measured change in consumption was simply ascribed to changes in viscosity. In Table 4, estimates of the change in consumption for a 10 SSU change in viscosity at 210 F are listed, based on data

[9] "How Do Volatility, Viscosity, and V. I. Improvers Affect Oil Consumption?" by R. L. Overcash, W. Hart, and D. J. McClure. Paper presented at SAE Annual Meeting, Detroit, January, 1956.

[10] ASTM Proceedings, Vol. 35, 1935, Part II, p. 608: "The Effect of Volatility on Oil Consumption," by L. L. Davis and R. D. Best.

[11] *Lubrication*, Vol. 9, February, 1957, p. 11: "Mechanism of Oil Loss Past Pistons," by P. de K. Dykes.

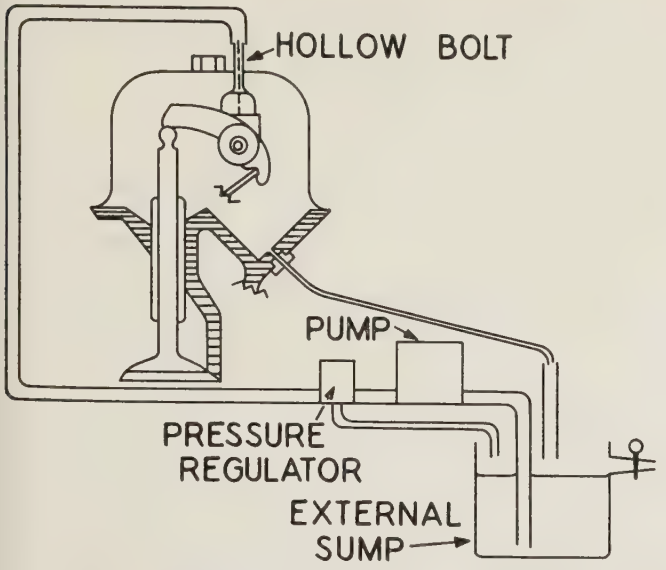

Fig. 4 — Schematic diagram of separate overhead lubrication system

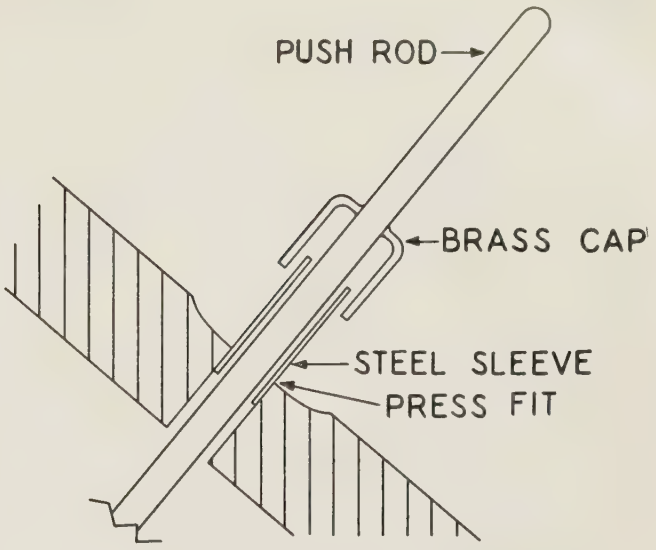

Fig. 5 — Details of oil baffle on push rod

from several recent papers. It appears from these data that limits of *15–35%* may be placed on mileage changes resulting from a 10 SSU as 210 F change in viscosity, but that the lower figure reflects viscosity changes alone, rather than changes in both viscosity and volatility.

Effects of Engine Design

Engine design is, understandably, the most important factor affecting the rate of internal oil consumption. Graphic proof of this was presented by Dykes[11] who showed with a motored engine that oil loss past rings can be raised by a factor of 2700 by installing a taper-faced ring in an inverted position.

It is not proposed to separate the effects of individual design changes. Rather the accumulated effects of design improvements will be shown by presenting oil consumption data for two engines. Both engines were operated under the same conditions which are shown together with descriptions of the engines in Table 1. At 3000 rpm, the average oil economy of the 1951 engine was 250 mpq, compared with 1400 mpq for the 1954 engine. The marked difference in oil economy between these two engines under these severe high-speed conditions is approximatly maintained, in terms of actual mpq, at less severe conditions.

Effects of Speed and Load

Oil consumption in the test engine increased rapidly with increasing speed and was reduced by increasing the load. These facts are demonstrated by the data of Table 5 obtained on the V-8 overhead valve engine just described and are seen graphically in Fig. 3. The figure was constructed by arbitrarily assuming that mph equals rpm/50. Each of these curves shows the variation of oil mileage with speed as a constant bmep. It is seen that oil mileage decreases very rapidly with increasing speed. The *decrease* in oil mileage at lower loads is also shown. This decrease is consistent with the higher manifold vacuum at lower load. Both of these effects are at least qualitatively in agreement with published information on the effects of speed and load.[1] The quantitative relationship between these factors is very heavily influenced by engine design variables, but it appears from Fig. 3 that advances in oil economy are obtainable over the entire useful speed range through improved design.

Consumption via Overhead Valve Assembly

With the rapid rise in popularity of the overhead valve engine and with improved control of oil flow past the rings, the relative importance of the routes of oil consumption in passenger-car engines has changed. Whereas oil consumption in the past was mainly by way of the piston-cylinder assembly, the liberal lubrication of overhead valve gear together with a major portion of all engine operation at part throttle and high manifold vacuum has caused oil loss via the valve assembly to assume major importance. This section describes tests run with the 1954 V-8 overhead valve engine to measure oil consumption via the overhead valve assembly separate from that occurring via the piston-cylinder assembly and bearings. These and other engine tests show that from one-third to two-thirds of the total oil consumed by modern engines is lost by way of the valve assembly.

Test Method

Description of Method — In order to measure the oil consumption that takes place past the valves a simple modification to the engine was required. This consisted of blocking the normal oil lines to the rocker arms and providing the external sump, pump, and oil lines as diagrammed in Fig. 4. Oil return to the crankcase through the push-rod openings was blocked by extending a sleeve from each opening and mounting a baffle on each rod to fit outside the sleeve, as shown in Fig. 5. The small external sump for the overhead oil system had a capacity of 7 lb, and was filled to an overflow level at the beginning of each test while the engine was running and oil circulating. At the end of each test the weight of oil required to refill the sump under the same conditions was measured. As with the normal engine, a 20-hr test period was used.

To determine the effects of operating conditions

and oil composition on consumption past the valves six different oils were tested, each under several operating conditions. The engine conditions used are shown in Table 6. Under each condition of speed and load, the oil temperatures and manifold vacuum remained fairly constant for the various oils tested. The oils in these tests included four of SAE 30 and two of SAE 50 grade and represented a wide range of volatilities. No SAE 10 grade oils were included because they leaked past the push-rod baffle at too high a rate to permit confidence in the measurements.

The fundamental assumption in this test procedure is that the oil flow to the overhead system is the same in the modified engine as in the normal engine. The oil pressure to the rocker arms in the normal engine was measured under various conditions of speed, load, and oil viscosity. In the tests with a separate overhead lubrication system, the oil pressure was adjusted to the appropriate value by means of a pressure relief valve in the external circulation system.

Corrections — Aside from the correction for fuel dilution described in the section for the normal engine tests, a small but significant correction for leakage of overhead oil to the crankcase via the push-rod openings was made. This correction was found necessary in spite of the baffle arrangement used in the test engine, and was made by tagging the overhead oil with oil-soluble sodium or zinc salts and measuring their concentration in the crankcase oil before and after test.

In these tests the cylinder consumption was corrected for engine wear by running an SAE 30 reference oil at the beginning and end of the series and adjusting the measured cylinder consumption values to the midpoint on a linear basis. The corresponding correction for the overhead consumption was not made because of insufficient reference runs.

Repeatability — The deviation of *cylinder* consumption measurements is presumed to be at least as good in these tests as in tests with the single lubrication system. Because in some cases only one result was obtained the estimated standard deviation of the reported cylinder consumption data is as much as 40% of the reported value.

The estimated standard deviation of the *overhead* consumption values reported is also 40% of the mean value. Nevertheless, it will be shown that the conclusions reported from tests with the divided engine are consistent with those from the normal engine.

A summary of results with the divided engine is given in Table 7.

Table 7 — Consumption in Modified Engine Equipped with Separate Overhead Lubrication System

Engine: 1954, V-8, overhead valve (two engines, designated 2a and 2b)

Engine No.	Oil[a]	Viscosity, SSU at 210 F	40% Point, F	Speed, rpm	Bmep, psi	Consumption, lb/hr	
						Cylinder	Overhead
2a	A	61	456	1500	0	0.032	0.020
				2250	0	0.032	0.013
				3000	0	0.075	0.044
2a	B	61	314	1500	0	0.013	0.027
				2250	0	0.056	0.027
				3000	0	0.167	0.032
				3000	25	0.092	0.072
2a	A	61	456	2250	0	0.019	—
				3000	0	0.075	—
				3000	25	0.043	0.027
2a	C	93	458	1500	0	0.002	0.014
				2250	0	0.009	0.002
				3000	0	0.041	0.019
2b	A	61	456	2250	0	0.048	—
				3000	0	0.077	0.016
				3000	25	0.033	0.013
				2250	25	0.029	—
2b	D	63	379	2250	0	0.040	0.031
				3000	0	0.070	0.044
				3000	25	0.018	—
				2250	25	0.005	—
2b	B	61	314	2250	0	0.087	0.022
				3000	0	0.103	0.011
				3000	25	0.087	0.030
				2250	25	0.071	—
2b	E	60	460	2250	0	0.041	0.006
				3000	0	0.064	—
				3000	25	0.035	—
				2250	25	0.013	—
				2250	44	0.012	0.031
2b	F	90	370	2250	0	0.014	0.025
				3000	0	0.025	0.032
				3000	25	0.023	0.019
				2250	25	0.014	0.012
				2250	44	0.017	0.016

[a] Oil compositions.

Oil	Base Stock	Polymer	
		Type	%w
A	HVI	—	
B	Wide Range MVI	X	7.5
C	HVI	X	6.0
D	HVI	X	9.0
E	MVI		
F	Light MVI + Heavy HVI	X	7.5

Effects of Speed and Load

In an earlier section of this paper it was seen that oil consumption increases sharply with increasing speed and decreasing load in an overhead valve V-8 engine. Results with the divided engine (listed in Table 7) show that both the cylinder and overhead oil consumption generally follow the same pattern. This is most easily seen by considering the average consumption for all the oils tested under the various speed and load combinations. The only result in Table 7 not included in the averages shown in Table 8 is a single abnormally high value for overhead oil consumption with a very volatile oil. In analyzing these results, it should be kept in mind that separate effects of volatility and viscosity have been ignored and that the data represent the average performance of a variety of oils.

The cylinder oil consumption consistently follows the same pattern shown for the single lubrication system in that oil consumption increases with increasing speed, but falls as the load is increased. The average manifold vacuum values corresponding to loads of 0, 25, and 44 bmep were 23, 19, and 16 in. of Hg. Thus, lower vacuum correlates generally with lower oil consumption.

The oil lost by way of the valve assembly shows the same general pattern but is less consistent. In particular, the values in italics do not confirm the trend. These values are the averages for only two or three oils and are too high to be consistent with values obtained previously with the single lubrication system.

Effects of Oil Viscosity and Volatility

The data of Table 7 may be analyzed from the standpoint of the effects on consumption of oil viscosity and volatility. A total of six oils of grades SAE 30 and SAE 50 were used, representing a range of base stocks from mineral seal oil to bright stock. The results are summarized in Figs. 6–8 for three operating conditions. The three figures show the operating conditions 3000 rpm at no load, 3000 rpm at 30 bhp, and 2250 rpm at no load, respectively.

In Fig. 6, the separate effects of viscosity and volatility are shown. By increasing the oil viscos-

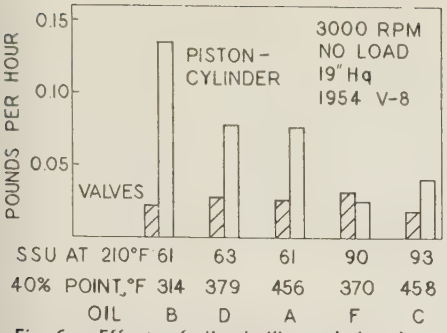

Fig. 6 — Effects of oil volatility and viscosity on oil consumption by two routes

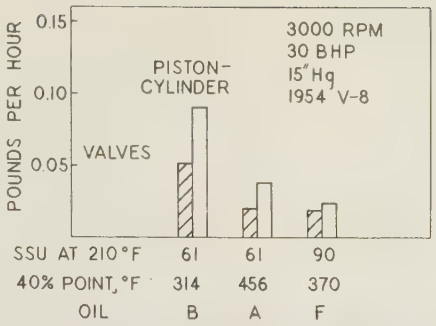

Fig. 7 — Effects of oil volatility and viscosity on oil consumption by two routes

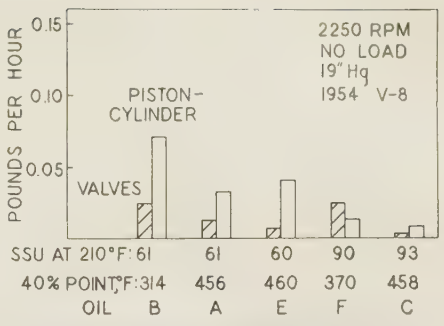

Fig. 8 — Effects of oil volatility and viscosity on oil consumption by two routes

ity from 61 to 93 SSU at 210 F (Oils A and C) the consumption via the cylinder was reduced by one-half. Conversely, keeping the viscosity constant and greatly increasing the volatility (Oils B and A) greatly increased the consumption via the piston-cylinder assembly. This is a reflection of the high temperatures encountered in the upper part of the cylinder, a condition under which a very volatile oil is rapidly flashed from the cylinder. Fig 6 also shows that the changes in oil consumption via the valves are too small to be significant with the present data. The sums of the separate consumptions for these oils show the expected downtrend with rising viscosity and lower volatility.

Fig. 7 shows the similar consumption pattern obtained at 3000 rpm and road load, the same conditions used in the standard tests with the normal lubrication system. Again, the total consumption figures show the expected relationship. However, in these tests, the use of very volatile stocks in Oil B caused an increase in the consumption by way of the valve assembly as well as via the piston-cylinder assembly. While this difference is of dubious significance with so few tests, it is possible that when the engine operates under load the increased average gas and valve temperatures are sufficient that the volatility of the oil on the exposed valve stem becomes important.

The results shown in Fig. 8, measured at 2250 rpm with no load, confirm the trends shown in Fig. 6 and reaffirm that with no load at least, consumption via the valves is not much affected by a large increase in volatility.

On the average, the ratio of valve consumption to total consumption for all oils and conditions was 0.39 for the 1954 overhead valve V-8 engine used in these tests. Thus, over one-third of the total oil consumed in this engine is lost by way of the valve assembly.

The results obtained with separate overhead lubrication are based on single tests and must be very conservatively interpreted. Nevertheless, it is encouraging to find considerable internal consistency and agreement with results from the unmodified engine. In summary, it was found that:

1. Under no load, increased viscosity reduces oil loss by way of the piston-cylinder assembly. Reduced volatility also reduces consumption by this route but does not significantly affect consumption by way of the valve assembly.

2. Under load, a more volatile oil is consumed more rapidly via the piston-cylinder assembly and possibly also by way of the valve assembly.

3. Consumption by way of the valves generally constitutes one-third to one-half of the total consumption.

Table 8 — Effects of Speed and Load on Cylinder and Overhead Oil Consumption

Speed, mph	Average Cylinder Oil Consumption, quarts/1000 miles			Average Overhead Oil Consumption, quarts/1000 miles		
	0 bmep	25 bmep	44 bmep	0 bmep	25 bmep	44 bmep
30	0.29	—	—	*0.36*	—	—
45	0.45	0.31	0.18	0.21	0.14	*0.29*
60	0.71	0.40	—	0.25	0.20	—

Table 9 — Effect of Valve Seals on Oil Consumption

Engine: 1955, V-8 overhead valve
Oil: SAE 10W-30

Run No.	Oil Consumption, lb/hr	
	Without Seals	With Seals
1		0.07
2		0.10
3	0.31	
4	0.30	
5		0.12
6		0.14
7	0.26	
8	0.24	
9		0.15
10		0.16
11	0.29	
12	0.24	
13		0.20
14		0.17
15	0.30	
16	0.30	
Average	0.28	

Effect of Engine Design

The last conclusion above, that consumption by way of the valves is of the same general magnitude as consumption by way of the piston-cylinder assembly, has been strongly reinforced by additional work with an engine equipped with valve seals. The engine used in this case was a low-priced 1955 V-8 overhead valve engine, arranged as in Fig. 1 with no separate valve lubrication. The engine was equipped with a set of experimental valve seals.[12] The seal took the form of an inverted Neoprene cup which fitted tightly around the top of the valve guide, and through the base of which passed the valve stem. A split cast-iron ring, mounted inside the base of the cup, surrounded the stem and controlled oil flow.

A total of sixteen 20-hr tests was run under the high-speed, moderate-load conditions listed in Table 1; half of these runs were with seals and half without seals. An SAE 10W-30 grade lubricant was used. The results of these tests are listed chronologically in Table 9 and shown graphically in Fig. 9. The

[12] Private communication from A. M. Brennecke, Perfect Circle Corp., Hagerstown, Ind.

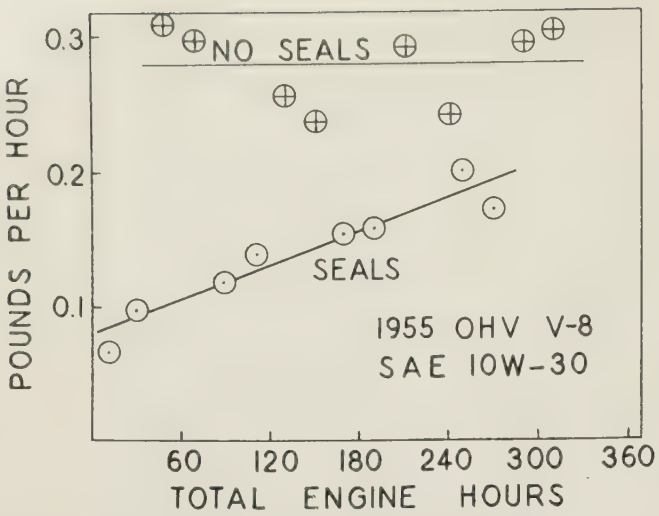

Fig. 9 — Effect of valve seals on total oil consumption

results show the very marked reduction in oil consumption which can be achieved by controlling the loss of oil by way of the valves. Fig. 9 shows that oil consumption with seals installed was increased as the seals were alternately removed and reinstalled. Nevertheless, after a period corresponding to 9000 miles of operation with seals there was still a 30% reduction in consumption with seals, while with unworn seals the reduction was 70%. It is expected that an improved version of this seal will offer a very significant reduction of oil consumption.[12]

Mechanism of Oil Consumption

The work described in this paper has demonstrated that internal oil consumption is the sum of losses via the piston-cylinder assembly and the valve system both of which are of major importance in overhead valve engines. Similarly, both the viscosity and the volatility of the oil were shown to be important in determining the consumption. Higher engine speeds were shown to increase consumption by both paths, while the design and condition of the engine were shown to influence oil consumption very critically.

The establishment of a detailed mechanism to bring together all the observed facts appears almost impossible to achieve at this time. This is primarily because of a lack of experimental information on oil film thicknesses, temperature gradients, and gas and oil turbulence in operating gasoline engines. Nevertheless, it is possible to discuss consumption mechanisms in a qualitative way.

Both the piston-cylinder assembly and the valve assembly act as pumps to transfer oil from a reservoir to the combustion space. The net flow of oil from the reservoir to the combustion chamber is promoted by various agencies. Putting aside the splash action of the crankshaft and the analogous force of the rocker arms in creating the reservoir for their respective pumps, the forces which affect the transfer are shown in Table 10.

Consumption via Valve Assembly

An oil film present on the lower valve stem and underhead, as a result of the forces enumerated above, is presented to the combustion chamber during the intake stroke and during the exhaust stroke. Oil presented during the exhaust stroke is presumed to be removed by the drying action of the hot exhaust gases as they pass from the combustion space. This action may be a combination of mechanical and evaporative removal. When the valve closes, the combined effects of gravity and capillary action cause the oil film again to wet the portion of the valve stem which had been partially or completely dried. Thus, there is a net flow of oil down the stem, which is removed by the action of the hot exhaust gases.

The data obtained with the separate overhead lubrication system show that this route of oil loss is an important one, accounting for one-third to one-half of the total consumption. The results also show that higher speeds raise the consumption rate via the valve assembly, in keeping with the higher rate of oil-film removal required by the drying hypothesis. Unfortunately, the data are not sufficiently repeatable to permit the separation of the effects of oil viscosity and volatility for consumption via the valve assembly.

Consumption via Piston-Cylinder Assembly

A mechanism which is viscosity-dependent has been proposed in the literature[13] on the basis of tests with a motored glass-cylinder engine. The basic feature of this mechanism is that oil flow up the cylinder takes place largely in the grooves behind the rings. Near tdc, the top ring and the oil which has been scraped into the top groove during the upward stroke experience an upward acceleration. The oil then flows out of the groove until the ring reaches the top of the groove and blocks this path, and the rate of oil flow rises with lower oil viscosity. Some of this oil is thrown into the combustion chamber and is lost. Oil flow by this path is a low-shear process and the viscosity conferred by a polymer is, therefore, effective in this mechanism.

While the glass-cylinder engine was motored, it was presumed that in a fired engine the effect of compression and combustion pressure would be to hold the top ring in the lower part of its groove, thus reducing oil loss. This led to the conclusion that, under firing conditions, most of the oil ejection must occur at the end of the exhaust stroke when the pressure is near atmospheric.

The present results are consistent with this, showing decreasing consumption with increasing bmep. Of course, it must be kept in mind that these results are also consistent with the hypothesis that the higher vacuum associated with operation at low loads causes increased transfer of oil on the intake stroke. The increase in oil transferred to the combustion chamber outweighs the decrease in rate of oil evaporation from the cylinder wall.

This discussion indicates that it is reasonable to associate the consumption which is viscosity-controlled with a mechanism of low-shear flow behind the rings. The data support this loss path in preference to that of oil passage between the ring face and the cylinder wall.[14] As further evidence on this subject, it appears established by Dykes[10] that

[13] SAE *Journal*, Vol. 54, October, 1946, pp. 60–67: "Piston Lubrication Phenomena in Motored Glass-Cylinder Engine," by S. J. Beaubien and A. G. Cattaneo.

[14] MIRA Report No. 1953/2, 1953: "Note on Oil Consumption in Internal Combustion Engine," by G. R. Oliver.

while oil *circulation* certainly occurs between ring and cylinder wall, oil *loss* or net upward flow is not to be expected by this mechanism. In fact, a normally tapered ring acts as a powerful force for returning oil to the sump.

A complete consumption mechanism would permit calculation of the effect of changes in oil volatility. However, much of the published work on consumption mechanisms has of necessity been done with a motored engine to simplify the interpretation of results. Under these conditions the role of volatility in consumption is, of course, not subject to study. In a firing engine it is evident that the oil film presented to the combustion space is subjected to a dynamic thin-film evaporation process by heat from the combustion gases. In this situation the gas and oil turbulence, the temperature gradient across the static gas film and through the oil film, and the volatility characteristics of the oil are the factors which determine the rate of evaporation of oil. In contrast to viscosity-controlled consumption, which is primarily initiated during the exhaust stroke, the volatility-controlled consumption is initiated during the power stroke. During this stroke the conditions of a large area of oil film exposed to hot combustion gases are most favorable for the evaporation of some of the lighter ends of the oil which escape with the exhaust gases. On the next upward stroke of the piston, a new supply of oil is carried up the cylinder wall, which mixes with oil remaining on the wall. On the next downward stroke, the rings accurately meter the oil film on the cylinder wall, restoring it to the same thickness as before the power stroke.

The oil remaining in the film is more concentrated in nonvolatile constituents and eventually returns to the crankcase. Continued use of such an oil must ultimately result in a more viscous, less volatile oil and a decreasing consumption rate. A decrease in volatility with use was demonstrated by Overcash, and McClure,[9] while a decreasing rate of consumption was observed in several of the tests described earlier in this paper.

Consumption of Multigrade Oils

The formulation of a crankcase lubricant represents a compromise between many conflicting requirements, even if only those factors affecting viscosity are considered. On the one hand, the need for easy starting and good fuel economy suggests an oil of low viscosity. On the other hand, the need for adequate protection of highly loaded engine components and for good oil economy dictates an oil of high viscosity and low volatility. The formulation of multigrade oils is governed by the same considerations but is considerably more complicated, owing to the presence of polymers. Since both the type and amount of polymer can be varied, and since oils which contain polymers undergo both temporary and permanent viscosity loss in an engine, simple measurements of the viscosity and volatility of an unused oil are not sufficient to predict the performance of multigrade oils in the field.

Considerable information on the effects of changes in multigrade oil formulation may be found in the literature. Estimates of the minimum viscosity required for adequate engine protection have been published. Several workers have reported data on how base oil viscosity and the polymer content and amount affect fuel economy and ease of starting.[5,6,13] From this work it is clear that easiest starting and best fuel economy are achieved by the use of thinnest possible base oil together with a polymer which has a maximum temporary viscosity loss at high shear rates. It appears that, at shear rates approximating those in engine bearings, oils made with this type of polymer can lose more than half of the polymer-conferred viscosity.[15]

With this brief review as a background, it is of interest to apply the conclusions of the present work to a consideration of the consumption rates of multigrade oils. The adequate viscosity of multigrade oils is no guarantee of low consumption, since the oil may consist of a volatile base stock thickened with a large amount of polymer. The general agreement that viscosity is the major factor governing consumption had led some workers to discount entirely the effects of volatility. This leads to noticeable errors when assessing the consumption characteristics of certain multigrade oils. Two recent papers reflect opposing viewpoints on this subject. The first[15] stressed the advantages of an SAE 10W-30 grade oil formulated from a 41 SSU at 210 F base oil thickened with a large amount of relatively inefficient V.I. improver. Oil consumption was regarded as no problem provided the base oil is "nonvolatile under engine operating conditions." The second paper[9] reported tests on an SAE 10W-30 grade oil made from a 37 SSU at 210 F base oil, and found that the consumption of the 10W-30 oil was decidedly greater than that of an SAE 20 grade oil. This result is *certainly* attributable to the higher volatility of the multigrade oil, since its viscosity at engine operating temperatures would be considerably higher than that of the SAE 20 grade oil.

By applying the consumption equations discussed in an earlier section of this paper, the relative oil mileages expected from various types of SAE 10W-30 grade oils can be calculated. Table 11 shows the consumptions of the two experimental oils discussed above, and with that of a commercial

Table 10 — Forces Affecting Oil Transfer from Reservoir to Combustion Chamber

Force	Effect on Transfer Via: Valve Assembly	Effect on Transfer Via: Piston-Cylinder Assembly
Force of Gravity	Promotes	Opposes
Force Due to Surface Tension of Oil	Promotes	Promotes
Differential Acceleration of Mechanical Parts	No effect	Promotes
Differential Pressure		
Compression & Combustion Pressure	No effect	Opposes
Intake Vacuum	Promotes	Promotes
Mechanical Pumping by Normal Ring Taper	No effect	Opposes

Table 11 — Consumption of Various 10W-30 Grade Oils

Oil	Reference	Viscosity, SSU at 210 F: Base Oil	Viscosity, SSU at 210 F: Blend	40% Point, F[a]	Per Cent Oil Mileage (SAE 30 = 100)
A	15	41	64	394[b]	50
B	2	37	60	350[b]	61
C	(commercial)	46	64	425	91

[a] 40% distillation temperature at a pressure of 1 mm of Hg.
[b] Estimated from values reported at higher distillation pressures.

[15] SAE Transactions, Vol. 64, 1956, pp. 608–624: "Cold Starting with V. I. Improved Multigrade Oils," by F. B. Fischl, H. H. Horowitz, and T. S. Tutwiler.

10W-30 oil, all relative to SAE 30 consumption.

The low oil mileage calculated for experimental Oil B is, of course, partly the result of the lower viscosity at 210 F of this oil. The reduced value for experimental Oil A is due solely to the fact that a highly volatile base oil was used to compensate for the inclusion in the blend of a large amount of inefficient V.I. improver.

Unfortunately, high molecular weight polymers undergo permanent viscosity loss from thermal, oxidative, or mechanical chain-breaking reactions. This permanent viscosity loss results in oil mileage less than that which would be predicted from the new oil viscosity[6] and is probably responsible for the fact that the *used* oil viscosity is more useful for predicting consumption rates than is the *new* oil viscosity.[1,6] Nevertheless, of two oils having the same ease of starting, a polymer-bearing oil will give better oil mileage than a nonpolymer oil. This is true even when the increased base-oil volatility and the permanent viscosity loss of the polymer-bearing oil are taken into account. To illustrate this point, the calculated oil mileages of two oils of equal startability are shown in Table 12. Calculations are based on published startability data[15] and on the consumption equation presented in the present paper. Thus, multigrade oils can show oil mileage advantages of 6–18% over a single grade oil of equal startability, the actual amount depending on the *permanent viscosity loss of the finished multigrade blend.*

The consumption data presented in this report are consistent with the idea that *consumption varies continuously* with oil volatility, and that there is no "magic volatility" below which the consumption is unaffected. The most careful field data also support this idea in that the consumption rates of oils thought to be "nonvolatile" on the basis of less accurate work have shown a dependence on oil volatility. This information permits the accurate design of a multigrade oil to the optimum standards both of startability (and fuel economy) and of oil consumption level.

Conclusions

Using primarily data obtained in laboratory gasoline engines equipped with external oil sumps the following conclusions have been reached.

1. Engine design is the most important factor affecting oil consumption.

2. The rate of consumption of an oil is a continuous function of both its viscosity and its volatility. A quantitative relationship among these three variables has been derived by statistical analysis of results for 21 oils studied under high-speed conditions. The equation is as follows:

$$M = -161 + 1.45V + 0.43T \qquad (2)$$

where:

M = Per cent relative oil mileage (SAE 30 = 100)
V = Used oil viscosity, SSU at 210 F
T = 20% distillation temperature, F at 1 mm of Hg

3. By providing a separate overhead valve lubrication system, it was found that oil consumption by way of the valve assembly constitutes one-third to one-half of the total consumption in the test engine. It is likely that in many modern engines this fraction is decidedly higher.

Table 12 — Mileages of Two Oils

Oil	Polymer	Base Oil Viscosity, SSU at 210 F	New Oil Blend Viscosity, SSU at 210 F	Used Oil Blend Viscosity, SSU at 210 F	Change in 20% Point, F	High Shear Blend Viscosity, SSU at 0 F	Per Cent Increase in Oil Mileage
1	Yes	50	64	—	−2.1	20,000	18
1	Yes	50	—	56	−2.1	20,000	6
2	No	51	51	51	0	20,000	0

4. Changes in engine speed and load appear to affect consumption via the valves in the same direction as they affect consumption via the piston-cylinder assembly, that is, increased consumption with higher speeds and with lower loads.

5. Oil consumption by way of the piston-cylinder assembly is governed by both the viscosity and volatility of the oil. The viscosity-dependent mechanism of oil loss involves primarily a low-shear path behind the ring. The volatility-dependent component involves the thin-film evaporation of volatile components and the return of less volatile oil to the sump.

6. Since the viscosity-dependent component of oil consumption involves a low-shear process the viscosity of polymeric V.I. improvers is effective in controlling oil consumption.

7. A well-designed multigrade oil will excel a single grade oil both in starting ease and in oil mileage. The economy of the multigrade oil is maximized by the use of an efficient V.I. improving polymer together with a base oil having the lowest volatility obtainable at the necessary viscosity level.

8. The consumption rate of a multigrade oil can be calculated from a knowledge of its volatility and from the viscosity of the *used* oil.

9. Because a major portion of oil loss from a modern overhead valve engine is by way of the valve assembly, mechanical design studies of the means of control of this component of consumption are indicated. An important increase in operating economy can be achieved by such work.

Additional Reference

1. SAE *Quarterly* Transactions, Vol. 3, July, 1949, pp. 431–443: "Motor Oil Consumption Characteristics," by C. W. Georgi.

DISCUSSION

System of Oil Consumption Determination Records Weight of Make-Up Oil Reservoir

— Vern C. Vanderbilt
Perfect Circle Corp.

THE authors indicated a method of oil consumption determination which is an improvement over drain-and-weigh methods. At Perfect Circle we believe that we have a method which is an improvement over even the authors' method. Our system was developed by the late Karl H. Effmann of our company a number of years ago. His paper entitled, "Engine Oil Consumption Determination," was not reported in the SAE publication; and thus, the system is not well-known. We would be happy to send anyone a copy upon request to the Engineering Division of Perfect Corp., Hagerstown, Ind.

Basically the system is one for continuously recording the weight of a make-up oil reservoir. Fig. A is a typical

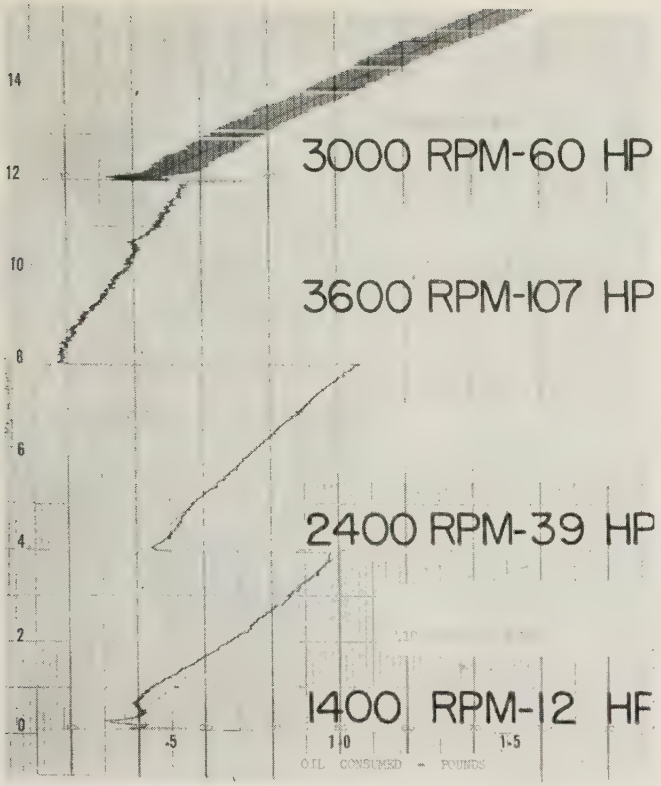

Fig. A — Oil consumption chart taken from recorder. Four hr checks run on a 1957 V-8 engine, SAE oil, 180 F water jacket temperature, 180 F oil out temperature

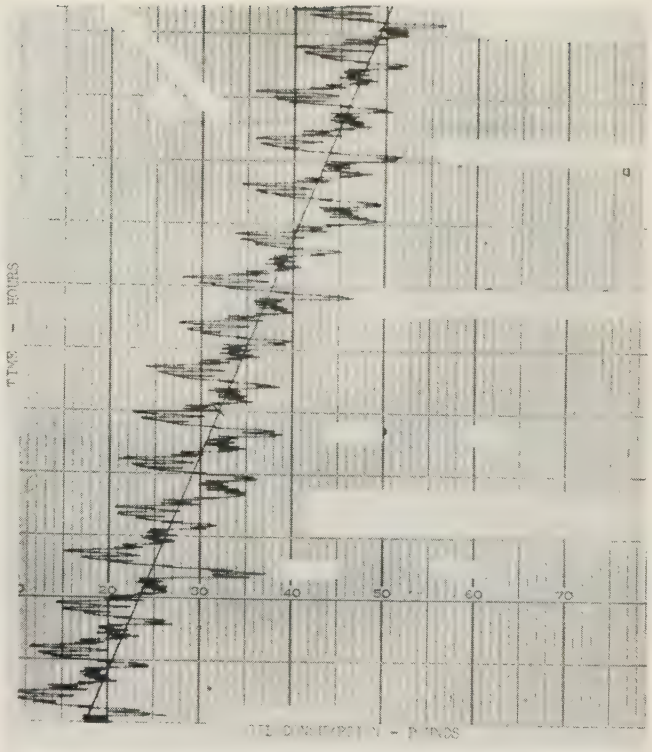

Fig. B — Proving ground. (Each horizontal division equals 0.05 lb of oil, each vertical division equals 1 hr)

chart obtained from the recording system. Thus, the trend of oil consumption during the test can be determined.

Fig. B is a similar chart taken of an engine undergoing a test which was controlled by an automatic dynamometer programed by a magnetic tape memory. The tape was recorded in a vehicle on the road so that actual loads with typical transients were included in the testing program.

Contrary to the authors' statement we have usually noted negative oil consumption during the first few hours of testing with a new oil. Fig. C shows this trend on two charts taken from a test on a large diesel engine. The same results have been encountered on gasoline-fired engines. We believe this to be due to fuel dilution.

A design problem affecting oil consumption which has not had much publicity is indicated in Fig. D which shows the exhaust port profiles for three different heads. The pressure in the port area will vary by the way the nozzle formed by exhaust ducting is shaped. It is possible to obtain pressures below atmospheric adjacent to the valve stem when the valve movement is downward.

We agree with the authors' comment on the amount of oil that is lost by the valve guides. Fig. E shows the oil consumption before and after the installation of a positive valve stem seal. Such a seal is shown in Fig. F installed on a head. We cannot agree with the wear trend as shown in Fig. 9 of the authors' paper. This trend could be attributable to the excessive number of times that the seals were removed. A teflon insert currently is used to

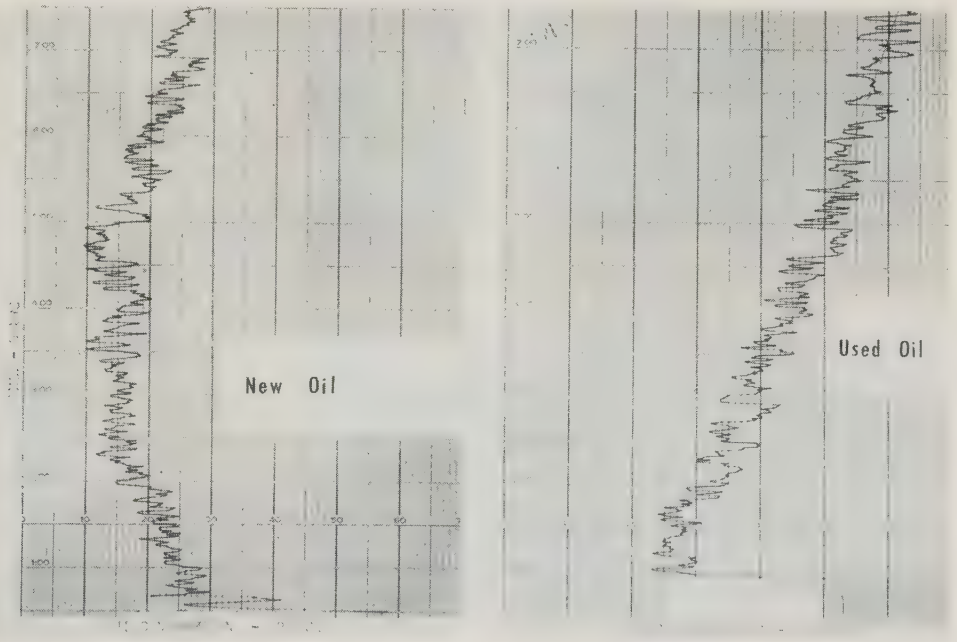

Fig. C — Oil make-up

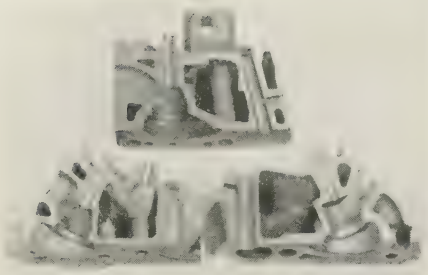

Fig. D — Exhaust port profiles of various heads

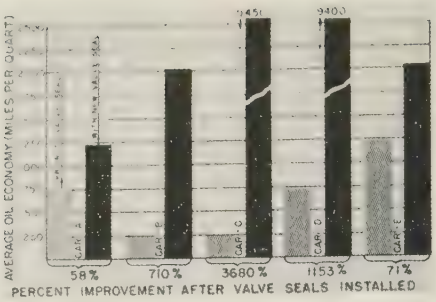

Fig. E — Oil economy with standard engines and normal road service

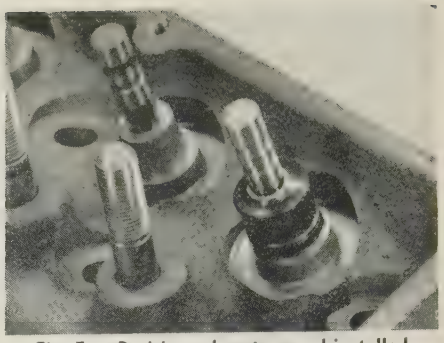

Fig. F — Positive valve stem seal installed on stem

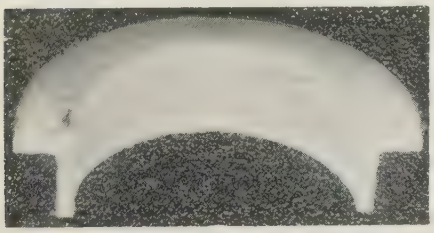

Fig. G — New teflon insert

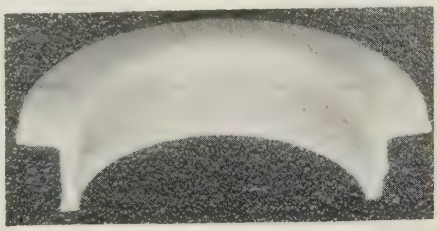

Fig. H — Teflon insert after 11,700 miles of service

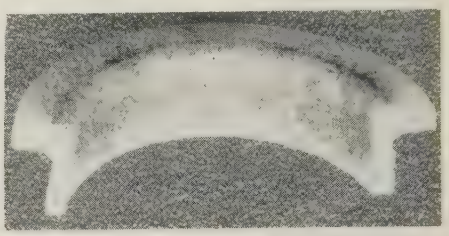

Fig. I — Teflon insert after 29,000 miles of service

Fig. J — Drops of oil on teflon insert, illustrating inhibiting of capillary action

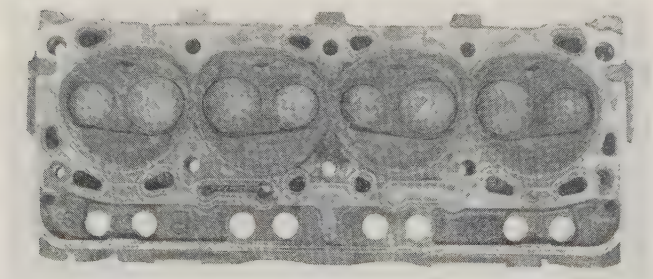

Fig. K — Head with positive valve stem seals after 15,000 miles of fleet service

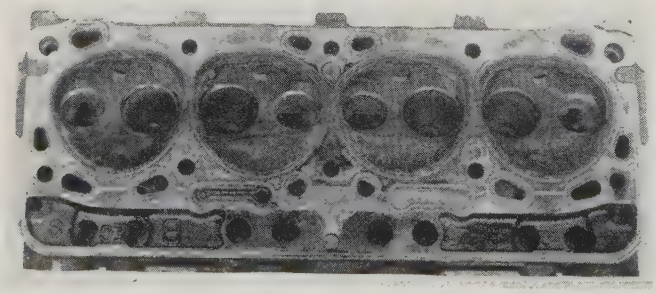

Fig. L — Head of Fig. K with valve removed

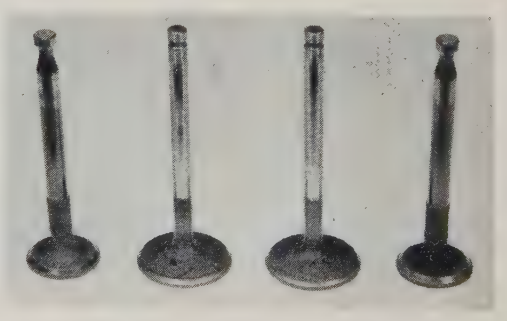

Fig. M — Valves of head shown in Fig. K

replace the cast iron. Figs. G–I show sections of the insert at 0, 11,700 and 29,000 miles of service, respectively. The insert shown in Fig. I was in taxi service. Machining can be seen on all inserts.

Teflon inhibits capillary attraction referred to in the authors' paper. (See Fig. J.) Equal drops of oil were placed on a ground cast-iron surface. One side of the disc was previously rubbed with Teflon while the other side was not. The photo was taken 30 min after the drops were placed on the disc. Note that the one drop is not attracted to the iron surface. This shows the inhibiting effect on the teflon rubbed surface as contrasted to the non rubbed surface.

With positive valve stem seals, the close fits between stem and guide should not be necessary to keep the fuel/air ratio correct on the exhaust gases from the rocker box. To prove this contention, three of our fleet cars were fitted with the rather ridiculous 0.015-in. stem to guide clearance. After 5000 miles on each of the cars, no one has been able to detect any differences between these cars and others. The compression pressures have continued to improve with each check. Two of the newer V-8's are averaging 145–150 psi gage and an older 6-cyl — 135 psi gage. Finally, a sodium-cooled valve engine was equipped with 0.015-in. stem to guide clearance heads. Fig. K is a photo of one of the heads after 15,000 miles of rather severe fleet service. Fig. L is the same head with the valves removed and Fig. M shows the valves from this head. The other head is continuing in service. The compression pressure remained high during the test and the valve stem wear was 0.0004 in. on the exhaust valve and 0.0006 in. on the intake. The guides were worn an additional 0.0002 in. on the intake and 0.013-in. on the exhaust port end over the initial clearance of 0.015 in.

New Industrial Tools Utilizing Phosphors

C. W. Wallhausen, United States Radium Corp.

This paper was presented at the SAE Summer Meeting, Atlantic City, June 9, 1958.

PHOSPHORS are of academic interest only to most people, beautiful to look at but of practical use only to the cathode ray tube, billboard advertising, and the novelty trades. Recent advances in phosphor technology, the increasing interest in automation, new military requirements, and the expanding atomic energy industry with its associated byproducts and problems, have combined to create new potentials which are radically changing the attitude toward these energy converting and light-emitting compounds. New developments in the fields of sensing, air tracers, infrared quenched, infrared stimulated, ultraviolet excited, and ultraviolet emitting phosphors are all industrially important and worthy of consideration. For discussion at this time, however, I have selected two specific developments which have fairly widespread and immediate industrial application — isotope-activated self-luminous light sources and thermographic phosphors.

The principles involved and the intended end uses of isotope-activated light sources and thermographic phosphors are entirely different and should perhaps be the subject of separate presentations. The former rely upon radioactive materials to produce a more or less permanent source of light; whereas, the latter involve the use of heat and ultraviolet light to produce a fugitive image on a light-emitting surface. However, both products utilize a phosphor, and it is possible that with further study, the principles of isotope activation to produce a permanent source of light can be incorporated into certain applications of thermography.

Isotope-Activated Light Sources

The excitation of phosphors by radiations from radioactive material to produce sources of light is an art which is as old as the history of radioactivity itself. Recent advances, therefore, are primarily concerned with the adaptation of new exciting agents, the improvement of phosphors, and improvement of techniques. A Canadian patent dated 1906 (shortly after the discovery of radioactivity) establishes the fact that advancement merely represents improvement in existing products, for it discusses an improved method for producing a spinthariscope, the basic principle of radioactively excited light sources.

Radium-excited self-luminous compounds were used commercially as early as 1910–1912 to illuminate the characters on clock and watch dials. Later, mesothorium and mixtures of radium and mesothorium were used for this same application, and the use was expanded to include military instruments. Between the time of the first use of self-luminous compounds and about 1946, improvements in the compounds were comparatively minor. Zinc sulfides were and still are the most efficient convertors of radioactive energy to light, and advances in luminous compounds were limited to improvements in the response of the sulfide to alpha radiation. During this relatively long period, the response of the sulfides was increased by a factor of two or three, but even this improvement did not permit the production of compounds of high brightness level. The limiting factors were the deleterious effect of alpha radiation on the phosphor, and the high cost of such compounds in relation to useful life. Beta-emitting radioactive elements were not considered, due to scarcity, cost, and comparative inefficiency as activators.

In 1946, the Atomic Energy Commission made available commercially, under very restrictive rules, certain byproduct fission materials resulting from the plutonium production program. The isotopes made available were all beta- or beta-and-gamma emitting, and they were initially released to permit study of their potential use in medical and certain limited commercial applications. It was during a program investigating sulfur 35 for a medical application that the feasibility of using beta radiation on a commercial scale to produce a luminous source first became apparent. This isotope of sulfur emits a beta ray of 0.167 mev energy, is relatively cheap compared to radium, and except for its short half life of 87 days, is a far better than predicted phosphor activator. It did establish the fact that accepted theories regarding the inefficiency of beta radiation and the resultant cost of luminous compounds incorporating beta emitters required further investigation.

The desirable features in radioactive luminous compounds are high brightness, long useful life, low toxicity, freedom from excessive external radiation, freedom from gaseous disintegration products, and costs which make their use practical. The crude experiments with sulfur 35 indicated the possibility of attaining, to various degrees, some or all of these features. Isotopes could be obtained which emitted only the relatively easily shielded beta radiation, had a long useful life, created no objectionable daughter products, and possessed less toxic qualities than radium. Preliminary investigation also indicated that destruction of the phosphor crystals so pronounced with alpha radiation was either nonexistent or for all practical purposes, negligible, and that decrease in light output was apparently di-

rectly related to the life of the radioactive material.

Early work was directed toward the use of isotopes such as strontium 90, thallium 204, promethium 147, and carbon 14, with half lives of 25 years, 4 years, 2.7 years, and 5000 years, respectively. These isotopes proved very effective and made it possible to produce useful luminous compounds of higher initial brightness, longer life, and of lower external radiation level than had ever been available in the past. There are many applications for these materials, they overcome most objectionable features of radium-activated compounds, and in some instances no good substitutes exist. However, they do have limitations. Being solid compounds, there are upper limits to the amount which can be advantageously added to a phosphor, and the law of diminishing returns controls the end result. There also exists that much overemphasized potential hazard to personnel, resulting from possible rupture of the light source capsule.

Recent work on light sources has been directed toward the use of gaseous radioactive isotopes; and while the choice of isotopes is quite limited, variation in source configuration and adaptation of well-known optical principles offer many opportunities for improving end results. Two isotopes which are of particular interest are krypton 85 and hydrogen 3 or tritium. The former is a byproduct material produced in quantity in the fission of uranium; and the latter is a product of neutron irradiation of lithium and, therefore, can also be produced in quantity. Krypton 85 has a half life of 10.25 years; it emits a beta ray of 0.695 mev energy and a small amount of gamma radiation at 0.54 mev. Tritium has a half life of 12.5 years, emits a beta ray of 0.018 mev, and does not emit gamma radiation. Both are low in the toxicity scale, can be procured at comparatively high specific activity, and when used in gaseous form, offer the advantage that they are easily diluted and dissipated in the atmosphere. Nearly all work at high brightness levels is currently being directed toward utilization of these gaseous isotopes, and the end use must be of such a nature that it can utilize a hermetically sealed unit of some shape or configuration. The high brightness materials cannot yet be supplied in a paint or dry pigment form and applied in the same manner as the better known radium-activated compounds.

It is as yet too early to make even an educated guess on upper limits of brightness that can be attained, ranges of visibility that can be achieved, or uses to which these sources can be put. Selection of suitable encapsulating materials and fabrication of such materials into acceptable containers for the radioactive gases are problems which, to a large degree, control the rate of progress. During recent months containers have been developed and tested which permit one to think of source brightnesses some five to six times greater than were available earlier this year. One now speaks in terms of millilamberts or foot lamberts rather than microlamberts. As these levels become higher, it will be necessary to investigate new binders for the phosphor used as the light source and to determine whether there will occur, at some point, a change in the unexpected resistance of the phosphor crystals to destruction by beta radiation. At all brightness levels attained so far, this resistance appears to be excellent; and where any decrease in brightness of gas filled sources has occurred, it can usually be traced to mechanical problems or degradation of encapsulation materials.

Considerable effort has been devoted to the adaptation of these light sources for use in various types of optical systems. This would appear to be an extremely simple problem since only well-known optical principles are involved. The major difficulties are those connected with maintaining high light output, while at the same time maintaining low external radiation level, reasonable size, and stability of the system under radioactive radiation. Light sources have been produced which use from one-tenth to one-third the radioactive gas required in the brightest sources available one year ago and which are, at the same time, several times brighter than the higher gas content sources. This has been done by designing sources and shielding which permit the use of spherical or parabolic mirrors, lens and lens combinations, edge lighting principles, and various methods of focusing or scattering light.

A question which is often asked is one regarding the light output compared to some standard type lamp. This we have not concerned ourselves with in the past simply because the applications on which we were working were more concerned with distance visibility in total darkness of a luminous area and, in general, this could be easily determined. Even this is becoming difficult to define because of the many variations possible in size, geometry, color, source intensity, and conditions under which interested parties wish to use the sources. Work is under way to attempt to define light output in some standard or easily understood terms.

While there are innumerable uses for these self-energized light sources, efforts have been concentrated on only a few which could have or do have immediate application. Typical uses include sources for photocell activation; escape hatch, emergency exit, and instructional markers for aircraft; trip lamps for use in mines; deck, personnel, vehicle, mine field, and bridge markers for military use; railroad switch lamps; harbor and barge markers; airstrip markers; and light sources for illuminating in-flight refueling equipment. Some work has also been done on general area lighting devices; illuminated street signs, house numbers, and mine markers; and instrument scale illuminators. The latest development is a high-intensity white-light source with which color filters can be used, making it possible to produce any color of the visible spectrum. This seemingly obvious and simple development is not as simple as it may seem. However, because of the compactness of such a source, the method opens many new fields.

Thermographic Phosphors

Since thermographic phosphors are comparatively new materials, their characteristics and applications are not as well-know as those of the self-luminous materials, and here the help and cooperation of groups which might find thermography of commercial interest is needed in development work.

Thermographic phosphors are special inorganic, crystalline materials of the zinc sulfide type which emit visible light under excitation by ultraviolet light, and which also exhibit marked change of brightness with change of temperature. Most phosphors exhibit some brightness variation with changes

in temperature; however, this is generally small and has nuisance value only. Based upon work originating at Eastman Kodak Co. special effort was devoted to producing materials in which temperature effect would be emphasized and would be reproducible. Preliminary work indicated that a zinc cadmium sulfide, silver-activated and containing a trace of nickel as a poison, would meet these requirements. Such a material is now available commercially for use in the near-room temperature range. When excited by near ultraviolet radiation, this phosphor emits broad-band radiation with a dominant wavelength in the yellow, and when subjected to heat, shows a change in brightness of 24% for each degree centigrade change of temperature. Such a brightness change is easily observable with the naked eye and can be accurately measured with proper photometric equipment. Thus, the phosphor can be used as a temperature indicator. To illustrate this temperature sensitivity, it has been used experimentally to detect small changes in body temperature.

The specific phosphor described above is most effective in the temperature range from room temperature to 90 C. For higher temperature operation, modified types of zinc cadmium sulfide phosphor are required. At the present time, the higher temperature materials have not yet been developed to the point where they exhibit the same temperature sensitivity as the near room temperature type, but their sensitivity is, nevertheless, adequate for most applications. Phosphors available for higher temperature operation and their corresponding temperature sensitivities include the following:

35–140 C	13% per deg C
130–290 C	7½% per deg C
250–430 C	7% per deg C

Thermographic phosphors applied to a surface act as a temperature indicator, and can be used to show heat flow patterns and variable electrical conductivity of thin surface layers. By causing heat to flow through the body of an object, discontinuities in the body may be visually revealed because of temperature differences at the surface. The phosphor provides, in effect, a nondestructive testing technique which in many cases is faster and more than adequate as a substitute for radiographic methods. It now appears that the technique is best suited to situations where the flaw is large or if small, near the surface, but further work may produce techniques whereby the field of application can be expanded. It is particularly effective for showing flaws in the bonding of laminates or the bonding of sheets to substructures.

The method of using the phosphor is simple and consists essentially of these steps:

1. The phosphor, mixed with a suitable binder, is uniformly applied to the surface being tested. Application may be by brush, spray, screen, settling, or by the recently developed phosphor decal method. Uniformity is necessary and optimum thickness depends to some extent on the accuracy required and the desired definition. An extremely thin coat results in low light output, whereas, a heavy application leads to loss of definition. A coating thickness of about 0.005 in. appears to give the best results.

2. After application of the phosphor, the coated surface is exposed to ultraviolet light. This activating light should uniformly expose the coated surface and should also contain a minimum of visible radiation in order to produce the best results.

3. While still exposed to the ultraviolet source, the coated surface should be exposed simultaneously to a source of heat. The heat source may be an infrared lamp or other suitable device, but again, heating should be uniform and devoid, as much as possible, of visible radiation.

Following the above procedure, defects in the material under test will appear as dark areas against a luminous background. Where contact of the phosphor coat with the test surface is good, heat conduction occurs and the area remains bright. Where a flaw exists, conduction is poor and quenching of the phosphor takes place.

Visual observation of the brightness is all that is necessary in many cases, especially if only qualitative results are required. By using suitable filters to exclude reflected ultraviolet and blue light, the pattern can also be photographed, making it possible to maintain a permanent record of the test. Photography also provides a good technique for quantitative work. A comparison film to serve as a standard can be calibrated by photographing the phosphor-coated surface of a simple calibrating device, the temperature of which can be varied in measured steps. In many cases, it is also possible to utilize photocell sensing, particularly if only spot areas are of interest or if certain types of assembly line operations are involved.

The preceding comments apply only to contact thermography where the object to be tested can be directly coated with the phosphor. Most work to date has been in applications of this nature. A field which shows very definite promise and should be further explored is that of projection thermography. Since these phosphors respond to infrared radiation, a screen of the phosphor can be used to detect distant sources of heat radiation, and by optically projecting an image of the source on the screen, a pattern of the source can be seen and photographed. This method can be used for the study of objects at very high temperatures.

It was mentioned earlier that there existed a possibility of combining certain features of isotope-activated light sources and thermographic phosphors, and if so, it would make discussion of the two subjects in a single paper appear more logical.

Many isotope-activated self-luminous compounds exhibit a pronounced quenching effect when exposed to infrared or other types of heat sources. It is conceivable, therefore, that a thermographic phosphor could be isotope-activated and applied to a surface as a paint or decal, giving a constantly glowing phosphor surface under normal conditions. In applications where a sudden rise in temperature might be undesirable, the extinction of the glow would serve as a temperature rise indicator. Applied to a heated surface, the change from extinction to a glowing surface could also be used to indicate visually unexpected or sudden drop in temperature. This particular combination of isotopes with thermographic phosphors has not been explored, but does offer some very interesting possibilities.

Although thermographic phosphors are not a strictly new development, it is only within recent months that they have been developed to a point where commercial applications appear feasible and practical. Many possible uses exist and much work remains to be done on development of techniques.

VEHICLE SUSPENSIONS
COIL

M. C. Turkish, Eaton Manufacturing Co.

This paper was presented at the SAE Summer Meeting, Atlantic City, June 9, 1958

THE use of coil springs to support a vehicle chassis on its wheels is nothing new, but it is very practical. With all of the recent discussion of revolutionary changes being made in vehicle suspension systems, the potent fact still remains that a steel spring is the most economical suspension means today. In today's competitive market the cost of an item to the consumer is of paramount importance, so that the suspension system which will prevail in the future is one which will offer at a lower cost many of the good characteristics featured by more expensive or elaborate systems.

Coil Spring Characteristics

Mechanical springs used for vehicle suspensions are basically of three types: leaf springs, torsion bar springs, and helical coil springs. Each of these springs possesses certain inherent advantages over others, and it is the purpose of this presentation to explain the basic merits of the helical coil suspension spring so that these advantages may be appreciated and utilized in the greatest degree possible.

The large scale adoption of the coil spring as a suspension media by the automotive industry in the 1958 automobiles serves to attest to the many advantages offered by this type of spring. The coil spring was first used in this country on the Brush Runabout which appeared in 1908. The frame was supported at all wheels on four extension-type coil springs; but the application proved to be limited, probably due to one of the many desirable characteristics offered by this type of spring, namely, friction-free action.

The compression type of suspension coil spring appeared in 1934 with the introduction of the independent front wheel suspension which was developed by Maurice Olley and his associates in General Motors Corp. This development came when an urgent need arose to uncouple the two front wheels to prevent wheel tramp and shimmy and to lower materially the rates of the front springs in order to improve the ride characteristics of the automobile of that day.

The independent front wheel suspension also permitted the design of an accurate steering mechanism even with the lower spring rates adopted, since the motion of the wheel was controlled by upper and lower control arms rather than by a stiff leaf spring as formerly. Also, the unsprung mass was reduced by going to independent wheel suspension. The basic qualities which led to the use of the coil spring over other types of springs for the independent wheel suspension was its comparatively

LEAF SPRING

$$\varepsilon_L = \frac{S^2 V}{6E}$$

$$\frac{\varepsilon_L}{W} = 2.02 \cdot 10^{-4} S^2 \quad \text{IN.\#/\#}$$

TORSION BAR

$$\varepsilon_T = \frac{S^2 V}{4G}$$

$$\frac{\varepsilon_T}{W} = 7.63 \cdot 10^{-4} S^2$$

COIL SPRING

$$\varepsilon_C = \frac{S^2 V}{4G} = \frac{S_M^2 \cdot V}{K_W^2 \cdot 4G}$$

$$\frac{\varepsilon_C}{W} = 4.88 \cdot 10^{-4} S_M^2$$

NOMENCLATURE

- ε = ENERGY - INCH POUNDS
- V = ACTIVE STEEL VOLUME - CU IN.
- W = ACTIVE STEEL WEIGHT - POUNDS
- V = 3.52W FOR SPRING STEEL
- S = STRESS P.S.I.
- S_M = MAXIMUM WAHL STRESS P.S.I
- K_W = WAHL STRESS FACTOR (1.25 TYPICAL)
- E = MODULUS IN TENSION $29.0 \cdot 10^6$ P.S.I.
- G = MODULUS IN TORSION $11.5 \cdot 10^6$ P.S.I.

ENERGY STORAGE RATIO AT GIVEN STRESS

$$\varepsilon_T / \varepsilon_L = 3.78$$

$$\varepsilon_C / \varepsilon_L = 2.42$$

Fig. 1 — Comparison of energy storage in steel springs

USING SPRINGS

THIS paper describes the characteristics of helical coil springs, particularly the less expensive ones. Comparisons of energy storage in steel springs are made.

The author demonstrates the method of calculating normal coil spring load and the rate required for independent front wheel suspension.

The author describes the use of the coil spring suspension in a variety of vehicles. He thinks that the system will continue to be used on a great number of the cars, trucks, and buses of the future.

small physical size and its friction-free action. The use of hydraulic shock absorbers permitted a controlled means of damping to provide proper control to the friction-free action of the suspension coil spring.

The adoption of the coil spring with the independent wheel suspension, together with the shifting of the engine and body weights forward, resulted in front and rear frequencies of about the same order. This produced a relatively horizontal ride with the elimination of most of the pitching, which was so prevalent in the earlier vehicles with their stiff front springs.

A leaf spring stores energy during spring deflection by bending, so that the material on one surface is stressed in tension, while on the opposite surface it is stressed in compression. A torsion bar and helical coil spring store energy by twisting the material so that the material is stressed in shear. Since a greater portion of the material in a spring which is twisted is stressed to a high degree, it is possible to store more energy per pound with a torsion bar or a coil spring as compared to a leaf spring. A comparison of the energy storage obtainable with steel springs is given in Fig. 1. Here it is shown that the energy storage per pound of active weight of steel is $2.02 \times 10^{-4} \times S^2$ for a leaf spring, $7.63 \times 10^{-4} \times S^2$ for a torsion bar, and $4.88 \times 10^{-4} \times S_M{}^2$ for a coil spring using a typical Wahl factor of 1.25. Considering some particular value of stress (tension for the leaf spring and shear for the torsion bar and coil spring), then the energy storage ratio of the torsion bar to the leaf spring is 3.78, and for the coil spring to the leaf spring is 2.42. Actually, these ratios do not show the true picture, since the torsion bar is generally not stressed as high as the leaf spring or coil spring.

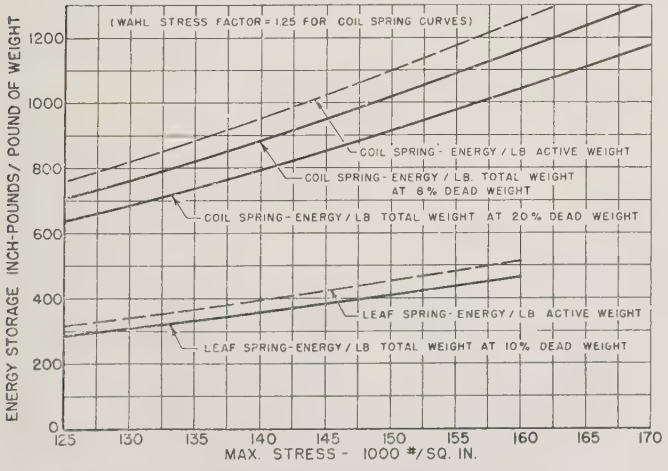

Fig. 2 — Relationship of energy storage to stress

A comparison of the coil spring to the leaf spring on the relationship of energy storage to stress is shown in Fig. 2. Here the energy storage per pound of active weight in the coil spring is shown to be 2.42 greater than in the leaf spring for a given stress. A coil spring made with alloy steel can generally be stressed to 130,000–140,000 psi at minimum operating height and designed to a solid stress of 145,000–160,000 psi when preset solid. A leaf spring made with alloy steel and designed with equal stresses on the front and rear sections can be stressed to 130,000–140,000 psi at maximum deflection without considering windup stresses. Unequally stressed springs with a conservative stress on the front section which ties the axle to the frame can have much higher stresses in the rear section, in the order of 160,000 psi maximum.

Since the coil spring can be designed and utilized as a perishable item, the hardness and stress can

be made sufficiently high to operate on only a small safety factor. A coil spring failure is not nearly so serious a matter as a leaf spring failure, since the steering control is always maintained by the control arms and links.

Fig. 2 also shows the energy storage per pound of the total spring weight. For the leaf spring 10% dead weight is added, which is the average amount for automotive applications with the usual size of spring eyes and clamped seat areas. For heavy-duty leaf springs this dead weight may reach values as high as 25%, due to the heavy clamped seat section. The lower curve of the coil spring group of curves with 20% dead weight represents a typical coil spring with two flat ends, while the higher curves with 8% dead weight represent a typical coil spring with two pigtail ends.

From these curves the weight advantage of the coil spring is readily apparent, especially when two pigtail ends are used and the spring is stressed quite high at solid height. As an example, a typical coil spring with pigtail ends stressed to 155,000 psi at solid height will have the same energy storage capacity as a leaf spring weighing three times as much and stressed to a maximum value of 140,000 psi at maximum deflection. This points to a large advantage of the use of coil springs on larger, heavy-duty vehicles, especially when independent wheel suspension is used.

Types of Coil Spring Ends

The different types of ends used for suspension coil springs are shown in Fig. 3. These springs are formed from alloy steel bars of approximately ¾ in. in diameter and, therefore, must be coiled red hot. The flat ends on the spring are made by hot taper rolling the ends of the bar before the spring is coiled. During the coiling operation the ends are positioned to produce the flat end structure shown. The tangent-tail end is an economy feature, but results in a somewhat higher solid height and requires a different type of seat to fit the tangent-tail end. The pigtail end offers the advantage of a lower solid height, a lower amount of inactive spring material, and a reduced cost as compared with the flat end.

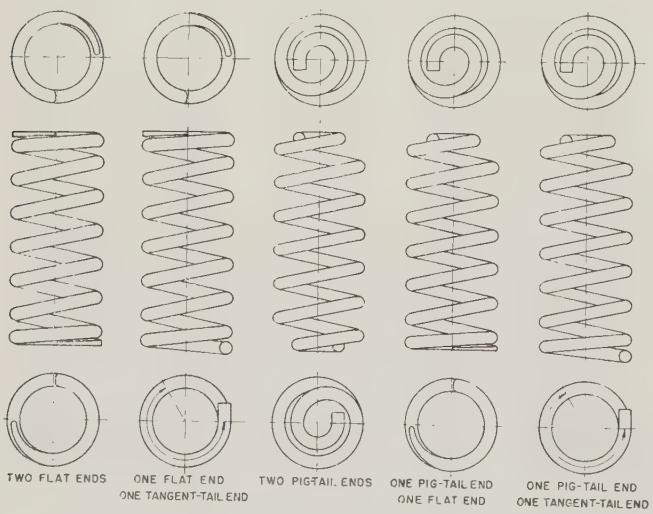

Fig. 3 — Typical ends for hot-coiled compression springs

The five different springs illustrated in Fig. 3 show the practical combinations of ends which are generally used. Fig. 4 shows the effect of these various end constructions on solid height, material cost, and total cost of a spring for a typical application. Since solid height is frequently a limitation on the spring design, this can be an important factor in determining the type of end to be used. From this bar chart it is apparent that the spring with one flat end and one tangent-tail end is the highest for solid height, whereas the spring with the two pigtail ends is the lowest. The material cost is highest for the spring with two flat ends, and is lowest for the spring with two pigtail ends. The total cost is highest for the spring with the two flat ends, and is lowest for the spring having one pigtail end and one tangent-tail end.

Spring Materials and Processing

Two types of alloy steels are in general use today for hot-coiled suspension coil springs; namely, chromium steels of the 5100 series and silico-manganese steels of the 9200 series. The most popular chromium steel for automotive applications is 5160 and contains 0.55–0.65 C, 0.75–1.00 Mn, 0.20–0.35 Si, and 0.70–0.90 Cr, with phosphorus and sulphur each held to less than 0.04. The only commonly used silico-manganese steel is 9260 and contains 0.55–0.65 C, 0.70–1.00 Mn, 1.80–2.20 Si, with phosphorus and sulphur each held to less than 0.04.

The silico-manganese steels are good from the standpoint of hardenability and tensile strength; however, generally they tend to be "dirty" with inclusions. If the inclusions happen to be large and near the surface, they can bring about early fatigue failures.

In addition to these two steels, other types can be used, such as SAE 4068 (Amola), SAE 6150 (Chrome-Vanadium), and SAE 9254 (Chrome Silicon). For heavier duty spring applications, the bar diameter may be in excess of 1.00 in. Then steels with greater hardenability are required, and this calls for the use of SAE 8660 or SAE 9262. The chemical composition of these steels is outlined in the new SAE Manual on Design and Application of Helical and Spiral Springs.

Alloy steel bars for use in manufacturing suspension coil springs are purchased from the mill either as precision-rolled bars with close dimensional tolerances or as centerless ground bars.

After the spring is hot coiled, it is quenched in

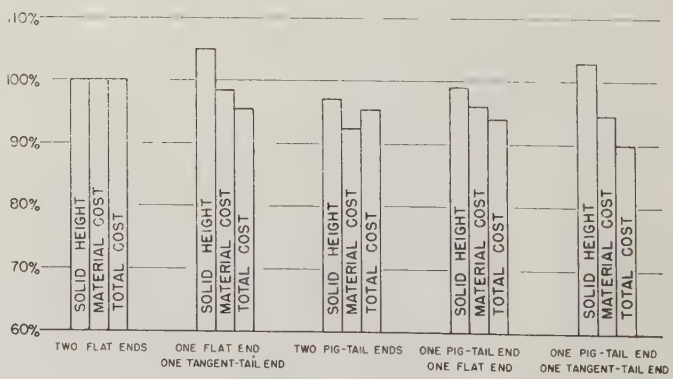

Fig. 4 — Effect of end construction of suspension coil springs on solid height and cost

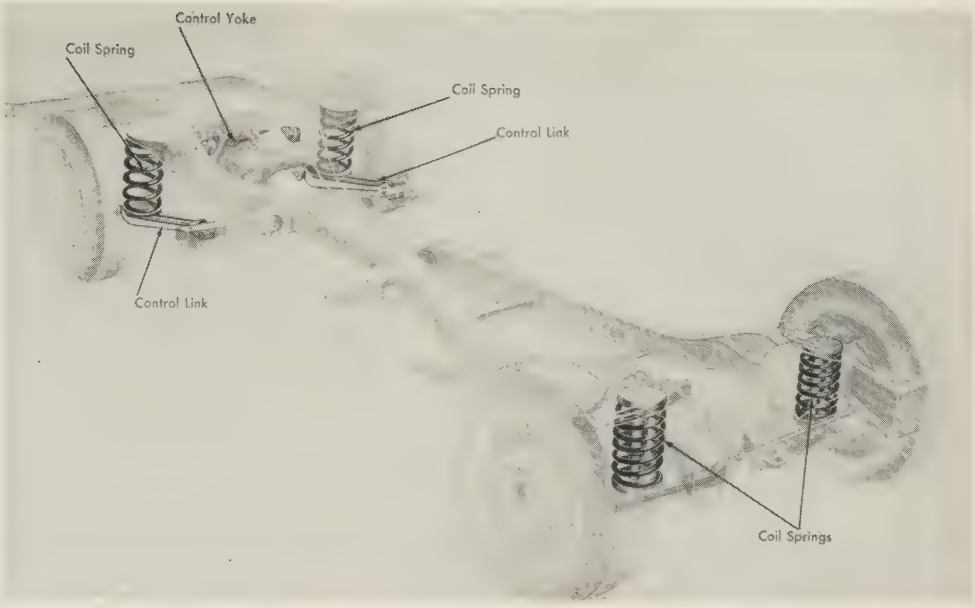

Fig. 5 — Automotive coil spring suspension (1958 Cadillac)

oil at approximately 1600 F. The spring is then drawn at a closely controlled temperature to obtain the specified hardness, which is generally within a narrow limit of the broad Brinell range of 387 to 512, with a typical range being 460–512.

The spring is then shotpeened. In this process the scale is removed and trapped compressive stresses are induced in the surface, thus considerably increasing the fatigue life. In the shotpeening process the spring is rotated and advanced linearly through the blast pattern, which consists of small steel particles that have a velocity of 200 fps. After shotpeening, the coil spring is dip-coated with a high-grade baking enamel as a corrosion preventive.

A final operation of presetting the coil spring is performed, which consists of compressing the spring to its solid height or slightly above. In a properly designed spring having a solid stress of 135,000–160,000 psi, the spring will take some set as a result of the surface yielding. In actual use the spring does not operate at the high stress, so usage at lower stress levels will produce little or no further settling. By this presetting operation the settling is practically eliminated and the fatigue life is improved.

A typical modern automotive vehicle suspension using coil springs for all four wheels is shown in Fig. 5. This photograph is for the 1958 Cadillac, which has independent wheel suspension for the front and control links to attach the rigid rear axle to the vehicle frame.

Springs for Front Suspension

A more detailed illustration of a typical front wheel independent suspension using a coil spring is shown in Fig. 6. This is for the 1958 Pontiac and shows the double control arm arrangement providing vertical motion to the wheels. The lower control arm is longer than the upper control arm, and the arms are positioned in such a manner as to obtain the best compromise in track variation, wheel tilt, roll center height, and high cornering force at the tire-road surface.

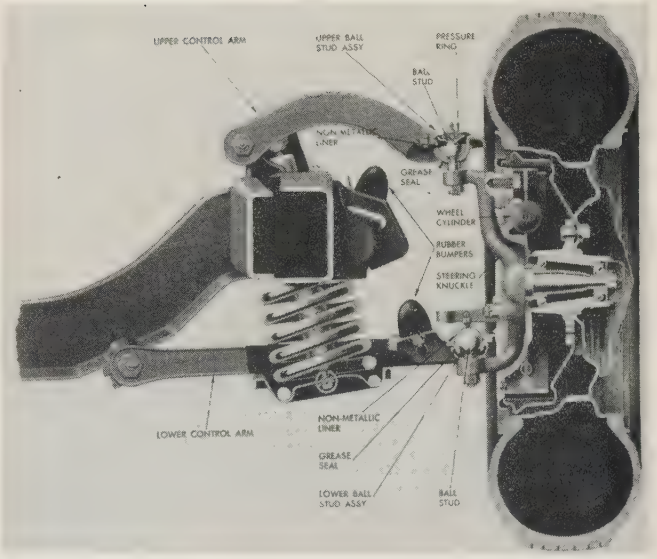

Fig. 6 — Independent front wheel suspension using coil springs on 1958 Pontiac

The coil spring is interposed between the lower control arm and the frame and is loaded in compression. The spring rests in a cupped seat properly contoured in the lower arm to take the tangent-tail end in this particular application. The spring load is considerably greater than the wheel load, due to the load magnification produced by the leverage action of the lower control arm.

The upper end of the coil spring reacts in the frame, and a bending couple is produced between the lower arm pivot point and the place where the spring load reaction is taken by the frame. The front cross-member must be stiff enough to handle this bending moment during wheel deflection without having undue response occurring at the other front wheel. This rigidity is imperative to eliminate all tendency for wheel tramp and shimmy, and this rigidity is obtainable in the modern welded automotive frame using channel and box sections.

The method of calculating the normal coil spring load and rate required for the independent front

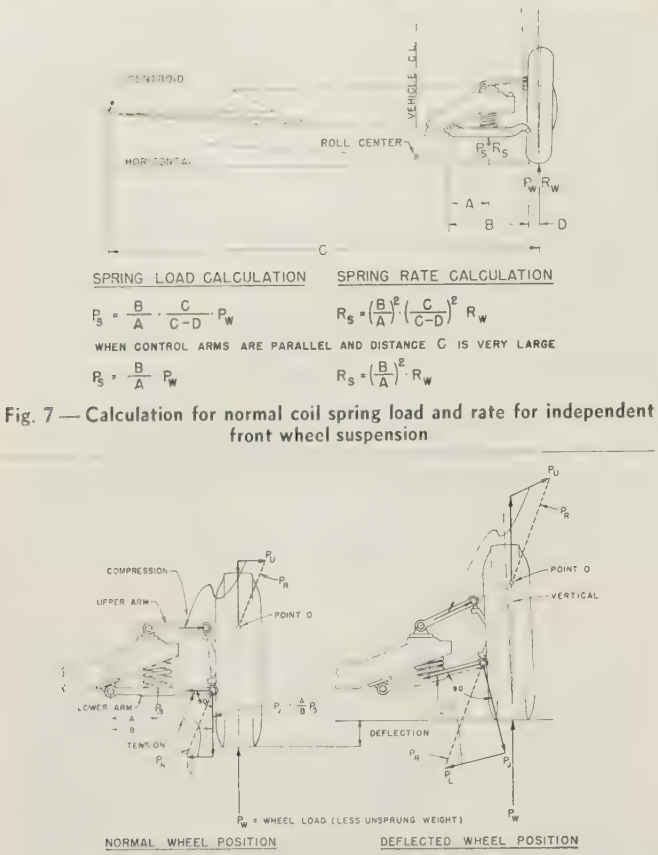

Fig. 7 — Calculation for normal coil spring load and rate for independent front wheel suspension

Fig. 8 — Graphical determination of loads in structure of independent front wheel suspension

Fig. 9 — Independent front wheel assemblies on cross-member that is attached to the vehicle structure (Jaguar)

Fig. 10 — Sturdy cross-member supporting independent front wheel assemblies as used on 12-ton London Routemaster bus

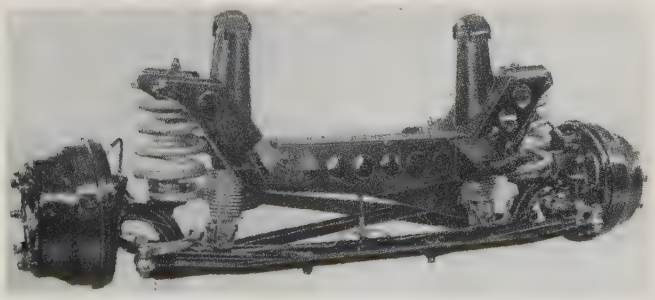

Fig. 11 — Heavy-duty beam axle front suspension using coil springs by Mercedes-Benz for a large bus (note internal booster coil springs)

wheel suspension it outlined in Fig. 7. For simplicity, a vertically acting coil spring is illustrated. When the spring acts at an angle from the vertical, then an angle correction must be applied to the load and rate calculations similar to that shown later in making calculations for the coil spring for the rear suspension (Fig. 13). For a given wheel load P_W, the required spring load can be calculated from the geometry of the double control arms. By first determining the location of the centroid point, which is at the intersection of the two lines drawn through the pivot points of the control arms, the spring load P_S can be calculated from the formula:

$$P_S = \frac{B}{A} \cdot \frac{C}{C-D} \cdot P_W \qquad (1)$$

When the control arms are parallel and the distance C is very large, the determination of the spring load does not require a consideration of the wheel offset dimension D.

Geometry of the control arms must similarly be considered when it is desired to calculate the normal coil spring rate from a given wheel rate. The spring rate R_S is given by the formula:

$$R_S = \left(\frac{B}{A}\right)^2 \left(\frac{C}{C-D}\right)^2 R_W \qquad (2)$$

This also simplifies when the control arms are parallel and distance C is very large, as shown in Fig. 7.

By extending a line from the centroid point to the tire-road surface, the roll center is readily established. This is at the intersection of the reference line and the vehicle vertical center line.

On automotive-type vehicles, a centroid distance of 200–300 in. with a roll center height of 1.5–3.5 in. above the road appears to give the best compromise in the various factors of tread variation, wheel tilt, roll center height, and high cornering force at the tire-road surface.

In developing an independent wheel suspension, the loads in the control arms must be determined to design these members properly for adequate strength and rigidity. These forces can be calculated analytically for various positions of the wheel; however, a much more rapid and very accurate approach is to employ the graphical method shown in Fig. 8, which was developed by W. D. Allison. The solution is begun by determining the downward force P_J on the lower ball joint at normal wheel position, which is calculated from the spring load to be equal to:

$$P_J = \frac{A}{B} \cdot P_S \qquad (3)$$

Point 0 is then established at the intersection of a line through the pivot points of the upper control arm and a vertical line through the center of the tire-road contact surface. A reference line is then drawn through point 0 and the lower ball joint. Vector P_L is then drawn (parallel to the lower control arm) to the intersection with the reference line. This establishes the magnitude of vector P_R which is drawn as a dashed line on the layout. Vector P_R is then laid out from point 0 along the reference line. The vector P_U is then drawn parallel to the upper arm, and its intersection with the vertical line establishes the vertical component of P_R, which is equal to the wheel load P_W less the unsprung weight. Vector P_L is equal in magnitude to the

tension load in the lower control arm, and vector P_U is equal in magnitude to the compression load in the upper control arm.

Similarly, the loads in the upper and lower control arms can be determined graphically for various positions of wheel deflection as shown in Fig. 8. Load vector P_J is determined first by calculation from the spring load as before; resultant vector P_R is then established, from which the control arm loads P_L and P_U are readily determined.

Independent front wheel suspension systems can be adapted to larger vehicles than the automotive type to secure many of the functional advantages over the rigid axle suspension. The chassis structure of trucks and buses is generally made with built-in flexibility to permit good load division between all four wheels when the suspension springs alone have insufficient flexibility to handle the load variation as the vehicle moves over a contoured surface. Since there is an absolute need for a stiff frame to carry the independently sprung front wheels, the solution lies in mounting these wheels on a rigid cross-member. This cross-member can then be attached to the usual type of relatively flexible frame. A construction of this type has been made by Jaguar, as shown in Fig. 9. This construction permits the use of rubber between the cross-member and frame to materially isolate the vehicle from wheel noises, without impairing the accurate position of the front wheels which is so important to secure an accurate steering mechanism.

An independent front wheel suspension of this type, employing a sturdy cross-member to support the front wheels, is shown in Fig. 10. This is the suspension used on a large 12-ton London Routemaster bus which uses coil springs at all wheels.

Another heavy-duty bus application using coil springs for the front suspension was made by Mercedes-Benz using a rigid type axle and is shown in Fig. 11. Here the axle positioning is accurately controlled by means of a V-link and a transverse panhard rod. This application is interesting from the standpint that it employs two coil springs for each wheel, one spring inside of the other. The inner spring is much shorter than the outer one and serves as a booster spring to carry heavy loads and to prevent bottoming through during large wheel deflection.

An interesting application of coil springs in an independent wheel suspension is shown in Fig. 12. This is for a German armored car built during the last war and employs two coil springs in parallel in each suspension unit. This vehicle had four wheels independently sprung and could be either 2- or 4-wheel steered.

Springs for Rear Suspension

Coil springs can be readily adapted for use in rigid axle rear wheel suspensions in place of the tried and proved leaf springs. Buick and Nash have done this for many years, and recently this system has found more widespread adoption because it permits the use of much lower spring rates. This also was one of the main reasons for adopting coil springs for the front suspension in 1934. The use of coil springs necessistates a construction using control links and yokes to guide the rear axle in its motion.

As previously pointed out, the coil spring will weigh considerably less than the leaf spring which it replaces. The leaf spring has the advantage, however, that it is positioned longitudinally with the frame and at a location where adequate space for the leaf spring is generally available. On the other hand, the suspension coil springs require more vertical space above or near the rear axle, so that the spring height can be a serious problem. For this reason, solid height is often of prime importance and pigtail-end springs are frequently used. Also, the pigtail ends generally are well-adapted to be fitted to the control link (Fig. 13).

This figure also shows the method of calculating for the normal coil spring load and rate required to give a known or desired wheel load and rate. In this drawing the spring is shown positioned at an angle from the vertical, and the spring load required is determined from the formula:

$$P_S = \frac{B}{A}\,\frac{1}{\cos\alpha}\,P_W \qquad (4)$$

The spring rate R_S is determined from a similar

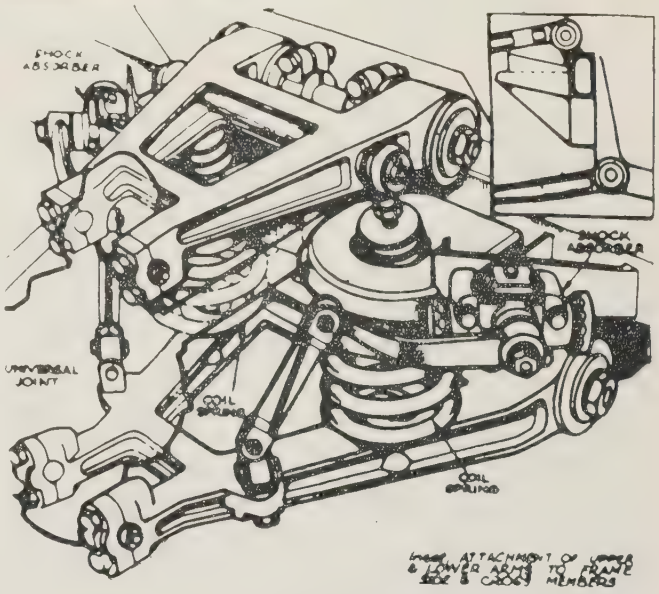

Fig. 12 — Heavy-duty independent wheel suspension using two coil springs in parallel on a German armored car

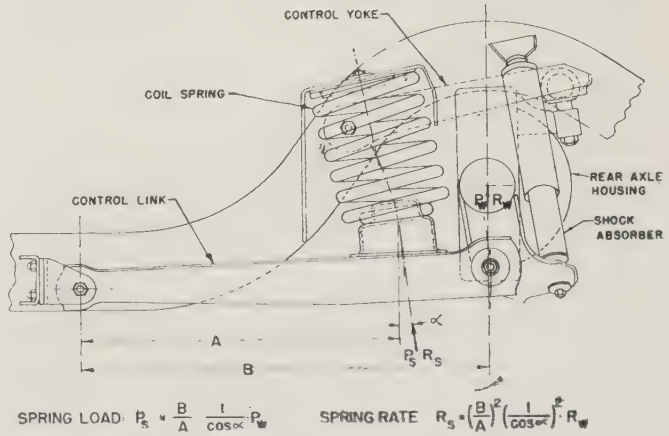

Fig. 13 — Calculation for normal coil spring load and rate for rear suspension

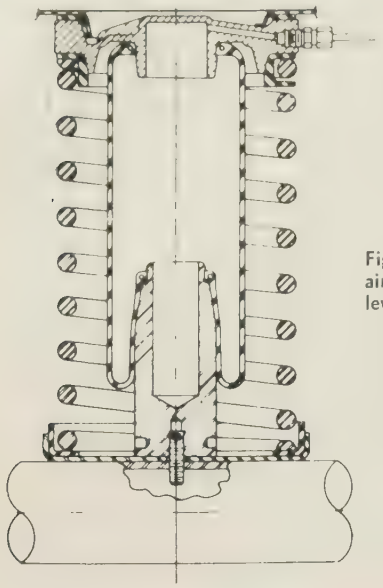

Fig. 14 — Coil spring used with air spring in rear to give vehicle leveling and variable rate (1958 Rambler)

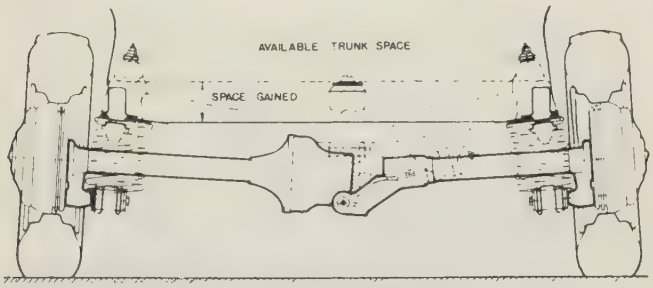

Fig. 15 — Rear swing axle using coil spring suspension (Daimler-Benz)

formula where the angle is taken into account, namely:

$$R_S = \left(\frac{B}{A}\right)^2 \left(\frac{1}{\cos \alpha}\right)^2 R_W \qquad (5)$$

Axle rotation during vertical axle motion is controlled by the lengths and positioning of the lower control link and upper control yoke and is readily determined by a graphical analysis by rotating the control link through small angle increments and then determining the resulting axle rotation.

In the layout of Fig. 13 only a single coil spring is shown which has uniform coil spacings in the spring. This spring has relatively constant rate for all positions of vehicle loading. Variable rate or increasing rate with vehicle loading can readily be obtained by having nonuniform coil spacings in the spring so that some coils close out during spring compression. As the spring is then compressed and some coils close out, a higher coil spring rate is obtained. A scheme using two coil springs similar to that shown in Fig. 11 for the front axle could readily be used for the rear springs to give an increased rate when the vehicle is heavily loaded.

Another very practical means of obtaining variable rate and also to give vehicle leveling is to employ an air spring together with a coil spring. The air spring, such as a Goodyear rolling lobe type, may be mounted adjacent to the coil spring on the control link or mounted internally within the coil spring as used in the 1958 Rambler station wagon (Fig. 14).

Fig. 16 — London Routemaster bus which uses coil spring suspension at all wheels

In the Rambler installation, the combination coil-air spring is employed in the rear only, where practically all of the load variation occurs when the vehicle is fully loaded. This spring combination is mounted directly over the rear axle. With the vehicle unloaded, the coil spring carries approximately 85% of the vehicle load, and the other 15% is carried by the air spring at a pressure of only 20 psi. When the vehicle is loaded and the leveling valve permits air to enter the air spring and level the vehicle, the load on the coil spring remains unchanged, and all of the added load is carried by the air spring at a pressure of about 100 psi. This higher air pressure in the air spring results in a much stiffer spring to give a higher total spring rate.

Coil springs are readily adaptable to DeDion and swing axles. A recent development is the Daimler-Benz low-pilot single-joint swing axle (Fig. 15).

The versatility of the coil spring exceeds that of torsion bars and leaf springs for both front and rear suspension applications. Whenever one wants to develop a low rate suspension for almost any application, coil springs can be made to do the job in one manner or another. A typical instance of this is the London Routemaster bus shown in Fig. 16. From the photograph it is readily apparent that the center of gravity is unusually high, so that a suspension with high roll resistance is imperative. This vehicle was built using coil-spring suspension at all wheels, and despite the softer riding characteristics obtained and the larger number of passengers carried on the top deck, the roll stability of the vehicle is better than has ever before been achieved.

The independent front wheel suspension used in this bus was previously discussed and shown in Fig. 10. The rear spring arrangement is shown in the plan view of Fig. 17, which allows the outboard location of the coil springs. The use of the coil spring permits such a spring installation to aid in giving good roll stiffness. A further roll-stiffening effect

is obtained from the two long trailing arms which support the axle and act as a roll-stiffening member. A similar application by Crossley for a double deck bus is shown in the photograph of Fig. 18.

Coil springs can be used in a variety of ways to secure variable rate, an interesting method being the use of a toggle device. A practical application of this principle is in the Gregoire suspension, which employs two small toggle springs in conjunction with a main support leaf or coil spring. A drawing of this type of spring assembly used with a leaf spring to obtain variable rate is shown in Fig. 19. This device has been used in several models of English buses in recent years with reportedly good ride performance.

The coil spring as a vehicle suspension means has gradually increased in popularity where today its usage in the modern automobile vehicle exceeds in quantity all other types of suspension springs combined. Its popularity should remain high in the future, as spring steels are improved to permit the use of even higher stresses than are used at present. The use of higher stresses can bring about further economies, which is bound to keep this type of spring competitive with others.

A more noticeable trend in the future should be in the usage of the suspension coil spring for the front suspension of light and medium trucks. It will also undoubtedly find some application to the rear suspension of some trucks with booster coil springs to provide the desired variable rate characteristics.

Acknowledgments

The author desires to gratefully acknowledge the guidance and engineering data given by Bernhard Sterne of Chrysler Corp. and the data and photographs given by John Hoban of the Cadillac Division of General Motors Corp. Also, acknowledgment is given to the Pontiac Division of General Motors Corp., Studebaker-Packard, Daimler-Benz, Jaguar, and the London Transport Co. for various photographs, and the sources listed in the bibliography for some information appearing in this paper.

References

1. *Automotive Industries,* Vol. 115, Oct. 15, 1956, p. 59: "Latest Vehicles Displayed at Britain's Commercial Motor Show," by W. S. Amos.
2. *Automobile Engineer,* Vol. 45, January, 1955, pp. 3, 71, 545: "London Transport Routemaster Bus."
3. *Automobile Engineer,* Vol. 45, January, 1955, p. 511: "Front Suspension."
4. Pp. 468, 494, 542 of "The Automotive Chassis," by P. M. Heldt. Third Edition. Pub. by Chilton Co., Philadelphia, 1952.
5. SAE *Quarterly* Transactions, Vol. 3, October, 1949, pp. 571–581: "Comparing Fundamentals of Spring Suspensions," by N. E. Hendrickson.
6. "Resume of Bus Suspensions," by A. B. Hirtreiter. Paper presented at SAE National Transportation Meeting, New York, October, 1956.
7. SAE *Journal,* Vol. 29, March, 1934, p. 73: "Independent Wheel Suspension—Its Whys and Wherefores," by Maurice Olley.
8. "Daimler-Benz Swing Axles," by H. Scherenburg, R. Uhlenhaut, and J. Miller. Paper presented at SAE Annual Meeting, Detroit, January, 1958.
9. SAE Transactions, Vol. 54, 1946, pp. 366–374: "Flexible or Spring Medium of Suspensions," by R. Schilling.
10. "Manual on Design and Application of Leaf Springs." SAE Special Publication No. 7.
11. "Manual on Design and Application of Helical and Spiral Springs." SAE Technical Report No. 9.
12. "Observations of Various German Suspensions and Steering Gears," by R. L. Weider. Paper presented at SAE German Engineering Evaluation Meeting, Detroit, March, 1946.

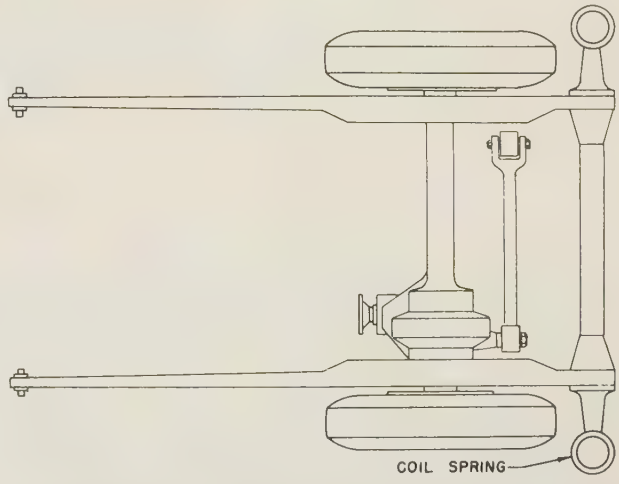

Fig. 17 — Plan view of London Routemaster bus suspension showing location of rear coil springs

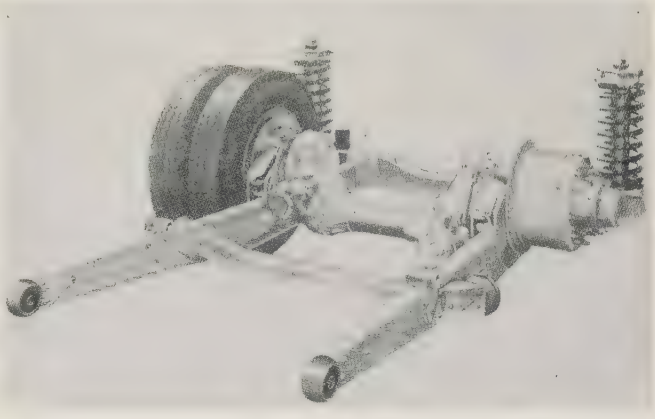

Fig. 18 — Crossley rear coil spring suspension unit

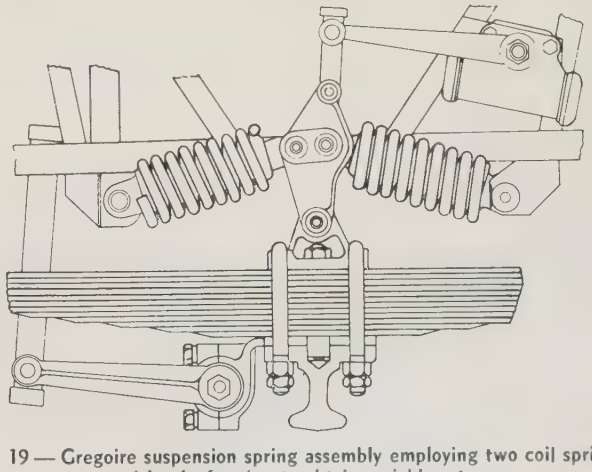

Fig. 19 — Gregoire suspension spring assembly employing two coil springs with a leaf spring to obtain variable rate

Possibilities and HIGH ENERGY

Walter T. Olson, National Advisory Committee for Aeronautics

This paper was presented at the SAE National Aeronautic Meeting, New York, April 9, 1958.

BORON compounds offer a heat of combustion 40% greater than that of aircraft fuels in current use. Diborane and pentaborane have burned satisfactorily in turbojets, afterburners, and ramjets. But boron compounds leave troublesome deposits and they present supply, storage, and handling problems.

This paper describes investigations into the use of boron hydrides as high-energy liquid fuel. Present results indicate that the ultimate fuel will be a boron-hydrogen-carbon compound.

The author also discusses other high-energy fuels of magnesium, aluminum, beryllium, and boron. Magnesium has been found to be a top fuel for short-time high-thrust applications, because of its high combustion temperature.

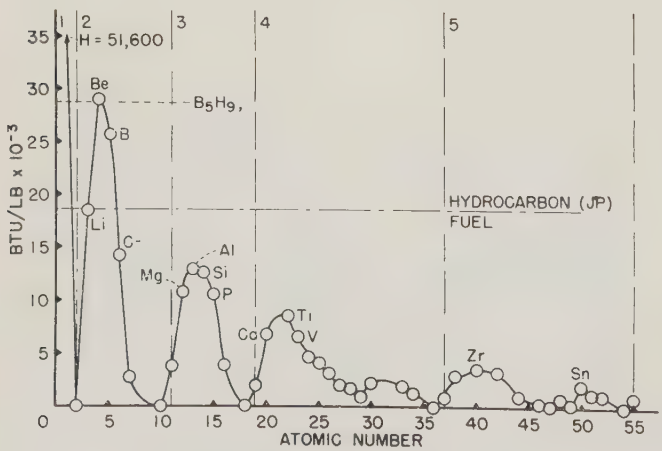

Fig. 1 — Heats of combustion of elements

THE interest in fuels other than conventional hydrocarbon types for jet engines stems from the desire to extend speed, altitude, and range of aircraft. These flight characteristics are so related, as will be shown later, that increases in, for example, speed or altitude, may be possible only at the expense of flight range. As a consequence, fuels having higher heat of combustion per pound are of particular interest; they offer the possibility of improved range or payload for flight in the atmosphere. To be sure, availability, physical properties, properties of exhaust products, flame temperature, and combustion characteristics are also important to fuel selection. Some research and development on nonhydrocarbon fuels has actually been undertaken, either to capitalize on high bulk densities of fuel for short-range missiles, or to increase maximum thrust of engines of fixed size, or to improve combustion at severe operating conditions. The primary concern, however, is to put the largest energy aboard in the fuel load that must be carried, and so most of the research and development on nonhydrocarbon fuels has been on fuels of high heating value.

It is the intention of this report to discuss factors leading to fuel selection, the chemical possibilities for high-energy fuels, and some of the problems attendant to their application to flight propulsion. Although many organizations have contributed to the field[1] illustrations are drawn largely from NACA research.

Chemical Possibilities

General Principles

The importance of fuel energy and the reasons for interest in high-energy fuels in the current aeronautical scene may be appreciated by examining the terms of the Breguet range equation, which may be

[1] NACA RM E51D23, 1951: "Status of Combustion Research on High-Energy Fuels for Ram Jets," by W. T. Olson and L. C. Gibbons.

Problems of Some FUELS FOR AIRCRAFT

written:

$$\text{Range} = H_c \eta_e \, L/D \, ln \frac{1}{1 - \frac{W_f}{W_0}} \quad (1)$$

or, since:

$$W_0 - W_f = W_{PL} + W_s + W_e \quad (2)$$

$$\text{Range} = H_c \eta_e \, L/D \, ln \frac{1}{\frac{W_{PL}}{W_0} + \frac{W_s}{W_0} + \left(\frac{W_e}{F}\right)\left(\frac{1}{L/D}\right)} \quad (3)$$

where:

H_c = Heat of combustion of fuel
η_e = Overall efficiency of engine
L/D = Lift to drag ratio
W_0 = Weight at take-off
W_f = Weight of fuel
W_{PL} = Weight of payload
W_s = Weight of structure
W_e = Weight of engines
F = Thrust

Obviously, range depends directly on fuel heating value. Normally expressed as Btu/lb, heating value is also ft-lb/lb, or miles for which a pound of fuel will produce a pound of thrust; ideally, for a hydrocarbon jet fuel of 18,500 Btu/lb, 2400 nautical miles. However, the engine and aircraft efficiencies and the log term involving the weight of fuel that can be carried are multiplied onto the energy in the fuel; thus, the effects of speed and altitude on these terms should be considered.

Engine efficiency for both turbojets and ramjets will increase with speed if cycle temperatures are correspondingly increased. Temperature limits do exist, however. In the turbojet they are set by turbine materials, and in the ramjet by the decreasing margin to which the fuel can heat the inlet air. Thus, engine efficiencies increase at a decreasing rate with speed, reach a maximum, and thereafter decrease. But lift-to-drag ratios decrease with speed. This decrease is most marked from subsonic speeds where L/D values in excess of 20 are easily achieved to supersonic speeds where values may be of the order of only one-fourth or one-fifth the subsonic value. The term L/D enters the range equation most strongly. Also, structural weights must be larger to sustain higher flight speeds. The net effects of aerodynamic efficiency and structural weight overpower engine efficiency in going to supersonic speeds; the result is that maximum obtainable flight ranges for supersonic flight are less than for subsonic flight. Further, as supersonic speed is increased, range may increase as engine efficiency increases, but these other terms again catch up to engine efficiency, and so the flight range obtainable maximizes at some Mach number.

The effect of altitude is most strongly felt in the term W_e/F, where thrust depends directly on air density. At successively higher altitudes this term eventually overpowers any increase in L/D, and flight range will maximize at some altitude.

Clearly, increase in range, speed, or altitude, alone or in combination, will come to various degrees from improvements in fuel energy, airframe and engine weights, or airframe and engine efficiencies. When about all that can be done with weights and efficiencies has been done, the only significant increase in flight performance can come from a fuel of higher heat content than the conventional hydrocarbon jet fuel. Thus, the significant interest in high-energy fuels.

Heat of Combustion

A search for high-energy nonhydrocarbon fuels emphasizes the excellence of hydrocarbon fuels. Hydrocarbons have high heats of combustion, yet their physical properties can be widely tailored and their exhaust products are clean, gaseous, and relatively harmless. The alternatives on an energy basis alone are few. Considering the heat of combustion of all the elements, only hydrogen, beryllium, and boron have higher values than hydrocarbons (Fig. 1). Note the periodicity of heating value, similar to the periodic behavior of numerous other properties of the elements.

Hydrogen, a light gas, requires temperatures near absolute zero to be a liquid. At present, economical sources of beryllium are too few and too limited to consider its use in fuel. Boron, a refractory material in the same group of elements as aluminum, is available. Between 750,000 and 1,000,000 tons of borax (as $Na_2B_4O_7$) are annually mined, mostly in California from underground deposits and from Searles Lake brine; proved reserves appear to be of the

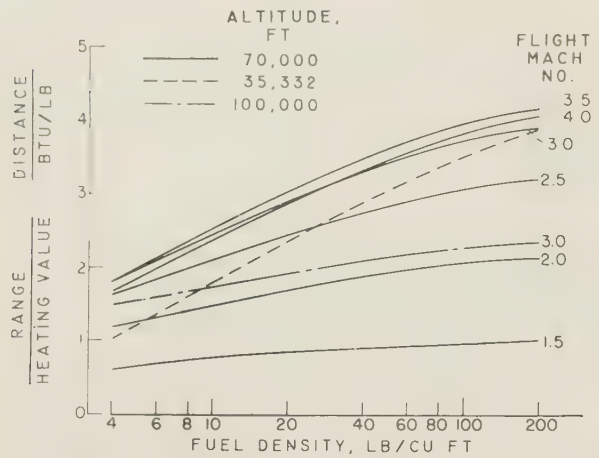

Fig. 2 — Effect of fuel heating value and density on range of ramjet aircraft (150,000-lb gross weight, 10,000-lb payload)

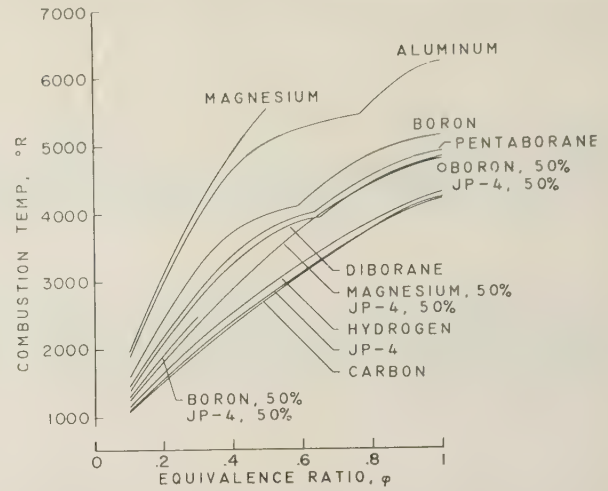

Fig. 3 — Theoretical combustion temperature of several fuels (560 R combustor inlet air temperature, 2 atm inlet air pressure)

order of 10 times this quantity. Possibilities for high-energy fuels thus narrow down to boron, or a few classes of compounds involving hydrogen, boron, and possibly some other light elements.

An important class of these compounds is the boron hydrides. Their chemistry dates from Stock[2] and Schlesinger.[3] A typical preparation from borax proceeds through boron trichloride or boron trifluoride. For example, evaporation of water from borax and dilute hydrofluoric acid produces a white powder, sodium fluoborax, $Na_2O(BF_3)_4$. This can then be treated with fuming sulfuric acid and BF_3 distilled off:[4]

$$Na_2B_4O_7 \cdot 10H_2O + 12HF(aq) \rightarrow Na_2O \cdot (BF_3)_4 + 16H_2O$$
$$Na_2O \cdot (BF_3)_4 + 3H_2SO_4 + SO_3 \rightarrow 4BF_3 + 2NaHSO_4 + 2H_2SO_4$$

Schlesinger and coworkers have reacted different hydrides with ether solutions of boron halides, for example:

$$6NaH + 8(C_2H_5)_2O \cdot BF_3 \rightarrow B_2H_6 + 6NaBF_4 + 8(C_2H_5)_2O$$

Various higher boron hydrides are made by pyrolysis of B_2H_6:

$$B_2H_6 \rightarrow B_5H_9,\ B_{10}H_{14}$$

Major has written a current review of the technology of the boron hydrides.[5]

Since 1952 the Navy's Bureau of Aeronautics and, since 1955, the Air Force's Air Research and Development Command have sponsored the preparation of experimental quantities of possible high-energy fuels that are compounds of boron, hydrogen, and carbon with heating values in the 25,000–27,000 Btu/lb range — Project ZIP. In early 1957 announcements were made of contract awards of about $40,000,000 each to the Olin-Mathieson Chemical Co. and the Callery Chemical Co. for semicommercial production of these ZIP fuels.

Table 1 lists pertinent physical and thermal properties of a number of materials of possible interest as fuels. The list is by no means exhaustive; it is representative of some of the main possibilities in the field. In addition to the materials already mentioned as having higher heats of combustion on a weight basis than jet fuel, a number of materials have a heating value based on volume. These materials include light metals such as aluminum, beryllium, boron,, magnesium, and titanium; hydrides of light metals; carbon, silicon, and boron carbide; and hydrocarbons such as 1-ethylnaphthalene. NACA has prepared and measured the physical properties of several series of hydrocarbons of greater volumetric heating value than conventional jet fuels.[6] These high-density hydrocarbons nearly always have less heat of combustion on a weight basis than jet fuel. It is to be noted that only beryllium, boron, and some boron compounds are listed as superior to jet fuel on both the bases of heating value per unit weight and heating value per unit volume.

The significance of heating value on a volume basis depends very much on the particular application. In general, for long-range flight, the drag induced by carrying fuel weight is more important to range than the drag of structural weight due to fuel storage. An illustration of this point is presented in Fig. 2, an analysis of the ultimate cruising range of a ramjet powered aircraft.[7] In the analysis an aircraft of 150,000-lb gross weight with a 10,000-lb payload was considered for only the cruising part of a flight. Every component of the aircraft was assumed to be designed specifically for each condition considered.

As fuel density decreases, the size and weight of the structure increase and the drag increases, shortening range. This influence of fuel density is seen to be greater at higher flight speeds and at lower altitudes. The heating value on a weight basis, nevertheless, overshadows the heating value on a volume basis for long range. For the hypothetical aircraft of Fig. 2 at a flight Mach number of 3 at 70,000 ft, the flight ranges relative to jet fuel are

[2] "Chemistry of Hydrides of Boron and Silicon," by Alfred Stock. Pub. by Cornell University Press, Ithaca, N. Y., 1933.
[3] *Chemical Review*, Vol. 31, August, 1942, pp. 1–75: "Recent Developments in Chemistry of Boron Hydrides," by H. I. Schlesinger and A. B. Burg.
[4] Pp. 8 and 14 of "Boron Trifluoride and Its Derivatives," by H. S. Booth and D. R. Ray. Pub. by John Wiley & Sons, Inc., New York, 1949.
[5] *Chemical Engineering Progress*, Vol. 54, March, 1958, pp. 49–54: "Technology of Boron Hydrides," by C. J. Major.
[6] *Journal of American Chemical Society*, Vol. 76, Feb. 20, 1954, pp. 1104–1106: "Dicylic Hydrocarbons. XI-Synthesis and Physical Properties of Monomethyldiphenylmethanes and Monomethyldicyclohexymethanes," by J. H. Lamneck, Jr., and P. H. Wise.
[7] NACA RM E51L21, 1952: "Effect of Fuel Density and Heating Value on Ram-Jet Airplane Range," by H. N. Henneberry.
[8] NACA RM E52L08, 1953: "Summary Report on Analytical Evaluation of Air and Fuel Specific-Impulse Characteristics of Several Nonhydrocarbon Jet-Engine Fuels," by R. Breitwieser, S. Gordon, and B. Gammon.

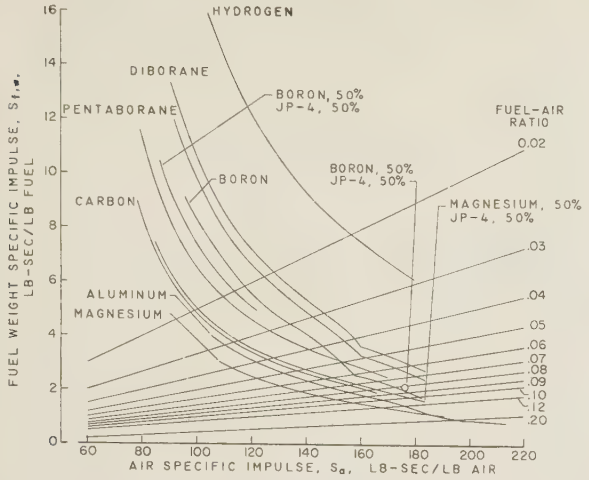

Fig. 4 — Variation of fuel-weight specific impulse with air specific impulse for several fuels (560 R combustion inlet air temperature, 2 atm inlet air pressure)

noted in Table 2. The values are rounded off, because they could be varied about these values by varying the assumptions of the flight analysis.

No provision was made in the analysis for insulation or pressurization to contain such low boiling fluids as hydrogen, diborane, methane, or acetylene.

Maximum Thrust

The maximum thrust that can be achieved from a given air mass flow is dependent on the specific heats, physical states, heats of phase changes, and the dissociation energies of the combustion products. These products establish a limit to the combustion temperatures and thrusts that can be obtained. There may be instances where, for a given engine size, higher thrusts than those available from hydrocarbons may be required even without regard to specific fuel consumption, as, for example, the short-range ramjet missiles for second-stage boosting of missiles, for acceleration of ramjets, or for maximum thrust augmentation of turbojets by afterburning during take-off or for superperformance.

Combustion-gas temperatures for several fuels of interest are summarized in Fig. 3. The inflections in the curves are due to heats of fusion and vaporization of the oxides. The lack of thermal data on magnesium oxide precludes other than an estimate at high temperatures. Some combustion temperatures noted for stoichiometric fuel/air ratios and combustion at 2 atm and 560 R are:

Fuel	deg R
Magnesium	——
Aluminum	6160
Boron	5100
Pentaborane	4850
Diborane	4750
Hydrogen	4256
JP-4	4180
Carbon	4173

These temperatures not only qualitatively indicate the maximum expected thrust, but also emphasize the problems to be expected in cooling and in the selection and use of materials.

Air specific impulse quantitatively indicates the thrust that can be obtained with a particular fuel.

Table 1 — Heating Values of Various Substances

	Melting point, F	Boiling point, F	Specific gravity	Heat of Combustion[a]	
				Btu/lb	Btu/cu ft
Acetylene	− 115.2	− 118.5	0.621 (− 119F)	20,740	804,000
Aluminum	1220	3735	2.70	13,320	2,246,000
Beryllium	2336	5013	1.816	26,950	3,055,000
Boron	4172	4622	2.32	25,500	3,680,000
Boron Carbide (B_4C)	4442	> 6332	2.54	25,200[b]	3,996,000[b]
Carbon	> 6332	7592	2.26	14,100	1,991,000
Decaborane	210	415	0.78 (212F)	28,300	1,379,000
Diborane	− 266	− 134.5	0.447 (− 134.5F)	31,330	872,000
1-Ethylnaphthalene	5	486	1.008	17,020	1,074,800
Hydrogen	− 434.8	− 423	0.0708 (− 423)	51,660	228,000
Jet Fuel (JP-4)	< − 76	135-484	0.777	18,620	900,000
Lithium	366.8	2502	0.53	18,450	610,500
Magnesium	1202	2025	1.74	10,810	1,174,000
Pentaborane	− 52.4	136.4	0.63	29,130	1,142,000
Silicon	2588	4712	2.4	13,176	1,974,000
Titanium	3272	> 5432	4.50	8192	2,301,000
ZIP	—	—	—	—	—

[a] Condensed phases of oxides at approximate room temperature, except $H_2O(g)$ and $CO_2(g)$.
[b] National Bureau of Standards, "Selected Values of Chemical Thermodynamic Properties."

Table 2 — Relative Range of Various Flight Fuels

Fuel	Relative Range
Beryllium	1.6
Diborane (− 134 F)	1.6
Hydrogen (− 423 F)	1.6
Boron Carbide	1.5
Pentaborane	1.5
Decaborane	1.5
ZIP	1.4
Boron	1.4
50% Boron in JP4	1.2
Methane	1.1
JP-4	1.00
Carbon	0.86
Aluminum	0.82
Magnesium	0.64
Titanium	0.51

Table 3 — Air Specific Impulse of Various Fuels (2 atm and 560 R)

Fuel	Air Specific Impulse, lb-sec/lb air (at stoichiometric)
Magnesium	220 (estimated)
Magnesium, 50 -JP, 50	184
Aluminum	213
Pentaborane	184
Boron	182
Boron, 50 -JP, 50	176
Diborane	184
Hydrogen	180
JP-4	170
Carbon	166

It is defined as the stream thrust, or total momentum (pressure × area + mass flow × velocity) per unit of air mass flow with the exhaust stream at a Mach number of 1.0. It may be translated into net thrust per pound of air at a given flight speed and altitude, first by adding any thrust derived by expanding from Mach 1.0 to Mach > 1 at the nozzle exit, and second by subtracting the stream momentum at the engine inlet.

Fuel specific impulse is simply the product of air specific impulse and air/fuel ratio. It indicates the duration for which a given air specific impulse can be maintained with a fixed fuel supply; it is a criterion of fuel economy.

Fig. 4 summarizes calculations of air specific impulse and fuel specific impulse for several fuels.[8] The air specific impulse theoretically available at stoichiometric ratio with combustion inlet air at 2 atm and 560 R for the fuels from Fig. 4 is shown in Table 3.

The higher values of air specific impulse possible with fuels such as magnesium or aluminum will, compared to jet fuel, give very appreciable percent-

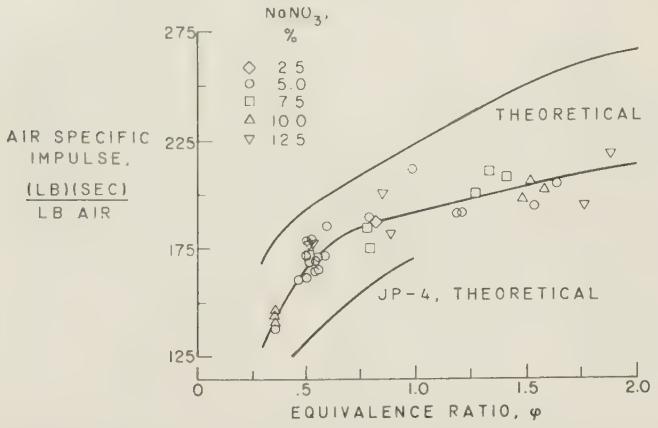

Fig. 5 — Variation of air specific impulse with equivalence ratio for magnesium fuel in 6-in. burner (airflow: 4.1-5.4 lb per sec, air temperature: 605-581 R, pressure: 24.4-36.2 psi, fuel: 2% boiled linseed oil + Mg + $NaNO_3$, charge: 6 in. OD × 4 in. ID, length: 62 in.

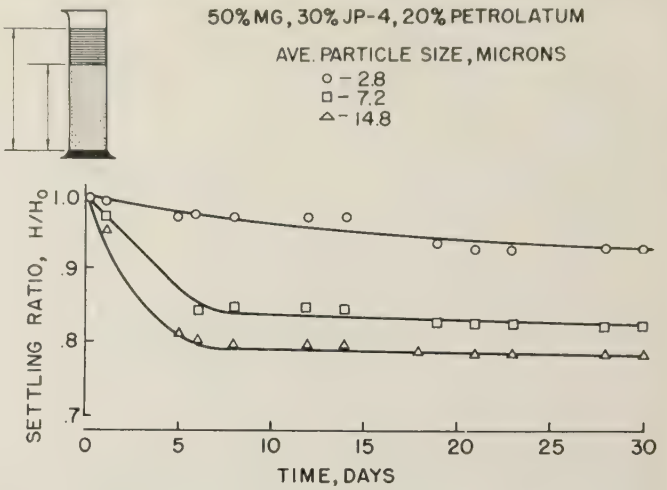

Fig. 6 — Settling characteristics of magnesium particles (H = height of column of settled particles, H_o = height of liquid column)

age gains in engine thrust or in thrust minus drag. Although high thrust from minimum engine size may be desirable for some short-range applications, for long range engines large enough to permit operation at high values of fuel specific impulse are preferred. It is seen in Fig. 4 that at low values of air specific impulse, 120 sec or less (low fuel/air ratios), the fuel specific impulse is in general agreement with the flight range predictions from heat of combustion alone.

In summary, the chemical possibilities for high-energy fuels for aircraft are narrowed by thermodynamics and fuel availability to boron and its compounds with hydrogen or with hydrogen and a few other light elements such as carbon. Some collateral interest exists in a few other light metals, such as magnesium or aluminum, as high-thrust producers or for their high volumetric heat of combustion; they actually give less range for sustained flight than hydrocarbons, however.

Problems with Light Metals

Fuel Handling

Obviously a big problem with a solid fuel is how to store it on an aircraft, deliver it to the combustion system at a metered rate, and prepare it for combustion.

Solid beds — The German Luftfahrtforschung prior to 1945 explored the possibility of burning coal in a fixed fuel bed in a ramjet.[9] The appeal of this approach is the inherent simplicity of the system, eliminating as it does fuel lines, pumps, and controls. This and related leads were further studied by the U. S. Bureau of Mines and others from late 1945 to 1954.[10,11,12] For example, at the Bureau of Mines hollow cylinders and longitudinally perforated cylinders were formed by compressing powdered carbon on coal with binders; charges up to 6-in. diameter and 36 in. long were tried. Solid fuel brequettes of powdered metals have also been studied in 2–6 in. diameter charges.

Boron powder, magnesium,[10,13] and aluminum[10,14] alone and in combinations, have been compacted into solid fuel grains with binders and oxidizers; combustion studies were performed in air ducts. Some free jet tests were also performed by NACA at Wallops Island.

Burning rates of these solid fuel charges were found, in general, to be governed by mass transfer and to be low. Addition of oxidizer was required to cause the fuel to sputter off the grain into the air stream and, thus, to increase burning rate. A continuing problem with solid-fuel beds was to prevent fragments of solid fuel from spalling off and leaving the engine unburned; this phenomenon has caused serious combustion efficiency losses. Fairly high values of thrust per unit of airflow were achieved in several studies of magnesium-based fuels for periods up to 10 sec (for example, Fig. 5); for comparison, the theoretical air specific impulse of JP-4 is 170 at stoichiometric. In no instance, however, has there been a successful solid-bed system having a higher heat of combustion than hydrocarbons.

Solid feed systems — Early experiments on continuously feeding metals as fuels were with aluminum. RAE fed aluminum flake powder to a 6-in. diameter combustor by fluidizing the powder with air.[15] Combustion temperatures to 5400 F were reported. NACA fed lightly compacted aluminum powder through a rapidly rotating, slotted disk, or cutter. The cloud of powder so produced issued into the combustion air stream of either a 2- or 4-in. diameter combustor. Aluminum wire was also burned by melting and atomizing it into a small combustor from a modified commercial metalizing gun.[16] In other experiments, aluminum-impregnated plastic wire was similarly burned.

These and similar feed systems appear to lack

[9] WADC Trans. Rep. No. F-TS-1021-RE, December, 1946: "Investigation of Suitability of Solid Propellants for Ramjets," by H. Schwabl.

[10] Bureau of Mines, Progress Report No. 19, NAer 01045, Oct. 1–Dec. 31, 1950: "Combustion of Solid Fuels for Ram Jets," by G. H. Damon and J. A. Herickes. (See also other progress reports in this series.)

[11] Progress Report 3–12, Powerplant Lab. Proj. No. MX527, Jet Prop. Lab., C.I.T., Sept. 27, 1946: "Solid Fuel Combustion as Applied to Ram Jets," by H. R. Bartel and W. D. Rannie.

[12] Meteor Report No. 55, Interim Progress Report of Meteor Project, Guided Missiles Program, M.I.T., June, 1950: "Meteor." (See also Meteor Report No. 29, March, 1950.)

[13] "Summary Report on Solid Fuel Ram Jet Development," by J .C. Squiers. Continental Aviation and Engineering Corp., July 30, 1950. (Contract W-33-038-ac-13371.)

[14] "Solid Fuels for Ramjet Engines," by R. L. Wolf. TM-229, Experiment Inc., June 30, 1950.

[15] Tech. Note No. AERO 1978, S.D. 86, British RAE, November, 1948: "Use of Sweat Cooling to Prevent Buildup of Oxide in Combustion Chamber," by A. G. Bowling.

[16] NACA RM E51B02, 1951: "Combustion Properties of Aluminum as Ramjet Fuel," by J. R. Branstetter, A. M. Lord, and M. Gerstein.

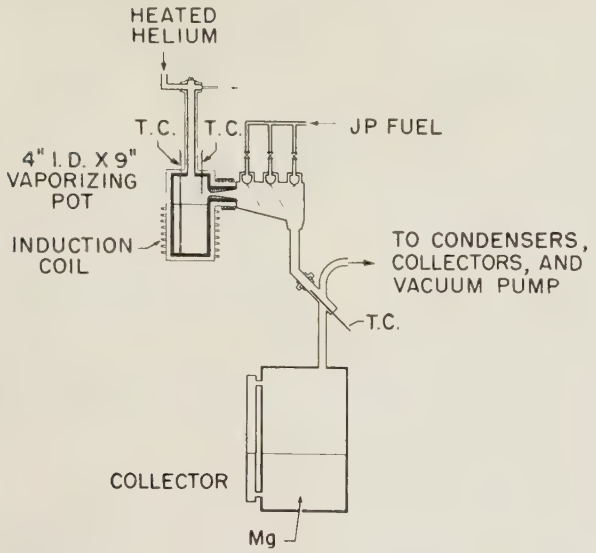

Fig. 7 — Preparation of small particles from magnesium vapor

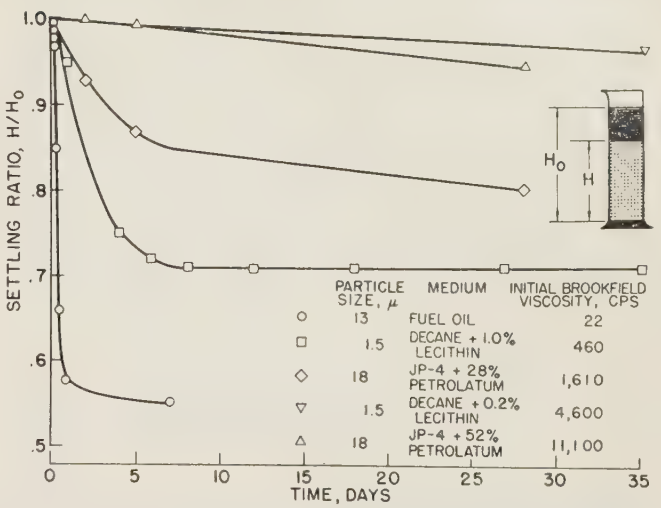

Fig. 8 — Settling characteristics of 50% magnesium in various media (H = height of column of settled particles, H_0 = of liquid column)

practicality for aircraft. Storage of powder or wire presents a difficult design problem, and some volume will be lost in the aircraft. Considerable invention and mechanical ingenuity would be required to insure adequate, reliable feed systems.

Slurry fuel systems — The simplest way to early application of metals as fuels would seem to lie with slurries, that is, suspensions of metal particles in hydrocarbons. Slurries could be used in tanks and fuel-feed systems similar to those existing and could be pressure-sprayed into the combustion space. Of course, part of the price is that heating values are now split with hydrocarbons.

The objective in slurry preparation has been to achieve a high metal concentration in a stable suspension that is still sufficiently fluid to be flowed, pumped, and sprayed. It was quickly learned that the quantities of material that could be suspended and the physical properties of the resulting suspension were functions of the particle sizes and shapes, the composition of the carrying medium, and the type and concentration of any additives. An empirical knowledge regarding the properties of slurries and what affects them has resulted from extensive experimentation.[17] Some of this lore about slurry preparation and properties can be briefly reviewed here.

Aluminum was early dropped from the program in favor of magnesium, because when aluminum was burned the sticky, molten aluminum oxide caused a very serious deposit problem in the combustor. Magnesium oxide does not melt appreciably at the flame temperatures encountered and does not stick to the combustor walls as aluminum oxide does.

A first point about metal slurries is that the finer the particles, the more stable is the slurry. For example, Fig. 6[18] shows that for spherical particles in a common carrier, the largest particle sizes settled most and the most rapidly, while the smallest settled the least and more slowly.

Attempts to produce fine magnesium particles by milling or grinding mainly resulted in flattening the particles without reducing their size. Pressure-spraying molten magnesium into an inert atmosphere produced spherical particles, although generally greater than 5 microns. Some grading could be done with cyclone separators. Really fine particles, 50% by weight smaller than 1.5 microns, were prepared by shock-chilling magnesium vapor. The cloud of particles so produced was washed down with excess jet fuel. Conventional centrifuges then concentrated the slurry. A laboratory-size plant is shown in Fig. 7; reduced pressure lowered the temperatures at which magnesium vaporized, and helium assisted the vapor flow out of the pot.[19] The Air Force sponsored development of a pilot plant along these lines at the Dow Chemical Co., work which has been concluded.

The present commercial methods of producing boron by reducing the oxide with magnesium at high temperatures yield particles that assay as 1–2 microns in size.

Concentrations of the order of 50–60% by weight of fine metal particles only form a muddy mass of wet metal powder in a carrier such as jet fuel. Addition of 1–2% of a surface active agent disperses the metals and produces suspensions that will flow and that have viscosities of 200–5000 centipoises as measured with a Brookfield instrument (consistency between glycerol and honey).

While surface-active agents make possible a fluid slurry, the experience is that the lower the viscosity of the suspending medium, the more rapidly and extensively do the particles settle (for example, Fig. 8).[17] Thickening agents (for example, petrolatum, or soaps such as aluminum octoate), added in less than 1% produced quite stable suspensions of either magnesium, with average particle sizes up to 18 microns, or boron (1 to 2 microns). In the case of boron, both a dispersant and a thickening agent were used. The ensuing high viscosities would preclude pumping and spraying, except that the viscosity of slurries made with gelling agents such as aluminum octoate decreases rapidly with increase in

[17] NACA RM E55B14, 1955: "NACA Research on Slurry Fuels Through 1954," by W. T. Olson and R. Breitwieser.
[18] NACA RM E54A22, 1954: "Effect of Magnesium Particles of Various Equivalent Diameters on Some Physical Properties of Petrolatum Stabilized Magnesium-Hydrocarbon Slurries," by J. M. Lamberti.
[19] NACA RM E55I20, 1955: "Design Considerations of Condensing System for Vaporized Magnesium," by W. R. Witzke, G. M. Prok, and T. A. Keller.

shear rate, as illustrated in Fig 9.[20,21] The Brookfield instrument measures viscosity at very low rates of shear, several orders of magnitude less than those with the Severs instrument. Glycerol illustrates a Newtonian fluid with viscosity independent of shear rate. At high rates of shear, the viscosity change with shear is small enough that fuel can be metered conventionally over limited ranges of flow, and loss coefficients for pipe line systems for Newtonian flow can be applied to these slurries.[22]

Thus, slurries can be made with 50–60% by weight metals of particles of the order of a micron in size. These slurries can be pumped, flowed, and sprayed, and have reasonable, if limited, storage life.

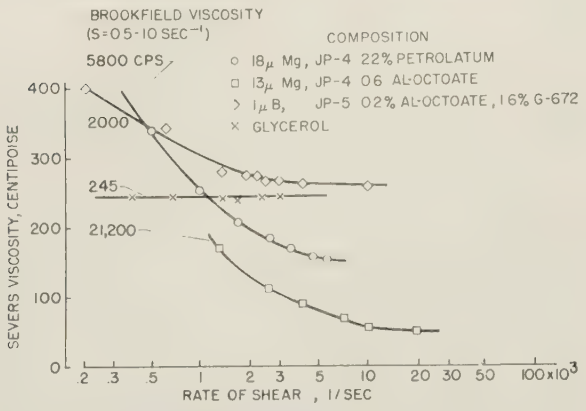

Fig. 9 — Effect of rate of shear on viscosity of 50% slurries

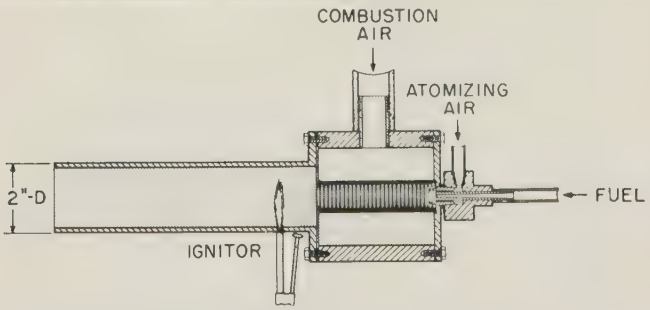

Fig. 10 — Blowout velocity apparatus

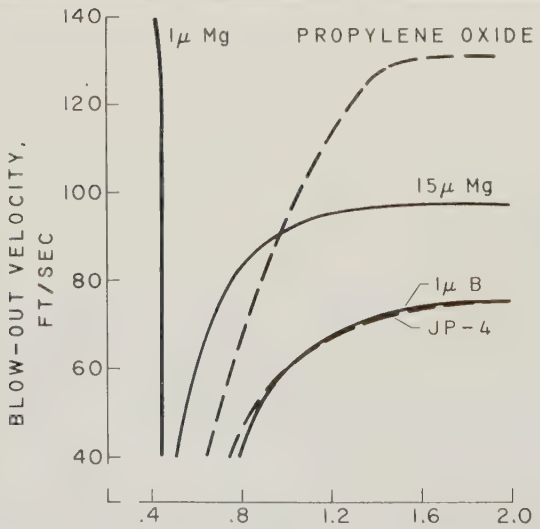

Fig. 11 — Flame stability of 50% metal slurries in JP-4 and of reference fuels

Two important problems were never completely solved, however. First, physical properties were uncertain from batch to batch. Perhaps quality control of materials and processes could minimize this problem. Second, storage life was of limited and uncertain duration. Satisfactory slurries were formulated of magnesium and boron with a storage life under the favorable conditions of a laboratory shelf for 30–60 days; some formulations for boron lasted 6 months. Vibration, contamination, or variable storage temperatures often produced particle settling, however. A settled slurry would not redisperse to give as good stability as it originally had. This problem of storage life probably could never be solved to a degree commensurate with the storage life of usual jet fuels.

Combustion

Combustion of metals as fuels was studied concurrently with work on fuel handling problems. Early studies on beds, powders, and wires have been mentioned. Extensive experimentation was performed on combustion of slurries mostly in small-scale burners, but included some work in full-scale jet engines.

Burning rates of solid particles — An analytical treatment of the combustion rate of single fuel particles in quiescent air provides insight into the burning rates of magnesium and boron. Magnesium ribbons were burned in various mixtures of oxygen with argon, nitrogen, and helium. Burning times calculated from a heat- and mass-transfer mechanism quite analogous to that used for calculating the burning time of liquid fuel drops were in excellent qualitative agreement with experiment; actual numerical values agreed within a factor of 2 or 3.[23] Experiments with the combustion of boron have supported the observation that evaporation of the oxides, rather than chemical reaction, is the rate-limiting step.[24]

General equations have been developed for computing the burning rates of small particles burning as diffusion flames.[25] These equations were applied to boron, carbon, hydrocarbons, and magnesium. In the analysis of a diffusion flame mechanism it is assumed that a steady state flame surrounds the particle, that oxygen diffuses inward, fuel vaporizes and diffuses outward, and reaction products diffuse outward. Chemical processes within the flame are presumed to be fast. Heat is assumed to be conducted inward from the reaction zone to vaporize and heat fuel, and to be conducted outward, in part preheating the inbound oxygen. Coffin and Brokaw[25] treated the effects of diffusion and dissociation quite rigorously. No artificial combustion zones were posited, and chemical equilibrium was assumed to exist throughout the system. Both rigor-

[20] NACA RM E54F18a, 1954: "Preparation and Properties of Concentrated Boron-Hydrocarbon Slurry Fuels," by I. A. Goodman and V. O. Fenn.
[21] NACA RM E54C10, 1954: "Stabilization of 50% Magnesium—JP-4 Slurries with Some Aluminum Soaps of C8 Acids," by R. M. Caves.
[22] NACA TN 3889, 1957: "Pressure Losses of Titania and Magnesium Slurries in Pipes and Pipeline Transitions," by R. N. Weltmann and T. A. Keller.
[23] NACA TN 3332, 1954: "Burning Times of Magnesium Ribbons in Various Atmospheres," by K. P. Coffin.
[24] "Combustion of Elemental Boron. Summary Report for June through October, 1957." Experiment, Inc., Richmond, Va. Report No. TM 1009, Nov. 1, 1957.
[25] NACA TN 3929, 1957: "General System for Calculating Burning Rates of Particles and Drops and Comparison of Calculated Rates for Carbon, Boron, Magnesium, and Isooctane," by K. P. Coffin and R. S. Brokaw.

Table 4 — Computed Burning Rates of Various Substances
(Temperature 300 K, air at 1 atm)

	Burning Rate			Evaporation constant, β', sq microns/sec	Lifetime of 1-micron particle t_l, sec
	moles/cm-sec	gm/cm-sec	cal/cm-sec		
Isooctane[a]	0.86×10^{-5}	99×10^{-5}	10.5	1.11×10^{6}	0.90×10^{-6}
Magnesium[a]	3.97	97	5.7	0.444	2.25
Boron					
Case A[a]	1.31	14.2	1.98	0.0492	20.3
Case B[a]	1.79	19.4	2.70	0.0673	14.8
Analytical	1.27	13.7	1.92	0.0477	21.0
Carbon					
Numerical	1.05	12.7	1.02	0.0505	19.8
Analytical	1.10	13.2	1.07	0.053	18.9

[a] Simplified calculation.

ous and simplified solutions for burning rate were carried out, and evaporation constants β, and particle lifetimes t_l were calculated for the relations:

$$d^2 = d_0^2 - \beta t \quad (4)$$

$$t_l = d_0^2/\beta \quad (5)$$

where:

d = Diameter at time t
d_0 = Diameter at time $t = 0$

Results are repeated from Coffin and Brokaw[25] in Table 4.

One significant result to note is that boron requires nearly ten times as long to burn completely as magnesium. These results do not, however, explain fully the difficulty of burning boron particles in situations where residence times are several orders of magnitude larger than the time indicated in Table 4. Perhaps the boron oxide near the particle surface becomes momentarily chilled by turbulent gases and coats the particle and thus prevents further combustion. Magnesium would appear to have plenty of time to burn in ramjets and afterburners, even for particle sizes up to 20 microns.

Boron — Boron slurries were evaluated for blowout velocity in a 2-in. diameter tube with provision for uniform mixing of fuel and air (Fig 10);[26] blowout velocities were compared to those of JP-4 fuel (Fig. 11).

Combustion efficiencies were studied in a 2-, 5-, and 16-in. diameter ramjet-type combustion systems.[17,27,28] The main observations can be summarized. Although heat outputs (Btu/lb mixture) higher than the theoretical for JP-4 fuel were attained with boron fuels at high fuel/air ratios, combustion efficiencies were generally below 85% and were particularly low at lean fuel/air ratios. Good fuel atomization, high local flame temperatures, and recirculation of boron fuel into the flame were required for even moderately high combustion efficiencies. The high local temperatures required for good combustion efficiency destroyed engine parts, however. On the other hand, attempts to keep combustor parts cool lowered efficiency and produced large deposits of boron oxide. Fuel composition and

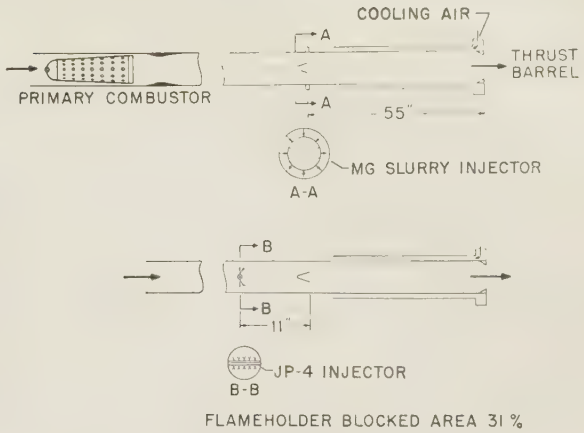

Fig. 12 — Simulated afterburner of 6-in. diameter

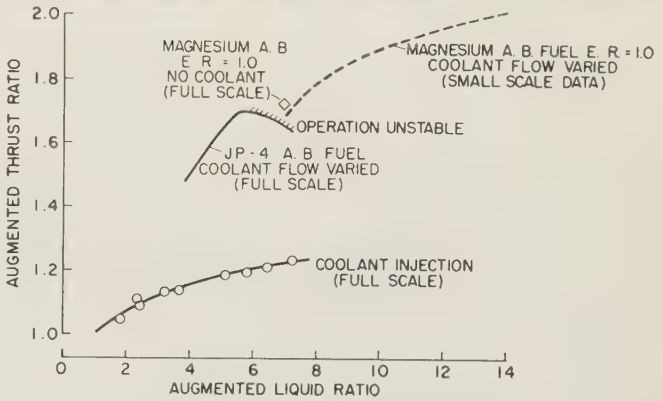

Fig. 13 — Turbojet engine thrust augmentation 60% magnesium slurries (sea level static, water or water-alcohol coolant)

combustor lengths 40–100 in. had little influence on combustion efficiency. In short, satisfactory combustion of boron was not achieved.

Magnesium — Magnesium slurries, in contrast to boron, proved easy to burn. Some idea of the difference between the combustion of boron and that of magnesium can be seen from measurements of blowout velocity (Fig. 11). Data for JP-4 and propylene oxide, whose flame speed is 1.8 times that of JP-4, are included for reference.

Magnesium slurries have been burned quite successfully and with high efficiencies in combustors of both afterburner and ramjet type. For example, Fig. 12 illustrates apparatus in which both jet fuel and magnesium slurries were burned at afterburner conditions. Magnesium slurry was injected from eight radial stations located at the downstream edge of a single V-gutter that spanned the 6-in. test section. JP-3 required upstream injection to burn; magnesium slurry injected upstream burned out the flameholder.

Some of the data are summarized in Fig. 13, along with data from a full-scale turbojet. Water injection alone gave 22% thrust augmentation at a liquid ratio of 7, that is, seven times the normal fuel-flow rate of the engine with no thrust augmentation.[29] Forty-three per cent augmentation was achieved by afterburning with about three times the normal fuel flow. These and subsequent data are for a low-pressure ratio engine; afterburner performance is thus low. Combined water injection and afterburning

[26] NACA RM E54A28, 1954: "Blow-out Velocities of Various Petroleum, Slurry, and Hydride Fuels in 1⅞-In. Diameter Combustor," by P. N. Cook, Jr., A. M. Lord, and S. Kaye.
[27] NACA RM E52B01, 1952: "Experimental Investigation of Combustion Properties of Hydrocarbon Fuel and Several Magnesium and Boron Slurries," by A. M. Lord.
[28] NACA RM E54D07, 1954: "Performance of Slurries of 50% Boron in JP-4 Fuel in 5-In. Ramjet Burner," by T. W. Reynolds and D. P. Haas.
[29] NACA RM E9K30, 1950: "Experimental Investigation of Thrust Augmentation of 4000-LB-Thrust Axial-Flow-Type Turbojet Engine by Interstage Injection of Water-Alcohol Mixtures in Compressor," by J. H. Povolny, J. W. Useller, and L. J. Chelko.

produced 70% thrust augmentation; a water flow limit was set by unstable operation and loss of combustion efficiency.[30]

The dashed curve on Fig. 13 represents data from the 6-in. apparatus plotted on the same basis as the data for the full-scale engines.[31] These data show nearly 70% thrust augmentation with magnesium afterburning alone; fuel flow was seven times that with no augmentation. Water injection combined with afterburning with magnesium slurry doubled the unaugmented thrust at a liquid ratio of 14. Combustion efficiency of magnesium slurry, in contrast to JP-3, was essentially unaffected by water injection to water rates as high as 12% of the airflow.

One short duration run of magnesium slurry was made in a full-scale afterburner. The data point for this run with no water injection and with stoichiometric combustion is also plotted on Fig. 13 and agrees quite closely with the results from the 6-in. diameter apparatus.

The high reactivity, high thrust potential, and high impulse characteristics per unit volume of magnesium slurry make this fuel a suitable possibility for short-range ramjet vehicles. Design and operating details of a 6.5-in. diameter ramjet combustor, 19-in. long, were established by experiments in a connected pipe and free jet tests. Typical data achieved in the configuration shown with them are plotted in Fig. 14.[32] A shroud around the fuel injectors prevented premature spreading of the fuel to the outside walls while still permitting time for atomization and evaporation of the carrier fluid; the flameholder was designed to deflect the magnesium component of the fuel into the piloting region. Maximum thrust coefficients for a simulated Mach number 2.3 and altitudes above 35,000 ft were well in excess of those obtained with hydrocarbons (ethylene, in this example) and those theoretically possible with hydrocarbons. Subsequently, several vehicles with dual 6.5-in. engines were flight-tested with magnesium slurry. Results of one flight, for example can be summarized: rocket boost to Mach 1.73 at 5900 ft; ramjet acceleration to a maximum of 6.1 g; maximum air specific impulse 150 sec; maximum thrust coefficient, 0.76; maximum Mach number, 3.84 after 13.2 sec and at 38,100 ft.[33]

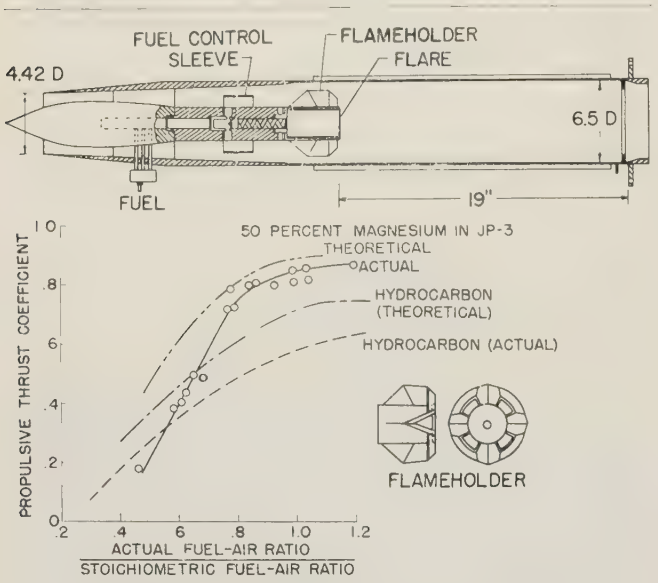

Fig. 14 — Performance of magnesium slurry in 6.5-in. ramjet engine (simulated altitude of 35,000 ft, Mach number 2.3)

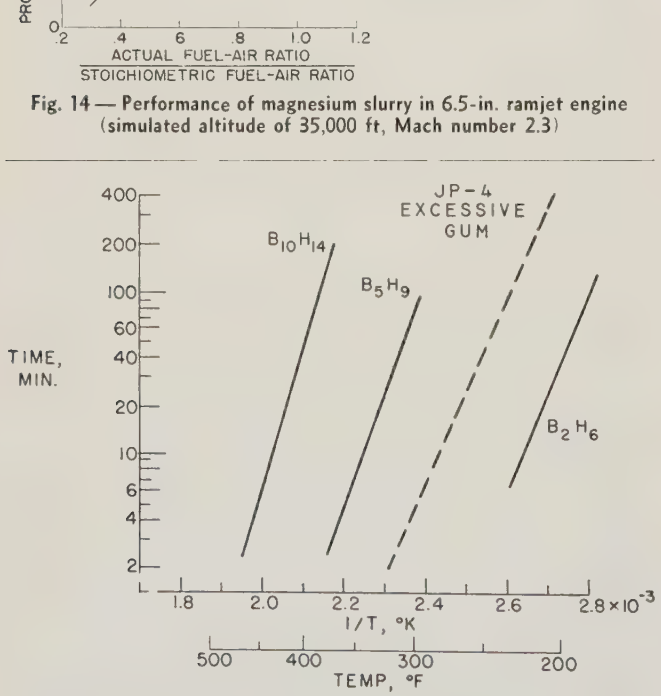

Fig. 15 — Five per cent thermal decomposition of boron hydrides (data of Bragg, et al., adapted for 1 atm of B_2H_6)

In summary, combustion characteristics of magnesium slurries are excellent. Not only have high thrust levels been demonstrated, but the fuel burns well under circumstances where hydrocarbons burn only with difficulty. Research has been concluded on magnesium slurry, however, and there does not at present appear to be an application where the high-thrust capabilities and good burning qualities of this fuel are a strong enough requirement to offset its reduced heating value and its handling difficulties.

Problems with Boron Compounds

In view of the imposing problems of handling metals or slurries of metal powders on the ground and in aircraft, most recent effort has been toward the attainment of a liquid fuel having high-energy content and acceptable properties. As noted, this effort is necessarily centered on boron compounds.

Among the earliest experiments on the application of boron compounds to aircraft[1] were combustion tests of diborane in a 2-in. diameter burner by the Applied Physics Laboratory of Johns Hopkins University (1947), flame speed and flammability studies by the General Electric Co. (1947–1949), and analytical and experimental studies of diborane as a ramjet fuel by NACA (1950). NACA has participated in Project ZIP since its inception in 1952 by assisting in measurements of fuel properties, especially thermal and combustion properties, by establishing combustor design principles, and by studying fuel performance problems in full-scale turbojets, afterburners, and ramjets.

A complete story on boron compounds cannot be

[30] NACA RM E51H16, 1951: "Experimental Investigations of Turbojet-Engine Thrust Augmentation by Combined Compressor Coolant Injection and Tail-Pipe Burning," by J. W. Useller and J. H. Povolny.

[31] NACA RM E52H25, 1952: "Effect of Water Vapor on Combustion of Magnesium-Hydrocarbon Slurry Fuels in Small-Scale Afterburner," by L. K. Tower.

[32] NACA RM E53E27, 1953: "Magnesium-Slurry Combustion Performance in 6.5-In. Diameter Ramjet Engine Mounted in Connected-Pipe Facility," by J. R. Branstetter, J. B. Gibbs, and W. B. Kaufman.

[33] NACA RM L56I24a, 1957: "Flight Investigation of Ramjet Burning Magnesium Slurry Fuel and Having Conical Shock Inlet Designed for Mach Number of 4.1," by W. A. Bartlett, Jr., and C. F. Merlet.

Table 5 — Physical Properties of Boron Hydrides

	Diborane B_2H_6	Pentaborane B_5H_9	Decaborane $B_{10}H_{14}$
Melting point, F	- 265.9	- 52.4	209.7
Boiling point, F	- 134.6	136.4	415
Specific gravity, 60/60	0.21	0.63	0.78[a]
Viscosity, centistokes - 40 F		1.11	
Lb B_2O_3/lb fuel	2.5	2.76	2.85
Lb B_2O_3/100,000 Btu	8.0	9.48	10

[a] At 212 F.

told yet, because much research still lies ahead. Further, military security curtails a full status report. Nevertheless, some of the general problems encountered in the application of these fuels can be discussed. These problems arise because the boron fuels differ from hydrocarbons in certain physical and chemical properties, in combustion characteristics, and in producing boron oxide, normally a solid. Specific illustrations are limited to such interim fuels as boron hydrides.

Properties

Physical properties — Some of the pertinent physical properties of boron hydrides are tabulated in Table 5. By combining alkyl groups with boron hydrides, whole ranges of properties, from volatile liquids to solids, can be met, analogous to hydrocarbons.

Although the usual physical properties pose no unfamiliar problems to aircraft operations, the boron hydrides are more reactive than hydrocarbons. They are more easily decomposed by heat, and react readily with air or moisture.

The boron hydrides are quite toxic; tolerable concentration limits are of the order of 1 part per million for an 8-hr day, about like chlorine.

Most of the usual engineering materials for fuel systems (that is, copper, aluminum, tin-lead solder, paper, asbestos, and graphite) appear suitable. Tests with pentaborane showed that most natural and synthetic rubbers absorbed pentaborane and lost strength; polyfluoroethylene plastics were much more resistant and are useful as gaskets and seals.

Thermal decomposition — Fuels for aircraft operating at Mach 3, for example, will be heated gradually to 300–400 F in uninsulated fuel tanks, and transiently, to temperatures as much as 100–200 F more if they are pumped and used to cool engine oil in the same way conventional fuels are currently. In general, thermal stability is one of the biggest problems with jet fuels for present and future military use.

Decomposition rates have been studied for several boron hydrides, particularly for diborane from which other boron hydrides can be made. The chemistry of many of these decompositions has been worked out, so that many of the products that result at different temperatures and pressures are known.[34] An example of the decomposition time of boron hydrides is in Fig. 15. Data were obtained by weighing the nonvolatile residue after heating about 0.25 cu in. of material in a closed, stainless-steel cylinder to the temperature and for the time indicated.[35] For comparison, some data from Bragg, McCarty, and Norton[36] on diborane are adapted and included; they tend to check the statement on page 10 of Schechter, et al.[34] that pentaborane is more stable than diborane by a factor of 100. Also for comparison is a curve indicating levels of gum formation in good-quality JP-4 fuels that may cause trouble in jet engines;[37] this quantity of gum represents only a small fraction of a per cent of the fuel, however.

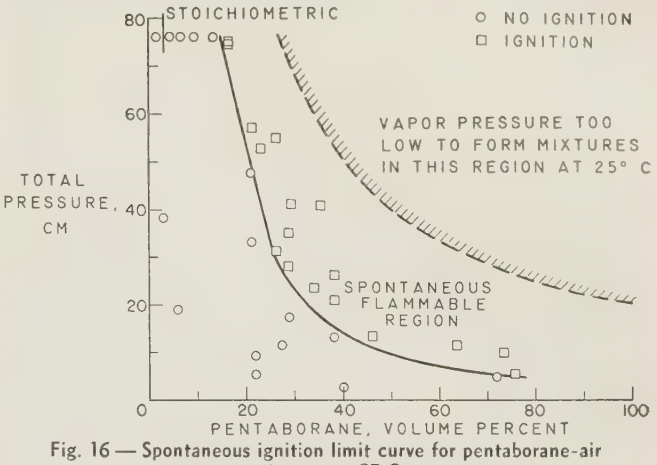

Fig. 16 — Spontaneous ignition limit curve for pentaborane-air mixtures at 25 C

Decomposition of boron hydrides produces insoluble materials that can plug fuel systems and gases that can cause vapor lock. Thermally stable boron compounds will be needed in the research program, and steps must be taken to minimize heat addition to the fuel; perhaps insulated fuel tanks will be required.

Flammability limits — The volatile boron hydrides have wide flammability limits. Price[38] has reported that 1–2% diborane in dry air at 1 atm will give self-sustaining flames, and 95% diborane – 5% oxygen will also burn. These limits were independent of moisture and tube size. A mixture of diborane with 22% dry air did not inflame in Schlesinger's early experiments. First and second pressure limits of explosion of diborane-oxygen mixtures were found, indicating a chain branching mechanism for the reaction. Diborane is not spontaneously flammable in dry air.

Pentaborane also has a lean limit of about 1–2% in air or air-nitrogen mixtures. Pentaborane, however, is spontaneously flammable in air. The limits for spontaneous ignition have been determined in a 6-cm diameter glass bulb[39] and are plotted in Fig. 16. The data required gradual blending of pentaborane into air by one of several possible techniques; the reverse procedure produced explosions. Rich flammability limits have not been found because vapor pressures of pentaborane are too low to prepare rich enough mixtures.

Flame speeds — The maximum flame speed of diborane in air has been reported to be about 17 fps.[40] That is about 13 times the flame speed of usual hy-

[34] "Boron Hydrides and Related Compounds," by W. H. Schechter, C. B. Jackson, and R. M. Adams. Callery Chemical Co. Second Edition, May, 1954.
[35] NACA RM E55H01, 1955: "Rate of Decomposition of Liquid Pentaborane from 85 to 202 C," by G. E. McDonald.
[36] *Journal of American Chemical Society*, Vol. 73, May, 1951, pp. 2134–2140: "Kinetics of Pyrolysis of Diborane," by J. K. Bragg, L. V. McCarty, and F. J. Norton.
[37] NACA TN 3276, 1956: "Properties of Aircraft Fuels," by H. C. Barnett and R. R. Hibbard.
[38] P. 9 of footnote 34.
[39] NACA RM E55B03, 1957: "Spontaneous Ignition Limits of Pentaborane," by R. L. Schalla.
[40] *Fuel*, Vol. 35, 1956, p. 323: "Properties of Diborane Flames," by W. G. Parker and H. G. Wolfhard.

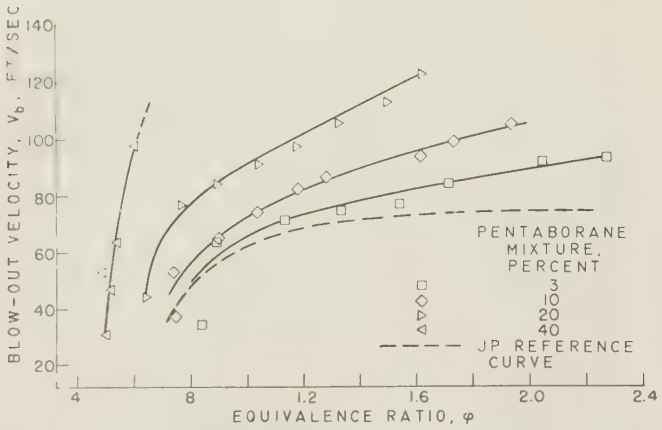

Fig. 17 — Blowout velocities of four mixtures of pentaborane in JP-4 fuel

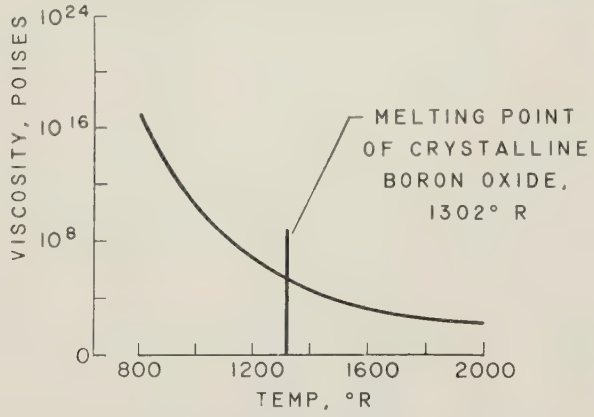

Fig. 18 — Viscosity of vitreous boron oxide B_2O_3

drocarbons. Detonations are readily produced.

Flame speeds for pentaborane are also quite high, about 18 fps at maximum.[41]

Data for blends of pentaborane studied in the apparatus depicted in Fig. 10 show the effect of the high flame speed and high reactivity of pentaborane on blowout limits (Fig. 17); these data may be compared to Fig. 11.

Hydrolysis — Boron hydrides react with water. Diborane is completely hydrolyzed to boric acid in less than a minute. Pentaborane and decaborane hydrolyze at rates governed largely by their rate of contact with water, since they are insoluble in water.[2,34,42]

From a consideration of the foregoing properties of boron hydride, it is evident that they will be more difficult to use than hydrocarbon fuels because of toxicity, thermal decomposition, flammability, and sensitivity to water. The high flame speeds and wide flammability limits should aid combustion in engines, however.

Application to Combustors and Engines

Turbojets — Early in the research program on project ZIP, diborane and pentaborane were burned in essentially unmodified turbojet combustors. A major problem encountered, of course, was that of dealing with B_2O_3. A lb of diborane produces 2.5 lb of B_2O_3; a lb of pentaborane, 2.76 lb. This glass-like oxide has a high viscosity at normal turbine operating temperatures, as Fig. 18 shows.[43]

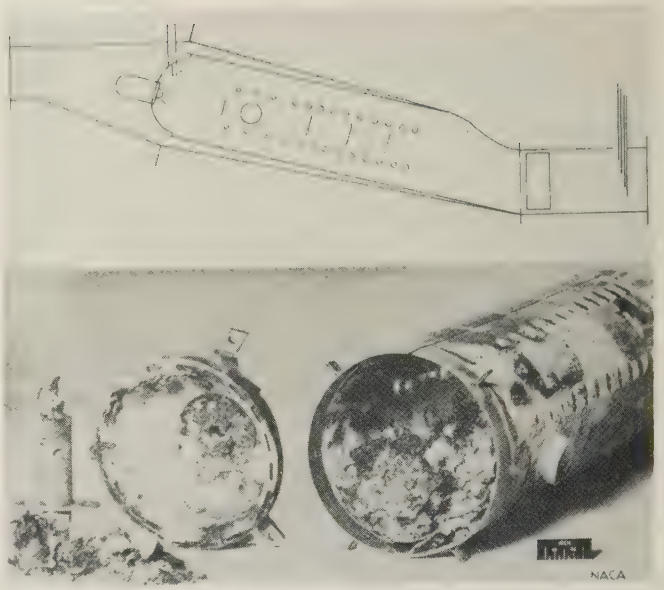

Fig. 19 — Boron oxide deposits in standard turbojet combustor

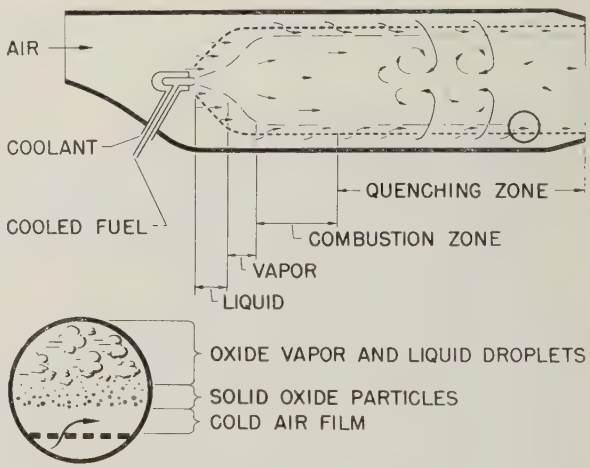

Fig. 20 — Illustrative principles for combustion of borane fuels

Results of an attempt to burn diborane in a standard turbojet combustor are shown in Fig. 19. Several factors contributed to the obvious problem. Fuel decomposed in the nozzle and fuel lines, partially plugging them and lowering the outlet temperature. Boron oxide clinkers rapidly developed in the combustor. Fuel decomposed in the chamber before it could burn and contributed to the deposit growth.

Consideration of these problems and a series of experiments have led to design features to be incorporated in a combustor for boron-hydride, or similar, fuels. Fuel must be kept cool until it enters the combustor to reduce thermal decomposition; air or other coolant may need to be used in a jacket around the fuel line. A fine spray and rapid mixing of fuel and air are required so that fuel will not thermally decompose in the combustion space before it burns; the pyrolysis products of volatile boron hy-

[41] *Combustion and Flame*, Vol. 1, December, 1957, pp. 420–430: "Determination of Burning Velocity of Pentaborane-Oxygen-Nitrogen Mixtures," by W. G. Berl, *et al.*

[42] *Journal of American Chemical Society*, Vol. 60, March 8, 1938, pp. 524–530: "Structures of Hydrides of Boron. IV. B_2NH_7 and $B_3N_3H_6$. The Structure of Dimethylamine," by S. H. Bauer.

[43] *Journal of Physical Chemistry* (USSR), Vol. 16, 1942, pp. 23–26: "Viscosity of Borox and Boric Anhydride in Interval of Softening," by B. V. Rabinovich.

Fig. 21 — Deposits in turbojet engine: combustor domes

Fig. 22 — Deposits in turbojet engine: combustor transition sections

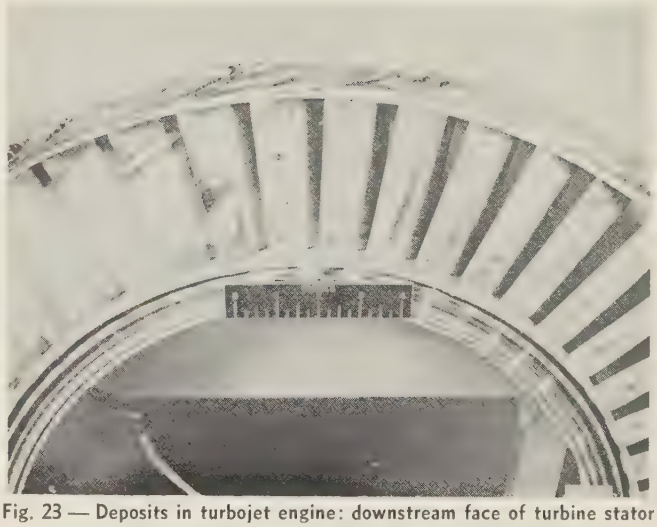

Fig. 23 — Deposits in turbojet engine: downstream face of turbine stator

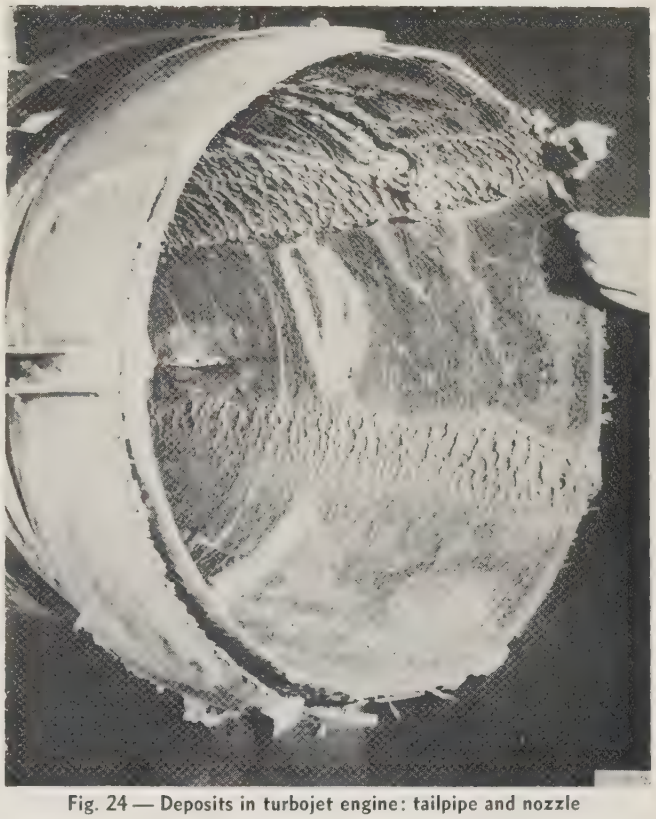

Fig. 24 — Deposits in turbojet engine: tailpipe and nozzle

drides are exceedingly difficult to burn completely. Air atomization is helpful in producing a finely atomized spray. The spray should also be well-defined and not impinge on walls, again to avoid thermal decomposition.

Deposits from boron oxide, or from cracked fuel can be minimized by avoiding the strong reverse flow that is usually designed into a high velocity combustor to provide flame piloting. The wide flammability limits and high flame speeds of boron fuels make it possible to reduce the piloting otherwise required by hydrocarbon fuels. Another step in minimizing deposits is to film the combustor walls with air to prevent impingement of fuel or boron oxide on the surfaces; various techniques are available: porous walls, louvers, step construction, and so forth. A final step is to keep any surface that must be contacted by boron oxide above 1070 F, the approximate melting point of the oxide. Fig. 20 helps to summarize these features.

Tests in full-scale engines have been performed at sea level and simulated altitude with borate esters, low-energy fuels that at least produce boron at about one-third the rate that a high-energy fuel would. Boron hydrides have been studied at simulated altitudes. Boron oxide deposits collect and flow along engine parts, including combustor walls and transition pieces, turbine stators and rotors, tailpipe walls, including any afterburner parts, and variable-area nozzles. Figs. 21–24 illustrate deposits in engines after operation with boron fuels. High-speed photographs of turbines show sheets of oxide flowing from the stators into the rotor, where much of it is then centrifuged onto the rotor shroud. Obviously, a lot is being required of a turbine, already designed to perform near its aerodynamic and mechanical limits. If boron fuels are to be used ahead of a turbine, redesigned engines are required.

Afterburners — Application of boron fuels to afterburners will require careful attention to the thermal decomposition problem, both in fuel lines that are necessarily around and in the hottest part of the engine and in the combustion gases where the fuel spray may crack before it burns. The good burning characteristics minimize flameholding re-

quirements. The oxide problem is less difficult, as experiment has shown, because no moving engine parts are present. A problem involving the thermodynamics of the exhaust gases should be mentioned here, however. At combustion temperatures much above 3000 F, considerable heat goes to vaporizing boron oxide. The loss of this heat from the kinetic energy of the exhaust system is reflected in the specific fuel consumption realized, as illustrated in Fig. 25. For engine operations that expand the exhaust gases to low pressure and low static temperatures, some, but not all, of these losses could be recovered. The exact amount of energy recovered in the expansion will depend on the condensation rate of B_2O_3 in the exhaust nozzle. Engine operation will be limited to temperatures below 3000 F if the benefits of boron fuels are not to be largely dissipated by this effect.

Ramjets — As in the case of afterburners, boron fuels offer range and combustion advantages for ramjets while posing less of a deposit problem than in turbojets. Combustion under ramjet conditions has been studied with pentaborane in equipment ranging from small ducts to a 48-in. diameter engine in an altitude facility.

For example, research on fuel handling, fuel injection, ignition, and flameholding was conducted in detail in a 9.75-in. diameter engine in connected pipe tests. Subsequently, flight tests were made of this engine. Fin-stabilized, unguided engines were launched at high altitude from a carrier aircraft. One flight was rocket boosted as well. Data were obtained during descent by radar tracking and by eight channels of radio telemetering (Fig. 26). The results indicated that the expected increase in performance of about 60% over a hydrocarbon fueled ramjet was achieved.

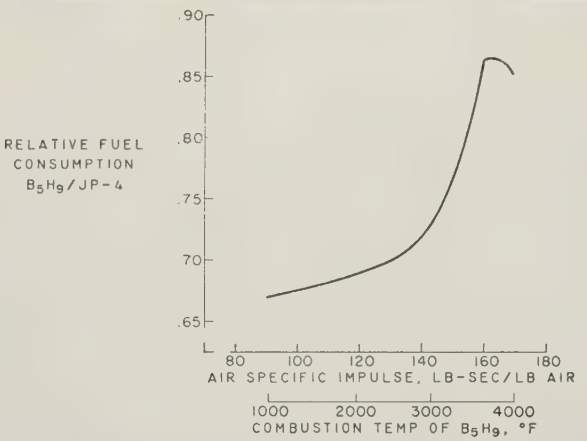

Fig. 25 — Consumption of pentaborane relative to JP-4 as a function of air specific impulses (combustor inlet air conditions: 2-atm pressure, 560 R, Mach 0.2)

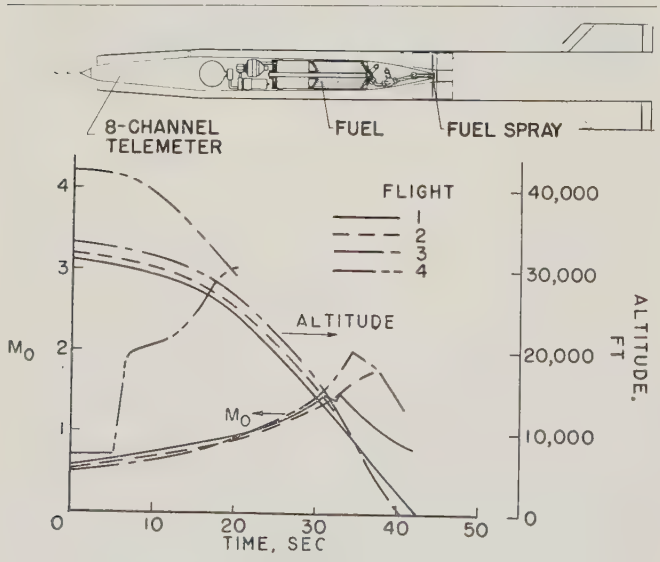

Fig. 26 — Ramjet flights with pentaborane

Conclusions

This report has reviewed some of the possibilities and problems of high-energy fuels for aircraft. A number of materials contain sufficient energy to make their use attractive. Central interest is on fuels of high heat of combustion for long-range flight. There has also been some interest in fuels that can produce high thrust to a given airstream, even at the expense of the heat of combustion. Properties of all of these potential fuels are such that handling on the ground and their use in aircraft will be more difficult than for hydrocarbon jet fuels, but not impossible.

Research on metals as fuels was centered on boron for long-range flight and on magnesium for high thrust. Metals as small particles have been made into high-concentration slurries; although reasonably stable and fluid for research and development, these slurries are far from ideal for practical aircraft operations. If slurry fuels are ever wanted for other than limited or experimental use, problems of producing, storing, and handling them must be solved.

Boron could not be burned to high efficiencies in jet engine combustors. Further interest in boron as an aircraft fuel is not warranted, especially in view of the possibilities of liquid boron compounds as fuels.

Magnesium slurries have burned quite well, even under conditions where hydrocarbon fuels burn only with difficulty or not at all. The high-thrust capabilities of magnesium slurry fuel have been realized experimentally in combustion systems, including ramjet flight. Laboratory research on its use has been concluded.

Current effort is directed toward attainment of a suitable liquid fuel with a heat of combustion of the order of 40% more than hydrocarbons. It probably will be a compound of boron, carbon, and hydrogen. Research aimed at applying boron fuels to engines has proceeded with boron compounds, including boron hydrides. Satisfactory combustion of diborane and pentaborane has been demonstrated in turbojets, afterburners, and ramjets. The anticipated reductions in specific fuel consumption have generally been observed. Deposits in the turbine engine are a continuing problem. Aircraft and engine fuel systems, and fuel supply, storage, and handling will also present problems.

Much research lies ahead to determine the experimental payoff on the thermodynamic promise of these fuels. After this research has been completed, the value of these fuels to military operations can be assessed. Then their importance relative to other military technology can be and will need to be evaluated properly.

THIS year the Chrysler Corp. has introduced a new V-8 engine designed to meet market conditions requiring larger displacements. Versions of the basic engine are available in several models of the Corporation's cars.

This engine provides increased vehicle performance with excellent economy, durability, and quietness. Emphasis on minimum weight and production economy led to many novel design features which should interest the automotive engineer.

The paper will include a review of the overall design considerations, as well as a description and discussion of the engine and its component parts.

CHRYSLER CORPORATION'S NEW V-8 ENGINE

R. S. Rarey and E. G. Moeller, Chrysler Corp.

This paper was presented at the SAE National Passenger-Car, Body, and Materials Meeting, Detroit, March 6, 1958.

BEFORE designing any new engine, it is necessary that the designer first fully explore and evaluate the prerequisites of the engine to be designed. Below are discussed some of the main design requirements and how they affect the Chrysler Corp. new V-8 engine.

Uppermost in the engine designer's mind must be structure. The structural rigidity of any new design must be uncompromised to provide the desired engine smoothness and necessary durability. The uncompromised structure must even be projected in the design to cover future structural requirements as engine size and performance are increased.

Secondly, weight is becoming increasingly more important in engine design. In addition to the use of larger engines in our cars, the engine position has been moved forward at the insistence of the stylist to a point where car weight distribution can be affected seriously unless the overall powerplant weight is reduced.

Studies made to decrease engine weight by reducing the size of existing power section components indicated a loss of structural rigidity or engine durability. It was finally decided that for greatest gains in engine weight reduction a new simpler lightweight head design should be pursued. Our investigation favored use of the conventional wedge-shape combustion chamber with side-by-side intake ports. With this as the first step and with features described later, we attained our objective with a minimum loss in power potential.

The new head design uses a simplified in-line valve arrangement and features reduced coolant sections in the head without loss of effective cooling. Moreover, it permits the use of high exhaust manifolds necessary for ease of installation.

Environment studies showed the need for the lowest possible engine to enable a lowering of hoods. This study dictated engine mount position, overall engine height and length, as well as the distributor drive and oil pump locations. It also became obvious that any oil pump location which extended below the crank throw of the engine would interfere with the steering linkage. This problem was resolved by moving the distributor to the front of the engine and placing it on a 45-deg angle parallel to the axis of the right cylinder bank. This made it possible to locate the oil pump, which is driven from the distributor driveshaft, on the front of the cylinder block above the lowest point of crank throw (Fig. 1). The arrangement relieved any steering linkage interference problems, and also a heater-to-distributor interference. In addition, it provided a more serviceable distributor location and an easily accessible line-free location for the oil filter which could be mounted directly on the oil pump cover.

Another design condition was ease of manufacturing. The greatest manufacturing cost savings can be obtained only if manufacturing methods are taken into consideration when the initial design is conceived. For example, the cylinder head was designed to provide a valve gear arrangement facilitating use of an economical stamped rocker arm mounted on a tubular rocker shaft as shown in Fig. 2. The rocker shaft not only provides a simple and trouble-free bearing for the rocker arms but also serves as an oil gallery to feed all valve gear parts. Moreover, with the new design it was possible to omit the conventional drilled cylinder head oil drain-back holes in both head and block. Thus, a foundry problem was alleviated and machining operations reduced. These savings were effected by the use of a "pie-shaped" coolant cross-section in the head design. As shown in Fig. 3, oil from the

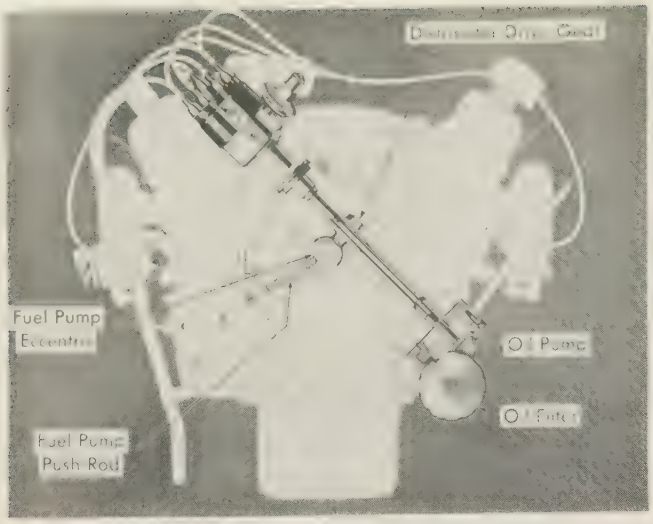

Fig. 1 — Distributor, oil pump, and fuel pump drive

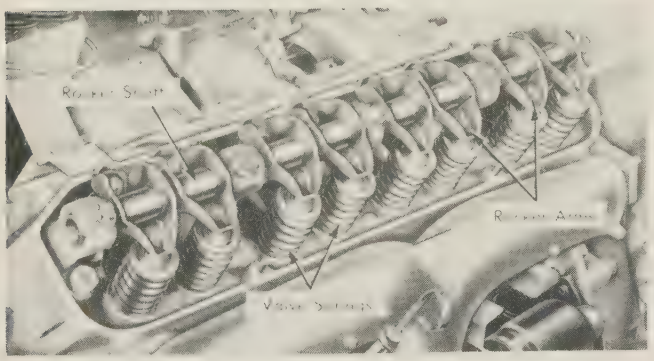

Fig. 2 — Rocker arms and valve train

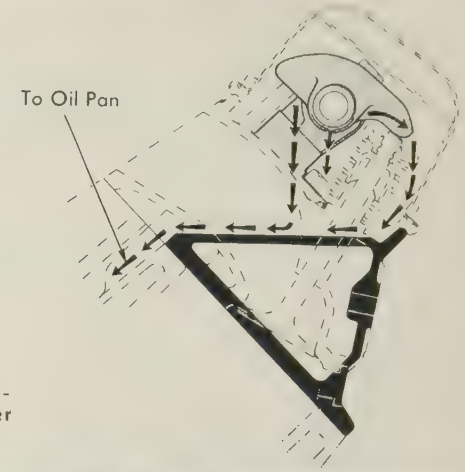

Fig. 3 — Oil drainage of cylinder head

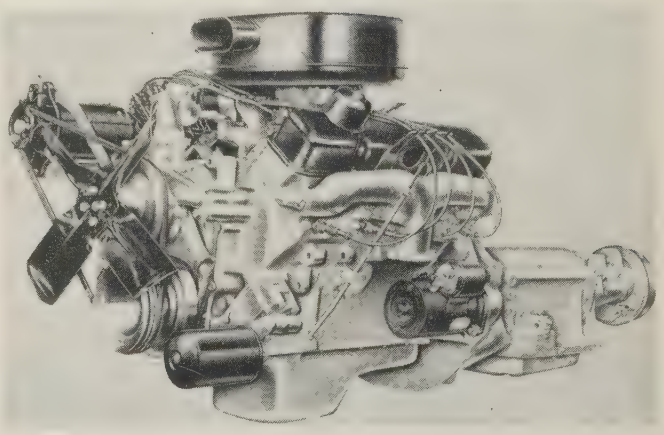

Fig. 4 — Engine assembly, ¾ front view

cylinder head is permitted to return to the tappet chamber by flowing across the nearly horizontal roof of the "pie-shaped" section.

In addition to the requirements discussed above, other important objectives of this new engine design are:

1. A high level of performance and fuel economy.
2. Simplicity of service.
3. Design flexibility for future size requirements.
4. Reduction of coolant for quick warmup.

The following description of the engine and its component parts will show how these factors have been satisfied in the new engine design.

Engine and Component Parts

This new engine is a 90-deg V-8 with a bore of either 4 1/16 or 4⅛ in. and a stroke of 3⅜ in. giving piston displacements of 350 and 361 cu in., respectively. The related design details and the location of the accessories are shown in Figs. 4–6.

Cylinder Block — The cylinder block, of gray cast iron, is of a rigid deep-skirt design (Fig. 7), its sides extending downward 3 in. below the crankshaft centerline. The cylinders are on 4.80-in. centers and have 0.96-in. offset between banks. While increasing the rigidity of the block itself, the deep skirt is primarily designed to improve the stiffness of the whole powerplant. The deeper skirt directly supports more of the torque converter housing, or clutch housing, so that the housing and block in combination are less apt to deflect under engine loads. The increased rigidity results in smoother, quieter engine operation. Also, the oil pan is easier to seal, requiring only a single cork gasket instead of the 4-piece rubber and cork gaskets used on previous designs. The cylinder block was developed to have outstanding durability and is capable of withstanding the most severe engine applications.

Cylinder Heads — The new compact design of the chrome-alloy cast-iron cylinder head (Fig. 8) features minimum bulk and exceptionally short, direct exhaust passages, offering virtually no obstruction to the flow of hot gases. Water-jacketing of the adjacent common-walled intake ports is greatly reduced, although careful attention has been given to the cooling of the valve seats, valve guides, and combustion chambers (Fig. 9). An air jacket around the exhaust crossover passage in the cylinder head, which is vented to the atmosphere, prevents overheating of the intake side of the head and prevents oil from contacting the exhaust crossover. The underside of the exhaust crossover is shielded by a projection of the cylinder head gasket.

Numerous benefits accrue from the new head design. The extremely short exhaust ports reduce heat rejection to the cooling system. The smaller mass of metal and coolant heats more rapidly and provides quicker engine warmup. The large cast openings around the push rods provide drainback of valve gear lubricating oil and accessibility to the hydraulic tappets (Fig. 10). The tappets can be replaced through these openings without removing the intake manifold and tappet chamber cover.

The combustion chambers (Fig. 11) have an "as-

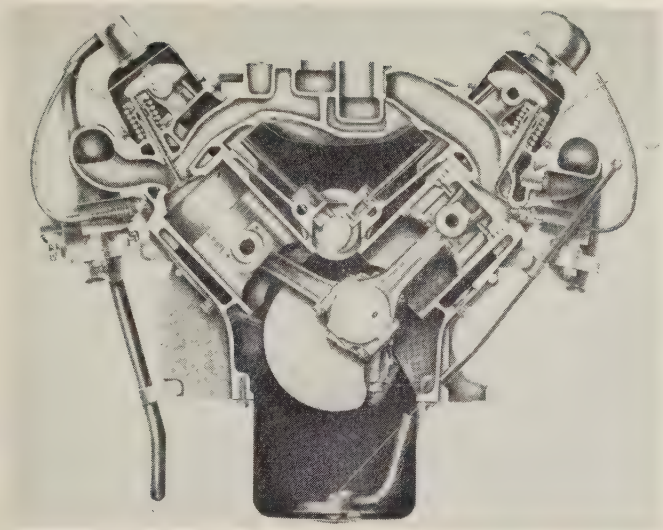

Fig. 5 — Engine assembly, cross-sectional view

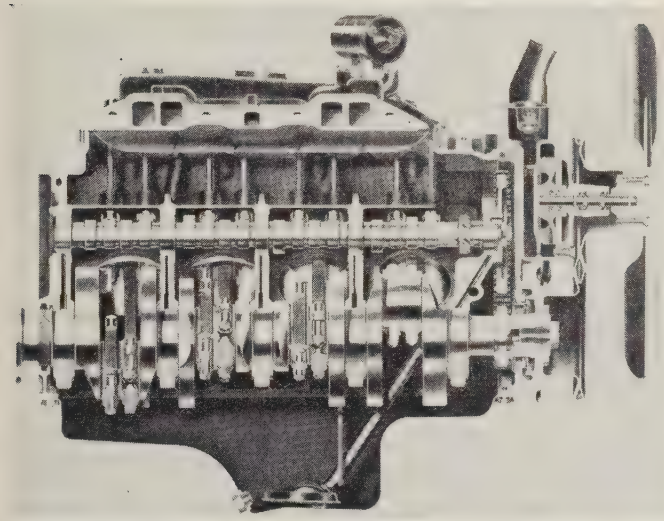

Fig. 6 — Engine assembly, longitudinal section

cast" contour and were designed to obtain 10/1 compression ratio with a desirable flat-head piston. Both exhaust and intake valve seats and guides are integral with the cylinder head. The horizontally positioned spark plugs are located at the wide end of the wedge-shaped combustion chambers. The valves are of generous size with valve head diameters being 1.95 in. for the intake and 1.60 in. for the exhaust, both having 3/8-in. diameter stems.

For less distortion and improved sealing, the number of cylinder-head bolts is increased from 10 to 17 in each head, so placed that five bolts are spaced symmetrically around each cylinder. This attachment of the cylinder heads provides better sealing, in conjunction with a 0.015-in. thick embossed-steel gasket.

Cylinder-Head Covers — The cylinder-head covers are attached to the cylinder heads by means of four screws along the gasket channel. A coated cork gasket is used to seal between the cylinder-head covers and the as-cast gasket rail on the top of the cylinder head. Provision is made in these covers for crankcase ventilation and the addition of engine oil.

Crankshaft — The forged-steel crankshaft is ex-

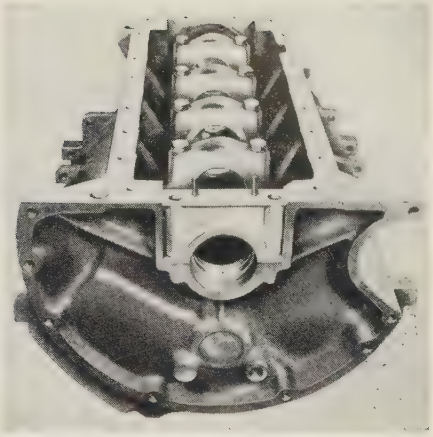

Fig. 7 — Cylinder block, rear view

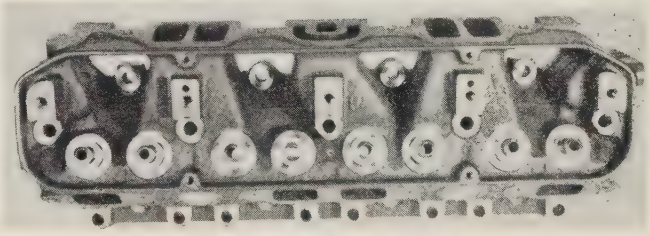

Fig. 8 — Cylinder head, top view

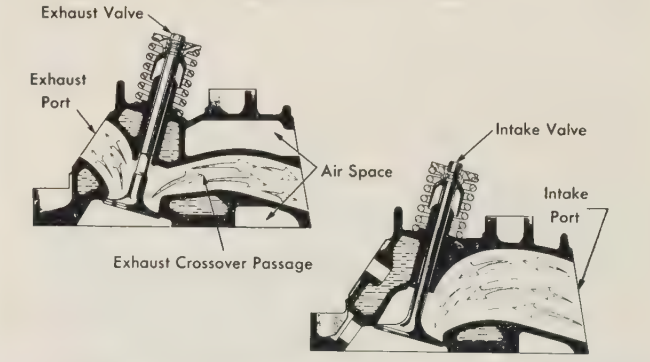

Fig. 9 — Cylinder head sections through valves

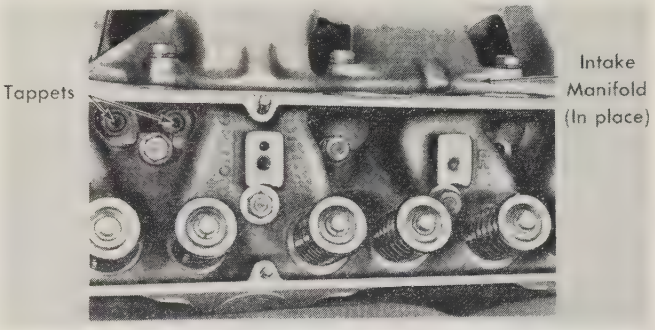

Fig. 10 — Installed cylinder head showing accessibility of tappets

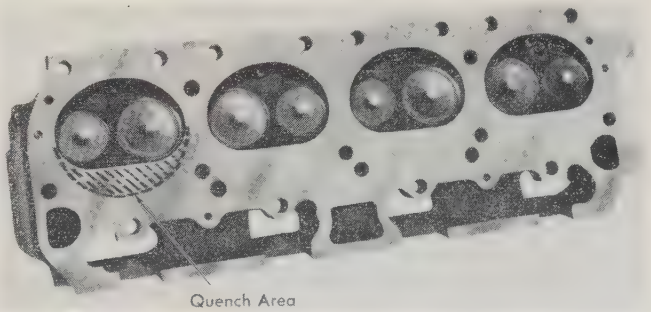

Fig. 11 — Cylinder head showing combustion chambers

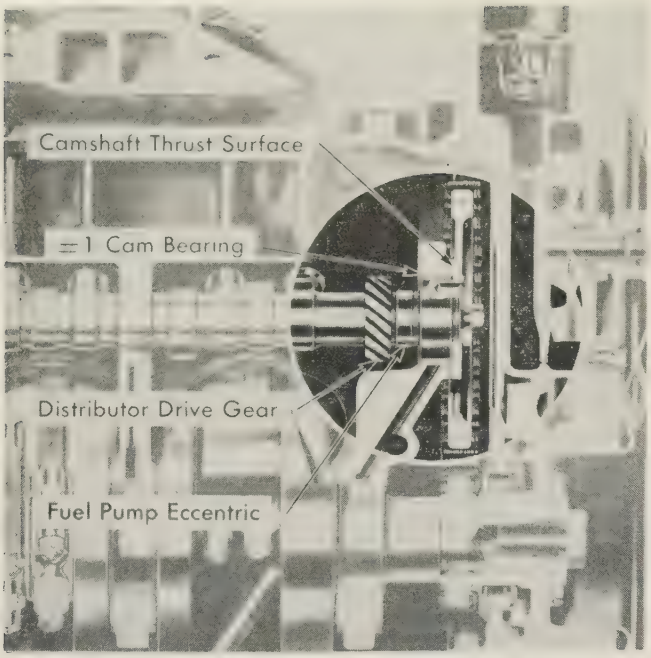

Fig. 12 — Longitudinal view of distributor drive

tremely stiff, minimizing engine noises originating from crankshaft vibrations. The stiffness is the result of having large journals, 2⅝-in. mains and 2⅜-in. rods, and a short 3⅜-in. stroke which provides 13/16 in. of crankshaft journal overlap. The crankshaft is 27-in. long and the torsional natural frequency is 333 cps. This rigid design results in lower imposed stresses, particularly in fillet areas. A new high-speed turning process provides very smooth fillets of controlled shape which greatly increase crankshaft strength. Axial crankshaft thrust is taken on the flanged No. 3 main bearing.

The large crankshaft journals are supported by five babbitt-on-steel main bearings. While the upper bearing shells have conventional oil holes and grooves, the grooves have been eliminated from the lower shells to increase their load-carrying ability. The resulting increase in the main bearing area is approximately 10% but the effect due to the more advantageous L/D ratio is much greater.

A torsional-vibration damper is mounted on the front end of the crankshaft.

The new engine is dynamically balanced during assembly to ensure vibration-free operation.

Connecting Rods — The short connecting rods of alloy steel designed on 6.36-in. centers are forged to a tapered I-beam section which combines maximum strength with minimum weight. The rods are conventional except for the use of piston pins which are pressed into the small ends with an interference fit of 0.0007/0.0012 in. This eliminates the need for a bushing in the rod and for lock rings in the piston. The rod bearings are babbitt on steel with a projected area of 2.23 sq in.

Pistons and Rings — The cam-ground, aluminum-alloy pistons incorporate a steel strut for expansion control of the piston skirts. Two 5/64-in. wide compression and one 3/16-in. wide oil-control rings, all located above the pin, are used on each piston. The oil ring is a conventional cast-iron type, spring loaded by a hump-type expander spring which is burred to keep the ring from rotating.

The 1.09-in. diameter piston pin is offset 1/16-in. from the piston centerline towards the thrust face and has a clearance of 0.00045/0.00075 in the piston bosses.

Camshaft — The hardenable cast-iron camshaft is located in the conventional position and is driven through a ½-in. pitch and ⅞-in. wide timing chain and sprockets from the crankshaft. The compact arrangement of this drive is shown in Fig. 12. It has an integral oil pump and distributor drive gear and fuel pump eccentric. The five replaceable bearings are babbitt on steel. Rearward camshaft thrust is taken by the rear face of the cast-iron camshaft sprocket bearing directly on the front of the cylinder block, thus eliminating the need for a separate thrust plate. Since the helical oil pump and distributor drive gear and the camshaft taper both tend to produce only a rearward reaction, no provision is made for a forward thrust. The camshaft lobes and fuel pump eccentric are hardened to 48 Rc minimum.

Valve Train — The overhead valves, operating at a 30-deg angle from the vertical, are actuated from the camshaft through a conventional train consisting of hydraulic tappets, 5/16-in. diameter solid push rods, and stamped-steel rocker arms.

Hydraulic Tappets — Integral-type hydraulic tappets having a spring-loaded flat check valve occupy a key position in the valve train. These tappets maintain zero clearance throughout the valve mechanism by means of a column of oil supplied from the engine lubrication system. Use of hardenable cast iron for the tappet body results in low wear and long camshaft life.

Rocker Arms and Shafts — New one-piece stamped-steel rocker arms, oscillating on tubular steel shafts, transmit valve train motion from the push rods to the valve stems with a 1.5/1 valve-to-cam motion ratio. The rocker arms are separated on the rocker shaft by means of Oilite spacers rather than by springs, as in previous designs, because push rod angularity tends to force the pairs of rocker arms together, rather than apart. Five small die-cast aluminum brackets attach each rocker shaft to the cylinder head.

The rocker arm, which bears only on the lower half of the shaft is made from a single-piece metal stamping (Fig. 13), commonly referred to as the "bath tub" because of its open design. The rocker arm is wide enough to permit forming the rocker shaft holes from the inside, thus facilitating the stamping operations and alleviating the possibility of any burrs on the shaft bearing surface. The bearing surface is coined to provide a uniform contact between shaft and rocker arm. A lubrication groove 90 deg to the shaft axis is formed at the same time the rocker arm shaft bearing surface is coined. Push rod lubrication is accomplished by feeding oil from a hole in the rocker shaft, through the coined oil groove in the rocker arm bearing to a small punched hole at the base of the concave 5/16-in. diameter spherical push rod seat. As the rocker arm is placed in the engine, it would appear that the lubrication of the push rod socket has been attained by making oil flow uphill. Actually this has been accomplished by damming the oil against the rocker shaft to a point where the oil level reaches the punched hole for lubricating the push rod as shown in Fig. 14. The valve end of the rocker arm is lubricated by gravity flow since the valve tip

is lower than the rocker shaft oil supply.

Stamped rocker arms were considered desirable because of their lower manufacturing cost together with equal or improved durability and consistent production quality as compared to arms made of cast malleable iron. The arms are stamped from 0.120-in. thick cold rolled (1010) steel and are subsequently carbonitrided and hardened to a depth of 0.007–0.012 in. With these specifications plus a lubrite coating on the rocker arm and rocker shaft, the durability and wear characteristics have been exceedingly good.

Valves — Since valve life is limited primarily by the ability of the metal to withstand heat, both intake and exhaust valves are made of special heat-resistant, high-alloy steels — silicon-chromium (8440) for intake valves, nickel-manganese-chromium (21-4N) for the exhaust valves. Further protection from high and nonuniform temperatures is provided by the ample supply of coolant supplied by the new series-flow cooling system.

Both intake and exhaust valves are "tulip" shaped, providing greater flexibility and, thus, better seating of the valves. It also reduces the weight of the valves, lowering their inertia and enabling them to be operated at high speeds by valve springs of moderate load (180-lb valve open) which do not impose excessive loads on the cams and tappets.

Rubber cup seals are used to shield both intake and exhaust valve stems from oil splash, thus avoiding excessive oil consumption and exhaust smoking.

Low-friction 4-bead valve locks, introduced on previous engines, are retained on exhaust valves to allow valve rotation with consequent longer valve life. The intake valve uses the 2-bead lock because it does not require appreciable rotation to ensure satisfactory life. Although no valve rotators are employed as such, the normal slight vibration of the valve train and springs is sufficient to overcome the low resisting torque of the valves and cause them to rotate, even at relatively low engine speeds.

Intake Manifold — A very compact and light intake manifold (Fig. 15) is used in conjunction with a separate tappet chamber cover. This cover — an inexpensive, single-piece, sheet metal stamping — aslo serves as the intake manifold gasket (Fig. 16). With the intake manifold relieved of its secondary function as tappet chamber cover, it is designed as an open series of branches without excess cast iron. Siamesing of adjacent branches also reduces weight and material.

For intake mixture heating, a crossover in the intake manifold conducts exhaust gases from the No. 4 exhaust port in the right cylinder bank to the hot spot, and out through the No. 5 exhaust port in the left bank.

A constant cross-sectional area of 2.0 sq in. is maintained in the intake system from the base of the carburetor risers to the intake valve seats. This has been found to be the best compromise for engine output and driveability over the speed range. Furthermore, there is no sump in the fuel-air passages between the carburetor and the valve seats, thereby avoiding "flash" and "puddling" problems.

The intake manifold has a low silhouette which, in combination with the lower engine and shorter carburetors, permits adoption of the more efficient concentric-type, paper-element air cleaners. The concentric design makes possible better airflow

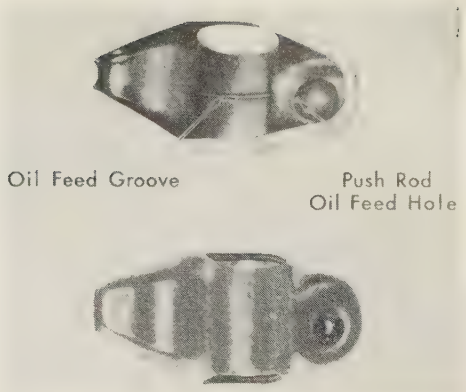

Fig. 13 — Stamped rocker arm

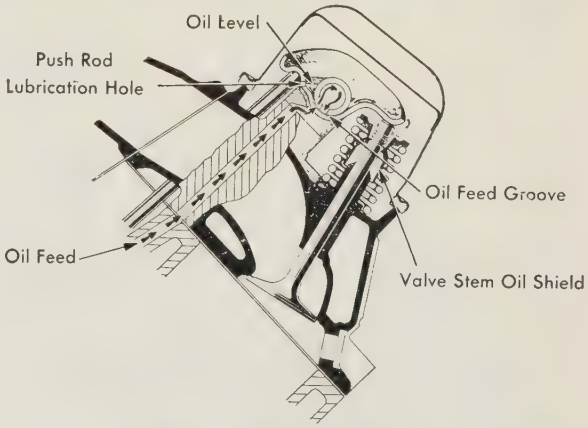

Fig. 14 — Cylinder head valve mechanism lubrication

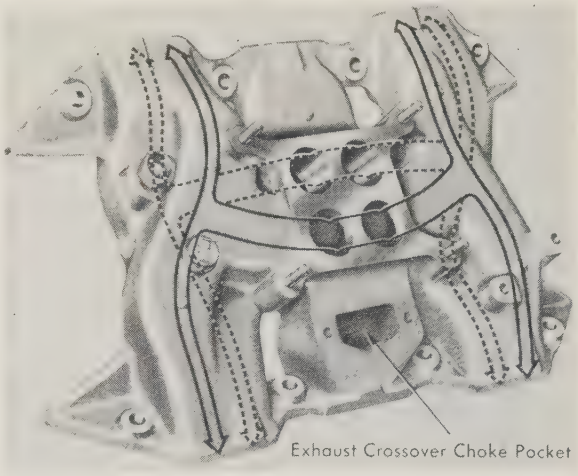

Fig. 15 — Intake manifold (4-barrel carburetor)

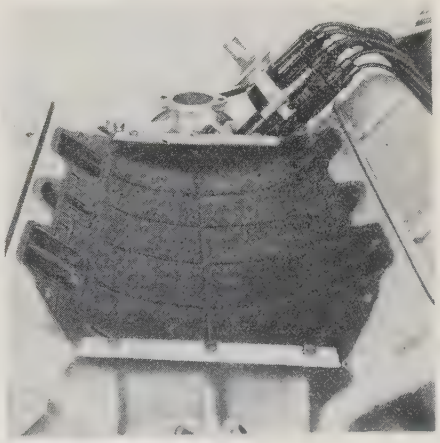

Fig. 16 — Intake manifold gasket and tappet cover

characteristics which in turn contribute to improved engine performance.

Exhaust Manifolds — The exhaust manifolds are located on the outer sides of the cylinder heads, immediately above the spark plugs. Their new, separated-branch design makes gaskets unnecessary because the branches are flexible enough to absorb the distorting effects of heat.

A shield at the heat-control valve on the right-side manifold prevents cold air from the fan from stroking the temperature-sensitive bimetal spring which controls the valve. This aids in maintaining intake manifold temperatures at the optimum level for peak performance and maximum fuel economy.

Cooling System — Uniform metal temperatures are maintained throughout the new engine because of the careful attention given to the design of the cooling system and its new series flow pattern. Series flow means that all of the coolant in each cylinder bank is forced to pass first around all of the cylinders and then, in its return through the cylinder head, around all of the valve seats.

The high-capacity centrifugal water pump, bolted to the front of the engine and belt-driven from the crankshaft pulley, assures an adequate supply of coolant at all engine speeds. Coolant from the radiator enters the pump from the lower left side and is directed to the front of both cylinder banks by a symmetrical scroll in the pump housing (Fig. 17). The coolant then flows around the cylinders to the rear of the block, and upward through matching holes in the block and cylinder head. Virtually all of the coolant circulating in each bank passes through these holes of about 1-sq-in. area at the rear of each bank. The flow is then from the rear of the cylinder heads, past all of the valves and seats in each cylinder bank, into passages in the forward end of each bank of the cylinder block, and thence into a common manifold which is an integral part of the water pump housing. The coolant then passes through a thermostat and into the radiator top tank. A permanent bypass in the water pump housing, between the engine discharge and the pump intake, maintains circulation through the engine during warmup. It should be noted in Fig. 17 that the high point of the cooling system is at the cylinder block water outlet, due to the cylinder bank angle and the design of the cylinder heads. This is desirable for proper elimination of air or vapor from the cooling system during filling and engine operation.

Fig. 17 — Engine cooling system

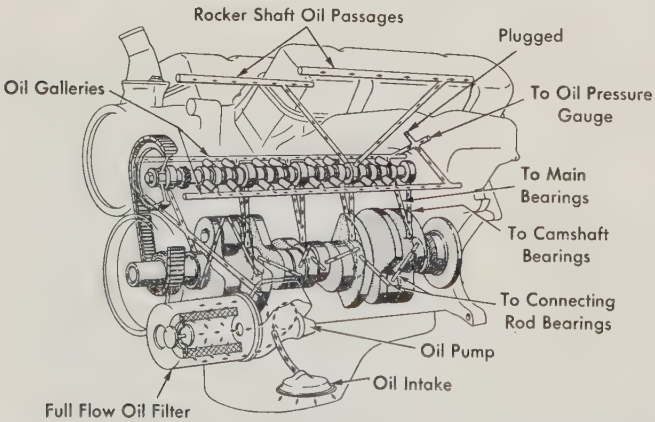

Fig. 18 — Engine lubrication system

Steam-relief slits in the cylinder head gasket are provided to prevent steam pocketing; with the exception of these and two ¼-in. drain holes for service draining (through which only a negligible amount of coolant short circuits), all of the coolant must first pass each cylinder and then must pass all of the combustion chambers in each head. In this series-flow system, the use of large passages instead of metering orifices provides greater coolant velocity which avoids clogging and hot spots. With fewer passages between the cylinder block and head, sealing is improved and there are fewer places where the coolant tends to stagnate.

Laboratory and vehicle tests of the engine indicate very good overall cooling performance. With a wide-open thermostat and at 2000 engine rpm, the coolant flow is approximately 300 lb per min. At wide-open throttle, the coolant temperature rise through the engine is 7–9 deg over the speed range. The heat rejection per bhp at wide-open throttle varies from 31 Btu/min at 2000 rpm to 28 at 4000 rpm.

The overall coolant capacity of the engine cooling system including the radiator is 16 qt. This is appreciably less than other V-8 engines of comparable displacement. A large part of this reduction is made in the cylinder heads as each head of the new engine contains only 1.2 qt. Figs. 8 and 9 illustrate the small water volume in the new head. The reduced amount of iron as well as the smaller coolant capacity provides a more rapid engine warmup than any former Chrysler-built V-8. This is important in cold weather car heater performance and also insofar as fuel economy is affected by engine warmup time.

Lubrication System — The lubrication system consists of an oil sump in the pan, a rotor-type oil pump, full-flow filter, and a series of passages to deliver the oil as explained below (Fig. 18). The oil pump draws the oil from the sump through a fixed screen suction pipe and forces it through the full-flow filter. From the filter, the oil moves across the front of the block through a drilled passage to the right oil gallery. The passage that carries the oil to the right gallery is intersected by holes which feed the No. 1 main bearing and the No. 1 camshaft bearing. The right oil gallery supplies the other mains and the camshaft bearings through drilled holes. The rod bearings are lubricated through holes drilled in the crankshaft to the nearest main journal. Squirt holes in the connecting rods spray oil on the cylinder walls. The piston pins are lubricated by splash oil which drains down from the underside of the piston heads through holes in the piston pin bosses. Intersecting holes through No. 4 camshaft journal meter oil to drilled holes in each

Table 1 — Dimensional and Weight Comparison

	1957 De Soto	1958 De Soto
Bore and Stroke, in.	3.78 x 3.80	4.125 x 3.375
Displacement, cu in.	341	361
Total Weight including T/C Adapter, lb	674	638
Weight per Cubic In. Displacement	1.98	1.76
Length — Fan to Rear of Block, in.	29.0	32.0
Height — Crank Centerline to Carburetor Pad, in.	15.2	13.3
Width — Across Exhaust Manifolds, in.	25.0	26.0

bank which carry it up through the cylinder block and heads to the rocker shafts. Holes in the rocker shafts oil the rocker arms. A crossover at the rear of the block transfers oil from the right gallery to the left. The tappet bores for both cylinder banks intersect the oil galleries so that oil is fed directly from the galleries to the hydraulic tappets. The gerotor-type oil pump, which has generous capacity, is mounted externally on the lower left-hand side of the block near the front. It is driven through a hexagonal joint by the oil pump and distributor driveshaft.

The new full-flow oil filter is located on the front of the oil pump body parallel to the engine centerline. It is a replaceable can-type filter and contains an integral anti-drainback flapper-type check valve and a relief valve which opens to supply oil to the engine if the filter becomes clogged. The filter can be replaced by hand without the use of wrenches from the underside of the car.

Engine crankcase ventilation is by road draft tube connected to the right cylinder head cover with the fresh air entering at the oil fill cap on the left cylinder head cover. A baffle is installed in both cylinder head covers below these openings to prevent oil loss.

Carburetors — Both the 350- and 361-cu-in. engines have models using Ball and Ball (BBD) dual carburetors and Carter AFB 4-barrel carburetors.

The *BBD dual carburetor* was especially designed for this engine and incorporates a 1½ in. SAE flange as compared to the 1¼-in. size used on all other Chrysler-built engines. This larger size provides more freedom in the selection of throttle bore and venturi diameters. For this engine size range, 1 9/16-in. throttle bores and 1 5/16-in. venturi are used.

In designing the carburetor, specific attention was given to obtaining a low overall height of 3.96 in. as compared to 4.53 in. on other Chrysler Corp. dual carburetors. To promote air cleaner interchangeability, the same 4.18-in. diameter air cleaner mounting pilot was incorporated as is used on the 4-barrel carburetors.

Vapor lock tests have shown that a large reserve of fuel in the carburetor bowl reduces vapor lock tendencies when accelerating after a short idle or soak period. This reserve provides a fuel supply to accelerate the car until much of the vapor has been purged from the pump and lines. In addition, a large area bowl enables the use of large floats which in turn allows the use of larger diameter needle valve seats (No. 34 versus No. 38) to give increased vapor and fuel handling properties. To gain these advantages, the bowl capacity of this carburetor was designed to have 90 cc of usable fuel as compared with 47 cc on the previous dual carburetors.

During hot weather testing, it was found desirable to incorporate an outside bowl vent which is opened when the throttle is closed for idle. The outside vent is opened only at idle to maintain complete internal balance under conditions of higher airflow when air cleaner restriction would influence carburetor metering. To reduce the heat transfer to the bowl, a ⅛-in. thick insulating gasket is used between the throttle flange and the main carburetor body containing the bowl.

The accelerating pump plunger passes through the bowl cover inside the air horn. This eliminates the effect of air leakage on internal balance and prevents dirt and water from entering the bowl at this point.

The carburetor was designed to allow all castings to be made of aluminum for reduced cost. Considerable effort was also expended to promote ease of manufacture and to use the minimum number of individual pieces.

Carburetor Choke — This engine uses a distinctive choke system for both the dual and 4-barrel carburetors. The bimetallic choke coil is located in a pocket in the exhaust crossover passage of the intake manifold. A rod connects the choke coil unit to the choke shaft in the carburetor air horn. This arrangement offers these advantages over the conventional choke heated by hot air drawn from a stove or heat tube in the exhaust manifold:

1. The rate of heating of the choke coil closely follows the rate of intake manifold warmup. Conventional chokes heated by drawing hot air across the coil tend to come off fastest when the car is running at light load and high manifold vacuum, due to the higher rate of heated air flowing across the coil. Conversely, the conventional choke comes off slowest when the engine is operating under high-load conditions and has little manifold vacuum to draw the heated air through the choke coil. Under these conditions with the engine heating up the fastest and the choke coming off the slowest, over-rich conditions can be encountered.

2. There is no problem of drawing dirt-laden air from an exhaust manifold heat tube through the choke mechanism and into the engine.

To obtain choke mixtures more nearly matching engine requirements, a staged vacuum piston is incorporated in the air horns of the dual and 4-barrel carburetors. The function of the vacuum piston is to pull the choke blade towards the open position to provide leaner mixture at part throttle. At the same time the conventional choke coil is developing an opposing force which is proportional to intake manifold temperature and wide-open throttle engine requirements. The principal innovation of the staged vacuum piston is that it has a finer degree of control to obtain the correct choke blade relationship between wide-open throttle and part throttle during the entire warmup cycle.

Tests during the first 5 miles of a start and warmup cycle have shown substantial fuel economy gains resulting from the use of this staged piston.

Engine Weight and Physical Size — The overall dry weight of the new engine as used in the 1958 De Soto is 638 lb including starter, generator, front engine supports, air cleaner, carburetor, distributor, vent pipe, spark plugs and wires, pulleys, and belts. The weight is complete from the fan to the crankshaft flange except for special accessories, such as the power steering pump and belt drive. This weight is for an engine which still has some space for future displacement increase. A comparison

with the 1957 De Soto engine is made in Table 1. The small ratio of weight per cubic-inch displacement is obtained with no sacrifice in ruggedness of the power section, as indicated by the generous sections in the cylinder block, crankshaft, and other power section components previously discussed. It is quite apparent that careful design work in the cylinder head, valve mechanism, water pump assembly, and many small components has resulted in appreciable weight savings in order to obtain this desirable overall result. The new engine has a weight per cubic-inch displacement which is equal to or better than other engines in the industry today and will improve as engine size is increased.

The external dimensions of the engine are also given in Table 1. As compared to the 1957 De Soto, the new engine is 3-in. longer, primarily due to increased cylinder bore spacing, 4.80 versus 4.31 in. It is almost 2 in. lower, due to the shorter stroke and compact intake manifold design. Finally it is 1 in. wider in spite of the short stroke and compact cylinder heads because of the longer individual branches of the exhaust manifold which improve engine performance.

Combustion Chamber and Engine Performance — A considerable review has already been made of the factors which led logically to the line-valve type of combustion chamber in this new engine. This design was predicated on factors involving weight, space considerations, and manufacturing economies. With this as a base, Chrysler standards of intake and exhaust manifold design, valve and port areas, and combustion-chamber detailed refinements were incorporated in the final development of the engine. The resulting performance and economy characteristics are very satisfactory.

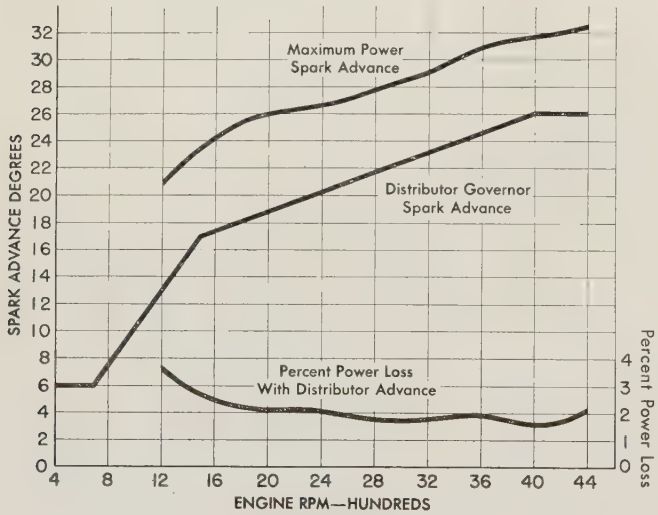

Fig. 19 — Spark advance characteristics

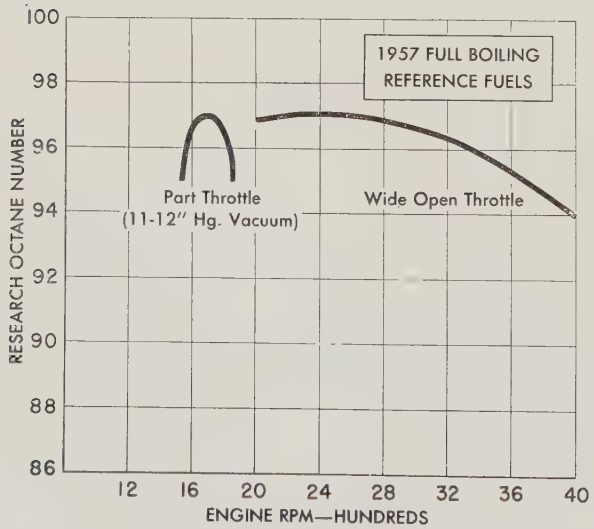

Fig. 20 — Road octane requirement

The camshaft in most models of the new engine is moderately conservative with 252 deg of intake and exhaust valve opening duration and 30 deg of top overlap. This combination provides good performance over the speed range and smooth idling characteristics.

Fuel Octane Requirement — The spark advance for maximum wide-open throttle power over the speed range is presented in Fig. 19. The distributor governor advance curve for operation on commercial premium grade fuel is also shown. In the lower part of the plot, the per cent power loss due to spark retard is shown.

The fuel octane requirement of the new engine is quite reasonable. Representative octane requirement data from production-built engines and using commercial reference fuels are shown in Fig. 20. Most of the engines used in this evaluation had less than 3000 miles of deposit accumulation. The part-throttle knock is a maximum in the 11–12 in. of Hg intake manifold vacuum range under which condition the vacuum spark advance is approximately 14 deg. Further reduction in vacuum spark advance will naturally reduce the part-throttle knock but will adversely affect fuel economy and driveability. Also, tests have shown that part-throttle knock is affected much more than wide-open throttle knock by high air and coolant temperatures of the engine (approximately one octane number increase per 10-deg increase in coolant temperature). This problem is becoming more apparent as compression ratios increase and is not a peculiar characteristic of this particular engine.

Conclusions

The preceding description and discussion have covered these important engine characteristics:

1. Excellent engine performance, on an output per cubic-inch displacement basis and particularly on an output per pound of weight basis.
2. A light weight engine with good durability and exceptional structural rigidity which assures quiet operation.
3. A new cooling system which provides very effective cooling of vital engine parts with a relatively low rate of heat rejection to be dissipated in the radiator. Also due to the small quantity of coolant in the system and the small mass of iron to be heated, engine warmup is more rapid than contemporary engines.
4. The latest manufacturing and assembly methods were utilized to promote maximum economy to the manufacturer as well as the consumer.

This engine is the newest addition to the Chrysler Corp. line of V-8 models and it represents a major forward step in the production of efficient and lightweight engines to power the modern automobile.

Oral discussion of this paper will be found on pp. 110-111.

Engineering the "W" Engine Chevrolet's 348-cu-in. V-8

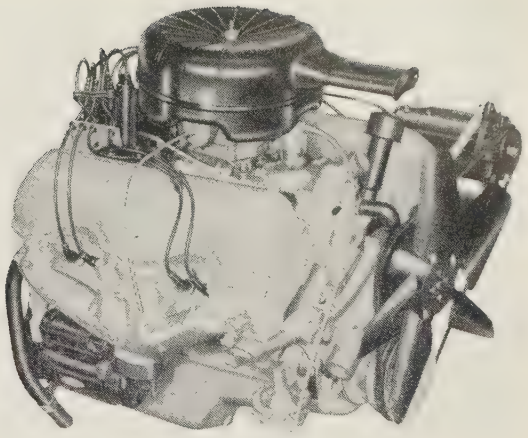

J. T. Rausch, H. H. Kehrl, and D. H. McPherson, General Motors Corp.

This paper was presented at the SAE National Passenger-Car, Body, and Materials Meeting, Detroit, March 6, 1958.

WITH the 1958 model, Chevrolet introduced a new 348-cu-in. V-8 engine. This engine — commonly referred to as the "W" — broadened the range of engine sizes, so that now Chevrolet makes available a 235-cu-in. in-line 6, a 283-cu-in. V-8, and the 348-cu-in. V-8 in all its passenger cars.

Conception and Design

In order to meet customer demand for the V-8 engine, it became necessary in 1955 to plan for an increase in our production facilities. Because of the rising demand for automatic transmissions in our deluxe line of cars, it was also necessary to look forward to increasing the engine displacement to provide optimum low-speed and mid-range vehicle performance. A larger engine with good low-speed torque, we felt, would make an exceptionally good teammate for the Turboglide transmission, then in the development stage. During the past ten years we all have seen numerous V-8 engines put into production. With very few exceptions, these have been single purpose engines, patterned very much like the V-8 engine first produced by Cadillac in 1949. During this decade we have seen many of these engines redesigned and retooled at great expense, because it became necessary to increase displacement to provide the performance necessary for safe and pleasant motoring.

Primary Objectives — Because of the importance of multiple usage to insure high volume production and to insure maximum usage of automated manufacturing equipment, we recognized the need for establishing a new set of ground rules and conceiving a design which would meet them. We decided that the new design must permit:

1. Adaptability to a broad range of displacement with a minimum number of different parts.
2. Adaptability to broad compression ratio range to match the octane trend of future fuels.
3. Dimensions compatible with the anticipated space limitations of passenger-car design.
4. Provisions for mounting accessories on engines for both passenger cars and trucks.
5. Flexibility of machine tools to accommodate future engine modifications.

Basic Dimensions — Fulfilling the first requirement, adaptability to a broad range of displacement, was a rather straightforward job. After establishing the bore and stroke to provide a displacement in line with passenger-car requirements, we deter-

SPECIFICATIONS of the new Chevrolet Turbo-Thrust V-8 engine described in this paper are:

Type	90-deg V-8
Valve Arrangement	In head
Bore	4.125 in.
Stroke	3.25 in.
Stroke-to-Bore Ratio	0.79/1
Displacement	348 cu in.
Compression Ratio	9.5/1 (passenger car)
Carburetor	Single 4-barrel
Maximum Gross Horsepower	250 at 4400 rpm
Maximum Gross Torque, lb-ft	355 at 2800 rpm
Maximum Bmep	152.3 psi at 2800 rpm

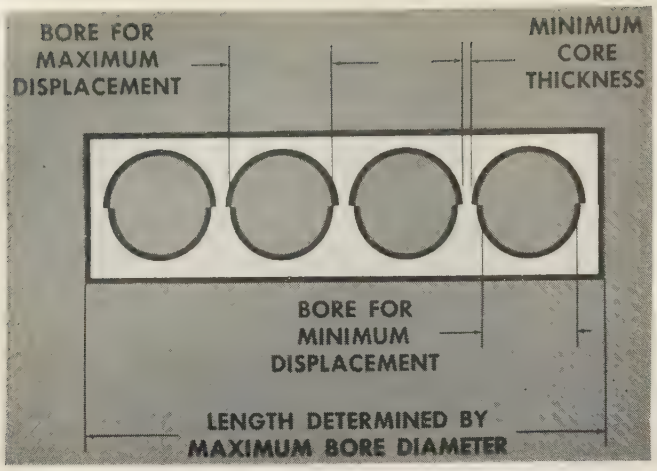

Fig. 1 — Determining basic dimensions of engine from cylinder bore size

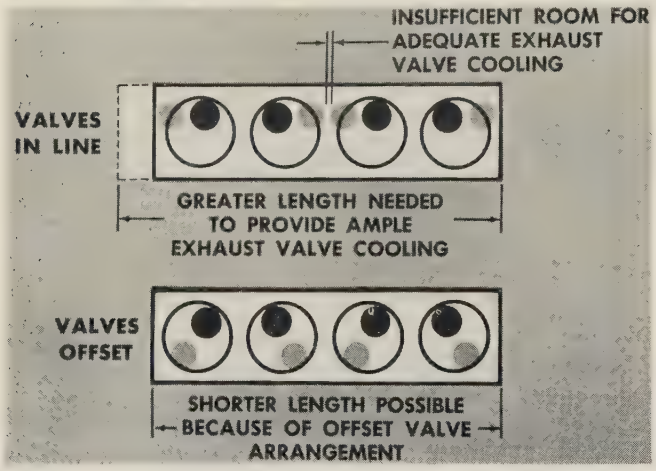

Fig. 2 — Determining basic dimensions of engine from valve arrangement

mined the bore size that would satisfy our maximum displacement truck engine requirements. The largest bore size then established the bore centers that would provide full circumference cooling and minimum core thickness between bores which would be acceptable to the foundry (Fig. 1).

Preliminary Studies — Starting in 1955, we made numerous design studies of engines having greater displacement than our then new 265-cu-in. V-8 engine. We built and tested two of these engines of approximately 300-cu-in. displacement, with the same basic external dimensions and configuration as the 265-cu-in. V-8. In one engine, increased displacement was obtained by increasing the bore to 4 in. while retaining the 3-in. stroke. This necessitated joining the bores, creating a difficult casting problem and preventing complete coolant circulation around the cylinder.

In the other engine, the stroke was increased from 3 to 3.3 in. and the bore from 3¾ to 3 13/16 in. In addition to necessitating completely new tools and equipment for crankshaft machining, both these designs would have severely limited further displacement and compression ratio increases that might be required in the future.

In 1956 the ratio of V-8 to in-line 6 engines at Chevrolet was increasing rapidly due to customer acceptance of the V-8. Management was confronted with the necessity of buying more lines for V-8 engine production by model year 1958.

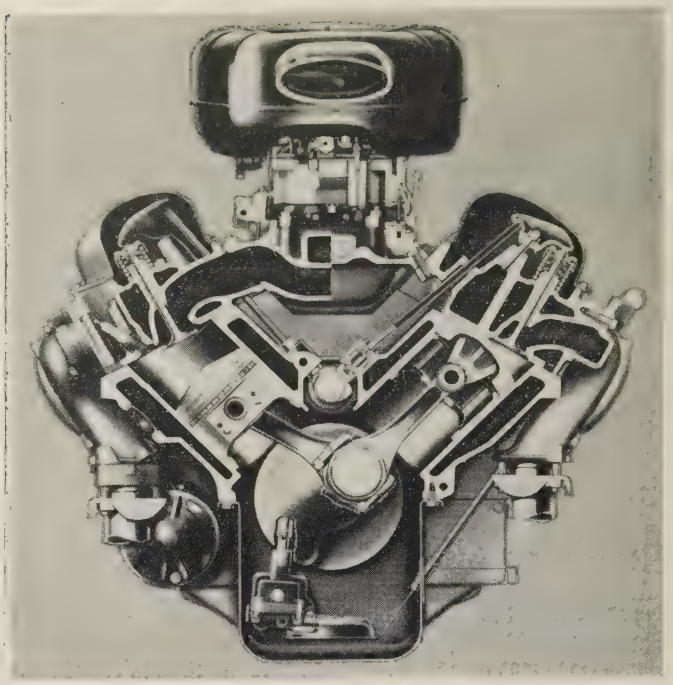

Fig. 3 — Cross-section of engine

The cost of new capital equipment would not be greatly increased by providing the added lines with a design which could add materially to the displacement range for passenger cars. The same basic engine could be used for the higher gvw truck models which Chevrolet is now building. As a result of these considerations, the proposal to develop an entirely new engine was approved.

Valve Arrangement — The basic length could then be maintained, provided that room was available for valves of the size needed for the maximum displacement engine, with spacing adequate for good exhaust valve cooling and freedom from valve seat distortion. Placing the valves in line would increase the length of the engine in order to provide sufficient space between valves. Staggering the valves, on the other hand, would allow for the necessary space while still maintaining the minimum overall engine length (Fig. 2). Advantageous location of the valves was relatively easy to achieve by means of individually mounted rocker arm mechanism that has been used successfully by Chevrolet and Pontiac since 1955. Flexibility of this design also permitted the use of a common rocker arm for all the valves.

The required piston proportions, counterweight radius, and connecting rod length established the basic height of the cylinder block (Fig. 3).

The established engine length permitted excellent proportions for bearing length and cheek thickness (Fig. 4). These features were combined with large overlapping journals to produce a stiff crankshaft.

Combustion Chamber — In order to meet the second objective, provision for a range of compression ratios, considerable design effort was expended Many manufacturing problems had to be investigated. It was obvious that with the combustion chamber placed in the cylinder head, the foundry must retool every time a compression ratio change is in order. The necessity of making special heads to provide a range of compression ratios and to per-

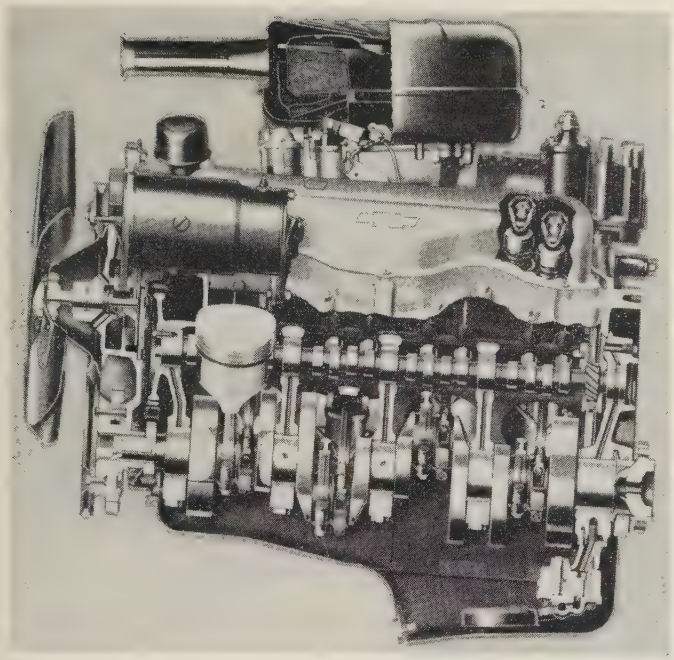

Fig. 4 — Lengthwise view of engine

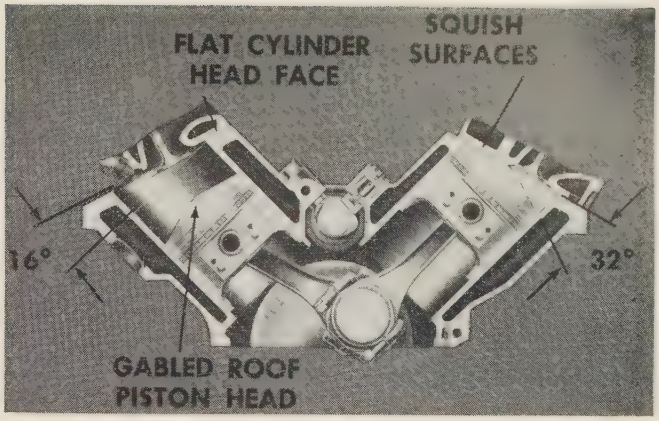

Fig. 5 — Engine block geometry for combustion chamber

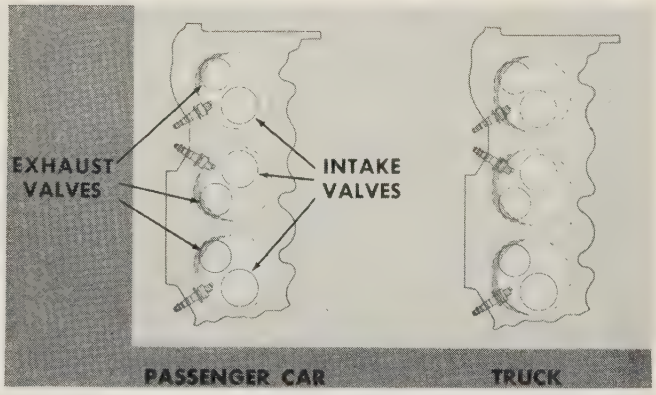

Fig. 6 — Combustion-chamber arrangement

mit attachment of accessory mountings for the various model applications is of serious concern to the manufacturing and service departments. Chevrolet manufactures and services eight different heads for the 283-cu-in. engine because of the requirements imposed by multiple model usage. It would be possible to reduce this number of cylinder heads. However, when the necessary tools and equipment are added to a previously established automated machine line, the cost becomes prohibitive because generally the volume of production for special requirements is low.

If the combustion chamber is placed in the head, the designer is also faced with a dilemma. For good volumetric efficiency at high speed, space for large valves must be provided. At the same time, the new engine needs to have the highest permissible compression ratio, and latitude to go still higher in the future. Unfortunately, these requirements are not compatible; eventually, it would become necessary to compromise at the expense of major cylinder head machine equipment changes.

Making the cylinder head with a flat bottom and placing the combustion chamber in the upper cylinder bore appeared to have possibilities of meeting our objective. Regardless of what changes might be made in piston shape, stroke, or bore size, the flat bottom cylinder head would remain the same. It would also lend itself to freedom from valve shrouding, promoting efficient flow characteristics. The actual combustion-chamber shape could be achieved by contouring the piston head, by angling the top of the block, or by a combination of both. How it was to be done depended on what we believed necessary to establish a sound combustion-chamber design:

1. Compactness, for fast burn rate.
2. Adequate quench and squish area, for turbulence.
3. Central spark-plug position, for minimum flame travel.
4. Latitude to obtain different combustion volumes for broad compression ratio range, without affecting piston shape or basic machining equipment.

Inclining the top of the block to 16 deg and shaping the top of the piston like a gabled roof with a 16-deg angle resulted in a 32-deg wedge-shaped combustion space. Approximately one-half of the piston top surface and the underside of the cylinder head, which are parallel, provided the desired quench area (Fig. 5).

The addition of two milled cutouts to extend the volume of the combustion wedge can provide a compression ratio of 7.5/1; one milled cutout produces a 9.5/1 compression ratio (Fig. 6).

Compression Ratio Flexibility — The difference between the volume of these cutouts provides a wide compression ratio range without making any changes in the piston or cylinder head. The number or size of cutouts is varied simply by adding or removing cutters.

Because of the position of the exhaust valve in relation to the cylinder bore, a definite minimum cutout is required to provide clearance for exhaust valve lift.

Future increases in compression ratio beyond 10/1 can be accomplished by modifying the top of the piston. The manufacturing equipment has been designed for this eventuality and changes can be made at reasonable cost.

The staggered valve positions were also advantageous in establishing the spark-plug position. The plug is in a favorable position for good scavenging, fast burn rate, and freedom from oil fouling.

Placing the plugs above the exhaust manifold permits shorter wires between the distributor and

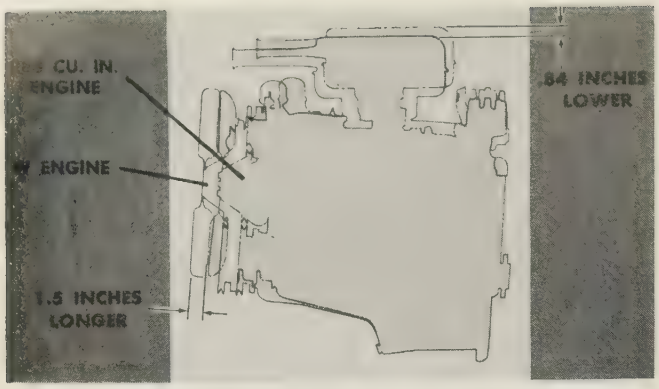

Fig. 7 — Overall size, "W" engine versus 283-cu-in. engine

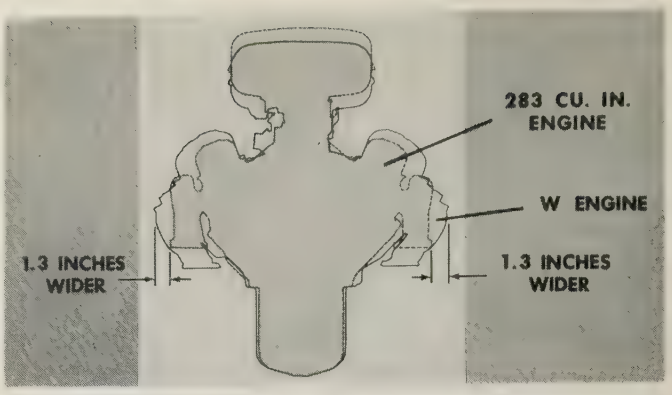

Fig. 8 — Overall size (width), "W" engine versus 283-cu-in. engine

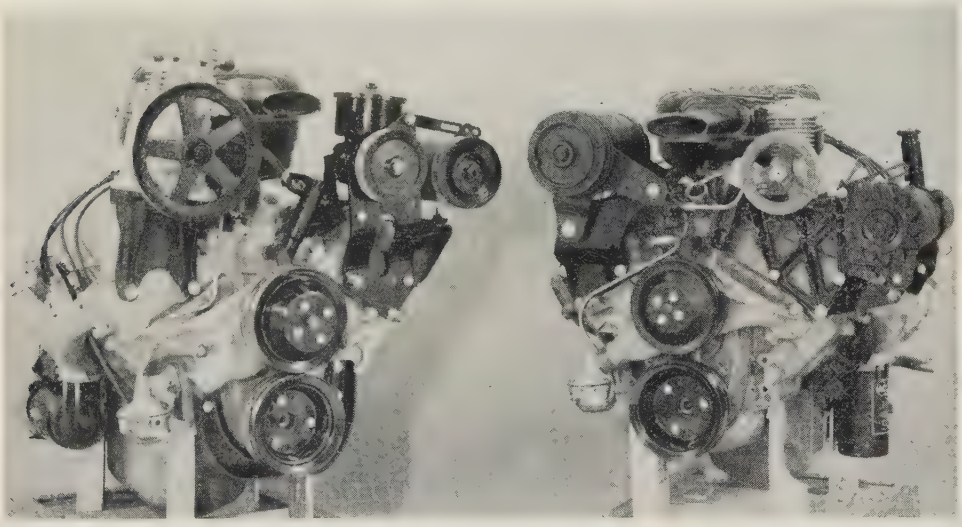

Fig. 9 — Mounting of compressors; left — truck engine, right — passenger-car engine

plugs and better arrangement of wires. This location eliminates the possibility of burned wires and makes the plugs easily accessible.

External Dimensions — During the entire design program, we kept in mind the space limitations imposed by passenger-car design, which had determined our third objective for the new engine. That we succeeded in meeting this limitation is indicated by the fact that the "W" engine assembly with a piston displacement of 348 cu in. is only 1.5 in. longer and 2.6 in. wider than the 283-cu-in. engine assembly. In height, we were able to effect a decrease of about 0.8 in. (See Figs. 7 and 8.)

To meet the requirements of the fourth objective, providing mountings for optional accessories, it was necessary to make composite studies of mountings for all the accessories deemed necessary for passenger cars and trucks.

Accessory Mounting — Placing three tapped holes in the end wall of the cylinder head and two tapped holes on the top of the inlet manifold made it possible to install durable mounts and brackets. These points of attachment are used to mount the compressors for air conditioning and Level Air ride for passenger cars and to mount the air-brake air compressor and the power-steering pump for trucks (Fig. 9).

The group of three holes is placed at both the front and the rear of the cylinder head to eliminate the need for a right- and left-hand unit.

By careful planning for both the present and the future, and coordinating this program with our manufacturing department, we automatically covered the requirements of the fifth objective. We believe we have taken a long stride toward achieving maximum flexibility in the use of automated manufacturing equipment, with resultant long-range economy.

Development Program

This completed the conception and initial design phase of our "W" engine program. Chronologically, we were now at the point when the first prototype engine was completed and ready for laboratory development.

In order to understand the initial direction of the development program, it is necessary to review the overall situation at that time. Chevrolet management felt it was extremely important that an engine meeting the design objectives be available for 1958 production. In view of production tooling lead time requirements, the primary objective of the initial development program was to determine if any problems existed in the design of the engine which might affect major production tooling. It was imperative that this question be answered in a minimum of time. The most serious questions recognized at this point were the following:

1. Was the basic combustion-chamber design satisfactory from the standpoint of specific power output, fuel octane requirement, and fuel economy?
2. Would the location of the combustion chamber

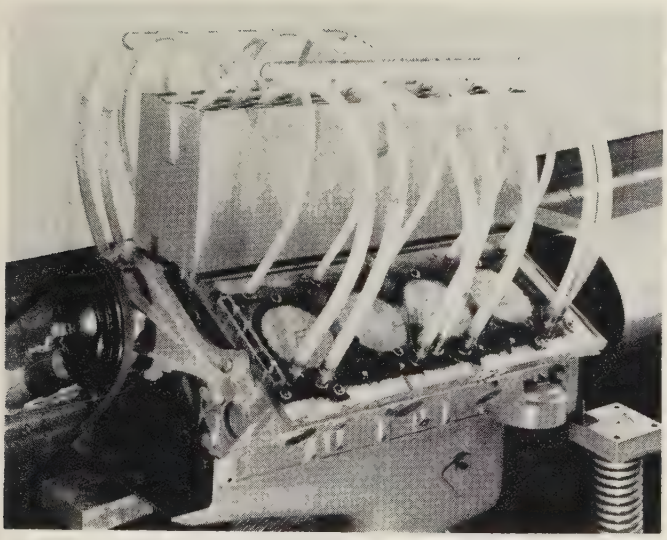

Fig. 10 — Setup enabling visual observation of water flow patterns

inside the cylinder block produce any special cooling problems requiring major tooling changes?

3. Would the larger piston crown area resulting from the gabled head design increase piston temperatures and durability problems?

Cooling System — In order to investigate any of the other questions, it was first necessary to insure adequate combustion-chamber cooling. A total of 40 thermocouples were installed in the first engine at suspected localized hot spots. In spite of an extended program to insure adequate water flow and proper distribution of metering holes in the top deck of the cylinder block, it was not possible by this means alone to eliminate hot spots adjacent to the combustion-chamber surfaces.

Inasmuch as water temperature is only a secondary approximation to heat transfer at a given point in the cooling system, the top deck of the cylinder head was removed and replaced with a plexiglass sheet for visual observation of water flow patterns (Fig. 10). Visual observation of water flow in these areas confirmed our suspicion that there was very little turbulence and, therefore, poor heat transfer along the outer wall of the cylinder block. The nature of the flow and turbulence patterns and hot spot temperatures are shown in Fig. 11.

An experimental modification was made to the water pump to direct the coolant discharge along the outer edges of the cylinder block. This arrangement showed a major improvement in turbulence in the critical areas and also eliminated the hot spots. Fig. 12 shows the turbulence patterns and typical temperatures with the modified water inlet. This arrangement was then released in place of the original design.

Performance Characteristics — With satisfactory combustion-chamber cooling assured, the next objective was to determine whether the performance characteristics of the combustion chamber were satisfactory. Dynamometer measurements of bmep, leanest best torque fuel requirements, minimum spark advance for best torque, and borderline knock characteristics indicated satisfactory combustion-chamber performance in comparison with our 283-cu-in. engine.

Combustion-chamber pressure cards were obtained and compared to our 283-cu-in. engine. Fig. 13 shows the comparative pressure cards; the indication was that combustion-chamber characteristics would be satisfactory. Mbt spark requirements as shown on Fig. 14 also were found to be acceptable.

Piston Durability — The next area of concern was durability of the gabled head piston design. Initial piston durability tests were not wholly satisfactory, but indicated potential for development. Subsequent modification, involving a slight increase in thickness of piston head and ring belt, gave us the needed strength and durability. These early durability tests also gave assurance that the mechanical structure of the cylinder head, block, and crankshaft would satisfactorily carry the imposed loadings. To verify further the conclusion that high

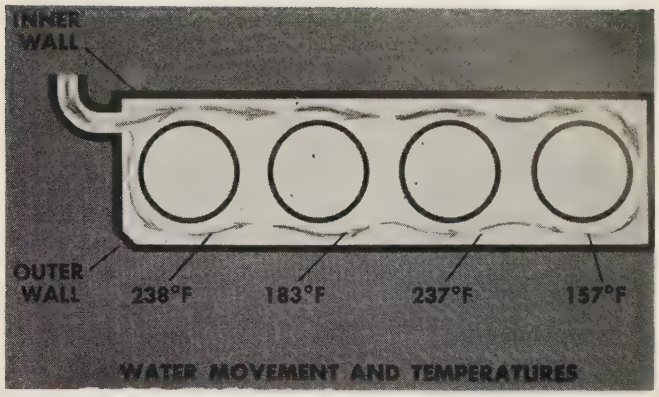

Fig. 11 — Cooling system of original "W" engine

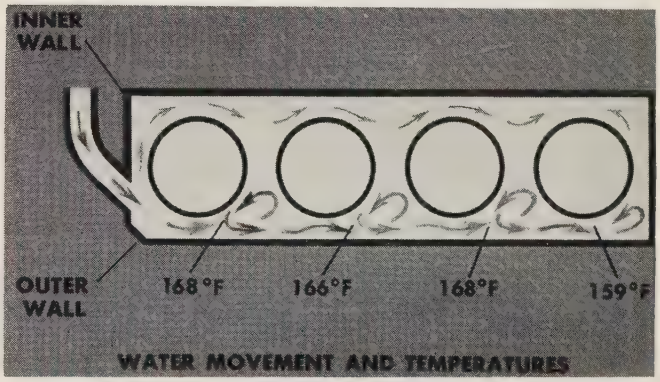

Fig. 12 — Cooling system of revised "W" engine

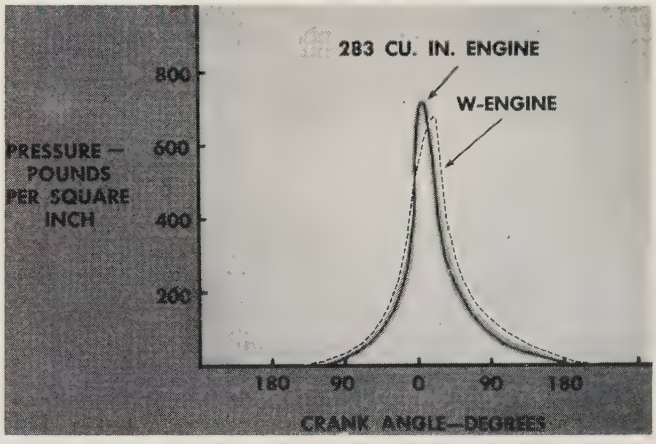

Fig. 13 — Cylinder pressures, 3000 rpm

piston head temperatures would not present a serious problem, actual piston temperature measurements were made. A comparison revealed that piston temperatures were higher in the "W" engine than in the 283-cu-in. engine. The difference, however, was not much more than might be expected with the greater heating to cooling area ratio inevitable from the larger piston diameter alone.

At this time it was felt that sufficient development work had been done to predict that the basic engine design would make a satisfactory product. This was also the point of no return insofar as the production tooling was concerned, as the basic production machinery was on order. If we made any major engineering changes after this, we would incur large cancellation charges and might find it impossible to meet production deadlines.

Most of the remaining development problems were solved by conventional techniques. However, certain aspects of the programs relating to valve train, camshaft selection, and crankcase ventilation system are worthy of discussion.

Valve Train — The valve train is similar to that used on the 283 engine with the exception that the rocker arm ratio has been increased from 1.50 to 1.75. This change reduces the effective inertia of the push rod and valve lifter, and also makes possible a substantial increase in cam nose radius with a resultant reduction in contact stresses. Modifications to valve springs, valve lifters, and valve train rigidity resulted in a final limiting speed of 5400 rpm. Limiting speed is defined as the speed beyond which the engine will not develop satisfactory power due to valve train malfunction.

A high limiting speed is very desirable to minimize the danger of valve-to-piston interference due to accidental engine overspeeding. The high limiting speed of the Chevrolet engine is a result of good lifter performance, the low weight and high rigidity of the stamped rocker arm construction, and the use of flat wire valve spring dampers. We first used the valve spring dampers in the 1956 models for the 265-cu-in. engine. Without dampers, the spring oscillations continue through the valve-closed portion of the valve train operating cycle, seriously affecting the dynamic characteristics of the valve train as well as the durability of the valve spring. With the dampers installed, the valve spring oscillations are quickly damped out, with a resulting improvement in valve train quietness and durability (Fig. 15).

Fairly late in the development program some difficulty was experienced with valve heads breaking off where the valve head joins the stem. It was suspected that the failures were caused by high dynamic seating loads resulting from excessive valve guide clearances or sporadic lifter leak-down.

A cylinder head was modified so as to include a strain gage load cell arranged to measure valve seating loads. This cylinder head was operated on a dummy setup and valve seating loads were measured with various tappet and valve guide clearances. Fig. 15 shows typical traces taken at 4500 rpm with normal production parts. The effect of valve seating and spring surge are clearly seen. No abnormal

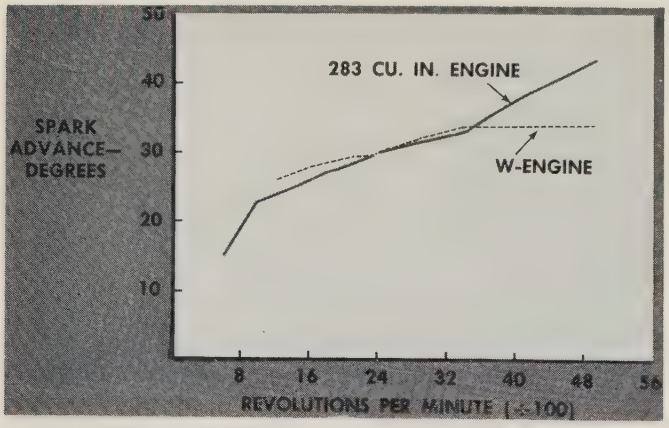

Fig. 14 — Spark requirement, minimum advance for best torque

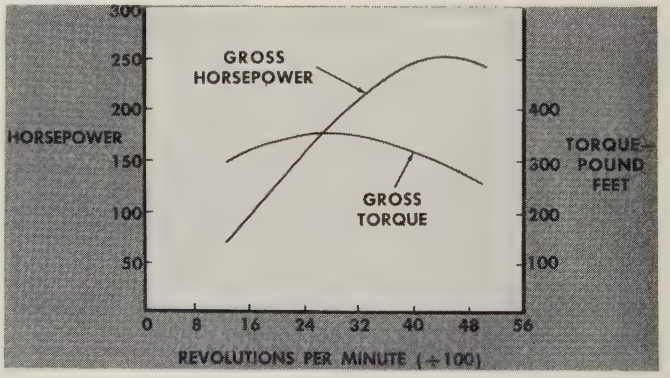

Fig. 16 — Engine characteristics of 348-cu-in. "W" engine with 4-barrel carburetor

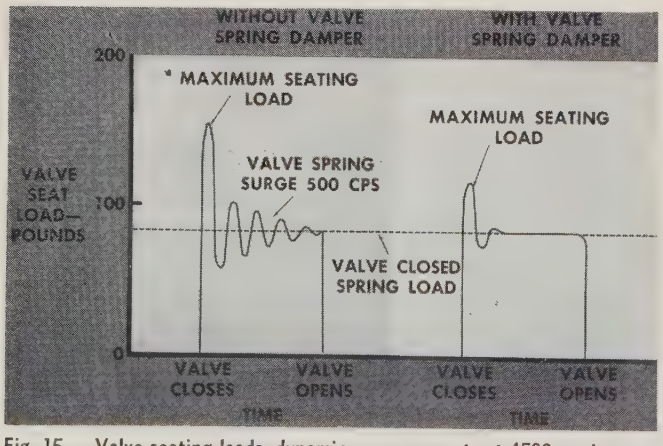

Fig. 15 — Valve seating loads, dynamic measurements at 4500 engine rpm

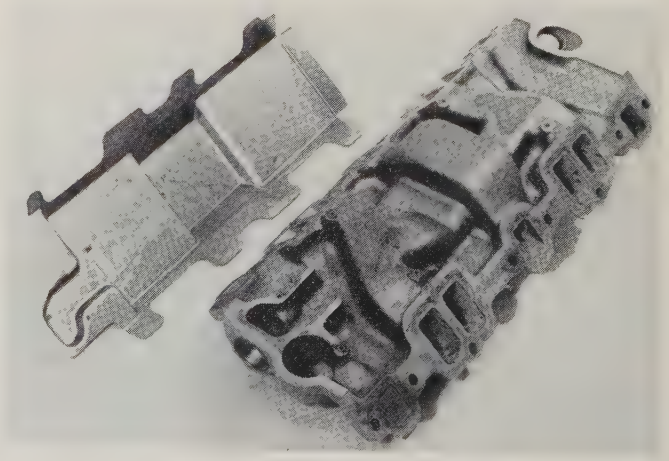

Fig. 17 — Cast rib and shield of manifold

loading was found with normal valve guide clearances. A combination of a badly worn guide and lifter leak-down was found to produce loads in the region of 2500 lb, approximately the hot strength of the valve. The valve guide wear problem was solved by careful attention to valve guide surface finish and valve stem lubrication. An additional factor of safety was obtained by a design modification to eliminate a stress raiser where the valve stem grind run-out blends with the underside of the valve head.

The final selection of the camshaft was based on a study of overall powerplant characteristics in combination with the Turboglide transmission. The speed range of 2400–3200 engine rpm was found to be vital in producing good low-speed and mid-range performance; therefore, an effort was made to provide ample torque in this speed range. The final powerplant performance accomplishes this objective as shown in Fig. 16.

Crankcase Ventilation — The original design crankcase ventilation was satisfactory, except that modifications had to be made in the oil separator. The oil separator was incorporated as part of the intake manifold assembly. It consists of integral cast ribs which serve as walls for air passages, plus an attached shield riveted to the underside of the manifold (Figs. 17 and 18). This simple design worked out well after two basic problems were solved: (1) entrance air velocity was too high for effective oil separation, corrected by deepening the rear section to provide more passage area; (2) drainage of the oil after separation. Effective drainage was achieved after we replaced the two original ¼-in. holes in the shield by two louvered slots extending the full width of the passages. With these changes, the oil separation characteristics had improved to the extent that air could be drawn through the separator at the rate of 10 cfm at 5000 engine rpm without oil pullover. This figure, when compared with normal engine blowby of approximately 2 cfm, gives a safety factor of 5.

Fuel Requirement — The distributor centrifugal advance curve is shown in Fig. 19. With this advance curve, loss from best torque is only 5% at 1200 rpm, 3% at 2400 rpm, and 2% at 3600 rpm. Fig. 19 also shows the fuel octane requirements of an engine with representative combustion-chamber deposits and cooling water temperature at 190 F. A gasoline with a Research octane number of 97 satisfies the engine's requirement throughout the usable speed range.

Durability Test Program

The extremely large volume of Chevrolet production makes it imperative that any product placed on the market be free from defects. Therefore, the durability testing of the engine was of paramount importance throughout the program. In the laboratory, two separate types of dynamometer durability tests were run. Valve train, pistons, crankshaft, and bearings were evaluated on a 4500-rpm full-throttle basis. Total engine test evaluations were made on a long-term cycling durability test.

By the time construction of pilot line engine had begun, more than 40 experimental engine assemblies had been put through tests of varying length and severity over a period of about 18 months. One of the engines built in the Chevrolet Engineering experimental shops had successfully completed a 200-

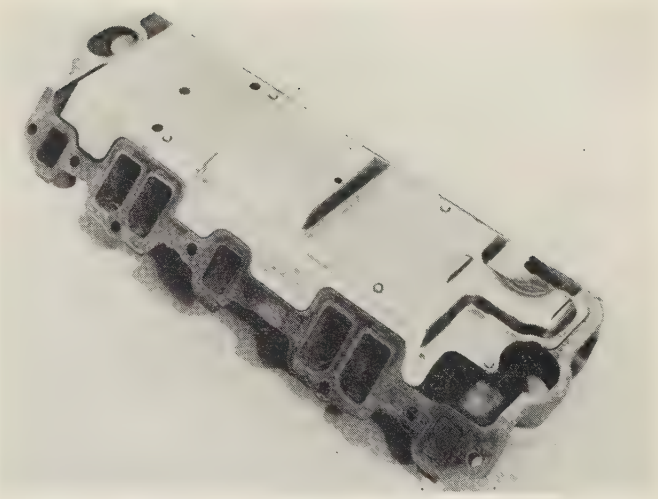

Fig. 18 — Shield riveted to underside of manifold

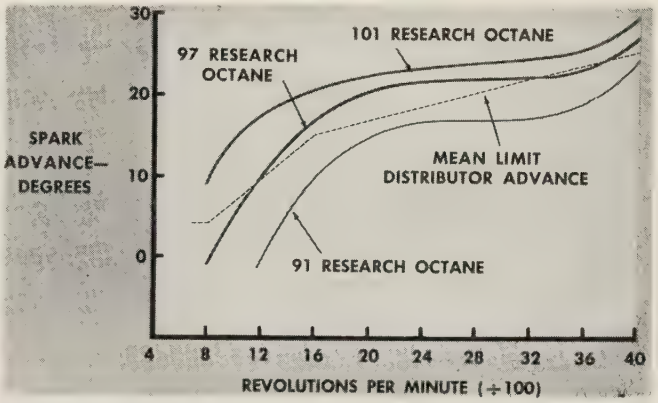

Fig. 19 — Fuel octane requirements of 348-cu-in. passenger-car "W" engine

hr wide-open throttle test at 4500 rpm — equivalent to 20,000 miles at 100 mph — as well as a 1000-hr cycling durability test.

The pilot line prototype engines were built by the Tonawanda engine plant, using production tools wherever possible. The purpose of the test program using the pilot line engines was to determine whether any durability problems might develop as a result of variations from experimentally built engines to production engines.

Tests were conducted independently by the Tonawanda engine plant and the Chevrolet Engineering Center. One result of this phase of the testing program was that minor changes were made in the cylinder head and block castings to correct for foundry core shift variations.

Durability testing of experimentally built and preproduction engines on the road was carried out both in General Motors Proving Ground passenger cars and trucks, and in fleet vehicles. Engines in commercial fleet vehicles underwent a wide variety of service conditions over almost 200,000 road miles. At the time it entered volume production, the new engine had a succesful durability test history equal to over a million vehicle miles of operation.

As a result of the advanced pilot engine test program and the manufacturing program at Tonawanda, we were able to supply this engine in the quantities required by our sales department for the start of the 1958 model year.

Customer acceptance of the new engine, which is

now known as the Turbo-Thrust V-8, has been excellent. Design, development, and timely release by production of the engine have been the outcome of cooperative effort by Chevrolet design, laboratory, and manufacturing groups.

ORAL DISCUSSION

Reported by Vincent Ayres
Eaton Manufacturing Co.

J. D. Turlay, Buick Division, General Motors Corp.: The new engines under discussion appear to be very well planned, sound designs, and I am sure they will prove to be excellent engines. The new Chrysler line is certainly more conventional than the hemispherical combustion-chamber models and does show the influence of other competitive engines. This is no reflection on the designers for the best products usually result from adoption of the best features of existing designs. We are all deeply involved in this game of comparing, refining, making improvements, and reducing cost, and we are all indebted to others for some of our design details. Also, once a general design is established, certain advantages and disadvantages inevitably accrue and in some cases desirable features cannot be adapted to a given design; for instance, we have not been able to work out a satisfactory stamped rocker arm for our engine.

Reference is made in both papers to the effect on design of the physical environment in which the engine is placed. We, too, have found that this is a most important factor, in fact in many cases chassis considerations seem to be more important than the ideal functioning of the engine components. The reduced height of the engines is very desirable in view of the styling trend toward lower and lower hood lines.

The weight saving of the new Chrysler engine is indeed worthy of comment. I agree that all materials cost something and that a reduction in weight usually results in overall manufacturing economy in addition to the many engineering advantages obtained. One feature influencing weight which was not mentioned is the necessity for designing for machine tool equipment. For example, we have had to increase the rigidity and weight of our crankcase considerably, not for durability reasons, but merely to withstand the rapid metal removal of the big broaches.

The Chrysler combined intake manifold gasket and push rod cover appears to be a very clever and inexpensive design. It is apparent that all the new "V" engines are adopting means of this sort to eliminate the necessity for dry sand cores in the push rod compartment of the cylinder block and thus make possible weight saving and foundry economies.

In all the new engines, the structural rigidity of the crankcase and crankshaft was evidently a major consideration, and they appear to be very adequate.

There are several features of the Chrysler engine of which I heartily approve since they were used in Buick straight eight and continued in the V-8, such as the series flow cooling system, the extended crankcase skirts, and the extended cylinder bores to shorten the water jackets. Evidently Chevrolet is not convinced of the value of series flow cooling or extended crankcase skirts as these features were not incorporated in their new engine.

The new Chrysler cylinder head design provides a minimum of water capacity and should reduce the heat rejection and yet provide high water velocity and excellent cooling with the series flow system. The exhaust ports are commendably short and the air jacketed exhaust crossover is a novel design.

Either there has been a complete reversal of opinion at Chrysler in regard to spark plug location or, as I think is more probable, the new location at the extreme edge of the chamber was a compromise which was found necessary in designing the remarkably compact and light new head. I would be interested in hearing the experiences of the Chrysler authors with this plug design as compared to their almost ideal centrally located and well-cooled plug in their hemispherical combustion chamber, especially in regard to fouling tendencies.

The new flat Chevrolet cylinder head would seem to provide manufacturing economies, as well as excellent breathing potential. I wonder how many recall that the Chevrolet "490" introduced in 1915 had a similar flat cylinder head with the combustion chamber in the upper cylinder bore. Of course, the 1915 version had a pancake-shaped combustion chamber with no squish area, as combustion-chamber development had not yet progressed very far.

The spark plug is more nearly centrally located in the Chevrolet than in the new Chrysler head, but like the Chrysler appears to be only partially water jacketed. It would seem that some difficulty might be encountered in keeping the combustion-chamber face flat and the valve seats square with their guides, because of the thermal and gas pressure effect on the large flat face of the Chevrolet chamber. Would the authors like to comment on their experience with these problems?

Apparently, the relative position of the spark plugs and exhaust manifolds has not been stabilized. In all the competing engines these two parts seem to be playing a game of leap frog; first one is on top and then the other. I note that in the new Chevrolet engine the plugs have moved from below the manifold to above, but in the Chrysler engine they have moved from above to below. They have also reversed positions on the new engines of another competitive line which is not at present under discussion. Undoubtedly, the plugs above the manifolds are easier to service, but with a full quota of engine accessories the engine is so completely covered that there is little advantage either way. Certainly by the time these engine accessories are removed to gain access to the plugs the exhaust manifolds should be cooled sufficiently to present no hazard to the mechanic.

A statement was made in the Chrysler paper as to the use of "desirable" flat top pistons. As one of the earliest users of bump-top pistons I feel we should rise to their defense. Pistons with contoured tops present no cost handicap as permanent mold top surfaces are satisfactorily smooth and accurate without machining, and compression heights can be held sufficiently accurately. We have found that with some piston dome shapes a considerable improvement in structural strength is achieved, permitting the use of a lighter head thickness and an actual saving in weight. The Chevrolet paper pointed out the manufacturing advantages of modifying the piston top instead of the cylinder head to obtain changes in compression ratio necessary with multiple model usage. Finally, piston bumps provide a very convenient method for changing the volume distribution of the combustion chamber and greatly increase the flexibility of the chamber design.

Both papers implied that provision had been made in the new designs for further displacement increases. Evidently, the displacement race is not over, despite all the statements to the contrary.

Mr. Moeller: Reference was made by Mr. Turlay of Chrysler having abandoned the hemispherical combustion-chamber design engine for one more conventional. This change is certainly admitted, but perhaps an additional comment is desirable. There is no change in the thinking that for maximum high-speed volumetric efficiency and power output, the larger valves and unrestricted port shapes in the hemispherical engine are ideal. However, the weight savings and general simplification possible with a line valve type of cylinder head made it attractive for consideration in the new engine. After development of the valve and port details of the new engine, it was found that engine output losses, as compared to the hemispherical engine, were negligible except for a small percentage difference at high speed in the range of 4000 rpm.

In regard to the spark-plug position in the new engine, it has been very satisfactory with no greater tendency towards fouling or overheating than any other engine we

have tested. The generally favorable characteristics of the series flow cooling system undoubtedly contributed to these desirable results. The flat top configuration of the piston reduced the heat input, which is desirable.

Mr. Rausch: The tendency of a flat-bottom cylinder head is to show most trouble with gaskets. The use of six bolts per cylinder successfully eliminates leakage of gas. There also is no excessive bore or cylinder head distortion.

The design of crankcase split at the crank centerline is used to reduce overall cost of manufacture. Its strength is adequate with the bulkhead as designed.

The metered-type water system is adequate based on past performance. Piston temperatures were not compared with those of other types of piston design, nor was it felt necessary since durability was satisfactory.

Spark-plug temperatures were checked as satisfactory and no problems arose as a function of new plug location. The problem of plug durability is best resolved by issuing bulletins recommending plug types to be used in the field for the type of service involved.

P. M. Clayton, Ford Motor Co.: The advantage to Chevrolet of using their valve location is probably related to their ability to machine the bores. The new combustion chamber used by Chevrolet appears to be satisfactory but Ford still prefer the in-line valve arrangement and see no disadvantages in it.

The engine compartment seems to be full regardless of make, which complicates service and is a challenge to the designer. Chevrolet engineers are to be congratulated on the excellent high-speed valve gear dynamics demonstrated in their motion photography. The use of high-speed photography to study this phenomena appears well-recommended.

The continued use of metal valve stem seals by Chevrolet might be questioned inasmuch as it seems like this could be improved by synthetic materials.

Ventilation of engines is usually last in any new design evaluation and, therefore, becomes a compromise.

In regard to fuel economy, the large displacement engines have an advantage when compared to smaller engines because of lower friction at their lower operating rpm assuming that proper axle ratios are used.

Mr. Rausch: The valve position adopted by Chevrolet was used to obtain necessary quench area in combustion chamber. The subject of valve stem seals is always under investigation for possible improvement. The design we are using is best for our conditions. I agree that ventilation is always a problem, one eventually resolved in a compromise.

Mr. Moeller: Large engines operating with low numerical axle ratios have a lower noise level than smaller engines running at higher speeds. However, our experience indicates that there is a limit where the combined effects of lower friction and poorer thermal efficiency of the slow speed engine have a detrimental effect on fuel economy. This result is particularly emphasized when automatic transmission torque converter slip is taken into consideration. Consequently, an engine size should only be large enough to obtain adequate car performance with an axle ratio which allows a satisfactory engine noise level.

W. D. Innes, Ford Motor Co.: The 1958 V-8 Chrysler engine has many new and novel features. It is interesting to compare this engine with its predecessor which, if memory serves me correctly, was introduced in the year of 1951. This new engine is relatively the same size engine in cubic-inch displacement as the 1951 engine; however, package-wise, it has changed considerably. The 1951 engine was essentially a square bore and stroke engine; this engine follows the modern trend of short-stroke design.

A major benefit of a short-stroke engine compared to an engine of similar cubic-inch displacement but with a square bore and stroke relationship is the increased efficiency of the engine itself. This generally will be indicated in increased usable power and should result in an improvement in fuel economy, provided the engines are placed in identical circumstances. No data has been presented on this comparison today; however, it would have been a very interesting comparison in basic engine design.

The novel features of this new Chrysler engine are: (1) cylinder head — reduced water jacketing, (2) new carburetors, (3) one-piece intake manifold gasket and valve chamber cover, (4) stamped rocker arm mounted on a rocker arm shaft, (5) cylinder block — rigid deep skirt design, and (6) throwaway-type oil filter.

The cylinder head design is unique in regard to the amount of water jacketing it has. This V-8 engine has approximately 6 qt less coolant than the conventional V-8's; however, in some areas of the cylinder head this reduction might be harmful. In looking at the design of the cylinder head in the intake port area, it is possible that water jacketing could be helpful in maintaining proper mixture temperatures particularly in the cold weather operation. The small water jacket section in the cylinder head would seem to create a foundry problem, handling water jacket cores with reduced sections—however, not knowing the casting procedure of this engine, it is difficult to tell. Another novel feature of this cylinder head is the air space around the exhaust crossover port. This certainly looks like an advantage in keeping heat out of the cylinder head proper.

Another feature of the new Chrysler engine is the cylinder block with its rigid deep skirt design. Our experience with this type of construction parallels the benefits mentioned in the paper.

The induction system of this new engine is more-or-less conventional with the exception of the carburetor and automatic choke combination. However, I did notice the bottom of the intake manifold risers has been squared-off now in comparison to rounded corners present in the 1957 engines. This, I feel, is an aid to better distribution with the heights of risers we now have to live with in these lower package heights.

The new carburetors used on this Chrysler engine have certainly been reduced in height. This new trend in carburetion opens entirely new concepts in the induction design field. I noticed in the paper that the dual carburetor has a mechanically operated bowl vent which is open only at idle and is closed at normal operating condition, making the carburetor fully balanced. This would certainly eliminate any air cleaner buildup or restriction from enrichening the fuel flow under operating conditions. However, in the 4-barrel carburetor a combination of internal and external vents are used, making an unbalanced carburetor, which could affect fuel flow under increased air cleaner restriction. In our experience with a similar type of air cleaner, restriction under normal driving conditions buildup is so slow that after 20,000 miles the increase is only 0.5–1.0 in. of water; therefore, I do not believe this is a serious problem.

The new econo-choke which we have heard so much about is certainly a novel arrangement. The two-staged vacuum piston mounted in the air horn is definitely a new feature. The basic premise of reducing the choke enrichment under operating road load conditions is excellent. The only difficulty would seem to be a possible hysteresis when operating under road load conditions and then suddenly going to wide-open throttle which could possibly cause a leaning out condition. This hysteresis is not the choke plate closing but is the metering system itself recognizing this change in plate closing. In regard to conventional chokes coming off fast under slow driving conditions and slow under fast driving conditions, it might be pointed out that the difference in manifold vacuum running road load at say 20 and 50 mph is 3 in. of Hg and the variance in total airflow over the choke bimetal spring is only 0.3 of a cfm. However, the amount of heat available to pass over the bimetal spring is determined by the road load condition at which the vehicle is being run. The heat available is generally the same for any type of choke arrangement excluding the possible losses in tubes to heat boxes and the like. The Chrysler setup, however, with its heated mass which will keep the choke off under warm engine conditions proves very beneficial.

a new look at High Compression Engines

D. F. Caris and E. E. Nelson, General Motors Corp.

This paper was presented at the SAE Summer Meeting, Atlantic City, June 11, 1958.

FOR over 75 years, engineers have realized that a fundamental method of improving the efficiency of the internal-combustion engine is to raise the compression ratio.[1] A fact that has become equally well-known is that an increase in compression ratio causes the knocking tendency to increase. Thus, from the early stages of development of the gasoline engine, higher compression ratios have by necessity been closely related to improvements made by the petroleum industry in fuel octane quality.

The development of Ethyl gasoline in 1923 provided a fuel that permitted substantial increases in compression ratio. The subsequent trend of increasing fuel antiknock value and compression ratio has recently been reported by J. M. Campbell.[2] The relatively rapid increase in the compression ratio of automotive engines in recent years gave rise to considerable speculation as to how far this trend may go. From basic thermodynamic considerations, it was known that thermal effciency is a function of compression ratio and that the magnitude of the gain becomes progressively less as compression ratio continues to increase. Thus, it became increasingly important to establish quantitative relationships between efficiency and compression ratio over a much wider range than previously has been possible.

The results of the work of C. F. Kettering and his associates in this area were presented before the SAE in 1947.[3] This paper presented data from tests on single-cylinder engines with compression ratios from 6/1 to 15/1 and on two 6-cyl engines with compression ratios of 6/1 and 12.5/1. From results of these tests, it was shown that very substantial gains could be obtained in thermal efficiency when the engine structure had sufficient rigidity to withstand the higher loads encountered.

Mr. Kettering's work foreshadowed the commercial development of present-day high-compression V-8 engines. Later studies, reported by C. L. McCuen[4], showed the relationship between thermal efficiency and compression ratio for multicylinder V-8 engines with compression ratios of 8/1, 10/1, and 12/1.

The results of these studies along with the increase in octane rating of commercial gasoline have resulted in increases in the compression ratio of production engines to the point where once again it is desirable to determine the effect that further increases will have on thermal efficiency. Therefore, the objective of the work presented in this paper was to study this relationship on engines with compression ratios from 9/1 to 25/1.

Although the original objective was to investigate part-load operation, the successful use of the manganese antiknock compound developed by the Ethyl Corp.[5] permitted full-throttle tests to be conducted on engines with compression ratios as high as 20/1. These full-throttle tests, along with pressure-time data taken at part throttle, helped to explain the difference between observed and theoretical relationships.

Procedure and Equipment

Test Engines

The seven engines used for this investigation were basically production V-8 engines with a displace-

[1] Institutions of Civil Engineering—Proceedings, Vol. 64, 1882, pp. 220–250; "Theory of Gas Engine," by Duglad Clerk.
[2] SAE SP 216, 1957: "Looking Ahead in Fuels for Automotive Transportation," by J. M. Campbell.
[3] SAE *Quarterly* Transactions, Vol. 1, October, 1947, pp. 669–679: "More Efficient Utilization of Fuels," by C. F. Kettering.
[4] Proceedings of American Petroleum Institute, Vol. 31, 1951, Sec. 3, p. 198: "1900 to 19xx—A Report on Automobile Engine Progress," by C. L. McCuen.
[5] "New Manganese Antiknock," by J. E. Brown and W. G. Lovell. Paper presented before Division of Petroleum Chemistry, American Chemical Society, San Francisco, April, 1958.

ment of 324 cu in. The main modifications consisted of changes in the combustion chambers and main bearing caps. The combustion chambers were formed by the use of pot pistons and flat cylinder heads similar to those shown in Fig. 1. The change in compression ratio was accomplished by varying only the depth of the pot; thus, the quench area, the quench thickness, and the position of the pot remained constant for each engine. The quench area is defined as the area of the flat portion of the piston, while the quench thickness is defined as the distance between the flat portion of the piston and the cylinder head. A quench thickness of approximately 0.060 in. was used in each of the test engines.

Since it was realized at the outset of this project that the loads on the crankshaft would be considerably higher than those for which the production engine was designed, it was decided that as a safety precaution, the main bearing caps should be reinforced. This was accomplished by removing the normal rounded portion on the bottom of the cap and adding a steel bar (Fig. 2).

Standard Tests

Preliminary Work — Test engines were first given a normal dynamometer break-in. The deposits were then removed from the combustion chambers and the valves were reconditioned to the extent necessary. The compression ratio was determined by the use of a Helmholtz resonator. Before fuel economy tests were made, compression pressures were taken. Normal compression gages were used on engines with compression ratios from 9/1 to 17/1. However, failure of the check valves in this equipment at higher compression ratios made it necessary to use a balanced diaphragm indicator for measuring the compression pressures of the 20/1 and 25/1 engines.

Part-Throttle Tests — Part-throttle economy data were obtained by running fuel fish hooks at fixed manifold depressions. The air/fuel ratio was varied in steps from ½ to 1 ratio, from over rich to very lean mixtures with the spark adjusted to mbt (minimum advance for best torque) for each adjustment of the air/fuel ratio. The minimum brake specific fuel consumption (bsfc) curves were obtained at each of the test speeds by drawing a curve tangent to the fuel fish hooks (Fig. 3).

The bsfc curves as shown in Fig. 3 were plotted on logarithmic graph paper to reduce the slope of the curves and hence improve the accuracy of plotting and reading. Establishment of these optimum fuel economy curves for each test engine permitted fuel consumption and thermal efficiency relationships to be studied at any desired load in the part-throttle region. The fuel used for these and other part-throttle tests was isooctane plus 3 ml of tel per gal. Engine speeds of 1200, 2000, and 2800 rpm were used, since they are about equivalent to car speeds of 30, 50, and 70 mph. Also, these speeds were chosen to provide data on how the parameter of engine speed affects the relationship between compression ratio and economy.

Full-Throttle Tests — Full-throttle power and economy tests were conducted at 2000 rpm. The power and economy data were taken from fuel fish hooks similar to those described above. The fuel used for all full-throttle tests was isooctane plus enough antiknock additives to permit the spark to

THE automotive and petroleum industries have been concerned for many years with the mutual problem of improving the thermal efficiency of gasoline engines. Great progress in refining technology, as well as advances in engine design in recent years, have made it desirable to take a new look at high-compression engines.

This paper describes an investigation of the effect of compression ratio on engine efficiency over a range of compression ratios from 9/1 to 25/1. The results show that the thermal efficiency of the multicylinder engines used in this study peaked at a compression ratio of 17/1. The decrease in thermal efficiency at higher compression ratios is due primarily to delay in the completion of the combustion process.

This paper received the 1958 Horning Memorial Award.

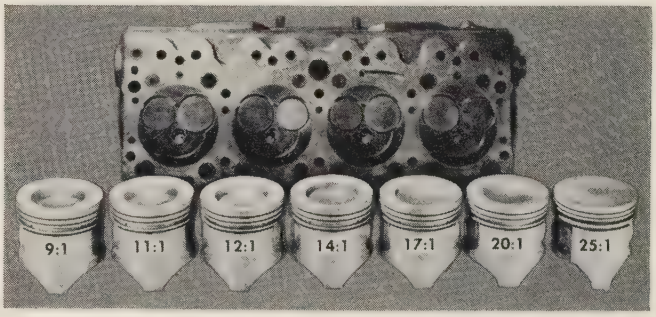

Fig. 1 — Experimental cylinder head and pistons

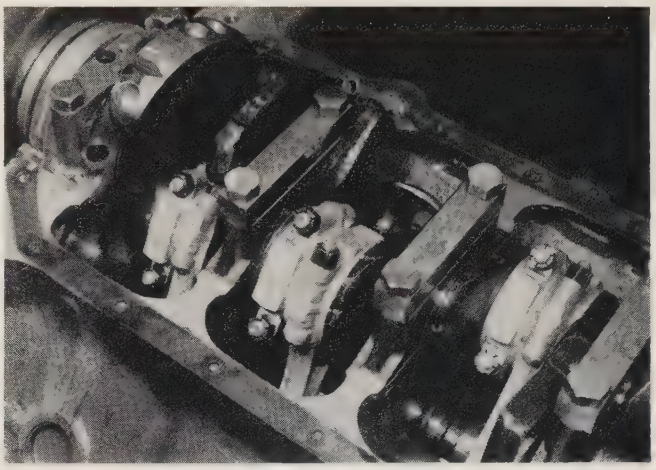

Fig. 2 — Reinforced main bearing caps

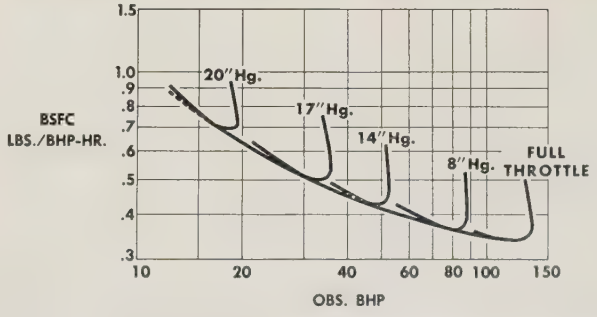

Fig. 3 — Minimum brake specific fuel consumption at 2000 rpm and 17/1 compression ratio

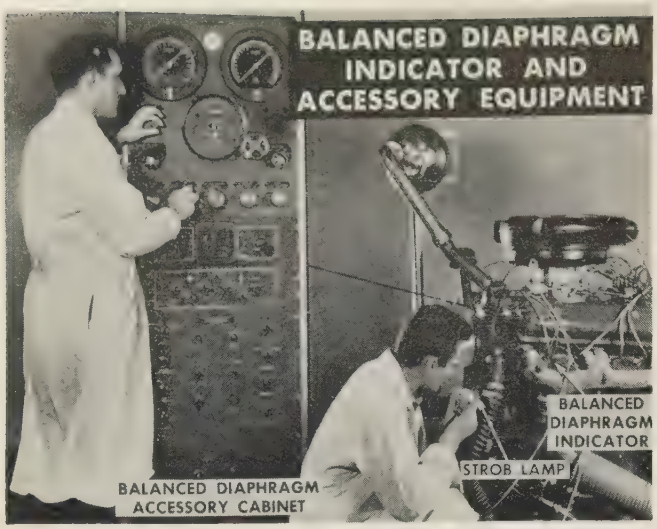

Fig. 4 — Balanced diaphragm indicator and accessory equipment

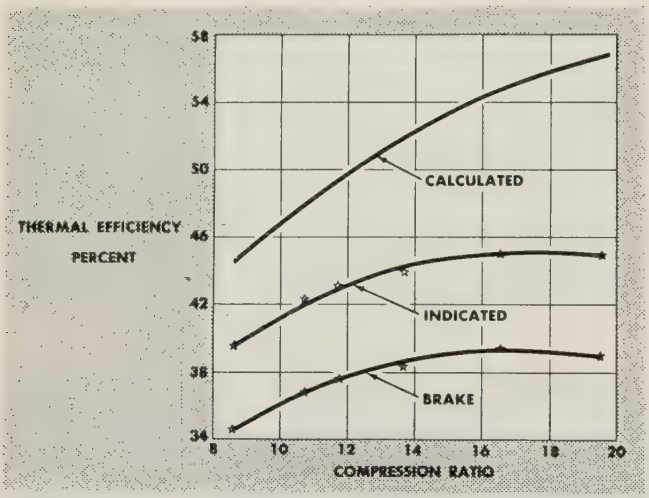

Fig. 5 — Full-throttle thermal efficiency at maximum economy settings and 2000 rpm

be adjusted to mbt without knock. The antiknock additives used were tel and the new manganese compound (AK-33X) developed by the Ethyl Corp.[5] These additives were used in concentrations as high as 6 ml tel plus 6 grams of AK-33X per gal of isooctane.

Other dynamometer tests such as normal power runs, volumetric efficiency, and heat rejection tests were run in accordance with the procedure set forth in the General Motors' Engine Test Code.[6]

Special Tests

Engine Indicator Tests — Extensive use was made of a balanced diaphragm indicator to study various thermodynamic and combustion characteristics. The balanced diaphragm indicator used was developed by General Motors Research Staff.[7] Fig. 4 shows this indicator installed in an engine and the associated accessory equipment.

The *p-t* (pressure-time) and *p-v* (pressure-volume) data presented in this report were obtained at part-load conditions at an engine speed of 2000 rpm. The air/fuel ratio and the spark advance were adjusted to give maximum economy.

Sound Recordings — Sound recordings were made with a magnetic tape recorder to provide a basis for comparison of the noise level and frequency over the range of compression ratios tested. Recordings were made at full load under both knocking and non-knocking conditions.

Processing Test Data

A digital computer was used to process a large portion of the test data. The normal data from power, volumetric efficiency, and heat rejection tests were put on "mark sense" computer cards by the dynamometer operator and processed by a program previously established to handle data from these tests.

A new computer program was established to process *p-t* data. This program was set up to convert *p-t* data to *p-v* data and to give the values of the work represented by the various loops of the *p-v* diagram.

Discussion of Results

Full-Throttle Thermal Efficiency and Power

Thermal Efficiency — The relationship between thermal efficiency and compression ratio of the test engines at full throttle was determined at 2000 rpm with the air/fuel ratio adjusted for maximum economy and also for maximum power. Thermal efficiency was calculated from specific fuel consumption data on the basis of the lower heating value of isooctane (19,065 btu/lb)[8]. The observed data shown in Fig. 5 represent the maximum thermal efficiency that could be obtained when both air/fuel ratio and spark advance were adjusted for maximum economy. Because of the high octane requirement, the 20/1 compression ratio engine was the highest that could be run under these conditions. The calculated thermal efficiency curve is included in Fig. 5 for comparison. It will be noted that the brake thermal efficiency curve reached a maximum at a compression ratio of about 17/1 and fell off at the higher ratios. The difference between calculated and observed efficiency values increased quite rapidly as compression ratio approached 17/1.

The maximum thermal efficiency at 17/1 compression ratio as shown in Fig. 5 was 39.3% which substantiates the statement by Kettering[3] in 1947:

> "At the present time, diesel engines are operating with a range of compression ratios between 14 and 17/1, and with brake thermal efficiencies as high as 38%. If equivalent compression ratios can be used in spark ignition engines, the same full-throttle brake thermal efficiencies should be obtained."

The indicated thermal efficiency values at full throttle were obtained from bhp data and from friction data as determined by the motoring method. It is interesting to note that indicated thermal efficiency values of 44.5% were observed on both the 17/1 and 20/1 test engines and that the indicated thermal efficiency peaked at a compression ratio of about 18/1.

The data on calculated thermal efficiency were

[6] "General Motors Corp. Automotive Engine Test Code," Fourth Edition. General Motors Corp., Detroit, 1953.

[7] ISA *Journal*, Vol. 2, September, 1955, pp. 348–351: "Recent Developments in Balanced-Diaphragm Pressure Transducers," by L. R. Voss, L. E. Baker, E. F. Weller, and G. M. Rassweiler.

[8] P. 90 of "Fuels and Combustion," by M. L. Smith and K. W. Stinson. First Edition. Pub. by McGraw-Hill Book Co., Inc., New York, 1952.

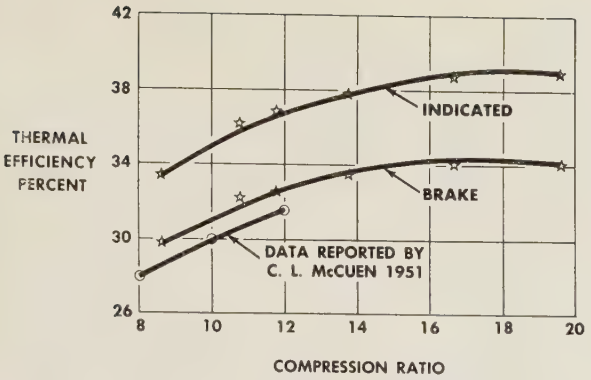

Fig. 6 — Full-throttle thermal efficiency at maximum power settings and 2000 rpm

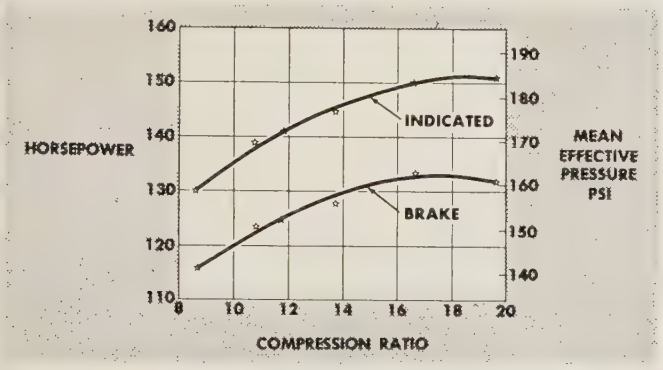

Fig. 7 — Corrected power and mep at full throttle and 2000 rpm

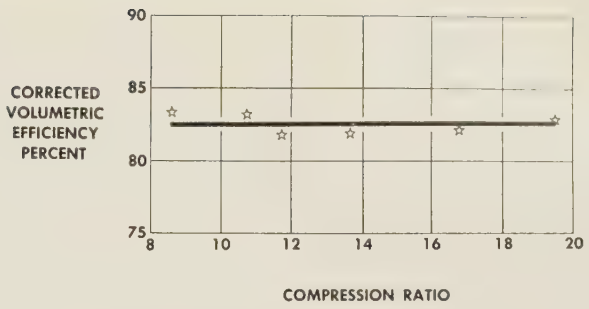

Fig. 8 — Volumetric efficiency at full throttle and 2000 rpm

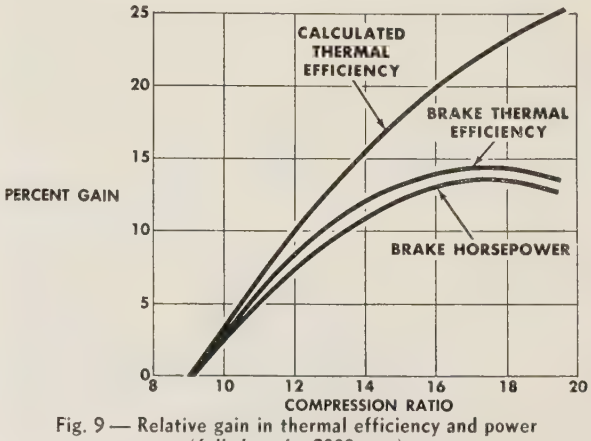

Fig. 9 — Relative gain in thermal efficiency and power (full throttle, 2000 rpm)

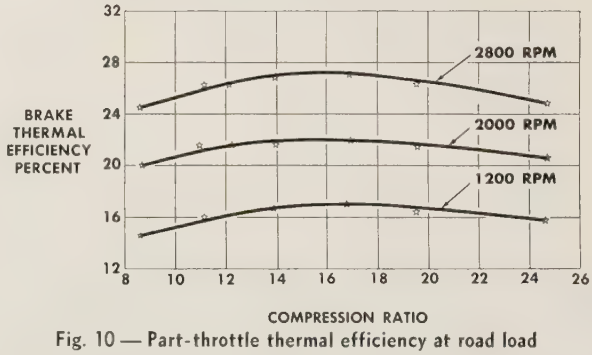

Fig. 10 — Part-throttle thermal efficiency at road load

computed from the thermodynamic charts prepared by Hershey, Eberhardt, and Hottel.[9] Thermodynamic charts for air/fuel mixtures with 110% of theoretical air were used for these calculations. The difference between the calculated and indicated efficiency represents losses due to valve timing, nonconstant volume combustion, and direct heat losses.

The thermal efficiency data that were obtained with the air/fuel ratio and ignition timing adjusted for maximum brake power are shown in Fig. 6. The brake and indicated thermal efficiency data shown in this figure followed the same general relationship that was established by the maximum thermal efficiency data shown in Fig. 5. Also included in Fig. 6 are thermal efficiency data reported by McCuen[4] at compression ratios of 8/1, 10/1, and 12/1. In general, there is good correlation with present data included in this chart.

Power — The relationship between full-throttle power and compression ratio at 2000 rpm is shown in Fig. 7. This relationship follows the same general trend that was observed between thermal efficiency and compression ratio. The data shown in this figure were obtained by operating the test engines with the air/fuel ratio and the spark advance adjusted to give maximum power. Ihp data were obtained using the motoring friction method.

Volumetric efficiency of the test engines as shown in Fig. 8 was essentially independent of compression ratio. Thus, volumetric efficiency was not a factor in the decreasing power observed in the higher compression ratio engines.

Air/Fuel Ratios — The data obtained during full-throttle power and economy tests at 2000 rpm indicate that the air/fuel ratio which gave maximum power was about 12.7/1 and the air/fuel ratio that gave maximum thermal efficiency was approximately 16.5/1. The power developed with the air/fuel ratio adjusted for best economy was about 88% of maximum power. Values of these optimum air/fuel ratios were not appreciably affected by changes in compression ratio.

Comparison of Relative Power and Economy Gains — The relative gain in full-throttle brake power and efficiency with a compression ratio of 9/1 as the base is shown in Fig. 9. The per cent gain in bhp and in thermal efficiency peaked at a compression ratio of 17/1 and then decreased at higher ratios.

Part-Throttle Thermal Efficiency

Brake Thermal Efficiency — The relationship between brake thermal efficiency and compression ratio of the test engines at part throttle is shown in Fig. 10. The engine load used at each of the engine

[9] SAE *Journal*, Vol. 39, October, 1936, pp. 409–424: "Thermodynamic Properties of Working Fluid in Internal Combustion Engines," by R. L. Hershey, J. E. Eberhardt, and H. C. Hottel.

speeds shown for this comparison was the calculated power that the engine would have to develop to propel a 1956 Oldsmobile over a level road. These engine "road load" requirements were determined by using an assumed drive line efficiency of 80% at each speed. The curves in this figure indicate that the compression ratio which gave maximum brake thermal efficiency under constant power output conditions was about 16/1.

The road load data shown in Fig. 10 can be used to predict the gain in economy that would be obtained if these engines were installed in identical cars and operated at constant speeds. However, in addition to the gain in economy, the cars with higher compression ratio engines would also have an increase in performance. Thus, if all of the potential advantages of the high-compression engines were to be taken in the form of an increase in mpg, the engine displacement and/or the axle ratio would have to be changed to keep performance constant.

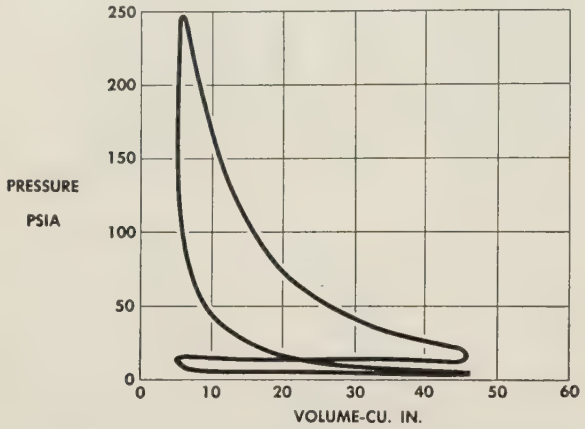

Fig. 11 — Typical pressure-volume diagram (17 in. of Hg, 2000 rpm, 8.7/1 compression ratio)

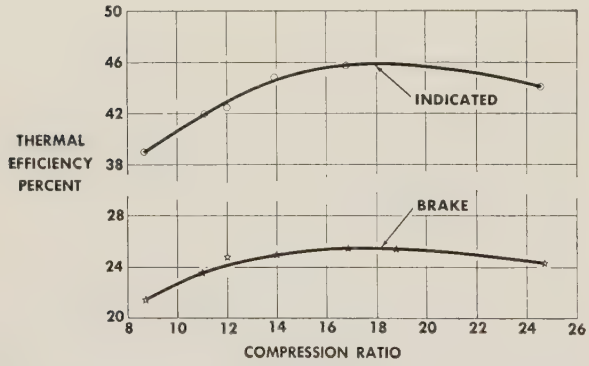

Fig. 12 — Part-throttle thermal efficiency (17 in. of Hg, 2000 rpm)

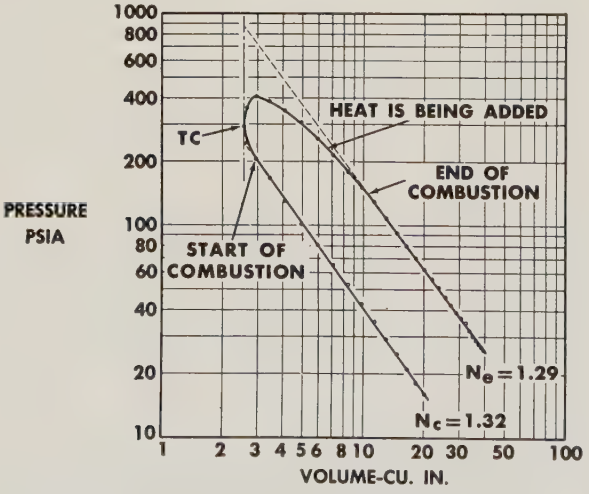

Fig. 13 — Typical logarithmic pressure-volume diagram (17 in. of Hg, 2000 rpm, 16.8/1 compression ratio)

Engine Indicator Data — The fact that the brake efficiency decreased after the compression ratio was increased above 16/1 or 17/1 requires an explanation. One of the first suppositions offered to explain this phenomenon was the possibility that engine friction increased in such a way as to nullify the expected gain. In addition to friction, changes in combustion and thermodynamic characteristics were also suggested as possible causes for the decrease in thermal efficiency. Extensive use was made of engine indicators at part-throttle conditions to determine how these factors were affected by changes in compression ratio.

Because of the amount of time required to run tests of this nature only one representative speed, 2000 rpm, was used. The cylinder pressure was measured in psi and time was measured in terms of crank-angle degrees. These data were then converted to a pressure-volume basis using a digital computer. Fig. 11 is a plot of a typical p-v relationship. In most cases complete p-v charts were not required since the computer was programmed to present indicated power data directly.

Indicated Thermal Efficiency — In regard to the absolute value of indicated thermal efficiency, it should be stated that the indicated power for this comparison was determined by measuring the indicated power (the upper loop of the p-v diagram) produced in cylinder No. 1 of each engine. Although it is agreed that this power for one cylinder multiplied by eight might not give the exact value of total indicated power of the engine, it is felt that the conditions of these tests were such as to produce valid trends. These tests were run with the same intake manifold and the same variable air/fuel ratio carburetor on each engine so that the proportion of air and fuel delivered to cylinder No. 1 at a constant manifold depression would be comparable from engine to engine.

Fig. 12 shows the relationship between indicated and brake thermal efficiency and compression ratio as calculated from data taken during p-t tests at a manifold depression of 17 in. of Hg. The air/fuel ratio and ignition timing were adjusted to give maximum economy. It is interesting to note that the indicated thermal efficiency curve peaked at a compression ratio of about 18/1 and then dropped off as the compression ratio was increased to 25/1. This indicated that friction was not the main factor which caused the reduction in the thermal efficiency of the higher compression ratio engines.

Combustion and Thermodynamic Characteristics

Pressure-Volume Relationships — In general, compression and expansion processes can be described by the expression $pv^n = c$, where p is absolute pressure, v is volume, n is the observed or apparent exponent, and c is a constant. With this relationship the compression and expansion processes can be represented

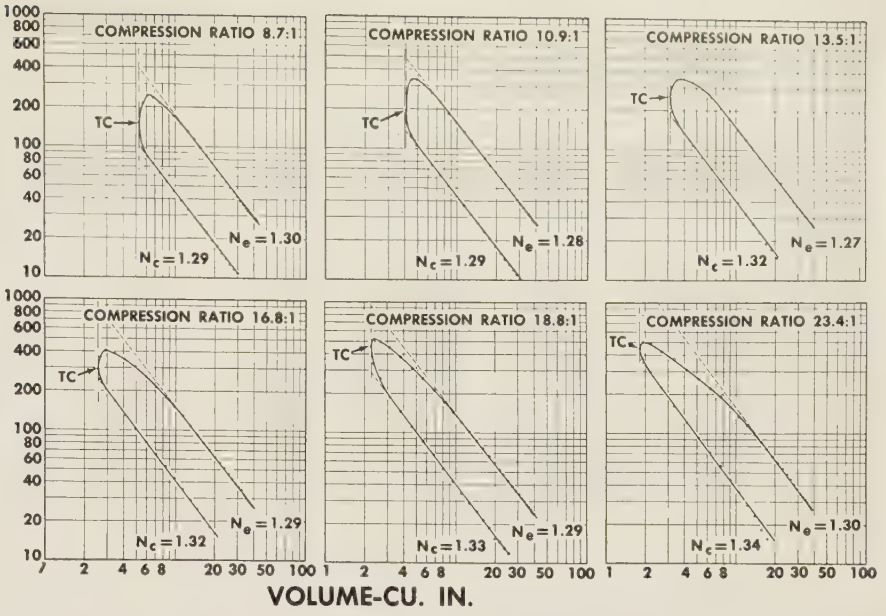

Fig. 14 — Comparison of logarithmic pressure-volume diagrams (17 in. of Hg, 2000 rpm)

by straight lines on a log p-log v plot. The logarithmic plot of p-v data provides an excellent opportunity to study both the value of the exponent n and the combustion portion of an actual engine cycle.

Fig. 13 shows a typical logarithmic p-v plot of the compression, combustion, and expansion portions of the engine cycle. The value of the exponent n for the compression and expansion portions of the cycle is determined by the slope of the respective straight lines.

Fig. 14 shows part-throttle logarithmic p-v plots of these compression, combustion, and expansion portions of engine cycles at different compression ratios. It should be remembered when viewing these diagrams that in each case the ignition timing and the air fuel ratio were adjusted for maximum economy. The main points of interest here are: (1) the values of the compression and expansion exponents n_c and n_e, (2) the time required for the combustion process, and (3) the pressure rise in the top center region.

Compression and Expansion Exponent — Fig. 15 is a plot of the compression and expansion exponents as determined from logarithmic p-v plots at different conditions of compression ratio and load. This figure shows that the exponent remained constant for the expansion process and increased for the compression process as compression ratio increased. A study of these data along with some p-v data that were taken at full throttle on the lower compression ratio engines, indicated that the value of n was essentially independent of load.

Late Burn Phenomena — Indicated thermal efficiency under firing conditions (Fig. 12) showed that the reduction in thermal efficiency at the higher compression ratios was not caused primarily by increased friction. Also, studies of the exponent n (Fig. 15) showed no important change with compression ratio. Therefore, in order to obtain data on other factors which were contributing to the reduction in thermal efficiency at the higher compression ratios, further study of the combustion portion of the engine cycle was necessary.

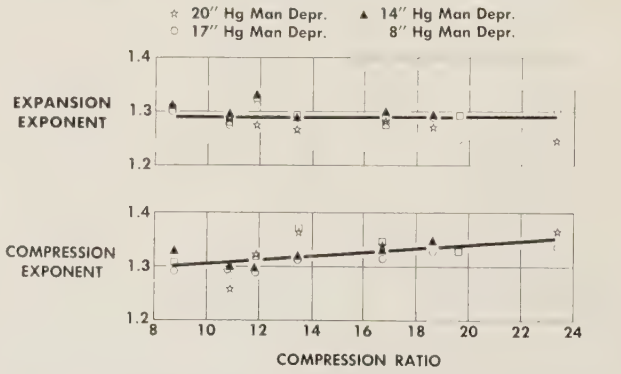

Fig. 15 — Compression and expansion exponents at 2000 rpm

Part-Throttle Evidence of Late Burning:

In addition to the exponent n, the logarithmic plot of p-v data provides an excellent opportunity for studying the combustion portion of an actual engine cycle. If the compression and expansion lines on a logarithmic p-v plot are extrapolated to the volume at top center and then connected by a constant volume line, the resulting diagram will represent the upper portion of what can be considered an "ideal engine" cycle.

Before the length of time required for the combustion process is studied, it is necessary to define the terms "start of combustion" and "end of combustion." The expression "start of combustion" refers to the time in the cycle when combustion of the charge has progressed enough to cause the pressure to rise over and above that due to normal compression. The expression "end of combustion" is used to define the point in the engine cycle where the heat released by the combustion process ceases to have an appreciable effect upon the slope or exponent of the expansion process.

Fig. 16 shows a plot of combustion data along with the time of peak pressure as determined from part throttle p-t and p-v plots. The time of peak pressure is shown to occur closer to tdc as compression ratio increases. This fact, along with the observation from Fig. 14 that the pressure rise in the top

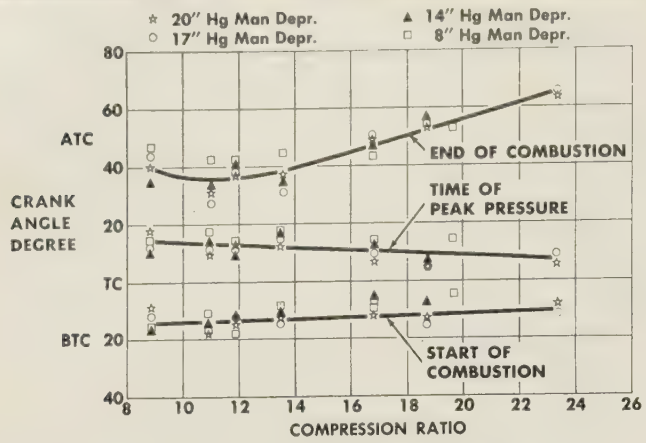

Fig. 16 — Combustion characteristics at 2000 rpm

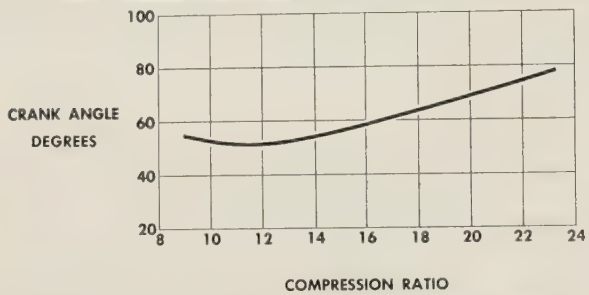

Fig. 17 — Time for complete combustion (part-throttle, 2000 rpm)

center region was less than might be expected for the high-compression engines, leads to the conclusion that the per cent of the charge that burns in the top center region decreases as compression ratio increases. This decrease is influenced by the mass distribution of the charge.

The time required for complete combustion, as determined by computing the difference in the crank-angle degrees between the start and end of combustion, is shown in Fig. 17. The combustion time shown in this figure is not significantly affected by load.

These observations on late burning are of considerable value in helping to explain why the higher compression engines tested did not give the high thermal efficiencies expected. When ideal cycles are analyzed, it is assumed that the heat energy is added at constant volume with the piston at tdc. If the heat is added either before or after tdc in the ideal cycle, the net result is that the effective compression ratio (or expansion ratio) is less than the conventionally defined compression ratio. In the engines tested the tendency toward nonconstant volume combustion increased as compression ratio increased, and the gain in thermal efficiency was less than predicted on the basis of the conventionally defined compression ratio. L. C. Lichty[10] summarizes a similar discussion as follows:

> "In all cases, it is the liberation of chemical energy at a condition which permits the largest possible expansion of the medium thereafter which results in the highest efficiency."

Although quantitative data are not available at this time, it is felt that the late burn tendency observed during this investigation was the major factor that caused the reduction in thermal efficiency

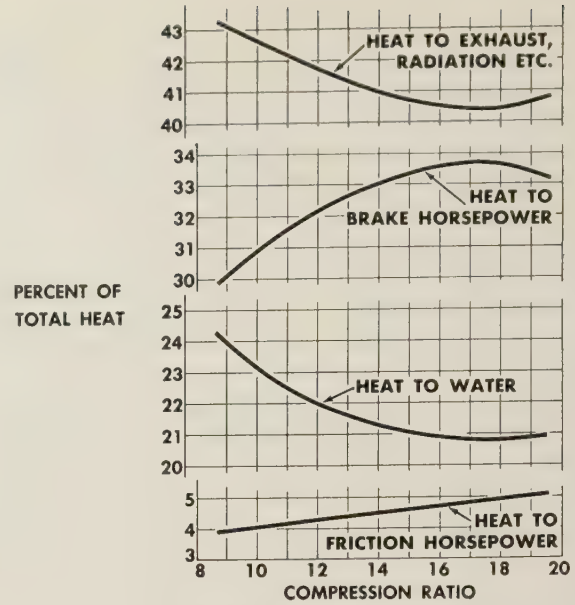

Fig. 18 — Heat distribution at full throttle and 2000 rpm

at the higher compression ratios. The fact, for example, that the effective expansion ratio of the 25/1 engine would be reduced to 20.3/1 if all of the heat energy were added at 10 deg atdc, points up the significance of late burning.

Full-Throttle Evidence of Late Burning:

The late burning tendencies that were disclosed by part-throttle p-v data have also been observed at full throttle. One of the full-throttle tests that shows this tendency is that of heat distribution. Fig. 18 shows the relationship between heat distribution and compression ratio. Theoretically, the per cent of heat rejected to the coolant and to the exhaust gases, radiation, and the like, should continue to decrease as compression ratio increases. Instead, the curves that represent the per cent of heat rejected in this manner level off at a compression ratio of about 17/1 and then start to increase. The amount of heat converted to bhp correlates with previously established relationships between bhp, brake thermal efficiency, and compression ratio. The per cent of heat or work going into friction as determined by the motoring method is shown to be a linear function of compression ratio.

Another approach, which was used to study the relationship between compression ratio and the energy in the exhaust gas, was to measure the exhaust gas temperature at full throttle. The data of Fig. 19, which show the relationship between exhaust gas temperature and compression ratio, were obtained with the air/fuel ratio and the spark advance adjusted to give maximum power. The fact that the exhaust temperatures at full throttle did not continue to decrease with the increases in compression ratio verifies the late burn tendencies that were observed at the higher compression ratios.

The relationship between spark advance and compression ratio is shown in Fig. 20. It is interesting to note that the spark advance required for maximum power did not continue to decrease as com-

[10] P. 82 of "Internal Combustion Engine," by L. C. Lichty. Sixth Edition. Pub. by McGraw-Hill Book Co., Inc., New York, 1951.

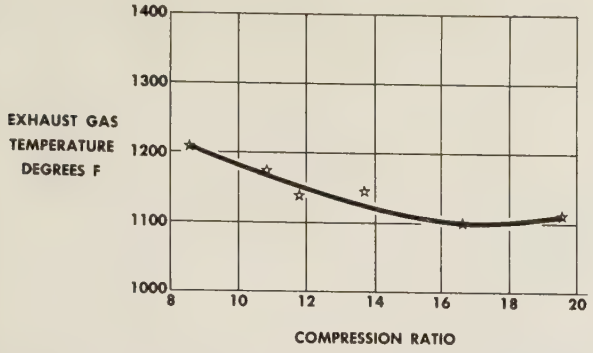

Fig. 19 — Exhaust gas temperature at full throttle and 2000 rpm

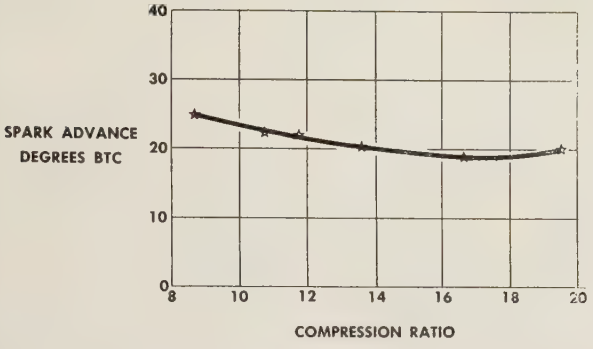

Fig. 20 — Maximum power spark advance at full throttle and 2000 rpm

pression ratio increased. This phenomenon is probably related to the mass distribution of the charge in the top center region. Apparently, in the 20/1 engine, the balance between the amount of the charge in the space around the spark plug and the charge in the quench zone with the piston at tdc was such that a slight increase was required in the spark advance for maximum power.

Factors Causing Late Burning:

One factor that determines the amount of charge that will burn in the top center region is the geometric shape of the combustion chamber. Fig. 21 shows cross-section views of the combustion chambers used in this study. The compression ratio of the test engines was changed by varying only the volume of the portion of the combustion chamber that was in the piston. Thus, the quench area and the quench zone, the space between the flat portion of the piston and cylinder head, were held constant from engine to engine. However, this configuration did not provide comparable distribution of the mass of charge in the combustion chambers as compression ratio increased.

As can be seen from Fig. 21, the per cent of the charge that was contained in the piston and the space around the spark plug decreased as compression ratio increased, which means that more and more of the charge was forced into the quench space. This lack of equal mass distribution of the charge in the combustion chambers as compression ratio increased probably accounted for most of the late burning.

Another factor which may contribute to the late burning is the overall area/volume ratio of the combustion chamber. Fig. 22 shows how this area/volume ratio changed with compression ratio. In Fig.

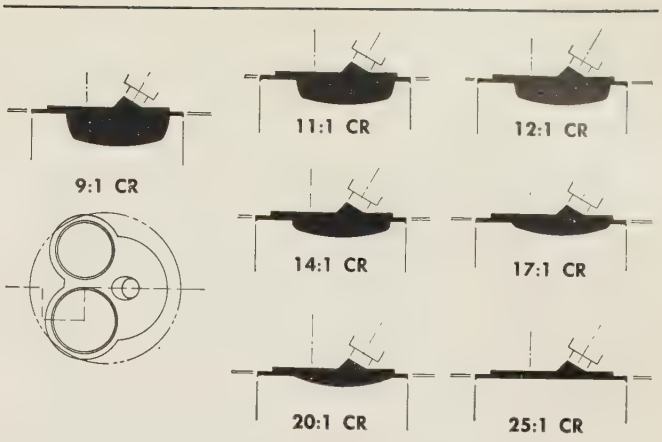

Fig. 21 — Sectional views of combustion chambers

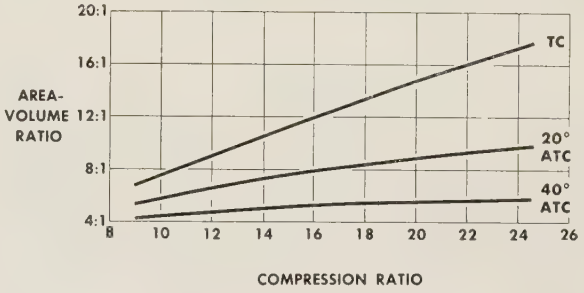

Fig. 22 — Area-volume ratio

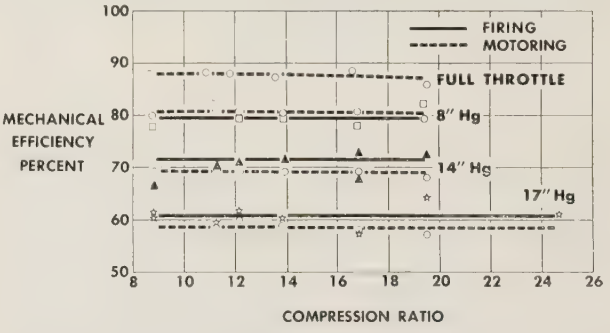

Fig. 23 — Mechanical efficiency at 2000 rpm

22, the combustion chamber was considered to be the space above the piston regardless of the position of the piston. With the piston at tdc, the area/volume ratio more than doubled when the compression ratio increased from 9/1 to 25/1. This resulted from a large decrease in volume with only a slight decrease in area.

Other factors such as lack of turbulence, for example, may also contribute to the late burn problem. Turbulence characteristics are primarily a function of the geometry of the combustion chamber. As can be seen from the section views in Fig. 21, the combustion chambers changed from very compact, turbulent chambers to "pancake" chambers as compression ratio increased.

Mechanical Efficiency

Motoring and Firing Mechanical Efficiency — Fig. 23 shows the relationship between mechanical efficiency and compression ratio at different throttle conditions. Mechanical efficiency as determined by the motoring friction method is shown at full-

throttle and at several part-throttle conditions. For comparison purposes, mechanical efficiency was also determined at several part-throttle conditions by the firing friction method using indicated power data (the upper loop of the p-v diagram) obtained during p-t tests.

The data shown in Fig. 23 indicate that mechanical efficiency remained constant as compression ratio increased. Although there was a difference in the magnitude of mechanical efficiency as determined from firing and motoring friction, it is interesting to note that the trends as established by both methods are substantially the same.

Motoring Friction — The motoring friction horsepower data at full throttle and at a manifold depression of 20 in. of Hg are shown in Fig. 24. The friction horsepower was linearly related to compression ratio. The increase in motoring friction with compression ratio was the result of the increase in compression pressures. The rate of increase of motoring friction with compression ratio was greater at full throttle than at a manifold depression of 20 in. of Hg. Thus, at the higher compression ratios and also at the higher speeds, the full-throttle and part-throttle motoring friction curves intersect.

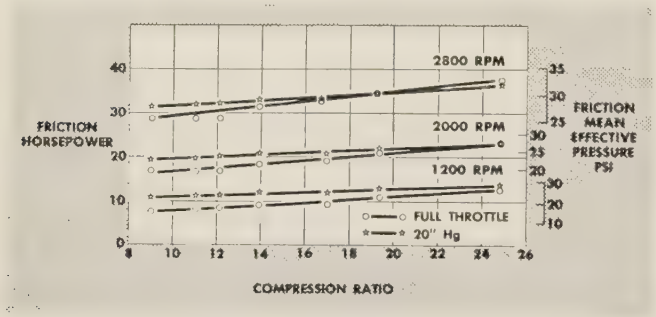

Fig. 24 — Motoring friction

The relationship between motoring compression pressures and compression ratio is shown in Fig. 25. Note that compression pressures were linearly related to compression ratio, and that the compression pressures of a 25/1 engine at 2800 rpm were approximately 1100 psi. These pressures are higher than peak firing pressures of today's engines and result in connecting rod loads up to 6.5 tons under motoring conditions.

Although the linearity between compression pressures and compression ratio has been shown by other investigators,[11] it is a somewhat surprising observation. In theory the pressure at the end of compression is a function of the initial pressure multiplied by the compression ratio raised to an exponent. As a check on this relationship, the compression pressures were calculated for the condition where the initial pressure was assumed to be 13.4 psia and the exponent 1.35. The resulting curve, which is included in Fig. 25, correlates quite well with the data observed at 2000 rpm.

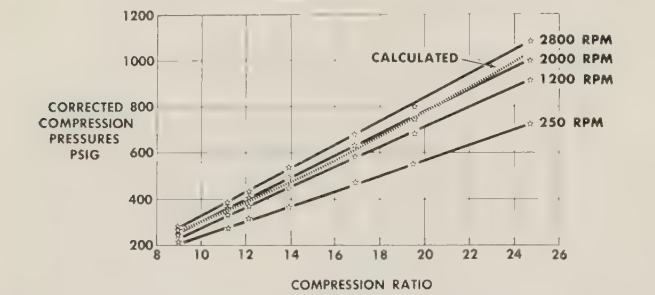

Fig. 25 — Compression pressures

Pumping Losses — In reference to Fig. 23, the mechanical efficiency as determined by the motoring friction method, is lower than that determined by the firing friction method in the light-load region. This relationship prevails at light loads primarily because of the difference in engine friction as measured under motoring and firing conditions. The difference in pumping losses is shown in Fig. 26. This figure shows the relationship between the shape and the magnitude of the pumping loops under motoring and firing conditions.

The characteristic shape of the part-throttle pumping loop while the engine is firing is familiar to all engineers who have studied engine cycles. However, the pumping loop that occurs while motoring may be less familiar. As can be seen in Fig. 26, the motoring pumping loop resembles a rectangle that has manifold depression as one dimension and cylinder displacement as the other. As a result of the differences in the pumping loops, the motoring loop is larger and thus represents more work than the firing loop. When part-throttle motoring friction, which includes pumping work, is added to brake power to get indicated power, this value of indicated power at light loads is higher than the value of indicated power taken from p-v data. Therefore, the mechanical efficiency at light loads as determined by the motoring method will be lower than that determined by the firing method.

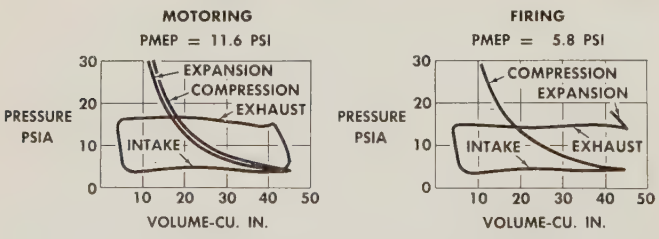

Fig. 26 — Characteristic pumping loops at 20 in. of Hg and 2000 rpm

The general relationship between motoring and firing pumping work and load is shown in Fig. 27. These relationships are not significantly affected by changes in compression ratio.

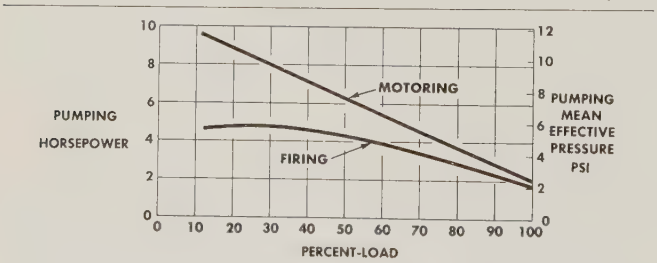

Fig. 27 — Motoring and firing pumping losses at 2000 rpm

Sound Recordings

A common consensus has been that engine roughness and noise level increase as compression ratio increases. However, during this investigation, the personnel that were closely associated with the op-

[11] "Combustion Chamber Geometry and Fuel Utilization," by J. C. Hughes. Paper presented at SAE Annual Meeting, Detroit, January, 1957.

eration of these engines could not detect a noticeable change in noise characteristics as the compression ratio was increased. In order to get a more permanent and quantitative basis for comparison, sound recordings were taken on each of the test engines.

The recordings were taken while the engines were being operated at 2000 rpm full throttle, and with the ignition timing adjusted to give maximum power. The engines were essentially clean or free of deposits when the recordings were made. The microphone was placed 5 ft from the left side of the engine.

Fig. 28 shows a plot of sound level and frequency data at one-half octave bands for the 9/1, 14/1, and 20/1 engines. It can be noted that there is a comparatively small change in the overall sound level and in the sound level at different frequencies. This substantiates observations that were made both in the test cell and from a jury playback method of evaluating the recordings. Thus, it is concluded that the sound level produced by the engines used in this study was substantially independent of compression ratio. It should be mentioned that this relationship may change as combustion-chamber deposits accumulate, and also it may change if the combustion efficiency or burn characteristics are improved at the higher compression ratios.

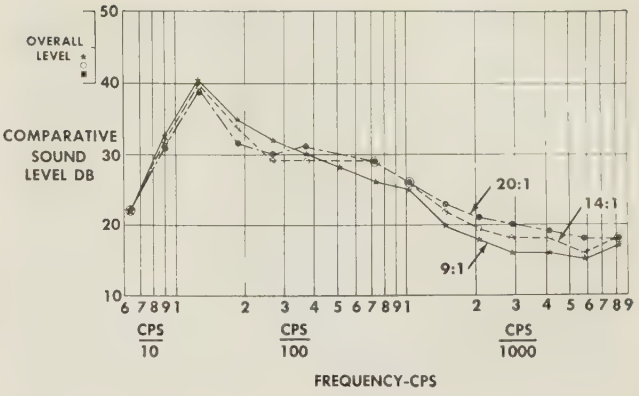

Fig. 28 — Sound level comparison at full throttle and 2000 rpm

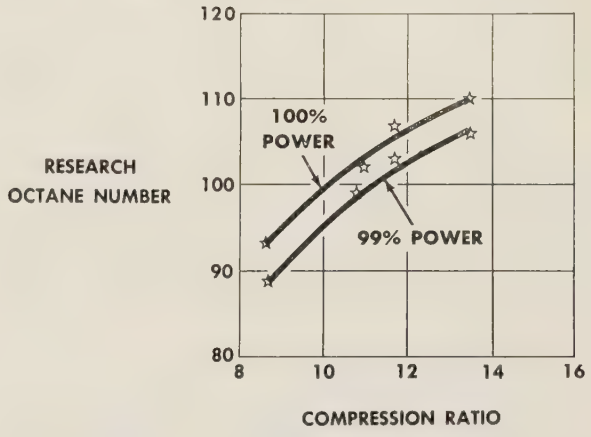

Fig. 29 — Octane requirement at full throttle and 2000 rpm

Octane Requirement

Determination of the octane requirement of the engines tested was not an original objective of this program. It is of interest, however, to observe the general area of octane quality required in a program of this nature. All tests were run on the engine dynamometer with essentially clean combustion chambers. For this reason, the octane requirement data do not have a direct relationship to car operation, but are included as a matter of interest.

Fig. 29 is a summary of observed octane requirement data. The octane requirement tests were run using commercial-type reference gasolines blended to have research octane numbers increasing in two number steps. The highest reference gasoline available for these tests has a research octane number of 110. Research octane numbers above 100 were determined by the proposed method given in the ASTM Standards on Petroleum Products and Lubricants.[12] Under clean conditions, gasoline with a Research octane number of 110 was sufficient for full-throttle operation at 2000 rpm of the 14/1 compression ratio engine with maximum power air/fuel ratio and mbt spark advance. The full-throttle octane requirement of this engine and lower compression ratio engines are shown in Fig. 29 with the spark adjusted for maximum power and also with the spark retarded to give 99% of maximum power. In both cases, maximum power air/fuel ratio was used.

No attempt was made during this investigation to determine the octane quality of the fuel used in the 17/1, and 20/1 engines when they were operated at full throttle. Sufficient antiknock quality to permit full-throttle operation with mbt spark advance was obtained by using different quantities of tel and the manganese compound (AK-33X).[5] These antiknock agents were added to isooctane in concentrations as high as 6 ml of tel plus 6 grams of AK-33X per gal.

It is recognized that combustion-chamber deposits present certain problems that must be overcome before higher compression ratios become commercially practicable. Some of these problems have been discussed in the past,[13] and they are discussed more fully in companion papers of this symposium.

Full-Throttle Operating Problems

Piston Failures — No major failures occurred during normal operation of these full-throttle tests. There was, however, one type of failure which occurred twice before the cause was discovered. This was the failure at full throttle of the piston in cylinder No. 1 of the 20/1 compression ratio engine. The failure of the replacement piston in the same cylinder seemed to isolate the problem and point to the cause. The cylinder heads used on this engine had an opening into the combustion chamber of cylinder No. 1 for an engine indicator. Since the indicator was not being used during full-throttle tests, it was replaced with a steel plug which apparently provided a hot spot that caused surface ignition. After the replacement piston failed in an identical manner (Fig. 30), cylinder heads without an opening for an engine indicator were used. This eliminated the abnormal combustion and permitted further full-throttle operation without any additional piston failures.

Ignition Problems — The only other problem encountered in operating the high compression ratio

[12] ASTM Standard on Petroleum Products and Lubricants. Appendix V-A. November, 1957.

[13] SAE Transactions, Vol. 64, 1956, pp. 76–100: "Mechanical Octanes for Higher Efficiency," by D. F. Caris, B. J. Mitchell, A. D. McDuffie, and F. A. Wyczalek.

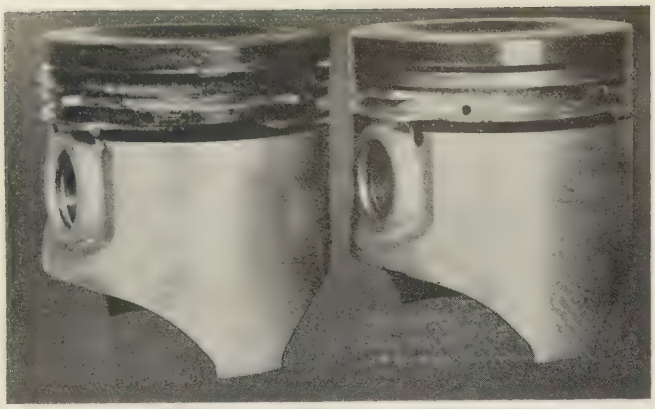

Fig. 30 — Piston failures

engines at full throttle was the short life of spark plugs. Extremely high concentrations of antiknock additives were added to isooctane to permit full-throttle operation. The use of these additives caused considerable difficulty due to spark-plug fouling. Since the study and permanent elimination of this problem were beyond the objectives of this investigation, a temporary remedy was sought. The most practical interim solution was that of reducing the spark-plug gap and changing the plugs as soon as the engine started to miss fire.

Compression Ratios in the Future

It should be remembered that the trend in thermal efficiency versus compression ratio as presented in this report was determined with engines of conventional present-day design. The fact that the brake thermal efficiency curve peaked at a compression ratio of 17/1 should by no means imply that this is a fixed relationship, nor that this report, therefore, defines the maximum useful compression ratio for spark-ignition engines. Proper application of the data obtained during this study may be instrumental in the development of engines that give thermal efficiencies which more closely parallel those predicted by theory.

One of the major problems which has been highlighted by this study is that of obtaining complete combustion in the top center region of "high" compression engines. A satisfactory solution to this problem is not known at this time; however, there are several possibilities that could be examined.

For example, the combustion chamber could be designed to keep the mass distribution of the charge constant as compression ratio increases. In other words, the geometric shape of the combustion chamber could be varied so that the per cent of mass at any given distance from the spark plug would be independent of compression ratio. If the stroke/bore ratio and displacement were held constant, as was done in this study, it would be necessary to decrease the quench thickness as compression ratio increases. However, there are some practical limitations which control the amount that the quench thickness can be decreased in production engines.

Another design change which may improve the combustion characteristics of the higher compression ratio engines would be to keep the area/volume ratio of the combustion chamber constant as compression ratio increases. This could be accomplished by use of a larger stroke/bore ratio (a long stroke engine). Here again, there are some practical limitations that govern the amount that the stroke/bore ratio can be increased without compromise or loss in other desirable properties. Engine breathing, friction, and inertia loads are some of the factors that are adversely affected by large stroke/bore ratios.

These ideas express some of the thinking that may contribute to future refinements of the internal-combustion engine. The ultimate goal from the engine designer and manufacturer's standpoint is to develop high compression ratio engines with efficiencies closer to those predicted by theory.

This study has shown that, although the gains are approaching a point of diminishing returns, a substantial improvement in thermal efficiency of modern engines is still possible through further increases in compression ratio. The development of these higher compression ratios in commercial engines is dependent on the ability of the petroleum industry to produce economically the higher octane gasoline required by these engines. Based on the paper by E. V. Murphree, et al.,[14] a significant increase in engine compression ratio and gasoline octane quality above current levels does appear economically possible. As in the past, further developments in engines and fuels must proceed in an orderly and evolutionary manner as permitted by advancing technology of the times.

Summary

This paper presents the results of an investigation which was conducted to determine the effect that large increases in compression ratio have on thermal efficiency. The engines used in this investigation were production V-8 engines of conventional design with modified combustion chambers.

The results of this study have shown that the thermal efficiency of the test engines peaked at a compression ratio of 17/1 and that further increases resulted in a decrease in thermal efficiency. The primary cause for the decrease in thermal efficiency at compression ratios above 17/1 was the delay in the completion of the combustion process. This delay, which means that more of the heat energy was added during the expansion stroke as compression ratio increased, is a function of combustion-chamber design. Although there are some changes in combustion-chamber design which may improve the combustion characteristics of very high compression engines, most of these changes either result in an undesirable compromise of other engine properties or they are limited by practical considerations.

This study has once again shown that substantial gains in thermal efficiency can be obtained by further increases in compression ratio. Whether these gains will be realized as an overall economic gain to the customer will depend upon the ability of the petroleum industry to continue to increase economically antiknock quality of commercial gasoline. In the event that future advances in petroleum technology result in the economic production of higher octane fuels, the results of this investigation point the way to further improvements in the efficiency of the spark-ignition engine.

[14] "Value of High Octane Number Gasolines," by E. V. Murphree, H. G. Codet, E. S. Corner, and W. A. Herbst. Paper presented before Division of Petroleum Chemistry, American Chemical Society, San Francisco, April, 1958.

Compression Ratio for Maximum Thermal Efficiency Stays Fixed As Engine Load Changes

— Prof. Jay A. Bolt
University of Michigan

THE data presented in this paper are especially valuable because the authors cover a wide range of compression ratios. The logarithmic diagrams of Fig. 14 are most useful for studying the combustion and heat flow phenomena of the gaseous engine medium.

Pressures, volumes, and values of the exponent n have been taken from Fig. 14, which make it possible to compute the charge temperature at the end of the compression stroke. These values are shown on Fig. A, which are in essential agreement with experimentally determined compression temperatures of Livengood.[a] Combustion temperatures and pressures were then computed with the following assumptions:

1. Complete combustion of a lean octane-air mixture of 0.0605 fuel/air ratio.
2. Constant volume combustion.
3. No heat losses.

Figs. A. and B show these calculated values and the authors' experimental results. The upper curve J of Fig. B indicates an almost linear increase in pressure as compression ratio is increased, if the charge consisted of air having variable specific heats, as obtained from Keenan and Kaye.[b] If a constant value of specific heat were used, the temperatures and pressures would be linear and even higher. Curve K was established by using the Hottel Charts,[9] which include the influence of variable specific heat of the real products of combustion and the effects of chemical dissociation.

Chemical dissociation is a process by which molecules decompose into smaller molecules, or atoms, at high temperature, with absorption of energy. For example, hydrogen and oxygen burn to form steam, with release of chemical energy. However, at high temperatures, the steam partially dissociates to form hydrogen and oxygen, with absorption of energy. In this manner, nature employs chemical dissociation to reduce extremely high combustion temperatures.

As the engine power stroke proceeds, the charge temperature is reduced by expansion, and recombination of the dissociated products occurs, with heat release. This delayed energy release, unfortunately, results in a loss of availability (the thermodynamic term for loss of ability of a substance to do work) because the expansion ratio for the recombined portion of the charge has been reduced. The effects of dissociation and subsequent recombination are the same as those of delayed combustion, and it is impractical from the authors' data to isolate the relative importance of each. The authors have commented upon the effects of delayed combustion.

Curve K is not continued to the higher compression ratios because the Hottel charts do not extend to these conditions. The differences between curves J and K on Figs. A and B indicate that the effects of chemical dissociation are substantial, as would be expected for these temperatures.

Curve L (Fig. B) shows that the actual pressure rise due to burning in the test engines did not change greatly with compression ratio. This reduced pressure rise, in comparison with curve K, includes many additional factors, including burning atdc, heat losses, and increased combustion-chamber surface/volume ratio as compression ratio is increased.

The authors state, ". . . the per cent of the charge that burns in the top center region decreases as compression ratio increases." From the information given, we do not know how much this observed result is due to dissociation, and how much to lack of the optimum combustion chamber shape for each compression ratio. In present practice the rate of combustion and pressure rise is greatly influenced by the combustion-chamber shape used. However, it seems reasonable to believe that chemical dissociation phenomena are having increased influence at increased compression ratio. This leads to the opinion that efforts to approach constant volume burning at increased compression ratios by combustion-chamber modification may meet with only limited success.

The authors' results show that the compression ratio for maximum thermal efficiency is not greatly affected by en-

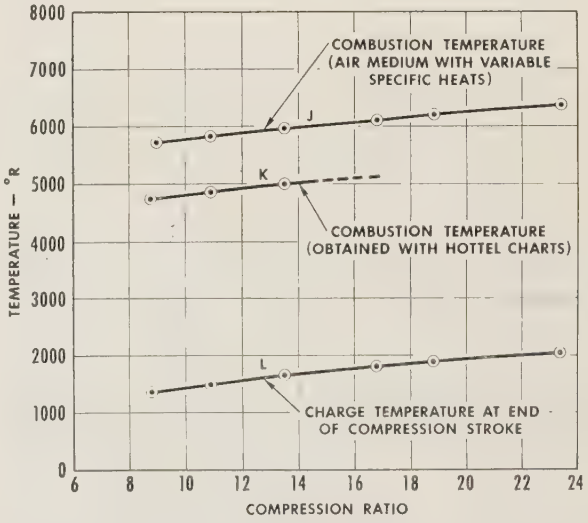

Fig. A — Computed temperatures for otto cycle engine at part load

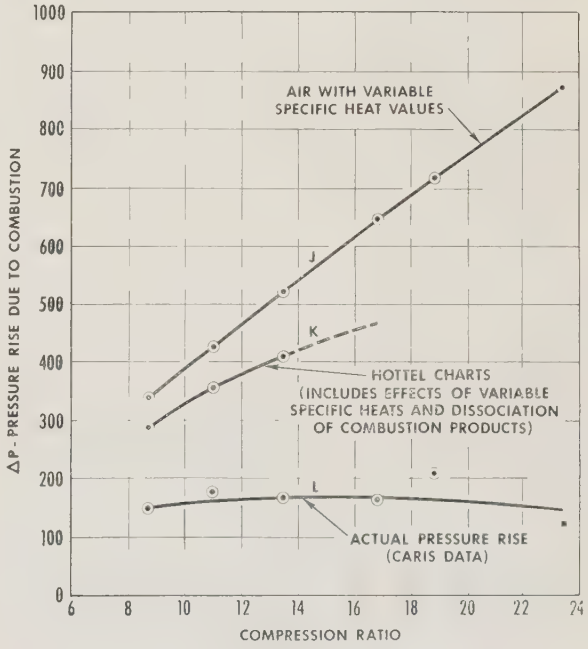

Fig. B — Pressure rise due to combustion at part load

[a] SAE Transactions, Vol. 66, 1958, pp. 683–699: "Measurement of Gas Temperatures in Engine by Velocity of Sound Method," by J. C. Livengood, C. F. Taylor, and P. C. Wu.

[b] "Gas Tables," by Keenan and Kaye. Pub. by John Wiley & Sons, Inc., New York.

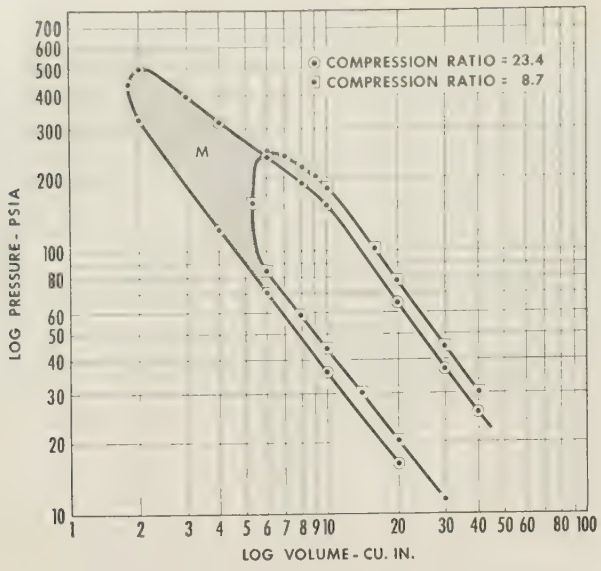

Fig. C — Superimposed logarithmic cycle diagrams, Caris data

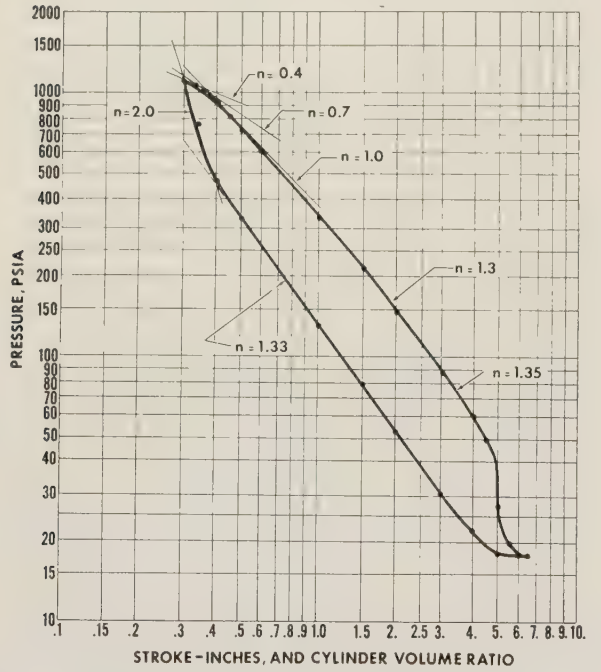

Fig. D — Log pressure versus log volume diagram of diesel power cylinder (Muntz free-piston air compressor, model P-42 — full load, cylinder bore of 4¼ in., 1038 cpm frequency, 2-stroke cycle)

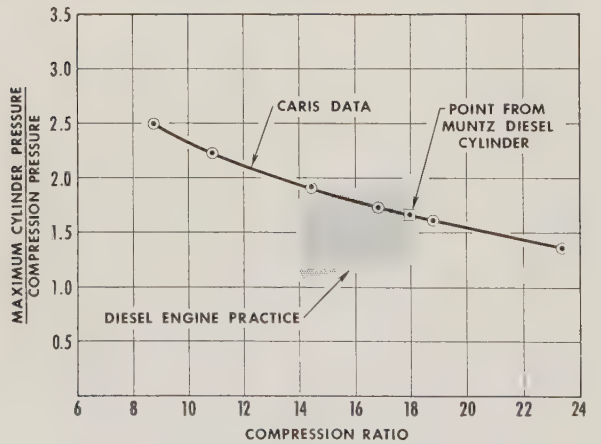

Fig. E — Pressure ratios for otto and diesel cycles

gine load. It is interesting to note that for spark-ignited engines with essentially constant fuel/air ratio, the charge temperature at the end of the compression stroke is a function of the charge temperature at the beginning of compression and the compression ratio, and not greatly influenced by load. During the combustion process the temperature rise will also be a constant increment independent of load (pressure). Therefore, the maximum cycle temperature of part and full load do not differ greatly. This near equality of maximum temperatures, and the fact that chemical dissociation is very predominantly a function of temperature, may partially explain why the optimum compression ratio is quite independent of load.

The use of very lean mixture ratios will minimize the tendency of the products of combustion to dissociate because they reduce the temperature rise due to normal combustion. Increase in charge temperature before ignition, resulting from increased compression ratio, also permits ignition of leaner mixtures.[c] These factors may be expected to make possible and enhance the merits of leaner mixtures at increased compression ratios.

Fig. C shows the superimposed logarithmic diagrams of the lowest and highest compression ratio engines of the authors. These diagrams show that the piston moved down on the power stroke to such a point that the pressure and volume (and, therefore, the temperature) were approximately equal when combustion was completed. The shaded area M represents added work accomplished by the engine of higher compression ratio with the same fuel quantity, and in general shows why increased compression ratio yields higher thermal efficiency.

A log-pressure log-volume diagram for a compression ignition cylinder is shown on Fig. D. These data, taken with a balanced-pressure type indicator, were supplied by the Detroit Diesel Engine Division of General Motors Corp., and have been plotted on logarithmic coordinates for comparison with the spark-ignition engine diagrams of the authors.

The small values of the exponent n during the early portion of the power stroke establish the known fact that a substantial amount of the fuel is also burned during the expansion stroke of diesel engines.

From the standpoint of the combustion of the authors' engines, as compression ration was increased the engines behaved less like ideal otto cycle engines and more like diesel engines. This is illustrated on Fig. E, showing a plot of the ratio of the maximum cylinder pressure/compression pressure for the authors' engines. This ratio diminishes as compression ratio is increased, as stated by the authors. For comparison, a zone of common practice for diesel engines is shown. A single point for the Muntz free-piston diesel cylinder, taken from the cycle diagram of Fig. D, is also shown.

Author's Closure To Discussion

SOME OF THE remarks that Prof. Bolt made in reference to the use of logarithmic pressure-volume diagrams warrant further discussion. We certainly do agree that these plots provide an excellent opportunity for studying combustion and thermodynamic characteristics of the actual engine cycle. It should be emphasized, however, that the areas of the logarithmic plots shown in Fig. C do not represent work directly as do the areas on a normal pressure-volume plot. The amount of work represented by a given area on logarithmic pressure-volume plots is a function of both the size and the location of the area.

[c] American Chemical Society *Journal*, Vol. 127, 1925, p. 672: "Limits for Propagation of Flame in Inflammable Gas-Air Mixtures," Part 3 of "The Effect of Temperature on Limits," by A. G. White.

Starting and Stopping Modern Engines

V. F. Massa, Esso Research and Engineering Co.

This paper was presented at the SAE Summer Meeting, Atlantic City, June 11, 1958.

PROBLEMS in combustion at low engine speeds have been created by the high levels of compression ratio in current U. S. passenger cars. These are: Hot-starting noise, hot-cranking difficulty, and after-running. These combustion irregularities are not major field problems at present, but their severity and frequency of occurrence will probably increase as compression ratio continues to rise.

An investigation of these low-speed combustion irregularities has been conducted in the laboratory and on the road. It has been found that hot-starting noise usually occurs during the first revolution the engine makes when being cranked. Although starting noise may result from compression ignition, it usually follows spark ignition. It can be influenced by engine operating conditions, compression ratio level, engine water jacket temperature, cranking speed, and fuel type. The starting noise behavior of a fuel has been related to its octane quality, volatility, and aromaticity.

Hot-cranking difficulty, the slowing down or stalling of the starting motor, is due to early compression ignition of the fuel, and appears related to cetane quality. After-running at low engine speeds, attributable to compression ignition following ignition cutoff, also appears related to fuel cetane quality. The three low-speed combustion difficulties were found to be worse when operating on a paraffinic fuel than with other fuel types of the same research octane number.

HISTORICALLY the development of the otto cycle engine has been accompanied by increases of compression ratio, upon which it depends to a large extent for improvements in thermal efficiency. During the postwar period the compression ratio of the average new U. S. car has increased from about 6.5/1 to about 9.5/1. This increase in compression ratio has represented challenges to both the engine builder and the petroleum refiner. To maintain this upward trend, it has been necessary to redesign engines and also refinery equipment to manufacture the high octane number fuels required for these new engines.

During this period there have been more subtle developments that are now beginning to emerge as potential problems. These developments concern combustion at low engine speeds and are associated with the starting and stopping of the engines. They are:

1. Hot-starting noise, which we define as any detonation noise observed during the cranking period.

2. Hot-cranking difficulty, which is the slowing down or stalling of the starting motor due to early compression ignition of the fuel.

3. After-running or key-off operation attributable to compression ignition, as distinguished from run-on resulting from surface ignition.

All three of these items are combustion problems in the approximate range of 50–500 engine rpm; like other combustion phenomena, they may be influenced by engine design, conditions of operation, and fuel quality. Since all three appear to be aggravated by high levels of compression ratio and since further increases of compression ratio appear likely, they were regarded and investigated as potential problems. To accomplish this the low-speed combustion characteristics of a group of late model cars were investigated. A specially instru-

mented laboratory engine and test car were also used to make detailed studies of engine and fuel behavior during engine starting and stopping periods.

Survey of Low-Speed Combustion Phenomena

Engine Starting and Stopping Characteristics, Survey of Late Model Cars — A survey of low-speed combustion phenomena was made in 38 late model cars. The objective was to assess the extent of hot-starting noise, hot-cranking difficulty, and after-running. Five of the cars had compression ratios that had been increased to the range of 11/1 to 12/1. The remaining cars were 1956 (8) and 1957 (25) production models, representing a wide variety of makes.

Preliminary studies had indicated that although starting noise was observed occasionally with a cold engine, it was usually more severe with a warm engine. For this reason, the cars were first driven 10 miles at normal speeds. Immediately following this warmup period, their starting noise requirements were established in terms of the Research octane numbers of a series of commercial-type reference fuels. Noise level was measured during a series of six successive starts using the Uniontown knock intensity scale. The results were then checked after an additional 2-mile temperature stabilization run. A moderate throttle opening was used during the starting periods. Throughout this test any tendency to give after-running or hot-cranking difficulty was also noted.

In general, hot-starting noise was observed to increase with increasing compression ratio. In terms of the Research octane number of commercial-type reference fuels it was observed that cars of 10/1 compression ratio were approximately 35 octane numbers higher in requirement than cars of 7/1 compression ratio. For the same increase in compression ratio, experience would indicate that road octane requirements would increase by about 10–12 Research octane numbers. These data are shown in Fig. 1 and indicate that the compression ratio increases that have occurred in recent years have been in a range where starting noise requirements were rapidly approaching the level of road antiknock requirements. The data also suggest that increases of compression ratio beyond today's levels may place starting noise requirements above road octane number requirements.

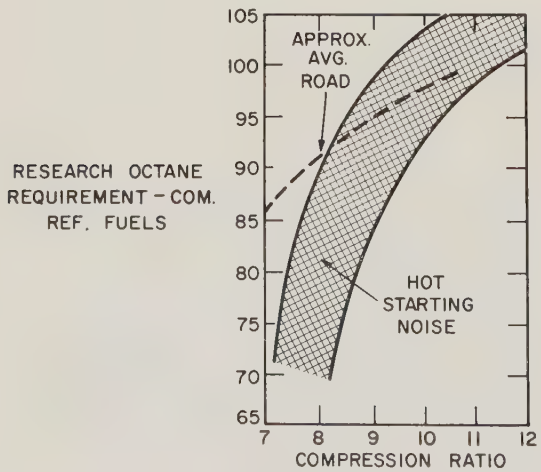

Fig. 1 — Hot-starting noise requirements increase as compression ratios rise

The different slopes of the octane requirement curves for starting noise and road antiknock quality, as influenced by compression ratio, may be due to the difference in engine speeds at which they occur. However, other factors should be considered. Increases in road octane requirements have not been controlled by compression ratio alone, but have been tempered by changes in ignition timing schedules, automatic transmissions, engine/transmission speed relationships, combustion-chamber design, and the like. On the other hand, there has been little need to consider starting noise requirements or to effect improvements in this direction.

The hot-starting octane number requirements of the 38 cars surveyed were determined for levels of noise ranging from "no-knock" to "light-medium." A comparison of the hot-starting and road octane requirements of these cars indicates that at some levels of satisfaction, the former exceeded the latter by as much as 4 units (Fig. 2). At about 90% car satisfaction, the noise requirements for starting exceeded those of the road by about 2½ units.

The maximum starting noise level observed was a "light minus" when the fuels used just satisfied the no-noise road requirements of the cars tested. This difference in noise level between these two requirements varies with the type of fuel used, as will be discussed later.

One production model and one 12/1 compression ratio test car showed a tendency to give after-running on fuels that would just satisfy their road octane requirements. The 12/1 compression ratio car gave hot-cranking difficulty, and on three occasions required 5-min intervals for cooling and decay of cylinder pressure before the engine could be restarted. Both the after-running and the hot-cranking difficulty appeared more objectionable to trained observers than did the starting noise.

Driver Reaction to Low-Speed Combustion Phenomena — An additional survey was conducted to obtain the reaction to these phenomena of persons not connected with engine test work. One hundred persons employed at the Esso Research Center were asked to start each of two cars six times. They were asked to compare the starting characteristics of late model cars with those of their own cars. Each time a start was made, the level of hot-starting noise was raised to a higher intensity by adjusting engine operating conditions. In this manner a level of starting noise eventually was reached that most people detected and objected to. The participants' comments about each start were recorded and later compared with the ratings made simultaneously by a trained observer. Approximately one-third of the participants detected and objected to hot-starting noise at or below a light intensity level. The participants objected to the same level of detonation noise in both cars, although background noise levels differed. In many instances, after-running was made to occur by adjustment of engine throttle position and engine operating temperature. Without exception, the participants in this phase of the experiment detected and objected to after-running whenever it occurred. In some cases they were alarmed by after-running.

While these studies indicate that hot-starting noise does not represent a serious field problem at

present, it could become a problem at higher compression ratio levels as a result of a greater increase in starting noise than in road octane number requirements. Hot-cranking difficulty and after-running are expected to occur more often as compression ratios rise. The ease of detection and high level of objection noted in the present survey suggest that they will also increase in importance.

Experimental Techniques

Equipment Used — Since hot-starting noise, hot-cranking difficulty, and after-running may represent potential field problems, their mechanism was studied further in the laboratory. Hot-cranking difficulty has been recognized by others as a potential field problem and the mechanism was discussed by Bowditch and Stebar.[1] Other investigators in the field of antiknock, and particularly those studies where motored engines were used,[2,3] contributed much that we considered helpful.

For our studies a 10/1 compression ratio V-8 engine was chosen. This engine was equipped with spark-plug type strain gages for the measurement of cylinder pressures in alternate cylinders. Suitable electronic equipment was employed to display the data on an oscilloscope. Ion gaps were installed in each combustion chamber opposite the spark plug to signal the arrival of the flame front. Crank angle position was measured by means of magnetic pickups located 45 deg before and after tdc. The relative load imposed on the starting motor as shown by the voltage in the starting motor and battery system was also measured. Magneto-striction-type pickups were used to record knock which was also observed and recorded simultaneously by trained observers. A comparison of the data observed on the oscilloscope with a recording made on a multipen Brush recorder indicated that for the purposes to which the data would be put the latter would be satisfactory.

A sample of the type of records obtained is shown for a typical engine start in Fig. 3. The data shown by the ion gaps indicate that the first and third cylinders did not fire. The second and fourth cylinders fired near tdc as indicated by the crank angle position and developed pressures much larger than normal at a very rapid rate. The first cylinder to fire actually did so slightly ahead of tdc which increased the load on the starting motor as shown by the drop in the battery voltage. This is also shown by the reduction in engine speed which is indicated by the wider interval between the 90-deg crank angle positions for this cylinder than for other cylinders. The rapid rates of pressure rise and the abnormally high pressures developed resulted in knock for both the first and second cylinders to fire. This is shown by the knock pickups at the bottom of the recording. Ignition timing was 2-deg btdc.

Other instrumentation included thermocouples for measurement of the temperatures of the air to carburetor, inlet manifold, water jacket, crankcase oil, and spark-plug tips. Intake manifold pressures, engine speed, ignition timing, and air/fuel ratios existing prior to shutdown were also recorded.

[1] SAE Transactions, Vol. 66, 1958, pp. 179–192: "Autoignition Associated with Hot Starting," by F. W. Bowditch and R. F. Stebar.

[2] SAE *Quarterly* Transactions, Vol. 4, July, 1950, pp. 438–454: "Precombustion Reaction in Spark-Ignition Engine," by E. R. Retailliau, H. A. Richards, Jr., and M. C. K. Jones.

[3] SAE Transactions, Vol. 61, 1953, pp. 386–401: "Some Factors Affecting Precombustion Reactions in Engines," by M. W. Corzilius, D. R. Diggs, and D. L. Pastell.

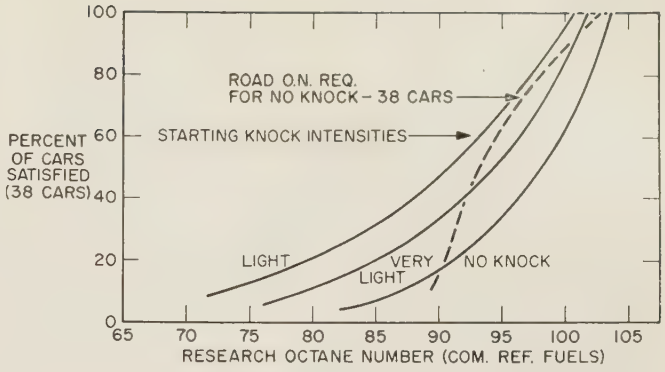

Fig. 2 — Starting knock intensity varies at different levels of road antiknock requirement

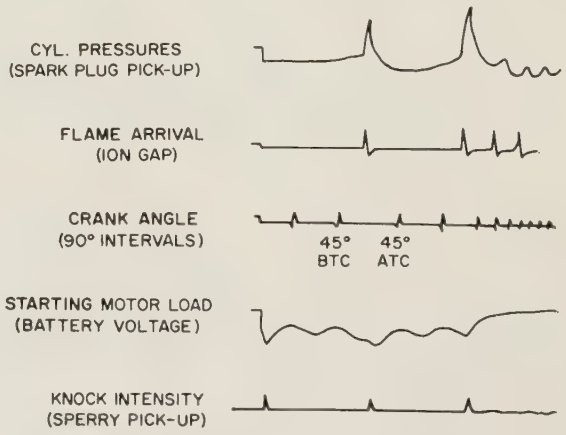

Fig. 3 — Data record-brush recording

Test Procedure — To simulate actual road conditions as closely as possible, the starting motor furnished with the engine was used for all starting tests. Only fully charged batteries were employed, and these were changed frequently to avoid voltage variations.

The engine was operated at 1500 rpm under no load conditions until the engine temperatures reached equilibrium. The water jacket and crankcase oil temperatures were maintained at 175 F. Upon reaching equilibrium temperatures, the engine was operated on the test fuel for 10 min under the same conditions used for warmup. The throttle was set for a fast idle when the ignition was turned off. It was reset to give 1500 rpm no load for the starting period. A series of six successive starts of the engine was then made to observe hot-starting noise. Following this, the engine was cranked over without spark ignition to examine the hot-cranking behavior of each fuel. Upon completion of these tests the engine was again run at the 1500 rpm condition for 2 min, before observing the after-running behavior of each fuel. Any tendency of a fuel to give hot-cranking or after-running difficulty during the starting test was also noted.

Experimental Results: Hot-Starting Noise

Influence of Engine Adjustment and Operating Variables — With the equipment and techniques that have been outlined, a study was made of some of the conditions of engine adjustment and operating variables that can influence starting noise, hot-cranking difficulty, and after-running. It was

found that hot-starting noise may be the result of compression ignition of the fuel or spark knock following spark ignition. Both of these phenomena at low engine speeds were studied and photographed by Bowditch and Stebar[1] who referred to the peculiar characteristics of knocking combustion at these speeds as "slow knock." Our studies indicate that whether starting noise will result from compression ignition or follow spark ignition will depend on the difference between engine octane requirement and fuel octane quality. Most of the hot-starting noise observed during the present study followed spark ignition. This was not the case when hot-starting noise was observed in conjunction with hot-cranking difficulty.

It would be expected that raising engine operating temperatures would accelerate the precombustion reactions of the fuels and increase starting knock. It was found that starting noise requirements increased by 12 octane numbers when the water jacket temperature was raised from 130 to 175 F. These results were obtained in terms of the Research octane numbers of commercial reference fuels: At 130 F water jacket temperature, the hot-starting noise requirement was 89 Research octane number; at 175 F, it was 101 Research octane number.

The higher engine water jacket temperatures also increased the tendency to give hot-cranking difficulty and after-running.

Increased combustion-chamber temperatures obtained by raising engine speed prior to shutdown resulted in a higher level of starting noise for a given fuel: At 800 rpm, the starting noise intensity was very light; at 2000 rpm, it was medium heavy.

Ignition timing was also found to influence hot-starting noise. Advancing the ignition timing of the laboratory engine from tdc to 10-deg btdc caused a significant increase in noise. Retarding the spark was beneficial up to 15–20 deg atdc; beyond that point compression ignition ignited the charge prior to the occurrence of spark ignition. A difference in the influence of ignition timing on hot-starting noise was also noted between fuels of different type. These data are shown in Fig. 4.

An examination of the traces of cylinder pressure, crank angle position, knock, and the like, indicate that the detonation noise heard during the starting period usually occurs during the first revolution of the engine. From one to four cylinders may knock, depending on the level of fuel quality; the lower the fuel quality, the more cylinders will knock. Examination of the data obtained during the cranking period showed that starting from rest the engine speed accelerated rapidly. As a result, the speed at which the engine was turning was vastly different for different cylinders in a position to fire for the first time. Although the engine used for this test had a constant cranking speed of about 125 rpm, it was found that the average speed for the first cylinder in position to fire might be as low as 50 rpm. If the first or second cylinders in a position to fire actually did so, then the speed reached at the end of the first revolution was about 250–500 rpm. Since starting knock was not usually observed after the first revolution, this suggests that the cranking speed of the engine may have a pronounced effect upon starting noise. No means for changing the cranking speed of the engine was readily available; however, a simulated higher cranking speed was obtained by raising the engine rpm to a level above that desired and then cutting the ignition. When the engine speed dropped to approximately 300 rpm, the ignition was turned on to simulate starting at higher cranking speeds. No knock was observed on fuels that gave medium-heavy knock

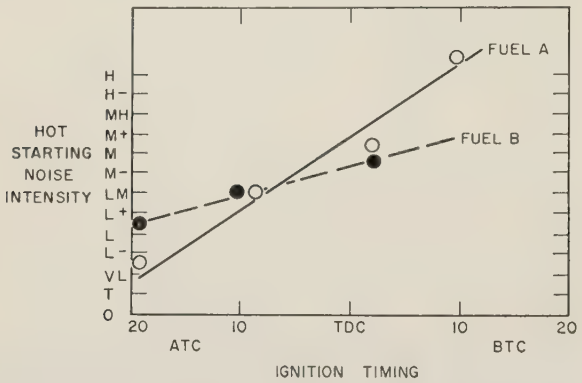

Fig. 4 — Hot-starting noise may be influenced by ignition timing

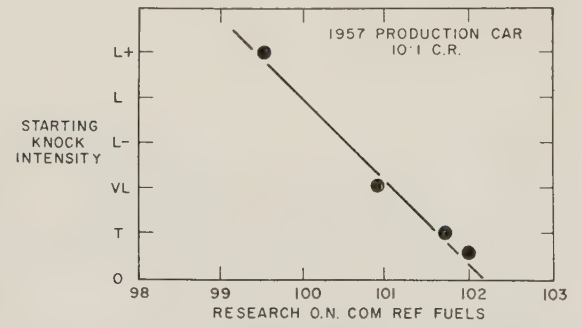

Fig. 5 — Starting knock is controlled by octane number when fuels are of similar type

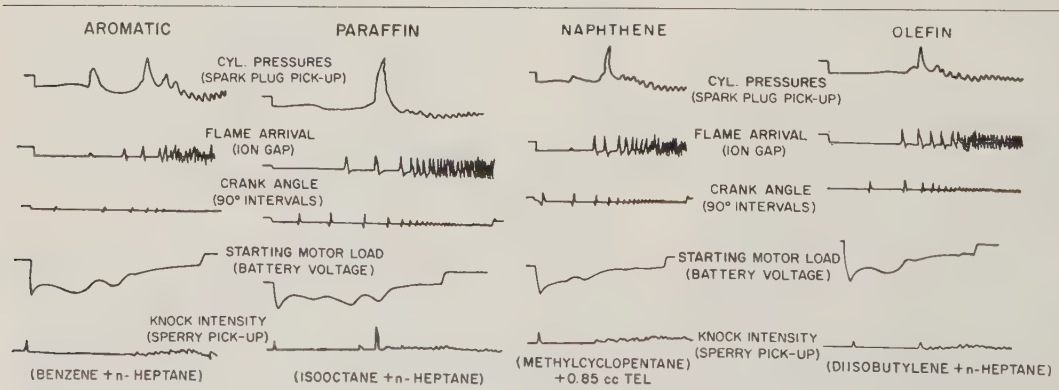

Fig. 6 — Hot-starting noise behavior of different fuel types (98 research octane number)

under normal starting conditions. A similar test was conducted on a car on the road in which the engine was allowed to come to rest prior to using the momentum of the moving car as a cranking force. The results obtained were similar to those noted in the laboratory engine. It is realized that there are limitations to the significance of such a test, but it does indicate that cranking speeds may influence starting knock. If so, it would be expected that the higher torque starters recently introduced to counteract hot-cranking difficulty may also be helpful in reducing hot-starting noise.

These observations, in conjunction with compression ratio effects discussed earlier, show that there are at least several factors of engine design, adjustment, and operation that have a significant influence upon hot-starting noise.

Influence of Fuel Composition — In addition to the factors previously discussed, the influence of fuel quality on low-speed combustion phenomena was investigated. For this purpose, a series of aromatic-type fuels was prepared at two levels of Research octane number. This was also done for fuels that were predominately olefinic, paraffinic, and naphthenic in character, and for mixtures of these fuel types. A number of these fuels were made in such a manner as to make it possible to observe the influence, if any, of tel on the combustion effects being investigated. As is usually the case when attempting to make a wide coverage of fuel type, pure compounds must be included. The fuels so made are subject to limitations imposed by volatility. However, a wide range of full-boiling gasolines was included among the 30 fuels investigated.

When considering fuels of similar type, it was found that hot-starting noise varied with the level of fuel octane quality. In Fig. 5 it may be seen that as the Research octane number of such a series of fuels was reduced, the hot-starting noise increased. However, differences were also found among a group of fuels of similar Research octane number but differing in other respects such as fuel hydrocarbon type, Motor octane number, and volatility. In Fig. 6 are reproductions of the actual data obtained under starting conditions with four different fuel types, all of approximately 98 Research octane number. The top line in each of these charts shows the cylinder pressures developed in every other cylinder. The bottom line shows knock, if any. These data show that the paraffinic fuel developed a much higher peak cylinder pressure than did the aromatic, olefinic, or naphthenic types. The bottom trace indicates that the paraffinic fuel also knocked quite hard (M+), while the maximum noise observed for the other three fuels was a trace knock for the olefin. Of interest also, as shown by the 90-deg interval markings on the middle trace, is that peak pressure and knock, if any, developed within the first revolution of the engine as discussed earlier. The four examples of fuel hot-starting noise behavior shown in Fig. 6 were chosen because they were representative. From this it may be seen that Research octane number alone is not a sufficient criterion of knock under starting conditions. Lack of correlation between Research octane number and hot-starting noise was also shown by Bender, et al.[4] Data of the type shown in Fig. 6 were obtained for all of the fuels included in this test.

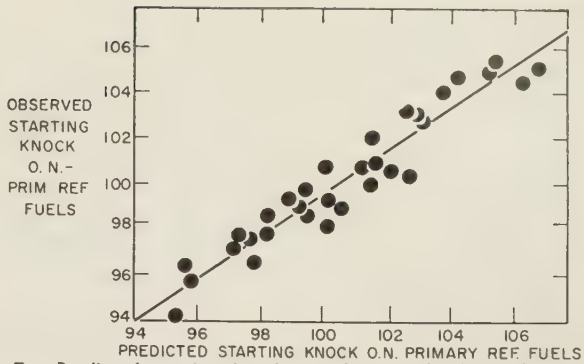

Fig. 7 — Predicted starting knock correlates with observed values in laboratory engine

A correlation of these data with various fuel qualities, such as tel content, octane number, volatility, type, and the like, was attempted. The statistical analysis indicated that when other fuel quality factors were equivalent, the use of tel to obtain a desired octane number level had no effect upon fuel hot-starting noise characteristics. Multiple regression analysis showed that Research octane number, Motor octane number, and volatility, and to a lesser extent, the aromatic content of the fuel, were the most important fuel qualities involved. A discussion of the regression technique employed is shown in the Appendix. Although there were other factors that gave a slight improvement when included in the correlations considered, they appeared to be of minor importance. The variables mentioned gave a "goodness of fit" by regression analysis of 91%. The equation that was developed is expressed in terms of the octane number of primary reference fuels:

$$\text{Hot-starting noise octane no.} = 1.036\,(\text{Research octane no.}) - 0.306\,(\text{Motor octane no.}) - 0.041\,(90\%\text{ point, F}) - 0.033\,(10\%\text{ point, F}) + 0.040\,(\%\text{ aromatics}) + 42.5 \quad (1)$$

When using this equation to predict fuel behavior under hot-starting noise conditions, the mean deviation was found to be one octane number. The predicted values based on this equation and the observed values as determined in the laboratory engine are compared in Fig. 7.

The laboratory-developed equation also showed reasonably good correlation in the prediction of the relative tendency of fuels to give starting noise with data obtained on two cars on the road. One of these cars was a 10/1 compression ratio production 1958 model, the other was one in which the engine compression ratio had been increased to 12/1.

The test technique used on the road for the determination of hot-starting noise was the same as that described in an earlier section of this paper. The fuels were the same as those used for laboratory studies of hot-starting noise. Their performance was compared with that of primary reference fuels. The observed hot-starting noise determined in these two cars did not show a one-to-one relationship with the predictions based on the laboratory studies but did show satisfactory correlation. It is possible that the differences in degree of emphasis on certain fuel qualities noticed between the road and the laboratory are not only due to differences in engine severity, but may also be a reflection of ambient

[4] "Combustion Irregularities at High Compression Ratios," by R. O. Bender, G. C. Meyer, and A. J. Pahnke. Paper presented at American Chemical Society Meeting, San Francisco, April, 1958.

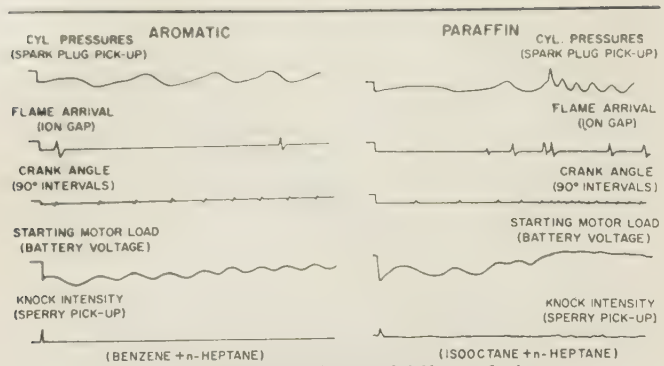

Fig. 8 — Hot-cranking behavior of different fuel types (98 research octane number)

temperature. The laboratory studies were conducted at temperatures of from 70–79 F, whereas the ambient temperatures prevailing during the road tests ranged from 10–40 F. The data obtained on the road, however, do show that hot-starting noise was influenced by essentially the same fuel quality factors as determined in the laboratory studies, but to a somewhat different degree. The equation developed by regression analysis from road data for the prediction of hot-starting noise is:

Hot-starting noise octane no. = 0.82 (Research octane no.) − 0.217 (Motor octane no.) − 0.02 (90% point, F) + 42.5 (2)

The "goodness of fit" for this equation is 77% and the mean deviation is 0.87 octane number. Aside from fuel aromaticity which was a relatively small although significant factor used in the laboratory-developed equation, both road and laboratory studies are in agreement that Research octane number, Motor octane number and volatility are the most important factors controlling fuel starting knock behavior. The fact that both studies indicate Motor octane number to have a negative coefficient also is of interest, but does not seem surprising. Our own studies and those of others[5] have shown that engine severity varies with speed, being more severe (approaching Motor octane number) at high speed and less severe (approaching Research octane number) at low engine speeds. The negative coefficient shown for the temperature at which a given per cent of fuel is distilled, indicates that high volatility is beneficial. However, the effects of fuel volatility are not completely separable from those of other fuel qualities. It may be that merely by being volatile more of the fuel reaches the cylinder, and gives a richer mixture than with a less volatile fuel. If so, the richer mixture would probably give less knock due to greater displacement from the air/fuel ratio for maximum knock. Other fuel qualities such as fuel aromaticity, olefinicity, and tel content when included in the regression analysis made only minor improvements that had little significance at confidence levels above 90%. For this reason, with the exception of aromaticity which seemed of importance in the laboratory developed equation, they were not used. Either of the equations presented permits a reasonable prediction to be made of the relative hot-starting noise performance of motor fuels. More data is needed to establish which is the more applicable.

Hot-starting noise requirements were determined in one of the road test cars and also in the laboratory engine before and after the accumulation of approximately 7000 deposit miles. The requirements in both cases were within 1 octane number of what they had been with a clean engine. This suggests that the influence of deposits on hot-starting noise may not be as great as their effect on road octane requirements. On the other hand, the tendency of fuels to give after-running and hot-cranking difficulty after the accumulation of deposits showed a marked increase compared with results obtained earlier in a clean engine. This is attributed to the thermal insulating effect of the deposits, leading to higher combustion-chamber temperatures.

Experimental Results: Hot-Cranking Difficulty

The application of the equation for the prediction of hot-starting noise to the prediction of hot-cranking difficulty and after-running met immediate failure. This was not surprising, since the starting noise equation is based largely on detonation following spark ignition while the other two phenomena were the result of compression ignition.

The length of time available during a normal engine starting period was usually too short to study the hot-cranking behavior of fuels. For this reason, a special test was used to obtain supplementary data. This test consisted of bringing the engine to the equilibrium temperature conditions described previously and then cranking the engine with no spark ignition. It was immediately obvious that there were big differences in the hot-cranking behavior of fuels. Some fuels would permit the starter to crank the engine at essentially constant speed, seemingly offering neither assistance nor hindrance to the cranking effort. Others, however, would ignite as the result of compression ignition and develop peak cylinder pressures sufficiently ahead of tdc either to impede seriously or to stall the starting motor. If this latter type of fuel did not ignite during the first few cycles thus allowing the starting motor to reach its normal speed, then compression ignition of the fuel usually would assist the starting motor, because peak cylinder pressures would be developed at a more favorable crank angle. In such cases, cranking speeds up to 375 rpm were reached with a starter capable of giving only 125–135 rpm without assistance. This assistance could not be counted upon, however, for the very same fuel might reduce the cranking speed to 20 rpm during the next cranking period. For this reason, a "hot-cranking index" was used as a measure of fuel tendency to give hot-cranking difficulty.

$$\text{Hot-Cranking Index} = \frac{\text{Maximum rpm reached during cranking}}{\text{Minimum rpm reached during cranking}} \quad (3)$$

A fuel with a high index would, therefore, be one that had shown erratic hot-cranking behavior. An example of the behavior of two different fuels typifying the hot-cranking behavior just discussed is shown in Fig. 8. In this figure, the aromatic-type fuel is shown developing normal cylinder pressures (top line) with little combustion shown by the ion gaps (second line) and reaching essentially constant cranking speed of about 125 rpm after the first revolution of the engine, as shown by the 90-deg intervals on the third line. The smooth pressure development of each of the cylinders, including those not monitored with pressure traces, are reflected in the voltage changes in the starting motor battery cir-

[5] SAE Transactions, Vol. 64, 1956, pp. 554–569: "Knocking Behavior of Fuels and Lubricants," by R. V. Kerley and K. W. Thurston.

cuit (fourth line).

In contrast to this, the paraffin-type fuel of the same Research octane number (both 98 Research) shows evidence of compression ignition as reflected by a high cylinder pressure (top line). This fuel also shows considerable combustion activity at the ion gaps (second line) and reached about 350 rpm as shown by the 90-deg crank angle intervals (third line). It will also be noted from the fourth line that the load imposed upon the starter, as reflected by line voltage, has been almost reduced to zero. The hot-cranking behavior of these two fuel types appears to be in agreement with the findings of Retailliau, et al.[2] concerning precombustion reactions shown for a paraffin (isooctane) and for an aromatic (benzene) during motored engine tests. For a given Research octane number, the hot-cranking behavior of the paraffinic fuels was also poorer than that of naphthenic and olefinic types. This is also in agreement with the findings of Bowditch.[1]

An examination of the hot-cranking behavior of over 30 fuels covering a broad range of fuel type and octane number quality, clear and leaded, did not show good correlation with such factors as Research and Motor octane numbers, volatility, and the like. With some exceptions, a correlation of hot-cranking behavior was obtained with cetane quality. Since the cetane quality of the fuels tested was below the normally used part of the cetane number scale, the values are expressed as the minimum compression ratio for sustained dieseling in an ASTM-CFR cetane engine. This relationship is shown in Fig. 9. These data suggest that the hot-cranking difficulty caused by different fuels may be related to cetane quality. Of course, hot-cranking difficulty can be related reasonably well to fuel octane quality which is the inverse of cetane quality for a given fuel type. However, this is not true for mixed fuel types.

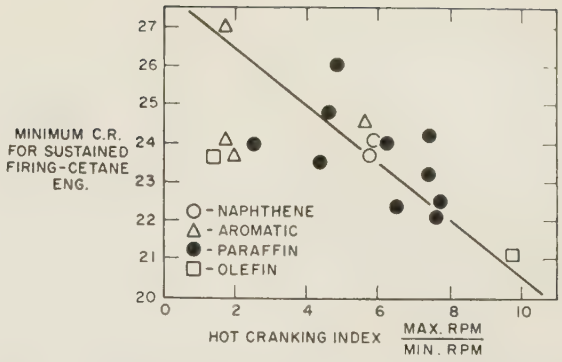

Fig. 9 — Hot-cranking difficulty is related to fuel cetane quality

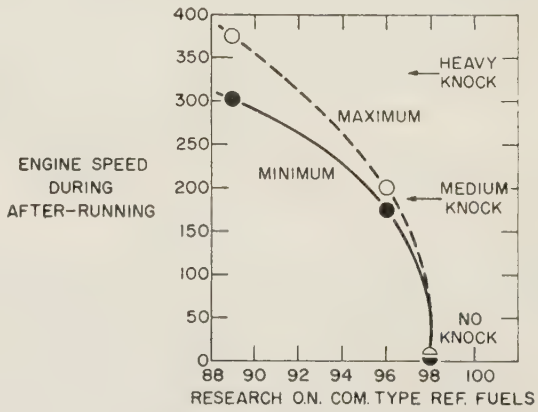

Fig. 10 — After-running is related to octane number when comparing similar type fuels

Experimental Results: After-Running

The after-running referred to in this paper is limited to that which occurs as the result of compression ignition. Spark-plug tip temperatures were measured and found to be much below those that would be expected to cause surface ignition. The absence of surface ignition may also be deduced from the maximum rpm obtainable during after-running. This requirement of a minimum residence time is consistent with compression ignition rather than with surface ignition (by a glowing particle).

It was possible to correlate the extent of after-running due to compression ignition with Research octane number for fuels of similar type. This is shown in Fig. 10, where Research octane number is correlated with engine speed existing after ignition cut off at a fixed throttle setting. Of interest in this plot is the fact that there is a band representing minimum and maximum after-running speeds that varied with Research octane number as did also the knock intensity that accompanied the after-running. For example, when fuel quality was 98 Research octane number, after-running was borderline. When the fuel quality was reduced to 96 octane number the engine speed cycled between a minimum and maximum of from 175–200 rpm. Reducing the octane number quality to 89 raised the engine speed of after-running and caused cycling to occur between 300 and 375 rpm. An examination of the cylinder pressures and combustion activity as indicated by the ion gaps gives a clue to this cyclic behavior. For example, with the 89 octane number fuel, the minimum after-running speed of 300 rpm was determined by the number of cylinders firing and the extent and position of the cylinder pressures developed. The maximum speed of 375 rpm was probably related to the minimum residence time within the cylinder required to produce compression ignition. When this minimum time no longer existed due to increased speed, the engine ceased to fire, thereby reducing speed and permitting sufficient time for compression ignition to be resumed. The 98 octane number fuel showed no high cylinder pressures and no abnormal combustion activity. The reduction of octane number quality to 96 and 89 increased the number of high cylinder pressures and erratic combustion activity and also caused a medium and heavy knock.

Increasing the charge density by opening the throttle probably raised the maximum speed for after-burning by reducing the minimum residence time required for compression ignition. The maximum speed that could be attained with the 89 octane number commercial reference fuel was 750 rpm.

Typical after-running behavior patterns obtained in the laboratory engine for an aromatic fuel and a paraffinic fuel of equivalent Research octane number show the latter to be far more prone to give after-running. This is illustrated in Fig. 11 in which the aromatic fuel developed normal cylinder pressures (top line) following ignition cutoff. Not many flame arrivals were shown by the ion gaps for the number of cycles involved (second line) and the engine came to a smooth stop without noise as shown by the knock pickup on the bottom line. The

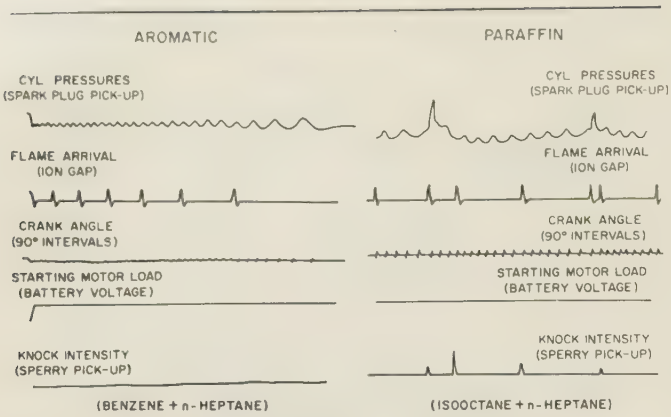

Fig. 11 — After-running behavior of different fuel types (98 research octane number)

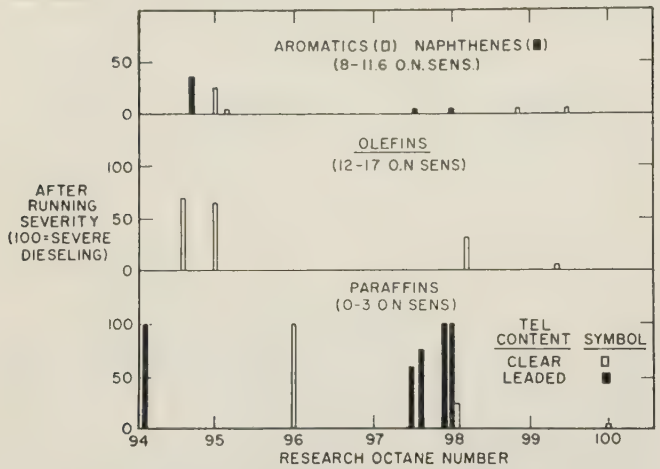

Fig. 12 — Paraffins increase after-running

Table 1 — Outline of the Stepwise Regression Procedure as Applied to Starting Knock in a Laboratory Engine

Regression Step	Variable Entered	Reduction of Original Variance, %	Standard Deviation about Regression, Octane Number
1	Research Octane Number	14.1	2.83
2	Motor Octane Number	54.7	2.16
3	Temperature at 90%	80.8	1.44
4	% Aromatics	87.1	1.21
5	Temperature at 10%	91.1	1.01

paraffin fuel in Fig. 11 shows the development of a sufficient number of abnormally high cylinder pressures attributable to compression ignition to keep the engine running on for some time. This was accompanied by knock as shown by the bottom line. Data of this kind showed that paraffins gave more after-running than other fuel types.

This is demonstrated by comparing numerical values for after-running severity assigned to the different fuel types tested. The after-running severity values were obtained by assigning equal importance to the following factors:

1. Number of abnormally high cylinder pressures developed.
2. Levels of peak cylinder pressures developed.
3. Maximum after-running speed attained.
4. Intensity of knock during after-running.

Each of these factors was rated on the scale 0 to 25, with the sum of the ratings taken as the after-running severity. The after-running behavior of various fuel types, as measured by this rating scale, is compared at given levels of Research octane number in Fig. 12. These data show the paraffins to be the most prone to give after-running, the aromatics and naphthenes least, and the olefins intermediate in this respect.

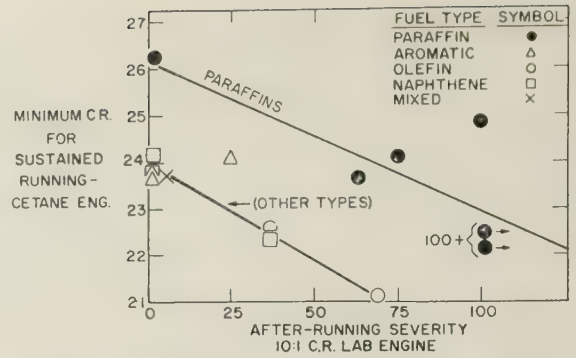

Fig. 13 — After-running is related to cetane quality (minimum compression ratio for sustained dieseling)

In general, the after-running severity of the fuels tested showed a correlation with cetane quality as represented by the minimum compression ratio for sustained firing in an ASTM-CFR cetane engine. Under these conditions the paraffinic-type fuels were again more prone to give after-running than other fuel types when compared at a given level of cetane (compression ratio) quality. These data are shown in Fig. 13.

Conclusions

The conclusions reached as a result of this work are as follows:

1. Hot-starting noise requirements increased more rapidly than did road octane requirements when compression ratios were increased from 6.5/1 to 9.5/1.
2. Hot-starting noise does not appear to be a significant field problem at present compression ratio levels but may be a potential one at higher levels of compression ratio.
3. The most significant fuel quality factors controlling hot-starting noise are: Research octane number, Motor octane number, volatility, and, to a lesser extent, aromaticity. These factors may be used to predict starting noise with reasonable accuracy.
4. Hot-cranking difficulty and after-running resulting from compression ignition were not as prevalent in late model cars surveyed as hot-starting noise. These difficulties, however, were more serious when they occurred: after-running was found to be objectionable to untrained observers.
5. Hot-starting noise, hot-cranking difficulty, and after-running are influenced by conditions of engine design or adjustment and operating conditions.
6. Increased levels of compression ratio above those now in use will tend to increase the frequency of hot-cranking difficulty and after-running. Both of these compression ignition phenomena are related to fuel cetane quality.
7. The three low-speed combustion difficulties were found to be worse with paraffinic fuels than with other fuel types of the same Research octane number.

Acknowledgment

The author wishes to acknowledge with thanks the assistance received from the many persons at

the Esso Research Center who contributed to the preparation of this paper. It is especially desired to thank J. A. Wilson for his assistance in the design and preparation of the electronic instrumentation and F. E. Steidler for his contributions in the statistical analyses.

APPENDIX

Development of Octane Index Equations for Starting Knock

A stepwise multiple regression technique was used to develop octane index equations for both a 10/1 compression ratio laboratory engine and two test cars. By means of this procedure the various factors such as Research octane number, Motor octane number, and the like, are introduced one at a time into the regression equation. The variable selected at any stage of the calculations is always that variable which results in the largest improvement in goodness of fit. The process continues until none of the remaining factors produces any statistically significant improvement. At this point all of the variables in the equations are retested to determine their significance.

The result of successive additions to the starting knock equation for the laboratory engine are outlined in Table 1. No other factors examined proved to be significant after the addition of the fifth term. Hence, the analysis was terminated at this point. The final standard deviation of 1.01 octane number approximates the repeatability of duplicate ratings in the laboratory.

The regression equation developed for the road data contained only three terms as compared with five for the laboratory studies. The reason for this difference is that the last two and least significant factors in the table did not significantly improve the goodness of fit for the road data. This is not surprising since the number of fuels tested on the road was less because the knocking range encompassed by the test cars was not as great as for the laboratory engine. The final standard deviation of 0.87 octane number for the test cars, however, is within experimental error. For the available data, therefore, the equation is adequate.

DISCUSSION

After-Running in Low-Compression Engines Due to Ignition by Hot Spot

— W. E. Morris
E. I. du Pont de Nemours & Co., Inc.

WE HAVE also carried out tests to measure hot-starting noise resistance of fuels. Results were obtained in terms of coolant temperature for hot-starting noise, and were related to a reference system composed of blends of toluene and normal heptane. We confirm Mr. Massa's finding that aromatics are good and paraffins poor from this standpoint. In fact, isooctane had mediocre hot-starting noise resistance.

As to after-running, we have found this phenomenon very sensitive to throttle opening. We do not obtain after-running in 12/1 compression engines when the throttle is closed. With a slightly opened throttle, many present-day engines will after-run. This refers to after-running due to compression ignition which is the type that Mr. Massa has discussed.

It might be of interest to take a quick look backward at after-running in lower compression ratio engines, which is due to ignition by a hot spot rather than to compression ignition. In 1954 we sent a questionnaire to 8340 employees which included the question "When you turn your ignition key off, does the engine ever keep running?" Of the 2251 returns, 1.7% checked, "Yes." The next question was "If yes, after what type of driving?" A number of the employees wrote that it occurred after high-speed driving. Older cars as well as later model cars were represented, and no model was significantly out of proportion to its registration. Chances are that almost all the 1.7% of owners had observed after-running caused by a hot spot. Considering car registration figures, these 1.7% would amount to about 1% of cars now on the road.

Hot-Starting Noise and Hot-Cranking Difficulty Related

— F. W. Bowditch
General Motors Corp.

THE author has discussed three low-speed engine operating problems: hot-starting noise, hot-cranking difficulty, and after-running. He has shown the effect of operating parameters to be somewhat different for each problem. We do not agree. Our experimental evidence shows the problems of hot-starting noise and hot-cranking difficulty are very closely related and that they were equally affected by operating parameters.

In contradiction to Mr. Massa's conclusions, we found from high-speed flame photographs that compression ignition invariably occurred whenever the hot-starting noise was heard. Spark advance was found to have very little, if any, effect on this phenomenon. In mild cases, the spark discharge provided the initial source of ignition, but subsequent ignitions produced by compression ignition also occurred. In general, the magnitude of the noise was found to be directly related to the time in the cycle at which compression ignition occurred.

And Mr. Massa points out, octane quality is not a good measure of the resistance of a fuel to compression ignition under starting conditions, unless any comparison of fuels is limited to one class of hydrocarbons at a time. This should not be surprising since low-speed operating problems occur under much different engine conditions than those used in determining octane quality. In order to determine successfully a fuel parameter which will indicate the ability of a fuel to cope with these problems, it seems probable that the determinations will have to be carried out under engine conditions approaching hot engine starting conditions.

Mr. Massa states that the hot-starting noise is caused by knock or detonation. I would be very interested in knowing the author's definitions of these two terms. If the author agrees with the CRC terminology,[a] then for knock he means in part, that "The flame speed is many, many times greater than that which follows normal spark ignition." If the author agrees with Messrs. Lewis and vonElbe,[b] then the term detonation means "a shock wave which is sustained by the energy of the chemical reaction in the highly compressed explosive medium in the wave."

In our own studies of the hot-starting problem,[c] we also studied the hot-starting noise. We went to great detail in our paper to explain the types of reactions occurring in our work during hot, low-speed engine operation. It was pointed out that under no conditions at cranking speeds did knock or detonation, as they were just defined, occur regardless of the octane quality of the fuels used. Therefore, I would be quite interested to know what new evidence the author has to substantiate his statements concerning the occurrence of knock and detonation.

[a] SAE *Journal*, Vol. 62, October, 1954, p. 46: "Combustion Terms for Use in Otto Cycle Engine Combustion."
[b] P. 227 of "Combustion, Flames, and Explosions of Gases," by Lewis and vonElbe. Pub. by Academic Press, Inc., New York, 1951.
[c] SAE Transactions, Vol. 66, 1958, pp. 179–192: "Autoignition Associated with Hot Starting," by F. W. Bowditch and R. F. Stebar.

THUDDING in High

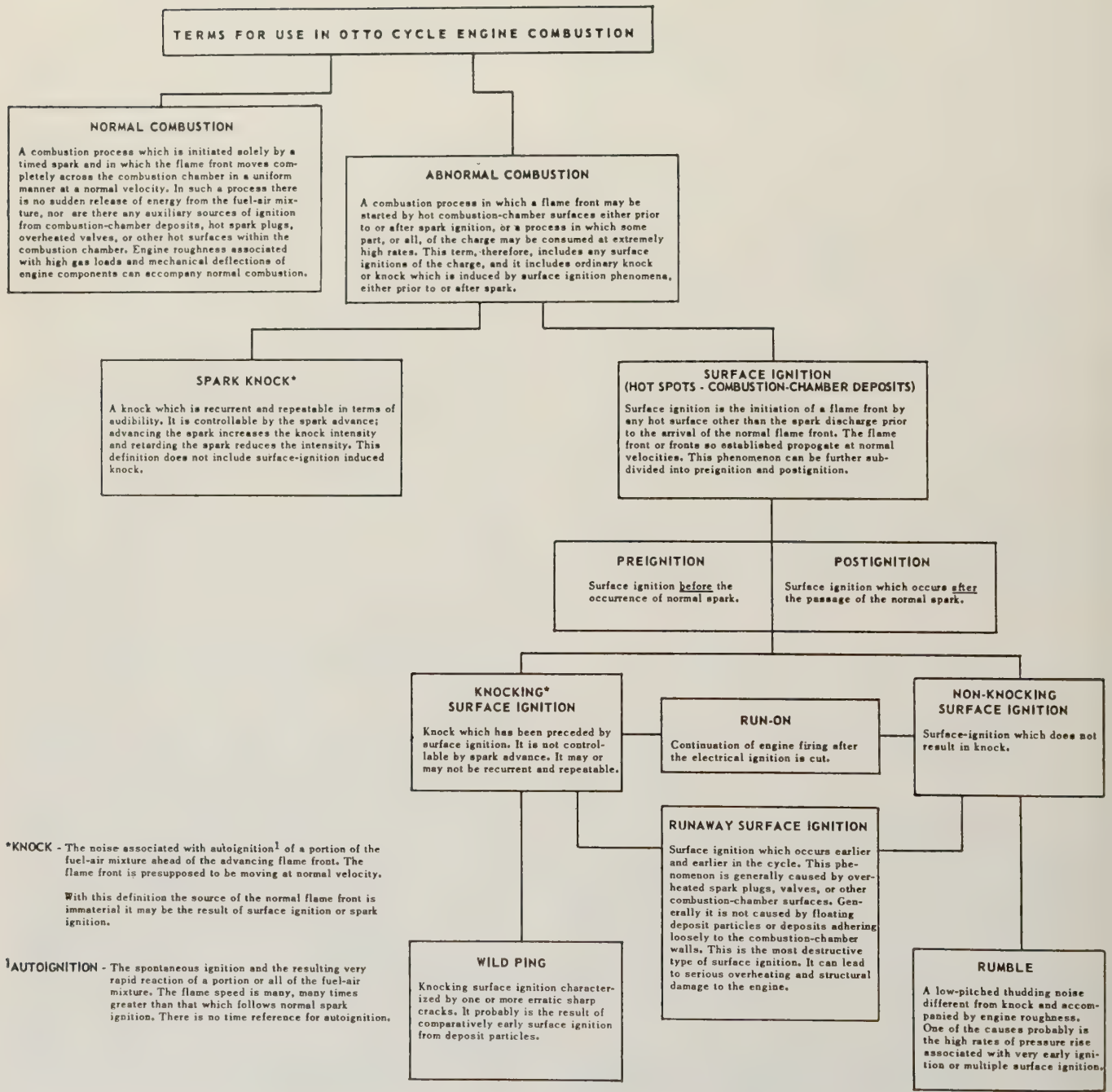

Fig. 1 — CRC definitions of terms for use in otto cycle engine combustion

Compression Ratio Engines

W. E. Morris and D. C. Fariss, E. I. du Pont de Nemours & Co.

This paper was presented at the SAE Summer Meeting, Atlantic City, June 11, 1958.

THREE types of abnormal combustion that have received considerable attention during the past few years are listed as spark knock, wild ping, and rumble under the CRC definitions of Terms For Use in Otto Cycle Engine Combustion (Fig. 1). Spark knock and wild ping are high-pitched engine noises caused by autoignition of a portion of the air-fuel mixture. Spark knock is recurrent and repeatable but wild ping is erratic, reflecting its initiation by surface ignition from combustion-chamber deposits. Rumble is a low-pitched engine noise caused by high rates of pressure rise during combustion of the air-fuel mixture. Like wild ping, rumble is erratic because it is brought about by surface ignition from combustion-chamber deposits.

Another low-pitched engine noise, which also is due to high rates of pressure rise can be obtained in the absence of surface ignition. This noise is called "thud" for the purposes of this paper because it is similar in mechanism to the "benzene thud" obtained in laboratory test engines. The relationship between thud and spark knock, wild ping, and rumble is indicated in Fig. 2. The terms "roughness" and "harshness" have been used by other investigators to describe the noise we define as thud.

Thud has been observed during high-speed, wide-open throttle operation of 1958 production engines as well as engines modified to 12/1 compression ratio. Even though thud was quite loud at high speed, its low pitch relative to the sharper sound of spark knock permitted determinations of road octane number in 12/1 compression ratio engines. In order to determine some of the characteristics of thud and how it is affected by fuel composition, a brief program was carried out using two test cars with engines modified to 12/1 compression ratio.

Thud Is Not Rumble

To illustrate the distinction between thud and rumble, the effect of combustion-chamber deposits on these noises was determined in a car of Make I

THUD—a noise due to high rates of pressure rise in the absence of surface ignition—is the subject of the investigations described in this paper. The tests were performed on 12/1 compression ratio engines.

The authors found that thud could be obtained both in engines with clean combustion chambers and those with deposits. Thud is most likely to occur in 12/1 compression ratio engines at least — at wide-open throttle, high speed, and high spark advance.

Table 1 — Rumble After Low-Duty Operation
("Standard" Spark Timing)

Test No.	Knock	Rumble
1	None	Very severe
5	None	Severe
10	None	Light
11	None	None
12	None	None

Table 2 — Spark Advance for Light Knock or Severe Thud at Wide-Open Throttle

Fuel	12/1 Car L Clean Combustion Chambers				12/1 Car I Heavy-Duty Deposits			
	3000 rpm		4000 rpm		3000 rpm		4000 rpm	
	Knock	Thud	Knock	Thud	Knock	Thud	Knock	Thud
Benzene	67	*45*	56	*38*	43	*36*	40	*23*
Toluene	54	*47*	55	*43*	33	33	36	34
Toluene Containing 3 ml Tel	68	*50*	60	*40*	42	45	46	45
Isooctane + 3 ml Tel	55	54	50	*39*	35	37	36	36
Catalytic Reformate + 3 ml Tel	49	50	46	44	27	27	28	27

[a] 105.1 research octane number, 100.5 motor octane number.

Notes: 1. Italicized figures denote severe thud occurring with spark retarded at least 5 deg from light spark knock.

2. "Standard" spark advance, deg btdc.

	3000 rpm	4000 rpm
Car L	24	24
Car I	21	23

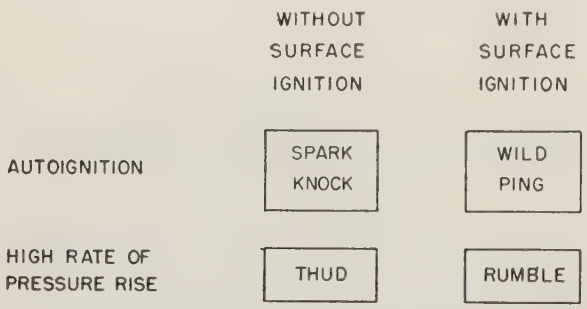

Fig. 2 — Relationships among combustion noises

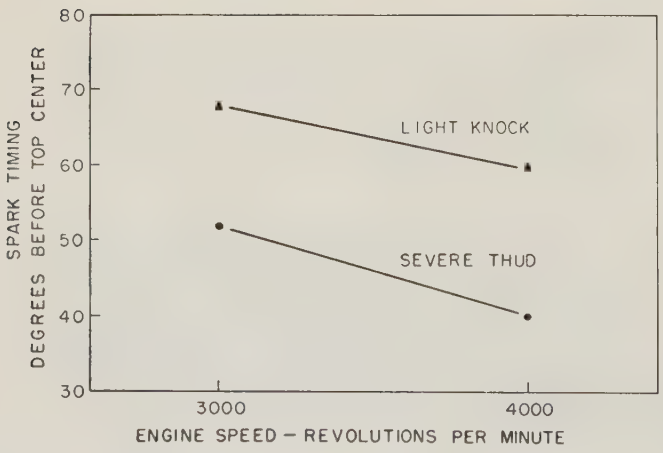

Fig. 3 — Effect of engine speed on spark timings giving knock and thud with 12/1 compression ratio Car L at wide-open throttle (toluene + 3 ml tel per gal)

modified to 12/1 compression ratio. After accumulation of combustion-chamber deposits under low-duty conditions, the car was operated on a chassis dynamometer for test periods of 10 sec at 2500 rpm with wide-open throttle. The effect of deposit condiction on rumble with toluene containing 3 ml tel per gal is shown in Table 1. Rumble decreased and then disappeared as low-duty deposits were scavenged by wide-open throttle operation. Thus, rumble is closely related to deposit condition.

Following these tests, the spark timing was advanced and the car was operated with continuous knock for 10 min to scavenge all but the most tenacious deposits. Tests were then carried out at 3000 rpm, wide-open throttle. Thud was obtained with a variety of fuels when the spark was advanced sufficiently. With toluene containing 3 ml tel per gal, thud was first noticed at 27 deg btdc spark timing and it became severe at 41 deg. Thud was repeatable and did not disappear with continued operation.

To determine whether combustion-chamber deposits are necessary to obtain thud, tests were carried out in 12/1 compression ratio car Make L after complete removal of all combustion-chamber deposits. Again, thud was obtained with a variety of fuels when the spark was advanced sufficiently. With toluene containing 3 ml tel per gal, at 3000 rpm, severe thud was obtained at 50 deg btdc spark timing, as compared to 68 deg required for light spark knock. Thud reported in the remainder of this paper was obtained in Car L with clean combustion chambers, or in Car I after sustained heavy knock to remove any loose combustion-chamber deposits. Thud in both cars was steady and repeatable and could be controlled by spark advance.

Thud and rumble sound the same and both probably emanate from low-frequency vibrations of engine parts. In both cases, the exciting force is probably a high rate of pressure rise in the combustion chamber. With rumble, the high rate of pressure rise is attributed to formation of additional flame fronts by surface ignition from combustion-chamber deposits. With thud, the high rate of pressure rise is due to rapid but orderly combustion of the fuel at a high rate, without the accelerating effect of surface ignition.

Effect of Engine Operating Conditions

At a constant throttle setting and speed, thud was obtained by advancing the spark timing and was eliminated by retarding the spark timing. An experienced observer can notice light thud at the "standard" spark timing of 24 deg and severe thud at 40 deg with toluene containing 3 ml tel per gal in Car L at 4000 rpm with wide-open throttle. Severe thud and light spark knock represent levels of noise that would probably be noticed by an inexperienced observer.

As engine speed is increased, the tendency toward thud increases so that less spark advance is required (Fig. 3). In Car L with clean combustion chambers both thud and spark knock occurred with lower spark advance at 4000 rpm than at 3000 rpm and severe thud occurred at 20 deg lower spark advance than required for light knock. The effect of manifold vacuum on the occurrence of knock and thud is shown in Fig. 4. Greater spark advance was

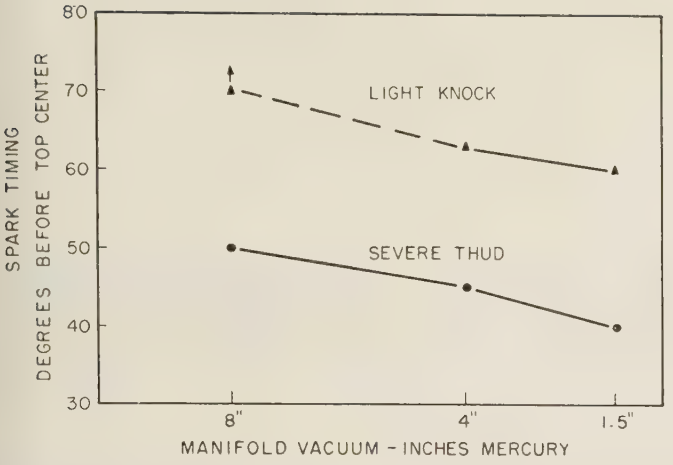

Fig. 4 — Effect of manifold vacuum on spark timings giving knock and thud with 12/1 compression ratio Car L at 3000 rpm (toluene + 3 ml tel per gal)

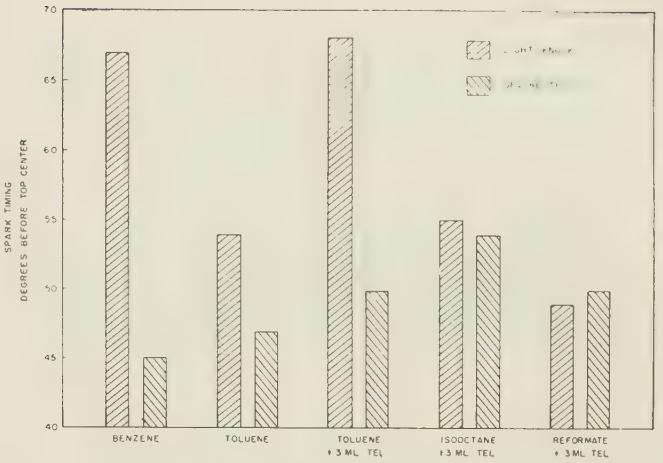

Fig. 5 — Influence of fuel on spark timings giving knock and thud with 12/1 compression ratio Car L at 3000 rpm

required to obtain thud at part throttle than was required at wide-open throttle. High speed, wide-open throttle operation, and high spark advance favor the occurrence of thud. This effect would be expected since all these factors tend to increase the rate of pressure rise.

Effect of Fuels

In the absence of spark knock, the spark advances required for severe thud fell within a fairly narrow range for a variety of fuels including benzene, clear and leaded toluene, leaded isooctane, and a leaded reformate. This result, obtained in 12/1 compression ratio Car L with clean combustion chambers, is illustrated in Fig. 5. Spark advances for thud and spark knock were greatly over-advanced from "standard" in Car L. Spark advances for knock and thud are shown in Table 2 for both cars.

Benzene was the only fuel giving thud in the absence of spark knock in Car I. The close agreement of spark advances for knock and thud for the other fuels indicates that the two phenomena are related in some manner.

Relationship Between Thud and Spark Knock

Either thud or spark knock can occur in the absence of the other. The behavior of fuels from the standpoint of spark knock alone is well-known. The behavior from the standpoint of thud alone is shown by the results in Table 2 obtained in Car L. For example, clear and leaded toluene have about equal thudding tendency. However, in Car I which gave knock and thud together, the spark advance required was considerably greater for leaded toluene than for clear toluene, which is characteristic of spark knock rather than thud. In fact, the spark advances for knock and thud in Car I with leaded isooctane and leaded reformate were also characteristic of spark knock rather than thud.

This suggests that spark knock or something associated with spark knock intensified thud in Car I. During a knocking cycle, precombustion reactions are taking place at an ever-increasing rate as autoignition is approached. The precombustion reactions presumably give combustion a "head start" and thus cause a slight increase in mass burning rate. That slight increase might be enough to cause thud at a given spark timing in an engine that would otherwise thud at a more advanced spark timing.

Control of Thud

When the combustion-chamber deposits that cause rumble are modified or minimized sufficiently to avert rumble, high compression ratio engines can still give thud. If the engine design and operating conditions lead to thud in the absence of spark knock, little can be done by changing fuel composition since fuels differ little in their tendency to thud in the absence of spark knock. Under such conditions, two measures can be taken to control thud:

1. Change in combustion-chamber design or operating conditions to decrease mass burning rate.
2. Change in engine structure to withstand a given mass burning rate without excessive vibration.

If precombustion reactions or some other factor associated with spark knock are inducing thud, two other measures can be taken to control thud:

1. Increase in high-speed road octane number of the gasoline.
2. Decrease in high-speed octane requirement of the engine.

Summary

Thud is defined as an engine noise caused by high rates of pressure rise in the absence of surface ignition. A brief investigation of thud leads to the following tentative conclusions:

1. Thud can be obtained in 12/1 compression ratio engines with clean combustion chambers or with deposits accumulated under heavy-duty conditions.
2. The tendency of an engine to produce thud is greatest at wide-open throttle, high speed, and high spark advance.
3. When thud occurs in the absence of spark knocks, benzene, clear and leaded toluene, leaded isooctane and leaded catalytic reformate differ little in thudding tendency.
4. Precombustion reactions or some other factor associated with spark knock can intensify thud.

RUMBLE —— a deposit at high compression

A. E. Felt, J. A. Warren, and C. A. Hall, Ethyl Corp.

This paper was presented at the SAE Summer Meeting, Atlantic City, June 11, 1958.

UNTIL recently, noises from abnormal combustion in automotive engines were classified as either spark knock or knocking surface ignition.[1] These two phenomena have also been termed normal knock and audible surface ignition. For both types, the sound is a high-frequency one — in the range of 4000–6500 cps.

Lately, however, a different type of noise has also been noticed in both commercial and experimental automotive engines having compression ratios above 9.5/1. It has a low-pitch in the range of 600–1200 cps. Cars with high-compression engines that contain deposits from light-duty operation are often bad offenders during full-throttle accelerations. The noise, generally heard at speeds above 2000 rpm, can be very objectionable, and may impose a limit on usable compression ratios.

A CRC Committee on Nomenclature[1] has classified the new sound as resulting from surface ignition and has designated it as "rumble." It defines rumble as "a low-pitched thudding noise different from knock and accompanied by engine roughness." Others have called the noise such terms as "thudding," "thumping," and "pounding." The CRC designation is used in this paper.

Rumble appears to be a phenomenon which cannot be solved by merely increasing fuel octane number unless knock-induced. Hence, it is worthy of considerable study by both the petroleum and automotive industries.

This paper discusses some studies of rumble made at our laboratories. Since rumble is another manifestation of the surface ignition caused by deposits, test procedures and special instrumentation were already available for these studies. However, some additional test techniques were developed, and they are explained in the paper.

What Goes on in the Combustion Chamber?

To study the combustion process with and without rumble, pressure-time diagrams and sound records have been obtained in both single-cylinder and multicylinder engines.

In one of the multicylinder engine studies, one cylinder of a 1957 V-8 engine of Make E was equipped with an extra hole for an 18-mm Li pressure pickup. This cylinder had a piston to provide 12/1 compression ratio, while the other seven cylinders had com-

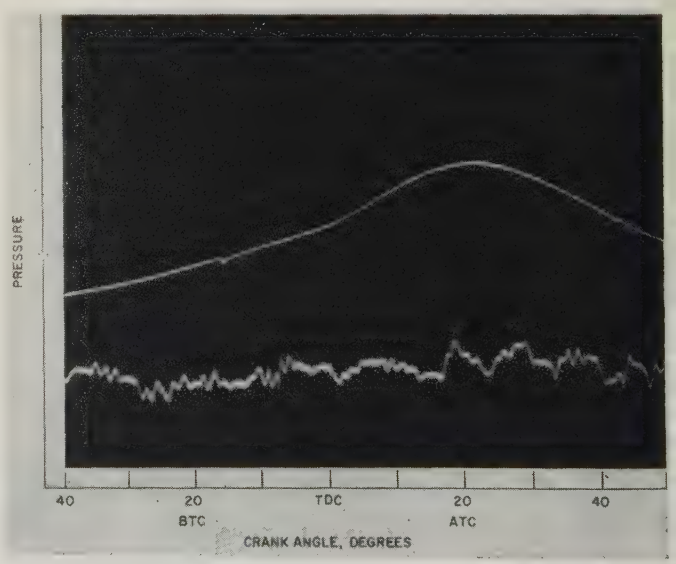

Fig. 1 — Normal combustion in clean engine (17-deg btdc ignition, Make E, 12/1 compression ratio)

[1] Coordinating Research Council, Report, No. 278, June, 1954: "Terms for Use in Otto Cycle Engine Combustion."

effect

ratios

RUMBLE is a type of abnormal combustion which may impose a limit on usable compression ratios if proper attention is not paid to fuel and lubricant factors. It is characterized by a low-frequency noise.

This noise is much more likely to be present in engines which have been operated on light-duty schedules than in those which have been used in heavy-duty operation. Once deposits are present, rumble generally occurs at wide-open throttle and high engine speeds.

Rumble does not appear to be confined to any particular type of combustion chamber, and increasing engine rigidity does not show promise of reducing the problem. Fuels with low deposit-forming tendencies help alleviate the problem. While not a complete cure, phosphorus fuel additives do a good job in reducing the incidence of rumble.

This paper presents the results of work aimed at defining the problem, together with data illustrating the influence of various fuel factors.

pression ratios of 8/1. This was done to insure that any abnormal combustion would occur in the instrumented cylinder. A dual-beam oscilloscope was used to display pressure-time records of cylinder pressure and a record of the sound picked up by a microphone held near the engine.

Fig. 1 shows normal combustion in a clean engine when operated on a primary reference fuel with an octane number considerably above the requirement of the engine. Test conditions were as shown in Table 1.

Ignition and tdc are indicated on the figure, and the wavy line below the pressure-time trace is a record of engine noise picked up by the microphone. The photographs were taken with a Fairchild strip-film camera operated at 10 fps. The pressure-time trace indicates a maximum rate of pressure rise of 16.5 psi per deg and a peak pressure of 600 psi.

Fig. 2 shows normal knock in the same cylinder operated in exactly the same fashion, except that a 96 octane number primary reference fuel was used. This fuel was about two octane numbers below engine requirement. The knock is indicated in two ways: (1) by the high-frequency vibrations on the pressure-time trace and (2) by the high-frequency noise picked up by the microphone. The frequency of the knock shown here is about 4800 cps. Up until the time in the cycle when knook occurred, the rate of pressure rise and pressures in the cylinder were essentially the same as those in

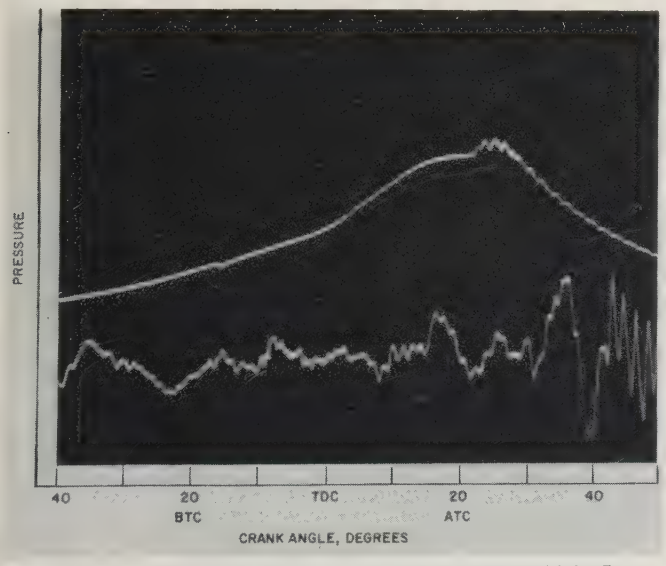

Fig. 2 — Knock in clean engine (17-deg btdc ignition, Make E, 12/1 compression ratio)

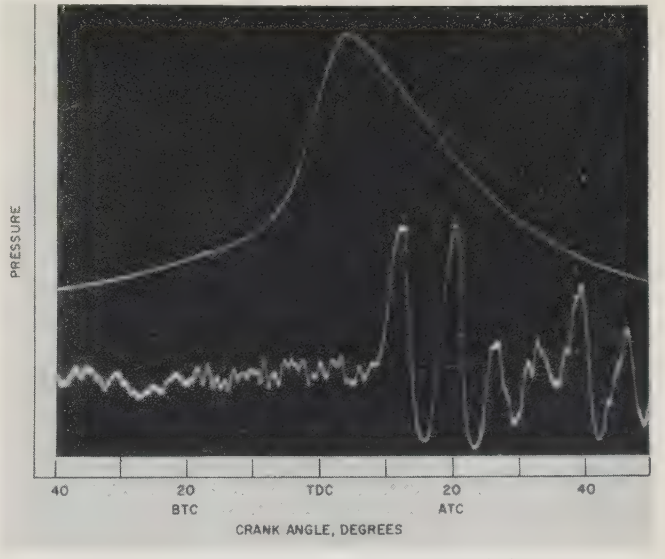

Fig. 3 — Rumble without knock in engine with deposits (17-deg btdc ignition, Make E, 12/1 compression ratio)

the previous figure illustrating normal combustion.

Prior to making the run from which the next two figures were obtained, the engine was operated for about 8 hr on a reasonably light-duty schedule with leaded commercial fuel containing about 43% aromatics. During the time that the pictures were made, the engine was run on the same fuel used to build up the deposits. Its quality was about eight octane numbers above the engine requirement.

Fig. 3 shows a cycle in which low frequency rumble occurred. There is no high-frequency knock. The rumble is indicated by the rapid rate of pressure rise following ignition and by the low-frequency noise (1100 cps) picked up by the microphone. The maximum rate of pressure rise illustrated in this figure is about 124 psi per deg. This is about eight times that measured from the pressure-time trace in Fig. 1 which illustrates normal combustion. The maximum pressure is about 1200 psi, as compared with 600 for normal combustion.

Fig. 4, from the same strip of film as Fig. 3, shows rumble and normal knock in the same cycle. The rumble is again indicated by both the rapid rate of pressure rise following ignition and the low-frequency noise picked up by the microphone. Superimposed on the low-frequency sound trace, and also readily seen on the pressure-time trace, is the high-frequency vibration which is characteristic of normal knock. Since the fuel was far above the normal engine requirement, it is believed that the knock was induced by the higher peak pressure which resulted from rumble.

During this same run, other cycles indicated all degrees of normal knock varying from none (as in Fig. 3) to much heavier than that shown in Fig. 4. The rapid rate of pressure rise characteristic of rumble was present in nearly all of the cycles. The noise that is heard may be rumble, knock, or both — depending upon the relative intensities of the two forms or abnormal combustion.

Table 2 summarizes pertinent data from these figures.

These results and others from similar studies in other engines strongly suggest that the low-frequency rumbling noises are caused by the extremely rapid rate of pressure rise and the high peak pressure attained when rumble occurs. The rapid rate of pressure rise generally starts earlier in the cycle than it does when normal knock occurs. The rapid rate of pressure rise and high peak pressure are probably caused by multiple ignition sources, such as might result from simultaneous firing of a number of spark plugs in the same combustion chamber. It has been seen that knock does not necessarily accompany rumble. Evidently, when rumble occurs without knock, ignition is from such a large number of sources that the fuel-air mixture is quickly consumed, leaving no end-gas pockets of mixture to detonate. There is no evidence to suggest that the rate of flame propagation at any one point is any different whether rumble is present or not. Whether normal knock accompanies rumble may be dependent on how many extraneous sources of ignition are present and active. The incidence of rumble appears to be a direct function of compression ratio, increasing as compression ratio increases. This suggests that rumble is a function of the increased tem-

Table 1 — Test Conditions

Engine Speed	1600 rpm
Ignition Timing 17-deg btdc—3% power loss from minimum best torque	
Compression Ratio	12/1
Throttle	Wide open
Fuel Air Ratio	Mean limit carburetor[a]
Intake Air Temperature	100F
Jacket Temperature	180F

[a] Midway between F/A limits specified by engine manufacturer.

Table 2 — Pressure and Noise Characteristics of Combustion Phenomena

	Normal Combustion	Normal Knock	Rumble	and Knock
Rate of Pressure Rise, psi/deg	16.5	16.5	124	124
Noise Frequency, cps	600	600[a]	1200	1200
Peak Pressure, psi	—	4800	1100	1100 & 4800

[a] Immediately prior to knock.

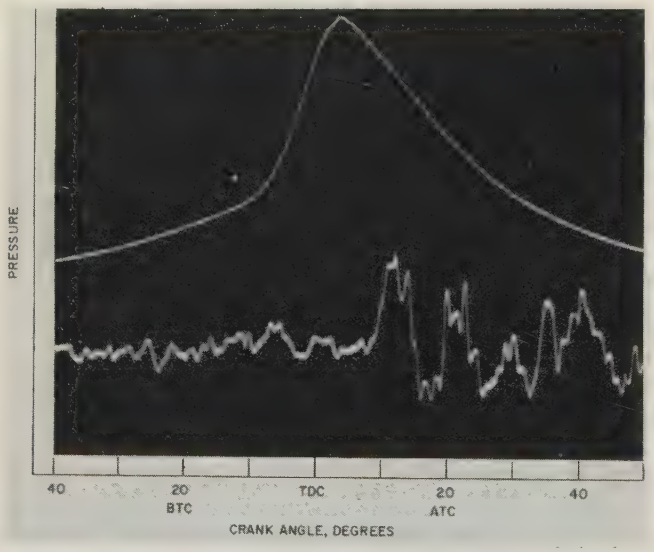

Fig. 4 — Rumble and knock in engine with deposits (17-deg btdc ignition, Make E, 12/1 compression ratio)

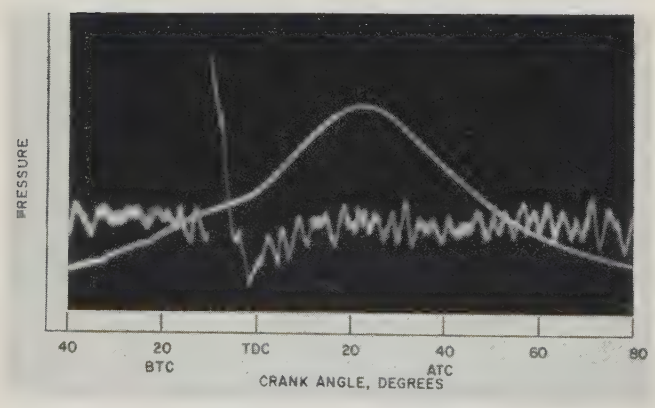

Fig. 5 — Normal combustion in clean single-cylinder engine (10 deg btdc, 11.3/1 compression ratio)

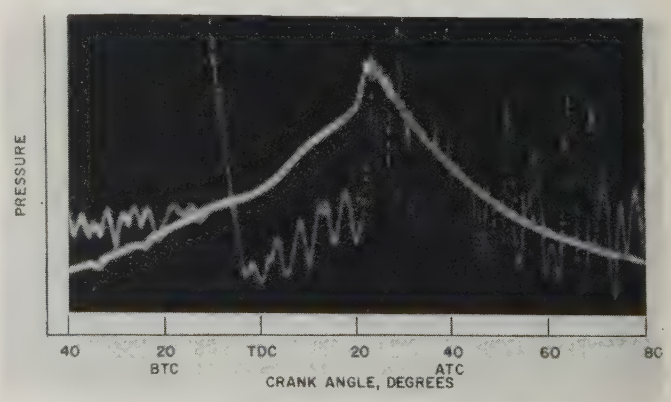

Fig. 6 — Knock in clean single-cylinder engine (conditions as in Fig. 5)

peratures and pressures which result when compression ratio is increased.

Rumble Induced in Clean Engine — The work already reported and other work done in both single-cylinder and multicylinder engines of high-compression ratio indicated that rumble is caused by high rates of pressure rise early in the combustion process. The higher than normal rates of pressure rise were undoubtedly the result of multiple ignition of the charge. These observations suggested that rumble could be induced in a clean engine by using more than one spark plug to ignite the charge, thus simulating the presence of hot deposits.

An investigation of induced rumble was conducted in a single-cylinder engine of 11.3/1 compression ratio having a hemispherically shaped combustion chamber and a domed piston top. The cylinder head was equipped with two 14-mm openings about 1¾ in. apart. These were located on opposite sides of a line connecting the centers of the valves. A combination spark plug and pressure-pickup indicator was used in one opening, and the standard plug in the other. This made it possible to ignite the charge at two different points and also to obtain pressure-time records. Other equipment, similar to that used in the multicylinder engine experiments provided a means of obtaining a photographic record simultaneously of both the pressure-time relationship in the combustion chamber and the sound effects of combustion.

Fig. 5 shows pressure-time and sound traces of full-throttle nonknocking combustion in the clean engine. Ignition was by the standard spark plug at 10-deg btdc, which is about 9 deg retarded from the minimum best torque (mbt) point. Fuel/air ratio was 0.08 and engine speed was 1140 rpm. The sound trace shows the background noise made by the engine and also the interference that resulted at 10-deg btdc when the spark occurred.

The records in Fig. 6 were obtained under the same engine conditions, except that a lower octane fuel was used so that the engine went into a rather heavy knock. Both the pressure-time and the sound traces show this effect quite clearly. Knock, occurring at about 20-deg atdc, was of the end-gas high-frequency type often referred to as normal knock.

Fig. 7 was obtained by simultaneously igniting the charge with both plugs at 10-deg btdc. The second spark plug simulated a hot deposit. The fuel was of sufficiently high octane number to prevent normal knock. That no such knock occurred is shown by the smooth pressure-time trace and the absence of a high-frequency record on the sound trace. However, the engine made the decided pounding or thudding noise typical of rumble. The sound trace shows that a low-frequency noise of about 800 cps was picked up by the microphone. This record is very similar to that obtained in the multicylinder engine when rumble is present. Decreasing the compression ratio of the single-cylinder engine to about 9.5/1 made it impossible to induce rumble by dual ignition. However, increasing the compression ratio to 13/1 made it possible to induce rumble by dual ignition at more retarded ignition timings.

Fig. 8 shows the pressure-time records of Figs. 5–7 superimposed upon each other. All three cycles were identical until tdc was reached. At this point the effect of the two ignition sources becomes apparent, the dual-ignition (rumble) cycle having a rate of pressure rise nearly three times that shown for normal combustion. The knocking cycle follows the normal combustion cycle until about 20-deg atdc when the end-gas effect from knock becomes apparent.

The increased work output suggested by the dual-ignition cycle is as expected, since the 10-deg btdc single ignition was about 9 deg retarded from the mbt point. The use of the second plug was equivalent to advancing the timing.

This work in a clean engine has provided additional evidence that rumble results from an abnormal rate of pressure rise and higher peak pressures.

Records showing rumble were obtained from the same engine when it contained deposits from mild-duty operation. These were almost identical to the multicylinder engine records discussed earlier.

Effect of Operating Conditions

During Deposit Accumulation — Operating conditions are quite important in laying down combustion-chamber deposits which are apt to cause rumble in vehicles. Rumble occurs oftener in engines operated on the light-duty driving schedules characteristic of much traffic driving than in engines used in heavier duty operation. In a 10/1 compression ratio dynamometer engine operated on a light-duty schedule, rumble occurred during a large percentage of the full-throttle tests of octane number requirement. When the same engine was operated on a schedule more characteristic of normal driving, rumble was much less frequent.

During Rumble Evaluation — Once deposits have

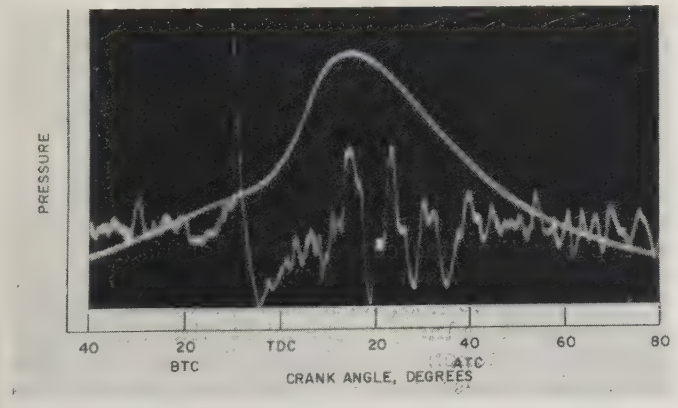

Fig. 7 — Rumble in clean single-cylinder engine (dual ignition at 10 deg btdc, 11.3/1 compression ratio)

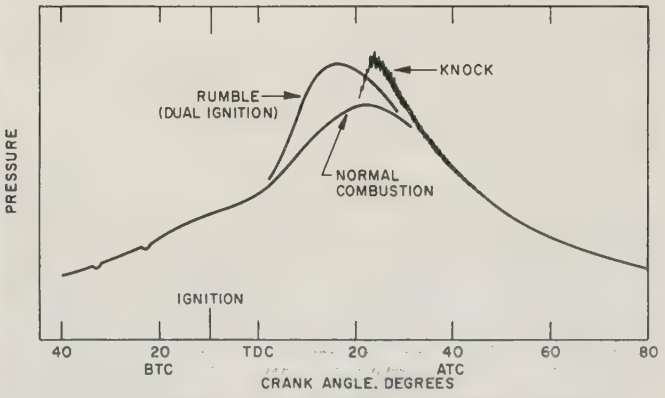

Fig. 8 — Normal combustion, knock, and rumble in a clean single-cylinder engine (11.3/1 compression ratio)

Table 3 — Rumble Data with Three Test Fuels

Fuel Composition	Fuel 1 23% Alkylate 68% Cat. Cracked 9% Polymer	Fuel 2 22% Alkylate 53% Cat. Cracked 25% Severe Reformate	Fuel 3 25% Straightrun 40% Cat. Cracked 35% Extracted Aromatics
Hydrocarbon Type			
Aromatics, %	18	30	48
Olefins, %	29	12	9
Inspection Data			
Gravity, deg API	61.9	58.8	52.1
ASTM 90% point, F	345	342	345
Rumble Data		Rumble, % of Observations	
3 Car Q	14	40	67
3 Car M	13	7	7
3 Car F	27	27	60
9-Car Average	18	25	45

Table 4 — Description of Two Blends of Fuel 2-E

	Blend A	Blend B
Composition, %		
Isopentane + alkylate	39	39
Toluene	22	41
High-boiling aromatics	20	20
Commercial solvent[a]	19	0
Aromatics, %		
Whole fuel	48	48
Last fraction (338 F and up)	29	20
ASTM Distillation		
90%, F	324	315
End point, F	395	375

[a] Boiling 300 410 F; 70% catalytic reformer bottoms.

been accumulated, the occurrence of rumble depends on how the evaluation is made. It is most likely to occur at wide-open throttle and high engine speed, and fuel/air ratio has a marked effect.

In a laboratory single-cylinder engine where fuel/air ratio could be controlled, there was no rumble at 0.095 F/A, light to medium rumble at 0.085, medium to heavy rumble accompanied at times by considerably advanced preignition at 0.075, and again no rumble at 0.060. In this case, fuel/air ratio was the only independent variable. The spread between 0.075 and 0.095 would probably not be wide enough to cover the fuel/air ratios prevailing in all eight cylinders of a vehicle under acceleration at wide-open throttle.

Increased cylinder temperatures and/or increased intake air temperatures also tend to increase rumble tendencies. With all other conditions remaining fixed, rumble is most likely to occur with a high barometer on a dry day.

Effect of Engine Design Factors

The rumble problem apparently is not confined to any one particular type of combustion chamber used in modern overhead valve engines; it has been observed in all types currently in use. At compression ratios of 11/1 and higher, rumble does not appear to be any worse with one combustion-chamber design than with another. However, this does not prove that combustion-chamber design cannot influence rumble.

Rumble has been observed and recorded in laboratory single-cylinder engines mounted on extremely rigid crankcases, and equipped with very rigid crankshafts, connecting rods, pistons, cylinders, and ample bearing capacity. Two different types of combustion-chamber design were operated on the same crankcase. One of these was a hemispherical chamber with a domed piston. The other was a wedge-type chamber designed for more turbulence. The rumble problem appeared to be equal in both cylinders at the same (12/1) compression ratio.

A shrouded intake valve was installed in the hemispherical-head single-cylinder engine referred to in the previous paragraph. This valve was expected to increase the tendency to rumble due to the increased rate of pressure rise resulting from faster burning of the more turbulent mixture. However, it was impossible to reproduce the same level of rumble readily obtainable with the standard intake valve. Longer periods of operation under light-duty conditions might have produced deposits which would have caused rumble. However, the same deposits which readily produced rumble with a standard intake valve would not do so with the shrouded intake valve. Air consumption was the same with both valves and ignition timing was at mbt in both cases. Apparently, with the shrouded intake valve, no portion of the rapidly swirling fuel-air mixture was in contact with hot deposits long enough for deposit-induced ignition to occur.

Effect of Fuel Hydrocarbon Composition

As mentioned, ignition of fuel-air mixture by hot combustion-chamber deposits (surface ignition) is responsible for the rumble noises in high-compression engines. From previous work by numerous investigators, it is known that fuel hydrocarbon composition and phosphorus can greatly affect the composition of combustion-chamber deposits and their tendency to produce surface ignition. Most of this earlier work was done at compression ratios which produced little or no rumble. Surface ignition was measured with ionization gaps or by audible means using the "key-off" technique. More recently, high-compression engines have been used in road and dynamometer tests, wherein rumble observations have been made on stabilized deposits formed with various fuel compositions.

Procedure — The general procedure was to operate the dynamometer engine or road vehicle on the deposit-accumulation fuel under light-duty conditions. At intervals of about 3 hr, after deposits had accumulated, a full-throttle acceleration was made on the "observation" fuel up to an engine speed of approximately 3000 rpm. The speed at which rumble started and the maximum sound intensity of the rumble were recorded. The intensity was noted as light, medium, heavy, and very heavy. Three "observation" fuels were generally used: (1) 105 octane number primary reference fuel (isooctane + tel), (2) 105 octane number 1957 CRC full-boiling reference fuel, and (3) deposit-accumulation fuel.

The data are reported as the percentage of the observations (accelerations) with a given fuel in which rumble of medium intensity or greater occurred.

Three 100 Research Octane Number Fuels — Earlier single-cylinder engine studies had shown that aromatic hydrocarbons tended to form the type of deposits that increase surface ignition. These laboratory findings were followed by a road test program. Three gasolines were selected to represent different refinery approaches which might be used for production of 100 Research octane number fuels. A brief description of the three fuels is presented in the upper portion of Table 3. Their overall composition varied in aromatic content from 18–

48%, and in olefinic content from 29–9%. Since the three fuels were very similar with respect to sulfur content, 90% ASTM distillation point and Research rating (100 octane number), their tendencies to form combustion-chamber deposits would be expected to be directly dependent on their hydrocarbon composition.

Each fuel was run until combustion-chamber deposits had stabilized (6000 miles) in each of nine vehicles (three makes) equipped with 10/1 compression ratio engines. The vehicles were driven over a controlled test course in the vicinity of San Bernardino, Calif. The driving schedule represented city-suburban passenger-car service and the top speed was limited to 40 mph.

In order to evaluate the rumble tendencies of the three fuels and their deposits, a full-throttle acceleration was made on the deposit-accumulation fuel each time the vehicle was knock-rated on the chassis dynamometer. The lower portion of Table 3 presents the rumble data in terms of per cent of the accelerations on the deposit-accumulation fuel in which rumble of medium intensity or greater occurred. While Car F did not produce knocking surface ignition, it did produce rumble noises, especially with Fuel 3. Very little rumble was encountered with Car M. Car Q's rumbling tendency varied directly with the aromatic content of the fuel.

The rumble obtained was affected not only by the deposits formed but also by the tendency of the fuel to be ignited by hot deposits. The findings were confirmed directionally, but at a lower incidence, by observations with primary reference fuels. Thus, increasing the aromatic content increased the formation of rumble-inducing deposits in those car makes which tended to produce this type of erratic combustion.

Effect of High-Boiling Aromatics — In another series of road tests at San Bernardino using 11/1 compression ratio engines, we were quite surprised to find that after a few hundred miles of operation, all of the vehicles were so rumble limited that they could not be knock-rated. Some of the vehicles produced highly objectionable rumble even during part-throttle acceleration.

An investigation of the cause of this excessive rumble disclosed that the test Fuel 2-E, blend A, contained 19% of a commercial solvent boiling from 300–410 F. Seventy per cent of the solvent (13.3% of the whole fuel) consisted of bottoms from a catalytic reformer. This solvent was not present in previous or subsequent blends. Table 4 lists composition and inspection data for blends A and B of Fuel 2-E. While both blends had the same total percentage of aromatics, the high-boiling solvent in blend A increased the percentage of aromatics in the last fraction of that fuel.

Table 5 compares the effects of two blends of Fuel 2-E in two different car makes in laying down rumble-inducing deposits. Observations were made both during full-throttle accelerations up a 7% grade and on the chassis dynamometer, using 105 octane number 1957 CRC full-boiling reference fuel and 105 octane number primary reference fuel. In every case there was less rumble in cars operated on blend B, clearly showing the effect of the higher boiling aromatics on the formation of rumble-inducing deposits.

In a single-cylinder engine, blend A produced approximately three times as much surface ignition as blend B, when both were evaluated by the ionization-gap technique.[2]

Alkylate versus Highly Aromatic Fuel — In order to further explore the effects of fuel type on rumble, two fuels of widely different composition were formulated. One was a full-boiling alkylate, the other a blend of light alkylate and catalytic reformate. This second blend, which contained 45% aromatics, is one possible route a refiner might take in making a high-octane fuel. Both fuels contained 3 ml tel and had Research octane numbers of about 106. The aromatic blend was somewhat higher boiling, as shown by the distillation data in Table 6.

Both fuels were run in an 11.6/1 compression ratio engine (Q) under a light-duty cycling schedule. The engine was connected to a dynamometer through a Hydramatic transmission. Knock and knocking-surface-ignition requirements were determined daily, using primary and full-boiling 1957 CRC fuels on alternate days. This was done during full-throttle accelerations in fourth gear. Rumble ratings were obtained every 3 hr during a wide-open-throttle acceleration on one of three reference fuels. The rumble data are expressed as the percentage of ratings in which rumble of medium intensity or greater occurred.

The results on the two fuels are presented in Table 6. When the engine was operated on a highly aromatic fuel until deposits had stabilized, the "noise" requirements could not be satisfied with 105 octane number fuels. Rumble occurred 100% of the time with commercial-type fuels and 89% with 105 oc-

Table 5 — Rumble Observations with Fuel 2-E, Blends A and B

105 Octane Number Reference Fuel	Rumble, % of Observations[a] 1957 CRC Full-Boiling Reference Fuel		Primary Reference Fuel	
Fuel 2-E, Blend	A	B	A	B
Car F—11/1 Compression Ratio				
7% Grade	87	80	63	25
Chassis Dynamometer	100	80	83	[b]
Car Q—11/1 Compression Ratio				
7% Grade	75	40	17	[b]
Chassis Dynamometer	100	[b]	100	[b]

[a] Medium intensity or greater.
[b] Data not obtained.

Table 6 — Knock and Rumble Requirements with Alkylate and Highly Aromatic Fuels

(Engine Q, 11.6/1 compression ratio; light-duty cycle, dynamometer tests; base fuels contained 3 ml tel)

Fuel Composition	Alkylate: 89% Full-Boiling Alkylate, 9% Straightrun, 2% n-Butane	Highly Aromatic: 55% Extracted Reformate, 33% Alkylate, 5% Light Straightrun, 7% n-Butane
Hydrocarbon Type		
Aromatics, %	0	45
Olefins, %	1	2
Saturates, %	99	53
ASTM Distillation, F		
10%	137	150
50%	213	255
90%	247	337
End point	419	418
Knock Requirements, Octane Number		
Primaries	99.9	Surface-ignition and rumble limited on 105 octane number
1957 CRC reference fuels	100	
Rumble, % Observations		
105 octane number primary	0	89
105 octane number 1957 CRC	0	100
105 octane number test fuel	0	100

[2] SAE Transactions, Vol. 62, 1954, pp. 40–49: "Deposit-Induced Ignition — Evaluation in Laboratory Engine," by D. A. Hirschler, J. D. McCullough, and C. A. Hall.

Table 7 — Effect of Phosphorous Additive on Rumble

(Controlled road tests, 40 mph top speed; fuel 2-E + 3 ml tel; multigrade oil)

11/1 Compression Ratio Vehicles	Rumble, % of Observations[a]	
	No Phosphorus	0.4 Theory Phosphorus
3 Car Q	33	7
3 Car M	53	40
3 Car F	53	7
9-Car Average	46	18

[a] 105 octane number '57 CRC reference fuel.

Table 8 — Effect of Phosphorous Additive in "On-Top-Of" Type Tests

(General transporation service; fuels contained 3 ml tel; multigraded oil)

Vehicle	Deposit Miles	Theories Phosphorus	Knock Requirement,[a] Octane Number	Rumble, % of Observations[b]
Car Q	4,160	0	103.2	75
11/1 compression ratio	3,714	0.4	103.3	17
	5,129	0	103.4	75
Car Q	13,355	0.4	103.1	50
12/1 compression ratio	3,871	0	104.5	100
Car E	11,870	0	103	75
12/1 compression ratio	2,000	0.4	103.3	40

[a] '57 CRC reference fuels.
[b] 105 octane number '57 CRC reference fuel.

tane number primary reference fuel. On the other hand, operation with the alkylate fuel resulted in a stabilized knock requirement of about 100 octane number, and no rumble occurred with any of the three reference fuels. This pair of tests illustrates the extreme importance of the type of fuel on which the deposits are accumulated.

Effect of Phosphorus Fuel Additives

It has been known for some time that phosphorous fuel additives are highly effective in reducing the tendencies of combustion-chamber deposits to ignite the fuel-air mixture. In view of this, one would expect phosphorous fuel additives to minimize rumble tendencies in high-compression engines. This has been found to be the case in both road and dynamometer tests.

Road Tests — In one series of controlled road tests in nine 11/1 compression ratio vehicles at San Bernardino, 0.4 theory of phosphorous additive reduced the incidence of rumble from 46% of the observations to 18%. These data are presented in Table 7. While Car M did not produce much rumble at 10/1 compression ratio (Table 3) it did produce considerable rumble at 11/1 compression ratio, compared with the other car makes.

Phosphorus fuel additives are also effective when added "on-top-of" stabilized combustion-chamber deposits. This is illustrated by the data in Table 8. Three high-compression vehicles were operated by various drivers in general transportation service until knock requirements had stabilized. The fuel-and-additive combinations were then changed, deposits were not removed, and the tests were continued until the deposit effects had again stabilized. These data show that phosphorous, while not completely eliminating rumble, does reduce its incidence. Furthermore, in these tests, phosphorous did not increase stabilized knock requirement.

The foregoing data show that phosphorous fuel additives are highly effective in minimizing rumble, even though they are not a complete cure for the problem.

Importance of Rumble Problem

To the Automotive Industry — Rumble may impose a limit on usable compression ratios. Possible solutions to the rumble problem via the fuel route have been discussed. At the present time, it is not clear whether the problem can be solved by engine design.

No case is known where engine damage has resulted directly from rumble. However, with sustained rumble, some portion of the combustion chamber, such as the spark plug or the exhaust valve, might get hot enough to take over as a source of ignition and cause runaway pre-ignition, with piston burning as the probable result.

To the Refiner — In the past, the refiner has been able to take care of erratic combustion noises by increases in fuel octane number. The advent of rumble in high-compression engines has posed a problem which cannot be solved in the same manner. As long as fuel octane number is high enough to satisfy the requirement of the engine for normal knock and knocking surface ignition, further increases in fuel quality do not help to reduce rumble.

The trend toward higher aromatic concentrations in gasolines will no doubt tend to increase rumble in the higher compression engines of tomorrow. While rumble tendencies can be greatly decreased by the use of highly paraffinic fuels, this may not be as economically attractive as the use of phosphorous fuel additives.

Summary

Data presented show that rumble is a surface-ignition phenomenon initiated by combustion-chamber deposits. It is a low-frequency noise in the range of 600–1200 cps, in contrast to the 4000–6500 cps resulting from normal knock and knocking surface ignition. There is evidence that the noise from rumble is caused by abnormally high rates of pressure rise and the resulting high peak pressures. Furthermore, these pressure effects are found to occur earlier in the combustion process than the end-gas type of reaction associated with normal knock and knocking surface ignition.

Rumble becomes increasingly more of a problem as compression ratio is raised above 9.5/1. It does not appear to be confined to any one particular type of combustion chamber. Also, making engines more rigid does not show promise of offering a solution to the problem.

Rumble-producing deposits are most likely to be produced by light-duty operating conditions. Once deposits are present, rumble generally occurs at wide-open throttle and high engine speeds. Such factors as fuel/air ratio, cylinder and intake air temperatures, and barometric pressure all influence the tendency of a given engine to rumble.

Unfortunately, increasing fuel octane number has little effect in minimizing rumble. However, other factors which reduce surface ignition also reduce rumble. Fuels with low deposit-formation tendencies have been shown to help alleviate the problem. While not a complete cure, phosphorous fuel additives do a good job in reducing rumble.

Acknowledgment

We are indebted to many of our associates for their contributions to this paper. Special recognition goes to D. L. Lenane, Owen Russell, and Edward Zelda for their assistance in obtaining the pressure-time combustion records, and to Larry Stinson for the San Bernardino road tests.

knock-knock:

Spark Knock, Wild Ping, or Rumble?

R. H. Perry, Jr., and H. V. Lowther, Socony Mobil Oil Co., Inc.

This paper was presented at the SAE Summer Meeting, Atlantic City, June 11, 1958

ENGINE noise has become an increasing problem with the higher and higher compression ratios of present-day automotive engines. Because fuel octane number cannot be raised indefinitely, the problem is one of engine design and selection of crankcase lubricating oils and gasoline formulations, the authors think.

This paper describes investigations into the cause of spark knock, wild ping, rumble, and the added problem of hot-spot surface ignition (which also intensifies as compression ratios increase). The authors have found gasolines with phosphorous additives, used with properly formulated multiviscosity lubricating oils, provide a partial answer to the problem of engine rumble.

The authors conclude that very exact tailoring of fuels, lubricants, additives, and engines will be necessary to prevent engine noise if compression ratios continue to rise.

COMPRESSION ratios of postwar cars have risen very rapidly. Since 1947 the top advertised compression ratio has increased by 2.75 units. During this time, the antiknock quality required to satisfy 95% of new model cars has risen about nine octane numbers. The joint efforts of the automotive and petroleum industries have made it possible to effect these increases and permit the American motorist to derive the benefits in the form of increased performance and/or fuel economy.[1]

If additional increases in compression ratio are to be practical, still further advances must be made in tailoring engines, fuels, and lubricants to function as a perfectly matched ensemble. In the past a great deal of emphasis has been placed upon minimizing spark knock requirement. However, with today's high compression ratio engines operating at higher and higher combustion temperatures, several forms of abnormal combustion are demanding considerable attention. Therefore, not only must work continue on minimizing spark knock requirement, but also efforts must be concentrated on minimizing abnormal combustion lest they become the limiting factor on further usable compression ratio increases.

In the Research Department of our company, a

[1] "Looking Ahead in Fuels for Automotive Transportation," by J. M. Campbell. Horning Memorial Lecture, 1957. SAE SP 216.

coordinated attack is underway to minimize the occurrence of wild ping, rumble, runaway surface ignition, and spark knock requirement increase. The purpose of this paper is to report on progress to date.

Spark Knock

Obviously, the most apparent way to control troublesome spark knock is to raise the octane number of the fuel. However, fuel octane numbers are extremely expensive and eventually a point of no return is reached where the engine performance gained is more than offset by the fuel cost. There are two other major ways to satisfy the demand for high octane numbers: one is through improved engine design and the other is through selection of the crankcase lubricating oil.

The subject of engine design should be left in the hands of the engine builders. However, the effect of engine lubricating oil on the stabilized octane number is of great interest. This phenomenon has been observed and reported by many investigators. L. Raymond and J. F. Socolofsky have presented considerable data illustrating differences between lubricating oils.[2]

Studies in later model, higher compression ratio engines have shown that significant differences are still present. Fig. 1 presents data obtained in nine 1956 passenger cars which had an average compression ratio of 8.3/1. An average clean engine octane number requirement at 93.4 was obtained. The cars were then driven under normal operating conditions with a multiviscosity SAE 10W-30 engine oil and it was found that the average stabilized octane number requirement was 95.9. At this point, without overhaul or any engine cleanup the oil was changed to a conventional SAE 20 grade product. The average stabilized octane number rose to 97.9. Thus, the multiviscosity engine oil provided a 2.0 octane number advantage over the conventional SAE 20 grade oil.

The differences in octane number noted above were believed to be due primarily to base stock characteristics and secondarily to chemical additive type. Further work, therefore, seemed justified on improving the combustion-chamber deposit tendencies of the multiviscosity oil. An experimental oil was designed which, although totally unrealistic from a commercial standpoint, had minimum combustion-chamber deposit forming tendencies.

This experimental oil was compared in eight 1957 cars with the same multiviscosity SAE 10W-30 oil used in the 1956 test. The 1957 cars were driven over a specific road course which included city, suburban, and high-speed driving. The combustion chambers were cleaned after stabilization on each oil before the next oil was tested.

The results of this test are shown in Fig. 2. The experimental oil had an average stabilized octane number requirement about 2.5 units below that of the multiviscosity SAE 10W-30 oil. These results illustrate that work on continued improvement of the combustion-chamber deposit-forming tendencies of engine oils is justified.

Wild Ping

One form of surface ignition is classified by the term "wild ping." These "wild pings" sound very much like spark knock to the uninitiated observer and probably would be called such by the average motorist. To the trained operator they sound sharper and clearer than spark knock and are erratic in nature — not reproducible on a cycle-to-cycle basis. Wild ping is believed to be due to ignition of the fuel-air mixture from overheated combustion-chamber deposits prior to spark ignition. This appears to result in a knock similar to that encountered when ignition timing is advanced — thereby increasing the octane number necessary to suppress noise. As might be expected, this form of surface ignition can be combated by minimizing the quantity of combustion-chamber deposits or altering the nature of the deposits. The L-head engine design, with its relatively high surface-to-volume ratio, proved to be an excellent tool for measuring the effect of deposit-modifying fuel additives. An example of the octane number savings that could be effected by altering the nature of the deposits in one make L-head engine of 7.7/1 compression ratio is shown in Fig. 3. In this case the engine, installed in a car, was driven to deposit stability on a commercial fuel and lubricant. It was found that this car had a spark knock requirement of 93 octane number. On 93 octane number fuel an average of five wild pings was heard on each acceleration. On 98 octane number fuel, an average of three wild pings would be heard on each acceleration. When 0.2 theory of phosphorous "A" was added to the base fuel and the combustion-chamber deposits restabilized (without removing combustion-chamber deposits between the two stabilization periods), the average number of wild pings per acceleration was reduced to a frequency slightly lower than three when using the 93 octane number fuel — less than was noted on the 98 octane number fuel before phosphorus was used. After using 0.2 theory phosphorus, only an occasional wild ping could be heard with the 98 octane number fuel. This reduction in wild ping was substantiated by a reduction in the number of preignitions visible on the Socony Mobil Cathode Ray Engine Analyzer.[3]

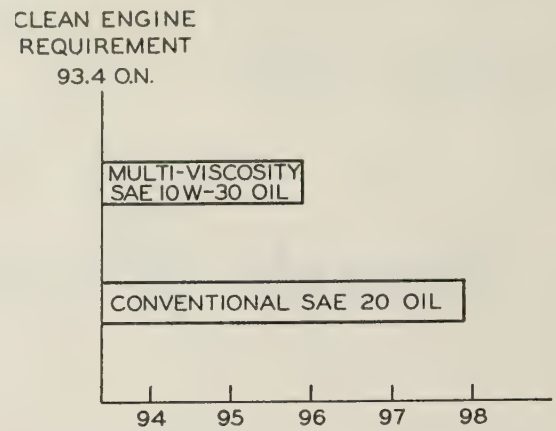

Fig. 1 — 1956 passenger-car test

[2] SAE Transactions, Vol. 63, 1955, pp. 132–144: "Designing New Performance into a Special Motor Oil," by L. Raymond and J. F. Socolofsky.

[3] "New Engine Analyzer," by E. A. Martin and J. H. Goffe. Paper presented at SAE Summer Meeting, Atlantic City, June, 1954.

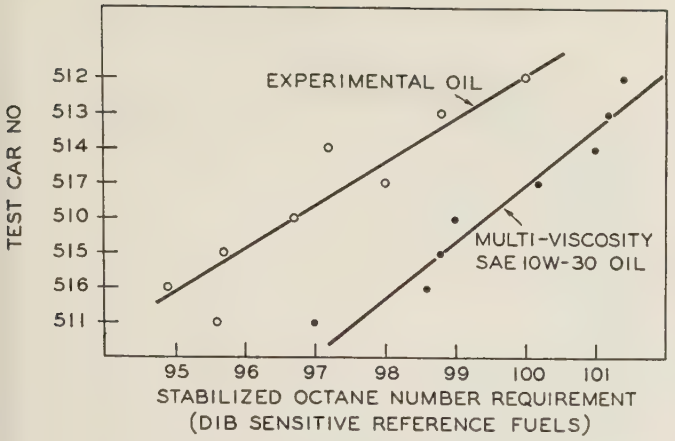

Fig. 2 — 1957 passenger-car test

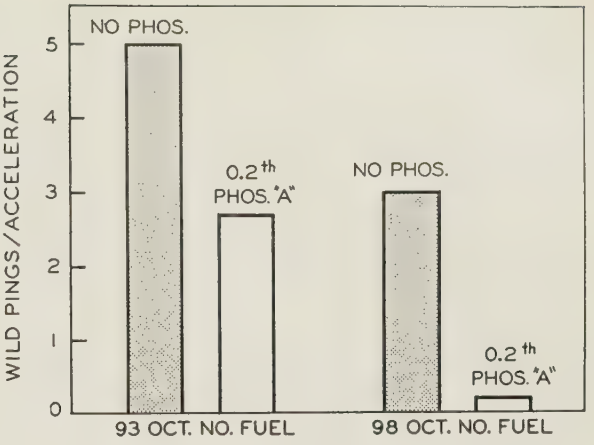

Fig. 3 — Effect of phosphorous additives on wild ping

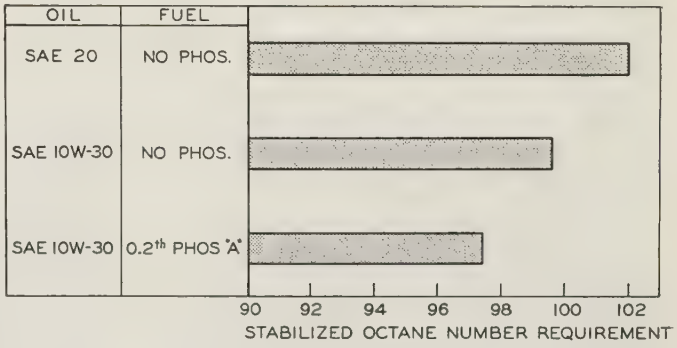

Fig. 4 — Octane number required to suppress wild ping 9.5/1 compression ratio engine

The example cited here is typical of that found in many other tests with similar design engines. In some cases the response to the additive was more dramatic; in others, less dramatic. Similar advantages have been shown for multiviscosity lubricants compared to conventional lubricants in this same type of test.

Laboratory tests with overhead valve V-8 engines of higher compression ratio have indicated similar advantages when combustion-chamber deposits are modified and/or reduced through the use of optimum fuel and lubricant formulations. For example, a 9.5/1 compression ratio V-8 overhead valve engine was operated on a low-duty cycle to build up deposits. Octane number requirements were measured once every 24 hr, or the equivalent of about every 600 miles of operation, for 240 hr or 6000 miles. Fig. 4 shows the reduction in requirement that was brought about through the use of multiviscosity lubricants and commercial gasoline containing 0.2 theory of phosphorus "A." When operated on nonphosphorus additive fuel and conventional SAE 20 grade engine oil, the stabilized requirement to suppress "wild ping" noise was 102 octane number. When operated on the same fuel but with a multiviscosity SAE 10W-30 engine oil, the requirement to suppress "wild ping" noise was reduced to 99.6. A still further reduction was accomplished when the engine was operated on the same fuel but containing 0.2 theory phosphorus "A" and the multiviscosity SAE 10W-30 engine oil — the requirement to suppress wild ping being lowered to 97.4 which was also the spark knock requirement. This dramatically illustrates the advantages to be gained by the combined use of fuels and lubricants designed to minimize the occurrence of "wild ping."

Rumble

Still another abnormal combustion phenomenon has reared its ugly sound as compression ratios have risen to their present level. Indeed, judging by its intensity in the engines modified to higher than standard compression ratio in the authors' laboratory, rumble appears to be a formidable hurdle that must be overcome before compression ratios can continue their upward trend.

Rumble is believed to be caused by unduly high rates of energy release resulting from too rapid burning of the fuel-air mixture. This rapid burning can be caused by multiple ignitions of the charge originating from overheated combustion-chamber deposits. It is influenced by fuel hydrocarbon type and appears to be related to the flame speed of the fuel being burned. It is believed possible to influence rumble tendency through combustion-chamber design. Based on studies carried out in a single-cylinder modified CFR supercharged engine, it is thought that the rumble noise emanates from vibration of engine parts at a cycle time approximating that when the piston is at bottom center following its power stroke. The engine was equipped to measure and record *P-T*, *dp/dt*, and aural noises. Slightly higher than normal combustion pressures and rates of pressure increase have been noted during the combustion cycle preceding this noise. It is hypothesized that these abnormally high pressures, or rates of pressure increase, result in bearing loads that exceed design capacity. It is thought that peak bearing loads would occur at about bottom center. Therefore, any increase in load would be expected to induce an overload at this time and might be the source of the rumble noise.

In multicylinder engines, concentrated efforts have been directed towards learning as much as possible about the effects of fuels and lubricants on rumble. Rumble has been encountered to a limited extent in several standard 1958 production cars. It has been found to be a formidable problem in all of the engines modified to higher than standard compression ratios. To date, tests have shown that rumble can be influenced by fuel hydrocarbon type,

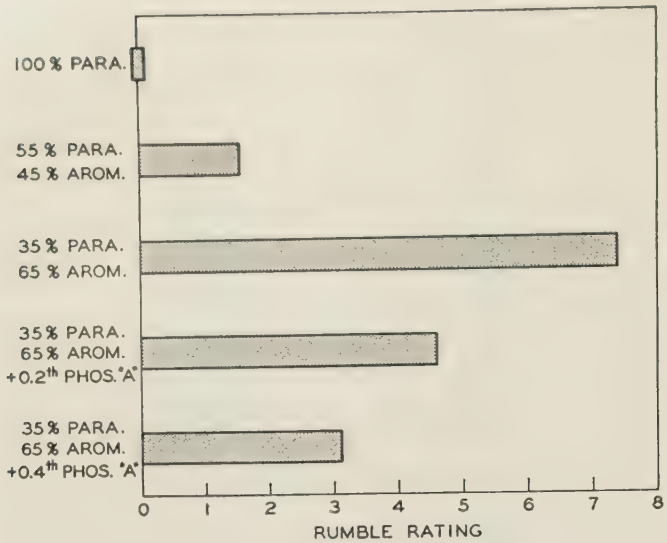

Fig. 5 — Effect of fuel composition on rumble

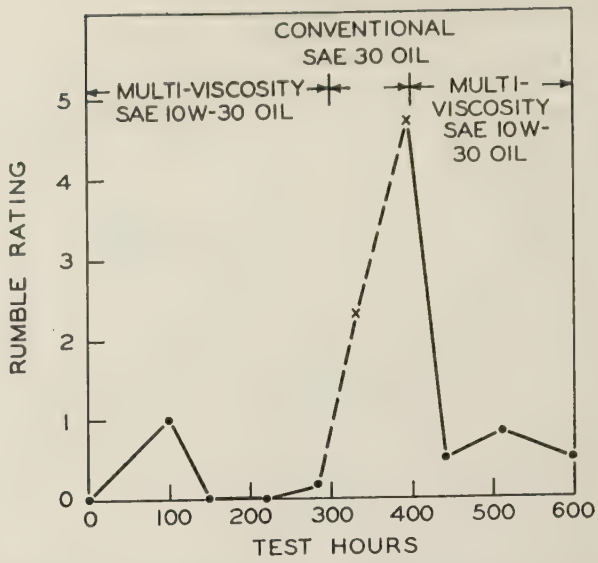

Fig. 6 — Engine rumble studies in 12/1 compression ratio engine

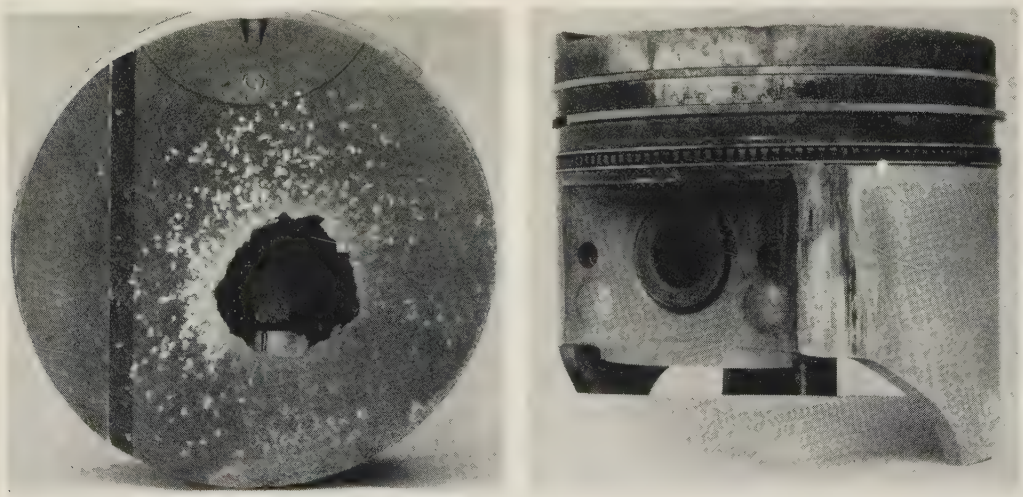

Fig. 7 — Hot-spot surface ignition

fuel additives, and lubricating oil formulation. But no commercially feasible fuel and lubricant combination has been found to completely eliminate this phenomenon in all engines. Therefore, assistance through the engine design will likely be required to prevent rumble.

One series of tests using a modified 11/1 compression ratio V-8 overhead valve engine installed on a laboratory stand illustrates the influence of fuel factors on rumble. The engine is operated on a light-duty cycle for about 220 hr or the equivalent of 7500 miles. Ratings are made once each 24 hr. A rumble number is assigned based on the average intensity of rumble encountered during 15 accelerations on primary reference fuel. A value of 10 would be assigned if heavy rumble were encountered on all accelerations. A value of zero would illustrate no rumble on any acceleration. Intermediate values indicate a rumble level between these extremes. A summary of the test procedure is attached as Appendix I. Results of the tests are shown in Fig. 5. In this series a multiviscosity SAE 10W-30 oil was used for all tests. As can be seen from the figure, a 100% paraffinic gasoline caused no rumble. A fuel containing 45% aromatics and 55% paraffins gave a rumble rating of 1.6, while a fuel containing 65% aromatics and 35% paraffins gave a rumble rating of 7.4. However, this relatively severe rumble was reduced through the use of phosphorus additive "A." At a concentration of 0.2 theory phosphorus, the rumble rating was reduced to 4.6; while at 0.4 theory the rumble rating was reduced to 3.2.

Tests in this engine and in road test cars have shown that fuel hydrocarbon type affects the rumble intensity that will be encountered in a given combustion-chamber environment. In a 1958 model car equipped with a standard 10/1 compression ratio engine, considerable rumble has been encountered when combustion-chamber deposits were stabilized using the nonphosphorus additive, high aromatic fuel shown in Fig. 5. With these stabilized combustion-chamber deposits, accelerations were made on a highly aromatic reformate gasoline just satisfying the no-knock spark knock requirement. The fuel used was 102 Research octane number and contained 59% aromatics. Heavy rumble was encountered on each of three successive wide-open throttle accelerations over a speed range from 2000 rpm to greater than 2900 rpm. Following these tests, ac-

Table 1 — Effect of Hydrocarbon Type on Rumble Tendency in 1958 Model 10/1 Compression Ratio V-8 Car

Order of Testing	Fuel			Rumble	
	Research Octane Number	Aromatic, %	Paraffinic, %	Intensity	Speed Range
1	102	59	41	Heavy	2000-2900 +
2	101	0	100	Trace on two accelerations	26000-2700
3	102	59	41	Light	2400-2900 +

celerations were made on other aromatic-type reference fuels with similar rumble experience, and the spark knock requirement was found to be 101 Research octane number in terms of this reference fuel system. Accelerations were then made using primary reference fuels (isooctane and tel). On 101 octane number primary reference fuel (which just satisfied the no-knock spark knock requirement), only a trace of rumble was noted on two or three accelerations over a speed range from 2600–2700 rpm. Since rumble intensity is known to be diminished by repeated wide-open throttle accelerations, the tests were repeated on the 102 octane number aromatic fuel to establish the degree to which rumble had been affected by the repeated wide-open throttle accelerations. In this case, the rumble tendency was found to have been reduced to a level where a light rumble was encountered over a speed range from 2400 to greater than 2900 rpm instead of the original level of heavy rumble over the range from 2000 to greater than 2900 rpm. These data are shown in Table 1.

Studies in another high compression ratio V-8 engine have shown that significant relief from rumble can also be obtained through engine oil formulation.

Several runs have been made in a 12.0/1 compression ratio V-8 laboratory engine running under the city-suburban type cycle described in Appendix II. The most interesting data illustrating rumble requirement are shown in Fig. 6. A paraffinic fuel containing 3 ml tel was the fuel for this run. For the first 282 hr a multiviscosity SAE 10W-30 engine oil was used and the rumble rating (described earlier) varied between 0 and 1. At this point the oil was changed to a conventional SAE 30 grade oil and at 330 hr (48 hr on the SAE 30 oil) the rumble rating rose to 2.3. At 398 hr (116 hr on the SAE 30 oil) a rumble rating of 4.7 was obtained. At this point the oil was changed back to the SAE 10W-30 product and by 430 hr the rumble rating was down to 0.5 and remained low until completion of the test at 600 hr.

When fuels of very high aromatic content are used in place of the paraffinic fuel in this engine, the rumble rating with the SAE 10W-30 oil rises by 3.0 to 6.0 numbers.

Hot-Spot Surface Ignition

As compression ratios and power outputs have risen, peak combustion temperatures encountered during periods of wide-open throttle operation have also arisen. This requires that all combustion-chamber parts be adequately cooled to prevent hot-spot surface ignition during periods of maximum power operation. If hot-spot surface ignition is not prevented, the motorist won't have to decide whether the knock that he hears is spark knock, wild ping, or rumble. His engine won't be operating long enough to matter!

Fig. 8 — Overheated spark plug

In the course of test work conducted by our company, destructive hot-spot surface ignition has been encountered on several occasions during periods of high output operation. An example of this is shown in Fig. 7. In this case the cause of surface ignition was believed to be overheated spark plugs which were aggravated by the overadvanced spark used during knock rating tests. This same type of trouble has been encountered in other makes of test cars. A picture of the spark plug, mounted in the head, is shown in Fig. 8. It will be noted that the center electrode is burned off well up inside the ceramic insulator. Also, the ground electrode is partially burned.

The spark-plug manufacturer is caught on the horns of a dilemma. On the one extreme, the plugs must be designed to dissipate the higher heat loads placed upon them by the higher combustion temperatures resulting from the higher horsepowers and higher compression ratios. On the other extreme, the plugs must also be designed to retain sufficient heat under low-duty stop-and-go driving to prevent fouling from combustion deposits. As engine power output has increased, the percentage of available power required to propel a car at light loads has decreased. With this reduction in power factor, the spark-plug manufacturer is forced to design present-day spark plugs to handle both higher and lower heat loads than were required in the past.[4] The plugs *must* be designed to handle the higher heat loads in order to prevent the hot-spot surface ignition. Then the designer does his best possible job to supply sufficient heat-retaining

[4] "New Engines Demand Tailored Spark Plugs," by R. C. Teasel. Paper presented at SAE Mid-Continent Section Meeting, Tulsa, October, 1956.

Table 2 — Laboratory Test Conditions — Spark-Plug Fouling

(10/1 Compression ratio V-8 overhead valve engine)

Deposit Buildup Cycle					
	Idle	Cycle Operation			
Time, min	15			45	
Time, sec	—	24	12	6	58
Speed, rpm	500	500	{ 500 / 1500	{ 1500 / 1200	1200
Condition	Idle	Idle	Road Acceleration	Deceleration	Road Load
Load, bhp	1	1	Mild	—	8
Water Out Temperature, F	140 ± 5				
Spark Plug	Champion J-7				
Air/Fuel Ratio (orsat)					
Idle (rich)	9/1				
1200 rpm Road Load	12/1				
Rating of Spark-Plug Performance					
Procedure	4 Wide-open throttle accelerations 800-2500 rpm				
Measure	1. Increase in acceleration time 2. Plug fouling shown by engine analyzer				

Table 3 — Road Test Conditions — Spark-Plug Fouling

Test Course	
Conditions	Heavy City Traffic
Miles per Lap	10.4
Average mph	20
Maximum mph (legal)	35
Maximum Acceleration	5 in. manifold vacuum minimum
Parked Idle Time	15 min per lap
Approximate Miles per 8-hr Shift	120
Air/Fuel Ratio	Rich as possible for smooth idle
Idle	
Orsat	10/1
Measured Fuel and Air	8/1 – 9/1
30 mph	12/1
Rating of Spark Plug Performance	
Procedure	8 Wide-open throttle accelerations, 10-60 mph
Measure	1. Increase in acceleration time 2. Plug fouling shown by engine analyzer

Table 4 — Operating Conditions for 11/1 Compression Ratio Laboratory Engine "A"

(test duration – 220 hr)

Type of Operation	Constant Speed	Cyclic[a]			
		Idle	Acceleration	Run	Deceleration
Time, min	60	1/2	1/2	2	1/4
Speed, rpm	1700	500	to 1700	1700	to 500
Inlet Air Temperature F	105	105	105	105	105
Coolant Temperature, F	180	180	180	180	180
Oil Temperature, F	200	200	200	200	200
Spark Advance, btdc	40	5	to 40	40	to 5
Intake Manifold Pressure, in. of Hg	11	12	22	11	Closed throttle

[a] Cyclic procedure repeated for 1 hr before returning to constant speed operation.
NOTE: Accelerations for ratings from 500–2800 hpm.

Table 5 — Test Operating Conditions

	City Cycle			Country Cycle	
	Idle	Accelerations	Run	Low Speed	High Speed
Time, sec	30	10	50	60	120
Engine, rpm	450	—	—	—	—
Dynamometer, rpm	0	to 1300	1300	900	2150
Dynamometer, bhp	—	—	10	5	30
Jacket Out Temperature, F	180 ± 5			180 ± 5	
Oil Sump Temperature, F	250 maximum			250 maximum	

Alternate between City Cycle and Country Cycle hourly.

properties to prevent combustion-deposit fouling under low-duty operation.

It is in this low-duty operation that the petroleum industry can make a significant contribution toward easing this problem. If sufficient antifouling properties can be provided through the fuel and lubricant, then the manufacturer can use a colder spark plug and minimize hot-spot surface ignition without encountering the troublesome plug fouling.

A previously published survey, conducted by the Ethyl Corp., has shown that one-third of late-model cars tested have plugs fouled enough to reduce engine performance by 20% or more.[5] A survey conducted by our laboratories in 1954 showed 62 of 150 cars tested (41%) had one or more plugs fouled or partially fouled.

Tests have shown this fouling tendency can be reduced through the use of fuel additives. One laboratory engine test used in our laboratory to measure spark-plug fouling is conducted on a 10/1 compression ratio V-8 overhead valve engine operated under low-duty cyclic conditions. In this test, spark-plug life has been defined arbitrarily as the engine operating hours to a 20% increase in wide-open throttle acceleration time. Details of the test procedure are shown in Table 2. Typical results are shown in Fig. 9. Using the defined criteria of spark-plug life, it can be seen that the base fuel caused failure after 12 hr. With the additive fuel, the spark-plug life was prolonged to 31 hr.

Tests in passenger cars have shown similar results. In one series of tests with passenger cars operated through heavy city traffic, results were obtained as shown in Fig. 10. In this case the car was a standard production 1956 model of V-8 overhead valve design having 8/1 compression ratio with a 2-barrel carburetor and automatic transmission. Details of the test procedure are shown in Table 3. It can be seen that after 1000 miles of operation on the base fuel, the time required to accelerate from 10 to 60 mph had been increased by 60% due to spark-plug misfiring. Using this same fuel containing 0.2 theory phosphorus "A," the acceleration time had been increased by only 15%. And approximately this same level of performance was maintained until the test was discontinued after 3500 miles of operation.

It is a well-known fact that sustained high-speed driving tends to reduce the deposits that cause plug misfiring. It is interesting to note this effect as seen with the two fuels shown in Fig. 10. After 10 miles of operation at 60 mph using the base fuel, the acceleration time was reduced. Instead of a 60% increase in acceleration time, there was only a 40% increase in acceleration time. Using the fuel containing 0.2 theory phosphorus "A," the acceleration time was reduced to almost the equivalent of that obtained with new plugs.

Conclusions

If significant increases are to be made in usable compression ratios, over and above those of today's highest compression ratio cars, astute engine design and tailor-made petroleum products must roll

[5] "Spark Plug Fouling: A Survey — Test Procedures — Fuel Factors," by C. A. Hall, R. C. Beaubier, E. C. Marckwardt, and R. L. Courtney. Paper presented at SAE Annual Meeting, Detroit, January, 1957.

back the abnormal combustion barrier that is blocking the avenue of progress. Fuel and lubricant composition and additive content, as well as engine design, determine how formidable this barrier will be. Very exact tailoring of fuels, lubricants, additives, and engines appears necessary to prevent engine noise, abnormal combustion, and/or spark plug misfiring. How successfully the automotive and petroleum industries meet these sometimes diverse but nevertheless exacting requirements will determine whether the knock heard will be spark knock, wild ping, or rumble.

APPENDIX I

Test Setup

Engine — 11.0/1 compression ratio engine "A."

Procedure — The engine is operated under light-duty simulated cyclic-city and suburban driving conditions. Every 24 hr the engine is rated for octane number requirement and rumble tendencies. The first five accelerations of each rating period are made on isooctane plus 3 ml tel per gal. If rumble is present, the intensity and speed range over which the noise is present are recorded. The octane number requirement is then determined. The occurrence of rumble, including speed range and intensity, is recorded when detected. (See Table 4.)

Interpretation of Rumble Data

A minimum of 15 accelerations is usually required to establish the spark knock and rumble requirements of the engine. To maintain a consistent approach, the occurrence of rumble is measured by the intensity of rumble occurring on the first 15 accelerations. A value is assigned for each rumble intensity as follows:

Heavy Rumble	10
Medium Heavy Rumble	7.5
Light Rumble	5
Trace Rumble	2.5
No Rumble	0

The rumble rating is then obtained by assigning each acceleration a number according to its rumble intensity, adding these figures, and dividing the total by the number of accelerations (15). For example:

	Rumble Value		No. Accelerations	
Heavy Rumble on Accelerations 1–3	10	×	3	= 30
Medium Heavy Rumble on Accelerations 4 & 5	7.5	×	2	= 15
Trace Rumble on Accelerations 6 & 8	2.5	×	2	= 5
No Rumble on Accelerations 7 & 9–15	0	×	8	= 0
Total				50

Rumble Rating = 50/15 = 3.3

The final rumble rating is the average of the individual daily ratings starting with the 48 hr rating. (The 0 and 24 hr ratings are not included.)

APPENDIX II

Engine — 12.0/1 Compression Ratio Engine B.

Outline — A special high compression ratio test engine is operated under cyclic city-and-suburban driving conditions to build up combustion-chamber deposits. Periodic octane number requirement determinations are made to observe changes in requirement, preignition, and rumble as deposits are accumulated. (See Table 5.)

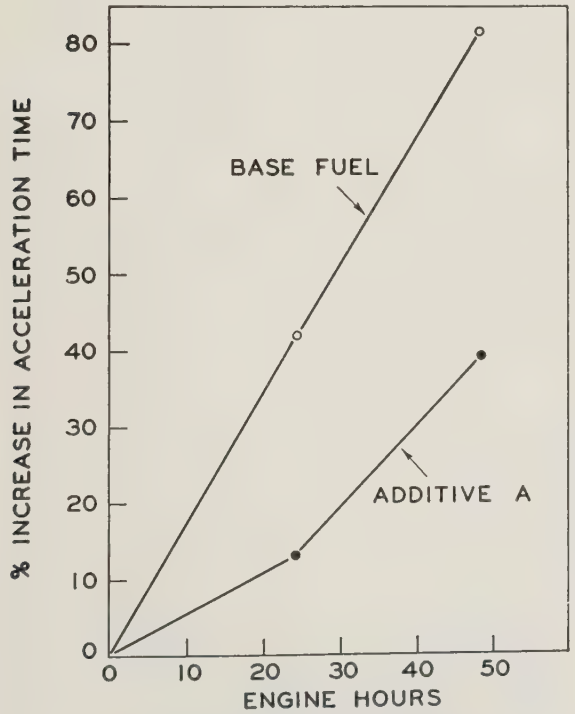

Fig. 9 — Laboratory spark-plug fouling test

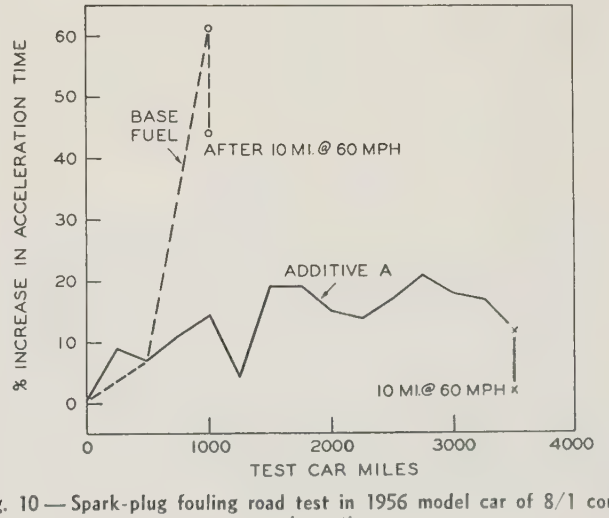

Fig. 10 — Spark-plug fouling road test in 1956 model car of 8/1 compression ratio

THIS paper summarizes a series of experiments to determine the cause of combustion noise in an automotive engine.

Results indicate that wild ping is associated with fuel octane number and rumble with surface ignition. Rumble can be reduced by careful selection of base stocks of fuels, although deposit-modifying additives also have a minimizing effect.

The author concludes by stating that higher and higher compression ratios will increase the problems of engine noise.

Knock, and

H. F. Hostetler and W. R. Tuuri,
The Standard Oil Co. (Ohio)

This paper was presented at the SAE Summer Meeting, Atlantic City, June 11, 1958.

IF A CAR develops combustion noise on the road, the motorist may get angry. Because he can blame the engine or the fuel, both the automotive and petroleum industries have a common interest here. More particularly, both industries wish to know exactly what these noises are and how they can be controlled or eliminated.

Road antiknock performance is a function of fuel octane quality and engine design considerations. Several excellent papers on this subject point out that by maintaining proper Research and Motor octane ratings of fuels and by judicious compression ratio, distributor vacuum, and centrifugal advance, and air fuel ratio selection, spark knock can be controlled.

Wild ping, the high frequency, randomly occurring, violent, spark-like knock evolving at low speeds with various engines, can be controlled by fuel composition, octane level, and vehicle design factors. Papers on this subject are noted in References. Recent tests run by our laboratories substantiate in general these findings. However, because little written reference material is available on rumble, this paper will cover recent findings relating rumble to fuels and engines.

Road Test Program

Our recent program involved 64 fuel combinations following a statistical design to study the deposit effects of base stocks and additives. The program was conducted in eight 1956 model vehicles with 10.3/1 compression ratio V-8 engines. Each cylinder of each engine was equipped with ionization probes to measure surface ignition activity. Each gasoline blend was used in the vehicle for 3600 miles. Deposits were accumulated under light-duty city driving conditions. In addition to octane and surface ignition requirements, occurrences of rumble were observed. Incidences of rumble were recorded when heard during periodic level road full-throttle accelerations throughout the test program. Rumble —the dull thudding noise much lower in frequency than either spark knock or wild ping—was generally observed at high vehicle speeds and with fuels having octane ratings considerably above the octane requirements of the test cars. One 10W–30 motor oil was used in all road tests.

In this program, it appeared that surface ignition, as measured with the ionization probes, correlated to a high degree with the incidence of rumble. This relationship is shown as Fig. 1 where the fuels were classified into four groups by surface ignition counts. These surface ignition counts were then plotted against per cent of fuels rumbling.

A correlation analysis was made between rumble noise and audible wild ping severity. The results indicated that there was little or no correlation between the two. However, a fair degree of correlation existed between the road octane level of the test fuels and the level of the wild ping activity.

Gasoline blending stocks affect rumble as shown in Fig. 2. In this chart, alkylate gave essentially no rumble. Fifteen per cent motor polymer showed only a 6% rumble incidence. Fuels containing 25% cat distillate had 36% more incidences of rumble than those not containing cat distillate. Fuels containing 25% cat reformate had an incidence of rumble 66% higher than when none was present.

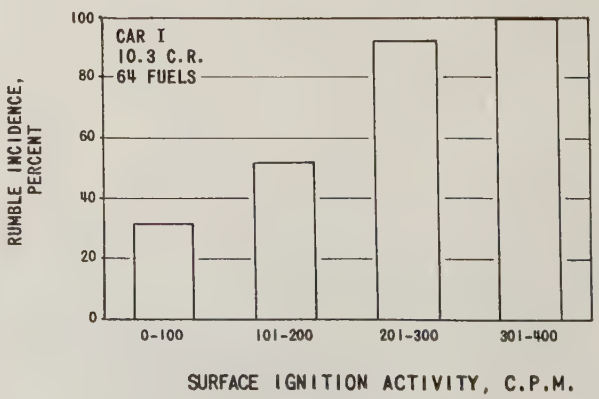

Fig. 1 — Surface ignition versus rumble

Rumble, Ping

Gasoline additives help control rumble. In the road test program, two chemically different popular deposit-modifying additives were investigated separately and in combination. Fig. 3 shows that additive A was effective in reducing the incidence of rumble from 94 to 54%. Additive B reduced the incidence of rumble to 44% while the two additives together reduced it to only 25% of that of the base fuels tested.

Laboratory Engine Tests

In order to obtain more quantitative data on rumble, a program was set up to develop a valid and reliable technique, to obtain more fuel-additive information, and to study engine operating variables as related to rumble. Two test methods were employed: (1) a determination of the maximum manifold vacuum at 3000 rpm at which rumble was observed and (2) a determination of the rpm at which rumble was first observed during wide-open throttle accelerations. A 1958 V-8 engine coupled to a dynamometer was used in this test. Three fuels of 102 Research octane, all containing 3.0 ml. tel per gal, were blended as shown in Table 1 below to study the effects of hydrocarbon type on rumble. These consisted of a highly paraffinic, a balanced, and a highly aromatic fuel.

During the laboratory tests, equilibrium deposits in the engine were accumulated with a commercial-type fuel containing tel but no other additives. This fuel was also used to restore deposits between ratings when the engine was operated for 15 min at 1500 rpm and 25% load.

An analysis of variance revealed that both test techniques separated the fuels and engine operating variables significantly. However, the vacuum-limiting technique was slightly more precise and somewhat more sensitive in separating test variables.

Theorizing that the dull thud (rumble) emanating from an engine was the result of connecting-rod bearing to crankshaft journal pounding, the viscosity of the motor oil was varied and changes in rumble severity noted. Fig. 4 indicates that as the oil viscosity (SSU at 210F) increases, the intensity of rumble severity decreases. Note the differences between fuels.

The effect of air/fuel ratio on rumble was studied. Fig. 5 illustrates the results. These data show an increase in the proneness to rumble as the air/fuel ratio was increased from 10/1 to 13.4/1. At a higher air/fuel ratio of 15/1, the severity of rumble decreased moderately. It is interesting to note that the peak rumble intensity appears to be about 12.5/1 air/fuel ratio. This is in the range of best power air/fuel ratio for this engine. Also, combustion-chamber temperatures are near their maximum here. The paraffinic fuel was practically innocuous to rumble at the three air/fuel ratios. The balanced

Table 1 — 102 Research Method Octane Number Blends
(3 ml tel per gal)

	Paraffins, %	Olefins, %	Aromatics, %
Paraffinic fuel	100	0	0
Balanced fuel	51	7	42
Aromatic fuel	18	0	82

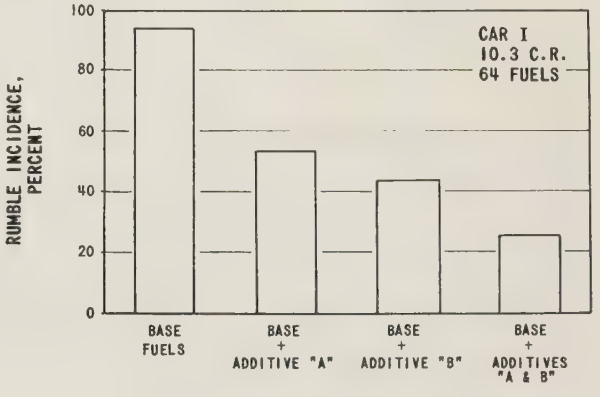

Fig. 3 — Gasoline additives

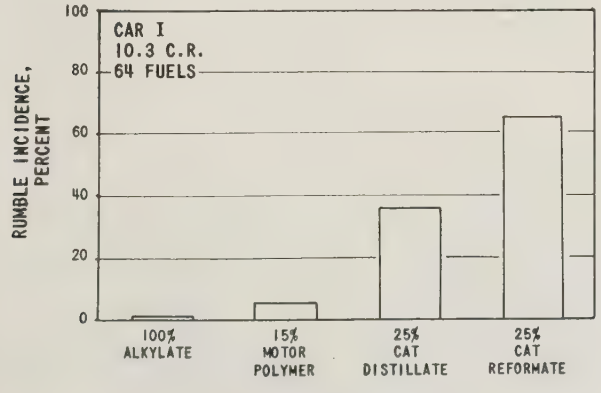

Fig. 2 — Gasoline blending stocks

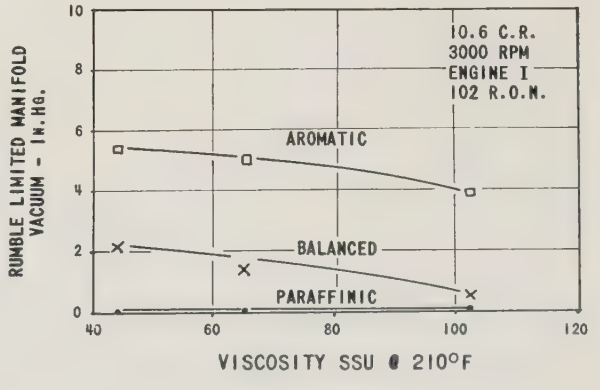

Fig. 4 — Oil viscosity

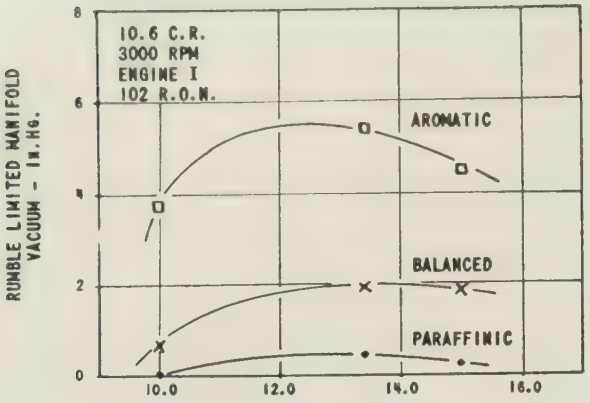

Fig. 5 — Air/fuel ratio

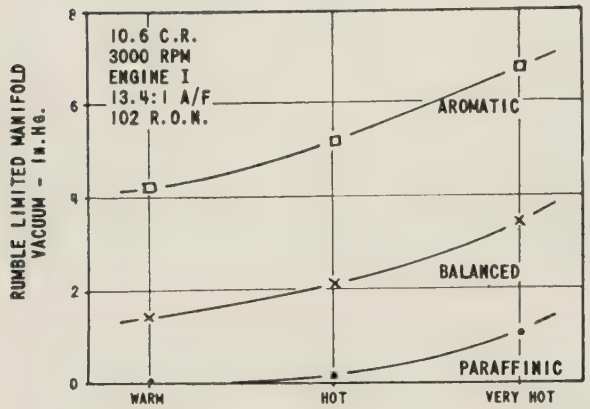

Fig. 6 — Spark-plug heat range

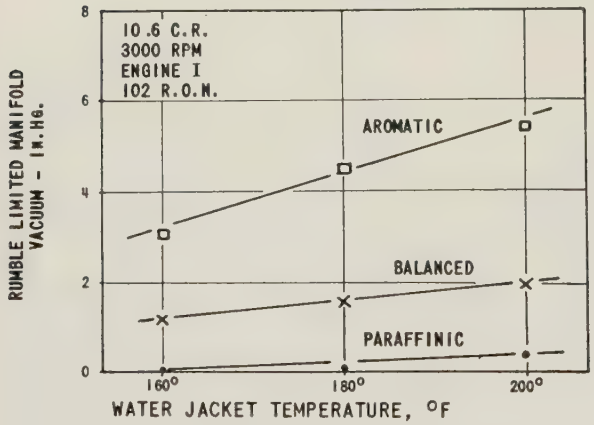

Fig. 7 — Water jacket temperature

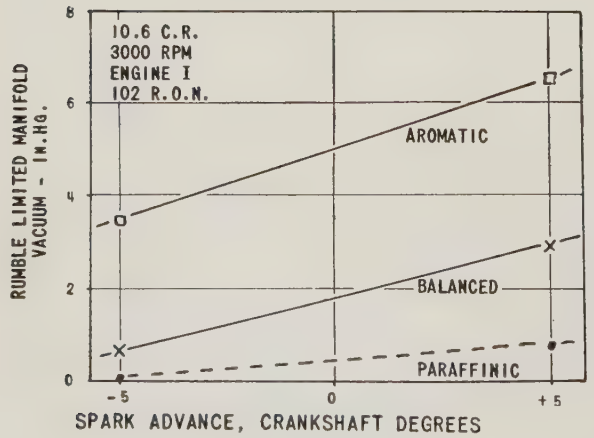

Fig. 8 — Spark advance

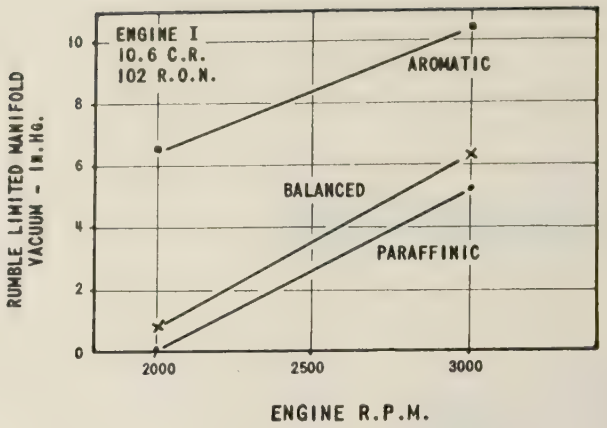

Fig. 9 — Engine rpm

hydrocarbon type fuel exhibited some rumble, while the aromatic fuel rumbled severely at the three air/fuel ratios examined.

The effect of spark-plug heat range on engine rumble was explored. These effects at 13.4/1 air/fuel ratio are shown as Fig. 6. These data indicate that as the heat range of the spark plug is increased from warm to hot to very hot, the severity of rumble increases significantly. In this study, the three fuels showed the same differences as described in the previous illustrations.

The effect of water jacket temperature on rumble was studied. Fig. 7 shows that the severity of rumble increases somewhat as the water jacket temperature is increased from 160 to 200F. This water temperature effect is more pronounced with the aromatic fuel.

The results of advancing and retarding engine spark ignition timing were investigated. Fig. 8 shows that the severity of rumble increases considerably as the basic ignition setting is increased from 5 deg atdc to 5 deg btdc.

In both the road and laboratory tests, it was observed that the severity of rumble increased as the engine speed was increased. Fig. 9 shows the data observed in the laboratory test.

Fig. 10 illustrates the effect of compression ratio changes on rumble severity. It can be concluded from this chart that an increase in compression ratio will seriously increase the severity of rumble for the paraffinic, balanced, and aromatic fuels tested.

Fig. 11 shows the rumble limited bhp which could be obtained from the test engine at the three compression ratios tested. Note that as the compression ratio is increased, the rumble limited bhp is significantly reduced. This is true through the range of hydrocarbon-type fuels investigated.

Conclusions

As a result of these studies, it is concluded that knock, rumble, and ping mean a lot — a lot of noise or a satisfied customer. In addition:

1. Wild ping is associated with octane number.
2. Rumble is related to surface ignition.
3. Fuels can be designed to provide minimum rumble through the proper selection and blending of base stocks.
4. Deposit-modifying additives reduce rumble.
5. The automotive manufacturer can minimize rumble by proper selection of compression ratio,

air/fuel ratio, thermostats, spark advance, and spark-plug heat range.

6. Higher compression ratios may increase nothing but customer complaints.

Acknowledgments

The authors wish to acknowledge their thanks for the efforts of N. Bender, R. Ewing, and W. Hutchings, whose assistance contributed to the work reported in this paper. The contributions of J. August, Jr., Chief of the Automotive Engineering Division, and E. H. Scott, Section Supervisor of the Automotive Engineering Division, have been particularly valuable.

References

1. *Petroleum Refiner*, Vol. 33, August, 1954, pp. 97–100: "How Effective Are Gasoline Additives?," by F. C. Burk, L. J. Test, and E. R. Jackson.

2. "Combustion Chamber Deposit Problem in High Compression Ratio Engines," by M. W. Corzilius, D. R. Diggs, and R. A. Hoffman. Paper presented at API 21st Mid-Year Meeting, Montreal, May, 1956.

3. "Laboratory Octane Ratings — What Do They Mean?," by R. B. Fell and H. F. Hostetler. Paper presented at SAE National Fuels and Lubricants Meeting, Cleveland, November, 1957.

4. SAE Transactions, Vol. 61, 1953, pp. 361–377: "Combustion-Chamber Deposition and Knock," by H. J. Gilson, C. A. Hall, and D. A. Hirschler.

5. SAE Transactions, Vol. 62, 1954, pp. 40–49: "Deposit-Induced Ignition — Evaluation in Laboratory Engines," by D. A. Hirschler, J. D. McCullough, and C. A. Hall.

6. "Result of Use of Boron as Gasoline Component," by E. C. Hughes and E. O. Hook. Paper presented at NPA Meeting, Cleveland, April, 1956.

7. "Future of Combustion Research," by E. C. Hughes. Paper presented at American Chemical Society Meeting, Dallas, April, 1956.

8. "Combustion-Chamber Geometry and Fuel Utilization," by J. C. Hughes. Paper presented at SAE Annual Meeting, Detroit, January, 1957.

9. SAE Transactions, Vol. 62, 1954, pp. 32–39: "Investigation of Preignition in Engines," by A. O. Melby, D. R. Diggs, and B. M. Sturgis.

10. "Preignition in Automotive Engines," by J. R. Sabina, J. J. Mikita, and M. H. Campbell. Paper presented at API Division of Refining Mid-Year Meeting, New York, May, 1953.

11. "Preignition Resistance of Fuels," B. M. Sturgis, E. N. Cantwell, W. E. Morris, and D. L. Schultz. Paper presented at API 19th Mid-Year Meeting, Houston, May, 1954.

12. SAE Transactions, Vol. 62, 1954, pp. 57–65: "Some Effects of Fuels and Lubricants on Autoignition in Cars on the Road," by R. K. Williams and J. R. Landis.

13. "Some Factors Involved in Surface Ignition in Spark-Ignition Engines," by D. B. Wimmer. Paper presented at SAE National Fuels and Lubricants Meeting, Tulsa, November, 1956.

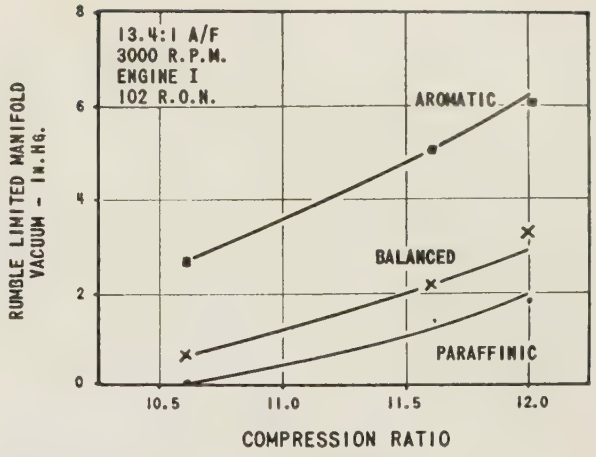

Fig. 10 — Compression ratio

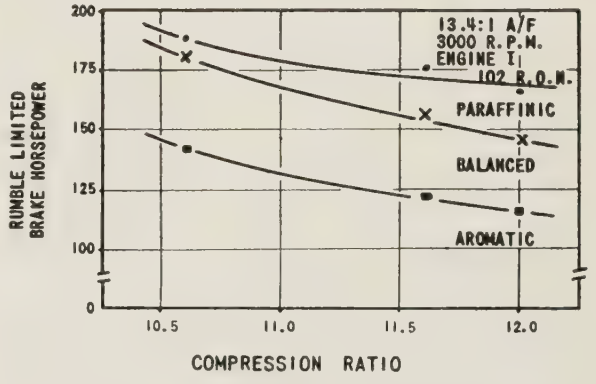

Fig. 11 — Compression ratio versus power

DISCUSSION

Rumble Varies With Engine Design

— F. T. Finnigan
Pure Oil Co.

IN CONDENSING such a research program to a brief presentation, it is logical to assume that many factors of interest had to be omitted. It would be appreciated if the authors would offer comment on the following questions:

1. What was the range of the sensitivity of the test fuels used and was any correlation noted between the incidence of rumble and fuel sensitivity?

2. Were any fuels blended using markedly different composition but the same sensitivity and Research octane number and if so, was there then a marked difference in the rumble tendency of the fuels?

3. Is it possible that the results of the investigation with increasing compression ratio using fuels of constant 102 Research octane number were affected by fuel octane quality as related to the engine's octane requirement?

4. Do the authors have data that would give some idea of the expected precision of the work carried out at 3000 rpm under conditions of increasing manifold vacuum for the measurement of rumble?

Many of my questions result from the fact that we have found rumble rather difficult to tie down in precision terms. We have also found it to vary with engine design.

At the suggestion of the Ethyl Corp., we refitted our 1956, 12/1 compression ratio Oldsmobile engine with alumi-

nized exhaust valves. This modification resulted in a very marked reduction in rumble in this engine, while the same fix in another engine has failed to produce measurable improvement. This may be due to the numerous other engine parameters pointed to by the authors. I suspect air/fuel ratio is an important one.

These authors tend to single out the petroleum industry's high-octane aromatics, greatly depended upon to assist in the operation of our high-power vehicles, as a source of much of the difficulty encountered. It should be pointed out that the aromatic fuel contained 82% aromatics, the source of which is not stated. I doubt very much if any of us will be concerned with fuel performance at that level of aromaticity. A look at the balanced fuel at the more realistically commercial level of 42% aromatics shows data more closely resembling that obtained with paraffins which rated "top billing" throughout. Would the authors care to comment on the source of the aromatics used in the highly aromatic fuel? Is it the same as that used in the balanced blend only at a higher concentration, or have specific aromatics been selected to obtain the 82% concentration? Work in this field by others as well as ourselves indicate that the aromatic hydrocarbons as a class are capable to providing extremely diversified performance characteristics. It is possible that this hydrocarbon type can be erroneously condemned, whereas actually the situation lends itself to correction.

If it can be assumed that we are all rating the same phenomenon — and this is open to some question, it has been our own observation that engines prone to rumble will do so even on primary reference fuels. However, it appears that test cell conditions are considerably more severe than those normally encountered on the road.

I am sure that the work reported by the authors will stimulate further investigations of a phenomenon which momentarily appears to be blocking progress to more efficient engines. This is not the first time and will not be the last that the automotive and petroleum industries have come to what appears to be a formidable roadblock. Look what has been accomplished in less than a decade in the fields of combustion research, crankcase lubricant quality, and fuel technology. In our highly competitive industries, it would appear that if it is to the advantage of our mutual customers and if it is economically sound, this problem, like many of its forerunners, will be solved resulting in benefit to all.

Engineers Will Solve Problem Of Rumble at High Compression Ratios

— H. T. Niles
Ford Motor Co.

THERE are several comments which I would like to make to the authors:

1. In the determination of rumble tendencies versus compression ratio, were engine spark and air/fuel ratios developed for maximum performance at each compression ratio? If not, it is probable that the rumble ratings were affected considerably by these limitations.

2. If the authors can visualize the design of fuels and engines which minimize rumble, as they suggest in the third and fifth conclusions, it is difficult to understand how they can imply in their final conclusion that abnormal combustion could continue in such proportion that it eventually hinders progress. Certainly, if under the present limited understanding of the chemical and mechanical factors which control surface ignition and rumble, the petroleum and automotive engineer can produce fuels and engines which minimize these abnormal combustion phenomena; these same people can, when the factors are better understood, design combinations that completely eliminate the problem, thus allowing further progress.

In conclusion, I would again like to compliment the authors on their descriptive approach. For I am sure that the final solution to the problem depends on the collective efforts of the petroleum and automotive engineer, each using his own specific skills to define the controlling factors of this phenomenon.

A Study of Engine "Rumble"

— L. A. McReynolds
Phillips Petroleum Co.

ENGINE rumble occurs at high speeds in high compression engines. Numerous investigators, who have been working on the problem of engine rumble, have reached the same general conclusion as to the origin of this high compression ratio phenomenon. Rumble is probably caused by an early release of a major portion of the energy of the charge. This produces a higher than normal rate of pressure rise and results in a low-frequency noise from vibration of one or more engine components. Rumble produces an objectionable noise, similar to the sound produced by "running a stick along a picket fence." Unless a fuel or engine design remedy is found, rumble may impose a ceiling on compression ratios.

The objective of this study was to evaluate various fuels and lubricants to determine if rumble could be eliminated with special commercial-type fuels or lubricants. The results of our limited investigation indicate that little can be done, within practical limits, toward eliminaton of rumble by changes in fuel and lubricant composition.

Figs. A and B show views of an inductor dynamometer stand equipped with a 12/1 compression ratio engine, transmission, and inertia wheel. The inertia wheel was designed so that the rotational kinetic energy is equivalent to the translational kinetic energy of a 5000-lb automobile with a 3.07/1 axle ratio. This inertia wheel provides the engine loading for both part-throttle and full-throttle accelerations and also makes possible high manifold vacuum decelerations. The dynamometer provides the engine loading for constant speed operations and also functions as a brake for the engine and inertia wheel.

An automatic engine cycler was utilized to control the engine through a city-suburban type of driving schedule to accumulate combustion-chamber deposits (Fig. C). After deposits were accumulated, rumble determinations were made under wide-open throttle acceleration conditions from 25 to 90 mph to determine aurally the existence and severity of rumble.

Several full boiling range fuels were prepared having Research octane numbers of approximately 100 and a range in aromatic content of 0–40%. Results of rumble determi-

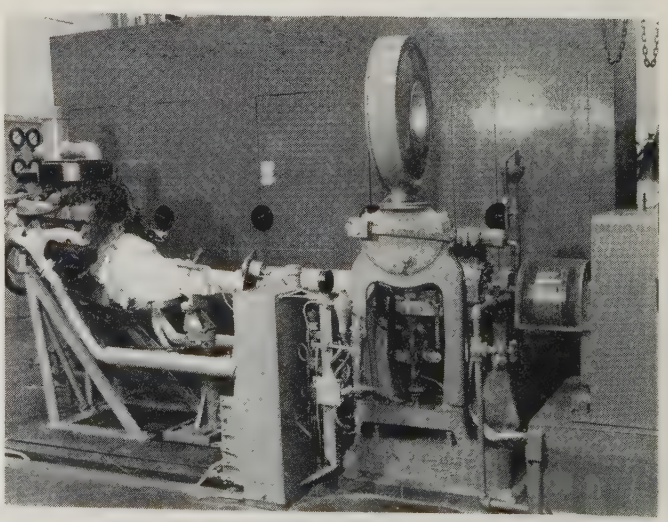

Fig. A — Side view of engine installation

nations on each of these fuels, after deposits were accumulated, are shown in Table A. The spark was retarded in several cases in order to eliminate knock as much as possible during the rumble determination. In addition, tests were conducted on reference fuel isooctane (clear and leaded to 3.0 ml tel) and a 50-50 blend of isooctane and benzene (3.0 ml tel). As may be noted, Fuel A (nonaromatic) was superior to Fuels B, C, D, and E with respect to rumble severity. The laboratory and full-scale ratings on these full boiling range fuels indicate that octane number is not the controlling factor in reducing or eliminating rumble. Since rumble was obtained with Fuel A (nonaromatic), it is also indicated that the presence of aromatics is not required for rumble. Tests conducted on noncommercial-type fuels indicated that hydrocarbon type was very important. The leaded benzene-isooctane blend produced severe rumble whereas isooctane plus 3.0 ml tel resulted in a smooth acceleration with no rumble.

Surface ignition and rumble were studied simultaneously with four of eight cylinders equipped with ion gaps. The engine was operated on a commercial nonphosphorus fuel on the deposit buildup cycle until deposit equilibrium had been reached. Without removing deposits, a phosphorus additive was added to the fuel in two different concentrations and the engine was operated on the test cycle for approximately 1200 additional miles in each case. Several surface ignition and rumble determinations were made prior to and after each change in test fuel. These determinations were made using a rumble reference fuel composed of 25% toluene, 25% mixed xylenes, and 50% isooctane leaded to 3.0 ml tel. The results of this study tend to confirm the theory that rumble is primarily a surface ignition phenomenon (Table B). As may be noted, a high concentration of a phosphorus fuel additive was required to reduce rumble severity substantially in the 12/1 compression ratio engine. A smaller concentration of a phosphorus fuel additive may control rumble in a lower compression ratio engine.

The introduction of water into the engine inlet air stream was found to be very effective in eliminating rumble (Table C). The minimum water-to-fuel ratio that eliminated rumble was found to be approximately 0.3. The introduction of water at this rate was also very effective in reducing the engine octane requirement but increased the acceleration time to 90 mph by 4–6%, indicating a power loss.

During the course of this experimental work, the following additional items were investigated to some extent:

1. Several types of motor oil, both multigrade and single grade, were evaluated as to their ability to reduce rumble. Multigrade oils were found to offer some advantages, making rumble less severe.
2. Moderate changes in spark advance had little or no effect on rumble.
3. The engine has not been damaged in any visual or operational way as a result of numerous rumble determinations.
4. Improved instrumentation is needed.

This is presented as a progress report. Many factors need to be investigated in future work. However, water injection and the use of a high concentration of a phosphorus fuel additive are two promising leads for reducing or possibly eliminating rumble in high compression ratio engines.

Table A — Effect of Fuel Type
(12/1 compression ratio engine)

Fuel Code No.	Composition P	O	A	Research Octane Number	Motor Octane Number	Full-Scale High-Speed Octane Rating[c]	Rumble Severity
Isooctane (clear)	100	—	—	100	100	100	None[b]
Isooctane (3.0 ml tel)	100	—	—	115.5	115.5	—	None
Fuel A[a]	100	—	—	99.6	101.6	103.5	Light
Isooctane-Benzene (3.0 ml tel)	50	—	50	116.8	103.4	—	Severe
Fuel B[a]	60	—	40	99.9	92.2	103.0	Heavy
Fuel C[a]	60	40	—	99.3	90.1	98.0	Heavy[d]
Fuel D[a]	20	40	40	99.7	87.3	97.2	Heavy[d]
Fuel E[a]	80	—	20	100	97.9	103.0	Heavy

[a] Full boiling range fuels (3.0 ml tel).
[b] Heavy knock was present.
[c] Primary reference fuels.
[d] Spark retarded to avoid excessive knock.
NOTE: Test oil—single grade MIL-L-2104A motor oil.

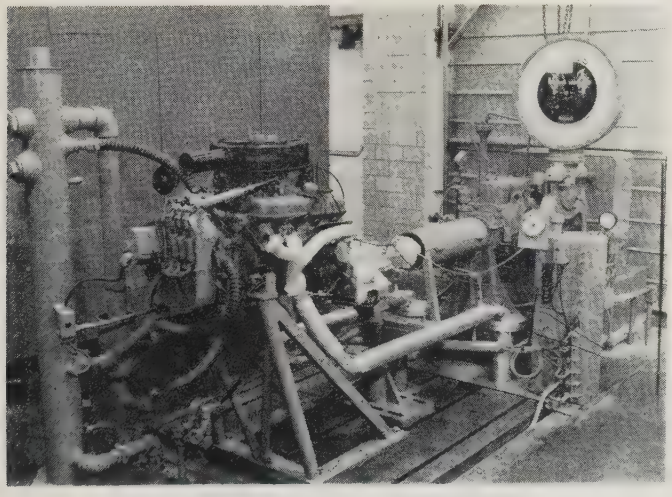

Fig. B — Front view of engine installation

Table B — Effect of Phosphorus Fuel Additive

Phosphorus Fuel Additive	Surface Ignition (counts per hr)	Rumble Intensity
0	219	Heavy
0.4T[a]	50	Light
1.0T[a]	1	Trace—practically eliminated

[a] T designates theoretical amount of phosphorus required to combine with the tel to form lead orthophosphate.
NOTE: Test oil—Supp. I multigrade motor oil.

Table C — Effect of Water Injection

Fuel	Rumble Severity
Rumble Reference Fuel[a]	Heavy
Rumble Reference Fuel plus Water Injection[b]	None

[a] Calculated Motor and Research octane numbers 114 and 117, respectively.
[b] Ratio of water to fuel approximately 0.3.
NOTE: Test oil—single grade MIL-L-2104A motor oil.

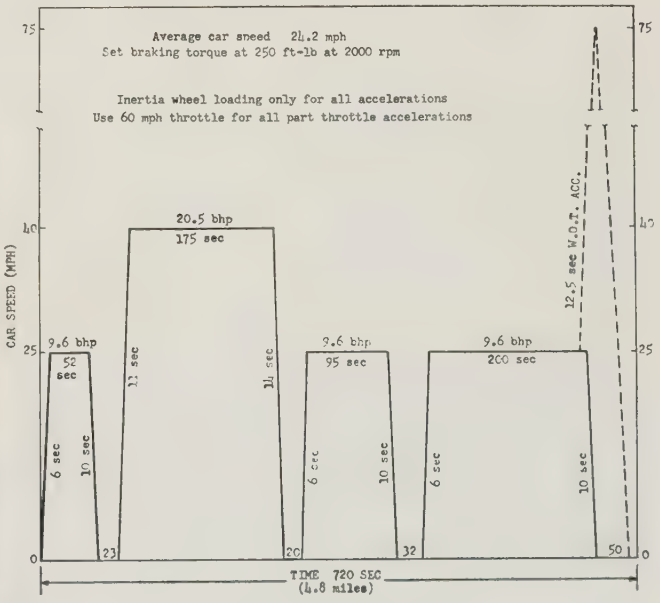

Fig. C — Deposit accumulation cycle

ENGINE POUNDING—

Its Causes and Control

J. L. Bame and R. G. Tuell, Shell Oil Co.

This paper was presented at the SAE Summer Meeting, Atlantic City, June 11, 1958.

ENGINE knock is an old problem which is fairly well recognized by everyone associated with the automotive and petroleum industry. Although much of the mechanism of this phenomenon still is not completely understood, it has been possible through constant research on engines, fuels, and lubricants to learn to control the noise, thus permitting the gasoline engine to evolve to its present stage. More recently a new noise, rumble — or as we prefer to call it — pounding, has been encountered in some of the higher compression ratio engines.[1,2,3,4,5,6,7] This noise, which is distinct from that of knock, would appear to pose a potential barrier to further engine development unless means are found for controlling it.

At the November, 1957, SAE Fuels and Lubricants meeting in Cleveland a brief summary of some of our studies of the pounding problem was presented in discussion of another paper.[8] This paper amplifies the discussion given at the Cleveland meeting and presents the results of more recent work. For the benefit of those who may not be familiar with the sound of pounding, it has been described variously as "a broomstick on a picket fence" or as being similar to the alarming clattering sound of worn connecting-rod bearings. Pounding is generally encountered when operating at relatively high power and may start at quite moderate speeds under heavy load. Thus, in passenger-car operation pounding is most likely to be encountered in rapid acceleration, such as when entering a boulevard or highway from an access road, overtaking and passing, or when climbing hills or grades which are steep enough to require a considerable amount of throttle. In severe circumstances pounding can begin at speeds as low as 30 mph during wide-open-throttle acceleration. Thus, pounding is not a laboratory curiosity but can occur under circumstances which are by no means foreign to normal passenger-car service.

Over the past several years we have observed and studied the pounding phenomenon in some 48 different makes and/or models of high compression ratio automotive engines, both in the laboratory and on the road. While detection on the road, so far, generally has been limited to experts, it would appear that 1958 may well be the year in which pounding begins to force itself on the attention of the average motorist.

The influence of pounding on fuel requirements as contrasted to that of knock is illustrated by the results of laboratory tests in 10/1 compression ratio overhead-valve V-8 Engine A shown in Fig. 1. This figure represents the average noise requirements under full-throttle accelerating conditions for 12

---

[1] SAE Transactions, Vol. 63, 1955, pp. 481–491: "Correlation of Engine Noise with Combustion Phenomena," by R. Meagher, R. L. Johnson, and K. G. Parthemore.

[2] Proceedings of API, Vol. 33, 1953, Part 3, pp. 137–150: "Preignition in Automotive Engines," by J. R. Sabina, J. J. Mikita, and M. H. Campbell.

[3] SAE Transactions, Vol. 62, 1954, pp. 32–39: "An Investigation of Preignition in Engines," by A. O. Melby, D. R. Diggs, and B. M. Sturgis.

[4] SAE Transactions, Vol. 62, 1954, pp. 40–49: "Deposit-Induced Ignition — Evaluation in Laboratory Engines," by D. A. Hirschler, J. D. McCullough, and C. A. Hall.

[5] SAE Transactions, Vol. 62, 1954, pp. 50–55: "Occurrence of Preignition in Present-Day Cars in Normal Service," by R. F. Winch.

[6] SAE Transactions, Vol. 62, 1954, pp. 56–65: "Some Effects of Fuels and Lubricants on Autoignition in Cars on the Road," by R. K. Williams and J. R. Landis.

[7] SAE Transactions, Vol. 66, 1958, pp. 549–556: "Investigating Combustion Phenomena in Unmodified Engines," by J. A. Robison, M. D. Behrens, R. G. Mosher, and J. M. Chandler.

[8] Discussion by L. S. Echols of "Interrelationship of Fuel Constituents, Combustion-Chamber Deposits and Automotive Engine Performance," by A. V. Mrstik and R. B. Payne. Paper presented at SAE National Fuels and Lubricants Meeting, Cleveland, November, 1957.

THIS paper describes studies of rumble with particular emphasis on the mechanism involved, the present and potential future extent of the problem, and means whereby the noise can be controlled or eliminated.

From the mechanism studies it is apparent that pounding is distinct from knock and is a form of combustion shock arising from too rapid burning of the charge as a result of secondary flame fronts introduced by deposit ignition. Objectionable levels of pounding have been observed in many of the 1958 model cars and, based on tests conducted in experimental high-compression engines, the problem can be expected to become worse as compression ratios are increased.

To date the most practical means which has been found for controlling pounding is the incorporation of tricresyl phosphate in the deposit fuel. The substantial increase in pounding-limited power afforded from the use of 0.3 theory of this additive is sufficient, in most cases, to eliminate pounding in 1958 and earlier model engines.

In more severe 11/1 and 12/1 compression ratio engines, however, pounding and other surface-ignition effects are only partially overcome. Thus, it would appear that unless further help can be provided from the standpoint of engine design, even more effective means for controlling surface ignition may have to be found for such engines.

engines after approximately 5000 miles of simulated urban driving. (The rating fuels and operating cycles for this and other tests which will subsequently be discussed are given in Appendices I and II, respectively.) In clean condition, knock was the only noise observed in the engines. With deposits, however, pounding was encountered at high speeds (as denoted by the crosshatched area to the right of the solid line) and could not be eliminated by increases in fuel antiknock quality. While reductions in fuel octane number below that required to prevent knock caused a marked decrease in the pounding-in speed (indicating that pounding very definitely can be knock induced), increases in fuel octane number above that sufficient to satisfy the knock requirement had only a minor influence on the speed at which pounding was encountered. Although the pounding noise could be diminished somewhat by repeated acceleration, it usually returned in force within 200 miles of additional simulated urban operation.

In view of the severity of the pounding noises and the lack of response to fuel antiknock quality noticed in our earlier encounters with the problem, a rather intensive investigation was initiated to determine the mechanism of the phenomenon, the current and probable future extent of the problem, and methods which could be employed to ameliorate it. Results of these studies are discussed in detail in the following sections of this paper.

Mechanism Studies

Our investigations of the mechanism of pounding have included both the use of instrumentation and observations of the effect of fuel, engine, and operating variables on the phenomenon. Very early in these studies it was confirmed that the mechanism of pounding is quite distinct from that of knock. For example, the conventional Sperry high-frequency magnetostriction vibration pickup which is quite commonly used for knock detection was found to be "deaf" to pounding as shown in Fig. 2. On the other hand, the Dumont vibration pickup,

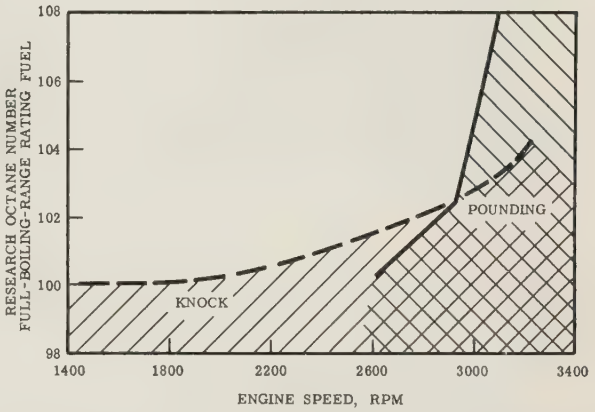

Fig. 1 — Response of knock and pounding to fuel antiknock quality in 10/1 compression ratio Engine A (wide-open throttle accelerations after about 5000 miles simulated urban operation)

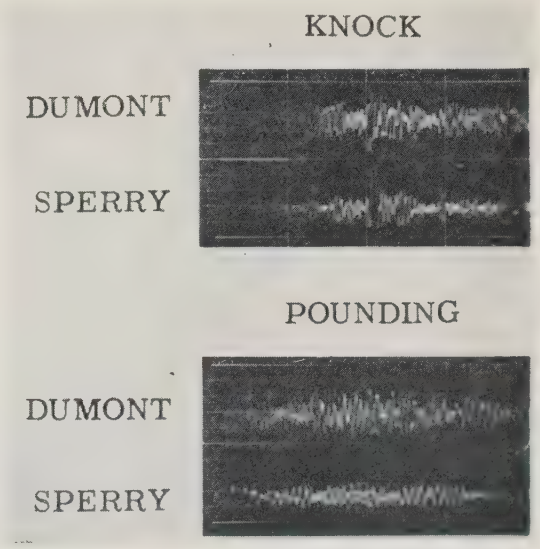

Fig. 2 — Difference in response of two different types of engine-mounted vibration pickups to knock and pounding

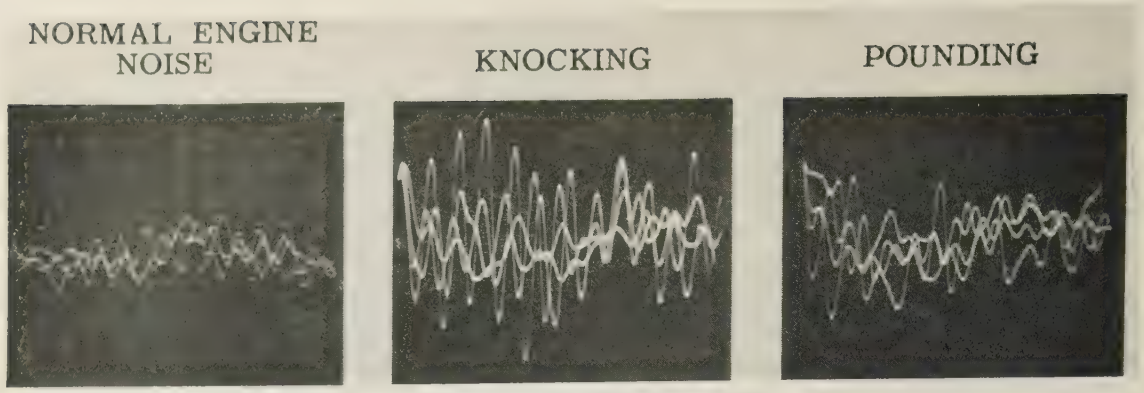

Fig. 3 — Oscilloscope traces of airborne noises observed during normal, knocking, and pounding operation at 3000 rpm full-throttle in a 10.4/1 compression ratio Engine B (each trace represents 2 millisec or 36 deg of crankshaft rotation)

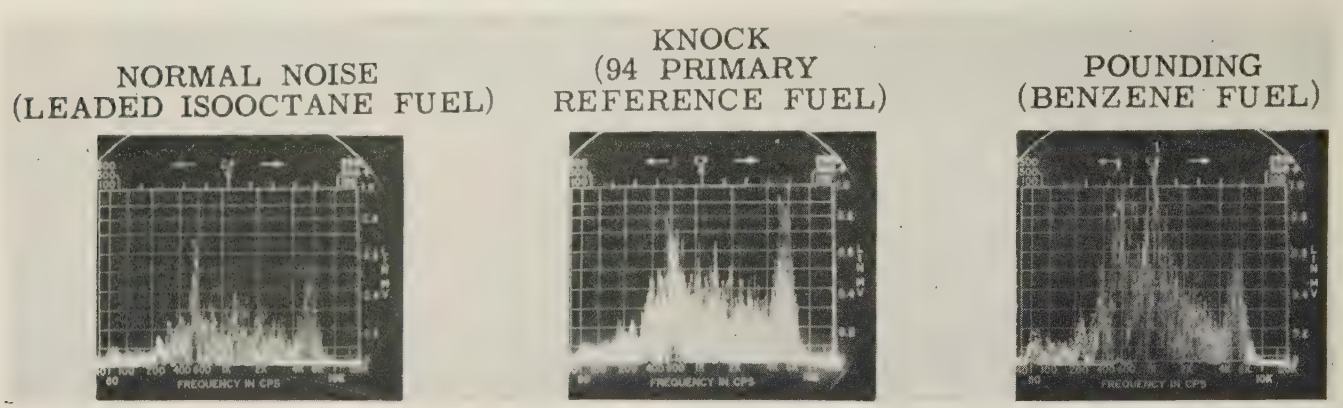

Fig. 4 — Analysis of airborne engine noises occurring at 3000 rpm full-throttle in 10.4/1 compression ratio Engine B during normal, knocking, and pounding operation

which has lower frequency "hearing," readily responded. This difference in response of the two instruments has proved quite helpful in distinguishing between high-speed knock and pounding in multicylinder engine studies.

As a follow-up to the foregoing observations, a brief study was made of the noise vibrations associated with pounding as compared to those with knock. Fig. 3 shows photographs of the airborne vibrations observed during normal, knocking and pounding operation in a 10.4/1 compression ratio Engine B (using a Turner Aristocrat Model TV50D dynamic microphone coupled via suitable amplifiers to a Hewlett-Packard Model 130A oscilloscope). It will be noted that the wave forms of the vibrations associated with the two abnormal combustion noises are rather complex, precluding accurate analysis by any casual observations. In general, however, it can be seen that a rather pronounced high-frequency vibration (at about 6000–7000 cps) occurs with knock, whereas the noise associated with pounding appears to be due to a general increase in intensity over a range of frequencies. A more thorough analysis of the noise vibrations was made using a Model LP-1a Panoramic Sonic Analyser. Due to the transient nature of knock and pounding (and the discrete sweep interval of the sonic analyser) it was necessary to record the noises on a closed-end magnetic tape and then recycle through the analyser. While this provided resolution of the transient noises, the characteristics of the recording circuits were such that all frequencies above about 8500 cps were eliminated. From the results of the sound analyses (Fig. 4), it will be noted that normal combustion in this engine produced noises throughout the scanned frequency spectrum with peaks in intensity at approximately 600 and 5000–6000 cps. Under knock conditions a pronounced increase in the intensity of the 5000–6000 cps noise was observed along with a somewhat smaller increase in the 600-cps vibration. In contrast, under pounding conditions a marked increase in sound intensity was noted at a number of the lower frequencies (in particular in the 400–1500 cps range) while only a moderate increase in intensity was noted in the 5000–6000 cps noise.

It is believed that the low-frequency noises observed with pounding represent vibration of power train components (such as the connecting rods, crankshaft, and the like). As suggested by the work of Robison et al.,[7] in order for this to be true the rates of energy release from the fuel during pounding would have to be lower than those with knock (where the energy is released so rapidly that it is primarily expended at the combustion-chamber level with resultant vibration of the relatively rigid combustion-chamber components). As indicated by our own studies and those of Meagher, et al.[1] this is, indeed, the case since the high-frequency gas vibrations seen with knock are not observed with pounding (unless knock is also present). This is illustrated by the pressure-time diagrams shown in Fig. 5 which were obtained during severe pounding in a 10/1 compression ratio Engine A (using an Autronic model COS-3K capacitance-type pressure sensor installed in the No. 2 cylinder).

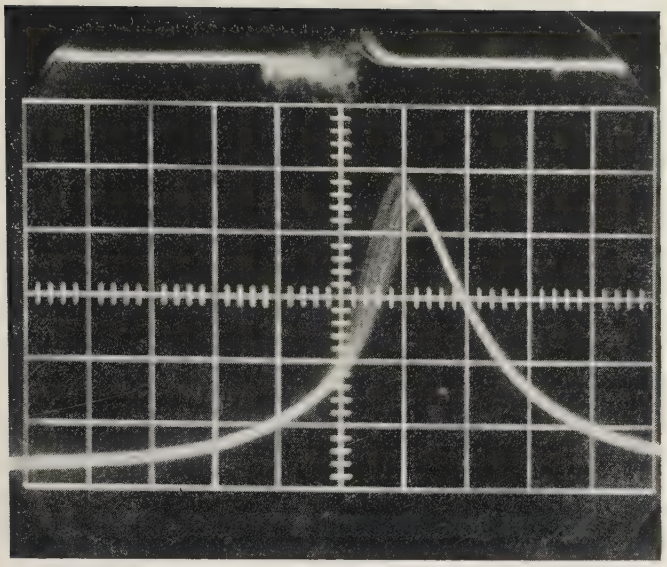

Fig. 5 — Pressure-time diagrams obtained during severe pounding operation in 10/1 compression ratio Engine A (3200 rpm, benzene fuel)

In addition to the foregoing engine vibration and noise analyses, there are several other observations which are quite pertinent to defining the mechanism of pounding. The first of these is the fact that evidence of early ionization was frequently seen during pounding operation (using the Sun ionization method[9]), suggesting that surface ignition was involved in the phenomenon. This is in contrast to knock where early ionization is rarely observed except where knock is surface-ignition induced. A second, but equally important observation, is the previously mentioned lack of response of pounding to changes in fuel octane quality. Coupled with this is the fact that spark retard (a common palliative for knock) has little or no effect on pounding unless the retard is of such magnitude as to appreciably lower engine power output. In contrast, the use of fuels of low surface-ignition resistance (such as benzene) markedly increases the tendency toward pounding, as does the presence in the combustion chamber of deposits with high surface-ignition activity. These effects are illustrated in Figs. 6 and 7, respectively.

The foregoing observations (which are summarized in Table 1) indicate that pounding is distinct from knock and suggest that surface ignition of the fuel-air charge is involved in the pounding mechanism. This was investigated further using the aforementoned Autronic pressure sensor (mounted in the No. 2 cylinder of the 10/1 compression ratio Engine A) to obtain pressure-time diagrams with two fuels of widely different surface-ignition resistance characteristics at several levels of operating severity. The results are shown in Fig. 8. The curves at the top represent the average pressure-time diagrams (for the 25% of cycles showing the most rapid pressure development) and the curves at the bottom represent the corresponding rate of pressure change-time values. The curves were obtained in the following manner: with the engine operating at 3000 rpm on leaded benzene, the throt-

[9] SAE Transactions, Vol. 61, 1953, 453–461: "Method for Identifying Preignition," by R. F. Winch and F. M. Mayes.

Table 1 — General Observations Regarding Pounding and Knock

	Pounding	Knock
Detection by:		
Conventional High-Frequency Vibration Pickup	No	Yes
Wide Frequency Band Vibration Pickup	Yes	Yes
Early Ionization	Frequent	Seldom
Gas Vibrations	No	Yes
Response to:		
Fuel Octane Number	Slight	Yes
Spark Advance	Slight	Yes
Surface Ignition Resistance of Fuel	Yes	No
Surface Ignition Activity of Deposits	Yes	No

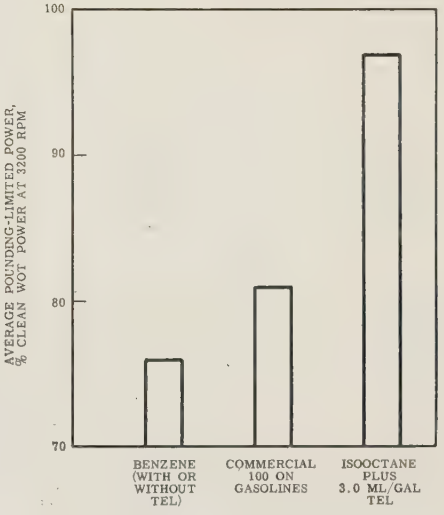

Fig. 6 — Resistance of fuels to pounding in twelve 10/1 compression ratio engines A (after about 10,000 miles simulated urban operation)

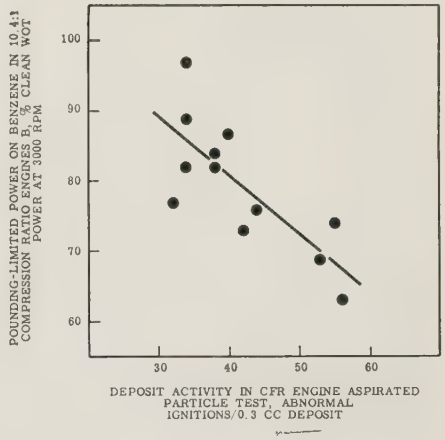

Fig. 7 — Relationship of pounding to deposit surface-ignition activity

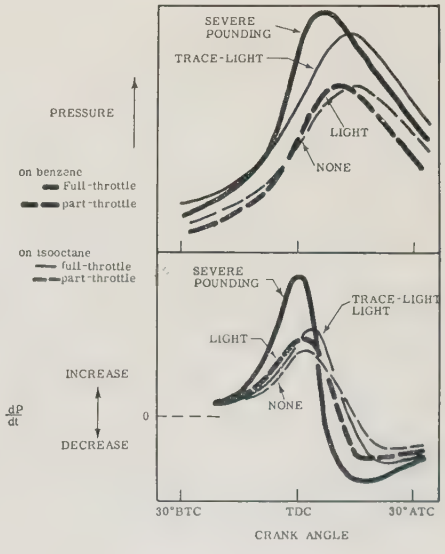

Fig. 8 — Pressure-time and dP/dt curves for varying degrees of pounding severity at 3000 rpm in a 10/1 compression ratio Engine A (values are averages for 25% of cycles showing most rapid pressure development)

tle was slowly opened until light pounding was encountered as represented by the heavy dashed line. At the same throttle setting, the engine was switched to leaded isooctane. This eliminated the noise and produced the pattern shown by the light dashed line. While still operating on isooctane the throttle was advanced to the wide-open position. At this condition trace to light pounding was encountered and the pattern shown by the light solid line obtained. While still at full throttle, the engine was switched back to benzene. Severe pounding and the pattern shown by the heavy solid line resulted. It will be noted that the maximum of the derivative of the pressure-time curves groups the severity of pounding better than the maximum of the pressure curves. As shown in Table 2 the second derivative of pressure with respect to time gives a still better correlation. In this we are reminded of the pioneer work of R. N. Janeway[10] and later L. L. Withrow[11] regarding combustion shock and, indeed, pounding would appear to be combustion shock — arising not from poor combustion-chamber shape as in the case of the earlier work but from an upset in combustion control resulting from surface ignition. A forced vibration of the engine structure is the classic result. Incidentally, it is perhaps of interest to note that the "thudding" noises associated with the rating of high aromatic content fuels in the CFR engine show the same relationship between pressure parameters and intensity as in the case of pounding, suggesting that "thudding" is combustion shock rather than knock.

From the foregoing observations, and leaning on the pioneer work in combustion shock, we have postulated a mechanism for pounding which is shown diagramatically in Fig. 9. Briefly, this mechanism attributes pounding to early or multiple ignition of the charge (usually by glowing deposits) which leads to excessive rates of burning. The resultant increase in the rate of energy release produces vibration in the power train and results in an audible noise. If this mechanism is correct, it is obvious that in addition to the noise problem, pounding may also constitute a potential threat to the engine structure by serving as a trigger for the development of runaway hot-spot preignition.

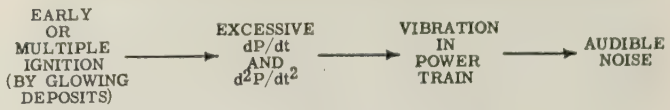

Fig. 9 — Postulated pounding mechanism

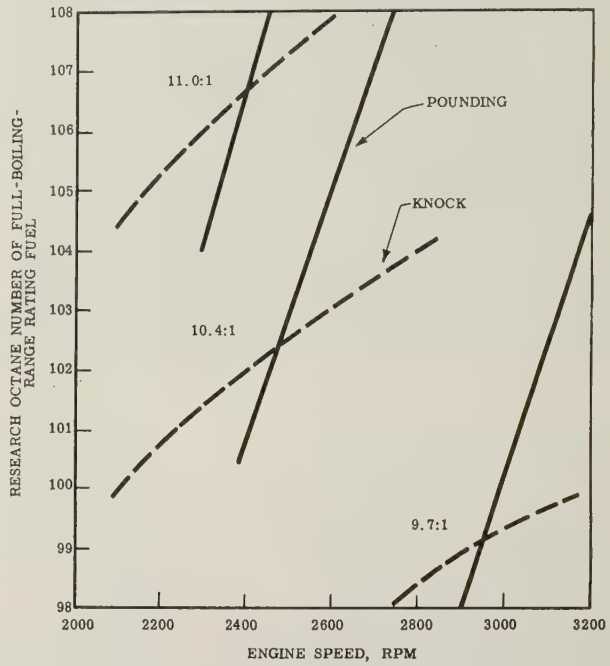

Fig. 10 — Effect of compression ratio on noise requirements in laboratory tests in Engine B (after about 2000-3000 miles of simulated urban driving on fuel containing 3.0 ml tel per gal with 0.3 theory tricresyl phosphate)

Extent of Problem

The extent and probable future severity of the pounding problem has been examined in both road and laboratory engine tests. Results obtained in several makes of laboratory-installed passenger-car engines are shown in Table 3. In these tests the engines were operated on leaded commercial-type fuels (containing no supplementary deposit modifiers) until deposit equilibrium was attained and then checked for pounding by determining the noise-limited power at 3000 rpm while operating on benzene (a fuel of low surface-ignition resistance selected to accentuate pounding). It will be noted that while pounding was not observed in 8.2 compression ratio 1954 model Engines C, it produced rather severe restrictions on the power which could be developed without encountering abnormal combustion noise in the 9.6 and higher compression ratio engines.

Similar results were obtained in passenger-car tests conducted on the road. In these tests the vehicles were operated under controlled driving conditions for deposit accumulation and then periodically checked for pounding tendencies by making full-throttle level road accelerations on either commercial-type rating fuels or leaded benzene. Table 4 shows the results of a series of tests conducted under urban driving conditions using leaded deposit fuels containing no supplementary deposit modifiers. It will be noted that no pounding was detected with commercial-type rating fuels in the 1957 and earlier cars. In the 1958 cars, however, some pounding was observed with the commercial-type rating fuel in six of the 10 vehicle makes tested with the severity being sufficient to be deemed objectionable (medium intensity or greater) in three of the cars. On the more severe benzene rating fuel, pounding was detected in nine of the ten 1958 vehicles and was deemed objectionable in five cases.

As shown by the results in Table 5, an even greater tendency toward pounding was noted when the deposits were accumulated under simulated severe metropolitan conditions. This is illustrated by the medium level of pounding encountered on commercial-type rating fuel in 1957 model Car A under severe metropolitan-type conditions as contrasted to the absence of pounding in the previously described urban driving test. Of perhaps even more

[10] SAE Transactions, Vol. 24, 1929, pp. 139–153: "Combustion Control by Cylinder Head Design," by R. N. Janeway.

[11] SAE Transactions, Vol. 52, 1944, pp. 106–112: "Physical Characteristics of Roughness in Internal Combustion Engines," by L. L. Withrow and A. S. Fry.

Table 2 — Correlation of Pounding Severity with Combustion Parameters in 10/1 Compression Ration Engine A

Fuel	Operating Condition, (3000 rpm)	Degree of Pounding Observed	Pressure maximum psi[a]	dp/dt maximum, psi/deg[a]	d^2p/dt^2 maximum, psi/deg/deg[a]
Isooctane	Part throttle (5½ in. of Hg)	None	560	23.7	1.6
Isooctane	Full throttle	Trace-light	740	34.5	2.3
Benzene	Part throttle (5½ in. of Hg)	Light	560	29.6	2.6
Benzene	Full throttle	Heavy	820	54.6	5.3

[a] Based on P-t curves obtained with Autronic sensor mounted in No. 2 cylinder. Data shown are averages of the 25% of curves showing highest values.

Table 3 — Pounding Observed in Laboratory Tests in Passenger-Car Engines

Make	Year	Actual Clean Compression Ratio	Deposit Buildup Cycle[a]	Pounding-Limited Power on Benzene at 3000 rpm, % Full-Throttle Power
C	1954	8.2	Urban	100.0
A	1955	10.0[b]	Urban	68.5
A	1955	10.0[b]	Interurban	70.0
B	1956	9.8	Urban	57.0
B	1956	10.4[b]	Urban	45.0
D	1957	9.6	Urban	73.5
P	1958	9.7	Urban	71.0

[a] In all cases the deposit fuel was a full-range commercial-type containing a nominal 3 ml tel (Motor Mix) per gal with no supplementary deposit modifiers.
[b] Raised from standard compression ratio using special pistons and/or heads supplied by the manufacturer.

Table 4 — Pounding Tendencies of Passenger Cars Following Deposit Accumulation in Urban-Type Driving[a]

Vehicle			Degree of Pounding Observed During 0–65 mph Full-Throttle Level Road Accelerations	
Make	Year	Actual Clean Compression Ratio	Commercial-Type Fuel[b]	Benzene + 3 ml tel
F	1955	8.1	None	—
E	"	8.2	"	—
C	"	8.3	"	—
D	"	8.7	"	—
A	"	8.8	"	—
E	1957	8.8	"	—
C	"	9.1	"[c]	—
H	"	9.1	"[c]	—
D	"	9.2	"[c]	—
F	"	9.2	"	—
G	"	9.3	"[c]	—
A	"	9.9	"	—
K	1958	8.4	None	Trace
E	"	9.2	"	"
G	"	9.3	Light	Medium
H	"	9.4	"	Light
O	"	9.4	"	Medium
D	"	9.5	Medium	"
B	"	9.6	None	None
F	"	9.6	Medium	Heavy
P	"	9.6	Heavy	"
A	"	9.8	None	Trace

[a] Deposit fuels were full-range commercial-types containing a nominal 3 ml tel (Motor Mix) per gal in all cases. Unless noted otherwise, no supplementary deposit modifiers were employed.
[b] Of sufficient antiknock quality to satisfy the knock requirement. In general, a greater tendency toward pounding was noted when fuels of submarginal antiknock quality were employed.
[c] Deposit fuel contained 0.3 theory tricresyl phosphate.

Table 5 — Pounding Tendencies of Passenger Cars Following Deposit Accumulation in Severe Metropolitan-Type Driving[a]

Vehicle			Degree of Pounding Observed During 0-65 mph Full-Throttle Level Road Accelerations	
Make	Year	Actual Clean Compression Ratio	Commercial-Type Fuel[b]	Benzene + 3 ml tel
		(Standard Compression Ratio Cars)		
E	1957	8.8	None	Medium
D	"	9.2	"	"
F	"	9.2	"	"
G	"	9.3	"	"
A	"	9.9	Medium	Heavy
		(Special High Compression Ratio Conversions)		
A	1955	10.0	None[c]	Light[c]
D	"	10.0	"	"
B	"	10.0	Heavy	Heavy
C	1957	11.9	Medium	"
E	"	12.5	Heavy	"

[a] The deposit fuel was a full-range commercial-type containing a nominal 3 ml tel (Motor Mix) per gal. Except where noted the fuel contained 0.3 theory tricresyl phosphate.
[b] Of sufficient antiknock quality to satisfy the knock requirement. In general, a greater tendency toward pounding was noted when fuels of submarginal antiknock quality were employed.
[c] The deposit fuel contained no supplementary deposit modifier.

interest is the marked pounding tendency exhibited by several of the cars which had been converted to higher compression ratios. Whereas the tendency toward pounding usually diminished greatly after three or four full-throttle accelerations in the standard compression ratio vehicles, in the special high compression ratio cars (particularly the 11.9 Car C and the 12.5 Car E) the pounding persisted after a large number of accelerations and frequently led to run-on with the ignition shorted. In fact, in several instances piston and gasket burning were encountered in the high compression ratio vehicles. This is believed to have resulted from hot-spot preignition induced by deposit ignition and would appear to confirm the suspicions mentioned earlier regarding the possibility of engine destruction which may be associated with or initiated by pounding.

In view of the greater tendency toward pounding noted in the higher compression ratio cars, the effects of raising compression ratio in a given make of engine was examined. Fig. 10 shows the influence of this parameter on combustion noise phenomena as observed in laboratory tests in a 1956 Engine B. In each case the engine contained stabilized deposits accumulated under simulated urban driving conditions. The onset of pounding occurred suddenly at the solid lines during acceleration and persisted at higher speeds. The dashed lines show the knock requirements of the engines in terms of octane numbers. Although not shown, at 8.5/1 compression ratio no pounding was observed at speeds up to 3500 rpm. At 9.7/1 and higher compression ratios, however, severe pounding was encountered. The comparatively small effect of increasing fuel antiknock quality on pounding and the marked adverse effect of increasing compression ratio is particularly notable. From this it would appear that with the trend toward increasing engine compression ratio we can expect the pounding problem to become acute unless steps are taken to ameliorate the problem.

Before leaving the subject on the extent of the pounding problem it should be emphasized that the foregoing results are not meant to imply that pounding is limited to operation at or near full-throttle or that pounding cannot be induced in some of the lower compression ratio cars. In three of the 1958 cars which had rather extreme spark advance characteristics pounding was encountered at manifold vacuum settings of 5–12 in. of Hg when operating on fuels of marginal antiknock quality. Further, in one of these cars (Car F) it was found that pounding could be induced with the engine in

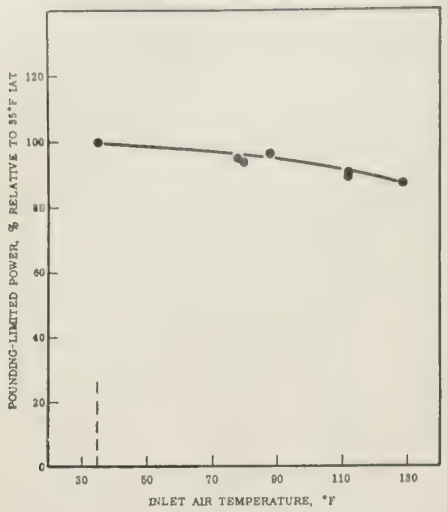

Fig. 11 — Effect of carburetor inlet air temperature on pounding in 10.4/1 compression ratio Engine B (at 3000 rpm on full-boiling-range rating fuel)

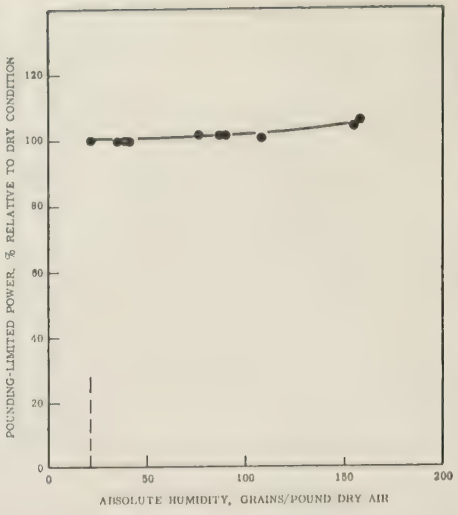

Fig. 12 — Effect of humidity on pounding in 10.4/1 compression ratio Engine B (at 3000 rpm on full-boiling-range rating fuel)

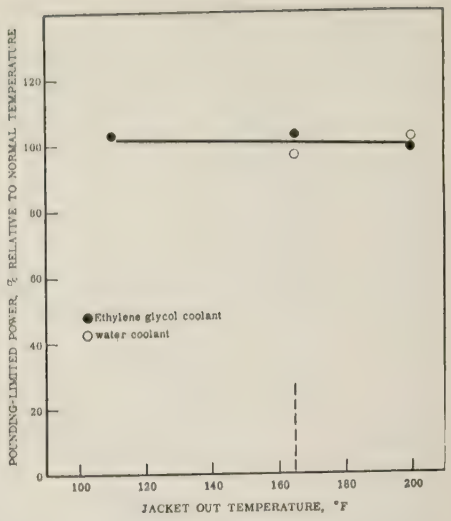

Fig. 13 — Influence of cooling water jacket temperature on pounding in 10.4/1 compression ratio Engine B (each point represents the average of 2-3 determinations)

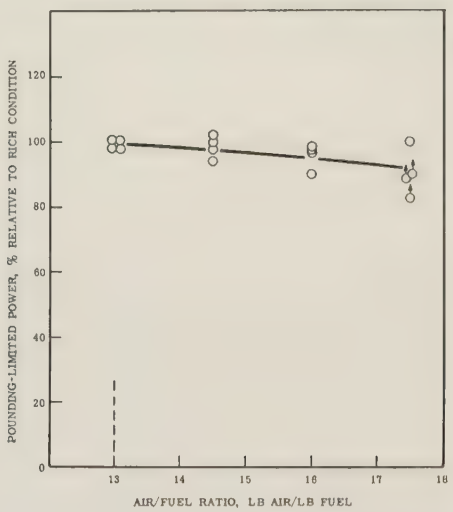

Fig. 14 — Effect of mixture strength on pounding in 10.4/1 compression ratio Engine B (at 3000 rpm on full-boiling-range rating fuel)

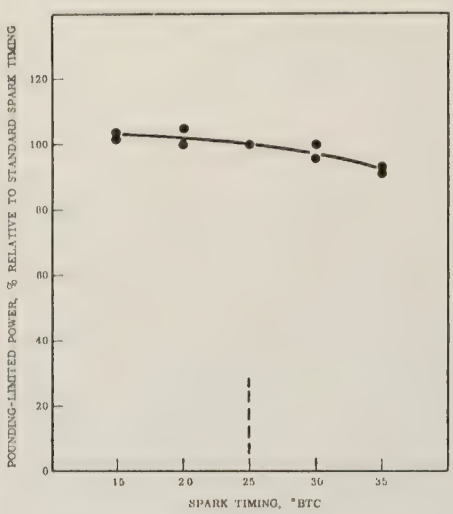

Fig. 15 — Effect of spark timing on pounding in 10.4/1 compression ratio Engine B (at 3000 rpm on benzene, vacuum advance inoperative)

clean condition by operating on a rapid-burning fuel (benzene) with an abnormally advanced spark timing. Similarly, under severe operating conditions such as hill climbing a greater tendency toward pounding is observed than during the level road accelerations reported herein and, indeed, pounding has been observed in some of the lower compression ratio vehicles under such conditions.

Influence of Atmospheric and Engine Operating Variables

The effect of changes in atmospheric and engine operating variables on pounding was explored briefly in laboratory tests in a 10.4/1 compression ratio Engine B which contained "stabilized" deposits from simulated urban driving. The results are shown in Figs. 11–15. With the exception of temperature, changes in atmospheric variables had little or no influence on the pounding-limited power which could be developed in the engine. Increasing engine intake air temperature (Fig 11) caused a significant decrease in pounding-limited power (approximately 14% for a 100 F increase in temperature). This is as would be expected since increases in intake air temperature would tend to be reflected in an increased tendency toward surface ignition at a given power level (due both to increased deposit temperature and an increase in fuel reaction rates). Increases in atmospheric humidity (Fig. 12) had a considerably smaller but beneficial effect. (Incidentally, the injection of water into the induction system had a fairly substantial beneficial effect, which is believed to have resulted from internal cooling.) Although not shown, changes in barometric pressure had no influence on the pounding-limited power but merely changed the manifold vacuum setting required for obtaining an objectionable degree of pounding.

Of the engine operating variables investigated, changes in jacket temperature and coolant type

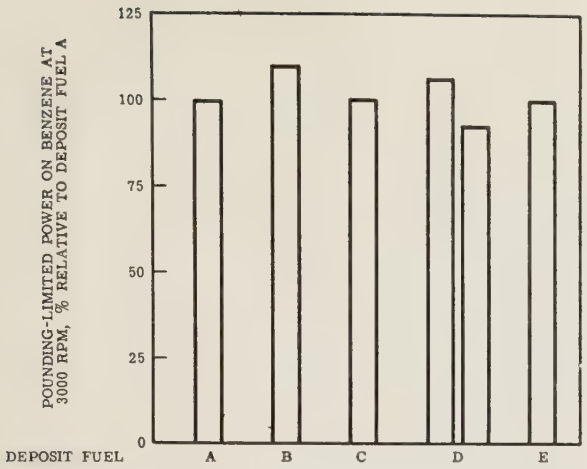

DEPOSIT FUEL	A	B	C	D	E
PRIMARY COMPONENT	1-STAGE CAT. CRK	2-STAGE CAT. CRK	LOW SEV CAT. REF	HIGH SEVERITY CAT. REFORMATE	
% SATURATES	54	33	52	52	32
% OLEFINS	20	29	NIL	NIL	NIL
% AROMATICS	26	28	48	48	68
% BOILING ABOVE 400°F (TRUE BOILING POINT)	2.4	1.1	0	2.2	3.4

Fig. 16 — Influence of fuel hydrocarbon composition on pounding in laboratory tests in Engines B

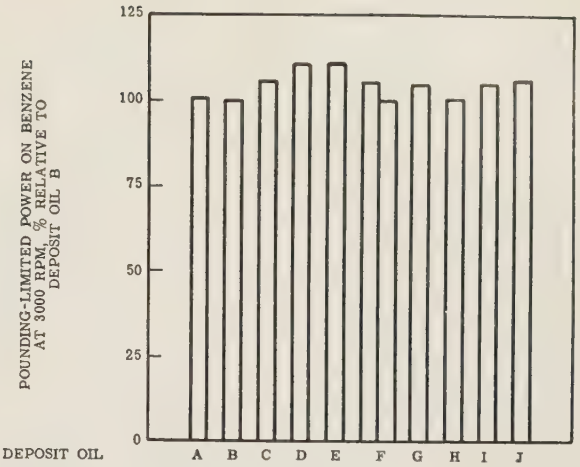

DEPOSIT OIL	A	B	C	D	E	F	G	H	I	J
SAE GRADE	5W-20 ←			10W-30			→	20W-40		30
% SULFATED RESIDUE	1.2	1.2	1.6	1.4	0.3	1.1	1.2	1.9	1.6	2.4
TBN-E	5.6	5.6	5.8	2.7	0.1	6.3	5.3	8.1	5.1	8.4
POLYMER	B	B	A	A	A, C	D	E	A	A	-
DETERGENT AND ANTIOXIDANT	N X Z	N X Z	N X Y	R	X Z	N X Z	N X Z	N V X Z	M X Z	M U W

Fig. 17 — Influence of deposit lubricant on pounding in laboratory tests in Engine B

had no effect on pounding-limited power (Fig. 13), and enrichening the fuel-air mixture (Fig. 14) or retarding the spark (Fig. 15) had only minor beneficial results. It should be noted that at a given speed and deposit condition the tendency of an engine to pound on a given fuel is largely dependent on the power level to which the engine is stressed. Thus, even though changes in such variables as barometric pressure, spark timing, and fuel/air ratio exert only a minor influence on pounding-limited power, they may be sufficient in borderline cases to eliminate pounding by reducing the full-throttle power output sufficiently to place the engine below a critical level.

Means for Controlling Pounding

So far we have been concerned primarily with the causes and extent of the pounding problem. Let us now turn our attention to methods which can be applied to control or ameliorate the pounding noise. These naturally fall into two categories, namely, changes in engine design and changes in fuels and lubricants. As regards the former, we will leave discussion to the automotive people except to note that: (1) we have observed pounding in engines representative of each of the major types of combustion-chamber design currently in vogue, and (2) we do not feel that stiffening of the engine structure to exclude the vibration from the normal operating range is a satisfactory solution, since this would merely mask the noise and not eliminate deposit-induced surface ignition as a potential source for exciting runaway hot-spot preignition.

As regards changes which come under the province of the petroleum refiner, there are two routes which immediately suggest themselves; namely, changes in fuel hydrocarbon structure to improve surface-ignition resistance characteristics and changes in fuels and/or lubricants to decrease the activity of deposits laid down in the combustion chamber. Possibilities offered by the first of these approaches are illustrated by the results from tests conducted in 10.4/1 compression ratio Engines B shown in Table 6. Each of the results shown in this table is an average of five determinations in each of six engines. Prior to determining the pounding resistance of the test fuels, the engines were operated the equivalent of approximately 5000 miles on a commercial-type fuel containing 3 ml tel per gal (Motor Mix) and 0.3 theory tricresyl phosphate. It will be noted that the effect of the test fuels on pounding-limited power bears a close resemblance to the well-known surface-ignition resistance characteristics of the fuels, with the pure aromatics being poor, isooctane somewhat better, and mixtures of the two intermediate. Although not shown in the table, a number of commercial-type gasolines were also rated with results similar to that shown for the 50/50 toluene/isooctane blend. It should be noted that even with isooctane (the best fuel tested) only 57% of the determinations were noise-free, indicating that even wide changes in fuel hydrocarbon composition beyond those of commercial feasibility offer little promise of solving the problem.

The possibilities of controlling pounding by decreasing the surface ignition activity of the combustion-chamber deposits have been investigated from three different standpoints, namely: (1) changes in hydrocarbon composition of the depositing fuel, (2) variations in lubricant composition and additive type, and (3) incorporation of deposit modifiers in the fuel. Within the range of commercial feasibility changes in the hydrocarbon type of the deposit fuel appear to offer little or no promise for relieving the pounding problem. This is illustrated by the results from tests conducted in 10.4/1 compression ratio Engines B shown in Fig. 16. In these tests

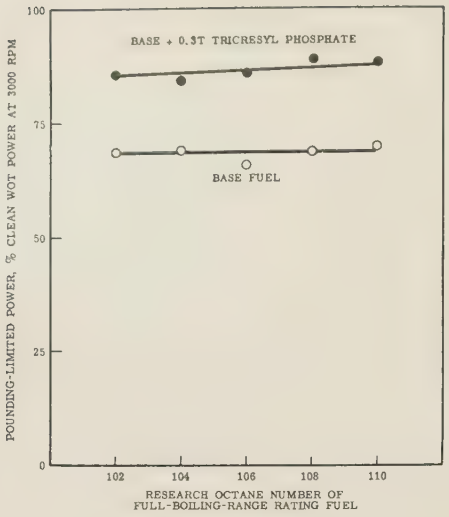

Fig. 18 — Efficacy of tricresyl phosphate in minimizing pounding in simulated urban driving tests in 10.4/1 compression ratio Engine B (pounding limited power is average obtained during 3000-6000 mile interval)

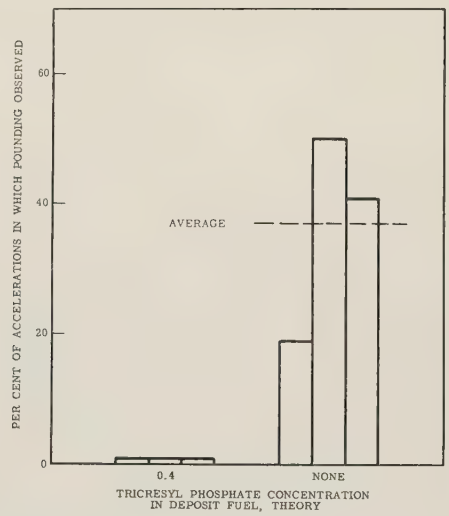

Fig. 19 — Incidence of pounding during full-throttle accelerations in 10/1 compression ratio Engines A operating under simulated urban driving conditions (during 2500-5000 mile interval at 3000 rpm on full-boiling-range rating fuels)

each of the deposit fuels shown were run in from three to six engines. In every case the fuels contained a nominal 3 ml tel per gal (Motor Mix) and 0.3 theory tricresyl phosphate. At periodic intervals the pounding tendencies of the engines were determined using a common rating fuel (benzene). The standard deviation for any given average on a deposit fuel is approximately 5%. Thus, it is seen that even wide variations in the hydrocarbon composition and/or boiling range of the deposit fuel had little or no significant effect on the pounding tendency of the engines.

Similar results with respect to lubricant composition are shown in Fig. 17. In this case the results represent averages obtained in from two to four engines, with a standard deviation of from 5–10%. Here again, it will be noted that even wide variations in lubricant viscosity grade and additive type had little or no effect on the activity of the combustion-chamber deposits formed.

Table 6 — Influence of Fuel Composition on Pounding in 10.4/1 Compression Ratio Engines B[a]

Rating Fuel[b]	Pounding-Limited Power, % Clean Wide-Open Throttle Power at 3000 rpm	Determinations in which Pounding Not Encountered at Wide-Open Throttle, %
Benzene	86	None
Cumene	90	None
Toluene, Xylene or 50-85% Benzene in Isooctane	96	None
50% Toluene in Isooctane[c]	97	None
5% Benzene in Isooctane	99 +	25
Isooctane	99 +	57

[a] Engines contained deposits from 5000 miles simulated urban operation on fuels containing 0.3 theory tricresyl phosphate.
[b] The addition of tel had no effect on the pounding resistance of the fuel.
[c] The addition of up to 15% olefins or naphthenes to this blend had no effect.

In contrast to the foregoing, the inclusion of tricresyl phosphate in the deposit fuel has been found to have a profound effect on pounding as might be expected from its well-known influence on deposit ignition. This is illustrated by the results in Fig. 18 which show, in quantitative terms, the improvement in pounding-limited power afforded in laboratory tests in a 10.4/1 compression ratio Engine B. It will be noted that in contrast to the almost negligible effect of fuel octane quality, the addition of 0.3 theory tricresyl phosphate to the deposit fuel provided approximately a 25% increase in the power which could be developed before objectionable levels of pounding were encountered. It is interesting to compare this effect with the somewhat analogous influence of tel on knock where, in current commercial-type fuels, the addition of 3 ml tel per gal is found to give increases of 22–28% in knock-limited performance number. In the case of the latter, of course, the effect is immediate, whereas deposit conditioning must take place in order for tricresyl phosphate to exert its effect on pounding.

The substantial increase in pounding-limited power afforded by the inclusion of tricresyl phosphate in the fuel has been found to be sufficient to eliminate pounding under most conditions in current (and lower) compression ratio engines. For example, in three 10/1 compression ratio Engines A run in the laboratory under simulated urban driving conditions, the addition of tricresyl phosphate to the fuel in 0.4 theory concentration completely controlled pounding as contrasted with the moderate to severe pounding observed in three identical engines which were operated on the base fuel. This is illustrated by the results in Fig. 19 which show the incidence of pounding observed in the engines during daily transient octane requirement determinations on full-boiling-range reference fuels during the 2000–7500 mile interval of the test.

In confirmation of these findings, field tests conducted on sixteen 1956 model cars of Makes A and C are of interest. In these tests the cars were operated by their owners in normal service on both base fuel and base fuel containing tricresyl phosphate with their performance being checked periodically on 100 octane number full-boiling-range reference fuel on a chassis dynamometer. (The chassis dynamometer checks were somewhat more severe than level road accelerations due to the greater tendency toward lugging the engine during the latter stage of the acceleration.) On the base fuel, pounding was experienced in both makes of cars. The average pounding behavior of the more

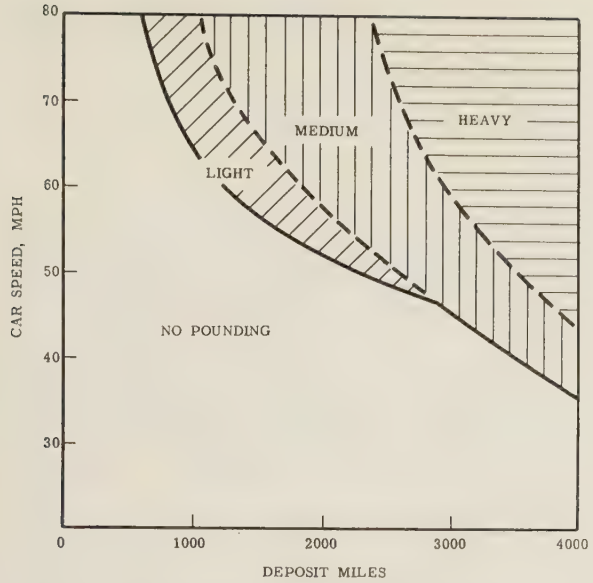

Fig. 20 — Average pounding severity noted in 1956 passenger Cars C in owner-driver service on base fuel (pounding checks made on chassis dynamometer during wide-open throttle accelerations using 100 octane commercial-type rating fuel containing 50% aromatics)

severe make (Car C) during full-throttle accelerations on the chassis dynamometer is shown in Fig. 20 as a function of deposit miles. It will be noted that as mileage accumulated the car speed at which pounding was encountered became progressively lower. The curves for the other less severe make of car were similar but shifted to the right. The same group of 16 cars when operated starting from clean engine condition on fuels containing 0.3 theory of tricresyl phosphate showed no evidence of pounding after 4000 miles of owner operation (Table 7). Further, two of the cars, which showed the most severe pounding at 4000 miles after the operation on the base fuel, were switched to fuel containing 0.3 theory tricresyl phosphate and after 2000 additional miles no evidence of pounding was observed.

The effect of tricresyl phosphate on the pounding tendency of preformed deposits was further demonstrated in tests conducted in the ten 1958 model vehicles mentioned previously. In these tests the cars were operated under urban conditions on a nominal 100 octane number commercial-type fuel containing 3 ml tel (Motor Mix) per gal until equilibrium deposits were obtained. Without disturbing the deposits, the cars were then switched to a similar fuel containing 0.3 theory tricresyl phosphate and operated an additional 2000 miles under urban conditions. Prior to and following the switch in fuels the pounding tendencies of the cars were assessed during 0–65 mph full-throttle level road accelerations on a commercial-type rating fuel. The results are shown in Fig. 21. It will be noted that with equilibrium deposits from operation on the base fuel six of the 10 cars exhibited some degree of pounding with the level being objectionable (medium or greater) in three of the cases. After 2000 miles additional operation on the fuel containing tricresyl phosphate, the intensity of pounding was significantly lower in four of the six cars which previously had evidenced pounding and was at an objectionable level in only one instance.

From the foregoing results it is seen that the in-

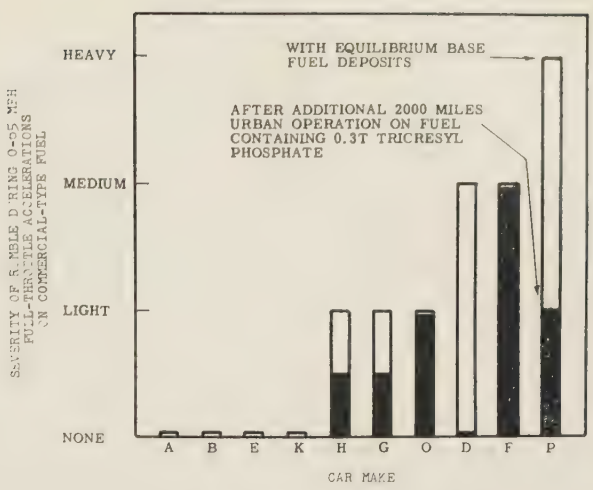

Fig. 21 — Efficacy of tricresyl phosphate in reducing pounding with preformed deposits in 1958 model cars

Table 7 — Effectiveness of Tricresyl Phosphate in Minimizing Pounding in Owner Service

Car Type	Pounding Intensity Noted During 0–65 mph Full-Throttle Accelerations on Chassis Dynamometer Using 100 Octane Number Commercial-Type Fuel After 4000 Miles Owner Service on	
	Base Fuel	Fuel Containing 0.3 Theory tricresyl phosphate
1956 Model C	Heavy in 7 cars, medium in 1 car	None in 8 cars
1956 Model A	Heavy in 1 car, medium in 4 cars, light in 3 cars	None in 8 cars

clusion of tricresyl phosphate in the deposit-forming fuel is an effective means for controlling pounding in engines of current and near-future compression ratio levels. Looking somewhat further into the future, results of road tests conducted in experimental 11.9 and 12.5/1 compression ratio engines (described earlier in Table 5) show severe pounding and other surface-ignition effects which are only partially ameliorated by phosphorus at presently used concentrations. Thus, unless the engine designers can provide help as compression ratios are increased, further improvement in the chemical control of pounding may be needed.

Summary

In summary, pounding—an abnormal combustion noise which is distinct from knock — has been observed with increasing frequency during high-load operation of late model engines. This noise, which is similar in sound to the alarming "clatter" associated with worn connecting-rod bearings, shows little or no response to increases in fuel octane quality. From studies of the phenomenon in instrumented engines and in tests designed to explore the mechanism, it is concluded that pounding is a form of combustion shock arising from too-rapid burning of the fuel due to secondary flame fronts initiated by deposit ignition.

Based on extensive laboratory and road tests it would appear that pounding constitutes a potential field complaint problem in current model vehicles and can be expected to become more severe as engine compression ratios are further increased.

Basically there are three factors which tend to promote pounding: (1) poor combustion-chamber

Table 8 — Urban Driving Cycle

	Cyclic: 30 sec Idle, 30 sec 30 mph	30 mph Boulevard Driving	60 mph Highway Driving	Engine Stopped[a]
Time, min	126.5	72	5.5	156
Miles	30.1	36	5.5	0
Mileage, %	42	50.3	7.7	—

[a] With forced cooling.

Table 9 — Operation During Urban Driving Cycle

Maximum Speed, mph	Approximate Average Speed, mph	Test Miles, %	Approximate No. of Stops
20-25	15	42	90
30	25	50	10
45	35	8	5

shape, (2) the use of rapid-burning fuels, and (3) deposit ignition. The first is in the hands of the engine designer. Although this factor appears to be under control in present-day engines, it may be possible to effect still further improvements. Within the range of fuel burning rates obtainable with commercially feasible compositions, little control of pounding can be effected. Of the methods investitigated for controlling pounding, the incorporation of tricresyl phosphate in the fuel was by far the most effective. Based on quantitative measurements, the addition of 0.3 theory of this additive was found to allow approximately a 25% increase in pounding-limited power. This substantial effect of tricresyl phosphate on pounding is similar to the marked beneficial effect of tel on knock and is sufficient in most cases to make the difference in whether or not objectionable pounding is encountered in current compression ratio vehicles.

Acknowledgment

The authors want to express their gratitude to the many people in the Shell organization whose encouragement and assistance made this paper possible. In particular, the authors wish to recognize the efforts of B. M. Henderson in collecting and analyzing much of the data reported herein.

APPENDIX

Rating Fuels Employed In Determining Engine-Pounding Tendencies

Full-Boiling-Range Reference Fuels (FBRF) — These fuels contained 50% aromatics, 50% saturates with 3.0 ml tel (Motor Mix) per gal, and had ASTM distillation characteristics similar to those of the average commercial premium-grade fuel. The Research octane ratings were varied by changing the antiknock quality of the saturate components while holding the sensitivity (Research minus Motor ratings) constant at 10.

Commercial-Type Rating Fuels — These fuels were blended from refinery streams in accordance with commercial practices and unless otherwise noted, contained 16–33% aromatics and a nominal 3 ml tel (Motor Mix) per gal.

Deposit Accumulation Cycles

Laboratory Simulated Urban Driving Cycle (Multiengine Tests) — This cycle is one devised to simulate urban-type driving in the Midwestern United States. The engines are automatically controlled by a series of cams and telephone-type stepping-relays to give the average operation during each 6-hr cycle, as shown in Table 8.

This results in the accumulation of 71.6 miles at an average running speed of 21.1 mph during each 6-hr period.

Laboratory Simulated Urban-Driving Cycle (Single Engine Tests in Engine B) — The operation in this test consists of a repetitive cycle of 5 min at 35 mph load interspersed with 1-min idle periods.

Road Urban Driving Conditions — The cars were operated on a test course in the Wood River, Ill., area which was selected to give urban operation with a high percentage of low-speed driving. The course gave the approximate operation during each 32-mile cycle shown in Table 9. This resulted in an overall average speed of about 19.8 mph with 3.1 stops per mile.

Road Simulated Severe Metropolitan Driving —In these tests the engines were operated (with the cars at rest on a test pad) by an automatic cycling device which produced alternate operation of 2-min at 600-rpm idle and 5 min at 1500 rpm. Prior to rating checks the cars were driven approximately 10 miles on the road to burn out any loose carbonaceous-type deposits.

ORAL DISCUSSION

— Reported by F. T. Finnigan
Pure Oil Co.

Edgar Rose, Kiekhaefer Corp.: Tcp tends to increase spark-plug fouling in 2-stroke engines.

Mr. Bame: In 4-stroke engines, where spark-plug failures are primarily due to lowered shunt resistance, TCP has proved to be an excellent control. We have also seen many cases where the additive was beneficial in 2-stroke engines. However, in some 2-stroke engines which suffer from plug cavity packing due to inability to digest ash, the additive is not completely effective.

Gilbert Way, Ethyl Corp.: In one of our research programs, the car with the highest compression ratio showed the least tendency toward rumble. Another vehicle of the same make reversed this finding in a later test. Retarded or advanced spark within reasonable limits did not affect rumble or surface ignition. In the presence of heavy deposits, retarded spark will cause pounding. Deposit warmup also affects this problem.

George Round, consultant: Richardo encountered rumble at 4/1 and 4.5/1 compression ratio using a high-turbulence head. Work by Midgley at high compression ratio with the spark plug located at the point of maximum turbulence resulted in a rapid pressure rise. In a clean combustion chamber, roughness and rumble resulted; and high turbulence and reduced compression ratio made matters worse. His conclusion was that turbulence aggravates the rumble problem.

Harry Bryan, Labeco: I think that rumble is related to turbulence and the rate of flame front area away from the spark plug. At no time should the exhaust valve lie between the flame front and the end of flame travel. High octane fuels mask the autoignition tendencies of an engine. Combustion-chamber walls and deposits rise in temperature and become ignition points, thus starting a flame front area; the rate of pressure rise is up and thud or diesel knock results. The Robison paper[a] verifies this. The unburned mixture is protected from preignition due to gasoline octane quality.

[a] This paper will be found on pp. 169–174.

Investigating *RUMBLE* in Single-Cylinder Engines

J. A. Robison, M. D. Behrens, and R.G. Mosher, Ford Motor Co.

This paper was presented at the SAE Summer Meeting, Atlantic City, June 11, 1958.

RUMBLE is a low-frequency noise heard in high compression engines and accompanied by high rates of pressure rise. Thus, rumble indicates a rapid combustion process. This paper describes a method of studying this problem: by detection of flame fronts by ionization gaps.

Results of experiments show that rumble is caused by deposit ignition in the end-gas region. These multiple ignitions occur after the normal flame front has progressed partially across the chamber. The authors conclude that this type of deposit ignition is generally a self-sustaining process, lasting until the deposits are burned out at a particular engine performance level. When the level is increased, the process repeats itself.

AN ENGINE noise, descriptively called "rumble" or "pounding," in high compression ratio engines has recently caused concern in both the petroleum and automotive industries. This low-frequency noise is most prevalent in automotive engines having deposits in the combustion chambers, but it has also been reported in clean engines. Observation of instantaneous cylinder pressures reveals that rumble is accompanied by high rates of pressure rise and thereby indicates a very rapid combustion process. These phenomena have also been observed in single-cylinder engines.

Rumble has been defined by the Coordinating Research Council as a "low-pitched thudding noise different from knock and accompanied by engine roughness." It is further stated that "one of the causes of this noise is probably the high rates of pressure rise associated with very early ignition or multiple surface ignition." In the investigation reported here, emphasis was was placed on studying the causes of the high rates of pressure rise. It is believed that this is a more basic approach than studying audible manifestations of high rates of pressure rise which might occur in many ways. To define the combustion phenomenon leading to rumble more clearly, flame propagation in a single-cylinder engine during normal combustion and rumble was measured by multiple ionization gaps.

Instrumentation

The detection of flame fronts by ionization gaps depends on the flame to ionize air gaps and thus to make them conductors of electrical current. An ionization gap, located at any point in the chamber, constitutes a break in an electrical circuit. The instant the flame front reaches the gap, the circuit is closed and current flows. This current flow, after it has been amplified, can be displayed on an oscilloscope or used to deflect an oscillograph galvanometer. With the ionization signal displayed against a time base, the exact time of flame arrival at the gap can be determined.

In 1933, Schnauffer[1] reported results obtained by the use of 24 ionization gaps spread over the combustion-chamber cylinder head surface. The ionization gaps used were "special units having an average electrode diameter of 2–2.5 mm set in 3-mm holes in the cylinder head." The signals were recorded by an oscillograph and "all the conditions affecting the speed of flame propagation in a high-speed spark ignition engine were determined." In 1953, Melby and others[2] installed 17 ionization gaps in an L-head

[1] SAE Transactions, Vol. 34, 1934, pp. 17–24: "Engine-Cylinder Flame Propagation Studied by New Methods," by Dr. Kurt Schnauffer.
[2] SAE Transactions, Vol. 62, 1954, pp. 32–39: "An Investigation of Preignition in Engines," by A. O. Melby, D. R. Diggs, and B. M. Sturgis.

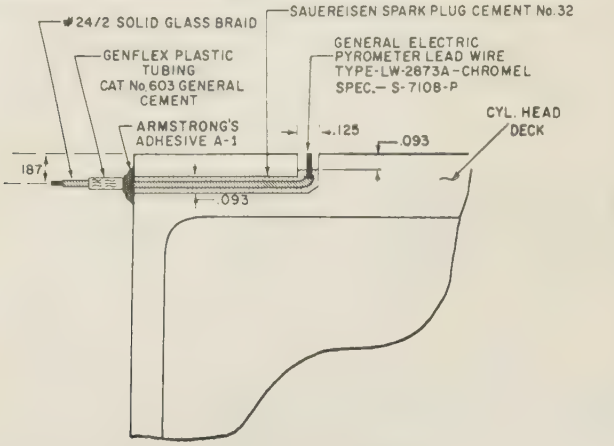

Fig. 1 — Ionization gap installation

Table 1 — Oscillograph Package

36 Channel Recording Oscillograph
Consolidated Electrodynamics Corp.
Type 5-119

Signal	Amplifier	Galvanometer
Ionization	Ionization Gap Pulse Amplifier (Fig. 4)	Consolidated 7-320 and 7-323 0-600 cps
Pressure/Time	Consolidated Type 1-112-C	Consolidated 7-326 0-3000 cps
60-Cycle Timing Pulse Generator	Consolidated Type 1-112-C	Consolidated 7-326 0-3000 cps.
Tdc, Magnetic	Timing Pulse Amplifier	Consolidated 7-325 0-1100 cps

CFR engine to investigate preignition.

In recent years, the use of single ionization gaps has gained prominence in surface ignition investigations. Single gaps located in the end-gas region are used to detect normal and earlier-than-normal flame fronts. The installation of these individual gaps in the end-gas of overhead valve engines could usually be accomplished by use of miniature spark plugs inserted through the top of the cylinder head and jacketed from the cylinder head coolant.

Use of this single gap technique revealed earlier-than-normal flame front arrival at the gap (located in the end gas) during rumble. This information merely supplemented the pressure development observations, however, and gave no clue as to the source of the rapid burning indicated. Whether there were indeed "multiple ignitions" or whether there might possibly be some other combustion phenomenon present during rumble remained unanswered. It was thought that flame propagation patterns such as those obtained by Schnauffer would provide further insight into the actual combustion process which produces rumble.

Many problems were encountered in developing a satisfactory ionization gap design and in finding a practical means of installing multiple gaps in an overhead valve, single-cylinder engine. Investigations of miniature gap design were made to find an optimum design which would give strong signals over a normal range of speed, load, and air/fuel ratio. Several methods of installing multiple ionization gaps were tried, and problems of sealing and insulating were solved before a satisfactory design was obtained.

The finalized ionization gap design and its multiple installation in the cylinder head deck is shown in Figs. 1 and 2. Insulated wires are led through drilled passages in the deck from the outside and project into the combustion chamber flush with the chamber surface. The metal surrounding this wire serves as the circuit ground. Spark-plug cement is forced into the passages using a specially constructed "caulking" gun. The cement was allowed to set for several hours and was then tamped down in the ionization gap cavity to the desired depth. The head was placed in an oven with the temperature slowly increased to 400 F over a period of 36 hr. Lead wires on the outside of the cylinder head were covered with plastic tubing and soldered to three Amphenol sockets. The instrumented cylinder head with 29 ionization gaps and a Kistler SLM pressure tranducer is shown in Fig. 3. Note that the wire in a gap adjacent to the spark plug is missing. This wire was accidentally broken off during the installation.

A 36 channel Consolidated oscillograph was used to record the 29 ionization signals, a 60 cycle per revolution timing pulse, a tdc pulse, and a cylinder pressure signal. The instrumentation, including amplifiers and galvanometers used for the various signals, is given in Table 1. The amplifier diagram for a single ionization gap pulse is shown in Fig 4.

Flame Propagation Studies

The instrumented cylinder head was installed on a 1955 Lincoln engine converted to single-cylinder operation. The combustion chamber was formed by a flat cylinder head and a piston which had a slightly dished dome and had a compression ratio of 12.0/1. This "open" chamber had previously been found to have a high rumble tendency. All flame propagation tests were conducted at 2000 rpm with lbt (leanest fuel flow for best torque) and mbt (minimum spark advance for best torque) conditions as required at wide-open throttle while operating on leaded alkylate fuel (3 ml tel per gal). The engine speed of 2000 rpm was chosen as a compromise between the increased rumble tendency at higher engine speeds and the increased time spread of oscillograph data obtained at lower engine speeds.

A portion of the oscillograph data showing the various signals is reproduced in Fig. 5. The peaks of the 60 cycle pulse represent 6 crankshaft deg. The accuracy of determing time of ionization from these records is within plus or minus one crankshaft degree. The oscillograph paper speed was 100 in. per sec. For all tests, oscillograph records were taken in 2 sec bursts, providing 16 2/3 engine cycles per record.

The average flame propagation pattern of 30 cycles of normal combustion with a clean chamber at wide-open throttle is shown in Fig. 6. Spark ignition occurs at 16 crankshaft deg btdc (16B), and the flame propagates almost symmetrically outward to the edges of the chamber. Rather slow flame propagation immediately after spark ignition is indicated by the area of combustion present at 5 deg atdc (5A). The signal of the broken gap previously mentioned was strong, but it had an obvious time lag due to the additional time required by the flame to burn down into the gap cavity. In all flame propagation plots, this biased signal was disregarded.

In plotting the flame propagation patterns obtained by determining the flame arrival time of 28

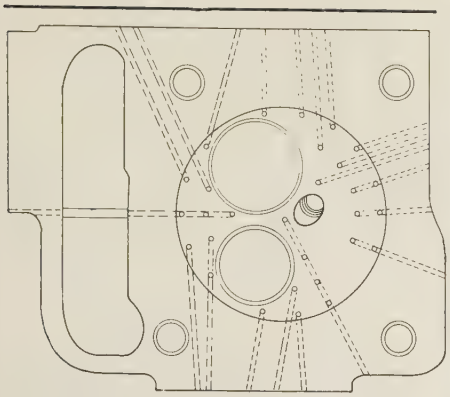

Fig. 2 — Ionization gap layout

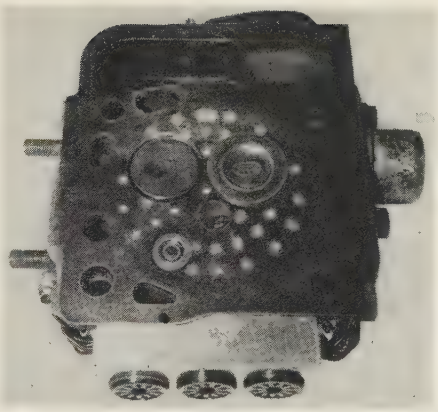

Fig. 3 — Instrumented cylinder head

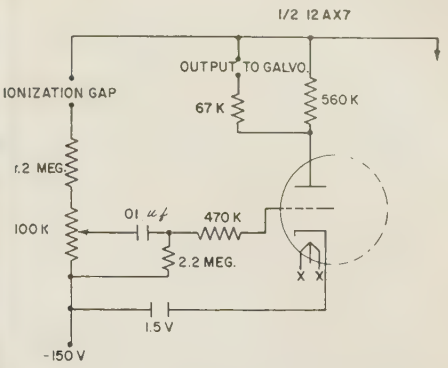

Fig. 4 — Ionization gap pulse amplifier

working gaps, it is realized that the result is only a crude approximation of the actual flame propagation. There is no information as to the flame location over valve areas or in the combustion chamber below the plane of the cylinder head and it is necessary to interpolate the flame location in areas between gaps. Nevertheless, the flame propagation patterns obtained are sufficiently informative to be extremely valuable in combustion work.

There had been discussions as to the possibility of the ionization gaps changing the actual combustion process and of the possibility of the gaps becoming hot spots. However, the run made with clean chamber duplicated a previous clean run with the unmodified head. There was no indication of surface ignition by noise, by pressure development, or (in the second run) by flame propagation. A visual inspection of the insulated wires was made and none were found burned.

Deposits were built up for 16 hr at 2800 rpm, 50% load on Indolene 30 fuel (3 cc tel per gal). At this time, the cylinder head was removed and photographs taken of the combustion-chamber deposits. The buildup was then continued for another 8 hr at 2000 rpm, 25% load on the same fuel. The lubricating oil used was a commercially available lubricant —Mil. Spec. 2104. The original intent was to remove the cylinder head after deposit buildup, and clean the ionization gaps. However, the circuits were first checked and found to be open, and it was decided not to remove the head. The engine temperatures were stabilized at 2000 rpm, 50% load on leaded alkylate fuel and the throttle slowly opened until rumble occurred. Rumble occurred at part throttle, and it was found to maintain rumble for any length of time it was necessary to continue opening the throttle. Rumble lasted approximately 3 min of the total operation and finally disappeared completely after about 30 sec of wide-open throttle operation. During the period of rumble, seven 1-sec records of oscillograph data were taken. A record was also taken after rumble had ceased. An identical test previously conducted using this same cylinder head but without ionization gaps resulted in identical rumble duration and time of encounter. It is definitely believed that there is no possibility that deposits in the gaps were contributing to the rumble condition. Photographs taken of the deposit formations on the cylinder head and piston after rumble further confirm this opinion.

Figs. 7–9 show typical flame propagation patterns obtained during rumble. These plots show conclu-

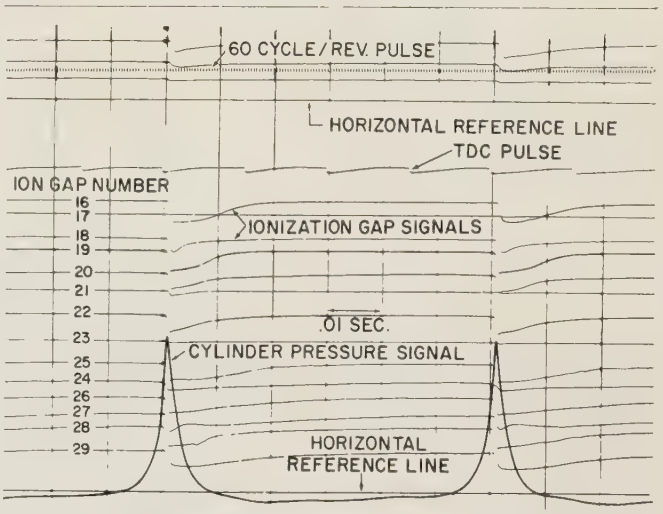

Fig. 5 — Oscillograph record sample, cycles 14-11 and 14-12

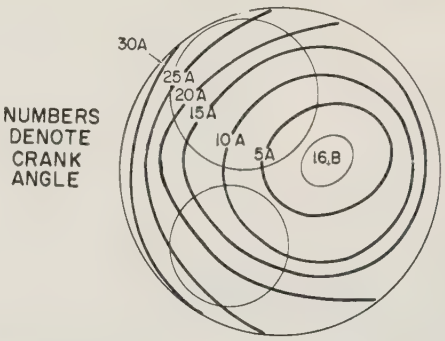

Fig. 6 — Flame propagation pattern of normal combustion with clean chamber, 30 cycle average. (Conditions: 2000 rpm, load — 1.8 in. of water manifold vacuum with wide-open throttle, leaded alkylate fuel)

sively that multiple flame fronts are present in the chamber. An analysis of the data shows that all rumble cycles (as determined by pressure development) had at least one secondary flame front. On some cycles, as many as four extra flame fronts were detected. In all cases, the additional flame fronts occurred in the end-gas region after the normal spark-ignited flame front had progressed part way across the chamber. At the start of rumble, all extra flame fronts started at the edge of the chamber in the end gas similar to those shown in Figs. 7 and 8. Toward the end of rumble, many of the cycles showed extra flame fronts originating at points inward from the edge of the chamber similar to those shown in Fig. 9. There are possibly other flame fronts present that were not detected. For

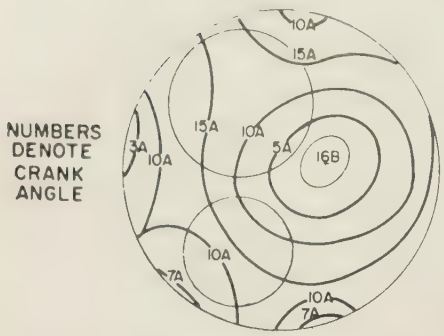

Fig. 7 — Flame propagation pattern of combustion during rumble with deposited chamber, cycle 14-15. (Conditions: 2000 rpm, load — 4.5 in. of water manifold vacuum, leaded alkylate fuel)

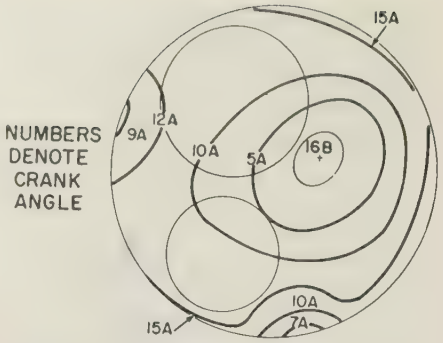

Fig. 8 — Flame propagation pattern of combustion during rumble with deposited chamber, cycle 14-10. (Conditions: 2000 rpm, load — 4.5 in. of water manifold vacuum, leaded alkylate fuel)

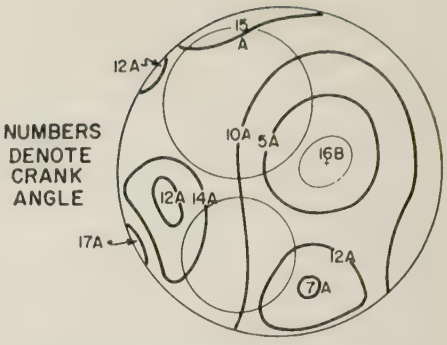

Fig. 9 — Flame propagation pattern of combustion during rumble with deposited chamber, cycle 14-1. (Conditions: 2000 rpm, load — 4.5 in. of water manifold vacuum, leaded alkylate fuel)

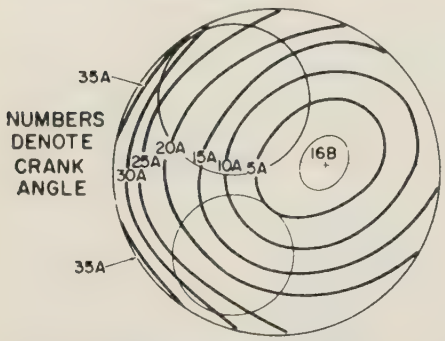

Fig. 10 — Flame propagation pattern of normal combustion with deposited chamber, 16 cycle average. (Conditions: 2000 rpm, load — 1.8 in. of water manifold vacuum, leaded alkylate fuel)

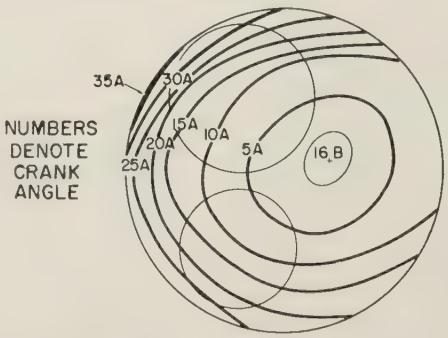

Fig. 11 — Flame propagation pattern of normal combustion with deposited chamber, cycle 15-10. (Conditions: 2000 rpm, load — 1.8 in. of water manifold vacuum with wide-open throttle, leaded alkylate fuel)

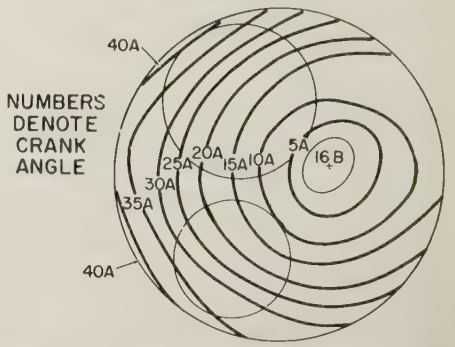

Fig. 12 — Flame propagation pattern of normal combustion with deposited chamber, cycle 15-8. (Conditions: 2000 rpm, load — 1.8 in. of water manifold vacuum with wide-open throttle, leaded alkylate fuel)

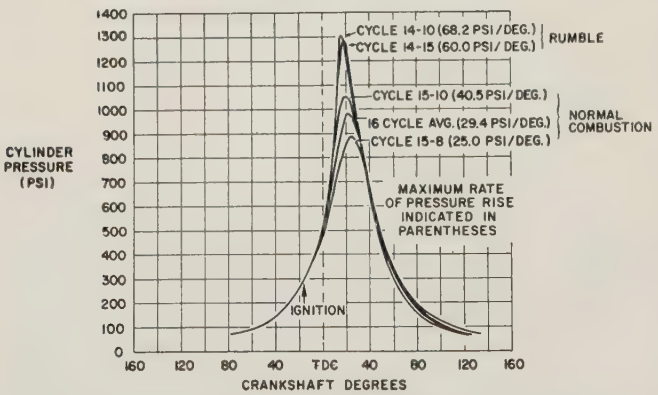

Fig. 13 — Pressure development, rumble compared with normal combustion

instance, the flame propagation of cycle 14-10 (Fig. 8) indicates extremely fast combustion between 10 and 15 atdc over the exhaust and intake valves.

After the engine had stopped rumbling at 2000 rpm wide-open throttle, oscillograph records were made. The flame propagation pattern (Fig. 10) of a 16-cycle average showed normal flame propagation. A particularly fast, normal flame propagation is shown in Fig. 11; and a slow, normal propagation is shown in Fig. 12.

Other Observations

The resulting pressure development of some of the cycles of flame propagation previously shown is given in Fig. 13. Note the difference between cycles 15-10 and 15-8, depicting fast and slow normal combustion. The pressure development during rumble results in an increase in peak pressure of approximately 300 psi and a doubling of the maximum rate of pressure rise when compared to an average normal combustion cycle.

Observations of the combustion-chamber deposits after 16 hr of buildup and after rumble (Figs. 14 and 15) indicate that piston deposits are the source of the extra flame fronts. The area of burned and cracked deposits on the piston correlates very closely with the areas of extra flame front sources noted on the flame propagation plots. The source of the largest percentage of the extra flame fronts was in the end gas region at a point farthest from the spark plug. Fig. 15 shows black carbonaceous deposits on the piston (arrows) in this region before rumble and their absence after rumble. Those deposits present after rumble represent a condition of deposit formation which did not produce rumble, even at wide-open throttle. The cylinder head deposits do not seem to be as severely affected.

The possibility that rumble is caused predominately by piston deposits had been suggested by previous tests conducted at 2800 rpm with an unmodified head. After a deposit buildup, the engine was found to rumble quite readily at part throttle. The moment rumble was established, the engine was shut down to preserve deposits. The deposits on the exhaust valve were removed, and the engine checked for rumble tendency. Rumble still occurred at the same throttle opening as before. All of the cylinder head deposits were removed next and again the engine rumbled quite readily, although slightly more throttle opening was required. Finally, the

piston deposits were removed, and rumble could not be obtained, even at wide-open throttle.

The effect of spark advance on rumble tendency was investigated in several ways. A deposit accumulation of 16 hr at 2000 rpm, 25% load on Indolene 30 fuel was used as a base for these tests. The engine was then operated on leaded alkylate fuel, and the throttle was slowly opened to a point just below rumble. Spark timing was retarded 5 deg, and temperatures were stabilized for 5 min. No rumble occurred. Spark timing was then returned to the original setting for 5 min without rumble. Upon advancing the spark timing 5 deg, severe rumble occurred almost immediately. Another test involved deposit formations which were "rumbled out"; that is, deposits which would not produce rumble even at wide-open throttle. Spark timings of 5 deg retard from mbt, (minimum spark advance for best torque), and at mbt did not produce rumble; but advancing the spark timing approximately 10 deg more than mbt resulted in severe rumble. It was also noted that once severe rumble had been established in the engine, the only way it could be stopped was by substantial closing of the throttle. The implication of these results will be discussed later.

To determine the effects of unleaded deposits on rumble tendency, deposit buildups were made on Indolene clear fuel (unleaded) and Indolene 30 fuel (3 ml tel per gal). In each case, deposits were accumulated starting with a clean chamber for 16 hr at 2000 rpm, 25% load. At the end of the deposit accumulation period, the fuel was switched to leaded alkylate and the throttle slowly opened. Rumble occurred at approximately 75% load with leaded deposits but could not be induced, even at wide-open throttle, with unleaded deposits.

Efforts to obtain "clean-engine rumble" failed except for very isolated bursts of mild rumble. These isolated bursts were attributed to deposits built up during the warmup periods. In any event, there was no sustained rumble such as that readily obtained with a deposited chamber.

There are several types of combustion processes which might occur in a clean engine that can result in a noise similar to rumble. One is rapid, normal combustion brought about by combustion-chamber design, fuel type, or engine operating conditions. We have referred to this engine noise as "pressure

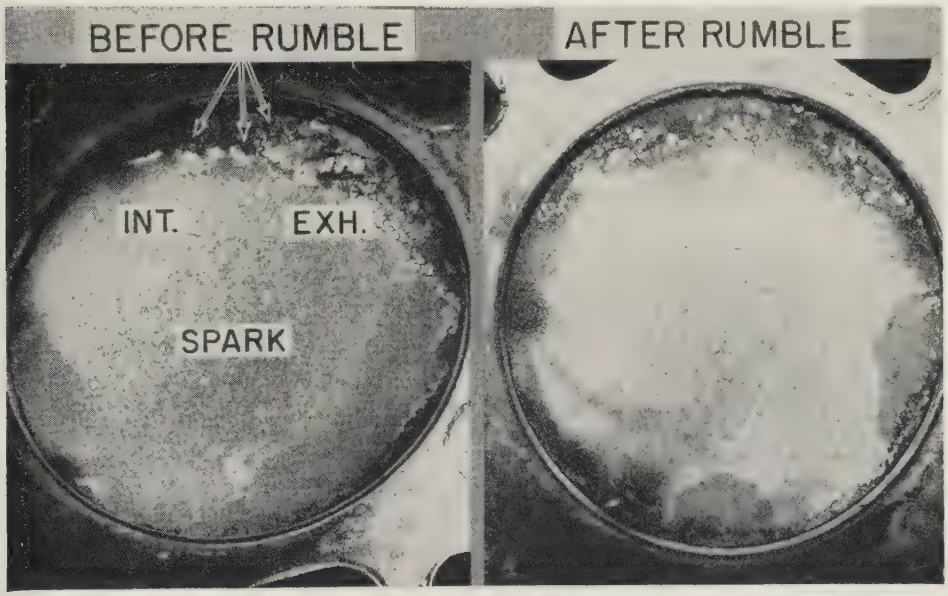

Fig. 14 — Piston deposit formation

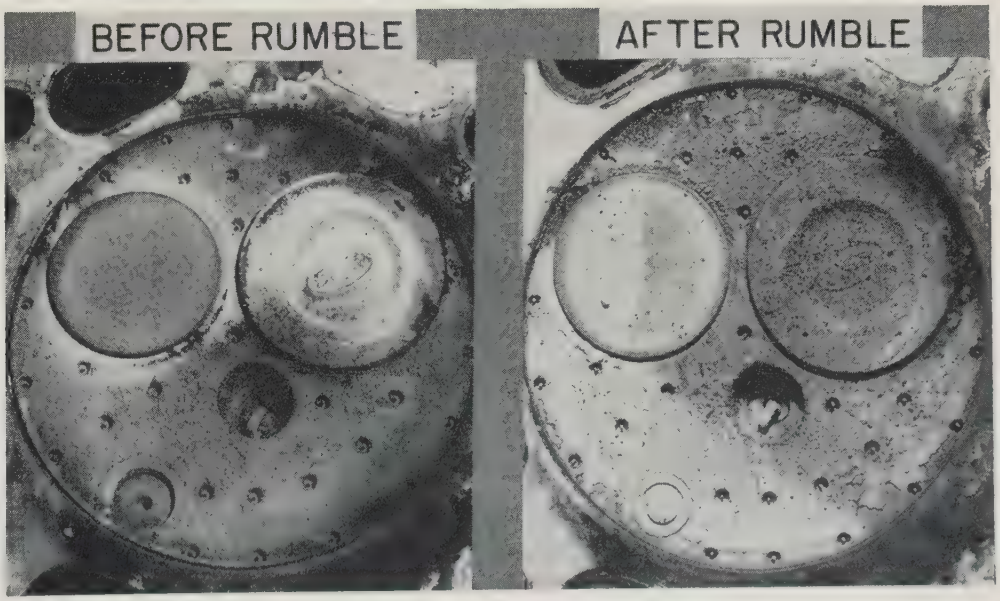

Fig. 15 — Cylinder head deposit formation

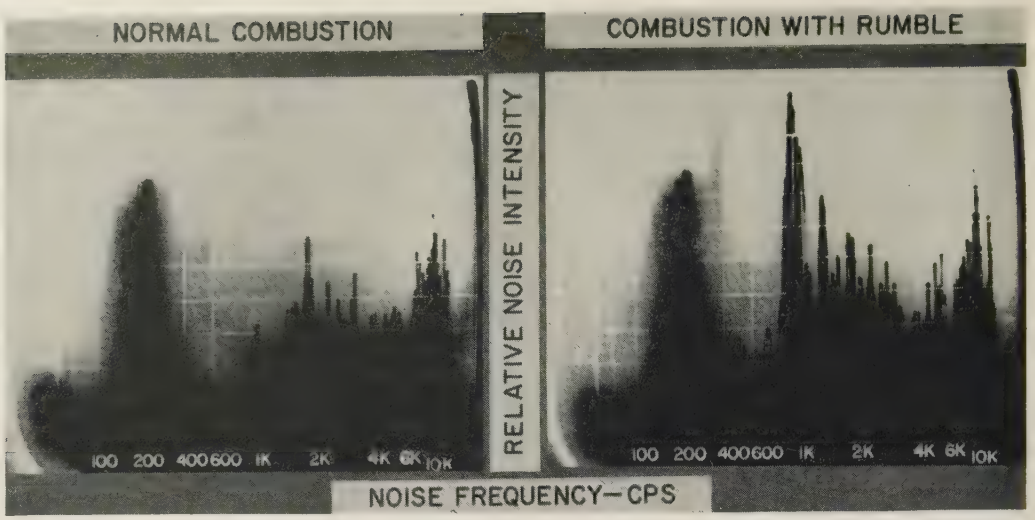

Fig. 16 — Noise quality by panoromic sonic analyzer, 2000 rpm, wide-open throttle

rap" or "thudding." Another combustion process which results in a thudding noise very similar to rumble is rapid, abnormal combustion caused by hot-spot ignition. In our experimental 12.0/1 compression ratio engines, we encountered a type of thudding noise which was found to be caused by hot-spot ignition from the exhaust valve. This combustion process not only caused engine noise but invariably led to engine damage. One particular fix for this type of hot-spot ignition is the use of sodium-cooled exhaust valves.

Noise analyses of rumble in a deposited engine and normal combustion were made with a panoramic sonic analyzer. The use of this instrument in analyzing spark knock was previously reported by the authors.[3] Fig. 16 shows that the amplitude of noise at 1000- and 1400-cps increases considerably during rumble. These two frequencies were also present in a much lesser degree during normal combustion. This evidence indicates that the audible sources of rumble are present even during normal combustion and are already contributing to the total engine noise. When rumble occurs, these same sources are excited to a greater noise intensity, producing the characteristic sound of rumble.

Conclusions Concerning the Mechanism

Analysis of flame propagation patterns and cylinder pressure development, observation of deposit structure before and after rumble, and interpretation of associated single-cylinder engine tests have shown that:

1. Rumble is caused by deposit ignition in the end-gas region from one or more sources.
2. Piston deposits are the major source of rumble.
3. These multiple ignitions occur after the normal flame front has progressed partially across the chamber.
4. Once started, the deposit ignition process continues almost steadily cycle after cycle, without developing into runaway preignition, until the deposits are incapable of glowing or burning at those particular engine operating conditions.
5. Deposits which have been "rumbled out" at a given level of engine performance and conditions can be induced to cause rumble by increased pressure and temperature stressing (usually by increasing the imep or by further advancing of the spark timing).

From the foregoing, an outline of the mechanism of continuous, multiple deposit ignition can be drawn. It seems logical to assume that a prerequisite to rumble is the presence of certain types of low-duty deposit particles usually formed in the end-gas region (such as shown in Fig. 15). As soon as these deposits are stressed by additional load and/or spark advance, their temperature increases. When the approaching normal flame front compresses the end gas and radiates additional heat to these deposits, they are incapable of further immediate heat transfer to the end-gas combustion-chamber surface; consequently, they reach their critical glowing or burning temperature. This glowing or burning causes ignition of the surrounding conditioned end gas. These glowing or burning deposits are probably cooled below their critical temperature by the incoming charge; however, the deposit temperature remains sufficiently high enough to be induced to glow or burn again by the advancing normal flame front of the next cycle. This particular type of deposit ignition is generally a self-sustaining process, lasting until the offending deposits are burned out at a particular engine performance level. Finally, should the imep or spark advance of the engine be increased after deposits have been "rumbled out" at a given engine performance level, the resulting increased pressure and temperature of the advancing normal flame front provides the additional thermal stress required to again initiate multiple deposit ignition.

We believe that multiple, continuous deposit ignition is an intensification of the deposit ignition problem that has been prevalent for years. The occasional occurrence of rumble in present-day engines is a warning that the problem is becoming more severe. Whether rumble stays with us will depend on how skilled we are in designing fuels, oils, and engines for the future.

Acknowledgment

The authors wish to thank the Instrument Development Unit of the Instrumentation Section, Engineering Research, and the Test Instrumentation Section of the Dynamometer Department, Product Engineering Office, for their work on the oscillograph package and for other technical assistance.

[3] SAE Transactions, Vol. 66, 1958, pp. 549–556: "Investigating Combustion Phenomena in Unmodified Engines," by J. A. Robison, M. D. Behrens, R. G. Mosher, and J. M. Chandler.

if you squeeze them, must they SCREAM?

W. M. Wiese, General Motors Research Staff

This paper was presented at the SAE Summer Meeting, Atlantic City, June 11, 1958.

NOT necessarily! At least not in the case of fuel and air molecules being squeezed together during the combustion process in a modern high-compression automobile engine. There appear to be several factors relating to gasoline composition which can be varied to help alleviate the screaming. (In this text the terms knock, surface ignition, and rumble[1] will be used synonymously with "screaming").

Spark knock has historically been the factor which limits utilization of the maximum efficiency potential of an engine.[2,3,4,5] The occurrence of spark knock is principally dependent upon the values of compression ratio, spark advance, air/fuel ratio, and the antiknock quality of the fuel. Spark knock can, therefore, be controlled by proper design of the engine to fully utilize available antiknock quality. During recent years, compression ratios have increased rapidly as the octane quality of commercial gasolines has increased. Unfortunately, at these higher compression ratios a different type of abnormal combustion has appeared on the scene — surface ignition.[6,7,8] Today this phenomena, as well as spark knock, limits utilization of the potential efficiency of an engine. Surface ignition (of which rumble may be a symptom) presents a more formidable obstacle than spark knock, because no way is known to control it directly by engine design. Since surface ignition as well as spark knock must be controlled in order to make further gains in engine efficiency, the potentiality of reducing surface ignition through changes in gasoline composition is of great interest. For this reason, the work reported in this paper was undertaken.

These studies were concerned with the influence of the following factors on the octane number requirement and the occurrence of surface ignition in high-compression automobile engines: (1) a change in gasoline tail-end volatility, (2) a change in gasoline aromatic content, and (3) the use of various ignition control additives in the gasoline. Nearly 300,000 miles of deposit-accumulation driving and testing were done, using eight cars having experimental engines with measured clean compression ratios of 10/1 to 10.25/1.

Statistical Test Method

The principal purpose of these tests was to determine the octane requirements and surface ignition

[1] Rumble is a low-pitched thudding noise which is different from knock but is associated with combustion. It is believed to be due to the high rates of pressure rise associated with very early ignition or multiple-surface ignition.

[2] *Journal of Institute of Fuel*, No. 9, 1935, pp. 10–15: "Progress of Internal Combustion Engine and Its Fuel," by H. R. Ricardo.

[3] SAE *Quarterly* Transactions, Vol. 1, October, 1947, pp. 669–679: "More Efficient Utilization of Fuels," by C. F. Kettering.

[4] SAE *Quarterly* Transactions, Vol. 3, April, 1949, pp. 341–353: "Increasing Thermal Efficiencies of Internal Combustion Engines," by J. M. Campbell, D. F. Caris, and L. L. Withrow.

[5] SAE Transactions, Vol. 64, 1956, pp. 76–100: "Mechanical Octanes for Higher Efficiency," by D. F. Caris, B. J. Mitchell, A. D. McDuffie, and F. A. Wyczalek.

[6] SAE *Journal*, Vol. 62, January, 1954, pp. 51–52: "Occurrence of Preignition in Present Day Cars in Normal Service," by R. F. Winch.

[7] Proceedings of API, Vol. 33, 1953, pp. 137–50: "Preignition in Automobile Engines," by J. R. Sabina, J. J. Mikita, and M. H. Campbell.

[8] "Fuel Quality Requirements of High Compression Ratio Engines," by J. K. Appeldoorn. Paper presented at API Lubrication Committee Meeting, Detroit, February, 1956.

TODAY'S high-compression engines present new problems of engine noise to automotive engineers. This paper deals with some of the factors which contribute to rumble, knock, and surface ignition.

The work was primarily concerned with the influence of fuel composition on the equilibrium octane number requirement and surface ignition tendency of high-compression engines. Both the effect of the combustion-chamber deposits formed by the fuel and the effect of the combustion characteristics of the fuel itself were considered.

The results indicate that a reduction in gasoline tail-end volatility or the use of an effective ignition control additive can reduce knock, surface ignition, and rumble; while use of gasolines containing high concentrations of aromatic hydrocarbons can increase these combustion difficulties.

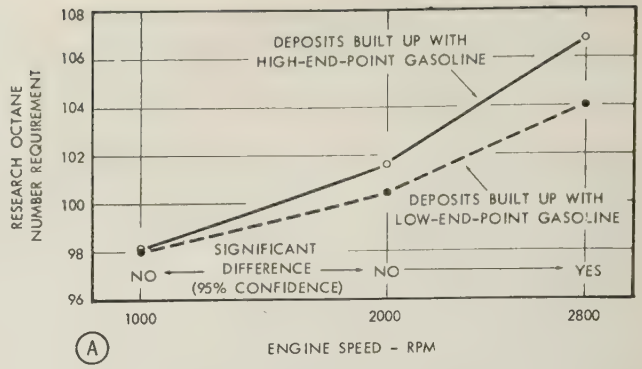

Average Octane Number Requirements With Deposits Built Up By the Use of High-End-Point Gasoline Compared to Those With Deposits Built Up With Low-End-Point Gasoline.

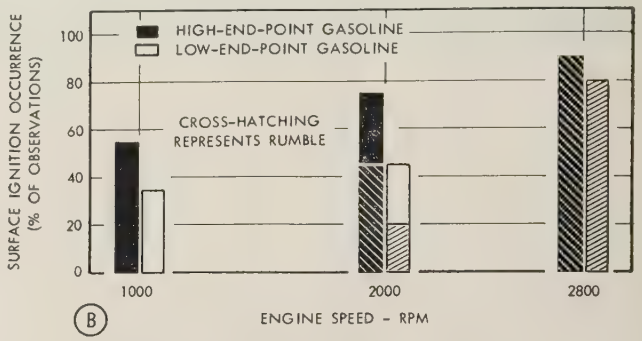

Surface Ignition Occurrence With Deposits Built Up by the Use of High-End-Point Gasoline Compared to That With Deposits Built Up With Low-End-Point Gasoline.

Fig. 1 — Tail-end volatility

tendency of high-compression engines when using various types of fuel to accumulate combustion-chamber deposits. Deposits were accumulated at the General Motors Proving Ground on a suburban-type deposit accumulation schedule with a 50-mph top speed.

During a test of this type, in which "normal" engine deposits are maintained, considerable deposit accumulation time is required. Unfortunately, the accompanying changes in atmospheric conditions often alter the octane requirement of an engine as much as the test variable (in this case gasoline composition). To compensate for this undesirable variability, *each test fuel comparison in this program was made in two "identical" automobiles using a latin square test arrangement.* Differences between the two test cars as well as atmospheric changes tend to cancel with this arrangement. A typical test arrangement is shown in Table 1 for a case in which the deposit forming characteristics of Fuel A are being compared to those of Fuel B in two test cars.

Each phase of this test consists of approximately 8000 miles of deposit accumulation driving per car. Observations of octane number requirement and occurrence of surface ignition were made at intervals of 500 miles between 3000 and 8000 deposit miles. Considering both phases, this test method provides 10 observations on each car when using each test fuel or a total of 20 observations for each test fuel. From these 20 observations, average differences in octane number requirement were calculated and the statistical significance of these differences were evaluated at the 95% confidence level.

Each fuel comparison reported in this paper was made using this general test method. Additional details of procedure are discussed as required in the following sections.

Gasoline Tail-End Volatility

High-boiling constituents or "dirty burning tail-ends" in gasoline have been singled out[9,10] as contributors to harmful combustion-chamber deposits. In these tests, the deposit-forming characteristics of two gasolines having a difference of 50 F in their distillation temperatures at the 90% point and 85 F difference in end point were compared. Analyses of both gasolines are shown in Table 2. Both gasolines had high aromatic content. A fully distilled mid-continent 20-20W engine oil was used during these tests.

Octane number requirements were determined at full throttle for three engine speeds; namely, 1000, 2000, and 2800 rpm. Test observations were made at constant engine speed over a period of 5 sec by holding car speed constant with the brakes. Octane number requirement was defined in terms of the Research octane number of the commercial reference fuel required to eliminate objectionable combustion noise. Surface ignition was considered to be objectionable when either (1) one or more cylinders would continue to fire after the ignition circuit had been grounded or (2) rumble was so loud as to be considered objectionable. These same criteria were

[9] "Control of Engine Knock Through Gasoline and Oil Composition," by C. L. Fleming, Jr., N. V. Hakala, L. E. Moody, R. W. Scott, and C. O. Tongberg. Paper presented at SAE Annual Meeting, Detroit, January, 1955.

[10] SAE Transactions, Vol. 62, 1954, pp. 40–49: "Deposit-Induced Ignition, Evaluation in Laboratory Engine," by D. A. Hirschler, J. D. McCullough, and C. A. Hall.

Table 1 — Typical Test Arrangement

Car	First test phase		Second test phase
1	deposit accumulation driving on Fuel A	deposits removed, test fuels reversed	Deposit accumulation driving on Fuel B
2	deposit accumulation driving on Fuel B		deposit accumulation driving on Fuel A

Table 2 — Test Gasoline Analyses for Tail-End Volatility Tests

	Low End Point Gasoline	High End Point Gasoline
Specific Gravity at 60 F	0.777	0.796
Tetraethyl Lead, cc per gal	2.15	2.14
Reid Vapor Pressure, lb	8.6	7.5
Gum, mg per 100cc	5.2	8.0
Sulfur, %	0.05	0.03
Motor Octane Number	88	89
Research Octane Number	99	100
Distillation, F		
Initial	88	92
10	127	129
20	157	159
30	192	204
40	234	254
50	257	287
60	270	296
70	278	316
80	288	328
90	304	358
End	339	424
Recovery, %	97.0	97.0
Residue, %	0.6	0.8
Hydrocarbon Content		
Paraffins, %	39.5	33.6
Olefins, %	13.3	11.8
Aromatics, %	47.2	54.6

used during all tests described in this report.

It is recognized that the occurrence of rumble cannot be controlled entirely by octane quality. During these tests, however, it was observed that rumble was reduced to an acceptable noise level when successive tests were run on fuels of increasing octane quality. The resultant octane number requirement may in some cases have been as much dependent upon the amount of full-throttle test operation preceding the test on the acceptable fuel as upon the octane quality of that fuel. This lack of response to octane quality caused greater variability of results when rumble was present. Better methods for measuring surface ignition and rumble in engines are currently being investigated.

The results of the tail-end volatility tests are shown in Fig. 1. The average octane number requirements are shown in Fig. 1A for both test gasolines at each of the three test speeds. On the average, use of the low end point gasoline resulted in octane requirements that were 1.2 and 2.8 numbers lower at 2000 and 2800 rpm, respectively, than when the high end point gasoline was used. However, only the difference shown at 2800 rpm is significant at the 95% confidence level. The unusually high octane requirements at 2000 and 2800 rpm are the result of rumble.

Surface-ignition occurrence is shown for both high end point and low end point gasolines in Fig. 1B. The length of each bar indicates the per cent of total observations during which surface ignition was objectionable. This includes both knocking surface ignition and rumble. At each speed the black bar indicates the frequency of occurrence of surface ignition with high end point gasoline and the white bar indicates the same for the low end point gasoline. The cross-hatched area in each bar indicates the portion of the observations during which rumble was objectionable. It is apparent that the low end point gasoline produced slightly less surface ignition and rumble than the high end point gasoline. These results are in general agreement with previously published data.[9,10]

Aromatic Content in Gasoline

The effect of gasoline aromatic content on the octane requirement and surface-ignition characteristics of an engine is of great importance at the present time because of the trend toward higher aromatic content in gasolines. Aromatic hydrocarbons produced by modern catalytic reforming processes have very high octane quality; therefore, the general outlook is for still higher aromatic content in gasolines as the octane quality goes up. To investigate the influence of aromatic concentration in gasoline, a road test program was set up to find the effect on octane number requirement and surface ignition of: (1) the combustion-chamber deposits built up by the use of a high-aromatic gasoline, and (2) the combustion characteristics of the high-aromatic gasoline itself when used in an engine containing aromatic deposits.

Two high-aromatic gasolines were compared to a low-aromatic blend in two separate tests. Both tests were arranged in a latin square consisting of 13,000 miles of deposit accumulation on each of two test cars with both the high-aromatic test gasoline and the low-aromatic blend. In order to observe the combustion characteristics of the aromatic fuels in an engine containing aromatic deposits, it was necessary to determine octane number requirements in terms of a set of aromatic reference fuels as well as the commercial reference fuels. Alternate observations of octane requirement and surface-ignition occurrence were made with aromatic reference fuels and with commercial reference fuels. The data obtained were then compared from three different viewpoints to determine the following information about the use of high-aromatic gasolines:

1. Effect of aromatic deposits.

The octane requirements and surface-ignition tendency with the high-aromatic combustion-chamber *deposits* were compared to those with the low-aromatic *deposits* on the basis of commercial reference fuels, and on the basis of aromatic reference fuels.

2. Effect of aromatic reference fuels.

The octane requirements and surface-ignition tendency with aromatic reference *fuels* were compared to those with commercial reference *fuels* when high-aromatic deposits were present, and when low-aromatic deposits were present.

3. Total effect; aromatic deposit plus aromatic reference fuel.

The octane requirements and surface-ignition tendency with high-aromatic combustion-chamber *deposits and* aromatic reference *fuels* were compared to those with low-aromatic *deposits and* commercial reference *fuels* to determine the total effect of using high-aromatic gasoline.

Results of tests evaluating the two high-aromatic gasolines are shown in the following two sections.

Test No. 1, Aromatic Gasoline A

Two gasolines were compared during the test: a high-aromatic 108 octane prototype gasoline (A),

Table 3 — Test Gasoline Analyses for Aromatic Gasoline Test No. 1

	Low-Aromatic Blend	High-Aromatic Gasoline A
Specific Gravity at 60 F	0.724	0.796
Tetraethyl Lead, cc per gal	3.00	3.01
Reid Vapor Pressure, lb	7.1	8.6
Gum, mg per 100cc	1.6	0.4
Sulfur, %	—	0.03
Motor Octane Number	94	97
Research Octane Number	99	108
Distillation, F		
Initial	94	96
10	132	151
20	156	172
30	176	184
40	195	195
50	211	207
60	222	226
70	236	259
80	252	302
90	289	346
End	364	389
Recovery, %	97.0	97.0
Residue, %	0.5	0.7
Hydrocarbon Content		
Paraffins, %	80.5	45.7
Olefins, %	5.0	2.5
Aromatics, %	14.5	51.8

Table 4 — Reference Fuel Data for Aromatic Gasoline Test No. 1

Aromatic Reference Fuels

Octane Number		Hydrocarbon Type		
Research	Motor	Paraffins, %	Olefins, %	Aromatics, %
108	97	45.7	2.5	51.8
106	95.5	47.3	2.2	50.5
104	94.5	49.0	2.2	48.8
102	93	51.2	2.2	46.6
100	91.5	53.2	2.1	44.7
98	90	55.6	2.0	42.4
96	89	57.7	2.0	40.3

Commercial Reference Fuels

Octane Number		Hydrocarbon Type		
Research	Motor	Paraffins, %	Olefins, %	Aromatics, %
108	98	66.1	12.6	21.3
106	95.5	62.5	14.6	22.9
104	93.5	60.3	16.7	23.0
102	91.5	54.8	20.6	24.6
100	89	59.6	16.5	23.9
98	87	48.4	23.5	28.1
96	85	58.4	18.7	22.8

and a special low-aromatic blend of aviation alkylate and commercial premium gasoline. The high-aromatic gasoline contained approximately 52% aromatics while the low-aromatic blend contained only 14%. Analyses of both gasolines are shown in Table 3. Table 4 contains Research and Motor octane number data along with hydrocarbon type data for the high-aromatic and commercial reference fuels used to define octane requirements during this test. The high-aromatic reference fuels were blended by adding increasing amounts of normal heptane to the high-aromatic gasoline A.

Details of the test technique were identical to those described in the section dealing with tail-end volatility. Octane number requirement and surface-ignition tendency were determined at full throttle for three engine speeds; namely 1000, 2000, and 2800 rpm.

Effect of Aromatic Deposits — The difference in average octane number requirement and surface-ignition occurrence when using either high-aromatic gasoline A or the low-aromatic blend to build up combustion-chamber deposits are shown on Figs. 2 and 3. Fig. 2 is based on observations with commercial reference fuels while Fig. 3 is based on observations with aromatic reference fuels. The oc-

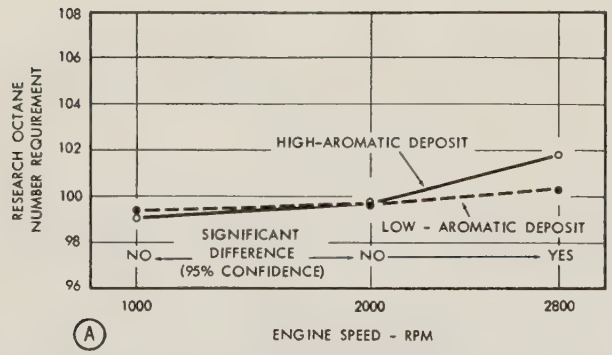

Average Octane Number Requirements With Deposits Built Up By the Use of High-Aromatic Gasoline Compared to Those With Deposits Built Up With a Low-Aromatic Blend. (Commercial Reference Fuels)

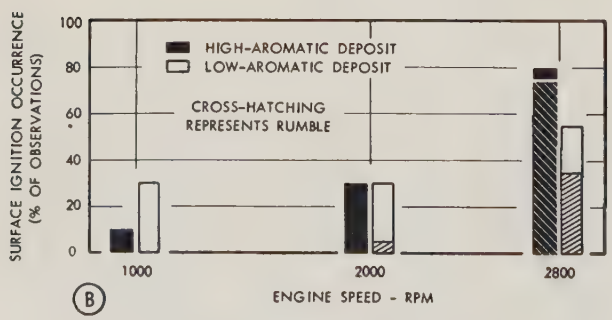

Surface Ignition Occurrence With Deposits Built Up By the Use of High-Aromatic Gasoline Compared to that With Deposits Built Up With a Low-Aromatic Blend. (Commercial Reference Fuels)

Fig. 2 — Effect of deposits from aromatic gasoline A, commercial reference fuels

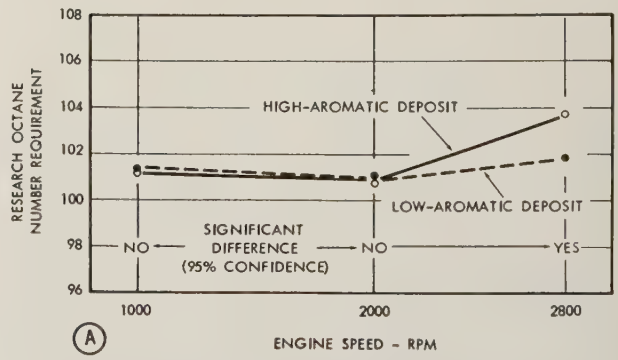

Average Octane Number Requirements With Deposits Built Up By the use of High-Aromatic Gasoline Compared to Those With Deposits Built Up With a Low-Aromatic Blend (Aromatic Reference Fuels)

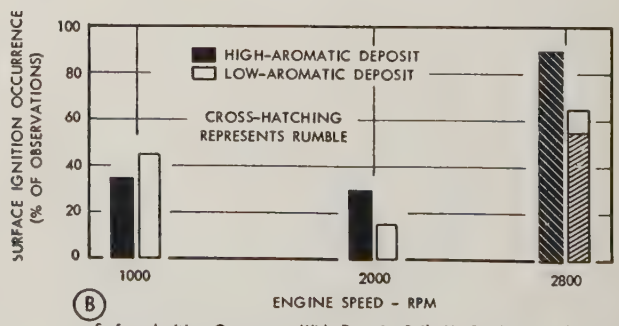

Surface Ignition Occurrence With Deposits Built Up By the Use of High-Aromatic Gasoline Compared to That With Deposits Built Up With a Low-Aromatic Blend. (Aromatic Reference Fuels)

Fig. 3 — Effect of deposits from aromatic gasoline A, aromatic reference fuels

tane requirements shown on Figs. 2A and 3A at 1000 and 2000 rpm are approximately the same for both types of deposit, but at 2800 rpm the average requirements when using high-aromatic gasoline A are higher by 1.5 and 1.9 octane numbers. These differences are significant at the 95% confidence level.

Differences in surface-ignition and rumble occurrence (shown on Figs. 2B and 3B) are not consistent among the test speeds. At 2800 rpm, however, the high-aromatic deposit appears to have caused slightly more surface ignition that the low-aromatic deposit.

Effect of Aromatic Reference Fuels — The effect of the use of aromatic reference fuels in defining octane number requirement is shown in Figs. 4 and 5. Fig. 4 is based on tests when high-aromatic deposits were present and Fig. 5 on tests when low-aromatic deposits were present. Both Figs. 4A and 5A show that average octane requirements were from 1.2 to 2.1 octane numbers higher when using aromatic reference fuels than when using commercial reference fuels. These differences are significant at the 95% confidence level at all three test speeds.

Surface-ignition and rumble occurrence are shown in Figs. 4B and 5B. No significant trends are apparent.

Total Effect, Aromatic Deposit Plus Aromatic Reference Fuel — The combined effect of using high-aromatic gasoline A both as a deposit builder and as a reference fuel is shown in Fig. 6. This corresponds to the case of a customer who would use an aromatic

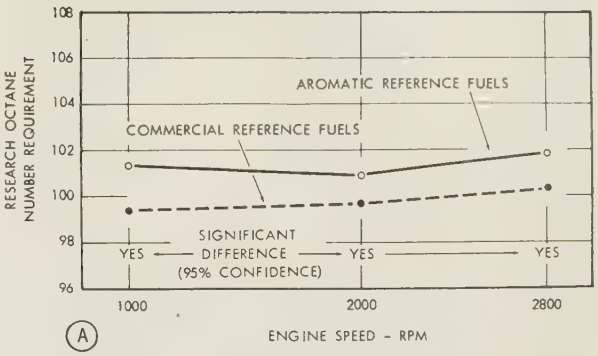

Average Octane Number Requirements Determined With Aromatic Reference Fuels Compared to Those Determined With Commercial Reference Fuels. (Low-Aromatic Deposits)

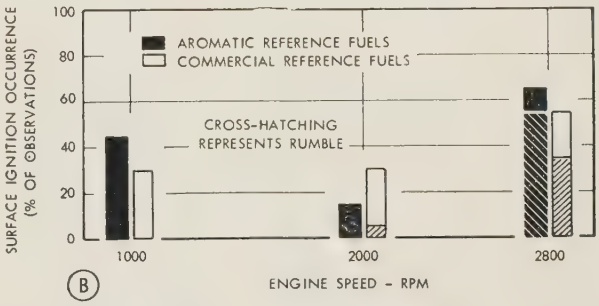

Surface Ignition Occurrence With Aromatic Reference Fuels Compared to that With Commercial Reference Fuels. (Low-Aromatic Deposits)

Fig. 5 — Effect of aromatic reference fuel, aromatic gasoline A with low-aromatic deposits present

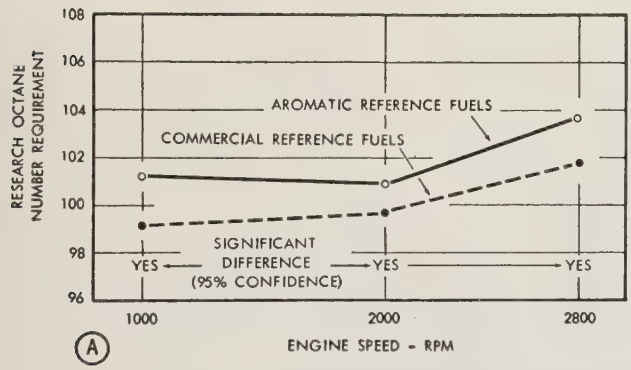

Average Octane Number Requirements Determined With Aromatic Reference Fuels Compared to Those Determined With Commercial Reference Fuels. (High-Aromatic Deposits)

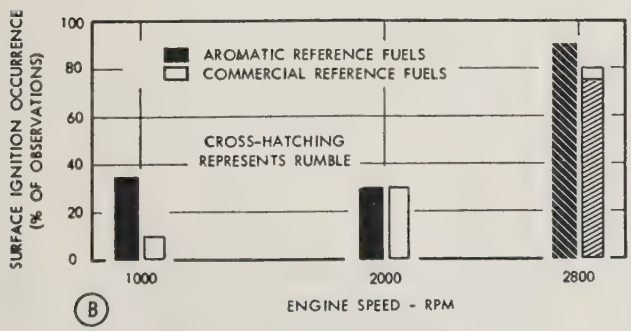

Surface Ignition Occurrence With Aromatic Reference Fuels Compared to That With Commercial Reference Fuels. (High-Aromatic Deposits)

Fig. 4 — Effect of aromatic reference fuel, aromatic gasoline A with high-aromatic deposits present

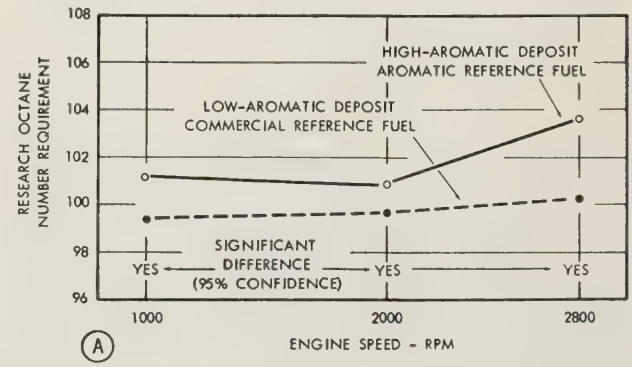

Average Octane Number Requirements With High-Aromatic Deposits and Aromatic Reference Fuels Compared to Those With Low-Aromatic Deposits and Commercial Reference Fuels.

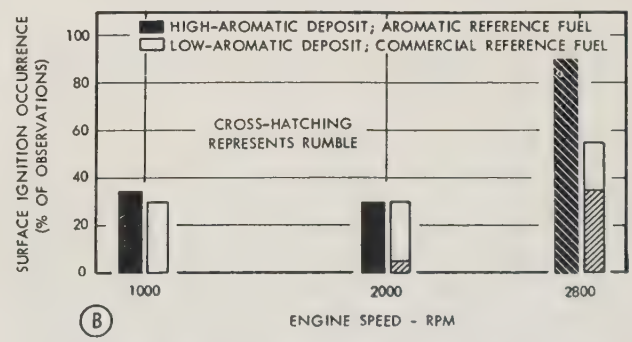

Surface Ignition Occurrence With High-Aromatic Deposits and Aromatic Reference Fuels Compared to That With Low-Aromatic Deposits and Commercial Reference Fuels.

Fig. 6 — Total effect: aromatic deposits plus aromatic reference fuel (aromatic gasoline A)

Table 5 — Test Gasoline Analyses for Aromatic Gasoline Test No. 2

	Low-Aromatic Blend	High-Aromatic Gasoline B
Specific Gravity at 60 F	0.718	0.774
Tetraethyl Lead, cc per gal	3.22	2.61
Reid Vapor Pressure, lb	8.7	8.8
Gum, mg per 100cc	1.4	1.8
Motor Octane Number	95	95
Research Octane Number	99	104
Distillation, F		
Initial	92	90
10	128	126
20	154	156
30	172	191
40	193	218
50	205	230
60	216	239
70	235	252
80	259	282
90	304	328
End	382	389
Recovery, %	98	96
Residue, %	0.3	0.3
Hydrocarbon Content		
Paraffins, %	82.4	54.4
Olefins, %	5.7	1.5
Aromatics, %	11.9	44.1

Table 6 — Reference Fuel Data for Aromatic Gasoline Test No. 2

Aromatic Reference Fuels

Octane Number		Hydrocarbon Type		
Research	Motor	Paraffins, %	Olefins, %	Aromatics, %
106	96.5	54.9	1.0	44.1
104	95	52.8	2.0	45.2
102	93	56.0	1.7	42.3
100	91	54.7	1.7	43.6
98	89	60.2	1.7	38.1
96	88.5	61.0	1.6	37.4

Commercial Reference Fuels

Octane Number		Hydrocarbon Type		
Research	Motor	Paraffins, %	Olefins, %	Aromatics, %
106	95	61.5	15.3	23.2
104	93	60.1	16.8	23.1
102	91	59.4	15.6	25.0
100	89	57.8	14.5	27.7
98	87	48.0	23.0	29.0
96	85.5	62.0	16.7	21.3

gasoline in his tank and would also observe knock or the lack of it on the same tank gasoline. From Fig. 6A it can be seen that the average octane number requirement when using aromatic reference fuels in the presence of high-aromatic deposits is from 1.2 to 3.4 octane numbers higher than when using commercial reference fuels with low-aromatic deposits. Differences at all three test speeds are significant at the 95% confidence level.

Surface ignition and rumble occurrence are shown in Fig. 6B. No differences are shown at 1000 and 2000 rpm, but at 2800 rpm the combined high-aromatic deposit and aromatic reference fuel appears to produce somewhat more surface ignition and rumble than when low-aromatic deposits and commercial reference fuels are used.

Test No. 2, Aromatic Gasoline B

In this test, a high-aromatic 104 octane prototype gasoline (B) was compared to a low-aromatic blend of aviation alkylate and commercial gasoline similar to the previous low-aromatic blend. Gasoline B contained approximately 44% aromatics while the low-aromatic blend contained only 12%. Analyses for both gasolines are shown in Table 5.

Special aromatic reference fuels were blended as before by adding increasing amounts of normal heptane to the high-aromatic gasoline, in this case Gasoline B. In order to blend a 106 Research octane

Table 7 — Effect of Aromatic Deposits

	Average Octane Requirement	Total Surface Ignition[a] and Rumble, %	Rumble, %[a]
Commercial Reference Fuels:			
High-Aromatic Deposit	99.3	65	25
Low-Aromatic Deposit	98.9	40	0
Difference	0.4	25	25
Significant Difference (95% confidence level)	no		
Aromatic Reference Fuels:			
High-Aromatic Deposit	100.3	65	35
Low-Aromatic Deposit	99.9	35	15
Difference	0.4	30	20
Significant Difference (95% confidence level)	no		

[a] Per cent of total test observations during which surface ignition or rumble was objectionable.

Table 8 — Effect of Aromatic Reference Fuels

	Average Octane Requirement	Total Surface Ignition[a] and Rumble, %	Rumble, %[a]
High-Aromatic Deposits:			
Aromatic Reference Fuels	100.3	65	35
Commercial Reference Fuels	99.3	65	25
Difference	1.0	0	10
Significant Difference (95% confidence level)	Yes		
Low-Aromatic Deposits:			
Aromatic Reference Fuels	99.9	35	15
Commercial Reference Fuels	98.9	40	0
Difference	1.0	−5	15
Significant Difference (95% confidence level)	Yes		

[a] Per cent of total test observations during which surface ignition or rumble was objectionable.

fuel, it was necessary to add aromatic Fuel A to aromatic Fuel B. Octane number and hydrocarbon type data are shown in Table 6 for both the aromatic reference fuels and the commercial reference fuels.

In contrast to the tests on aromatic Gasoline A, octane number requirement and surface-ignition occurrence for Gasoline B tests were determined during vehicle accelerations rather than at constant speeds. Test accelerations were made at maximum throttle from 1000–3200 rpm in fourth gear on level road. The same fully distilled mid-continent 20-20W engine oil was used as in the Gasoline A tests.

Effect of Aromatic Deposits — The effect of using high-aromatic Gasoline B to accumulate combustion-chamber deposits is shown in Table 7. Average values of octane number requirement and surface-ignition occurrence are shown for both the high-aromatic deposits and the low-aromatic deposits as determined with both sets of reference fuels.

From Table 7 it can be seen that there were only small differences between the average octane number requirements with the high-aromatic and low-aromatic deposits. These differences were not significant at the 95% confidence level. Surface ignition and rumble appear to occur more often when deposits are accumulated with the high-aromatic gasoline.

Effect of Aromatic Reference Fuels — The average octane requirements and surface-ignition occurrence when using aromatic reference fuels as compared to commercial reference fuels is shown in Table 8. Results are shown for tests with both high-aromatic and low-aromatic deposit accumulation.

From these data it can be seen that average octane number requirements were higher when the requirement was defined in terms of aromatic ref-

Table 9 — Total Effect: Aromatic Deposit Plus Aromatic Reference Fuel

	Average Octane Requirement	Total Surface Ignition[a] and Rumble, %	Rumble, %[a]
High-Aromatic Deposits			
Plus Aromatic Reference Fuels	100.3	65	35
Low-Aromatic Deposits			
Plus Commercial Reference Fuels	98.9	40	0
Difference	1.4	25	35
Significant Difference (95% confidence level)	yes		

[a] Per cent of total test observations during which surface ignition or rumble was objectionable.

Table 10 — Ignition Control Additives

Additive	Chemical Composition	Additive Concentration
A	chloropropyl thionophosphate	0.5 theory
B	triphenyl phosphine	0.5 theory
C	unknown (non-phosphorus)	commercial
D	dimethyl methoxymethyl phosphonate	0.5 theory
E	unknown (phosphorus containing)	0.26 theory

erence fuels than when it was defined in terms of commercial reference fuels. In other words, the aromatic reference fuels were depreciated by an average of 1.0 octane number as compared to the commercial reference fuels. Maximum knock speed occurred between 1600 and 1800 rpm for nearly all test observations. There were no large differences between the amounts of surface ignition and rumble occurring with the aromatic or commercial reference fuels.

Total Effect, Aromatic Deposit Plus Aromatic Reference Fuel — The total effect of using high-aromatic Gasoline B both as a deposit accumulation fuel and as a reference fuel to define octane requirement is shown in Table 9. The octane requirements with high-aromatic deposits and aromatic reference fuels are compared to those with low-aromatic deposits and commercial reference fuels.

On the average, the octane number requirement is 1.4 octane numbers higher when high-aromatic Gasoline B is used both in the tank and to define octane requirement than when the low-aromatic blend is used in the tank and commercial reference fuels are used to define octane requirement. Surface ignition and rumble were somewhat more frequent in occurrence when the high-aromatic combination of deposits and fuels were present than with the low-aromatic deposits and commercial reference fuels.

On the basis of the two road tests just described, it appears that the use of gasolines having high-aromatic content (as opposed to low-aromatic content) in high-compression automobile engines may cause increases of 1–3 octane numbers in the antiknock quality required. Surface ignition and rumble are also increased by the use of high-aromatic gasolines. A part of this increase can be attributed

[11] SAE Transactions, Vol. 63, 1955, pp. 53–62: "Practical Yardsticks for Deposit Effects," by C. A. Hall, J. A. Warren, and J. D. McCullough.

[12] "Fuel Antiknock Performance in High-Compression Engines," by C. J. Domke, N. D. Esau, D. S. Gray, and H. R. Taliaferro. Paper presented at SAE Summer Meeting, Atlantic City, June, 1956.

[13] "Laboratory Qualities as Predictors of Road Octane Number," by I. A. Caputo, K. J. Sewell, and H. A. Toulmin. Paper presented at SAE Fuels and Lubricants Meeting, Cleveland, November, 1957.

[14] "Effect of Hydrocarbon Type and Distribution in Boiling Range on Road Antiknock Performance," by W. A. P. Meyer and R. G. Goldthwait. Paper presented at SAE Fuels and Lubricants Meeting, Cleveland, November, 1957.

Table 11 — Effect of Using Ignition Control Additive E

	Average Octane Requirement	Surface Ignition, %[a]
Base Gasoline Only	98.3	100
Base Gasoline Plus Additive E	97.5	93
Difference	0.8	7
Significant Difference (95% confidence level)	yes	

[a] Per cent of total test observations during which surface ignition was objectionable.

to the combustion-chamber deposits built up by the aromatic gasoline, but the major share appears to be due to octane depreciation of the aromatic fuel when used in an engine containing equilibrium suburban-duty deposits. The small increase in octane-number requirement found with high-aromatic deposits is in agreement with previous laboratory engine data;[11] however, the apparent octane depreciation of the aromatic gasoline is inconsistent with the results of other investigators.[12,13,14] These investigators have reported superior road octane performance for gasolines containing high percentages of aromatics. Those studies, however, were limited to modified borderline or modified Uniontown road octane rating comparisons with very few combustion-chamber deposits present. The presence of surface ignition and rumble during the tests described in this paper may be the reason for the poorer performance (depreciation) of the aromatic gasolines.

Ignition Control Additives for Gasoline

Many gasoline additives have been introduced by the petroleum industry over the past few years to reduce or eliminate surface ignition in high-compression engines. This section describes the results of several tests evaluating gasoline additives with respect to their ability to reduce octane number requirement, surface ignition, and rumble.

Five additives were evaluated in latin square deposit accumulation tests. Each additive was evaluated by determining the octane requirement and surface-ignition occurrence in test cars operated both on a base gasoline containing 3 cc tel and on the same base gasoline plus the additive. The chemical composition of each additive and the concentration at which it was tested are shown in Table 10.

Since these additives are believed to act by modifying the combustion-chamber deposits, no attempt was made to measure the effect of the additive on the combustion characteristics of the fuel. The effectiveness of each additive was determined by the reduction in octane number requirement and surface-ignition and/or rumble occurrence when the additive was used in the tank gasoline. Octane requirements were found in terms of commercial reference fuels. During tests on Additives A, B, C, and D, octane requirements were found at 1000 rpm-2 in. of Hg. manifold vacuum, 2000 rpm-full throttle, and 2800 rpm-full throttle by the same technique used in the tail-end volatility tests. Requirements were found during maximum throttle accelerations from 1000–3200 rpm in fourth gear during the tests on Additive E.

A Pennsylvania base 20-20W-30 engine oil was used during all of the additive tests to increase the occurrence of surface ignition when using the base

gasoline, thereby providing a surface-ignition problem for the additive to "cure."

Additive A

Results of the tests on Additive A are shown in Fig. 7. Use of Additive A in the gasoline reduced the average octane number requirement by amounts ranging from 0.4 octane numbers at 1000 rpm to 4.2 octane numbers at 2800 rpm. The differences shown at 2000 and 2800 rpm are significant at the 95% confidence level.

The occurrence of surface ignition and rumble was reduced markedly at all three test speeds by the use of the additive as shown in Fig. 7B. Even though use of Additive A resulted in large reductions in octane requirement and surface ignition, the octane number requirement shown at 2800 rpm in Fig. 7A was still abnormally high for an engine having 10/1 compression ratio.

Additive B

As shown on Fig. 8, the octane number requirement was reduced by only a small amount when Additive B was used. Average reductions ranged from 0.3 octane numbers at 1000 rpm to 2.2 octane numbers at 2800 rpm. Only the difference shown at 2000 rpm is significant at the 95% confidence level. At 2800 rpm the lack of significance is caused by the erratic nature of rumble.

Surface ignition was reduced at all speeds when the additive was used, although the reduction appears to be small at 2800 rpm. Rumble was very prevalent at 2800 rpm both with and without use of the additive.

Additive B is unsuitable for use as a commercial gasoline additive because excessive intake manifold and valve deposits were formed during its use.

Additive C

Octane number requirements both with and without the use of Additive C are shown in Fig. 9. No advantage is shown at 1000 or 2000 rpm, but an average reduction of 2.2 octane numbers is shown at 2800 rpm. This difference is signicant at the 95% confidence level. The occurrence of surface ignition and rumble did not appear to be affected by the use of Additive C.

Additive D

The results of tests on Additive D are shown in Fig. 10. The average octane number requirement was reduced by 0.5 octane number at 1000 rpm, by 1.4 octane numbers at 2000 rpm, and by 1.3 octane numbers at 2800 rpm. Only the difference shown at 2000 rpm is significant at the 95% confidence level. The occurrence of surface ignition was reduced at all speeds by the use of this additive.

Additive E

The results of tests on Additive E are shown in Table 11. Octane number requirements were found only at the speed for maximum knock during test accelerations. Maximum knock usually occurred between 2500 and 3000 rpm.

From these data it can be seen that the use of

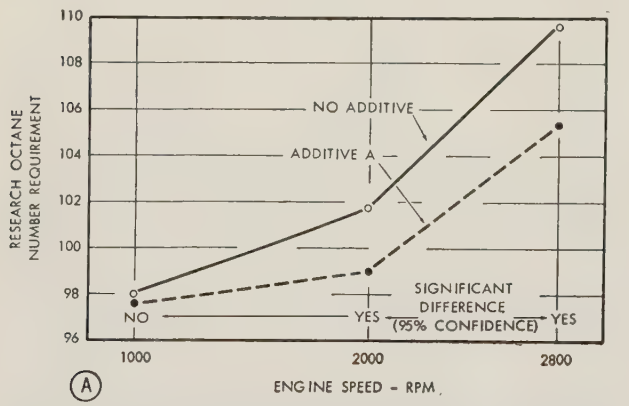

Average Octane Number Requirements When Using 0.5 Theory of Additive A in the Tank Gasoline Compared to Octane Number Requirements When Using Base Gasoline Only.

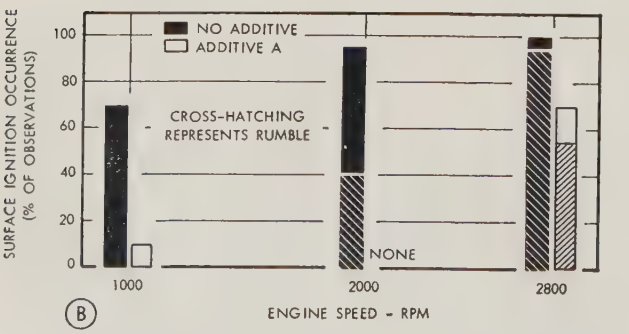

Surface Ignition Occurrence When Using 0.5 Theory of Additive A in the Tank Gasoline Compared to Using Base Gasoline Only.

Fig. 7 — Ignition control additive A

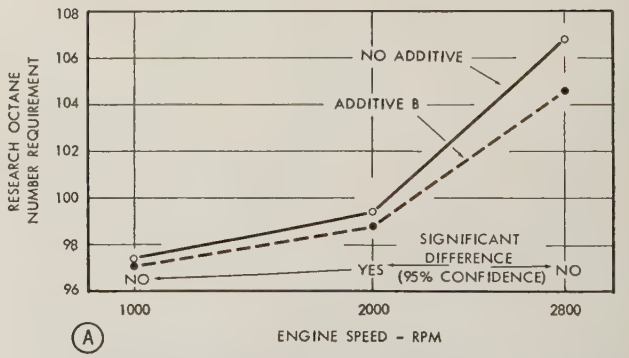

Average Octane Number Requirements When Using 0.5 Theory of Additive B in the Tank Gasoline Compared to Octane Number Requirements When Using Base Gasoline Only.

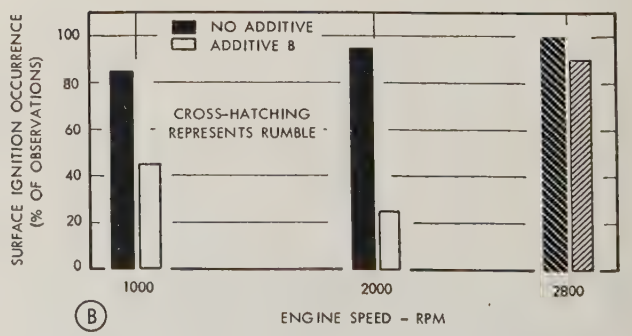

Surface Ignition Occurrence When Using 0.5 Theory of Additive B in the Tank Gasoline Compared to Using Base Gasoline Only.

Fig. 8 — Ignition control additive B

Additive E reduced the octane number requirement by an average of 0.8 octane number. This reduction is significant at the 95% confidence level. The occurrence of surface ignition was reduced only slightly. Rumble was not apparent during this test.

From the results of these tests on ignition-control type additives certain general observations can be made. The most important is that some of these additives are capable of reducing octane number requirements by substantial amounts through the reduction of surface ignition and rumble. Almost equally important is the observation that even the most effective of the additives tested did not eliminate surface ignition entirely. This is reflected in the very high average octane requirements and the prevalence of surface ignition and rumble at 2800 rpm even when ignition-control additives were used (Figs. 7–10). The additives were not completely effective in spite of the fact that several of the phosphorus-type additives were tested at concentrations of 0.5 theory, which is approximately double the average commercial concentration. Still further reduction or, preferably, elimination of surface ignition through additive treatment of gasolines has great potential to facilitate improved engine efficiency through increased compression ratio.

Summary

It appears that gasoline composition has an important bearing on the "screaming" that may emanate from a modern high-compression automobile engine. Deposit accumulation type road tests evaluating fuel composition factors in the presence of "normal" combustion-chamber deposits indicate that gasoline tail-end volatility, aromatic content, and additive treatment have measurable effects on the octane number requirement and surface-ignition tendency of 10/1 compression ratio cars.

A reduction in gasoline tail-end volatility (approximately 50 F at the 90% distilled temperature) resulted in a 1–2 octane number average reduction in equilibrium octane number requirement. Surface-ignition and rumble occurrence were also reduced.

The use of gasolines containing 45–50% aromatic hydrocarbons increased the average octane number requirements by 1–3 octane numbers over the requirements when using gasolines having lower aromatic content. Surface ignition and rumble were also increased. A part of the increase in octane requirement can be attributed to the combustion-chamber deposits built up by the aromatic gasoline, but the major share of the increase appears to be due to octane depreciation of the aromatic fuel when used in an engine containing normal equilibrium deposits.

Ignition-control additives in the gasoline reduced average octane-number requirements by as much as four octane numbers. Corresponding decreases were found in the occurrence of surface ignition and rumble. Further reduction or elimination of surface ignition through the use of gasoline additives could benefit the customer by allowing higher engine efficiencies to be reached through higher compression ratios.

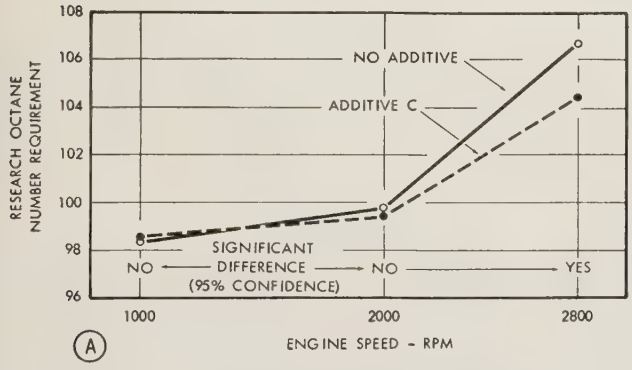

Average Octane Number Requirements When Using Additive C in the Tank Gasoline Compared to Octane Number Requirements When Using Base Gasoline Only

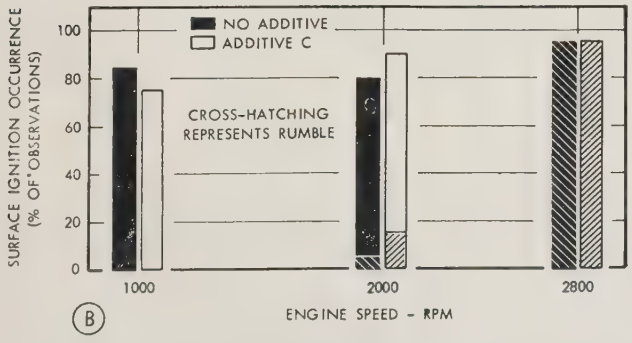

Surface Ignition Occurrence When Using Additive C in the Tank Gasoline Compared to Using Base Gasoline Only.

Fig. 9 — Ignition control additive C

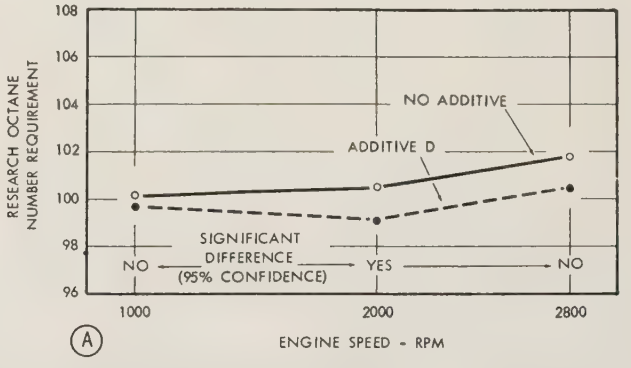

Average Octane Number Requirements When Using 0.5 Theory of Additive D in the Tank Gasoline Compared to Octane Number Requirements When Using Base Gasoline Only

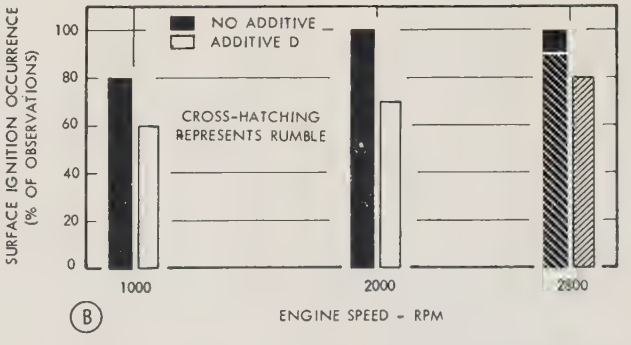

Surface Ignition Occurrence When Using 0.5 Theory of Additive D in the Tank Gasoline Compared to Using Base Gasoline Only

Fig. 10 — Ignition control additive D

PYROCERAM

W. W. Shaver and S. D. Stookey, Corning Glass Works

This paper was presented at the SAE Summer Meeting, Atlantic City, June 11, 1958.

THE automotive industry has made effective use of glass for many years. In the past few years this use has increased greatly, with the development of safety glass, tempered glass, curved windows, and multiple headlamps. However, until very recently, no serious thought has been given to employing glass or ceramics in the working parts of an engine (except as spark plugs) or as load-bearing parts of an automobile. These functions have been the exclusive domain of metals, because glasses and ceramics have not had sufficient strength and flexibility to fulfill the requirements. If it were not for these shortcomings, such materials might well have found applications, because some of them are superior to most metals in hardness, corrosion resistance, and resistance to high temperatures. In addition, their weight per unit volume is lower than most of the commonly used metals, except aluminum and magnesium.

Two important new fields of development are beginning to change this picture in such a way that automotive engineers and planners of the cars of the future are looking to glass and ceramics as potential engineering materials. One of these is the progressive development of new kinds of engines for the car, whose parts will operate at much higher temperatures than any metals, except the most expensive alloys, can stand.

The second might be called a breakthrough in glass technology which gives us hope of producing new materials having the physical properties required to serve where present materials are not satisfactory. This report is intended to serve two purposes: to outline this new development in general terms, pointing out the directions it may be expected to follow; and to describe the properties of two of the new materials.

PYROCERAM signifies a new family of fine-grained crystalline materials called glass-ceramics. These materials are made by a process of controlled crystallization from special compositions containing nucleating agents.

The materials are valuable particularly because of their resistance to high temperatures and chemical attack. They are classed as heat and electrical insulators.

A major use of these new materials is in the structural parts for hypersonic aircraft.

Glass-Ceramics

In May, 1957, Corning announced the discovery of a new family of fine-grained crystalline materials made from glass. These materials are called glass-ceramics, and products made from them are designated by the trade-mark Pyroceram. They are made by a process of controlled crystallization, from special compositions containing nucleating agents.

Glass-ceramics appear worthy of attention for their new and useful combinations of properties, for their basically new manufacturing process, and for the broad range of potential compositions and properties open for exploration.

Manufacturing Process

Melting — The batch ingredients, including the nucleating agent, are mixed and melted to a homogeneous molten glass. Depending upon the composition, the glass may be nearly as fluid as molten metal or extremely viscous. The glass is held uniform in composition by stirring and other methods, just as optical glass is made.

Forming — The molten glass is formed by conventional glass-forming methods, such as pressing or blowing into molds; drawing as tube, rod or pipe; rolling or drawing into flat sheet; or centrifugal casting. The more fluid glasses may be cast into intricate shapes by methods similar to metal casting. Sizes and shapes that can be made are virtually without limit.

The glass ware then is cooled. At this point it is transparent and readily inspected for flaws or bubbles. Some compositions can be reheated and reworked into new shapes while still in the glassy state.

Heat-Treatment — A carefully controlled high-temperature heat-treatment causes first the precipitation of billions of submicroscopic crystal nuclei; then growth of these nuclei until the glass

Table 1 — Comparison of Properties of Pyroceram with Glass and Ceramics

	Glass-Ceramic Pyroceram		Glass		Ceramic
	Code 9606	Code 9608	Code 7900 96% Silica Glass	Code 7740 Boro-silicate Glass	High-Purity Aluminas
General					
Specific Gravity, 77 F	2.60	2.50	2.18	2.23	3.6
Water Absorption, %	0.00	0.00	0.00	0.00	0.00
Porosity (gas permeability)	gas tight	gas tight	gas tight	gas tight	gas tight
Thermal					
Softening Temperature F	2282	2282	2732	1508	3092
Specific Heat, 77 F	0.185	0.190	0.178	0.186	0.181
Mean Specific Heat, (77–752 F)	0.230	0.235	0.224	0.233	0.241
Thermal Conductivity (77 F mean temperature), Btu/hr-ft-F	2.10	1.13	—	0.626	1.25–1.40
Linear Coefficient (77–572 F) of thermal expansion $\times 10^7$	31.6	3.9–11.1[a]	4.45	17.8	40.5 (68–932 F)
Mechanical					
Modulus of Elasticity, (psi $\times 10^6$)	17.3	12.5	9.6	9.5	40
Poisson's Ratio	0.245	0.25	0.17	0.20	0.32
Modulus of Rupture, abraded psi $\times 10^6$	20	16–23	5–9	6–10	40–50[b]
Hardness					
Knoop, 100 g	698	703	532	481	1880
500 g	619	588	477	442	1530
Electrical					
Dielectric Constant					
Frequency $\times 10^6$, 77 F	5.58	6.78	3.8	4.6	8.81
572 F	5.60	—	3.9	5.9	—
932 F	8.80	—	—	—	9.03
Frequency $\times 10^{10}$, 77 F	5.45	—	3.8	4.5	8.79
572 F	5.51	—	—	—	—
932 F	5.53	—	—	—	9.03
Dissipation Factor					
Frequency $\times 10^6$, 77 F	0.0015	0.0030	0.0005	0.0046	0.00035
572 F	0.0154	—	0.0042	0.0130	—
932 F	—	—	—	—	0.012
Frequency $\times 10^{10}$, 77 F	0.00033	—	0.0009	0.0085	0.0015
572 F	0.00075	—	—	—	—
932 F	0.000152	—	—	—	0.0021
Loss Factor					
Frequency $\times 10^6$, 77 F	0.009	—	0.0019	0.0212	0.0031
572 F	0.086	—	0.0164	0.0566	—
932 F	—	—	—	—	0.108
Frequency $\times 10^{10}$, 77 F	0.002	—	0.0036	0.282	0.0132
572 F	0.004	—	—	—	—
932 F	0.008	—	—	—	0.019
Volume Resistivity					
Log_{10}, ohm-in. 482 F	9.6	7.7	9.3	7.7	13.6 (212 F)
662 F	8.2	6.4	7.7	6.2	12.5 (572 F)

[a] Depending on heat-treatment.
[b] Unabraded values.

article is converted, substantially unchanged in size or shape, to the fine-grained crystalline product Pyroceram. The crystals in Pyroceram are normally smaller than 0.0001 in, in diameter and are randomly oriented. Usually a small proportion of glass is interspersed with the crystals.

Finishing — Although it is possible to form reproducibly glass-ceramic articles to reasonably close tolerances requiring no further finishing in many cases, some high-precision shapes do require finishing. Glass-ceramics are capable of being ground and polished to very accurate dimensions by the methods used for glasses, ceramics, and hard metals.

Properties

Glass-ceramics are nonporous and generally have an opaque white appearance in the finished state, though some compositions may also be transparent like glass. They are resistant to high temperatures in terms both of strength and oxidation. They are like glasses in their ability to resist chemical attack with measured durabilities in weight loss ranging in values comparable to the durable chemical glasses. They are lighter and harder than most metals. In thermal conductivity they are classed as heat insulators. The thermal expansion coefficients range from negative values, through zero, to positive values of 110×10^{-7} per deg F. Hence, extreme heat shock resistance may be had by choice of composition.

In electrical properties glass-ceramics are classed as electrical insulators having dielectric constants from 5 to 10 and power factors at high frequencies ranging down to extremely low values. In mechanical properties these materials are generally higher in Young's modulus than glasses, ranging from 12.5 to some 20×10^{6} psi with strengths higher than glasses and most ceramics. Glass-ceramics are not ductile or malleable as are most metals, but are classed as brittle materials.

Various compositions can be tailor-made to meet desired properties, with the final control depending on special heat-treatment. Two compositions in various forms and types of product are now available commercially. These have code numbers 9606 and 9608 and their properties are listed in Table 1 together with values for two commercial glasses and high purity alumina for comparison.

Properties of Pyroceram code 9606 indicate that it is suitable for high-temperature high-frequency applications in the electronics field. The maximum usable temperature under load is 1560 F for 1000 hr. This glass-ceramic has been successfully used as a missile radome. Its hardness and ability to withstand high temperatures make it suitable for consideration as an abrasive binder and for bearing parts.

Special glass-melting techniques are used on Pyroceram code 9606 to assure uniform composition, constant density, freedom from bubbles and striations, and uniform electrical properties. Code 9606 is most easily formed by gravity and centrifugal casting. With certain limitations, it can be pressed and rolled.

Pyroceram code 9608 is a white, opaque, fine-grained crystalline material with high mechanical strength, extremely low coefficient of thermal expansion, and a hardness substantially higher than that of glass. Developed primarily as a general-purpose material, Pyroceram code 9608 can be formed by all automatic glass manufacturing processes. It can be blown, drawn as tubing, pressed, and rolled. It is believed to have a wide range of applications in scientific, industrial, and consumer fields.

The hardness and low expansion coefficient of Pyroceram code 9608, plus its ability to be easily formed, have brought the material to the attention of bearing manufacturers. Tests indicate Pyroceram 9608 bearings will operate under varying conditions at temperatures as high as 1000 F, at loads approximating half that expected of standard steel bearings. The advantage over steel is that Pyroceram bearings under actual running conditions will operate at high temperatures without the corrosion, deformation, and softening.

Applications and Directions of Future Development

This new field of materials obviously opens many opportunities for applications where presently available materials are unsatisfactory. Applications now under consideration include such products as air compressor blades, abrasive binders, radar antenna housings, brake shoes, structural parts for hypersonic aircraft, piston heads, high-temperature bearings, and heat exchangers where severe abrasive conditions exist.

Recent laboratory developments give promise for the near future of substantial increases in mechanical strength at temperatures up to at least 2200 F, increased hardness and wear resistance, tailor-made compositions having a range of expansion coefficients to match various metals, and transparent materials many times stronger than present glasses. These Pyroceram materials with their variety of forms and combinations of properties undoubtedly will find application in process and service functions providing better performance and/or lower cost. They provide a new opportunity to reconsider industrial processes with the possibility of answering unsolved problems or developing better methods to accomplish the desired result.

ORAL DISCUSSION

— Reported by G. H. Seaver
Ford Motor Co.

C. L. Burton, Aluminum Company of America: Would Pyroceram be a suitable material for crucibles for melting metals?

Mr. Shaver: If the temperature were below 2000 F and there were no chemical attack of the metal, slag or flux on the crucible, Pyroceram might be suitable.

C. Neely, International Harvester Co.: How can Pyroceram be bonded to metals?

Mr. Shaver: The problem of bonding Pyroceram to metals is being investigated. The composition of the metal must be considered; and a 17% Cr-Ti stabilized stainless grade is one on which considerable work is being done. Pyroceram can be metallized and the attachment made to the metallized surface. It is not yet feasible to bond Pyroceram in the original glassy state to metals by fusion, because of the large difference in expansion encountered.

F. A. Franklin, General Motors Corp.: What methods of finishing or machining are employed to obtain close dimensional tolerance with Pyroceram?

Mr. Shaver: Abrasive grinding is used, either with a diamond wheel or with carborundum wheels.

ION ROCKET ENGINE DEVELOPMENT

Donald L. Eschner, Boeing Airplane Co.

This paper was presented at a meeting of the SAE Metropolitan Section, New York, March 4, 1958.

DRS. Werner Von Braun and Ernst Stuhlinger have advocated a rather interesting concept for travel to Mars. The trip would involve transport in three separate vehicles. The first, a conventional liquid or solid fueled 3-stage vehicle, escapes from the Earth's atmosphere and terminates at an orbiting space station 1000 miles from the Earth's surface. The second vehicle, the space cruiser, leaves the satellite orbit and enters an orbit 600 miles above Mars. The third vehicle, the landing vehicle, would be detached from the space cruiser, reduce its orbiting speed by rocket power and enter a downward trajectory thru the Martian atmosphere.

To return, the landing vehicle would leave from Mars to the orbiting cruiser, the crew transfer to it, and begin the return flight to the Earth's satellite. Return to the Earth is made in the crew-cargo portion of the third stage rocket that made the trip from Earth to its satellite.

The space cruiser would of necessity be assembled at the orbiting space station and due to the large investment in fuel for the commuter rockets to transport the component parts for both the space station and the cruiser, lightweight construction is an absolute necessity. Because the largest part of the weight of the space cruiser will be taken up by fuel, the investigation of a suitable propulsion system is imperative.

INTERPLANETARY travel long talked about by the science fiction writer has become the subject of grave concern to our engineers, scientists, and to those concerned with the defense of our economy. Since the much publicized work of the Russians, greater emphasis has been placed on the necessity of knowing the environments experienced during space travel, the development of a vehicle capable of such travel, and the support of life for sustained periods in outer space.

Propulsion Systems

Basic rocket equations determine the performance mainly by the exhaust velocity of the gases from the combustion chamber.

$$V_F = V_o + V_E ln \left(1 + \frac{M_F}{M_P}\right) \qquad (1)$$

where:

V_F = Final velocity of vehicle
V_o = Original velocity of vehicle
V_E = Exhaust velocity
M_F = Mass of fuel
M_P = Total vehicle mass less fuel mass
$\frac{M_F}{M_P}$ = Mass ratio

With chemical fuels this velocity is related to the gas temperature. Present rocket combustion chambers operate at temperatures close to the maximum expected from the chamber materials. Significant performance improvements are not expected.

Four basic propulsion methods (chemical, heated gas, electric, and photonic) fall into two categories: (1) those where the propulsion system is the primary power source and (2) those requiring a primary power source for the propulsion system to

operate. Only the chemical system falls into the former category.

Both chemical and gas heating systems are limited by the temperature resistivity of structural materials. The maximum temperature that these systems can tolerate is 3500 C, without atomic modification. Gas heating systems all rely upon a separate primary energy source. This is true of solar energy, high-intensity electric arc, and nuclear reactor heating of gas generating chemicals. The additional weight penalties imposed over chemical propulsion systems can be compensated only by higher exhaust velocities. The exhaust velocities of all three basic heated gas systems from 4500 to 6000 meters per sec as opposed to 2500–3000 meters per sec for chemical rocket motors.

The electric propulsion system relies upon ionization of a gas and consequent acceleration of the ions. A primary power source is necessary to cause ionization and ion acceleration. The ionization propulsion concept is not restricted by temperature limitations of the structure as there is no random heating of gas molecules which are free to strike the walls of the thrust chamber and heat it. An electric or magnetic field will cause the particles to be directed away from the chamber walls. The exhaust velocity will be in the neighborhood of 80,000–100,000 meters per sec. As ions are formed and ejected from the vehicle, it will assume a large negative change, causing the positively charged ions to be attracted back to the vehicle and the net thrust will drop to zero. A possibility for elimination of the space charge effect is to cause recombination of the ions and electrons in the exhaust stream just aft of the thrust chamber.

Photonic propulsion employs the emission of a unidirectional beam of photons. This process assumes that photons can be created by direct conversion of matter into radiation energy. This conversion can be observed in nuclear processes in the annihilation of an electron and a positron to form a pair of gamma quanta. Einstein's theory of relativistic mechanics shows that the relation between energy and momentum of a body is given by:

$$E^2 = c^2p^2 + m^2c^4 \qquad (2)$$

where:

E = Energy
m = Rest mass
p = Momentum
c = Velocity of light

For radiation with zero rest mass the equation reduces to:

$$E = cp \qquad (3)$$

and the thrust is given by:

$$F = \frac{1}{g}\frac{d}{dt}\left(\frac{E}{c}\right) \qquad (4)$$

A thrust of one gram requires a rate of working of 2943 kw or 1.3×10^6 kw per lb of force.

The total energy available from the complete fission of 1 lb of uranium 235 is about 10^7 kwhr or a thrust of 1 lb for 7½ hr if a 100% conversion efficiency is achieved. Conventional energy converters and light sources are unlikely to provide more than 2–3% efficiency — enough to provide 1 lb of thrust for 1 min. The impulse obtainable from 1 lb of uranium used to drive a photon motor is unlikely to be more than 100 lb sec — much less than conventional propellants. If the photons are generated within a container, the walls must have transmissivity of the order of 0.99999999 as must be the reflecting power of the collimating mirror to form an almost parallel bundle of photons. With lower transmissivity and reflectivity, the chamber walls and mirror would absorb such great amounts of radiative energy as to be immediately vaporized. The exhaust velocity of photons is 300,000 kmps.

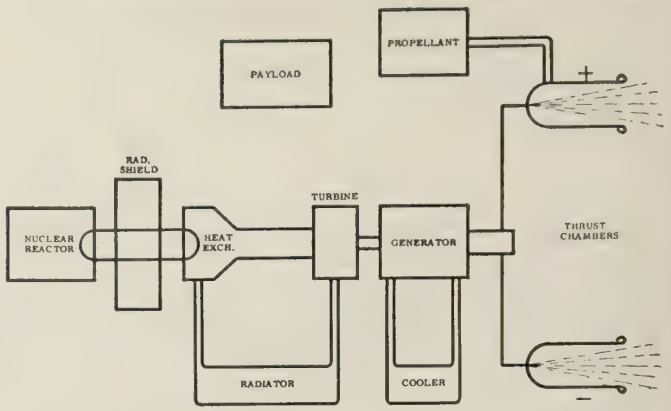

Fig. 1 — Components of electrical powerplant of space cruiser

Electric Propulsion System

Dr. Stuhlinger has proposed a propulsion system of significant promise for a space cruiser. High exhaust velocities can be obtained by electrically accelerating gas particles. The amount of electrical energy that can be applied to a given mass of exhaust material is significantly greater than the energy given to the same mass by chemical reactions. If we assume for a chemical-propelled vehicle that $V_E = 3 \times 10^3$ meters per sec with $V_o = 0$ and the mass ratio 1, the mass ratio for an electric-propelled vehicle can be calculated and compared. Substituting in Equation 1 for chemical-propelled vehicle:

$$V_{F(CP)} = 3 \times 10^3 \ ln\ (2) = 2.08 \times 10^3 \text{ meters per sec} \qquad (5)$$

$$V_{F(CP)} = V_{F(EP)} \text{ (assumed)} \qquad (6)$$

$$V_{E(EP)} = 8 \times 10^4 \text{ (known)} \qquad (7)$$

$$V_{F(EP)} = V_{E(EP)}\ ln\left(1 + \frac{M_{F(EP)}}{M_{P(EP)}}\right) \qquad (8)$$

$$ln\left(1 + \frac{M_{F(EP)}}{M_{P(EP)}}\right) = \frac{2.08 \times 10^3}{8 \times 10^4} = 0.026 \qquad (9)$$

$$1 + \frac{M_{F(EP)}}{M_{P(EP)}} = 1.026$$

$$\frac{M_{F(EP)}}{M_{P(EP)}} = 0.026$$

We can, thus, accelerate 1000 lb of payload with 26 lb of fuel using electrical propulsion to the same final velocity that 1000 lb of chemical fuel could propel this same payload. The electrical field is capable of preventing exhaust particles from striking the thrust chamber walls, thereby reducing chamber heating problems. To accelerate the exhaust particles electrically requires that they be ionized; therefore, the propellant must be capable of efficient ionization and high yields of ionized particles. The

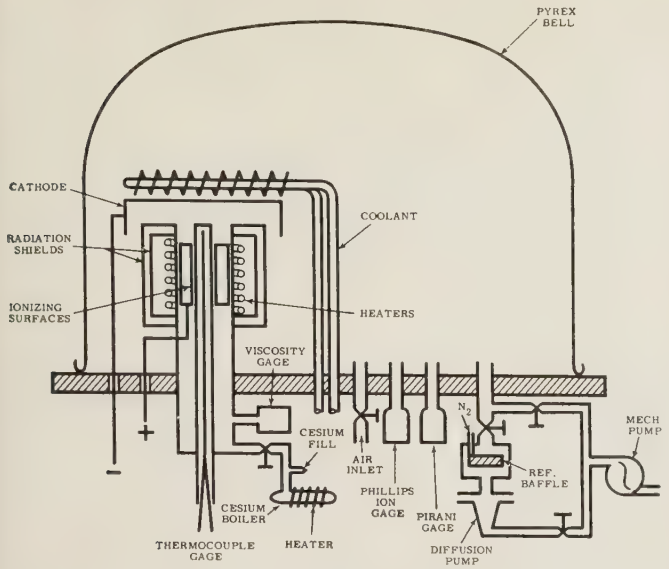

Fig. 2 — Ion source test unit

electrical propulsion system will require a primary power source, conversion of the primary power into electric power, and a thrust chamber in which electric power is applied to accelerate the ions. Dr. Stuhlinger's feasibility study has proved that an electrically propelled space cruiser would be much lighter than one having a chemical propulsion system. The electrical system would be restricted to space vehicles traveling between satellite orbits because of the low thrust inherent with this system. The propulsion system will operate continuously, first accelerating and later decelerating the vehicle. The primary power source must generate power throughout the time the cruiser is traveling. The duration of a journey to Mars and the return trip is in the order of two years. The payload for such a journey is 150 tons with an acceleration of 10^{-4} *g*'s. The total weight is 730 tons with a propellant mass of 365 tons.

A space cruiser using an electrical powerplant is comprised of several distinct parts (Fig. 1).

The payload includes the crew and quarters, stored atmosphere, food, water, instruments, landing vehicle, and exploration equipment. A considerable amount of research and development work is currently being conducted that will apply to the support of life in a space vehicle. Medical research tells us the minimum requirements for survival; aircraft cabin design determines the crew quarters construction requirements, air distribution, and temperature control. Radiation shielding work has allowed us to install a crew within a submarine and is applicable to the space cruiser.

A fast nuclear reactor is chosen as the primary power source. Reactor heat is absorbed by a liquid metal cooling system and transferred by a heat exchanger to a working fluid driving a turbine. This fluid is cooled by means of a large radiator and returned to the heat exchanger. The turbine drives an electric generator which is likewise cooled by liquid metal with the heat rejected by a radiator and the coolant recirculated. The reactor contains 12 tons of uranium 235 enriched to 1.7%. This type of reactor is within present state-of-the-art knowledge. Work on aircraft nuclear powerplants is directed at lightweight systems which are critical for the space vehicle.

A more difficult problem is the design of a radiator to cool the heat exchanger fluid. The radiator will probably be of large surface area as heat loss will be solely by radiation. Evaporative cooling techniques may be employed to minimize size and weight. This problem resolves into a design optimization study and conventional methods will be employed. We are currently cooling airborne electronic equipment by evaporative techniques achieving significant weight savings. The fact that the flight of a space vehicle will be in near-perfect vacuum may prove advantageous to a sublimative cooling system, where heat exchange is performed by expelling vapors from a sacrificial material having a high latent heat of sublimation. This sacrificial material may be the fuel which is to be vaporized.

Control will be performed by gimballed thrust units. As the acceleration is very low, response of this type of control system does not appear critical; therefore, guidance can be accomplished by the crew who will rely on star tracking to navigate. I do not believe that guidance and control are as serious a problem for the space vehicle designer as they are for current ballistic and guided missile developments.

Thrust unit development appears to be the significant problem area. The electrical propulsion concept, which is attractive because it lies within present technical capabilities, is capable of providing thrust for long periods and is more economical from a weight standpoint than a chemical system. Specific impulses for ionic propulsion systems are 20–50 times greater than those of chemical rockets, although the first trip to a celestial body will probably be made with a chemically propelled vehicle. An electrical system is capable of being developed relatively soon that will prove to be more practical than all other systems and will be the replacement for chemical systems in long-duration space flight.

Ion Generation

Positive ion generation is possible by a variety of methods, including canal rays, capillary arcs, radio frequency, and magnetic field augmentation. These methods are dependent on electron-atom collision producing a plasma with a negative electrode to remove positive ions. Other methods of positive ion generation include photoelectric effect, heating, and chemical reactions. The Langmuir method of ion production is simpler than all the above methods and its power requirements are low.

Atoms of the alkali metals are easily and efficiently ionized. The gaseous metal is made to impinge on a heated metallic surface where the atoms lose one electron. The probability of ionization is assumed to be as high as 90% because the ionization potentials of the alkalis are low and the contact potentials high.

A neutral alkali metal atom contacting a hot metal surface will share its most loosely bound electron with the conduction band of the metal. The alkali atom's identity is momentarily lost and a surface alloy is formed. The base metal is hot and the alkali ion evaporates with a high probability that the outer electron is left behind. The positively charged ion creates an electrostatic field between it and the metal; the strength of this field is dependent upon the ionization potential. When

the ratio of this ionization potential to the work function of the ionizing surface is low enough the probability that an electron will be extracted from the ionizing surface is very small.

Thrust Unit Development

The work of Langmuir, Kingdon, and Ives indicated that alkali vapor becomes ionized when contacting a high work function electrode, such as tungsten. Later work has presented data on surface interactions between the alkalies and platinum, oxygenated tungsten, and a platinum-tungsten alloy. The Langmuir or surface contact method of ion generation require further analysis and experimentation before it can be applied to an ionic propulsion system. Of primary importance is the choice of the anode material and its operating temperature. As the temperature of a specific material is lowered the power requirements are also lowered, due to the associated reduction of radiation. This lowering of anode temperature may be accompanied by a decrease in the percentage of ionization. It will thus be necessary to weigh power requirements against fuel loss in the final selection of anode material. Consequently, the first part of a study is the establishment of design criteria for the anode. Cesium is vaporized and passed over anodes made of tungsten, platinum, platinum-rodium, iron, and tantalum. The temperature of these materials is varied as is their shape and configuration. Ions are collected on a cathode and the ion current measured. The percentage of cesium atoms ionized is determined and is the basis for comparing materials and anode temperatures. A large voltage gradient is maintained between the positive ion emitter and the cathode to obtain high ion current densities in the ion source. Ion currents in excess of 100 milliamp are to be supplied.

The second portion of the study will consist of the construction of an ion source and an accelerator for the generated ions. Pulse techniques may be employed in ion acceleration to eliminate space charge problems and increase the average current density. Linear accelerator methods may prove applicable for increasing ion velocities.

Cesium was chosen from the alkali metals because of its high ionization potential. There is little likelihood that cesium will be used as fuel for a space vehicle as the known free world's ore supply will probably not produce more than 100 tons of the pure metal. After an operating ion motor has been produced and tested, a substitute for cesium will be sought. Potassium can be used but is less efficient due to its higher ionization potential and lower molecular weight. It is believed that this search for fuel can best be accomplished after an ion motor has been demonstrated to be practical.

The first part of the study can be divided into two problem areas: (1) the development of a technique for measuring percent of ionization, and (2) the collection of design criteria for an ion source.

The measurement of percentage of ionization can be made by condensing both ionized and unionized cesium on a cathode. Ion current is measured at the cathode. The condensate is accurately weighed and the per cent ionization calculated after determination of ion current. This method is complicated by the reactivity of metallic cesium with oxygen and water and, therefore, weighing must be accomplished in a vacuum or an inert atmosphere. Between 1 and 4 mg of cesium will be evaporated in an hour; consequently, the accuracy of weighing must be high. This weighing is accomplished in a secondary chamber within which is installed the ion source in its own sealed chamber. Manipulation of the balance and cathode is done using rubber gloves, whose wrists are attached and sealed to the secondary chamber walls. This secondary chamber is at atmospheric pressure and contains dry nitrogen.

The ion source test unit is schematically displayed in Fig. 2. It consists of an evacuated bell jar within which is mounted the ionizing surface contained within a vapor stack, radiant heaters, and the cathode assembly.

The vacuum system employs a liquid nitrogen baffle, oil diffusion pump, and mechanical pump. The vacuum obtained is in the 10^{-5} mm of Hg range. Vacuum pressure is measured with Pirani and Phillips gages.

Cesium metal is vaporized in an electrically heated boiler. Its pressure is measured with a Langmuir viscosity gage and temperature by the thermocouple. The cesium vapor rises within a tube in which is placed the ionizing surfaces. These surfaces are heated by radiation between 1000 and 1200 C. Heat loss is minimized by highly polished tantalum radiation shields and a very thin-walled vapor stack cuts conductive losses. Temperature of the anode is measured by a thermocouple installed within a central anode support tube. Ions are collected on the cathode. The cathode is chilled so that cesium atoms and ions are condensed.

The use of ionic propulsion for flight through outer space is dependent upon an orbiting earth satellite space station. Conventionally propelled rockets to carry prefabricated parts of this satellite along with equipment and personnel to assemble it are outside the range of current developments. There are indications that an early effort will be made to establish a manned orbiting space station. Our effort to develop a new propulsion system to be used from this space station, consequently, does not appear to be premature.

Acknowledgment

The author gratefully acknowledges the guidance and assistance of his associate, Dr. Paul Leliak, in the preparation of this paper.

References

1. *Journal of Astronautics,* Vol. 2, Winter, 1955, pp. 149–152; Vol. 3, Spring, 1956, pp. 11–14; Vol. 3, Summer, 1956, pp. 33–36: "Electrical Propulsion System for Space Ships with Nuclear Power Source," by E. Stuhlinger. Also in *Missiles and Rockets,* June, 1957.

2. "The Mars Project," by W. Von Braun. Pub. by The University of Illinois Press, 1953.

3. "The Exploration of Mars," by W. Von Braun. Pub. by Viking Press, New York, 1956.

4. Vol. 2 of "Orbital and Satellite Vehicles," by A. J. Gale. Pub. by Department of Aeronautical Engineering, Massachusetts Institute of Technology.

5. *Physical Review,* Vol. 21, April, 1923, pp. 408–418: "Methods for Neutralization of Electron Space Charge by Positive Ionization at Very Low Gas Pressure," by K. H. Kingdon.

a progress report—

Dry-Type Air Cleaners on Farm Tractors

J. C. Siemens and J. A. Weber, University of Illinois

This paper was presented at the SAE National Farm, Construction and Industrial Machinery, Meeting, Milwaukee, Sept. 10, 1958.

GREATER ease of servicing is one of the ultimate goals in the development of dry-type air cleaners. The authors acknowledge, however, that the oil-bath cleaner is a rugged proved component that has done a good job for the farmers who serviced it properly.

This paper describes studies made in Illinois of oil-bath and dry air cleaners in field service. At the same fuel/air ratios, the maximum horsepower of a test engine was greater with the dry-type filter than with the oil-bath cleaner.

It was found that with AC fine dust and steady airflow, the oil-bath cleaners had significantly lower efficiencies than the dry-type filter. At less than rated airflow the efficiency of the oil-bath cleaner decreased while that of the dry filter remained high.

THE life of tractor engine parts is primarily dependent on the design of the air cleaner and the service it receives by the operator. Elements of good design include high efficiency, low restriction, adequate capacity, and ease of service. Since farm-tractor air cleaners are serviced by individual operators, the ease of service is a most important factor.

The Illinois Farm Supply Co. has been sponsoring a study of improvement of farm tractor maintenance in the Agricultural Engineering Department at the University of Illinois since 1955. One of the first steps in this project was the inspection of 60 farm tractors to find out how well they were being maintained. Results of this study are given in Station Bulletin 624. Seventy-eight different items were inspected on each tractor and after analysis of the conditions of the items and their importance, the air cleaner was one of the items chosen for further study.

Field Study

Condition of Oil-Bath Air Cleaners — A review of the condition of oil-bath air cleaners in the field shows that 16 of the 60 tractors inspected had more than 0.5 in. of dirt in the cup. In 21 cleaners the oil level was more than 0.25 in. low. Seven of the 60 cleaners showed excessive restriction to airflow due to chaff, soybean fuzz, and dirt that had accumulated in the cleaner body due to lack of complete cleaning of the cleaner. In another study 3 of the 28 had restrictions above 15 in. of water at rated airflow compared to 5–7 in. after they had been thoroughly cleaned.

So in Central Illinois, about 1 of every 10 tractors cannot produce full power because of excessive restriction of a dirty air cleaner.

Operators' Servicing of Cleaners — The operators of the 60 tractors knew that daily service was recommended for the cleaner cup; however, most of them were servicing the cleaners at engine oil change or once or twice a week. These practices are in line with the more recent and realistic recommendation of servicing the cup when the dirt accumulates to 0.5 in. Manual recommendations for complete cleaning of the air cleaner varied from 60 hr to once a year; however, 35 of the 60 operators

had never performed this maintenance chore. Operators of 6 of 7 tractors with restricted air cleaners were in this group. Many farmers and mechanics said that it was almost impossible to clean bean fuzz and chaff from the wire element by recommended procedures. Many oil-bath cleaners are being dismantled for cleaning by breaking the spot welds that hold the wire element in place. When the wire element is reinstalled, free air channels are formed that permit high-velocity airflow and oil pull-over.

Research on Dry-Type Paper Filters — The successful application of dry-type filters in the automotive industry and their relative ease of service justified exploring their use on farm tractors. The study was divided into three areas:

1. Dynamometer tests to determine the effects on engine performance of changing from an oil-bath cleaner to a dry paper filter.
2. Laboratory bench tests to determine efficiency, restriction, and capacity of oil-bath and paper cleaners.
3. Field tests of the paper filters under farm conditions to determine rate of restriction buildup, service requirements, and other field characteristics.

Engine Tests

Dynamometer tests were made on a carbureted, $3\frac{1}{2} \times 4\frac{1}{2}$, 4-cyl engine with a rated engine speed of 1650 rpm. Tests were made with both the original oil-bath cleaner and with the paper filter cartridge assembled with a hat-type hood and intake pipe like the cleaner shown in Fig. 1.

Effect of Type of Cleaner on Maximum Horsepower — All tests were run at 1625 rpm. For each type of air cleaner a complete carburetor curve was run. Fuel/air ratios were also determined. The equipment used is shown in Fig. 2. The blower was used to maintain atmospheric pressure in the 30-gal barrel over the air cleaner inlet. The orifice was isolated from the engine and blower with surge chambers to get accurate airflow measurements.

At all fuel/air ratios, the maximum horsepower was greater with the dry-type air filter (Fig. 3). The maximum horsepower with the paper filter was 37.7 compared to 36.5 with the oil-bath cleaner, an increase of 3.2%. The maximum horsepower for both air cleaners occurred at a fuel/air ratio of 0.086 and a specific fuel consumption of 0.575 lb per hp-hr. At other fuel/air ratios the percentage increase in horsepower with the dry-type over the oil-bath was approximately the same, with no significant difference in exhaust temperature or specific fuel consumption.

The increased horsepower for the dry-type cleaner is due to increased airflow which is attributed to two factors: (1) the lower restriction of the dry-type cleaner and (2) the effect of the long tube that was used to connect the dry cleaner to the engine carburetor. The restriction of the dry cleaner and its hood was 2 in., compared to 6 in. of water for the oil-bath cleaner. The increase in horsepower due

Table 1 — Carburetor Adjustment Required When Oil-Bath Air Cleaner was Replaced with Dry-Type Air Filter
(full load, full throttle, 1625 rpm)

	Carburetor Setting (Turns Open)	Fuel/Air Ratio	Hp	Fuel Consumption, gal/hr	Specific Fuel Consumption (lb/hp-hr)	Airflow (lb/min)
Oil-Bath	4	0.072	35.4	2.82	0.495	4.06
Dry	4	0.078	37.4	3.08	0.512	4.29
Dry	1¾	0.074	37.2	2.97	0.495	4.22

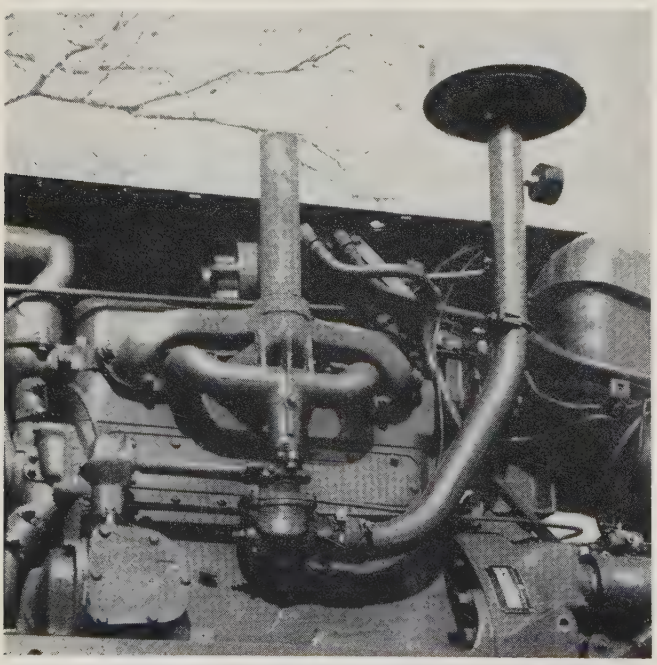

Fig. 1 — Dry cleaner mounted on tractor with restriction gage on inlet tube

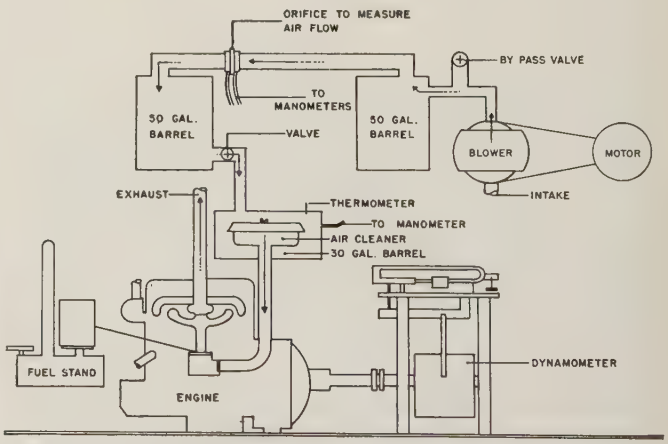

Fig. 2 — Equipment used for determining effect of air cleaners on fuel/air ratio and engine performance

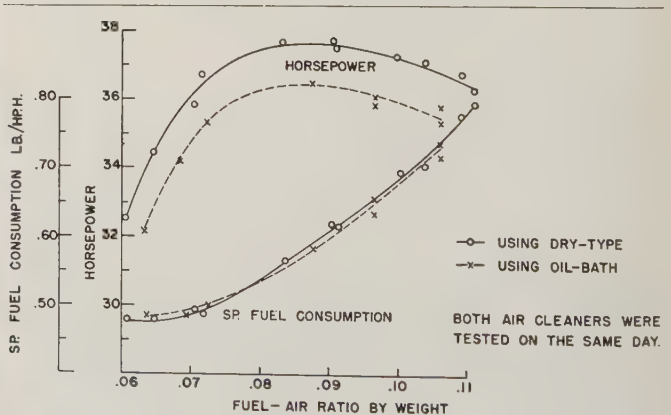

Fig. 3 — Engine performance with dry-type and oil-bath air cleaners (conditions: 3½-in. bore, 4½-in. stroke, full load, 1625 rpm)

to the lower restriction can be estimated using the formula:

$$HP_2 \text{ (dry type)} = HP_1 \text{ (oil bath)} \left(\frac{P_2}{P_1}\right)\left(\frac{T_1}{T_2}\right)^{\frac{1}{2}} \quad (1)$$

P is the absolute pressure and T the absolute temperature between the air cleaner and the carburetor. With an atmospheric pressure of 399 in. of water (29.4 in. of Hg), a constant temperature of 540 R, and the maximum of 36.5 hp with the oil-bath cleaner, the horsepower with the dry-type cleaner would be:

$$HP_2 \text{ (dry type)} = 36.5 \left(\frac{399-2}{399-6}\right)\left(\frac{540}{540}\right)^{\frac{1}{2}} = 36.9$$

Thus, the increase in horsepower due to the lower restriction of the dry cleaner was only 0.4 hp or 33% of the total increase of 1.2. The other 0.8 increase was due to the long tube connecting the dry cleaner with the carburetor. The tube permits inertia of the intake air stream to increase the airflow due to "ramming effect." Also, if the tube is of such a length that it is 'tuned" to the opening and closing of the intake valves, there will be an additional increase in airflow. The actual increase in airflow due to lower restriction, ramming effect, and tuning was about 5% (Table 1).

Effects of Paper Filter on Fuel/Air Ratios — Changing from the oil-bath cleaner to the dry cleaner and long intake tube increased the fuel/air ratio at full load for a given carburetor setting. For example, at an economical carburetor setting of 4 turns open, the engine had a fuel/air ratio of 0.072 with the oil-bath cleaner and 0.078 with the dry filter (Table 1). It was necessary to turn the carburetor needle valve in 2¼ turns to get a fuel/air ratio of 0.074 with the dry-type installed.

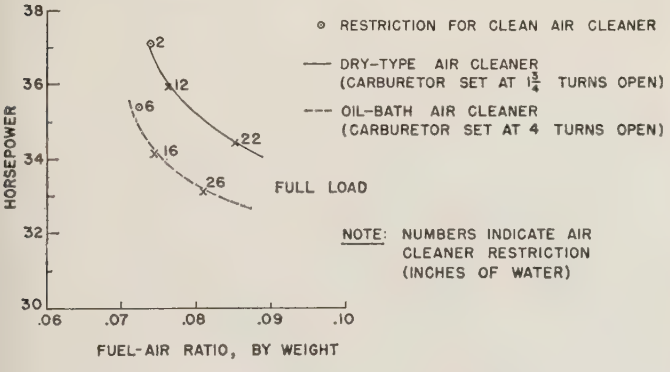

Fig. 4 — Effect of restriction on hp and fuel/air ratio for oil-bath and dry-type air cleaners

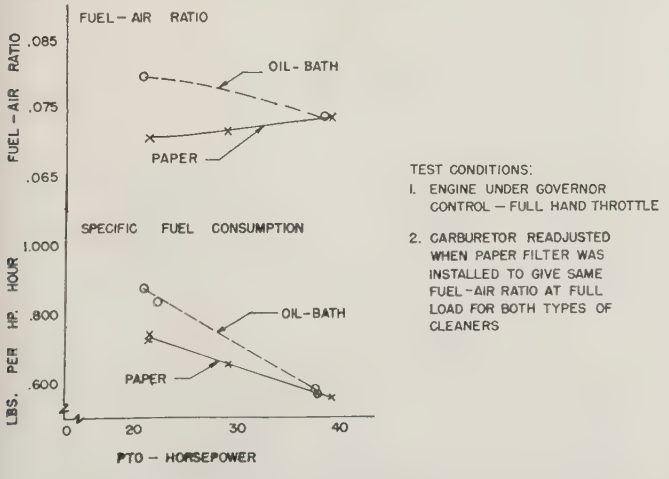

Fig. 5 — Effect of paper filter on fuel/air ratio and specific fuel consumption

How Partially Clogged Cleaner Affects Engine Performance — A partially clogged (or restricted) air cleaner was simulated by artificially reducing the pressure in the 30-gal barrel surrounding the cleaner inlets (Fig. 2). Carburetor settings were used that gave the same fuel/air ratio for both types with "clean" air cleaners.

Effects of air cleaner restriction on engine horsepower and fuel/air ratio were similar for both types of cleaners at full load. The horsepower decreased and the fuel/air ratio became richer with increased restriction (Fig. 4). The maximum horsepower was nearly proportional to the change in absolute pressure in the inlet pipe between the air cleaner and carburetor. An increase in air cleaner restriction of 10 in. of water decreased the maximum horsepower at 1625 rpm by 3% with the dry-type cleaner and 3.4% with the oil-bath cleaner. It would seem that the restriction of any air cleaner should not be allowed to increase more than 10 in. of water above its original restriction at full load, if optimum performance is to be obtained.

When the effect of air cleaner restriction was checked at three-quarters of full load, the decrease in horsepower due to restriction was less than at full load. Restriction at part load was compensated by the governor opening the throttle plate and maintaining engine speed as the air cleaners were restricted.

Part-Load Operation — In addition to the tests on the 3½ × 4½ engine, tests were also made on three current tractor models. At maximum horsepower, all three showed richer mixtures at the same carburetor setting when changing from the oil-bath to the dry-type cleaner. At the same fuel/air ratio, a greater maximum horsepower was obtained with the dry-type.

These three tractors were also tested at part load with both types of cleaners. The carburetor of each tractor was adjusted to the manufacturer's recommended setting or to a fuel/air ratio of approximately 0.074 at full load with the oil-bath cleaner installed. The needle valve in each carburetor had to be turned in to give the same fuel/air ratio at full load using the dry-type filter. As the horsepower was reduced from a maximum, the fuel/air ratio became richer with the oil-bath cleaner and leaner with the dry-type (Fig. 5). At part loads some of the effects of increased airflow and air pulsations that cause richer mixtures at full load are cancelled out by the closing of the throttle plate. The fuel/air ratios at part load are not seriously affected by the type of cleaner and, therefore, are determined primarily by the adjustment of the carburetor load needle.

Air Cleaner Efficiency and Capacity

A tractor engine operates at less than full load most of the time. Fig. 6 shows the distribution of hours at various percentages of full load for one year of operation. This data is an average for nine tractors operated on Central Illinois farms. Each

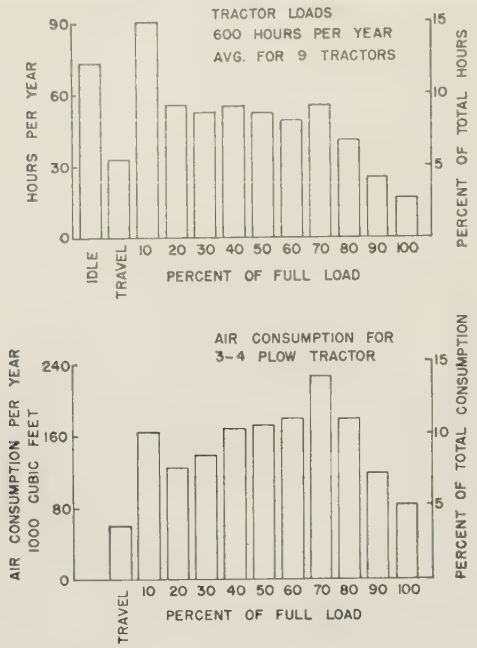

Fig. 6 — Air consumption for farm tractor at various loads for one year

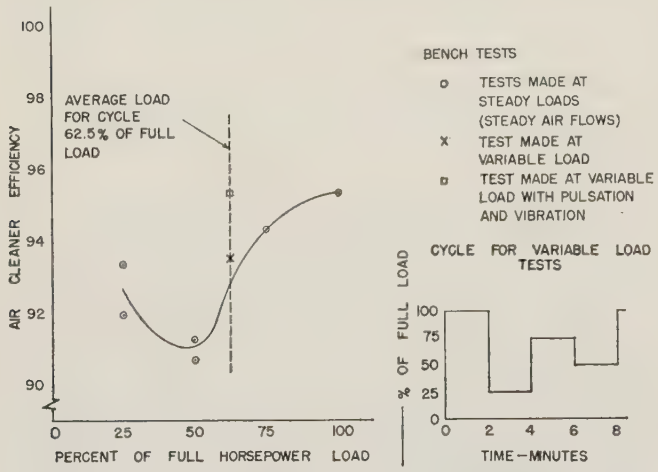

Fig. 7 — Oil-bath air cleaner efficiencies

tractor was brought to the laboratory for a dynamometer test to determine fuel consumption versus per cent of full load. The nine farmers then kept records of hours of operation and fuel consumption for each operation during the year. The distribution of air consumption obtained by using the volumetric efficiency at the various loads shows the importance of high air cleaner efficiency at part loads.

Equipment Used for Efficiency Tests — An apparatus was set up in the laboratory according to the SAE test code for determination of air cleaner efficiency, restriction, and capacity. Standardized AC fine and AC coarse dusts were fed by using a floating dust feeder. A deagglomerator was also used to help feed the dust in individual particle sizes. The dust feed rate and other recommendations of the SAE code were used where they were applicable.

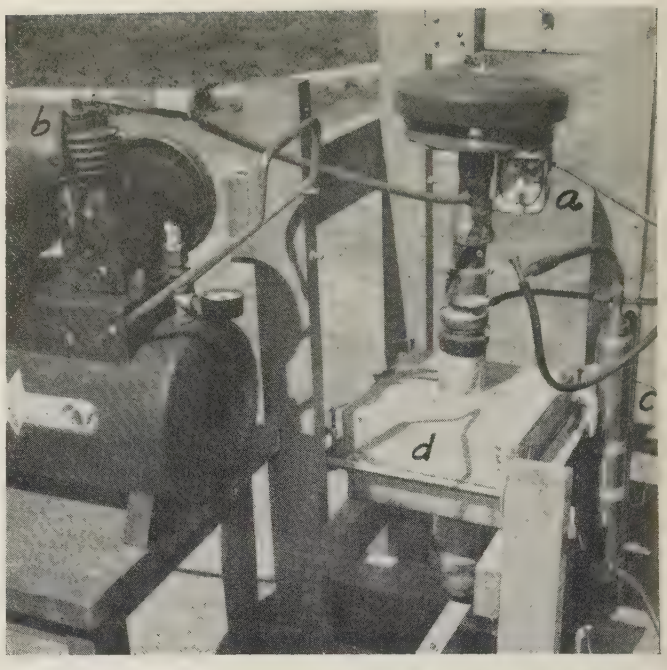

Fig. 8 — Laboratory equipment for efficiency tests with filter shroud removed (a-vibrator, b-reciprocating piston, c-dust feeder, d-absolute filter

Efficiency at Steady Airflow — The oil-bath and paper cleaners had nearly the same efficiency at full and one-half load airflows with coarse dust (Table 2). In these tests, the airflow was constant and no special attention was given to assure that all of the elements of the oil-bath cleaners were saturated with oil. With fine dust, the oil-bath cleaners had significantly lower efficiencies than the dry-type at full-load airflow. Also, while the efficiency of the paper element remained constant at less than full load, the efficiency of both oil-bath cleaners decreased. The rated airflow of oil-bath cleaner *A* did not pull all of the oil from the center of the cup up into the element. This may account for its lower efficiency compared to cleaner *B* in the full and one-half load tests. The efficiencies of cleaner *B* for steady airflow are shown by the curve in Fig. 7.

Efficiency at Varying Airflows — To investigate further the efficiency of the oil-bath cleaner *B* at less than rated airflow, a test was made according to the cycle shown in Fig. 7. The average airflow for the cycle is 62.5% of full-load airflow. Using this cycle, the oil-bath cleaner was slightly more efficient than indicated by the curve for steady airflow.

Addition of Pulsation and Vibration to Efficiency Test — When mounted on the tractor, the dry-type cleaner was subjected to vibration that had a frequency of twice engine speed and a maximum vertical amplitude of 0.012 of an in. Also, when used as a primary filter the element is subjected to the pulsations of the intake airstream. To make the laboratory tests more realistic, these conditions were added to the test apparatus by using an electric vibrator adjusted to the frequency and amplitude found on the tractor and pulsating the airflow by connecting a reciprocating piston of 5.5 cu in. displacement operating at 900 cpm between the element and absolute filter (Fig. 8). The efficiency of the paper filter was not affected by the addition

of vibration and pulsation, even when dust was fed very slowly over an 8-hr period.

Using vibration and pulsation of airflow on oil-bath cleaner *B*, along with the variable airflow cycle, the efficiency increased from 93.5 to 95.3%. This improved efficiency with air pulsation is probably more representative of actual field operation than steady airflow bench tests.

Capacity and Restriction in Laboratory Tests — Fig. 9 compares the increase in restriction and dirt capacity of oil-bath cleaner *B* and dry filter *A*-3 (1200 sq in. of paper surface). In the laboratory practically all of the dust that had been fed to the paper filter could be removed by tapping it against a flat surface. The capacity before excessive restriction was about 250 grams. This is about one-third the capacity of the oil-bath cleaner and would seem to indicate that a dry filter of a practical size would not have sufficient capacity.

Capacity for Bean Fuzz — Bean fuzz was collected from combine radiator screens and laboratory capacity tests were made on oil-bath filter *B* and dry filter *A*-3. It took 50 grams of fuzz to increase the restriction of the dry-type from 2 to 11 in. of water. At rated airflow 25 grams increased the restriction of the oil-bath cleaner from 6 to 48 inches of water. A test made with a centrifugal pre-cleaner on the oil-bath increased the capacity of the main cleaner to a satisfactory amount; however, the fuzz that found its way to the wire element of the main cleaner was very difficult to remove. Also, the pre-cleaner nearly doubled the initial restriction of the air-cleaner system.

Field Test

Four sizes of paper elements were used in the field tests (Fig. 10). Each cleaner was mounted on a long intake pipe that was equipped with a diaphragm restriction gage reading in inches of water as shown in Fig. 1. The tractor operators kept a daily record of hours of use, the farming operation and conditions, and the highest restriction during the operation.

In September, 1957, 10 of the size *A*-3 filters were installed on privately owned 45-hp tractors. These filters were used until May, 1958, then were removed for efficiency tests. Farming operations included plowing, discing, combining, and corn picking. None of the 10 filters exceeded a restriction of 4 in. of water, though some had over 300 hr of service. The farmers were particularly pleased with the ability of the dry filters to maintain low restriction when working in chaff, especially bean fuzz.

Only one filter was serviced or tapped out during the test period. Table 3 gives hours of operation of the filters and the weight of dirt they retained. To some extent the filters were self-cleaning, as some dirt vibrated off of the elements. Their effective field capacity exceeded that predicted by laboratory tests and the filters had a satisfactory period of service before excessive restriction. Compared to laboratory work a smaller amount of the dirt retained could be tapped out.

Three filters that were not tapped out before efficiency tests had higher efficiencies than a new paper filter (Table 3). Those that were tapped out, however, had lower efficiencies. It was not determined whether these lower efficiencies were due to a change in the paper or damage to the gasket sur-

Table 2 — Efficiency and Restriction Oil-Bath and Paper Air Cleaners
(laboratory tests, steady airflow)

Type of Air Cleaner	Airflow, cfm	Equivalent Engine Load	Standardized Dust Efficiency, %		Initial Restriction, In. of Water
			Fine	Coarse	
Oil-Bath	90[a]	Full	92.8	98.5	5.3
A	55	One-half	91.1	97.4	3.8
Oil-Bath	70[a]	Full	95.3	99.5	7.6
B	45	One-half	91.3	98.6	3.6
Paper	90	Full	99.2	99.7	2.0
A-3	45	One-half	99.4	99.7	1.4

[a] Rated airflow.

Table 3 — Field Test Results of 10 Dry-Type Air Cleaners from September, 1957, to May, 1958

Tractor No.	Maximum Pressure Drop (in. of water)	Hr of Operation	Dust Collected (grams)	% Tapped Out	Efficiency,[a] % (fine dust)
		Efficiency Test Made Before Tapping Out			
1	4	205	43	—	99.5
2	3	283	95	—	99.9
3	3	235	70	—	99.6
		Efficiency Test Made After Tapping Out			
4[b]	4	378	218	67	97.7
5	3	272	121	63	97.2
6	3	154	40	75	99.2
7[c]	4	407	118	73	99.1
8	3	295	81	76	96.2
9	3	190	110	67	98.7
10	3	300	68	43	96.0

[a] Efficiency of new filters was 99.2%.
[b] Cartridge tapped after 150 hr and again after 378 hr.
[c] Cartridge tested with variable and pulsing airflow and with filter vibration.

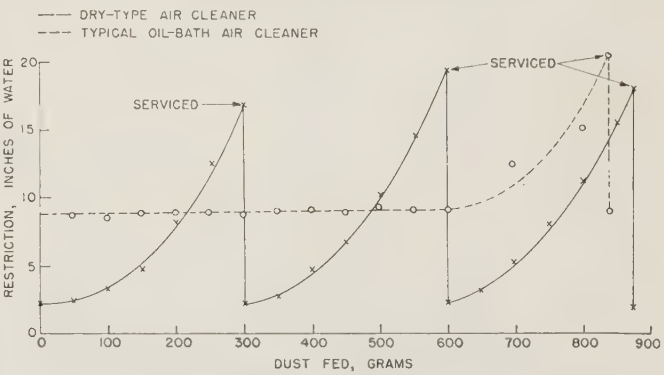

Fig. 9 — Restriction buildup of oil-bath and dry-type air cleaners (laboratory test using coarse dust)

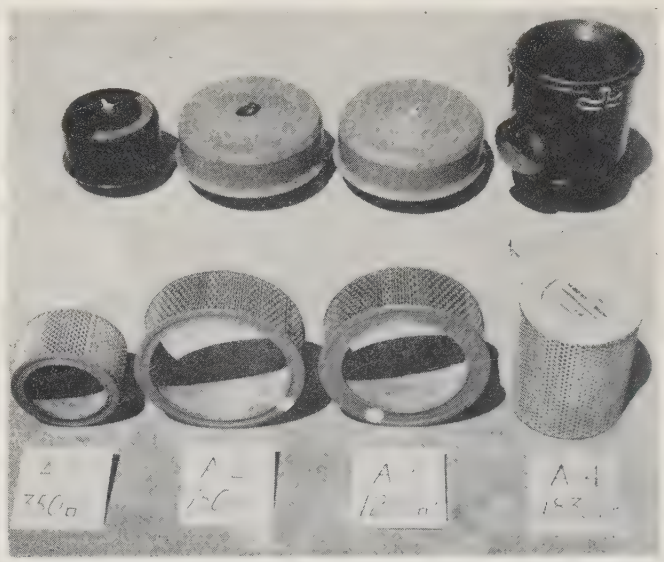

Fig. 10 — Four sizes of dry filters used in field studies (paper elements are in foreground, assembled cleaners in background)

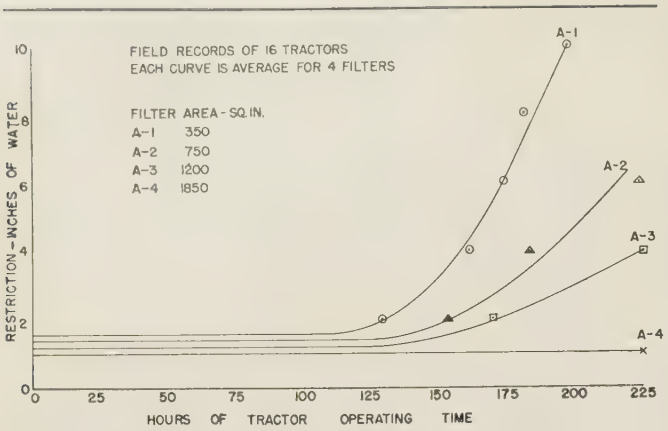

Fig. 11 — Restriction buildup of four different paper filter sizes versus tractor operating time

faces that allowed dirt to bypass the filter element. Microscopic examination of the paper showed no aparent change with service and subsequent efficiency tests in which caulking compound was used to assure gasket sealing did not show this decrease in efficiency after use and tapping out.

It was concluded that paper elements similar to A-3 cannot be tapped out by farmers without damage to the sealing surfaces and when an element becomes restricted it should be replaced with a new one. This makes it essential that the operator be provided with a restriction gage which will tell him when replacement is necessary and keep his handling of the cleaner to a minimum.

Tests of Different Sizes — In the spring of 1958, 16 more tractors were equipped with four different sizes of paper elements (Fig. 10). These filters experienced a dustier than average spring work period. Fig. 11 shows that the paper area has a direct bearing on the hours of service before excessive restriction. The four *A*-1 filters were excessively restricted after 200 hr and are probably too small. On the other hand, the *A*-4 filters have not increased in restriction and are probably larger than necessary.

Excessive restriction of the *A*-1 filters occurred during disc harrowing. This seems to be the dustiest farming operation in central Illinois. It is of interest that agronomists are recommending less working of the soil and that minimum tillage practices now being accepted call for little or no discing. The dirt load of the tractor air cleaner in the Midwest will probably be reduced in the future and chaff and fuzz will make up a larger percentage of the material the cleaner must handle.

Other Observations

Even though the paper elements had high laboratory efficiencies after as much as 300 hr of service, the field service cannot be considered completely satisfactory. What was considered to be an excessive amount of dust was observed in the intake pipes of some of the tractors with *A*-1, *A*-2, and *A*-3 filters. Three of the four tractors with *A*-1 filters had excessive piston ring and sleeve wear. Dust may have entered in three ways: through the paper, around the gaskets of the element, and through connections between the hood and intake pipe. Even on filters that had not been disturbed since installation, dust had penetrated the outer sealing ring of the gaskets. This suggests that dirt also penetrated the inner ring.

The paper filter as it is now being used by the automotive industry cannot be recommended for use on farm tractors. The paper elements and hoods must be more rugged and foolproof than those in filters *A*-1, *A*-2, and *A*-3. It is felt that many complaints on dry filters that were sold can be attributed to leaks and damage to the filter element caused by tapping them out.

The metal cylinder that provides support for the paper element must be heavier to prevent deformation and the gaskets should be designed to provide wedging action between the hood and cartridge that will assure a positive seal. Filter *A*-4 has these requirements but seems larger than necessary for Illinois conditions. A centrifugal pre-cleaner principle used in conjunction with a smaller element reduces the dirt load on the element but loses the advantage of the self-cleaning experienced in the Illinois tests.

Future tests will include determination of the amount of dirt that tractor air cleaners must handle and the composition of this material. More work is planned on study of airflow to engines with low restriction and "tuned" inlet tubes. Paper filters that have been sold and used, and are blamed for engine destruction because of visible holes, still have high laboratory efficiencies. The authors feel that the laboratory procedure for determination of air cleaner efficiency must be improved and made more realistic to solve this discrepancy.

The uncertainty of continuous high efficiency is an inherent disadvantage of present-day dry filters. Nevertheless, the advantages of the dry-type cleaner indicate that its development for use on farm tractors should be continued.

Acknowledgments

The Agricultural Engineering Department wants to thank the Fram Corp. for supplying some of the cleaner hoods and all of the paper elements that were used in the field study; and the M & W Gear Co. for supplying intake pipes and hoods. We also appreciate the technical help of the United Specialties Co. and the Donaldson Co.

References

1. SAE Handbook, 1956, pp. 1091–1095: "Air Cleaner Test Code."

2. "Air Cleaners — The Why of Wet and Dry," by H. M. Turner. Paper presented at SAE West Coast Meeting, Seattle, August, 1957.

3. "Air Cleaners for Military Vehicles," by Edward Blackburne and C. R. Denton. Paper presented at SAE Automotive Ordnance Day, Center Line, Mich., February, 1955.

4. "Maintenance Inspections of Sixty Farm Tractors," by J. A. Weber. University of Illinois Agricultural Experiment Station, Bulletin 624, February, 1958.

5. "Dry-Type Air Filters for Farm Tractors — Efficiency, Restriction, and Service Requirements," by J. C. Siemens. Unpublished thesis for master's degree, University of Illinois, 1958.

Discussion of this paper and of the Turner-Anderson paper is on p. 202.

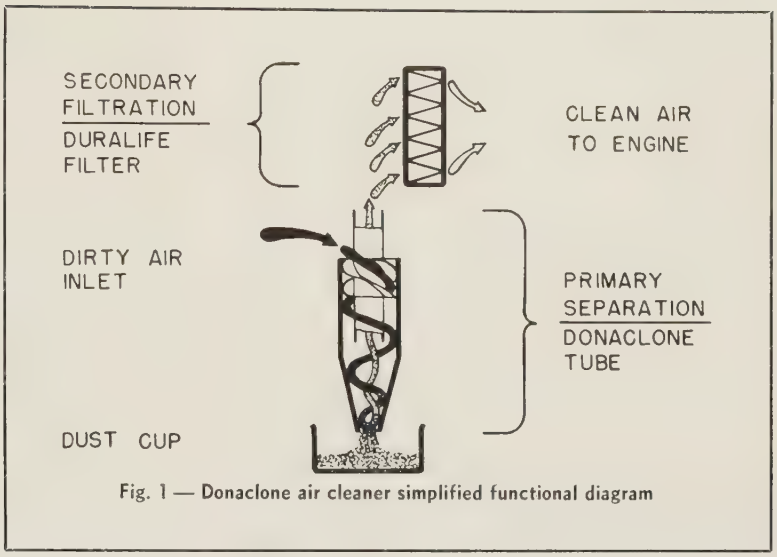

Fig. 1 — Donaclone air cleaner simplified functional diagram

NOW—

Practical "Double Dry" Filtration with *DONACLONE*

H. M. Turner and D. K. Anderson, Donaldson Co., Inc.

This paper was presented at the SAE National Farm, Construction, and Industrial Machinery Meeting, Milwaukee, Sept. 10, 1958.

OVER the years, air cleaner improvements have kept pace with the demands imposed by new engine and equipment designs. Chronologically, we have seen the dry-contrifugal, the oil-wetted, the oil-washed, and the dry paper element systems. Each of these systems represents a performance compromise. However, do they meet your needs today? Can they fulfill the demands of tomorrow?

The engines of today run at higher speeds and with closer tolerances — a problem of more air and more wear. In the last 10 years, the air demand for a basic engine has more than doubled. The use of superchargers, and more recently turbochargers, has accounted for a major portion of this increase in airflow. Further, it is recognized that oil mist and dirt are natural enemies of the turbocharger. Changes in vehicle design and use have produced severe conditions of bounce, shake, and angle operation detrimental to the function of the oil-washed air cleaner. Since equipment costs rise each year, maintenance is more important; however, these maintenance costs are also rising. These are the problems of the engine manufacturer, equipment manufacturer, and the equipment user. As an air

DRY-TYPE air cleaners are considered to be easier to service than the oil-bath type. This paper describes one such cleaner, the Donaclone developed by Donaldson Co.

Field and performance tests on the cleaner on farm tractors, trucks, military tanks, and similar vehicles are described. Maintenance of the three sections of the cleaner (dust cup, tube section, and filter element) is also outlined.

The authors consider the Donaclone to give positive engine protection, long service life, installation flexibility, and service economy.

cleaner manufacturer, we accept them as a challenge that demands satisfaction.

The solution to these problems must lie in the practical combination of these features in an air cleaner:

1. No oil.
2. The efficiency of the better paper elements.
3. The service life of the best oil-washed air cleaner.
4. The service simplicity of the centrifugal or paper designs.

Another desirable feature is installation flexibility — the air cleaner should not be sensitive to attitude, but function in any position dictated by style, space, or terrain. The practical union of these features is the salient characteristic of the Donaclone air cleaner.

Operation of Cleaner

Operation of the Donaclone air cleaner is shown in Fig. 1. The dirty air is drawn through a conventional inlet into a chamber, which is a common entrance to the Donaclone tubes. The dirt-laden air enters these tubes and is rotated by the helix vane to create centrifugal force on the dust particles. The air spirals down the coned section of the tube and reverses direction at the bottom. As the air reverses within the cyclone tube, dust is ejected to the cup. The cleaned air then moves through the cyclone outlet tube and to the Duralife filter element for final filtration before entering the engine.

The heart of the Donaclone air cleaner is the specially designed Donaclone tube which meets rigid manufacturing and environmental specifications. These specifications are necessary for the practical service life of the secondary filter. An extensive laboratory and field investigation of many methods of primary separation indicated a dry, centrifugal approach was required. The centrifugal separators used to date as "pre-cleaners" are 70–80% efficient on AC coarse test dust. The Donaclone tube efficiency is 96–98% — an average reduction in dust to the secondary filter of 88%.

To take advantage of the efficiency of the Donaclone tubes, the secondary or final filter must provide high dust-holding capacity and high efficiency resulting in minimum dust to the engine (Fig. 2). Also, an air filter element must function satisfactorily in the normal environment of an air cleaner — that is, oil vapors, exhaust carbon, lint, chaff, and moisture. Further, engine protection suffers if an element does not consistently provide its engineered performance and have the durability to withstand abuse, mishandling, and subnormal service. A special filter media, purposeful design and construction, and strict manufacturing control provide the best balance for these requirements in the Duralife element.

The composite performance of the tubes and Duralife filter, which is the Donaclone, is shown in Table 1. The union of long life and high efficiency is borne out by these tests. As indicated, the paper element in the primary dry air cleaner must be serviced nearly nine times during the life of a single paper element in the Donaclone air cleaner (Fig. 3). The Donaclone service life also greatly exceeds that of the better oil-washed air cleaner. The allowable "service point" restriction directly affects the Donaclone service life. As an example, for a typical Donaclone, increasing the "service point" restriction from 20 in. water to 30 in. water will increase the service life 55% at 750 cfm (Fig. 4).

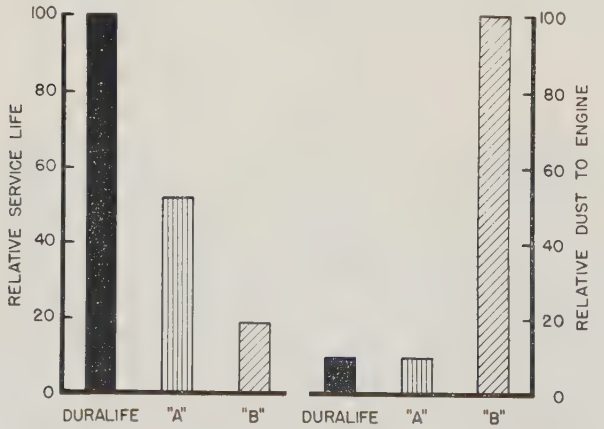

Fig. 2 — Laboratory performance comparison of filter elements

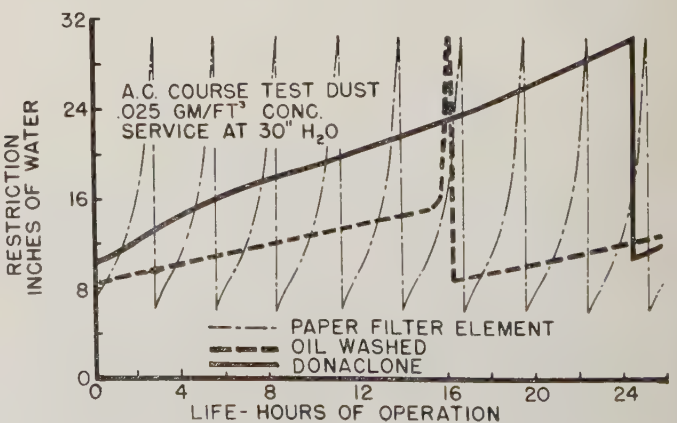

Fig. 3 — Laboratory comparison of air cleaner service life

The long service life of the Donaclone is combined with a high and level efficiency over the entire airflow range (Fig. 4). This is important from the standpoint of engine protection because varying airflow and reduction of engine speed settings occur in normal field use. A typical Donaclone applied to an engine with an air demand of 750 cfm at full governed speed and 250 cfm at idle has an efficiency of 99.9% throughout this airflow range. Because of this feature, an increase or decrease of governed engine speed by the user or the use of an over- or under-size air cleaner will not result in loss of engine protection.

Only after successful field trail can a product be considered for general application. It was imperative that field experience be gained over a wide range of engines, vehicles and operating conditions. Actual field tests of 150,000 hrs have been completed on Donaclone air cleaners to date (Table 2). The first stages of field tests were conducted under closely controlled conditions at the Phoenix, Ariz., Proving Grounds of Caterpillar Tractor Co. Later, this work was expanded to Caterpillar's Peoria Proving Grounds; the General Motors Proving Ground at Milford, Mich.; the International Harvester Co. Proving Grounds at Phoenix and the Army Ordnance Testing Grounds. Realizing final proof of performance reliability and structural durability would come only through normal operation and maintenance by the ultimate user, over 150 Donaclone air cleaners were installed on commercial equipment and on vehicles operated by the military forces. Test vehicles were farm tractors, over-highway trucks, off-highway construction equipment, rockcrushers, and military tanks.

Over 10,000 operating hr have been accumulated on individual test Donaclone air cleaners without excessive engine wear. Visual inspection in these field tests supports the efficiency improvements shown by laboratory tests. The air transfer pipes following the Donaclone air cleaners were found to be clean and dry. A substantial reduction in upper engine wear is indicated. The magnitude of this decrease will not be recorded until a complete pattern of engine wear is established.

Maintenance

Dust Cup Service — Service periods of the dust collection cup on test air cleaners have varied according to dust concentrations encountered. The maximum dust cup service interval on the field test air cleaners was 6 months. The minimum period, on a rockcrusher operating in very severe dust conditions, was 8 hr. To obtain an 8-hr service period on an oil-washed air cleaner in the same installation, it was necessary to remote the inlet to a point of minimum dust concentration. A distinct advantage of the Donaclone air cleaner is its simple dust cup service: Remove the dust cup, empty it, and replace it. The attitude of field service personnel emphasizes the need for simple service.

Tube Section Service — Field results have shown special and regular servicing is not necessary on the Donaclone tubes. A stiff brush inserted in the tube normally will remove any unusual deposits.

Filter Element Service — Service life on new paper elements ranged to 2000 hr depending on the type of application and operating conditions (Table 3). For example, 21 new filter elements, in Donaclones installed on off-highway trucks on the Mesabi Iron Range, varied in service life 753–2115 hr — with an average of 1144 hr. In the same test location, the regular service period for oil-washed air cleaners ranged from 8 to 40 hr.

Service life on new elements used in a Donaclone air cleaner operating under severe dust conditions, such as rockcrusher installations, ranged 34–489 hr with an average of 213 hr. Compare this to the service period of less than 8 hr for an oil-washed air cleaner in the same application.

Although a paper filter is normally considered as an expendable cartridge, proper and careful cleaning can extend its original life. In these field tests, elements have been serviced up to five times without

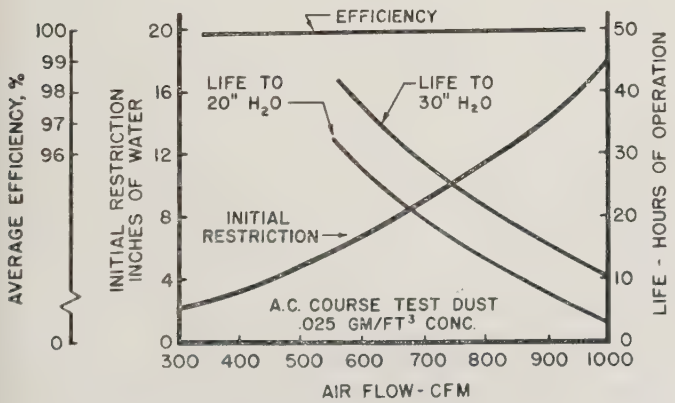

Fig. 4 — Laboratory performance curves of typical Donaclone air cleaner

Table 1 — Comparative Air Cleaner Performance Laboratory Tests

	Oil-Washed	Donaclone	Primary Paper Element
Efficiency			
AC Fine Test Dust, %	98.5	99.9	99.9
Service Life to 30 in. of H_2O			
AC Coarse Test Dust, hr	16	24[a]	2.75

[a] Based on filter element service only.

Table 2 — Donaclone Field Test Experience

Type of Equipment	Type of Work	Field Test Locale[a]	Test Hours to Date
Crawler Tractors	Dozing, pushing, ripping, logging, land clearing, land leveling	North and South Central, North and Southwest, Northeast	57,780
Earthmoving	Scrappers, dumpers, graders	North Central, North and Southeast, Southwest	28,140
Trucks (off-highway)	Ore hauling, logging, earth hauling	Southwest, North Central	41,180
Power Units	Rock crushers, asphalt plant	North and South Central, Southeast	14,660
Front-End Loaders	Cement, fertilizer, and smeltering plants	North Central, Southwest	6430
Trucks (over-highway)	Road construction	Northwest	1350

[a] Field test locale selected to provide environmental conditions of rain, snow, lint, chaff, dust temperature extremes, and vibration to insure complete test coverage.

Table 3 — Service Life Donaclone Filter Elements

Type of Equipment	Hours of Operation[a]		
	Maximum	Minimum	Average
Crawler Tractors	108	1505	492
Scrapers	355	899	557
Trucks (off-highway)	753	2115	1144
Front-End Loaders	974	1473	1224
Rock Crushers and Asphalt Plants	34	489	213

[a] Based on actual field data on new elements to 30 in. of H_2O.

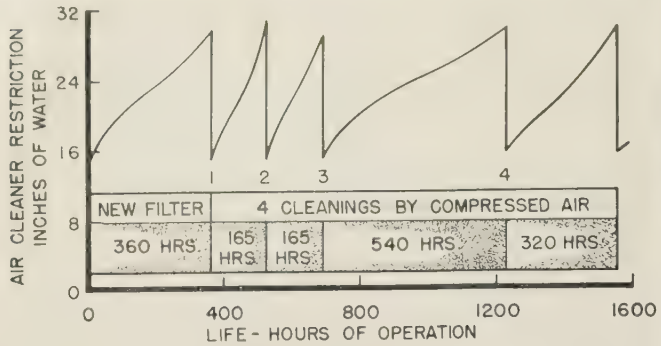

Fig. 5 — Donaclone filter element service life (crawler tractor operation in Southwest United States)

Fig. 6 — Comparative air cleaner service costs, field data of medium to heavy-duty operation

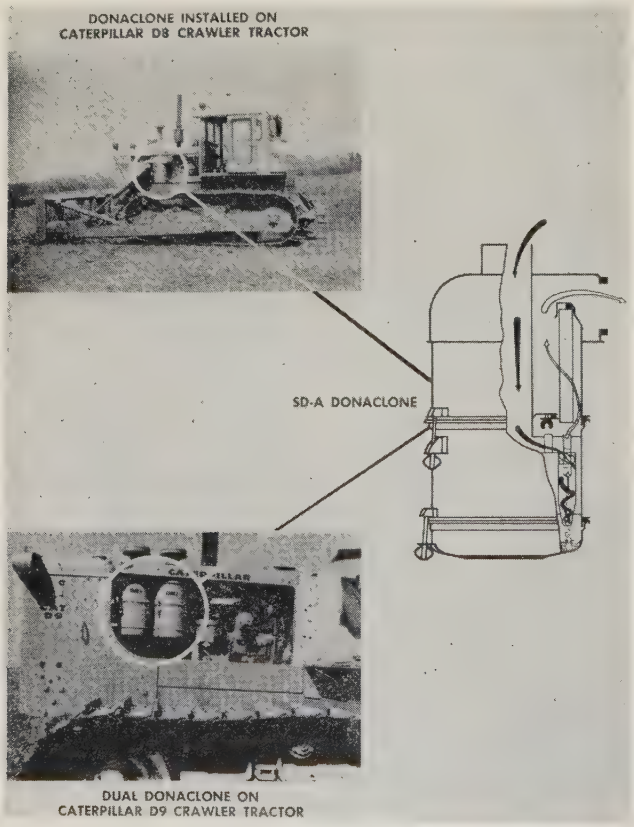

Fig. 7 — SD-A Donaclone installed on two configurations

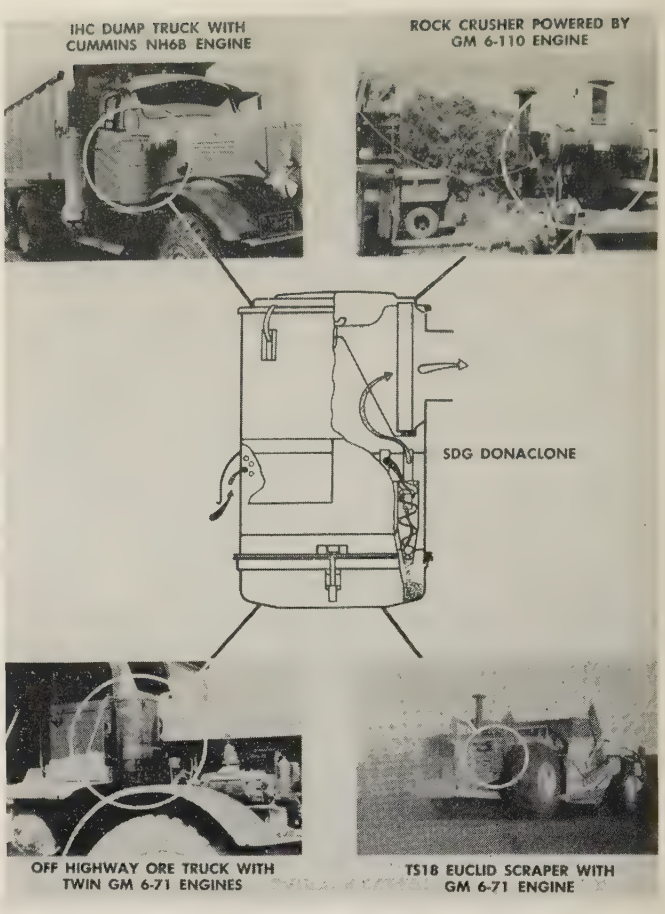

Fig. 8 — Installation of SDG Donaclone

Table 4 — Factors in Service Cost Comparison of Oil-Washed and Donaclone Air Cleaners

Oil-Washed	Donaclone
1. Cost of oil	1. Cost of filter element
2. Labor to service oil cup and tray	2. Labor to service dust cup
3. Labor to service body assembly	3. Labor to serivce tubes
4. Dust capacity	4. Filter element life
5. Need for service (safety)	5. Need for service (safety)

damage (Fig. 5). We have found as high as 100% additional element operating life after an element cleaning. Of course, this additional operating life is dependent on a number of factors, including dust particle size, type, and concentration.

In the field several methods have been used to clean paper elements. A jet of compressed air in the direction opposite to the normal airflow is most successful for element cleaning.

On a Donaclone air cleaner the need for service can be measured accurately. The time for element service can be determined by a vacuum gage or service indicator; therefore, the "calendar" service period, common to oil-washed air cleaners, is not necessary. Service periods determined by vacuum indicator provide the most economical use of filter elements.

The service cost of any air cleaner must include the cost of the necessary materials plus the cost of time required to service each air cleaner component. When comparing service costs of the Donaclone air cleaner to the oil-washed air cleaner, we must consider the factors shown in Table 4.

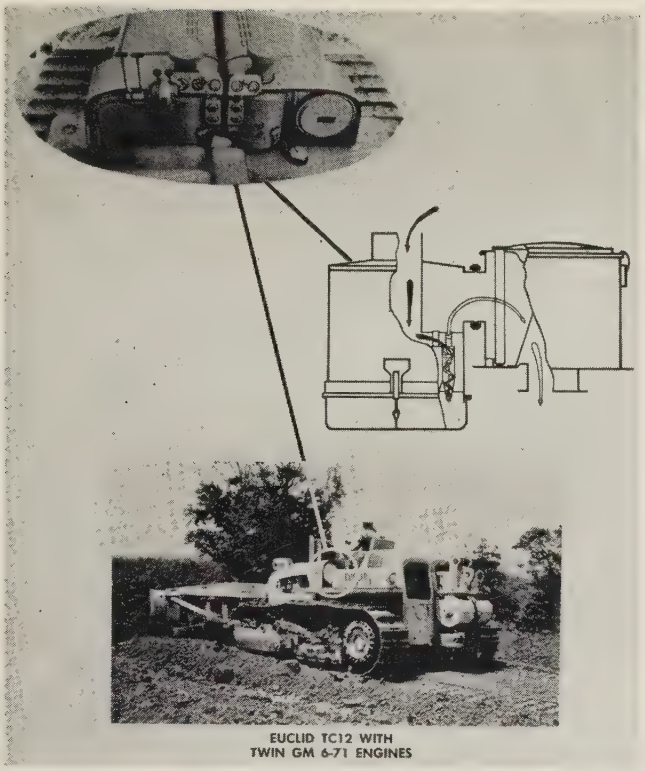

Fig. 9 — Donaclone installed on Euclid TC12 with twin GM 6-71 engines

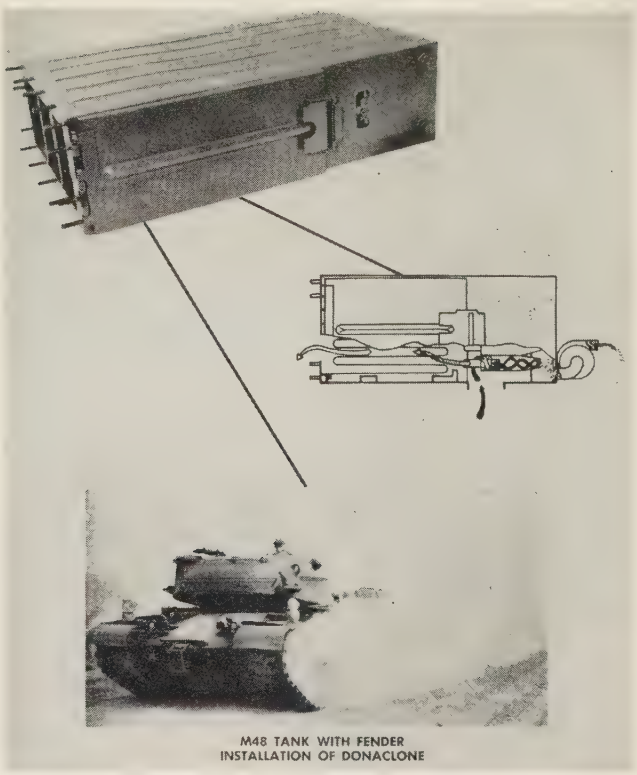

Fig. 10 — M48 tank with fender installation of Donaclone

As mentioned previously, the need for service from a safety standpoint has made common the practice of a "calendar" service period on the oil cup of the oil-washed air cleaner. On the Donaclone air cleaner a "calendar" service period need apply only to the dust cup.

On the basis of data obtained in a field test program involving 47 Donaclone air cleaners, one leading construction equipment manufacturer has found a reduction of over 45% in service costs of the Donaclone air cleaner compared to an oil-washed air cleaner. A large mining company operating a fleet of 150 off-highway trucks has found a 66% reduction in service costs. Based on all the field test results, the reduction in service cost is approximately 60% (Fig. 6). The full magnitude of savings which the Donaclone provides by reduction in engine wear and service costs will not be realized until future vehicle maintenance records provide the necessary amount of data.

The use of an engine in a dusty application is not limited to a particular engine size or type. Consequently, the Donaclone has been engineered for application to all sizes and types of engines. Successful installations have already been made on engines of 35–800 hp — carbureted and diesel engines; naturally aspirated, supercharged, and turbocharged.

The installation flexibility of the Donaclone is clearly shown by the four different designs which were used in the field test program. One design has the center tube inlet and side outlet typical of many oil-washed air cleaners. The Donaclone tube section is completely removable from the filter section, and the filter element is serviced from the bottom (Fig. 7). Another design has a side inlet which can be shrouded or tubular, a side outlet, and the filter element is serviced from the top (Fig. 8). In the third design, the Donaclone tube section and the Duralife filter section are separated into individual units and are connected by ductwork (Fig. 9). Splitting the sections into separate and distinct units further allows installation of the Donaclone sections in areas remote from each other. The fourth Donaclone design is rectangular in cross-section in contrast to the cylindrical cross-sections previously described (Fig. 10). The rectangular air cleaner can be of any practical dimensions for the cross section as long as the proper area is maintained. The outlet is usually at one end with the inlet located on any of four sides. Filter element access is through a specially designed door.

Worthy of special mention is the rectangular Donaclone developed to meet special military requirements (Fig. 10). The problem of logistics peculiar to the military has dictated a "minimum service" design. An electric dust exhauster automatically ejects the collected dust; and a special fabric filter media and unique element construction provide extra long service life and field service without cleaning equipment.

Donaclone is a practical air cleaner. Its combination of positive engine protection, long service life, installation flexibility, and service economy is creating a new air cleaner performance standard. The Donaclone air cleaner has been thoroughly performance tested and appears as standard equipment on many engines and vehicles today.

References

1. "Advantages of Well-Chosen Air Cleaner Inlet System," by R. E. Larson. Paper presented at SAE

National Tractor Meeting, Milwaukee, September, 1952.

2. "New 3-D in Engine Air Cleaners — Dry Design Developments," by R. J. Lunn. Paper presented at meeting of SAE Twin City Section, November, 1955.

3. "Air Cleaners — Why of Wet or Dry," by H. M. Turner. Paper presented at SAE West Coast Meeting, Seattle, August, 1957.

4. "Dust and Engine Wear," by E. S. Dahl and K. H. Rhodes. Paper presented at SAE National Tractor Meeting, Milwaukee, September, 1952.

5. "New Methods of Securing Improved Air Cleaner Efficiency," by D. P. Eastman. Paper presented at SAE National Tractor Meeting, Milwaukee, September, 1952.

6. "Engine Wear as Affected by Air and Oil Filters," by W. S. Jones and B. G. Brown. Paper presented at SAE Summer Meeting, French Lick, Ind., June, 1950.

7. "Air Cleaners for Military Vehicles," by Edward Blackburne and C. R. Denton. Paper presented at SAE Ordnance Day, Center Line, Mich., February, 1955.

DISCUSSION

Dry-Type Air Cleaners Easier To Service than Oil-Bath Cleaners

— Howard M. Knight
International Harvester Co.

THESE papers show that we are getting closer to the ideal air cleaner that will remove all the dirt from air entering the induction system, require no servicing and maintenance, and need the minimum of space.

As Messrs. Siemens and Weber state, the oil-bath cleaner is a rugged proved component that has done a good job for those who have serviced it properly, but it is difficult to get the owners to do this. As everyone knows, it is very messy to service.

The cellulose type of air cleaner can, if properly made, give a higher dirt removing efficiency than the oil-bath type, throughout the airflow range. It will also, as a rule, be less affected by chaff, fuzz, and lint, but have less dirt capacity. If a break or leak develops though, damage to the engine can occur without warning. And it is difficult to get owners to service it properly or replace it when necessary.

They describe the effect on power of the cellulose and oil-bath cleaners. We regret they did not make tests of the dry-cleaner intake pipe and element container without the element, to determine the effect of "tuning" and also to determine how much loss was due to the element. We would also suggest that they make dust capacity tests on the engine, as it does not seem possible to simulate the pulsations on a bench test. We have not found that the absolute filter appreciably affects the pulsations, especially if PF105 is used as the media.

The territory in which the tractor tests were made either had very little dust at the cleaners or the dust was of a type that did not stick to the cellulose and that would unload. We have found places where the dust would not unload and could be only partially removed even with the use of compressed air. Recently, at Phoenix, Ariz., after 15 min use of an air hose, we were able to reduce the increase in restriction by only 50%.

We have found that the standardized air-cleaner dusts do not have all of the same characteristics in the laboratory as the dust collected on cleaners at Phoenix.

Also, these tractors evidently did not have smoky exhausts, or the exhaust was so located that the smoke did not enter the cleaner. Smoke particles can plug a cellulose type of element very quickly and they cannot be removed. Fibrous plastic wraps show promise, but our experience is not sufficient to recommend them.

We have also found as stated by Messrs. Siemens and Weber that the sealing between the elements and containers is often not good. The container must be rigid and have very good seats for the element. The element must be able to resist the "crush" and retain a resilience that will maintain the seal even when the restriction of the element is very high. Many of the automobile-type containers are too flimsy for tractor use.

They state that an indicator based on restriction is needed to tell when the replaceable element should be serviced or replaced. A regular vacuum gage can be used, but its life on farm or industrial equipment is usually too short. A type that is fully protected from dust and that uses a micro-switch on a diaphragm has proved satisfactory. Other types are on test and show promise. However, these indicators will not necessarily show when a break, leak, rupture, or collapse of an element occurs.

It must be remembered that the restriction of the cellulose element can rise very high and if the unit is operating on part load, the power loss can go unnoticed. This high restriction will tend to rupture the cellulose, and will tend to force dirt into the induction system past the element seals, through the connections, cracks, pores, and the like. Siemens and Weber recommend 10 in. of water as a limiting restriction; and since this is substantially the same as given by a good oil-bath cleaner, the "permissible" pressure drop would not be higher. We can realize though that higher pressure drops will exist, which are not due to using warning devices, or the malfunctioning or ignoring of such devices. Therefore, the induction system must be airtight and have good connections, and the rupture strength of the cellulose element must be high.

The authors state that pre-cleaners are available. What is the overall efficiency with them? We know that with oil-bath air cleaners the overall efficiency is reduced and that more dirt enters the engine when they are used than without them, due to the cyclonic action reducing the size of the dirt particles. Is this also true with the cellulose type of cleaner?

To date, we do not feel that we can recommend the general use of the straight cellulose type alone, but believe it has advantages when used as a pre-cleaner for an oil bath cleaner. The latter acts as a safe guard if the cellulose fails.

The Donaclone air cleaner does not give much advantage in size but it can be separated into two parts and fitted in where otherwise there would be no room. It is far less messy to service than the oil-bath type. The dust cup must be properly serviced or the cyclone action will stop and the cellulose element's life shortened.

It is also affected by smoke but to a lesser degree than the straight cellulose, as the Donaclone tube section removes a good portion of the smoke particles.

If the Duralife element should fail, the engine would still be protected to a fair degree by the tube section.

Summarizing, the chief advantage of dry cleaners over the oil-bath type of cleaner is the easier and less messy servicing required. They can all give higher efficiencies *if properly made and serviced* but it is difficult to tell when they are properly made on a production inspection basis. It will be difficult to get proper servicing.

They all require a warning device to tell when the replaceable element should be serviced. Care must be taken to keep smoke out of the cleaners. The induction system must be kept airtight, as the higher differential pressures possible will tend to force more dirt in.

LIMITED SLIP DIFFERENTIALS

R. P. Lewis and L. J. O'Brien, Dana Corp.

This paper was presented at the SAE National Passenger-Car, Body, and Materials Meeting, Detroit, March 5, 1958.

WITH the increasing power of today's automotive engines, the limited slip differential is coming into more general use. The conventional differential has been found to be inadequate for many driving conditions.

The limited slip differential is one in which the amount of slipping is controlled. This paper discusses three of this type: cam, variable velocity gear, and the friction. The authors describe most fully the latter, concentrating on the Powr-Lok. They include a detailed load and force analysis of the friction-type differential.

The authors believe the limited slip differential greatly increases the utility and safety of a vehicle.

THE SUBJECT of locking differentials has been before the automotive engineer since the very beginning of the industry. The shortcomings of the conventional differential were recognized early, as testified by the hundreds of patents that have been issued both here and abroad. Many of these have been manufactured, found wanting, and have long since fallen by the wayside. However, during the past few years the limited slip type of differential has been adopted as optional equipment by the passenger-car and light-truck industry.

The purpose of this paper is not to cover the complete story of locking differentials and thereby review past history, but rather to bring everyone up to date on what is being done today and what we might expect in the future. Therefore, we will cover only the limited slip type, confining our material to those being used at the present time. Since the heavy-duty field are even more vitally interested, we have included all types of applications.

Because a limited slip differential employs practically all of the features and principles of the conventional differential, it is necessary to understand these first.

Conventional Differential

Early in the development of power-driven vehicles two requirements were recognized: First, that the wheels of the vehicle travel at different speeds; second, that it is desirable to provide equal force to the driving wheels. In order to understand the function of a differential, let us analyze these two principles in detail. First of all, the wheels must travel at different speeds because they travel different distances in the same length of time. In Fig. 1 the calculation of the difference in speed between two wheels of a vehicle rounding a 90-deg turn is outlined. Assuming a 60-in. tread and 13-in. tire, the outer wheel makes 1.15 revolutions more than the inner wheel. In order to understand the relative motion of parts in the differential which we later will install between these two wheels, consider a maximum condition of a car traveling 60 mph on a 1-mile track when the outer wheel will make 4.6 more rpm than the inner wheel. This appears to be very small, and maybe somewhat insignificant; however, when considered in tire wear or tire scrubbing, it would definitely be an important factor in the operation of a vehicle. Secondly, in a 4-wheel vehicle with two wheels driving, when the force is greater on one side than on the other, the driving force has a tendency to steer the vehicle. Therefore, it is desirable to have an equal division of load to the driving wheels. This will also equalize wear and fatigue on the driving parts.

In order to obtain differences in speed and to

supply equal driving forces to each wheel, a solid shaft between the two driving wheels is not the answer. By separating the shafts which drive each wheel and by connecting these two shafts with a gear set that makes them interdependent, we can accomplish the requirements as outlined above. In Fig. 2 is shown a schematic diagram of a conventional bevel gear differential commonly used in automotive vehicles today. With the vehicle going in a straight direction, the ring gear No. 1, which transmits the main driving force to the axle, and the differential side gears No. 2 and 3 all travel at the same speed. In making a right turn, the left wheel is at the outside of the curve and must travel further than the inside wheel. Therefore, in a right turn the left wheel and side gear travel faster than the ring gear, and the right wheel and right side gear travel slower than the ring gear. The reverse is true in making a left turn. In a condition of the left wheel spinning and the right wheel stationary, the side gear attached to the right gear is stationary and the side gear attached to the left wheel and ring gear are rotating. And with the right wheel spinning, the reverse is true. If with the engine stopped and the ring gear stopped, the right wheel were to be rotated forward, the right side gear would also rotate forward; but the left side gear and the left wheel would rotate in the reverse direction. In other words, with the conventional differential, the two wheels are geared together with an independent compensating gear set which permits independent rotation of the wheels, but prevents applying more power to one wheel than the other. It should be remembered that the conventional differential will always drive the wheel easiest to turn.

The fact that the conventional differential divides the power equally to both wheels is a major disadvantage. In everyday driving, we encounter a variety of conditions that present poor traction to one wheel. For example, the coefficient of friction on concrete can equal only one under the best circumstances; while the coefficient on wet ice under the worst conditions can be as low as 0.15. With the conventional differential or compensating gear set, the total driving force on a vehicle can never be more than twice that which can be applied to the wheel with the poorest coefficient of friction. As an example, let us consider a 4000-lb automobile with weight equally distributed front and rear. Under ideal conditions, this vehicle with two driving wheels could have a force of 1000 lb available at each wheel. This means that a total force of 2000 lb could be applied to move the vehicle. With a coefficient of friction of 0.5 the available driving force has been reduced 50% to 1000 lb, and with a 0.15 coefficient of friction it is down to 300 lb. A coefficient of friction of 0.5 is considered good. With a conventional differential the loss in traction at one wheel results in the same loss of traction as if the condition occurred at both wheels. With a differential in which the load to the slipping wheel can be multiplied, the driving force can be appreciably increased; and the performance and usefulness of the vehicle will be greatly improved under all adverse driving conditions.

The second disadvantage of the conventional differential is that under a number of conditions there is uncontrolled load application at the driving wheels. For example, if we are driving down the highway and one wheel encounters poor traction such as sand, mud, or ice, either on or off the road, the power we are applying may easily spin the wheel with poor traction. When this wheel regains traction, the inertia of the spinning wheel plus the power which we are applying to the wheel will suddenly apply an extra large force to one of the driving wheels. This force will often have sufficient magnitude to affect the stability and control of the vehicle. Another example of this condition is very obvious when driving on a rough (corduroy) road, where the wheels are constantly leaving the road due to the bumps. As a wheel leaves the road, the major portion of the power is applied to this wheel, causing the wheel to spin. When the spinning wheel regains the road, a suddenly applied driving force is introduced at one wheel. We have all tried

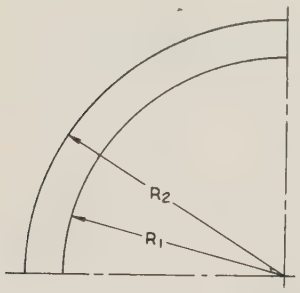

$$\text{DIFFERENCE IN DISTANCE-90 TURN} = \frac{2\pi R_2}{4} - \frac{2\pi R_1}{4} = \frac{\pi (R_2 - R_1)}{2}$$

$$R_2 - R_1 = \text{TREAD}$$

$$\text{REVOLUTIONS} = \frac{\text{DIFFERENCE}}{2\pi \times \text{TIRE RADIUS}}$$

$$\text{REVOLUTIONS 90° TURN} = \frac{\pi \times \text{TREAD}}{2} \div 2\pi r = \frac{\text{TREAD}}{4r} \qquad (r = \text{TIRE RADIUS})$$

60" TREAD 13" TIRE RADIUS

$\frac{60}{4 \times 13} = 1.15$ REVOLUTIONS DIFFERENCE IN 90° TURN

THE OUTER WHEEL MAKES 1.15 REVOLUTIONS MORE THAN THE INNER WHEEL.

$$\text{DIFFERENCE IN REVOLUTIONS-360° TURN} = \frac{2\pi (R_2 - R_1)}{2\pi r} = \frac{\text{TREAD}}{r} = \frac{60}{13} = 4.6$$

A CAR TRAVELING 60 M.P.H. ON A 1 MILE TRACK MAKES ONE 360° TURN PER MINUTE. THEREFORE THE OUTER WHEEL WILL MAKE 4.6 REVOLUTIONS PER MINUTE MORE THAN THE INNER WHEEL.

Fig. 1 — Relative wheel speed on curves

Table 1 — Limited Slip Differentials

Make	Name	Type	Differential Action	Transfer (Bias) Ratio	Application	Model	Torque Rating, lb-ft
Mack Truck	Mack Power Divider	Cam and plunger	Yes	3.00	Heavy-duty trucks Bus	C model	20,000–65,000[a]
Zahnradfabrik, Germany	Z-F	Cam and plunger	Yes	2.50	Off-highway vehicles, race cars	I	1200
						I_A	1800
						II	2200
						II_A	3600
						III	5000
						IV	9000
Timken-Detroit Axle Div.	High Traction	Variable velocity gears	Yes	1.50	Trucks		
Le Tourneau Westinghouse	Tournamatic	Gear thrust friction	Yes	3.00	Extra-heavy-duty vehicles	D	5500
						C	16,500
						B	32,500
Dana Corp.	Powr-Lok	Controlled friction clutches	Yes	From 2.00 to 5.00	Passenger cars Trucks	44	3000[a]
						45	3500
						53	4000
						60	5000
						70	7500

[a] Load (lb) on tires.

to accelerate a car with a conventional differential down a rough road, and know that the car has a very great tendency to fish-tail. There are also times we attempt to make a rapid start at a traffic light and find our progress retarded due to poor friction under one of the driving wheels. A limited slip differential prevents the wheel from spinning while it is in the air, and returns the wheel to the road at the same speed as the driving wheel, eliminating this condition.

Limited Slip Differential

A limited slip differential is basically a conventional differential in which the amount of slipping is controlled. They are also called bias or controlled differentials and may be further subdivided into their own individual types, such as: inertia, variable leverage, hydraulic, cam, variable velocity gear, and friction.

The first three of these have never proved practical and none are being used at present.

Table 1 shows a few of the characteristics of the limited slip differentials that are now available for all types of applications. A few of these have been made for several years and are still continued in limited quantities. All have been designed to retain differential action. The transfer or bias ratio varies from a low of 1.50 to a high of 5.00, with an average between 2.00 and 3.00.

Cam Type — There have been many versions of the cam type of differential all employing the same general principle — the use of sliding plungers, balls, or rollers over two cam surfaces in place of the usual differential gears. All of these have been abandoned except the Mack Power Divider and the Z-F in Germany.

The Mack Power Divider was originally designed in 1929 as a third differential on 4-wheel drive bogies and approximately 100,000 have been used for that type of application (Fig. 3). At present it is standard equipment as an interaxle unit on all 4-wheel drive bogies ranging in capacity from 32,000–100,000 lb. In 1948 it was also adopted as an interwheel differential for truck rear axles, as an extra cost item. It is now available on 18 tractor models, 33 truck models, and all transit bus models.

The driving member is a ring or cage carrying 24 radial plungers in two rows which are free to slide radially. An inner and an outer cam constitute the two driven members. The plungers are in contact with both the inner and outer cam surfaces. The two rows of plungers are staggered, as are the two rows of cam lobes on the inner cam. The outer cam, however, is indexed uniformly across its width.

Relative motion between the driving ring and either of the cams will cause the plungers to reciprocate as they ride over the surface of the cams. Because the two cams are opposed, inward motion of a plunger, as it surmounts the crest of one lobe, causes outward motion on its other end; thus, it forces the other cam to turn in the opposite relative direction. This action is exactly like a conventional differential, except being accomplished by cams and plungers instead of by gears.

In operation, the drive causes the cage to turn, carrying with it the 24 plungers. These plungers are at all times in contact with both cams; because of the angles of contact, they cause the two cams to be carried around with the cage, so that for normal straight driving the whole Power Divider revolves as a unit, driving both wheels at the same speed.

When differential action is required, as in rounding a curve, one cam will tend to overrun the speed of the cage while the other lags behind. The overrunning cam moves ahead of the plungers, either

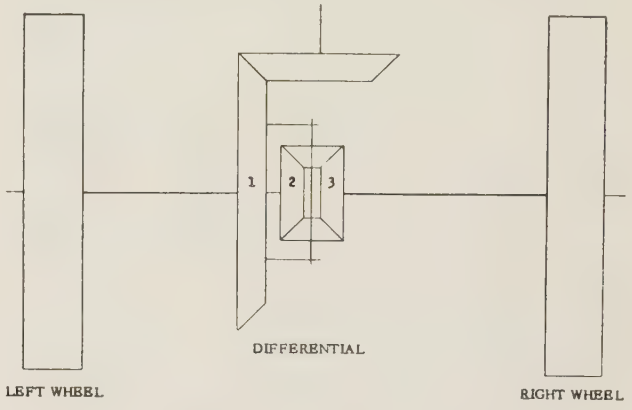

GEAR 1 = RING GEAR
GEAR 2 = L.H. DIFFERENTIAL SIDE GEAR
GEAR 3 = R.H. DIFFERENTIAL SIDE GEAR

SAME SPEED BOTH WHEELS STRAIGHT DRIVING	GEARS 1, 2 & 3 SAME SPEED
L.H. WHEEL FASTER RIGHT TURN	GEAR 2 FASTER THAN GEAR 1 GEAR 3 SLOWER THAN GEAR 1
R.H. WHEEL FASTER LEFT TURN	GEAR 3 FASTER THAN GEAR 1 GEAR 2 SLOWER THAN GEAR 1
L.H. WHEEL SPINNING	GEAR 3 FIXED GEARS 1 & 2 ROTATING
R.H. WHEEL SPINNING	GEAR 2 FIXED GEARS 1 & 3 ROTATING
GEAR 1 FIXED ENGINE STOPPED	ROTATE R.H. WHEEL FORWARD GEAR 3 ROTATES FORWARD-GEAR 2 & L.H. WHEEL ROTATE IN REVERSE

Fig. 2 — Schematic diagram of conventional differential

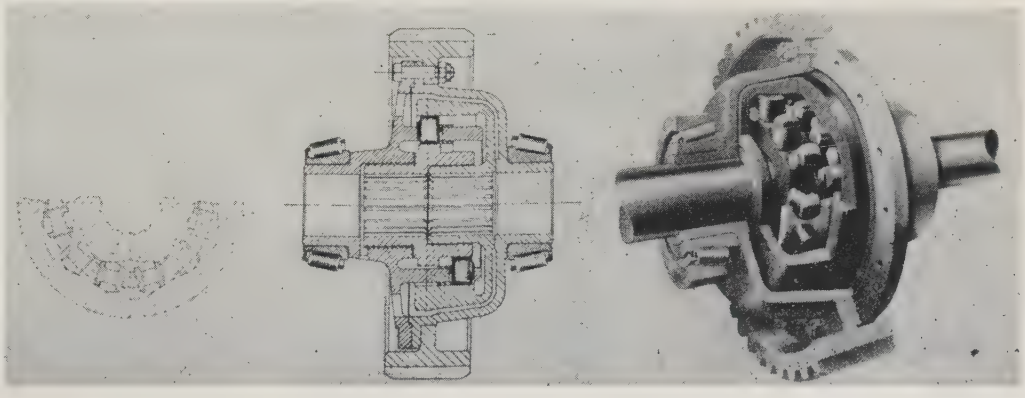

Fig. 3 — Mack Power Divider

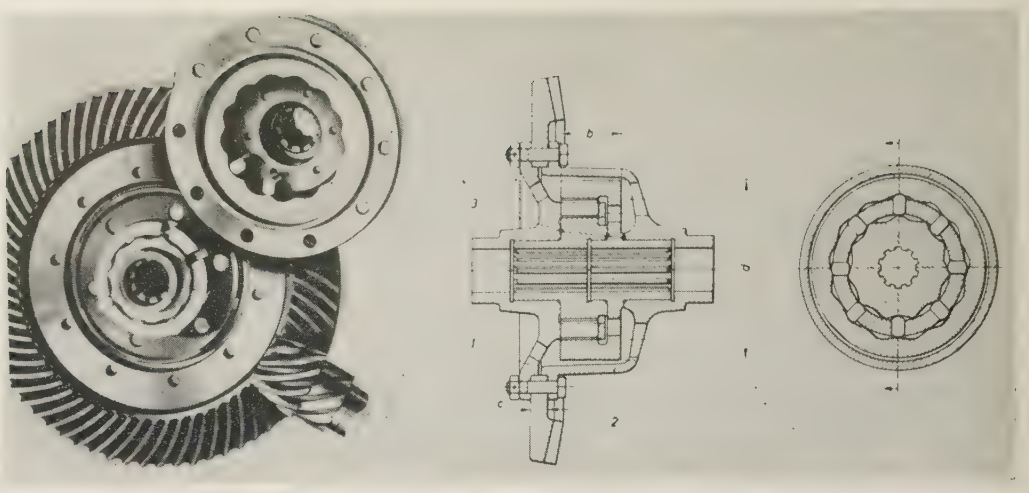

Fig. 4 — Z-F differential (Germany)

forcing them inward or allowing them to move outwardly as they travel over the cam surfaces. At their opposite ends they similarly work on the inclined surfaces of the lagging cam, forcing it to turn at a speed slower than the cage, which exactly corresponds with the overrun of the other cam. Thus, true differential action is effected, the average speed of the two cams being always equal to that of the cage, regardless of the difference in speed between the two cams.

Under immobile conditions, with one wheel slipping because of the cam angles, the torque required to drive the slipping wheel is multipled so that three times this amount of torque is made available at the opposite wheel. In other words, the cams and plungers provide a fulcrum effect favorable to the wheel with the greatest traction.

This action is controlled by the angularity of the cams and plungers; the angles may be changed in the design to suit requirements.

Fig. 4 shows the Z-F differential made in Germany by Zahnradfabrik Friedrichschafen, which is also of the cam and plunger type. These have been produced in various sizes for the past 25 years and many thousands were used during the last war in military vehicles by the German army. They are now principally being used in off-highway vehicles and racing cars.

Although the design and construction is slightly different, the principle and method of operation is the same as that described for the Mack Power Divider.

Variable Velocity Gear Type — Fig. 5 shows a comparison of the Timken High Traction Differential with a conventional differential. This has been used since the early 1930's and is the only one now available of the variable velocity gear type.

A special tooth form is used which causes the leverage between the mating teeth to vary at different indicies of rotation and in such manner that variations from minimum to maximum occur alternately with respect to the two sides.

Thus, when the left side has the maximum leverage from the pinion the right will have the least and vice versa. This alternation of leverage from side to side takes place every time the pinion turns one tooth.

When going forward, this has no effect when the whole differential turns together. In rounding a curve, also, there is no noticeable difference between

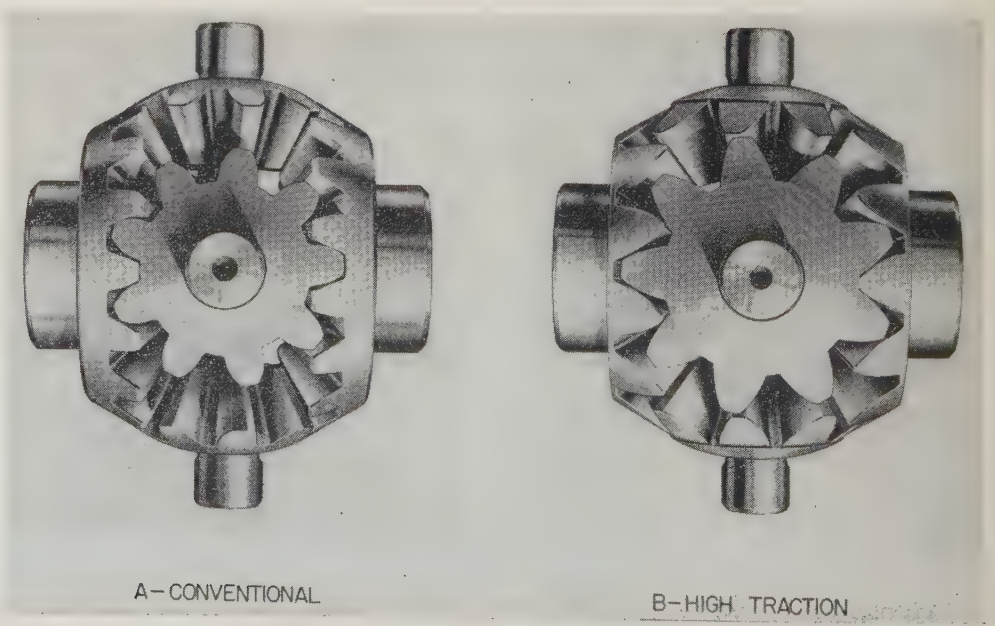

Fig. 5 — Timken conventional and high-traction differential

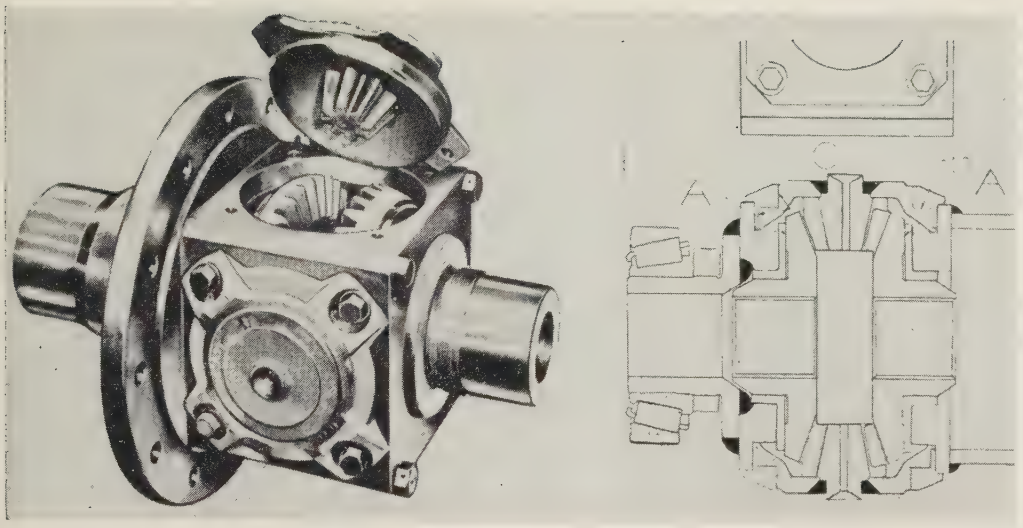

Fig. 6 — LeTourneau Tournamatic differential

its action and that of a conventional differential. Upon loss of traction by one wheel, however, the action is a pulsating one: first, one side and then the other being given for a part of a turn, thus providing an improvement in traction.

Friction Type — Probably one of the first methods of limiting the slip of differentials was to apply friction in the form of clutches or brakes to the side gears and pinions. Various methods of doing this have been employed and then discarded. Shown in Table 1 are two of the friction type that are now being used, the Tournamatic made by LeTourneau-Westinghouse and the Thornton Powr-Lok manufactured by the Dana Corp.

Fig. 6 shows the Tournamatic differential which has been used for several years for very-heavy-duty applications such as earthmoving equipment and off-highway vehicles. This is essentially a conventional differential which has been so designed as to incorporate as much internal friction as possible. In order to do this, special oversize bearings and thrust surfaces are used for the differential pinions and side gears. The differential functions the same as a conventional differential. However, under immobile conditions, advantage is taken of the total amount of friction available which includes the thrust on surfaces "A" from the two side gears and that from the four pinions, which includes the thrust load on surfaces "B" and the radial load on "C." It is claimed that from this accumulated friction a transfer (bias) ratio of as high as 3/1 is made available. All wearing surfaces have been made easily removable so that they may be conveniently replaced.

Fig. 7 shows the Powr-Lok differential. To explain the design, application, and accomplishments of a limited slip differential, we will use this as an example, as it is the unit with which we are most familiar. The problem of retaining the two main functions of the differential (namely, that it permit the wheels to travel at different speeds, and that the load be divided between the driving wheels) can be somewhat simplified if we maintain the conventional differential parts and merely add some device to restrict the differential operation under certain conditions. In the Powr-Lok we do this by attaching clutch members which will retard the rotation of the side gears under certain conditions. These clutches are actuated by the cam surfaces on the cross-pins, which in turn are actuated by the amount of load applied to the differential. The torque is transmitted from the differential case to the cross-pins and differential pinions to the side gears in the same manner as torque is applied in the conventional differential. The driving force moves cross-pins "B" up the ramp to the cam surface "C," applying a load to the clutch rings "D," and restricts turning of the differential through the friction surfaces of the clutches at "E."

Load Analysis

Let us now analyze the loading and forces that are encountered. For the purpose of this analysis, we are neglecting friction at the functional points as

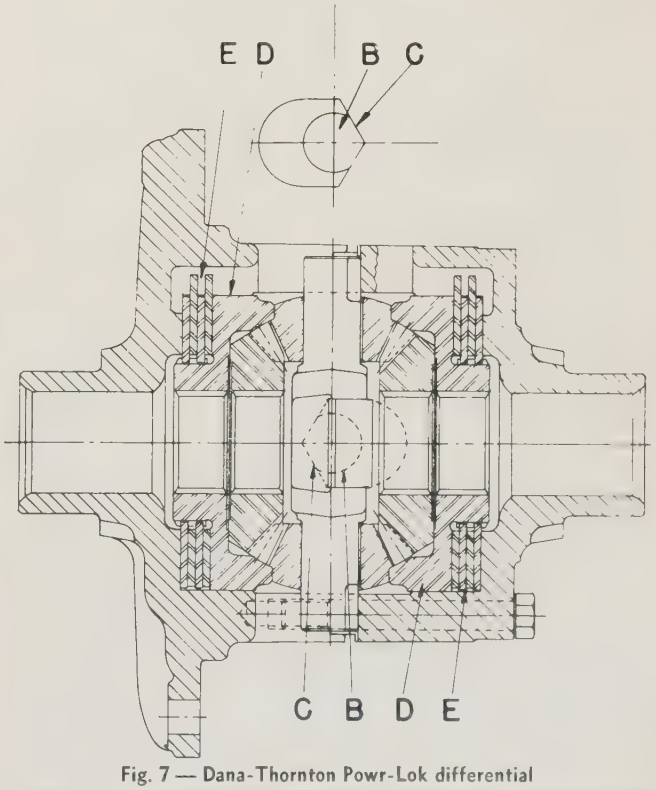

Fig. 7 — Dana-Thornton Powr-Lok differential

these are all well-lubricated. First, we must select the amount of transfer (bias) ratio we would like to use, then determine the size and capacity of the clutches that will be required to obtain this ratio. Since the clutch action is always relative to the applied load, this transfer ratio will remain the same for all loads and applications provided the clutches are not changed. Therefore, to determine the clutches required we need only to analyze the loads and forces under normal straight driving operation. The symbols we will use are given in Table 2. As shown by the power path diagram Fig. 8 and the force diagram Fig. 9, the torque is divided equally between both wheels and is being transmitted through both the clutches and the differential gears. The per cent of the load transmitted by each will be relative to the clutch capacity and the transfer ratio.

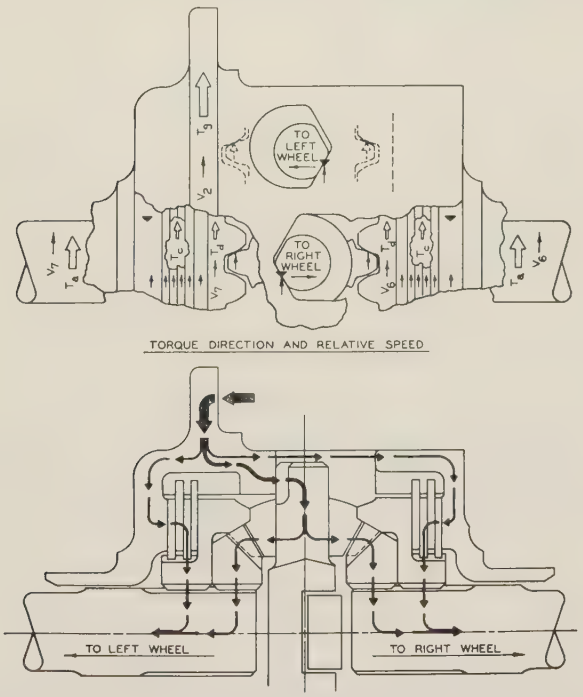

Fig. 8 — Power path diagram, Powr-Lok differential — straight driving

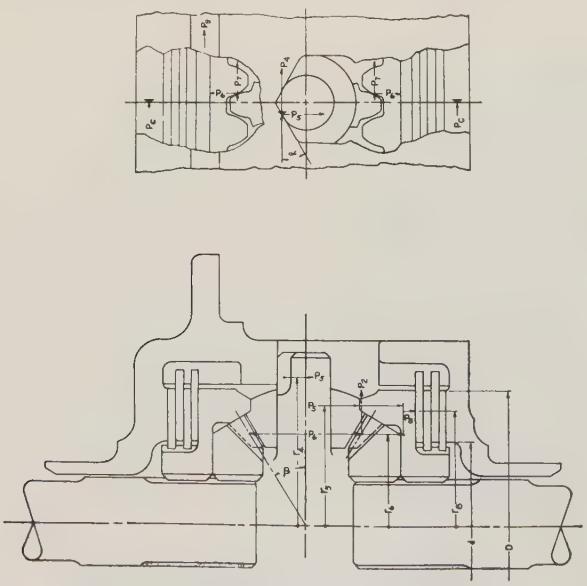

Fig. 9 — Force diagram of Powr-Lok differential

The torque capacity required by each (1) clutch to obtain the desired transfer ratio:

$$T_c = T_a - \frac{T_g}{R_t - 1.00} \quad (1)$$

The remaining amount of torque is transmitted thru the differential gears:

$$T_d = T_a - T_c \quad (2)$$

The load used to apply the clutches is controlled only by the force P_4 at the cam which in turn is determined by the amount of torque that is being transmitted only thru the differential gears T_d:

$$P_4 = \frac{T_d}{r_4} \quad (3)$$

The total clutch pressure P_8 is the sum of the force P_5 from the cam and the side gear axial thrust P_6:

$$P_8 = P_5 + P_6 \quad P_5 = P_4 \cot \alpha \quad P_6 = P_7 \tan \phi \cos \beta \quad (4)$$

$$P_7 = \frac{P_4 r_4}{r_6}$$

The torque capacity available T_{c1} at each clutch must equal that required T_c, if we are to obtain the desired transfer ratio:

$$T_{c1} = P_8 N f_8 r_8 \quad (5)$$

To determine the number of friction surfaces required to obtain the desired capacity:

$$N = \frac{T_c}{P_8 f_8 r_8} \quad (6)$$

The unit pressure against the friction surfaces may be determined by:

$$U = \frac{P_g}{A} \qquad A = (D^2 0.7854) - (d^2 0.7854) \quad (7)$$

Under immobile conditions with one wheel slipping the torque at stationary axle shaft and wheel is:

$$T_{a3} = T_{a4} R_t \qquad T_{a3} = T_{a4} + 2T_c \quad (8)$$

This analysis reveals a limited slip differential which can be made very flexible to fit a number of conditions. Locking action or load division in the differential can be controlled by the number of surfaces used, or it can be controlled by the cam angle on the cross-pins. These two items, of necessity,

Table 2 — Load and Force Symbols

All loads and forces are computed in lb, dimensions in in., and torque and moments in lb-in.

α = Cam angle
β = ½ pitch cone angle, differential pinion
ϕ = Tooth pressure angle, differential gears
A = Effective friction area of clutch disc
D = Outside diameter of clutch disc
d = Inside diameter of clutch disc
f_8 = Coefficient of friction, clutch surfaces
N = Number of effective friction surfaces for clutch
P_4 = Tangential force at cams
P_5 = Thrust force at cam and at pinion hub diameter
P_6 = Axial thrust force of side gear
P_7 = Tangential force at side gear
P_8 = Clutch pressure force
r_4 = Tangential force radius at cam
r_6 = Tangential force radius of side gear
r_8 = Mean radius of clutch friction surfaces
R_t = Transfer ratio (bias), the ratio of the torque available at the stationary wheel relative to the torque required to drive the slipping wheel
T_a = Torque at each (1) axle shaft and wheel, normal straight driving
T_{a3} = Torque available at stationary axle shaft or gripping wheel
T_{a4} = Torque required at the spinning axle shaft or slipping wheel
T_c = Torque capacity required by and transmitted through each (1) clutch
T_{c1} = Torque capacity available at each (1) clutch
T_d = Torque transmitted through each (1) differential side gear
T_g = Applied torque at the drive gear and differential case flange

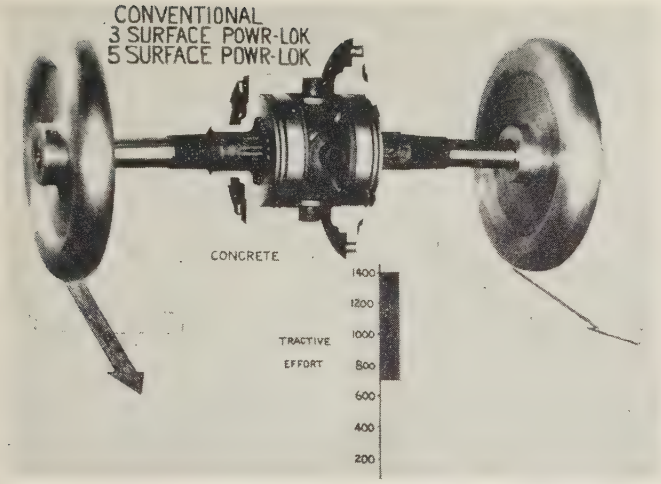

Fig. 10 — Equal traction performance of conventional and Powr-Lok differentials

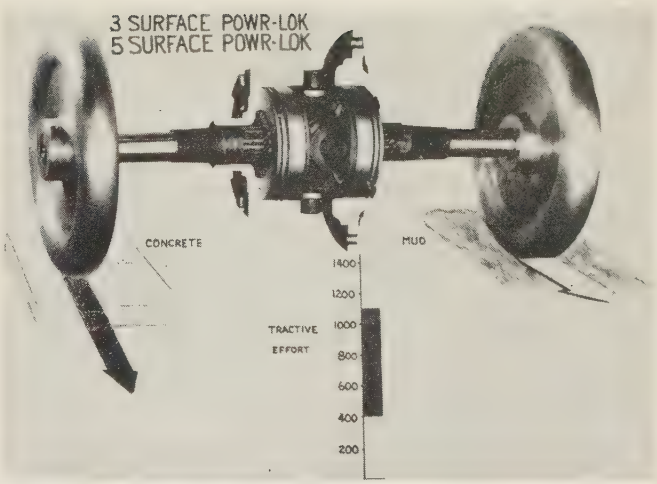

Fig. 11 — Concrete-mud performance of 3/1 and 5/1 Powr-Lok differentials

must be designed to give a unit which will operate in a satisfactory manner under today's passenger cars. We have found that a 45-deg pressure angle at the cross-pin with five friction surfaces in the clutch stack offers the best condition in this type differential. We also note from our load analysis that when no load is applied to the differential, there is no resistance to its operation, which is exactly the same condition we would encounter in the conventional differential. In other words, with no load applied to this differential, the wheels are free to rotate at their independent speeds.

All of the automotive vehicles that are in use today have sufficient power to provide full traction or to slip the wheels under some conditions of loading. In fact, most American cars have sufficient power to slip the wheels under almost all conditions of driving and loading. As the power is increased in the automotive vehicle, we need more traction to be able to use this power.

In Fig. 10 is shown a differential with equal traction under both wheels and a chart indicating an assumed total available traction and the traction under each wheel. Under these conditions the results are the same with both the conventional differential and the Powr-Lok using either the 3/1 or the 5/1 multiplication factor. Fig. 11 shows Powr-Lok with the 3/1 load multiplication factor under the condition of driving in mud. The total available driving force is now 1100 lb. This is 300 lb more than the conventional differential had under the same conditions. With a 3/1 differential, up to three times the load of the slipping wheel can be applied to that which has good traction. We have also included the differential having a 5/1 multiplication factor, which provides an available tractive force to move the vehicle of 1100 lb. This is 300 lb better than the conventional differential; however, it is equal to the differential with a 3/1 multiplication factor under this same condition of driving. This is due to the fact that the difference between the available force at the two wheels is not more than 3/1. In Fig. 12 is shown the 3/1 differential under the same conditions. With the 3/1 differential, the driving force is increased to 400 lb which is double that obtained with the conventional differential. Fig. 13 shows the differential with a 5/1 load division. Under the worst condition of driving the driving force is increased to 600 lb as against 200 lb with the conventional differential. In other words, we now have three times the force available to move the vehicle. Under this condition of driving, the full capacities of the 5/1 differential can be used. Fig. 14 is a summation of the charts indicating the tractive effort available with each differential, and their comparison to the conventional dif-

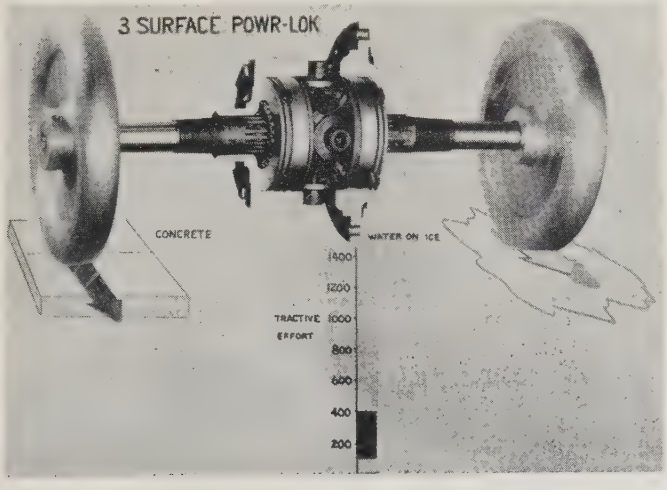

Fig. 12 — Concrete-ice performance of 3/1 Powr-Lok differential

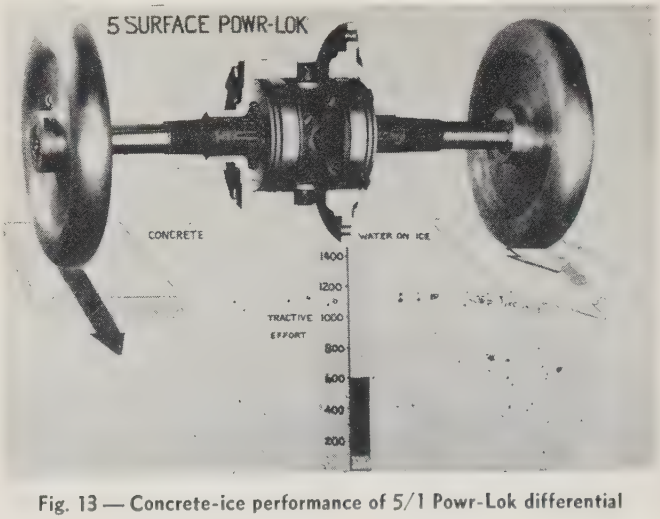

Fig. 13 — Concrete-ice performance of 5/1 Powr-Lok differential

ferential under various conditions of driving. With the 3/1 Powr-Lok the full available driving force can be applied to the vehicle with coefficient of friction as low as approximately 0.23. This range will cover approximately 80% of all driving conditions. With the 5/1 load division, full available driving force can be applied to the vehicle with a coefficient of friction down to as low as 0.14 under one wheel. With this differential the full effective driving force can probably be applied to the vehicle under 94% of all driving conditions. In fact, our experience has indicated that with a differential which has a load division of 5/1 it is almost impossible to find a driving condition where it is not fully effective, and where a full load cannot be applied to the wheel with the best traction.

With Powr-Lok limited slip differential, one wheel of the vehicle can be jacked up and run without providing traction to the wheel on the ground, as with a conventional differential. We do not recommend this procedure with the Powr-Lok; because if a load were applied to the differential by some external force, the differential would become effective and the vehicle would move. A study of this condition is interesting, as it illustrates that under some conditions of loading the limited slip differential becomes much more effective. As load is applied to the cross-pins of Powr-Lok, thrust is applied to the clutch members. This load can be applied in a number of ways. As weight is applied to the driving wheels, the load increases at the cross-pins, a vehicle going up an incline requires more driving force than a vehicle on the level, we may also apply a force to our clutch pins by applying a brake load at the wheels. For the purpose of this analysis, we are assuming that we apply additional load with brakes at the rear wheels only; and that the load is also equally divided at both rear wheels.

In Fig. 15 is shown the total traction available with a conventional, a 3-surface differential, and a 5-surface differential having additional load at the rear wheels. First, let us examine the conventional differential. We have a condition of 100 lb of traction at one wheel which is on ice, and 700 lb traction at the wheel which is on concrete. With no external force applied to the axle except that provided by the wheel on ice, a total traction force of 100 lb is available at each wheel, or a total of 200 lb. We now increase the load on the differential by applying 50 lb of brake load at each wheel. (We have loosely considered this 50 lb as being equivalent to 50 lb of traction at the wheel.) In this case, 150 lb of force is applied to the axle shaft with the wheel on ice. With equal division in the differential, this also means that 150 lb is applied to the axle shaft for the wheel on concrete. However, because an equal load is applied to both brakes at the wheels we must subtract the 50 lb from the 150 lb at the axle shaft, giving a resultant force of only 100 lb at the wheel. This again, gives us a total force of 200 lb of traction with our conventional differential. For further analysis, we apply a braking load of 400 lb at each wheel, which applies a total force of 500 lb to the axle shaft. However, again, we must subtract 400 lb of brake loading from each of the shafts and, again, the resultant force is only 200 lb in traction.

Now let us study the differential with the 3/1 locking action. In this case with the 100 lb traction at each wheel and on external load applied, we have a total traction force of 400 lb to move the vehicle. However, this is not sufficient and the difference in the coefficient of friction between the two wheels is such that the wheel is spinning on ice. We now add a brake load of 50 lb at each of the rear wheels as we did with the conventional differential. We find that the load on the axle shaft for the wheel on ice is now 150 lb but the load on the axle shaft for the wheel on concrete is now 450 lb. Subtracting the 50-lb brake load, we have the original 100 lb on ice plus 400 lb on concrete, or a total of 500 lb to move the vehicle. Again, this is not sufficient, so we increase the brake load to 200 lb. We now have 900 lb on the shaft for the wheel on concrete; and removing 200 lb of the brake load for a total of 700 lb, we have a total tractive force of 800 lb. In other words, we have doubled the effectiveness of the 3/1 differential in moving the vehicle. An increase in the brake load to 400 lb increases the axle shaft torque on the wheel on concrete to a total of 1500 lb. Removing the 400 lb of brake load, we could have 1100 lb for the wheel on concrete. However, the total capacity of the wheel on concrete is only 700 lb, so this is all that can be effective in driving the vehicle. The other 400 lb would be merely used in slipping the wheel on the concrete.

To complete this analysis, let us look at the differential with a 5/1 locking action with a load applied at the rear wheels. Again, with zero load applied we have five times 100 lb on ice, or a total of 500 lb for the wheel on concrete. This gives a total force

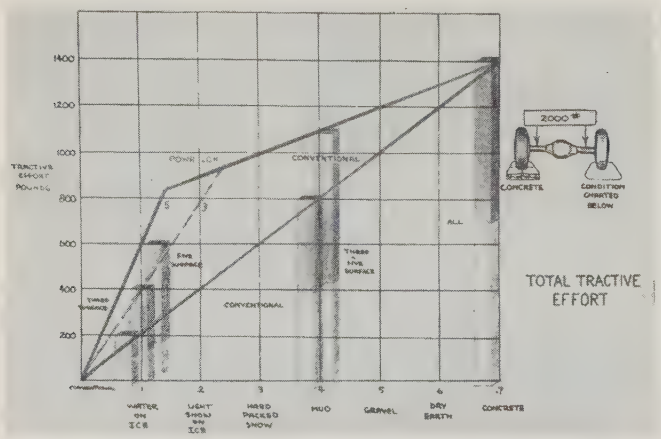

Fig. 14 — Total tractive effort, Powr-Lok versus conventional differential

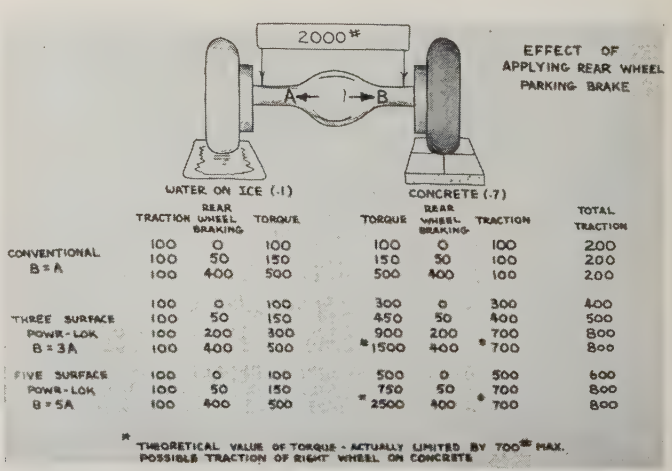

	TRACTION	REAR WHEEL BRAKING	TORQUE	TORQUE	REAR WHEEL BRAKING	TRACTION	TOTAL TRACTION
CONVENTIONAL B=A	100	0	100	100	0	100	200
	100	50	150	150	50	100	200
	100	400	500	500	400	100	200
THREE SURFACE POWR-LOK B=3A	100	0	100	300	0	300	400
	100	50	150	450	50	400	500
	100	200	300	900	200	700	800
	100	400	500	*1500	400	*700	800
FIVE SURFACE POWR-LOK B=5A	100	0	100	500	0	500	600
	100	50	150	750	50	*700	800
	100	400	500	*2500	400	*700	800

* THEORETICAL VALUE OF TORQUE - ACTUALLY LIMITED BY 700# MAX. POSSIBLE TRACTION OF RIGHT WHEEL ON CONCRETE

Fig. 15 — Additional torque from braking

of 600 lb. Assuming that this is not sufficient to move the vehicle, we again apply a brake load of 50 lb as with the other two differentials. With the 50-lb load applied with this differential, we now have 750 lb at the axle shaft for the wheel on concrete. Subtracting 50 lb of brake load, we have 700 lb at the wheel or a total of 800 lb to move the vehicle. In this case it takes very little load to increase greatly the effectiveness of this differential. Again, we have shown the case of 400-lb load applied in comparison with our conventional unit, in this case we have a total available force on the axle shaft for the driving wheel of 2500 lb or 2100 lb at the wheel, which is three times the load necessary to slip this wheel on concrete.

In conclusion, we think it is clear that this type of unit definitely increases the utility of a vehicle, and makes available much more of the power being built into the vehicles. We do not believe that the point of increased safety can be stressed too highly. The fact that the driver has complete control of the driving force under all conditions eliminates one of the factors that has been considered a cause of accidents. The Powr-Lok differential has been in production for over 3 years. There are some 200,000 of these units in the field in all parts of the country, and reports from the owners have been extremely satisfactory.

Acknowledgment

We want to acknowledge and thank those who have so kindly contributed to this paper: Dana Axle Engineering and Testing Departments; W. M. May, Mack Trucks Inc.; N. R. Brownyer, Timken Detroit Axle Division; E. W. Spannhake, LeTourneau Westinghouse Co.; Karl Fischer, Zahnradfabrik Friedrichshafen, Germany.

References

1. SAE *Quarterly* Transactions, Vol. 5, July, 1951, pp. 359–375: "Automotive Differentials," by L. R. Buckendale and L. G. Boughner.

2. SAE Transactions, Vol. 66, 1958, pp. 364–382: "Rear Axles — Today-Tomorrow," by R. P. Lewis and L. J. O'Brien.

3. *La Vie Automobile* (France), October, 1956: "Self-Locking Differentials."

DISCUSSION

Suitable Lubricant A Major Problem With Limited Slip Differential

— Frank Daley
General Motors Corp.

AS MESSRS. Lewis and O'Brien pungently indicate, there have been nonspin differentials as numerous as perpetual motion machines and some about as sensible. At least, we can now see plainly that we are finally out of the Land of Rube Goldberg with Spicer's Powr-Lok and a few of its contemporary designs.

My own experience, both literary and practical, shows the great effort made from the time of the "Krohn Kompensator" and before down to the present in simmering this kind of device down into something simple, producible, durable, and reliable. It further amplifies in the sense of practical contact with experimental units the advances in the last 10 years toward these same goals.

At Buick we have experimented with several of the different units mentioned in the paper, the most practical being the old Thornton No-Spin and the Z-F. We designed a Z-F unit for use in our experimental cars Le Sabre and XP-300 which worked admirably, but which was quite complex and somewhat lacking in good noise-free life. I think our recent experience with experimental Spicer units is much more favorable and supports the described advantages in traction power in marginal situations which can be of considerable assistance.

We have also observed certain other effects on handling and maneuverability which are a noticeable departure from the characteristics of the conventionally equipped car. Please note that I say these effects are different, not better or worse. They are things which I believe are readily "learned" by the driver in most cases and can be conceived as differences which are probably acceptable in the light of special advantages obtained with a unit such as Powr-Lok. Some of the observed differences in handling and response are:

1. Inadvertent loss of lateral rear-end stability. Both rear wheels break traction and hind-end swerves. This is most noticeable when starting and turning on ice, and requires deft application of throttle or a spin results.

2. Inside wheel drive on curves and turns. This increases tendency to understeer and requires a different technique of steering curves. It is advantageous in my opinion in a drift or slide type of turn, but there is some slight disadvantage in "feel" on normal curves.

Probably the greatest problem involved is that of establishing a suitable lubricant for use with the unit and ensuring against contamination with improper oils during the life of the car. The lubricant seems to be a factor in most cases of reported malfunction. Although somewhat deficient in antiscoring properties by our normal standard, we have worked successfully with one lubricant, as initial fill, without resorting to lubricating of axle drive gears. Careful initial break-in in this oil has given adequate scoring resistance on our test schedules, without undue chatter or noise in the differentials up to moderate test mileage. I do feel that, should we release a nonspin unit as an option, it would be necessary to attach a permanent tag to the axle filler plug which says in large letters, "*Whoa! — read Service Instructions,*" or words to that effect.

The marketing of a lubricant to insure field availability of a material entirely suitable to all the requirements of these special differentials is in a state of flux, and probably will require that the automobile manufacturer take special steps at least for the present and near future.

The interest shown so far in sales of the Powr-Lok unit indicates that the differences in cost, car handling, and special requirements which exist appear to be outweighed in the mind of the customer by the advantages obtained, especially in marginal traction conditions.

Lubricant Also a Problem at Studebaker-Packard

— M. P. deBlumenthal
Studebaker-Packard Corp.

WE OF Studebaker-Packard, as users of the limited slip differential manufactured by the Dana Corp. would like to augment the authors' paper by describing briefly our service experience with these units during the past 3 years.

The basic design of the limited slip differential, which we call Twin Traction, has not been changed since its adoption by Studebaker-Packard in 1956 on the Packard and Clipper cars. Modifications to improve the performance, however, have been made. The original design utilized a cone clutch to restrict rotation of differential and

was known as a 30-30 unit in that the cross-pin ramp angle and a friction ring cone angle were both 30 deg. Although the performance of the unit was satisfactory, it did possess one inherent weakness — that of chatter under a condition of surge of torque with one wheel on a low-friction surface. This chatter was caused by stick-slip action between the contacting friction surfaces of the cone clutch ring and the differential case. In the second design, which we are now using, a multiple disc clutch replaced the cone clutch. This unit uses a 30-deg ramp and three friction surfaces in each of the disc clutch packs. The latest design, which we will be using shortly, changes the differential cross-pin ramp angle to 45 deg and the number of effective clutch friction surfaces to five. This latest change increases the multiplication factor to 4/1 from the previously used 3/1.

With the use of these units in our passenger cars and trucks, we were concerned with the hazard involved in balancing of either rear tire and wheel assembly by a procedure which raises one of the rear wheels and spins it. Obviously, any normal friction in the spinning assembly, brake drag as an example, would cause a torque transfer to the stationary wheel and resulting movement of the vehicle. Our service manuals warn of the danger of this practice and all cars equipped with Twin Traction differentials carry an identification decal on the instrument panel. A few complaints have been received from service stations equipped with this type of wheel-balancing equipment.

We were also concerned that the limited slip differential be taken as a "cure-all" for all types of driving conditions. It is entirely possible that a vehicle thus equipped may encounter abnormal road conditions wherein it will become stalled in spite of the best efforts of the driver. It follows in these cases that when the force resulting from the coefficient of friction between the driving wheels and the road surface is less than the force required to move the vehicle, stalling will occur. This limitation has not proved to be a deterrent. This is evidenced by the fact that more and more car manufacturers are offering the limited slip differential and also by our own experience where the percentage of cars that we build with Twin Traction differential is constantly increasing. Currently, we install Twin Traction differentials in 12.8% of all of our 6-cyl models and in 52% of all of the 8-cyl models. It might be interesting to note that a police department in the Midwest and a taxicab fleet in the East, after operating a limited number of cars last year equipped with Twin Traction differentials, now have stipulated that all cars purchased hereafter shall be equipped with the limited slip differential.

The multiple-disc limited slip differential possesses many advantages over the original cone type. However, it does present a new problem; that of chatter on sharp turns under drive load conditions. Due to the low noise level of the chatter, it was believed that it would not become a source of owner complaints or concern. It was also determined that the "stick-slip" action between the clutch plates, the source of chatter noise, caused no material damage to the plate surfaces. Consequently, when it was released for production in January, 1957, we specified a sulfur-chlorine-lead base type of hypoid lubricant. The clutch plates, however, proved to be more sensitive than expected and in the field approximately 50% of the units had chatter that was considered highly objectionable by the owners. We then changed our initial fill and service lubricant specifications to a hypoid lubricant having a sulfur and phosphorus extreme pressure additive, along with a considerable percentage of properly compounded fatty oils. The special care to specify lubricity additive stemmed from the experience of the Packard Division, who were first to make available a production limited slip differential, plus experience in our own South Bend test cars. The problem of selecting the proper lubricant for the Twin Traction differential is complicated by the presence in one housing of two different mechanisms. The gearing demands an extreme pressure lubricant while the clutch plates, which provide limited differential action, seem to be satisfied only when fed lubricity agents which provide a film of low shear strength on the clutch friction surfaces.

Summarizing briefly, our lubrication road test data and field experience indicates the following:

1. To date we have only one lubricant that successfully eliminates all objectionable clutch chatter noise.
2. This lubricant cannot serve as a "break-in" lubricant to be replaced at a later date with an approved multipurpose gear lubricant.

We are concerned, therefore, that only one lubricant is currently available and even that one is available only as the initial fill or in service through our dealer organization. To our knowledge, there is no 100% satisfactory lubricant available at a filling station level. Further, not even one satisfactory service product is available in the export fields in view of the many import restrictions that are applied against service lubricants in countries such as Mexico.

Since the limited slip differential results in customer satisfaction, it is here to stay. Hence, the answers to lubrication problems must be found. Certainly, the primary antiscore emphasis that has been placed on rear axle lubricants will have to be modified to a compromise lubricant suited to the appetite of this rapidly growing infant, the limited slip differential.

Need for Limited Slip Differential on Passenger Cars Questionable

— W. R. Rodger
Chrysler Corp.

THE paper treats the subject of limited slip differentials quite thoroughly. Not having run any quantitative tests, we cannot confirm absolute values of traction obtained. We expect they vary widely with the lubricant used.

I believe the subject of limited slip differentials in passenger cars is a controversial one among engineers. Therefore, the statement that they are a necessity is debatable. They are probably a convenience whose advantages are realized occasionally by some drivers.

ORAL DISCUSSION

— Reported by V. J. Jandasek
Ford Motor Co.

Mr. Lewis: In the limited slip differential, the power transfer ratio affects the power going through the differential gears and, consequently, may be advantageous from the standpoint of durability. For instance, with a transfer ratio of 3/1, 50% of the power is transmitted through the gears and 50% is transmitted through the clutches.

O. J. Wolfer, Pure Oil Co.: Three of eight vehicles in my company's fleet have limited slip differentials. In tests with these, it has been observed that a difference of 0.25 in. in diameter of rear tires results in increased steering effort. This is attributed to the effect of the limited slip differential. As a result, it may be desirable to replace tires in pairs in order to maintain equal diameter and eliminate any additional steering effort which might otherwise occur.

In view of the potential problems which can occur with the installation of a wrong lubricant, it is necessary that all axle units be identified properly for field service.

Mr. O'Brien: Presently, considerable progress is being made in the direction of identification of units and it is anticipated that in the near future all differentials will be identified to insure installation of proper lubricant.

W. Baugh, General Motors Corp.: What is the effect of clearance between the parts of limited slip differential?

Mr. O'Brien: There is no difference in torque or torque multiplication as a result of clearance in the differential.

Mr. Rodger, Chrysler Corp.: What is the variation in torque with different lubricants?

Mr. O'Brien: There is no significant difference in torque multiplication factor as effected by lubricants.

How a Diesel Engine Rates Itself

W. J. McCulla, Caterpillar Tractor Co.

This paper was presented at the SAE Summer Meeting, Atlantic City, June 12, 1958.

BEYOND what point, or level of operation, will an internal-combustion engine break, melt, or rapidly wear out? Here are the elements of "rating" — a controversial subject to say the least, controversial because seldom does the experience of each of us extend beyond a limited range of engines and a limited set of conditions. A "rating" is often based upon theoretical considerations such as fuel/air ratio or some other index related to thermal loading. These factors are quite useful in making a rational selection of preliminary ratings. The approval of the engine, however, is essential before a rating can be considered final.

As spokesman for the engine, the manufacturer is required to say, in some sort of words, about how much engine he thinks he has created. Usually, he does this in terms of maximum allowable speed (rpm) and output (hp) both of which values may be accompanied by time limitations and environmental factors such as barometric pressure, temperature, allowable fuels, and the like.

But the engine manufacturer is not the only party who has ideas. The engine user is also involved, and in our experience he often knows more about what the engine can and will do *for him* than does the manufacturer. So the engine user, through use of the engine, also puts a rating upon it. Although this may be more modest than the engine manufacturer's rating, in our experience it more often far exceeds the manufacturer's rating as to speed, load, or both.

A typical user operates his engine at the load that returns the highest net profit. To illustrate by exaggerated example, this user might (to the horror of the designer) so rate and use his engine as to make rebuilding mandatory every weekend — and our experience persuades us that the user would do just that if he were convinced it would make him the utmost in profit.

We would like to make the long-term experience of users a direct factor in the rating of an engine. Unfortunately, before the engine is sold to the first customer, its abilities must be made known. The manufacturer, then, has no choice but to publish some sort of "rating," some sort of guide which says what he thinks the engine will do under certain conditions. He can guess at this, he can determine it in the laboratory with a limited number of engines and a selected set of conditions, or he can combine laboratory information with past field ex-

SETTING ratings for diesel engines takes laboratory testing and field experience for critical parameters such as smoke, piston temperature, and exhaust temperature.

Rating is based upon theoretical considerations, plus the approval of the engine itself. Factors in rating considerations include a knowledge of the application of the engine, and whether its use is to be intermittent or continuous.

Ratings by the manufacturer are not always accepted by the engine user, however. The user will run the engine at the load most profitable for him, which may be above or below that recommended by the manufacturer.

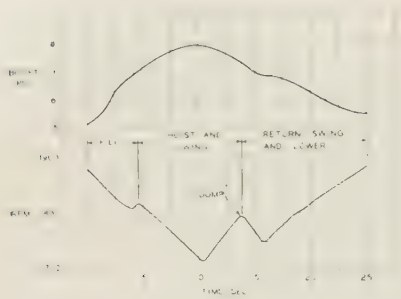

Fig. 1 — Power shovel load cycle

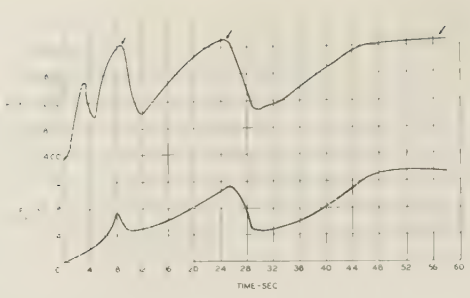

Fig. 2 — Wheel tractor load cycle

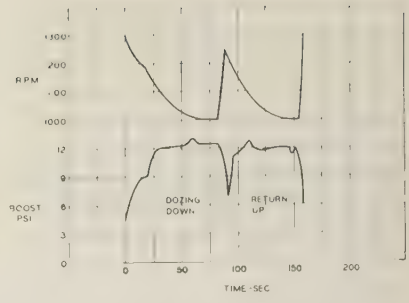

Fig. 3 — Load cycle of track-type tractor with bulldozer, 40% grade

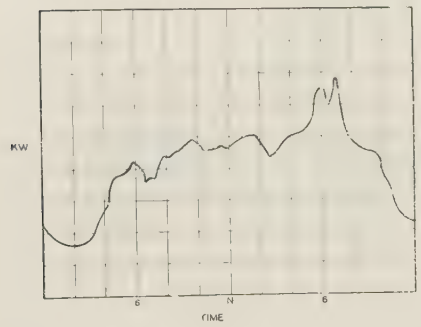

Fig. 4 — Typical kilowatt demand curve of small town

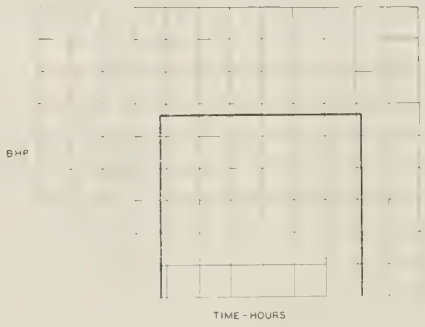

Fig. 5 — Standby power demand

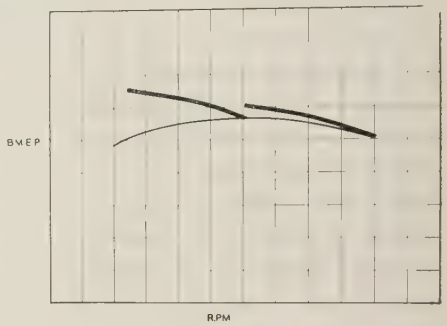

Fig. 6 — Torque rise from rating points

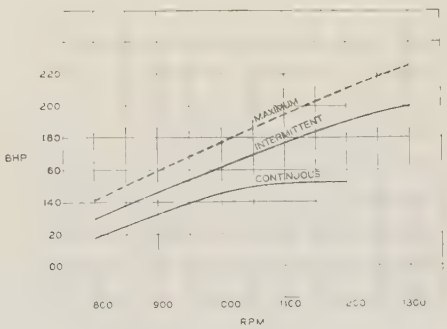

Fig. 7 — Rating curves of D342 engine

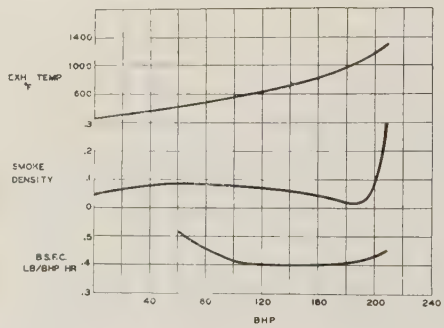

Fig. 8 — Typical part-load curve naturally aspirated engine

perience to aid him in interpreting what the engine is saying.

At our company we do not guess; we spend a lot of time and a lot of money letting the engine talk to us in the laboratory and in the field before we sell it, and we then publish a rating. But the rating the engine finally gets in the market place is the rating it establishes for itself in the user's hands — and this is to a large degree an economic, not an engineering, determination.

Applications and Road Cycles

In order to know what questions to ask the engine, the manufacturer must have an intimate knowledge of the applications for which the engine will be used. In a small to medium size, medium to high speed engine of the type built by Caterpillar, applications range from those having variable speed and variable load requirements to those of constant speed and constant load. First consider those highly variable both in speed and load. A typical example would be an excavator or power shovel. Operations involved here (Fig. 1) are filling the bucket, the swing, dump, and the return swing. Periods of high load occur during the filling of the bucket and at the beginning of the swing and return swing portions of the cycle, while periods of no load occur during deceleration, as at the end of the swing or when lowering the bucket.

Another example of highly variable speed and load occurs in the wheel tractor with a scraper or wagon. The load cycle shown in Fig. 2 is a simple one for this machine, involving only operation in four gears during acceleration from a stop with a loaded wagon. Even so, three times in less than a minute the load drops to zero and the engine speed is reduced, with alternate periods of heavy load and increasing speed. Add to this the effect of loading a scraper, of traveling up and down grade, loaded and empty, and you have a normal earthmoving cycle. Overspeed up to 50% over rated speed is common when traveling downhill pushed by a loaded wagon or scraper.

We see an example of less variable speed and more consistently high load in the track-type tractor, whose load cycle when equipped with bulldozer (Fig. 3) shows forward and reverse operation without intermediate shifting of the gears, with the load absorbed suddenly and held at a high value.

An example of constant speed and variable load is that of an electric generator set taking the full residential lighting load of a small community (Fig. 4). Here the speed is constant, load variations are large but occurring in relatively small

increments to give a slow rate of change throughout the day.

Constant speed and constant load are typical of a generator set installed as the standby power unit in, for instance, a municipal water works, as indicated by the load cycle in Fig. 5. Here, except for periodic check starts, the engine does not operate at all until power is suddenly not available from the normal source. Although the load is continuous, it can be much higher than the normal continuous load since the engine will operate very few hours in a year's time. A higher rate of wear or tendency to promote deposits is not critical because of the few hours involved, provided that the engine is mechanically stable and can be depended upon to hold the load for any required period.

An irrigation pump typifies applications where both speed and load may be absolutely constant for days at a time.

An engine performance characteristic which is essential to the earthmoving applications described is that of a rising torque curve as engine speed is decreased. Most applications of this type require at least a 10% increase in engine torque as the engine speed is reduced to about two-thirds rated speed, as shown in Fig. 6.

Preliminary Ratings

Since obviously not all of these applications can be described in detail by a rating curve we separate them into two groups and describe them as either intermittent or continuous in nature (Fig. 7). Since, in general, an intermittent application requires appreciably less fuel per hour than a continuous application, the intermittent rating can be appreciably higher. On our specification sheets we describe intermittent horsepower as a rating for use in variable load applications where the duration of sustained full power output is 1 hr or less. We have intentionally omitted a "rated" output curve from this figure because of its gradual elimination from our specification sheets. As we learn to make engines live at consistently high ratings, there seems little reason to differentiate between unlimited continuous operation and that of 12-hr duration. Even the well-known British Standard Specification No. 649 is being revised to eliminate the 12-hr rating in favor of a continuous rating plus 10% overload capacity. The continuous curve in Fig. 7 is obviously not a fixed percentage of the intermittent curve. For reasons to be discussed, this relationship is not the same on different engines or at different speeds of the same engine.

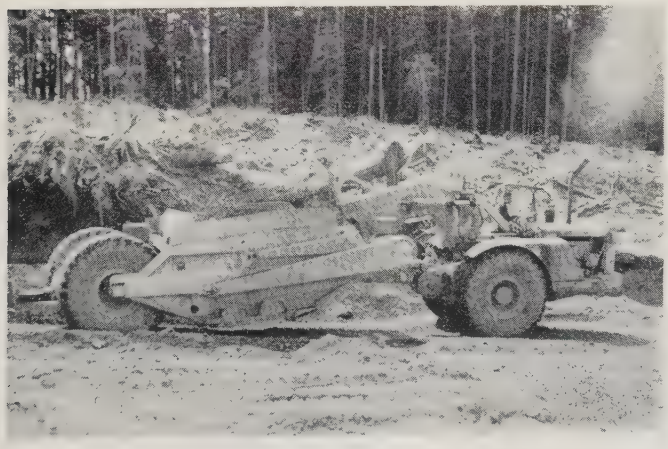

Fig. 9 — Exhaust smoke beyond acceptable limits

With loads of this type in mind we then ask the engine for its help in establishing preliminary ratings. The engine is far from a silent partner in this rating procedure. It is willing to talk to those skilled in its language. Its eloquence is limited, however, to that of its interviewer, in that it normally answers only those questions that it is asked. The questions that we ask turbocharged engines on the one hand, and naturally aspirated engines or those with mechanically driven blower on the other hand, are somewhat different because of the inherent difference in these engines and in the type of limits which apply.

Rating Unblown Engines

Let's consider first the more familiar type of engine, that is, the naturally aspirated or that with a mechanically driven blower. Part-load curves (Fig. 8) run on these engines on the dynamometer will have a very consistent form for engines of the same type and operating in their normal speed range. One thing noticeable on the part-load curve of pre-combustion-type engines such as built by Caterpillar is that the smoke density curve shows a very distinct break at a point near maximum output. At loads below this point the smoke is not visible in the exhaust. At loads above this point it rapidly becomes more and more dense until maximum load is reached. This type of engine can operate, therefore, comparatively close to its maximum output with a smoke-free exhaust. Here, if we choose an arbitrary value of smoke density such as 0.3 on the Caterpillar smoke meter, a point beyond the knee of the curve where the smoke is becoming clearly visible in the exhaust, it becomes a useful starting point for selecting ratings.

Normal atmospheric variations of temperature and pressure can cause changes in atmospheric density of up to about 8%. Therefore, to avoid operation with objectionable smoke in the exhaust at rated speeds and loads under normal variations of ambient conditions, the intermittent rating is tentatively selected at 8% below the load at which 0.3 smoke appears as measured on the Caterpillar smoke meter under standard laboratory conditions of 29.6 in. of Hg and 90 F. Fig. 9 is an example of a smoke level somewhat over 0.3. This machine is operating with excess fuel for the ambient conditions, caused possibly by altitude or by opening the fuel rack beyond normal settings. The tentative rating at 92% of the 0.3 smoke point is checked to see that 10% torque rise at two-thirds rated speed is possible at any selected point along the rating curve. If not, then the rating is reduced as required. If the initial performance is not what we consider normal for our engines, further development takes place on a single-cylinder test engine and results are checked on the multicylinder engine before ratings are selected.

Obviously, we're not going to run extensive tests at every point on this proposed rating curve. It's necessary, therefore, that we know what the most critical points are with reference to many of the factors which can affect operation. Fortunately,

there are certain family characteristics of engines which tell us about how certain limiting factors will vary with speed and load. Therefore, only spot checks are necessary on each engine to see that these things are behaving normally before our test points are selected.

Fig. 10 shows, overplotted on our proposed rating curve, some constant piston temperature lines. Piston temperature affects deposits, wear, and ring sticking; and since there is a point where piston temperature begins to increase rapidly, we can choose a level below this point. From the standpoint of piston temperature alone, any point to the left of this constant temperature line is a safe continuous rating. Similarly, a higher piston temperature can be selected as a limiting value for an intermittent rating where strength and fatigue life for the piston are still adequate to meet the greater loads. On either rating curve the piston becomes cooler as speed is reduced. The continuous curve could even blend with the intermittent at lower speeds with a safe margin of piston temperature.

Fig. 11 shows a line of constant exhaust temperature and its relation to the proposed ratings. The curve of exhaust temperature shows a trend similar to that of piston temperature but much less pronounced. It is the shape of the exhaust temperature curve that keeps us from raising the continuous curve to match the intermittent at lower speeds. Exhaust temperature is not as much a limiting factor in any case as is piston temperature, since we have valve materials and facings that will function at present exhaust temperatures. However, we can select a value that is reasonable for the materials that we choose to use. Operation below this particular curve then is acceptable from the standpoint of exhaust temperature.

The rate at which heat is released in the cylinder, of course, has a definite effect upon the temperatures of the various parts of the combustion system. Therefore, a plot of constant fuel rate in lb/hr/cu in. displacement of the cylinder is another useful line limiting operation. Since fuel rate is closely related to thermal loading, note that on both rating curves the fuel rate (and, therefore, the heat load) is reduced as speed is decreased (Fig. 12).

Smoke, as indicated by the dotted line in Fig. 7, although of itself not harmful for short periods, is a useful visual aid to limiting the rating. Smoke joins with exhaust temperatures in cautioning us to keep the continuous rating at low speeds somewhat below the intermittent rating to avoid any possibility of a smoky exhaust under extremes of climatic conditions.

Acceptable peak pressure (Fig. 13) although subject to change depending upon piston, piston ring, bearing, and connecting rod design, is a definite limit at any stage of development of an engine.

If the engine is operated for long periods at loads and speeds where oil deterioration becomes excessive, then harmful deposits can be formed and oil viscosity can become dangerously high. This can make ring sticking a problem and even reduce oil flow and impair engine lubrication. The general location of this region is shown in Fig. 14. Its extent is greatly affected by the quality of the lubricant.

If we bring all these factors together into a single curve (Fig. 15), we can see that our rating curves are pretty well circumscribed by limiting conditions. Intersection of various limiting points are obvious locations for test. To operate test engines under conditions worse than those proposed for ratings, both for safety factor and to accelerate the test, it seems obvious that an increase in speed at full load will offer the most promise.

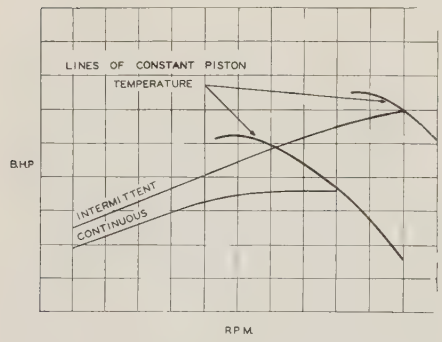

Fig. 10 — Constant piston temperature

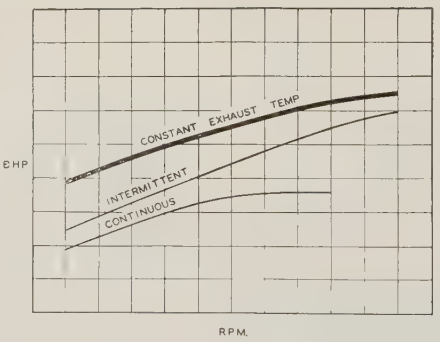

Fig. 11 — Constant exhaust temperature

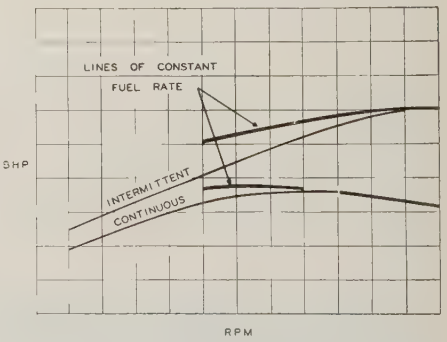

Fig. 12 — Constant fuel rate

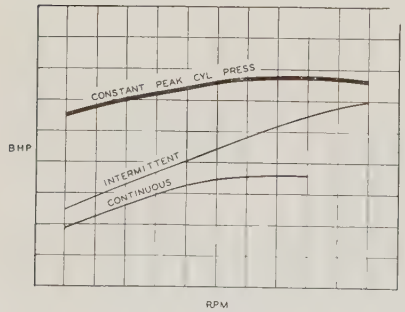

Fig. 13 — Constant peak cylinder pressure

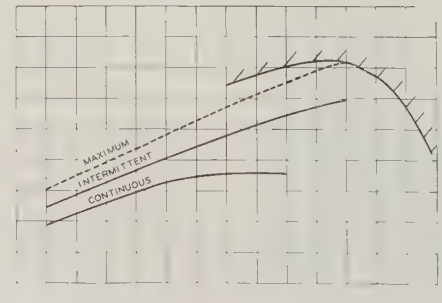

Fig. 14 — Region of excessive oil deterioration

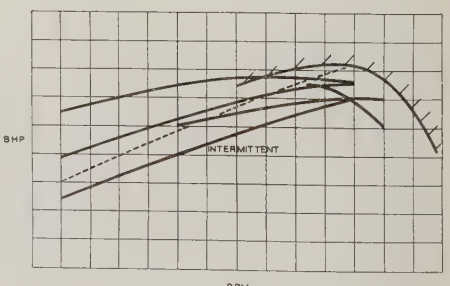

Fig. 15 — Combined limits from previous figures

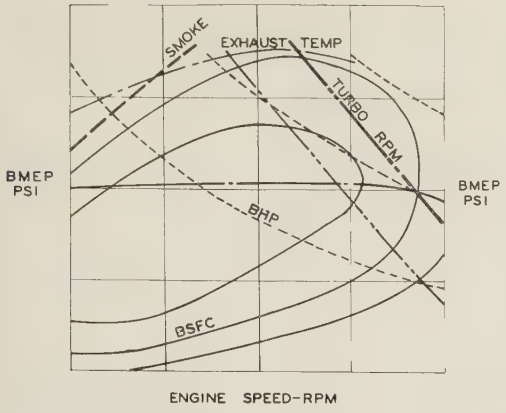

Fig. 16 — Performance of turbocharged engine (constant value lines)

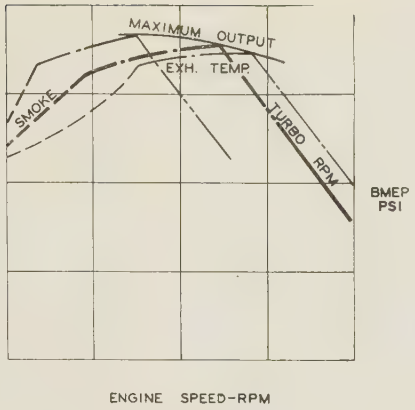

Fig. 17 — Umbrella curves of performance limits with three turbine nozzles

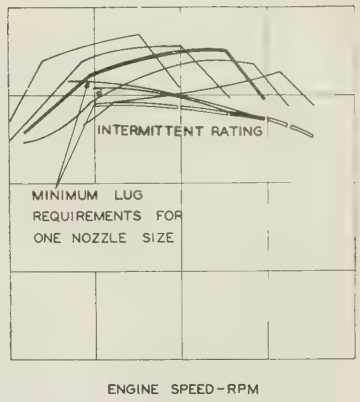

Fig. 18 — Lug performance of turbocharged engine from intermittent ratings

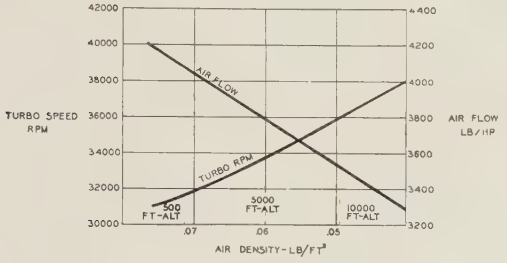

Fig. 19 — Constant bhp altitude performance of turbocharged engine

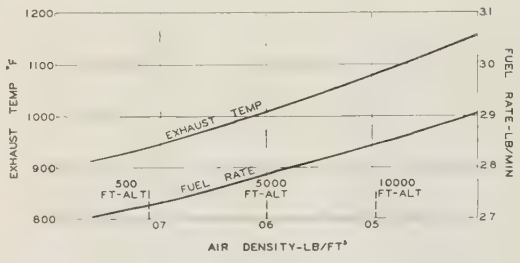

Fig. 20 — Altitude performance of turbocharged engine, constant hp

Altitude effects do not concern us greatly in choosing ratings for the naturally aspirated engine provided that the proposed ratings are suitable for a specified altitude. Maximum output of the naturally aspirated engine changes almost in direct proportion to air density, while part-load operation is unaffected to rather high altitudes. Since the lug curve from any point on the intermittent curve reaches 0.3 smoke under normal ambient conditions, a reduction in air density waves an obvious black flag if fuel delivery is not adjusted accordingly. This is actually a favorable situation, in that even customer-adjusted racks will approximate the intermittent rating. The operator accepts the appearance of smoke on lug as a sign that the engine is working. There is small wonder that the rack limiting nut has since the early 1930's been called a "smoke screw."

Rating Turbocharged Engines

Other limits become significant as we look at some of the characteristics of turbocharged engines. Here in Fig. 16 we have part-load curves plotted into a composite form showing the addition of turbocharger speed as a matter for consideration. Manufacturers of turbochargers, of course, have certain limits which they specify based upon design considerations. These limits are expressed as rotational speed, exhaust temperature, and, in some cases, surge of the compressor. At times, exhaust smoke becomes a limit at a lower bmep than does surge and thus becomes the controlling factor. This grid of curves is characteristic of an engine with a single fixed nozzle in the turbocharger. A change in nozzles to favor operation at some other speed in effect makes this a different engine altogether.

If we plot the so-called umbrella curve of turbocharger rpm, exhaust temperature, and exhaust smoke or surge for a particular nozzle, that is, if we lift it from Fig. 16 and plot it by itself we have something as shown on Fig. 17. From other tests we add umbrellas depicting operation with two additional nozzle sizes. If we connect the points of intersection of exhaust temperature and turbocharger rpm or, as in the case of some boundary matching conditions, exhaust smoke or surge and turbocharger rpm, we can plot a line representing maximum output of the engine at these limiting points. Obviously, to operate on every point along this curve we would have to have either an infinite variety of nozzles or a continuously variable nozzle, neither of which at present appears quite practical.

Ratings for the engine with free-running turbocharger must, therefore, be chosen within the bounds of a practical number of fixed nozzles. At any rated engine speed the turbocharger speed must be within limits. During lug from any rating the exhaust temperature or smoke must be within reason. In Fig. 18 the dark lines represent the umbrella curve of a representative nozzle and the section of the intermittent curve where this nozzle is applicable. A similar relationship can be envisioned for the other umbrella curves and the associated segments of the intermittent rating curve.

It is well-known that the turbocharged engine tries to be self-compensating where altitude is concerned. This characteristic demands consideration when ratings which use the full capability of the turbocharger are being considered. Figs. 19 and 20

show how the Caterpillar D397 engine behaves with a change in air density when the output is held at a constant 400 bhp at 1200 rpm. Turbocharger speed increases quite noticeably as the turbo tries to make up the weight of air lost per unit volume. That it fails to quite do so is shown by the reduced weight flow. With the loss of air, additional fuel is required to produce the same power. Since the fuel rate increases while airflow decreases, the exhaust temperature must rise. If, on the other hand, we hold turbocharger speed constant (Fig. 21) we must decrease fuel rate to do so. Thus, horsepower and, of course, airflow are reduced while exhaust temperature is nearly constant.

To permit some flexibility of movement, intermittent and vehicle ratings of our turbocharged engines are such as to permit operation at full power up to a 2500-ft altitude without exceeding limits of exhaust temperature or turbo rpm. Ratings are reduced for each 2500-ft increase in altitude beyond that point to hold the same turbo speed and exhaust temperature. Operation at continuous ratings is, of course, possible at much higher altitudes, since the margin of turbocharger potential is greater.

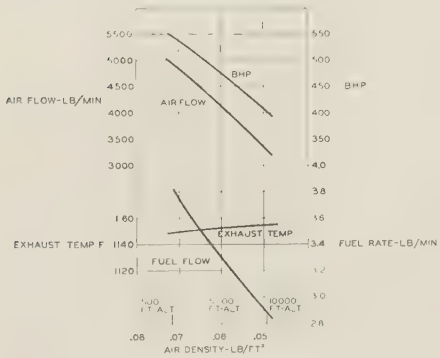

Fig. 21 — Altitude performance of turbocharged engine, constant turbocharger rpm

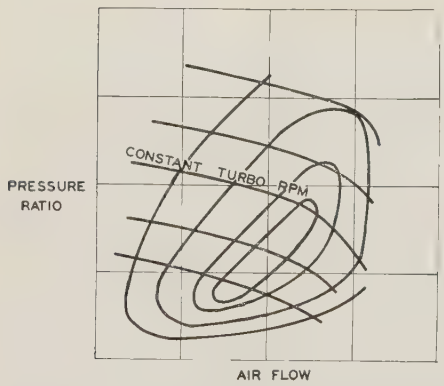

Fig. 22 — Turbocharger compressor map showing near parallelism of speed and pressure ratio

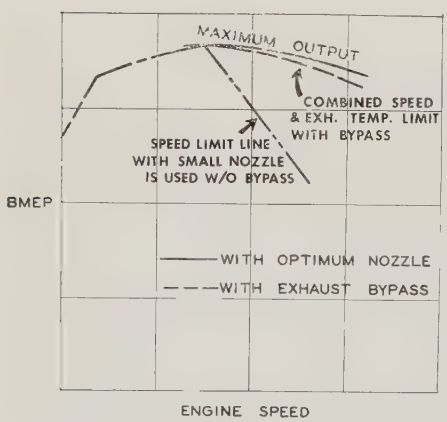

Fig. 23 — Reduction of maximum output with use of small nozzle and exhaust bypass

Testing is done with oversize nozzles, giving lower turbocharger speed, in order to operate at fuel/air ratios and exhaust temperatures equal to those at 2500 ft.

An additional type of engine that requires special rating consideration is that with a speed-limited turbocharger. We have mentioned the lack of a continuously variable nozzle to maintain high air delivery over a wide engine speed range. Much the same effect can be had by using a small nozzle in the turbine and bypassing excess exhaust gas to limit the speed. We use an automatic device sensitive to pressure ratio to control turbocharger speed. Reference to Fig. 22 shows that, in the useful operating range of a typical compressor, pressure ratio and speed are closely related. Under constant ambient conditions a boost control would be equally effective. The pressure ratio control has the added advantage of preventing turbocharger overspeed at altitudes above normal limits.

As you may suspect, the gain in operating range is accompanied by the loss of performance at full speed. The small nozzle causes higher back pressure and somewhat higher exhaust temperature, so that the maximum output line drops as shown in Fig. 23. On this plot the dashed line represents the combined limit of exhaust temperature and turbocharger speed when the control is used. The dot-dash line extending downward to the right is the speed limit line when the small nozzle is used without the control. Although a separate test evaluation is not required, the rating must be reduced to compensate.

Durability Tests

We are not concerned in this discussion with testing intended only to evaluate mechanical components or engine parts not affected by load. However, it is pertinent to describe certain tests related to rated speed.

A new engine is first tested for mechanical stability, fluid flows, and running clearances, and any obvious faults are corrected. We then run preliminary part-load curves from which to set the tentative ratings for laboratory running. I don't mean to imply that we had no idea up to this point what the ratings would be. No serious marksman shoots without first setting up a target. These first runs, however, do tell us whether our sights need adjustment.

When we are satisfied that the engine is behaving normally we determine the fuel rack setting to produce the proposed intermittent horsepower at the highest rated speed. It is obvious from the discussion of engine limits and load cycles that this is the most critical point of operation. All of our testing with reference to loaded operation is related in some way to this one rating point. Our actual test is run, however, at a higher speed. This puts us in the criti-

cal area of operation described in Figs. 10–14. This is done basically to provide an accelerated test and show up weak points in need of further development as quickly as possible.

We aren't surprised if the engine grumbles a bit. We're asking it, in effect, "Isn't this load a little too high for continuous operation?" On this run, with respect to highest rated load, we are using more fuel, the piston and rings are hotter, the peak pressure slightly higher, oil flow is greater, and its heat absorption more rapid. The valves are running hotter and seating more violently. Tendencies that should appear in this test include piston and valve deposit formation, exhaust valve dishing, and oil deterioration. We are deliberately working the engine harder than we expect it to be used by the customer. We still expect the engine to give a good account of itself to provide an extra margin of performance for abnormal conditions it may encounter.

The piston in Fig. 24 is from an engine that did not accept the rating at its existing state of development. Too close a clearance with the liner restricted lubrication, causing overheating, deposit formation, stuck rings, and scuffing.

The valve in Fig. 25 shows unacceptable dishing from the same test.

Certain abnormal conditions of field operation can cause the engine to run hotter than is usual. Testing at a generally high temperature level tells us how the engine will react to such conditions. The high temperature level causes piston-to-liner clearances to become closer. Oil viscosity becomes lower, oil films thinner in bearings and on cylinder walls. Temperatures are higher and temperature gradients steeper in the cylinder head. Oil deterioration with its side effect of deposit formation is more likely. The piston in Fig. 26 shows light scuffing and uneven bearing after this test.

I laid some stress on the variability of load that rubber-tired earthmovers undergo. We once had a mild epidemic of piston top land and top ring breakage in such a machine. You know what an epidemic is. It's the occurrence of the same trouble in two engines in one distributor's territory. The common factors relating these failures were rapid load cycles, altitude (about 7000 ft), and cold weather. These factors appeared to be related to rates of pressure rise in the cylinder. This problem resulted in the development of a test to duplicate field failures in the laboratory. By controlling the

Fig. 24 — Piston after overload test

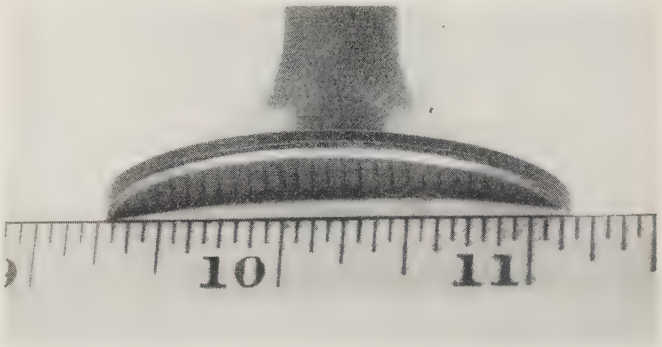

Fig. 25 — Dished valve after overload test

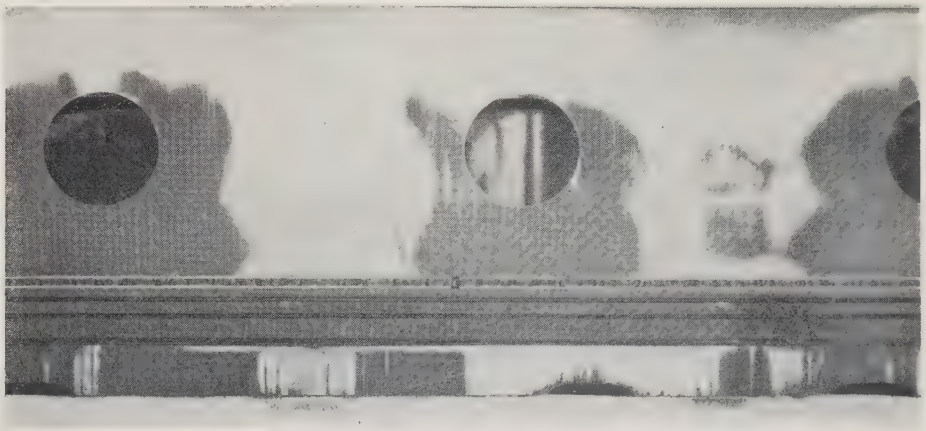

Fig. 26 — Piston after high engine temperature test

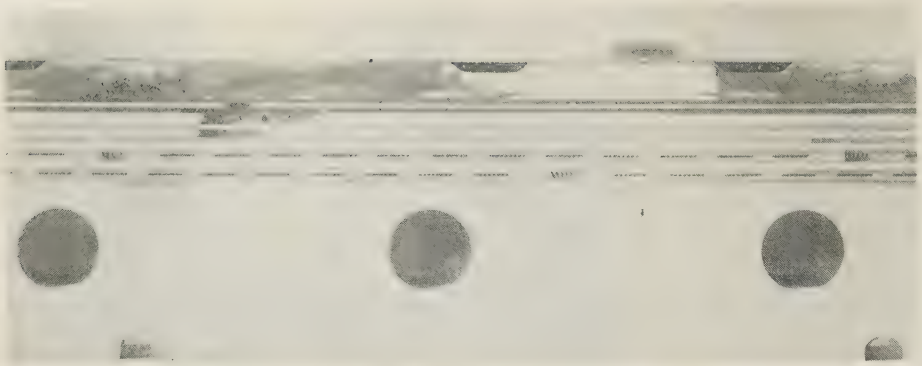

Fig. 27 — Piston after shock load test

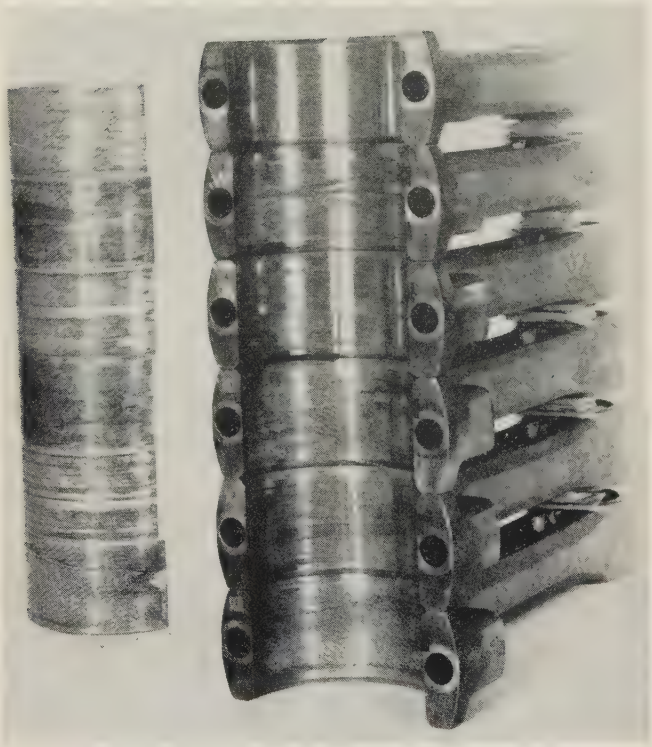

Fig. 28 — Fretted bearing backs and connecting-rod bores after overspeed test

ratio of rate of pressure rise during combustion to rate of pressure rise during compression, we were able to break the piston that failed in the field and to develop a design that did not fail in the field. All new piston designs are now subjected to this test. The piston in Fig. 27, needless to say, did not pass.

Since any proposed rating involves both load and speed and since vehicles are subjected to overspeed, the engine must be asked how it likes typical overspeed conditions. This is a stringent requirement and we would much prefer to avoid it. We haven't found, however, that a red mark or even the scale limit pin on a tachometer will hold back an engine on a long downhill run. So, failing to lick 'em, we must join 'em, and design the engine to live under a reasonable, but not unlimited, overspeed condition. Operation at such a speed gives valuable information on general structural strength, valve train separation, flexure of parts and their side effects, such as fretting of bearing backs, and oil oxidation under the violent pumping and splashing conditions.

The rods and bearing backs in Fig. 28 show extreme fretting resulting from flexure. Redesign of the connecting rod was required.

If the laboratory engine hasn't turned thumbs down on our proposed ratings we are ready for proving ground tests in vehicles under actual load cycles. Even here we run at overspeed to accelerate the test. Vehicle testing includes both normal earth-moving cycles and high load-factor high rolling resistance operations where fuel burned per hour is 50–100% more than normal. If an engine has no application in our own vehicles we put a number into regular industrial service on selected field jobs.

As you may have inferred from my opening remarks, years of experience have taught us that our customers can do things to our machines by chance that we cannot do on pupose. Accordingly, test units, both vehicles and engines, are turned over to established customers for evaluation. It is rare for any results of these limited field tests to affect ratings. Rather, we would expect to learn about accessibility, leaks, mud pockets, response, governing, cooling and other matters of mechanical design.

Future Ratings

Neither combustion development nor mechanical development is static. As we learn to put more air through an engine or to use it more efficiently, ratings will keep pace. Although at any stage of development structural considerations can limit ratings, these are temporary limitations. We are confident that advances in combustion limits can be matched by the necessary stamina for the jobs our engines must do. To be sure that we are ready for each rating advance, we will again go to the engine for approval.

ORAL DISCUSSION

— Reported by Carl H. Meile
International Harvester Co.

James F. Blose, Naval Engineering Experimental Station: Manufacturers do not push toward the potential limits inherent in a design. For example, I know of a case where an engine was rated not to exceed 180 F maximum water temperature. This engine was operated up to 280 F water temperature with the system under pressure. The engine apparently was not harmed by this temperature, although after 5 hr of operation the feed water pump failed.

Mr. McCulla: Five hr is not enough time for conclusive evidence of engine distress at the higher temperature. Placing the cooling system under pressure does tend to more effective cooling, however.

Pneumatic Power Control Systems for • Trucks • Trailers • Buses

Stephen Johnson, Jr.,
Bendix-Westinghouse Automotive Air Brake Co

This paper was presented at the SAE Summer Meeting, Atlantic City, June 9, 1958.

THE principles of the basic air brake system for trucks, trailers, and buses are reviewed in this paper. The author emphasizes especially the dual-pressure and high-pressure systems, which are able to supply air not only to the brakes, but also to other power functions.

Some additional applications are air suspension, air-powered steering, antiskid devices, transmission shifters, crane and shovel controls, and engine auxiliary controls such as air assist booster for clutch control.

AIR-POWERED brakes have been used for many years on trucks, trailers, and buses. Because there is a source of compressed air on these vehicles for air brakes, it suggests that it can be used to power functions other than brakes. It is the purpose of this paper to review a limited number of these additional functions or applications.

Air Brakes

The piping diagram of an air brake system with auxiliaries for a two-axle tractor and a tandem-axle semi-trailer combination is shown in Fig. 1. With this system, "vehicle by vehicle" brake protection is obtained. The tractor protection valve is automatic and when the pressure in the tractor system drops for any reason below 45 psi the tractor protection valve closes, retaining pressure in the tractor system and causing the trailer brakes to apply automatically.

Load Compensation — Brakes on a vehicle are considered balanced when the brake details are so designed and calculated to obtain a predetermined ratio between the retarding force per wheel and the weight per wheel on the ground.

The components that actuate the brakes are usually selected on the basis of stopping distance per-

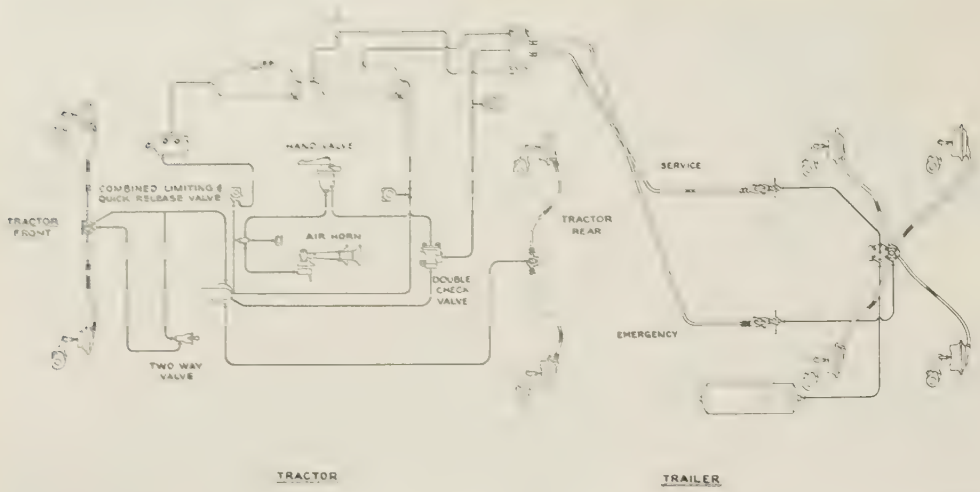

Fig. 1 — Air brake system of two-axle tractor and tandom-axle semi-trailer

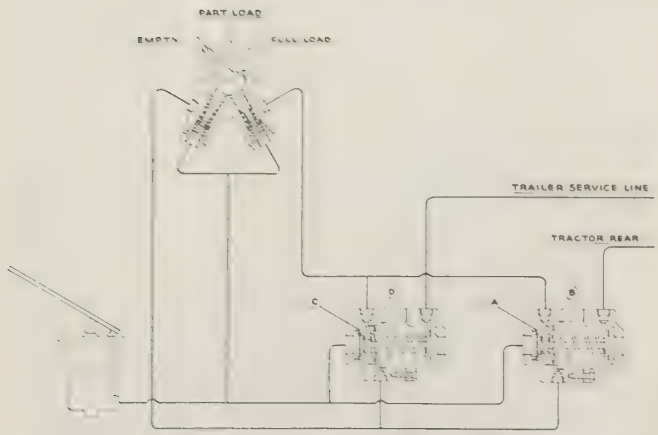

Fig. 2 — Braking adjustment on tractor-trailer combination

formance under maximum rated load conditions. When the vehicle or vehicle combination is empty or partly loaded, different brake performance and control conditions prevail.

Recently industry has given consideration to "load proportional" braking, "light and load" braking, or "load compensation" braking, and considerable study has been given to a means of adjusting the braking effort for the variable axle loads.

Fig. 2 shows a relatively simple system for adjustment of the braking effort on tractor-trailer combination as the payload is reduced. This system can be described as "manual load compensation" and is essentially a system wherein the driver can easily adjust the braking effort for part-load or empty-load conditions.

Limiting valves are installed in the air brake system on the tractor to control the air pressure delivered to both the tractor rear axle and the trailer axles. The limiting valves are similar to those used on the front steering axles for dry or slippery road conditions and are manually regulated with a control valve. The control valve delivers air to the various ports of the limiting valves and thus proportions brake valve pressure delivered to the respective axle brake chambers.

Automatic means of sensing axle weights on the vehicle while in operation are also worthy of consideration.

Dual-Pressure Systems — In an effort to maintain the brake system at its present pressure level and at the same time provide a source of high air pressure for air suspension, air steering, and the like, some interest has been shown in dual-pressure systems.

Fig. 3 shows a dual-pressure pneumatic system. In this system air from the conventional single-stage compressor is delivered to the low-pressure reservoir. A feed valve spills air to the second-stage cylinder which delivers high-pressure air to its reservoir. The second-stage cylinder is of the balanced pressure type and will continue to deliver air until a fixed balanced pressure is reached in the high-pressure reservoir. Control of pressure in the low-pressure reservoir is by the normal governor and unloader mechanism. The maximum pressure in the high-pressure reservoir is controlled by the supercharge pressure supplied from the low-pressure reservoir and assuming a second-stage compression ratio of 3/1 the following pressures can be obtained:

Low-Pressure Reservoir, psi (gage)	High-Pressure Reservoir, psi (gage)
85	285
100	330
105	345

The advantage of the dual-pressure pneumatic system lies in the fact that the air brake system components stay as they are and by so doing retain interchangeability and compatibility of hundreds of thousands of vehicles now in operation.

High-Pressure Air Brake Systems — The chief advantage of a high-pressure air brake system is the reduction in size of the brake actuating units — brake chambers or rotochambers.

To obtain this advantage, of necessity a two-stage compressor, which obviously is more complicated than the single-stage design, is required. The reservoirs would be smaller to store the same amount of energy but the design must have added strength. The power units would be reduced in size but the concept of a rubber diaphragm such as now used in

brake chambers and rotochambers might have to be abandoned. All of the other system components necessarily require redesign.

A high-pressure air brake system can be successfully developed but the big problem to resolve is the matter of trailer interchange — means must be worked out so that the high-pressure system on the tractor can operate with the present low-pressure system on the trailer and vice versa.

Other applications of compressed air, either actually in use or being contemplated, are many. You are familiar with such applications as air horns, air windshield wipers, two-speed axle shifters, snow-plow lifts, and differential lock-out devices. Other applications such as air suspension, power steering, radiator shuttle controls, engine air starters, engine throttle control, clutch control, antiskid devices, and transmission shifters are worthy of discussion.

Air Suspension

Successful application of air suspension to buses was made a few years ago. Field service experience has been highly satisfactory. Several hundred trailers have been equipped with air suspension and to a lesser degree, some trucks and truck tractors. The advantages to be gained by using air suspension for buses, trucks, truck-tractors, and trailers have been discussed in previous SAE papers. Therefore, we will confine our remarks to an item in which we have been directly involved — the leveling control valves.

Every engineering group has its own concept as to what characteristics or functions the leveling valve should have. Consequently, we have designed and built many different varieties, some of which will be described.

In all air-suspension systems to date, the leveling valve is bolted to the frame or body of the vehicle. The valve is equipped with an actuating lever which is connected by some means to the axle. Thus, relative movements between body and axle cause the valve to operate. Most of the installations on trucks and buses used one valve for the front axle, two valves for the rear axle, one for each side. On trailers, one valve for each side is used.

All of the valves we will describe function in the same basic manner. Upward movement of the valve actuating lever, which is downward movement of the vehicle body from the normal ride position, admits air to the bellows at a rate depending on the amount of movement of the valve lever and the type of valve. Downward movement of the valve

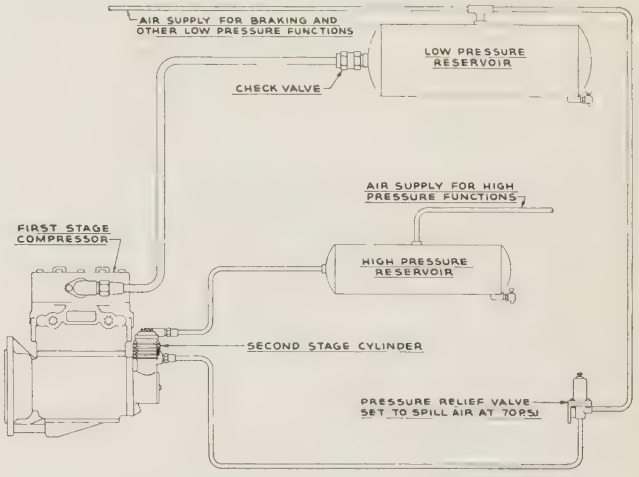

Fig. 3 — Dual-pressure pneumatic brake system

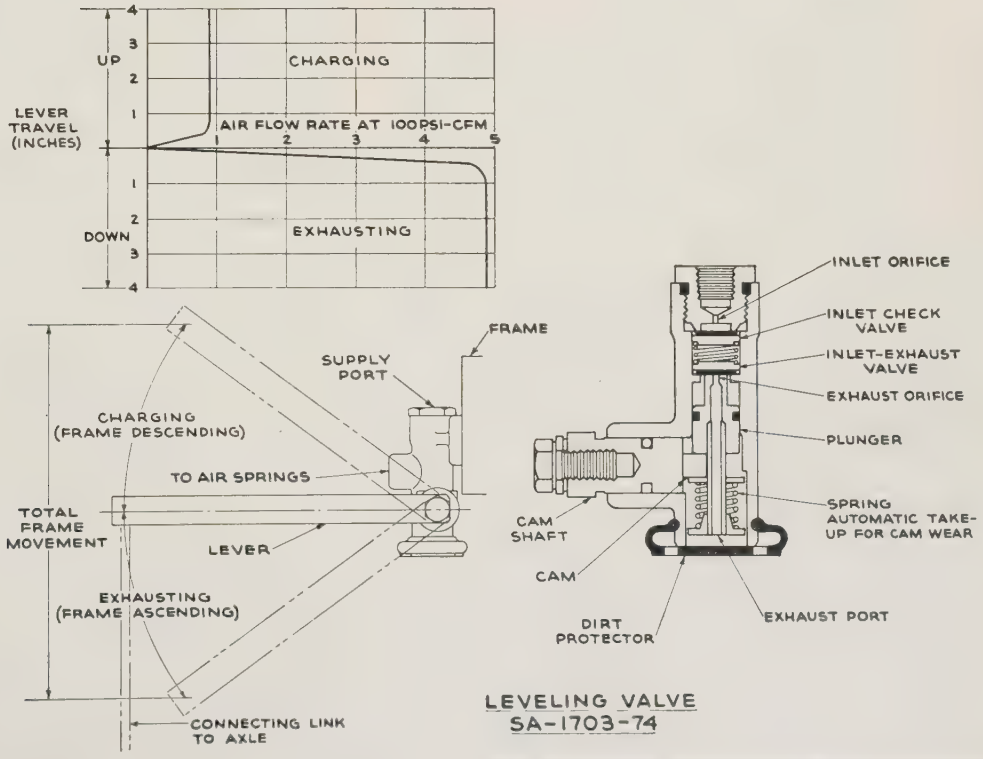

Fig. 4 — Leveling valve with single-stage inlet and single-stage exhaust

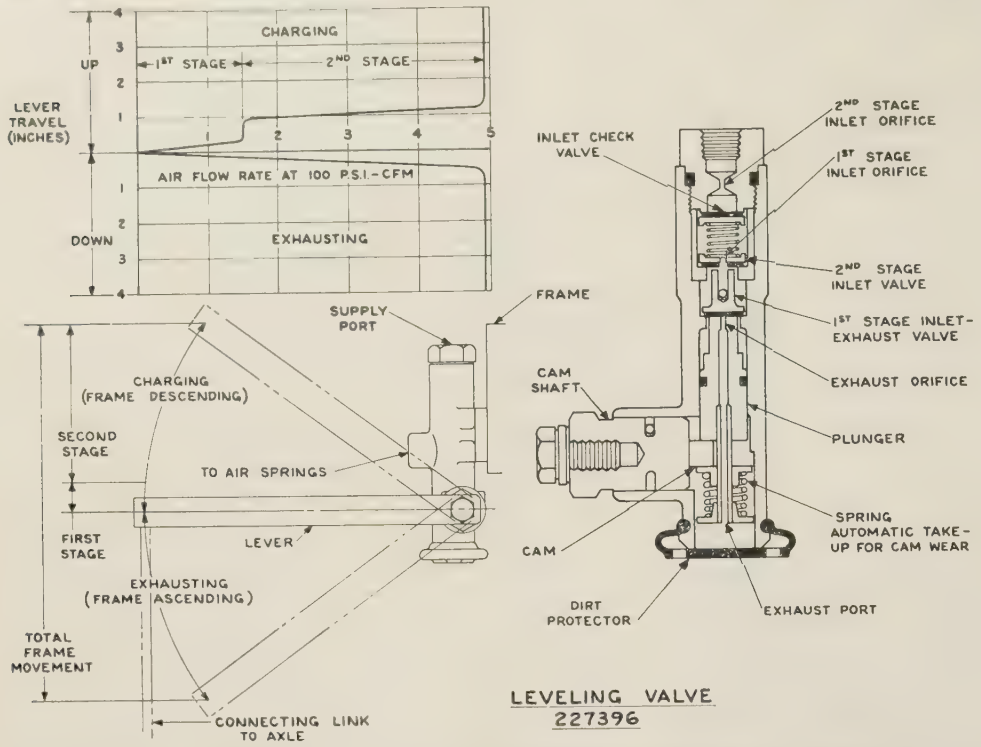

LEVELING VALVE
227396

Fig. 5 — Leveling valve with two-stage inlet and single-stage exhaust

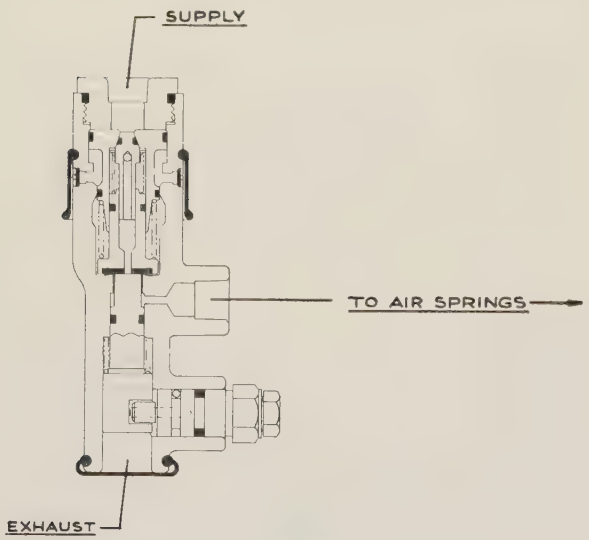

Fig. 6 — Leveling valve, isolation type

actuating lever, which is upward movement of the vehicle body from the normal ride position, exhausts air from the bellows at a rate depending on the type of valve.

Fig. 4 shows the simplest form of leveling valve which is a single-stage inlet and single-stage exhaust type wherein flow rates through the valve are controlled by orifices. Flow rate chart of a typical valve is shown in the upper left hand corner and you will note that little movement of the actuating lever on the charging side results in full flow of air to the bellows, while exhaust is at a slower rate. It is obvious that when such a valve is solidly linked to the axle the result will be considerable air consumption as the vehicle runs along the road, depending of course on the air pressures and the orifice sizes.

Fig. 5 shows a leveling valve having two-stage inlet and single-stage exhaust. The flow chart shows the contrast with the valve shown in Fig. 4. While the exhaust rate remains the same, the inlet rate is in two steps and full flow of air into the bellows is not accomplished until after a considerable travel of the actuating lever. Thus, on normal over-the-road operations the amount of air in and out of the bellows is reduced and if fast charging is required, such as in initial buildup, the valve is full open.

Fig. 6 shows an isolation type of leveling valve. When this valve is in the position as shown, air is trapped in the bags and cannot be exhausted or replenished. When control air is applied to the top of the stepped piston, this piston moves down and the air bags are reconnected to the air supply and to exhaust.

Fig. 7 is a diagram of a system including the valve shown in Fig. 6. In this system a solenoid valve is actuated by a treadle switch. When the treadle is released the solenoid valve opens, permitting air to pass to the leveling valve and normal leveling of the vehicle is accomplished. With a depressed treadle, air is exhausted from the control portion of the leveling valve and air in the bags is trapped.

We have covered only some of the schemes that are being considered but these certainly indicate that air-suspension systems are many and varied, particularly when the various air leveling valves are linked with the several types of bellows.

In addition to the above, there is some interest in applications of what may be called air suspension in track laying vehicles. One of these was to use an air ride seat cushion controlled by a leveling

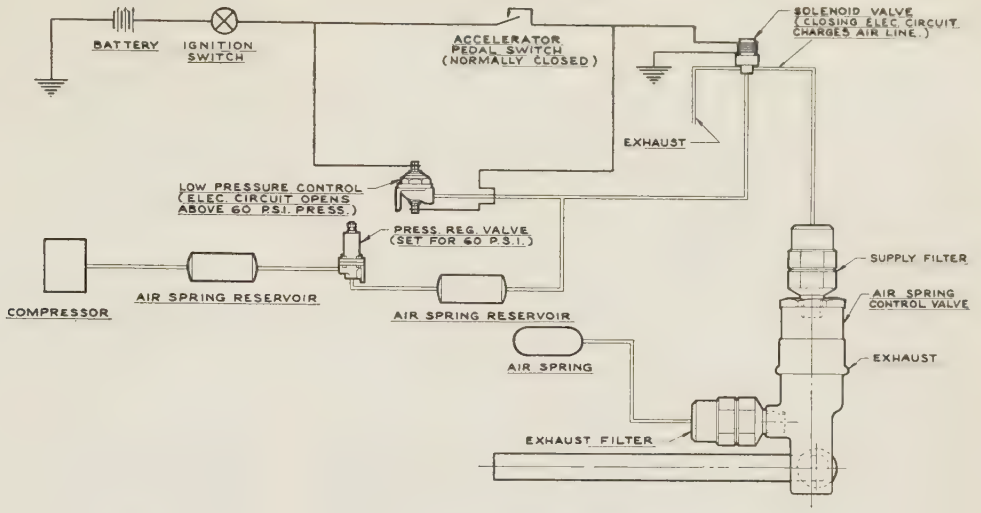

Fig. 7 — Bus air-spring control system

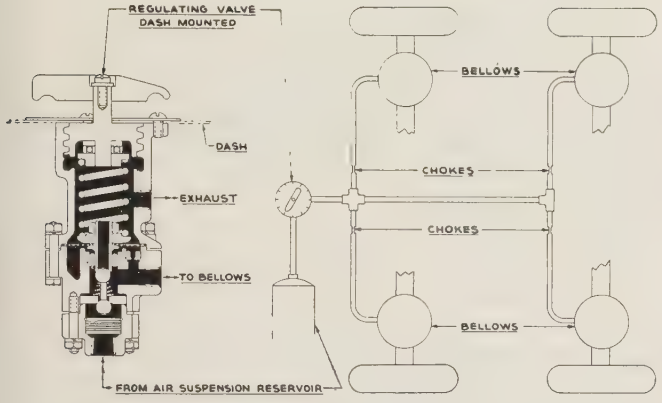

Fig. 8 — Air-suspension system

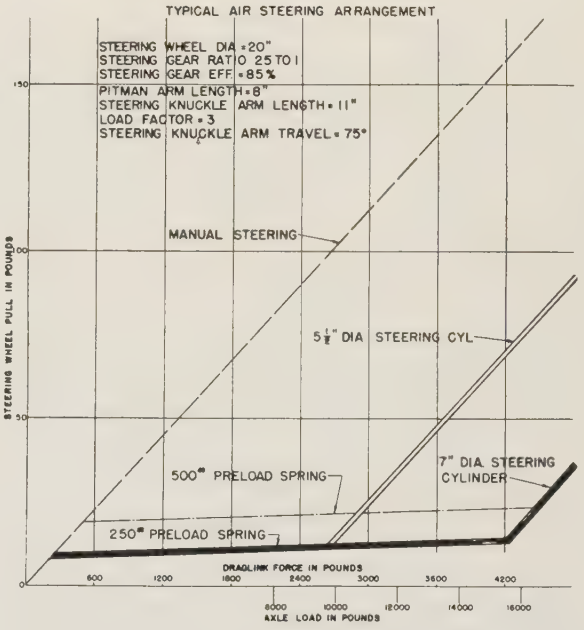

Fig. 9 — Wheel efforts using different sizes of power cylinder

valve and the other was to suspend the entire operator's compartment on air springs.

All concepts of air suspension today include automatic leveling by means of leveling valves. However, there has been some thought given to a much simpler system which provides a manual control and eliminates the leveling valves. The simplified form of such a system is shown in Fig. 8 wherein all of the air bellows are connected to one regulating valve which, when the driver turns the handle, controls the pressure in the bellows to provide any ride or level he may desire. By the addition of other valves, this system can be modified to provide independent adjustment for any axle or any bellows.

Air-Powered Steering

The basic elements of a booster type air-powered steering system are a double-acting piston type power cylinder and a control unit containing twin valving and preloaded spring. The cylinder is anchored to, and reacts against, some point on the front axle or chassis frame, while the cylinder piston is pivotably connected to a convenient point on the steering knuckle arm or steering linkage. The control unit is usually interposed in the drag link between the pitman arm and the steering knuckle arm. When the induced force on the control unit and drag link does not exceed the load of the preloaded spring in the control unit, the air valving does not function and steering will be without power assist. When the drag link force exceeds the load of the preloaded spring, the air valving functions and a power assist is provided. Full manual steering can be accomplished by more wheel effort, since mechanical connection is maintained.

A typical example of resultant wheel efforts using two different sizes of power cylinder is shown in Fig. 9.

Engine Auxiliary Controls

Cooling Shutters — With this type of coolant control, the amount of air passing through the radiator is regulated by a thermostat-air valve with an air cylinder or brake chamber connected to the shutters. Coolant water temperature maintenance within high and low limits of 8 F is possible with this type of control.

Starters — Many of these are currently being used

in trucks and consist of a vane-type air motor connected to a Bendix friction clutch and housing.

Throttle Control — The air throttle control consists of a graduating-type air valve actuated by a suitable foot treadle and connected by an air line to the throttle cylinder. The throttle cylinder piston movement is in direct proportion to the air pressure applied or released by the throttle valve.

Of particular interest in the design of the air throttle cylinder is the fast idle feature whereby the throttle is mechanically advanced to the fast idle position when the reservoir air pressure is depleted.

Clutch — For clutch control the air assist booster type is used on some trucks and heavy off-the-road vehicles where the pedal load to disengage the mechanical clutch is too great for driver comfort. This arrangement consists of a pull-type air valve placed in the clutch pedal rod and a clutch cylinder operating on the clutch shaft lever. The linkage can be arranged so that an acceptable clutch pedal pad force, usually 50 lb maximum, can be obtained.

Antiskid Devices

Most of you are aware of the development and application of automatic devices to prevent wheel slipping or skidding of railroad and aircraft equipment. These automatic devices detect a change in the condition of wheel rotation and transmit this information or signal to an intercepter device to release or apply the brakes, thus preventing wheel slippage or skidding.

There is some current interest in antiskid devices for trucks, trailers, and buses.

The means to accomplish the end result appear complicated at the present time but engineering development will simplify them. As we see it, each wheel would be equipped with a sensing device and an intercepter valve to regulate brake pressures.

The sensing device must be able to detect sudden changes in wheel or tire velocity and thus must be designed into the wheel structure in some manner. There appear to be several means which could be used to provide the sensing function, such as:

1. Mechanical means that would compare the rotation of a wheel driven flywheel with the rotation of the vehicle wheel.
2. Electrical means such as a generator driven by the vehicle wheel plus electric circuitry and relays sensitive enough to detect rapid changes in velocity.
3. Electronic means such as a wheel driven generator plus circuit interrupter or pulse generator.
4. Pneumatic means using a compressor driven by the wheel.

The intercepter device would be designed using the same means as the sensing device and thus it could be operated pneumatically, mechanically, electromagnetically, or electropneumatically.

Regardless of the means employed and to arrive at a satisfactory answer, the end results obtained by such devices must be balanced against economics.

Transmission Shifters

The shifting of gear box transmissions by air power has been used in various applications. Both full air power and air power assist means have been employed.

With full-power shifts the shift rails of the transmission are mechanically linked to some form of air actuators which are controlled by a valve or a valve cluster which can be remotely located or attached to the air cylinder structure and operated by such means as a bowden wire. The full-power shifting of auxiliary transmissions is a simpler application than one for the main transmission, because only the fore-and-aft shifting of usually one rail is involved. The full-power shifting of the main transmission is more complex and to afford a fully remote control the cross-shifts must also be accomplished by air and valving. Also, some interlocking device is required to insure the air power is applied at the proper time. All full-power shifts must, of course, rely on the presence of air pressure.

With air power assist shifting, the shift lever is retained and a mechanical connection between the shift lever and the shift rails is maintained, permitting the possibility of shifting even though air pressure is not available. Air power assists have been applied to main transmissions and is accomplished by an air cylinder and valving contained in a structure which mounts in the linkage between the shift lever and the shift rails. Its action is the same as the air steering and valve combination I have described and power is supplied only when needed. The overall effect is to considerably reduce the shift stick effort. In fact, this effort has been reduced sufficiently to permit the use of a steering column mounted shift lever, a feature which has been desired in trucks with the heavy transmissions for some time.

Crane and Shovel Controls

When operating power cranes or shovels it is necessary for the operator to manipulate and control various devices, many of which are friction clutches. It has been found that compressed air controls (valves and actuators) provide the operator with precise and fast control of these devices. One manufacturer has arrived at a design wherein the air control valves are arranged in two clusters operated by only two levers which control the following operations: boom derricking, boom brake, swing, crowd, retract, hoist, clam holding, drag-in, power load lowering, and third drum. On self-propelled rubber-tired machines, the travel is also controlled by metered air.

On crawler machines additional air controls actuate all crawler operations such as tread and travel locking pawls, shifting of jaw clutches for selection of travel or swinging, steering and turntable swing lock. On shovels the dipper trip is also air operated. Sometimes air booster operation of secondary hoist drum brake and main drum brake is used.

Conclusion

Compressed air as a source of power has long been used in our industry to perform a large number of tasks. Air in its free state is abundant in nature and is, therefore, an ideal medium. Compressed to relatively high pressures, its energy can be stored in a small space. It is considered by many to be the best form of power for certain specific applications. For other applications, its efficiency and economics will determine whether or not it should be used.

The *ION* ROCKET ENGINE

R. H. Boden, Rocketdyne Division, North American Aviation, Inc.

This paper was presented at the SAE National Aeronautic Meeting, New York, April 9, 1958

THE ion-propulsion rocket system, its possibility and its basic theory, have been discussed at length by many writers. North American Aviation, Inc., has performed several informal studies on electrical powerplants. The objective was to seek a jet propulsion powerplant of high performance which would supplement the capabilities of chemical and nuclear rocket engines. A powerplant was sought which would have good performance after the capabilities of other types were exceeded.

The Directorate of Advanced Studies, Air Force Office of Scientific Research, Pasadena, Calif., has sponsored a formal theoretical investigation of the ion rocket engine at Rocketdyne during 1957. The results of this program have indicated that an ion rocket engine in which the propelling ions are accelerated by an electrostatic field has the capability of producing usable thrust levels and will supplement other rocket engines in applications to space vehicles.

The results of this study program conclusively show that three major problem areas exist in the development of the ion rocket engine. These are the ion thrust chamber, the propellants, and the development of a high specific power generator. These three areas have been delineated and apply to electrical propulsion systems in general (Table 1).

The ion-propulsion research program is to continue for the coming year at Rocketdyne under the sponsorship of the Directorate of Advanced Studies, AFOSR. In addition to the theoretical work, a limited experimental program is to be performed to verify partially the data presented here.

The direct objective of this paper is to analyze the ion thrust chamber, establish the significant overall design parameters, establish criteria for selection of the propellant, and point out the direction toward a working model. The interest of the report is not in the feasibility of the system as a whole, but primarily in the development of the thrust chamber itself.

Discussion

Chemical rocket development has shown that the important performance functions are the thrust F exhaust velocity C, specific impulse I_s, thrust coefficient C_f, characteristic velocity C^*, and propellant flow rate w.[1] For a thrust chamber fitted with a

THE significant design parameters of an ion-propellant rocket engine are developed in terms of three independent parameters. These are: the ratio of the acceleration voltage to atomic or molecular weight of the propellant, gross weight of the vehicle, and thrust-to-weight ratio.

Engineering trends are presented which will lead toward advanced study of ion thrust chambers, power generation systems, and propellants.

This paper received the 1958 Manley Memorial Award.

[1] "Rocket Propulsion Elements," by G. P. Sutton. Second edition. Pub. by John Wiley and Sons, Inc., New York, 1956.

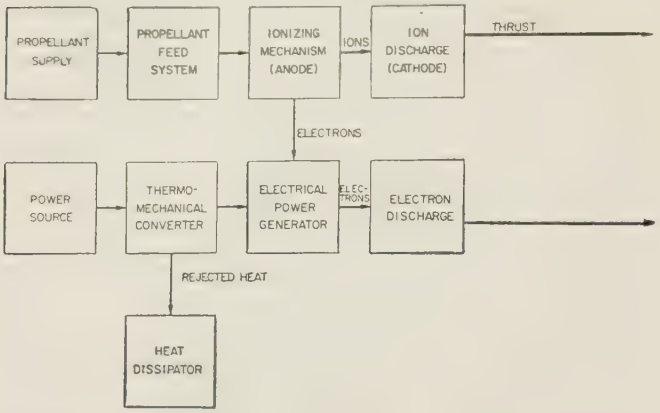

Fig. 1 — Ion propulsion system schematic (present conception)

Table 1 — Major Problems of Ion Rocket Engine Development

- Ion Thrust Chamber
  - Power requirements
  - Ion source
  - Electron source
  - Ion acceleration
  - Efficiency
  - Design and operating parameters
- Propellants
  - Ion weight
  - Weight to fit mission
  - Charged particles and compounds
  - Physical properties
  - Chemical properties
- High Specific Power Generator
  - Mechanical conversion of heat to electrical power
  - Direct conversion of heat to electrical power
  - Heat rejection

fully expanded nozzle, these functions can all be expressed in terms of the ideal exhaust velocity:

$$C = \sqrt{\frac{2\,g\,k}{k-1}\,\frac{RT}{M}\left(1-\frac{P_o}{P_c}\right)^{\frac{k-1}{k}}} \qquad (1)$$

and the propellant flow rate:

$$\dot{w} = \frac{P_c A_t k g \sqrt{[2/(k+1)]^{(k+1)/(k-1)}}}{\sqrt{kg\,\frac{RT}{M}}} \qquad (2)$$

where:

C = Exhaust velocity, fps
$\dot{w}$ = Flow rate, lb/sec
g = Acceleration due to gravity, ft/sec² = 32.174 ft/sec²
R = Gas constant = 1544/lb molecule
T = Gas temperature, deg R
M = Molecular weight, lb
k = Ratio of specific heat
P_c = Chamber pressure, psia
P_o = Ambient pressure, psia
A_t = Thrust area, sq in.

The significant variables upon which these functions are dependent are the chamber pressure, gas temperature, molecular weight, thrust area, and pressure ratio parameters P_c/P_o. Parallel electrical relations exist for the ion thrust chamber. These are developed in this report.

The ion rocket engine model upon which this analysis is predicated is outlined in the schematic diagram of the ion-propulsion system (Fig. 1). Propellant is carried in a convenient form (solid, liquid, or gas) in a supply system. In its passage through the feed system it is vaporized and then introduced into the ionizing chamber at a controlled rate. The ionizing mechanism is an electric arc or heated metallic plate, for example, of tungsten or platinum. The body of the ionizing chamber collects the electrons, and they in turn pass through the electrical power generator. The ions are extracted from the ionizing chamber by an electrostatic field and accelerated to a suitable velocity to produce the major component of thrust from the rocket engine. The electrons, after passing through the generator, are reproduced by thermonic emission. They, in turn, are accelerated by a second electrostatic field of a strength sufficient to bring the electron velocity to approximately that of the ions. This portion of the ion rocket engine is discussed in this report. The power source, thermomechanical converter, heat dissipator, and details of the electrical power generator will be discussed in other technical reports.

The state of the art of the ion rocket engine is in the pre-engineering phases. As a result, performance calculations occur in a variety of fundamental systems, both mechanical and electrical. For this reason, this report presents the performance parameters in two mechanical systems, the centimeter-gam-second (cgs) and the foot-pound-second (fps). Practical electrical units are used along with electrostatic units for many of the basic constants, for example, the charge of an electron. In order to avoid confusion, use of each system of units is carefully indicated.

Fundamental Relations of Ion Rocket Engine

Thrust is the main consideration of a jet propulsion powerplant. For a device in which the propellant is self-contained, Newton's laws of motion formulate the relation for thrust:

$$F = Ma = \sum \dot{N}_i\, m_i\, C_i \text{ dynes} \qquad (3)$$

In the fps system:

$$F = M_g\, G = \sum \dot{N}_i\, m_i\, C_i \text{ lb} \qquad (3a)$$

where:

F = Thrust, dynes (lb)
M = Mass of vehicle, gams (pound mass)
a = Acceleration of vehicle, cm/sec² (ft/sec²)
$\dot{N}_i$ = Flow rate, particles per sec
C_i = Particle velocity relative to vehicle, cm/sec (ft/sec)
M_g = Weight of vehicle, lb
G = Thrust/weight ratio in the fps system
m_i = Mass of particle, grams (lb)

Three variables, N_i, m_i, and C_i, depend upon the propellants selected and the performance of the thrust chambers. Each is discussed in turn.

The ion rocket ejects both ions and electrons in order to maintain an electrically neutral vehicle. Both are ejected in a direction opposite and parallel to the direction of thrust. The ion is frequently conceived of as an atom stripped of one or more electrons. Numerous investigators have shown that ions are not necessarily atoms, but may be submolecular or molecular species or combinations of several atoms. The ions $UC1_2^+$ and SF_6^- are examples. For convenience in discussion, the atomic weight A is

used and defined as the sum of the atomic weights of the elements in the ion. These atomic weights, in grams, are readily available in scientific and engineering literature. The ion may also carry a charge greater than that of the electron. The ion charge of a multiply ionized particle is an integral number h of electron charges.

Expressed in terms of the atomic weight of the propellant, the mass of the ion is:

$$m = \frac{A}{6.0248 \times 10^{23}} h m_e \text{ gram} \tag{4}$$

The thrust of the ion rocket, in dynes is then:

$$F = Ma = \frac{A\dot{N}C}{6.0248 \times 10^{23}} + (\dot{N}_e C_e - h\dot{N}C) m_e \tag{5}$$

where:

$\dot{N}$ = Ion flow, ions per sec
$\dot{N}_e$ = Electron flow, electrons per sec
Avogadro's number = 6.0248×10^{23}
m_e = Mass electron = 9.1084×10^{-28} gram
A = Atomic or molecular weight of propellant, gram
C = Velocity of ion, cm/sec
C_e = Velocity of electron, cm/sec
h = Number of electrons stripped from ion

The particles ejected from the engine influence the behavior of the vehicle because of electrical image forces resulting from induced charges on the conduction surface of the vehicle.[2] If the relative velocity of the ions and electrons is large, the probability of their combination or the formation of a neutral plasma is small.[3] The precise effect of these image forces on the vehicle is not discussed in this report. It is believed, but subject to verification, that the ion and electron velocities should be of nearly the same magnitude and that more electrons than ions should be ejected in order to give the vehicle a slight positive surface charge. Under these conditions, the approximate thrust is given by the relation:

$$F = \frac{A\dot{N}C}{6.0248 \times 10^{23}} \text{ dynes} \tag{5A}$$

Since the difference $(\dot{N}_e C_e - h\dot{N}C)$ from the above considerations, is small and the mass of the electron is very small in comparison to the mass of the ion:

$$\frac{m_e}{m} = \frac{1}{1836A - h} \cong \frac{1}{1836A} \tag{6}$$

The particle flow rate is directly proportional to the current:

$$\dot{N} = \frac{2.9979 \times 10^9 I}{he} = 6.246 \times 10^{18} \frac{I}{h} \tag{7}$$

where:

e = Electron charge = 4.8029×10^{-10} esu
I = Current in amperes

If the particles are electrons, h is unity.

The coefficient 2.9979×10^9 is the factor to convert the current I, in practical units, to current in electrostatic units (esu).

The particle exhaust velocities are obtained from the change in kinetic energy imparted to them by the electric field. If the initial velocity is zero, the kinetic energy is:

$$\tfrac{1}{2} m_i C^2 = \frac{heV}{300} \text{ ergs} \tag{8}$$

and the exhaust velocity is:

$$C_i = \left(\frac{heV}{150\, m_i}\right)^{\frac{1}{2}} \text{ cm/sec} \tag{9}$$

where:

V = Potential difference across which particle is accelerated, volts
m_i = Mass of particle, gram

The potential difference V is the total work done on a particle of unit charge by the electrostatic field. In the case of a linear field (for example, between two plane, parallel, accelerating electrodes with guard rings), V is the voltage difference between the two electrodes.

For the ions, the exhaust velocity is:

$$C = 1.389 \times 10^6 \left(h\frac{V}{A}\right)^{\frac{1}{2}} \left(1 - \frac{h}{1836A}\right)^{-\frac{1}{2}} \text{ cm/sec} \tag{10}$$

or:

$$C = 4.557 \times 10^4 \left(h\frac{V}{A}\right)^{\frac{1}{2}} \left(1 - \frac{h}{1836A}\right)^{-\frac{1}{2}} \text{ ft/sec} \tag{10a}$$

The ratio $\frac{h}{1836A}$ is so small for all propellants to be considered that the coefficient $\left(1 - \frac{h}{1836A}\right)^{-\frac{1}{2}}$ is assumed to be unity in the following development.

For electrons the exhaust velocity is:

$$C_e = 5.952 \times 10^7 (V_e)^{\frac{1}{2}} \text{ cm/sec} \tag{11}$$
$$C_e = 1.953 \times 10^6 (V_e)^{\frac{1}{2}} \text{ ft/sec} \tag{11A}$$

The thrust is then in terms of the accelerating voltages and current:

$$F = 14.39 \left[I \left(\frac{AV}{h}\right)^{\frac{1}{2}} + I_e \left(\frac{V_e}{1836}\right)^{\frac{1}{2}} \right] \text{ dynes} \tag{12}$$

$$F = 3.235 \times 10^{-5} \left[I \left(\frac{AV}{h}\right)^{\frac{1}{2}} + I_e \left(\frac{V_e}{1836}\right)^{\frac{1}{2}} \right] \text{ lb} \tag{12A}$$

The contribution to the thrust by the electrons is small because the vehicle is maintained at a neutral electrical level. This procedure requires equal total charges and velocities of ions and electrons, that is, the same current in both the ion and electron thrust chambers, and a voltage ratio (from Equation 9) of:

$$\frac{V_e}{V} = \frac{m_e}{m} = \frac{1}{1836A - h} \sim \frac{1}{1836A} \tag{13}$$

The last fundamental relationship required is the power in the exhaust jet. At this time, it is emphasized that the power requirements discussed here are net requirements for the power that must go into the exhaust of both the ion and electron accelerators, *not* the power developed by the elec-

[2] P. 350 of "Introduction to Theoretical Physics," by L. Page. Pub. by D. Van Nostrand & Co., Princeton, N. J., 1929.
[3] Pp. 618–646 of "Electronic and Ionic Impact Phenomena," by H. S. W. Massey and E. H. C. Burhop. Pub. by Oxford University Press, New York, 1952.

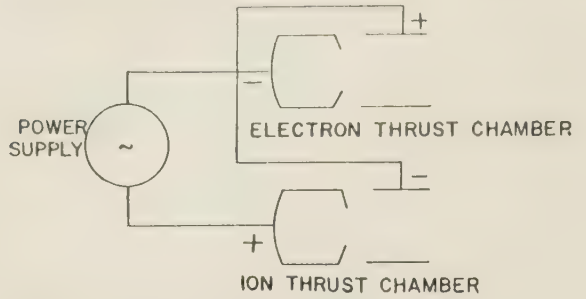

(A) ION ROCKET ENGINE, SERIES CONNECTION

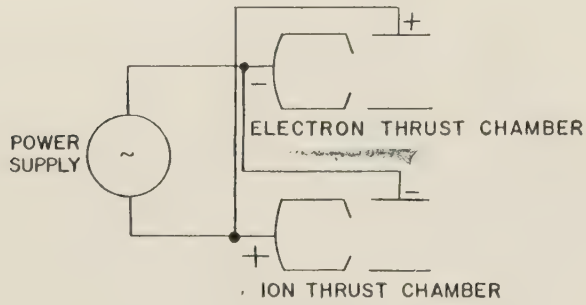

(B) ION ROCKET ENGINE, PARALLEL CONNECTION

Fig. 2 — Ion rocket engine arrangements

trical power generating equipment. The efficiency of conversion of electrical energy to kinetic energy of the exhaust is influenced by the configuration of the particle accelerators, dispersion of the exhaust jet, resistance losses in the power transmission system, and losses due to collisions of the particles with the structure of the thrust chamber.

The power in the exhaust of the ion rocket is:

$$P = (\tfrac{1}{2}\dot{N}mC^2 + \tfrac{1}{2}\dot{N}_e m_e C_e^2)10^{-7} \text{ watts} \qquad (14)$$

The first term is the contribution from the ion flow, the second due to the electron flow. In terms of the atomic weight, the jet power becomes:

$$P = \tfrac{1}{2}\left[\frac{\dot{N}AC^2}{6.0248 \times 10^{23}} + (\dot{N}_e C_e^2 - h\dot{N}C^2)m_e\right] 10^{-7} \text{ watts} \qquad (15)$$

If velocities are expressed in terms of the accelerating voltages:

$$\frac{C_e^2}{C^2} = 1836A\,\frac{V_e}{hV}\left(1 - \frac{h}{1836A}\right) \qquad (16)$$

the power in the jet becomes:

$$P = \tfrac{1}{2}\frac{\dot{N}AC^2}{6.0248 \times 10^{30}}\left[1 + \left(\frac{1836\ V_e}{V/A}\,\frac{I_e}{I}\left\{1 - \frac{h}{1836A}\right\} - h\right)\frac{1}{1836A}\right] \text{ watts} \qquad (17)$$

Two methods of connecting the ion and electron accelerators are possible: series and parallel (Fig. 2). Neither requires voltage transformers, a consideration in minimizing weight. Both can be operated directly from the supply.

If a series arrangement is used (Fig. 2A), voltages can be adjusted to produce the same ion and electron velocities. The power in the jet then becomes:

$$P = \tfrac{1}{2}\frac{\dot{N}AC^2}{6.0248 \times 10^{30}} \qquad (17A)$$

since the currents in both thrust chambers are equal.

For voltage ratios of 0.01 and greater, the power is given very closely by the relation:

$$P \cong \tfrac{1}{2}\frac{\dot{N}AC^2}{6.0248 \times 10^{30}}\left(1 + \frac{V_e}{V}\right) \text{ watts} \qquad (17B)$$

For a parallel arrangement (Fig. 2B) the power becomes:

$$P = \frac{\dot{N}AC^2}{6.0248 \times 10^{30}}\left(1 - \frac{h}{1836A}\right) \text{ watts} \qquad (17C)$$

Since the contribution to thrust by the electron is negligibly small (Equation 12), and the power required increases rapidly with electron accelerating voltage, a series arrangement of the two particle accelerators begins to appear the more promising arrangement. This will become more apparent from study of the design parameters.

The presence of the different ion species in the exhaust jet changes the value of the parameter A. From the basic thrust equation it is easily proved that the effective value of A is:

$$A^{\frac{1}{2}} = \sum_K \frac{I_K}{I}\left[\left(1 - \frac{h_K}{1836A_I}\right)\frac{A_K}{h_K}\right]^{\frac{1}{2}} \qquad (18)$$

where:

A = Effective weight of ions, gram
$\dot{N}_k$ = Particle flow of the K'th ion species, particles Kw
I_k = Ion current of the K'th ion species, amp
I = Total ion current, amp
A_K = Atomic, or molecular, weight of K'th ion species, gram
h_K = Number of electrons stripped from K'th ion species

This value of A is the atomic weight of a singly ionized atom equivalent in effectiveness to the ionized propellant.

Unless otherwise noted, A is defined by Equation 18 in the derivations and charts which follow.

Design Parameters

The design parameters are developed from the fundamental relations developed previously. Included in these parameters are the specific impulse, thrust per unit power, power per unit vehicle weight, mass ratio, propellant flow rate, and the like. It is shown that these parameters are governed by the vehicle weight, thrust-to-weight ratio, and the ratio of accelerating voltage to atomic weight of the propellant. The last parameter corresponds to the chamber pressure in conventional chemical rocket analyses.

Power-to-Mass Ratio — The power in the exhaust jet can be expressed in terms of the mass and acceleration of the vehicle. From Equations 14 and 3, the general expression for the exhaust power is:

$$P = \left[\tfrac{1}{2}MaC + \tfrac{1}{2}m_e\dot{N}_e C_e^2\left(1 - \frac{C}{C_e}\right)\right] \times 10^{-7} \text{ watts} \qquad (19)$$

The power in the electron exhaust P_e is:

$$P_e = \tfrac{1}{2}\dot{N}_e m_e C_e^2 \times 10^{-7} = XP \text{ watts} \qquad (20)$$

in which X is the fraction of the total exhaust power

in the electron beam.

It is convenient to express all of the design parameters in terms of the ion variables, for example, velocity, accelerating voltage, weight, and the like. However, the electrons removed from the ions affect all the parameters. Analytically, these effects are expressed in the correction factor:

$$E = 1 - X\left(1 - \frac{C}{C_e}\right) \tag{21}$$

This factor is a correction to the ion velocity and the ratio C/E is the effective efflux velocity of the ions and electrons. For convenience in presenting the parametric charts of the design variable, the total power P and E are associated as a product.

The power-to-mass ratio then becomes:

$$\frac{P}{M} = \frac{aC}{2\left[1 - X\left(1 - \frac{C}{C_e}\right)\right]} = \frac{aC \times 10^{-7}}{2E} \text{ watts/gram} \tag{22}$$

or:

$$\frac{P}{M_g} = \frac{GC}{1100\left[1 - X\left(1 - \frac{C}{C_e}\right)\right]} = \frac{GC}{1100E} \text{ hp/lb} \tag{22A}$$

The thrust-to-weight ratios which can be achieved by the ion rocket for various exhaust-power vehicle weight ratios are shown in Fig. 3 as a function of the ion exhaust velocity. The velocity range covers the operation of conventional liquid propellant rockets, 3000–6000 fps, through the highest velocity expected from the ion thrust chamber. The significant point of this chart is that the power demand of the exhaust jet rapidly outstrips the ability of the vehicle to produce power. For example, the modern transport aircraft develops 0.05–0.08 hp per lb of gross weight. With this range as a yardstick, the thrust-to-weight ratio of the ion rocket is 10^{-4} to 10^{-3} for exhaust velocities of 10^5 to 10^6 fps. The modern rocket engine develops between 1–2 hp per unit vehicle weight, but only for short periods. Therefore, the chemical rocket engine cannot be directly compared to the ion rocket engine.

These ratios may be expressed in terms of the accelerating voltages. For the same current through both thrust chambers, previously mentioned to be desirable, the fraction X becomes the ratio of electron acceleration voltage to the total voltage in the system, and the velocity ratio C/C_e is obtained from Equation 10:

$$\frac{PE}{M} = 0.0695a\left(\frac{V}{A}\right)^{\frac{1}{2}} \text{ watts/gram} \tag{23}$$

in cgs units, or:

$$\frac{PE}{M_g} = 41.42G\left(\frac{V}{A}\right)^{\frac{1}{2}} \text{ hp/lb} \tag{23A}$$

in fps units, or:

$$\frac{PE}{M_g} = 3.089 = 10^4 G\left(\frac{V}{A}\right)^{\frac{1}{2}} \text{ watts/lb} \tag{23B}$$

If the ion exhaust consists of multiply ionized atoms or several species, the atomic weight is replaced by the equivalent value of Equation 18.

When the electron and ion velocities are equal, the factor E becomes unity and the power-to-mass ratio has a minimum value. If the accelerating voltages of the two exhausts are the same, the power-to-weight ratio is doubled. Therefore, a series arrangement of the ion and electron thrust chambers (Fig. 2A) in which the accelerating voltages are adjusted to produce equal exhaust velocities in both thrust chambers is preferable to the parallel arrangement of Fig. 2B. A secondary advantage to the series arrangement is that lower currents are used, resulting in a weight and power loss saving in the electrical conductors and generating equipment.

The power-to-weight ratio parameter increases directly with the thrust-to-weight ratio and the square root of the ratio of the accelerating voltage and atomic weight of the propellant, but varies inversely with a factor accounting for the effects of electron exhaust. This factor:

$$E = 1 - X\left[1 - \frac{C}{C_e}\right] = 1 - \frac{I_e V_e}{I_e V_e + IV}\left[1 - \left(\frac{1}{1836A}\frac{V}{A}\right)^{\frac{1}{2}}\right] \tag{21}$$

is a correction factor to the ion velocity. In this report it is associated with the total power in the exhaust jet P rather than with the ion exhaust velocity.

The power-to-weight ratio parameters PE/M_g is always equal to or less than the actual power-to-

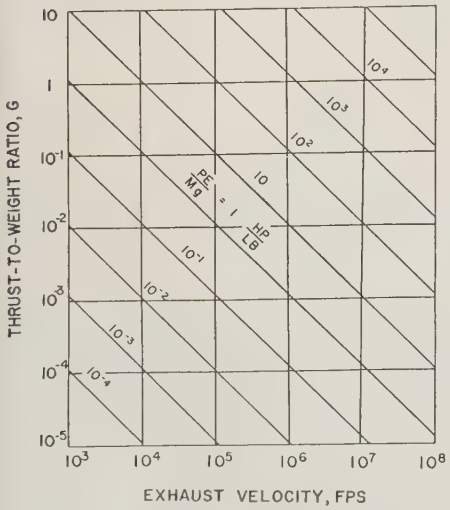

Fig. 3 — Thrust-to-weight ratio of ion rocket vehicle

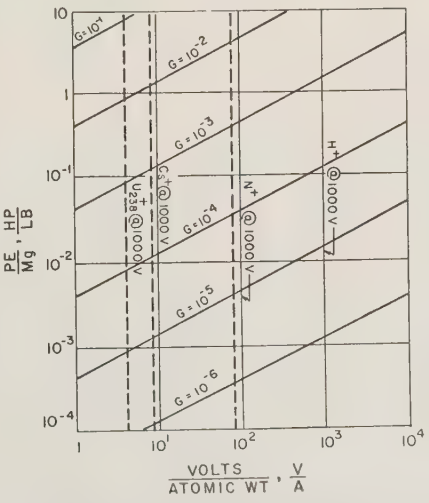

Fig. 4 — Power-to-vehicle-weight ratio of ion rocket

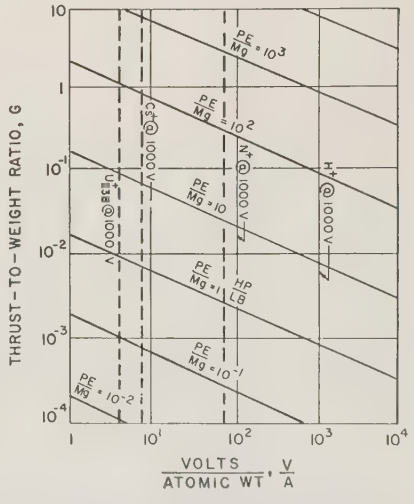

Fig. 5 — Thrust-to-weight ratio of ion rocket vehicle

weight ratio. The corrected power-to-weight ratio is shown as a function of V/A for several values of thrust-to-weight ratio G (Fig. 4).

In Fig. 5 the decrease of G with V/A is shown for several different values of PE/M_g. Later, it will be shown that the cross-sectional areas of the ion and electron thrust chambers vary inversely as the square of the accelerating voltages, V and V_e. The design of the thrust chambers will demand a compromise judgment between achievable power-to-weight ratios and permissible thrust chamber areas. A high atomic weight propellant reduces the requirements for the power-to-weight ratio. For example, if a constant accelerating voltage is applied, singly ionized uranium ions, U^+_{238}, theoretically produce 15.4 times the thrust obtainable from hydrogen ions, H^+, at the same accelerating voltage.

Thrust Per Unit Power — The thrust of the ion rocket and the power in the exhaust jet have a direct relationship. Since the electrical power in the exhaust is:

$$P = IV + I_e V_e \text{ watts} \tag{24}$$

The thrust becomes, from Equation 12:

$$F = 14.39 \left[(P - P_e) \left(\frac{V}{A}\right)^{-\frac{1}{2}} + P_e \left(\frac{1}{1836 V_e}\right)^{\frac{1}{2}} \right] \text{ dynes} \tag{25}$$

In cgs units as:

$$F = 3.235 \times 10^{-5} \left[(P - P_e) \left(\frac{V}{A}\right)^{-\frac{1}{2}} + P_e \left(\frac{1}{1836 V_e}\right)^{\frac{1}{2}} \right] \text{ lb} \tag{25A}$$

in fps units. The thrust per unit power in the jet is then:

$$\frac{F}{P} = 14.39 \left(\frac{V}{A}\right)^{-\frac{1}{2}} \left[1 - X \left\{ 1 - \left(\frac{1}{1836 V_e} \frac{V}{A} \right)^{\frac{1}{2}} \right\} \right] \text{ dynes/watt} \tag{26}$$

when:

$$X = P_e / P$$

or:

$$\frac{F}{P} = 0.02414 \left(\frac{V}{A}\right)^{-\frac{1}{2}} \left[1 - X \left\{ 1 - \left(\frac{1}{1836 V_e} \frac{V}{A} \right)^{\frac{1}{2}} \right\} \right] \text{ lb/hp} \tag{26A}$$

or:

$$\frac{F}{P} = 3.235 \times 10^{-5} \left(\frac{V}{A}\right)^{-\frac{1}{2}} \left[1 - X \left\{ 1 - \left(\frac{1}{1836 V_e} \frac{V}{A} \right)^{\frac{1}{2}} \right\} \right] \text{ lb/watt} \tag{26B}$$

The inverse of these ratios are of engineering use and are evaluated here:

$$\frac{PE}{F} = 0.06949 \left(\frac{V}{A}\right)^{\frac{1}{2}} \text{ watts/dyne} \tag{27}$$

or:

$$\frac{PE}{F} = 41.44 \left(\frac{V}{A}\right)^{\frac{1}{2}} \text{ hp/lb} \tag{27A}$$

or:

$$\frac{PE}{F} = 3.089 \times 10^4 \left(\frac{V}{A}\right)^{\frac{1}{2}} \text{ watt/lb} \tag{27B}$$

The variation with the ratio V/A of the corrected exhaust power-to-thrust ratio in units of hp/lb and watt/lb are shown in Fig. 6. The power that must be expended in the exhaust jet increases rapidly with the ratio of accelerating voltage to atomic weight of the propellant. The power-per-unit-thrust parameter again demonstrates the desirability of a propellant having a large atomic weight.

Exhaust Velocity — The exhaust velocities of the ions and electrons have been discussed. These are the ion velocities:

$$C = 1.389 \times 10^6 \left(\frac{V}{A}\right)^{\frac{1}{2}} \text{ cm/sec} \tag{10}$$

or:

$$C = 4.557 \times 10^4 \left(\frac{V}{A}\right)^{\frac{1}{2}} \text{ ft/sec} \tag{10A}$$

and the electron velocity is:

$$C_e = 5.952 \times 10^7 V_e^{\frac{1}{2}} \text{ cm/sec} \tag{11}$$

or:

$$C_e = 1.953 \times 10^6 V_e^{\frac{1}{2}} \text{ ft/sec} \tag{11A}$$

The ion and electron velocities should be very nearly the same in order to minimize undesirable charge effects in the vehicle and to reduce the power requirement in the exhaust jet. The ion velocity is shown in Fig. 7 as a function of $\frac{V}{A}$.

Exhaust Current — The total exhaust current from the ion rocket engine will be different depending upon whether a series (Fig. 2A) or parallel (Fig. 2B) arrangement is used. In the series arrangement, the same current passes through both the ion thrust chamber and the electron thrust chamber. In this case the current is:

$$I = \frac{P}{V + V_e} \tag{28}$$

From Equation 26:

$$I = \frac{0.06949 F}{\left(1 + \frac{V_e}{V}\right) \left\{ 1 - \frac{V_e}{V + V_e} \left[1 - \left(\frac{1}{1836 V_e} \frac{V}{A} \right)^{\frac{1}{2}} \right] \right\} A \left(\frac{V}{A}\right)^{\frac{1}{2}}} \text{ amp} \tag{29}$$

if F is in dynes, and:

$$I = \frac{3.091 \times 10^4 F}{\left(1 + \frac{V_e}{V}\right) EA \left(\frac{V}{A}\right)^{\frac{1}{2}}} \text{ amp} \tag{29A}$$

if F is in lb.

Two special cases are of interest. If the electrons are allowed to bleed off the vehicle, V_e vanishes and the current is:

$$I = \frac{0.06949 F}{A \left(\frac{A}{V}\right)^{\frac{1}{2}}} \text{ amp} \tag{30}$$

in cgs units and:

$$I = \frac{3.089 \times 10^4 F}{A \left(\frac{V}{A}\right)^{\frac{1}{2}}} \text{ amp} \tag{30A}$$

in fps units. These relations define the current in the ion thrust chamber alone. If the electrons are ejected at the same velocity as the ions, the correction factor E becomes unity, but a small fraction of the total power is taken by the electrons. From Equation 13:

$$V_e = \frac{V}{1836A - 1} \text{ volts}$$

and the current is reduced slightly.

$$\frac{0.06949F}{\left(\frac{1836A^2}{1836A-1}\right)\left(\frac{V}{A}\right)^{\frac{1}{2}}} \text{ amp} \qquad (31)$$

for the thrust in dynes, and:

$$I = \frac{3.089 \times 10^4 F}{\left(\frac{1836A^2}{1836A-1}\right)\left(\frac{V}{A}\right)^{\frac{1}{2}}} \text{ amp} \qquad (31A)$$

for F in lb. The minimum current is required in a series arrangement in which the exhaust velocities of the ions and the electrons are the same.

The voltages and currents are the same in both the ion and electron thrust chambers for a parallel arrangement (Fig. 2B), and the total current is:

$$I = \frac{P}{V} \text{ amp} \qquad (32)$$

which becomes in cgs units:

$$I = \frac{0.06949F}{\left\{1 - \tfrac{1}{2}\left(\frac{1836A-1}{1836A}\right)^{\frac{1}{2}}\right\} A \left(\frac{A}{V}\right)^{\frac{1}{2}}} \text{ amp} \qquad (33)$$

and:

$$I = \frac{3.089 \times 10^4 F}{\left\{1 - \tfrac{1}{2}\left(\frac{1836A-1}{1836A}\right)^{\frac{1}{2}}\right\} A \left(\frac{V}{A}\right)^{\frac{1}{2}}} \text{ amp} \qquad (33A)$$

in fps units.

The parallel arrangement of the thrust chambers requires twice the current and power that is expended in the exhaust of the series connection. There is little gain in the thrust from the electrons, roughly 1/43 of that from the ions.

For a given thrust level the current diminishes with increasing atomic weight of the propellant and the ratio of accelerating voltage to atomic weight. The variation of the corrected current per unit thrust of the ion rocket engine, $\frac{IE'}{F}$, is shown in Fig. 8. The correction factor E' is defined as:

$$E' = \left(1 + \frac{V_e}{V}\right)\left[1 + X\left\{1 - \left(\frac{1}{1836V_e}\frac{V}{A}\right)\right\}^{\frac{1}{2}}\right] = \left(1 + \frac{V_e}{V}\right)E \qquad (34)$$

for the series connected engine (Fig. 2A).

$$E' = E \qquad (35)$$

for the parallel connected engine (Fig. 2B). The current per unit atomic weight is shown for four representative ions: H^+, $A = 1.008$; N^+, $A = 14.008$; Cs^+, $A = 143.91$; and U^+_{238}, $A = 238.07$. The ordinate of these figures gives the exhaust current in amps directly for an ion thrust chamber of unit thrust.

A point of particular interest demonstrated by these curves is that the exhaust current for a given thrust ion rocket is diminished by two magnitudes if uranium is used as the propellant rather than hydrogen. The use of the heavier elements as propellants greatly reduces the size of electrical transmission lines within the engine.

Propellant Weight Flow — The propellant weight flow is calculated from the ion flow and the weight

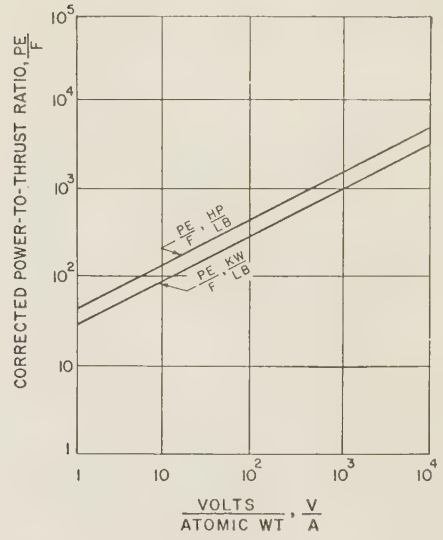

Fig. 6 — Exhaust jet power of ion rocket engine

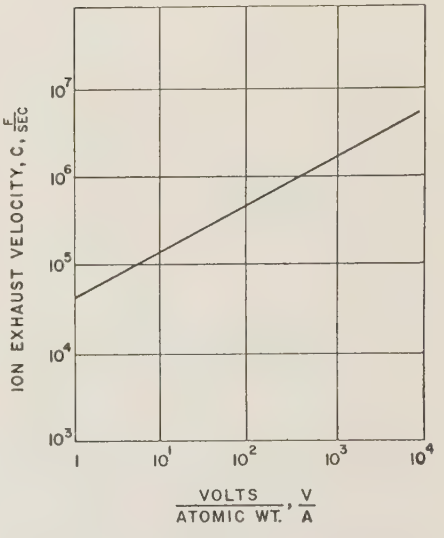

Fig. 7 — Ion exhaust velocity

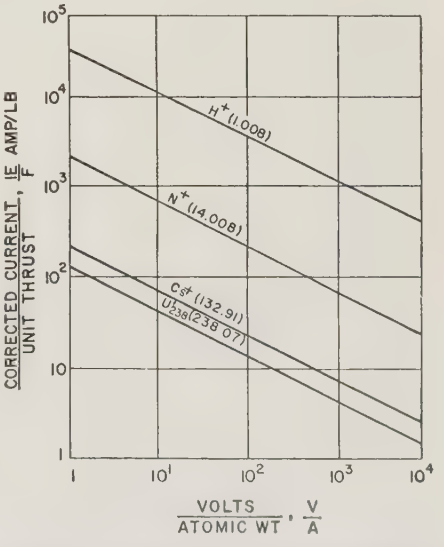

Fig. 8 — Ion rocket exhaust current for representative ions

of the atoms used for propellant:

$$\dot{w} = \dot{N}m + h\dot{N}_e m, \quad \frac{2.997 \times 10^9 IA}{6.0248 \times 10^{23} e} \tag{36}$$

where:

$\dot{w}$ = Propellant flow, gram/sec
I = Current in ion thrust chamber, amp
e = Charge of electron = 4.8029×10^{-10}, esu

In cgs units, the propellant flow is, if A is given by Equation 18:

$$\dot{w} = 1.038 \times 10^{-5} IA \text{ gram/sec} \tag{37}$$

and in fps units:

$$\dot{w} = 2.286 \times 10^{-8} IA \text{ lb/sec} \tag{37A}$$

The flow rate can also be expressed directly in terms of the vehicle gross weight and the thrust-to-weight ratio. From Equations 30 and 37:

$$\dot{w} = 7.199 \times 10^{-7} Ma \left(\frac{V}{A}\right)^{-\frac{1}{2}} \text{ gram/sec} \tag{38}$$

and:

$$\dot{w} = 7.060 \times 10^{-4} M_g G \left(\frac{V}{A}\right)^{-\frac{1}{2}} \text{ lb/sec} \tag{38A}$$

in cgs and fps units, respectively.

The flow rate per unit thrust is plotted as a function of the parameter V/A in Fig. 9.

Specific Impulse — The specific impulse of the ion propellant is by definition the thrust per unit weight flow of the propellant. This is obtained directly from Equation 38A:

$$I_s = 1417 \left(\frac{V}{A}\right)^{-\frac{1}{2}} \text{ sec} \tag{39}$$

or from the ratio of C/g. This parameter has the same value in both cgs and fps units, as does the specific impulse of the electrons:

$$I_{se} = 1417(1836V_e)^{\frac{1}{2}} = 6.072 \times 10^4 V_e^{\frac{1}{2}} \text{ sec} \tag{40}$$

The specific impulse is shown as a function of the ratio V/A in Fig. 10.

Dimensions of Ion Thrust Chamber — The ion rocket thrust chambers carry a high current. The density of this current is limited by Child's law[4]. From the particle current and the limiting current density an estimate of the minimum dimensions of the thrust chambers can be obtained.

A quantitative analysis of the problem is not practicable except when it can be expressed in terms of a single dimension, that is, when the particle paths follow the lines of electric force as they do when the thrust chambers are of rectangular, cylindrical, and spherical symmetry. In the case of the ion rocket thrust chamber, it is assumed that the following conditions hold:

1. The electrodes are assumed to be infinite, plane, equipotential surfaces.
2. The number of charged particles emitted at the repelling electrode exceeds the demand.
3. The particles start from rest at the repelling electrode.
4. Particles have simple positive or negative charge, only one species present in the thrust chamber.
5. The accelerating voltage is constant and has been constant sufficiently long for the current to reach its steady-state value.

Under these conditions the current density of the particles is given by the relation:

$$2.997 \times 10^9 J = \frac{1}{9\pi d^2} \left(2\frac{e}{m}\right)^{\frac{1}{2}} \left(\frac{V}{299.7}\right)^{\frac{3}{2}}, \tag{41}$$

where:

J = Current density, amp per unit area
e = Charge on the particle, esu
m = Mass of the charged particle, grams
V = Accelerating voltage, volts
d = Separation of accelerating electrodes, cm or ft

The dimensions of J are amp/cm^2 or amp/sq ft depending upon whether d is expressed in cm or ft.

Evaluated in terms of the parameter V/A, the current density becomes:

$$J = 0.5468 \times 10^{-7} \frac{A}{d^2} \left(\frac{V}{A}\right)^{\frac{3}{2}} \text{ amp/unit area} \tag{42}$$

The cross-sectional area of the ion thrust chamber is then, from Equations 30 and 42:

$$A_t = \frac{I}{J} = 0.1271 \times 10^7 Ma \left(\frac{V}{d}\right)^{-2} \text{ cm}^2 \tag{43}$$

in cgs units:

$$A_t = 5.651 \times 10^{11} M_g G \left(\frac{V}{d}\right)^{-2} \text{ sq ft} \tag{43A}$$

in fps units:

A_t = Cross-sectional area of ion thrust chamber

The current density of the electron thrust chamber:

$$J_e = 2.334 \times 10^{-6} \frac{V_e^{\frac{3}{2}}}{d_e^2} \text{ amp/unit area} \tag{44}$$

Since the dimensions of the electron thrust chamber have a specific relation to those of the ion thrust chamber, rather than discuss the dimensions of the former directly, it becomes more convenient to relate dimensional ratios of the two thrust chambers. The area ratio of the electron and the ion thrust chambers is:

$$\frac{A_{te}}{A_t} = \frac{I_e J}{I J_e} = \frac{J}{J_e} \tag{45}$$

because it is desirable to have the same current in both chambers in order to minimize effects of external charges on the vehicle. From Equations 42 and 44, the area ratio for the same currents is expressed in terms of the design parameter V/A:

$$\frac{A_{te}}{A_t} = \frac{0.02334A}{V_e^{\frac{3}{2}}} \left(\frac{V}{A}\right)^{\frac{3}{2}} \left(\frac{de}{d}\right)^2 \tag{46}$$

Conclusions about the dimensions of the ion rocket thrust chambers are limited by the assumptions upon which the analyses are based. Parallel flat plate electrodes are assumed. Since the charged particles are ejected from the vehicle to obtain thrust, the accelerating electrodes of the thrust chambers are grid of ring types rather than plates. An accelerating grid has been found to be impractical in the linear accelerator field. Short grid life results from collisions of the ions with the structure, which destroy the grid.[5] Dispersion of the ions results in an attendant waste of power.

An extrapolation from the flat plate configuration

[4] "Applied Electronics," by staff of Electrical Engineering Dept., M.I.T. Pub. by John Wiley and Sons, Inc., New York, 1943.

[5] *Review of Scientific Instruments*, Vol. 27, November, 1956, pp. 907–909: "High Current Ion Injector," by W. A. S. Lamb and E. J. Lofgren.

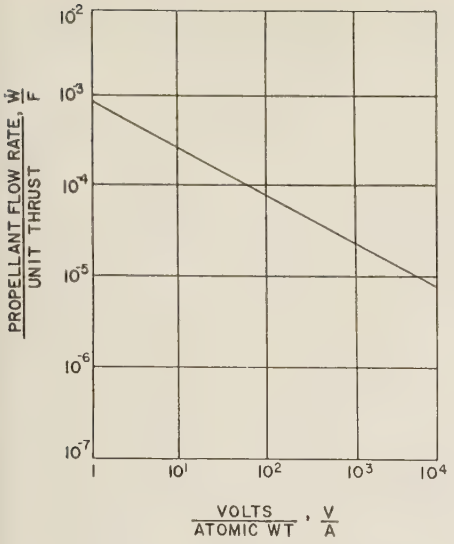

Fig. 9 — Ion rocket propellant flow rate

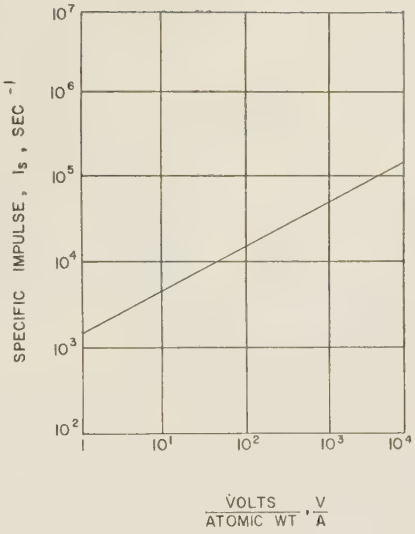

Fig. 10 — Ion rocket specific impulse, I_s

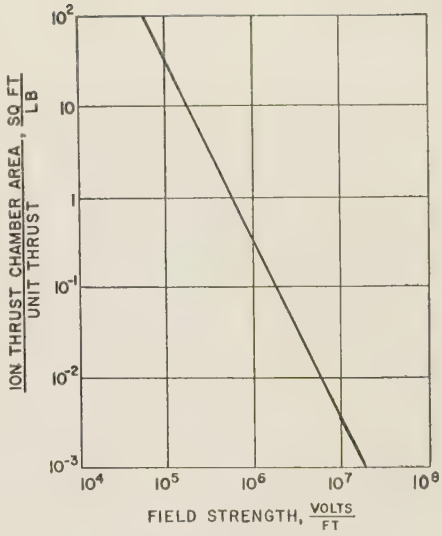

Fig. 11 — Influence of field strength on ion thrust chamber cross-section

to the ring configuration of Fig. 2 can be made by considering the accelerating field strength. The ratio V/d is the field strength between flat plate electrodes. The electric field of the thrust chambers (Fig. 2) can be adjusted to be parallel over a considerable distance, then sharply curved, terminating on the ring accelerating electrode. If the parallel portion of the field is sufficiently long, the field drops in strength outside the ring and the particles reach a high velocity. They will continue on an approximately parallel path and be ejected from the thrust chamber. Under this situation, d is the distance the charged particles travel within the electric field, V is the potential difference between the repelling electrode and the point where the charged particle leaves the electric field. The voltage drop between electrodes is, thus, greater than the accelerating voltage which acts upon the charged particle. Therefore, this analysis gives an estimate of the minimum area required for the ion rocket thrust chambers.

The area of the ion thrust chamber will be proportional to the thrust and inversely proportional to the square of the field strength V/d. The decrease of the ion thrust chamber cross-section per unit thrust with increasing field strength V/d is shown in Fig. 11. It is believed that the proportionality constant will be greater than the values given in Equation 43. The area is independent of the propellant used. The design problem is to adjust the accelerating voltages and the electrode spacing to minimize the cross-section of the thrust chambers, yet not to force the power-to-weight ratio into the region which is impractical to achieve (Fig. 4).

The dimensions of the electron thrust chamber are selected with the compromise in mind to obtain a minimum dissipation of power with the acceleration of electrons. Production of electrons by a heated tungsten or oxide-coated cathode is believed to be sufficient for the ion rocket application. Temperature variation of the heated cathode offers a method of control of the electron emission to maintain the current through the electron thrust chamber. If the accelerating voltage of the electron thrust chamber is selected to make the electron and ion velocities equal, the area ratio of the thrust chambers becomes:

$$\frac{A_{te}}{A_t} = 1836A\left(\frac{d_e}{d}\right)^2 \tag{47}$$

This implies that the effective electrode spacing in the electron thrust chamber is very small to keep the area of this component of reasonable size. The electron field strength must be high.

The cross-sectional dimensions of the electron thrust chamber will be of the same order of magnitude as, or greater than, the cross-section of the ion thrust chamber. This problem can be solved by discharging negatively charged particles having a mass comparable to that of the positive ions. This technique has a further virtue in that power will not be dissipated in discharging particles of small mass.

Comparative Performance

The velocity change of the rocket vehicle, which is assumed to be in gravity-free space, gives a measure of the performance of the rocket engine. The development of this change convincingly demonstrates the influence of the propellant and accelerating voltage on the thrust chamber.

The velocity change of the rocket vehicle, neglecting the small effect of the electron flux, in gravity-free space is:

$$\Delta v = C l n \frac{M_g}{M_o} \tag{48}$$

The vehicle gross weight to empty weight ratio M_g/M_o is expressed in terms of the thrust-to-weight ratio G and the parameter V/A and the operating time t (Equation 38).

$$\frac{M_g}{M_o} = \frac{M_g}{M_g - \dot{w}t} = \frac{1}{1 - 7.060 \times 10^{-4} G \left(\frac{V}{A}\right)^{-\frac{1}{2}} t} \tag{49}$$

The operating time of the ion rocket engine to achieve a given velocity change V of the vehicle is the significant parameter upon which to judge the

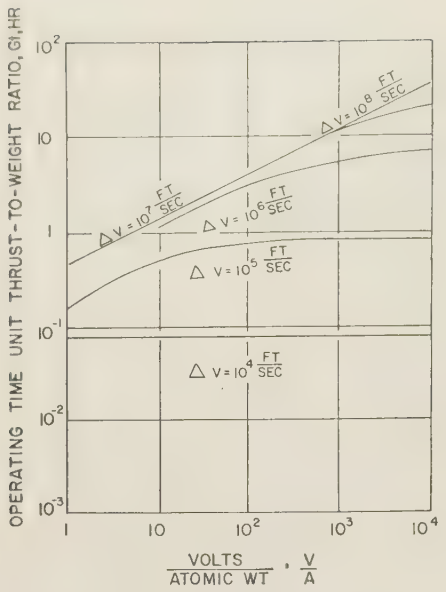

Fig. 12 — Operating time for ion rocket engine of unit throat-to-weight ratio

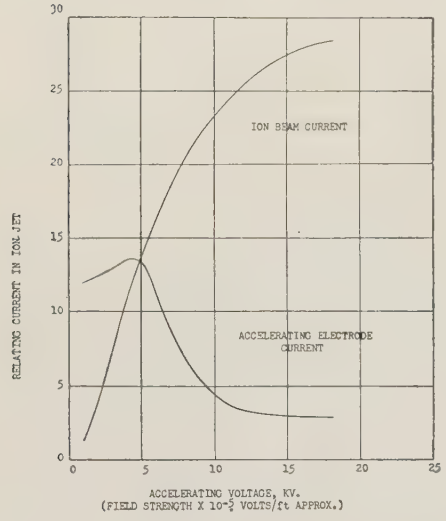

Fig. 13 — Typical current variation of ion rocket engine

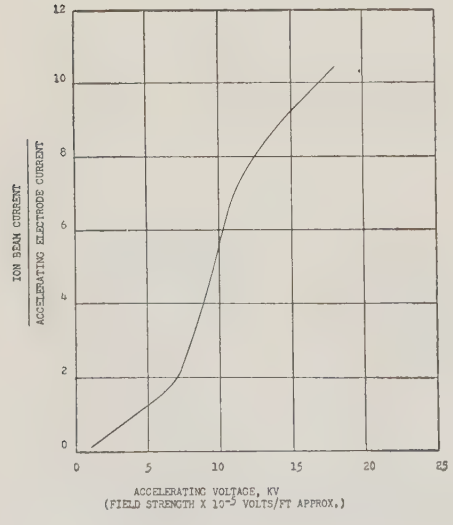

Fig. 14 — Comparison of currents of ion rocket engine

engine performance. From Equations 10A, 48, and 49, the operating time is:

$$t = \left[\frac{1 - e^{-\frac{\Delta v}{4.557 \times 10^4 \left(\frac{V}{A}\right)^{\frac{1}{2}}}}}{7.060 \times 10^{-4} G} \right] \left(\frac{V}{A}\right)^{\frac{1}{2}} \text{ sec} \qquad (50)$$

This parameter increases with decreased thrust-to-weight ratio and increased operating voltage. A propellant of heavy atomic weight decreases the operating time.

For large velocity changes for which the ratio:

$$\frac{\Delta v}{4.557 \times 10^4 \left(\frac{V}{A}\right)^{\frac{1}{2}}} > 5$$

the vehicle velocity does not exceed one-tenth the velocity of light, that is, 10^8 fps, the operating time is:

$$t = 1416 G^{-1} \left(\frac{V}{A}\right)^{\frac{1}{2}} \text{ sec} \qquad (51)$$

Comparative operating times for an ion rocket engine developing the same thrust and operating under the same accelerating voltage but using different propellants differ markedly. For example, to achieve a high vehicle velocity change an electron rocket engine must operate 650 times longer than one using uranium ions to achieve a velocity change of 10^8 fps. A hydrogen ion engine must operate 15.5 times as long as the uranium ion engine.

If the ratio:

$$\frac{\Delta v}{4.557 \times 10^4 \left(\frac{V}{A}\right)^{\frac{1}{2}}} < 0.07$$

the operating time becomes nearly independent of V/A and depends only on G:

$$t = 0.0311 \frac{\Delta v}{G} \text{ sec} \qquad (52)$$

Selection of the operating voltage and the propellant is of small consequence so far as the operating time to achieve a small change in vehicle velocity is concerned.

The operating times for a range of vehicle velocity changes are summarized as a function of the parameter V/A in Fig. 12.

Minimum Accelerating Voltage

The minimum accelerating voltage used in the ion thrust chamber determines, in conjunction with the weight per unit electron charge of the ion, the maximum thrust-to-weight ratio of the vehicle (Figs. 4 or 5), the minimum total power requirement (Fig. 6), and influences all of the other design parameters summarized in this paper. The importance of this voltage in overall engine design and its application to a vehicle is immediately evident.

Theoretical determination of this minimum voltage is an involved problem including the solutions of Poisson's and LaPlace's equations with boundary conditions, which describe the electrical potentials and space rate of change for the particular accelerating electrode configuration used.[6]

[6] *Journal of Applied Physics*, Vol. 11, August, 1940, pp. 548–554: "Rectilinear Electron Flow in Beams," by J. R. Peirce.

In conjunction with these, the equations of motion of the ions must be solved. From these solutions the number of ions passing through the accelerating electrode are then computed. This task is sufficiently formidable that resort to experimental methods has been taken to obtain initial estimates of the minimum accelerating voltage. Early efforts of an experimental program on accelerating system configurations should be the determination of this voltage.

Experience of investigators of heavy ion sources furnish data upon which a preliminary estimate of the minimum accelerating voltage can be made.[7] These data are summarized and related to the ion rocket engine in Figs. 13 and 14.

The ion beam passes through an electrode with a slotted aperature which is designed to satisfy the Peirce Conditions.[6] In Fig. 13 the ion current is plotted as a function of the accelerating voltage in kilovolts. The electric field strength of this system is directly proportional to this voltage. At low voltages the ion beam current is very low, most of the ions being deflected to the electrode. The current rapidly increases with voltage and approaches a limiting value established by the capability of the source to furnish ions. As this emission limitation is approached, the ion source becomes degenerative and unstable, eventually being extinguished at excessive accelerating voltages.

The accelerating electrode current starts at a high level for low voltages because most of the ions extracted from the source strike the electrode.

The current steadily increases, reaching a maximum at 5000 volts. Above this voltage the current rapidly diminishes, approaching a minimum value at approximately 12 kv. The electrode current at the higher voltages is developed from photoelectrons, thermionially emitted electrons, secondary electrons, and collection of ion pairs generated in the gap between the accelerating electrode and the ion source. The configuration of the curve describing the variation of accelerating electrode current is independent of the type of ion. The maximum can be shifted somewhat by modifying the operating conditions. The minimum current can be reduced further by optically shielding and cooling the accelerating electrode. The shape and alignment of the ion thrust chamber system affects the efficiency of ion acceleration as well as the angular divergence of the exhaust jet which causes a loss of thrust.

The ratio of the ion beam current to the accelerating electrode current (Fig. 14) further defines the accelerating voltage range over which an accelerating electrode system of good design changes from an inefficient to a relatively efficient system. This voltage range is 6,000–12,000 volts. Above 12 kv the ion output can be increased at will without ion loss to the accelerating electrode. The voltage limit is that voltage at which the ion source becomes degenerative.

From these data the minimum accelerating voltage is tentatively established at 12 kv. The minimum accelerating field is approximately one million volts per foot.

[7] *Review of Scientific Instruments*, Vol. 27, October, 1956, pp. 809–817: "Ion Source for Production of Multiply Charged Heavy Ions," by C. F. Anderson and K. W. Ehlers.

If vehicle thrust-to-weight ratios greater than 10^{-4} are desired with power plants of presently achievable specific power, research on ion accelerating techniques in the voltages range of 5–12 kv will be rewarding since the design parameter V/A becomes less for a given ion.

Conclusions

Three parameters, the ratio of the accelerating voltage to the effective atomic or molecular weight of the propellant per unit charge (V/A), the gross weight of the vehicle M_g, and the thrust-to-weight ratio G, determine the design characteristics of the ion rocket engine.

The maximum thrust-to-weight ratio to be expected from an ion rocket engine using presently available power generators is less than $10^{-4}G$.

Propellants of the highest possible atomic or molecular weight which form singly charged ions are most efficient for use in the ion rocket engine.

Power is wasted if lightweight ions or electrons are used to develop thrust.

Ions having atomic or effective molecular weights of less than 100 grams produce thrusts too low to be of use.

The major problem of the ion-propelled space vehicle is the continuous development of high specific power.

The Linac linear accelerator, which uses a radio-frequency resonant cavity to achieve extremely high ion velocities, is impractical for application as an ion thrust chamber.

The ion thrust chamber is basically a simple device consisting of an ion source with an accelerating electrode, and an electron source also with an accelerating electrode.

Productive avenues of research, directed toward achieving a successful high-thrust ion rocket engine, are high specific power electrical generators and heavy ion propellants.

The design of the thrust chamber demands a compromise judgement in the selection of the accelerating voltage, the propellant, and the thrust-to-weight ratio of the vehicle to achieve the optimum balance among specific power demands, size, weight, and operating time of the rocket engine.

The minimum accelerating voltage for an ion thrust chamber is now estimated to be 12,000 volts.

Additional References

1. "Problems of Physics in Ion Source," by A. H. Barnes, S. M. MacNeille, and C. Starr. TID-5219, Clinton Engineer Works, Tennessee Eastman Corp., Oak Ridge, Tenn., 1951.

2. "Sources and Collectors for Use in Calutrons," by A. Guthrie and R. K. Wakerling. TID-5218, University of California, Berkeley, Calif., June, 1949.

3. *Journal of Chemical Physics,* Vol. 25, September, 1956, pp. 389–394: "Ionization on Platinum and Tungsten Surfaces, Part I — The Alkali Metals," by S. Datz and E. H. Taylor.

4. *Journal of Chemical Physics,* Vol. 22, September, 1955, pp. 1711–1718: "Study of Chemical Reaction Mechanisms with Molecular Beams, Reaction of K with HBr," by E. H. Taylor and S. Datz.

5. *Journal of Applied Physics,* Vol. 28, January, 1957, pp. 7–15: "Formation of High-Density Electron Beams," by G. R. Brewer.

AN ENGINEERING evaluation of six automobile head-on collision experiments is presented for impact speeds ranging from 21 to 52 mph. An analysis of the relative collision performances of unit-body and frame-type construction is made. Anthropometric dummy subjects facilitate determination of force systems for restrained and unrestrained motorists, their dynamic and kinetic responses to impact, and the causative factors associated with motorist injury production.*

The systems of instrumentation which enabled a comprehensive analysis to be made from an event lasting only 0.25 sec are briefly presented.

Specific data include deceleration patterns for different locations on the car underbody and body; gross and localized elastic and permanent deformations of structures; the relationship of repair costs to impact velocity; motorist injury analysis including the contributions of the steering wheel, seats, and other parts of the car interior; statistical significance of differences in collision performances observed for unit-body and frame-and-body construction; and the physics of the automobile head-on impact. Lap belt performance is presented in terms of efficiency, loadings, and elongation as a function of impact velocity.

Automobile

THE purpose of the experiments described in this paper was to determine through engineering research the injury-producing and related factors associated with the automobile collision, in order to provide a sound basis on which appropriate engineering revision of the automobile may be accomplished. Additionally, this study was conducted to determine head-on collision performances for vehicles of unit-body and of frame-and-body type construction at impact velocities between 21 and 52 mph.

Facilities and Equipment

Vehicle Control Systems — A 2860-ft asphalt runway, a portion of a former airfield, was selected as the site for conducting head-on collision experiments. The exacting requirements of photographic instrumentation made it essential to have a predesignated nonshifting point of impact. Previous studies involving vehicle-to-fixed-barrier and car-to-car rear-end collisions, as well as the subject head-on collisions, were all planned to assure that the impact would occur in full view of all cameras (Fig. 1). Our specifications for head-on collision experiments were as follows:

1. An allowable error of ±2 in. lateral displacement of one car relative to the other (directional control) throughout all collision-speed ranges.[1]
2. An allowable error of ±6 in. from point of impact along the 1400 ft pre-crash parallel axes of approach.
3. Both cars to have identical speeds.
4. Impact speed to be within ±2 mph of the designated crash speed.
5. Both cars completely free of speed and directional constraining influences during impact.

During the past seven years of collision research, directional control of experimentally crashed vehicles has been accomplished from remote positions, by radio control, electrical control by selsyn motor, and a single steel cable which simultaneously pulled and grossly guided the car. By direct control, cars have been guided to impact using a human driver. Of these systems, the use of the human operator was the most accurate but the necessary limitation of the human operator to certain types of collisions at speeds generally below 30 mph made it necessary to devise another system for these experiments.

Specification 1 for vehicle directional control was met, therefore, by the installation of an aluminum

* The research described in this report was conducted in the Institute of Transportation and Traffic Engineering, Department of Engineering, University of California, Los Angeles. Financial support for the experiments was provided by Parish Pressed Steel Co. (a division of Dana Corp.), Reading, Pa.

[1] Which means that each car must be steered within 1 in. of the prescribed course, a degree of precision neither consistently nor generally possible by human operation.

Head-On Collisions — — series II

Fig. 1 — Head-on collision

D. M. Severy, J. H. Mathewson, and A. W. Siegel, University of California

This paper was presented at the SAE National Passenger-Car, Body, and Materials Meeting, Detroit, March 5, 1958.

ground-level monorail guide system extending 1400 ft in opposite directions from the point of impact (Fig. 2[2]). Specification 2, the allowable deviation from the point of impact with respect to the axis of approach, was met through the use of a 3/8-in. steel cable connected to the rear of Car No. 1 (the power car), thence passing through a sheave anchored at the end of the track behind Car No. 1 and back under Car No. 1 to the front end of Car No. 2 positioned at the other end of the 2800-ft track. By proper length adjustments, Car No. 1 pulled Car No. 2 into mutual collision at the prescribed point of impact (Fig. 3[3]).

Specification 3, identical speed for both cars, was satisfied by physically linking the two cars together by means of the cable-sheave assembly; and Specification 4, relating to the speed of impact, was met by equipping Car No. 1 with a governor. To meet Specification 5 the cars were guided along the monorail by a phenolic shoe which slid along inside the U-shaped rail. This shoe was fastened by a yoke extending from the shoe to the front bumper. The tow cable was released a fraction of a second before

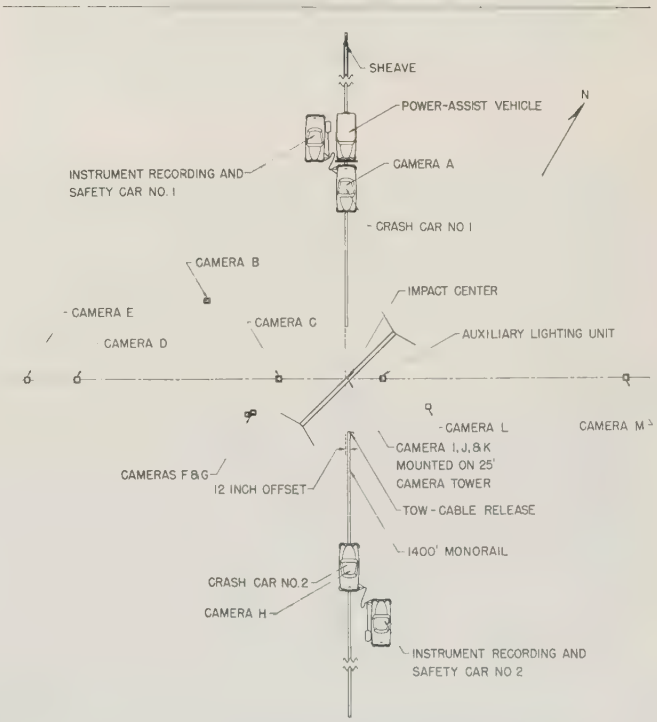

Fig. 3 — Vehicle control and photographic systems

[2] Deleted in the interest of brevity. Microfilm copy of complete paper including appendices available by writing to the Library Photographic Service, University of California, Los Angeles 24, Calif.

[3] The camera data of Fig. 3 will be referred to in the section on instrumentation.

impact by a disconnector hook on the track engaging the cable release lanyard located under the front end of Car No. 2. The track, in both directions, terminated 20 ft from the impact point, thus eliminating the constraining influence of the track during the impact event. These factors, cable release and termination of the track, satisfied the final specification requiring that vehicles be free from speed- and direction-constraining influence at time of impact.

Camera Tower — The dependability of the vehicle control system permitted cameras to be moved in as close as desired to the impact area and to be positioned at every important camera angle about the perimeter of the impact area. Two important dimensions were, however, still excluded from photographic coverage, one being vertically upward to provide opportunity to study the collision performance of the car underbody and the other vertically downward to provide a bird's-eye view of the collision. The underbody photography will be described in a later section. To accomplish photography of a collision event in a vertically downward direction, two 30-ft high steel towers and a 50-ft horizontal cross-span were designed and erected to support vertically oriented cameras 26 ft above ground level (Fig. 4[2]). To facilitate tower camera photography of the impact of car occupants with the cars' interiors, the sheet metal roofs above the front seat area were cut away (Fig. 5).

Fig. 5 — Tower camera view of collision

Instrumentation

Impact phenomena are difficult to instrument. A practical degree of accuracy is attainable only after proper attention has been given to the many related variables. The essential identifying and descriptive data for the different systems of instrumentation applied to these head-on collision experiments are presented in Table 1. As frequently as practical, deliberate overlapping of coverage by independent systems of instrumentation provided duplicate data to permit evaluation of reliability of data.[4]

Experimental Procedure

Following several weeks of buildup time, the two days immediately preceding each experiment are utilized by the entire research team for setting up and operationally checking equipment at the test site. A control board is used to record the current status as preparations proceed (Fig. 8). When the control board shows that all preparations have been completed, the project engineer takes his station at the power control unit situated adjacent to the impact point. He is in telephone communication with instrument recording vehicles, each positioned adjacent to its respective crash car at opposite ends of the track (Fig. 9). At this time, the project en-

[4] This is the "principle of redundancy" commonly used in missiles systems and other expensive experiments to ensure reliability and to guard against loss of data. Further instrumentation details are given in Appendix III. Reference is also made to 14 previous papers by the first two authors, some of which describe these systems of instrumentation in detail. Several of these papers are listed in footnotes.

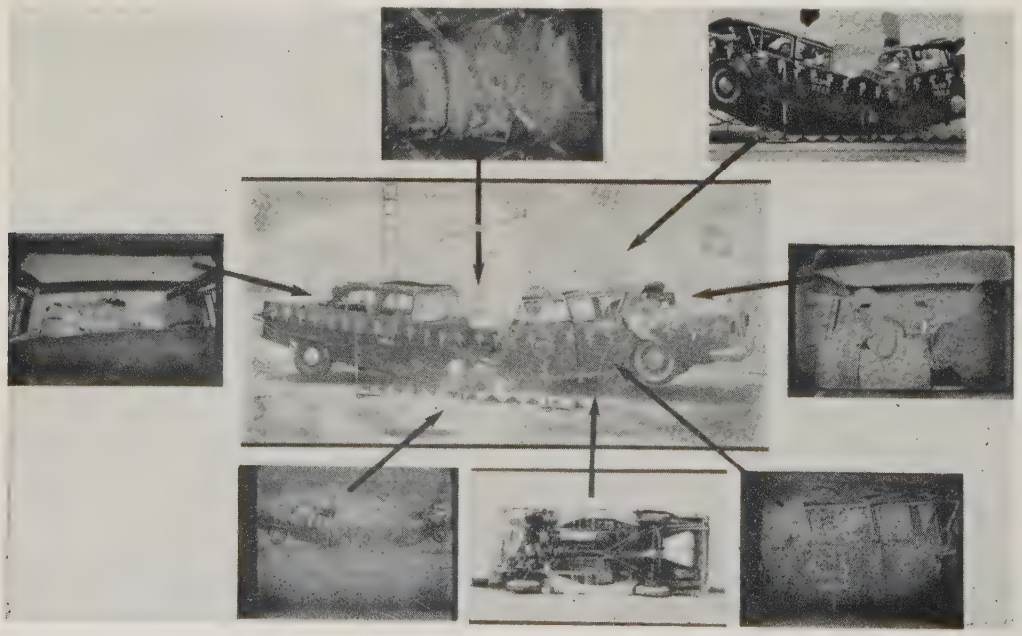

Fig. 6 — Three-dimensional photographic coverage

Table 1 — Instrumentation

Item	Device	To Provide	Location	Specifications
I	High-speed motion picture cameras	Time displacement and auto-dummy kinematic data	Cameras D, E, F, J, and M, Fig. 3	Eastman I high-speed camera, Eastman II high-speed camera, Fastax WF-3 high-speed camera, 16 mm Superior 4 negative film, 800–1400 frames per sec (f/s)
II	Moderately high-speed motion picture camera	Kinematics of dummies from within car	Cameras A and H, Fig. 3, Fig. 6	Urban Engr. Co. GSAP MBH 200-16 High-G Tolerance, 16 mm Superior 4 negative 200 f/s
III	Standard-speed motion picture cameras	General photographic coverage	Cameras B, I, and L, Fig. 3	Kodak Cine Specials I and II, 16 mm, DuPont 914A, 24 f/s
IV	Still camera	Precision-timed photographs of car at instant of maximum collapse	Cameras C, G, and K of Fig. 3; Fig. 6	Speed Graphic, 4 x 5, Royal Pan 1/500 sec with electronic timer to trigger camera precalculated millisec after start of collision
V	Calibrated reference boards	A calibrated and fixed reference positioned at photographic range of subject	See Figs. 1 & 5	1/4 x 6 x 96 in. plywood; calibrated black and white in alternate 1 ft increments, positioned both vertically and horizontally
VI	Anthropometric dummy and engine reference lights	Point source of light for high-speed photography	Head and shoulders of dummy; principal points on the engine and adjacent frame structures	1.5 volt lens-type bulb secured to target and operated at over-voltage
VII	Reference targets	Precision photographic references for micromotion analysis	On points of interest for both the car and occupants, Figs. 1, 5, and 6	4 x 4 in. black-and-white targets
VIII	Electrical accelerometers	Time-deceleration data	Stations 2, 5, 8, and 10 of car; driver's chest and passenger's hip	B & F LF 50-50; Statham A38a-60-350, specifications detailed in Appendix III
IX	Seat belt tensiometer	Force-time applications to seat belt by dummy	Between floor pan anchorage and belt webbing, rear seat occupant	Provided in Appendix III
X	Recording oscillograph	Time-deflection record of transducer signals	Carried by instrument recording vehicle (Fig. 7[a])	24-channel Hathaway oscillograph type S 8-C used with power supply units and strain gage control unit, type MRC-15
XI	Electronic delay timer	Precision timing for still photography	At impact center, Fig. 3	184-millisec time delay device built by I. T. T. E.
XII	Pulse generator	Timing for high-speed cameras	Between camera and power source	Wallensak Optical Co., 100 and 1000 cycles per sec
XIII	Anthropometric dummy	Human simulation	Driver and right rear seats	One Model 120 and three Model 157, Sierra Engineering, Sierra Madre, Calif.
XIV	Car underbody position indices	Permanent deformation data	On principal structures of car underbody Figs. 6 and 11	White 3/8-in. diameter painted dots for optical comparator analysis and pre-crash/post-crash superposition photographs of underbody
XV	Displacement recorders	Measurement of differential motion of certain body components	See Fig. 14	2½-in. bronze stylus arm mounted by bracket to one part of car body with stylus spring-loaded against carbon-blacked polished chrome plate secured by its bracket to adjacent part of car body
XVI	Repair cost appraisals	Comparative repair cost analyses	See Fig. 25 of repair cost analysis section	Not less than 3 independent appraisals for each car by qualified repair agencies

[a] See footnote 2.

gineer announces "minus 5 min" which initiates a series of last minute instrumentation and general operational checks. These are concluded with an "all clear to commence run" by the project engineer after which the operator of the power-assist vehicle commences to push the power crash car (Car No. 1) up to cruising speed. As the power crash car (in gear, ignition on) is pushed forward, its engine starts and thereafter contributes to the acceleration to cruising velocity. The cable-pulley linkage connecting the two collision cars prevents any speed differences from developing within the system. When the crash cars reach the pre-designated cruising velocity it is maintained as a steady state by means of a governor on the power crash car. Meanwhile, the power-assist vehicle has dropped back from its pushing position as cruise velocity is approached.

If a malfunction occurs during a run, the instrumentation engineers riding in the pacing data-recording vehicles, may stop the collision vehicles by remote-controlled air brakes. A position 10 sec before impact is signalled by the passing of a stationary marker at which time the instrumentation engineers start the recording oscillographs in their cars and the cameras in the crash cars. The instrument-recording cars commence decelerating from their slightly leading position so as to permit the crash cars, now maintaining a constant speed, to forge ahead of the instrument cars just before impact (Fig. 5). The instrument-recording cars brake

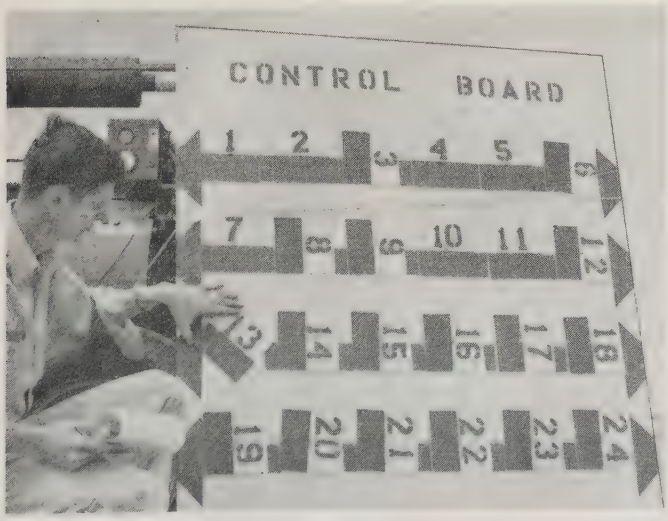

Fig. 8 — Operations control board

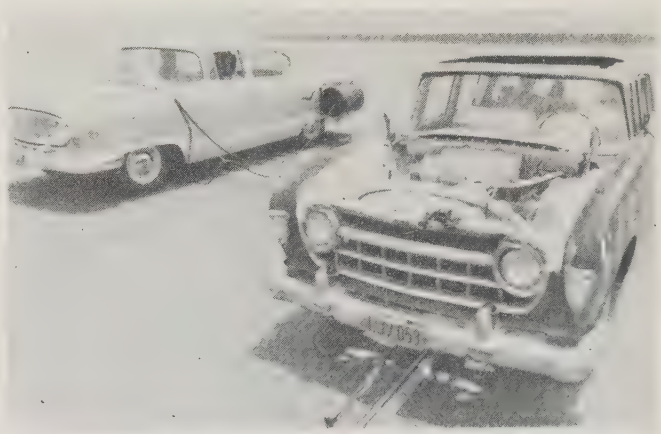

Fig. 9 — Crash car is paced by instrument recording car

Table 2A — Automobile Impact Analyses

Item Number	Description	Derived from	Experiment 37		Experiment 41		Experiment 39		Experiment 40		Experiment 43		Experiment 44	
			1949 Ford 4-door sedan	1950 Nash 2-door sedan	1956 Nash Rambler 4-door sedan	1956 Nash Rambler 4-door sedan	1956 Ford 4-door sedan	1956 Nash 4-door sedan	1956 Ford-1 4-door sedan	1956 Ford-2 4-door sedan	1956 Ford 4-door sedan	1956 Nash Rambler 4-door sedan	1956 Pontiac 4-door sedan	1956 Nash Statesman 4-door sedan
1	Measured weight of car with dummy, lb	Weighmaster certificate	3110	2930	3440	3370	3730	3330	3680	3610	3660	3530	4000	3580
2	Velocity before impact, ft/sec	Film analysis	+ 31.4	− 30.8	+ 29.0	− 30.9	+ 39.0	− 39.6	+ 39.9	− 40.0	+ 68.7	− 68.2	+ 76.3	− 75.5
3	Velocity after impact, ft/sec	Film analysis	− 3.3	− 2.3	− 2.6	− 2.0	+ 3.3	+ 5.1	− 2.8	+ 4.3	− 1.5	+ 2.0	− 5.0	− 5.0
4	Peak deceleration rate, G	Transducers	26	22	22	18	32	27	30	45	53	79	> 50	66
5	Duration of impact, sec	Transducers	0.100	0.092	0.083	0.095	0.125	0.125	0.075	0.085	0.105	0.077	0.132	0.107
6	Maximum amount of collapse, ft	Film analysis	1.71	1.61	1.29	1.43	1.73	1.78	1.57	1.54	3.50	3.08	4.50	3.69
7	Mass (w/g), slugs	(#1) /32.2	96.6	91.0	106.8	104.7	115.8	103.5	114.3	112.2	113.7	109.7	124.2	111.2
8	Momentum before impact (mv), lb-sec	(#7) × (#2)	+ 3030	− 2805	+ 3100	− 3240	+ 4520	− 4100	+ 4570	− 4490	+ 7810	− 7480	+ 9470	− 8400
9	Momentum after impact, lb-sec	(#7) × (#3)	− 318	− 209	− 278	− 209	+ 382	+ 528	− 320	+ 483	− 171	+ 219	− 622	− 556
10	Total change in velocity, ft/sec	(#3) − (#2)	− 34.7	+ 28.5	− 31.6	+ 28.9	− 35.7	+ 44.7	− 42.7	+ 44.3	− 70.2	+ 70.2	− 81.3	+ 70.5
11	Kinetic energy before impact ($\frac{1}{2}$ mv^2), ft-lb	$\frac{1}{2}$ (#7) × (#2)^2	47,500	43,200	44,800	49,900	88,000	81,000	91,000	89,700	267,000	254,000	362,000	317,000
12	Kinetic energy after impact, ft-lb	$\frac{1}{2}$ (#7) × (#3)^2	530	240	360	210	630	1300	450	1040	130	220	1600	1400
13	Coefficient of restitution (v_2/v_1) (dimensionless ratio)	Δ(#3)/Δ(#2)	$0.016 = \left(\frac{1.0}{62.2}\right)$		$0.010 = \left(\frac{0.6}{59.9}\right)$		$0.023 = \left(\frac{1.8}{78.6}\right)$		$0.089 = \left(\frac{7.1}{79.9}\right)$		$0.026 = \left(\frac{3.5}{136.9}\right)$		$0 = \left(\frac{0}{151.8}\right)$	
14	Change in momentum, lb-sec	(#9) − (#8)	− 3348	+ 2596	− 3378	+ 3031	− 4138	+ 4628	− 4890	+ 4973	− 7981	+ 7699	− 10,092	+ 7844
15	Loss of kinetic energy during impact, ft-lb	(#11) − (#12)	46,970	42,960	44,440	49,690	87,370	79,700	90,550	88,660	266,870	253,780	360,400	315,600
16	Average force acting on car, lb (ΔKE/S = work/S)	(#15)/(#6)	27,400	26,700	34,400	34,700	50,500	44,800	57,700	57,600	76,300	82,300	80,200	85,500
17	Average rate of energy dissipation (ΔKE/t), ft-lb/sec	(#15)/(#5)	470,000	467,000	535,000	523,000	698,000	637,000	1,208,000	1,045,000	2,540,000	3,295,000	2,730,000	2,950,000
18	Crash horsepower, hp	(#17)/550	855	850	973	950	1270	1158	2195	1900	4620	5980	4970	5370

to a stop 10–30 ft short of the point of impact (Fig. 10). This procedure ensures that the 100-ft transducer cable running between each crash car and its respective instrument vehicle will not become detached just prior to or during impact. At zero minus 4 sec to impact, the project engineer sequentially energizes all high-speed cameras.

Technical Findings: Collision Performance of Automobile Structure

Automobile Impact Analyses

The physical factors relating to the six head-on collision experiments included in this study are presented in Table 2A. Experiment 37 represents vintage vehicles (1949-50) crashed at 21 mph. Experiments 39 and 43 involve identical impact conditions, except that Experiment 39 was conducted at 27 mph and Experiment 43 at 47 mph. Experiment 40 involves two 1956 Fords each with a speed of 27 mph at time of impact; and Experiment 41, two 1956 Nashes each at 21 mph at time of impact. Experiment 44 was conducted with two medium-weight vehicles, a 1956 Nash Statesman and a 1956 Pontiac, each having a speed of 52 mph at time of impact.

The coefficients of restitution for these six head-on collisions varied from zero to 0.089. The highest coefficient obtained for a head-on collision was 0.102, recorded in an earlier study. These values indicate that for the direct or near-direct head-on collision, the impact is essentially inelastic, if each car is viewed externally as a single unit.

These low coefficients of restitution for the automobile impact are favorable collision characteristics because they indicate reduced probability of:

1. The motorist striking the car interior with a velocity higher than the initial impact velocity of the car as a result of the car's velocity being re-

Fig. 10 — Post-collision positions of instrument recording cars

Table 2B — Automobile Impact Analyses

Experiment Number		37 F1 N2		41 N1 N2		39 F1 N2		40 F1 F2		43 F1 N2		44 P1 N2	
Speed, mph, both vehicles same pre-impact speed		21		21		27		27		47		52	
Year		1950	1949	1956	1956	1956	1956	1956	1956	1956	1956	1956	1956
Make		Ford	Nash	Nash Rambler-1	Nash Rambler-2	Ford	Nash Rambler	Ford-1	Ford-2	Ford	Nash Rambler	Pontiac	Nash Statesman
Weight of vehicles including dummies, lb		3110	2930	3440	3370	3730	3330	3680	3610	3660	3530	4000	3580
Underbody Station ↓		Peak G	Peak G	Peak G	Peak G	Peak G	Peak G	Peak G	Peak G	Peak G	Peak G	Peak G	Peak G
Deceleration, maximum (peak G)	2	[b]	30	95	105	100[d]	[b]	100	85	[a]	[a]	[a]	[a]
	4	24	23	[a]	[a]	[a]	[a]	[a]	[a]	[a]	[a]	[a]	[a]
	5	[a]	[a]	13	17	27	25	27	32[c]	51	72	70[d]	100
	6	26	22	[a]	[a]	[a]	[a]	[a]	[a]	[a]	[a]	[a]	[a]
	8	[a]	[a]	22[c]	18	32	27	30[c]	45	53	79[e]	> 50[b]	66
	10	[a]	[a]	[a]	[a]	[a]	[a]	[a]	[a]	45	46	50[c]	54
Roof over driver 7R & 6R[g]		21	28	19	29	35	35	52	32	39	45	34[h]	46[h]
Passenger, rear seat	Hips G	44	40	30	34	48	38	> 34[b]	[b]	55	60[b]	72[e]	73[e]
	Belt load, lb	7000	5000	[b]	4500	7500	5000	8000	8000	9000[f]	[b, f]	9000	15000
Driver	Hips G	[a]	[a]	24	39	45[d]	54	[a]	65	57[b]	64[e]	[b]	[a]
	Chest G	[a]	[a]	> 80[e]	31	32	45	60	44	75[e]	68[e]	[b]	72[e]
	Head G[g]	[a]	[a]	38	36	54	38	61	70	> 100	> 100	> 200	> 350
Permanent centerline deformation, ft		1.2	1.5	1.2	1.1	1.1	1.7	1.1	1.1	2.3	2.0	3.5	2.5
Average cost between two independent repair shops, $		[a]	[a]	940	960	1110	1290	1150	1350	2560	2800	3570	2925

[a] Not instrumented.

[b] Data incomplete for this channel because of crash damage to transducer or its leads, or malfunction of amplifier or oscillograph.

[c] Differences of ± 2G were recorded for pre-post-crash calibrations.

[d] Partial trace which does include the significant data.

[e] Reading approximately correct although beyond calibrated range of the transducer (60G). Manufacturer states that transducer functions to 125% (75G) of rated load.

[f] Lap belt anchorage failed because of attachment lug shearing at floor pan.

[g] Deceleration obtained by micromotion analysis.

[h] Readings are for station 9R because of destruction of 7R & 6R.

versed in direction from elastic rebound.[5]

2. Involvement in a secondary (spring back) impact with another vehicle or structure.

3. Injuries resulting from extended duration of deceleration forces.

In order to enable the reader to readily make comparative analyses of results, some of the more significant findings from the six head-on collision experiments are summarized in Table 2B. Each type summarized is presented and discussed in detail elsewhere in the paper.

Vehicle Deformation

Permanent Deformation of the Underbody — Three independent systems of instrumentation were used to obtain permanent deformation data for the automobile: (1) micromotion analyses of high-speed motion picture film of the collision event,[6] (2) precision still photography of the car underbody before and after collision to permit photographic superposition of these negatives for direct comparison of every part of the underbody deformation (Fig. 11), and (3) data obtained directly from dis-

[5] This condition has been identified with automobile-to-fixed-object type impacts.

[6] The tower high-speed camera J (Fig. 3) provides accurate centerline deformation of cars during the collision event as seen in Fig. 5, and described later in connection with Fig. 13.

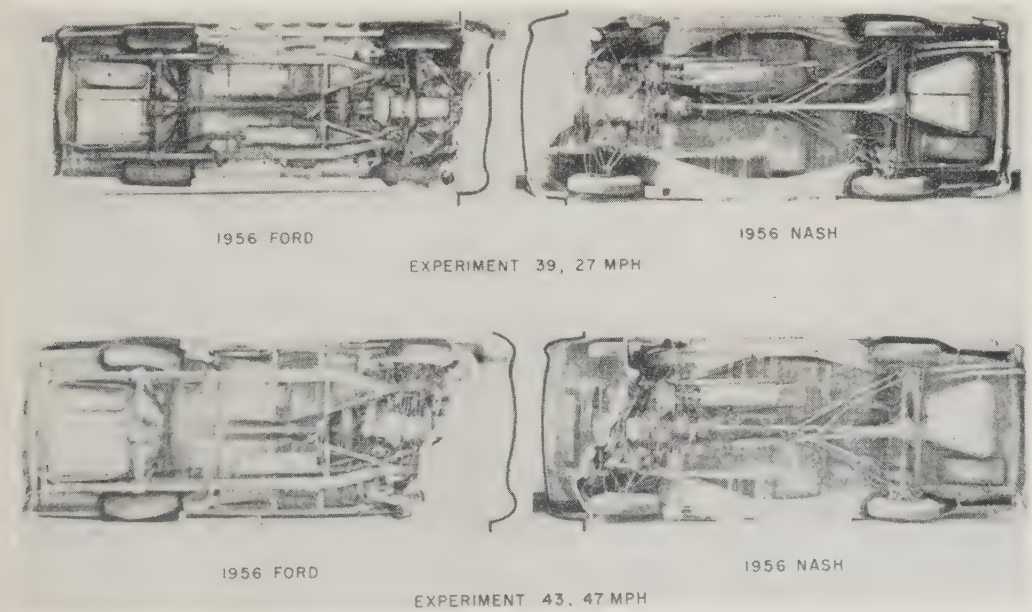

Fig. 11 — Photographic superposition of underbody, before and after collision

placement recorders which were applied at specially chosen locations on the car body (discussed following the next section). Systems 1 and 3, in addition to giving permanent deformation, also provide a very satisfactory method for obtaining maximum and elastic deformation.

For system 2, the camera position relative to the car underbody was exactly duplicated for each photograph. Consequently, a single calibration may be used for approximate comparative measurements between photographs or, by using the 1-ft calibration marker in each photograph of Fig. 11, precise measurements may be made. Underbody superposition photographs for the other four experiments are provided in Appendix 4. The application of $\frac{3}{8}$-in. diameter white dots to principal points on the underbody structure facilitate observation and measurements of deformation for different portions of the underbody.

Underbody permanent deformations with opposing cars superimposed are shown in Fig. 12. Relative to permanent deformation of underbody, the following observations may be made:

1. Experiments 40 and 41 each involved identical cars in head-on collisions. Since their impact speeds were also identical, deformations would be expected to match, as is shown by the data.
2. The 1949-50 vehicles used in Experiment 37 appear to have deformation properties comparable to new vehicles of the same type, used for Experiment 39, especially when allowance is made for the impact speed of 27 mph for Experiment 39 in contrast with 21 mph for Experiment 37.
3. Experiments 39 and 43 are identically matched except that their speeds are 27 and 47 mph, respectively. However, a reversal in collision deformation of the frame relative to the unit-body type is clearly evident with this change of speed. In the diagram for Experiment 39 F_1N_2 the frame-type car is deformed the least whereas in the diagram for Experiment 43 F_1N_2, the unit-body type is deformed the least. Deformations for Experiments 37 and 44 reinforce this observation.

Maximum and Elastic Deformation of Vehicle — High-speed photography provides an excellent means for measuring large deformations. Micromotion analysis utilizes position-time measurements taken from high-speed motion picture photography. The maximum deformation is the initial distance between the impact surface and the point, minus the shortest corresponding distance that develops during the impact event. Elastic deformation is this closest distance subtracted from the corresponding distance at the moment the cars break away from each other as a result of restitution. The inelastic or permanent deformation is the difference between the maximum and elastic deformation. Considering the deliberately built-in 12-in. offset from centered head-on impact in these collision experiments, it will be clear that the location of the tower high-speed camera is essentially the only point from which photographic coverage of maximum centerline deformation could be obtained. The maximum, permanent, and elastic deformations are presented in Fig. 13 for the several impact speeds of unit and frame type vehicles.

Based on the somewhat limited data provided by

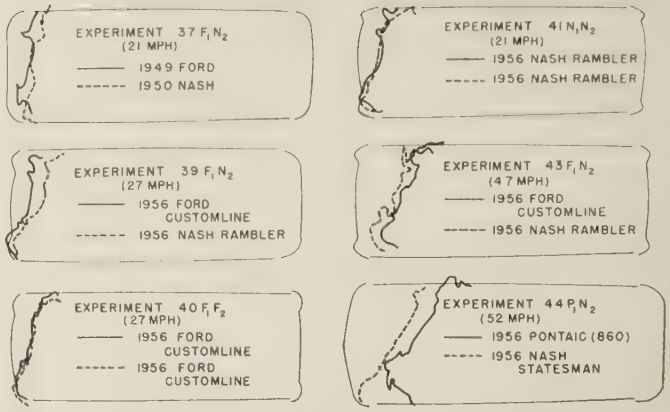

Fig. 12 — Comparisons of underbody permanent deformation, head-on collisions

six head-on collisions, the following observations may be made for Fig. 13. Compared with frame-type construction the unit-body appears to:

1. Undergo a greater maximum deformation for impact speeds below 35 mph and smaller maximum deformations for speeds over 40 mph.
2. Develop greater permanent deformation at speeds below 45 mph, and less at speeds above 45 mph.
3. Have less elastic deformation for head-on impact speeds up to 50 mph.

Displacement Recorder Analysis — Gross deformation of the contacting areas characterizes the head-on collision, even at the comparatively low impact speed of 21 mph. The attending decelerative forces are high, sufficiently high to be fatal or serious-injury producing. In portions of the structure more remote from the impacting surfaces, small deformations may also be identified with the production of high decelerative forces and these, too, may lead to fatalities. For example, the small deformation in a sharp-edged dash panel may account for a dangerous head injury. Because of elastic properties, some deformations are not apparent on post-collision examination, making it difficult to identify the cause of injury. Small deformations that occur in door frames during impact permit doors to open when sufficient lateral forces prevail. This condition frequently leads to ejection of motorists from the car with fatal or other serious consequences.

In the instrumentation developed by A. G. Gross[7] for recording car-body transient deformations, the recording device consists of a $1\frac{1}{2}$-sq-in. polished metal plate and a companion jeweled stylus. The polished plate is smoked by exposing it to a pure acetylene flame, and is attached to one structural member of the car while the stylus is mounted directly opposite on an adjacent structural member. The stylus is held firmly in contact with the plate. In the mounted assembly shown in Fig. 14, the recorder plate was mounted on the center door post and the stylus on the adjacent edge of the front door. The scribed record, therefore, portrays the movement, resulting from collision deceleration forces, of the front door relative to the center door post.

For control purposes both parts of another re-

[7] Gross Research Laboratories, Inglewood, Calif.

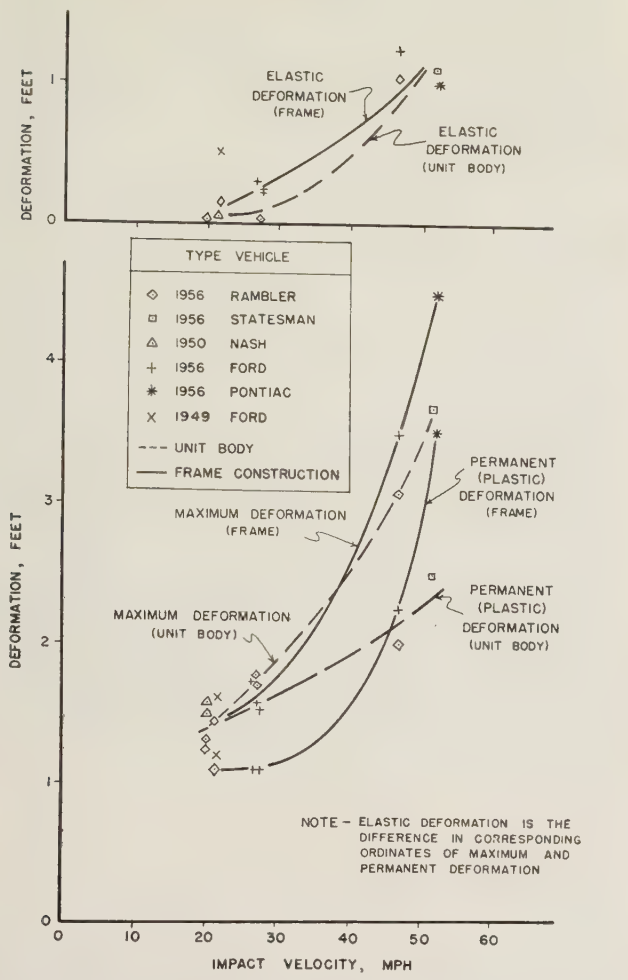

Fig. 13 — Maximum, elastic, and permanent deformations as functions of velocity for unit-body and frame construction

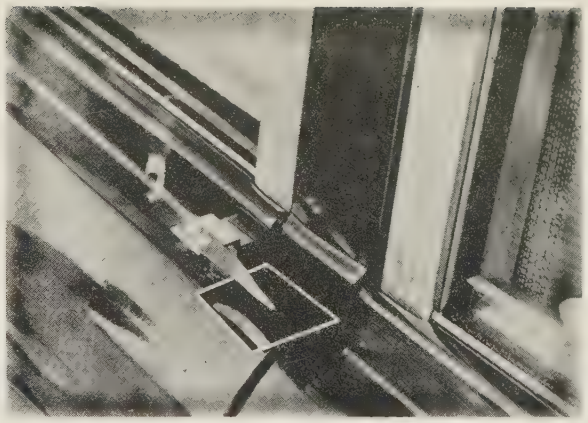

Fig. 14 — Displacement recorder, door relative to door frame

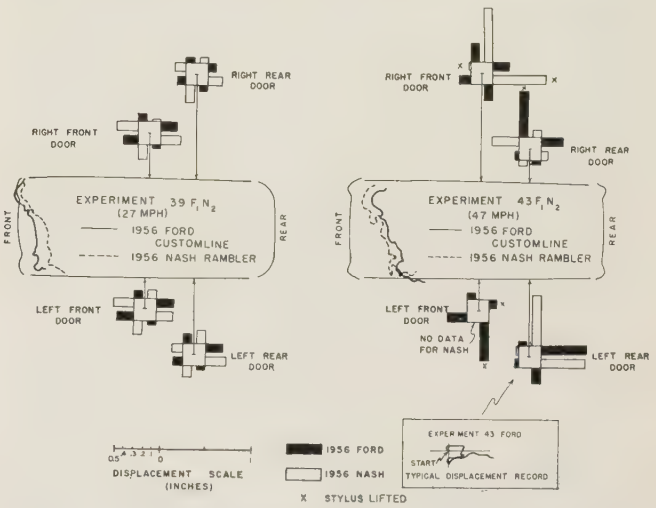

Fig. 15 — Door displacement relative to car body at door latch level

cording unit were mounted on the same structural member of a rear panel which probably would not undergo any relative deformation. This permitted determination of the presence or absence of any elastic deformation of the device itself. No deflection reading was obtained on the control device so that it may be concluded that the device mounted on the door and door post recorded a valid measurement.

The data obtained for two experiments are presented in Fig. 15. These experiments were selected because they were identical, each being a head-on collision between a 1956 Ford and a 1956 Nash, except that Experiment 39 was conducted at 27 mph and Experiment 43 at 47 mph. In contrast with the unit-body construction (Nash) the frame-type construction (Ford) was deformed the least in the 27 mph impact and the most in the 47 mph impact. Displacements are represented in Fig. 15 by bar graphs oriented relative to the plan views of the car bodies to correspond with the orientation of the displacement recording surface mounted near the rear edge of the front and rear doors at the position indicated by the arrows. The shaded bars represent displacements recorded for the Ford and the open bars displacements for the Nash. In Fig. 15 the displacement scale, in inches, is shown in the lower left corner and a typical displacement record in the lower right corner. The left-hand diagram shows in superimposed form the two cars used in Experiment 39. It will be noted that the Nash door deflections are generally greater than those of the Ford but the differences, as such, do not appear to be significant. For the same type cars colliding at 47 mph, significant differences are evident (right-hand diagram). The door to door-frame deformations appear to be sufficient to permit the Nash right front door to open but it actually remained closed. The door to door-frame deformation appears to be sufficient for the Ford right rear door to become unlatched but it also remained closed. For both the Ford and Nash, the left rear door deformations in a fore-and-aft direction were of the same order of magnitude. In this experiment, however, the Nash door opened but the Ford did not. The opening of car doors during collisions stems principally from the action of those forces that bring about differential movements of car doors with respect to door frames. Such openings generally mean loss of protection in that they readily permit the ejection of car occupants. In recent years, improvements in door latch mechanisms by automobile manufacturers have been shown to have reduced significantly the probability of doors opening

during collision events.

These experiments disclosed the possibility of doors opening even when the differential movements described above are prevented by the improved types of door latch mechanisms. In certain cases, for example, the forces of collision deceleration are sufficient to open doors as a result of the inertia of door latch mechanisms in a manner comparable to normal operation. Under these circumstances, therefore, a door may open during collision without post-collision evidence of door versus doorframe deformation. In order to get some further notion of such action, displacement recorders were mounted on the latch mechanism and behind door handles to record the respective linear and angular displacements that occur during impact. In Experiment 43, the displacement recorders on the Ford did not show evidence of door latch movement due to the inertia effect (Fig. 16[2]). A single test is not, of course, conclusive but it is possible that the mechanical components of the latch system were designed to prevent opening by inertia action. In the same collision experiment, the data obtained for the Nash door latch mechanisms showed positive inertia action of a magnitude sufficient to operate the latch and thus permit the doors to open. As was previously stated, the left rear door did open but the high-speed motion picture coverage of this incident shows excessive body deformation in the vicinity of the rear edge of the door. Accordingly, either or both of the following possibilities could account for the door opening: (1) inertia effect operated the door latch, thus permitting the door to be forced open by the compressive forces acting across the door frame; and (2) the door latch could have remained in position until after the door was forced slightly open by the compressive force of the door frame on the door. If the latter did occur, the door latch would be expected to show evidence of a forced opening, but there was no evidence of malfunction following impact.

The potential for three of the four doors of the Nash to have opened is indicated by the data of Table 3[2]. The fact that only one door opened may in part be attributed to the smallness of the spin force by virtue of the shift of the rear of the car laterally occurring considerably after the peak longitudinal deceleration. The high-speed motion picture film shows a rearward shift of the front fender panel partially over the front door; also, the front door shifted rearward to partially cover the rear door. These two shifts may have had some effect in keeping the doors from opening. The left rear door of the Nash opened only after substantial deformation of body and door had occurred in the vicinity of the latch.

Post-Collision Observations, Car Exterior

Following an experimental collision and before the cars are removed from their positions of impact, a tabulation is made of observable items of interest. These observations are presented in detail in Appendix 5. The following statements constitute a brief summary of these post-collision observations:

1. During the 47 and 52 mph impacts, the rear of each car shifted laterally, counterclockwise when viewed from above, 4 and 6 ft respectively. All cars

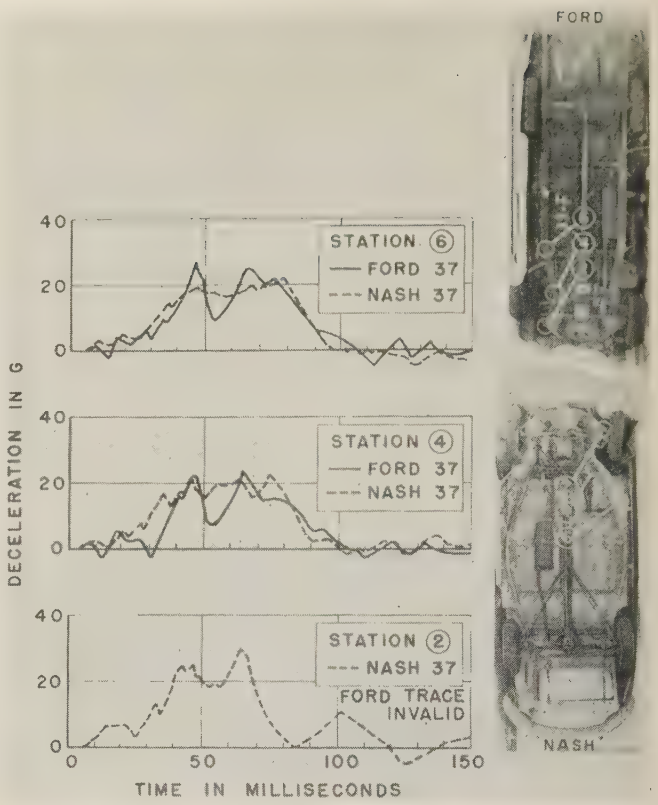

Fig. 17A — Frame deceleration patterns, Experiment 37

were crashed with a 12-in. offset to the right of the opposing car. However, no lateral shift occurred for the four collisions conducted at the lower impact velocities of 21 and 27 mph. A 12-in. eccentricity from centered head-on collision does not produce significant spin forces for impacts to 27 mph. Even with the 12-in. eccentricity, the spin forces generated in the 47- and 52-mph impacts were not excessive and occurred late in the impact event.

2. In some collisions there was evidence of vertical displacements sufficient to permit the opposing front bumpers to pass over or under each other without significant mutual contact during impact.

3. Engines shifted permanently rearward relative to their mounts for all six collision experiments. In the 52-mph impact, the engine in both cars shifted rearward until the firewall was pushed approximately even with front surface of the dash. The excessive collapse of cabin structures around the driver precluded the possibility of survival for the driver. Such collapse was greatest in the case of the Pontiac.

4. For the two higher speed impacts, 47 and 52 mph, the left front wheel was forced through the floor against the driver.

5. Windshields generally shatter excessively with pieces of glass falling mainly outside and to the front of the car. No windshield popped out of mounts intact. Generally, the front of the windshield shattered outward with the wrap-around portion remaining partially or substantially mounted.

6. The doors of the 1949 Ford and 1950 Nash would not open without the application of considerable force following their 21 mph impact. The

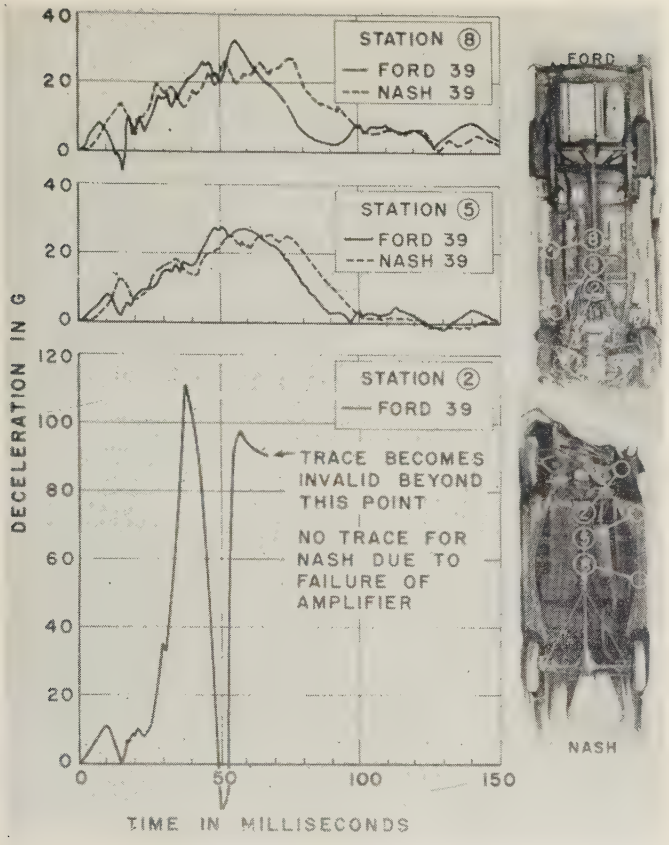

Fig. 17B — Frame deceleration patterns, Experiment 39

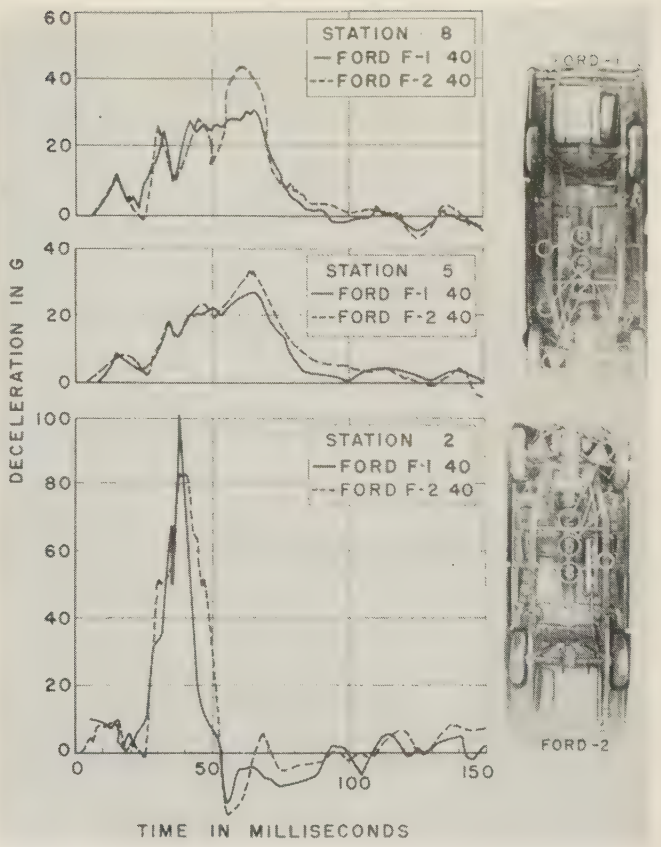

Fig. 17C — Frame deceleration patterns, Experiment 40

improvement in door structure and latching mechanism for the 1956 cars was evident, even in the higher velocity impacts.

7. In the 47 mph head-on collision, body deformations were evident in the Nash Rambler as far to the rear as Station 13. In the 52-mph collision, cabin collapse about the driver was considerably more severe for the Pontiac than for the Nash. (See Figs. 1 and 5).

Deceleration-Time Patterns

Of paramount interest in this study was the relative collision performances of unit-body and frame construction. One method of evaluation is to record the deceleration-time relations obtainable during a collision through the use of transducers mounted at specific points on the car underbody. Variations in collision performance of the car structure 2 ft from the front bumper may have a significant effect on the performance of the remaining collapsible structure separating the motorist from the point of impact. Instrumentation of the underbody at Station 2 (2 ft back from the front bumper) was possible for impact speeds to 27 mph but it was visualized that total destruction of the transducer would occur for the 47-mph head-on collision (Experiment 43). Consequently, the 47- and 52-mph head-on collisions were instrumented at Stations 5, 8, and 10 in contrast with Stations 2, 5, and 8 for the lower speed impacts.

The deceleration-time patterns derived from corresponding positions of instrumentation of the car underbody are presented for each of the six head-on collisions in Figs. 17A–17F. Malfunction of equipment prevented obtaining data for the Ford, Station 2, Experiment 37 and Nash, Station 2, Experiment 39.

In Experiments 40 and 41, identical vehicles were paired for the purpose of determining the magnitude of differences in collision performance for essentially identical exposures. A further purpose in the case of Experiment 40 compared with Experiment 39 was the provision for determining the influence on collision performance of the type structure of the opposing vehicle. The extent to which the corresponding curves of Experiments 40 and 41 differ is attributable essentially to errors of instrumentation and to structural variations in production models.[8] With respect to instrumentation error, two transducers were mounted side by side on the frame of one of the vehicles subjected to a head-on collision for experimental control. The data from this control over transducer-sensed information is presented in Fig. 18 and demonstrates the reasonably faithful interpretation of the same deceleration pattern by different type transducers whose signals are recorded independently and simultaneously. The mean deviation of peak decelerations was 2.5 *G* (4%) and of area under the curve 0.015 *G* sec (0.5%).

In Experiments 40 and 41, where identical cars opposed each other, errors of instrumentation may account for as much as twice the mean deviation or

[8] The pairs of vehicles in Experiments 40 and 41 were identical and, therefore, no collision performance variations may be attributed to any lack of symmetry on the part of the opposing vehicle structure.

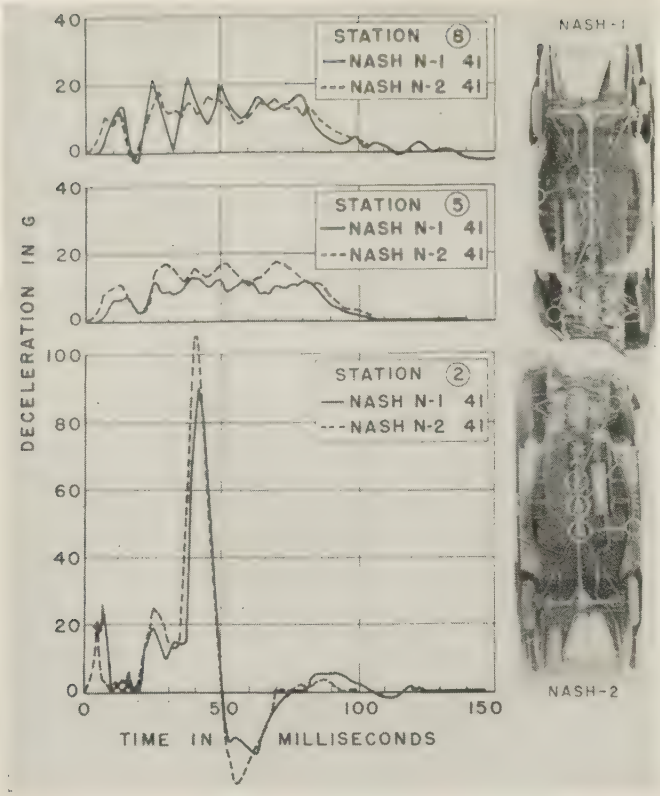

Fig. 17D — Frame deceleration patterns, Experiment 41

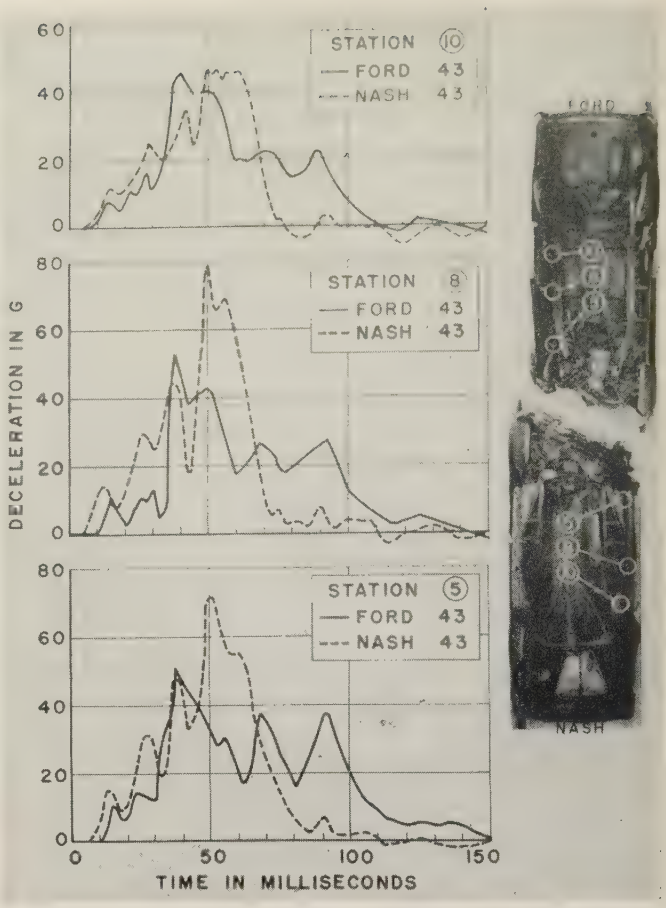

Fig. 17E — Frame deceleration patterns, Experiment 43

8% of the discrepancies indicated for corresponding stations of identical vehicles symmetrically opposed in a head-on collision. This leaves unaccounted differences in peak decelerations ranging from zero to 8% and these differences are attributed to the variation in collision performances even though the opposing vehicles are the same make, model, and year.

Rather than to attempt to interpret the significance of the relative deceleration patterns (Figs. 17A–17F) for each collision experiment separately, some of the more important information has been abstracted for composite presentation in Fig. 19. Deceleration patterns are characterized by the following variables: rate of onset, peak value, and duration of deceleration. For the head-on collision, the rate of onset of deceleration of the vehicle is of little consequence with respect to motorist safety because the motorist, even when restrained by a lap belt, experiences no force effect from the collision until well after the car-deceleration peak has passed. The duration of automobile impact seldom exceeds 200 millisec (0.2 sec) and the duration of motorist injury-producing decelerations seldom exceeds 100 millisec (0.1 sec). Consequently, the production of injuries attributable to prolonged deceleration is not, for the most part, a matter of concern in automobile collisions except that the duration of peak deceleration is an important consideration. Peak deceleration values having durations exceeding 1 millisec provide a realistic basis for comparing the collision performances of equivalent positions in opposing cars.

Peak values of deceleration for six head-on collisions involving different vehicle types and different impact speeds are presented in Fig. 19. In this figure the "zone of preferred collision performance" has been added to provide a reference for values which exceed the deceleration peak of 27*G* sustained by a human volunteer decelerated with a lap belt as his only means of restraint.[9] The zone of 27*G* has been extended parallel to the abscissa to include the passenger compartment and will be seen to increase rapidly in deceleration value from the windshield forward to the front bumper. The deceleration value of the front bumper contacting the opposing bumper of a car of comparable mass and velocity would approach infinity (zero time for deceleration) if the bumpers under this extreme force of impact did not deflect vertically from their normal positions sufficiently to permit them to deform beyond each other. (See Fig. 1.) Consequently, while deceleration values of the front end are extremely high because of limited deceleration distances, these values do not approach infinity for the head-on collision because of mutual penetration of opposing structures. When we consider successive positions from the front bumper toward the passenger compartment, the relatively undeformed collapsible distances, if utilized, would permit reduced peak decelerations. As shown in Fig. 19, all Station 2 peak deceleration values considerably ex-

[9] Stapp, John, Col. USAF, as reported before the Special Sub-Committee on Traffic Safety of the Committee on Interstate and Foreign Commerce, House of Representatives, 85th Congress, 1st Session Union Calendar No. 493, Report No. 1275, U. S. Government Printing Office, Washington, D. C., Aug. 30, 1957. 7 pp.

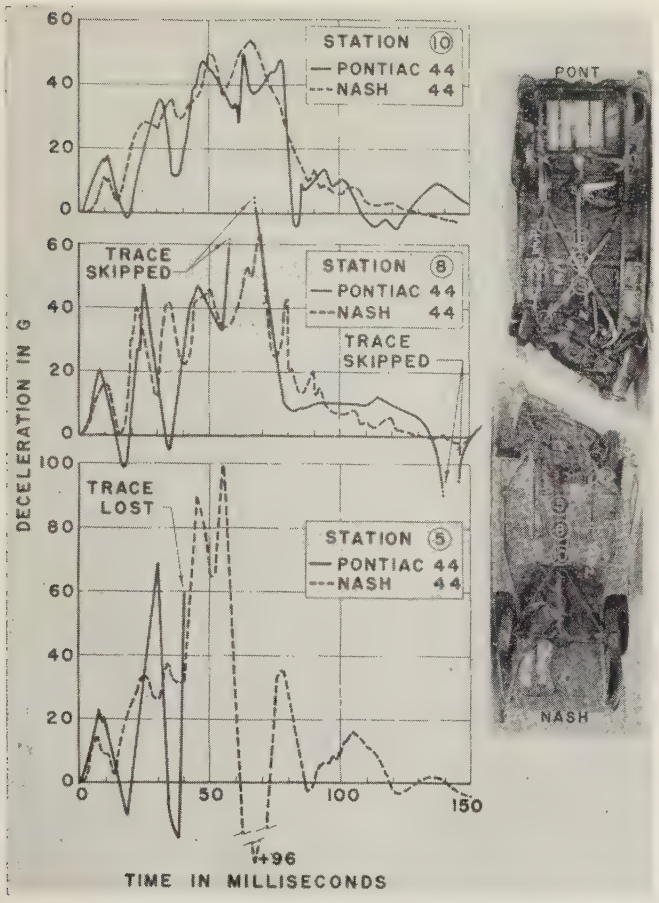

Fig. 17F — Frame deceleration patterns, Experiment 44

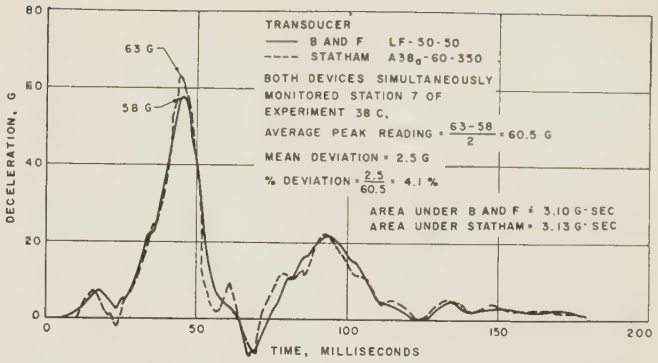

Fig. 18 — Correlation between two different type transducers mounted side by side sensing same deceleration event simultaneously and independently

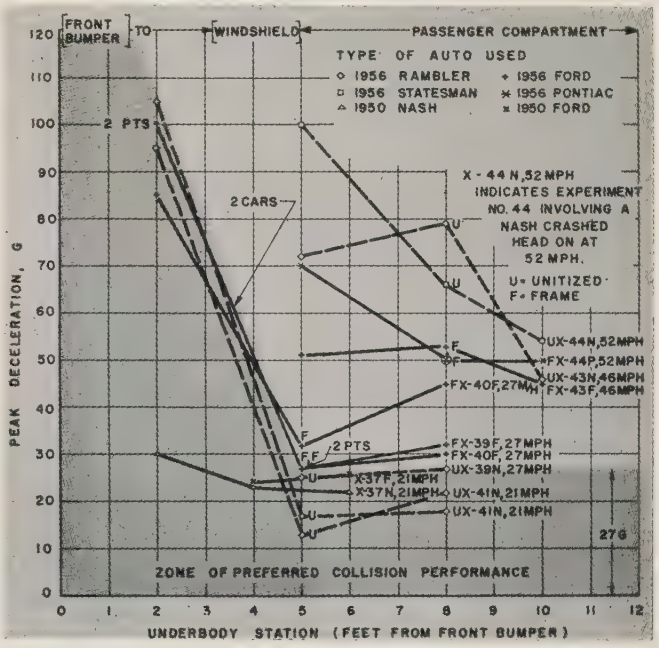

Fig. 19 — Relation of peak deceleration of underbody to distance from front bumper

ceed Station 4 values. For head-on collisions under 30 mph, the structure at Station 2 is severely collapsed compared with the minor deformation occurring at Station 4 (Fig. 20[2]). Also, as shown in Fig. 19, there are several instances in which the underbody peak deceleration at Station 8 (driver's position) exceeds values for Station 5, 3 ft closer to the point of impact. This condition has been identified in earlier studies[10] and is at least in part attributed to the changes in structural rigidity of the passenger compartment in contrast with the engine section and is common to both the frame and unit-body construction.

The peak deceleration values of Section 8 for each head-on collision vehicle represented in Fig. 19 have been further identified by a letter *U* for unit-body construction and *F* for frame-and-body construction. Note that for the two lower velocity collisions Experiment 37 at 21 mph (Station 6) and Experiment 39 at 27 mph (Station 8) in which frame and unit-body structures are in opposition, the peak deceleration is lower for the unitized than for frame construction. (See also Table 2B.) The reverse situation appears to exist for the 47- and 52-mph head-on collisions, in which the two unit-body construction vehicles show higher peak decelerations for the three stations (5, 8, and 10) monitored than for corresponding values of the frame-type vehicles. This difference in peak decelerations for the two higher speed impacts is not as significant for Station 10 as for Stations 5 and 8. Referring to Table 2B, the values of peak deceleration for underbody Stations 2, 5, and 8 are the same for the 1956 Ford in Experiment 39 as for the 1956 Ford in Experiment 40. Since both experiments were conducted at identical speeds, the only difference between them is that the Ford in Experiment 39 struck a 1956 Nash (unitized) and the Ford in Experiment 40 struck a 1956 Ford (frame). The results of these two experiments suggest that the nature of the opposing structure per se (whether unitized or conventional) has no effect on the collision performance of a vehicle. Further, referring to Table 2B, we note that for the three Fords, seat belt loadings were comparable as would be expected for identical cars undergoing essentially identical deceleration rates. However, the driver of the Ford in Experiment 39 received only half the chest loading received by the driver of the Ford in Experiment 40 under seemingly identical conditions. This marked difference is attributed primarily to the po-

[10] *Clinical Orthopaedics*, Vol. 8, Fall, 1956, pp. 275–300: "Automobile-Barrier Impacts, Series II," by D. M. Severy and J. H. Mathewson.

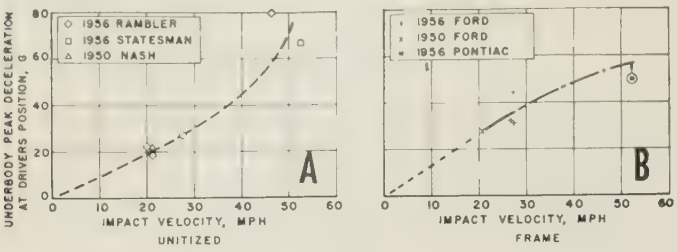

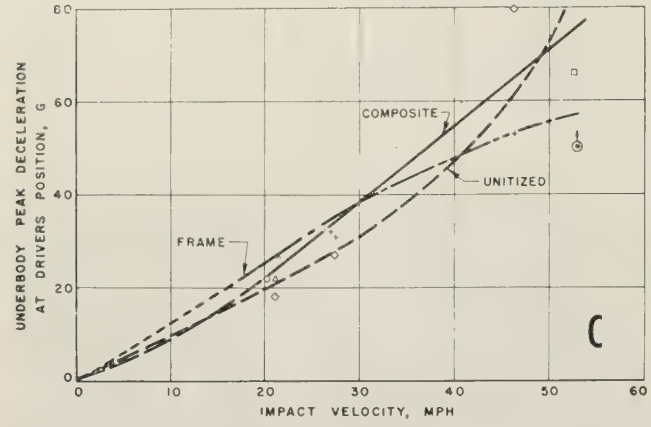

Fig. 21 — Underbody deceleration peaks for driver compartment

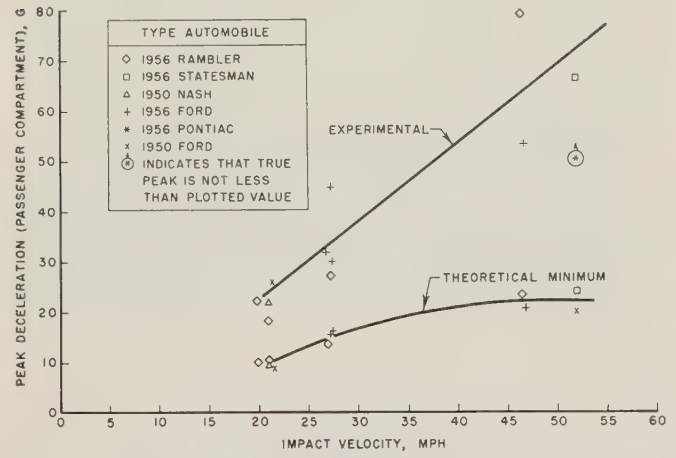

Fig. 22 — Peak decelerations, passenger compartment, compared with theoretical minimums

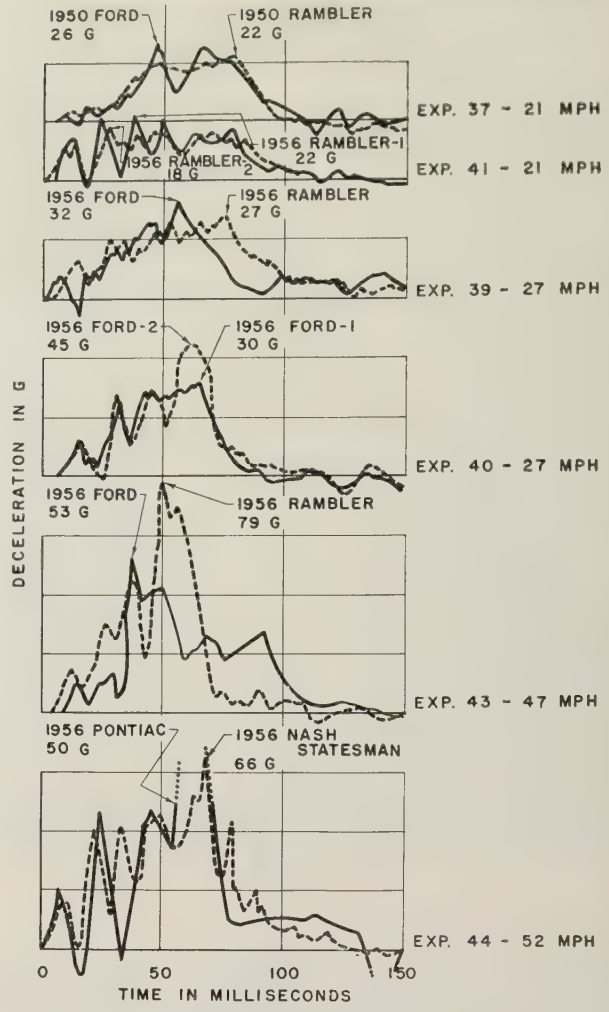

Fig. 23 — Passenger compartment deceleration for variations of impact speed, type and age of vehicles

sition of the driver behind the wheel and when we refer to collision photographs of the steering wheel for these Fords in later sections we shall see that peak deceleration loads are the highest where the driver squarely struck the wheel and lowest where the driver struck sufficiently off center to crowd to one side of the wheel.

The variation of peak deceleration for the underbody at the driver's position is shown for unit-body construction in Figure 21A and for frame construction in Fig. 21B. The two curves are superimposed in Fig. 21C and a third "composite" curve is shown fitted to the combined data points for these two curves. These curves should be regarded only as approximations of the relation of the driver's compartment peak deceleration to changes of impact velocity for unit-body and frame construction. With respect to Fig. 21, the following observations are made:

1. The collision performance of the unit-body construction appears to be slightly better than frame construction for impact velocities in the 20–30 mph range and slightly poorer for impact velocities in the 45 to 55 mph range.[11]

2. The difference in collision performance between unit-body and frame construction is small at any velocity, as shown by the rather close correspondence of the frame and unit-body curves to the composite curve fitted through data for both.

The absence of clearly defined differences in collision performances of unit and frame construction suggest the application of statistical analysis for further evaluation of the data.

Automobile head-on collision performances have been evaluated in terms of motorist's compartment peak decelerations for a specified impact speed and vehicle type (Figs. 19 and 21). A further evaluation of automobile collision performance is provided by using the composite curve of Fig. 21C for comparison with a corresponding theoretically minimum peak deceleration curve (Fig. 22).

[11] For the 45–55 mph range, at least, these differences in peak G become negligible for the rear seat passenger position (See Fig. 19, Station 10).

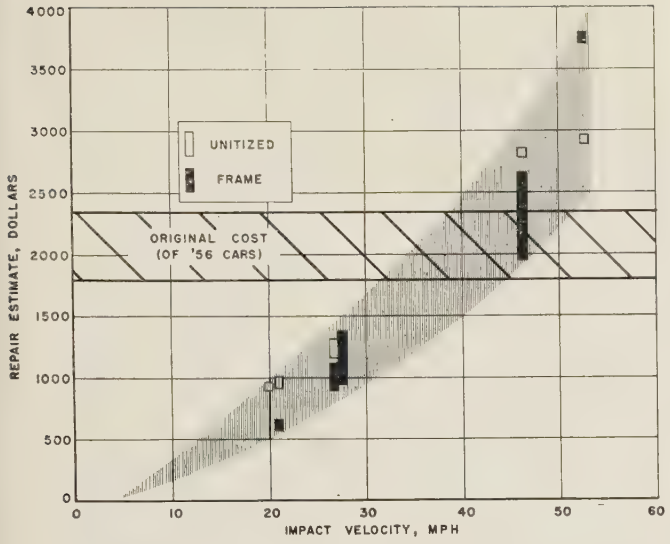

Fig. 25 — Relation of repair cost to impact velocity and type construction

In Fig. 22, the experimentally determined peak deceleration values are represented by the line labeled "experimental." Each deceleration value corresponds to a car whose maximum (centerline) deformation[12] has been presented in Fig. 13. For the maximum deformation and impact speed for each experiment, there may be calculated a theoretical minimum peak deceleration value which would result if the car decelerated uniformly throughout the entire collapse distance up to maximum deformation. These "theoretical minimum" values of peak deceleration are represented by the lower curve of Fig. 22. Comparison of these two curves provides the following information:

1. At 21 mph, the experimentally determined peak decelerations of the automobile are more than double their theoretical minimum value and at 52 mph triple their theoretical minimum. Collision performance decreases with increases in impact speed from 20–50 mph.

2. The experimental peak decelerations appear to increase uniformly with increases in impact velocity whereas the theoretical minimum decelerations appear to reach a plateau at about 47 mph, because of the relatively large maximum deformations occurring for impact speeds of 47 and 52 mph.[13]

Relation of Repair Cost to Impact Velocity and Type Construction

An additional means for evaluating the relative merits of unit-body and frame construction results from comparing the cost of repairing the cars damaged in a controlled collision. The experimental collision series included in this study provide a reasonably accurate evaluation because all of the factors which influence vehicle damage could be accurately determined or were prevented from affecting the data.

In order to reflect a realistic repair cost schedule for the impacted vehicles, not less than three separate repair estimates were made of each vehicle. Reputable independent appraisers and automobile dealer firms submitted detailed repair estimates. The administrative aspects of securing estimates were conducted in such a manner as to avoid biasing the data.

The vehicles underwent, prior to impact, minor modifications. These modifications were performed in order to facilitate data collection. For example, the engine hoods, air cleaners, and batteries were removed. Other modifications included cutting a viewport in the top of each vehicle, and mounting instruments and accessory equipment in various sections of the vehicle. These pre-impact modifications were in some cases considered by the estimators and in other cases excluded from their evaluation. This made it necessary to adjust all estimates to a common base, which was not difficult to accomplish using the itemized cost data submitted with each estimate.

A detailed tabulation of all estimates is presented in Appendix VI. The relation of repair cost to impact velocity and type of vehicle construction is shown in Fig. 25.

For reference purposes Fig. 25 includes the original cost of the vehicles,[14] represented by the horizontal cross-hatched band. The intersection of this horizontal band, with the shaded area (repair cost) indicates the region where it becomes uneconomical to repair a car. For purposes of this study, carefully itemized repair estimates were secured for all cars including those damaged beyond repair and having salvage value only. The bar graph data indicate the range of repair estimates submitted for each vehicle. The original costs of all cars, except the Pontiac and Statesman used in the 52-mph collision, are approximately represented by the lowest value, and the Pontiac and Statesman by the highest value of the horizontal band. Repair costs for these more expensive cars (the 52-mph impact) may be expected to be proportionately higher and this in part accounts for the more pronounced upsweep at the high-speed end of the repair cost curve.

Technical Findings: Collision Performance of Occupant with Car Interior

The number of variables associated with an automobile collision are many, each with a rather wide range of magnitude. The speed, mass, and structural properties of the vehicle, the point of impact, impact eccentricity and type of object struck, together with associated factors such as secondary or tertiary impacts and the post-collision environmental circumstances all have their influence on the extent of injuries to the car occupants. Within the car, another group of factors further complicates the motorist survival picture. The collision forces which prevail within the motorist compartment for the majority of fatal accidents are of orders of magnitude which would be survivable if two precautions were taken. The first relates to interior design. All surfaces should be designed to avoid protuberances of relatively small area whenever their material is sufficiently rigid to generate injury when struck by

[12] Maximum deformation is the total deformation occurring during impact and, therefore, is elastic plus permanent deformations.

[13] Section on Statistical Analyses deleted in the interest of brevtiy. Section includes omitted Tables 4 and 5, and Fig. 24. Fig. 23 shows the deceleration patterns for Station 8 of the passenger compartment for each of the 12 cars. Microfilm copy of complete paper available by writing to the Library Photographic Service, University of California, Los Angeles 24, Calif.

[14] The original cost of vehicles is the Advertised Dealer's Price (ADP) for these cars, new.

the occupant. Since an occupant can be violently forced against any surface of the car's interior, there should be no exceptions to this design principle.[15]

In addition, then, to the many variables of collision operating from outside the car, there are many features within the car which become death dealing even when the external factors are of sublethal caliber. Also significant are the height, weight, age, and general physical condition of the individual as well as the particular surface of the car interior against which certain parts of his anatomy are crushed.

The second precaution necessary for motorist protection is the responsibility of the driver to ensure, to the extent possible, that he and his passengers control (through the use of seat belts, for example) the part of the body on which the collision-deceleration forces are concentrated. Even with the many different factors which influence survivability from the automobile impact, some conditions stand out as frequent offenders, as would be expected. It will be the purpose in this section to identify the more common motorist environmental factors leading to injuries and, in a general way, the nature of the injuries. For the purpose of providing guidance to the reader in the interpretation and use of medico-engineering material of the nature presented in this paper, the following paragraph is quoted from an earlier paper:[16]

> "It is recognized that a medical authority cannot be expected to translate, without qualification, structural damage occurring to an anthropometric dummy into injuries to which the human counterpart would have been subjected. It is also impractical for an engineer to attempt to evaluate precisely the structural failures and other more subtle indications of abuse to which an anthropometric dummy is subjected during collision in terms of human injury data. Until more basic data are procured concerning the average strength and resistance to injury of the various components of the human body, the combined judgment of the medical and engineering researcher appears to be the most practical approach to applying this type of instrumentation to the experimentally crashed car." (See Fig. 26.)

The physical consequences of dummy[17] damage evaluated by the research engineer and interpreted by the medical scientist in terms of physiologic consequences of the inferred body injury are presented in Table 6.

Table 6 — Summary of Collision Injury Findings

		State of Injured Motorist (Dummy)[a]	Loading on Safety Belt, lb	Peak Deceleration of Dummy, G	
				Hips	Chest
Experiment 37	Driver[b]	Possible fatality	N.B.[c]	—[d]	—
Ford	Passenger	Survived	7000	44	—
21 mph	Driver	Probable survival	N.B.	—	—
Nash	Passenger	Survived	5000	40	—
Experiment 39	Driver	Possible fatality	N.B.	45	32
Ford	Passenger	Survived	7500	48	—
27 mph	Driver	Probable fatality	N.B.	54	45
Nash	Passenger	Survived	5000	38	—
Experiment 40	Driver	Possible fatality	N.B.	—	60
Ford-1	Passenger	Survived	8000	34	—
27 mph	Driver	Probable fatality	N.B.	65	44
Ford-2	Passenger	Survived	8000	M[e]	—
Experiment 41	Driver	Probable survival	N.B.	24	80
Nash-1	Passenger	Survived	M	30	—
21 mph	Driver	Probable fatality	N.B.	39	31
Nash-2	Passenger	Survived	4500	34	—
	Driver	Fatality	N.B.	57	75
Experiment 43	Passenger	Probable fatality	9000	55	—
Ford	Driver	Fatality	N.B.	64	68
47 mph	Passenger (rt)	Survived	M	60	—
Nash	Passenger (lt)	Fatality	N.B.	—	—
Experiment 44	Driver	Fatality	N.B.	M	M
Pontiac	Passenger	Probable survival	9000	72	—
52 mph	Driver	Probable fatality	N.B.	—	72
Nash	Passenger	Probable survival	15000	73	—

[a] Classes of inferred injuries are: Minor, Moderate, Serious, Critical.
[b] Driver and passengers (rear seats) were anthropometric dummies, which accounts for their "injuries" being described as "inferred."
[c] N. B. indicates that no belt was worn.
[d] — indicates that no instrumentation was applied at that point.
[e] M indicates malfunction of instrumentation, no data.

The information presented in Table 6 provides a basis for some conclusions. The reader is cautioned against generalizing from Table 6 because, in addition to the many underlying subtleties, the data are deficient in two ways: the smallness of the sample and the somewhat subjective process leading to inferred physiological consequences for a traumatic event are obviously less exacting than most systems of instrumentation. However, the following three readily apparent conclusions (based on Table 6) are consonant with the exacting data presented elsewhere in this paper:

1. The chances of survival are approximately the same in either a unit-body or frame-structured vehicle.

2. The chances of survival decrease with higher speeds of impact.[18]

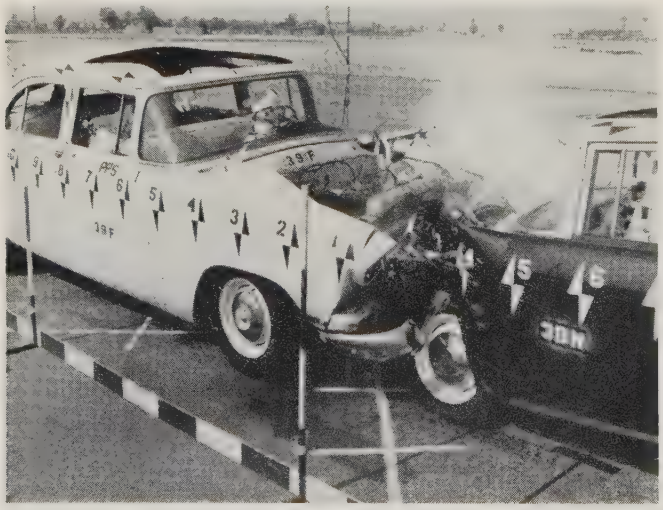

Fig. 26 — Impact at 27 mph forces drivers of both cars to collapse steering wheels and columns

[15] For example, the rigid sharp-edged visor over the instrument cluster at first appears to be positioned too remote for the driver to contact because of the presence of the steering wheel situated between the visor and driver. In Experiment 43, the driver collapsed the deep-dish steering wheel and column against the dash where his head struck the visor resulting in his very strong (solid plastic) nose being cut off completely. In Experiment 44, the decapitation of the dummy occurred on contact of the neck with the instrument visor. This instrument visor would be as functional and decorative if made of materials such as flexible rubber or vinyl, the practice by aircraft manufacturers for many years.

[16] P. 290 of "Automobile Barrier Impacts," by D. M. Severy and J. H. Mathewson. See footnote 10.

[17] The anthropometric dummy: For a complete description of this mechanical substitute for the human body refer to "A Technical Description of Sierra Sam and Family." Pub. by Sierra Engineering Co., Sierra Madre, Calif., 1955. For details of how dummy is used to obtain meaningful data on collision injuries, refer to pp. 39–54 of "Automobile Barrier Impacts," by D. M. Severy and J. H. Mathewson. Highway Research Board, Bulletin 91, January, 1954.

[18] It should be borne in mind that the 8000-lb (loop strength) seat belts in Experiment 43 failed and that partial failure of floor pan structure occurred with the 16,000-lb belts used in Experiment 44. These belts are double and quadruple, respectively, the strength of the better automobile seat belts. Consequently, dummy damage would have been considerably greater had ordinary seat belts been used, especially for the higher speed impacts.

Recognition should also be given to the fact that it is entirely possible that no human being could survive a lap belt loading of 15,000 lb. Visceral shift leading to herniations and the development of extreme hydrostatic pressure in the vicinity of the heart may, for single lap belt loadings of this order of magnitude, preclude survival. An evaluation of this nature is beyond the scope of this study.

3. The chances of survival are greatly increased with the use of a lap belt.[19]

Dynamics of Injury Production — Anthropometric Dummies

The dynamic sequence of injury production is contained in the following descriptive analysis of the dummy's reaction to impact. The basic data are derived from the analysis of high-speed motion picture film. Supporting data are provided by electronic instrumentation, medical analyses,[20] and post-collision observations and photographs. Zero time refers to that instant when the bumpers of the two vehicles make contact.

Experiment 39 (Ford) Driver — As the driver, seated at Station 8, shifted his position toward the steering wheel, 25 millisec after the initiation of impact, the two colliding vehicles have decelerated to nearly zero velocity. The total front-end deformation was sufficient to force the frame-anchored steering column into the driver as he moved forward. His chest struck the lower rim of the steering wheel (50 millisec), which has shifted toward the driver approximately 12 in., causing moderate contusions to the lower anterior chest and right upper chest (Fig. 26). With the chest forced against the lower half of the steering wheel, the upper half was deflected into the driver's face, forcing the head to the right and backwards (65 millisec) with the probability of a serious fracture or dislocation of the cervical spine. Also, the blow from the wheel generated a moderate 0.5-in. laceration just anterior to the superior portion of the left ear.

Just prior to the time the head was forced to the right, the extended steering wheel hub was struck by the mid-anterior chest (65 millisec). The chest continued crushing forward, causing the exposed steering wheel hub to penetrate the chest during the next 40 millisec (65–105 millisec) resulting in a deep 1-in. long laceration. The peak *G* reading recorded in the chest cavity was 32. The combined action of the extension of steering column toward the driver as the driver's chest moved into it, forced the steering wheel and column upwards approximately 4–5 in. (100 millisec). The dashboard was simultaneously elevated 3 in.

Both knees were violently jammed into the dashboard (75 millisec) causing moderately serious lacerations and contusions and probable fractures. The peak *G* reading at the driver's hips was 46 *G*, which indicates that the femur of each leg was loaded to approximately 2300 lb or slightly in excess of 1 ton, as the knees were crushed into the dash. Moderate contusions and lacerations were sustained by the right mid-forearm and abrasions by the dorsum of the right hand due to their impact with the dashboard (Fig. 27).

The front seat and back rest, a single structure, followed the driver from the instant he began his forward movement, relative to the car interior, until he reached his maximum forward position at about Station 6 (135 millisec). (See Fig. 28.) The seat structure and driver returned to Station 7 after the impact. This seat, static weight almost 100 lb, had torn free from its anchorage at about the beginning of the impact and followed the driver forward to load him with an additional 1500 lb against the forward structure.

Experiment 39 (Ford) Rear-Seat Passenger — The rear-seat passenger seated at Station 11 began to move forward in a normal seated posture about the

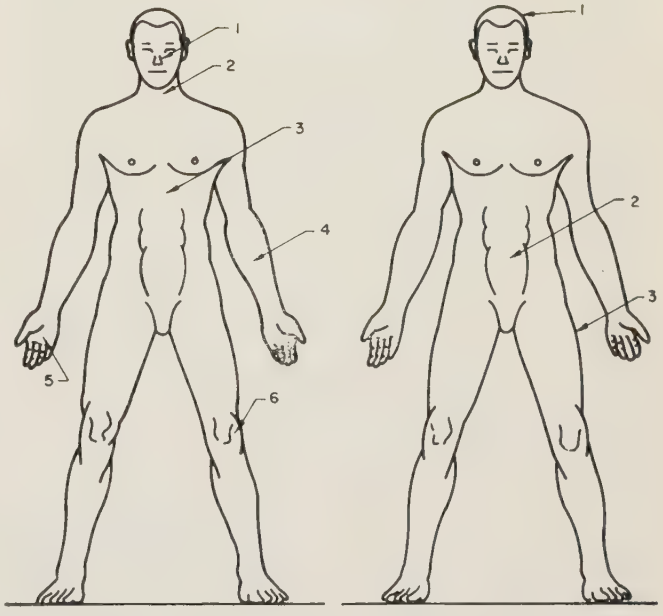

DRIVER (NO LAP BELT) – POSSIBLE FATALITY
1. MODERATE 1/2" LACERATION – LEFT EAR. ABRASION; NOSE.
2. SERIOUS, PROBABLE SPINAL FRACTURE OR DISLOCATION.
3. SERIOUS, DEEP LACERATIONS, CONTUSIONS LEFT OF STERNUM.
4. MODERATE, LACERATIONS ON MID FOREARM.
5. MODERATE, ABRASIONS ON RIGHT HAND.
6. MODERATE – SERIOUS, KNEES CONTAIN MULTIPLE LACERATIONS, PROBABLE FRACTURE.

REAR-SEAT PASSENGER (LAP BELT) – SURVIVED
1. MODERATE, ABRASION OVER OCCIPUT.
2. MODERATE, SMALL CONTUSION-LACERATION NEAR BELT BUCKLE LOCATION.
3. MODERATE – MINOR, CONTUSION-LACERATION NEAR BELT LOCATION.

Fig. 27 — Dummy injury pattern, Experiment 39 (Ford)

Fig. 28 — How seat anchorage failures contribute to motorist injuries

[19] In this study evaluation was limited to the use of a lap belt for rear-seat occupancy.

[20] Medical interpretations were made by Wendell Severy, M.D., Los Angeles, Calif.

same time (50 millisec) that the driver struck the lower rim of the steering wheel. Upon reaching Station 10 (85 millisec) the restraining action of the lap belt (8000-lb loop strength) was noticeable. The passenger's head swung forward and downward and his back inclined forward (145 millisec) to a position between Stations 9 and 8. The maximum load recorded by the lap belt tensiometer was 7500 lb. The hip accelerometer recorded a peak deceleration of 44 *G*.

As the restraining action of the lap belt took effect, the arms lifted from their lap position (80 millisec) and became outstretched from the shoulders pointing towards the dashboard. His head and back then became nearly parallel to the road surface (135 millisec). The passenger was then lifted 3–4 in. from the rear seat (150 millisec), the lap belt sliding down to his upper thighs. Moderate injuries, small contusions, and lacerations occurred to the left and right of the lower abdomen, just above the belt buckle, and also to the upper left and right thighs. These injuries were produced by the lap belt buckle. The passenger reached his maximum forward position at 180 millisec. Both occupants returned to near pre-collision positions at 440 millisec. The rear seat and back rest were torn from their anchorages (Fig. 28).

Experiment 39 (Nash) Driver — The initial relationship of driver to steering wheel during the onset of impact (20 millisec) was similar to the description given for the Experiment 39 Ford. In Experiment 39 Nash, the driver was also seated at about Station 8. The driver's lower mid-chest and upper abdomen contacted (40 millisec) the lower rim of the steering wheel which caused the upper rim to deflect (50 millisec) into the chin and throat region. The dummy continued his forward motion, thereby forcing the steering wheel column hub up and along the sternum (50–75 millisec) until it reached the throat and chin region (75 millisec). There were moderate scattered contusions over the lower mid-chest and upper abdomen. The steering wheel hub caused serious marked lacerations and contusions on the mid-upper chest. The chest accelerometer recorded a peak deceleration of 45 *G*, indicating that the head and chest were loaded to approximately 2200 lb.

The driver continued forward another 2–3 in. (75–110 millisec) while the steering wheel hub forced his head (110 millisec) into acute dorsiflexion. The action caused serious and extensive lacerations about the chin, lower lip, left jaw, and throat region. Moderate to minor lacerations occurred on the right side of the nose. The hip accelerometer recorded a peak deceleration of 54 *G*. Both knees were contused and lacerated by being crushed

(a) FAILURE OF SEAT ANCHORAGE, STEERING WHEEL RIM DEFLECTED INTO FACE.

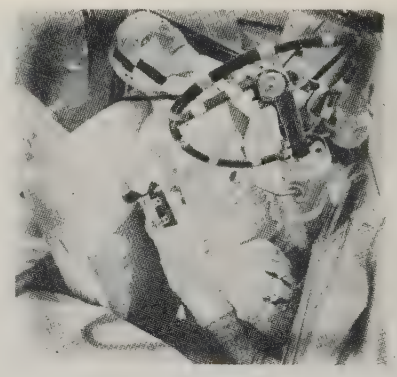

(b) KNEE INJURIES FROM DASH PROTRUSIONS. CHEST INJURIES FROM EXTENDED SHATTERED END OF STEERING COLUMN.

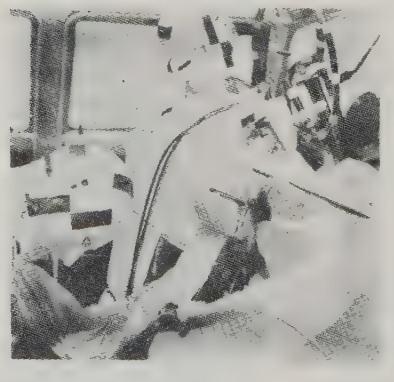

(c) HEAD DEFLECTED FROM ASH TRAY THEN HEAD AND ARMS PENETRATED SEAT BACK.

(d) FLOOR PAN FAILURE AT LAP BELT ANCHORAGE.

Fig. 29 — Post-collision evidence of structural failure and some conditions responsible for motorist injuries

against the dashboard, each under a loading of approximately 4000 lb. The left knee was presumed fractured due to excessive crushing. The dorsum of the right hand showed minor contusions.

Experiment 39 (Nash) Rear Passenger — The movement of the rear-seat passenger during impact was similar both with respect to the kinematics and to the injury production reported for the rear-seat passenger of Experiment 39 (Ford). Differences in seat belt loading and in peak deceleration of the hips were, however, recorded. The seat belt tensiometer registered a maximum of 5000 lb while a peak deceleration of 38 *G* was reached.

In all experiments all front seats tore loose from their anchorages, thus adding critically to the injury producing loadings on the driver.

Post-Collision Observations — Motorist Compartment

In this study 12 cars, representing three makes, were experimentally crashed at four different impact speeds. Each collision produced some car interior collapse features not in common with others. This fact is more readily appreciated after considering the following two examples:

1. It was found that a slight variation in driver posture will alter the damage on impact to the steering wheel and change the chest loading on the driver by as much as a factor of two.
2. For the comparable conditions of Experiments 39 and 40, the rear-seat Ford occupant (Experiment 40) received no head injury in contrast to a moderate head injury for the rear-seat occupant of Experiment 39.

Thus, some of the observations were singularly significant while others were altogether characteristic of the head-on collision. The post-collision observations for the car interior are presented in Appendix 5. (See also examples in Fig. 29.)

In order that the importance of post-collision observations may not be underestimated, consider for a moment the caption of Fig. 29C, "Head Deflected from Ash Tray." The edge of the ash tray cut a long, wide, and deep V-groove into the scalp of the dummy.[21] This ash tray location, common to most cars, should be eliminated in favor of the flush mounted armrest trays.

[21] Under similar circumstances, a 9-year old boy was killed from what the police report described as a head injury caused by his head striking the ash tray mounted in the center of the front-seat backrest.

Fig. 30 — Characteristic collision performance of steering wheel and column

Steering Wheel and Column

Six head-on collision experiments were performed in this study. In all, 12 vehicles, representing three makes of cars, were employed. The general collision performance of the steering wheel and column was essentially the same for 11 out of 12 cars. Characteristically, the wheel structure was forced back towards the driver as the driver moved forward into the wheel and column (Fig. 30). The movement of the steering column into the driver's chest is the result of the terminal of the steering column being mounted onto the frame or underbody a short distance from the front end of the car. The collapsing of the front end forces the rigid steering column axially rearward along the column mounts into the motorist compartment.

At the instant illustrated by Fig. 30 the steering

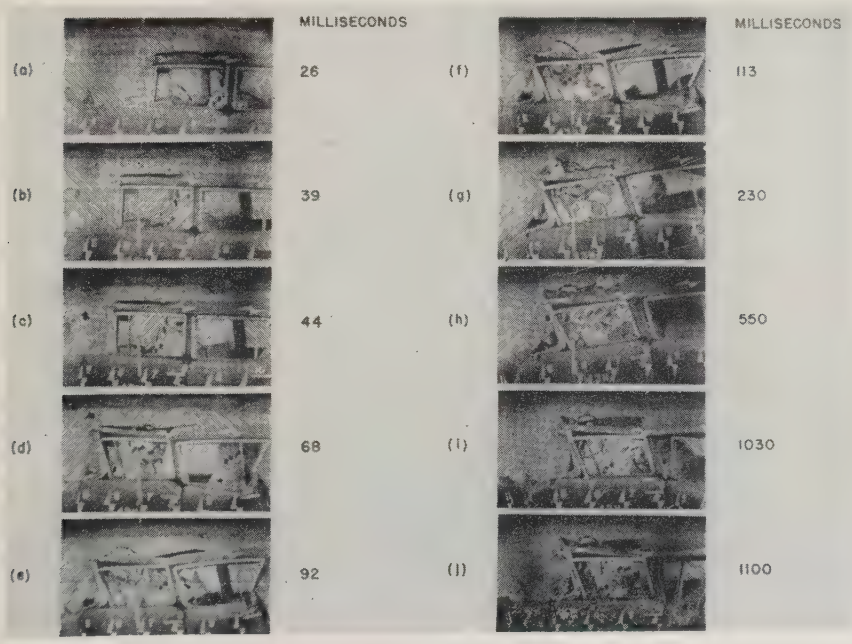

Fig. 31 — Kinetics of driver and steering wheel during impact

column violently struck the chest, resulting in a chest deceleration in excess of 80 *G*. The chest accelerometer for the driver of the opposing Nash exposed to comparable collision conditions was only 31 *G*. Minor variations in posture and in collision performances of the same production make of car can lead to considerable variation in the injury potential for a given collision configuration, even for the controlled collision. The collision performance of the steering wheel is best illustrated by the high-speed motion picture sequence taken of the driver-dummy of the Nash during the 47-mph impact of Experiment 43 (Fig. 31).

The film sequence of Fig. 31 shows (A) the front bumpers collapsing but steering wheel and driver still in normal position; (B) the driver and front seat shifted forward a few inches and the steering column and wheel extended even further toward the driver than he has moved forward; (C) the steering wheel hub in contact with the sternum and the lower rim, contacted earlier, deflecting the upper rim of the wheel almost into the eyes of the driver, rim subsequently strikes head and hub is thrust deeply into his chest; (D) driver ramming past and to the left of the wheel and column as they are pushed upwards; the rear-seat passengers moving forward, the passenger in back of the driver having no restraint, the other wearing a lap belt (8000-lb loop strength); (E) driver crushing against windshield and dash, and wheel extending through the viewport in roof, the restrained passenger has sheared the anchor clevis of his 8000-lb lap belt causing him to lag slightly behind the unrestrained rear-seat passenger who crushes against the driver; (F) and who crowds on to the right of the driver and has rotated counterclockwise, the formerly restrained passenger has collapsed the front-seat backrest against the dash; (G) his head strikes the mid-windshield header-board; (H) the rear door opening and the driver returning to his former position, the unrestrained rear-seat passenger has collapsed onto the floor of the rear-seat area and the formerly restrained right rear-seat passenger (head through roof) returning to his former seated position; (I) rear door opened further; and (J) the post-collision status.

The post-collision status of the steering wheels and columns for 27- and 47-mph head-on collisions are shown in Fig. 32 for both the frame (parts A and C) and unit body (parts B and D) type construction. Except for minor variations, the steering column performances for the two types of cars are the

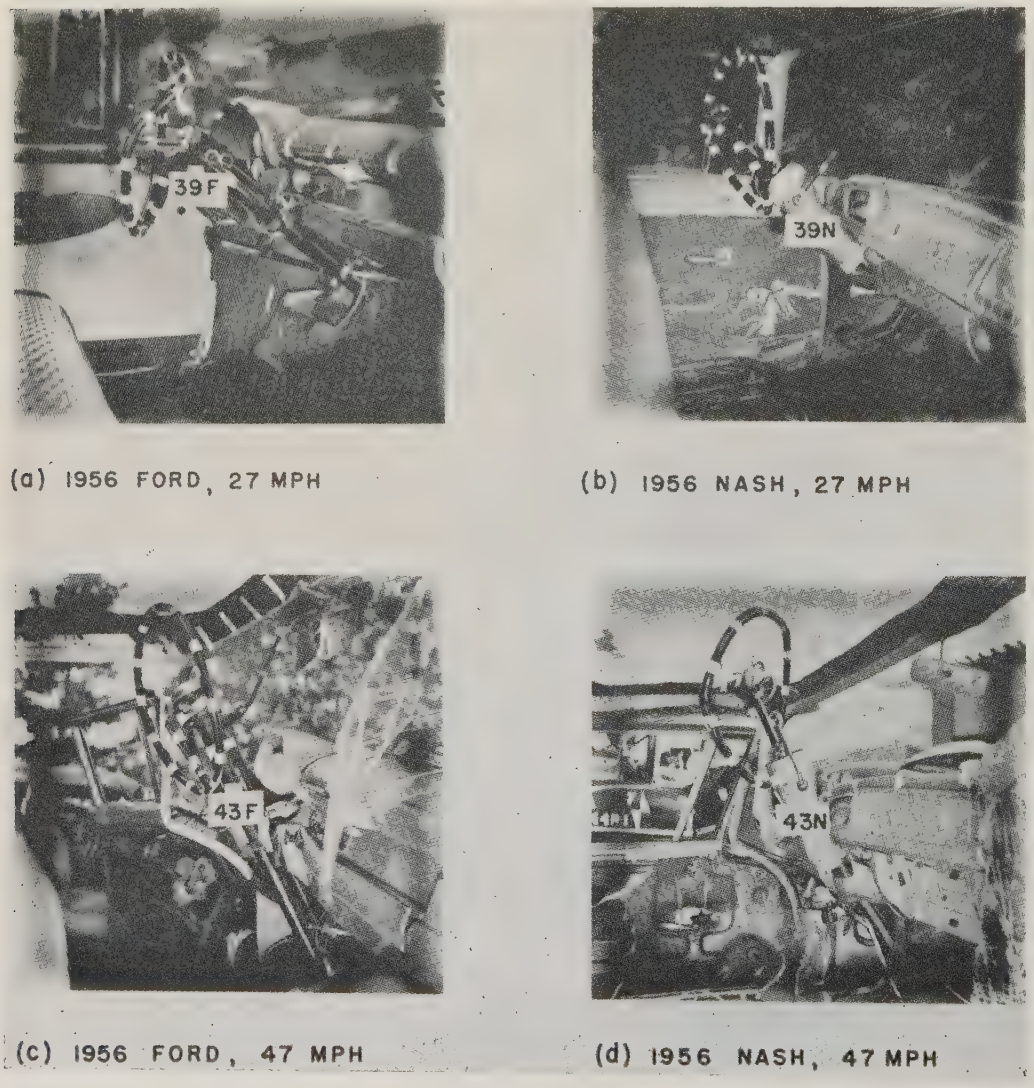

(a) 1956 FORD, 27 MPH

(b) 1956 NASH, 27 MPH

(c) 1956 FORD, 47 MPH

(d) 1956 NASH, 47 MPH

Fig. 32 — Steering wheel and column, post-collision

same. While not conclusive, the data obtained for this series of head-on collision experiments failed to establish an advantage with respect to force reduction for the deep-dish steering wheel compared with the wheel having the hub, spokes, and rim in the same place. A slight recession in the hub accomplishes little since the motorist will still collapse the rim to the hub. Upon impact, the hub and column are thrust into the driver.

The deceleration values for the drivers' chests encountering the steering wheels, (Fig. 32), are respectively (A) 32 G[22], (B) 45 G, (C) 75 G, and (D) 68 G. Considering that approximately half the weight of the dummy driver is restrained when impaled by the steering wheel, the lowest load to the chest was 3200 lb and the highest 7500 lb. For the two Experiments 39 and 43 the post-collision medical analysis of the dummy drivers for the 27 mph impact, Figs. 32A and B, listed inferred driver injuries as "probable-critical" and for the 43 mph impact, parts C and D, as " critical." After considering the transducer, micromotion, and post-collision medico-engineering analyses in relation to each other, it was concluded that for the Ford-Nash head-on collision at 27 and 47 mph, the collision performances of the steering wheel (two types) and column were not significantly different.

The single departure in steering wheel collision performance already referred to was observed in the high-speed motion picture film of the 1956 Pontiac during its 52-mph head-on collision. Instead of the steering column being rammed into the driver's chest, the action was quite different (Fig. 33). Part A shows normal position of driver and steering wheel, B that the wheel shifted up towards the windshield before the driver, now moving forward, could contact the wheel, and part C the upper most position the wheel assumed. Post-collision examination of the Pontiac steering wheel and column (Fig. 33D) provided an explanation for this action. The steering column is securely anchored at the dash by a steel bar extending to the top of the firewall. The lower end of the column, attached to the gearbox, is secured to the frame in the conventional manner. During the initial stages of impact, the Pontiac frame first buckled about 4 in. to the rear of the point of attachment of the gearbox. This rearward movement of the base of the column, together with pivoting at the dash, resulted in the rotation and elevation of the column and steering wheel. The characteristic performance of the steering wheel and column (depicted in Fig. 30) shows how dangerously concentrated loads are applied to the head and chest of drivers during collisions (Fig. 34A). An approach to the solution to this problem for existing automobiles is indicated in Fig. 34B. Since structures are more amenable to modification than people, the following two design changes appear to merit consideration:

1. Employment of a flat board-surfaced hub approximately two-thirds the diameter of the wheel to provide for a distributed rather than concentrated load to the motorist violently forced against it.

2. A splined shaft connection on the firewall side of the steering column to eliminate the dangerous collision-generated axial thrust delivered to the column through its base attachment.[23]

Kinetic Analysis

The basic objective in collision research is to determine a feasible means for minimizing motorist injuries. At some risk of oversimplification, findings from this research indicate that the greatest possible gain in motorist protection will be derived

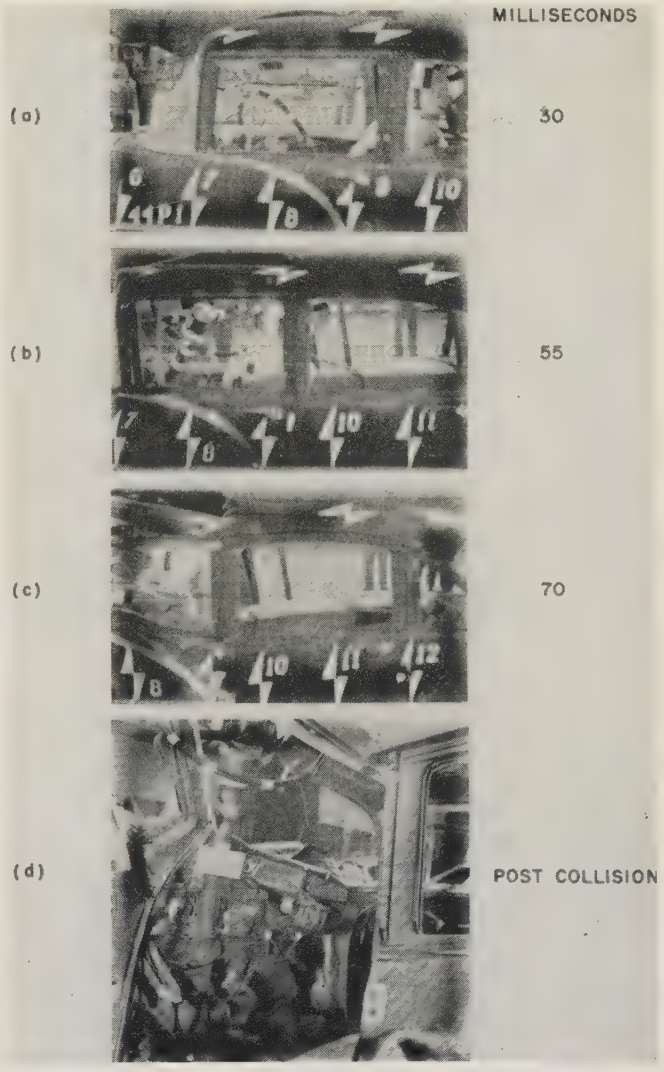

Fig. 33 — Collision performance of Pontiac steering wheel and column

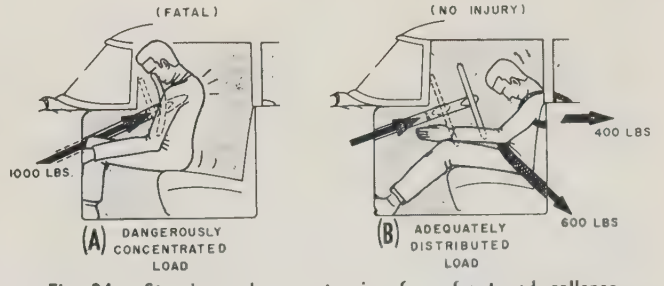

Fig. 34 — Steering column extension from front-end collapse

[22] In Experiment 40, in which two Fords were crashed head-on at this same speed (27 mph), the chest decelerations were 60 G and 44 G for 225- and 185-lb dummies, respectively.

[23] In essence, this recommendation was made by the authors in "Automobile Impact Research," National Safety Council *Transactions*, Vol. 28, 1954, pp. 93–101.

from (1) redesigning the car interior to minimize injuries to motorists thrown against the car interior following impact, and (2) restraining the motorist at least at the hips by a high performance belt to control more effectively the forces applied to the motorist. Relationships between car deceleration, belt loadings developed in restraining the rear-seat passenger, and the motion of the restrained passenger during impact, are shown in Fig. 35. The posture of the dummy is accurately depicted by the figure silhouettes,[24] each posture conforming to the time after impact appearing directly below the hips. The corresponding distance which the hips have moved forward during impact is indicated at the top of Fig. 35. This forward hip movement reached a maximum at 100 millisec or shortly after the peak belt loading was reached.

The deceleration of the motorist compartment (shaded portion of graph) commenced a few millisec after contact was made by the front bumpers of the opposing cars. Even after the initial peak deceleration of 20 G is reached by the car, the passenger shows no change in his posture although as soon as the car started its deceleration, the motorist commenced to move forward relative to the car interior. At 20 millisec, the mechanical slack[25] has been taken up by the occupant moving forward 0.16 ft and significant belt loading commences to occur. At 60 millisec, the belt has reached 1600 lb before the dummy's posture shows a reaction. The peak loading is reached at 85 millisec which is 8 millisec after the final car peak deceleration and about 1.4 in. short of the maximum forward position the hips attain. At this belt peak load, posture is normal except that the dummy has moved 10 deg from a slightly reclined toward an erect seated posture. The restraining action has decreased to nearly one-half its peak load as the upper torso flexes past vertical on its way to a leaning-forward-in-seat posture.

Even when the belt is fitted snugly across the lap, slack in the restraining device still prevails and thereby leads to an appreciable delay in restraining the motorist. At 40 millisec, the car is decelerating at 15 G and if this passenger were able to decelerate with the car, his belt load would be 15 × 210 lb × 65% body weight restrained or 2000 lb. However, because of slack, the belt reading at 40 millisec is only 300 lb. This means that the restrained motorist is decelerating inefficiently by not making use of the deceleration potential provided by the collapsing of the vehicle front-end structure. Furthermore, this inefficiency further shifts the force attenuation problem to the belt system. The deceleration pattern associated with belt restraint, while generally of comparable efficiency for the rear-seat passenger, has the following disadvantage. In order for the belt to attenuate the motorist deceleration force — in the manner the collapsing of the front-end structure of the car attenuates the motorist compartment decelerative forces — the belt must elongate considerably. For the rear-seat occupant, substantial belt elongation presents no serious problem but, for the limited forward distance available to the front-seat occupant, belt elongation is critical.

This loss in the restraining efficiency becomes evident when the peak deceleration of the compartment, 22 G, is converted to an equivalent belt load

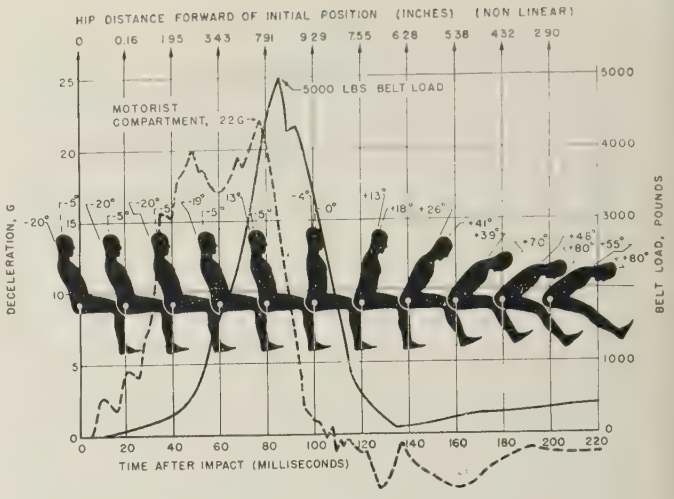

Fig. 35 — Kinematics of restrained occupant as related to belt loadings, head-on collision (Nash, 21 mph)

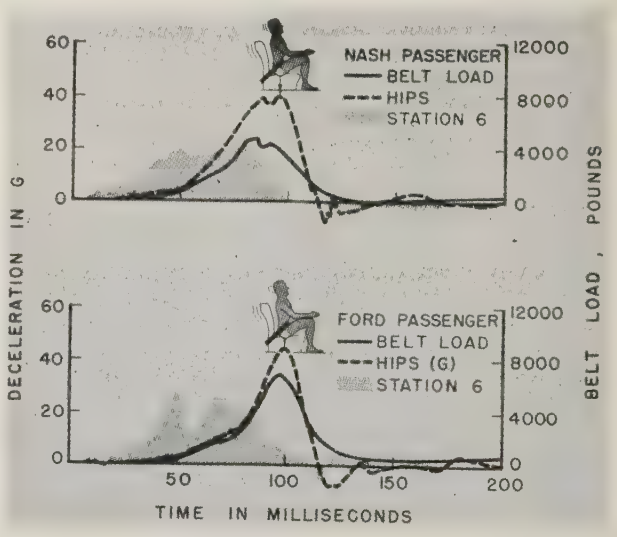

Fig. 36A — Occupant deceleration and belt load, Experiment 37

(22 G × 210 lb body weight × 65% body weight restrained at peak G) of 3000 lb compared with the belt peak load of 5000 lb. Even though this experiment included a properly installed 3-in. nylon belt, the flexure and flailing actions of the passenger, his body extension, body compression under the belt loading, stretch in the belt and belt anchorages, deflection of the floor pan and to a small extent longitudinal compression of the cabin structure all contribute to the phenomena called slack.[26]

Both the occupant and the passenger compartment have the same pre-crash and post-crash speeds but the occupant's deceleration is character-

[24] Upper torso posture angle appears to the left and head position angle appears to the right, both just above the head. The data for Fig. 35 were derived from Experiment 37 (Nash) by removing sheet metal on one side of the car to facilitate accurate micromotion analyses of high-speed motion picture film taken during impact.

[25] Looseness inherent in any belt even when, as in this case, it is fitted snugly about the occupant.

[26] It will be clear that slack may be considered as the inevitable result of the inability of the human body to conform to a deceleration force field in a manner comparable with a securely fastened rigid structure. To the extent that slack contributes to force moderation slack will be desirable except where: (1) Avoidable slack leads to further delay in onset of motorist deceleration so that the force moderation provided by the vehicle is correspondingly less useful to the motorist. (2) The presence of avoidable slack permits motorist to shift position far enough forward to induce injury by contact with forward interior surfaces of the cabin structure.

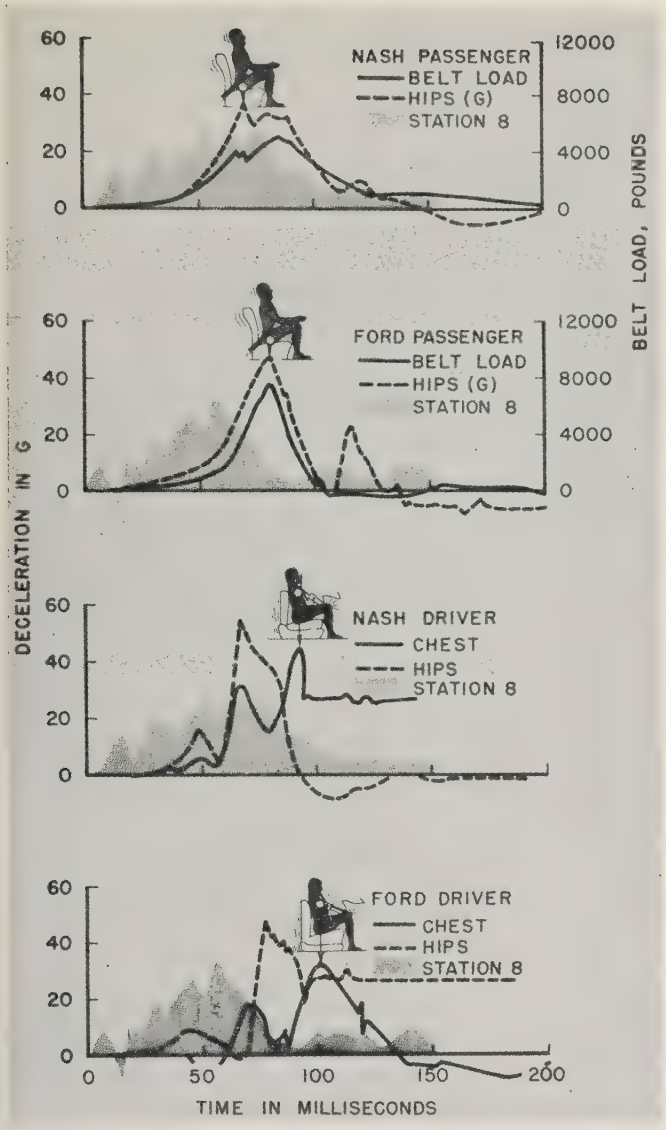

Fig. 36B — Occupant deceleration and belt load, Experiment 39

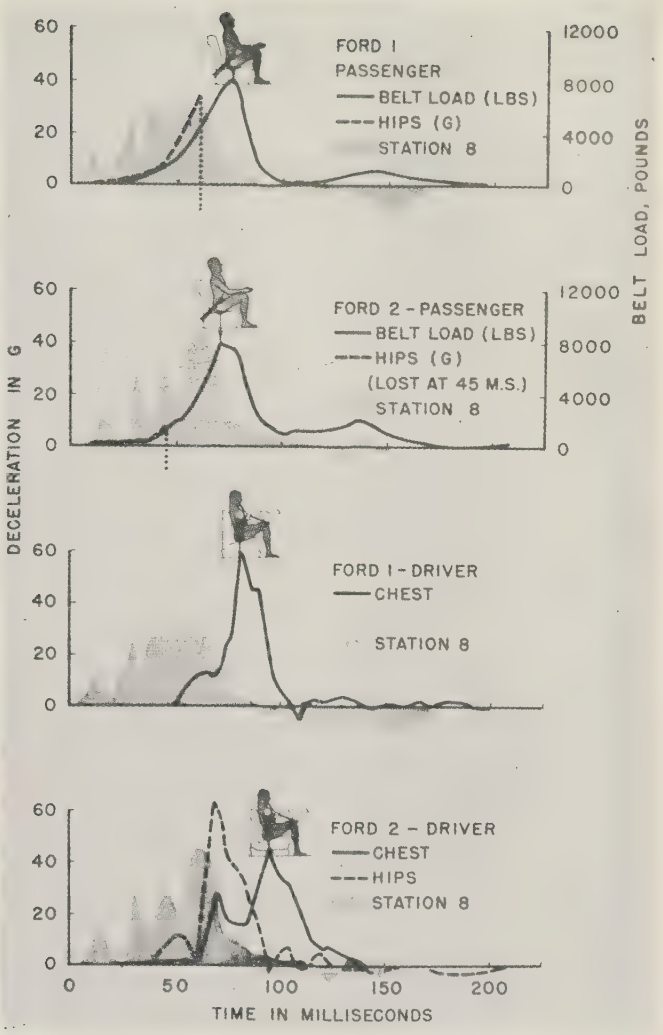

Fig. 36C — Occupant deceleration and belt load, Experiment 40

istically delayed and thus prevents him from deriving much advantage from the moderated deceleration of the passenger compartment. The foregoing discussion may be summed up as follows:

1. A well-engineered and properly installed lap belt worn comfortably snug minimizes loss in restraining efficiency.

2. In contrast with the 3000–4000 lb, 3-in. lap belt currently used by motorists, an 8000 lb loop strength, 3-inch wide nylon[27] lap belt will increase motorist protection by (a) reducing contributions to slack such as those identified as belt stretch and body deformation; (b) reducing restraining unit pressure applied by the lap belt to the motorist because of the greater surface area provided by a 3-in. belt;[28] (c) providing a restraint having a loop strength more in keeping with the loadings encountered in automobile collisions and, therefore, less likely to fail during impact; (d) reducing front-seat occupants' leg injuries by reducing the belt elongation that permits the knees to contact the dash for moderately severe front-end collisions.

The car deceleration, occupant deceleration, and belt loading for the 12 experimentally crashed cars are presented in Figs. 36A–36F. In the case of the top graph of Fig. 36A, these Nash passenger data have been presented in greater detail by Fig. 35 so that the reader would have no difficulty interpreting the remaining data presented in more simplified manner by Figs. 36A–36F. Although the Fig. 36 graphs are self-explanatory, the reader will be particularly interested in the following observations:

1. The peak belt load and peak hip deceleration occur for the restrained passenger substantially later than the peak car deceleration (shaded curve) and before the passenger's erect posture has been changed.

2. Peak belt load and peak hip deceleration occur at approximately the same time as would be expected for the restrained rear-seat occupant whose knees do not encounter the car interior forward structure, as in the case of the front-seat occupant.

3. The relative time and magnitude of driver

[27] Nylon is recommended because of its strength and availability. Materials with improved properties having at least comparable strength may replace nylon.

[28] The argument that the advantages of wider belt webbing are offset by the webbing folding (becoming ropelike) as the body jackknifes about the restraint appears invalid since this study has established that the peak load applied by the occupant to the belt occurs before significant body pivoting about the hips commences.

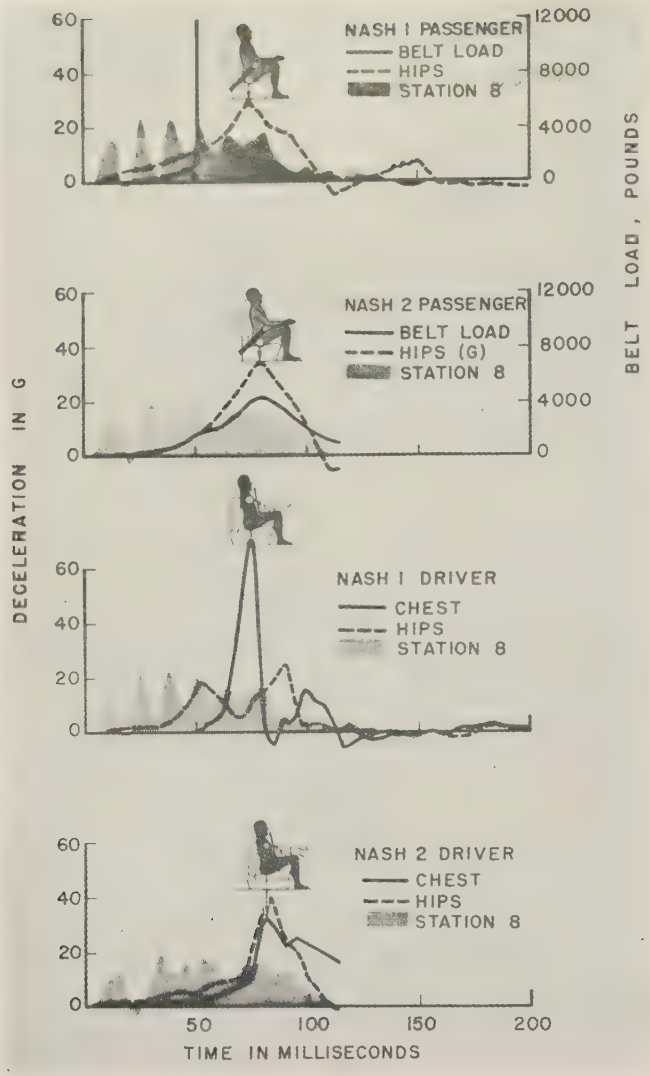

Fig. 36D — Occupant deceleration and belt load, Experiment 41

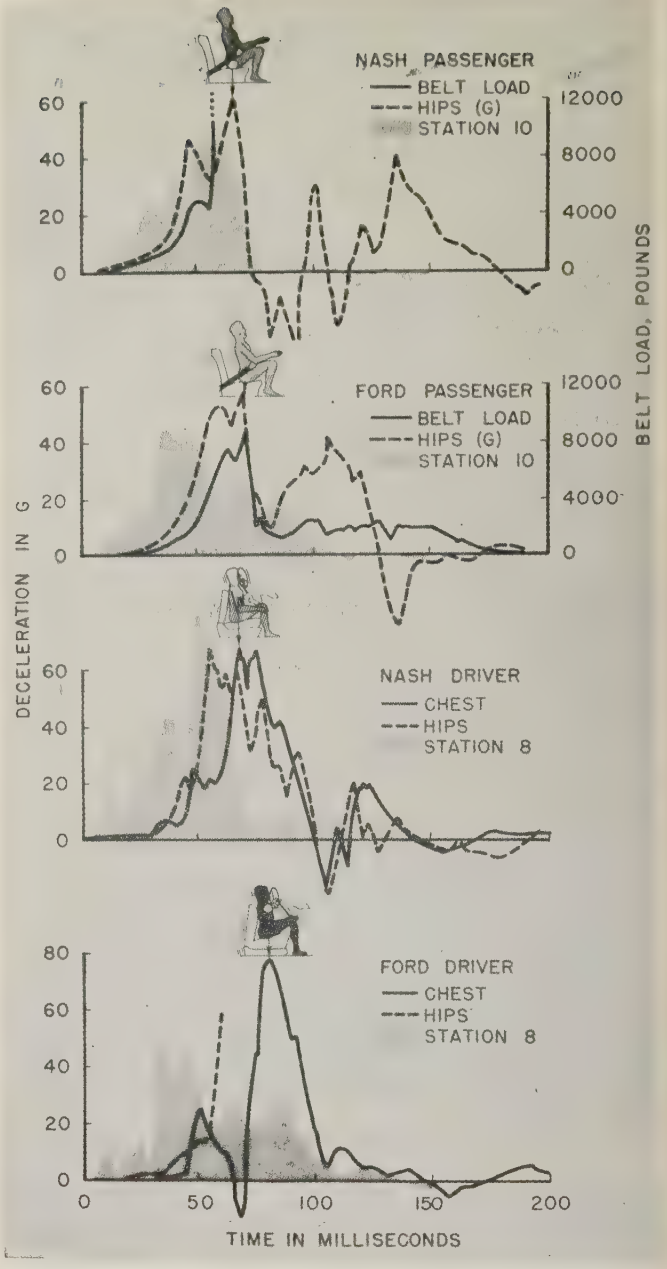

Fig. 36E — Occupant deceleration and belt load, Experiment 43

peak decelerations for chest and hips appear to be random. The driver's weight and position, car type, and impact speed are the significant variables in operation.

Some concept of the magnitude of forces encountered by motorists in collisions is provided by Fig. 37. The values shown are conservative because (1) the motorist is properly restrained and (2) the motorist is favorably positioned (rear seat). Notwithstanding these advantages, the force systems are extremely high, even for the 20-mph impacts. Without the restraint, the passenger is hurled against the front interior of the car with the probability of serious to critical injuries. In Fig. 37, belt tensiometers with hip (femur) accelerometers register their peaks between 70 and 95 millisec for the 21, 27, and 52 mph head-on impacts.[29] The full extension of the lap belt occurs appreciably later (125 to 210 millisec). Consequently, the simultaneous relationship between approximately erect posture and peak belt loadings, as shown in Fig. 35, applies for speeds ranging from 21 to 52 mph. The increased elongation of the belt[30] with higher impact speeds demonstrates the adaptability of the nylon belt to varying conditions of impact.

The belt tensiometers registered 5500 lb for the 21-mph impact at the same time that the hip transducer registered a peak deceleration of 40 *G*. Deceleration loading for a 210-lb dummy at 40 *G* amounts to 8400 lb. The seeming inconsistency between 5500 and 8400 lb can be resolved by reference to Fig. 35 and noting that at 85 millisec the peak belt load occurs even though the upper torso is moving forward with no restraining influence, other than that of the pivot point of attachment at the waist and hips. Consequently, the peak belt load relates to the mass being restrained at that instant, that is, approximately the mass from the waist down or 60% of the total body mass (0.60×210 lb

[29] The 47-mph collision is not represented here because failure of the 8000-lb restraint precludes direct comparison with the data presented in Fig. 37.
[30] Part of this elongation was due to partial failure of floor pan.

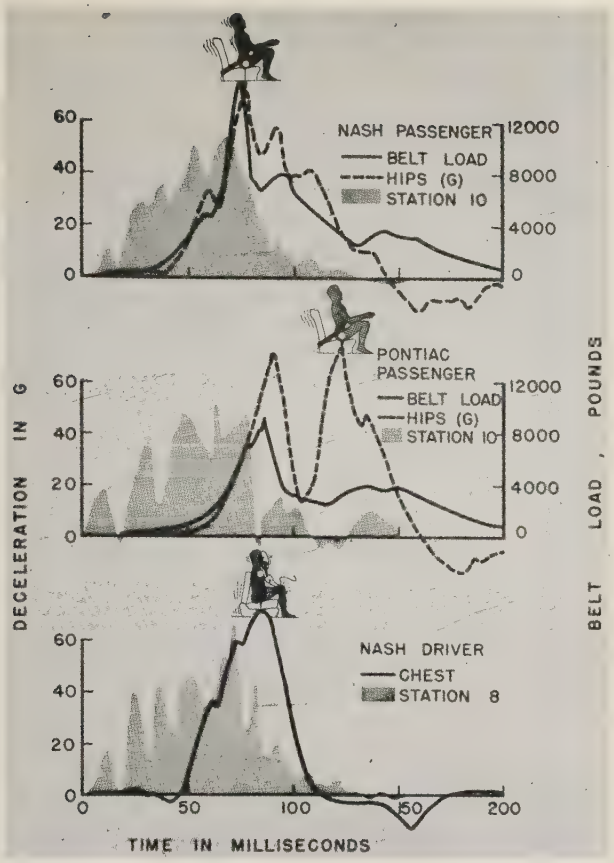

Fig. 36F — Occupant deceleration and belt load, Experiment 44

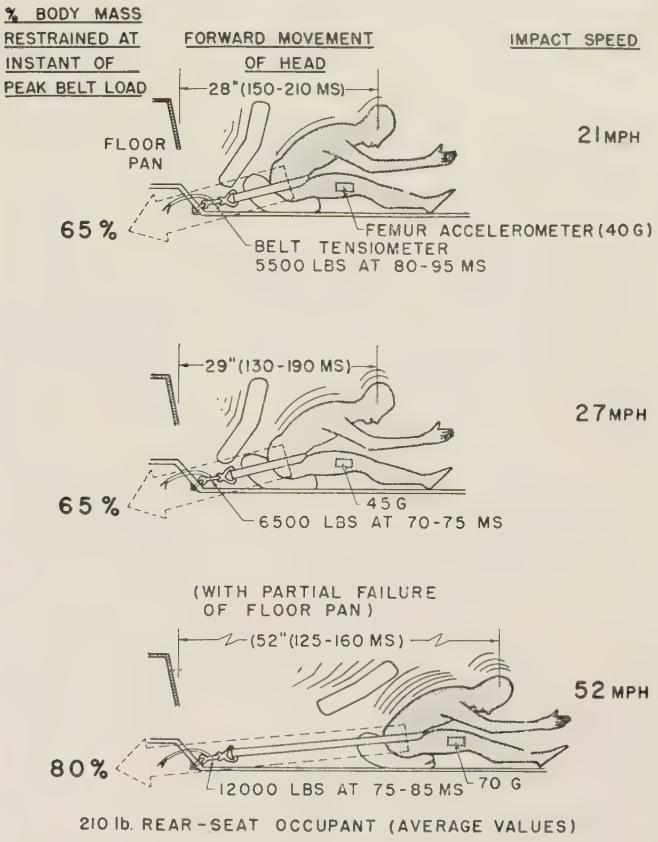

Fig. 37 — Lap belt performance, 3-in. nylon (Air Force Specification)

$\times 40\ G = 5040$ lb). When adjustment is made for the cosine error between the small downward angle[31] the belt makes with the point of attachment at the floor pan, the 5500-lb load correlates with the 5040-lb hip deceleration equivalent loading. The per cent body mass restrained at the instant of peak belt load is given to the left of each sketch (Fig. 37).[32]

In the foregoing analyses, it has been established that even for the adequately restrained motorist, deceleration of the car has reached advanced stages before significant motorist deceleration commences. This will be true even when the effects of slack are held to a practical minimum. This means that the mechanism of collapse of the front-end structure, while important, is not as critical as was once believed; contrariwise, the type of restraining configuration and material, and the manner in which the restraint is installed are correspondingly more important. Although some contributions to slack are unavoidable,[33] it was considered at least of academic interest to compare the theoretical passenger restraining load[34] with the actual passenger belt load (Figs. 38A and B).

For purposes of correlation, the hip deceleration was converted to load and is shown in Fig. 38C. No attempt was made to correct the per cent actual body mass restrained; thus, the values presented assume 100% in contrast with the 65–80% body mass indicated in Fig. 37. In Figure 38D the upper graphs A, B, and C are superimposed for comparison. With the correction in per cent body mass, the correlation load would correspond closely to the actual load. For speeds below 30 mph, slack creates no disadvantage with respect to the amount of restraining load. At impact velocities above 30 mph, slack appears to reduce the load. The contributions to slack above 30 mph, which differ from those below 30 mph, essentially relate to orders of magnitude of belt and anchorage elongation (partial failure of floor pan).

Conclusions

Specific findings and conclusions have been stated within the various sections of this paper. In large measure these conclusions are valid only when considered with the qualifying remarks which precede them. Accordingly, the authors have deemed it inadvisable to separate the findings and conclusions from the text for the purpose of providing a summary. Although such a summary has some desirable aspects, the feeling persists that the interpretation of isolated findings and conclusions would impose an unreasonable responsibility upon the reader.

Acknowledgment

The authors wish to acknowledge the valuable engineering consultation service given by John Leggat, Parish Pressed Steel Co. consultant for the

[31] The angle the belt makes with the horizontal axis is small after most of the slack has been removed, as would be the case for a peak loading (Fig. 35).

[32] For this approximation, the small cosine error due to the shallow belt angle has been neglected.

[33] For example, the contribution of flesh compressibility and body mass displacements common to any restrained subject.

[34] Where slack is eliminated by the assumption that the passenger is decelerated as though he were a rigid structure securely attached to the car body.

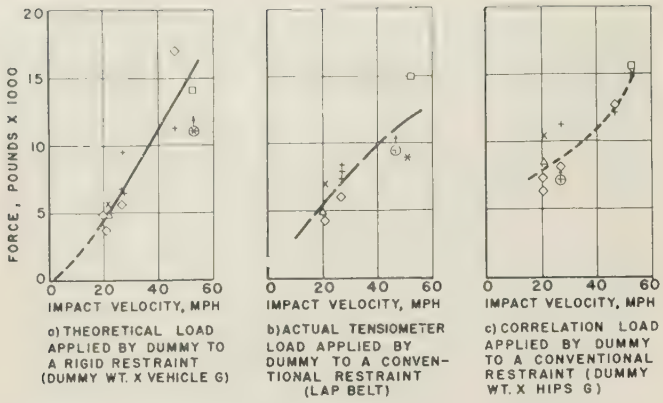

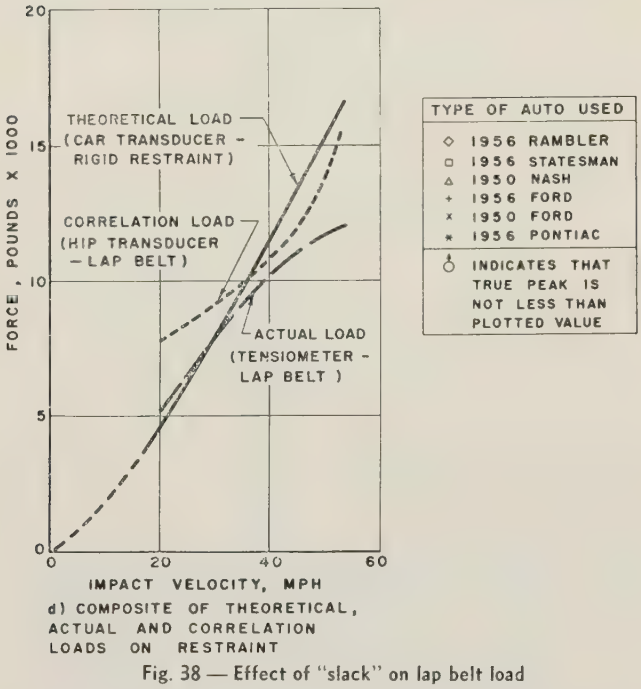

Fig. 38 — Effect of "slack" on lap belt load

project, and to express sincere appreciation to Arthur G. Gross for original contributions in the instrumentation systems used in this research. The authors also wish to take this opportunity to acknowledge, and express their appreciation for, the sustained and efficient performance of all of the project personnel and, in particular, the following: Paul Barbour, engineer, micromotion analyses; Robert Brenner, engineer, statistical; Richard B. Sheridan, engineer, data reduction; David M. Blaisdell, technician, electronic instrumentation; James J. Currey, technician, mechanical systems; James Halverson, technician, photography; and Robert K. Roberson, technician, automotive.

Appendices

Data not essential to the presentation and understanding of the experimental findings for six head-on collision experiments have been organized into eight appendices. An abstract of each of these appendices is provided.[35]

Appendix I: Physical Facilities

Specifications and description of the vehicle control systems and camera tower structure. The description of the control systems includes information on speed control, position synchronization, and directional control of the two vehicles crashed in each experiment.

Appendix II: Inferred Injury Diagnosis

Detailed injury patterns are presented for each experimental collision subject based on the medical scientist's post-collision analyses of anthropometric dummies. Initial examination is made before the dummies are removed from this collapsed vehicle. Following their removal under medical supervision they are re-examined in greater detail.

Appendix III: Instrumentation

Description of the instrumentation developed and utilized to obtain experimental collision data. New techniques are explained in detail — previously used techniques being indicated with appropriate reference where they are explained in detail. Instrumentation for collision injury research consists of five categories: mechanical, electrical, photographic, physiological, and repair cost.

Appendix IV: Underbody Deformation

Underbody photographs were taken before and after each impact for each of the 12 collision vehicles included in this study. A technique is presented whereby these photographs may be superimposed to provide a single photograph. A two-dimensional analysis of underbody deformations can be made directly from the superimposed photograph.

Appendix V: Post-Collision Observations

An investigation of the two wrecked vehicles is conducted immediately following impact to provide a photographic and written record of all observable phenomena of interest. Final positions of motorists, seats, doors, and of the cars themselves are noted. Structural failures and deformations are likewise included. These and other observations are presented in detail for each vehicle.

Appendix VI: Repair Cost Analysis

The cost to repair each experimentally wrecked automobile was obtained independently from several qualified sources and these are tabulated.

Appendix VII: Statistical Analysis

An example of the tests used and calculations supporting statistical findings reported in the text are presented.

Appendix VIII: Automobile Impact Analyses

Table 2B of this paper has been expanded to include rate of onset and peak deceleration data.

---

[35] Complete appendices deleted in the interest of brevity. Microfilm copy of complete paper including appendices available by writing to the Library Photographic Service, University of California, Los Angeles 24, Calif.

DISCUSSION

Unit-Type Body Construction Found Superior in Side Impacts

— Carl W. Cenzer
American Motors Corp.

THE authors are to be complimented for the comprehensive instrumentation setup, and the exhaustive analysis of the data on the high-speed car-to-car crashes reported in this paper. The procedures used represent several technical advances in equipment and methods over those employed in the crash tests performed for American Motors during the preceding year.

It is interesting that the authors point out the relatively slight differences in "collision performance" between the unit-body construction and the frame bolted-body construction. In this connection, we would like to make two general observations:

1. The advantage of the unit-body construction, at relatively low car speeds (in the 20–30 mph range), seems to be significant, due to the fact that survivable accidents on the road are largely in this low speed range. Superiority of the frame-type construction at higher crash speeds, if present, may be largely of theoretical interest, due to the fact that at these high speeds occupants are not likely to survive, regardless of the construction used.

2. The experiments described in this paper, represent car-to-car crashes involving front ends only. In actual field experience, cars are involved as well in front corner impacts, side-swipes, side impacts, rear-quarter, and rear-end impacts, as well as roll-overs. A full examination of the two types of car construction would involve tests under these varied conditions, each configuration involving a number of crash speeds. Such a program would require the destruction of a large number of cars, and would be quite expensive.

At American Motors, we consider the unitized type of construction to have major crash worthiness in several of these other types of impacts. Specifically, the sturdy underbody structure, at the extreme outside edges of the car between the wheels, has definite advantages in side impacts. In addition, the front wheelhouse structure offers added protection in front corner blows, and in those cars, where major impacts occur at a sufficiently high level to override the bumper and frame side sills.

Education May Be Best Approach To Passenger-Car Safety

— O. Edward Kurt
Educational and Technical Consultants, Inc.

THE large amount of information and the detailed interpretation presented in this outstanding paper reflect unusually comprehensive planning and preparation. Other discussers will, no doubt, point out the value of this information and its obvious application in the engineering design of automobiles. This discusser wishes to point out some less obvious but nevertheless important areas of application.

As an independent consultant, I have investigated automobile accidents and have aided legal counsel in the interpretation of evidence to reconstruct accident situations and determine responsible causes. The data in this paper provide positive quantitative confirmation of a number of factors I have previously deduced less accurately from inspection of wrecked automobiles and photographs of accident sites. With fundamental information such as developed by Mr. Severy and his associates, and more extensive investigation of accidents by qualified engineers, there would certainly be further improvements in the design for safety of automobiles.

The experiments described in this paper are beyond the financial resources of the individual engineer and most appropriately were supported by a member of industry. This study deserves further continued support from the industry, financially and in the form of freer exchange of experimental findings. Certainly safety is a subject in which there should be unrestricted dissemination of information; and this has been recognized in other industries, notably the chemical industry. Mr. Severy's papers will serve a very valuable cause if they encourage or prod members of the industry to release their findings.

It may not be feasible by engineering design to meet every hazardous situation created by driver carelessness and thoughtlessness. Education may be a more practical approach and there may already be enough information available to initiate such an approach. There is some evidence of a need for such education within the industry before initiating a program for the driving public. Some of the measures taken by the industry to increase performance and to reduce cost have actually increased the driver and passenger hazards. The overloading of passenger-car tires is an example which culminated about a year ago in an increase in the maximum load ratings. This definitely reduces the margin of safety which the unsuspecting driver has been led by advertising to believe had been developed by tire improvements.

Term "Head-on Collision" Covers Wide Range of Accidents

— Roy Haeusler
Chrysler Corp.

NOT only has the authors' research been remarkable for its elaborateness and for the amount of information provided but it has also provided vivid illustration of the violence of a 50-mph collision. The extreme destruction shown is all the more thought-provoking when we are reminded that a 50-mph collision into a barrier would be considerably more severe! In some quarters within industry there has been more sympathy with our efforts to minimize the likelihood of accident rather than to deal with its consequences. We can better understand why that might be so when we see these pictures.

The data presented by Mr. Severy and supplemented by Mr. Fredericks of the Ford Motor Co. and the material offered in connection with this discussion greatly emphasized the importance of describing accident severity in terms of units of deceleration rather than in terms of impact speed. I mentioned this because the question is very frequently asked as to what speed range is thought to be covered by one or another of the protective devices, such as safety belts, instrument panel padding, or other interior padding. These data remind us again that we can talk about a relationship between speed and severity only in so far as we are able to hold a number of other conditions constant, as was done in the investigations reported. When, however, we attempt to talk about speed alone without specifying the nature and properties of the object with which the vehicle collides—whether barrier, another car head-on, another car in a broadside impact, or another car in a sideswipe accident—we have no basis whatever for judging what the severity will be in terms of g's of deceleration.

Whenever such data as these are presented, the question is certain to arise as to the permissibility of generalizing on it and of applying the findings to other comparisons that are superficially similar. It is very much to the credit of the author that he went out of his way to remind us that the results he obtained could be related only to the specific cars and conditions which he established as part of the control in this test. This seems most important in view of the fact that attempts may be made to appraise the merits of other frameless cars and other cars with conventional frame construction, and in view of the fact that attempts will be made to generalize on the features of head-on colli-

sions without regard to amount of overlap or offset between the colliding cars. It should be clear that a head-on collision involving a greater degree of offset might produce radically different results even though left front wheels interlock.

Furthermore, in this connection we will all want to recognize the need for assessing the importance of these results in terms of the frequency with which this particular kind of head-on collision occurs. Such assessment would presumably be based on a study of the distribution of injury-producing accidents such as can be obtained through the Cornell Automotive Crash Injury Research Program. It is recognized, for example, that while roughly half of all injury-producing accidents involve forward collision, this category includes collisions from 45 deg to the left through those which are frontal to those which are at 45 deg to the right. Furthermore, it includes all degrees of overlap from hood ornament to hood ornament matching to a bare sideswipe involving primarily the left front wheels. It will be recognized that a relatively minor proportion of highway accidents involve so severe a collision as has been portrayed here tonight. This is indeed fortunate since there would be far more injury and death if it were not so. This applies not only to the direction of impact and the amount of overlap of cars but also to the impact speeds.

On a point of detail I would like to call your attention to the fact that Mr. Severy's data showed the peak safety belt load occurring appreciably sooner than did the maximum forward hip movement. This serves as a reminder of an important difference between static and dynamic testing. Under the dynamic conditions prevailing it is apparent that the floor pan of the car was continuing to deform even after the peak loading had been passed, thus emphasizing the important role played by car body deformation at the seat belt anchors in reducing the peak decelerations and peak loadings experienced by the occupants held by the seat belts. It is also interesting to note that the peak value of deceleration experienced by the seat belt occupant occurred after the peak deceleration seen by the car itself. In consequence, it could be expected that the occupant's deceleration peak might be higher than that experienced by the car. This would suggest that if we were able to decelerate the occupant with a higher spring rate system, such as would keep the occupant's deceleration more nearly in a phase with the car's deceleration, we might expect the occupant to be subjected to an even lower deceleration peak than he now sees.

Reduction of Buckling Is Not A Difficult Design Problem

— D. W. Sherman
A. O. Smith Corp.

CONSIDERING the fact that only a very short section of the car can be crushed before collapse of the passenger compartment which, in itself, can cause serious injury to the passengers, the potential for design improvement for anything in excess of very low speeds is obviously limited. The benefits from removing sharp projections, maintaining door closure, and the like, are, of course, self-evident for all speeds. Under the circumstances then, the very small differences between structure types is not surprising.

As compared to structural differences the effect of the large engine mass must obviously be of prime importance. Here we have a powerful battering ram leading the way. An impact test on equivalent cars but with rear-mounted engines would be interesting. Here the passengers would be in the middle, so to speak. I have never heard this point mentioned in discussions of the merits of rear-engine cars.

Perhaps the old-fashioned cars with lengthy hoods had some merit from the collision standpoint. Certainly, we wouldn't want to be located at station No. 1 during a head-on collision.

In any event, considering impact damage from the standpoint of basic design, we have two somewhat contradictory factors for consideration. For deceleration force destruction should occur over a maximum distance. On the other hand, collapse of the passenger compartment and rearward movement of the engine can crush the passenger, and the extent of such will presumably increase as the length of the collapse area increases. Such considerations apply in the case of head-on crashes between vehicles with passengers in each. The situation, however, will be different in the case of a car striking an inanimate but movable object such as a telephone pole. Here a heavier stronger car structure might displace the pole with less resulting car damage than for a more collapsible vehicle. A good design for one condition, in other words, may not be so good for another.

Comparing unitized construction with the separate frame vehicle we would expect the heavy-gage rigid frame rails to restrain momentarily damage at initial impact, which results perhaps in higher initial deceleration, depending upon the penetrability of the body struck. Then, as the frame sections buckle, the deceleration should be greater. The tests appear to support this. Modification by design of the force required to produce buckling, should not be difficult and may warrant some thought.

The fact that frame buckling can influence steering column action is interesting. Perhaps favorable column action can be provided intentionally without design penalty.

ORAL DISCUSSION

— Reported by John W. Leggat
Engineering Consultant

Kenneth Coppock, General Motors Corp.: The automotive industry for some time has been appraising, evaluating, and developing safety features for their vehicles. The data submitted in this paper is of inestimable value to the industry. It will also be of value to the U. S. Congress if they attempt to establish safety standards to which automobiles will have to be built. All safety features considered by that body will have to be tested before they can be approved. The cost of such testing and evaluating the many features that have a possibility of contributing toward passenger safety will be very heavy. It appears that all such testing would be a logical field for the government to enter.

D. J. Schrum, Studebaker Corp.: At the higher speeds it appears that there is little that the automotive industry can do to nullify the forces developed. However, much can be accomplished, particularly at the lower speeds. Proper attention can be given the locating of items such as ash trays, instrument boards, instrument controls, and the like; also, by design control the behavior of the steering wheel and column. Front-seat anchorage can and should be of a more secure design.

Robert Knickerbocker, General Motors Corp.: Current styling trends indicate that the passenger compartments will continue to be moved forward in the vehicle. Is this not the wrong direction?

Mr. Severy: If the distance from the dash to the front bumper of today's cars is maintained, there should be no extra injury hazard. If it is shortened, then indications are that the hazard would be increased. Front passengers are now located close to the optimum position considering front- and rear-end collision conditions.

R. McLedy, General Motors Corp.: There have been many proposals for devices to allow axial translation of steering column and wheel during crash deceleration conditions. Considering the direction and nature of steering column failure as shown in the high-speed pictures, do you feel that such devices could be of value?

Mr. Severy: Yes.

C. W. Schwartz, Ford Motor Co.: Was there an attempt made to make equal the test weights of the mated crash cars?

Mr. Severy: The difference in the weights of the mated cars was fully considered before the crashes and taken into account in preparing the paper.

"DELRIN" ACETAL RESIN

—a new engineering material

H. H. Goodman and J. D. Young, E. I. du Pont de Nemours & Co.

This paper was presented at the SAE Summer Meeting, Atlantic City, June 11, 1958

THERMOPLASTIC resins of formaldehyde have been known for a long time, but they lacked either the long-chain length, necessary mechanical properties, or sufficient thermal stability to be of practical interest. As a result of an extensive program of fundamental research, (it has been roughly estimated that one man alone would have needed 300 years to complete the research carried out on this material), Du Pont has been able to make from formaldehyde a new plastic which is called "Delrin" acetal resin. This new material differs from previous resins of formaldehyde because of its very long chains and excellent thermal stability. Our laboratory evaluations of this new material showed it to have an excellent combination of properties. For example, it exhibited high strength, good fatigue life, low creep, and excellent solvent resistance. It also showed the ability to retain these properties at elevated temperatures. However, this laboratory testing was not enough — we had to know if practical application could be made of these properties. To get this answer, an extensive end-use evaluation program was carried out within Du Pont. This has now been expanded to a test program with end users and plastic processors throughout the country, a tremendous amount of the work being done in the automotive industry. Results of these tests confirm the suitability of "Delrin" for a wide variety of mechanical applications in a number of industries, including automotive, machinery, appliances, plumbing and hardware. Its colorability, decorative features, and strength have also attracted much attention for consumer and packaging applications.

"Delrin" is not yet commercially available, but it is being produced now in limited quantities in a small semi-works unit. This material is being used in a planned field program to obtain even more data on product properties, processibility, and suitable end uses. A large full-scale plant is now under con-

"DELRIN" is a new thermoplastic which offers high strength, excellent thermal stability, good fatigue life, low creep, and excellent solvent resistance. This paper describes the physical and chemical properties of the material, and the range of possible uses.

The material is easily fabricated into complex shapes by standard injection-molding techniques. Also, it can be easily joined to itself or to other materials. The authors think that the material offers advantages over metals in its good frictional properties, abrasion resistance, and corrosion resistance.

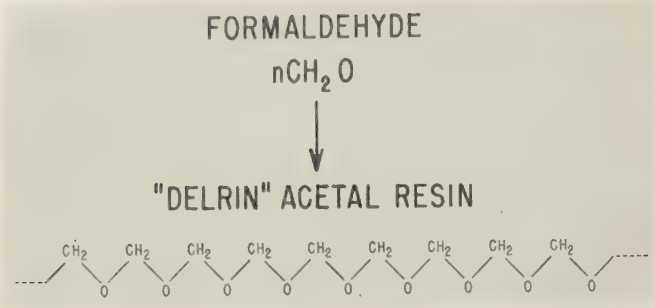

Fig. 1 — Formaldehyde units

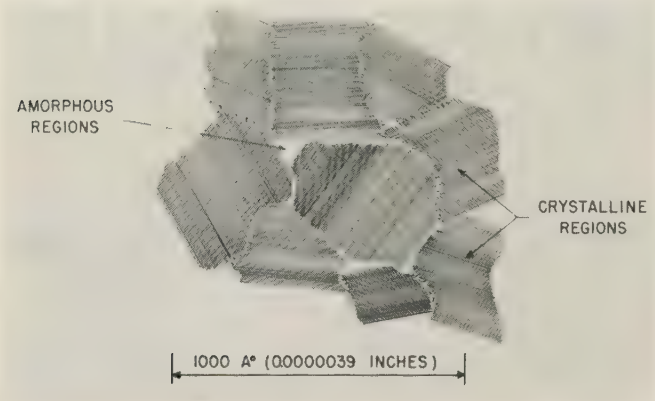

Fig. 2 — Crystalline and amorphous regions

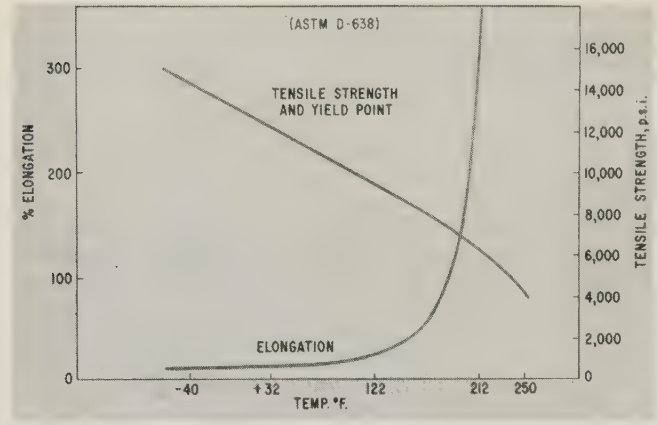

Fig. 3 — Effect of temperature on tensile properties

struction in Parkersburg, West Va., and the material will be available commercially in mid-1959 on a large scale.

Physical Properties

As we mentioned earlier, "Delrin" is made from formaldehyde, a simple chemical with exceptional reactivity. In "Delrin," the formaldehyde units are combined in long, unbranched chains (Fig. 1) normally averaging more than 1000 units per chain.

The generic name, acetal resin, comes from the fact that the chain is made up of repeating carbon oxygen units, as shown in the figure. Because of the nature of the carbon-to-oxygen linkages in this polymer, the chains can pack closely together in a dense uniform pattern. As a result, the chains arrange themselves into strong, solid crystals interspersed with small areas of amorphous material (Fig. 2). This dense crystalline structure is responsible for many of the key properties of "Delrin" — especially strength and stiffness, high temperature behavior, and solvent resistance.

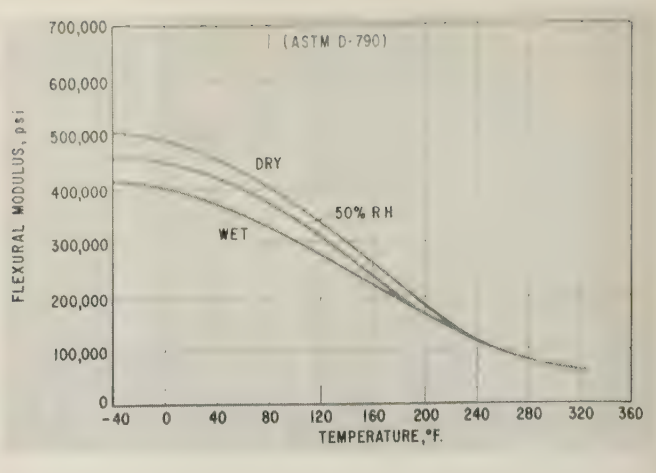

Fig. 4 — Flexural modulus versus temperature

At room temperature, "Delrin" has an elongation of about 16% and a tensile strength of 10,000 psi. The effect of temperature on these properties is shown in Fig. 3. You will note that as the temperature is increased, tensile strength falls off while elongation increases. However, at 250 F the tensile strength of "Delrin" is higher than that of any of the present commercial thermoplastics. Tests to date indicate that this acetal resin is satisfactory for use at 250 F for the life of an automobile. Although some of the people with whom we have worked in field tests have successfully applied cyclic loads for short times to parts at 300 F, parts operating above 250 F should not be considered except in cases where the temperature might momentarily go higher only two or three times during the life of the car.

In Fig. 4, the flexural modulus is plotted at various temperatures and humidity conditions. The modulus value in the range from −40 to 300 F is among the highest available in present thermoplastics. The difference in stiffness under extremes of humidity is small at room temperature and essentially nonexistent at elevated temperatures.

All plastics exhibit gradual deformation called "creep" or "cold flow" when they are subjected to a continuously applied load. This creep does not continue indefinitely at a constant rate but levels off as the time increases. Typical curves for deformation under load of "Delrin" with time are given in Fig. 5.

If the load is removed, the inherent elasticity of the material will effect nearly complete recovery in time. Thus, the amount of deformation which will occur in a part that is loaded intermittently is dependent upon the amount of load, the length of time under load, and the length of time no load is applied. This is illustrated in Fig. 6, which shows bars of "Delrin" which were loaded for five cycles to the indicated tensile stress, with load being completely removed after each cycle. At stresses below 5000 psi, there was negligible permanent deformation.

At normal temperature and humidity, "Delrin" exhibits about the same kind of creep behavior as the most rigid of the present thermoplastics. But at elevated temperature and humidity, this acetal resin

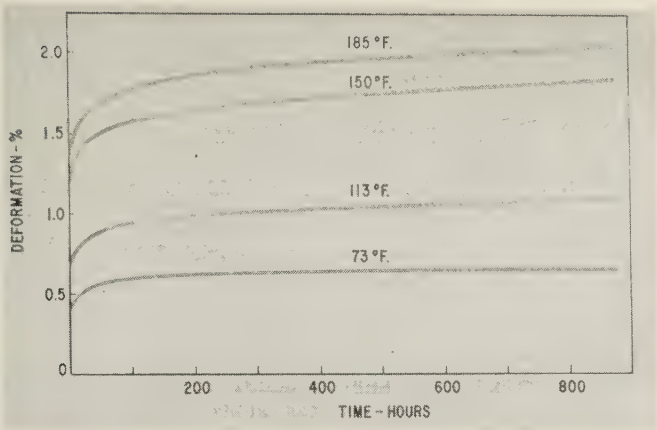

Fig. 5 — Total deformation versus time at 1500-psi stress

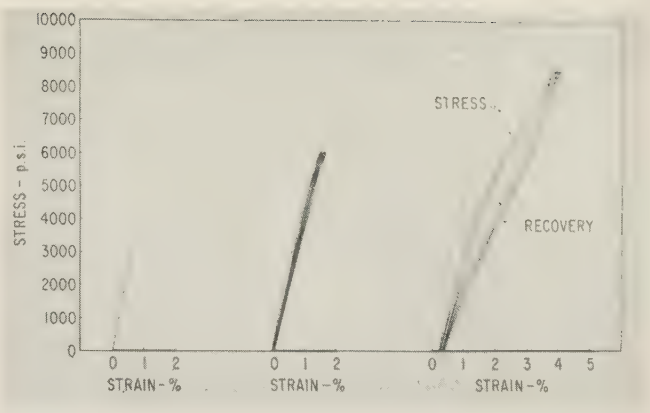

Fig. 6 — Tensile stress and recovery under repeated loadings

exhibits exceptional resistance to creep.

The resistance of "Delrin" to creep is important in many applications. One good illustration would be where interference fits are used to hold components together. The experimental data we have obtained indicate that at stress levels up to 5000 psi, the rate of stress relaxation or creep soon becomes asymptotic, assuring continued strength of the fit. This was illustrated by a test conducted to show the force required to remove a 0.25-in. rod of "Delrin" from a hole in a "Delrin" block with a 0.007-in. interference fit. Initially, a force of 400 lb was required to remove the rod. After heating the assembly for 70 hr at 200 F (to accelerate stress relaxation), the parts reached an equilibrium stress level. Upon cooling to room temperature, 180 lb was required to remove the rod from the hole, demonstrating good retention of the interference fit.

When subjected to a repeated cyclic stress, all materials will ultimately fail at a stress lower than the apparent tensile strength of the material. This phenomenon is known as fatigue failure. Our experiments indicate that there is a stress value below which this new resin will not fail, no matter how many times the load is applied. This stress is called the fatigue endurance limit. Fig. 7 shows the fatigue life under two environmental conditions. Thus, at 150 F and 100% relative humidity, "Delrin" will have an infinite fatigue life as long as the stress level does not exceed about 3000 psi.

Fatigue endurance is important in gear applications since each tooth is subjected to repeated cyclic stresses. Our evaluation of "Delrin" in a gear test mechanism, as well as practical applications such as the speedometer and windshield wiper gears, indicates that it is an excellent gear material. As other factors such as abrasion and environmental conditions can affect gear operation, many additional tests are needed to establish a practical limit of the load-carrying capacity of gears of this material. This limit will lie somewhere between the points representing tested applications and the theoretical fatigue limit.

For its stiffness, "Delrin" is a very tough, resilient material. This has been confirmed by evaluation of its toughness in many practical applications. However it cannot take as much deformation as the more flexible materials like nylon or polyethylene. When thinking about the toughness or resilience of this material, it should be compared to the resilience

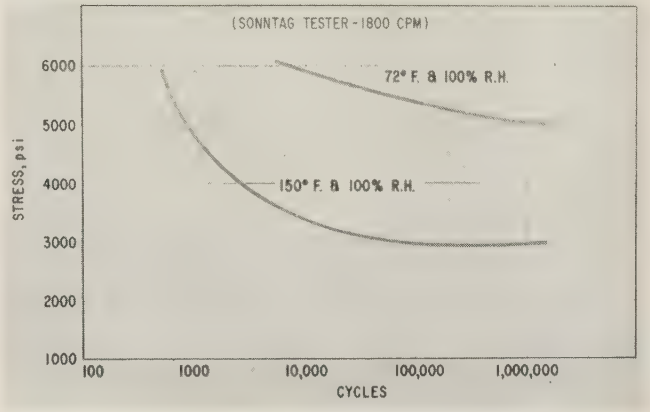

Fig. 7 — Fatigue life

of a steel spring rather than the elasticity of a rubber ball.

Izod impact tests on unnotched bars of polyoxymethylene show it to have an impact strength of about 20.5-lb per in. Notching the bar reduces the impact strength to about 1.4–1.6 ft-lb per in. Although this latter value is still quite good for a rigid thermoplastic, the marked drop in impact strength emphasizes the need to eliminate sharp corners and other stress raisers in designing parts of "Delrin."

Temperature has almost no effect on the notched izod impact strength of the plastic. From −40 to 260 F, the range of temperatures which would normally be encountered in an automobile, the impact strength remains essentially constant. All of our toughness and impact data lead to the conclusion that "Delrin" is tough in the sense of "strong and rigid." It should be used where high strength and resistance to bending is required and not where severe deformation must be tolerated in service.

Dimensional stability is an important property of any engineering material. Dimensional changes in plastic materials are caused by four major factors: Expansion or contraction resulting from temperature changes, volumetric changes resulting from water or solvent absorption or loss, changes in shape due to stress relief, and deformation under continued load. The last of these has already been discussed.

The effect of temperature on this resin is defined by the coefficient of linear thermal expansion which

is 0.00005 in. per in. per F. This value is approximately equal to that of most other plastics. This coefficient is several times greater than that of ferrous and nonferrous metals, a factor which must be taken into account in part design. Numerous design techniques are available for overcoming this difference in thermal expansion.

The effect of moisture and other solvents on dimensions and strength properties is shown in Table 1. Test length varied from 180–365 days, and exposure from 122–158 F. In all cases, the per cent change in tensile strength and length are relatively minor. Thus, "Delrin" can be considered suitable for use in contact with most fuels, lubricants, and other chemicals normally associated with the automobile.

Locked-in stresses in an injected-molded thermoplastic part will vary with molding conditions and with the geometry of the part. Experience to date with this new material has shown that no allowance need be made for dimensional changes caused by release of these stresses so long as the parts are to be used at temperatures below 120 F. If service temperatures are higher and if close dimensional control (in the range ± 0.001–0.003 in. per in.) is required, it may be necessary to anneal the parts after fabrication.

The smooth hard surface of "Delrin" is slippery to the touch, which would indicate good frictional properties. The coefficient of friction of the resin against steel is shown in Table 2. Of special significance is the fact that under identical conditions of measurement, there is little, if any, difference between the static and dynamic coefficients of friction. Elimination of slip-stick tendencies will be especially important in automotive applications where intermittent rotational or sliding motions are encountered, such as ball-joint seats, steering linkage bushings, and other mechanical linkage bushings. The absence of slip-stick may also be responsible for the absence of squeak when this material is rubbed against many mating surfaces even without lubrication.

The frictional properties of "Delrin," coupled with its strength and low-creep rates, have led to its being tested in a variety of bearing applications. Some bearings made of this acetal resin which have operated successfully in our test program include: Portable gasoline engine camshaft and connecting-rod bearings, door hinge bushings, storeroom cart wheel bushings, bicycle steering bushing, and electric shaver cams.

Processibility

Processibility of an engineering material is just as important as its physical properties. Being a thermoplastic, "Delrin" can be easily fabricated into complex shapes by standard injection-molding techniques. This moldability has been conclusively demonstrated in many tests within our own laboratories and in our customers' plants. Parts successfully molded have included internal and external threads, undercuts, helical gears, wall sections of 0.040–0.375 in. and large pieces weighing up to 2½ lb. To obtain test parts of large complex pieces, we have even molded "Delrin" in molds made for die casting. This is not usually practical for commercial production of parts, but it has been of great value in obtaining parts for evaluation.

"Delrin" can be extruded into a variety of shapes and forms, but our work in this area has not been as extensive as in molding because of limited availability of material. We have demonstrated that the material can be handled on conventional equipment used to extrude other thermoplastics.

While usually not necessary in production of molded parts, "Delrin" can be machined by conventional metal-working techniques such as sawing, milling, turning, reaming, threading, and tapping. The machinibility of the material can be compared to that of soft brass. This machinibility is especially important in the production of prototype parts from rod stock for use in test programs.

"Delrin" can be joined to itself or other materials by a wide variety of techniques. Several forms of welding may be used. These include hot-plate welding, hot-gas welding, resistant wire welding, induction welding, and spin welding. In the latter case, heat required to melt the material to effect the bond is generated by rotational friction. Bonds formed by these methods have in many cases approached the basic strength of the material itself.

Data to date indicate that mechanical fasteners such as self-tapping screws, bolts, explosive rivets, and other types of rivets will give very strong joints. In one particular test, a 400-lb pull was required to remove a self-tapping screw from a piece of "Delrin." The high creep resistance of the material should insure that the pieces joined in this way will remain tight.

Two other methods of joining made use of the resilience of the plastic; these are snapfits and interference fits referred to previously. In many instances, properly designed snapfits can be used to save assembly time and cost.

Several of the applications visualized for "Delrin" will require some form of finishing. Since the material is naturally a white translucent color, it can be integrally colored by pigmentation in a wide range of shades and hues. Parts which previously had to be painted can be made of "Delrin" with the color molded throughout the part.

Where painting is desirable, suitable techniques are available for this new plastic. Its good temperature resistance will permit bake-outs at 300 F to insure good adhesion and a durable surface.

Interesting strides have been made recently in the field of first-surface metalizing of plastics. Several bright finish parts in today's automobiles are made of plastic with a vacuum-metalized surface protected by a suitable organic coating. Such systems are available for "Delrin," and we fully expect that, as a result of the research now under way in this field, even more durable surfaces will be forthcoming. Objectives of this research are to provide bright finished parts for use in high-wear areas such as interior hardware and in exterior applications. In this latter field, "Delrin" could provide definite advantages in weight reduction and reduced production cost in some items, such as heavy lamp housings, grille sections, and trim.

We have considered "Delrin" as an engineering material and have approached the possible applications for this material in the automotive industry with careful consideration of the design requirements involved. One area of application is the interior hardware, such as door handles, window crank handles, and the like. An analysis of the

stresses involved in the operation of an interior door handle was made to determine what changes in design, if any, would be required to provide the same strength in "Delrin" as now available in the metal handle. This analysis is summarized in Fig. 8. The calculations were based on a maximum torque of 250 in.-lb which was assumed to be concentrated at a point 5.0 in. from the shaft centerline. The upper line represents the stress levels incurred in present production models, and the lower line the stress present in a design with some modified sections. The stress reduction was accomplished by widening the handle slightly. The volume of material in the new design was kept the same as that of the present design by eliminating unnecessary material from the back of the handle. Because injection molding eliminates secondary operations such as trimming and buffing required for die-cast parts, it appears possible to make handles at a cost saving from "Delrin."

A spectacular area for the application of this acetal resin is housings for automotive instrument clusters. These are parts that traditionally have been made of die-cast metals — in fact, the parts in Fig. 9 were made in die-cast molds. The additional strength of "Delrin" at elevated temperatures combined with its toughness permits it to challenge the use of metals for such applications as these. "Delrin" offers a number of advantages over other plastics as well as die-cast metals that make it quite attractive for construction of these parts. First fabrication by injection molding eliminates several secondary operations, such as trimming and buffing required for decorative die-cast pieces. Weight reduction, important in the vehicle itself, would also make for greater ease in handling during assembly and shipping. The fact that the material is an electrical insulator will allow the incorporation of improvements such as stamped circuits on the back of the housing itself. And finally, properties such as translucence and resilience of the material allow new and novel approaches to the design of future housings.

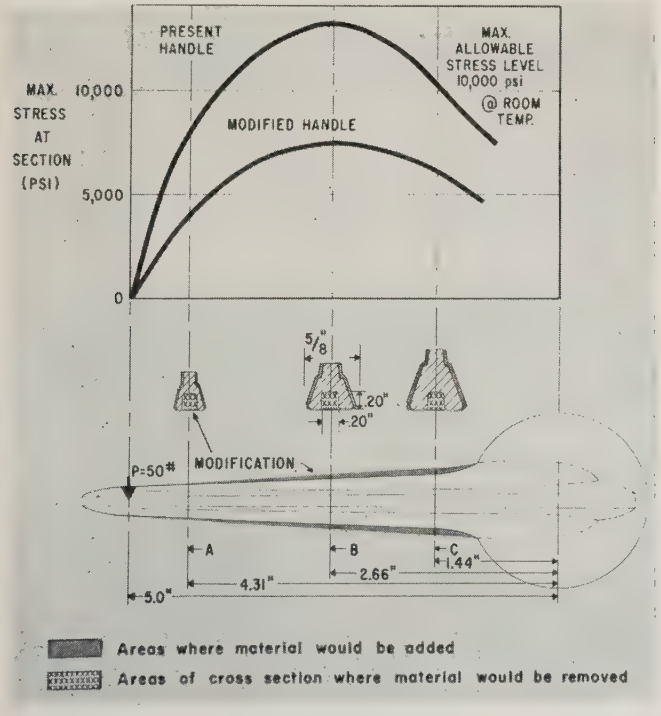

Fig. 8 — Calculated stress levels in current production door handle and as it might be modified for molding in "Delrin" acetal resin

Use of the new material in such an application obviously poses problems, but there appear to be good solutions for them. For example, "Delrin" does not have the same degree of stiffness or rigidity as the metal it replaces. However, as we demonstrated in our discussion of the door handle, proper redesign of the housing will give adequate strength. With the present design of housings, opacity is also a problem. This too can be eliminated by painting or use of properly pigmented polymer.

Strictly functional housings such as sections of the fuel pump, carburetor, control valves for air suspension, and windshield wiper transmission housings also offer attractive areas for the application of "Delrin." One of the reasons for its consideration is its retention of mechanical properties in automotive fluids at elevated temperatures. Another is the precision with which parts can be molded directly, offering real cost savings by eliminating secondary machining and finishing operations. In some applications, the good bearing properties of "Delrin" allow the housing and bearing to be made as an integral unit. A separate bearing insert is, therefore, not required.

During the past few years a lot of work has gone into the development of ball-joint suspension systems. To get a joint with optimum operational

Table 1 — Resistance of "Delrin" Acetal Resin to Selected Fluids

Material	Test Length, Days	Test Temperature, F	Tensile Strength, % Change	Length, % Change
Heavy Mineral Oil ("Nujol")	365	158	+2	−0.4
Motor Oil — 10W30 ("Uniflo")	365	158	+3	−0.3
100% Aromatic Fuel (toluene)	365	122	−7	+1.2
Ethyl Alcohol, 100%	365	122	−5	+1.0
Acetone	365	122	−7	+1.1
Brake Fluid ("Super" 9)	365	158	−6	+0.6
Water	275	140	+2	+0.5
10% Salt in Water	180	158	0	0.0

Table 2 — Coefficient of Friction of "Delrin" on Steel

Conditions	Coefficient of Friction[a]	
	Static	Dynamic
Dry (73 F)	0.1-0.3	0.1-0.3
Dry (250 F)	0.1-0.3	0.1-0.3
Lubricated with Water (73 F)	0.2	0.2
Lubricated with Oil (73 F)	0.1	0.05-0.1

[a] Measurements were made by the inclined plane method.

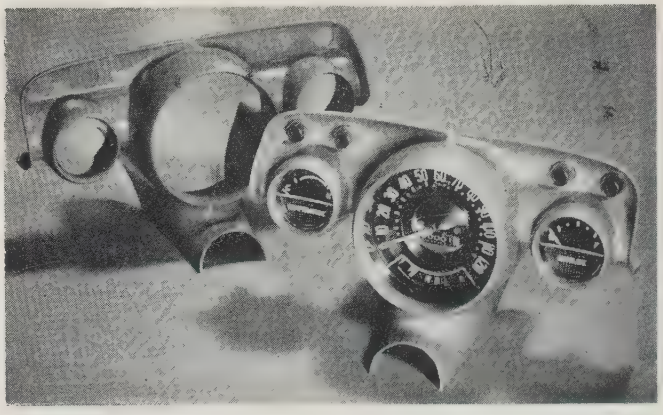

Fig. 9 — Parts of automotive instrument panel made of "Delrin"

qualities, a material is needed for the seat which has a low coefficient of friction, no stick-slip, low creep, and good impact resistance. The properties of "Delrin" appear to meet these requirements and, as a result, it is being examined by a number of manufacturers for such applications. An artist's conception of such a joint is shown in Fig. 10, along with other samples of low-speed intermittent action bearings.

Casings for rotary and push-pull mechanical controls (Fig. 11) are applications where a combination of good frictional properties and strength are required. Use of "Delrin" would eliminate problems of rust and corrosion. With the inherently good frictional properties, grease may not be necessary to assure continued smooth, squeakless operation.

"Zytel" nylon resin has been used successfully in small squirrel cage blower wheels for some time (Fig. 12). As a light-weight unit which could be molded complete in one operation, it saved money by eliminating both assembly and balancing costs required for metal blowers. The greater stiffness of "Delrin," particularly at temperatures of around 200 F, makes it attractive for even larger blower wheels. Tests are under way to determine the extent which "Delrin" will broaden the application of plastic blower wheels and make them more useful to automotive needs.

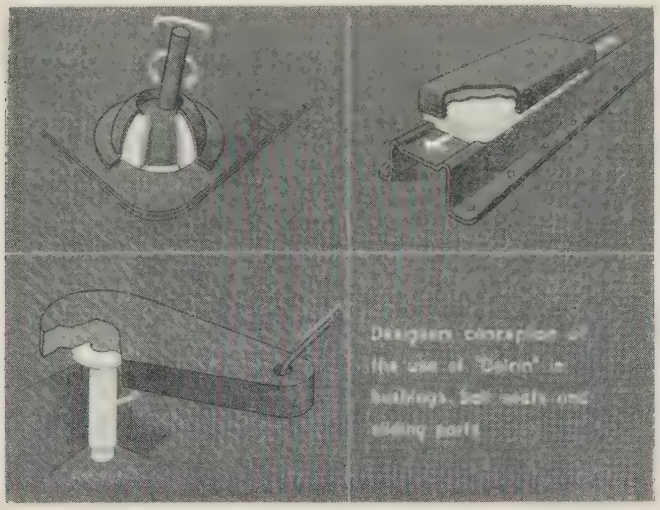

Fig. 10 — Intermittent, heavy-load bearings

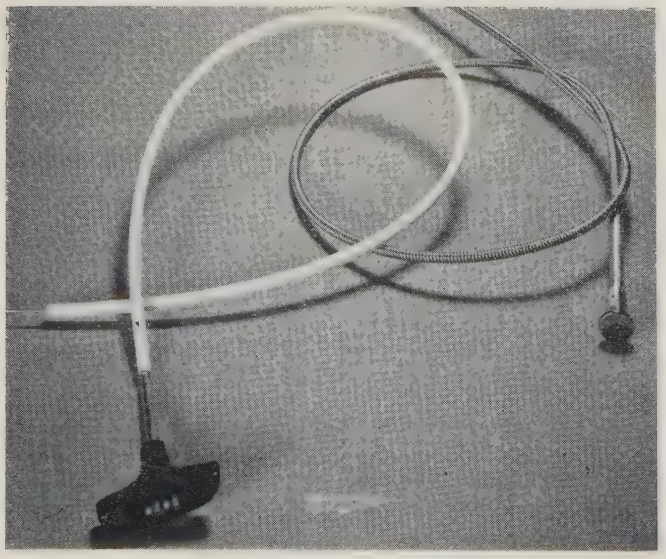

Fig. 11 — Casings for mechanical controls made of "Delrin"

In conclusion, "Delrin" is a new thermoplastic, chemically unlike any material now on the market. Propertywise, its strength, low creep, and resilience help to bridge the gap between metals and existing plastics. In addition, it offers definite advantages over metals in ease of fabrication by injection molding, good frictional properties, abrasion resistance, and corrosion resistance. We feel the future will see an ever-increasing use of this versatile, new engineering material in the automotive industry.

ORAL DISCUSSION

— Reported by G. H. Seaver
Ford Motor Co.

R. Sergeson, Jones and Laughlin Steel Corp.: Can "Delrin" be applied to steel and wood with good adherence in, for example, the manufacture of shuttles and other parts for textile machinery?

Mr. Goodman: The problem of developing adhesives for "Delrin" is being worked on at present; due to its resistance to solvent action, this is a difficult area in which to work. Probably the best solution to attaching "Delrin" to other materials for such applications would be to use inserts molded into the part itself.

R. D. Chapman, Chrysler Corp.: Is there any evidence of anisotropy in "Delrin?"

Mr. Goodman: There could be some differences between transverse and longitudinal properties in the extruded material or in very thin sections, but "Delrin" is essentially isotropic in most molded parts.

P. Allmendinger, Stewart-Warner Corp.: What is the coefficient of expansion of "Delrin?"

Mr. Goodman: The coefficient of thermal expansion is essentially the same as for most other plastics, 5×10^{-5} in. per in. per deg F.

B. W. Keese, Rockwell-Standard Corp.: What would be the maximum load which could be applied to a "Delrin" bushing, where the relative motion is low; for example, a king pin bushing? Also, can this material be applied to unlubricated mechanisms or where the lubrication is poor, such as clutch pedals, clutch throw-out bushings, and the like?

Mr. Goodman: In such applications, the load is dependent on the speed, so that at low speeds a maximum load of 4000–5000 psi is possible. In answer to the second question, "Delrin" should be very suitable for unlubricated mechanisms because of the absence of "stick-slip." It may not have the abrasion resistance of Zytel, but it has better creep properties.

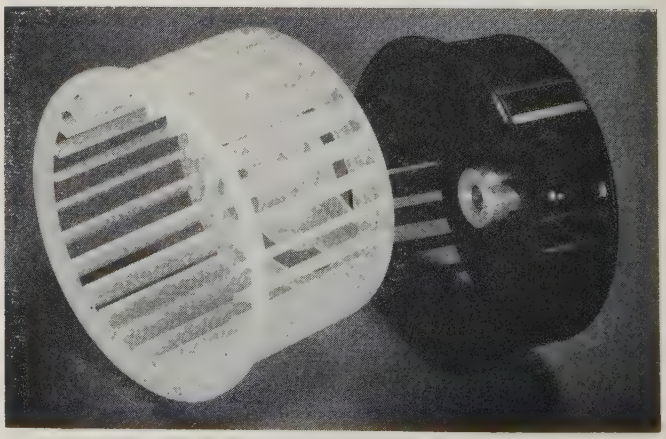

Fig. 12 — Blower wheels of "Zytel" nylon resin

Single-Cylinder Engine Fuel Research

A. W. Pope, Jr., Waukesha Motor Co

This paper was presented at the SAE Summer Meeting, Atlantic City, June 11, 1958.

THIS REPORT on single-cylinder engine fuel research will cover a period starting with the first automotive and pertoleum industry joint efforts to measure fuel antiknock quality. The continued cooperation of the two industries has resulted in the establishment of world standards of knock rating for motor gasolines: the ASTM Motor and Research methods. This accomplishment took 30 years of the combined efforts of many individuals, companies, and industry associations. [My own small part in this program was inspired by H. L. Horning in whose honor this award is made.]

The true measure of a man can be seen only in the life of his works. Mr. Horning, along with a few other industry greats, gave his full energies to establishing an organization through which the automotive and petroleum industries could work together on mutual problems. This was successfully accomplished through the Cooperative Fuel Research Committee (CFR) which developed a knock test engine and an industry-accepted method of knock rating motor gasolines in the period 1928–1932. This was only one of the many automotive-petroleum mutual problems solved by the group. The mushroom growth of the CFR activity was clear evidence of the success of the work of Mr. Horning and the other founders of this activity. The program quickly expanded to such a degree that the informal nature of the original CFR organization seemed inadequate, and a more formal organization with directors and bylaws was incorporated in 1943 as the Coordinating Research Council (CRC). The organization's list of projects is long, but only time will tell how effective the new organization will be. A reorganization of the entire technical committee structure is being put into effect this year. By this action the residue of the old CFR committee has finally been formally liquidated. It would be interesting to have heard Mr. Horning's advice on these matters. Perhaps recalling some of his qualities will give a clue to what he would have done.

The quality in Mr. Horning which stands out clearest in my mind is that he was a thinker and a doer. There are many thinkers in the world and many men of action, but the combination is rare. Mr. Horning's mind seemed to be always working, and he quickly put his thoughts into action. He radiated action. Anyone in his presence immediately was stimulated to spring to the job. I was first attracted to him in 1924. *Automotive Industries* carried an article about a Waukesha truck engine which gave 100 ton miles per gallon. The illustration showed a modern looking Ricardo head engine, and indicated unusual things were being done at Waukesha. So I went to see, and it was "love at first sight."

In 1928 the CFR Committee had reached the decision that a standardized single-cylinder engine must be produced as the first step in developing a gasoline knock test method. But there was a deadlock on the issue of L-head versus variable-compression overhead-valve type. Although designs of each type were under consideration, agreement was impossible because of the great popularity of the

THE AUTHOR outlines the research and development work on single-cylinder fuel research engines resulting from the industry cooperative program which grew out of the Cooperative Fuel Research Committee. The establishment of world standard methods of gasoline knock rating have resulted from this work.

Six types of single-cyclinder laboratory engines produced for motor, aviation, and diesel research are described as well as instrumentation for indicating gasoline knock and diesel fuel ignition quality.

The current problem of rating aromatic-type fuels in the range above 100 octane is explained as being an instrument characteristic which gives "knockless knock ratings" on certain fuels. A new electromechanical detonation indicator is described.

This paper was the 1957 Horning Memorial Lecture.

L-head Ricardo type and the equally strong preference for the overhead-valve variable-compression engine by some important producers. At the critical moment I had the good fortune of dreaming up a very simple valve gear linkage which permitted interchangeable L-head and variable-compression overhead-valve cylinders to be installed on the same basic crankcase. Mr. Horning succeeded in breaking the committee deadlock with this design. Early in December, 1928, after the committee meeting in New York he wired Waukesha to make detail drawings at once and have an engine built for display in Detroit on Jan. 14, 1929, at the SAE Annual Meeting. The engine was designed, built, tested, and delivered to Detroit in about 45 days. Mr. Horning really was a doer.

The engine became known as the CFR engine, and many of the original engines are still giving good service after nearly 30 years. The cylinder and valve gear linkage have remained practically unchanged. Fortunately, top management at Waukesha has continued Mr. Horning's research policy by giving full support to the laboratory engine development program. The CFR engine was the forerunner of a number of single-cylinder laboratory test engines developed at Waukesha. Since the basic nature of the Waukesha business is to build engines in limited quantities to fit special applications, the organization was well-equipped to design and build these very special engines.

Fig. 1 is a sectioned assembly view of the original CFR engine in the variable-compression overhead-valve version.

The original CFR engine was intended for low-speed operation, 600 rpm. Therefore, vibration was not a serious problem. But when the 900 rpm Motor method was established in 1932, need for a balancing system arose, particularly for engines which were mounted above ground level. A crankcase with reciprocating counterweights was produced to meet this need. Fig. 2 shows the detail of the balancing system operated from eccentrics on the crank cheeks. This gave a compact engine with good balance capable of operating over the full passenger-car engine speed range. The design was arranged so that the new high-speed crankcase was interchangeable with the original low-speed engine.

The high-speed crankcase expanded the usage of the engine beyond the original intent of a standardized knock test engine, and laboratories throughout the world started using it for general engine research and instruction purposes. During World War II the high-speed CFR engine was used for the Aviation Gasoline Test Method at 1200 rpm, and the Supercharged Aviation Test Method at 1800 rpm. These methods have since become ASTM standards.

As a result of the high combustion pressures resulting from supercharged aviation fuels and the postwar trend toward high compression ratio and high octane engines, there was need for a more rigid crankshaft design than was provided in the CFR high-speed engine with crank eccentrics for reciprocating counterweights. Therefore, a new design was produced with rotating counterweights. This permitted maximum rigidity of the crankshaft with closely spaced main bearings. This design is known as the CFR 1948. Fig. 3 shows the arrangement of the counterweights and the larger shaft and bearing details. While the balance with this system is theoretically not as good as the reciprocating counterweight earlier design, it balances the main primary reciprocating forces and permits speeds up to 4500 rpm with reasonable smoothness. This crankcase was designed to be interchangeable with the original low-speed engine and, therefore, was readily adapted to the standard fuel test meth-

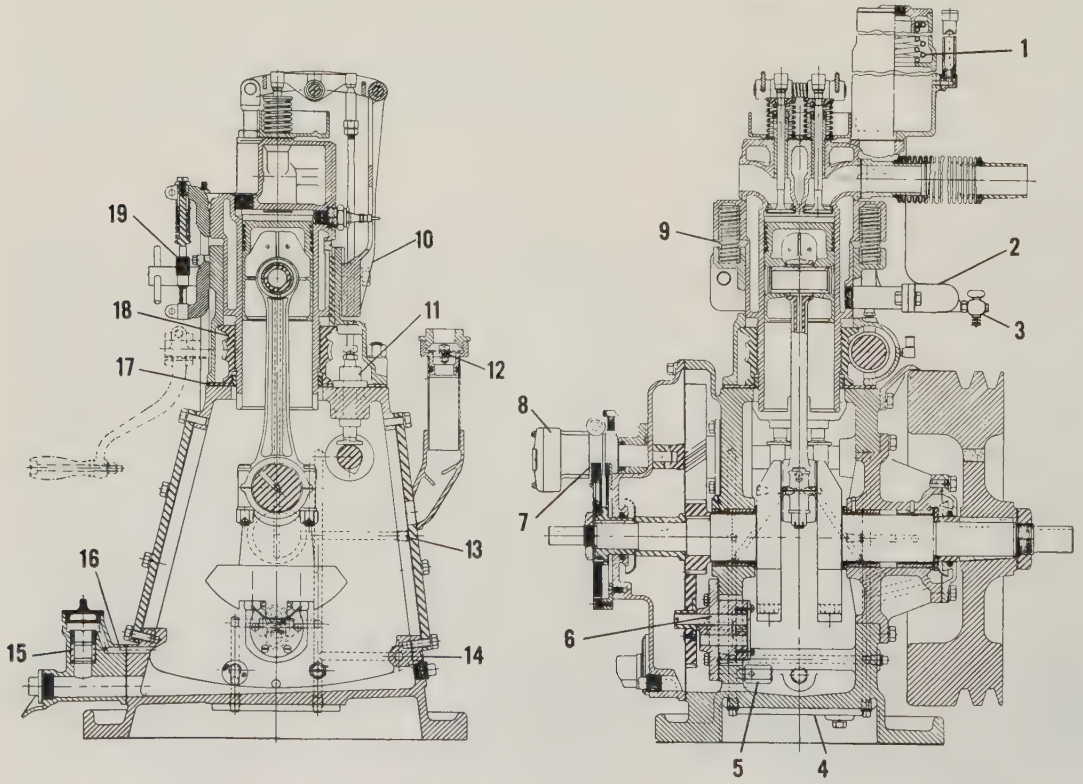

Fig. 1 — Sectional assembly view of original production design CFR engine

ods. It has now completely superseded the earlier low- and high-speed designs, which are no longer produced. This is now the standard crankcase for the ASTM Motor and Aviation gasoline test methods and also the Diesel Fuel Cetane method.

In 1931 the CFR variable compression ratio engine, which had proved useful for gasoline knock rating, was adapted for studying the ignition quality of diesel fuel. This involved applying an injection pump and a special piston with a pear-shaped chamber to fit the fuel spray from the injector which was located in the side sparkplug hole of the standard variable-compression gasoline cylinder. The critical compression ratio of the diesel fuel was determined by motoring the engine under standardized conditions and then injecting fuel for a 3-sec period. The compression ratio was varied until the critical ratio, at which audible combustion in the exhaust was produced, was determined. This was considered to be the critical compression ratio required to ignite the fuel. It gave a very practical measure of fuels ignitability under actual engine conditions. It was the equivalent of a dynamic bomb test, and gave a better measure of the fuels ignitability in an engine than a static bomb test or the ignition delay test in a running engine. The critical ignition compression ratio determined by this method clearly demonstrated why high antiknock carburetor engine fuels are hard to ignite in a diesel engine. Eighty octane gasoline has a critical compression ratio of about 14/1 compared with 8/1 for average diesel fuel.

As the number of cycles fuel injected had an effect on the critical compression ratio, the personal variable in the manual control of this factor was eliminated by providing an automatic engine-driven control valve, which made two injections every 30 cycles. This improved the accuracy of results and convenience in running the test. The critical ignition compression ratio of a diesel fuel has always seemed a more significant property than its operating ignition delay period, as it has a closer relation to the fuels starting and cold light load operation. These are the two operating conditions most affected by the fuels ignition quality. In spite of these fundamentals, the standard test method was developed using the ignition delay in a running engine instead of the critical ignition compression ratio as the index of ignition quality.

The variable-compression diesel cylinder used on the CFR engine for determining the cetane number by the ignition delay method is unique. The design was first worked out by Shell Laboratory in Holland. They were interested in correlating their original large fixed compression ratio engine cetene method to the CFR engine. Note the original diesel test reference fuel proposed by the Shell laboratories was cetene, not cetane. Later, when attempting to obtain a supply in this country the DuPont laboratories pointed out that cetene was unsaturated and unstable, and that cetane would be a better reference fuel as it was stable and reproducible. Cetane was, therefore, adopted as the standard ignition quality reference fuel. The variable-compression combustion chamber is cylindrical in form with a tangential throat at one end connecting it to the cylinder barrel. A moveable plug piston adjusts the length of the cylindrical-shaped combustion chamber and, thus, its compression ratio. The plug piston seal is made by expanding the piston. This eliminates piston rings and provides a positive reliable seal. Injection is in an axial direction, which provides automatic compensation for the change of combustion-chamber length when compression ratio is changed. The lower the ratio, the longer the chamber and greater the spray penetration. This permits operating over a wide range of compression ratio without seriously upsetting combustion. The tangential throat provides rotary air swirl which

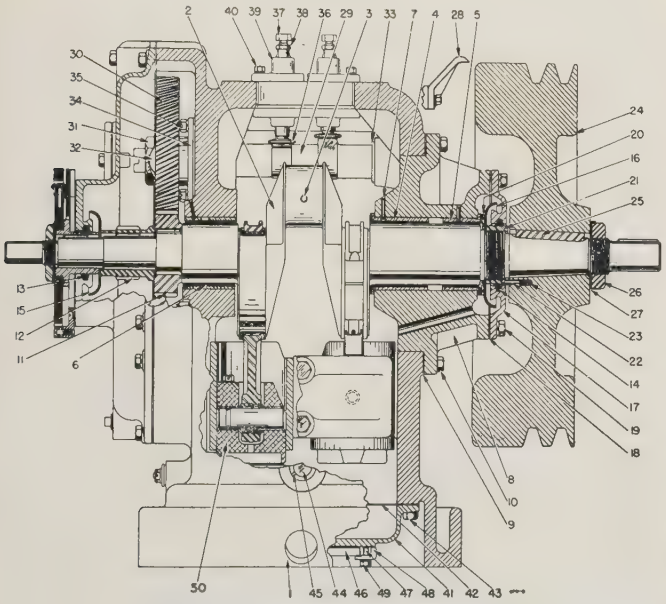

Fig. 2 — Detail of balancing system

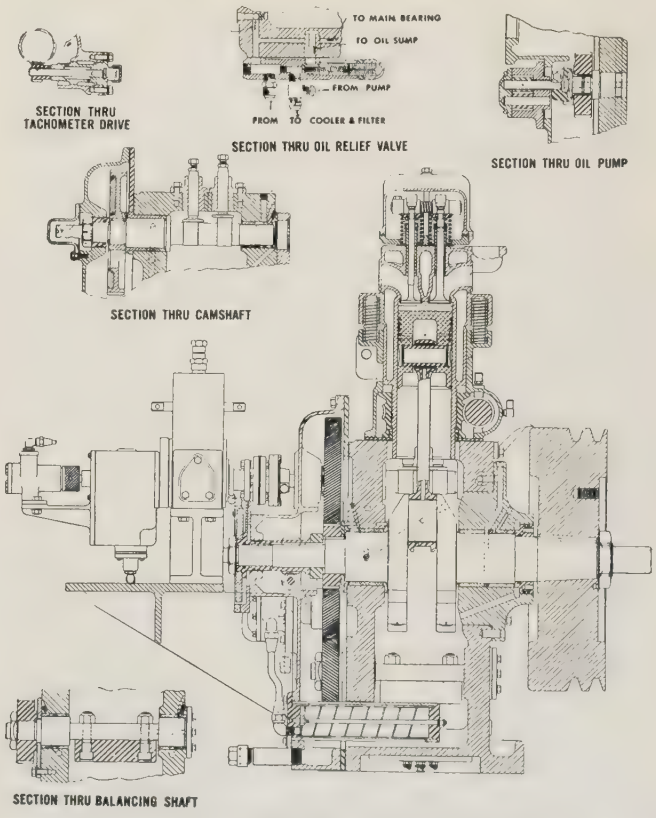

Fig. 3 — 1948 model high-speed ASTM-CFR crankcase

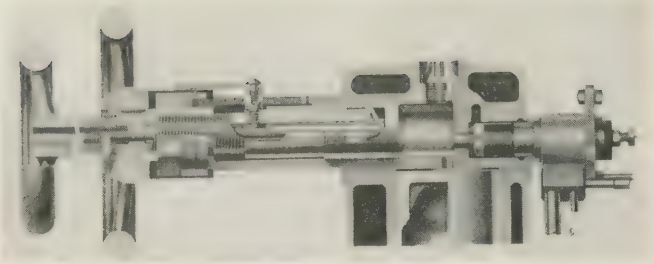

Fig. 4 — ASTM variable compression diesel cylinder

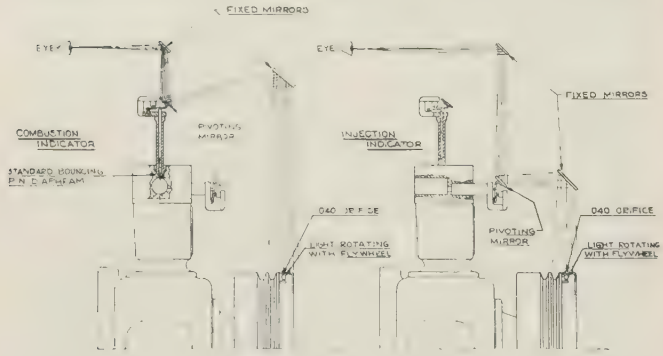

Fig. 5 — Diagram of optical system

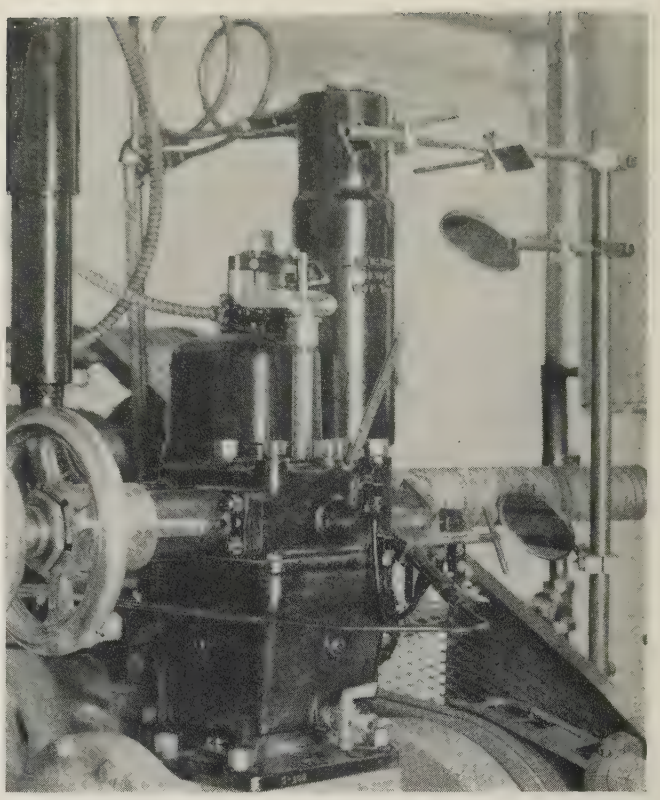

Fig. 6 — Optical system installed on engine

also helps to make the engine less sensitive to injection and combustion-chamber detail variables. Fig. 4 shows the standard ASTM variable-compression diesel cylinder, as used for the ignition delay cetane method.

The standard instrumentation for many years consisted of neon lights rotating with the flywheel and controlled by contact points on a combustion indicator and injection indicator. The angular position of the light flash indicated the start of injection and combustion, and permitted setting the compression ratio to cause the engine to operate with a standard 13-deg delay period. The compression ratio setting for the sample and the bracketing reference fuels was used to calculate the reference fuel blend which would match the sample.

Instrumentation for the ASTM Cetane method has finally evolved into an electronic package which indicates the fuel ignition delay period on a meter scale. The instrument was developed and supplied by the Solatron Corp. of England.

At Waukesha our aim in developing test engines and equipment has always been to keep the apparatus as simple as possible, in order to let the user run tests without being distracted by complicated instruments. With this in mind, a simple direct optical method of measuring ignition delay was developed and used for many years in our laboratory. However, we were never able to generate enough interest to have it adopted for the ASTM Cetane method. Fig. 5 is a diagram of the optical system, consisting of a set of mirrors arranged to observe a light beam emitted by a small light bulb attached to the flywheel rim. The light beam is observed on a path passing through a pivoted mirror attached to the combustion indicator or through a pivoted mirror attached to the injector indicator. Deflection of the mirror, either by combustion pressure or by injector needle valve lift, deflects the light beam; thus giving a diagram of combustion pressure rise or needle valve lift.

Fig. 6 is a photograph of the system installed on the engine. A reference marker line controlled by a micrometer screw permits accurate measurement of the ignition delay period, as shown on the optical diagram. An advantage of a mechanical optical indicator of this type is that it gives a direct diagram without need of any calibration device. The injection and combustion events are observed directly without chance of deviation due to adjustment variables. A surprising thing about its operation is that vibration of the mirror support does not distort the observed diagram. Apparently, the entire diagram image deflects as a unit and, therefore, is undistorted. The precision of ratings with this indicator is about twice as good as the original neon light system. When our laboratory started using it on the committee exchange sample program, their ratings went from near the poorest of the group to near the best. While this instrument has proved to be a simple reliable tool for measuring ignition delay, it has apparently not appealed to routine operators because observing a moving diagram is much more tiring than reading a stationary meter needle.

Experience with the earlier CFR knock test engines proved the value of standardized single-cylinder laboratory engines in several respects not anticipated. The intent of the original design was to provide a rigidly standardized knock test engine which would be a common yardstick for measuring gasoline antiknock quality. As the engines came into use for knock testing, it was soon apparent there were many advantages in using a standardized engine for general engine research. It made possible a better understanding of results obtained in different laboratories and permitted a freer ex-

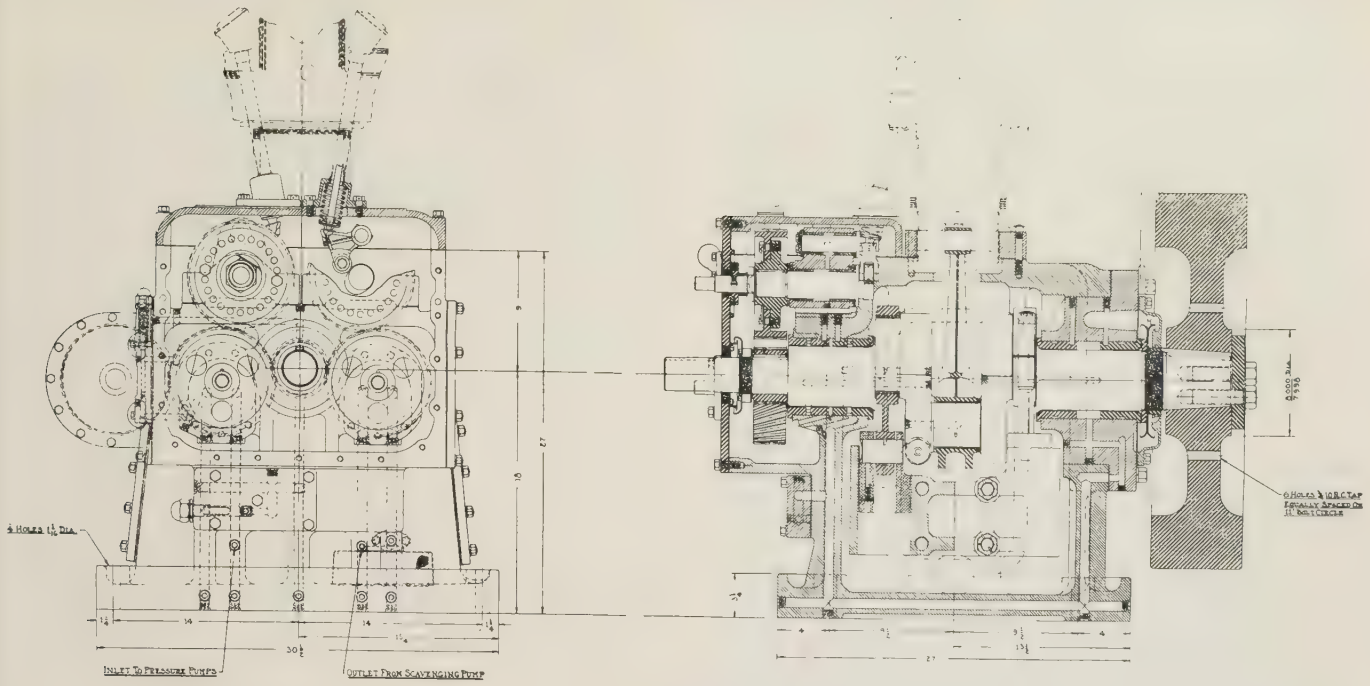

Fig. 7 — Single-cylinder test engine

change of technical data. The availability of standard research engines also made it unnecessary for individual laboratories to design and build their own test engines. This gave a twofold gain by letting the technical staff devote their full energies to the specific problem in hand and also providing a well-developed engine at a great cost saving.

There is a mysterious charm about engines which tempts every engineer to try his hand at creating a design. Therefore, unless the laboratory staff is kept pretty well-occupied by the main objective, they are pretty sure to be led astray by the desire to design their own special laboratory test engines. Recognition of this situation prompted Waukesha to develop a number of single-cylinder laboratory engines in addition to the CFR engine. Prior to World War II there was urgent need for a single-cylinder crankcase to run spark-plug tests on full-scale aviation cylinders. The SAE Ignition Committee made this need known, and in 1937 we designed and built in 90 days a reciprocating counterweighted engine model CWA (Counterweighted Aviation) to operate the Wright aircraft engine cylinder. Fig. 7 illustrates the engine. It was used effectively by one of the major spark-plug companies in developing spark-plug types which were soon required for our military planes. Only one engine was produced to this design, as it did not meet requirements for aviation lubricating oil tests.

Therefore, a new design was developed, known as the CUE (Cooperative Universal Engine). This design attempted to cover as wide a range of features as possible in order to make it useful for general research on lubricants, fuels, and mechanical elements of full-scale aviation cylinders. Fig. 8 shows the design detail with the rotating counterweight system located in a subbase structure independent of the engine crankcase. Full-scale cylinders from all of the military aviation engines of World War II were applied to these engines, and it would be interesting to know how many petroleum and mechanical problems were solved by their use. It is certain, however, that they permitted running a great many more tests under more accurately controlled conditions than would have been possible with full-scale engines or improvised single-cylinder engines.

The CWA and CUE are interesting examples of individual and cooperative design results. The CWA design was based on the dominating objective of simple rugged structure with perfect balance. The CUE design was dominated by the need to meet a wide range of applications and to permit rigid control of the lubrication. Five designs were made before committee approval was obtained. It took over a year to design and build. The CWA project handled by an individual took much less time, but its use was very limited. The CUE project, a cooperative effort, took longer to accomplish, but the engine had a very much wider application and longer life. In fact the engines are still being used today, 20 years later, for engine development work. This suggests that the cooperative method might be considered a way of making haste slowly. It takes a little longer to get started, but it finds the best solution sooner.

The CUE engine was extremely useful for testing full-scale aircraft engine cylinders under rigidly controlled conditions and cost much less to run than a full-scale multicylinder engine. But it still involved the use of rather expensive laboratory facilities which made routine lubricating oil test fairly expensive. Consequently, there was interest in obtaining a small engine to be used for aircraft lubricating oil screening tests. In 1942 a small single-cylinder oil test engine design was developed to meet the specifications laid out by an Air Force representative with the help of an industry advisory committee. This engine was known as the COT (Cooperative Oil Test) engine. It had a 2¾-in. bore and 2¾-in. stroke with domed combustion chamber. It was instrumented with thermocouples in the piston head, the connecting rod journal, and

the cylinder sleeve. Fig. 9 shows a sectioned view of the engine. The primary reciprocating forces on this engine were not balanced; but due to its small size, it was possible to run at high speeds by using a heavy subbase and foundation. A standard supercharged aviation oil test procedure number L-30 was worked out for this engine by the COT Engine Group of the CLR Engine Oil Division. This test method never came into commercial use. Apparently, the switch from piston to jet military aircraft engines relieved the urgency and the petroleum industry escaped the establishment of an aircraft lubricating oil test method. However, a considerable number of these engines were built for petroleum laboratories, and we are told they were very useful as a small engine for screening tests.

Recently, a new use has been found for this crankcase by designing a small variable-compression cylinder similar to the standard ASTM knock test cylinder, but with 2¾-in. bore instead of 3¼ in. This served two main purposes: (1), it gave a small rugged variable-compression knock test engine of half the weight of the standard ASTM engine which could be used in portable laboratories, and (2), it permitted studying the size scale effect on fuel knock characteristics. By adjusting the temperature, time, density factors, it was found possible to get knock ratings which correlated with standard ASTM method larger engines.

A supercharged method for aviation fuels was also worked out for use on this engine with very much simplified instrumentation, since it was desired to use it in a mobile laboratory which did not have room for the standard ASTM dynamometer and fuel/air ratio measuring equipment. By using an exhaust gas analyser to indicate percentage of unburned hydrogen in the exhaust and manifold pressure as an index of the knock limited power, it was possible to do away with the dynamometer, the fuel weighing device, and the airflow orifice meter of the standard unit. Basically, the ratings with this method are made at a constant chemical air/fuel mixture ratio in contrast to a physical weight ratio as with the ASTM method. For fuels of normal type the two systems will correlate, but if the chemical type of fuel varies, the two methods will be quite different. It seems that a method which will rate at a constant percent of chemical over enrichment will give results more significant of a fuel's true ability than the standard method based on fuel/air ratio by weight. Therefore, the standard ASTM Supercharged Aviation Gasoline

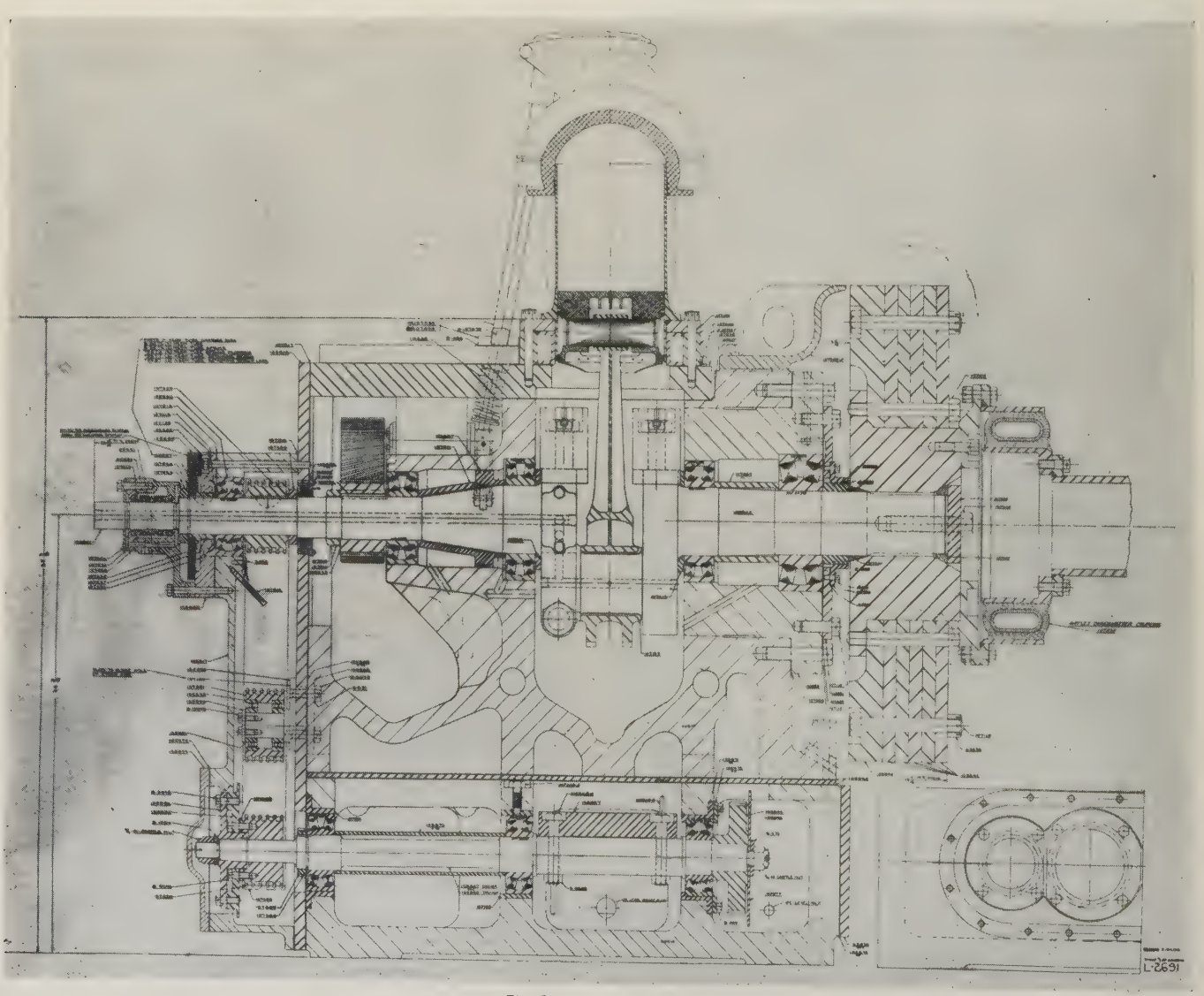

Fig. 8 — Design detail

Test method might be made more significant and at the same time very greatly simplified by replacement of the fuel/air weight measuring equipment with a conductivity type of exhaust analyser to measure the chemical over enrichment. It is true that exhaust analysers are generally considered unreliable, but this is because they are usually used to indicate in the lean mixture range. Exhaust analysers of the thermal conductivity type depend upon the relatively high conductivity of the hydrogen in the exhaust to produce the meter reading. With lean mixtures there is very little hydrogen in the exhaust. With rich mixture there is an appreciable quantity of hydrogen present and the meter readings, therefore, are quite reliable. As the aviation supercharged knock test method is run with overrich mixture, an exhaust analyser of the thermal conductivity type gives very reliable and reproducible readings; and, therefore, is a practical instrument for indicating the percentage of chemical fuel-air enrichment.

The laboratory test engines described above were made possible by Mr. Horning's activity and success in getting individuals, companies, and industries to work together on their mutual problems. The engines have spread throughout the world, and have done their bit toward solving fuel engine problems and instructing students in this field.

I believe the intent of the Horning Award is to provide an incentive for others to think and work at the fuel engine problems which Mr. Horning was forced to leave to younger men. The practice of occasionally making the award to older men such as myself, therefore, seems to carry the obligation of presenting information which may be of value and help to the younger men who are working on the problem. With this in view I will leave the single-cylinder engine subject, and outline my experience first with research on the instrument for knock measurement and second with the functions of committees for cooperative research.

Mr. Horning used to tell about the boy in the laboratory who first noticed that a coin lying on an engine cylinder head would bounce when the spark was advanced enough to produce an audible ping. This was at the same period when Midgely had made the same observation in his optical indicator, and as a result had constructed the Midgely bouncing pin to indicated knock by arranging the pin to close electric contact points. The current flow was proportional to the audible knock intensity. This ballistic-type indicator was excited by the same type detonation shock wave which rattled the coin lying on the cylinder head of Horning's engine. It was used successfully for a number of years by operators who developed a skill in bending the springs to obtain proper tension and frequency to give consistent knock indications.

When Waukesha was given the problem of producing the bouncing pin for the standard test method, something had to be done to reduce the art of bouncing pin adjustment to more of a science. This was accomplished by designing graduated screw adjustments for the leaf spring tension, the inner coil spring tension, and the gap setting. With these four graduated adjustments it was possible to establish a standard pin setting which would at least tell the operator how to start. With a little practice it was then fairly easy to master the art of making the final adjustment to correct for the numerous variables in the bouncing pin ballistic system. The adjustable bouncing pin became an ASTM standard and held its own against all competitors for many years. Fig. 10 shows the original nonadjustable Midgley bouncing pin and the improved adjustable-type bouncing pin.

Finally, in 1954 the magnetostrictive-type pressure pickup developed by the Standard Oil Co. of California, in conjunction with the electronic meter developed by the Phillips Petroleum Co., was adopted by ASTM as standard equipment to replace the bouncing pin. The electronic meter had been de-

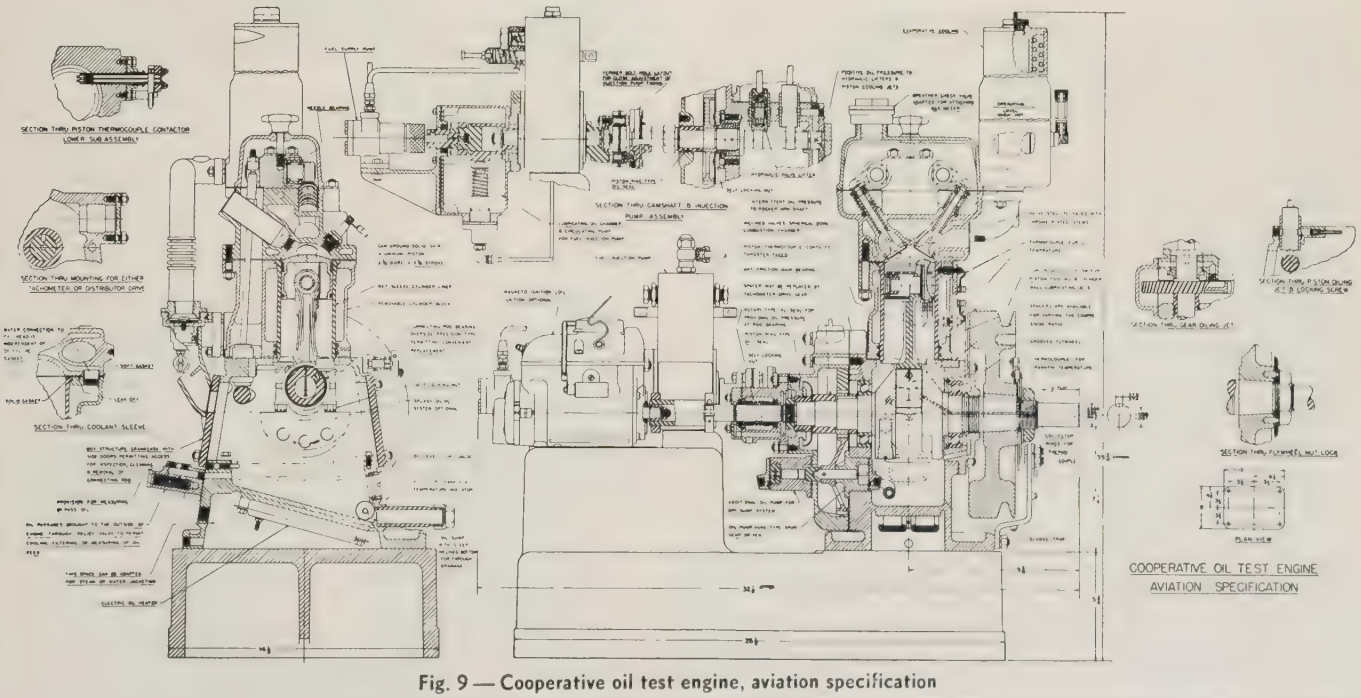

Fig. 9 — Cooperative oil test engine, aviation specification

veloped to give ratings to agree as closely as possible with the bouncing pin and astonishingly close agreement was obtained. However, statistical analysis of a large number of ratings showed that with certain fuels there was a real difference. Therefore, it was not practical to permit the optional use of the bouncing pin and electronic meter in the standard method.

In 1956 Waukesha was given the problem of producing the magnetostrictive pressure pickup and electronic meter. The situation was a little similar to the earlier one when we were required to reduce the bouncing pin operation from an art to a science. However, there was a difference. In the case of the bouncing pin there was no manufacturing difficulty, but a big operating problem. With the electronic system there was nothing for the operator to do, but a big manufacturing problem in finding the engineering design details which were critical to the performance of the pressure pickup and meter. The pressure pickup has numerous critical mechanical and metalurgical details which require close control in order to obtain standard performance. The filter circuit at the entrance to the electronic meter requires extremely rigid control to produce standard knock ratings. The adjustment of this filter circuit is the means of controlling knock ratings to agree with the bouncing pin. It is astonishing that the developers of this meter obtained such close agreement with the old ballistic type of bouncing pin.

Things went well with the electronic knockmeter until it was attempted to extend the octane scale above 100. Isooctane plus lead is used as the reference fuel above 100; and the octane number is an emperical scale extending to 120, which approximates the relative knock limited performance ability in a nonsupercharged engine. The electronic knockmeter gives an indication of the knock intensity of leaded reference fuel which agrees fairly well with the audible knock; but with aromatic-type fuels, the meter may indicate knock when there is no audible knock present. This means that a nonknocking fuel is indicated to have the same knocking tendencies as a heavily knocking references fuel. In other words, the meter may give "knockless knock ratings." Obviously, the method is invalid for some fuels in the extended octane range. This puts the industry in the predicament of having an extended octane scale reference fuel, without a method of test.

When this situation was first noticed, the test engine was suspected of being the cause. After all, it was designed nearly 30 years ago, and might not conform to modern design principles. However, tests made by others with modern wedge-shaped chambers and domed chambers have shown the same characteristics. This proves that "knockless knock ratings" are an instrument and not an engine design problem. The original variable-compression CFR cylinder is fundamentally a sound design to measure fuel detonation properties under controlled turbulence, temperature, and compression ratio conditions.

Although all signs pointed to the instrumentation as the key to the knock test problem, there was considerable interest in the characteristics and possibilities of the inclined-valve domed-head combustion chamber with large valves and short stroke similar to modern passenger-car practice. Therefore, a cylinder of this type has been designed and supplied to a number of laboratories. It has a 3 13/16-in. bore and 3⅝-in. stroke, and has a variable compression ratio mechanism. The valve gear, which permits lowering the cylinder to raise the compression ratio and fits the CFR-48 crankcase, utilized the same type linkage as the standard CFR cylinder. However, the inclined-valve layout required a rearrangement of the supports and careful design of lever angles and lengths to provide a linkage which would maintain constant valve clearance over a reasonable range of cylinder movement. Fig. 11 shows the design. This cylinder permits variable compression fuel research on the CFR 48 crankcase with a cylinder and porting of modern passenger-car proportions.

As it became apparent that knock rating in the range above 100 is an instrument rather than a cylinder problem, we have directed most of our attention to the pressure pickup and the electronic meter, and have developed what appears to be a simple and practical solution. Observation of the pressure pickup output with an oscilloscope showed that a nondetonating aromatic-type fuel might show a diagram with the same voltage peak as the detonating reference fuel, and the meter would show the same knock rating for the nonknocking fuel as the knocking reference fuel. This meant the meter was responsive to voltage peak which could be the same for a knocking reference fuel as for a nonknocking aromatic-type fuel. Apparently, the combustion rate of pressure rise on the aromatic fuel was as steep as the reference fuel detonation rate of pressure rise which reached the pickup. This suggested that what was needed was an output signal voltage proportional to the detonation intensity. It also seemed probable the slope of the rate of change of

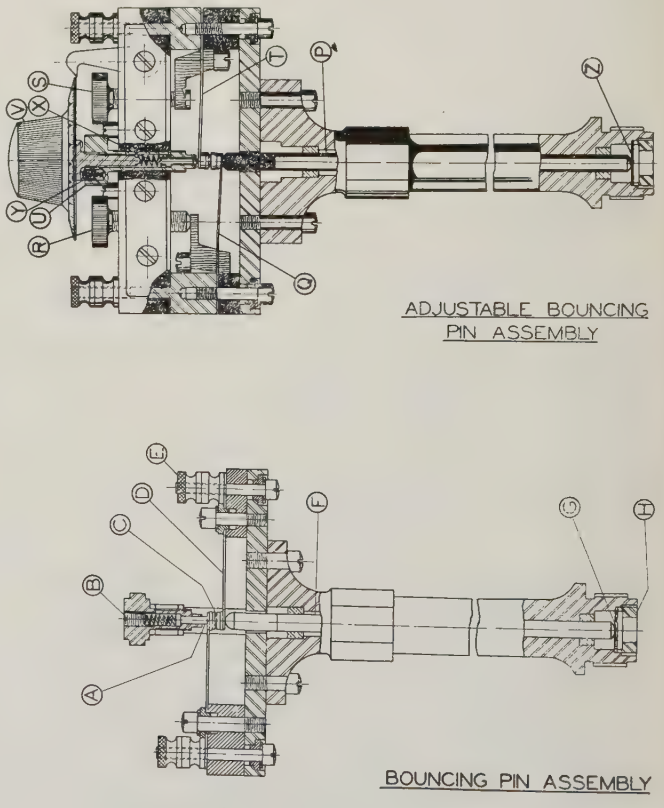

Fig. 10 — Pin assemblies

pressure curve would be an index of the detonation shock intensity. In other words, the differential of the ordinary rate of change of pressure curve should give a diagram with a peak voltage proportional to detonation shock. Attempts to differentiate the pickup output by introducing capacity and resistance in the output circuit seemed to attenuate the signal strength too much for use with the standard meter. Therefore, a simplified combination mechanical ballistic and electric pressure pickup was applied to the problem.

This new experimental pickup seemed to be a happy combination of the mechanical ballistic principles of the original Midgely bouncing pin with a modern barium titanate magnetostrictive material of such high output that no magnet or coils are required to obtain a satisfactory output signal. Fig. 12 illustrates the simplicity of the device with the barium titanate capsule mounted at the upper end, isolated from the engine heat and bearing on the upper end of the bouncing pin which rests on a diaphragm exposed to the combustion chamber. The voltage output from this pickup is about double that of the standard ASTM pickup, and can be increased if needed by the size of the barium titanate capsule. The output signal shape differs from the standard pickup in that the high frequency wave following the main pressure peak is absent. The pin's mechanical inertia is probably the cause.

The output signal voltage peak from the barium titanate pickup on reference fuel and aromatic-type fuel shows the same characteristic as the standard pickup — namely, that the reference fuel will knock much harder than an aromatic-type fuel which puts out the same signal strength. To correct this situation it is necessary to differentiate partially the output with a shunt resistance across the pickup output leads. When this is done, the signal voltage from the low-knocking fuel is lowered more than the voltage from the heavy-knocking reference fuel. The shunt can be adjusted until the voltage output from the pickup corresponds with the audible knock intensity. Having produced a signal strength proportioned to the audible knock intensity, all that is then required is a meter to measure the signal strength. This is in contrast to the standard rate of change of pressure signal which might or might not show a peak proportional to the detonation intensity.

The standard meter required a filter system to select the part of the signal most affected by detonation. The need of any filter is eliminated with the new mechanical electric pin, as the main signal peak is directly proportional to audible detonation. Therefore, the meter is very much simplified by completely eliminating the filter system. Briefly, the new electromechanical detonation pickup in conjunction with the simplified electronic meter accomplished the following results:

1. Meaningful knock ratings can be made in the range above 100 octane on aromatic-type fuels.
2. Positive control is provided to permit establishing the rating level of the highly aromatic-type fuels at a point to correlate with average full-scale engine ratings.
3. The electromechanical detonation pickup is an extreme simplification of both the mechanical bouncing pin and the magnetostrictive pressure pickup. It eliminates all the adjustment valuables of the old bouncing pin and the intricate metalurgical, electrical, and mechanical manufacturing details required for the magnetostrictive type pickup.

The automotive and petroleum industries are faced with the necessity of a change in the gasoline knock test procedure for rating fuels above 100 octane. A reference fuel scale up to 120 octane has been

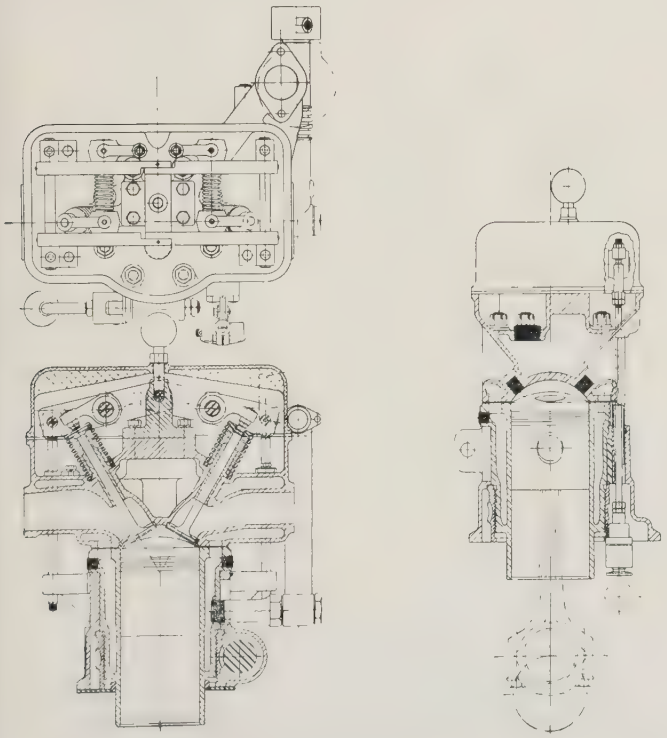

Fig. 11 — Inclined-valve domed-head combustion chamber

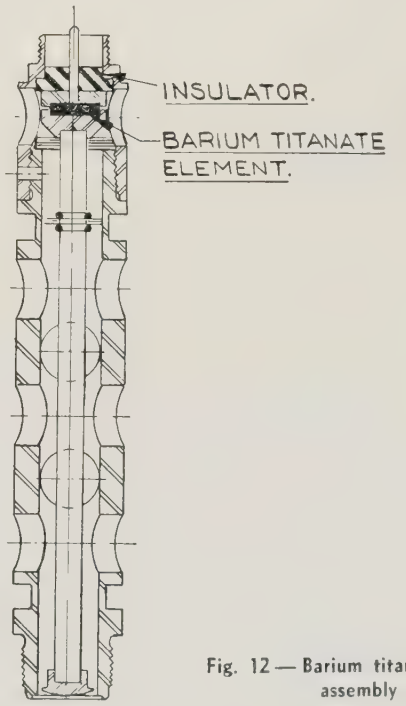

Fig. 12 — Barium titanate pickup assembly

established, but the standard instrumentation fails to give ratings which agree with the audible knocking tendencies of some fuels. This situation is an excellent example of the need for and value of technical cooperation between the two industries. Fortunately, through the foresight of men like Mr. Horning, we now have highly developed organizations such as CRC and ASTM ready to act on problems of this type. These agencies now operate so smoothly they may not be appreciated by those who did not see the sweat and strife that went into their making. For example, in a recent conversation, a prominent older SAE member stated that he never could understand why SAE should contribute to the financial support of CRC. He thought API should carry the full expense. Fortunately, those who think this way are in the minority, and so cooperative research can continue.

Since my work in the development of single-cylinder engines and equipment for fuel research has put me in rather a unique neutral position between the two industries, my viewpoint may be different from an automotive member who is entirely interested in engine problems, or a petroleum member who is completely absorbed by the fuel problems. Therefore, I am taking advantage of this opportunity to make a few observations regarding SAE policy and cooperative research.

The SAE was founded before my day, but I became a member early enough to catch a glimpse of the spirit of dedication shown by man like Clarkson, Horning, and others in steering its progress during the critical period it was adjusting to bigness. Our present general manager, John Warner, had the good fortune of growing up with Clarkson and the long list of distinguished past presidents who have left their mark. It has been a great success story as gaged by every physical measure; number of members, number of technical papers, number of technical sessions, number attending meetings, and finally number of dollars income. It is, therefore, necessary to look and search for the trends which might cause trouble.

A point of SAE policy which may need clarification is the status of the individual member. It has always been a basic policy that SAE was an association of individual members speaking and voting as individuals and not as company representatives. This of course is a very simple and easy method of preventing the encroachment and domination by commercial interests, but the policy is not entirely realistic, as the interests of the individual and his company are usually the same. Therefore, most individuals do speak and act in a manner approved by their company. In the few cases where an individual finds himself out of step with the policy of his company, he is likely to have little influence.

Since individuals do speak and act in a manner approved by the company for which they are working at any given time, that fact should be fully recognized. Present policy should be redefined, if necessary, to assure the continuation of the high technical prestige SAE has established for itself in the world. This high position has been attained in part by individuals acting as individuals, but chiefly by the respect for sound technical facts as opposed to commercial expediency. In other words, decisions must always be based on technical rather than commercial grounds. If such a policy can be firmly established, the high prestige of SAE should live and grow in our expanding scientific world.

Another SAE basic policy has been the belief in cooperative research. In the early days, problems of common interest were relatively simple, and it was easy to get a group to work together on the solution of a simple problem. As technical progress has been made, an expanding horizon has uncovered almost an infinite field for activity, and it is now necessary to define a limited field in which cooperative research fits our competitive industrial system. There has been much said and written attempting to define research and to distinguish between basic and applied research. The common definitions have never meant much to me, as it has always seemed that research could not be set apart for a few "egg heads" working alone in isolated laboratories. It applies to every living individual, and he starts research at birth. If you want to see research in action, watch a year-and-a-half old boy use the experimental method pulling and tugging and twisting on anything which will move until it gives. Watch the glow of satisfaction when the thing does give, and he has gained knowledge. This process continues through life in every field of activity, and is not confined to specialized technical laboratories specifically organized for the solution of problems in a definite field. About the only broad classication of research that has ever meant much to me has been long range as opposed to short range. The time factor is the significant one, rather than a definition of basic or applied.

There is much confusion and great difference of opinion as to where cooperative research can be applied effectively. It seems obvious that corporations should not pool their laboratory facilities to develop devices they are working on to improve their competitive position, nor is there any definite distinction between long- and short-range projects which would mark them as being suitable for cooperative research. However, there does appear to be a definite clearly defined field well-suited to cooperative research. This is the field of MEASUREMENT.

Analysis of most successful cooperative research projects shows them to be basically measurement problems. In the case of CFR gasoline knock test method, the petroleum and automotive industries had the mutual problem of measuring antiknock qualities of gasoline. Individual laboratories were each measuring antiknock by their own methods, but there was no common measure which would permit meaningful interpretation of information between the petroleum and engine companies. This was an ideal cooperative project, and a continuing and expanding one. The problem of controlling and assigning research projects for cooperative solution would seem to be much simplified if they were gaged on the basis of whether they were directed toward solution of common measurement problems, rather than determining whether they interfered with competitive industry or commercial interests.

I have explained the field for cooperative research as it has appeared to me. To others in different positions it will look quite different, and our only chance of getting mutual understanding and agreement is to find those who are able and willing to look at a problem from all sides. SAE seems to be blessed with men seeking the true facts, and the truth is always there for those who look.

SUPERCHARGING

in the FREE-PISTON CYCLE

H. G. Spier, Baldwin-Lima-Hamilton Corp.

This paper was presented at the SAE National Diesel Engine Meeting, Baltimore, Oct. 23, 1958.

THE EVER-INCREASING power output of the modern diesel engine has in great measure been made possible by advances in the science of supercharging. Experience has shown that, through supercharging, cycle temperatures and thermal loads may be controlled to the extent that remarkable increases of cycle pressure and power output are safely obtainable.

Applying this principle to gas power-producing free-piston engines seems logical enough, except that the necessary cycle energy balance in free-piston machines must be maintained by the basic arrangement. This is important if design simplicity is properly evaluated as a competitive necessity.

In order to visualize the subject on hand, Fig. 1 shows the diagrammatic cycle stages of our simple cycle 2-stage compression free-piston gasifier. In this machine the scavenging air and bounce air volumes are combined. This eliminates separate bounce control by making the bounce energy a function of delivery pressure, and the pressure stresses are thereby reduced to a point where even the highest load pressures will result in less strain than would occur on a machine with separate bounce

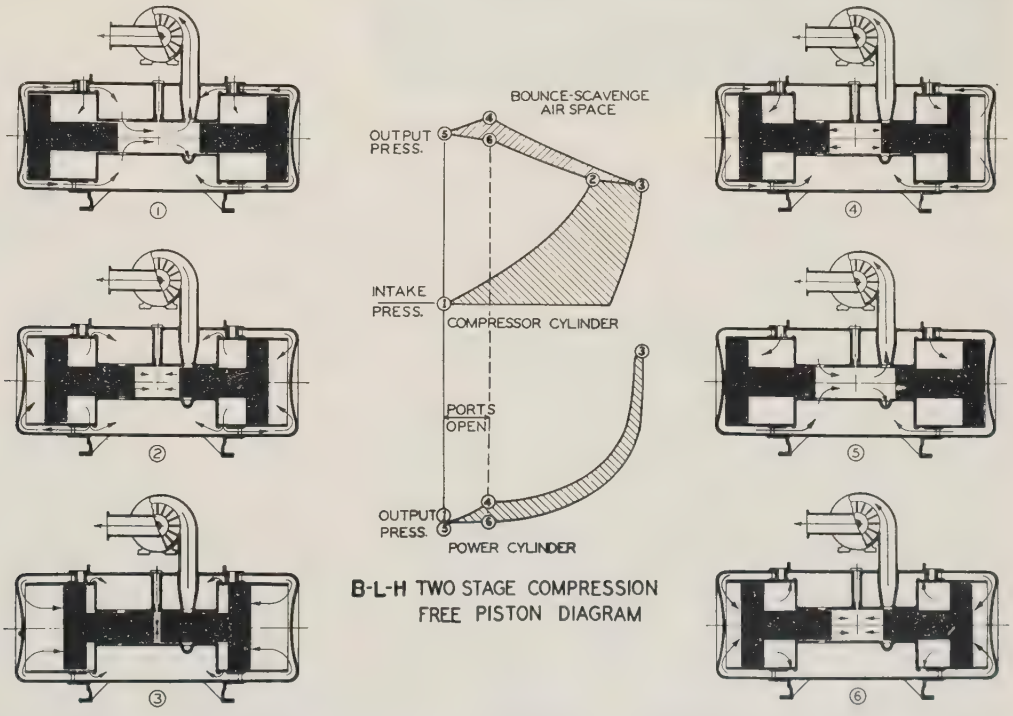

Fig. 1 — Two-stage gasifier diagrams

THE RESULTS of analytical studies backed by actual tests concerning the use of supercharging in the free-piston cycle are reviewed. They indicate that, under conditions of increased cycle pressure ratio and of adequate cooling of the air, supercharging has power possibilities far beyond those which might even optimistically be hoped for from naturally aspirated operation. Also, supercharging can be used to effect a significant reduction in part-load fuel consumption.

Also discussed are: The possibility that further developments beyond present pressure and lubrication borders can further raise the goal of maximum practical power gain through supercharging; series operation of supercharger and gasifier, and the mutually related problems of supercharger drive and of matching the characteristics of the plant components. The elimination of intake air pulses is a factor in adaptability of the free-piston powerplant to almost universal applications.

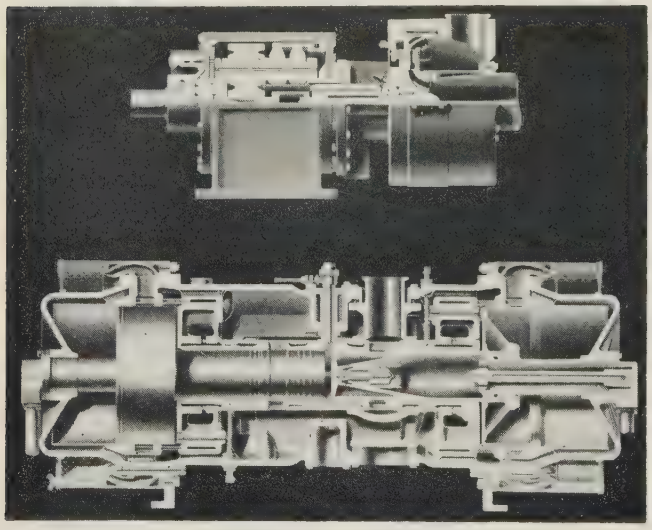

Fig. 2 — Cross-section of 2-stage compression gasifier

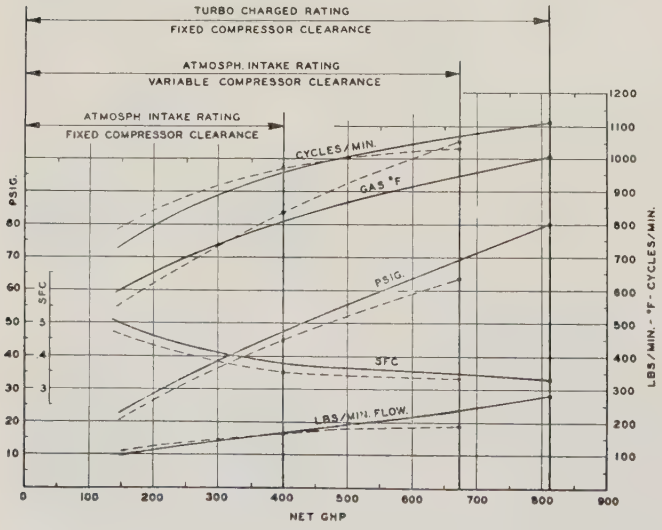

Fig. 3 — Comparative test curves on 8-in. bore gasifier

spaces. A 2-stage compression machine and turbine with reduction gear of corresponding capacity are shown at the same scale in Fig. 2.

Although this lowers the natural stroke frequency somewhat, the load capacity is regained by supercharging. Fig. 3 shows the performance gain between natural aspiration, adjustable compressor and clearance and supercharging. This is also graphically expressed in Fig. 4.

Other advantages are also decisive in the choice of this 2-stage compression configuration.

The time coincidence of maximum scavenging air pressure with the opening of the scavenging ports for the practical elimination of blowdown losses, the lower pressure and temperature at which the compressor valves operate, and the avoidance of lubricating oil deterioration spaces by the full sweep of scavenging air throughout the machine, are the main points that can be made.

Also, the slightly longer dwell of the piston at the outer stroke end allows more time for the inflow of air into the all important compressor cylinders.

It is well-known that, as free-piston gasifier and turbine pressure ratios are increased, more useful power can be obtained from a gasifier operating at maximum gas flow in the naturally aspirated (or simple) cycle. This higher power is accompanied not only by lower specific fuel consumption but also by higher scavenge air temperature and turbine inlet temperature. In other words, thermal loads increase concurrently with pressure loads and power and, conceivably, output cannot be thus raised indiscriminately without exceeding practical limitations. We may, therefore, conclude that a rating limit exists for simple cycle operation, which is not exactly defined because it is a function of development progress, practical safety factors, and of the specific application.

	A	B	C	D	E
Gasifier Type *	PESCARA GS-34	BLH DL	BLH DLS	BLH DLS	BLH FP-165
Gasifier Compressor Stages	SINGLE	SINGLE	SINGLE	SINGLE	TWO STAGES
Gasifier Compressor Head Position	FIXED	VARIABLE	FIXED	FIXED	FIXED
Gasifier Intake Air Pressure Temperature	ATMOSPHERE ATMOSPHERE	ATMOSPHERE ATMOSPHERE	SUPERCH'D NOT COOLED	SUPERCH'D COOLED	SUPERCH'D COOLED
Rated Gauge Pressure	45	62	62	73	80
Percent Rating Effect Over "A" (as 100%)	100% HP, 100% W	164% HP, 67% W	152% HP, 70% W	182% HP, 61% W	200% HP, 55% W

HP = NET GAS HP W = WEIGHT - APPROX. COST PER HP
RATING LIMITATIONS = VOLUMETRIC OR 450° F TEMPERATURE AT COMPRESSOR DISCHARGE VALVES.
* VALUES BASED ON EQUAL DESIGN STRESS LEVELS

Fig. 4 — Rating progress through development

For supercharged operation, however, the limitations due to physical compressor clearance and the temperature can be extended far enough to exceed the results obtained with the diesel engine. Therefore, close analytical and experimental study of supercharging in the free-piston cycle has been made.

Supercharging in the free-piston cycle has been generally interpreted along the idealized lines of the definition:

> "Supercharged, as opposed to naturally aspirated, operation of a free-piston gasifier is that operation in which air at above-atmospheric pressure is supplied to the gasifier compressor cylinders and in which the pressure ratios of the gasifier itself are equal to those of the naturally aspirated condition, as far as the free-piston energy cycle balance requires it."

This is the concept with which this paper is primarily concerned.

General Evaluation

The several variations of the supercharged cycle can be compared to each other and to the simple cycle by means of a semi-idealized study which incorporates basic simplified assumptions. Because these assumptions are reasonable, the results are sufficiently accurate to show trends, as proved by actual tests at our plant in Hamilton, Ohio, under the auspices of the U. S. Navy.

Bearing in mind that cycle pressure ratio equals the product of supercharger pressure ratio and gasifier pressure ratio, supercharging may be considered only with increased overall cycle pressure ratio. To consider a pressure ratio limited to the simple cycle ratio would not provide the necessary trapped air fuel in the power cylinder and in praxis defeat the purpose.

There is a possibility of bleeding off the excess of scavenging air created by supercharging and retaining a limited pressure ratio. If all exhaust gas power is used for supercharging, such a machine would become one of many desirable turbocharged air compressor configurations. Since we are concerned with only a true gasifier cycle, however, we can concentrate on the supercharged cycle with increasing pressure ratio.

Three primary cases of supercharging have been evaluated (Fig. 5). In the "supercharged, uncooled cycle" a supercharger supplies air to the compressor cylinders without benefit of any coolers. In the "supercharged, intercooled cycle" the supercharger feeds the compressor cylinders through an inter-

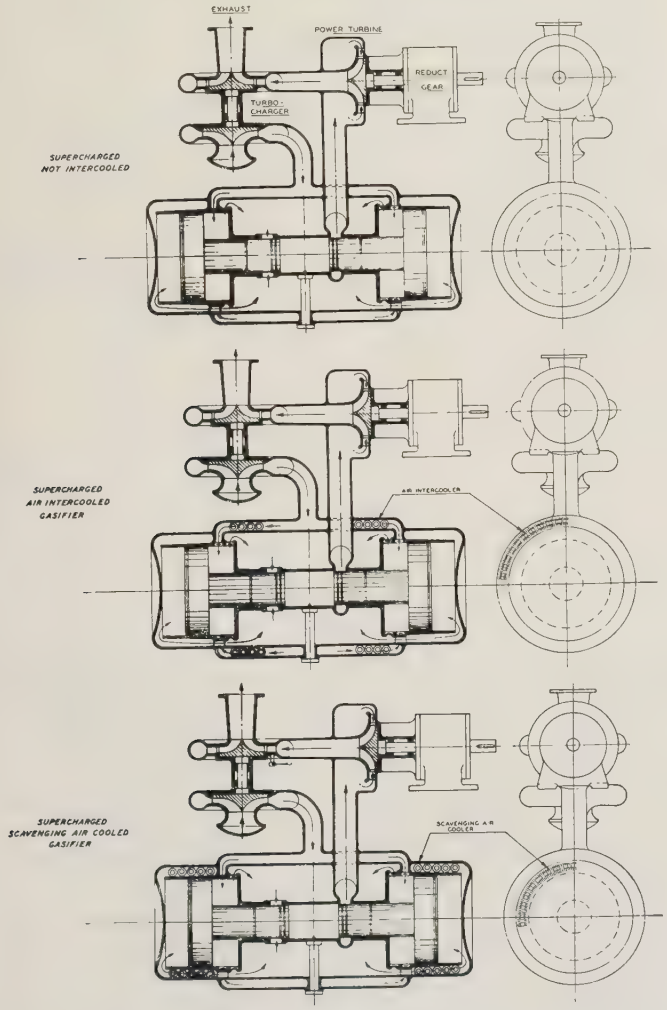

Fig. 5 — Diagrams of supercharged uncooled, intercooled, and scavenged aircooled cycle

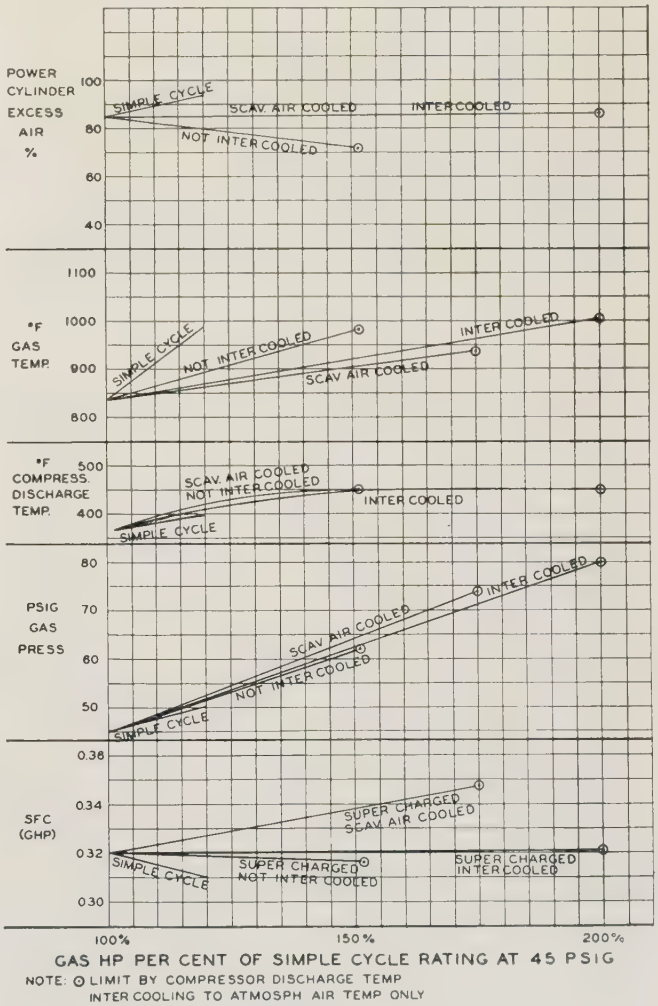

Fig. 6 — Curves of characteristics of above cycles

cooler. Perfect intercooling, in which the compressor inlet temperature is maintained equal to the supercharger inlet temperature, is assumed. In the "supercharged, scavenge-aircooled cycle" the supercharger supplies air directly to the compressor cylinders, but a cooler is placed in the scavenge system between the compressor and power cylinders. Here scavenge-aircooling to the scavenge temperature of the simple cycle base is assumed.

Curve sheet (Fig. 6) shows the results. Quantities of interest, for various levels of supercharge, are plotted against per cent net power. Simple cycle operation at 45-psig gasifier exhaust or turbine inlet pressure is taken as the base point, because this rating is generally accepted for the Pescara-type gasifiers now in commercial service.

In view of the beneficial temperature reductions, we find that if temperatures and thermal loads can be controlled, we may expect legitimate power boosts from increased pressures and pressure loads. This has been the guiding philosophy of the supercharged diesel engine and proves to be that of the supercharged free-piston gasifier.

Taking notice now of the solid-line curves, which illustrate the constant gasifier pressure ratio-increased cycle pressure ratio concept, we find that supercharging has theoretical power possibilities far beyond those which might optimistically be hoped for from the simple cycle.

Supercharged, Uncooled Cycle — A good power gain would be obtained with uncooled supercharging, with a slight drop in fuel consumption. However, because the temperatures rise rapidly and the power cylinder excess air drops appreciably, the supercharged, uncooled cycle has practical limitations. The most important one is the air compressor delivery temperature on lubricating oil.

Since most of the difficulty with lubricants centers around the reciprocating compressor valves, the 2-stage compression configuration was devised by our company. This allows the final air delivery temperature to be raised, because the compressor valves do not have to pass this second stage compression air delivery.

This method raises the practical limitations of uncooled supercharging to a point where the practical output capacity is raised as much as 60% over the accepted standard of naturally aspirated gasifiers.

For higher power and whenever a sufficient cooling medium is available, we can consider the supercharged, intercooled Cycle.

Supercharged, Intercooled Cycle — The supercharged, intercooled cycle can actually supply as much power as the supercharged, uncooled cycle without the expense of a specific fuel consumption increase, because of the inherent reduction in power cylinder cooling losses over those of the simple cycle base condition, which was proved by tests. The significant difference between these two methods of supercharging is that the intercooling controls the cycle temperatures and the excess air to the extent that they are the same as those of the base condition. The supercharged, intercooled cycle is, therefore, very attractive. Of course, because the temperature of the compressor intake air must be reduced to or near to that of the ambient from the comparatively low value at the supercharger discharge, and adequate supply of low-temperature coolant must be available. For marine and even for most stationary applications, this is possible.

Supercharged, Scavenge-Aircooled Cycle — Where it is not, the supercharged, scavenge-aircooled cycle might possibly be used. This cycle supplies appreciable power also, but at a higher fuel rate than the supercharged, intercooled cycle, because the compressor cylinder temperatures are higher, a difficulty that can be circumvented only by additional cylinder and valve cooling. In praxis, these conditions might be found economically desirable in relatively few applications.

Effect on Gasifier Cyclic Speed — The stroke frequency and piston speed change from a naturally aspirated gasifier to a supercharged gasifier is proportional to the change in rate of pressure rise

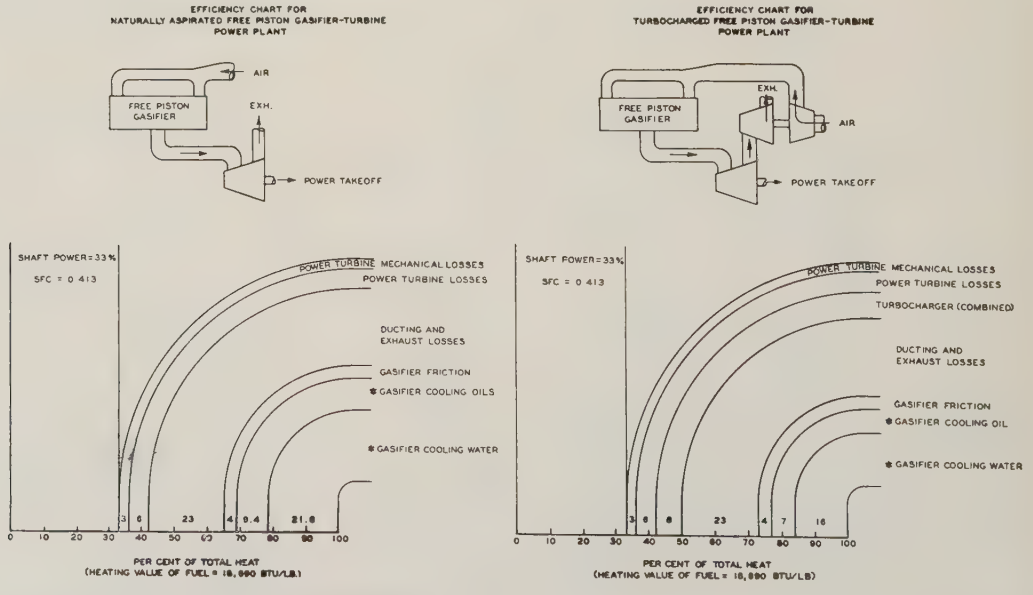

Fig. 7 — Comparative heat balances

* POWER CYLINDER COOLING LOSSES SHOWN ARE PRESENTING REQUIREMENTS FOR USE OF STANDARD DIESEL LUB OILS MIL-L-2104-A. LUB OILS WITH HIGHER SPREADABILITY, FILM STRENGTH AND DETERGENCY PERMIT LESS COOLING AND THE GASIFIER EFFICIENCY CAN THUS BE RAISED ACCORDINGLY

during the compressor cylinder cycle.

Since the rate of this pressure change is lower in a supercharged machine, the cyclic frequency for a given pressure is also lower.

Consequently, a higher pressure is required to retain the unsupercharged frequency.

This has the effect that the low load and idling range of the machine is extended downward from a full load to idle ratio of 4.22–5.57 without re-circulation of compressor air.

At the same time, the frequency rises only 8.3% and the gas temperature only 20% if the power is doubled by supercharging.

This clearly indicates the advantage of supercharging for increased gasifier power against using afterburners or frequency stimulation where either the temperature or the piston speed would reach undesirable values.

Effect on Specific Fuel Consumption Characteristic — Curve sheet Fig 6 indicates that, for either of the two more desirable forms of supercharging, the specific fuel consumption changes less than expected, because of the favorable changes in heat balance over the naturally aspirated cycle, which counterbalances the energy rejected by intercooling, as shown in the heatbalance (Fig. 7). This tested fact shows the similarity with the turbocharged crankshaft diesels. In addition, supercharging can result in appreciably reduced fuel consumption when prolonged operation at part load is involved. Let us assume, for example, that a ship powered by a simple cycle free-piston gasifier plant has the specific fuel consumption power characteristic shown in Fig. 8. Because of the maximum power requirement, this ship operates most of the time (cruising and below) at less than its peak efficiency. If its powerplant were replaced with a smaller plant containing only half as man gasifiers, cruising power could be obtained through simple cycle operation and maximum power could still be obtained when necessary through supercharging. The specific fuel consumptions are now 6% lower at cruising power and 14% lower at one-quarter power. The smaller supercharged plant with its lower effective fuel consumption should, therefore, result in substantial reduction in weight and volume of machinery plus fuel.

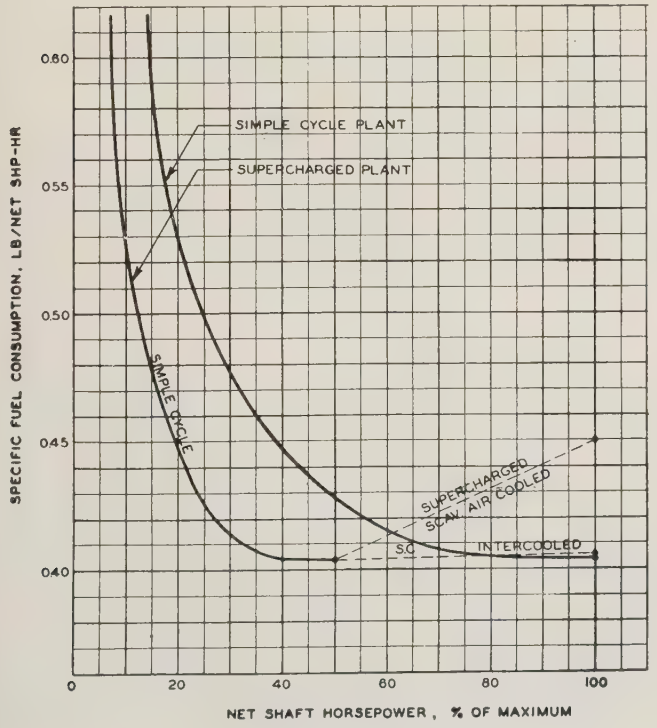

Fig. 8 — Part-load fuel savings

The effect of intercooling on specific fuel consumption is quite marked. The resulting reduction in compressor work is in approximate proportion to an increase in efficiency.

Highly efficient intercooling to below ambient temperature can lead to specific fuel consumptions competitive with crankshaft diesels if the required cooling medium is available.

Practical Application

Although the general evaluation indicates that supercharging in the free-piston cycle effects remarkable improvements in specific power, such knowledge is the more meaningful, because these gains were practically achieved without apparent difficulties. The fact that an increase of 20% and more in power can be obtained at the same gas temperatures over the simple cycle machine indicates the basic tendency in supercharging of free-piston gasifiers.

With a gas temperature rise of only 100 F (1000 to 1100 F) over the simple cycle gasifier, the power of our tested Model DL was increased 65% over established 60-psi rating without exceeding conservative temperature and pressure limits, even though this machine was not originally designed for turbocharged performance. Rather it received its higher output rating only through the compressor clearance control, typical for this type machine.

Intake Air Pulse Confinement — A very gratifying solution to the intake pulse problem, common to all gasifiers, was also found in supercharging.

Due to the typical velocity characteristic of the free-piston compressors and their large intake stroke volume, the resulting intake pulses are difficult to dampen to an acceptable degree without serious effect on gasifier efficiency, particularly if any amount of ducting is involved in the installation of naturally aspirated gasifiers.

Efficient ducts must be so short that engine room air intake is usually used, with the result that the most annoying if not harmful pressure pulsations, particularly in enclosed spaces, become very objectionable to operating personnel. Turbocharging eliminates these outward pulses completely at all loads, even on single gasifier installations. Cycle phasing of multiple gasifiers for dampening intake pulses becomes, therefore, unnecessary.

Series Operation of Supercharger and Gasifiers — The second topic stems from the fact that a gasifier is an intermittent flow machine, whereas a rotary supercharger is a steady flow device subjected to severe flow system pulses. Therefore, unless a suitable air receiver is used, supercharging can be at its best only in multigasifier plants in which the gasifier intake pulses are combined to approximate steady flow at the supercharger discharge. We thus infer that supercharging must be planned originally in the design of the powerplant.

Supercharger Drive and Matching of Component

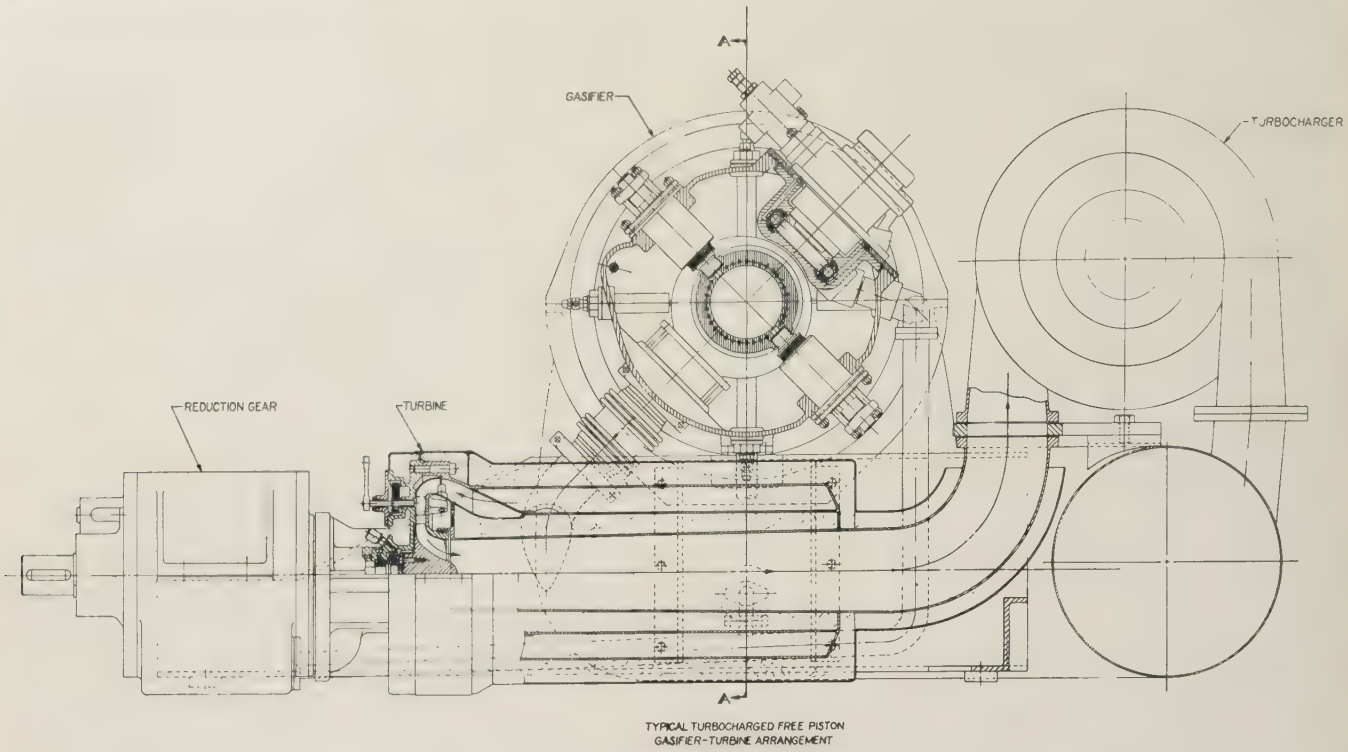

Fig. 9 — Typical supercharged gasifier-turbine unit

Characteristics — Two other points in question are that of supercharger drive and that of matching the flow, pressure, temperature, power, and speed characteristics of supercharger, gasifiers, and turbine. Because these two problems are mutually related, they will be studied as if they were one.

In consideration of the results of the general evaluation, we would for maximum efficiency, prefer to operate a supercharged plant in the following manner, if reconcilable with reasonable system simplicity.

1. We would use the simple cycle, without effect from the supercharging system, for operation up to an approximate pressure ratio of four at a medium load. This would obtain for us a part-load specific fuel consumption characteristic similar to that illustrated by Fig. 8.

2. Then we would cut in the supercharging system gradually and efficiently and, while holding the gasifier pressure ratio and stroke clearance conditions reasonably constant, increase power to the maximum or to the intermediate load desired.

Mechanical drives for the supercharger are, of course, possible; but they present definite limitations in controllability, except in the rare case of fixed power output. Mechanical drives are not practical.

By placing a turbocharger in series with the main turbine, two of the best arrangements are possible.

In the first one, the turbocharger is placed in the main turbine exhaust. This permits the use of standard diesel-engine-type turbochargers. As the turbocharging ratio increases with increasing load, the power turbine pressure ratio can then stay practically constant. Such a powerplant arrangement is shown in Fig. 9.

In the second arrangement the turbocharger is placed in the gas flow ahead of the main turbine. The turbocharger then requires shaft seals against full pressure, but the nearly constant pressure ratio on the main turbine is retained. However, the gas flow pulses will be smoothed out and thereby aid in the efficient performance of the main turbine. The pulse dampening is especially important when longer ducts to the main turbine are required, or when axial flow main turbines with greater pulse sensitivity are used.

This placing of the turbocharger at the gas outlet point of the gasifier is also applicable when direct gas power is delivered without conversion into turbine shaft power. This applies particularly to gas jet pumps or evacuators for large volume, low-pressure fluids or gases of almost unrestricted composition.

Although this last arrangement for supercharging seems to offer the most universal benefits, the other arrangements for supercharging are available if their characteristic seems desirable.

Conclusions

1. Supercharging in the free-piston cycle is definately attractive as a means of increasing power and of reducing part-load fuel consumption.

2. For the achievement of these advantages, the total cycle pressure ratio must be increased. Adequate cooling of the air, preferably between the supercharger and the gasifiers but alternately between the compressor and power cylinders, is necessary for control of temperatures and of power cylinder excess air in the maximum power ranges.

3. In consideration of the history of the diesel engine, the increased cycle pressure ratio concept of gasifier supercharging is realistic. However, in contrast with the case of the diesel engine,

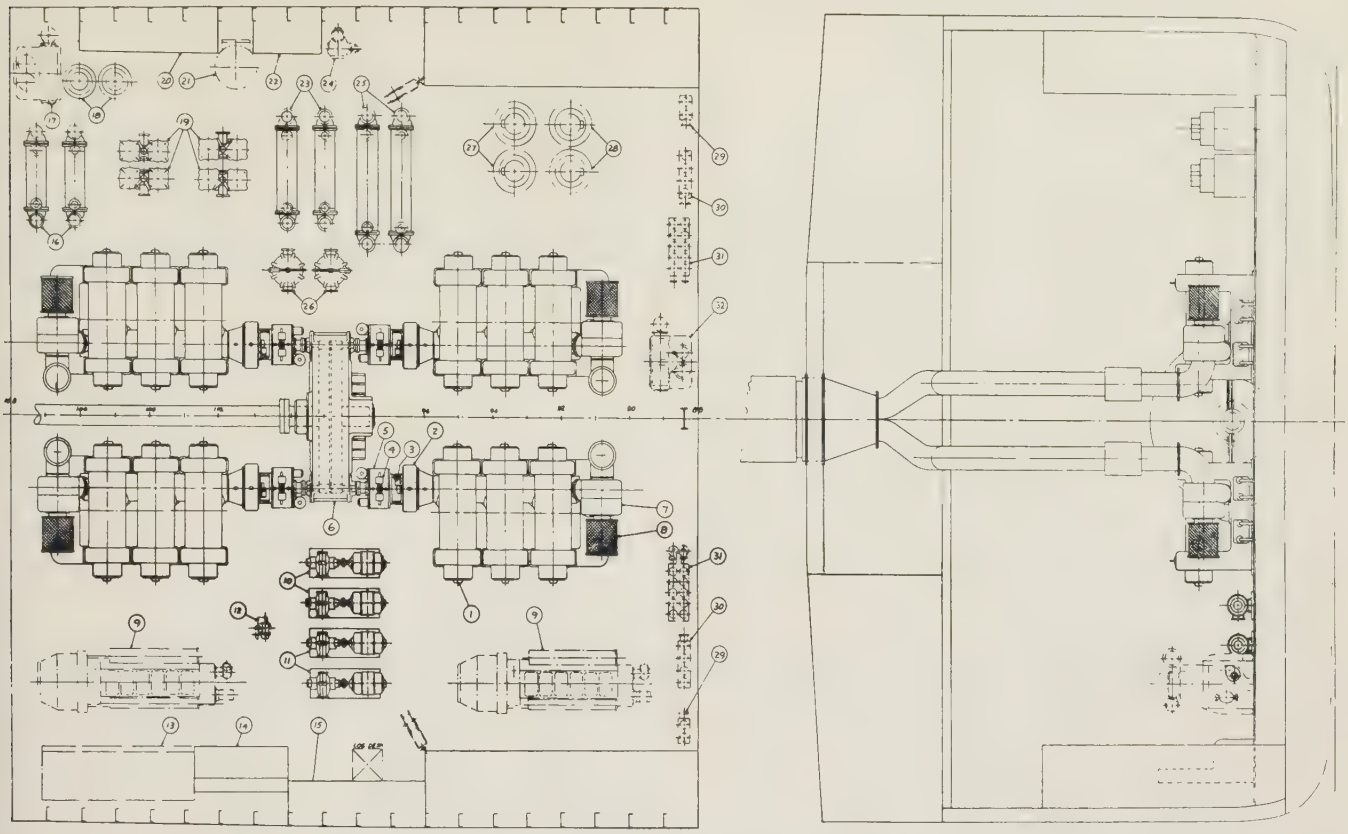

Fig. 10 — 8000-shp ship propulsion plan

a considerable amount of variation can be developed for industrial demands.

4. A mechanical supercharger drive appears simple, but practically excludes the part-load specific fuel consumption advantage. At least a variable nozzle area main turbine will be required.

5. An independent supercharger drive or the use of a turbocharger results in better performance than that obtainable with a mechanical drive. In conjunction with a variable nozzle area main turbine, a turbocharger permits all the performance gains of which supercharged gasifiers are capable. The most practical arrangement appears to be a turbocharger powered in series with the power turbine, because it reduces the individual turbine pressure ratios, requires simple ducting, and can reduce cost by the use of standard equipment.

6. The general picture of supercharged free-piston gasifier power that presents itself is highly encouraging. It shows that a high specific power weight ratio of a value between that of diesel engines and gas turbines is possible without the latter's excessive loss in efficiency over the diesel engine, especially at smaller power ratings.

Basic improvements and simplifications like the combining of scavenging air and bounce air space for what is termed 2-stage compression and its effect of lowering valve temperatures, can develop these machines to a degree of competitiveness in cost performance that is bound to demand commercial recognition. Although the pursuit of developments towards further elimination of all critical design elements and the realization of maximum power and efficiency is on its way, supercharging definitely has contributed more to the economically possible rise of free-piston power than any choice of configuration in the gasifier itself can accomplish.

7. The economics of turbocharging of free-piston gasifiers are, of course, all important.

Since a 100% rise in power can be achieved by turbocharging, it follows that this is the thing to do as long as the cost of the turbocharger plus intercooler is less than that of an additional gasifier.

Actually, it is approximately 50% or less of the gasifier cost, while the turbocharged gasifier is approximately 47% lighter than a naturally aspirated machine. In addition, however, the pulse dampening and in many cases the increased load range due to turbocharging are vital factors in increasing the fields of applications and therefore the economic potential.

The installation of multiple units does not necessarily present a problem as shown in Fig. 10, which represents an 8000-shp ship proposal, using 12 gasifiers in four turbocharged groups.

It is, of course, very difficult to evaluate the competitive cost status of free-piston engines without focusing the problem to given circumstances.

This refers not only to potential production volume alone, but also to the general recognition of free-piston power in its variety of forms as direct gas power and its conversion to shaft power. To obtain this recognition is the major and complex task confronting us now.

Discussion of this paper will be found on p. 288.

DISCUSSION of Spier paper

Two-Stage Compression Free Piston To Bring Many Development Problems

— Cdr. O. A. Templeton, Bureau of Ships, Navy Department

THE AUTHOR has put supercharging of the free piston in proper perspective. The primary advantages of supercharging are in improving part-load efficiency, and providing higher power weight ratios, without exceeding practical temperatures in the compressor lubricant. These factors have been ignored by previous authors in discounting supercharging. The additional advantage of reduced intake pulses is important.

The 2-stage compression free-piston cycle is extremely interesting and appears to be relatively simple. However, based on past experience, each new configuration of the free piston introduces a new set of development problems. This factor should not be ignored in planning a development program.

The advantages of free-piston engines and compressors for a number of applications are well-known. It is to be hoped that the mammoth task of developing a reliable and commercially competitive free piston can soon be accomplished in this country.

Prefers Outward Compressing Gasifiers And Separate Bounce Control in Supercharger

— W. A. Morain, Cooper-Bessemer Corp

IT IS GRATIFYING to learn that actual test work has been undertaken in supercharging free-piston gas generators and that the predicted improvements in performance as described in the earlier studies of London,[a] Soo and Morain,[b] and others have been confirmed. It would have been most helpful if the author had chosen to include more of the actual test data, such as inlet pressure boost, compression and maximum pressures experienced, and similar details; nevertheless, the results shown are encouraging.

The concept of scavenging air intercooling was discussed earlier by Soo and Morain[b] in which a reduction in jacket water heat rejection was anticipated. In many cycle studies, cooling of the scavenging air before it enters the power cylinder has been found to be most desirable, if not actually necessary.

With regard to the basic assumptions listed by the author, the assumption of 100% scavenging efficiency can lead one astray. Uniflow scavenged cylinders, even with substantial quantities of excess air, will not show scavenging efficiencies exceeding 90% and are frequently lower. When one accounts for the presence of 10–15% exhaust gas in the cylinder and takes into account the consequent mixing between this and the incoming fresh air, the temperature levels throughout the power cylinder cycle are substantially elevated. This is an often-neglected feature which leads to erroneous judgment in determining the permissible peak loading without exceeding safe cylinder wall temperature limits.

The B-L-H gasifier described in the article is quite interesting, and the reduction in discharge valve temperature with this arrangement is appreciated; however, it seems that one sacrifices a certain desirable flexibility of control with this arrangement, especially when considering supercharged operation. The writer has always preferred outward compressing gasifiers and separate bounce control. The use of a separate bounce control does not present any particularly difficult development problem. With such a device, the inner dead point is variable at the choice of the designer or operator.

It is logical to assume that the present, unsupercharged gasifiers are already operating at or near their maximum permissible peak pressures in the interest of high fuel economy. As the supercharge pressure is increased, the inner end clearance should be increased more than the usual amount to confine the peak pressures to reasonable limits, and this practically dictates an independent bounce control. Otherwise, there would be a pressure increase beyond the established safe limit. With outward compression gasifiers, this required increase in toe end clearance volume has very little effect. On the other hand, since the compressor discharge pressure is steadily rising, further increase in the head end clearance of inward acting compressors becomes more and more difficult to accommodate, with a practical limit clearly in the picture. However, I am inclined to agree with the author in his sixth conclusion that the advantages of supercharging are more important to us at this time than any argument concerning configuration of the gasifiers.

The writer does not feel that the required increase in the inner end clearance under highly supercharged conditions will have too much effect on the fuel economy. At least, theoretical studies do not indicate any pronounced efficiency loss. The peak pressures carried in the free-piston cycle are already quite high and the advantage of going higher is debatable in view of diminishing returns.

Of all the supercharging schemes discussed, the writer is most interested in series turbochargnig with the turbocharger set located at the exhaust of the power turbine. This arrangement does not entail expensive components and a conventional internal-combustion engine turbocharger may quite often be found to fit one's needs. Some variation in the nozzle area of the turbocharger turbine is usually all the flexibility needed to obtain a suitable match.

Occasionally, a gasifier application arises where a source of hot, high-pressure gas is the end requirement rather than turbine shaft power. Many of these schemes entail supercharging, since the pressures required often exceed those available with natural aspiration. It would appear that the supercharged free piston has a number of applications of this nature.

It would be interesting to learn how far B-L-H went with their supercharging tests and how many of the possible schemes the author discusses were actually tested.

Author's Closure to Discussion

THE DESIRABLE test data are presented in Fig. 3. The boost pressure used for the given data was 3 psig at 65 psig turbine inlet pressure, and the maximum firing pressures were held to 2000–2200 psig, which we found in many tests to give the best efficiencies.

We have used these firing pressures through all our naturally aspirated, as well as supercharged, tests and found them very acceptable, although the power cylinder and piston crown design must, of course, be compatible with these pressure.

The scavenging efficiency is to a large extent a formation of port design. The inward compression machine has the advantage of starting the scavenging cycle with peak scavenging air pressure. The 8-in. power cylinder machine on which the paper is based had a scavenging efficiency of up to 96%.

In the two-stage compression machine the bounce energy can be either initially or operationally controlled by the turbine inlet vanes to any necessary degree.

On turbocharged gasifiers, the compressor piston end clearance becomes largely unimportant; therefore, inward or outward compression configurations show the same benefits from supercharging.

Since we have built both types of configurations, we have found that the inward compression gasifiers are somewhat simpler, less costly, and more compact in design and more constant in operation, because both the power piston and the compressor piston end clearances are very constant.

---

[a] ASME Transactions, Vol. 78, October, 1956, pp. 1757–1764: "Supercharged and Intercooled Free-Piston and Turbine Combination — Cycle Analysis," by A. L. London.

[b] "Some Design Aspects of Free-Piston Gas Generator Turbine Plant — Part I, 'Thermodynamic and Component Characteristics,'" by S. L. Soo and W. A. Morain. Paper presented at ASME Meeting, November, 1955.

Optimization Study

Missile Auxiliary Power Systems

(as viewed by the equipment supplier)

E. I. Brown and R. W. McJones, Vickers, Inc.

This paper was presented at the SAE National Aeronautic Meeting, New York, April 11, 1958.

VARIOUS energy sources applying to self-sufficient power units for aircraft and missiles using ramjet and/or rocker powerplants are discussed in this paper. Most of the systems mentioned require a 5-20 hp hydraulic supply and enough electrical energy for durations up to 1½ hr.

Within the limitations of this study the flywheel system has been shown to have some surprising weight advantages for durations up to 1–2 min. The reciprocating engine powered by hot propellant gas, or by air fuel, is lighter for longer durations. Monopropellant turbines and silver-zinc cells powering electrical motorpumps are generally competitive on a weight basis for the intermediate durations.

The authors also discuss several types of power conversion units: hydraulic, alternator and d-c motors, turbines, hot-gas servo systems, and invertors.

AUXILIARY power provision in aircraft and missiles can be divided into two major categories: Provision for airborne vehicles using rotating main powerplants and those using ramjet and/or rocket powerplants. For vehicles using rotating main powerplants which operate throughout the flight, experience has shown that weight, reliability, and economy point toward extracting auxiliary power from the main engines. For vehicles using ramjet and/or rocket powerplants, a different approach is required. Provision must be made for a completely self-sufficient auxiliary power unit. Thus, "APU" becomes attractive and, in many cases, mandatory.

The general plan of this study is first to consider the various energy sources which may be applied to a self-sufficient APU, then to consider the power conversion units necessary to provide the specified form of power output, and finally to synthesize and compare complete systems in relation to typical overall requirements. The typical system requirement in the study calls for 5–20 hp hydraulic supply and electrical energy for durations up to 1½ hr.

Energy Sources

The more promising energy sources are: electric cells, monopropellants, compressed gas, mechanical energy storage, and reciprocating engines. The assumptions and considerations involved in preparing

the summary of Table 1 are presented in the ensuing paragraphs.

Electric Cells — A brief survey of battery characteristics is summarized in Fig. 1. In general, only the silver-zinc cells offer an attractive energy-to-weight ratio; so they have been selected for detailed study later in this paper. It should be noted that silver-zinc cells of 75 whr/lb (10 lb/hp-hr) are believed possible with sufficient development, whereas currently available cells offer about 50 whr/lb (15 lb/hp-hr).

A distinction should be made between primary (one-shot) and secondary (rechargeable) batteries. Silver-zinc cells can be provided in either form, the primary version being stored in a dry-charged condition with the electrolyte injected automatically just before use. Secondary silver-zinc cells have only 1–3 months reliable standby life, hence the expense of maintaining a missile system on a standby basis with these cells is considerable. Incidentally, they have a salvage value of only about 10% of their initial cost. Primary silver-zinc cells have a standby life of about 5 years, and are approaching the point of 100% operational efficiency. Primary cells tend to be heavier than secondary cells in sizes less than about 10 hp, because of the electrolyte injection equipment. If injection can be performed from the launcher outside of the missile, the battery weight should be reduced by approximately 40–50%.

Additional considerations involved in battery selection include: (1) the maximum current which may be drawn from a given cell, and (2) the effect of absolute cell size on specific output. These factors are illustrated in Fig. 2, which shows that, even for zero duration, a cell weight of about 2 lb is required to provide an output of 1 hp. Fig. 2 also shows that a significant improvement in specific weight is realized with the larger cells. For a given application, the number of cells is established by the required total voltage; and the hp-hr per cell is obtained from the required total output and the number of cells. The arbitrary line (14 lb/hp-hr plus 2.0 lb/hp) shown on Fig. 2 has been used in later portions of this paper as representing silver-zinc cells — either primary or secondary.

Another possibility is a cell which converts fuel directly to electricity. The Union Carbide Corp. has announced tests of such a cell which uses gaseous oxygen and hydrogen at a stated efficiency of 65–80%. This corresponds to a specific fuel consumption (sfc) of about 0.5 lb/hp-hr. The primary limitation on this cell is its larger weight per whr.

Cells utilizing various forms of nuclear energy are under development but are believed to be presently handicapped (like the fuel cell) by a large fixed

Table 2 — Relationship of Pressure and Power Output

Pressure Ratio	Theoretical Specific Fuel Consumption, lb/hp-hr
2/1	18
5/1	8
10/1	6
20/1	5
40/1	4.3

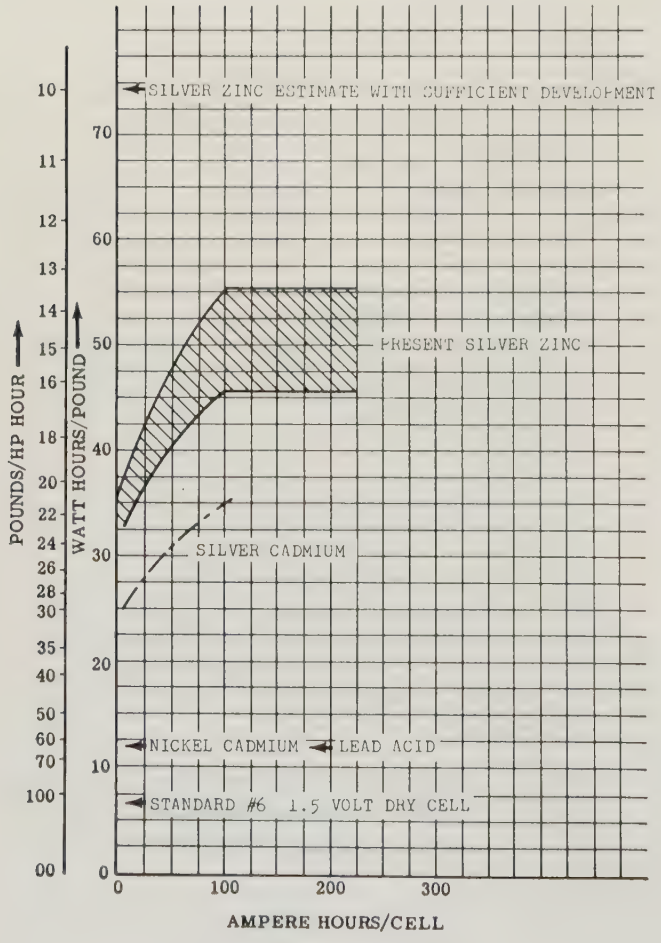

Fig. 1 — Battery comparison

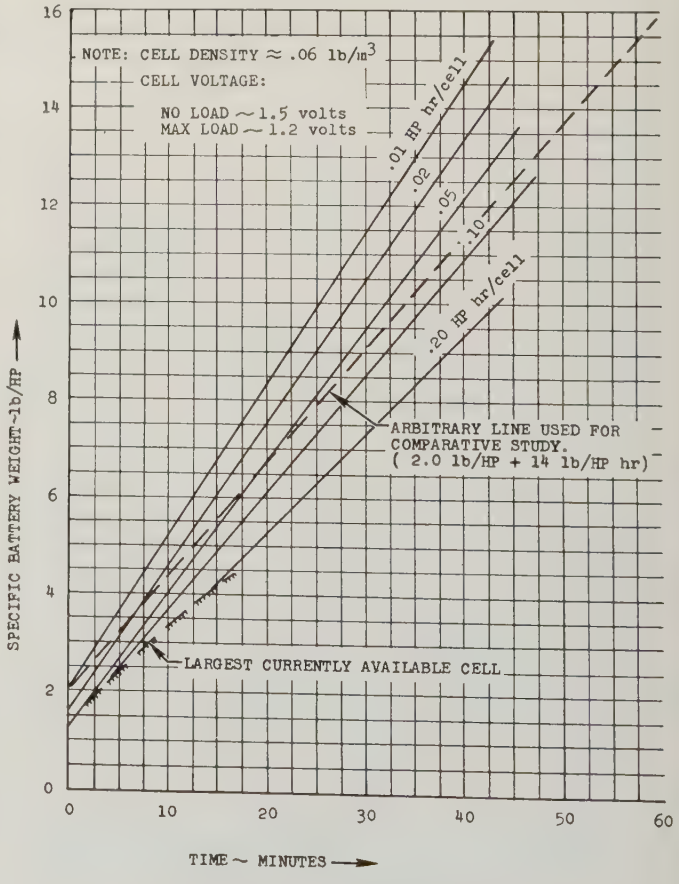

Fig. 2 — Silver-zinc cell weight

Table 1 — Energy Source Summary

Energy Source	Form of Output	Fixed Weight lb/hp	Duration Factor or sfc, lb/hp-hr	Comments
Ethylene Oxide	Ideally expanded gas	Nil	5.0	Theoretical sfc at pressure ratio of 20/1 (perfect turbine)
Ethylene Oxide	Ideally expanded gas	Nil	8.75	With allowance for pressurized tank at 75% fuel weight (perfect turbine)
Ethylene Oxide	Turbine drive	See Fig. 3	35.0	With allowance for pressurized tank at 75% fuel weight, turbine efficiency = 25%
Ethylene Oxide (or assumed solid propellant)	Hot gas servo actuators	See Fig. 3	70	Includes tank weight as above, servo valve-actuator efficiency = 12%
Silver-Zinc Cell	Direct current	2.0	14	See graphical presentation of battery data
Air Bottle	Ideally expanded air	Nil	77	3000 psi, bottle weight[a]
Air Bottle	Constant pressure air	Nil	690	Assumes air throttled to 1500 psi
Hydraulic Accumulator	Constant pressure fluid	Nil	1400	Assumes separate air bottle with air regulated into spherical accumulator
Hydraulic Accumulator	Constant pressure fluid	Nil	2500	Spherical accumulator 3000 psi maximum output throttled to 1500 psi
Hydraulic Accumulator	Variable (± 10%) pressure fluid	Nil	3200	Spherical accumulator riding on system
Flywheel	Variable speed shaft	Nil	74	Constant stress wheel at 100,000 psi, 25% allowance for unavailable work (2/1 speed range), 25% allwoance for housing and gears
Spring	Variable torque shaft	Nil	75,000	100,000 psi stress, 25% allowance for mounting
Gasoline Engine (piston or turbine)	Shaft	2.0	0.60	Requires ambient air for combustion

[a] Bottle weight from p. 685 of *Interavia*, Vol. 12, July, 1957.

weight per unit output. A startling Russian comment comes from the daily newspaper *Soviet Aviation* for July 29, 1957, in an article on nuclear propulsion for aircraft which says: "Presently existing radioactive sources of current are still very ineffective. They can be used only for supplying airplane accessories."

Monopropellants — Ethylene oxide, one of the more popular monopropellants, is a volatile liquid which decomposes exothermically into a mixture of hot gases which may be expanded through a turbine to produce useful power. The specific power output is a function of the pressure at which the decomposition process takes place, as shown in Table 2.

Since the sfc improvement becomes very slight beyond a pressure ratio of 20/1, this value has been taken as typical for the study. A serious practical problem associated with the use of ethylene oxide results from its high volatility, which makes storage and pumping extremely difficult. Current practice is to store the fuel in a pressure vessel and to use a high-pressure flild (nitrogen or hydraulic fluid) to displace it during operation of the power unit. Allowance for tankage and pressurizing means used herein amounts to 0.75 times the fuel weight, which is actually considerably less than is found in several current production units. Since the tank weight is proportional to the total amount of fuel, it may be totaled with fuel weight to yield an equivalent theoretical sfc — which becomes 8.75 lb/hp-hr for 100% turbine efficiency for the present study. This value must be further increased to account for turbine efficiency in a given application. A typical turbine efficiency of 25% would give an sfc of 35 lb/hp-hr, including fuel tank weight.

The possibility of using the hot gas from an ethylene oxide decomposition chamber or a solid propellant as a working fluid in flight control actuators is frequently mentioned and is considered in this study as an alternative to the use of hydraulic actuators. When utilized in this way, the gas is used at a constant pressure and only a portion of its available energy is realized. The speed of response has been shown to be adequate for many systems investigated. The load stiffness may be insufficient in certain cases. Presently visualized hot-gas systems maintain a continuous pressure on both sides of the actuator and also meter gas flow out of the two sides through a servo valve. This system effectively makes the hot gas work against itself in the actuator and further decreases the overall system efficiency. Considering these factors, an sfc of 40 lb/hp-hr is considered reasonable for a typical hot-gas servo system — which, corrected for tank weight yields an overall value of 70 lb/hp-hr for 2000 F and short durations. For longer durations and lower temperatures, the sfc will be 170 lb/hp-hr.

The use of solid propellants to avoid the logistics and tankage problems of ethylene oxide is frequently mentioned. The solid propellant burning rate is highly sensitive to the propellant temperature at the time of ignition. This leads to requirements for storage temperature control if serious efficiency losses are to be avoided. Nonuniform burning problems impose an upper limit upon the power duration of a single solid propellant grain. This leads to multile chambers with accompanying weight, complexity, and reliability problems. A third limitation on solid propellants is the difficulty of modulating the burning rate to match the power demand of the system. This, in turn, leads to significant decreased overall efficiency in most applications. In general the slow growth of solid propellant APU acceptance suggests that any advantages they offer over ethylene oxide must be relatively minor. Weight and performance information available for solid propellants indicates that the ethylene oxide systems offer a reasonable approximation of solid propellant weight characteristics.

Similarly, there are several liquid fuels which offer different compromises between energy content, logistics, cost, and the like, but their lack of general acceptance suggests that they do not offer significant improvements and that they may be grouped with ethylene oxide and the solid propellants for study purposes.

Compressed Gas — Compressed-gas storage systems include two major subdivisions based on the final working fluid, namely air bottles and hydraulic accumulators. The characteristics of both types are summarized in Table 1.

Air bottle weight is based on two Bristol Aircraft (England) units;[1] moreover, this weight is in good agreement with general values quoted by Wright[2]

[1] P. 685 of *Interavia*, Vol. 12, July, 1957: "Paris Air Show."
[2] "Why Hate High Pressure Pneumatics?" by H. E. Wright. Paper presented at SAE National Aeronautic Meeting, Los Angeles, October, 1957.

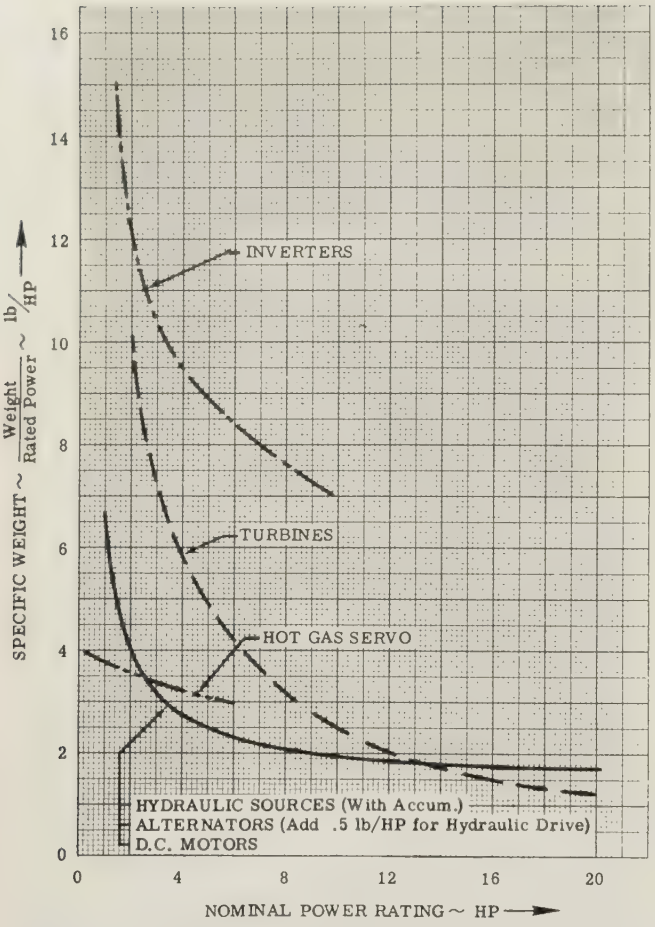

Fig. 3 — Power conversion weights, short-duty cycle and limited life

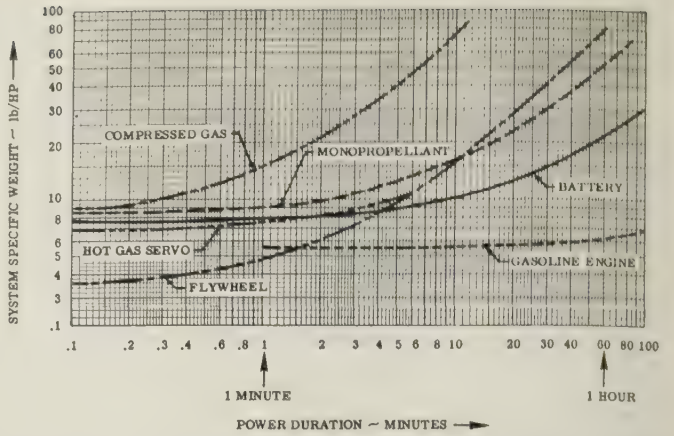

Fig. 4 — 5.0 hp auxiliary power unit, 50% hydraulic (provision for 100% overload for 1 sec) and 50% electric (all a-c, or one-half a-c and one-half d-c, as convenient). System summaries will be found in Fig. 6

and Kline, et al.[3] The ideal expansion specific weight of 77 lb/hp-hr may be compared with the value of 8.75 for ethylene oxide plus tankage, and indicates the reason for their relative acceptance in current power units.

When stored air is used at constant pressure, only about one-half of the total air can be used and only a small fraction of the available energy of that air can be realized, because of the problems mentioned previously under hot-gas servos. Accordingly, the specific weight is increased almost tenfold to 690 lb/hp-hr for perfect actuators and would be further increased for a real servo system.

The most efficient hydraulic accumulator involves a compressed air bottle followed by a pressure regulator and a hydraulic vessel which is initially filled with oil and operates at constant pressure while the oil is displaced by air. This system starts with an ideal constant pressure air system weight of 690 lb/hp-hr and adds the weight of oil and oil accumulator to reach a total of 1400 lb/hp-hr. The more conventional single-unit accumulator is still heavier since the oil vessel must be stressed to the maximum storage pressure and the air vessel pays a weight penalty for the diaphragm installation; the resulting specific weight is 2500 lb/hp-hr based on throttling the output oil to a constant value of one-half the maximum pressure. A single accumulator riding on the system and operating over a 20% variation in pressure would weigh about 3200 lb/hp-hr.

Mechanical Energy Storage — Mechanical energy storage may take the form of kinetic energy (flywheel) or potential energy (spring) systems. The values of Table 1 are based on the calculations of Kline, et al.[3] with certain practical allowances, as shown. Only the flywheel offers a specific weight small enough to be interesting, and it may become highly attractive for short to medium durations.

The configuration envisioned involves a hydraulic pump/motor which utilizes energy from an external source to bring the flywheel up to speed and maintain speed until missile launching. Then, the flywheel drives the unit as a pump to provide hydraulic power for flight control actuators and a hydraulically driven alternator. The instantaneous power output from the flywheel is limited only by the pump and gearing, so an accumulator is not necessary for hydraulic overloads and only a small surge accumulator is provided in later system comparisons. The gyroscopic effect of the flywheel may be an asset in stabilizing a missile during flight; however, if it is not desired, it may be eliminated by employing two counter-rotating wheels geared together. The wheel(s) would probably be enclosed in a sealed, partially evacuated housing and would offer a virtually infinite shelf life.

Reciprocating Engines — Although they operate on chemical heat release as do the monopropellant systems described earlier, the reciprocating engines are sufficiently different to warrant separate consideration.

The conventional air-breathing gasoline engine is well-known and its characteristics as shown in Table 1 are based on current practice. Engines of about 2.0 lb/hp are available in a variety of sizes from the model airplane, chain saw, outboard engine, aircraft target drone, and imported automobile industries. At about 50 hp, the gas turbine becomes competitive with the reciprocating engine and begine to dominate the scene above about 200 hp.

In the larger sizes, specific weights much less than 2.0 lb/hp are readily available, but are not reflected here since this study is primarily aimed at the 5–20 hp field. A reciprocating engine using self-contained fuel and oxidizer may be developed within

[3] "Work Capacities of Energy Storage Systems on Basis of Unit Weight and Unit Volume," by L. V. Kline, S. M. Marco, and W. L. Starkey. Paper No. 57-SA-7 presented at ASME Meeting, San Francisco, June, 1957.

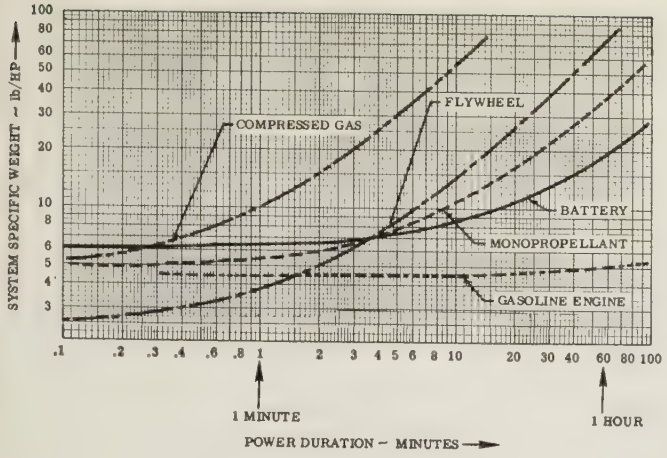

Fig. 5 — 10.0 hp auxiliary power unit (conditions same as Fig. 4). System summaries will be found in Fig. 6

the next few years. Since such an engine will probably use only liquids, it will not require a compression stroke and hence will yield more power per unit piston displacement than is currently available. On the other hand, it may require rather elaborate injection equipment. The sfc is a function of the fuel(s) selected and may be as low as 2.0 lb/hp-hr or as high as 8.75 lb/hp-hr — the latter would provide ethylene oxide in a pressure tank. In the system comparison charts which follow, the effects of different assumptions for the weight and fuel consumption of internal reaction engines can be estimated by interpolating between the monopropellant turbine and the air-breathing engine lines.

Power Conversion Units

Power conversion units for this study involve small units operating for short-duty cycles with limited overall life requirements. Units discussed in this study are hydraulic sources, alternator and d-c motors, turbines, hot-gas servo systems, and inverters and are plotted in Fig. 3.

Hydraulic Sources — The hydraulic source weight includes a pump, reservoir, mounting hardware, pressure regulating and relief valves, and an accumulator sufficient to double the rated output for a period of 1 sec. The accumulator requirement varies markedly in different applications, and the 100% overload for 1 sec used here is merely an arbitrary approximation. This accumulator provision adds about 1.0 lb/hp to the system weight, which is over one-half the total hydraulic source weight for the larger systems.

It should be noted that the servo valves, connecting lines, and actuators are *not* included anywhere in this study, since they are assumed to be independent of the means used for providing the working fluid.

Alternators and D-C Motors — The weights shown are based on recent firm proposals made by reputable manufacturers and are believed to be realistic. It is rather surprising that the electric and hydraulic units fall on the same weight curve; however, the actual data points are so overlapped as to make separate fairings pointless.

Turbines — Turbine weights include control systems, gear boxes, and decomposition chambers and are based on available data for current ethylene oxide fueled APU packages.

The sharply rising specific weight for small units reflects the fact that minimum wheel sizes are encountered at about 20 hp — with smaller units using smaller turbine nozzles (and yielding poorer operating efficiencies).

Hot-Gas Servo Systems — The weight shown includes fuel control system components and an estimated allowance for the weight differential between the hot-gas servo valves and actuators and their hydraulic counterparts as used in the other systems. This weight penalty arises out of the decreased effective pressure and increased temperature in the hot-gas system.

Inverters — The inverter weights shown are based on currently available units with arbitrarily increased ratings to take advantage of the reduced life requirement. It is possible that lighter units could be developed, but no current effort is known in this field. A side investigation conducted as part of the present study shows that an alternator driven by a constant-speed hydraulic motor taking fluid from the main hydraulic source will be both lighter and more efficient than even an improved inverter, since the integrated hydraulic drive allows the use of a single large d-c motor with relatively poor speed regulation. Both effects are in the direction of reduced motor weight. Solid-state inverters show an interesting potential but are not believed ready for actual consideration.

System Comparison

To obtain a final evaluation of the various energy sources and conversion units, it is necessary to combine them into complete systems to meet particular design specifications. For purposes of the present study, three typical system requirements have been established and the various APU types are compared against each requirement.

System power ratings of 5, 10, and 20 hp bracket current missile requirements according to our experience — a finding which agrees with a General Electric survey of the missile APU market.[4] Within each system, a power breakdown of 50% hydraulic and 50% electric is generally consistent with Vickers and GE experience. Further detailed considerations are: (1) the provision of 100% hydraulic overload for 1.0 sec and (2) the acceptance of a 50–50 split between a-c and d-c electric power where batteries are employed and d-c can be provided more efficiently.

The results of the system studies are presented graphically in Figs. 4–6. It will be noted that system specific weight (lb/hp) is used rather than absolute system weight, even though each figure is concerned with systems of a constant power rating. The use of specific weight permits ready evaluation of scale effects by comparing the three sizes studied, and interpolated specific weights may be used for calculating the weights of intermediate size systems. General conclusions which may be drawn from Figs. 4–6 are discussed in the following paragraphs.

Flywheel — A flywheel system is the lightest available for durations up to 1 min and is competitive with most currently available systems up to about 6 min. The reliability, simplicity, low development cost, and excellent storage characteristics of the

[4] *Aviation Age*, Vol. 28, November, 1957, p. 101: Staff item.

flywheel, coupled with its excellent weight characteristics, recommend it for additional consideration.

Reciprocating Engines — Where ambient air is available for combustion and cooling, the conventional reciprocating gasoline engine is the lightest powerplant for all but the very shortest durations, where the flywheel takes over. The superiority of the reciprocating engine has long been recognized for automotive and aircraft applications where duration is measured in hours. It is, however, surprising to find that these same engines remain unchallenged down to durations of a minute or two.

Silver-Zinc Cells — While a silver-zinc cell system is never the lightest possible, its competitive weight position over the entire spectrum, coupled with certain other advantages, makes it highly attractive. These cells are in current production in a wide variety of sizes by several reputable manufacturers. The freedom from lengthy development programs makes them attractive for many applications. Also, the d-c motors and other required components are readily available so that prototype systems can be built and demonstrated at costs which are at least an order of magnitude less than that of, for instance, an ethylene oxide turbine package.

Hot-Gas Supplies — The hot-gas supply to servo valves and actuators is generally heavier than a battery-powered system, and is slightly heavier than monopropellant turbine system in the 10- and 20-hp sizes. In addition to the weight disadvantage shown, the hot-gas system has at least two other fundamental limitations:

1. To provide a-c power, two complete power systems with their development problems would be required. This would necessitate maintaining two types of prime mover. The hot-gas system for flight controls and perhaps a battery inverter or turbine drive system for a-c power.

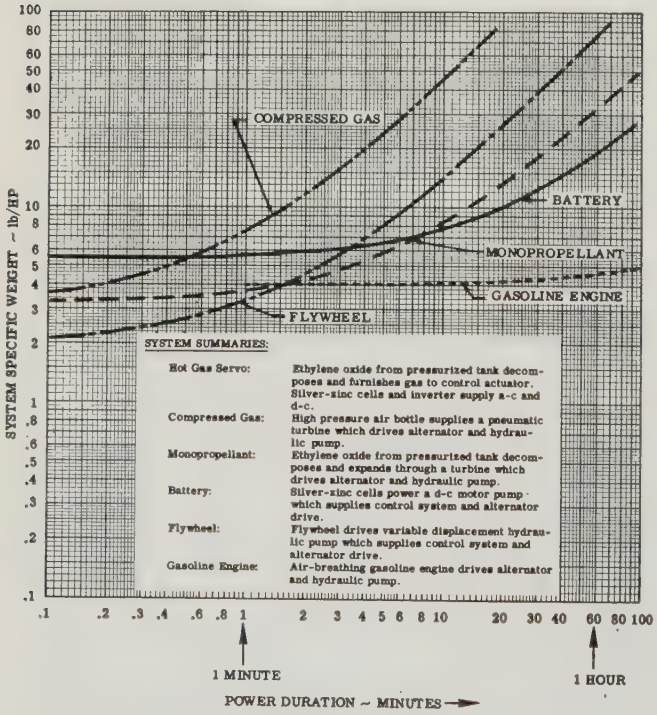

Fig. 6 — 20.0 hp auxiliary power unit (conditions same as Fig. 4)

2. The hot-gas system is not at a comparable development status with either battery or turbine driven systems and would, therefore, require development program before adequate reliability could be demonstrated.

The primary reason for considering hot-gas actuators has been the threat of high-temperature problems in hydraulic systems; however, this threat has not yet materialized as a result of successful high-temperature hydraulic system developments on the one hand, and the surprisingly adequate thermal lag of missile hydraulic systems in actual flight on the other hand.

Ethylene Oxide Turbine — The relatively poor weight showing of this system and the known difficulties in handling monopropellant fuels suggests that the large development effort required is a poor investment.

Compressed-Gas Systems — These systems could have been eliminated immediately on the basis of the results shown in Table 1. The air bottle plus turbine, which is one of the better combinatnions, is included here for comparison only.

Typical System Schematic — Fig. 7 illustrates a typical system based on silver-zinc cells. The d-c motor driven hydraulic pump and the hydraulically driven alternator are shown as they are included in the comparative system weight curves.

Conclusions and Recommendations

Within the limitations of this study the flywheel system has been shown to have some surprising weight advantages for durations up to 1–2 min. The reciprocating engine powered by hot propellant gas, or by air fuel, is lighter for longer durations. Monopropellant turbines and silver-zinc cells powering electrical motorpumps are generally competitive on a weight basis for the intermediate durations. Hot-gas servo systems are unattractive on the basis of weight, and have several other limitations. Compressed gases and mechanical springs are too heavy to be competitive.

The weight advantages of the flywheel and the reciprocating engine are obvious, and these systems should be considered whenever they are applicable. Silver-zinc cells appear to offer a favorable combination of characteristics over a wide range of applications and are recommended for further study.

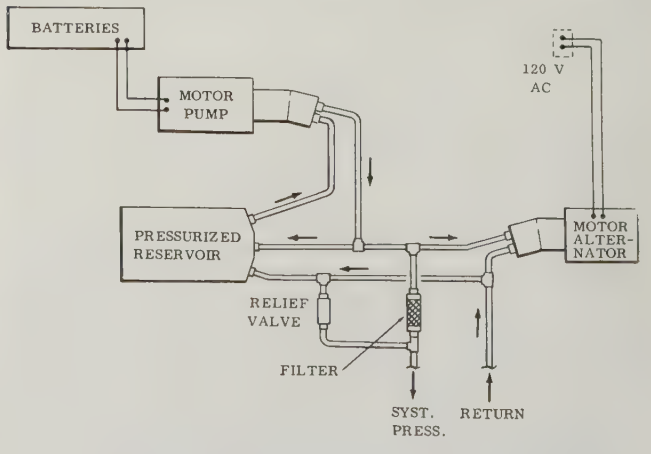

Fig. 7 — Schematic of typical system based on silver-zinc cells

ALUMINUM ENGINES—

design for modern fabrication

J. M. Smith and R. M. Smith, Aluminum Company of America

This paper was presented at the SAE Summer Meeting, Atlantic City, June 13, 1958.

INTEREST in application of aluminum in major components of the automotive engine has mounted rapidly in recent years, stimulated by an attractive horsepower/weight ratio and the possibilities of production economies.

The all-aluminum engine is not new. In 1917 an all-aluminum engine using Northway components was designed, built, and dynamometer tested by Alcoa (Fig. 1). About 1924, several all-aluminum cars powered by 6-cyl all-aluminum engines were designed and built (Fig. 2). These vehicles were road tested up to 100,000 miles with excellent perfomance for that day. One of these engines is on exhibition in the Ford Dearborn Museum in an all-aluminum sedan built as part of this same program. An all-aluminum version of a 1942 6-cyl Pontiac pleasure car engine (Fig. 3) has been viewed and tested by many automotive people. During a 14-year program, periodic examinations verified design and alloy selection.

In 1950, experimental all-aluminum V-6's and V-8's, using cylinder blocks and heads of aluminum sandwich brazed construction, were successfully tested (Fig. 4). About 7 years ago, Alcoa had the opportunity to cooperate in the design and production of the all-aluminum engines in the futuristic Le Sabre and XP-300 cars.

Such experience with the all-aluminum automotive engine has demonstrated the many advantages it has over the now conventional ferrous unit. A partial list would include:

1. Reduction in engine weight — assists in solving critical vehicle weight distribution problems. Lighter engine supporting members enhance the overall weight reduction with resulting improvement in vehicle performance and economy. Reduction in weight contributes to the solution of the serious braking problem, and also makes possible the use of smaller and, therefore, cheaper tires.
2. Production cost savings and reduction in capital investment — realized by employing the higher machining speeds and feeds, lower finish allowances, and ease of handling possible with aluminum.
3. High thermal conductivity — affords excellent paths for dissipation of heat. Volumetric efficiency and specific engine performance are improved. Moderate temperature gradients and elimination of local hot spots in thermally loaded parts reduce thermal strains and distortion.

There can be no doubt of the successful applica-

ALUMINUM engines promise a gain in the power/weight ratio and possibilities of production economies. Aluminum has already proved its value for some parts; only the adaptation of design for high production methods delays full realization of the metal's potentials.

This paper describes the problems encountered in adapting the V-type engine to fabrication methods using aluminum alloy parts. Applications of aluminum in crankcase and cylinder block, cylinder liners and heads, intake manifold, pistons, and bearings are also discussed.

tion of aluminum alloys to automotive engine parts. Some parts are now in production which were proved on the early experimental engines. The full realization of the advantages of this versatile metal awaits design adaptation to high production methods.

No attempt is made here to develop a complete engine design in all its detail. This paper will present some problems encountered in adapting the modern automotive V-type engine to modern fabrication methods where aluminum alloy parts are used.

Production Process

In the integrated organization that conducted this extensive testing program, all the methods of aluminum fabrication economically applicable are employed. It is, therefore, possible to select without prejudice the process most suitable from economic and engineering standpoints.

The very nature of engine castings dictates the application of the several aluminum foundry processes. Considering the two common high production casting methods, the issue can be stated very simply: Where thin sections are indicated, the die casting is preferred; when relatively thicker sections are required for strength and rigidity and internal soundness is important, the permanent-mold process is the proper choice. If all design efforts fail to produce a part suitable for production by either of these two methods, the semi-permanent-mold or the sand-mold process should be considered because of their relative versatility. These general statements assume production quantities warrant consideration of all these methods. Economics will quickly dictate the choice, engineering considerations being equal.

Design requirements for sand castings in aluminum and iron are similar. The usual allowances for core shifts and finish must be observed.

When designing for permanent-mold or die-cast manufacture, these or similar considerations must also be satisfied. Since these are more precise processes, allowances need not be so generous as in sand. Furthermore, the fear of broken or washed cores is eliminated. Since the mold, or die, and cores are not expendable as in sand casting, the part must be designed without backdrafts or undercuts. Thus, the cores must retract, and the part must be ejectable from the mold or die.

At this point, a feature of the permanent-mold process should be noted in which it differs from the die-cast process. In the former, where backdrafts and undercuts are unavoidable, collapsible cores may be used. In the interest of economy, such design should be a last resort. In die casting, because of the pressures used when filling the die, fins would develop between collapsible cores if used. In die castings, loose core pieces are sometimes employed to produce undercuts, adding to the cost and retarding the operating cycle.

The semi-permanent-mold process utilizes a multipiece iron mold and disposable cores. This process shows promise as another possible high production method for producing aluminum castings of the conventional crankcase geometry. Work is progressing on suitable economical core materials which could be easily and completely removable from the casting.

The engineer accustomed to designing in iron or steel should bear in mind, when designing in aluminum, the moduli of elasticity of these materials. Also, the designer must satisfy one or more of the following: strength, rigidity, and process requirements. Frequently, depending upon the process adopted, wall sections may be moderately reduced below those customarily required in similar iron parts, since section proportions are frequently dictated by foundry practice.

During many years of designing with aluminum, certain design details have been found particularly important. These would include: (1) blending at severe section changes, (2) marginal distance at bolt holes, (3) bolt boss diameters and threaded depth of holes, (4) broad, flat, low ribs in general, as contrasted to narrow, round, and high (these are frequent causes of failure), and (5) bolt fastenings located in, or near supporting wall sections to minimize eccentric loading, inducing bending.

Crankcase and Cylinder Block

In the production of modern engines, the largest single engine component is restricted to the integral crankcase and cylinder block construction. The merit of this design has been well-demonstrated and mere mention of its advantage over the two-piece construction will suffice: economy and inherent rigidity. Interest in the overhead valve engine, which eliminates the complicated coring of valve and port passages from this large casting, enhances its attractiveness as a one-piece casting. Stresses from gas loading are more uniformly carried into the crankcase from the cylinder than could be accomplished by the bolted assembly of two separate pieces. Hereafter, the term "crankcase" will imply the integral cylinder block as well, although this paper will present one solution involving the multipiece construction.

The crankcase is a classic example of a structure defying rational design procedures and analysis. The loading, while extremely fluctuating in nature, is susceptible of accurate determination at several crankshaft speeds, together with its phasing with crankshaft position. The direction of the most severe loads may then be used judiciously in so proportioning the bearing bulkheads or bridges to carry these loads, in the most direct fashion possible, to the structure as a whole.

Because of the involved nature of the crankcase and the varying loads applied, adequate mathematical stress analysis is not possible, even though the nature of the loading and its direction are accurately known. Therefore, no attempt will be made here to present a stress analysis; instead, attention is directed to the experimental tools, Stresscoat (the brittle strain indicating lacquer), and electric strain gages, available for proving the design.

All American pleasure-car engines are of the integral sleeve and cylinder block construction. Such a construction in sand is possible for aluminum, as well as for iron. It will be obvious from Fig. 5 that the aluminum crankcase as conventionally produced in sand for dry-liner installation cannot be produced by permanent-mold or die-casting methods. The top deck prevents metal water jacket core withdrawal; but by removing this top deck and the integral cylinder wall, substituting an insertable wet liner, the design is made practical for production in permanent mold or die casting. Two satisfactory liner arrangements are shown in which the upper

end of the cylinder is closed by a plate into which is inserted in one case, a liner with a shoulder resting against the plate. An alternate type of construction has been advocated in some quarters in which the liner is brazed into the cover plate. In the case of the all-aluminum engine, an aluminum plate instead of an iron or steel plate better equalizes expansion of the top and bottom portions of the crankcase. Into this aluminum plate, iron or aluminum liners may be assembled by known methods. The stiffness of this cover plate must be adequate to sustain the gasket load on application of the cylinder head. In constructions "A" and "C" the liner should extend 0.002–0.005 in. above the cover plate in order to produce an effective seal against combustion pressures.

Wet liners are conventional with many heavy-duty transportation and tractor engines. Fear of water leakage has often prevented adoption of such construction. The cylinder center distance in the conventional iron engine without liners is less than that of a wet-liner engine of the same bore. When considering an aluminum engine with liners, this difference in cylinder center distance is reversed and, as in Fig. 5, the wet-liner construction may permit an even smaller cylinder center distance than with the dry liner. The proportions of the drawing from which these figures were prepared

Fig. 1 — Early V-8 aluminum engine (1917)

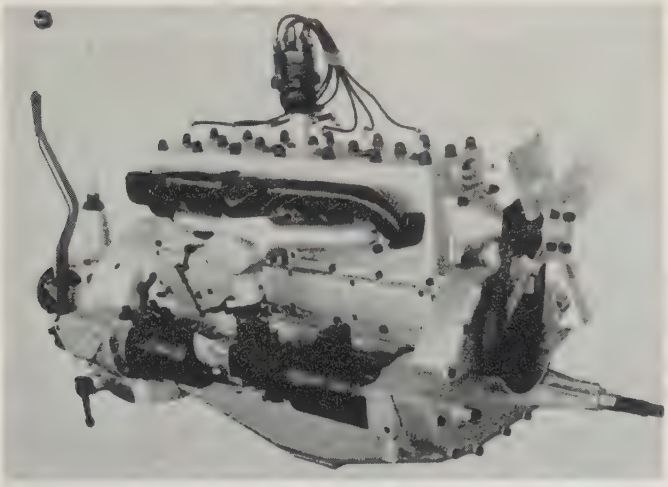

Fig. 2 — Early 6-cyl aluminum engine (1924)

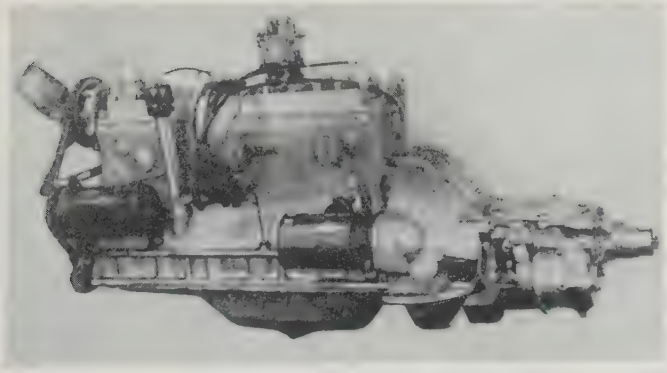

Fig. 3 — Six-cylinder aluminum engine (1942)

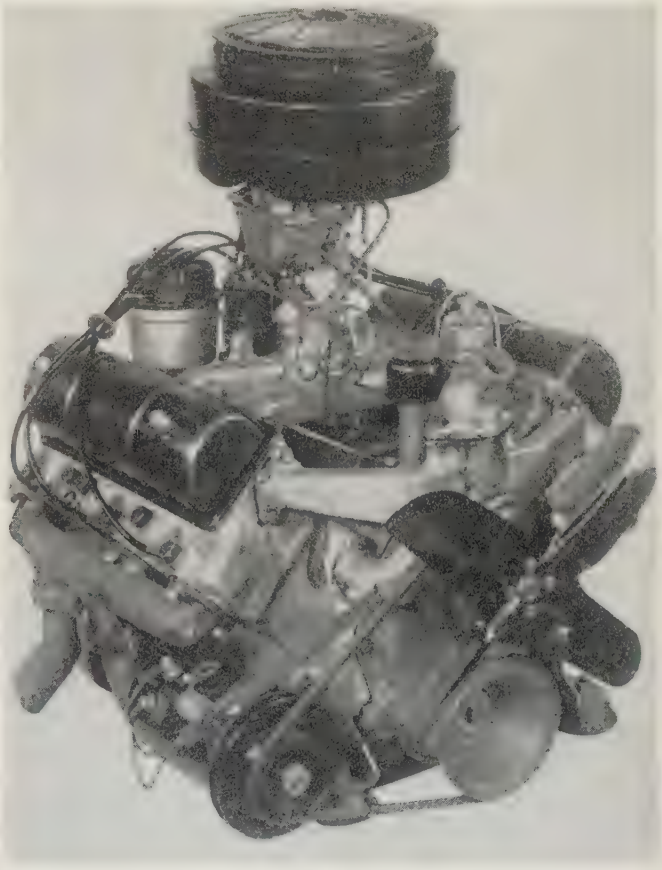

Fig. 4 — Aluminum V-6 engine — furnace brazed sandwich construction

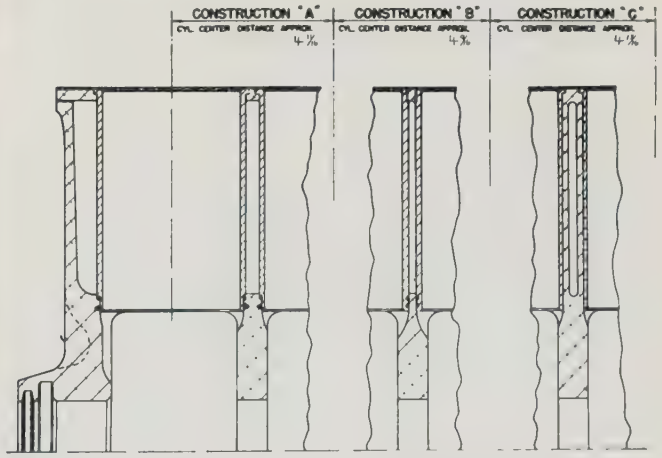

Fig. 5 — Wet and dry liner constructions, longitudinal section showing influence of design details on cylinder center distances

were for a 4-in. bore present production engine. On the basis of a comparative design, the cylinder center distances are approximately 4 11/16 and 4 9/16 in. for wet-liner construction "A" and "B" respectively, as against 4 13/16 in. for the dry-liner sand cast-aluminum engine.

Attention is directed to methods for sealing the lower end of the wet liner. A single rubber ring of square section has been suggested which is confined within the counterbore and shoulders at the bottom of the liner. In addition to the square section ring, an "O" ring confined in a "V" groove should be added since most engine people will not be sufficiently assured of water tightness by a single ring.

Fig. 6 shows two other wet-liner constructions requiring no top deck on the crankcase. On the left, the upper end of the liner is retained in a counterbore in the cylinder head. In the right-hand view, the upper shoulder is supported by the cylinder head bolt bosses. Both methods require a shoulder at the lower end to resist the head hold-down load. Other arrangements for supporting the liner and for sealing the bottom end will occur to the engine designer, since specific layouts and space available will establish particular features. Attention is called to the fact that rubber is relatively incompressible and when using this material for sealing, as here applied, space must be allowed for the rubber to flow. Thus, undue pressure will not cause collapse of the lower end of the liner. Deformation of the rubber ring section is sufficient to exert sealing pressure.

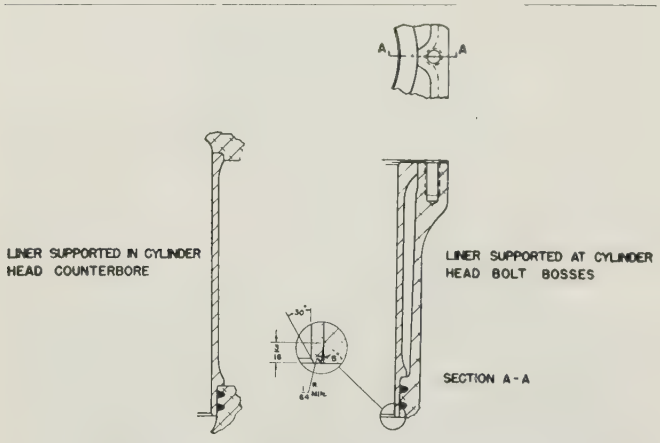

Fig. 6 — Wet liner constructions, no top deck

Fig. 7 of the Italian Lancia 6-cyl, 60 deg "V" engine, the crankcase being made as a permanent-mold aluminum casting. The arrangement is somewhat of an abridgement of the wet-liner construction, in which the upper end of the liner is supported against the cylinder head bolt bosses, and conventional dry-liner construction. In Fig. 8, a close-up of the liner indicates that water flow is from the water jacket proper into a space between the liner and the aluminum barrel, upwards with high velocity and then out through slots at the upper shoulder. This is an ingenious design providing high water velocity for good heat transfer but, admittedly, it is expensive.

Fig. 9 shows possible dry-liner constructions, again with a comparison of minimum cylinder centers. Construction "C", indicates sections for the conventional dry-liner sand-cast engine, again

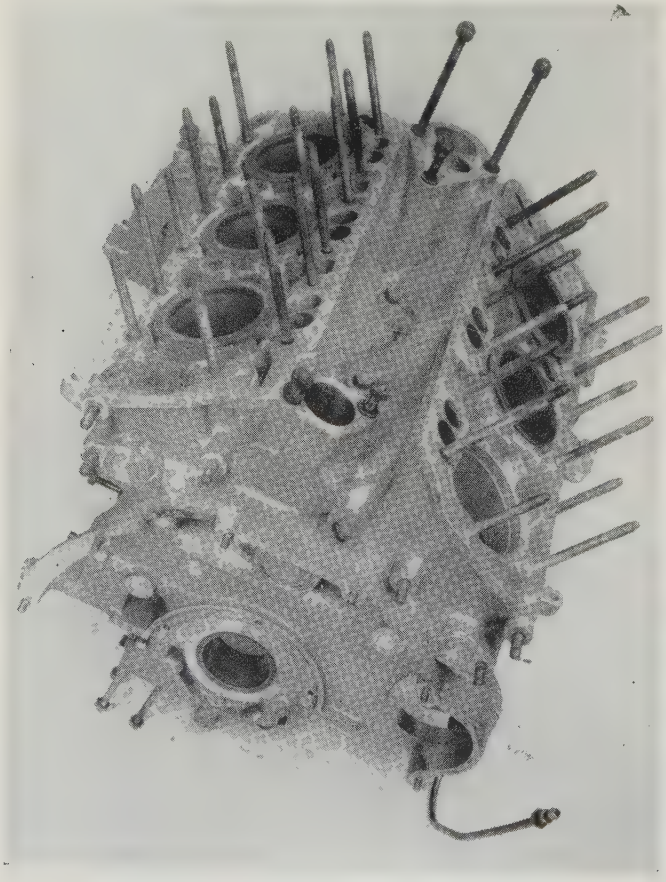

Fig. 7 — Crankcase of Italian Lancia V-6 engine

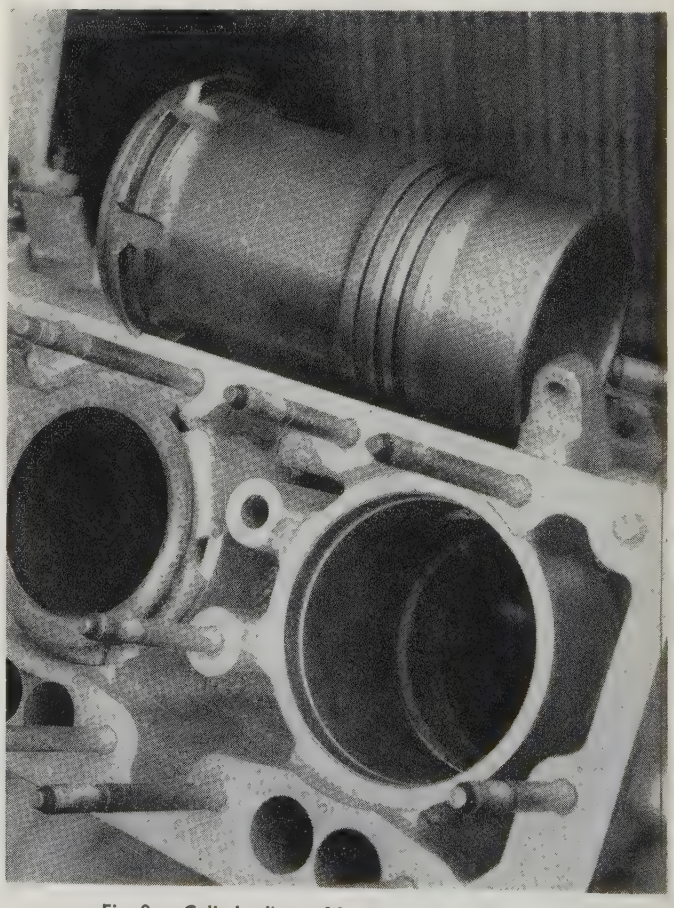

Fig. 8 — Cylinder liner of Italian Lancia V-6 engine

based on a 4-in. bore. In construction "B" no top cylinder deck is used, permitting the metal jacket core to be withdrawn from the casting. Water seal at the top is accomplished by a conventional cylinder head gasket. Construction "A" is similar to construction "B" with the application of a top plate into which the liners are inserted. Both constructions require a center distance of 5 3/16 in., 3/8 in. greater than the minimum sand-cast engine.

Treatment of the outside lower edge of the liner (Fig. 9) is important. In the case of the dry liner, the purpose is to avoid scoring of the aluminum bore during assembly with a recommended fit of 0–0.002 in. tight. In the case of the wet-liner construction, a similar treatment is recommended to permit easy insertion of the liner past the rubber seal rings. Application of a mild soap solution will facilitate this assembly.

In a dry-liner engine, the aluminum bores should have a finish of 10–20 microin. rms. The use of a lubricant of the colloidal graphite type is suggested to permit insertion and removal of the liners without scoring the aluminum bore.

Since present conventional practices in aluminum engines require the use of a liner, it is apparent that attempting a dry-liner construction with permanent mold or die casting calls for an engine of greater overall length. Adoption of the wet-liner construction simplifies the crankcase casting, makes the operation of the mold or die equipment more rapid, and reduces overall engine length.

Fig. 10 illustrates a transverse section of a basic "V" engine crankcase designed for permanent-mold or die-cast manufacture. Referenced to the plane of the pan rail, the mold or die pieces forming the sides and ends move in parallel planes, lifter chamber cores move in a perpendicular plane, and water jacket cores move in the plane of the cylinder centerlines. Local heavy sections frequently result through avoiding undercuts or backdraft. This condition is indicated near the cylinder head bolt hole on the extreme right, alternate "B." This situation may sometimes be relieved by resorting to the construction shown in alternate "A." A wavy contour results on the inside edge of the crankcase upper deck which is not suitable for the application of a sheet-metal valve lifter cover. Generally, the cover can be attached to the cylinder head, or the inlet manifold can be used as the cover. It is not possible with this type of mold construction to core the lifter holes completely. The bores for the camshaft will be left solid at this juncture in the interest of equipment simplicity. The oil gallery passages will be drilled, because it is impractical to core so long and so small a hole. The bearing bridge is a solid section lacking ribbing or lightening holes. Such detail is impossible without expensive collapsible cores.

Fig. 11 shows a top view of the crankcase employing recessed pockets at certain cylinder bolt bosses, as indicated in Fig. 10. Note also the intricate parting between the cores forming the lifter chamber and the crankcase. Attention is directed to the fact that any contour appearing in the direction of the draw of the core must continue to the bottom of the recess to permit core withdrawal. Thus, where the water jacket wall is recessed between cylinders, an advantageous reduction of casting weight and water jacket volume is accomplished.

Fig. 12 illustrates a transverse section of a "V" engine with the lower crankcase flange below the crankshaft centerline typical of many production engines today. Means for ribbing the outside of the casting are shown as a contribution to overall rigidity. These ribs follow the wavy wall section intro-

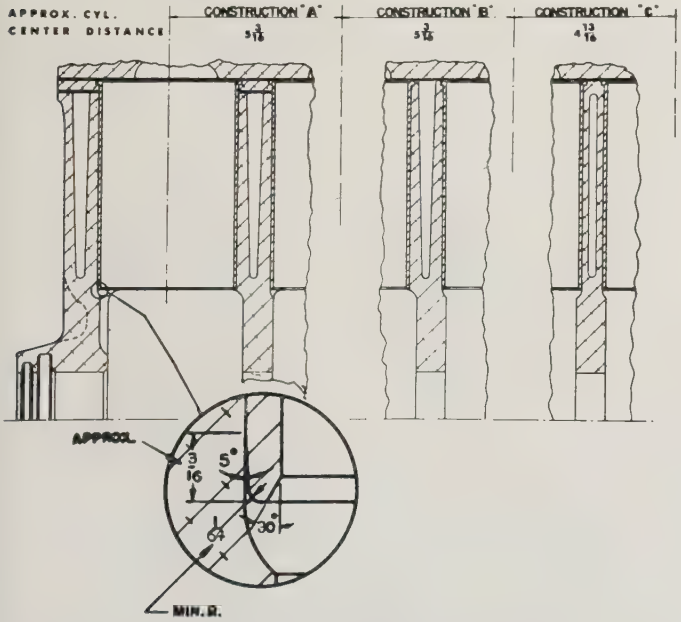

Fig. 9 — Dry liner constructions, longitudinal sections showing influence of design details on cylinder center distances

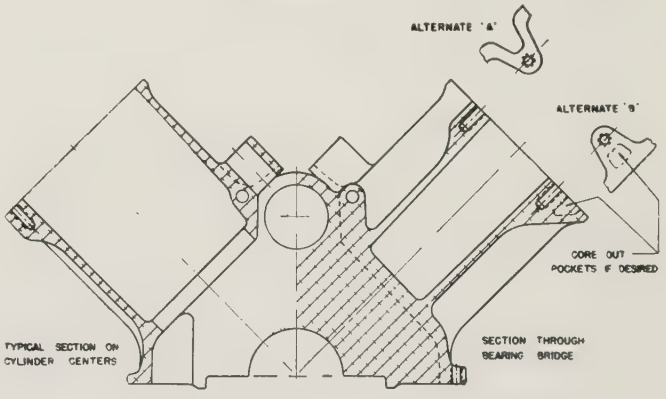

Fig. 10 — Transverse section of aluminum crankcase

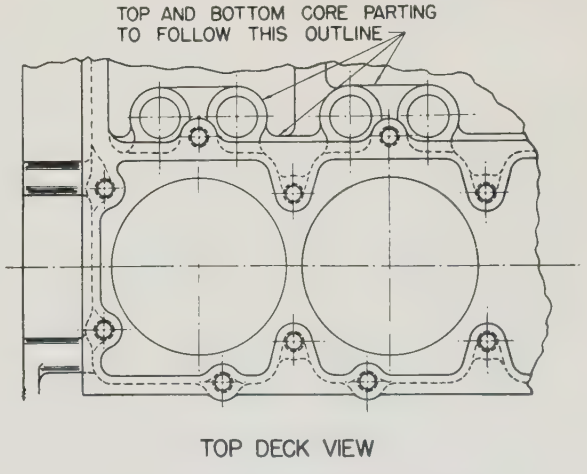

Fig. 11 — Top-deck view aluminum crankcase

duced as a weight-saving measure.

Fragmentary views in Fig. 13 indicate two possible methods for reducing the heavy metal sections near the main bearing bridge. On the left, unnecessary metal is cored from below and this core piece draws with the main crankcase core. In type "B" the wavy outside wall contours accomplish the same result.

In Fig. 14, a method is presented for further reducing the heavy metal sections in main bearing bridges by coring from above utilizing an extension of the water jacket core.

Ribs, bosses, or other detail appearing on the ends of the crankcase offer no problem provided no undercuts are present, since slides producing these contours move longitudinally.

Simplification of a crankcase may be accomplished by providing a camshaft bearing and lifter boss cluster assembled to the crankcase by bolts, as shown in Fig. 15. This accomplishes the removal of considerable detail from a rather large casting, permitting less expensive coring and eliminating the local heavy section in the uncored camshaft bores. In this casting, two oil galleries are provided, thus eliminating two drilled holes in the crankcase proper. The assembly could consist of two identical clusters, front and rear.

Fig. 16 illustrates still another simplification in which the camshaft is removed from the crankcase and an overhead camshaft design results. A small oil gallery is located in the vertex of the "V." Oil return holes to the crankcase would be necessary. On the left is shown a weep hole between the two "O" rings at the bottom end of the liner. This is common practice where more than one "O" ring is used; should the top one leak, static pressure is relieved from the lower ring preventing leakage into the crankcase.

Fig. 16 also shows recommended main bearing bolt practices. The purpose, here, is to illustrate design principles rather than design proportions. Bolt load should be carried well up into the bridge by counterboring the threaded hole, achieving improved stress distribution. On the left, location of the main bearing cap is attained by a body fit bolt. As an alternative, this is accomplished by interference of the cap in the bridge, shown on the right. Such a stud when installed to a predetermined torque will be prestressed to a value such that no fluctuating stress may be applied to the threads by main bearing loading. An undercut stud or bolt is recommended so that extension will occur in the body of the bolt and not in the threads. Use of hardened and ground steel washers under bolt heads and nuts is highly important, not only in this location but on other critical fastenings in aluminum as well. The reason is obvious: the bearing area is increased to the point at which aluminum can sustain the bolt load without setting and at which the bolt load, once applied, remains at the initial value.

The bearing cap design illustrated is not intended to be typical. They may be made as permanent-mold castings in a cluster or as forgings, depending upon the properties required. It should be mentioned that, in addition to the applied bearing loading, the crush load of the bearing inserts is also applied to the cap. The edge distance between the bolt hole and housing bore should be ample so that no deformation of the bore is caused by bolt's installation.

In the interest of the best utilization of the most suitable aluminum alloys, a multipiece design is proposed which admittedly is costly.

Recent interest in hypereutectic aluminum-silicon alloys suggests this possible design. These alloys have demonstrated good wear resistant qualities in cylinder bore applications. A wear comparison of standard cast-iron and aluminum alloys and various coatings will be made later in this discussion.

If hypereutectic aluminum-silicon alloys satisfy the cylinder bore wear and crankcase structural requirements, the sand- or semi-permanent-mold processes could be utilized to produce a one-piece conventional casting. The semi-permanent-mold process requires that backdrafts and undercuts be eliminated on outside surfaces. It is preferred that the expendable water jacket core material be kept to a minimum. Again, this is in the interest of foundry economy, rigidity, and reduction of cooling water volume.

Should these high-silicon-type aluminum alloys not fulfill the requirements of the crankcase but satisfy the needs of the cylinder bore, a multipiece construction is proposed. Fig. 17 previews a possible design solution. The cylinder blocks with integral liners are to be made as permanent-mold or die castings in hypereutectic aluminum-silicon alloy. The crankcase is designed for the permanent-mold or die-cast process, but in a suitable aluminum alloy.

Note is made of the cast in oil gallery with the necessary drilled supply passages to the integral lifter bosses. Two methods of assembling the cylinder blocks to the crankcase are suggested. On the right, a shoulder stud is suggested. This method

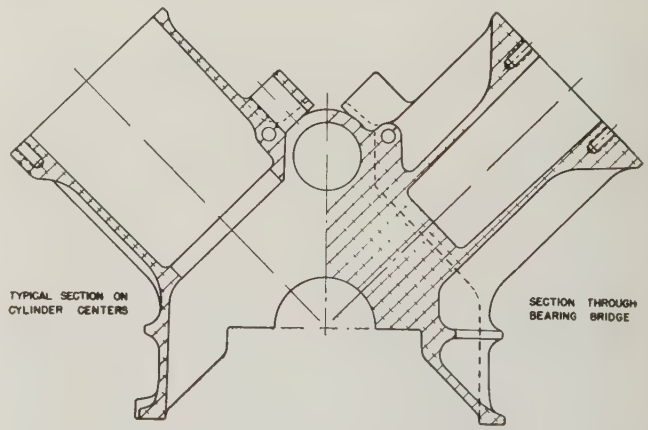

Fig 12 — Transverse section of aluminum crankcase

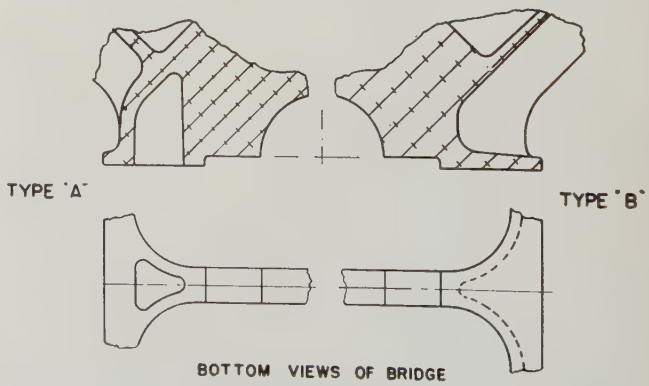

Fig 13 — Design treatment of main bearing bridge for optimum metal distribution

requires cast reliefs in the cylinder head to accommodate this shoulder. In the fragmentary view, a recessed head bolt is proposed with a cap screw threaded into it as means of assembling the cylinder. Locating dowels are required for alignment in assembly.

Conventional gasket practice is called for at the junction of cylinder block and crankcase.

The omission of the top deck on the cylinder block is in the interest of previously discussed casting process requirements. The cylinder head structure around the combustion chamber must be rigid to provide sufficient gasket load to effect a seal.

An attempt was made in discussing the design details of the crankcase to show examples of the problems encountered, rather than the complete solution of all problems that may be met in a crankcase design. An extension of the principles illustrated applies to other details such as bosses, ribbing, and local coring to remove excess metal. Such local coring, in addition to saving weight, may reduce the cost of the casting and certainly contributes to an improvement of casting quality.

Before leaving this discussion of the crankcase, consideration should be given to the differential expansion between the crankshaft and the aluminum case. To reduce clearance allowance, it is preferable that end thrust be taken at the center main bearing. This is not always practicable, in which case sufficient allowance should be made that the crankshaft never rides the fillet at the end opposite the thrust bearing location.

Cylinder Liners

Previously, aluminum-alloy automotive engine crankcases universally used separately installed cylinder liners. Design considerations and methods of installing wet and dry liners in aluminum crankcases have been discussed.

Ferrous liners have been used almost exclusively in the past because of their availability, wear resistance, and economy. Aluminum-alloy liners have a decided advantage over iron — weight saving, superior heat conductivity, and a coefficient of expansion the same as the crankcase and piston are all in their favor. Further, in the case of aluminum-alloy wet liners, dissimilar metals in the cooling system would be avoided. However, a wear resistant surface has been required on the usual aluminum-alloy liner. Chrome plate has enjoyed the greatest success in past years. Chrome-plated aluminum-alloy liners were successfully tested in an all-aluminum car in the 1930's. European engine manufacturers have successfully produced chrome-plated

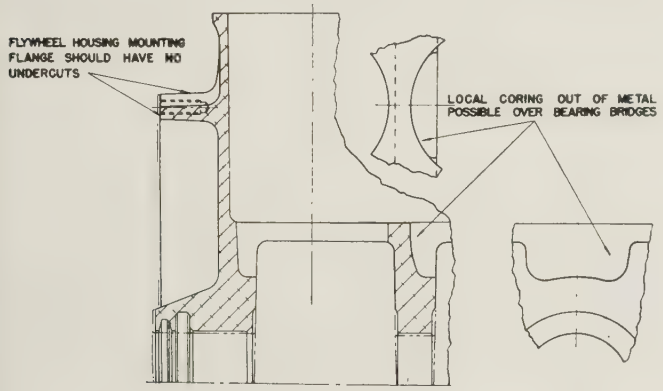

Fig. 14 — Longitudinal section on cylinder centers

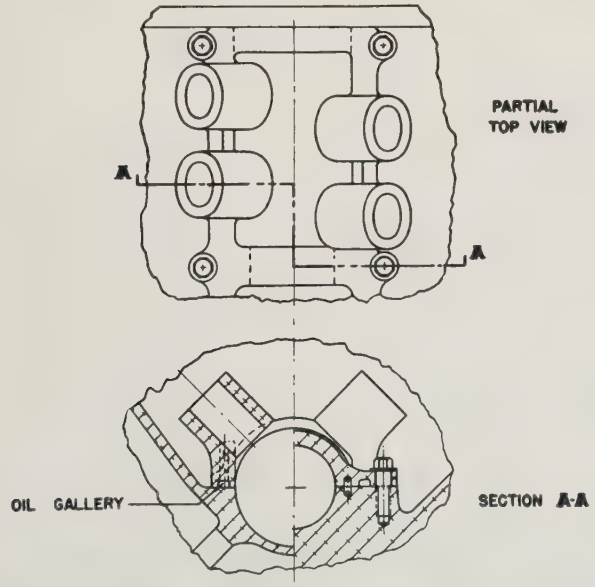

Fig 15 — Partial section showing aluminum lifter boss and camshaft bearing cluster

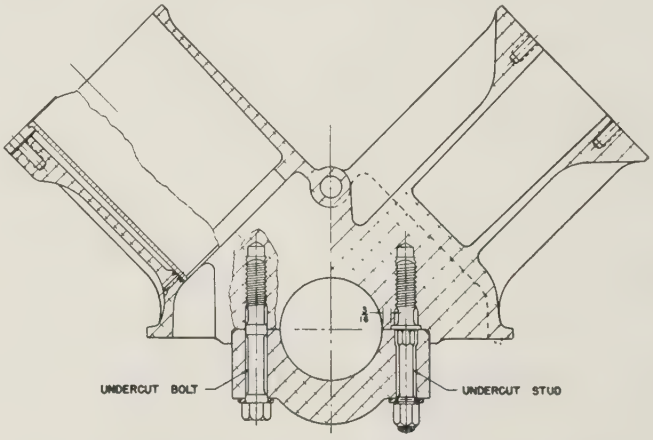

Fig. 16 — Aluminum crankcase construction for overhead camshaft engine and recommended main bearing cap assemblies

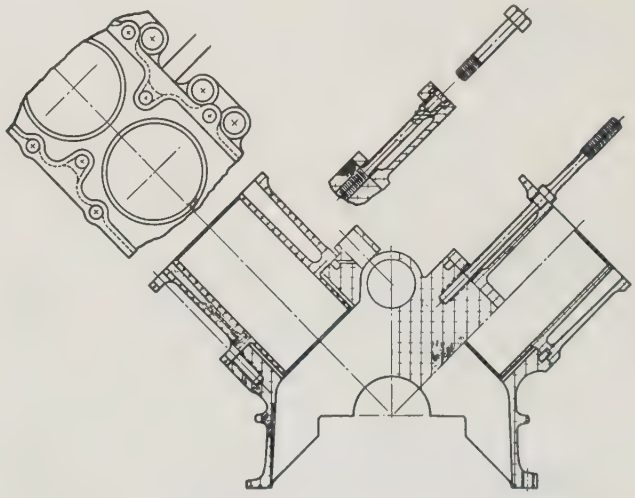

Fig. 17 — Aluminum cylinder block and crankcase assembly

aluminum-alloy cylinder bores for automotive aircooled engines. Some small 2-stroke, aircooled, industrial engines in the United States employ chrome plate on die-cast aluminum-alloy cylinders. The success of the chrome-plated aluminum-alloy cylinder wall depends largely on the quality of the plating.

Highly successful tests have been conducted on aluminum cylinder walls with metallized coatings from 0.005 to 0.015 in. in thickness. The sprayed metal coating is compatible with aluminum pistons and the wear resistance is excellent. The coating is porous in nature possessing good oil retention properties. Problems of production spraying and final finishing of the metallized surface are being studied. The economics are expected to be favorable considering advantages gained.

The porous nature of the sprayed coating introduces the possibility of galvanic corrosion between the dissimilar metals at the interface. By impregnating the coating with a resin dissolved in a suitable vehicle, the moisture resulting from condensation is excluded from this area. Tests have proved the effectiveness of this treatment. Finish honing is performed after sealing and the operation benefits from the sealing procedure.

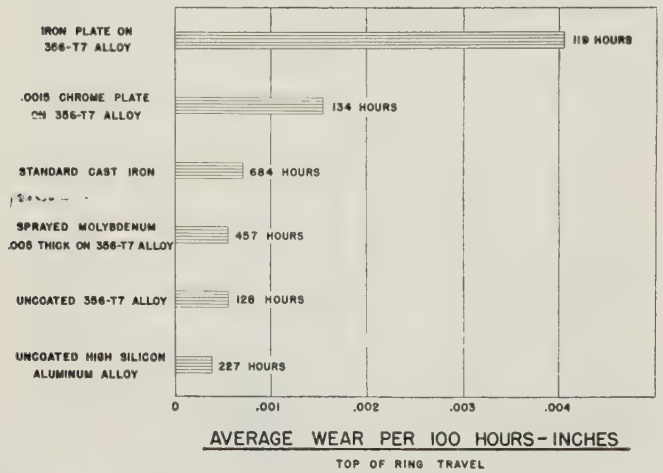

Fig. 18 — Cylinder liner and coating materials

The wear-resistant qualities of hypereutectic aluminum-silicon alloys have long been known. Only limited application was realized because of their relatively poor machining and foundry characteristics. Improvement in metal cutting tools and development of silicon constituent refining techniques have resulted in a renewed interest in this class of alloys.

Exploratory tests of a few promising alloys and coatings have been conducted in a wet-liner truck engine. The program is not yet finished but preliminary results are shown in Fig. 18. Average rate of wear in the ring pocket is shown, together with the number of hours of operation on the following cycle: 30 min at 3500 rpm, full throttle; 20 min at 1400 rpm, full throttle with ignition set to produce medium to heavy detonation, followed by 10 min at 500 rpm, no load. Water and oil sump temperatures were controlled at 180 and 200 F, respectively. Testing was carried on in four cylinders; the remaining two in standard cast iron for control.

Initial testing of 356-T7 alloy liners used uncoated, step-cut compression rings with bevelled edges. The last 50 hr were with chrome-plated torsional compression rings. The piston skirts were flash chrome plated in these liners only, all others were immersion coated with tin. Chrome-plated torsional compression rings were used in testing the high silicon-aluminum alloy liners; all other liners were operated with unplated torsional compression rings.

Although laboratory conditions can hardly be considered to be comparable to service, the exploratory nature of these tests warrants the conclusion that aluminum alloys are promising as a cylinder material. Uncoated alloy 356-T7 with 7% silicon is very comparable to the cast-iron liner material standard in this engine. A hypereutectic aluminum-silicon alloy containing a nominal 20% silicon developed an even lower rate of wear when run as an uncoated

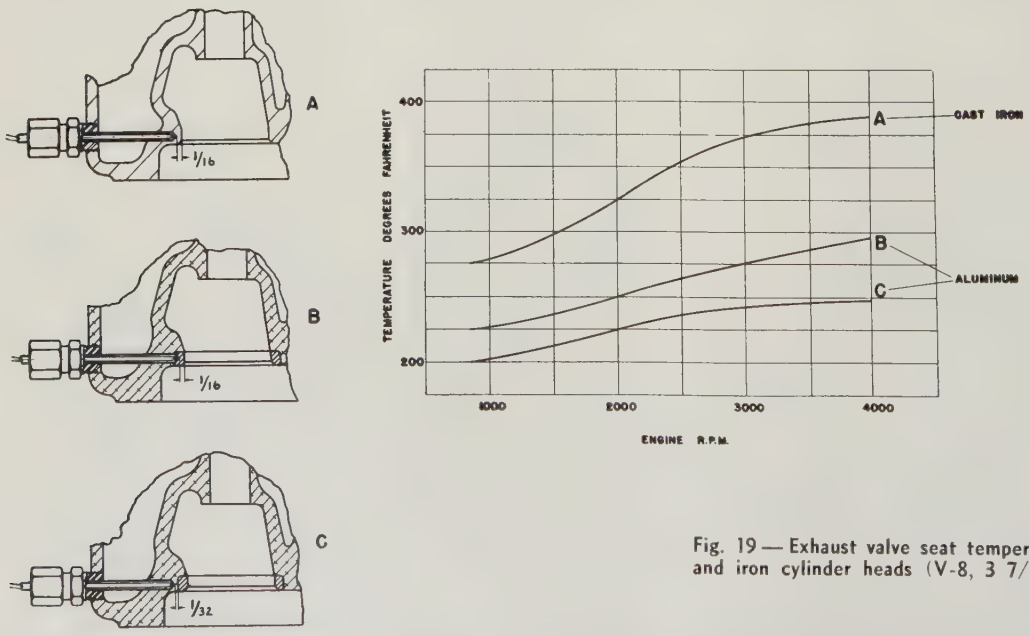

Fig. 19 — Exhaust valve seat temperatures at full throttle of aluminum and iron cylinder heads (V-8, 3 7/8 × 3 7/16 overhead valve engine)

liner surface. The wear rate of the sprayed molybdenum coating is shown to be approximately the same as that of the standard iron liner, and the electrolytic iron plate developed an extreme wear rate in the ratio of 5/1 compared with cast iron.

These engine tests will be continued to include other coatings and aluminum alloys, operation with low water temperatures to promote corrosive wear, and with ingested dust to simulate service conditions more nearly.

Liner temperatures were taken at the top of ring travel 1/16 in. under the inner surface. With the water and oil temperatures controlled at 180 and 200 F, respectively, and the engine developing full load at 3500 rpm, the aluminum-alloy liners operated 40 F cooler, on the average, than cast iron. It can be expected that piston-ring groove and crown temperatures will be lower when operating in aluminum-alloy liners.

Cylinder Heads

The high thermal conductivity of aluminum makes it a desirable material for cylinder heads and its application in this part is not a new one. Its disappearance from the American scene may have been for several reasons: cost, the almost universal adoption of the overhead valve engine, and corrosion. Let us consider these three factors briefly.

The valve-in-head arrangement transfers the complicated water jacket and port coring to the smaller of the two heaviest engine parts. It thus has rendered the crankcase relatively less complicated and the head more intricate than in the side valve design. In the latter, the semi-permanent-mold casting process found ready application, with a simple, easily operated, book-type mold and a one-piece (usually) sand core forming the water jacket. By contrast, water jacket and inlet and exhaust port passages of the overhead valve cylinder head require lacey, multi-piece and fragile coring. A high production specialized foundry should produce aluminum-alloy cylinder heads at an added cost over cast iron of little more than is represented by the metal value involved.

Aluminum alloys suitable for cylinder head production are virtually free from corrosive attack by most natural waters. Aluminum-alloy heads installed on iron crankcases are subject to galvanic attack caused by coupling of dissimilar metals producing an effective electrolytic cell. Although this problem does not appear in the all-aluminum engine, a brief review is in order.

The practical elimination of the problem of galvanic corrosion has been accomplished by many years of labortory and road testing. The answer to this phase of aluminum-alloy cylinder head application to iron crankcases lies in the satisfaction of three requirements:

1. The selection of the proper alloy and heat-treatment having a low solution potential when coupled with iron.
2. Introduction of metered flow of coolant by design of water port passages, preventing the scrubbing removal of the protective oxide and the continuous exposure of fresh metal to attack.
3. Inhibitors are not required to prevent corrosion of aluminum-alloy cooling system parts. When they are essential to reduce rusting and scaling of iron parts, the addition of 1% of napthenic-base soluble oil will accomplish the desired result without serious galvanic attack of the aluminum.

Another problem associated with aluminum-alloy cylinder heads, which many will recall, is known as "head sticking." Seepage of the coolant past the gasket caused galvanic corrosion product to form between the studs and stud holes, on occasion making head removal extremely difficult. This trouble can be eliminated by using bolts instead of studs and providing 1/16-in. diametral clearance of bolt in bolt hole. Head locating dowels should permit longitudinal freedom by using a slightly elongated dowel slot at one end, when aluminum-alloy heads are applied to iron crankcases. As a further precaution, we recommend coating the bolts with a high flash point, bright stock petroleum product on assembly.

Iron and steel valve seat inserts should be provided in aluminum-alloy cylinder heads to withstand the impact of the valve seating. To obtain the highest possible volumetric efficiency, the largest valves that can be accommodated in combustion chambers are now being installed. The result: an absolute minimum bridge between valves, in some cases precluding the installation of seat inserts. This has stimulated work by some investigators aimed at eliminating the inserts, thus seating the valves directly on aluminum. It is not yet possible to report on the progress made, but the use of slower cam seating ramps may be at least a partial solution. Head castings of the harder high silicon-type aluminum alloy may permit this simplification together with elimination of valve guides.

An interference shrink of steel or iron valve seats of 0.0035 to 0.0045 in. per in. of port diameter is recommended.

Hydraulic lash adjusting valve lifters permit use of aluminum in both crankcases and heads without requiring long cam ramps. The expansion in the distance from camshaft to rocker arm shaft, cold to hot, is thus automatically permitted.

The thermal conductivity of the aluminum alloy more than compensates for the thermal barrier introduced at the interface of the shrink fit. Cast-iron and aluminum-alloy heads were instrumented as shown in Fig. 19. Thermocouples were located as closely as feasible to the valve seating surface in both cases. Curves of temperatures over the speed range, engine operating at full throttle, show that the barrier to heat flow at the interface, while appreciable, is much more than offset by the high thermal conductivity of aluminum. At 4000 rpm the seat temperature in the aluminum head is 95 deg cooler than in the iron head.

The cooler valve seat benefits the valve temperatures, as Fig. 20 indicates. These curves show a remarkable reduction of 125 F in exhaust valve temperatures in an aluminum head compared to those experienced in an iron head of identical design without inserts. Substantial improvement in valve life is indicated. These data were obtained using shielded chromel-alumel thermocouples with beads copper-brazed in the valve heads as shown. The leads were silver soldered in a slot milled in the valve stem and brought out through the valve cover. The life of this instrumentation was remarkable and relatively trouble-free.

It must be emphasized that the curves of Figs. 19

and 20 were developed from two engine designs. A significant difference is that one employed directed water flow. This is a desirable feature and makes the most effective use of the high thermal conductivity of aluminum.

Temperatures of the hottest parts of a combustion chamber materially affect the volumetric efficiency of an engine. Investigations have indicated an increase in power when an aluminum cylinder head replaces one of cast iron. This improvement, at equal compression ratios, accompanied by a reduction in specific fuel comsumption, is credited, at least partly, to an improvement in cylinder filling.

Sizable reductions are obtained in octane number requirement, when aluminum heads are used. The curves of Fig. 21 show this improvement. The aluminum and iron heads again were identical and of equal compression ratio. The reduction in maximum requirement of three octane numbers is extremely interesting to the petroleum industry. A material cost reduction in refining processes is indicated, particularly in this octane range. The curves represent trace knock requirement at full throttle using primary reference fuels. It is important to note that this improvement is not at equal power ratings but includes the power gains observed with aluminum heads at equal compression ratios.

Aluminum-alloy and cast-iron cylinder heads each of 9/1 compression ratio are compared in Fig. 22 on the basis of surface ignition characteristics. It was expected that a lower temperature level would prevail throughout the casting. The more effective cooling of the hottest parts of the assembly could beneficially affect the tendency toward surface ignition. Further, it was conjectured that the combustion chamber in aluminum alloys might be self-scavenging. The high thermal expansion would cause deposits to flake off and be cleared through the exhaust port. The procedures used in building up combustion-chamber deposits and methods of evaluating the deposits failed to disclose these expected results.

The usual rating procedure was used and evaluation was by audible means. The engine was operated on a deposit buildup cycle as follows: 2 min idle at 600 rpm and 10 min at 2000 rpm road load. Water temperature was controlled at 180 F and oil sump temperature allowed to seek its own level but limited to a maximum of 200 F.

Starting with clean combustion chambers with valves reseated, the engine was rated at 5-hr intervals of cyclic operation. The ignition was set at top center manually and the engine operated at 1000 rpm, full throttle on primary reference fuel of octane number above the expected rating. Fuels of successively lower rating by 2½ octane numbers were admitted until surface ignition occurred establishing the rating for the period. Operation was resumed on the cycle for another 5-hr period, the entire procedure being repeated for a total of 50 hr.

The observed difference in surface ignition rating of 2½ octane numbers in favor of aluminum-alloy cylinder heads is assumed to be attributable to the lower temperatures of the hottest parts of the assembly. This seems reasonable since no significant difference was assigned to the character or amounts of deposits in the heads of the two materials.

Temperatures of the spark-plug bosses were determined using solid copper gaskets fitted with thermocouples. Fig. 23 shows average plug boss temperatures for aluminum and iron cylinder heads at full throttle and part throttle. The appropriate power curves accompanying the temperature data appear on this chart.

Not only is the level of the boss temperature from 70–165 F lower in the aluminum than in the iron heads for full load, but the variation of temperature for the speed range shown is 35 deg for the aluminum head and 125 deg for the iron head. The spread of boss temperature from part load to maxi-

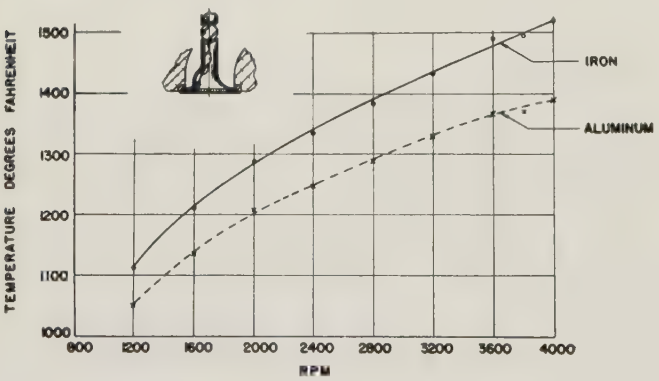

Fig. 20 — Average exhaust valve temperatures of aluminum and iron cylinder heads (6-cyl, 3½ × 4⅜ overhead valve engine), thermocouple measurements at full throttle

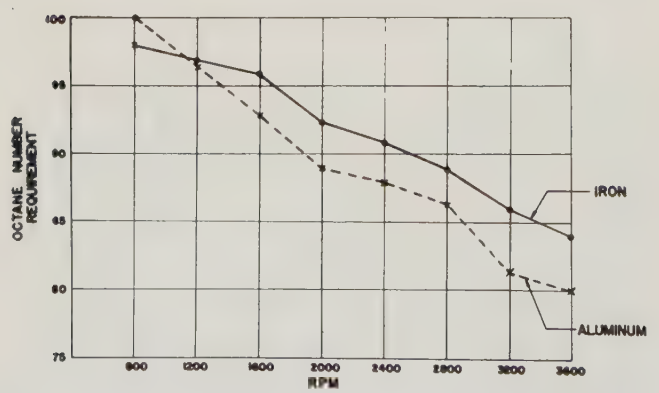

Fig. 21 — Octane requirement of aluminum and iron cylinder heads at full throttle (6-cyl, 3½ × 4⅜ overhead valve engine)

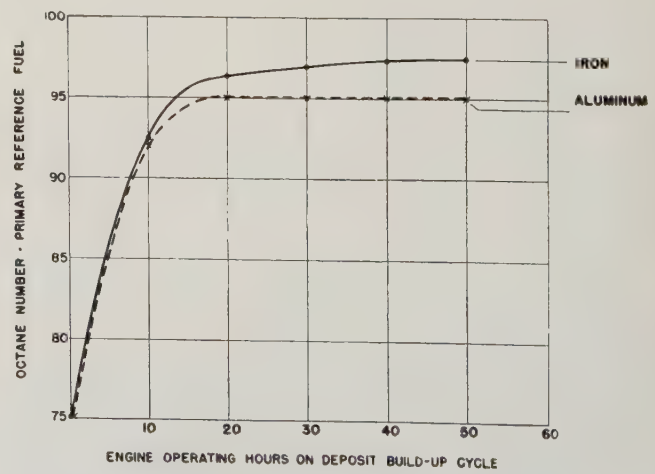

Fig. 22 — Surface ignition rating of aluminum and iron cylinder heads (V-8, 3 7/8 × 3 7/16 overhead valve engine, compression ratio 9/1)

mum horsepower of 60 deg for aluminum and 180 deg for iron is of perhaps greater significance. The more effective cooling of the spark plug not only reduces its temperature level but the range of temperature caused by load and speed variations.

Fig. 23 also indicates the power comparison of aluminum and iron heads of identical compression ratio. As reported elsewhere, the gain in power is attributed, in part at least, to improved volumetric efficiency caused by lower prevailing temperatures in the aluminum head assembly.

The high thermal conductivity of aluminum makes it an admirable choice for cylinder heads in still another respect. Temperature distribution throughout the casting is more uniform. Therefore, thermal strains are at a low level resulting in reduced valve seat distortion and better gas-sealing conditions. This factor undoubtedly contributes to the reduced exhaust valve temperatures referred to previously.

The traditional method of producing cylinder heads has been by sand casting. The more compact the designs, the more fragile and intricate the cores become. Broken and washed cores result in increased foundry scrap, or defective parts in service causing poor cooling. These difficulties would be greatly reduced were it possible to produce the cored cavities by metal cores and by so designing the cylinder head that these cores can be withdrawn from the casting. Consideration of this problem in some of its phases follows.

Inlet and exhaust port contours are conventionally designed for good fluid flow in the interest of high volumetric efficiency. This is accomplished by smooth area and shape transitions along the flow path.

Three possible port treatments are shown in Fig. 24. Solid lines indicate port contours for a conventional sand-cast iron head. Dash lines show contours from which metal cores may be withdrawn. It is obvious that the cores forming the passages draw toward the sides and the valve port cores draw generally downward with or through the combustion-chamber cores. The two core sections meet at the diagonal dash line, and this must, by the draw and draft requirements, be the minimum area. Referring to the inlet port section of View A, the restriction is most serious but is relieved somewhat by disposing the passage generally upward to the left as in View B.

In both Views A and B the passage cores draw on straight lines. Considerable improvement in layout and amount of restriction is obtained in such a design as C of Fig. 24. Here the passage cores roll out, rotating about a center. The centers of the arcs forming the top and bottom of the passage are displaced from the roll center so that adequate draft facilitates core removal.

In Fig. 25 a port design for straight-draw cores is shown together with a horizontal section along the port centerlines. Here, also, the conventional sand-cast design is shown in solid outline with the die-cast or permanent-mold design by dash lines. Interference with push rod and bolt holes is caused by the straight draws in Section A-A and represents a challenge to the engine designer. The discontinuity in area transition at the juncture of the passage and valve port cores is again clearly apparent. The necessary compromise which is the solution to the valve port problem for permanent-mold or die-cast production will no doubt be distasteful to designers also faced with the task of extracting the ultimate in power per cubic inch of displacement. Offsetting the limitations of the process to some extent is the

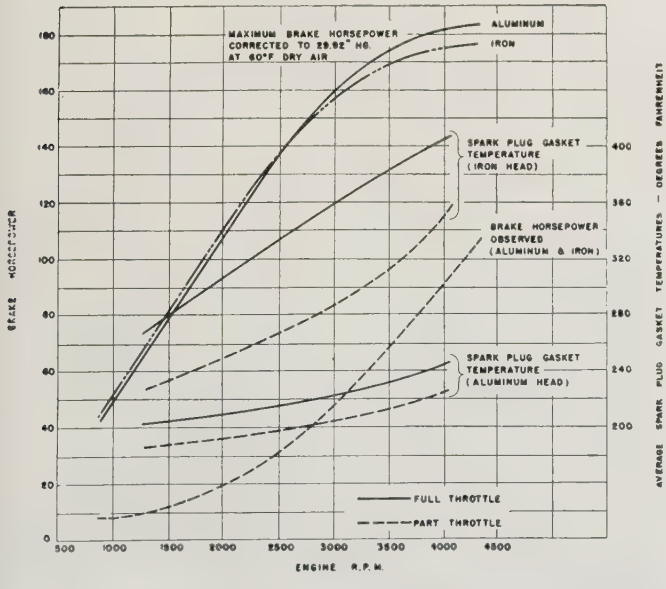

Fig. 23 — Spark-plug gasket temperatures of aluminum and iron cylinder heads (V-8, 3 7/8 × 3 7/16 overhead valve engine)

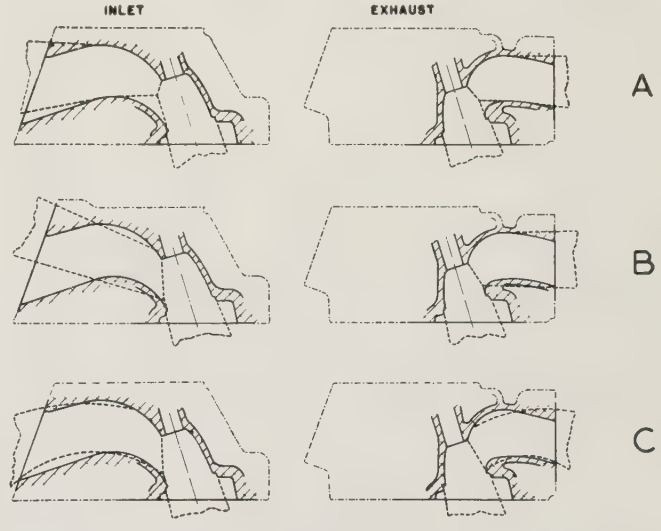

Fig. 24 — Port treatment

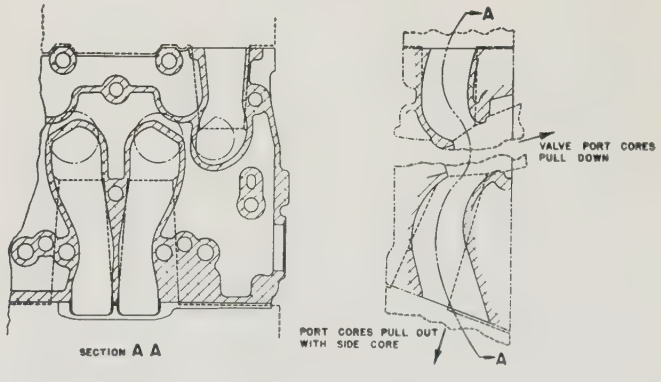

Fig. 25 — Valve port details

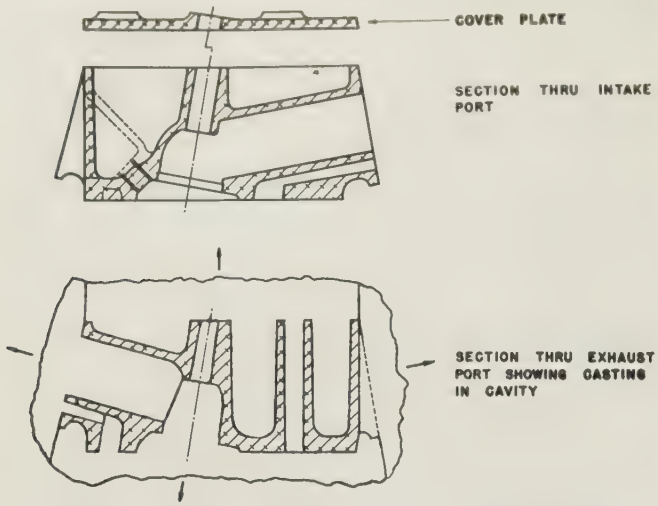

Fig. 26 — Aluminum cylinder head, die cast or permanent mold

smooth passage surface attainable.

Proceeding now to the water jacket and outside walls of the head, Fig. 26 shows a die-cast or permanent-mold casting. The lower view is a section through an exhaust port of a casting in the mold or die cavity. Directions of the draws are shown by arrows. The usual considerations of draft and undercuts apply.

The upper view is a section through an intake port with a spark-plug pocket shown dotted. A cover plate to close the water jacket cavity and support the valve rocker arm mechanism is retained by the head hold down bolts. Leakage is prevented by a gasket or resin-bonded seal.

The water jacket is completed around the port passages by a core piece extending into the cavity from the mold or die side pieces. These fingers draw with, or through, the side pieces, together with the port passage cores. The exterior openings will be closed by the manifold gasket and flanges.

To complete the discussion on cylinder heads, and repeating the statement made elsewhere in this paper, hardened and ground steel washers should be used under bolt heads and nuts. A valve spring retaining washer should be used between the spring and cylinder head.

Intake Manifold

This part as presently designed for V-8 engines cannot be made by permanent-mold or die-casting practices. Passages are usually so involved that iron or steel cores cannot be withdrawn. Opening the passages, by designing multiple pieces to be resin-bonded into a completed assembly, renders the part possible of casting by these processes.

Exhaust heated manifolds represent a problem in high temperatures. Finning the exhaust passage, so disposing this portion that it may receive airflow from the cooling fan, may be a solution. Yield of this hot passage under thermal and installation stresses presents a serious leakage problem. A stuck heat valve controlling manifold temperature can be disastrous unless effective cooling can be accomplished. Intake manifolds for fuel injection engines do not present this high temperature problem and may be simpler in configuration and be assembled from permanent mold or die cast pieces.

Jacket water heated intake manifolds are receiving attention. This design relieves the high-temperature problem but adds passages to an already involved part. The cored water passage under the intake port in Fig. 26 could admit hot water to heat the manifold which then could function as a water-collecting manifold as well. Mixture temperature control might be difficult, however.

Furnace Brazing

Reference has been made to the furnace-brazing assembly of aluminum castings to produce major components of an experimental engine. This method is admirably suited to production of experimental engine crankcases, cylinder heads, and intake manifolds. However, the designs must be capable of being easily broken down into sections that can be readily cast in green sand molds. Cost of pattern equipment is relatively reduced over conventional sand-casting requirements and design changes are readily made as the engine development requires. The production of certain parts requiring smooth passages and having complicated involved coring can be economically accomplished by furnace-brazed assembly of component slices.

Pistons

The adoption of aluminum engines should not significantly influence piston designs. Under operating temperatures a reduction of differential expansion can be expected between cylinder and piston, with an aluminum cylinder, as compared to an iron cylinder. This may not be true under transient or warmup conditions. The clearance requirement, or the range of clearance, starting cold to operating temperatures may be different in aluminum engines than those to which we are accustomed in iron engines.

The thermal control characteristics which may be required by the aluminum engine can be furnished by features well-known to those skilled in piston art. To explore this fully would require a paper in itself.

Aluminum Bearings

Common aluminum alloys have been used for some years as bearings in light-duty, low-speed applications. Special aluminum bearing alloys were developed to satisfy the requirements of high-duty bearing service and several years of successful commercial experience is now a matter of history. Aluminum-tin bearing alloys in sand, permanent-mold and die-cast, and wrought forms are now available possessing excellent bearing characteristics. Many production engines now employ all-aluminum bearings or aluminum-alloy steel-backed bearings.

Differential expansion between the aluminum crankcase and steel crankshaft presents the problem of maintaining bearing clearance at low temperatures without exceeding standard clearances at operating temperatures. The problem is solved using the steel-backed bearing by the provision of a heavier backing and an increase in parting line height. The solution is a high prestress to resist the contraction of the aluminum housing with reduction of temperature.

For steel-backed aluminum bearings in aluminum

housings, an increase in backing thickness from usual practice by two gage numbers is suggested. A parting line height should be selected which will maintain a normal crush stress at operating temteratures. It will be found that such practice will resist the decrease of bearing clearance due to differential expansion at normal low starting temperatures, and engine starting torque requirements will not be materially increased.

Camshafts or accessory drive shafts may be run directly in the aluminum crankcase without the use of bushings as required in cast iron.

Miscellaneous Parts

Many engine or related parts are being made in aluminum abroad or in the United States in which problems of design and manufacture have already been solved. Production of these items requires only selection of the production process, design for that process and selection of the proper aluminum alloy. In this category can be included:

Front cover	Valve cover
Water pump body and cover	"V" belt pulley
Water outlet housing	Distributor housing
Oil pump body	Fuel pump parts
Oil filter adapter	Carburetor parts
Rocker arm	

Structural members, now produced in aluminum, such as flywheel and torque convertor housings, transmission cases and transmission extensions present problems, the solution for which involves design for adequate rigidity, attention to the elimination of discontinuities and stress concentrations. Such parts should be subjected to rigorous tests in the laboratory for stress distribution and deflection, as well as on the proving ground.

Conclusion

We have presented the reasons for the use of this versatile metal in lightweight engine construction and have developed means for realizing its advantages. Solutions of all the problems likely to be encountered in even a single aluminum engine design could hardly be presented in a paper of such general scope as this one. Some problems have been stated and methods of solution indicated for the V-type engine, with particular reference to modern production aluminum-casting processes. The same principles can be applied to other engine configurations such as the opposed cylinder and in-line arrangements. Modifications may be required to suit the particular problems presented by the aircooled engine.

The supply of aluminum warrants the present interest in automotive circles in lightweight engines. The appearance of aluminum engines on the American scene is imminent.

DISCUSSION

Corrosion Resistance Remains Big Problem in Aluminum Engines

— F. A. Gundlach
National Carbon Co.

THE AUTHORS pointed out advantages of recently available cast-aluminum alloys and fabricating methods in building new high output engines. In their paper the question of cooling system corrosion is briefly discussed and the so-called "soluble oils" recommended as corrosion inhibitors. Our experience with insoluble polar film inhibitors to date would suggest that these recommendations are the right direction but we are convinced that there is still a serious corrosion problem to be solved before these new alloys and engine fabrication techniques can be completely satisfactory.

We must not overlook the interference tendencies of inorganic water soluble chemicals such as chlorides, which can be particularly corrosive toward aluminum . . . these can be introduced by the tap water. Other sources of corrosive materials are exhaust gas leakage and chemical cooling system treatments which, although they may have been satisfactory for current design engines, could contain ingredients that tend to attack the new aluminum alloys.

We still have serious reservations regarding complete aluminum corrosion inhibition in multimetal cooling systems — particularly where design considerations contribute to so-called "crevice attack," a phenomenon which we fear is difficult of practical control by currently known corrosion inhibitor techniques.

Although automotive cooling system aluminum parts may not always fail due to corrosion penetration, we must draw attention to the potential clogging problems from the voluminous nature of aluminum corrosion products, at usual pH levels in the neutral range, when circulating through the narrow water passages of radiators, car heaters, and the like. There are also cavitation erosion problems which can develop from high-frequency vibration of nonrigid cylinder liners. Even when these liners may be made corrosive resistant, they have been known to transmit their vibration-erosion problems to an adjacent aluminum water jacket.

We trust that the aluminum fabricators will also consider optimum corrosion resistance when selecting alloys for other design properties and the engine designers will endeavor to minimize the known galvanic corrosion problems inherent in multimetal engine cooling system design when planning assemblies.

Vibration of Crankcase Causes Serious Corrosion of Aluminum Engines

— J. E. Witzky
White Motor Co.

MESSRS. SMITHS' introduction that the application of aluminum in major components of the automotive engine is rapidly increasing in recent years is certainly true. Aluminum as a construction member for automotive engines has certainly a great future. However, it may be appropriate to point out some limitation or, let's say, some difficulty encountered in an all-aluminum diesel engine — difficulty which still requires a solution.

In both papers very little was mentioned about corrosion, and the word "cavitation" was not even mentioned. A discouraging experience occurred on an aluminum crankcase of a wet-sleeve 300-hp 6-cyl engine and on a 600-hp V-12 diesel engine. After relatively long service in marine installation, peculiar pittings occurred in the water side of the aluminum crankcase. The attack was most severe approximately 1-in. below the shoulder support of the

liner and around the lower "O" ring seals. Numerous investigations were conducted to find the solution for this very serious condition. The first question which arose was — Is it corrosion or cavitation? Sample pieces exposed to a chemical or electrolytical attack created smooth well-rounded pittings. Sample pieces tested in a magnetostriction cavitation test machine produced sharp ravine-like pittings. Section pieces through a corroded crankcase showing a combination of both indicated that corrosion as well as cavitation must be the cause of the destruction. Corrosion is considered a chemical action; cavitation a mechanical action of a vibrating wall in connection with water. The corrosion encountered in the sealing area of the lower "O" rings is considered a crevice corrosion produced by squirting water in and out of the small clearance volume between the vibrating liner and the crankcase. The vibrating condition in a diesel engine, due to the higher peak pressure and the high rate of pressure rise, certainly aggravates the situation; however, I can imagine that, by considering the further tendency in the gasoline engine field to increase the compression ratio, similar phenomena will occur.

As a resume of this discussion I, as a diesel engineer, would recommend to my friends in the gasoline engine field that the wall vibration of the aluminum crankcase be reduced to a minimum by designing stiff and rigid cases. As I mentioned in the beginning, these phenomena occur after a long time in service. In some cases, the first attack was recognized after 2000 hr of operation which would indicate that the second-hand car buyer would be in trouble. I feel that this fellow should be protected as well as the original buyer.

Chrysler Laboratory Wear Tests Agree With Authors' Results

— R. D. Chapman
Chrysler Corp.

AT CHRYSLER, we in the Metallurgical Research Department become intrigued with the use of aluminum for powerplants, and especially with coatings and the hypereutectic silicon alloy for possible cylinder liner use. For several years we have been investigating the phenomenon of wear. A reciprocating wear test machine was constructed and is shown schematically in Fig. A. In essence, this machine consists of a slider with a wearing surface of approximately ¾ in. × 8 in. The slider is attached to an eccentric which imparts a reciprocating action to the slider. A rider, which is loaded by an air cylinder, is held against the slider. This machine was designed primarily for measuring wear resistance; but we found that we were able, under full lubricating conditions, to reproduce scoring. Preliminary tests have indicated that an SAE 51100 rubbing against an SAE 51100 has a scoring load that appears to fit an equation $L \times F^{0.58}$, where L is the load in psi and F is the surface finish in microin.

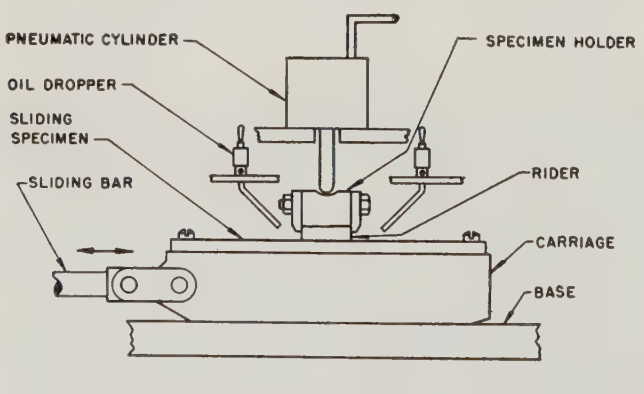

Fig. A — Reciprocating wear machine

It is interesting to note in the cylinder wear figure presented by the authors that several materials were tested which we also had tested for scoring resistance.

Rating of the materials that we have tested, we likewise show that a 20% aluminum-silicon alloy showed the greatest score resistance; next came molybdenum coated, followed by cast iron. We were very pleased to see the direct correlation between laboratory tests and the actual engine tests.

If our design engineers were to have any comments in regard to these papers, I am sure they would like to encourage the die-casting industry to continue the development of their process in order that good sound castings could be produced along with their high mechanical properties.

Die Casting Most Economical for Mass Production of Aluminum Parts

— A. F. Bauer
National Lead Co.

THIS paper gives many design details and suggestions for solutions to problems which we face in the changeover of a gray iron engine into an all-aluminum engine.

We find that here, as well as across the ocean, the lighter weight and the high thermal conductivity of aluminum, combined with its adaptability to modern casting methods and its ease of machining, are recognized as its most important advantages while its higher coefficient of expansion and its low wear resistance are considered as its main disadvantages, especially with regard to the cylinder sleeve arrangement.

The authors state that the automotive engineer has at his disposal several aluminum foundry processes such as sand casting, permanent mold, semi-permanent mold, and die casting, and that the nature of the engine castings warrants consideration of all these casting methods. This statement seems to me an easy way out of the design problems which the introduction of aluminum for large engine parts will of necessity entail.

In my opinion, aluminum sand casting cannot replace gray iron castings because it does not offer any foundry advantages which would compensate for the higher initial metal costs of aluminum. Semi-permanent mold is also relatively costly because of the high manufacturing costs for disposable cores. *The successful introduction of aluminum for engine castings depends on the development of a design which lends itself to mass production in either the die-casting or permanent-mold process by eliminating all undercuts and backdrafts.* The earlier the automotive engineer realizes that the undercuts of the present gray iron castings must be eliminated, the sooner will we have aluminum engines on a large production scale.

Considering the two high production casting methods for aluminum, the authors state: "Where thin sections are indicated, die casting is preferred; when thicker sections are required for strength and rigidity, the permanent-mold process is the proper choice."

The old story that die castings are only suitable for thin-walled parts, that they are more porous and, therefore, not so strong as permanent-mold castings, is a thing of the past. Higher injection pressures and other improvements have increased the properties of die castings so much that today properly designed die castings compete quite well in strength with permanent mold and are generally considered stronger, in spite of the fact that their center sections may have some finely dispersed porosity. The fatigue strength of aluminum die castings is appreciably higher than that of the best permanent mold castings. This superior fatigue strength of aluminum die castings was confirmed in papers given by Messrs. R. L. Templin and C. O. Smith in 1954. One of these papers stated that a die casting can be reduced in its walls and total weight

by about 20% and still be as strong as a permanent mold casting of the same design.

The die-casting industry has taken full advantage of these superior properties of aluminum die castings and has successfully converted such highly stressed parts as torque converter housings and transmission cases. Since die casting is also the more modern process which produces more castings per hour at a greater accuracy with less machine stock and at a lower weight, it has a distinct price advantage over permanent-mold parts and has proved this with the many aluminum die castings which are now used on cars. Their only limitation in the past was the size of the existing die-casting machines. Since large die casting machines were not available in the past and since the older casting methods, sand casting and permanent mold, could not compete with gray iron castings, the large castings of the present-day engine remained in gray iron. The erection in 1954 of large die-casting machines capable of producing castings up to 75 lb of aluminum and the development of a 45-lb 6 cyl in-line engine block in aluminum die casting have aroused new interest in an all-aluminum engine and have given these large aluminum applications new impetus. Since the creation of the 6-cyl engine block in die casting, a number of water-cooled V-8 engines with blocks and heads in aluminum die casting have been designed and some of them tested on sand-cast prototypes.

While the V-8 engine block resulted in a design which is somewhat easier to die cast than the 6-cyl in-line engine block, it was soon recognized that the real problem of introduction was in the cost of machining the wet sleeves and in the difficulties of their assembly.

Most of the suggestions and proposals shown in the paper and several more were carefully investigated and some of them tested, but none found approval as an economical solution for high production. While most of the wet-sleeve designs are technically acceptable, we were told that their costs just simply are too high.

Based on the reluctance of the automotive industry to accept any of the different designs of wet or dry sleeves, a new approach is being investigated at the present time. The new approach calls for a single sleeve or a battery of sleeves connected with a deck plate made in aluminum die casting and produced with such a high accuracy that they can be resin-bonded or soldered into the engine block without any prior machining. With this new method the engine block assembly could be machined on transfer machines in a similar fashion as the present gray iron engine block.

Die-cast cylinder sleeves without any taper in the bore and with unusual accuracy and soundness have already been produced on a small test run basis and have shown remarkable results. The alloys chosen for these tests are the conventional die-casting alloys SC-84, SC-114, and the hypereutectic aluminum-silicon alloy with 22% silicon and 2% nickel. Research work will continue to produce these sleeves with a thin coat of a wear-resistant material, a method which is expected to be appreciably cheaper than chrome plating or molybdenum spraying of the bores. *This new method of die casting a cylinder sleeve with a wear-resistant coat or insert may open the door for a more economical design of light-metal engine blocks; for water-cooled as well as aircooled engines.*

While this new method for the production of low-cost wet sleeves may bring the die-cast V-8 engine block closer to a solution, the two other major castings — the cylinder head and the intake manifold — still present serious conversion problems because of their many internal channels and pockets now made with disposable cores. The most acceptable solution and the most economical approach for die casting of these parts, in my opinion, is to split the intake manifold and the cylinder head into several sandwich-type sections, which may be welded or resin-bonded into the assembled piece. It must be admitted that the joining of these sections has its problems which are not completely solved yet. On the other hand, such a split design would create smooth passages and eliminate sand pockets and uncontrollable core shifts. Through high accuracy obtainable in die casting, this sandwich-type design may well be the most economical solution for these parts in the future.

To sum up: Just as the most modern machining methods are used when large quantities justify the expenses for tooling, so should the most modern casting method — the die-casting process — be used when large quantities of aluminum castings have to be produced. Aluminum sand castings are only competitive for extremely short production runs. For medium production the permanent-mold process with it relatively low tooling costs often is best suited. Where, however, the higher tooling cost for die-casting dies can be amortized over a large number of parts, the die-casting process is the most economical casting method. This holds true even for those parts which like the cylinder head and intake manifold have to be completely redesigned for die casting.

In these days when the U. S. automotive industry has its eye on the European small cars, many a U. S. visitor returns from his European trip astonished and full of praise of the large tonnage and outstanding quality of permanent-mold castings which are used in the European cars. They recommend that we, too, set up large permanent-mold facilities here, but they do not realize that what they have seen is already obsolete and on its way out.

The European automotive industry is well under way to introduce light-metal engines with engine blocks and other large parts made in aluminum die casting and even in magnesium die casting (for aircooled engines only). The passenger-car production in England, France, Italy, and Germany has increased so much that die castings are considered more economical than permanent-mold castings for large engine parts. The major conversion from permanent mold to die casting took place in the Volkeswagen plant a few years ago and resulted in appreciable savings. Most of the major European automotive companies have completed the design stage for die-cast engine blocks and heads. Since Europe has little experience in the manufacture of these large parts, and since the necessary large die-casting machines are not available in Europe, they try to get some kind of an arrangement to have the die-casting dies and the die-casting equipment of these large engine parts built and tested here.

Negotiations along these lines are under way. If the U. S. automotive industry continues its conservative attitude, it may well be that the first light-metal engines with all major parts in die casting will be produced in Europe on large die-casting machines which have been developed in this country.

Use of Aluminum Cuts Costs

— A. D. Reynolds
Reynolds Aluminum Sales

AS THE AUTHORS so aptly point out, aluminum engines and engine components are being used extensively abroad. An approximate idea of just how extensively is revealed in the number of foreign automotive companies presently using aluminum engine components: Crankcase and cylinder blocks, 12; cylinder heads, 19; intake manifolds, 30; oil pans, 22; timing gear covers, 26; valve covers, 23; water pump bodies, 18; connecting rods, 5; and steering box housings, 7.

From these figures we can see that aluminum engines are certainly acceptable for production.

The European manufacturers' greater use of aluminum in relation to the total weight of the automobile has been motivated by the desire for operating economy.

Aluminum's economy has also been the motivating factor behind American automobile manufacturers' accelerating consumption — a 400% increase in just the past few years. Increasingly, engineers, designers, and purchasing agents have come to realize that they can lower the cost

of many parts by switching to aluminum. Cost saving results when aluminum's initial price penalty is overcome by directly related cutbacks in production tooling, machining, assembling, handling, shipping, and other costly operations.

In many recent instances aluminum has been adopted after someone took a fresh look at costs. What this look reveals is that the raw-material price gap may actually be much smaller than is often assumed, and that hasty cost comparisons are apt to be misleading.

Further economies have resulted from a growing awareness that casting tolerances for aluminum need not be as wide as for iron. By breaking with tradition and writing more exacting foundry specifications, some master mechanics have lopped as much as 10% from the material and conversion costs chargeable to each unit.

In additional cases aluminum was able to demonstrate a price advantage when its more favorable scrap-reclamation yield was credited to the part instead of to the shop.

In considering a part for aluminum, basic material costs do not determine final part cost. Techniques and processes applicable to aluminum often can give a better product at a lower final cost.

Generally, aluminum is at a disadvantage against ferrous materials only on the basis of the metal content of the part involved. All foundry and subsequent processing operations favor aluminum and, frequently, these advantages are so great that the final parts cost less in aluminum.

In the case of aluminum engines with their tremendous weight reduction, the ultimate savings to the automobile manufacturer will probably not be realized until the automobile is redesigned to take advantage of this weight reduction. The result will be greater operating economy to the public and greater manufacturing economy to the automobile producer.

General Motors Tests New Aluminum Engines

— D. F. Caris and R. F. Thomson
General Motors Corp

THE automotive powerplant of the future has been the concern of General Motors Research and Engineering Staffs for many years. Much of the thinking has previously been presented before SAE as, for example, the Whirl Fire gas turbine engines in the Firebird cars, the Turbocruiser bus, and the Turbo-Titan truck. Another possibility was the Hyprex free-piston engine used in the XP 500. There have been various reasons for exploring these powerplants, always with the objective of supplying, in the future, that type of motive power which gave the American car buyer the type performance and operating characteristic he desires.

There have been other developments such as the high-compression otto-cycle engine which has resulted in either more economy or more performance at minimum loss in economy.

For the past several years we have been interested in long-term trends in material utilization, especially as long-term buying habits of the American motoring public can be forecast. At the same time we have paid attention to strategic material consideration, material availability, and material cost.

One of the metals which has received considerable attention has been aluminum because of its low specific gravity, with its lighter car weight possibilities. Outside of the body and frame, the largest single component part is the cylinder block. Present cast-iron blocks and heads weigh between 200 and 300 lb. The possibility of removing significant weight from the powerplant has properly focussed attention on the cylinder block.

Our work to date has shown that the weight of the block and head, when made in aluminum, is less than half the weight of cast-iron components resulting in an overall

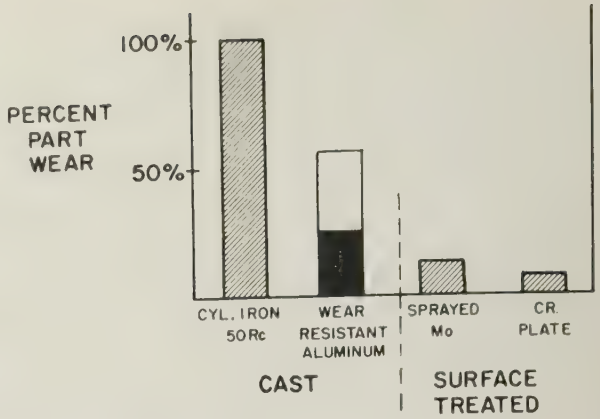

Fig. B — Relative wear resistance of wear-resistant aluminum compared with other wear materials

powerplant weight reduction of 30%.

One might properly ask why this is really significant and Mr. Caris' answer is, "This results in a cumulative process because as the engine becomes lighter, the supporting structure can be lightened decreasing overall car weight and as this happens smaller engines may be used to give the same performance. One conceives this leads to more economical and lighter weight vehicles."

Aluminum engines are not new but generally they have been made with either a ferrous liner or a coating, such as chromium plate, for the bore material. Both of these procedures are expensive and impose processing difficulties. The probable future use of aluminum in cylinder blocks is largely dependent on minimizing these two problems.

While the GM Automotive Engines section was exploring the engineering problems and performance characteristics of aluminum engines, the Metallurgical Engineering Department was directing efforts to solving the problem of finding an improved bore material.

It has been obvious that the simplest solution would be to develop a wear-resistant aluminum alloy which could be cast in a manner similar to that used in current cast-iron production. This material must have the same, or improved, wear and frictional characteristics as cast iron, while maintaining comparable castability, machinability, corrosion restistance, strength, and the same or lower processing costs. (The latter may involve other foundry processing methods than currently used for grey iron.) We have come a long way toward this goal and research is continuing to find even more suitable materials. The principle of wear-resistant aluminum-alloy combinations leads to application to other components than blocks and heads with further weight reduction. This is a very brief report on some of the progress we have made. Some of the progress has been possible through new adaptations of old material, of more recent materials, and some new ones which we have developed.

Many materials have been investigated in the laboratory and have showed varying degrees of promise. These have included coated as well as uncoated materials.

Among the more promising coatings investigated were: chromium plate, iron plate, electroless nickel plate, oxide-type coatings, sprayed steel, sprayed molybdenum, and sprayed aluminum and its alloys. Some of these coatings were investigated in both the as-plated and "surface conditioned" state.

A number of aluminum alloys without coatings have been investigated, including high-silicon alloys similar to those tested by the authors as well as some new ones developed by General Motors Research.

These alloys are first investigated at GMR on a number of bench tests, which evaluate in a relative manner the frictional characteristics and the wear resistance of various materials.

Fig. B shows some comparative wear data on various

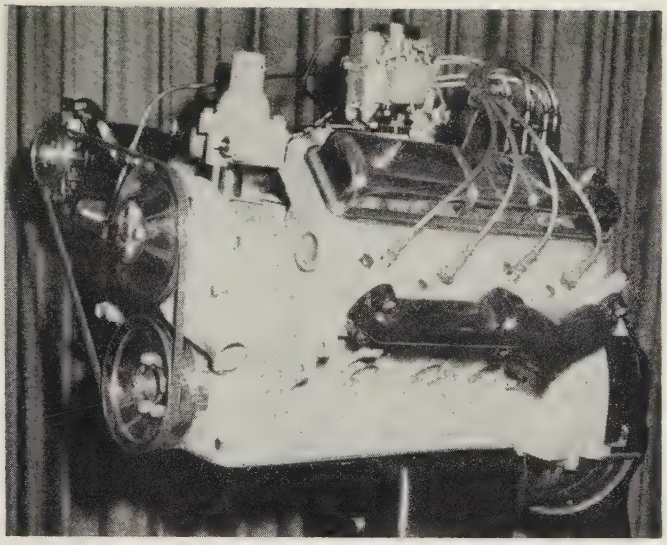

Fig. C — Experimental 253-cu-in. engine utilizing aluminum-base alloys

cylinder bore materials run on the constant friction wear test machine. It will be noted that all of the materials shown have better wear resistance than wear-resistant cast iron and approach chromium plate.

Following bench test evaluation, a new experimental 253-cu in. engine (Fig. C) was used to investigate the performance of various materials and coatings on the dynamometer durability test which consists of 100 hr at maximum power and 140 hr at maximum torque. A number of materials have satisfactorily passed this test including plated coatings, sprayed coatings, and the wear-resistant aluminum alloys.

The sprayed coatings have generally run successfully. Fig. D(a) shows a molybdenum-sprayed bore which satisfactorily passed this endurance testing. The wear-resistant aluminum alloys have been similarly successful with regard to wear resistance in these tests.

Fig. D(b) shows the condition which may result predominantly at the top of the ring travel. Within 80 hr, as much as 0.003–0.006 in. radial thickness may be worn off. This amount of wear has even been experienced on cast-iron bores, chromium plated, which removed the possibility that this may have been due to lack of support by the lower modulus aluminum alloy.

In addition to dynamometer tests, we have installed experimental engines with several combinations of the above materials in cars. Fig. E shows the 253-cu in. experimental engine being installed in a 1952 Chevrolet car. To date we have accumulated more than 120,000 miles on this and similar cars in road testing.

One should not conclude that all of the problems have been satisfactorily solved because it takes many years, millions of passenger-car miles, and large production experience to point up all problems and find satisfactory solutions to them. Some of these are technical, others economic and still others customer reactions to the end product.

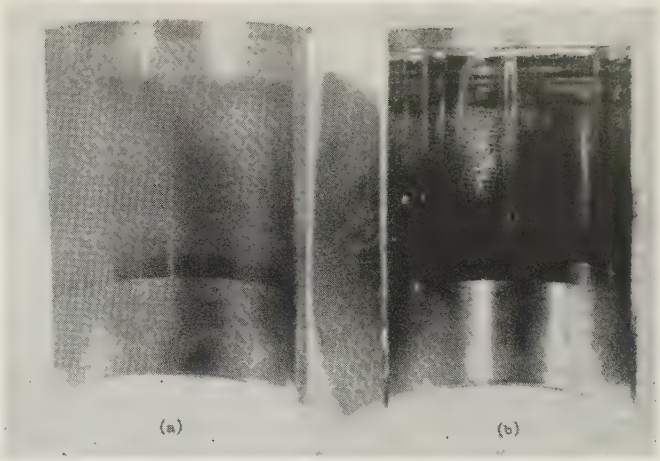

Fig. D — Samples of aluminum bores after dynamometer test, (a) molybdenum-sprayed and (b) chromium-plated

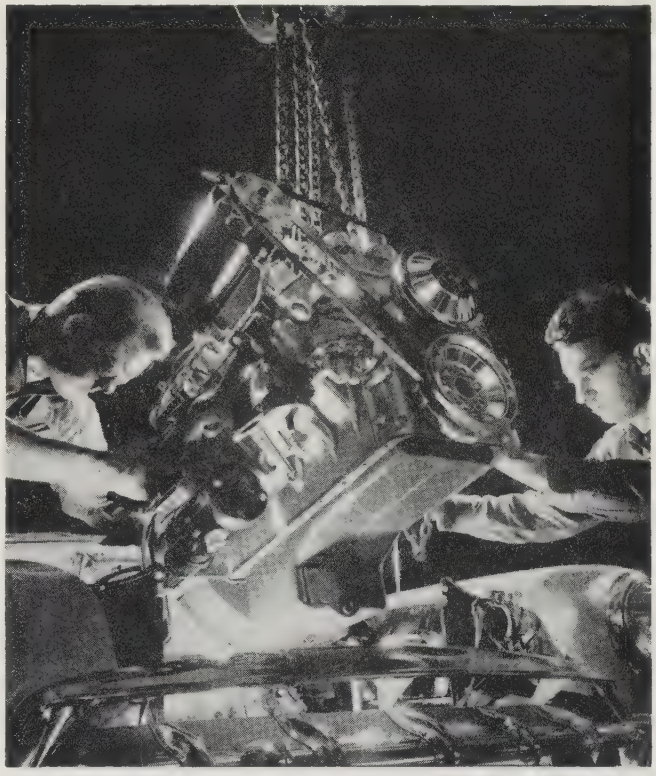

Fig. E — Experimental 253-cu-in. engine being installed in 1952 Chevrolet car

Inhibitors Necessary for Operation of Aluminum Engines

— J. C. Crawford
Commercial Solvents Corp.

IN THE section entitled Cylinder Heads, the authors deal with important service and maintenance factors which influence consumer acceptance of aluminum engines.

While water as a coolant may be satisfactory in an all-aluminum cooling system, current designs and those in a transition period do not offer this environment. A wide variation in water quality is experienced throughout the United States alone. Motor vehicles operated with ambient temperatures below the freezing point of water continue to require an antifreeze.

The water, the antifreeze, and the service life contaminants in the engine require a proper balance of inhibitors for satisfactory operation. Field experience with aluminum components in cars of foreign or domestic manufacture, and the literature on corrosion itself suggest greater demands on inhibitor performance rather than the authors' finding that "inhibitors are not required. . . ."

There is insufficient evidence that a soluble oil would do more than contribute the disadvantages of this type material to the heat transfer medium in the case of an aluminum engine.

As present practice is to ship automobiles from the factory with a sealer compound installed and (in winter) an antifreeze as well, some realistic test and development work in which auto makers, aluminum suppliers, and the chemical industry participate is in order.

Fig. 1 — Research vehicle arranged for rubber-tired skid steering, 48-in. wheelbase

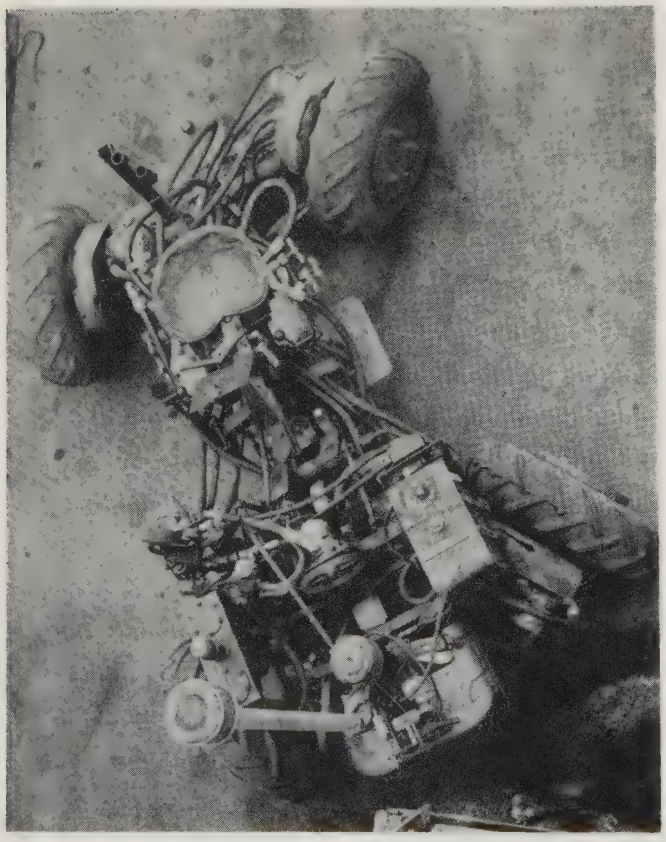

Fig. 2 — Research vehicle arranged for 4-wheel steering (Ackerman type), 74-in. wheelbase

Steering and

of Rubber-

ALTHOUGH we are in the age of jets and rockets, off-the-road vehicles will continue to be the work horses for industry and the military. Further development is needed to design better vehicles for pulling various types of loads; and plows, agricultural implements, and scrapers for road building. We also need better vehicles for transporting men and material with greater mobility on cross-country terrain.

The first off-the-road vehicles utilized solid wheels. In the tractor field, grousers or lugs were added to improve traction. Shortly before World War I, the crawler tractor was developed in California for farm use. About this same time, the military started applying the crawler principle to armored carriers or tanks.

In 1932, the first pneumatic tires were used on farm tractors. The use of rubber tires in agriculture has increased to the point where approximately 96% of tractors on farms today are rubber-tired. The use of the rubber tire in the earthmoving equipment field has also been increasing at a rapid rate.

Rubber tires generally are considered to have the advantage of permitting higher speeds, greater mobility, less maintenance, and lower first cost. Crawler vehicles, on the other hand, generally excel in their traction characteristics under a wide range of soil conditions, in their greater flotation or lower ground pressure, and in their utilization of the entire weight of the vehicle for tractive effort. But have wheels or rubber tires been applied in a way to obtain the optimum in off-the-road performance?

Objectives of Study

The broad objective of our research effort was to answer this question by comparing the traction and steering characteristics of 4-wheel drive vehicles of various steering and drive systems with conventional 2-wheel drive and crawler vehicles. Although much data has been developed on the characteristics of particular vehicles, it is difficult to compare quantitatively the performance of the various systems because of the many variables that cannot be readily controlled.

The specific objectives of the program were to

Traction Characteristics

Tired and Crawler Vehicles

W. J. Adams, Jr., Food Machinery and Chemical Corp.

This paper was presented at the SAE National Farm, Construction, and Industrial Machinery Meeting, Milwaukee, Sept. 11, 1958

determine and evaluate quantitatively the influence of the following on performance:

1. Traction Systems — (a) tires, (b) tracks.
2. Steering Systems — (a) geometric wheel steering, (b) skid steering, both wheel and crawler.
3. Drive Systems — (a) 2-wheel and 4-wheel, with differential or locked axle, for geometrically steered vehicles, (b) variable ratio, clutch-brake, and differential-brake for the skid steer vehicles.
4. Suspension Systems — (a) oscillating wheels, transversely, (b) rigid wheels, transversely.

To obtain some indication of the flexibility or adaptability of the various vehicle systems, the evaluations were conducted under the following three ground conditions at speeds ranging from approximately 1–20 mph: Macadam (asphalt) pavement, loose ground (disced dry adobe), and mud (sprinkler irrigated adobe).

No attempt was made in this program to evaluate the economics of the various vehicle configurations.

Research Vehicle

Initially, consideration was given to the thought of purchasing a number of vehicles and modifying them in some manner to obtain the 17 different combinations of drive, steering, and traction means that were felt to be the most representative of the present or anticipated art. Obviously, such an approach would have introduced many variables and additional parameters, such as differences in total weight, weight distribution, tire sizes, tire inflation pressures, tread width, wheelbase, and the like.

In the interest of reducing parameters and variables, it was decided to build a research vehicle which was so flexible that it could be adjusted or changed in any one of at least 17 combinations quickly.

Drive Systems

The research vehicle uses a gasoline engine in combination with two variable-displacement hydraulic pumps and four fixed-displacement hydraulic motors, one on each driving wheel. By combinations of series and parallel connections between the hydraulic pumps and motors, by varying the displacement of the pumps, and by different valving of the circuits, it is possible to change from one to another of the following basic drive systems in a matter of seconds:

1. Variable ratio drive between the right and left wheels, with full reversing one side possible for making spot or c. g. turns.
2. Clutch-brake, fixed ratio drive with simulated

THIS paper describes evaluations made of several drive and steering combinations of 4-wheel, 2-wheel, and crawler vehicles on macadam, loose ground, and mud.

Tests revealed that geometrically steered 4-wheel drive and steer vehicles closely approach the drawbar characteristics of crawler vehicles. High-speed tests on macadam showed the geometrically steered vehicles to be superior to skid-steered wheeled vehicles.

The variable ratio type skid-steer drive came closest of all configurations tested to approaching the pulling and steering characteristics of the geometrically steered vehicles.

clutch release.

3. Simple differential drive.
4. Locked axle drive.

Any of the above drive systems can be used by the manipulation of other valves to power the vehicle for: front or rear 2-wheel drive, 4-wheel drive, and crawler drive.

Steering Systems

The wheels of the research vehicle are mounted on Ackerman-type king pins with hydraulic cylinders to control the front and rear steering linkages. The frame is hinged in the center about a vertical axis with a hydraulic cylinder to control the angular position between the front and rear portions. The front and rear axle assemblies are slidably mounted on the tubular frame portions to facilitate varying the wheelbase. The rear frame is made on a single tube so as to permit the rear axle assembly to oscillate freely or to be locked. This basic arrangement of frame and wheel design makes possible the evaluation of the following steering systems:

1. Two-wheel steer, front or rear.
2. Four-wheel steer with the front and rear wheels articulating in opposite directions for minimum radius turns or in the same direction for diagonal steering.
3. Frame or broken-back steering with the front and rear wheel steering linkages locked.
4. Skid steering, with the frame pivot locked and wheel steering linkages locked, for tires or tracks.

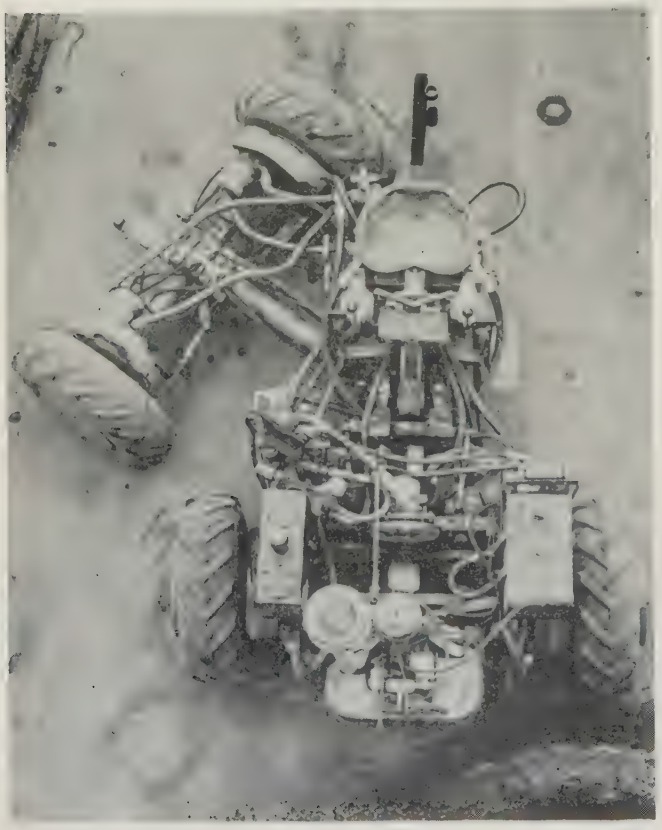

Fig. 3 — Research vehicle arranged for frame steering, 74-in. wheelbase

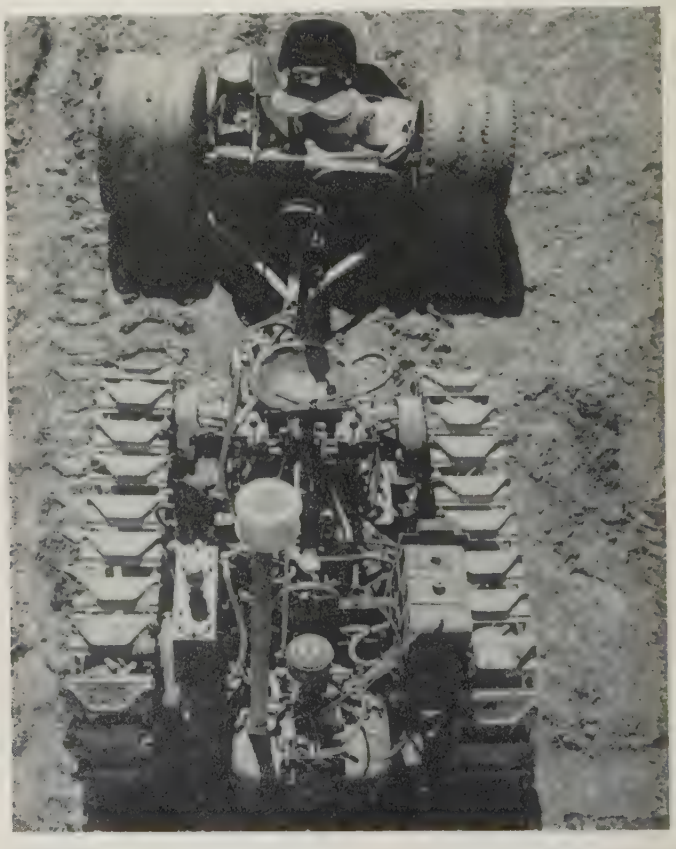

Fig. 4 — Research vehicle arranged for crawler skid steering, 48-in. wheelbase

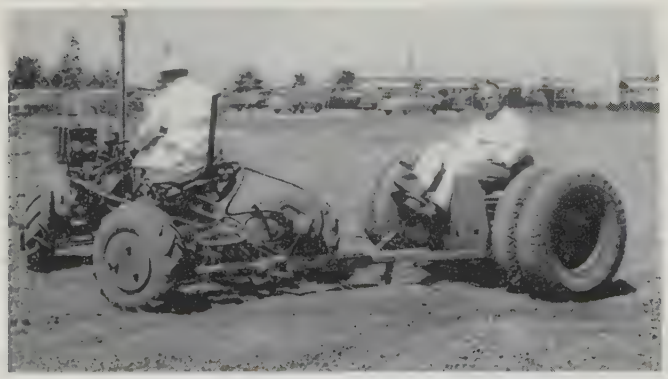

Fig. 5 — Rubber-tired version of research vehicle undergoing drawbar tests, pulling dynamometer trailer on loose ground

Fig. 6 — Crawler version of research vehicle under mud tests

Table 1 — Specifications of Research Vehicle

Engine — Approximately 26 hp at 3600 rpm. Engine was calibrated, after run-in, to determine bhp versus speed, throttle position, and manifold vacuum.

Hydraulic Pumps — Variable volume, piston wobble plate type.

Hydraulic Motors — Fixed displacement, piston wobble plate type.

Chain Drive — Ratios, approximately: Low 63/1; Second 37/1; Third 23/1; High 9/1

Tread Width — 60 in.

Wheelbase — Variable, 48–74 in.

Tires — 8–16 ground grip, mounted on 8 × 15 rims. 12-psi pressure unless otherwise noted.

Tracks — Galanot, ground pressure 2.5 psi.

Total Weight for Low-Speed Wrawbar Tests — 3600 lb, including operator. Wheel weights were added equivalent to the weight of the tracks for the wheeled vehicle low-speed tests.

Total Weight for High-Speed Steering Tests — 3360 lb, including operator.

Weight Distribution — 35% rear, 65% front for 4-wheel drive and crawler drawbar tests. — 65% rear, 35% front for 2-wheel drive drawbar tests. — 50% front, 50% rear for high-speed steering and transporting tests.

Drawbar Dynamometer — Dual-wheel truck axle modfied to form a dynamometer trailer. Hydraulic cylinder was placed in the tongue and arranged with pressure gage calibrated directly in lb. Loads above rolling resistance of the trailer were added by applying hydraulic brakes within wheels of dynamometer.

Overhead views of the research vehicle arranged for rubber-tired skid steering, 4-wheel steer, frame or broken-back steering and crawler skid steering, respectively, are shown in Figs. 1–4.

Specifications of the research vehicle are shown in Table 1.

Low-Speed Drawbar Load Tests

Low-speed traction tests were made to determine the average ground speed, gross input horsepower, maximum drawbar pull ability, and traction characteristics under varying drawbar loads. The highest chain drive ratio was selected for these tests so that maximum drawbar pull was limited solely by traction rather than engine power.

Tests were made varying the drawbar load in 200-lb increments while observing the calibrated engine throttle position (with the engine governor set at 3600 rpm) and the time required to negotiate the following level courses:

1. Pulling *straight* ahead for 50 ft.
2. Pulling around a *moderate turn* of 22½-ft mean radius (equivalent to a steering ratio[1] of 1.25/1) for 90 deg.
3. Pulling around a *sharp turn* of a 7.4-ft mean radius (equivalent of steering ratio of 2/1) for 180 deg.

These test runs were made under the ground conditions of macadam, loose ground, and mud (where possible. Figs. 5 and 6 show the vehicle under loose ground and mud conditions.

Fig. 7 shows relative tractive ability as drawbar pull in per cent of total vehicle weight (including the operator) for the 2-wheel drive, 4-wheel drive, and crawler versions of the research vehicle when pulling straight. The abscissa of this curve was scaled arbitrarily to give some indication of the relative tractive ability as traction conditions become poorer, going from the left to the right. In the case of the crawler tractor, the steel grousers were removed when testing on macadam, which explains the dotted line drop off of the crawler curve. The peak point of the crawler curve was taken as

[1] Steering ratio is defined as the ratio of the theoretical speed of the outside wheels and the inside wheels to accomplish a given radius of turn.

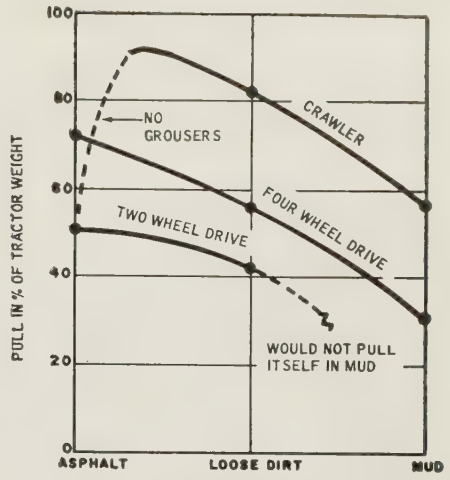

Fig. 7 — Relative tractive ability of traction and drive systems when pulling straight

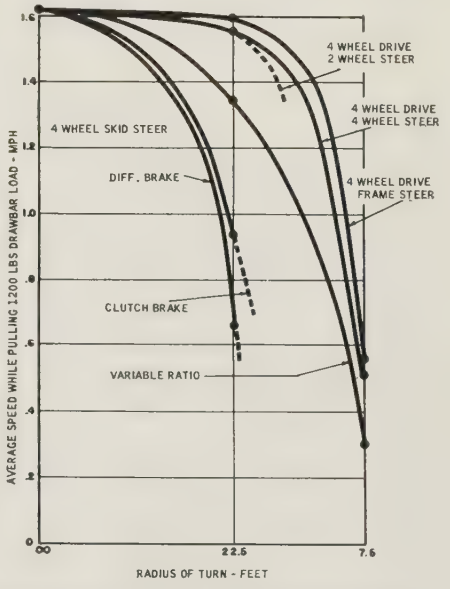

Fig. 8 — Effect of radius of turn and steering systems on speed of pulling moderate load on macadam

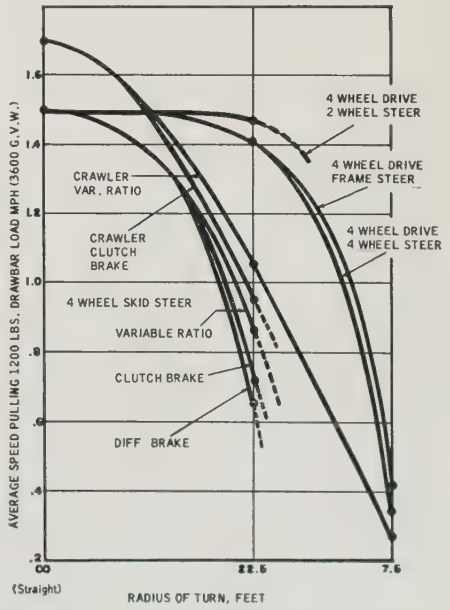

Fig. 9 — Effect of radius of turn and steering systems on speed of pulling moderate load on loose dirt

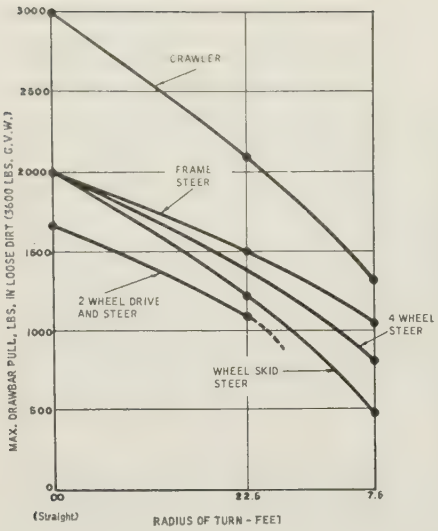

Fig. 10 — Effect of radius of turn and steering systems on maximum drawbar pull that can be developed on loose dirt

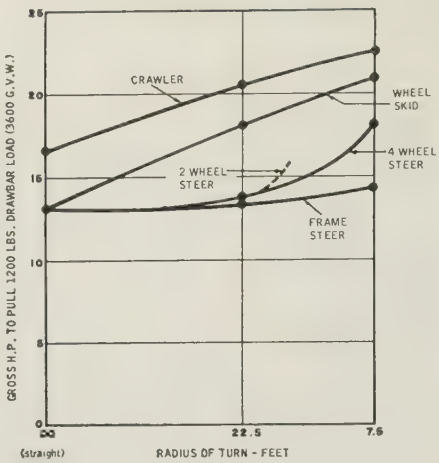

Fig. 11 — Effect of radius of turn and steering system on gross hp to pull moderate load in loose dirt

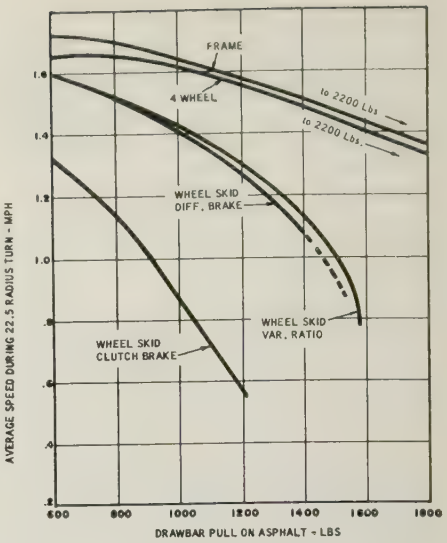

Fig. 12 — Effect of pull and steer systems on speed of making moderate turn on macadam

an average of Nebraska Tractor Test data determined on hard-packed ground.

Figs. 8 and 9 show the effect of turning on the speed of pulling a moderate 1200-lb drawbar load (33 1/3% of the gross vehicle weight) on macadam and loose ground with the various 4-wheel and crawler drive and steering systems. As would be expected, the performance while pulling straight for all of the wheeled systems is the same, but the crawler speed is higher due to the tracks having a larger rolling radius and probably a somewhat lower ground slip. The speed of rubber-tired and crawler skid systems drops off much more rapidly than the geometric steering systems as the radius of turn is reduced. The 2-wheeled steering systems were not capable of making the 7.4-ft mean radius turn.

Fig. 10 shows the effect of radius of turn and steering system on the maximum drawbar pull that can be developed on loose dirt by the various 4-wheel drive and crawler steering systems. Here again it will be noted that the skid systems suffer more than the geometric steering systems while negotiating turns.

Fig. 11 shows the effect of radius of turn and steering system on the gross horsepower required to pull a moderate load (one-third of the gross vehicle weight) in loose dirt. It will be noted that the crawler version of the research vehicle required approximately one-fourth more power than the wheeled vehicles when pulling straight. About half of this increase is due to the larger rolling radius of the tracks. Fig. 11 indicates that wheel skid vehicles compare favorably with crawler skid vehicles, but both require more power than geometrically steered vehicles.

Fig. 12 shows the effect of pull on the speed of making a moderate 22½-ft mean radius turn on macadam. Here again, it will be noted that the skid vehicles are not capable of pulling as much as the geometrically steered vehicles on macadam. This curve also shows that the variable ratio and differential brake systems, which maintain a positive drive on all wheels while turning, have a definite advantage over clutch-brake steering. The characteristics of the differential-brake steering system are quite similar to variable ratio, but the maximum pull ability is limited by available engine horsepower due to the added losses of braking the inside wheels. The geometrically steered vehicles show a definite advantage on speed as drawbar pull increases. They also have a maximum drawbar capability while turning that is 40–80% higher than the wheeled skid-steer systems.

Side Hill Performance

To examine the effect of differential and locked axle action, limited tests were conducted on macadam of varying side or cross slopes. The results are shown on the upper part of Fig. 13. The drop off due to differential action is not as great as it theoretically should be. This is due to the fact that the hydraulic friction losses in the research vehicle amount to approximately 5–10 times the losses of an equivalent mechanical differential. Thus, there is considerably more of a locked differential effect to aid in maintaining a more equal distribution of power to the drive wheels under adverse traction conditions.

During these and other side slope tests, it was noted that the frame steer vehicle was considerably more unstable while turning uphill than the skid or 4-wheel steer versions. Stability tests were made and are tabulated on the lower part of Fig. 13.

Rigid Versus Oscillating Axle

Limited tests were conducted to compare the performance of wheeled skid-steer versions of the research vehicle with the rear frame assembly locked to give rigid wheel mounting and with it free to oscillate. The tractor was operated on a prepared course with split telephone poles laying approximately 60 deg relative to the path of travel. The spacing was such that, theoretically, when diametrically opposite wheels were on top of the logs, the other two wheels would have little or no load im-

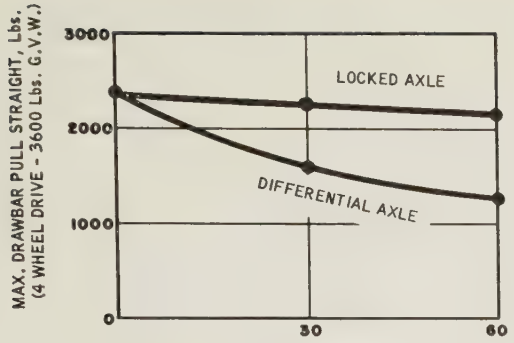

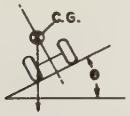

4 WHEEL DRIVE STEER SYSTEM		STABILITY ANGLE STEERING RATIO 1.25:1	2:0
SKID		55°	55°
4 WHEEL		55°	55°
FRAME	UP HILL TURN	45°	35°
FRAME	DOWN HILL TURN	58°	65°

Fig. 13 — Four-wheel drive vehicle side-hill pull and stability characteristics versus per cent slope

posed upon them. Fig. 14 shows there was no significant difference in the pulling ability as measured in terms of the average speed required to traverse the course. The higher tire pressures resulted in a rougher ride in both instances. It is important to emphasize that the wheels on each side of the rigid wheel skid steer vehicle must be locked or positively driven to perform equal to the oscillating wheel arrangement. With differential action between the right and left or front and rear wheels, wheel spinning was observed which momentarily caused the vehicle to slow down or stop.

High-Speed Steering Tests

The wheelbase for the research vehicle for the high-speed tests was adjusted to 48 in. and weights were added to the rear wheels to obtain a 50–50% weight distribution. The chain drive was changed to the lowest ratio for maximum travel speed. Having the wheelbase 48 in. made it possible to test the high-speed steering characteristics (with a wheelbase-to-tread ratio or L/t of 0.8), of wheel skid steering, of 4-wheel steering, and of frame steering without any other changes or variables introduced.

Steady state high-speed tests were conducted by observing the amount of time required for the vehicle to traverse, without any drawbar loading, the following runs on level macadam: straight run for 500 ft, 150-ft mean radius turn for 180 deg, and 50-ft mean radius turn for 360 deg.

Fig. 15 shows the results of this test with the tire pressure held constant at 12 psi. Here again, the geometric steering systems show the highest average speed and the least amount of drop off with decreasing radii turns. Of the wheel skid systems,

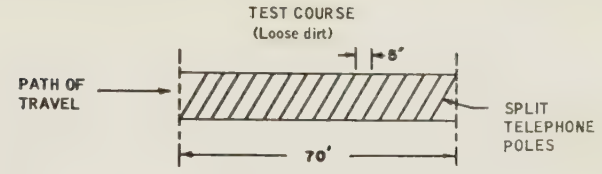

DRAWBAR LOAD LBS	AVERAGE SPEED ON 70 TEST COURSE			
	RIGID AXLE		OSCILLATING AXLE	
	12 PSI	20 PSI	12 PSI	20 PSI
600	1.68	1.74	1.72	1.72
800	1.72	1.60	1.72	1.66
1000	1.60	1.58	1.55	1.55

Fig. 14 — Comparison of rigid versus oscillating axle on performance of 4-wheel drive skid-steer vehicle

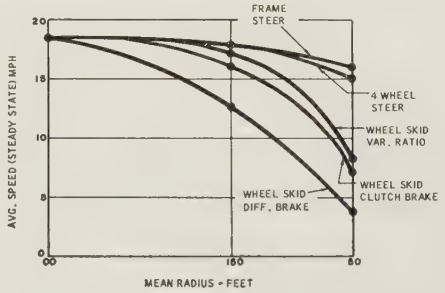

Fig. 15 — Effect of radius on turn on high-speed maneuvering of 4-wheel drive vehicles under maximum throttle conditions

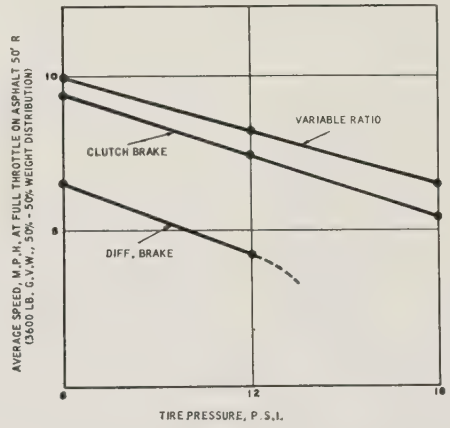

Fig. 16 — Effect of tire pressure and steering systems on speed of turning 4-wheel drive skid-steer vehicle

the variable ratio drive is the best and the differential brake system is the worst, which parallels the ratings determined by the low-speed drawbar test. During these high-speed tests, performance was limited by engine horsepower rather than tractive ability of the tires as in the case of the low-speed drawbar tests. The output of the hydraulic pumps was varied in an effort to maintain full throttle for maximum horsepower at 3600 rpm at all times. In the case of the differential-brake runs, however, it generally was not possible to prevent

the engine from lugging down while making the 50-ft radius and sharper turns.

Fig. 16 shows the influence of tire pressure on the steering ability of skid-steer wheeled vehicles under the conditions of variable ratio, clutch-brake, and differential-brake steering. This data confirms the belief that the resistance to skid steering is not constant, but rather it decreases with increasing speed and decreasing tire pressure. If it were not for this, the skid-steer vehicles would not have been able to negotiate steady state turns when the chain drive ratio between the hydraulic motors and the wheels was dropped from 63/1 to 9/1, or by a factor of 7. This was further confirmed by observing that the vehicle, with the 9/1 ratio, was physically incapable of turning, except for slight movement due to the deflection of the tires, when attempting a spot or c. g. turn with the vehicle at rest.

In order to check the relative performance and efficiency of these wheel systems under dynamic conditions, a 1018-ft test course was laid out on relatively level macadam pavement (Fig. 17). The turn radii vary from the very gradual curve of approximately 500 ft to as sharp as 10 ft. Again, the output of the pumps was varied in an effort to maintain full engine power at 3600 rpm. With the geometric-steered vehicles, it was necessary to reduce speed to prevent skidding while negotiating the sharp turns. The bar charts of this figure show the average speed capabilities of the various vehicle systems based on the time to make one complete circuit of the test course. Again, the relative performance of the geometric-steered systems was the best with the variable ratio skid steering being superior to clutch-brake and differential-brake, in that order.

Miscellaneous Tests

During the mud tests, it was observed that the frame-steered vehicle was capable of traversing mud better than either the 4-wheel steer or skid-steer versions. This is attributed to the ability of the frame-steered vehicle to be jack-knifed or "wiggled" forcibly to place the wheels into new and different traction spots, whereas with the other arrangements, the wheels tend to remain and "wallow" in one spot.

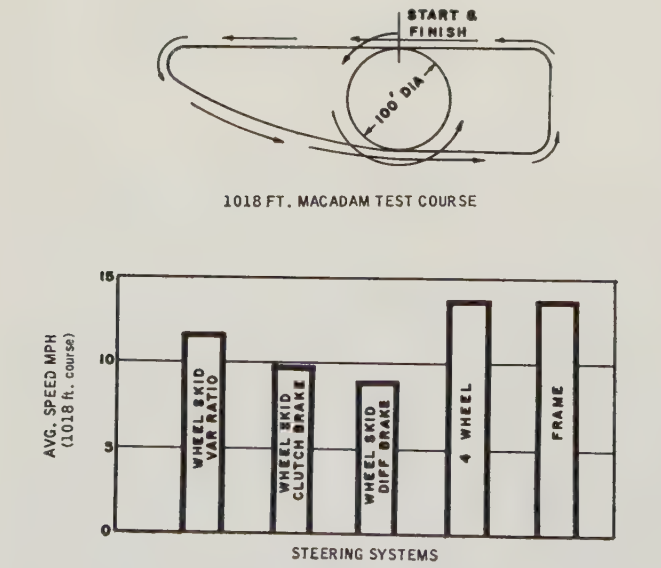

Fig. 17 — Effect of steering methods on average speed capability of 4-wheel drive vehicle to run test course

While the crawler showed the best performance pulling straight in mud, the frame-steered wheel vehicle matched its performance pulling on turns, especially the sharp turns.

Limited tests were also conducted to determine the steering ability of the wheeled skid-steer arrangements with the wheelbase stretched out to give wheelbase-to-tread ratios (L/t) of 1/1 and 1.25/1. With the 1/1 ratio, compared with an L/t of 0.8, the vehicle required around 15% more power when turning a given load, and displayed 15–30% less pull ability when making the same turns. Although the vehicle with the L/t 1.25/1 ratio displayed more skidding and difficulty while turning, it did turn satisfactorily and would even make spot or c. g. turns.

Reducing the wheelbase to an L/t of 1/1 as compared with 1.25/1 for the 4-wheel steer test, showed a slight gain in drawbar pull ability without any measurable gain in power. Except for the high-speed test, no runs were made with the frame steer version set with the wheelbase shortened below an L/t 1.25/1. The reason for this is that, with the shorter wheelbase, the vehicle would not have been capable of making the tight 7.5-ft mean radius or 2/1 steering radius turns.

Although the tightest turns evaluated by test runs were of 2/1 steering ratio, some limited testing was done to check tighter turning. The skid-steer vehicles demonstrated their superiority to maneuver in close quarters. The variable-ratio drive version (reversing one side) accomplished "spot" or c. g. turns with ease. The clutch-brake and differential-brake versions would make "pivot" turns (pivoting about one side) with somewhat greater difficulty. Near the conclusion of this program, the clutch brake with reversing feature was tried. Due to the quick action of the valves, the steering control was somewhat jerky but otherwise the vehicle made "spot" or c. g. turns with the same ease as the variable-ratio drive.

Summary

A research vehicle was developed which was so flexible it could be adjusted or changed to evaluate 17 drive and steering combinations quickly. Vehicle and test parameters and variables were thereby reduced to a minimum.

The results of the low-speed drawbar tests on macadam, loose ground, and mud showed that the geometrically steered 4-wheel drive and steer vehicles most closely approached the drawbar characteristics of crawler vehicles. The frame-steered wheel vehicle showed a superiority in its ability to traverse mud.

The high-speed tests on macadam showed the geometrically steered vehicles to be superior to the skid-steered wheeled vehicles.

The variable-ratio type skid-steer drive comes the closest to approaching the pulling and steering characteristics of the geometrically steered vehicles.

The skid-steered wheeled and crawler vehicles demonstrated their basic superiority to turn in less space than geometrically steered 4- and 2-wheeled vehicles.

the potential of *Unconventional Powerplants* for Vehicle Propulsion

Peter Kyropoulos, General Motors Corp.

This paper was presented at the SAE West Coast Meeting, Los Angeles, Aug. 12, 1958.

SCOPE of the discussion is reasonably well-defined by the title of this presentation. We shall consider primarily *commercial vehicles* and use the *diesel engine* as a basis for comparison. Commercial vehicles shall include highway as well as off-the-road applications. Military vehicles are not considered here since their requirements and specifications are basically different from commercial trucks (that is, start on a 60% grade, air transportability). A comparison of gasoline engine and gas turbine in a military truck is presented in Turunen, et al.[1]

In making forecasts, we shall not try to extrapolate beyond 1975.

In appraising the potential of any powerplant, we should keep in mind that, in order to supplant present piston engines, the new engine must: occupy less space, weigh less, operate more economically, be cheaper to produce, be cheaper to maintain, and give better vehicle performance. To succeed, the new engine cannot merely break even but must surpass present achievements and it must do so in the face of continued improvement of present engines.

How Unconventional Can We Get?

Just what is meant by *unconventional* powerplant? First, we shall examine means of storing energy and transforming it into thrust at a controlled rate.

We are accustomed to the use of liquid hydrocarbons as a source of energy, transformed into work in a heat engine. This is certainly not the only way to obtain energy. Is this method good? Have we overlooked a better solution?

Tables 1 and 2 show a comparison of energy

Table 1 — Comparison of Work Capacity Per Unit Mass[a]

	Ft-Lb/Lb	Lb/100 HP-Sec
Liquid Hydrocarbon (fuel only)	14,500,000	0.004
Solid Propellant (fuel only)	1,050,000	0.053
Diesel Engine	660,000	0.083
Lead — Acid Battery	38,000	1.45
Flywheel (uniform-stress disc with rim)	26,700	2.1
Compressed Gas (spherical container)	22,600	2.4
Flywheel (cylindrical)	18,000	3.1
Compressed Liquid (ether)	300	183
Compressed Solid (steel)	49	1120
Compressed Solid (coil spring)	15	3670

[a] Data adapted from footnote 2.

Table 2 — Comparison of Work Capacity Per Unit Volume[a]

	Ft-Lb/Ft³	Ft³/100 HP-Sec
Liquid hydrocarbon (fuel only)	682,000,000	0.00008
Solid Propellant (fuel only)	105,000,000	0.00048
Diesel Engine	100,000,000	0.00056
Flywheel (uniform-stress disc with rim)	8,780,000	0.00626
Flywheel (cylindrical)	8,750,000	0.0063
Lead — Acid Battery	5,000,000	0.011
Compressed Gas (spherical container)	2,500,000	0.022
Compressed Liquid (ether)	90,000	0.495
Compressed Solid (steel)	24,000	2.290
Compressed Solid (coil spring)	5000	11.000

[a] Data adapted from footnote 2.

[1] "Aspects of Automotive Gas Turbine for Military and Commercial Vehicles," by W. A. Turunen, R. Schilling, and E. L. Baugh. Paper presented at SAE Summer Meeting, Atlantic City, June, 1957.

COMPARISON of work capacity per unit mass and volume of different energy carriers shows that liquid hydrocarbons are superior to other energy sources. Solar and nuclear powerplants as well as their use in conjunction with a steam engine are examined in this paper.

Suitability of an electric drive is discussed. Using a production 2-stroke diesel engine and its development forecast, a comparison is made of spark ignition, diesel, and gas turbine engines.

The status of the free-piston engine turbine combination is reviewed.

storage capacity of several systems.[2] Although these tables are admittedly not the whole story, they nevertheless indicate that a thermal engine using liquid hydrocarbon fuel leads other energy sources by a ratio 12/1. It is quite apparent that the flywheel-powered bus and the electric car are not optimum solutions.

Solar, Nuclear, and Steam Powerplant

The capabilities of steam engines for vehicles have been examined repeatedly.[3, 4, 5, 6, 7] Although they present some attractive characteristics, the disadvantages are overwhelming in the face of readily available high-grade hydrocarbon fuels and the high level of development of the internal-combustion engine.

The fundamental disadvantage of the steam engine is a thermodynamic one: the available enthalpy drop across the engine is limited, since low condenser pressures cannot be used in a steam engine. A combination of steam engine and low-pressure turbine is feasible in stationary or marine applications, but does not lend itself to small installations. I do not say that a steam engine cannot be used. I *do* say that it is an inefficient way to transform chemical energy into thrust at the wheels of vehicles. The availability of cheap sources of energy would possibly change this situation. *Solar radiation,* in principle, is such a source of energy. However, it is not consistently available and no ready and compact means of storing the energy has yet been developed.

Average energy received at sea level between latitudes 20–40 deg is 0.17 hp/ft^2. A typical trailer (40 × 8 ft) has a roof area of 320 ft^2, which corresponds to an energy input of 54.5 hp. This example shows how marginal, at best, the available solar energy is for vehicle propulsion.

Direct conversion of solar energy into electricity is an active field of research. The energy storage problem is not solved. Even if electrical energy could be produced and stored, the basic unsuitability of electric propulsion for high-powered vehicles rules out solar propulsion on the road.

If *nuclear energy* became a feasible source of thermal energy for vehicles, the steam engine would probably be the most suitable converter. There are two basic obstacles to the use of atomic power in small powerplants:[8, 9, 10, 11] large size and weight because of shielding requirements; and high cost of fissionable material.

Using data from Ormsby,[10] the shielding weight of a 250-hp reactor powerplant would be of the order of 90,000 lb. Minimum fuel cost is estimated to be $20,000–30,000 per vehicle.

Electric Drive

In considering propulsion systems, it is in order to examine the potential of the electric drive. Strictly speaking, this is a form of power transmission and could be combined with several types of prime movers.

Electric Motors — The d-c series motor has good characteristics for traction service and has, consequently, been developed highly. In vehicle applications, the duration of full power is generally limited in time. A wide range of operating power is required.

Aircraft gas turbine starter motors havebeen developed for short duration overloads and may serve to illustrate the potential. They are used for a maximum duration of 30 sec with one-third to one-half of this time under maximum current condition. They will stand two consecutive cycles without being allowed to cool.

Weight data for such starter motors are shown in Fig. 1. Normally, maximum current is maintained only to 50–60% of rated motor speed. The line "normal rating" is based on this operation. If cooling were provided, it is estimated that the line "possible overload rating" could be obtained. Rated speeds are of the order of 10,000 rpm. Conceivably, such motors could be designed to drive individual wheels. The power range of Fig. 1 is, therefore, realistic. Reduction gearing would be needed which would add weight. A line for 400-cps aircraft induction motors is also shown. These motors, by themselves, are lighter than d-c motors. If they are to be used for variable-speed operation, a very complex frequency control system is needed which makes cost and weight unattractive for vehicle application.

Electric Generators — Although d-c motors have

---

[2] ASME Transactions, Vol. 80, May, 1958, pp. 909–914: "Work Capacities of Energy Storage Systems on Basis of Unit Weight and Unit Volume," by L. V. Kline, S. M. Marco, and W. L. Starkey.

[3] SAE *Quarterly* Transactions, Vol. 2, April, 1948, p. 288: "Thermodynamics of Vapor Powerplants for Motor Vehicles," by E. B. Neil.

[4] Zeitschrift, Verein Deutscher Ingenieure, Vol. 92, June, 1950, p. 401: "Die Schnellaufende Kolbendampfmaschine," by V. Reinhold.

[5] Automobiltechnische Zeitschrift, Vol. 48, January, 1946, p. 21: "Dampfangetriebene Kraftfahrzeuge," by O. Eichmann.

[6] Automobiltechnische Zeitschrift, Vol. 46, 1943, p. 351: "Entwicklungsmoglichkeiten des Dampfkraftwagens," by M. Hubmeier.

[7] Zeitschrift, Verein Deutscher Ingenieure, Vol. 78, January 20, 1934, p. 65: "Neue Dampffahrzeuge," by K. Imfeld and R. Roosen. (Report on Doble-Henschel Car)

[8] SAE *Journal,* Vol. 66, March, 1958, p. 69: "Atomic Powerplants," by E. D. Reeves.

[9] SAE Transactions, Vol. 65, 1957, pp. 436–451: "Automotive Nuclear-Heat Engines and Associated High-Temperature Materials," by F. L. Schwartz and H. A. Ohlgren.

[10] *Aeronautical Engineering Review,* Vol. 17, January, 1958, p. 20: "Airborne Nuclear Powerpropulsion System Design Considerations," by R. B. Orsmby, Jr.

[11] "Materials in Automobile of Future," by A. L. Boegehold. Paper presented at ASTM Meeting, Cleveland, April, 1956.

characteristics suitable for traction applications, d-c generators are unsuited. A d-c generator capable of delivering the required starting and acceleration (high current flow at low voltage) and high speed, low load running (low current and high voltage) is too heavy for vehicles other than locomotives.

Aircraft alternators (400 cps), possibly cooled and fitted with cooled silicon rectifiers, appear to have the right magnitude of weight. Control of the drive motors could be achieved by changing the voltage reference for a transistor regulator which controls the field strength of the alternator. Fig. 2 shows weight estimates for this type of alternator.

Although no complete design proposal using electrical components has been presented here, there are indications that electrical power transmission is not out of the question. Our study is not complete enough to indicate whether this scheme is merely feasible or whether it promises substantial gains.

Comparison of Prime Movers

We have made it reasonably plausible that for some time to come a hydrocarbon-fueled air-breathing engine will be most suitable for vehicles.

Three types of engines are available: (1) captive piston (diesel and spark-ignition engine and their modifications, 2-stroke, 4-stroke, turbocharged, aluminum, cast iron); (2) free-piston; (3) regenerative gas turbine.

Comparisons of these engines have been made repeatedly and many of the pros and cons are common knowledge. It is, therefore, sufficient to revise the data in the light of recent developments. However, a note of caution is in order. Comparisons of engine weights and outputs may be misleading if they are not based on similar assumptions. The following section will illustrate the wide variety of data which can be quoted for a single engine.

Case of Diesel Engine

The diesel engine has approximately 50 years of development behind it. After this long a period, changes are relatively slow and gains small. This does not mean the end of the line. For our comparison and forecast, we shall use General Motors Detroit Diesel Division's bread and butter engine, the 6-71. This engine has three ratings which are determined primarily by the life requirements in each application. These are defined as follows:

1. Continuous — This rating is used in applications where load factors are high and life between overhaul is far more important than high specific output (marine work boats and continuous duty generator sets).

2. Intermittent — The intermittent rating covers a wide range of load factors and, therefore, all overhaul intervals in applications where specific output and life are both of considerable importance (highway vehicles, earth moving equipment, and most industrial applications).

3. Maximum — The maximum rating is used where the highest possible specific output is desired. Life in terms of engine hours at this rating is relatively lower (typical applications: marine pleasure crafts and certain military engines).

The marine engines are included here since they are indicative of the development potential.

Typical data for this engine are shown in Table 3. Each rating is based on the permissible modifica-

Table 3 — Present Engine 6-71 In-Line

Rating	Continuous	Intermittent	Maximum
Maximum Hp (gross)	170	210 (+24%)	310 (+82%)
Maximum Rpm	1800	2100	2300
Weight (fan to flywheel), lb	2190	2070 (−5.5%)	1780 (−19%)
Plus Turbo (lb)	None	None	175
Total (fan to flywheel), lb	2190	2070	1955
Specific Weight, Total lb/max hp (gross)	12.9	9.85	6.3
Fuel Consumption, lb/gross hp-hr	0.396	0.410 (+3.5%)	0.423 (+7%)
Volume, ft³/100 hp	23.3	18.9	12.8
	Cast iron	Cast iron plus some aluminum	Aluminum cylinder block

"Fan to flywheel" includes: Blower, starter, generator, exhaust manifold.
Truck accessory power (fan and generator) not included:

1800 rpm	6.8 hp
2100 rpm	9.8 hp
2300 rpm	12.0 hp

The weights include: Blower, starter, generator, and exhaust manifold.
The running engine would require:

Coolant:	78 lb (truck)	70 lb (stationary)
Oil:	38 lb (truck)	51 lb (stationary)
Radiator:		
Industrial		67 lb
Truck		122.75 lb
Air Cleaner, Truck (2)		37.5 lb

These weights are not customarily included.

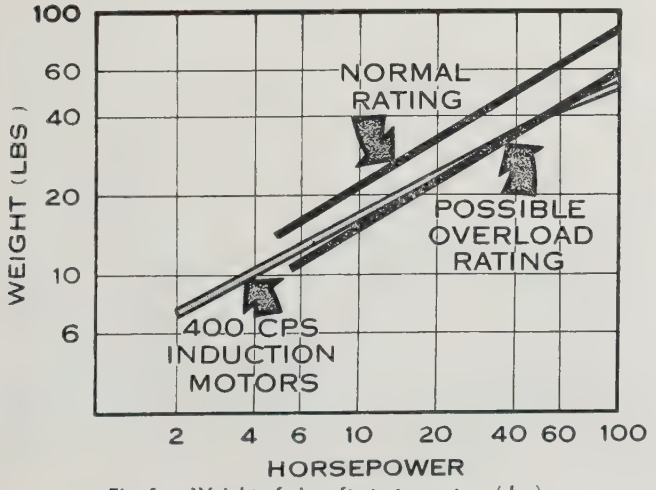

Fig. 1 — Weight of aircraft starter motors (d-c)

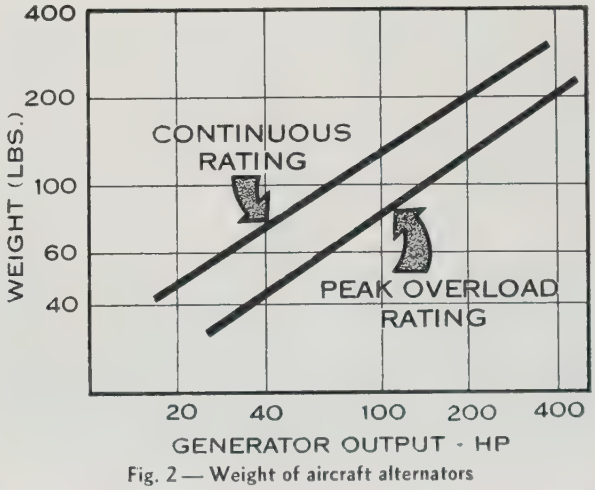

Fig. 2 — Weight of aircraft alternators

tions. The continuous rating is based on an all cast-iron engine (except for the blower, which is aluminum). The maximum rating is based on an engine with an aluminum block in addition to the other aluminum parts.

Engines of Immediate Future (1962)

Horsepower — While there is always a desire for maximum output from a given size engine, the trend in this direction is not very strong in most applications. Considerations of engine life and fuel economy, together with legal weight and speed restrictions, tend to keep horsepower down in highway vehicles. In earthmoving equipment the demand for increased power is great, but again considerations of engine life made larger engines, rather than extremely high specific outputs, preferable. Only in the area of "maximum rated" engines is high specific output very desirable. We do not expect to make radical increases in specific output in the next few years.

Weight — Minimum engine weight is, of course, very desirable in all applications. Even in track-laying equipment where weight is needed for traction, it is cheaper to use pig iron than heavier engine castings. A new family of engines was designed to keep weight to an absolute minimum. Weights of the new 6-71 engines shown in Table 4 reflect this weight consciousness.

Fuel Economy — From a practically insignificant factor in 1948, fuel economy has become one of the most important single items governing the salability of engines for highway vehicles. We believe that this trend is certain to continue in highway vehicles and to become more and more important in other areas as well. We do not expect major breakthroughs in improved thermal efficiency, but rather a relatively steady progress in improved economy through careful attention to design detail.

Table 4 summarizes data for the engines planned for the immediate future.

Crystal Ball Engines

Horsepower — There are two known methods of increasing engine output: by raising engine speed, or by raising bmep, or by a combination of both. Both methods increase thermal and mechanical loads on engine components and, therefore, require either hot-strength materials or improved design to maintain life. Turbosupercharging of diesel engines has been and probably will continue to be the major method by which bmep increases are obtained. With improved high-temperature materials and rotor design made possible by gas turbine progress, higher pressure ratio and higher efficiency turbos will become available which will permit higher engine ratings.

Several years ago, a 6-71 engine was turbocharged to an output of 425 bhp or 1 hp per cu in. of displacement. This was done with a turbo of relatively low efficiency. Today, it could be done more easily with lower stress on cylinder components because of better turbos, but the engine would still not have commercially acceptable life using materials and design techniques which would produce a commercially priced engine. The day when this can and will be done will certainly come. We can predict for the future a 6-71 turbocharged engine weighing 1600 lb and having an output of 400–450 bhp at a speed of 2500 rpm. Fuel consumption will be of the order of

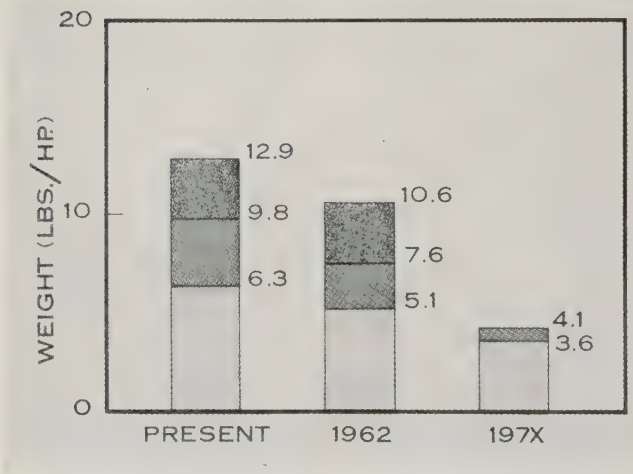

Fig. 3A — General Motors 6-71 diesel, present and future weight

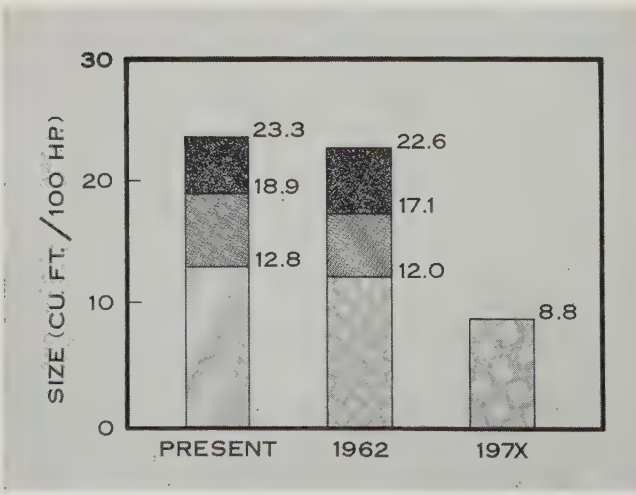

Fig. 3B — General Motors 6-71 diesel, present and future size

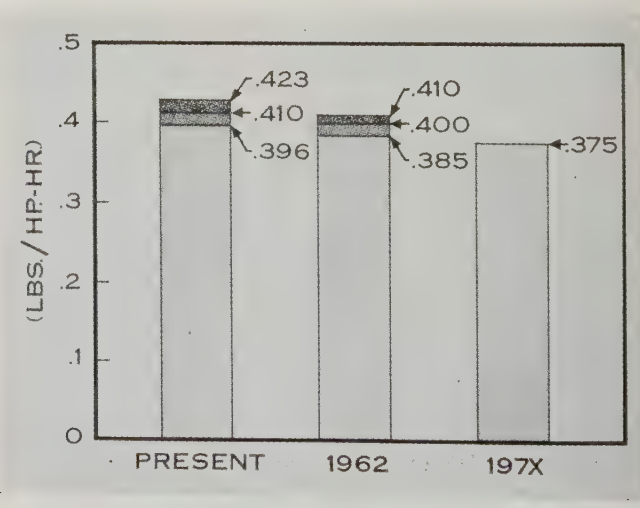

Fig. 3C — General Motors 6-71 diesel, present and future fuel consumption

0.375 lb/bhp-hr. Table 5 summarizes data expected for this engine.

Figs. 3A–3C summarize the data of Tables 3–5 in bar charts. It becomes immediately apparent that a single bar cannot represent the full range of engine capabilities. For this reason, some engine comparisons have been criticized (Fig. 6 of Boegehold[11]).

Case of Spark-Ignition Engine

Although primarily designed for passenger-car service, the modern V-8 engine can be used for commercial vehicles. Table 6 shows a comparison of data for a typical V-8 cast-iron engine and its aluminum counterpart. The rating corresponds to the maximum rating of Table 3.

Case of Gas Turbine

The suitability of the gas turbine has been established.[1] Fig. 4 shows an experimental gas turbine truck. Fig. 5 shows a schematic cross-section through the regenerative engine. Fig. 6 shows the engine (GT 305). Fig. 7 compares the torque curve of a gas turbine and a piston engine. Fig. 8 shows a typical plot of turbine temperatures and their effect on brake specific fuel consumption. Fig. 9 shows the development of turbine performance (bsfc) and a forecast of possible future fuel consumption.

Table 7 shows observed data for the GT 305 truck turbine.

The great attraction of the turbine lies in the fact that high outputs can be obtained in relatively small

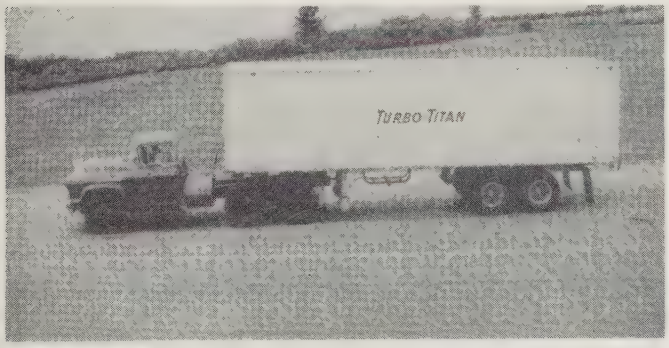

Fig. 4 — Gas turbine truck-trailer combination

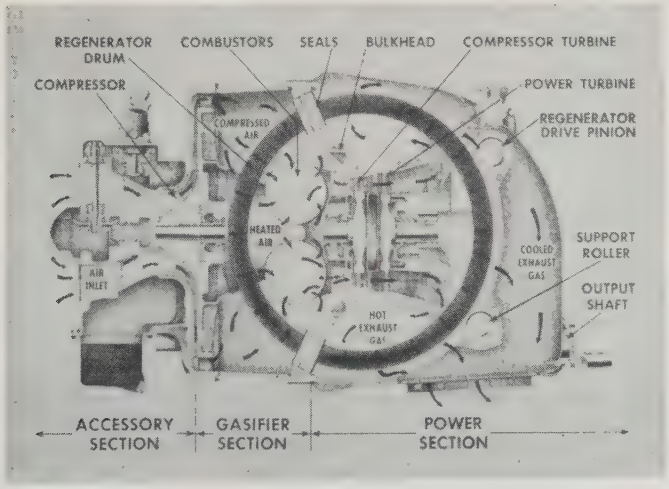

Fig. 5 — Schematic cross-section of GM research regenerative gas turbine (GT 304)

Table 4 — Engines of Immediate Future (by 1962)

Rating	Continuous	Intermittent	Maximum
Maximum Hp (gross)	175	232 (222)	330
Maximum Rpm	1800	2300 (2100)	2300
Weight (fan to flywheel), lb	1855	1760	1505
Plus Turbo, lb	None	None	175
Total (fan to flywheel), lb	1855	1760	1680
Specific Weight, Total lb/max hp (gross)	10.6	7.6	5.09
Fuel Consumption lb/gross hp-hr	0.385	0.410 (0.398)	0.400
Volume, ft³/100 hp	22.6	17.1	12.0

Table 5 — Crystal Ball Engine (197X)

Rating	Maximum
Maximum Hp (gross)	400–450 + 165%[a]
Maximum Rpm	2500
Weight (fan to flywheel), lb	1450
Plus Turbo, lb	175
Total (fan to flywheel), lb	1625 (– 26%[a])
Specific Weight, Total lb/max hp (gross)	4.06–3.61
Fuel Consumption, lb/gross hp-hr	0.375
Volume, ft³/100 hp	8.8

[a] Based on Table 3, continuous rating.

Table 6 — V-8 Spark-Ignition Engine (283 cu in.)
(Rating Corresponds to Maximum of Tables 3–5)

	Power, (max bhp)	Weight, (lb)[a]	Fuel Consumption, (lb/hp-hr)	Lb/hp	Cu ft/100 hp
Cast Iron (10/1 compression ratio)	200	562	0.401	2.81	5.86
Aluminum (11/1 compression ratio)	205	413	0.390	2.02	5.74
Aluminum (Turbocharged)	285	443	0.370	1.55	4.21

[a] Dry Weight, but including radiator (Copper 22 lb, Aluminum 12 lb)
Coolant Weight, 50 lb
Oil Weight 10 lb
Fan hp – 8 at 4400 rpm, not included in rated power
Octane Requirement: 98.

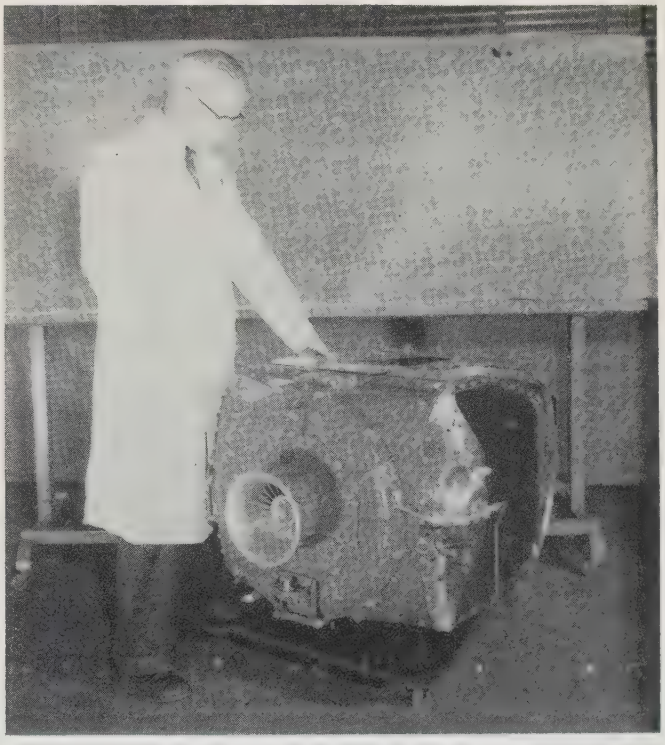

Fig. 6 — GM research gas turbine (GT 305)

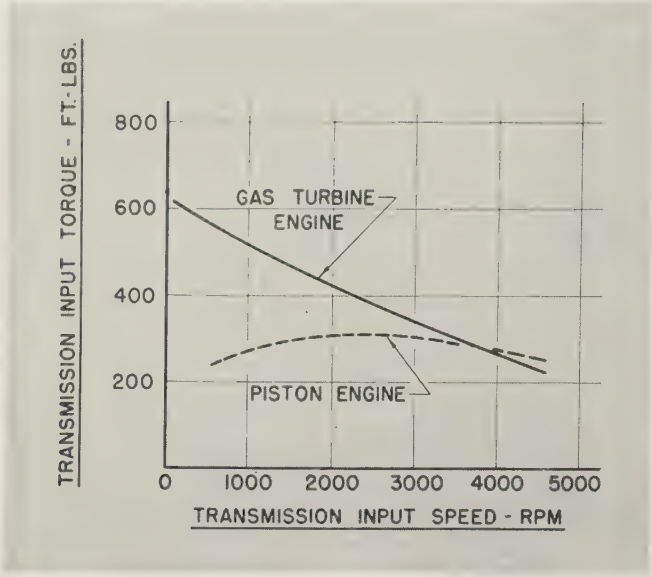

Fig. 7 — Comparison of gas turbine and piston engine torque

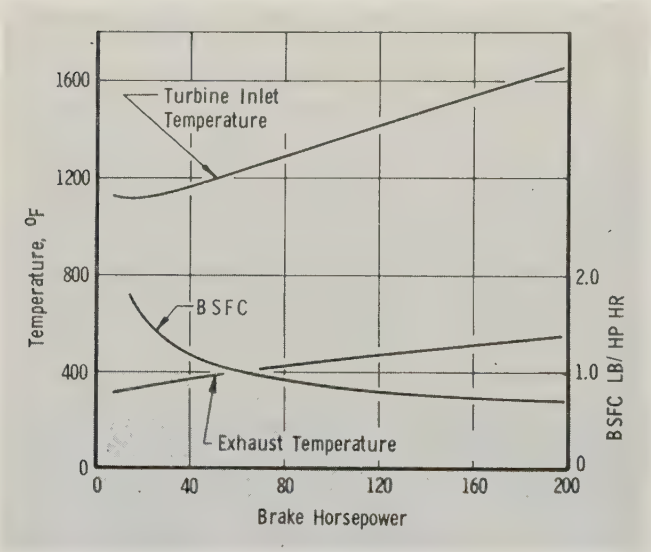

Fig. 8 — Effect of turbine inlet temperature on fuel consumption (GM research GT 304)

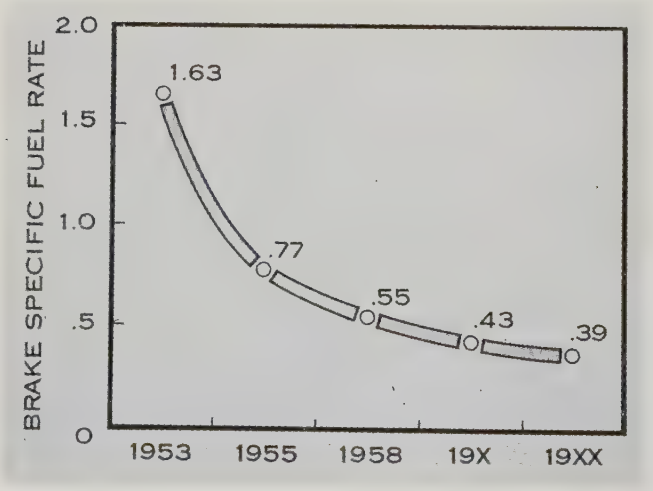

Fig. 9 — Gas turbine fuel consumption: past, present, and future

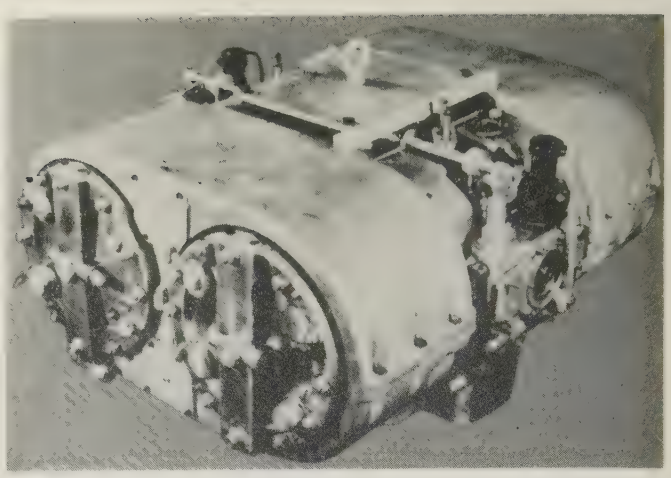

Fig. 10 — GM research free-piston gas generator

and light engines. Specific weights of 3–4 hp/lb are attainable in the 200-hp range. Jet engines (corresponding to the gasifier section of the vehicle turbine) delivering an equivalent of 1000 hp weigh 250 lb and have a fuel consumption of 0.6–0.7 lb/hp-hr. This, then, promises to be an engine for very large earthmoving equipment, logging and mining operations, as well as mountain highway hauling.

A 60,000-lb truck going up a 6% grade at 45 mph requires approximately 1100 hp. A turbine can readily furnish this much power. Since level road power requirements are much lower, the part-load fuel consumption of a turbine, operating far below the design point, would be very poor. A compound powerplant may be attractive in which level road consumption is provided by a diesel engine of appropriate capacity.

Considerable progress has been in the design for production. The cost of turbine engines, if built in quantities similar to truck engines, is estimated to be of the same magnitude as present diesel engines.

Case of Free-Piston Gas Generator

Free-piston engines have been under development for 30 years and many large engines (1000 hp and more) are in operation. Interest in smaller engines for vehicles is relatively recent.[11,12,13,14]

The power producing part of the "free-piston engine" is a turbine. The free-piston device proper is essentially an air compressor run by a diesel cycle. The exhaust from the diesel cycle runs the power turbine. The diesel cycle has a high compression ratio (30/1 to 50/1) and runs with much excess air (400%). It is, therefore, relatively insensitive to fuel quality. The turbine runs at a low temperature of 450–900 F compared with 1500–1600 F in the conventional gas turbine. In spite of the low turbine inlet temperature, the overall specific fuel consumption is good (0.40–0.45 lb/bhp-hr) with an estimated future value of 0.35 lb/hp-hr.

Fig. 10 shows an existing free-piston gasifier and

[12] SAE Transactions, Vol. 65, 1957, pp. 377–391: "GMR 4-4 Hyprex Engine, A Concept of Free-Piston Engine for Automotive Use," by A. F. Underwood.
[13] SAE Transactions, Vol. 65, 1957, pp. 628–634: "Automotive Free-Piston-Turbine Engine," by D. N. Frey, P. Klotsch, and A. Egli.
[14] SAE Transactions, Vol. 65, 1957, pp. 508–515: "Observations on 25,000 Hours of Free-Piston Engine Operation," by G. Flynn, Jr.

Fig. 11 — Schematic proposal for free-piston gas generator and turbine for truck installation

Table 7 — Truck Gas Turbine (GT 305)

Power, max hp	Dry Weight, lb	Fuel Consumption, lb/hp-hr	Lb/hp	Cu ft/100 hp
225	590	0.55	2.6	6.85
Oil Cooler	10 lb			
Oil	10 lb			

Fig. 11 a proposed truck installation.

Only limited experience has been published to date. Consequently, an appraisal of the engine's capabilities must be rather qualitative. Size and weight are slightly greater than cast-iron spark-ignition engines (3.5 ft^3/100 hp, 3–5 lb/hp). Gasifier and power turbine can be located quite far apart. They are connected by hot gas ducts only. It must be allowed that, in principle, this could be done with a conventional gas turbine.

Low turbine temperatures result in long turbine wheel life and this is an advantage. On the other hand, the gasifier has peak pressures of 200 psi which poses problems of piston-ring sealing. The varition of efficiency with load is said to be moderate so that good fuel consumption is expected over a wide range from cruising to full power. This would be highly desirable for vehicles. Free-piston engines have been run on a wide variety of fuels, from gasoline to crude oil. This may be a definite advantage under certain circumstances. However, diesel engines also will run on gasoline as well as on diesel and jet engine fuel, an important fact for military applications.

In summation, a conclusion from Frey, et al[13] will be quoted verbatim:[14]

> "The free-piston-turbine engine is a possible contender for the engine of the future because it does not suffer by comparison to the piston engine in regard to throttle response, fuel economy, or cost of manufacture. It has a superior torque curve and allows for split passenger vehicle installation with important vehicle advantages. Currently, it has a serious weight disadvantage. The free-piston-turbine engine must develop, if successful, into a machine of much higher gasifier cyclic speeds than the 2400 cpm presently attainable." This statement was made in October, 1956, and so far has not been contradicted.

Conclusion

These are the facts as they appear in August, 1958. The principal conclusion which is in order is that the diesel engine has by no means exhausted its potential for development. The turbine is here in a competitive form and shows great promise in the size range beyond (larger than) the diesel engine. Other powerplants do not show promise in the foreseeable future.

Acknowledgments

The author is indebted to the following colleagues at General Motors for data and helpful discussion:

K. L. Hulsing and H. S. Ford, Detroit Diesel Engine Division.

W. A. Turunen and E. E. Flanigan, Research Staff.

G. Flynn, Research Staff.

Dr. C. Marks, Engineering Staff.

ORAL DISCUSSION

—Reported by Mark Ogden, Cummins Service & Sales

Earl Klinge, Ford Motor Co.: Most comparisons of engine performance, in order to be valid, must be on a net installed basis. It is necessary, for example, to consider the size or bulk of air cleaners. My studies of aircooled engines lead me to agree with your weight comparisons, Dr. Kyropoulos, but I disagree on bulk and volume. In making comparisons, a volume of fuel used for say a 1000-mile range should be used throughout. Then, too, cooling system components should be considered in computing weight and bulk.

Dr. Kyropoulos: I agree that all the factors you mention should be taken into consideration. One of the hardest problems to solve is that of volume, or space — how to accommodate all the accessories, especially in a passenger-car application where there is a limited amount of room. Your air-cleaner point is also well taken.

Unidentified Member, Standard Oil Research & Engineering: Were your comparisons based on full-throttle or part-throttle operations?

Dr. Kyropoulos: Full-throttle.

Henry Ard, Potlach Forest Industries: Bmep's of as high as 200 have been mentioned. My question is, are these coming soon?

D. T. Marks, Cummins Engine Co.: Our plans for the future include gradually increasing Bmep's but at a slow rate. The rate will be that required to meet increasing demands for higher horsepower.

Homer Wood, Consultant: The charts shown us indicate that spark-ignited engines have 1.55 specific weight in pounds per horsepower compared to nearly twice as much for diesel engines. My question is, why consider diesel at all, or does life expectancy enter into your comparisons? Also, I recently read of captive piston-type generators being used to propel Swedish locomotives. Are we lacking in imagination?

Dr. Kyropoulos: As you surmised, the answer to your question "Why diesels?" is largely because of its longer life expectancy. The life expectancy of a spark-ignited passenger-car engine is much less than for a diesel. Although the possibility of using captive-piston type gas generators has been kicked around a lot, there is little evidence of this type of powerplant being adopted widely.

Mr. Marks: The captive piston-type generator can be considered for rail cars because the designers have more space available and weight is not an important factor. In your convenience, but we are talking here about vehicular a rail car, you have room to arrange your components to powerplants where space and weight are vital factors.

some thoughts on optimum

Wings and Vertical in VTOL

W. Z. Stepniewski, Vertol Aircraft Corp.

This paper was presented at the SAE National Aeronautic Meeting, Los Angeles, Oct. 3, 1958.

THIS PAPER reviews VTOL problems, indicating probable ways toward optimization of whole lifting and propelling system. Also discussed are the power and thrust requirements for optimum cruise and vertical take-offs and landings for propeller-driven and jet-propelled aircraft.

Three speed ranges offer the most promise for VTOL aircraft, if thrust requirements for cruise and take-off are to match. The ranges are centered around Mach numbers of 0.65, 0.8, and 2.0+. There is a possibility of overcoming the high thrust needed for hovering by use of bypass augmentation, special hovering jets, or favorable ground effects, the author reports.

FOR ANY MISSION defined either in terms of distance flown or endurance, an efficient aircraft design requires that the combined weight of the propelling and lifting systems, plus the fuel required for this mission, be at a minimum. In conventional fixed-wing aircraft, it is often necessary to deviate from the optimum size of the wing (make it larger) because of the take-off and landing requirements. Take-off requirements also force to install more power, or to provide more thrust than required for the optimum cruise.

In VTOL aircraft, where the lift necessary for take-off and landings is provided by special vertical thrust generators, the take-off and landing aspects can be, at least in principle, removed from the design considerations of the wing and this latter can be optimized for the cruising condition.

Greater freedom in optimizing the wing of VTOL aircraft also may be helpful in solving another problem which may be encountered in the future. Constantly increasing conjestion of the airspace may necessitate the restriction of some aircraft to low-altitude flying. It becomes interesting to get some feeling whether that freedom of wing optimization can counterbalance in VTOL aircraft the disadvantages of cruising at lower altitudes.

Although VTOL aircraft may be at an advantage (by comparison with the conventional ones) as far as the wing size is concerned, they are definitely in a worse position with respect to the difference between power or thrust requirements in an optimum cruise and that in a vertical take-off or landing.

Power and Thrust Requirements

Airscrew-Type Aircraft — As far as airscrew-type (tilt wing, deflected slipstream) VTOL aircraft are concerned, the disparity of power requirements at take-offs and landings versus optimum cruise can be narrowed down through a proper selection of such parameters as wing loading and aspect ratio

combinations of

Thrust Generators

Aircraft

on one hand, and propeller disc loading on the other combined with the highest cruising altitude.[1] Nevertheless, it seems that in spite of the best possible selection of design parameters this gap may still exist.

One possible solution to this problem is simply to install less power than required for VTOL maneuvers and thus resign to take-offs and landings with a short run (STOL). Another solution would be to overload VTOL aircraft above their hovering gross weight.

Technical feasibility of the above approach stems from the fact that in the airscrew-type configurations (tilt wing for instance) power required to sustain a given gross weight rapidly decreases with forward speed. Allowing, hence, for a short run necessary either to accelerate to, or decelerate from, those speeds would permit a considerable reduction in the power installed requirements resulting from the take-off and landing conditions. Analytical and wind tunnel studies[2] of that decrease in power required with forward speed were confirmed by power measurements in actual conversions of the VERTOL 76 flight research aircraft from hovering and back to hovering (Fig. 1).

Still another solution to the design economy problem was suggested by C. Zimmerman.[3] In this approach auxiliary jet engines are installed on the propeller-driven VTOL aircraft, in order to provide additional vertical thrust during take-offs and landings, thus permitting the selection of the main powerplant closer to the cruising requirements.

Jets — In jet-propelled aircraft the discrepancy between vertical thrust at take-offs and landings ($T_v \cong W$), and that required to propel the aircraft at optimum L/D is even more striking. Lower part of Fig. 2 gives the relationship between $(L/D)_{max}$ and flight Mach number (based on wind tunnel tests

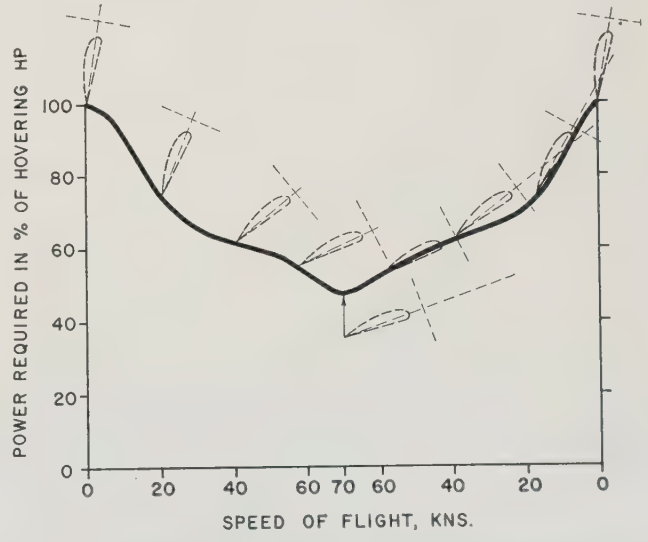

Fig. 1 — Relative power requirements in actual conversion flight of VERTOL 76 tilt wing flight research aircraft

[1] *Journal* of Helicopter Association of Great Britain, Vol. 11, December, 1957, pp. 299–339: "Tilt Wing Aircraft in Comparison with Other VTOL and STOL Systems," by W. Z. Stepniewski.

[2] "Take-Off and Landing Distance and Power Requirements of Propeller-Driven STOL Airplanes," by R. E. Kuhn. Paper presented at meeting of Institute of Aeronautical Sciences, 1957.

[3] *Journal* of Helicopter Association of Great Britain, Vol. 12, August, 1958, pp. 141–168: "Powered Lift Systems," by C. H. Zimmerman.

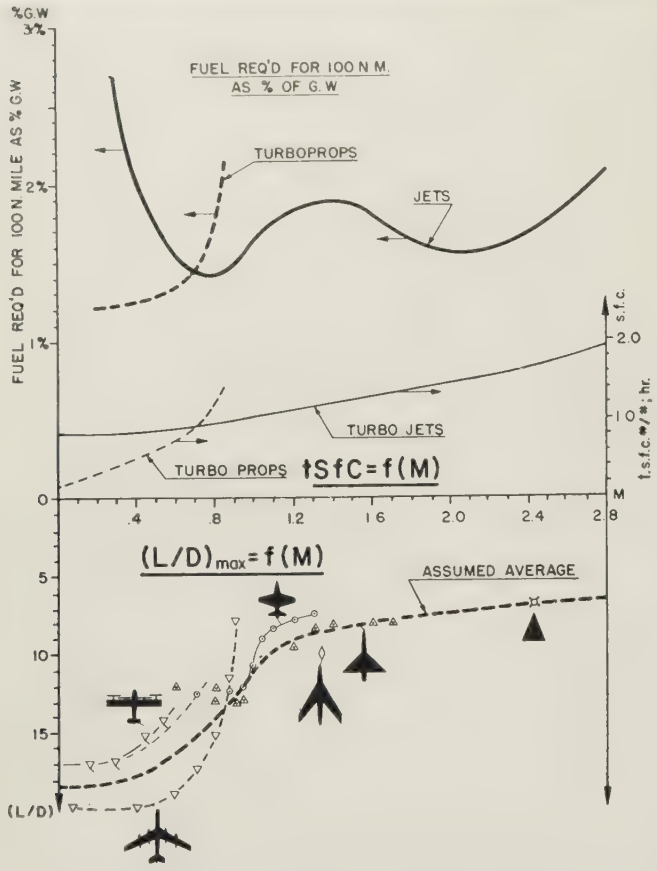

Fig. 2 — Optimum lift-to-drag ratios and relative fuel required per 100 n. miles versus Mach number

as reported by various investigations [4, 5, 6, 7, 8] and supplemented by some results of studies by Stepniewski[1] and Jones[9]). A glance at Fig. 2 will indicate that for properly designed aircraft optimum thrust required even at supersonic speeds will amount to only a small fraction (1/11 at $M = 1.0$ and 1/6 at $M = 2.8$) of the gross weight.

In order to minimize the weight penalty resulting from this disparity of the thrust requirements in hovering and in cruise, the following sum should be made a minimum:

$$W_{F_f}/W + W_{F_h}/W + W_{TG}/W + W_W/W = \min \qquad (1)$$

where:

W_{F_f}/W = Relative weight of fuel for forward flight
W_{F_h}/W = Fuel required in hovering
W_{TG}/W = Relative weight of the thrust generating system (vertical and propelling)
W_W/W = Relative wing weight

In Fig. 2 (top) relative fuel weight (per cent of gross weight) required for 100 nautical miles is shown versus Mach number for turboprops and turbojets. In establishing this relationship the $(L/D)_{max}$ versus M shown in the lower part of Fig. 2, and thrust specific fuel consumption (tsfc; lb/lb of thrust, hr.) as shown in the middle of Fig. 2 were assumed. Thrust specific fuel consumption for the turboprops was computed assuming sfc = 0.6 lb/hp-hr and the following propeller efficiencies: $M = 0.2$–0.4, $\eta_{pr} = 0.85$ *gradually decreasing to* $\eta_{pr} = 0.65$ at $M = 0.85$. Thrust specific fuel consumption for the turbojets was taken from Morgan.[10] It can be seen from Fig. 2 that up to approximately $M = 0.7$ turbines, even with conventional propellers, show the lowest fuel consumption. With supersonic propellers this region of the turboprop superiority can probably be extended to still higher Mach numbers.[11] However, it looks that optimum region of the airscrew-type aircraft, as far as the cruise fuel economy is concerned, extends approximately to $M = 0.5$.

It is interesting to notice that turbojets (which show poor performance at low Mach numbers up to $M = 0.5$ or 0.6) indicate two distinct optimum regions. One of them is around $M = 0.8$ and another at $M = 2.1$. It should be further noticed that the forward flight fuel requirements at the second optimum are only slightly higher than those for the high subsonic ($M = 0.8$) region. This is in spite of the fact that at the higher Mach number $(L/D)_{max} = 7$ and at $M = 0.8$, $(L/D)_{max} = 14$.

It may be concluded, hence, from the examination of Fig. 2 (top) that unless structural weight of the wing and hovering aspects reflected in the weight of powerplant and hovering fuel would upset the trend, three distinct speeds regions should be of interest for VTOL aircraft:

1. Medium subsonic region, up to $M = 0.6$ where the airscrew-type VTOL aircraft should be most advantageous.
2. High subsonic region, around $M = 0.8$ where the turbojet-propelled aircraft show optimum fuel consumption in forward flight.
3. The Mach 2+ region, where again the turbojet-propelled aircraft look promising.

Optimization of Thrust Generating System and Hovering Fuel Weight

Thrust generating systems based on the jet principle can be considered as composed of the hot gases generator and a bypass system. Energy of the hot gases produced by the gas generator can be either used directly for production of thrust (Fig. 3*A*), or part of that energy can be taken with the help of a turbine to drive an arrangement producing a secondary (bypass) flow. These arrangements for the secondary flow may take various forms: Fig. 3*B* represents a ducted fan located close to the gas generator itself. Fig. 3*C* shows a case where ducted

---

[4] NACA, TN 3789, 1956: "Results of Wind-Tunnel Tests to M.N. of 0.90 of Four-Engine Propeller-Driven Airplane Configuration Having Wing with 40 deg of Sweepback," by G. G. Edwards, J. K. Dickson, F. B. Sutton, and F. A. Demele.

[5] NACA, TN 4279, 1958: "Effects of Fixing Transition on Transonic Aerodynamic Characteristics of Wing-Body Configuration at R.N. from 2.4 to 12 Million," by L. W. Hunton.

[6] NACA, RM A51D30, 1951: "Lift, Drag, and Pitching Moment of Low-Aspect-Ratio Wings at Subsonic and Supersonic Speeds — Plane Triangular Wing of AR 4 with 3% Thick, Biconvex Section," by J. C. Heitmeyer.

[7] NACA, RM A52202, 1953: "Lift, Drag, and Pitching Moment of Low-Aspect-Ratio Wings at Subsonic and Supersonic Speeds — Comparison of 3 Wings of AR = 2 of Rectangular, Swept-Back, and Triangular Platform, including Effects of Thickness Distribution," by R. C. Hightower.

[8] NACA, RM L51H06, 1951: "Effects of R.N. on Aerodynamic Characteristics of Delta Wing at Mach Number of 2.41," by J. E. Hatch, Jr.

[9] "Possibilities of Efficient High-Speed Transport Aircraft," by R. T. Jones. Paper presented at Conference on High Speed Aeronautics, Polytechnic Institute of Brooklyn, 1955.

[10] Journal of Royal Aeronautical Society, Vol. 61, September, 1957, pp. 561–593: "Some Thoughts on Aeronautical Research and Design," by M. B. Morgan.

[11] To what extent the high-speed propeller capabilities will affect its static thrust characteristics is another question.

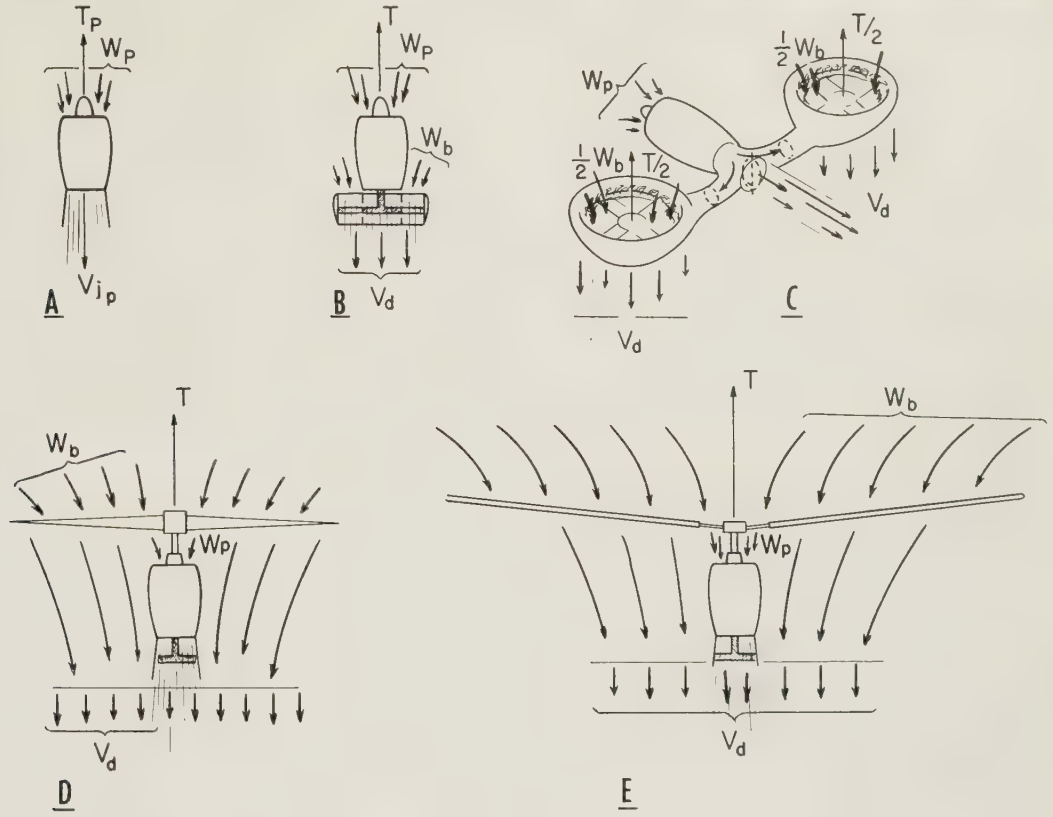

Fig. 3 — Various schemes of the bypass arrangements

fans are physically separated from the gas generator and located, say, in the wings. There, they can be driven either by hot gases ducted to the turbine wheels mounted on the perimeters of the fans (Breguet-Kappus system) or through mechanical shafts, as proposed by this author as an interim solution until the hot gas drive can be developed.

The bypass system may also consist of a propeller as shown in Fig. 3*D*, or finally of a rotor as in Fig. 3*E*.

In all of the above schemes one thing is common: Part of energy, represented by the hot gases leaving the prime gas generator at the initial exhaust velocity V_{jp}, is taken by the turbine and a secondary (bypass) flow is induced at a lower down-wash speed (V_d) than the original one.

Assuming for simplicity that energy from the prime flow of gases is taken in such a way that gases after passing through the power turbine have the same speed as the ultimate downwash velocity of the bypass system,[12] it is easy to develop very simple relationships showing how the thrust specific fuel consumption changes with downwash velocity and how the original thrust is augmented through this arrangement.

Thrust (T_p) which can be obtained from the prime gas generator by discharging directly the gases at their jet velocity V_{jp} will obviously be:

$$T_p = \frac{W_p}{g} V_{jp} \tag{2}$$

where:

W_p = Rate of flow (lb/sec) through the prime system.

Thrust developed by the bypass system plus the prime gas generator will be:

$$T = \frac{(W_p + W_b)}{g} V_d \tag{3}$$

where:

W_b = Rate of flow through the bypass arrangement (Fig. 3)

The ratio of the thrust obtained through the bypass arrangement to that which could be obtained from the prime system, or in other words the thrust augmentation ratio becomes:

$$T/T_p = (1 + W_b/W_p)(V_d/V_{jp}) \tag{4}$$

As to the flow rate ratio (W_b/W_p), it can be determined by the following considerations: Assuming that efficiency of the power turbine (including efficiency of the transmission between the turbine and the bypass flow generator) placed in the stream of gases produced by the prime source of power is η_t and aerodynamic efficiency[13] of the device producing the secondary (bypass) flow of air is η_a, the energy balance can be written as follows:

$$\frac{1}{2}\frac{W_p}{g} V^2_{jp} = \frac{1}{2g}\left(W_p + \frac{1}{\eta_t \eta_a} W_b\right) V_d^2$$

[12] For ducted arrangements it will be equal to the jet exit velocity. For free propellers and rotors it will amount to twice the induced velocity at the disc.

[13] The aerodynamic efficiency is defined as a ratio of ideal induced power required to produce a given thrust to that actually absorbed by the secondary (bypass) flow generator.

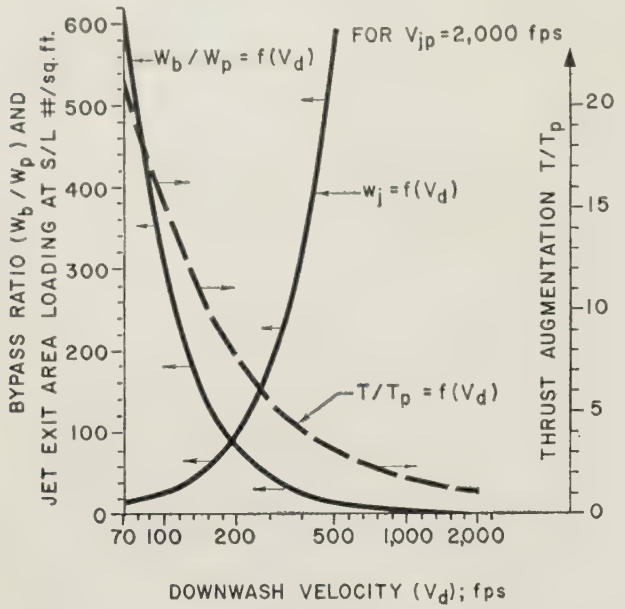

Fig. 4 — Thrust augmentation ratio, bypass rate of flow ratio, and jet exit area loading at sea level shown versus downwash velocity

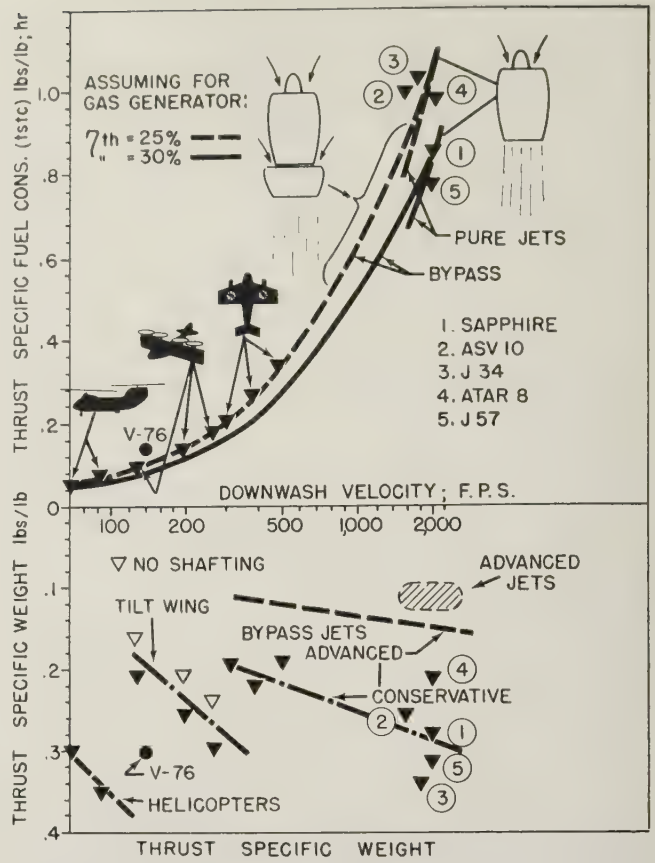

Fig. 5 — Thrust specific fuel consumption and specific weight trends versus downwash velocity

and the flow ratio:

$$W_b/W_p = [(V_{jp}/V_d)^2 - 1]\ \eta_t\ \eta_a \qquad (5)$$

while downwash velocity expressed in terms of the flow ratio becomes:

$$V_d = V_{jp}\sqrt{\frac{1}{1 + (W_b/W_p)\ \eta_t\ \eta_a}} \qquad (6)$$

The W_b/W_p flow ratio is shown versus downwash velocity in Fig. 4. In establishing this graph it has been assumed that jet velocity of the prime source of gas power is $V_{jp} = 2000$ fps, $\eta_t = 0.87$, and for bypass fans $\eta_a = 0.87$. For the airscrew-type bypass devices (unshrouded propellers and helicopter rotors) the aerodynamic efficiency is defined as:

$$\eta_a = 1/\left[k + \frac{3}{4}(\bar{c}_{d_o}/\bar{C}_L)\left(V_t/\frac{1}{2}V_d\right)\right] \qquad (7)$$

where:

k = Ratio of the ideal induced power to the actual one
$\bar{c}_{d_o}$ = Average blade profile drag coefficient
$\bar{C}_L$ = Average blade lift coefficient
V_t = Blade tip speed

It can be seen from Fig. 4 that when downwash velocity comes down to the level, characteristic of helicopters ($V_d = 70$ fps), the bypass flow rate is about 600 times higher than that passing through the prime source of gas power.

As to the thrust augmentation ratio (T/T_p) it can be seen from Fig. 4 that by using a helicopter rotor as a bypass arrangement the original thrust of a gas generator ($V_{jp} = 2000$ fps) can be augmented more than 20 times. For propellers with downwash velocities between 150 and 250 fps, the thrust augmentation ratio will be between 10 and 5, respectively. In order to give some idea regarding loading of the bypass devices, the jet exit area, or the ultimate slipstream loading (w_j)[14] is also shown in Fig 4.

For the VTOL aircraft an important problem lies not only in the proper augmentation of the prime thrust, but also in the fuel consumption associated with this process. The specific fuel consumption per pound of total thrust generated can be developed as follows: Calling η_{th} thermal efficiency of the prime gas power generator, and assuming that fuel lower heating value is 18,600 Btu/lb, the hourly fuel flow becomes:

$$W_F/\text{hr} = \frac{1}{2}\frac{W_p}{g}V^2_{jp}\frac{3600}{778.26 \times 18{,}600\ \eta_{th}}$$

This divided by thrust of the whole bypass system as given by Equation 3, with V_d expressed by Equation 6 becomes:

$$\text{tsfc} = \frac{V_{jp}}{8000\ \eta_{th}} \times \frac{\sqrt{1 + (W_b/W_p)/\eta_t\ \eta_a}}{1 + W_b/W_p} \qquad (8)$$

or, in terms of the downwash velocity:

$$\text{tsfc} = \frac{V_{jp}}{8000\ \eta_{th}} \times \frac{V_{jp}/V_d}{1 + [(V_{jp}/V_d)^2 - 1]\ \eta_t\ \eta_a} \qquad (8A)$$

[14] This is thrust divided by the cross-section of the fully developed slipstream. For ducted fans and ducted propellers (with constant duct area), this will be equal to the disc loading, while for the unshrouded propellers and rotors it will amount to the doubled disc loading.

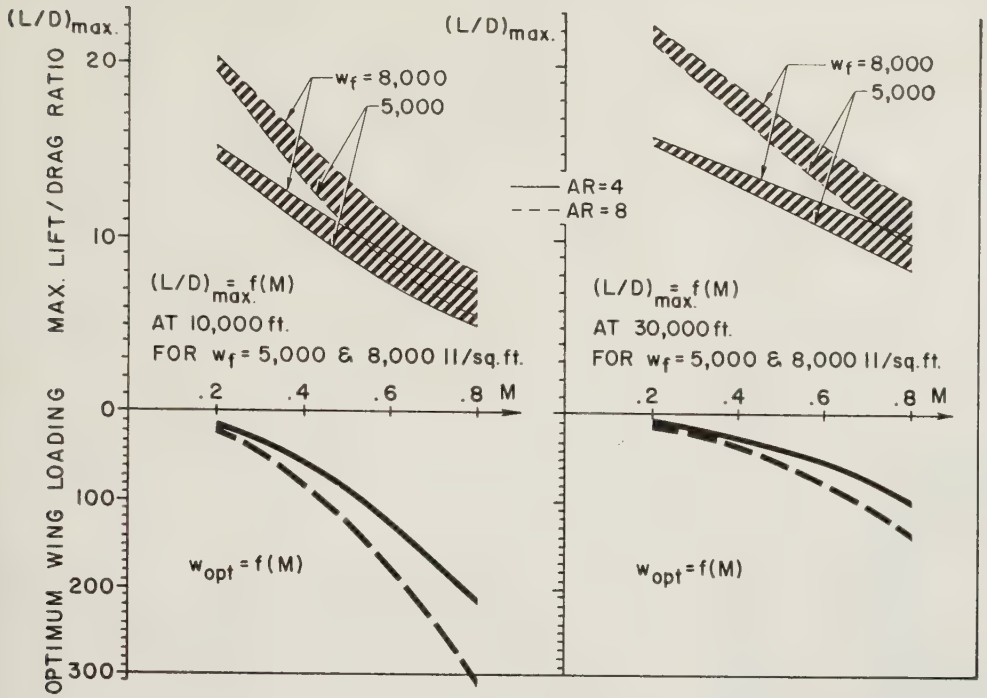

Fig. 6 — Maximum lift/drag ratios and optimum wing loadings of subsonic aircraft

When there is no bypass flow ($W_b = o$, and $V_d = V_{jp}$) the thrust specific fuel consumption becomes (for pure jets):

$$\text{tsfc} = \frac{V_{jp}}{8000\ \eta_{th}} \qquad (8B)$$

The thrust specific fuel consumption is plotted in upper part of Fig. 5 versus downwash velocity for pure jets and bypass arrangements. Two values of thermal efficiency of the prime gas power generator were assumed: $\eta_{th} = 0.30$ and $\eta_{th} = 0.25$.

By inspecting specific thrust fuel consumption values obtained from the designs based on the contemporary turboprop engines it can be seen that they rather follow the $\eta_{th} = 0.25$ curve. The same is true of the older type jet engines. But tsfc of more modern jet engines is located closer to the $\eta_{th} = 0.30$ curve.

Specific weights of the thrust-producing systems are also shown in Fig. 5 (in its lower part). For rotor or propeller equipped aircraft, weight of the thrust-producing system is considered as composed of the weight of the rotors, or propellers, shafting, and powerplant. For jet bypasses, it includes weight of fans and their driving system plus that of the prime gas power generator. This specific weight is defined as a ratio of the above described structural weights to the static thrust developed by the system.

It can be seen that specific weight patterns versus V_d are not as regular as those of the thrust specific fuel consumption. Furthermore, it can be noticed that there are rather separate trend lines for helicopters and tilting wing aircraft with a tendency (within each group) toward decreasing specific weight with the decreasing downwash velocity.

Specific weight trends for the jet propulsion systems can be established in the following way: Design studies of the wing-submerged ducted fans (Vertodyne[15]) give a few points of the specific weights at lower downwash velocities. Those studies were based on rather conservative jet engine designs; it may be assumed, hence, that the corresponding specific weight trend curve will assume a shape shown by the dash-point line at the bottom of Fig. 5. Whether the same general slope versus decreasing downwash velocity will be maintained in the bypass arrangements based on more advanced, light (about 0.10 lb per lb of jet thrust) prime hot gases generators, it is difficult to predict at this time. However, it may be assumed that, allowing for some initial jump in the specific weight due to the bypass installation, this specific weight value will, in general, decrease with the decreasing downwash velocity (dashed line at the bottom of Fig. 5).

Optimization of Vertical Thrust Generator Plus Wing System

Having established tsfc and specific weight trends as shown in Fig. 5, the problem of an optimum combination of the vertical thrust generator and wing for speed regions of $M = 0.8$ and $M = 2.0+$ can be considered. Possible weight penalties resulting from cruising at lower altitudes than normally considered

[15] *Aero Engineering Review*, Vol. 16, September, 1957, pp. 60–68: "Evaluation of VTOL Systems Suitable for Transport Aircraft," by W. Z. Stepniewski and J. Mallen.

as most suitable for jets can also be investigated.

M = 0.8 Region — Maximum lift-to-drag ratio trends in the subsonic region shown in Fig. 2 are based on models of conventional aircraft where wing area in proportion to the fuselage cross-section may be larger than in VTOL aircraft. In order to obtain a more realistic picture for this latter category, two values of equivalent flat-plate area loading of $w_f = 5000$ and 8000 psf were assumed and maximum lift-to-drag ratios have been computed up to $M = 0.8$ for flight altitude of 10,000 and 30,000 ft and aspect ratios of AR = 4 and AR = 8 (Fig. 6).

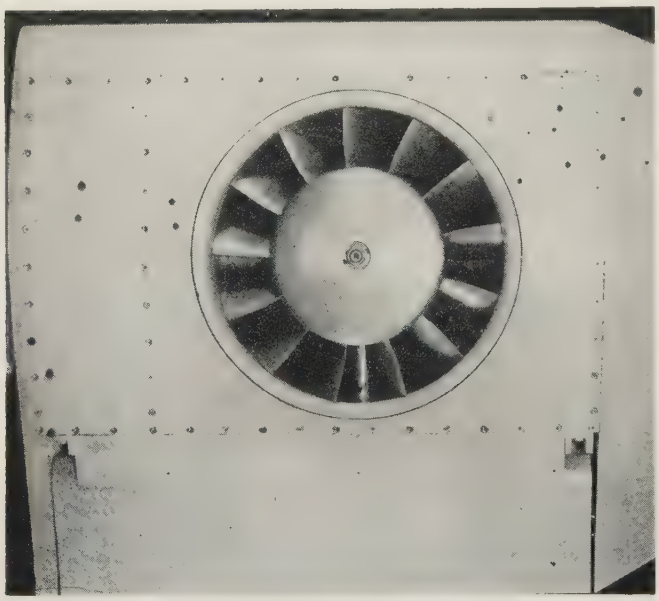

Fig. 7 — Wind tunnel model of the Vertodyne wing and fan

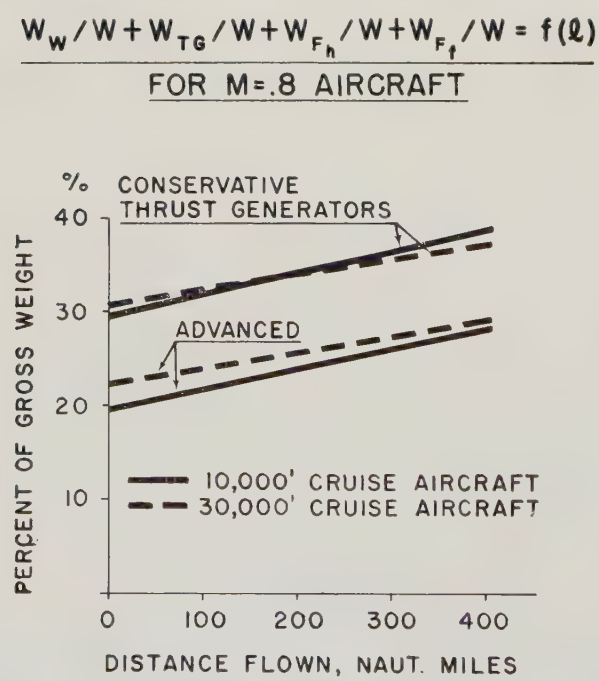

Fig. 8 — Comparison of sum of relative weights of wing, thrust generators, and fuel versus distance flown for VTOL aircraft designed to cruise at 10,000 and 30,000 ft

A glance at Fig. 6 will indicate that at high subsonic speeds the aspect ratio is of a lesser importance than the aerodynamic cleanliness. Attention will be concentrated, hence, on the combination of AR = 4 and $w_f = 8000$ psf.

For the above selected values $(L/D)_{max} = 7.2$ is obtained for the 10,000-ft cruise aircraft and $(L/D)_{max} = 10.2$ for the 30,000 ft.

Accounting for the loss of thrust with altitude ($T_{10000} = 0.76\ T_{SL}$ and $T_{30000} = 0.455\ T_{SL}$) and assuming that actual cruise is performed at 85% of the thrust available at an altitude, sea level thrust installed requirements (dictated by cruising) can be established. These values as well as minimum hovering thrust requirements and the resulting thrust augmentation ratios are shown in Table 1.

It can be seen from Table 1 that in order to hover and maneuver at take-offs and landings, a vertical thrust more than four times larger than that resulting from the cruise considerations is required. Various solutions may be considered for closing that gap:

1. Favorable ground effect.

Advantage can be taken of the favorable ground effect by discharging vertical thrust generating gases along the periphery of the wing. According to von Glahn[16] thrust augmentation ratio of about 2 can be obtained for annular nozzles. Whether the same effects can be obtained for other than circular planforms of the wing, it is not known. But even for the circular shape the disadvantage of this method lies in a rapid decrease of the augmentation ratio with the elevation from the ground. At h/D ratio of about 0.6 the augmentation factor drops to 1.2 only. This means than an aircraft with a circular wing of say 30-ft diameter hovering 24 ft from the ground would little benefit from this favorable ground effect. Furthermore, even maximum thrust augmentation which can be obtained through the ground effect is still not sufficient to close the gap between the cruise and take-off and/or landing thrust requirements. This means that still some additional means of thrust augmentation and/or generation would be required.

2. Special hovering jets.

This solution has been discussed more thoroughly in Stepniewski.[15] It may be mentioned here that in many types of practical operations an impingement of high-speed hot gases on the ground may be objectionable.

3. Thrust augmentation through Bypass.

This method offers a great variety of the thrust augmentation ratios; hence, it will be examined more closely.

Last two columns of Table 1 give downwash velocities and loadings of the bypass thrust generators. Those last values amount to 210 psf for the 10,000-ft cruise aircraft and to 310 psf for the 30,000-ft one. The optimum wing loading as given by Fig. 6 would be 210 and 100 psf, respectively.

This means that for the 10,000-ft cruise aircraft a jet exit area equal to that of the wing should be provided, while for the 30,000-ft one it would

[16] NACA, TN 3982, 1957: "Exploratory Study of Ground Proximity Effects on Thrust of Annular and Circular Nozzles," by U. H. von Glahn.

amount to only 31% of the wing area. Provision for the bypass flow with a jet exit area as large as that of the wing may be rather difficult. By contrast a bypass flow jet exit area equal to say one fourth or perhaps one third of the wing area can be realized in the wing submerged ducted fan concepts shown in Fig. 3C and Fig. 7. Wing submerged ducted fans may be considered, hence, as a possible direct solution for the thrust augmentation problem for the 30,000-ft cruise aircraft. For the 10,000-ft cruise aircraft, however, application of the wing ducted fan concept would require one of two things:

a. Maintain the bypass thrust generator loading as given in Table 1 and increase the wing until it can accommodate the fans, or

b. Retain the optimum wing loading and increase loading of the ducted fans until they can be located in the wing. This obviously would require installation of a larger prime gas generator than dictated by cruise.

An investigation of the two above approaches regarding weight of the wing-thrust generator combination should be quite instructive. Assuming that weight of the wing is 10 psf, it can be easily seen that say doubling of the wing area would increase the relative weight of the wing from 4.8 to 9.6% while doubling of the jet exit velocity (reduction to the ½ of the original jet exit area) would increase the relative weight of the thrust generating system by 2.5% only (from 19.5 to 22%) for the conservative specific weight trend of Fig. 5 and by 1% (from 11 to 12%) for the advance designs.

It may appear, hence, that whenever a conflict exists between the optimum wing loading and size of the bypass flow generator, the wing loading assuring the smallest wing should be retained and loading of the thrust generator increased.[17]

The above conclusion may be modified, however, when due to a long time in hovering weight of fuel required for this regime of flight becomes significant. But as it can be seen from Table 2 this is not the case in the considered example where 5-min hovering time has been assumed.

Using values indicated in Table 2, Fig. 8 was prepared. In this graph the sum of the relative weights of wing, thrust generating system, fuel for 5-min hovering, and fuel required in forward flight is shown versus distance flown for the 10,000- and 30,000-ft cruise aircraft. It can be seen from Fig. 8 that due to the greater freedom in selecting wing size of the VTOL aircraft, it will probably be possible to design special aircraft for the low-altitude operations (at high subsonic Mach numbers) which for a few hundred mile range will have payload capacities equal to those of the VTOL aircraft designed to operate at higher altitudes, generally more suitable for jet-propelled aircraft.

M = 2.0 plus Region — Some problems of the high-speed VTOL aircraft have been discussed by O'Malley.[18] At this point it may be mentioned only that due to the noise problem and temperature rise

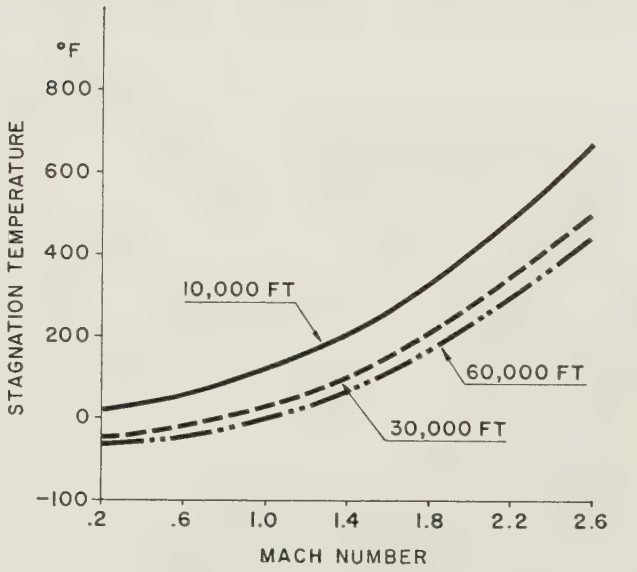

Fig. 9 — Stagnation temperature versus Mach number

Table 1 — Thrust at Two Altitudes

Cruise Altitude, ft	S/L Thrust from Cruise	Hovering Thrust Required	Thrust Augmentation Ratio	Downwash Velocity, fps	Bypass Thrust Generator Loading, psf
10,000	0.23 W	1.10 W	4.8	300	210
30,000	0.27 W	1.10 W	4.1	360	310

Table 2 — Fuel Requirements at Two Cruise Altitudes

Cruise Altitude, ft	Wing Weight, W_W/W, %	Thrust Generating System Weight, W_{TG}/W, %		Fuel Requierd	
		Conservative	Advanced	for 5 ft Hover, W_{F_h}/W, %	for 100 N. Miles W_{F_f}/W, %
10,000, optimum wing and thrust generator[a]	4.8	19.5	11.0	1.65	2.05
10,000, optimum wing, larger thrust generator	4.8	22.0	12.0	3.10	2.05
30,000	9.0[b]	20.0	11.5	1.85	1.60

[a] Aircraft structurally not feasible.
[b] Assumed structural weight of 9 psf.

(Fig. 9) those Mach 2 + VTOL aircraft will probably operate at altitudes higher than 30,000 ft. Due to this fact and lower $(L/D)_{max}$ values than for the 0.8M aircraft, the gap between the sea level thrust requirements as dictated by cruise and those resulting from hovering will be narrower than for the previously considered cases. With a low augmentation ratios and a short time required in hovering it may be more advantageous to install special hovering jets than to resort to the bypass arrangements. (See specific weight trends for advanced designs in Fig. 5.) Should, however, the bypass system be required, then ducted fans can be located either in the wings, or somewhere else.

Even if the wings had their optimum loading (Fig. 10), it should not be difficult to submerge fans in them. This is due to the fact that in spite of low airfoil thickness ratios required at Mach 2 speeds, there should be enough space for the fans because

[17] STOL considerations and ease of transition from hovering to forward flight may dictate selection of a lower wing loading than optimum.

[18] "Supersonic Civil Air Transports wtih Considerations of Potential VTOL Capabilities," by J. A. O'Malley. Paper presented at meeting of Institute of Aeronautical Sciences, 1958.

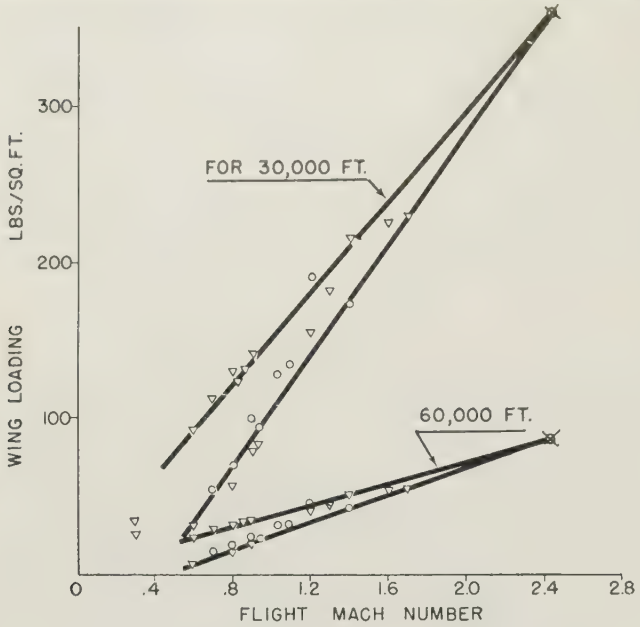

Fig. 10 — Optimum wing loading trends up to high Mach numbers

of the relatively large wing chords resulting from the delta, or "paper arrow" planforms. Location of the bypass arrangements in the wing may be preferrable to other solutions due to the fact that it would not increase the aircraft frontal area, and this may be an important factor as far as drag at those high speeds is concerned.

Concluding Remarks

Considerations presented in this paper are not detailed design studies. It can be expected, hence, that actual designs may deviate from the trends indicated here. Nevertheless, it is believed that keeping in mind the above reservations some general conclusions can be made.

1. Reviewing a large spectrum of VTOL aircraft, from low subsonic to Mach 2+, it can be seen that (as in conventional airplanes) three speed regions, favorable because of the cruising fuel consumption, can be identified:

a. Low and medium subsonic, up to $M = 0.6$ or 0.7, where airscrew-type VTOL aircraft seem to be most promising.

b. High subsonic (around $M = 0.8$) where jet-propelled VTOL systems become more advantageous and where a large disparity exists between the installed thrust requirements as resulting from cruising and those dictated by the take-off and landing maneuvers.

c. Mach 2+ region, where turbojets still seem to represent the most suitable powerplants and where the gap between the installed thrust requirements from cruise and that from take-off and landing is narrower.

2. Technique of the vertical take-off and landing offers an opportunity to reduce the wing to its optimum size as dictated by the cruising conditions. This should reduce to some extent weight penalties resulting from the necessity of providing a thrust generating system capable of developing thrust much higher than required in cruise.

3. In order to decrease the weight penalty associated with the thrust generator, the bypass system (automatically incorporated in all airscrew-type turbine-powered VTOL aircraft) should be used up to the Mach 0.8 VTOL machines. Under some conditions it may be advantageous even for the Mach 2 VTOL airplanes.

4. Whenever in jet-propelled aircraft large bypass flow ratios are required, wing submerged ducted fans may be superior to other systems.

5. Should a conflict exist between an optimum size of the wing and thrust augmentation ratio, then from the weight point of view it would probably be advantageous to lean toward retaining this optimum wing and to compromise on the thrust augmentation ratio.

6. The greater freedom in selecting wing size opens a way toward at least partial compensation, (through lower structural weight) of the higher fuel consumption resulting from low cruising altitudes, which may be imposed on VTOL aircraft as a result of the airspace congestion, or for tactical reasons.

APPENDIX

Symbols

$\bar{C}_L$ = Blade average lift coefficient
$\bar{c}_{d_0}$ = Blade average profile drag coefficient
D = Drag, lb; or diameter, ft
L/D = Lift to drag ratio
M = Mach number
V_d = Downwash velocity, fps
V_{jp} = Jet exit velocity of the prime gas generator, fps
V_t = Tip speed, fps
W = Gross weight, lbs
W_{F_h} = Fuel weight in hovering, lb
W_{F_f} = Fuel weight in forward flight, lb
W_{TG} = Weight of the thrust generating system, lb
W_W = Weight of the wing, lb
W_p = Rate of flow through the prime gas generator lb/sec
W_b = Rate of flow through the bypass arrangement lb/sec
w_j = Jet exit area loading, psf
w_f = Equivalent flat plate area loading, psf
T = Thrust of whole thrust generating system, lb
T_p = Thrust from the prime gas generator, lb
g = Acceleration of gravity, 32.2 ft/sec^2
h = Height, ft
k = Ratio of the ideal induced power to the actual one
sfc = Specific fuel consumption, lb/hp, hr
tsfc = Thrust specific fuel consumption, lb/lb, hr.
η_{th} = Thermal efficiency
η_a Aerodynamic efficiency
η_t = Power turbine and transmission efficiency

Iron-Aluminum Base Alloys— cheap stainlesses of the future?

Blake King, J. J. Mueller, N. N. Ida, and F. G. Tate, The Martin Co.

This paper was presented at the SAE Summer Meeting, Atlantic City, June 11, 1958.

DESIGNERS are faced today with an increasing number of applications requiring alloys that resist atmospheric corrosion and high-temperature oxidation. Unfortunately, in shopping around for materials that meet our needs we come face to face with some stern economic realities. The conventional corrosion-resistant alloys are expensive, and in these troubled times they can become scarce overnight because of the strategic metals they contain. The newer alloys, particularly those developed under military sponsorship for nuclear or aircraft applications, tend to be costlier still and of more uncertain availability.

A positive statement would be premature, but there are indications that iron-aluminum base alloys can be developed that will be exceptions to the tendency for better materials to command higher prices and be harder to get. Several laboratories are engaged in developing and testing Fe-Al base alloys, and have succeeded in producing many experi-

IRON-aluminum base alloys have shown great resistance to high-temperature oxidation, the authors report. These alloys can be made to exceed the resistance of any stainless steel.

Several problems exist in connection with the alloys: room-temperature brittleness, only moderate high-temperature strength, and susceptibility to grain growth. However, the authors think these problems will probably be solved with further experimentation.

The principal advantages of the alloys are their low cost and availability, factors in case a chromium shortage affects the availability of straight-chromium stainless steels.

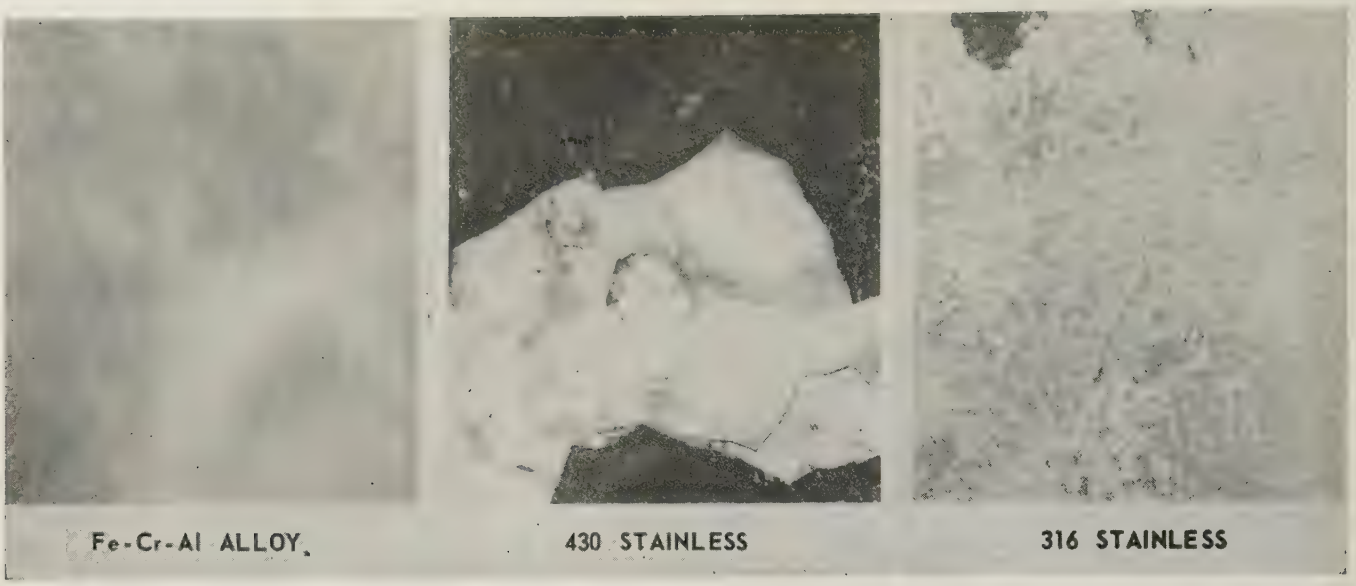

Fig. 1 — Appearance of specimens after 68 hr in air at 1850 F.

mental materials that exhibit attractive properties.

The most striking characteristic of Fe-Al base alloys is their phenomenal resistance to high-temperature oxidation, which can be made to exceed that of any stainless steel. Fig. 1 shows the apperaance of a 5.5 Al, 9.5 Cr, 0.5 Ti, 0.03 C, balance Fe alloy, a ferritic stainless steel, and an austenitic stainless after a week's exposure to still air at 1850 F.

Aluminum alone seems not to be as effective as chromium in inhibiting room-temperature corrosion, but a combined aluminum-plus-chromium addition appears on the basis of preliminary tests to be nearly as influential as straight chromium in this respect. In Fig. 2 are photographs of the Fe-Cr-Al alloy described above and Type 430 stainless steel after being subjected to a salt-spray test.

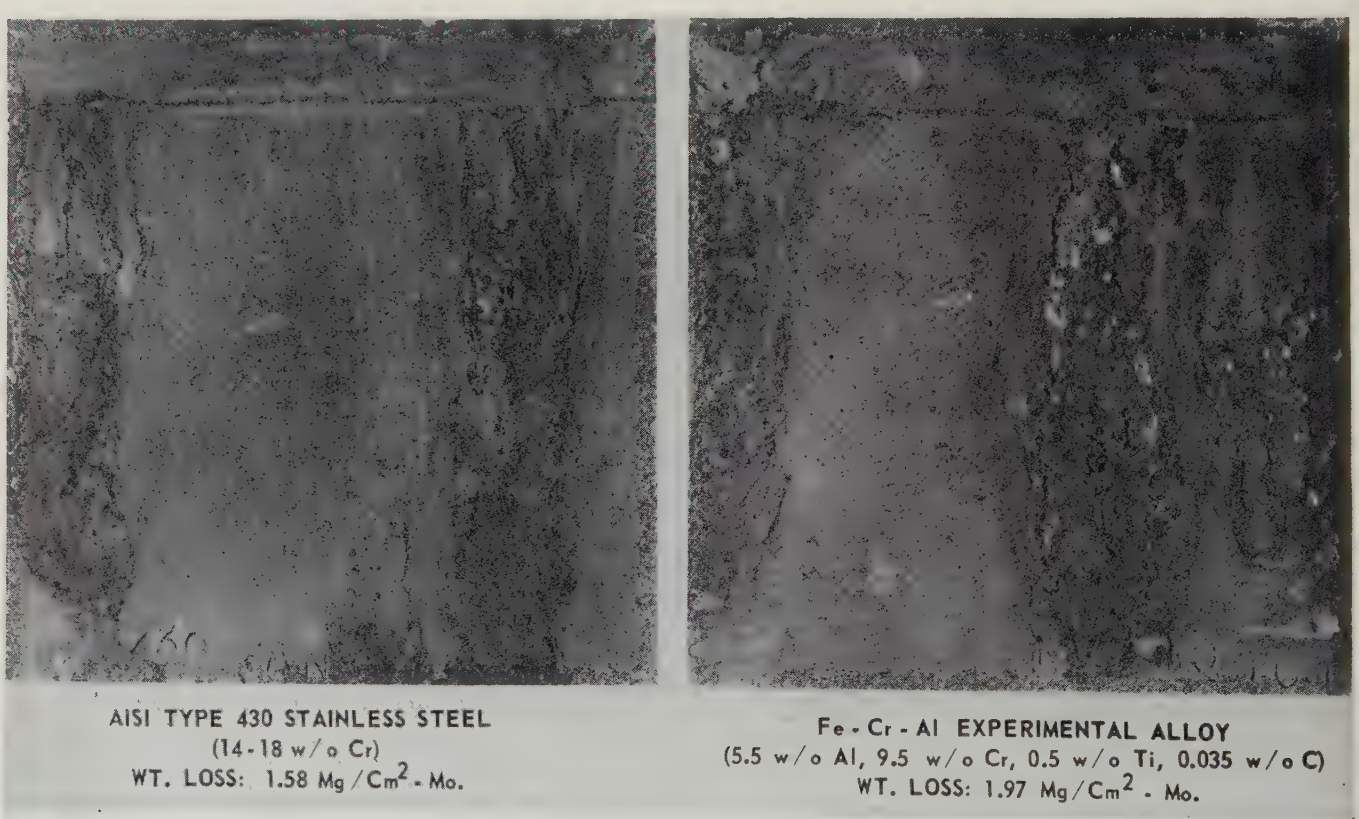

Fig. 2 — Appearance of specimens after salt-spray test of 672-hr exposure of 20% NaCl at 95 F.

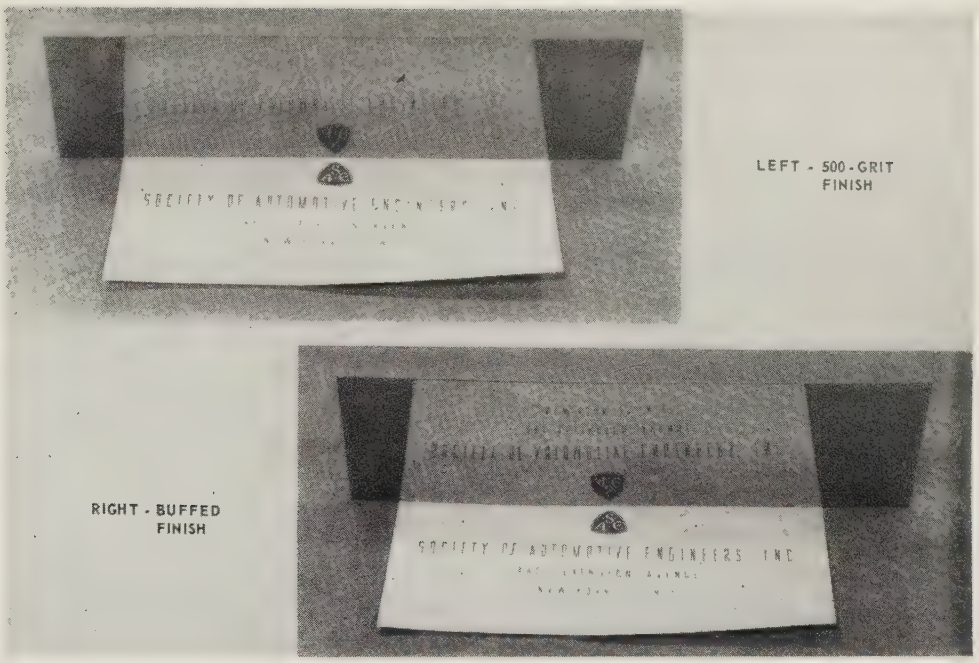

Fig. 3 — Quality of surfaces produced on cold-finished 5.5 Al, 9.5 Cr, 1 Ti, balance Fe alloy

Iron-aluminum base alloys are capable of taking a high polish: the highly reflective finish shown in Fig. 3 was produced by buffing. While the polished surface does not have the blue-white color of chromium plate, it is a considerable improvement over the faint yellowish cast of some stainless steels.

Cost-wise, it is probable that Fe-Al base alloys could be made competitive with straight-chromium stainlesses, and being nickel-free, they are inherently cheaper than the austenitic varieties of stainless steel. In Fig. 4 the prices of several types of stainless sheet are compared with prices predicted for some Fe-Al base alloys if they were to be produced commercially in sheet form. These latter prices were arrived at with the aid of the following formula, and are admittedly only roughly approximate:

Predicted Price of Fe-Al Base Alloy Sheet =

$$\text{Current Market Price of Stainless Steel} \times \frac{\text{Cost of Raw Materials for Fe-Al Base Alloy}}{\text{Cost of Raw Materials for Stainless Alloy}} \quad (1)$$

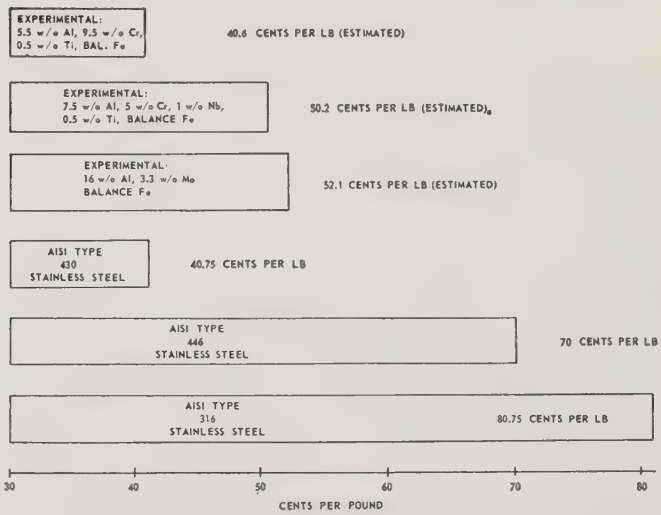

Fig. 4 — Relative costs of certain Fe-Al base experimental alloys and competitive stainless steels

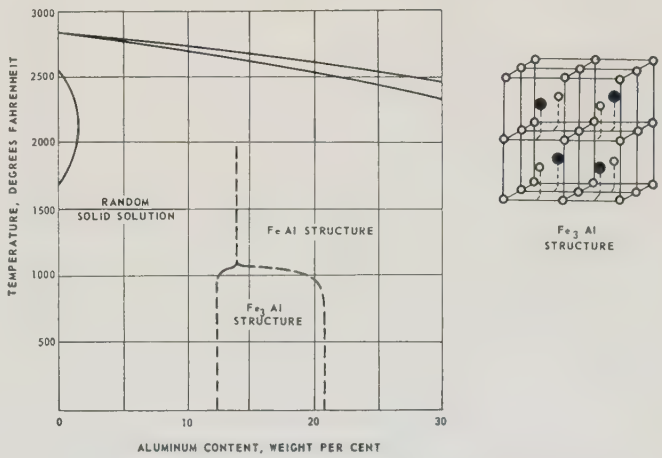

Fig. 5 — Iron-aluminum equilibrium diagram (after Fink and Willey, 1948 Metals Handbook)

Problems in Iron-Aluminum Alloy Development

The use of binary iron-aluminum alloys in the past has been severely limited by their room-temperature brittleness, and this brittleness is still a formidable problem. While there is much to be learned about the basic physical metallurgy of the Fe-Al system, some agreement exists that these interrelated factors contribute to poor room temperature ductility:

1. The appreciable difference between the ion diameters and crystal structures of iron and aluminum.
2. The tendency of an Fe_3Al type ordered structure to come into being in alloys containing 13–21 w% aluminum (Fig. 5).
3. An apparent sensitivity of these materials to

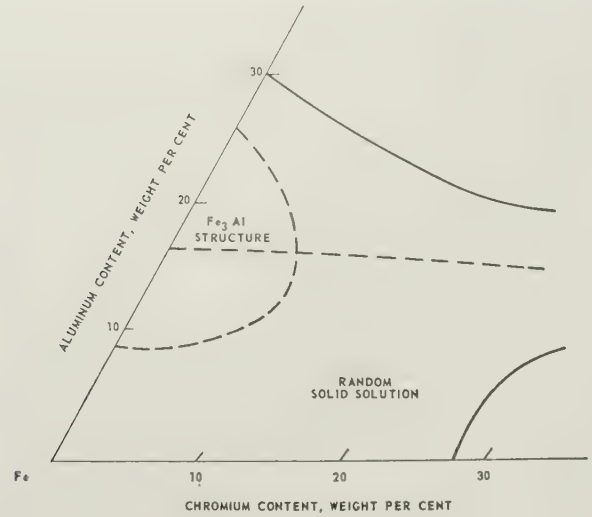

Fig. 6 — Iron-rich corner of Fe-Cr-Al ternary diagram (after Kornilov)

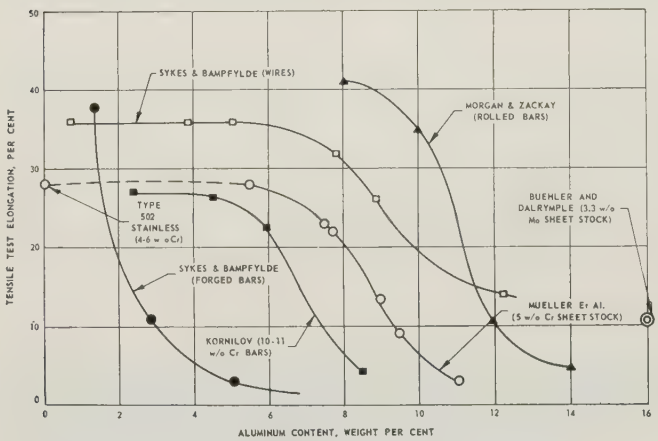

Fig. 7 — Effect of aluminum on ductility of annealed alloys

the effects of interstitially dissolved elements.

4. A considerable propensity for grain growth at high temperatures.

A second inherent deficiency of binary Fe-Al alloys lies in their only moderate high-temperature strength, a fault which they share with the ferritic stainless steels. Aluminum additions tend to prevent the allotropic transformation in iron, and Fe-Al base alloys retain a body-centered cubic structure at all temperatures.

The susceptibility of Fe-Al alloys to grain growth also makes them very difficult to weld. The weld zone is usually characterized by a coarse, columnar structure when Fe-Al filler metal is used. The use of an austenitic filler metal results in a ductile deposit, but the heat-affected zone next to the weld becomes brittle.

Development Program

The general plan of attack adopted by the authors to overcome these disadvantageous properties involves first the employment of a fairly sizeable addition of a third element, selected principally for its ability to eleminate the superlattice as a source of difficulty. Fig. 6 is a portion of a room-temperature isothermal section through an Fe-Cr-Al ternary equilibrium diagram,[1] showing the back boundary of the ordered state space. In the more promising alloys prepared by the writers, chromium has been used to insure compositions well away from those in which the superlattice might form. In addition, chromium contributes to corrosion resistance. The fact that a moderate amount of information on the metallurgy of the Fe-Cr-Al system exists in the literature[2, 3] also influenced the choice of chromium as a ternary addition.

So that the compositions of the exploratory alloys could be controlled closely and atmospheric contamination disregarded in correlating compositions and properties, it was decided to vacuum-melt the experimental heats.

Other alloying elements in addition to chromium and aluminum are added in small quantities to impart specific characteristics to the alloys. The effects of these metals on the properties of an iron-aluminum base are described in the literature. Additions of titanium, silicon, tantalum, molybdenum, and beryllium are thought to promote high-temperature strength and good creep properties.[3, 4, 5] Titanium, tantalum, and niobium (columbium) tend to improve room temperature ductibility.[6, 7] We have found zirconium additions to have a beneficial effect on the way in which certain alloys respond to heat treatment.

A unique feature of the development program is the adaptation of statistical techniques to the design of experiments. The use of factorial schemes in planning series of melt compositions has made it possible to evaluate independently the effects of single additives in five- and six-component alloys with all the components being varied from heat to heat.

Properties of Experimental Alloys

As noted above, the principal problem involved in the development of Fe-Al alloys is that of ductility. In Fig. 7 curves are plotted showing the ductilities reported by some of the investigators who have studied the properties of these materials. It should be noted that specimen size and shape as well as aluminum content have an appreciable effect on specimen ductility; rounds are considerably more ductile than sheet materials, and wires have an advantage over rods. The curve on the left is from the results of tests conducted by the British metal-

[1] Pp. 38–50 of "Zheleznye Splavy," Vol. 1, by I. I. Kornilov. Moscow, 1945. (Brutcher Translation No. 1966)

[2] "Alloys of Iron-Chromium-Aluminum," by I. I. Kornilov. Pub. by Polygrafkniga, Moscow, 1945.

[3] Battelle Memorial Institute Report No. BMI-922, 1954: "Investigation of Wrought Iron-Chromium-Aluminum Alloys for Service at 2200 F," by H. A. Saller, J. T. Stacy, and N. S. Eddy.

[4] *Metal Progress*, Vol. 68, October, 1955, pp. 126–128: "Ductile Iron-Aluminum Alloys," by E. R. Morgan and V. F. Zackay.

[5] NAVORD Report 3700, U. S. Naval Ordnance Laboratory, June, 1954: "Thermenol, Non-Strategic Aluminum-Iron Base Alloy for High-Temperature Service," by J. F. Nachman and W. J. Buehler.

[6] Archiv Eisenhüttenwessen, Vol. 13, 1942, pp. 539–542: "Influence of Alloy Additions upon Some Properties of Heat Resistant Iron-Aluminum Alloys," by H. Cornelius and W. Bungardt. (Brutcher Translation No. 965)

[7] NAVORD Report 5744, U. S. Naval Ordnance Laboratory, October, 1957: "Metallurgical Factors Affecting Tensil Properties of Fe-Al Base Alloys," by W. J. Buehler and C. G. Dalrymple.

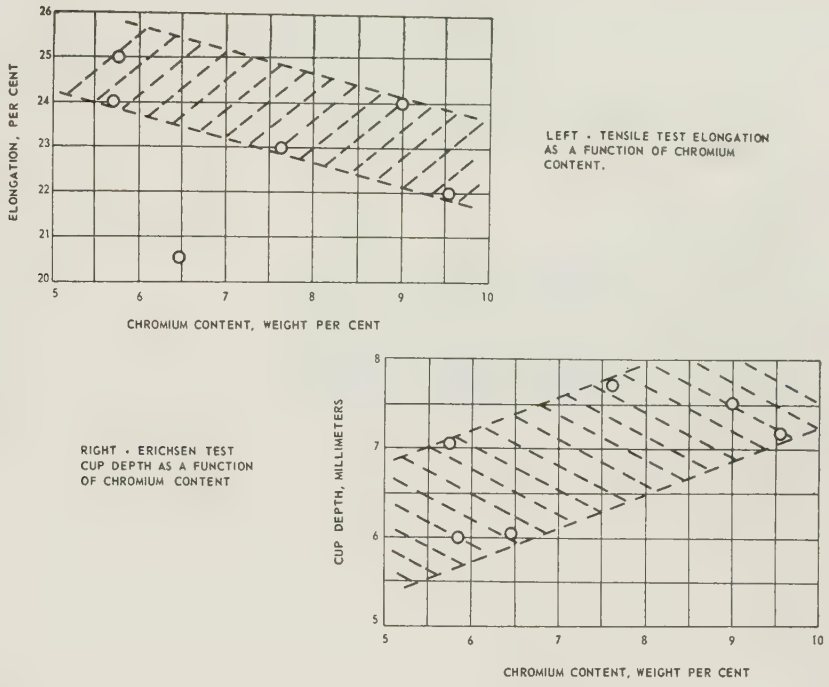

Fig. 8 — Effect of chromium content on ductility of 4.14-5.85 Fe-Al alloys

lurgists Sykes and Bampfylde[8] in 1934 on forged bars of air melted material which were annealed at 1380F and furnace-cooled. Sykes and Bampfylde also tested 0.043-in. diameter annealed wires drawn from air-melted alloys and obtained much higher ductilities than those exhibited by their forged bars. Data reported by Kornilov,[2] a contributor to the very considerable Russian effort in this field, are plotted to indicate the effect of chromium on ductility; it is probable that air-melted annealed bar-stock specimens were used. Morgan and Zackay[4] reported the results plotted in the right-hand curve; it is understood that the specimens were machined from $\frac{5}{8}$-in. diameter vacuum-melted rolled bars which had been annealed at 1400 F, and that the gage-length diameter was 0.250 in. The single point plotted at 16 aluminum represents the ductility that personnel at the Naval Ordnance Laboratory[7] have been able to induce in 0.020-in. Thermonel sheet (16 Al, 3.3 Mo, balance Fe); this piece of data is significant in that it is the impressive result of an investigation of heat-treating procedures.

The results of some preliminary work carried out by the writers are reflected in the center curve; the tests were performed using annealed sheet stock specimens 0.030–0.040 in. thick. This material contained 4.95–5.57 chromium. That it exhibits lower ductility is attributed to (1) its chromium conent, (2) the fact that heat-treatments and rolling procedures, to which the properties of Fe-Cr-Al alloys seem to be very sensitive, were not completely optimized for each of the alloys, and (3) the use of sheet-stock tensile specimens. A point is plotted to indicate the ductility of a 5 Cr alloy so that the effect of aluminum may be better evaluated.

[8] *Journal* of Iron Steel Institute, Vol. 130, 1934, pp. 389–418: "Physical Properties of Iron-Aluminum Alloys," by C. Sykes and J. W. Bampfylde.

Table 1 — Properties of 5.5 Al, 9.5 Cr, 0.5 Ti, 0.03 C, Balance Fe Alloy Compared with Those of AISI Type 430 Stainless Steel

	Experimental Alloy[a]	AISI Type 430
Yield Strength (0.2% Offset), psi:		
Annealed Material	64,000	35,000 min[b]
30% Cold Worked Material	108,400	—
Ulitmate Tensile Strength, psi:		
Annealed Material	82,900	70,000 min[b]
30% Cold Worked Material	109,450	—
Elongation, % in 2 in.:		
Annealed Material	22.0	20 min[b]
30% Cold Worked Material	4.0	—
Erichsen Cup Depth, mm (Annealed Material)	7.2	7–9[c]
Minimum Bend Radius (Annealed Material)	½ T	½ T[b]

[a] Martin Co. test data—0.030–0.040 in. sheet.
[b] ASTM A 176-54.
[c] AISI Steel Products Manual.

Two experimental alloys prepared by our Nuclear Division will be described. The second of these shows such promise that application has been made for a patent on a range of compositions in which it is included.

The first of these is 5.5 Al, 9.5 Cr, 0.5 Ti, 0.03 C, balance Fe material that appears to possess properties comparable to those of Type 430 stainless steel. The salt-spray corrosion resistance of this alloy is indicated in Fig. 2. Its mechanical characteristics are shown in Table 1, and are compared with values for corresponding properties of Type 430 stainless. It will be noted that the material shows a decided tendency to work-harden.

Chromium has been found to have an interesting effect on the ductility of low-aluminum alloys of this type. Plotted in Fig. 8 are curves correlating chromium content with tensile-test and Erichsen Cup Test ductility. A tendency on the part of chromium to reduce tensile ductility is indicated; on the other hand, chromium additions seem to enhance the deep-drawing capability of these alloys.

The second alloy contains a nominal 7.5 Al, 5 Cr,

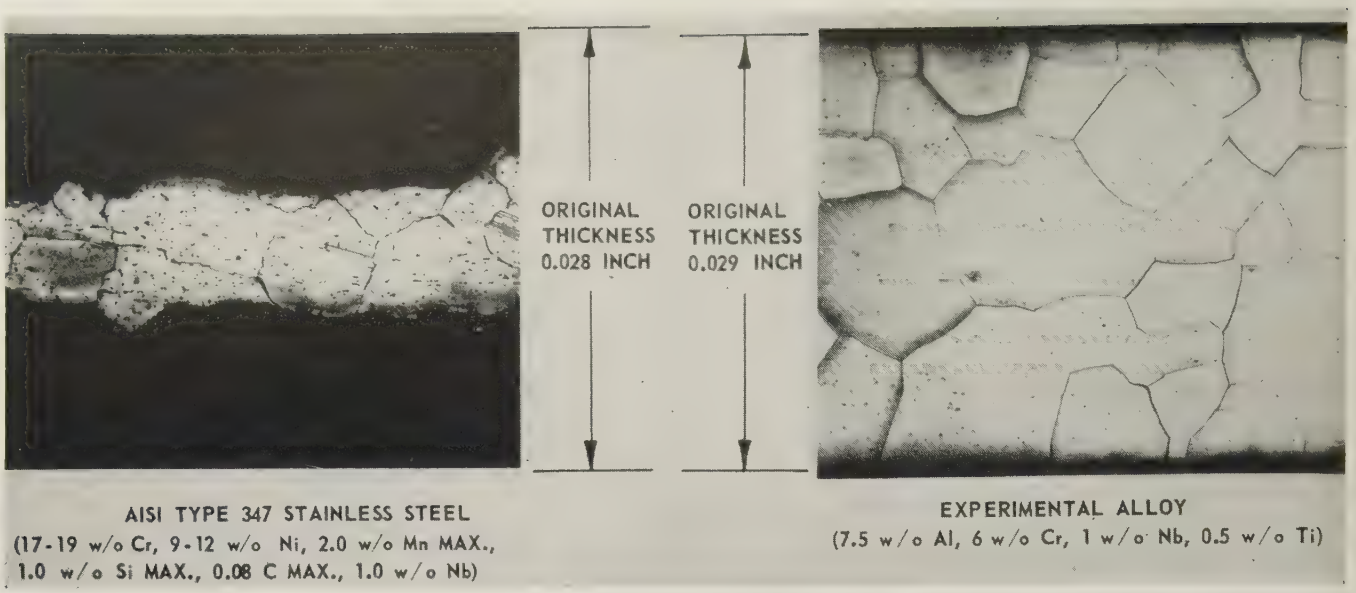

Fig. 9 — Photomicrographs of sections through specimens exposed to still air at 2000 F for 400 hr (magnified 100 times)

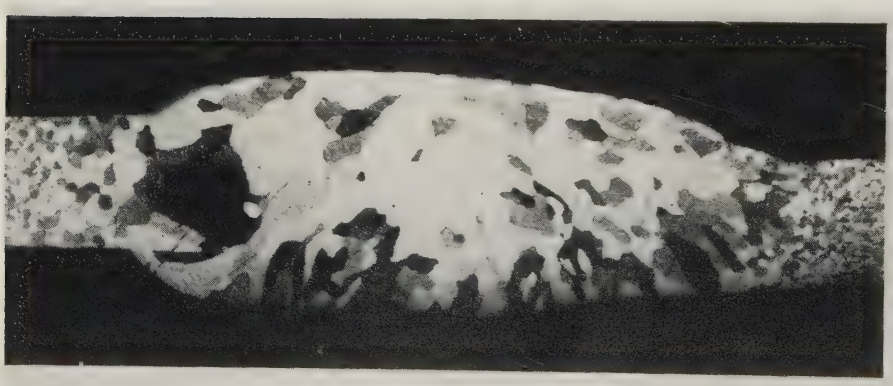

FUSION WELD MADE WITH INERT-GAS SHIELDED-ARC EQUIPMENT; FILLER METAL OF SAME ANALYSIS AS BASE. 25X.

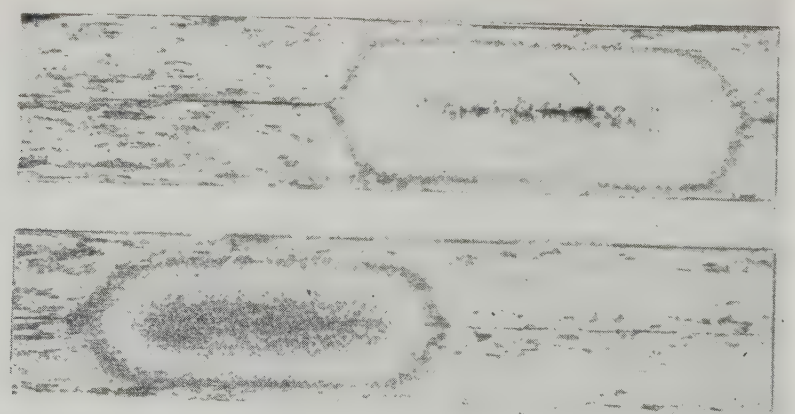

RESISTANCE SPOT WELDS. TOP: WELD INVOLVING FORMATION OF MOLTEN NUGGET. BOTTOM: SOLID-STATE RECRYSTALLIZATION BOND. 14X.

Fig. 10 — Welds in 7.5 Al, 5 Cr, 1 Nb, 0.5 Ti experimental alloy

1 Nb, and 0.5 Ti in an ingot-iron base, and was the forerunner of a family of alloys currently being developed for gas-cooled reactor applications. No deliberate attempt was made to impart good high-temperature properties in the design of this particular alloy; the primary concern was to make a material having sufficient ductility to be fabricated into cladding for fuel elements and other core components. Its mechanical properties, together with those of some competing alloys, are listed in Table 2; all the data apply to annealed material. The exceptional oxidation resistance of this alloy in illustrated in Fig. 9.

Neither of the alloys described above can be successfully fusion-welded. A transverse section through a weld shows the coarse, brittle structure that results when the metal is melted and solidified (Fig. 10). Resistance welds, particularly those made without producing a molten "nugget" are, on the other hand, strong and ductile. (See Fig. 10.)

There is good reason to believe that the high-temperature strength problem is not insurmountable. The decided improvement brought about by a molybdenum addition to an Fe-Al base alloy is illustrated by data obtained from stress-rupture tests on two alloys developed by Nachman and Buehler of the Naval Ordnance Laboratory. Stresses required to rupture sheet-stock specimens in 100 hr at 1500 F were 890 psi for "Alfenol" (16 Al, 84 Fe), and 2100 psi for "Thermenol" (16 Al, 3.3 Mo, 80.7 Fe). High-temperature strength can also be developed by means other than solid-solution effects. In the current Martin program, consideration is being given to two possibilities: the formation of precipitated phases that are stable at high temperatures, and the admixture of a finely divided insoluble refractory.

Considerable success has been had in hot-roll bonding the 7.5 Al, 5 Cr alloy to other materials, including some of the high-hot-strength alloys. Photomicrographs showing bond interfaces between an Fe-Cr-Al alloy and other materials can be seen in Fig. 11. Composite materials made in this fashion combine the oxidation resistance of an aluminum-bearing clad with the high-temperature strength of the base material.

Summary

Iron-aluminum base alloys exhibit unsurpassed oxidation resistance. There are indications that

Table 2 — Properties of 7.5 Al, 5 Cr, 1 Nb, ½ Ti, Balance Fe Alloy, and Certain Other Materials

	Experimental Alloy (sheet stock specimens)[a]	Type 446 Stainless (wrought bar specimens)	Type 316 Stainless (wrought bar specimens)	Thermenol, 16 Al, 3.3 Mo, (sheet stock specimens)
Room Temperature Properties:				
Yield Strength (0.2% Offset), psi	60,000	51,500[c]	38,500[c]	—
Ultimate Tensile Strength, psi	87,500	83,000[c]	85,500[c]	129,000
Elongation, % in 2 in.	24	25	60	10.5[c]
Properties at 1500 F:				
Yield Strength (0.2% Offset), psi	5,000	3500[c]	18,500[c]	—
Ultimate Tensile Strength, psi	11,000	8000[c]	27,500[c]	23,000[d]
Stress to Produce Rupture in 1000 hr at 1500 F	1000	1100[b]	7000[b]	1000[a]

[a] Martin Co. test data.
[b] Metals Handbook, 1948.
[c] Footnote 7.
[d] Interpolated from "Investigation of Mechanical Properties, Corrosion Resistance, and Oxidation Resistance of Thermenol, an Iron-Aluminum-Molybdenum Alloy," by K. L. Kojola. NAVORD Report 5190, U. S. Naval Gun Factory, August, 1956.
[e] United States Steel Corp. Published ADV-18566 (S).

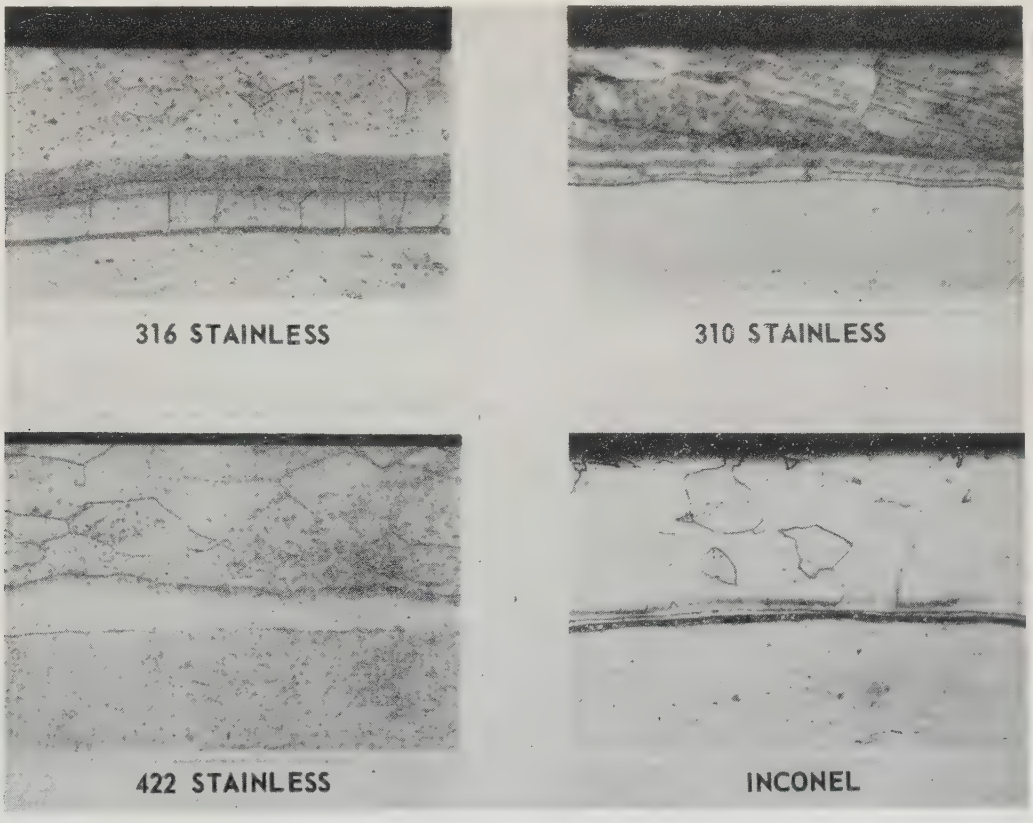

Fig. 11 — Photomicrographs showing appearance of bonds between experimental alloy (7.5 Al, 5 Cr, 1 Nb, 0.5 Ti, balance Fe) and various high-hot-strength materials (magnified 100 times)

aluminum and chrominum in combination impart room-temperature corrosion resistance to iron in much the same manner that chromium alone does. Fe-Al base alloys tend to be deficient in room-temperature ductility, in weldability, in high temperature strength, and in their susceptibility to work-hardening; however, their qualities can be improved by means of alloying additions and through refinement of preparation and heat-treat methods. The experimental alloys prepared by the authors compare favorably in strength and ductility at both high and low temperatures with the ferritic stainless steels.

It is unlikely that Fe-Al or Fe-Cr-Al base alloys can compete at present with the straight-chromium stainless steels in applications requiring only resistance to atmospheric corrosion. In event of a chromium shortage, however, they would probably enjoy an advantage with regard to cost and availability. In high-temperature service, their superior oxidation resistance recommends them for immediate use; where high-temperature strength must be combined with oxidation resistance, presently developed alloys can be used to clad high-hot-strength materials.

Further development of Fe-Al base alloys can be carried out profitably by means of semi-empirical methods, though a great need exists for basic data on the metallurgical peculiarities of the Fe-Al system. Our immediate goals include the development of air-melting procedures, the substitution of low-carbon scrap steel for the ingot iron used in experimental work, and the maximization of aluminum content.

DISCUSSION

Oxidation Resistance Dependent Upon Aluminum Content

— E. D. Marande, V. F. Zackay, G. H. Seaver

Ford Motor Co.

THE authors are to be commended for their recognition of the need for a nonstrategic, inexpensive alloy having a good combination of oxidation and corrosion resistance. Considerable research and development work has been done at our company's Scientific Laboratory on the properties of iron-aluminum alloys; both the binary system and more complex alloys based on the binary iron-aluminum system have been investigated.

Our own work on the oxidation of both iron-aluminum and iron-aluminum-chromium alloys at elevated temperatures (in the range 2000–2200 F) shows that the oxidation resistance is primarily dependent on the aluminum content. The effect of chromium at levels below about 7–8% appears to be negligible, while at higher aluminum contents and still higher temperatures (above 2200 F) chromium appears actually to have a deleterious effect on the oxidation resistance of the alloy. Due to this effect, it might be more suitable to use a binary iron-aluminum for cladding higher strength alloys.

The corrosion resistance of iron-aluminum-chromium alloys depends much more on the chromium content than does the oxidation resistance. This was found to be true for the corrosive media employed in our laboratory, which were 40% boiling nitric acid, 10% acetic acid, 1% ferric chloride, 20% sodium hydroxide, 10% sodium chloride (immersed testing), 5% salt spray and intermittent immersion in Detroit city water. However, chromium and aluminum were not necessarily found to be additive in conferring corrosion resistance; for example, a combined chromium and aluminum content of 15% (8% Al and 7% Cr) was not nearly as corrosion resistant as Type 430 stainless (14–18% Cr) in 40% boiling nitric acid.

For the past several years, considerable welding research has been conducted on iron-aluminum alloys by the Manufacturing Research Group of our company and successful fusion welding techniques have been developed for alloys containing up to 8% aluminum.[a] It is possible that these techniques or a slight modification of them might prove applicable to the authors' iron-aluminum-chromium alloys.

The authors properly contend that "more basic data on the metallurgical peculiarities of the iron-aluminum system" be determined. Some of this data has already been published by Kayser[b] and by Justusson, Zackay, and Morgan,[c] although more work remains to be done.

Last, the authors suggest the development of air-melting techniques for iron-aluminum-chromium alloys. Considerable work has been done in this field by Scientific Laboratory,[d] and a specialty steel company, with the aid of our personnel, has developed techniques for air-melting iron-aluminum and iron-aluminum-chromium alloys in the composition range similar to that mentioned by the authors. The size of the heats made in this way varied 1–5 tons.

ORAL DISCUSSION

— Reported by G. H. Seaver

Ford Motor Co.

F. E. Moskovics, A. O. Smith Corp.: Has flash welding been tried with these iron-aluminum alloys?

Mr. King: No attempts have been made to flash weld the alloys.

A. W. Laird, New York Air Brake Co.: Has there been any recognition by the Navy in connection with these alloys?

Mr. King: The Bureau of Ships is interested in the alloys from the standpoint of their resistance to attack by V_2O_5 at elevated temperatures.

Porter Wray, U. S. Steel Corp.: Were the cost estimates made on the basis of vacuum-melting methods or air-melting procedure?

Mr. King: The estimates were made on the basis of air-melting procedure only.

Robert Sergeson, Jones & Laughlin Steel Corp.: It would seem that the costs should not be based on raw material alone, but on increased costs of cold-rolling because of greater work hardening, and similar **processing** costs where the iron-aluminum alloys would be different from ferritic stainless grades.

---

[a] WADC TR 57-298, Part 3, May, 1957: "Iron-Aluminum Alloy Systems, Welding of Iron-Aluminum Alloys," by R. Burthwick and S. Goodman.

[b] WADC TR 57–298, Part 1, May, 1957: "Iron-Aluminum Alloy Systems, Fundamental Studies and Alloy Development," by F. X. Kayser.

[c] Transactions of American Society of Metals, Vol. 49, 1957, pp. 905–921: "Mechanical Properties of Iron-Aluminum Alloys," by W. Justusson, V. F. Zackay, and E. R. Morgan.

[d] *Journal of Metals*, Vol. 10, April, 1958, p. 203: "Air Melting of Iron-Aluminum Alloys," by V. F. Zackay and W. A. Goering.

the economics of *HIGH-OCTANE GASOLINES*

F. W. Kavanagh, J. R. MacGregor, R. L. Pohl, and M. B. Lawler, California Research Corp.

This paper was presented at the SAE National West Coast Meeting, Los Angeles, August 13, 1958

IT IS well-known that horsepowers, compression ratios, and octane requirements of American passenger-car engines have continued to rise throughout their history. So have the octane numbers of the gasolines produced for them. Fig. 1 shows where octane numbers have been; and the dotted, straight-line extrapolations show where we might be going. The more sophisticated predictions of future octane trends which have been published[1,2,3] also show higher octanes in the future. We know that octane numbers are becoming more expensive and that the theoretical, incremental improvement in gasoline mileage for each compression ratio becomes smaller as compression ratio goes up. It is evident, therefore, that there must be an optimum octane number from economic considerations—or a series of optima depending on the bases used. This paper analyzes our data on this subject as well as other published data and a number of private communications. It is concluded that the octane number of today's premium gasoline is at or somewhat beyond the most economical point for present-day, commercial processes. Octane numbers of premium gasolines should stay at or near present levels until new developments make it possible for the customer to get more for his money.

The bases on which this study is made have a profound effect on the end results. They will, therefore, be discussed in some detail as follows:

1. Only present, commercial technology was applied. The petroleum industry is expending great effort to develop more economical processes for making high-octane gasolines. However, such developments are not here yet.

2. All improvements were taken in terms of gasoline mileage at constant performance; that is, constant accelerating ability. We realize that this does not represent the history of the automobile — most engineering developments have been taken in the form of bigger cars with bigger engines, better accelerating ability, and in power-consuming "luxury" items such as automatic transmissions, power

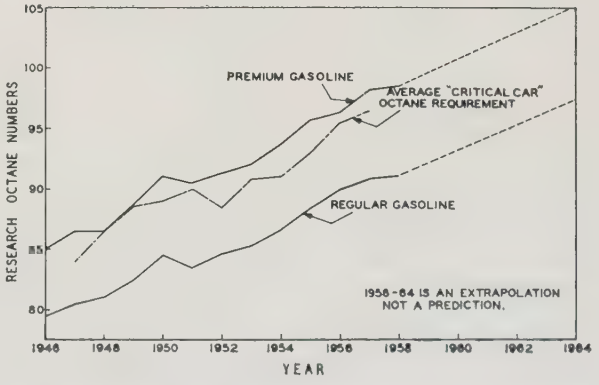

Fig. 1 — Trends in octane numbers and average octane requirement

[1] Du Pont Technical Conference Notes, 1957: "Tomorrow's Cars, Gasolines, and Refineries."
[2] "Future Automobile Engines and Their Fuel Requirements," by Bartholomew and Kass. Ethyl Corp., 1956.
[3] "Automotive Fuel Requirements," by R. I. Potter. Ford Motor Co., 1958.

FUEL of 97 + octane number gives the most miles for the dollar, present calculations show. At this point, increased efficiency from high compression ratios equals the rising cost of high-octane fuel. For town driving about 95 octane is inherently the least expensive, and over-the-road cars can benefit from gasolines up to almost 99 octane number.

This paper describes an analysis made by California Research Corp. of the costs and the value of high-octane gasolines. The economics of octane numbers was based on current commercial practices regarding improved efficiencies of higher compression ratio cars and higher manufacturing costs of higher octane gasolines. The authors believe that if compression ratio and octane number stay in proper relation to each other, the consumer will benefit.

steering, power brakes, power windows and seats, and refrigeration. However, as the value of improved acceleration and of power equipment is almost impossible to calculate, we have taken all our gasoline improvements in gasoline mileage. The effects of mechanical octane numbers are considered, and a separate section on effects of octane numbers on power is included.

3. Compression ratios were adjusted perfectly to the gasolines in all cases. This can never apply to all cars on the road but has been approached, on a statistical basis, by the average octane requirement of the more expensive cars each year and the premium gasolines of that year. This was shown in Fig. 1.

4. Improved gasoline mileage from higher compression ratios was based on experimental data from eight cars of three different makes. The engines in these cars were either special modified engines obtained from the manufacturer or were modified after consultation with the manufacturer. Average driving conditions were used to determine the most economical octane number. This is not so favorable to high octane numbers and compression ratios as the over-the-road condition used in all previous papers on this subject coming to our attention. Nor is it so unfavorable as the condition of short trips from a cold start in which extra gasoline is consumed because the engines are too cold and higher compression ratios are of no particular benefit.

5. Octane number costs were calculated on the basis of adding equipment to a hypothetical, typical U.S. refinery. This gives costs higher than a series of grass roots refineries each designed for a specific octane number of the premium gasoline. But it is the practical case and the one that will be used if octane numbers go up.

6. Increased costs of producing gasolines were added directly to the retail gasoline prices. Only increased manufacturing costs were used, and these were calculated for a U.S. average refinery.

7. The overall U.S. average condition of 30% premium plus 70% regular grade with the present-day average spread in octane number between them was used in the refinery economics and usage calculations. Cheaper, low octane fleet gasoline as well as expensive, superpremium gasolines are also sold but in small volume. However, the same economics will apply.

Several relationships must be developed as a basis for determining the optimum octane number. These are the effects of compression ratio on octane requirement and gasoline mileage plus the relationship between octane number and manufacturing costs.

Octane Requirements

Octane requirement data were used in accordance with the method developed by the Coordinating Research Council. This means the octane requirement of a car is the octane number of a gasoline that will give trace knock in a level road acceleration. Most drivers will not discern trace knock, and practical octane requirements are somewhat lower than the curves shown.

There is no simple relationship between compression ratio and octane requirement. Cars coming off the same production line and seemingly identical in every respect will nevertheless differ in octane requirement over a range of 8–10 octane numbers. This is due to the manufacturing tolerances of critical engine parts. Fig. 2 illustrates the variation in primary reference fuel octane requirement among cars of the same make and model as well as among cars of different makes and models. Each of the five 1957 models represented in Fig. 2 has a nominal compression ratio of 10/1. The average octane requirement distribution for the five car makes is also shown. Data from Fig. 2 were used as the basis for the relationship between compression ratio and octane requirement, shown in Fig. 3. Base points for the lines on Fig. 3 are for 10/1 compression ratio using the data on the 120 1957 model cars from Fig. 2. The lines were then extrapolated in both directions, using nine performance numbers per compression ratio. This extrapolation is consistent with historical data in the 6/1 to 10/1 compression ratio range. Our data on 13 cars converted to 11/1 and 12/1 compression ratio also confirm the extrapolations in Fig. 3, as shown on Fig. 4. The data on Figs. 3 and 4 were obtained using primary reference fuels; and for this study, it is necessary to convert

Table 1 — Effect of Compression Ratio on Gasoline Mileage

Car	Displacement, cu in.	How Modified	Mpg City Driving		Increase, %	Mpg at 50 mph, Constant Speed		Increase, %
			9/1 Compression Ratio	12/1 Compression Ratio		9/1 Compression Ratio	12/1 Compression Ratio	
A-1	324	Special engine	13.6	13.8		18.7	19.1	
A-2	324	Special engine	14.1	14.4		—	—	
A-3	324	Special engine	14.6	14.8		18.4	18.7	
A-4	324	Special engine	14.9	15.6		17.4	19.2	
A-5	324	Special engine	15.2	16.1		18.4	19.0	
A-6	324	Special engine	15.7	16.6		14.6	19.4	
B-1	316	Head conversion	13.6	14.4		17.8	18.5	
C-1	392	Head and piston conversion	13.8	14.2		19.0	21.7	
Average			14.44	14.99	3.8	17.76	19.37	9.1

these to octane requirements in terms of the F_1 of commercial-type gasolines. This cannot be done, because the road response (road rating minus F_1) for different commercial gasolines in different cars of varying compression ratio covers a wide range (Fig. 5). In view of this scatter, we conclude that there is no effect of compression ratio on road response for production cars. However, road response is a function of fuel sensitivity (F_1 minus F_2). Based on extensive data from eight late-model cars, we have used the following relationship relating road octane rating to fuel sensitivity:

$$\text{Road Rating ON} = 3.2 + 0.52\,F_1 + 0.48\,F_2$$

Based on fuel sensitivity information developed in a later section for gasolines up to 104 octane number, Fig. 6 was constructed relating F_1 octane requirement and compression ratio for commercial gasolines at the 90% satisfied level by the CRC method. Experience has shown that this level of satisfaction is historically correct for premium gasolines. This chart was used in subsequent calculations unless stated otherwise.

Gasoline Mileage

The effect of compression ratio on gasoline mileage used in this study was to a considerable extent based on data from eight cars of three makes recently tested and shown in Table 1. Six of these cars, Make A, were 1956 models converted to 12/1 compression ratio by using factory built replacement engines. Car B was converted by using a factory-supplied, high compression ratio cylinder head, and Car C was converted by following manufacturer's recommendations with special pistons and cylinder heads. These cars gave the following average results:

	Gasoline Mileage, mpg		Increase, %
	9/1	12/1	
Constant Speed (highway) 50 mph	17.8	19.4	9.1
Stop-and-Go Service (city)	14.4	15.0	3.8

The per cent increase in mileage going from 9/1 to 12/1 compression ratio was essentially the same at all speeds tested from 30–60 mph. The city cycle

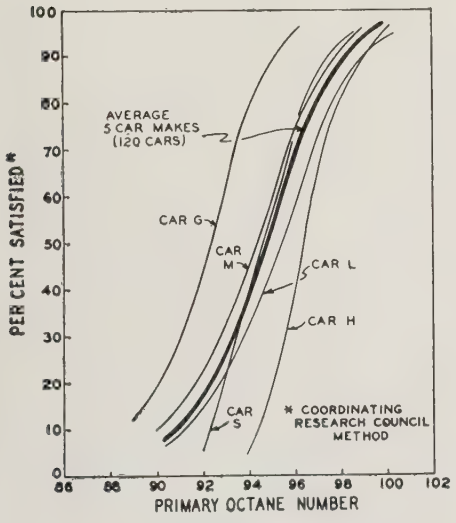

Fig. 2 — Octane requirements of 10/1 compression ratio cars, 1957 production models

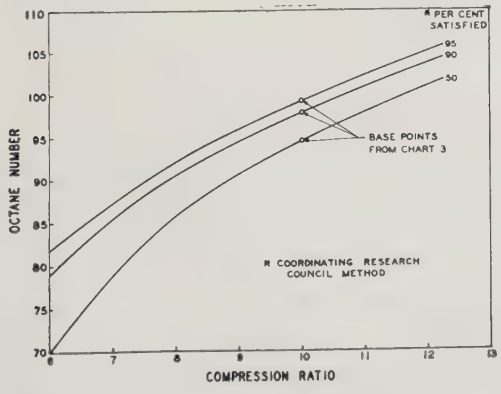

Fig. 3 — Primary octane requirements of passenger cars

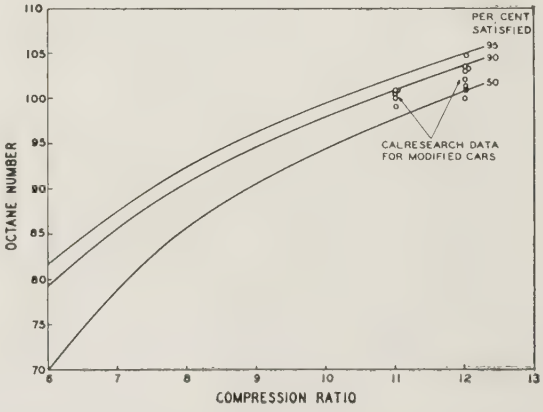

Fig. 4 — Primary octane requirements of passenger cars

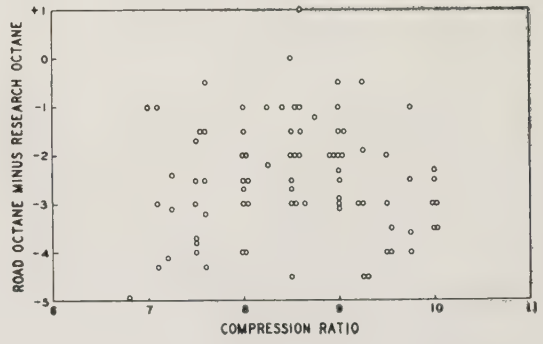

Fig. 5 — Effect of compression ratio of road response

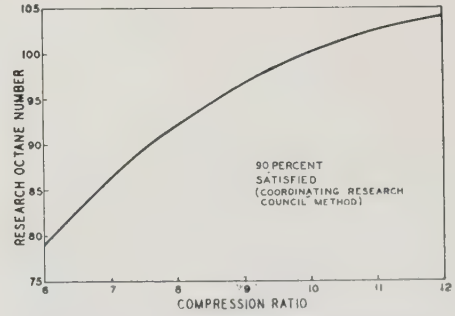

Fig. 6 — Commercial octane requirements of passenger cars

Table 2 — Description of Town Driving Course

Course Type	Speed, mph Maximum	Speed, mph Average	Miles Traveled	% of Total
Level	35	19.3	9.0	67
Hills	25	22.0	4.4	33
Total		20.6	13.4	100
Stops	No.		Average Wait	
Signs	16		5 sec	
Lights	14		(Average 8 red) 23 sec	

Table 3 — Miles Traveled by Passenger Cars in 1956 (including taxicabs)[a]

	Miles Traveled (millions)	% of Total
Main Rural Roads	185,901	36.5
Local Rural Roads	89,923	17.7
Urban Streets	231,791	45.8
Total	507,615	

[a] Source: U. S. Bureau of Public Roads, Table VM-1, 1956.

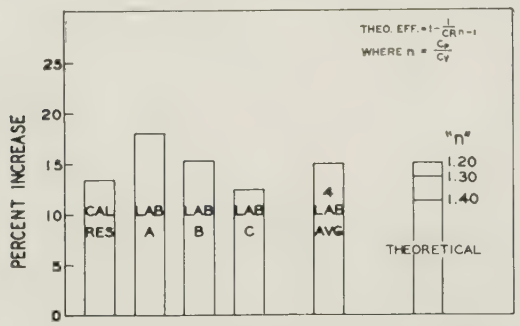

Fig. 7 — Increase in mpg. Conditions: 8/1 to 12/1 compression ratio, constant rear axle ratio, constant speed driving

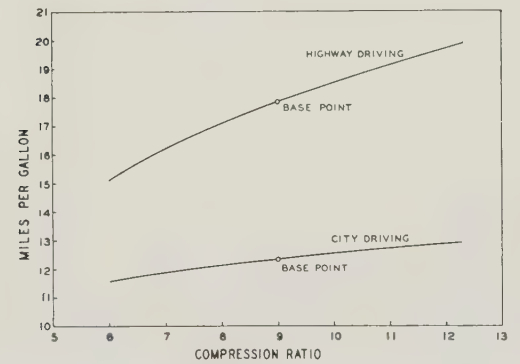

Fig. 8 — Improvement in fuel mileage at constant rear axle ratio

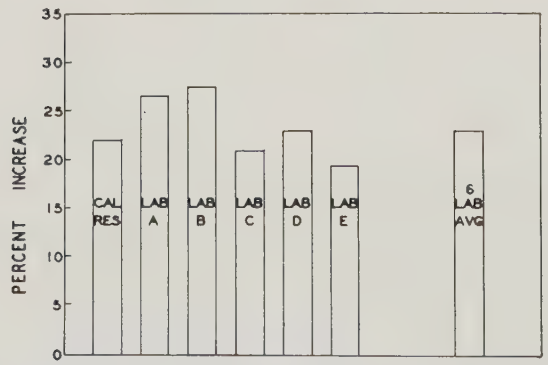

Fig. 9 — Increase in mpg. Conditions: 8/1 to 12/1 compression ratio, constant performance, constant speed driving

(Table 2) included 8 miles of stop-and-go driving in city traffic plus 5 miles of suburban operation, permitting maximum speeds of 35 mph and was made with warmed-up engines. The small effect of compression ratio under city driving conditions is due to the high percentage of gasoline consumed at idle and while accelerating. At the rich mixtures supplied under these operating conditions, the maximum benefits of compression ratio are not obtained.

There are considerable economy data published for highway-type driving. Fig 7 summarizes such data from three laboratories in addition to our data. The data for the four laboratories show excellent agreement and are also consistent with the theoretical increase for an operating engine. The four-laboratory average value given in Fig. 7 was used for highway driving in all subsequent calculations.

No published data for the compression ratio range of interest could be found for city-type driving. Thus, our data tabulated above were used as a basis for all calculations involving city driving. In order to have the absolute miles per gallon consistent with respect to average late model cars, we obtained published mileage data[4,5,6,7,8] for 1957 model passenger cars and weighted these mileage data in accordance with car registration. This gave base points for Fig. 8. We then ran the lines through these base points using the percentage increases for highway and city driving described above.

Constant Performance

Thus far in our discussion of gasoline mileage, we have compared engines of the same size and cars with the same rear axle ratios. However, increasing the compression ratio of an engine increases its horsepower and, consequently, the accelerating ability of the vehicle. Inasmuch as we are looking for the effect of compression ratio on gasoline mileage at constant performance, we must correct for this increase in horsepower either by using a smaller engine or a numerically lower rear axle ratio. This has been calculated by several laboratories assuming a lower rear axle ratio as shown on Fig. 9 for a change from 8/1 to 12/1 compression ratio. Our calculations for constant performance assume that average rear wheel torque for the speed range (road speed) of interest is held constant. A relationship between rear axle ratio and compression ratio can then be obtained. Data for these calculations were obtained from Roensch.[9] These data are for highway driving (constant speed), and the six-laboratory average was used as a basis for the highway curve in Fig. 10. The same percentage improvement for constant performance was applied to the city driving conditions shown. This is believed to be an optimistic assumption.

Average Driving

City driving, or at least city-suburban driving, represents the most common use of gasolines. A survey by the U.S. Bureau of Public Roads (Table

[4] *Motor Trend*, 1956–1957 issues.
[5] *Hot Rod Magazine*, 1956–1957 issues.
[6] *Consumer Reports*, 1957 issues.
[7] *Motor Life*, 1957 issues.
[8] *Motor Guide*, 1957 issues.
[9] "Thermal Efficiency and Mechanical Losses of Automotive Engines," by M. M. Roensch. Presented at SAE National Passenger-Car, Body, and Production Meeting, Detroit, March, 1949.

3) shows that approximately 46% of the miles traveled by passenger cars in 1956 was on urban streets, 18% on local rural roads, and 36% on main rural roads. This breakdown is also typical of earlier years reported by this same source and is considered a reliable prediction of the driving habits of U.S. motorists. For this study, one-half the local rural road mileage was considered as town driving and one-half as highway driving. Using the base points from Fig. 8 for city and highway miles per gallon, the per cent of gasoline consumed for each type of driving was calculated as 63% city and 37% highway. We can now construct Fig. 11 for average driving conditions by weighting Fig. 10 data on the above basis of 63% city-37% highway driving. It is significant that no other investigators of octane economics have to our knowledge used city driving in their calculations.

Cost of Octane Improvement

Historically, refinery installations for gasoline processing have been of two types, those whose function is to produce gasoline from lower value feed stocks and those whose function is to increase the quality of a stock already in the gasoline boiling range. Thermal and catalytic cracking represent the former, and thermal and catalytic reforming represent the latter.

When thermal cracking was introduced commercially in 1913, the main incentive was to produce more gasoline. The fact that the thermal gasoline was higher in octane than most other gasoline components of its day came as a bonus. The octane improvement came at little cost because the refiner could convert fuel oil to gasoline. It may be seen in Table 4 that the value of the products from thermal cracking is greater than the feed value. This pays for the investment and operating expense of the thermal cracker. In arriving at the above value ratio, no credit was assigned for the higher octane level.

Much the same situation is true for catalytic cracking. It converts fuel oil to gasoline more effectively than thermal cracking. Not only does the process make more gasoline but also higher octane, 90–100 F_1 instead of 75–80. Here again, the octane increase comes at a reasonable cost to the motorist because the products from catalytic cracking have more than feed value.

Thermal reforming was introduced in the middle 1930's for the purpose of improving octane number of a stock already in the gasoline boiling range. It consumes gasoline instead of making more gasoline as do thermal and catalytic cracking. Thus, gasoline is simply converted into less gasoline for the sake of increasing its octane number. This is quite expensive.

Since about 1950, catalytic reforming has been displacing thermal reforming as a gasoline improvement process because of its ability to achieve higher octane numbers. Because of decreased gasoline yield, it is relatively expensive. Furthermore, because its installation has been much more extensive than thermal reforming, the impact of catalytic reforming on the cost of gasoline manufacture has been much greater.

The cost of octane as a function of octane level is shown in Fig. 12. For octane numbers below 99, the cumulative cost at different octane levels is based on lowest Gulf Coast cargo prices for a 10-year period corrected to 1957 dollars. Although the gasoline price in cents per gallon fluctuates, the curve of the cumulative cost versus octane level

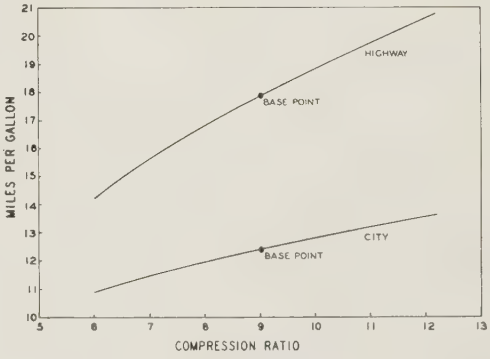

Fig. 10 — Improvement in fuel mileage at constant performance

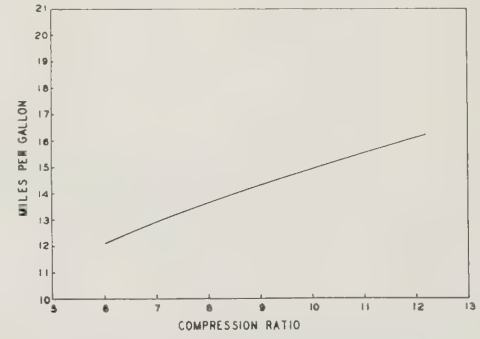

Fig. 11 — Weighted average improvement in fuel mileage at constant performance

Table 4 — Major Gasoline Process Developments

Process	Year of Widespread Usage	Feed	Product	Typical Value Ratio[a]	Reason for Use
Thermal Cracking	1920	Gas oil and residuum	Gas gasoline fuel oil	About 1.4/1	Make gasoline
Catalytic Cracking	1940	Heavy gas oil	Gas gasoline gas oil	About 1.8/1	Make gasoline
Catalytic Reforming (Platinum Type)	1954	Gasoline	Gas gasoline	Less than 1/1	Raise octane

[a] Exclusive of octane number value.

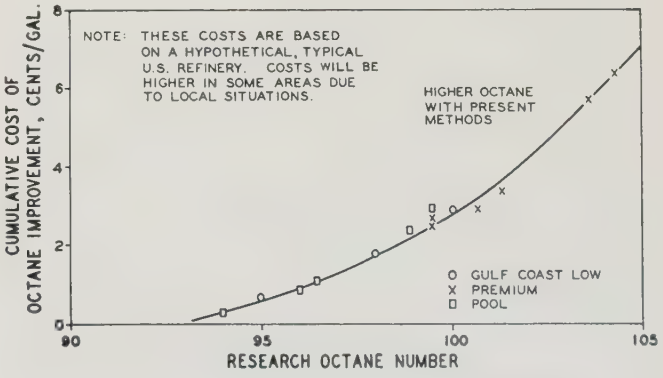

Fig. 12 — Cost of premium gasoline octane improvement

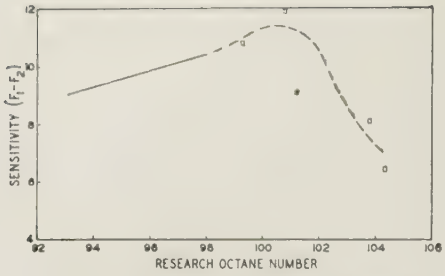

Fig. 13 — Sensitivity of premium gasoline

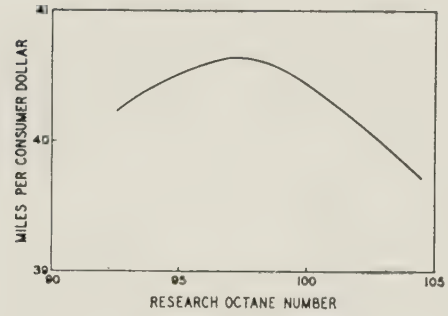

Fig. 14 — Effect of octane level on gasoline economy

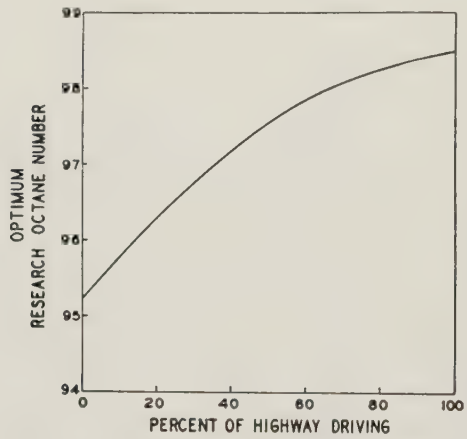

Fig. 15 — Effect of highway driving on optimum Research octane number

remains essentially fixed in shape.

Costs of octane improvements above 99 are based on the addition of equipment and processing plants to a hypothetical typical 100,000 BPCD U.S. refinery. This refinery and the subsequent steps were designed to give octane numbers at the minimum cost that can be obtained. Clearly, these costs will be higher in some areas where the optimum conditions cannot be realized. The processing in the base refinery consists of crude distillation, two-stage catalytic reforming, fluid catalytic cracking, thermal cracking of residuum and cycle oil, butene alkylation, and propene-butene polymerization. Excess alkylate above that needed for aviation is used in motor gasoline. The process units are sized in proportion to the U.S. installed capacity as shown by the National Petroleum Council report of 1958. Refinery input and products are based upon U.S. Bureau of Mines national average figures. Motor

Table 5 — Minimum Cost of Premium Octane Improvement Average 100,000 BPCD U. S. Refinery
(70% regular, 30% premium)

Process Addition	Premium F_1	Sensitivity ($F_1 - F_2$)	Cumulative Cost Over Base, cent/gal	Pool Gasoline Produced BPCD
1. Base refinery	99.3	10.8	—	46,800
2. Increased reforming severity plus reformate splitting	100.8	11.9	0.47	45,860
3. Additional butene alkylation	101.3	9.1	0.88	47,430
4. New high severity reformer	103.8	8.1	3.31	44,840
5. Isopentane recovery and n-pentane isomerization	104.3	6.4	3.89	44,780

Total added investment over base refinery — $22,000,000.

gasoline consists of 30% premium and 70% regular. The catalytic reforming severity is set at the current average. It has been further assumed that the existing reformer is at its limit and can go to higher severity only by adding more reactors. This is necessary in order to place a cost on any octane improvement obtained from higher reforming severities.

Process units added to the base refinery to raise octane were in order: (1) reformate splitting by distillation, (2) facilities for increased reformer severity, (3) alkylation of butenes formerly polymerized, (4) a new high severity catalytic reformer, and (5) pentane isomerization. Crude input and products other than gasoline were held constant. Gasoline production, refinery gas, and purchased isobutane varied according to the processing step employed.

From the above series of process cases, a cost curve was determined for the gasoline pool. The pool costs did indeed verify the shape of the Gulf Coast price curve in the region 95–100 F_1 octane number; and for that reason, it is considered that the Gulf Coast curve does reasonably represent favorable, average manufacturing costs. This curve was then used to place a value on regular gasoline. The cost of premium octane improvement was derived by backing this value for regular out of the pool cost. A summary of the cost of premium gasoline is shown in Table 5. The cost of making 104 F_1 premium will be at least 3.9 cents per gallon over the present premium of 99 F_1 octane number.

It should be emphasized that the cost curve for the hypothetical, typical 100,000 BPCD refinery cannot be applied directly to an existing refinery for several reasons. These are:

1. Everthing in the hypothetical refinery was of the size to represent minimum costs. This rarely, if ever, happens commercially.
2. The latest and best processes were used, and the base refinery was designed (on paper) to utilize these processes to the maximum.
3. The product demand proportions were favorable to minimum cost octane numbers.

On the West Coast where premium represents about half of the total gasoline and where the demand for the very high octane aviation gasoline is far higher than the national average, costs are higher. Therefore, the cost curves represent the minimum, not the average, and should not be applied directly to any area without verification. It is significant that this minimum cost curve gives

the highest "optimum" octane number.

Premium sensitivities are also summarized in Table 5 and shown on Fig. 13. We have drawn an average curve through the sensitivity points. This curve was used in calculations described earlier in this paper. The reason for drawing an average rather than stepwise curve is that the nationwide change in sensitivity will be gradual; whereas, installation of a new process in a specific refinery produces a sudden change. As an example, all refiners will not move to alkylation of total butenes at the same time.

Optimum Octane Number

Economics of octane numbers to the motorist is best given by considering the miles traveled per dollar of gasoline purchased. Such a relationship can be developed from information in Figs. 6, 11, and 12. For this purpose, it is more convenient to consider absolute values rather than percentage changes over an arbitrary base point; and a price of 36 cents per gal was, therefore, assigned. This is a typical U.S. service station price for premium gasoline and includes a typical 9-cent tax. The relationship between miles per dollar and F_1 octane number for premium gasoline is shown in Fig. 14. This shows that for the conditions used the optimum is about 97 octane number. The motorist will not benefit in terms of lower fuel costs if fuels above this octane level are supplied even though his car is exactly designed to use the higher octane gasolines. It is implicit from Fig. 14 that maximum economy would be obtained in the idealized situation where all cars on the road were at the same compression ratio and all required gasolines of 97 octane number. This ideal situation, of course, never will be realized for reasons given in our discussion of Fig. 2. However, this does not alter the conclusion that approximately 97 octane is optimum for gasoline economy. It simply means that there should always be a place for a second structure gasoline.

Effects of Bases on Optimum Octane Number

Although the curve in Fig. 14 peaks, the change between 93 octane and 100 octane is relatively small, suggesting that the bases used could easily shift the optimum point. The effect of several of these bases on this optimum point has been considered as follows.

Fig. 15 shows the effect of operating conditions on the optimum octane level. When city driving conditions are used exclusively, the peak is lowered about 2 octane numbers. On the other hand, the optimum is increased to almost 99 octane number for highway driving exclusively.

Fig. 16 considers the effect on the optimum octane number of the level of octane requirement satisfaction selected. Fig. 14 is for 90% satisfied. However, Fig. 16 shows that a change in this level would have only a small effect on the optimum point because the slope of the relationship between octane requirement and compression ratio is not a function of the level of satisfaction chosen. Fig. 16 can also be used to illustrate the influence of knocking level in octane requirement determinations on the optimum octane number. Reducing the per cent satisfied from 90% to 60% reduces the optimum octane number from 97 to 96. This change

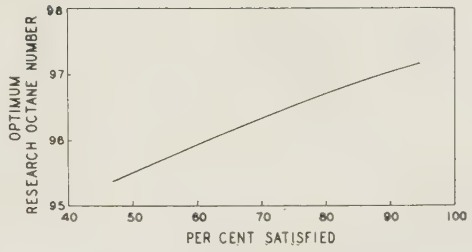

Fig. 16 — Effect of per cent satisfied on optimum Research octane number

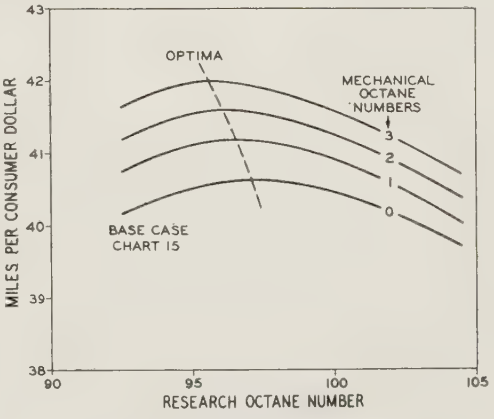

Fig. 17 — Effect of mechanical octane numbers on optimum Research octane number

in per cent satisfied was shown in Fig. 2 to represent 3 octane numbers. Three octane numbers on a noise basis covers the range from "trace" to "heavy."

The service station price of the gasoline, 27 cents plus 9 cents tax, also influences the peak octane number. Decreasing by 5 cents lowers the optimum to about 95 and increasing by 5 cents raises the optimum to about 99.

It is possible that there will be a further lowering of octane requirement for a given compression ratio from the efforts of the engine manufacturer. This improvement is discussed by the trade in terms of "mechanical octane numbers" as contrasted to the "chemical" octane numbers obtainable through refinery processing. It is anticipated that any design change giving additional "mechanical" octane numbers will apply equally at any compression ratio. Making this assumption, we have investigated the effect of "mechanical" octane numbers on the optimum octane number as summarized in Fig. 17. In constructing this curve, we consider first a given change in primary fuel octane requirement for each compression ratio. The new curve can then be converted to commercial fuel requirements by the same procedure used to go from Fig. 4 to Fig. 6. Fig. 17 shows that additional "mechanical" octane numbers raise miles per consumer dollar for any compression ratio. However, there is a slight adverse effect of "mechanical" octane numbers on the optimum octane number. Note that the line connecting the optima covers the same range shown in Fig 16.

The cost of octane improvement (Fig. 12) was chosen at the minimum level to determine the maximum level to which octanes could rise with

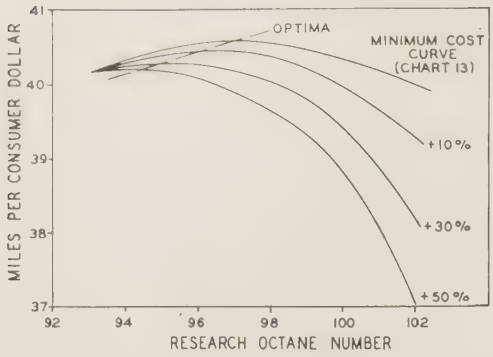

Fig. 18 — Effect of octane improvement cost on optimum octane number

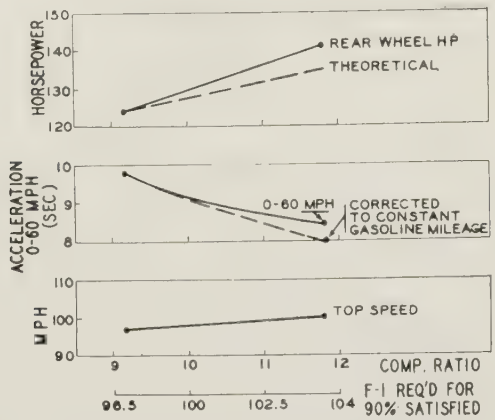

Fig. 19 — Improvement in performance with octane number, car B-1

benefit to the consumer. But, as pointed out, octane improvements cannot always be obtained this inexpensively. The influence of these more costly situations was analyzed and is shown on Fig. 18. All costs are the same at the 93 octane level and so is the miles per dollar. And as the cost of octane improvement increases, the points at which the miles per dollar start to drop off also decrease. It may be noted that an increase of 50% in the cost of obtaining high octane numbers decreases the optimum octane number from about 97 to about 94.

Improvement in Power with Octane Number

One basis for this study was to take all improvements from octane number with higher compression ratios in terms of increased gasoline mileage. But it is possible to take all improvements in terms of increased power. Fig 19 shows the effect on performance of increasing compression ratio from about 9/1 to 12/1 in one test car. On a 90% satisfied basis, this raises the octane requirement from 97 to 104. Maximum rear wheel horsepower was increased from 124 to 141, and acceleration time from 0 to 60 mph was reduced from 9.8 to 8.4 sec. The increase in rear wheel horespower increased calculated top speed from 97 to 100.5 mph. These values are consistent with predicted values from theoretical considerations.

In the previous sections of this report the improvement in power with higher compression ratio was corrected back to constant performance, which further improved the gasoline mileage. Likewise, the improvements in power with increasing octane number and compression ratio can be corrected back to constant gasoline mileage by raising numerically the rear axle ratio. This results in an additional small improvement in acceleration and brings the 0–60 acceleration time down to 8.0 sec.

Summary

Historically, both the octane numbers of gasolines and the compression ratios of automobiles have climbed steadily. The performance of automobiles has improved greatly, whether that improvement be taken in the form of power for acceleration or to drive accessories or in economy. Whereas, the cost of producing the higher octane gasoline was originally justified by increased production, recent improvements in octane number at the high levels have been much more costly because of the necessity of consuming gasoline fractions in their processing.

An analysis has been made of the costs and the value of high-octane gasolines. It has been shown that the most economical octane number of motor gasolines by present processing methods is around 97 for the average driver when the compression ratio is adjusted to the gasoline. For town driving about 95 octane is inherently the least expensive, and over-the-road cars can benefit from gasolines up to almost 99 octane. The same octane economics apply, whether improvement in performance with increasing compression ratio and higher octane number is taken in the form of power for acceleration or to drive accessories or in economy. With the present octane numbers of premium and super-premium gasolines, it is apparent that the point of maximum economy to the motorist has already been reached or passed. If all advantage of octane number is taken in power, the result of increasing from present levels to 104 octane is 12% more power, slightly more than the calculated improvement.

The economics of octane numbers is based on present commercial practices regarding improved efficiencies of higher compression ratio cars and higher manufacturing costs of higher octane gasolines. Both of these can change and, indeed, are expected to do so. Better engines will come from the automotive industry. Also, more economical methods for manufacturing higher octane gasolines will be developed by the petroleum industry, but not rapidly nor in the immediate future because the invention and commercialization of new additives and new processes are time-consuming developments. If compression ratio and octane number stay in proper relation to each other, the consumer will benefit. It is sincerely hoped that this will be the case and that compression ratio and octane number will not be forced up too fast and result in economic disadvantage to the motorist.

Acknowledgments

The authors wish to express their appreciation to J. H. Macpherson, R. K. Stone, D. R. Olson, J. Govits, and F. C. Franklin of the California Research Corp. for their assistance in preparing this paper. Recognition is also expressed for the helpful comments from our many friends in the automotive and petroleum industries.

PRIMING AIDS for Cold Starting Diesel Engines

J. J. DeCarolis and W. E. Meyer, The Pennsylvania State University
P. W. Espenschade, U. S. Army Ordnance Corps.

This paper was presented at the SAE National Diesel Engine Meeting, Baltimore, Oct. 23, 1958.

IN REVIEWING the events, or their absence, which led to the investigations reported in this paper, it is appropriate to begin by acknowledging the persistence with which the Society of Automotive Engineers has continued to program at its national meetings since 1950[1] sessions and papers devoted to the broad environmental field of which the subject matter of this paper is a part. Research and equipment design have assuredly benefited from the related and consistent interest and activity of the Society's Construction and Industrial Machinery Technical Subcommittee on Winterization, organized in 1952 at the instigation of the U. S. Army Corps of Engineers.[2]

It seems also appropriate here to recall several significant developments which have in large measure through the past 15 years set the stage for an ultimate solution to the low-temperature, quick-start problem, which is a matter of real concern to the military and industry. For example, there was the farsighted installation in October, 1943, of the multipurpose climatic test chamber at Fort Belvoir, Va., for what was then the Engineer Board, U. S. Army Engineer Corps (forerunner of the U. S. Army Engineer Research and Development Laboratories[3]). Much of what eventually materialized, pertinent to this discussion, was spawned there.

Post World War II circumstances, for reasons even more evident today, gave rise to staff directives in 1948 concerning a range of temperature requirements specified for operation as – 65 to 125 F and

THIS PAPER reports progress in a current research program on the use of secondary fuels as ignition promoters, to aid cold-weather starting of diesel engines.

The best method, the authors report, is to supply ether to the intake manifold in vapor form. The amount of ether reaching the manifold can be controlled easily, and any condensed vapor is carried along by the cold intake air. Thus, the difficulties resulting from ether accumulation are prevented.

There is a minimum starting temperature for each engine type, even with the vapor introduction of ether. Therefore, further work is needed to assure cold starting in all engines.

[1] "Winterization of Construction Equipment," by R. W. Beal. Paper presented at SAE National Tractor Meeting, Milwaukee, September, 1950.
[2] First Progress Report on SAE CIMTC Subcommittee on Winterization, by J. E. Jass, Chairman. Jan. 7, 1953.
[3] "Low Temperature Engine Testing and Facilities," by P. W. Espenschade. Paper presented at SAE National Diesel Engine Meeting, Cleveland, October, 1954.

for storage as – 80 to 160 F of U. S. Army equipment and supplies. One implementing plan, announced in October, 1948, by the Office of the Chief of Engineers, authorized selective tests to investigate the engine cold-starting capabilities of high-volatility fuels (Project No. 8-50-02-001, Engine Accessories, Cold Weather Starting and Operations, subsequently Project No. 8-49-13-102) in connection particularly with a special objective in the then designated low-temperature aspects of the military matériel requirements. This plan originally included an important provision: "all combat, combat support and shelter equipment and supplies produced for the U. S. Army for use in the temperate zone areas, excluding clothing, will have designed and built into them the capability to operate satisfactorily from the top temperature limit down to an ambient of – 40 F." Regulations were issued shortly thereafter to clarify and/or modify these provisions.[4]

Eventually, the term "winterization" became identified with the special preparation (featuring preheating up to one hour) of equipment for starting, operating, or functioning in the extreme temperature range of – 25 to – 65 F (associated geographically with subarctic, arctic, and polar areas), when such equipment could be reasonably expected to function at such low temperatures. For the range from – 25 F upward, involving the greater volume of equipment, the use of preheating (with its attendant delays) was ruled out; and highly complex accessories (with complications for operators and mechanics) were minimized on logistical and tactical grounds, thus narrowing the options for fast cold starting to simple aids and fundamentals.

These basic operational requirements were supplemented by the issuance of military specifications for gasoline and diesel industrial-type engines (MIL-E-11275 and MIL-E-11276 series, respectively). However, a review of typical starting characteristics curves for representative diesel engines indicates that starting is a problem which must be realistically faced by users of such components. Although arctic engine oil[5] and fuel[6] will generally alleviate the problem of handling, circulating, and filtering these materials down to – 65 F, and more effective cranking speeds are feasible, eventual combustion for positive starting will require additional measures.

Fig. 1 shows that without priming fluids or preheating, standard engines could be started satisfactorily on the arctic fuel available in 1951 at 60 F with 10–100 sec of cranking at 125 rpm; but under the same conditions none would start at 40 F, leaving a considerable gap to be bridged for satisfying the military requirements. This was hardly news even then. (See Appendix.) But the scientific and engineering challenge of dealing with the fundamentals of the problem was ignored or bypassed by many, often in favor of opposing the temperature limitation itself, or promoting preheating in one form or another as the sole palliative.[7] Other methods proposed at that time offered mere remedies for spot situations rather than permanent solutions and results for specific engine categories under controlled conditions at specific temperatures.

Preliminary cold-starting investigations within the U. S. Army Corps of Engineers,[8] in conjunction with the earlier findings of the U. S. Army Ordnance Corps[9] and of the U. S. Navy Bureau of Yards and Docks,[10] were reported for the Army to the trade through the Society of Automotive Engineers in 1952,[11] and by the former Research and Development Board at a comprehensive symposium for industry contractors in the same year.[12] Significant data presented then and obtained in later operations of military cognizance are matters of record and available to contractors through ASTIA (Armed Services Technical Information Agency, Arlington 12, Va.). The reaction in many quarters, particularly to the evidence presented in favor of diethyl ether as a priming fluid, was still one of skepticism and hesistancy. Quick starts to – 50 F were considered fantastic goals. Difficulties with the application of the priming fluid and engine damage encountered with crude priming systems were thought to be insurmountable problems.

Considerable significance attaches to the Navy's success with, and qualification of, the pressurized primer capsule (per Military Specification MIL-P-16912, Ships, dated Dec. 18, 1951) for certain purposes (per Military Specification MIL-E-11278, which outlines engine qualification tests). This solution and its implications were not fully accepted by all military agencies because some of them considered successes with conventional priming systems on gasoline engines as the basis of universal answers. The special problems of the conventional and field-expedient primary fuels themselves, regarding their vaporization characteristics for start-

---

[4] "Research and Development of Materiel — Operation and Protection of Material Under Adverse Conditions of Temperature," Department of Army Special Regulation SR705-70-5, Dec. 26, 1950. Superseded by "Research and Development of Materiel—Operation of Materiel Under Extreme Conditions of Environment," AR 705-15, Aug. 14, 1957.

[5] "Oil, Engine, Sub-Zero," Military Specification MIL-0-10295 (ORD), May 5, 1950; and Amendment 1, Dec. 11, 1950. Ultimately superseded by "Lubricating Oil, Internal-Combustion Engine, Sub-Zero," MIL-1-10295A, July 17, 1956 (designated OES, and coded under Federal Sotck Class 9150).

[6] "Fuel Oil, Diesel," Military Specification MIL-F-896, Oct. 25, 1950 (Class 3, Low Temperature, 35 Cetane). Subsequently superseded by Federal Specification VV-F-800, Dec. 17, 1954 (Grade DF-A, Arctic, 40 Minimu Cetane; pour point – 70 F, maximum; coded under Federal Stock Class 9140).

[7] "Cold Weather Operation of Diesel Engines, Part III," by M. W. Ayton and J. A. Shea. October, 1951. Prepared as annotated bibliography for Office of Naval Research by Library of Congress.

[8] "Low Temperature Starting and Operation of Engines." USAERDL Report 1215 (Projects No. 8-48-09-001, 5-50-02-001, and 8-68-08-020), Aug. 31, 1951.

[9] "Preliminary Investigation of Diesel Engine Fuel Requirements at Low Temperature," Report No. 2, Office Chief of Ordnance Research and Development Project No. TB5-8403E, March 15, 1949 (conducted at USAERDL, Fort Belvoir, Va., for ORDTB-F & L).

[10] "Chevron Fluid Starting Aid Report." U. S. Naval Experiment Station Report No. 2B71703, Oct. 19, 1951.

[11] SAE *Quarterly* Transactions, Vol. 6, October, 1952, pp. 689–709; "Sub-Zero Winterization of Diesel Engine Power Equipment," by P. W. Espenschade, R. C. Navarin, and W. W. Van Ness.

[12] "Problems Related to Starting Diesel Engines at Low Temperatures." Restricted Symposium by Committee on Fuels and Lubricants, and Equipment and Supplies, Washington, D. C., May, 1952, Report FAP 201/10. Session papers on starting aids and fuels comprised:

(a) "Problems Encountered in Cold Room Study of Diesel Starting Fluids at Sub-Zero Temperatures," by H. D. Young.

(b) "Field Performance of Fuels in Arctic Winter Operation of Diesel Equipment," by J. A. Miller.

(c) "Deficiencies in Existing Low Temperature Diesel Engine Fuels," by J. P. Qualey.

(d) "Fuel Vaporization, the Neglected Combustion Factor—Discussion of Problem," by R. W. Hurn.

(e) "Effect of Fuel Ignition Quality on Low-Temperature Diesel-Engine Operation," by M. J. Anderson and G. C. Wilson.

(f) "Development and Application of Starting Fluids for Internal Combustion Engines," by E. F. Griep.

(g) "Effect of Special Fuels on Starting Diesel Engines at Low Temperatures," by H. E. Vermillion.

(h) "Border Temperature and Pressure of Intake Air When Misfiring Occurs in Compression Ignition Engine, as Function of Cetane Value," and "Cranking Speed with Uniform and Irregular Angular Velocity, as Function of Fuel Ignition Quality at 30 F, Temperature Increments from – 30 to + 120 F," by O. D. Treiber.

ing and warmup, have added to the confusion.[13] At the same time, a trend developed to promote variations of the ether fluids or blends developed for the military, and application systems for them did not take cognizance of the demands imposed by the military temperature requirements. (See Appendix.)

This situation appeared to justify an objective research program to provide answers which would lead to a solution for military purposes. Eventually, in 1953, this need was translated into a coordinated research program on secondary fuels as ignition promoters and other aspects of cold-starting diesel engines at subzero temperatures,[14,15] leading to a contracted series of investigations[16,17,18] on part of which this paper reports.

The Problem

Starting is the most difficult problem encountered in the operation of diesel engines at low temperatures. Successful cold starts depend on satisfying two fundamental requirements:

1. Sufficient torque must be available to crank the engine at a speed that will produce suitable conditions within the cylinders.
2. An aid must be provided for initiating combustion and keeping the engine firing until it is warm enough to run without the aid.

The latter requirement can be satisfied in one of two ways:

1. By supplying heat to the engine from an outside source, such as a torch, a combustion, electric, or other heater, or by glow plugs. Open heaters are dangerous and often unreliable. Coolant and engine-block heaters present installation problems. Heating the entire engine or part of it requires time and is, therefore, undesirable from the military viewpoint, since quick starting is essential for attaining maximum mobility and availability of materiel. Glow plugs and intake air heating require less time, but glow plugs are unsuitable for most types of combustion chambers and neither method makes starting possible at low enough ambient temperatures.
2. By introducing into the engine a fluid that will promote ignition of the regular fuel.

This paper deals with the latter method. Assuming that the engine can be cranked, whether or not ignition takes place during a starting attempt depends on whether sufficient heat is generated by the heat of compression to vaporize and ignite the fuel. Since in a given engine the compression temperature decreases with the initial air temperature, starting becomes impossible when the autoignition temperature of the fuel is no longer attained. By using a starting fluid with a sufficiently low autoignition temperature, the minimum temperature at which starts are possible can be lowered.

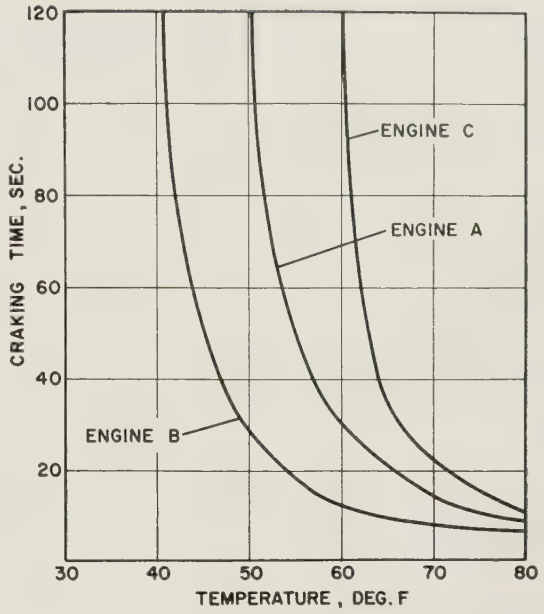

Fig. 1 — Startability of three commercial engines without aids (fuel: MIL-F-896, 35 cetane number; oil: MIL-O-10295; cranking speed: 125 rpm)

Successful starting with priming fluids depends on combining a satisfactory fluid with a suitable method of applying it. The priming fluid must have a relatively high vapor pressure and low self-ignition temperature to be able to initiate combustion and promote ignition of the regular fuel at temperatures at which the regular fuel will not ignite by the heat of compression alone. The applicator must supply the engine cylinders with priming fluids at the proper rate to start the engine quickly and keep it running until the engine has warmed up sufficiently to operate on regular fuel alone.

Many earlier investigations have shown that diethyl ether is the most promising priming fluid, but the problem of applying priming fluids has never been studied systematically. (See Appendix.) The research on which this paper reports attempts to make a contribution to the solution of this problem.

The various methods of applying priming fluids fall into three major categories:

1. Direct cylinder introduction, including intermittent port injection.
2. Spray introduction into the air intake system.
3. Vapor introduction into the air intake system.

Before proceeding with a thorough study of priming fluid application, it was decided to obtain general information on the priming fluid requirements of the engine in order to understand the applicator problem better.

The following information was desired:

1. Effect of priming fluid injection rate on crank-

---

[13] "Emergency Fuel Studies," final report, July 13, 1956. Contract No. DA-44-009-ENG-1679, sponsoring agency U. S. Army Engineer Research and Development Laboratories with Southwest Research Institute.

[14] Third Progress Report on SAE CIMTC Subcommittee on Winterization, by M. G. Mardoian, Chairman. May, 1957.

[15] Conference of R & D Board Fuels and Lubricants Committee "Panel on Fuels for Air-Breathing Power Plants." Pennsylvania State College. April, 1953.

[16] "Low Temperature Cranking of Gasoline and Diesel Engines." Contract No. DA-44-009-ENG-765, Project No. 8-50-02-001, sponsoring agency U. S. Army Engineer Research and Development Laboratories, with The Pennsylvania State College. (Reference: SAE Transactions, Vol. 63, 1955, pp. 515–530: "Engine Cranking at Arctic Temperatures," by W. E. Meyer, J. J. DeCarolis, and R. L. Stanley. Also, Final Report, Part II, June 15, 1956, by J. J. DeCarolis and W. E. Meyer.)

[17] "Priming Fluids for Cold Starting Diesel Engines." Contract No. DA-44-009-ENG-765, Project No. 8-50-02-001, sponsoring agency, U. S. Army Engineer Research and Development Laboratories, with The Pennsylvania State University. (Final Report Sept. 30, 1955, by J. J. DeCarolis and W. E. Meyer.)

[18] "Priming Methods for Cold Starting Diesel Engines," Contract No. DA-44-009-ENG-3123, Project No. 8-49-13-102, sponsoring agency, U. S. Army Engineer Research and Development Laboratories, The Pennsylvania State University.

ing time.

2. Priming fluid requirements during the warmup portion of the priming period. We here define this period as the time during which the engine is running with the aid of priming fluid.

3. Effect of atomization on startability.

4. Influence of the primary fuel.

5. Startability of various priming fluids and blends.

To obtain this information an intermittent port injection system for introducing the priming fluid was used. This system was selected because it gives positive delivery to the cylinders and permits controlling and evaluating the amount of priming fluid reaching the cylinders.

Intermittent Port Injection Applicator

An intermittent port injection system for applying priming fluid was installed on a 4-cyl, 4-stroke, naturally aspirated, precombustion-chamber engine. This applicator consisted of a multiplunger pump, including a governor, and pintle nozzles set to open at 2000 psi. The intake manifold was removed, and the nozzles were installed to inject into the intake ports. The priming fluid pump was driven by the engine at half crankshaft speed and was timed to inject during intake valve opening.

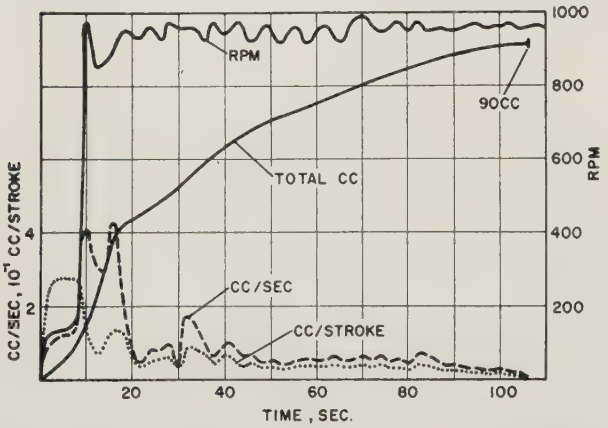

Fig. 2 — Complete starting cycle with high-pressure intermittent port injection of ether (Engine A, cranking speed: 125 rpm, temperature: −40 F)

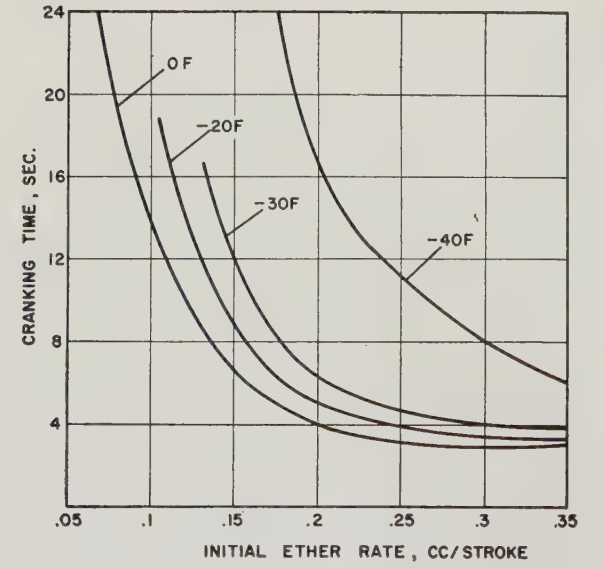

Fig. 3 — Startability with high-pressure intermittent port injection of ether (Engine A, cranking speed: 125 rpm, regular fuel injection at rated maximum)

The results of a typical test are illustrated in Fig. 2. This is a plot of ether rate in cc per stroke, cc per sec, total ether injected, and engine speed versus elapsed time in seconds. The ambient temperature was −40 F and cranking speed was 125 rpm. The regular fuel governor was set at about 1000 rpm, and the priming fluid pump governor at about 850 rpm, so that the priming fluid would be shut off when the engine would run on regular fuel only. The lubricating oil was MIL-O-10295 and the regular fuel was MIL-F-896 with a cetane number of 35.

The plot shows that the engine started to fire after being cranked for about 7 sec, as indicated by an increase in engine speed, ran without aid of the starter at about 10 sec, and reached the warmup speed at 11 sec. The ether rate during cranking was 0.27 cc per stroke, which is a little below the stoichiometric rate for this engine (calculated without considering the presence of regular fuel). This rate was selected before the start by limiting the travel of the pump rack. As soon as the engine started gaining speed, the governor began reducing the ether rate. When the engine reached warmup speed, the ether rate was about 0.10 cc per sec, and it was gradually reduced until the engine was running without the aid of ether after 106 sec. The total amount of ether required was 90 cc.

Effect of Priming Fluid Injection Rate on Cranking Time — The effect of ether rate on cranking is shown in Fig. 3 These results were obtained with the regular fuel governor set at full rated speed. The curves show that if cranking time is to be kept short the priming fluid rates must be relatively high. The quantity, of course, increases as the temperature decreases. The curves, if extended to the left far enough, become asymptotic to the y-axis. This indicates that there is a minimum priming fluid rate below which the engine cannot be started, even with prolonged cranking. Tests at −50 and −55 F (not shown in this graph) with 0.35 cc per stroke, the maximum capacity of the pump, gave cranking times of 10 and 45 sec, respectively. The minimum starting temperature for this engine is about −55 F.

These values are typical for this particular engine model. They will vary considerably with compression ratio, combustion-chamber type and design, engine size and type, and the like. The same reservation applies to other data concerning the priming and starting process.

Priming Fluid Requirements for Warmup Portion of Priming Period — After an engine has been started with priming fluid, it must be kept running for some time until the cylinders become warm enough for the engine to run on regular fuel only. During this period, priming fluid acts primarily as an ignition promoter, with the regular fuel furnishing most of the power. The required rate diminishes as the cylinders warm up, and is less with higher temperatures. If higher rates than the minimum required to promote ignition are introduced, the

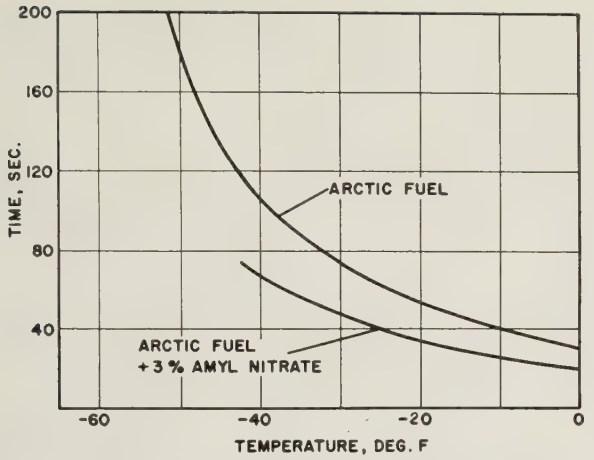

Fig. 4 — Duration of priming period, high-pressure intermittent port injection of ether (Engine A, fuel: MIL-F-896, 35 cetane number, oil: MIL-O-10295)

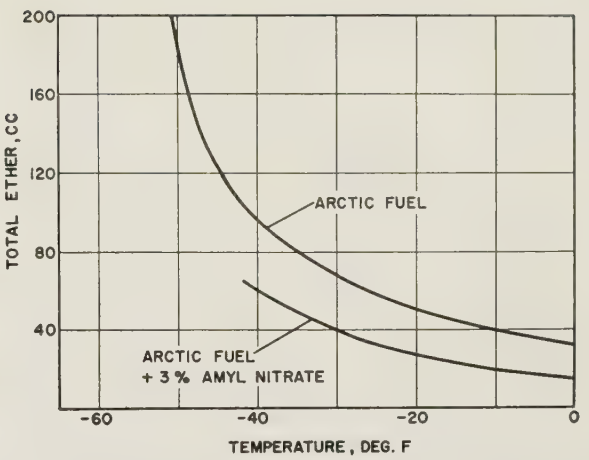

Fig. 5 — Total ether required per start, high-pressure intermittent port injection of ether (Engine A, fuel: MIL-F-896, 35 cetane number, oil: MIL-O-10295)

regular fuel governor reduces the quantity of regular fuel to maintain governed speed. Tests in which no regular fuel was injected showed that about three times the minimum required amount of ether can be introduced before the engine exceeds its maximum rated speed.

The length of the priming period and the total quantity of priming fluid required increase appreciably with decreasing temperatures and also vary somewhat for starts at the same conditions. The average duration of priming fluid application increased from 30 sec at 0 F to 180 sec at – 50 F for the test engine (Fig. 4). For the same temperature span, the total required quantity of priming fluid increased from 30 to 175 cc (Fig. 5).

Effect of Atomization on Startability — The effect of priming fluid atomization on startability was determined with two different types of nozzles which gave widely different spray characteristics. One was the high-pressure pintle type, which gave a fine spray, and the other was a low-pressure, outwardly open, variable orifice type, which gave a coarse spray. The comparison between these nozzles is made in Fig. 6 on the basis of cranking time at – 20 F for various ether injection rates. Only slightly longer cranking times were required for the coarse-spray nozzle. These results are surprising in view of the fact that larger drops provide considerably less surface area for evaporation than do the smaller ones.

Noteworthy is the fact that the engine was severely damaged by only a few tests with coarse atomization. Piston rings and lands were broken, and the pistons were badly scuffed. This was in sharp contrast to the experience with other methods of priming fluid introduction. Ninety starts with port injection through the high-pressure nozzles and with spray introduction into the manifold produced only slight scoring of the piston skirts.

Influence of Primary Fuel — The influence of the quality of the primary fuel on starting with ether as a priming fluid was investigated by adding a cetane improver to the arctic test fuel in an amount that increased its cetane number from 35 to 60. Cranking time with the "doped" fuel was about the same as with the basic arctic fuel, and the ether injection

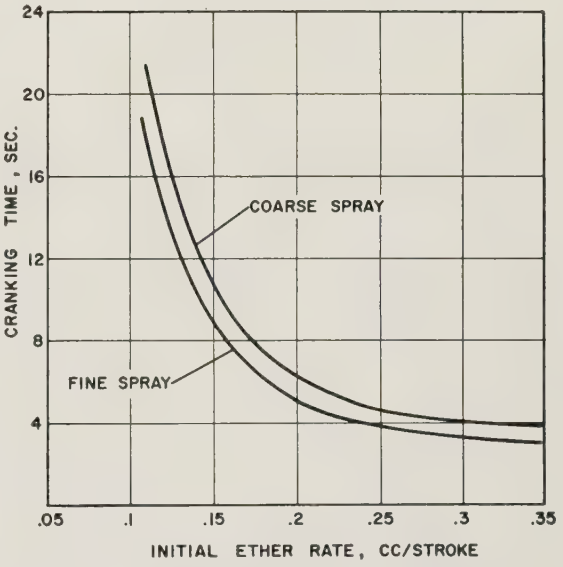

Fig. 6 — Effect of atomization, intermittent port injection of ether (Engine A, cranking speed: 125 rpm, temperature: – 20 F)

rate at the beginning of the warmup portion of the priming process was also about the same as with the basic fuel. This indicated that adding a cetane improver to the fuel had little or no influence while the cylinders were still relatively cold. After the cylinders began to warm up, however, less ether was needed and the engine was able to run without the aid of ether within a shorter time than with the basic fuel. For example, at – 40 F the priming period was 105 sec with the basic arctic fuel and 65 sec with the "doped" fuel (Fig. 4). The total quantity of ether used was 90 and 60 cc, respectively (Fig. 5).

Startability with Various Starting Fluids and Blends — Tests with a number of different combustible fluids, including carbitol, propylene oxide, and several commercial starting fluids, reconfirmed that diethyl ether excels in producing starts at low temperatures. It combines high volatility with low self-ignition temperature. These qualities, however, cause ether to detonate severely if an exces-

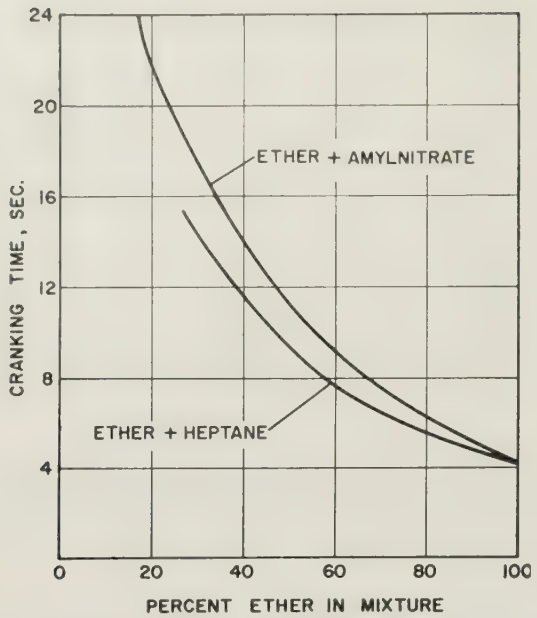

Fig. 7 — Startability with ether mixtures (high-pressure intermittent port injection, Engine A, cranking speed: 125 rpm, 0.3 cc priming fluid per sec, temperature: – 20 F

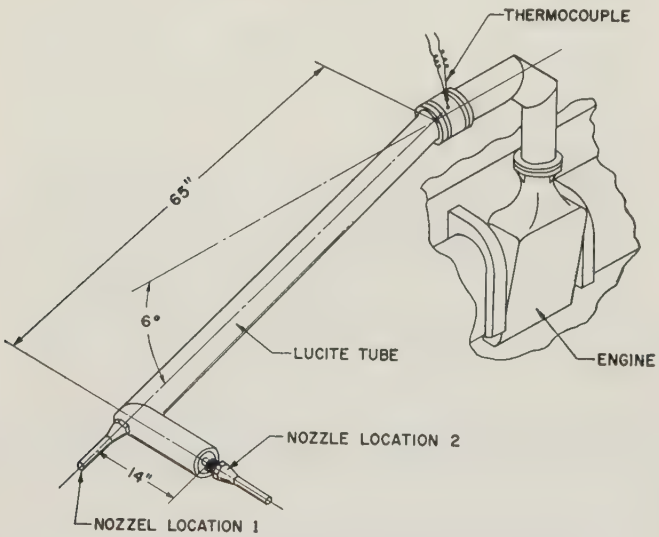

Fig. 8 — Setup for visual study of ether introduction into manifold

sive amount of it is applied to warm cylinders.

Blending the ether to make it less apt to detonate was found to reduce its effectiveness in initiating combustion. This is borne out by the data of Fig. 7, which show the cranking time at – 20 F for various proportions of ether in mixture with n-heptane and with amyl nitrate. The cranking time was increased appreciably as the percentage of ether in the mixtures was decreased. A little more ether was needed in the amyl nitrate mixture than in the heptane mixture to obtain starts within the same cranking time.

After the engine started running on its own power, the quantity of starting fluid required with the blends was only slightly more than with straight ether. Therefore, when introduced directly into the cylinders, the blends have only one advantage: there is less likelihood of severe detonation during warmup.

The fact that ether has the undesirable characteristic of causing detonation, when too much is introduced for the temperature condition of the cylinders, imposes an additional requirement upon the priming fluid applicator in that it must control the priming fluid rate so as to limit the severity of detonation to prevent engine damage.

Practicability of Direct Cylinder Introduction — The intermittent injection priming fluid applicator used in this program served as a satisfactory instrument in obtaining general information on engine priming fluid requirements. As a practical applicator, it is not recommended. It requires expensive components and its installation is expensive, since the pump must be driven and timed to the engine.

In addition, serious detonation can result if means are not provided to limit automatically the amount of fluid per stroke in accordance with the temperature condition of the engine. Therefore, a thermostatic device for limiting the rate per stroke must be provided, adding further to the cost and complexity of the system.

Another shortcoming is that this type of application system does not lend itself to 2-stroke engines or to 4-stroke engines with siamese intake ports.

Spray Introduction into Air Induction System

Another general method of applying priming fluids is that of spray introduction into the intake air stream. Any device that divides the fluid into droplets at the point of introduction belongs in this category. This is the method employed by all the applicators on the market at present.

The priming fluid is transported by the intake air. Small droplets remain suspended in the moving air and thus reach the engine cylinders; large droplets precipitate and collect in the induction system, and some of the fluid is vaporized and carried into the cylinders in this form. The mass mean droplet diameter is relatively large even with the best of atomizers, on the order of 30 microns for pneumatic and 50 microns for hydraulic atomization. Since, for good delivery, droplet size should be 5–8 microns or less, only a small portion of the fluid reaches the cylinders during cranking.

The fact that delivery of priming fluid is poor with spray introduction limits the minimum starting temperature, since higher cylinder rates are required at the lower temperatures. At the higher temperatures, acceptable starts can be obtained because the engine requires ether at low rates only, the ether vaporizes more readily, and the saturation limit of the air is higher.

Another undesirable feature of this application method is that fluid accumulated in the induction system during cranking is rapidly taken into the cylinders after the engine starts, due to the much higher air velocities. When a considerable amount of fluid accumulates in the air induction system as a result of a long cranking period, dangerous engine overspeed and engine damage can result.

To obtain some idea of the amount of ether that collects in the manifold, a simple experiment was performed in which ether was sprayed into a Lucite

tube, as shown in Fig. 8. The tube, with an inside diameter of 2½ in., was connected to the intake of an engine in order to provide typical engine airflow conditions. The tube was inclined about 6 deg against the horizontal in order to permit collection of precipitated ether at the air entrance of the tube. The spray nozzle, when located in Position 1, injected in the direction of the airflow into the 65-in. long straight section of the tube. A thermocouple was located at the downstream end of the tube for obtaining an indication of the mixture temperature.

For a test at – 40 F the engine was cranked at 120 rpm to give an airflow of approximately 18.7 cfm. With a swirl-pin nozzle having a spray angle of about 18 deg in still air, ether was sprayed at a rate of 2.30 cc per sec for 30 sec, for a total of 69 cc. The following observations were made:

1. Fallout from the visible spray occurred within 14 in. from the nozzle.
2. Liquid ether collected in large quantities at the bottom of the tube.
3. The air moved the liquid along the bottom of the tube as far as the end of the tube.
4. The temperature at the end of the tube was 5–6 F below the ambient.
5. The amount of liquid ether collected at the tube entrance was 44 cc at the end of the test.

These observations clearly show what small portion of the injected ether would reach the engine cylinders. Actually, the liquid fallout was more than the 44 cc collected, since some liquid remained on the wall of the tube at the end of the experiment. It is estimated that at best about 15 of the 69 cc were carried through the tube, or less than one-quarter of the introduced amount. This represents an effective ether/air ratio of about 0.03. The ether transported by the air was in the form of small droplets and vapor. That there was evaporation was indicated by the observed temperature drop at the end of the tube. No attempt was made to determine the proportion between vapor and floating droplets.

To obtain an indication of how much ether can be vaporized when the air supplies the latent heat, the adiabatic saturation at different temperatures was computed (the "no heat added" curve in Fig. 9). At – 40 F an ether vapor-air ratio of 0.028 is obtained under these idealized conditions. With spray introduction, however, it is doubtful that ether vapor saturation is ever obtained, because the available liquid surface area is not large enough for efficient vaporization.

This experiment demonstrates forcefully that with spray introduction the transportation of priming fluid at the lower temperatures is far from satisfactory. The nonpositive delivery of the fluid to the cylinders limits startability and can create conditions that might result in engine damage.

Vapor Introduction into Air Intake System

The third method of priming fluid application is that of vapor introduction. In this method the priming fluid is supplied to the engine manifold in vapor form and mixed with the intake air. The air then carries the fluid to the cylinders as a mixture of vapor and aerosol, the latter being formed by condensation of some of the vapor around nuclei in the air. Only an insignificant portion of the vapor condenses on the induction system surfaces at the vapor rates required for starts down to the lowest temperatures.

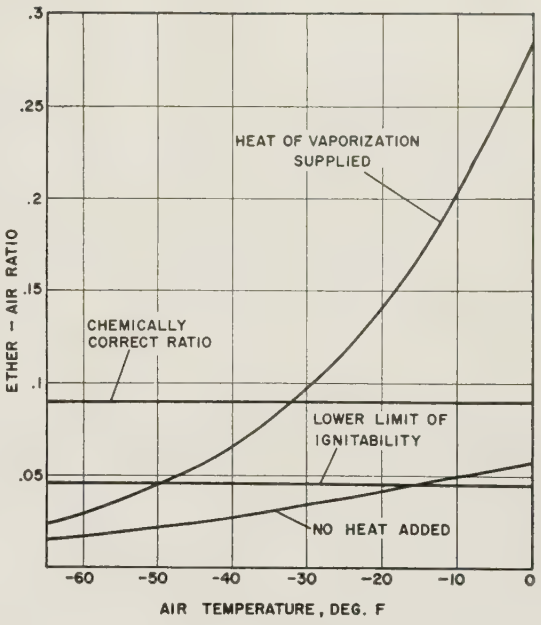

Fig. 9 — Ether/air ratios at saturation

Forming an aerosol by mixing a jet of vapor with a relatively low-temperature airstream is a known process.[19] The mixing will produce supersaturation and, in the presence of nuclei, condensation into extremely small droplets will take place. This process occurs frequently in nature in the atmosphere and is often employed in the laboratory and in technology. When an aerosol is generated by jet mixing, it is relatively stable if the substance has a sufficiently low vapor pressure at normal temperatures. This is not true for ether, however, because it has a relatively high vapor pressure.

When a jet of ether vapor emerges into cold air, large volumes of air are drawn into the jet; and because of the internal turbulence, masses of vapor are thrown out, mixed with air, and then drawn back into the jet. A large number of droplets are formed in this process, the smallest ones re-evaporating and recondensing while still in the turbulent zone. At some distance from the nozzle, aerosol formation ceases. As the droplets are carried along by the air, they will evaporate if the air is not saturated. Also, coagulation takes place, forming larger droplets. The rate of coagulation is proportional to the number of droplets present.

In applying this principle to priming fluid application, how much of the ether remains in vapor form and how much condenses into droplets is not too important as long as the ether can be transported properly by the air and condensation on the walls stays within reasonable limits.

To compare priming fluid delivery with vapor introduction to that with spray introduction, ether vapor was introduced into the Lucite tube of the

[19] "Particulate Clouds: Dusts, Smokes and Mists. Their Physics and Physical Chemistry and Industrial and Environmental Aspects," by H. L. Green and W. R. Lane. Pub. by E. & F. N. Spon., Ltd., London, 1957.

setup of Fig. 8. The Penn State vapor applicator (to be described later) was used to supply the ether vapor.

Several tests were conducted at – 30 and – 40 F with several constant ether rates and vapor nozzle locations. The engine was again cranked at 120 rpm. The capor nozzle orifice was 0.133 in. and elliptical in shape. The ether rates were varied from 2.15 to 5.0 cc per sec for vapor velocities at the nozzle from 290 to 625 ft per sec and ether/air ratios from 0.13 to 0.29. The temperature of the vapor leaving the nozzle was about 100 W. Results with the vapor nozzle at Position 1 (at the elbow) were as follows:

1. At – 40 F with an ether rate of 3.15 cc per sec, a slight amount of wetting in the form of small drops on the tube wall appeared after 10 sec of cranking, beginning about 20 in. from the nozzle. Aerosol was visible in the center of the tube from about the same point on. The temperature rise at the downstream end of the tube was 20 F.

2. At – 40 F with an ether rate of 2.15 cc per sec, a very fine mist covered the last foot of the tube wall after 10 sec. This light wetting moved towards the front of the tube for a very short while, then the tube cleared up throughout. The temperature rise was 17 F.

3. At – 30 F with an ether rate of 5.00 cc per sec, there was considerable wetting throughout the tube but liquid ether did not collect at the bottom of the tube.

4. At – 30 F with an ether rate of 3.80 cc per sec, some wetting developed on the wall of the tube near the downstream end after about 3 sec. After 20 sec, wetting started to appear over about 40 in. of the tube, and at about 28 sec the tube became clear throughout. No aerosol was noticeable under ordinary lighting.

5. At – 30 F with an ether rate of 3.15 cc per sec, the tube remained clear throughout.

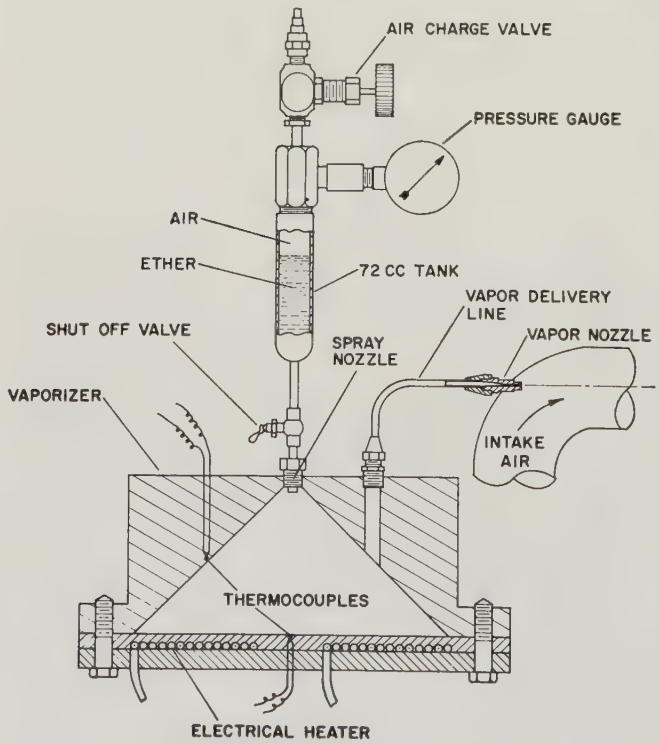

Fig. 10 — Penn State vapor applicator

Table 1 — Starting Performance of Precombustion-Chamber-Type Engine 18.5/1 compression ratio, 125 rpm

Temperature, F	Initial Ether Rate, cc/sec	Ether Duration, sec	First, Fire, sec	Cranking Time, sec
0	0.95	8	1	2
– 25	1.15	11	1	2
– 40	1.40	15	2	3
– 50	1.58	19	2	3
– 55	2.10	29	2	4
– 62	4.45		8	38

With the vapor nozzle in Position 2 the results were essentially the same except that there was light wetting at the outside radius of the elbow for a distance of 6–8 in. A few tests were conducted with the vapor nozzle located 4 in. from the far wall of the elbow to obtain the effects of severe impingement. With an ether rate of 2.15 cc per sec at – 30 and – 40 F, there was more wetting at the elbow than with the nozzle in Position 2 (15 in. from elbow), but otherwise there was little difference. At higher rates wetting occurred throughout the tube.

The results of these experiments clearly show that with vapor introduction, delivery of ether is positive with an insignificant amount of wetting for rates up to 2.4 times the stoichiometric ether/air ratio at – 30 F and 2.0 times at – 40 F. All indications are that these rates are adequate. For example, a start on a precombustion chamber engine at – 40 F within 4 sec of cranking required ether at a rate only slightly in excess of 1.5 times of the stoichiometric rate.

The reasons for the excellent transportation characteristics of vapor introduction method are:

1. Only small droplets are formed, which do not precipitate.
2. A large portion of the ether remains in vapor form.
3. The ether which is transformed into droplets gives up its latent heat, thereby increasing the temperature of the air and thus improving its vapor-carrying capacity.

The "heat of vaporization supplied" curve in Fig. 9 shows how much ether can remain in the air in vapor form under these conditions. For example, at – 40 F ambient, if the air temperature is increased 20 F in the induction system, saturation occurs at an ether/air ratio of 0.14, or better than 1.5 times the stoichiometric ratio.

The quantity of ether that can be carried by the air as droplets depends on their size and number. On the basis of the reported visual experiments it is difficult to say how much of the supplied ether was transported as aerosol and how much as vapor. The answer to this question is not important, because at the ether rates which are required in practice the transportation is entirely satisfactory.

Penn State Vapor Applicator — In developing a vaporizer for experimental work, the requirement was laid down that vaporization should be rapid so that the vapor rate to the engine could be controlled

Table 2 — Starting Performance of Precombustion-Chamber-Type Engine at Various Cranking Speeds

Temperature, F	Cranking Speed, rpm	Initial Ether Rate, cc/sec	Ether Duration, sec	First Fire, sec	Cranking Time, sec
0	95	0.95	8	1	2
– 25	85	1.15	11	2	3
– 40	85	1.40	15	2	7
– 50	98	2.35	29	15	17
– 50	85	2.35	29	2	29 (no start)
– 55	112	2.35	29	16	40 (no start)

Table 3 — Comparison of Vapor Introduction and Spray Introduction

Ambient Temperature, F	Ether Rate, cc/sec	Spray Introduction		Vapor Introduction	
		First Fire, sec	Cranking Time, sec	First Fire, sec	Cranking Time, sec
– 55	2.40	38	40 (no start)	2	6
– 50	2.40	13	24	2	3
– 40	1.15	9	16	3	4
– 40	1.84	3	5	1	2

by the liquid rate to the vaporizer. The hot-plate vaporizer shown in Fig. 10 was designed to satisfy this requirement. It consists of a conical chamber with a spray nozzle at the apex and a heated plate at the base. Its operating principle is simple: liquid ether is sprayed onto the hot plate by a swirl nozzle that divides the liquid into small droplets and distributes them evenly over the plate. The vapor flows from the chamber through a short delivery line to the vapor nozzle in the engine intake manifold. The plate is heated by an electrical-resistance wire embedded in a spiral groove on the underside of the plate.

Bench tests have shown that vaporization lag is very small. For all practical purposes the vapor rate can be considered equal to the spray rate after the first second of operation.

At – 40 F the amount of heat required for vaporizing ether is 0.36 Btu per cc. In practice a somewhat higher rate of heat supply will be needed, since there will be heat losses from the vaporizer; but these can be kept low by proper design. In the laboratory model no special attempt was made to control these losses.

Ether is delivered to the spray nozzle from a tank pressurized by air. By selecting the tank just large enough for a single start at the minimum temperature, a decreasing ether rate is obtained as the tank is discharged. With suitable charging pressure this rate will approximate the engine requirements for which an example was given in Fig. 2. The ether rates and application durations required at other starting temperatures are obtained by corresponding choice of the ether quantities and the air pressures with which tank is charged.

Results with Vapor Introduction — Tests with vapor introduction have been conducted on three different engines. The engines differ in combustion-chamber designs and air induction system configurations, and, therefore, cover some of the variables encountered in cold starting with priming fluids.

The lowest temperature at which starts were obtained with a precombustion-chamber-type engine having a compression ratio of 18.5/1 was – 62 F. The starting permformance of this engine at various temperatures when cranked at 125 rpm is given in Table 1. The initial ether rates given in the table are optimum values for minimum cranking time. The rates diminished with time in a predetermined fashion so as to approximate engine requirements during warmup.

The data show that starts with only 4 sec of cranking are possible down to – 55 F. It should be noted that the given temperatures are those of the air in the cold room and of the engine throughout. Thermocouples were placed in the engine at numerous strategic spots. The temperatures at these points were held constant for several hours before making a test.

Table 2 gives data on starts with the same engine at different cranking speeds.

At the higher temperatures good starts were obtained with cranking speeds as low as 85 rpm, which was the minimum rate at which the engine could be cranked at uniform speed. At – 50 F a start was obtained in 17 sec at 98 rpm, but it failed to start with 85-rpm cranking speed. At – 55 F the engine failed to start with 112-rpm cranking speed although, as Table 1 shows, it started quite well at 125 rpm with an even lower ether rate. These data indicate that, in the minimum temperature region, starts become very marginal or impossible below a certain cranking speed.

The lowest starting temperatures for the other two engines tested were considerably higher than for the precombustion-chamber engine. One of these engines was an open-chamber type. It could be started down to only – 25 F. The other, a Lanova type, would not start below – 20 F. Differences in compression temperatures, due to cylinder size, surface-to-volume ratio, and the like, are doubtlessly the major reason for such differences in startability; but other influences may also play a part. Therefore, we are now studying the relationship between compression temperature and startability by measuring instantaneous cylinder charge temperatures with thermocouples made of wire having a diameter of 0.0008 in. Such wires, thin as they are, still show some temperature lag, but tests have shown that temperatures so obtained are close enough to the true ones to make direct comparisons valid. We will report on the results of this study at some later date.

Comparison Between Results of Vapor and Spray Introduction

To compare startability with vapor introduction to that with spray introduction several tests were conducted on the precombustion chamber engine under identical conditions. The cranking speed was 125 rpm. The ether rate was maintained constant during a test. The results are given in Table 3.

It is evident from these data that startability at the very low temperatures is considerably better with vapor introduction. What the data do not show is the much better behavior of the engine when it is started with vapor. Since puddling in the induction system does not occur, overspeeding after the start is absent and so is excessive detona-

tion. At higher temperatures there is little difference in cranking time for the two methods, because the ether rates which the engine requires are much lower.

Engine Damage

From time to time, laboratories and operators report serious damage to engines started with priming fluids. It is, therefore, of interest to note that the precombustion chamber engine, when dismantled after 100 starts with vapor application of ether (usually at very low temperatures which require high rates) showed no ill effects except for very slight scuffing on two of the four pistons. This absence of significant damage can be attributed to the fact that the ether reaching the cylinders causes a minimum of dilution of the lubricant on the walls, and that overspeeding and excessive detonation are avoided by good control of the ether admission to the cylinders.

This indicates that if vapor application is used, the full low-temperature starting potential of engines can be exploited without fear of harming the engine.

Summary and Conclusions

For starting a diesel engine with priming fluid, the fluid must be supplied initially at a high rate in order to keep cranking time short. After the engine has started and accelerated to warmup speed, the rate should gradually decrease and become zero when the regular fuel will ignite without assistance from the priming fluid. For every temperature-engine combination a minimum initial rate exists for a start within a given number of seconds.

At very low temperatures the required initial rates can be quite high. The problem is to provide the cylinders with priming fluid at these rates. This can be accomplished by injecting it directly into the cylinders, but means for accomplishing this are prohibitively complex and costly.

Spraying fluid into the intake manifold is the simplest method, but precipitation of the larger drops of the spray makes it difficult, if not impossible, to deliver enough fluid to the cylinders during cranking. In addition, the fluid which has accumulated in the induction system during cranking will be rapidly drawn into the cylinders once the engine starts, leading to overspeeding and possible damage.

These undesirable effects can be somewhat lessened by the priming fluid composition. The most effective practical fluid is diethyl ether. Diluting it with less volatile, slower burning materials will improve engine operation after cranking, but dilution of the ether reduces its effectiveness during the crucial cranking period.

A better method is to employ plain ether and supply it to the intake manifold in vapor form. Part of the introduced vapor will condense in the cold intake air and form small droplets that are carried along by the air without difficulty. This means that delivery to the cylinders is positive. They receive ether at the rate at which it is supplied to the manifold, making it easy to provide adequate rates. The difficulties attendant to accumulation of ether in the induction system are prevented.

Results are reported that illustrate the improvement in startability which can be obtained by vapor introduction of ether. Even with vapor application, however, there is a minimum starting temperature for each engine type. In some cases the minimum temperature can be quite high, indicating that further work must be done if quick starts are to be obtained on all engine types throughout the military temperature range.

The advent of Alaskan statehood should focus the serious attention of trade interests on the complexities of arctic operation and the full utilization of automotive and construction equipment in military as well as commercial service. Economic forecasts about the northern frontier and its expanding commercial possibilities emphasize the scope of the opportunities, yet the man-made potential continues to be seriously handicapped by the seasonal difficulties with internal-combustion engines.

Every effort to minimize the starting problem should pay ample dividends. Numerous and costly gadgets must be eliminated and elaborate and time-consuming procedures avoided. The authors hope that this paper will contribute to dispelling the factors of mystery and ignorance concerning cold starting, and advance the state of the art in the spirit of an approach outlined "way back then."[11]

Acknowledgment

The authors gratefully acknowledge the support by the U. S. Army Engineer Research and Development Laboratories of the research[17,18] on which this paper is based.

APPENDIX

Selected Publications and Technical Reports (1943-1958)

1. *Automotive Industries,* Vol. 88, May 1, 1943, pp. 24–26, 64; and May 15, 1943, pp. 30–32: "Cold Starting for Diesel Engines," by P. M. Heldt.

Survey of entire problem based chiefly on papers given at the SAE Symposium on Cold Starting at the SAE War Engineering Production Meeting, 1943. Later originally referenced in SAE *Journal,* February, 1943, pp. 74–75, including abstracts of nine papers of which the following were later published in SAE Transactions: Cloud and Ferenczi, 1944; Porter, 1943; Roensch, 1943.

2. SAE TRANSACTIONS, Vol. 51, 1943, pp. 277–279: "Effects of Injection Pumps on Cold Starting," by M. M. Roensch.

Reports on tests which show that for starting, pumps should give about 75% more fuel than at full load and that good distribution among cylinders is very important.

3. SAE Transactions, Vol. 51, 1943, pp. 356–357, 368: "Cold-Starting Tests on Diesel Engines," by H. R. Porter.

Reports on tests with laboratory and full-scale engines, indicating that starting improved with higher cetane number, but that this does not hold true for "doped" fuels. Starting improved by injection of various substances into intake. Service starting believed predictable from laboratory tests.

4. SAE Transactions, Vol. 52, 1944, pp. 233–237: "Special Cold-Starting Fuels for Diesel Engines," by G. H. Cloud and L. M. Ferenczi.

Various additives were found to be mildly effective but ethyl ether introduced with intake air allowed starting down to −40 F. Characteristics described for ethyl ether versus pentane.

5. SAE Transactions, Vol. 52, 1944, pp. 276–280: "Oper-

ating Automotive Equipment at – 50 F," by R. W. Goodale.

Fuel and lubricant problem under arctic conditions (Alaska). Trouble with high pour-point fuel; stove oil proved to be a satisfactory diesel fuel. Ice formation in fuel tanks and its prevention. Special starting fluid (forerunner of "Chevron") and methods of introducing it into intake manifold. Reference: U. S. Patent No. 2, 431, 322 (Applicant — R. Wayne Goodale, May 1, 1944), "Diesel Engine Starting Fluid," issued Nov. 25, 1947.

6. *Diesel Power and Diesel Transportation,* Vol 24, October, 1946, pp. 1190–1193, 1230: "Cold Starting of Diesel Engines," by P. H. Schweitzer.

Tests conducted with variable compression CFR engine at Pennsylvania State College showed that of all known methods the most effective way to start a diesel engine in cold weather is by introducing diethyl ether into the intake air. Ether carburetion utilizing plastic capsules for fluid described.

7. Institution of Automobile Engineers *Journal,* Vol. 41, November, 1946, pp. 51–82: "Recent Developments in Low-Temperature Starting of Petrol and Compression-Ignition Engines," by R. Barrington, W. A. Bevis, and K. Brook.

Lack of preparedness in 1939 for low-temperature starting due to no economic necessity; how in short time and under unpleasant conditions the big task was undertaken of ensuring that all internal-combustion engines intended for the land forces should start at 0 F or lower. General similarity of problems for both gasoline and diesel engines, excluding differences in detail. Objective for gasoline engine boils down to effective ignition with a minimum speed necessary to attain appropriate mixture ratio, augmented at very low temperatures by use of specially volatile fuel for starting; for compression-ignition engine, a sufficient cranking speed to prevent heat losses to cylinder walls and other parts which can preclude self-ignition, or an ignition promoter (priming fluid) to augment burning reaction. Steps to – 40 F comparatively easy once main principles had been grasped. Ultra-cold starting obtained by direct frontal attack without supporting school of thought which urged easy way of keeping vehicle warm when faced with service in cold climates. Hazards of fuel dilution of sump oil in false starts. Desire to avoid use of nonautomatic starting aids. Adoption of capsule containing 13.5 cc of ether, pressurized in 3-cc air space by inert gas compressed to 550 psi ("Sparklet Ethalet Bulb") for use with carburetor, and 100% excess fuel setting for injection pump during cranking and low-speed running.

8. *Journal of Research,* Vol. 39, July, 1947, pp. 39–47: "Cold Starting Abilities of Various Substitute Motor Fuels," by R. E. Streets. U. S. National Bureau of Standards Research Paper No. RP1811.

Tests of various nonhydrocarbon fuels in a standard 8-cyl auto engine showed the starting abilities of single constituent fuels to be rather limited, but the addition of small percentages of more volatile fuels lowered the minimum starting temperature to a marked degree. Under altitude conditions, also showed a further reduction in minimum starting temperature of each fuel used; should compensate to some degree for the lower average temperatures generally encountered at higher altitudes so that for any one area it would be possible to obtain satisfactory starting with a minimum amount of blend changes. Test method was that outlined in "CFR Procedure for Testing the Starting and Warming-Up Characteristics of Fuels," CRC designation F-6-943. Most effective and desirable additive appears to be diethyl ether.

9. *Diesel Power and Diesel Transportation,* Vol. 25, November, 1947, pp. 49–51: "Frigid Starting and Operation," by E. W. Goodale.

Review of investigations in Alaska during latter two years of World War II related to diesel and gasoline-engine powered trucks, tractors, and stationary units. Development of starting fluid and priming system.

10. *Commercial Car Journal,* Vol. 4, December, 1949, pp. 72, 120, 122: "Diesel Cold Starting — Problem of Design and Fuel," by F. L. Nelson and C. S. Ulzheimer.

Reports on investigation of a variety of priming fluids, showing ethyl ether best for use as low-temperature starting aid. Also referenced under title "Ethyl Ether Best for Cold-Starting Diesels," in SAE *Journal,* Vol. 58, March, 1950, pp. 42–50.

11. *Diesel Power and Diesel Transportation,* Vol. 28, February, 1950, pp. 52–53: "Sinclair Markets a Diesel Starting Aid."

Flexibility in the methods of application and availability of the fluid in bulk or in capsules makes usage possible over a wide range of engines (to – 11 F).

12. *Caterpillar Service Magazine,* Vol. 19, Nov. 30, 1950, pp. 45–47: "Ether — An Aid for Cold Starting."

Introducing ether steel capsule injectors as a fast and convenient method of aiding diesel-engine starting in cold weather; connected to inlet manifold opening formerly used for manifold air heater.

13. *Standard Oiler,* Vol. 13, February, 1951, pp. 8–9: "Hot Product for Cold Engines — Starting Fluid Aids Military Operations."

Description and development of "Chevron Starting Fluid," for commercial production based on service tests.

14. *Diesel Power and Diesel Transportation,* Vol. 29, May, 1951, pp. 54–56, 79: "Cold Weather Starting and Operation," by D. P. Herron, A. C. Scurlock, and A. W. Sloan.

Condensation of survey made for the Office of Naval Research, involving interviews and correspondence with numerous U. S. diesel research centers and literature references. Ether injection favored as best means of ignition.

15. *Diesel Power and Diesel Transportation,* Vol. 29, February, 1951, pp. 58–59: "For Winter Operation — A Cold Starting Aid," by J. A. Jones, Jr.

Physical properties and characteristics of "Chevron Starting Fluid" developed for the military.

16. *Diesel Progress,* Vol. 16, April, 1951, pp. 64–65: "Cold Starting of Diesel Engines," by H. Ferguson.

C.A.V. ether starting device employing plastic capsules and providing a high rate of ether supply at beginning of cranking.

17. SAE *Quarterly* Transactions, Vol. 6, October, 1952, pp. 689–709: "Sub-Zero Winterization of Diesel Engine Power Equipment," by P. W. Espenschade, R. C. Navarin, and W. W. Van Ness.

Problems encountered in winterization of Army Corps of Engineers equipment and description of techniques developed. Analysis of successful cold starts of 831-cu-in. displacement, 4-stroke diesel engine at temperatures as low as – 40 F, using hydraulic cranking, military arctic lubricants and fuel, and ether priming fluid in capsules.

18. *Diesel Progress,* Vol. 17, March, 1952, p. 82: "Report on Chevron Starting Fluid."

Heavy equipment owners' and operators' replies to questionnaire on performance.

19. SAE *Journal,* Vol. 60, April, 1952, pp. 40–44: "Factors Affecting Diesel Engine Starting," by J. F. Blose.

Condensation of unpublished paper "A Summary of Seventeen Years of Diesel Engine Starting Tests at the U. S. Naval Engineering Experiment Station," reviewing work done on cold starting based on investigation of such factors as engine design, fuels, lubricants, and starting aids.

20. "Starting Cold Diesels," by E. E. Kilty, N. K. Lammers, and K. J. Fleck. Paper presented at SAE National Tractor Meeting, Milwaukee, September, 1952. Condensation in SAE *Journal,* Vol. 61, February, 1953, pp. 36–40.

Tests using full-scale caterpillar diesel engines to develop cold-starting methods. Combinations of glow plugs, ether injection, and standby heating (to – 65 F).

21. *Petroleum Engineering,* Vol. 25, February, 1953, p. C10: "Cold-Room Study of Starting Fluids," by H. D. Young.

Problems encountered in cold-room study (Sinclair Research Laboratories, Inc.) of starting fluids at subzero temperatures. Results obtained in cold starting tests of diesel single-cylinder 4-stroke engine and 3-cyl 2-stroke

engine to explore effects of different primary fuels. Injector and valve malfunctions. Optimum points for starter fluid application.

22. *Product Engineering,* Vol. 24, July, 1953, pp. 202–204: "Operation Eager Beaver I — Arctic Testing."

Success of arctic lubricants, starting aid, and related products in combined United States-Canadian Army Engineer exercise from December, 1951, until May, 1952, in the Yukon, Canada.

23. *Diesel Power and Diesel Transportation,* Vol. 32, September, 1954, p. 65: "Cold-Engine Starter."

Introduction of Ampco-Sinclair self-contained pneumatic starting fluid applicator which operates on "aerosol" principle and is designed for cold-engine starting down to – 40 F.

24. "Low Temperature Engine Testing and Facilities," by P. W. Espenschade. Paper presented at SAE National Diesel Engine Meeting, Cleveland, October, 1954. (Condensation in SAE Journal, Vol. 63, April, 1955, p. 95: "Seven Precautions for Cold Room Safety.")

Key points for reasonable prediction of performance in the field and assurance to user for service as intended. Climatic test facilities of large capacity in U. S. universities, research installations, industry, and government. Cold-room safety precautions. Instrumentation. Descriptive questionnaire for rating and evaluating environmental test chambers.

25. "Engine Starting Tests," by J. F. Blose. Part 1 of "Effect of Low Ambient Temperature on Cranking and Starting of Diesel Engines," by Blose, J. P. Qualey, J. T. Duck, and L. G. Schneider. Paper presented at SAE National Diesel Engine Meeting, Cleveland, October, 1954. (Condensation in SAE *Journal,* Vol. 63, May, 1955, p. 112: "Diesel Cranking Studied at Arctic Temperatures.")

Low-temperature starting data based on tests at U. S. Naval Engineering Experiment Station with 2-stroke engines indicate relative effectiveness of various starting aids and cranking systems is not constant. Starting performance improved by adopting higher voltage (that is, 24–30) for electrical cranking systems. Best aid for each application can only be determined by trial and error.

26. "Application of Starting Fluids to Internal Combustion Engines," by W. G. Ainsley and H. D. Young. Paper presented at SAE National Diesel Engine Meeting, Cleveland, October, 1954. (Condensation in SAE *Journal,* Vol. 63, May, 1955, p. 110: "New Starting Fuels Excel Di-Ethyl Ether.")

Discussion of starting fluids, problems of application, and philosophy of specific requirements for Sinclair Research version of applicator, and formulation of blended starting fluids which retain the advantages of straight diethyl ether but have none of its disadvantages.

27. SAE Transactions, Vol. 63, 1955, pp. 515–530: "Engine Cranking at Arctic Temperatures," by W. E. Meyer, J. J. DeCarolis, and R. L. Stanley.

Based on Contract No. DA-44-009-ENG-765, Project 8-50-02-001, with the Pennsylvania State University sponsored by the Engineer Research and Development Laboratories. Determination of breakaway torque and cranking requirements of representative industrial and automotive gasoline and diesel engines, with and without accessories, for different speeds at 0, – 25, – 40, and – 65 F utilizing arctic engine oil (MIL-O-10295) and speed ranges between 50, 100, and 150 rpm (gasoline) and 100, 200, and 300 rpm (diesel engines). Copies of original data released to all participating engine manufacturers.

28. *Oil Engine and Gas Turbine,* Vol. 23, July, 1955, pp. 92, 93: "Safe Low Temperature Starting Without Detonation."

High cetane number and peroxide content characteristics of throw-away fuel capsules ("Start Pilot") to – 35 F.

29. *Caterpillar Service Reporter,* October, 1955, pp. 2–3: "Ether Safely Contained — Off to Quick Start."

Quote "Considering all the requirements, the ether starting aid offered for all Caterpillar Diesel Engines provides the safest, surest method of ether starting assistance in cold weather. If a starting aid is required, consider it as a sure way to get off to a better start."

30. "Diesel Fuels for Cold Starting and Warmup." Report No. 617-23E, Texas Co. Beacon Laboratories.

Not for public disclosure except by reference to and with express authorization by The Texas Co.

31. *Oil Engine and Gas Turbine,* Vol. 23, January, 1956, pp. 345: "Low Temperature Startability Proved."

Starting tests on 4- and 6-cyl Dorman engines with "Start Pilot" equipment under simulated arctic conditions (– 25 F).

32. *Diesel Progress,* Vol. 21, July, 1956, pp. 56, 61: "Automotive Diesel Progress: Low-Temperature Diesel Starting," by M. C. Horine.

Resume of "solutions" to problems of cold-weather starting of diesel engines, including glow plugs, dual fuel arrangements, electric resistance heaters, fuel-burning heaters, ether injection, and shotgun shells. Quote "Considering the cost in fuel and unnecessary wear and tear on the engine involved in the all-too-prevalent practice of overnight idling of engines, these auxiliary starting aids merit the consideration of every user of dieselized equipment in cold climates."

33. *Diesel Power and Diesel Transportation,* Vol. 34, September, 1956, p. 54: "Cold Starting Made Easier."

Description of "Start Pilot" device.

34. "Primer, Pressure, Internal Combustion Engine (Cold Starting Aid) and Primer Cartridges." Interim Federal Specification F-P-00666 (GSA-FSS), Revision 2, Oct. 1, 1956.

35. *Aviation Week,* Vol. 65, Dec. 3, 1956, pp. 111–113: "New Primer Aids Engine Starts in Chill South Pole Temperatures."

Discussion and tests regarding "Reichhelm Gasifier" (Patent No. 2,197,347).

36. *Diesel Progress,* Vol. 23, January, 1957, p. 50: "What's Going On in England — An Aid to Cold Starting."

Discussion of C.A.V. Ltd. "Thermostart," which makes use of the primary engine fuel as a starting aid for diesel engines.

37. "Cold Weather Operation of Diesel Engines," Part II. A bibliography of reports by Technical Information Division, Library of Congress, January, 1958, issue (Card No. 53-60028). Also available from the Office of Technical Services, U. S. Department of Commerce, Washington 25, D. C., as PB No. 131492.

38. *Diesel Power and Diesel Transportation,* Vol. 36, March, 1958, p. 32: "Using Starting Fluids Properly."

Discussion of "Spray Products" priming fluid packaged in pressurized cans, and associated kit.

DISCUSSION

Starting Fluids with Diethyl Ether Found to be Most Satisfactory

— J. F. Blose

U. S. Naval Engineering Experiment Station

THE NAVAL Engineering Experiment Station was introduced to starting aids for diesel engines when the first units were received for test in the early 1930's. These engines used glow plugs, air intake heaters, or compression changing valves to obtain minimum starting temperatures of 10–20 F. Starting fluids containing diethyl ether were first tested in 1943 when experience gained during the war showed the need for starting engines at subzero temperatures. While other types of starting aid are often effective, the use of starting fluids containing diethyl ether has been found to start most of our engines with a minimum of

wear and tear on the engine, the cranking system, and the operator.

We have not directly investigated the effect of spray particle size or rate of fluid injection on engine starting; however, the different types of commercial applicators tested have covered a wide range of both of these variables. The minimum starting temperature has been found to be about the same, on our test engine, for any make of starting fluid or design of applicator except when the ether has been diluted with excessive amounts of less active materials. The duration of cranking required and the amount of fluid used do appear to be a function of particle size and rate of injection as reported by the authors. The incorporation in the fluid of ingredients to improve ignition quality or promote combustion has not, in our experience, improved engine starting, although it may have improved engine operation during warmup. Our best starting results were obtained with commercially pure diethyl ether.

We have had no experience with vaporized ether as a starting aid. This method of application appears to offer important advantages since it eliminates fuel puddling in the intake manifold, heats the intake air slightly, and produces a more intimate mixture of air and fuel than can be obtained with spray. It is hoped that a suitable commercial version of the applicator will soon be offered on the market.

The reported starting performance of the precombustion-chamber engine is excellent. The authors are requested to state whether the other test engines gave better starting with vaporized fluid than with sprayed fluid. The reported minimum starting temperatures, – 25 and – 20 F, respectively, appear to be about the same as would normally be obtained with commercial methods of fluid application on these engines.

Even Firing with Ether Dependent On Good Distribution of Starting Fuel

— V. C. Reddy
General Motors Corp

THE AUTHORS are to be congratulated for presenting an interesting and timely paper on the subject of starting diesel engines at low ambient temperatures. It is timely for two reasons. First, this is the time of year when operators begin to experience difficulty in starting their diesel engines and are interested in better starting methods. Secondly, it is necessary to remind the engineers engaged in the design and development of diesel engines that starting a diesel engine in cold weather can be a problem. Many engineers become so engrossed in raising the horsepower and improving the fuel consumption of their engines they forget about starting difficulties. Increasing the turbocharger pressure ratio and lowering the engine compression ratio does not help a customer get his engine started. The most efficient engine is of little value if it cannot be started.

The superiority of vaporized diethyl ether over an atomized ether spray for starting diesel engines should be of considerable interest to both engine builders and users. The vaporizing apparatus described in the paper appears rather bulky and complicated for commercial use. We would like to know if a simple, compact vaporizer suitable for field installation has been developed?

The authors have not given very much information on the exact starting procedures used during their tests. During the many cold-starting tests conducted by Detroit Diesel, we have found that small changes in technique sometimes mean the difference between success and failure. We agree with the authors that better starts are possible if the cylinders are each insured of an adequate supply of ether during the starting cycle. Fig. A shows the method used to direct ether to the inlet ports of a Model 2-71 engine equipped with a hydraulic starter during starting tests at – 25 F. The hydraulic starting system provides relatively high cranking speeds for a very short interval of time (Fig. B). With this system the engine must run under its own power after a very short cranking period. For our starting tests, strain gages are attached to the cylinder head to indicate which cylinders are firing. By this method misfiring due to the uneven distribution of the starting fluid is easily detected, as shown in Fig. C. In addition to good distribution of the starting fluid, it is very important the throttle remain closed until the engine is firing evenly on ether. An injection of cold fuel oil into the cylinder during the initial starting cycle depresses the

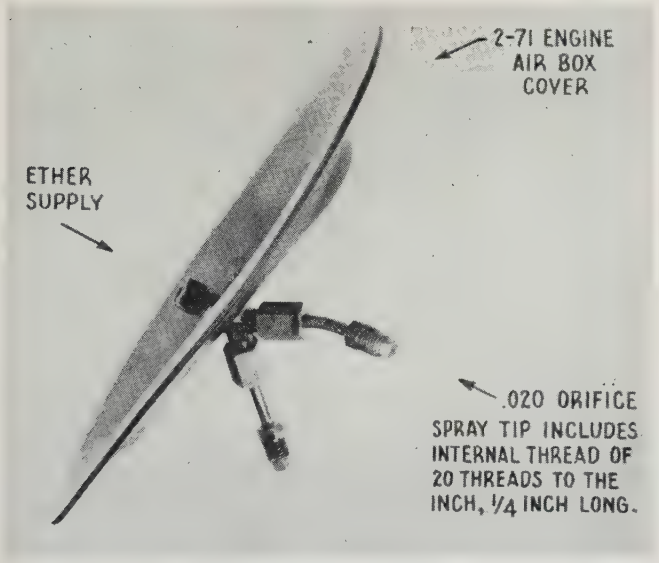

Fig. A — Ether injection nozzles (2-71 engine) for starting at – 25 F

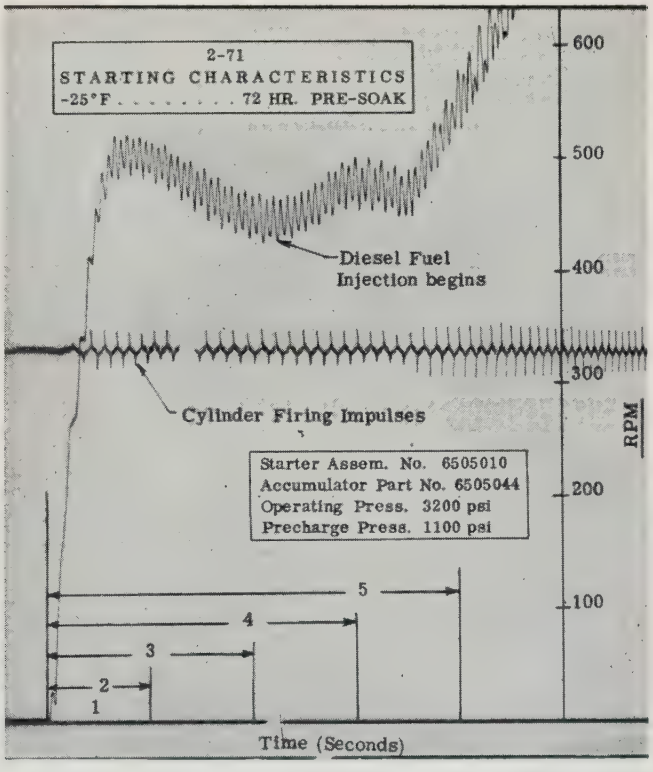

Fig. B — Starting characteristics of 2-71 engine at – 25 F and 72-hr pre-soak

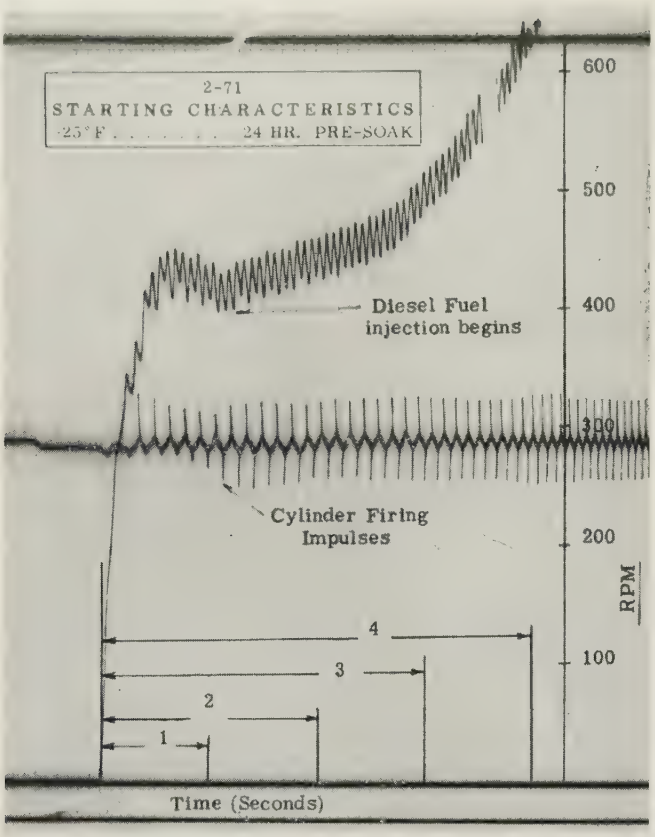

Fig. C — Starting characteristics of 2-71 engine at −25 F and 24-hr pre-soak

temperature of the compressed air ether mixture. For example, injecting 90 cu mm of fuel oil at 0 F with an ambient temperature of −20 F lowers the temperature of compression approximately 54 F in a Series 71 engine cylinder. This may be calculated as follows:

Heat given up by air = Heat taken up by (liquid fuel + latent heat of vaporized fuel + vaporized fuel (negligible) (A)

$$W_a \times C_{pa} (t_a - t_m) = \%V \times W_f \times C_{pf_1} (t_m - t_f) + \%V \times W_f \times C_{pf_2} (IBP - t_f) + \%V \times W_f \times L_f \quad (B)$$

where:

t_a = Initial boiling point of fuel = 300 F
t_f = Temperature of air at time of fuel injection = 450 F[a]
IBP = Temperature of fuel being injected = 0 F

W_a = Weight of air trapped in cylinder $= \frac{1.326 \times 29.5}{-20 + 460} \times \frac{71}{1728}$
$= 366 \times 10^{-5}$ lb

W_f = Weight of fuel injected $= \frac{90 \text{ mm}^3 \times 0.808}{1000 \times 453} = 16 \times 10^{-5}$ lb

C_{pa} = Specific heat of air at 450 F = 0.1759
C_{pf_1} = Specific heat of fuel between t_m and t_f = 0.527
C_{pf_2} = Specific heat of fuel between IBP and t_f = 0.505
L = Latent heat of vaporization of the fuel at the IBP = 104 Btu/lb
$\%V$ = Percent of fuel vaporized at the final t_m (from distillation curve)

Calculation

$$366 \times 10^{-5} \times 0.1759 (450 - t_m) = 0.85 \times 16 \times 10^{-5} \times 0.527 (t_m - 0) + 0.15 \times 16 \times 10^{-5} \times 0.505 (300 - 0) + 0.15 \times 16 \times 10^{-5} \times 104$$

$$450 - t_m = \frac{16 \times 10^{-6}}{366 \times 10^{-5} \times 0.1759} (0.85 \times 0.527\, t_m + 0.15 \times 0.505 \times 300 + 0.15 \times 104)$$
$$= 0.249 (0.448\, t_m + 22.7 + 15.6)$$
$$= 0.1118\, t_m + 9.52$$
$$1.1118\, t_m = 440.48$$
$$t_m = 396 \text{ F}$$

Temperature drop due to injection of 90 mm³ of fuel into air at 450 F = 450 − 396 = 54 F

The calculated values are, of course, only approximate, as some of the unburned fuel is deposited on the walls of the combustion chamber and never reaches the temperature of compression. The unburned fuel may also have a detrimental effect on starting by reducing ring lubrication and sealing. This detrimental effect of early fuel oil injection on the starting ability of a diesel engine has been demonstrated in the cold room on numerous occasions.

Author's Closure To Discussion

IN ANSWERING Mr. Blose we have to state that we have made no direct comparisons between spray and vapor introduction of ether on engines, other than that on which we have reported in the paper. Reasoning would indicate, however, that engines of inherently poorer startability will not be improved as much by a change to vapor priming. This is so because vapor priming excels principally on account of the improved transportation of the ether from the point of introduction to the cylinders. The lower the temperature in the induction system, the more difficult it is to transport ether properly at higher rates. Consequently, starts at lower temperatures will exhibit greater improvement due to vapor introduction than starts at higher temperatures.

However, even when the minimum starting temperature of an engine is quite high, vapor priming is the preferred method of ether introduction because it is positive and can, therefore, be controlled closely in accordance with the engine requirements. Furthermore, the ether vapor and aerosol mixture is much less apt to cause dilution of the lubricant film on the cylinder walls than the inevitable precipitate from sprays.

Mr. Reddy asks what starting procedure was employed. In the described tests the engine governor was set prior to a starting attempt to the proposed warmup speed, so that no manipulation of the throttle would be required during the starting process. This, of course, resulted in diesel-fuel injection during cranking at the maximum rate permitted by the rack stop. The stop was always left in the position dictated by the manufacturer's rating of the engine. With the priming methods described in detail in the paper, either introduction was always begun simultaneously with cranking.

Mr. Reddy found that better starts are obtained on the 2–71 engine when diesel fuel is not injected until the engine fires evenly. We have made no similar tests on Series 71 engines, but on another engine we found cranking time to be essentially the same whether diesel fuel was injected during cranking or not. The engine was of the precombustion-chamber type and this may explain why our findings differ from those of Mr. Reddy's who worked with an open-chamber engine.

It may be well to point out that the vapor applicator shown in Fig. 10 represents an early experimental model and only one means for producing the desired results. Our experience and data are available to any one desiring to develop it into a commercial unit. Vapor application should be of particular interest in connection with hydraulic cranking, because it is capable of insuring ignition within the few revolutions which such systems produce.

[a] Report S3-30, by J. J. May. General Motors Corp.

THE *TERACRUZER*

—a high mobility vehicle

G. D. Simonds, The Four Wheel Drive Auto Co.

This paper was presented at the SAE West Coast Meeting, Los Angeles, Aug. 13, 1958.

THE REPORTS of the new low-pressure high-flotation tire developed by the Goodyear Tire & Rubber Co. had intrigued us. So when Army Ordnance invited bids on a Research and Development contract to develop a vehicle to use this tire, we bid on the business and were successful. The contract was signed on Dec. 11, 1954.

Early Vehicles

Fig. 1 pictures the first vehicle on our proving ground, showing the articulation of the bogie supports and the drive rollers (A). These terra tires were driven by friction rollers on top of the tire so that neither the load nor the rotating force went through the axle. The only purpose of the axle was to mount the tire and transmit its rotation to forward thrust, driving the vehicle through radius arms (B). The pressures in the tire affected the ability of the vehicle to negotiate the various types of ground conditions. Thus, it was decided that this pressure should be variable in each tire either individually or as a group, and that this pressure should be regulated from the driver's seat in the cab while the vehicle was in motion.

With a free working bogie going over very soft terrain, such as loose dry snow, the first tires would tend to sink further into the undisturbed snow, throwing up a big windrow which hindered the vehicle's forward progress. If the angle of approach of the bogie were controlled to take some of the load off of the leading tire, the front tire would partially compact the snow making a better track for the rear tire. Thus, the mobility would be greatly enhanced. The air cylinders (C) control this angle of attack. They are controlled individually from the driver's compartment, where an indicator shows the angles at which they are being held.

Fig. 1 — First model of Teracruzer

The early trials showed that both of these concepts of air pressures and angle of approach contributed greatly to the mobility of the vehicle.

Preliminary tests on our premises and with the Army in Greenland showed that there was great promise for this type of tire, but also that many improvements could be made. In fact, even before we had finished building the first prototype Goodyear had discovered a way to make this type of tire with

THE DESIGN and operating characteristics of a new ground support vehicle is described in this paper. Built for the Air Force, the Teracruzer weighs only 16,000 lb and has a maximum payload of 16,000 lb.

The vehicle uses Goodyear high-flotation tires of 42-in. diameter, the air pressure of which is controlled by the driver. All wheels have axle drive. Angle drive brings the drive down through the centerline of the steering fifth wheel.

a carcass which would permit loading and driving the tire by means of the central axle. The roller drive, being a friction drive, had its limitations; for example, in mud the tire became coated with slime which, of course, cut down the coefficient of friction between the tire and the roller. Slippage occurring at this point was more prevalent than that between the tire and the ground. Also, the free-wheeling possibilities were very limited and the power loss between the engine and the ground was such that excessively high horsepower was required to move the loads. We found that with a gross load of 36,000 lb all of the 350 hp in the engine was required to move it over the highway at its maximum speed of 25 mph. There also seemed to be a definite limitation of maximum speed that could be obtained with this roller drive. Goodyear's preliminary test with axle drive showed a possible speed of better than 60 mph and an efficiency reasonably comparable with conventional tires when using the axle drive.

Another feature on this vehicle that proved a detriment to its high mobility was the type of center differential, which was essentially an overrunning clutch, where the power to the front bogie was not connected until the rear bogie tires slipped. When the rear tires slipped, they lost much of their footing and, in fact, would start digging a hole; the power to the front wheels was not enough to move the vehicle.

The U. S. Air Force was looking for a vehicle of high mobility to take care of the ground support for their Matador guided missile. They became interested in the Teracruzer for use with the Goodyear Aircraft concept of load packs. They wanted the entire ground support system to utilize a standard vehicle on which they could mount all of the various packs and tools to support, assemble, and shoot the missile, regardless of the terrain surrounding the launching site.

Goodyear Aircraft presented a concept which would be a combination of their removable packs and a specially designed Teracruzer. The Air Force ordered one experimental prototype of this Teracruzer for test evaluation. Needless to say, the axle drive on the tires presented many problems in design. This prototype also presented design deficiencies in vehicle weight and transmission. (See Fig. 2.)

Construction

The requirements set up in the specifications for five pre-production prototypes was a joint problem between the Air Force, Goodyear Aircraft, and the Four Wheel Drive Auto Co. The Air Force, of course, knew what they wanted. Goodyear Aircraft knew the requirements for handling their various ground support equipment packs and we, through our experience with Teracruzers in general and the first prototype for the Air Force, were well-aware of limitations in production.

The main problem, of course, was to rectify the mechanical and operational deficiencies, and to lower the weight so that the concept of the ground support with these vehicles could be successfully met. The requirements of the vehicle are shown in Table 1.

I believe that the best way of describing this vehicle would be to take a trip through the assembly floor in our factory. Fig. 3 shows three frame skeletons in various stages of assembly. The one in the background is as it comes to the assembly floor with the various brackets and cross members installed.

Fig. 4 is a close-up showing the various air, hydraulic, and electrical quick disconnects. The cab can be removed without making laborious disconnects of the various circuits. An entire cable is disconnected through multipronged plugs and receptacles.

Fig. 5 shows where the outrigger framework made

Fig. 2 — First prototype of Teracruzer for Air Force

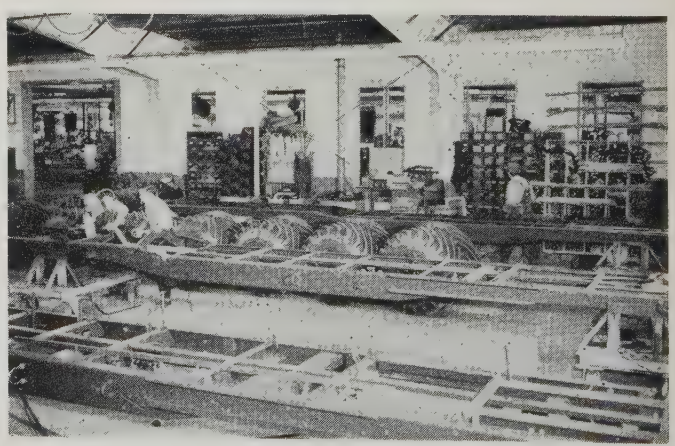

Fig. 3 — Frame skeleton of Teracruzer on assembly floor

of alloy aluminum is bolted onto the frame preparatory to installing the aluminum platform deck.

Fig. 6 shows the instrument panel installed in the cab which is mounted on the frame. This shows the cab with the windshield, the upper part of the door and sides folded over, and the rear panel removed, reducing the height to that necessary to load it onto a freight-carrying airplane.

Fig. 7 is a close-up view of the instrument panel on a work bench, illustrating the complexity of instruments necessary for the operation of the Teracruzer. The bogie tilt indicators (A) show the degree of tilt to the two front bogies and the two rear bogies, and the toggle switches (B) control the tilt, one each for the front and rear. The tilting is done by air pressure in power cylinders. Gages show the pressure for the right tires (C) and for the left tires (D). The top gage is for the front tires and the lower gage for the rear. A pair of toggle switches (E) control the air pressure in the two front tires, other pairs adjacent to the various gages control the air pressure in the pair of tires represented by the gage. When the toggle is in the upper position, air is being admitted to the tires. When it is in the lower position, air is being exhausted from the tires, and when in the middle the tire pressure is held constant. The two toggle switches (F) control the air pressure in the tires in a group. The left one will raise or lower the pressure in the entire group of lefthand tires and the righthand toggle will do the same for the righthand tires. This is valuable in leveling when operating on an appreciable side slope. The multiconnector plugs (G) go into recep-

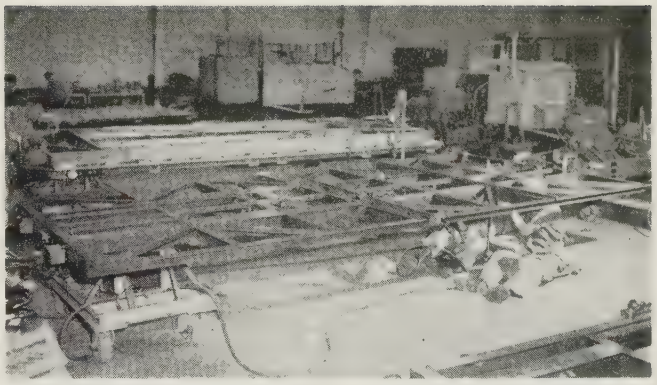

Fig. 5 — Outrigger framework

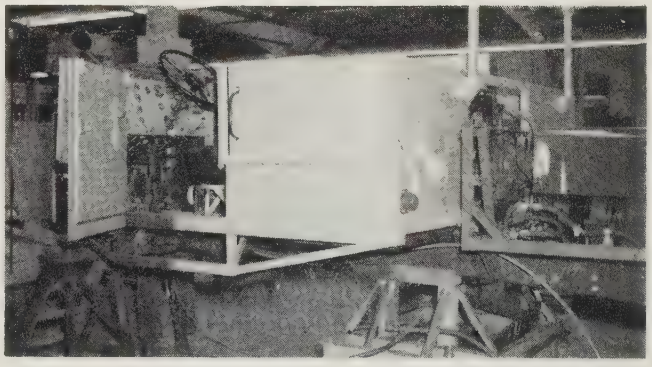

Fig. 6 — Instrument panel installed in cab

Table 1 — Specifications of the Teracruzer

Vehicle Weight	16,000 lb
Maximum Payload	16,000 lb
Overall Length	374 in.
Overall Width	108 in.
Operational Height	122 in.
Reducible Height (for loading in aircraft)	101 in.
Platform Length	216 in.
Power Output (stationary)	
Continuous	125–150 hp
30 min	175 hp
1 min	190 hp
Maximum Speed	40 mph
Maximum Grade, full payload, without trailer	60%
Grade with Trailer, at 25 mph	2%
Turning Radius	40 ft

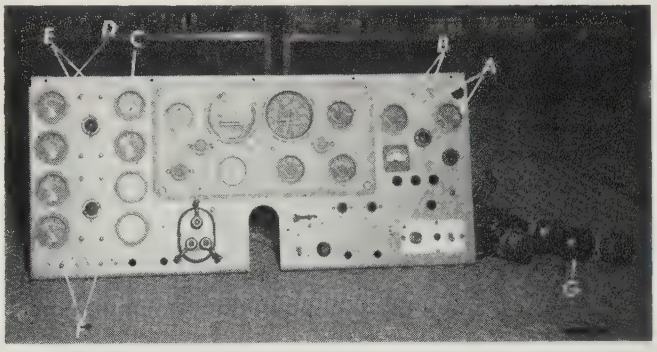

Fig. 7 — Close-up of instrument panel

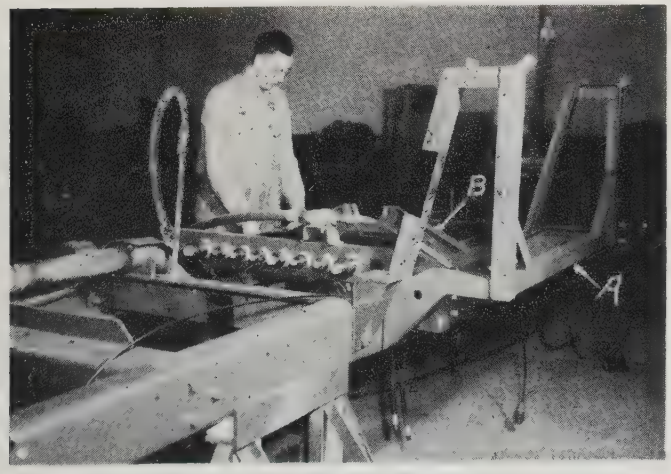

Fig. 4 — Quick disconnects

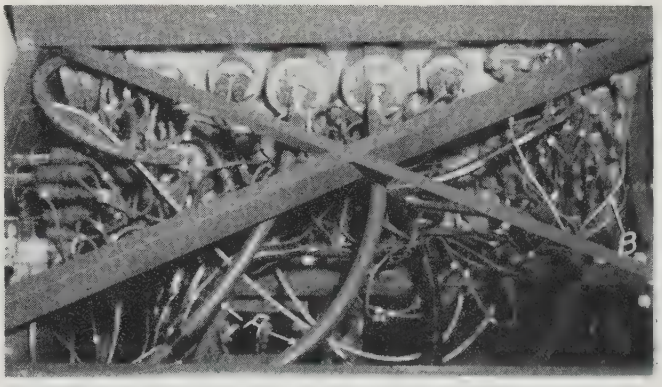

Fig. 8 — Back of instrument panel mounted in truck

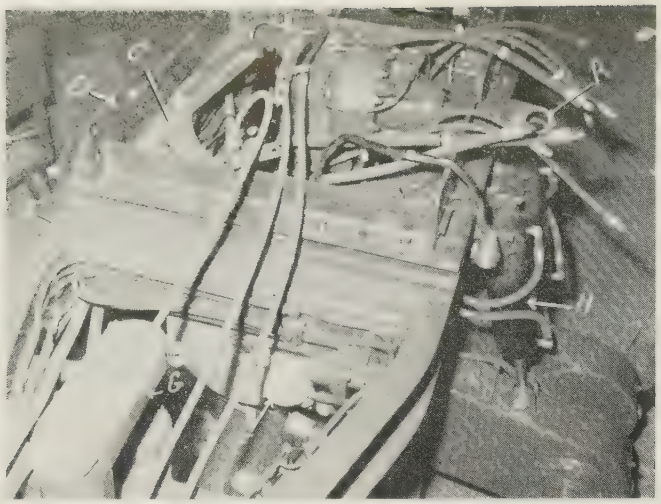

Fig. 9 — Front bogie

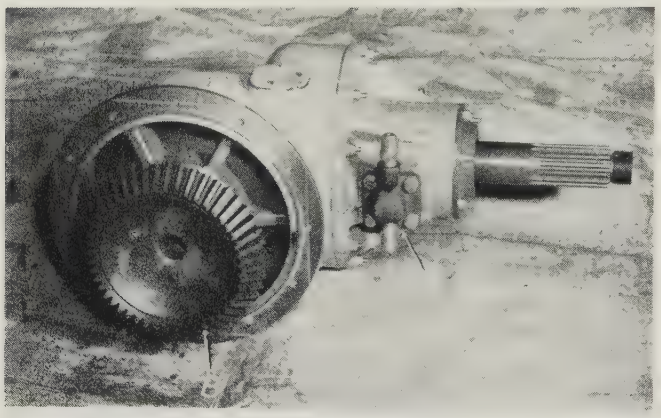

Fig. 10 — Angle drive gear case

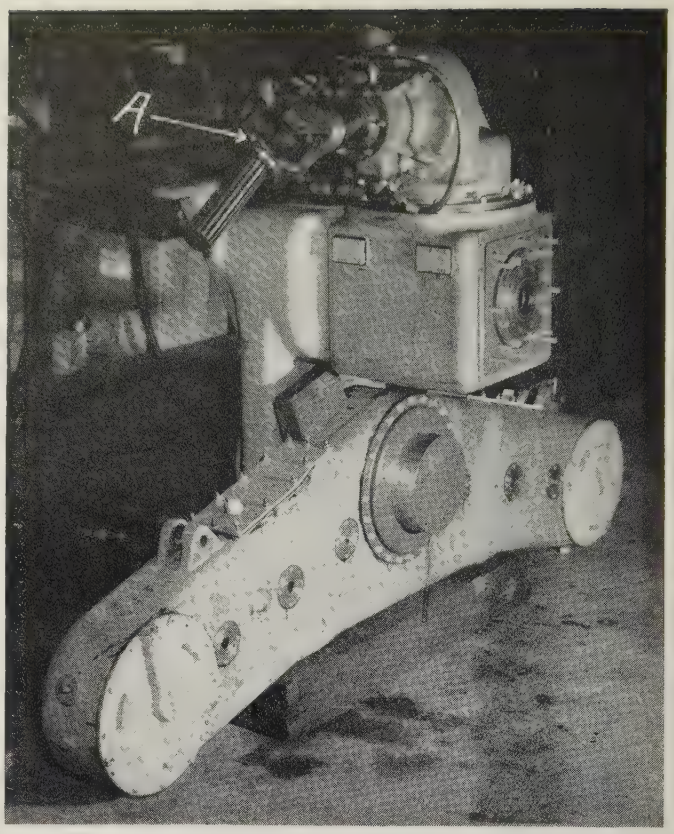

Fig. 11 — Drive train of front bogie

tacles mounted on the cab. This will permit the complete disassembly of the instrument group without any complicated electrical circuits being disconnected.

Fig. 8 shows the back of the instrument panel mounted in the truck. It illustrates the difficulty that would result if this wiring harness and assembly procedure with the quick disconnect receptacles were not used. The installation of the cables to the tachometer and speedometer at (A) illustrates the ease in which they can be connected. The ⅛-in. tubing brought up in a protective loom is connected to the individual pressure gages at (B).

In Fig. 9 the front bogie is about to be installed, the front propeller shaft is connected to the universal yoke (A) which goes into the angle drive gear box (B). The fifth wheel (C) is of the roller-bearing type, the upper portion of which is secured to the frame work (D) which in turn is attached to the main frame of the Teracruzer. The lower portion is secured to the bogie frame (E). This illustration shows the service brakes which are of the aircraft disc type at (F), the trunnion mounting bracket for the steering rams at (G), the mass of wiring, air lines, hydraulic lines, and the air cylinders controlling the tilt of the bogie at (H). The vertical centerline of the angle drive case (B) is laid out so that it falls in the vertical centerline of the fifth wheel. Although this angle drive is a part of the main drive assembly, it is free to rotate while the angle drive remains stationary in relation to the main frame. The entire bogie gear box, drop gears, and the rest rotate with the bogie frame.

Bogie Gear Assembly

To illustrate the type of drive on the Teracruzer, I have taken a series of pictures of various parts as they are assembled into the bogie driving gear assembly.

Fig. 10 is the angle drive gear case just before it is installed on the differential gear box. The universal yoke of the front propeller shaft is installed on spline shaft (A); and the output pinion meshes with a bevel gear in the differential gear case at (B). A small plunger pump (C) driven by a balanced eccentric on the input shaft sucks the oil from the differential gear case and distributes it to the gears and bearings in the angle drive.

Fig. 11 shows the drive train of the front bogie about half assembled. The propeller shaft joint is shown installed on the input shaft at (A).

Fig. 12 is the inside mechanism in the cross-differential gear box. The driven bevel gear (A) meshes with the bevel gear pinion at the bottom of the angle drive. The free-working bevel gear differential (B) and the jaw clutch (C) is used to lock out the differential action when slippage occurs and a solid drive to all of the tires is desired.

Fig. 13 shows one of the drop gear cases that takes the drive down to the swivel point of the bogie walking beam gear case from the cross-shafts that come out of the cross-differential gear box.

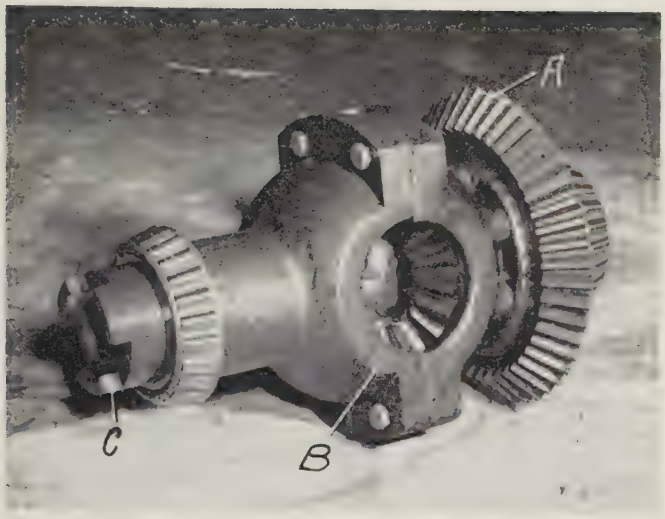

Fig. 12 — Inside mechanism in cross-differential gear box

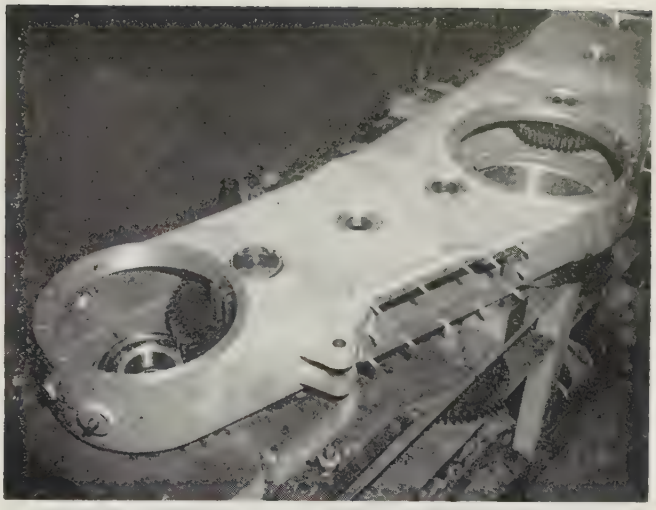

Fig. 14 — Walking beam gear case

Fig. 13 — Drop gear case

Fig. 15 — Complete gear train

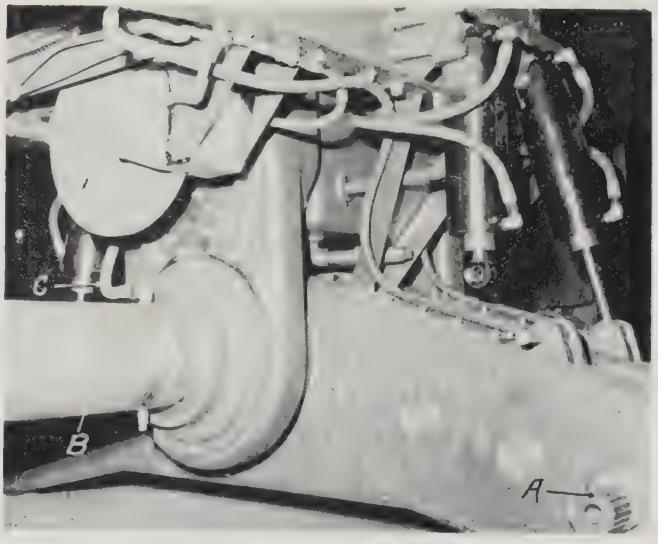

Fig. 16 — Complete drive assembly

Fig. 14 is the walking beam gear case with the gear trains partially mounted, ready to be installed on the drop gear case. This is the inside portion.

In Fig. 15 the complete gear train in the drop gear case and the bogie walking beam gear case has been laid out on the floor. Drive pinion (A) is splined to the end of the cross-differential shaft on one side. This same shaft goes through the differential and is splined into the side gear. (B) is an idler gear. A gear cluster (C) takes the drive out of the drop gear case and through the swivel joint between housings to the walking beam gear case which is allowed to swivel or oscillate in relation to the drop gear case. Gears bringing the drive out to the center of the tires on the bogie serve as reduction as well as idler gears (D). A stub shaft and gear (E) brings this drive out of the walking beam gear case and drives the tires.

Fig. 16 shows the complete drive assembly mounted on a bogie frame. The splined shaft that drives the tire is now shown in its proper relation at (A). A heavy torque tube (B) connects the walking beam gear case and the outer walking beam framework of the bogie so that they oscillate to-

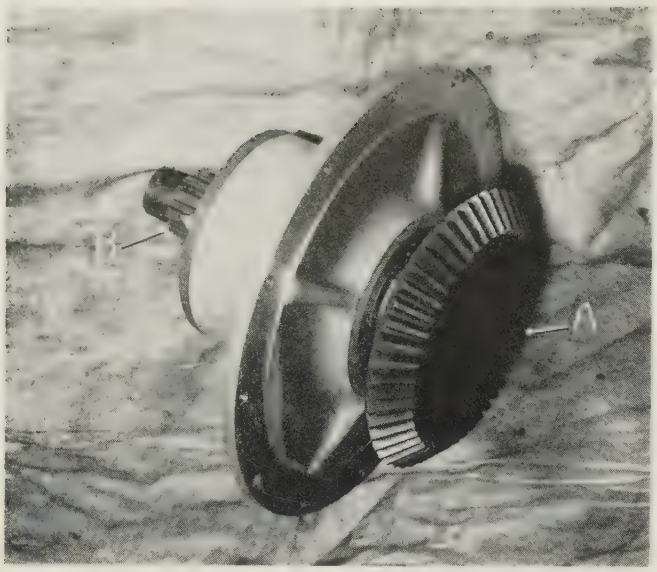

Fig. 17 — Input drive shaft of rear bogie

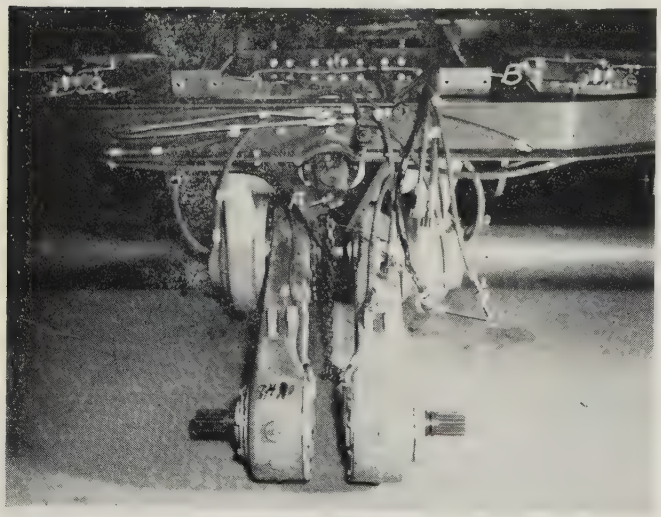

Fig. 18 — Rear bogie

gether and are tied together torsionally. This arrangement keeps the tires always in alignment regardless of their oscillation. With the high torque involved, a rather large section of tubing is required. To make full use of this generous section the torque tube is sealed up at both ends and is utilized as an air tank. The air connection is shown at (C).

Rear Bogie Drive

The rear bogie is identical to the front except that the angle drive is not required. In place of this drive the cross-differential gear case is mounted so that the input opening comes to the forward side of the assembly. In place of the angle drive gear case the simple input drive shaft is used (Fig. 17). Also shown is a bevel gear drive pinion (A) and the input spline (B) on which is mounted the rear propeller shaft.

Fig. 18 is a view of the partially assembled rear bogie, showing the yoke for the rear propeller shaft (A) and the brackets for rigidly mounting this frame work to the frame of the Teracruzer (B). The rear of the mechanism is identical with the front. This shows quite clearly the quick disconnect for air lines and electrical cables at (C). Thus, the complete bogie assembly can be removed from the Teracruzer without complicated disconnections of electrical circuits and air lines.

Tire Assembly

Fig. 19 is a sectional drawing through one of the tires and wheels, illustrating how the tire is mounted on the wheel, how the wheel is mounted in the bogie, and how air is controlled in the tire during operation of the vehicle. The wheel, an alloy aluminum casting (A), has a tapered seat for the bead of the tire, similar to that used in conventional tire casings (B). The tire (C) is clamped on the wheel by clamping rings (D). On the inner side of the wheel is bolted a flange (E) which has an internal spline fitting over the stub shaft (F) that comes out of the walking beam gear case and drives the wheel. The

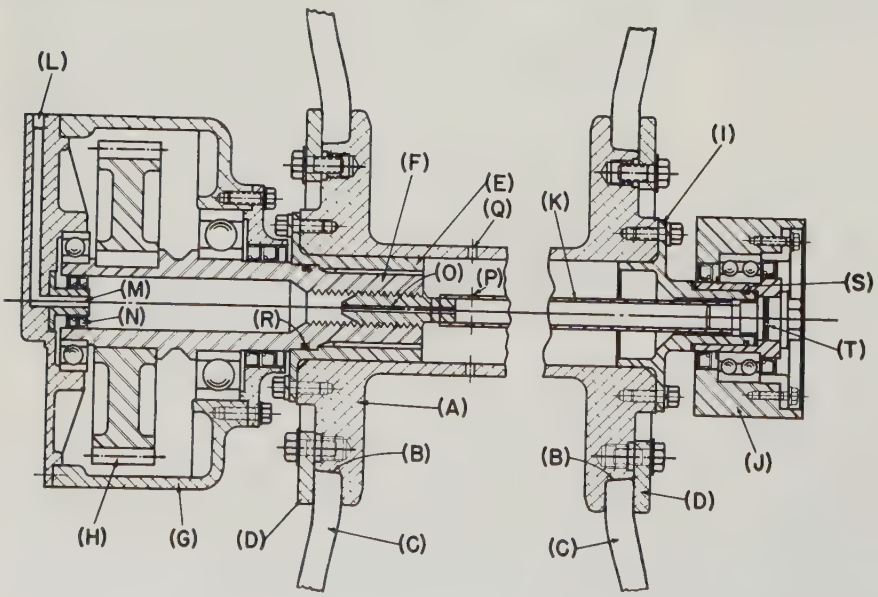

Fig. 19 — Mounting of tire on wheel

walking beam gear case is shown in its lower extremity in section at (G). The gear (H) is the one which was seen when all of the gears were laid out on the floor. A stub spindle (I) that is bearinged in the removable part of the outside walking beam framework (J) is bolted to the outer ends of the wheels.

The mounting and dismounting of the complete tire assembly is very simple. (J) is removed from the outer walking beam, the complete wheel and tire assembly is slipped over the driving spline and (J) is slipped over the stud shaft and secured to the outer walking beam. To hold this assembly securely and to take some of the lateral strain from the walking beam, a special draw bolt (K) draws the complete assembly together and is screwed to stub shaft (F). The way air is admitted or expelled from the tire is very simple. All of the parts are integral with the mechanism or are located in a nonvulnerable position. The air line from the control valve is attached at (L) and enters the hollow portion of the stub shaft at (M). At this point we have regular oil seals (N) to seal the pressure in the central portion of this assembly and keep it from going into the gear case. This is the only rotating seal in the air line. Because of the external air line, the air hose that connects with the central tire inflation system entering at (L) is on the inside of the bogie, it is well-protected. The air goes into the hollow section of the draw bolt through air opening (O) and enters the center of the wheel through a multiplicity of radial openings (P) and in turn reaches the tire itself through a multiplicity of radial openings in the wheel (Q). There are O-rings (R), (S), and (T) that seal other joints in the air system to guard against leaks.

Fig. 20 is a front view of the front bogie complete and ready to be installed under the Teracruzer. The air hoses for tire inflation (A) are in the protected positions.

Fig. 21, taken as the Teracruzer is coming over a 60% test grade, shows the steering arrangement very clearly. The Pitman arm on the steering gear (A) is connected through a drag link to a bell crank (B) which is pivoted on bracket (C). The bell crank is connected by means of an additional drag link to the power steering valve (D) and the power steering valve is connected to the bogie frame. The steering valve is of the free center flow type used on practically all truck linkage power steering devices. If it were connected directly to the linkage at the steering gear Pitman arm, a 0.015 in. travel of the steering gear arm would have a ⅛-in. travel of the bogie. We found this to be satisfactory at slow speeds; but above 30 mph, the tendency was to wander quite violently from one side of the highway to the other. The purpose of the linkage is to keep the hydraulic steering valve on the bogie so that it corrects immediately any tendency to wander and then reduce by means of the unequal arm bell crank the bogie travel down to normal travel of a steering gear Pitman arm.

This practice has worked out very well: it is possible to drive this truck at its maximum speed of 45 mph with utmost confidence and security.

Fig. 22 is a view of the Teracruzer going up the 60% test grade.

Fig. 23 shows the Teracruzer going over the rick-

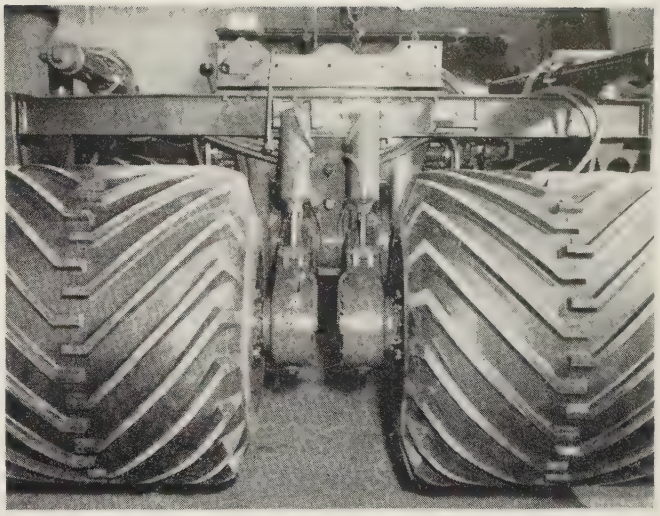

Fig. 20 — Front view of front bogie

Fig. 21 — Teracruzer coming over 60% test grade

Fig. 22 — Teracruzer going up 60% test grade

rack portion of our Proving Grounds, illustrating the articulation of the bogies and giving a good view of the outer walking beam. The outer bearing and portion of the walking beam frame work is readily removed by detaching two capscrews (A) so that the tire can be conveniently changed.

Mobility

In order to compare the load-carrying ability of various types of terrain we use a penetration instrument which consists of a prod presenting 1 sq in. of area to the surface of the ground, accurately guided in a vertical position and on which can be mounted either weights or an accurate impact can be applied. One of our standard impact loads is a 20-lb weight allowed to drop with an acceleration of gravity a distance of 1 ft, or roughly 20 ft-lb of impact energy. This prod will sink 1/10 in. into dry clay fill which has not been tamped. On the undisturbed sand in this particular sand hole, the 1-sq-in. prod penetrated 4.6 in. under the 20-ft-lb impact load. Where the sand had been disturbed by churning of vehicles the figure was over a foot, which is as deep as the instrument can penetrate; therefore, we do not know exactly how far it would have gone in if it were not restrained.

To this test ground we took the Teracruzer fully loaded with 4000 lb per tire. We also took a conventional 4 × 4 truck with 11.00 × 20 tires loaded to 4400 lb per tire, a 6 × 4 truck with 11.00 × 20 in. tires loaded with 1744 lb per tire, and a special logging tractor with 14.00 × 20 tires loaded to 2150 lb per tire.

Fig. 23 — Teracruzer going over rick-rack course

The 6 × 4 truck would not pull itself into the test course, even with the relative light load on the tires. The 4 × 4 truck with 11.00 × 20 tires would pull itself through the sand at about 0.25 mph — just enough for you to say that it was moving. The logging tractor with the 14.00 × 20 would not only negotiate the sand but also was able to pull slightly at the drawbar. The Teracruzer, of course, would go anywhere. We measured the rolling resistance of the Teracruzer tires with various inflation pressures against the 11.00 × 20 tired truck on which the tire pressure was much lower than recommended. Then we measured the drawbar pull of the Teracruzer at various inflation pressures and of the logging tractor with 14.00 × 20 earthmover tires (the only other vehicle that would pull anything so that we could get a comparative measurement).

Fig. 24 shows results of this test. We made at least three tests for each vehicle and averaged the results. Generally, they were quite uniform.

The rolling resistance of the terra tire decreased as the inflation pressure increased up to 16 psi, where the rolling resistance increased considerably. This, we feel, is due to the smaller foot print of the tire as the pressure increased. When it got to a point where it broke through the load-carrying ability of the sand to such a point that it sunk in, it built up quite a windrow in front of it. When you compare the rolling resistance of this terra tire with a conventional 11.00 × 20 you can begin to understand the reason for the greatly increased drawbar possibility of this tire.

On the drawbar scale, the terra tire shows almost a lineal increase in drawbar possibilities as the inflation pressure goes down. Also, with the low pressure in the terra tire, the drawbar is practically four times as great as with the 14.00 × 20 earthmover tire.

We have not had the opportunity to measure accurately the relationship between the foot prints of this tire at various loads and inflation pressures but approximately the pounds per square inch of footprint area is very slightly more than the inflation pressure of the tire itself. As the load on the tire increases, the loaded radius decreases and the area of the footprint increases until they very nearly balance. Of course, the carcass of the tire will support some load but it is not appreciable and does not affect this balance.

Another peculiarity of this tire is that the speed and rim pull is not a function of the loaded radius but is a function of the circumference.

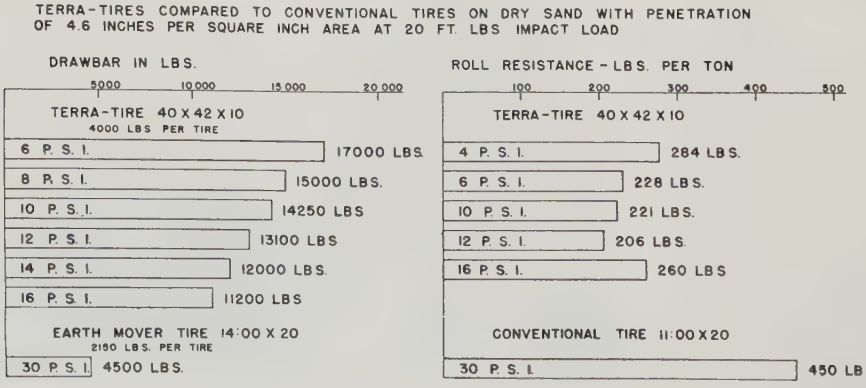

Fig. 24 — Performance characteristics

FORD *FREE-PISTON ENGINE* DEVELOPMENT

Paul Klotsch, Ford Motor Co.

This paper was presented at a meeting of the SAE Texas Gulf Coast Section, Houston, Jan. 10, 1958.

THE Free-Piston Engine Program at the Ford Motor Co. was started in February, 1954. The objective was to obtain basic thermodynamic and design information on small high-speed free-piston engines. This information was to be a basis for designing an industrial or automotive-size powerplant. This objective has been realized.

Operating Principle

Fig. 1 shows the operation of the free-piston engine. In Phase 1, the pistons are moving outward in the direction of the arrows due to combustion in the central diesel cylinder. The pistons uncover the exhaust ports, first allowing blowdown of cylinder pressure to the turbine. As the intake ports are opened, air previously compressed into the scavenge box (the central chamber surrounding the diesel cylinder) blows through the cylinder, out the exhaust ports, to the turbine. During this stroke, air is also drawn into the compressor "C" through the intake valves. In Phase 2 the pistons have stopped in the outboard position. During the previous stroke, air has been compressed in the bounce chamber "B" which stops the pistons and forces them inward. On the inboard stroke (Phase 3) the ports are closed, starting the diesel compression process. The compressor cylinder intake valves have closed and air is forced into the central scavenge box through the compressor exhaust valves. When the pistons reach the innermost position, fuel is injected into the diesel cylinder, starting combustion. The outward stroke then begins, starting Phase 1 again.

Fig. 2. is a photograph of the first Ford free-piston

THE Free-Piston Engine Program described in this paper was concerned with determining thermodynamic relationships of small, high-speed engines. The purpose was to establish proper engine geometry and mechanical design which could then be applied to developing larger automotive engines.

The author outlines the problems encountered during the Program's beginnings: starting system, powerplant assembly, cooling system, and lubrication.

The results indicated that the free-piston engine would be particularly applicable to the farm tractor. The author thinks that such a powerplant may equal or better the diesel engine in economy.

engine. This engine has a 2-in. power cylinder and a 5-in. compressor, operated at frequencies up to 3600 cpm according to piston weight, and developed up to 16 ghp. Complete measurements were made on this test engine, establishing the piston motion diagram and the pressure-volume relationships in the three working chambers. The engine was run on many different hydrocrabon fuels ranging from zero to 100 octane number gasoline, and on gaseous fuels such as propane. Operation was successful with either carburetion or fuel injection, and with either spark ignition or compression ignition.

This program verified an opinion that successful, small free-piston engines could be built, and many of the design features of these small engines were incorporated in the present free-piston engine.

Work was then started on a larger automotive size free-piston turbine engine. A design power of 120 shaft hp or about 160 ghp was set. Some preliminary research was first done on compressor valves. It was recognized that the compressor inlet and exhaust valves had to be as foolproof as possible, offer minimum pressure drop, and have adequate life expectancy. Experience gained from the small engine program dictated the selection of a reed-type valve.

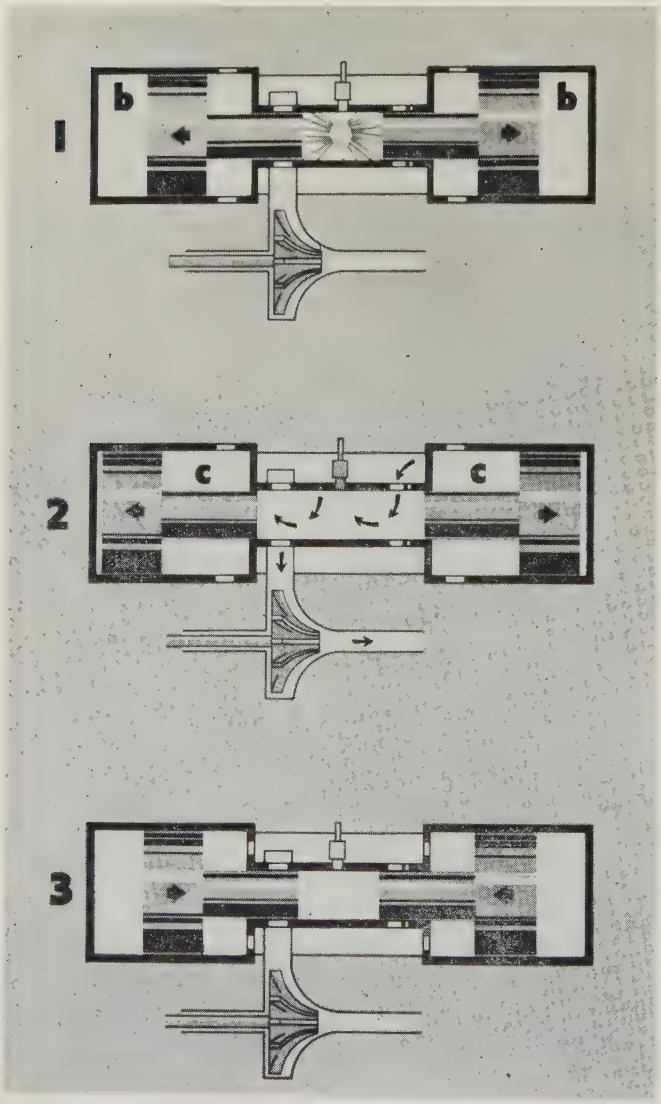

Fig. 1 — Free-piston operating cycle

Fig. 3 is a section through this valve.

A test rig was built which simulated the valve operation as closely as could be predicted by calculation. The valve was operated at engine frequency against calculated back pressure and temperatures. The 120-hp engine has 144 intake valves mounted in 24 pads, 12 for each compressor cylinder. The compressor discharge valve plates have 40 valves per cylinder.

The development of this valve consisted of establishing the proper clearances, determining the material, developing the backup plate shape, and determining the flow-restriction. The particular valve design chosen was characterized by low flow restrictions. During the testing program, the valve life was progressively improved until valves were developed which would run 1000 hr without failure at conditions approximating full-load engine operation. The real worth of this valve program has been realized in the engine test program. During the engine development period, there have been no valve failures of any type.

Engine Development

The Program was a dual effort. One concentrated approach was directed toward determining the thermodynamic relationships for the engine which would establish the proper engine geometry. From this analysis, the bore, stroke, port relationships, and area ratios as well as cyclic frequency were obtained. The second and concurrent effort was con-

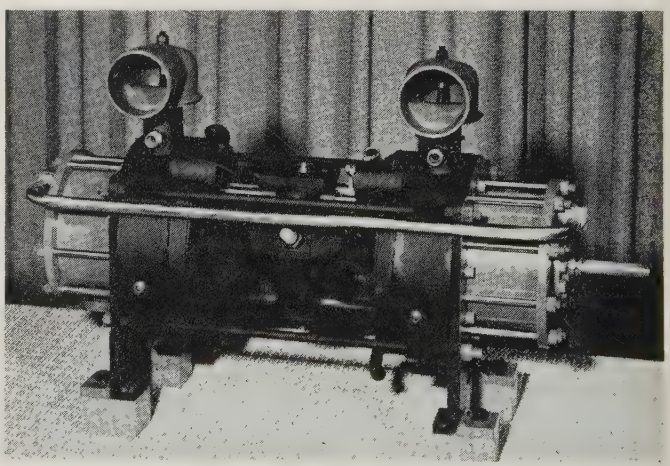

Fig. 2 — First Ford free-piston engine

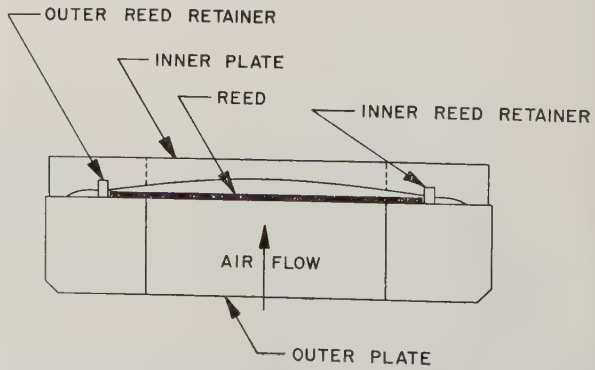

Fig. 3 — Sectional view of reed-type valve

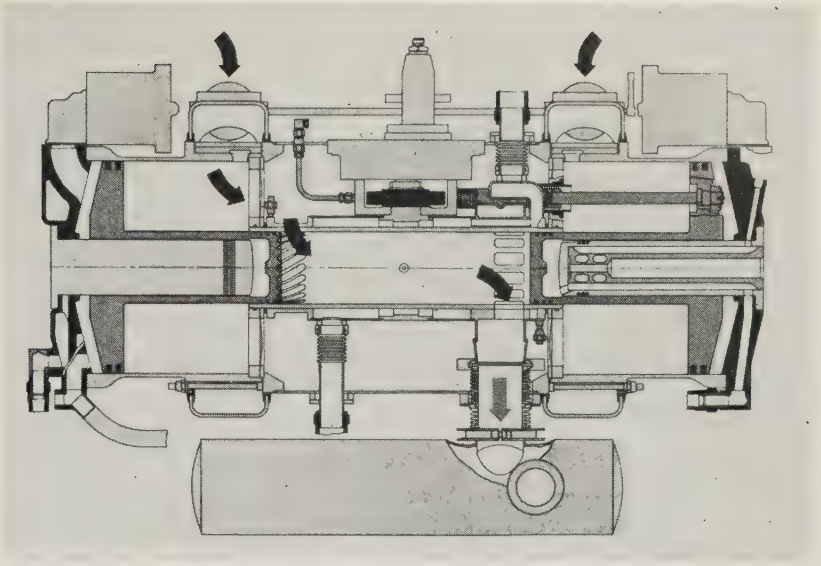

Fig. 4 — Model 519 free-piston gasifier

cerned with the mechanical design of the power-plant. From this second effort, synchronizing means, injection pump actuation, valve design, piston design, power cylinder construction, engine materials, and a multitude of small but important design features were determined.

During the preliminary phase of the program, performance design calculations were made by hand. These calculations established the basic geometry to which the engine was built. Concurrent with these design efforts, a complete and detailed performance analysis was programmed for the IBM 702 computer. After applying this analysis to a number of basic engine configurations, one of which was the 120-hp engine, the computer verified the results of the hand calculations and justified the basic engine geometry.

Fig. 4 is a cross-sectional view of the engine which evolved from the small engine testing and the computer work. The diesel bore is 3.75 in., compressor bore 11 in., total mechanical stroke 6.8 in., and the effective stroke 4.2 in. Other features of the engine which can be plainly seen in this view are the diesel cooling jacket, piston cooling oil system, port and exhaust collector arrangement, and the air path shown by the arrows.

Fig. 5 shows the exterior of the gasifier with the inlet manifolds removed. The three-piece shell consisting of two compressors and a welded scavenge box is quite evident in this picture. The intake valves and fuel pumps can be plainly seen. The small cylinders located above each compressor are the starting tanks which will be described later.

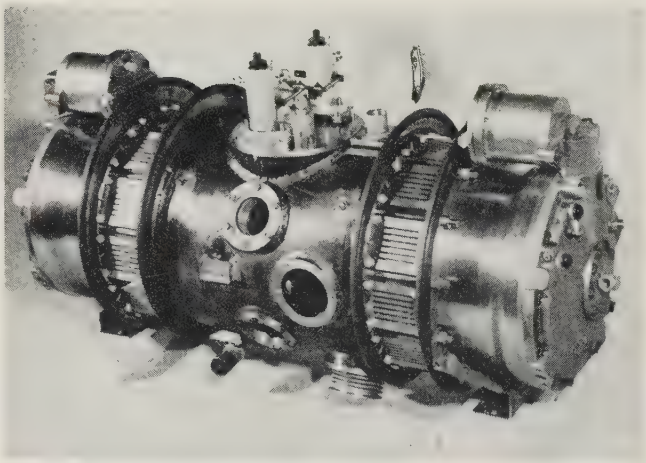

Fig. 5 — Gasifier with inlet manifolds removed

Fig. 6 shows an exploded view of the major engine parts. The major parts are described from left to right: Cylinder head including bronze piston guide and piston oil cooling passages, compressor cylinder and valve assembly, pistons of the one- and two-piece type, compressor exhaust valves, diesel cylinder, scavenge box assembly, and in the foreground,

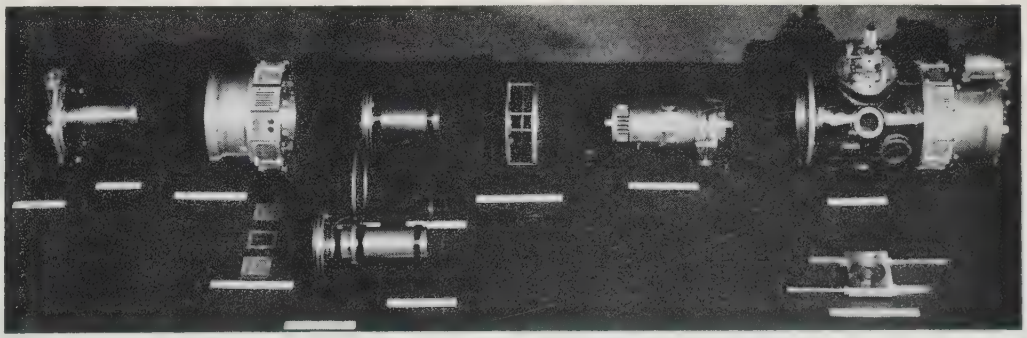

Fig. 6 — Exploded view of major free-piston engine parts

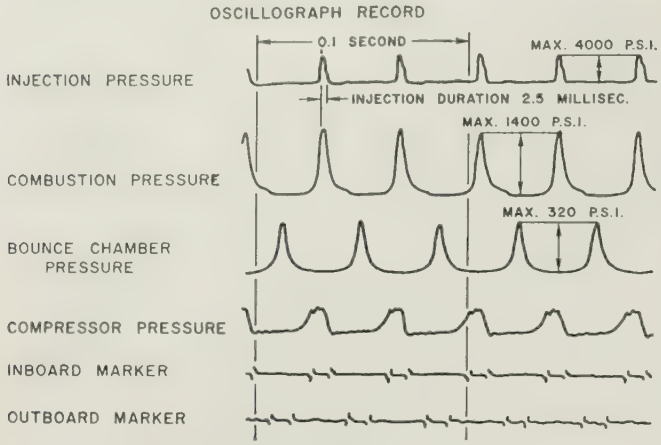

Fig. 7 — Free-piston gasifier cycle events

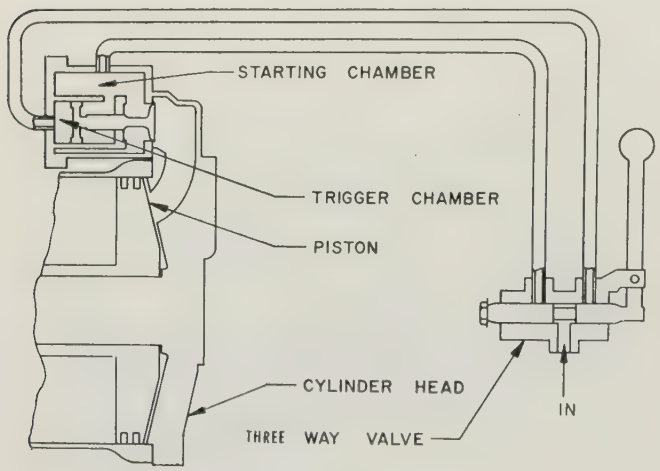

Fig. 8 — Diagram of starting system

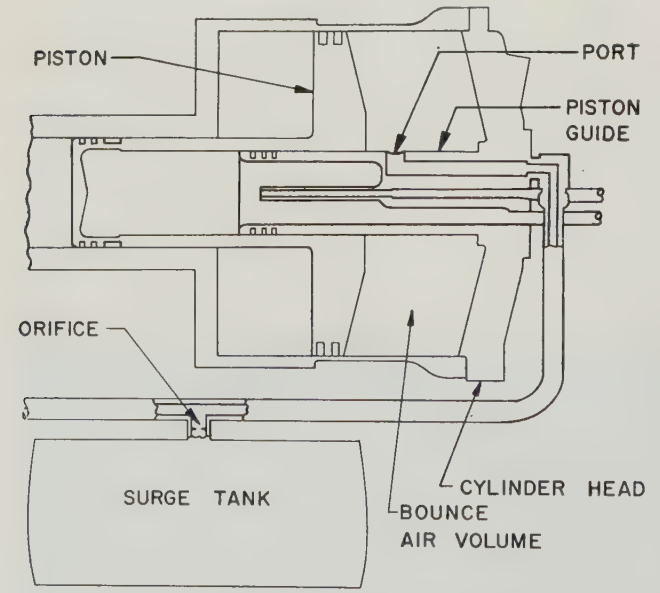

Fig. 9 — Diagram of stroke control system

the synchronizing racks and pinion. The injection pumps are driven by cams on the synchronizing rods.

During the development of the engine, many difficulties were encountered. Piston ring life was initially very short. Flow losses from the gasifier to the turbine were unusually high and, occasionally, unreasonable temperatures were encountered. Most of these problems have been solved. Piston ring life has been greatly extended by proper material selection and ring design. A chrome-plated, steel ring is used in the power cylinder, which has shown acceptable durability.

Fig. 7 is a typical pressure trace showing the injection, combustion, bounce, and compressor pressures versus time with piston marker pips at known piston positions. These are all recorded simultaneously as the engine is running. Every cycle of operation, whether stable, erratic, or transient can be recorded, studied, and analyzed.

As soon as the gasifier was running, test data were fed into the computer program to reconcile the computer results to the test stand results. This reconciliation involved programming adjustments for actual scavenging efficiency, port losses, valve losses, combustion efficiency, temperatures in the working chambers, and other related factors, so that test data and computer results were essentially the same over the load range of the engine. With the basic analsis locked in with the gasifier test program, it became possible to make changes in engine geometry on the computer with the expectation that the engine would faithfully reproduce the results. This expectation has been realized in practice.

The lack of a finite stroke and clearance volume, and the absence of rotating parts to actuate the injection pumps posed two of the most difficult problems. In an effort to minimize the shock loading on the cams and followers, two linear cams with cycloidal contours operating two pumps were selected. These cams, mounted on the synchronizing rods, move exactly as the pistons move, creating a timing problem.

The major difference between pumps is in the configuration of the plungers, which are upper, lower, or double helix. Most of the engine development has been with a lower helix plunger pump which starts delivery at the same cam position in each stroke, and varies the termination of injection by the position of the helix relative to the spill port. Further work is planned with an upper helix pump, since preliminary analysis indicates that this pump should reduce the duration of injection to suit engine requirements better.

Much work has gone into finding the correct atomization, penetration, and distribution of the fuel spray to yield optimum combustion performance in the combustion chamber. A 3-hole tangential nozzle has resulted in the longest nozzle life, while a 7-hole fan appears to give slightly better engine performance. The search continues for a spray pattern which will improve both performance and nozzle life. The present injection system is reliable and reasonably efficient, but there are modifications yet to be made before the system is adequate.

Another major problem in the design of the engine was the development of the starting system.

Most commercial starting systems studied were cumbersome, lacked reliability, and were costly. The small free-piston engine was started by positioning the pistons near the inner dead point, filling the combustion chamber with a fuel-air mixture, and igniting the charge with a spark. This system served its purpose on the small engine, but was unsuitable for the larger gasifier.

Throughout the Program, starting has been a major problem. Unlike conventional engines, the free-piston engine cannot be motored through a repetitive cranking cycle. A free-piston engine must start on the first stroke of a starting cycle. The pistons must be brought together with sufficient energy to compress the air in the power cylinder to a pressure and temperature which will ignite the fuel as it is injected. Many systems were tried before the following system was evolved:

1. The pistons are retracted to their outermost position by means of a vacuum pump or an air piston.
2. The starting chambers are filled to about 300 psig from an air bottle.
3. The starting valves are triggered by admitting bottle pressure into the trigger chambers.
4. The starting valves open, allowing the stored air to expand into the bounce chamber to drive the pistons together.
5. As the pistons travel inward, the control ports are opened and the excess air in the bounce chamber is allowed to escape.
6. The starting valves close and the engine runs.

The entire starting operation is accomplished in a simple and direct manner. Fig. 8 is a schematic diagram of the starting system showing the 3-way valve and the pressure-operated trigger valves. The starting system may be actuated by a solenoid or manually as shown. The pressure supply for the starting system is automatically recharged by the engine through a tapping valve in the combustion chamber.

Stub shaft piston supports on the bounce cylinder head perform two important functions. These shafts provide a means of supplying cooling oil to the underside of the piston crowns by a nozzle within the piston guide, and the return flow is scavenged from the guide by a scavenge pump driven by the turbine. This oil is used to cool the power pistons and to lubricate the compressor pistons through a controlled leakage path. The power pistons are lubricated by applying oil directly to the ring belt through four small holes. Oil is supplied to the power pistons by a metering pump, and the total consumption is regulated to 1/200 of full-load fuel flow.

The stub shaft piston guides serve a second important function by providing means for stroke control. Fig. 9 is a schematic diagram of the stroke control system, showing the bounce control ports located in the stub shafts. These ports are opened on the inward stroke of the pistons at about the mid-point of the piston travel. The control ports are connected to the surge tank which is at turbine inlet pressure. At a predetermined point in the bounce chamber cycle, the bounce pressure is adjusted by the action of the control ports. When the bounce volume has been properly selected, in relation to the position of the control ports, automatic stroke control is maintained over the full-load range of the engine. An orifice in the connecting passage allows air to flow between the bounce chamber and the surge tank according to the relationship between turbine pressure and the pressure in the bounce chamber while the ports are open.

As the power level is increased, the surge tank pressure increases. When the control ports open, this increased pressure causes air to flow into the bounce chamber. Thus, as more fuel is put into the combustion chamber, more air is put into the bounce volume to absorb this additional energy. The control system is self-compensating and has no moving parts. Throttle response is instantaneous and positive.

Load control of the engine is accomplished by a single link to the compressor inlet throttles, which are mechanically connected to the fuel injection pump racks through an adjustable ratio linkage. This system provides air and fuel metering to the gas generator in predetermined proportions dictated by the gas horsepower required. There is no control connection between the turbine and the gas generator, except as provided by the turbine speed governor.

The philosophy behind this control system is based on the independence of the gas generator and turbine. Though the pressure-flow relationship does change slightly with turbine speed, this change is negligible. Therefore, aside from governor influence, the gas generator is independent of turbine speed and the gasifier may develop its maximum gas horsepower in conjunction with any speed of the turbine. This contributes to the excellent torque-speed relationship of the power plant.

When the throttle-rack linkage is properly adjusted, the fuel/air ratio follows a predetermined schedule over the load range of the engine. A primary criterion of proper adjustment is turbine inlet temperature. The turbine inlet temperature range is 600–900 F. Rated turbine speed is 43,000 rpm and, at full load, the turbine inlet pressure is 53 psia.

This engine has no provision for recirculation. Compressor inlet throttling provides the necessary control and maintains air-box temperatures through thermodynamic processes quite similar to recirculation, but with added advantages of simplicity and directness. Basically, compressor inlet throttling allows the pressure ratio of the compressor to remain almost constant over the load range. This provides high air-box temperatures to insure compression ignition even at low compression pressures. With reduced airflow to the compressor, total flow losses are small. This control system works well in actual practice, and provides simple, complete, and positive control of the powerplant.

Applications

After a study of the characteristics of the free-piston turbine engine, it seemed that it would be an ideal powerplant for the farm tractor. It has economy equivalent to a diesel-piston engine. It has the response and flexibility of a gasoline engine. An auxiliary starting engine is not required, such as those necessary with most diesels of equivalent size in mobile use. A wide range of engine sizes can be

economically produced from the same manufactured parts. It is adaptable to a wide range of fuels. Most important is the ideal torque characteristic. There is a growing trend toward the diesel engine for farm tractor powerplants, particularly in the larger sizes. Industrial users have been taking advantage of the diesel engine, with its good economy and lugging characteristics, for many applications. Preliminary tests have shown that the free-piston engine may equal or surpass the diesel in economy.

Much design time and engine development work is done on reciprocating engines to get a flat torque curve. The best of these cannot approach the torque curve of the turbine engine in its application to farm tractor work. Due to the varying load encountered in field work with the farm tractor, this is a very important characteristic and one that gives the free-piston turbine engine a big advantage over conventional farm tractor engines.

Fig. 10 illustrates the torque curve for a crank engine tractor and Fig. 11 for a turbine-powered tractor. It can be seen that the turbine engine will deliver increasing drawbar pull up to stall speed. For most practical applications, the increased drawbar pull would allow the tractor to move through the conditions in the field that caused the increased load, without a change in gear ratio or without stalling the engine.

When it was decided to install a free-piston turbine engine in a tractor, a conventional tricycle configuration was selected because it is typical and because it was easily adaptable to the free-piston engine powerplant. Fig. 12 shows the arrangement of the gasifier, turbine, gear box, and accessories in the tractor.

The performance of the tractor power unit has been satisfactory in tests to date. The engine operates very smoothly and is practically vibration-free. Mufflers are not necessary, as the noise level is low. A turbine whine is perceptible at idle speeds but is not audible at working speeds. Many changes and improvements are constantly being made as the tests progress.

The free-piston engine is now entering a more advanced stage of development. The problems of engine weight, accessory drive, engine braking, noise level, high rotative speeds, acceleration lag, and fuel economy are quite minor in nature. The first four items primarily concern the passenger vehicle application shown in Fig. 13. The latter three pertain to most applications, but experience has shown that careful design can eliminate these problems.

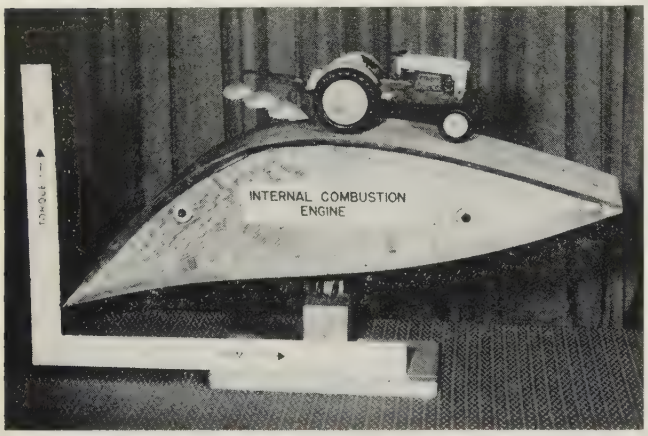

Fig. 10 — Torque curve for crank-engine tractor

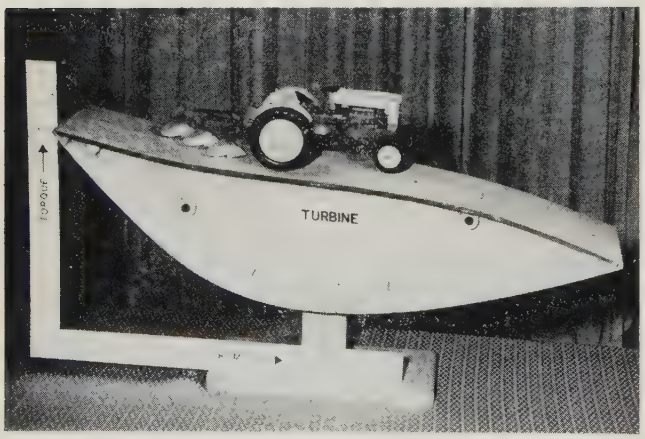

Fig. 11 — Torque curve for turbine-powered tractor

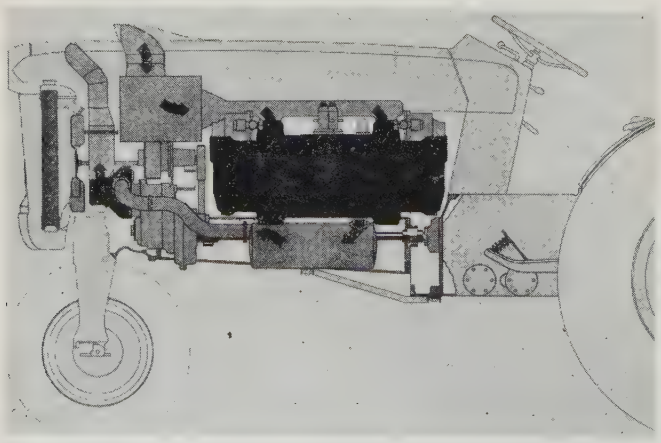

Fig. 12 — Model 519 free-piston turbine engine tractor installation

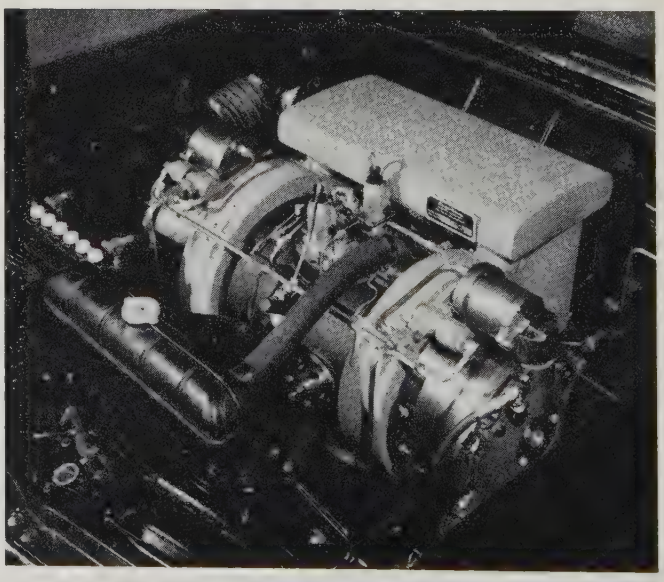

Fig. 13 — Passenger-vehicle application of free-piston engine

recent developments make ENGINEERING SPECIFICATIONS more realistic

Dorian Shainin,
Rath & Strong, Inc.

This paper was presented at a Southern New England Section meeting, Windsor Locks, Conn., Oct. 7, 1958

SPECIFICATIONS that are realistic for production and result in a product that functions properly can be set with a three-step method evolved from statistical control techniques. The tolerances thus established reduce production costs, as well as costs arising from faulty products, the author states.

The author applies the method to a leakage problem encountered on mechanical-hydraulic units. Through the use of statistical control techniques, the cause of the leakage was discovered.

FROM AMONG the techniques of statistical quality control have come logical approaches which contribute to solving a problem of long standing — deciding when a tolerance is just right. These developments, unfamiliar to most engineers, can be used to set up specifications that optimize the combination of component production ability and product operational capability.

Among the costs that such particular combinations reduce will be those associated with:

1. Customer service adjustments.
2. Warranty replacements.
3. Inspection screening of items beyond specification.
4. Material review board activity.
5. Special manufacturing equipment.
6. Unusual training of personnel.
7. Uneconomical feeds and speeds.
8. Scrap and rework.
9. Selective assembly practice.

Because current engineering practice usually misses the optimum combinations, a company may

well consider the present level of these costs as characteristic of their particular kind of manufacturing activity and product requirements.

A few engineering managements, to the considerable profit advantage of their firms, now know how to avoid specifications which are either too loose or too tight. This paper presents a sample of "statistical engineering" techniques that reconcile the two different objectives in setting specifications — amenability to production processes and ability to function as intended. Fundamentally, the methods add objectivity to the procedure for evaluating specifications by providing basic factual information previously considered too expensive to acquire.

Table 1 describes the objectives more specifically as *practical* versus *realistic*.

Manufactured quality characteristics inherently vary item to item. Functional outputs also vary, assembly to assembly. Fig. 1 shows a typical frequency distribution of many such characteristics or outputs.

The distance *A* represents the "process capability" when we are considering the inherent spread of the results, of a single quality characteristic of a component, from the action of process variables. Alternatively, it can be the "product capability" when the distribution shows the variation of a functional output from supposedly identical products or assemblies. So *A* measures numerically the practical or the realistic nature of an engineering specification.

Making Product Practical and Realistic

Reconciliation of the two points of view readily occurs for a rather simple product — say a fastener. It may have one or two functional requirements, and three or four contributing quality characteristics. A few samples can represent the planned tolerance ranges, and be tested under the conditions the product can be expected to be used.

Much industrial and military equipment is sufficiently complex to make this common-sense approach quite impractical. There can be several output requirements, perhaps severe environments, and certainly manufacturing operations involve many tolerances and usually have to deal with a large number of material variations.

Typically, even years after initial deliveries, engineering changes continue to be made because some specification originally was to rigid, too liberal, or had been omitted. Now statistical engineering contributes a major upset to the philosophical acceptance of such conventional experiences. Here are the basic steps that aid in more rapidly bringing specifications to the best attainable combination of being practical and realistic with the existing basic product design, materials, and manufacturing equipment:

1. Isolating the relatively few quality characteristics, *whether specified or not*, that contribute most to the product's variability of output. The first important steps here need only two assemblies, usually experimental ones representing the first attempts to convert the design to the physical article. Control of these vital few characteristics is the objective of this step.

2. In the early stages of production, say after nine assemblies are made, additional changes can be detected that will further reduce the variation of outputs. Here, for the first time, it is possible to estimate how much of the total variation is separately associated with each of three parts of total variation: that within the assembly (lack of repeatability); assembly to successively built assembly; time to time. Reducing the two largest (of the three parts of total variability coming from manufacturing) to equal approximately the variability of the smallest becomes the objective of this step.

3. When at least 30 sets of components are available, so that most of each tolerance range has been used (considering only the specifications determined to be important from the previous two steps), the vital tolerances can be evaluated. This work leads to changes that make them at once practical and realistic. The technique separates the single effect upon output of each tolerance, as well as showing any combination effects that might exist (called interactions).

An alternate version of Step 3 uses at least three sets of components, representing close to high, medium, and low parts of the tolerance range for the important specification. They are then reassembled 30 times, but in completely random sets of tolerance position each time.

Case histories will illustrate the application of the approach in each of these three steps.

Step 1 — Early Reduction of Output Variation

Among the various outputs analyzed statistically, the one serving best to illustrate the power of this method was a requirement for no external leakage for a mechanical-hydraulic unit. At first, it seemed there was no variation between the two units. They both leaked slightly at the cover O-ring seal. A gradual wetting of the joint between the cover and body was noticeable after 10-min operation on the test rig.

A thin bluing check showed the body and cover faces of both assemblies to be flat and smooth. The seal diameters and the width of the seal groove in the cover were measured at several places along their lengths and found to be within specification. Although the widest permissible groove width and the smallest seal diameter on the drawing showed an adequate interference fit, by the conventional engineering approach it was planned to increase the nominal seal diameter or to reduce the groove width in the cover.

Statistical engineering starts with the variation of output between the two units. Two means of measuring are the insensitive method of "attributes" and the more revealing method of "variables." The former classifies this type of output in two categories, it leaks or it does not leak. It calls these two units alike. The latter measures the leakage on a continuous scale from zero through fractions of a drop per minute on to several drops per minute.

We know many statisticians, and some engineers, who at this point would state that this slight leakage wetting the entire length of the cover-body joint cannot be practically measured by variables. So they would suggest producing several more units in the hope that one would not leak at all. Failing

Table 1 — Engineering Specifications

Practical	Realistic
Product can be manufactured and can be measured	Product will function as intended
Measured by:	
Process capability — an expected spread of results from the action of many process variables	Product capability — an expected spread of functional outputs from combinations of many tolerances and other variables
Tend to Result in:	
Tolerances which are too wide, or in selective assembly practice.	Tolerances which are conservatively tight.

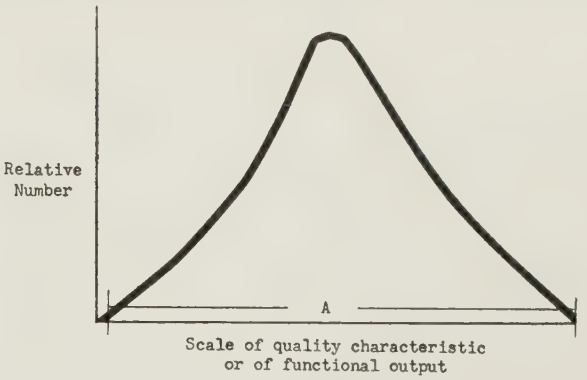

Fig. 1 — Frequency distribution of manufactured quality characteristics

this good fortune, they would propose classifying the several units as light, moderate, and heavy leakers.

But the statistical engineer on this job, with only the two units available, set out to find a way of measuring the amount of leakage. He came up with small, equal-size rectangles cut from a sheet of blotting paper. A single drop of oil was deposited on a metal surface from an eye dropper. The short side of the rectangle soaked up the drop of oil, discoloring the paper for a given distance from that side. The test was repeated for another drop using a piece cut fom a location on the large sheet away from the first. The soak distance was the same.

One rectangle soaked up 10-min worth of leakage from one unit, and another similarly was applied around the other units at the leaking joint. There was a difference between the units: one leaked a drop and a half, the other three drops.

The Latin Square approach can now be used for isolating the component having the quality characteristic responsible for most of the difference in leakage. The three-drop unit was labeled *HI*, and the other *LO*. *C* stands for cover, *S* for seal, and *R* for the rest of the unit, which in this case was the body assembly. Four assembly combinations from these components of the two assemblies are indicated by the designed experiment shown in Table 2.

Table 2 — Organization of Latin Square

	C_{LO}	C_{HI}
S_{LO}	7 R_{HI} 3	1 R_{LO} 8
S_{HI}	2 R_{LO} 6	5 R_{HI} 4

Each of the four indicated combinations was put together twice, in random sequence as shown by the numbers at the right of each box. The 10-min leakages found from these eight trials are shown in Table 3.

Table 3 — Leakages of Eight Trials

Test	Combination	Drops per 10 Min
1	$C_{HI}S_{LO}R_{LO}$	3.2
2	$C_{LO}S_{HI}R_{LO}$	1.7
3	$C_{LO}S_{LO}R_{HI}$	1.8
4	$C_{HI}S_{HI}R_{HI}$	3.2
5	$C_{HI}S_{HI}R_{HI}$	3.0
6	$C_{LO}S_{HI}R_{LO}$	1.4
7	$C_{LO}S_{LO}R_{HI}$	1.6
8	$C_{HI}S_{LO}R_{LO}$	2.9

Arranging the leakages in their proper positions in the Latin Square:

1.6	3.2
1.8	2.9
1.7	3.0
1.4	3.2

The use of a random sequence has, with a high probability, forced all other factors that could also affect leakage to show their net effect in the lack of repeatability between the pair of trials of exactly the same combination of components. Some of these factors would be the method of assembly, temperature of oil, influence of humidity difference on the blotting paper, variation in the skill of the engineer in touching all spots to pick up oil with the blotter. These factors and others like them can change with time. If each combination is done again at some random, later time, the influence of such factors can be measured. But if the testing were done in systematic rather than random order, some factors changing with time would have their effect "confounded" with the effect of one or more of the components of the test. For example, note that in systematic order the last four tests could have been the ones giving the higher leakages close to three drops per 10 min. And the real cause could have been the test rig temperature stabilizing at some much higher value than it had during the first four runs. But because they all used C_{HI}, we would have associated the higher leakages with that cover.

The average of the differences between the pairs of results comes out to be 0.25 of a drop, properly called experimental error only from a randomized experiment. With this measure of the effect of all other factors can be compared the separate effects of the difference between the two covers, the two seals, and the two body assemblies—much information obtainable statistically from only four combinations.

The vertical average of the four readings under C_{LO} 1.6 can properly be compared with the average

under C_{HI} 3.1. The influence of any difference between the two seals has been neutralized here, since two of the readings under C_{LO} were with S_{LO} and the other two were with S_{HI}. Similarly, in the C_{HI} column are two contributions each from S_{LO} and S_{HI}. Whatever the effect of S, it does the same thing to each of the vertical averages, because the contribution is similar. Since the *difference* between those two averages cannot be influenced by S, it represents the influence of C. The rest of the unit R is similarly balanced out or neutralized. And a statistical table of odds will give the chances that the lack of repeatability 0.25 can explain the 1.5 difference between the averages for C_{LO} and C_{HI}. Since these odds are low, it is an intelligent engineering decision that a valid cause-and-effect relationship is probably being shown by this statistically designed approach.

The difference between the horizontal averages, 2.4 and 2.5, for S cannot be affected by the balanced-out influence of C and of R. And the diagonal averages show the effect of the rest of the assembly R, 2.3 and 2.4, with S and C neutralized. So 1.5 clearly predominates the other two differences, 0.1 and 0.1. The statistical table shows the odds are high that the 0.1 differences could have come entirely from the lack of repeatability, meaning that S and R could even have no effect at all on leakage.

The two covers were carefully inspected visually and dimensionally to detect the quality characteristic causing the leakage difference. When nothing could be found and when the leakage using C_{HI} did not go down at all after the cover, a casting, had been impregnated to seal a very fine porosity it might have, several engineers close to the project wanted to go to work trying seals of different diameter and of different durometer hardness. After years of thinking about problems in the conventional way, an engineer generally does not change because he is exposed once, or even a few times, to the logic of a new approach—especially when the new approach seems to run into a snag!

The statistical engineer had to insist that the elusive quality characteristic was represented by some difference between those particular covers. The designed experiment clearly eliminated the body and the seal.

Further attention was given to the covers. One engineer made the statement that the fact that they had been anodized did not seem logically to influence leakage. Upon hearing that, another engineer looked in the groove for the seal and remarked that the anodic coating had not been masked from the groove. But he, too, could not think how that would make any difference. A third engineer offered the information that some coatings seemed a bit rougher than others; perhaps the coating itself was porous. The coating was removed from the groove of C_{HI}, exposing the bare metal. It did not leak at all! When similarly cleaned C_{LO} also did not leak. The performance specification of no external leakage was now practical and realistic.

Other outputs (such as gallons per hour delivery, and change in flow with the application of a given back pressure) were checked in the two experimental units with Latin Squares consisting of the relief valve subassembly, the pump subassembly, and again R for the remainder of the unit. One by one the approach gave basic factual information leading to the early reduction of output variation.

Step 2 — Making Three Parts of Variation Almost Equal

During early production of the units, records were kept of certain performance outputs at final test. For one day, in each of three weeks, three successively assembled units were run three times each to get a figure for within-unit variation, unit-to-unit variation (within a day), and a third figure for time-to-time variation (the average of all readings one day compared to that in another week, and to that in the third week). The time-to-time figure was the smallest; and so attention was directed to the largest variation, which was unit to unit.

From these nine units, the two extreme performance ones were then given the previously described Latin Square analysis. Unexpectedly, the bellows spring rate was found to affect an important output rather severely. The next to the largest variation, within unit, was then analyzed for what could contribute to the observed amount of lack of repeatability. Four logical, plausible causes were then checked out in a factorial experimental design, which is a variation of the Latin Square approach. The edge condition of the sleeve ports and valve lands was found to be much more important than the other three plausible causes. After changes to these specifications, successively made units were found to have unit-to-unit and within-unit variation about equal to time-to-time.

Step 3 — Checking Important Tolerances for Size

In this approach, evaluating and changing tolerances to obtain a final overall balance between part tolerances and performance outputs, an analytical tool called "Random Balance" was used. It separates the effects of each of the 12 tolerances found from the previous two steps to have been influential, and makes it possible to find out which is the most important, next to the most important, and so on. The 12 tolerances turned out to be far from equally important. Controlling three rather closely, permitted sizable increases in the remainder of the tolerances originally set conservatively tight. These were many more than the remaining nine used in the Random Balance Analysis. The resulting manufacturing economies from this liberalizing were substantial.

If the Factorial Experimental Design had been used to investigate all the combinations of just high and low values of the twelve tolerances, 4096 test combinations would be involved. Random balance, in effect, takes a random or representative sample of 30 combinations to estimate the important effects. And just the values of each tolerance that normally occur during the production of 30 assemblies can serve better than specially made extreme values.

Conclusion

Teaching statistical engineering to groups in many firms around the country has clearly brought out that this more objective way of thinking is well within the capabilities of almost all the engineers, regardless of their area of specialization. Such analytical thinking becomes a fitting, modern addition to their experience and knowledge in their field to bring research and development work to new levels of accomplishment.

selection of

Optimum Modes of Control

for aircraft engines

THE optimum mode of control for an aircraft engine is dependent on both the configuration of the engine and its application. Each engine application requires several detail modes of control, one for each definable regime of operation of the engine. Discussions of control requirements can be simplified by classifying these regimes by objectives: physical limiting, thrust, and transient control. The turbojet engine is the basis for the discussion in this paper.

Acceptable modes of control can often be selected by inspection of the engine and its application. Selection of an "optimum" control mode requires investigation of the operation of the engine and weapons system at every stage of its use.

The selection of a "mode" of control requires a compromise between performance and other design factors. The need for simplicity and accuracy must be balanced against the stability requirements. The availability and flexibility of control components may limit the modes of control considered. The need for reliability and full-range performance must be considered in terms of system weight.

A. J. Sobey, Allison Division, General Motors Corp.

This paper was presented at the SAE National Aeronautic Meeting, New York, April 11, 1958

THE design of a control system for an aircraft engine proceeds logically along the following steps:

1. Evaluation of engine characteristics to determine control requirements.
2. Evaluation of aircraft application requirements to determine the necessary control functions.
3. Selection of a mode of control to establish how the controls will operate.
4. Selection of a control system configuration to provide the necessary control functions.
5. Design of components to convert the "mode" to "hardware."
6. Development of the control system to insure proper life and eliminate "bugs."

This paper is a discussion of the third step. The particular mode of control selected for each engine will give it a personality of its own. Practically

everyone connected with the aircraft, from the pilot to the service and operating personnel, will be affected by this initial choice.

The mode of control selected defines what the controls can do; how they will use available "handles" (such as fuel flow) to provide the regulation of variables (such as rpm), and the way these are altered as a function of reference parameters (such as the power lever position, temperature, or altitude).

On early turbojet engines control modes were selected to provide the best possible engine performance at any condition where the engine might be used. Consequently, the same control system has been used on a fighter, a bomber, a trainer, and a guided missile. The performance of these powerplants (when considered in terms of all performance parameters, including weight, complexity, and reliability) was not optimum. Increased performance demands on aircraft have made the "general purpose systems" unacceptable. That the operating modes and control systems are closely related to the performance requirements of the aircrafts will be shown by the following examples.

Basic Factors in Selecting Mode of Control

Fig. 1 illustrates the range in possible control modes for turbojet engines. In this figure a basic turbojet of the J35 class is shown in solid lines while the added features, such as might be included in a supersonic afterburning 2-spool engine, are shown by the dashed lines.

The table at the bottom of the figure shows the order of complexity of possible control mode choices for the two engines.

1. The first line lists the number of individual control functions which must be provided by the control system. The simplest aircraft rocket would have only two (starting and full thrust); the basic engine has at least nine, including: starting, acceleration, deceleration, maximum thrust, idle thrust, overspeed limit, overtemperature limit, overpressure limit, and shutdown. The more complex engine may have 17 or more.

2. The second line lists the number of independent control variables, or handles for each powerplant. The basic engine has only one (fuel flow), while the more complex engine is indicated to have six (variable inlet secondary, variable compression geometry, main fuel flow, afterburner fuel flow, and convergent and divergent jet nozzles). This number may increase substantially in specific installations and 10 independent control variables could be found on some powerplants.

3. The third line lists the basic reference parameters available for control purposes in each powerplant. This number includes only pressure and temperature at various engine stations and the magnitude of primary engine elements, such as throttle position and rotor speed. Many other parameters are possible, such as the derivatives of these functions, total and static pressures, and airframe flight performance.

4. The fourth line lists the required modes of control. Where possible similar regimes, such as starting and acceleration, can be combined into one mode. The simplest combination for a manned turbojet would be starting, idle, maximum thrust, and transient modes.

5. The fifth line is an indication of the number of theoretically possible modes of control based on simple relationships of independent variables and reference parameters. This number increases further, because each mode can be used with different classes of control, such as proportional or integrating governors.

6. The last line is an estimate of the probable number of workable modes of control and combinations, based on the actual performance requirements of the system.

With so many choices, the selection of the best mode of control for each operating regime by inspection would be a difficult task. Fortunately, the problem of selecting acceptable modes of control is not as difficult as this algebraic exercise could indicate. A large number of the alternates include redundancies. Many analytical techniques can be used to eliminate the unpromising modes.

Classes of Control Modes

Since the basic mode of control divides into individual modes of control for different operating regimes, it is convenient to classify them by their objectives:

Class I—Physical limiting control modes: to protect the engine against damage or malfunctions which could result in loss of power.

Class II—Thrust control modes: to provide the desired engine performance at all expected operating conditions.

Class III—Transient control modes: to provide starting and power changes at all specified conditions.

The selection of a specific mode of control requires consideration of both the engine and airframe in which it is to be used, and consequently, optimum control modes cannot be generalized for all applications. However, some examples of problems and general solutions can be discussed.

Class I: Physical Limiting Control Modes

The first problem facing the control designer is to select control modes that insure safe operation over the expected range of conditions.

The functions which must be regulated to insure the physical integrity of the engine include stress limits such as overspeed of the rotors, maximum combustion-chamber pressure, and temperature limitations (for example that of a turbine, which is very sensitive to any period of overtemperature). Basic limits of the performance cycle, such as combustion blowout and functions which are normally out of the operating range of the control system, must also be considered.

Two examples which include representative problems in the selection of physical limiting modes of control for a turbine engine are: (1) the prevention of rotor overspeed on an afterburner shutdown, and (2) the prevention of destructive overstressing of parts subject to full compressor discharge pressure during high Mach flight at low altitude.

Overspeed Limitation During Afterburner Blowout—On a conventional jet engine with a variable jet nozzle area, engine overspeed is prevented either

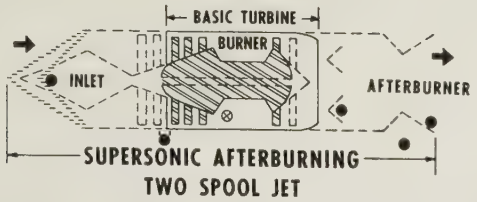

TURBO-JETS	BASIC	SUPERSONIC
DEFINABLE REGIMES OF OPERATION	9	17
INDEPENDENT CONTROL VARIABLES	1 ⊗	6 OR MORE ●
REFERENCE PARAMETERS	10	18 +
MODES OF CONTROL REQUIRED	4 TO 9	11 TO 17
POSSIBLE PARAMETRIC COMBINATION	(3.6×10^6)	(6.3×10^{15})
EST. USEABLE MODES OF CONTROL	200	200,000,000

Fig. 1 — Growth of control variables for typical turbojet engines

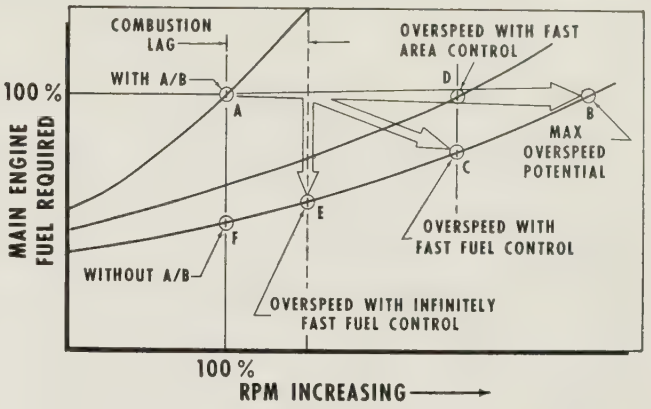

Fig. 2 — Engine overspeed potential on afterburner blowout

by reducing engine fuel flow or by closing the jet nozzle area. Steady state control performance requirements will usually support either choice. However, certain restricting functions will be found in the prevention of overspeed on an afterburner blowout.

Fig. 2 is a sketch of the basic relationships of engine fuel flow to engine speed during afterburning (point *A*) and immediately after an afterburner blowout (point *F*). An afterburner blowout is equivalent to a step change in engine fuel requirements of approximately 50% due to the sudden elimination of the "restriction" downstream of the turbine caused by the afterburner combustion.

As neither the fuel flow nor the exhaust nozzle area can change instantaneously, the engine will attempt to overspeed. If the engine time constant is small, or the controls are slow, the engine could overspeed to point *B*. If the jet nozzle remains fixed, a reasonable fast fuel control will prevent overspeed in excess of point *C*. However, even an infinitely fast fuel control cannot reduce the overspeed below point *E*, due to the combustion delay time of the fuel already in the burners. The magnitude of this overspeed is a function of the particular engine time constants and related fuel flow and area gain terms. The trend to lighter engines is making this problem more serious, as much shorter time constants (one-tenth of present production times) can be expected on future engines.

An infinitely fast jet nozzle has the potentiality of reducing the overspeed to its minimum value. Most jet nozzles operate against significant forces and a jet nozzle area control system which would just equal the performance of an "ordinary" fuel governor (point *D*) might weigh 100 times as much as a system which would satisfy all other nozzle control requirements. Consequently, the main engine fuel governor is used for most afterburning turbojets.

Compressor Discharge Pressure Limitation—The second example of physical limiting modes is the control required to prevent excessive compressor discharge pressure during high-speed flight at low altitude.

Fig. 3 illustrates the effect of flight Mach number on compressor discharge pressure and engine

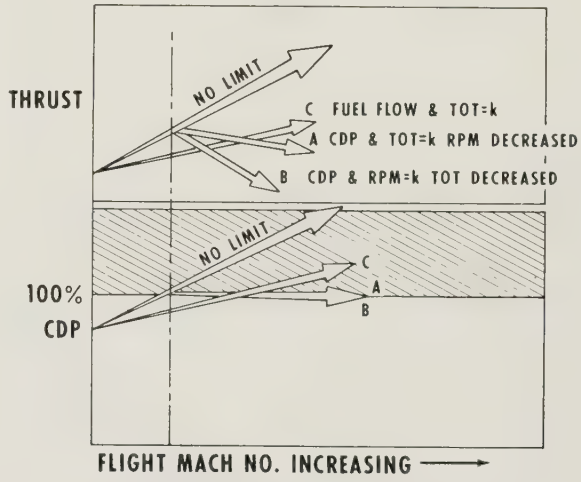

Fig. 3 — Methods of limiting compressor burst pressure

thrust for the conditions in question. When the compressor discharge pressure (cdp) starts to exceed its maximum value either (*A*) engine speed or (*B*) turbine inlet temperature can be reduced to limit its value.

In this case it will be seen that if the turbine temperature is reduced (line *B*), there will be a greater loss in available thrust than if rpm is reduced (line *A*). Consequently system *A* is usually preferred. Both of these systems will allow the engine and airframe to operate safely. However, if the airframe is "Q" limited so that operation in this regime is not expected during its mission, a simple limit of maximum fuel flow will provide some protection with a reduction in weight and complexity and only a minor loss in available performance (line *C*). This problem is more complex in multispool engines where different overspeed limits may be required for each rotor.

Class II: Thrust Control Modes

The acceptability of a powerplant depends on its ability to provide the thrust required for the airframe with the desired fuel consumption. Any control system which would limit the desired per-

formance of the aircraft would be unacceptable. On a turbine engine, control of engine speed, jet nozzle area, afterburner fuel flow, or water injection, and related functions (such as divergent nozzle area and other variable engine geometry) are part of the thrust control mode.

If we take the classic definition of optimum thrust control we will find that there are five different regimes:

1. Take-off maximum power with only minor consideration for specific fuel consumption.
2. Cruise operation where the most range (miles per pound of fuel) is desired.
3. Loiter operation where the most time of flight per pound of fuel is desired.
4. Idle, where lowest thrust within the requirement of the engine and airframe is desired.
5. Reverse or braking thrust, for stopping the aircraft after landing or ground maneuvering.

Any specific powerplant may have one or more of these requirements, depending on its design and application. The most common problems include design for optimum performance considering the range of control, available from each handle, design for optimum system weight, compatibility with airframe installations (such as inlet ducts), and the requirement for minimum thrust or idle.

Different modes of control will often provide similar engine performance in the normal operating regimes of the powerplant. The specific thrust modes of control selected will be limited by the necessity for insuring compatibility between the thrust control and other control modes.

Optimum Control System Weight to Satisfy Specific Missions—Considerable emphasis has been placed on the desirability of obtaining a control system which will provide the best ratio of specific fuel consumption to weights. A control system cannot improve sfc but only degrade it by inaccuracies; then, if the additional fuel required for operation with a simpler, less accurate control system is less than the weight saving in control hardware, the more inaccurate system may be acceptable.

Fig. 4 is a generalized plot of aircraft operating at constant Mach number to indicate the improvement in per cent sfc required to offset a 1% increase in the total weight of the engine. Since the controls are a small portion of the weight of the engine (10–25%), it is usually difficult even on short-range missions to substantiate deviations from "optimum" performance by this method.

Weight saving and performance gains can be obtained by restricting the altitude capabilities of the engine to the region actually flown by the aircraft. Fig. 5 shows a typical flight spectrum (guarantee limits) for a turbojet engine in terms of Mach number and altitude. The region of operation required for a modern turbojet aircraft is indicated by the

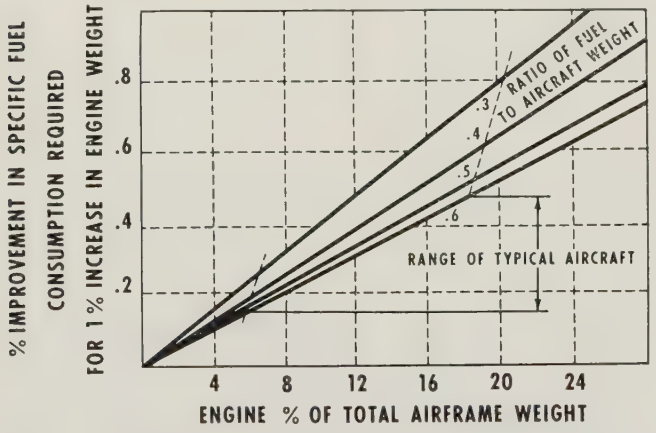

Fig. 4 — Weight and specific fuel consumption trade-off factors for constant range

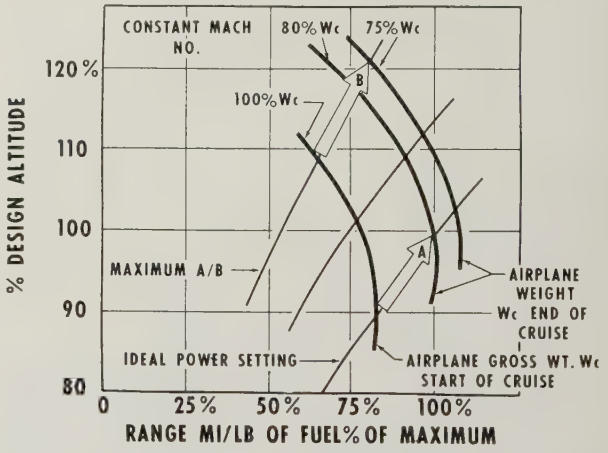

Fig. 6 — Effect of specific operating mode on maximum range

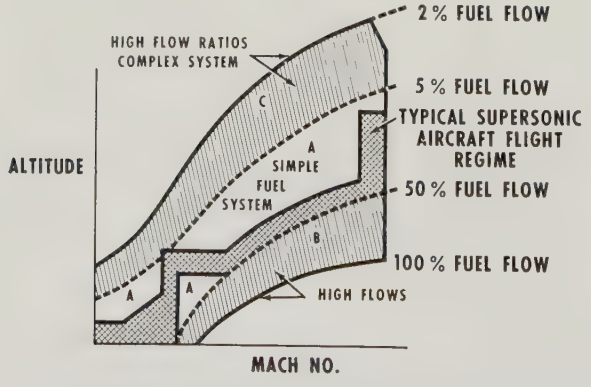

Fig. 5 — Performance regimes of turbojet engine fuel system

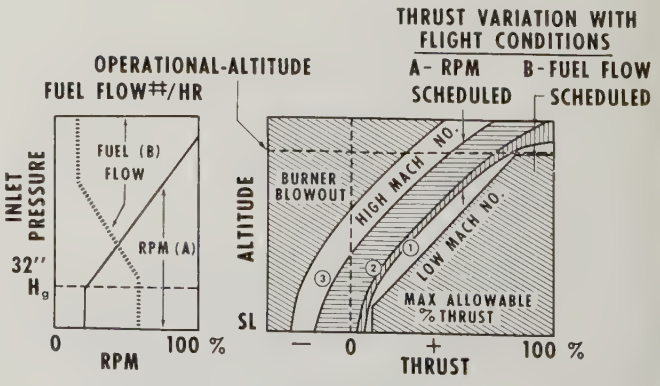

Fig. 7 — Turbojet idle control modes

cross-hatched region. A control system which will supply the fuel flows for this aircraft will be satisfactory for operation anywhere within area *A*. If it is necessary to operate at low altitudes and high speeds (region *B*), higher fuel flows will be required with an increase in control system weight. An increase of approximately 1% in control weight may be expected for 3% increase in fuel flow. In this region, operation also is approaching the structural limiting condition shown in Fig. 3, which requires additional control functions and increased control complexity.

If operation at high altitudes and low Mach numbers (region *C*) is desired, there will be a further increase in system weight and complexity due to the increased ratio between maximum and minimum fuel flows. Simple pumping and metering systems are generally limited to a flow range of 10/1. Consequently, staged pumping systems or variable displacement pumps may be required and maximum system pressure may increase greatly. Minimum power limitations for both the primary engine and afterburner become more restrictive as combustion limits are approached. Operation in region *C* will result in engine and control cooling problems, due to the low fuel flow and consequent limited heat sink. In extreme cases these requirements may result in a 50% increase in the weight of the control system.

Optimization of Control System Functions—It is possible to reduce the weight and improve performance and reliability of a control system by eliminating complex functions which do not significantly improve the operation of the weapons system. For example, Fig. 6 is a plot of the performance of a supersonic aircraft in terms of range in miles per pound of fuel and altitude at the cruise Mach number for two modes of operation of the same basic turbojet engine:

1. Use modulated afterburner setting with improved fuel consumption (mission *A*) in cruise.
2. Use maximum afterburning throughout the entire mission with a simplified control system (mission *B*).

A study of the range of the aircraft is necessary to make a decision. At a given altitude the modulated afterburner has a fuel consumption of approximately half of the maximum setting. When the differences in altitudes are considered, the advantage drops to less than 20%. Additional fuel equivalent to 5% of the weight of the aircraft is required, counterbalancing a higher altitude (20%) which is probably superior from a combat standpoint.

To offset this increase in fuel, the weight savings by elimination of the modulated afterburner would have to be at least 20% of the basic weight of the engine. While this is more than can usually be obtained, it illustrates the necessity of considering alternate systems in order that the airframe designer can have a choice in his approach to the mission.

Idle Thrust Requirements—The lower limit to the thrust spectrum of an engine is the idle thrust. The idle thrusts for a turbojet, desired by the military, have in the past been established in terms of per cent available thrust versus altitude. The control design problem has been to insure that the thrust did not exceed this value and still retain desirable engine operating characteristics (avoiding lean combustion blowout at altitude, or in the case of high Mach number vehicles, avoiding regions of unstable inlet operation).

Fig. 7 illustrates two typical control modes which may be selected by the turbojet engine designer. In system *A*, minimum engine speed is scheduled as a function of inlet pressure to approximate the desired thrust levels at low flight speeds (line 1). The ram effect on engine fuel requirements and scheduled speed will result in a high negative net thrust at high flight speeds (line 3).

Control mode *B* provides more nearly the desired performance by scheduling the minimum engine fuel against inlet pressure. In this instance changes in fuel requirements with increasing Mach number (line 2) are compensated for by equivalent changes in thrust. Unapparent in the curves is the fact that deceleration times will be greater with the second mode and that certain airframe missions may desire high negative thrust.

Class III: Transient Control Modes

The engine must be capable of starting at any normal operating condition and responding to any power transient which a pilot or guidance system may require from it.

The transient control modes include the regulation to start and accelerate the engine. Afterburner fire-up and shutdown, as well as normal decelerations, are factors in the transient mode of control, as is the control of other devices specifically required for transients (such as surge modifying variable compressor geometry).

The most publicized factor in the design of turbojet engine control systems is the control of acceleration time. The allowable acceleration fuel flow is a narrow band limited on the bottom by the maximum time allowable and on the top by physical engine limits of surge (or stall), overtemperature, and burner blowout.

Basic Modes of Acceleration Control—A number of control systems have been devised for circumventing the limits and accelerating an engine within a reasonable time.

The simplest acceleration system used on early engines might be called the "calculated risk" system. The pilot calculated how fast he could move the throttle, then took the necessary "risk." Even on simple engines this proved to be excessively dangerous and automatic acceleration control became necessary. With the careful sequencing of controls required for more complex "modern" engines, it is doubtful if the average pilot could obtain maximum performance from both the engines and the airplane under combat conditions.

Fig. 8 shows the four most common acceleration control modes in terms of their basic parameters, plotted against engine speed. In each case the upper lined zone is a composite of the acceleration limits of surge, overtemperature, or blowout. The lower line represents the stabilized values of the parameter.

Mode *A* is the most commonly used mode. It incorporates arbitrary biases of inlet pressure and inlet temperature to compensate the control schedule for predictable decreases in fuel requirements

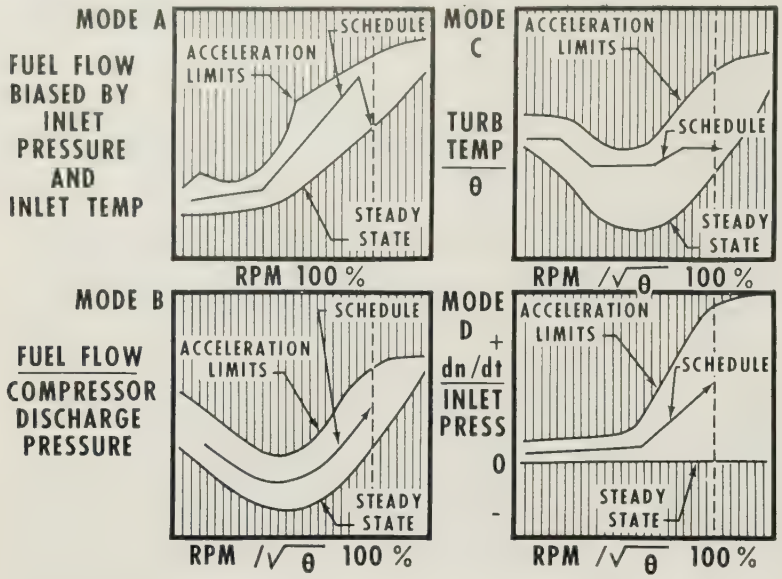

Fig. 8 — Turbojet engine acceleration control modes

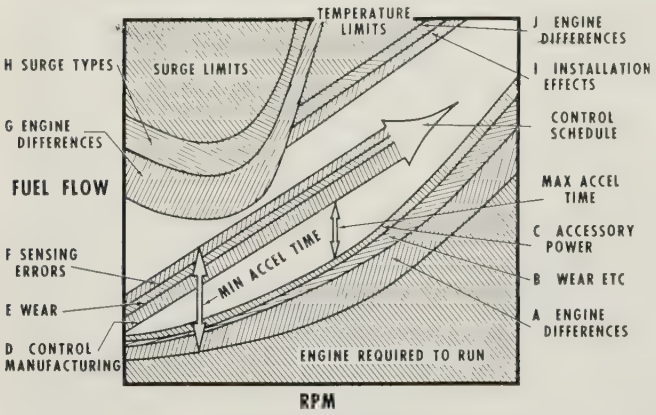

Fig. 9 — Factors affecting acceleration schedules

with increasing altitude and increasing temperature. Schedule inaccuracies can result in a large variation in acceleration times between individual engines.

Mode *B* is commonly used on 2-spool engines. In this case the fuel flow is biased by compressor discharge pressure rather than inlet pressure. The fuel flow is scheduled against corrected engine speed defined by rpm/$\sqrt{\theta}$. This results in a simpler control mechanical design (less cam lift) and certain operational advantages (such as a tendency to reduce fuel flow during a stall). This control mode can introduce instability as a result of the interaction of regulated fuel flow and measured cdp. It shifts in the wrong direction with many changes in engine performance. An increase in compressor discharge pressure, due to an incipient stall condition, results in an increase in fuel flow causing a further increase in compressor pressure, thus moving the engine toward stall.

Mode *C* is a "closed-loop" acceleration mode that measures an engine parameter (in this case, turbine temperature) and adjusts fuel flow to obtain the desired value of that parameter. This is particularly useful where the fuel energy content is variable, or where precise compensation for all required variables is unknown. It is more accurate and consistent in its operation than the previous modes. It has certain limitations, as it requires a thermocouple with its inherent time delay and complex electronic equipment.

Mode *D* is also a "closed-loop" acceleration mode. In this case the rate of change of engine speed itself is scheduled. This will provide the most consistent and fastest average acceleration time of the listed control modes. While the sketch indicates that the control should be biased by inlet pressure and temperature for optimum performance, these biases are not critical. The mode can be used for simple applications without any biasing parameters. It was found that one early version of the J33 (now using a fuel scheduled control) could meet the present acceleration limits using this control mode with no biases. This system has some limitations in application to 2-spool engines, due to the change of coupling between the spools during a gross transient. If referenced to low-pressure rotor speed it could require a negative initial dN/dt. The acceleration temperature limiting mode or simple hydromechanical system may be preferred for many applications.

None of these systems will provide the most rapid acceleration time possible with any given engine. A number of studies have been made to find a system which will be responsive directly to the limiting parameters of the engine, particularly stall. Such investigations have helped greatly in our understanding of stall phenomena, but to date have disclosed little promise of a satisfactory solution.

Effect of Tolerances on Acceleration Performance —These systems have certain inherent tolerances and limits which result in less than "optimum" acceleration time. Fig. 9 shows some of the variables which must be considered:

1. The engine variations caused by production tolerances, deterioration, and aircraft accessory power loading may have significant effects on the

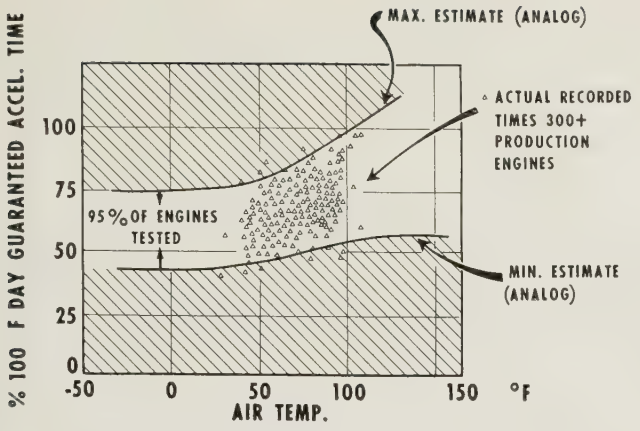

Fig. 10 — Predicted variations in acceleration time

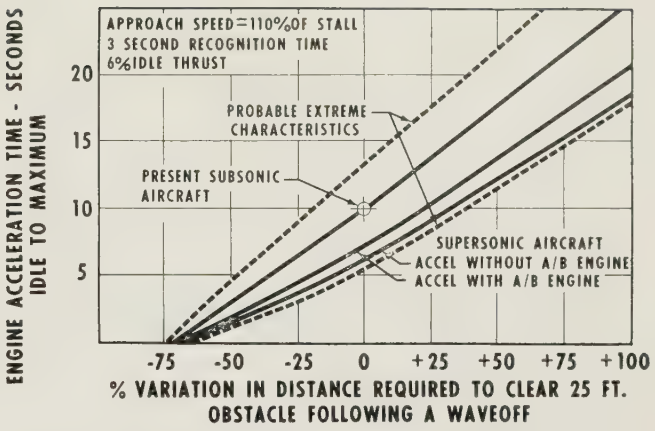

Fig. 11 — Effect of acceleration time on wave-off distances based on typical jet aircraft characteristics

acceleration times.

2. Control manufacturing tolerances, wear, and sensing accuracy must be considered in the control tolerances.

3. The effect of engine surge and temperature variations and unusual engine surge characteristics must be included in the definition of the surge margin. Thus, the narrow "limit stack" of engine and control tolerances may require twice as long to accelerate as the wide margin combination.

Fig. 10 shows the maximum and minimum acceleration times obtained for one type of engine which uses a fuel-scheduled control system. These data are plotted against the predicted acceleration times from the analog computer to provide character for this figure.

Effect of Acceleration Time on Aircraft Performance — The fastest possible acceleration is not necessarily the optimum acceleration. For example, on a twin-engined aircraft with a substantial spacing between the engines, unequal acceleration would result in aircraft yaw. The correction required could more than offset any time advantage making uniform acceleration characteristics desirable.

The most critical acceleration requirements occur during an aborted landing, where the pilot must accelerate an aircraft from a point just above stall to a reasonable climbing rate as quickly as possible. Fig. 11 is a comparison for a family of jet aircraft of the distances required to clear a 25-ft obstacle following a wave-off. This comparison is based on the performance of a typical large subsonic aircraft used with engines which accelerate from idle to maximum in 10 sec.

For comparison an assumed supersonic aircraft is included. The effect on its wave-off distance caused by the use of afterburning is shown. The extreme variation which might be expected from conceivable turbojet aircraft is shown by the dotted lines.

It can be seen that the wave-off distance is quite sensitive to the acceleration rate of the engine. Since there is a minimum acceleration time for any engine this means that dive brake, thrust reversers, or spoilers could be required on applications where the wave-off time is critical. A secondary point illustrated by this curve might be the

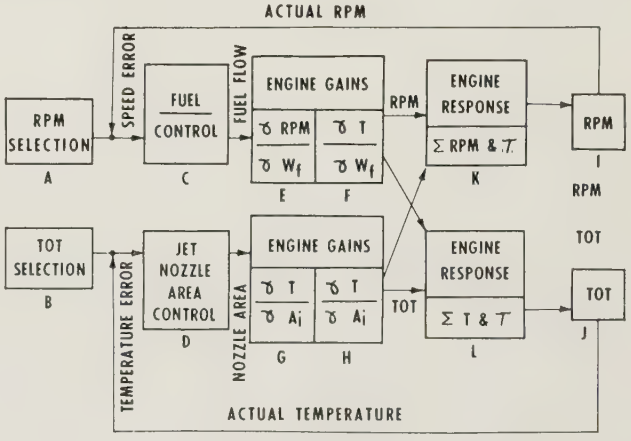

Fig. 12 — Simplified control interaction diagram

desirability of using smaller engines. With geometrically similar powerplants the acceleration time decreases approximately as the square root of the airflow. Thus, the wave-off distance of a 4-engine aircraft might be 35% less than an equivalent single-engine aircraft.

If an airframe, such as a missile, does not have a critical acceleration time, simple acceleration schemes can be used. These advance the engine speed so slowly that safe accelerations are always obtained.

System Compatibility Requirements

In selecting a mode of control there is also the choice of the type of regulation which will be used, that is, whether the system will be open or closed loop, proportional or integrating.

Where more than one closed-loop system is used in a control system, the problem of providing the necessary stability will become much more difficult. Two systems, which are by themselves acceptably stable, may interact in an unacceptable manner when used on the same engine even though they have no parts directly in common.

For example, Fig. 12 is a simplified block diagram showing the interrelationships involved where two proportional controls are used on a simple turbojet engine with variable jet nozzle area control. In

this case, a specific engine speed (A) and temperature (B) are selected by the pilot. Any errors in actual engine speed (I) as indicated by the control will result in a change in fuel flow as a function of that speed error and the proportionality of the fuel control (C). This change in fuel flow will then cause an equivalent change in engine speed (E) and turbine-out temperature (F) as defined by the specific "gain" terms of the engine. The latter change will result in a change in the observed turbine temperature (J) which will be sensed by the jet nozzle area control as an error which must be corrected. The control will then adjust the jet nozzle area an amount defined by its own gain of area to temperature (D) and force appropriate changes in engine speed (G) and turbine-out temperature (H).

The speed error so created will then be sensed by the fuel control, and if the timing is right (or wrong, depending on your viewpoint), the entire process will repeat indefinitely. In this figure the "area control" could be replaced by a propellor, an afterburner fuel control, or other similar control elements.

The effects of this interaction on the stability of a practical control system (with hysteresis) are shown graphically on Fig. 13. In this figure the slope of the fuel flow governor is plotted against the gain of the temperature area control system. Very low proportionalities as indicated by the ruled zones would be unacceptable for control purposes as they would result in excessive errors with changing conditions. As the gain of either system increases it will first reach a point of conditional stability as indicated by line *A*, then pass through a zone of increasing but marginally acceptable limit cycles (line *B*) until complete or divergent instability is found at line *C*. The tool which we have found most useful in evaluating these problems is the analog computer. It is now standard procedure for Allison to simulate the engine before control hardware is designed to establish special interrelationship problems, and try out the effects of various modes of control.

By use of the analog and digital computers, it is possible to investigate the operation of the engine and control system as it would be expected in the airframe environment, including the effects of inlet ducting, fuel supply conditions, mission requirements, and other factors which must be considered in order to establish the basic requirements, and thus, the optimum mode of control for any specific application.

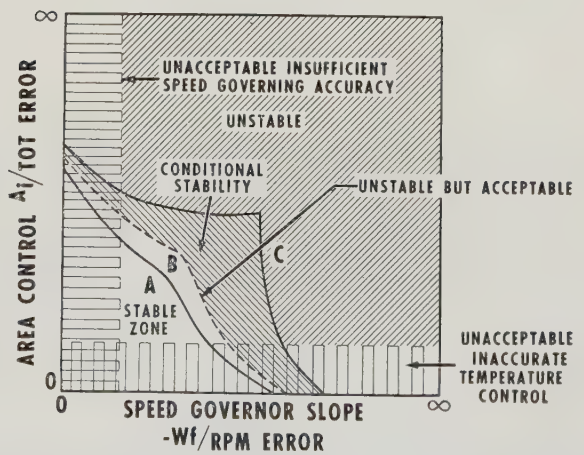

Fig. 13 — Typical stability interactions of two proportional engine control systems

Practical Control Design Considerations

The final mode of control selected must include consideration of the mechanical design components available. Frequently in the past, the control mode selected for an engine has been tailored to existing control devices. Time schedules frequently force this type of decision, as the development time for an entirely new control system is probably greater than the time required to develop a new powerplant.

Consequently, flexibility is of major importance. Where schedules are used, ease of schedule change with changes in performance and engine development and growth is extremely important.

Reliability considerations dictate selection of modes of control which operate by the most direct method possible to avoid excessive numbers of parts. Fail-safe philosophies for manned aircraft make it necessary to select modes which, in case of the mal-operation of a single component, will not cause loss in performance to the extent that the airframe and pilot are endangered.

Summary

This discussion has reviewed the basic problems in the selection of an initial mode of control for an engine. The necessity for flexibility of setting and operation of basic control systems and components in order to tailor the control system for "optimum" performance of the weapon system has been emphasized. The degree of refinement will vary from the highly integrated problems of the VTO, where the attitude and speed of the aircraft depend on the control of the engine, to simple "boost" engines which operate under very limited conditions of flight. Much originality and development effort will be required to find and develop the engine control systems which will provide the maximum performance potential for the weapons systems.

Symbols Used in Text and Illustrations

cdp = Compressor discharge pressure
tot = Turbine-out temperature
K = Constant value
sfc = Specific fuel consumption, lb fuel/lb thrust/hr
A/B = Afterburner
A_j = Jet nozzle area
d_N/dt = Rate of change of engine speed
$\frac{\partial N}{\partial W_f}$ = Partial differential of rpm to fuel flow
$\frac{\partial T}{\partial W_f}$ = Partial differential of temperature to fuel flow
$\frac{\partial N}{\partial A_j}$ = Partial differential of rpm to jet nozzle area
$\frac{\partial T}{\partial A_j}$ = Partial differential of temperature to jet nozzle area
Σ = Summation of changes
τ = Time response
θ = Temperature ratio $\frac{T_{\text{observed}}}{518\ \text{F}}$

Engagement Characteristics of Wet-Type Clutches

L. P. Ludwig, Twin Disc Clutch Co.

This paper was presented at the SAE National Farm, Construction, and Industrial Machinery Meeting, Milwaukee, Sept. 9, 1958

WET–TYPE clutches, as referred to in this paper, are those having the friction surfaces oil lubricated by splash, spray, or forced methods. Briefly, this paper contains a mathematical analysis of the slip (dynamic) torque curve of the engagement period, and a presentation of some related experimental work.

The torque capacity of disc-type clutch is expressed by the following formula:

$$T = F\kappa R_m n = PA\kappa R_m n \qquad (1)$$

where:

T = Torque capacity
F = Clamping force
κ = Coefficient of friction
R_m = Effective mean radius
n = Number of surfaces engaged in transmitting torque
P = Pressure on friction surfaces
A = Area of one surface

Mean Radius

Under static conditions (when the relative velocity is zero at the friction surfaces) the mean radius derivation is based on the assumption that uniform pressure exists on the friction surfaces, and the differential torque is:

$$dT = R\kappa_s P dA$$

where:

R = Mean radius of incremental area dA
κ_s = Static coefficient of friction
dA = Incremental area

(n is unity, since only one surface is under consideration.)

Noting that the incremental area (dA) is equal to $2\pi R dR$ (Fig. 1) and integrating from R_i *to* R_o:

$$T = 2\pi\kappa_s P \int_{R_i}^{R_o} R dR = 2/3\pi\kappa_s P(R_o^3 - R_i^3) \qquad (2)$$

Further, for one surface ($n = 1$), Equation 1 can be expressed as:

$$T = \pi P(R_o^2 - R_i^2) R_m \kappa_s \qquad (3)$$

Combining Equations 2 and 3 and solving for R_m:

$$R_m = \frac{2(R_o^3 - R_i^3)}{3(R_o^2 - R_i^2)} \qquad (4)$$

Under slipping conditions (dynamic) the mathematical derivation of the mean radius is based on

THIS PAPER presents a mathematical analysis of clutch engagement under certain idealized conditions and the related experimental work. The analysis is divided into several cases concerning pure inertia load acceleration and inertia load with a superimposed "work" torque load.

The author also discusses the "wear in" process which occurs in some clutch materials, such as phosphor bronze mated to steel plates; the effect of grooving; and the static coefficient of friction.

the principle of uniform wear. This implies that each surface particle performs the same amount of work; and since the particles near the OD travel further than those near the ID, the pressure distribution must vary proportionately so as to provide equal work. Therefore, the relationship between pressure and radius is:

$$PR = P_1R_1 = C$$

The incremental clamp force can be expressed as:

$$dF = PdA = C/R(2\pi RdR) = 2\pi CdR \qquad (5)$$

The incremental torque is:

$$dT = \kappa_k RdF = 2\pi C\kappa_k RdR$$

and the torque of one surface (assuming the dynamic coefficient of friction, κ_k, is constant) is:

$$T = 2\pi C\kappa_k \int_{R_i}^{R_o} RdR = \pi C\kappa_k (R_o^2 - R_i^2) \qquad (6)$$

Noting that the total clamp from Equation 5 is:

$$F = 2\pi C(R_o - R_i) \qquad (7)$$

and combining Equations 1, 6, and 7, we have:

$$R_m = \frac{R_o + R_i}{2} \qquad (8)$$

For the majority of clutch plates, the ID to OD ratio is such that Equation 8 may also be used for calculating the static mean radius without introducing significant error.

Theoretical Analysis of Inertia Load Acceleration by Clutch

During the slipping phase of clutch engagement the energy input is partly converted into heat at the friction surfaces, and the remaining part appears as useful work.

$$E_i = Q + E_o \qquad (9)$$

where:

E_i = Energy input
Q = Heat energy liberated at the friction surfaces
E_o = Useful work

This investigation of heat energy and useful work in clutch engagements is divided into several cases, and is based upon the following assumed conditions:

1. Schematically, the system consists of a prime mover, a clutch, and a flywheel inertia load. (An external "work" torque requirement is added in one case.)
2. The prime mover speed remains constant, and the angular velocity of the flywheel inertia load is zero at the first instant of engagement. (The case, in which the clutch is used as a brake, is pure inertia deceleration.)
3. The slip torque of the clutch is constant over the full engagement period.
4. The system is frictionless for pure inertia acceleration or deceleration.

The first case is that of pure inertia load acceleration to the speed of a prime mover. By Newton's Law:

$$T_c = I_f\alpha = I_f \frac{dw_f}{dt} \qquad (10)$$

where:

T_c = clutch slip torque
I_f = Polar moment of inertia of flywheel
α = Angular acceleration of flywheel
w_f = Angular velocity of flywheel

The instantaneous flywheel velocity is then:

$$dw_f = \frac{T_c}{I_f}\,dt$$

and the velocity at any time t is:

$$w_f = \frac{T_c}{I_f}\,t \qquad (11)$$

The instantaneous slipping velocity is then:

$$w_s = w_i - w_f \qquad (12)$$

where:

w_s = Slipping velocity or relative velocity at clutch friction surface
w_i = Prime mover velocity

The energy liberation at one friction surface in time t is:

$$Q = fs = F_{k_k}s = \frac{T_c}{R_m}\,\mathrm{s} \qquad (13)$$

where:

Q = Heat energy
f = Tangential force
s = Distance traveled by force f during time t

Since

$$s = \theta R_m \qquad (\theta = \text{Radian displacement})$$

$$Q = \frac{T_c}{R_m} \qquad \theta R_m = T_c\theta \qquad (14)$$

and since $w_s = \frac{d\theta}{dt}$

$$\theta = \int w_s dt = \int (w_i - w_f)\,dt$$

When integrated:

$$\theta = w_i t - \frac{T_c t^2}{2I_f} \qquad (15)$$

Combining Equations 14 and 15:

$$Q = T_c w_i t - \frac{T_c^2 t^2}{2I_f} \qquad (16)$$

From Equation 16, at $t = t_e$ (engagement com-

pleted) the total amount of heat liberated (Qe) is:

$$Q_e = \frac{T_c^2 t_e^2}{2I_f} \tag{17}$$

The flywheel kinetic energy is:

$$\text{K.E.} = \tfrac{1}{2} I_f w_f^2 \tag{18}$$

since:

$$w_f = \frac{T_c t}{I_f}$$

$$\text{K.E.} = \frac{T_c^2 t^2}{2I_f}$$

The rate of heat generation $\dot{Q}$ is:

$$\dot{Q} = \frac{dQ}{dt} = \frac{d}{dt}\left(T_c w_i t - \frac{T_c^2 t^2}{2I_f}\right) \tag{19}$$

$$\dot{Q} = T_c w_i - \frac{T_c^2 t}{I_f} \tag{20}$$

Since:

$$w_f = \frac{T_c t}{I_f}$$

$$\dot{Q} = T_c w_s \tag{21}$$

A study of the preceding equations and of the plot of these equations in Fig. 2 leads to the following conclusions:

1. The total amount of heat generated (Q_e) is exactly equal to the final flywheel kinetic energy.
2. At any time t the heat energy liberated (Q) is equal to the total input energy (E_i) expended minus the flywheel kinetic energy (K.E.).
3. The rates of heat generation ($\dot{Q}$) and of flywheel energization are not equal.
4. Fifty per cent of the heat generated (Q) at the friction surfaces is liberated in the first 30% of the total engaging time.
5. The maximum rate of heat generation ($\dot{Q}$ max) occurs at the first instant of engagement and diminishes linearly, reaching zero at the last instant of slip.

The second case is that of a clutch being used as a brake to decelerate an inertia load. Similar analysis, as was applied to acceleration of an inertia mass, leads to the following set of equations.

The flywheel velocity (w_f) at any time t is:

$$w_f = w_i - w_d \tag{22}$$

where:

w_d = Decrease in velocity from $t = o$
w_i = Initial flywheel velocity

The decrease in velocity is:

$$w_d = T_c t / I_f \tag{23}$$

The energy liberated in the form of heat is:

$$Q = T_c w_i t - \frac{T_c^2 t^2}{2I_f} \tag{24}$$

The flywheel kinetic energy is:

$$\text{K.E.} = \frac{I_f w_i^2}{2} - Q \tag{25}$$

and the rate of heat generation is:

$$\dot{Q} = T_c w_f \tag{26}$$

Equation 26 is exactly equal to Equation 21; therefore, the rate of heat generation is the same for either case of flywheel acceleration or deceleration by a clutch. This suggests that certain test data obtained in using the clutch as a brake can be reliably applied to clutch design. Other data, such as effect of grooving on the coefficient of friction (which is probably influenced by the effect of centrifugal force on fluid flow) is reliable only on a comparative basis. Fig. 3 is a plot of Equations 22–26 for the case of deceleration of a flywheel by a brake.

The third case is that of acceleration of an inertia load with a superimposed "work" torque load. This "work" torque load includes all resistances not of an inertial origin, such as bearing friction, windage, and compressor or engine gas forces, and is presumed constant in time. The following equation holds:

$$T_c = T_s + T_f \tag{27}$$

$$T_c = T_s + I_f \alpha$$

in which:

T_c = Clutch slip torque
T_s = Torque required to overcome the superimposed "work" torque
T_f = That part of the clutch slip torque which is available for acceleration of the inertia mass

An analysis similar to that applied in pure inertial

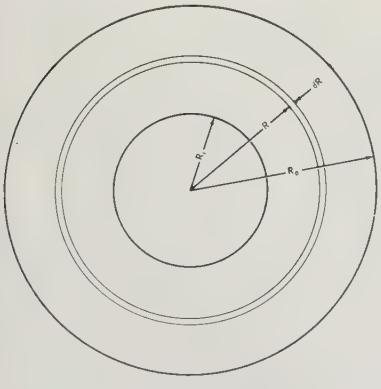

Fig. 1 — Mean radius quantities

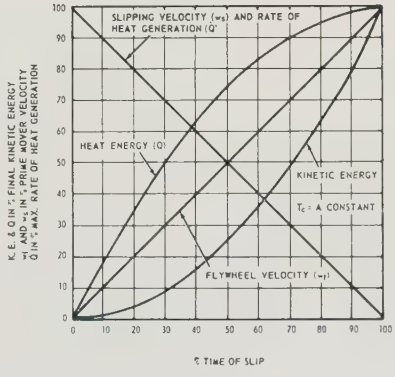

Fig. 2 — Theoretical variation of interrelated functions during clutch engagement when accelerating flywheel mass

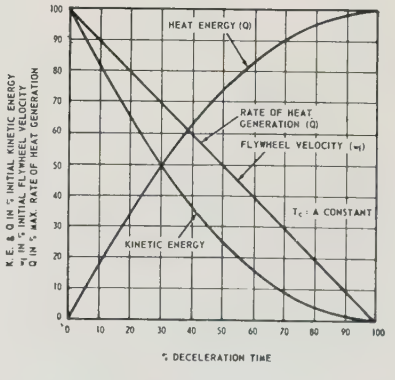

Fig. 3 — Theoretical variation of interrelated functions during clutch engagement when decelerating flywheel mass

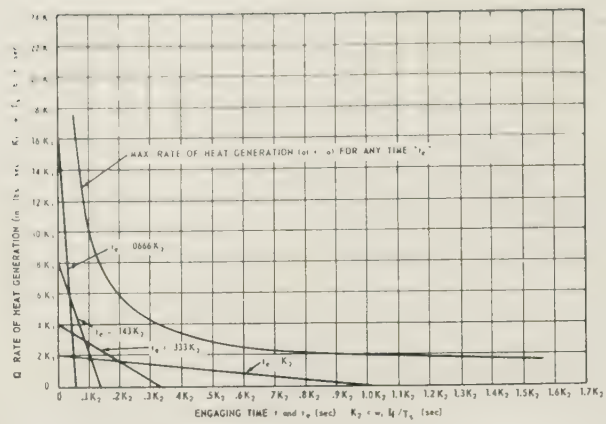

Fig. 4 — Heat generation curves for acceleration of inertia load with superimposed "work" torque load (T_s)

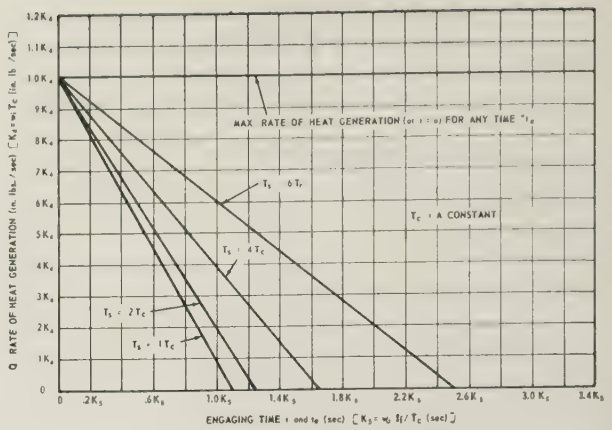

Fig. 6 — Heat generating curves for acceleration of inertia load with superimposed "work" torque load

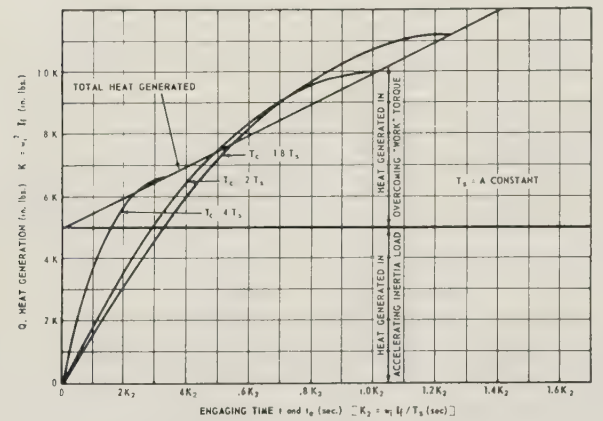

Fig. 5 — Heat generation curves for acceleration of inertia load with superimposed "work" torque load (T_s)

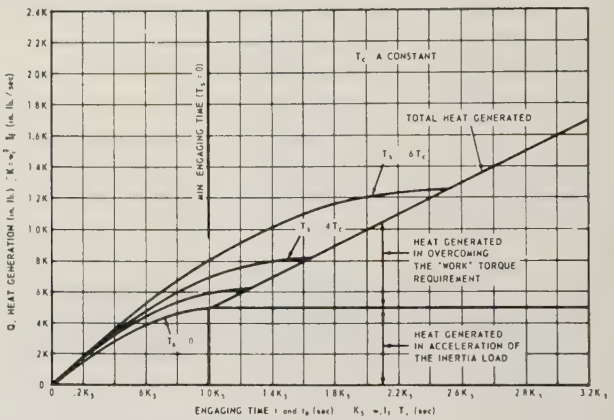

Fig. 7 — Heat generating curves for acceleration of inertia load with superimposed "work" torque load

acceleration leads to the following set of equations:
The flywheel velocity is:

$$w_f = (T_c - T_s)\, t/I_f \tag{28}$$

The kinetic energy of the flywheel is:

$$\text{K.E.} = (T_c - T_s)^2 t^2/2I_f \tag{29}$$

The heat energy liberated up to time t is:

$$Q = w_i t T_c - T_c(T_c - T_s)\, t^2/2I_f \tag{30}$$

and the rate of heat generation is:

$$\dot{Q} = w_s T_c \tag{31}$$

The curves in Figs. 4–7 show the heat generation curves for this third case. It should be noted that the amount of heat energy liberated which is attributable to acceleration of the flywheel is constant for all engaging times.

Comparison of Heat Generation Characteristics

The varied clutch applications cover a gradation in ratio of superimposed "work" torque over clutch slip torque. Obviously, for a given clutch slip torque (the inertia mass and prime mover speed being constant for each engagement) as this ratio increases the clutch torque capacity remaining to accelerate the inertia load decreases and the length of engagement time increases. From a heat generation standpoint, several general cases exist and comparison of the heat versus time curves illustrates pointedly the many possibilities.

The first case (Figs. 8 and 9) is that of pure inertia load acceleration. The conditions of operation are:

1. The prime mover speed and inertia mass are the same for each engagement and the prime mover speed is constant during the engagement.
2. The clutch slip torque is varied in order to produce various engagement times. (This slip torque is held constant during any one engagement.)

Inspection of Figs. 8 and 9 (see Equations 16 and 21) demonstrates that as the length of engagement time approaches zero, the maximum rate of heat generation approaches infinity; and that as the slipping time approaches infinity the rate of heat generation approaches zero. However, the total energy released at the friction surfaces is the same for every length of engagement time. The important factor here is the possibility of surface destruction or thermal distortion under the high rates of heat generation associated with the extremely short en-

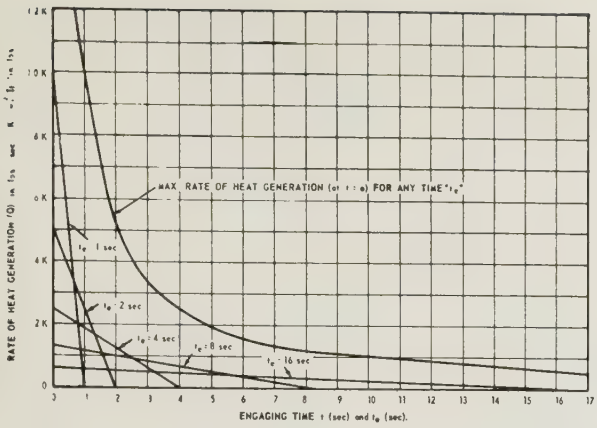

Fig. 8 — Heat generation curves for pure inertia acceleration

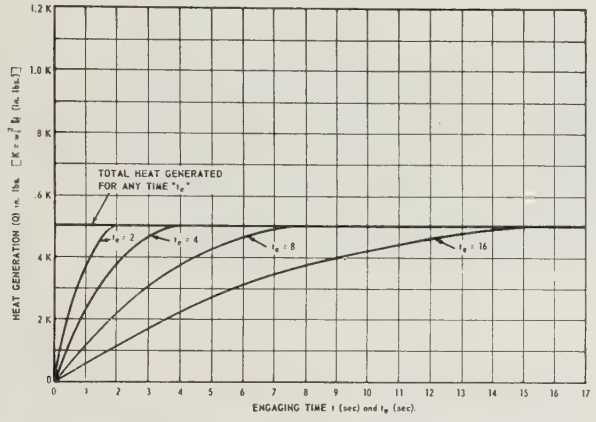

Fig. 9 — Heat generation curves for pure inertia acceleration

gagement periods. Theoretically then, for pure inertia acceleration, the longer periods of engagement time are less abusive.

The second general case (Figs. 4 and 5) is acceleration of an inertia load with a superimposed "work" torque load. Here the conditions of operation are:

1. The superimposed "work" torque is the same magnitude for each engagement.
2. For each engagement a different clamping force is selected, hence providing various engagement times. T_c is constant during any one engagement.
3. The final flywheel velocity and the flywheel mass are the same for each engagement.

Figs. 4 and 5 (Equations 30 and 31) show that the amount of heat generated, which can be attributed to acceleration of the flywheel remains constant for all engaging times and is equal to the final flywheel kinetic energy. However, the total heat liberated increases with increasing engagement time. Dependent upon the magnitude of superimposed "work" torque and clutch slip torque, this case has a definite optimum engaging time. The reason for this is suggested in Fig. 4, in that when t_e is extremely short, the rates of heat generation are high, and when t_e becomes relatively longer, the total amount of heat generated (as shown in Fig. 5) becomes greater. The minimum amount of heat would be generated for $t_e = o$. At this point the energy released is equal to the flywheel kinetic energy, but the rate of heat generation is infinitely great and prohibitive. For any one particular application, the solution for optimum engagement time is a heat-transfer problem, and beyond the scope of this paper.

The third case (Figs. 6 and 7) is similar to case 2 except that the clutch torque capacity is constant and the magnitude of the superimposed "work" torque is allowed to vary in order to vary the length of the engagement. Here the maximum rate of heat generation remains constant, for all lengths of engaging time and the total heat liberated and length of engaging time increases as the "work" torque requirement is increased. Again, that part of the heat generated attributable to inertial acceleration remains constant.

Practical Implications from Preceding Theoretical Analysis — An inspection of the theoretical acceleration and heat generation curves suggest that the ability to absorb high energy loads can be improved if the clutch torque varies such that the peak rates of heat generation are reduced. Thus, by employing an initially low clutch clamping pressure and gradually increasing to a final high pressure at the end of the engaging cycle, a reduction in the peak rates of heat generation is effected, and the heat load is spread over the entire engaging cycle. The optimum condition, although impractical, would be a constant rate of heat generation over the entire engaging period. The torque variation (or pressure variation) necessary to produce this ideal rate of heat generation can be derived from the basic equations discussed previously.

The basic condition is that the rate of heat generation is constant in time:

$$\dot{Q} = T_c w_s = c \tag{32}$$

From Newton's law:

$$T_c = I_f \alpha = I_f \frac{dw_f}{dt} \tag{11}$$

where:

$$T_c = f(t)$$

Since:

$$T_c = c/w_s$$

$$dt = \frac{I_f w_s}{c}\, dw_f = \frac{I_f}{c}\,(w_i - w_f)\, dw_f \tag{33}$$

and the relationship between time t and flywheel angular velocity (w_f) is:

$$t = \frac{I_f}{c}\left(w_i w_f - \frac{w_f^2}{2}\right) \tag{33A}$$

The total heat liberated Q in time t is obtained from Equation 32:

$$Q = t_c w_s t \tag{34}$$

The input energy to any time t is:

$$E_i = w_i \int T_c dt \tag{35}$$

combining Equations 33 and 35:

$$E_i = w_i I_f w_f \tag{35A}$$

From Equation 9 we have:

$$\text{K.E.} = E_i - Q$$

$$\text{K.E.} = w_i I_f w_f - T_c w_s t \tag{9A}$$

The relationship of the slipping velocity (w_s) and the time t is obtained by combining Equation 33A

and the relationship, $w_s = (w_i - w_f)$.

$$t = \frac{I_f}{2c}\,(w_i^2 - w_s^2) \qquad (36)$$

or:

$$w_s = \left(w_i^2 - \frac{2ct}{I_f}\right)^{1/2} \qquad (36A)$$

Also from Equation 36 the relation between T_c and t is

$$t = \frac{I_f}{2c}\left(w_i^2 - \frac{c^2}{T_c^2}\right) \qquad (37)$$

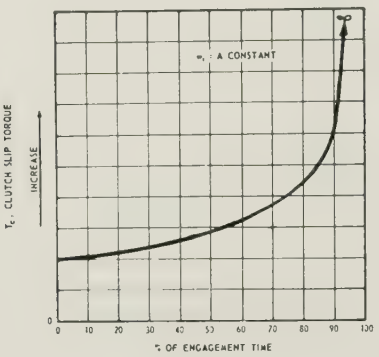

Fig. 10 — Torque variation necessary to produce constant rate of heat generation

Fig. 10 shows this theoretical variation of torque necessary to produce a constant rate of heat generation. Of course, in practice the curve must be altered in order to keep the clutch pressure within limits. Fig. 11 is a plot of the variation of clutch parameters under this condition of constant rate of heat generation and a comparison of this plot to Fig. 2, which is for clutch torque constant in time, demonstrates the differences in energy rates between the two systems.

Test Results on Engagement Characteristics

Briefly, the test data presented here was taken with a hydraulically actuated clutch being used as a brake to decelerate a flywheel. The test plate was 5 in. in outside diameter and 3.75 in. at the inside diameter. The two steel mating plates were 0.06 in. thick and had a 35 to 45 a.a. surface roughness (ground) measurement. Splash lubrication at 75 to 105 F was used, the lubricating oil being Socony Vacuum D.T.E. heavy-medium-type oil.

"Wear In" Process — Fig. 12 contains some test results demonstrating the "wear in" process which occurs in some common clutch materials. In each case, during the initial engagements, the coefficient of friction steadily decreased to a level off value. The Sanborn traces in Fig. 13 illustrates this "wear

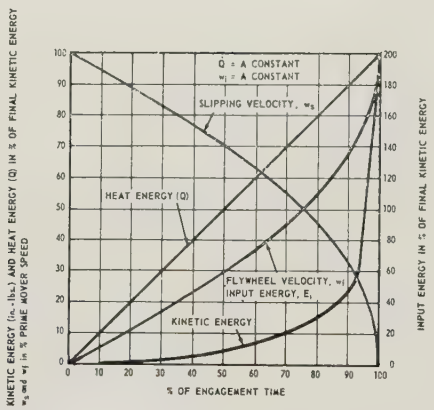

Fig. 11 — Theoretical variation of interrelated functions during pure inertia acceleration for condition of constant rate of heat generation

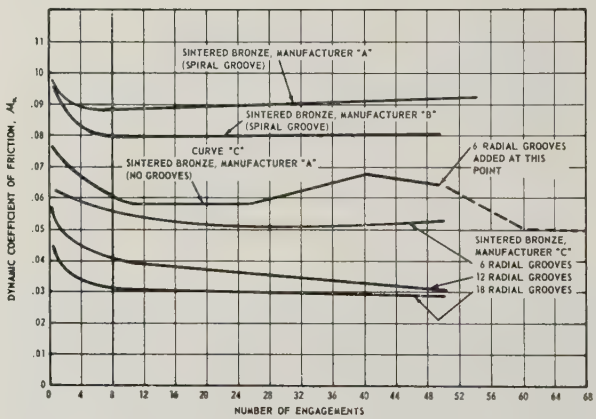

Fig. 12 — Dynamic coefficient of friction versus number of engagements (120-psi swept area pressure)

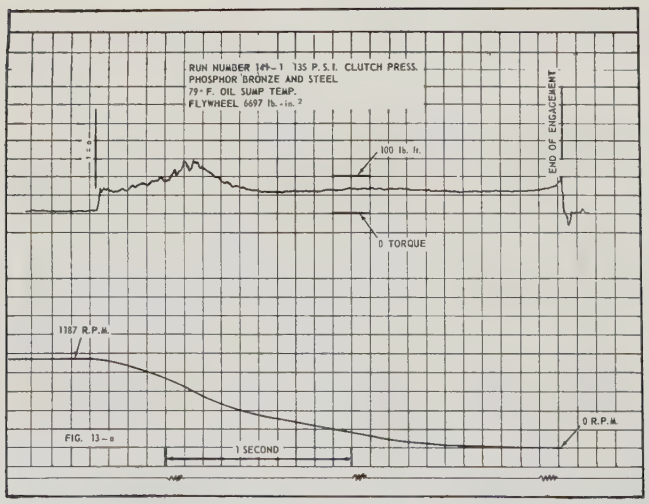

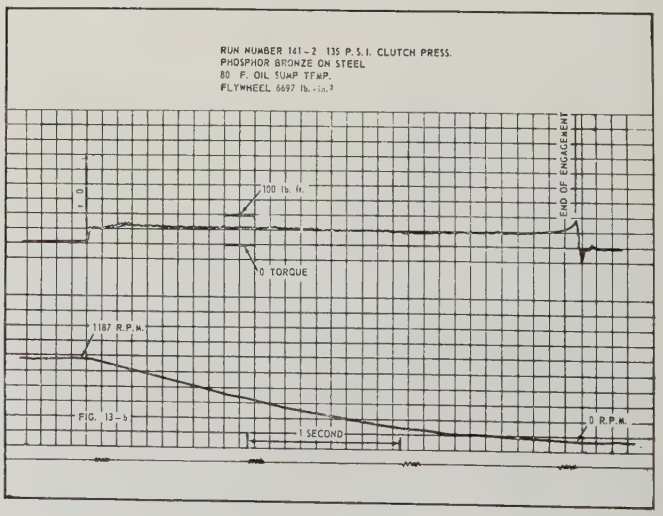

Fig. 13 — Sanborn traces illustrating "wear in" process for phosphor bronze plates mated to steel plates

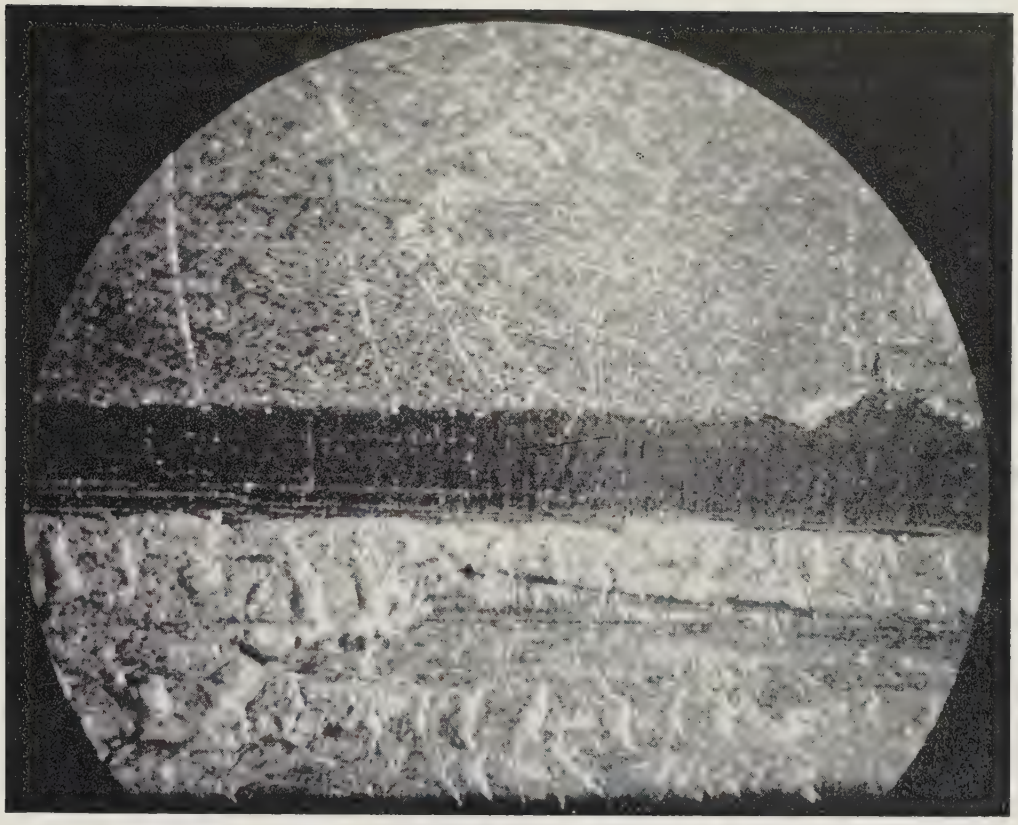

Fig. 14 — Phosphor bronze surface: untouched area (top), polished area (center), and light plastic deformation (bottom). (Original photograph magnified 35 times)

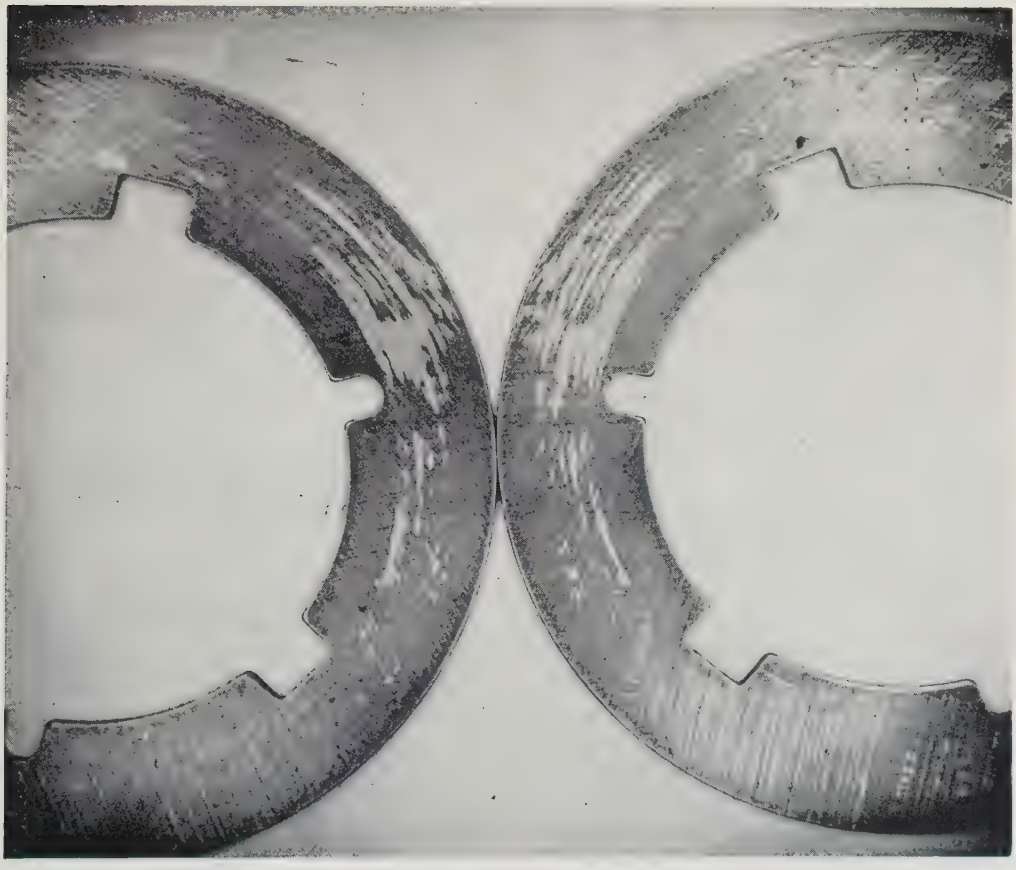

Fig. 15 — Heavy bronze transfer to steel plates

in" process for phosphor bronze plates mated to steel plates. The first trace, on a new previously unused plate, indicates some metal transfer or welding of bronze to steel. The trace of the next run shows that the more prominent high spots have been "worn off" and the engagement proceeds without appreciable indication of metal transfer. At this point, it should be pointed out that the torque trace shows steep pressure rise to full clutch pressure in 0.02 sec, and that this closely approaches the assumption of "clutch slip torque constant in time" used in the theoretical analysis.

The photomicrograph of the rolled phosphor bronze surface in Fig. 14 shows the following damage and "wear in" characteristics of this type of material:

1. Plastic deformation of the surface due to welding (lower section).
2. "Wear in" polishing of the surface (center portion).
3. Nonuniformity of contact pressure, as is indicated by an area which has no evidence of rubbing (upper portion).

Welding results in transfer of metal to the steel plates, as shown in Fig. 15. An interesting observation is that the transfer pattern is the same on each steel plate, which leads to the conclusion that this combination of materials is very sensitive to surface discontinuities, and that a discontinuity on one surface can be reflected through to the others.

The energy absorption capacity for a single engagement of phosphor bronze or steel was vastly greater for "worn in" plates as compared to new plates. This energy absorption capacity was found to be a function of both rate of heat generation and total heat generated.

Effect of Grooving — The tests indicated that the type of grooving on the friction face has a tremendous influence on the dynamic coefficient of friction, and no appreciable influence on the static coefficient of friction. This study was incomplete but the presence of the gross effect of grooving configuration suggests a detailed analysis (including effect of such variables as pressure, temperature, and oil flow) will yield fruitful results.

Certain engagement characteristics, such as the rate of torque increase or the torque magnitude, can be partially controlled by grooving configurations. Fig. 12 contains some examples. These examples concern a spiral groove, a ⅛ in. wide radial groove equally spaced in the basis of 6, 12, or 18, and a plate with no grooves. The main conclusion is that a plate with a small number of radial grooves will have less dynamic coefficient of friction than a spiral grooved plate or even a plate with no grooves. (This may not be true for all temperatures and pressures, and certainly is not true for a plate with a large number of radial grooves.) In Fig. 12, the addition of six radial grooves (per face of the test plate) to a plate with no grooves immediately dropped the dynamic coefficient of friction. Also, 12 radial grooves had less dynamic coefficient of friction than 6, and 18 less than 12. The spiral grooved plate, as indicated by the two top curves in Fig. 12, produced the highest coefficient. In general, the evidence indicates that radial grooves tend to introduce a hydrodynamic component, or at least to cause an increase in average thickness of the boundary lubricating film.

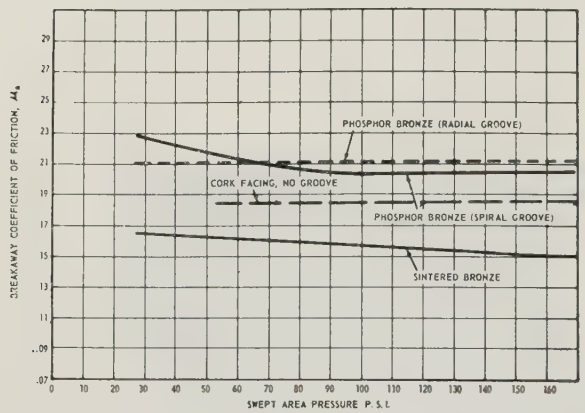

Fig. 16 — Variation of breakaway coefficient of friction with pressure

Static Coefficient of Friction—The "breakaway" or static coefficient of friction (Fig. 16) shows very little change over the tested range of pressures. These results are in good agreement with the classical law of friction, which states that the coefficient of friction is independent of load. It is noteworthy that the static coefficient of friction of rolled phosphor bronze is approximately 30% greater than sintered bronze, and that the type of grooving on the phosphor bronze plates makes little difference on the magnitude of the coefficient of friction. The greater static coefficient of friction of rolled phosphor bronze can probably be attributed to stronger welded junction at the tips of the surface asperities, whereas sintered bronze, being more heterogeneous and having low friction contaminating constituents of lead, tin, and graphite, probably has welded junctions of less strength and of less numbers.

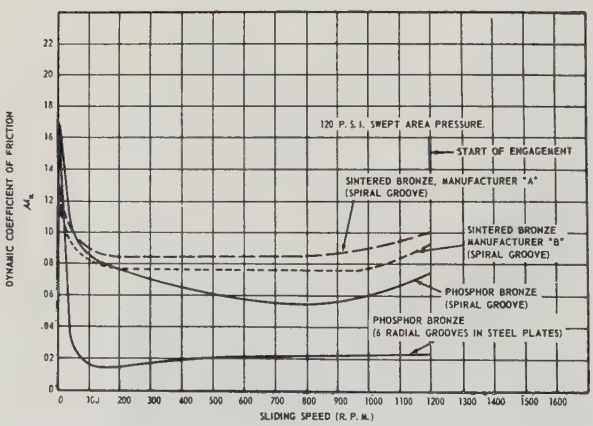

Fig. 17 — Variation of dynamic coefficient of friction during clutch engagement

Effect of Sliding Speed — The results plotted in Fig. 17 show the coefficient of friction is constant during a large portion of the engaging cycle. It should be noted that the coefficient increases rapidly between 100 rpm (115 fpm) to 0 rpm and approaches (but does not reach) the value of the breakaway coefficient of friction.

DISCUSSION

Shows Effect of Plate Load On Dynamic Coefficient of Friction

— F. E. Kronenberg
Caterpillar Tractor Co.

MR. LUDWIG has done an outstanding job in presenting a thoretical approach to the problem of heat generation in a clutch during engagement. As indicated in his paper, the heat transfer aspect would necessarily have to be considered in solving for the optimum engaging time. Control of the clutch mass temperature will influence the frequency with which the clutch can be engaged and still maintain its capacity characteristics.

In the overall analysis, the mechanism in which the clutch is installed usually dictates its requirements. The heat energy involved can be spread to a satisfactory degree during initial engagement by modulating the applied load and in the total cycle by sufficient surface area and cooling oil flow.

The experimental data presented in this paper has some interesting sidelights. It is rather surprising to us that all coefficient curves versus number of engagements start with the higher value than that for stabilized conditions. This may be an indication of too high an energy rate.

Our experience with single-disc, small-scale clutch testing results in about as many low, as there are high values.

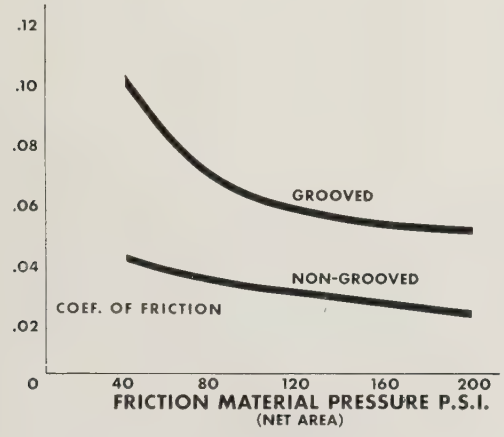

Fig. A — Friction material operating in oil

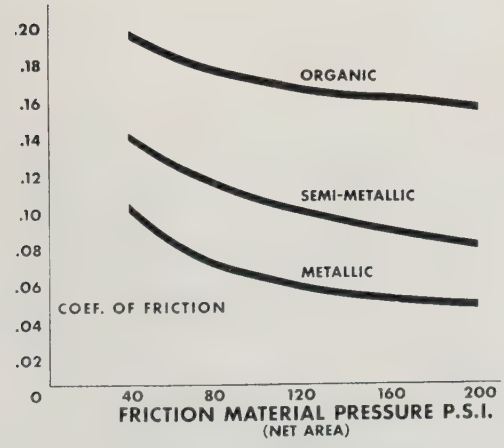

Fig. B — Grooved friction materials operating in oil

We attribute this varying condition to a change in the effective mean radius during the "wear in" process. We have not experienced the metal transfer shown for the rolled phosphor bronze material and wonder if other materials tested exhibit this condition during the initial engagement at 135 psi. Our test specimens are made reasonably flat to avoid high spots that can cause localized heating. Following a drag run for 2 hr at 20-psi load, several runs are made through a variable pressure range at two different engaging speeds to establish the material characteristics.

Grooving a material operating in oil does have a tremendous influence on the dynamic coefficient of friction. Fig. A shows a comparison of grooved and non-grooved metallic material. Note that the dynamic coefficient of friction of the grooved material is almost doubled at 200-psi net area and has an increasing trend as the pressure is reduced. The static coefficient of friction is usually in a range of 1¼ to 2½ times the dynamic. This variation has to do with the type of material and the dynamic value realized by the groove pattern selected.

We do not fully agree with the author as to the effect of plate load on dynamic coefficient of friction. Fig. B shows a comparison of three different types of friction materials. The dynamic coefficient of friction for these spiral grooved materials indicates a definite increase in the same general order as the pressure is reduced. Experimental data have shown that the more effective a groove pattern is in raising the coefficient of a material, the greater the load effect can be on the dynamic coefficient of friction.

Effect of Grooving Configuration On Engagement of Tractor Clutches

— K. C. Adams
Allis-Chalmers Mfg. Co.

ONE PHASE of our subject which Mr. Ludwig has presented so ably is the effect of grooving. I would like to add briefly to this phase of the discussion by relating some problems encountered in the development of the Allis-Chalmers Power Director clutches for the Model D14 and D17 tractors.

The Power Director is a system for transmitting power consisting of a dual-range transmission which includes two multiple-disc clutches that are selectively and alternately engageable with either range irrespective of ground speed and the pto drive. A neutral position between the ranges is provided. These two clutches must engage quickly to permit rapid speed changes without stopping the forward motion of the tractor, to permit the driver to start smoothly for inching the tractor, and to permit the driver to slip the clutches for short periods to provide infinite speed ratios.

These engagement characteristics obviously are conducive to large amounts of heat generation with the resulting wear and distortion of the friction and separator plates. Therefore, major problems in the development of the clutches were the selection of material which had an acceptable wear rate and provision of grooving and slotting configurations for cooling the plates. Determination of the proper material and grooving required patient and methodical testing of plates in both tractors in the field and clutch tester apparatus in the laboratory.

The clutch plates first tested were very similar to those used in the Model WD-45 transmission clutch. These plates were faced with a sintered bronze material with a dynamic coefficient of friction of 0.090 and a static coefficient of 0.123. The facing was spiral grooved 13 grooves per inch 0.020-in. wide. In addition, the facing had two pair of ⅛-in. wide wagon track grooves cut 90 deg to each other and crossing the spiral grooves. Although this clutch plate worked well in the Model D14 tractor, it proved to wear and warp excessively in the D17 clutches. Patient

and methodical testing of numerous plates of varying design followed.

The plate finally developed for the D17 also has a sintered bronze facing with dynamic and static friction coefficients of 0.099 and 0.121, respectively. The D14 spiral grooving was used; however, instead of two pairs of wagon track grooves, it was necessary to cut six parallel ⅛-in. wide grooves across the plate vertically and horizontally. In addition, it was necessary to provide six internal radial slots about a third through the facing.

Mr. Ludwig has stated that the presence of the gross effect of grooving configuration suggests a detailed analysis will yield fruitful results. I'd like to think that our work in developing clutch plate grooves has yielded such results.

However, it is apparent that much time and effort were involved in the development of satisfactory plates since a theoretical approach to the design of grooves for clutches, which would permit accurate design without much trial and error, had not been developed. Devising such a system should be a challenge to be met successfully in the near future.

Finds Author's Theory Impractical in Practice

— J. R. Ludwig
Dana Corp.

THE MATHEMATICAL analysis given in this paper is straight-forward. The theory is based on ideal conditions which in certain cases are impractical. I refer to a paragraph starting on p. 391 following Equation 4: "Under slipping conditions (dynamic) . . . pressure distribution must vary proportionately so as to provide equal work."

In practice, it is impractical to vary the pressure across the friction face to provide equal work by each surface particle.

The results described by Mr. Ludwig in tests which he had conducted are similar to our experiences. The type of grooving on the friction face not only has a tremendous influence on the dynamic coefficient of friction but also has an appreciable effect on dynamic drag encountered in multiple disc clutches.

Other factors which are very important on the engagement characteristics of wet clutches are surface finishes and treatments, type of lubricants, unit pressures, and types of friction material.

Rate of Heat Generation More Critical than Total Heat

— J. B. Snoy
Borg-Warner Corp.

THE USUAL wet-clutch engineering program consists of testing various friction materials, groove configurations, and apply pressure control systems. These methods, though producing results, are relatively crude. There is something to be gained from analyzing what is going on inside of a clutch during a shift as Mr. Ludwig has done. Mr. Ludwig's paper is a good, basic primer for any engineer who wants to think like a clutch, and you must think like a clutch if you are to develop a clutch.

I would like to comment on some of the analyses made in this paper and then some variations encountered in actual practice.

Two assumptions are made in the development of the formulas for mean radius: uniform pressure per unit area under static conditions, and uniform work per unit area under kinetic conditions. I do not see why the assumption of uniform pressure does not hold true both statically and kinetically. As pointed out in the paper, there is little difference in the final result and in actual practice the location of the mean radius and uniformity of unit pressure is influenced to a more pronounced extent by the deflection of the backing plate.

Mr. Ludwig's studies of total generated heat and rate of heat generation are of great interest since they are related to the most common type of failure in multidisc clutches, that is, a cremated clutch pack.

We have obtained data at Rockford Clutch that indicates that rate of heat generation is much more critical than total heat. In most cases the shift cycle occurs so fast that ability of the oil to do any cooling during the shift itself can be neglected. The oil *does* lower the average temperature of the pack, reduces wear rate, and also—unfortunate in this case—lowers the dynamic coefficient of friction.

In multidisc clutch packs with shift engagements of short duration, successful durability depends on the ability of the pack to carry the heat away from the surface of generation so that failure temperatures are not reached at that surface. In metallic plates this is determined by the specific heat and conductivity of the plate materials. Recently, nonmetallic, porous friction materials have been developed which *do* permit the oil to cool the surface of heat generation. The material is oil soaked and cooling is accomplished by the latent heat of evaporation—I am quoting. However, test results are very promising and it is not out of order to look forward to greater use of such materials in heavy-duty clutches since other benefits are obtained—namely, hard cores, conformability, and higher kinetic coefficients.

Another interesting study is the ideal clutch slip torque curve for constant rate of heat generation shown in Fig. 10. Mr. Ludwig states that a clutch with such an engagement characteristic is impractical. It is impractical only at two points—the beginning and the end—for you cannot go from zero torque to some value instantaneously nor can you have an infinite torque. An infinite torque, as well as being impractical, would be undesirable. With some modifications of the end points, such a curve can be duplicated and such a clutch is being produced today. Along with minimum rate of heat generation, a remarkably smooth shift is obtained and a study of the curves will tell you why.

At the present state of the art, all heavy-duty hot-shift transmissions consist of torque converters in series with a hydraulically shifted gear set. Now every one is fairly well-agreed that a torque converter is hard to beat for getting a heavy load moving, but once it is moving a solid gear train is more efficient to get the power from the engine to the wheels. The development of compact, durable, fast, and smooth clutches will soon bring us to the day where all heavy-duty hot-shift transmissions will be solidly shifted with converter used only for starting. This function of the converter may even be eliminated by the development of a good slipping clutch and studies such as the one reported by Mr. Ludwig will show the way.

Author's Closure To Discussion

I WANT TO THANK Messrs. Adams, Ludwig, Snoy and Kronenberg for their discussion of this paper and for the interesting and valuable comments on their related practical and experimental data.

I would like to comment briefly on several points. In the mean radius deviation for dynamic conditions, wear measurements form the basis for the assumption of uniform work per unit area. However, as pointed out by Mr. Snoy, deflections of the backing members often appreciably influence the pressure distribution and the mean radius location becomes unknown.

Mr. Kronenberg's comments on the influence of plate load on dynamic coefficient of friction is interesting and agrees with other experimental data which has come to my attention.

an evaluation of *AFTERCOOLING* in Turbocharged Diesel Engine Performance

J. E. Mitchell, Caterpillar Tractor Co.

This paper was presented at the SAE National Diesel Engine Meeting, Baltimore, Oct. 23, 1958

DURING the history of the internal-combustion engine and especially during the last 20 years, there has been a continuous and increasing pressure toward higher specific output. Within the diesel engine portion of this field, this drive toward more power for less bulk and weight has precipitated various approaches to the problem. Most of these have concentrated on supplying the engine with more air in one way or another, such as increased engine speed, refined engine air and gas handling systems for better breathing, and pressure charging with mechanically or turbine-driven compressors. This last approach brought with it the practicability of cooling engine charge air after its pressure and temperature were increased by the compressor to achieve another increase in air density and, in turn, an increase in the weight of air supplied to the engine. Using present-day engines as a basis greatly narrows the range of methods for developing higher output. Engine operational speed, for example, with a given engine and application would probably be limited by either the engine manufacturer or the user. Thus, any output increase would be largely dependent upon an increase in air supply by means of larger displacement or an increase in the density of the air supplied to the engine.

Turbocharging and Aftercooling

In the diesel industry at present, the turbocharger with a pressure ratio capacity of about 2/1 is just about the standard package for use on small and medium-size 4-stroke engines. Fig. 1 shows a cross-plot of the capabilities of the compressor of such a turbocharger relating the ratio of air density in-

AFTERCOOLING, coupled with higher pressure turbocharging can increase vehicle engine output. The author thinks that it is possible to anticipate diesel engines being run with compressors supplying air at pressure ratios higher than 2/1.

Density ratio is the most important consideration in increasing pressure ratio, since the engine's output is dependent upon weight rather than volume of air supplied. Because the density of the compressed air is dependent upon its temperature at any pressure level, cooling the air after compression results in density increases.

This paper describes various methods of aftercooling which increase engine output and fuel economy.

crease across the compressor to its pressure ratio, efficiency, and discharge air temperature, all for 90 F ambient air. Since the engine's output is dependent upon weight rather than volume of air supplied, the density shown here is the most important consideration. In turn, the density ratio is dependent upon compressor efficiency as well as pressure ratio for, as shown, an improvement in compressor efficiency from 60 to 80% at a pressure ratio of 2/1 produces a 6% higher density ratio and potentially 6% more air for the engine. Because the density of the compressed air is obviously dependent upon its temperature at any pressure level, cooling the air after compression to a pressure ratio of 2/1 results in the density increases shown in Fig. 2. Here a compressor efficiency of 75% is shown, with aftercooling of the compressed air to 200, 150, and 100 F. Air densities after such cooling are 7, 16, and 26% higher, respectively, with potentially a proportionate increase in engine air supply. Thus, there is good reason to consider aftercooling with superchargers presently in service.

It does not require any really long-range daydreaming to anticipate diesel engines being run with compressors supplying air at pressure ratios higher than 2/1. Expansion of the density, pressure, and temperature considerations to higher pressures are shown in Fig. 3. Here again a 75% efficient compressor was used with cooling after compression to 200, 150, and 100 F. At a pressure ratio of 3/1 the increase in density ratio by use of aftercooling to the above temperatures is 23, 35, and 45%, respectively, compared to the density ratio at a 3/1 pressure ratio with no cooling. A more reasonable consideration from an engine operational standpoint would be to compare the increase in density ratio of the high pressure ratio air with aftercooling, to lower pressure air without aftercooling. Use of the high pressure is generally contingent upon use of aftercooling to avoid high air-to-engine temperature which would result in a relatively small increase

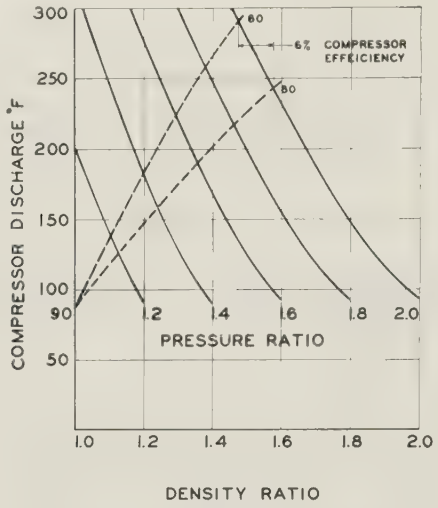

Fig. 1 — Compressor pressure ratio and efficency effect on density ratio

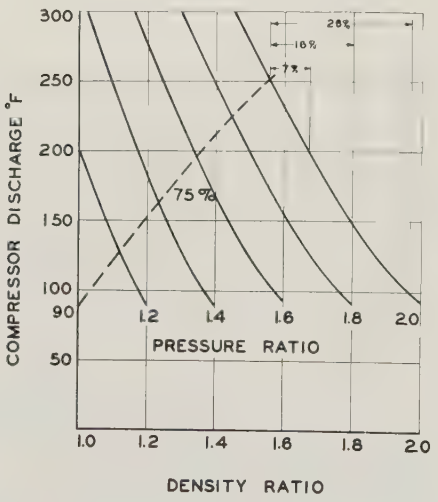

Fig. 2 — Aftercooling effect on density ratio of medium-pressure turbo

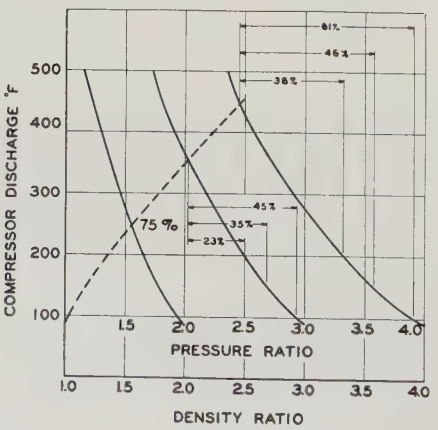

Fig. 3 — Aftercooling effect on density ratio of high-pressure turbo

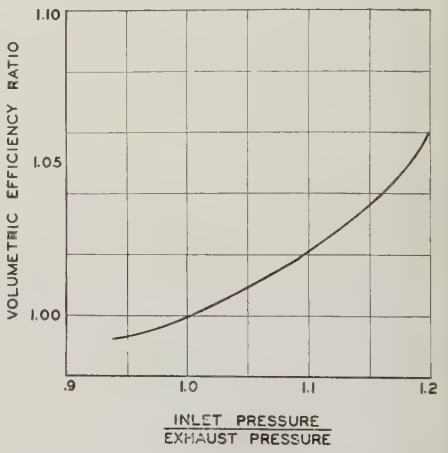

Fig. 4 — Engine volumetric efficiency related to inlet and exhaust pressure

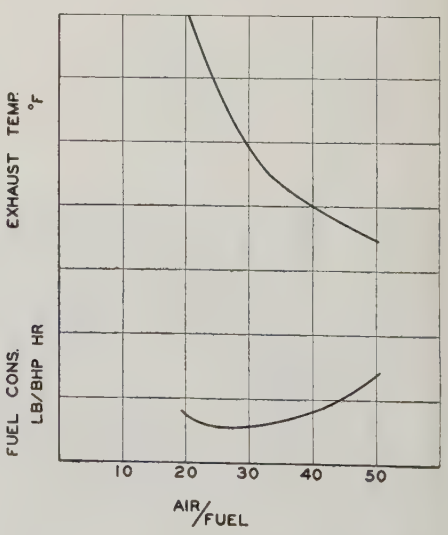

Fig. 5 — Exhaust temperature and fuel consumption at constant engine speed

in air supply achieved by a large increase in engine system temperature and pressure. For example, consider the density ratio of 1.55 achieved at a 2/1 pressure ratio without aftercooling as a base point. Use of a 3/1 pressure ratio machine with aftercooling to 200, 150, and 100 F will increase the density ratio to 2.50, 2.68, and 2.94. These reflect percentage increases in density ratio of 61, 73, and 90% which are very substantial gains. The increases attainable at a 4/1 pressure ratio are even greater (Fig. 3).

Diesel Engine Output and Thermal Load

This potential in air supply must be used by the diesel engine to produce power in order to be of use to the engine manufacturer or user. The engine development sequence described here used standard Caterpillar diesel engines. Since differences in basic engine types and sizes can make material differences in the precise numbers involved in the development of an aftercooled engine, the following data are presented on a comparative rather than an absolute basis for the sake of increasing their generality. A medium-pressure turbo will be considered as one with a pressure ratio potential up to about 2/1 and, in general, will be used in the range of ratios of 1.8/1 to 1.9/1. A high-pressure turbo will be considered as one with a pressure ratio potential over 2/1 with the operational data presented in the 2.2/1 to 2.5/1 range. Generalized background data presented in the following work cover a considerably broader range of pressure ratios.

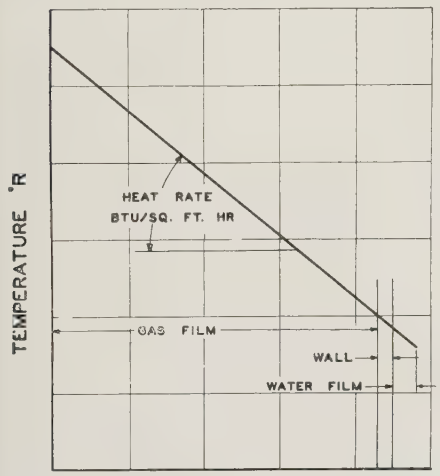

Fig. 6 — Wall temperature at given heat rate

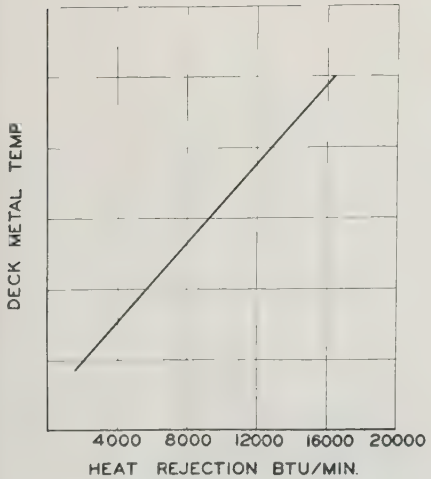

Fig. 7 — Deck temperature versus heat rejection

Engine volumetric efficiencies based on inlet manifold air conditions were checked over a wide range of engine loads, manifold pressures, and temperatures at constant engine speed (Fig. 4). On this engine, volumetric efficiency is basically a function of the pressure ratio across the engine cylinders. Since this is the case, it is quite simple to calculate engine airflow for any pressure level with any degree of aftercooling when turbo compressor and turbine efficiencies are known from manufacturer's data or have been found from tests. This air supply may be further tied into engine output through air/fuel ratio, specific fuel consumption, and exhaust temperatures at a given engine speed (Fig. 5). Brake specific fuel consumption is shown here since indicated conditions are extremely difficult to establish over a wide range of turbocharged engine operating conditions; also, the use of this approximation has been found to be sufficiently accurate. Exhaust temperature data are more useful if reduced to a given pressure level, which may be done with a simple isentropic expansion from the engine test condition pressures. Figs. 4 and 5, then, together provide a simple means of estimating engine output at any exhaust temperature, air/fuel ratio, turbo pressure level, turbo efficiency, and even with or without aftercooling. Again, tests have shown the calculation to be sufficiently accurate.

This completes the information needed to make engine output predictable within a practical range of engine test accuracy. However, it does not provide any insight into the thermal loading of the engine or any means of establishing control of thermal loading. Fig. 6 shows a relatively conventional picture of temperature distribution in and near an engine combustion space. The vertical scale is temperature and the horizontal scale is resistance to heat transfer, on which the gas film resistance, the metal wall resistance, and that of the water film are all plotted. The line joining the mean cylinder gas temperature and the coolant temperature has a slope equal to the heat rejection rate. So long as the coolant temperature remains relatively fixed, as it normally would on an engine in service, the wall temperature will vary with the mean cylinder gas temperature in the simple relationship of similar triangles. Also, since the coolant temperature remains constant, changes in the mean cylinder gas temperature or gas film resistance change the slope of the line, which means a change in heat rejection as pointed out above. Thus, the temperature of a given point in the metal wall is directly related to engine heat rejection. This relationship has been verified on engine tests over a broad range of operating conditions with the results as shown in Fig. 7. This relationship would, of course, break down if the characteristics of the heat transfer process at the metal-to-coolant surface should change materially. However, this did not occur within the range tested. These data were based on metal temperatures within the lower deck of the cylinder head directly above the main combustion space. Although actual temperatures would vary with the thermocouple location, relative temperatures around the combustion space are helpful in esti-

mating valve life and material requirements, piston heat loading and its influence on ring sticking, ring life, clearances, and the like, on a given engine configuration. The data indicate that on the engines tested, thermal loading can be controlled by limiting heat rejection from the engine. No alterations were made to the engine cooling system during these tests.

This, then, reduces the engine thermal load problem to one of heat rejection which can be measured with relative ease and over which we can maintain some control, as shown in Fig. 8. These data compare engine heat rejection to the cooling system for a simple turbocharged engine to that for the same engine equipped with an aftercooler which maintains a constant air-to-engine temperature. Notice that at a given output the engine without the aftercooler has a higher heat rejection rate than the engine with the aftercooler when the heat carried off by the aftercooler is considered separately. However, when the heat to the aftercooler is added to the engine heat rejection, the total heat rejected is found as shown, which is very nearly identical to that for the original engine. Engine data have verified this over a wide range of conditions. Thus, it provides a useful tool for predicting engine heat rejection and, in conjunction with Fig. 7, thermal loading for various engine ratings, degrees of supercharge, and aftercooling.

Table 1 — Aftercooler Summary

Aftercooler Type	Air to Engine Water	Air to Air	Air to Cold Water
Air Temperature from Cooler, F	200	150	100
Relative Size	Small	Large	Small
Installation on Engine	Simple	Complex	Simple
Usable on Vehicle	Yes	Yes	No
System Used in This Development	V		

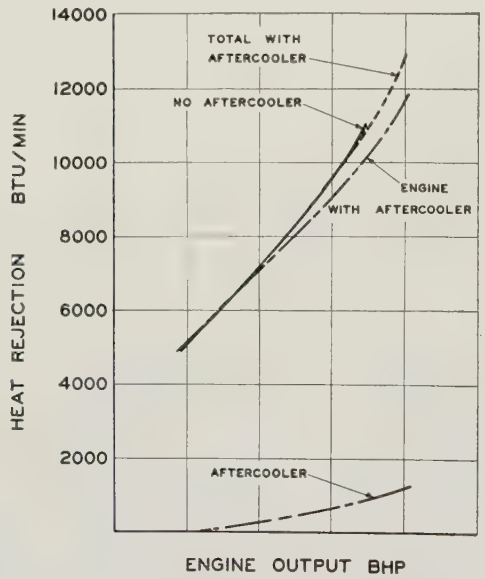

Fig. 8 — Heat rejection with and without aftercooler

Fig. 9 — Engine output at constant exhaust temperature and constant engine speed

Fig. 10 — Engine heat rejection at constant exhaust temperature and constant engine speed

Fig. 9 carries the engine output characteristics shown in Figs. 4 and 5 along further and indicates output attainable from a turbocharged engine with and without aftercooling as a function of turbocharger pressure ratio with constant engine speed and constant pre-turbine exhaust temperatures. Engine output is shown as a multiple of the output of a naturally aspirated engine running at the same exhaust temperature. The constant pre-turbine exhaust temperature condition that was used here as a basis for comparison is a logical one in that it is one of the limitations under which a turbocharged engine operates and which may be dictated by the metallurgy of engine parts exposed to exhaust gases, as well as turbine parts in the hot gas stream. It is a more realistic limitation than air/fuel ratio, since exhaust temperatures rise at constant air/fuel ratios with increasing pressure levels from higher pressure turbocharging. All work in this report has been held to this temperature limitation so that it is comparable. Within this limitation the engine output increase attainable with turbocharging, with and without aftercooling, is clear.

In the same manner, Fig. 10 shows engine heat rejection to coolant, excluding heat to the aftercooler, as a function of turbocharger pressure ratio at constant engine speed and with the same fixed pre-turbine exhaust temperature as that used in Fig. 9. Heat rejection is also given as a multiple of that rejected at the same exhaust temperature by the naturally aspirated engine. Note that this is total heat per minute, not specific heat rejection, since total heat rejection is a measure of thermal loading and that is the major point of interest. Notice also that this total heat rejection rate increases with both pressure charging and aftercooling with the

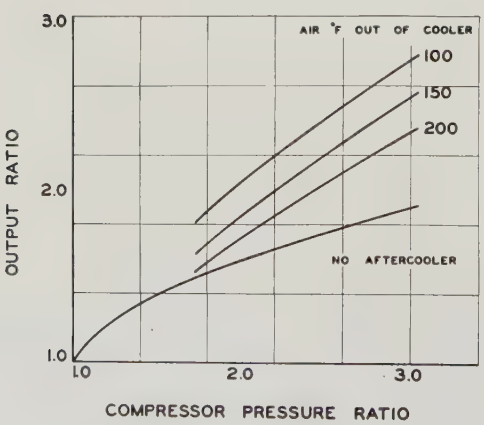

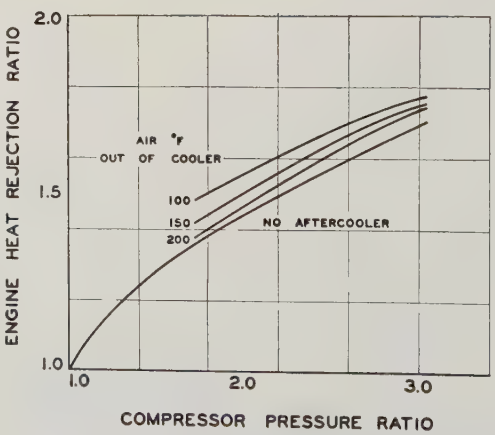

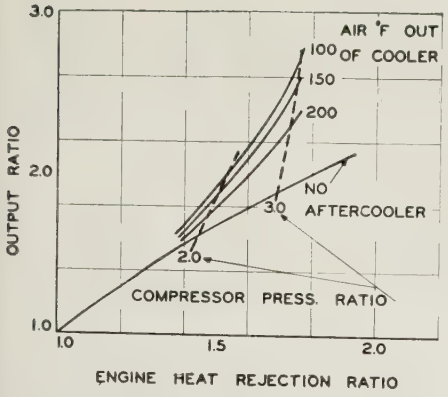

Fig. 11 — Engine output and heat rejection at constant exhaust temperature and constant engine speed

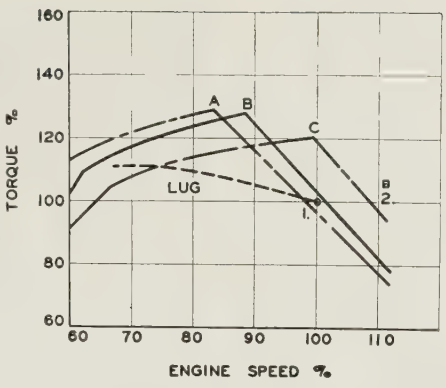

Fig. 12 — Engine torque of medium-pressure turbocharger without aftercooler

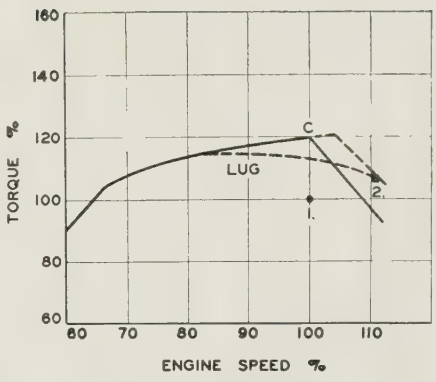

Fig. 13 — Engine torque of medium-pressure turbocharger without aftercooler

constant exhaust temperature maintained, even though we know that the specific heat rejection rate would decrease. This is important since it indicates a method of increasing turbocharged engine output without or with a controlled increase in engine heat rejection, by use of aftercooling. However, it would require more excess air and a reduction in exhaust temperatures.

Fig. 11 shows the interrelationship of output and heat rejection from Figs. 9 and 10 for the same exhaust temperature limitation and engine speed. A vertical line on this sheet is a line of constant heat rejection. Thus, control of engine heat rejection may be established by use of this type curve by relating desired output to the acceptable thermal loading and the degree of turbocharging with aftercooling that are considered practical. Further, these curves may be drawn for several exhaust temperatures and that variable may also be considered. From these data, the output gain attainable at a 2/1 pressure ratio is seen to be appreciable, but it is small compared to the potential at higher ratios.

Aftercooler Application

Applying these principles to an actual engine, the most logical place to begin is the nonaftercooled turbocharged engine. Fig. 12 shows the output limits of such an engine turbocharged to a pressure ratio between 1.85/1 and 1.90/1 without an aftercooler. The three limit curves A, B, and C show the operational limits of this engine when three turbine nozzles with different areas are considered. The lines sloping down to the right represent the limitation due to maximum acceptable turbocharger rotational speed, the central portion of each curve represents the limits set by maximum acceptable exhaust temperature, and the curves sloping sharply down to the left represent an engine exhaust smoke limitation. These limits are those considered acceptable in view of desirable life, available materials, and customer acceptance, and are generally somewhat below the true maximum for any of them. The exhaust temperature limit is the same as that used earlier. A vehicle rating of this engine is shown at point 1 as 100% speed and torque, while engine lug operation is indicated by the dashed line. Notice that this engine operational curve fits nicely under limit curve B, which is that turbine nozzle used for this engine application. Curve A, then, represents operational limits with a smaller turbine nozzle and C a larger turbine nozzle. This rating is satisfactory for this engine-turbocharger combination. However, suppose a rating at point 2 were required. This rating could not be reached within the limits shown for these three nozzles. It could, however, be reached by nozzle C as shown in Fig. 13, if the limiting turbocharger rotational speed could be increased as shown by the dashed line. Even if that were done, lugability for vehicle operation or the characteristic of an increase in torque with decreasing engine speed would not be sufficient for satisfactory operation and its altitude capability would be decreased.

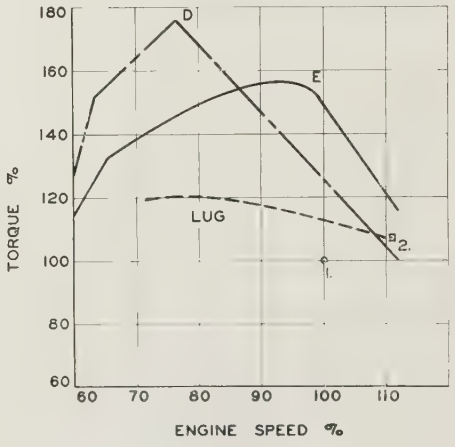

Fig. 14 — Engine torque of high-pressure turbocharger without aftercooler

The next logical method of achieving the desired output increase would be the application of a turbocharger capable of higher pressure ratios and associated higher airflow. The limits established by such a turbo are shown in Fig. 14 where the limits are similar to those discussed previously for the lower pressure turbo of Fig. 12. Here, turbine nozzle E could completely satisfy the engine output demand at rating point 2 as well as supply adequate part speed lugability, at least as far as turbine speed, exhaust temperature, and smoke are concerned.

Another logical method of achieving the higher rating would be the use of aftercooling with no increase in turbo pressure ratio. However, the practical application of aftercooling to a vehicle engine leads to many considerations. First, within reasonable limits, the cooler the air supplied to the engine, the higher its potential output. However, the problem of obtaining cool air on a vehicle becomes rather complex. Table 1 shows a summary of the more

logical cooler configurations with some of their assets and liabilities. The simplest cooler for vehicle use is the one using engine water, which is easy to install, and could provide the engine with air at about 200 F. A direct air-to-air cooler would probably be larger and its installation more complex; however, it could supply the engine with air at 150 F or less. To achieve 100 F air at maximum pressure to the engine, a cold water source would be required. This is impractical for vehicle use, but could be quite practical for many industrial applications. In the overall view of the problem, it was decided that the air-to-engine water cooler could best be used for immediate development needs. That is the type unit considered here.

Engine output limitations using the medium-pressure turbo with the air-to-engine water cooler are shown in Fig. 15. The maximum output was materially improved over the nonaftercooled engine which was shown in Fig. 12 and now the desired output at point 2 may be obtained with relative ease using turbine nozzle size J. However, using this nozzle the engine has a limited high torque operating range, since the largest gain by aftercooling occurs at high turbo pressure output while there is little gain at low output. Thus, engine lug operation as shown with nozzle J would not be satisfactory for vehicle use.

Considering only engine constant speed and part-load data as shown in Fig. 16, there are real advantages for the aftercooled engine compared to the nonaftercooled engine which was turbocharged high enough to obtain the same output. These data were run on standard Caterpillar engines of the same type modified, only to the extent necessary to manifold the two different turbochargers and the aftercooler properly. All of these data are important to the engine. Notice the relatively high airflow with low inlet manifold pressure obtained with cooling and the resultant low exhaust temperatures. The lower heat rejection to the engine coolant with the aftercooled engine is, of course, quite significant in itself, but even more so since it reflects lower metal temperatures around the combustion chamber. Fuel consumption also shows some advantage for the cooled engine over most of the range. From just about all viewpoints then, the engine indicates that it prefers to run aftercooled rather than at a high pressure to achieve the same output.

Fig. 17 shows why the deficiency in lug occurs and why achieving satisfactory lugability with a turbocharged engine requires careful consideration. This shows the engine air demand over the lug range as pictured in relation to a turbocharger compressor characteristic. At rated engine speed, represented by the right edge of the engine operating range, the turbo is run up to the pressure ratio necessary to provide air for the desired output of the engine at its rating. Operation at this condition is quite satisfactory. However, as the engine is overloaded and lugged down (as it frequently is in tractor operation), the engine air supply decreases as shown across the top of the engine operating range. This is due not only to loss of engine speed but is compounded by a decrease in turbo pressure output, which to varying degrees characterizes free-running turbocharger operation. This results in a decreased air supply per engine cycle under lug where the specific engine output requirement is highest. This problem may be handled in several ways. For example, a turbocharger capable of operation considerably above the engine requirement at rated output may be used so that sufficient air for engine lug may be supplied with the result of excess air at rating. This, of course, is the most used approach.

Turbocharger Control

From the standpoint of maximum lugability it would be desirable to have the engine air supply as shown in Fig. 18, where the turbo speed is shown constant over the engine lug range with the increase in pressure and airflow (as shown by the cross hatched area). This would result in a more-than-adequate air supply for the engine during lug and could materially improve that type operation.

Fig. 19 shows the operational limit curves for the aftercooled engine with four turbine nozzles, as discussed previously. With any one of these nozzles it is clear that the wide high output range indicated in Fig. 18 would be unattainable. Notice that each of these limit curves reaches a maximum point where the turbine speed and exhaust temperature limits intersect. A line drawn through these peaks then represents the simultaneous limits for an infinite number of turbine nozzles or a variable nozzle. This could, of course, produce the desired range of operation. However, such a mechanism would quite possibly be somewhat expensive, especially on relatively small engines, as well as being difficult to maintain from a functional viewpoint in the engine exhaust atmosphere.

A substitute for this rather complex mechanism

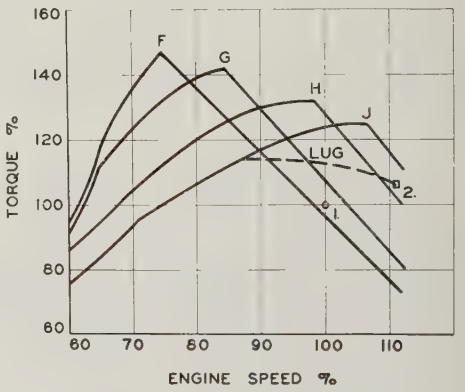

Fig. 15 — Engine torque of medium-pressure turbocharger with engine water aftercooled

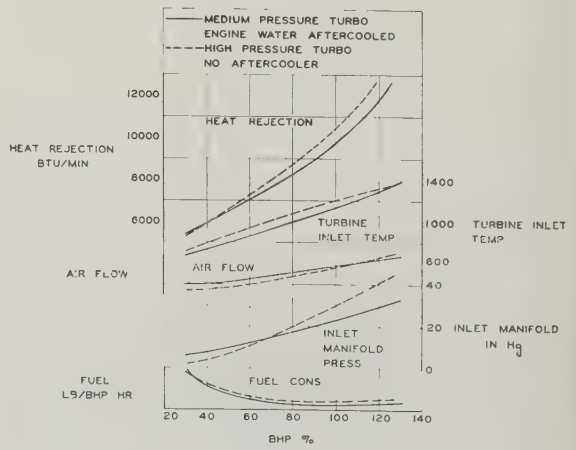

Fig. 16 — Constant speed and part load data

has been in use for years on turbocharged aircraft engines in the form of a controllable bypass around the turbine. This type control is used in conjunction with a small turbine nozzle such as F in Fig. 19. The exhaust bypass opens sufficiently to prevent turbine overspeed at high engine output. With such a unit installed, engine maximum output is slightly less than that with a variable nozzle and is shown as the dashed line in Fig. 19. Thus, while it does not duplicate the performance of the variable nozzle, it approximates it with a much simpler mechanism.

Use of this type of control on an engine produces an airflow requirement as shown in Fig. 20. The unit used by Caterpillar actually measures and controls compressor pressure ratio. The exhaust gas bypass valve is of a simple poppet type and is actuated hydraulically by engine fuel pressure. This control has shown itself capable of producing the desired range of operation and was adopted for that purpose. The increase in engine airflow at reduced engine speed is evident compared to that when the control was not used, as shown in Fig. 17.

Aftercooler and Control Application

Engine operational limits with the proper turbine nozzle and using the aftercooler in conjunction with the exhaust bypass control are shown on Fig. 21. The lug curve shows very good vehicle operation from the new higher rating at point 2.

Fig. 22 shows a comparison of engine lug data for this engine with the medium-pressure turbo rated at 100% speed and output. Also shown are the two methods of achieving the increased rating: (1) the same medium-pressure turbo plus exhaust bypass control with aftercooling and (2) the higher pressure turbo with neither control nor cooler. All these data are plotted against engine speed, and in all cases the aftercooled and controlled engine shows up very well. The increase in rating is evident from the horsepower output curves, but the horsepower at part engine speed of the controlled and aftercooled engine is considerably above that achieved with the high-pressure turbo. A comparison of the airflow data to a large extent explains this with the aftercooled engine considerably superior. Exhaust temperatures on the aftercooled engine are lower than the nonaftercooled engine. The output increase with the aftercooled engine did not require

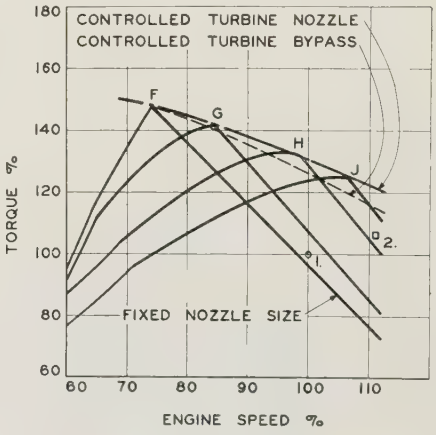

Fig. 19 — Engine torque

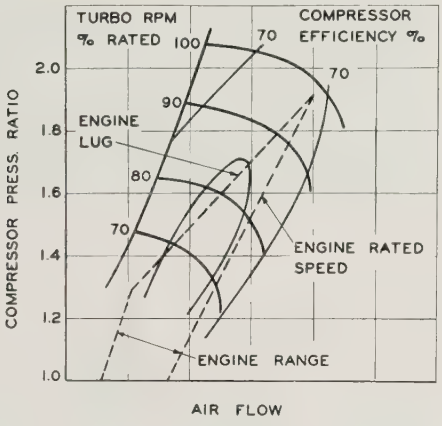

Fig. 17 — Engine-turbo relationship, medium-pressure turbo with engine water aftercooled

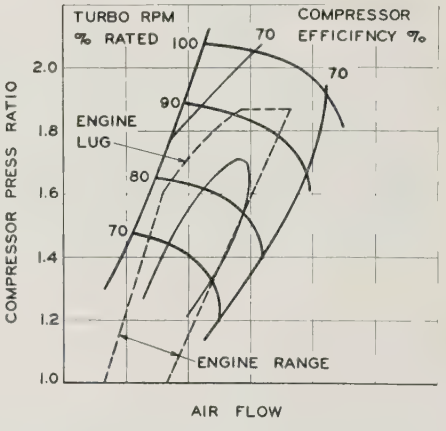

Fig. 20 — Engine-turbo relationship, medium-pressure turbo with controlled turbine bypass and engine water aftercooled

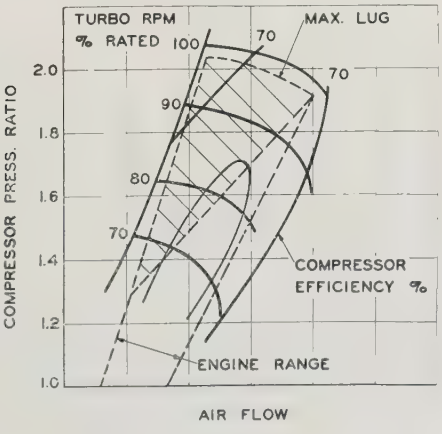

Fig. 18 — Engine-turbo relationship, medium-pressure turbo with constant speed control and engine water aftercooled

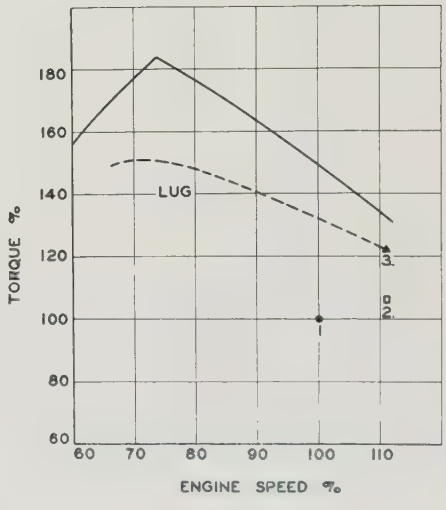

Fig. 21 — Engine torque of medium-pressure turbo with engine water aftercooled and controlled turbine bypass

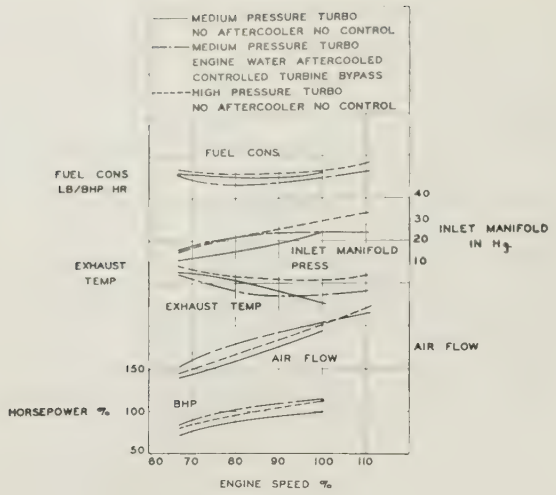

Fig. 22A — Engine lug

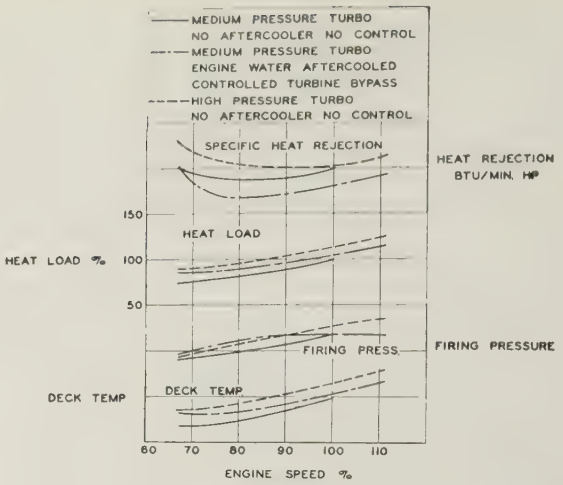

Fig. 22B — Engine lug

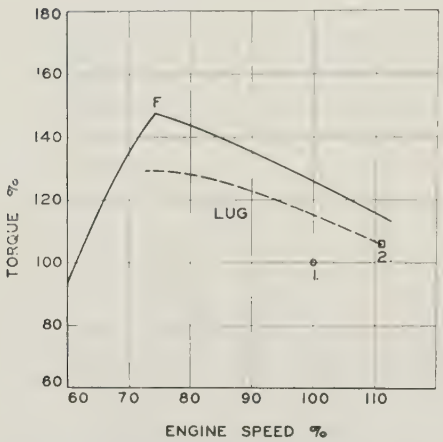

Fig. 23 — Engine torque of high-pressure turbo with engine water aftercooled and controlled turbine bypass

any increase in engine inlet pressure, a significant factor from the viewpoint of engine mechanical loading as well as demand on the turbocharger. Finally, in Fig. 22 fuel consumption on the aftercooled engine is improved over either of the other engines. In Fig. 22A, deck temperatures and heat load or heat rejection go together as was developed earlier; and the advantage of the aftercooled engine is evident. Notice the advantage of the aftercooled engine as far as specific heat rejection is concerned. Finally, there is a definite advantage for the aftercooled engine as far as firing pressures are concerned — a significant item in engine design.

While all these data show a very definite advantage for the aftercooled engine with its medium-pressure turbo as compared to the nonaftercooled engine with the high-pressure turbo, it certainly does not indicate that the high-pressure turbo should never be considered. Quite the contrary, Figs. 3 and 11 show that higher pressure turbocharging has much to offer, but it should be used in conjunction with aftercooling to reach its best potential. Without aftercooling, the engine pays a heavy price in terms of increased mechanical and thermal loads for a limited output increase. Fig. 23 shows a limit curve and engine lug curve from

Table 2 — Engine Development Summary

Engine	1	2	3	4
Turbo Pressure Ratio	1.9	2.2	1.9	2.2
Controlled Turbine Bypass	No	No	Yes	Yes
Engine Water Aftercooled	No	No	Yes	Yes
Engine Rated Rpm, %	100	111	111	111
Rated Bhp, %	100	118	118	136
Rated Bmep, %	100	106	106	123
Lug Torque Rise, %	100	108	175	191
Exhaust Temperature, %	100	108	104	107
Air/Fuel at Rating, %	100	97	100	98
Firing Pressure, %	100	115	100	120
Specific Heat Rejection, %	100	106	97	92
Heat Load, %	100	124	115	125
Deck Temperature, %	100	106	104	106

a still higher rating at point 3 achieved by use of the high-pressure turbocharger in conjunction with the aftercooler and exhaust bypass control. This again is a sound and very satisfactory operating condition, as shown in the comparative engine lug data in Fig. 24. These data compare the medium- and high-pressure turbocharged engines, both with aftercoolers and exhaust bypass controls. In this case both mechanical and thermal loads have been increased, requiring careful reconsideration of engine parts affected. But with proper design the result is a sound, high output engine that makes good use of the pressure potential of its turbo and operates very well for the vehicle application.

Summary

Table 2 shows a summary of comparative data on this engine with the medium-pressure turbocharged engine, with neither turbo control nor aftercooler as the reference unit. The direct comparisons of this chart help point up the applicability of the aftercooler to this type vehicle engine.

Fig. 25 shows a Caterpillar production engine currently applying these principles of turbocharging, turbo control, and aftercooling. Notice the rather simple installation of the pressure ratio control, the exhaust bypass valve, and the aftercooler.

The information presented in this report shows the successful application of a well-known basic principle, namely aftercooling, to vehicle engines in conjunction with higher pressure turbocharging to achieve increased output, and use of a simplified turbocharger control to expand greatly the utility of the power-producing package.

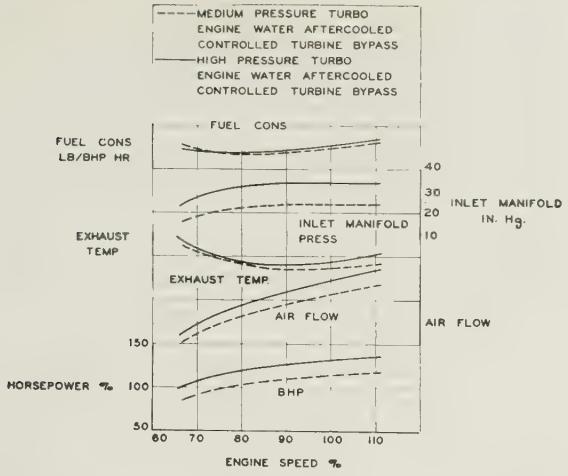

Fig. 24A — Engine lug

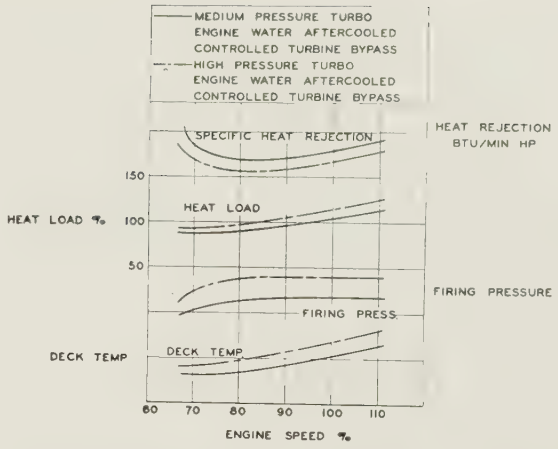

Fig. 24B — Engine lug

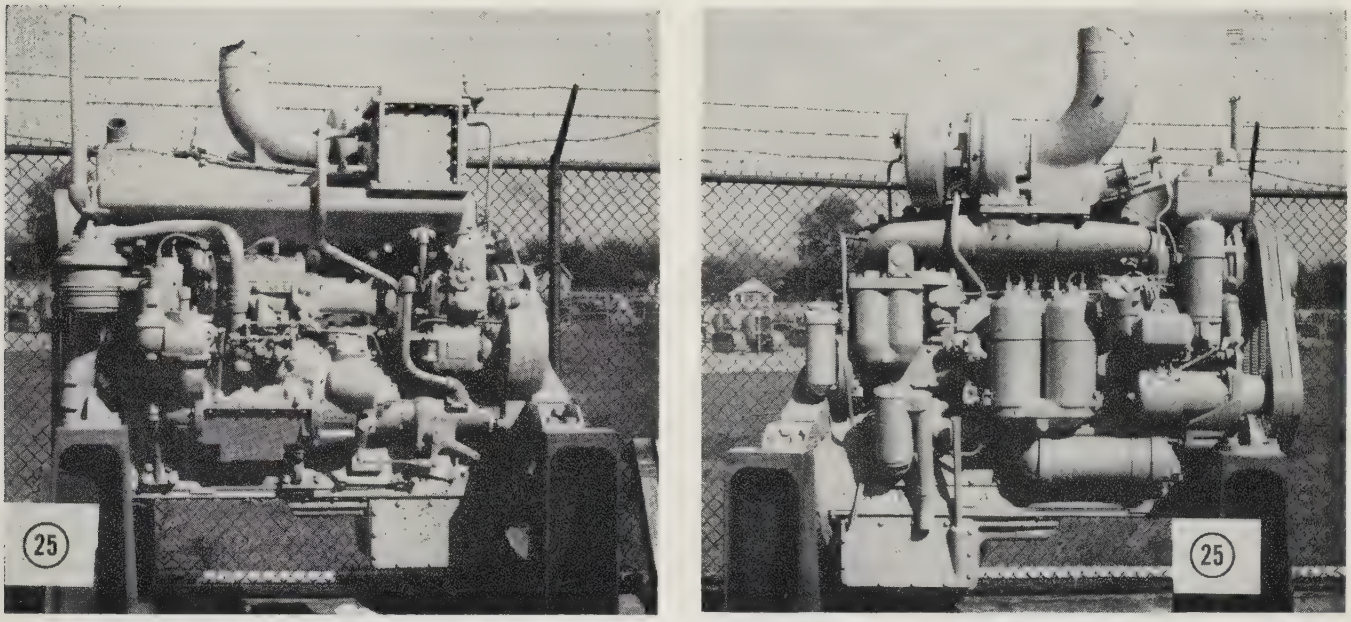

Fig. 25 — Caterpillar production engine applying principles of turbocharging, turbo control, and aftercooling

DISCUSSION

Charge Aircooling Increases Turbocharger Compressor Operating Range

— Hans Egli

AiResearch Industrial Division
Carrett Corp.

THE SPEAKER is to be congratulated for his very comprehensive presentation of the advantages of charge aircooling for turbocharged 4-stroke high-speed diesel engines. Whereas this basic principle is fairly old and has been used successfully for many many years, mainly on large stationary and marine engines, Caterpillar Tractor Co. has really pioneered its application to high-speed engines for vehicle usage.

I presume that Figs. 9, 10, and 11 apply to one and the same engine with always the same engine compression ratio resulting in increasing firing pressures with increasing degree of turbocharging. Fig. A shows a similar graph, indicating maximum engine output on the basis of constant exhaust temperature for constant firing pressure instead of constant engine compression ratio. This graph has been made some time ago, essentially for the purpose of showing what power increases can be obtained by turbocharging with and without charge aircooling without an increase of peak pressures and exhaust temperature. Obviously, the

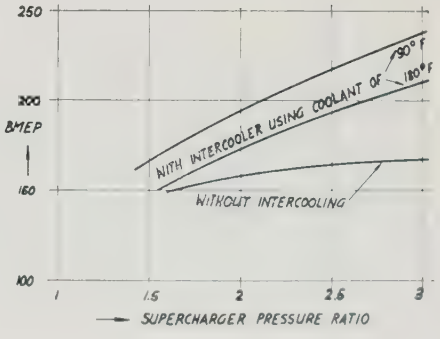

Fig. A — Engine performance as affected by intercooling

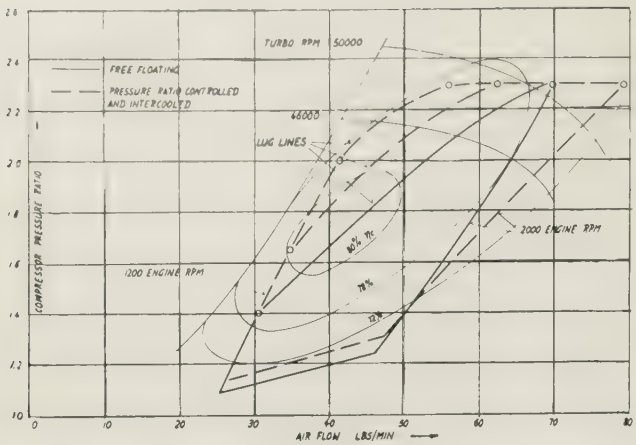

Fig. B — Effect of turbocharger controls and intercooling on selection of turbocharger

power increase is smaller than shown in Fig. 9. The graph points out even more drastically the need for charge air-cooling for high-pressure turbocharging.

Peak firing pressures will always be a very important criteria in engine mechanical loads. Therefore, the system with the lowest permissible boost pressures for a given output will permit the highest engine compression ratio with a correspondingly better specific fuel consumption and better cold-starting characteristics. Aftercooling, as well as turbine bypass control, also helps considerably in this respect.

People often say that the approach of turbine bypass system wastes exhaust gas energy in a certain operating region. In this respect I would like to re-emphasize the small difference in output obtainable with an ideal variable area turbine nozzle in comparison to a turbine bypass, as has been shown on Fig. 19. One of the reasons for this small difference is, of course, the very large kinetic energy loss of the turbine discharge gases of today's small automotive-type turbochargers. The bypass controlled turbine has a more favorable discharge loss which compensates, to quite some extent, for the bypassed energy.

Charge aircooling makes high-pressure turbocharging feasible with respect to thermal loading. It will, however, in conjunction with the necessary lugging characteristics, increase the requirements for broadness of the turbocharger compressor characteristic. Fig. B basically indicates this trend already for a pressure ratio of only 2.3. I do not mean to say, however, that this should be a reason for not using charge aircooling—it represents merely a challenge for developing high-pressure turbochargers suitable for engines having lugging requirements. It, of course, points out the increasing necessity for looking at engine, turbocharger, charge aircooling, controls, and possibly other components from an overall system point of view with very close cooperation of the different manufacturers of components.

Describes Diesel Tests With Turbocharger Using Blowdown Exhaust Manifold System

— J. P. Matthews
Cooper-Bessemer Corp.

SEVERAL of us at Cooper-Bessemer read this paper with particular interest since we have been concerned with various combustion air-conditioning systems and their influence on engine performance variables since about 1950. Mr. Mitchell's paper is concerned primarily with results obtained from tests of a relatively high-speed automotive-type 4-stroke diesel engine employing a medium-pressure turbocharger and a steady flow or constant pressure exhaust manifold system. Our most similar product is a 9×10½ 4-stroke diesel engine with a medium-pressure turbocharger using the pulse or blowdown exhaust manifold system. This engine is rated 197 bmep at 1000 rpm. Its primary application is in diesel-electric locomotive service. For this service an air-to-engine water aftercooler is used.

We have performed rather extensive tests on this basic engine in order to determine its sensitivity to combustion air temperature. Results of these tests were almost identical to those shown by Figs. 8–11.

Much of our work with combustion air-conditioning systems since 1950 has been done with our lines of low-speed, heavy-duty, 4-stroke turbocharged high-compression gas engines in mind. Combustion air conditioning, more than any other single factor, has permitted a rating increase of more than 43% for our line of 15½ × 22 engines of this type.

Fig. C is a plot of percentage rating versus manifold air temperature for 4-stroke supercharged gas engines, reflecting data obtained from a number of tests on different engines. Detonation or rough combustion will occur if the engine is operated in regions above the curve. The change in slope of this "detonation limit" line is rather difficult to explain. It should be pointed out that, during our tests at air manifold conditions below approximately 100 F, the air was approaching or had become supersaturated and the benefits of wet compression were realized. We do not feel that this accounts for the total change in slope indicated, but we have no other explanation at this time.

Fig. D is a cross-section wash drawing of a turbo machine which we call a turbocooler. This machine is used to obtain the low-combustion air temperatures necessary for the higher rated turbocharged gas engine.

The unit mounts in the combustion air line between the turbocharger and the air manifold. The rotor is composed of a booster impeller and a radial inflow turbine or expander wheel mounted back to back on a common shaft supported by two end bearings. Appropriate casings are used to enclose the rotor.

Combustion air from the turbocharger enters the booster impeller as shown. The booster impeller recompresses the air and discharges it at a considerably higher pressure and temperature. From the booster impeller, the air enters an air-to-water heat exchanger where, by virtue of the high air temperature, it is possible to transfer much more heat to the cooling water than would have been possible with the air temperature reached after only one stage of compression as in normal aftercooling. Cooled air from the heat exchanger is expanded through the turbine wheel; and since the turbine does work by driving the booster impeller, the air is cooled upon expanding. The turbine expansion ratio (and the booster compression ratio) is varied by adjustment of the expander nozzle area. Nozzle area adjustment is accomplished automatically by the engine air/fuel ratio control system.

The turbocooler is capable of producing combustion air temperatures considerably lower than the temperature of the water available to the air-to-water heat exchanger.

A considerable part of Mr. Mitchell's paper is devoted to turbocharger matching for maximum or adequate engine

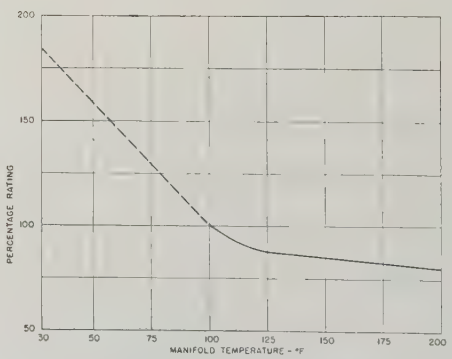

Fig. C — Percentage rating versus manifold temperature for 4-stroke supercharged gas engine

lug. Lug torque rise—or lack of it—has long been a problem to manufacturers and operators of automotive-type internal-combustion engines. Conventional turbocharger matching, rather than improving engine response rate, has magnified the problem. Any solution short of controlled nozzle area and controlled diffuser width is a compromise. Controlled turbine bypass appears to be a good compromise, the only apparent disadvantages being: (1) wider turbo blower operating range requirements dictating impeller designs which are not applicable to higher pressure ratio machines, and (2) slightly higher brake specific fuel consumption during operation at and above engine rated speed and torque conditions. We would like Mr. Mitchell's observations on these two points.

An alternative solution to the problem of supplying adequate combustion air for maximum engine response to rapid and extreme torque increases is one that we have recently used quite successfully. This particular job involved the application of one of our basic $9 \times 10\frac{1}{2}$ turbocharged 4-stroke diesel engines to an engine generator set for welding continuous rail. The unit was to operate at 900 rpm, at which speed a maximum of 211 bmep would be required.

A complete load cycle consisted of a rail-heating cycle followed by the rail-welding cycle. The heating cycle required 15 repetitions of subcycles composed of 1.8 sec at full load and 1.4 sec at no load. The welding cycle involved a 12-sec period composed of momentary full load, a period of approximately one-half load, and ending with momentary full load.

By equipping the engine with a crankshaft-driven centrifugal blower, piping the discharge air from this blower to the inlet of a high-pressure turbocharger, and employing air-to-jacket water aftercooling, the unit was capable of handling the extreme load fluctuations with practically no speed droop and no exhaust smoke. Also, no controlled turbine bypass was required. A supercharging system such as this provides a higher engine response rate than that which is obtainable from a purely turbocharged unit. The major disadvantage of the system is the parasitic load imposed by the engine-driven blower—another compromise.

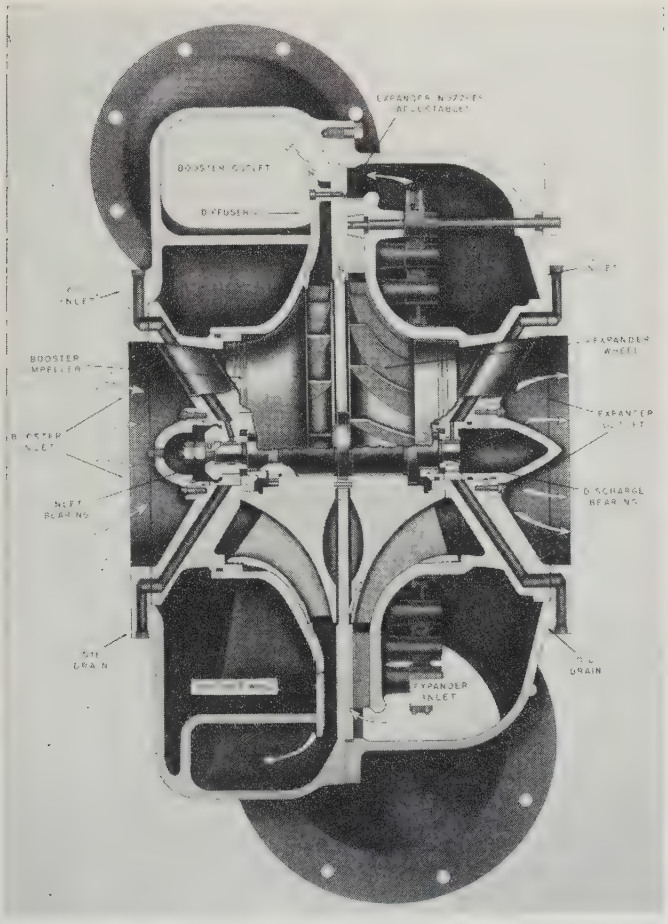

Fig. D — Turbocooler used to obtain low combustion air temperatures

Aircooling and Turbine Bypass Control Improve Output and Fuel Economy of Diesel

— G. W. Phillips
Detroit Diesel Engine Division
General Motors Corp.

IT IS APPARENT from this paper that aftercooling combined with turbocharging has provided another step toward raising the specific output of the diesel engine.

At Detroit Diesel this type of cooling has been successfully applied to the 2-stroke 6-71 turbocharged engine. Because of the greater cooling potential with cold water, we have concentrated on the marine application where an ample supply of cold water is always available. Tests have indicated that approximately two to four times more gain in performance is obtainable with 80 F raw water than with 180 F engine water as a source of cooling.

In comparing the application of aircooling to both the 2- and 4-stroke engines, I would like to point out that on the 6-71 engine the aircooler is mounted between the turbo compressor and the Roots blower as shown in Fig. E and, therefore, we refer to this as intercooling rather than aftercooling.

The 6-71 turbocharged engine, however, has a natural aftercooler built into the airbox. After compression by the compressor and the Roots blower, the air is discharged into the airbox, which is partially bounded by the cylinder water jacket which extends the entire length of the cylinder and airbox and contains cooling water at approximately 180 F. With no intercooler the air temperature leaving the Roots blower is sufficiently high so that the jacket water lowers the temperature of the incoming air and is, in effect, an aftercooler using engine water as a coolant. With an intercooler installed ahead of the Roots

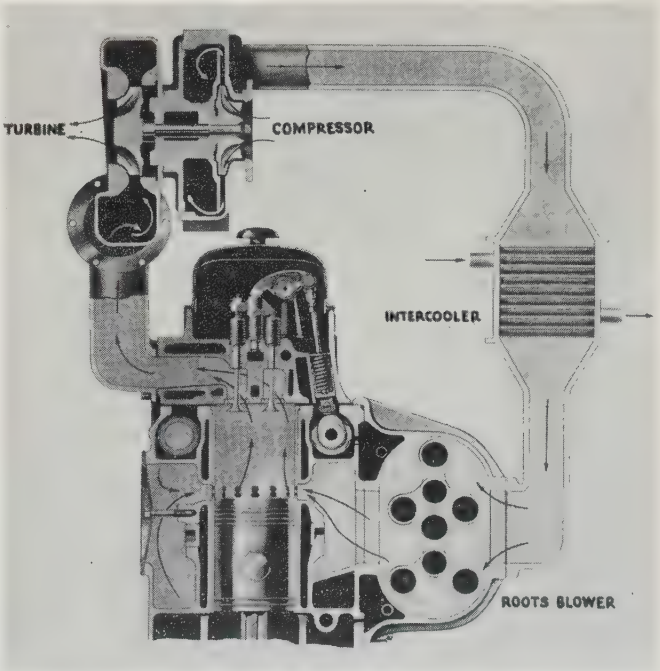

Fig. E — General Motors 2-stroke 6-71 turbocharged diesel engine with intercooler

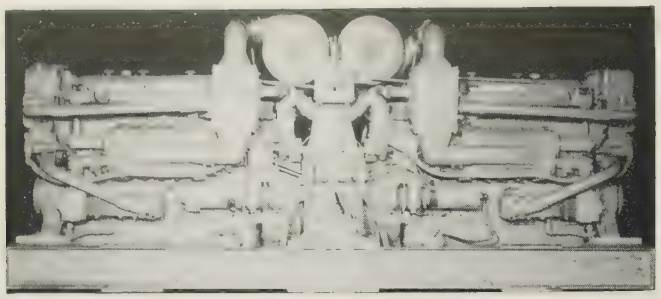

Fig. F — Tandem twin 6-71 turbocharged marine unit with intercooling

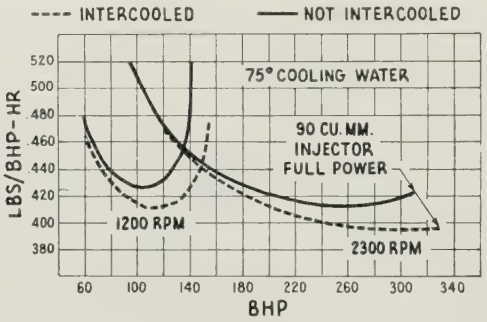

Fig. G — Effect of intercooler between compressor and Roots blower 6-71 turbocharged engine

blower, however, the temperature into and out of the blower is lowered considerably. The effectiveness of the airbox aftercooler is then greatly reduced, since the air-to-jacket water differential is reduced.

It can be seen that this would be an advantage in the nonintercooled engine where the air-to-water temperature differential is great but would show a reduced net gain when intercooling is applied. Additional aftercooling has been tested using water tubes with cooling fins installed in the airbox, however, the additional gain in performance was small when used in conjunction with intercooling and the added cost has not been justified.

A production tandem twin intercooled marine unit is shown in Fig. F. The two 6-71 engines are coupled together and driven through a reduction gear and a single output shaft. Each engine has a separate turbocharger, intercooler, Roots blower, and raw water pump. The intercooler takes the full engine raw water flow of about 80 gpm in a single pass and the water is then discharged into the engine heat exchanger.

Improvement in full power performance with intercooling on the 6-71 turbocharged engine is about 6% using 75 F water supply, as shown in Fig. G. This improvement was obtained without any increase in fuel input and, therefore, resulted in lower operating temperatures. The air temperature into the Roots blower as well as the pre-turbine exhaust temperature were both lowered approximately 100 F.

The maximum pressure ratio at full load was 1.9/1 and, as Mr. Mitchell shows in Fig. 9, even greater gains in performance would be possible at higher pressure ratios. However, it should be noted that as the pressure ratio is increased the compressor efficiency generally decreases.

The improvements in engine performance and torque characteristics obtained by combining aircooling and controlled turbine bypass are very impressive. The bypass arrangement also offers the added advantage of turbine overspeed protection at high altitudes, not mentioned by Mr. Mitchell. A unit very similar to that used on the Caterpillar engine has operated satisfactorily on a 4-71 turbocharged engine at simulated altitudes up to 16,000 ft in our Laboratory altitude chamber. As Mr. Mitchell pointed out, the turbine bypass control is actuated by a pressure ratio sensing device. We found that at no time was the pre-set pressure ratio exceeded at high altitudes

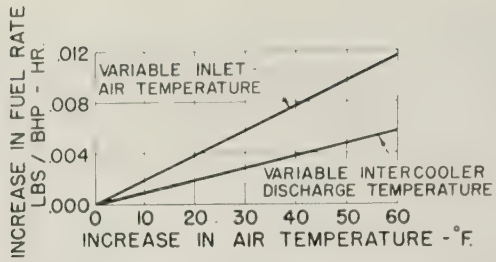

Fig. H — Effect of variable pre-cooled and intercooled temperature

and the turbine did not overspeed above the sea level setting when going to 16,000 ft.

While adding to the complexity of the diesel engine the combination of turbocharging, aircooling, and turbine bypass control have shown very real and worthwhile gains in raising the output, and improving the fuel economy of the diesel engine.

Agrees that Parts Life and Engine Economy Improved with Use of Scavenging Aircooling

— W. C. Arnold
Fairbanks, Morse & Co.

THE GENERAL results of the benefits of cooling the engine scavenging air prior to admitting it to the engine cylinders, have been corroborated by our tests. Our testing, however, has been confined to constant-speed variable-load turbocharged 2-stroke diesel engines of considerably more horsepower output. This does not appear to change the trends resulting from the use of aftercooling. It should be pointed out that aftercooling can not always be used, due to size limitations, cooling mediums available, and the like. But, it should be used whenever possible.

Fig. H shows just how effective scavenging aircooling can be. This plot shows that while cooling inlet air is the more effective per deg F, large improvements may be obtained through aftercooling, due to the greater reductions in temperature that may be achieved. These data were obtained from controlled air temperature tests conducted on an $8\frac{1}{8} \times 10$ turbocharged diesel engine operating at 900 rpm and 135 bmep. The compressor pressure ratio was about 1.9/1 and the discharge temperature approximately 280 F. This air temperature allows large gains to be made through aftercooling. Also, the heat load on an engine is reduced in two ways: (1) from lower specific fuel inputs as indicated by this curve, and (2) from lower cycle temperature levels resulting from the lower initial charge temperatures. These two factors show that aftercooling a turbocharged diesel engine which is operating with airbox pressures nearly twice atmospheric are effective for improved parts life and engine economy.

However, the fact that some aftercooling is good does not mean that more aftercooling must be better. Fig. I shows the inside of a liner. Section A is a view of a chrome-plated bore after several hundred hours operation at 185 F cooling water temperatures, 110 F air from the aftercooler, and operation on No. 2 fuel oil which contains about 0.6% sulfur. The large white areas are sulfur corrosion patches. B is the same bore after another 150-hr operation at identical conditions except that the aftercooler discharge temperature was held at 130 F. Note that the sulfur corrosion areas are nearly gone. This corrosion resulted from condensation of the sulfur combustion products. The improvement shown was obtained by increasing the average cycle temperature levels at 20 F, a quantity sufficient to stop the condensation. This occurred at a slight cost to the engine fuel economy. Another method for combating this corrosive action is now under test: The jacket water temperatures have been increased to 215 F which holding the aftercooling discharge temperature at 110 F. When the engine

was torn down for inspection, not one patch of corrosion could be found. This means that where this method is used, aftercooler discharge temperatures may be held as low as is possible with the cooling mediums available and gain all the potential in fuel economy that is possible.

Some of our testing has included turbine bypass tests using a turbocharger sized for approximately 75% load. From this up to 110% load, the bypass holds the turbine speed nearly constant. This was a major improvement in helping the 2-stroke engines at low speeds and loads. Actually, it made it possible to start and run up to full speed and load without benefit of any auxillary air supply, once the starting air was shut off. While it is still in the early experimental stages with us, we feel that this will be an important factor in removing auxillary air-supply systems from 2-stroke turbocharged diesel engines.

Why does the author feel that the total heat rejected to the engine cooling water with aftercooling plus the heat absorbed by the aftercooler water is exactly equal to the total heat rejected without aftercooling? This is shown in Fig. 8. It would seem that the efficiency of cooling with jacket water would very likely be different than that of cooling with scavenging air. If this is true, somewhat different total heat figures would be expected.

In Table 2, is the column "per cent heat load" a total of engine plus aftercooler rejected heat? If not, it would appear that a 23% increase in torque results in a 25% increase in engine heat load with only a 6% increase in engine deck temperatures. These figures are somewhat difficult for me to understand.

My last question is: What increase in maximum cylinder firing pressures were required as turbocharger pressure ratios were increased? The maximum mechanical loading that any one engine can withstand would set the high limit of boost pressure unless maximum firing pressures were maintained in some way.

Author's Closure To Discussion

THE DISCUSSERS are to be commended on their interesting and informative additions to this presentation. It is always helpful to hear of the results of the application of a principle, in this case aftercooling, to as wide an engine range as possible. The comments presented certainly achieved that end. Their confirmation of our reported data is most encouraging.

In answering the questions that they have presented, we should re-emphasize the fact that our test and development work was carried out on a limited size range of engines, all of which had a definite family resemblance. Since engine size, design concepts, and use vary and affect the application of aftercooling, we would expect the results of such applications to vary as well. However, we do expect the basic principles to be consistent. With that in mind we may proceed to the questions as they were presented.

Mr. Egli is correct in his assumption that Figs. 9–11 relate to the same engine without change to its compression ratio. Fig. A is interesting and could be of direct importance on some engines. Over the range of pressure charging considered, maximum pressures have not been a limiting consideration, although eventually they may reach that category. This is one of the items that depends on engine size and design as noted earlier. In any case, we agree that the minimum boost to attain a given output from the engine is most desirable.

As Mr. Egli noted and Fig. B shows, the range problem for high-pressure turbocharging can become acute. This certainly is a field worthy of considerable development by engine and turbocharger manufacturers.

Mr. Matthews' confirmation of our data is appreciated, as is his presentation of Fig. C describing an aftercooler application to a large gas engine. The "Turbocooler" of Fig. D is an interesting extension of the aircooling principle for use on large gas engines. Again, this is a different engine type lending itself to different application techniques.

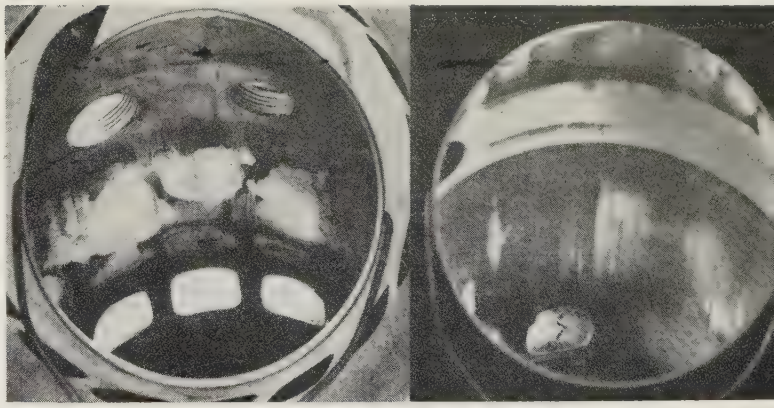

Fig. 1 — Chrome-plated bore (left) after operation at 110 F aftercooler discharge temperature and (right) after another 150-hr operation at 130 F aftercooler discharge temperature

Mr. Matthews noted in connection with the use of a controlled turbine bypass that its advantages are: (1) wider turboblower operating range with requirements for a blower design of less than optimum efficiency and perhaps not applicable to high pressure ratio output, as well as (2) slightly increased fuel consumption. Theoretically he is right in (1), although to date our problems of range have been solved by careful engine and turbo matching without sacrifice of pressure ratio potential. With reasonable ranges of control application we expect to be able to work within the limits imposed by high-pressure turbochargers. In part (2) again he is right at rated engine speed and output. However, when considered on the basis of the percentage of the input energy to the engine that is bypassed around the turbine, the loss in fuel consumption is very small. If the fuel consumption over the range of engine operation with the turbine bypass control is compared to a free-running turbo application, the controlled turbo is, of course, superior.

Mr. Matthews' comments on their engine that was tailored for very high output and very exacting response illustrate another application of pressure charging and cooling.

The extension of this subject to include relatively small 2-stroke engines by Mr. Phillips is greatly appreciated. He has noted that the pressure ratio control limits turbine speed at altitude and prevents turbocharger overspeed. That, of course, is true and was one of the basic requirements set in the development of the control. It was perhaps second only to attaining the required engine lug characteristic.

Mr. Arnold's basic confirmation of our results as extended to larger 2-stroke engines is also interesting, as is his note of caution on very severe aftercooling and related corrosion. We have not encountered this problem but clearly we all must be aware of it.

In reply to the question of the equality of total heat rejected by an aftercooling engine to that rejected to the engine coolant of the nonaftercooled machine (as shown in Fig. 8), we would like to make the following comments. First, we can agree that at a given output, the aftercooled engine will reject less heat to its coolant than the nonaftercooled engine. The exactness of the equality of total heat rejection on the two engines seems somewhat problematical. However, on the engines tested, this was found to be a very definite characteristic within the range of test accuracy. In that sense it is useful. Just how other engine types and sizes would react on a similar basis would be very interesting.

The question of maximum firing pressures was considered previously in reply to Mr. Egli's comments.

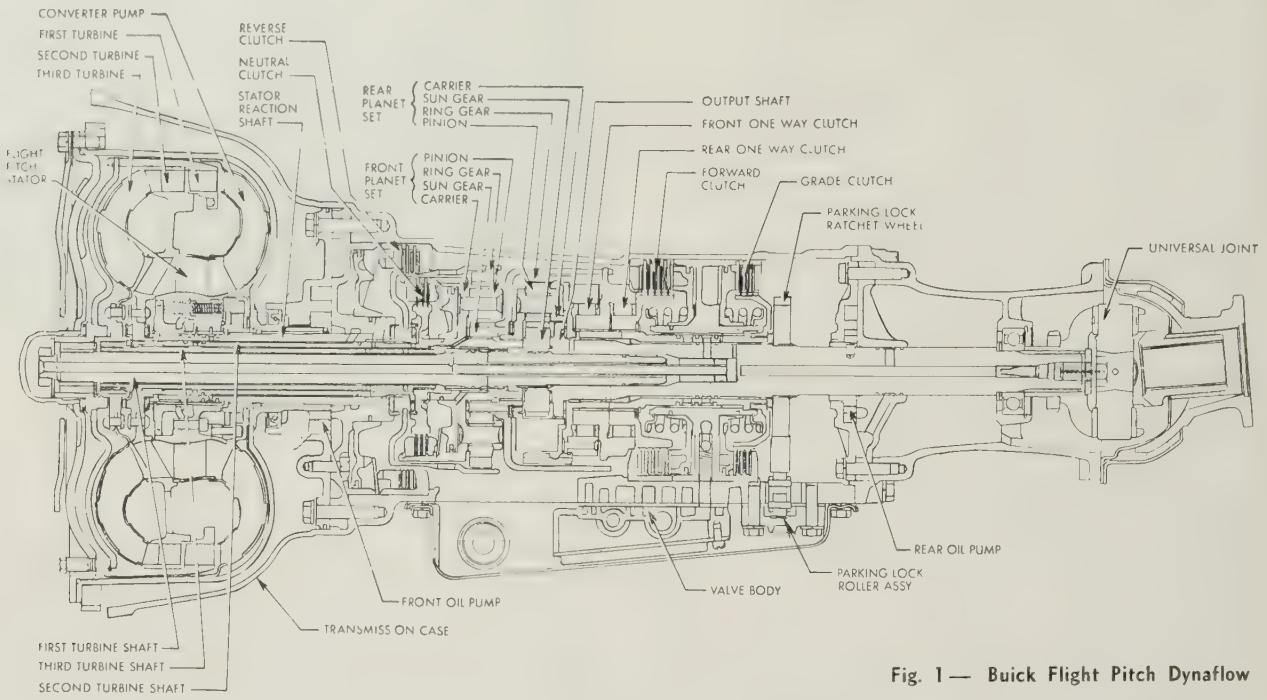

Fig. 1 — Buick Flight Pitch Dynaflow

THE BUICK *FLIGHT*

Forest McFarland and Charles S. Chapman,
Buick Motor Division, General Motors Corp.

This paper was presented at the SAE National Passenger-Car, Body, and Materials Meeting, Detroit, March 5, 1958.

AUTOMATIC transmission design and development for American automobiles after the early days of inertia, variable crank, hydrostatic, pneumatic, electric, and friction drives, narrowed down to two successful types of design: the stepped gear design first exemplified by the Hydramatic in 1939 and the torque converter design first introduced by Buick in 1948. We have seen five other car manufacturers follow with torque converter designs. All of these now, however, employ shifts putting them in the modified step gear classification. Chevrolet is one exception to this pattern in that one of its transmissions, the "Turboglide" employs no shifts.

Buick, alone, has stayed strictly with a transmission employing no shifts but has depended upon a series of improvements in the converter to maintain competitiveness in design. This has consisted of introduction of a geared first turbine in 1953, variable angle reactor blades in 1955, and a second reactor between the first and second turbine in 1956, all to improve performance and efficiency. A definite further step has been taken in the introduction of the "Flight Pitch" transmission in 1957 employing three turbines, each geared at its own speed ratio to the driven shafts and still employing no shifts in the design.

General Description

The Buick Flight Pitch Dynaflow (Fig. 1) is a triple-turbine transmission with a stator control which allows continuous variation of the stator blade pitch. The unit contains a 5-element torque converter in combination with two planetary gear-

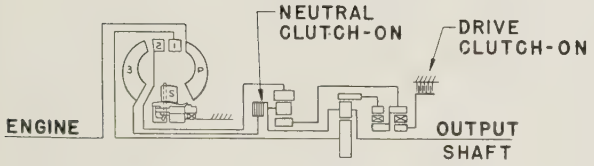

Fig. 2 — Drive range

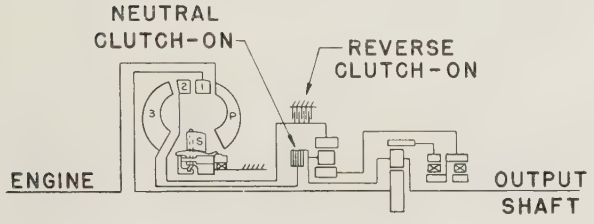

Fig. 3 — Reverse range

THE Buick Flight Pitch Dynaflow is unique among automatic transmissions in that it contains no gear shifts. Rather, it employs three turbines, each geared at its own speed ratio to the driven shafts.

The transmission contains a 5-element torque converter — an engine-driven pump member, three turbines, and the stator — combined with two planetary gearsets. The total transmission weighs about 200 lb, a result of the extensive use of aluminum.

The authors outline in detail the design of the unit and its functioning.

PITCH DYNAFLOW

sets. The elements of the torque converter are shown schematically in Fig. 2 and consist of an engine-driven pump member, three turbines, and the stator.

Drive Range — The drive and neutral clutches are engaged in drive range, as shown in Fig. 2. The first turbine is connected to the sun gear of the rear planetary gearset, which multiplies the turbine torque by 2.86/1. The ring gear is the reaction member being grounded through both one-way clutches and the drive friction clutch. The planet carrier, which is the output member, is connected to the transmission output shaft. The second turbine is connected to the ring gear of the front planetary gearset, which multiplies the turbine torque by 1.54/1. The sun gear is the reaction member and is grounded through the rear one-way clutch and the drive friction clutch. The carrier of the front gearset is again the output member and is connected to the output shaft through the rear carrier. The third turbine is connected directly to the output shaft through the neutral friction clutch. The stator is grounded to a reaction shaft through a one-way clutch. The stall torque ratio in drive range is 4.75/1.

Reverse Range — The reverse and neutral clutches are engaged in reverse, as shown in Fig. 3.

The first turbine and rear sun gear drive the rear ring gear rearward since the carrier is connected to the output shaft. This results in a forward torque on the carrier. The rear ring gear drives the front sun gear rearward through the front one-way clutch. This sun gear drives the front carrier rearward since the outer ring gear is grounded through the reverse friction clutch. The reverse torque on the front carrier is considerably higher than the forward torque previously mentioned on the rear carrier. Since they are connected, this results in a net reverse torque to the output shaft. The reverse torque ratio at stall is 4.50/1.

Grade Range — Fig. 4 shows the grade range. Since the performance in drive range requires no additional gearing for hill climbing and the like, there is no low range in this transmission. This leaves no hill retarding without making special provision for it. Many combinations were tested to arrive at the most suitable hill retarding mechanism that could be provided considering cooling problems,

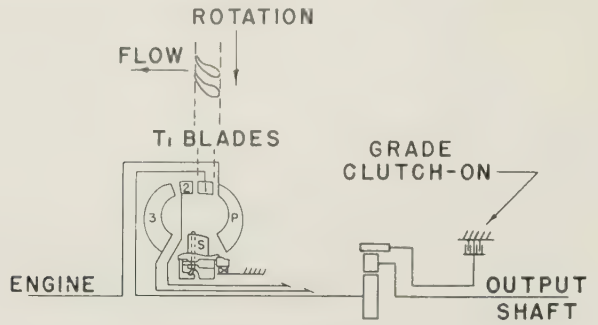

Fig. 4 — Grade range

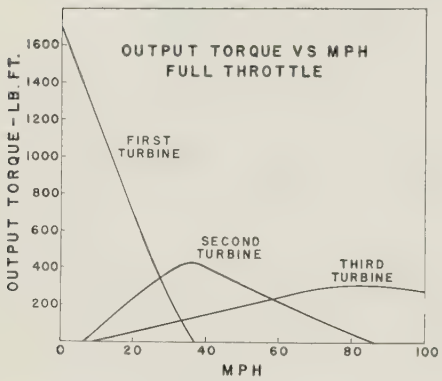

Fig. 5 — Turbine and gear output torques

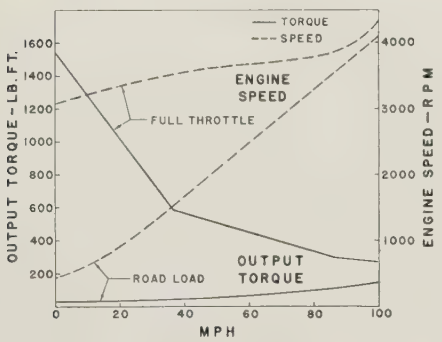

Fig. 6 — Road-load and full-throttle speed and torque comparison

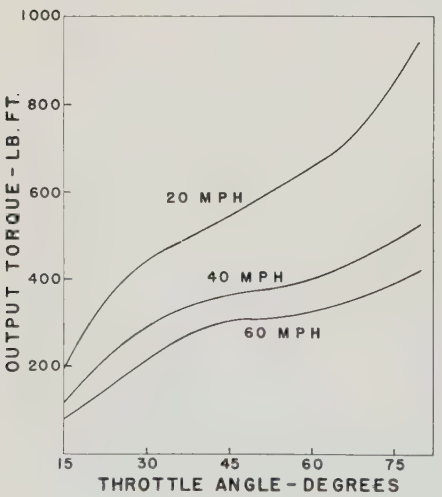

Fig. 7 — Output torque versus throttle angle

complication, and production costs. The device which proved the best solution was the addition of the grade clutch.

In grade range, the grade clutch is engaged and the other friction elements are released. The grade clutch is necessary to hold the rear ring gear from rotation since the one-way clutches allow it to turn forward in drive range. The gearset turns the first turbine at 2.86 times output speed. The first turbine acts as an axial flow pump driving the fluid in the same direction as the pump of the converter in drive. The flow established by the first turbine drives the torque converter pump which drives the engine, effecting engine braking. Varying the throttle opening will change the amount of braking, although the car cannot be driven in grade range since the first turbine free wheels at low vehicle speeds in normal driving operation.

In neutral and park, all of the friction elements are disengaged.

Performance

Fig. 5 shows the individual contributions of three turbines and their gearing to the total output torque at wide-open throttle in drive range. The figure illustrates that at stall the first turbine is contributing all of the torque with the second and third turbines having slight negative torques. As the vehicle accelerates, the second turbine torque increases until it reaches a maximum at 1390 output rpm or 35 mph. The third turbine torque also increases with increasing output speed and reaches a maximum at 3400 rpm or 88 mph.

The stator reaction torque is a maximum at stall and reaches the coupling point at 3490 rpm or 91 mph at full throttle. The total output torque curve is the summation of the three turbine torque curves.

Fig. 6 shows the wide-open throttle output torque and input speed at high stator angle in comparison with the road load torque and input speed. The difference between the two torque curves indicates the torque available for acceleration. The continuously variable stator blade pitch enables the driver to select any value of torque between the curves he desires at any given speed.

The essential reason for developing an automatic transmission is to eliminate the necessity for the use of controls other than the accelerator pedal in obtaining different levels of performance. Further refinements require that as the driver varies the accelerator pedal position, the requested changes of performance level take place at the rate that he wants them to rather than in abrupt or sudden changes. Therefore, it is very desirable to have the output torque vary linearly with the carburetor opening so that the movement of the accelerator pedal can be controlled easily to select the exact level of performance the driver desires.

Fig. 7 shows the output torque versus carburetor opening at various road speeds for the Flight Pitch Dynaflow. It illustrates that the output torque is nearly linear with the carburetor opening over the speed range.

Hydraulic Controls

The transmission controls shown in Fig. 8 are relatively simple by industry standards. There are two valves which are common to all automatic transmissions, these being the manual or selector valve and the line pressure regulator valve. The

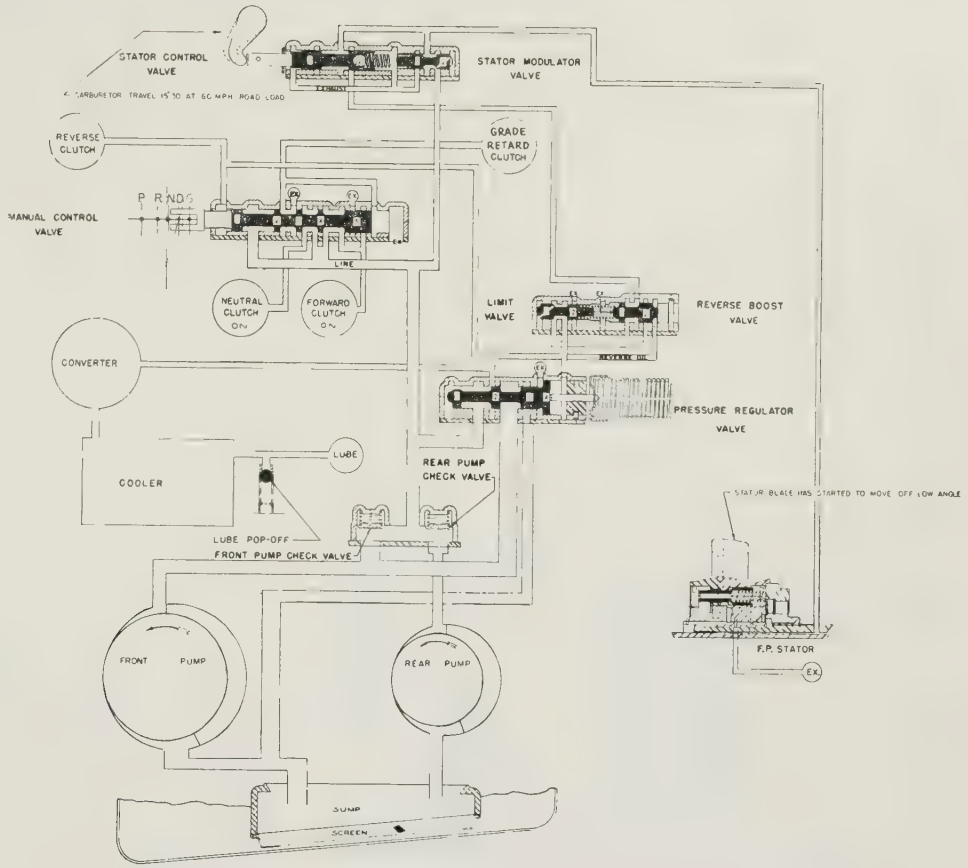

Fig. 8 — Hydraulic control diagram in drive range at 60 mph road load

stator modulator valve is similar to the throttle pressure valves in many automatic transmissions in that it produces a pressure proportional to throttle movement. This pressure is directed to the continuously variable stator where it controls the movement of the stator, as will be explained. The stator pressure is also used to increase the line pressure to provide sufficient torque capacity for the friction clutches as engine torque increases. The limit valve provides a means of limiting the maximum line pressure to that value required to hold wide-open throttle torque at stall. The stator modulator pressure is routed through the stator valve in such a manner that minimum line pressure is carried at road load at normal road speeds.

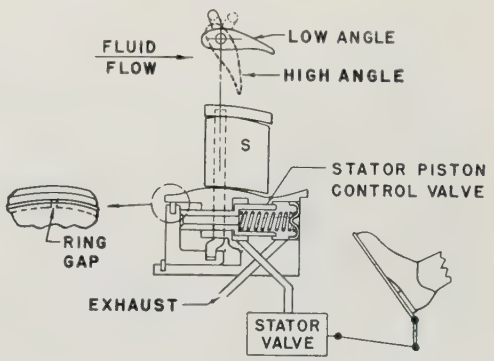

Fig. 9 — Stator blade control mechanism

Stator

Fig. 9 shows a cross-section of the continuously variable stator. The stator blades have steel cranks with the crank throws inserted in a groove of the stator piston similar to the arrangement of the Variable Pitch Dynaflow. The axial movement of the stator piston rotates the stator blades about the center of the crank. The position of the piston is determined by the stator piston control valve. In the low angle or normal driving position, the end of the hollow valve is touching the stator piston, sealing the chamber behind the stator piston. The torque converter charging pressure is equalized on both sides of the piston, and the fluid flow forces on the stator blades tend to turn the cranks in a direction to force the piston to the left against the snap ring. There is a gap in the sealing ring at the outer diameter of the piston which permits the torque converter charging pressure to fill the piston cavity and balance the pressure on the two sides of the piston. As the stator modulator valve increases the stator pressure, the pressure acts on the valve area moving the stator piston control valve to the right against the valve spring. When the stator piston control valve leaves the piston, it opens the exhaust hole in the center of the valve. This allows the oil pressure in the piston cavity to be vented, which unbalances the pressure forces on the piston. The pressure unbalance is maintained by the orifice effect of the gap in the piston sealing ring which prevents the converter oil from escaping in excessive quantities. The piston moves to the right until it nearly touches the valve, forming a partial seal of the piston cavity. The oil flowing through the gap in the piston sealing ring produces a pressure

in the cavity of the piston such that the differential force on the piston balances the fluid flow forces of the stator blades acting through the cranks on the stator piston. Therefore, the piston moves toward the valve in such a manner as to regulate a pressure in the cavity until this force balance is reached. The area of the piston is such that the forces involved are large enough to minimize friction effects.

When the stator pressure drops as the driver lifts his foot from the accelerator, the stator piston control valve spring forces the valve to the left against the piston. This seals the exhaust opening in the valve. The torque converter charging pressure acting through the gap in the piston sealing ring balances the pressure on the piston and the stator blade forces acting through the cranks force the piston to the left toward the snap ring.

The valve areas and spring force are set up to allow the stator blades to leave the low-angle position at half throttle and complete the change to high angle just before the throttle is wide open. The total travel of the piston is approximately ¼ in. and the stator blade angle change is 55 deg.

The outer diameter of the stator assembly is machined spherically with its radius at the intersection of the centerline of the stator blade crank and the axis of rotation as shown in Fig. 10. The bottom of the stator blade is cut off to form an arc slightly larger than the sphere on the stator hub and tangent to it at the crank. This keeps the clearance between the hub and the pivoting stator blade to a minimum as the blade turns to the various positions. The outer core ring is also formed as a sphere about the same center as the stator hub. The outer end of the stator blade is cut off at a slightly smaller radius so that the stator blade touches the ring only at the crank and not at the tip of the blade. This prevents any slight out-of-round condition in the outer core ring from causing a sticking condition as the stator blades turn.

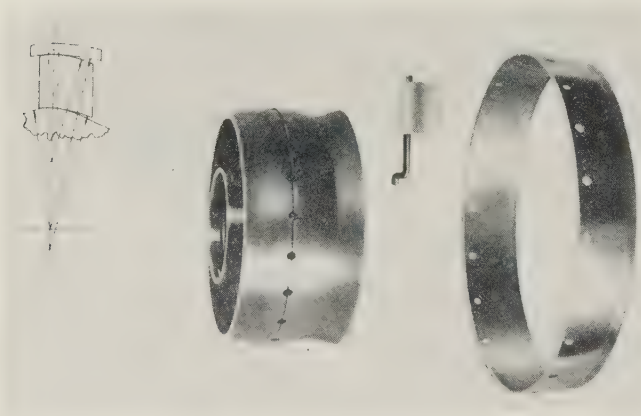

Fig. 10 — Stator blade geometry

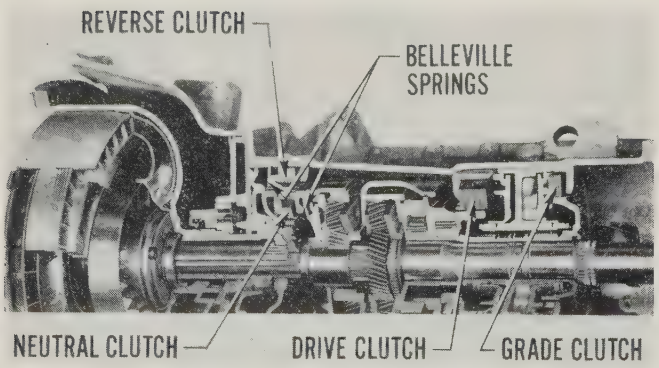

Fig. 11 — Multiple disc clutches

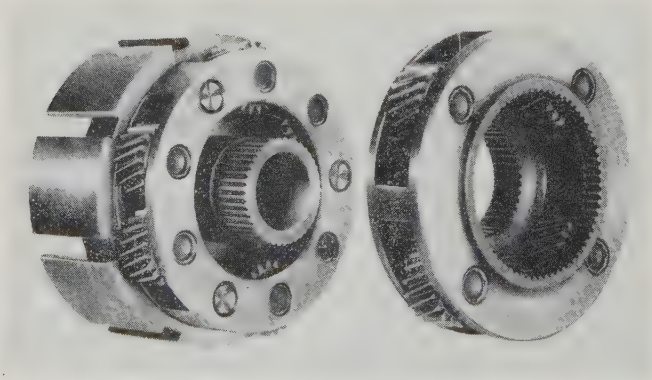

Fig. 12 — Planet carrier assemblies

Clutch Design

The friction elements are multiple disc clutches as shown in Fig. 11. Since the reverse and grade clutches are disengaged and spinning freely in drive range, a careful investigation was made to keep the clutch drag losses to a minimum. The effects of grooving, plate clearance, and type of friction material were carefully studied. The most critical factor influencing these losses is the amount of oil used to cool the clutch plates. The outer chambers in which the clutch plates turn were carefully vented to prevent the oil from accumulating between the plates. The chamber of the grade clutch was effectively dammed by the clutch backing plate since the lower portion of the clutch plates are below the normal oil level. The oil vents are at the sides and top of the clutch backing plate for this

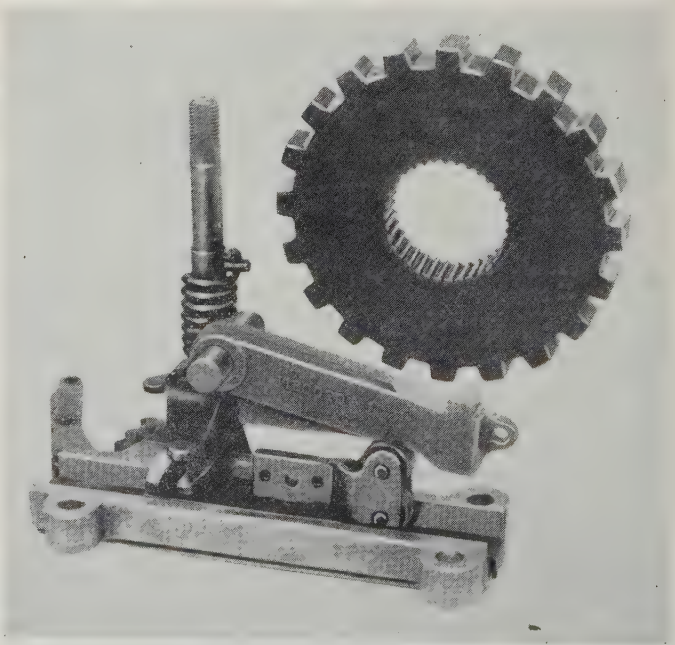

Fig. 13 — Parking lock mechanism

reason. The reverse clutch backing plate has oil vents around its periphery since it is above the oil level.

The neutral and reverse friction clutches have three friction plates as well as belleville springs, which serve as piston return springs and also as levers to multiply the piston force. The belleville springs have a "flat" characteristic after reaching the peak in the initial part of the curve. This flat portion of the curve allows a constant spring force with the normal variation in clutch pack tolerances. Both belleville springs were designed without any fingers or slots, which are difficult to control in production as far as the removal of sharp edges and burrs is concerned.

The grade clutch has three friction plates with a direct-acting piston. The forward clutch has five friction plates, also with a direct-acting piston.

Gears

It was felt that gear noise would be a major problem with a unit that has two gearsets that do not lock up in any range. During the design stages, there was considerable discussion of the problem. The basic design configuration made it difficult to pilot the ring gears. Therefore, it was decided to pilot them flexibly and let them seek their own centers located by the planet pinions. The planet pinion carriers and sun gears were well piloted with respect to one another. While the experimental units were being built, some alternate designs and "fixes" were studied in case noise trouble were encountered. The experimental gears were cut in the production plant to acquaint the production personnel with any problems occurring during the development period. Surprisingly, very little gear noise difficulty was encountered in the experimental transmissions. When production started, the transmissions were also very good in this respect. While the engineering department would like to take credit for an ingenious design, the real contribution was made by the production department for turning out high-quality, quiet gears. The years of experience in producing the gearset in the torque converter of the Variable Pitch Dynaflow have proved to be of considerable value.

The four planet pinions in the rear gearset shown in Fig. 12 take just under five times engine torque at stall in drive range. The six pinions in the front gearset also shown in Fig. 12 take nine times engine torque in reverse at stall. The number of teeth and helix angle in the front and rear ring gears is the same and this is also true of the sun gears. The planet pinions in the two gearsets are identical.

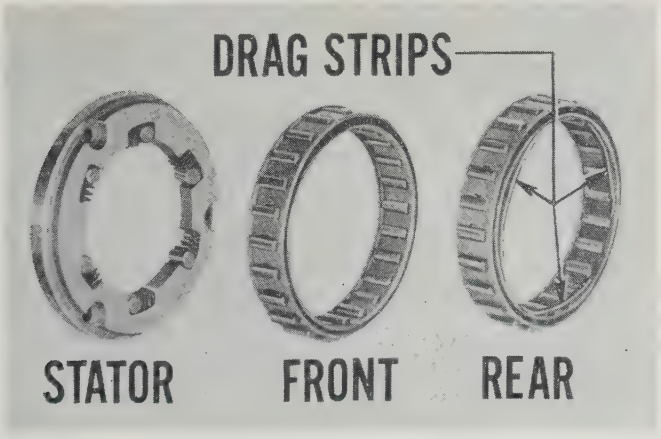

Fig. 14 — One-way clutches

Parking Lock Mechanism

One of the features that was introduced with the early automatic transmissions was the transmission parking lock. Such a device was desirable because the fluid elements of the transmission have no capacity at zero speed and the feature of leaving a car parked "in gear" was lost. Since many customers are not careful to have the emergency brake adjusted periodically as it should be, there is a safety hazard in not having a more positive mechanism to hold the car on a grade. For this reason, the transmission parking lock came into general use. All of the presently used transmission locks consist of a pivoted pawl engaging a gear on the output shaft. The mechanisms for actuating the pawl differ.

The most difficult problem involved in the design of a parking pawl actuating mechanism is the reduction of release effort when the pawl tooth is heavily loaded, which occurs when the car is parked on a grade.

A roller mechanism was developed to minimize this effort which has proved highly effective. Fig. 13 shows the parking lock mechanism. The shift lever on the wheel is connected to the roller slide through the transmission linkage. When the rollers move the pawl into engagement, the rollers are wedged between the flat on the pawl and the flat surface of the bracket retaining the roller assembly by the separating forces between the gear tooth and the pawl tooth. The two surfaces bearing on the roller are parallel so that the main forces to overcome in releasing the pawl are the friction forces of the roller contact points. The pins in the rollers are pressed into the rollers and are a loose fit in the slide assembly. Since they are of relatively small diameter, their friction forces are negligible.

One-Way Clutches

The three one-way clutches in the Flight Pitch Dynaflow are shown in Fig. 14. The stator one-way clutch located in the torque converter is an internal cam and roller clutch with waved individual energizing springs. This one-way clutch does not carry much torque (about 170 lb-ft) and is of conventional design.

The two one-way clutches located inside the transmission consist of sprag assemblies and circular races. Work was done with internal cam and roller designs which had some shortcomings. They were borderline on capacity under shock loading and have centrifugally disengaging characteristics which were highly undesirable in this application. The sprag clutches were used because the sprag contours can be made in such a manner that the sprags tend to "tuck in" or engage as the sprag assembly is rotated. They also have good capacity for a given space. The rear or "T-2 sprag assembly" has three bronze drag strips on the inner cage which tend to make the assembly rotate with the inner race. Since the inner race is stationary in drive range, these drag strips hold the sprag assembly stationary and cause the rubbing velocity between

the sprags and race to take place at the outer race where centrifugal force tends to throw the lubricating oil. The front or "T-1 sprag assembly" has centrifugally engaging sprags with no drag strips. The drag strips were not used because of the fact that the outer race is stationary in grade range with the inner race rotating at high speed. Anchoring the sprag assemblies to the rotating inner race would allow centrifugal force to throw the individual sprags against the outer race, causing excessive sprag wear in grade range. Since both the inner and outer races freewheel in the same direction in drive range, the rubbing speeds between sprags and races are not so high that drag strips are needed.

The required static torque capacity of the sprag one-way clutches is 1080 lb-ft.

Thrust Bearings

Needle thrust bearings (Fig. 15) were used extensively throughout the transmission because of their excellent capacity and antifriction characteristics. These antifriction characteristics were helpful in keeping the spin losses to a minimum.

One of the most troublesome items during the development of the transmission was the large num-

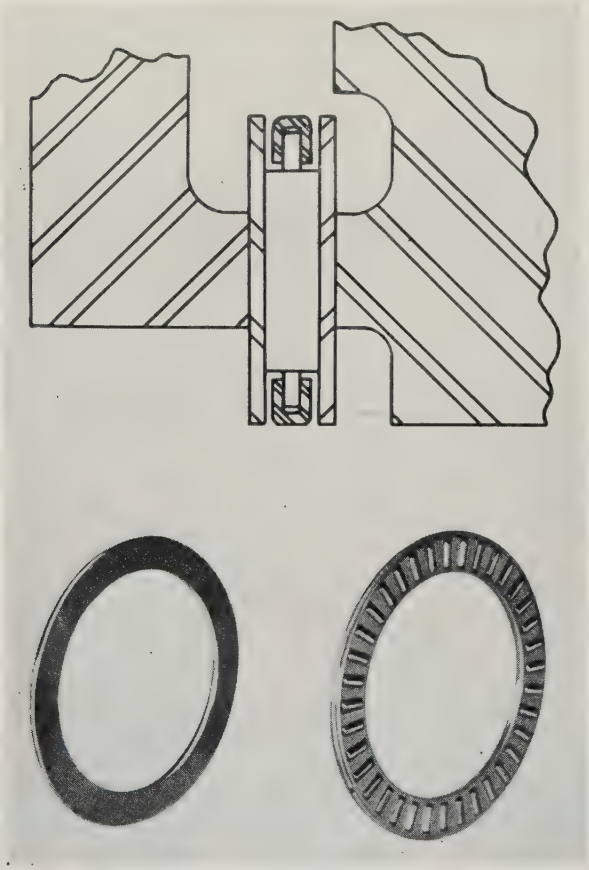

Fig. 15 — Stator thrust bearing mounting

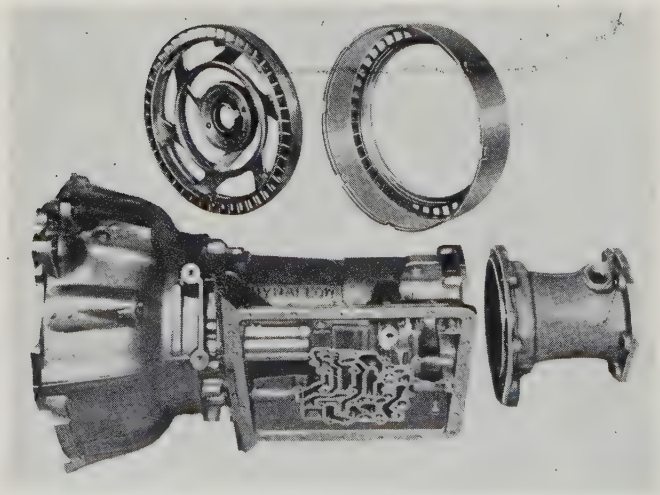

Fig. 16 — Aluminum permanent mold castings

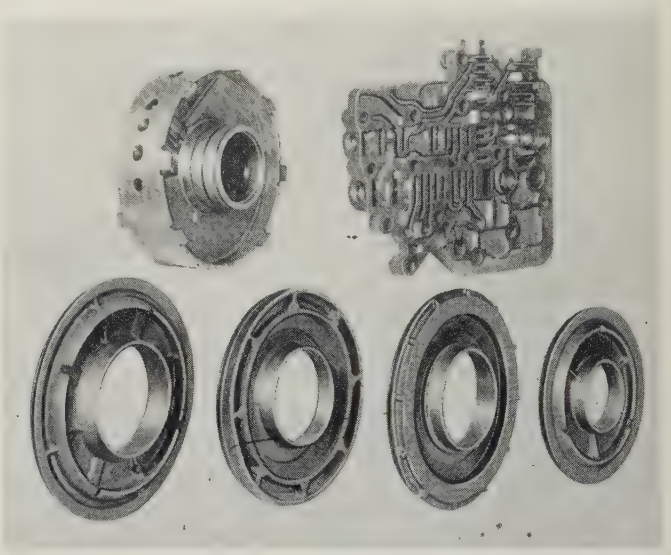

Fig. 17 — Aluminum die castings

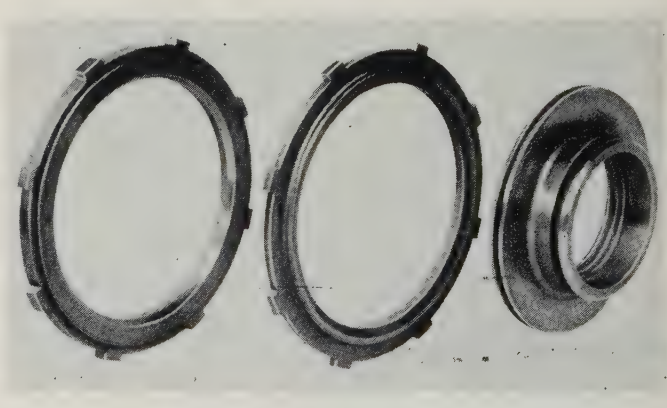

Fig. 18 — Powdered iron parts

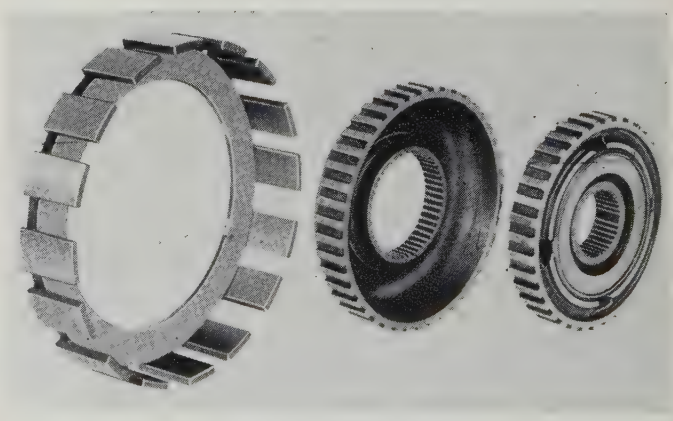

Fig. 19 — Pearlitic malleable iron castings

ber of needle thrust bearing failures at the location between the stator and the converter pump. While these bearings did not disintegrate causing a "basket case," the tips of the needles and the races pitted causing a very unpleasant noise in the unit.

After many unsuccessful attempts, two steps were taken which ultimately made this bearing trouble-free. The bearing races were backed up at the center of the needle roller path only, and the areas in back of the roller tips were relieved. This allowed the races to deflect enough to relieve the heavy bearing at the roller tips. This was the biggest factor in increasing the bearing life. The needle roller diameter was increased from 0.078 to 0.125 in. which also helped.

Materials and Fabrication

Aluminum was used extensively throughout the design to reduce weight and facilitate machining. Fig. 16 shows a number of aluminum parts.

The transmission case is an aluminum permanent-mold casting with an integrally cast torque converter housing. The valve body transfer ditches are cast in the bottom of the case. The weight saving in this finished piece compared to an identical cast iron piece is 42 lb.

The rear bearing retainer or extension case is also an aluminum permanent-mold casting. The first and second turbines are permanent-mold aluminum castings with C-resin cored blade sections. Die-cast aluminum parts shown in Fig. 17 include the valve body, four clutch pistons, the output shaft support, and parking brake roller bracket.

We have found powered iron parts to have cost advantages in several locations. Fig. 18 shows the stator piston, the neutral clutch backing plate, and the neutral clutch pressure plate. The front and rear pump check valves and the converter outlet check valve are also made from powdered iron.

Pearlitic malleable cast iron is used in the second and third turbine hubs, the neutral clutch hub, the grade clutch hub, and the forward clutch backing plate at the present time. Three of these parts are shown in Fig. 19.

Grey iron is used in the front pump casting, the mating casting which holds the stator reaction shaft and in the stator hub castings, (Fig. 20). It is also used in the reverse and grade clutch backing members, the rear pump body, and rear pump cover castings.

Stamped members (some of which are shown in Fig. 21) include the torque converter cover, the torque converter pump outer shell and blade assembly, the third turbine blade assembly, first turbine disc, the clutch pack steel plates, belleville springs, valve body plate, regulator valve spring retainer, the oil pan, parking pawl roller and slide assembly, parking pawl roller slide retainer, and the stator ring. The front ring gear drum and front sun gear drum are machined from hot stampings.

The stator blades are made from extruded aluminum. The cranks are made from upset steel wire with rolled serrations and are then pressed into the hole in the blade.

The use of these materials yields a total transmission weight of 200 lb which is about 24 lb lighter than the Variable Pitch Dynaflow. The assembly is shown in Fig. 1.

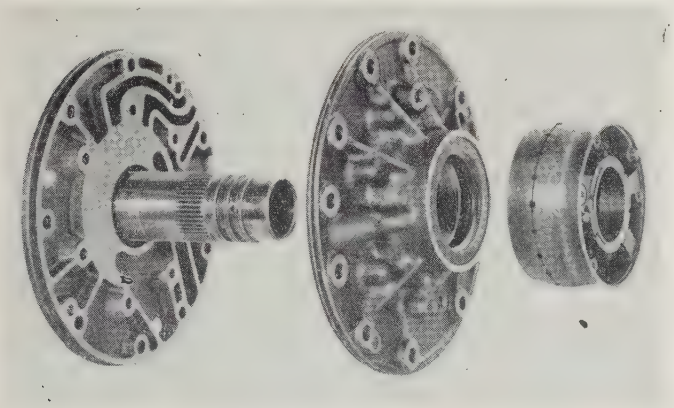

Fig. 20 — Grey iron castings

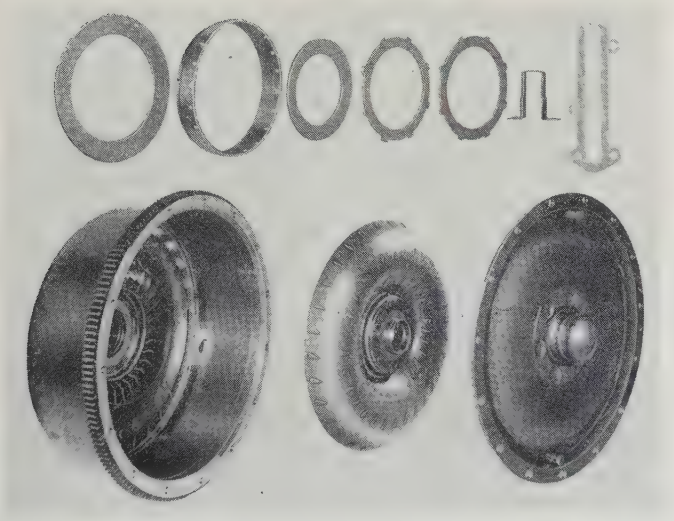

Fig. 21 — Stamped parts

Development Problems

There are lugs on the aluminum support which take the forward clutch reaction torque. During the durability testing, these lugs cracked off time and again. Each design improvement helped but it was not until die castings replaced the experimental sand castings that we were out of trouble. If the aluminum casting suppliers could produce prototype castings which had the fatigue characteristics of die castings without building costly production dies, a lot of ulcers would be saved in product engineering departments.

During the development period there was considerable difficulty encountered in cooling the transmission, particularly on our hill schedules at the proving grounds where the cars are going up and down the hills 24 hr a day at wide-open throttle. The problem was caused by insufficient torque converter and cooling oil flow. The flow was increased from slightly over 2 gal per min to 4½ in high stator angle. This was accomplished by revising the torque converter oil circuit to take full advantage of the natural pump action of the torque converter. The flow in low angle is slightly over 2 gal per min at the higher engine torques.

There was also some difficulty in properly venting the transmission, which made our experimental cars strong competitors in the road oiling business for a short time. The difficulty was eliminated by im-

proving the drainage and venting between the different compartments in the transmission case.

Acknowledgment

We wish to acknowledge the contribution of the General Motors Engineering Staff for their excellent work in the initial stages, the guidance of J. D. Turlay during the development program, and the fine work of R. J. Gorsky and the production group in solving the inevitable problems of introducing a new unit into production. Our suppliers have also been particularly cooperative. The tireless efforts of the various project engineers working on this program cannot be over-emphasized and it was these efforts which solved the many problems.

DISCUSSION

Describes Tests with Flight Pitch And Other Transmissions

— R. W. Wayman
Borg-Warner Corp.

IN MY opinion the most obvious feature of this transmission is that it is essentially an enlarged version of the Chevrolet Turboglide with a different method of controlling the variable pitched stator blades.

The changed manual control pattern wherein reverse position is placed between the park and neutral has not gone unnoticed as we in Borg-Warner were the first to do this commercially and are glad to see so much company, even in an era of push button controls.

In general, the various parts do not appear easy to build and, in fact, some are quite complicated. The lubrication oil tube in the first turbine shaft appears of unusual construction and particularly vulnerable as it projects beyond the end of the shaft.

The use of belleville springs for multiplying clutch piston engaging forces, and also supplying the release spring requirement, was pioneered commercially by Borg-Warner and the use of these springs is duly noted in the reverse and neutral clutches. These allow the use of smaller clutch packs although complicating the control problem of engagement smoothness.

The positioning of the stator blades with throttle pressure is carried out by an ingenious method. Our tests show some problem with repeatability of setting with a given throttle pressure although these seem to work sufficiently well for the purpose.

Once again the ability of planetary gearing to handle high torques in small packages is well-demonstrated in this transmission. The two planetary sets appear almost insignificantly in the overall package.

One of the most striking advantages of this type transmission is the lack of torque shifting friction members, the only one being the grade retard clutch. This also provides the rather simple hydraulic control as shown in Fig. 8. I notice the converter, cooler, and lube circuits are shown in series. Our experience indicates good results by placing these in parallel and, in particular, large cooler flows can be obtained which is difficult in the series circuit.

Preliminary road testing indicated very acceptable acceleration and deceleration performance. Not being used to this type of drive, I felt a noticeable "engine float" feel. Investigating further, I noticed that in the 30–50 mph range the engine rpm difference between road load and coast was better than 600, whereas a typical 3-element converter showed about 200 rpm. This difference is accentuated when the change is made from accelerating conditions to coast conditions.

Dynamometer checks revealed rather disappointing efficiencies, not only in reverse but also in the driving range.

Of interest to me, in going over some prior art, was an item in the patent literature (F. T. Fawcett 2,055,895) in 1936 describing fairly well this type of transmission, although using a multiturbined coupling instead of a converter.

In maintaining a no-shift feel type of transmission Buick has utilized a number of converter modifications, some of which create considerable compromise. In going to the Flight Pitch Dynaflow definite gear assistance to the converter is supplied. We are pleased to see this trend as Borg-Warner pioneered gear-assisted converters in the automatic driving range in 1950.

Outlines History Of Automatic Transmissions

— W. B. Herndon
General Motors Corp.

THE Buick Division is to be congratulated on the attainment of a new goal in automatic transmission design — the ultimate in smoothness. Flight Pitch is the first wide ratio spread high-performance automatic transmission to be completely free from all sudden torque changes in the driving range. While the Flight Pitch is similar in some respects to other transmissions on the market, it is different from all others in that it has achieved "infinitely variable" or "continuously variable" ratio change control.

This is certainly an engineering accomplishment. No one ever questions the desirability of smoothness. From an engineer's point of view, however, all engineering solutions have their compromises and Flight Pitch is no exception. Increased complication and cost, higher engine speed, and no engine drive in the braking range are some of the characteristics the critics may call compromises.

The Flight Pitch is a very ingenious combination of gears, torque converter elements, and controls. The solution to the difficult gear problem, the use of a one-piece aluminum case, the use and control of the four plate clutches are only a few of the many problems that have been solved.

The history of the automatic transmission, while it has not been long, has been a very interesting one. Hydra-Matic, the pioneer, appeared in 1939. It had a 4-speed planetary gearbox, fluid coupling split torque drive, and fully automatic controls.

After 19 years and approaching 10 million units, Hydra-Matic today has a 4-speed planetary gearbox, fluid coupling split torque drive, and fully automatic controls. The substitution of the controlled coupling and overrunning clutches for the original band clutch control has greatly improved the smoothness and overall pleasability of Hydra-Matic, but the basic principle remains unchanged. For the maximum performance and economy, this fluid coupling split torque geared drive principle has worked out so well that none better has been found.

The first converter transmission, the Buick Dynaflow, made its appearance in 1948. It was followed soon by a number of other automatic transmissions. All of them used converters. The original converter transmissions did all the torque multiplying in the drive range with the converter only. Then engineers began to add gearing to converters to obtain better performance and economy. A converter transmission appeared with one gear ratio plus direct, with automatic control. In other words, it was a 2-speed transmission with a converter. Then another gear set was added which made a 3-speed transmission with a converter, all automatically controlled. Then there was dual turbine and now the triple turbine. The dual turbine added one gear set and the triple turbine added two geared ratios to assist the converter.

It is an interesting fact that most of the automatic converter transmissions on the market today have sufficient pure gear ratio in them to drive the car very well without using the converter at all. They have a low gear ratio of around 2.5/1 and a second gear ratio of about 1½/1 plus a 1/1 drive. These ratios are approximately equal to those

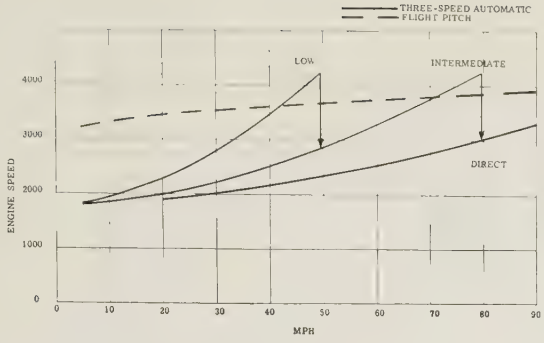

Fig. A — Three-speed automatic transmission versus Flight Pitch Dynaflow full-throttle engine speed

found in the average synchromesh transmission. No one questions the ability of a synchromesh car to perform well or to give good economy. Why then do we need the converter? The answer to this question is that the converter has graduated from its original role of the torque multiplier to a new assignment.

Gears now do most of the necessary torque multiplying and the converter has taken over the job of varying the ratio between the geared steps, so that torque multiplication can be had in small increments instead of in perceptible stages.

Questions Fuel Economy Of Flight Pitch Transmission

— Martin G. Gabriel
Ford Motor Co.

THE automatic transmission, as well as playing an important part in vehicle performance, will also influence vehicle fuel economy. For example, fuel economy will be affected by transmission efficiency, both at road load and full throttle. In addition, the level of engine speed at various throttle angles as controlled by the transmission will also affect economy.

Flight Pitch transmission efficiencies were not discussed in the paper. Since values of 80% efficiency or less are not uncommon for a transmission of this type, it would be interesting to hear of the authors' experience as to vehicle tank fuel economy with the new Flight Pitch as compared to the 1957 Dynaflow transmission.

Fig. A shows a full-throttle engine speed curve of the Flight Pitch compared to a 3-speed automatic transmission.

Comments on Car Control During Grade Descent

— William R. Roger
Chrysler Corp.

OUR experience with the 1958 Buick cars with this transmission have been generally good: the cars have been pleasing to drive, they are very responsive to the throttle, performance is adequate although not outstanding, and the car is quiet. It goes without saying that the smoothness of no shifts is very enjoyable.

Our only criticism lies in the means for controlling the car during grade descent or mountain driving. The convenience of a mountain driving range and even the flexibility required for steep hill descent are noticeably missing. The braking requirement on these cars must penalize the brakes considerably. We have run several dynamometer checks and confirm the performance results. These results were somewhat difficult to obtain due to the frequency of mechanical failures.

We note with satisfaction that there is now another adherent to the now almost universally accepted quadrant positioning of P-R-N-D-L.

We have been somewhat curious about the following:

1. What is the natural pumping action which is different from that used in most other converters to produce cooling flow?

2. Does the use of up to 220-psi charging pressure result in any structural penalties in the converter?

3. It appears that contrary to the authors the car could be driven in grade retard range. The authors indicate that first turbine free-wheels.

Is there any significant loss in performance or efficiency by going into high stall stator position above the coupling point?

In conclusion, I must say that we certainly admire the Buick Division for its tenacity in adhering to the principle of a "shiftless" transmission. On the other hand, we wonder if it is worth the cost.

Author's Closure To Discussion

SEVERAL of the written discussions questioned the effect of a high stator blade angle efficiency on the overall fuel economy of the vehicle and seem to assume that it is the major factor in determining the tank mileage. This occurs only at wide-open throttle where the driver is asking for the ultimate in performance. The percentage of time spent at wide-open throttle is very small, and there are other compensating factors. The fact that the engine speed increases as the engine approaches wide-open throttle enables the engine designer to modify the valve timing, spark timing, carburetion, and compression ratio to increase performance and economy at all throttle positions with less tendency for detonation, since the engine cannot be "lugged" at low speed. The gains to be made in this respect can best be illustrated by comparing synchromesh transmission efficiency with any automatic transmission on the transmission dynamometer and then in a vehicle with engines set up as they are in production vehicles. The synchromesh transmission will excel on the dynamometer, but by the time the cam, spark, carburetor, and compression ratio are modified to make the car run smoothly, it will generally show less tank mileage than a car equipped with an automatic transmission. Another benefit that the Flight Pitch Dynaflow has is a high torque ratio at stall which allows the use of a lower numerical axle ratio in order to improve economy.

Mr. Roger asked if the natural pumping action of the Flight Pitch Dynaflow is different than other torque converters. It is not; but originally another circuit was used for convenience of feeding off to and from the torque converter, which due to low flow was abandoned in favor of the present design.

In answer to Mr. Roger's question on the 220-psi torque converter charging pressure and a structural problem, the actual charging pressure in the torque converter does not exceed 135 psi because of flow restrictions between the valve body and converter. However, this pressure is still high and requires a stiffer front cover and pump shell than is normally used.

We do not follow Mr. Wayman's comments. The Borg-Warner design is of the step-gear type, substituting a torque converter of conventional type with two mechanical shifts for the fluid coupling with three mechanical shifts, as originally introduced by Hydramatic. Hydramatic now uses fluid entirely in its 1 to 2 shifts and 3 to 4 shifts and partially in the 2 to 3 shifts. Buick, in introducing the first torque converter transmission in 1948 in passenger cars, used the "no shift" principle and still does, but has increased performance by adding a second and third turbine, gearing the first and second turbine each through its own gear ratio with the third driving directly. The Buick development since first introduction as cited in the paper has been along its own unique independent line. We hope to continue with further improvements.

the behavior of

RADIATION-RESISTANT

RADIATION effects on lubricants is perhaps as broad a subject as a paper could possibly undertake, so this presentation will be limited to what we can expect of some of the better present-day experimental lubricants operating under conditions of oxidative, thermal, mechanical, and radiation stress.

The designer of a propulsion unit that will operate under high-level radiation stress must know what to expect from the lubricants he will have available, and it is difficult to form a clear picture by reviewing the results from the static irradiation of lubricants performed under a nitrogen blanket at ambient temperatures. Foreseeing this problem, Pratt and Whitney Aircraft, in the fall of 1955, requested Southwest Research Institute to initiate a study of the problems involved in testing lubricants and fuels under dynamic conditions supplemented by the additional stress of high-level radiation. The purpose of the program was to develop, as closely as possible, a "best estimate" of projected propulsion unit conditions.

After a thorough investigation of the available means of producing high-level radiation, it was finally determined that high specific activity Cobalt-60 emitting gamma radiation would be the most practical solution to the problem. Although neutron irradiation would probably be more damaging, it was reasoned that if the hydrocarbon material could not resist gamma radiation, it could be assumed that it would also perform poorly under neutron irradiation. Also, gamma radiation has the prime advantage of leaving the test equipment and test fluids "clean" with no induced radioactivity to make detailed inspection difficult.

Upon selecting the type of radiation to be used and the lubricant test equipment to be employed in the evaluation, a facility was designed and constructed to allow the most flexible use of the equipment and radiation source. This facility (Fig. 1) consists of a pair of operating cells with dry storage of the Cobalt-60 between the cells. The Cobalt-60 source differed in concept from other similar installations in that it was divided into a number of small point sources that could be arranged in virtually an infinite number of radiation configurations. The sources, or "tapes," each consist of four discs of Cobalt-60, 1 cm in diameter by 2 mm thick, encapsulated in a flattened stainless-steel tube which is heliarced closed on the ends. The Cobalt-60 had an initial specific activity of about 45 curies per gram, giving each tape (Fig. 2) a total activity of 290 curies.

RADIATION can produce almost instantaneous failure of modern aircraft lubricants, tests at Southwest Research Institute show. Two types of failures demonstrated are rapid viscosity rise and loss of heat conductivity. Furthermore, it was found that lubricants can become excessively corrosive under high-level radiation.

Generally speaking, the better lubricants appeared to improve in performance while marginal ones deteriorated to a greater extent under radiation. When the better lubricants were subjected to static irradiation prior to the deposition test, there was a minor increase in deposition number as the total dose was increased.

ANP TURBINE LUBRICANTS

J. M. Clark, Jr., and G. C. Lawrason, Southwest Research Institute

This paper was presented at the SAE National Aeronautic Meeting, Los Angeles, Oct. 3, 1958.

The reasoning behind the use of the expensive high-activity Cobalt-60 was based on the reduction of the inverse square loss and circumvention of attenuation by the intervening layers of a low specific activity source in attempting to create a high-level radiation field. The maximum available flux from a Cobalt-60 source is a function of the specific activity of the source and within reasonable limits is relatively independent of the total number of curies. Hence, it is possible to attain fields of 10 times the flux level with one-tenth the total number of curies by using high specific activity material having a specific activity 30–40 times the usual low specific activity source.

When the initial study was planned, it was decided that standard lubricant stability tests that have found general acceptance by the petroleum industry would be conducted under high-level radiation. The simplest thermal stability screening test showing good correlation with engine data was to be investigated first. The WADC deposition test was to be modified as slightly as possible to allow the use of radiation so that baseline or unirradiated data would be comparable to background data on the standard test.

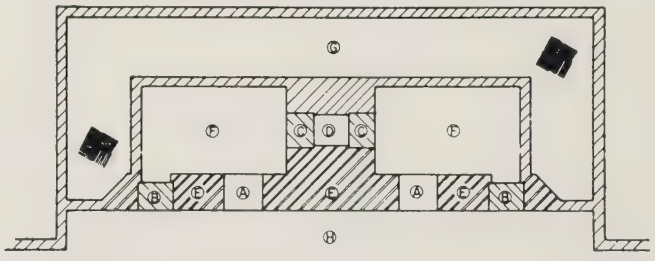

Fig. 1 — Plan view of hot cells

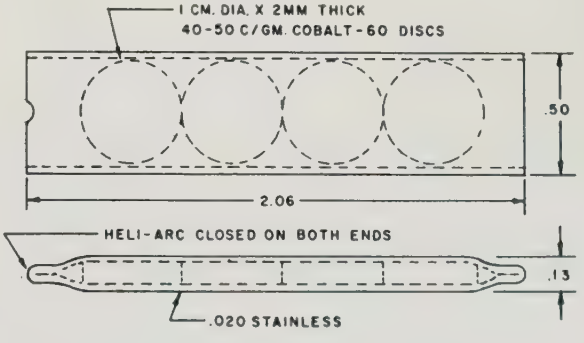

Fig. 2 — Cobalt-60 encapsulation or "tape"

Irradiated Deposition Test

The arrangement of the irradiated deposition test is shown in Fig. 3. In the standard WADC deposition test, an aluminum tube heated to 590 F is used in the glass-walled coker sump; the lubricant is pumped through this sump from the top down, passes down through a cooler, a circulating pump, and a filter, and returns to the coker sump. Moist air is bubbled through the lubricant as it passes

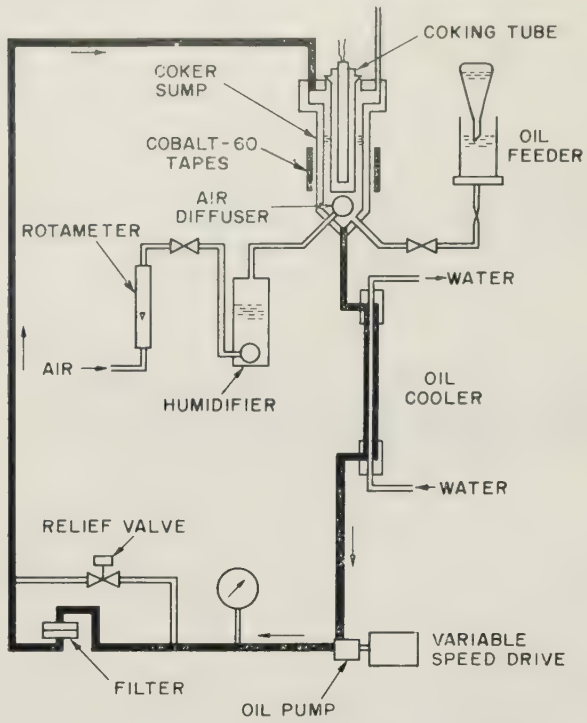

Fig. 3 — WADC deposition test modified for irradiation

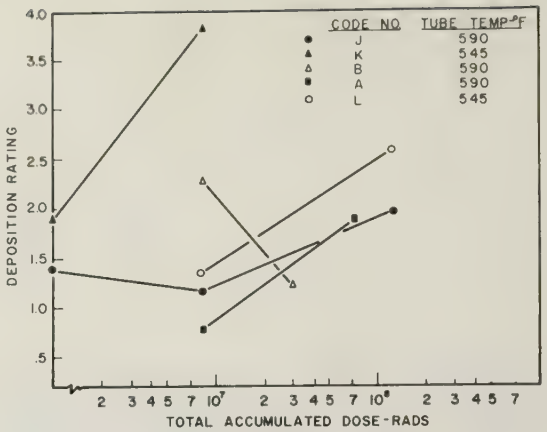

Fig. 5 — Deposition rating as function of accumulated dose

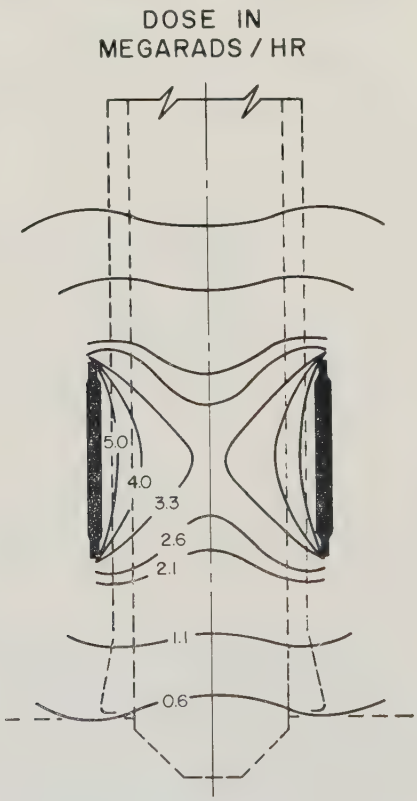

Fig. 4 — Isodose lines in irradiated WADC deposition tests

down through the coker sump. The air provides an oxidation accelerator and improves the heat transfer from the heated tube by agitating the oil. The thermal stability of the lubricant is rated by the amount of sludge deposited on the filter, plus the adjusted weight of hard coke deposited on the heated tube in the coker sump during a 12-hr test. The weight of the sludge in grams plus 10 times the weight of the hard coke in grams on the heated tube is given as the deposition number and is used as an index of the lubricant's thermal stability. In the modified test, the arrangement of the circuit was altered slightly to allow the Cobalt-60 sources to be placed quite close to the surface of the pyrex glass wall of the coker sump. This brought a high-level radiation field to the point of maximum thermal stress. If the high-level radiation should accelerate the thermal degradation of the lubricant, it would be afforded an excellent opportunity with this arrangement. Fig. 4 gives the isodose lines through the deposition tester sump.

The first results from this modified deposition test appeared a little disappointing to those of us who had been working on the development of these dynamic radiation tests. It is hard to say what we expected from these first exploratory runs, but we certainly presumed that there would be a sharp increase in the sludge and coke weights with a resultant high deposition number. Curiously enough, the deposition number dropped in many cases and showed but a slight gain in others. As a generalization, the better lubricants appeared to improve in performance while the marginal lubricants deteriorated to a greater extent under the radiation. But we were employing the "old ground rules" to this screening test, and we knew only a small part of the story, as we later learned.

As the tests progressed, we tried a little harder to damage the lubricants and subjected the better lubricants to considerable static irradiation prior to the deposition test. The results of some of these tests are shown in Fig. 5. The dynamic radiation dose applied under test is 8.4×10^6 rads[1] on this plot,

[1] A rad represents approximately 7% greater energy absorption by the lubricant than a roentgen of radiation.

so that any higher accumulated doses were added by static irradiation. As can be seen from this graph, there is a minor increase in the deposition number as the total dose is increased.

One important point did emerge from this pre-irradiation — there was evidence of considerable attack of the pure aluminum coking tube, particularly in the area directly over the diffuser ball where the humidified air is introduced. Heavy pits and corroded areas appeared on the tube, in addition to overall etching of the tube as evidenced by a weight loss for the coking tube. It was decided that the corrosivity of the fluid might be altered considerably due to the radiation damage during the dynamic test. To check this possibility, a revised sump was constructed as shown in Fig. 6.

Irradiated Corrosion-Deposition Test

The corrosion-deposition tester was designed to take six of the standard 400 F corrosion metal samples mounted on a stainless-steel support clip. The metal samples were: copper, silver, aluminum, magnesium, iron, and lead. The radiation field was moved lower to place the high flux field on the metal samples as they are soaked in the hot lubricant descending from the coking tube. Placing the high flux field around the metal samples insures that the production of unstable free radicals, if any, will be given ample opportunity to combine with the metal samples. The isodose flux field for the sump is shown in Fig. 7. As in the WADC deposition tester, the moist air is bubbled up into the lubricant through a ceramic diffuser ball. The remaining system is identical to the previous tester.

Severe corrosion weight losses were observed dur-

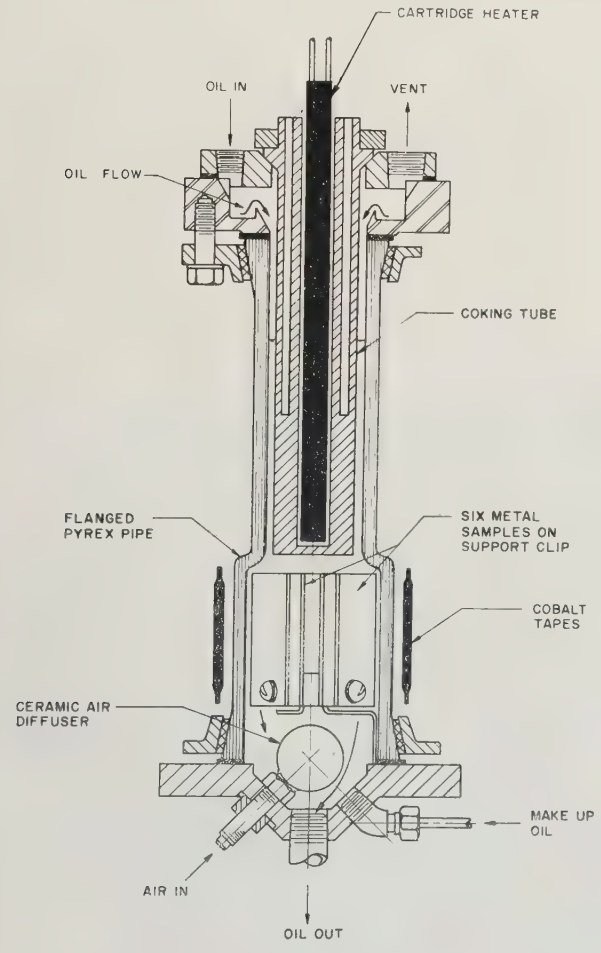

Fig. 6 — Corrosion-deposition tester

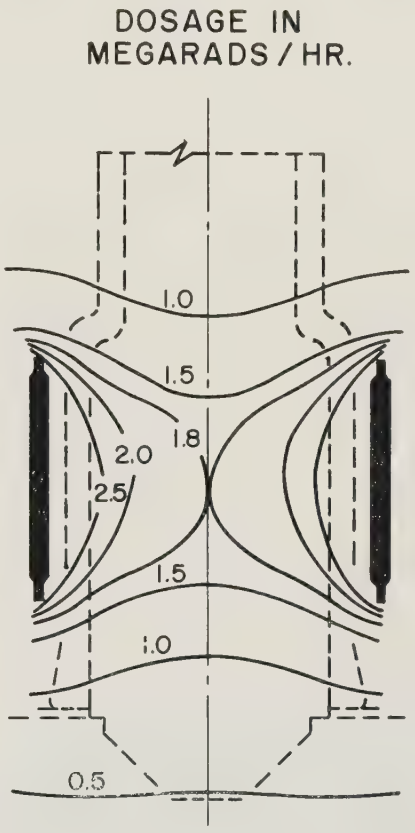

Fig. 7 — Isodose lines for corrosion-deposition tester sump

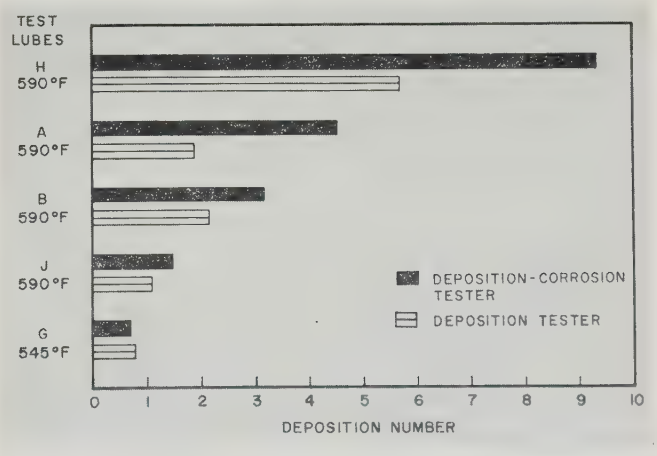

Fig. 8 — Deposition numbers for several lubricants in two types of deposition testers

ing 12-hr runs — 300–400 mg/in.^{2} being common for lead, copper, or silver. A particularly unusual result with one lubricant was the plating of the copper onto the surface of the aluminum specimen. The plating was thick enough to require an acid strip to remove the copper to obtain the true weight of the aluminum specimen. The corrosion-deposition tester tended to increase the deposit-forming characteristics of those lubricants that had increased deposit-forming characteristics in the irradiated deposition test, as illustrated in Fig. 8. Notice that the word stability is avoided at this point, because, as we presently know, the deposition number is an unreliable index of the stability of a lubricant operating under radiation.

An interesting sidelight brought forward by the corrosion-deposition tester is the seeming independence of the neutralization number relative to the corrosivity of the lubricant under dynamic test. The neutralization number has been regarded to some degree as an index of the comparative corrosivity of an oil. Static irradiation data normally show a sharp increase of the neutralization number with increased dose; but Fig. 9, showing total accumulated dose versus neutralization number on a number of oils operated on the first tests in the irradiated deposition tester, shows that generally there is little or no increase in the neutralization number as the dose is increased. Perhaps light acids formed as a result of the irradiation are evaporated during the test.

The effect of neutralization number on corrosivity is shown in Fig. 10. These data were obtained on the corrosion-deposition tester. The total metal attack plotted as the abscissa is the sum of the milligrams of metal removed from all six metal specimens and serves as a rough parameter to evaluate the overall corrosivity of the lubricant. The "shot gun scatter" seems to indicate that the neutralization number bears no relation to the total metal attack when the test is conducted under radiation. The total metal attack is not a simple function of the neutralization number, however, since there would be many other controlling factors.

Table 1 — Operating Conditions of 100-mm Bearing Under Radiation

Lubricant Flow	480 cc/min
Total Lubricant in System	1180 cc
Bearing Load	500 lb radial
Bearing rpm	10,000
Bearing Temperature	500 F
Dose Rate	2×10^6 rads/hr average

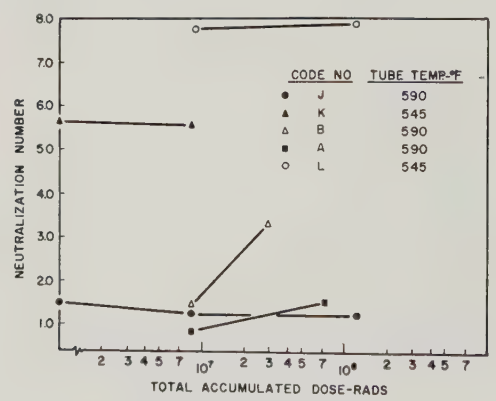

Fig. 9 — Neutralization number as function of accumulated dose of several lubricants

Irradiated Bearing Head

After a considerable number of oils had been screened in the irradiated deposition tester and the irradiated corrosion-deposition tester, tests were started on an irradiated version of the WADC high-temperature bearing head. This bearing head was modified to maintain the maximum percentage possible of the total test lubricant volume of the system in a high-level radiation field. As a result, the detail design of the bearing head was modified to a considerable extent, particularly to incorporate a pressure sump on the face of the bearing head where the oil could be subjected to radiation prior to being jetted onto the 100-mm test bearing. The remainder of the system was miniaturized to reduce the amount of oil outside of the high flux level zone.

Fig. 11 is a schematic of the high-temperature bearing head configuration. The housing supporting the 100-mm test bearing was milled with 20 slots around the periphery of the outer race to allow 20 Cobalt-60 tapes to be inserted close to the mechanically stressed inner surface of the outer race. A

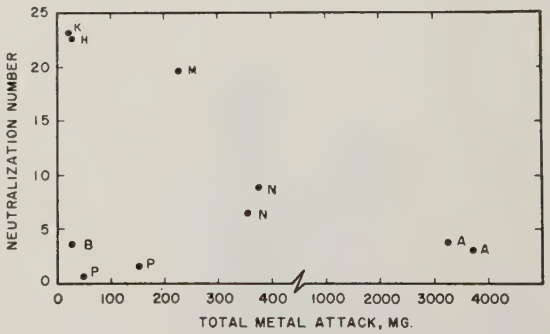

Fig. 10 — Effect of neutralization number on total metal attack

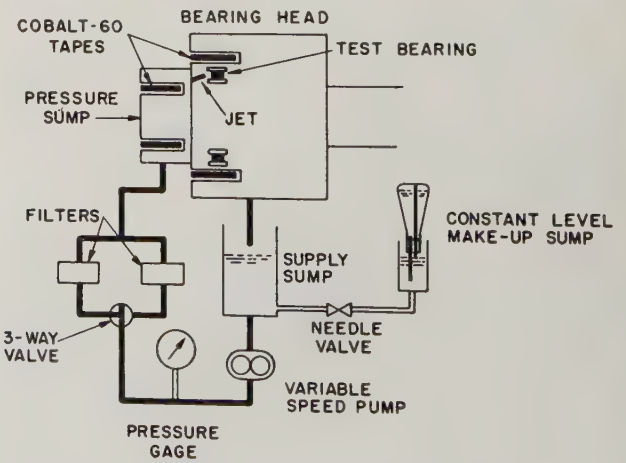

Fig. 11 — Schematic of high-temperature bearing head

considerable portion of the total lubricant in the system was contained in a pressure sump on the front face of the bearing where it was subjected to high-level radiation by a matrix of 10 Cobalt-60 tapes. Fig. 12 illustrates the isodose lines in megarads per hour obtained through the bearing and the pressure sump area. The bearings, in spite of the attenuation of the small amount of intervening supporting housing, were subjected to approximately 2 megarads per hr, while the pressurized sump area varied between 2–3 megarads per hr average flux level. The average overall dose accumulated by the lubricant in circulating through the entire system was approximately 2×10^6 rads per hr. A more detailed section of the high-temperature bearing head can be seen in Fig. 13, showing the radiation matrix of Cobalt-60 tapes used to create the high-level flux field.

The conditions used for operation of the 100 mm bearing under radiation conditions are shown in Table 1.

The first oil operated in the bearing rig under radiation conditions was a paraffinic mineral oil that had shown a comparatively low deposition number under irradiation at 590 F. At the end of 25 hr and 15 min of testing in the high-temperature bearing rig under dynamic radiation conditions, the test oil pressure increased suddenly and sharply from 20 to 60 psig, and the bearing head temperature climbed rapidly without the addition of external heat. The pressure sump was removed from the face of the bearing head within a few minutes of shutting down the test, and the lubricant dripping from the pressure sump solidified before hitting the floor of the test cell. The interior of the pressurized oil reservoir is shown in Fig. 14. The material within the reservoir was a tough, tarry substance that resisted the efforts of hot degunking baths and required re-

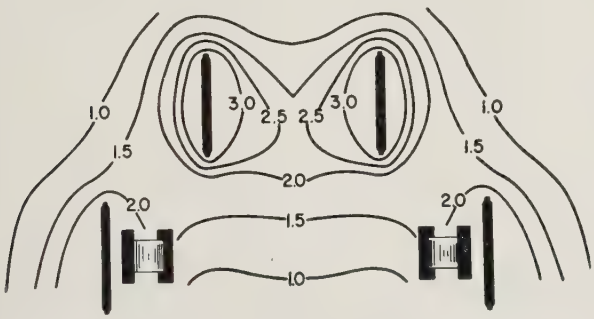

Fig. 12 — Isodose lines for high-temperature bearing head (dosage in megards/hr)

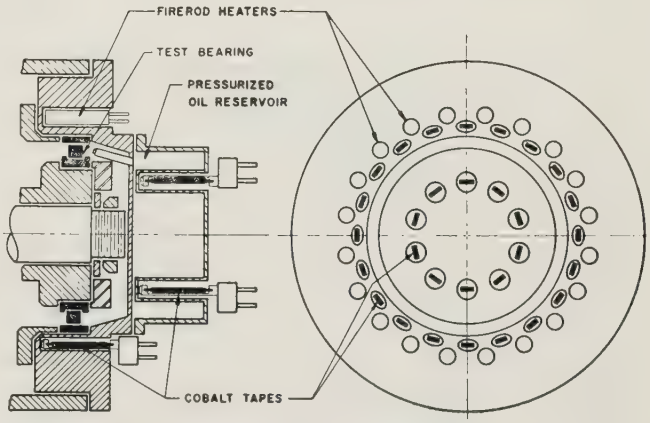

Fig. 13 — Cross-section of high-temperature bearing head

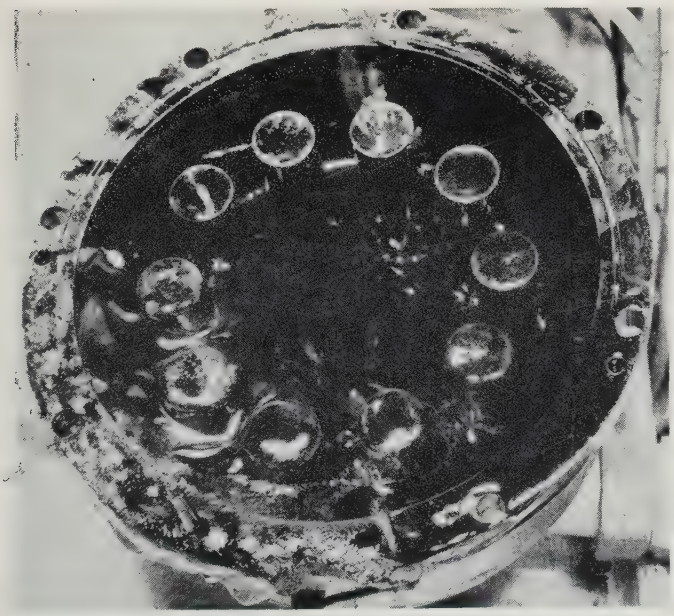

Fig. 14 — Interior of pressurized oil reservoir after lubricant solidified on test

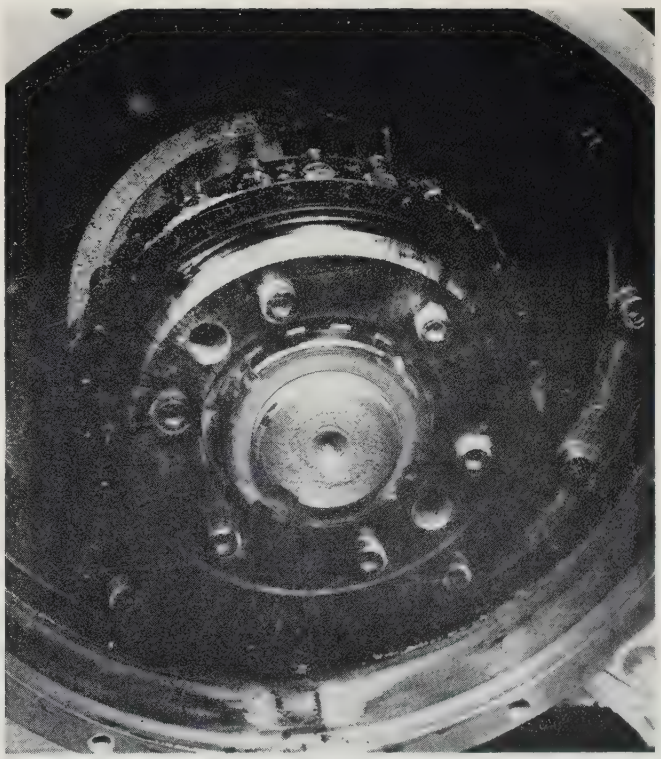

Fig. 15 — Rollers and cage after irradiated bearing test on paraffinic mineral oil

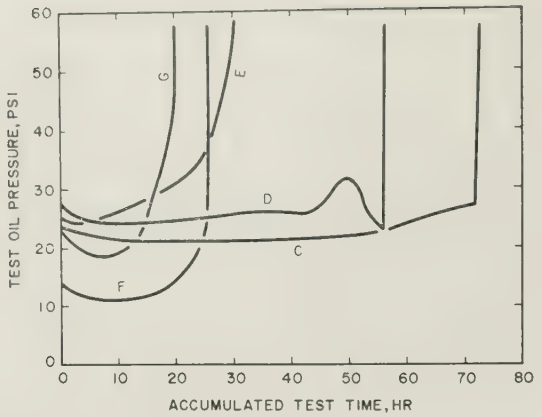

Fig. 16 — Test oil jet pressure as function of test time

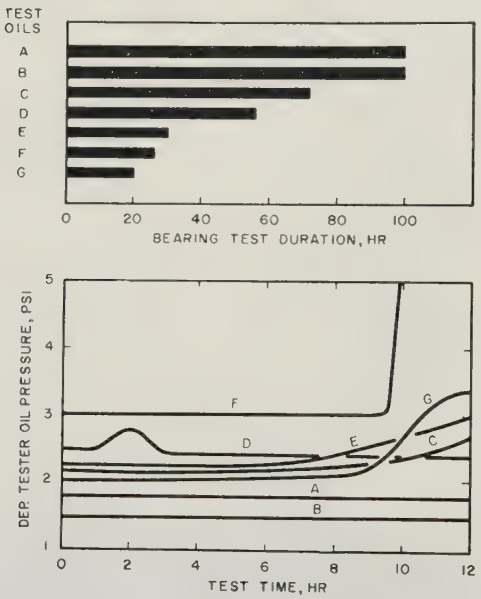

Fig. 17 — Correlation between corrosion-deposition tester and high-temperature bearing head test duration time

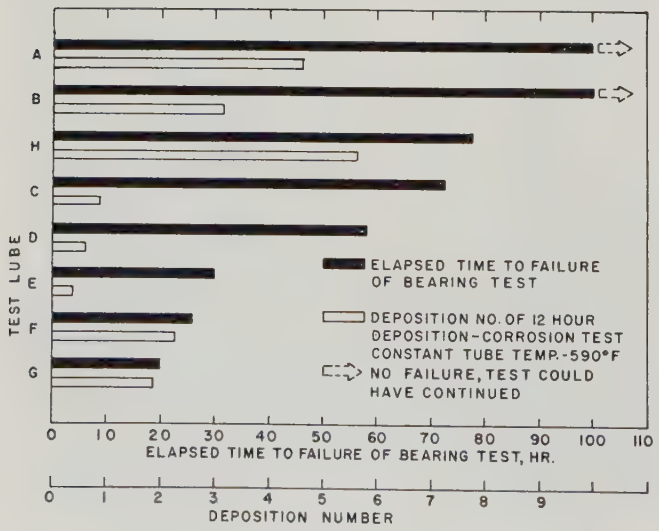

Fig. 18 — Comparison of deposition rating of 12-hr corrosion-deposition test and duration of high-temperature bearing test

moval by chipping and scraping from the interior of the reservoir, with a final clean-up using emery and crocus cloth. Although it is difficult to see in Fig. 15, the rollers and cage were amazingly clean and free from coke or sludge deposits.

The mechanism of failure was sudden; quick action by the operator averted damage to the test oil pressure gage. Up to the moment at which the lubricant started to solidify, its performance appeared to be completely satisfactory with little or no prior indication of the impending failure, other than a slow, unimpressive increase of the test oil pressure. A number of other lubricants, including synthetic, were run after this first test, and the pattern of failure was quite similar to this paraffinic mineral oil. During the three years or more of screening experimental lubricants with the unirradiated 100-hr WADC high-temperature bearing test in our laboratories, there has been no instance in which a lubricant has exhibited such sharp viscosity changes.

Fig. 16 shows the test oil pressure as a function of test time, and the pattern of failures illustrates the sudden pressure increase demonstrated by the first lubricant. The test lubricant pump is a gear-type, constant displacement pump driven by a variable speed drive and discharging through a fixed jet orifice. Although the filter lies between the oil pump and the oil jet, the sudden pressure increase is due to a viscosity increase and not due to sludge formation or hard coke in the jet or the filter. This possibility was eliminated during the first few tests by stopping to clean the filters and orifice at the first indication of a sharp pressure rise. No undue blocking or plugging was evidenced, and the oil pressure started off again at approximately the same level at which the test had been interrupted. There is normally only a small amount of sludge formed during the dynamic radiation bearing test; in fact, there appears to be a definite reduction of sludge and coke formation when this test is operated irradiated as compared to unirradiated. This is not a general rule for all lubricants but only those that show a high degree of thermal stability.

Correlation of Test Procedures

A study was made of all of the variables of each of the deposition tests to determine if there was a single or a combination of parameters that could be used to predict the duration of the high-temperature bearing test. Fig. 17 shows the only parameter that bore any correlation whatsoever. The corrosion-deposition tester oil pressure is a function of the pressure required to force the lubricant through the small filter and the 0.25-in. tubing between the pump and the sump. With the exception of lubricant "F" that plugged the oil filter with sludge to bypass at 7 psi, the remainder of the oil pressure increases are due to viscosity increases.

It was noticed during some of the corrosion-deposition tester runs that a considerable reduction in energy input to the coking tube was required toward the termination of the test to maintain a constant coking tube temperature. With this in mind, another look was taken at our method of stressing the lubricant. If a physical change was occurring in the lubricant so that it was unable to remove a constant amount of heat energy from the coking tube,

why should the heat input be reduced during the test to maintain a constant tube temperature? The engine uses the oil as a heat transfer medium to remove heat energy generated by the gears and bearings; therefore, if the lubricant suffers a physical change that will not allow it to remove this fixed amount of generated heat, then it is simply going to have to face a higher temperature differential until a heat balance is obtained. In the light of this elementary bit of logic, a constant heat energy input test certainly seemed to offer more realistic data than the conventional constant temperature type of test. Lubricants with high specific heats and good heat-transfer coefficients should not be penalized in screening tests by being forced to remove a larger amount of heat energy by virtue of these desirable characteristics.

A new set of test conditions was, therefore, established for the corrosion-deposition tester. A lubricant that had shown excellent stability during irradiated tests was selected and several tests were run maintaining a 590 F coking tube temperature in the corrosion-deposition tester. The heat energy delivered to the lubricant per hour was measured with an integrating wattmeter. An average heat energy input figure of 900 watts was obtained, and this was selected as the input level for the new test. The lubricants were operated on test until one of three events occurred: 40 hr elapsed test time, cross-linking or polymerization of the lubricant so that it could no longer be pumped, or a change in the heat acceptance capability of the lubricant so that it could no longer maintain a reasonable coking tube temperature. A limiting coking tube temperature of 750 F for the test was established, since the rise in temperature generally appeared to be virtually asymptotic at this level. Forty hours of test duration was selected as a compromise figure, since it appeared from preliminary data that 40 hr would be equivalent to 100 hr, the duration limit of the bearing test. This duration was sufficient to screen the majority of the lubricants, but not all of them, since lubricating ability enters into the bearing test and is not evaluated in the corrosion-deposition test. Lack of lubricating ability at elevated temperatures has eliminated a number of promising thermally stable lubricants in unirradiated bearing tests. With these new test conditions, the comparative duration time of the corrosion-deposition screening test was almost in perfect correlation with the irradiated high-temperature bearing test duration. Fig. 18 illustrates the lack of correlation between the deposition number of the first 12-hr corrosion-deposition test and the duration of the irradiated bearing test. If the deposit-forming characteristics of the lubricants had been truly indicative of the radiation stability of the lubricant, then a small deposition number should accompany a bearing test of extended duration. Fig. 19 illustrates the comparison of the duration of the new constant heat input corrosion-deposition tests and the duration of the irradiated high-temperature bearing head test. A good correlation is obtained between the relative duration of the two tests. With this new screening test, a more definitive means of screening the lubricants prior to the bearing test was obtained.

With the improved correlation of the constant heat corrosion-deposition tester in predicting the

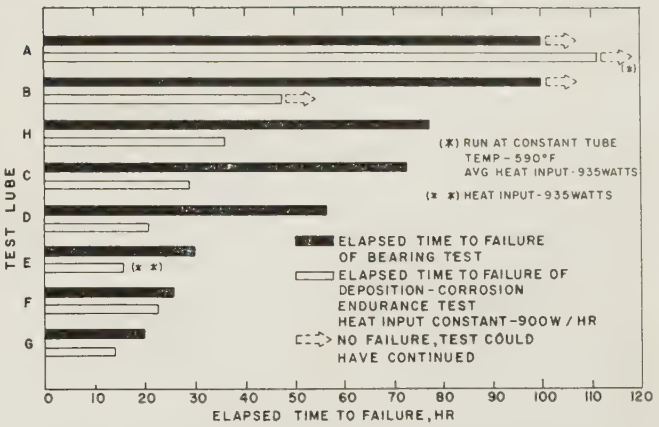

Fig. 19 — Comparison of duration of constant heat input corrosion-deposition test and high-temperature bearing test

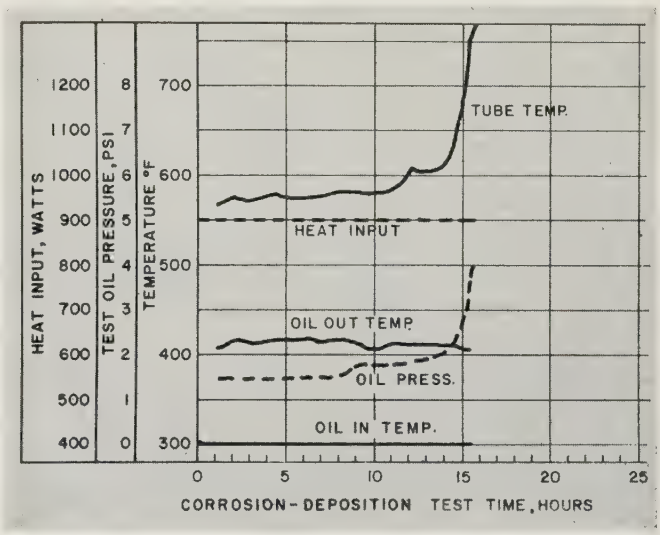

Fig. 20 — Performance of unstable lubricant in corrosion-deposition test using constant energy input

lubricant performance, the constant heat energy input concept was extended to the irradiated high-temperature bearing rig. To some extent this test had been perfroming as a constant heat input device due to the heat generation of the 100-mm bearing running at 10,000 rpm under a 500-lb radial load. The same lubricant "A" was used to establish the constant heat energy input to the bearing rig, as in the case of the corrosion-deposition test rig. Holding a constant bearing temperature of 500 F, an input of 2400 watts was selected as the best compromise for a constant heat input. Failure of the lubricant in this constant energy input test was subsequently defined as a bearing temperature of 650 F, a test lubricant pressure of 100 psig, or any unusual vibration or noise generated by the bearing. These conditions were selected because total failure of the bearing was imminent if these conditions were exceeded to any extent. The bearing test was to be operated for 100 hr only to permit the screening of more lubricants during the available test time.

Fig. 20 illustrates the performance of a relatively unstable lubricant in the constant energy input cor-

rosion-deposition tester. Once the properties of the lubricant began to change, the failure generally occurred within a short period of time. As the heat acceptance capability of the lubricant decreases, the temperature of the coking tube starts to increase and accelerates the degradation of the lubricant. In contrast, the constant temperature type of test reduced the energy input to maintain a constant tube temperature and prolonged the test by favoring the immediate capability of the lubricant to remove energy from the coking tube.

Fig. 21 shows what happens to a lubricant that displays marginal stability in the constant energy input corrosion-deposition tester when it is operated in the irradiated bearing test. The steady test pressure increase and coking tube temperature increase indicate a considerable degradation of the lubricant in the screening test. Undoubtedly, if the corrosion-deposition test had been continued for a few more hours, the coking tube temperature would have reached the 750 F limit of the test. The instability of this lubricant was verified by its performance in the bearing test where it was determined at 29-hr elapsed time that the lubricant would fail within a short period of time, so the test was terminated. The appearance of the rollers and cage as well as the outer bearing housing can be seen in Fig. 22. There was little or no hard coke on the cage but a considerable quantity of soft sludge on the surface of the outer bearing assembly. The rollers were free in the cage, although the temperature of the bearing was climbing rapidly at the time the test was terminated.

Fig. 23 illustrates the behavior of a stable lubricant in the screening and the bearing test. The corrosion-deposition test indicated a high degree of stability with the heat-transfer characteristics improvng slightly during the test, as shown by the decrease in the coking tube temperature. The lubricant survived the 100-hr bearing test, but it is evident from the increasing test oil pressure and bearing temperature data that failure was imminent. Fig. 24 shows that even after a 100-hr test the rollers, cage, and all of the rotating parts are clean, while the outer bearing housing assembly shows some accumulation of soft sludge.

Conclusion

At this point it would be well to emphasize that the data generated in this program was of a "cataloging" nature where the maximum number of lubricants was screened to determine how many of them and to what extent each would be stable under these severe conditions. If there appear to be unanswered questions and areas requiring better defi-

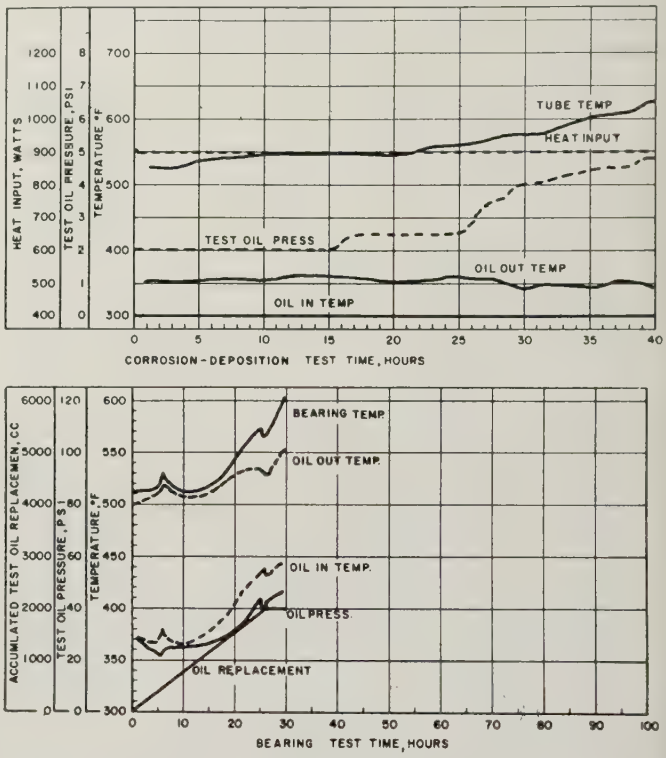

Fig. 21 — Performance of marginally stable lubricant in corrosion-deposition test and high-temperature bearing test using constant energy input in both cases

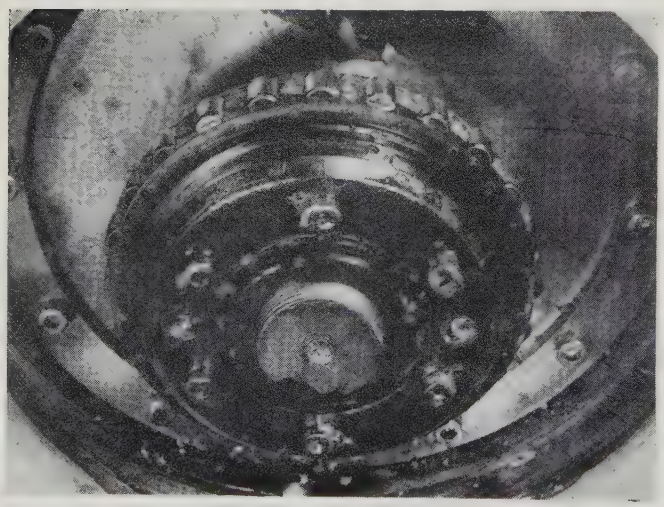

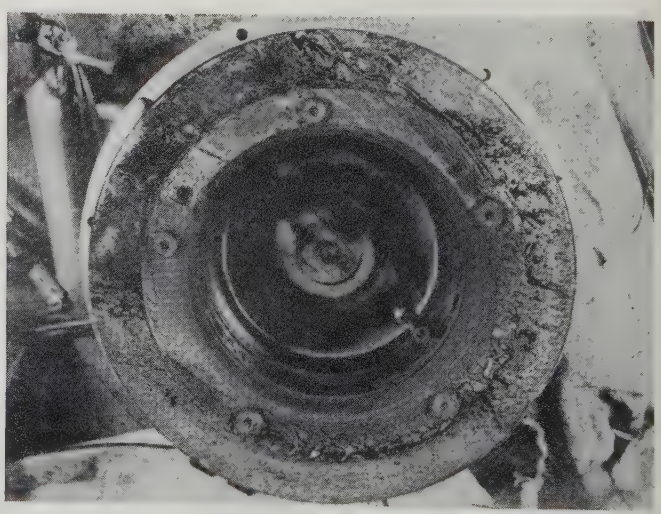

Fig. 22 — Rollers and cage and outer bearing housing assembly after failure of marginally stable lubricant

nition, and there are a considerable number of both, time and funds did not permit the thorough exploration of the interesting sideroads revealed during the planned screening runs.

In review, what are some of the things we have learned about the lubrication of a propulsion unit under high level radiation? First, we must be extremely careful about the selection of engine materials, because the lubricants can become excessively corrosive under high-level radiation. Lead, copper, silver, magnesium, and to some extent aluminum, may be heavily attacked and in approximately that order. Second, the lubricants may fail quite suddenly with no prior warning; the failure may result from either cross-linking to a solid material or from an almost complete loss of heat acceptance capability, either of which would be sufficient to initiate engine failure. As to fatigue, one test was run for a total of 300 hr and there did not appear to be any damage to the bearing. This lubricant, however, had a high replacement loss rate, and it is possible that as it became damaged by radiation it was evaporated before it could affect the fatigue life of the bearing by surface corrosion or some allied phenomena. There was one incident that lends a note of caution: One of the qualified MIL-L-7808 lubricants that has consistently shown high stability under radiation demonstrated a surprising fatigue or corrosion phenomenon. After approximately 72 hr of running, the temperature of the bearing started climbing at a precipitous rate and upon examination it was found that the 100-mm roller bearing had approximately 1/16 of an inch total clearance. The surface of each of the rollers had spalled or flaked off to a depth of 0.015. The races appeared unchanged by visual inspection and the damage had occurred to the rollers only. The only indication of this failure had been a sudden rise in bearing temperature, so it is difficult to define the pattern of the failure. Nevertheless, it is a little unnerving to view this type of phenomenon and realize it may happen with other lubricants at some unpredicted dose level.

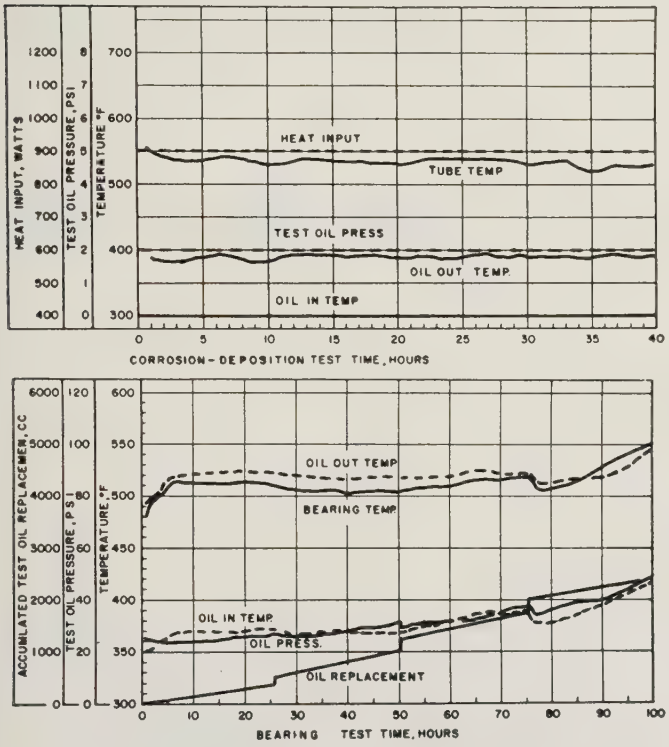

Fig. 23 — Performance of stable lubricant in corrosion-deposition test and high-temperature bearing test using constant energy input in both cases

Looking back over the work that has been accomplished prior to the termination of the program, it is possible to see that the surface of dynamic testing work has only been scratched. A comprehensive investigation of one of the ill-defined areas would constitute in itself a major research effort. This is not surprising when we consider that decades of research have been spent in defining and improving the stability of lubricants in high-temperature applications. We have added the additional dimension of radiation with its accompanying array of unknowns — why shouldn't the picture be complex?

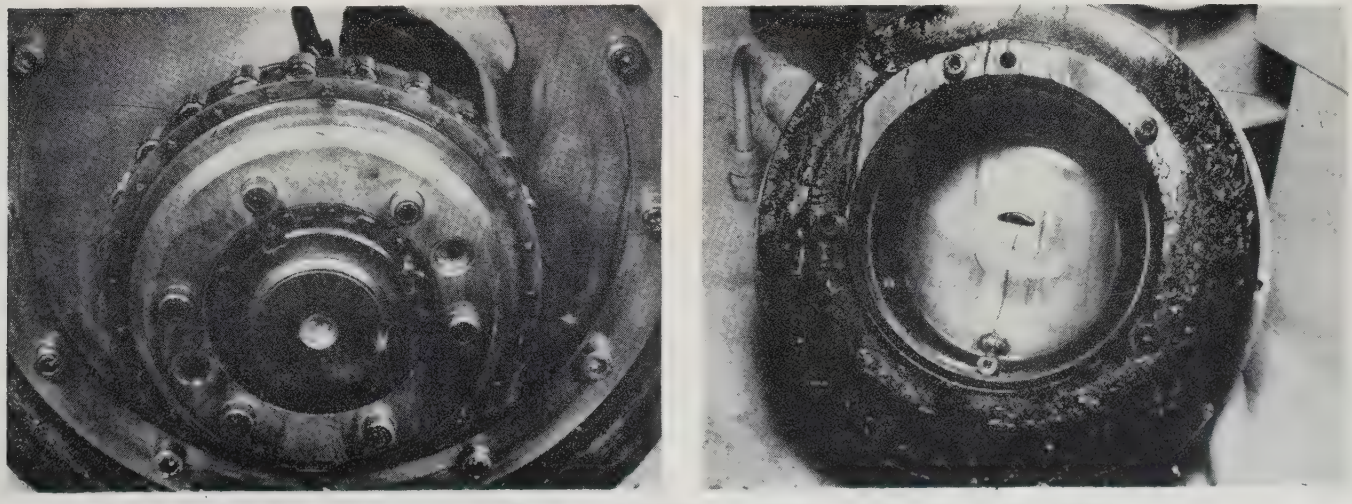

Fig. 24 — Rollers and cage and outer bearing housing assembly after 100-hr run on stable lubricant

status of the VIBRATION of Aircraft

THIS PAPER outlines progress to October, 1958, on the new Shock and Vibration Manual. At that point, the methods of solving vibration isolation problems had been established. After further refinements and expansion, the manual will be issued by SAE Committee S-12 on Shock and Vibration.

The manual will set up procedures to be followed by engineers who don't have extensive experience in the field. It will give procedures for problems having up to six degrees of freedom.

The procedure, as described in the paper, now consists of three steps:

1. Specification of the data required for the solution of a given problem.
2. Calculating whether vibration isolators are needed.
3. Determining the dynamic properties of the isolation system when the above step indicates isolation mounts are needed.

AT THE October, 1957, National Aeronautic Meeting of the SAE technical sessions on Shock and Vibration were sponsored by the S-12 Committee. One of these sessions was devoted to the activities of S-12 and its approach to the problem of vibration isolation of electronic equipment in aircraft. The purpose of the present paper is to summarize progress made during the past year and to outline the current approach, which has evolved from S-12 efforts to develop a satisfactory design procedure for vibration isolators.

As originally conceived,[1] the problem of vibration isolation concerned the interrelationship of three subsystems: the vibration source, the equipment to be isolated (designated as the "receiver"), and the vibration isolator which is interposed between the source and the receiver. This breakdown of the problem is shown in Fig. 1.

In order to focus the attack on the problem, the S-12 Committee was organized into working subcommittees designated as the Subcommittee on Sources, Isolation Systems, and Receivers, respectively, corresponding to each of the components of the general problem. The function of these subcommittees was to explore the significant factors and problem areas associated with each sub-system, to collect pertinent information on these factors, and to develop the proposed approach to the isolation problem from the standpoint of the designated sub-system. In addition, a Subcommittee on Complex-Wave Excitation was formed to consider the problems involved in, and the techniques required for, treatment of the situations involving excitation with random and/or complex periodic vibration.

In addition to the subcommittees, there is a Steering Committee consisting of the committee officers and the subcommittee chairmen. The results of the efforts of the subcommittees are discussed and compared at the committee meetings. Fig. 2 shows the current organization of the S-12 Committee.

1957 Status Summary

To provide a background for assessing progress, the status of the problem as presented at last year's meeting will be summarized.

1. The vibration source[1] at the equipment mounting point in the airplane is characterized mainly by its vibratory motion and by its pertinent mechanical properties, particularly the mechanical impedance, which is determined by the mass, stiffness, and damping factors of the structure. Since all aircraft mounting structures have finite flexibility, the motion of the source (which is the input to the isolator-receiver combination) is affected by the load impedance (mass, stiffness, and the like). This implies a requirement for two types of information which are not now readily available.

a. Information on mechanical loading at the

[1] "Describing Aircraft as Vibration Source," by W. W. Harter. Paper presented at SAE National Aeronautic Meeting, Los Angeles, September–October, 1957.

SAE S-12 approach to

ISOLATION

Electronic Equipment

Fred Mintz, Lockheed Aircraft Corp.

This paper was presented at the SAE National Aeronautic Meeting, Los Angeles, Oct. 1, 1958.

point of measurement should be included with all vibration data obtained in aircraft (and much more vibration data are needed).

b. Of utmost urgency is the need for data on the mechanical impedance (as a function of frequency) of typical aircraft mounting points.

2. The Subcommittee on Isolators[2] has listed the following categories of isolator properties as significant, and has begun to accumulate information on them:

a. Linearized dynamic performance — along and about three axes (the concept of "elastic center" of the isolator is highly useful in this connection).
b. Loading and deflection capabilities.
c. Strength and endurance.
d. Ability to withstand environmental influences, such as temperature, oil, ozone, and the like.
e. Features of installation and construction.

3. With respect to receivers,[3] the important in-

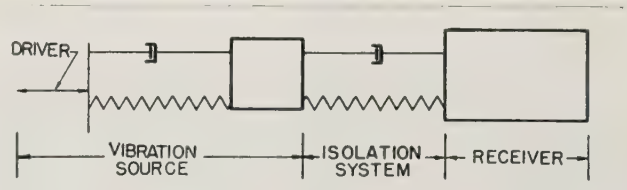

Fig. 1 — Schematic representation of aircraft equipment installation dynamic system

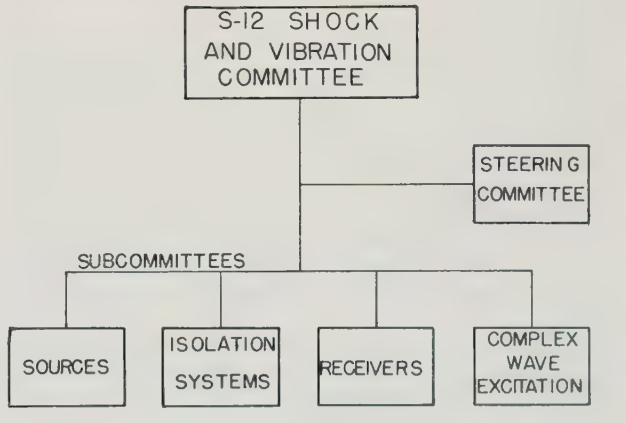

Fig. 2 — S-12 Shock and Vibration Committee organization

[2] "Selection of Shock and Vibration Isolators," by S. Rubin. Paper presented at SAE National Aeronautic Meeting, Los Angeles, September–October, 1957.
[3] "Subcommittee on Receivers Report on . . .," by H. Himelblau, Jr., et al. Paper presented at SAE National Aeronautic Meeting, Los Angeles, September–October, 1957.

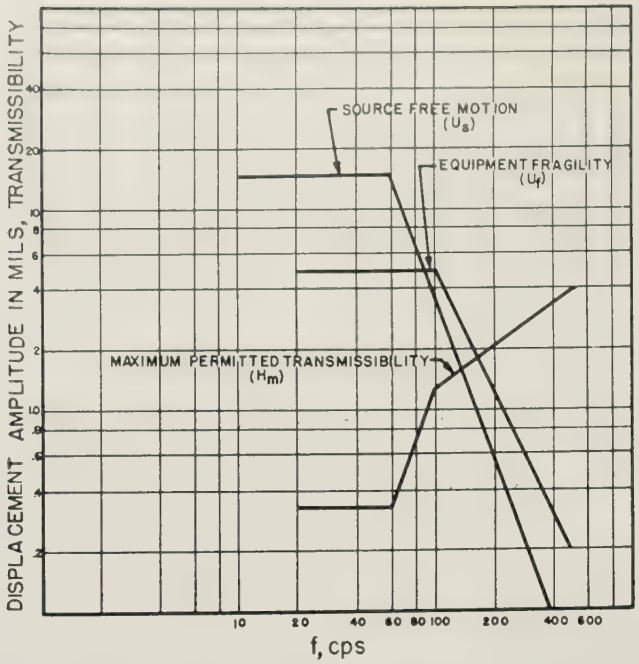

Fig. 3 — Fragility curve (U_f), source free motion (U_s), and maximum permitted transmissibility (H_m)

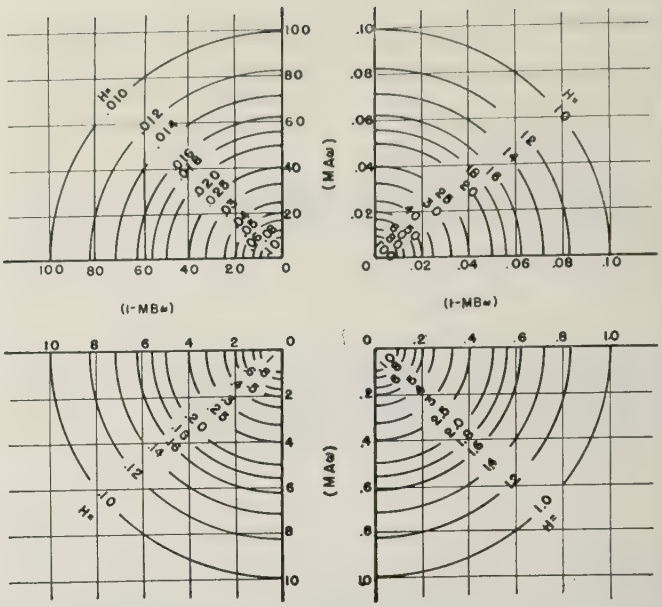

Fig. 4 — Curves of (MA_ω) versus ($1\text{-}MB_\omega$) for constant H (in four ranges: 0-0.1, 0.1-1.0, 1-10, 10-100)

Table 1 — Tabular Form for Calculation of H_o

f, cps	A_s,[a] in./lb-sec	B_s,[a] in./lb-sec	$2\pi mB_sf$ $(=\omega B_s)$	$1-m\omega B_s$	$2\pi mA$ $(=m\omega A_s)$	H_o (from Fig. 7)

[a] Obtained from the given source admittance data:

$$\text{(admittance } \varepsilon_s = \frac{1}{Z_s} = A_s + iB_s)$$

formation needed for design of an isolator system is the receiver's mechanical impedance and its fragility. To make the design problem reasonably tractable, the initial approach considers the receiver impedance to be represented adequately by a simple mass load. Consideration has also been given to the matter of location of a fragile component inside a receiver and how this location affects isolation system design. A concept of fragility has been developed, summarized as follows:

The vibration environment and the fragility are both described as "lumpy" blankets on a three-dimensional plot, the length and width of the blanket corresponding to the vibration frequency and time axes. The height of the blanket and the thickness of the lumps represent the mean amplitude of the vibration and its standard deviation, respectively. Probability of damage is minimized when the "fragility blanket" is much higher than the "environmental blanket" and both blankets are relatively thin.

4. In its consideration of complex disturbance, the Subcommittee on Complex Excitation has developed the following views:[4]

Given the source impedance and mechanical properties of the isolator-receiver combination, it is possible to compute the sinusoidal components at the receiver from those in the source. Likewise, it is possible to compute the random part of the receiver vibration from the power spectral density curve for the random part of the source. To establish that the receiver will survive the excitation, it may be possible to set up some arbitrary rules for converting "fragility" to a single curve or single probability distribution.

What is now done is to combine the effect of the several sinusoids and the random components by applying an appropriate margin of safety, and to see whether the receiver is adequately protected within this margin of safety.

1958 Developments

Since the October, 1957, meeting, the S-12 Committee has, through the subcommittees, continued to explore the problem areas outlined earlier, to develop and clarify the techniques used in analyzing and solving the problems and to solicit and collect available information from their own industrial contacts, through government sources and from Committee consultants.

Among other significant items, terminology, and definitions have been thoroughly considered; a great deal of detail labor was eliminated when draft copies of the proposed new Standard Shock and Vibration terminology became available and were adopted by the Committee for its use. The question of transient excitation was considered and presented in detail at one of the Committee meetings by one of its members. The matter of designing an isolation system to protect against shock, however, has been deferred until the problem of isolation against

[4] "Role of Complex Wave Excitation in Equipment Protection Problem," by R. S. Bradford. Paper presented at SAE National Aeronautic Meeting, Los Angeles, September–October, 1957.

steady-state excitation is more nearly under control.

Analytical treatment has been developed, yielding the performance equations for the general isolation case of the suspended rigid body with six degrees of freedom.

Of perhaps greatest significance, however, has been the institution of a series of "shirt-sleeve sessions" at which has been carried out the arduous task of extending the theory, molding it into a simple and effective design procedure, and working out numerical examples. Although much effort is yet needed, and additional revisions in the design procedure have to be adopted before an acceptably simple and reliable design procedure is at hand, encouraging progress has been made at these work sessions. The results of these sessions have been presented to and considered by the various subcommittees, with subsequent feed-back of results and suggestions.

Today, the outline and philosophy of the proposed procedure have assumed a visible shape and the direction of further development seems reasonably clear. It seems appropriate, therefore, to consider the design procedure in some detail.

Tentative Design Procedure

This section is devoted to a presentation of the isolator design procedure in its state of development at the time of writing. For purposes of clarity, attention will be focused on the case of a simple center-of-gravity mounting system in which only vertical vibration is of interest; the major intent here is to show how the design problem is treated when the finite mechanical impedance of the source is a significant factor.

In this approach, the first item of interest is the statement of data required to define the problem. The next step is to determine whether isolation is required. If it turns out that isolation is indeed necessary, suitable dynamic parameters for the isolator must be selected by a repetitive trial process.

1. *Data Required*

1.1 Equipment Inertia Parameters
(Weight W in lb and location of c.g.)

1.2 Equipment Fragility

A single continuous curve of sinusoidal amplitude versus frequency, defining the limits of motion below which failure or malfunction will not occur (covering the entire frequency range of interest and including necessary adjustment of factors for fatigue, super-position of several sinusoidal inputs, and the like).

1.3 Source Data

1.3.1 Free motion . . . amplitude of sinusoidal displacement, velocity, or acceleration versus frequency.

1.3.2 Mechanical impedance or admittance of source versus frequency.

2. *Determination of Need for Isolation System*

When the source impedance is finite, the load of the equipment affects the source motion, making it different from that of the unloaded source. This is, in fact, precisely the reason that source impedance must be considered in determining the need for isolation and in designing the isolation system.

In order to treat this situation in a simple manner, it becomes convenient to define a new kind of "transmissibility," H, as the equipment amplitude divided by the source free amplitude. As the source impedance approaches infinity (or the source admittance aproaches zero) H approaches, in value and in meaning, the conventional "transmissibility."

2.1 The maximum permitted transmissibility H_m is determined as the ratio of the maximum permitted amplitude, μ_f (fragility amplitude), to the source free amplitude, μ_s. H_m is plotted as a function of frequency. (If μ_f and μ_s are plotted together on log-log coordinates, H_m can be determined graphically as the difference between the μ_f and the μ_s curves and plotted on the same scale, as shown in Fig. 3).

In order to ascertain whether isolation is needed, it must be determined whether the amplitude of the equipment mounted directly on the source exceeds the maximum permitted (fragility) amplitude.

The effect of the load impedance, $m\omega i$, on the source motion is given by the equation:

$$\frac{\mu_o}{\mu_s} = \frac{|Z_s|}{|Z_s + m\omega i|} \tag{1}$$

where:

μ_o = Amplitude of motion of the equipment mounted directly on the source
μ_s = Amplitude of free motion of the (unloaded) source
$|Z_s|$ = Absolute value of the source impedance
$m\omega i$ = Impedance of the equipment of mass m

If the source parameters are expressed as admittances, Equation 1 can be written:

$$\frac{\mu_o}{\mu_s} = [(1 - mB_s\omega)^2 + (mA_s\omega)^2]^{-\frac{1}{2}} \tag{2}$$

where:

A_s = Real part of the source admittance
B_s = Imaginary part of the source admittance
$\omega (= 2\pi f)$ = Frequency in radians per sec

The ratio μ_o/μ_s of amplitude of equipment mounted on source to free amplitude of source, may also be thought as a transmissibility H_o. If this ratio H_o exceeds the maximum permitted transmissibility, H_m (this is another way of saying that μ_o exceeds μ_f) at any frequency, then isolation is required. If not, then isolation is not needed.

2.2 Calculate H_o, the transmissibility achieved when the equipment is mounted directly on the source, as a function of frequency. The calculation of H_o from Equation 2 is systematized by the use of the tabular form shown in Table 1 and the curves of Fig. 4, which is a plot of $(1\text{-}mB_s\omega)$ versus $(mA_s\omega)$ for constant values of H.

Plot H_o on the same coordinates as H_m and compare the two. If H_o exceeds H_m at any frequency, isolation is required. Proceed to Step 3.

3. *Determination of Required Dynamic Properties of Isolation System*

Since there is no unique, closed-form design equation, selection of the dynamic parameters of the isolation system ordinarily is made initially on the basis of intuition and experience. One useful general rule which may serve as a guide is based on simple vibration theory, assuming infinite source impedance.

Transmissibility of a simple isolation system is

always greater than one at frequencies below $\omega/\omega_o = 1.4$ and always less than one above $\omega/\omega_o = 1.4$. Consequently, the natural frequency of the isolation system should be no higher than 0.7 times the lowest frequency at which transmissibility less than one is required. (Once the natural frequency ω_o has been determined, the total stiffness of the isolation system is given by $K = \omega^2_o m$ for infinite source impedance.)

More generally, the behavior of simple isolation systems may be seen graphically from Fig. 5, in which transmissibility is plotted as a function of the dimensionless frequency α $(= \omega/\omega_o)$ for various values of damping β (= per cent of critical damping value $2\omega_o m$). If the maximum allowable transmissibility H_m is plotted on a log-log scale and the simple isolator transmissibility H_{th} is plotted on a transparent overlay to the same scale, the H_{th} curve may be slid along until the H_m curve lies everywhere above it. If this is done in such a way that the H_m curve barely touches the H_{th} curve, the natural frequency of the isolation system is that frequency, on the H_m curve scale, which coincides with $\alpha = 1$ on the H_{th} curve scale. This reasoning leads to step 3.1.

3.1 Place a transparent overlay of the H_{th} versus α curve (Fig. 5) over the H_m versus f curve so that the vertical scales coincide. Slide the overlay along until the H_m curve lies at all points above the H_{th} curve for a suitable value of β (usually 0.1). The first trial natural frequency f_1 of the isolation system is the highest value of f on the H_m curve, coinciding with $\alpha = 1$ on the H_{th} curve, for which H_m exceeds H_{th} everywhere.

3.2 Compute the imaginary part of the isolation system admittance at f_1 from the following equation:

$$\frac{\omega_1}{K_1} = \frac{Z\pi f_1}{K_1} = \frac{1}{2\pi f_1 m} - B_s(f_1) \qquad (3)$$

K_1 is the first trial value of stiffness. Using $\beta = 0.1$ as isolator damping, compute the real and imaginary parts of the isolator admittance as a function of frequency from Equations 4 and 5.

$$A_1'(f) = \frac{2\beta(\omega_1/K_1)}{4\beta^2 + (f_1/f)^2} = \frac{0.2(\omega_1/K_1)}{0.04 + (f_1/f)^2} \qquad (4)$$

$$B_1'(f) = \frac{(f_1/f)(\omega_1/K_1)}{4\beta^2 + (f_1/f)^2} = \frac{(f_1/f)(\omega_1/K_1)}{0.04 + (f_1/f)^2} \qquad (5)$$

The tabular form shown in Table 2 is useful in carrying out this computation.

3.3 Compute the transmissibility achieved by this isolation system in combination with the source admittance by use of Equation 6:

$$H_1 = \frac{\mu_1}{\mu_s} = [(1 - mB_1\omega)^2 + (mA_1\omega)^2]^{-\frac{1}{2}} \qquad (6)$$

where:

$$A_1 = A_s + A_1'$$

$$B_1 = B_s + B_1'$$

The tabular form is similar to that used in step 2.2 and the H curves of Fig. 4 also apply in this computation.

3.4 Plot H_1 on the same graph as H_m.

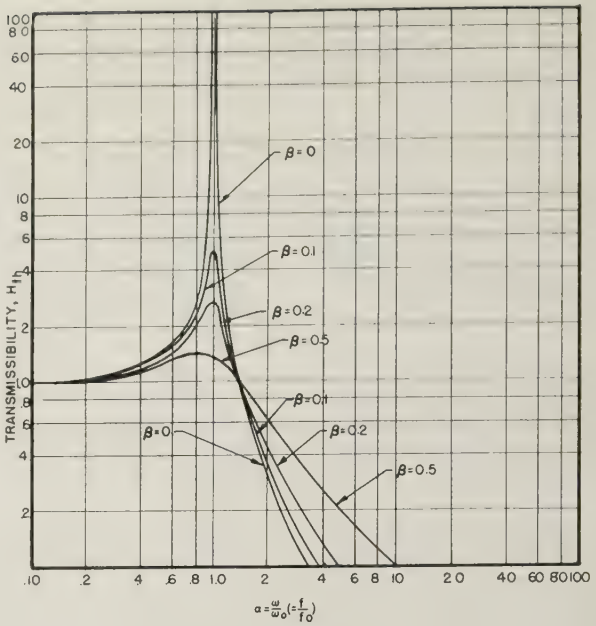

Fig. 5 — Transmissibility (H_{th}) of isolator on source of infinite impedance

If H_1 is less than H_m at all frequencies, then the necessary isolation has been achieved. If H_1 exceeds H_m at any frequency, the isolation is not adequate and a new trial resonant frequency should be selected.

To show this procedure in more explicit detail, two examples will be given and the computations carried out in detail.

Example 1

Step 1 — Data

1.1 Weight, $W = 100$ lb (c.g. of receiver is at geometric center and four symmetrically disposed mounts will be used; only vertical vibration is considered).

1.2 Equipment — Fragility curve is shown in Fig. 3 (determined by measurement or by specification test).

1.3 Source Data — 1.3.1 The measured (or computed or assumed) free motion of the source is also shown in Fig. 3.

1.3.2 The mechanical impedance and corresponding admittance values of the source are listed, for various frequencies, in Table 3 and are plotted in Figs. 6 (impedance) and 7 (admittance).

Step 2 — Determination of the Need for Isolation

2.1 The curve of maximum permitted transmissibility, H_m, is determined graphically by subtraction of the μ_s curve from the μ_f curve. The H_m curve is shown in Fig. 3.

2.2 The computation of H_o (as given in Equation 2 is carried out in Table 4, for frequencies between 10 and 500 cps. Note that the H values are found in Fig. 4 for various values of $(1-2\pi m B_s f)$ and $(2\pi m A_s f)$. The H_o values are plotted in Fig. 8, together with the H_m curve determined previously. It is apparent that isolation is required, since the H_o curve is above the H_m curve in part of the frequency range.

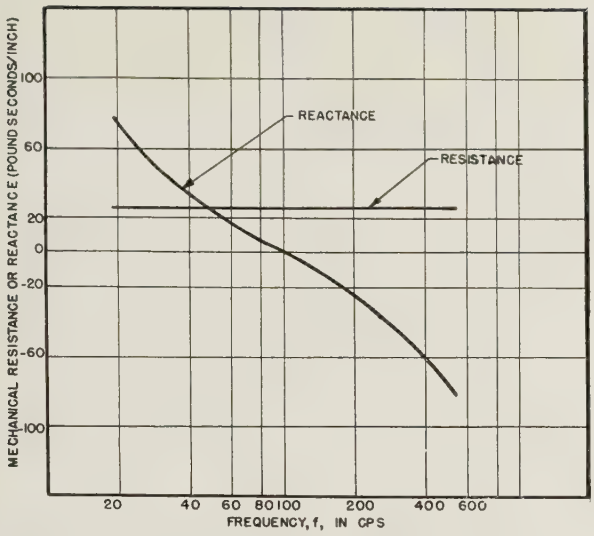

Fig. 6 — Source impedance

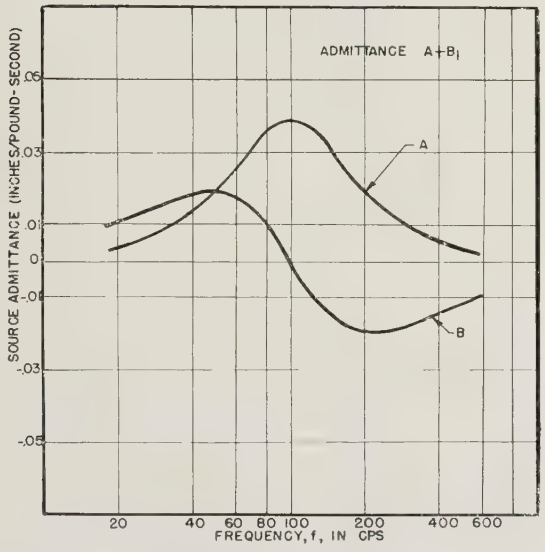

Fig. 7 — Source admittance

Step 3 — Determination of Dynamic Properties of Isolator

3.1 A transparent overlay of the H_{th} versus α curve (Fig. 5) is placed over the H_m versus f curve (in Fig. 8), and slid along until the H_{th} curve for $\beta = 0.1$ lies entirely below the H_m curve. This first occurs when the $\alpha = 1$ line of Fig. 5 coincides with the $f = 9.5$ cps line of Fig. 8. Consequently, the first trial frequency f is 9.5 cps.

3.2 The imaginary part of the isolation system admittance is computed by substituting 9.5 for f_1 in Equation 3. B_s at 9.5 cps is found, by extrapolating the curve of Fig. 7, to be about 0.009. For weight, $W = 100$ lb, $m = 100/386 = 0.263$ lb-sec^2/in.

Therefore:

$$\frac{\omega_1}{K_1} = \frac{1}{2\pi(9.5)(0.263)} - 0.009 = 0.055$$

The computation of A_1 (f) and B_1 (f) (from Equations 4 and 5) is carried out in Table 5. From these values and Equation 6, H_1 is computed. This cal-

Table 2 — Form for Computing Equation 5

Trial natural frequency $= f_1$; ω_1/K_1 from Equation 3; $\beta = 0.1$

f_1, cps	f_1/f	$(f_1/f)^2$	$(f_1/f)^2) + 0.04$	$\frac{A_1'}{0.2\ \omega_1/K_1}$ (4)	$\frac{B_1'}{(2)\ \omega_1/K_1}$ (4)

Table 3 — Source Impedance and Admittance

$$A = \frac{R}{R^2 + X^2} \qquad B = \frac{-X}{R^2 + X^2}$$

Frequency, cps	Impedance (lb-sec/in.) $R + Xi$		Admittance (in./lb-sec) $A + Bi$	
	R_s	X_s	A_s	B_s
10	25.9	− 160	0.001	0.009
20	+ 25.9	− 77.5	0.00388	0.0116
30	"	− 48.8	0.0085	0.0160
40	"	− 33.8	0.0143	0.0187
50	"	− 24.2	0.0206	0.0193
60	"	− 17.2	0.0268	0.0178
70	"	− 11.7	0.0321	0.0145
80	"	− 7.25	0.0358	0.0100
90	"	− 3.4	0.0380	0.0050
100	"	0	0.0386	0
150	"	+ 13.4	0.0305	− 0.0158
200	"	+ 24.2	0.0206	− 0.0193
300	"	+ 42.9	0.0103	− 0.0171
400	"	+ 60.4	0.0060	− 0.0139
500	"	+ 77.3	0.0039	− 0.0116

Table 4 — Computation of H_o

$W = 110$ lb $\qquad m = 0.259$ lb sec^2/in. $\qquad 2\pi m = 1.63$

$$\frac{\mu_s}{\mu_o} = [(1 - m2\pi f B_s)^2 + (2\pi m A_s f)^2]^{-1/2}$$

f, cps	A_s	B_s	$2\pi m B_s f$	$1 - 2\pi m B_s f$	$2\pi m A_s f$	H_o[a]
10	0.001	0.009	0.150	0.850	0.016	1.14
20	0.00388	0.0116	0.378	0.622	0.126	1.58
30	0.0085	0.0160	0.780	0.220	0.415	2.10
40	0.0143	0.0187	1.22	− 0.22	0.932	1.7
50	0.0206	0.0193	1.57	− 0.57	1.68	5.6
60	0.0268	0.0178	1.74	− 0.74	2.62	0.37
70	0.0321	0.0145	1.65	− 0.65	3.66	0.27
80	0.0358	0.0100	1.63	− 0.63	4.67	0.215
90	0.0380	0.0050	0.735	0.265	5.58	0.18
100	0.0386	0	0	1.00	6.30	0.158
150	0.0305	− 0.0158	− 3.86	4.86	7.45	0.113
200	0.0206	− 0.0193	− 6.29	7.29	6.71	0.102
300	0.0103	− 0.0171	− 8.36	9.36	5.04	0.096
400	0.0060	− 0.0139	− 9.06	10.06	3.91	0.092
500	0.0039	− 0.0116	− 9.45	10.45	3.18	0.090

[a] From Fig. 4.

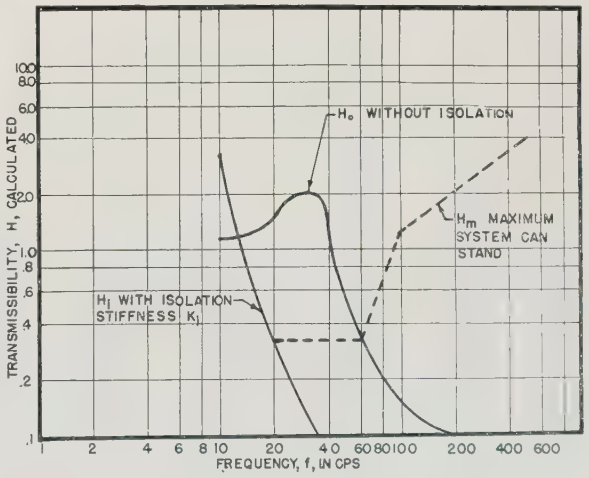

Fig. 8 — Transmissibility with and without isolators

culation is shown in Table 6. The values of H_1 in this case are computed only to 50 cps, since the trend of the curve, which is similar to the H_{th} curve for $\beta = 0.1$, is established. The H values are plotted in Fig. 8; since the H_1 curve does not lie above the H_m curve at any frequency, the isolation system is adequate dynamically, and no further steps are necessary to prescribe the desired dynamic properties of the isolators.

Example 2

The influence of source impedance on the equipment motion has already been mentioned. That this factor may affect the need for isolation is demonstrated by a second, more hypothetical, example shown plotted out in Fig. 9. In this case, the equipment fragility (maximum allowable amplitude) curve is appreciably different from that of the first example. By the graphical procedure described earlier, the H_m curve is determined and plotted from the fragility and free displacement curves.

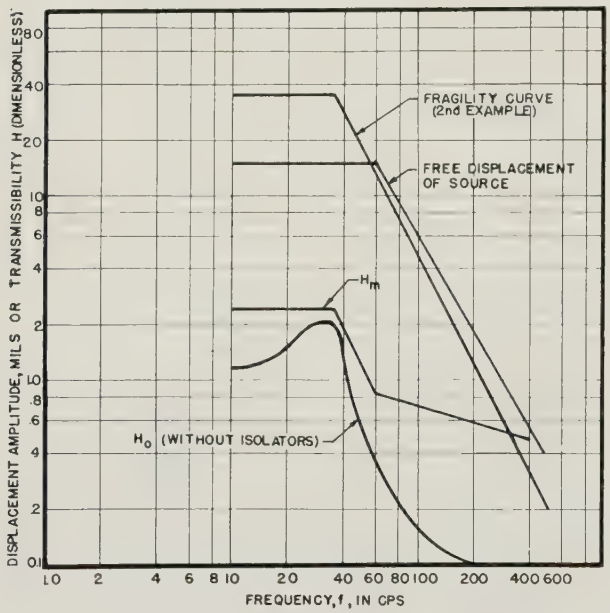

Fig. 9 — Effect of source impedance on need for isolators

The allowable transmissibility H_m is greater than unity below 55 cps, but is less than unity above 55 cps. If the source impedance were infinite, the transmissibility H_o with the equipment mounted directly on the source would have a value of unity at all frequencies and isolation would be needed. The computed H_o curve for the source impedance of the example, however, shows a transmissibility less than one above 42 cps; in fact, since H_o is everywhere less than H_m, isolation is not required in this case.

Closing Comments

At the present stage of development of the procedure, the selection of the new trial frequency, if one is needed, depends on intuition and experience. Inspection of the H_{th} curves of Fig. 5 should provide guidance as to selection of the new trial value.

It is hoped eventually to develop a definite procedure which will not require experience to make the sequential selection of trial frequencies converge on the optimum value. The S-12 Committee is working on a variety of trial examples, covering what is hoped to be a reasonable range of problem values. It is hoped that this will develop sufficient understanding of the behavior of isolation sysytems on finite-impedance bases to permit the evolution of a definite closed-form procedure.

Meanwhile, analyses are going ahead on the more general isolation problem, covering translational motions along three axes, and a combination of this condition with rotational motions about the three axes.

It is intended eventually to incorporate the simple repetitive-graphical techniques outlined here into the more general procedures for the multi-degree-of-freedom systems, once we are satisfied with its simplicity and reliability for the simple case.

The SAE S-12 Committee will welcome comments relative to the utility and practicality of the proposed procedure and suggestions leading to its simplification and application to the more general problem. The author would like to express his appreciation to his colleagues on the S-12 Committee for their cooperation and assistance in the preparation of this paper and particularly to Dr. C. T. Molloy, who has guided the S-12 Committee with consistent, effective leadership, and to Dr. S. Rubin, who is in large part responsible for the evolution of the computational procedure to its present form.

Table 5 — Computation of A_1' and B_1'

$f_1 = 9.5$ cps

$$A_1'(f) = \frac{(0.2)(0.055)}{0.04 + \left(\frac{9.5}{f}\right)^2} = \frac{0.011}{0.04 + (9.5/f)^2}$$

$$B_1'(f) = \frac{(9.5)(0.055)\frac{1}{f}}{0.04 + \left(\frac{9.5}{f}\right)^2} = \frac{0.55\frac{1}{f}}{0.04 + \left(\frac{9.5}{f}\right)^2}$$

f	$\frac{9.5}{f}$	$\left(\frac{9.5}{f}\right)^2$	$\left(\frac{9.5}{f}\right)^2 + 0.04$	A_1'	B_1'
10	0.95	0.90	0.94	0.019	0.056
20	0.475	0.2255	0.2655	0.042	0.099
30	0.317	0.1006	0.1406	0.079	0.125
40	0.238	0.0566	0.0966	0.115	0.136
50	0.190	0.0361	0.0761	0.146	0.139
60	0.158	0.0249	0.0649	0.171	0.135
70	0.136	0.0185	0.0585	0.190	0.129
80	0.119	0.0141	0.0541	0.206	0.119
90	0.106	0.0112	0.0512	0.217	0.114
100	0.095	0.0090	0.0490	0.227	0.108
150	0.0634	0.0040	0.0440	0.253	0.080
200	0.0475	0.0023	0.0423	0.263	0.063
300	0.0317	0.0010	0.0410	0.271	0.043
400	0.0238	0.0006	0.0406	0.274	0.033
500	0.0190	0.0004	0.0404	0.275	0.026

Table 6 — Computation of H_1

($2\pi m = 1.63$)

f	A_1'	B_1'	A_1	B_1	$1.63B_sf$	$1 - \frac{1.63}{B_sf}$	$1.63A_sf$	H_1
10	0.019	0.056	0.020	0.062	1.01	− 0.01	0.32	3.1
20	0.042	0.099	0.046	0.112	3.65	− 2.65	1.5	0.34
30	0.079	0.125	0.088	0.141	6.9	− 5.9	4.3	0.14
40	0.115	0.136	0.129	0.155	10.1	− 9.1	8.4	0.08
50	0.146	0.139	0.166	0.158	12.8	−11.8	13.5	0.055
60	0.171	0.135	0.198	0.152				
70	0.190	0.129	0.222	0.143				
80								
90								
100								
150								
200								
300								
400								
500								

METALLURGICAL DEVELOPMENTS IN BRAKE DRUMS

V. A. Crosby, Climax Molybdenum Co.

This paper was presented at the SAE Annual Meeting, Detroit, Jan. 14, 1959.

HIGHER SPEEDS and heavier automobiles have put added demands on today's brake drums. This paper is a review of the braking problem as applied to materials, considering the metallurgical, structural, and chemical properties that account for mechanical properties required.

The discussion includes: (1) the use of higher carbon materials, such as malleable iron, graphitic steel, and high-carbon high-strength gray iron to obtain increased resistance to thermal shock and heat checking; (2) properties and structures of cast-iron drums; (3) brake drum wear data; and (4) typical compositions that meet mechanical properties.

IN MANY CASES, ability to stop a car may be much more important than the power to accelerate. Industry-wide acceptance of this premise has resulted in a continuing program of brake research and development, not only by the automobile industry itself but by suppliers as well.

Better braking requires consideration of two basic problems: (1) design of the braking system, and (2) selecting the right material for the job. In this paper, consideration has been given only to material selection: strength requirements, wearing qualities, microstructure, and, particularly, the unique and important role of free carbon in cast-iron brake drums are discussed in detail. In addition, consideration is given to the specific factors that must be evaluated in choosing brake drum material. Some suggestions are offered concerning the types of material that are most likely to be used in tomorrow's passenger cars and trucks.

In the first 25–30 years of the automotive era, pressed steels of various compositions were used for brake drums, starting with SAE 1008 cold-formed. Because of unsatisfactory performance, steels of higher carbon contents were tried. This change permitted an increase in yield, tensile, and hardness. During the final stages of this 25-year era some companies were using SAE 1070 hot-formed steel.

In those days, driving speeds were comparatively slow and motor vehicles were light. For these reasons, the materials mentioned above were fairly satisfactory. However, during the 1928–1932 era, motor-car speeds were increasing, and car weights were rising steadily. These imposed a more severe braking problem. The most important change was the generation of higher temperatures in the brake drum itself.

These higher temperatures resulted in softening the steel drum so that severe scoring resulted in the lower carbon drums. In the higher carbon grades, a very hard martensitic skin would often result from

severe service. This came about because the surface became very hot followed by a quick cool. Both conditions were unsatisfactory. In the latter case, a glass-hard surface often resulted in "fading."

Simultaneously with the above usage, some car manufacturers were testing and using much higher carbon materials, including malleable iron, graphitic steel, and low-carbon high-strength gray iron. The latter was usually made in malleable iron shops, using a graphitizing technique. Table 1 shows the composition of several of these materials.

The malleable iron drum consists largely of soft ferrite, and possesses many of the disadvantages of the steel drum previously used. While it has a much larger amount of graphite, the graphite is nodular in form and insufficient quantities are present to overcome the scoring tendencies prevalent in braking.

Graphitic steel drums offer much promise because the harder matrix is admirably suited to resist scoring, and provide better wear resistance. However, because of the greater metallic continuity and the rounded shape of the graphite particles, this material too is susceptible to heat checking and to "Martensitic spot" formation. These conditions have been aggravated with our advanced designs of motor vehicles of greater weight traveling at higher and higher speed.

Ermalite, a heat-treated malleable iron — a forerunner of pearlitic malleable iron as we know it today — also found appreciable acceptance as a suitable material for drums in the 1930's. It has good strength, good resistance to scoring and wear, but is lacking in resistance to heat checking.

Low-carbon gray iron, while recognized as an excellent braking material, was looked upon with grave misgivings by many automotive engineers because of its lack of ductility or "brittleness" as compared to steel. Nevertheless, numerous braking tests were made, and this material was ultimately adopted by a few manufacturers. These earlier low-carbon, cast-iron drums had good frictional characteristics, and they were competitive with the types of materials previously used. Surprisingly, these early low-carbon gray iron brake drums showed 229 to 269 Bhn, and had tensile strength in the order of 50–60,000 psi. At the time, these drums met the requirements of braking loads without scoring or scuffing and showed no evidence of thermal checking, and were considered quite satisfactory.

While there were those enginers who had become quite complacent with the development and success of low-carbon, high-strength gray iron, there were those who thought many cast-iron drums were harder and stronger than was necessary to do the job. Experiments were initiated with irons containing more graphitic carbon, but having lower strength and hardness. These irons could be made readily by cupola melting and at a substantial saving in metal cost. Practical tests substantiated the soundness of this approach to the brake drum problem. Today, cupola-melted gray cast iron, having total carbon contents of 3.20–3.80% and hardnesses of 180–250 Bhn, makes up the majority of brake drums used in the automobile, truck, bus, and trailer industries. To say that these drums today are entirely satisfactory for all applications would be an overstatement.

With the advent of still greater loads and higher

Fig. 1 — Increased graphite content in random form

driving speeds, new braking problems have been introduced. In addition, passenger-car wheels are smaller, and no provisions for better cooling have been provided. For this reason, brake drums are being given unusual consideration by engineers — along with linings and auxiliary equipment included in "retarders" of all types.

Many engineers believe we are approaching an era where a whole new aproach to the problem of automotive braking is necessary. Brake drums will be only one of the many retarding mechanisms studied and reviewed. A study of this kind requires detailed examination of the basic qualities required in brake drum materials. These qualities include:

1. Stable coefficient of friction — to resist "fading" and "stick slip."
2. High specific heat — so the drum can act as a reservoir for the storage of heat which can be dissipated to the air later.
3. High thermal conductivity — to avoid high temperatures in the thin surface of the brake drum face.
4. Resistance to heat checking — to avoid failure of the drum.
5. Resistance to scoring — to avoid lining wear and uneven braking.
6. Strength at room and elevated temperatures — to prevent bursting.
7. Good wear resistance — to secure long life.

A rather extensive elaboration dealing with the seven properties shown above is given in two papers that have been widely disseminated to the automotive engineers.[1,2] These subjects will be dealt with only briefly in this paper.

There are a great number of requirements for

Fig. 2 — Undesirable dendrite form of graphite

Table 1 — Composition of Various Brake Drum Materials

Material	Total Carbon	Si	Mn	S	P	Cu	Cr	Mo	Bhn	Tensile Strength, psi
Malleable	2.60	0.90	0.35	0.06	0.08	—	—	—	143	50,000
Graphitic Steel	1.50	1.30	0.40	0.03	0.03	—	—	—	240	110,000
Ermanite	2.45	2.10	0.50	0.06	0.15	—	—	0.40	248	62,000
Low-Carbon Gray Iron	2.75	2.50	0.70	0.06	0.08	—	—	0.50	269	55,000

Table 2 — Effect of Carbon and Alloys on Strength at Room and Elevated Temperatures

	Analysis							Tensile Strength, psi		
	Total Carbon	Combined Carbon	Si	Mn	Cr	Ni	Mo	Room Temperature	932F	1000F
Plain Iron A	3.29	1.10	1.27	0.28				34,300		22,200
Cr-Ni	3.19	0.65	2.13	0.58	0.34	0.67		29,800		21,000
Plain Iron B	3.63	0.73	1.15	0.54	0.03	0.03		33,000		24,800
Cr Iron	3.46	0.87	1.36	0.68	0.54			42,000		34,200
Plain Iron C	3.36		1.82	0.40				41,200	24,200	
Mo 1	3.32		2.04	0.46			0.21	42,500	26,200	
2	3.36		2.00	0.48			0.42	45,000	27,800	
3	3.25		1.80	0.40			0.60	48,500	33,200	
4	3.25		1.81	0.40			0.86	53,400	39,400	
5	3.27		2.08	0.44			1.05	52,800	37,800	
Cr-Mo 1	3.40		2.00	0.53	0.29		0.24	43,000	26,200	
2	3.30		2.02	0.55	0.29		0.34	45,200	28,900	
3	3.40		2.00	0.55	0.29		0.72	50,200	32,700	
4	3.30		1.90	0.51	0.27		0.84	52,600	36,000	
5	3.45		2.00	0.55	0.29		1.00	53,500	37,400	
Climax										
1790	3.39		1.93	0.83	0.22		0.50	41,300		28,700
1791	3.36		1.93	0.83	0.24		1.03	52,800		38,900
1808A	3.79		1.06	0.82			0.51	31,700		21,900
B	3.82						1.00	33,900		23,300
C	3.80						1.88	42,200		32,600
D	3.80						2.70	45,800		39,300

brake materials. Any choice of material to meet these varied properties must result in a compromise. Some car manufacturers, because of type and use of the vehicle, might well emphasize one of the categories listed over some of the others. For instance, one user might value resistance to heat checking as paramount; another would prefer outstanding resistance to wear. Different compositions would be indicated to meet these respective needs.

To assist in obtaining the above characteristics, both the SAE[3] and the ASTM[4] have set up chemical, mechanical, and metallurgical specifications for drums. These are known as SAE 113, 114, and 115, and A-159 of ASTM. The one mandatory feature in both chemical specifications is the total carbon content 3.40% minimum in the first two specifications and 3.50% in the SAE 115.

The basis for using high total carbon is to obtain increased resistance to thermal shock and heat checking. Physical and road tests over a number of years clearly substantiate this deduction, but a compromise is inevitable, taking into account the weakening effect of graphitic carbon and the necessity for providing adequate strength in the drum.

We are indebted to Messrs. Toghill and Angus[1] for the following statement:

> "Increasing the graphite content in the random form (Fig. 1) strengthens the resistance to thermal shock, increases the thermal conductivity, both general and local, and decreases the tendency for rapid solution of the carbon in the iron at temperatures above the critical. (For sake of comparison, Fig. 2 shows undesirable dendritic form of graphite.) The tensile strength and hardness of cast iron are, however, reduced as the graphite content increases, so that a limit is presented to the increase in resistance to thermal shock and the increase in effective thermal conductivity which can be obtained by raising the graphite content. Some degree of compensation can be obtained by the addition of alloys, such as molybdenum, nickel, copper and chromium which, by increasing the matrix strength, may counteract the weakening effect of increased graphite. Alloy additions, however, reduce the thermal conductivity, and there is a limit to the degree to which the loss of strength caused by high graphite contents can be offset by increasing the matrix strength through alloying."

The problem of obtaining sufficient tensile strength is important from the viewpoint of both safety and weight reduction. In service, the drums must withstand high pressures exerted by power-applied brake shoes, pressures which readily may produce stresses within the drums as high as 30,000–40,000 psi. Drums often may be subjected to these stresses at elevated temperatures. Therefore, the material must possess as high an elevated temperature tensile strength as is possible without sacrificing other important properties. Most data indicate that the irons which exhibit higher strengths at elevated temperatures also possess correspondingly higher strengths at room temperatures.

Table 2 has been compiled to illustrate the effects of carbon content and alloy content on the tensile

[1] *Automobile Engineer*, October, 1953, p. 409: "Cast Iron Brake Drums," by E. C. Toghill and H. T. Angus.
[2] *The Foundry*, Vol. 68, July, 1940, pp. 32–35: "Metallurgical Aspects of Brake Drums," by G. A. Timmons and V. A. Crosby.
[3] SAE Handbook, 1957, p. 175.
[4] ASTM Standards, 1955, Part I, Ferrous Metals, p. 1365.

properties of cast iron at room and elevated temperatures. Some of the irons had not been developed specifically for brake drum applications but are included here for the purpose of comparison only.

Properties and Structures of Cast-Iron Drums

Since gray cast iron will consist, essentially, of pearlite, graphite, some free ferrite, and some free carbide, it is difficult to determine the true value of thermal conductivity. Transfer of heat from the braking surface of the body of the drum, where it can be dispersed, depends upon this property. This factor is, therefore, a matter of primary importance. The thermal conductivity of the constituents mentioned above in calories/cm^3 per sec per deg C has been given as follows:[1]

Ferrite	0.17	Carbide	0.017
Pearlite	0.12	Graphite	0.33

While ferrite has a higher conductivity than pearlite, it is a highly undesirable constituent because of its tendency to score. Graphite offers more promise but, because of the comparatively small amount, it would not seem to be sufficient to account for the excellent job the drum does in dispersing high-temperature gradients when brakes are applied.

If the entire brake drum could be heated uniformly, normal thermal expansion would not be so important as it is in the case of a rapidly heated surface layer, say 0.005-in. thick, which attains during braking temperatures in the range of 1400–1800 F, while the metal immediately beneath it is still at a temperature in the range of 70–300 F. Under these circumstances, the heated surface layer expands while the cooler adjacent layers maintain their original dimension. The heated metal becomes weak in compression, while cold metal beneath it is strong and highly resistant to deformation. This causes the surface metal actually to upset itself in localized areas. Because of their prominence on the surface of the drum, these areas now become the main contacts between brake shoe and drum and, therefore, carry the frictional load. This serves to increase further the temperature of the metal at these spots, and a further volume increase results. When the metal in these localized areas cools, contraction produces stresses in excess of the tensile strength of the material, resulting in failure which is manifested by a network of fine cracks or crazing. Observations made subsequent to the first few applications of the brakes show that such spots are present on the surface of the drum and that they are the origins of these heat checks.

Convinced that these areas were definitely a factor in the thermal checking of brake drums, one organization interested in the brake drum problem used an abrasive material in their test brake shoes in quantities sufficient to remove these spots as soon as they were formed. While this caused complete elimination of heat checks, it increased drum wear appreciably.

It has been stated by various sources that the most frequent causes of failure in cast-iron brake drums are: (1) wearing and scoring, and (2) heat checking, cracking, and breakage. The first is usually associated with ferritic soft iron and the latter with low graphitic content irons having pearlitic-carbide matrices.

Toghill and Angus[1] have commented on this matter as follows:

> "So long as brakes are designed and fitted which rely on the conversion of the kinetic energy of the vehicle by friction into heat energy which requires it to be absorbed and dissipated through the brake drum, it should be fully realized that such a part is a highly loaded bearing which is to run without a coolant or lubrication. As such, therefore, it must be accepted as a wearing part which should, after reasonable life, be replaced."

We are indebted to the Gunite Corp. for the information given in Table 3 showing the differences in wear of identical materials used on the right side and left side of trailers. These wear data are tied in with the composition used in each case and serve to show how difficult it is to determine the merits of any particular composition through the medium of road tests. The high-carbon iron alloyed did, however, show appreciably less wear.

Some typical compositions that meet the mechanical properties set forth in SAE 113, 114, and 115 and in ASTM A-159 for gray iron brake drum usage

Table 3 — Brake Drum Data

Material	No.	L.S.[a]	R.S.[b]	Average, in.	Miles	Producer
C	6609	0.086–0.102	0.094–0.125	0.102	145,000	Gunite
C	6631	0.060–0.085	0.086–0.087	0.080	135,000	"
E	6578	0.084–0.103	0.039–0.065	0.073	128,000	"
E	7564	0.125–0.132	0.120–0.127	0.125	145,000	"
High-Carbon Iron		0.054–0.073	0.047–0.056	0.057	120,000	"

	C MedC—Low Alloy	E Med C—Med Alloy	H.C. Hi C—Hi Alloy
C	3.20–3.50	3.20–3.50	3.60–3.90
Si	1.70–2.10	1.70–2.10	1.20–1.60
Cu	0.15–0.25	0.35–0.45	0.75–1.00
Cr	Residue	Residue	0.40–0.60
Mo	0.05–0.15	0.25–0.35	0.40–0.60
Maximum	207	217	255

[a] Left side of trailer.
[b] Right side of trailer.

Table 4 — Typical Analyses of Cast-Iron Brake Drums

Elements	1	2	3	4	5	6	7	8	9	10	11	12	13
Total Carbon	3.35	3.35	3.45	3.40	3.70	3.40	3.40	3.50	3.50	3.90	3.80	3.25	3.40
Si	2.15	2.15	1.65	2.00	1.80	2.10	1.50	1.90	1.60	1.40	2.15	2.20	1.60
Mn	0.65	0.65	0.75	0.80	0.80	0.75	0.80	0.60	0.80	0.65	0.85	0.85	0.80
Sul max	0.12	0.12	0.12	0.12	0.13	0.09	0.18	0.12	0.12	0.09	—	0.12	0.10
Phos max	0.25	0.25	0.12	0.15	0.15	0.12	0.20	0.15	0.12	0.12	—	0.20	0.15
Ni	—	—	—	1.50	0.20	—	—	—	0.25	1.25	2.65	—	0.20
Cr	0.65	0.65	0.35	0.50	0.80	—	0.20	0.35	0.40	0.50	—	0.30	0.20
Mo	—	0.35	0.35	—	0.75	—	0.50	1.00	0.60	—	0.70	—	0.30
Cu	1.25	1.25	0.60	—	—	—	—	—	0.60	1.25	—	—	—
V	—	—	—	—	—	—	—	—	—	—	—	—	0.20
Bhn	228	241	248	241	269	207	228	241	—	—	—	220	241
Tensile Strength, psi	32,000	45,000	40,000	40,000	42,000	30,000	40,000	40,000	—	—	—	—	40,000

are shown below in Table 4. These specifications are set up mainly for truck, trailer, and bus usage. Over the years these applications have demanded a great deal of attention because of the severity of the service requirements. For the opposite reason, little attention has been given to passenger-car drums. However, we may be approaching a period when it might be well for passenger-car brake engineers to look at the truck, trailer, and bus specifications.

So far as alloying elements are concerned in the SAE and ASTM specifications, the field is wide open and the choice is up to the producer or a matter of agreement between the producer and user. Usually, a combination of elements is more effective than a single alloying agent.

Much thought has gone into the design of brake drums to meet the requirements of rigidity, strength, and good heat dissipation. Some excellent examples of such designs are shown in Figs. 3–7.

Some idea of the matrix structures may be obtained from Figs. 8–11 which are reproduced from etched micrographs at 1000 magnification.

Fig. 8 shows a typical structure in an unalloyed gray iron drum having 3.56 total carbon (a pearlitic structure with some free ferrite).

Fig. 9 shows a pearlitic structure free of ferrite and carbide (a typical example of low-alloy combination).

Fig. 10 shows a very fine pearlitic structure with some carbide interspersed. This structure would be more highly alloyed and expected to offer greater wear resistance than the unalloyed or low-alloyed iron.

The structure shown in Fig. 11 results from severe surface temperature, followed by rapid cooling. When this condition occurs, very hard spots are formed having low coefficient of friction and ultimately no brakes. This structure is designated as martensite and may occur in either unalloyed or alloyed irons under the conditions stated.

Passenger-car drums at the present time are unalloyed gray iron having carbon contents of 3.25–3.50% and hardnesses of 180–220 Bhn. However, with the advent of smaller wheels and higher speeds there are indications that something in the way of improved materials may be necessary in the near future. One of the motor-car companies is featuring the flared-rim type of construction, using gray iron for the construction. A great improvement in the dissipation of heat is claimed for this design

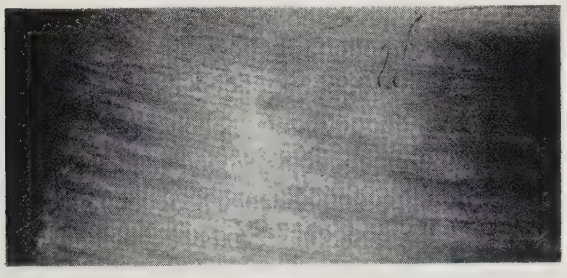

Fig. 3 — Cast-iron trailer drums, right side

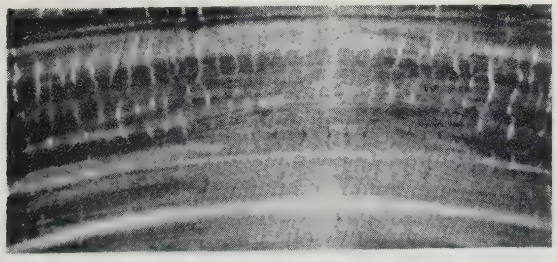

Fig. 4 — Cast-iron trailer drums, left side

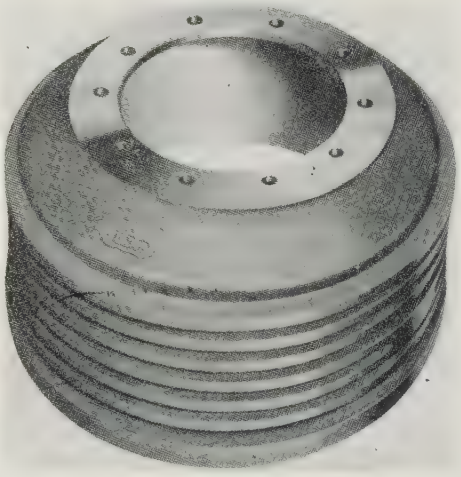

Fig. 5 — Cast-iron truck drum, Gunite Foundries Corp.

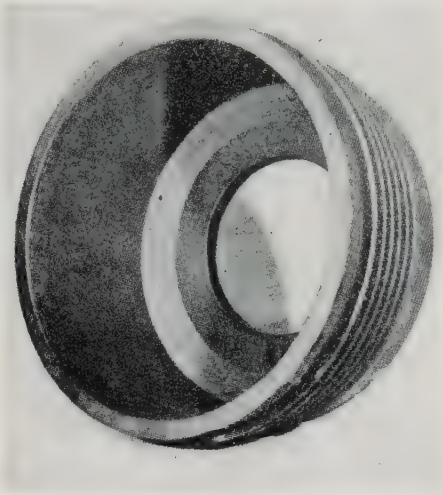

Fig. 6 — Cast-iron truck drum, General Foundry & Mfg. Co.

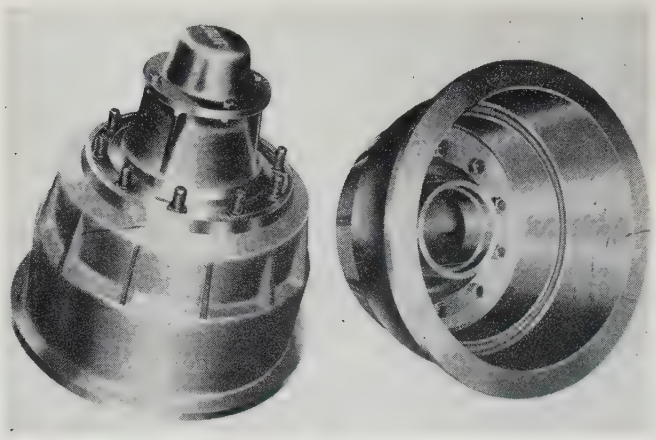

Fig. 7 — Alloyed drum that has given good service life (courtesy of Utility Trailer Mfg. Co.)

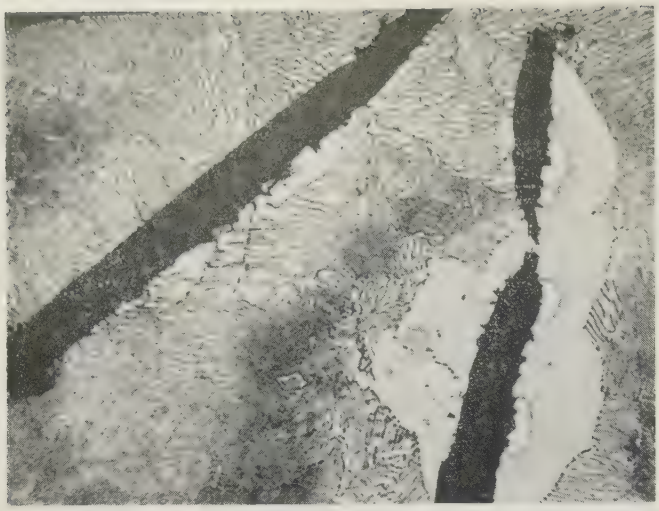

Fig. 8 — Structure of unalloyed gray iron drum having 3.56 total carbon

Fig. 9 — Pearlitic structure free of ferrite and carbide

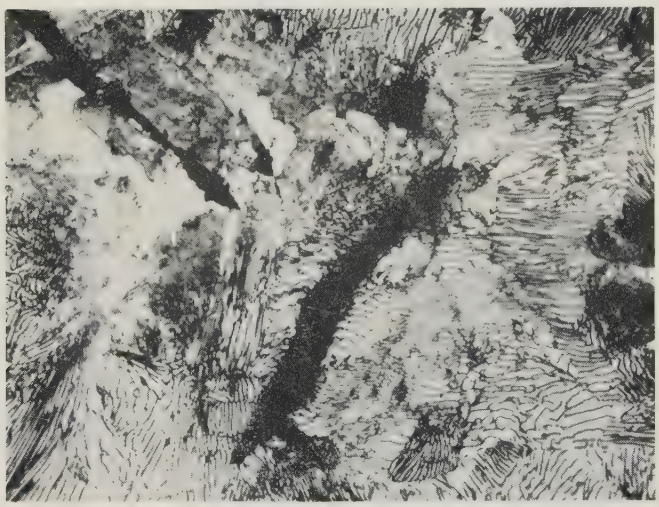

Fig. 10 — Pearlitic structure with some carbide interspersed

Fig. 11 — Results of severe surface temperature, followed by rapid cooling

which is shown in Fig. 12.[5] Another design is shown in Fig. 13[6] that involves a bimetallic construction utilizing aluminum as a drum material and a cast-iron insert for the braking surface.

Because of the high rate of conductivity and high capacity for dissipating heat to the air, aluminum offers many advantages. So far it has not been effective as a wear resistant material and, therefore, some material like gray cast iron must be inserted for the braking contact. It would seem feasible that some effort might be, or is being made, to develop satisfactory sprayed coatings which would have good wear resistance, and sufficiently high melting point to resist scoring and scuffing.

Along the line of future developments we are indebted to the Raybestos Division of Raybestos-Manhattan, Inc. for the following comment:

> "The key to the success of the Raybestos water cooled brake is the complete elimination of heat build-up, regardless of the frequency of high-speed stops, making it impossible for the brake to fade. Dissipation of heat is accomplished by the channeling of liquid from the engine cooling system through tunnels in copper lining fused to a variation of conventional brake shoes. The copper linings contact conventional brake drums lined with special Raybestos friction material."[7]

As indication of future promise through the use of aluminum drums and a sprayed wear-resistant surface, we have the following information to offer on molybdenum sprayed aluminum drums tested in France. The brake drums tested were of the type used on a passenger car. The molybdenum-sprayed surface of the aluminum had been previously lathe-grooved, and the coating thickness after machining was about 0.015 in. A French brake manufacturer carried out successive testing cycles with these brake drums (Table 5).

The braking tests were conducted with a deceleration of 13 ft/sec/sec. The best of the cast-iron brake drums withstand the second cycle but crack badly on the third. The molybdenum-sprayed drums withstood the three tests with excellent performance, although the linings had not been specially

---

[5] "Studebaker Flared Cross-Rib Drum Brake," by W. B. Love and D. E. Hobson. Paper presented at SAE National Passenger-Car, Body, and Materials Meeting, Detroit, March, 1956.

[6] *Sports Car Illustrated*, Vol. 3, February, 1958, p. 3.

[7] *Firing Line*, June 21, 1957, p. 6. Pub. by Raybestos-Manhattan, Inc.

Table 5 — Testing Cycles on Molybdenum-Sprayed Brake Drums

Cycle	Initial Speed, mph	Load, lb	Temperature, F	Number of Brake Applications
1	43.5	1,102	302–320	2,000
2	74.5	1,102	392	100
3	74.5	1,102 + 25% Extra	392	100

chosen. After the tests the sprayed surface showed checks but the bonding remained perfect.[8]

The author has attempted to present a brief review of the braking problem over the years as it has applied to materials, giving some consideration to the metallurgical, structural, and chemical properties that account for the mechanical properties required. The author has not been unmindful of the theoretical and practical considerations that must receive attention.

Additional Reference

1. SAE *Quarterly Transactions,* Vol. 4, July, 1950, pp. 369–380: "Brake Drum Materials," by F. J. Walls.

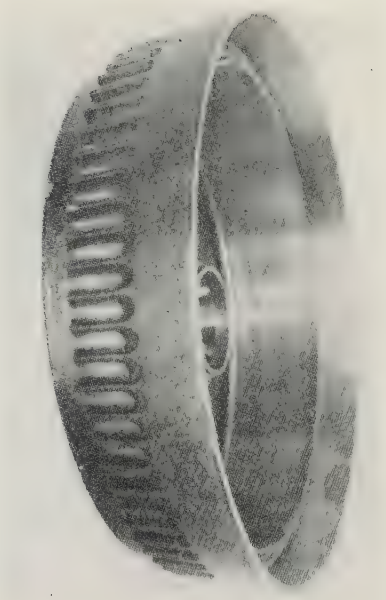

Fig. 12 — Flared-rib drum

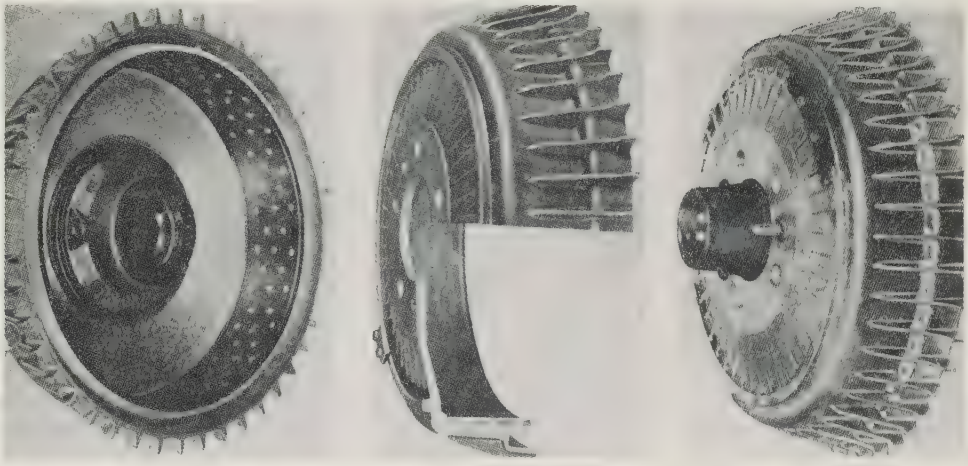

Fig. 13 — Bimetallic construction — aluminum drum and cast-iron insert for braking surface

DISCUSSION

Describes Metallurgical and Design Considerations of Cast-Iron Brake Drums

— Garnet P. Phillips
International Harvester Co.

MY EXPERIENCE with Frank Foundries Corp. of Moline, Ill., and, more recently, with International Harvester Co. confirms pretty much the data given by Mr. Crosby on cast-iron drums. We also established from experience that low-carbon, low-graphite, high-strength gray irons produced largely in the air furnace were inferior from a heat cracking point of view to high-carbon, high-graphite irons produced largely in the cupola for heavy-duty service. We found it necessary to alloy the higher carbon iron to obtain the necessary mechanical properties and a pearlitic structure to resist wear and scoring.

Metallurgical Considerations

The metallurgical investigation of brake drums led to the need for low coefficient of thermal expansion and good heat conductivity. In order to check some of these factors, we produced some austenitic iron drums with a high coefficient of thermal expansion which heat cracked very rapidly. An extensive investigation of thermal conductivity led to the conclusion that no great change could be accomplished with any particular metallurgical composition. A variety of special compositions were tried which were produced in the electric furnace. One of these was a very high carbon (about 4.00%), low silicon (1.25%) iron alloyed with nickel and molybdenum for adequate strength. Drums were produced with a variety of alloy contents.

In the early 1930's, the brake drums used on the front wheels of busses presented no particular problem from heat cracking; while those on the rear wheels, which were pretty well shrouded from the cooling air, were the ones that caused us most trouble. The research carried on then led to the production use of a cupola-melted iron containing about 3.50% total carbon, about 2% silicon, with a low phosphorus content, with a tensile strength of about 35,000

[8] Private communication, Climax Molybdenum Co., June, 1958.

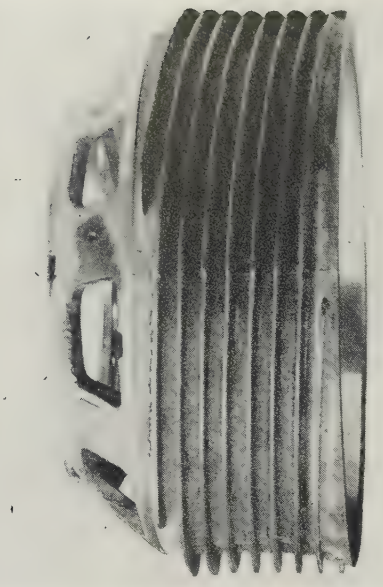

Fig. A — Helical cooling fin drums produced in 1932

psi. For heavy-duty service, alloys were added consisting of about 1.25% nickel and 0.65% chromium. The hardness of these drums would run in the range of Bhn 200–245. It should be pointed out here that regardless of composition that any drums made could be heat cracked if the service imposed on them were severe enough. This was found to be true particularly in mountainous country.

The material used in truck brake drums by International Harvester was a low-carbon, low-graphite, high-strength iron produced in air furnaces for many years. The material was changed to a cupola melted high-carbon, high-graphite type around 1940. The heavy-duty sizes were alloyed with copper-chrome (1.25% Cu and 0.60% Cr) alloy for strength and wear resisting structure.

Mr. Crosby gives values for the thermal conductivity of the constituents of gray iron including those for ferrite, pearlite, carbide, and graphite. The thermal conductivity values given in calories/cm^2 per sec per deg C per cm of thickness were as follows:

Ferrite	0.17	Carbide	0.017
Pearlite	0.12	Graphite	0.33

The values given for the first three items check very well with the values given by various investigators in Cast Metals Handbook. The value for graphite, however, is very much higher than that given in that handbook, which is 0.057. This is important in that the high conductivity reported for graphite in Mr. Crosby's paper is stated to be responsible for the better performance of the high-carbon high-graphite cast irons. We do not feel that this is the case, but do agree that high-carbon high-graphite irons are to be preferred for brake drum service due to their heat cracking resistance.

Design

Up until this time, that is — in the early 1930's, brake drums with reinforcing ribs of various types were used. We began to give thought to the more efficient dissipation of heat and tried the use of cooling fins, particularly on the rear drums used on busses. It was found that circumferential fins made very little difference, due to the fact that cooling air could not get to the rear drums. We next tried the use of helical cooling fins and this proved to be very helpful in preventing heat cracking. Fig. A illustrates the design of one of the first helical cooling fin drums produced in 1932, on which a mileage in excess of 100,000 was obtained in a year's operation on a bus.

Some time later, while carrying on work on truck brake drums for International Harvester, we made extensive tests on thermal conductivity and expansion of cast irons of various compositions and were unable to affect these properties materially. At this same time, we cast some drums with a cast-iron braking surface and with an aluminum outer wall which had helical cooling fins. The aluminum outer wall was not bonded metallurgically to the cast-iron braking surface but was locked mechanically in place, since the cast-iron brake surface ring was machined with serrations on the outside diameter and the aluminum cast around it. On severe dynamometer testing, the cast-iron brake surface ring actually twisted inside the aluminum outer wall and proved unsatisfactory both from a mechanical strength point of view and from a heat conductivity point of view. If these drums had had a metallurgical bond between the cast-iron brake surface and the aluminum outer wall, they probably would have proved quite satisfactory.

In conclusion, we confirm the findings given by Mr. Crosby in regard to cast-iron brake drum materials and feel that this is a timely subject at present as there is increasing engineering thought being given to the design of brake drums and brake drum systems to dissipate heat more effectively.

Stresses on Brake Drums Often Severe

— J. V. Bassett
Raybestos-Manhattan, Inc.

THE QUALITIES listed are the ideals. Our Central Laboratory ran some tests several years ago on four different makes of drums, using the same friction material for all tests. The results showed that each make of drum had a different friction value, rate of wear on friction materials, and fade characteristics. The higher carbon irons appeared to have less resonance and less tendency to develop the stick-slip phenomena known as "brake squeal."

Today, too many drum manufacturers are making drums that are too light in weight or have too little mass for the job they have to do. They heat check badly and quickly, then crack or break in service. Either the manufacturer does not realize, or does not consider, the stresses incurred under severe brake requirements. For example, the 16½ × 6 in. brake, such as used in over-the-highway equipment (two on the tractor and four on the trailer) with a gvw of 56,000 lb, from 50 mph must absorb approximately 9½ million ft-lb of energy, which develops over 12,000 Btu. And it must do this in 5½ sec. This heat is about the same as derived by burning 0.58 lb of gasoline or 0.68 lb of diesel fuel. With a No. 36 brake chamber and 7-in. slack adjuster at 90-psi application pressure, the bursting stress on the drum is more than 45,000 psi from each shoe, or over 90,000-psi total internal pressure. This stress is applied while the drum is at elevated temperature where the iron has lost a large percentage of its strength.

Reply to Discussion

— Frederick P. Bens
Climax Molybdenum Co. of Michigan

ON BEHALF of the late Mr. Crosby, I wish to thank the discussors for their comments on this paper.

Mr. Phillips points out a discrepancy in the thermal conductivity value for graphite (0.33 cal/cm^2 per sec per deg C) compared with what is published in the Cast Metals Handbook (0.057). The latter is apparently accepted as the proper order of magnitude in this country. These data for thermal conductivity for ferrite, pearlite, carbide, and graphite are taken directly from the British publication by Toghill and Angus.[1] These authors state quite flatly that the thermal conductivity increases with graphite content and they discuss this point at some length as it relates to cast-iron brake drums. I believe this discrepancy should be explained and I may be able to obtain further information on the subject.

DIESEL ENGINES

for use in

Light Delivery Vehicle and Taxi Service

J. S. Bright, F. Perkins (Canada) Limited

This paper was presented at the SAE National Transportation Meeting, Baltimore, Oct. 21, 1958.

THE FOUR 99 is a relatively new powerplant intended for use in cars and light commercial vehicles. It develops 43 bhp at 4000 rpm with a maximum torque of 73 ft-lb at 2200 rpm. It is a 4-cyl, in-line engine with a bore of 3 in. and a stroke of 3.5 in. (99-cu-in. capacity).

Performance reports of experience in Europe have been favorable: A Bedford C. A. half-tone van equipped with the engine gave 31.6 mpg when operated over a route that included 115 vehicles starts per day. (A gasoline engine in the same capacity gave 12.5 mpg.)

The author describes some of the design problems encountered in the Four 99 development, including noise, vibration, and cold starting.

IN NORTH AMERICA the application of the diesel engine has lagged seriously behind that in Great Britain and Western Europe. While it has become firmly established in the larger sizes of U.S. trucks, the use of the diesel engine in small commercial vehicles and cars is still regarded as just a novelty and an interesting experiment. On the other side of the Atlantic, however, the use of the diesel engine in cars, taxicabs, and light commercial vehicles down to below 5000 lb gvw is increasing rapidly (Fig. 1).

While this trend was initially set by economic causes, the development of engines suitable for these lighter vehicles has kept pace with the demand. Engines of 200-cu-in. and under capacity, operating at speeds of 3000 rpm and above, have been developed, which are suitable for vehicles of gvw up to 10,000 lb. We intend to confine our attention in this paper to these.

As the demand for diesel engines for use in smaller and smaller vehicles increases, so it becomes more important to abandon our old concepts of

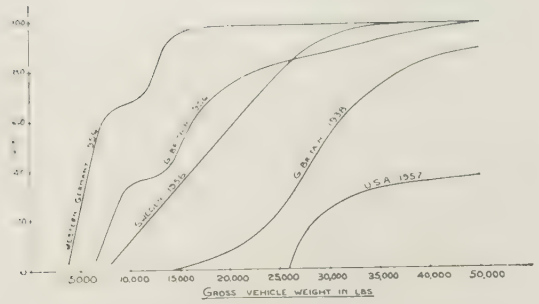

Fig. 1 — Comparison of diesel vehicle percentages of total new truck registrations in various world markets

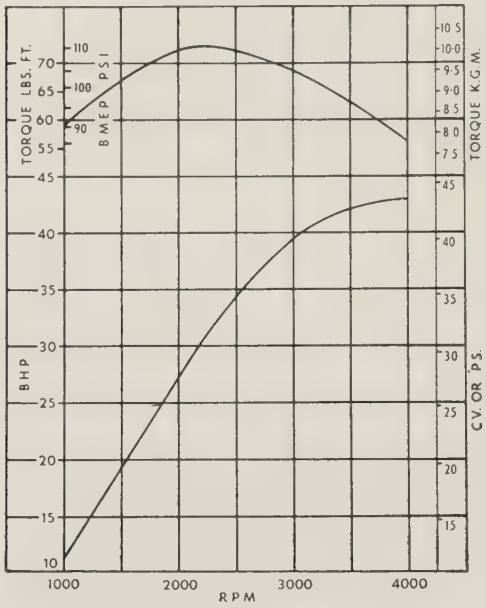

Fig. 2 — Four 99 vehicle engine

heavily built diesel engines with comparatively low rotational speeds. Engine manufacturers must strive to achieve reduced engine weights and volume per horsepower to enable the engines to be installed in the smaller vehicles, and increased engine rpm to give increased flexibility in operation.

My company has had many years' experience on one engine which has met the requirements sufficiently well for it to be used in a wide range of both car and light commercial vehicle applications. This is the P4 engine, a 4-cyl engine of 3½-in. bore and 5-in. stroke (192-cu-in. capacity) which is operated at 55 bhp at 2400 rpm in vehicles up to 10,000 lb gvw, and at 59 hp at 3000 rpm in cars and taxicabs.

This experience has been embodied in the design of an even smaller unit intended for vehicles below 5000 lb gvw, and for cars and taxicabs based on the medium-sized British and European cars, rather than for the larger American cars in which the P4 engine mentioned previously is particularly suitable. Five years of intensive development and field testing in Britain (and in Canada, Rhodesia, and Western Europe where the engine was submitted to a wide range of severe operating conditions) has enabled us recently to put into production a Four 99 engine

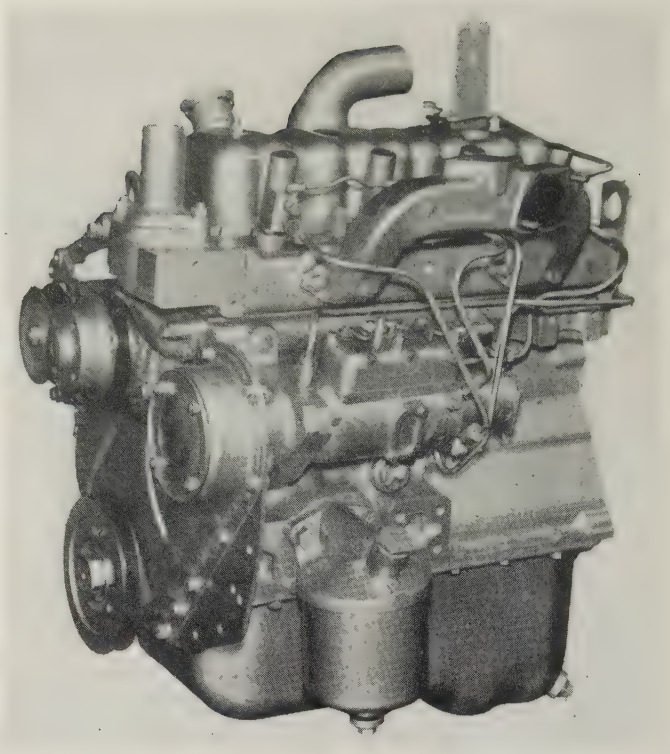

Fig. 3 — Four 99 1.6-liter diesel engine

which develops 43 bhp at 4000 rpm with a maximum torque of 73 lb-ft at 2200 rpm (Fig. 2). This engine (Fig. 3) is a 4-cyl in-line engine with a bore of 3 in. and stroke of 3.5 in. (99-cu-in. capacity). The dry weight of the bare engine less flywheel, flywheel housing and starter motor is only 320 lb. This enables a typical installation to be carried out with a weight penalty as compared with the corresponding gasoline engine of only 100–150 lb, including allowance for the increased size of batteries necessary. Sectional arrangements of the engine are shown in Figs. 4 and 5, while an enlarged cross-sectional view of the combustion chamber is shown in Fig. 6.

By reduction in the inertia of the moving parts and in the development of the combustion system, a serious attempt has been made with this engine to give a flexibility in use which is as near as possible equivalent to that of a gasoline engine. It is felt that this has been substantially achieved, and that at least this engine sets a new standard for diesel engines in this respect.

Engine Requirements

It is of interest to examine how closely the engine meets the general requirements of the applications for which it has been designed.

Installation — Fig. 7 shows the overall dimensions of the Four 99 compared to a typical 91-cu-in. gasoline engine. The differences are such that we anticipate no serious difficulties in installation. Installations have in fact been carried out in a wide range of typical cars and small commercial vehicles, both British and European, without serious difficulty and with very successful results. The comparatively small weight increase of 100–150 lb in

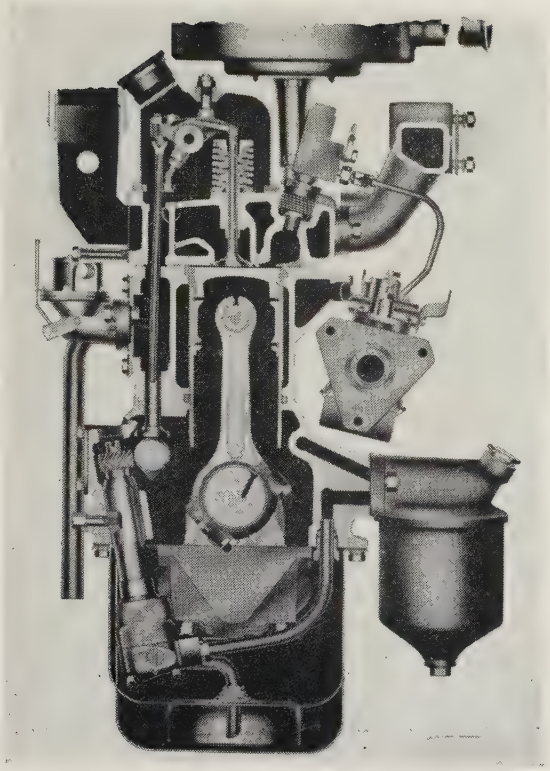

Fig. 4 — Front cross-sectional view of Four 99 diesel engine

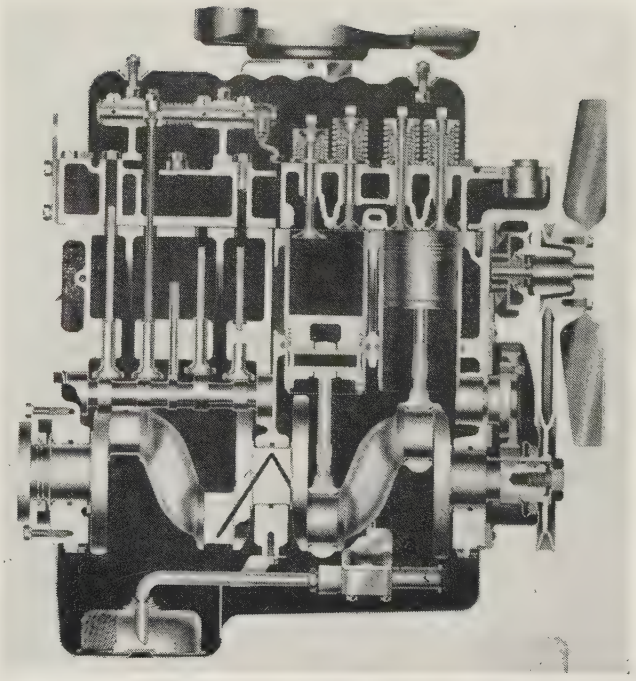

Fig. 6 — Combustion system of Four 99 diesel engine

the complete installation likewise has presented no serious difficulties.

Noise and Vibration — It cannot be claimed that the noise level is as low as that of a gasoline engine under all conditions. Provided that reasonable attention is paid to the soundproofing of the engine compartment, the noise level inside the vehicle at normal and high road speeds is similar to that of a gasoline-engined vehicle. At idling and accelerating from rest there is some increase in noise, but not to an extent that is considered unacceptable.

Vibration at all road speeds is again little or no different from that with a gasoline engine; vibra-

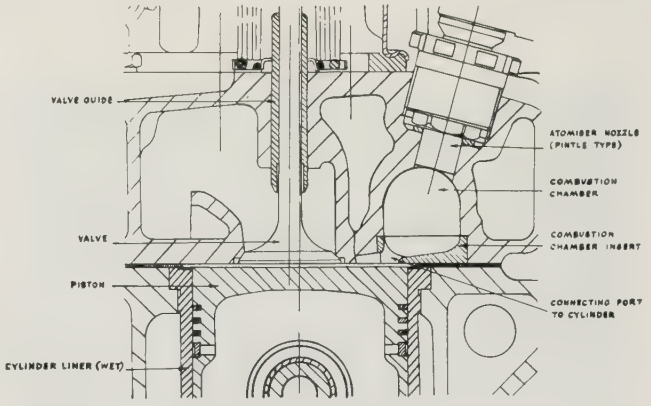

Fig. 5 — Longitudinal view of Four 99 diesel engine

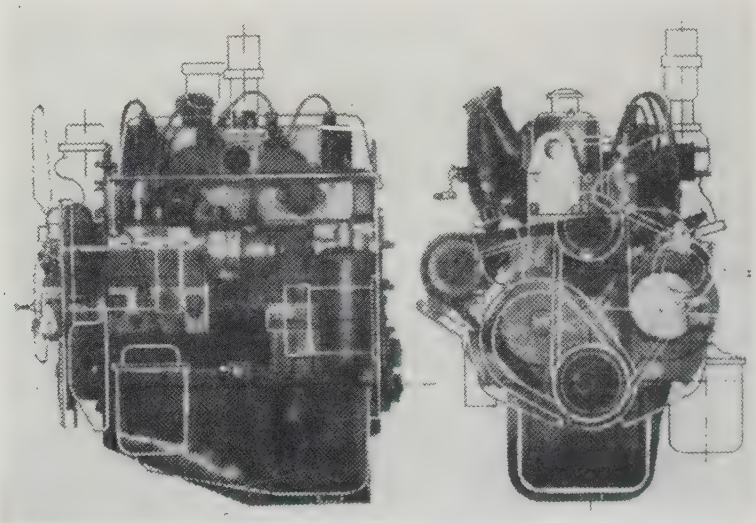

Fig. 7 — Size comparison of 99-cu-in. capacity diesel engine and 91-cu-in. gasoline engine

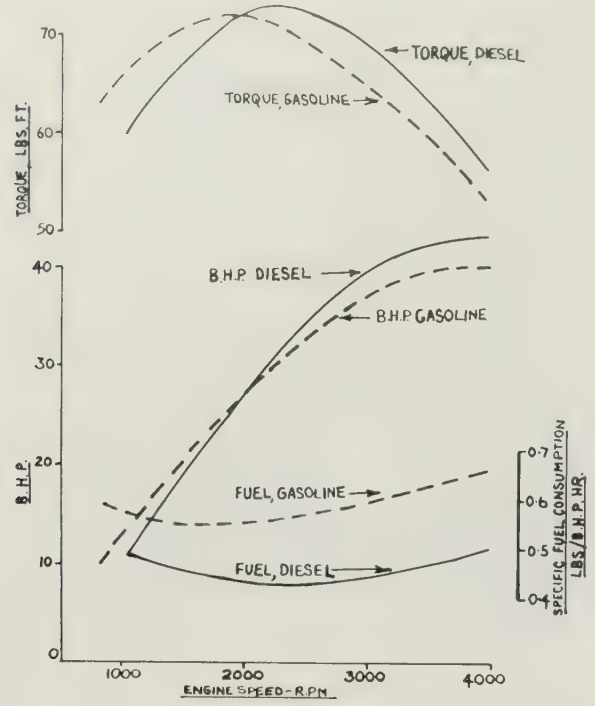

Fig. 8 — Comparison of fuel-load performance curves of diesel and gasoline engines of same maximum torque

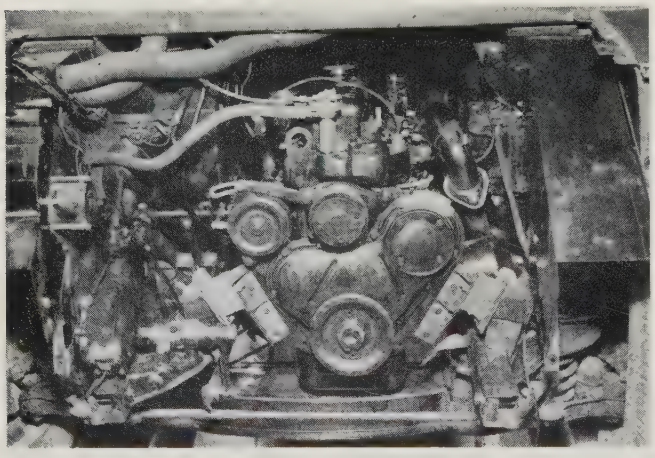

Fig. 9 — Conversion of 1956 Bedford C. A. half-ton van with Four 99 diesel engine, showing front view

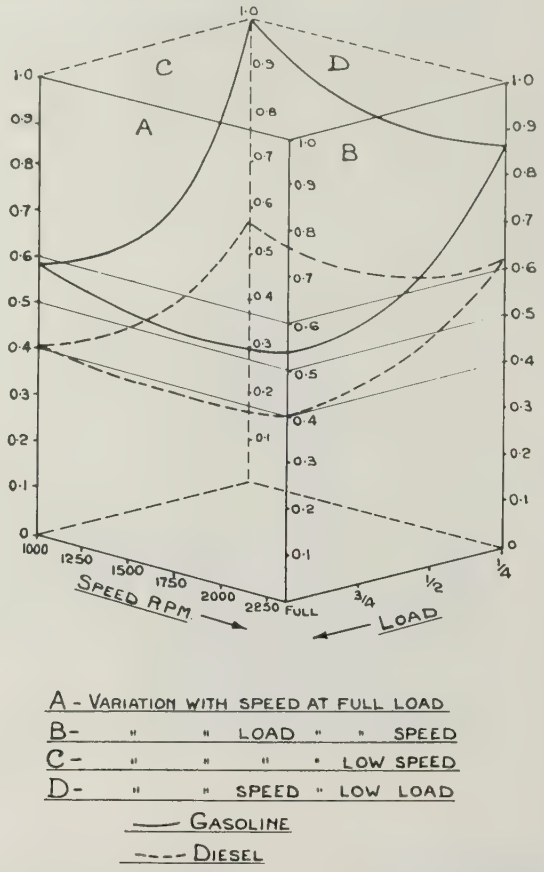

Fig. 10A — Comparison of specific fuel consumption under varying conditions of load and speed between typical gasoline and diesel engine for given vehicle installation

tion can be worse under idling conditions, but the development of suitable engine mountings has eliminated this difficulty.

Cold Starting — As cylinder size is reduced, so the increased heat losses during the operating cycle increase the ambient temperature at which starting is possible without external aids. During the development of our engine a new type of starting aid, simple and reliable in operation, became available, and all engines are fitted with it. The C.A.V. Thermostart starting aid is a heating unit situated in the induction manifold which is operated by means of a simple switch which can in fact be combined with the starter switch.

Depending on the starter motor and battery used, starts can be obtained at temperatures below 0 F with no aids other than this induction heater. For temperatures of the order of – 20 F the use of ether is necessary.

Smoke — Much development work has been carried out to reduce combustion smoke from the engine to a level which is entirely satisfactory for city operation. The efficiency of the combustion system is such that no problem was encountered in achieving the required performance with a clean exhaust, and the engine has, in fact, got something in hand in this respect. However, difficulty was experienced in eliminating white smoke under cold-starting conditions, and at high engine speeds when operating at light loads. To overcome this, a special auto advance device has been developed for the fuel pump, which is sensitive to engine load as well as to engine speed, advancing the injection timing as the engine load is reduced. This eliminates the difficulty.

Performance — A comparison of the Four 99 engine output with that of a typical gasoline engine of the same maximum torque is shown in Fig. 8, which indicates that no great difference is to be expected in the performance of the vehicle, whether fitted with the diesel or gasoline engine. Much of the early test work on this engine was carried out in cars which were originally fitted with gasoline

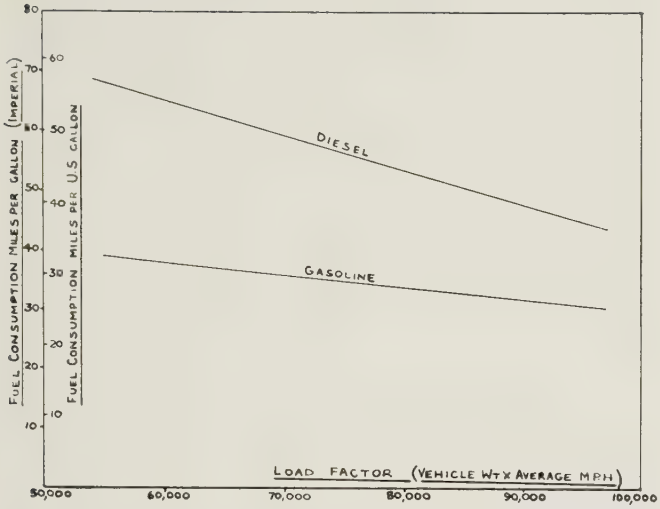

Fig. 10B — Comparison of fuel consumption under varying conditions of load and speed for typical gasoline and diesel engine (1.6-liter capacity) in similar vehicle installation

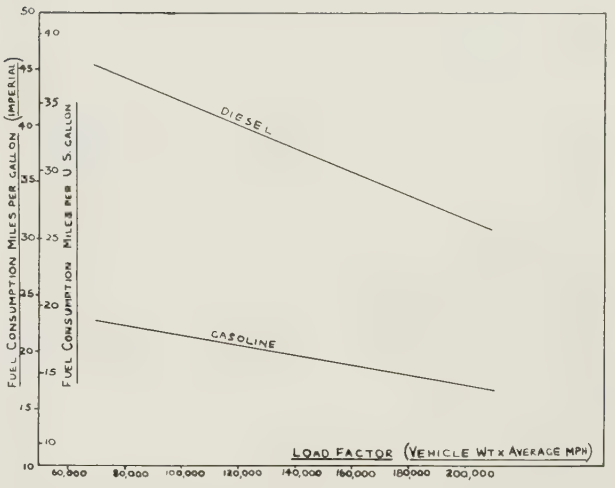

Fig. 10C — Comparison of fuel consumption under varying conditions of load and speed for typical gasoline and diesel engine (3.14-liter capacity) in similar vehicle installation

engines of practically identical output, and the performances of the vehicles with both diesel and gasoline engines were practically identical.

Much of our later performance work has been carried out in Ford Mark II Consul cars, and the relative performance details of these when fitted with the standard gasoline engine and the Four 99 diesel engine are shown in Table 1. In this case, the Four 99 engine was replacing a larger gasoline engine of considerably greater output, but the performance is nevertheless acceptable for the type of operation for which this engine is intended.

Consumption — Tests have been carried out on a wide range of commercial vehicles and cars under widely different operating conditions. On one proving endurance test a light van of approximately 3900 lb gvw converted to take the Four 99 engine completed more than 100,000 miles, partly on the road but mainly operating on the MIRA proving ground at maintained speed of 56 mph. The fuel consumption at 30 mph at the commencement of the test was 36.6 miles per U.S. gallon and at the end of the test 36.4 miles per U.S. gallon.

Fig. 9 shows a 1956 right-hand drive Bedford C. A. half-ton van converted to use a Perkins Four 99 diesel. Note the front mounting brackets shown in this front view of the engine installation. When this vehicle was used on normal delivery service, it returned a fuel consumption of 31.6 miles per U.S. gallon when operated over a route which included 115 vehicle starts per day. On 50% of the vehicle stops the engine was stopped and restarted. The average fuel consumption of a gasoline engine used on the same application was 12.5 miles per U.S. gallon, the diesel installation thus being about 2.5 times as economical as the gasoline.

The Royal Automobile Club of Great Britain conducted official tests on a Vauxhall Velox car fitted with the Four 99 engine over a distance of 218 miles, consisting of fairly narrow, twisting, and hilly roads with a number of small towns and city driving. The fuel consumption officially recorded for the distance was 47.2 miles per U.S. gallon at an average speed of approximately 34 mph.

Maintenance — A considerable bulk of evidence now exists to support the claim for reduced maintenance on diesel engines by comparison with gasoline. The Four 99 engine is too new to have built up experience over a large number of engines, but already engines have achieved a 100,000 miles without overhaul and are continuing satisfactorily.

A much greater experience on the P4 engine in light vehicles indicates that while the average life obviously depends on the treatment the engine receives from the operator and the standard of maintenance, an average period between major overalls of between 120,000 and 150,000 miles is normally obtained and mileages far in excess of 150,000 miles have been experienced under good operating conditions.

This is not intended to imply that the diesel engine can do without maintenance, as these mileages can only be achieved if strict attention is paid to normal maintenance procedure, and the recommendations with regard to changing oil filters, air filters, and fuel filters, and to the regular servicing of injectors.

Future Applications

The main reason for using diesel engines in vehicles is economy in operation, but against this must be set the increased price of the engine. The economies to be achieved by a diesel engine in a vehicle carrying out high annual mileages are well-known, but less well-known are the economies which can be achieved in light vehicles doing quite modest annual mileages. Fig. 10A which is taken from a paper by J. Scott shows specific fuel consumption curves for gasoline and diesel engines plotted on a basis of both speed and load. While the reduction in specific fuel consumption of the diesel engine as compared with the gasoline is quite substantial at full load, the greatest difference occurs under low-speed light-load conditions. This difference is also shown up in road fuel consumption tests, and Figs. 10B and 10C are derived from actual road tests of Four 99 and P4 engines. As the load factor is reduced, so both the actual and percentage economy of the diesel engine improves.

Applying this to actual operating conditions, it follows that the diesel engine should show a greater

saving on light door-to-door, stop-start delivery duties than long distance haulage. This is, in fact, borne out in practice.

By dividing the miles per gallon obtained on a given vehicle operating with a diesel engine by the miles per gallon obtained with the same vehicle operating with a gasoline engine, a ratio is obtained which indicates the increased mileage which the vehicle will cover when fitted with a diesel engine over the mileage obtainable by the vehicle when fitted with the gasoline engine for a given quantity of fuel. For reference purposes we will refer to this as an increased mileage factor (imf).

Manufacturers have compiled a number of statistics covering operating results over a wide range of operating conditions in the class of engines and vehicles which we are now considering, and from which the following figures have been extracted:

1. For long- and medium-distance haulage in medium-duty trucks an imf of 1.70 to 1.8 is obtained.
2. For short-distance work, that is, taxi and suburban work, an imf of 1.8 to 1.9 is obtained.
3. For door-to-door, stop-start delivery work, and short-distance operations where auxiliary gear is operated by the vehicle engine (for example, refuse collectors), an imf of 2 to 2.1 is obtained, while in many cases this figure may be as high as 2.3 to 2.5.

On studying these figures, it will be seen that the applications for small diesel engines in light commercial vehicles can most advantageously be considered for:

1. Taxi service.
2. Municipal vehicles such as road sweepers, gulley emptiers, and refuse collectors.
3. Delivery vans for city door-to-door and suburban operation.

With regard to taxi service, the percentage increase of diesel cabs in new annual registrations in Great Britain over a 5-year period 1953–1957 is quite remarkable (Fig. 11). From less than 2% in 1953 the figure has risen to 86% in 1957, which is conclusive evidence of the suitability of small high-speed diesel engines to meet requirements of this type of operation.

In Brussels, Belgium, a 360-strong fleet of Chevrolet taxis owned by S.A. Bruxelloise d'Auto Transports are 70% dieselized with Perkins P4(c) diesels (Fig. 12).

In Baltimore, Md.. three P4 diesel engines were installed in Plymouth taxicabs in 1956 in order to gain experience of this type of operation. One engine completed over 100,000 miles and the other two engines were in the region of 70,000 miles before the ownership of the cab company changed hands and the cars were sold (Fig. 13).

During this period of operation, no major overhauls were required and the diesel-equipped Plymouths were returning an average fuel consumption of 23 mpg which gave an imf of 1.85 over the performance previously obtained from the gasoline engined vehicles (12.5 mpg).

Further diesel engine conversions have recently been carried out in Los Angeles in two 1957 Chevrolet taxicabs, and in Detroit in both Chevrolet and Ply-

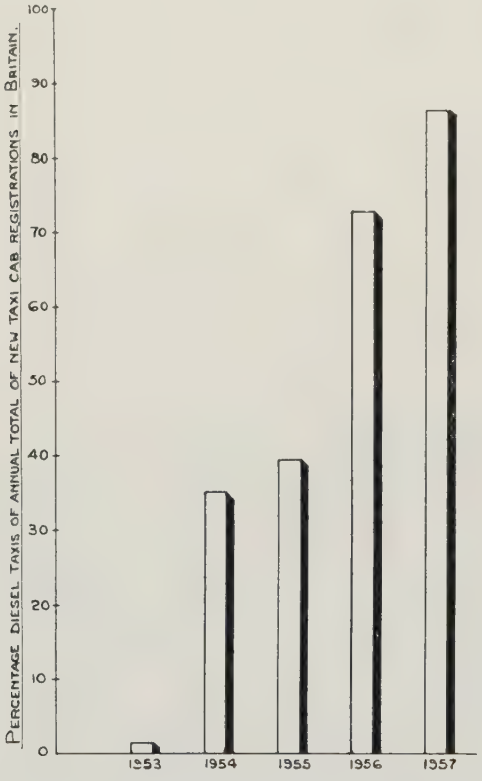

Fig. 11 — Percentage of diesel cab registrations in Great Britain, 1953-1957

Fig. 12 — Some of 250 Brussels American Chevrolet taxis which are powered by Perkins P4(C) type diesels. Taxis are operated by Bruxelles Taxi Verts et Camionette Verts

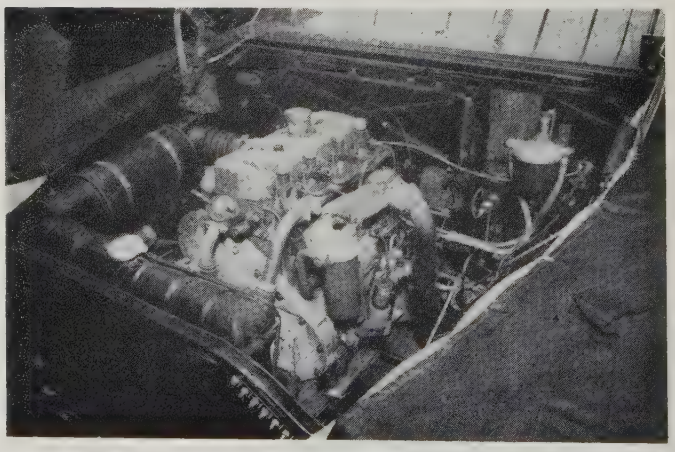

Fig. 13 — Conversion of 1957 Plymouth Plaza car with Perkins P4(C) type diesel engine, showing nearside view with top radiator hose connection removed

mouth conversions. Reports to date indicate that these engines are operating extremely well and yielding fuel savings similar to the Baltimore cabs.

In considering the engine for taxi service and taking the average life of a stock car taxicab to be 2–3 years with a mileage of between 150,000 and 200,000, it should be possible for the cab operator to recover the additional cost of a diesel installation within one-third to one-half the life of the vehicle, and, for the remaining life of the cab, operate at approximately a 50% reduction in fuel costs, based on current gasoline and diesel fuel prices. In a large fleet operating 100 cars or more, it will be appreciated that the saving would be very considerable.

With regard to municipal vehicles, it is interesting to note that in Britain in 1952 only 29 municipalities were operating diesel-engined public cleansing vehicles, whereas today 596 municipalities are now operating dieselized vehicles. In assessing the results of fuel savings from returns made by over 200 municipalities operating under varying conditions throughout Great Britain, an imf of 2.1 was obtained using a 6-cyl engine of 288-cu-in. capacity. The imf, however, can be as high as 2.4 or more, depending on local conditions.

With regard to applying diesel engines for milk delivery door-to-door work, and short-distance surburban routes for parcel delivery service, and the like, a substantial saving in operating costs would also be achieved.

Assuming an average vehicle life of 10 years for a milk delivery truck, for example, with a total life mileage of 100,000 miles, recovery of the additional first cost of a diesel engine should be made within 40% of the total vehicle life and for the remaining 60% period of operation fuel costs would be approximately halved.

On a light-delivery panel van for parcel delivery service, where short distances are experienced with a total annual mileage of, say, 25,000, it should be possible to recover the extra first cost of the diesel engine within 2–3 years of operation. As the average life of this class of vehicle is between 6 and 7 years, the remaining one-half to two-thirds of the life of the vehicle should show approximately 50% reduction in fuel costs.

These savings are based on prices of engines as conversion units and fuel cost savings, only. It is our experience that further savings can be made in maintenance and general operations, but the most important saving and reduction in break-even mileage would be obtained if the engines were offered as first equipment instead of conversions.

Conclusion

In summarizing, we can say that engines are available with the characteristics required for operation in light commercial vehicles and taxis, and these have been thoroughly proved in a wide range of applications. The economies already being achieved in Great Britain and Western Europe can also be achieved in a number of North American applications, even though these applications do not call for high-load factors or high annual mileages. The full benefits can only materialize from cooperation between the vehicle manufacturers and the diesel-engine manufacturers to allow the offer of the vehicles fitted with the diesel engine as first equipment. It would be wrong to suggest that the diesel engine will ever displace the gasoline engine completely in the light commercial vehicle, but there is no doubt that we shall see a very considerable increase in the use of the diesel engine in this field within the next few years.

Acknowledgments

The kind permission of the directors of F. Perkins Ltd. to publish this paper is acknowledged, as is the ready assistance of the author's colleagues.

APPENDIX

Relative Performance Diesel Fuel and Gasoline Consumptions

Engine and Vehicle Details

	Perkins Four 99-Diesel	Ford Consul Mark II-Gasoline
Rating:	43 bhp at 4000 rpm gross (actual)	59 bhp at 4200 rpm (published)
Capacity:	1621 cc (99 cu in.)	1702 cc (104 cu in.)
Weight as tested:	2688 lb	2548 lb
Batteries:	1 × 12 volt 64 amp hr	1 × 12 volt 45 amp hr
Axle Ratio:	4.11 – 1	4.11 – 1
Tyres:	590 × 13	590 × 13
Miles per hour per 1000 rpm in top gear:	16.6	16.6

Diesel Fuel and Gasoline Consumptions — Over 57.5-Mile Course

Average Speed, mph	Four 99 Diesel, mpg (U. S.)	Gasoline Engine, mpg (U. S.)
30	44.6	27.0
35	41.2	24.2
40	31.0	22.6

Accelerations

Through Gears, mph	Diesel, sec	Gasoline, sec
0/30	9.2	6.8
0/50	24.2	15.8
Top Gear, mph		
30/40	7.8	6.0
30/50	17.2	12.8
Maximum Speed		
Mean, 2 directions, mph	67	76

ORAL DISCUSSION

— Reported by D. E. Woomert
U. S. Army Ordnance Corps.

William Kaplan, American Oil Co.: Three of the P4(c) engines were operated in the Baltimore Taxi Fleet on an experimental basis. They saw approximately 120,000, 70,000 and 80,000 miles and gave 22–24 mpg. Because it was an experimental operation, parts were a problem and they were taken out of service for this reason.

Question: What fuels and oils are used?

Mr. Bright: No specific distillation, sulfur, or analysis is immediately available; but the engines have operated with no difficulty on standard No. 2 oil found in Canadian service stations. Three engines operating in the Baltimore Taxi Fleet used No. 1, 40 cetane, diesel oil.

SAE 30 weight oil is recommended above 80 F and SAE 20 below 80 F down to 30 F; and SAE 10W below 30 F.

Question: What service is necessary on the injectors?

Mr. Bright: At 10,000–20,000 miles the injectors should be removed and cleaned and possibly reset. It would be no more than a spark-plug change. The pintle nozzle in the Four 99 engine probably has an advantage over the nozzles used in our larger engines in this respect.

Question: Are complete conversion packages available?

Mr. Bright: For most European vehicles, conversion packages are available. The engine is designed so it can simply be incorporated in any vehicle.

INDOOR CLIMATIC of Automotive and

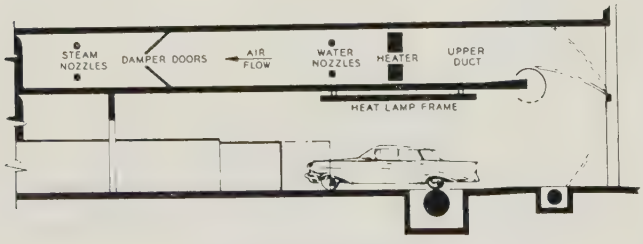

Fig. 1 — Hot tunnel

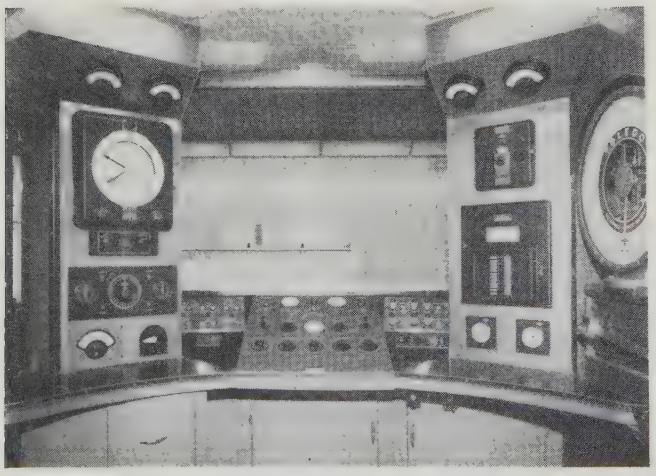

Fig. 2 — Control booth for dynamometer

CONTROLLED CLIMATIC testing is essential for the orderly design and development of automotive engine cooling and air-conditioning systems. Road testing, which in the final analysis is the true test of any design, does not offer the flexibility which is required during development stages. Outside temperature variations, seasonal and diurnal, wind direction and velocity changes, instrumentation difficulties, and road traffic interferences all contribute to this situation. Indoor climatic testing facilities permit properly instrumented year-round testing under controlled reproducible conditions.

The first part of this paper will be devoted to engine cooling. It will include a description of hot-tunnel test facilities at Harrison Radiator Division, a description of test procedures, and a comparison of results obtained in the tunnel with actual road tests at the Desert Proving Ground near Phoenix, Ariz.

Engine Cooling

Test Facilities — Fig. 1 shows a cutaway sketch of one of our automotive hot tunnels. The tunnel consists of two parallel ducts communicating at each end. Located in the lower duct to the far left are six fans which discharge air through a rectangular duct to the front of the car. The end of the discharge duct telescopes in order to accommodate cars of different wheelbases. Located in the far right end of the tunnel are electrically operated doors and turning vanes, which make it possible to recirculate all of the air or discharge part to the atmosphere

TESTING

Engine Cooling

Air-Conditioning Systems

C. V. Hawk and J. W. Godfrey, Harrison Radiator Division, General Motors Corp.

This paper was presented at the SAE Annual Meeting, Detroit, Jan. 15, 1959.

and replenish with an equal amount of fresh air. The six fans — three counterrotating sets of two each — are 10 ft in diameter. Each pair is controlled by a variable speed 100-hp motor. These variable speed motors, along with the damper doors in the upper duct, make it possible to obtain air velocities at the front of the car varying from 5 to 110 mph.

Steam heating coils in the upper duct provide the means for regulating tunnel air temperature. Temperatures from atmospheric up to 125 F can be obtained.

Test Procedures — The car is anchored on the rolls of a chassis dynamometer directly in front of the air discharge duct. The dynamometer is operated from the control booth (Fig. 2), and serves as a load or brake on the car wheels and also measures the brake horsepower at the rear wheels. The control booth is completely equipped with instruments, which indicate or record all required temperatures and pressures throughout the engine cooling system and the tunnel. Included are the following:

1. Coolant temperature to radiator.
2. Coolant temperature from radiator.
3. Fuel temperature to carburetor.
4. Fuel pressure to carburetor.
5. Oil temperature to transmission oil cooler.
6. Oil temperature from transmission oil cooler.
7. Carburetor air temperature.
8. Radiator top tank pressure.
9. Engine block pressure.
10. Water pump inlet pressure.
11. Fan air temperature.
12. Tunnel air temperature to radiator.
13. Engine oil temperature.

Fig. 3 shows instrumentation as provided on the

INDOOR CLIMATIC testing provides a 24-hr-a-day means for continuing developmental work on engine cooling, car heating, and air conditioning throughout the year. This paper describes one such test facility at General Motors.

The authors discuss engine cooling, including a description of the hot-tunnel test facilities, test procedures, and a comparison of results with actual road tests. In the second part of the paper, they treat the development of air-conditioning systems, describing the simulation of outdoor conditions and correlation with road tests.

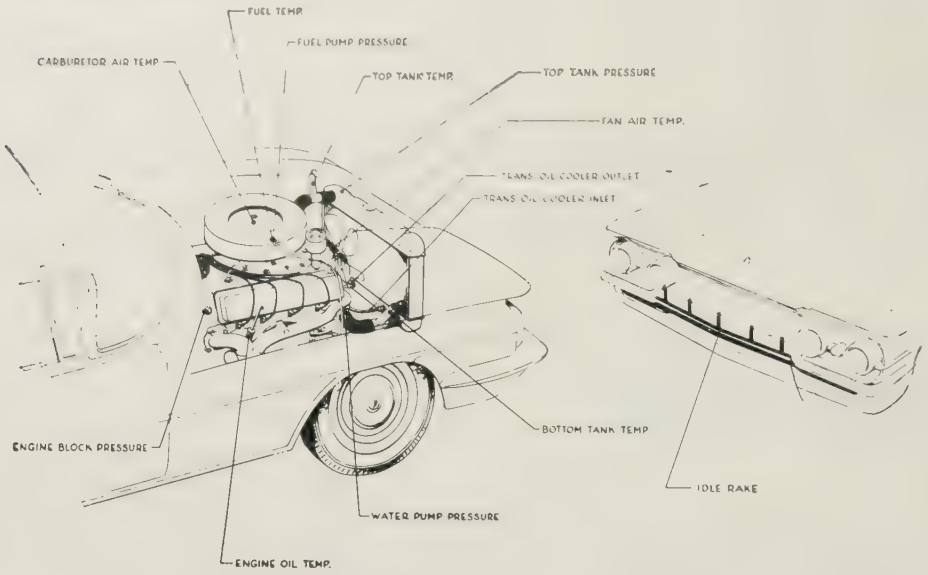

Fig. 3 — Instrumentation provided on test car

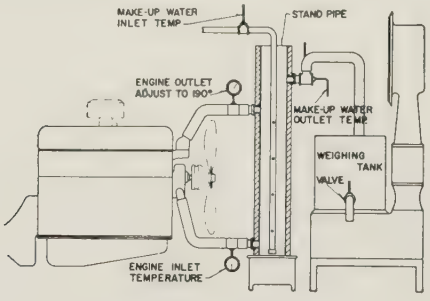

Fig. 4 — Heat rejection setup

Table 1 — Cooling Test Procedures

Heat Rejection	— 90 F ambient, 20 mph wind velocity, 70 mph wide-open throttle break-in, to be recorded at 30 min and 1 hr 40, 60, 80 mph wide-open throttle Idle at manufacturer's recommended rpm
Standard Cooling	— Wide-open throttle 40, 60, 80 mph at 90 F ambient or 10 F below expected air temperature to boil
Grade Cooling	— 7.2% Grade (previously 6% Grade) 25, 40, 60 mph at 100 F ambient or 10 F below expected air temperature to boil
Road Load	— 25, 50, 70, 90 mph at 100 F ambient or 10 F below expected air temperature to boil
Idle Run after 70 mph Road Load	— rpm to manufacturer's recommendation — in drive — brake on. Record top tank temperature every 3 min to 250 F or 30 min, whichever is sooner. Normal specified boiling point will be noted and recorded. 100F ambient temperature and full solar load.

car.

As you can see, there is an infinite number of conditions under which a car can be tested. We agreed jointly with the various car manufacturers on the standard cooling test procedures shown in Table 1.

When checking engine cooling in the hot tunnel, it is usual practice to determine engine heat rejection to the cooling water first. In this test, a tunnel air velocity of 20 mph and air temperature of 90 F are maintained. The car, with the radiator removed, is set up on the dynamometer rolls and piping connections made as shown in Fig. 4.

The cooling water inlet and outlet on the engine block are connected to the standpipe mixing chamber, into which city water is added in sufficient volume to control the outlet water temperature from the engine block at 190 F. Overflow water from the standpipe is measured in the weigh tank, and provides the means for calculating heat rejection in Btu when substituting in the formula:

$$\text{Btu} = \text{Lb of water} \times \text{temperature rise} \times \text{specific heat of water} \quad (1)$$

Generally, after heat rejection tests are run, standard cooling tests at wide-open throttle are conducted. These tests determine the full capacity of the cooling systems at wide-open throttle conditions for various selected speeds. These tests also show the influence of different types of grilles, bumpers, baffles, and the like, and underhood conditions affecting airflow. In these tests, as also with the grade cooling tests and road-load cooling tests, we encounter the term "air temperature to boil." This is the maximum ambient air temperature at which the car may be operated at any specified engine load for a particular speed without the engine coolant outlet temperature exceeding the boiling point. It is commonly referred to as the "Cooling Index."

The next tests to be conducted in the tunnel are the partial-throttle tests, usually simulating a 7.2% grade. It is rare in a modern automobile with the installed high horsepower engine, that all of the horsepower is required. For this reason, many engineers favor the adoption of a cooling index at some partial load less than full throttle.

After partial-load tests, it is customary to run road-load cooling tests. These are tests run at horsepowers necessary to move the car down a level road at the desired speed.

The last test to be run is the idle cooling test. The car is operated at 70 mph road-load horsepower until stabilization has been reached. The rear wheels

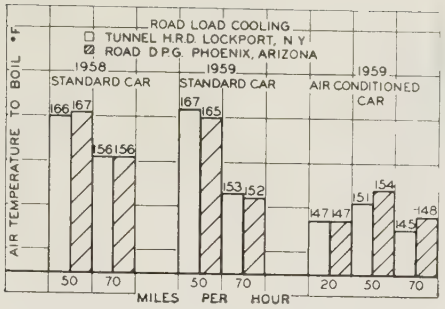

Fig. 5 — Engine cooling, road versus hot tunnel test — road-load cooling

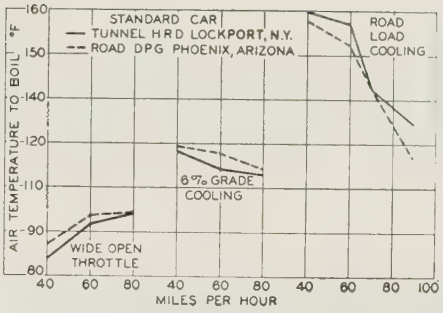

Fig. 6 — Engine cooling, road versus tunnel test — standard car

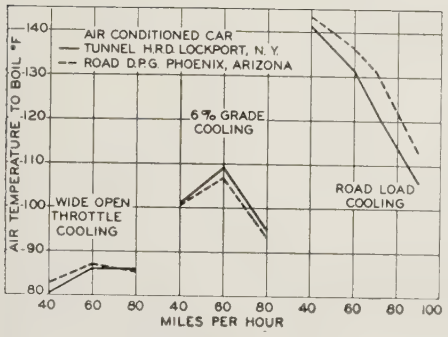

Fig. 7 — Engine cooling, road versus hot tunnel test — air-conditioned car

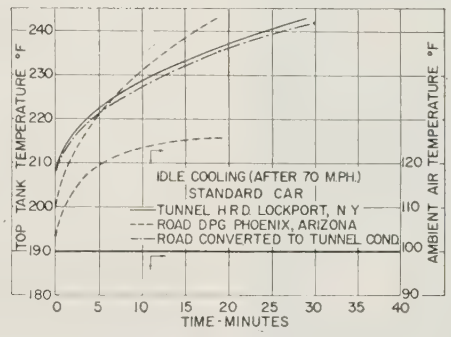

Fig. 8 — Engine cooling, road versus hot tunnel test — idle cooling (after 70 mph), standard car

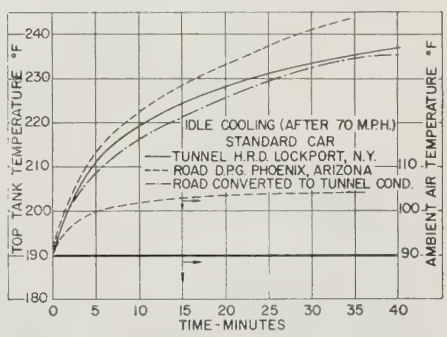

Fig. 9 — Engine cooling, road versus hot tunnel test — idle cooling (after 70 mph), standard car

are then stopped, transmission placed in drive with brake on (Synchromesh transmission cars are placed in neutral), tunnel air discharge blocked, and recordings are made every 3 min until the boiling point is reached, or until a period of 30 min has elapsed. This test is conducted at 100 F ambient with full solar load and with air conditioning operating if so equipped.

Correlation of Tunnel Tests with Road Tests — For this purpose, we conducted tests on several cars in the hot tunnel, then transported these cars to Arizona, where road tests were conducted at the Desert Proving Ground. In all instances, we endeavored to conduct Proving Ground tests under the same conditions that prevailed in the hot tunnel. As you will see, this was not altogether possible, due to outdoor atmospheric changes during the tests.

Fig. 5 shows road load air-to-boil temperatures obtained on three cars. Tests were conducted both at 50 and 70 mph. We consider this comparison excellent, with a maximum variation of only 3 deg.

Figs. 6 and 7 show comparisons of tests made on two cars — one a standard car and one an air-conditioned car — at wide-open throttle, 6% grade, and road load. These comparisons, though not as good as those shown in Fig. 5, still are considered to be within acceptable limits.

Figs. 8 and 9 show idle cooling test comparisons. Here, the effect of wide variations in ambient temperatures is most evident. The tunnel ambients were maintained at 90 and 100 F; whereas at the Proving Ground measured temperatures at the grille increased during the idle period as much as 23 F.

Inasmuch as the cars tested at the Desert Proving Ground were the same as those previously tested in the hot tunnel, our next step was to convert Proving Ground conditions to tunnel conditions. In making this conversion, the following assumptions were made, and for all practical purposes, should give accurate results:

1. Idle rpm is constant.
2. Engine heat rejection is constant.
3. Water flow through the radiator is constant.
4. Airflow through the radiator is constant.

Therefore, the effectiveness of the radiator, that is, temperature change of either fluid per 100 F inlet temperature difference, is also constant.

Using heat rejection and water flow values obtained previously in the tunnel and assuming a water effectiveness of 4.38, tunnel test results were converted to road test conditions using the following formulas:

$$H = M\,cp\,\Delta t = M\,cp\,N\,(ITD) \qquad (2)$$

where:

H = Heat rejection, Btu/min
M = Fluid flow — Lbs/min
cp = Specific heat, — Btu/min/F
Δt = Temperature change, F
N = Effectiveness, ratio
ITD = Inlet temperature difference, F

$$T_{in_{(1)}} = T_{in_{(0)}} - N_w(T_{in_0} - t_{in_0}) + \Delta t \qquad (3)$$

T = Water temperature
t = Air temperature
(0) = Zero time
(1) = One min later

As you can see, in each of the Figs. 8 and 9, when

Fig. 10 — Hot tunnel No. 1

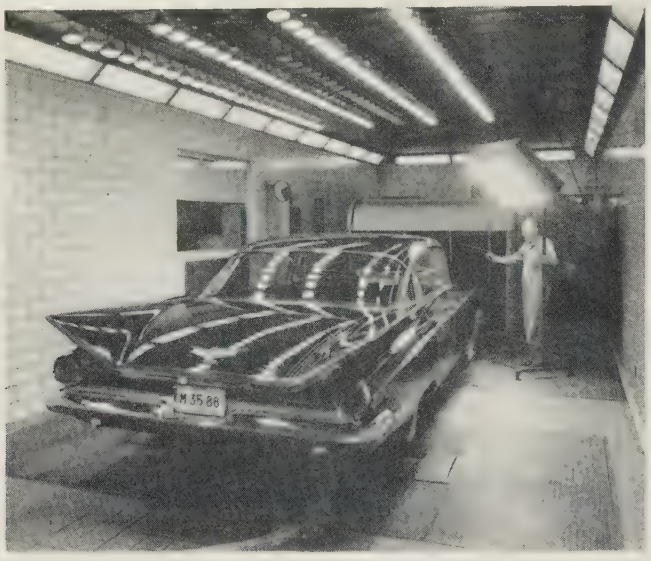

Fig. 11 — Infrared heat lamps in hot tunnel

tunnel conditions and road conditions are the same, excellent correlation of test results can be obtained.

Automotive Air Conditioning

Since people ride in automobiles out-of-doors, the final evaluation of air-conditioning performance must be made under actual road and weather conditions. However, as pointed out earlier, road testing is not satisfactory for design and development of new systems and new features. Among the reasons for this are the variations in the weather from day to day, the relatively few hours each day during which high ambient conditions prevail, traffic interferences, and instrumentation difficulties.

For these reasons, indoor test facilities which permit around-the-clock and around-the-calendar tests under carefully controlled and reproducible conditions are necessary for the design, development, and preliminary evaluation of automotive air-conditioning systems.

The three weather factors having the greatest effect on the performance of an automotive air-conditioning system are the dry bulb temperature, the relative humidity of the ambient air, and the intensity of the heat from the sun. In addition to these weather factors, we have found that engine heat load and wind velocity have significant effects on air-conditioning performance.

Simulation of Outdoor Conditions — Considering all of these factors, test equipment and procedures have been developed for evaluating air-conditioning systems with the automobile mounted on a dynamometer in a wind tunnel. Tests are conducted at road load with car and tunnel air speeds synchronized at speeds up to 100 mph.

The control of the dry bulb temperature has already been discussed under the testing of engine cooling systems.

Referring to Fig. 10, it will be noted that steam and water jets have been placed in the return air duct above the ceiling. The moisture content of the air flowing around the automobile is controlled by sensing the wet bulb temperature of the air with a platinum resistance thermometer encased in a wick connected to a reservoir of water. Deviations from the prescribed wet bulb temperature control the rate at which steam is injected, and thus maintain the wet bulb temperature with an accuracy of ±1 F. The injection of water is controlled manually, and is used only when supplementary capacity is required.

The importance of having accurate and reproducible humidity control can be demonstrated by the fact that, to obtain the discharge air temperature required for good performance, approximately twice as much cooling capacity is required to cool 100 F air which is 40% saturated with moisture as would be needed if this same air were only 10% saturated. For this same reason, an evaluation of an air-conditioning system by road testing in a hot and dry climate only cannot be relied upon, since a system which works well under these conditions may not be adequate when hot and humid weather is encountered. This is especially true of systems which use an appreciable percentage of outside air.

Fig. 11 also shows the infrared heat lamps which have been placed over and alongside the automobile to simulate the effect of solar heat. The heat intensity and arrangement of these lamps is based upon very comprehensive data obtained with three cars in Texas in the summer of 1955. These tests included such variables as angle of incidence to the sunlight, car body color, and car speed, as well as the day-to-day and hour-to-hour variations of temperature and humidity. Cool-down tests, after prolonged soaking in the sunlight, were included in these studies.

When sufficient data had been accumulated in Texas, the cars were returned to the car tunnel and the Texas conditions were duplicated. The heat lamps were adjusted to give comparable breath level air temperatures, which are most significant in relation to passenger comfort.

It was found that the roof, hood, and trunk temperatures were higher those obtained in Texas, at corresponding breath level air temperatures, for two reasons:

1. The wave length of the solar radiation is different from that of the heat lamps, which affects the transmittance of radiant heat energy through the glass.

2. Because the sun is at a great distance, the unit solar radiation received by various areas on the car is constant. This cannot be exactly duplicated in

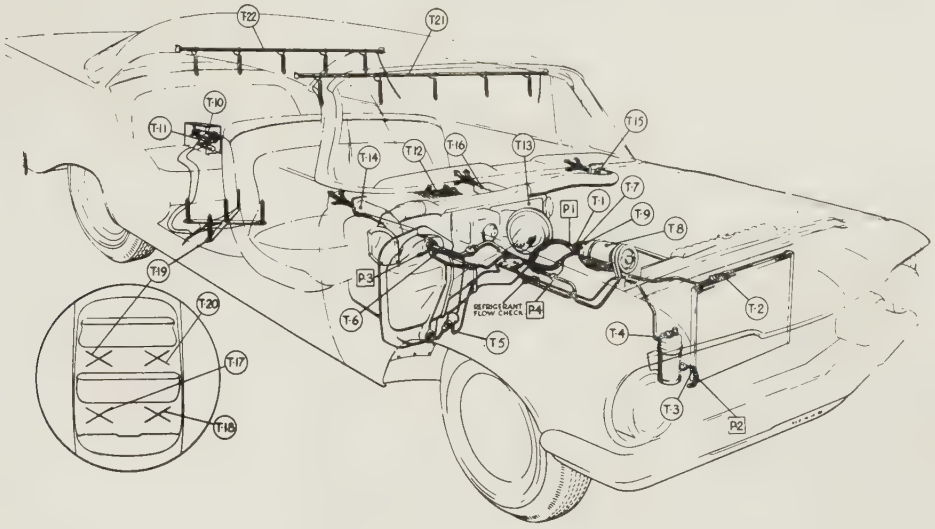

Fig. 12 — Instrumentation of car

the car tunnel because the heat lamps are relatively close to the car surfaces, and small differences of distance effect differences in the heat intensity.

Upon completion of the tests and analysis of the data, it was concluded that the best simulation of the Texas sun was obtained by the use of 96 overhead lamps, 250 watts each, arranged in four rows of 24 lamps per row, plus a side bank, shining in from the right front, of 20 lamps of 375 watts each, giving a total of 31,500 watts. The spacing of the lamps in the rows is 8 in., and the row spacing is approximately 2 ft. The lamps are approximately 4 ft above the top of the car. The instrumentation of the car is shown by Fig. 12. Significant temperatures and pressures are read and recorded, as well as the flow rate of the refrigerant. The flow rate of the cooled air is determined separately, by the use of a calibrated orifice.

Test Procedures — For performance evaluation at high ambient conditions, three types of tests are used. Ambient conditions of 100 F dry bulb temperature and 40% relative humidity with a simulated sun load have been selected for the design conditions.

1. Stabilized Performance Across the Speed Range

These tests are made with no passengers and are usually at speeds of 15, 25, 40, and 60 mph. The car is operated until all temperatures and pressures become stabilized before any readings are recorded.

2. Soak and Cool-down —

These tests are also made with no passengers. The car is soaked under simulated sun load without engine running and with no tunnel air until average interior air temperature is at a prescribed level, usually 135 F. The car and tunnel are then operated at 25 mph for 1 hr with data being recorded at 5-min intervals.

3. Comfort Evaluation —

Comfort evaluations are made with four passengers. The car is soaked as described above for a soak and cool-down test. At the end of the soak, the passengers are exposed to tunnel ambient conditions, under the heat lamps, for about 10 min before entering the car. At the end of this period, the passengers enter the car, opening and closing the doors quickly. The car is started and operated at 25 mph for 45 min, followed by 15 min of operation at 60 mph. Fig. 13 shows the results of a typical comfort ride. Each passenger records a numerical value representing how he feels at the time, according to a scale of 9 (cold) to 1 (hot).

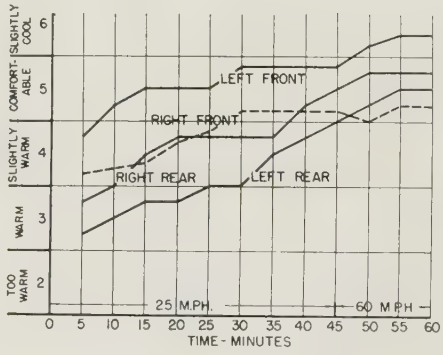

Fig. 13 — Comfort evaluation
(100 F, 40% R.H., 135° breath level, full sun load, prod. rec. air)

We do not expect that the results obtained from comfort rides will be exactly reproducible. Experience has shown that the same person will react differently on different days or even at different hours of the same day. Also, different people tend to emphasize different features of comfort and, therefore, vary considerably in their reactions. Nevertheless, the comfort rides do provide valuable information beyond that which can be obtained by readings from the instruments.

Correlation with Outdoor tests — The accuracy which has been achieved in the simulation of out-of-door conditions, and the reproductibility of the test results, were again verified by a comparison obtained during the 1959 development program.

During the autumn and winter of 1957, the design and testing of the 1959 General Motors air conditioning systems was completed, and verification of the tunnel test results was obtained by operating these systems under actual road and weather conditions. A test car was prepared which duplicated the 1959

automobiles in the areas where the equipment would be installed, and provisions were made for quickly installing each of the five 1959 air-conditioning systems. Extra glass areas were incorporated, again simulating the 1959 cars. After the performance of all of the systems had been established by car tunnel tests of both actual temperatures and comfort, the test car and an escort car were driven to the vicinity of Verz Cruz, Mexico, during early February.

Fig. 14 shows a comparison between the results obtained in Mexico and the previous results from the car tunnel. Fig. 15 shows a comparison on the basis of passenger comfort. These may be considered to be excellent correlations, especially when we consider the fact that the cars had been operated for several thousand miles between the two tests, different instrumentation was used, and two of the four passengers were different people.

Looking to the future for a moment, consideration is now being given to the addition to the car tunnels of equipment which will allow control of temperature and relative humidity at lower than ambient conditions. This is required to obtain service data satisfactory for the various systems, over a considerable range of temperature and humidity, as would be encountered in the field. As much as 200 tons of refrigeration equipment would be required to dehumidify the air and to lower its temperature.

Further work is being done to determine the exact effects of driving over very hot pavements, where the air temperature to the condenser and radiator may be considerably higher than the ambient air temperature. Data was obtained on a test car in Texas and Arizona during the past summer, and this will be used as a basis for further investigations of this effect in the car tunnels, and for the development of methods of simulation.

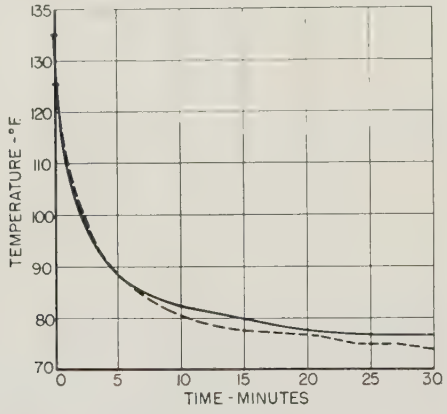

Fig. 14 — Road test versus hot tunnel test, 25 mph cool down
— Tunnel, 100 F, 40% R.H.
— — Road (Vera Cruz, Mex.), 102 F, 35% R.H.

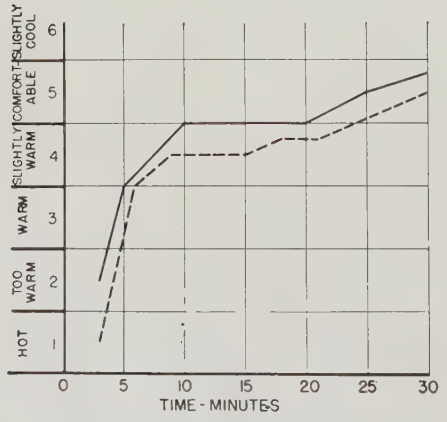

Fig. 15 — Comfort appraisal
— Tunnel, 100 F, 40% R.H.
— — Road (Vera Cruz, Mex.), 102 F, 35% R.H.

Conclusion

In conclusion, indoor climatic testing has provided the engineer with a means whereby he can continue his developmental work on automotive engine cooling, car heating, and air conditioning throughout the entire year. His facilities are close at hand at all times, and he can use them for the full 24 hr of every day.

DISCUSSION

Comments on Authors' Heat Rejection Equations

— J. P. Lindsay
Chrysler Corp.

EQUATION 2 in the text is a general engine heat rejection expression, $H = M\ cp\ \Delta t = M\ cp\ N\ (ITD)$, when Δt and ITD are equilibrium temperature differences. For automotive radiator application, M, cp, Δt, and N may be in consistent units for either the air or water side. From the above equation we obtain:

$$\Delta t = N\ (ITD) \tag{A}$$

$$N = \frac{\Delta t}{ITD} \tag{B}$$

Using the authors' symbols of t for air temperature and T for water temperature, we may obtain values of N for either the air or water side:

$$N_A = \frac{\Delta t}{ITD} = \frac{t_{out} - t_{in}}{t_{in} - T_{in}} \tag{C}$$

$$N_W = \frac{\Delta t}{ITD} = \frac{T_{out} - T_{in}}{t_{in} - T_{in}} \tag{D}$$

Experience idicates that N_W is roughly 0.05 at idle and that the authors' stated value of 4.38 is more likely 0.0438.

Equation 3 is apparently derived from the following relationship for an engine cooling system at a nonequilibrium condition:

Engine heat rejection during the time from 0 to 1 min = Heat transferred from the radiator to the air + heat to raise the water temperature from T_{in_0} to T_{in_1}, or using the authors' symbols:

$$H = M_{cp} N_W\ (T_{in_0} - t_{in_0}) + M\ \text{cp}\ (T_{in_1} - T_{in_0}) \tag{E}$$

Rearranging:

$$M\ cp\ (T_{in_1} - T_{in_0}) = H - M\ cp\ N_W\ (T_{in_0} - t_{in_0}) \tag{F}$$

Substituting the waterside equivalent for H:

$$M\ cp\ (T_{in_1} - T_{in_0}) = M\ cp\ \Delta T - M\ cp\ N_W\ (T_{in_0} - t_{in_0}) \tag{G}$$

The above substituted value of ΔT is an equilibrium value but the nonequilibrium ΔT is very nearly equivalent.

Since all values used above of M and cp are those for water, dividing both sides of the equation by $M\ cp$ yields:

$$T_{in_1} - T_{in_0} = \Delta T - N_W\ (T_{in_0} - t_{in_0}) \tag{H}$$

Rearranging:

$$T_{in_1} - T_{in_0} - N_W\ (T_{in_0} - t_{in_0}) + \Delta T \tag{I}$$

This is similar to the authors' equation except that ΔT replaces Δt.

Theory and instrumentation of inertial navigation systems

J. Statsinger, American Bosch Arma Corp.

This paper was presented at a meeting of the Southern New England Section, Springfield, Mass., Nov. 5, 1958.

INERTIAL NAVIGATION is a highly refined dead-reckoning technique which utilizes as its basic data the measured acceleration of the vehicle being navigated.

A new suspension principle has made such navigation practical for aircraft and missiles. It is the fluid immersion technique and has reduced nearly to zero the friction forces that caused errors in previous systems. A gyroscope and an accelerometer are the heart of inertial guidance. The first provides a stable platform for the second. By integrating the accelerations experienced during flight, the system can give position and velocity at any time.

This paper describes the design and operation of several inertial navigation systems.

FOR PURPOSES of this discussion, the navigation problem will be defined as the problem of determining the position coordinate and the velocity vector of a moving vehicle with respect to some well-defined frame of reference. Common frames of reference are earth coordinates (latitude and longtiude) and various types of grid coordinates used over limited areas. There are, of course, an infinite number of conceivable coordinate systems and many different schemes have been used in special purpose application. And, by the use of suitable mathematics, information furnished in one coordinate reference system can generally be transformed into any other system.

Before going into a specific discussion of the principles of inertial navigation, it is probably valuable to mention briefly some of the more familiar types of navigation devices.

Historically, navigation techniques were first developed primarily to meet the requirements of travel by sea. Prior to the introduction of the magnetic compass in the middle ages, the most common method used was the observation of coastal land-

marks as a means of determining position. Out of sight of land, steering could be managed for short distances by naked eye observation of the pole star.

Position fixing remained very crude until the eighteenth century when both the sextant and the first marine chronometer were introduced. The determination of position by crude means nevertheless enabled the navigator to form some estimate of his direction and speed by means of successive position observations and a rough knowledge of elapsed time. On the other hand, the introduction of the magnetic compass coupled with means for estimating speed enabled the navigator, starting from some known position, to estimate subsequent positions by a dead-reckoning process.

In many applications today, the navigation problem is solved by what are essentially refinements of these early techniques. The gyrocompass has in many areas replaced the magnetic compass, excellent water and air speed measuring devices are in general use, precise sextants and chronometers are commonplace, and so on. In addition, many of the operations and computations which are required are now performed by automatic equipment.

However, there are many applications where their techniques are inadequate and a great many otherwise intractable problems are solved today by the use of the varied systems of radio navigation. These systems provide precise means for determination of position and velocity under a variety of conditions and have greatly increased the scope of the navigation art.

It is worth noting that certain basic principles are common to many of the navigational means which have been used in the past or are used at present. For example, differentiation of position data to obtain velocity, or the converse process of integration of velocity data to obtain position, is characteristic of many navigation systems. It will be seen later that inertial navigation involves similar mathematical techniques.

Another characteristic common to all of the navigation systems mentioned thus far is that their utility depends more or less on the availability of data from external references. Some systems require up-to-date and precise knowledge of winds or ocean currents in order to maintain accurate performance; others must receive electromagnetic radiation either in the form of light signals from astronomical objects or in the form of radio signals from known sources. Unfortunately, the availability of these data is dependent to some degree on atmospheric and other conditions and, consequently, there are circumstances under which the utility of these systems is more or less curtailed.

It seems clear that for most military and many civilian applications it is highly desirable to have available a navigation system which would be independent of external information. One of the prime advantages of inertial navigation systems is exactly this: they are inherently self-contained and independent of external data sources.

Inertial navigation is, in essence, a highly refined dead-reckoning technique which utilizes as its basic data the measured acceleration of the vehicle being navigated. Assuming that sufficiently accurate accelerometers can be appropriately mounted in the vehicles, and that the velocity vector and position coordinates of the vehicle are known at one instant of time (for example, at the time of starting), then a continuous reading of subsequent velocity can be obtained by a single integration of accelerometer outputs, and continuous position data is obtained from a second integration. In mathematical terms:

$$V(t) = Vo + \int_o^t a(t)dt$$
$$D(t) = Do + \int_o^t V(t)dt$$

where:

$V(t)$ = Instantaneous velocity as a function of time
Vo = Initial velocity
$a(t)$ = Acceleration as a function of time
$D(t)$ = Instantaneous displacement as a function of time
Do = Initial displacement

This arrangement is certainly self-contained since the accelerometers and integrators are located in the vehicle; and the navigation information is derived without reference to external data sources, except for the reading of velocity and position which may be made before starting travel.

The arrangement which has been presented is highly oversimplified, but does nevertheless illustrate the basic concepts of an inertial navigation system. In order to refine the description, it is necessary to consider in some detail the requirements for mounting and orienting the accelerometers. Before doing so, however, it should be pointed out that the system which will be described does not necessarily represent any presently existing or proposed inertial navigator. Many different configurations are possible, and the one selected for presentation was chosen because it provides a convenient means of illustrating principles and requirements common to substantially all inertial navigation systems.

One possible way of measuring the total acceleration vector of a vehicle is to measure the three components of the acceleration in a three-axis orthogonal coordinate system, using three orthogonally mounted accelerometers.

The integration performed on these acceleration components will then provide corresponding velocity and displacement components, provided that the coordinate system is properly chosen. One basic requirement for such a coordinate system is that its orientation in space (either fixed or variable) must be known at all times. Otherwise, the reference directions for the acceleration, velocity, and displacement components are not defined, and the data are useless for navigation purposes. This implies specifically that the coordinate system must be stabilized against angular motions of the vehicle since those motions are, in general, arbitrary and unpredictable. In other words, the three accelerometers used to measure the acceleration components must be mounted on a stable platform. The only device known today which is capable of providing a reference of sufficient accuracy for a stable platform is the gyroscope, which is essentially a flywheel rotating at high speed, and which has the property that it maintains the orientation of its axis of spin fixed in space unless acted upon by a torque. Gyros are, thus, essential components of an inertial navigator, since they provide the means whereby a well-defined coordinate reference sys-

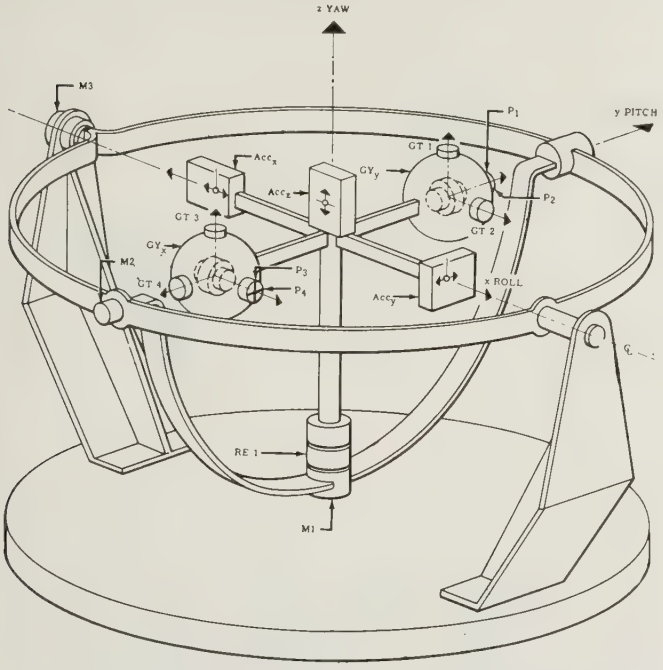

Fig. 1 — Functional view of inertial platform

tem can be physically realized in the form of a stable platform mounted in a vehicle. A gyroscopically stabilized platform which has three mutually orthogonal accelerometers mounted on it is frequently termed an inertial platform and is the basic sensing element for an inertial navigation system (Fig. 1).

Another factor, which must be taken into consideration in measuring the components of vehicle acceleration, is that for all of the applications under consideration here, the measurements are made in the presence of the earth's gravitational field. It is a fundamental principle of mechanics that an accelerometer cannot distinguish between gravitational acceleration and an acceleration due to motion in space. Consequently, each accelerometer output will, in general, consist of a component of vehicle acceleration and a component of the gravitational field. A direct integration of such an output will not, therefore, provide the desired velocity information since the velocity is the integral of vehicle acceleration only, and the integral of the gravity component constitutes an error term.

In order to describe the way in which the proper velocity and displacement components may be obtained from the accelerometer outputs, we will consider a reference coordinate system which has a fixed orientation in space. For the moment, an arbitrary gravity field will be assumed. Such a field may be described completely at each point in space by its three components in the directions of the reference axes. Each component is a function of the position coordinates.

If we let (1) The gravitational field components in the x, y, z, directions be: $g_x(x, y, z)$, $g_y(x, y, z)$, and $g_z(x, y, z)$, respectively; (2) the vehicle accelerations in the x, y, z directions be a_x, a_y, a_z, respectively; (3) the accelerometer readings in the x, y, z directions be A_x, A_y, A_z, respectively; the following equations are obtained:

$$\begin{aligned} A_x &= a_x + g_x(x, y, z) \\ A_y &= a_y + g_y(x, y, z) \\ A_z &= a_z + g_z(x, y, z) \end{aligned} \tag{1}$$

These equations merely express the fact that each accelerometer reads the sum of the gravity component and the vehicle acceleration component along its axis of measurement.

Inasmuch as the coordinate system maintains a fixed orientation in space, the components of vehicle acceleration a_x, a_y, a_z, are the second derivatives of the displacement components with respect to time, or:

$$a_x = \frac{d^2x}{dt^2} \qquad a_y = \frac{d^2y}{dt^2} \qquad a_z = \frac{d^2z}{dt^2} \tag{2}$$

Substituting Equations 2 into Equations 1, these result:

$$\begin{aligned} A_x &= \frac{d^2x}{dt^2} + g_x(x, y, z) \\ A_y &= \frac{d^2y}{dt^2} + g_y(x, y, z) \\ A_z &= \frac{d^2z}{dt^2} + g_z(x, y, z) \end{aligned} \tag{3}$$

Equations 3 form a set of three differential equations in three variables and can, theoretically at least, be solved for the displacements x, y, z, and the velocities $v_x = \frac{d_x}{dt}, v_y = \frac{d_y}{dt}, v_z = \frac{d_z}{dt}$, provided that the functions g_x, g_y, g_z are known. The method of instrumentation of a computer for this purpose would depend on the specific form of the functions g_x, g_y, g_z.

The case of most immediate interest is concerned with navigation on or near the surface of the earth. In discussing this case, it will be assumed that the earth is a perfect, homogeneous sphere, and that the altitude of travel, if any, is negligible by comparison with the earth's radius.

Under these conditions Equations 3 can be shown to assume the following form:

$$\begin{aligned} A_x &= \frac{d^2x}{dt^2} + \frac{g}{r}x \\ A_y &+ \frac{d^2y}{dt^2} + \frac{g}{r}y \\ A_z - g &= \frac{d^2z}{dt^2} + \frac{g}{r}z \end{aligned} \tag{4}$$

where:

g = Gravitational acceleration at surface of earth
r = Earth's radius

(Both g and r are constants for a perfectly spherical homogeneous earth, as shown in Fig. 2.)

Each of Equations 4 is a second order linear differential equation with constant coefficients, and with the first derivative term (that is, the damping term) absent. This implies that the transient portion of the solution is a sinusoid which maintains constant amplitude, or in other words, a computer which solves one of these equations would, if subject to a sudden disturbance, break into an oscillation,

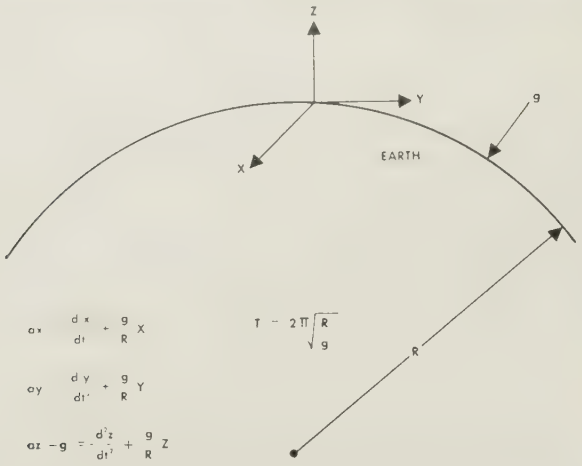

Fig. 2 — Conditions of perfectly spherical earth of Equations 4

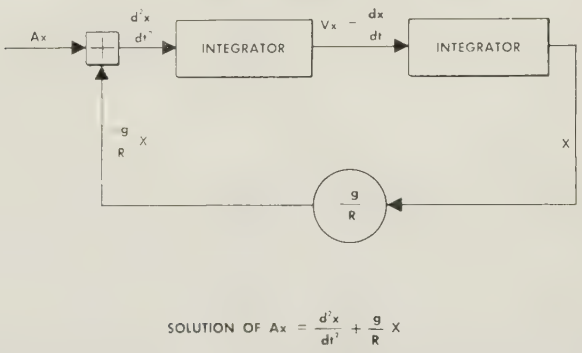

Fig. 3 — Computer with two cascaded integrators

the amplitude of which (theoretically) would neither increase or decrease with time. From the equations, it can be seen that the period of such oscillation is given by:

$$T = 2\pi\sqrt{\frac{r}{g}} \qquad (5)$$

The computer shown in Fig. 3 involves two cascaded integrators in a closed loop with no damping connections and, consequently, can at best be quasi-stable. In fact, a practical computer will be somewhat unstable because of component imperfections, frequency response, and the like. These factors must be very carefully controlled in order for the computer to be usable.

The system equations which have been discussed in a theoretical manner can, of course, be set up in more elaborate form to take into account the physical properties and performance characteristics of both the inertial platform and computer components. The analysis of these equations leads to a set of accuracy specifications for the various components of the system. The analysis will not be presented here, but some of the results can be generally described.

For most applications, it is necessary that the accelerometers and the major computer components maintain an extremely high level of accuracy and that the gyros maintain their theoretical orientation within very close tolerances. The requirements

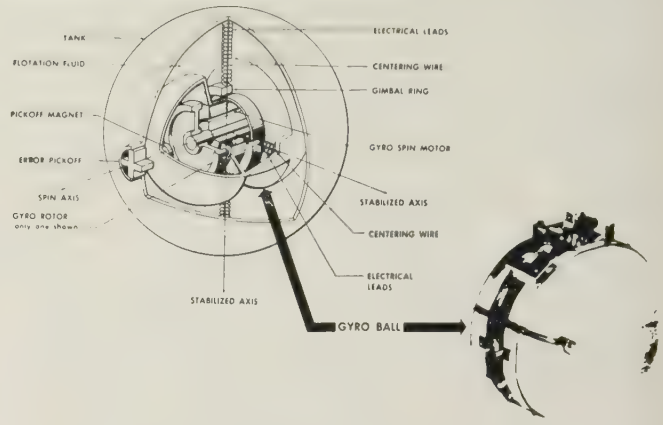

Fig. 4 — Functional view of inertial gyro

are generally quite severe, but are not impossible to meet. It is of interest to note that shipboard gyrocompasses which have been made for many years have had component accuracy requirement of the same order. However, most of the applications for inertial systems are in aircraft of various types and there are many problems which arise in achieving shipboard performance in an airborne component. The two most obvious problems are the considerably greater restrictions on size and weight demanded of airborne equipment and the tremendously increased severity of environmental conditions such as acceleration, shock, vibration, and temperature range.

Some of the approaches which have been used to solve these problems will be discussed, along with the success which has been achieved.

Inertial navigation has become feasible and attractive over the past few years because of a number of new components and instrumentation techniques which have been developed. We shall attempt to illustrate the special features which are of value to inertial systems.

Gyros

The principal new component is the high-precision fluid immersion gyro. On the surface, this device bears no obvious resemblance to a typical gyro with its rotating wheel. It appears rather as a sealed container with several electrical terminals. Actually, of course, a rotating wheel is contained within this assembly. This wheel, with its spin axis mounted on ball bearings, is hermetically sealed in a spherical shell which is then completely submerged in neutral buoyancy in a container of fluid. It is this container which we observe with its electrical terminals. The spherical shell is centered in the fluid container by very light wire filaments which are maintained at zero angle of twist by an external servo system. Thus, torques due to wire twist are kept at a zero level and the friction of conventional pivot bearings is not present. Since the spherical shell is in neutral equilibrium, it is buoyed up completely by the fluid and in accordance with Archimedes' principle this will be true under any accelerating forces. Thus, the gyro has no tendency to move and hit the walls of the tank, even under extremely high shock loads. The wire filaments are

not subject to any load (other than a minute amount caused by lack of perfect buoyancy). This arrangement gives us an essentially frictionless suspension for the gyro so that very high accuracies are maintained even with rather small gyros. (See Fig. 4.)

This is in contrast to older gyros which used gimbal pivots such as ball bearings, which were required to take the entire load of the gyro and hence caused considerable friction. Ingenious suspensions were frequently developed in order to give low friction but these invariably deteriorated under acceleration forces and did not offer the basic solution which has been provided by the fluid immersion gyro.

Pickoffs — Since the new gyro derives its accuracy by virtue of negligible friction torques, it must not be permitted to drive output devices, platform, and the like, which would exert a reaction back on the gyro. Rather, it provides an electrical signal which is then used to actuate a servo drive. This signal is obtained from a magnetic-type pickoff which measures angular deviation between the gyro (that is the spherical shell) and the fluid container. This pickoff employs an exciting winding on the spherical shell to create an alternating magnetic field and a pickoff winding on the fluid container which generates a voltage in proportion to the relative position between the winder and the magnetic field. The pickoff has been designed so as not to create any reaction torques. The fluid container is then mounted on a set of motor-driven gimbal pivots (that is, the platform) and the motor drives are actuated through amplifiers by the pickoff signal. The motor drives to position the fluid container and platform to the point where the pickoff signal is zero. Thus, the platform always follows the gyro in angular position and becomes a power-driven space-stabilized platform of high precision. This same servo drive, of course, maintains the wire filaments at zero twist as mentioned previously.

The pickoff acts as a low-impedance, high-precision signal source at the reference frequency of the system (typically 400 cycles).

Two Axis Design — Since it is possible to observe angular deviations from the spin axis of a gyro in two perpendicular directions, we may double the effective stabilizing ability of a given gyro. For example, a vertical spin axis gyro can detect both roll-and-pitch motions and a horizontal spin axis gyro can detect azimuth and tilt motions. To accomplish this, the gyro pickoff is built as a two-axis device with two windings wound at right angles to each other, each one capable of sensing one of the motions. This arrangement gives rise to the two-axis gyro which serves as the heart of the modern inertial navigation system. Each one of gyro pickoffs operate an appropriate servo drive on the platform.

Other Features — Because of the hermetically sealed nature of the design, reliability and life become of extreme importance. Careful attention to mechanical design has resulted in a permanently lubricated device which has a minimum 10,000-hr life. Manufacturing procedures which involve proper running-in tehniques and lubrication checks assure this long life.

Installation of the gyro on the platform is somewhat similar to installation of a synchro or resolver. The gyro actually employs a synchro-mounting flange and need merely be aligned by a standard zeroing procedure before being placed in operation.

Accelerometers

The development of a precision accelerometer has been as necessary and as difficult as the development of the precision gyro. Current components have attained this goal partly by using similar frictionless support methods to those used in the gyro.

Early accelerometers were essentially pendulous masses on a pivot bearing, and coupled to an electrical pickoff. They would move off the vertical during acceleration and actuate the pickoff. To eliminate the pivot friction, bearings have been replaced with thin flexing metallic tapes. It would be possible to use the tape as a spring and obtain motion proportional to aceleration. Such a system, however, would not give the required high precision, since a tape stiff enough to take maximum acceleration would invariably have too much hysteresis and the desired low threshold acceleration would not be attained. The tape is, therefore, designed with a low stiffness in order to eliminate hysteresis and the mechanical spring is supplemented with an electrical spring.

Pickoffs — Pickoffs have generally been of the a-c electromagnetic type similar to those used in the gyro. They are characterized by high accuracy, low impedance, low drift, and negligible reaction torque. Designs have also been made using capacity-type pickoffs operating at higher frequencies. These appear to give very satisfactory results although requiring somewhat more complex instrumentation.

The entire assembly is immersed in a viscous damping fluid and sealed in a container. The fluid provides effective damping and shock protection for the system while permitting rapid response to applied accelerations.

Velocity-Type Accelerometers — Much effort has been expended by various people to produce an accelerometer having an output proportioned to velocity. This automatically smooths out rapid acceleration functions which would otherwise have to be done elsewhere in the system. One method employs viscous drag of a damping fluid on the moving assembly to give output proportioned to the time integral of the acceleration. This arrangement is limited by viscous drag linearity obtainable with most fluids and configurations.

A more promising approach is use of resonating vibrating systems in which the application of an acceleration force will alter the resonant frequency. This frequency deviation is a measure of acceleration and if total cycles of the frequency deviation are counted over time interval, this is proportional to total velocity change. Another approach employs an unbalanced gyro with servo follow-up platform for the gyro. Application of an accelerating force will cause the gyro (and platform) to process at a rate proportional to acceleration. Hence, the total precession angle will be proportional to velocity. There is general promise in approaches of this type in the accuracy which can be attained. One disadvantage of this type is its mechanical complexity since it does require both a gyro and a servo.

Computer

To utilize the outputs of the inertial platform,

moderately extensive and quite precise computations must be performed. Both analogue and digital computers have been utilized successfully, the preference for one or the other depending on the particular application. Analogue computation involves such specific items as integration, multiplication, and trigonometric computation.

Integrators — Integration may be performed on an a-c or d-c analogue basis. The a-c integrators make use of induction tachometer generators in a feedback circuit. In this circuit, the tachometer is forced to drive at such a speed that its voltage is equal and opposite to the input voltage. Therefore, its speed is proportional to the input voltage and the number of revolutions is proportional to input voltage and time, being actually the integral of the voltage with respect to time.

The large range of input signal voltage may cause a number of difficulties. The minimum voltage to be integrated may be lower than spurious signals caused by drift, and the like, in tachometer and amplifier, thus causing errors. The minimum speed of the tachometer shaft may be so low as to cause erratic motion. Conversely, the maximum speed may be so high as to exceed the linear range of the tachometer. To overcome these difficulties, special tachometers with low noise and low shaft friction are employed. In addition, two-stage integrators are employed. These utilize two tachometers at different speeds and voltage ranges with a suitable switching scheme to use either one or the other.

The d-c integrators make use of high-gain operational amplifiers with a feedback capacitor. The operation is analogous to that described for the a-c integrator. As in the case of tachometer feedback, the use of high gain makes the system insensitive to variations in gain. The precision item in this type of computation is the capacitor. Modern, high-accuracy capacitors are sufficiently low in leakage current, dielectric hysteresis, and capacitance drift to be suitable for inertial computations. The extreme range of input signals requires that special attention be given to circuits to minimize noise and drift.

Multipliers — Multiplication is generally performed by means of servo-type multipliers in which the position on a resistance potentiometer is set up to watch one voltage while the other voltage is applied across the potentiometer. The output of the potentiometer is then the product of the two voltages. Use of high-gain amplifiers for the set-up servo reduces the error to that present in the potentiometer. With modern, small, multiform potentiometers, accuracies of a few hundredths of a per cent are practicable.

Trigonometric Computations — These make use of electrical resolvers which are variable coupling transformers having voltage ratios proportional to sine and cosine of their rotation. By using two primary and two secondary windings, great flexibility is obtained in that any distance or velocity vector represented by its components on one set of space axes can be transformed into the voltage components along any other set of space axes. When driven by high feedback amplifiers, the resolver permits computation to better than 1 part in 1000. The feedback circuits also permit applying the proper voltage for the primary so as to get a desired value at the secondary winding. This reverse problem effectively gives us any of the inverse trigonometric functions and combinations of them.

Digital Computers — Digital computers come up for serious consideration because of the high-accuracy requirements. Countering this advantage is the relative complexity and unreliability which has been typical of digital computers in the past. One envisions a general purpose computer with card punching equipment, thousands of tubes, and an operating staff. Actually, however, special-purpose digital computers have been developed which are a far cry from this picture.

These computers have only one set of equations to solve. This means that there is no need for card punch equipment or other means of external programming. The schedule of additions, multiplications, and other operations for the problem is stored in a permanently wired diode matrix array. At most, certain numerical constants are inserted for different flight application. This is accomplished by means of plug-in printed circuit cards with constants stored on diode matrices. Alternate means such as magnetic core storage registers are also employed. Since results in decimal form are ordinarily not required, a simple binary code is generally used for simplicity of equipment. For similar reasons of economy, serial-type computation is generally employed and parallel computation with its duplication of equipment is utilized only where absolutely necessary.

Modern digital computers are completely transistorized and utilize printed circuit techniques for compact packaging. (This, of course, is also true of analogue computers.) Thus, current techniques and design approaches are producing digital computers which are no more complex and no larger than the analogue computer required for the same problem.

Certain computation problems with a low order of complexity may still find the digital computer at a disadvantage since a certain minimum number of parts, such as an arithmetic unit and a control unit, are always required. On the other hand, most problems that are likely to arise in the future will involve considerable complexity. Thus, they may involve integration of the navigation comutations with those for weapons and aircraft control, logical decisions, modes selections, and the like. Here the advantages of the digital computer stand out strongly, since the high computing rate of modern equipment permits considerable computation beyond that of the navigation problem without duplexing of such equipment. Thus, one million counts per second is not difficult to obtain in a number of the modern computers.

Outputs from the computer are used for controlling and directing the aircraft. This information is generally in the form of scaled electrical signals which are obtained from the digital information. These signals are tied in to the aircraft controls by conventional techniques, such as used in autopilot controls.

While considerable problems still remain in many areas of hardware development, we see that a great deal has been accomplished and we can state that practical hardware exists today for inertial navigators in all applications.

the advantages of the new SAE standard for

INVOLUTE SPLINES

from a design standpoint

L. N. DeVos, Ford Motor Co.

This paper was presented at the SAE Annual Meeting, Detroit, Jan. 16, 1959.

INVOLUTE SPLINES enjoy three major advantages over their straight-sided counterparts:

1. New design concepts have given a more rational approach to clearances and errors.

2. Manufacturing is cheaper and more accurate.

3. Gaging is simpler. Thus, the involute spline standard of SAE and ASA continue to take precedence over the older straight-sided standards.

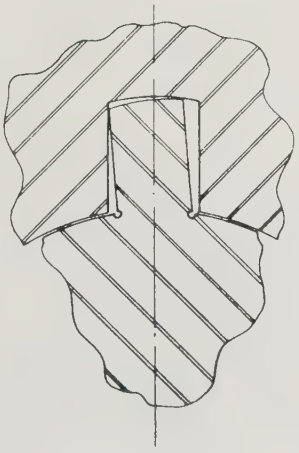

Fig. 1A — Line contact

FROM AN engineering standpoint, standards must be formulated to provide sound basis for selection of design that will satisfy assembly needs and yet be flexible enough to allow adjustments for specific performance and/or production conditions. The new SAE Standard for Involute Splines, Serrations, and Inspection was compiled with this objective in mind.

The involute-type spline was selected because of its basic advantages from a design standpoint as well as manufacturing and inspection advantages.

The involute-type splines provide the greatest amount of contact along the tooth profiles regardless of the amount of backlash in the splined connection. This backlash or clearance is usually necessary in order to assure assembly under a variety of conditions.

Fig. 1A shows that straight-sided splines, where the sides of the shaft tooth are parallel to the centerline, have only line contact on the side of the tooth when clearance is provided between the mating parts; the shaft rotates against the internal spline when under load, and the points at the major diameter travel farther than the points near the minor diameter. Therefore, the tip of the tooth on the shaft reaches the side of the space of the internal spline before any other point of the tooth side is contacted.

The problem can be overcome by making the amount of clearance proportional to the distance from the center. In Fig. 1B this condition is satisfied since the clearances C_1 and C_2 are in proportion to the diameters D_1 and D_2. Such splines, however, with tooth sides that fall on the radius, are by no means a solution of the problem, due to the weak cross-section of the shaft tooth at its root and the impractical shape of the internal spline.

Fig. 2A shows how this condition may be corrected with straight-sided serrations. The clearances C_1

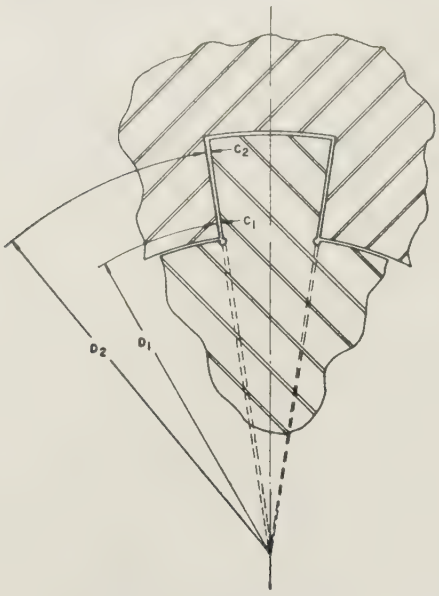

Fig. 1B — Impractical design

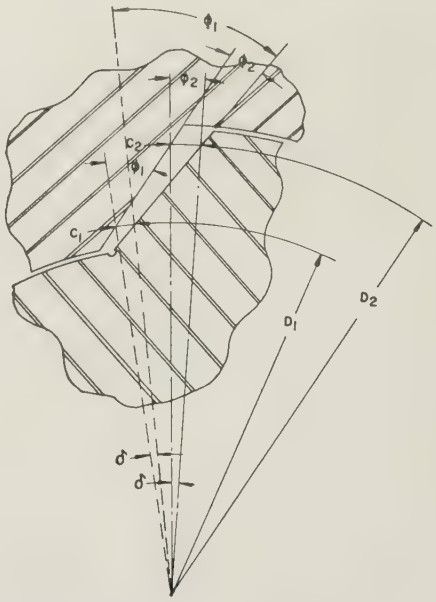

Fig. 2A — Serration spline

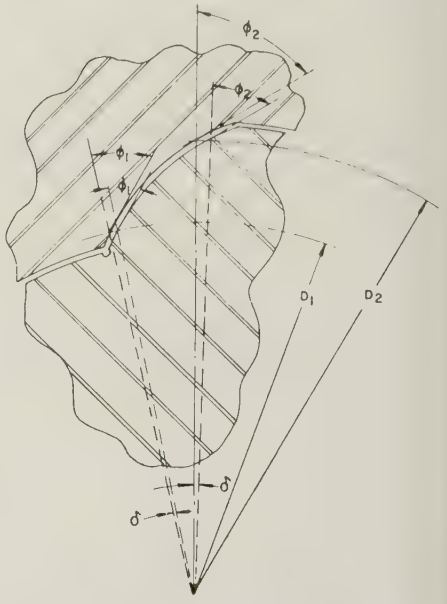

Fig. 2B — Involute spline

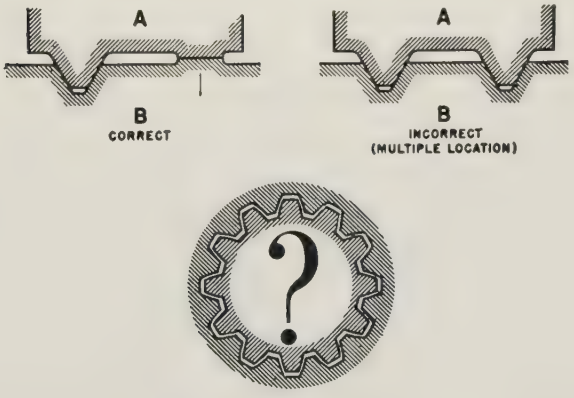

Fig. 3 — Problem of splines

and C_2, subtending the same angle are in proportion to the diameters D_1 and D_2 at which they are measured. When the spline tooth rotates under load against the side of the internal spline space, it matches along its whole active depth. Consequently, after it is rotated back into the position shown in Fig. 2A the angles ϕ_1 and ϕ_2, which represent the angles between the profiles and radial lines through the intersections of these profiles with a reference diameter are equal on the internal and the external spline tooth. These angles are commonly called the pressure angle. Thus, the requirement of surface contact demands equal pressure angles at the same reference diameter for both splines. The application of this principle to the general case of splined teeth with curved (involute) sides is shown in Fig. 2B. The pressure angles ϕ_1 and ϕ_2 are the same on both mating spline profiles.

The design (Figs. 2A and B) provides not only maximum tooth contact, but does so with an increased minor diameter and a wide-base tooth which in turn provides greater shaft and spline tooth strength.

The involute form as shown in Fig. 2B was selected because of manufacturing and inspection advantages.

The SAE Standard for involute splines is based upon a 30-deg pressure angle in order to give a wide-base tooth for strength and yet be of a nature that will slide along its length under normal torque loads. The 30-deg pressure angle is also advantageous on fine pitch splines that are case hardened. The tooth configuration allows a soft core at the base of the tooth, providing resistance to breakage.

The 45-deg pressure angle for involute serrations was selected for use on splines of close fits which are not subjected to sliding while in use. These splines have greater contact pressures along with increased radial forces and resistance to sliding. They are generally used when a manufacturing advantage can be gained.

The new standard also makes available to the designer a method of specification that assures the final assembly will be of a quality and fit range necessary to its proper function. This is accomplished through the use of "effective" and "actual" dimensions.

Splines are designed to provide location on a multitude of matching tooth surfaces. This basic requirement represents a rather flagrant violation of an elementary rule of machine design which requires that multiple locating surfaces be avoided. Fig. 3 illustrates this rule. In the upper left-hand view, the slide "A" is located on bed "B" by a V-groove and a pad. The V-groove provides horizontal location and support for part of the weight; the raised pad carries the remaining weight. Two V-grooves, as shown in the right-hand view, create a problem of fitting due to slight differences in the width, the spacing and the parallelism of the V-members in "A" and "B". The third view of Fig. 3 shows the spline as a rank offender with as many as 8, 12, 16, and sometimes many more teeth acting or expected to act as locators.

To meet the problem of multiple location, it was

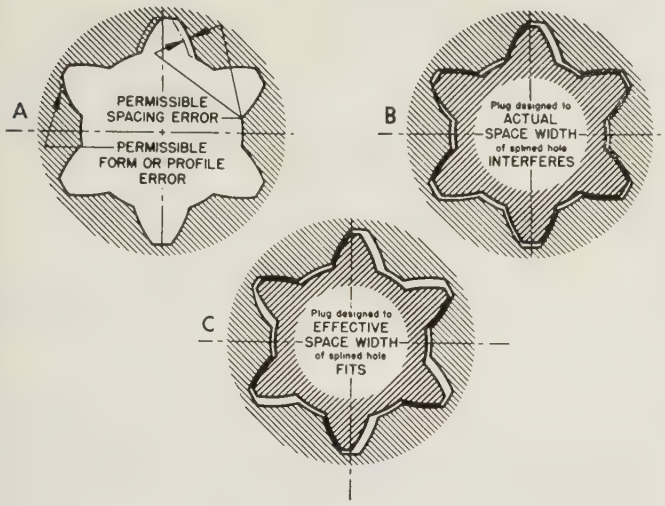

Fig. 4 — Mating of splines

necessary to adopt a system of dimensioning which is peculiar to splines. No consistent solution seemed to be available to the problem of dimensional control of splines until the concept of "effective" and "actual" dimensions was presented, which is further explained in the following paragraphs. This concept was first proposed by The Vinco Corp. in their 1945 catalog and was accepted on a national scope through the 1950 revision of the American Standard B5.15 for Involute Splines.

It must be recognized that the fit between mating splines is not sufficiently defined by just the space width of the internal spline and the tooth thickness of the external spline; the fit is also affected by errors in spacing, profile, out-of-roundness and lead. Fig. 4A shows an internal spline with pitch and profile errors; out-of-roundness and lead errors are not illustrated. Fig. 4B shows that an ideal spline contour, without errors does not fit the internal spline even though each tooth has the same width as the corresponding mating space. To allow the ideal spline contour to fit in any position, its teeth must be reduced in thickness by the amount of interference shown in Fig. 4B. The effective space width of the internal spline is equal to this reduced width as shown in Fig. 4C.

The same reasoning when applied to the external spline leads to the concept of effective tooth thickness of an external spline as a dimension equal to the circular space width, on pitch circle, of a theoretically perfect internal spline which would fit the external spline without clearance or interference.

The effective space width of the internal spline minus the effective tooth thickness of the external spline is the effective clearance, which establishes the fit between mating parts.

The width of individual spaces, which is greater than the effective space width, is termed the actual space width of the internal spline. The actual tooth thickness of the external spline is the circular thickness on the pitch circle of single teeth.

The difference between effective and actual dimensions represents the accumulated effect of the spline errors and is termed the effective error, and the amount of permissible effective error is the error allowance.

A clear understanding of the distinction between "effective" and "actual" dimensions permits the construction of part specifications which are consistent with service requirements and provide a clear path for the processing and inspection of splined components.

The above, along with tables giving all of the spline specifications and basic engineering information listed in the appendix of the standard, makes it possible for the designer to select a standard spline that will usually fit the needs of the end product. In the rare case where a standard spline is not applicable, the engineering information included makes it possible for the designer to follow the standard practice for specifications. By following this standard specification practice, the designer is assured of the same tool and inspection equipment control as provided for standard designs.

Reference

1. *Tooling and Production,* October, 1953, "Quality Control of Involute Splines," by A. S. Beam and L. N. DeVos.

ORAL DISCUSSION

— Reported by A. P. Trowbridge
General Motors Corp.

S. L. Buckay, Buick Motor Division, General Motors Corp.: Can the sides of straight-sided splines be biased like the straight-sided serration shown in Fig. 1B to eliminate line contact due to backlash?

Mr. DeVos: This can be done, but the form is not as desirable as the involute from the design manufacturing and measurement standpoints.

D. Nichols, Vickers, Inc.: What are the wear characteristics of involute serrations as compared to involute splines when both are operated under the same conditions?

Mr. DeVos: I do not know of any comparative tests that have been performed. But I assume that as the mating splines and serrations wear in toward maximum contact, the subsequent wear out should be comparable. Because of the greater angle of the serrations, a higher bursting pressure would result and, therefore, the sliding force would be greater.

I. K. McAdam, Sundstrand Machine Tool Co.: What are the advantages and pitfalls of the major diameter fit splines?

Mr. DeVos: The major diameter fit in the involute spline standard is a carry-over from the earlier straight-sided spline standards where there was a requirement for centralization which is now met by the use of the involute form. Currently, I am discouraging the use of the major diameter fit because of the manufacturing problems encountered in holding the close tolerances. However, there are probably areas where the major diameter fit is still required, particularly where problems of concentricity of the spline with other components is a requirement of the design.

G. K. Pickering, Buick Motor Division, General Motors Corp.: Are straight-sided splines continuing in use primarily because of better sliding action or is this better sliding action indeed a fact?

Mr. DeVos: Under ideal conditions of manufacture, when the straight-sided splines are produced with parallel sides and assembled with no backlash, they would probably slide under torque load with less effort than the comparable involute splines; this being due to the expanding pressures inherent in the involute spline. Since these conditions are not obtainable in practice, the result will be as shown in Fig. 1A. The involute spline will be more satisfactory from a practical standpoint, as shown in Fig. 2B.

SIX BASIC suggestions are offered on how to design for practical, producible, economical structures of brazed honeycomb sandwich.

The author illustrates the application of some of these design suggestions and explores the step-by-step theoretical reasoning a designer might use to arrive at a satisfactory design for a hypothetical large missile wing.

The final design of a honeycomb sandwich component must take into account the process as well as structural and configuration requirements.

practical for Brazed

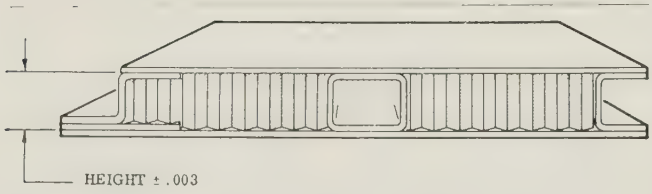

Fig. 1

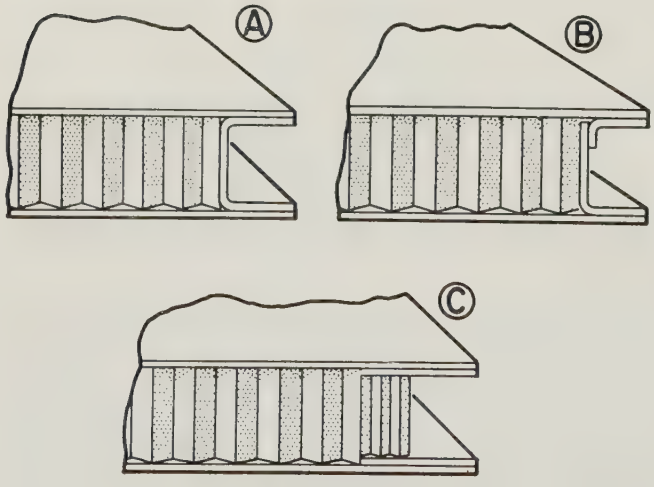

Fig. 2

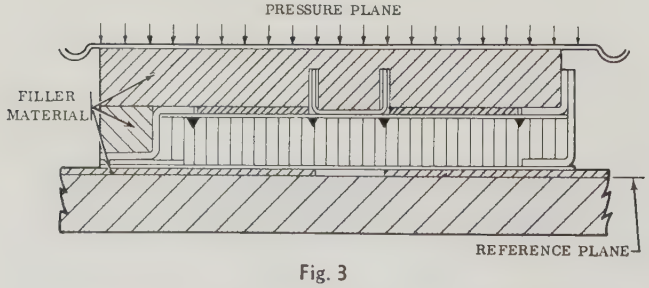

Fig. 3

THE problems and requirements of both the analytical designer and the fabricator must be reflected in the ultimate design of brazed honeycomb sandwich structures. The finished product must be both structurally functional and producible.

The following six points are basic keys to practical and economical honeycomb sandwich designs. The first four are requirements of the process which can influence the ultimate design; the last two are manufacturing characteristics which can be utilized to increase the efficiency of the honeycomb structure.

1. Minimize detail design subject to the extremely tight tolerance requirements of the brazing process.

To achieve intimate contact between all members being brazed together, height tolerances in the order of ± 0.003 in. must be obtained on all integral parts. Maintaining these tolerances, especially in the case of formed sheet metal parts, greatly influences producibility and cost. The edge members, spar, and core blanket of the panel shown in Fig. 1 all share the same ± 0.003-in. tolerance. In addition, the core at the doubler must have a step machined in it to within ± 0.003 in. of the doubler thickness. This tolerance problem is amplified if the honeycomb sandwich panel has curvature.

The influence of these tight dimensions can be relieved by careful attention to detail design. A basic fact to remember is that the core blanket can easily be surfaced to an accurate dimension by electromechanical methods of machining. A practical design approach, therefore, would be to concentrate height tolerances on the core and try to eliminate formed members with fixed heights.

By accepting a small weight penalty, the fixed height channel (shown at A in Fig. 2) could be redesigned as two adjustable angles (illustrated at B), which could be positioned to match the accurately machined core height, with no detail tolerances required. A further improvement would be to eliminate the vertical legs completely and substitute dense core to transmit panel loading, as shown at (C).

The ultimate objective, in all cases, is to reduce

design suggestions

users of

Honeycomb Sandwich

F. F. Rechlin, Solar Aircraft Co.

This paper was presented at the SAE National Aeronautic Meeting, Los Angeles, October 1, 1958.

the design as closely as possible to that of a simple sandwich consisting of core and facings with no full depth members.

2. Make allowances in design for uniform brazing pressure and temperature distribution.

Pressures must be applied on the faces of a panel being brazed to insure intimate contact of all parts at brazing temperatures. Any deviations from a uniform flat sandwich surface must be compensated for by filler sheets or filler material in order to provide equal pressure planes on both sides of the sandwich. A small amount of filler material can be tolerated. If, however, the design configuration extends too far from the normal plane of the sandwich, the compensating filler material tends to become a heat sink, causing undesirable brazing temperature gradients.

Fig. 3 shows a design that incorporates extended edge members, an external channel along the center of the panel, and a doubler located on the opposite face. Massive filler material must be added, as shown, creating varying temperatures around the part. This still does not guarantee perfectly distributed pressures on the sandwich face, as allowances must be made for differing thermal expansions at brazing temperatures and areas could occur, as shown by the dark triangles, where minimum brazing pressures would be experienced.

External stiffening members or attachment fittings sometimes cannot be avoided, but projections away from the face of the sandwich can be minimized through careful design. Fig. 4 shows the attachment of two angle sections to a doubler by indirect resistance welding, effectively forming an external channel section. By using such secondary attachment after brazing, only a filler sheet is needed to compensate for the added thickness of the external doubler, rather than the massive material illustrated earlier.

3. Consider brazing temperatures and pressures in the choice of structural material.

Normal structural design considers only flight or applied loads at stipulated temperatures. As mentioned before, an additional set of temperatures and loads must be considered for brazed honeycomb sandwich structures. Brazing pressures in no way equal in magnitude those imposed on the structure during service. They occur, however, at temperatures as high as 2200 F, which, being near the plastic state of the metal, makes their effect a definite consideration in the selection of core density.

Fig. 5 shows typical compressive strength curves

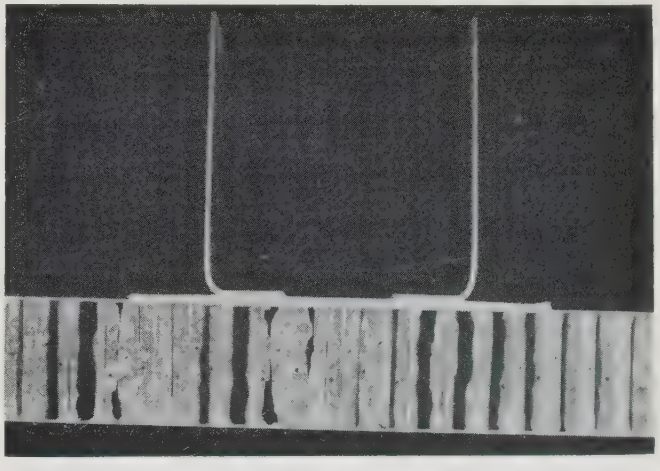

Fig. 4

for 17–7PH and Inconel honeycomb core at various temperatures. In most designs, the physical property values to the left of the shaded area will dictate the structural material choice. For brazed honeycomb sandwich designs, however, the core must also meet the standards shown in the shaded area. Thus, a structure that may be adequate for flight loadings could be incapable of withstanding brazing pressures at temperature.

So far, little information is available on the strength properties of honeycomb core at high temperatures. The problem is further complicated in that each design requires its own pressure range. Greater pressures than those needed for skin-to-core brazing are usually required for heavy gage faces and incorporated members. These pressures, due to uniform distribution, must also be withstood by the core, which may result in core failure. One suggestion is to avoid foil thicknesses of 0.001 in. or less, unless the facings and edge members are relatively thin.

The designated brazing alloy may also govern the selection of core density, when service temperatures beyond the limits of silver-base alloys are needed. The metallurgical effect of high-temperature braze alloys on the core foil should always be investigated.

4. Insure that the design can be assembled for brazing.

Designers sometimes forget that honeycomb sandwich must be pieced together, literally as a "sandwich." As part of this layup procedure, sufficient access must be available for mechanical or weld attachment of those faying surfaces in the assembly not affected by the vacuum pressures.

To illustrate this point, Fig. 6 shows some structural spar designs for a honeycomb component. Conventional airframe design practice has established the I-beam section (shown at A) as a normal choice for this spar. No access, however, is available to establish a shear tie between the core and the spar. In addition, it is impossible to slip the core between the caps of the I-beam section with only a 0.003-in. gap available, due to required brazing tolerances.

The ideal spar construction for honeycomb sandwich, therefore, would be a box section. The box spar design (shown at B) consists of two fusion-welded channels, joined after the core has been spot-brazed in place. The design at (C) is a refinement, intended to eliminate height tolerances. The weight penalty introduced by the two box beam webs can be alleviated through the use of extruded or forged material, or by brazing doublers on top of thin-gage channel sections.

The structural spar design (shown at D) would weigh approximately the same as an I-beam by substituting dense core for the I-beam web. The spar caps are simple doublers, spaced by the accurately machined core between them.

Fig. 7 is another illustration of this design philosophy. Here, a smooth closeout member is required at the edge of a honeycomb panel. The channel section shown at (A) is a good structural selection, but, again, a proper shear tie cannot be obtained between the core and the channel face. One solution (shown at B) is to spot-tack the core to a closeout angle, after which a doubler is welded in place, forming the desired channel before brazing. This design could be further simplified to two doublers, separated by dense core, if a corrugated panel edge is permissible.

5. Incorporate varying core densities to transmit loads internally.

The use of varying density core presents unlimited design opportunities. Ideal lightweight structures can be created, with high rigidity and shear resistancy concentrated exactly where needed. Splicing is always necessary to achieve the final size and shape needed for a core blanket; hence, it costs little more to incorporate different densities, beyond the cost of the core itself. Densities can be varied by inserting areas of smaller cell or heavier gage core, or sections of the normal core blanket can be shaped or crushed during the layup stage

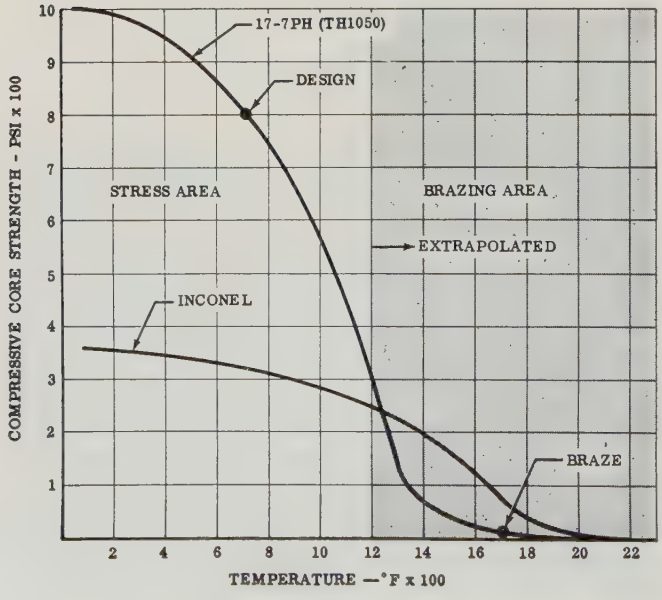

Fig. 5

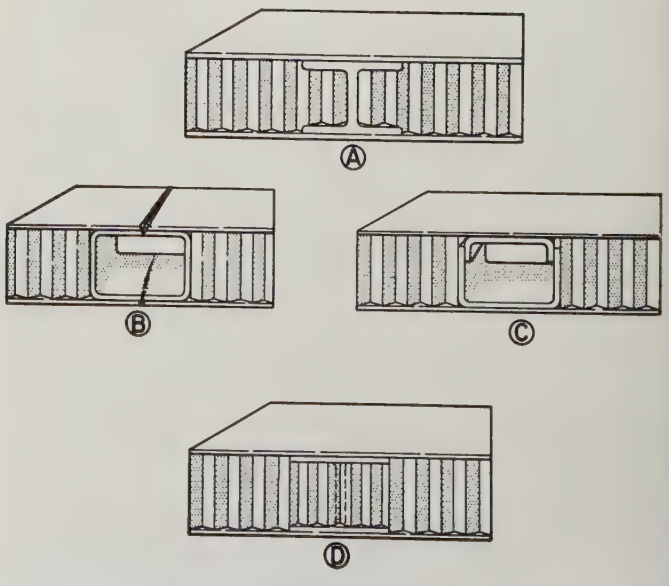

Fig. 6

to form load-carrying paths. Once spliced in place, the core is machined and brazed as a unit, resulting in a permanent internal structure.

Fig. 8 shows varying core densities applied to the edges and core blanket of missile flipper. Core is compressed in a fan-shaped pattern to concentrate the loads. The sharp trailing edge uses small-size cell core to insure maximum skin stabilization. If the larger cell core were carried out to the trailing edge, little or no face stabilization would be available.

Integral load-carrying paths in a sandwich can sometimes be separate prebrazed assemblies (Fig. 9). The main cylinder framing here was a brazed assembly of dense core and doublers, with the main core blanket and facings added later by a second brazing operation.

When sandwich fasteners are needed, a small area of dense core can provide local compressive and bearing strength.

6. Attempt to treat honeycomb sandwich as a material. The time is approaching when honeycomb sandwhich should be regarded as a material, rather than a built-up structure varying with each application. It may soon be feasible to rough cut large, flat, brazed panels to size, form them to a desired shape or curvature, finish machine, and attach the required edge members by brazing, welding, or mechanical joining. By using variations of present-day techniques, it is already possible to standardize basic panel design, thereby greatly reducing costs.

Attachment of edge members to simple brazed panels can be accomplished in a number of ways. My company has been investigating secondary brazing methods. Fig. 10 shows the cross-section of a typical secondarily brazed edge member, and a sketch showing how the various components were added. The completed unit was structurally sound, including shear ties. The doubler itself was secondarily brazed in place within 0.050 in. of the faces,

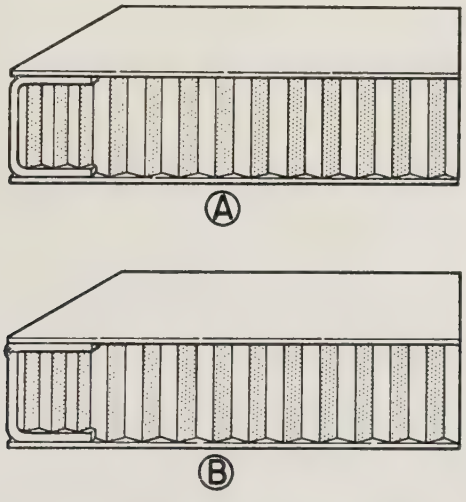

Fig. 7

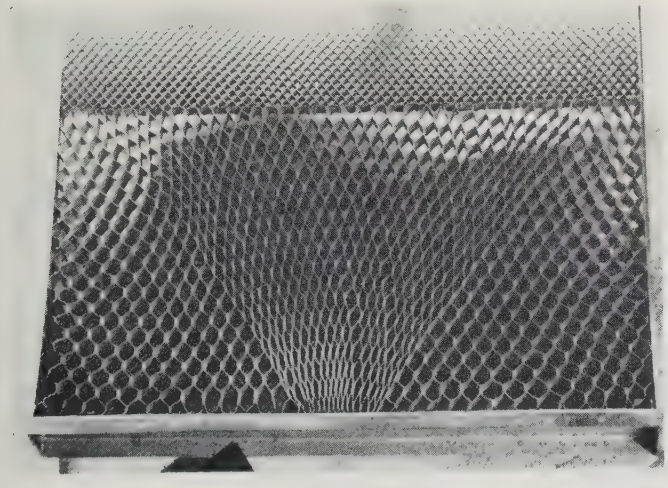

Fig. 8

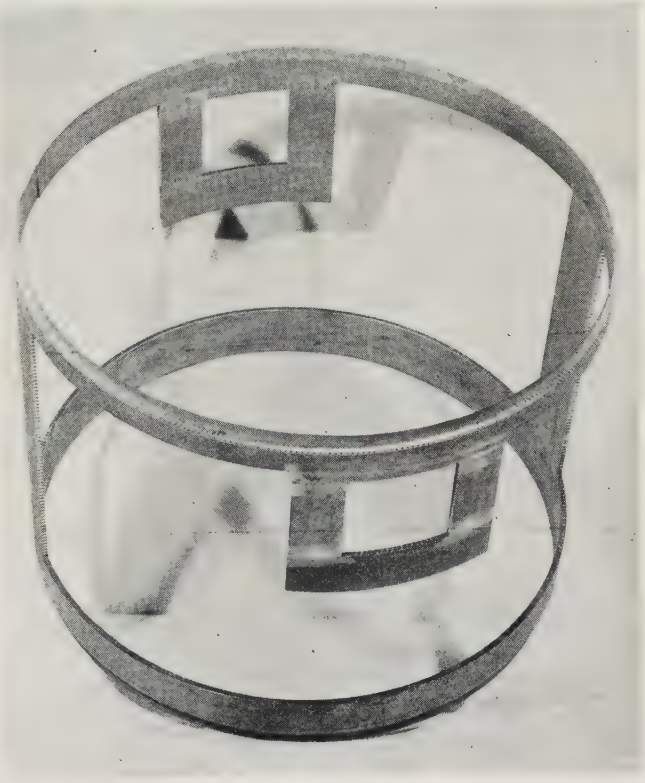

Fig. 9

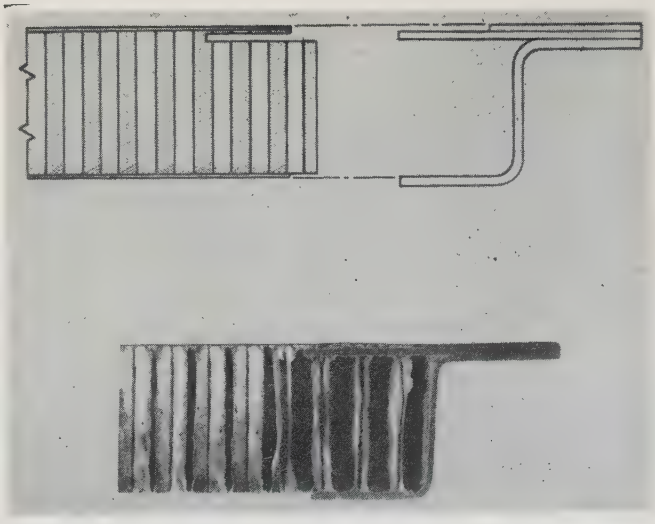

Fig. 10

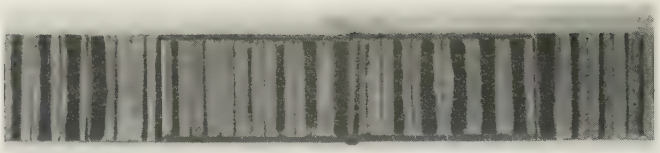

Fig. 11

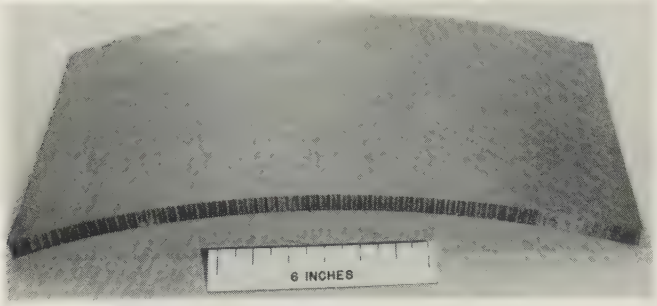

Fig. 12

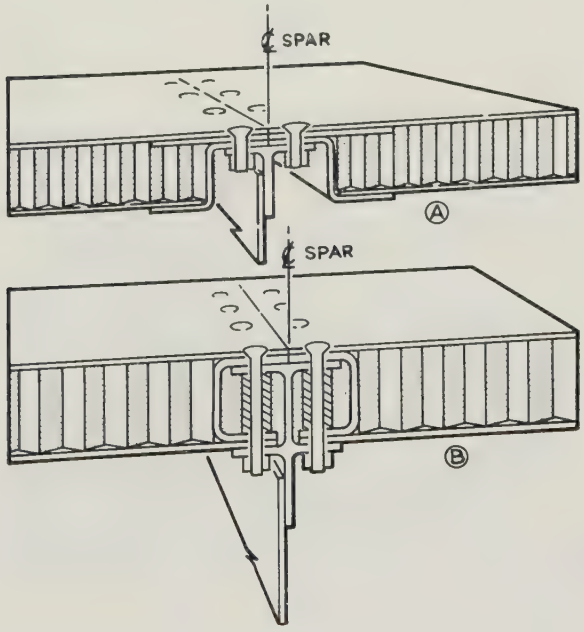

Fig. 13

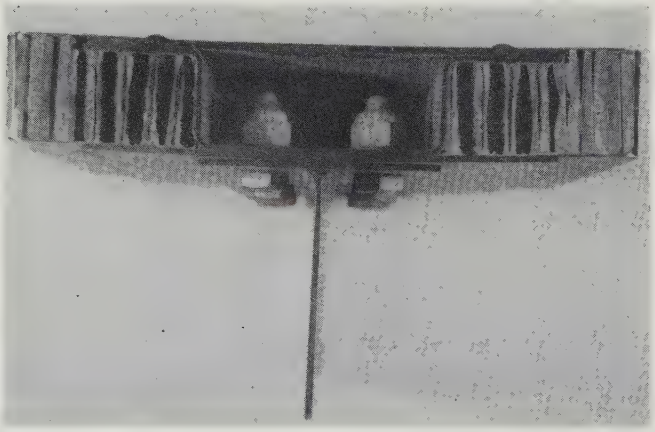

Fig. 14

with no reduction in load transfer strength.

To acquire extremely large honeycomb sandwich panels, a facility large enough for brazing would have to be found or built, or the designer could attach smaller panels together at a slight increase in weight. The design approach shown in Fig. 11 was to treat the sandwich as material and employ weld joining techniques. To make up for the lack of a shear tie, the core along the edge of each panel was densified. Doublers were used to transfer loads and to make up for the loss of heat-treat due to welding. Weld joining is entirely practical, but weld technicians should be consulted due to the lightness of the structure.

As part of this basic material concept for honeycomb sandwich, Solar, in cooperation with the Hufford Corp., has been engaged in a stretch-forming program on honeycomb sandwich. Fig. 12 shows a 17–7PH panel, formed in the full TH 1050 condition, with only 5% elongation available. Eighteen-inch radius panels have so far been successfully stretched with no discernible core crushing. Many problems are yet to be solved, but the process shows promise for future designs.

One final characteristic of honeycomb sandwich that should be remembered is that, once brazed, it becomes a material of finite thickness. Transferring loads through mechanical joints, while still accommodating this established thickness, is a challenge to the designer's ingenuity. Fig. 13 depicts a typical honeycomb panel wing-to-spar intersection. Access is usually not available for mechanical fastening on the inside, because of sealed "wet" wing requirements. The design at (A) is inefficient and introduces a weight penalty. The Zee-section doubler combination must be sufficiently heavy to transfer inner skin loads from one panel, up over the spar cap and down to the adjacent panel. The most efficient way would be to transfer loads directly through the spar cap with no directional change, as shown at (B). This design, however, requires spacers to insure a mechanical tie. The added weight of the spacers and bolts, along with a severe assembly problem, makes this design also impractical.

One possible solution is shown in Fig. 14. Here, loads are transferred through a cap strip, which is welded in place after the panels are bolted to the spar cap. The cap strip can be ground off, and another strip welded in place if panels need replacing. Care, however, should be exercised in the design of such joints to minimize shrinkage and thermal stresses in welding.

Summary

These design suggestions can be summarized by applying them to an illustrative problem, such as the missile wing envelope (Fig. 15). Let us assume the following design criteria must be met:

1. A high strength-to-weight ratio with minimum flutter is desired.
2. Service temperature is around 1600 F for a few minutes.
3. Surface discontinuities are permissible at the root, and only the leading edge need be sharp.
4. Major loads are to be carried by a central spar and a root edge member, with a shear fitting located near the forward edge.

Applying the design suggestions previously discussed, the following line of reasoning might be used to arrive at a finished design:

1. Honeycomb sandwich construction is picked for its light weight, high rigidity, and multidirectional properties. Basic honeycomb core densties and facing thicknesses are determined for a suitable high-temperature material, with the core density checked for its ability to withstand anticipated brazing pressures and temperatures and its metallurgical compatibility with the selected high-temperature brazing alloy.

2. In starting the detail design, basic protuberances or deviations from the desired flat sandwich plane, such as the large spar fitting, should be noted. This fitting, because of its large mass, can also greatly influence heat distribution, and an attempt should be made to incorporate it after brazing.

3. The integral spar configuration is the design keystone for this wing. A number of spar cross-sections, such as those shown in Fig. 6, should be studied to determine which one will best satisfy the design and brazing requirements. A spar cross-section similar to (D) could be picked, where bending moments are carried by the doublers, with shear transmitted through the connecting dense core.

4. Final attachment of the spar fitting must still be provided for. One solution is shown in Fig. 16. Here, the doublers are formed at the inboard ends as a receptacle for the fitting and the core attached to the back of this pocket before brazing to transmit shear.

5. Having established the spar design, the basic edge member and facing combination would be considered next. To eliminate the close brazing tolerances to which a formed sheet metal channel would be subjected, a densified core-doubler combination could be picked for the root edge member design.

6. The resulting wing design could be as shown in Fig. 17. Here:

(a) The basic core blanket has a thin band of small cell core at the leading edge for maximum skin support.

(b) The skins are welded together to form a sharp leading edge.

(c) A shear fitting is buried in the core during layup.

(d) Loads are carried along the root by densified core and external doublers, with the doublers resistance-welded to the face prior to brazing to avoid machining an internal tapered step in the core.

(e) The trailing edge is also dense core for surface rigidity.

(f) The spar fitting is attached to the brazed wing by secondary brazing, welding or mechanical means.

7. As a final step, it is recommended that all designs be checked for manufacturing feasibility by engaging in a mental step-by-step layup, to insure that all parts can be assembled satisfactorily.

To summarize, the final design of a brazed honeycomb sandwich component must take into account the process as well as structural and configuration requirements. By combining a knowledge of both aspects of sandwich design, a component will be produced that will not only be structurally functional, but producible.

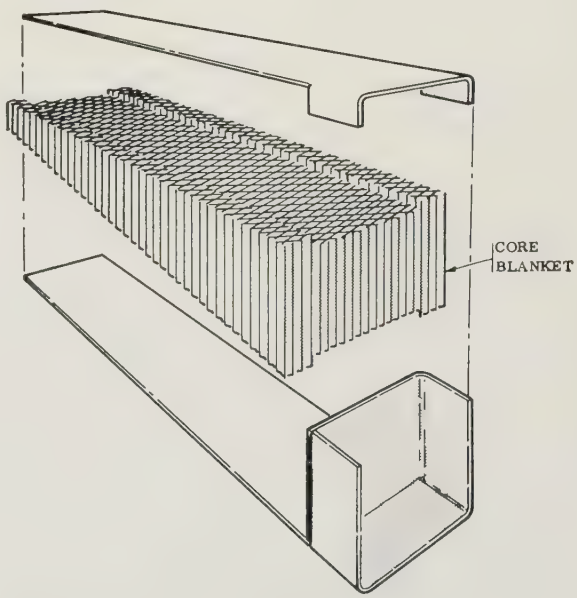

Fig. 16

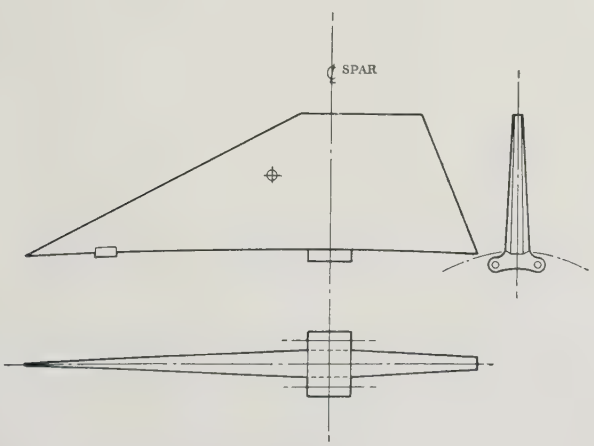

Fig. 15

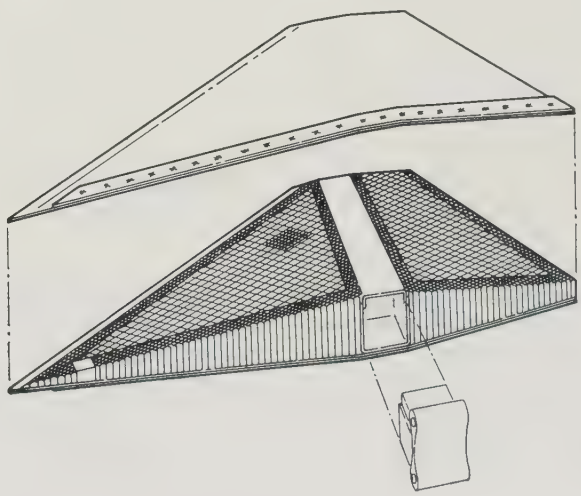

Fig. 17

THERMAL LOADING AND as functions of Turbocharged Compression-

E. T. Vincent, University of Michigan
N. A. Henein, University of Alexandria, Egypt

This paper was presented at the SAE National Diesel Engine Meeting, Baltimore, Oct. 24, 1958.

TURBOCHARGING and aftercooling are direct means of increasing the power output of diesels. Higher specific power outputs and lower thermal loads and wall temperatures result from turbocharging.

This paper describes a method by which internal surface temperatures of cylinder walls can be predicted from knowledge of cycle pressure and temperatures. The thermal load and wall temperature were found to be related to indicated power output and affected to a lesser degree by intake manifold conditions and the engine speed.

Test results also showed that the turbocharged engine performance was improved by increasing the air density and reducing its temperature in the intake manifold. The result was higher specific power outputs and lower thermal loads and wall temperatures. Aftercooling is one method to achieve this.

THE FIRST APPROACH to turbocharging dates back to the early 1900's and some practical applications occurred at that early date. The demand for high-duty engines of the compression-ignition type has increased enormously since the end of World War II to such an extent that most engine manufacturers now offer models equipped for turbocharging. This development is due to the following factors:

1. The demand for higher power outputs at maximum fuel economy.
2. The availability of improved heat-resisting alloys and technology, which has resulted in exhaust gas turbine chargers having the desired degree of reliability and life for the service conditions encountered.
3. Improved engine materials, bearings, and oils to carry the extra loads, temperatures, and the like.

The factors which limit the output of the oil engine are many and varied, including: (1) cycle of operations, (2) combustion system (open chamber, precombustion chamber, and the like), (3) bearing capacities, (4) stress levels, (5) heat disposal, (6) breathing capacity, (7) durability, and (8) reliability.

It is believed that the most important factors regarding output are three:

1. Mechanical stressing of parts and bearings.
2. Oxygen content of cylinder.
3. Internal temperature of working surfaces.

If the above three items are controlled in a satisfactory manner, little doubt exists that a successful engine be built. Little need be said regarding the first item, which is well-understood, much work having been published regarding it.

The oxygen content of the cylinder determines the amount of fuel that can be burned per cycle and, thus, the power output or indicated mean effective

WALL TEMPERATURE

performance of

Ignition Engines

pressure. Here the reason for turbocharging is found—it is a means of increasing the oxygen of the cylinder at little or no expense in burning some of this oxygen to supply the additional charge of oxygen. The energy for supercharging is obtained from the exhaust gases, not from the power output of the cylinders, and thus the oxygen supply as in the case with mechanically driven superchargers. This observation is true, provided that the application of the turbine in the exhaust stream does not impose power drop of any magnitude on the engine output.

The application of supercharging of itself does not assure increased performance. The combustion process can change for the worse when little improvement in output or economy is to be expected. Under such conditions, resulting from poor combustion, the combustion extends late into the expansion stroke, producing mainly an increased temperature of the parts and heat loss to the jackets with failure of the lubricating oil film and piston seizure to be expected.

If turbocharging is applied correctly (resulting in improved specific fuel consumption) the cylinder pressures and gas density increase, as can also the maximum gas temperature. All these factors also lead to increased heat transmission to the jacket, despite a reduction of the percentage heat loss to the coolant. It follows that the internal surface temperature of the cylinder must also increase, reducing the margin of safety provided by the oil film. It follows that the designer should have means available for the calculation of heat flow problems, as well as those for pressure, power output, and the like.

As a result of a cycle analysis investigation carried out during World War II, a method was developed whereby the effect of heat transfer on specific fuel consumption and power output could be calculated in a very satisfactory manner for both spark and compression-ignition engines.[1] As a further advance in the heat flow problem, the authors looked into the possibilities of solving the problem of the actual surface temperature of the engine cylinder, in the hope of supplying means of determining this important missing limitation on modern engine output. Then, with the combination of modern stress calculation and measurement accurate cycle pressure and temperature estimation, plus working surface temperatures, it would be possible to predict all of the major parameters for any proposed engine design.

It is too optimistic to conclude that this present attempt is the final answer to the problem. However, it presents a method by which the internal surface temperatures of cylinder walls can be predicted from a knowledge of the cycle pressure and temperatures when such is available (or by the use of Vincent[1]), together with the present method, it would be possible to examine with some degree of accuracy the stresses, power possibilities, and heat limitations of any proposed engine type operating on any type of cycle.

The results presented here show reasonable agreement between the calculated and measured mean surface temperature over a wide range of operation, so much so that it is believed possible to predict limiting power output due to heat flow if a maximum wall temperature is known or assumed (at least for the type of engine tested).

Heat Transfer Between Gases and Walls

The rate of heat transfer between a gas and a surrounding surface is, in general, a function of the surface area, the temperature difference between the

[1] "Supercharging the Internal Combustion Engine," by E. T. Vincent. Pub. by McGraw-Hill Book Co., New York, 1948.

gas and the surface, and a coefficient of heat transfer. For any internal-combustion engine, these factors change from instant to instant throughout the cycle.

The surface exposed to the gases in the cylinder varies from a minimum at top dead center to a maximum at bottom dead center. When the piston is at top dead center, the surface exposed to the gases consists of that of the combustion chamber plus the piston top. As the piston moves toward the bottom dead center, the cylinder bore is exposed to the gases. The surface area variation follows a curve similar to that of Fig. 1. The area during the intake and exhaust strokes includes those portions of the intake and exhaust manifolds enclosed in the cylinder head casting, since these manifold walls transfer heat between the gases and the cooling water during the corresponding strokes.

The temperature of the gases in the cylinder varies widely during the different strokes. At the beginning of the intake stroke, the temperature is that of the clearance gases, but falls rapidly as the fresh air is brought in. It rises during the compression stroke, reaches its maximum at the end of the combustion process, then decreases with expansion, and drops rapidly after the exhaust valve opens. There is a small drop in temperature during the exhaust stroke.

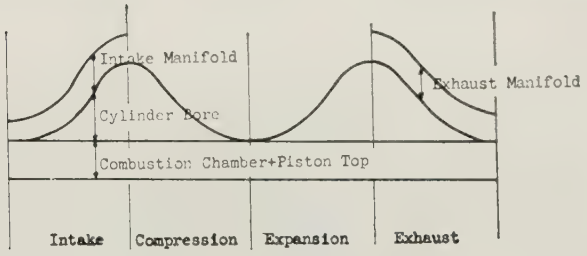

Fig. 1 — Area of heat transfer

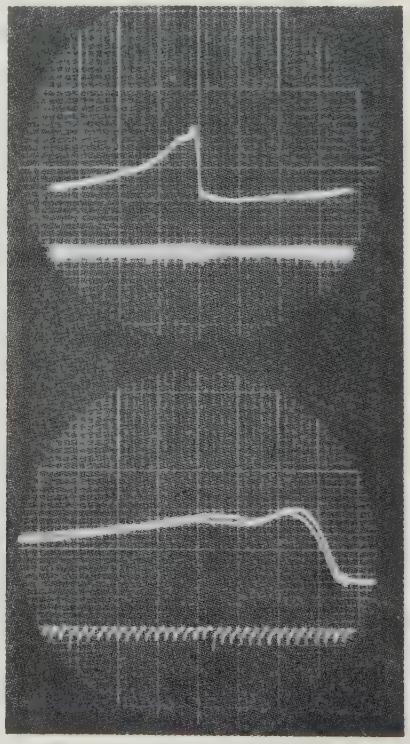

A — Wall temperature and crank angles over the whole cycle (with 3 amplifiers)

B — Wall temperature and crank angles for the combustion period (with 3 amplifiers)

Fig. 2 — Combustion-chamber surface transient temperature

It follows that the temperature of the inside surface of the cylinder wall will also fluctuate during the cycle, following the variation of the gas temperature. The wall temperature reaches its maximum at the end of the combustion process, then drops continually during the exhaust and intake strokes, and reaches its minimum during the early part of the compression stroke. Fig. 2 shows a picture of the wall temperature variations for the whole cycle of the engine during one of the runs.

The change in the coefficient of heat transfer, during the cycle, follows the variations in the gas temperature and pressure. At any instant of the cycle, this coefficient is a function of the instantaneous pressure and temperature of the gas. This function as given by G. Eichelberg, in terms of Btu and ft-lb units is:

$$\alpha_g = 0.0564\sqrt[3]{S}\sqrt[2]{PT}_g \frac{\text{Btu}}{\text{hr-sq ft-deg}} \qquad (1)$$

where:

S = Mean piston speed in ft per sec
P = Pressure in lb per sq in.
T_g = Deg Rankine

It follows that the equation for the heat transfer to a wall becomes:

$$Q = \int_0^t \alpha_g A_g (T_g - T_{wg})\, dt \qquad (2)$$

where:

A_g = Area of wall on gas side
T_{wg} = Temperature of wall on gas side

This equation applies to that portion of the combustion-chamber wall continually exposed to the heat from the gases. At the same time, heat transfer is occurring to some part of the cylinder wall uncovered by the piston. If it is assumed that T_{wg} of Equation 2 can be considered constant (its variation as compared with that of the gas temperature is negligible, as can be seen by inspection of the test results), then the overall heat transfer through the combustion-chamber walls can be represented by:

$$Q = A_{\text{c.ch.}} \alpha_m (T_{me} - T_{wg}) \qquad (3)$$

where:

$A_{\text{c.ch.}}$ = Total area of combustion-chamber walls (including piston crown)
α_m = Mean coefficient of heat transfer from gas to wall over the whole cycle
T_{me} = Gas mean effective temperature over the whole cycle
$= \dfrac{(\alpha_g T_g)_m}{\alpha_m}$

Heat Transfer Through Walls — The heat reaching the walls of the cylinder passes by conduction through the wall by the following equation:

$$Q = A_m \frac{k_w}{X} (T_{wg} - T_{wc}) \qquad (4)$$

where:

A_m = Mean area of wall
k_w = Thermal conductivity of metal of wall
X = Thickness of wall
T_{wc} = Wall temperature on coolant side

For the reasons given above, T_{wg} and T_{wc} can both

be considered constant.

Heat Transfer to Coolant — Heat transfer through the wall is followed by transfer to the coolant, which is mainly considered as convective when:

$$Q = \alpha_c A_c (T_{wc} - T_c) \tag{5}$$

where:

A_c = Area of wall on coolant side
α_c = Coefficient of heat transfer from wall to cooling water
T_c = Cooling water temperature

The value of α_c will be some function of the rate of flow of the cooling medium, its physical properties, and the actual mechanism of cooling. It was assumed that for a water-cooled engine α_c can be calculated by using Nusselt's equation:

$$\frac{\alpha D}{k} = C_1 \left(\frac{VD\rho}{\mu}\right)^m \left(\frac{c\mu}{k}\right)^n \tag{6}$$

where:

D = Constant for a given engine
k = Thermal conductivity of water
V = Velocity of flow
ρ = Density
μ = Dynamic viscosity
c = Specific heat

On the basis that $(V\rho)$ is proportional to the rate of flow of the coolant and that k is a constant at the given temperature maintained by the thermostat, then Nusselt's equation becomes:

$$\alpha_c = C_1 \left(\frac{W_c}{\mu}\right)^m \left(\frac{c\mu}{k}\right)^n \tag{7}$$

The values of the exponents m and n were given by B. Pinkel[2] as $m = 0.6$ and $n = 0.4$ while the constant C_1 is to be determined for each engine.

The heat flow to the wall from the gas, through the wall and to the coolant, is of constant magnitude. It follows that by equating and rearranging Equations 3, 4, and 5, Equation 8 is obtained:

$$\frac{k_w}{\alpha_m (T_{me} - T_{wg})} = \frac{A_g}{A_m}\left(\frac{X}{T_{wg} - T_{wc}}\right) = \frac{A_g}{A_c}\left(\frac{k_w}{\alpha_c (T_{wc} - T_c)}\right) \tag{8}$$

Combustion-Chamber Wall Temperature

Examination of Equation 8 shows that if an imaginary thickness $\left(\frac{k_w}{\alpha_M}\right)$ be placed on the gas side of the combustion-chamber wall and another one of thickness $\left(\frac{k_w}{\alpha_c}\right)\left(\frac{A_g}{A_c}\right)$ on the cooling side with the conductivity of these imaginary walls equal to that of the chamber wall, then a straight line between the mean effective temperature of the gas and cooling water temperature, will intersect the wall at a temperature equal to that of the wall, as shown in Fig. 3. The equation for this temperature is:

$$T_{wg} = T_{me}\left(\frac{Z}{Z + \frac{k_w}{\alpha_M}}\right) + T_c\left(\frac{\frac{k_w}{\alpha_M}}{\frac{k_w}{\alpha_M} + Z}\right) \tag{9}$$

[2] "Heat Transfer Process in Liquid-Cooled Engine Cylinders," by B. Pinkel, E. G. Mangancello, and E. Bernardo. NACA ARRNOES g31, 1955.

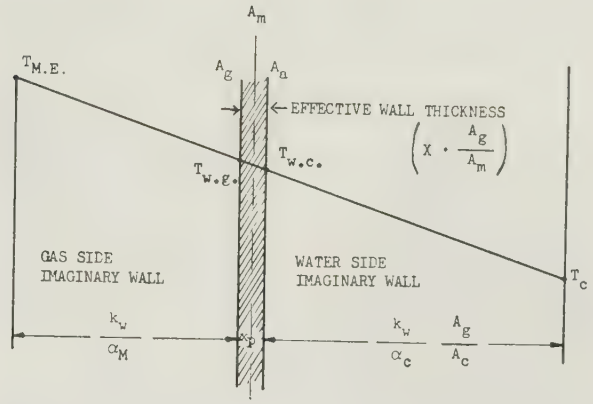

Fig. 3 — Graphical construction of imaginary walls

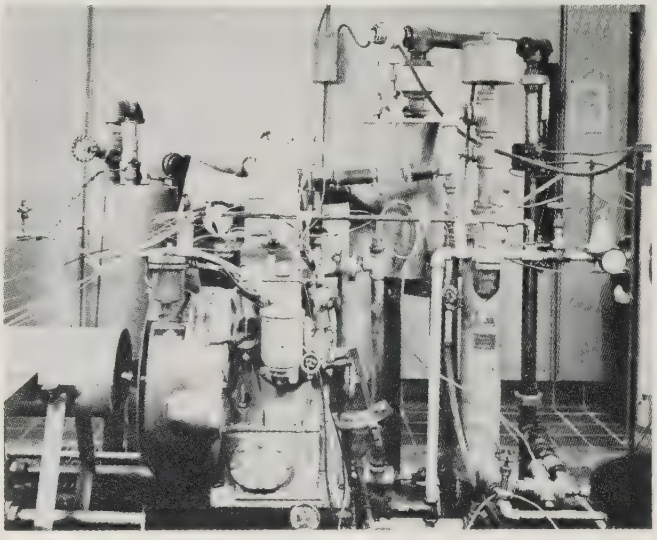

Fig. 4 — General layout of experimental setup

where:

$$Z = \frac{A_g}{A_m} x + \frac{A_g}{A_c} \cdot \frac{k_w}{\alpha_c}$$

While the thermal load on the cylinder walls is given by the amount of heat transfer to the wall per unit time, namely:

$$Q = A_M U (T_{me} - T_c)$$

where:

A_M = Mean effective area of heat transfer
U = Overall coefficient of heat transfer between gases and cooling medium. U can be calculated from the following equation:

$$\frac{1}{U} = \frac{1}{\alpha_m} + \frac{A_g}{A_m} \cdot \frac{X}{k_w} + \frac{A_g}{A_c} \cdot \frac{1}{\alpha_c} \tag{10}$$

Similar equations were set up for the piston heat flow and temperature.

Experimental Apparatus

A single-cylinder, 4-stroke cycle, liquid-cooled Nordberg diesel engine was used for the tests. The cylinder had a bore of 4½-in. and stroke of 5¼-in. with a compression ratio of 14.5/1. The general test setup is shown in Figs. 4 and 5.

The airflow to the engine together with its pres-

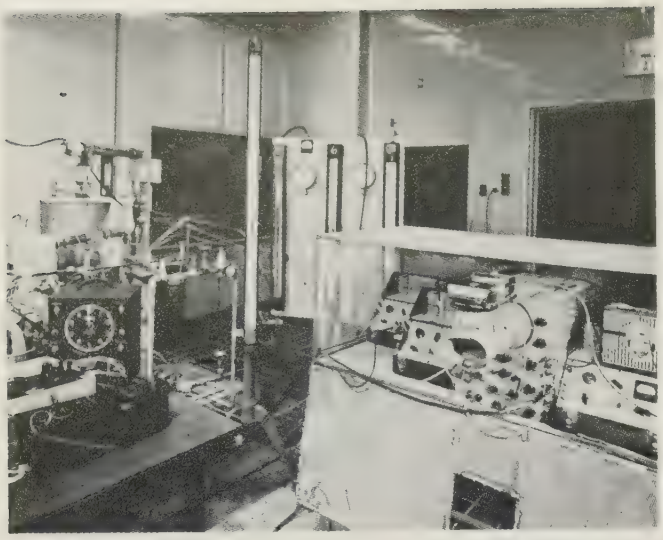

Fig. 5 — General view of oscilloscope and amplifiers

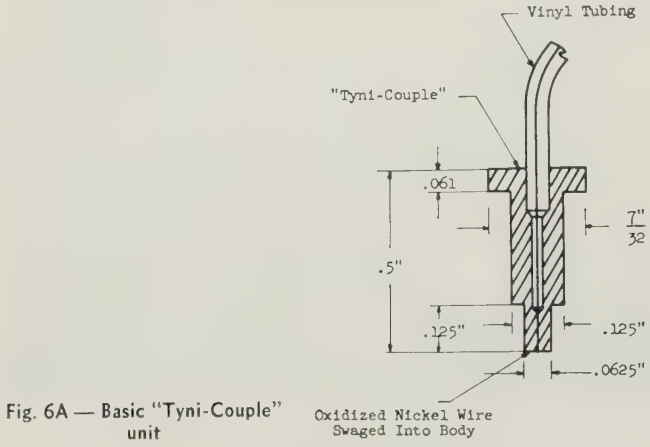

Fig. 6A — Basic "Tyni-Couple" unit

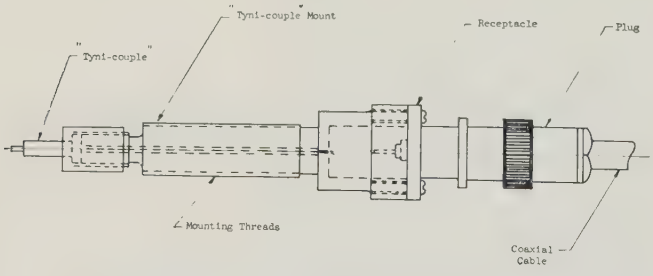

Fig. 6B — "Tyni-Couple" assembly

sure and temperature could be measured and controlled. Surge tanks were fitted at both inlet and exhaust. Conventional controls and measuring devices were employed for water, oil, and fuel flows and temperatures. Complete details of the equipment employed are given in Henein.[3]

In addition gas pressure was recorded by a catenary-type pressure pickup and timing marks provided for every 3 deg of crank rotation.

The special equipment for wall surface temperature consisted of a special nickel-steel thermocouple manufactured by the Detroit Controls Corp. It is shown in Fig. 6 and consists of a "Tyni-couple"

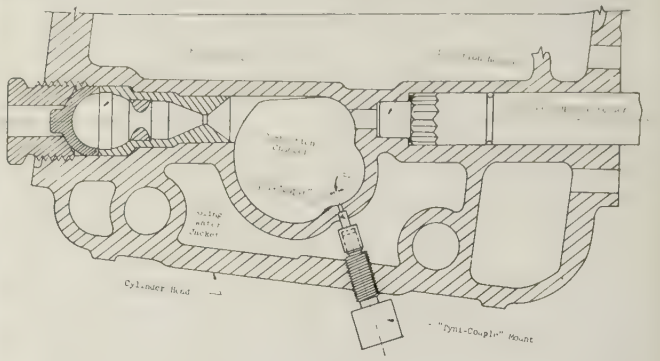

Fig. 7 — Sectional plan of cylinder head showing combustion-chamber thermocouple

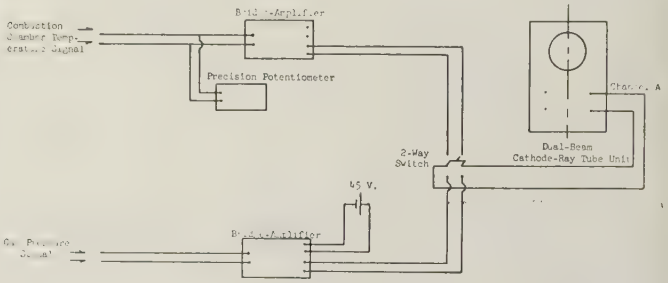

Fig. 8 — Layout of electrical circuits for pressure and temperature recording

basic unit, "Tyni-couple" mount, receptacle plug and coaxial cable. The basic unit was mounted with its tip flush with the inside surface of the combustion chamber. The thermocouple junction was at a distance of 0.00025 in. from the tip. Fig. 7 shows the details of the thermocouple as it is mounted in the combustion chamber. The position of the thermocouple was chosen in a part of the wall where the above mentioned analysis could be applied.

Shielded copper wires were used to carry the signal to a bridge-amplifier and a cathode ray oscilloscope. The layout of the temperature recording system being used in the tests is shown in Fig. 8. The oscilloscope trace, together with the crank angles, were photographed simultaneously with a polaroid camera. The reference junction of the thermocouple circuit was at the ambient temperature, which was measured for each test. A sample of the pictures taken for the change in the wall temperature is shown at the top of Fig. 2. The lower trace in the same figure is the crank-angle marks.

The theoretical response time, as given by the manufacturer: (Time to reach 62.3% of the imposed surface step change) = 4.5 microsec. This time is quite short as it is equal to the time required for the crankshaft to rotate 0.034 of a crank angle at an engine speed of 1200 rpm.

Experimental Procedure and Results

The tests covered fuel/air ratios from 0.0134 to 0.055, air manifold pressures up to 45 in. of Hg, air

[3] "Thermal Loading and Wall Temperature of Turbocharged Compression Ignition Engines," by Naeim A. Henein. Universtiy of Michigan Publication IP-229, July, 1957.

A — Gas pressure and crank angles for the whole cycle

B — Gas pressure and crank angles for the compression and expansion strokes

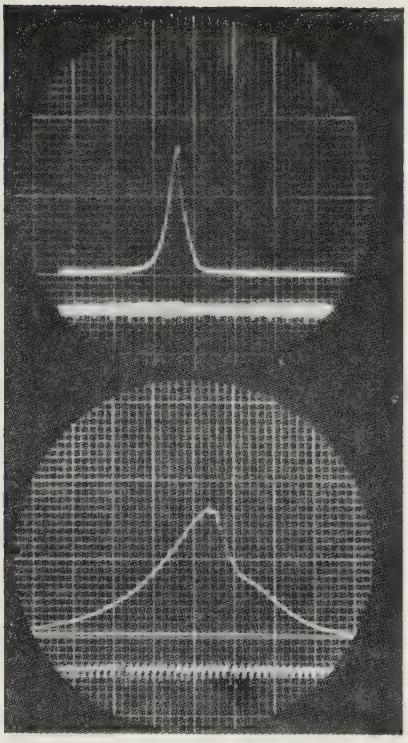

Fig. 9 — Gas pressure during cycle

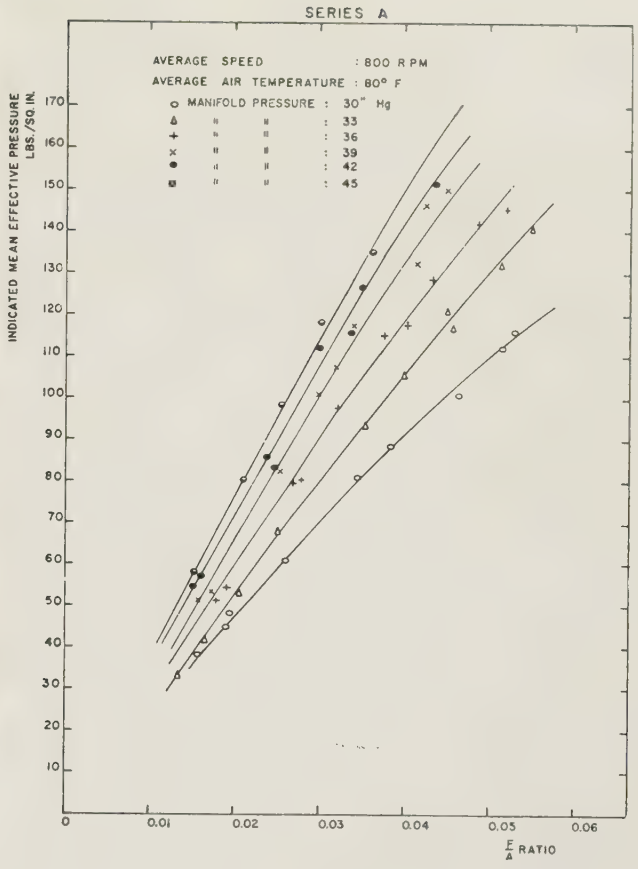

Fig. 10 — Effect of fuel/air ratio on imep for various manifold pressures

manifold temperatures up to 204 F, and engine speeds from 560–1770 rpm. The experiments included two series of tests, each of them with one variable changed at a time. The first series of runs was at variable manifold pressure; the manifold temperature and engine speed were kept constant. The second series of tests was at variable manifold temperatures at another engine speed.

Since the engine was designed to run under natural aspiration conditions, to avoid troubles due to overloading by supercharging, the following limits were observed: the exhaust temperature not to exceed 1000 F and the gas peak pressure in the cylinder not to exceed 1200 psia. The engine at the end of the tests was in a satisfactory condition, without any sign of failure in any of its parts.

For each test the data necessary for the calculation of the brake output, fuel consumption, air consumption, cooling water losses, wall temperatures at the different points in the engine, and the gas pressure inside the cylinder were taken. Pictures for the following traces were also taken:

1. Gas pressure and crank angles for the whole cycle, a sample is shown in Fig. 9A.
2. Gas pressure and crank angles for the compression and expansion strokes (Fig. 9B).
3. Combustion-chamber wall temperature and crank angles for the whole cycle (Fig. 2A).
4. Combustion-chamber wall temperature and crank angles for the combustion period only (Fig. 2B).

Some of the interesting experimental results are shown in form of graphs in the figures included in this article. The following is some of the conclusions reached from the experimental results:

1. The measured instantaneous change in the

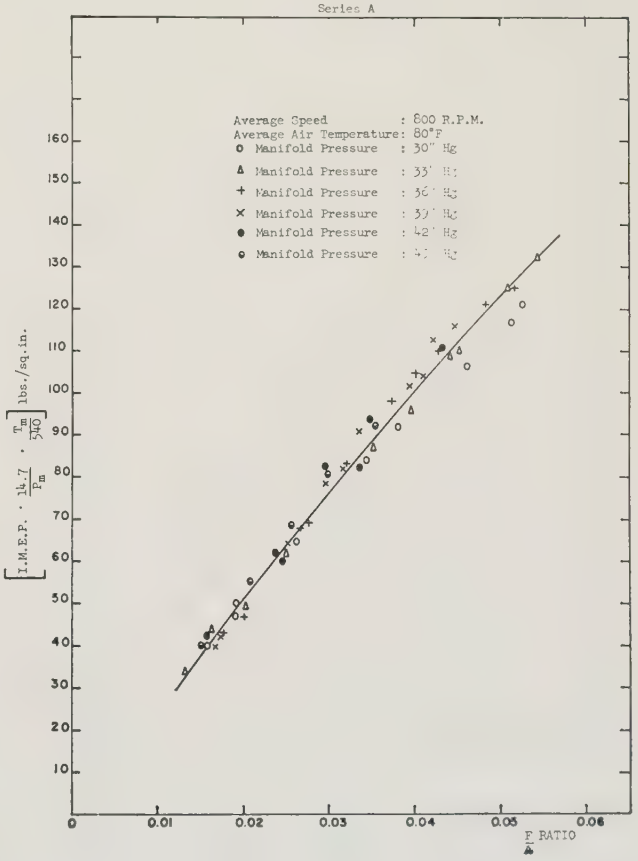

Fig. 11 — $\left(\text{imep} \cdot \frac{14.7}{P_m} \cdot \frac{T_m}{540}\right)$ versus fuel/air ratio for various manifold pressures

temperature of the inside surface of the wall of the combustion chamber is very small compared to the change in the temperature of the gas. For the picture shown in Fig. 2, this change is 49 F while the change in the gas temperature is 2167 F.

2. The indicated power output of the engine at a constant fuel/air ratio changes in direct proportion with the intake air pressure and inversely with its absolute temperature. When the results shown in Fig. 10 were reduced to the same pressure and temperature they resulted in one curve shown in Fig. 11.

3. The heat losses change in a straight-line relationship to the indicated mean effective pressure at constant engine speed and intake air temperature. Fig. 12 shows the heat losses measured for runs at variable manifold pressures but at constant engine speed and manifold temperature.

4. At constant indicated mean effective pressure and engine speed, the heat losses change roughly in a straight-line relationship to the intake air temperature.

5. The cooling losses change in proportion to the cube root of the mean piston speed, with the other conditions kept constant. The data obtained were reduced to an engine speed of 800 rpm and air temperature of 80 F, and plotted in Fig. 13. The curve in the same figure is for another series of tests under the same reduced conditions.

Heat-Transfer Analysis of Experimental Results

The purpose of this analysis is to calculate the combustion-chamber wall inside-surface temperature and the thermal load on the cylinder walls, and to check the calculated values with those measured. Equations 9 and 10 will be used for the calculations after finding a relation between both the mean effective gas temperature and the mean coefficient of heat transfer, and the running conditions of the engine. The running conditions include the manifold temperature, the manifold pressure, the mean piston speed, and the indicated mean effective pressure.

The mean effective gas temperature (T_{me}), and the gas mean coefficient of heat transfer (α_M) were calculated for each run. For the calculations, the temperature along the cycle was evaluated from the measured gas pressure and the measured air and fuel consumption. This enabled the coefficient of heat transfer (α_g) to be calculated from Equation 1, for the whole cycle as shown in Fig. 14. The mean value of α_g was then calculated from the same figure by integration. The mean effective gas temperature could then be calculated by integration of the $\alpha_g T_g$ curve over the whole cycle and Equation 4. (See Fig. 15.)

The mean coefficient of heat transfer and the mean effective gas temperature were then correlated to the mean piston speed, the manifold pressure, and temperature. The best correlation of the results was found to give the following relation:

$$T_{me} = \frac{T_m}{\sqrt[3]{P_m \cdot T_m}} \frac{[14.71 + 0.233(\text{imep})]}{[0.48 + 0.00157(\text{imep})]} \qquad (11)$$

$$\alpha_M = \sqrt[3]{S}\sqrt[3]{P_m \cdot T_m}[0.48 + 0.00157(\text{imep})] \qquad (12)$$

The consant C of Equation 7 for the coefficient of heat transfer from the walls to the cooling water was found experimentally to be equal to 3.15.

Calculation of Combustion-Chamber Wall Temperature — This temperature could be calculated for each run from the above equations and the values for the air manifold pressure, air manifold temperature, engine speed, indicated mean effective pressure, rate of flow of cooling water, temperature of cooling water, and other constants for the engine. The mean effective gas temperature, calcu-

Table 1 — Combustion-Chamber Wall Temperatures Calculated and Measured (Constant speed, 800 rpm, constant T_m)

Run No.	P_m, in. of Hg abs.	T_m, F	N, rpm	F/A Ratio	Imep, lb per sq in.	T_{wg} Calculated, F	T_{wg} Measured, F	Error, F	Error, %
				$P_m = 30$ in. of Hg					
1	28.75	83	807	0.0261	61.2	192.5	212.8	20.3	9.5
2	28.78	84	800	0.0463	101	225.2	231.9	6.7	2.9
94	29.55	90	826	0.0515	112.5	273.8	245	- 28.8	- 11.7
4	28.56	72	810	0.0528	116.2	251	258.3	7.3	2.8
				$P_m = 33$ in. of Hg					
81	32.84	86	796	0.0205	56.4	198.5	219	20.5	9.4
93	32.55	87.5	832	0.0455	118.2	261.8	237.9	- 23.9	- 10
36	32.3	87	790	0.0444	121.5	237.2	231.6	- 5.6	- 2.4
95	32.62	90	821	0.0511	132	249.3	243.6	5.7	2.34
37	31.93	77	830	0.0546	141.6	242.7	241.6	- 1.1	- 0.5
				$P_m = 36$ in. of Hg					
47	35.12	73	828	0.0179	51.3	188.2	200.4	12.2	6.1
51	35.25	80.5	850	0.0431	129	240.8	227.2	- 13.6	- 6
52	35.17	81	847	0.0519	145.7	250.8	229.7	- 21.1	- 9.2
				$P_m = 39$ in. of Hg					
83	38.54	87	820	0 0174	53.3	200.4	208.5	8.1	3.9
97	38.47	83	814	0.0412	132.5	250.1	237.9	- 12.2	- 5.1
64	39.24	82	807	0.0424	146.5	241.8	246.2	4.4	1.8
71	39.27	90	789	0.0448	149	255.2	260.7	5.5	2.1
				$P_m = 42$ in. of Hg					
66	41.47	76	827	0.0154	54.8	193.1	206.7	13.6	6.6
90	41.8	72.5	837	0.0336	116	234.3	245	10.7	4.4
69	41.72	86.5	805	0.035	127	240.5	252.2	11.7	4.6
70	41.97	88.5	815	0.0434	152	262.5	260.4	- 2.1	- 0.8
				$P_m = 45$ in. of Hg					
72	44.25	83.5	823	0.0154	58	186.6	211.1	24.5	11.6
74	44.05	88	832	0.0257	98.6	220.2	244.9	24.7	10.1
75	44.55	89.5	815	0.030	118.6	234.2	254.6	20.4	8
76	44.70	90	815	0.0357	135.2	237.7	250.4	12.7	5

lated from Equation 11, and the mean coefficient of heat transfer, calculated from Equation 12, were substituted in Equation 9 to get the wall temperature. Table 1 records some of the results so obtained.

When the calculated values of the wall temperature (T_{wg}) were compared with the values measured by the thermocouple, they were found to be in good agreement. The maximum error was 12.7% with an average of about 4%. Some of this deviation of the measured temperature from that calculated was thought to be due to the following experimental errors:

1. The wall temperature and the cooling water temperature were not measured simultaneously and a change in the water temperature might have taken place between the two readings. The change in the water temperature could not be held less than ± 5 F during the run, due to lack of sensitivity in the thermostatic control.

2. The indicated mean effective pressure used to calculate the wall temperature was evaluated by adding the friction load measured at the end of the day's tests to the load for the run. The friction load, being a function of the lubricating oil temperature, was not exactly constant for all the runs of the day, with the result that small errors exist in the indicated mean effective pressure.

3. The average cooling water temperature used in the calculations would be lower than the water temperature near the combustion-chamber wall, resulting in the majority of the calculated wall temperatures being lower than those measured by the thermocouple.

Calculation of Thermal Load on Engine — The thermal load on the cylinder walls was also calculated, and compared with the measured heat losses. As was to be expected, the calculated thermal loads were in general lower than the measured cooling water heat losses. Attention is called to the fact that the thermal load as defined in this paper is not the same as the heat rejected to the coolant, since the latter includes the friction heat. The following

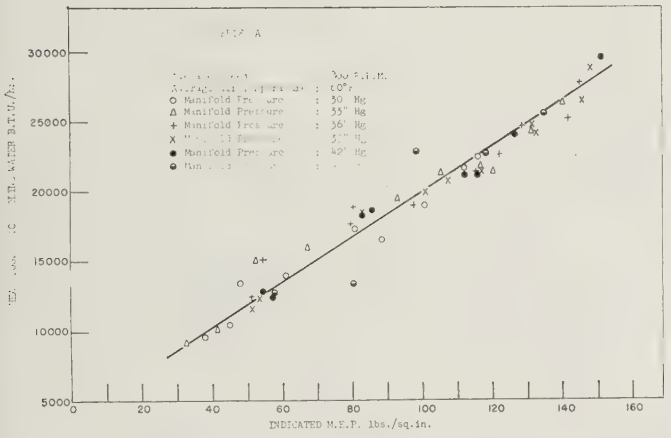

Fig. 12 — Heat losses to cooling water versus imep for various manifold pressures

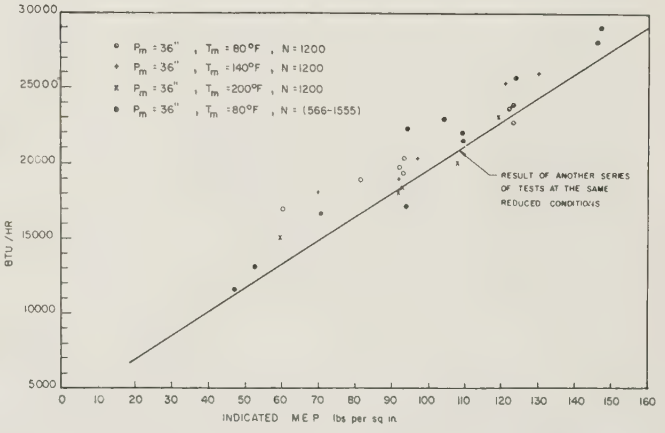

Fig. 13 — Heat losses to cooling water reduced to same speed and intake air temperature ($N = 800$, $T_m = 80$ F)

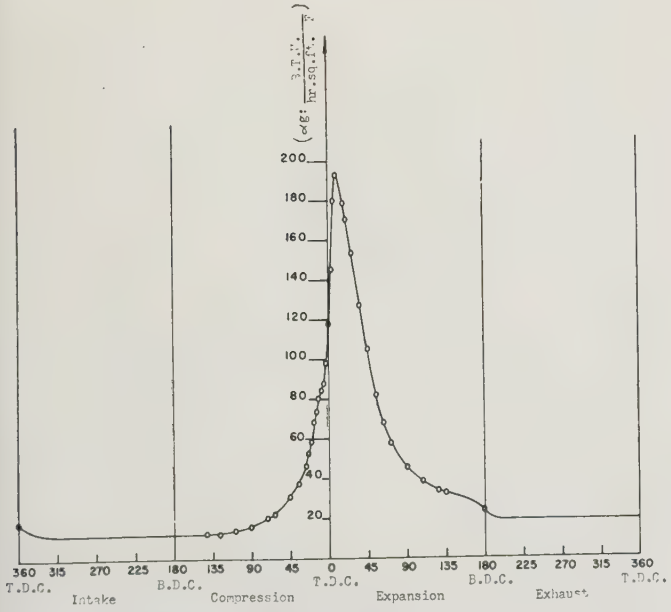

Fig. 14 — Coefficient of heat transfer from gas to walls for cycle, Run No. 95

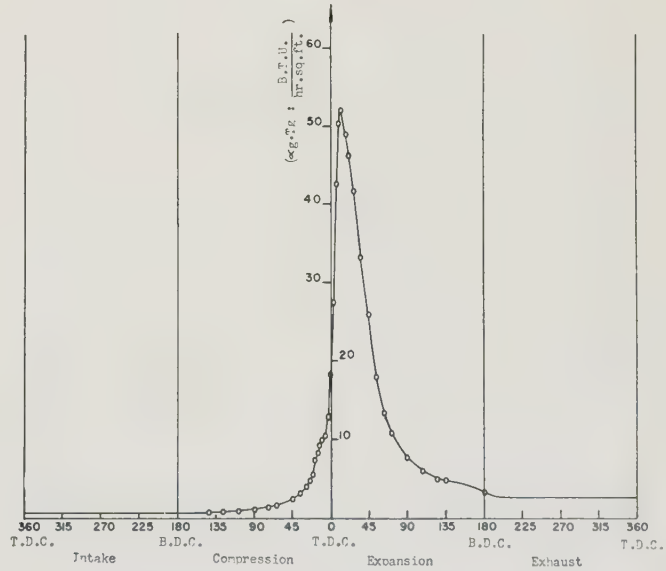

Fig. 15 — $(\alpha_g \cdot T_g)$ for cycle of Run No. 95

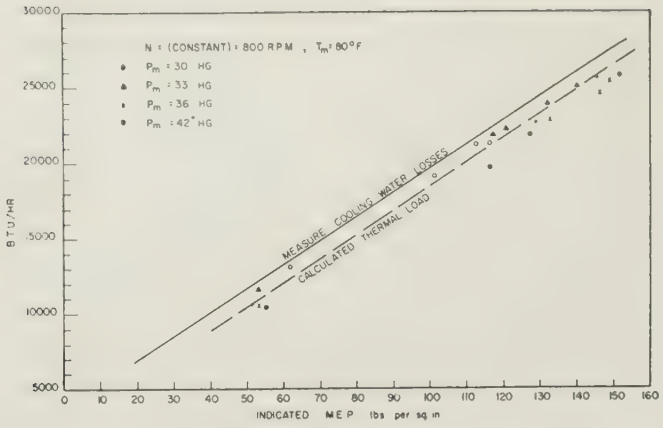

Fig. 16 — Comparison between calculated thermal loads and cooling water losses

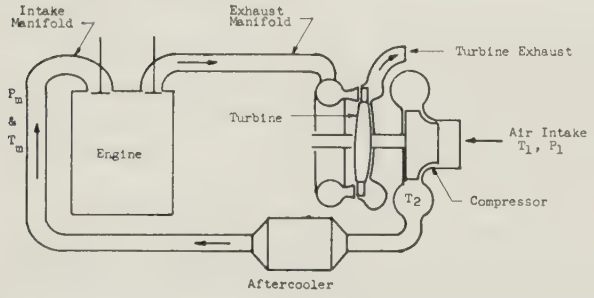

Fig. 17 — Diagram of assumed turbocharged compression-ignition engine

equation gives the relation between these heat flows:

$$\text{Thermal load} + \text{Friction heat} = \begin{matrix}\text{cooling}\\ \text{water}\\ \text{losses}\end{matrix} + \begin{matrix}\text{Heat lost}\\ \text{from engine}\\ \text{outside surface}\end{matrix}$$

Again it is pointed out that the friction heat to be accounted for is not equal to the motoring work. In these investigations the friction heat was calculated by extrapolating the cooling losses curve to zero indicated mean effective pressure, as shown in Fig. 12. This amounted to 3750 btu/hr, while the motoring work for the same series of runs was in the range of 6500 btu/hr.

The difference between the cooling water losses and the thermal load as indicated from the above equation equals the difference between the friction heat and heat lost from the external surfaces of the engine. From Fig. 16 this difference amounts to 1250 btu/hr, from which the heat lost from the engine outside surface was found equal to 2500 btu/hr. This value was thought to be reasonable for the engine used in the tests.

Another way to check the derived equations was to reduce the heat losses to the cooling water, to the same conditions of manifold and engine speed. From the previous equations the thermal load is proportional to:

$$Q\alpha(\alpha_M \cdot T_{me} - \alpha_M \cdot T_{wg})$$

Since T_{wg} is small compared to T_{me} and the change in the wall temperature is negligible compared to that of the mean effective gas temperature, the thermal load could be considered proportional to $\alpha_M T_{me}$ or in terms of the other variables:

$$Q\alpha\sqrt[3]{\overline{ST}_m}(14.71 + 0.233 \text{ imep})$$

It can be seen then that Q changes in direct pro-

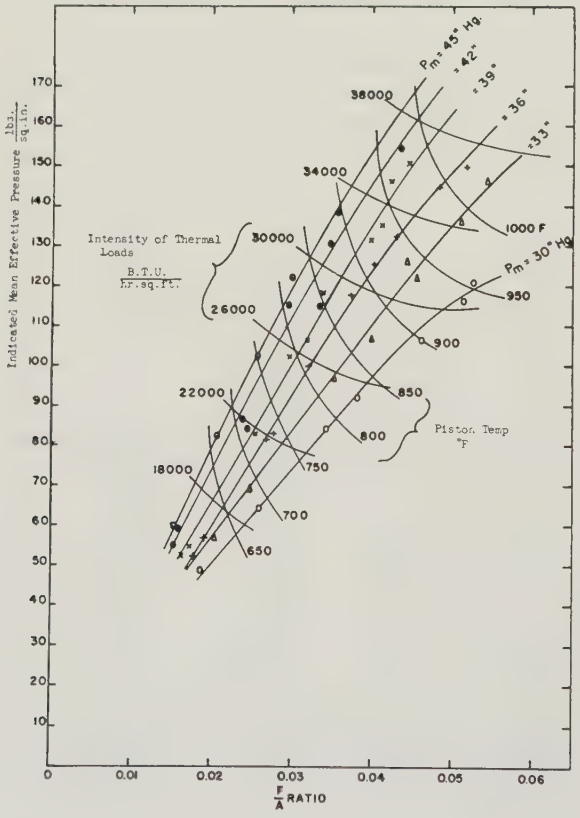

Fig. 18 — Performance with 100% aftercooler effectiveness

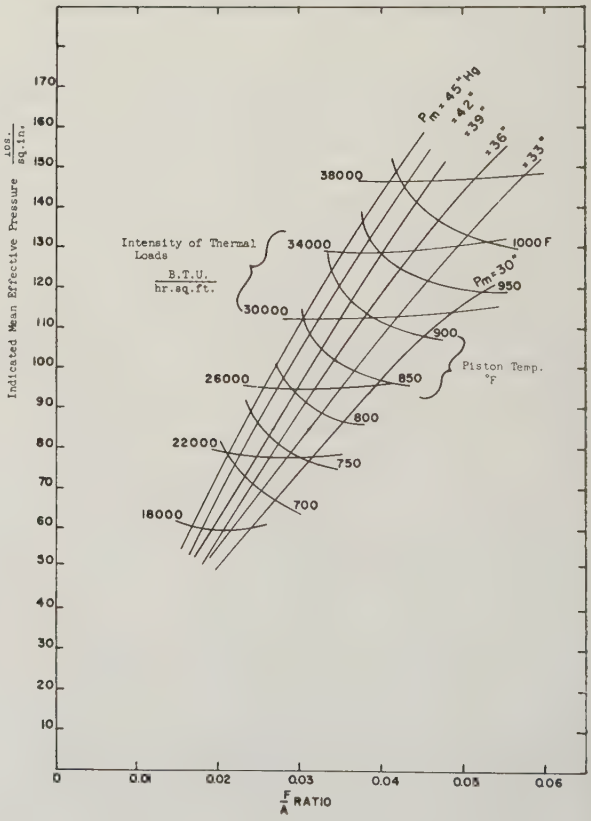

Fig. 19 — Performance with 50% aftercooler effectiveness

portion to the cube root of the mean piston speed and the manifold absolute temperature. These conclusions agree fairly well with the experimental results mentioned before.

Investigation on Effect of Aftercooling — An investigation was made to find the effect of aftercooling on the engine operation. The arrangement on which calculations were based is shown diagrammatically in Fig. 17. The conditions of operation assumed were as follows:

Compressor efficiency	= 0.80
Atmospheric pressure	= 30 in. of Hg
Atmospheric temperature	= 80 F
Drop in pressure between compressor and engine manifold	= 0.5 psi

The calculations were made for three aftercooler effectiveness 0, 50, and 100%. Other details and method of calculation are given in the original thesis.

The results of the above calculations are shown in Figs. 18–20. To illustrate more clearly the effect of aftercooling, Figs. 21–23 were drawn.

The effect of aftercooling on the output (mep) is shown in Fig. 22. It is interesting to notice that the same mean effective pressure could be obtained by supercharging to 45 in. of Hg without aftercooling, or by supercharging to 41.2 in. of Hg with an aftercooler effectiveness of 50%. This means that it would be better, in the interest of lowering the thermal load, to use an aftercooler with an effectiveness of 50%, which might result in an additional pressure drop up to 3.8 in. of Hg, rather than to exclude the cooler and keep the pressure at 45 in. of Hg.

The effect of aftercooling on the thermal load is indicated by plotting the intensity of the thermal load versus the manifold pressure for different effectiveness (Fig. 21). Supercharging at effectiveness 100% has a reducing effect on the thermal load, while supercharging without aftercooling increases the thermal load under the conditions of test. The increase in the air temperature is seen to have a much greater effect on increasing the thermal load than the reducing effect of the increased air pressure. An increase of 87 F due to turbocharging to 45 in. of Hg caused an increase of 22.3% in the thermal load.

It is worthwhile to point out here that for a mep of 140 and a speed of 800 rpm, the thermal load on the cooling system is reduced by an amount twice as much as the heat removed from the air in the aftercooler. This is illustrated in Fig. 23.

The effect of aftercooling on the piston maximum temperature is shown in Figs. 21 and 23, which indi-

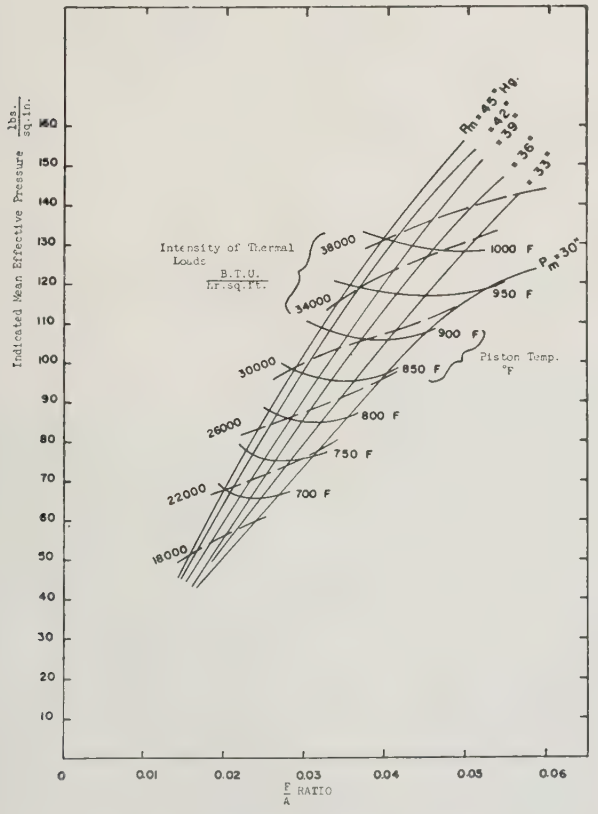

Fig. 20 — Performance without aftercooling

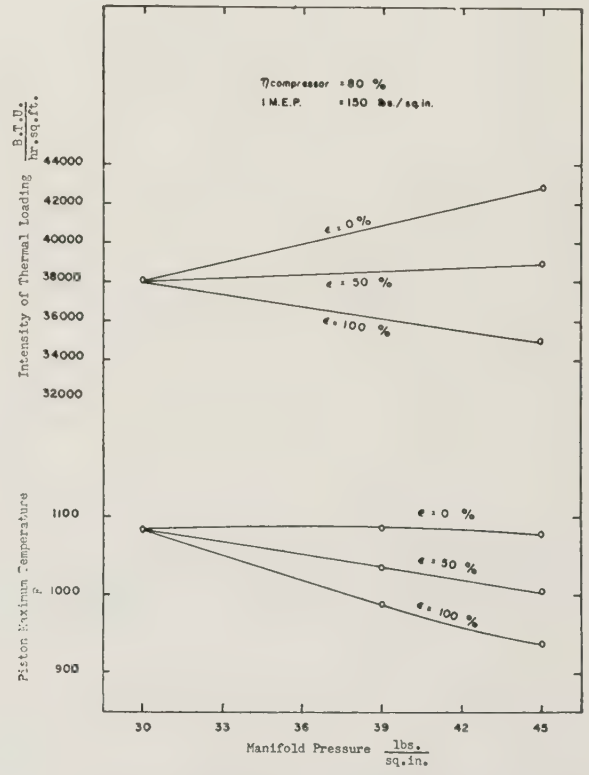

Fig. 21 — Effect of aftercooling on intensity of thermal loading and piston maximum temperature

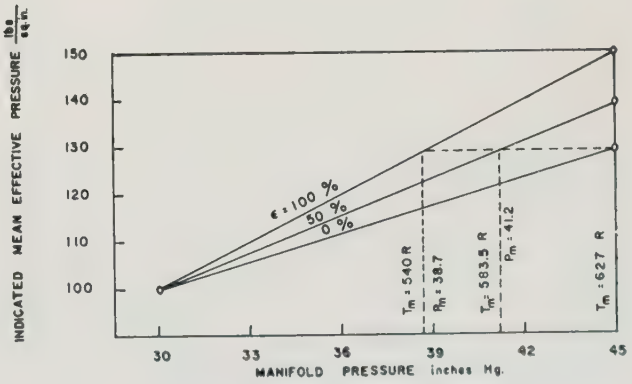

Fig. 22 — Effect of aftercooling on output mep

cate that the temperature drops with aftercooling. A drop of 140 F is a result of aftercooling with effectiveness 50% at a mep of 140 and 800 rpm.

Conclusions

It was concluded that:

1. The thermal load and wall temperature of a turbocharged compression-ignition engine are primarily related to the indicated power output and affected to a lesser degree by intake manifold conditions and the engine speed. Results of this investigation show that:

a. The thermal load and wall temperature are straight-line relationships to the indicated mean effective pressure.

b. For the same indicated mean effective pressure:

—Boosting the intake manifold pressure without a corresponding heating of the air will reduce the thermal load and wall temperatures.

—Raising the intake air temperature will increase the thermal load and wall temperature.

—Thermal load changes in direct proportion to the cube root of the mean piston speed.

c. For the same intake manifold pressure the wall temperature changes in direct proportion to the thermal loading.

2. For the operation of turbocharged engines at constant power output and no aftercooling, one of the following two conditions prevails: (a) High supercharging resulting in better fuel economy; or (b) low supercharging resulting in poor fuel economy, but reduced thermal and mechanical loads, without any reduction in the mean wall temperatures.

3. The turbocharged engine performance is improved by increasing the air density and reducing its temperature in the intake manifold resulting in higher specific power outputs and lower thermal loads and wall temperatures. Aftercooling is one method used to increase air density by decreasing the air temperature. Even though the pressure drop increases as the aftercooler effectiveness increases, general engine performance will be improved by using an aftercooler with high effectiveness.

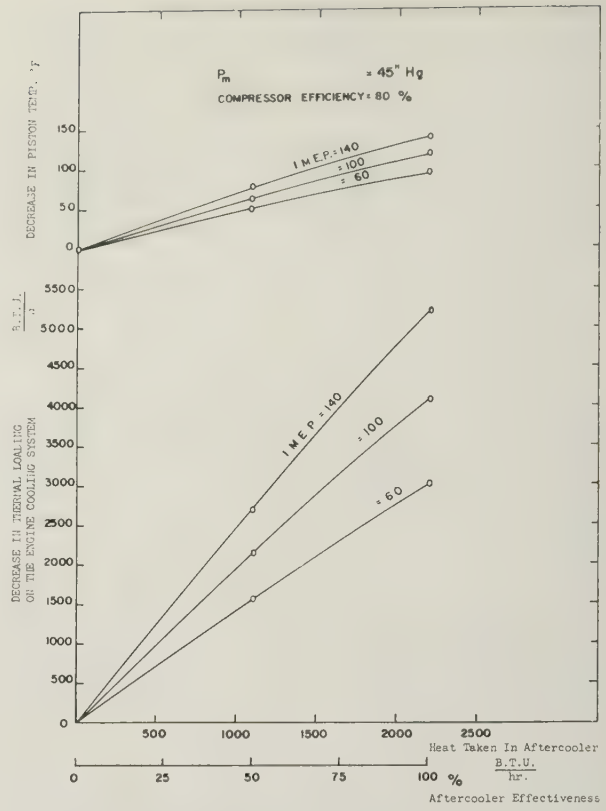

Fig. 23 — Effect of aftercooling on reduction of thermal loading and piston maximum temperature

It should be added here that the above investigation was done on one type of combustion chamber. It is believed that similar types of engines will give similar results. But for other types of engines a similar investigation might be needed before using the derived formulas.

DISCUSSION

Shows Heat Rejection In Precombustion-Chamber Engine

— E. W. Landon
Caterpillar Tractor Co.

IN STUDYING the paper, the writer observed that some of the piston temperatures plotted in Figs. 18–20 were above 1000 F which is much higher than we experience with aluminum pistons. We assume that some type of iron pistons were used in this engine, since the thermal conductivity of iron was used in calculating the piston temperatures. With iron pistons and only aircooling on the underside of the piston as indicated in the thesis, one would expect a high temperature on the gas side. The writer would like to ask the authors if it is possible with their method to come up with a realistic piston temperature on the gas side when jet oil cooling is employed?

We have measured heat rejection in a precombustion-chamber engine and I would expect this to be somewhat similar to an energy-cell-type engine in that some of the combustion gases go into an auxiliary chamber. Our engine was set up in such a way that we could measure the heat rejected from various heated surfaces independently. The heat rejected to the liner, the heat rejected to the bottom deck of the head and the exhaust port, and the heat rejected to the precombustion chamber were all measured independently. A plot of these data indicates that the total heat rejected to the liner and the heat rejected to the head have approximately the same slope (Fig. A). The heat rejected from the precombustion chamber, however, has a different slope. In a small auxiliary chamber of this type approximately 18% of the heat is rejected. However, the area is 6.8% of the heat-conducting area in contact with the hot gases. There is probably a velocity and temperature factor here which does not follow the main combustion chamber. It would seem to me that an error would

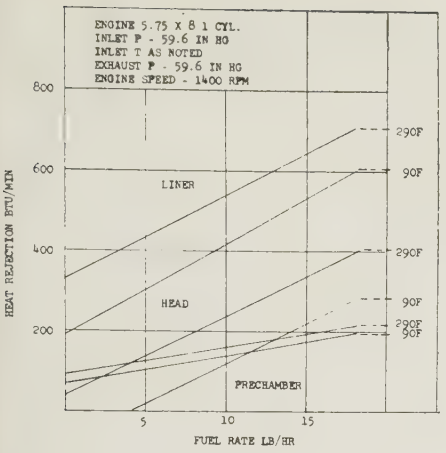

Fig. A — Heat rejection in precombustion chamber engine

be made by assuming the heat loss in the antechamber would follow the remainder of the exposed wall areas. Some elucidation of this aspect of the heat rejection may assist in evaluating this type of engine. The turbulence factor in auxiliary chamber engines undoubtedly has an effect on the calculation of heat-transfer coefficients on the gas side.

Thermal Load Capacity Remains a Design Problem

— Harold Holler
Norberg Mfg. Co.

THE AUTHORS are to be complimented for an excellent paper which together with another paper by D. H. Brown[a] represent valuable contributions to the understanding of thermal load limitations of engines and afford methods of predicting thermal loads on proposed engine designs.

It is most interesting to note the close comparison between calculated thermal load and measured cooling water losses. This confirms that heat to cooling water is a true measure of thermal load and affords a relatively simple method of determining thermal load on an existing engine by means of an ordinary heat balance.

First, the writer would like to make several comments relative to the Nordberg engine used in the tests. The engine, at a naturally aspirated rating of 80 bmep (approximately 105 imep) is rated at 10 bhp at 1200 rpm and normally operates with a peak firing pressure of 800 psi and exhaust temperature of 700 F. The fact that the engine withstood loadings up to 160 imep (approximately 120 bmep) with firing pressures up to 1200 psi and exhaust temperatures to 1200 F without any sign of failure in any of its parts attests to the reliability of the engine at normal ratings. This is borne out by the fact that engines of this type have been operated for as much as 40,000–50,000 hr in unattended oil pumping applications without major overhaul.

While the theory of G. Eichelberg, which states that the heat-transfer coefficient is a function of the cube root of the piston speed and the square root of the cylinder gas pressure has been verified by both of these papers, considerable mystery still surrounds the actual thermal load capacity of an engine.

The heat losses to cooling water for the test engine shows (Fig. 13) that at 105 imep (coresponding to normal full load of 10 bhp) the heat loss is approximately 2000 btu/bhp-hr when engine is supercharged to 36 in. of Hg manifold pressure. Nordberg tests at normally aspirated conditions resulted in 2870 btu/bhp-hr to cooling water or 32% of total heat input which seems quite high for an engine with an uncooled exhaust manifold. Yet this engine has a proved record of reliability and a 50% increase in total heat load during tests conducted by the authors apparently was still within the thermal load capacity of the engine.

It has been our experience that as engine bore increases, the thermal load capacity in terms of btu/bhp-hr decreases for equivalent reliability. For naturally aspirated engines of other sizes, we have found the following heat loads to cooling water to give desired reliability:

9	× 11½ in.	4-cycle — 1400	btu/bhp-hr
13	× 16½ in.	" " — 1100	"
21½	× 31 in.	2-cycle — 1100	"
29	× 40 in.	" " — 1000	"

Thus, some other parameters such as combustion-chamber surface/volume ratio must affect thermal load capacity. This area needs much further study.

When turbocharging is to be considered for any given engine, the total thermal load capacity of an engine for equal reliability remains constant. Thus, if we wish to double the output, the heat to cooling water in terms of btu/bhp-hr must be halved. As pointed out by the authors, an increase in output will increase heat load in a straight-line relationship regardless of manifold conditions and engine speed. This condition, known to some but ignored by many, has led to many costly failures in attempts to turbocharge a particular engine.

The authors point out the advantages of aftercooling on reduction of thermal load. Certainly anything done to reduce charging temperature and thereby reduce mean cycle temperature will assist in reducing thermal load. Other schemes, such as providing adequate scavenging to move residual gases, reduction in compression ratio, and the like, will assist in this goal. To show what can be accomplished in this direction, Nordberg has recently developed a 3600 bhp, 16-cyl, 11-in. bore × 12-in. stroke high-supercharged engine rated at 174 bmep at 900 rpm for the U. S. Navy. The engine was reported on in an ASME paper[b] and from the heat balance we note a heat to cooling water rate of 655 Btu/bhp-hr corresponding to only 10% of the total heat input.

Besides thermal load problems mentioned in the paper, mechanical load problems created by higher firing pressures also are to be contended with in supercharging of a particular engine. Thus, attempts to supercharge existing engines, if they already are at their thermal and mechanical load capacities when nonsupercharged, invariably result in failure. While design for increased mechanical loads can usually be accommodated, design for increased thermal loads is not easily accomplished.

Much of our future design work will depend upon the thermal load of an engine because the mechanical sciences have progressed to a state where it is reasonably simple to design a structure for suitable mechanical loading, but the thermal loading problem still requires a considerable amount of research in order to develop a satisfactory engine.

Cylinder Head Temperatures In Turbocharged 2-Stroke Diesel

— A. R. Schrader
U. S. Naval Engineering Experiment Station

ANALYSIS OF THE heat-flow relationships in a diesel engine is a tremendously complicated procedure. Many of the factors are difficult or impossible of precise measurement and the critical temperatures vary from point to point in the engine and from instant to instant in the cycle. The authors of this paper are to be congratulated on their development of logical analysis methods for a difficult problem.

The paper contains a wealth of information, but there

[a] SAE Transactions, Vol. 66, 1958, pp. 522–531: "Diesel Cylinder Heat Transfer Design Criteria," by D. H. Brown.

[b] "Development of a Lightweight, High Output Four Cycle Diesel Engine for Naval Service," by L. Wechsler and H. Holler. ASME Paper No. 58-OGP-2.

are several points on which data are incomplete, as follows:

1. Equation 3 represents the overall heat transfer to the gas side of the walls. However, this expression appears to cover only the combustion-chamber walls and not the surfaces swept by the piston. Would the authors comment on this apparent discrepancy?

2. In the engine setup to simulate turbocharging, reference is made to a valve in the exhaust line for the purpose of throttling the exhaust gas flow. Would the authors describe the basis used for adjusting the exhaust pressure to correlate with the airflow rate and thus simulate self-sustained turbocharging?

3. What method was used to calibrate the sensitive thermocouple mounted in the combustion-chamber wall? Was a single such thermocouple used or were others mounted elsewhere?

4. Would the authors define the term "aftercooler effectiveness"?

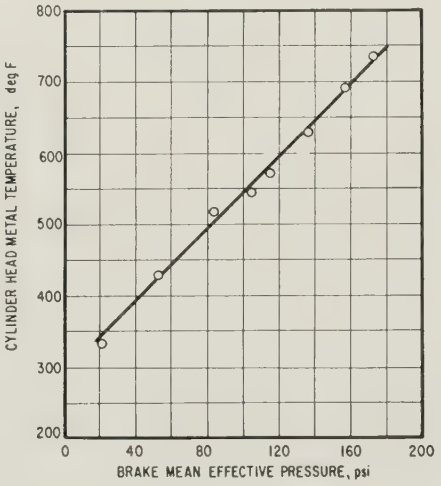

Fig. B — Relation of cylinder head metal temperature to engine power output

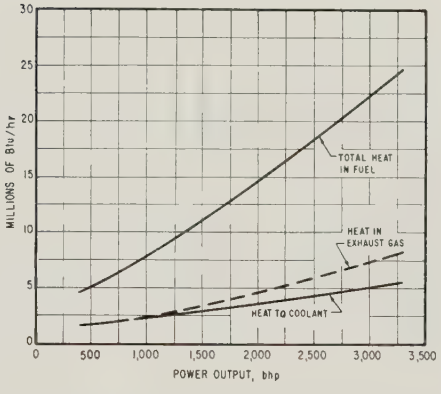

Fig. C — Heat balance data

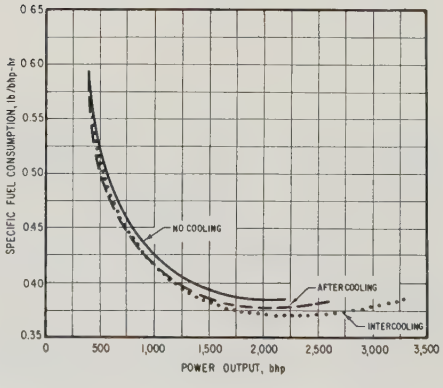

Fig. D — Effect of combustion aircooling on engine performance

5. What method was used to compute the piston temperatures shown graphically in Figs. 18–20, inclusive?

It is regrettable that the paper does not include some of the actual temperature measurements made by the sensitive thermocouple installation. Its usefulness would have been increased by these data.

We have not used an experimental temperature measurement method as described. However, we have recently measured cylinder head temperatures in a turbocharged, 2-stroke cycle diesel engine. The thermocouples, of a conventional type, were installed in holes drilled in the head lower deck parallel to the combustion-chamber surface. The thermocouple junction was located between a pair of exhaust valves at a distance of ¼-in. from the combustion-chamber surface. Fig. B shows the average temperatures measured in several cylinders. A straight-line relationship is indicated, with temperatures reaching rather high values at the maximum loads. We are not yet certain of the significance of the measurements, but we are using them as an indication of relative thermal loading in a critical area.

Thermal load analyses, as developed in the authors' paper, produce overall or average values of heat flow intensity. These are valuable for purposes of study or comparison. But too much reliance should not be placed on them when assessing the capabilities of a particular engine. Unfortunately — or perhaps I should say fortunately — engines are not built like the famous one-horse shay where every part was made as strong as every other part. In the usual engine, there are thermal load weak points due to imperfect localized cooling or excessive localized overheating. It is at those points that failure is initiated. Average or overall values of thermal loading may, therefore, lead to an unfounded confidence.

It is stated in the paper that heat losses to the coolant occur in direct proportion to the indicated mean effective pressure and reference is made to the curve shown in Fig. 12 in support. Actually, this curve shows that the heat losses to the coolant are somewhat less than directly proportional to the imep. For example, when the imep is trebled from 40 to 120 psi, the heat loss is only a little more than doubled. This is as it should be in a turbocharged diesel engine. Actually, if the engine had employed a valve timing more suitable for turbocharging, with increased valve overlap, more of the rejected heat would have gone to the exhaust and there would have been still less in the coolant.

Fig. C shows heat balance data on a turbocharged, 2-stroke cycle diesel engine tested at the Naval Engineering Experiment Station. As the engine load is increased, the greater amount of heat rejected to the exhaust, as compared to the coolant loss, is shown by the difference in the slopes of the curves.

In this test, when the engine load was trebled, the heat rejection to the coolant increased 2.3 times. The coolant included that used in the engine jackets, turbocharger jackets, and intercooler. If the coolant in the engine jacket only had been considered, as was apparently the case in the tests reported in the paper, the heat rejection to the coolant increased only 1.6 times when the engine load was trebled.

This easing of the coolant system loading in a turbocharged engine, by reason of the greater amount of heat carried away in the exhaust, is well-recognized in the engine industry. In many instances, it has been possible to use the same heat exchange equipment in a turbocharged engine as was used in the naturally aspirated version of the same engine.

The authors' analyses show the considerable benefits in improved engine performance and lessened thermal loading that are obtainable by cooling the air charge going to the engine cylinders. Our experience has borne this out fully.

Fig. D shows the results of comparative tests made on a turbocharged 2-stroke cycle diesel engine. The supercharging was done in two stages, with the turboblower as the first stage of air compression and an engine-driven, Roots-type blower as the second stage. With no cooling

of the air, the lowest specific fuel consumption was 0.385 lb/bhp-hr and the maximum power output was held to 2200 bhp by an aribtrary exhaust temperature limitation.

With aftercooling to 100 F, the specific fuel consumption was lowered and the engine developed 2600 bhp before reaching the exhaust temperature limitation. With intercooling to 100 F, the optimum specific fuel consumption was lowered to 0.370 lb/bhp-hr and 3300 bhp was developed without reaching the exhaust temperature limit.

The relationship shown in these curves applies to a specific engine arrangement and should not be construed as representing an absolute evaluation of the relative benefits of intercooling and aftercooling. The engine performances shown for the several conditions can be varied somewhat by a better matching of the turbocharger and the engine driven blower capacities to suit the type of cooling chosen.

The opinions or assertions made above are those of the author, and are not to be construed as official or reflecting the views of the Navy Department or the naval service at large.

Compares Heat-Transfer Data of Authors and Own Cycle Analysis

— H. A. Cook
Thompson Ramo Wooldridge Inc.

I AGREE WITH the authors on the three important limiting factors as regards engine output: (1) mechanical stressing of parts and bearings, (2) oxygen content of cylinder, and (3) internal temperature of working surfaces.

The authors experimental results obtained on cylinder wall temperature and heat transfer between gases and the walls are greatly appreciated. In analyzing turbocharged diesel engine performance, I am using a digital computer at Thompson Products to calculate the turbocharged diesel cycle. The information presented is very useful to me because I am calculating the same things that they discuss in their report. Fig. E is an example of calculated turbocharged diesel engine cycles. Peak cylinder pressure can be related to stressing of parts and bearings. The various pressures and temperatures existing during the exhaust and intake are most important for effective turbocharging. The temperature in the cylinder is the factor effecting the heat transfer to the cylinder walls.

Fig. F presents a comparison of heat transfer data from Fig. 15 of the subject report and calculated results in my cycle analysis. The major differences are that I am calculating negative heat transfer during some of the intake and compression strokes based on a constant wall temperature and a greater hump in the curve during the power stroke. The time of the peak is related to the combustion timing and is not of particular concern.

I would like to have the authors discuss the two differences I have noted above and indicate why their heat transfer remains positive and why it drops off so rapdily on the power stroke.

Present Own Test Data On Thermal Loading

— Ralph Miller
Consulting Engineer

THERMAL LOADING of internal-combustion engines as a research subject has long been neglected—probably because we do not have sufficient data on limiting internal surface temperatures nor the relation of these temperatures to the thermal load as measured by the heat flow to the water jackets.

In 1943 I conducted an extensive series of heat balance tests using a 6-cyl 12 × 14 in., 600 rpm Worthington engine. The data from these and more recent tests conducted with a 4.875 × 6 in., 6-cyl diesel at 15.18 C.R. and 2100 rpm are not in agreement with conclusions listed on page 10 of the

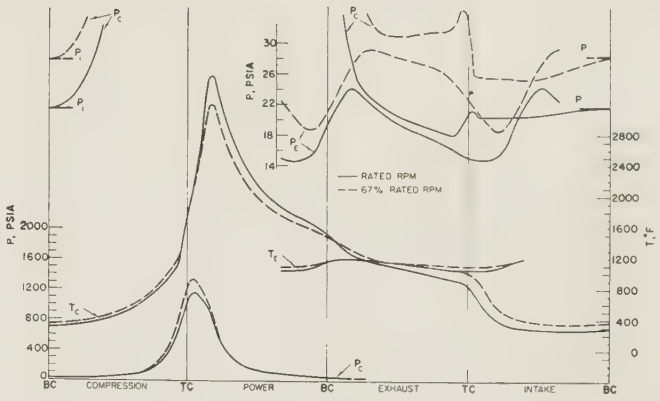

Fig. E — Effect of engine rpm and constant fuel

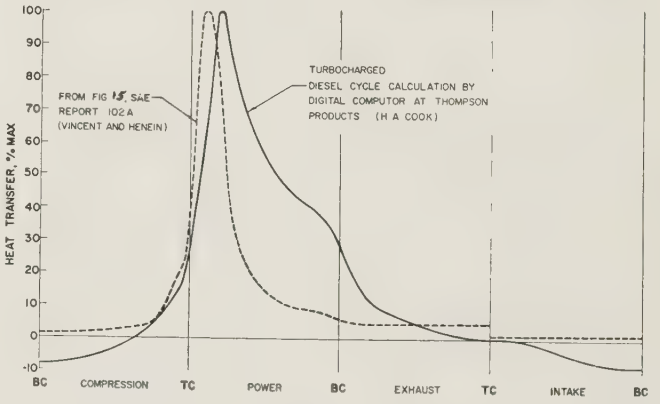

Fig. F — Comparison of heat transfer

paper. Neither does the author's test data support these conclusions.

The imep is proportional to the absolute pressure in the manifold and inversely proportional to the isfc as shown in Fig. 10, but not directly with the manifold pressure alone as concluded.

The third conclusion on p. 484 states that heat losses change in direct proportion to the indicated mean effective pressure at constant rpm and intake air temperature. This conclusion is in conflict with the data plotted in Fig. 12, which shows an increase of 50% in heat load for an imep increase from 91 to 150 or 65%.

The data plotted in Fig. 12 agrees with observations I have made in heat balance tests conducted with many different types and sizes of engines.

It can be stated very simply that the heat flow to the water jackets or the thermal load is proportional to the total heat released, and further that the total heat released is proportional to a factor which is the product of engine rpm, isfc, and imep.

For 91 and 150 imep on the 0.04 fuel/air ratio line these factors become 27600 and 41400, respectively, and the heat to cooling water then rises from 18,800 at 91 imep to 28,200 at 150 imep and falls on the line in Fig. 12.

The fourth conclusion states that at constant imep and rpm the heat losses change in direct proportion to the intake air temperature.

An 11 × 12 in., 16-cyl, 900 rpm, 4500-ihp engine recently tested showed a drop in heat to cooling water from 2,620,000 to 2,320,000 when the manifold temperature was reduced from 160 to 100 F. This cooling at constant manifold pressure increases the weight of the air charge from 8.5 to 9.4 lb per hr per ihp and reduced the isfc from 0.304 to 0.298 lb.

The heat to water jackets was shown to be proportional

to the isfc times the absolute inlet temperature. At constant cylinder charge pressure the per cent of total heat rejected to the water jackets decreases with the manifold temperature and is directly proportional to the absolute temperatures. In this test heat rejection to cooling water was 9.9% of total heat at 160 and 8.95% at 100 F manifold temperature.

The engine was operating on the Miller system of supercharging with a net compression ratio of 9.5 at full load and a cylinder compression ration of 11.8. The cylinder charge temperature at the beginning of the compression stroke is therefore $620 \times \left(\frac{9.5}{11.8}\right)^{0.4} = 568$ deg absolute or 108 F at 160 F manifold temperature and 513 deg absolute or 53 F at 100 F manifold temperature.

The authors' conclusion that cooling losses increase with the cube root of the piston speed is not proved by the data which seems to show that the increase in cooling loss is due to increased isfc.

The test with the 4.785 × 6 in. engine showed the same per cent of total heat in heat loss to water jacket when the speed was increased from 1800 to 2100 rpm.

The data presented confirms observations I have made and reported in several technical papers in recent years — namely that the most effective method of increasing the weight of air in the cylinder charge is by reducing its temperature, because neither thermal load nor compression pressure is increased by this method of increasing air weight and thereby imep.

With the Miller system the ultimate power increase obtainable by this method is achieved by lowering the actual compression ratio and thereby the temperature of the air in the combustion chamber. When supercharging by pressure at constant temperature the thermal load and the compression pressure both increase directly with the cylinder charge pressure as the imep is increased.

Heat Transfer Affected by Both Wall Temperature and Radiation

— Dr. Franz Jaklitsch
U. S. Army Ordnance Tank-Automotive Command

I HAVE SEVERAL comments:

1. The influence of the wall temperature on the heat transfer coefficient.

This question was asked during the discussion following the presentation of the subject and answered negatively by the speaker because the Eichelberg formula shows no relationship to the wall temperature.

The Nusselt formula[c] for the heat transfer by convection in engines:

$$h_c = 0.99\sqrt[3]{p^2 T} \cdot (1 + 1.24S) \qquad \text{(A)}$$

also does not include the influence of the wall temperature.

[c] "Heat Transfer in Engines," by W. Nusselt. Forsehungsarbeiten No. 264, 1923. Verein Deutscher Ingenieure.
[d] "Heat Transfer in Engines," by F. Jaklitsch. Pub. by Oldenbourg, Munich, 1929.

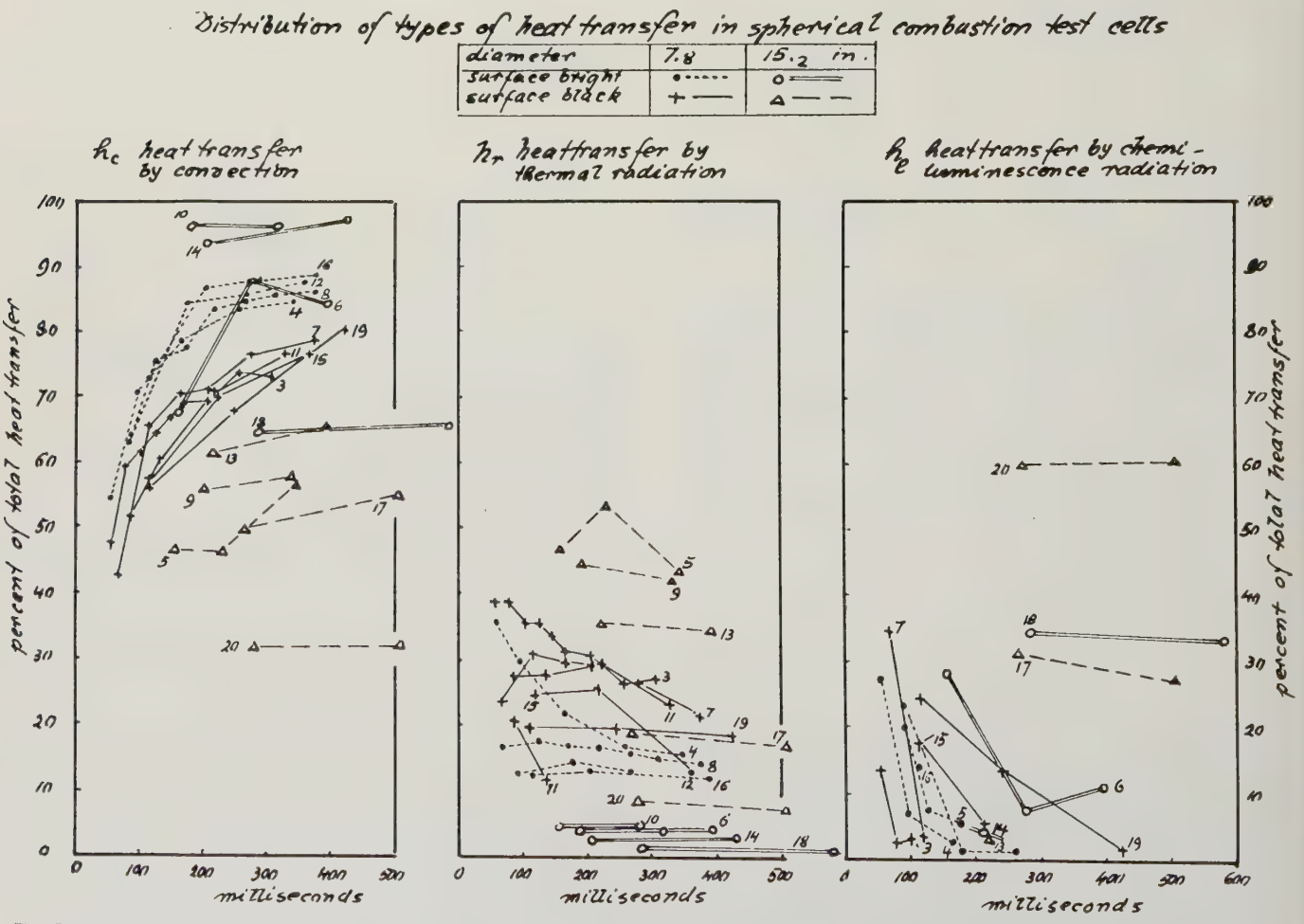

Fig. G — Percentage of heat transfer by convection Fig. H — Percentage of thermal radiation Fig. I — Percentage of radiation caused by chemiluminescence

However, as a matter of fact, there exists a positive influence of the wall temperature on the heat-transfer coefficient of convection and of thermal radiation also.

This dependency was evidenced by an analysis[d] of test results of W. Nusselt[e] obtained by a series of combustion tests in spherical combustion chambers resulting in the formula for heat transfer by convection:

$$h_c = 2.35 w_w + 4.9 \cdot \frac{w_w}{w_o} \qquad (B)$$

or

$$h_c = 23500 \cdot \frac{p}{R T_w} + 4.9 \cdot \frac{T_o}{T_w} \qquad (C)$$

where:

p = Gas pressure in kg/cm²
R = Gas constant
T_w = Absolute wall temperature in deg. Kelvin
T_o = Absolute gas temperature at the end of cooling in deg. Kelvin
w_w = Specific weight of the gas on the wall in kg/m³
w_o = Specific weight of gas at end of cooling in kg/m³

Equation C demonstrates that the heat-transfer coefficient increases in a linear relationship with decreasing absolute wall temperature and this is easy to interpret. The physical phenomenon of heat transfer by convection takes place in the immediate gas layer on the wall. Since the heat transfer is a mutual interchange of kinetic energy between individual molecules at every collision, it is obvious that it will increase with the number of collisions and, therefore, with the density in the boundary layer at the wall.

The second term $4.9 \cdot \frac{w_w}{w_o}$ shows the influence of migration of molecules into the boundary layer by the density variation during combustion.

2. The heat transfer by radiation in engines.

In Figs. G–J the results of an analysis of combustion tests made by W. Nusselt[e] in regard to the heat-transfer coefficients versus time are shown.

Fig. G discloses the percentage of heat transfer by convection affected by the size of the test spheres (7.9 in. and 15.4 in. of inside diameter) and the condition of the inner surface.

Fig. H demonstrates the percentage of thermal radiation determined by Nusselt as follows:

$$h_r = \frac{0.362}{\frac{1}{A_1} + \frac{1}{A_2} - 1} \cdot \frac{\left(\frac{T}{100}\right)^4 - \left(\frac{T_w}{100}\right)^4}{T - T_w} \qquad (D)$$

where:

h_r = Heat transfer coefficient for thermal radiation in kcal/m², h, o_c
A_1 = Absorption capacity of gas
A_2 = Absorption capacity of the internal surface of the combustion chamber
T = Absolute gas temperature in deg Kelvin
T_w = Absolute wall temperature in deg Kelvin

The wide variation caused by the size and the surface condition is of particular interest. An additional influence in this respect will be induced by the shape modification of the combustion chamber.

Fig. I shows the percentage and the time history of a special kind of radiation caused by chemiluminescence, which is influenced greatly by the amount of humidity and the type of mixture before ignition and, to a certain extent, by the size of the test specimen also. The shape of the combustion chamber is expected to have some influence too, but the present knowledge of it is very limited. The existence of this category of radiation was evidenced in combustion tests by W. Nusselt[e] and interpreted by an analysis[f] by F. Jaklitsch. Under special conditions, this kind of heat transfer can increase up to 60% of the total heat transfer and should, therefore, not be overlooked.

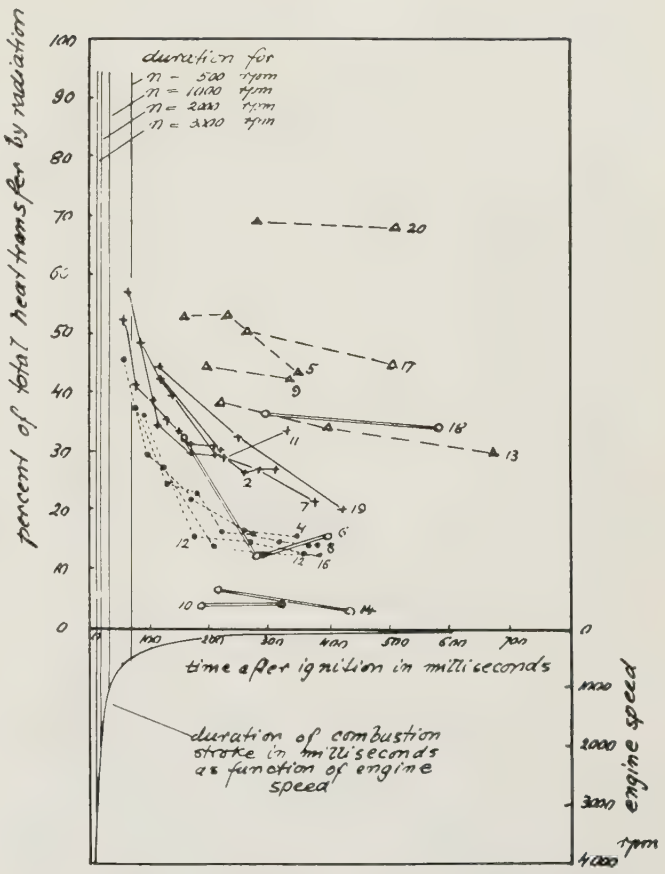

Fig. J — Influence of combustion time of total heat transfer by radiation ($h_r + h_c$) in comparison with duration of combustion stroke in reciprocating engines

Fig. J shows the total percentage of heat transfer by radiation varying between 5 and 55% of the total heat transfer.

This diagram demonstrates, furthermore, that the duration of a combustion stroke is below the investigated time range in the tests by W. Nusselt for engine speeds above 700 rpm that is for all smaller internal-combustion engines. The influence of the engine speed is, therefore, still an open problem.

The influence of the engine was found to be:

by Nusselt $f(s) = 1 + 1.24 \cdot 5$ (E)
by Eichelberg $f(s) = \sqrt[3]{s}$ (F)
by Conrad $f(s) = 5(1 + 1.24 \cdot 5)$ (G)

which demonstrates, therefore, a wide variation of opinions.

The paper presented does not mention the role of radiation in the investigated Nordberg diesel engine. A supplementary pertinent statement would be highly appreciated.

The authors' closure to the discussion will be found on page 494.

[e] Page 361 of "Heat Transfer in Gas Engine. Part I — Its Functional Relationship with Time," by W. Nusselt. Zeitschrift Verein Deutscher Ingenieure, 1914.
[f] Page 11 of "Heat Transfer in Engines," by F. Jaklitsch. Pub. by Oldenbourg, Munich, 1929.
[g] Page 610f "Fuel and Engine at Start of Automotive Engines," by W. Rixmann, E. Schaub, and H. J. Conrad. Deutsche Kraftfahrt Forshung, No. 55, Verein Deutscher Ingenieure, Berlin, 1941.

Authors' Closure To Discussion

MR. LANDON's statement regarding piston temperatures of 1000 F is correct, aluminum pistons would fail before reaching this temperature. As a matter of fact, it is believed that a cast-iron one would not be too happy either. It must be remembered that the piston temperature given was a completely calculated one, with not even one check point on which to base assumptions. Its accuracy is, thus, somewhat doubtful but does indicate the range of temperature to be encountered. In the case of oil-jet cooling, it is believed that the same method could be used, provided that the jet supplied a stream sufficiently large to flood the piston head to give uniform cooling similar to that in the water jacket. The oil temperature would substitute for that of the air and a heat transfer coefficient for oil should be employed.

With regard to heat transfer in the energy cell, Mr. Landon's statement about some variation here is probably correct since the high velocities in the location would have considerable effects upon the coefficients.

Mr. Holler's comments are appreciated and the authors agree that engine size does have considerable influence on the rate of heat transfer. When dealing with engines of the size employed in the experiments reported in the paper, heat transmission alone is believed to be the limiting condition. As the size increases, metal thickness increases and on top of heat transmission, thermal stresses become involved and they alone may limit the rate of heat transfer. Soon after World War I one of the authors conducted some tests on cylinders 20–25 in. in diameter, operating at bulk high piston speeds and high mean effective pressures. Here, special designs were worked out for handling heat stress and considerable success was obtained in increasing heat transmission beyond the normal standards, rates probably comparable with those now employed in small high-speed engines were required. These gains were at an increase in costs of construction, naturally; since the engine was for submarine purposes this was somewhat of a secondary consideration.

The statement given by Mr. Schrader regarding combustion-chamber wall area is correct. However, the location of the thermocouple was in the surface continually exposed to gas temperature and Equation 3 was based on this fact. Equation 2 covers the case where the cylinder surface is varying from point to point.

The exhaust manifold pressure P_e, was adjusted by the valve to be a constant fraction of the intake manifold pressure P_m; say $P_e = 0.85\ P_m$ to provide sufficient pressure difference for cylinder scavenging.

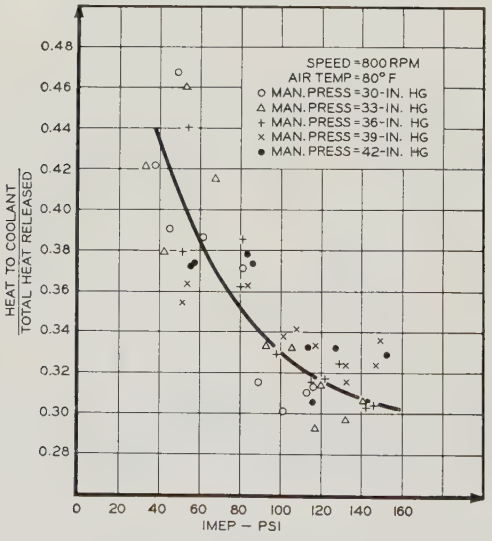

Fig. K — Variation of per cent *ht* to coolant with imep (speed constant)

The calibration curve of the thermocouple was delivered by the manufacturer with the couple. This curve was not checked by the authors.

Aftercooler effectiveness is the ratio of the heat removed by the cooler from the supercharge air leaving the turbo charged to the maximum possible that could be removed if cooled to the ambient temperature.

$$\text{Effectiveness} = \frac{T_2 - T_3}{T_2 - T_a} \qquad \text{(H)}$$

where:

T_2 = Temperature of air delivered by supercharger
T_3 = Temperature of air delivered to manifold
T_a = Ambient air temperature

The piston temperature calculations were made in the same manner as the cylinder wall. Reference to University of Michigan Publication IP-229[3] (the original thesis) will give all details.

Temperature measurements have been added to the paper to supply the material asked for.

The imbedded thermocouple described by Mr. Schrader does indicate critical conditions and gives a good guide to limiting powers; as a practical tool it is of great value, more so perhaps than the author's type placed for heat flow data rather than maximum temperatures.

The differences of Fig. F of Mr. Cook and the author's Fig. 15 seem to be that in Fig. 15 is shown the product of α_g and T_g not heat transfer. To obtain heat transfer the product $\alpha_g\ T_w$ should be subtracted from the values in Fig. 15 when the negative transfer will show up.

It is difficult to tie some of Mr. R. Miller's remarks into the paper since at no point have isfc been given for the engine tested; thus the manner in which he included this factor into his calculations is not known.

Fig. 10 of the paper where corrections proportional to P/T have been made do support the conclusion of the authors, which was that the correction was proportional to manifold pressure and inversely as the temperature — not manifold pressure alone.

The conclusions drawn cover the independent variables. True, there are some others of secondary effects not mentioned, such as volumetric efficiency, indicated thermal efficiency, and the like.

Conclusion 3 questioned by Mr. Miller, is perhaps a conflict of what is to be understood, the text states that we are considering the *change* of losses, not the losses. What is intended could perhaps be better expressed by the following:

$$\frac{dQ}{d(\text{imep})} = \text{Constant} \qquad \text{(I)}$$

where Q = heat flow, that is a straight-line relationship exists.

The heat loss to the coolant as a fraction of the total heat release has been calculated and plotted versus imep on Fig. K. It is seen that this is far from a straight-line relationship mentioned by the discusser.

The material contributed by Mr. Jaklitsch is of interest and should receive some consideration. However, at the moment, without a very careful analysis it is difficult to separate out the various types of heat transfer from the author's tests. The work quoted by Dr. Jaklitsch appears to be for a bomb and the first readings begin some 50–100 millisec after the start of combustion; in our case the engine would have made some 2–3 revolutions in such a time. During these revolutions temperatures capable of providing much radiation would only exist for ⅛ to ¼ of the time.

It is stated that the heat transfer coefficient increases linearly with decreasing wall temperature. Is this what is intended? If the heat transfer increases, then in order for more heat to flow with the same external temperature the gradient through the metal must increase, not decrease — the internal wall temperature must go up.

the design of

Planetary Gear Trains

Oliver K. Kelley, General Motors Corp.

This paper was presented at the SAE Annual Meeting, Detroit, Jan. 14, 1959.

THE usefulness of planetary gear trains and the engineering techniques necessary for optimum design are discussed in this paper. A simple method for calculating planetary gear ratios is described which can be used to determine quickly the potential usefulness of any planetary configurations.

The author lists criteria which help to evaluate the potential of a planetary gear train schematic from the standpoints of gear noise and structural viewpoint.

Detailed design of individual members include spacing of the pinions, mounting considerations, thrust direction, lubrication, and stress evaluation.

WHY do the millions of American automatic transmissions use planetary gears exclusively in all passenger cars and almost exclusively in the heavy-duty automatic transmissions? Obvously, there must be important reasons for this, and I would like to point out, first of all, what some of them are.

Advantages of Planetary Gears

1. The planetary gear train is obviously more compact than the countershaft gear train designed for the same function. The planetary gear train accomplishes the entire design arrangement (lengthwise) within the length of one gear's face width only, plus a small additional dimension for the carrier's flange thickness. The countershaft arrangement of necessity must use separate input and output gearsets, which must occupy greater length.

As the planetary gear train provides three or more meshing gearsets concentrically arranged around the input gear, their load sharing reduces the gear width in proportion to the number of planetary pinions. (Tooth contact surface stress determines the fatigue life for quiet operation; thus, the longer the working contact line, the lower the stress.) Although slightly lower stress must be used in the planetary design to accommodate the more-than-one-gear-meshing contact per input gear revolution which tends to reduce the hours of life, the overwhelming advantage results from lower stress of multiple pinions. This is a very significant factor.

A planetary gear train also eliminates the length required to place radial load-carrying bearings for both input and output gearsets of the countershaft design. In planetary gears there is no radial load on the input or the output member, as the multiple pinion arrangement automatically cancels it. Each pinion does carry a radial load, but here the design picture provides a natural place for locating the bearings directly under the load on the pinion shafts, thus occupying the same space as the pin-

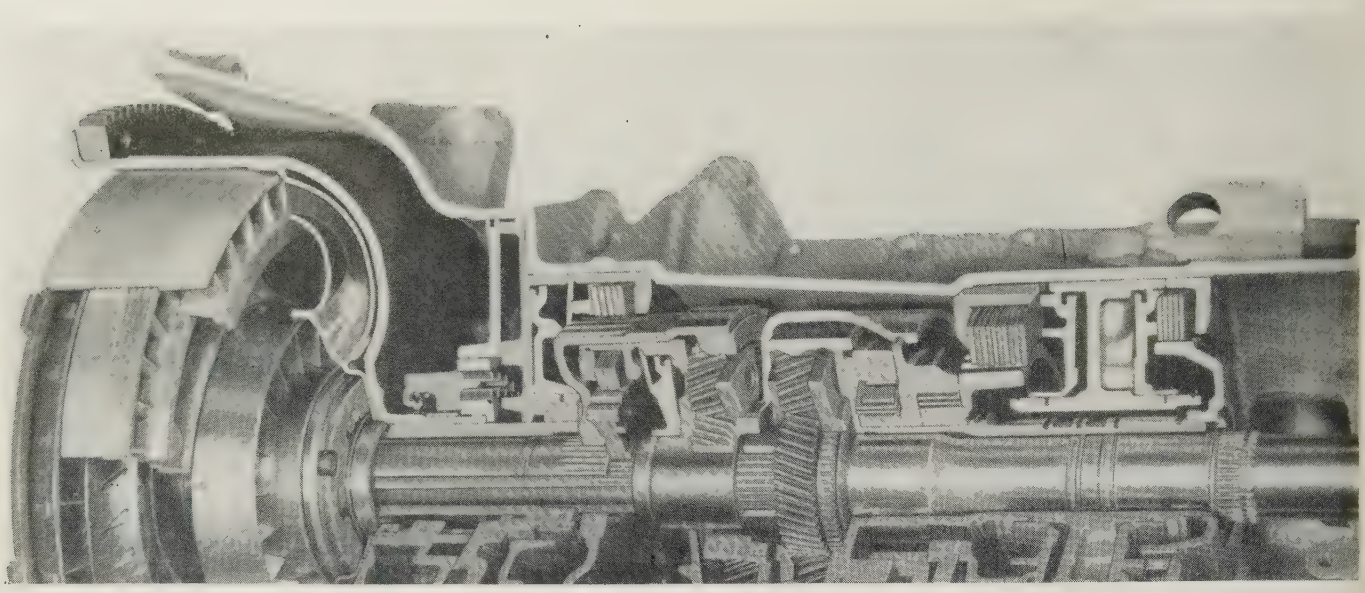

Fig. 1 — Gear train of Buick Triple Turbine transmission

ions. This is also a significant factor in reducing the overall length of the design.

Although the radial dimensions in some cases may be less favorable than in countershaft design where the countershaft can be placed at will in the most advantageous position for radial space considerations, there can be no doubt about the general advantages of the planetary gear design in space savings.

Fig. 1 pictures the gear train in the latest American automatic transmission — the Buick Triple Turbine. Note the small space required for the gear train, which is connected to two axial flow turbine members to give two forward gear ratios and reverse within the same set.

2. The planetary gears are more efficient in gear action. A fixed countershaft dictates the existence of two sets of gears transmitting the full power and suffering the sliding action loss of the involute gear teeth twice. The two losses are: (1) the input gear train loss in proportion to the input speed times input torque, and (2) the output gear train loss in proportion to the output speed times output torque. They are substantially equal.

In the planetary arrangement the gears handle only the differential power; first, there is the input gear loss in proportion to *the input speed minus the output speed times the input torque;* and second, the reaction gear loss in proportion to the *output speed times the reaction torque.* Again, as we will see, the two losses are substantially equal. The output member is the "countershaft" carrier, which reduces the operating gear action speed as compared to a fixed countershaft design. The resultant gain is very substantial in planetaries designed for small reduction ratios where the input speed minus the output speed is small and the reaction torque is also small.

Let us examine this more closely in a 4/1 planetary train and a 1.33/1 planetary. Both ratios are obtained from the same gears, depending on whether the input member is the sun gear or the ring gear.

In the 4/1 arrangement, the input gear action loss is in terms of one minus one-fourth times the input torque, totaling only *three-quarters* of the input train loss of an equivalent countershaft design. The reaction gear action loss is in terms of one-fourth times the reaction torque which is three in this case, totaling also *three-quarters* of the output train loss of an equivalent countershaft design.

In a 1.33/1 arrangement the input gear action loss is in terms of one minus three-fourths times the input torque, totaling *one-fourth* of the input train loss of an equivalent countershaft design. The reaction gear action loss is in terms of three-fourths of one-third of the input torque, also totaling *one-fourth* of the output train loss of an equivalent countershaft train. The input loss and the reaction loss are the same in planetary trains, regardless of the gear ratio. This is true because the pitch line velocity and the tooth load are equal at all points within the set.

A simple picture emerges here. The planetary gear loss is in terms of twice the input torque multiplied by the input speed minus output speed, whereas the countershaft gear train loss is always in terms of twice the input speed times the input torque, no matter what the output speed is. This gives the planetary gear a substantial plus, especially for small reduction ratios where the input speed minus the output speed becomes a small multiplying factor.

3. The planetary train is more efficient because of smaller bearing losses. The bearing P-V values are a direct reflection of the "gearing P-V" values, if one may use such an expression. If pounds per square inch bearing stresses as well as pounds per square inch tooth-load surface stresses are kept on the same basis in all cases, we can say that the advantages of planetary gear designs over the countershaft gear designs are of the same general order in bearing P-V losses as they are in gear tooth action losses.

4. Planetary gearing is easier to make quiet than countershaft gearing.

In countershaft gearing there is no artificial helping factor to keep pitch line velocities down. What-

ever driving gear diameter the tooth-load considerations demand will unavoidably set the pitch line velocity. First of all, because of the multiple pinion arrangement, the planetary gear trains permit the use of a smaller diameter driving gear. There is also the artificial helping factor of the planet carrier rotation which reduces the velocity of the gear action, thus further decreasing the pitch line velocity.

Another important factor aids the planetary gear designer in obtaining quieter gears. Countershaft support bearings can be difficult and expensive if the tooth-load induced bending moments on the shaft are to be properly carried for good gear alignment. This is hardly a problem in planetary gearing designs where the only bearing loads are on the straddle-mounted pinions directly on the pinion shafts. As long as the carrier is torsionally rigid so that the output torque cannot twist the carrier, there is little difficulty in obtaining gear alignment.

5. Planetary gears lend themselves readily to power-shifting designs. The classic 3-element planetary gear train (Fig. 2) consists of three concentrically placed elements, one of which is the reaction member. When in reduction, this member must be held from rotation. This is easily done by a friction band, a ground clutch, or a free-wheel unit. When in 1/1 direct drive, this reaction member can be clutched to the input member by a rather low-torque friction clutch which seldom results in anything but a simple design.

To obtain two speeds in a countershaft design, there must be two rotating clutching members and they invariably carry higher torque and must occupy more space and are more complicated than in planetary designs. The planetary gear train is a "natural" for friction element and free-wheel unit placements for power shifting.

There are other less important points of design comparison that could be made, but the five that I have enumerated are the fundamental reasons for the popularity of planetary gears in power transmission designs in America today.

To repeat: Compact design, more efficient gearing and bearing design, easier to make quiet, and more suitable for designs of uninterrupted power shifting are the principal advantages.

Design Limitations

Let us examine some of the design limitations of planetary gearing as to easily available ratios.

Where the sun gear is driving and the ring gear is the reaction element (Fig. 2B), there is generally no difficulty in obtaining reduction ratios of 3/1 or greater. The trouble comes in getting good gear and planet pinion bearing design when reduction ratios of less than 2.8/1 are attempted. The pinions get to be too small, the number of teeth gets to be less than 15 (resulting in difficult tooth modifications for minimum overlap), and the space left for the bearing gets too small.

When the ring gear is driving and the sun gear is the reaction member (Fig. 2A), the trouble point of the small pinion begins to show up when reduction ratios of 1.55 or more are attempted. On the other hand, the ring gear input reduction gears run into oversize problems when the reduction ratios of less than 1.35/1 are attempted. Generally, the reaction sun gear must always be large enough to permit the output shaft to run through it. This imposes diametral size problems for the ring gear, which in the case of 1.28/1 ratio must have a pitch diameter 3.57 times larger than that of the sun gear, and will very likely get to be too large to fit in. The most commonly used ring gear driving planetary reduction ratios are between 1.35/1 and 1.55/1. Although these ratios are exceeded in some cases where ratios greater than 1.55/1 or less than 2.8/1 must be obtained, there are always problems of extremely accurate control of all factors that influence quiet gear action and satisfactory bearing life.

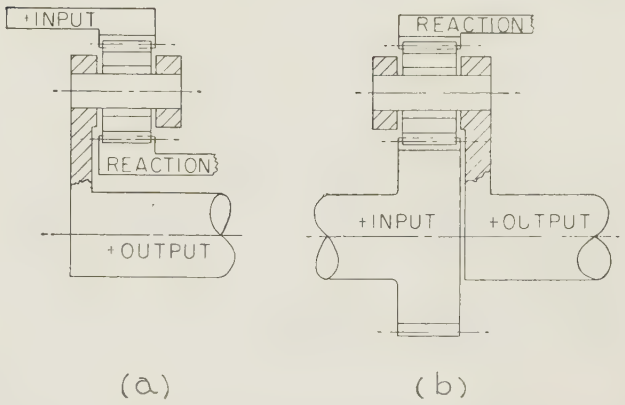

Fig. 2 — Classic 3-element planetary gear train

Taking a quick look at the extreme limiting conditions of ratios available, one might mention the impossibility of obtaining a 2/1 ratio for either the sun gear driving or the ring gear driving, as these require zero pitch diameter pinions.

Compound Planetaries

This is where compound planetaries come in. Let us look at a compound gear train design for the "impossible" 2/1 reduction ratio (Figs. 3A and 3B).

This compound train makes use of one planetary set to reduce the full-speed gear action of the other set, thus also reducing the other set's final drive ratio. It is a near ideal example of load and speed dividing to accomplish a gear ratio unobtainable in a single planetary gear train. Each planetary does about the same amount of work. (See Fig. 3A.)

Let us look at another compound planetary gear train which also produces a 2/1 reduction ratio. In this arrangement the left-side ring gear input planetary drives the right-side planet carrier at a reduction ratio of 1.5/1. The planet pinions of the right-side carrier deliver the carrier torque two ways. The portion going to the output ring gear is 0.666 and the remaining 0.333 is delivered back to the original input shaft to increase the input torque artificially. This is a good example of a regenerative planet gear train where the tooth loads are higher than in the first example and the gear and bearing losses are slightly higher.

Both designs are useful. The first design obviously would be a good way of obtaining two different reduction ratios through use of either the first ring gear or the first carrier as the reaction member, thus getting optimum efficiency. The sec-

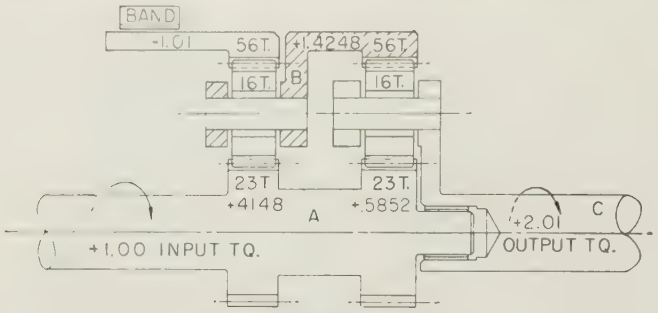

Fig. 3A — Compound gear train design, load dividing, 2/1 forward reduction

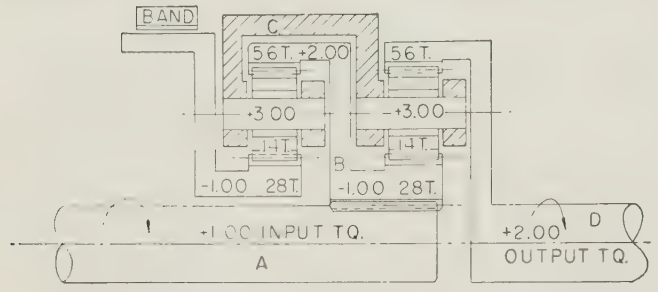

Fig. 3B — Compound gear train design, regenerative, 2/1 forward reduction

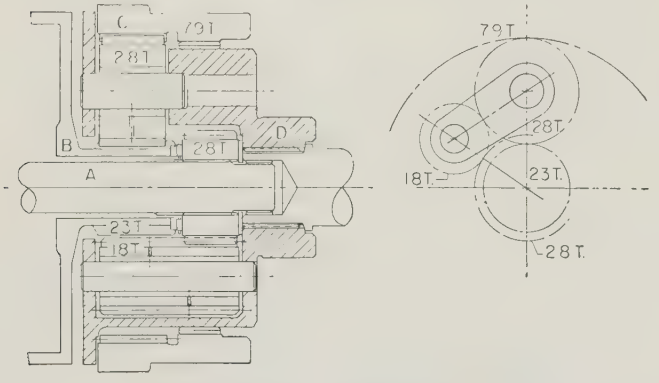

Fig. 4 — "Ravigneaux" compound planetary gears

ond design obtains a single reduction ratio and approximately equal reverse ratio by using either the first sun gear or the carrier combination as a reaction member, resulting in reasonable efficiency.

When nearly 2/1 ratios are sought, the "Ravigneaux" compound planetary design (Fig. 4) offers good solutions and has some structural advantages because it uses a single carrier only. In this design, there are two sun gears, three long pinions, three short pinions, and a ring gear which is used for reverse reaction. The 28-tooth sun gear is the input gear, the 23-sun gear the forward reduction reaction gear, the 79-tooth ring gear is reverse reaction gear, and the planet carrier is the output member. Both forward and reverse reduction ratios are 1.82/1.

Since the same tooth load prevails throughout this train, the reaction gear tooth load equals the driving gear tooth load and the reaction torque is directly proportional to the number of teeth in the reaction gear and the input gear.

Where less than 2/1 reduction ratio is involved, the reaction gear is smaller than the input gear and where more than 2/1 reduction ratio is involved, the opposite is true. Exact 2/1 ratio is unobtainable as the long pinion would not clear one of the sun gears and the side-by-side double pinion action would be impossible.

This design is extensively used in several automatic transmissions today, and while not quite as efficient as the simple planetary gear trains, does offer one of the better ways of keeping the pitch line velocities down. It is also compact in design and lends itself well to popular transmission gear ratios.

The number of possibilities of compound planetaries of two or more interconnected trains is almost infinite. In searching for the required results, it is very nice to know a quick and easy way of computing compound gear train ratios. The simple planetary ratios are so easy to compute that they hardly need to be mentioned here. When the ring gear is driving, the ratio equals the sun plus the ring divided by the ring; and when the sun gear is driving the ratio equals the sun plus the ring divided by the sun. In other words, take the total number of teeth in the sun and ring gears and divide by the number of teeth in the driving gear. But when regenerative and other less obvious phenomena occur in the gear train, the designer can spend a lot of time in studying and analyzing all the possibilities contained in planetary arrangements unless he knows this easy way. I first learned it from Earl A. Thompson who was my boss when he directed the early automatic transmission design activity for General Motors Corp. until 1939.

It goes as follows:

1. Hold any member of a gear train and turn another member one turn. Record the speed for each rotating member of the gear train when the speed of the member you are holding is zero. (Note: The calculation is easier if the initial member held is common to each gearset in the train.) The resulting figures disclose the speeds of all the members of the gear train.

2. Choose any of the rotating members for the next possible stationary member and add an equal quantity of opposite sign to its speed value. This makes its speed value zero. Then, add this same quantity to all the other members' speed value. This gives the original arrangement's zero members a definite speed value and changes all the other members' speed values all over.

3. Repeat this procedure until every member has been equated to zero, while the other members have changed their speeds to corrseponding new values.

4. Now examine the potential speed relations of the compound gear train for usable forward and reverse ratios. The full potential of the gear train is revealed quickly by this simple algebraic addition method.

Two examples will illustrate the method.

Fig. 5 shows the complete analysis of a load-dividing double planetary and Fig. 6 shows a similar analysis of the "Ravigneaux" train.

	A	B	C	D	STEP 4 REDUCTION RATIOS FORWARD	REVERSE
STEP 1	+1.00	$-.5393 = \frac{19}{56}$	0	$+.2533 = \frac{19}{75}$	$\frac{A}{D} = 3.947$ TO 1	$\frac{A}{B} = 2.947$ TO 1
	-.2533	-.2533	-.2533	-.2533		$\frac{B}{D} = 1.34$ TO 1
STEP 2	+.7467	-.5920	-.2533	0	$\frac{B}{C} = 2.337$ TO 1	$\frac{A}{B} = 1.261$ TO 1
	+.5920	+.5920	+.5920	+.5920		$\frac{A}{C} = 2.947$ TO 1
STEP 3	+1.3387	0	+.3387	+.5920	$\frac{A}{C} = 3.947$ TO 1	
					$\frac{A}{D} = 2.26$ TO 1	
	-1.3387	-1.3387	-1.3387	-1.3387	$\frac{D}{C} = 1.747$ TO 1	
STEP 3a	0	-1.3387	-1.00	-.7467	$\frac{B}{C} = 1.3387$ TO 1	
					$\frac{C}{D} = 1.3387$ TO 1	
					$\frac{B}{D} = 1.793$ TO 1	

OBVIOUSLY WE WOULD HAVE TWELVE OVERDRIVE RATIOS BY TAKING THE RECIPROCAL OF THE ABOVE RATIOS

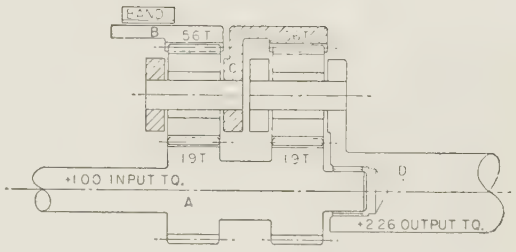

Fig. 5 — Analysis of load-dividing double planetary gear

	A	B	C	D	STEP 4 REDUCTION RATIOS FORWARD	REVERSE
STEP 1	+1.00	$-1.2174 = \frac{28}{23}$	$+.3544 = \frac{28}{79}$	0	$\frac{A}{C} = 2.821$ TO 1	$\frac{B}{C}$ 3.435 TO 1
	-.3544	-.3544	-.3544	-.3544		$\frac{B}{A} = 1.2174$ TO 1
STEP 2	+.6456	-1.5718	0	-.3544	$\frac{B}{D} = 4.435$ TO 1	$\frac{B}{A} = 2.434$ TO 1
	+1.5718	+1.5718	+1.5718	+1.5718		$\frac{A}{D}$ 1.821 TO 1
STEP 3	+2.2174	0	+1.5718	+1.2174	$\frac{A}{C} = 1.410$ TO 1	
					$\frac{A}{D} = 1.821$ TO 1	
	-2.2174	-2.2174	-2.2174	-2.2174	$\frac{C}{D} = 1.291$ TO 1	
STEP 3a	0	-2.2174	-.6456	-1.00	$\frac{B}{C} = 3.435$ TO 1	
					$\frac{B}{D} = 2.2174$ TO 1	
					$\frac{D}{C} = 1.549$ TO 1	

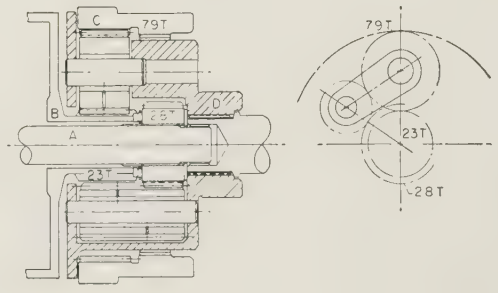

Fig. 6 — Analysis of "Ravigneaux" gear train

The next thing the designer must determine is the number of pinions to use. Less than three pinions are seldom worthwhile unless extreme reduction ratios are required (the two pinion design provides the most space for large pinions and sometimes makes possible otherwise impossible designs). More than three pinions are often used; 4- and 6-pinion planetary gear trains are found in many contemporary automatic transmissions. Today's production machinery has little difficulty in boring the pinion shaft locating holes accurately enough to produce actual load sharing for all pinions.

Simple rules govern the number of teeth in the sun and ring gears and the pinion center locations on the carriers so that all the pinions mesh simultaneously.

First of all, if standard or only slightly modified addendum-dedendum tooth proportions are used, the pinion will not fit at all if the number of teeth in the sun is odd and in the ring is even, or vice versa. They both must be either odd or even. Each simple planetary gear train has a number of places for the pinions where they will fit into the sun gear mesh and the ring gear mesh simultaneously. This number is equal to the sum of the teeth of the sun gear and the ring gear.

Fig. 7 illustrates the "least mesh angle" of a

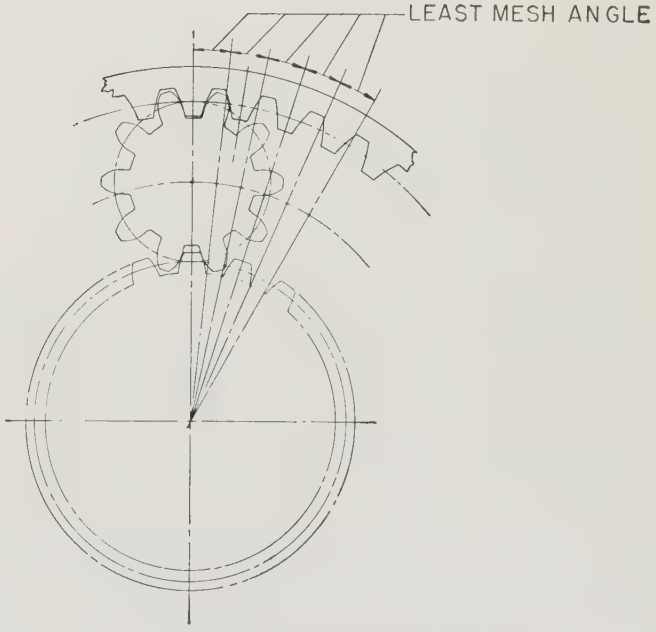

Fig. 7 — Least mesh angle of simple planetary gear

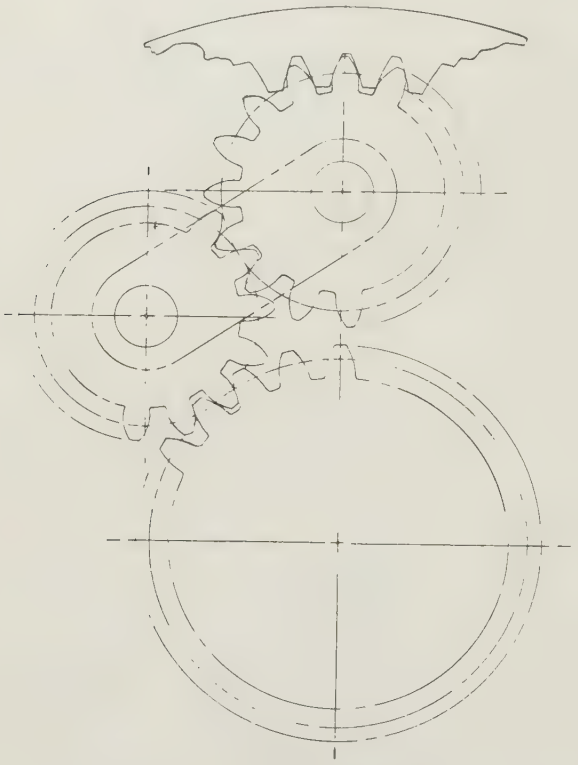

Fig. 8 — Double pinion gearset.

simple planetary set. The pinions must mesh in increments of the least mesh angle in order to assemble both the sun and ring gears.

The least mesh angle for a simple planetary gearset is:

$$\frac{360^\circ}{R+S} \tag{1}$$

where:

R = Number of teeth in ring gear
S = Number of teeth in sun gear

In order to have evenly spaced pinions, the angle between them must equal:

$$\frac{360^\circ}{N} \tag{2}$$

where: N = Number of pinions to be used

Then, for evenly spaced pinions, this angle must be an integral multiple of the least mesh angle, or:

$$\frac{\frac{360^\circ}{N}}{\frac{360^\circ}{R+S}} = \text{Whole number} \tag{3}$$

or:

$$K = \frac{R+S}{N} \tag{4}$$

For a double pinion gearset (Fig. 8):

$$\text{Least mesh angle} = \frac{360^\circ}{R-S} \tag{5}$$

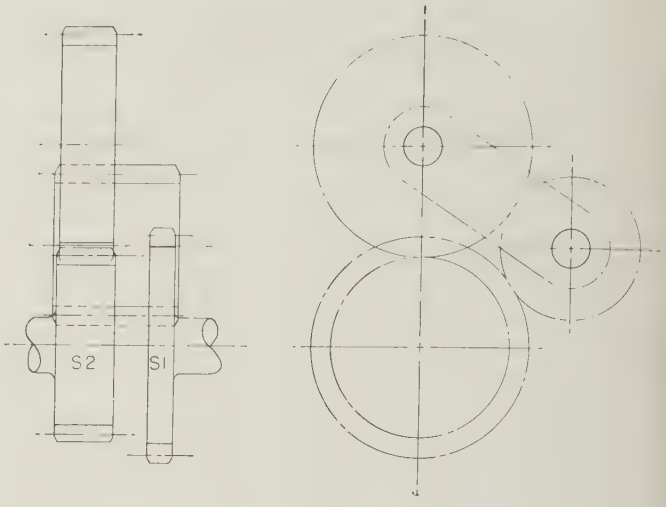

Fig. 9 — Long and short pinion meshing with two sun gears

For evenly spaced pinions whole number:

$$K = \frac{R-S}{N} \tag{6}$$

For a long and short pinion meshing with two sun gears (Fig. 9):

$$\text{Least mesh angle} = \frac{360^\circ}{S_1+S_2} \tag{7}$$

For evenly spaced pinions whole number:

$$K = \frac{S_1+S_2}{N} \tag{8}$$

For a development of the preceding formulae, see Appendix.

The Ravigneaux planetary set with a ring gear mounted to the large pinion (Fig. 4) must meet all of the foregoing formulae. If the requirement for a double sun and a double pinion is met, then the requirement for a simple planetary set is met.

Gear Noise

Quiet operation of planetary gears is near mandatory on today's passenger-car automatic transmissions. Fundamentally, gear noise is caused by the impact of two imperfect involute cams engaging each other in space. The impact is proportional to the degree of imperfections, first of all. This means that there must be accurate tooth spacing, accurate helix angle in the case of most designs today, accurate involute shape (all these must be so after heat-treat), and sufficient tooth overlap to minimize the spacing distortions caused by tooth deflection.

It is also necessary to have accurate parallelism of the meshing gears, especially when helical overlap is a major consideration. Gear center distances must be as nearly right as possible. This is naturally more important in fine pitch gears.

Obviously we are not going to get a 100% score on all of these points.

The first thing to remember is that whatever imperfections we have to inherit in the final product, the noise-making impact is proportional to the

square of the meshing pitch line velocity. Everything else being equal, the greatest single help comes from reduced pitch line velocities. This is the advantage of planetary gears. They offer many choices of designing a gear train for most needs that still give low pitch line velocities and are easier to make quiet in operation.

Helical gear planetary designs which depend on the helix overlap for tooth engagement are often noisier when carrying light loads only. This is caused by slight misalignment of pinions, which tends to cause gear edge loading only, thus losing all help from the helical overlap. Load application on the pinion teeth at both the sun gear and the ring gear contacts will deflect the structure sufficiently in many cases to establish the contact across the face of the gear, thus bringing into full advantage the helical overlap.

Bearing Problems

Planetary gears in most cases are free from any serious bearing problems, but when they do occur, they present some interesting new design considerations.

The needle bearing has come to wide use in the planetary pinions and many bearing companies have gained clear understanding of the problems involved. A relatively flexible long bearing needle trying to roll on a deflected-at-the-middle shaft and also on the inner surface of a rigid pinion bore does not behave like a true roller bearing. High helix angle thrust loads, especially in the larger size pinions, impose a sizeable cocking couple on the bearing that shifts the load to a spiral pattern on the sides of the deflected shaft. The resultant spiral rolling pattern can cause the roller to have a high end thrust that is difficult to cope with.

Helix angle induced end thrusts of both the driving gear and the reaction gear need to be carefully studied for thrust washer design and lubrication.

I would like to pay tribute to the engineers of Torrington Co. who pioneered the needle bearing thrust washer, which has been the biggest aid in many cases of difficult planetary thrust load situations. It has saved many a case of short-life thrust washers in American automatic transmissions as the engines were increased in power, for there was no other way to increase the transmission gear train thrust capacity.

Heavy-duty, high-horsepower, and especially high-speed planetary gear designs have revealed some bearing problems that ordinarily do not plague the automatic transmission designers for passenger cars.

When the planet carrier increases in size or speed, the centrifugal force on the pinions becomes a problem. At the same time, the centrifugal force on the pinion bearing rollers becomes a problem. The bearing load pattern shifts toward the underneath portion of the pinion shaft, aggravating the centrifugal misbehavior of the bearing rollers or needles. Fig. 10 shows a case where the centrifugal load on the pinion is nearly equal to the tooth loads on the pinion.

At the underneath of the shaft where the bearing load is carried, the rollers are loaded and rotate as bearing rollers should. There is no clearance between the pinion bore, the rollers, and the shaft.

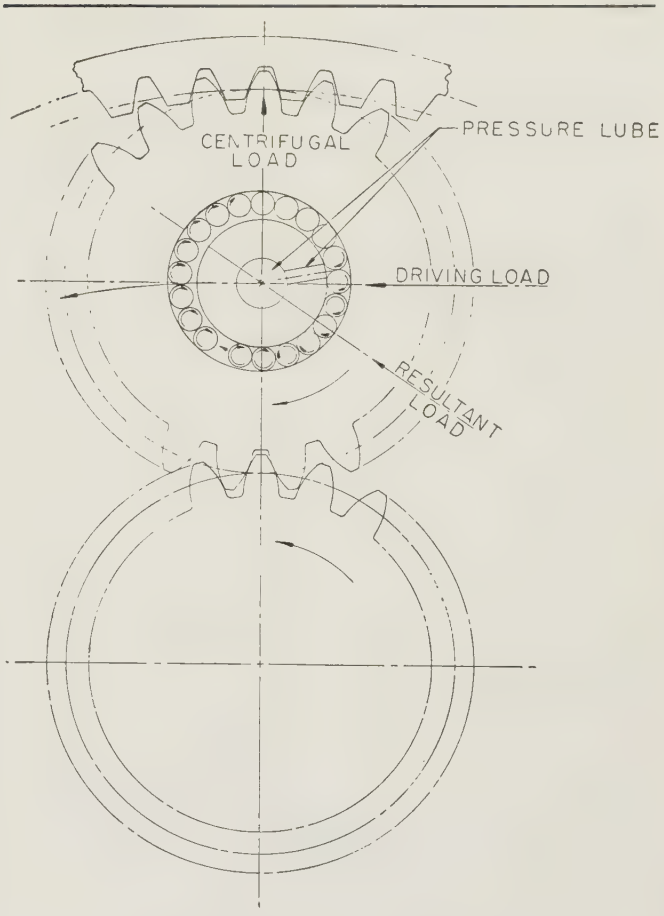

Fig. 10 — Centrifugal load on pinion gear

The maximum clearance now exists near the top opposite the combined load point, and the actual side clearances increase toward this point on both sides. As the rollers roll out of the loaded spot, the centrifugal force due to high carrier speed tends to expedite their travel toward the top and retard their travel back down again on the other side. The entire stack of rollers tends to accumulate tightly packed against each other at the top side and then tend to lose their private rotational speed because of the side friction of the neighboring rollers.

The rollers, tightly packed, are forced into bearing contact down below one at a time; and when they have to enter the actual working part of the path, they need to be reaccelerated to full rotational speed of the roller bearing action all at once. It is very much like a jet landing on the landing strip and yanking the wheels to speed at the wheel contact point.

Plenty of cooling oil fed to the bearing may save the day. However, I had to work out a tank transmission design once where nothing that we could do was enough. A special roller retainer to stop the side-by-side friction had to be developed. This retainer had to be designed as a plain bearing, running on the pinion bore to sustain its own centrifugal force without crowding the rollers. It finally lived after proper lubrication for this plain bearing surface had been developed.

Gas turbine reduction gears offer plenty of similar

situations. In the automotive gas turbine applications it isn't easy to tame down a 30,000-rpm, 300-hp turbine shaft so that you can get a hold of it to make it drive the car and do this quietly. Side-by-side gearing invariably leads into pitch line velocities that are extremely difficult to handle quietly.

We had this problem recently and tackled it with a first-stage planetary gear of 5.6/1 reduction (Fig. 11).

The input gear was as small as possible for a minimum respectable number of teeth (15). Twenty pitch helical gears were used to balance the turbine thrust and to give a pitch diameter of about 0.75 in. This resulted in an acting pitch line velocity of 4680 fpm, which isn't too far from the upper limit of passenger-car automatic transmission figures. Small carrier size and not much over 5000-rpm speed kept the centrifugal forces of the pinions and bearing needles within reasonable bounds. Moderate oil flow introduced to the shaft centers proved satisfactory for the bearing life.

It is interesting to note, however, that we really had to go all out to cool the input gear. Two per cent of the 300 hp was just too many Btu's to radiate out of this already hot shaft. We had to pass almost a gallon of oil per minute through the input gear to make it live.

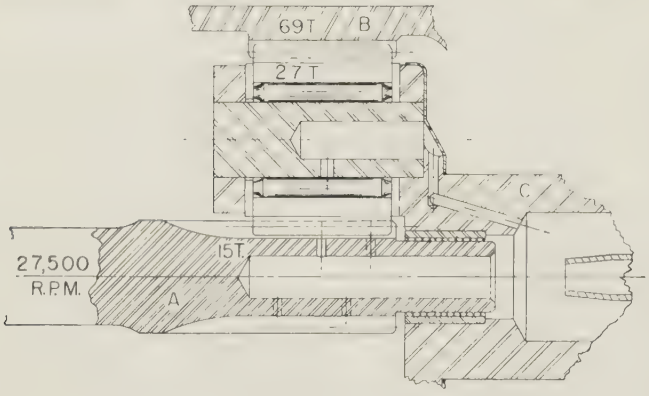

Fig. 11 — First-stage planetary gear of 5.6/1 reduction

Torque Requirements

As planetary gears are most frequently used in power shifted transmissions, let us discuss the design of friction elements for ratio changing.

Assuming that the output speed does not change during the shift, the clutching action for shifting into 1/1 drive, must absorb the difference in the kinetic energy of the engine, plus the engine torque multiplied by the lost engine revolutions during the shift. During a smooth shift the engine speed does not change instantaneously. A time element of, let us say, 1 sec is allowed to slow the engine down to the new speed. During the shift interval the engine speed averages halfway between high and low, and it is this speed minus the output speed that equals the lost revolutions during the shift. The Btu's ab-

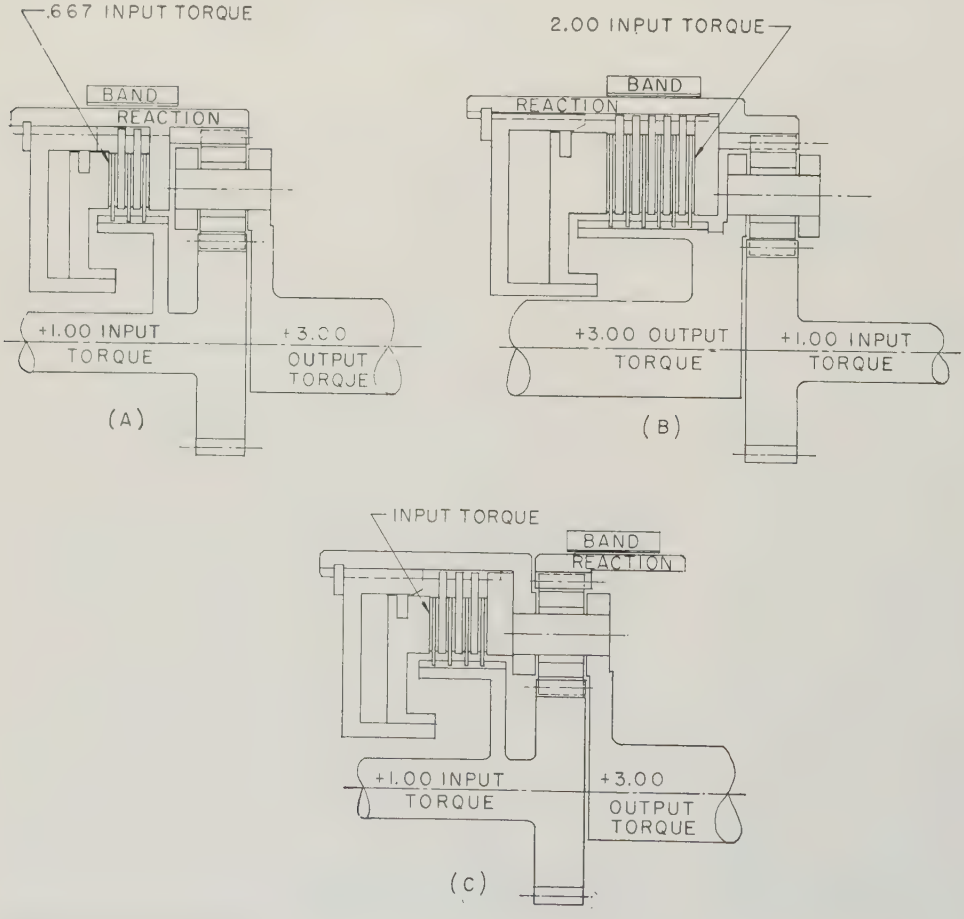

Fig. 12 — Clutch positions in gear train

sorbed during a shift are the same regardless of where the clutch is placed in the gear train. This is true because of the inverse speed and torque relationship.

The one rule to remember in determining torque requirements of the clutch in its positioning within the gear system is that the clutch torque is in inverse proportion to the speed difference between the clutched elements.

The torque capacity of the clutch is, therefore, determined by the inertia of the powerplant and its connected masses and the clutch's share of the driving torque under which the shift is to be made. The torque capacity of the clutch should be limited so that the inertia torque impulse $I \times \alpha$ imposed on the powerplant during the shift will not be greater than one-third or one-fourth of the powerplant output torque, otherwise the shift will be "rough," meaning that the transmission output shaft will feel a momentary overtorque during the shift that leaves the driver with an unpleasant shift feel.

Fig. 12 shows different clutch positions in the gear train. Using the rule that the clutch torque is in inverse proportion to the speed difference between clutched elements, we have these simple relationships:

Clutch Connection	Clutch Torque
Input to reaction	$\left(\frac{\text{Torque Ratio} - 1}{\text{Torque Ratio}}\right)$ input torque
Output to reaction	(Torque Ratio – 1) input torque
Input to output	Input torque

For a simple planetary set having a torque reduction of 3/1, a clutch between the input and reaction member requires 0.667 times input torque; whereas a clutch between reaction and output requires two times input torque or three times as much torque capacity. The amount of heat dissipated would be the same in a given shift time for either clutch.

A large torque capacity clutch requires more plates, a larger apply force, larger plates, or some combination of these.

From the foregoing discussion we can conclude that the preferred location for a clutch in an underdrive gear train is between the input and forward reaction member.

The reaction member of a planetary gearset is generally held to the ground member, usually the transmission case, by a brake band. Where the band is used in conjunction with a gearset lockup

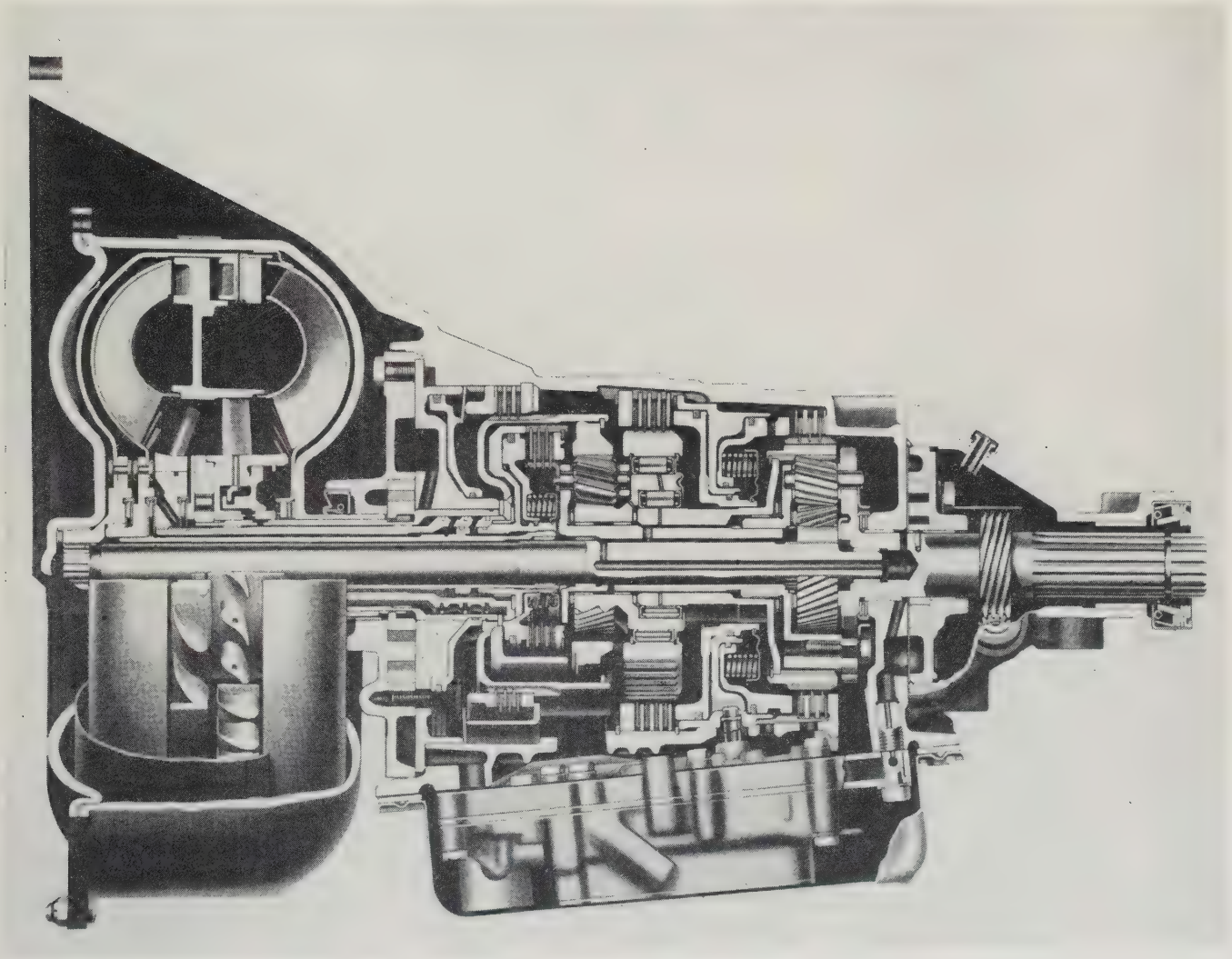

Fig. 13 — Chevrolet Turboglide transmission

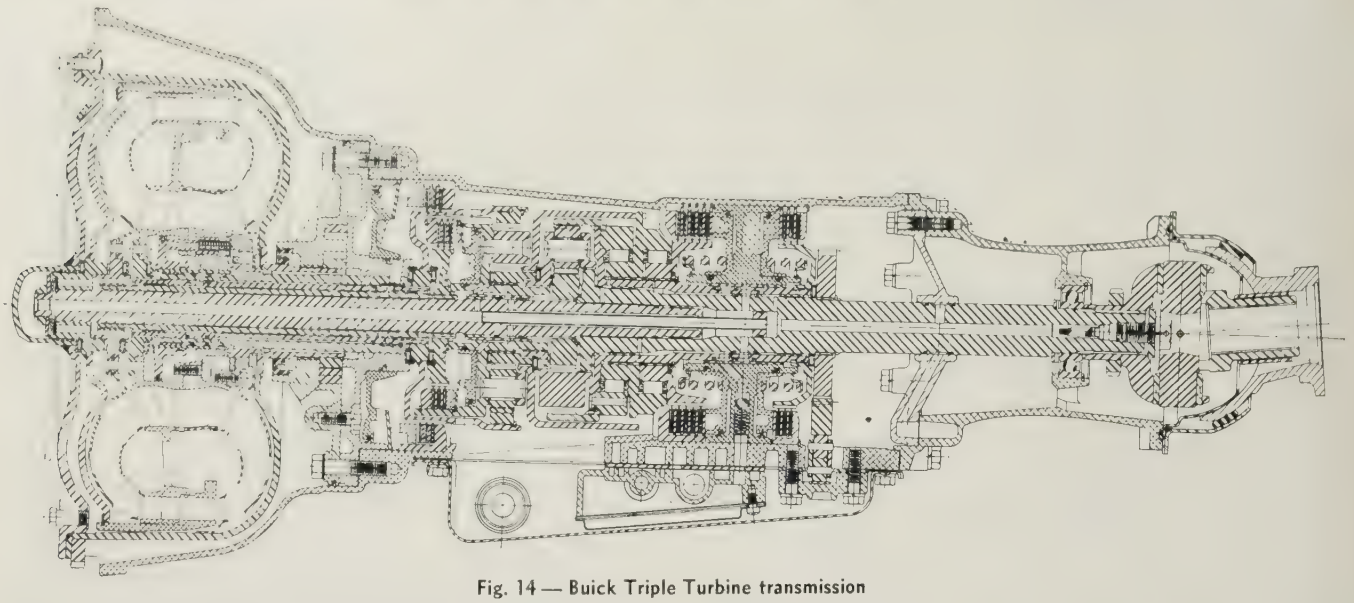

Fig. 14 — Buick Triple Turbine transmission

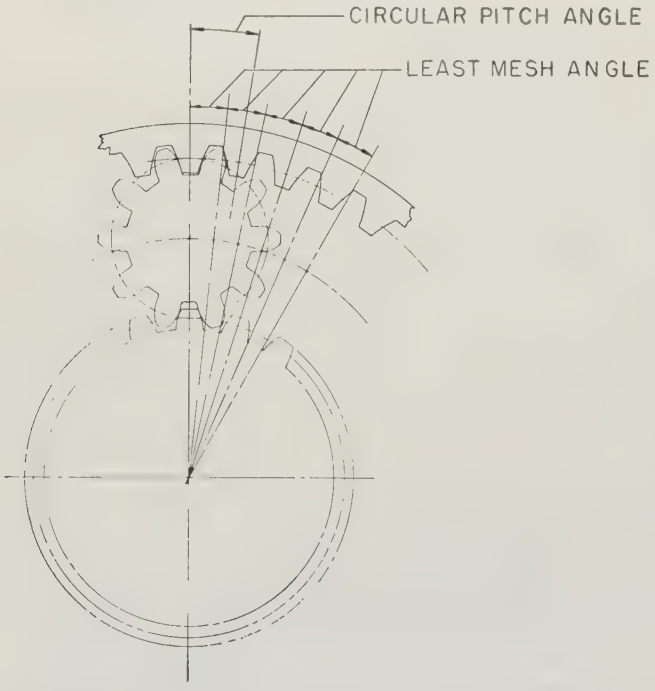

Fig. 15 — Simple planetary gearset

clutch, its release must be so timed with the clutch application that there will be a minimum of "dog fight" and still prevent "runaway" where both friction elements are momentarily off, thus permitting the powerplant to "spin up." A wrong timing of the friction elements as outlined above will result in unpleasant shift feel. When downshifting back onto the band, the timing should be such that the band is applied at the point where the reaction member is just ready to reverse its rotation. A late application of the band will cause the brake drum to spin backward with a consequent increase in friction, which results in increased heat and wear for the brake lining. This condition also results in an unpleasant shift feel. A double wrap band has been helpful in providing better timed band to clutch power shifts. It is less sensitive to mistiming on the upshift and thus minimizes "dog fight" as it wants to unwrap in the non-energized direction. It is more effective in the energized direction than a single wrap band and can, therefore, be applied with less force permitting better timing for application on the downshift.

In recent years the free-wheel unit has found wide application as a means for grounding the reaction member. It is a "natural" for perfect timing with the gearset lockup clutch for power shifting either up or down.

The free-wheel unit which is a one-way clutch has permitted the exploitation of the planetary set to where it has made possible a broad torque range nonshifting multiturbine torque converter transmission, as exemplified by the Buick Triple Turbine and the Chevrolet Turboglide automatic transmissions (Figs. 13 and 14).

APPENDIX

Spacing the Planets

In order to begin the design of the planet carrier, it is necessary to determine the number of planets and their spacing. The number of planets is determined from stress evaluation. The spacing is a function of the number of pinions and the number of teeth in the gears mating with the pinions. The spacing analysis and formulae will be shown for the three most common gearsets and the method can be used to derive the spacing for any arrangement of planetary gears.

Fig. 15 shows a simple planetary gearset. In considering the gearset, we assume that a single pinion is meshed with the sun gear and ring gear. It is desired to find the smallest angle between the meshing positions of the pinion as we lift it out of mesh with the gears and move it around the sun gear. It can be seen by inspection that the smallest

angle is found by pulling the pinion out of mesh with the ring gear and rotating while still in mesh with the sun gear teeth until it meshes with the ring gear again. Since the planet teeth turn about the center of the planet pinion, the size of this "least mesh angle" is affected by the direction of rotation of the planet as we turn the carrier around the sun. The fact that the planet turns in the same direction as the carrier when we turn the carrier around the sun gear makes the least mesh angle of the simple planetary gearset quite small. This analysis assumes for the convenience of calculation that the ring gear turns one tooth or one circular pitch and the angle through which the carrier moves is the angle required to move from one tooth to another on the ring gear (Fig. 16).

$$\angle POA' = \frac{360^\circ}{R}$$

$$\angle AOB + \angle A'OB' = \angle POA'$$

but: $\angle A'OB' = \angle AOB\left(\frac{S}{R}\right)$ since: $A'B' = AB$

$$\angle AOB + \angle AOB\left(\frac{S}{R}\right) = \angle POA' = \frac{360^\circ}{R}$$

$$\angle AOB\left(1 + \frac{S}{R}\right) = \frac{360^\circ}{R}$$

$$\angle AOB = \left(\frac{R+S}{R}\right) = \frac{360^\circ}{R}$$

$$\angle AOB = \frac{360^\circ}{R+S}$$

where:

R = Number of teeth in ring gear
S = Number of teeth in sun gear

Having found the least mesh angle ($\angle$ AOB), the pinions must be meshed in increments of this angle in order to assemble both the ring and sun gears. Failure to space the pinions accordingly will result in gears that will not assemble.

In order to have evenly spaced pinions, the angle between them must equal 360 deg/N, where N is the number of pinions to be used. If the pinions can be evenly spaced, then this angle must be an integral multiple of the least mesh angle, or:

$$\frac{\frac{360^\circ}{N}}{\frac{360^\circ}{R+S}} = \text{Whole number}$$

$$\frac{R+S}{N} = \text{Whole number} = K$$

For a double pinion gearset (Fig. 17):

$$\angle AOB = \angle POB'$$

$$\angle POA' = \frac{360^\circ}{R}$$

$$\angle POA' = \angle POB' - \angle A'OB'$$

$$\frac{360^\circ}{R} = \angle AOB - \angle AOB\left(\frac{S}{R}\right)$$

$$\angle A'OB' = \angle AOB\left(\frac{S}{R}\right)$$

$$\frac{360^\circ}{R} = \angle AOB\left(\frac{R-S}{R}\right)$$

$$\angle AOB = \frac{360^\circ}{R-S}$$

Evenly spaced pinions:

$$\frac{\frac{360^\circ}{N}}{\frac{360^\circ}{R-S}} = \text{Whole number} = K$$

And:

$$K = \frac{R-S}{N}$$

The next example will derive the spacing for a

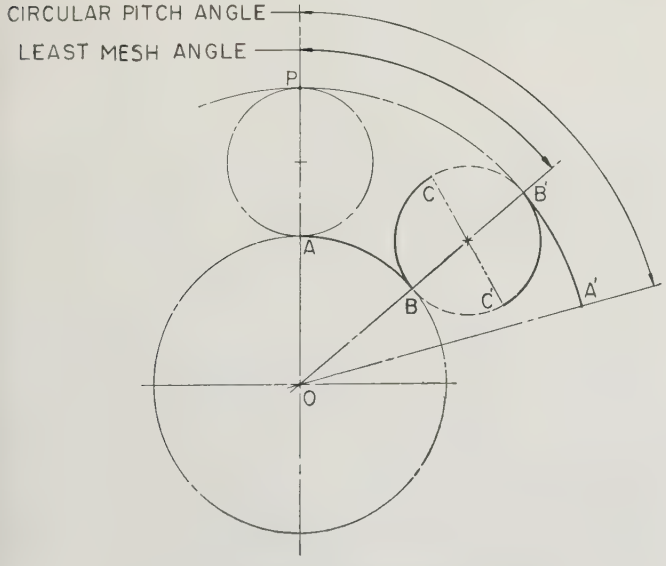

Fig. 16 — Analysis of simple planetary gearset

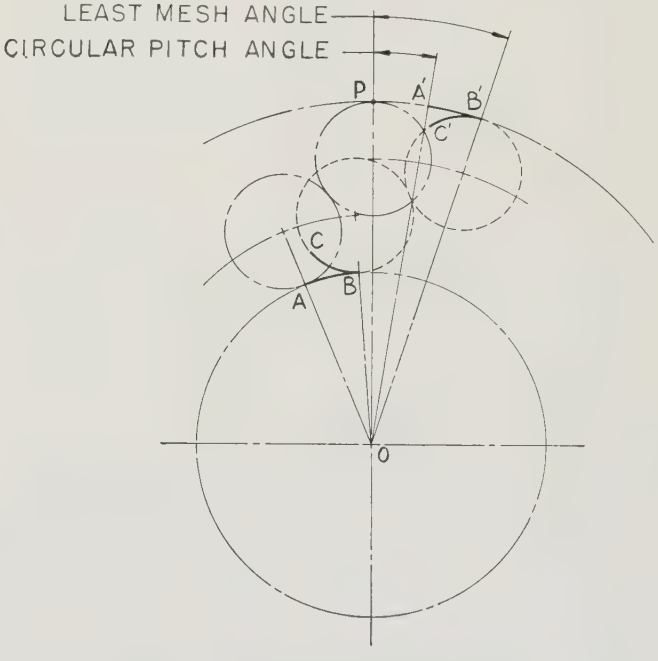

Fig. 17 — Analysis of double pinion gearset

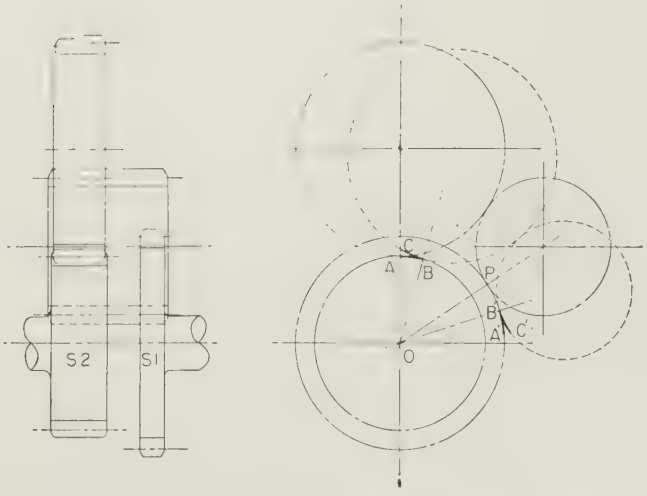

Fig. 18 — Analysis of long and short pinion meshing with two sun gears

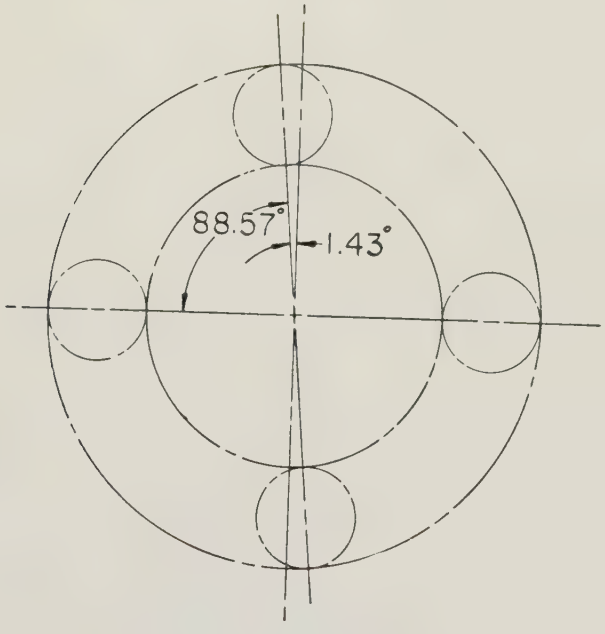

Fig. 19 — Spacing of pinions on Buick Dynaflow torque converter gearset

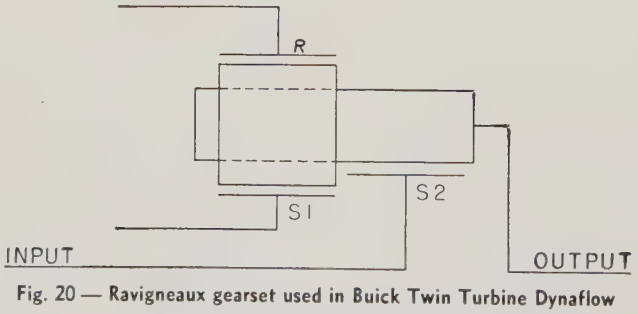

Fig. 20 — Ravigneaux gearset used in Buick Twin Turbine Dynaflow

long and short pinion meshing with two sun gears (Fig. 18):

$$\angle POA' = \frac{360^\circ}{S_1} = \angle POB' + \angle A'OB'$$

$$\text{but } \angle POB' = \angle AOB$$

$$\text{and } \angle A'OB' = \angle AOB\left(\frac{S_2}{S_1}\right)$$

$$\therefore \frac{360^\circ}{S_1} = \angle AOB + \angle AOB\left(\frac{S_2}{S_1}\right)$$

$$= \angle AOB\left(\frac{S_1 + S_2}{S_1}\right)$$

$$\therefore \angle AOB = \frac{360^\circ}{S_1 + S_2}$$

where:

S_1 and S_2 = Number of teeth in sun gears

And for even spacing:

$$\frac{\frac{360^\circ}{N}}{\frac{360^\circ}{S_1 + S_2}} = K$$

And:

$$K = \frac{S_1 + S_2}{N}$$

Let us examine some commercial examples to illustrate the use of these relationships.

1. Buick Dynaflow torque converter gearset (Fig. 19).

Ring gear teeth = $R = 79$
Sun gear teeth = $S = 47$
No. of pinions = 4

$$K = \frac{R + S}{N} = \frac{79 + 47}{4} = \frac{126}{4} = 31.5$$

The resultant K is not an integer and the pinions cannot be evenly spaced.

$$\text{Least mesh angle} = \frac{360^\circ}{R + S}$$

$$= \frac{360^\circ}{126}$$

$$= 2.857143^\circ$$

It should be noted that two pinions can be placed opposite to one another, since two pinions can be equally spaced from our formula:

$$K = \frac{R + S}{N} = \frac{79 + 47}{2} = 63$$

Since the four pinions cannot be equally spaced, the number of "least mesh angles" between the two opposite pinions is an odd number. Therefore, we can arrive at the spacing by subtracting one-half of the least mesh angle from 90 deg or by multiplying the least mesh angle by whatever integer which makes the product nearly 90 deg. In the example shown, these angles are 1.42857 and 88.571433 deg (equals 31 times 2.857143 deg), respectively.

2. The Ravigneaux gearset used in the Buick Twin Turbine Dynaflow (Fig. 20).

The front gears form a simple planetary gearset:

$$\frac{R + S_1}{N} = \frac{79 + 23}{3} = 37$$

The pinions can be evenly spaced considered from the simple planetary viewpoint. The rear sun gear (S_2), the two pinions, and the ring gear form a double pinion gearset:

$$\frac{R - S_2}{N} = \frac{79 - 28}{3} = 17$$

This again will permit even spacing.

The two sun gears and the pinions form another gearset which must be considered:

$$\frac{S_1 + S_2}{N} = \frac{23 + 28}{3} = 17$$

This also meets the requirements.

The above gearset illustrates how the tooth numbers in a single gearset may require checking for planet spacing in several different arrangements before we are sure that the unit will assemble without interference.

Thrust Considerations

Because of the high tangential loads usually encountered in planetary gearsets, high thrust loads result where helical gears are used. Thrust loads on the order of 4000–4500 lb at stall are not uncommon in automotive practice. In the case of converter-type transmissions, these thrust loads fall off quite rapidly when the vehicle is in motion, but are still substantial.

The preparation of surfaces for thrust washers or bearings to run against and the cost of the washers themselves can become a substantial part of the total cost of the unit. Each thrust surface contributes to the parasitic losses within the unit: therefore, a careful analysis should be made of the thrust forces within the complete system to determine the minimum number of thrust washers or bearings required. Normal practice is to contain the thrust of the planetary set within the gearset, as the thrust load is equal and opposite between an internal and sun gear. Coast thrusts, where they exist, being opposite in direction to drive thrusts, must be considered in the tolerance stack-up within the unit so that adequate clearance is provided for relative movement of the parts.

A coefficient of friction of 0.015 is used on bronze or babbit-type thrust washers for P-V values up to 125,000 and a well-lubricated surface. With higher unit pressures and speeds, the coefficient of friction will reach 0.04. The P-V value limit for a high-density high-leaded bronze washer is 900,000[1] (psi × fpm). For values over this, an antifriction bearing of the needle or ball-type is required. Quite often for many thrust applications where service is not severe, various nonmetallic washers can be used to a good cost advantage.

Gear Stress Evaluation

Where there is no shock loading of gear teeth, gear tooth bending stresses may be 30–50% higher than where ratio changes are accomplished by automatically applied friction-type clutches. For example, a nonshifting converter-type transmission such as used in some automobiles will operate satisfactorily with Almen and Straub bending tooth stresses of 100,000–125,000 psi for low gears that are in the normal operation of the transmission. For reverse gear and where low gear is used only for emergency conditions, gear tooth bending stresses may range between 150,000 and 175,000 psi.

Lower stressed gears are required on power-shift-type gearsets where the $I\alpha$ torque value of the powerplant, determined by the capacity of the clutch and the inertia of the clutched members, is mechanically imposed on the gearset in addition to the regular torque value of the power unit. This is generally kept to one-third of the normal torque value. (See discussion of friction element design.) This sudden "overtorque" adds to the fatigue of the transmitting members and must be considered by strengthening the members involved.

For the bending stress values given above, compressive tooth stresses will be sufficiently low to avoid scuffing or pitting when the operating pressure angle is 23 deg maximum and when the internal gear has a Brinell hardness range of 241–302 and the sun and pinion gears have a thin case (0.008–0.025) of R_C 50 to 60 in such steels as SAE 5140H, 5160, 4063, 1330, or 8620. Internal gears may be made of preheat-treated steels or castings such as the pearlitic-malleable type.

For balanced design, gear teeth are modified to balance the bending stress between the sun and pinion. This is done by spreading operating centers (increasing the operating pressure angle) or by increasing the addendum of the pinion, where the pinion is smaller than the sun gear, with a corresponding decrease on the sun gear (increases tooth thickness of the pinion), or, a combination of both.

The limiting condition for modification would be 23-deg operating pressure angle and a contact ratio of at least 1.25.

For a multipinion planetary set (three or more) a good example of tooth modification would be a Lewis form factor of 0.024 on the pinion and 0.026 on the sun gear. The sun gear tooth is slightly stronger to withstand the greater number of tooth loadings per cycle.

[1] Recommended limit for passenger-car automatic transmission type service.

DISCUSSION

Various Factors in Use Of Planetary Gearing

— B. W. Cartwright
Chrysler Corp.

THAT AUTOMATIC TRANSMISSIONS have found widespread acceptance by the motoring public is shown by recent figures which indicate that approximately 80% of all passenger cars sold are now so equipped. The success of these units, which has been acclaimed as the most outstanding automotive achievement in the past 20 years, has taken place even though automatically controlled transmissions have several important disadvantages — increased cost, weight, size, and poorer efficiency as compared to the manually controlled type. The major reason for public approval lies in the fact that, as the name indicates, these transmissions are "automatic" and require practically no

effort on the part of the operator, thus lessening driving fatigue and leaving him free to concentrate on other driving functions. In several units, only the touch of a button is required to place the vehicle in the "drive" range, and the driver is not required to use the transmission controls again until reverse, neutral, or coast range is desired.

This popular acceptance of the automatic transmission has led to a corresponding increase in the use of planetary gearing. In fact, it is the only type of gearing used for passenger-car automatic transmissions. The outstanding reason why planetary gears are preferred above all others for this application is that they lend themselves far more readily to power shifting. The application and release of hydraulically actuated friction elements is all that is required to accomplish a ratio change. There is no need for axial shifting of gears with the resultant gear clash and synchronizer problems.

The major disadvantage of planetary gearing lies in its cost. A manually operated planetary transmission would be more expensive than its countershaft complement.

Simple planetary gear trains are used in both of Chrysler's automatic transmissions. This factor, together with the selection of the same number of teeth for both front and rear sets of the compound trains, has made possible widespread interchangeability between planet pinion, planet pinion carriers, and other associated parts. These cost advantages, which also include the use of aluminum for the planet pinion carriers, are not normally possible with Ravigneaux compound planetary gears.

As Mr. Kelley suggests, the stresses on internal gears are usually quite low and permit consideration of more economical materials such as pearlitic malleable iron. When the service life requirements are low, such as for reverse, this material may be used without subsequent heat-treatment. However, our experience has shown that for forward-drive applications, a Rockwell hardness of 50 c is necessary to prevent wear and spauling. Both flame and induction hardening were tried, but in all cases, the resulting distortion was so great that the gears were excessively noisy and impractical for volume production. These gears had vertical flange sections which prevented uniform heat treatment. However, it is possible that annulus gears made in tubular sections without the flange would be satisfactory.

The method described in the paper for exploring the ratio possibilities of planetary gear systems is the one most widely used today by transmission engineers and it should always be used for compound trains.

Power shifting of a planetary transmission must be accomplished smoothly if the operation is to be considered satisfactory by today's standards. During the power upshift, however, a disturbance in output shaft torque is unavoidable and good shift quality is obtainable only by precise control of friction element capacity during the transition period. During power downshifts, a disturbance in output shaft torque is again unavoidable because the transmission must be placed in a neutral or near neutral condition to permit the engine to accelerate to a speed compatible with the lower ratio. The Chevrolet Turboglide and the Buick Flight-pitch transmissions are testimonials of the extent to which some transmission designers are willing to go to avoid the problems of power shifting.

The planet pinion needle bearing generally receives well-deserved attention; however, other bearings in the gear train are also deserving of consideration.

These bearings which support the rotating parts and maintain alignment are often overlooked because of the inherent balanced nature of planetary gearing. Life problems on support bearings become particularly severe in units which use brake bands as reaction members. In these units, the side loads produced by the bands deflect the brake drums, thus causing the problems of misalignment and concentricity to be accentuated. If sufficient backlash is not provided in gear trains where deflection cannot be controlled, a condition of "tight gear mesh" occurs and it results in increased noise and in reduced gear and needle bearing life.

The questions which I have are with respect to 4- and 6-pinion simple planetary gear trains. How effective are the extra pinions as to load-carrying ability? Also, if two units were being designed to the same torque capacity, one with three pinions and the other with six, which would be expected to be the most expensive?

Comments on Equal and Unequal Spacing of Gear Teeth

— H. W. Simpson
Consultant, Planetary Transmissions

THE SIMPLE METHOD described for determining the position of unequally spaced planets can save a designer a lot of figuring.

The question arises, why have unequal spacing involving odd angles, when it is so easy to obtain equal spacing? Equal spacing can always be obtained by slight changes in the number of teeth without appreciably changing the gear ratio or diameter of the gears.

I am sure Buick engineers had a very good reason for the spacing converter gearset shown in Fig. 19. Mr. Kelley states that in the case of the Buick Dynaflow converter gears, the space limitation was a factor.

With equally spaced planets and with the sun and ring each divisible by the number of planets, the instant at which any one tooth starts to engage another is the same for each planet.

If the teeth are not divisible by the number of planets but still equally spaced, this uniform timing is broken up when three planets are used, but with four planets each pair has one planet meshing in harmony with the other. If then, in addition, the planet spacing is unequal (as in Fig. 19) the engagement pattern is scrambled still more.

In view of the above, I have followed the practice of using three planets with even spacing, but with the number of teeth in the sun and ring not divisible by three. Where diameters must be kept small, four or more planets, of course, must be used. Would Mr. Kelley give us his views on this?

Does unequal spacing of planets reduce harmonic vibrations and, therefore, noise in high-speed planetaries?

I am glad Mr. Kelley brings out the fact that the horsepower at the tooth meshes of planetary gearing is much less than the actual horsepower being transmitted, and that tooth losses are, therefore, correspondingly less. This makes it possible to put a lot of power through a comparatively small set of gears.

The simple formula which he gives for comparing losses in gear trains is admirable for simple gear trains, but may be confusing for regenerative trains such as the Chrysler Powerflite low gear or for gear train like the Fordomatic in second speed, where tooth loads are not the same at all four meshes.

The system I have used in such cases is to assume an input of one unit of torque at 100 rpm, determine the corresponding torque and rpm at each gear mesh, and then multiply them together. This gives the horsepower at each mesh in per cent of input power. Then by adding these for all the meshes in the transmission you get a figure which permits comparison of tooth losses in other transmissions.

For instance, the sum of the horsepowers for a countershaft transmission would be 200% of input. In comparison, the figure for Chrysler TorqueFlite in second gear is 62%, and for the Hydramatic in third speed is 71% of input. In other words, the total horsepower at the working meshes is only 71% of the horsepower which would occur at a single tooth mesh if there were no planetary action.

Mr. Kelley makes no mention of variations in the coefficient of friction when tooth speed is reduced. I have seen data which show the coefficient reduced somewhat when tooth speed went down but doubt if it was based on actual test data. Can Mr. Kelley give us more information on this aspect?

WHAT'S NEW in

Brake Linings

N. H. McCuen, Chevrolet Motor Division, General Motors Corp.

This paper was presented at the SAE Annual Meeting, Detroit, Jan. 14, 1959.

THE DEVELOPMENT of brake linings capable of meeting all the requirements of the progressive American passenger cars is one of the most pressing problems of automotive engineering. Great effort is expended annually by the automobile industry to develop the most effective braking systems possible. It is in the development of improved linings that the greatest effort is being made. Millions of dollars are spent on experimental engineering, and millions of miles of brakes tests are made each year to produce efficient, dependable brake linings.

There are numerous brake designs currently being carried on in the industry, both here and abroad. These engineering designs cover disc-type, band-type, water-cooled, and oil-immersed brake systems. However, regardless of the brake design under discussion, a review of friction materials today is essentially a study of two linings — the organic type and the metallic type. Therefore, this paper will restrict its subject matter to these two basic lining materials.

To be acceptable to the automobile manufacturers, present-day linings must have the following characteristics:

1. Wearing ability — Without sacrificing any other attributes, a brake lining must have a low wear rate.
2. Minimal friction variations — Brake linings

A COMPARISON of the capabilities and weaknesses of organic and metal linings shows that neither is completely satisfactory. The author analyzes advantages and disadvantages of both.

Organic linings are more than equal to the demands of average daily driving. The metallics are equal to demands of "heat problem" braking of police cars, sports cars, and other vehicles subjected to high-speed, prolonged deceleration.

The author believes that the competition between organic and metallic friction materials will produce the effective brake lining of the future.

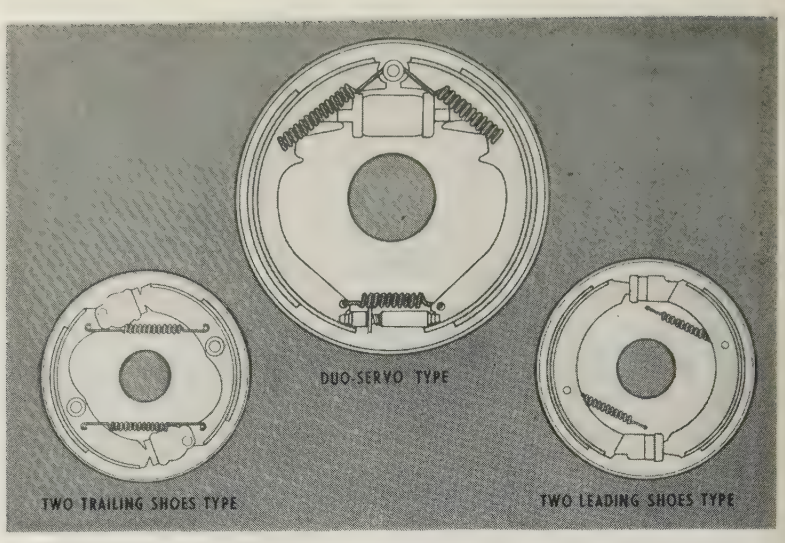

Fig. 1 — Basic brake designs

must have a high coefficient of friction that is equal at all four wheels and consistent on all cars to prevent pull, "grabbiness," or other erratic braking conditions.

3. Resistance to high temperature and fading — Linings must be capable of withstanding and dissipating heat to prevent brake fade, which is a temporary reduction of brake effectiveness resulting from heat, and linings must have adequate mechanical strength through all operating temperatures.

4. Lining surface must be compatible with mating surface to prevent galling, excessive wear, or heat checking of the drums.

5. Consistency of performance in all braking systems — The majority of cars are still equipped with unassisted brake systems. Therefore, brake linings must engage smoothly with low effort and operate effectively with both standard and power brakes.

6. Quietness of operation — Quietly operating brakes are an important comfort factor in passenger cars; therefore, lining and drum engagement sounds must stay below the audible level.

7. Low cost — In this era of cost-conscious engineering, it is essential that the expenditures for brake lining fabrication and warranty servicing be controlled.

For purposes of clarity, all data presented herein apply to a drum-and-shoe brake of the duo-servo type. The two other drum-and-shoe brake designs generally employed are the two-leading-shoe type and two-trailing-shoe type. (See Fig. 1). There is also a one-leading-one-trailing-shoe type in general use which is not shown.

Organic Brake Linings

All American passenger cars use organic brake linings. There are two organic linings which are classified by their method of fabrication. Organic dry mix is basically a gray-white compound of asbestos, filler materials, and powdered resins which is thoroughly mixed, preformed to shape, and placed under heat and pressure until it forms a hard, slate-like board. Then it is cut and bent into individual arcuate segments and attached to the shoe.

Organic wet mix is a compound of asbestos, organic fillers, and liquid resins that has a gray-brown color when blended. The compound is processed by any of several different methods which include high-pressure extruding, screw extruding, calendering, and other processes.

Organic linings are generally composed of six basic ingredients:

1. Asbestos, with its high heat resistance and high coefficient of friction in contact with iron and steel, is the basic material.
2. Friction modifiers, such as the oil of the cashew nut shell, give linings desired friction qualities.
3. Fillers are a wide variety of materials, such as rubber scrap, which are added to linings to control noise, wear, or other brake characteristics.
4. Curing agents and/or accelerators are added to a lining compound to produce required chemical reactions in the ingredients.
5. Materials for special effects are added to compounds to improve overall braking performance. They include powdered lead, brass chips, and aluminum powders.
6. Binders, which are predominantly phenolic resins, hold all the other ingredients together and are selected to govern the physical strength of the material at high temperatures.

Organic brake linings have several distinct and important characteristics, regardless of how they are compounded:

1. The fabricating cost is low in general.
2. A high initial friction is inherent with organic linings, along with a light pedal effort which hardens with usage.
3. They vary only slightly in effectivenes with speed.
4. They show a moderate change in effectiveness with temperature.
5. Organics do not have a buildup at end of stops.
6. They protect themselves from heat damage by fading at high temperatures.
7. Organic linings do not require extremely

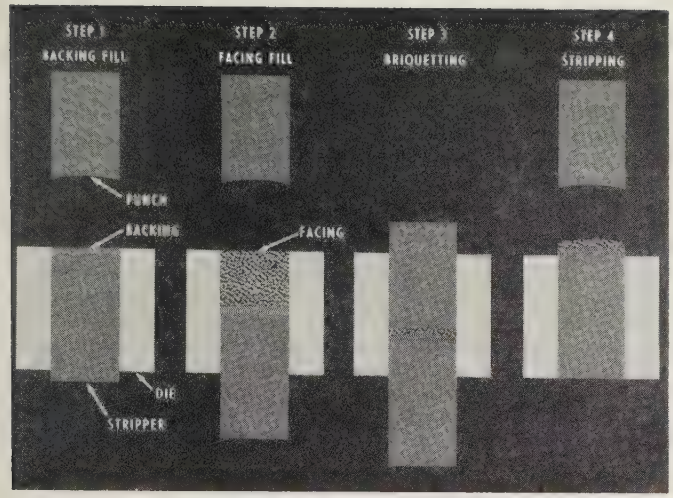

Fig. 2 — Metallic-lining briquetting process

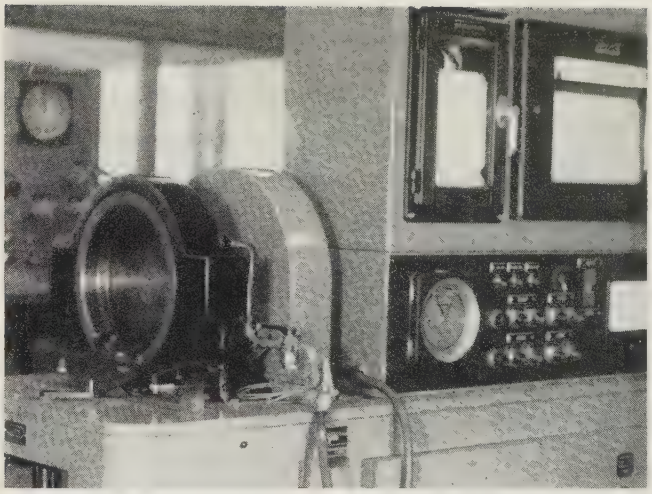

Fig. 3 — Chase friction machine

smooth lining facing or drum finishes (60–150 micro-in. range permissible on drums), but organic surfaces are sensitive to moisture and contaminants.

Metallic Brake Linings

The other lining compound under wide development is the sintered metallic type. Metallic linings represent the most important new development in brake lining.

Metallic linings are composed of finely powdered iron or copper, graphite, and lesser amounts of inorganic fillers and friction modifiers. The dry powders are accurately weighed, placed in a sifter in a specific order, and mixed in a tumbling cone type blender for 30–50 min. A lubricating oil is added to prevent segregation of the individual ingredients which are of different sizes and densities.

The powders are then put through a briquetting process in which the backing and friction material powders are compressed between a punch and a stripper to form the lining. In the first step, the stripper is lowered slightly and the powder that forms the backing of the lining is poured into a cavity, as shown in the schematic drawing in Fig. 2. The stripper is lowered again and the lining facing powder is poured into the cavity. Then, the powders are compacted under high pressures. During the briquetting stroke the two layers of powder are pressed into an integral unit with green strength. The briquettes then are automatically conveyed into a furnace and sintered in temperatures well over 1000 F. The furnace creates exothermic atmosphere generated from 1000 Btu natural gas that protects linings from oxidation. This heat-treatment forms sintered bonds between particles that give linings great strength and durability. The manufacture of metallic linings is highly automatic, a fact that will lead to more competitive pricing as production increases.

Present-day metallic linings have several distinct and important characteristics:

1. In comparison with organic linings, the metallics are relatively high cost. At present, the cost factor is one reason the application of metallic linings is restricted to the "heat-problem" brakes.
2. Metallic linings have a low initial friction, and a resultant hard pedal that lightens with usage.
3. They have reduced effectiveness at low speeds and temperatures.
4. They are extremely heat and fade resistant.
5. Only slight roughness is detectable at high speeds with metallics.
6. Metallics are not affected by wetness.
7. They do require a smooth facing grind and drum finish. The metallic-lining brake drum has a mirror-like finish with a uniformity of surface that is required to assure stability of braking.

The compounder must select the exact combination of ingredients from hundreds of possibilities to produce linings that have all the required characteristics. His success is measured by the manner in which his linings stand up under a battery of tests.

Laboratory Testing of Brake Linings

To complete the comparision of organic and metallic linings, it is necessary to evaluate the performance characteristics of both types as established by the wide range of laboratory and road tests being conducted by the automotive industry. Laboratory testing provides fast, low-cost evaluation of the wide range of linings developed annually. Over 1500 compounds of various metallic combinations already have been developed by one manufacturer and organic-lining compounds run into the thousands.

The Chase machine shown in Fig. 3 is invaluable in quickly comparing friction materials for durability, wear, and the effects of temperature on friction and wear characteristics. The Chase machine consists of a heavy iron brake drum that is rotated by a variable speed motor and magnetic clutch assembly. A specimen of friction material is held against the drum by dead weights. Instruments record all test results.

The curves in Fig. 4 indicate the basic differences between metallic and organic linings throughout their rise in temperatures caused by their own friction plus external heat applied to the drum within the Chase machine. The friction coordinate is

shown at left, drum temperature at the right, and time at the bottom of the chart. The organic lining curve shows some increase in friction up to about 550 F and then a rapid fade out. The metallic lining curve indicates a constant, lower friction that increases at high temperatures. Metallic lining drum temperature goes higher than the organic.

Dynamometers of the type in Fig. 5 provide an excellent evaluation of a brake on an accelerated laboratory schedule of tests including effectiveness, fade, recovery, durability, drum score, and odor. The dynamometer duplicates the energy load of the automobile.

Only linings that prove worthy in the laboratory receive further testing.

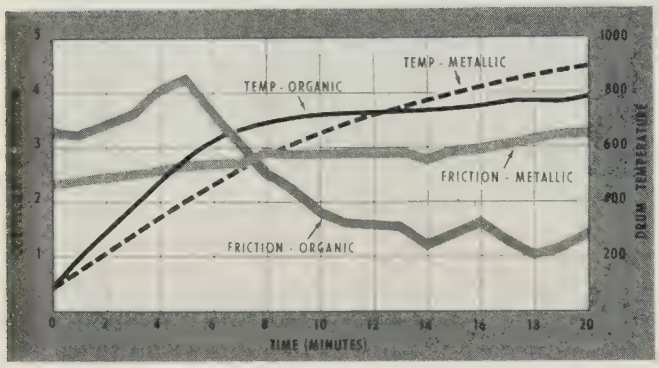

Fig. 4 — Friction evaluation (load — 200 psi, speed — 20 fps)

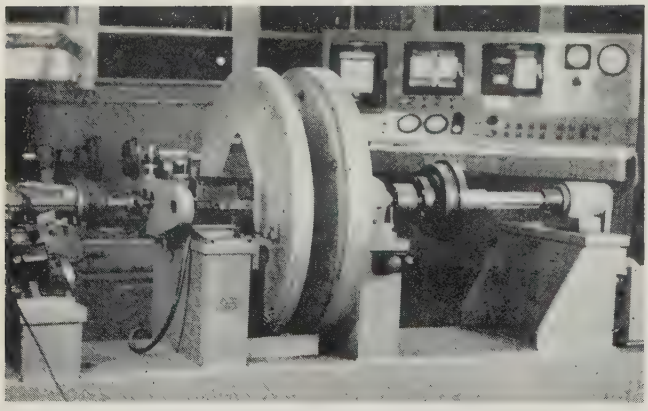

Fig. 5 — Brake dynamometer machine

Road Testing of Brake Linings

As is true of all automotive development, the vehicle itself must produce the final verification of laboratory brake findings. Tests of every type on Chevrolet brakes totaled 1,680,000 miles from October, 1957, to October, 1958.

The results of brake road tests described herein apply to organic lining bonded to the shoes, as contrasted to the riveted type, both of which are shown in Fig. 6.

Tests on metallic linings apply to the type shown in Fig. 7, with the lining riveted to the shoes in segments. The metallic segments on the shoe are flexible in their application in that they can be varied

Fig. 7 — Metallic brake shoe

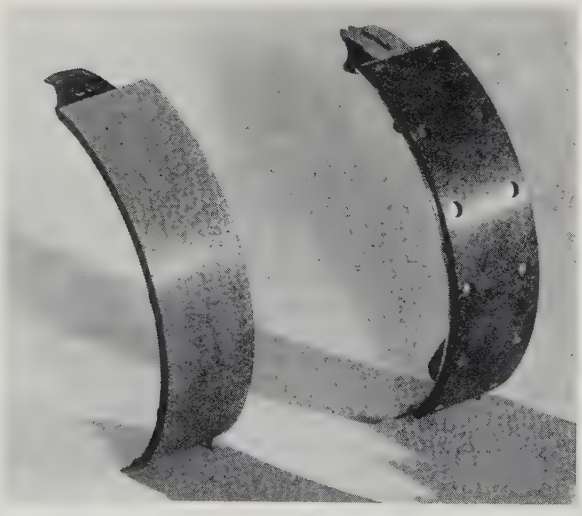

Fig. 6 — Organic brake shoes

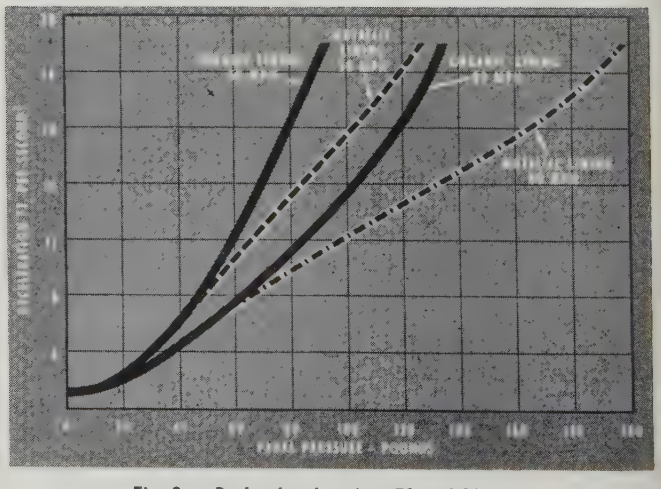

Fig. 8 — Brake deceleration, 50 and 80 mph

in number, position on shoe, or material formula to produce the braking effort desired.

The ultimate structure of all linings is determined by test. A brake lining material that has progressed from laboratory to road testing first undergoes a "general feel" test. Brake development engineers try the facings for an overall impression.

If the findings are good, an effectiveness test is made. The 50- and 80-mph brake deceleration test results shown in Fig. 8 depict the effectiveness of high-speed emergency stops with organic and metallic linings. This test requires the use of a load applicator, decelerometer, and recording unit. Load is applied to the brake pedal automatically and the recording unit indicates pedal load, deceleration, pedal travel, and time required to make test stops. The 50- and 80-mph brake deceleration curves show the brake effectiveness of the organic and metallic linings. The rate of load application on the brake pedal to obtain the curves is 30 lb per sec and each curve represents a single stop. The curves reveal that the organic material is less speed sensitive and more effective in this test. It should be pointed out that the metallic lining curves are those in which the brakes were cool at the start of the stop. For the organic lining, the pedal load required at a deceleration rate of 20 ft/sec^2 from 50 mph is 80 lb, and from 80 mph is 118 lb. Under the same conditions for metallic lining, the pedal load from 50 mph is 103 lb, and from 80 mph is 165 lb.

If linings perform well in the effectiveness test, they are subjected to the fade test. The chart in Fig. 9 illustrates a brake fade test comparison of organic and metallic linings. Line pressure is indicated by the coordinate at the left, and stop numbers at the bottom of the chart. The stops were made from 60 mph at 15 ft/sec^2 deceleration. The interval between fade stops was 0.4 mile, or about 40 sec. Initial feel and recovery stops were made from 40 mph at 8 ft/sec^2 at one mile intervals. The organic curve shows a slightly decreasing initial to

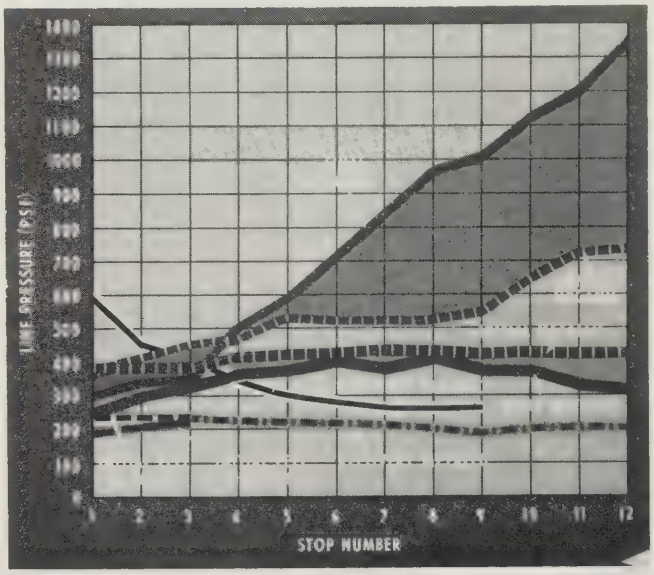

Fig. 9 — Fade test

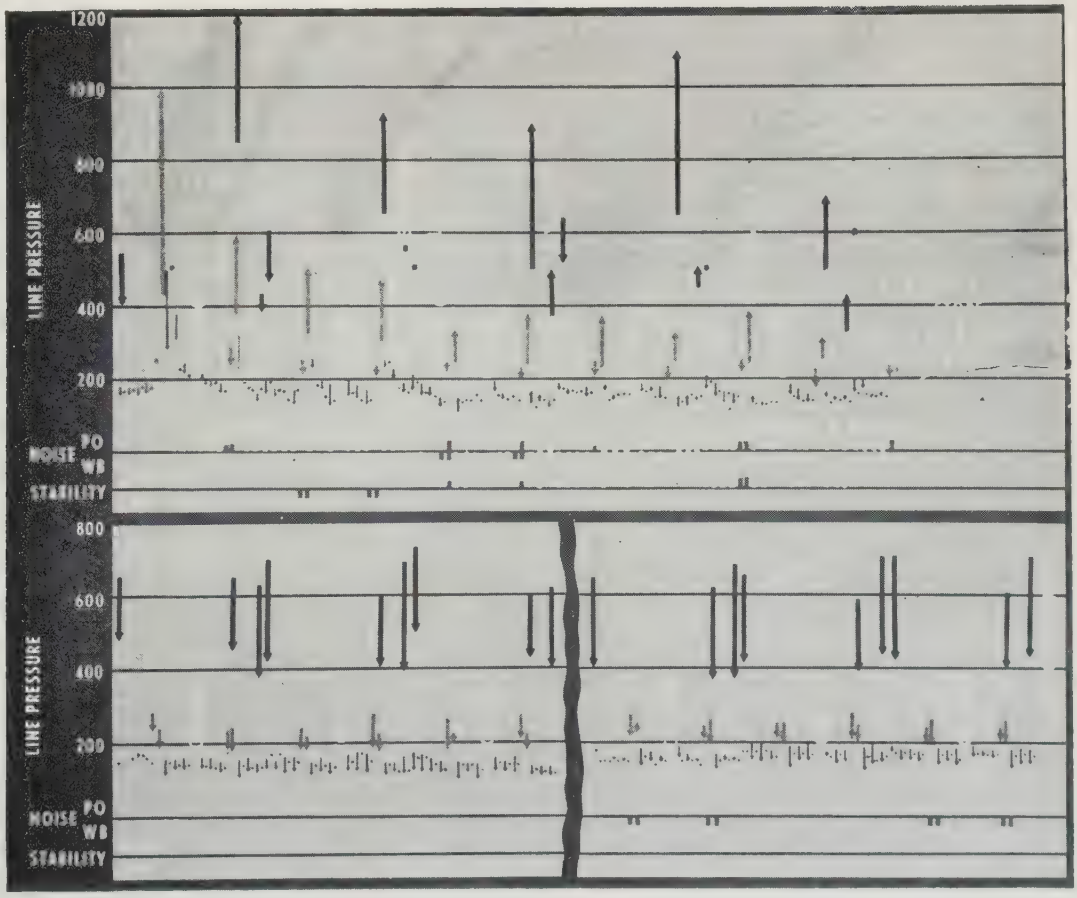

Fig. 10 — Police durability schedule

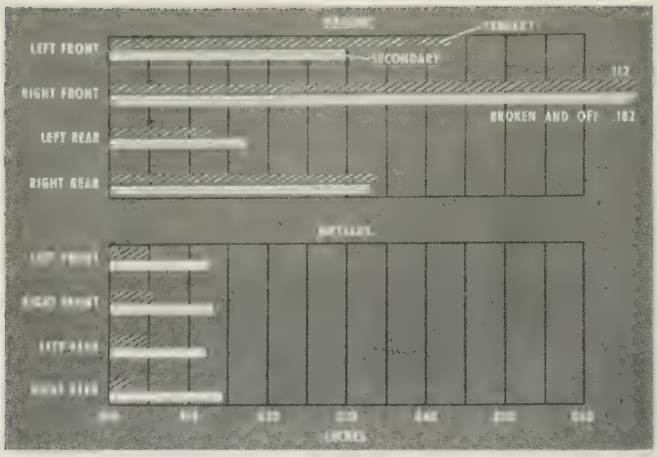

Fig. 11 — Police durability schedule, lining wear per 1000 miles

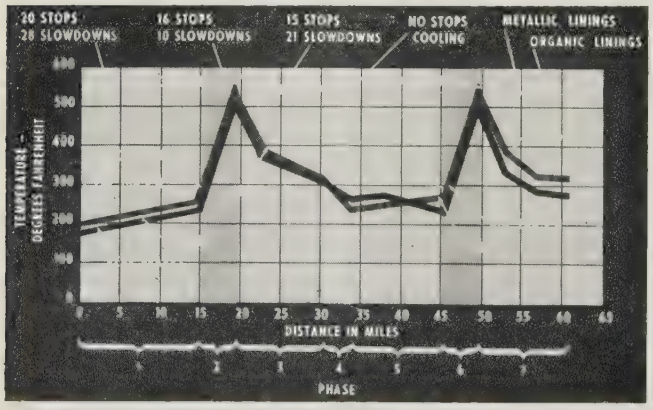

Fig. 12 — Los Angeles brake schedule

final line pressure during the first three stops with each successive stop becoming harder. This is indicated by the shaded distance between the broken and solid line curves. By the fourth stop, the line pressure increases progressively during each stop and the pedal becomes harder. By the seventh stop, line pressure is over 800 psi and fade continues with each stop. Recovery is slow and requires 7 miles to level out to within 20 psi of the initial. As the metallic lining curves indicate, the line pressure increases only 50 psi during entire test. The line pressure decreases during each stop with no recovery being required. Tests such as this show the need for organic linings that have less heat buildup and, thereby, less fade. Therefore, some organic linings are being grooved down the middle to ventilate the lining and mitigate the heat problem. Grooving of the linings also reduces heat spotting of the drum. In addition, lining areas are being increased, because for a given rate of vehicle braking, the pressure per square inch of lining area decreases as total area increases, and heat concentration is reduced.

Following the fade test, the brake linings are checked for general durability. This is accomplished by installing linings on vehicles scheduled for the 25,000-mile durability run. Consistency of effectiveness is observed during periodic stops which occur about every two miles throughout the 25,000-mile run.

Concurrently with the tests described, linings are subjected to a steam room humidity test, wet brake tests, grade parking checks, and others. In addition to the many standard tests for brakes, the brake development engineers conduct many special tests to collect performance data.

One of the most comprehensive and revealing special tests of organic and metallic brake linings was conducted recently on a 1000-mile police vehicle schedule (Fig. 10). On the chart, line pressure is shown at left, and the fifth and twelfth stop and slowdown of each test cycle are shown. The length of each arrow indicates the range of line pressure during a stop or slowdown. The wide range of line pressure during stops and slowdowns shows the effectiveness of organic linings to vary much more than metallic linings, especially during the first 200 miles. A much greater difference shows up on the fade stops. Note that with organic linings, the 35 mph at 8 ft/sec^2 stop fades from 425 to 1000 psi. Also, during the first stop at 60 mph at 15 ft/sec^2 with brakes hot, line pressure reaches 1200 psi. This fade condition gradually improves as long as the lining lasts, but is always present. Note the arrows at the end of fade schedules pointing upward, indicating increasing line pressure during decelerations. With the metallic, fade is absent because the arrows in metallic part of test are pointing downward. Organics developed considerable noise, odor, roughness, pulls, and near the last grabbiness. Failure occurred at 396 miles, while the metallic linings remained constant throughout the 1000-mile schedule. The police schedule is extremely rugged and shoe temperatures usually go above 600 F during the fade stops.

The letters PO at the noise test line stand for "pinch out," a short noise at extreme end of stop. WB stands for "wire brush," a scraping noise through the entire last part of a stop. The length of each noise line indicates intensity of sound.

The stability line on the chart indicates vehicle pull to right or left during stops. The length of lines indicates amount of pull. Notice the superior stability of vehicles with metallic lining in this test.

Wear was another measurable differential between the two linings indicated by the police schedule. Notice the extent of organic lining wear shown in Fig. 11. The right front primary lining wore 0.112 in. and the right front secondary lining wore 0.182 in. and broke off at 396 miles to end the test. As the chart shows, a maximum wear of only 0.014 in. occurred on the right rear secondary metallic lining at the end of 1000 miles of high-speed stops. The police durability schedule emphasizes the inadequacy of organic linings on heat-problem brakes.

What about a brake test for the average passenger car in one of America's urban areas? To establish such a test, General Motors engineers studied the necessary slowdowns and stops on several routes in cities throughout the country and finally decided on a Los Angeles route. The Los Angeles schedule is shown in Fig. 12. It calls for seven phases of stops, slowdowns, and cooling periods of varying duration over a 60-mile run. The first phase is 20 stops at speeds ranging between 20 and 30 mph at 5 ft/sec^2, and 28 slowdowns from 30 to 20 mph at the same rate in a distance of 15 miles. The second phase is 16 stops from 35 mph to 0 at 8 ft/sec^2, and 10 slowdowns from 35 to 15 mph at 8 ft/sec^2 in 5 miles. The

third phase calls for 15 stops and 21 slowdowns at 5 ft/sec² in a distance of 10 miles. Phase 4 is a cooling period of no stops for 5 miles. Phase 5 is a repeat of Phase 3, Phase 6 a repeat of Phase 2, and Phase 7 a repeat of Phases 3 and 5.

As the curves illustrate in Fig. 12, the organic and metallic lining temperatures for front and rear brakes follow almost parallel plots. The significant fact depicted here is that at each given temperature reading for both organic and metallic linings, the metallic lining pressure is considerably below the organic. The metallic lining brakes are operating more efficiently with less effort required. This test does not mean that organic linings are unsafe during severe stopping conditions encountered in everyday driving. Organic linings are capable of meeting all the requirements of safe stopping. The test does establish the superiority of metallic linings in stopping a vehicle with ease under severe and prolonged braking requirements.

There are tests also that call for braking ability far beyond the requirements of everyday driving. The long winding descent of the road from the summit of Pikes Peak, Colo. is the site of a special brake test of this type. Fig. 13 indicates the result of separate runs down Pikes Peak to measure the comparative braking effectiveness of metallic and organic linings. The car with metallic linings descended Pikes Peak in drive range. Speeds were kept in a 20–30 mph range. Brake checks were made every ½ mile at 8 ft/sec², regardless of the braking that was required to maintain the speed range. In the lower portion of the chart, you can see that the metallic line pressure remained practically constant for the entire descent.

A vehicle with organic brake linings making a similar descent failed at 10½ miles with brakes entirely gone.

In comparing wheel cylinder temperatures, it can be noted that the cylinders with organic lining brakes increased slightly more than the cylinders on metallic-lining brakes. The thermocouples were exposed in the end of the bleeder screws on the cylinders.

The secondary shoe temperatures shown were measured at the back of rim-web juncture near the horizontal center of the shoe. Notice that the temperature in metal shoes tends to flatten out when work is lighter. When the work load is severe, temperatures in the front shoes go above the rear shoes. The organic fronts cannot take the load and fade holds down the temperature increase.

Metallic fronts continue to work and temperature rises steadily. Note that the highest temperatures on the metallic are still below the organic lining readings. It must also be kept in mind that when considering comparative temperatures, the thermocouples in metallic-lining shoes respond faster due to conductivity.

Both the police durability and the Pikes Peak brake tests are extremely severe and prove the value of metallic linings for vehicles that must withstand abnormal braking requirements.

Field testing[1] of brake linings on police and taxi

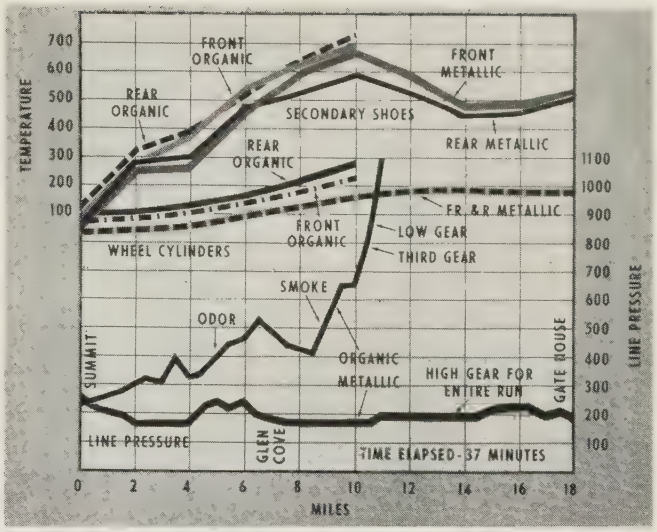

Fig. 13 — Pikes Peak test, 20-30 mph, 8 fps² checks

fleet vehicles is also a most important method of gathering important test data. Chevrolet has installed metallic linings on police vehicles in three different areas of the country. The police departments participating reported actual operational observations, including facts on wear, feel, fade noise and additional data, to Chevrolet field service engineers that confirmed company test results. As a result of their superior performance in heavy-duty operations, Chevrolet has released metallic linings as optional equipment.

Conclusion

The postwar trend in automobile developments has been a veritable nightmare for the brake engineer. As cars have become heavier and far more powerful, his working area has been reduced with the size of wheels. Yet his brakes, and particularly his linings, have proved equal to the test.

In comparing the overall capabilities and weaknesses of today's organic and metallic linings, it has been shown that both have their good and bad characteristics. Today's organics are more than equal to the demands of average daily driving. The metallics are equal to the demands of the "heat problem" braking of police cars, sports cars, and other vehicles subjected to high-speed, prolonged decelerations.

However, in striving for the perfect brake friction material, engineers are not completely satisfied with either the organic or metallic linings. In defense of the metallics it should be kept in mind that they have undergone intensive development work only in the last 3½ years, and great progress has been made in that short period in improving their objectionable characteristics. On the other hand, organics have been under intensive development for over 30 years and, although further deficiency improvement may be obtained, they have possibly reached their peak of perfection with the ingredients to which they are now restricted. The competition between the organic and metallic friction materials is a healthy condition that points to rapid progress in the attainment of the versatile, highly effective brake lining of the future.

[1] "Dragnet for Defects — Field Testing," by Edward Gray. Paper presented at meeting of SAE Metropolitan New York Section, February, 1958.

some aspects

Operation of Utility

E. C. Paige and H. T. Mueller, Ethyl Corp.

This paper was presented at the SAE National Transportation Meeting, Baltimore, Oct. 20, 1958

SOME of the problems encountered in the operation of utility or auxiliary engines are associated with the accumulation of combustion-chamber deposits. These deposits are common to all types of internal-combustion engines. Their deleterious effect on the operation of both automotive and stationary-type engines has been recognized since early days. The many excellent papers on this subject published in the 1920's and 1930's, and the many patents covering "Carbon Removers" issued in the same era, offer convincing evidence of the efforts that were being made to overcome the difficulties encountered. As a typical example, we might quote from a book[1] published in 1919. In a chapter titled "Diseases of Combustion Engines" the author discusses valve burning and engine knock. He states in part:

> ". . . The two chief reasons why valves burn are because (a) carbon gathers in a film on the valve seat and (b) the valves get warped by the heat. . . ."

and, on engine "knock", he says:

> ". . . There is an even dozen diseases that make an engine knock, and, specified these are (1) the spark is advanced too far; . . . (3) the spark plugs need cleaning; (4) the compression is too high; . . . (6) the fuel mixture is not proportioned right; . . . (10) there is carbon in the cylinder; (11) premature ignition caused by red-hot particles of carbon."

It is interesting to note that this publication, which describes in vivid detail the common ills of modern engines, is dated some two years before the discovery of tetraethyl lead as an antiknock agent, and well before the general use of any type of additive in either fuels or lubricants.

The effects of combustion-chamber deposits on engine operation are still under active investigation. This paper discusses some of the factors that have been investigated, including the mechanism of deposit formation, the effect of deposits on engine operation, engine design factors, maintenance problems, and possible methods of deposit removal.

Deposit Effects on Engine Operation

The major effects of combustion-chamber deposits on engine operation can be classified into four basic categories. In order of their overall importance, these are:

1. Increase in octane requirement.
2. Tendency to promote abnormal forms of combustion.
3. Decrease in available power.
4. Reduced durability of some engine parts.

The first three of these effects are interrelated. In most instances, anything that is done to reduce the magnitude of any one effect also improves conditions in respect to the other two. This is true whether the modification is by means of engine design or through changes in formulation of the fuel and lubricant.

At the present time, the effect of deposits in increasing engine octane requirements and in causing abnormal combustion are of major importance. This effect is under intensive investigation by all laboratories associated with the petroleum and

[1] "Gasoline and Oil Engines," by A. Frederick Collins. Pub. by D. Appleton & Co.

of the

Engines

THE EFFECTS of deposit power loss are most severe in the constant-speed, constant-load service common to the auxiliary or utility-type engines. This paper describes studies made of this problem. Factors investigated are: mechanism of deposit formation, the effect of deposits on operation, design and maintenance problems, and deposit removal.

Since the greatest part of this loss results from decreased air consumption, proper attention to engine design can materially reduce such loss. The new multigraded oils may offer some relief from deposit problems because they form less resinous material. Carbon removal by physical or mechanical means also may be beneficial in some cases. Proper engine application and conscientious maintenance, however, can go a long way toward reducing deposits.

The authors also discuss the problem of heavy-duty truck operation and passenger-car service.

automotive industries. Due largely to the advanced engine designs of recent years, problems of power loss and engine durability are considered of little consequence today in normal passenger-car and motor-truck service.

In recent years there has been a marked increase in the use of all types of gasoline engines for a myriad of utility purposes. In many instances these engines are required to operate for extended periods at constant load. It will be shown later that, under these operating conditions, combustion-chamber deposits form more rapidly and to a greater extent than in the varying speed and load operation common to passenger cars and motor trucks. In utility engines, power loss and sometimes reduced durability are problems of major importance. To summarize, we can say that combustion-chamber deposits are common to all engines but differences in operating conditions determine their effects on engine operation.

Mechanism of Deposit Formation — When hydrocarbon fuels such as gasoline are burned as fuel-air mixtures in engines, residual deposits are left on the surfaces of the combustion chamber. Contributing to the formation of these deposits is the partial combustion of lubricating oil that finds its way into the combustion chamber. Early investigators pointed out the importance of engine design, mechanical condition, and operating conditions in determining the type and quantity of deposits that are formed. However, a summary of their work shows that they considered the resinous deposits remaining from the partially burned oil as being the binder or "fly-paper" which caught and held the fuel deposits and other materials, such as road dirt.

A similar summary of more recent reports indicates that the deposits from modern fuels and lubricants are different in appearance and physical character. However, the resinous deposits from partially burned motor oil are still considered to be the materials that catch and hold the decomposition products from modern fuels and lubricants. These resinous materials are of fundamental importance, and will be discussed in greater detail later.

Causes of Deposit Power Loss — Deposits cause power loss by reducing both thermal efficiency and volumetric efficiency or breathing capacity. It is generally agreed that roughly two-thirds of the deposit power loss results from decreased air consumption which, in turn, results from physical and thermal restriction of the intake charge.

Investigations of the physical restrictions have shown that this is a highly variable effect, and is dependent largely on engine design. "Thermal restriction," the term used to identify a reduction in the weight of the incoming charge caused by the transfer of heat from deposits to the charge, is also a highly variable effect. It is largely dependent on engine design factors. However, thermal restriction is of primary importance with respect to deposit power loss in all engines.

Effect of Tel Concentration

Probably no other fuel or oil variable has received more blame for power loss or other engine effects than has tetraethyl lead. Since the presence of tel in the fuel increases deposit weight over that with clear fuel by several times, it is commonly believed that power loss also is increased several times. As will be apparent from the following data, the effect of deposits on power loss is highly variable, and is almost entirely dependent on the type of service or engine operating conditions encountered. For illustrative purposes, data are shown from tests conducted under three types of operating conditions: (1) heavy-duty truck operation, (2) normal passenger-car service, and (3) constant-speed and constant-load service such as operation of refrigerators, fans, pumps, or generators.

The data to be shown are the results of many

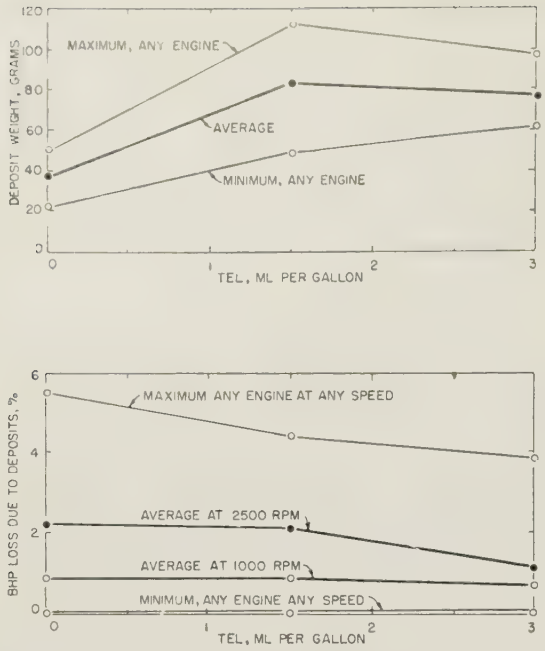

Fig. 1 — Effect of fuel tel content on deposit power loss and deposit weight in heavy-duty truck operation (engine: 18 Make C and 12 Make D truck engines; operating conditions: 15,000 miles of heavy-duty car haulaway service, power loss measured at 1000-3000 rpm, full throttle)

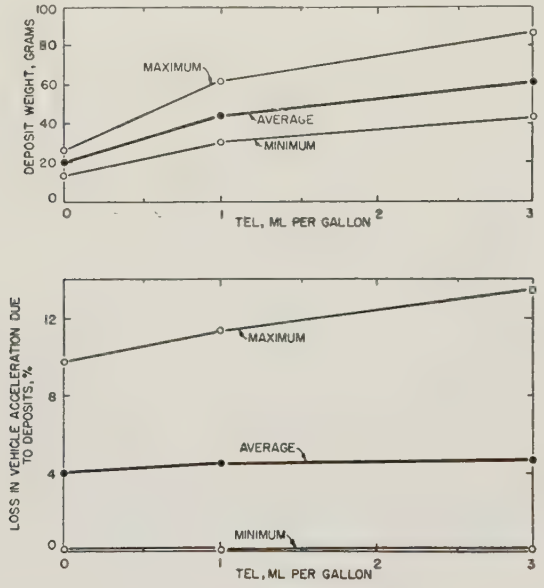

Fig. 2 — Effect of fuel tel content on loss in vehicle acceleration due to deposits and deposit weight in passenger-car service (vehicles: fleet of 66 1946 cars A, B, C, and D; operating conditions: 12,500 miles of normal city and country driving)

repetitive and carefully conducted tests. For studies of passenger-car or heavy-duty truck operation, large numbers of vehicles were used to provide statistically significant data. Complete details of these tests have been reported in a previous paper.[2]

Heavy-Duty Truck Operation — The effect of tel concentration on power loss in heavy-duty truck service is shown in Fig. 1. All engines were new at the start of the test. At the end of 15,000 miles of deposit accumulation, each engine was removed from its tractor and mounted on an engine dynamometer. "Before and after" deposit-removal studies were made at speeds of 1000–3000 rpm.

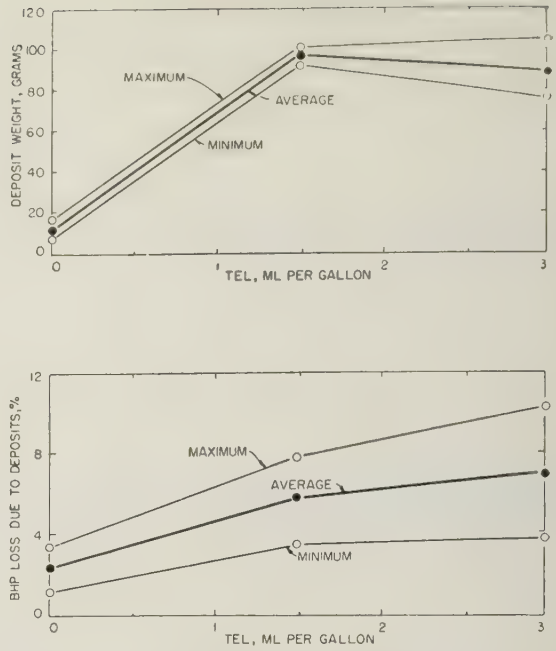

Fig. 3 — Effect of fuel tel content on deposit power loss and deposit weight in constant speed and load dynamometer tests (engines: Makes C and D; operating conditions: 100 hr at 3000 rpm, 75% load)

The power loss is plotted for both 1000 and 2500 rpm to show the effect of engine speed and also to make possible a comparison with constant-speed operation to be shown later. Values shown are an average for all vehicles operated on each tel concentration. The maximum and minimum power losses in any engine at any speed are also shown.

Power loss at 2500 rpm was about 2%, roughly double that at 1000 rpm. At either speed, however, the data show that the loss of power caused by deposits was independent of tel concentration. It is also important to note that operation on clear fuel is no guarantee of freedom from power loss. Although deposit weight is shown to be affected by tel concentration, it bears no relation to the observed power loss.

Passenger-Car Operation — In this test a group of 66 new passenger cars were operated in a fleet. The service, which included both city and suburban-type driving, was considered typical of normal "owner" operation. Each vehicle was operated for 12,500 miles at which time "before and after" deposit-removal tests were conducted. Included in the tests were observations of the time required to accelerate from 10 to 30 mph and from 10 to 50 mph. These observations, which provide a direct measure of the power loss, are shown in Fig. 2. Here again, it is seen that tel concentration has an insignificant effect on power loss, and that deposit weight bears no relation to vehicle performance. Operation on lead-free fuel does not eliminate power loss effects.

Operation at Constant Speed and Load — Because it is impractical to make direct power measurements of these engines when connected to their normal loading devices, these tests were conducted in the

[2] SAE *Quarterly* Transactions, Vol. 6, October, 1952, pp. 594–605: "Combustion-Chamber Deposition and Power Loss," by H. J. Gibson, C. A. Hall, and A. E. Huffman.

laboratory. The engines were the same makes and models as used in the truck operation previously described. Operating conditions were set to simulate field operation of equipment such as generators, blowers, refrigerating equipment, and the like.

Fig. 3 shows the power loss and deposit weight as functions of tel concentration. As in the previous studies, maximum, minimum, and average values are shown for the two makes of engines used in this program. It is apparent that deposit power loss is affected by tel concentration in service of this type; however, operation on clear fuel does not eliminate the effects of deposits on power loss.

It is important at this point to remember that the average power loss due to deposits in truck service was about 2%. In passenger-car service the average loss was shown to be about 4%. In service at constant speed and load, including the effect of tel concentration, the loss is shown to be about 7%.

Effect of Operating Conditions

The important effect of variations in operating conditions on the magnitude of deposit power loss is shown in the left-hand portion of Fig. 4. In these studies, all other variables were eliminated insofar as possible. Here, the relative power losses due to deposits are shown to be approximately 10, 4, and 2% for constant-speed, cycling, and heavy-duty types of operation, respectively. Comparison of deposit effects when a wide variety of fuels and lubricants were used are shown in the right-hand portion of Fig. 4. Here, the relative amount of power loss is similar to that shown in the other portion of the figure when fuel and lubricant types were controlled. However, the absolute magnitude of the effect is somewhat greater.

The larger effects of deposit power losses shown to be associated with operation at constant speed and load can present maintenance problems in some applications of this type of service. Therefore, studies have been made in an effort to determine the factors influencing deposit formation under these operating conditions.

Engine Design

Of all the factors studied that may influence the magnitude of power loss effects due to combustion-chamber deposits, engine design is probably the most important from the practical standpoint of minimizing deposit effects. The effects of combustion-chamber design are readily observed in the data shown in Fig. 5. Four different engines were used in this investigation. Two engines, AE and AB, were of L-head design and two engines, AC and AF, were of overhead-valve design. The general superiority of the overhead-valve design is clearly shown by the relative amount of the deposit effects. Also, certain designs within each of these two general design classifications are definitely superior. This was more clearly defined in a series of tests of a certain small single-cylinder L-head engine. As received, this engine could not produce rated power after 150 hr of constant-speed operation. Investigation showed that deposits in the block around the intake valve reduced the effective valve opening and caused physical restriction of the incoming charge. The condition was remedied by increasing the valve lift from 1/8 to 3/16 in., with the result that power loss was insignificant even after 1000 hr of operation. Here is definite evidence that minor design details can have major effects on deposit power loss. It is also further proof that both good and poor designs are possible regardless of basic engine configuration.

Lubricating Oil

Tests carried out in many research laboratories have shown that the choice of motor oil used in the crankcase may affect the increase in engine octane requirement to a marked extent. Therefore, it is natural to suspect that the choice of motor oil also may affect deposit power loss. Tests have confirmed this suspicion. The variations in motor oils that occur because of differences in crude source, refinery processes, distillation and viscosity characteristics, additive type, and additive quantity are too numerous to mention. However, the data shown in Fig. 6 indicate the probable extremes that may be expected in the effect of deposits on power loss when using commercial-type lubricants. Many oils having

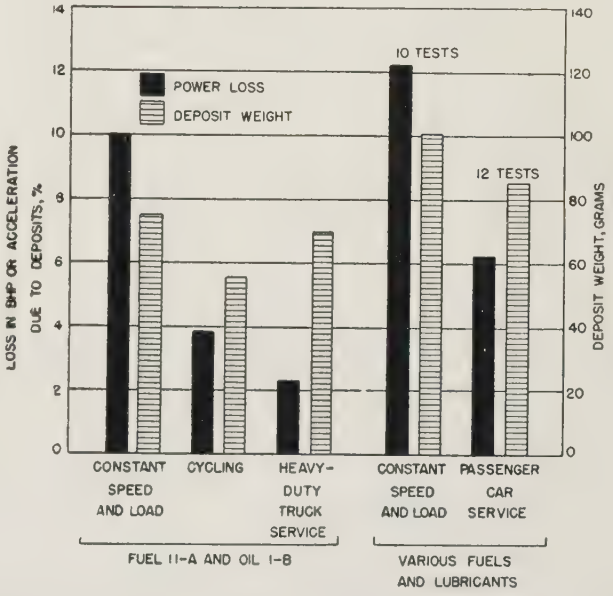

Fig. 4 — Effect of various operating conditions on deposit power loss and deposit weight (engine: Make C; fuels contained 3 ml tel)

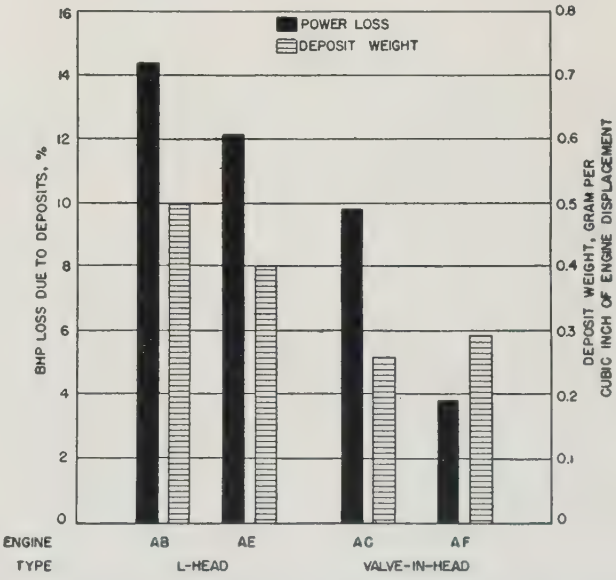

Fig. 5 — Effect of design on deposit power loss in tractor engines (operating conditions: 100 hr at governed speed, 75% load)

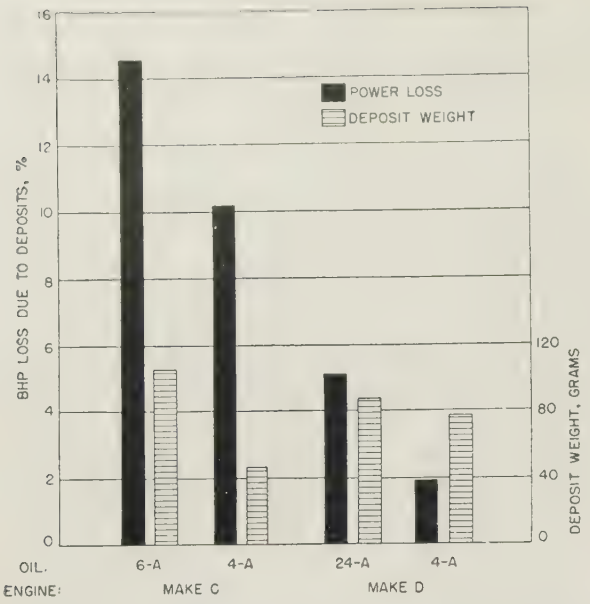

Fig. 6 — Effect of lubricating oil type on deposit power loss and deposit weight (operating conditions: 100 hr at 3000 rpm, 75% load)

characteristics similar to those of oil 4A are now commercially available. It would seem desirable to use oils of this type in utility engines.

Carbon Removers

The preceding portion of this discussion has shown that modern fuels and lubricants are eminently suited for use in the engines that power our modern passenger cars and motor trucks in their normal service. It also has been shown that these fuels and lubricants may contribute to the effects of deposits on power loss when the fuels and lubricants are used in service applications for which they are not specifically designed. In addition, it has been shown that the choice of engine type and, of equal importance, minor changes in engine design are major factors affecting the magnitude of the power loss to be expected when operating at constant speed and load. These conclusions are supported by the thousands of engines now operating in such service without any apparent difficulty. However, some problems do exist. The following discussion covers other investigations and observations made in an effort to reduce the effects of deposit power loss in those instances where the power loss adversely affects engine operation.

Simple and easily applied methods of either removing or loosening combustion-chamber deposits have been sought for many years. Two lines of attack — chemical removers and physical removers — have been followed in approaching the problem.

Chemical Removers — In earlier days, before the widespread use of fuel and lubricant additives, combustion-chamber deposits were composed largely of fuel soot or carbon, foreign contaminants such as road dirt and metallic particles from engine wear, and resinous products from the partial oxidation of the motor oil. Today, deposits are composed largely of ash from burned fuel, fuel and lubricant additives, road dirt and wear particles, and resinous products from the partial oxidation of the motor oil. Present-day deposits are different in appearance and physical structure from those of former years. There are no known compounds that will dissolve either carbon or additive ash without also dissolving the engine. The use of such a compound, while effective in removing deposits, obviously would be highly impractical. Therefore, chemical carbon removers must attack only the resinous products from the partially oxidized motor oil which catch and hold the other materials.

Some 30 years ago the Ethyl Laboratories carried out an extensive investigation which led to the development and patenting of several practical carbon-remover fluids. These fluids were designed to dissolve the gummy binders. In this manner, the carbon and other deposits were left loose in the combustion chamber, and were expelled from the engine with the normal exhaust. The fluids were effective in removing the type of deposits found in engines at that time. One fluid was marketed by AC Spark Plug Division of General Motors Corp. under the trademark name "Remo" together with a means of applying the fluid to an engine, the "Remo Injector." Oldsmobile used the injectors as standard equipment during one model year. Since the actual treatment of the engine was left in the hands of the car owner, the use of Remo never became widespread. Some field tests were carried out at that time in commercial-truck operations. Remo was found to be effective not only in removing combustion-chamber deposits but also in cleaning piston skirts, rings, and ring lands. Since there were some serious objections to the use and handling of these fluids in bulk in garages, it was not felt practical to pursue the matter further.

With the advent of the new engines having high octane requirements and the resulting knocking complaints, interest in carbon removers was revived. Therefore, a second project was initiated in 1950 to investigate carbon-remover fluids and means of applying them to an engine. At the same time, plans were made to investigate their use in stationary and utility engines since these engines were then starting to be widely used with a consequent increase in complaints of deposit power loss.

In this development program it was soon found that fluids of the "Remo" type were relatively ineffective in loosening or removing the current type of deposits composed largely of ash from fuel and lubricant additives. In general, these deposits are hard and dense. The "Remo" fluids could not penetrate sufficiently to attack and dissolve the binders and thus loosen the deposits.

In all, over 250 compounds and combinations were tested. From this work, patent protection was requested on a family of fluids that effectively removed from 60 to 90% of the deposits formed in a wide variety of engines and under many types of operating conditions. Like the "Remo" compounds, the new fluids had the beneficial side effects of also cleaning pistons, piston rings, and the like. They were found to be from two to four times more effective than other products then on the market.

There are many reasons why these new superior fluids never reached the market, including a few disadvantages that are common to all effective materials of this type. Some of the disadvantages are:

1. They have a highly unpleasant and tenacious odor that is hard to remove, and the exhaust odor after treating an engine is highly disagreeable.

2. They are somewhat toxic and are highly flammable. Special precautions must be observed when using them indoors.

3. Oil must be changed after treatment because material reaching the crankcase promotes oil oxidation.

4. Pieces of loosened deposit often lodge on valve seats and hold the valves open. This may make starting difficult on 4-cyl engines and impossible on single-cylinder engines.

Other attempts at developing carbon removers that could be added to the fuel or lubricant to provide automatic action have met with failure to date.

Physical Carbon Removers — Many proposals have been made involving physical or mechanical means of dislodging deposits so that they could be expelled through the exhaust system. Most have had some form of disadvantage that has limited their use or prevented commercial application. The disadvantages in some cases were with the process proposed and in others in the inconvenience and labor cost involved in the application.

At present, we know of only one device on the market that offers possibilities of carbon removal by physical or mechanical action. This device is employed by many laboratories to remove combustion-chamber deposits from the CFR engines which are used to determine the octane numbers of motor fuels. Deposit removal is accomplished by "blasting" the deposits loose by means of compressed air and some material that will not harm the engine. Materials used have been rice and finely ground walnut shells. Although the efficiency of deposit removal is believed to be somewhat less than that of a superior liquid solvent, this method does not have many of the disadvantages previously outlined. It is believed that this method of carbon removal might be practical for use by some large fleets.

Field Investigations of Deposit Problems

The foregoing sections of this discussion have covered laboratory tests and laboratory-controlled field tests used to determine the causes of combustion-chamber deposits, their effects on engine operation under a wide variety of operating conditions, and possible methods of deposit removal. In addition, many studies have been made of field conditions in operations where the effects of deposit accumulation have been felt to be a problem. These studies have covered a wide variety of operating conditions where the engines have been used to power equipment such as generators, fans, pumps, and air-conditioning and refrigerating systems. Some of the observations made are pertinent to this discussion. Since time is not available to discuss all of the items investigated, only a few typical examples will be cited.

Choice of Engine — In one operation, 9.5 hp was required to operate a compressor. The engine chosen would produce 11.0 hp when it was clean and operating at best efficiency. Deposit power loss and other maintenance deficiencies caused difficulty in many cases after 300–500 hr of operation. The removal of a 50-amp generator, which was being driven by the engine unnecessarily, provided a reserve of power and improved the operation. Subsequently, a larger engine of the same design was used to power similar equipment. This provided trouble-free service for periods ranging from 1500 to 3000 hr.

Spark-Plug Selection — Many instances have been found where power loss attributed to combustion-chamber deposits actually was caused by fouled or "missing" spark plugs. Here, deposits on the insulator of the spark plug were to blame. The choice of a plug having a different heat range often alleviated the problem. In this connection, it might be mentioned that spark plugs used in 2-stroke engines are subject to severe accumulations of deposits. Spark plugs of special design have been very effective in combating this problem and are currently available. It is possible that their use in other types of engines may be very beneficial.

General Maintenance — Unfortunately, it has been observed in many instances that the lack of satisfactory maintenance is responsible for many complaints attributed to deposit power loss. Even when adequate maintenance schedules are programmed, it has been observed that shop personnel frequently will not touch the utility engine if time runs short during an inspection period. In one operation having serious complaints of deposit power loss in air-conditioning engines, arrangements were made to test a carbon-remover fluid at the request of the fleet operator. Forty vehicles were chosen for the test. Twenty were to receive regularly scheduled treatments and the other 20 were to receive normal routine maintenance services. At the end of a 6-month trial period, the shop records revealed that not one engine of the 40 had received maintenance service (except oil change done by another group) unless the equipment failed to operate.

In another operation having complaints of deposit power loss, the fleet management insisted that prearranged maintenance programs be carried out during the test period. Although the results indicated little advantage for the use of the carbon remover, observance of a good maintenance program significantly improved the general fleet operation.

In such cases as those just cited we might paraphrase an old saying to read: "Neither the Lord nor an engineer can help those who won't help themselves." To be fair to the maintenance groups, we hasten to point out in these instances that the designer of the equipment had made adequate maintenance very difficult.

Summary

The deleterious affects of combustion-chamber deposits on engine operation have been recognized since the earliest days of internal-combustion engines. In spite of ever-increasing research budgets directed toward alleviating these effects, much still remains to be done. The present discussion has been confined to power-loss effects.

It has been shown that all engines suffer from deposit power loss and that the magnitude of the effect is a direct function of the type of operating conditions or engine service involved. Power-loss effects are most severe in the constant-speed, constant-load service common to the use of auxiliary or utility-type engines.

The effect of tel in motor fuel on deposit power loss problems has been explored, and is shown to be an influencing factor only in constant-speed, constant-load service common to the use of auxiliary or utility-type engines. Engine type and factors of engine design also have been shown to have major

effects on deposit power loss.

Considerable time and research effort has been expended in the development of so-called chemical "carbon removers." Although effective to a significant extent, these products have not achieved widespread use because of certain inherent disadvantages and problems associated with their proper application to an engine. Such products depend on their solvent action to attack the gummy binders resulting from partially burned motor oil. It is suggested that the use of the new multigraded oils may offer some relief from deposit problems because they form less resinous material. It is also suggested that carbon removal by physical or mechanical means may be beneficial in some applications.

Finally, direct investigation of field conditions involving problems of deposit power loss has shown that lack of adequate maintenance and improper engine application are often important factors in determining the magnitude of the deposit effect.

The total power loss is the sum of the deposit effect and the effects of many other factors influencing engine operation. Study of each of these other effects can often alleviate the power loss problem in constant-speed, constant-load operation.

DISCUSSION

Engine Design Must Meet Needs of Utility Engine Users

— George S. Kelm
American Telegraph & Telephone Co.

WHILE we in the telephone business are still having considerable difficulty with engine deposits in our utility engines, generally speaking, we have learned to live with our problems and our operations have been greatly improved as a result. In our automotive equipment it was quite common, just a few years back, to have an engine out at 25,000 miles due to deposits. Now we realize double and even triple that mileage regularly. In our utility engines, pumps, blowers, and small generator sets we frequently have to overhaul to remove deposits in a range between 800 and 1500 hr of running. We have had numerous occasions where the engine cannot turn over.

Just one brief comment on the chemical removers. We have found some that have been comparatively easy to use and quite effective. However, their use is not practical in our shops because of the toxic aspects of some chemicals themselves and the smoke problems encountered. A garage foreman would have to wait until after dark to purge the engine or face serious complications from the smoke abatement authorities.

All our engines are operated by telephone craft people. We have learned from experience not to expect too much from them in the way of careful operation or preventive maintenance work to minimize such problems as engine deposits. It is obvious from this paper that there is something wrong. It appears that the difficulties lie with the engine themselves, if they do not operate with sufficient satisfaction and reliability without more preventive maintenance than should be necessary. Certainly, 600 hr or less of satisfactory operation without considerable preventive maintenance servicing is far less than should be expected. The finger of blame is pointed, particularly, at the utility engines because our difficulties are being experienced with the same fuels and engine oils which we use in the operation of motor vehicle engines. In utility operations such as ours, it is out of the question to provide and use special fuels and special oils for limited number of pieces of equipment, even if such fuels and oils would extend appreciably the period of trouble-free use. We must be able to operate all engines with satisfaction on the fuels and lubricants which are readily available to us.

One can thus only reach the conclusion that engine design is at fault. If it cannot function satisfactorily under the conditions it is required to operate with the fuels and lubricants which the operator desires to use. It is, therefore, up to the engine designer to find out why his engines won't operate as desired and make the necessary changes so that it will.

In conclusion, while we greatly appreciate the efforts of the fuels, lubricants, and engine manufacturers to minimize our troubles, as operators we are still looking for a "cheap and dirty" solution to the combustion-chamber deposit aspect of the operation of utility engines.

Deposit Removal Possible Without Engine Disassembly

— Robert Best
Southwest Research Institute

IN 1956 WE made some experimental studies on the subject of deposit removal which may be of interest. Our work was done under contract with the U. S. Army Corps of Engineers who early recognized this problem in many military installations throughout the United States and overseas and requested that Southwest Research Institute conduct a program directed toward developing a practical method of alleviating the deposit power loss problem.

Stationary gasoline engines which operate at governed speeds and fixed loads tend to form heavier equilibrium combustion-chamber deposits than would ordinarily be formed if the load and speed conditions were variable. When occurring in certain L-head engines, such deposition oftentimes results in serious power losses, and occasionally heavy deposition may cause physical restriction between valve tops and cylinder heads. The more common occcurrence, however, is a gradual loss of power until it finally becomes necessary to shut down the engine.

The program conducted at Southwest Research Institute was separated into three phases:

Phase 1 was an extensive literature survey supplemented by personal interviews to compile data on as many commercial and experimental deposit removal methods as possible. Some 400 such methods were thus investigated and reported.

Phase 2 consisted of a laboratory investigation of 32 deposit-removing methods selected on the basis of Phase 1 as showing promise toward alleviating deposit power losses in stationary gasoline engines. The selected methods were evaluated on the basis of their ability to remove combustion-chamber deposits.

Phase 3 was a laboratory investigation to evaluate the three best methods from Phase 2 and select the one most suitable for Army field use. These three materials and tchniques were each applied to the removal of combustion-chamber deposits in two similar 4-cyl gasoline engines of small size. One of these engines was modified for radioactive wear measurements. Both of these engines were operated for a sufficient length of time to build up equilibrium deposits (200–400 hr), which would result in maximum power loss. The fuel contained 5 mg ASTM gum.

At the completion of the deposition run the engines were disassembled for inspection of the deposits and then reassembled. At this time, maximum power was obtained on each engine and compression pressure checked. The radioactive engine was run an additional period of 4–5 hr to permit establishing and stabilization of the wear rate, so that wear resulting from the use of the treatment could be distinguished from normal wear. Both engines then underwent deposit-removal treatment following which each engine was again disassembled for inspection.

With respect to the three compounds selected, the following is a brief outline of the type of material in each:

No. 1 was a "below zero" octane fuel which when burned in the engine removed deposits by the combined thermal and physical shock attendant on detonation and autoig-

Table A — Results of Deposit-Removal Tests

	No. 1	No. 2[a]	No. 3
Power loss by deposit, %	15	18	19
Recovery by treatment, %	68	44	55
Deposits removed			
Piston tops	21	57	45
Heads	36	43	26
Intake valve tulip	19	19	49
Amount required	8 oz	160 ml	1/5 lb
How introduced	Through fuel line connection to carburetor	Through spark-plug hole	Through butterfly valve to carburetor
Treatment time required, min	18	45	20
Personal hazard	Skin irritant	Volitile toxic irritant	None
Side effects	None	Slight increase varnish piston skirt[b]	Beneficial to intake valve
Intake manifold and parts effect	None	Some cleaning	Some cleaning
Wear as result of treatment	Small	Small	Small

[a] Note large deposit removal but not in the places causing loss of power.
[b] Bad odor—must be done outdoors.

nition. It is introduced through the fuel line connection to the carburetor and application is by successive full-throttle no-load accelerations of the engine.

No. 2 operates by chemical action on the deposits and is introduced through the spark-plug holes. The exhaust pipe is blocked to stop airflow through the engine, and the engine is cranked for 5 sec with throttle closed. After a 10-min rest period the engine is again cranked for 3 sec. This step is repeated twice more with a total treatment time of 30 min. After treatment the exhaust block is removed and the engine started and run for 10 min with frequent accelerations and then run under normal conditions for an additional 10 min. The crankcase oil is changed.

No. 3 is a mechanical treatment consisting of uniformly sized granular material which is slowly poured into the carburetor air intake of a running engine. The pellets buffet about inside the combustion chambers, blasting the deposits loose and expelling them through the exhaust system. About 1/5 lb of material is required which is introduced in small batches past the butterfly valve as it is snapped momentarily into wide-open position. The wide-open throttle position aids in the even distribution and the resulting acceleration increases the deposit removal action. Crankcase oil is changed following the treatment.

From the results shown in Table A it is apparent that considerable is possible in removal of deposits without engine disassembly. In addition, there is one other type of shock treatment which we and others have found to be effective. This consists of water poured into the carburetor of a rapidly running engine in spoonful amounts just insufficient to kill the engine. A combination of water with chemical agents has proved to be quite effective.

Our radioactive techniques have shown that even head removal caused considerably increased wear rates. Therefore, a deposit-removal agent such as those enumerated yields twofold benefits by eliminating labor expense for teardown and its consequently increased wear rate.

Unquestionably, high output engines in steady service lay down deposits in the greatest quantity and are the most difficult to remove.

Old long-standing deposits are also more difficult to deal with.

Deposits may be very harmful to valves, particularly exhaust valves, and this appears to be more prevalent in single-cylinder engines where small pieces of deposit may wedge in between the valve and its seat.

A very good description of this action was given by D. Downs in a paper on exhaust valve life in small industrial gasoline engines.[a] Apparently, overhead-valve engines are somewhat superior to L-head engines and exhaust valve life can be considerably improved by flush valve guides with generous counterbores, and by the use of valve rotators.

[a] Automobile Division of Institution of Mechanical Engineers (Great Britain), General Meeting of Automobile Division, London, March, 1956.

ORAL DISCUSSION

— Reported by L. C. Kibbee, American Trucking Associations

A. K. Hannum, Thompson Products, Inc.: I am interested in combustion-chamber removers that promote sharp detonation in the engine. They warrant more study and I am investigating such a product for possible use through nationwide jobbers for this application. In these studies, I have found that with this type of application, not all of the deposits were removed. Rather, in some specific instances subsequent to detonation removal of combustion-chamber deposits, that the engine spark time could be advanced once more, having previously been retarded to prevent normal detonation of the engine. The one difficulty encountered with this type of application seemed to be that the benefit derived after combustion-chamber deposit removal through detonation did not seem to have a lasting effect, but the engine treated was back to its previous octane requirements in approximately 5000–6000 miles. The material used in the test was basically normal heptane, a material too dangerous to trust for general application in automotive repair shops. Further, the material made such a violent knocking of the engine that many shop operators are afraid to use it. A side line complication was the concern of the vehicle owner if he heard the vehicle detonating to the extent necessary to do any good in deposit removal.

Mr. Paige: The engines discussed in our paper were typical of engines generally. Thus, the results shown are representative for big or small engines, and the effects of deposits are much the same in all types of engines. In summary, there is no panacea for easy carbon removal, either for practical daily application or for research application in the near future. One aspect not mentioned, and which I think important, is the deleterious effect of crankcase breathers which vent into the intake manifold. The oil fumes thus burned in the combustion chamber are a very serious factor in the accumulation of combustion-chamber deposits. Also, valve guide seals used by one manufacturer helped considerably by preventing lubricating oil from entering the combustion chamber and contributing to combustion-chamber deposits. Some progress can be made in reducing combustion-chamber deposits by using special fuels, but this is an expensive and confusing way to handle the problem in fleet operation.

F. K. Glynn, Automotive Consultant: A great deal of the combustion-chamber deposit problem is due to the utility engines involved operating at their maximum capacity almost all the time. If automotive vehicles were so operated, they too would be involved with serious combustion-chamber deposits. It appears that utility engines can be increased in capacity for their specific application, such that they will not need to be operated at full horsepower; and with such a cut-back in power, would be less susceptible to chamber buildup. This has been prominently brought out by engines operated in marine applications. Often in the desire to keep the engine small relative to the size of the boat, the result was that it worked at full horsepower almost constantly. Such engines in marine use were subject to the same ills of carbon deposit as are the small utility engines. Manufacturers of "package applications" which include both the working tool and the engine applied to it should consider using larger engines which can work at lower horsepowers.

D. R. Jones, California Research Corp.: I have had some experience with chemical deposit removers operated in service stations. In spite of the problems of toxic fumes and hazardous material, but I think there is some merit in the operation. There are still some service stations which are using this method, and they have been successful in removing some deposits that decrease engine power, but not so successful in removing material that increases octane requirements. All of my work has been aimed at passenger-car application, and not to the small utility engines under discussion. But, I think that a qualified man using such chemical removers can do an acceptable job.

development

SUPPRESSOR AND

FOR THE

L. R. Jordan and C. M. Auble, Douglas Aircraft Co., Inc.

This paper was presented at the SAE National Aeronautic Meeting, Los Angeles, Oct. 1, 1958.

EARLY in the DC-8 program, our company undertook the development and design of a jet-noise suppressor and thrust brake for the DC-8 airplane. A summary of this work is presented herein.

Although the exact requirements of a jet-noise suppressor have not been established, it has long been known that large jet transports would require noise suppression in airline service. Early in the development program it was estimated that a 9–12 db suppressor could be developed for the DC-8. When considered from a sound energy standpoint, this meant about a 90% reduction in energy. Obviously, the solution to the problem was not a simple one.

In addition to the noise problem, it was felt that aerodynamic braking after touchdown would be required by high-speed jet transports, as has been the case with piston-engine aircraft. An added advantage was anticipated in the use of an aerodynamic braking device in flight. Accordingly, thrust braking was considered a requirement for the airplane. A braking force equivalent to that obtained

THIS PAPER presents the development of the DC-8 suppressor and thrust brake unit from initial test work through the final design. The selection of the production unit was based on a wide background of test work using both model and full-scale facilities. On the basis of this work, the configuration selected for production consisted of a fixed, corrugated, suppressing nozzle with a retractable ejector. A target-type thrust brake, mounted in the ejector, was chosen for the thrust brake production unit. Approximately 12-db suppression and 44% reverse thrust are provided by the unit.

The ejector is hydraulically operated and the thrust brake air actuated. Both actuation systems obtain power from the aircraft systems which provides for operation during engine-out conditions. Alternate methods of actuation are provided in case of a primary system failure.

Mechanically, the suppressor-thrust brake was designed to provide high reliability and to be capable of operation anywhere within the flight envelope of the airplane. Particular attention was given to component failures and their effect on safety of the unit.

of the

THRUST BRAKE

DC-8 AIRPLANE

with reversing propellers on present-day aircraft was considered the minimum requirement for landing. Consequently, reversed thrust equal to approximately 40% forward gross thrust at maximum continuous power setting became the target for the DC-8. The DC-8 suppressor and thrust brake development goal thus became: (1) jet noise suppression of 9–12 db, and (2) at least 40% thrust in reverse. This goal was to be accomplished with a minimum penalty to thrust, drag, and specific fuel consumption during take-off and cruise.

In view of the lack of theoretical methods of analysis for either suppressors or thrust brakes, selection of a design configuration was based on a wide background of test work. This test work was accomplished on both model and full-scale test facilities, utilizing 10%, 20%, and full-scale models. In addition, wind tunnel tests were conducted using 6.87% scale models.

The final design was selected on the basis of test results with some compromises being necessary to:

1. Obtain the best balance between sound reduction, thrust loss, drag, and thrust braking performance.
2. Make an installation compatible with our reliability and safety standards.

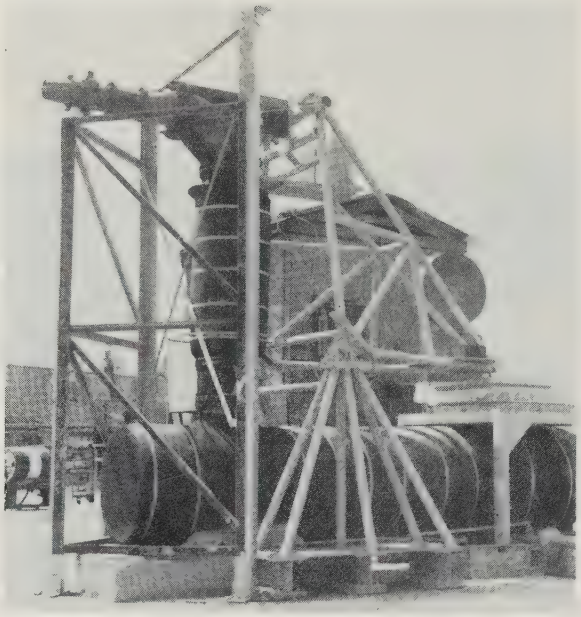

Fig. 1 — Douglas Santa Monica 20% scale test facility

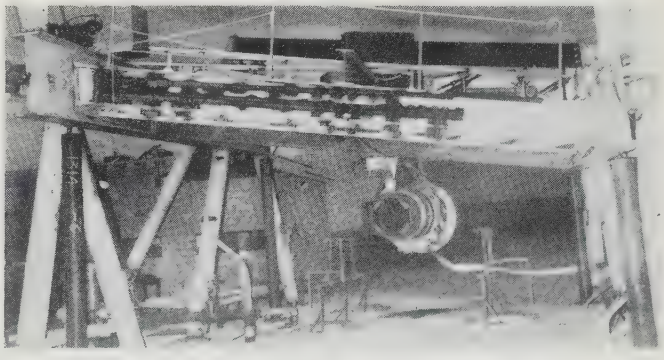

Fig. 2 — Douglas full-scale test facility

Development Test Program

The test program was started in 1955, using the 10% scale static test facility. The following year, the 20% scale facility shown in Fig. 1 became available and has since been used for all static model test work. Full-scale test work was first carried on with the help of Pratt and Whitney and NACA at their respective facilities. In 1957, the Douglas full-scale test stand shown in Fig. 2 became operational. Wind tunnel thrust and drag tests were conducted in the United Aircraft high-speed wind tunnel with 6.87% scale models. These tests were conducted

over a wide range of exhaust nozzle pressure ratios and aircraft speeds.

Sound suppression characteristics of suppressing nozzles were evaluated by observing overall sound pressure levels at a given radius from the nozzle. The data were plotted versus jet velocity to indicate sound levels at various power settings. This noise level, when subtracted from that of a reference nozzle (convergent bulleted nozzle), tested under identical conditions, afforded a measure of the suppressor's acoustic effectiveness. The curves in this paper present sound reduction at an angle of 30 deg to the jet axis. In most cases, this was the angle of maximum sound pressure level.

Thrust performance of a suppressing nozzle was also compared to that of a reference nozzle. Suppressor thrust loss was defined as the per cent loss in specific thrust (thrust per unit gas flow) with respect to the reference nozzle operating at the same pressure ratio and temperature. The thrust minus drag characteristics of a given nozzle and its nacelle fairing were evaluated in the wind tunnel. These data were compared to those of the reference nozzle on a specific thrust basis. In all cases a convergent, bulleted nozzle design was used as the reference. This reference nozzle is shown in Fig. 3. It is similar in many respects to that recommended by the engine manufacturer for installations where sound suppression is not required. In all test work, both the reference and suppressing nozzles were tested over as wide a range of exhaust nozzle pressure ratios as possible.

In thrust brake tests, the amount of reverse thrust was compared to the forward thrust of the reference nozzle operating at the same pressure ratio. The effect of the thrust brake on engine airflow was noted in all tests. Thrust brake stability characteristics were visually observed. All models which showed promise for final designs were tested for actuating and linkage loads over a wide range of nozzle conditions. These tests were accomplished under both static and simulated flight conditions wherever possible.

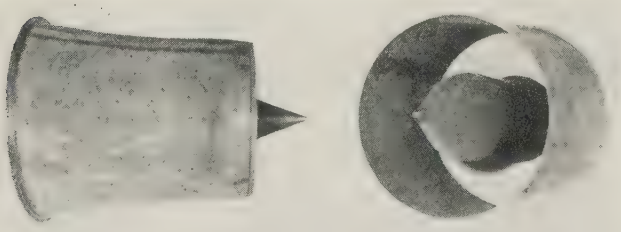

Fig. 3 — Douglas reference exhaust nozzle

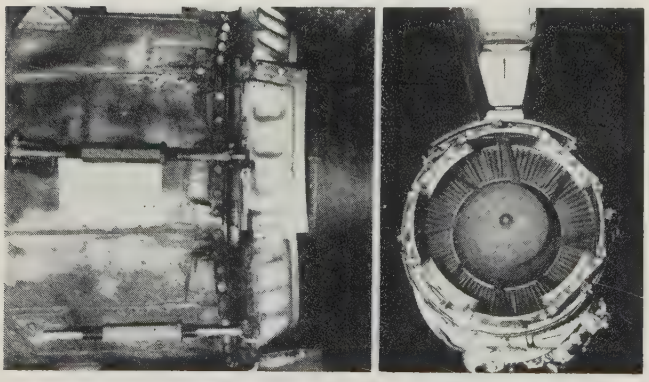

Fig. 4 — Adjustable-type suppressing nozzle (flaps shown in suppressing position)

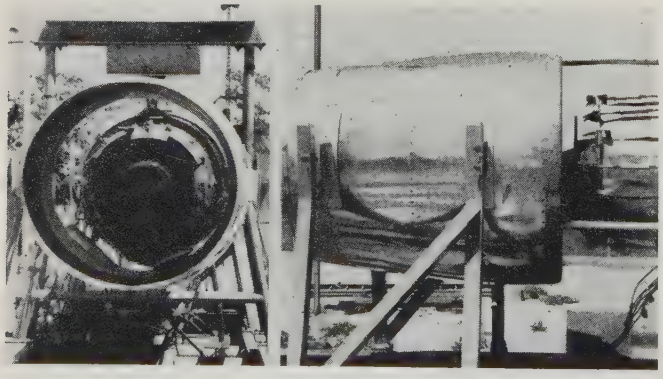

Fig. 6 — Adjustable-type suppressor with ejector (flaps shown in suppressing position)

Selection of Design Configuration

Selection of Suppressor Design — In the test program, two basic types of suppressing nozzles were studied simultaneously. These were adjustable and fixed types. Both types were tested with and without a retractable ejector. It was found early in the program that, if an ejector were to be used, retraction would be necessary because of the performance

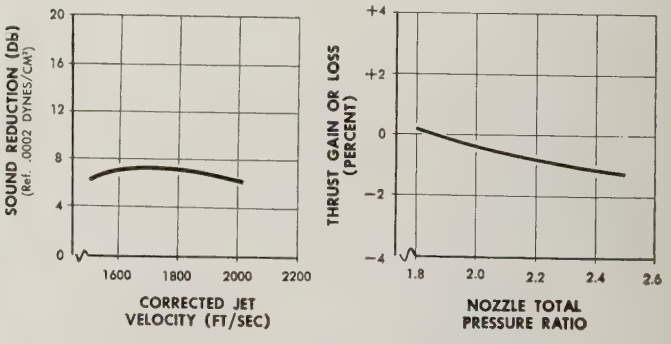

Fig. 5 — Sound and thrust performance of adjustable suppressing nozzle

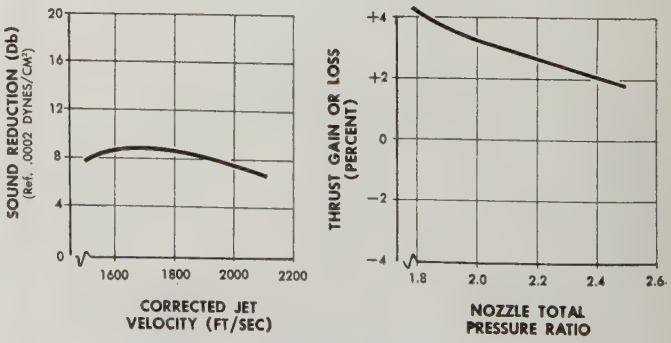

Fig. 7 — Sound and thrust performance of adjustable suppressing nozzle with ejector

loss at cruise in the extended position.

A typical adjustable suppressing nozzle is shown in Fig. 4. It is fitted with flaps which form a simple convergent cone in the retracted position. The flaps are hinged about 4 in. forward of the nozzle exit plane. In the suppressing position, alternate flaps are rotated in the direction of and away from the thrust axis, respectively. Thus, although the effective nozzle area is not changed, the exit has a castellated appearance. Sound reduction and thrust loss characteristics of this nozzle are shown in Fig. 5. The nozzle fell short of the sound reduction goal, although a relatively small thrust loss was incurred over most of the operating range. Fig. 6 shows this nozzle with an ejector. The addition of an ejector improved sound and static thrust performance, as can be seen in Fig. 7. However, the noise suppression was still considered to be inadequate.

Many different models of this nozzle and other adjustable types were tested. It became apparent during the course of the test work that much development effort would be required before adjustable suppressing nozzles could be designed to give the desired performance. In addition to the performance problem, it was anticipated that many reliability and safety problems would result from a design which placed moving parts continuously in the hot exhaust gases. Therefore, adjustable suppressing nozzles were abandoned in favor of fixed suppressing nozzle configurations.

Two types of fixed nozzles were tested: the multitube and corrugated types, respectively. A typical multitube nozzle is shown in Fig. 8. This particular nozzle was originally designed by Rolls-Royce and is temporarily in use on the first DC-8 test airplane. As shown in Fig. 9, the acoustic performance of this nozzle is much better than that of the adjustable type.

A typical corrugated nozzle and its performance is shown in Figs. 10 and 11, respectively. Corrugated

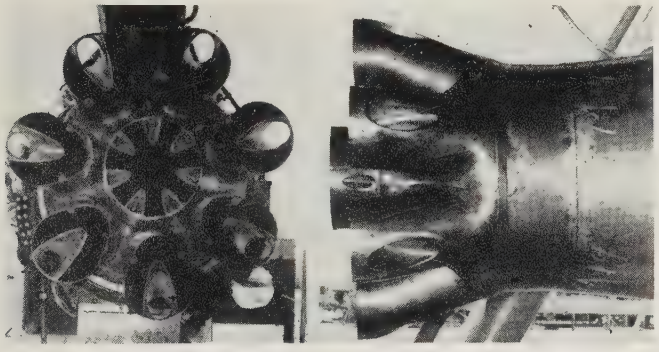

Fig. 8 — Fixed multitube-type suppressing nozzle

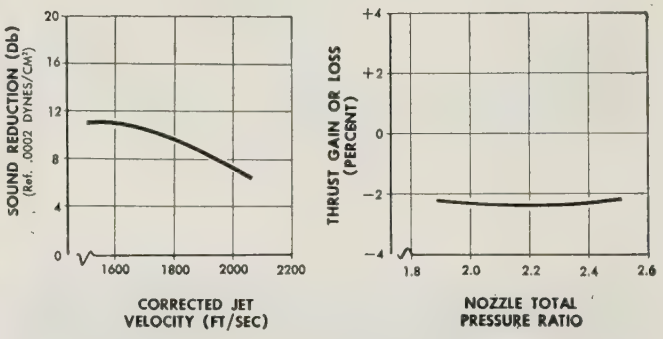

Fig. 9 — Sound and thrust performance of multitube suppressing nozzle

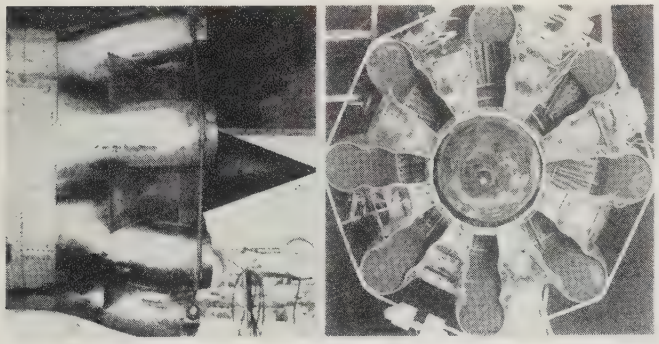

Fig. 10 — Fixed corrugated-type suppressing nozzle

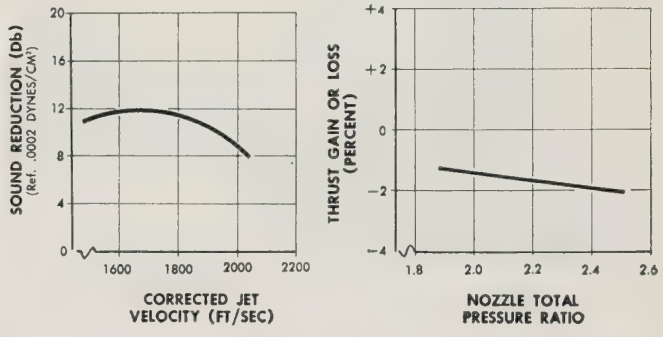

Fig. 11 — Sound and thrust perfromance of corrugated suppressing nozzle

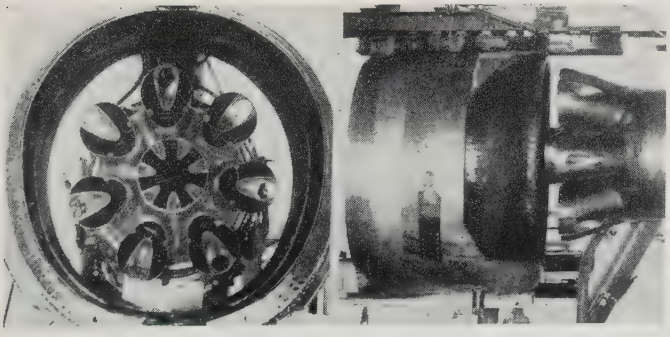

Fig. 12 — Fixed multitube-type suppressor with ejector

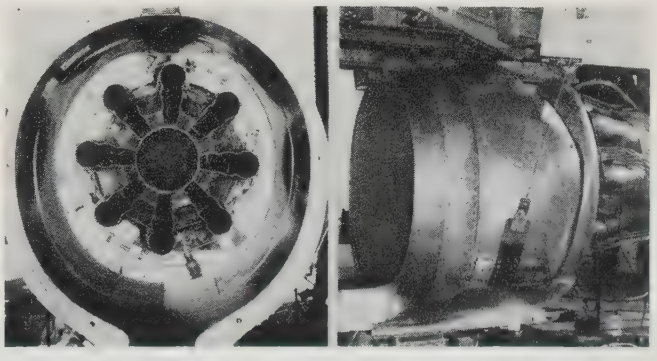

Fig. 13 — Fixed corrugated-type suppressor with ejector

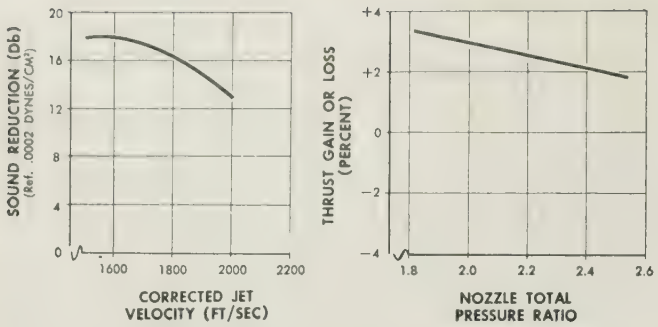

Fig. 14 — Sound and thrust performance of multitube suppressing nozzle with ejector

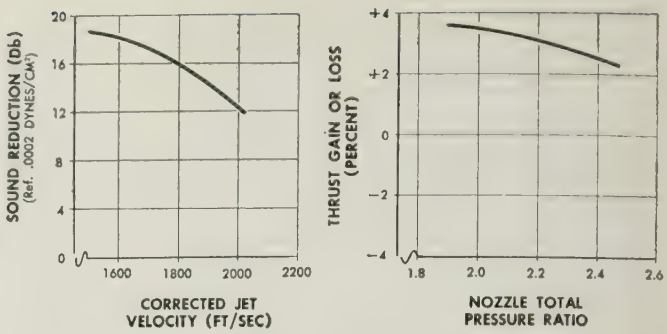

Fig. 15 — Sound and thrust performance of corrugated suppressing nozzle with ejector

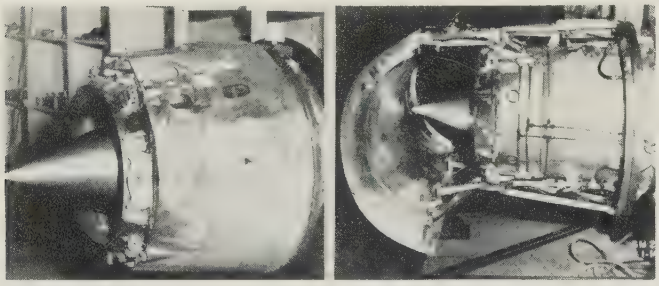

Fig. 16 — Adjustable-type suppressor with thrust brake in forward and braking positions

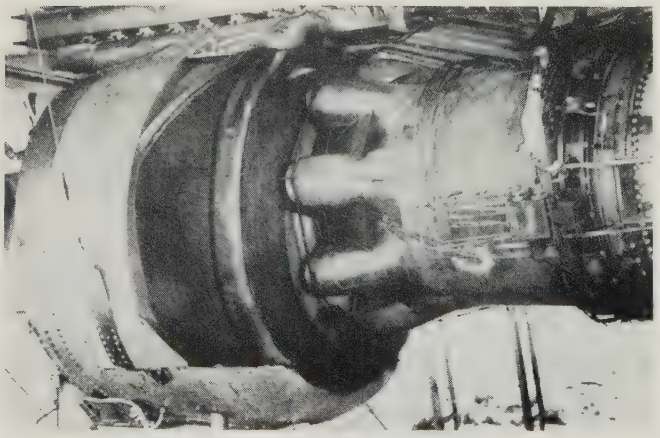

Fig. 17 — Fixed corrugated-type suppressor with ejector thrust brake

types show sound suppression and thrust loss characteristics similar to those of the multitube nozzle.

Both fixed types of nozzles showed promise as suppressors but did not produce the sound reduction desired. The addition of an ejector improved the sound performance of both types sufficiently to meet the design objective. In addition, the ejector augmented the thrust sufficiently to offset the supressor thrust loss for take-off operation. The multitube and corrugated nozzles with an ejector added are shown in Figs. 12 and 13, respectively. Fig. 14 shows sound reduction and static thrust performance of the multitube nozzle with an ejector. Similar curves for the corrugated nozzle are shown in Fig. 15. As can be seen in the figures, both nozzle types give comparable sound reduction and thrust performance with an ejector. For final design, the corrugated type was chosen because wind tunnel tests showed it had less drag than the multitube type.

To provide design data, a program was established to optimize the sound and thrust performance of corrugated nozzles. The results of this work indicated that for optimum sound reduction characteristics a nozzle should have:

1. As large an outer diameter as possible at the exit plane.
2. Lobes which increase in cross-sectional area at the exit plane with radial distance from the thrust axis.
3. No fewer than eight lobes.
4. A relatively small center body or bullet.
5. At least 90% of the exhaust area distributed in the lobes. In other words, less than 10% of the exhaust area should be located in the annular passage near the bullet.

For minimum thrust loss, it was found that:

1. The nozzle should have a cross-sectional flow area that is constant or slightly converging over most of its length. Convergence to the final flow area should take place rapidly in the final few inches of gas travel.
2. The fewer the number of lobes, the less the thrust loss.
3. Center body or bullet size has little effect on static thrust of the nozzle.

In designing the ejector, the geometry was largely determined by installation considerations. However, tests were made which indicated that in installations where some design latitude is available, optimum sound and/or thrust performance is obtained when the ejector:

1. Is made as long as possible.
2. Internal lines are smooth and unbroken.
3. Exit diameter is equal to or slightly greater than the outer diameter of the nozzle.
4. Is as nearly cylindrical as possible.
5. Leading edge thickness is sufficient to eliminate separation in static operation.
6. Leading edge is placed slightly aft of the nozzle exit plane.

Selection of Thrust Brake Design — In selecting a thrust brake design, three types of thrust brakes were considered. These were the internal cascade,

external target, and target-type mounted in the ejector. The internal cascade consisted of turning vanes mounted in the tailpipe with doors which block the tailpipe in the braking configuration. The target type consisted of contoured doors which mount behind the exhaust nozzle in the braking position. Early in the program a decision was made to use the target rather than the cascade type for the following reasons:

1. The internal cascade thrust brake requires a gas seal between the tailpipe and the nacelle. It was anticipated that this seal would present a formidable design problem, with some leakage in service being unavoidable. This leakage would result in a thrust loss not experienced by the target-type thrust brake.
2. The target-type thrust brake is isolated from the engine by a nozzle which is choked when reverse thrust is applied, and thus should have negligible effect on engine operation.
3. The internal cascade thrust brake requires that moving parts be placed continuously in the hot gas stream. Furthermore, its position makes accessibility difficult. Maintenance problems were expected to be more frequent and difficult than with a target-type thrust brake.

As a result of this decision, a minimum of test work was carried out on cascade-type thrust brakes.

The external target-type thrust brake was tested only in combination with adjustable-type suppressing nozzles. A typical installation is shown in Fig. 16. This type of thrust brake was found to provide acceptable performance from the standpoints of reverse thrust, engine operation, and stability. However, with the decision to use an ejector in the final suppressor design, integration of the thrust brake with the ejector was considered desirable in the interest of both simplicity and weight.

A typical ejector thrust brake installation is shown in Fig. 17. Two thrust brake buckets rotate so as to close off the ejector completely in the braking configuration. In the forward thrust position, the bucket surfaces form the inner liner of the forward ejector wall. A cross-section of the ejector center section is shown in the thrust braking position in Fig. 18. The following design criteria were established during the test work on this type of thrust brake:

1. Moderate aft sweep (Fig. 18) on the buckets in the braking position has little effect on the reverse thrust. Aft sweep was found to be desirable to stabilize the gas flow during the braking operation.
2. One per cent of unblocked area in the ejector results in approximately 2% loss in braking thrust.
3. The length of the aft lip extension which serves to turn the flow in a forward direction (Fig. 18), has a relatively small effect on performance. The optimum length was found to be approximately one-third of the reference nozzle diameter.
4. Corrugated nozzles with large center bodies produce less reverse thrust than corrugated nozzles with small center bodies.
5. The ejector leading edge shape and geometry has little effect on reverse thrust.
6. The per cent of reverse thrust is relatively insensitive to power setting under static operating conditions.
7. This type of thrust brake has negligible effect on engine operation.

The performance of this thrust brake installation in an ejector is shown in Fig. 19. The curve shows that the reverse thrust decreases slightly as nozzle pressure ratio decreases. The airflow curve in Fig. 19 indicates that the thrust brake has negligible effect on engine operation over the entire operating range.

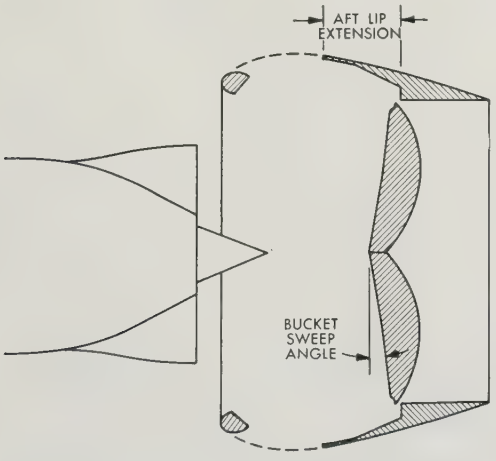

Fig. 18 — Cross-section of ejector thrust brake

Design, Operation, and Safety Features of Production Suppressor-Thrust Brake

Production Suppressing Nozzle — A photograph of the production suppressing nozzle is shown in Fig. 20. The nozzle design requirements were established

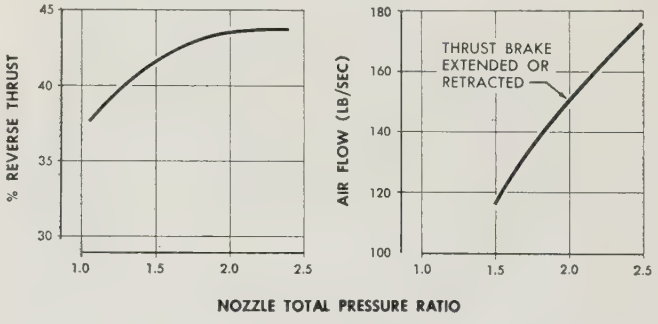

Fig. 19 — Reverse thrust and airflow performance of ejector thrust brake

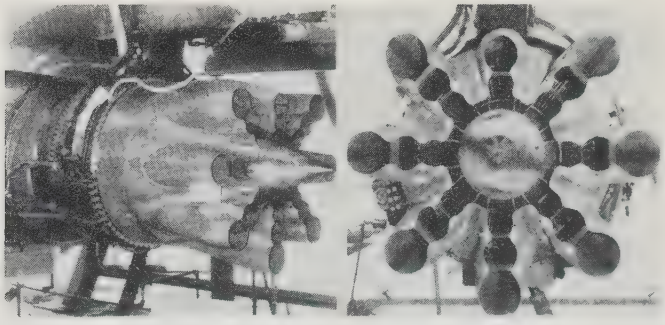

Fig. 20 — DC-8 production suppressing nozzle

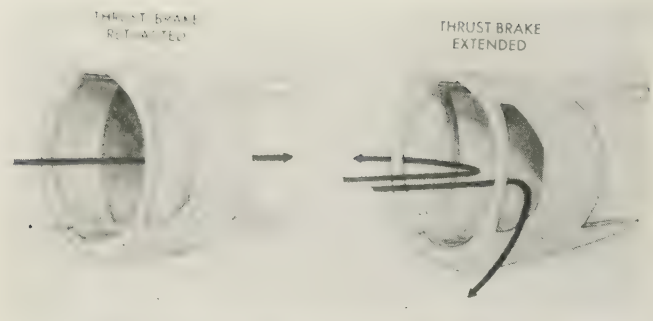

Fig. 21 — DC-8 production ejector and thrust brake

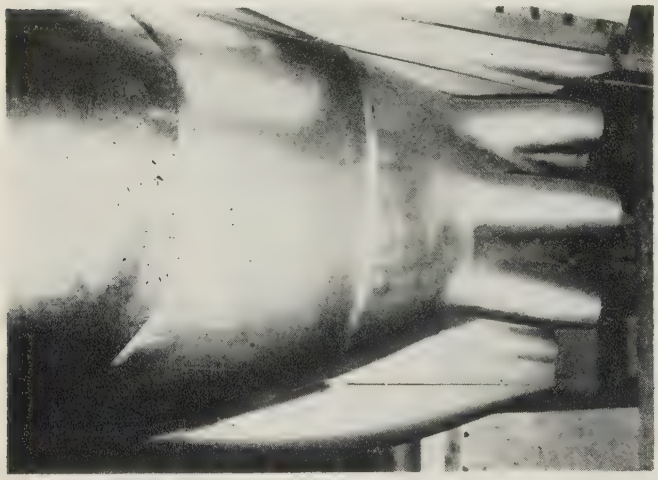

Fig. 22 — Mockup of production suppressor-thrust brake (ejector retracted)

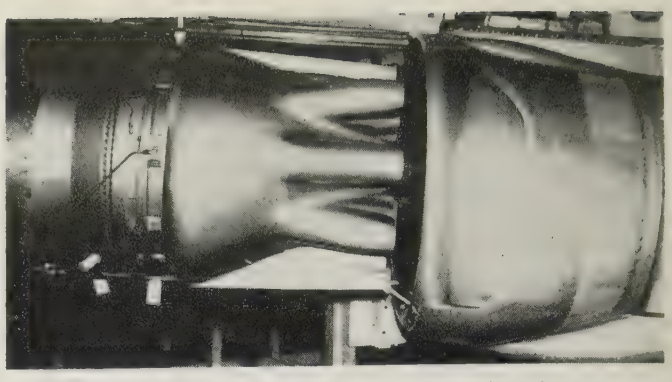

Fig. 23 — Mockup of production suppressor-thrust brake (ejector fully extended)

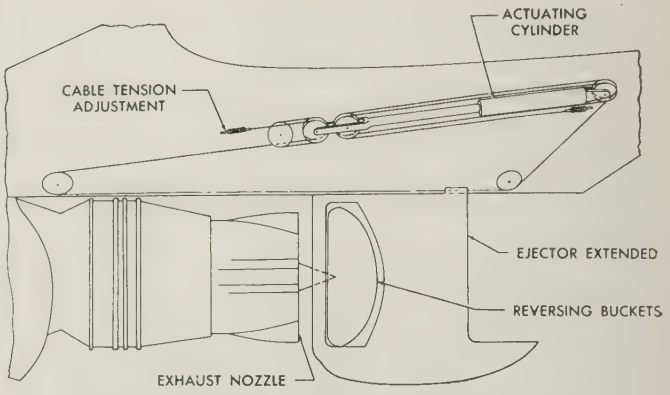

Fig. 24 — Schematic of ejector actuating mechanism

as: (1) high reliability, and (2) good dimensional stability.

To meet these requirements, the nozzle was designed to have negligible distortion due to temperature and pressure under service conditions. This was accomplished with a "triple bubble" design incorporating internal vanes and radial struts to place stress-carrying material in tension. Construction is of welded 19-9 DL stainless steel. Relatively light sheet is used for the outer portion of each lobe. Heavier material is used in the "valley" between the lobes. Radial struts, welded to the heavier material and bolted to a ring inside the bullet fairing, are used to retain the corrugated shape. The top lobe is reduced in height to eliminate washing of exhaust gas over the pylon. Nozzle area adjustment is provided by means of an adjustable bullet cone.

Production Ejector — A sketch of the production ejector is shown in Fig. 21. The ejector structure is designed to withstand:

1. Full aerodynamic braking for any condition within the flight envelope of the airplane.
2. Forces which may ocur in the event of a bucket failure in the thrust brake.

The ejector is supported from a track mounted below the pylon firewall. Longitudinal and vertical loads are taken out through the pylon structure. Lateral stability is provided by means of a link attached to the lower leading edge of the ejector. This link rides a lower track supported from the engine and nozzle. The highly stressed structural members are heat-treated 17-7 PH stainless steel. The balance of the ejector is constructed of 19-9 DL stainless steel. The inner skins on both the thrust brake buckets and the aft portion of the ejector are slip-joint supported to allow for differential thermal expansion.

Photographs of the installation mockup are shown in Figs. 22 and 23 for the retracted and extended positions, respectively. In the retracted position, the forward portion of the ejector including the thrust brake openings is covered by the engine access doors. A fixed cowl completes the aft nacelle fairing. The fairing on the underside of the ejector houses the thrust brake actuator and linkage.

A sketch of the ejector actuation system is shown in Fig. 24. The ejector rides on two sliding carriage assemblies and is positioned fore and aft along the pylon track by a 5/16-in. steel cable. Power is supplied through a piston operated by the aircraft hydraulic system. The actuator extends the ejector in 3 sec and retracts it in 6 sec. The ejector is held in either position by locking hydraulic fluid in the cylinder. Provisions are made for adjusting cable tension, cylinder stroke, and ejector position. Two bayonet-type disconnect valves are fitted in the aft slide assembly. When the ejector is fully extended, these connect with valves in the pylon at the rear of the ejector track and thus supply air for the thrust brake actuator. A shock absorber is installed

in the aft track assembly at the ejector stop to absorb impact energy in case of an actuating system failure. Latches are provided on the pylon track to prevent inadvertent extension in flight.

Emergency actuation is possible in case of a hydraulic system failure by means of stored high-pressure air. Air capacity is provided for one extension or retraction of each ejector. The system is cable operated from the cockpit.

A positive cam mechanism is incorporated which precludes ejector retraction with thrust brake buckets extended. This mechanism retracts the buckets as the ejector is pulled forward by means of cam action between the upper bucket pivots and the track. This system operates only in the event of failure in the thrust brake actuating system.

The ejectors are operated by two overhead switches in the cockpit. One switch operates both outboard ejectors, the other the inboard units. These switches energize solenoid valves which port hydraulic fluid to the actuating cylinders. Lights in the cockpit indicate full extension.

Production Thrust Brake — The thrust brake buckets and their actuating system are shown schematically in Fig. 25. They are mounted on stainless-steel shafts which rotate in self-aligning bearings attached to shear plates at the top and bottom of the ejector. The thrust brake pivot axes are located outboard of the bucket center of pressure. This location provides for bucket retraction by jet forces in case of an actuator power failure.

The buckets are actuated by a pneumatic piston and cylinder mounted at the bottom of the ejector. As shown in Fig. 25, the piston is connected to the bucket lower pivots through a bell crank linkage system. This system operates the buckets in 1–2 sec. Air is supplied to the thrust brake actuator through the bayonet valves previously mentioned. Thus, the thrust-brake may not be actuated until the ejector is fully extended, since high-pressure air is not otherwise available. The air used for actuation is taken from either the aircraft pneumatic manifold or the engine high-pressure bleed system. This system allows reverser bucket actuation on any engine, whether or not the engine is in operation. In the event of a thrust brake pneumatic system failure, the thrust brake buckets may be retracted by retracting the ejector, in the event they have not previously been faired due to pressure loading.

Since the thrust brake cannot operate until the ejector is fully extended, provision has been made to extend the ejector automatically when thrust braking is selected. This is accomplished by pressure switches which energize the ejector solenoid valves when the thrust brake pneumatic supply line becomes pressurized.

At the present time, no thrust brake bucket position modulation is provided. The thrust brake must be in either the full-open or full-closed position. Variation of reverse thrust is accomplished by throttle setting.

Thrust brake operation from the cockpit is controlled by the thrust brake throttles which are pivoted from the main throttles. Operation of the reverse throttle is possible only when the main throttles are in the idle position. Selection of thrust braking directs engine bleed air to the actuating cylinder. This is accomplished through an engine mounted pilot valve which takes its signal from a cam on the engine throttle shaft. The thrust brake actuating valve is a slide-type valve allowing pressurization on either side of the piston. Thus, normally the thrust brake buckets are retracted by the actuating piston when forward thrust is selected. A cockpit light indicates full-braking bucket position.

Both the thrust brake and ejector are operable from the normal ground power plugs. Thus, engine operation is not necessary for ground check-out.

Summary and Conclusions

Design features of the DC-8 suppressor thrust brake configuration can best be seen in the exploded assembly sketch shown in Fig. 26. The design consists of a fixed, corrugated-type nozzle with a retractable ejector. The target-type thrust brake is mounted in the ejector. This design, which is the culmination of test work on many suppressor and thrust brake configurations, meets or exceeds the performance objectives originally set up in the development program. Work is continuing at Douglas, however, to improve both thrust and sound suppression performance of the suppressor-thrust brake unit.

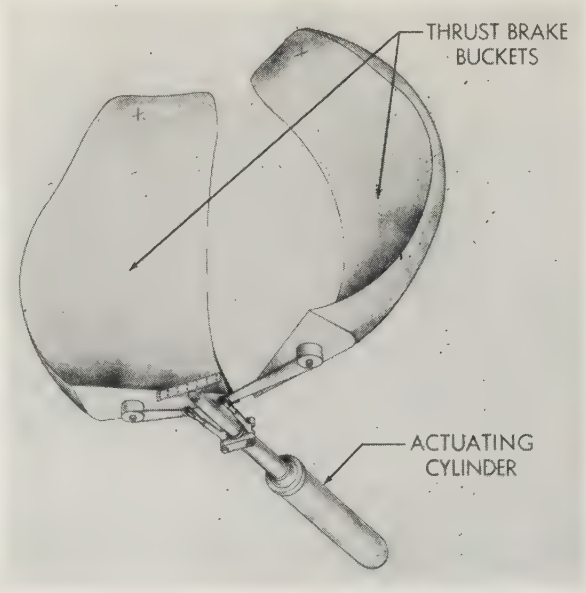

Fig. 25 — Thrust brake actuating system (thrust brake partially extended)

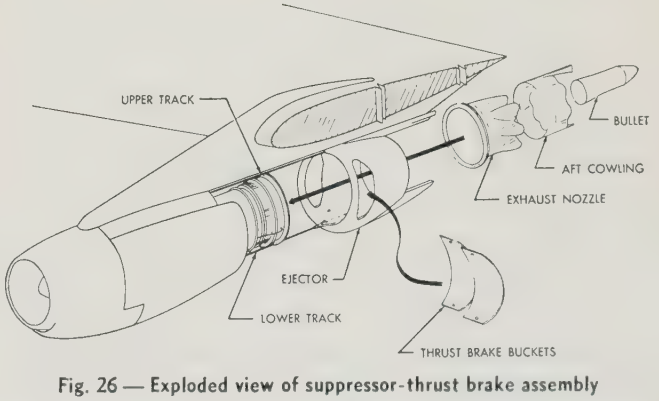

Fig. 26 — Exploded view of suppressor-thrust brake assembly

Digital Computer Analysis and Turbocharged

H. A. Cook, Thompson Ramo Wooldridge, Inc.

This paper was presented at the SAE Annual Meeting, Detroit, Jan. 12, 1959.

THE MATERIAL for this paper is the accumulated results of cycle analysis on turbocharged diesel engines initiated in 1954. The interpretation of results and conclusions are important to both engine manufacturers and users of turbocharged diesel engines. The subject can be discussed from a number of view points, for example:

1. Diesel cycle calculation on a digital computer.
2. Interpretation of results.
3. Application of analysis to an engine development program.
4. Evaluation of new engine design concepts in the planning stage.

The digital computer is used in the diesel cycle analysis presented herein because of its speed and ability to retain a high degree of accuracy in calculations involving small differences in relatively large numbers. Hand calculations would be too inaccurate and the time would be measured in years compared to hours or minutes on the 650 IBM Digital Computer. I believe current developments in faster and greater capacity digital computers should be utilized to the fullest extent for the solution of the engine designer's engineering problems, particularly where a turbocharger is involved. The emphasis in this paper will be to present useful results obtained by turbocharged diesel cycle calculations rather than the method used to make the calculations. Although calculation programs on both 4-stroke and 2-stroke turbocharged diesel engines are being used, only results of 4-stroke cycle studies are presented herein.

The interpretation of results of cycle calculation is of necessity dependent on the input data, the degrees of detailed analysis incorporated in the calculation, the required accuracy, and the nature of the turbocharged diesel operation being investigated. A variety of ways of treating the physical processes in the cycle calculation of a turbocharged diesel are available to the engineer. The selection of the particular mathematical treatment of various parameters will depend on the engineer's preference and the characteristics of the digital computer to be used.

In setting up the turbocharged diesel cycle calculations, particular detailed attention was given to the scavenging and charging processes as related to valve operation and turbocharger characteristics. This included the possibilities of backflows as well as mixing processes. Rather than to elaborate on how such things as heat transfer, mixing, compression, combustion, expansion, and inlet and exhaust flows were treated, I believe it is more important at this stage to look to the results obtained in investigations of various engine parameters with the present method and then if necessary incorporate improvements in the future.

The application of the cycle analysis to an engine development program entails first a correlation of calculated and test results and then the study of some design or operating parameters. This

Interpretation of Diesel Engine Performance

was done in the early stages of turbocharger development and satisfactory results were obtained. Encouraged by these results, an investigation of design concepts was undertaken on the problem of the best way to match a turbocharger to a V-8 diesel engine. Results of these V-8 studies where certain results are predicted for various designs of intake and exhaust manifolding, illustrate the potential usefulness of cycle analysis using the digital computer. The paper is concluded with an example of how a new engine design concept can be evaluated in the preliminary planning stages for an engine.

Subjects of interest to both turbocharger users and engine designers will be discussed in the following categories:

1. Operating and design variables.
2. Matching a turbocharger to a V-8 diesel engine.
3. Inlet manifold pressure study.
4. Evaluation of a new design concept.

Operating and Design Variables

The results of cycle analysis are comparable to data obtained on a very completely instrumented test engine and operating and design variables are studied the same way as the test engineer would conduct a test program. Results of cycle calculations are obtained in two forms: (1) Cycle data which is the time history of pressures, temperatures, gas flows, and work done for every increment (5 deg) of crankshaft rotation; and (2) final results which are the net effects of the cycle in terms of engine output. Cycle data are most easily studied by plotting variables with crank position as shown in Fig. 1, where the effects of engine rpm with constant fuel per stroke are shown for a 6-cyl engine with a 2-way divided exhaust system. The 2-way divided exhaust creates an exhaust pressure wave in each half of the exhaust system (front three cylinders divided from rear three cylinders) which has three complete cycles for the two revolutions required for one engine cycle. The cycles for exhaust pressure (P_e) and exhaust temperature (T_e) are only shown for the period they are effective for the cylinder being studied. Cylinder pressure (P_c) is plotted on the expanded scale for the exhaust pressure (P_e) during the exhaust and intake strokes and a dif-

THIS PAPER describes the application of computer analysis to an engine development program in one firm. Such cycle analysis can lead to specific recommendations in the matching of turbochargers to V-8 diesel engines and the designing of intake and exhaust manifolds.

The author discusses the correlation of the calculated data and the test results. He believes that clearer insights into engine test results and development problems are obtained when the effects of operating and design changes are studied analytically as well as experimentally. The result can be a saving of development time and a reduction in costly experimentation, he believes.

ferent scale to show peak pressure. Cylinder temperature (T_c) is on the same scale as (T_e). Intake manifold pressure (P_i) is the turbocharger compressor outlet pressure.

The accuracy obtained in these cycle calculations can be judged by the degree to which the various quantities match where the cycles are supposed to close. For the data of Fig. 1, all cycling variables close (final calculated value equal to starting value) with a maximum deviation of less than 0.4%. All results of cycle calculations presented herein have been refined by repetitive calculation until closing of cycling variables show less than 1% maximum deviation. Thus, in contrast to the difficulty of repetition of results in an engine laboratory, cycle calculations are stable and repeat to as fine a degree as the operator may desire.

The results shown in Fig. 1 indicate a difference in cylinder pressure variation during the exhaust stroke. At rated rpm, the closing of the exhaust valve is throttling the flow to the extent that cylinder pressure increases during the last half of the exhaust stroke. The pressure then drops from above inlet manifold pressure (P_i) to below it due to a

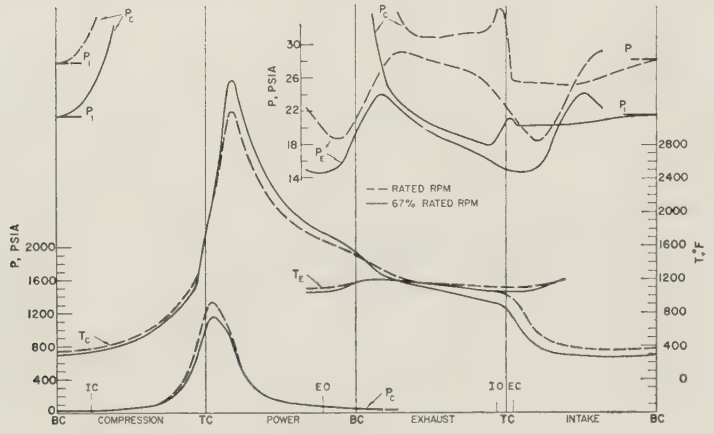

Fig. 1 — Effect of engine rpm, constant fuel

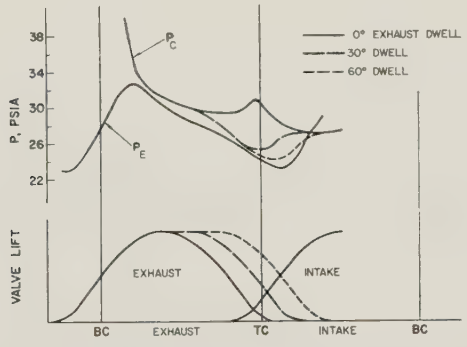

Fig. 2 — Effect of exhaust valve closing time

Table 1 — Effect of Advancing Camshaft (5 deg) on Engine Performance

	Rated Rpm	71% Rpm
Bhp	101.1%	100.7
Bsfc	98.8	99.2
Cfm, Air	98.5	99.5
Blow Through, Air	73.6	85.7
Boost Pressure	101.2	102.0

Table 2 — Six-Cylinder Engine Performance with 2-Way Divided Exhaust Compared to Nondivided Exhaust

Ihp	100.2%	Cfm, Air	111.1
Fhp	108.3	Boost Pressure	112.9
Bhp	99.5	Turbocharger, rpm	122.6
Bsfc	100.3		

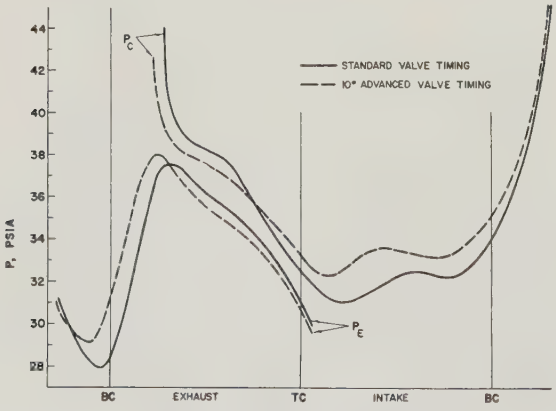

Fig. 3 — Effect of valve timing

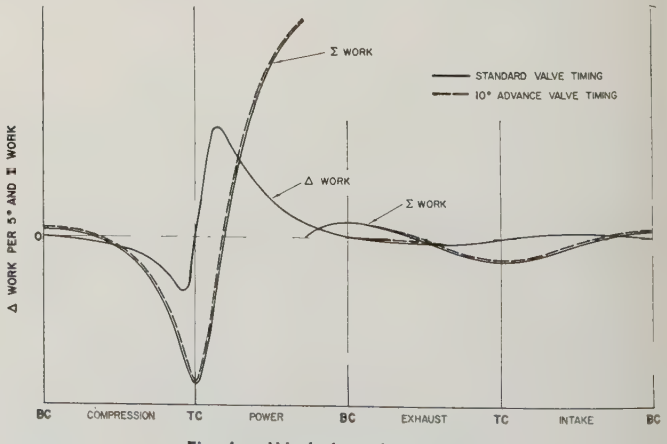

Fig. 4 — Work done during cycle

backflow into the inlet manifold before top center and then the downward motion of the piston on the intake stroke. Note that at both rated and 67% rated rpm, the cylinder pressure becomes equal to the inlet manifold pressure at the bottom of the intake stroke and again some backflow into the intake is found as the piston starts up on compression. The effects of these backflows will be discussed later. The main effect of engine rpm shown in Fig. 1 is the change in the characteristic of the cylinder pressure cycle during the exhaust stroke, the pressure rising and then dropping as noted above for rated rpm in contrast to more closely following the pressure in the exhaust manifold (P_e) and rising to inlet manifold pressure upon opening of the inlet valve for 67% rated rpm.

The above results suggest the possibility of improving the situation during the exhaust stroke by varying the valve timing. Data on another engine in Fig. 2 shows the effect on cylinder pressure of adding first 30 and then 60 deg crankangle of open dwell on the exhaust valve, thereby retarding its closing. These results illustrate how effects of valve timing changes can be studied by changing only one parameter at a time in the cycle analysis. The detail to which a valve timing change can be studied is indicated by another case where the camshaft of an engine was simply advanced 5 deg, thereby advancing all valve action 10 deg of crank rotation. The differences in exhaust and cylinder pressures during the exhaust and intake are shown in Fig. 3 with the net effect on engine performance shown in Table 1. A small increase in bhp of 1.1–0.7% is noted but differences of 98.5–99.5% in cfm, and 73.6–85.7% in air blown through during valve overlap are noted. The increase in bhp is attributed to the reduced cylinder pressure at the beginning of the exhaust stroke. This is shown to be the case by the study of the incremental work on the piston per 5 deg of crank rotation and its summation which are plotted in Fig. 4. The only noticeable difference occurs in the summation of work during the exhaust stroke and this difference persists to the end of the calculation resulting in the slight increase in power. The calculated cylinder pressure was correlated quite well with pressure measured in the cylinder, as shown in Fig. 5. The change in the calculated peak pressure (30 psia) with this valve timing change is insignificant but illustrates how peak pressure is changed by a design parameter.

An improvement in fuel economy, although it is small, would help to improve operating economy. A 1% reduction in a large monthly fuel bill can be dollars saved. The potential use of cycle calculations for optimizing performance of an engine is indicated by the possibility of correctly combining a number of small improvements resulting from a series of changes in design or operating parameters, which can be defined by cycle analysis far more precisely than by engine tests.

Previous data have all been with a divided exhaust on a 6-cyl engine, the effect of running nondivided is to modify the pressure variation in the exhaust gases supplied to the turbine. Two engine tests in our laboratories were run under identical setup and operating conditions with only the substitution of a 2-way divided flow turbine housing for a nondivided flow turbine housing. The results showed a remarkable increase in turbocharger rpm and an increase in compressor pressure ratio of about 25% at rated engine rpm. Thus, the different routing of exhaust gases through the same turbine and nozzle resulted in a much improved utilization of the energy in the exhaust. Cycle analysis of the nondivided turbine flow are compared in Fig. 6 with 67% rpm data presented in Fig. 1. Note the pressure changes at end of exhaust. The net effects on increased airflow and engine performance are compared in Table 2. Obviously, the comparison of nondivided and divided exhaust is affected by the entirely different situation imposed on the engine by the different level of turbocharging. A more correct basis of comparison would be to use a slightly larger nozzle with the divided flow so that a comparison at equal compressor pressure ratios is obtained. This will be discussed later under study of the division of exhaust for matching a turbocharger to a V-8 diesel. Note the lower exhaust temperature and cylinder temperature with the divided exhaust is due to increased airflow.

The basis of comparison of effects of variables must be considered carefully. For example, in a comparison of effect of turbocharger efficiency, the higher efficiency increased ihp but decreased bhp, because the resulting higher compressor pressure ratio resulted in higher pressure on the piston throughout the cycle which increased fhp. This is another case where the basis of comparison could well be equal pressure ratios obtained by selection of appropriate turbine nozzle sizes.

A preliminary check of the effect of altitude on a specific engine at 67% rated rpm indicated, at 7000

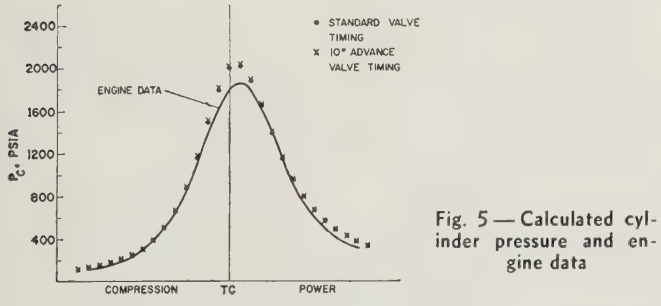

Fig. 5 — Calculated cylinder pressure and engine data

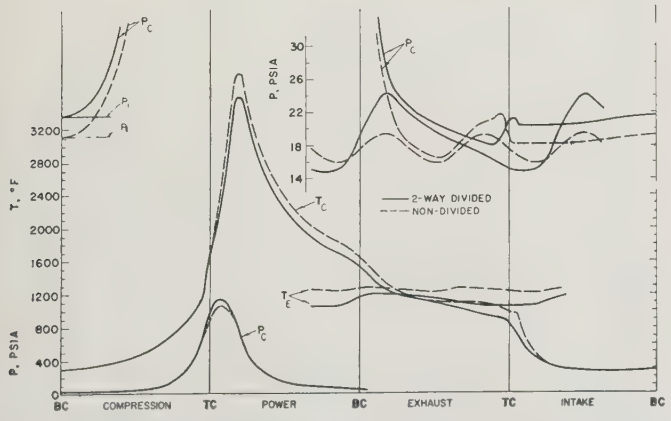

Fig. 6 — Divided and nondivided exhaust on 6-cyl engine (A_T constant)

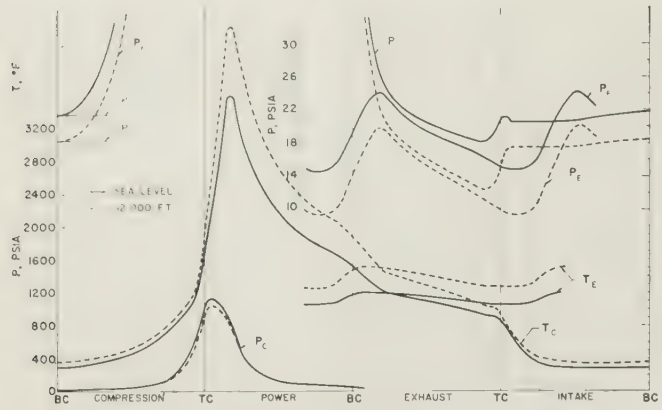

Fig. 7 — Effect of altitude, constant fuel at 67% rated rpm

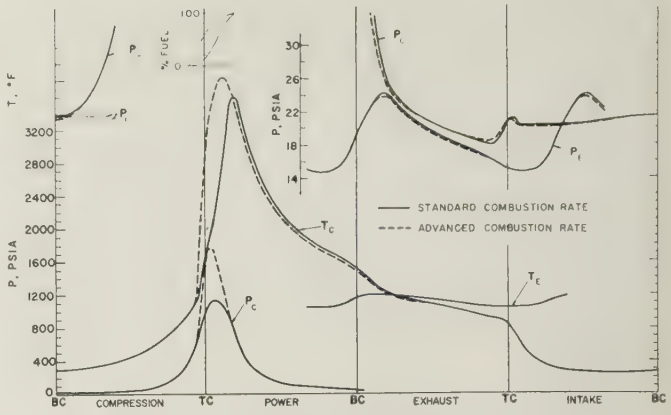

Fig. 8 — Effect of rate of burning on engine cycle

Table 3 — Altitude Performance Compared to Sea Level Performance (67% rated rpm)

	7000-Ft Altitude	12,000-Ft Altitude
Bhp	100.8%	101.1
Bsfc	99.3	98.7
Cfm, Sea Level Air	85.7	78.8
Exhaust Temperature	110.6	116.4
Inlet Pressure	89.5	84.4
Ambient Pressure	76.6	63.1
Turbocharged Rpm	120.4	136.0

Table 4 — Percentage Change in Performance with Accelerated Rate of Burning Fuel

Ihp	110.8%	Cfm, Air	99
Fhp	117.9	Boost Pressure	98.3
Bhp	110.0	Turbocharger, Rpm	97.5
Bsfc	91.1	Peak P_c	154.5

and 12,000-ft altitudes respectively, an alarming increase in turbocharger rpm (120% and 136% sea level rpm) and an increase in pressure ratio, but an actual decrease in weight of airflow (86% and 79% sea level airflow); thus indicating an inherent cutback in rated power would result due to over-rich fuel/air ratio. Altitude data without any other change than the inlet pressure are presented in Fig. 7 and Table 3 and illustrate the effect of going to 7000 and 12,000 ft altitude. The amount of fuel used in this altitude study was the maximum that could be burned theoretically at 12,000 ft. Devices to alleviate the effect of altitude on overspeeding of the turbocharger will be discussed later. Altitude operation imposes serious effects on engines, particularly with turbochargers, and each engine will have its individual characteristic depending on both the engine and the turbocharger.

Many of the variables discussed so far would have complex effects upon combustion in the engine cycle. Experience has shown that small changes to the injection timing, nozzle spray pattern, or the combustion chamber (even cutouts for value clearance) can alter peak firing pressure and the entire engine cycle. The effects of varying the rate of heat release due to combustion are shown in Fig. 8 and Table 4. The start, the duration of combustion, and the difference in rate of heat release as per cent fuel burned are shown at the top of Fig. 8. The beneficial effect of increased bhp must be weighed against the increased peak cylinder pressure. The situation in the engine can be more complex if consideration is given to differences in the compression stroke, resulting from a change in combustion rate, interacting on ignition timing.

Fig. 9 presents bomb test data on ignition delay of a mid-continent fuel oil. The compression pressure and temperature for a typical cycle are plotted to show the shortening of the ignition lag as the top of the compression stroke is reached. Note how initial burning will change the slope of the curve. Ignition delay in millesec is replaced by delay in degrees of crankangle rotation for several operating conditions and plotted against crankangle ahead of top center in Fig. 10. The upward sloping lines represent accumulated elapsed crank rotation after the ignition delay has become reasonably short. The results show that theoretically ignition timing could be changed one half a degree for the difference in combustion rate reported in Fig. 8. The effect of lowering inlet temperature was similarly studied and results show that a 40-deg drop in inlet temperature could retard ignition 5 deg. Rating an engine at different conditions showed almost 5 deg change in ignition timing. Results such as these aid in the interpretation of engine performance as affected by operating and design variables.

The versatility of cycle analysis by digital computer to correlate and use findings in diverse situations is well-illustrated by the above application of bomb fuel test data. Subjects such as engine friction[1] and thermal loading and wall temperature[2] are other examples of types of many diverse investigations that can be correlated and their findings used collectively in the development of turbocharged diesel engines. The remaining discussion will center about the application of cycle analysis to engine development and evaluation of new engine design

[1] SAE Transactions, Vol. 66, 1958, pp. 649–667: "Determination of True Engine Friction," by R. E. Gish, J. D. McCullough, J. B. Retzloff, and H. T. Mueller.

[2] SAE Transactions, Vol. 67, 1959, pp. 478–494: "Thermal Loading and Wall Temperature as Functions of Performance of Turbocharged Compression-Ignition Engines," by E. T. Vincent and N. A. Henein.

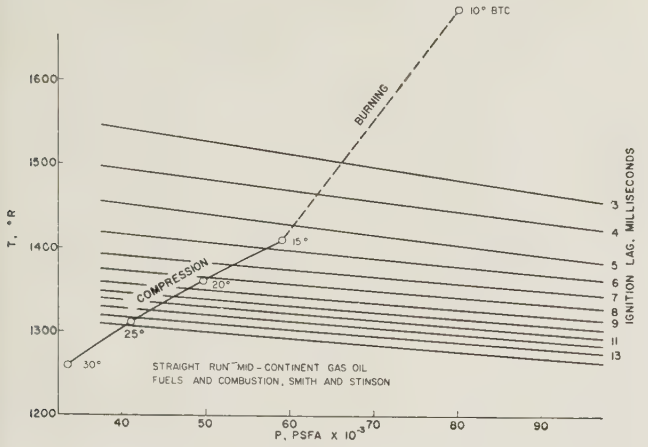

Fig. 9 — Correlation of compression with bomb data on ignition lag

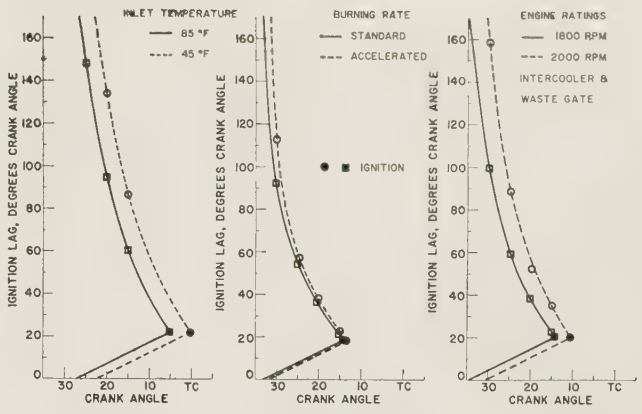

Fig. 10 — Ignition lag versus crankangle for various conditions

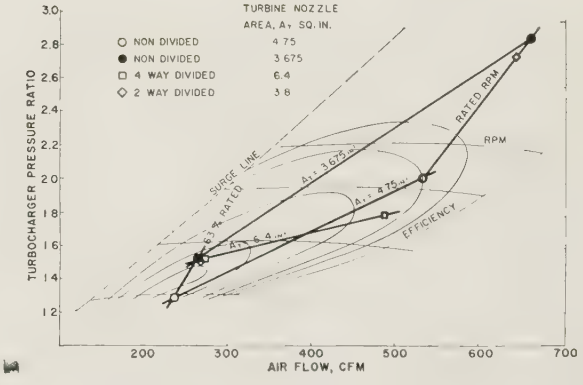

Fig. 11 — V-8 diesel pressure and airflow with various exhaust manifolds

concepts in the planning stage. The discussion and results presented so far have shown how the digital computer was used to analyze and interpret turbocharged diesel engine performance, as effected by operating and design variables.

Adapting Turbocharger to Exhaust of V-8 Diesel

Analysis of the V-8 engine cycle with a turbocharger was made in order to show the difference in matching of a turbocharger to an engine that results from dividing the exhaust in various ways.

Matching of a turbocharger to an engine is herein defined as the determination of the best configuration of exhaust division and the proper turbine nozzle area to give the desired engine performance over a specified speed range (from about 60 to 100% rated speed) and not exceed recognized temperature and pressure limits.

The firing order of V-8 engines is determined by crankshaft design and vibration considerations. In order to achieve various divisions of the exhaust, the practicability of the necessary manifold and ducting must be considered.

V-8 exhaust manifolding considered:

1. Nondivided.
2. Division into effective two 4-cyl engines.
3. Practical 4-way division.
4. Division right bank from left bank.

The nondivided and division of left and right banks of cylinder are generally considered because of the simplicity of manifolding. The effective division of the engine into two 4-cylinder engines with the same even firing sequence in each, is possible by joining a pair of cylinders from one bank with the appropriate pair from the other bank. In this way a 2-way divided turbocharger may be used. The further division of these cylinders to effectively divide the two 4-cyl groups into four pairs of cylinders is not feasible with the manifolding considered in (2) because paired cylinders from each bank fire successively.

A practical 4-way division of the exhaust is considered which will allow the use of two turbochargers with 2-way divided turbine housing (one on each side of the engine) or a single 4-way divided turbocharger. The cylinders from each bank are paired in such a way that a minimum of two other cylinders fire between the cylinders of each pair. This grouping of the cylinders for a 90-deg V-8 engine firing order is shown in the diagram at the top of Fig. 16.

The practical 4-way division is a logical step in the direction of approximating the ideal divison where three other cylinders fire between firing of each cylinder of a pair. As indicated before, the ideal 4-way division would require an elaborate cross-over exhaust manifold and is, therefore, considered impractical except for V-8 engines with exhaust ports on the inside of the V, which is an uncommon arrangement.

V-8 Exhaust Utilization

The pressure ratio and airflow in cfm for various operating conditions are presented in Fig. 11 on a typical turbocharger compressor map. The differences in operation at rated rpm and 63% rated rpm are clearly shown for the nondivided V-8 with turbine nozzle areas of 4.75 and 3.675 sq in. and for the 4-way and 2-way divisions of the exhaust flow to the turbine. The pressure ratio of 1.52 at 63% rated rpm with the 3.675-sq-in. area nondivided turbine was used as a basis for comparison of the 4- and 2-way division exhaust, because the airflow was adequate to burn the amount of fuel intended to be burned at 63% rpm. Note, comparison of divisions of exhaust starts with equal compressor pressure

ratio, at this engine rpm, by proper selection of turbine nozzles.

The fuel/air ratio and other pertinent data for the same operation points shown in Fig. 11 are presented in Fig. 12. Note, that the fuel/air ratio at 63% rated rpm with the 4.75-sq-in. turbine nozzle is above the chemically correct fuel/air ratio and, therefore, constitutes an unrealistic operating condition. Although operation with a nondivided turbine with the smaller turbine nozzle is feasible, the increase in pressure ratio upon going from about 63% rated to rated rpm is high (87% increase), whereas a much smaller increase is shown for the 4-way division (17%). The 2-way division is only slightly better (81%) compared to 87% for the nondivided. The advantage of using the lower pressure ratio afforded by the 4-way divisions of the exhaust is reflected in the lower peak cylinder pressure. Comparable operation in all respects is obtained at 63% rated rpm with generally improved performance with the 4-way division at rated rpm. These data clearly show that the 4-way division of the exhaust on the V-8 engine is very desirable for obtaining a good matching of turbocharger to the engine.

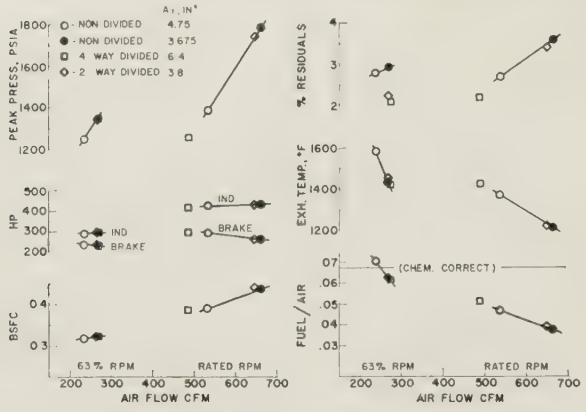

Fig. 12 — Engine performance with various exhaust manifolds on V-8 diesel

Fig. 13 shows the differences in the exhaust pressure cycles for the nondivided, 4-way divided and 2-way divided turbines at 63% rated rpm. The resulting lower cylinder and exhaust pressure during scavenging accounts for the per cent residuals being less with the divided turbine. Fig. 14 presents similar cycle data for operation at rated rpm. The same characteristics are observed as for the lower rpm, but operation is now at different inlet pressures as determined by the divisions of the exhaust.

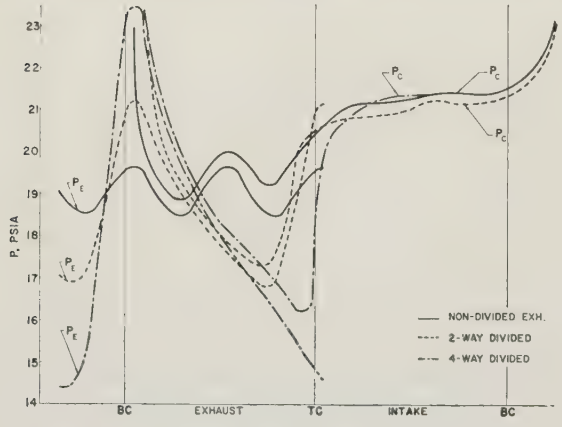

Fig. 13 — V-8 diesel exhaust cycles, 63% rated rpm

Because actual engine friction horsepower data were not available, the relationship of bhp to ihp shown in Fig. 12 is only approximate. A trend of the higher pressure ratio turbocharging to cause fhp to increase faster than the ihp increases is evident. This is but another reason for using as low turbocharger pressure ratio as is consistent with the engine application.

The simplicity of collecting the exhaust from each bank of cylinders and using a single-entry turbocharger on each side of the engine or a dual-entry turbocharger at the back of the engine has been considered by many engine designers. These configurations result in an uneven exhaust pressure cycle which is shown in Fig. 15. The effect on scavenging various cylinders is quite drastic, the analysis showing that No. 7 cylinder would have only 69% of the average cylinder airflow. This 2-

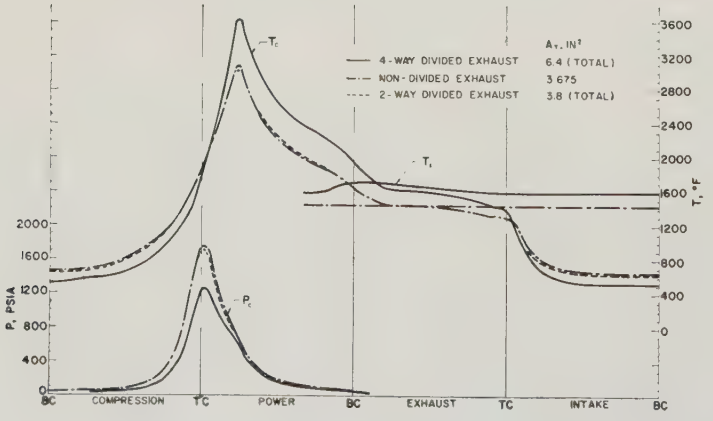

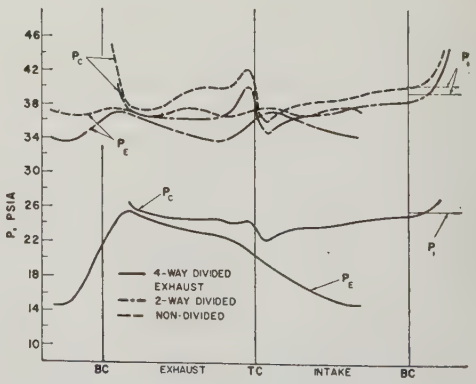

Fig. 14 — V-8 diesel cycles at rated rpm

way division of the exhaust of the V-8 engine by the separation of the right bank and left bank for turbocharging is, therefore, not recommended.

The degree to which the practical 4-way division suggested herein minimizes the effect of one cylinder upon the other is illustrated in Fig. 16. The blowdown of the exhaust of No. 1 cylinder is nearly complete before No. 3 cylinder starts exhausting. No. 3 cylinder has about 2.5% less airflow than No. 4 because of the slightly higher exhaust pressure during the scavenging period. The practical 4-way division of the V-8 greatly reduces the effect of one cylinder upon the scavenging of another and is recommended for use where a 4-way division of exhaust is desired.

The results of this analysis are indicative of the advantages and disadvantages of dividing the V-8 exhaust in various ways. Different engines having various degrees of valve overlap and different valve timing should be expected to show similar results to those discussed herein. The advantage shown for the 4-way divided V-8 over the 2-way indicates that a 4-cyl engine would be improved by division into pairs of cylinders.

Matching Turbocharger to V-8 Engine Exhaust

1. The data clearly show that the 4-way division of the exhaust on the V-8 engine is very desirable for obtaining a good matching of turbocharger to the engine.
2. The 2-way division of exhaust (effectively two 4-cyl engines) appears to accomplish practically none of the improvement in matching that results by using the 4-way division to reduce the increase in turbocharger pressure ratio with increase in engine rpm.
3. A 2-way division of the exhaust of the V-8 engine by separation of the right bank and left bank for turbocharging is not recommended.
4. The practical 4-way division of the V-8, suggested herein, greatly reduces the effect of one cylinder upon the scavenging of another and is recommended where a 4-way division exhaust is desired.
5. Different V-8 engines may be expected to show various degrees of improvement in matching of a turbocharger to an engine by using the recommended divided exhaust flow systems due to differences in valve timing.
6. Results on 4-way and 2-way divided V-8 engine indicate that 4-cyl engines would be improved by division into pairs of cylinders.

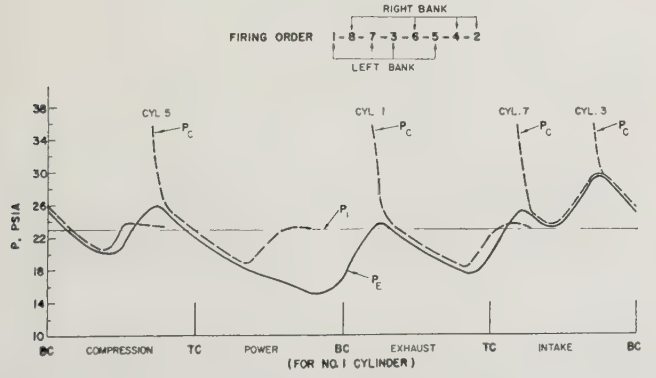

Fig. 15 — Uneven pressure in exhaust manifold for one bank of V-8 diesel

Inlet Manifold Design Study

The division of the exhaust has shown varied effects on diesel performance and in a similar manner the division of the inlet of a V-8 diesel inlet manifold into the equivalent of 2- and 4-barrel carburetor engine type manifolds might aid the flow of air into the cylinders. The pressure variations produced in inlet manifolds were studied for the following configurations:

1. V-8 engine nondivided.
2. V-8 engine 2-way divided (equivalent to two 4-cyl engines).
3. V-8 engine 4-way divided.
4. Six-cylinder nondivided.
5. Six-cylinder 2-way divided.
6. V-8 naturally aspirated separate manifolds on each bank.

The pressure fluctuations analyzed for the various configurations of turbocharged diesel engines were produced by the effects of a steady flow of air to the inlet manifold volume and an unsteady flow out according to the airflow to the different cylinders involved. Pressure effects due to resonance, inertia of flowing gases, or turbocharger characteristics are not included in the pressure variations presented herein. Fig. 17 presents the pressure variations of

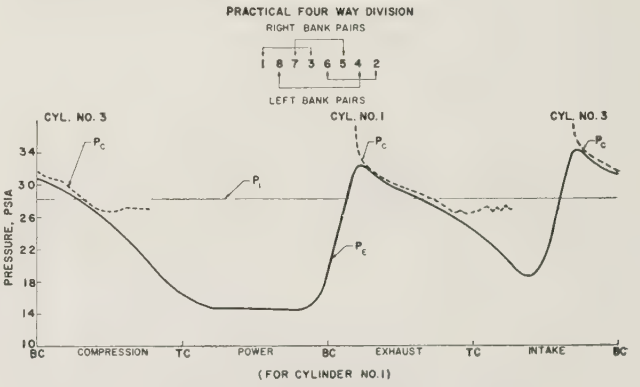

Fig. 16 — Similarity of cylinder scavenging with practical 4-way divided V-8 exhaust

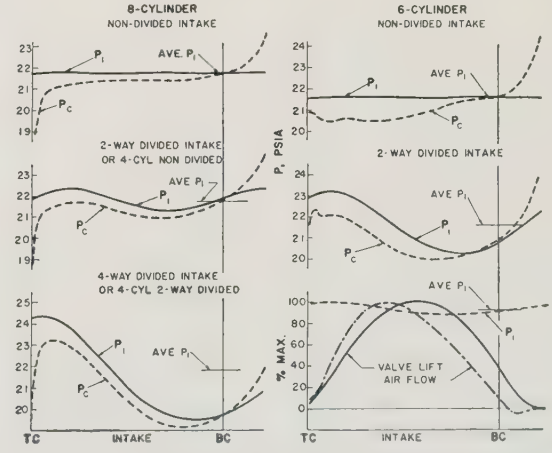

Fig. 17 — Effect of division of inlet manifold on V-8 and 6-cyl diesels

Table 5 — Effect of Separate Inlet Manifolds for Each Bank of V-8 Diesel (naturally aspirated)

	Engine Data			Calculated
	Motoring Compression Pressure, %			Inlet Pressure at Closing of Inlet Valve, %
	Cast Manifold		Large Steel Manifold,	500-cu-in. Manifold,
Cylinder	2000 rpm	2200 rpm	2200 rpm	2100 rpm
1	93	93	100	100
7	80	83	95	89
3	100	100	98	96
5	89	93	99	99

Table 6 — Performance with Throttled Compressor Outlet or Wastegated Turbine Compared to Baseline Run

	Wastegate	Throttle
Ihp	99.4%	99.2
Fhp	90.5	93.3
Bhp	100.7	100.1
Bsfc	99.4	100.0
Cfm, Air	90.9	90.9
Exhaust Temperature	103.6	105.1
Boost Pressure	86.0	98.4
Turbocharger Rpm	83.2	98.4

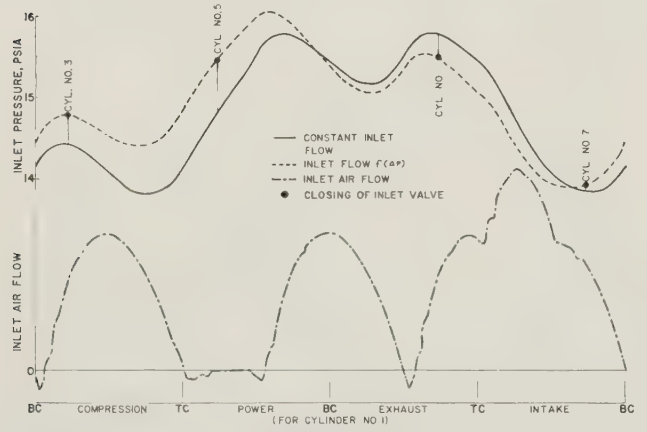

Fig. 18 — Effect of separate inlet manifolds for each bank of V-8 diesel (naturally aspirated)

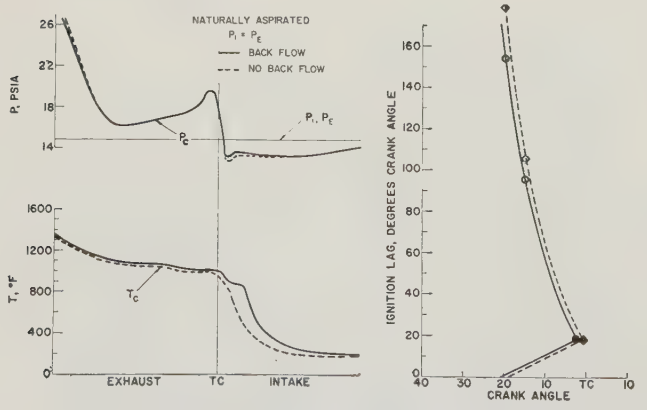

Fig. 19 — Effect of inlet manifold backflow on engine cycle and ignition timing

all the turbocharged configurations and in every case the inlet pressure is rising at the time of closing of the inlet valve but the peak pressure or a pressure appreciably greater than average is not obtained until after the inlet valve closes.

Fig. 17 also shows the relationship of valve lift, flow through the inlet valve, and pressure in the inlet for the 2-way divided 6-cyl engine. The difference in phase of the pressure wave compared to the airflow is obvious and unless some advantage of tuning or ram effect can be utilized, the division of the inlet alone does not increase airflow. These results for divided inlet manifolds show that the above pressure fluctuations are not beneficial and, therefore, a large volume nondivided inlet manifold is recommended for turbocharged 4-stroke cycle engines.

An inlet manifold study on a V-8 was made to evaluate some data obtained with a naturally aspirated engine using separate manifolds on each bank. The results are presented here as an example of how analysis contributes to the understanding of test results and to substantiate the conclusion that separate inlet manifolds on each bank (non-even firing) of a V-8 are not recommended. The uneven intake sequences results in the inlet airflow for one bank of the V-8 shown in Fig. 18. This study starts with naturally aspirated engine cycle calculations where inlet and exhaust pressure are equal and constant. Using the airflows and backflows into the inlet manifold, the pressure waves shown in Fig. 18 were calculated using a steady air supply from the air cleaner and an air supply calculated as a variable flow depending on a resistance through the air cleaner and the existing pressure drop. The resulting wave shows the various inlet pressures at the time of closing of the intake valve for each cylinder. These pressures correlate with the observed engine data where motoring compression pressures show trends that agreed with the pressure variation as calculated. (See Table 5). More refined differences in performance of cylinders could be obtained, if desired, by applying the pertinent portions of the composite inlet pressure wave to specific cycle calculations for each cylinder. This technique is the one that was applied in the study of the nonuniform exhaust pressure wave for the single exhaust manifold on each bank of the turbocharged V-8. This refinement was not made in this inlet study because the preliminary wave already explained the situation and, obviously, the single inlet manifold for each bank is not recommended because of unevenness of airflow distribution. Note, that the same cylinders of each bank are adversly effected by the above inlet manifold as are effected by the single exhaust manifold per bank.

The nature of the effect of backflows into the inlet manifold for even the naturally aspirated idealized case of equal inlet and exhaust pressure is illustrated in Fig. 19, where a delay in drop in cylinder temperature results from the reswallowing of the hot gases that had just backflowed into the inlet. The data are compared to a cycle where the backflow was not reswallowed but by some means crossflowed into another cylinder. This difference in backflow resulted in a 14-deg difference in charge temperature at the start of compression (inlet valve closing) and a 20 F difference near the end of com-

pression where burning starts. Analysis presents sufficient justification for the engine to run rough, which it did, considering the possibility of the irregular inlet pressure wave (Fig. 18) exaggerating the differences in backflows for various cylinders and interacting on combustion by presenting different pressures, temperatures, and amounts of residuals. Reports on combustion studies indicate[3] that when combustion gets off to a good start, it continues well and even differences from cycle to cycle in a spark-ignition engine can be attributed to the nature of the initial phase of combustion. The way the initial diesel fuel burns is important, (Fig. 9) because temperature and pressure increase rapidly and thereby accentuate the conditions for burning the remaining fuel. Therefore, diesel engine combustion can be expected to reflect the effects of the detailed differences that can be shown by digital computer analysis to occur in the compression stroke. This result indicates the potential usefulness of cycle calculations for correlating cold-starting data and determining correction factors for rating engines at standard conditions or at altitude.

I believe that cycle calculations on a digital computer presents a clearer insight into engine development problems than can be obtained by even a very elaborate and extensive testing program. Cycle calculations should be used to correlate data from a wide variety of sources and apply the findings of many experiments to current problems in engine development.

Conclusions on Inlet Manifold Design

1. Large nondivided inlet manifolds with generous size connections to the turbocharger and air cleaner are recommended on 4-, 6-, and 8-cyl engines, because pressure fluctuations resulting from restricted volume divided inlet manifolds produce no beneficial effect in themselves.

2. A single manifold for each bank of a naturally aspirated V-8 engine is not recommended where an uneven firing sequence will cause nonuniform cylinder charging pressures.

3. Cycle analysis should be used to study valve timing to minimize inlet air heating by backflows and possible crossflows between cylinders and should include the effect of inlet manifold design on inlet pressure variations.

Evaluation of New Engine Design Concepts in Planning Stage

The substitution of a throttle in the turbocharger compressor outlet in place of a wastegate in the turbine inlet is presented as an example of the new engine design concepts that can be evaluated by cycle analysis. The object of the throttle in the inlet or the wastegate is to improve the matching of the turbocharger to the engine. By using these devices, a smaller turbine nozzle for better performance at part load can be used and overspeeding of the turbocharger at rated engine rpm or at altitude is controlled by regulation of throttle or wastegate.

Fig. 20 shows the change in compressor operating conditions when a throttle or a wastegate is used to limit turbocharger rpm below that which would otherwise be obtained with reduced fuel at rated engine RPM. The two devices have reduced the airflow equal amounts but the turbocharger rpm's are 98% and 83% of normal rpm with the throttle and wastegate respectively. (See Table 6.) The wastegate does a better job of reducing rpm but the throttle moves the operating point on the compressor map in a more favorable direction, narrowing the required operating range of the compressor and moving toward a high efficiency region when the turbocharger is matched for best efficiency at some engine rpm below rated rpm.

For the amounts of throttling and wastegating shown, constant inlet manifold pressure could be maintained down to 87 and 80% rated engine speeds for the respective devices. Although throttling is less effective in controlling turbocharger rpm, it is almost equally effective in limiting peak cylinder pressure as shown in Fig. 21. In accelerating from 80% rated rpm, the compressor operating point would move along the dashed arrows. As noted before the compressor is kept in a more favorable operating condition by the use of a throttle than by the use of the wastegate. The advantages of

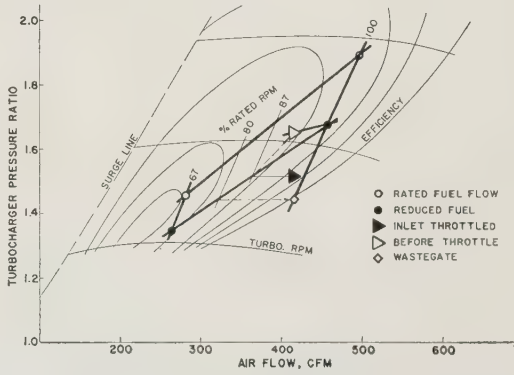

Fig. 20 — Comparison of operation with throttled compressor outlet and wastegated turbine

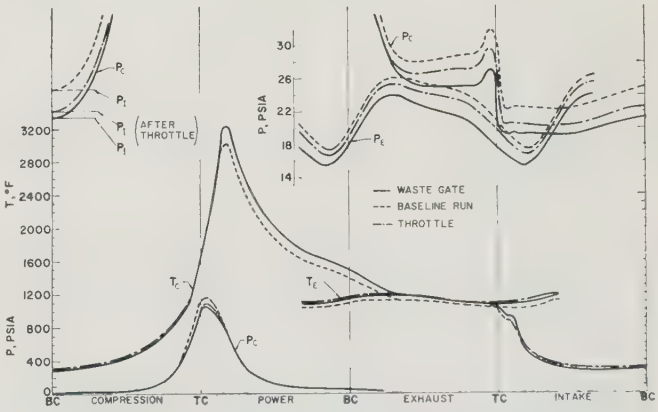

Fig. 21 — Engine cycles with throttled compressor outlet and wastegate turbine

[3] SAE Transactions, Vol. 62, 1954, pp. 514–530: "Practical Application of Engine Flame Temperature Measurements," by G. H. Millar, O. A. Uyehara, and P. S. Myers.

using a throttle in relatively cool air compared to a wastegate in hot gases is another factor to consider.

The evaluation of the throttled inlet should be extended to include the beneficial effects of aftercooling because this would eliminate the disadvantage of the higher inlet air temperature when the throttle is used. The requirement for extended compressor operating range with a wastegate is clearly pointed out by Mitchell.[4]

The preliminary study of the above use of a throttle indicates that a throttle can act to a degree like a wastegate but with different characteristics in regard to compressor operation. These results suggest that for some engine applications a throttle in the compressor outlet can be used as a pressure limiting control and improve matching of the turbocharger and engine and provide required desirable engine characteristics.

Conclusion

Turbocharged diesel engine cycle calculations by a digital computer promises to advance the art of new engine design by providing a means for funneling important detailed findings of many apparently distantly related investigations to apply their combined and interacting effects on a new situation, thereby aiding in developing specific engine characteristics.

Clearer insights into engine test results and development problems are obtained when effects of operating and design changes are studied analytically as well as experimentally. The result can be a saving of development time, and a reduction in costly experimentation.

Cycle analysis during various phases of an engine development program can lead to specific recommendations such as:

Conclusions on Turbocharged V-8 Engine Exhaust Design — 1. The 4-way division of the exhaust of a V-8 engine is very desirable for obtaining a good matching of turbocharger to the engine.

2. The 2-way division of exhaust (effectively two 4-cyl engines) appears to accomplish practically none of the improvement in matching that results by using the 4-way division to reduce the excessive increase in turbocharger pressure ratio with an increase in engine rpm.

3. A 2-way division of the exhaust of the V-8 engine by separation of the right bank and left bank for turbocharging is not recommended.

4. The practical 4-way division of the V-8, suggested herein, greatly reduces the affect of one cylinder upon the scavenging of another one and is recommended where a 4-way division of exhaust is desired.

5. Different V-8 engines may be expected to show various degrees of improvement in a matching of turbocharger to engine by using the recommended divided exhaust flow system due to differences in valve timing.

6. Results on 4-way and 2-way divided V-8 engine indicate that 4-cyl engines would be improved by division into pairs of cylinders.

Conclusions on Inlet Manifold Design — 1. Large nondivided inlet manifolds with generous size connections to the turbocharger and air cleaner are recomended on 4-, 6-, and 8-cyl engines because pressure fluctuations resulting from restricted volume divided inlet manifolds produce no beneficial effect in themselves.

2. A single manifold for each bank of a naturally aspirated V-8 engine is not recommended where an uneven firing sequence will cause nonuniform cylinder charging pressures.

3. Cycle analysis should be used to study valve timing to minimize inlet air heating by backflows and possible crossflows between cylinders and should include the effect of inlet manifold design on inlet pressure variations.

Evaluation of New Design Concept — Cycle calculations can be used to evaluate new design concepts in the planning stage for example, the effect of using a throttle after the compressor in order to achieve a result similar to a wastegated turbocharger but with different compressor operating characteristics.

DISCUSSION

What Assumptions were Made In Programming for Author's Work?

— C. F. Taylor
Massachusetts Institute of Technology

IN COMMENTING on Mr. Cook's paper, I would like to invite attention to previous work along the same lines done in the laboratories at M.I.T.[a,b] This work showed that it is possible to predict cylinder and manifold pressure versus time curves with a fair degree of accuracy, provided sufficient information is available regarding flow coefficients, physical dimensions, and the likes. In this work, pressures were carefully measured by means of the M.I.T. balanced diaphragm indicator[c] and were compared at all points with the computed results.

There is no doubt at all that the digital computer can be a very useful tool in predicting engine performance, provided the programs fed into the computer are a realistic representation of the characteristics of the real components which they represent.

While the results obtained by Mr. Cook seem plausible, they would be far more convincing if more data were included comparing measured with calculated results. It would be especially interesting to see actual pressure measurements taken in the cylinder and exhaust pipe, compared with the curves shown in the paper. Without such

[4] SAE Transactions, Vol. 67, 1959, pp. 401–413: "Evaluation of Aftercooling in Turbocharged Diesel Engine Performance," by J. E. Mitchell.

[a] NACA TN 1446, 1949: "Theory of Inlet and Exhaust Processes of Internal Combustion Engine," by T. C. Tsu.

[b] ASME Transactions, Vol. 77, October, 1955, p. 1133: "Dynamics of Inlet System of Four-Stroke Single-Cylinder Engine," by C. F. Taylor, J. C. Livengood, and D. H. Tsai.

[c] *Mechanical Engineering*, March, 1933: "New High-Speed Engine Indicator," by E. S. Taylor and C. S. Draper.

comparisons, it is difficult to have full confidence in the computed results.

It would also be of great interest if the author would include a list of the assumptions made in programming the computer for this work. The value of computations of this kind depends entirely on the validity of the simplifying assumptions which must be made to make such computations possible.

Wants More Information For Comparison of Experimental and Calculated Data

— P. S. Myers and O. A. Uyehara
University of Wisconsin

THE IMPORTANCE of papers such as the one presented by Mr. Cook cannot be over-emphasized from either a theoretical or a practical standpoint. It will indeed be a "red-letter day" when we become as "intelligent" as an engine and can "run" the engine on a computing machine prior to building the engine. And before this, even if we cannot obtain completely precise answers by running the engine on a computing machine, if we can decrease the experimental development time for a new engine, a significant monetary saving will be achieved. This point is of even greater importance in turbocharged engines where the additional variable of the turbocharger more than doubles the already large number of variables that must be investigated if the new engine design is to be optimized.

The value of such computations, however, varies greatly with their ability to predict the behavior of the engine. Judgment on this point can be formed both by inspecting the assumptions made during the computations and by inspecting the results. Thus, while it is perhaps not necessary to present the technique in detail, it would have been helpful in forming this judgment if the author had stated some of his basic assumptions. For example:

1. Was quasi-steady flow assumed, or were pressure wave phenomena considered?
2. When gases of different composition and temperature were brought together, such as occurs during backflow and filling of the cylinder, was immediate and complete mixing assumed?
3. What assumption was made concerning rates of heat transfer, both during the cycle and with changes in operating conditions?
4. What assumption was made concerning the variation of friction, both during the cycle and as rotative speed and cylinder pressures were varied?

The list is obviously incomplete but it does illustrate the type of information that would be helpful in forming the required judgment of the closeness of the computations to reality.

Turning next to the results, two specific comparisons are presented between experimental and calculated results. The first of these is presented in Fig. 5 where computed and experimental pressure-time diagrams are shown. The agreement is reasonably good, although the difference of approximately 200 psia in the peak pressure is not negligible.

The second comparison between experimental and calculated data is presented in Table 5 and Fig. 18. These data are replotted in Fig. A. There is good agreement between computed and experimental results when the "large steel manifold" was used. The agreement between Cylinder Nos. 1 and 5 is not good for the other two manifolds. The manifold volume assumed for the computations was stated — the volumes of the other manifolds were not. Thus, one's enthusiasm for the computations and the possible use that might be made of them is considerably lessened by his inability to determine exactly how closely the experimental and computed results compare.

The author states that "the accuracy obtained in these cycle calculations can be judged by the degree to which the various quantities match where the cycles are supposed to close." As a final question, does this statement refer to the accuracy with which the computations were performed or the accuracy with which the computations predict the events in the engine?

In conclusion, with the increased use of computing machines, and our understanding of such basic phenomena as heat transfer, friction, and the like grows, we will be able to "run" our engines on computing machines rather than the dynamometer. The author is to be congratulated for having the foresight and the courage to do the necessary work and demonstrate how close we are to this very desirable goal.

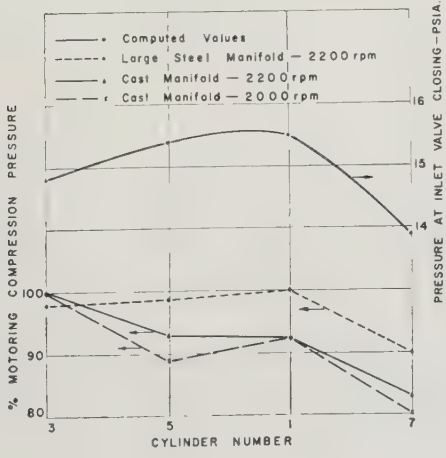

Fig. A — Plot of data from Table 5

Computers Can Shorten Engine Development

— C. R. Maxwell
Caterpillar Tractor Co

MR. COOK certainly enters a fertile and challenging field when he attempts to compute diesel engine performance. He shows good judgment in starting with the induction and exhaust systems, which can be reduced to mathematics. But reducing the mathematics to an answer, or a series of answers, is a formidable task by longhand. So formidable, in fact, that only the crudest empirical approximations are commonly used. Apparently, this paper is only a step toward the eventual possibilities of computers in relation to diesel engines.

However, a computer can do no more than operate on the data which is fed into it, and that data contains many assumptions, such as valve coefficients, bend effects, thermal effects, friction, and the like. Considering this, it is necessary to exercise a great deal of caution in using the absolute values of the results. Computed results are not flywheel horsepower. But the ease with which factors can be changed permits the examination of many variables, for trends and general effects.

While it is usually easy to find your mistakes after an engine is built, it is much cheaper to find them while the engine is still on paper. If computers can shorten the engine development time by paper analysis, they will certainly pay their way.

In view of the dynamic nature of inlet and exhaust flows, perhaps they might more easily be analyzed on an analog computer. Has the author considered this?

Fig. 18 shows the variation in inlet flow in one bank of a 90-deg V8 engine, from zero to almost double the average rate. When calculating the effectiveness of separate inlet manifolds, has the author taken into account the effect of this tremendous flow range on compressor efficiency, pres-

sure ratio, surge, and delivery?

A word of caution: Ignition delays and combustion times as determined in a bomb are probably considerably longer than those that occur in an engine, where turbulence becomes a major factor.

Source of Data Fed Into Computer Is Questioned

— E. T. Vincent
University of Michigan

CYCLE ANALYSIS by various means has been employed for a very long period of time to predict changes in engine performance. The results obtained depend to a large extent upon the factors taken into account in the analysis. It is believed that the present paper is just another way of obtaining the same results; its main advantage being that a wide range can be covered with far less effort.

Some years ago the speaker developed a method of cycle prediction which was quite effective in matching power output, fuel economy, and the like, with actual engine performance. The analysis of one set of data took perhaps 2–3 hr; about the time the work was going well, a machine calculator became available and the equations were somewhat modified to suit this means of calculation, with the result that 2-3 hr work (after the setup) produced all one could desire in the way of results; results that still checked the engine's performance.

It is seen that the writer is not against machine methods, but does question what is fed to the machine. Mr. Cook has presented a wide spread of data, so much so that it seems hard to find a starting point for a discussion even though the paper is limited to the scavenging and charging processes. Incidentally, these processes are considered to be the most difficult.

The chief point on which issue is taken is that no method is outlined as to how or where, much of the data came from that was fed to the machine: Were they pure guesses, were some calculated, and how? As an example, nice curves of exhaust gas temperature are shown with no explanation of how they were obtained. To the writer this is one of the most difficult factors to determine by pure thermodynamic calculation (and be right); a temperature can be obtained in several ways, but it does not agree by a long way with that actually measured.

Again, peak temperatures of the supercharged cycle reach only some 3000 F. This is low for most practical engines even of the naturally aspirated type, using modern thermodynamic properties of gases. Does this result from some assumed indicator diagram, or was an actual diagram used?

It is believed that a great help and a better understanding of the paper would be achieved by some presentation of the methods employed in approaching the problem rather than giving so many of the results. It would then be possible for other people to employ the work on their own problems.

Much of the paper hinges on the shape of the pressure waves in the intake and exhaust systems, but no indication is given of how these waves are obtained. They are extremely important in engine operation and are associated to some extent with the valve timing, as the author states.

One other general remark is perhaps that sufficient distinction is not drawn to what is actually measured from an engine and what was machine calculated. Fig. 5 gives measured and calculated pressures. The agreement is very good in this case. But how were the calculations made, how were heat loss and the like allowed for? Without this or similar allowances the agreement shown could not be obtained.

An advantage of the computer is given as a means of optimizing the engine performance and correctly combining a number of small improvements in the final results. Unfortunately, it has been the writer's experience that a number of definite individual improvements never add up, there is always some negative factor somewhere; the resultant gain of the whole group is far less than the individual gains.

Turning to particular points: Fig. 9 is not clear. It shows ignition lag, gas temperature, and compression pressure. Is the compression line shown that which would occur after fuel injection at 30-deg btc with rapid combustion at 15-deg btc? If so, what is the ignition lag? The diagram does not show it for a gas temperature of 1260 R. Or does the diagram show that the lag will be 5.7 millisec at the state labeled 15 deg; if so, the burning rate will not begin at 15 deg.

Again, Fig. 10 does not mean anything to the writer; taken at its face value it says the ignition lag is zero at 85 F if the injection is 27-deg btc or it could be 150 deg of crank rotation. It is felt that this interpretation is not what is intended, but without further explanation little else can be concluded.

There are a number of interesting conclusions drawn from the analysis and it is believed that they represent the results of the cycle analysis based on the information fed to the machine. However, the author definitely excluded the ram and dynamic effects from the program; to include them would be a very difficult problem, but it is believed that without them the results do not mean much, since they contribute so much to any engine's performance.

In conclusion it is believed, with the author, that the use of the computer in engine anaylsis is something that must not be neglected; it is a useful tool, and is as good as the data furnished for analysis. The paper would be of much greater value if some details of how the job was done, the background theory, were presented also.

The paper does present a formidable amount of analysis work for which the author is to be congratulated.

Author's Closure To Discussion

THE AUTHOR believes: Discussion accentuates the main purpose of paper.

One object of my paper was to present a summary of the useful results that we had accumulated over a period of about four years. Our digital computer programs for analysis of 4-stroke and 2-stroke turbocharged engines have been revised a number of times and improvements and additions are still being made. Many of the results are still predictions because, although 90-deg V-8 diesel engines are being developed rapidly, tests with the recommended turbocharger configurations are not yet complete. The difficulties and delays in obtaining complete and detailed test data from engines is the best justification for use of the digital computer analysis. As more engine data becomes available with indicator cards and measured inlet and exhaust pressure variation, these will be compared with our calculated results.

The assumptions and data fed into the computer are optional and should be selected by each engineer to meet his specific problem requirements. The digital computer does not object to doing things the hard way. By this I mean, simplifying assumptions need not be made when means for calculating given phases of a complex problem are available. I believe my most important conclusion in my paper is "Turbocharged diesel engine cycle calculations by a digital computer promises to advance the art of new engine design by providing a means for funnelling important detailed findings of many apparently distantly related investigations to apply their combined and interacting effects in a new situation, thereby aiding in developing specific engine characteristics."

new

FLUOROESTER LUBRICANTS

for high-temperature applications

E. C. Ballard and E. E. Sommers, E. I. du Pont de Nemours & Co., Inc.

This paper was presented at the SAE Annual Meeting, Detroit, Jan. 13, 1959.

THE INTRODUCTION of the turbojet engine signaled the start of a new era in lubrication. Although the early engines ran satisfactorily when lubricated with light mineral oils, it was not long before the need for improved lubricants was evident. The search for a turbojet engine lubricant which would pour below – 65 F and be an effective lubricant in systems where the bulk oil temperature was 300 F resulted in the development of synthetic ester lubricants based on di-2-ethylhexyl sebacate. The military engine oil specification MIL-L-7808 was written around the physical properties of this ester. Several million gallons of lubricants meeting this specification have been produced during the past 8 years; these oils are reported to lubricate 80% of the turbojet engines now in the air.[1] However, as aircraft speeds increase beyond Mach 1, significant improvements are required in the oxidative and thermal stability of engine lubricants. At Mach 2.3, a ram air temperature rise of 400 F is encountered. At this speed, the bulk engine oil temperature is expected to be in the neighborhood of 400 F and temperatures as high as 650–700 F will be reached occasionally in the main engine bearings.

A tentative Military Specification (MIL-L-9236) was written in August, 1954, describing a desired, but nonexistent, oil for turbojet engine lubrication at a bulk oil temperature of 400 F. Great progress has been made in the development of such oils and there is reason to believe that one or more 9236 oils will be available in the near future.[2]

Specification MIL-L-25968, describing an oil suitable for operation at a bulk temperature of 350 F, was issued in January, 1958. This specification, primarily for use in engine design, indirectly acknowledges the difficulties encountered in reaching the 9236 level of performance. Oils not quite meeting the 9236 specifications probably will be satisfactory for use under the conditions described in the 25968 specification.

Although 400 F oils are still under development,

THE NEED for greater speed in military aircraft and missiles is, without question, the primary force behind the current quest for lubricants of increased thermal and oxidative stability. Turbojet engines soon to be available will require improved lubricants for trouble-free operation. Once developed, these oils may find use in the engines of future civilian aircraft as well as in a variety of special applications.

It is the purpose of this paper to discuss the results of an experimental program in the field of high-temperature lubricants. Problems of relating chemical structure to the physical properties and performance of highly fluorinated ester lubricants will be described. Background information in the field of turbojet engine lubrication will be presented.

[1] "Developments in Aircraft Turbine Lubricants," by T. F. Davidson and J. H. Way. Paper presented at SAE National Aeronautic Meeting, New York, April, 1957.

[2] *Aviation Week*, Vol. 69, Sept. 29, 1958, p. 51: "USAF Developing High-Temperature Oils," by Michael Yaffee.

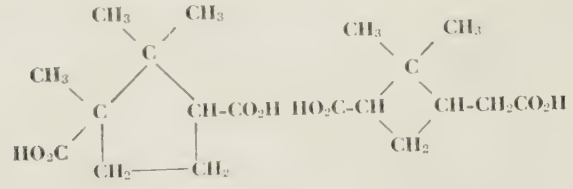

Camphoric Acid

Pinic Acid[7]

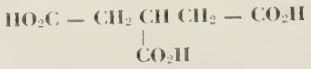

Tricarballylic Acid[7]

Fig. 1 — Three compact acids giving fluoroesters of excellent oxidative stability

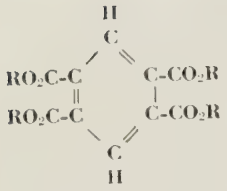

(R = fluoroalkyl)

Fig. 2 — Structure of tetrafluoroalkyl pyromellitate

Table 1 — Desired Properties for a MIL-L-9236 Oil

1. Thermally and oxidatively stable for operation at bulk oil temperatures of 400 F and bearing temperatures of 500–600 F.
2. Lubrication and load-carrying ability considerably better than that of nonadditive mineral oils.
3. Minimum viscosity at 400 F of 3.0 centistokes (cs).
4. Minimum use temperature of – 65 F.
5. High specific heat.
6. Noncorrosive to metals.
7. Nontoxic
8. Stable against hydrolysis.
9. Compatible with engine seals.

Table 2 — Classes of Compounds for High Temperature Lubricants

400 F Oils
Diesters
Polyhydric esters and glycol derivatives
Super-refined mineral oils
500 F Oils
Synthetic hydrocarbons
Chlorinated aromatic hydrocarbons
Chlorinated silicones
Silicates
Aryl phosphates

Table 3 — Oxidative Stability of Aliphatic Esters[a]

	Structural Formula	$C_7H_{13}F_{12}O_2C-C(CH_3)_2-CH(CH_3)-CO_2C_7H_{13}F_{12}$	$C_7H_{13}F_{12}O_2C-(CH_2)_8-CO_2C_7H_{13}F_{12}$	$C_8H_{17}O_2C-(CH_2)_8-CO_2C_8H_{17}$
		C_7-Fluoroalkyl Camphorate	C_7-Fluoroalkyl Sebacate	Di-2-Ethylhexyl Sebacate[b]
Viscosity Change, %				
210 F		– 9	+ 5	+ 160
100 F		– 12	+ 8	+ 120
Acid No. Increase		1.9	9.0	> 25
Copper Corrosion, mg/cm²		0.4	0.7	0.4
Used Oil:				
Color		Red-Brown	Black	Black
Sludge Content		None	Trace	Heavy

[a] Twenty-four hour oxidation tests at 500 F in which 25-ml samples of the fluids were blown with 25 ml dry air per min. The oxidations were run in glass cells in the presence of 10 sq cm copper surface as the oxidation catalyst. Similar results were obtained using oxidation cells of copper, steel, stainless steel, and aluminum.

[b] Contained 0.5 weight per cent phenothiazine as an antioxidant.

the need for oils of even greater stability is already being discussed. Within the next few years, some military aircraft will require oils to operate at a bulk temperature of 500 F and be suitable for bearing temperatures of 750 F and hot-spot temperatures of 900 F.[3]

Background

The general requirements for a 9236-type oil are listed in Table 1.

Various government and industrial laboratories working on high-temperature lubricants have surveyed many classes of compounds in their search for 9236-type oils. Those reported to have the most promise at the present time are listed in Table 2.[3]

Candidates for 9236 oils must possess excellent lubricity as well as excellent oxidative, thermal, and hydrolytic stability. In addition, they must meet the general physical properties required of a lubricant useful from below 0 F to 500 F and even higher. All these lubricant requirements are related to the basic properties of their molecular composition and structure. Of these, only lubricity, oxidative stability, and temperature-viscosity relationships are subject to possible improvement through the use of additives.

Antioxidants are being tested extensively by various laboratories in an effort to increase the oxidation resistance of MIL-L-7808-type oils to the level required by the 9236 oil specification. Another route to 9236 oils may be with structures of improved basic stability.

One possible route to structures of improved stability involves a series of highly fluorinated alcohols very resistant to oxidative and thermal degradation.[4, 5, 6] Such alcohols are prepared from tetrafluoroethylene and methyl alcohol by a very interesting reaction called telomerization:

$$CF_2 = CF_2 + CH_3OH \rightarrow H(CF_2CF_2)_XCH_2OH$$

$X = 1, 2, 3, 4, 5,$ and higher.

As will be discussed later, these alcohols can be reacted with selected di- or polybasic acids to form very stable esters.[7, 8, 9] The highly fluorinated groups have profound effects on the physical and functional properties of their esters. These effects are discussed in the following sections.

Oxidation Stability of Esters

The resistance of various esters to oxidation was generally determined in a small-scale adaptation of the procedure given in the 9236 specifications. The tests were run on the base esters (no additives) to permit conclusions to be drawn on the stability of the ester structure rather than on the performance of the antioxidant. Since small concentrations of impurities have a considerable influence on the sta-

[3] "Lubricants and Hydraulic Fluids," by L. T. Taylor. Paper presented at 25th Annual Meeting of Institute of Aeronautical Sciences, New York, January, 1957.

[4] U. S. Patent 2,559,628, by R. M. Joyce, Jr., 1951.

[5] U. S. Patent 2,559,629, by K. E. Berry, 1951.

[6] "Tetrafluoroethylene-Methanol Telomer Alcohols," by D. R. Baer. Paper presented at 132nd meeting of American Chemical Society, New York, September, 1957.

[7] *Industrial and Engineering Chemistry*, Vol. 48, March, 1956, pp. 445–454: "Partially Fluorinated Esters and Ethers as Temperature-Stable Liquids," by P. D. Faurote, C. M. Henderson, C. M. Murphy, J. G. O'Rear, and H. Ravner.

[8] "Preparation and Properties of Some Fluorine-Containing Diesters," by J. F. O'Brien, R. Filler, J. V. Fenner, and G. Rappaport. Wright Air Development Center Technical Report 56-11, December, 1956.

[9] U. S. Patent 2,840,593, by E. E. Sommers and B. M. Sturgis, 1958.

bility of esters (Appendix III of McTurk[10]), all samples were carefully purified before evaluation.

Several series of esters prepared from a single acid and the individual fluoroalcohols, as well as from several mixtures of these alcohols, were evaluated in this test procedure. The data indicate that esters prepared from $H(CF_2CF_2)_XCH_2OH$, where $X = 1$ (3 carbon atoms in the alcohol), tend to be less resistant to oxidation than those prepared from the higher alcohols. This is undoubtedly related to the lower fluorine content of the short chain esters and the lesser shielding of the acid portion of the ester by the small alcohol groups. Within each series, the esters from the higher alcohols are similar in oxidation resistance. Since those prepared from the fluoroalcohol with $X = 5$ (C_{11}) possess high pour points, they are not of great interest as lubricants. Esters prepared from C_5, C_7, and sometimes C_9 alcohols, or some combination of these three alcohols, offer the best compromise in low volatility and pour points coupled with excellent oxidative stability.

There is little information in the literature concerning systematic studies on the effect of the acid portion of the ester on the physical properties and oxidation performance of ester lubricants. Most of the work has concerned the effect that variations in the alcohol have on these properties when used in conjunction with a few readily available acids. The current investigation covers fluoroalkyl esters of the more common polybasic acids and also a number of acids which, at the present time, are not commercially available.

The oxidation performance of a series of fluoroesters of straight chain dibasic acids:[7]

$$HO_2C—CH_2(CH_2)_XCH_2—CO_2H$$

where $X = 0, 1, 2$, and 6

indicate that the repeating and unprotected CH_2 groups in such acids are subject to attack. Although considerably better than nonfluorinated esters, none of this series exhibits outstanding oxidation resistance.

Esters prepared from compact acid structures possess higher viscosities than straight-chain esters (for example, fluoroalkyl sebacate). In addition, the oxidative stability of these compact esters can be considerably better than that of straight-chain esters. Structures of three compact acids giving fluoroesters of excellent oxidative stability are shown in Fig. 1. The oxidative stability of the fluoroalkyl camphorate (as representative of the three compact structures in Fig. 1) and the fluoroalkyl sebacate are indicated in Table 3. The performance of di-2-ethylhexyl sebacate, a representative nonfluorinated ester, is also given in this table. These data illustrate how fluoroalkyl groups increase the oxidation resistance of a straight-chain dibasic ester and also how compacting the acid structure increases the oxidation resistance of fluoroesters.

Acids based on the stable structure of the benzene ring are logical starting points for the preparation of stable fluoroalkyl esters. Some of these esters have been described in the literature.[7, 11] Esters of 11 polybasic aromatic acids were included in this investigation. In general, ring substitution by nonacid groups decreases the oxidation resistance of the corresponding fluoroester. The tetrafluoroalkyl pyromellitate is one of the most interesting aromatic esters tested. It possesses extremely good resistance to oxidation (considerably better than the camphorate), has the highest V.I. of the aromatic esters, and is low in volatility. Its structure is shown in Fig. 2 and its oxidation resistance is indicated in Table 4.

Fig. 3 shows a visual indication of the degrees of oxidation resistance encountered in this program.

Thermal Stability of Esters

The temperature at which thermal decomposition of esters becomes significant is primarily a function of the alcohol. Esters of secondary alcohols begin decomposition in the range of 450–500 F.

$$RC(=O)—OCH(R')—CH_2R'' \xrightarrow[450–500\ F]{\text{Heat}} RC(=O)—OH + R'CH = CHR''$$

Esters of primary alcohols are thermally stable into the range of 500–600 F.

$$RC(=O)—OCH_2—CH_2R' \xrightarrow[500–600\ F]{\text{Heat}} RC(=O)—OH + CH_2 = CHR'$$

This reaction occurs via a cyclic intermediate and involves a hydrogen on the second (beta) carbon atom in the alcohol.[12] The resistance of an ester to

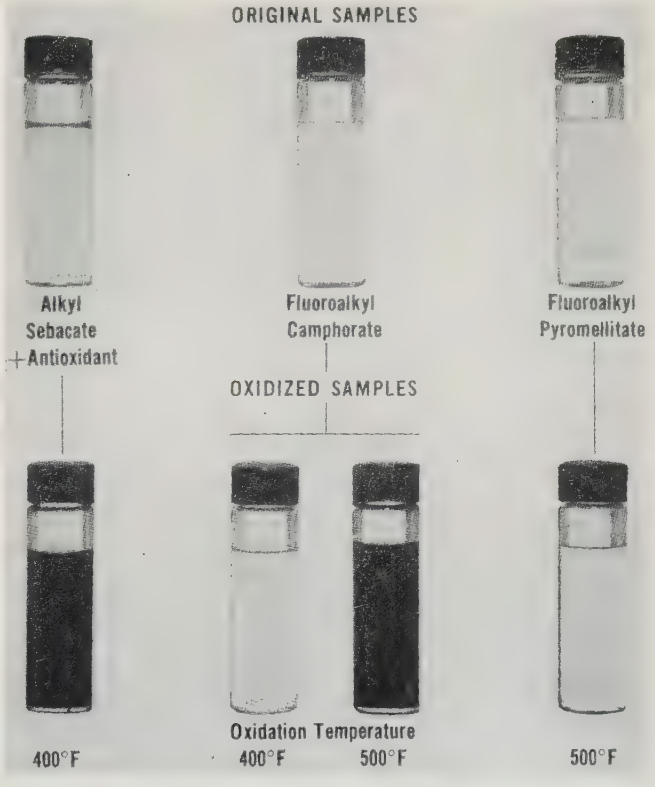

Fig. 3 — Change in appearance of fluoroalkyl and alkyl esters during 24-hr oxidation tests at 400-500 F

[10] "Synthetic Lubricants," by W. E. McTurk. Wright Air Development Center Technical Report 53-88, October, 1953.

[11] "High-Temperature Lubricants from Aromatic Acids and Fluoroalcohols," by C. M. Murphy, J. G. O'Rear, H. Ravner, P. J. Sniegoski, and C. O. Timmons. Paper presented at meeting of Division of Chemical Marketing and Economics Section, American Chemical Society, Chicago, September, 1958.

[12] *Journal* of American Chemical Society, Vol. 77, 1955, p. 5443: "Rate of Pyrolysis of Di-(2-ethylhexyl) sebacate," by E. E. Sommers and T. I. Crowell.

Table 4 — Comparison of the Oxidative Stability of Two Fluoroalkyl Esters[a]

	Fluoroalkyl	
	Camphorate	Pyromellitate
Viscosity Change, %		
210 F	− 9	+ 1
100 F	− 12	+ 1
Copper Corrosion	0.4	0.4
Used Oil:		
Color	Red-brown	Light amber
Sludge Content	None	None

[a] Test conditions described in a footnote to Table 3.

Table 5 — Thermal Degradation[a] of Esters in 24 Hr at 600 F

Ester	Weight Loss, %	Acid No. Increase	Decomposition, %[b]
Fluoroalkyl Camphorate	1.8	0.4	0.3
Di-2-Ethylhexyl Sebacate	7.4	41.7	14.0

[a] Exposed to the atmosphere but not blown with air.
[b] Based on Acid No. and corrected for material loss.

Table 6 — Physical Properties of Esters

	Viscosity at 210 F, cs	V.I.	Pour Point, F
Sebacate:			
n-octyl ester	3.56	183	+ 72[a]
1-methylheptyl ester	3.29	151	− 10
2-ethylhexyl ester	3.31	154	− 70
n-Octyl Ester of:			
adipic acid	2.85	187	50
alpha-methyladipic acid	2.66	137	− 26[a]
beta-methyladipic acid	2.90	180	− 33[a]
di-2-Ethylhexylphthalate	5.04	35	− 54[a]

[a] Freezing point.

thermal degradation can be increased through the use of alcohols which do not have hydrogen on the beta carbon atom.

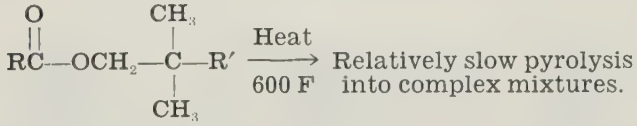

Hindered esters of this type, either prepared from monoalcohols and polybasic acids or from polyhydric alcohols and monobasic acids have been extensively studied as high-temperature lubricant candidates.[13, 14]

Since the fluoroalcohols do not possess hydrogen on the beta carbon atom and are fundamentally stable materials, they should form esters which resist thermal decomposition. The data given in Table 5 agree with this prediction. They show that a fluoroester prepared from a stable acid structure possesses excellent thermal stability as compared to a typical nonfluorinated ester prepared from an alcohol containing beta hydrogen.

Hydrolytic Stability of Esters

Hydrolytic stability is an important requirement for jet engine lubricants because they are exposed to the atmosphere during use and can come into contact with appreciable quantities of water. The hydrolytic stability of esters decreases with increasing strength of the acid portion of the ester. Highly fluorinated acids are considerably more acidic (due to the inductive electron withdrawing effect of CF_2 groups) than their nonfluorinated analogs. They yield esters not too desirable as high-temperature lubricant candidates because of the tendency to hydrolysis. However, esters prepared from highly fluorinated alcohols and nonfluorinated acids are quite resistant to hydrolysis.[7, 8] Thus, while the ester of a fluorinated acid and a nonfluorinated alcohol

is readily hydrolyzed by hot 5% KOH, the corresponding fluoroalkyl ester of a nonfluorinated acid

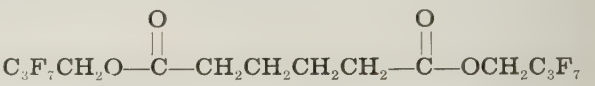

is not hydrolyzed by 5% KOH.

The hydrolytic stability of esters also is affected by the degree of actual physical (steric) hindrance which exists within the molecule near the ester grouping.[15] This hindrance is a function of the relative size of groups in the molecule close to the ester linkage. If these groups are sufficiently bulky, they can prevent the close approach of the hydrolyzing molecule (water, an acid, or a base) to the ester group and thus prevent hydrolysis. The effect of steric hindrance on the resistance of fluoroesters to hydrolysis can be illustrated with data on the two esters shown in Fig. 4.

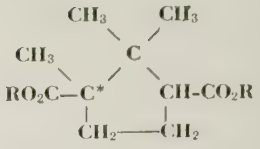

Fluoroalkyl Camphorate

*Center of steric hindrance

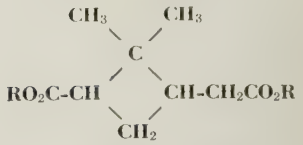

Fluoroalkyl Pinate

Fig. 4 — Structures illustrating steric hindrance

Alkaline hydrolysis of the camphorate using the procedure described in ASTM D-94-56T[16] reaches 50% within 24 hr, but does not proceed further during an additional 48 hr. This is due to the resistance toward hydrolysis of the highly hindered ester group attached to the carbon atom marked by the asterisk in Fig. 4. The fluoroalkyl pinate, lacking complete steric hindrance around either ester group, was completely hydrolyzed within 12 hr.

Similar data are not available on the pyromellitate but the esters of pyromellitic acid are, in general, resistant to hydrolysis because of steric hindrance. The fluoroalkyl pyromellitate can be blown with

[13] "High-Temperature Hydraulic Fluids," by E. S. Blake, et al. Wright Air Development Center Technical Report 54-532, Part 2, January, 1956.
[14] *Lubrication Engineering*, Vol. 13, August, 1957, p. 454: "Synthetic Ester Lubricants," by M. Z. Fainman and R. S. Barnes.
[15] P. 121 of "Physical Organic Chemistry," by L. P. Hammett. Pub. by McGraw-Hill Book Co., Inc., New York, 1940.
[16] A weighed sample of the ester is dissolved in methylethyl ketone and then is refluxed with a known quantity of alcoholic KOH. The consumption of KOH is determined after 30 min (or more extensive periods) of refluxing. The loss of KOH due to saponification of the ester is a measure of the hydrolytic stability of the ester under these alkaline conditions.

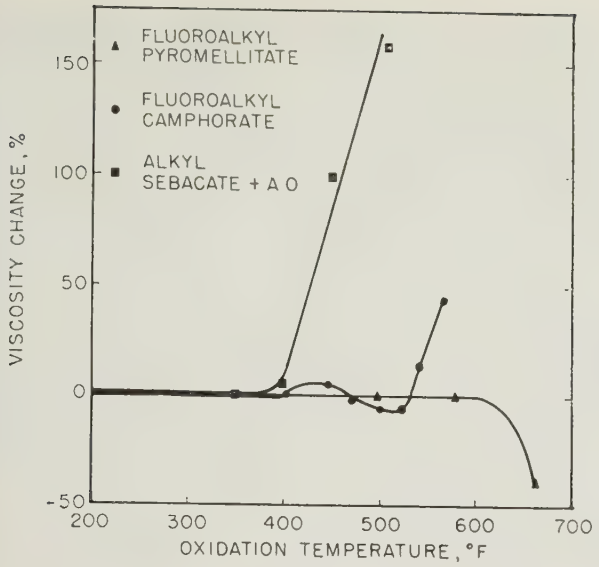

Fig. 5 — Change in 210 F viscosity of fluoroalkyl and alkyl esters during 24-hr oxidation tests at 350-650 F

live steam for several hours without undergoing significant change.

Physical Properties of Esters

Candidate lubricants for 9236 oils and other high-temperature applications should possess high V.I., low pour points, and low volatility. In addition, their viscosity at high temperature must be in the range required for proper lubrication performance. All these properties are functions of the structure of the lubricant molecule and its molecular weight. In the case of ester lubricants, these properties are affected by both the acid and alcohol used in their preparation. Long carbon chains with little or no branching in either the acid or the alcohol contribute to high V.I. and high pour points. The compact and rigid structure of aromatic acids in general causes their esters to have poor V.I. These factors are illustrated in Table 6.[10]

Fluorine is a more bulky atom than hydrogen and repeating CF_2 groups contribute to undesirable rigidity in the molecule and poor physical properties.[8, 17] Thus, as indicated in Table 7, esters based on the fluoroalcohols will have poorer V.I. than the corresponding alkyl esters. The problem is difficult to overcome. The harmful V.I. effects of the fluoroalkyl groups are minimized in esters of long-chain dibasic acids, but only at the loss of some oxidative stability. (See Table 3.)

Volatility of lubricants at high temperatures can become a limiting factor in their application. The weight loss of di-2-ethylhexyl sebacate in a 2-hr, 400 F test is approximately 12%.[18] This level of volatility apparently does not cause excessive oil consumption in high-altitude flight. Highly fluorinated esters are somewhat more volatile at high temperature than their nonfluorinated analogs.[8]

Table 7 — Effect of CF_2 Groups on Ester Viscosity and V.I.

	Viscosity, cs		V.I.	ASTM Slope
	210 F	100 F		
C_7 Fluoroalykyl Camphorate	8.21	113.6	2	0.86
n-Hexyl Camphorate	3.40	15.68	100	0.77
C_7 Fluoroalykyl Sebacate	4.49	28.37	62	0.80
n-Heptyl Sebacate	3.25	11.3	174	0.66

Table 8 — Physical Properties of Fluoroester Lubricants

	Fluoroalkyl Camphorate	Fluoroalkyl Pyromellitate	Di-2-Ethylhexyl Sebacate
Viscosity, cs:			
400 F	1.3	2.5	1.1
210 F	8.4	29.0	3.3
100 F	120	716	12.7
V.I.	0	58	154
Temperature where Viscosity = 13,000 cs, F	0	47	−65
Pour Point, F	−25	−5	−75
Specific Gravity	1.60	1.76	0.92
Volatility, 400 F Test, Weight Loss, %	65	1	12

Table 9 — Performance of Lubricants in the "Rapid" Falex Test

	Max. Load Carried, lb	Torque at Fail, lb/in	Maximum Bushing Temperature, F
Fluoroalkyl Camphorate	3700	90	545
Fluoroalkyl Pyromellitate	> 4500	75	450
Di-2-Ethylhexyl Sebacate			
Base Fluid	1150	45	260
+ 5.0 Weight % tcp[a]	1500	45	275
Experimental Esterlubricant			
Base Fluid	1200	51	320
+ 7.5 Weight % tcp[a]	2600	52	400

[a] Tricresyl phosphate.

Volatility studies on a wide variety of fluoroesters indicate that diesters should be prepared from acids containing at least 10 carbon atoms (for example, camphoric, sebacic, and the like) if they are to have reasonably low volatility. Triesters prepared from acids having six carbon atoms are considerably less volatile than the 10-carbon dibasic acid eters and, in this respect, are more desirable. All the tetrafluoroalkyl esters tested had very low volatility.

Fluoroester Lubricants

The fluoroalkyl camphorate and pyromellitate were selected for further evaluation as high-temperature lubricants. This selection was based on their relatively good physical properties, outstanding resistance to oxidation, and the availability of the acids. Their physical properties are shown in Table 8. As indicated in this table, their viscosity-temperature properties are not equal to those of a typical nonfluorinated ester lubricant.

Oxidation tests on these fluoroesters without additives indicate that the camphorate can be used at bulk oil temperatures up to 450 F. The pyromellitate, in turn, can be used at temperatures 100 F over the camphorate's limit. This is illustrated by the oxidation test data presented in Fig. 5. Di-2-ethylhexyl sebacate (plus 0.5 weight per cent phenothiazine) is included in this series.

Load-carrying ability was determined in the "Rapid" Falex Test.[19] The data are summarized in Table 9. As might be expected on the basis of their high halogen content, the performance of the fluoroesters was considerably better than that of typical nonfluorinated esters. The ability of the pyromellitate to carry higher loads than the camphorate may, in part, be due to its higher viscosity

[17] *Industrial and Engineering Chemistry*, Vol 42, December, 1950, p. 2415: "Structural Guides for Synthetic Lubricant Development," by C. M. Murphy and W. A. Zisman.

[18] Volatility data were obtained in a small-scale, open-dish test which correlates with the full-scale ASTM D972-56 volatility test used in the 9236 specifications.

[19] P. 153 of "Lubricant Testing," by E. G. Ellis. Pub. by Scientific Publications, Ltd., London, 1953.

Table 10 — Heavy-Duty Radioactive Piston-Ring Wear Test Conditions

Speed, rpm	1800
Load	Wide-open throttle
Test length, hr	14
Air/Fuel Ratio	13.5/1
Coolant Temperature, F	
Inlet	105 ± 2
Outlet	202 ± 2
Oil Temperature, F	150 ± 2
Spark Advance, btdc	20

Table 11 — Performance of Fluoroesters in ERDCO Bearing Test

	Camphorate	Pyromellitate
Bulk Oil Temperature, F	438	500
Oil at Jet-to-Bearing, F	400	437
Bearing Temperature, F	500	600
Oil Flow, lb/min	1.5	1.4
Used Oil Data:		
Viscosity Increase at 100 F, %	6	10
Acid Number	3.7	4.8

Table 12 — Operating Cycle of J-57 Engine Test

1. Alternate during 60 min:
   5-min idle thrust
   5-min maximum thrust
2. Ninety minutes normal rated thrust.
3. Thirty minutes accelerations and decelerations, 5 cycles maintaining maximum thrust for 30 ± 3 sec.
4. Sixty min at 90% normal rated thrust.
5. Thirty min at military thrust.
6. Thirty min at 75% normal rated thrust.

   Repeat for 20 cycles totaling 100 hr.

at the temperatures reached within the test pieces. The viscosity of the camphorate is approximately 1.0 cp at 450 F. When the camphorate reaches temperatures much above that figure, its viscosity may be insufficient for proper lubrication. Other workers have reported on the satisfactory boundary lubrication and low wear performance of fluoroesters.[20]

The Ryder Gear test performance of the camphorate without additive (2800 lb per inch of gear tooth width) equalled that of the experimental esterlubricant (Table 9) containing 7.5 weight per cent of tcp.

The bench test data on the lubricity of the camphorate were confirmed in a heavy-duty radioactive ring wear test in a COT (Cooperative Oil Test) engine. The wear rate obtained during operation of the engine lubricated with the camphorate was approximately 0.03 mg of iron per hr. This performance equaled that of typical high-detergency crankcase oils which had been run in the same test. The engine operating conditions are given in Table 10.

Both fluoroesters were evaluated in the Erdco Universal Tester by the Pratt & Whitney Aircraft Division of United Aircraft Corp. This test employed 100-mm roller bearings under a 500-lb radial load. The test duration was 100 hr at 10,000 rpm.[21, 22] The bearing was maintained at temperature with a "Calrod" heater which was wound around its outer race. Hot oil from a reservoir was pumped through an orifice to spray against and lubricate the bearing. The bearing housing was continuously swept with air at a rate of 30 cu ft per hr to promote oxidation of the oil. The oil was scavenged by pump from the bearing housing and returned to the reservoir for recycle. A summary of the conditions used during tests on the two

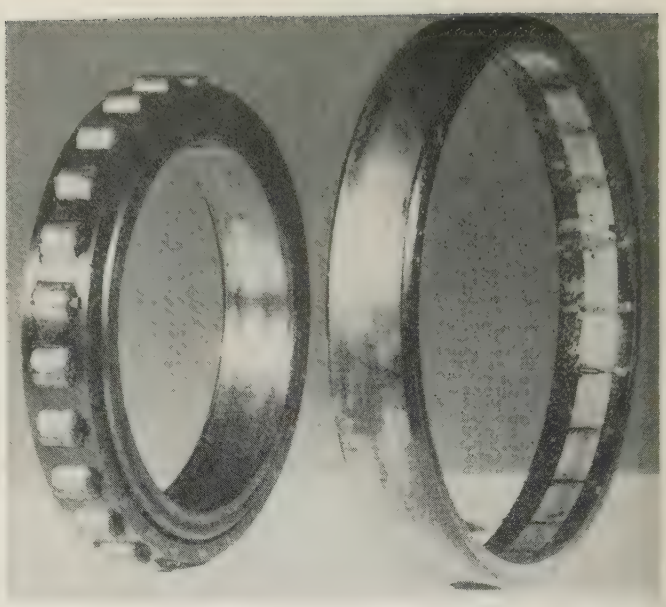

Fig. 6 — Bearing after 100-hr endurance test on fluoroalkyl camphorate (bulk oil temperature — 438 F, oil-in temperature — 400 F, bearing temperature — 500 F)

fluoroesters is given in Table 11 and photographs of the bearings after the tests appear in Figs. 6 and 7.

The camphorate test with 400 F oil-to-jet, 438 F bulk oil, and 500 F bearing temperature showed less oil stress than encountered with typical MIL-L-7808 oils run with 300 F oil-to-jet, 400 F bulk oil, 500 F bearing temperature. The 500 F bulk oil pyromellitate test was run at approximately the limits of the equipment and bearing. Under these very severe conditions, it equaled or exceeded the performance of the 438 F bulk oil camphorate test.

Oil consumption with the camphorate was considered to be undesirably high, while the pyromellitate showed low oil consumption. The oil consumption data were in agreement with the volatility data given in Table 8. However, as will be discussed below, test-stand operation of a turbojet engine on the camphorate did not show unusual oil consumption. The problem of oil volatility in jet engines may become significant at high oil temperatures or in high-altitude use of the lubricant.

The fluoroalkyl camphorate was evaluated by the U.S. Naval Air Material Center as a turbojet engine lubricant.[23] The test was run 100 hr in a J-57-P6A engine using a bulk oil temperature of 300 F. The operation conditions of the test are given in Table 12 and are essentially those used in the engine qualification of MIL-L-7808 oils.

When disassembled at the end of this test, the engine was found to be very clean. A photograph of the No. 6 engine bearing is shown in Fig. 8. This bearing is in the hot section of the engine and is one

[20] *Lubrication Engineering*, Vol. 12, July–August, 1956, pp. 245–253: "Boundary Lubrication Studies of Typical Fluoroesters," by R. C. Bowers, R. L. Cottington, T. M. Thomas, and W. A. Zisman.

[21] "Third Evaluation of du Pont Fluoroester Lubricant FCD-1664 in ERDCO High-Temperature Bearing Head," by H. W. Reynolds. Pratt & Whitney Aircraft Report FL-58-9, March, 1958.

[22] "Evaluation of du Pont Fluoroester Lubricant DV-5902 in ERDCO High-Temperature Bearing Head," by H. W. Reynolds. Pratt & Whitney Aircraft Report FL-58-19, July, 1958.

[23] "J-57 Turbojet Engine Evaluation of Fluoroalcohol Ester of Camphoric Acid, DV-5248," by A. L. Lockwood. U. S. Naval Air Material Center, Aeronautical Engine Laboratory, Phase A, Report NAMC-AEL-1515, August, 1957.

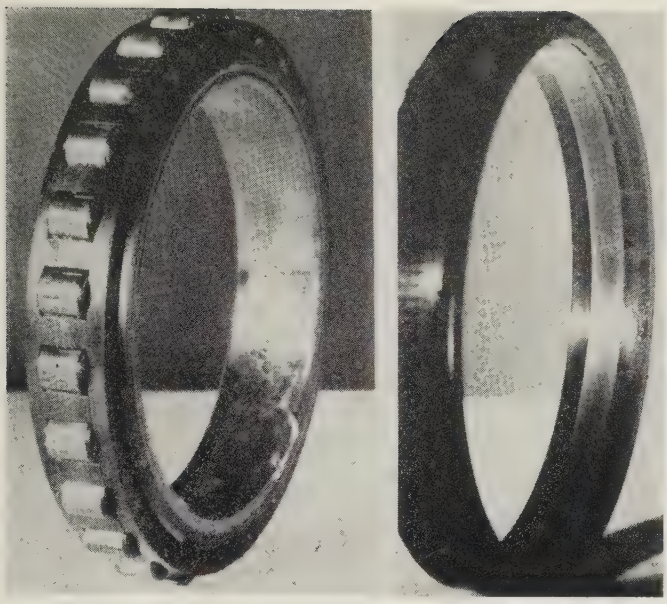

Fig. 7 — Bearing after 100-hr endurance test on fluoroalkyl pyromellitate (bulk oil temperature — 500 F, oil-in temperature — 437 F, bearing temperature — 600 F)

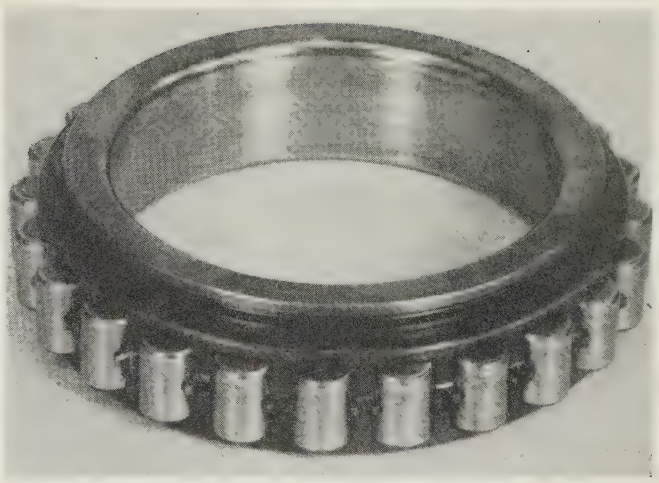

Fig. 8 — No. 6 bearing from 100-hr 300 F J-57 engine test on fluoroalkyl camphorate

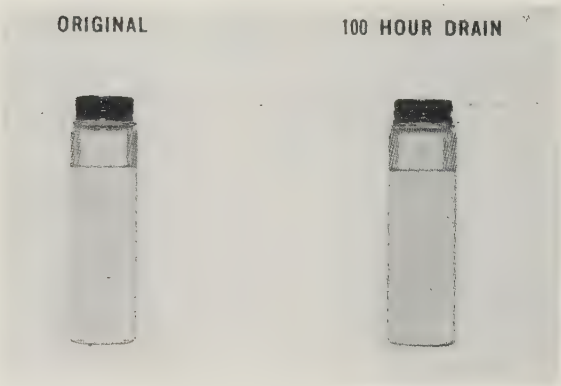

Fig. 9 — Effect of 100-hr 300 F J-57 engine test on fluoroalkyl camphorate used as engine lubricant

of the components which suffers during tests on marginal lubricants.

The used engine oil was a light-amber color essentially equal to the original oil in its physical properties. It possessed an acid number of only 0.1. Pictures of samples of the new and the used oils are given in Fig. 9. Oil consumption of the camphorate was not excessive, averaging 2.4 lb, or 0.19 gal, per hr. This was the same volumetric oil consumption rate (0.19 gal per hr), given by the reference MIL-L-7808 lubricant used during the 5 hr of preliminary operation to establish average bearing running temperatures and oil consumption figures. The only difficulties encountered related to some oil leakage through elastomeric "O" ring seals. The fluoroester tended to shrink and harden the "O" rings in the high temperature section of the engine. Work both before[24] and since this test indicates that elastomer formulations compatible with fluoroesters at high temperatures can be developed.

The J-57 engine test was not run under sufficiently severe conditions to establish the maximum performance limit of the camphorate. However, the engine results do confirm the data obtained in the laboratory on the excellent oxidative stability and lubricity of the camphorate.

Summary

1. Certain esters prepared from a class of highly fluorinated alcohols extended the maximum use (bulk oil) temperature of ester lubricants up to as high as 550 F.

2. Fluoroester lubricants discussed in this paper do not possess the excellent V.I. and low-temperature properties desired in the 9236 oils.

3. The good lubricity and oxidation resistance of two fluoroalkyl esters predicted by laboratory tests has been confirmed by limited rig and engine testing.

4. Additional field evaluation of these esters will have to be completed before their final usefulness is established.

Acknowledgment

The writers are indebted to the Pratt & Whitney Aircraft Division of United Aircraft Corp. for their permission to use photographs and data from their tests on fluoroesters. They are indebted to the Naval Research Laboratory and the U.S. Naval Material Center, Aeronautical Engine Laboratory at Philadelphia, Pa., for their permission to use data and photographs of the J-57 engine test on the fluoroalkyl camphorate.

DISCUSSION

Fluoroester Lubricants Promise Stability Above 500 F

— C. M. Murphy and H. Ravner
U. S. Naval Research Laboratory

THE CONDENSED aromatic acid ester, tetrafluoroalkyl pyromellitate, has a V.I of 58 as compared to zero V.I. for the condensed aliphatic acid ester, difluoroalkyl camphorate. In fact, the V.I. of the pyromellitate is only slightly smaller than that of the C_7 fluoroalkyl sebacate, a linear type ester with a V.I. of 62. This V.I. of the pyro-

[24] *Industrial and Engineering Chemistry*, Vol. 48, March, 1956, pp. 466-467: "Effects of Partially Fluorinated Diesters of Elastomers," by F. X. Cunningham, R. C. Taylor, and L. B. Lockhart, Jr.

mellitate is in contradiction to the generalization that aromatic esters would have poor V.I.'s. Do the other aromatic acid esters studied, but not reported here, have low V.I.'s as would be inferred from the generalization? Do the authors have any theories or care to speculate as to the reasons for the apparent anomaly in the viscosity-temperature properties of the pyromellitate? It is hoped that the data on the other fluoroesters will be published, as this information will be of interest to those studying the relationship between chemical and molecular structure, and bulk properties.

Information on the thermal stabilities of the fluoroesters was presumably obtained in glass systems. Some metals, particularly iron, catalyze thermal breakdown. Do the authors have information as to the catalytic effect of the common metals of construction on the pyrolysis of fluoroesters?

According to the generalization relating the hydrolytic stability of esters to the strength of the acid from which it was derived, the pyromellitic ester should be less stable than the corresponding ester of camphoric acid, as pyromellitic acid is about 1000 times as strong. Steric effects and the solubility of water in the ester also influence hydrolysis rates. As it is difficult to relate these factors, hydrolytic stabilities should be determined under service-simulating conditions.

Data on the lubricating properties of the fluoroesters indicate that they are good lubricants and are superior to conventional esters in load-carrying ability. This could obviate the use of load-carrying agents which frequently have an adverse effect on the properties of the finished oil, particularly oxidation stability.

This paper may well stimulate further work on improved fluoroesters. The authors have shown that the generalizations relating molecular structure to viscosity-temperature properties are inadequate to predict accurately the properties of fluoroesters. It is possible that new fluoroesters with higher V.I.'s will result from additional research.

Describes Test of Fluoroalkyl Camphorates at 350 F Oil-in Temperature

— Kerry L. Berkey
Wright Air Development Center

I SHOULD LIKE TO congratulate Messrs. Ballard and Sommers on an excellently prepared paper in which they covered the work on fluoroester lubricants quite thoroughly. The only revision I feel is necessary is in Table 1, item 3. Present thinking has lowered the minimum viscosity to 1.5 cs. In fact, we have satisfactorily run oils with a viscosity of around 1.0 cs.

The Government is interested in the fluoroesters as engine lubricants due to their apparently good thermal and oxidative stability.

As noted in the paper, the fluoroalkyl camphorates have been run in a J-57 engine at 300 F oil-in. A 350 F oil-in run has also been made since the paper was written. Before test termination, 43.5 test hr were accumulated at 350 F. During the testing, the oil entrained in breather air broke down in the rear engine breather to form either hydrogen fluoride or free fluorine which caused extensive corrosion damage in an aluminum cooler in the downstream breather line. A stainless-steel cooler which replaced the aluminum one also was badly corroded. Ferrous corrosion products were found in the No. 6 breather compartment. These products clogged a sump pump inlet causing the bearing compartment to flood which resulted in the failure of a smaller bearing fed off this compartment. It was this bearing failure which terminated the test. The iron oxide came from extreme corrosion of the No. 6 breather tube which comes out of the engine through a strut which crosses the engine exhaust stream. Gas temperatures around the strut can exceed 1100 F under maximum power conditions. There is no heat shielding between the strut and the breather tube. We feel that heat shielding in this area may relieve the problem. Both the 300 F and the 350 F engine testing were accomplished by the Naval Air Material Center at Philadelphia.

The Navy is currently preparing another J-57 engine to test the fluoroester at 400 F oil-in. Of great interest in this test will be the oil consumption. As noted in the paper, evaporation at 400 F is high. However, in both the 300 and 350 F engine testing, oil consumption was normal. An attempt may be made to provide heat shielding in the No. 6 breather line area to prevent oil breakdown into corrosive elements. The nature of the fluoroester program will probably be determined by the outcome of the 400 F testing. We are looking forward to this testing with great interest.

Authors' Closure To Discussion

THE PYROMELLITATE possessed the highest V.I. of the aromatic fluoroesters tested in our laboratory. We believe its relatively good viscosity-temperature performance is due to its overall symmetrical and rather long molecular shape.

In respect to the thermal degradation of fluoroesters, we have not observed any significant effect of metal catalysis. Our tests were of 24- or 48-hr duration and covered temperatures up to 600 F. Results were similar, whether obtained in test cells made of glass, steel, stainless steel, copper, or aluminum.

The hydrolytic stability of the pyromellitate fluoroester, under alkaline conditions, is not as good as that of the camphorate. This is undoubtedly due to the greater acid strength of the pyromellitic acid, as suggested by Messrs. Murphy and Ravner. However, under neutral conditions which approximate those of actual use, the fluoroalkyl pyromellitate has been blown with steam for over 18 hr with no signs of hydrolysis.

There were two areas of corrosion observed in the 350 F engine test mentioned by Mr. Berkey. One area was in the terminal end of a line attached to the oil tank breather vent for the purpose of collecting in an ice tower the volatile fractions from the lubricant breather system. This line is not part of a standard engine system. The corrosion observed here was due to low concentrations of hydrogen fluoride in the vent gases. This hydrogen fluoride probably occurred as the result of very high-temperature oxidation of the fluoroester at some hot spot in the engine.

Corrosion in the engine itself was observed in only one isolated section — the No. 6 breather pipe. Here there was no evidence of hydrogen fluoride. The corrosion produced was a scale-like material which proved to be a mixture of iron oxides (Fe_3O_4 and alpha Fe_2O_3) and a small amount of chromium oxide. Laboratory attempts to duplicate the corrosion observed in the No. 6 breather pipe at temperatures up to 575 F were not successful.

The excellent appearance, that is, the total absence of any sludge or corrosion, of all other sections of the engine lubricant and breather sections has prompted the "go-ahead" for a 400 F test, despite the fact the 350 F test was terminated after 43.5 hr.

It should be pointed out that Mr. Berkey's reference to the "fluoroester program" in connection with the 400 F test is in reference to the fluoroalkyl camphorate only.

It should be pointed out also that the ultimate usefulness of any new lubricant type can only be proved by actual service tests, and much additional testing is required with respect to the fluoroesters as high-temperature lubricants.

Muffler Corrosion

— its cause and control

R. A. Heath, Walker Manufacturing Co. of Wisconsin

This paper was presented at the SAE National Passenger-Car, Body, Materials Meeting, Detroit, March 18, 1959.

WHY THE current interest in mufflers . . . corrosion . . . and life?

Let's retrace our steps to 1940–1944 when mufflers were round, straight-through designs as compared to today's oval triflow mufflers. Fig. 1 shows a schematic comparison of these basic types. These straight-through designs, which usually ran cooler than today's triflows, often used coated steels for their heads, partitions, and shells. The coated steel used by the industry at that time was usually terne plate. Because terne plate, though somewhat inert, is a porous material, our company in 1944 pioneered with Buick and other car companies, the development and use of hot-dipped zinc material for mufflers. This material is "sacrificial" in character and will sacrifice itself to the condensate before allowing the condensate to attack the base metal. Aluminized steel, developed by Armco, was also tested and pioneered by Walker for mufflers but was not used on passenger-car mufflers at that time because of its higher cost.

Fig. 2 shows some of these mufflers tested in conjunction with the Buick Motor Car Co. in 1944 and the relative corrosion results. Even at this time, merely adding heavier gage steel for longer life was recognized as not the complete answer.

Later tests on hot-dipped zinc mufflers gave better results than terne plate. Reports written in 1945 by several G.M. divisions substantiated these data. Hot-dipped zinc was then often used on shells,

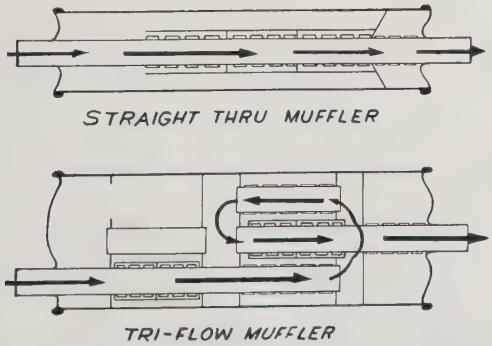

Fig. 1 — Comparison of straight-through and triflow mufflers

ACID CONDENSATE and its effect on mufflers is being controlled to an acceptable limit by a combination of three methods:

1. Use of hot-dipped zinc.
2. Use of aluminized steel.
3. Improved design.

The author describes the materials tests and temperature tests on single and dual exhaust systems, which are used to evaluate various muffler designs. He also describes the use of condensate drainage.

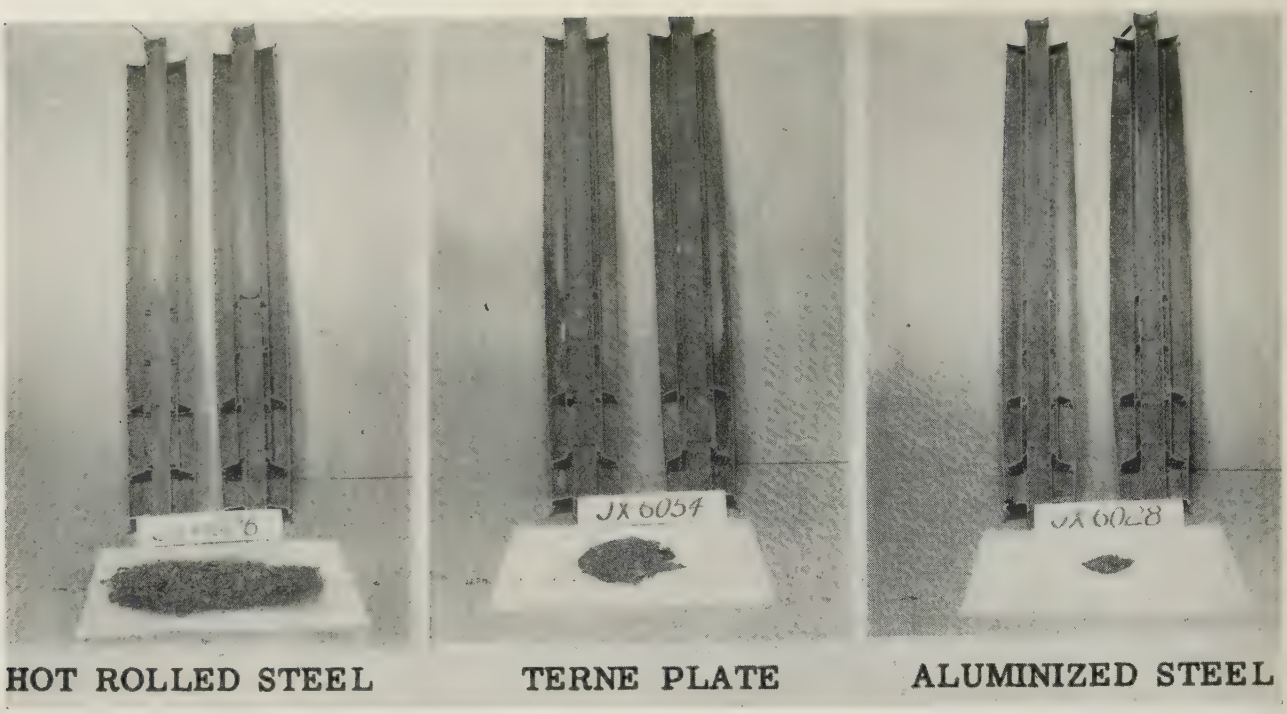

Fig. 2 — Muffler corrosion test, 1944 (accelerated test of approximately 80 hr each over 3-month period)

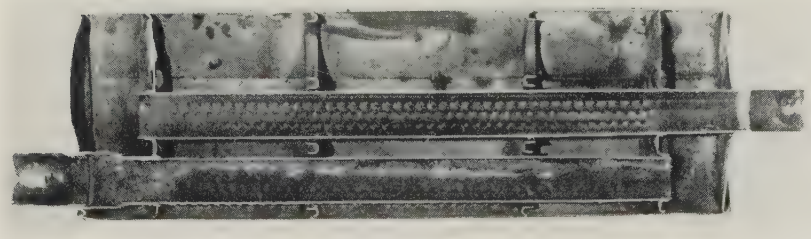

Fig. 3 — 1954 single system, which ran 31 months and 36,500 miles or 1180 miles per month

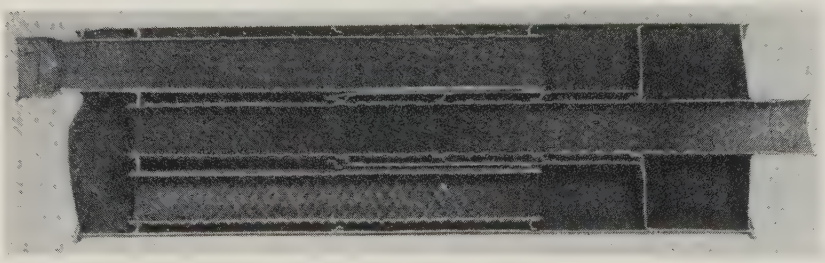

Fig. 4 — 1955 single system, which ran 36 months and 36,783 miles

heads, and partitions until the straight-through design was obsoleted, largely due to space limitations. For most car installations after 1950, triflow oval mufflers became necessary because cars were being lowered and mufflers had to be shorter. These oval triflow mufflers run warmer than most straight-through mufflers and often were made entirely of plain steel and gave very satisfactory life.

An example of this is Fig. 3 which shows a single exhaust system muffler made entirely of plain steel and which ran 31 months. This muffler is in excellent condition and would have run much longer if we had not cut it open for inspection. The driving was about 1000 miles per month which is about the national average.

Fig. 4 shows a similar result on another plain steel single system muffler after 36 months of life. These mufflers are all taken from privately owned cars—part of a large fleet of over 250 cars on which we maintain records and conduct endurance tests. This muffler is also in good condition.

Sometimes it became necessary to put tuned chambers in these mufflers to silence the car properly. In these cases, hot-dipped zinc heads, shells, and partitions were often used by the industry to protect these chambers. Seldom was the car owner who drove 1000 miles per month or more bothered with muffler problems. Fig. 5 shows a typical result of this type of design.

To determine what temperatures are actually in a muffler, we ran many temperature tests on single and dual exhaust systems. We also compared plain

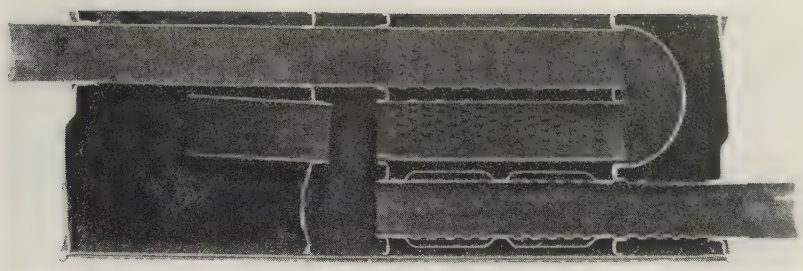

Fig. 5 — 1957 single system (type of muffler which often had coated parts, ran 21 months and 22,790 miles)

and asbestos-covered shells. A typical car installation is shown in Fig. 6. Surprisingly enough, the size of the engine seems to have little effect on the muffler temperatures or warmup time for the same driving conditions on the same muffler. Muffler design, however, has a pronounced effect on warmup time and running temperatures. Mufflers with long flow tubes or those using Walker's development of return-flow volume passage, called "Dynamic Wiping Action," ran warmer and warmed up faster than mufflers with tuned or closed chambers. Both types of designs are used by the industry on various cars for proper silencing. A long volume passage muffler "warms up" to its maximum temperature in about 3 min; the tuned design in about 6 min, rather independent of a car speed under 50 mph on single systems. The benefit of an asbestos-covered muffler is measured by faster warmup time and by shell temperatures ranging 50–100 F above the shell temperatures on the same design of muffler without asbestos. Asbestos is also beneficial on duals but to a less degree. These data were observed during sustained road load driving conditions.

Fig. 7 shows shell temperatures of various chambers in a long unit volume passage single system muffler at various sustained road load driving speeds. Notice, after 20-mph car speed, temperatures are above 202–210 F, which is the critical range of condensate boiling.

Fig. 8 shows shell temperatures of a tuned muffler for test purposes on the same car as the previous

Fig. 6 — Typical car installation

test. It will be noticed that the shell temperatures of the various chambers run colder in this design. As mentioned, both types of designs are common and when a muffler design is required which includes a cool chamber, it is often protected with hot-dipped zinc heads, shells, and partitions.

We have found it difficult to collect condensate above approximately 170–180 F and, therefore, we believe the largest quantity of condensate is formed below these temperatures. We feel that, under normal driving conditions (1000 miles a month or more), the muffler corrosion problem on single exhaust systems is under control.

At about the time of the advent of duals, mufflers

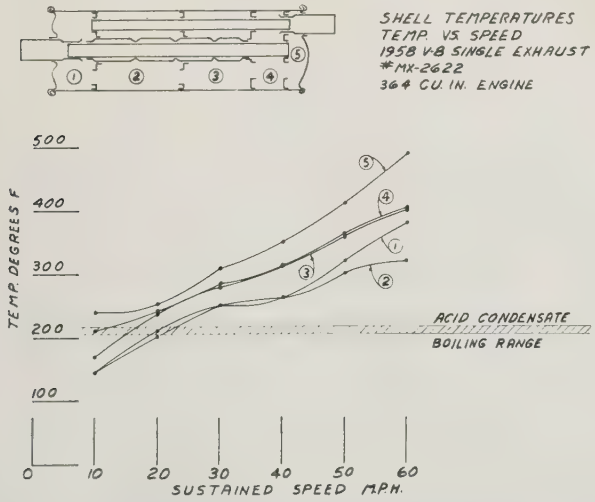

Fig. 7 — Shell temperatures, temperature versus speed, of 1958 V-8 single exhaust No. MX-2622, 364-cu-in. engine

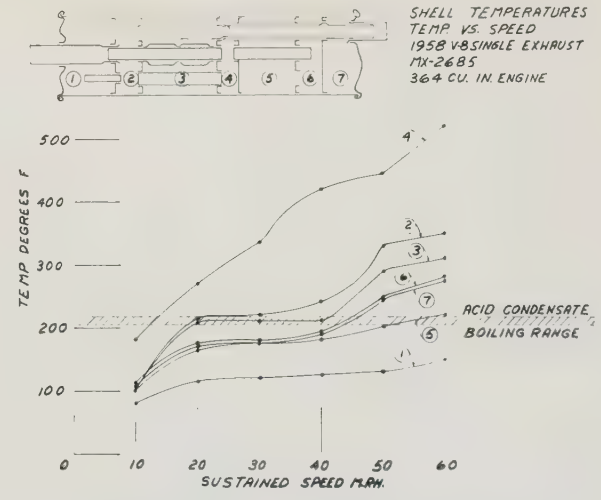

Fig. 8 — Shell temperatures, temperature versus speed, of 1958 V-8 single exhaust No. MX-2685, 364-cu-in. engine

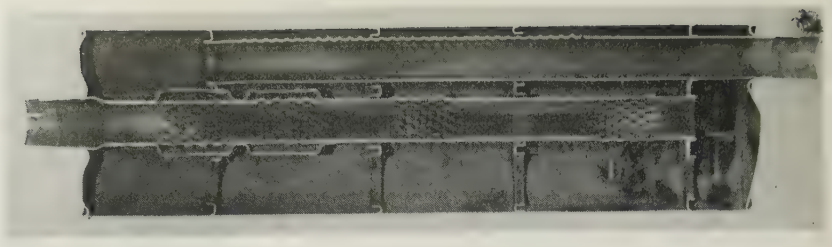

Fig. 9 — Typical single system muffler after 24 months and 19,456 miles

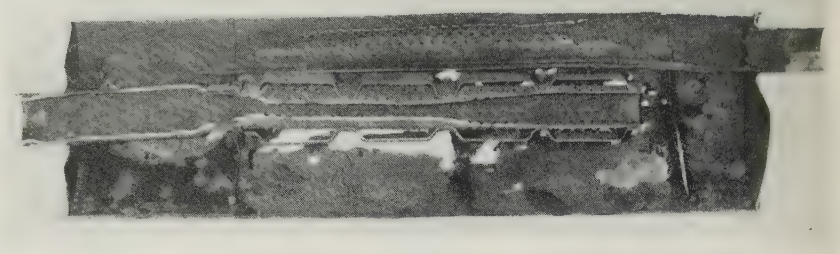

Fig. 10 — Single system design used as dual, after 7½ months and 5636 miles of service

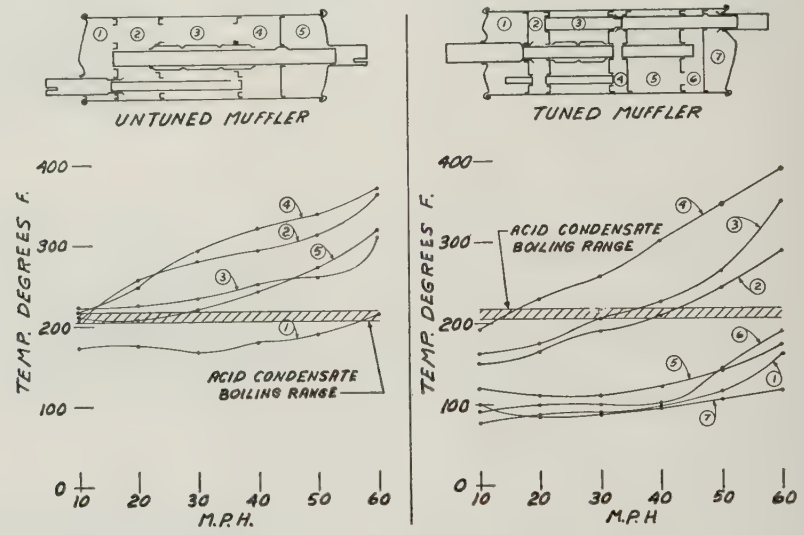

Fig. 11 — Shell temperatures, temperature versus speed, of hot side of dual system

became an everyday topic for several reasons:

1. The general increasing number of car registrations, which doubled in the last 10–12 years.
2. More start and stop driving on today's crowded roads.
3. Two-car families — and resulting short trips.
4. Dual exhaust systems on new cars as compared to hot-rod dual installations.
5. Short life of duals experienced by some drivers.
6. Muffler specialists, as new names entered an expanding market.

Duals are, many times, required on modern cars to assure full engine output and performance, for styling, and for proper underbody clearance. To have single exhaust systems with the same pipe flow area as a dual, would require exhaust and tail pipes of 2½–3½ in. diameters and mufflers up to 6 × 10 ovals. There isn't this much room under cars — at least not on the layouts we have seen.

Fig. 9 shows a plain steel single exhaust system muffler which gave excellent life as expected (24 months and 19,456 miles). Now let's see what happened when this same design of muffler was run experimentally on a privately owned dual exhaust system car. Fig. 10 shows such a muffler after 7½ months and 5636 miles. The vicious attack is clearly shown.

In most dual systems, there are "hot" and "cold" sides. The "hot side" takes most of the exhaust gas during city or suburban driving. The "cold side" is caused by a heat valve which forces most of the exhaust gas over the engine and under the carburetor. This heat valve permits a "solid" driving during engine warmup. Fig. 11 shows the shell temperatures of the "hot side," showing comparison of two designs. Again, these are current basic designs used by the muffler industries as the car needs dictate. These hot side temperatures run as much as 100 deg cooler than corresponding temperatures for the same designs on single exhaust systems.

Fig. 12 shows shell temperatures of the same mufflers on the "cold side." Notice neither design is sufficiently warm to drive off the condensate which boils around 202–210 F. These mufflers will often burn you if you touch them. You can hold your hand on objects up to about 120 F and it's hard to

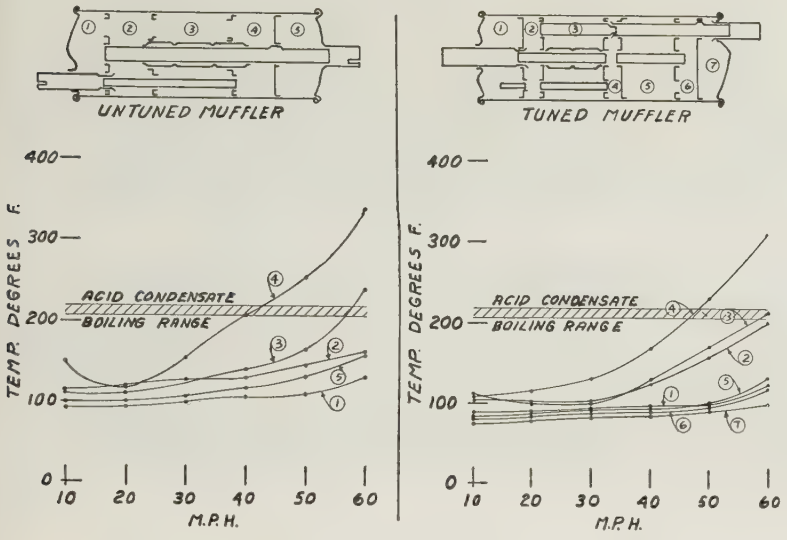

Fig. 12 — Shell temperatures, temperature versus speed, of cold side of dual system

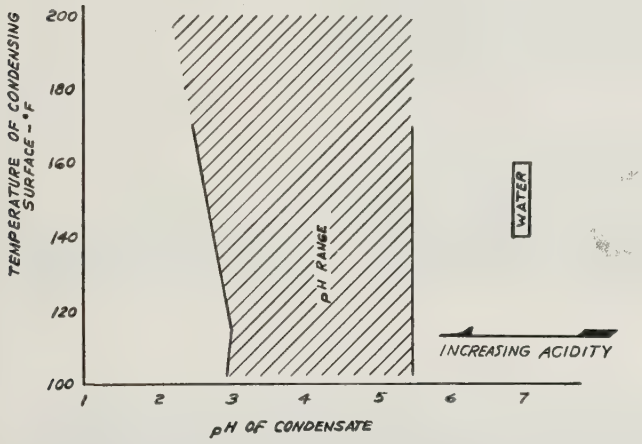

Fig. 13 — pH values of exhaust gas condensate

Table 1 — Acid Content of Typical Exhaust Gas Condensate Based on Its Chemical Analysis

Chemical Formula	Common Name of Acid	Concentration, Milligrams Per Liter
HCl	Hydrochloric	580
H_2SO_4	Sulfuric	141
H_2SO_3	Sulfurous	17.5
HBr	Hydrobromic	35.5
H_3PO_4	Ortha phosphoric	5.2
H_2CO_3	Carbonic	423

In addition to the above the condensate had suspended solids of 256.

tell people that these mufflers are cold. But they are too cold for their own good, and acid condensate is formed in quantities in these mufflers. Because it is acid condensate in the muffler, working from the inside out, which must be controlled, let's look at some typical condensate analyses.

Table 1 shows the composition and relative parts by weight of acids in a sample of exhaust condensate. The amount of the H_2SO_4 and the HCl varies greatly in different samples, but this one is typical. This chart gives the parts by weight only, and not acidity. We have no evidence to prove that today's fuels are any more acid than those of 10 years ago.

Fig. 13 shows the range of pH readings found in various condensates from laboratory and road tests. PH is a relative logarithmic term to define acidity in terms of the hydrogen ion. A reading of pH_7 has the same action as water and is considered neutral. The lower the pH number, the more acid is the solution, and normal solutions of acids would range from pH_1 and below. This chart shows the range of acidity only and does not attempt to rate different fuels at various temperatures. We did find, however, a great variation between brands of fuel; and there was no relation between regular and ethyl.

The pH of some fuels remained fairly constant regardless of temperature of condensing surface and condensing rate. On the other fuels it is varied widely within the range shown.

As previously mentioned, we have found it difficult to collect condensate in volume above 180 F and chambers below this point form condensate quite rapidly. Condensate can be formed in a cold chamber of a muffler at the rate of over ½ pt per hr.

Top view of Fig. 14 shows an early experimental dual with more use of hot-dipped zinc-coated steels than was normally used by the industry at that time and was decided upon after much investigation. Obviously, not enough coated steel or protection was used. It became apparent that the condensate built up had to be controlled by removal either through heat or drainage — or both.

The lower picture shows the control that was obtained with further use of coated steels (hot-dipped zinc plus aluminized steel), together with a properly engineered drainage system. This muffler had very severe service — 500 miles per month.

Fig. 15 shows both "hot" and "cold" sides of a dual muffler system which gave satisfactory life using proper coated steels and a drainage system. Drainage systems are controversial in the industry; however, when carefully engineered, we believe drainage of condensate to hotter sections — or from the muffler entirely — gives considerable benefit. Condensate drainage is being used, or is under con-

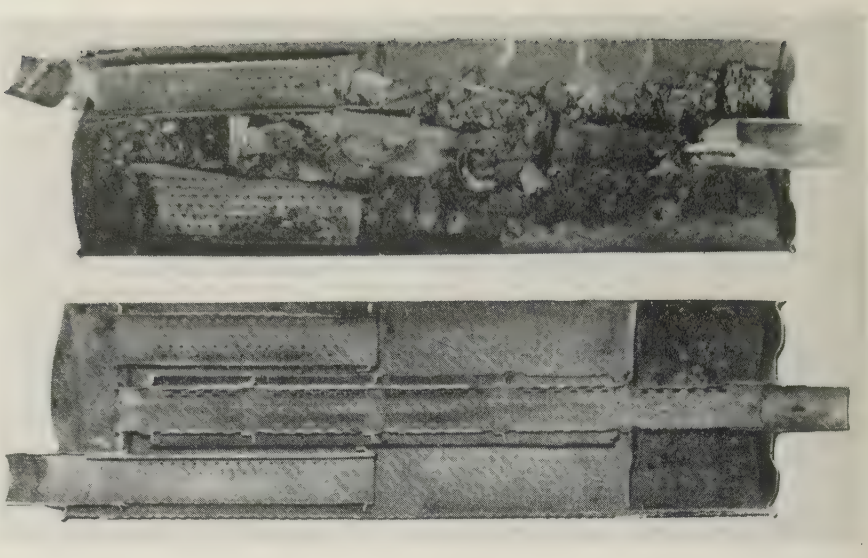

Fig. 14 — 1954 dual system

Experimental early dual muffler, has hot-dipped zinc heads, partitions, and shells, no drain holes, after 8 months service and 6688 miles total

Muffler with hot-dipped zinc shell, aluminized steel heads, partitions, and outlet tubes, and a drainage system, after 16 months service and 8820 miles total

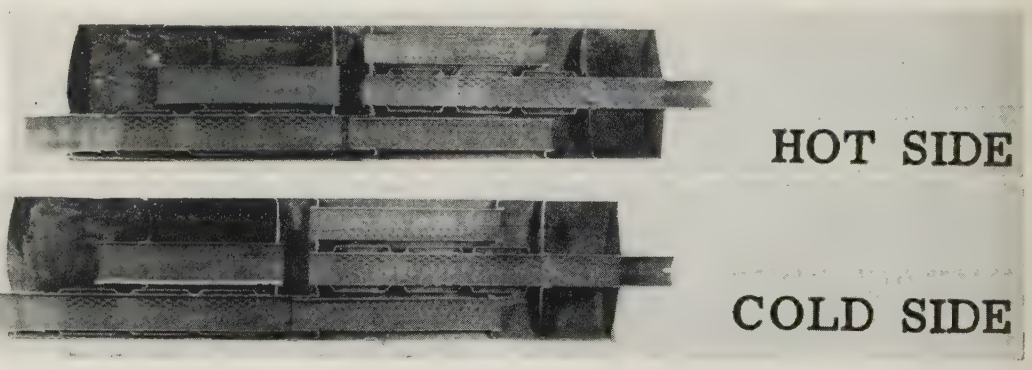

Fig. 15 — 1956 dual system

Both sides of dual exhaust are in excellent condition after 19 months and 19,669 miles of service

Mufflers protected with hot-dipped zinc and aluminized steel parts, and drainage system

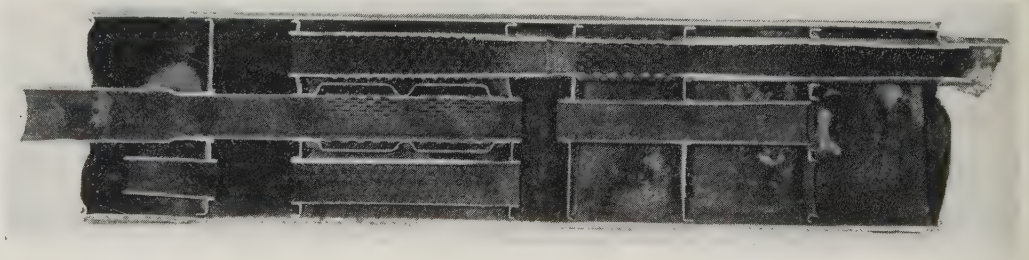

Fig. 16 — 1956 dual system, muffler has hot-dipped zinc and aluminized steel parts with modified drainage system, after 18 months and 19,653 miles

sideration, at most car factories.

Currently, all aluminized steel mufflers are being used by some car factories to further increase average life. The balance of aluminized and hot-dipped zinc must be worked out for each design.

Fig. 16 shows another dual muffler with good life after 18 months through the extended use of hot-dipped zinc and aluminized steel parts, and a modified drainage system. This muffler was in good condition when removed and had many months of life left in it.

Stainless steel, we believe, would be good for mufflers. However, in addition to being hard to form and weld, its price is very high. We have stainless-steel mufflers on cars that are in excellent condition after 1–1½ years and we are continuing these on test.

We believe that the acid condensate and its attack on mufflers can and is being controlled to an acceptable limit by the use of hot-dipped zinc and aluminized steel and by design. However, we are looking for better metals to improve muffler life even further, as are other muffler and car companies. We have at the present time over 39 different metals, coatings, and alloys under development and test. We are attempting to obtain metals which will give the same protection at a lower price — or if you prefer, better protection at a commensurate price.

Oral discussion of this paper will be found on p. 568.

EXHAUST SYSTEMS

fundamentals and design considerations

L. E. Muller, Buick Motor Division, General Motors Corp.

This paper was presented at the SAE National Passenger-Car, Body, and Materials Meeting, Detroit, March 18, 1959.

THIS PAPER will try to record some of the progress made over the years in the design of mufflers, and the equipment to test and study them.

Today, our equipment and facilities are much better than 25 years ago, perhaps they should be discussed.

Fig. 1 shows the dynamometer setup used in these studies. The engine was standard production and the pipes were of regular diameter and length. As will be noted, the pipes extended through the roof to the atmosphere where the microphone was located. A 3-way valve was used to give almost instantaneous comparative noise loudness values between any two exhaust systems merely by shifting the valve. It eliminated any climatic, speed, or engine condition that might affect the noise readings due to time lapse. A fan was used to cool the exhaust system in an attempt to approach car operating temperatures. The speed of the engine must be maintained exactly: therefore, it was electronically controlled.

The sound was analyzed and recorded by means of an Electrical Research Products, Inc. Sound Analyzer and Recorder, or a Techno Sound Analyzer and Recorder. Precise frequency was measured by means of a cathode oscilloscope and counter.

Velocity of Sound

One of the most fundamental requirements of noise work is to know the velocity of sound in the medium in which the work is to be done. In this case, it was exhaust gas at high temperatures and at high velocities.

How to measure its velocity defied solution for a long time due to the relatively high temperature of the gas. However, a very simple solution pre-

TWO TEST TECHNIQUES are helping the muffler designer keep ahead of the growing demands on the muffler system — cold acoustical testing and resonant pipe sound velocity measurements. The first is a method of screening new configurations and the second a means of finding the velocity of sound of hot exhaust gases during a full-scale muffler test.

The author discusses the design factors to be considered in designing mufflers, such as chamber location, resonators and multiple chambers and louvers; and the selection of the type of cross-section for the muffler.

sented itself in the form of the tuner, as shown in Fig. 2.

The tuning tube, which was made the same diameter as the exhaust pipe, was placed at right angles to the exhaust system with the open end exposed to the exhaust gases. It was basically a "closed organ pipe" whose effective length could be changed by means of a movable piston. The adjustable piston was connected to a calibrated rod that indicated the piston's location from the "open" end of the tube. The theory of the tube's operation is that when the piston is adjusted to give maximum attenuation for silencing of a given frequency, the distance from the piston to the center of the exhaust pipe is ¼ wave length of the frequency being attenuated.

However, a correction must be made for the difference in the temperature of the gas in the tube and the exhaust pipe. Therefore, thermocouples were installed in the tuning tube as well as the exhaust pipe for recording these necessary temperatures. To keep the gas temperature in the tuning tube as uniform as possible, it was covered with an insulating material.

In this test, data to determine the velocity of sound was taken at engine speeds from 900 to 3000 rpm at 300-rpm intervals under full- and part-throttle conditions. Since engine firing frequencies gave such a strong signal, they were used in calculating the velocity of the sound.

Fig. 3 shows the attenuation of firing frequency attained by the use of the tuning tube while the engine was running at 1200 rpm under road load conditions. Also shown are the temperatures recorded in the exhaust pipe and tuning tube. This attenuation curve shows the measured quarter wave length to be 48.5 in. long for an 80-cps sound.

Since:

$$V = F\,W_L$$

where:

V = Velocity of sound, fps
F = Frequency of Sound, cps
W_L = Wave length, ft

$$V = \frac{80\ (48.4)\ (4)}{12}$$

V = 1292 fps

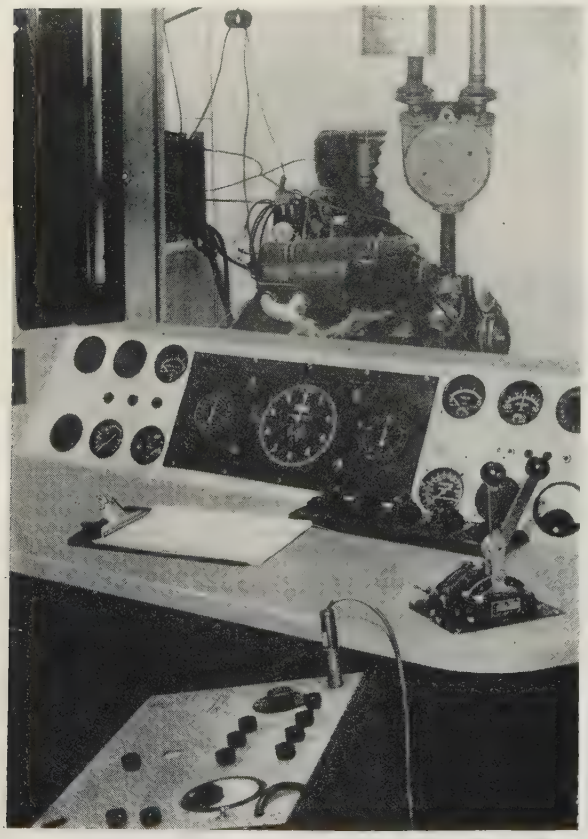

Fig. 1 — Dynamometer setup used in studies

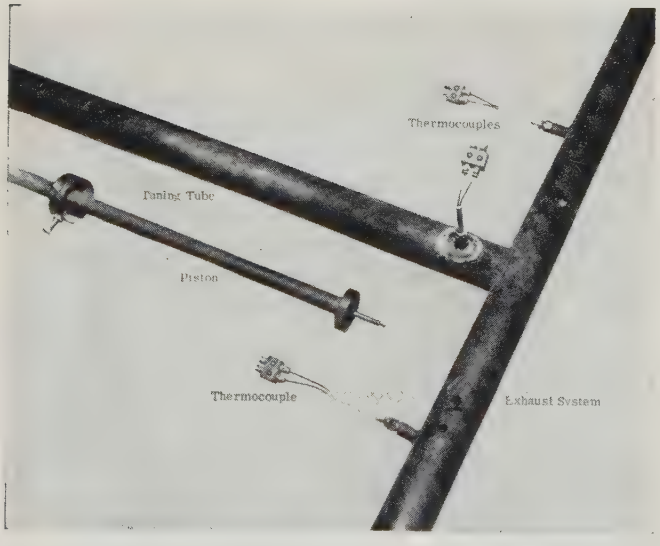

Fig. 2 — Tuning tube for velocity of sound study

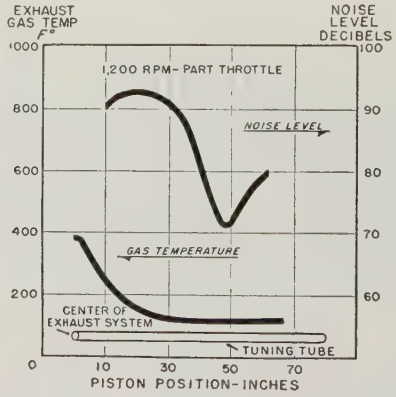

Fig. 3 — Chart tuning tube data for velocity of sound study

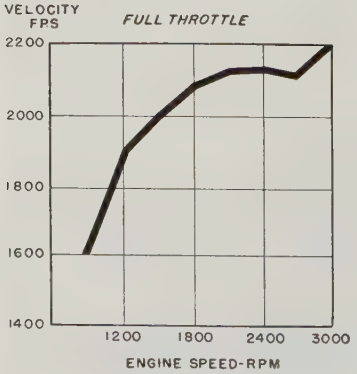

Fig. 4 — Full-throttle velocity of sound

However, since the temperature of the gas in the tuning tube is less than the temperature of the gas in the exhaust system, and since the velocity of sound varies as the square root of absolute temperature, a more correct velocity will be found by use of the following equation:

$$\frac{V_E}{V_T} = \sqrt{\frac{T_E}{T_T}} \qquad (2)$$

$$V_E = V_T \sqrt{\frac{T_E}{T_T}}$$

where:

V_E = Velocity of sound in exhaust system, fps
V_T = Velocity of sound in tuning tube, fps
T_E = Absolute gas temperature in exhaust system
T_T = Absolute gas temperature in tuning tube

It will also be noted that the temperature in the tuning tube varies from one end to the other. The average temperature was determined by the following formula:

$$T_{\text{avg.}} = \frac{T_1 + T_2 + T_3 - - - - - - - - T_N}{N} \qquad (3)$$

$$T_{\text{avg.}} = \frac{845 + 705 + 610 + 580 + 580 + 575}{6}$$

$$= \frac{3895}{6}$$

$T_{\text{avg.}} = 649$ deg absolute
$T_{\text{avg.}} = 189$ F

$$V_E = V_T \sqrt{\frac{T_E}{T_T}}$$

$$V_E = 1292 \sqrt{\frac{460 + 385}{649}}$$

$$V_E = 1292 \times 1.14$$

$V_E = 1460$ fps, the apparent velocity of sound

Fig. 4 gives the apparent velocity of sound for a particular location in the exhaust system as measured under dynamometer conditions for full-throttle loads. It should be borne in mind that the velocity of sound varies throughout the length of the exhaust system due to variations in the temperatures encountered.

Fig. 5 shows the temperatures recorded along the exhaust system at various loads and under full-throttle conditions.

Exhaust Noise Spectrum

With the advent of the sound analyzer and recorder, it is now possible to break down the exhaust

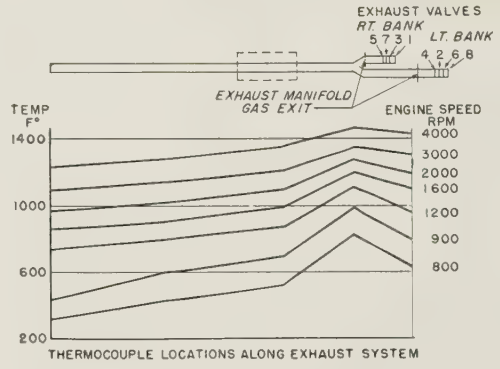

Fig. 5 — Full-throttle exhaust gas temperatures

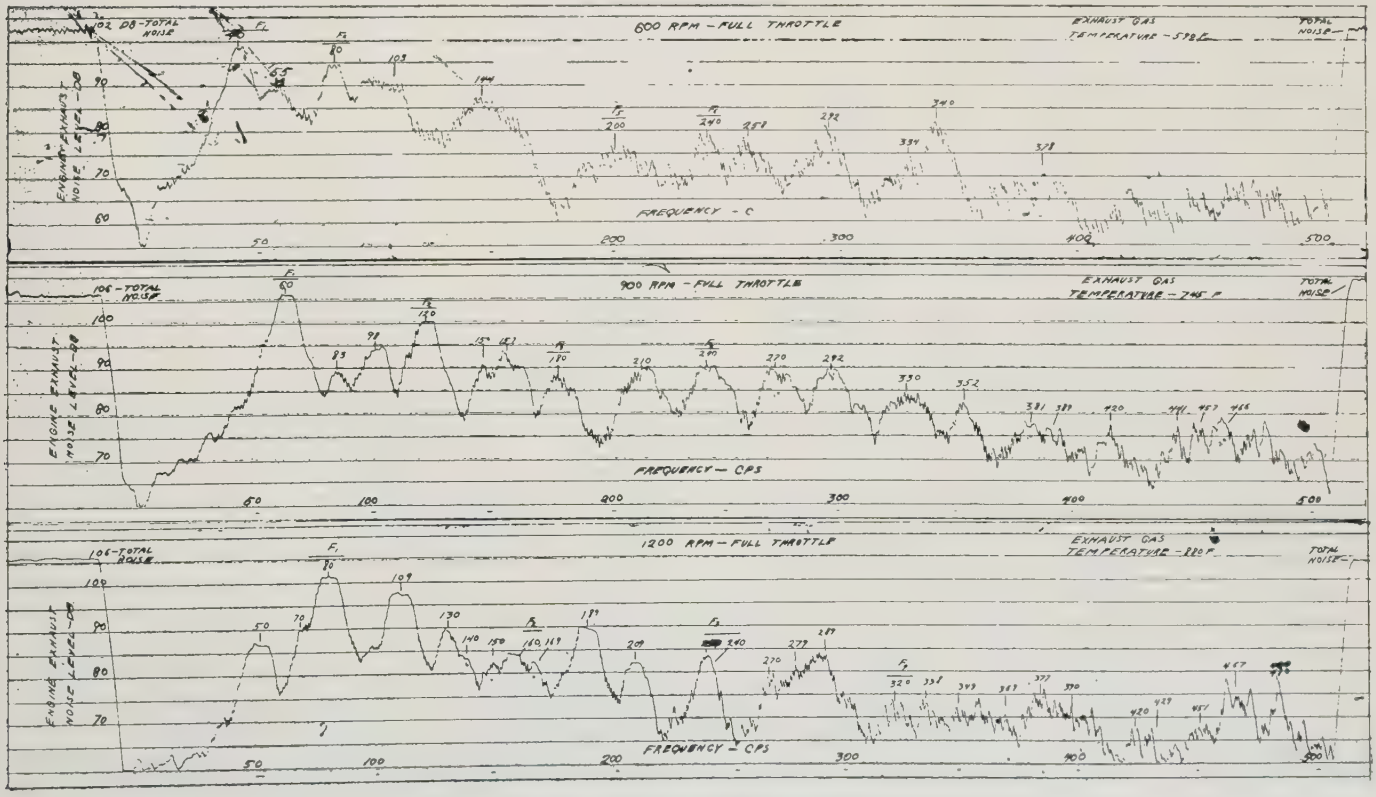

Fig. 6 — Noise spectrum (full throttle, 600 rpm, 900 rpm, 1200 rpm)

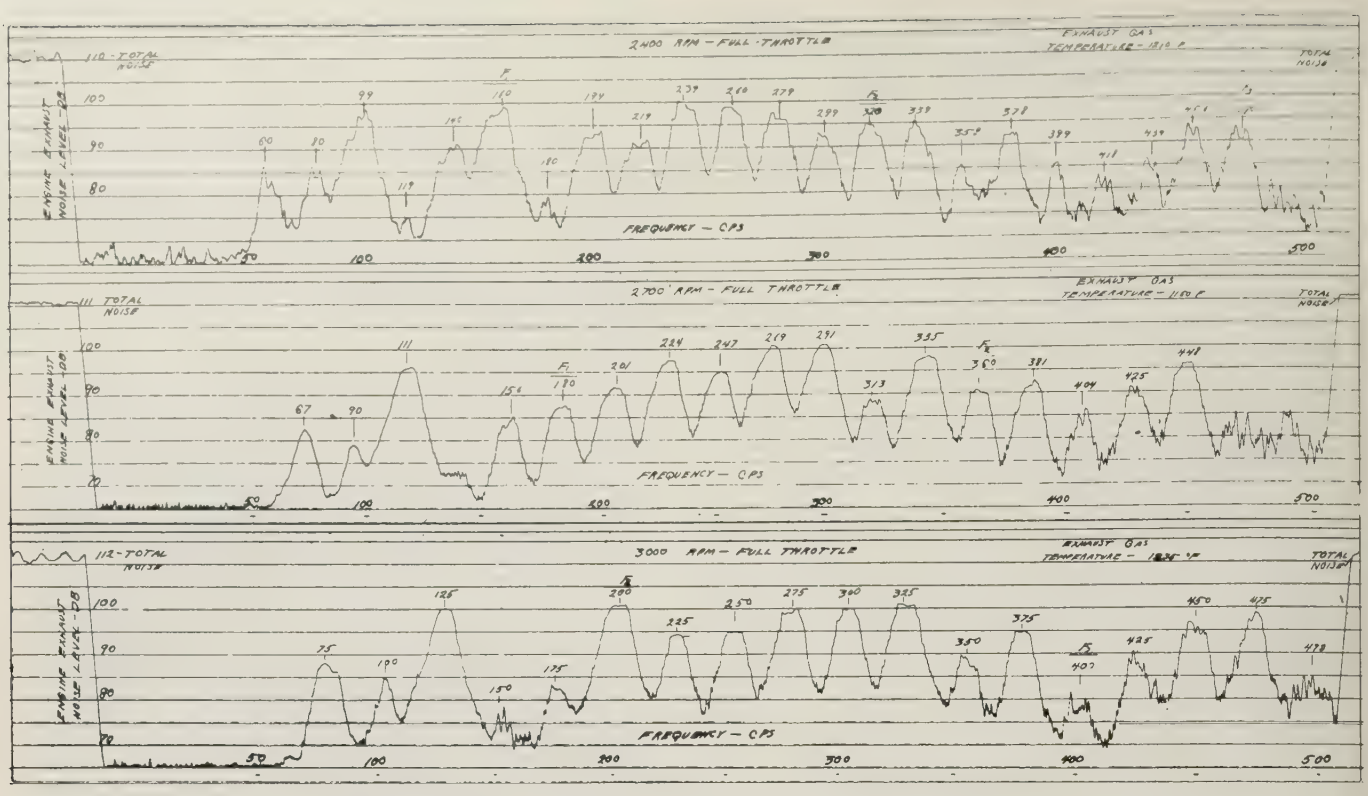

Fig. 7 — Noise spectrum (full throttle, 1500 rpm, 1800 rpm, 2100 rpm)

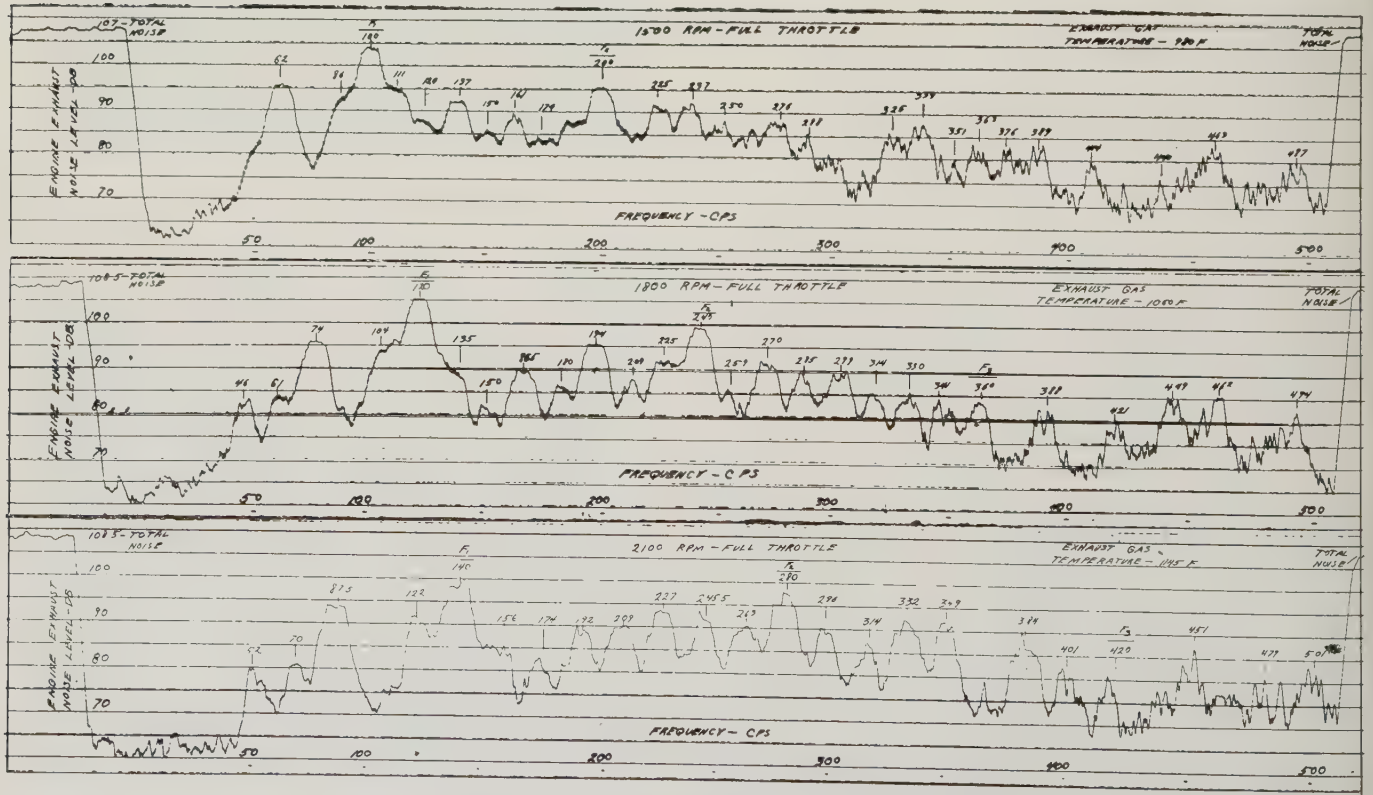

Fig. 8 — Noise spectrum (full throttle, 2400 rpm, 2700 rpm, 3000 rpm)

noise into its spectrum and determine the frequencies of which it is composed.

Figs. 6–8 show the spectrum of the exhaust noise produced by an engine running under full power at several speeds when only a straight pipe and no muffler was used. The speed range is 600–3000 rpm. The peaks present under road load conditions are essentially the same as those found under full load, except that their intensities are less. The rise and fall of the intensity of each of these peaks may be visualized if its loudness is plotted against its frequency, as shown in Fig. 15. In this illustration, firing and twice firing frequencies were used.

These curves are very interesting and help to answer many question: (1) that the exhaust sound at low speeds is composed of a few low notes and not many overtones, but a great deal of "hash" of low intensity; (2) that in many cases the sound peaks vary directly as the speed of the engine; and (3) that these peaks, at the higher engine speeds, are spaced one-eighth $\frac{F}{8}$ firing frequency apart. It will be noticed that as the engine speed increases, the overtones become more discernible, and of more equal intensity, with practically no harshness recorded within the frequency range scanned.

Chamber Location

Another basic requirement is that resonant chambers must be located properly in the exhaust system. This requirement was noticed many years ago when an unsatisfactory straight-through resonant-type muffler proved satisfactory when it was installed backwards. It has been found that the chamber must be located at or near a sound pressure antinode — that is, point of maximum pressure change.

Fig. 9 charts the attenuation that was obtained from a single Helmholtz resonator when it was placed in each of the 6-in. locations along the exhaust system. As will be noted, the chamber's effectiveness varied from zero attenuation in some locations to as much as 20 db in other locations.

In these curves, the ordinate is the amount of either positive or negative attenuation produced by the addition of the resonator. The "O" line represents the reference noise made by the engine when no silencer was used. The curved line represents the noise attenuation that was caused by the use of a silencer when it was placed in the exhaust system at any of the locations shown along the abscissa.

The resonator used had a volume of 247 cu in. with a neck that was 9 in. long and 1½ in. in diameter.

In Fig. 10 the enclosed area indicates where a Helmholtz resonator must be located on the exhaust system to attenuate firing frequency from 50–100% of the resonator's capacity under full-throttle conditions.

In order to be able to forecast the locations of the pressure antinodes or velocity nodes for chamber locating purposes, the data available was scrutinized to determine if a mathematical correlation could be established with actual measured results. If data from a complete run, in steps of 100 rpm over the complete speed range of "resonator location versus attenuation" as shown in Fig. 9, is

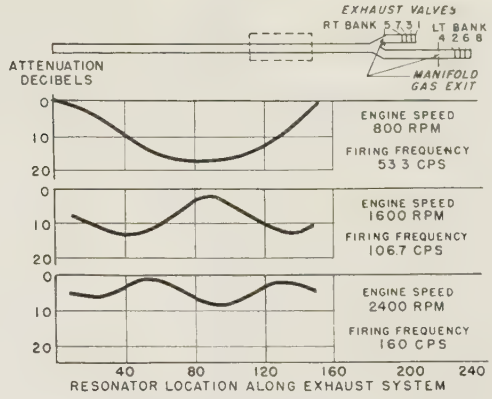

Fig. 9 — Effect of locations on resonator's attenuation

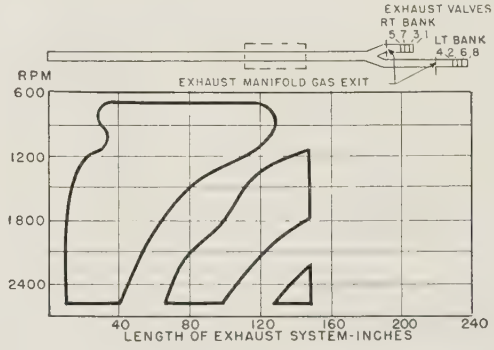

Fig. 10 — Resonator location producing 50-100% attenuation

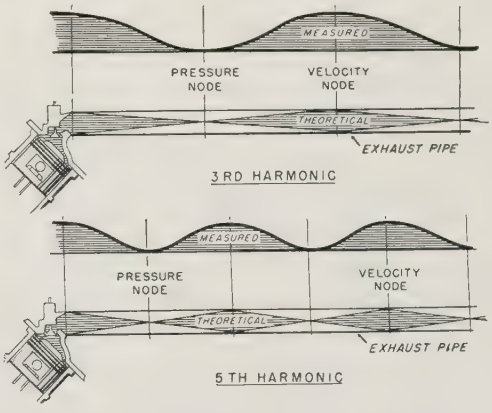

Fig. 11 — Comparison between calculated and measured nodal points

studied, it will be found that an agreement will exist between measured and calculated locations of these nodal points if the system is assumed to follow the laws of a pipe closed at one end.

This data indicates that the system, at least for this purpose, has overtones of the 3–5–7 . . . etc. order and the fundamental note has a wave length of four times the length of the entire system.

Fig. 11 is a comparison between the calculated and the measured locations of these points when the closed pipe assumption is used. As the chart shows, a perfect agreement is obtained.

It was also found that a pressure node always

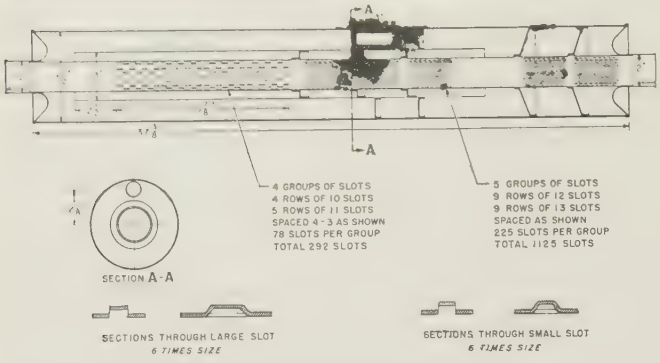

Fig. 12 — Straight-through resonant-type muffler

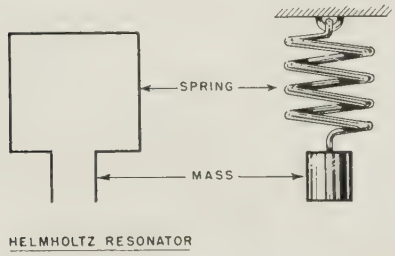

Fig. 13 — Comparison of Helmholtz resonator to spring-mass system

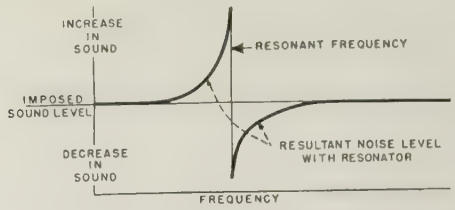

Fig. 14 — Response of resonator when excited in open air

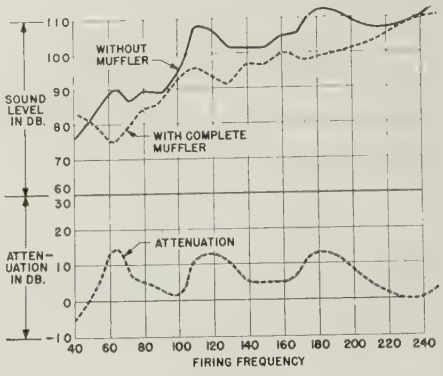

Fig. 15 — Comparison of exhaust noise with and without muffler, firing frequency

exists at or near the exit end of the pipe and a velocity node exists at or near the exhaust valve.

Resonators

In 1932, the high restriction type of muffler was replaced with the straight-through resonant type. This change decreased the power loss due to the exhaust system from 25 to 2½%. Fig. 12 shows a typical resonant muffler of this design.

As the name implies, all silencing was done by means of modified Helmholtz chambers. In general, the larger the chamber the more it will attenuate the lower frequency noises, providing it is at or near a pressure antinode. The higher frequency noises are removed by the smaller chamber and we, therefore, say they produce softness of sound.

This muffler has the feature of "compound chambers" in which the smaller chamber reacts on the exhaust noise through the 13/16-in. tube, then through the larger chamber and the 3-in. annulus tube, thence through the louvers and into the pipe.

Enough louvers are used so that their conductivity is so great as to cause the 2½ in. long, 3-in. annulus space to be the governing factor or neck of the chambers.

The resonant frequency of a single Helmholtz resonator may be predicted by the following formula:

$$F_R = \frac{V_s}{2\pi}\sqrt{\frac{\pi R^2}{Q\left(L+\frac{\pi R}{2}\right)}} \qquad (4)$$

where:

F_R = Resonant frequency, cps
V_s = Velocity of sound, fps
Q = Volume of chamber, cu in.
L = Length of entrance neck, in.
R = Radius of entrance neck in.

These chambers may be compared to a spring and mass system, as shown in Fig. 13. The chamber acts as the spring and the neck acts as the weight. It is realized that this comparison is much simplified, but it does illustrate a ready and simple reference. These chambers respond as in Fig. 14 when excited in the open air by a loud speaker. To determine how they act in an exhaust system, many hundreds of part-and full-throttle runs were made on the dynamometer and on road cars.

Figs. 15 and 16 illustrate the method used to determine what a given muffler would do to the "firing frequency" and "twice firing frequency" sounds.

In these graphs, the sound emanating from the tailpipe is plotted in decibels above the line "30–70" and the difference between the sound level with and without a muffler is plotted below this line and represents the noise removed at the various frequencies by the muffler or chamber. The frequency or engine speed in rpm is plotted along the abscissa and the noise removed in decibels is plotted below the "30-70" line along the ordinate. A more complete picture may be obtained by plotting not only the above frequencies but all orders of firing frequency. It should be noted that this muffler did not silence the 200-CPS twice firing frequency at all, but in fact actually increased the noise over no muffler conditions.

In another study of resonators, the location of the chamber remained constant, but the tuning was changed. The results obtained are shown in Figs. 17–22. It will be noted that there is no peak at-

tenuation at the chamber's calculated tuning frequency. As the chamber's resonant frequency is lowered, the attenuation at low frequencies is increased and decreased at higher frequencies. However, if the lowering of the resonant frequency of the silencer is accomplished by extending the neck beyond certain limits, even some of the lower frequency attenuation will be lost. This decrease is illustrated by the loss of attenuation between 100 and 160 cps frequencies that is recorded when the neck is extended from 6 to 10 in. Below the 100-cps frequency though, a marked gain is recorded. The shape of the curves remains similar in all cases, and the maximum attenuation usually remains at the same frequencies.

To demonstrate further the effect of raising the resonant frequency of the silencer on the exhaust sound, Fig. 23 shows how the attenuation curves may rotate within limits about a point when this is done.

Multiple Chambers

When more than one chamber is used, it becomes more difficult to calculate or predict the reaction or effect of these chambers on the exhaust system noise. Obviously, it is impossible to show the effect

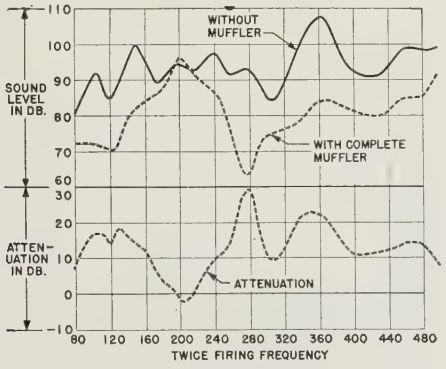

Fig. 16 — Comparison of exhaust noise with and without muffler, twice firing frequency

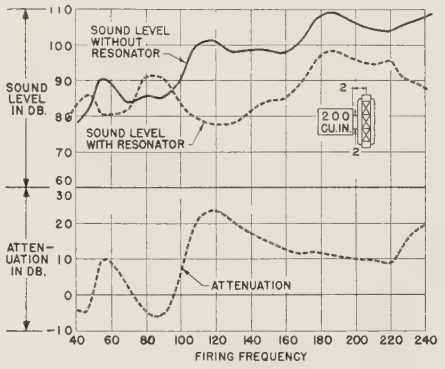

Fig. 17 — Attenuation curve of resonator

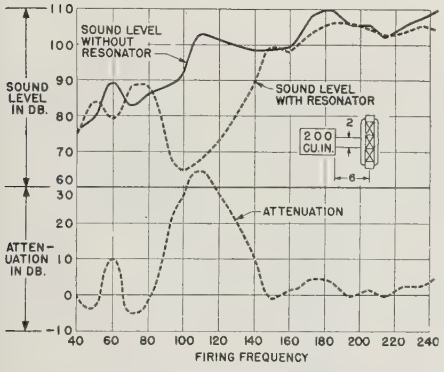

Fig. 18 — Attenuation curve of resonator

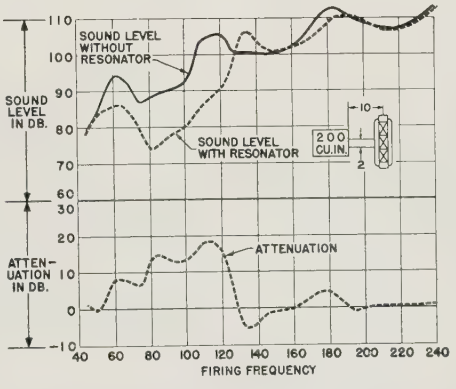

Fig. 19 — Attenuation curve of resonator

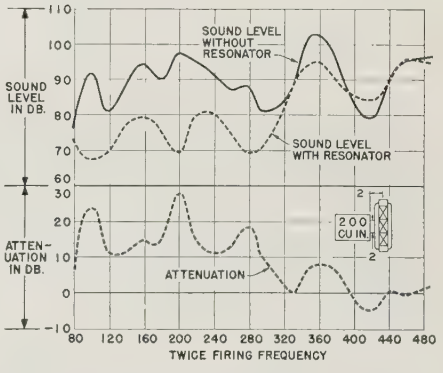

Fig. 20 — Attenuation curve of resonator

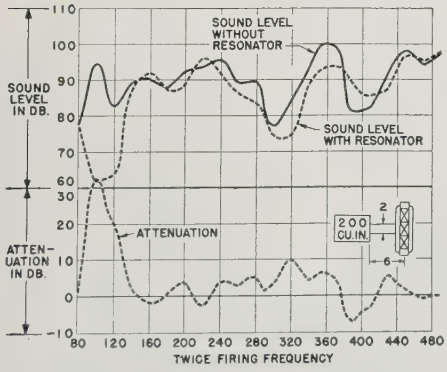

Fig. 21 — Attenuation curve of resonator

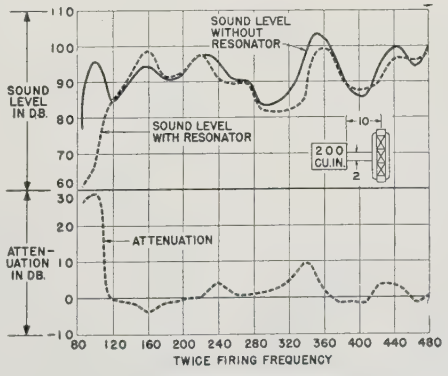

Fig. 22 — Attenuation curve of resonator

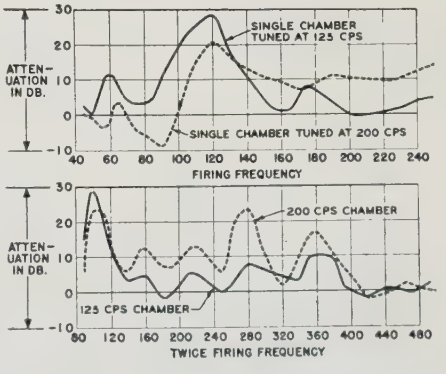

Fig. 23 — Comparison between attenuation of 125-cps and 200-cps resonator

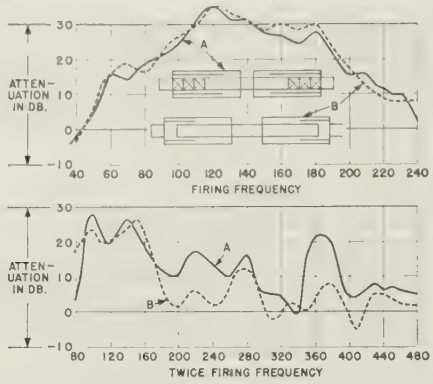

Fig. 24 — Attenuation of double chambers, showing effect of louvers

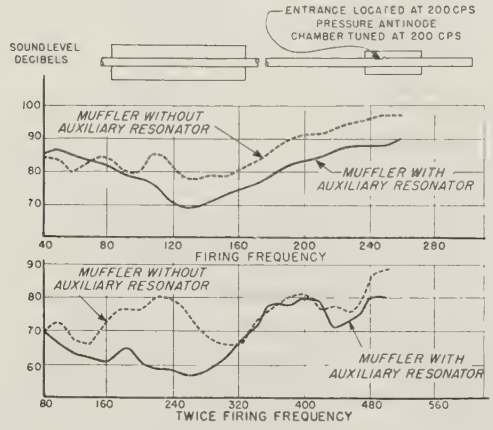

Fig. 25 — Effect of auxiliary resonator

of all possible chamber arrangements, but Fig. 24 gives the attenuation obtained from some double chambers.

It is believed that these two chambers tend to obey the following formula:

$$\text{Attenuation} = -8.69M \cosh^{-1}$$

$$\left[\cos\left(k_r l_1 \frac{f}{f_r}\right) + \frac{\frac{\sqrt{c_o V}}{2S}}{\frac{f}{f_r} - \frac{f_r}{f}} \sin\left(k_r l_1 \frac{}{f_r}\right)\right] \qquad (5)$$

Cut-off frequency (the frequency beyond which the resonator appreciably reduces the sound intensity):

$$f_c = \frac{c}{\pi}\sqrt{\frac{S}{l_1 V}\left(\frac{1}{1 + \frac{4S}{l_1 c_o}}\right)} \qquad (6)$$

These double chambers produced the best coverage of firing frequency noises of any combination that it has been our pleasure to test. The 34-db attenuation is as much as was obtained on any run made. This combination was tried on a car and, while it was good for low notes, it was quite harsh due to the higher overtones.

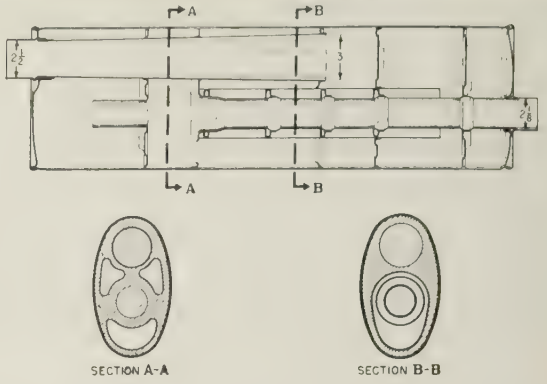

Fig. 26 — Reverse-flow muffler showing tapered tube for low restriction

While the data cannot be presented due to time and space limitations, it was found that, as the chambers were brought closer together and shortened to make room for the high-frequency chambers, a great deal of attenuation was lost, particularly at firing frequency. The higher frequency noises, though, were softened. These small 3-in. high-frequency chambers seem to kill the interaction between the two large low-tuned chambers. Thus, they probably tune higher and, therefore, do not attenuate the low notes as well.

On a particular exhaust system, a hole or lack of attenuation was found at 200 cps twice firing frequency. One of the things tried in correcting this difficulty was the use of an auxiliary resonator tuned at approximately 200 cps and its opening located near the 200 cps antinode.

The results obtained were tremendous, as a reduction of about 21 db was achieved at the desired frequency with this very small volume auxiliary silencer. (See Fig. 25.) Unfortunately, there was an untenable increase in the 40–70 cps firing frequency sound. This increase in noise created an off-idle boom that completely filled the car and made the resonator unacceptable for use. This result is not an unusual occurrence, so care should be exercised to check these lower off-idle frequencies whenever an auxiliary resonator is used.

Louvers

First, the question as to whether the use of louvers as the entrance to a resonate chamber affects its efficiency should be answered. Fig. 24 is a comparison between a silencer with louvers and one without. Very little difference has been found in the attenuation caused by a silencer on the low and heavy frequencies, such as firing frequencies when measured by instrumentation, if sufficient louver area is used. However, the ear does tell us that the louvers do react on the higher harsh notes. The curves show in Figs. 17–22 were obtained while using louvers at the entrance to the chambers.

Much work has been done on the size and shape of louvers. In general, to the ear, the area of each louver opening should be between the area of a 1/16-in. and a ⅛-in. hole. As the area approaches the lower limit 1/16-in. hole, the exhaust noise will become relatively softer, but the low-frequency noise will be slightly louder. If the upper limit ⅛-in.

hole area is used, the exhaust noise will be relatively harsher but the intensity of the low notes will be lower. Mufflers have been built with the ⅛-in. hole area louvers at the entrance to the low frequency chambers and 1/16-in. hole area louvers in the entrance to the high frequency chambers to realize the full advantages of each size louver. (See Fig. 12.) Today, however, it is the practice to use a compromise size louver for convenience and economy.

The primary reason for the various shapes and configurations of the louvers is an attempt to prevent the whistling noise that is present when a plain round hole is used and still meet other requirements, such as manufacturing.

Power Loss

As previously stated, the straight-through resonant-type muffler reduced the power loss from 25 to 2½%. In 1953, the muffler shown in Fig. 26, which was used with a 2⅛-in. tail pipe and a 2½-in. exhaust pipe, reduced the power loss to zero, as compared to no exhaust system at all. To help accomplish this, the inlet tube was tapered from 2½ in. at the inlet up to 3 in. at the outlet. This reduced the velocity of the gas and the restriction in making the 180-deg reversal of the gas flow. The gas passages at Sections A-A and B-B were made large and were streamlined by curling the edges of the holes over.

A generous radius and a larger than tube size opening were used at the entrance to the outlet tube to give a good gas flow factor at this point. The 1¾-in. resonator tube was entirely enclosed in the front chamber to reduce turbulence at this point.

Type

In picking the cross-section for a muffler, it should be borne in mind that a round section is the most economical and least troublesome shape to manufacture. If the shape becomes too wide and flat, an excessive number of baffles will be required to prevent drumming of the shell, and to give it strength to resist bursting by backfires.

When engines were smaller, the round section straight-through resonant muffler was the most economical with the least power loss. Since engines have become larger and space limited, the reverse flow elliptical cross-section muffler has become a necessity regardless of its increased cost. So far, it has been possible to get more attenuation per cubic inch from a reverse-flow than from a straight-through muffler.

Corrosion

Cold corrosion has been the second big problem of the exhaust system and a great deal of time and money have been spent solving it. The first advance on cold corrosion was made about 1937 when Terne plate material was used. This material, if made with sufficient tin to prevent pin-holing, gave about 1½ times the life of cold-rolled steel. The next advancements were zinc- and aluminum-coated steels that could be die formed without peeling the coating off of the parent metal.

Our method of testing a material for cold corrosion was to install a muffler of known weight on a privately owned car and check for weight increase each six months of operation. The driving habits of the

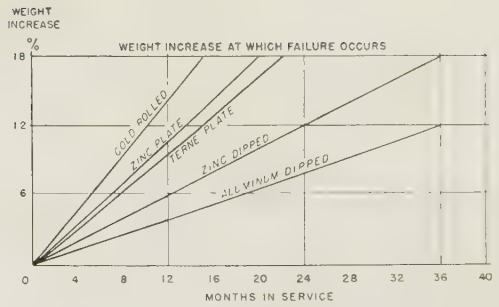

Fig. 27 — Muffler weight increase versus month in service for various types of materials

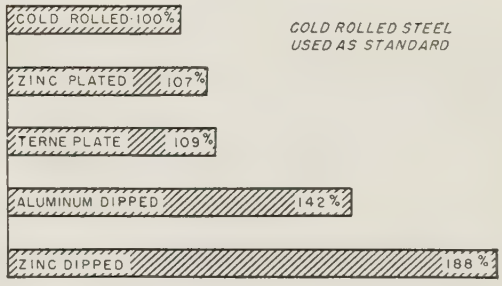

Fig. 28 — Comparative life per unit cost of various muffler materials

owner and the life of a cold-rolled steel muffler on this vehicle were known. It was found that a round straight-through muffler would be rusted out when its weight had increased 18%. This was true in all cases except those coated with aluminum and these increased only 12%; thus, the life of the material could be predicted without running the full life of the material.

Fig. 27 shows the weight increase versus time of several common materials when used with a "straight-through" muffler on a single system. The comparative life in months per unit of cost of several basic materials found on the above tests is given in Fig. 28. In general, where only cold corrosion is encountered and high temperatures are not a problem, zinc-coated steel is usually used, but if high temperatures are encountered, aluminum-coated steel is used.

There have been many corrosion tests proposed and tried, but they are too numerous to mention here.

Connections

For a connection to be satisfactory, it should fulfill the following requirements:

1. Must not leak.
2. Must permit easy removal of parts in service.
3. Must be economical.
4. Must allow parts to be aligned for clearance with other parts of the car without strain.

Many connections fulfill some of these requirements, but the ball type is the only one that meets all of them. As cars have become lower, more compact and quieter, it has become more difficult to install the exhaust system without interferences or strains, both of which cause owner dissatisfaction because of noise.

It was with this thought in mind that the ball-

type joint was developed, as it permits the exhaust system to be aligned for proper clearance without strain. It also does not leak, allows easy servicing, and is more economical than the joint it replaced.

Isolation

To prevent exhaust system vibrations from being transferred in the body, care should be exercised to use not only a very soft mount, but to locate the mount on the system at the point of least motion. An attempt should be made to design the exhaust system so the hangers may be placed as close as possible to the axis of rotation of the power plant.

Acknowledgments

The author wishes to acknowledge the assistance he has received from Harvey Barkley of GMC's Buick Motor Division, The Hayes Industries, Inc., Arvin Industries, Inc., and the Walker Michigan Co. for their help in this program. The formula used for Fig. 24 was taken from the NACA Report No. 2893.

Symbols for NACA Formula

c_o = Conductivity of connector between exhaust pipe and branch chamber, $\frac{\pi a^2}{\iota c + Ba}$

f = Frequency

f_r = Resonant frequency

$k_r = \frac{2\pi f_r}{c}$.

ι_1 = Length of pipe between connectors of two successive branches in a multiple chamber resonator or length of pipe between two chambers of a combination muffler

S = Cross-sectional area

V = Volume of resonant chamber

M = Number of chambers in multiple-resonator muffler.

ORAL DISCUSSION OF HEATH AND MULLER PAPERS

— Reported by A. C. Bodeau
Ford Motor Co.

R. F. Kohr, Palmer Products, Inc.: What part of the cost of a muffler is in the material? In other words, if we were to use a material twice as expensive as that currently in use, what per cent price increase could be expected in the purchase price of the muffler?

Mr. Heath: Approximately 50% of the cost of a muffler is in the materials. Thus, if we were to double the price of the material, we could expect approximately a 50% increase in the cost of the muffler. This assumes, of course, that the new material would not be appreciably more difficult to process than the current materials. On stainless-steel mufflers, the material costs, plus the increased processing difficulties, increase the cost to 3 or 4 times that of the mufflers made of conventional materials.

P. H. Richards, E. I. DuPont De Nemours & Co., Inc.: Assuming that muffler life can be greatly increased through corrosion-resistant materials, are we likely to encounter a condition of louver clogging which would then be the limiting factor of muffler life?

Mr. Heath: I doubt that this would be a problem, except in vehicles that are used almost exclusively for slow driving.

A. H. Purdy, AC Spark Plug Division, GMC: I feel the discussions have not considered the acoustical system in its entirety and have not looked at the problem as a complete system. I would suggest, on the basis of some work which we have conducted at AC Spark Plug, that the complete system be examined and that digital computers be used to calculate the theoretical results. We have found, on this basis, that we could compute the desired attenuation curves and design the muffler on the basis of computer calculations which could then be experimentally evaluated by means of the cold test. We have also found in the cold test that the test installation must simulate the system's impedances very closely.

Mr. Muller: There is still a good deal of art remaining in the design of mufflers and the reason for the investigations and studies presented today was to introduce more science into the design procedures by increasing our scientific knowledge. This is a rather complex problem. One must also consider the response of the car body to exhaust noise. We have problems in the area of body panels which are influenced by the temper of the body steel and the drawing properties of the dies. Considerations such as these are not possible in the basic laboratory studies discussed today and are most efficiently tested on the car installation. We also have the problem of the muffler noise preferences of the engineer specifying mufflers. Some engineers like mufflers which will give a low tone to the muffler noise, whereas others prefer muffler noise that contains more of the high notes. Thus, in designing the muffler, one must consider the noise preference of the specifying engineer.

P. J. Kent, Consultant Engineer: My personal experience with mufflers indicates that corrosion holes form from the outside of the muffler, possibly being brought about by the salt used to deice streets.

Mr. Heath: Our testing has indicated that exterior corrosion is negligible to interior corrosion, unless the service is such that the mufflers are operating very hot. In this case, interior corrosion would not be a problem and the muffler life would be very long.

J. S. Voigt, American Motors Corp.: Mr. Muller mentioned a 25% horsepower loss with early types of mufflers. It appears to me that this would constitute a considerable source of heat in the muffler.

Mr. Muller: Up to 1932 on the 60–100-hp engines of that era, we used baffle-type mufflers with holes in the baffles which were approximately ⅛–¼ in. By introducing the straight-through mufflers, we were able to increase our top speed approximately 5 mph and in those days our top speeds were around 60 mph.

Mr. Voigt: What are the possibilities of using porcelain coatings to eliminate corrosion?

Mr. Muller: Porcelain coatings present some rather difficult manufacturing problems but studies have indicated they give very good control of corrosion. We have found that some of the coatings are water soluble and all are quite brittle. The water soluable ones are washed off by the water product of combustion and the brittleness of the coatings make them susceptible in chipping by road stones. Where the coating chips off, the muffler has no more protection than it would have if no coating were used. We have found that the viscosity of the porcelain frits is such that it cloggs the louvers in the muffler tubes when the coating is applied after assembly. Application of the porcelain before assembly has been considered. This presents trouble in welding. Masking of the weld areas has been considered but this approach is expensive, and would locally eliminate the corrosion protection.

the use of

BENCH WEAR TESTS

in Materials Development

G. H. Robinson, R. F. Thomson, and F. J. Webbere, General Motors Corp.

This paper was presented at the SAE Annual Meeting, Detroit, Jan. 14, 1959.

TWO TYPES of bench wear tests employed by the General Motors Research Laboratories are described, and examples are given to illustrate the application of the tests to material development problems.

It is shown that correlation of a bench test with service may be achieved even when the laboratory test conditions do not appear to duplicate service conditions exactly. It is postulated that this behaviour is related to the formation of certain types of surface films during the wearing process. Some preliminary results are given of a study of the influence of lubricant type and material composition on the formation of anti-wear films.

ACCELERATED WEAR testing is frequently regarded as an unwanted stepchild — rarely trusted but assigned over and over to do the dirty work. We propose that accelerated bench-type wear tests may be trusted, providing the limitations for any particular application are understood.

The subject of wear and wear testing has few rivals among the varied interests of the automotive engineer. It is in this area that the durability of his product is most severely judged, since most consumers are keenly intolerable of failure by wear in service. Furthermore, modern design is often hard pressed to assure acceptable wear performance at a competitive price.

The advance in automotive engineering is now proceeding at such a rapid pace that it is possible to evaluate fully only a limited number of materials in actual component testing, prior to setting down production specifications. Some means must be provided to screen out the best of the potentially useful materials for a given application — and this must be done with sufficient discrimination to justify the expensive and time-consuming field tests which must certainly precede a production release.

It has long been recognized that there can be no universal wear test which will select materials for all wear applications. It is even unlikely that an accelerated wear test will be developed which will reliably predict the endurance of various materials in even a single application when the product is in the hands of the general public. The factors which influence wear are too dependent on environmental conditions, as well as outright abuse or neglect on the part of the operator. But when large margins of difference are being sought, and this is often the case when contemplating a material change, an accelerated wear test is an indispensable tool.

The purpose of this paper is to describe some of the wear testing facilities at Research Laboratories which have proved extremely valuable in material development programs. There are many types of wear tests at GM Research, each tailored to a particular kind of service. Our discussion will be limited to two tests distinguished primarily by the

magnitude of the contact stress.

Contact stress in the range of 15,000–30,000 psi is represented by a "constant friction" rotating drum test. Very high stresses, such as encountered at the interface between cam and valve lifter in an automotive engine, are produced by an actual cam arrangement where the Hertz stress in mating parts of ferrous materials may reach 300,000 psi. Both of these tests are basically empirical, but the record of accomplishment resulting from their use justifies a closer look by those responsible for the selection of wear material.

It is fortunate for the research metallurgist that he is often looking for differences of considerable magnitude. His assignment is usually to progress by "giant steps." The test facility, then, need not guarantee 1 or 2% reproducibility. The aim is 100% improvement or more, and time cannot be devoted to exploring shades of difference in wear rate. It is this philosophy that justifies the accelerated test, in as much as reproducibility within 10% is rarely achieved in a wear test no matter how elaborate the control features.

Constant Friction Test

Our "constant friction" drum-type machine, first conceived by Boegehold and Jominy,[1] has a remarkable history in selecting materials for a variety of wear applications. It was originally designed as a screening device in the development of ferrous materials for automotive and diesel cylinders. By coincidence, it has aided in the development of unrelated nonferrous materials as well. A few examples of actual correlation with service results will illustrate this versatility.

Cast-Iron Cylinder Liners — A series of controlled laboratory wear tests had revealed the superior wear resistance of a titanium-phosphorous containing iron over all other compositions investigated. This iron, designated GMR 125, gave less than one-half the wear rate of carburized and hardened 4615 steel in the laboratory tests. The comparison with service results in an actual engine is shown in Fig. 1. The durability in the road tests was 6600 miles per 0.001 in. of bore wear for the "improved" iron compared to only 1200 miles per 0.001 in. of bore wear for the surface-hardened 4615 steel. These tests were conducted in a 120-cu-in. wet sleeve engine. This degree of correlation with service results under road conditions is ample reason for using the laboratory test to screen the hundreds of compositions that were considered on the basis of other favorable properties.

This comparison reveals a characteristic of accelerated wear testing which should not be overlooked. While the factor of improvement in the laboratory test was less than 3/1, the improvement in the engine was greater than 6/1. Accelerated wear tests will often rate materials in a preferred order which will correlate with service results, but the magnitude of difference in wear in service between any two materials may not show a proportional relationship to the difference observed in the laboratory. This is probably the result of the artificial test conditions used to achieve measureable wear in a reasonable length of test time.

The improved GMR 125 iron was proof tested in numerous engines of the same type and later became the basis of a cylinder material used in an auxiliary aircooled power unit for U. S. Army tanks with a 10-year history of satisfactory performance. The wear rate finally achieved in a further modification of this iron having a hardness of 225 bhn in the as-cast condition was better than that of the standard diesel cylinder iron hardened to 46–50 Rockwell C. The bench test rig was entirely adequate to pave the way for a material change in this application.

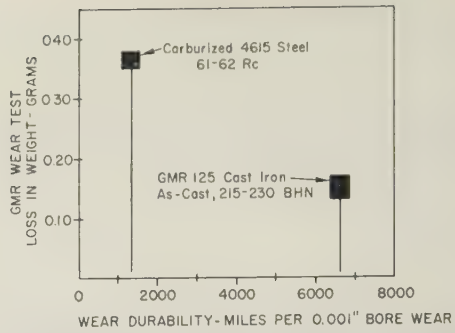

Fig. 1 — Correlation between GMR wear test and cylinder wear in 120-cu-in. engine

A more discriminating selection was achieved in distinguishing between cylinder irons from three different sources furnished to a manufacturer of diesel engines. Although the castings were supplied to the same chemical specification, field service had indicated definite differences in performance. Iron from supplier B-1 was reported to have excessively high wear. B-2 furnished material which showed a definite tendency to score. Service performance of material from B-3 was wholly satisfactory. Fig. 2 shows the correlation with results from the laboratory constant friction wear test. B-1 is definitely a high-wear iron in the bench test. B-3 is within the wear range which long experience has indicated to be satisfactory for cylinder application. The erratic behavior of B-2 is typical of materials which tend to gall or score. Again, the accelerated test demonstrated ability to select the material most likely to perform well from a wear standpoint in actual engine operation.

Sheet-Metal Forming Dies — An extreme case where a test designed for one type of service properly rated materials for a totally unrelated service is illustrated in the development of soft-metal dies for short-run sheet-steel stampings. A zinc-base alloy had become the accepted material specified for such dies and considerable amounts were used by GM Overseas Operations in runs where the greater durability and cost of cast-iron or steel dies was not justified. The constant-friction rotating-drum machine was used out of sheer expediency as a screening device in an alloy development program aimed at incorporation of hard particles in the zinc matrix to improve die life. Early results indicated that the addition of 0.5% silicon and 0.9% manganese to the original zinc alloy would reduce the wear rate to approximately one-tenth the value of the unmodified alloy. Fig. 3 shows the correlation with actual die life. Included are dies for many different parts, some representing more severe forming operations

[1] "Wear of Metals from Automotive Viewpoint," by W. E. Jominy. Paper presented at ASTM Symposium on Wear of Metals, April, 1937.

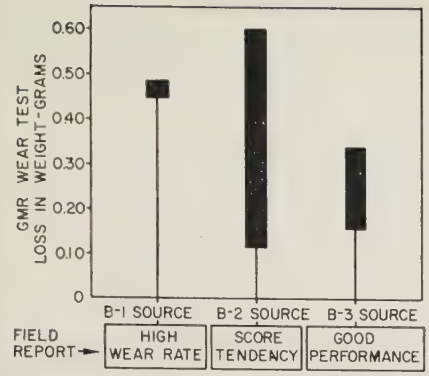

Fig. 2 — Correlation of GMR wear test with field reports for diesel cylinders from three different sources

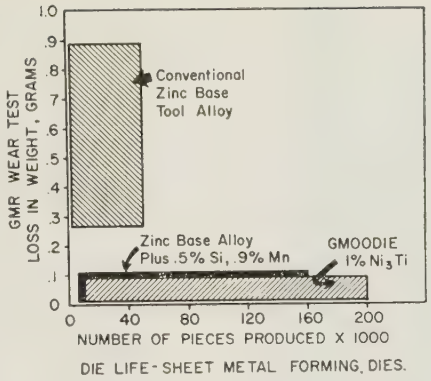

Fig. 3 — Correlation between GMR wear test and production experience on zinc-base dies

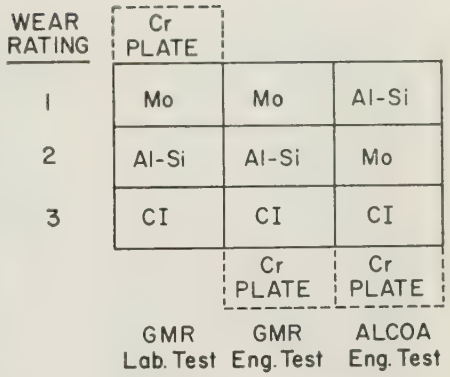

Fig. 4 — Wear rating of bore materials by three different tests

than others. The variation in die design accounts for the large spread in die performance. Obviously, when localized areas of the relatively soft zinc-base die are subjected to heavy unit loading, failure will be due to plastic deformation. This accounts for the low die life values included in the chart. For moderate unit pressures where plastic flow is not encountered, the improved wear resistance of the modified alloy results in greatly improved die performance. A later variation in the zinc alloy having improved foundry characteristics incorporated 1% Ni_3Ti in the composition. This material, given the name "Gmoodie," also showed some further improvement in both the laboratory wear test and in die performance.

The cost of evaluating in production the many experimental compositions which led to Gmoodie would have been prohibitive; but equally significant, a comparison in service would have been totally unreliable because the dies were used only for short runs which meant that only a few dies were made for any given part. Service conditions were constantly changing and a base line was impossible to establish.

Piston Rings — In any wear application the intereffect of mating materials upon each other must be considered. Changes which improve the wear resistance of one member may be detrimental to the mating surface. A bench test such as the constant friction machine, which evaluates only the specimen material, may sometimes give overly optimistic results. When comparing materials having wide differences in physical and mechanical properties, a good service correlation for one of the basic material types does not establish correlation for all materials.

For example, the development of grooved and tinned piston rings for diesel engines was conducted on the constant-friction machine with good results in the field and eventual production acceptance. Similarly, the GM Research test had shown that chromium plate was an outstanding candidate for piston rings — an observation later confirmed by wide use of chromium-plated rings in the automotive industry.

But a radical change to a sintered powdered metal ring created a new problem which could not be predicted from the laboratory test. The bench tests showed good wear resistance for certain sintered iron piston-ring compositions, in which the objective was to inhibit wear by incorporating hard particles in the iron matrix. The initial tests in the dynamometer were also good, but the results in actual vehicle operation in road tests were unsatisfactory due to high bore wear, although ring wear was still low.

This example is cited to emphasize that performance predictions based on laboratory tests must include the possibility of a change in the limiting criterion. This limit may be (as in the case of the sintered piston rings) something other than the wear resistance of the part being studied, such as abrasive action against the mating part, electrolytic corrosion, or other causes of incompatibility with contacting members.

Nevertheless, when correlation with service has been established, and where the materials have similar chemical and physical characteristics, the constant-friction type test has proved to be a reliable sorting tool.

Aluminum Cylinder Bores — A recent achievement of high current interest was the early indication that certain aluminum alloys might be suitable as cylinder materials without the need of any wear coating. Considerable engine testing in dynamometer and road tests have been made on aluminum alloys, which tested well under the same conditions used in the laboratory development of wear-resistant cast iron for cylinder bores.

Results obtained several years ago at GM Research, have been recently confirmed by Alcoa[2]. A comparison of the wear rating of several different bore materials is shown in Fig. 4.

Sprayed molybdenum, 20% aluminum-silicon alloy, and regular cylinder iron are rated in this same order of wear resistance by both the GMR constant friction test and the GMR engine tests. The Alcoa engine tests on similar materials agree reasonably well, since the difference between the sprayed molybdenum and the 20% aluminum-silicon alloy is marginal.

However, there is a marked discrepancy between the laboratory test and the engine tests when evaluating chromium plate. As already noted for piston rings, the normal laboratory test gives chromium plate a high rating, but the engine tests at General Motors and at Alcoa show chromium-plated bores to be worse than cast iron. While chromium-plated

[2] "Hypereutectic Aluminum-Silicon Alloys," by R. M. Smith. Paper presented at SAE Summer Meeting, Atlantic City, June, 1958.

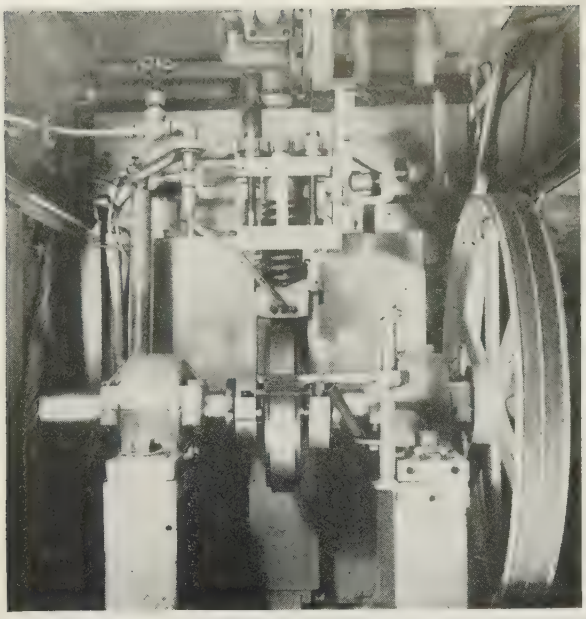

Fig. 5 — Constant friction wear test for selecting cylinder bore materials

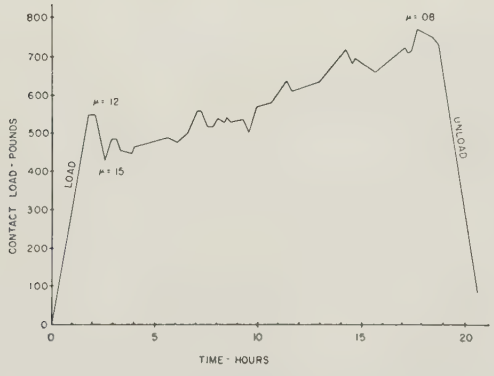

Fig. 7 — Typical load curve for cast iron versus cast iron in constant friction wear test

aluminum bores have shown good performance in several small European automotive engines, electroplated chromium has not been satisfactory as a bore material in the greater output and higher compression engines investigated at General Motors.

The bore measurements used in the above comparison are taken at the top of the piston-ring travel. If average bore wear is considered, the chromium plate rates well in the engine test, but there appears to be a condition associated with the reversal of motion at the top of ring travel which is particularly detrimental to chromium plate. High wear has also been observed by German investigators[3] in testing chromium-plated bores. Apparently, the constant friction test in its present form is not sensitive to the influences which promote failure of chromium plate in high output engines. An interesting observation, however, is that chromium plate does give very poor performance on this laboratory test when tested as a deposit on the 8-in. diameter rotating drum rather than on the stationary sample. This would suggest that the geometry of the contact surface may be extremely important when evaluating relatively thin coatings for wear resistance.

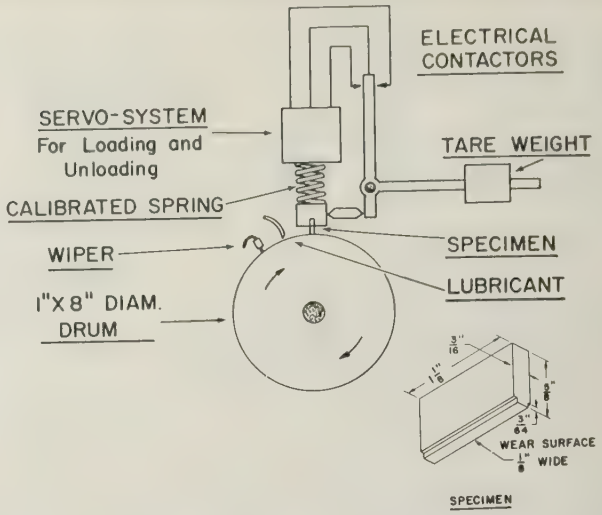

Fig. 6 — Mechanical principle in GMR constant friction wear test machine

Description of Constant Friction Test — The principle of the constant friction drum test shown in Fig. 5 is illustrated schematically in Fig. 6. A flat sample $\frac{1}{8} \times \frac{5}{8} \times 1\frac{1}{8}$ in. is loaded in contact with a rotating cast-iron drum (8 in. diameter × 1-in. wide) in such a manner that the reactive force due to friction drag can be measured and any deviation from a preset value translated to a servo-mechanism which will increase or decrease the pressure load holding the sample in contact with the drum. By this means, any change in the dynamic coefficient of friction which may occur during the test period is compensated by a proportional change in the contact load. A dilute lubricant consisting of 40 parts mineral oil and 60 parts kerosene is applied to the drum just ahead of the sample at a rate of 80 drops per minute. S-075 mineral oil has been used to avoid the variations associated with commercial detergent-type oils. The friction drag, which for a cast-iron drum and a cast-iron sample is held constant at 64 lb, will call for a perpendicular load between 500 and 900 lb. Thus, the dynamic coefficient of friction may vary from 0.13 to 0.07 during the 18½-hr duration of the test. It is this compensation for the change in dynamic coefficient which is the essential feature of the machine and which has resulted in better reproducibility and improved correlation with service than achieved with tests run at constant normal load.

There is no explanation at this time why such an improvement should result. It is certain that none of the applications cited above operate with the friction force constant. Nevertheless, the record of the machine is too impressive to deny that the beneficial effect is real.

Further details of the test may be of interest. The rotational speed of the drum is 145 rpm, giving a linear speed of 304 fpm at the periphery. The change in pressure load is continuously recorded by measuring the compression of a calibrated spring through which the load is applied. A typical load

[3] "Mercedes-Benz Experience with Aluminum Parts in Automotive Engines," by Eberhard Hundt. Paper presented at SAE Summer Meeting, Atlantic City, June, 1958.

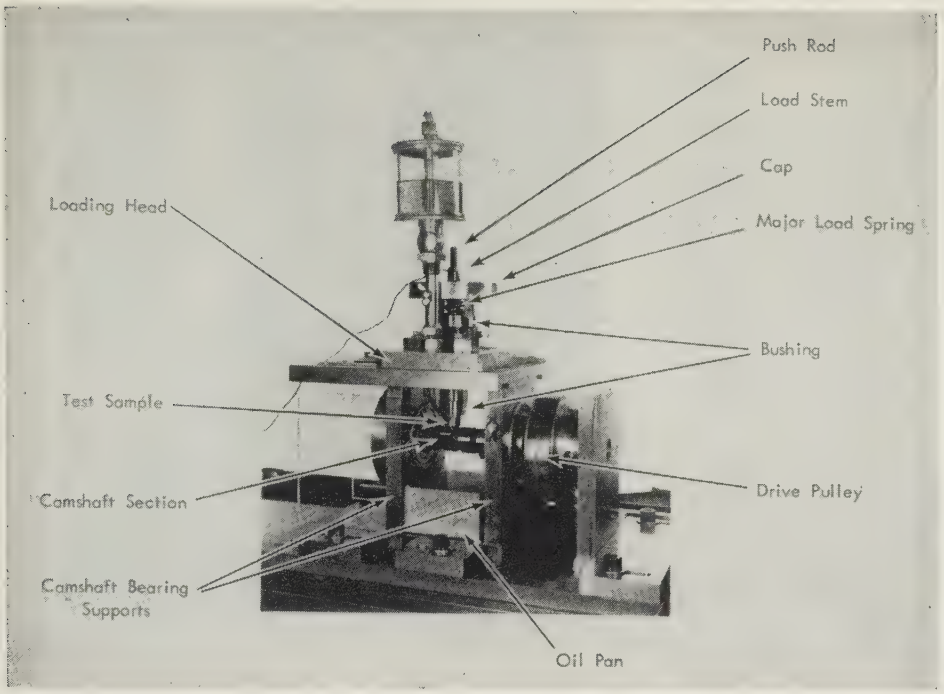

Fig. 8 — General view of tappet test machine

curve for cast iron versus cast iron is shown in Fig. 7. After start-up the load is increased at a steady rate until the preset frictional force has been reached. At this point the system appears to stabilize for a few minutes. Then the dynamic coefficient increases calling for less contact load. In a series of fluctuation adjustments the dynamic coefficient reaches a maximum and then decreases gradually over the remainder of the test time. The normal load which varies inversely with friction reaches a maximum near the end of the test time. The explanation of this phenomenon has not been fully investigated, but no doubt the transition from Hertz contact to actual wear contact, the increasing temperature of the specimen and drum, the formation and breakdown of surface films, and the response time of the servo-mechanism all have significant roles in the frictional changes observed.

The temperature of the sample is measured by a thermocouple located 3/16 in. from the wear surface. This is primarily a safety feature. Should scoring occur while the machine is unattended, the sudden rise in temperature will automatically shut off the power to the drive motor. Under normal conditions, since the friction is constant, the temperature of the sample should stabilize at some steady level inasmuch as the rate of work input at the wear surface is constant. Any irregularity in temperature is attributable only to inadequate response of the servo-system.

Wear rate is indicated by weight loss of the stationary sample. When testing porous samples such as sintered compacts or sprayed surfaces, accurate weight determinations cannot be made and volume loss becomes a more reliable parameter. The test has been demonstrated to give reproducible results with a deviation of 10% when the metallurgical quality of the samples is carefully controlled. In cast materials this is difficult to assure, and frequently a regrinding operation on the same sample will expose metallurgical differences which result in significant differences in wear performance. This is partially the result of the small contact area which is a maximum of only $\frac{1}{8}$ sq in. when worn completely across the face of the sample. At the beginning of the test, the Hertz contact area could be as low as 0.035 sq in. Most wear applications will generally present a larger contact surface, which will average out inhomogeneities in the metal structure. Because of the limited area being tested it is desirable to run duplicate or triplicate samples. However, in developing materials it is frequently the occasional poor result which limits the use of a material rather than its average performance. In such an instance, a single low test result may be sufficient cause to disqualify the material.

Experience with several thousands of tests on this equipment had indicated that the test is most discriminating when a moderate amount of wear occurs. For materials having very good wear resistance, the effect of the surface films may be predominant and the reproducibility from sample to sample of the same material may not be within several hundred per cent. Furthermore, the mechanical response and the effect of minor irregularities in the test become more significant when the wear loss is small. When extremely rapid wear occurs reproducibility is again poor — attributable to the violent effect of metal transfer and irregular lubrication.

To achieve the optimum amount of wear the preset friction load may be varied as different service applications are being investigated. Obviously, for relatively soft materials like the zinc-base Gmoodie, the load must be low enough to prevent "mushrooming" due to plastic deformation. On the other hand, extremely high loads may interfere with lubrication and create conditions so different from service conditions that good correlation is impossible. For combustion cylinder bore materials, a moderate wear rate with cast iron versus cast iron is achieved using a tangential friction load of 64 lb at the circumference of the 8-in. diameter drum. This produces approximately the same amount of wear in

18½ hr as obtained in normal road service after about 100,000 miles in a passenger car.

High Contact Load Tests

An example of wear testing under high contact load conditions is found in the Tappet Test Machine, where the range of maximum calculated contact stress is about 100,000–300,000 psi. This apparatus, as the name implies, was originally developed to study the wear behavior of automotive valve tappets and cams under simulated service conditions. Some of the early work on this machine was reported to SAE in 1955.[4] Since that time, the test machine has been redesigned, and its scope of application has been expanded to include general studies of the effects of materials and lubricants on wear and scuffing at high loads.

Equipment — A general view of the test machine in its present form is shown in Fig. 8. The test sample is attached to the end of a holder (tappet) and is held against a rotating cam by a spring-loaded push rod. The cam sample is a section of a production automotive camshaft, containing four cam lobes, and the loading head is moved to position the wear specimen over the desired lobe. Lubricant is metered to the contact area from the oil cup. The bushing which guides the specimen holder or tappet, together with the loading mechanism, fits in a well in the loading head so that the entire assembly can be removed for examination of the wear specimen and replaced without disturbing the alignment of the system, as shown in Fig. 9.

Use of a production cam as one of the wearing parts provides an economical and quite reproducible base sample. Preparation of the sample involves simply cutting a camshaft through the journals and slotting one of the journal ends of the section to take a drive key. The wear specimen to be evaluated is in the form of an insert which fits into the specimen holder, as shown in Fig. 10.

The method of loading is indicated in Fig. 11. Two separate loads are involved. The minor load is a constant force holding the wear specimen against the cam and is applied by a small spring inside the specimen holder. As the cam begins to lift the sample, the minor load alone acts until the mechanical lash is removed. At this point, the tappet sample, push rod, and load stem begin to move together, compressing the major load spring until, at maximum lift, the full major load is applied. The major load is usually measured at maximum lift, by means of strain gages cemented to the thin-walled load stem, and is adjusted by turning the threaded cap, which compresses the major load spring.

The type of load cycle obtained on the machine is shown schematically in Fig. 12. The time per cycle is approximately 0.05 sec. The operating conditions thus may be summarized as:

1. Relatively high rubbing velocity (approximately 500 fpm).
2. Boundary or quasi-hydrodynamic lubrication.
3. High load applied intermittently, superimposed on low constant load.

These conditions obviously duplicate most closely the operation of automotive valve gear, as the machine was originally designed to do. However, the apparatus should be of value in material development studies for other components which operate under somewhat similar conditions, for example, rear axle gears.

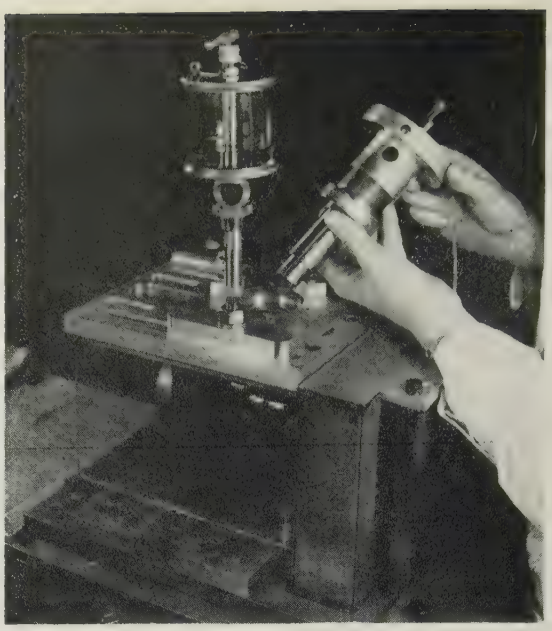

Fig. 9 — Showing location of bushing and loading assembly in test machine

Test Procedure — The test is conducted by operating a set of samples under progressively higher major loads, starting at 200 lb and increasing the load 50 lb after each run until a load of 550–600 lb is reached. The samples are run 15 min at each load. Lubricant is added dropwise at 1–2 drops per sec. The rate of lubication does not appear to be critical; varying the rate from one drop every 3 sec to about 2 cc per sec does not affect the results significantly.

Wear measurements are made after each test run. On the insert wear specimen, this is done by measuring the thickness of the insert with a micrometer to the nearest 0.0001 in. Cam wear may also be measured by a special dial gage which fits in the well on the loading head.

In addition to normal progressive wear, a catastrophic type of failure, termed scuffing, is sometimes encountered. This failure occurs very suddenly, usually within 1 or 2 min after starting the run. It is evidenced by heavy smoking and the appearance of large quantities of wear debris, and the foot surface of the wear specimen shows a very rough appearance. Metallographic examination of scuffed steel specimens reveals a layer of fresh martensite on the surface with a severely tempered layer immediately beneath, indicating very high surface temperatures. In contrast to the normal wear process, which is believed to proceed by welding and rupture of small asperities on the contacting surfaces,[5] scuffing appears to involve welding of relatively large areas. The action is catastrophic because the rough surface remaining after rupture of the weld and the relatively large amount of heat involved both favor additional gross welding.

Reproducibility and Correlation with Service — There are two principal items of concern in the de-

[4] SAE Transactions, Vol. 64, 1956, pp. 161–181: "Interrelationship of Design, Lubrication, and Metallurgy in Cam and Tappet Performance," by E. B. Etchells, R. F. Thomson, G. H. Robinson, and G. K. Malone.

[5] Pp. 285 ff of "Friction and Lubrication of Solids," by F. P. Bowden and D. Tabor. Pub. by Oxford, 1954.

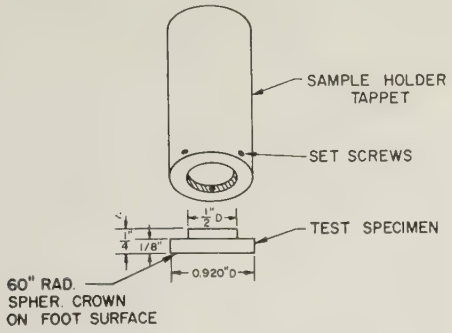

Fig. 10 — Tappet specimen and specimen holder

velopment of a bench wear test for material development studies. First, the reproducibility must be adequate, so that reliable answers can be obtained with a reasonable number of tests. Second, and of paramount importance in applied research, the results obtained on the bench test must have some degree of correlation with results observed in actual service of the mechanism or components of interest. As discussed earlier, the primary function of a bench wear test in materials development is to act as a sieve or strainer, discarding the poor materials and retaining only the good ones for further evaluation in service tests. The principal danger in lack of correlation is, obviously, that potentially good materials may be discarded by the bench test.

An indication of the reproducibility of tappet machine results is given in Fig. 13, which shows the data obtained in tests of six lubricants on two test machines by three different operators. The tests were made using carburized-steel tappet samples and hardened cast-iron cams. With the possible exception of the tests made with Oil No. 3, the results obtained on the two machines check satisfactorily, and the scatter is not excessive.

The material combination used in these tests is obviously very sensitive to the type of lubricant. Two of the oils appear to be very good in this application, and three others are relatively poor. The behavior of Oil No. 3 indicates that it is "borderline" with respect to antiwear properties.

Oils 1, 2, 3, and 4 have been evaluated with respect to their effects on valve train wear by CRC in 1955–56.[6] The results of these field tests, which required over a year to complete and involved a total of 295 automobiles, provide an excellent baseline for determining the degree of correlation of the bench test results with service.

Results obtained with the four oils on one cam-tappet material combination in the field tests are compared to the bench test rating obtained with the same materials in Fig. 14. A very definite correlation is evident, Oil No. 2 performing the best and Oils No. 1 and 4 giving the poorest results on both the bench test and the field tests. Only Oil No. 3 shows any discrepancy and, as noted earlier, the bench test rated this oil as borderline.

In Fig. 15, service wear data for four cam-tappet material combinations employed in the field tests are plotted separately, and it should be noted that,

[6] "Field Equipment Survey of Valve Train Wear." Coordinating Lubricant and Equipment Research Committee, Coordinating Research Council, Inc., January, 1957.

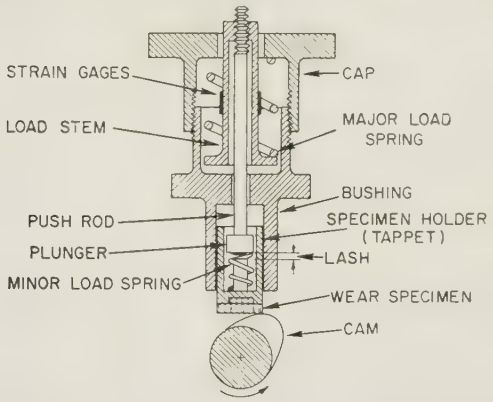

Fig. 11 — Schematic diagram of tappet test machine showing method of loading

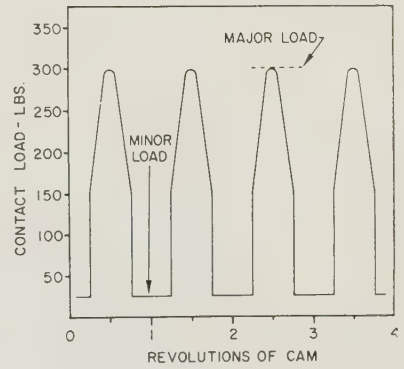

Fig. 12 — Load cycle on tappet machine (schematic)

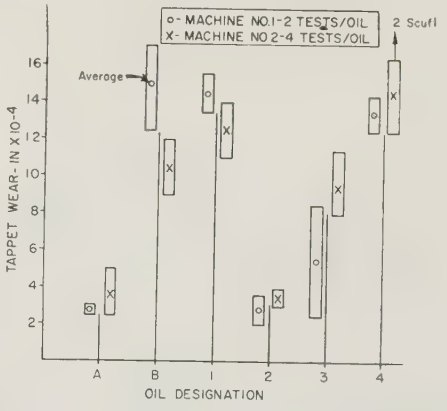

Fig. 13 — Reproducibility of tappet machine test results

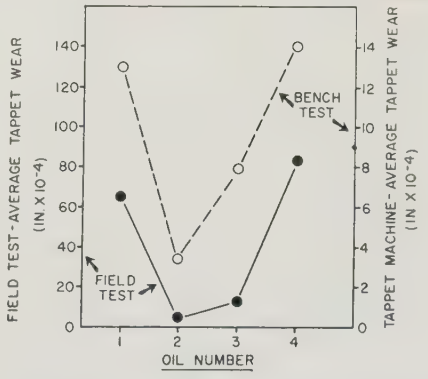

Fig. 14 — Correlation of tappet machine results with field tests (CRC Field Survey, 1956)

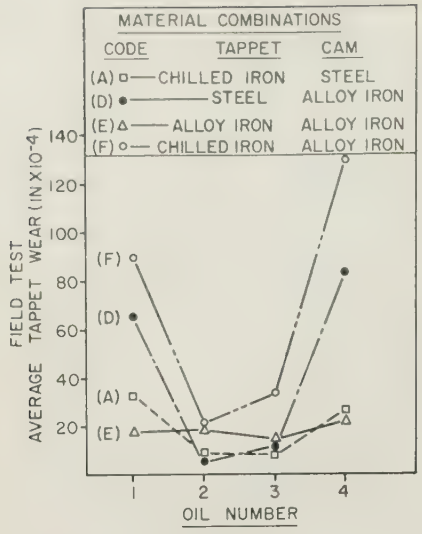

Fig. 15 — CRC field test results, showing sensitivity of various materials to type of lubricant

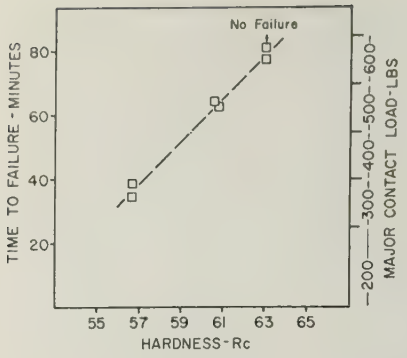

Fig. 16 — Effect of hardness on scuffing of alloy cast-iron tappets

Table 1 — Solubility of Visible Film on Alloy Cast Iron

Solvent	Results
Ethanol	Film not affected
Xylene	" " "
Benzene	" " "
Concentrated NaOH	" " "
50% HCl	Film removed
4% Nital	" "

Table 2 — Effect of Nital Treatment on Alloy Cast-Iron Specimens

Test No.	Treatment	Results
1	Nital	Scuff in 1 min at 300 lb
2	Nital	Scuff in 1 min at 350 lb
3	None	No failure at 600 lb

Table 3 — Effect of Used Engine Oil (10 total acid no.)

Test No.	Oil	Maximum Load (lb)	Total Wear	Appearance of Wear Surface
1	Used	400 — scuffed	Not measured	Bright — no visible film
2	Used	450 — no failure	0.0002 in.	" " " "
3	New	600 — no failure	0.0004 in.	Visible film (formed at 300 lb)

as would be expected, the degree of sensitivity to type of lubricant depends to a great extent on the composition of the wearing parts. The lack of sensitivity of combination E (alloy cast-iron tappet and cam) has been observed previously on the tappet test machine.[7] In material evaluation tests on the tappet machine, a standard lubricant, prepared by adding 4% of a commercial phenate-type inhibitor-detergent to a 10W base oil, is employed.

Typical Applications — The application of a bench wear test to material development, once its reliability has been established, may be made in two ways; investigation of production materials to determine means of improving their performance, and development of entirely new materials.

An example of the first type of application is given in Fig. 16, which shows the tappet machine results obtained on a series of production tappets of three different hardnesses. The data indicate that with this material, an alloy cast iron, increasing the hardness of the tappet increases its resistance to scuffing failure. Service tests have confirmed these results, and hardness specifications for these particular tappets have been increased.

Current work on the tappet machine is concerned with a more fundamental study of the wear process under high-contact loading, and has as its ultimate goal the development of improved materials. The investigation was started by examining conventional tappet materials in an attempt to gain some understanding of the reasons for the observed differences in behavior of these materials.

The superiority of hardened alloy cast iron over carburized steel as a tappet material is widely recognized. The difference in performance of the two materials has been attributed to various causes. For instance, it has been proposed that the graphite in the cast iron acts as a lubricant, or that the massive carbide particles in the cast iron prevent softening of the rubbing surfaces during operation. Neither of these explanations appears to be entirely valid. Tappets containing much graphite have given poorer results on bench and engine tests than those containing very little graphite. On the other hand, although performance of alloy cast-iron tappets tends to improve as the relative amount of massive carbide in the microstructure is increased, high carbon tool steels, containing considerable amounts of massive carbide, do not perform appreciably better than conventional carburized steels. It appears that something other than general microstructure is the controlling factor in this application. Observations made on the tappet machine have suggested that this controlling factor may be the type of film which forms on the rubbing surfaces during operation.

The rubbing surfaces of carburized steel and alloy cast-iron wear specimens operated under similar test conditions differ considerably in appearance, as may be seen in Fig. 17. The steel has a uniformly clear surface, while the surface of the cast iron appears to be partially covered with a dark film. Since steel specimens wore rapidly (approximately 0.0003–0.0004 in. in 15 min) or scuffed, while alloy iron showed no scuffing and almost no wear (approximately 0.00005 in. in 15 min) under these test conditions, it seemed possible that the visible film might be associated with the difference in performance of the two materials. The appearance of the foot surfaces of steel and cast-iron specimens at 500x magnification is shown in Fig. 18. The steel surface appears to be relatively clean, while the cast iron is covered with a film.

The chemical nature of this visible surface film was investigated in a preliminary manner by testing

[7] SAE Transactions, op. cit., p. 177–178.

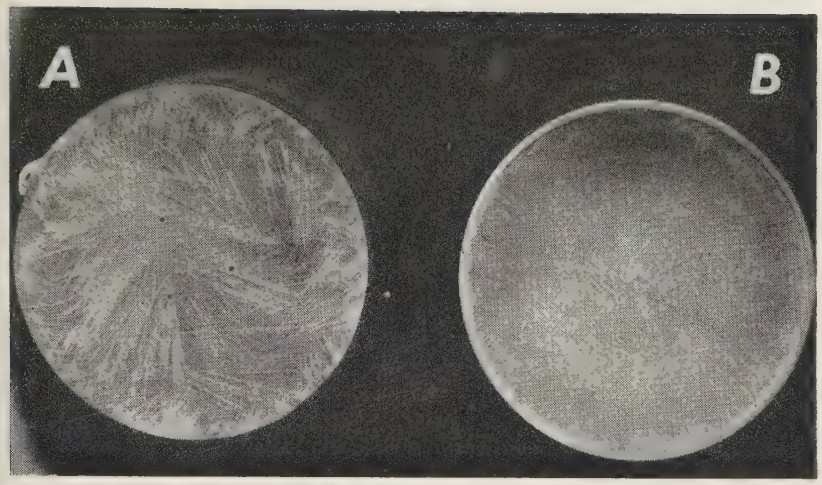

Fig. 17 — Comparison of hardened alloy cast iron (A) and carburized steel (B) wear specimens, showing surface film on cast iron (original magnified 2 times)

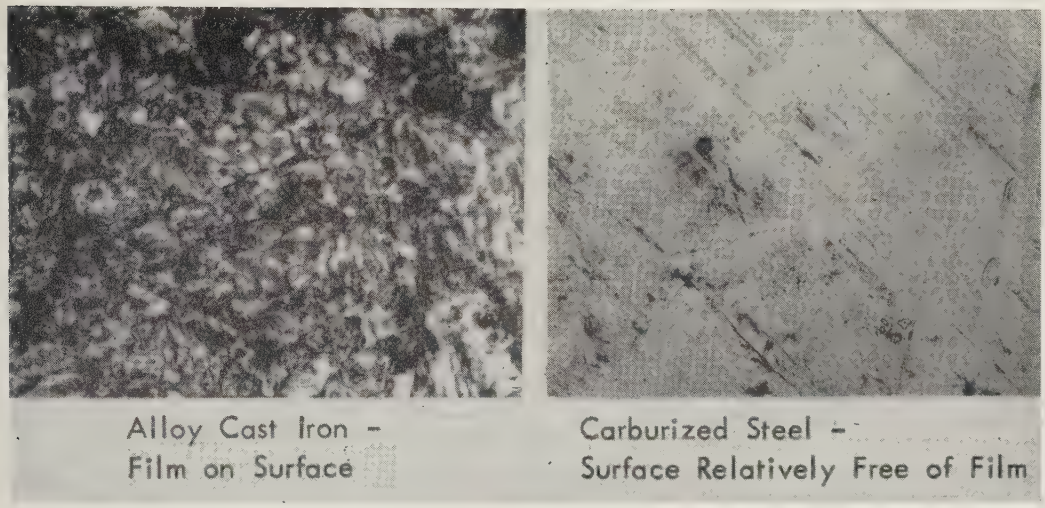

Fig. 18 — Wear surfaces after operation at 350 lb in tappet machine, using standard test oil (magnified 500 times, not etched)

the solubility of the firm in various liquids. The wear surface was examined microscopically to determine the extent of dissolution of the film. The results, listed in Table 1, indicate that the film is soluble in acids, but insoluble in bases or organic solvents.

This chemical behavior suggests that the film may be an oxide of iron. Other investigators[8, 9, 10] have reported that certain types of oxide films have a beneficial influence on friction and wear, both dry and in the presence of lubricants. The reason for the formation of a film on alloy cast iron and not on steel, however, is not apparent.

To check the hypothesis that the visible surface film on alloy cast iron is responsible for the superior wear and scuff resistance of this material, tests were made in which the specimen was immersed for 1 min in 4% nital before each run on the tappet machine. Other than this treatment, which was employed to remove the acid-soluble film from the rubbing surface, the test procedure was as described earlier. The results showed that removal of the film increased considerably the tendency of the specimen to fail by scuffing (Table 2).

In addition to removing the acid-soluble film, the nital treatment produced a slight roughening (etching) of the wear surface. To determine the influence of this roughening, an additional test was made by operating a specimen according to the standard procedure through the 450-lb run. The specimen was then immersed in nital and subsequently polished with 6-micron diamond paste to remove the etched surface. When the specimen was replaced in the machine at the same load, it scuffed in 1½ min after starting, indicating that surface roughness was not a major factor in the effect of the nital treatment.

The action of a weak acid such as nital in removing the film from alloy cast-iron specimens suggested that organic acids in the lubricant might have a similar effect. Accordingly, additional tests were made with a used engine oil having a total acid number of 10. The used oil was introduced at the 300-lb load portion of the test, after breaking in at 200 and 250 lb with the standard lubricant. The results, summarized in Table 3, showed that use of a highly acid oil does retard formation of a visible film.

The fact that one of the specimens tested with the used oil scuffed, while the other did not, indicates a borderline condition. Since the wear in Test No. 2 was not excessive, it seemed possible that a protective film was still present on this specimen, but did

[8] NACA TN 1578, 1948: Paper by R. L. Johnson, D. Godfrey, and E. E. Bisson.
[9] NACA TN 3444, 1955: Paper by E. E. Bisson, R. L. Johnson, M. A. Swikert, and D. Godfrey.
[10] Transactions of Faraday Society, Vol. 46, February, 1950, pp. 93–102: "Importance of Surface Oxide Films in Friction and Lubrication of Metals," by E. D. Tingel.

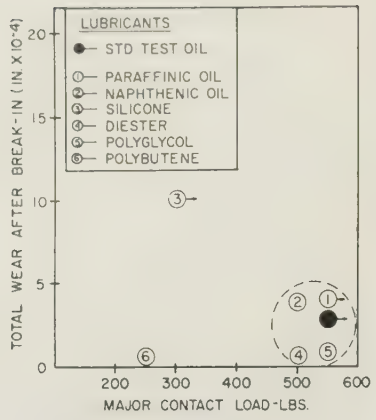

Fig. 19 — Effect of lubricant on wear

Table 4 — Effect of Lubricant on Film Formation

Lubricant	Load at which Visible Film was Detected (lb)
Polyglycol	250
Paraffinic Oil	200
Silicone	250
Naphthenic Oil	200
Polybutene	— (failed at 250 lb)
Diester	350–400
Standard	300–350

not attain the thickness necessary to make it visible because of its continual dissolution by the organic acids in the lubricant. To test this possibility, the specimen from this test was immersed in nital, to remove any acid-soluble film remaining, and rerun at 450-lb load. The specimen scuffed 1½ min after starting, suggesting that the surface film in this case, although not visible, was heavy enough to prevent gross metal-to-metal contact.

Since the most obvious environmental factor in this study was the lubricant, a number of tests were made with unconventional lubricants to investigate the influence of this factor on film formation. The normal test procedure was employed, except that the samples were prerun 15 min at 200 lb with the standard base oil prior to operation with the test lubricant.

The results are shown graphically in Fig. 19 in terms of total specimen wear and maximum load attained before failure by scuffing or excessive wear. With the exception of the polybutene and the silicone fluids, wear was not greatly affected by type of lubricant. The loads at which visible films were detected with the various lubricants are shown in Table 4.

It is interesting to note that carburized-steel tappets, which wear excessively when operated with the standard test lubricant, perform as well as alloy cast iron when the CRC Oil No. 2 is employed. The latter oil is treated with a zinc-dithiophosphate additive, which presumably functions by depositing a chemical film on the steel surface.

It was, of course, not possible to determine visually that the films formed with the unconventional lubricants on alloy iron were actually the same as that observed with the standard test oil. However, it appeared that the formation of a visible film on the rubbing surface was more a function of the specimen material than of the type of lubricant. Accordingly, work has been started to study the effect of material composition on film formation. This is

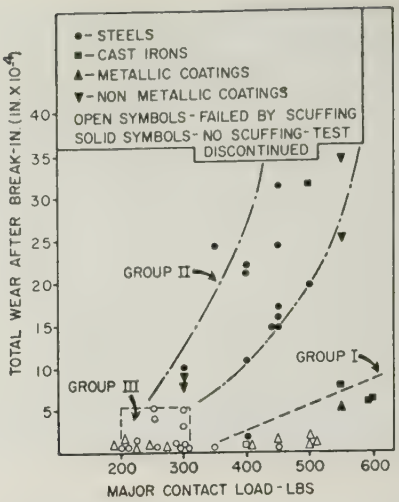

Fig. 20 — Effect of material on wear

being done both by visual examination of the rubbing surfaces and by observation of the wear and scuffing behavior of the various materials.

Four general classes of materials have been investigated to date: steels, cast irons, metallic coatings on steel, and nonmetallic coatings on steel. The test results, presented graphically in Fig. 20, indicate that the various materials fall into three groups, based on performance.

Group 1, characterized by low wear, and no scuffing at loads below 400 lb, includes two types of cast iron, two steels, and a metallic coating. All of the Group 1 specimens developed a visible film on the rubbing surface. The Group 2 samples showed considerable wear and no scuffing. Included in this group are a third type of cast iron, several steels, and the nonmetallic surface coatings. A visible film was detected on only two materials of this group — both nonmetallic coatings. Either these films were of a different type than that observed on the Group 1 materials, or some other factor was influencing the wear process, since both materials wore excessively. The specimens in Group 3 failed by scuffing at such low loads that a valid estimate of the wear resistance was not obtained. This behavior may reflect a tendency of these materials to form an antiwear film which prevents proper wearing-in of the parts and yet is not sufficiently stable to prevent failure under slightly more severe conditions of operation.

As yet, no explanation for the observed grouping of materials in these tests is apparent. Work is continuing in hopes that some common factors will emerge to indicate which material variables are important in determining whether or not a stable antiwear film will form.

Discussion

Results obtained on both of these bench wear tests emphasize the importance of surface condition on wear phenomena. Studies on the tappet machine have suggested that wear resistance is associated with the formation of surface films. The fluctuations in coefficient of friction on the constant friction test probably reflect changes in the average shear strength of the welded junctions, in accordance with the theory of Bowden, et al., and this

variation in shear strength is primarily an effect of the formation, transformation, and removal of surface films. In view of the importance of surface films, it appears probable that these tests correlate with service experience only because the test conditions are such as to develop the same types of surface films as are produced in the service environment. Sometimes this can be achieved by duplicating service conditions closely on the bench test, but often changes in test procedure are required to implement the test which make the wear conditions entirely different. This is obviously the case in the constant friction machine, since it is improbable that any natural wear phenomenon occurs with friction constant.

The state of knowledge in the field of wear has improved considerably in recent years, but the theory is not yet sufficient to permit design of bench tests with absolute confidence; the development of a laboratory test which correlates with service is still a matter of trial and error. This is particularly true in tests involving lubrication, where the surface reactions are undoubtedly exceedingly complex.

DISCUSSION

Describes Wear Pattern Of Chromium on Engine Cylinder

— Stanley Jacoby
The Superior Plating Co.

SINCE THERE has been so much contradictory evidence concerning the wear pattern of chromium on gasoline engine cylinder applications, we felt that it was extremely important that the facts pertaining to our experience over a period of 10 years be presented to this meeting.

We feel qualified to speak on this subject since we have had the good fortune to have been closely associated with the engine field over a long period of time and had the opportunity to hard chrome plate more aluminum than anyone in this country and perhaps in the world. For over 20 years, chromium has had a successful production experience to the engine field in cylinder applications and is widely used in the small aluminum engine field and European automotive engines. The railroads have for years salvaged their diesel liners with chromium and I have examined records of railroads indicating that the chrome liner outlasts by three times the original liner. It is a common procedure of all airlines and the Navy to salvage aircraft cylinders of high output engines through the use of chrome plating. Despite all of the applications, I have had other occasions to attend meetings where it has been disclosed that chromium plating cannot do an adequate job on cylinder applications. There is a logical explanation to all these unsatisfactory performances and I can best illustrate the point by citing our experience at one of the large automotive companies.

When Alcoa introduced us to the engine people at this company who were examining the application of aluminum to the engine field, we advised the group that it would be less expensive to plate a sleeve that it would be to handle the bore of a cylinder block and much could be learned in this way. We produced the first sleeves under normal plating conditions such as fixturing, current density, temperature of both, and baumé of solution. The sleeves were tested in engines of a compression ratio of 12/1 and were found to wear through at the top of the ring travel. There are some things strikingly familiar in this wear pattern. When chromium runs dry against iron, it polishes rather rapidly. The normal crack pattern of chromium decreases and instead of being the excellent lubricating material that it normally is, we found it actually resists oil. At this point globs of oil dropped on the plated surface will just lie there and not run. Then chromium wears rapidly and might, in this state, be considered a poor wear material. On these sleeves it appeared that the lubrication at the top of the ring travel was extremely poor and once the chromium began to polish it did not stand up well.

We had some sleeves which had been plated and stripped. In stripping, a severely etched condition was prevalent. We plated this etched sleeve which produced a very spongy like surface. When these sleeves were tested, they showed little sign of wear but produced high oil consumption.

Since our experience with this automotive company, we have been associated with enough tests to be able to state that chrome plate can be produced to give adequate wear life in any cylinder application. In order to be successful, however, the nature of the chrome deposit must be adapted to the wear pattern that the engine demands. The basic answer lies in producing a chrome pattern that gives adequate lubrication to the cylinder wall.

The paper indicates the true position of the poor fellow assigned to bench wear tests who always feels inadequate because he cannot simulate the true conditions and so much is dependent upon his vision. Perhaps he will take some comfort in our statement since bench tests indicate that chromium should do well, and there was adequate evidence in the field to substantiate this. To us, this looks like the shoe being on the other foot. When this occurs, ought not the bench tester inquire what was wrong with testng which did not support his findings?

ORAL DISCUSSION

— Reported by C. R. Lewis, Chrysler Corp.

Dr. F. P. Bowden, Cambridge University: Chromium is often considered incompatible with oil because it is difficult to attack chemically. Most lubricants work by attacking the metal to form a soap or some solid film on them. Chromium, because of its oxide layer, is very resistant to attack. Therefore, it seems quite probable that while you have rough chromium with the cracking in it, it will work; but if you get chromium very highly polished and smooth, it would lead to difficulties. But I haven't anything at all constructive to add to it. I was very interested in the point about the surface film present in these wear experiments. Could I ask whether you've looked at it or considered looking at it with electron diffraction or some method of that sort which should tell you very easily what is the nature of the film?

Mr. Webbere: We do not say that further investigation of chrome plating is not in order, we are merely citing our own experience. At the present time, we have no engine data which would indicate that the art of chrome plating as it now stands is suitable in the particular type of engine we are investigating. This was an aluminum bore engine with chrome plate on the bore surface.

Mr. Jacoby: It's our thought that the basic materials are not too critical in this particular application. We're expecting the coating to do the job, and so long as the basic material has all of the basic qualities it needs for pressures and things pertaining to pressures, we think that if the chromium is actually deposited properly for that cylinder application it should do its job. So we're not sold on this idea of whether it's aluminum or iron, because as you know, for example in the end cylinders, chromium has done beautifully and probably it's the most widespread practice that I can think of in this country where chromium has been really successfully used and accepted. I believe that our industry feels that the base metal is not going to be important because the problem basically with chromium and aluminum is to be sure that the adhesion is proper.

Mr. Robinson: In answer to Dr. Bowden's question, we have not examined the surfaces by electron diffraction.

THIS PAPER describes 20 years experience in developing and using die-cast aluminum cylinder blocks in outboard motors.

Several different types of cylinder blocks, ranging in size from 1½ to 50 hp, are described, with an outline of the design procedure of the 50-hp V-4 block. Production details included are: die construction method and casting data, process for impregnating, machining and air testing, use of dry liners, and plated and sprayed coatings.

Aluminum in

THE LIGHTWEIGHT low-cost powerplant is the engineering objective of all industries engaged in building private transportation vehicles. In no other field is it as important as in the marine industry — particularly the outboard motor industry.

The outboard motor industry built its foundation on a lightweight, portable fishing motor with which most of you have, no doubt, had personal experience and are completely familiar. The industry has now expanded into pleasure boating and is making powerplants that, in a small scale, rival the automotive engine. It produces more power per pound, and more power per cubic inch, than most piston engines. Part of these advantages start with the wide acceptance of die-cast aluminum parts throughout the entire unit. The principal part, and largest, is the cylinder block, which is also made of die-cast aluminum.

This paper will cover our experience in developing and using this type cylinder block over the past 20 years.

Beginning of Die-Cast Outboard Cylinder Block

It was the need for an extremely low cost, lightweight, 1-hp engine for the 1938 market, that first instigated our use of the die-cast cylinder block. Prior to having any practical experience with the die-cast cylinder block, it was felt to be inferior to the cast-iron block currently in use at that time. It was considered a compromise for cost considerations.

There were many fears concerning the success of the first die-cast cylinder. The areas of concern were the differential expansion between the aluminum and the cast iron, the strength of screw threads, whether or not the cylinder could be successfully die cast, structural strength of the die-cast aluminum, and cylinder bores going out of round. There was considerable reluctance on the part of die casters even to quote on the 1-hp cylinder because of their fear of whether or not it could be successfully cast.

Fig. 1 shows a cross-section view of the 1-hp die-cast cylinder block. The cast-iron cylinder sleeve and top journal bearing were cast in place. The sleeve thickness is ⅛ in. The outside diameter of the sleeve was rough turned to get good anchoring of the aluminum to the sleeve. The sleeve was retained by aluminum extending over each end of it. All holes were cored. The finish stock on flat surfaces and the cast-iron sleeve was 0.030 in.

This was our company's beginning in die-cast cylinder blocks.

As a result of this first die-cast cylinder, many advantages became apparent over cast iron, some of which contributed greatly to lower cost. These advantages are as true today, as they were in 1938, and have been substantiated over the past 20 years:

1. Production control — Scrap due to shifted cores, porosity, leaks, and the like, was reduced substantially. Scrap percentage in grey iron cylinders was very unpredictable and made production scheduling a difficult task, which was reflected in the end cost.

2. Easier machining — The amount of finish stock was reduced from 3/32 and ⅛ in cast iron to 0.030 in aluminum. This, coupled with the difference in materials, gave a surface machining rate differential of approximately 4 to 1.

3. Less machining required — Holes are cored, surfaces are cast flat, ready for use without machining in many cases.

4. Uniform product — Wall thicknesses in die casting are uniform, and can be thinner than cast iron where strength is not a factor. Close cast tolerances can be held easily. Boss sizes are uniform and accurately located. An example of this uniformity is the 3/64–1/16 crankcase-to-connecting-rod clearances held on engine after engine in production. In cast iron, this same clearance had to be ⅛ in.

5. Cleanliness — Substantial improvement in plant cleanliness was achieved. Working conditions improved; thus, it was a more desirable place to work.

6. Bearings and inserts can be die cast in place — This reduces the total machining required and gives more design latitude.

7. Less capital equipment required — Since the amount of machining and machining time is reduced, the total amount of capital equipment required is also reduced. This also results in less required machining floor space for the same amount of production output.

8. Corrosion resistance improved — Outboard motors are operated in salt water, and this water is pumped directly through the water jacket. In the case of cast iron, corrosion deposits and salt buildup were very severe. Water passages would become

Die-Cast Cylinder Blocks Outboard Motors

W. C. Conover and R. C. Nelson, Outboard Marine Corp

This paper was presented at a meeting of the SAE Detroit Section, Dec. 8, 1958

blocked and cause the engine to overheat. Aluminum exhaust covers would corrode through, because they were sacrifical to the cast-iron cylinder block. The die-cast aluminum cylinder has virtually eliminated these problems.

9. Intricate designs — Die casting offers greater design perimeters for casting intricate shapes.

10. Accuracy of locating in machine fixtures is good without primary machining operations.

11. Better heat transfer.

12. Floor space for die casting is substantially less than for the same volume in cast iron.

13. Better suited to mass production because of uniformity and production control. Also, there can be closer integration between die casting and machining departments. They can be housed in the same building.

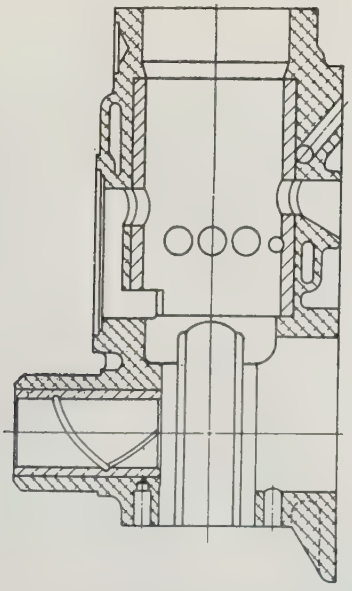

Fig. 1 — 1-hp die-cast cylinder block, 1938

14. Easier cleaning on the raw casting. No core wires or sand to get out of water jackets.

Since the advantages to the die-cast cylinder became quite definite, and our paper fears over differential expansion, thread strength, and structural strength did not materialize, larger motors with larger volume production were developed for the 1939. market These were the 2½- and 5-hp, 2-cyl, alternate firing engines.

As you can see in Fig. 2, a section through the 5-hp cylinder block, the construction is similar to the 1 hp, except it has two cylinders. The three bronze journal bearings were cast in place and anchored by the aluminum. Production die casting rate for the 2½- and 5-hp cylinders was 25 and 22 pieces per hr respectively. This 5-hp cylinder block replaced the 4.2-hp cast iron one shown in Fig. 3, and was interchangeable with it. The weight saved by the die-cast block was approximately 5¾ lb.

For the 1940 market, a 16-hp engine was produced

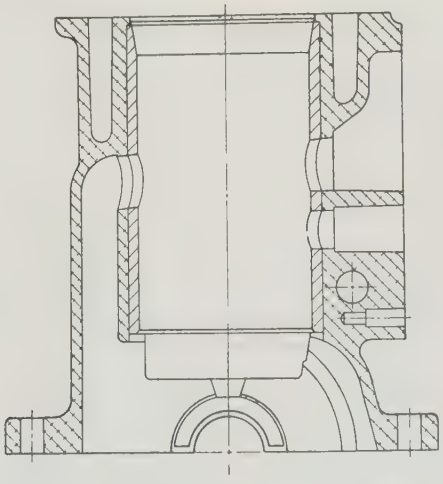

Fig. 2 — 5-hp die-cast cylinder block, 1939

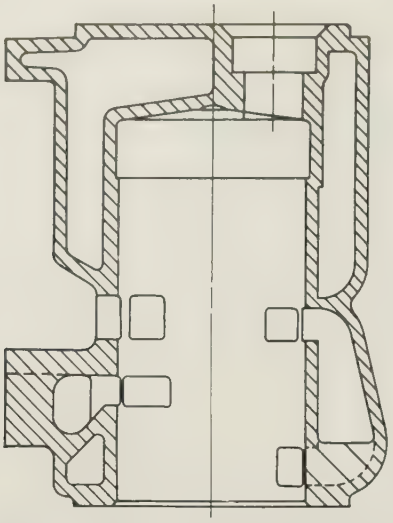

Fig. 3 — 4.2-hp cast-iron cylinder block, 1938

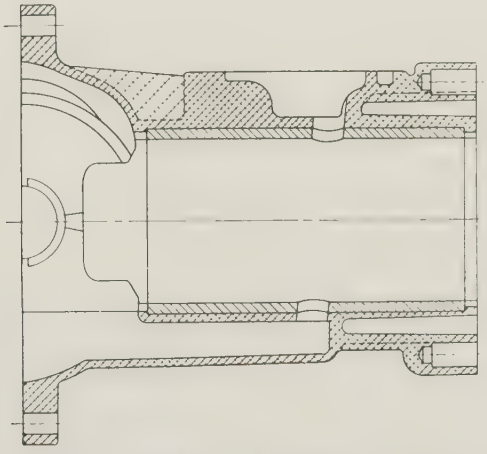

Fig. 4 — 16-hp die-cast cylinder block, 1940

(Fig. 4). This was the first all-new engine making full use of the die-cast cylinder block. The construction of this block is dry sleeve, the same as the previous cylinders. The weight of the aluminum in the finished block is 7.75 lb. Production casting rate was 17 pieces per hr. At this stage in our development of the die-cast cylinder blocks, cast iron was no longer given design consideration. The advantages of die casting were definitely established and there were no major technical handicaps.

Since 1940, there have been approximately 16 different die-cast cylinder blocks produced by the Corporation. These varied in horsepower between 1½ and 50. Some of these blocks are shown in Fig 5.

Fifty-Hp V-4 Cylinder Block

Design Procedure — The first question to be answered was how should the cylinder block be designed for die casting. After lengthy consideration, three possible methods evolved:

The first method was to split the banks of cylinders in the middle of the 90-deg V, indicated by line A-A in Fig. 6. The advantage to this method was the ease of die casting.

The disadvantages were:

1. Overall length of the block would have to be increased because of screw fastenings to hold it together (approximately 2½ in.).

2. The machined surfaces which accepted the exhaust cover and crankcase must be machined and located to line up perfectly.

3. Assembly would be difficult.

4. Manufacturing cost would be high.

The second method was to separate the cylinders from the crankcase along lines B-B and C-C in Fig. 6.

The advantages were:

1. Easier die casting.

2. If a cylinder bore is machined wrong, or one is damaged in service, it can be replaced without losing the whole block.

The disadvantages were:

1. The block is larger in all directions.

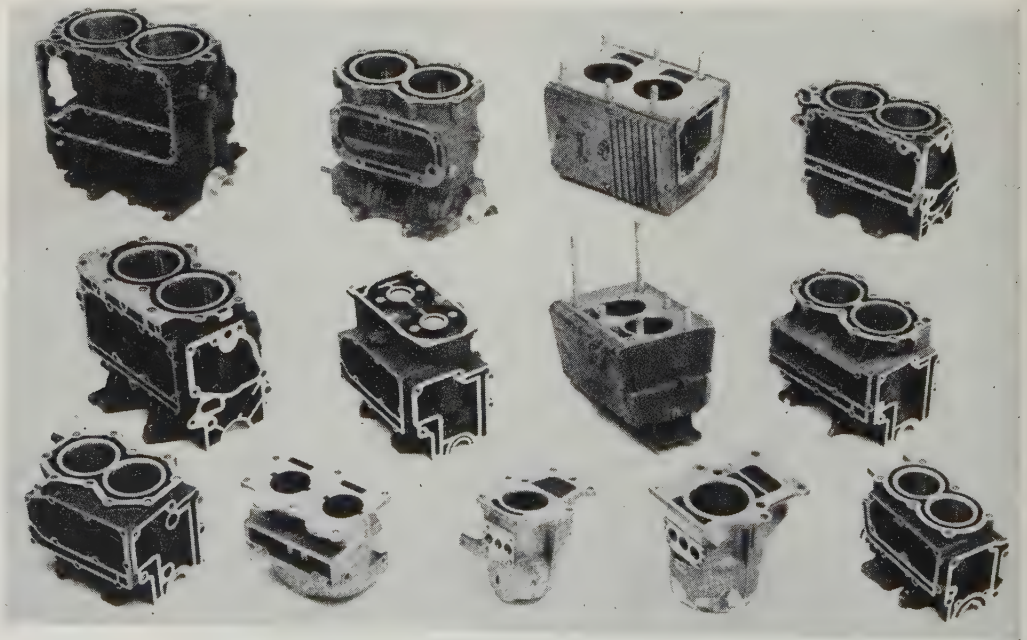

Fig. 5 — Several die-cast cylinder blocks produced by Outboard Marine Corp.

2. The crankcase volume becomes larger, which is detrimental to 2-stroke engine operation.

3. Manufacturing cost would be high.

The third method was to cast the block in one piece. The advantages were: simplest design, least costly to fabricate and assemble, smallest physical size, and lightest weight.

The disadvantages were:

1. Die casting would be more difficult.

2. If part of the casting is scrapped in fabrication, the whole block would be lost.

In order to resolve the block design for die casting, a full-scale wooden model of the cylinder was made for die design study. It was concluded that the one-piece cylinder block could be die cast.

The V-4 50-hp cylinder has a 90-deg V (Fig. 7), The use of seal rings, similar to piston rings between crankcases makes it possible to have only three journal bearings instead of five. This was done in order to reduce the overall length of the engine, and to give easier machining of the cylinder. This design feature has proved very successful. In the 2-stroke engine used in outboards, the crankcase forms a pump for scavenging the combustion chamber, which makes it necessary that the crankcase for each cylinder be separated and sealed from the others. The seal rings perform this function. The crankpin arrangement is such that primary inertia forces are completely balanced by counterweights on each end of the crankshaft (Fig. 8).

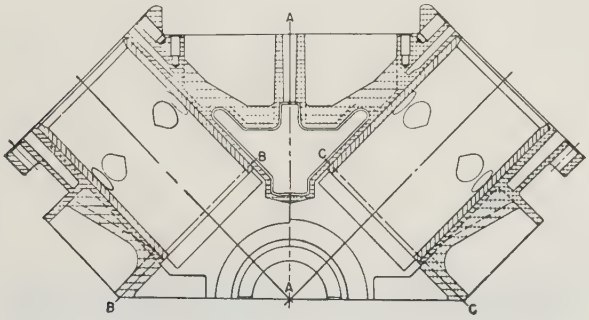

Fig. 6 — 50-hp die-cast cylinder block, 1958

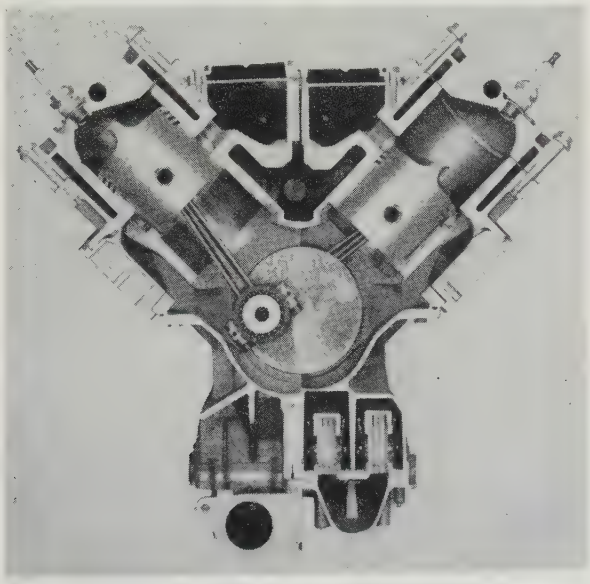

Fig. 7 — V-4 50-hp engine cross-section

Die Construction of V-4 50-hp Cylinder Block — To study the problem of die construction further, a full-scale wooden model of the proposed die, with movable slides, was constructed. This die was then placed in a wooden model of the die-cast machine frame. Fig. 9 shows the wooden model and one of the methods studied of positioning the die in the machine. In this manner, a more accurate study could be made of the various clearance problems, loading of inserts into the die, removing the block from the die, method of locking the die, and methods of moving the slides. This method of study proved to be very helpful, and it is believed that it

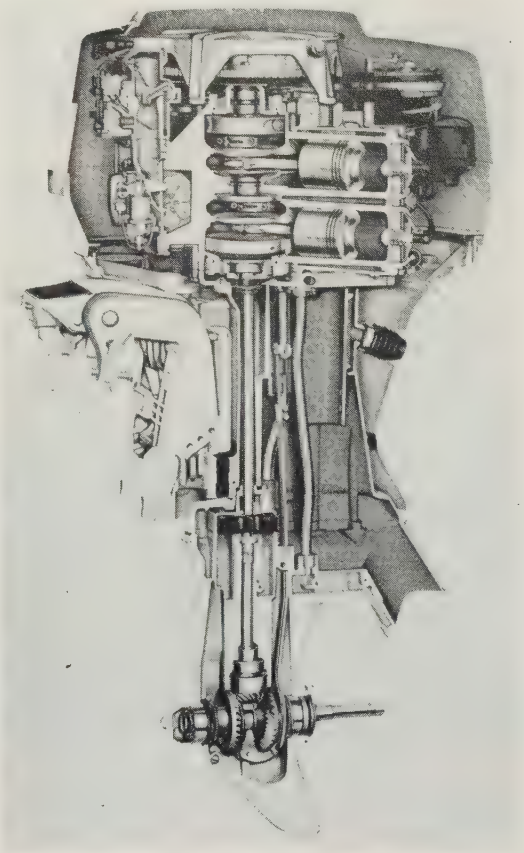

Fig. 8 — V-4 50-hp outboard motor cross-section

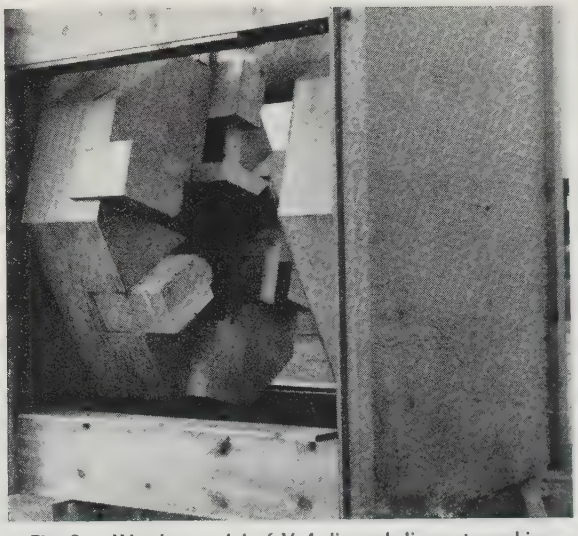

Fig. 9 — Wooden model of V-4 die and die-cast machine

saved thousands of dollars through the elimination of costly errors. Fig. 10 shows the ejector half of the die and the core slides.

The die is made in small sections so as to minimize the possibility of die cracking, and also because several small portions of the die can be replaced more readily, and for less money, than one larger one. This type construction is possible on parts such as cylinders where flash lines are not important. The die is made of a 5% chrome alloy, die steel, Type H-13, and cost approximately $75,000.00. The total weight of the die is approximately 20,600 lb. Six slides are incorporated, moving in the directions shown in Fig. 11. Stripper plates are used on core slides Nos. 5 and 6. These stripper plates support the casting after the core slides have been pulled back and the casting is ready for ejection. Internal locks were selected to hold the slides in position when die is closed, because of their inherent rigidity.

A very important feature in this die construction is the method of aligning the core slides. It is important that each core slide be accurately located so as to produce a uniform casting for subsequent machining operations. In order to achieve this, three gibs are used to locate each core accurately. (See Fig. 12.) Since these gibs are narrow, their total expansion is small. Therefore, they can be operated with much smaller clearances than the conventional method of positioning off the sides of the core slide. In the cold state, these gibs are fitted with 0.001 clearance, as compared to approximately 0.012 if the core slides were to be positioned from their sides. With this construction, the relationship between core slide faces on the casting is held to within ± 0.006 total variation on cylinder block after cylinder block. This ± 0.006 total variation is also held between the core slide faces and the ejector half face of the casting. The total variation in the castings across the parting of the die is approximately – 0.000 + .015.

In order to support the movable part of the die and the core slides, it is rested on the ways of the die-cast machine. The clamps normally used for securing the die to the platen would not be sufficiently strong, nor give enough rigidity with this extreme weight and overhang. The weight of this portion of the die is approximately 12,000 lb.

The casting is gated along the exhaust cover

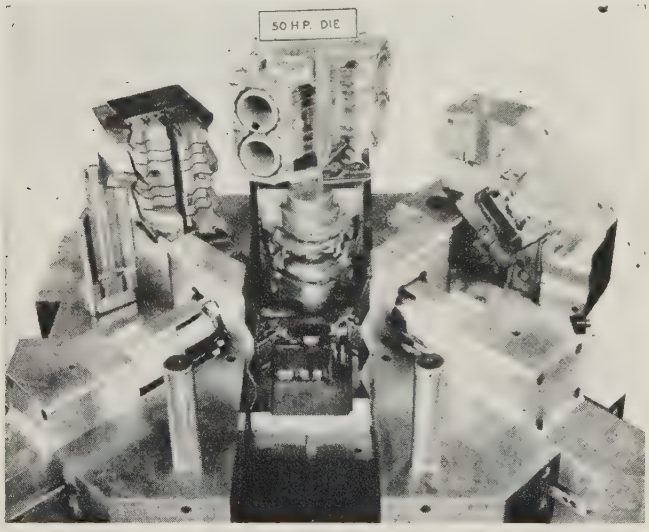

Fig. 10 — 50-hp die

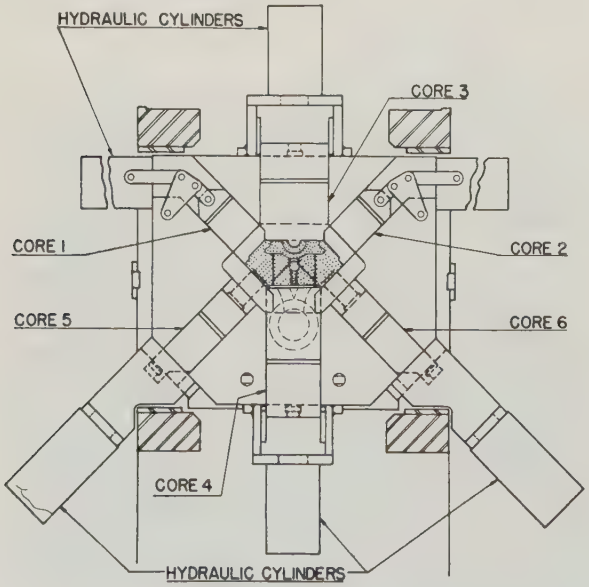

Fig. 11 — 50-hp V-4 die-cast cylinder die, core slides, and ejector half

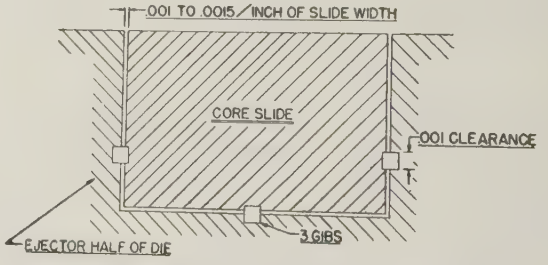

Fig. 12 — Method of positioning core slides in V-4 die

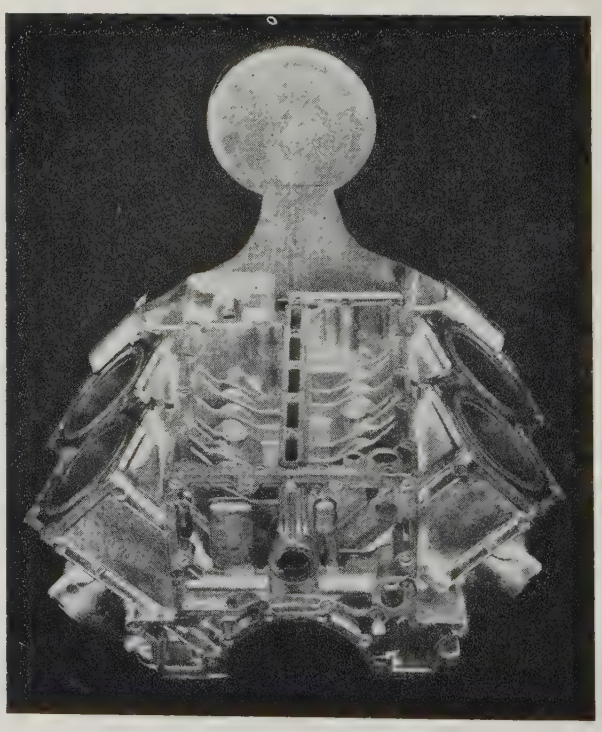

Fig. 13 — Casting for V-4 50-hp cylinder block with gate

flange and both cylinder head flanges (Fig. 13). The gate is about 15-in. long and 0.075-in. wide.

Lading of V-4 Cylinder Block — Automatic ladling is employed for casting the V-4 cylinder block. Manual ladling of 25.5 lb of aluminum offered problems, and would reduce the production rate, or else increase the piece cost per casting by requiring extra manpower. The automatic ladling is accomplished as shown in Fig. 14. Two 100-kw furnaces are hooked together in series by a 1-in. line below the surface of the aluminum. Aluminum coming from the smelter is poured into furnace No. 1. No. 2 furnace is sealed and has a pressure line attached to the top. After the die has closed, a 2-psi. air pressure is applied over the aluminum surface of furnace No. 2. This raises the level of the aluminum and the metal spills out the spout in furnace No. 2 into the plunger cavity. The pressure is removed after the correct time has elapsed. In order to compensate for the variation in aluminum level in the furnaces, the time the pressure is applied is varied. This is done automatically by a float level sensing device in the furnace, which relays the information to time control equipment. The average time required to ladle is 5 sec. This method of ladling has proved very successful. The maximum variation in the amount of aluminum poured, one shot to another, is approximately $\pm \frac{1}{4}$ lb.

Ejection and Removal of the Casting from the Die — In order to eject the casting completely from the movable part of the die, an auxiliary hydraulic ejection piston is used. The die-cast machine has a normal ejection length of 8 in. and the auxiliary ejector has another 5 in. for a total of 13 in. of ejection. At the time of ejection, a platform on an overhead track is inserted manually into the die to receive the casting as it is ejected. (See Fig. 15.) The casting is then removed from the die.

Insert Loading into V-4 Die — The four cast-iron cylinder sleeves and bronze center bearing seal are loaded into the die by fixture. This fixture is moved manually into the die on a long, jackknife arm, and the inserts are hydraulically positioned in the die. This eliminates the necessity of the operator having to get into the die.

Die Temperature Control on V-4 Die — Hot water is used to maintain a uniform die temperature. The water is thermostatically controlled to add heat or take it away. All six of the main core slides are water-cooled.

Treatment of Cast-Iron Sleeves Prior to Casting — All sleeves are cleaned by degreasing before casting, and heated to approximately 300 F in an electric furnace. A number of years ago, sleeves were heated with a torch. This deposited soot on the outside surface and sometimes gave poor heat transfer between the aluminum and cast iron.

Aluminum Alloy Used for Die-Cast Cylinder Blocks — An 11% silicon die-cast aluminum is used for cylinder blocks. This alloy is used because of its good casting qualities, good resistance to corrosion, and its characteristic of producing sound castings which will not leak under fluid pressure. The analysis is shown in Table 1.

Casting Data on V-4 Cylinder Block —

1. Production casting rate is 24 piecs per hr.
2. Weight of aluminum poured per shot — 25.5 lb.
3. Weight of sleeves and center bearing seal insert — 9.2 lb.
4. Weight of cleaned casting (less biscuit and gate) — 30 lb.
5. Total weight of casting with gates and biscuit — 34.7 lb.
6. Total floor space required for the die-cast machine, furnaces, furnace controls, and the like is approximately 1000 sq ft.
7. Peak injection pressure inside the die cavity is 8500 lb.
8. Holding time after shot is made is 23 sec.
9. Mean die temperature during operation is approximately 500 F.
10. A Lester-Phoenix $3\frac{1}{4}$–40 special die-cast machine is employed in casting the V-4 block. It is rated an 800-ton minimum clamp pressure. Fig. 16 shows a 1500-ton Lester-Phoenix die-cast machine, which was originally purchased for casting the V-4 cylinder. It is the largest unit — frame die-cast machine ever built. The frame casting was

Table 1 — Analysis of Aluminum Alloy Used in Cylinder Blocks

	Per Cent
Silicon	10–12
Copper	0.6 Maximum
Magnesium	0.1 Maximum
Manganese	0.3 Maximum
Zinc	0.5 Maximum
Iron	0.4–0.8
Nickel	0.5 Maximum
Chromium	0.3 Maximum
Titanium	0.3 Maximum
Others	0.2 Maximum

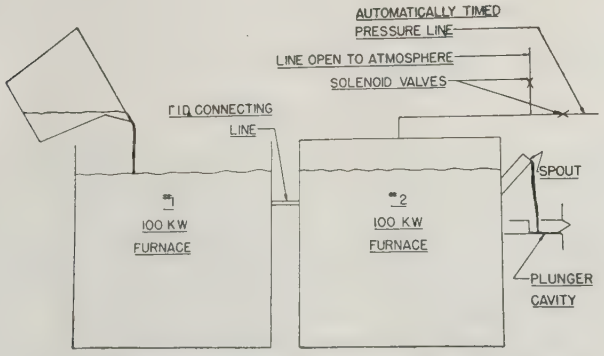

Fig. 14 — Automatic ladling for die casting 50-hp V-4 cylinders

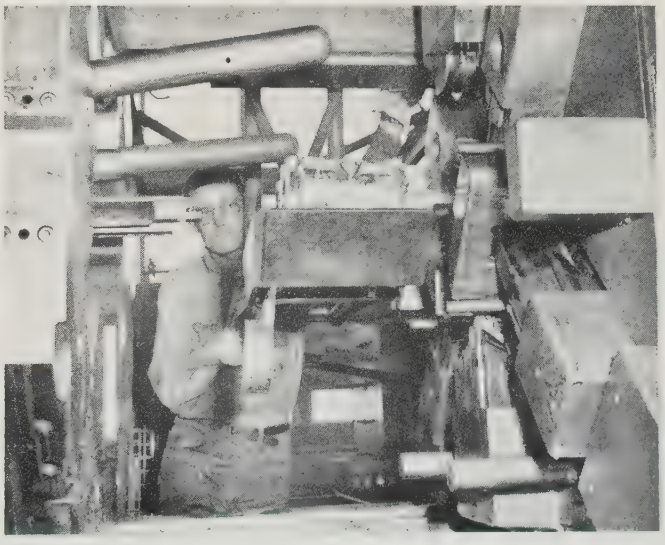

Fig. 15 — Ejection of casting from die

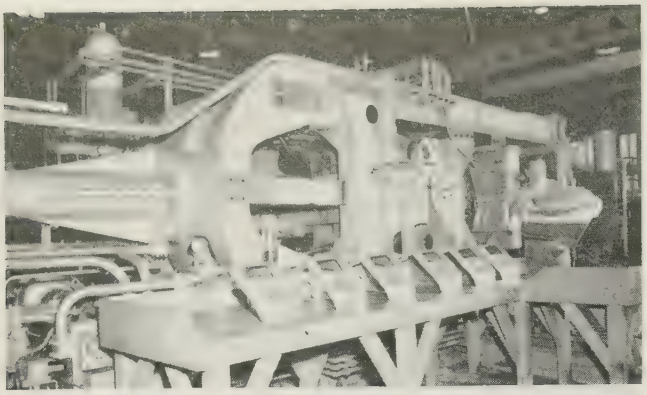

Fig. 16 — 1500-ton Lester-Phoenix die-cast machine

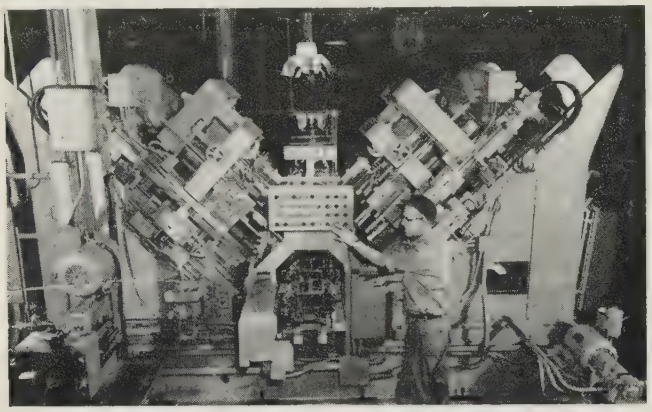

Fig. 17 — Machine which does rough and finish boring of cylinder bores

made in Germany. It was used to cast 50-hp engine covers last year, and will be used for casting future cylinder blocks. This machine will cast up to 47½ lb of aluminum per shot, with maximum injection pressure of 20,300 psi. It will take dies measuring 4½ ft high and 6 ft wide.

Impregnating Die-Cast Cylinder Block

After die casting and cleaning, all die-cast cylinder blocks are impregnated with a sealer. This serves the purpose of improving salt water corrosion resistance and sealing the casting to prevent water leaks. It also seals the crankcase against possible fuel leakage.

The process for impregnating is to place the clean castings in a container and pull a vacuum of 28 in. of Hg for 15 min. The impregnating compound is then admitted and an air pressure of 95–100 lb is placed on the compound and the cylinders for 15 min. The castings are then removed, drained, and baked at 300 F for 5 hr on a continuous conveyor oven. The sealer consists of 39.8% pigment and 23.2% binder. The details of the composition are shown in Table 2.

Machining and Air Testing V-4 Cylinder Block

The machine tools used for machining the V-4 are, for the most part, conventional machines which have been adapted for special purpose machining. An example is shown in Fig. 17. This machine does the rough and finish boring of all four cylinder bores. During the machining operation, the water jackets of every cylinder are air tested for leaks at 20 psi under water.

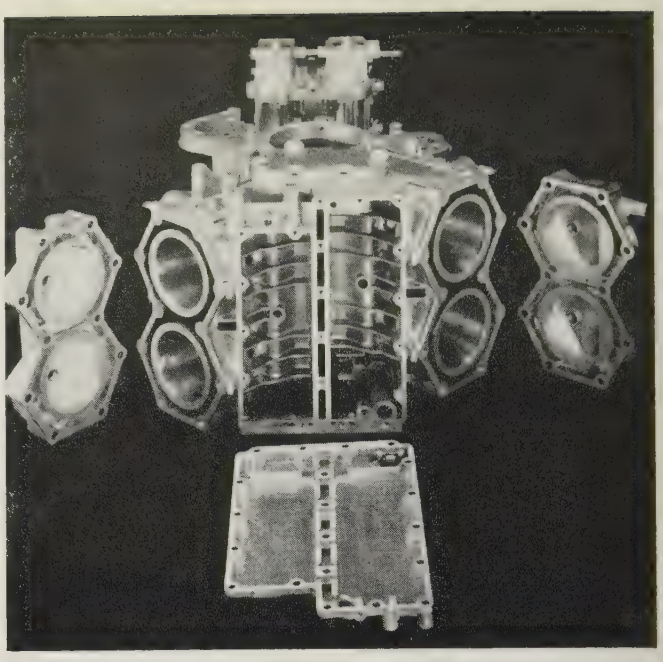

Fig. 18 — Machined V-4 cylinder block and other parts

Fig. 18 shows a machined V-4 cylinder block (less impregnating) and other die-cast parts.

Why Dry Liners?

Dry liners are used for the following reasons:

1. Corrosion problems are considerably less. As was mentioned previously, the die-cast cylinder has practically eliminated the problem which was so prevalent in cast-iron cylinders.
2. More rigid construction. With the sleeve cast in place, it becomes a structural member for the cylinder block and, therefore, results in more rigid construction.
3. Simplicity of design. Since there are no close tolerances on the OD of the liner, no "O" rings required, and no extra machining in the cylinder block required to accept the liner, the overall design is much simpler. Also, the manufacturing cost is lower for the dry sleeve construction.
4. Intake and exhaust port dimensions can be held closer. Since the intake and exhaust ports are machined while they are in a fixed position in the casting, the port dimensions can be held much closer than in the case of wet sleeve construction.
5. The need for cylinder liner replacement in the field is very low. Field experience over the past years indicates that there would have been very little advantage to the wet-liner construction from the standpoint of salvaging cylinder blocks due to scoring or other damage.

Differential Expansion

First of all, differential expansion between aluminum and ferrous materials in the cylinder block is not a problem. Trouble with loose sleeves and poor heat transfer has not been a problem. There are two reasons which appear to explain this. First, in the casting process, a strain is placed in the cast aluminum around the cast-iron sleeve. In order for the sleeve to become loose, this strain would have to be relieved by the difference in thermal expansion between the two materials. Second, the

Table 2 — Composition of Sealer

Pigment — 39.8%	
Zinc chromate and other inhibitive pigments	73.6%
Inert Filler	24.0%
Tinting Pigment	2.4%
	100.0%
Binder — 23.2%	
Phenolic Varnish & Plasticizing Agents	100%
Drier and Thinner — 37.0%	

Table 3 — Failure Torque and Torque Limit of Die-Cast Aluminum Screws

Screw Size	Failure Torque, ft-lb	Torque Limit, ft-lb
10–24	6½	2– 3
¼–20	14	5– 7
5/16–18	21	10–12
⅜–16	31	18–20

temperature gradient across the cast-iron sleeve and the aluminum surrounding it is such that the actual difference in total expansion is less than would occur if both materials were at the same temperature. The cast iron is hotter than the aluminum which is in contact with the water jacket. It is believed that these items, strain in the aluminum and temperature gradient, are the contributing factors to a successful job.

In the case of antifriction bearings in journal bearing applications, the outer race of the bearing is squeezed between the crankcase halves a sufficient amount to prevent the race from becoming loose when the cylinder block reaches operating temperature. The mean squeeze on most of our bearings is 0.001 on the diameter, but this may vary depending on the size of the bearing and the temperature of operation. Again, differential expansion is not a problem here.

High Silicon Alloy Cylinder Sleeves

Considerable experimenting and testing with high silicon cylinder sleeves has been done. The material used was Alcoa's No. 526, which is 20% silicon. The sleeves were die cast in place. From a production standpoint, this material is extremely hard to machine because of its abrasiveness. The other disadvantage found with the use of this material is its affinity for scuffing. It appears that any small pickup of carbon at the ports, or other foreign material, will start scuffing on the piston which, in turn, is transferred to the sleeve. Once scuffing has started, it feeds on itself and will not heal, as in the case of cast iron.

Screw Thread Strength in Die-Cast Aluminum

All screws used in die cast aluminum are heat-treated steel, or high-strength stainless steel, in order to obtain maximum strength in the die-cast material. Experience has indicated that when a screw yields in aluminum, it loads the thread non-uniformly. As the screw starts to elongate, it progressively pulls the aluminum thread out a portion at a time. This occurs because the load becomes excessively high on the first thread. If the screw does not yield excessively, the load is taken over all of the threads. This is the reason for using high-strength screws exclusively. Normal practice for thread engagement into the die-cast aluminum is twice the thread diameter.

Tests have been conducted to determine the strength of die-cast threads. In this test, all screws were coated with wool grease, which is used for corrosion protection. In almost all cases, the heat-threaded screw will break rather than strip the threads. Table 3 gives the torque required to either break the screw or strip the threads in the aluminum die casting, and the torque limits generally used in production in die-cast aluminum.

For special applications, such as 14-mm spark plugs and 5/16 cylinder head bolts, the torques held regularly in production are 20 and 15 ft-lb respectively.

Plated and Sprayed Coatings Cylinder Bores

Chrome Plating — We have twice set up pilot plants for chrome plating directly on die-cast aluminum cylinder bores (1940 and 1953), but have never gone into production with this process, because of the large number of manufacturing problems experienced, and also because there is no apparent advantage from an engineering standpoint. Also, the cost was equal to or higher for the chrome plating compared to cast-iron sleeves. Two different types of chrome plating were investigated in cooperation with two major chrome platers.

Other Plating and Sprayed Coatings — A number of different type platings and sprayed coatings directly on the die-cast aluminum bore, other than chrome, have been tested. In general, all types of plating materials and sprayed coatings tested are prone to scuff more easily than with the cast-iron sleeve. When the scuffing starts, it perpetuates itself, because the plating or coating is destroyed almost immediately, leaving aluminum on aluminum.

Some of the coatings tested were hard anodize, iron plating, sprayed steel over molybdenum, sprayed iron, and pure molybdenum.

Die-Casting Plant

1. Total number of die-casting machines — 117.
2. Average quantity of castings produced per month — 3–4 million.
3. Both primary and secondary aluminum are used. The secondary 2S and 3S aluminum is alloyed in the company operated smelter into No. 13 and other die-cast alloys.
4. Die casting floor area — 71,500 sq ft.

Smelter area — 15,000 sq ft.

Die storage area — 15,000 sq ft.

Conclusion

In conclusion, Outboard Marine Corp. is very optimistic about the future of die-cast cylinder blocks and, at the present time, sees no other fabrication process which will obsolete die casting. There appear to be a number of good possibilities of improving casting techniques. A recent improvement is the use of vacuum die casting, which has made it possible to cast No. 218 alloy successfully. It is anticipated that there will be improved alloys for ease of casting and improved physical properties in the near future. Last, there does not appear to be a die casting limitation to cylinder size, or design, that may be used by the outboard motor industry.

Discussion of this paper will be found on p. 588.

DISCUSSION of Conover-Nelson paper

Describes European Experience With Aluminum Die Casting

— A. F. Bauer
National Lead Co

THIS PAPER shows how the introduction of aluminum *has already been accomplished* on a large-scale production in the closely related field of outboard motors. This outstanding success was achieved through the exclusive use of the most modern casting method, the die-casting process. Aluminum die castings for outboard motors have been used almost from the beginning and showed their first satisfactory results on small engines of only 1 hp. As larger outboard motors were developed, the die castings just simply grew with the engines into very intricate and highly stressed structural parts.

The V-4 engine block, which discussed by the authors is a fine example of the adaptability of aluminum die casting to the mass production of extremely complicated and highly stressed castings. By properly designing for die casting, the Outboard Marine Corp. was able to solve the undercut problem and to use aluminum die casting for practically all of its castings. Since almost all outboard motors are designed for and constructed in aluminum die casting, we believe that the outboard motor industry today uses more aluminum die castings than any other industry.

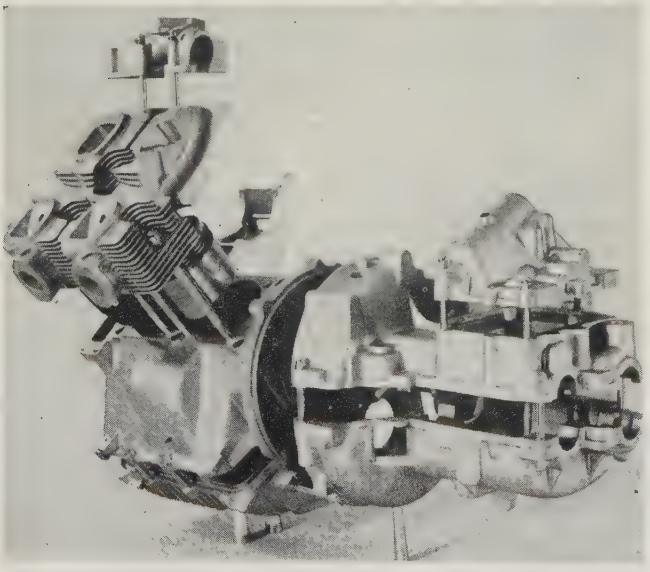

Fig. A — Lloyd-Alexander 600-cu-cm engine with 68 lb of aluminum permanent-mold castings (made by Karl Schmidt of Hamburg, Germany)

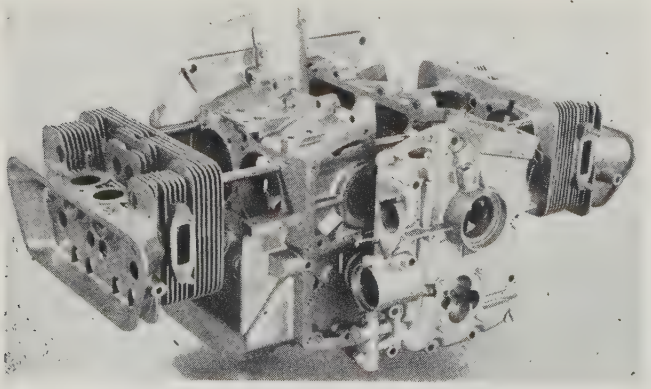

Fig. B — 1.5-liter Porsche engine with 70 lb of aluminum permanent-mold castings (made by Karl Schmidt)

Compared with this successful development, the automotive industry is *really far behind* in the use of aluminum for passenger cars and for its engines in particular. The average 1959 car contains only about 58 lb of aluminum, mostly for transmission castings, pistons, and decorative parts, or approximately 1.3% of the total car weight, while European cars average about 5–15% of their total weight in aluminum.

In these days when the American automotive industry has its eyes on the European small cars, the impression was created that European light-metal specialists, as well as European automotive engineers, consider the permanent-mold process as the most economical and best suited casting method for aluminum engine blocks and other large castings.

The fact is that European automotive companies *have used* aluminum permanent-mold castings quite extensively *in the past,* because they were best suited for their relatively small production rates. However, with increased car production, quite a few European companies are now changing to die castings to take full advantage of their lower manufacturing costs and reduced weights.

This latest European trend to retool for die castings, where large production rates justify this move, may best be explained on two engines — the small Lloyd-Alexander engine and the Porsche engine.

The Lloyd-Alexander 600 cucm engine, shown in Fig. A, is an unusual design of a 2-cyl aircooled engine for an extensively small car. All castings, with the exception of the gray-iron cylinder barrel, have been made in aluminum permanent mold by the Karl Schmidt Co. in Hamburg, Germany. Total weight of the aluminum castings is 68 lb. Since production has increased, the parts have been retooled for aluminum die castings.

Fig. B shows the major permanent mold castings of the 1.5-liter Porsche engine with a weight of 70 lb. These castings are also produced by Karl Schmidt. For the relatively small production rate of Porsche cars, the permanent-mold process is probably the most economical one.

The cylinder barrels for this engine are not shown because they are not made as aluminum castings. For their more expensive models, Porsche buys these barrels machined from extruded aluminum with the bore protected by a porous chrome plate. In the standard Porsche model, the cylinder barrels were changed back to gray iron to reduce costs.

This engine is shown because of its similarity to the Volkswagen engine which is also an aircooled opposed-type 4-cyl engine. The Volkswagen engine is somewhat smaller, but the main difference is that all its major castings for crankcase and transmission are made in magnesium permanent mold, except the cylinder barrels which are gray iron and the cylinder head which is aluminum permanent mold. After a careful study of the economics, which started two years ago, the Volkswagen plant decided to change all magnesium permanent-mold castings to magnesium die casting. This conversion has now been completed and all large castings (some 40 lb) are now being produced in magnesium die casting. I was told that the changeover to die castings resulted in tremendous savings of up to 30% of the manufacturing costs. This development to go to die castings to reduce manufacturing costs is very much in line with the 20 years of die-casting experience of the Outboard Marine Corp., expressed in the paper.

Of course, the castings shown in these two models and even the V-4 engine block for outboard motors are still relatively small in comparison to a 6-cyl or a V-8 cylinder engine block for passenger-car engines. On these large water-cooled engine blocks and cylinder heads it is not an easy task to eliminate all undercuts for die casting or to find a solution for the wear problem in cylinder bores as well as the expansion problem in the crankshaft bearings. However, with an open mind these problems can be solved, in fact have already found satisfactory solutions on some die-cast engine blocks.

Hypereutectic Al-Si alloys, with their low coefficient of expansion and increased wear resistance, have been suggested as material for cylinder sleeves and possibly complete engine blocks. Utilizing the sand casting or semi-permanent mold process, some engineers believe that a one-piece conventional engine block can be mass produced in these high Si alloys with water channels just like the present gray-iron blocks.

Based on present manufacturing practice, sand castings and semi-permanent mold for one-piece engine blocks would be much too expensive. From a technical standpoint, it has to be said that the first satisfactory wear results may be somewaht misleading. Europeans, who have been using hypereutectic Al-Si alloys for pistons for many years, have also tried hard to use them for cylinder sleeves and barrels. All their tests, however, showed the same questionable results as mentioned in the paper. None of the aluminum alloys tested, including the hypereutectic group, was 100% foolproof. While satisfactory results were obtained under normal operating conditions, failures occurred with excess dirt in the oil, also during cold starts and low oil levels, because the aluminum alloys generally do not have the same capacity as gray iron to retain the oil.

It is, therefore, safer to equip the cylinder bores of aluminum engine blocks with gray-iron inserts, as shown in the V-4 engine block of Outboard Marine Corp., or to protect them with some kind of a coating. The simple design of a shrunk-in gray-iron sleeve for a 2-cyl block, as shown in Fig. C, has proved itself for many years on hundreds of thousands of portable engines. Since some hot spots may develop when the aluminum shrinks away from the sleeve on heavy sections, a later and improved method to create a bimetallic interlock bond between gray iron insert and aluminum is shown on the right side in Fig. C. The enlarged view shows how the B. M. I. bond is accomplished by the die-cast aluminum penetrating fine undercut-like crevices of the rough surface of the centrifugally cast sleeve.

Other methods to protect the aluminum surface with a wear-resistant coating, and mentioned in both papers, are chrome plating and metal spraying of the bore. In addition, a new method of wear-resistant coating on aluminum die castings has been developed by Doehler-Jarvis Division of National Lead Co.

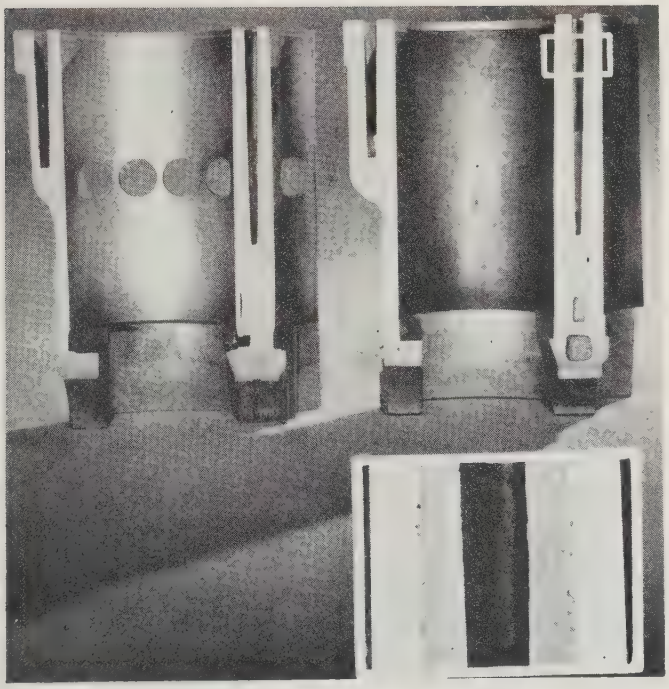

Fig. C — Sections of 2-cyl, 2-stroke water-cooled cylinder block for 40-hp outbroad motor (Left — cast-in gray-iron sleeve held by shrinkage only; right — cast-in gray-iron sleeve interlock bonded with aluminum as shown in enlarged view on right)

In Fig. D are shown two wet sleeves of water-cooled engines and a cylinder barrel of an aircooled engine coated by the new process with a porous iron coat of high wear resistance and only 0.020-in. wall thickness. This coat can be produced in almost any material and in any thickness, but is held relatively thin for economical reasons. Since the coat is first created on the core and then transplanted to the die casting, the part comes from the die with a coated bore of extreme accuracy and without any taper. The accuracy of the coated bore can be held with ± .003 in., and such a smooth surface finish that honing is the only finishing operation necessary.

Die-cast sleeves and cylinder barrels with this transplant coat can be produced very economically on semi-automatic equipment and create a product of highest quality.

The enlarged view of Fig. E shows that an excellent mechanical bond exists between the wear-resistant coat and the aluminum. Since the coat is hard and porous, there are indications that it will retain oil for cold start conditions. Short test runs of only 50 hr have given extremely satisfactory results, but have to be continued on a much broader basis before final conclusions of the wear resistance of this coat can be drawn.

I hope that the mentioning of these new methods of coating aluminum cylinder bores does not confuse the issue and that they will help the automotive engineer to find solutions for the engine problems in the design for aluminum engines.

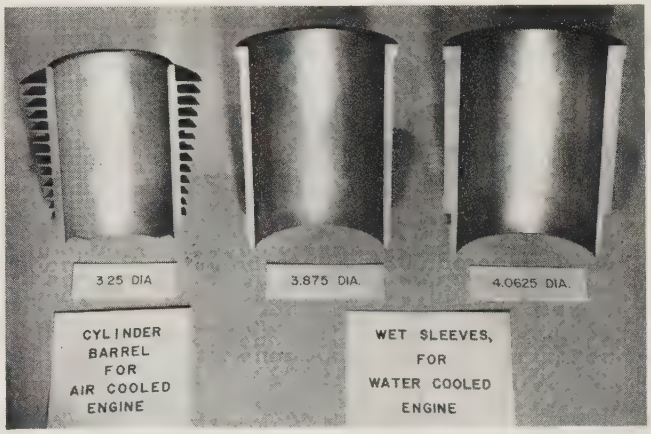

Fig. D — Cylinder barrel and two wet sleeves with 0.020-in. thick wear resistant iron coat in bore

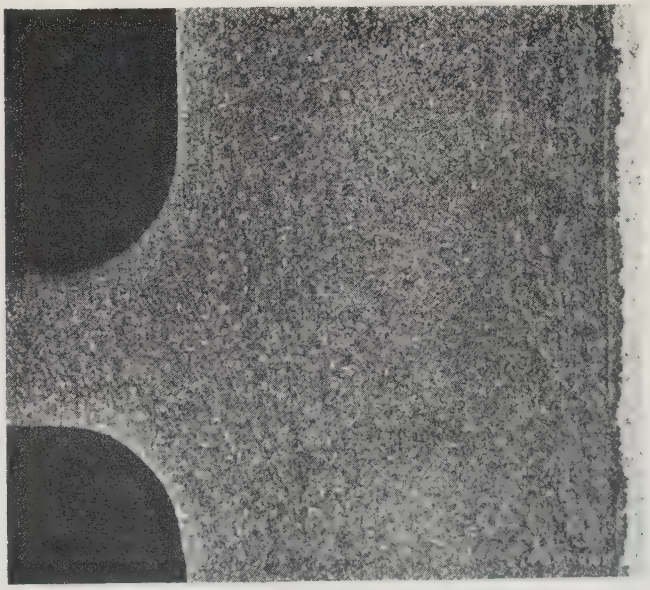

Fig. E — Enlarged section of cylinder barrels show excellent mechanical bond created by this translant cast

Strength and of Materials

THE PROPERTIES of presently available and advanced development alloys are reviewed in each of the following groups: (1) magnesium alloys, (2) aluminum alloys, (3) titanium alloys, (4) low-alloy steels, (5) corrosion resistant steels, and (6) nickel, cobalt, and mixed-base alloys.

The strongest materials in each group are selected to make comparisons of the strength of typical airframe components at various temperatures. From these comparisons, material-efficiency curves are made to show the strength and thermal limitations of each material group.

THE ADVENT of supersonic aircraft has created formidable problems for the airframe designer. These problems arise because the aerodynamic heating associated with high-speed flight imposes significant thermal loads on the aircraft structure. The temperature conditions encountered preclude the use of aluminum alloys which have long been the mainstay of the aircraft industry. Therefore, at the outset the designer is confronted with the predicament of selecting a material to withstand the severity of this thermal environment.

The material selection problem, of course, has many ramifications. Some of the salient factors requiring perusal are the cost, availability, producibility, fabricability, serviceability, and structural efficiency. Of course, each factor merits the designer's utmost scrutiny. However, it is not intended here to examine each facet of the problem, but only to consider the item of structural efficiency; that is, to select the material that will render the lightest weight structure.

For a specific problem, a study should be made to collate the efficiency of all suitable materials on the basis of the loads and temperatures given. In this way the majority of the materials can usually be eliminated from contention. The final choice will be made after considering the other factors mentioned previously.

To make such a study, it is convenient to divide all the materials into alloy groups. The predominant alloy in each group can then be used to establish the strength and thermal limitations of that group. Having done this, it is then easy to decide which materials should be regarded for the final design. This approach will be used to show the limitations of certain alloy groups on the basis of strength criteria usually found in airframe design.

Classification of Materials

The materials are divided into alloy groups as designated in Table 1. The alloys in each group have approximately the same moduli and densities. It is necessary to group materials with the same moduli together, since the load-carrying capacity of compression members is a function of the modulus of elasticity as well as the strength of the material.

The steel alloys are divided into two groups, those which are resistant to atmospheric corrosion and those which are not. The low-alloy steels are defined here as those containing less than 12% alloying elements. To be used in aircraft structures, these alloys require some means of corrosion protection. Included in this group are the 4340 or modifications of 4340-type steels and the hot-work tool-and-die steels.

The Group 5 alloys are the steels containing between 12 and 50% by weight of alloying elements. Included in this group are the martensitic, ferritic, and austenitic stainless steels as well as the age-hardenable and precipitation-hardening steels.

The nickel, cobalt, and mixed-base alloys are grouped together because over 50% of the composition is elements which are declared critical by the government. Therefore, none of these alloys would be used for major aircraft components unless they were the only alloys that could fulfill the design requirements.

In this study an attempt is made to present all materials that might be contemplated for aircraft stuctural applications. Beryllium and some of the refractory metals were omitted for two reasons. First of all, there is insufficient information to evaluate these materials, and secondly, these alloys are undergoing further developments.

Strength Criteria Considered

In designing any structure there is some strength criterion which establishes the dimensions of the part. To minimize weight it is desirable to use the material that has the highest strength-density ratio on the basis of this strength criterion. In some cases it may be necessary to compare the structural weight based on more than one criterion in order to ascertain which one will govern the final design. Also, the material may be selected as a compromise between several strength criteria.

The strength criterion which governs a structural design depends upon the type and magnitude of the loads, the type of structure, and the temperature conditions. In this paper the material groups are compared on the basis of strength criteria usually encountered in aircraft design.

These comparisons are based on the short-time elevated temperature strength for temperatures to 1200 F, that is, the strength determined by testing materials at temperature after ½-hr temperature exposure. The effect of exposure time and creep is

Thermal Limitations for Airframe Components

J. C. Ekvall, Lockheed Aircraft Corp.

This paper was presented at a meeting of the SAE Southern California Section, March 24, 1958.

not considered. The temperature range covered will be adequate for most structures heated, either by the engine or aerodynamically.

The strength criteria evaluated for these comparisons are listed in Table 2. The tensile strength and yield strength are probably the most prevalent strength criteria utilized, since this data is more readily available than any other material property. For the stiffness criterion, the modulus of elasticity of the material will be used. The buckling strength depends upon the type of structure; therefore, some of the most common types that occur in aircraft structures were picked, for example, columns, plates, and flanges. Simply supported edge conditions are assumed for the plate- and flange-type elements. Other edge conditions could be studied, but the relation between the material efficiencies would be similar to these. The ability of a plate to carry load, however, may not be limited by the buckling strength. The load a plate can support is dependent upon the ratio of the plate width to the plate thickness. For high values of this ratio, the ultimate load is considerably higher than the buckling load. This ultimate load is referred to here as the crippling strength. Only the crippling strength of plates with simply supported edges will be assessed, since the equation for this type of plate has been experimentally verified.[1] These strength criteria then will be discussed to show the limitations of each material group.

Tensile Strength Criterion

The ultimate tensile strength is the property most frequently applied for comparing materials for tension applications. To insure that the structure will not yield excessively in service, the design stress is limited to two-thirds of the ultimate tensile strength. This is based on the assumption that the tensile yield stress of the material is greater than two-thirds the ultimate tensile strength. For most materials, this is true. Assuming that the same factor of two-thirds will be used regardless of the material, the efficiency of tension members is indicated by the ultimate tensile strength-density ratio.

Tension members often contain joints, cutouts, and discontinuities which may produce high local stresses. In such places, the material is assumed to have enough ductility so that the points of stress

Table 1 — Classification of Materials

Alloy Group	Densities, lb/in^3	Moduli of Elasticity, 10^6 psi
1. Magnesium	0.064–0.065	5.9– 6.6
2. Aluminum	0.098–0.102	10 –11.4
3. Titanium	0.159–0.172	15 –17.4
4. Low-Alloy Steels	0.280–0.284	29 –30.5
5. Corrosion-Resistant Steels	0.278–0.292	29 –32.5
6. Nickel, Cobalt and Mixed-Base Alloys	0.290–0.334	29 –33

Table 2 — Strength Criteria

1. Tensile Strength
2. Yield Strength
3. Stiffness
4. Buckling Strength
   a. columns
   b. plates
   c. flanges
5. Crippling Strength
   a. plates

Table 3 — Materials Used for Tensile Strength/Density Comparisons (Fig. 1)

Material Group	Material Designation	Temperature Range, F
1. Magnesium	ZE11-H26	70– 580
	HK31A-T6	580– 650
2. Aluminum	X2020	70– 475
	2024-T86	475– 515
	2024-T81	515– 580
3. Titanium	Ti-4Al-3Mo-1V	70– 200
	Ti-16V-2.5Al	200– 725
	Ti-7Al-3Mo	725–1000
	Ti-8Al-2Cb-1Ta	1000–1200
4. Low-Alloy Steel	Thermold J	70– 500
	Peerless 56	500–1200
5. Corrosion-Resistant Steel	419	70– 330
	422(TH900)	330– 870
	419	870–1100
	A-286	1100–1200
6. Nickel, Cobalt, and Mixed-Base Alloys	Udimet 500	70–1200

[1] "Determination of Plate Crippling Strengths at Elevated Temperature," by J. C. Ekvall. Structures Research Memorandum No. 390, Jan. 31, 1957. Lockheed Aircraft Corp., Burbank, Calif.

concentrations will not cause failure. For many of these high-strength materials, the strength has been obtained at the expense of ductility. Just how much ductility is required is a moot question. However, a ductility corresponding to a 10% elongation from a tensile test coupon is usually adequate, and in some cases a 5% elongation may be sufficient. Most of the alloys used for the comparisons have greater than a 10% elongation and none of them have less than 5%.

The maximum tensile strength-density ratios for each material group are shown in Fig. 1. Table 3 lists the alloy designations and their applicable temperature ranges. The marked superiority of the low-alloy steels, Thermold J and Peerless 56, is evident for temperatures below 1000 F. The strength of the Groups 3, 4, and 5 alloys deteriorates rapidly above 1000 F. For temperatures above 1100 F Udimet 500 emerges as the superior alloy. Also, note that the F_{tu}/d ratio is higher for the Groups 3, 4, and 5 alloys at 650, 1000, and 800 F, respectively, than the aluminum alloys at room temperature. This indicates that tension structures could be built to operate at elevated temperatures for about the same or less weight as present aluminum structures.

Yield Strength Criterion

The compressive yield stress is applied as a criterion for the compressive strength of a structure if buckling or crippling does not occur. For instance, sandwich panels can be designed to develop the compressve yield stress of the material in the face sheets. The most efficient face material, then, is the one with the highest F_{cy}/d ratio.

Often the compressive yield stress is not given for a material. In these cases the tensile yield stress is used, since this information is usually available for all materials. The assumption that the compressive yield stress equals the tensile yield stress is reasonably accurate for materials which are annealed or heat-treated. However, it can be quite misleading for materials which obtain their strength by cold-work.

The curves of Fig. 2 indicate that the yield strength-density curves are not in the same order as the tensile strength-density curves. Again, these are composite curves of the strongest alloys in each group (Table 4). Here the titanium alloys have higher values up to about 750 F, low-alloy steels from 750–1130 F, and the Group 6 alloys, above 1130 F. The titanium alloys and low-alloy steels would be limited to temperatures of 800 and 1000 F, respectively, since the strength diminishes rapidly above these temperatures. The inferiority of the corrosion-resistant steels is attributed to the low yield strength-ultimate strength ratio of these materials. Future research should provide corrosion-resistant steel alloys with yield strengths approaching 90% of the tensile strength.

Stiffness Criterion

The modulus of elasticity-density ratio is used for comparing materials where the elastic stiffness of the structure is the design criterion. If the maximum allowable defomation is the criterion, the affects of creep, plasticity, and thermal expansion must also be accounted for. Thermal expansion, creep, and plastic strains may nullify any advantages obtained from a material with a high modulus-density ratio. Also, by comparing materials on a modulus-density ratio basis, the assumption is implied that the geometry is fixed. Although the external dimensions of the structure are usually set for aerodynamic reasons, there is some latitude as to the internal dimensions. The internal dimensions will depend upon the material selected, since

Table 4 — Materials Used for Yield Strength/Density Comparisons (Fig. 2)

Material Group	Material Designation	Temperature Range, F
1. Magnesium	ZE 11-H26	70– 590
	HM21XA-T8	590– 750
2. Aluminum	7178-T6	70– 130
	X2020	130– 360
	2024-T86	360– 600
	M276(APM)	600– 700
3. Titanium	Ti-6Al-4V	70– 900
4. Low-Alloy Steel	Thermold J	70–1000
	Peerless 56	1000–1140
	Thermold J	1140–1200
5. Corrosion-Resistant Steel	PH15-7Mo(RH950)	70– 500
	419	500–1000
6. Nickel, Cobalt, and Mixed-Base Alloys	M-252	70– 600
	Udimet 500	600–1200

Table 5 — Materials Used for Modulus of Elasticity/Density Comparisons (Fig. 3)

Material Group	Material Designation	Temperature Range, F
1. Magnesium	HM21XA-T8	70– 600
2. Aluminum	M276(APM)	70– 700
3. Titanium	Ti-5Al-2.5 Sn	70– 250
	Ti-6Al-4V	250– 600
	Ti-8Mn	600–1000
	TI-6AI-4V	1000–1200
4. Alloy Steel	Hy-Tuf	70– 425
	4340	425– 600
	Vascojet 1000	600–1200
5. Corrosion-Resistant Steel	422	70– 900
	A-286	900–1200
6. Nickel, Cobalt, and Mixed-Base Alloys	Inconel 700	70–1200

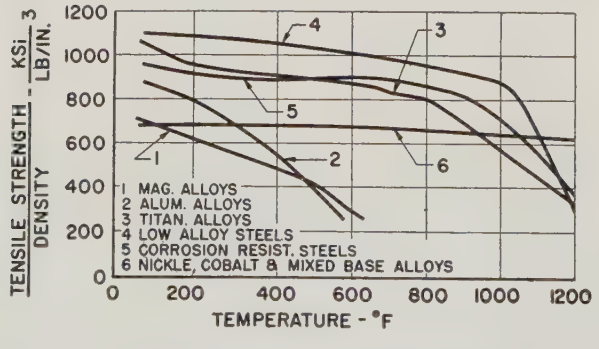

Fig. 1 — Comparison of maximum tensile strength-density ratios of each material group

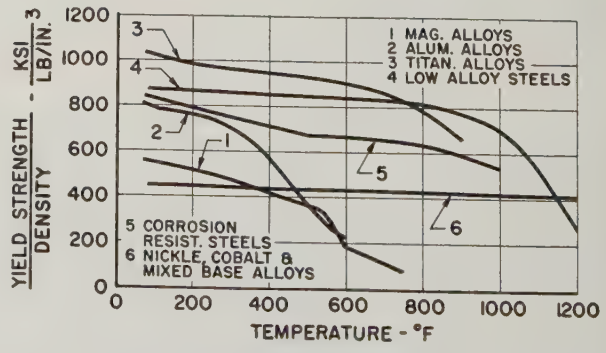

Fig. 2 — Comparison of maximum yield strength-density ratios of each material group

it is necessary to optimize each design consistent with the strength properties. For these reasons, the modulus-density ratio is probably not the most significant factor for comparing the stiffness of structures. Material is seldom selected on this basis alone.

In Fig. 3 it can be seen that the difference between the modulus-density ratios of the various groups is more significant at the higher temperatures. Table 5 lists the materials for these comparisons. Up to 775 F the corrosion-resistant steels are predominant, and above this temperature the Group 6 alloys are better. The titanium alloys have the lowest modulus-density ratio of all the groups. The modulus of elasticity is one material property that cannot be changed appreciably by alloying. Therefore, little improvement in the modulus-density ratios of these alloys can be expected in the near future.

A material with a high modulus density ratio is not always desirable. This is particularly true of structures which are subjected to thermal stresses. The thermal stress caused by temperature gradients in a structure is directly proportional to the modulus of elasticity and coefficient of thermal expansion. Therefore, a material with a low modulus and coefficient to expansion to minimize thermal stresses and a high strength-density ratio to minimize weight would be preferable. The high-strength titanium alloys are outstanding in this respect.

Buckling Strength and Crippling Strength Criteria

The buckling strength or crippling strength of a structure is dependent, among other things, upon its size and shape. Therefore, the type of structure should be given so that materials can be evaluated on the same basis. Columns, plates, and flanges have been selected for these comparisons. Usually, a complex structure can be subdivided into combinations of columns, plates, and flanges for calculation purposes. Then the materials can be compared by considering the composite efficiency of these structural elements.

Usually the designer is given the loads and the length or width over which the load must be carried. Therefore, the buckling equations are put in a form so that this given information is put on one side of the equation. The term containing the load and a given dimension of the structure is referred to as the "structural index." The other side of the equation contains the terms which are a function of the material properties and the critical buckling stress. Then for a given structural index and a given material, the critical buckling stress can be determined and hence the buckling stress-density ratio.

The equations relating the structural index to the buckling or crippling stress and material properties are summarized in Table 6. The moduli applied to account for the effects of plasticity was E_t for column buckling, $(EE_t)^{\frac{1}{2}}$ for plate buckling, and E_s for flange buckling. These plasticity reduction factors have been experimentally verified by various investigators.[2,3,4,5,6,7] The crippling equation was developed by Ekvall[1] and was found to check the test data for several different materials.[8,9]

To evaluate a material on a buckling or crippling strength basis, the material stress-strain curve at various temperatures is needed. From the stress-strain curves, the various moduli can be determined as a function of the buckling or crippling stress. However, instead of using the stress-strain curve, it is more convenient to use the Ramberg-Osgood parameters as denoted in Fig. 4. Using these parameters, the calculations can be done easily by automatic computer.

The materials in each group with the highest yield strength-density ratio were selected for these com-

Table 6 — Buckling and Crippling Equations

Type of Element	Strength Criterion	Equation
Column	Buckling	$\frac{P_{crcf}}{L^2} = \frac{0.101 F_{cr}^2}{E_t}$
Simply Supported Plate	Buckling	$\frac{P_{cr}}{b^2} = \frac{0.516 F_{cr}^{3/2}}{(EE_t)^{1/4}}$
Simply Supported Flange	Buckling	$\frac{P_{cr}}{b^2} = \frac{1.58 F_{cr}^{3/2}}{(E_s)^{1/2}}$
Simply Supported Plate	Crippling	$\frac{P_{max}}{b^2} = \frac{0.516 F_{max}^2}{K_r (E_s F_{0.7})^{1/2}}$

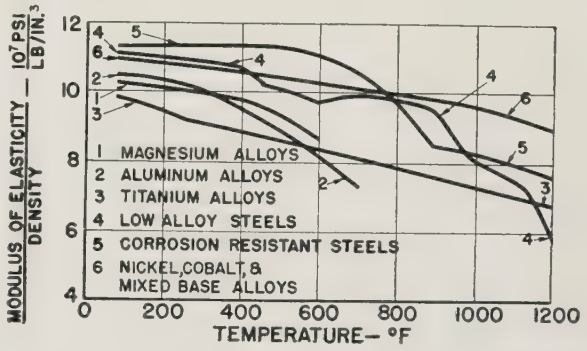

Fig. 3 — Comparison of maximum modulus of elasticity-density ratios plates with edges simply supported

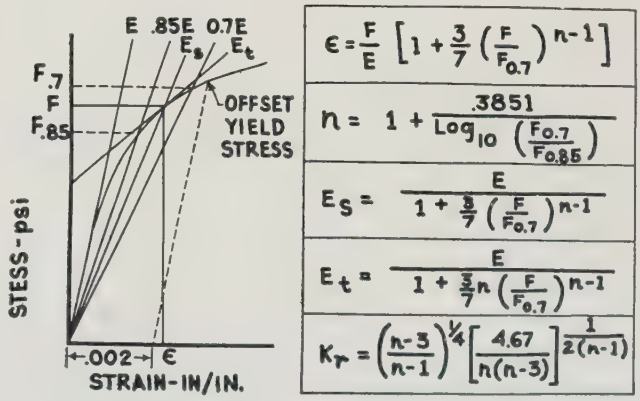

Fig. 4 — Ramberg-Osgood method of representing stress-strain curve

[2] *Journal of Aeronautical Sciences*, Vol. 14, May, 1947, p. 261: "Inelastic Column Theory," by F. R. Shanley.
[3] *Journal of Aeronautical Sciences*, Vol. 13, January, 1946, p. 38: "Secant Modulus Method for Determining Plate Instability Above Proportional Limit," by George Gerard.
[4] "Preliminary Thin Wing Study for P-80 Airplane," by C. Heilbron and Paul Sandorf. Report No. 5404, Lockheed Aircraft Corp., Burbank, Calif., August, 1945.
[5] "Factors Affecting Design of Thin Wings," by W. J. Conway. Paper presented at SAE National Aeronautic Meeting, Los Angeles, October, 1954.
[6] NACA TR 1029, 1951: "Compressive Strength of Flanges," by E. Z. Stowell.
[7] NACA TR 898, 1948: "Unified Theory of Plastic Buckling of Columns and Plates," by E. Z. Stowell.
[8] NACA TN 3600, January, 1956: "Correlation of Crippling Strength of Plate Structures with Material Properties," by R. A. Anderson and M. S. Anderson.
[9] NACA TN 3552, January, 1956: "Investigation of Compresisve and Creep Lifetime of 2024-T3 Aluminum Alloy Plates at Elevated Temperature," by E. E. Mathouser and W. D. Deveikis.

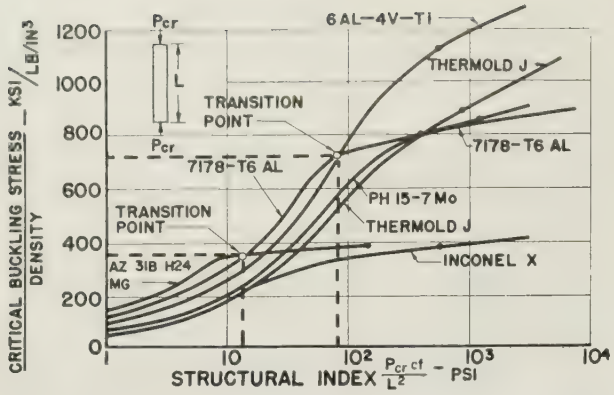

Fig. 5 — Structural efficiency for simple columns at room temperature

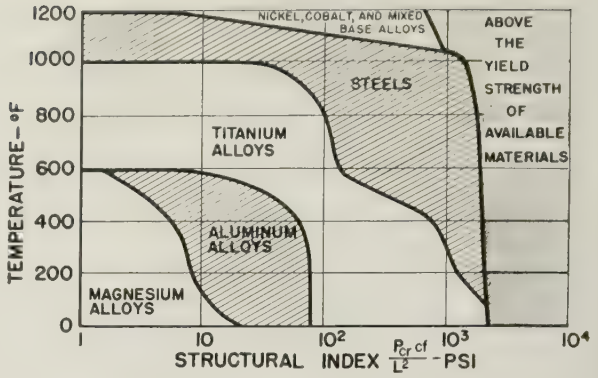

Fig. 6 — Strength and thermal limitations of materials for buckling of columns

Table 7 — Materials Used for Buckling and Crippling Comparisons

Material Group	Material Designation	Temperature Range, F
1. Magnesium	AZ31B-H24	70– 200
	HK31A-H24	200– 580
	HK31A-T6	580– 600
2. Aluminum	7178-T6	70– 210
	2024-T86	210– 500
	2024-T3	500– 600
3. Titanium	Ti-6Al-4V	70–1000
4. Low-Alloy Steel	Thermold J	70–1200
5. Corrosion-Resistant Steel	PH15-7Mo(RH950)	70– 800
	419	800–1000
	A-286	1000–1200
6. Nickel, Cobalt, and Mixed-Base Alloys	Inconel X	70–1200

parisons and are tabulated in Table 7. In some cases, the stress-strain curve for the best material was not available, such as ZE11-H26 magnesium and M-252 and Udimet 500 nickel-base alloys. The titanium alloy was 6Al-4V heat treated to 160–180,-000 psi ultimate tensile strength.

In Fig. 5 the materials in each group are compared as simple columns at room temperature. For any given structural index, the most efficient material is the one with the highest critical buckling stress-density ratio. As shown in the figure no one material is efficient over the whole range of structural indices. Points where two materials are equivalent are called transition points. The magnesium alloy is superior for a structural index between 1 and 13, the aluminum alloy between 13 and 80, and the titanium alloy above 80. The compressive yield stress of each material is indicated by the black dot on each curve. If the design stress was limited to the compressive yield stress, the curves would terminate at the black dots. Then the titanium alloy would be limited to a structural index of 500, and the steel alloys, Thermold J and PH15–7Mo, would be the most efficient from 500 to about 1000.

To discern how the material efficiency varies with temperature, curves similar to those shown in Fig. 5 would have to be made at temperature intervals, and cover the range of temperature of interest. To see how one material contrasts with another at a specific temperature, reference would have to be made to plots such as Fig. 5. However, if only the most efficient materials are of interest, the data can be presented in more simplified form. At each temperature the transition points are determined for the most efficient materials. These transition points are then plotted as temperature-structural index curves, forming a boundary or limit for which a given material is efficient.

A plot of the transition points for the buckling of columns is presented in Fig. 6. This shows for what ranges of structural index and temperature each material group is the most efficient. For low loads or long columns, the light alloys are foremost for temperatures up to 600 F. For high loads or short columns the titanium and steel alloys are better. The nickel, cobalt, and mixed-base alloys are efficient only for temperatures above about 1100 F. The area to the right of the steel alloys is above the yield strength of presently available materials. As higher strength steel alloys are developed, the boundary line will move to the right. If more temperature resistant alloys are developed, the boundary lines will move up.

Similar curves were constructed for the other types of compression elements. The strength and thermal limitations of materials for buckling of plates is shown in Fig. 7. The structural index for plates is the critical load divided by the square of the plate width. For long plates the buckling strength is independent of the plate length. Again, each alloy group is efficient for certain ranges of structural index and temperature. The nickel, cobalt, and mixed-base alloys are efficient only for temperatures above 1100 F. The titanium alloys have the largest region of application.

In Fig. 8 the strength and thermal limitations of materials for buckling of flanges is given. The material efficiency curves are further to the right than in the comparison for plate buckling. This is because a flange requires a smaller width to support a given load than a plate and, therefore, the flange would have a higher structural index. Many types of structures are composed of combinations of plates and flanges. A good example of this is an integrally stiffened skin which can be thought of as a combination of interconnecting plates and flanges. Since the plates and flanges are made of the same material, a higher structural index would be used for the flanges than for the plates to get the most efficient overall structure.

The final comparisons in Fig. 9 are based on the crippling strength of plates. These curves are similar to those for the buckling strength of plates. Since the crippling load for a plate is higher than the buckling load, the curves are further to the left than in the plate comparisons. The region of application for the magnesium alloys is small here. Actually, the magnesium and aluminum alloys are

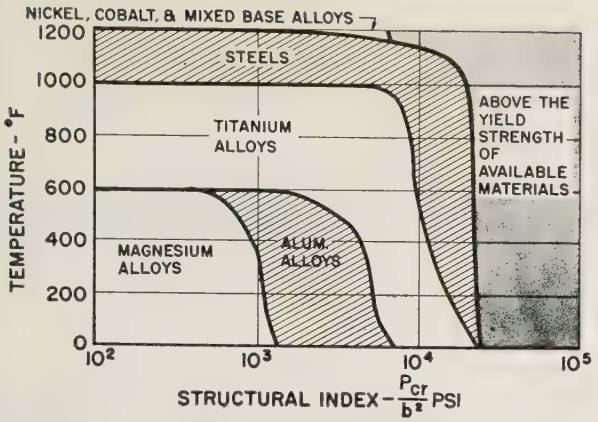

Fig. 7 — Strength and thermal limitations of materials for buckling of plates with edges simply supported

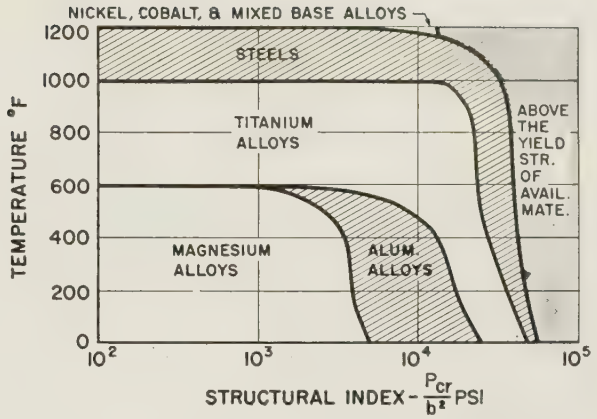

Fig. 8 — Strength and thermal limitations of materials for buckling of flanges with one edge simply supported

about equivalent for structural indexes between 100 and 1000 and temperatures below 600 F, the aluminum alloys being a little more efficient above 200 F.

The material limitations shown in Figs. 6–9 are for a ½-hr temperature exposure. To account for the effect of exposure time, the material stress-strain curves at various exposure times would have to be utilized. For longer exposure times the strength and thermal limitations of these materials would be reduced.

Conclusions

From these comparisons, it can be seen that no one material is a panacea for high-temperature structural problems. The most efficient material depends upon the temperature requirements, the loads, and the type of structure selected. Each group of materials has an efficient region of application, and comparisons such as shown here can aid the designer to select the most efficient material for a particular application.

Symbols

A = Cross-section area
b = Plate width
c = Coefficient of end restraint for columns
d = Density
E = Modulus of elasticity
E_s = Secant modulus of elasticity
E_t = Tangent modulus of elasticity
ϵ = Strain
F = Stress
F_{cr} = Critical buckling stress
F_{max} = Crippling stress
$F_{0.7}$ = 0.7 secant yield stress
$F_{0.85}$ = 0.85 secant yield stress
$f = \frac{\rho^2}{A}$ = Shape factor
K_r = Coefficient used in plate crippling formula
L = Column length
n = Ramberg-Osgood parameter
P_{cr} = Critical load
P_{max} = Crippling load
ρ = Radius of gyration

Additional References

1. "Weight-Strength Analysis of Aircraft Structures," by F. Shanley. Pub. by McGraw-Hill Book Co., Inc., New York, 1952.

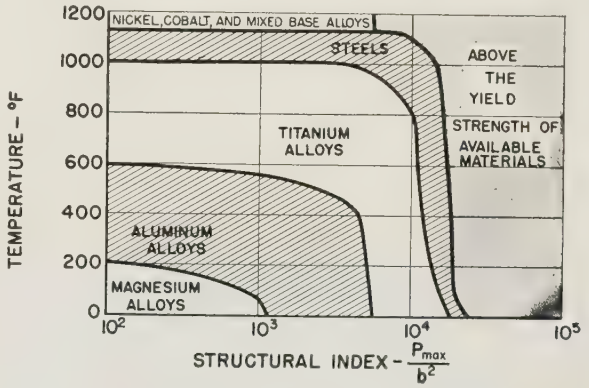

Fig. 9 — Strength and thermal limitations of materials for crippling of plates with edges simply supported

2. "Thermostructural Efficiencies of Compression Elements and Materials," by George Gerard. Paper presented at ASME Aviation Division Conference, Los Angeles, March, 1956.

3. "Use of Titanium Alloy Sheet in Airframe Components," by L. R. Jackson. TML Report No. 5A, July 29, 1955.

4. "Determination of Physical Properties of Ferrous and Nonferrous Structural Sheet Materials at Elevated Temperature," by D. E. Miller. AF TR 6517, Part 2, April, 1954; and Part 1, Supplement 1, February, 1957.

5. "Determination of Physical Properties of Ferfous and Nonferrous Structural Sheet Materials at Elevated Temperature," by D. D. Doerr. AF TR 6517, Part 2, April, 1954; and Part 1, Supplement 1, February, 1957.

6. NACA TN 3315, November, 1954: "Tensile and Compressive Stress-Strain Properties of Some High Strength Sheet Alloys at Elevated Temperatures," by P. J. Hughes, J. E. Inge, and S. B. Prosser.

7. "Strength-Density Comparisons of Materials at Elevated Temperatures," by J. C. Ekvall. Report No. 12532, Lockheed Aircraft Corp., Burbank, Calif., August, 1957.

8. "Problems in Design of Aircraft Subjected to High Temperatures," by F. R. Steinbacher and Louis Young. Paper presented at ASME Annual Meeting, New York, November-December, 1954.

9. "Optimum Stresses of Structural Elements at Elevated Temperatures," by A. Schmitt, M. A. Brull, and H. S. Wolks. Paper presented at ASME Aviation Division Conference, Los Angeles, March, 1956.

GM Diesel's Additional NEW VEES AND

K. L. Hulsing and C. E. Ervin, Detroit Diesel Engine Division, General Motors Corp.

This paper was presented at the SAE Annual Meeting, Detroit, Jan. 12, 1959.

IN 1937 General Motors introduced the two cycle Series 71 diesel engines. These engines are characterized by optional rotation and remarkable versatility of external component mountings (Fig. 1). Together with sound power and speed ratings, this adaptability of configuration built a wide acceptance for these engines in the small and medium diesel field. As is evident from a study of this chart, almost any engine configuration of exhaust and air intake location can be achieved with either direction of rotation. Starter, oil cooler, and other accessories may be placed on either side of the engine, enabling engines of a mirror image to be built for marine units and other applications where this type of engine is desirable from a servicing or operating standpoint. Over the years the 2, 3, 4, and 6-71's were complemented by Models 6-110 and 4-51 to give single engine coverage from 33 to 325 hp, and multiple engine coverage up to the 875 hp of the well-known 6-71 Quads (Fig. 2). The versatility previously indicated is apparent from units such as the Quad, which permitted a deep penetration of the traditionally large engine field by multiple engine configurations. Through 1958 the total horsepower produced by the Detroit Diesel Engine Division was over 78,000,000, representing the combined horsepower of the $4\frac{1}{4} \times 5$ in. Series 71, the 5×5.6 Model 6-110, and the 4.1×4.1 Model 4-51.

With the advent of turbocharging on a commercial scale, our company was among the first to apply turbos in truck and marine applications (Fig. 3) where more power was needed in a small space. Since in itself a turbocharger contains no magic for making an engine more durable, a conservative 25% was accepted as the power advantage to be obtained by fueling no higher than established nonturbocharged engines.

The net result of the turbocharging program was to extend our coverage to 375 hp in a single engine, and to realize some economies of operation in truck and marine applications where high specific outputs were advantageous.

In late 1955 Detroit Diesel was faced with three customer requirements:

1. Greater economy and durability.
2. Broader power range.
3. More complete power coverage.

The truck and coach industry was demanding more efficient and durable engines in order to offset to some extent uncontrollable rising costs of vehicle operation. The earthmoving industry, while expressing a desire for greater economy, actually wanted more horsepower than we could furnish in single engines. The third problem was the market below our smallest engine, the 2-71, and power gaps in the present line.

General Motors' answer was first the development of the free breathing "71E" engine, "E" standing for economy; this was closely followed by turbocharging as already indicated; and now by an all-purpose power line of 2-stroke "V's" and "in-lines."

The 71E engine when first released was lower in output per cylinder than the standard 71. However, continued development of the basic "E" concept has brought the "E" engine up to the power of the standard engine, while retaining a fuel advantage of 10–15% throughout the operating range. Developments now well along have convinced us that further sub-

Engines — —

IN-LINES

THIS PAPER describes two new series of diesel engines produced by Detroit Diesel — a smaller 53 Series and the V-71 Series.

The V configuration was chosen for all the new engines (except the very small 2-, 3-, and 4-cyl 53 Series) because of its inherent size and weight-saving characteristics. For example, the new 6V-71 engine is 40% shorter and 15% lighter than the in-line 6-71 engines.

Development of the Series 71E engine to date has yielded cleaner exhaust with equal power, improved fuel economy, longer life, and superior altitude performance.

The authors present design features of both series of engines.

stantial improvement can be achieved with the "E" configuration.

It was not, therefore, surprising that we elected to introduce two new engine lines based on the "71E" principle. Realizing that many of our present customers would prefer to remain with the engine they are now using, the new engines have been integrated with our present engines in such a manner as to offer new features of speed, torque, and configuration necessary to meet new applications, especially in the truck, farm tractor, and earthmoving industries. Particular attention was also given the design of these engines so that they might eventually become very lightweight, high-output engines, suitable for many military requirements and others where high specific output is demanded.

The first basic requirement of our new line of engines was, therefore, that a broad power range would be covered without turbocharging, but that all of the new engines could be turbocharged when the appli-

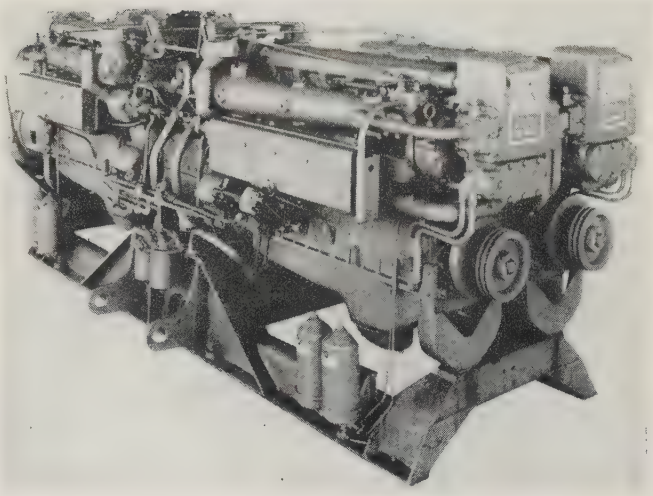

Fig. 2 — 6-71 quad

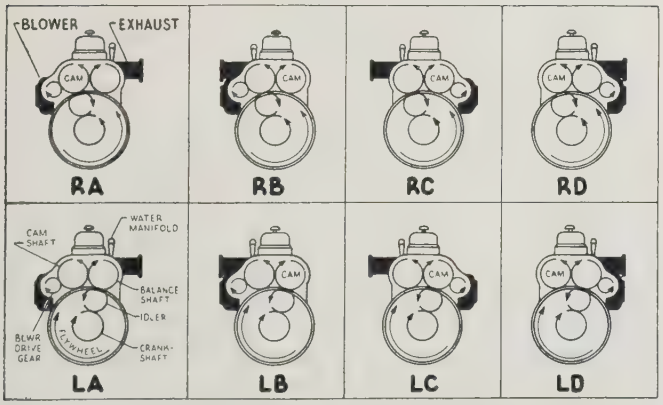

Fig. 1 — Series 71 basic engine arrangements (crankshaft rotation — R-counterclockwise, L-clockwise; type A, B, C, D designates location of blower and exhaust)

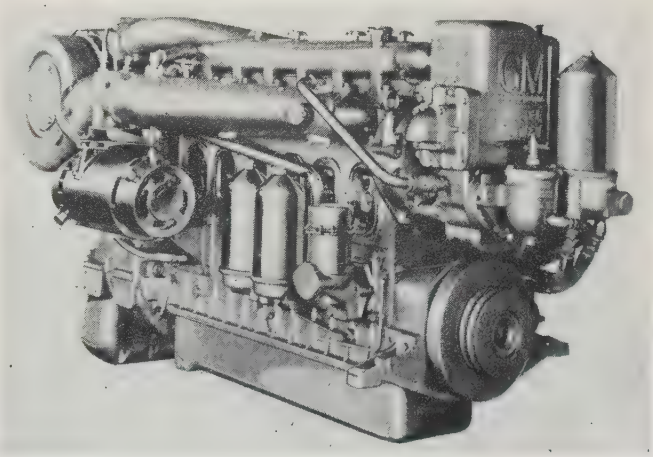

Fig. 3 — Marine 6-71 turbo

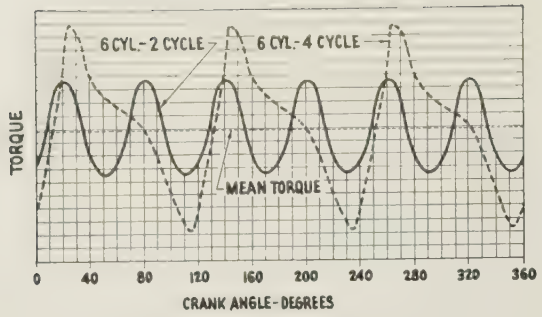

Fig. 4 — Engine torque variations, 2 stroke versus 4 stroke

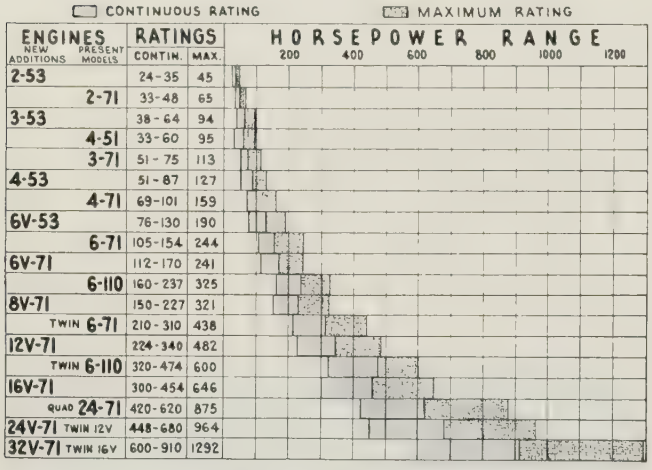

Fig. 5 — Power comparison, complete power line

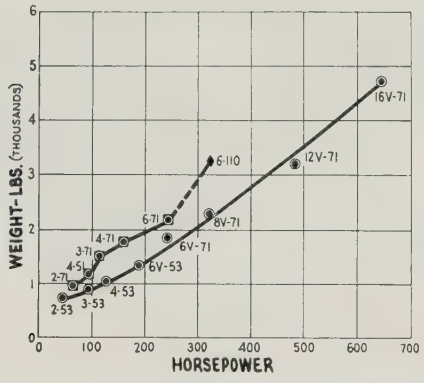

Fig. 6 — Weight and horsepower of new and present F-to-F cast-iron engines

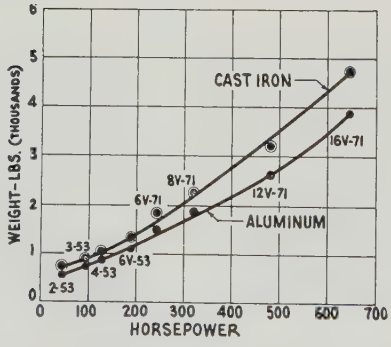

Fig. 7 — Weight and horsepower of new F-to-F engines, aluminum versus cast-iron

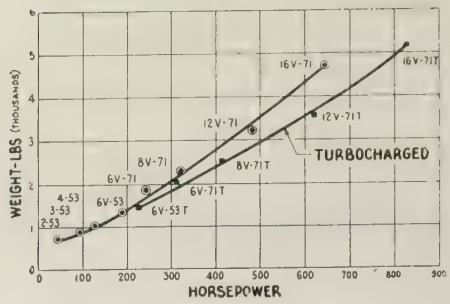

Fig. 8 — Weight and horsepower of new F-to-F cast-iron engines, turbocharged

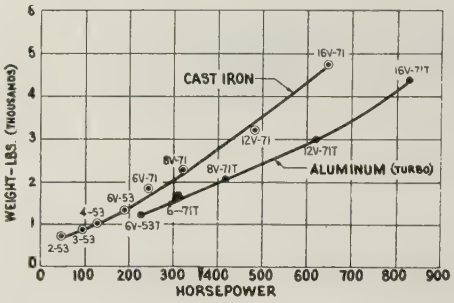

Fig. 9 — Weight and horsepower of new F-to-F engines

cation required it. Inasmuch as the mechanics of turbocharging a diesel is a subject in its own right, no attempt will be made to cover it in this paper.

The second basic requirement was that all of our new engines would be as versatile as the present 71 line. They are, infact, even more versatile because the balance and/or cam shafts are exposed on the front of the engine and available for driving accessories.

The third requirement was that the new engines be conservatively rated and, therefore, give life between overhauls equal to or better than present production engines. This we believe has been fully achieved and will be claried later in the paper.

For these two new lines of engines the 2-stroke cycle, uniflow design, was again chosen because we believe it has three major advantages:

1. More horsepower per cubic inch displacement.
2. Higher horsepower-to-weight ratio.
3. Higher horsepower to physical volume ratio.

These advantages are further amplified by the inherent size and weight-saving characteristics of the "V" configuration.

The 2-stroke design is also particularly suited to a series of engines all having the same vee angle, which has an obvious and important tooling advantage. The standardized vee angle is practical, as illustrated in Fig. 4, because the 2-stroke engine has a firing impulse in every cylinder for each revolution of the crankshaft, and is equivalent in torque smoothness to a 4-stroke having twice as many cylinders. As a result, unequal firing order is not as significant in the 2-stroke as in the 4-stroke engine.

The uniflow design was chosen in preference to the loop or cross-scavenged design, because of its increased effective stroke and ability to develop between 30 and 35% more power per cubic inch of dis-

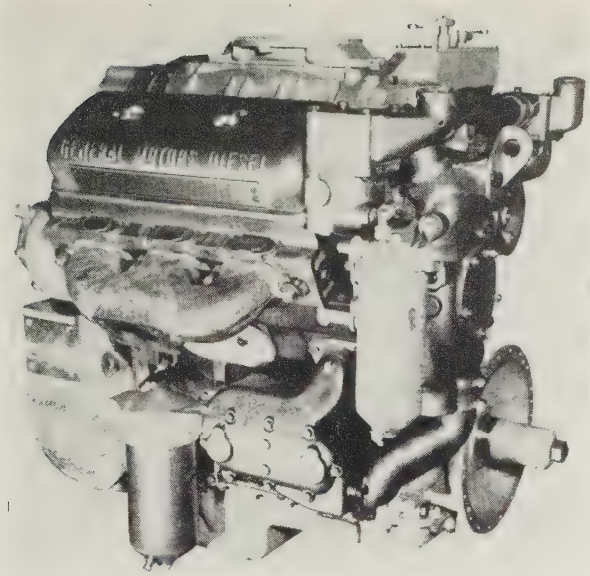

Fig. 10 — 6V-71

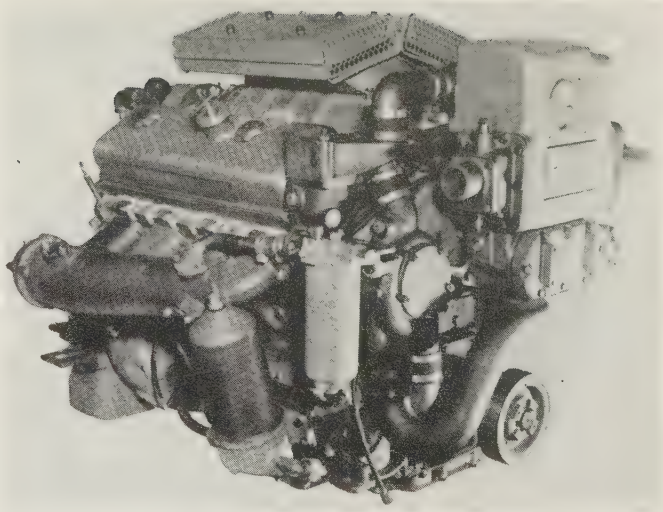

Fig. 11 — 8V-71

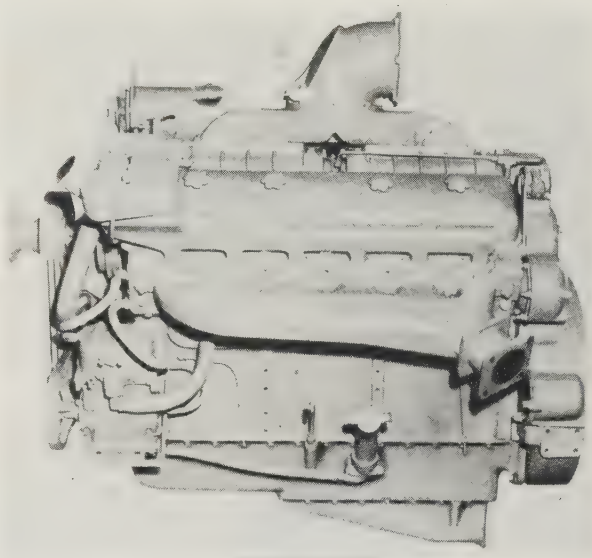

Fig. 12 — 12V-71

placement.

We wish to point out at this time that all horsepower ratings given in this paper, whether indicated on the chart or not, are at 0.0684 lb/cu ft, dry air density at an air temperature of 90 F and barometric pressure (dry) 28.33 in. of Hg. This base line is very comparable to the one proposed by the SAE Diesel Engine Test Code Committee which recommends: barometric pressure (dry) 29.5 in. of Hg, 500-ft, altitude, 50% relative humidity, and 85 F air temperature, which gives 0.07 lb/cu ft dry air density. We believe base lines such as these are more realistic for comparison of diesel engines.

The graph of Fig. 5 shows the power range of the new, all-purpose engine line. The length of the bar covers the horsepower range over which each engine will be applied, starting with the lowest continuous rating and progressing to its maximum output. The horizontal cross-hatched portion represents the range of continuous ratings and the stippled portion the range of industrial, intermittent, and maximum ratings. As is evident from this graph, the power range from 24–1292 hp is well-covered.

A graphic picture of the weight-to-horsepower comparison between present engines and new engines, and new engine combinations, is made in Figs. 6–9. Fig. 6 shows the relative horsepower and weight of our new engines as compared to production engines. "F to F" means a fan-to-flywheel engine, which includes such items as starter, generator, fan and drive, flywheel and housing, air and exhaust manifold, and fuel and lube oil filters. The curves graphically reflect weight reductions achieved in the new line, and the horsepower range which has been approximately doubled for single engine configurations. The curves of Fig. 7 illustrate a further weight reduction of approximately 20% by use of an aluminum block, flywheel housing, and various small castings. Fig. 8 illustrates the additional power that can be obtained by turbocharging the new engines, which would reflect approximately 25% increase in output throughout the line. The economics of turbocharging the new line of engines below the 6V-53 does not appear justifiable at the present time. Fig. 9 represents the ultimate that we believe can be achieved at the present time by turbocharging the aluminum engines mentioned previously. This reflects approximately 40% increase in horsepower per pound over the basic cast-iron engine.

The new 6V-71 (Fig. 10) is 40% shorter and 15% lighter than the in-line 6-71 and is particularly suited to new truck design trends. Intermediate between the 6-71 and 6-110 models, the new 8V-71 (Fig. 11) will provide for many applications a compact higher powered engine than is now available, especially for marine use, and for transit and parlor coach applications with their rising air-conditioning and propulsion requirements. The 12V-71 (Fig. 12) is a conservatively rated "work horse" to meet earthmoving, petroleum, and marine applications above the turbocharged 6-110T line. A graphic example of space and weight saving is obtained in Fig. 13 by comparing the new 12V-71 with the present 6-110, itself smaller and lighter than its competition. This comparison shows a 30% increase in power and

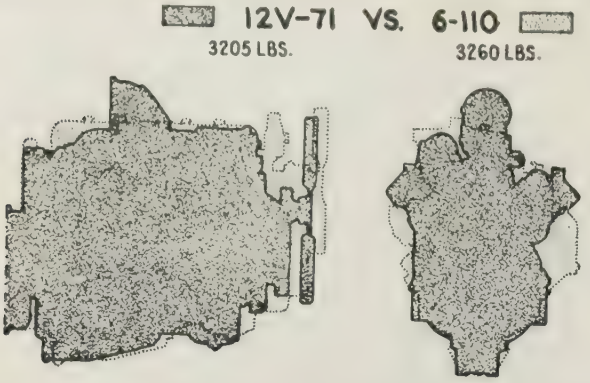

Fig. 13 — Size comparison of 12V-71 (3205 lb) versus 6-110 (3260 lb)

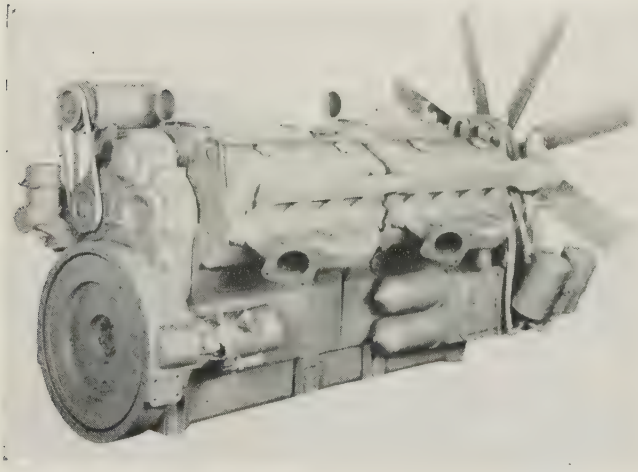

Fig. 14 — 16V-71

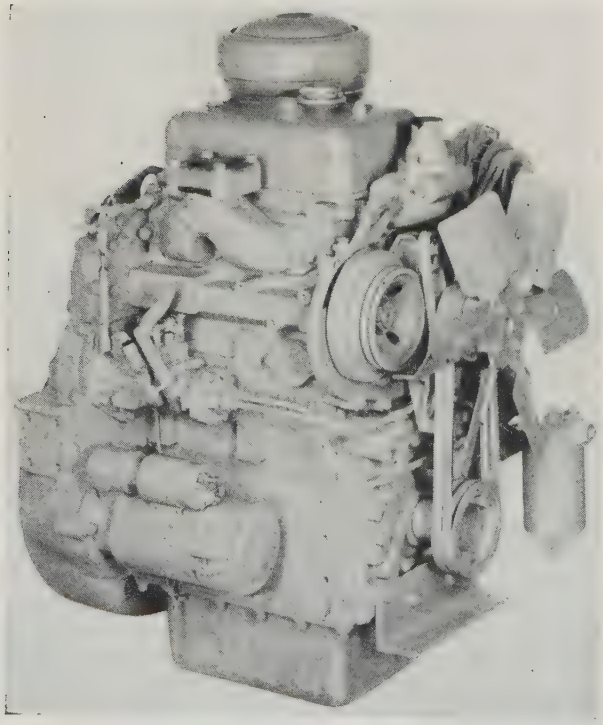

Fig. 15 — 2-53

displacement for the vee engine, but with overall weight and volume virtually unchanged. The 16V-71 (Fig. 14) now under development will extend the single-engine line to 646 bhp nonturbocharged and ultimately to 826 bhp turbocharged.

The need for small, light, versatile models in a wide speed range is met by the $3\frac{7}{8} \times 4\frac{1}{2}$ in. Series 53, also made up of durably rated, economy designed engines. An in-line 2-53 (Fig. 15) offers a small low-cost engine for applications below the 2-71 power range, such as lift trucks, small generator sets, and the light tractor field. The 3- and 4-53 in-lines (Fig. 16) replace the Model 4-51, and are compact, higher speed complements to the 2-, 3-, and 4-71 models, retaining their features of optional rotation and component location with added provision for front-end accessory drives.

The new 6V-53 (Fig. 17) is a small, high-speed engine with power intermediate between the 4-71 and 6-71, particularly suited to medium-truck and marine applications. The 2800-rpm ratings of the 3-, 4-, and 6V-53 bring them into contention with gasoline competition.

Up to this point we have discussed the engines in rather general terms in order to give you a picture of our overall program. The balance of the paper will be devoted to "specifics" of the engines.

Engine Details

Three principle ground rules were laid down for the new Series V71 and 53 engines:

1. Maximum fuel economy at conservative ratings.
2. Maximum use of standard parts, particularly those of higher service usage.
3. Minimum weight and space per horsepower.

1. Maximum Fuel Economy at Conservative Ratings

To achieve maximum fuel economy at conservative ratings, it was decided that the design and performance characteristics of the existing 71E engine would be incorporated in the new V71 and 53 engines.

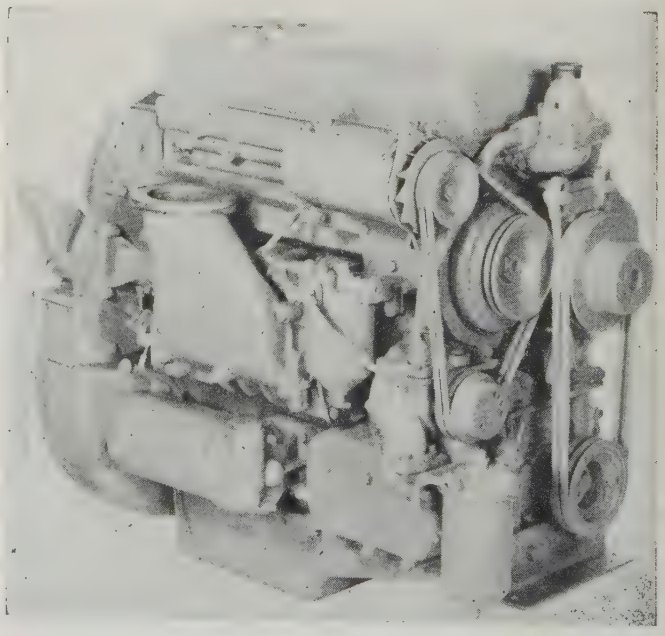

Fig. 16 — 4-53

Design Features

Scavenging — A uniflow scavenged 2-stroke cycle engine has one unique advantage over all other reciprocating powerplants of commercial design. By inducting air through inlet ports around the entire lower periphery of the cylinder and exhausting through the cylinder head, maximum airflow areas are achieved and pumping losses minimized. This feature of the uniflow engine was exploited as fully as possible in the development of the 71E engine as shown in Fig. 18. Inlet ports were changed from our standard "Figure 8" design to a longer, oval design in the "E" engine, and total inlet port area increased by 58%. Exhaust areas were increased by 23% in the four-exhaust-valve cylinder head compared to the two-valve design used in the standard engine. The combined effect of the enlarged inlet and exhaust areas increased the effective orifice area of the engine from 2.69 to 3.42 sq in., or 27%. With the increased area provided for airflow, the discharge pressure against which the scavenging blower worked was reduced and engine air consumption would have been increased. However, since the amount of fuel the "E" engine is required to burn is substantially reduced, air delivery would have been far higher than necessary, and this made possible a reduction in blower speed. On the in-line 71E a major reduction in blower drive ratio could not be achieved by gear train changes without a revision in gear centers, which would destroy interchangeability of timing gears, flywheel housing, and blower components between the standard and "E" engine. It was decided, therefore, to incorporate a set of reduction gears within the blower assembly itself. The reduction chosen changed the blower drive ratio from twice engine speed to approximately 1.7 times engine speed. Fig. 19 shows that by means of these changes in flow area and blower, a reduction of 18.5 hp (57%) in power required to drive the Model 6-71 scavenging blower was achieved at rated speed, while still maintaining more than ample air delivery as indicated by the scavenging ratio curves shown.

Fire Ring Piston — In a uniflow scavenged engine such as the 71, it is usually assumed that the top edge of the piston controls the intake port timing, and while this is true qualitatively, the piston does not provide a complete seal as shown in Fig. 20. There is a finite clearance between the rim of the piston and the cylinder wall which provides a leakage path until the compression rings seal the ports. The area of this leakage path varies with the rim temperature and its major location is opposite to the direction of piston side thrust. In order to provide a sharper port cutoff in the "E" engine, a fire ring was added ⅛ in below the top of the piston. In addition to providing the maximum possible effective compression and expansion strokes for any given inlet port height, the fire ring has several other beneficial effects:

1. As the piston approaches upper dead center on the compression stroke, all of the air in the cylinder is trapped above the fire ring and is readily available for combustion. Radial air velocity into the combustion chamber is also increased.

2. Early in the expansion stroke when gas temperatures and pressures are highest, the fire ring reduces the area of cylinder wall exposed to the burning mixture, thereby minimizing heat losses. The surface to volume ratio of the 71 cylinder at upper

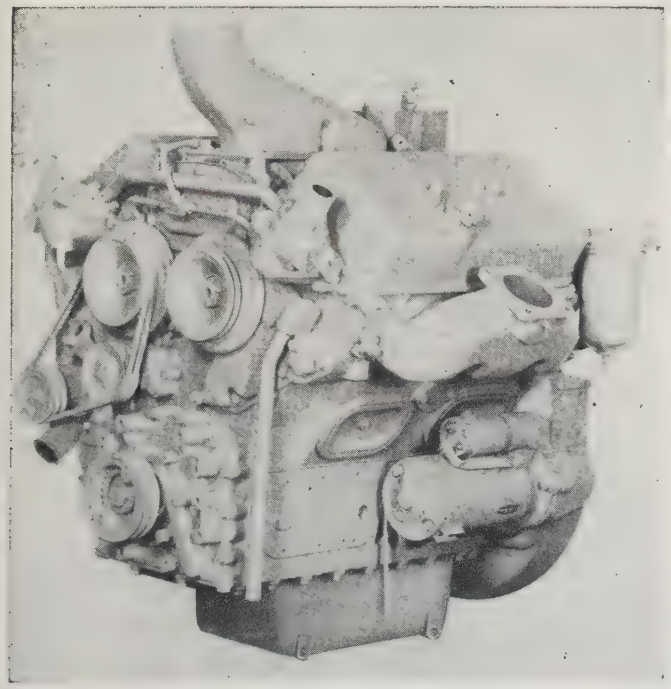

Fig. 17 — 6V-53

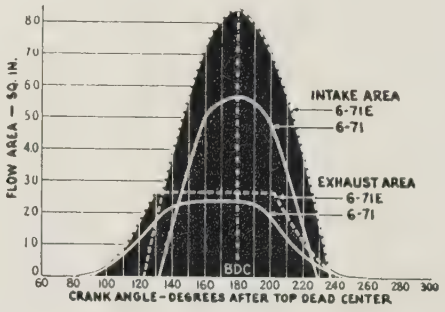

Fig. 18 — Intake and exhaust flow areas, 6-71 versus 6-71E

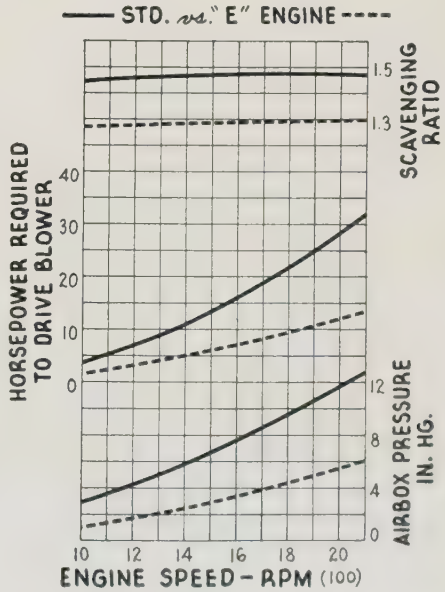

Fig. 19 — Scavenging data of 6-71

dead center was reduced 31% by addition of the fire ring.

3. The rim of the piston is normally its hottest spot because it receives heat from the hot gas on all sides; and under heavy load, it is subject to some "wiredrawing" effect after the rings uncover the inlet ports on the expansion stroke. Both of these effects are greatly reduced by the fire ring, and it was found that its addition to the "E" piston brought the temperature of the rim down to the same level that existed in the center of the bowl, thereby providing a uniform temperature distribution across the entire combustion chamber.

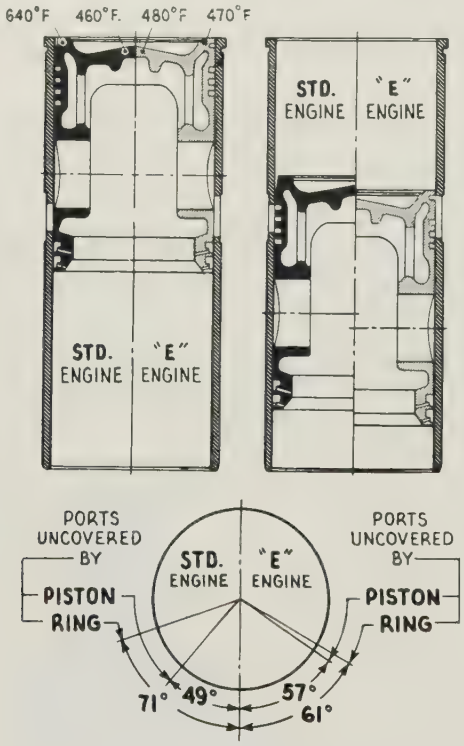

Fig. 20 — Effect of fire ring on port timing and piston temperature (60 cu mm, 2100 rpm)

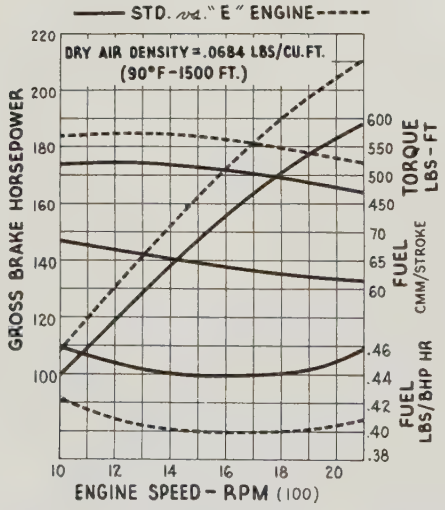

Fig. 21 — Full-throttle performance of 6-71 at equal fuel input

The above effects tend to improve indicated thermal efficiency, particularly under heavy load; and, therefore, permit a given horsepower to be developed with less injected fuel.

Injection — With the greatly increased airflow areas and reduced blower delivery which were discussed previously, the whole scavenging pattern of the engine had been changed. Pressure drop across the inlet ports had been reduced and, therefore, the inlet velocity and its tangential component were also reduced and made more uniform throughout the engine speed range. In addition, conditions of radial velocity into the combustion chamber and temperature distribution across the chamber had been greatly changed, all of which required that the injection characteristics be rematched to the new conditions of velocity and temperature. While all of these conditions are known qualitatively, precise data as to instantaneous temperatures, pressures, and velocities at all points in the combustion space under varying speed and load conditions are not known, and complete knowledge of the mechanism of combustion in a diesel cylinder is lacking. Matching injection characteristics to a given set of combustion-chamber conditions is, therefore, a most unscientific process of trial and error with only slight guidance from what is known of combustion-chamber conditions. Optimum combustion in the "E" engine was obtained with eight spray holes of 0.0055-in. diameter and an included

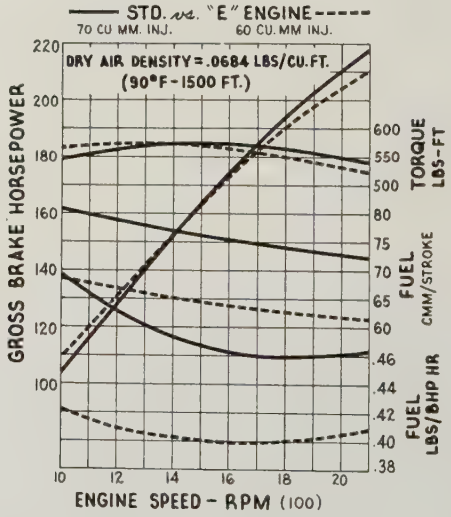

Fig. 22 — Full-throttle performance of 6-71 at approximately equal power

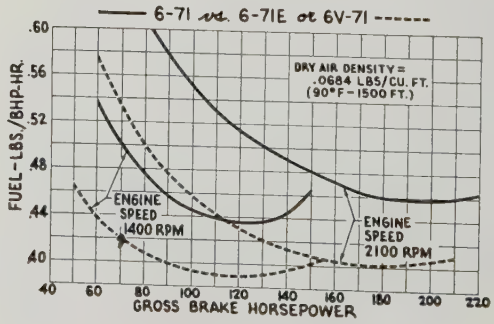

Fig. 23 — Comparative fuel consumption of 6-71

spray angle of 165 deg. The spray tip used in the standard engine has seven spray holes of 0.006-in. diameter with an included angle of 155 deg.

Performance Features

The cumulative effect of the design changes discussed above is indicated in the next group of figures. In the full-power comparison of Fig. 21, it is seen that with an equal rate of injected fuel, the "E" engine develops between 9 and 12% more brake horsepower than does the standard engine, which, of course, results in a 9–12% improvement in fuel economy. Of perhaps greater importance is the comparison of the standard and "E" engines in Fig. 22. We would call this a comparison of the engines at equal performance, for although the "E" engine develops some 8 hp less at rated speed, its improved torque and altitude performance make it the equal, performance-wise, of the higher power, standard engine. All further comparisons of the standard and "E" engines will be made on the same basis as shown in Fig. 22, that is, a 70-cu-mm standard engine versus a 60-cu-mm "E" engine. The magnitude of the part-throttle fuel consumption improvement at engine speeds of 1400 and 2100 rpm is shown in Fig. 23. Based on a typical highway hauling operation of 3000 hr or 100,000 vehicle miles per year, the annual fuel saving obtained with the "E" engine amounts to about 4000 gal per vehicle.

Thermal Efficiency — The improvement in full-throttle indicated and brake thermal efficiency (Fig. 24) has several benefits in addition to the obvious ones of reduced fuel costs and cleaner exhaust. The first of these additional benefits is superior performance at the higher altitudes, which is shown in Fig. 25. Because it burns less fuel and burns it more efficiently, the "E" engine needs less air for combustion; therefore, the rate of power loss with increasing altitudes and decreasing air density is considerably less than for the standard engine.

Fig. 26 shows the second additional benefit of the improvement in thermal efficiency. Reduced internal friction makes it possible for the "E" engine to develop brake mean effective pressures approximately equal to the standard version at very much reduced indicated mean effective pressures. Fig. 27 shows representative pressure-time diagrams of the two engines at a brake output of approximately 197 hp and at a speed of 2000 rpm. The reduced peak compression pressure of the "E" engine

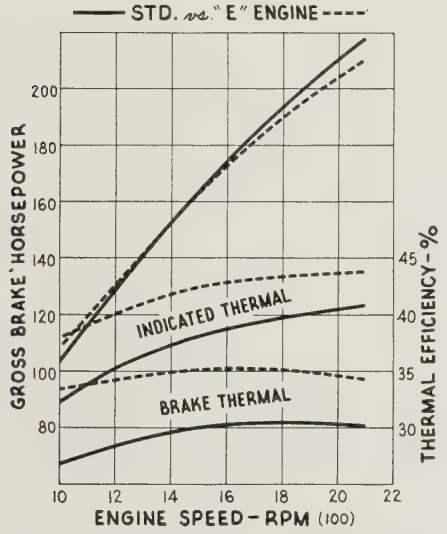

Fig. 24 — Full-throttle thermal efficiencies of 6-71

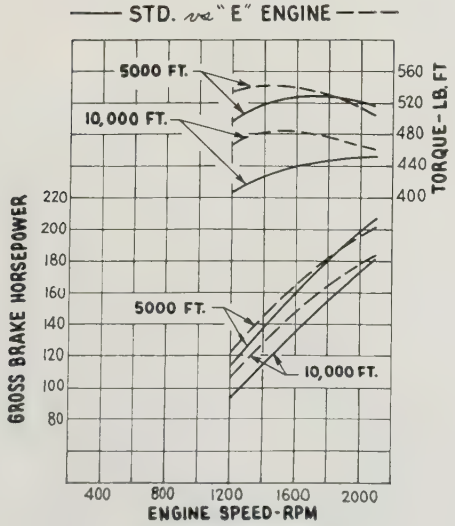

Fig. 25 — Altitude performance of 6-71

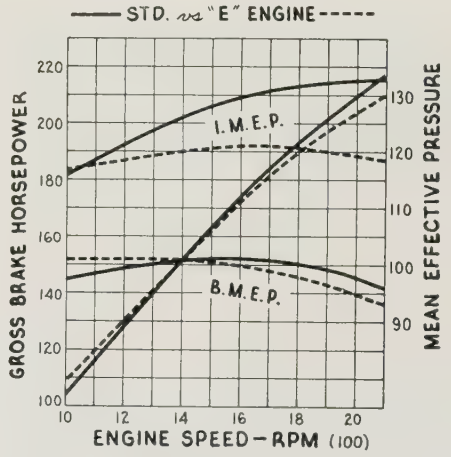

Fig 26 — Mean effective pressures at full throttle of 6-71

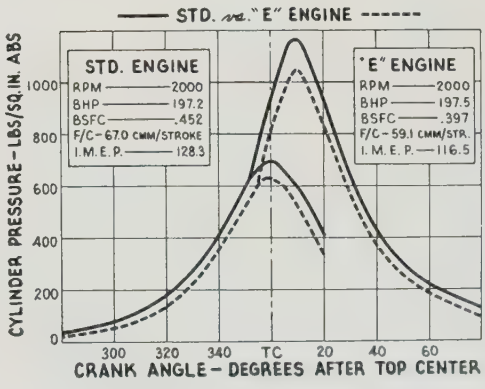

Fig. 27 — Pressure-time diagrams of 6-71

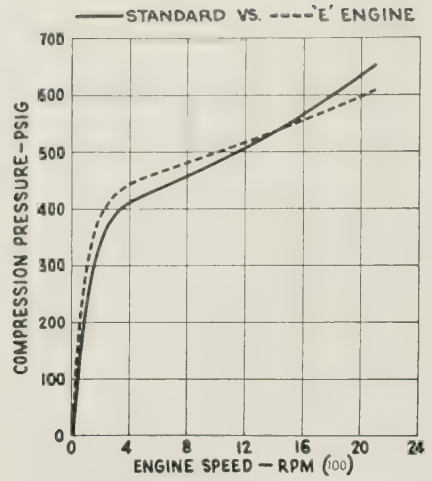

Fig. 28 — Motoring compression pressures of 6-71

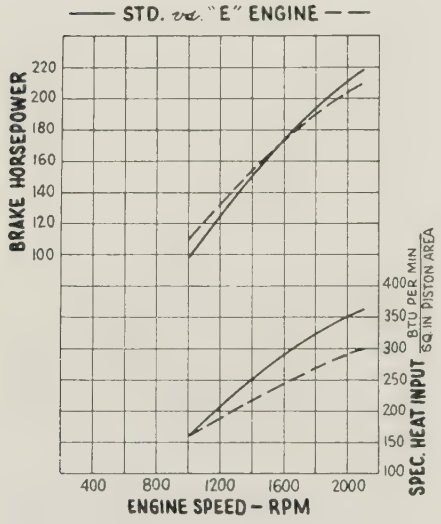

Fig. 29 — Relative thermal loading of 6-71

is attributable to its lower cylinder pressure at the start of compression resulting from its lower charging pressure. The lower peak and mean firing pressures are, in turn, due partly to the lower compression and partly to a reduced fuel rate. The mechanical compression ratio of the engine, on the other hand, has actually been slightly increased and compression heat losses minimized. Both of these effects are due entirely to the use of the fire ring. The combination of increased mechanical pressure ratio, plus reduced charging pressure, alters the shape of the motoring compression pressure curves as shown in Fig. 28. At cranking speeds, charging pressure is so nearly atmospheric that it does not affect the peak compression to any extent. The increased mechanical compression ratio of the "E" engine, therefore, provides appreciably higher compression at cranking speeds as shown, and therefore, easier starting. For an unaided 20-sec start, the "E" engine can tolerate an ambient temperature 15 F lower than the standard engine. It has, thus, been possible to improve the starting ability of the engine, while at the same time reducing gas pressures in the high power range.

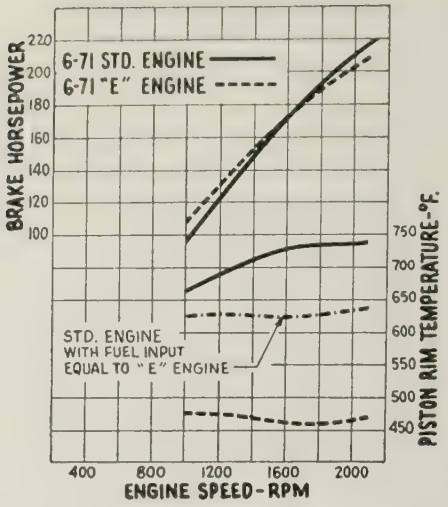

Fig. 30 — Effect of reduced thermal load and design changes on maximum piston temperature at full throttle

The third additional benefit of the thermal efficiency improvement is reduction in thermal load. In Fig. 29 thermal load on the firebox components is expressed in terms of the heat equivalent of the injected fuel rate per unit of exposed area. The reduced fuel rate of the "E" engine is shown to result in 15% less maximum thermal load on the piston, cylinder head, and cylinder walls. The effect of this thermal load reduction on one of the firebox components is shown in Fig. 30. It is seen here that the reduction in thermal load lowers by 100 F the maximum piston temperature occurring at the rim. An additional reduction of 170 F is obtained through use of the fire ring as explained previously. Similarly, the maximum rate of heat transfer to the cylinder head and exhaust valves has been decreased, thus reducing the temperature range through which they cycle.

New Engine Performance

Development of the GM Series 71 "E" engine to date has yielded the following:

1. A cleaner exhaust with equal power.
2. Greatly improved fuel economy.
3. Longer life.
4. Superior altitude performance.

These features made it mandatory that the design of the new V71 and 53 Series engines be predicated on the basic 71E design concepts. It was anticipated that the performance characteristics of the new 6V-71 would be identical to those of the in-line 6-71E, and tests of the new engines have borne this out (Fig. 31).

Since the 53 engine was designed to be geometrically similar to the 71E, the preliminary performance estimates assumed that for equal fuel input per cycle per cubic inch, the 53 and 71E cylinders would develop equal bmep at equal mean piston speeds. In Fig. 31 a comparison is made of the 6V-53 and 6V-71 performance with equal fuel input per cycle per cubic inch. The principle conclusion to be drawn is that if true geometric similarity with an existing engine is maintained, the performance of

a new engine design can be predicted with remarkable accuracy. In Fig. 32 a similar comparison is made for variable throttle at two different piston speeds.

We have shown performance data for 6-cyl engines only, and rather than present data for the entire line of 53 and V-71 engines, let it suffice to say that performance per cylinder of the other engines is the same as the sixes, except for small variations in mechanical efficiency with different numbers of cylinders.

2. Maximum Use of Standard Parts

Standardization on present 71E engine pistons, rings, wrist pins, and cylinder liners was carried further in the V-71's to make maximum use of parts already in production and widely distributed in the field (Fig. 33). Interchangeability was extended to cylinder heads, rocker covers, exhaust manifolds, timing gears, injectors, valves, injector and valve operating mechanisms, flywheels, and many other high volume items, providing obvious manufacturing and service advantages. The Series 53 follows a similar pattern of standardization and even uses some "71" parts and subassemblies such as the injector, push rods, cam followers, throttle control parts, and rear-mounted accessories.

Much existing equipment and tooling was utilized for similar new engine parts, including flywheel housings, Roots blowers, connecting rods, and camshafts. This high degree of design standardization has permitted and justified extensive new multistation machine tooling (Fig. 34), particularly in the case of the cylinder block and head lines.

3. Minimum Weight

Minimum weight was achieved in the new lines by a general reduction of casting walls to 3/16 in. wherever consistent with good structure and foundry requirements. It is interesting to note in

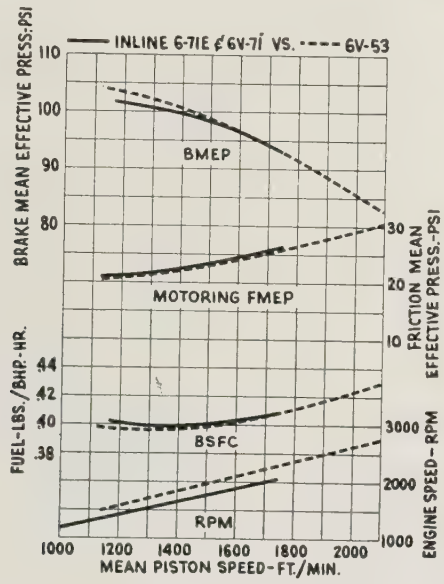

Fig. 31 — Full-load performance comparison at equal fuel input/cu in./cycle

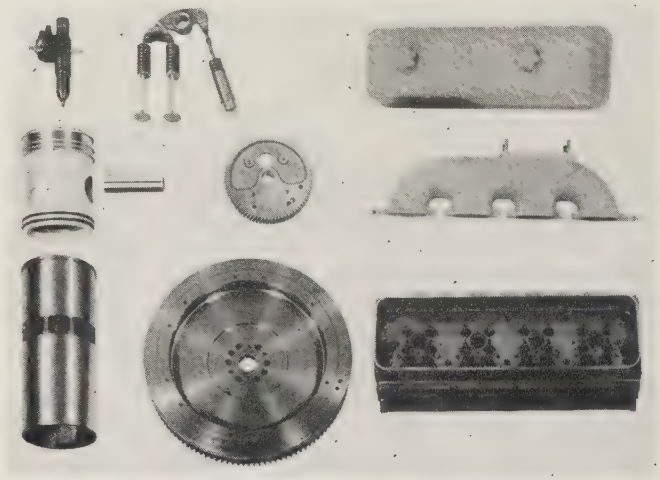

Fig. 33 — Standardization, V-71 and 71E parts

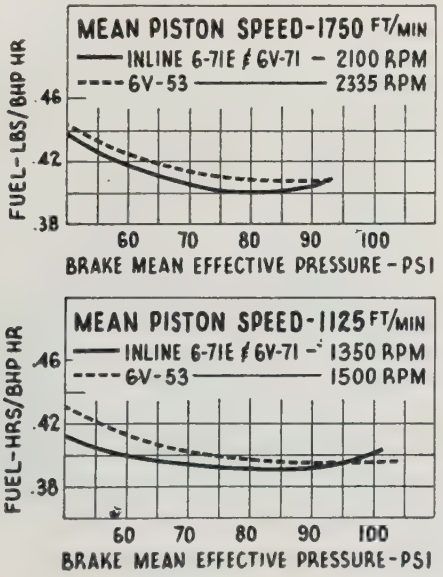

Fig. 32 — Part-throttle performance

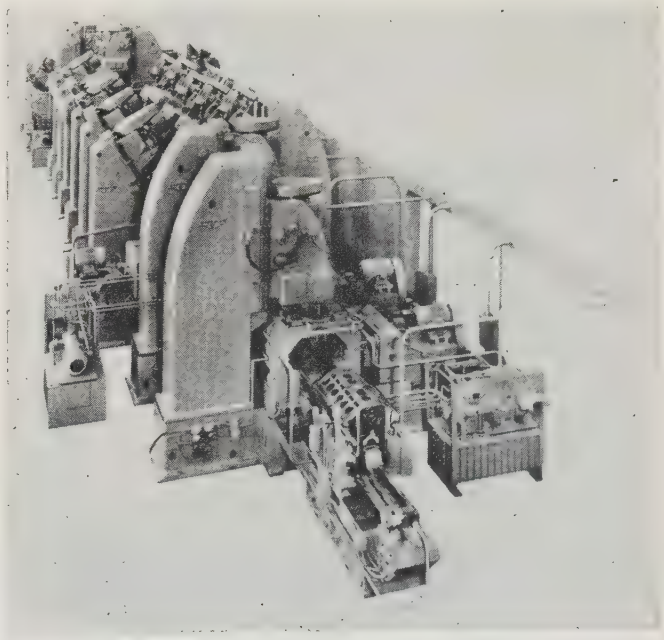

Fig. 34 — Special drilling machine, V-71 block

Fig. 35 that in a weight breakdown of a typical 6-cyl "iron" engine, almost 50% of the total weight lies in the cylinder block, cylinder head, crankshaft, and flywheel housing. In the new 6V-71 engine the inherent weight savings of the vee block configuration, the short crankshaft, and careful attention to lightweight construction, all combined to reduce total weight more than 300 lb. The results (shown in Fig. 36) are pounds per horsepower figures as low as 6.7 for the 12V-71, dropping to less than 5.5 with an aluminum block, flywheel housing, and various small castings, as previously mentioned.

The new 3-53 and 4-53 engines show sizable weight per horsepower gains not only at their 2800-rpm rating, but at the lower speeds of the present in-line engines as well. However, a high specific weight in the case of the smallest engine in the lines, the 2-53, plainly stems from a small displacement, coupled with the necessary full complement of external components (Fig. 37). In addition to having one of everything that the big engine has, the small engine's flywheel and housing constitute a greater proportion of its total weight.

Series V-71

With the ground rules of Series 71E engine configuration, maximum parts interchangeability, and minimum weight, the V-71's actually began to design themselves. The transverse cross-section of Fig. 38 shows how the Roots blower was placed on top of the block in the middle of the vee; use of existing 71 cylinder heads then placed the exhaust manifolds on the outboard sides and the push rods and camshafts on the inboard sides of the banks. The two contrarotating camshafts, permitting complete balance of primary rocking couples, dictated the 63½-deg vee angle by virtue of their established timing gear size and fixed location relative to the crank center. By use of this slightly unconventional vee angle, the goals of parts standardization and minimum engine width were achieved with no loss in operating smoothness.

The three basic box sections of the block consist of the crankcase, airbox, and water jackets, with internal tension members tying through from the head bolt bosses to the main bearing bulkheads. For added longitudinal and transverse rigidity and bore alignment, the tension members are tied in by a "shelf" at the tops of the lower cylinder liner bore stock.

Cylinder Liners — The dry cylinder liner used in the in-line Series 71 was selected for the V-71 because of paramount considerations of production and service standardization. It should be noted that water cooling is utilized only above the cylinder air inlet ports. Cooling of the lower cylinder section is aided by scavenging airflow and by oil jet cooling of the piston crown by means of a drilled connecting rod and spray orifice.

The length of the vee engines (Fig. 39) was set up by the established 3-, 4-, and 6-71 cylinder heads

ENGINE PARTS	6-71	6V-71
CYL. BLOCK ASSEM.	600	430
CYLINDER HEAD	168	171
CRANKSHAFT	162	138
FLYWHEEL HSG.	112	112
PISTON & ROD ASSEMS.	87	80
FLYWHEEL	75	75
BLOWER ASSEM. (ALUM.)	69	64
STARTER & GENERATOR	117	117
CRANKSHAFT DAMPER	52	NONE
VALVES & GEAR	49	53
GEAR TRAIN & BRGS.	45	42
CYLINDER LINERS	44	44
FRONT COVERS	46	28
EXHAUST MANIFOLD	32	32
CAM &/or BAL. SHAFTS	40	25
WATER MANIFOLD	19	NONE
OIL PUMP & OIL PAN	34	20
OIL COOL'R HSG & ADAPT'R	28	20
INJECTORS & GOVERNOR	22	20
MISCELLANEOUS	389	384
TOTAL	6-71 – 2190 LBS.	6V-71 – 1855 LBS.

(CAST IRON - LBS)

Fig. 35 — Weight breakdown, 6-71 and 6V-71

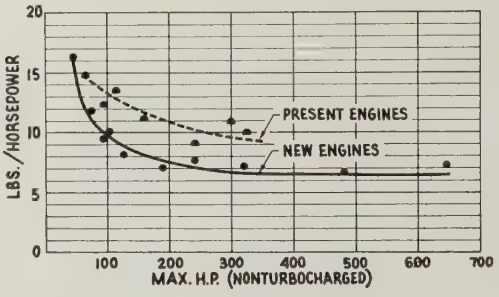

Fig. 36 — Weight versus maximum horsepower of new and present engines

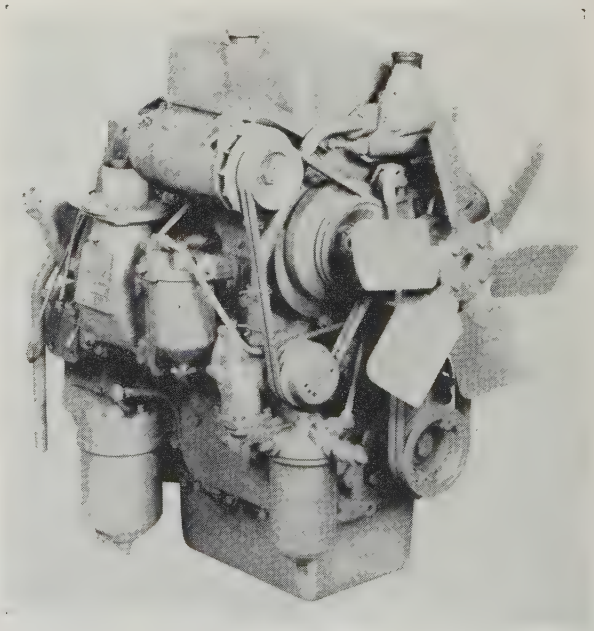

Fig. 37 — 2-53

with their 5¾-in. cylinder center distance. Even with the left bank staggered 1.2 in. ahead of the right bank and some additional length due to necessary water passage coring at the front, the V-71 blocks are less than 2 in. longer than their in-line counterpart with half the number of cylinders. The V-71 blocks are made in three sizes, 6V, 8V, and 12V; the 16V consists of two 8-cyl blocks attached together "front to front."

Initially a barrel-type crankshaft was considered to meet the fixed cylinder center limitations, but a conventional, large journal, side-by-side rod configuration proved both practical and more economical. With the cylinder spacing (Fig. 40) maintained the same as the standard Series 71 engine, the crankcheek thickness of the V-71 engine was necessarily reduced. This reduction was required to increase the length of the crankpin to accommodate the two side-by-side connecting rods. In addition to the reduced crankcheek thickness, the useful length of the crankpin journal was increased by using minimum fillet radii and allowing minimum grinding wheel-to-crankcheek clearance. The minimum fillet radius from a manufacturing standpoint was determined to be 0.100–0.130 in., which represents 1/32-in. reduction from the standard in-line engine practice.

Since each crankthrow of the new engines was required to carry the loads of two cylinders instead of one, both the crankpin and main journals were increased in size. This increase in diameters was from 3.5 to 4.5 in. on the main journals and from 2.75 to

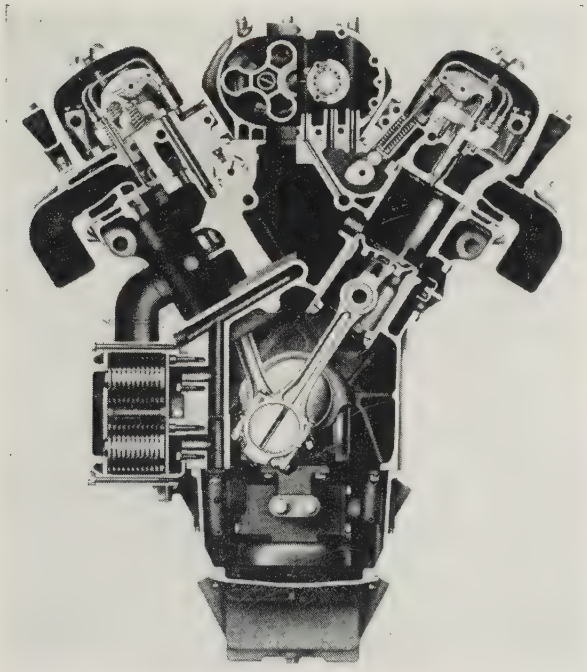

Fig. 38 — Transverse cross-section of 12V-71

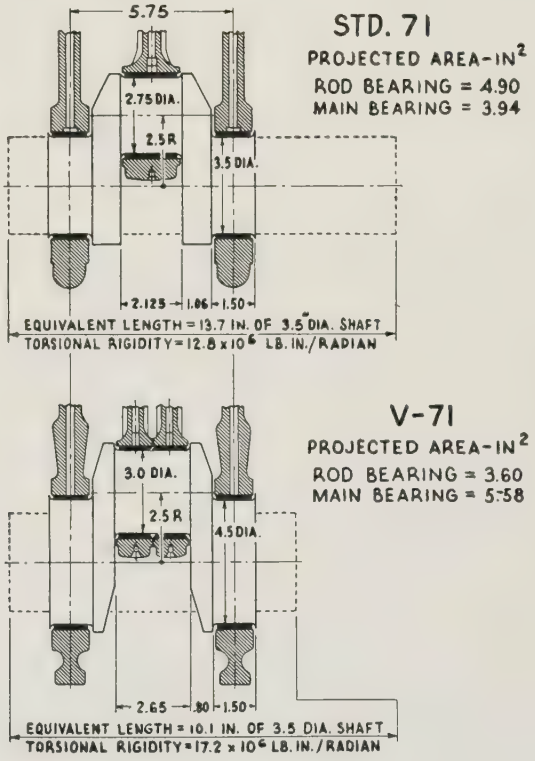

Fig. 40 — Comparison of crankthrows

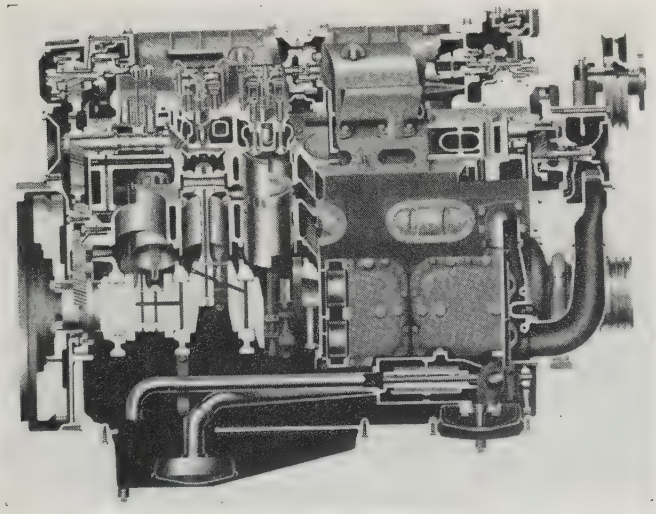

Fig. 39 — Longitudinal view of 12V-71

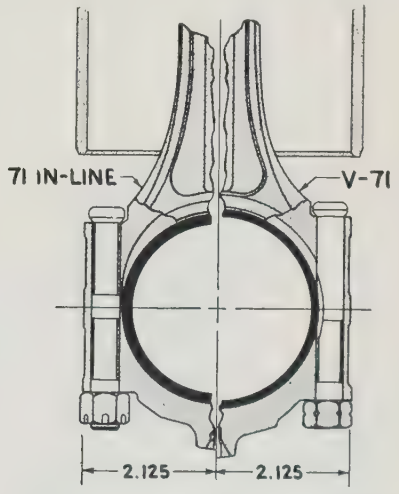

Fig. 41 — Connecting rod comparison

3.0 in. on the crankpins. The diameter of the crankpin had a definite limitation (Fig. 41); the big end of the connecting rod had to be able to pass through the 4¼-in. cylinder bore. By decreasing the bearing shell thickness 1/32 in. and notching the bearings at the split line for clearance with the cap bolt, the ¼-in. increase in rod bearing diameter was achieved. It was necessary, however, to equalize areas on the joint face of the cap to eliminate bearing distortion that resulted from unbalanced unit loading by the cap bolt.

Stress analyses were made to determine if the strength of the new crankshaft with its reduced crankcheeks would be satisfactory. The resistance of the crankshaft to bending fatigue (Table 1) was evaluated for the critical section, from the crankpin fillet through the crankcheek to the main journal fillet. This showed that a section modulus could be obtained to reduce bending stress 10% below that of the proven in-line 6-71 crankshaft. The ability of the crankshaft to transmit torque was evaluated by comparing the shear stresses in the crankcheeks nearest the flywheel end, when the maximum instantaneous torque was being transmitted. The increased shear also shown in Table 1 was secondary, since the shear stresses were of much lower magnitude than the bending stresses.

The large overlap obtained with the increased journal diameters, and the increased width of the elliptical crankcheek are shown in Fig. 42. Following current practice, the resistance to bending fatigue was increased by rolling the fillet areas of the journals to create a residual compressive stress in the crankshaft where the maximum bending stress occurs. It is of interest to note here that our standard method used to evaluate the quality of fillet rolling on sample 6-71 engine crankshafts is to operate the engine at full load with the No. 2 main bearing removed. This imposes a stress almost three times the normal, and 100-hr operation without fracture constitutes proof that the crankshaft processing is satisfactory.

Main and Connecting Rod Bearings — After the crankshaft was judged to be sufficiently strong to carry the loads to be imposed upon it, bearing loads were calculated to insure that the unit bearing pressures agreed with accepted practice on our standard engines; Fig. 43 illustrates this to be true. Many calculations were made to determine the highest loaded bearings, and to determine if it would be desirable to decrease the loads by placing counterweights on the crankshaft adjacent to the heaviest loaded bearings. These tedious and time-consuming calculations were only practical because the actual calculations were carried out by an I.B.M. 704 electronic computer.

Table 2 shows that by taking advantage of the increased journal diameters and by the strategic placement of counterweights, conservative peak unit bearing pressures were obtained, and mean pressures were achieved that were within the 1000–1400 psi limits of good practice, even for engine loads 15% above normal intermittent ratings.

Another consideration of prime importance in the design of a crankshaft is the torsional vibration characteristic. Usually it can be said that a crankshaft that is torsionally correct will not lack in strength in either bending or torsion. The torsional vibration characteristics of the Models 6-71 and 12V-71 crankshafts compared favorably as shown in Table 3. Use of a single, viscous damper of the large size presently in production, cut the 12V-71 torsional amplitude in half, bringing it to a satisfactory 0.42 deg double amplitude.

V-71 Engine Balance — In the balance of 2-stroke engines, it is important to consider disturbances due to the reciprocating action of the piston masses. These disturbances are of two kinds: unbalanced forces and unbalanced couples. These forces and couples are considered as primary or secondary according to whether they occur at engine speed or twice engine speed. Although it is possible to have unbalanced forces or couples at frequencies higher than the second order, they are of small consequence in comparison to the primary and secondary forces and couples.

Since it was desirable to maintain the same vee angle in all the engines in the new series, an extensive investigation was made of balance requirements of 63½ deg vee angle engines having 6, 8, 12 and 16 cyl. Many crankthrow arrangements were considered and the resulting effects upon crankshaft balance, firing interval, and engine balance were evaluated. The final selection for each engine was that which gave the best balance among all the considered factors.

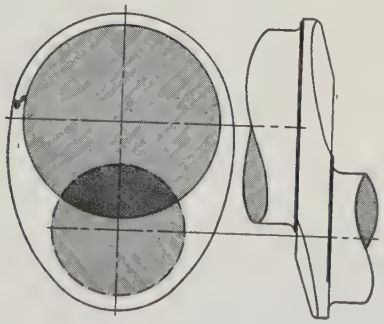

Fig. 42 — Crankshaft web construction and journal overlap

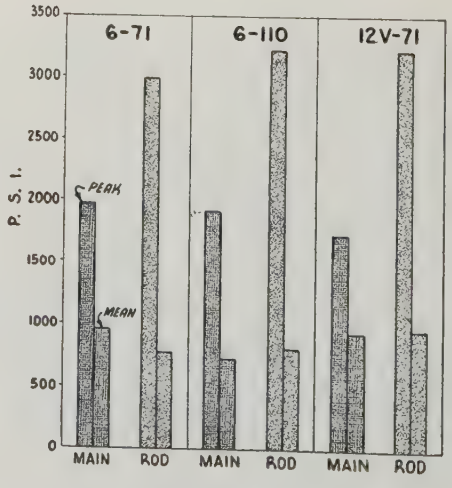

Fig. 43 — Bearing load comparison at maximum nonturbocharged ratings (maximum loaded bearings shown)

The Model 6V-71 engine crankshaft throw arrangment shown in Fig. 44 results in an engine which has inherently balanced primary and secondary forces and has a firing interval which deviates by only 3.5 deg from an even 60 deg. Balance of the primary rocking couples is accomplished by balance weights placed on the crankshaft and on the two camshafts, where they are conveniently made integral with the camshaft drive gears in the rear, and the accessory drive gear and pulley on the front of the engine. Rotating balance of the crankshaft is accomplished by the placement of counterweights as shown.

The selected crankshaft throw arrangement used in the Model 8V-71 engine (Fig. 45) resulted in balanced primary and secondary forces, and a balanced secondary rocking couple. The throws are equally spaced at 90 deg which results in an unequal firing order of 23.5 and 63.5 deg. The unequal firing order does not affect the engine torque fluctuation curve significantly because all cylinders fire during each engine revolution. The balance of primary rocking couples is accomplished in the same manner as on the Model 6V-71 engine. The rotating unbalance of the crankshaft again is corrected by the placement of counterweights. Additional counterweights are added on the second and forth main bearings to reduce the bearing loads.

On the Model 12V-71 engine crankshaft (Fig. 46), the three front and the three rear throws are equally spaced at 120 deg, but there is a phase angle of 30 deg between the two groups. This arrangement results in a firing interval which deviates by only 3.5 deg from 30 deg even firing. Both the primary and secondary forces are balanced by this arrangement, and the residual secondary rocking couple is small enough to be left unbalanced. The primary rocking couple is balanced, as before, by balance weights on the crankshaft and the two camshafts. Additional counterweights are placed on the crankshaft to balance the rotating weights and to reduce the magnitude of the bearing load on the center main bearing.

The Model 16V-71 engine is essentially two Model 8V-71 engines placed front to front. The first crankshafts have been fabricated by welding two 8V-71 crankshafts together with the fourth and fifth throws at a phase angle of 45 deg and spread apart by a distance 1.88 times the cylinder spacing. This gives a crankshaft that for all practical purposes is in rotating balance when the front, rear, No. 1 and No. 8 cheek counterweights are removed from each 8V-71 crankshaft. The physical balance of the crankshaft and additional balance weights on the

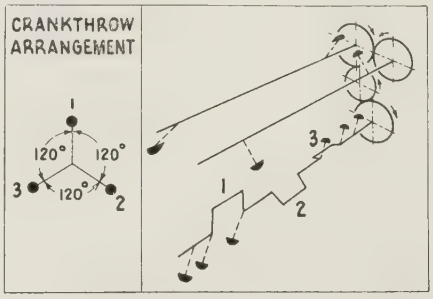

Fig. 44 — 6V-71 balancing system (primary couples are balanced with counterweights on camshafts and crankshaft; counterweights on crankshaft are for rotating and reciprocating balance)

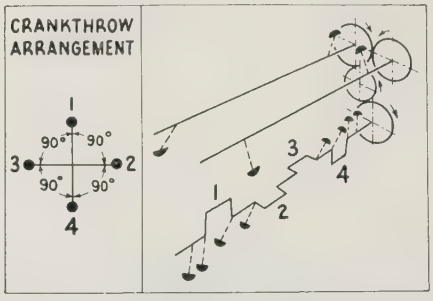

Fig. 45 — 8V-71 balancing system (primary couples are balanced with counterweights on camshafts and crankshaft; counterweights on crankshaft are for rotating and reciprocating balance and to reduce bearing loads on No. 2 and 4 bearings)

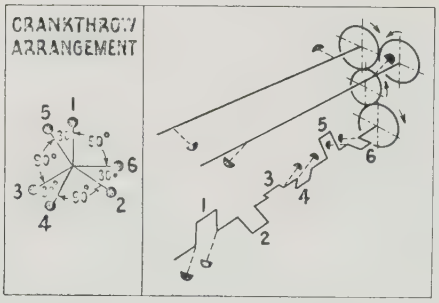

Fig. 46 — 12V-71 balancing system (primary couples are balanced with counterweights on camshafts and crankshaft; counterweights on crankshaft are for rotating and reciprocating balance and to reduce bearing loads on No. 4 main bearing)

Table 1 — Crankshaft Strength Comparison of 6-71 and 12V-71

Engine	6-71	12V-71
Crankcheek Section Modulus, cu.	0.93	1.18
Relative Bending Stress, %	100	90
Polar Section Modulus, cu. in.	1.57	2.00
Relative Maximum Shear Stress, %	100	122

Table 2 — Engine Bearing Load Comparison

Bearing	Highest Peak Pressure, psi	Highest Mean Pressure, psi
Connecting Rod	3220	960
6V Main	1790	965
8V Main	1810	900
12V Main	1740	990
16V Main	1810	970

Table 3 — Torsional Vibration Characteristics of 6-71 and 12V-71

Engine	6-71	12V-71
Crankthrow Stiffness, lb-ft/deg	18,700	25,000
Crankshaft Stiffness, lb-ft/deg	2,710	3,300
Crankshaft Natural Frequency (no dampers) vpm	13,000	12,000
Sixth Order Critical (no dampers), rpm	2,107	2,000
Crankshaft Natural Frequency (one large viscous fluid damper), vpm	8,400	9,000
Sixth Order Critical (one large viscous fluid damper), rpm	1,400	1,500
Amplitude at Front End of Crankshaft, deg double amplitude	0.40	0.42

camshafts balance the small primary couple; there are no primary or secondary forces. Fig. 47 is included for general reference to illustrate cylinder nomenclature and firing order.

Cylinder Heads — Of particular interest is the four-valve operating mechanism of the cylinder head (Fig. 48), which features the short push rod design and the standard roller cam followers of the in-line Series 71, but incorporates a new, stamped clevis-type bridge, actuating transverse pairs of valves. This simplified bridge eliminates difficult service adjustment procedures by automatically balancing valve lash, and reduces spring and high-speed-follow problems by virtue of its lightweight.

Only three different cylinder heads serve seven basic engines. A 3-cylinder head is used on the 6V-71; 4-cylinder heads are used on the 4-71E, 8V-71, and 16V-71; and 6-cyl heads are used on the 6-71E and 12V-71. In all designs, fuel supply and fuel spill passages (Fig. 49) are drilled in the head supplanting previous external, fabricated fuel manifolds. Greater flexibility of connection is achieved, and vulnerable parts are eliminated. Fig. 50 illustrates how the shorter 3- and 4-cyl heads accommodate either the separate, side-outlet water manifolding of the present in-line 71's, or a front end outlet for the 6V and 8V-71's. The separate, side outlet manifold and cross-flow through the cylinder head is employed on the 12V-71, as well as the in-line 6-71.

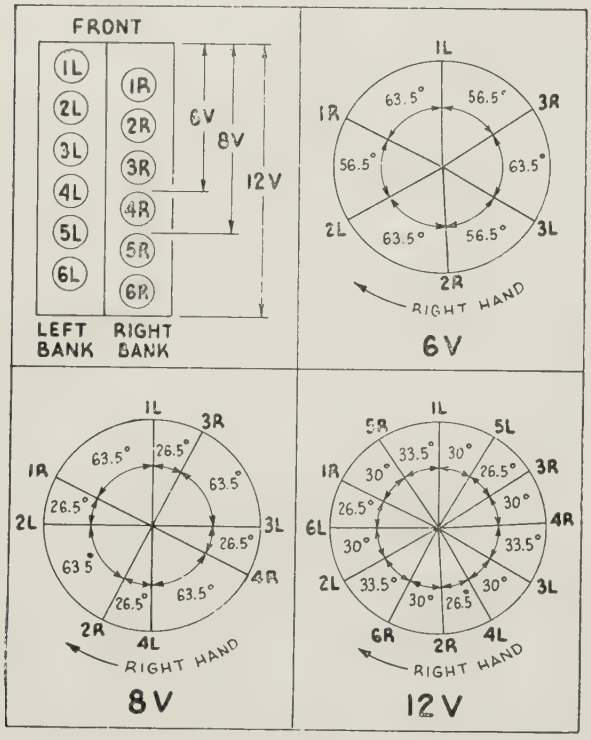

Fig. 47 — V-71 firing order

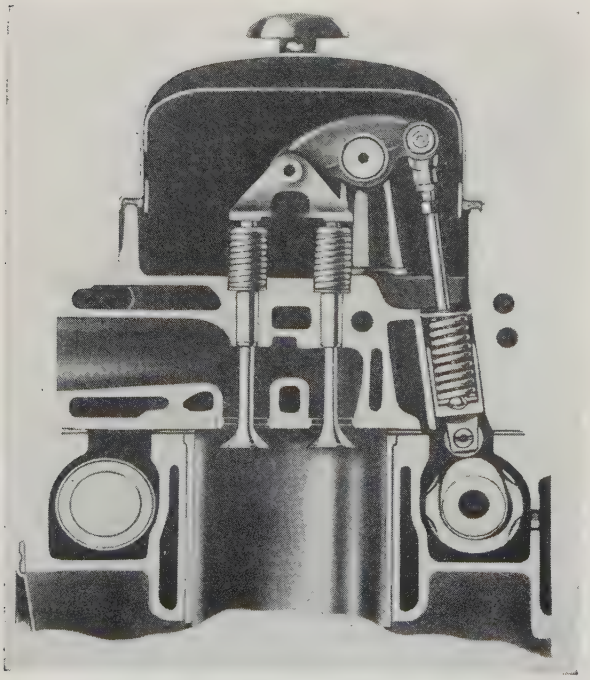

Fig. 48 — Four-valve operating mechanism

Fig. 49 — In-line 71 and V-71 fuel manifolding

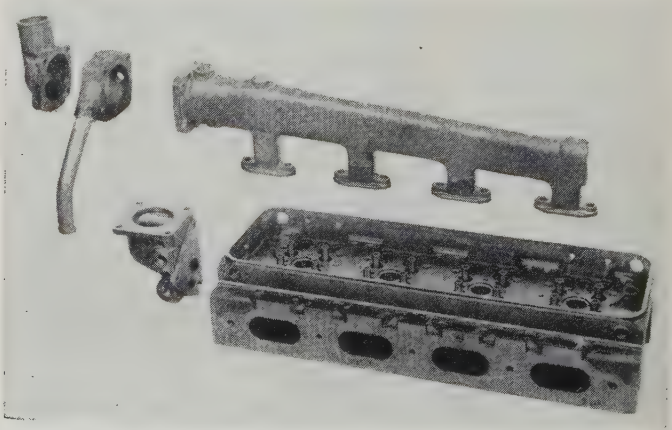

Fig. 50 — In-line 71 and V-71 water manifolding

This is done to obtain better coolant distribution in the relatively longer 6-cyl head where transverse water jacket area and increased coolant flow become limiting factors.

Lubricating System — The V-71 engine lubrication system shown in Fig. 51 has been designed to accommodate the same tooling for the 6-, 8-, 12-, and 16-cyl engines. Except for the oil pump, the 12V-71 system illustrated is typical of all the engines. The 12V and 16V oil pumps are located in the oil pan and mounted on the main bearing caps optionally at the front or the rear of the engine. Pump design is such that it will accommodate either left- or right-hand rotation merely by switching the positions of the drive and driven shafts, while internal body passages accommodate connection to the oil coolers and filters mounted on either the right or the left front corner of the block. The design also permits tandem installation of a scavenging pump section when required for such applications as earthmoving vehicles.

Full flow filters are placed in the system ahead of the plate-type oil coolers to protect them along with the rest of the engine. External oil coolers, common to all present in-line engines, have been retained on the new engines due to their versatility of configuration and capacity as required for high output engines and oil-cooled application components.

All cylinder block oil passages are drilled and are necessarily large since the 16V's oil flow rates exceed 50 gpm; there are no external oil lines subject to breakage which can so easily occur in the heavy-duty operation for which these engines are designed.

Oil flows from the coolers to the main, longitudinal gallery in the middle of the block; thence, each main bearing is individually pressure fed, passing oil to an adjacent pair of connecting rods by way of grooves in the unloaded halves of the main and rod bearings and appropriate crankshaft drilling. The rifle-drilled connecting rods carry oil to the piston pin bushings and provide the oil jet cooling spray for the piston crown.

Additional vertical passages off the main gallery carry oil to the camshaft end bearings in each bank and out the top of the block to the cylinder heads. Longitudinal galleries paralleling the camshaft connect with leads to the blower for drive gear and bearing lubrication.

Oil entering the rifle-drilled camshafts through the end bearing journals passes to the intermediate bearings, where it is jetted against the camshaft lobes and cam rollers running in an oil bath. This jet lubrication of lobes and rollers is very important immediately after starting with cold oil, before camshaft bearing oil flow, and oil drainage from the head have had time to build up.

Cylinder head and cylinder block oil drainage provisions were designed for adequate drainback under extreme operating angles and have proved satisfactory for inclinations over 45 deg in any direction. Consequently, the V-71 engines are capable of being permanently mounted with either bank laid over as far as horizontal by modifying only the oil pan and oil pump inlet.

Since the 6V and 8V-71 engines are intended for highway vehicles as well as earthmoving and stationary applications, oil pan clearance with front axles was a major consideration. To permit greater design freedom, the 6 and 8V oil pump (Fig. 52) was taken out of the sump and placed in the crankshaft front cover in a somewhat unique arrangement employing easily manufactured spur gears. The main pumping gear is concentric with, and spline driven on the front end of the crankshaft. The pump idler gear is much smaller than the main gear, and it runs on a well-lubricated copper-lead bushing and hardened steel shaft. With careful attention to inlet porting, the pump has been developed to give over 90% volumetric efficiency, a characteristic, no doubt, of better tooth filling with a large diameter, narrow-width gear running no faster than engine speed.

Cooling System — The gear driven, curved vane

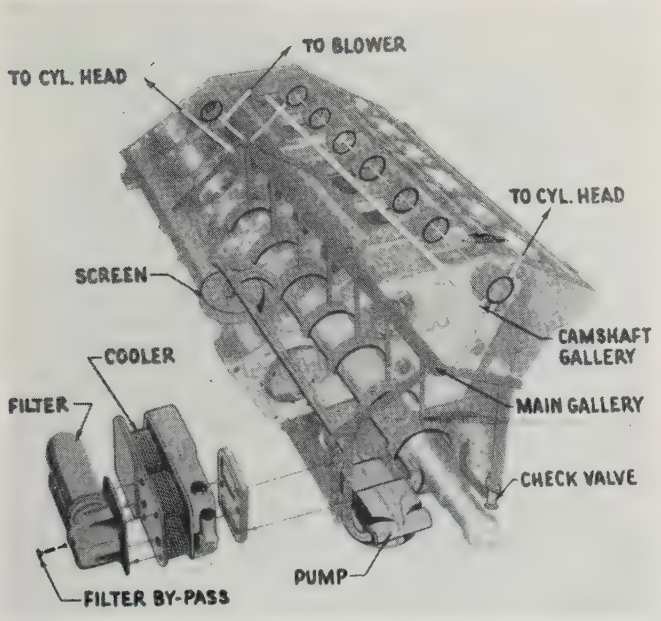

Fig. 51 — 12V-71 lubrication system

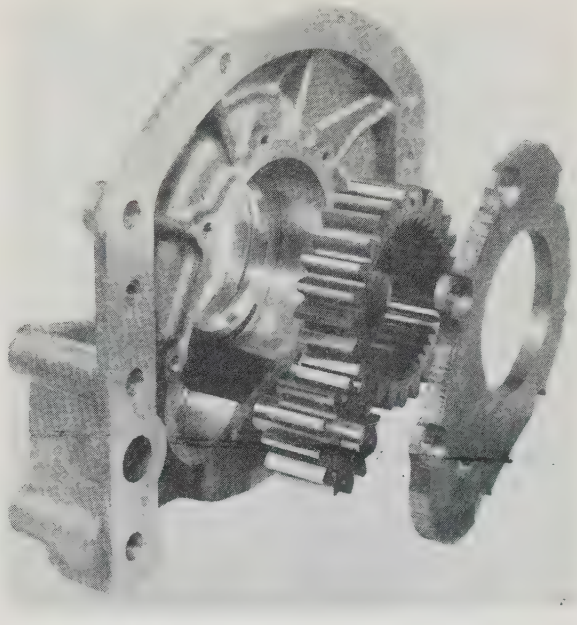

Fig. 52 — V-71 lubricating oil pump

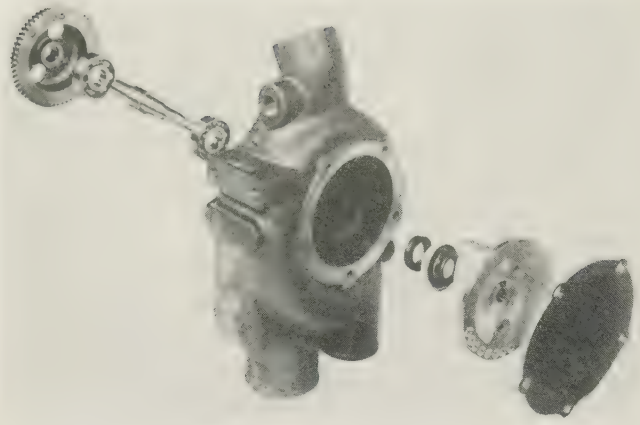

Fig. 53 — V-71 water pump

Fig. 54 — V-71 cooling system

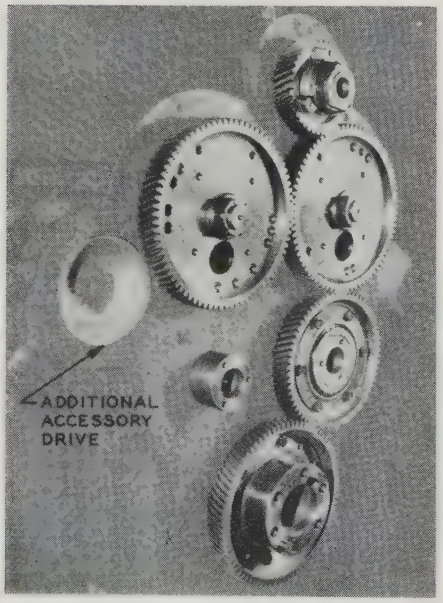

Fig. 55 — Timing gear train

water pumps (Fig. 53) are designed to deliver a maximum of 20 gpm per cyl. It was felt that this high capacity should be available to minimize costly radiator size and meet the ever greater cooling requirements of special application components, such as torque converters, marine gears, and torquematic brakes. Simple substitution of lower output impellers permits tailoring of water flows for specific applications where flow requirements are lower and an economy of pump horsepower is desirable.

A "full-flow," blocking-type bypass system, shown in Fig. 54, protects the engine from excessively choked-down coolant flow during high-load operation under cold-weather conditions. About 80% of maximum pump delivery obtains through the bypass with the thermostats closed, and modulation of water temperatures into the block is provided by the large bypass capacity. An added dividend of the system is equalization of coolant flows and temperatures through the two vee cylinder banks; since each bank has its own thermostat and housing tied into the common bypass, complete closure of one thermostat with the other open, only results in a 56% versus 44% division of pump delivery between the banks with practically no difference between the two "water out" temperatures.

Gear Train and Accessory Drives — As mentioned previously, the V-71 timing gears (Fig. 55) are standardized with the in-line 71. Separate balance weights are bolted to the two camshaft gears suitable for the engine involved. The idler gear runs on a preloaded roller bearing; bearing and hub are both standard in-line engine parts.

The combination gear train cover and flywheel housing (Fig. 56) is not only machined on present in-line 71 tooling, but is even cast with the same pattern equipment using various optional loose pieces. For this reason, a large number of existing production accessories and drives are directly applicable to the new V-71 line. Engine speed drives are available on both camshaft gears, while the blower

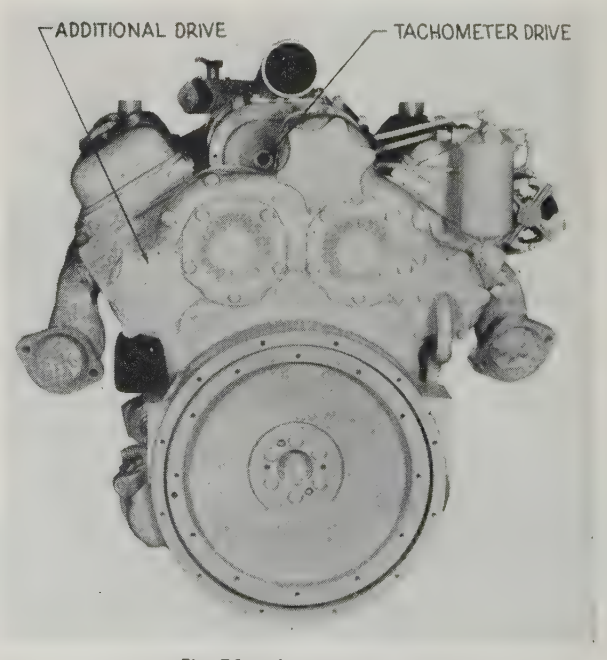

Fig. 56 — Accessory drives

and one optional gear offer two, twice-engine-speed drives. In addition, three multisheave pulley drives are available on the front ends of the camshafts and crankshaft.

Scavenging Blower — The Roots blower's location on top of the block assures equal distribution of scavenging air to both banks, and has obvious advantages for air cleaner piping and service accessibility. Furthermore, by nesting the blower between the two cylinder heads, a minimum silhouette is attained, while the sides of the block are left clear for optional accessory location and maximum frame clearance. Relatively shorter blowers for given capacities were possible because the blower to block joint face location and resulting drive gear centers permitted designing for a 2.05/1 drive ratio, compared to the standard 71E 1.69/1 ratio. Using the blower rotor contour and housing bores established by existing volume tooling, it was practical to design a tandem blower configuration (Fig. 57) for the 12V-71 and 16V-71, so that only two basic blowers serve all four V-71 engines. Further, on the same gear centers, it is possible to provide a blower drive gear to give a 1.95/1 ratio more closely tailored to the requirements of a turbocharged version of the engine.

The top-of-block location of the blower also offers a convenient mounting and 2/1 drive for the fuel pump and governor. The governor housing is integral with the blower front cover and is so located that simple linkages can connect directly through the sides of the cylinder heads to the standard Series 71 bellcrank and injector rack control mechanisms.

Crankcase Breathing — Crankcase breathers always present a problem; regardless of where they are installed on an engine, they always interfere with some accessory, frame member, engine mount, or other special condition in the multitude of varied applications encountered. Fig. 58 shows how, in an effort to get away from this once and for all and to approach a design insensitive to installation and operating angles, an internal crankcase breather has been incorporated in the rear end of the cylinder block. Only a stub breather tube sticks out of the top of the block, suitably located for a piping connection in any convenient direction.

Breathing is through two openings in the rear main bearing bulkhead of the crankcase, into a chamber shielded by a semi-circular cast wall and covered by the rear cylinder block end plate. Cast passages connect vertically with a generous breather cavity, which provides two breather essentials, large cross-sectional area, and maximum height. A large air handling capacity, unaffected by operating angle, results by breathing from this central, high crank-

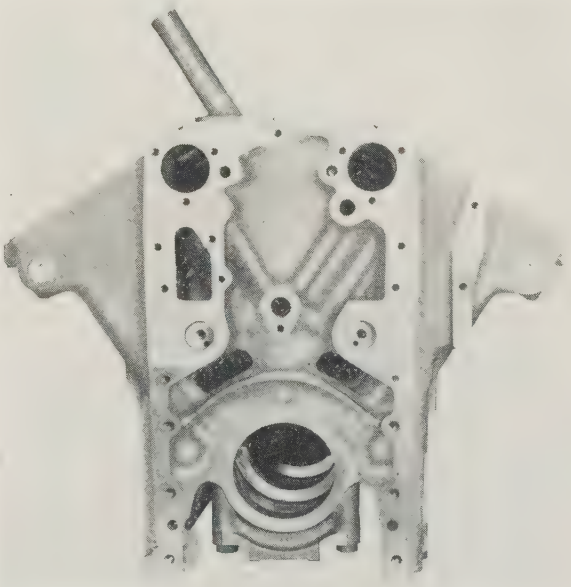

Fig. 58 — V-71 internal crankcase breather

Fig. 57 — 12V-71 blower and governor

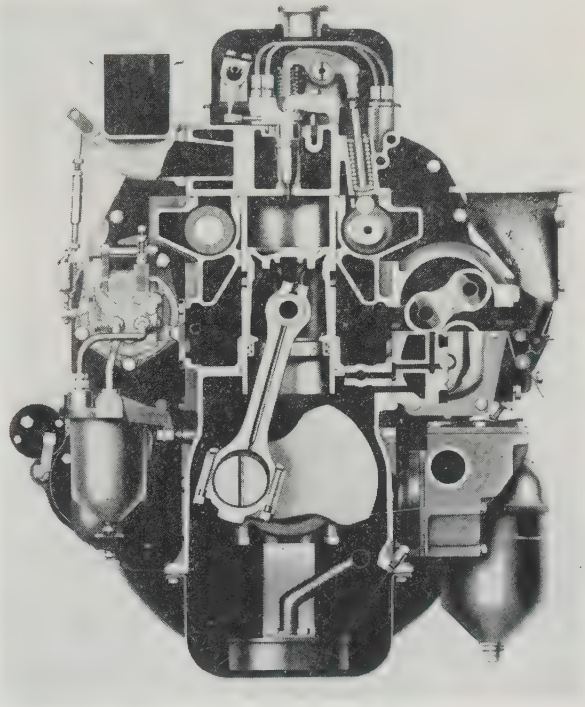

Fig. 59 — Transverse cross-section of 4-53

case location which cannot be flooded, and where air rising to the breather exit does not rise past and impede the drainage of oil from some higher section of the engine.

Series 53

It was initially decided that the smaller, lighter Series 53 must retain the model versatility of the Series 71, as well as the basic 71E combustion design principles. Therefore, the in-line 53 cylinder block was made symmetric (Fig. 59) with left and right sides machined identically to permit locating the Roots blower, water pump, oil cooler, and full-flow lube filter on either side of the engine. The cylinder block rear end plate is reversible to provide a blower drive mounting on the appropriate side, with the governor drive opposite. Like the in-line Series 71, the in-line 53's block accommodates turning the cylinder head end for end, accompanied by a switch of the cam and balance shafts, in order to place the exhaust manifold in optimum location. Unlike the Series 71, by separately driving the water pump the 53's pump and oil cooler location was made independent of the Roots blower, thereby doubling the number of optional model configurations.

Cylinder Liners — A wet cylinder liner construction was both feasible and desirable in the Series 53, where there was design flexibility. The open, internal structure of the Series 53 block eliminated a great deal of weight and offered good core support and casting ease that reduced core shift problems and made minimum wall thickness practical. The cylinder liners seal the water jacket in the block by a flange at the top and by high temperature synthetic "O" rings just above the ports. To avoid damaging the "O" rings during liner installation, the liner OD is stepped down slightly, starting just above the air inlet ports so that the latter do not drag across the seal rings when lowering the liner into position. An additional small diameter step occurs ⅜ in. below the cylinder liner flange to facilitate removal if scale or rust have accumulated on the surface of the liner exposed to the water jacket.

Oil Drainage and Crankcase Breathing — Lacking the space to accommodate the V-71's internal crankcase breather, special attention was given the Series 53 blocks with respect to oil drainage, and to breathing passages leading upward to rocker cover or flywheel housing vents. Generous head drains (Fig. 60) open directly into the camshaft pockets, which are paralleled on both sides of the block from front to rear by cast drainage galleries. In front, these galleries connect with the upper front cover, which in turn opens into the crankcase. In the rear, the galleries drain directly into the gear train housing, which is, of course, open at the bottom to the crankcase. Thus, both ends and both sides of the engine

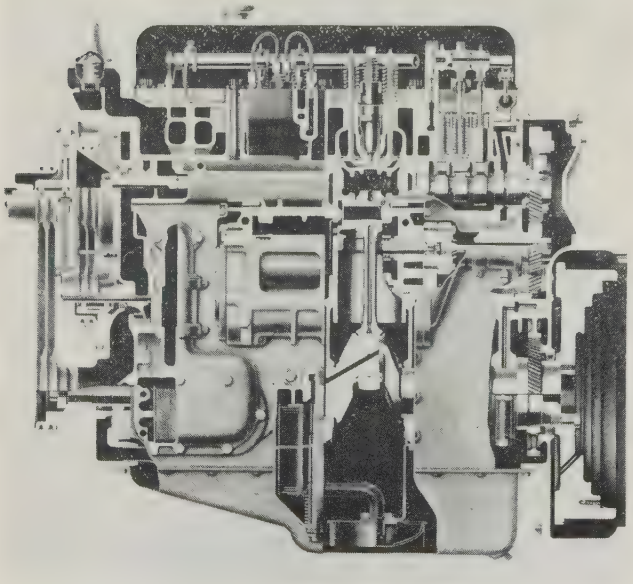

Fig. 60 — Longitudinal view of 4-53

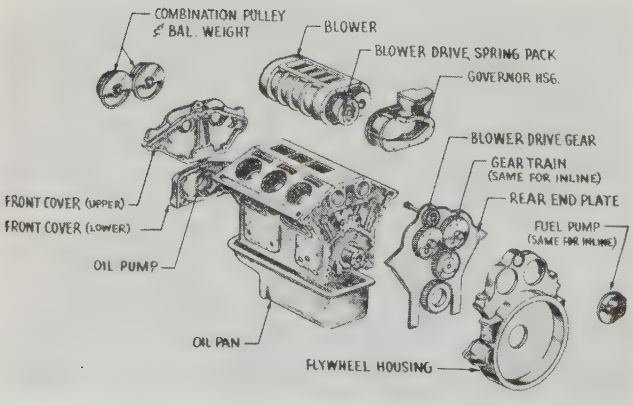

Fig. 61 — Series 53 V-design

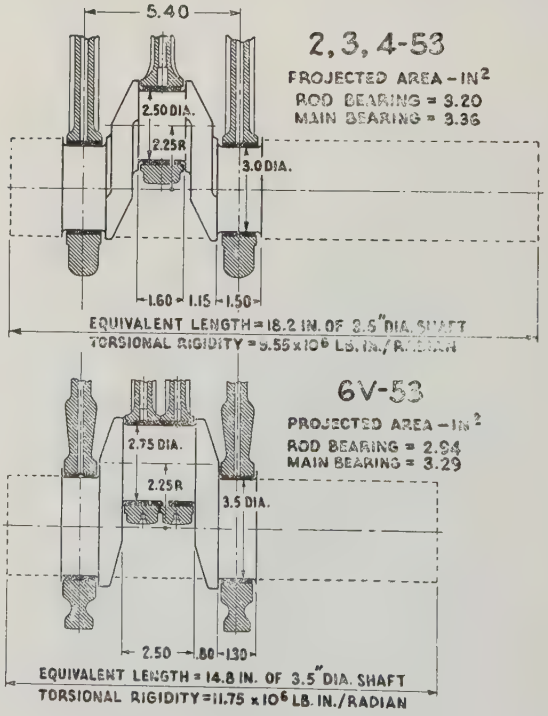

Fig 62 — Comparison of crankthrows

are so designed that regardless of the angle of operation, there are separate ways for oil to drain down and crankcase breathing to come up.

Camshaft and Bearings — Large diameter, press fit camshaft bushings of proven long-life in the high speed G.M. Model 4-51, have OD sizes stepped for ease of assembly. The rifle-drilled camshaft carries oil from the ends to the intermediate bearings where broached slots in the cylinder block bearing bores supply jet lubrication to the cam lobes and rollers.

Model 6V-53 — Fig. 61 shows in exploded view some basic elements of the 6V-53 design, which was incorporated in the engine line to provide a short, powerful, compact package with speeds up to 2800 rpm. Here, again, a vee-angle of 66¾ deg was established by the standard gear train, flywheel housing tooling, and cylinder heads of the in-line Series 53. The design is essentially that of two siamesed 3-53 banks joined by water passages, and utilizing a top Roots blower configuration closely resembling the 6V-71. Standardization was adhered to in piston assemblies, cylinder liners, heads and head gear, pumps, and timing gears.

Crankshaft and Balancing — The first in-line Series 53 engines were 4-53's designed and built with a cylinder spacing of 5.12 in., but this was increased to 5.40 in. (Fig. 62) to obtain more reasonable bearing loads when it was decided to extend the Series to include a 6V-53 engine. Analyses were made of the crankshaft bending and shear stresses and compared to those of the standard Model 6-71 engine. The bending stresses were found to be within 5% of those in the 6-71, and the shear stresses were 15% lower, all calculations being based upon the same peak cylinder pressures.

The 5.4-in. cylinder centers not only permitted the economy of uncheeked crankwebs on the in-line crankshafts, but, as shown in Table 4, also gave 6V-53 mean bearing loads within the range of current engine practice and peak loads considerably below those commonly encountered. As on the Model 6V-71 engine, no special crankshaft counterweighting was felt necessary to reduce Series 53 bearing loads.

The natural frequencies of each of the Series 53 engine crankshafts are sufficiently high so that the critical speeds of the major harmonic orders do not occur within the operating speed range of the engines.

In the balancing of the Models 2, 3, and 4-53 engines, shown in Fig. 63, the standard Series 71 engine practice was followed. Counterweights are placed on the crankshaft to accomplish rotating balance of the shaft, and balance weights are placed at the front and rear of the cam and balance shafts to balance the primary rocking couples that are inherent in the engine. The unbalanced secondary force in the Model 2-53 engine and the secondary couples of Models 3-53 and 6V-53 engines are not of sufficient magnitude to be of any consequence. There is no secondary force or couple in the Model 4-53 engine.

The 6V-53 balance, illustrated in Fig. 64, has primary horizontal and vertical rocking couples balanced by weights placed on the crankshaft and on the two camshafts similar to the Model 6V-71 engine.

Cylinder Heads — Like the new Series 71 and V-71 designs, the 53's cylinder heads (Fig. 65) have in-

Table 4 — Engine Bearing Loads of Series 53

Bearing	Highest Peak Pressure, psi	Highest Mean Pressure, psi
4-53 Connecting Rod	2090	1030
6V-53 Connecting Rod	2240	1150
4-53 Main	1755	880
6V-53 Main	1965	1295

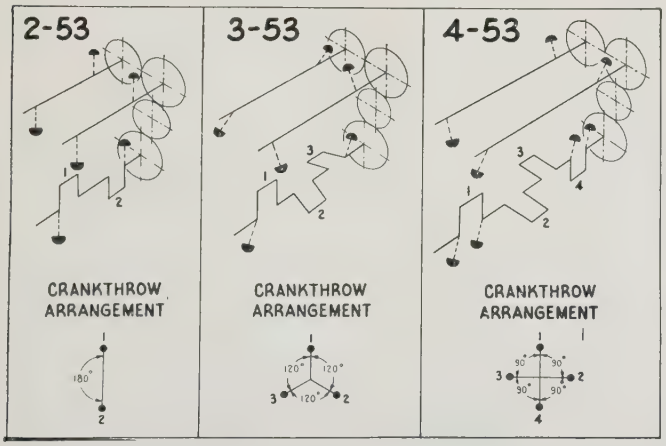

Fig. 63 — 2-53, 3-53,4-53 balancing systems (primary couples are balanced with counterweights on camshafts, counterweights on crankshaft are for rotating balance of crankshaft)

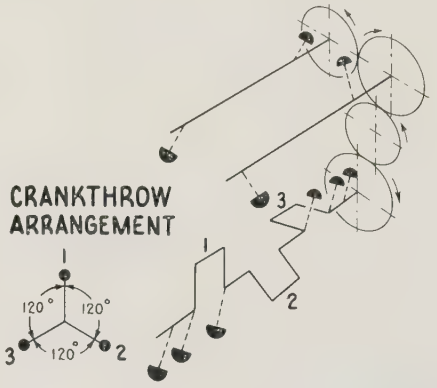

Fig. 64 — 6V-53 balancing system (primary couples are balanced with counterweights on camshafts and crankshaft, counterweights on crankshaft are for rotating and reciprocating balance)

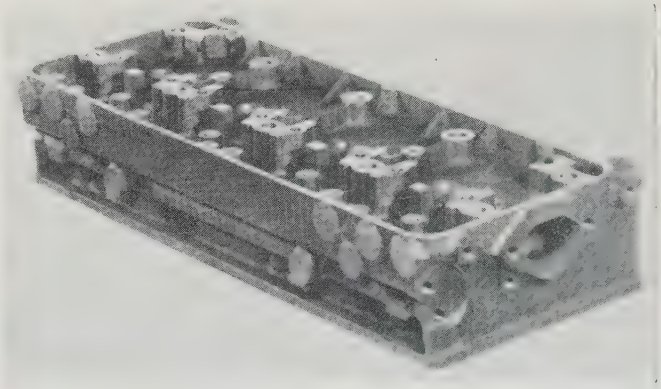

Fig. 65 — 4-53 cylinder head

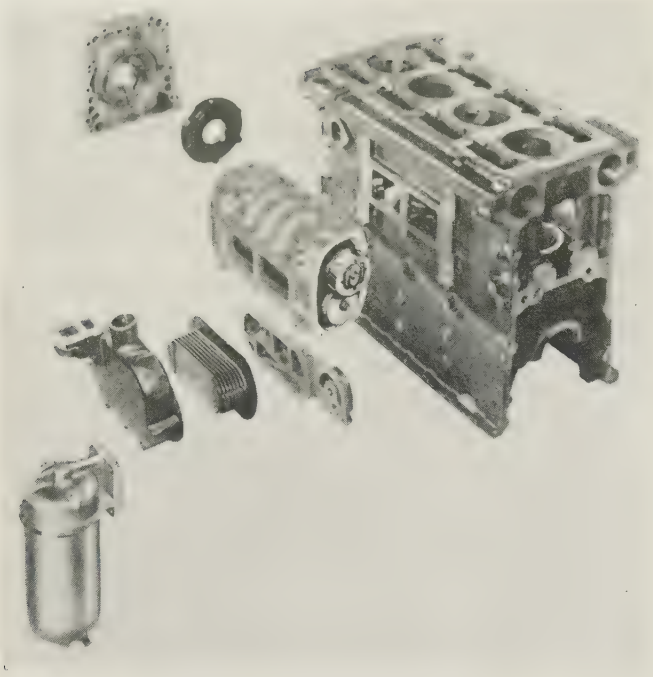

Fig. 66 — 4-53 lubricating system

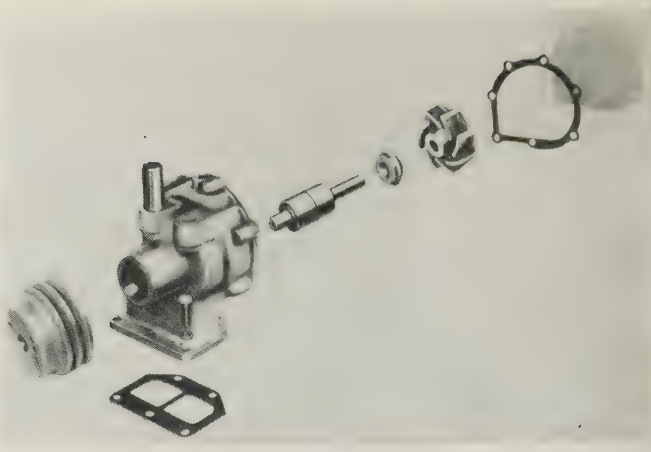

Fig. 67 — Series 53 water pump

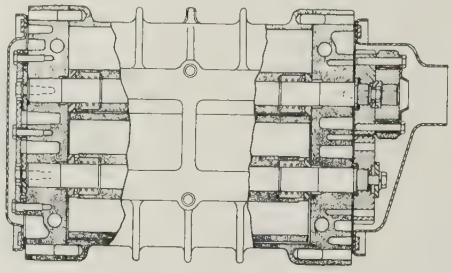

Fig. 68 — 4-53 blower

ternal lube oil and fuel galleries. These short heads lend themselves particularly to longitudinal coolant flow and elimination of an external water manifold; being symmetrical about their longitudinal center, they are completely reversible, with provision for mounting a water outlet and thermostat housing on either end. The heads are of 5/16-in. "thin fire deck" design with hardness up to 207 Bhn for maximum strength and resistance to cracking under adverse operating conditions.

The height of the Series 53 head was established by standardization on the Series 71E fuel injector configuration, which also led to similarity of injector and valve operating parts and throttle control mechanisms. Profile milling of the top deck was avoided by raising up all of the bosses for head bolts, rocker supports, and throttle control brackets flush with the structurally important side rails, so that all top side surfaces are finished by one milling cut. Additional transverse cylinder head rigidity was obtained by ½ in. wide transverse struts between head bolt bosses above the top deck.

As in the case of the in-line 3-71 and 6V-71 engines the 3-53 and 6V-53 cylinder heads are interchangeable.

Lubrication System — The Series 53 lubrication system (Fig. 66) is basically the same as the V-71's, with full pressure-fed main, rod, cam and balance shaft, and rocker arm bearings, and with jet-cooled pistons. The aluminum blower bearings, discussed later, are also pressure fed. An internal-external gear pump, mounted in the crankshaft front cover and running concentrically on the crankshaft is a type proved very successful on the high speed Model 4-51. One pump serves either right or left hand engine rotation merely by rotating the pump assembly 180 deg in the front cover so that appropriate inlet and outlet passages align. All pumps in the series are identical, except for gear thickness and corresponding depth of body machining.

The standard 53 line utilizes a full-flow lube filter and oil cooler. However, in the case of the Model 2-53, for applications with lower power and speed requirements, it has been practical to operate without oil cooler or piston jet cooling.

Water Pump — The pulley-driven 53 engine water pump, shown exploded in Fig. 67, is noteworthy in that it represents very nearly the ultimate in standardization; there is only one right-hand and one left-hand rotation pump for the whole line. Although different pulley ratios can be made available, this has not been judged necessary for two reasons. First of all, the cylinder block-to-head water holes at each end of the engine and between cylinders are the chief restrictions to coolant flow; the 6V-53 has 16 such holes to six for the 2-53, and consequently, it takes a fair-sized pump to meet the requirements of flow in one case and pump discharge head in the other. Secondly, radiator economics are usually quite significant in small engine applications such as the 2-53 and 3-53 where somewhat higher water flow can often permit smaller radiators and less fan horsepower.

Scavenging Blower — Since the general cooling system, gear train design, and accessory drive provisions are quite similar to the V-71, the Series 53 configurations require no further comment. However, the two lobe, straight rotor, Roots blower design, shown in the partial longitudinal section of Fig. 68, represents a departure from the conventional 71 engine design, and incorporates several novel features.

The chief characteristics of the aluminum design, illustrated by the Model 4-53 blower, are its adapta-

bility and use of standardized parts. Symmetrical configuration permits its use on either side of the in-line engine block simply by inverting the drive connection and gear cover. The rotor gears, end plates, shaft seals, thrust plates, and end cover are common throughout the line. All 53 blowers are driven at approximately two and one-half times engine speed.

While the rotor gears drive directly off the main gear train in the case of the short 2-53 and 3-53 blowers, the greater rotating masses of the longer 4-53 and 6V-53 versions call for a quill shaft and flexible drive coupling of spring-loaded cam type, piloted directly on one rotor gear. The rotor shaft journals ride directly in bearing bores in the aluminum end plates, and are pressure lubricated through drilled passages from the cylinder block mounting face.

Drained counterbores keep the phenolic face-type seals from being subjected to oil presure, and equalize longitudinal oil flow fore and aft in the bearings. The rotor drive gear thrust is taken by a hardened and ground washer on the end of the rotor shaft, running between the aluminum end plate and a stack molded, cast-iron thrust plate.

Conclusion

In conclusion, it would seem an achievement of some consequence to develop and tool eight different engines at once. Within three years, over 75,000 hr of laboratory development and field testing, and over a million Engineering and Processing man-hours have been expended on the new engines. With the addition of the Series 53 and V-71 engines to the present in-line Series 71 and 6-110, Detroit Diesel has one of the broadest and most complete horsepower coverage of any diesel engine manufacturer.

New production tooling and assembly lines, and 287,000 square feet of additional factory and block testing facilities have been furnished to produce the present and new lines. Production has started and programming established to make available the many model variations required by the users of these versatile new engines.

ORAL DISCUSSION

— Reported by R. W. Bristol
Curtiss-Wright Corp.

L. D. Evans, International-Harvester Co.: A statement made at the conclusion of the paper about the number of man hours that went into this development should make many of us take notice. Taking the figure of 1,000,000 man hours of engineering and processing time on this project boils down to an average of 166 men working full-time over the 3-year period. We would like to know if this is an accurate picture, and if it includes all Planning Department's time as well as Tooling, or just the Design and Test Engineering?

Mr. Ervin: The one million man hours includes tool design and layout, and product design and test man hours. It does not include time expended by outside machine builders or suppliers. This is an accurate figure based upon the average number of men actively assigned over the 3-year period to the new engine projects, amounting to over 50% of the Processing and Engineering personnel.

Q: Getting down to the engine line itself, if we can refer back to Fig. 5, there appears to be very heavy duplication of horsepower ranges. Is it planned to weed these out and drop from the line the older engines which overlap the new? If not, what advantage either economic or technological will there be of one over the other?

A: Any reduction in the number of engines in the line will be based upon sales requirements. With the exception of the Model 4-51, we will continue to produce all of our present engines as long as our customers want to buy them.

Careful examination of Fig. 5 will reveal that there is deliberate overlap, but no duplication of horsepower ranges, with the exception of the in-line Model 6-71 and the 6V-71: there are definite application limitations and customer requirements for this size engine that can make an in-line preferable to a V-engine, and vice versa.

Q: Since the piston fire ring is so high on the piston, we wonder, first, what type and material the ring is, and secondly, what difficulties have been encountered with the durability of this ring? In the past the recommendations of the ring manufacturers have always been to lower the belt to get out of ring distress.

A: The piston fire ring is a 5/64-in. thick, 5/32-in. wide chrome-plated steel ring. SAE 52100 and 9254 materials have been used successfully. Troubles encountered were chiefly mechanical rather than thermal, as indicated by solutions found with closer clearances, closer tolerances, and improved physicals. It goes without saying that the efficacy of lowering the ring belt to get out of ring distress depends upon the type of distress.

Q. What oil flow is used in piston cooling and what has been your experience with rifle-drilled connecting rods at high speeds? We find and have noted in literature studies that the inertia forces reduce the oil flow drastically above 2000 rpm, so that we cannot depend on it for cooling at higher speeds.

A: The rifle-drilled connecting-rod oil flow for piston pin lubrication and piston cooling amounts to approximately 1 gal per min per piston for the Series 71 and approximately half that for the Series 53. Piston cooling flow does vary inversely — but not drastically — with speed, and has been adequate for Series 53 durability operation at 3000 rpm continuously.

Q: The geometrical symmetry between the engines is very interesting. How far was this carried in porting, piston configuration, injection rate, and the like between 71E Series and the 53 Series?

A: Series 53 pistons are as close to scaled 71E pistons as permitted by casting and machining considerations. The cylinder intake ports give the same area-time to displacement ratio as the 71E within 2%.

The Series 53 uses the same exhaust valve cam profile, timing, and rocker arm ratio as the Series 71E. However, the exhaust area-time to displacement ratio is approximately 15% greater in the 53. Both engines use the same injector cam profile, timing, and rocker arm ratio, and the same injector except for output, helix timing, and spray hole size.

Q: With regard to the balance, we question a statement made about the insignificance of the unbalanced secondary forces and secondary couples in several of the engines. Do you suggest rubber mountings to isolate the vibration on these engines?

A: The secondary unbalanced forces and couples are low, but in those cases requiring a higher degree of isolation, rubber mountings are recommended.

Q: Referring to the aluminum block engines, are special lines being set up for machining since speeds, feeds, cutting tools are different for cast iron than aluminum, and what

structural changes are being made in the case?

A: The same production line tooling is used for aluminum and cast iron. There are conventional and appreciable structural changes and increases in wall thicknesses and load-carrying members in the aluminum blocks.

Q. How were piston temperatures measured as shown on Figs. 20 and 30?

A: Piston temperatures were measured with thermocouples silver soldered into the piston from the underside. Thermocouple lead wires were connected to contact points mounted on an insulating block secured to the lower skirt ID. Near bottom center these points contacted springs secured to an insulating block on the inside of the crankcase. Leads from the springs were taken out thru the crankcase wall to a potentiometer. Contact between points and springs occurred for a period of about 60 deg of crankshaft rotation.

In the ultimate rating of the engines, we feel that the 2-stroke engine may be more limited than the 4-stroke on the ability to take very high thermal loads. The time allowed for heat dissipation is one half that of a 4-stroke engine and gas flows have to be generated entirely by the blower, since none is generated by piston motion. In the past the durability and fuel economy of the 2-stroke engine have always been criticized by 4-stroke advocates, but the new series appear to have at least the fuel economy problem solved, and only time will tell about durability.

With reference to the 2-stroke versus 4-stroke controversy, our feelings after some 20-odd years of uniflow, 2-stroke experience are best summed up by our investment in eight new uniflow, 2-stroke engines.

C. F. Taylor, Massachusetts Institute of Technology — I am pleased to see a further confirmation of the theory of geometric similitude. Our work was done with 4-stroke spark-ignition engines, but now you have shown similar results with 2-stroke diesel engines. Were the same injection pump or fuel flow settings used for comparison between standard and "E" engines?

Mr. Hulsing: The standard and "E" engines were compared both at equal fuel input in Fig. 21 and at equal power output in Figs. 22–26. Industrially, the standard engine employes a nominal 70 cu mm/cycle injector; the "E" engine gives equal performance with a nominal 60 cu mm injector.

Q: Were measurements made of the reduction in heat flow?

A: Normal heat rejection tests have been run in addition to the piston temperature tests. Heat rejection was reduced about 10%.

Q: Is the fire ring different from or constructed the same as a piston ring?

A: Construction of the fire ring is the same as a chromium-plated piston ring except it is thinner axially. It is 0.093 in. thick, whereas the compression ring is ⅛ in. thick.

H. G. Braendel, Wilkening Manufacturing Co.: We tested fire rings 10–12 years ago and found a significant improvement in performance of 5%. A scalloped wear pattern formed above the ports and the rings formed carbon deposits in line with the ports. The wear was due to torching of the carbon deposits. I would like to ask what the stink rating is of the new engines?

A: The effect of the fire ring on performance depends on a great number of factors among which are engine load and speed. A simple statement as to the percentage improvement in overall performance cannot be made.

Since we are unfamiliar with the type of wear pattern described by Mr. Braendel, we will have to take his word for its cause, and simply point out that he is talking about a completely different engine and a fine ring of much less favorable configuration and quality.

Short of a carefully controlled statistical survey of a sniff panel, we know of no way to evaluate the relative odor of exhaust. Such tests have not been conducted on the new engines. Total air and total fuel have been reduced for a given brake output; however, we would not anticipate any marked change in exhaust odor.

W. I. Hamilton, Allis-Chalmers Manufacturing Co.: I wish to comment that the uniflow scavenging was a good choice for the 53 size engine, since loop scavenging would be difficult to accomplish in such a small cylinder. What is the turbocharged engine performance data?

Mr. Hulsing: In limited turbocharger work to date, the Series 53 has equaled the performance gains of the V-71T and in-line 71T engines.

Q: Are there any cooling system venting problems when operating the "V" engines with one bank horizontal?

A: Cooling system venting problems were anticipated, but did not materialize with longitudinal water flow through the head, equipped with a front water outlet connection.

P. H. Schweitzer, Schweitzer & Hussmann: Are sections in the aluminum engines the same as used for cast iron?

Mr. Hulsing: The aluminum engine sections are "beefed-up" over those in the cast-iron engines.

Q: Does the 53 Series have cooling below intake ports?

A: Neither the V-71 or 53 engines have liquid cooling below the intake ports.

Q: Does the fire ring ever stick?

A: The fire rings are sometimes cold stuck, but not hot stuck.

Q: Would you change the term "scavenging ratio" to "delivery ratio" to agree with SAE nomenclature?

A: Yes, we will change the term to agree with SAE nomenclature.

R. D. Best, Southwest Research Institute: What do you mean by a 20% reduction in air for the "E" engine?

Mr. Ervin: The delivery ratio of the "E" engine was reduced by nearly 20 *percentage points*, that is, from 1.47 to 1.30. Total air delivered was reduced by 1 minus $\frac{1.30}{1.47}$ or 11.6%.

Q: What is the effect on fuel/air ratio?

A: Because the fuel input was reduced for equal performance with the "E" compared to the standard engine, the full-throttle air/fuel ratio, based on total air delivered, was increased approximately 5%.

We do not have precise data on the "trapped-air" to fuel ratio differences between the two engines, but based on the following considerations, it is evident that the "E" engine is not suffering a shortage of trapped air:

1. Indicated thermal efficiency improved from 3 to 5 percentage points at full load as shown in Fig. 24.
2. Performance at high altitude greatly improved as shown in Fig. 25.
3. Exhaust smoke reduced throughout the speed range, and particularly at low speeds.

R. Cramer, Nordberg Manufacturing Co.: Your use of an rpm base for your performance curves makes it a little difficult to compare with bmep base which I am used to. What is your criterion for maximum horsepower?

Mr. Hulsing: Maximum horsepower is the power developed with the largest capacity injectors with which the engine will be sold for particular types of service, and is based primarily on exhaust condition and engine life requirements for that service. In no case does it even approach the "ultimate" power that the engine would develop with unlimited fuel input.

Q. In large engines our friction mep is in the order of 10–12, but your friction mep is in the order of 20–22. Why is the friction higher?

A: It is a rather well-accepted fact that friction mean effective pressure at constant mean piston speed decreases with increasing displacement. In our experience this decrease is quite gradual between displacements of 53, 71 and 110 cu in. per cyl, but we would expect it to be quite significant if extended to the 26,400 cu in. per cyl to which you might be referring.

Q. Why does the fire ring effect such a lowering of piston temperature? Is it due to its location or due to the reduced fuel?

A: As stated in the paper itself, the effect of the fire ring on piston rim temperature is due to both its location and to reduced fuel input.

RADIOACTIVE TRACERS

Cast New Light on

FUEL DISTRIBUTION

RADIOACTIVE TRACERS have been used to study the fuel distribution among individual cylinders in two modern V-8 engines. Individual fuel components (both hydrocarbons and fuel additives) were "tagged" with radioactive hydrogen (tritium) or carbon-14. These "tagged" components were blended into a commercial-type fuel, and their distribution to engine cylinders was determined by measurements of exhaust-gas radioactivity. The quantity of fuel distributed to the cylinders was measured by an exhaust-gas analyzer of the catalytic-cell type.

The results reported include the effect of various fuel factors, operating factors, and engine design factors on the distribution of both whole fuel and its components. A study of octane placement within the boiling range of the fuel revealed differences among fuels when rated under accelerating conditions (with "manifold lag") and when rated at constant-speed conditions with poor fuel distribution.

Also discussed briefly are the improvements in engine power, economy, octane requirement, and fuel ratings which resulted from improved fuel and tel distribution obtained with a modified carburetor.

D. E. Cooper, R. L. Courtney, and C. A. Hall, Ethyl Corp.

This paper was presented at the SAE Annual Meeting, Detroit, Jan. 13, 1959.

THE PROBLEM of distributing fuel from the carburetor to individual cylinders in multicylinder engines has received considerable study and is one of the most intriguing in the field of engine-fuel relationships.

Certain performance problems which appeared early in the history of the multicylinder gasoline engine could only be attributed to imperfect fuel distribution. Such performance characteristics as power, economy, durability, octane requirement, and any others that are influenced by the fuel quantity or composition in a single cylinder can be dependent upon fuel distribution.

Mock[1] was one of the first to observe that the gas-

[1] SAE Transactions, Vol. 15, 1920, Part 1, pp. 983 999: "Design of Intake Manifolds for Heavy Fuels," by F. C. Mock.

oline traveling from carburetor to cylinder via the intake manifold was primarily liquid at near-atmospheric manifold pressures. It has since been widely concluded that poor fuel distribution is due to the unequal distribution of the portion of the fuel that does not vaporize and remains in a liquid state in the manifold.[1-7] Most investigators found that engine design and operating conditions influenced distribution more than did fuel factors, such as volatility, whose limits are imposed by other considerations.[1-3,6,8] Increased fuel-air velocity and turbulence within the intake manifold improved distribution.[1,3,5,9] Minor carburetor modifications which changed the course of the liquid fuel caused major differences in fuel distribution.[1,3,6,10] Increasing fuel vaporization by applying more heat to the intake air or manifold "hot spots" significantly improved distribution.[1-3,5,11,12] Other ways of improving distribution by lowering the quantities of unvaporized fuel in the manifold included reducing fuel flow[3,12] and increasing fuel volatility.[2,3,9,11,12]

As the state of the art improved, it became possible to study the differences in fuel composition that existed between cylinders. Bartholomew, Chalk, and Brewster,[2] through a laboratory-road study of fuel-octane location with respect to boiling range, demonstrated that the richer cylinders could receive progressively greater proportions of the heavy ends of the fuel. Tel (tetraethyl-lead) distribution studies by Shell Thornton Laboratories (England)[4] indicated that the heavy ends of fuel distributed in amounts somewhat proportional to cylinder richness. Donahue and Kent[6] chemically analyzed the composition of special fuels arriving at each cylinder and found that the heaviest cuts of the fuel components distributed unlike the whole fuel. The specific properties of a fuel component which determine its distribution were unknown, although volatility in general was known to be important.

Chemical analysis techniques were employed to study the distribution of tel and ethylene dibromide, a chemical scavenger for tel. Tel was found to concentrate most heavily in the richest cylinders[4,6], but other test conditions indicated differently.[11] Ethylene dibromide was found to distribute much differently than tel, presumably because of the much higher volatility of ethylene dibromide.[4,11] Knowledge of factors influencing the distribution of fuel additives was scarce, because, as in the case of fuel component studies, adequate experimental techniques were lacking.

For many years, the greatest stumbling block in assessing distribution of whole fuel was the need for accurate methods of measurement. A review of the techniques employed includes the use of glass manifolds[1]; measurement of individual cylinder performance by firing pressures[13], indicator cards[10], and spark plug[12,14] and gasket[15,16] temperatures; chemical analysis of unburned fuel-air sampled from individual-cylinder intake ports;[11] and individual-cylinder exhaust-gas studies involving comparisons of flame colors.[16] Orsat analyses of exhaust gas as sampled[2,6,9,11,15,17] and after complete oxidation[16], and also exhaust-gas CO_2 detection by continuous reading analyzers.[9,12] Exhaust-gas analysis was found to be the fastest and most accurate method for obtaining fuel/air ratio, provided a representative gas sample was obtained.

The methods employed to sample the quality of each cylinder's charge were interesting. Unburned mixture was sampled through tubes installed in the intake manifold ports[11], through small poppet valves installed in each combustion chamber,[6] or through a small bleed-orifice in each chamber.[18] For exhaust-gas sampling, automobile engines were most often fitted with tubes inserted through the exhaust manifold so that the point of collection was between ½ and 1½ in. from the exhaust valve.[6,9] For positive assurance that samples were uncontaminated by gases from other cylinders, combination spark plugs and electrically actuated sampling valves for each cylinder were used effectively.[2,19,20] Aircraft engines with long individual exhaust stacks from each cylinder allowed sample probes to be installed downstream of the exhaust port and samples to be taken without contamination.[3,11,15,16]

Thus, much of the ground work had been completed, but for want of better techniques there still existed many unknowns in the problem of the distribution of fuel components and additives. Chemical or radioactive tracers appeared useful for studying the distribution of fuel components.

This paper will discuss not only the techniques which our laboratories have used for studying the distribution of fuels and their components, but also some of the fundamentals of distribution confirmed or discovered. Also presented is a demonstration of these techniques as they were used to evaluate the effects of modifications in carburetor design.

Background in Tracer Studies

In these methods, a single component in the fuel is "tagged" in such a way that it will produce a dis-

---

[2] SAE Transactions, Vol. 33, 1938, pp. 141–156: "Carburetion, Manifolding, and Fuel Antiknock Value," by E. Bartholomew, H. Chalk, and B. Brewster.

[3] NACA ARR E5105, October, 1945: "Study of Mixture Distribution of Double-Row Radial Aircraft Engine," by F. E. Marble, H. F. Butze, and R. O. Hickel.

[4] *Engineering*, Vol. 168, Dec. 30, 1949, pp. 710–716: "Fuels and Lubricants for Petrol, Diesel and Gas-Turbine Engines," by F. L. Garton.

[5] "Fuel Distribution in Multicylinder Engines and Its Effects on Knocking and Performance," by H. J. Gibson and C. Walcutt. Paper presented at SAE Annual Meeting, Detroit, January, 1940.

[6] SAE *Quarterly* Transactions, Vol. 4, October, 1950, pp. 546–558: "Study of Mixture Distribution," by R. W. Donahue and R. H. Kent, Jr.

[7] SAE Transactions, Vol. 31, 1936, pp. 257–266: "Engine Types and Requirements for Preparation of Fuels," by F. C. Mock.

[8] Proceedings of API, Vol. 32M (III), 1952, pp. 174–184: "Effects of Engine Variables on Octane-Number Requirements of Passenger Cars," by H. A. Bigley, Jr., A. E. Cleveland, and G. E. Onishi.

[9] SAE Transactions, Vol. 34, 1939, pp. 125–140: "Multicylinder Engine Detonation and Mixture Distribution," by A. J Blackwood, C. B. Kass, and O. G. Lewis.

[10] SAE Transactions, Vol. 24, 1929, pp. 102–109: "Balancing Power Output in Multicylinder Engines," by H. M. Jacklin.

[11] SAE *Quarterly* Transactions, Vol. 1, July, 1947, pp. 185–191: "Fuel Volatility — Its Effect on Performance and Distribution," by W. L. Hull and N. A. Parker.

[12] National Bureau of Standards, Vol. 35, 1945, p. 1681: "Utilization of Nonpetroleum Fuels in Automotive Engines," by J. T. Duck and C. S. Bruce.

[13] SAE Transactions, Vol. 26, 1926, pp. 269–301: "Laboratory Technique, Methods, and Equipment," by F. Jehle.

[14] *Automotive Industries*, Vol. 66, 1932, pp. 450–454, 486–491: "Mixture Distribution in Engine Studied by Spark Plug Temperature," by H. Rabezzena and S. Kalmar.

[15] NACA TN 583, October, 1936: "Mixture Distribution in Single-Row Radial Engine," by H. C. Gerrish and F. Voss.

[16] NACA ARR E105, September, 1944: "Effect of Fuel Volatility on Performance of Wright R-2600-8 Engine as Influenced by Mixture Distribution," by H. J. White and H. W. Englemann.

[17] *Nucleonics*, Vol. 15, June, 1957, p. 136: "C-14 Tracer Measures Fuel Distribution," by D. E. Cooper.

[18] *Automobile Engineer*, Vol. 44, March, 1954, pp. 103–107: "Mixture Sampling," by A. L. Wachal.

[19] "Recent Developments in Engine Instrumentation," by J. M. Chandler. Paper presented at SAE Summer Meeting, Atlantic City, June, 1953.

[20] "Automotive Engine Test Code," Standard Test Numbers 13, 13a. Fourth Edition, General Motors Corp., 1953.

tinctive combustion product which can be measured in the burned gases. Sampling and analyzing the gases from individual cylinders will then show the concentrations of this component that each received in its fuel charge. Any number of representative fuel hydrocarbons or additives may be selected and tagged for such tests. With enough of these tagged components, we can assemble a picture of the fuel make-up in every cylinder.

It needs to be made clear that all of the tracer studies to be described here were designed to show the compositions — *not* the relative quantities — of the fuel charges received by the cylinders. In each test, it is the *concentration* of the tagged component in the gasoline charge of a cylinder which is reflected by a similar *concentration* of tagged combustion product in the burned gas. Collectively, these concentrations can describe the complete make-up of the charge in a cylinder, but can tell us nothing of its amount. The amounts of the different fuel charges are always obtained in separate fuel-air measurements.

Synchronized Sampling Valve — For such tracer studies, and also for determining cylinder fuel/air ratios, we needed reliable samples of the combustion gases from each cylinder. The review of earlier work mentioned a sampling valve which had been developed by our engineers in collaboration with the Commercial Engineering Co. This valve simply replaces the spark plug of any cylinder and is attached to an appropriate sample receiver. As shown in Fig. 1, it comprises a small poppet valve for intermittently withdrawing combustion gases, and it also incorporates spark electrodes.

The valve is actuated by a solenoid timed with the combustion cycle. In the present work, the valve was set to open (for about a millisec) late in the power stroke, just after combustion was complete and before the gases were exhausted. This very useful device obtains its samples without disturbing the normal operation of the engine in any appreciable way.

Organic Halides as Tracers — In our first application of the tracer principle, we did not actually "tag" a fuel component; instead, we substituted a similar component which had a "built-in" tag. Trichlorobenzene has a high boiling point (near that of tel), and it was, therefore, presumed to distribute in much the same way as tel. Its chlorine atoms burn to hydrogen chloride, which we could readily analyze. We hoped that the concentrations of HCl found in the combustion-water condensates of the cylinders would tell us the different concentrations of trichlorobenzene that the various cylinders received in their fuel charges.

The first approach did not succeed. Because the HCl was subject to varying amounts of hold-up in the cylinders, consistent results could not be obtained. No way was found to overcome this problem, so we turned to isotopes as tracers.

Deuterated Compounds as Tracers — Our first success with tracing methods was achieved when we "tagged" some hydrocarbons with deuterium (heavy hydrogen) as the tracer isotope. In each case, the ordinary hydrogen atoms were replaced with deuterium, producing a compound with almost identical boiling point and other physical properties, but yielding "heavy water" upon combustion. Relatively small quantities of such a labeled hydrocarbon were blended in a typical gasoline. A set of sampling valves was used to obtain aqueous condensates from the cylinders of the test engine. The deuterium content of these condensates was determined by reducing them to a mixture of free hydrogen and deuterium, then analyzing the gas in a mass spectrometer.

Fig. 1 — Combination spark plug and sampling valve

The ratio of deuterium to hydrogen provided a measure of the concentration of deuterated additive in the fuel charge. This ratio was known for the fuel being fed the engine, and lower or higher ratios found in individual cylinder charges meant corresponding deviations from the original concentration in the fuel. Tests were run on three deuterated hydrocarbons boiling from 121 to 231 F, blanketing the lower and middle boiling range of the fuel in which they were blended. The interesting findings obtained with these compounds were confirmed in detail later with tritium tracers, so they will not be discussed here.

Although fruitful, this deuterium tracing technique had discouraging weaknesses. Preparation of the compounds was expensive. All samples had to be reduced to gaseous hydrogen, and the analytical work proved expensively slow. An inherent limitation was that the method could not be used to follow the distribution of additives such as tel. The tel content of gasoline is only about 0.1%, and the combustion water from fuel containing this amount of deuterated tel has too little deuterium for accurate analysis. The same situation precluded studies on lead scavengers and other gasoline additives.

Carbon-14 as a Tracer Element — For these reasons, we turned to the radioactive isotope carbon-14 to label fuel additives. The detection equipment

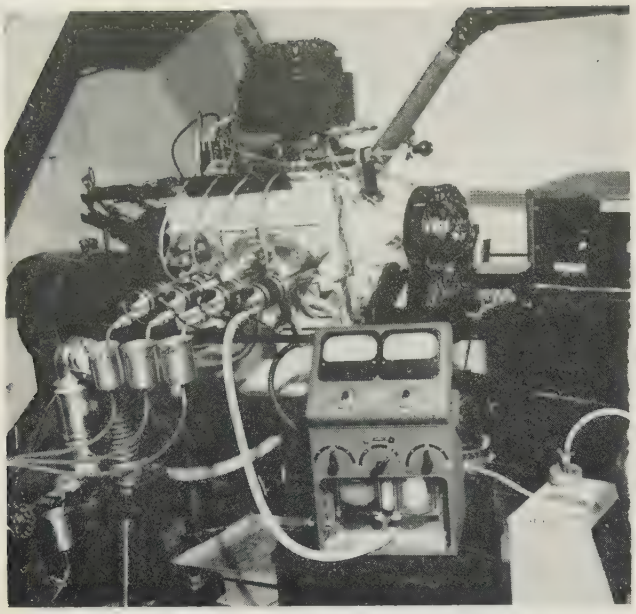

Fig. 2 — Engine equipped to measure fuel distribution and collect exhaust-gas condensates from individual cylinders

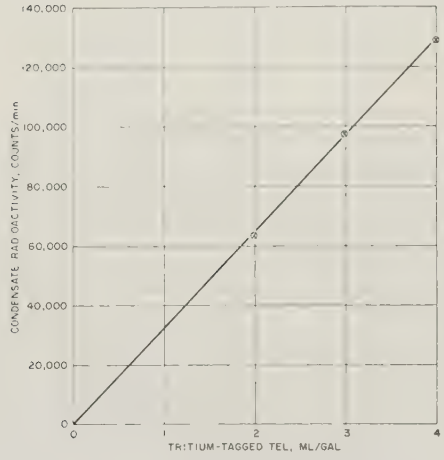

Fig. 3 — Relation of exhaust-condensate activity and tel concentration (Cyl No. 8 of Engine D)

for this beta emitter is sensitive enough to determine accurately the ratio of C-14 to ordinary C-12 atoms even when this ratio is as low as 1 in 10^8, and no additive is ordinarily employed in a lower concentration than this. A specific activity of only 0.05 millicurie per ml in the added tel will provide this proportion of carbon-14. With this isotope we measured the activity of the carbon dioxide in the combustion gas.

This technique, which had been published,[17] showed a remarkably high precision. This was established when one cylinder was fed separately with fuels containing varying concentrations of the tagged tel. The carbon dioxide radioactivity reflected the tel concentration in an almost perfectly linear manner. The method was used to follow the distribution of tel under a variety of conditions. Fuels of different volatility characteristics were used, and the effects of speed and throttle settings were studied. Since subsequent work showed that our findings here were part of a much broader picture, we will discuss them together later.

Tritium Tracer Technique

At about this time in our program, another radioactive isotope, hydrogen-3 or tritium, became available at a strikingly low cost. Almost simultaneously, some very efficient equipment for measuring the radioactivity of weak beta emitters of this kind was introduced commercially. Also, we learned through a private communication that the Shell Martinez Laboratory had been using tritium tracers in fuel-distribution studies. The advantages of a technique based upon tritium were so attractive that we changed to this isotope for the remaining (and major) portion of our studies.

Tritium-labeled compounds are much less expensive and more easily prepared than carbon-14 compounds. The raw isotope is available for $0.002 per millicurie as compared with $28 for carbon-14. The replacement of hydrogen by tritium atoms in a molecule does not require disturbing the carbon skeleton, since ordinary compounds can often be tagged simply by catalytic exchange or by the Wilzbach reaction. In the latter method the inactive form is merely exposed to tritium gas at room temperature, and the radioactivity of the gas induces replacement of the H-1 by the H-3.[21] In addition to these methods, ordinary synthesis procedures can be employed, and with tritium these also are usually simpler than with C-14. When using any of these approaches, the low cost of the raw tritium makes it unnecessary to make numerous blank runs to establish the most efficient reaction conditions.

The engine setup used for tracing tritiated components of gasoline is shown in Fig. 2. Each of the eight cylinder-sampling valves is connected with a stainless-steel condenser containing a 3-turn spiral of tubing chilled by powdered dry ice. A ninth condenser to sample the overall exhaust is connected to a probe in the exhaust pipe. Usually all the condensers are "filled," that is blocked with a slug of ice, after about 2 gal of fuel have been consumed. The collection of aqueous samples proved very much simpler than the system of CO_2 absorbers needed in the carbon-14 work.

Furthermore, the regeneration and tedious purification steps needed with the carbonate samples is avoided. Instead, we need only to treat the thawed-out condensates, about 1–3 ml each, with a little activated carbon and then filter. For the activity measurement, about 0.25 ml of the sample is added to 15 ml of a clear "phosphor" solution in a glass vial. This solution contains small percentages of certain organic compounds which have the property of emitting tiny flashes of light when excited by beta particles.

The beta particles from tritium are much too weak to penetrate the walls of the vial. However, the light scintillations they produce are readily transmitted and perceived by a photomultiplier

[21] *Journal* of American Chemical Society, Vol. 79, 1957, p. 1013: "Tritium Labeling of Organic Compounds with Gaseous Tritium," by K. E. Wilzbach.

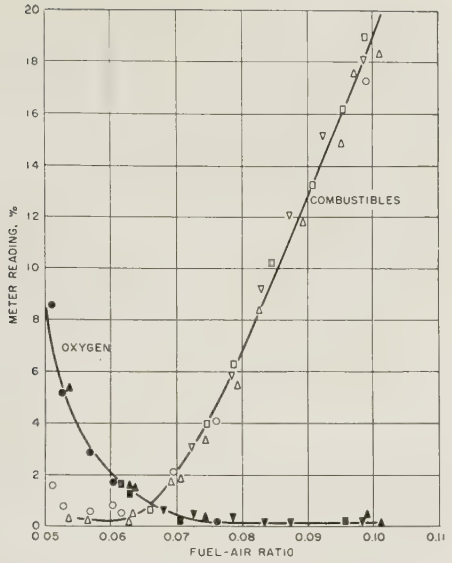

Fig. 4 — Calibration curve of exhaust gas analyzer for Fuel A (Engine D, Cyl No. 8 independently carbureted, various speeds and airflows)

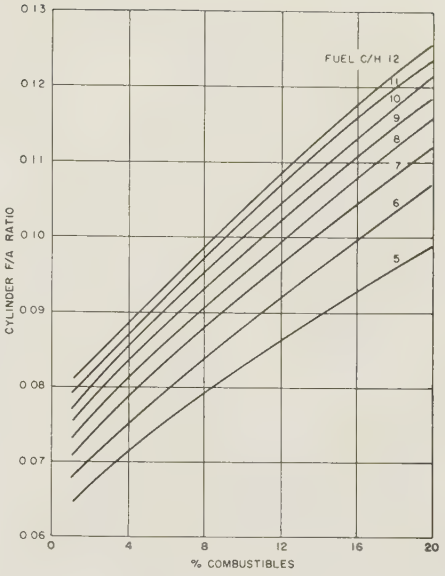

Fig. 5 — Calibration of exhaust-gas analyzer for fuels of different carbon-hydrogen ratio (Engine D, Cyl No. 8 independently carbureted)

tube. The detection instrument incorporates two such photo tubes and the additional elements needed to count the light emanations. Counting-samples prepared as described will run up about 50,000 counts per min. with 5 millicuries of activity incorporated in 6 ml of tel in the usual 2 gal of fuel (3 ml tel per gal). The minute or so of counting time required in this procedure is almost negligible compared to the several hours usually required with the CO_2 in the ion chamber. A complete description of this tritium-tracing procedure will be published elsewhere.

One-Cylinder Test of Technique — As with the carbon-14 method, we needed proof that the activity of the combustion sample, water in this case, was always proportional to the concentration of tagged additive in the fuel burned. To establish this, we blocked off one cylinder from the intake manifold and fed this cylinder from a miniature carburetor. When test fuels containing different concentrations of tritiated tel were fed, the activities of the condensates varied linearly (Fig. 3). Other tests showed that the sample activities were independent of fuel/air ratio.

There was some question as to whether the concentration of tel in the combustion-chamber charge was homogeneous enough to sample it reliably at only the one zone near the spark gap. In a special single-cylinder engine equipped with a sampling valve in the spark-plug hole, we tapped another hole in the remote end of the combustion chamber. This hole was fitted with a similar valve, and the engine was operated on a fuel containing tritiated tel. Samples taken from the two zones showed no significant difference in their activities.

A full program of tracer studies was then carried out in a multicylinder engine fitted with sampling valves. In each test we also obtained the cylinder fuel/air ratios to tell us the quantities, as well as the qualities, of the charges in individual cylinders. A description follows of the method used for this.

Measurement of Fuel/Air Ratio

For determining fuel/air ratio by exhaust-gas analysis, the absorption Orsat method has been most favored in the past. However, this method requires careful sample collection and handling, plus time-consuming analysis. In addition, interpretation of the Orsat data is rather critical.[22] For many years, continuous-reading electrical analyzers were not satisfactory for precise fuel/air measurement, primarily because of instrument error at fuel/air ratios leaner than 0.070 or circuit instability.[9,23]

For the studies reported herein, we used an exhaust-gas analyzer of the catalytic-cell type.[24] This gave accurate results over a range of 0.05 to above 0.10 fuel/air ratios. The instrument which is portable, continuously and simultaneously indicates the percentage of both the oxygen and the combustible gases in a flowing sample. Basically, the instrument combines part of the drawn-in sample with air in a catalytic cell. The resultant burning varies the resistance in one leg of a bridge circuit, and the imbalance is recorded as per cent combustibles. Another part of the sample is mixed with hydrogen in another catalytic cell where any oxygen present in the sample is detected as the result of its reaction with the added hydrogen and is indicated on another meter as per cent oxygen. Fig. 2. shows the instrument in a photograph of the test equipment.

Calibration of the instrument was necessary, since it does not indicate fuel/air ratio directly. Also, the combustible-analyzing circuit is sensitive to the carbon-hydrogen ratio of the fuel. The exhaust-gas analyzer was calibrated using Cylinder No. 8 which was carbureted independently of the rest of

[22] SAE Transactions, Vol. 38, 1936, pp. 90–98: "Relation of Exhaust Gas Composition to Air Fuel Ratio," by B. A. D'Alleva and W. G. Lovell.
[23] SAE Transactions, Vol. 48, 1941, pp. 234–238: "Characteristics of Exhaust Gas Analyzers," by J. L. Dilworth.
[24] *Steel* Magazine, Vol. 117, Dec. 10, 1945, p. 134: "Combustion Control: Cities Service Heat Prover."

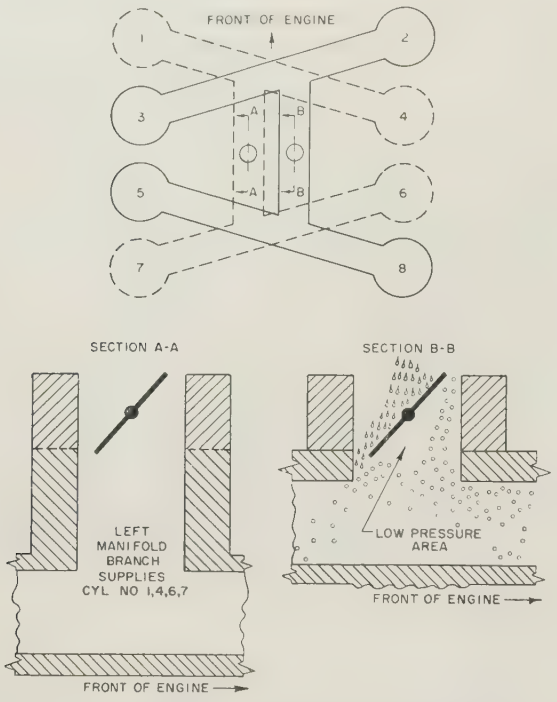

Fig. 6 — Schematic sketch of intake manifold design (Engine D)

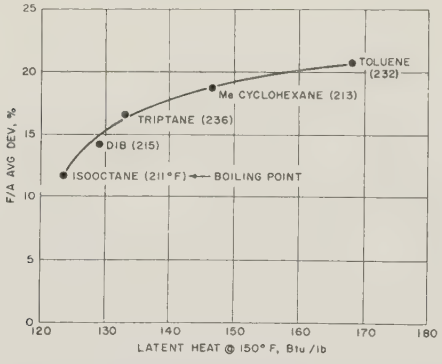

Fig. 7 — Effect of fuel latent heat on fuel distribution (individual hydrocarbons run as entire fuel, Engine D, 2400 rpm, 40-deg throttle)

Table 1 — Fuel Inspection Data

Fuels	A		D	E
Hydrocarbon Type				
Olefins, %	20.5		—	—
Aromatics, %	19.7		—	—
Saturates, %	59.8		—	—
Gravity, deg API	58.1		52.4	53.3
ASTM Distillation Temperature °F,				
Ibp	102		91	94
10%	137		138	151
30%	182		203	202
50%	241		273	244
70%	301		327	309
90%	354		363	361
End Point	401		408	412
TEL, ml/gal	0	3.0	0.75	0.47
Octane Number				
Whole Fuel				
Research	81.8	92.9	88.3	88.0
Motor	75.7	84.4	81.0	80.1
Front 55%				
Research	88.8	97.9	81.8	101.5
Rear 45%				
Research	67.5	81.9	96.9	71.4

the engine and was fitted with a timed sampling valve. Fig. 5 shows the relation of meter readings and measured input fuel/air ratio for Test Fuel A at a variety of operating conditions. The instrument was also calibrated for seven pure hydrocarbons and two commercial fuels with carbon-hydrogen ratios ranging from 5.0 to 12.0. The results are shown in Fig. 5.

Calculations based on component-distribution studies presented later indicated that the maximum variation in the carbon-hydrogen ratio of the Test Fuel A among the individual cylinders was 0.4. At an input fuel/air ratio of about 0.080, this variation in carbon-hydrogen ratio can cause a deviation of ± 0.001 in fuel/air ratio. The instrument accuracy of the analyzer is within $\pm 0.5\%$ of the meter reading which is less than ± 0.001 in fuel/air ratio. Thus, measurements of fuel/air ratio among the cylinders using the analyzer should be within ± 0.002 fuel/air ratio.

Besides minimizing sampling and operator errors, of the instrument responds very rapidly. A complete survey of the fuel/air ratio among all eight cylinders can be performed in less than 20 min for one operating condition by successively connecting the analyzer to the various cylinder sampling valves.

Selection of Test Conditions

The engine chosen for the distribution studies using tritium tracers was a 1956-model V-8 truck engine of Make D. It was known to have relatively poor distribution under some operating conditions. This engine was equipped with a two-barrel downdraft carburetor with throttle-body heat "off," exhaust crossover passage restricted but "open," and heat valve in "heat off" position. Each barrel of the carburetor supplied four cylinders. The intake-manifold design, illustrated in Fig. 6, provided equal-length passages to each cylinder.

An engine speed of 2400 rpm was used for most of these tests, because that speed is in the range that durability problems often occur and is also near the speed range of maximum knock for this engine. For most of the tracer studies, the throttle blade was set at the position which caused poorest fuel distribution. This setting, 40 deg angle from vertical or wide-open throttle, resulted in a manifold vacuum of 3.0 in. of Hg at 2400 rpm and 90% of wide-open throttle power. All of the tritium-tracer studies in this engine were conducted at a constant speed of 2400 rpm. Inlet air temperature was held between 80 and 90 F in all tests.

The fuel used for most of the test work was blended to be representative of the heavier commercial fuels. Inspection data on this Fuel A appears in Table 1 along with data on two other fuels which will be discussed later. Approximately 40% of the regular-grade fuels marked in the summer of 1958 had ASTM-distillation 90% points which were above that of Fuel A.

It is well at this point to review the index or measure of fuel distribution used frequently throughout this paper. Rather than expressing a set of data from eight cylinders as the maximum spread between them, the average deviation was used to represent the set of data with less partiality for extremes. Average deviation is simply the average of the deviations of all cylinders from the value that

would be expected if distribution were perfect. Thus, from the fuel/air ratio data shown in Table 2, Cylinder No. 2 was 27% richer and cylinder No. 6 was 14% leaner than the carburetor or average fuel/air ratio. Summing the per cent deviations (regardless of arithmetic sign) and computing the average for all eight cylinders gives an average deviation of 18.9%. The maximum spread among cylinders for all whole-fuel and fuel-component distribution tests was within ±8% of being 3.13 times the average deviation. This method of expressing distribution as percentage of average deviation will be used widely in the remaining paper for both fuel/air ratio and concentration of individual fuel components among the cylinders.

Effect of Fuel Factors

This section discusses the effect of fuel factors on the fuel/air ratios in the various cylinders and on the concentrations of the various fuel components in the cylinder charges.

Distribution of Whole Fuel — It is well-understood that the principal cause of maldistribution is that the fuel does not vaporize completely. The fuel vapor distributes fairly uniformly, but the liquid residue flowing along the walls of the intake manifold does not get divided equally among the cylinders.

Any fuel characteristic which allows increased vaporization will tend to improve distribution. Either higher volatility (lower boiling point) or lower heat of vaporization will help. A fuel with a lower latent heat means of course more fuel evaporated per Btu of heat transferred to the liquid in the manifold. When pure hydrocarbons are compared as single-component whole fuels, their distribution tends to improve with lower boiling points. We have been able to demonstrate improvements resulting from lower latent heat of vaporization. This was done by comparing the distributions of five pure hydrocarbons of similar boiling points but varying latent heats, as shown in Fig. 7. Other investigators [9,12] found that alcohols distributed much more poorly than hydrocarbons of similar boiling points. This was because the alcohols had much higher latent heats.

We next undertook to correlate the distribution of 23 typical commercial gasolines with their volatilities and latent heats. These fuels ranged wider in volatility and specific gravity than those from a 1957 Premium Fuel Survey.[25] Since it is difficult to assign a definite value of latent heat of vaporization to such a mixture as gasoline, we used specific gravities in our correlations. A close relationship has been found between gasoline specific gravities and latent heats.[26] This is undoubtedly because throughout the hydrocarbon family the specific gravities parallel the latent heats with remarkable consistency.

We fed the distribution data for these fuels, along with their specific gravities and various indices of volatility, into a digital computer in the form of linear regression equations. We discovered a very

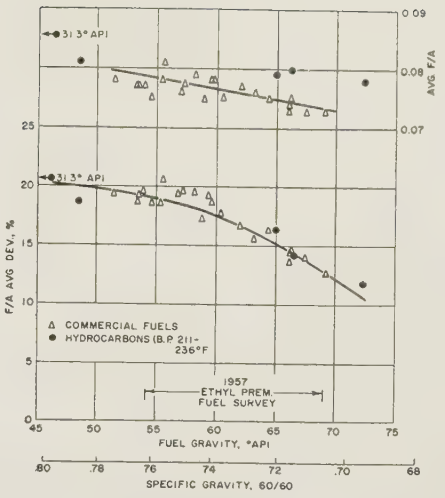

Fig. 8 — Relationship between fuel distribution and fuel gravity (Engine D, 2400 rpm, 40-deg throttle)

Table 2 — Computation of Fuel/Air Ratio Average Deviation
(Engine 1956 Make D, 2400 rpm, 40-deg throttle, Fuel A)

Cylinder	Fuel/Air	Deviation, %
1	0.0845	+ (8.6)[a]
2	0.0985	+ (26.6)
3	0.1020	+ (31.1)
4	0.0850	+ (9.3)
5	0.0560	− (28.1)
6	0.0670	− (13.9)
7	0.0670	− (13.9)
8	0.0620	− (20.3)
Average	0.0778	18.9%

[a] Example: $\frac{0.0845 - 0.0778}{0.0778} = 8.6\%$

pronounced correlation between uniformity of distribution and lower specific gravity (higher deg API gravity), as shown in the lower curve of Fig. 8. There was only a slight additional correlation with the ASTM 90% point. Previously, some investigators found that distribution could be correlated with ASTM distillation data[9,11] while others found little or no correlation.[6,8].

The specific gravities of commercial fuels vary rather widely, depending upon the proportions of aromatics and naphthenes used in the blend. These formulations are dictated, of course, by such factors as refining processes and sources of crude. Gasoline volatility is also dictated by other important engine performance requirements. Hence, it would appear that refiners can do very little to improve the distribution characteristics of gasolines.

Tracer Studies of Distribution of Individual Hydrocarbons in Gasoline Blends — In the first phase of our program with tritium, we followed the distribution of a series of six hydrocarbons whose boiling points were spaced evenly over the entire boiling range of the test fuel. In each case, a very small quantity, usually about 2 cc, of the tritiated hydrocarbon was blended into each gallon of a typical full-boiling gasoline (Fuel A). This quantity is far too small to change noticeably the other character-

[25] "Antiknock Behavior of Premium Motor Fuels," by I. A. Caputo and H. J. Sewell. Report No. RT-34, 1957, Ethyl Corp.
[26] *Petroleum Refiner*, Vol. 37, October, 1958, p. 123: "Find Latent Heats Quickly," by D. S. Davis.

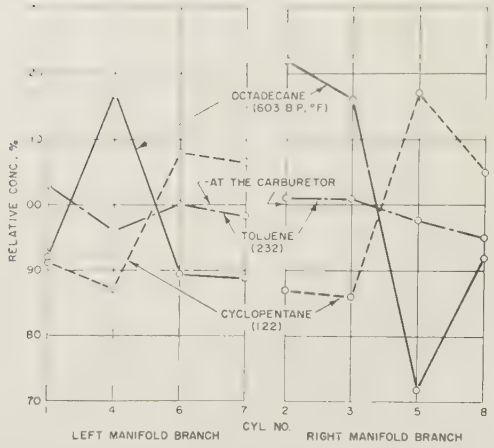

Fig. 9 — Distribution of octadecane, toluene, and cyclopentane in Fuel A (Engine D, 2400 rpm, 40-deg throttle)

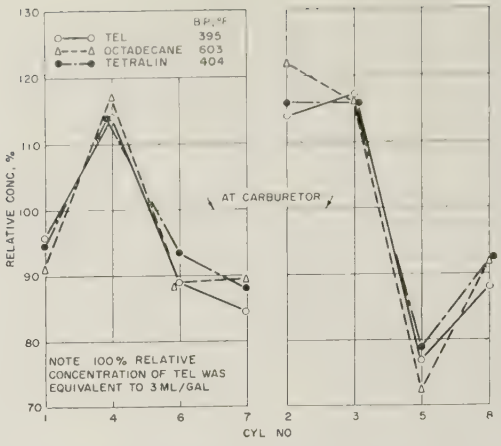

Fig. 11 — Distribution of three high-boiling components in Fuel A (Engine D, 2400 rpm, 40-deg throttle)

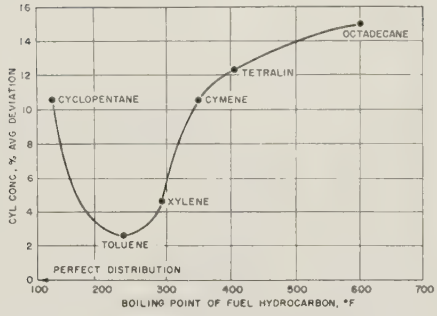

Fig. 10 — Average cylinder deviation for concentration of various fuel hydrocarbons blended in Fuel A (Engine D, 2400 rpm, 40-deg throttle)

istics of the gasoline. Because the technique is extremely sensitive, however, this amount is entirely adequate to tell us how material in the boiling range of the particular tracer hydrocarbon distributes in relation to the rest of the fuel.

In these tests, we again used Engine D at the 40-deg throttle position. Aqueous condensate samples were collected from the eight cylinders and also from the overall engine exhaust. The specific radioactivity of the condensate from the overall engine exhaust furnished a baseline value corresponding to the concentration of tritiated component in the fuel fed to the engine. The activities of the cylinder condensate could then be translated into concentrations of the tagged component in individual cylinder charges. A complete knowledge of the concentrations of this and other tagged components in a cylinder charge describes the overall composition of the cylinder charge. For many purposes, this knowledge can be more important than knowing fuel/air ratios. It is especially important in interpreting antiknock performance. For example, in later work we will be more interested in the concentration of tel (ml/gal) in the cylinder charge than in mass flow (ml/hr) to a cylinder.

The concentrations of the tagged component found in the various cylinders can be expressed relative to the original concentration in the engine fuel. In Fig. 9, this has been done with each of three hydrocarbons of widely scattered boiling points. The graph shows the role of volatility in determining how a particular hydrocarbon in the fuel gets disproportionated with respect to the whole fuel. Let's compare first the results with three hydrocarbons of widely scattered boiling points. The fuel charge received by Cylinder No. 2 contains 122% of the original concentration of octadecane, only 87% of the original of cyclopentane, but a near-original 101% of toluene. These relative concentration figures are based on the very nominal original concentration in the fuel. Cylinder No. 5 shows a complete reversal of this. When we examine in Table 2 the whole-fuel distribution characteristic of this engine condition, we see that Cylinder Nos. 2 and 5 were rich and lean, respectively.

How richness and leaness lead to these different fuel compositions becomes clear when we consider the different make-ups we may expect of the liquid and vapor feeds from the manifold.

A lean cylinder, such as No. 5, receives very little liquid, and so the overall charge will be high in cyclopentane, like the vapor. On the other hand, the rich No. 2 cylinder receives a large fraction of its fuel as liquid containing little or no cyclopentane. The converse is true with octadecane contrations in the cylinders. Toluene distributes evenly because of its normal concentration in either the liquid or the vapor.

The relative concentration values for the cylinders shown in Fig. 9 may be expressed as percentage deviations from the original concentration in the fuel. When these deviations are averaged for the eight cylinders, they furnish a single number which may be taken as an index of the spread in concentrations among the cylinders. These average deviations for the six tritiated hydrocarbon tracers are plotted versus their boiling points in Fig. 10.

The quite uniform distribution seen earlier with toluene places it at the minimum of this curve. The cylinder concentrations of cyclopentane vary widely from normal, for the reasons given earlier. The plateau beginning near tetralin shows that compounds having boiling points at 400 F or more exhibit

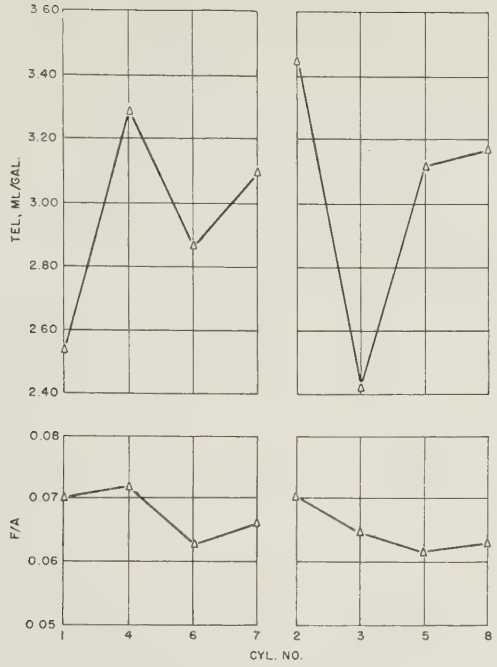

Fig. 12 — Distribution of tel and Fuel A at road load (Engine D, 2400 rpm, 65-deg throttle)

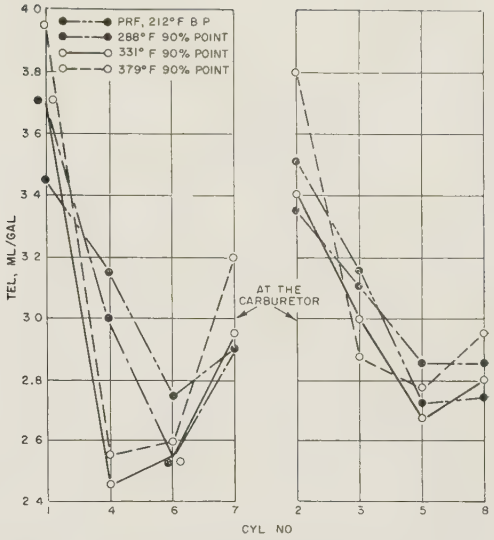

Fig. 13 — Distribution of tel in fuels of various distillation ranges (Engine Q, 800 rpm, 10-deg throttle)

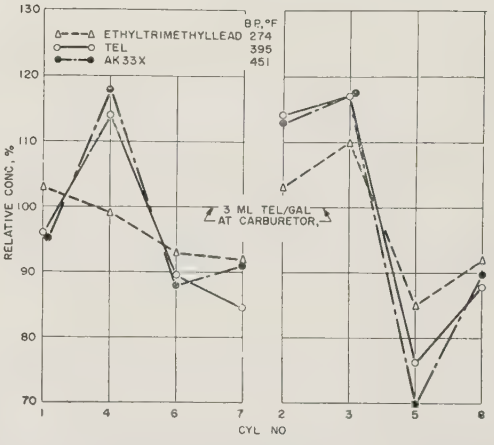

Fig. 14 — Distribution of three antiknock compounds (Engine D, 2400 rpm, 40-deg throttle, Fuel A)

about the same unevenness in their cylinder concentrations. Such substances are all effectively nonvolatile, and they are carried almost exclusively in the liquid portion of the feed.

As will be shown to be the case also with fuel additives, the distribution of a single component in a blended fuel appears to depend almost solely on its volatility. The reason for this will be discussed later.

Distribution of Tel — We shall see that fuel additives belonging to various chemical families distribute very much the same as hydrocarbons of the same boiling point. On the curve shown in Fig. 10, tel (boiling at 395 F) would fall on the plateau with high-boiling hydrocarbons. The resemblance of the tel pattern to that of two such hydrocarbons is seen in Fig. 11. Thus, the same relationship shown between high octadecane concentration and cylinder richness, discussed with Fig. 9, extends also to tel. Considerable indirect evidence for this correlation between fuel/air ratio and tel concentration was accumulated by earlier workers.[4,6]

However, we find that this correlation which occurs at high output conditions, where there is considerable liquid feed carrying tel to rich cylinders, does not occur at low output conditions such as road load. At road load, the high manifold vacuum and low fuel consumption result in much more complete vaporization of the gasoline, and this of course greatly evens out its distribution, as seen in the lower part of Fig. 12. However, the tel distribution is about as irregular as before, and the pattern no longer corresponds to the fuel/air ratios. We believe that at road load the tel is carried along in residual trickles of heavy ends of the fuel which drift erratically along the manifold surfaces. This phenomenon was observed repeatedly during the early work with the glass manifold. The courses of the trickling streams are so sensitive to slight changes in throttle setting and other parameters that no consistent pattern would be expected.

Effect of Fuel Boiling Range on Tel Distribution — One of the questions investigated during our earlier work with carbon-14 was whether tel distribution could be improved by changing the boiling range of the fuel. Fig. 13 shows the patterns obtained in Engine Q when the baseline fuel was replaced by fuels of lower and higher end points, and also by a flat-boiling primary reference fuel. It is clear that the distillation range of the fuel made little difference in the tel concentration picture. Even though the heavier fuels gave poorer fuel distribution, their tel patterns were much the same as with the lightest of the gasolines.

Why this happens becomes clear after we consider the extreme case of a completely nonvolatile fuel. This would remain entirely liquid and yet, regardless of how unequally the fuel was distributed, the same original tel concentration would be delivered to every cylinder. With all our actual test fuels of normal volatility, the tel concentrates in the liquid residue, and rich cylinders thus receive

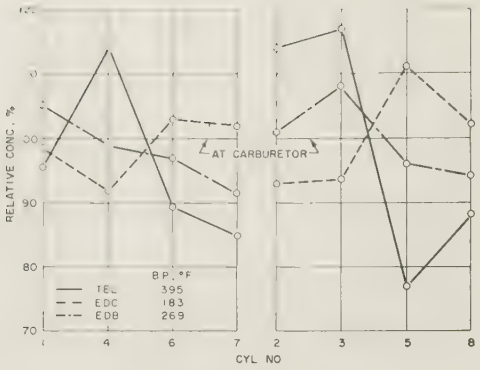

Fig. 15 — Distribution of tel and its Motor mix scavengers (Engine D, 2400 rpm, 40-deg throttle, Fuel A in carburetor contains — 3 ml tel, 0.5 theory ethylene dibromide, 1.0 theory ethylene dicholoride)

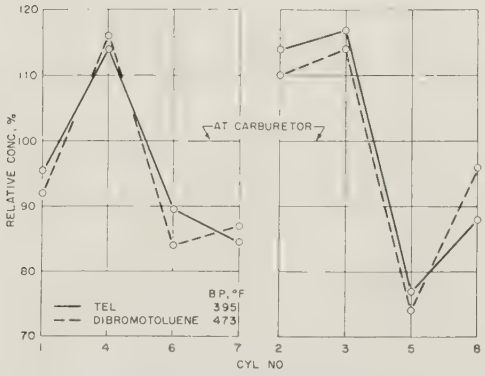

Fig. 16 — Distribution of dibromotoluene and tel (Engine D, 2400 rpm, 40-deg throttle, Fuel A)

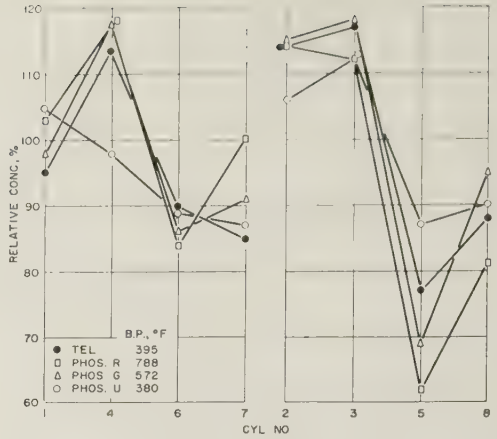

Fig. 17 — Distribution of phosphorus additives (Engine D, 2400 rpm, 40-deg throttle, Fuel A)

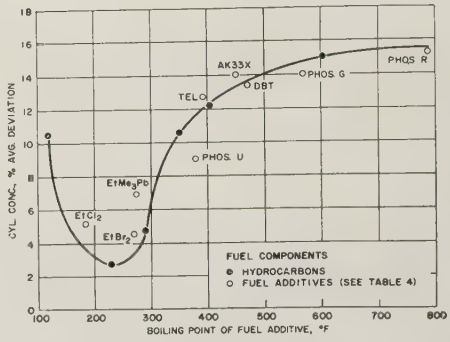

Fig. 18 — Average cylinder deviation for concentration of various fuel additives blended in Fuel A (Engine D, 2400 rpm, 40-deg throttle)

excessive shares. However, as we have seen, this disproportionation of tel is not especially poorer with our lightest fuels.

Distribution of Other Antiknocks — The attractiveness, from a distribution standpoint, of an antiknock having an intermediate volatility was recognizable from the patterns in Fig. 9, where toluene looked so good. Ethyltrimethyllead ($EtMe_3Pb$) boils somewhat higher (274 F) than toluene, but its improvement over the tel pattern may be seen in Fig. 14.

A new antiknock called AK-33X under commercial development by our company has a boiling point of 451 F, about 50 deg higher than tel. Its distribution is practically identical with that of tel as shown in Fig. 14.

Distribution of Lead Scavengers — Ethylene dibromide and ethylene dichloride boil, respectively, above and below the midrange of the fuel. Their distribution patterns, shown in Fig. 15, are essentially inverse, much as with cyclopentane and octadecane. It may be observed that these patterns balance one another in such a way that with 62 Mix (1 theory halogen as chloride and 0.5 theory as bromide) the total concentrations of halogen would be fairly uniform among the cylinders.

However, it has been generally supposed more desirable to keep the concentration of scavenger proportional to the tel concentration in the fuel charges. A number of years ago it was suggested that this might be accomplished by using halides with much higher boiling points, closer to that of tel.[27] The pattern for such a compound, dibromotoluene, is compared with that of tel in Fig. 16.

Phosphorus Additives — Most commercial phosphorus fuel additives for gasoline have very high boiling points. The distributions of two of these, boiling at 572 and 788 F, are seen in Fig. 17 to be much like that of tel. A third additive, which boils a bit below tel, is seen to distribute somewhat more uniformly.

Summary of Fuel-Component Distribution Relative to Volatility — The work just described shows that rich and lean cylinders of a maldistributing engine receive fuel charges of very different compositions with respect both to additives and to hydrocarbons of different boiling points. Whether a given component will be found in higher concentrations in the rich or the lean cylinders, and how much difference between these there will be, depends solely on the component's boiling point. This is because its concentration in the gasoline vapor (and thus also its concentration in the remaining liquid) depends only on its partial pressure in the liquid mixture flowing through the manifold. It is the latent heat of the entire mixture during the process of vaporization that controls the amount of vapor that is formed. Any single component is but

[27] U. S. Patents 2,479,900, 2,479, 901, and 2,479,902, by J. S. Wintringham and G. Calingaert. Aug. 23, 1949.

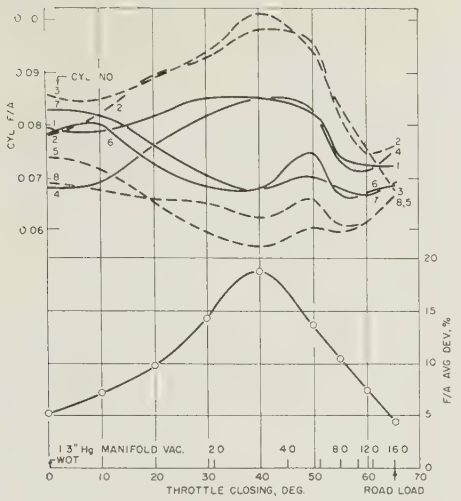

Fig. 19 — Effect of throttle position on distribution of Fuel A (Engine D, 2400 rpm)

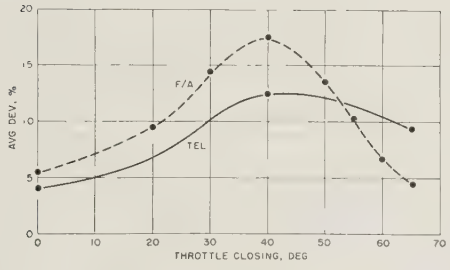

Fig. 20 — Effect of throttle position on distribution of tel and Fuel A (Engine D, 2400 rpm)

a fraction of this mixture, which comprises varying proportions of every substance present in the distilling liquid.

The boiling points and the average deviations from normal of the cylinder concentrations are listed in Table 3 for all the components we have studied. It is interesting to note in Fig. 18 that these deviations for all the additives, which are of widely different chemical nature, fall quite closely to the curve for hydrocarbons which was shown earlier as Fig. 10.

Because many commercial gasoline additives have high boiling points, it is worth observing that above a boiling point of about 400 F these reach a limiting degree of maldistribution.

Effect of Operating Conditions

Engine operating conditions influenced distribution more than the fuel factors. This is illustrated below where the effects of throttle-blade position, engine speed, carburetor fuel/air ratio, and accelerating conditions are discussed.

Throttle-Blade Position — Of the operating variables investigated, throttle-plate position had the greatest effect on distribution. Fig. 19 shows a plot of individual cylinder fuel/air ratio as a function of throttle-plate angle at 2400 rpm with Fuel A. The cylinders in dashed lines were fed through the right manifold branch. Each cylinder of the engine responded differently to throttle-plate angle.

At wide-open throttle (0 deg) distribution was

Table 3 — Summary of Distribution Data on Fuel Components

	Boiling Point (F)	Average Deviation, %[a]
Cyclopentane	122	10.6
Toluene	232	2.7
Xylene	291	4.5
P-Cymene	349	8.1
Tetralin	404	12.2
n-Octadecane	603	14.7
Tetraethyllead, TEL	395	14.0
Ethyltrimethyllead, $EtMe_3Pb$	274	6.9
AK-33X	451	14.3
Ethylene dichloride, $EtCl_2$	183	5.1
Ethylene dibromide, $EtBr_2$	269	4.7
Dibromotoluene, DBT	473	12.4
Phosphorus "R"	788	15.4
Phosphorus "G"	572	14.0
Phosphorus "U"	380	9.1

[a] For the concentrations in the eight cylinder charges, as compared to that originally blended in Fuel A.

relatively good, despite low manifold vacuum and consequent poor vaporization. Maximum maldistribution occurred with a throttle closing of 40 deg which corresponds to 3.0 in. of Hg manifold vacuum and 90% wide-open throttle power. At this throttle setting, the front four cylinders were over supplied with fuel, and the rear cylinders ran lean. Closing the throttle beyond 40 deg improved distribution significantly, and fuel distribution at road load was better than at wide-open throttle.

Two mechanisms apparently caused this throttle position effect — deflection and vaporization. The throttle plates, when set at an angle to the flow stream, are believed to have a low-pressure area on the underside of the trailing edge of the plates. This low-pressure area tended to deflect fuel toward the front cylinders (Fig. 6). The 40-deg angle, midway between closed and wide-open throttle, resulted in maximum deflection. From wide-open throttle to the 40-deg throttle position, the manifold vacuum increased by only 1.6 in. of Hg. The slightly increased fuel vaporization caused by the greater vacuum, was over shadowed by the effect of throttle-plate angle. The improvement in distribution at throttle closings greater than 40 deg resulted from improved vaporization caused by increased manifold vacuums (approximately 16 in. of Hg vacuum at 65-deg throttle) and better atomization due to fuel impingement on the nearly closed throttle.

Fuel-additive distribution was also importantly influenced by throttle-plate position. Fig 20 shows average-deviation curves for both fuel/air ratio and tel concentration as a function of throttle-plate angle. The tel distribution was poorest under the conditions that gave poorest fuel distribution. However, although fuel distribution improved at the greater throttle angles and higher manifold vacuums, the tel concentration distribution did not improve to the same degree.

Other work with carbon-14 in the 1949 Make Q engine showed that throttle-plate position drastically changed the pattern of tel distribution at the same manifold vacuum. Fig. 21 shows a comparison of the distribution patterns obtained at throttle settings of 10 deg before vertical and 10 deg after vertical. The effect is a general reversal between the front and rear cylinders. The data on fuel/air ratio showed that, in all cases, the cylinders with high tel concentrations were the rich cylinders, supporting the familiar relationship between liquid

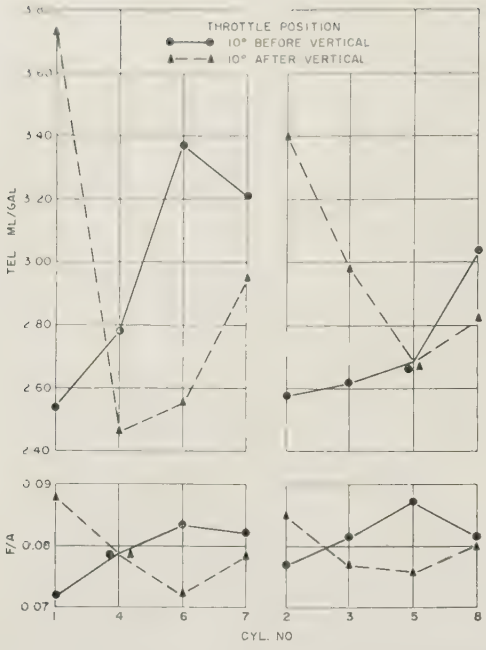

Fig. 21 — Effect of throttle position on distribution of tel and Fuel B (Engine Q, 800 rpm)

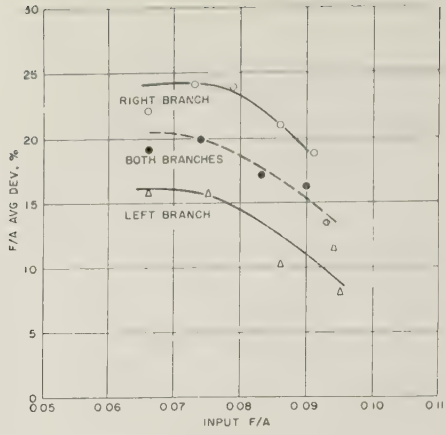

Fig. 22 — Effect of input fuel/air ratio on distribution of Fuel A (Engine D, 2400 rpm, 40-deg throttle)

cylinder feed and high concentrations of nonvolatile components at low manifold vacuums.

As mentioned, throttle-plate position had the greatest influence on distribution of any operating or fuel variable investigated. Later, it will be shown how the concept of throttle-plate deflection was used to modify the throttle so that these deflection effects were minimized.

Effect of Carburetor Fuel/Air Ratio — Increasing fuel flow in this engine improved fuel distribution in both manifold branches at the condition of poorest fuel distribution. Fig. 22 shows the average deviation of fuel/air ratio in both branches as affected by the input-mixture ratio at 2400 rpm and a 40-deg throttle. The overall fuel/air ratio was limited between 0.095 and 0.065, because the rich and lean limits of combustion were reached in Cylinder Nos. 3 and 5, respectively. There was little change in distribution between fuel/air ratios of 0.065 and 0.080. However, at ratios above 0.080, fuel distribution improved significantly. This response may be due to the same factors discussed under throttle-position effect, namely, deflection and vaporization. It is probable that greater fuel flow tended to move in the shortest path around the throttle plates, thereby reducing the deflection effects due to low pressure areas and thus improving distribution. Test conditions which do not emphasize throttle-plate deflection may show that reduced fuel flow results in improved distribution. Fuel-distribution improvements due to lean mixtures have been reported by others.[3] It should be stressed, however, that small variations in carburetor fuel/air ratios (that might be caused by differences in fuel specific gravity, see Fig. 8) did not significantly change distribution.

Increased engine speed has been reported to improve fuel distribution in some engines.[3,9] Complete fuel-distribution surveys over the load range at speeds from 1600–2400 rpm indicated that 40-deg throttle was the setting for poorest distribution. Fig. 23 shows the average deviation in fuel/air ratio at speeds of 800–2800 rpm with a 40-deg throttle position. About 1200 rpm appeared to be the speed for poorest distribution, and improvement was small at speeds beyond 1600 rpm. It is interesting that this V-8 test engine experienced significantly poorer distribution at 1200 rpm than at 800 rpm. A similar speed effect in a six-cylinder engine was observed by Donahue and Kent.[6] The previously discussed "deflection" caused by a low-pressure area beneath the throttle plate is dependent upon the mixture velocity over and around the throttle plate. Because of lower flow rates at the lower engine speeds, the "deflection" tendency may not have been as great at 800 rpm as at the higher speeds. However, there were other factors which tended to make distribution worse at the lower speeds. For instance, fuel "atomization" was poorer due to lower velocities. Furthermore, vaporization was less due to lower manifold vacuums. At 800 rpm the manifold vacuum was 3.5 in. of Hg less than at 2800 rpm. Thus, it is possible that these opposing factors caused 1200 rpm to be the speed for the poorest distribution.

Increasing speed improved tel distribution in the 1949 Make Q engine. Fig. 24 compares the tel-distribution patterns obtained at speeds of 800 and 2000 rpm with a throttle setting of 10 deg before vertical. The same overall fuel/air ratio was maintained. Although the whole fuel distribution was not greatly smoothed out, the tel-concentration pattern was appreciably better at the higher speed. Calculations indicated that at the higher speed all of the cylinders received much more fuel in liquid form. Since this liquid had not been as concentrated in tel as it was at the lower flow rate at 800 rpm, the rich cylinders received larger shares of liquid and also received more normal proportions of tel at 2000 rpm.

In general, the influence of speed on fuel distribution was not as great as would be anticipated with a lengthy manifold uncommon to V-8 engines. Furthermore, the advent of modern automatic transmissions has limited the wide-open throttle speed range of engines on the road. In the two V-8 engines studied, the influence of throttle position

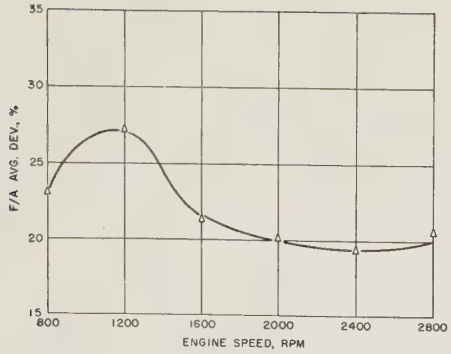

Fig. 23 — Effect of engine speed on distribution of Fuel A (Engine D, 40-deg throttle)

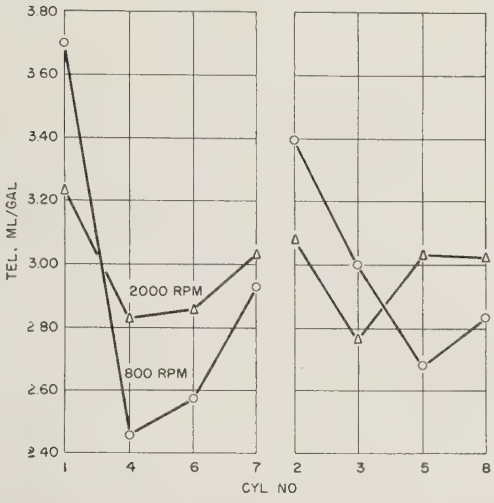

Fig. 24 — Effect of engine speed on tel distribution (Engine Q, throttle position 10 deg before vertical, Fuel B)

overwhelmed any effect of speed.

Distribution During Acceleration — In order to ascertain the significance of studying fuel and additive distribution under constant-speed (steady state) conditions, fuel distribution was measured on the engine dynamometer during accelerations, using more responsive instrumentation (infrared gas analyzers). (See Appendix for a description of techniques.)

Among the factors investigated under accelerating conditions were throttle position, engine speed, and fuel volatility. These accelerations, over a range of 20–65 mph, were similar to those obtained in a passenger car of Make D, equipped with an automatic transmission (allowing a stall speed of about 1750 rpm). The upper curve in Fig. 25 shows the change in fuel/air ratio during acceleration with a 20-deg throttle. There was little initial change in fuel/air ratio immediately following the throttle opening, but overenrichment occurred at about 4 sec. The period between the start of acceleration and the first time the value of the stabilized fuel/air ratio was reached can be termed (for purposes of this paper) "manifold lag." It was during this "lag" period that the fuel in the liquid state lagged behind the vapor and air. The length of the manifold lag for the three settings was between 2.5 and 3.0 sec.

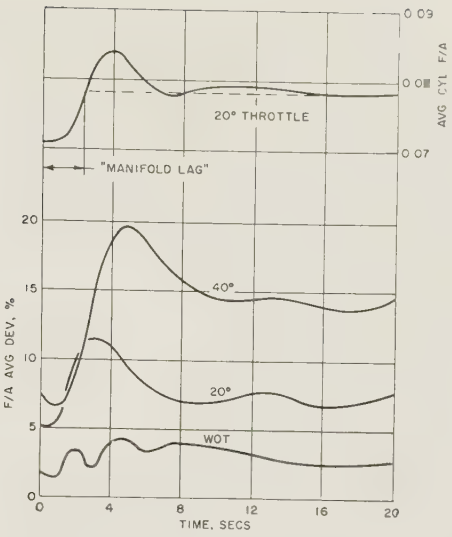

Fig. 25 — Effect of acceleration on distribution of Fuel A at three throttle settings (Engine D, acceleration from 1750 rpm)

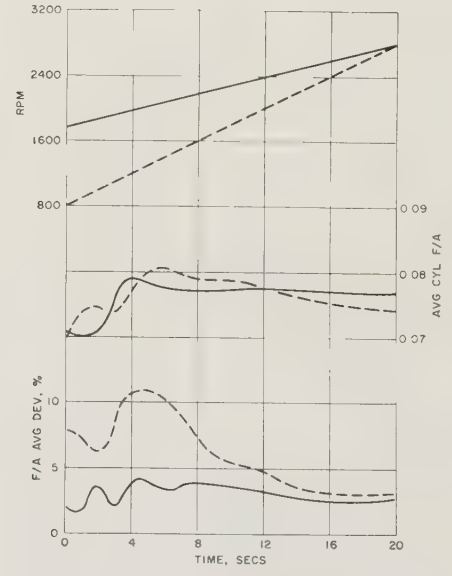

Fig. 26 — Effect of acceleration from different speeds on distribution of Fuel A (Engine D, wide-open throttle)

The lower three curves in Fig. 25 show the average deviation in fuel/air ratio among the cylinders for three throttle settings. At both the 20 and 40-deg throttle positions, poorest distribution existed during the acceleration at about the same time that the cylinders received over-enrichment. It is significant that the acceleration tests indicate the same relative effect of throttle position as did the constant-speed tests.

Fig. 26 compares the average fuel/air ratio and average deviation during wide-open throttle accelerations started from 1750 (previously shown) and 800 rpm which is representative of a third-gear acceleration (with a manual transmission) from about 10 mph. The start from 80 rpm caused longer manifold lag and also poorer distribution during the early part of the acceleration. The speed effect on distribution was greater under accelerating condi-

tions than it was at constant speed. Obviously, automatic transmissions with high stall speeds have minimized manifold lag and reduced the distribution problem involved in low-speed accelerations.

The distribution of very volatile commercial Fuel C was compared with that of Fuel A under the third-gear-type wide-open throttle accelerations. Fig. 27 shows that differences existed in distribution and also mixture ratio effects at the carburetor. The heavier and less volatile fuel A ran slightly richer, exhibited a greater manifold lag and distributed more poorly. Under constant speed 2400 rpm, 40-deg throttle conditions, the more volatile Fuel C distributed better than Fuel A. Under accelerating conditions, the more volatile fuel demonstrated an even greater superiority. Here again, while the accelerating tests show somewhat greater differences between variables, the constant speed, 40-deg throttle conditions compare effects very favorably in a directional manner.

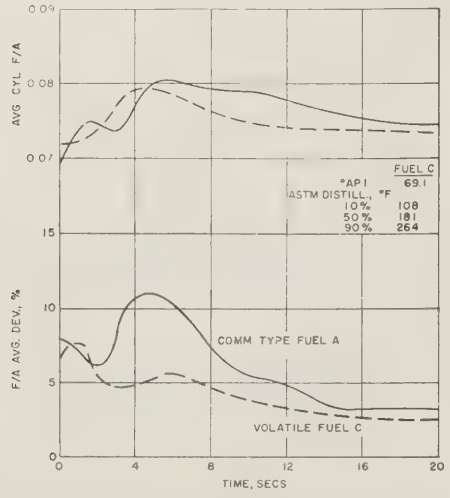

Fig. 27 — Distribution of two fuels during wide-open throttle accelerations (Engine D, acceleration from 800 rpm)

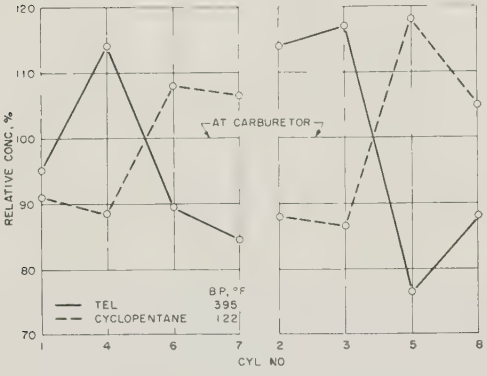

Fig. 28 — Distribution of cyclopentane and tel (Engine D, 2400 rpm, 40-deg throttle, Fuel A)

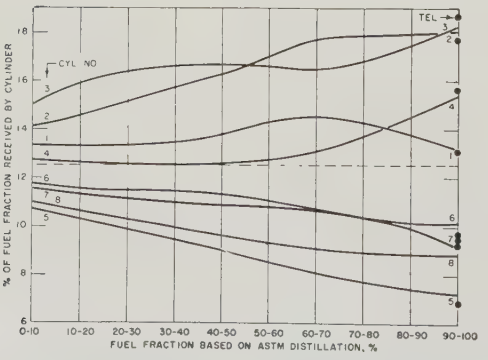

Fig. 29 — Composition of fuel received by each cylinder (Engine D, 2400 rpm, 40-deg throttle, Fuel A)

The general agreement found between the constant-speed and the accelerating test of whole-fuel distribution supports the validity of our fuel-component and additive distribution studies which were conducted under constant-speed conditions. The constant speed tests were easier to control and also allowed the use of more accurate and less complicated instrumentation.

Distribution of Octane Quality

The placement of octane quality within the boiling range of fuels has been responsible for the octane depreciation of some fuels in multicylinder engines.[2, 5, 28, 29] This phenomenon is caused by differences in fuel composition between individual cylinders and also "manifold-lag" conditions. Earlier data showed that lean cylinders are generally lower in tel under the high-output conditions where knock is most likely. However, as shown in Fig. 28, the tel-poor cylinders received high concentrations of the volatile front-end fuel components such as cyclopentane.

Fig. 29 shows the percentage of each 10% cut of Fuel A received by each cylinder at a constant speed of 2400 rpm and 40-deg throttle. Perfect quantity and quality distribution would result in exactly one-eighth (12.5%) of each fraction getting to each cylinder. Cylinder No. 2, while oversupplied with fuel, received a greater proportion of heavy-end material than front-end material. On the other hand, lean Cylinder No. 5 received a greater proportion of the front ends than the heavy ends. This indicates, for example, that a fuel with a high-octane front end would compensate the lean cylinders for the lower tel concentration.

Effect of Octane Placement in Base Fuel — The cylinders of Engine D were knock-rated independently at a constant speed of 2400 rpm and 40-deg throttle, in order to study octane-quality differences. Two fuels were prepared to provide the same whole-fuel distribution but to be radically different in octane placement within the boiling range. Table 1 shows that, although the Research and Motor octane numbers were about the same for both fuels, the rear 45% of fuel D rated 96.9 Research octane number, while the counterpart of Fuel E rated 71.4 Research octane number. These fuels were run at the condition of poorest distribution at 2400 rpm, and Fig. 30 shows the knock-limited spark advance plotted against the fuel/air ratios of the individual cylinders. Although both fuels were knock-limited

[28] *Petroleum Processing*, Vol. 6, June, 1951, pp. 618–621: "Bonus Fuels from Selective Blending," by T. H. Risk and D. MacDonald.

[29] "Road Antiknock Performance and Boiling Range of Hydrocarbon Types," by F. D. Buerstetta, W. C. Healy, Jr., L. A. McReynolds, R. Rohde, and H. C. Walters. Paper presented at SAE National Fuels and Lubricants Meeting, Tulsa, November, 1958.

at about the same spark advance in the lean cylinders, the rich cylinders differentiated best between these two fuels. This is because the rich cylinders received greater relative proportions of the heavy ends of the fuel (especially tel), than the proportion of front ends received by the lean cylinders, as shown earlier in Fig 29. Other investigators[9] also found little difference in cylinder octane quality due to composition differences under constant-speed conditions with full-boiling fuels.

Knock-rating under accelerating conditions clearly demonstrated the importance of octane placement in the fuel. The two widely different fuels, D and E, although they had similar Research and Motor octane numbers, differed by 9.1 octane numbers when rated by the Modified Borderline technique in accelerations of 750–2800 rpm at wide-open-throttle. Fig. 31 plots the engine rating of these fuels in terms of primary reference fuels over the speed range. The fuel with the high-octane front end was superior to the fuel with the low-octane front end at speeds below 2300 rpm. These accelerations were started from idle with high manifold vacuum. Upon quick opening of the throttle, the vaporized portion of the fuel arrived at the cylinder earliest and, as shown in Fig. 26, distribution did not stabilize until the engine speed was above 2000 rpm. Thus, Fuel D with its low octane in the most volatile part of the whole fuel, depreciated much more because its high-octane components were in the liquid portion which "lagged" behind the vapor. Gibson and Walcutt[5] have reported similar manifold lag effects.

To summarize, the importance of octane placement in the boiling range of the fuel is more evident under accelerating conditions than at constant speed. Fuels with high octane quality in the front end provide high road ratings,[29] especially in engines with bad cases of manifold lag.

Effect of Volatility of Antiknock Additive — The distribution of tel under accelerating conditions was found to undergo manifold lag effects similar to those experienced by the heavy ends of the fuel. Fuel A was knockrated both with and without 3 ml of tel per gal, and the octane-number gains due to tel are shown in Fig. 32 under both wide-open throttle accelerating and constant-speed conditions. Under constant-speed conditions, the increase in octane number due to 3 ml tel ranged from 8 to 10 octane numbers, depending on the speed. Under accelerating conditions, manifold lag was clearly demonstrated by a gain of only two octane numbers due to tel at 800 rpm as compared to 8.8 octane numbers under constant-speed conditions. At speeds above 1500 rpm, the gains exceeded those obtained at constant speed. This was due to an oversupply of tel in the cylinders during the latter part of the acceleration.

Differences between lead-alkyl antiknocks of different boiling points were found at a constant speed of 2400 rpm and 40-deg throttle. Because the additive-distribution patterns were very distinct, differences between the boiling points of the antiknocks were reflected in individual cylinder octane quality. Individual cylinders were knock-rated using Fuel A without lead and with sufficient lead alkyl to provide a Research octane number of 90.

Fig. 30 shows the increase in knock-limited spark advance allowed in the knocking cylinder, the cyl-

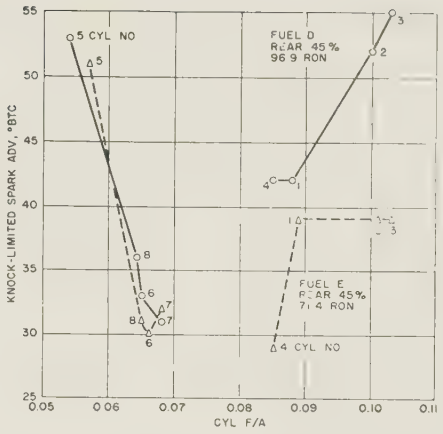

Fig. 30 — Knock-limited spark advance versus fuel/air ratio for individual cylinders (Engine D, 2400 rpm, 40-deg throttle)

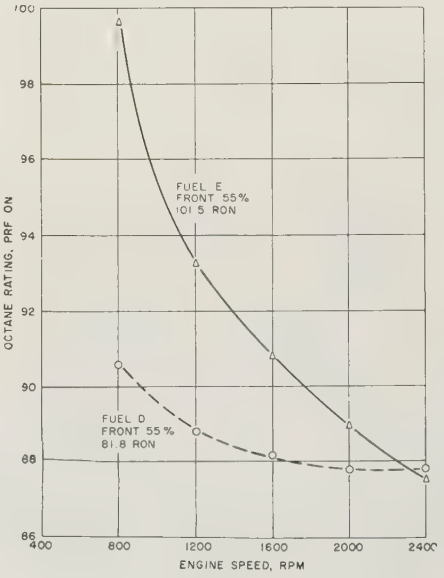

Fig. 31 — Octane ratings of two fuels with different octane placement under accelerating conditions (Engine D, wide-open throttle, modified borderline ratings)

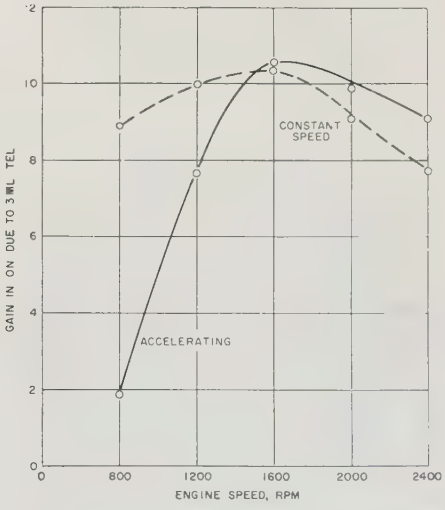

Fig. 32 — Octane gain due to 3 ml tel in Fuel A (Engine D, wide-open throttle)

inder of least increase, and the average of seven cylinders. (Cylinder No. 3, due to its richness, did not knock with all antiknocks.) In general, the lighter, more volatile antiknocks allowed larger increases in spark advance than did the higher boiling antiknocks. The mixture used in this test was composed of five lead alkyls varying in boiling points of 240–395 F, with a mean of 328 F. It is worthwhile to note that the greatest difference between the alkyls in terms of spark advance existed in the knock-limiting cylinder. The average spark-advance increase of the seven knocking cylinders shows this effect with more confidence than when observations were based on only one cylinder. The cylinder with the least increase in spark advance was the leanest cylinder (No. 5); it also showed a beneficial effect from the more volatile lead alkyls.

The relative effectiveness of these lighter alkyls would be expected to be greater when rated under accelerating conditions with manifold lag. Such advantages for the more volatile antiknocks have been demonstrated in some car-gasoline combinations in road-rating programs.

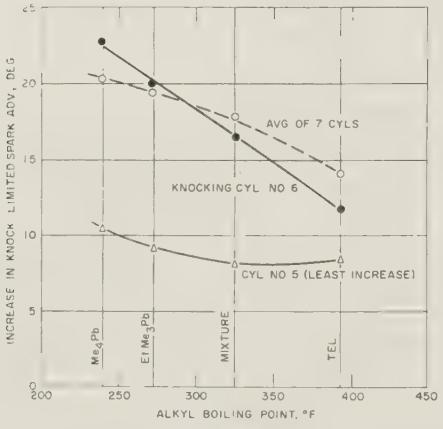

Fig. 33 — Effect of lead alkyl volatility on knock-limited spark advance due to antiknock addition to base fuel (Engine D, 2400 rpm, 40-deg throttle, Fuel A with 90 Research octane number with antiknock)

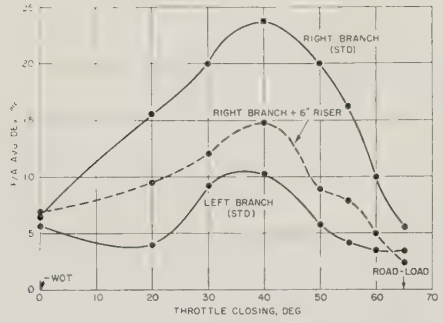

Fig. 34 — Effect of throttle position on distribution of Fuel A with additional manifold riser (Engine D, 2400 rpm)

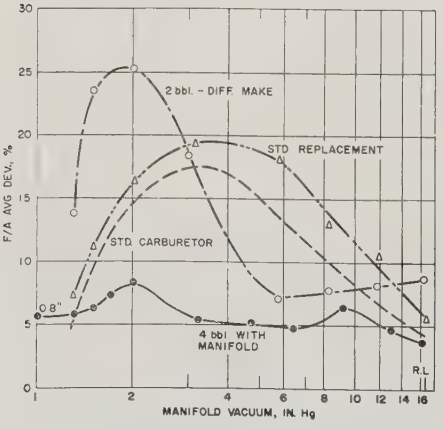

Fig. 35 — Distribution of Fuel A with production carburetors (Engine D, 2400 rpm)

Effects of Carburetor Design

The techniques presented should find use in development of both fuels and engines. The engine used for most of these studies was found to be particularly sensitive to carburetor design. Differences in the heat applied to the manifold branches were also found to play an important role.

The large differences in fuel distribution between the left and right manifold branches shown in Fig. 19 are attributed to differences in heat application and riser height. Fig. 34 shows that mounting an unheated 6-in. high riser section with an inside diameter the same as the manifold bore between the carburetor and manifold greatly improved distribution in the right branch at 40-deg throttle. Presumably, this is due to straightening of the mixture flow and improved fuel vaporization. However, it is more important to note that the unmodified left branch distributed fuel even better than the right branch with the 6-in. riser. Thus, the major differences between branches can be attributed to vaporization differences. Conventional manifold-design limitations are imposed by other considerations, such as tuning, volumetric efficiency, and engine compartment space.

Fuel Distribution with Production Carburetors — We also compared the fuel-distribution characteristics of other production carburetors specified for this 1956 Make D engine. Fig. 35 shows their average deviations of fuel/air ratio over the load range from wide-open throttle to road load at 2400 rpm. The manifold-vacuum scale is logarithmic because such plotting gives a curve of much the same shape as obtained when distribution with the standard carburetor was plotted against degrees throttle and because it tends to emphasize the importance of heavy-load operation (low manifold vacuum).

A supposedly identical replacement carburetor caused slightly poorer fuel distribution than the standard carburetor, but it gave the same general distribution characteristics over the load range. A carburetor of another design built by another manufacturer was run because it was specified as a replacement for use on this engine. The distribution at wide-open throttle was not as good as the standard carburetor, probably because its design stopped the throttle plates about 20-deg before reaching vertical. The magnitude of the poorest distribution was much greater than that with the standard carburetor. At higher manifold vacuums (above 3 in. of Hg), the distribution was significantly better.

A four-barrel carburetor and manifold which were offered as an option on the passenger-car version of this engine were also run. As with the other

carburetors, the throttle body heat was "off." This carburetor allowed a wide-open throttle manifold vacuum of 0.8 in. Hg, and the low level of average deviation at all manifold vacuums is particularly impressive. The slight increase in maldistribution at about 2 in. of manifold vacuum was caused by closing of the secondary throttle plates, and the slight increase at 9.5 in. of manifold vacuum was due to the closing of the power jet. This carburetor had smaller primary barrels than the two-barrel carburetor, and this improved mixing of the fuel and air.

Effect of Various Methods of Throttling — Because the carburetor had a tremendous influence on fuel distribution, we studied the effects of some modifications of a two-barrel carburetor. Small changes in the geometry of the diffusers below the fuel nozzles had large effects on distribution, but the areas of improvement were often offset by worsened distribution at other load settings.

The previously discussed concept of throttle-plate deflection of liquid fuel was used as a basis for planning throttle modifications of the two-barrel carburetor. Further exploration of the large effect of throttle-plate position demonstrated that a "nondeflective" throttle had some advantages. The throttle plate was maintained in the wide-open throttle position so as to minimize deflection effects, and the inlet air was throttled as it entered the air cleaner. The fuel distribution given by this "air throttle" is shown in Fig. 36. Over the range of manifold vacuums where large quantities of liquid fuel would be expected, definite improvements were obtained by eliminating the mixture deflection. It was believed that the fuel distribution became poorer at the higher manifold vacuums due to the pressurized fuel-discharge stream needed to control fuel flow and also because of the absence of fuel breakup by fuel impingement on the throttle plate at small throttle openings. Tel distribution using the "air throttle" was measured at two manifold-vacuum conditions. At 3 in. of Hg manifold vacuum (condition of poorest distribution with the standard carburetor), the average deviation in tel concentration as reduced from 12.7 to 1.7%, which was better than any tel distribution we had measured. At road load, however, the average deviation in tel concentration was reduced from 9.8 to 6.7%, which was still poorer than that at wide-open throttle.

The results with the "air throttle" encouraged an experiment with an iris-type throttle. This was another means of providing throttling without a tilting plate in the mixture stream. The standard throttle body was replaced by an assembly of two notched flat plates geared together and arranged horizontally so that one plate slid atop the other. At wide-open throttle, the plates allowed a fully circular opening, and closing the throttle resulted in square openings with the center at the bore center. At road load, a maximum impingement surface was obtained, and fuel distribution with the iris was much better than it was with the air throttle, as shown in Fig. 36. Reduced manifold vacuum caused successively poorer distribution; and at wide-open throttle, distribution was again poorer than with the standard carburetor. It appeared that fuel "breakup" or a mixture obstruction was necessary even at wide-open throttle.

The most uniformly successful throttle modification involved the use of standard butterfly throttle plates arranged to relocate the low-pressure area so that fuel was not deflected toward the front cylinders. Fig. 37 shows a photograph of the throttle arrangement in which the axes were relocated to be parallel with the engine crankshaft. The two throttle axes were geared together to maintain con-

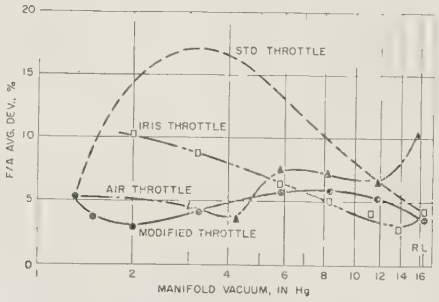

Fig. 36 — Distribution of Fuel A with four throttles (Engine D, 2400 rpm)

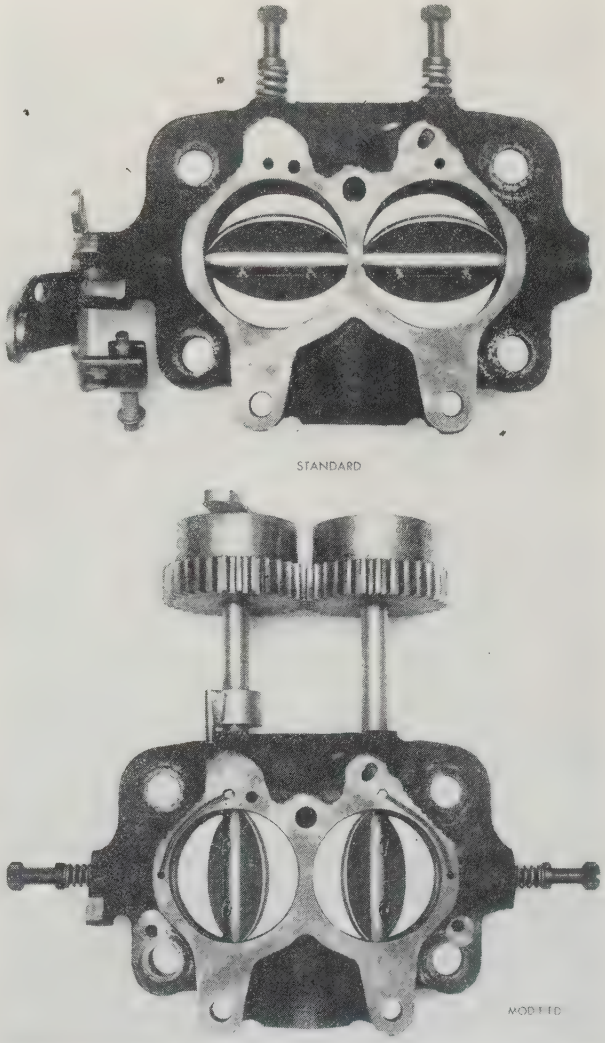

Fig. 37 — Comparison of modified throttle body with standard carburetor throttle body (Engine D)

stant angular relation. The plates of the *modified throttle* tilted so that the mixture deflection was lateral instead of front-to-back. Thus, the side walls of the main manifold plenum of each branch interrupted the deflected fuel. It was necessary to recalibrate the carburetor and reposition the standard fuel-nozzle diffusers.

Fig. 36 shows that this modified throttle gave a fuel distribution over the load range comparable (and even superior under some conditions) to that with the four-barrel carburetor and manifold. Fig. 38 compares the distributions of fuel and tel obtained with the standard and "modified-throttle" carburetors. Both fuel and tel distribution were importantly improved over the load range between wide-open throttle and road load, and their average deviations were of the same order.

The practicality of making such modifications in production carburetors was not considered in this demonstration of techniques. However, of the three throttle changes, the modified throttle appeared the least complicated. An idle system was most readily adapted to the modified throttle. Furthermore, subsequent tests indicated that the throttle plates could be simply linked together for constant parallel movement, and yield substantially the same improved fuel distribution.

Advantages of Improved Distribution

The benefits of uniform fuel distribution are well-known. However, it was of interest to determine in this particular 1956 Make D engine the effects of improved fuel and tel distribution on power, fuel economy, octane requirement, and tel effectiveness. Data obtained with the modified throttle, which provided most uniform fuel distribution, were compared with the results obtained with the standard two-barrel carburetor under constant-speed conditions only.

Power and fuel economy were increased with the modified throttle, particularly at part-throttle where the greatest distribution improvements were effected, as shown in Table 4. The maximum improvement was 6.9% at 2400 rpm and 3 in. of Hg manifold vacuum. There was no improvement at wide-open throttle or road load, since at these conditions distribution was good with both throttles. Another indication of increased engine efficiency was reduction of the combustible material exhausted. Measurements showed that between 2.5 and 5.5 in. of Hg manifold vacuum, at 2400 rpm, the combustibles exhausted were reduced from 7.1 to 5.1%. At manifold vacuums above 7 in. of Hg, there was no difference between carburetors. Others have observed similar effects with improved distribution.[30]

The knocking tendency of the engine was increased with the modified-throttle carburetor at similar manifold vacuums. However, power was also increased and this allowed greater knock-limited power with fuels of the same octane number as shown in Fig. 39. At the condition of greatest improvement in fuel and tel distribution, 3 in. of Hg manifold vacuum (40-deg throttle), the knock-limited power was increased about 7.5% for fuel of a given octane number.

The effect of carburetor throttle-type on the octane ratings of both clear and leaded fuels is of interest. Table 5 summarizes the ratings for three

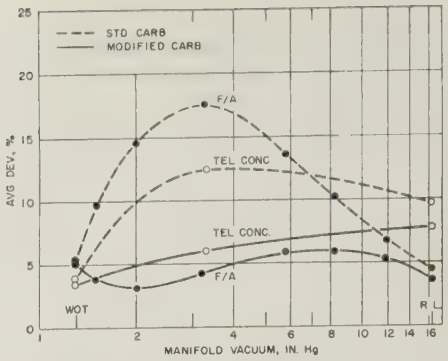

Fig. 38 — Distribution of tel and Fuel A with modified carburetor (Engine D, 2400 rpm)

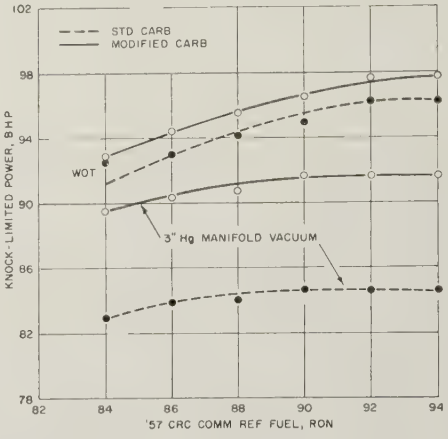

Fig. 39 — Effect of octane number on knock-limited power (Engine D, 2400 rpm, knock-limited spark advance)

fuels measured at 40-deg throttle (3 in. of Hg manifold vacuum) at 2400 rpm. As can be observed, changing to the modified throttle decreased the ratings of the clear fuels and increased the ratings of the leaded fuels. These two effects combined to produce greater tel effectiveness with the modified throttle. Other Ethyl studies on comparison of fuel injection with carburetion have shown these same effects from improved distribution.[31]

The decrease in clear fuel ratings and the improved effectiveness of tel found with the modified throttle resulted from three factors:

1. By improving distribution, the modified throttle caused the fuel/air ratio in some cylinders to be in the range of maximum knock, whereas no cylinders were in this range with the standard carburetor.
2. Tel response was greater at maximum-knock fuel/air ratio than at lean ratios.
3. The borderline spark-advance framework for the primary reference fuels was approximately the same with both throttle types. The primary reference fuels are quite volatile, and hence they distrib-

[30] Comptes rendus hebdomadaires des seances de l'academie des sciences, (6/2/58), pp. 3156, 3167: "Effect of Homogeneity of Fuel-Air Mixtures on Thermal Efficiency of Automobile Engines and on Carbon Monoxide Content of their Exhaust Gases," by H. Griffon and H. Heim.

[31] "Effect of Fuel Injection on Knocking Behavior," by A. E. Felt, D. L. Lenane, and K. W. Thurston. Paper presented at SAE Annual Meeting, Detroit, January, 1958.

Table 4 — Effect of Carburetor Throttle Type on Power and Fuel Economy

Engine D, Commercial Fuel F, Maximum Power Ignition Timing

	1600 rpm		2400 rpm	
Manifold Vacuum, in. of Hg	3.0	5.8	3.0	5.8
Bhp[a]				
Standard Carburetor	56.7	51.4	84.9	76.8
Modified Throttle	59.7	52.6	91.2	80.3
Fuel Consumption, lb/hr				
Standard Carburetor	31.7	29.3	46.6	42.6
Modified Throttle	31.7	28.8	46.7	42.6
Brake Specific Fuel Consumption, lb bhp-hr				
Standard Carburetor	0.559	0.570	.549	.555
Modified Throttle	0.531	0.548	.512	.531
Decrease, %[b]	5.0	3.9	6.9	4.3

[a] Corrected to 60 F carburetor air temperature; 29. 53 in. of Hg barometric pressure.
[b] With modified throttle.

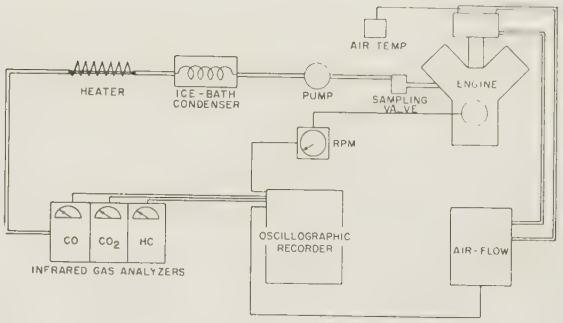

Fig. 40 — Schematic of equipment used for measuring fuel distribution during acceleration

Table 5 — Effect of Carburetor Throttle Type on Fuel Octane Rating

Engine D, 2400 rpm, 3 in. of Hg Manifold Vacuum (40 deg throttle)

Fuel	Tel ml/gal	Octane Rating: Standard Carburetor	Octane Rating: Modified Throttle	Change Due to Modified Throttle
A	0	80.9	80.0	− 0.9
	3	88.3	89.5	1.2
		7.4	9.5	2.1
D	0	84.4	81.4	− 3.0
	3	88.7	89.8	1.1
		4.3	8.4	4.1
E	0	84.8	82.8	− 2.0
	3	88.2	88.8	0.6
		3.4	6.0	2.6

uted nearly alike with both throttle types.

It was evident from this limited investigation that improved distribution can increase power, fuel economy, and tel effectiveness. The mechanical octane gains are real under certain operating conditions, and they have been measured in terms of increased knock-limited power. Thus, it can be observed that improved fuel and additive distribution through better carburetion would yield many of the benefits of fuel injection.

Summary

Techniques have been developed for accurately determining the distribution of both whole fuels and their individual components. These components were tagged with tritium and blended, one at a time, in the whole fuel. The radioactivities of the exhaust-gas condensates from the individual cylinders accurately reflected the concentrations of the tritiated components.

The distribution of whole commercial fuels can be correlated better with specific gravity than any other measurable fuel property. Distribution improves as specific gravity is decreased. The actual determining fuel characteristic is, no doubt, the latent heat of vaporization, of which specific gravity provides a convenient index. Higher latent heats increase the liquid in the manifold and result in poorer distribution.

The relative distribution of either additives or individual fuel hydrocarbons when blended in relatively low portions in the whole fuel was dependent only on their boiling points. Components of both very low and very high boiling points showed poor distribution based on their concentration in the cylinder charge. Best distribution was obtained with components in the mid-boiling range of the fuel. All fuel components, including additives, boiling above 400 F showed approximately the same maximum maldistribution. Fuel additives boiling below 400 F should have approximately the same boiling points if they are to distribute similarly.

Those cylinders deficient in high-boiling fuel components show an excessive concentration of low-boiling materials (and vice versa). Thus, the low octane quality in cylinders having low tel concentrations can be compensated for by providing high octane numbers in the volatile portion of the fuel. The gain in antiknock performance offered by having a high octane number in the front end of a leaded fuel is somewhat evident under conditions of maldistribution at constant speed, but is especially so during wide-open throttle accelerations. In the latter case, there is a lag in the delivery of the high-boiling fuel components including tel from the manifold to the cylinders.

If engines are to use gasoline with maximum efficiency, variations in the quantity and quality of fuel going to the various cylinders must be minimized. This can be done best by careful attention to carburetor and manifold design.

In both of the engines investigated, distribution was more affected by the position of the throttle plates than by any other operating variable. In one engine, the adverse effects of throttle-blade position were greatly minimized by shifting the throttle-plate axes 90 deg in the horizontal plane. The resulting improved fuel distribution increased power and fuel economy, reduced octane requirement for a given power output, and gave higher tel effectiveness.

APPENDIX

Measuring Fuel Distribution

Because the exhaust-gas analyzer which was used in the constant-speed tests did not have a uniform instrument lag, infrared gas analyzers were employed to measure exhaust gas composition under accelerating conditions. This instrument was used in the 1956 CRC field survey of exhaust gas composition conducted in Los Angeles for continuously

recording CO_2, CO, and hydrocarbon concentration exhausted.[32, 33] Fig. 40 shows the schematic layout of the equipment. Exhaust gas was sampled using the timed sampling valve and about 16 ft of sampling line including 6 ft of ¼-in. copper tubing condenser in ice water.

Passenger-car acceleration rates were simulated on the engine dynamometer through automatic throttle and load controls. One cylinder was sampled during each acceleration and simultaneous records of engine speed, airflow (using a viscous flow element in the air cleaner), CO_2, CO, and hydrocarbon were taken by an oscillograph recorder.

Interpretation of the records involved a lengthy procedure. The deflections of all the traces in one-second intervals were measured and tabulated. The zero or starting point for each of the CO_2 and CO or hydrocarbon traces were taken at the first change in the curve from its pre-acceleration level. The analyzer readings were converted to mole per cent values using a procedure similar to that used by Way and Fagley.[33]

The conversion of the data into terms of fuel/air ratio involved the assumption that variations in input cylinder fuel/air ratio were accompanied by total carbon-output variations in direct proportion.

The "total carbon" content was computed at each second from the start by summing the mole per cent CO_2 and CO together and adding 5.0 times the mole per cent hydrocarbon. Although the hydrocarbon cell was hexane sensitized and propane calibrated, it was found that in order to obtain best consistency and rationality in the end results, it was necessary to assume the hydrocarbon recorded was C_5. The fuel/air ratios indicated by the per cent CO and per cent CO_2 were determined from Orsat curves ($CH_{1.86}$ fuel; water gas constant 3.8).[33] The time that both CO and CO_2 agreed within 0.003 fuel/air ratios was usually near the end of the acceleration where composition was constant. The fuel/air ratio at the instant of agreement was divided by the total carbon content at the same point. That ratio was then multiplied by the total carbon content computed at any time during the run and the result was interpreted as the fuel/air ratio.

Manifold lag usually referred to involves the length of time between the start of the fuel flow at the carburetor and the reception of it at the cylinder. Because the start of the composition measurements was taken at the first change of cylinder composition indicated, this reported manifold lag is, therefore, actually the difference between the time of the air arrival and the fuel arrival at the cylinders.

DISCUSSION

Distribution Characteristics of Full Boiling Range Fuel Found Good

— J. A. Edgar
Shell Oil Co.

THE NUMBER and gravity of the compromises which must be made in a fuel-air distribution system are well-known. Exceptions to any of the rules of behavior which apply to a single carburetor-manifold combination or to a class of distribution systems will be too numerous to describe even in a report of widest scope. Mention of one or two observations which differ from those described may have some value for emphasis and background.

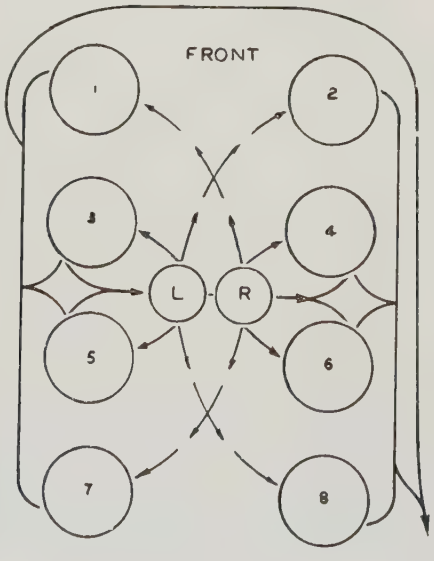

Fig. A — Arrangement of intake and exhaust manifolding, GMR engine

We should like first to recall the discussions in previous meetings which dealt with the problems of air distribution in engines where accurate fuel quantity delivery to the cylinders was assured by the use of liquid injection systems. Variations of mixture strength similar to those shown today arose from the vagaries alone of airflow through branched pipes.

The authors show that the route of the liquid phase through the manifold is strongly influenced by the direction taken by the air as it passes the throttle plate. To this must be added the effect of the shape and turbulence of the air stream above the throttle plate. The induction system certainly includes the air cleaner — and particularly any elbow connections — among the factors which influence distribution.

Distribution studies in our laboratory centered on the General Motors Research Engine, which had a somewhat less symmetrical manifold (Fig. A) than that which was used in a large part of the author's work. Exhaust sampling was accomplished (Fig. B) without use of external valves. Only the four-corner cylinders were sampled. The influence of volatility on distribution to these cylinders was clearly demonstrated, as in Fig. C. Tritiated butane reached these cylinders in comparatively greater quantities than did p-cymene (boiling point 350 F). By difference,

[32] "Application of Continuous Infrared Instruments to Analyses of Exhaust Gas," by B. M. Sturgis, W. F. Biller, J. W. Bozek, and S. B. Smith. Paper presented at SAE Annual Meeting, Detroit, January, 1958.

[33] "Field Survey of Exhaust Gas Composition," by Gilbert Way and W. S. Fagley. Paper presented at SAE Annual Meeting, Detroit, January, 1958.

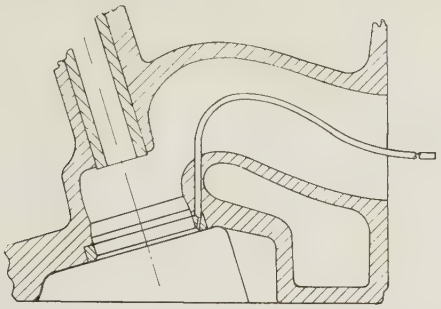

Fig. B — Valve seat exhaust sampling port, GMR engine

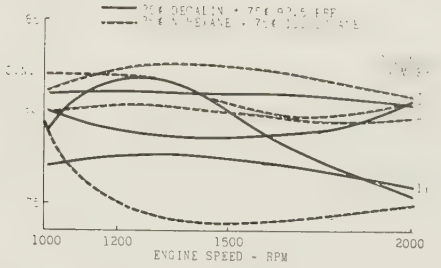

Fig. D — Effect of boiling point on octane quality distribution

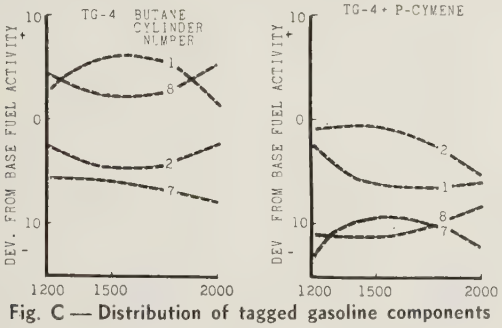

Fig. C — Distribution of tagged gasoline components

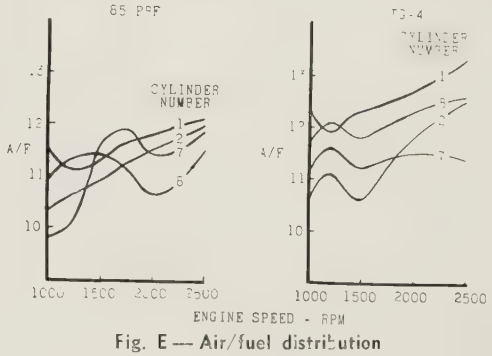

Fig. E — Air/fuel distribution

the inside cylinders received less butane and more of the heavier component. The interesting observation of these figures is the strong influence of speed (at road load corresponding to each speed) on the apportionment of the components to the cylinders.

Using the technique of knock-limited spark advance of individual cylinders, the distribution characteristics of decalin (boiling point about 380 F) and normal hexane are compared. The effect of speed/load is again strongly felt (Fig. D). It cannot be concluded from these data that a component of "front end" volatility (hexane) will be more satisfactorily handled by this engine than the heavier decalin.

Our firmest and at the same time most unexpected conclusion was that, for this engine, it is almost impossible to improve on a normal full boiling range gasoline respecting distribution characteristics. Even the constant-boiling primary reference fuel (Fig. E), shows little advantage over a normal full boiling range gasoline. This is not to say that the distribution is perfect, but rather that a compromise plumbing system had been achieved which would meter within 10–15%. Although this figure for an old-fashioned engine is better than the values found by the authors, it is one in which economy-minded manufacturers can have little satisfaction.

General Motors Data Agrees with Authors' Findings

— J. R. Landis
General Motors Corp.

MOST OF THE observations in this paper concerning the engine are in exact agreement with our own data; in particular, the almost overwhelming effect of the carburetor itself in deflecting or directing the liquid fuel streams. Other items of agreement include the following:

1. Mixture distribution does not always improve with increasing engine speed and decreasing throttle opening and in many instances does the reverse.

2. Mixture distribution improves with increasing riser depth, increasing manifold heat, and reduced venturi size.

3. Mixture distribution patterns are affected by the overall mixture ratio; that is, if the mixture is richened, some cylinders will richen up more than others.

Now for a moment, let us recall that the title of this paper was "Casting New Light on Fuel Distribution." There are two important aspects of casting light as we were reminded from this platform several years ago, when a speaker said "and those that had been in darkness had seen the light." In other words, here we have uncovered a new light, but in order that any benefit may come from this work, someone must see that light. In this paper it is clearly shown that the combination of low volatility tetraethyl lead with high volatility scavengers results in a considerable mismatch in the resulting deposits. Thus, lean cylinders are overscavenged, leaving excess halides; and rich cylinders are underscavenged, leaving excess lead deposits. This may be passed over lightly for passenger-car operation but in high volumetric efficiency truck engines, serious durability problems from the excess halide can result, particularly in valve seat wear. It will be interesting to see whether the light of this paper will uncover future improvements in antiknock additives and scavengers.

In conclusion, this paper has shown two major areas in which the overall engine-fuel relationship may be improved by further study and development:

1. Fuels and fuel additives should be tailored so that additive components distribute accurately with the fuel components and with one another.

2. The engine manufacturer should endeavor to obtain the best possible mixture distribution in the critical speed and load ranges, although with the number of engines in production today and the frequency of changes, this is a monumental task. For example, at Chevrolet alone, there are eight different truck carburetors and seven major passenger-car carburetors in production. This provides a bountiful supply of mixture distribution work, some of which closely parallels that done by the authors. Unfortunately, in development work of this type, expensive solutions such as the transverse-opening throttles are usually met with the request, "now go back and see if you can't do the job without spending any money."

AUTOMATIC TRANSMISSION

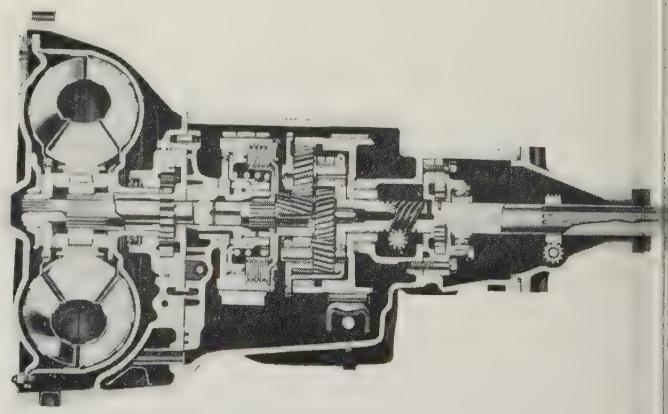

Fig. 1 — Powerglide automatic transmission

Three element torque converter with automatically controlled planetary gear system in drive range. Manual selection of reverse and low.

Maximum Converter Torque Ratio (at stall)	2.1/1
Planetary Gear Ratio in Low	1.82/1
Planetary Gear Ratio in Reverse	1.82/1

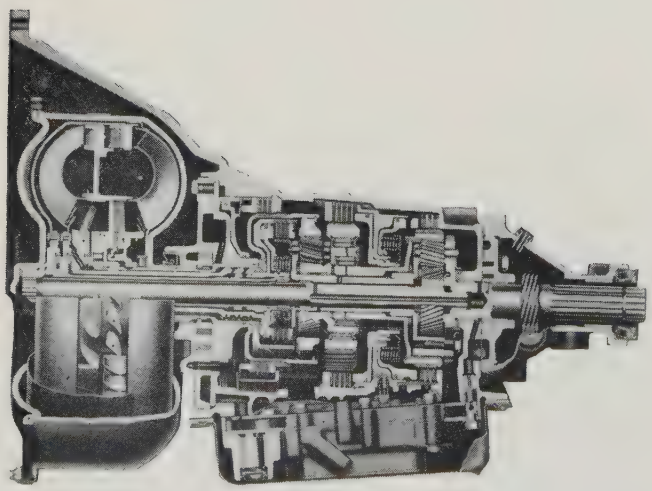

Fig. 2 — Turboglide automatic transmission

Five element, triple turbine torque converter. First and second turbine drive output shaft through planetary gear-sets. Third turbine drive output shaft directly. Manual selection of Reverse and Grade Retarder

Maximum Converter Torque Ratios (at stall)	
Stator Low Angle	3.8/1
Stator High Angle	4.3/1
Front Planetary Gear Ratio (second turbine)	1.63/1
Rear Planetary Gear Ratio (first turbine)	2.67/1
Reverse Gear Ratio	1.78/1

TESTING

H. H. Kehrl,

M. R. Marsh,

and R. A. Gallant,

Chevrolet Motor Division, General Motors Corp.

This paper was presented at the SAE National Passenger-Car, Body, and Materials Meeting, Detroit, March 16, 1959.

THE LABORATORY has been described as an "indoor" proving ground. However, laboratory investigations are not intended to substitute for proving ground activities, but rather are a necessary counterpart. Interrelation between the two becomes more clear when considering some of the laboratory's inherent advantages:

1. It permits close investigation of the operation of inaccessible parts.

2. Small differences in design performance may be evaluated through precise control and measurement of test conditions.

3. Road conditions, due to inclement weather, are of no concern.

4. The delay of transmission tests due to failure of other vehicle components is eliminated.

5. By utilizing automatic shut down features, it allows close inspection and pin-pointing of source of failure.

6. It allows accelerated testing since measured proving grounds data may be adjusted a given percentage before being put into a fixture.

This paper describes the laboratory testing of automatic transmissions.

THE NEED for modern laboratory methods and facilities is perhaps nowhere better exemplified than in the development of the automatic transmission.

Transmission refinement has been accelerated in recent years due to three primary factors: the transmission is called upon to deliver nearly three times its originally assigned horsepower; styling trends have confined it to its original package size; and competition has continuously raised its pleaseability standards.

To meet this challenge, designers have come to place greater emphasis on the facilities and methods of investigation that replace the educated guess with quantitative measurement.

Transient phenomena once were held accountable for the rather generous application of safety factors, experience factors, and fudge factors. Today's requirements call for accurate identification and quantitative measurement of the magnitude, duration, and effects of these transient phenomena so that designs may be based on more known quantities, and fewer unknowns.

The basic laboratory approach is to:

1. "Ask the machine" what the actual requirements of a new component design should be.
2. Set up test machinery to inflict these requirements on a proposed design and record its performance.

The "machine" referred to in the first step may be a complete transmission or any one of its components. In either case, the needed information is gathered by use of instrumentation with the test piece operating in its normal environment. This usually means it is installed in a test car running through an appropriate schedule, or in a machine designed to duplicate these conditions. These actual, rather than theoretical, requirements then be-

come the design baselines for both the component and the test machine.

The second step, the ability to duplicate accurately the normal operating conditions, allows the engineer to bring a variety of harsh outdoor realities inside where he can get a quantitative evaluation of their effects, on his own terms. Adherence to this approach ensures close correlation of laboratory test results with performance in a vehicle.

The laboratory work discussed herein is limited to Chevrolet Powerglide and Turboglide transmissions (Figs. 1 and 2). Detailed coverage of the Turboglide design has been described by Messrs. Winchell, Route, and Kelley.[1]

Component Testing

Friction Elements, Static — Evaluation of friction element capacities, both static and dynamic, is one of the laboratory's most exacting assignments. Fig. 3 shows a typical plate clutch. This particular clutch is used in Turboglide and has only to transmit a fixed amount of torque. It does not have a high energy input requirement.

The equipment used for evaluating static torque capacity of a clutch is shown in Fig. 4. At the left is a large gear reduction unit driven by a small variable speed motor to give a variety of slip speeds ranging from 0.03 to 1.4 rpm between the driving and driven members of the clutch. A 2-ft torque reaction arm, cradled in needle bearings, bears against a load cell on a dead weight scale. The load cell feeds information to the X-Y recorder on the right to provide a plot of torque versus degrees of rotation, while the scale gives a nominal check of torque capacity at a fixed slip rate.

Before the test is run, the clutch is installed and operated at maximum pressure and slow speed to burnish and stabilize surfaces. Plates are soaked in transmission fluid, and oiled during the tests.

A series of capacity checks at various operating pressures is made, and plotted either as torque capacity versus pressure, or friction coefficient versus unit pressure. The accuracy of these measurements makes the machine useful in determining the effects of various transmission fluids on the coefficient of friction.

Many of the materials tested do not have a sharply defined static coefficient, but rather show an increasing coefficient with increase in slip speed until the dynamic coefficient is reached. This characteristic is of value in that it may permit the designer a smaller safety factor.

Friction Elements, Dynamic — When high-energy absorption capacity is needed, as in the Powerglide high clutch, friction element requirements are more demanding. These materials must perform under extreme pressure and temperature conditions with a predictable coefficient of friction.

The energy capacity required is dependent upon engine torque, kinetic energy change of input system, and shift feel. Because of these requirements and the inherent variations in friction materials, the facilities for careful evaluation are mandatory.

The energy input to a clutch during a shift can be determined from an oscillographic record similar to Fig. 26. The energy entering the transmission during the shift is calculated from the engine torque and input system kinetic energy changes. The energy leaving the transmission during the shift is calculated from the propeller shaft speed and torque. The difference between these two quantities is the approximate energy dissipated in the clutch. The energy quantities thus determined then become the basis for the laboratory energy capacity test.

The basic test setup is shown schematically in Fig. 5. A 10-hp motor continuously drives a large flywheel and the input members of a clutch. With this clutch applied, selected inertia weights are brought up to a predetermined speed. After the

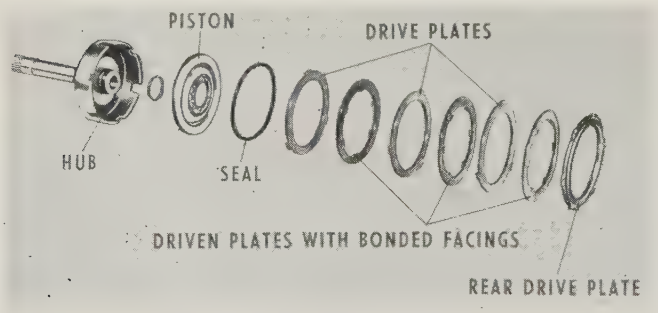

Fig. 3 — Turboglide neutral clutch

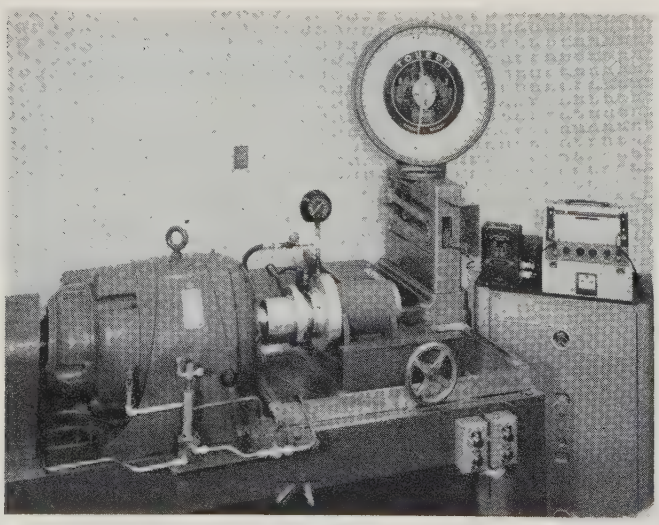

Fig. 4 — Static torque fixture

[1] SAE Transactions, Vol. 66, 1958, pp. 167–178: "Chevrolet Turboglide Transmission," by F. J. Winchell, W. D. Route, and O. K. Kelley.

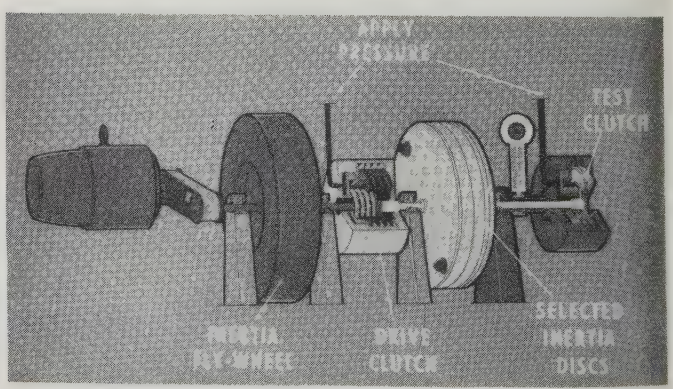

Fig. 5 — Mechanical diagram of dynamic clutch test fixture

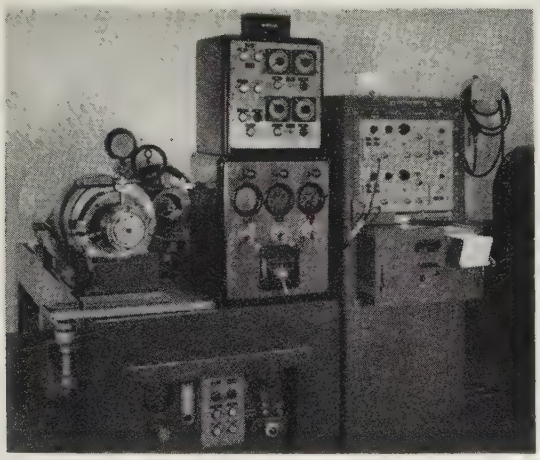

Fig. 6 — Dynamic test fixture

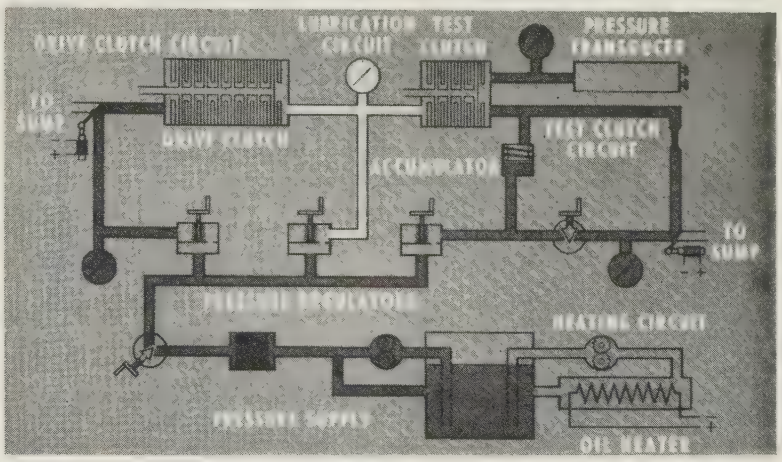

Fig. 7 — Hydraulic diagram of dynamic clutch test fixture

The accuracy required makes the actual fixture considerably more complex than the mechanical schematic might indicate. The unit consists of a hydraulic power supply, a control console, a 10-hp electric motor, a drive clutch, a test clutch, fixed and a variable inertia weights, a pressure transducer, a strain gauge and an oscillograph recorder. The oil supply unit contains an oil sump, a 10-gpm oil pump, heat exchanger, a filter, and two pressure control valves. This unit supplies oil at 200 psi to the control console.

The control console has three pressure regulator valves, four automatic timers set up in series, a manual control switch for the drive and test clutch. The 10-hp AC motor is used to supply energy to the fixed inertia weight through a timing belt. This flywheel is attached to the drive plates of a Powerglide clutch assembly. The driven plates of this clutch are attached to a shaft which carries the variable inertia weighs, a shear pin, and the hub of the test clutch. The driven plates of the test clutch are placed in a fixture grounded to the man structure. A strain gage transducer is placed between the clutch drum and the supporting structure to measure clutch torques. The pressure transducer is placed behind the test clutch piston. When instantaneous speed is required a tachometer generator is attached to the test clutch driven plate shaft.

In operation, the oil supply unit (Fig. 7) delivers oil at a preselected stabilized temperature, at 200 psi to the three pressure regulator valves in the console. From left to right: the first regulator supplies oil for the drive clutch at a predetermined pressure; the second reduces the oil to the desired lube pressure to cool the drive and test clutches; and the third supplies oil to the test clutch.

drive clutch is released, the test clutch is applied at a controlled pressure rise. The dynamic torque reaction is recorded on an oscillograph through a strain gage transducer on a fixed output shaft.

Inertia weights and speed are selected to duplicate the kinetic energy previously determined in an instrumented car. The apply rate of the test clutch is also established by "in car" measurement of the rate at which this energy is absorbed under actual operating conditions. The complete installation is shown in Fig. 6.

The automatically controlled sequence of events follows:

1. A timer activates a solenoid which directs oil to the drive clutch.
2. Engagement of this clutch accelerates the selected inertia weights and the test clutch drive plates to the test speed.
3. The first timer then releases the drive clutch, and a second timer causes a 3-sec delay.
4. This permits disengagement of drive clutch. A third timer activates a solenoid valve to supply oil to the test clutch. Any accumulators or orifices are placed between this valve and the test clutch. The oscillographic recorder is started before test clutch engagement and records clutch pressure rise and engagement torque against time.
5. The test clutch is released and cycle repeated.

This equipment can be used to check the dynamic coefficient of new friction materials, to evaluate life at a given energy level, or to determine energy ab-

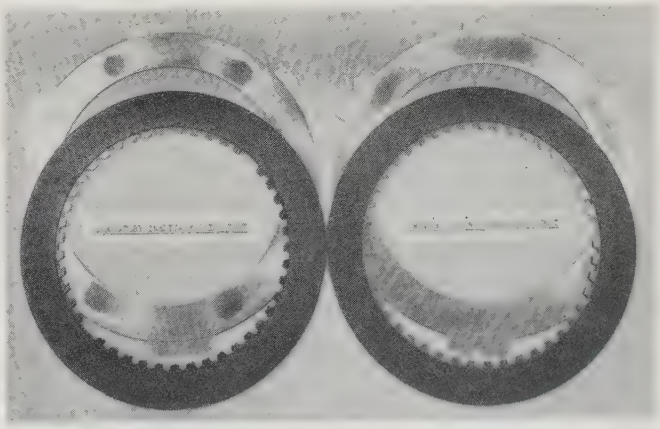

Fig. 8 — Correlation of test results on Powerglide clutch plates

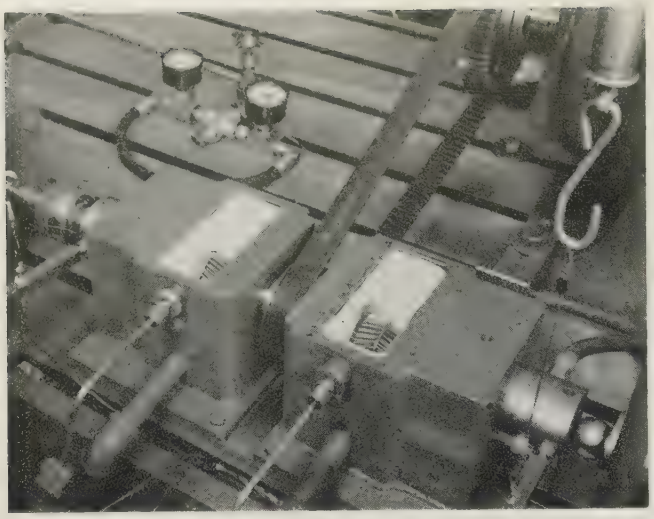

Fig. 9 — Thrust washer test fixture

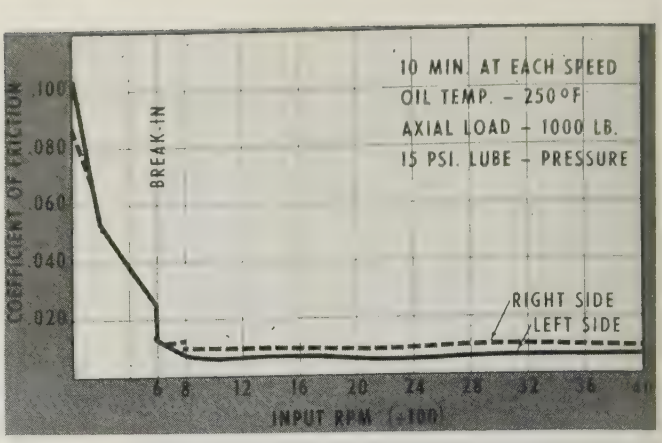

Fig. 11 — Friction coefficient

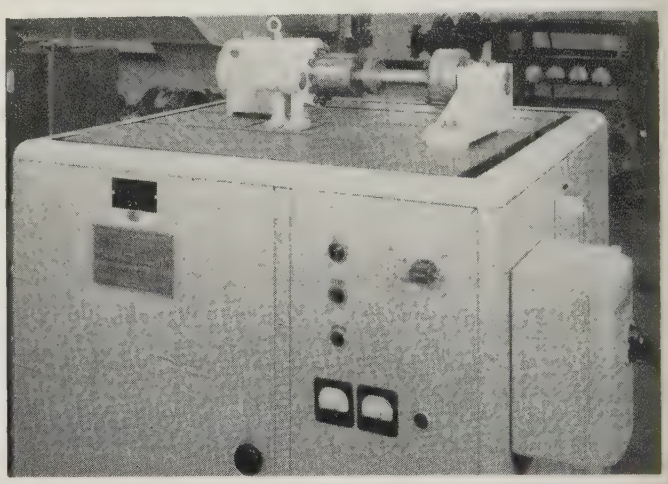

Fig. 12 — Fatigue testing T_2 shaft

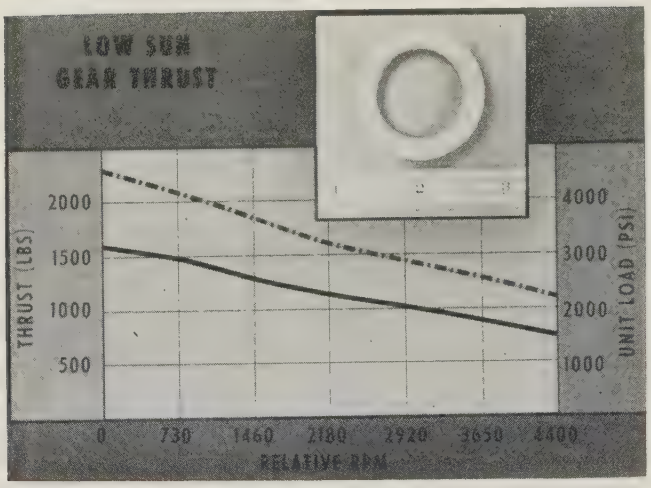

Fig. 10 — Low sun gear thrust

sorbing capacity of the given clutch design. Since the machine accurately measures small torque differences, it is also used to determine the effect of various transmission fluids on the dynamic coefficients.

This test provides good correlation with field performance. Fig. 8 shows a comparison of two pairs of Powerglide clutch plates. One pair is taken from a proving ground durability car, the other from a laboratory test designed to duplicate car conditions. The similarity in physical appearance, wear rate, and set-down time verifies the accuracy possible in duplicating a normal operating condition.

Thrust Washer Testing — As horsepower has increased, so has the problem of thrust loads imposed by helical gears. A typical thrust washer test fixture (Fig. 9) places the Powerglide input sun gear in its normal environment so that the effects of lubrication, oil grooves, fluids, materials, and designs may be studied.

Test conditions are determined by plotting a load-speed curve from the torque converter absorption curve (Fig. 10). These values are verified by means of a strain gage transducer in the transmission to determine the presence and magnitude of any transient loads.

Using these values, axial load is applied through a hydraulic cylinder. The input sun gear is driven at various speeds up to 4500 rpm. Friction torque of the washer is measured by a spring scale through a lever arm. Lube oil from an external pumping unit is temperature controlled and filtered.

The fixture provides accurate measurement of friction coefficients as indicated by the curves in Fig. 11. It is interesting to note that the coefficient of friction of the washer is approximately 0.01, as compared with normal dynamic coefficients of friction elements of 0.09–0.15. Apparently the difference between a thrust washer and a friction element can be only one decimal point.

Table 1 is a summary of the effects various oils had on the durability of transmission thrust washers. Close correlation is evident between the results obtained from proving ground schedules and laboratory tests.

Torsional Strength of Converter Shafts and Elements — Strength and fatigue life of shafts and converters are evaluated on the basis of engine torque loadings and transient loads induced by severe vehicle operation. Accurate determination of transient values is entirely dependent upon modern dynamic recording equipment such as that used in the

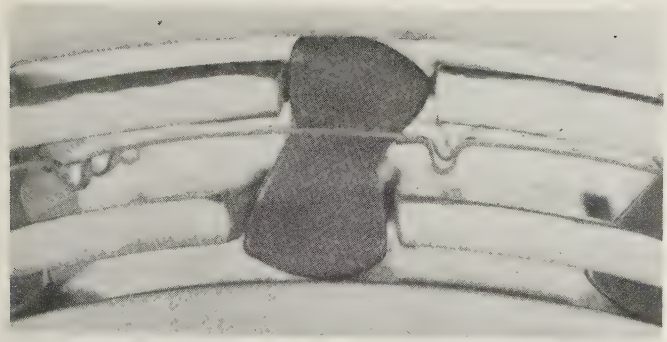

Fig. 13 — Turboglide sprag clutch

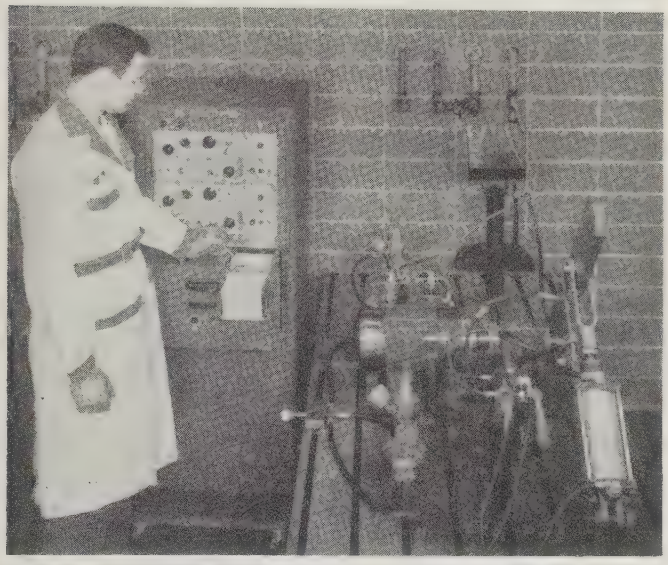

Fig. 14 — Overrunning clutch static test

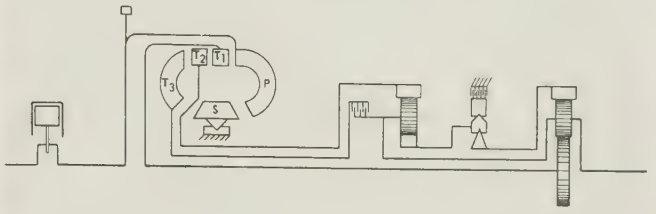

Fig. 15 — Turboglide neutral-to-drive shift

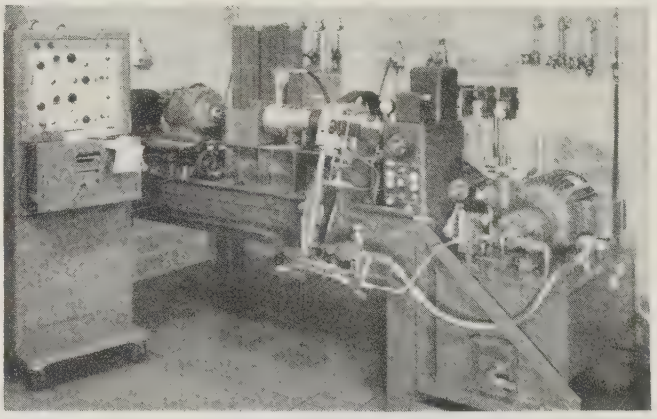

Fig. 16 — Overrunning clutch dynamic test

Table 1 — Powerglide Thrust Washer Tests

Fluid	Laboratory Tests		Proving Ground Schedules	
	Number of Tests	Success	Number of Tests	Success
A	8	0	10	0
B	4	1	4	2
C	8	5	5	4
D	8	7	6	5

abuse test described later.

Fig. 12 shows the Turboglide T_2 shaft mounted in a fatigue testing machine of the controlled-load type. The splined drum on the right normally carries reverse clutch plates. In this test, the drum is grounded. Input torque is applied to the splined shaft on the left which normally carries the T_2 turbine. The equipment shuts down automatically in the event of shaft failure.

The strength of die-cast turbines is established by stress coat, strain gage measurements, and torsional fatigue tests. Because turbine loads are applied through a large number of blades, care must be exercised in securing the test part to the fixture to assure proper load distribution.

Overrunning Clutch Testing, Static — The overrunning clutch shown in Fig. 13 is part of the geared converter arrangement of Turboglide. Its function is to permit a particular element to freewheel when it is no longer contributing to converter output. This eliminates the drag and loss of efficiency that would otherwise occur. Its assignment in the transmission calls for high torque capacity in a small space.

The stroking fixture shown in Fig. 14 is used to determine fatigue life of overrunning clutch elements, such as the sprag type used in Turboglide, or the cam and roller clutches used under the stators of both the Turboglide and Powerglide transmissions.

The operation is completely automatic, provides for repeated application of a predetermined torque, and provides sufficient rotation to establish new sprag-to-race contact points on each cycle.

Load is applied by the air cylinder on the right through a torque arm where it is monitored by strain gages and recorded on the oscillograph.

Apply load is limited by the known static breakaway capacity of two double wrap transmission bands attached to the outer race. The resulting rotation prevents brinnelling of the races due to repeated application in a fixed position.

Overrunning Clutch Testing, Dynamic — In the Turboglide neutral-to-drive shift, the T_1 sprag clutch must accept the sudden change from a high-speed overrunning condition to a high torque lockup (Fig. 15). The T_2 sprag has a similar assignment when the change is made from road load to full-throttle acceleration in the mid-speed range.

The machinery shown in Fig. 16 was specifically developed to duplicate either of these conditions by providing: high-speed rotation of the inner race,

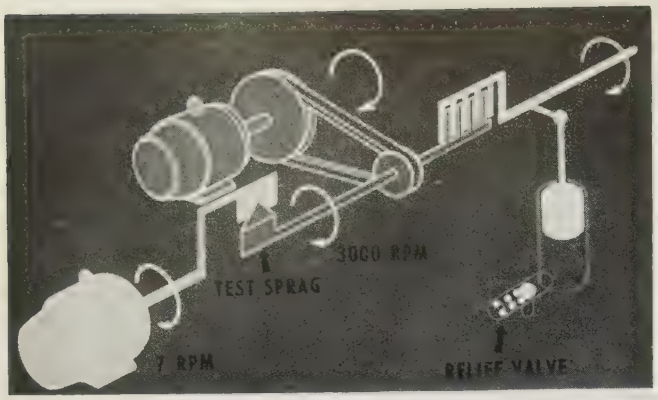

Fig. 17 — Overrunning clutch, dynamic test schematic

Fig. 18 — Converter performance

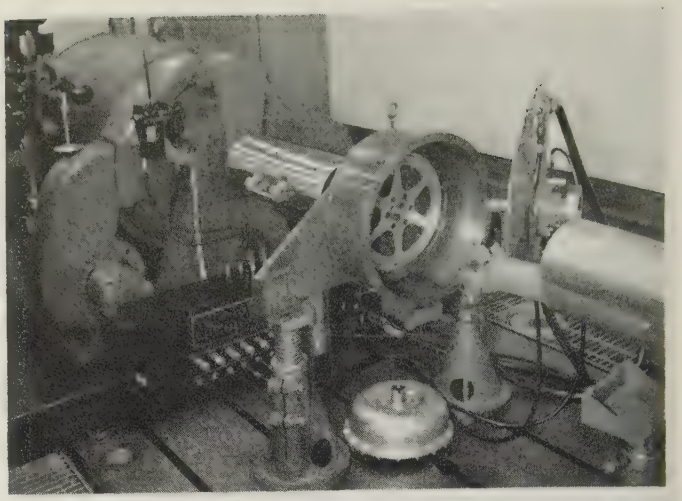

Fig. 19 — Powerglide converter fixture

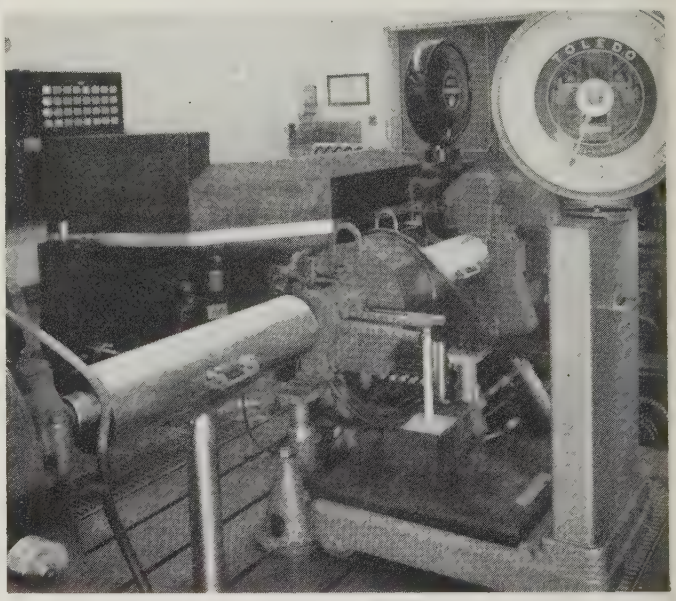

Fig. 20 — Equipment for relative torque test

predetermined input torque to the outer race, the means of grounding the inner race, and a measure of the reaction torque.

Testing is done on a single clutch, either the T_2 outer or T_1 inner sprag assembly. In either case the test piece is measured for strut angles, race diameters, and drag torque before entering the test machine.

The cycle begins with the outer race being driven through a reduction unit at 7 rpm (Fig. 17). The inner race is driven in the same overrun direction. When it reaches 3000 rpm, the driving motor is deenergized. A timer then engages a clutch (actually a Powerglide clutch pack) between the inner race and a torque arm attached to a hydraulic cylinder. The rapid torque buildup on the sprags due to the abrupt lockup is limited to a specified value by a relief valve in the cylinder. Movement of the torque arm then trips a microswitch to disengage the clutch, and the cycle is automatically repeated.

An interesting problem in the design of this fixture was the repeated failure of the belt that brings the inner race up to speed. Failure was caused by the decelerating torque of the Powerglide clutch, and was eliminated by installing a small slip clutch between the pulley and the race to limit belt tension.

Wear characteristics are also evaluated by a simple high-speed overrun test.

Converter Testing — In converter work, small changes in labyrinth seals, blade angles, and spoke designs exhibit nonlinear effects on converter performance and efficiency. Evaluation of these effects necessitates a high degree of accuracy in the measurement of input and output speed and torque. The equipment used to accomplish this is shown in Fig. 18.

A test converter is mounted in a fixture designed to simulate the "in car" condition (Fig. 19) and connected between two 250-hp dynamometers through rubber bushed propeller shafts. Direct current input and eddy current absorption dynamometers measure torque. The corresponding speeds are measured by digital counters. Frequent calibration of the dynamometers ensures the necessary accuracy.

To minimize the influence of oil temperature on indicated performance, converter outlet oil temperature is controlled within ± 2 F. The heat generated at the lower speed ratios necessitates a 25-gpm oil

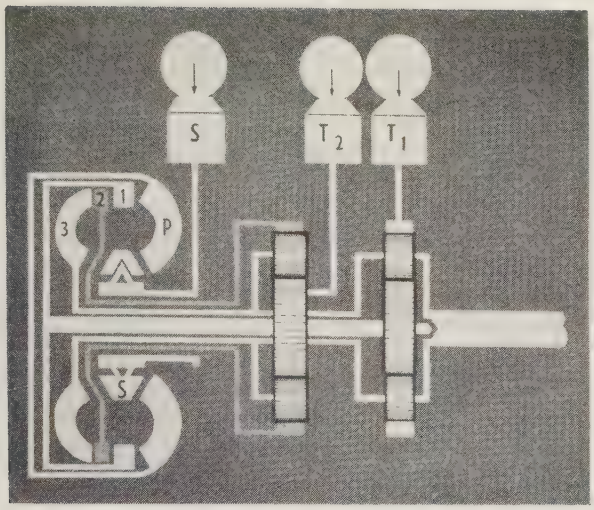

Fig. 21 — Turboglide relative torque test

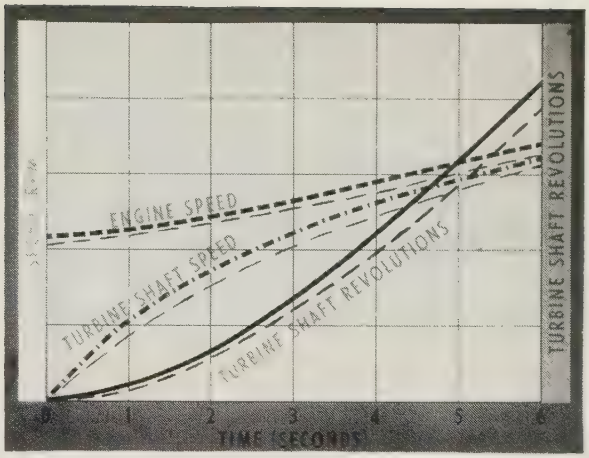

Fig. 22 — Torque converter turbine acceleration

supply and a large heat exchanger, which is located in the equipment room. Converter charging pressure is held constant by automatic controls.

Provisions are made for measurement of ballooning of the converter hub and flywheel at each output shaft speed. A light flat plate attached to the hub permits measurement by manual operation of a depth micrometer. Since the converter flywheel design does not lend itself to this simpler method, an electronic micrometer is used.

In Turboglide converter work, accurate measurement of the torque distribution between the three turbines throughout the operating range is essential to the evaluation of the effects on performance of small changes in design. This same base equipment is used to make both steady state and dynamic measurements of these quantities.

Fig. 20 shows the relative torque fixture designed for this use, and Fig. 21 shows it schematically. The gear set is actually part of the fixture which includes reaction arms for the T_1 and T_2 gear sets and the stator support shaft. The output shaft is connected to the dynamometer.

Constant input torque is supplied by a direct current dynamometer. At each output speed, gear reaction torque is determined by the lever arm and the load on a precision platform scale. A single scale is used, reactions being measured one at a time at each speed, while the other arms are simply grounded to the case. Readings are readily convertible to individual turbine torque contributions.

Dynamic measurements can be made with this setup simply by attaching strain gages to grounded lever arms and feeding the results to a multichannel oscillograph.

The usual method of converter performance testing at constant input torque and a series of output speeds produces data which can be converted into car performance after lengthy calculation. Recently, this equipment was used to compare vehicle performance of two converters by direct measurement of full throttle acceleration characteristics.

An engine was substituted for the input dynamometer, and inertia weights for car inertia. With the converter output shaft held by a manually controlled brake, the engine throttle was adjusted to give the desired input torque. The brake was then released, and the converter input and output shaft speed and revolutions recorded against time on an oscillograph. The information obtained (Fig. 22) corresponded closely with car measurements.

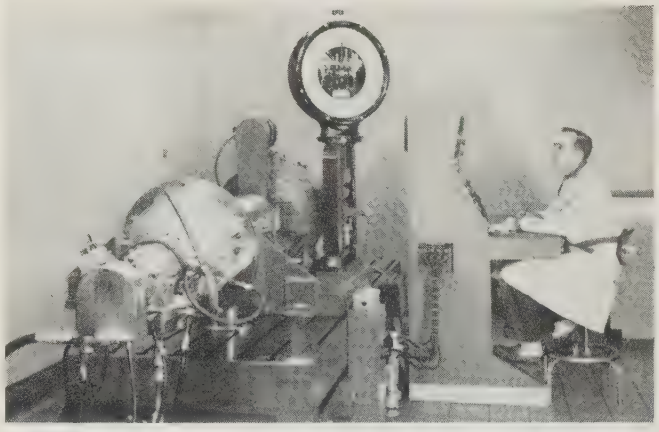

Fig. 23 — Spin dynamometer

Hydraulic Test Facilities — Basic equipment in a transmission laboratory must include the means for evaluating pump and valve body performance, and parasitic losses.

Pumps are tested on a 15-hp dynamometer, as shown in Fig. 23. The transmission is reworked to permit the normal pumping operation through suction and discharge passages. Oil pressure is controlled, and flow is measured by a positive displacement meter.

A separate temperature controlled pumping unit supplies oil to an open sump beneath the transmission where a constant level and temperature are maintained.

Pump performance is gaged by measuring flow, pressure, input torque and speed, and vacuum at the suction side of the pump. Any restriction in either the suction or pressure passages which affects pump delivery or horsepower requirements is readily isolated.

This equipment is also used to measure parasitic loss. Measurements are made of input torque and speed. From this, the horsepower required to drive

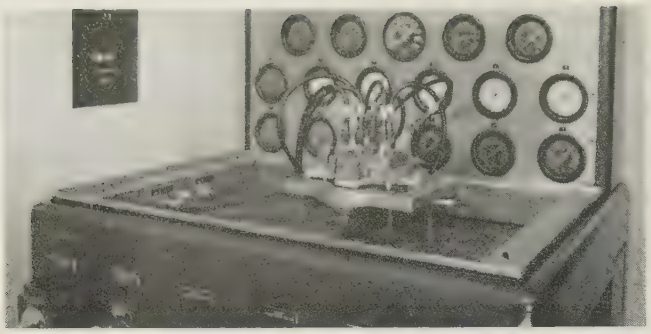

Fig. 24 — Hydraulic flow bench

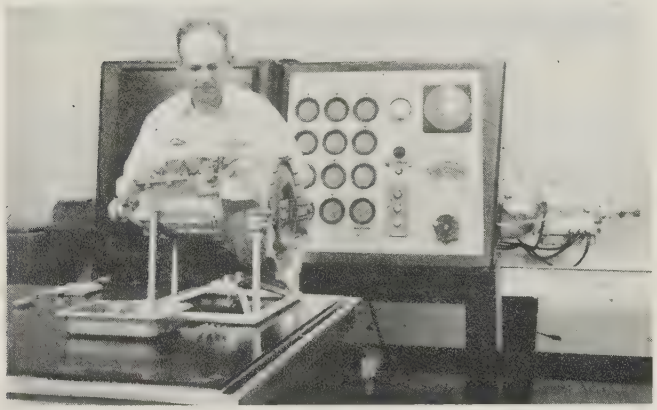

Fig. 25 — Spin rig

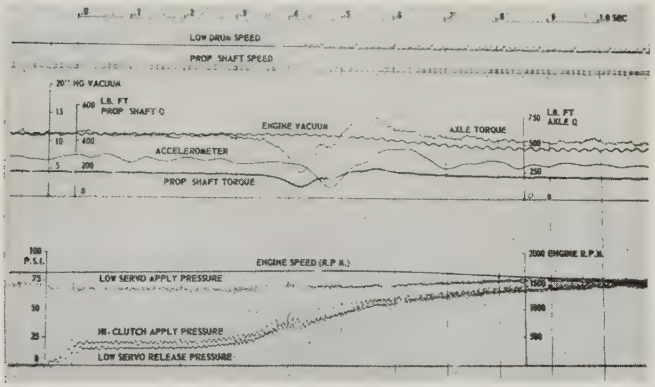

Fig. 26 — Automatic shift oscillogram

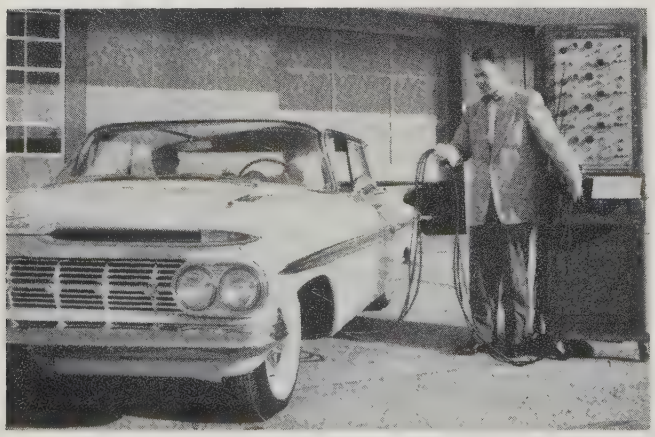

Fig. 27 — Abuse test

the transmission at various speeds is plotted.

The hydraulic flow bench (Fig. 24) is an all-purpose tool for valve body investigations, providing two sources of pressure and oil flow. It also includes necessary measuring devices for trouble shooting leaks, continuity of flow passages, regulation, shift valve calibration, and manual valve operation.

Oil is supplied by a 12-gpm pump through pressure and flow control valves. Pressure gages on the back wall can be connected through quick disconnect fittings to various taps on the test piece, in this case a Turboglide valve body.

Another test fixture that has been of great value in automatic transmission testing, is a spin rig, shown in the background of Fig. 25. This piece of equipment permits variable speed input to the transmission (on the right) and convenient measurement of associated pressures and input speed. This equipment is used for normal checkout on newly designed or newly revised transmissions, and also for trouble-shooting in the event of malfunction.

Complete Transmission Testing

Instrumentation — Final transmission performance must, of course, be evaluated on the basis of tests run in actual vehicles. In this activity, it is always desirable to supplement the "seat of the pants" evaluations with quantitative data. An example of a complete oscillogram used for analyzing an automatic shift is shown in Fig. 26.

These traces allow the transmission designer to study the torques, speeds, and hydraulic functions throughout the complete event. Records are available on low drum speed and torque, engine vacuum, propeller shaft speed, accelerometer readings, axle shaft and propeller shaft torque, engine speed, line pressure and high clutch apply pressure. The information gained is also useful in determining the input energy to the high clutch during engagement.

Accuracy in pressure and torque recordings made it necessary to utilize temperature compensated strain gage transducers. Care must be taken to remove all trapped air from the pressure transducers and their lines so that transient response is not impaired. Engine speed is recorded from an integration of the ignition voltage pulses. A magnetic pickup is installed near milled slots in the clutch drum to get accurate digital speed traces as well as the time at which the drum begins to rotate.

Abuse Test — This test measures the abuse capacity of the transmission, and consists of a series of manual shifts from drive to reverse to drive, continuously, at wide-open throttle (Fig. 27). Recordings are made on the first series of shifts. In this case, a 4-channel direct-writing oscillograph is used to produce the records shown in Figure 28. This record shows the timing relationship of the clutch pressures and propeller shaft torques, as well as clutch capacity and peak torque values. Such a performance record provides baseline information for strength tests.

Programmed Durability Testing — Extensive testing of complete transmissions is carried out at our proving ground. However, to get needed results year around without undue reliance upon favorable weather conditions, the laboratory is equipped to duplicate established proving ground schedules with

the installation shown in Figs. 29 and 30. This dynamometer facility is equipped with various size inertia discs, a magnetic brake, a pneumatically operated quick disconnect in the drive shaft, a failure sensing safety shut down unit, a closed loop servo-controlled throttle on the engine, a transmission range selector and a master controller, or programmer, incorporating a timer, stepping switches, and safety interlocks.

The programmer receives input information in the form of engine speed and throttle angle, vehicle speed, time required to reach various car speeds, transmission range (neutral, drive, or reverse), and transmission oil temperatures and pressures. The information fed to the programmer is taken from actual measurements on proving ground durability schedules.

Transmission input loads are simulated by control of the engine throttle angle. Output loads and speeds are controlled by selected inertia discs and the dynamometer load. Transmission oil temperature and pressure safety interlocks are incorporated so that the programmer automatically stops cycling the transmission in the event that any of these physical quantities exceed the proper operating range.

In this test a shock sensing transducer and associated electronics instantly stop the test if vibrations exceed a pre-set level. When this happens the transducer generates a signal which operates a relay that cuts the engine ignition and decouples the transmission from the dynamometer. The immediate removal of both input and output transmission loads, by means of a quick disconnect coupling, prevents excessive component destruction. This is important from two standpoints: it preserves expensive test pieces that have not failed but that would be destroyed in the normal grinding halt of a test; and it pinpoints the initial cause of the failure.

A case in point is shown in Fig. 31, wherein a cracked pinion was caught before final failure occurred.

Similar programmed tests, although on a smaller scale, are finding widespread application in the laboratory both on transmission clutch tests and engine durability tests.

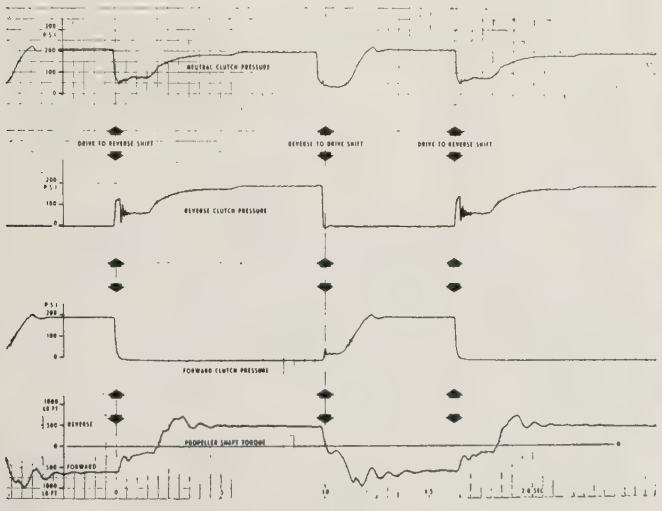

Fig. 28 — Abuse test oscillogram

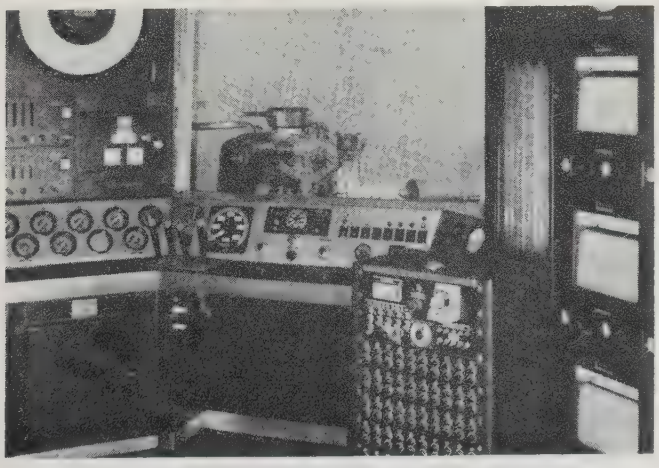

Fig. 29 — Transmission programming

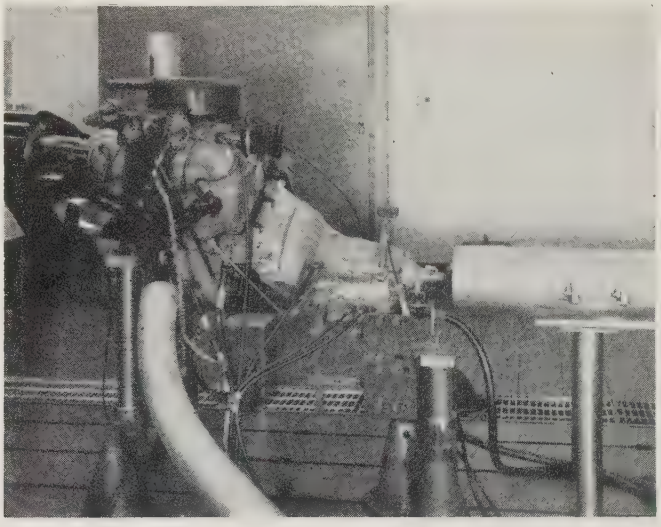

Fig. 30 — Programmer test stand

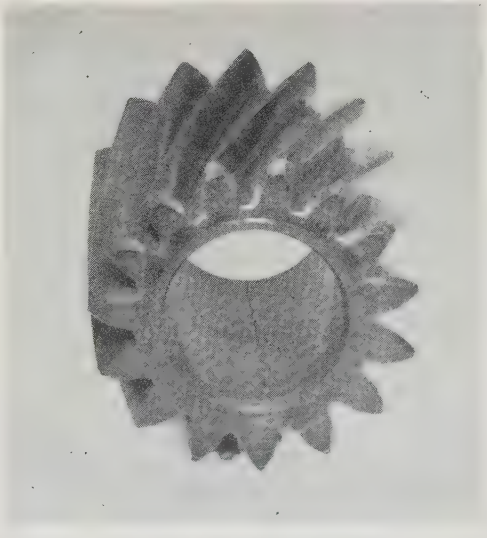

Fig. 31 — Arrested failure

some recent

FRICTION, WEAR, AND

THIS PAPER will give an account of some recent experiments which we have been carrying out in Cambridge. The first part will deal with the sliding friction and wear of nonmetals, particularly wood, diamond, glass, rubber, and metallic carbides. Some of these experiments are carried out at high temperature.

This is an age of high speed. The jet airliners are carrying people comfortably across the Atlantic at speeds of 600 mph. Many military aircraft can penetrate the sound barrier — 700 mph — and new ones are being developed which can fly at speeds greater than 2000 mph. Satellites and Sputniks are circling the earth at speeds of nearly 18,000 mph, and space rockets must reach a speed of about 25,000 mph. The second part will discuss some high-speed problems which arise when solids are deformed very rapidly. The friction and shearing of metals at high speeds (ca 2000 mph) and damage of metals and nonmetals under high-speed liquid impact are considered.

EXPERIMENTS have been conducted at Cambridge University which probed the sliding friction and wear of nonmetals, and the deformation of soilds at high rates of strain. The author was particularly interested in the deformation and damage of metals and nonmetals under high-speed liquid impact. The findings will contribute to the development of materials that can withstand the friction of high-speed space flight.

The author discusses the sliding friction and wear of wood, diamond, glass, rubber, and metallic carbides. In the last part of the paper, he describes the high-speed problems arising when solids are deformed very rapidly.

Friction and Wear of Nonmetals

Friction of Wood — Earlier work, especially on metals, has shown that the friction of unlubricated solids is largely due to strong adhesion occurring at the regions of real contact. In addition, part of the friction may arise from the ploughing of the softer surface by asperities on the harder. Experiments by Drs. Atack and Tabor[1] show that the friction of wood may be explained in a similar way, that is, it arises from an adhesion term and a deformation or ploughing term. In particular, it is found that the moisture content may have a profound effect — not necessarily a collateral one — on each of these terms.

The friction was studied between balsam wood (Abies Balsomea) and surfaces of steel and polytetrafluoroethylene (PTFE). The most revealing results are obtained when steel or PTFE spheres are slid or rolled over the wooden surface (Fig. 1). The rolling friction is found to be due to internal friction or hysteresis losses in the wood, and not to surface interaction. It is essentially the same for both steel and PTFE spheres. As the moisture content is raised from 0 to 30%, the rolling friction increases and then remains constant. This is apparently due to changes effected in the mechanical, rather than the surface properties of the wood.

In contrast, the sliding friction is found to depend both on the moisture content of the wood and on the chemical nature of the other surface. For a hard slider of a given material under specified moisture conditions, the sliding friction F_s may be expressed as the sum of two terms:

$$F_s = F_D + F_A \qquad (1)$$

F_D is the tangential force involved in deforming

[1] Proceedings of Royal Society, Series A, Vol. 248, 1958, pp. 539–555: "Friction of Wood," by D. Tabor and D. Atack.

experiments on the

DEFORMATION OF SOLIDS

F. P. Bowden, Cambridge University

This paper was presented at the SAE Annual Meeting, Detroit, Jan. 14, 1959.

the wood and is directly related to the internal friction or hysteresis losses in the wood itself: it corresponds to the rolling friction, F_A is the tangential force required to overcome interfacial adhesion, and is specific to the surfaces. It is high for steel whatever the moisture content of the wood, showing that the adhesion, which is probably due to hydrogen bonding, is strong in both cases. For PTFE the friction is fairly high when the wood has a low moisture content, implying a relatively strong adhesion; but it is very low when the moisture content exceeds 30–40%. This emphasizes the importance of surface structure in the adhesion term of friction in contrast to the deformation term, which is essentially a bulk phenomenon.

Friction and Abrasion of Diamond on Itself — In most abrasion processes an abrasive which is harder than the material to be worked is employed. With diamond this has not been possible and the material itself is normally used. This process is unusual in that there is a very large directional variation in the resistance to abrasion of diamonds abraded with diamond powder. The wear rates for different crystallographic directions vary by a factor of 500 or more. An attempt has been made by M. Seal[2] to determine whether the abrasion of diamond by diamond is primarily mechanical or thermal, that is, whether it occurs by fragmentation of the diamond on a microscopic scale or by some change caused by the local high temperatures produced by friction.

The experimental work described is in two sections: track formation on diamond and the friction of diamond. The work on track formation, carried out at low sliding speeds with a rounded diamond slider and a plane diamond surface, was done in an attempt to reproduce on a macroscopic scale the damage occurring on a microscopic scale during abrasion. It was found that, according to the conditions of sliding, tracks of three main types can be produced, and that on an individual diamond face there is no variation of the ease of track formation with sliding direction. This last result contrasts with the large directional variation in the ease of

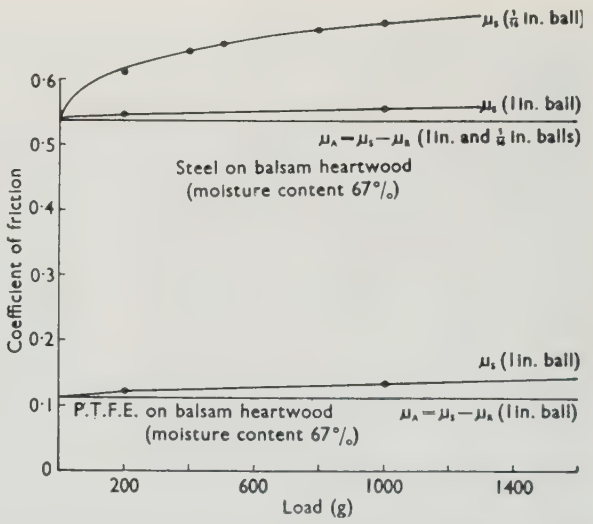

Fig. 1 — Sliding friction of wood, μ_S, can be resolved into two components, friction due to elastic hysteresis loss in deforming the wood μ_R (this is same as rolling friction), and friction due to adhesion between the sufaces, μ_A. μ_A follows same laws as friction of metals and is probably due to hydrogen bonding between surfaces

[2] Proceedings of Royal Society, Series A, Vol. 248, 1958, pp. 379–393: Article by M. Seal.

abrasion, and indicates that high sliding speeds introduce some effect which causes the anisotropy in abrasion resistance.

During high-speed sliding the points of contact between the abrasive and the diamond will become intensely hot. Local temperatures may reach 1000 C or more, which will be sufficient to change the diamond into amorphous carbon. This change is thought to be the cause of wear, the soft carbon being scraped away by the oncoming diamond dust. The following explanation of the anisotropy in high-speed wear rate is suggested. The work on friction shows that there is a variation with sliding direction of the coefficient of friction between diamond and diamond. Directions in which the friction can be high are directions of easy abrasion. The local surface temperatures during abrasion will depend on the coefficient of friction and will be greater when the friction is high. These directions would thus be expected to be those of easy abrasion. (See Fig. 2.) Furthermore, a small anisotropy in friction would account for a large anisotropy in abrasion resistance. Experiments by Dr. E. Freitag[3] show that even the hardest face of a diamond can be readily polished by a metal if the *rubbing speed is sufficiently high.* Again, there is evidence that this is due to the transformation of diamond to carbon at the high surface temperature which is attained. (See Fig. 3.)

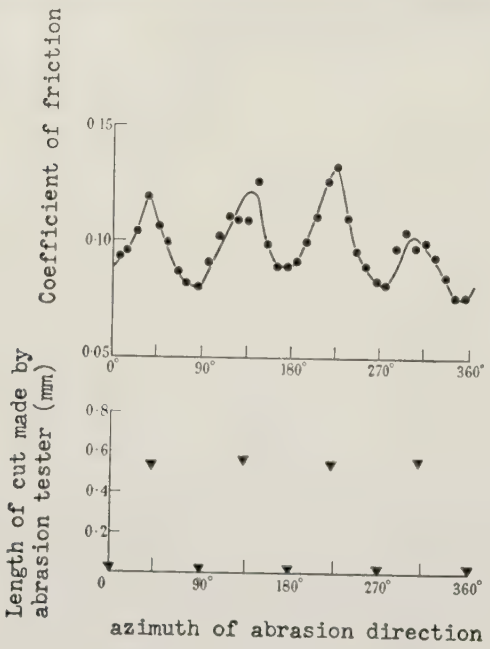

Fig. 2 — Friction and abrasion resistance in different azimuths on polished (100) diamond face. Crystallographic axes in face are at azimuths 45, 135, 225, and 315 deg. Diamond is readily abraded in high friction directions

Polishing, Surface Flow, and Abrasion of Diamond and Glass — Experiments by Dr. H. Scott[4] show that a diamond sliding on glass can under suitable conditions induce surface flow of the glass. The speed (v) and load (W) necessary to cause this flow have been studied and it is found that flow only occurs if $v\sqrt{W}$ exceeds a critical value which depends on the type of glass (Fig. 4). There is evidence that flow occurs when a critical surface temperature is reached and approximate calculations indicate that this temperature corresponds to the softening point of the glass. It is suggested that this type of thermal softening and flow may occur on a submicroscopic scale when glass is polished.

Heavy wear of a diamond sliding on glass has been observed. This wear is very dependent on the humidity of the atmosphere; in a dry atmosphere it may be 100 times greater than it is in a humid one. The wear rate of diamond on glass in dry air is greater than that on a scaife (diamond impregnated grinding wheel) as shown in Table 1. The wear is accompanied by the production of a detritus of amorphous carbon so that the process appears to be

[3] Proceedings of Royal Society, Series A, Vol. 248, 1958: Article by F. P. Bowden and E. Freitag.

[4] Proceedings of Royal Society, Series A, Vol. 248, 1958: Article by F. P. Bowden and H. G. Scott.

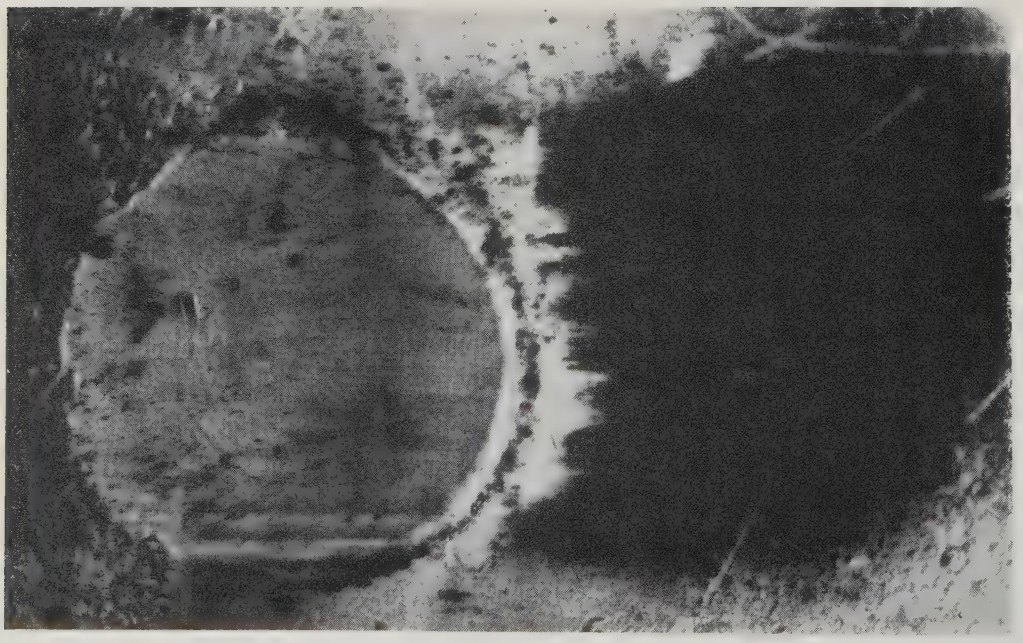

Fig. 3 — Abrasion mark and carbonaceous detritus produced by rotating steel ball on diamond surface. Sliding speed 100-200 m/sec (original magnified 230 times)

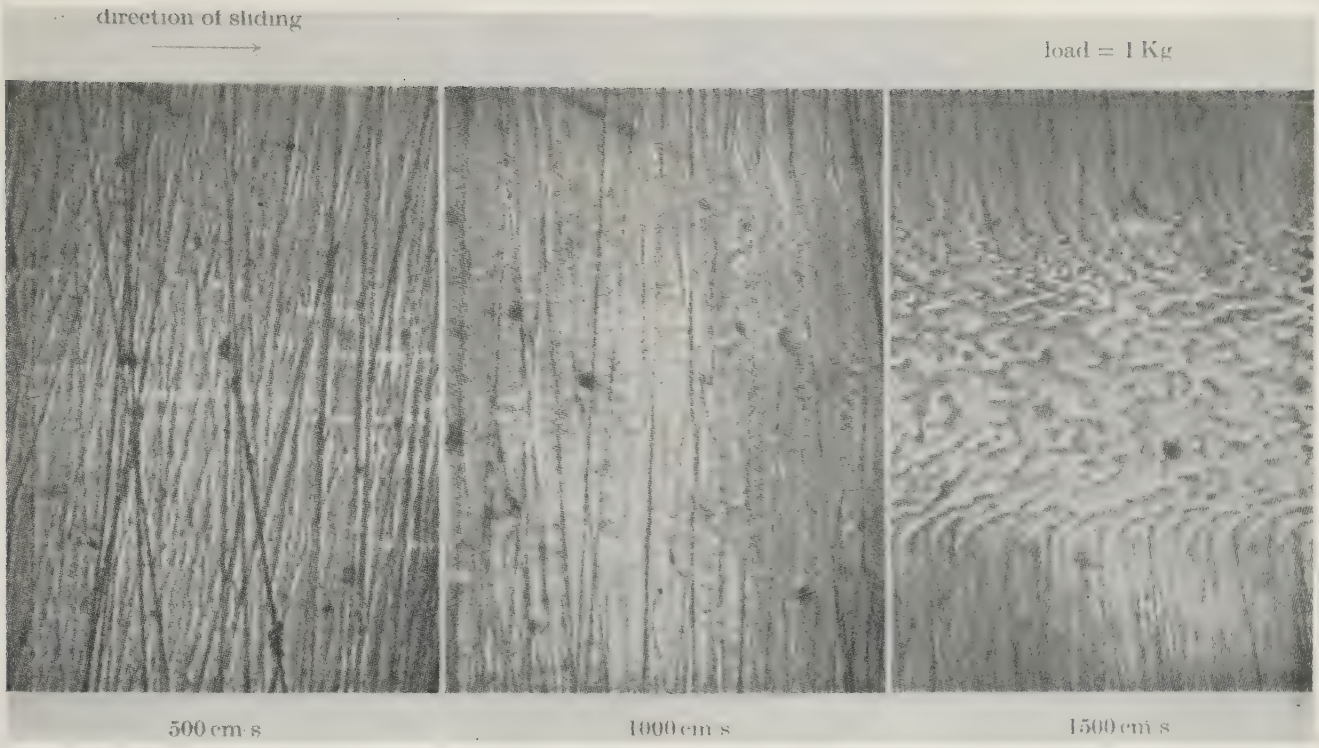

Fig. 4 — Wear tracks on glass, showing onset of flow. Surface flow of glass produced by rubbing with diamond at critical speed (magnified 100 times)

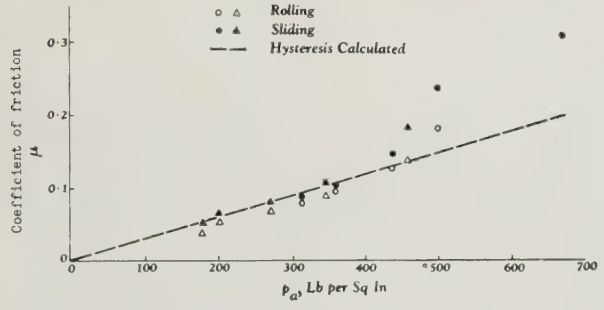

Fig. 5 — Coefficient of friction of steel spheres on black tread rubber as function of mean contact pressure p_a. Rolling friction and lubricated sliding friction are almost identical. Value agrees with that calculated from internal hysteresis loss

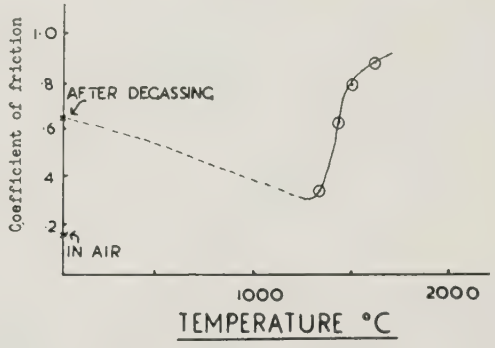

Fig. 6 — Graphic coefficient of friction/temperature C, titanium carbide on titanium carbide

primarily one of degradation of diamond to amorphous carbon. This degradation is aided by the temperature rise at the rubbing interface and there is evidence that it can occur at temperatures lower than those required when the diamond is heated without rubbing.

Friction of Rubber — Earlier experiments by Dr. Tabor[5] has shown that rolling friction on metals and other solids is not primarily a surface effect but is due, in a large measure, to elastic hysteresis loss within the solid. He and his colleagues have extended their experiments to the *sliding* friction of rubber. The work shows clearly that the *sliding* friction of solids on well-lubricated rubber is also due primarily to elastic hysteresis loss within the rubber.[6,7] (See Fig. 5.) These observations may be important in the friction skidding and wear of motor-car tires.

Table 1 — Rapid Wear of Diamond on Glass in Very Dry Atmosphere

Speed	840 cm/sec	Load	½ kg		
Sliding	in "soft"	direction	on	cube	face
		Wear	rate	of	diamond
			cm^3/hr		$\times 10^6$
In	"normal" air		ca 5		
In	dry air		500		
Diamond	on scaife		ca 50		

Friction of Metallic Carbides at High Temperature — We have done some work on the frictional behavior at high temperature of carbon sliding on itself, or on metal. Measurements were made at temperatures up to about 2000 C. It was shown that — with graphite sliding on itself or on copper or silver — the friction fell steadily as the temperature was raised. With graphite on many other metals, however, the friction at about 1000 C rose to

[5] Proceedings of Royal Society, Vol. 229, 1955, p. 198: Article by D. Tabor.
[6] Proceedings of Physical Society, Vol. 71, 1958, p. 989: "Sliding Friction of Rubber," by D. Tabor.
[7] Engineering, Vol. 186, 1958, pp. 838–842: "Hysteresis Loss in Friction of Lubricated Rubber," by D. Tabor.

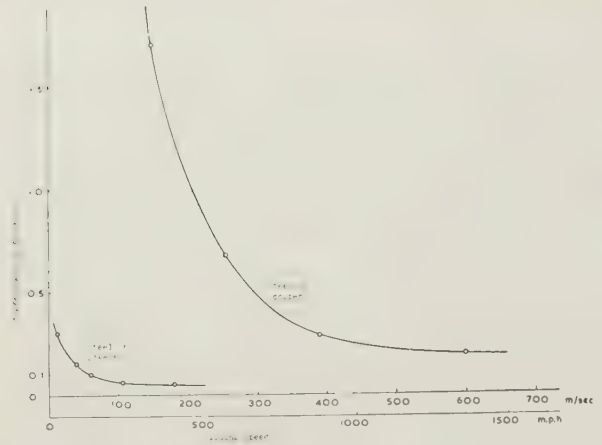

Fig. 7 — Friction of metals at very high speeds. At high sliding speeds, friction falls to low value because of the formation of very thin surface layer thermally softened or melted in metal

a high value. It was shown that this was due to the formation of metallic carbides at the interface.

We are continuing our studies of the physical properties of solids at high temperature and extending the range to about 3000 C. Mr. B. Mordike has been studying the friction behavior of the refractory carbides. Preliminary measurements on boron, tungsten, and titanium carbides show that the friction first falls as the temperature is increased and then at about 1000 C the friction rises steeply to a high value (Fig. 6). The reason for this is not certain and it is clear that one must learn more about the behavior of solids at very high temperatures.

Deformation and Damage of Solids at High Rates of Strain

Friction of Solids at High Speeds — We have described earlier[3] a method (based on Prof. J. W. Beams ultracentrifuge) for measuring the friction of solids at speeds up to 800 m/sec (ca 1800 mph). The results show that the sliding resistance of metals decreases as the speed increases and reaches very low values (Fig. 7). There is evidence that frictional heating produces high surface temperatures and a softening and melting of the metal at the regions of contact.

An analysis of the heat flow in a specimen shows that the area of intimate contact is very small compared with the apparent interface. Since the temperature falls very rapidly with increasing distance from the shearing zone, the metal behaves like a combination of a thin film of low shear strength supported by a hard substrate. This can explain the low friction at high sliding speeds. It is also suggested that the real area of contact depends on the velocity with which plastic strains are propagated in the metal. The shearing occurs so rapidly that full plastic yielding under the normal load is not possible. Some metals disintegrate in a brittle fashion when a critical speed is exceeded.

This experimental method has some limitations if the surface of the specimen breaks up into a multitude of fragments or if large-scale melting occurs. The metal which is ejected from the area of contact

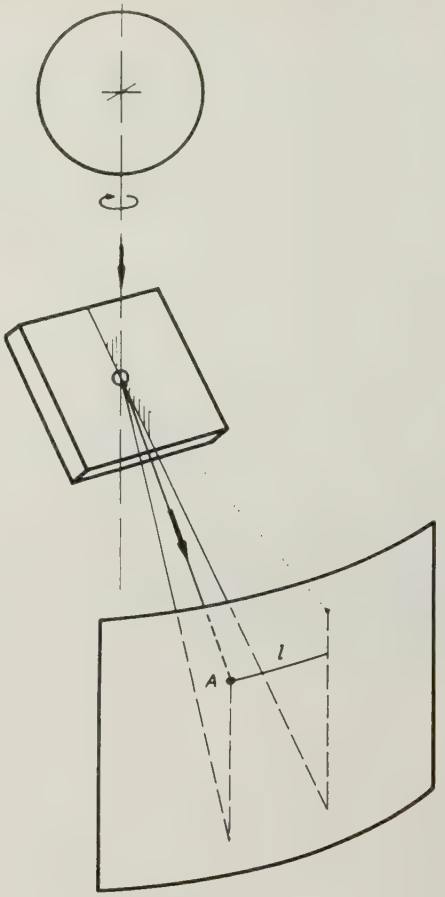

Fig. 8 — Measurement of friction at very high speeds. Fast spinning ball is dropped onto inclined plate and angle at which it bounces off is determined by coefficient of friction. μ is proportional to distance *l*

will cut off the beam of light used to measure the friction. Also, a soft metal with a low melting point will experience a considerable amount of wear, although the time of contact may be of the order of only a few seconds (this corresponds to a sliding distance of a mile or more). If excessive wear occurs, the load applied to the specimens changes appreciably during sliding and in an uncontrolled manner.

In these cases, therefore, a technique is wanted which does not depend upon a beam of light for the friction measurements and is suitable for contacts of very short duration to keep the wear small.

A new method has recently been developed by Per-Anders Persson which satisfies both these requirements. The steel ball is first suspended and accelerated in the same way as before and then dropped on to a flat specimen which is set at an angle of 30 deg with respect to the axis of rotation. The spinning ball then bounces off, but not in the plane normal to the specimen surface (Fig. 8). The sliding friction causes a deflection sideways, and it is easy to show that the angle of deflection is directly proportional to the coefficient of friction and independent of the load. Essentially, the measurement of friction consists simply in finding the spot where the spinning ball hit a certain target after the rebound. The time of contact during which the ball slides on the inclined specimen is measured by means of a piezo-crystal.

The results obtained in this way agree remarkably well with those found by the older method. In

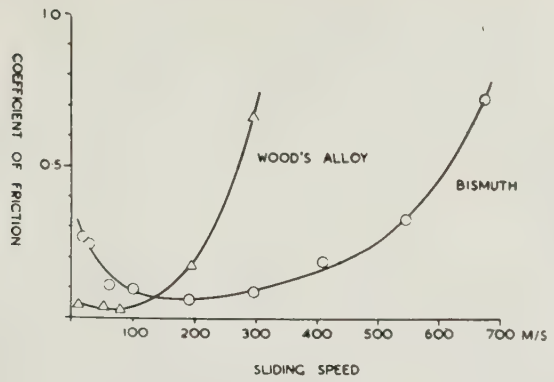

Fig. 9 — Increase of friction at high speed when excessive surface melting occurs

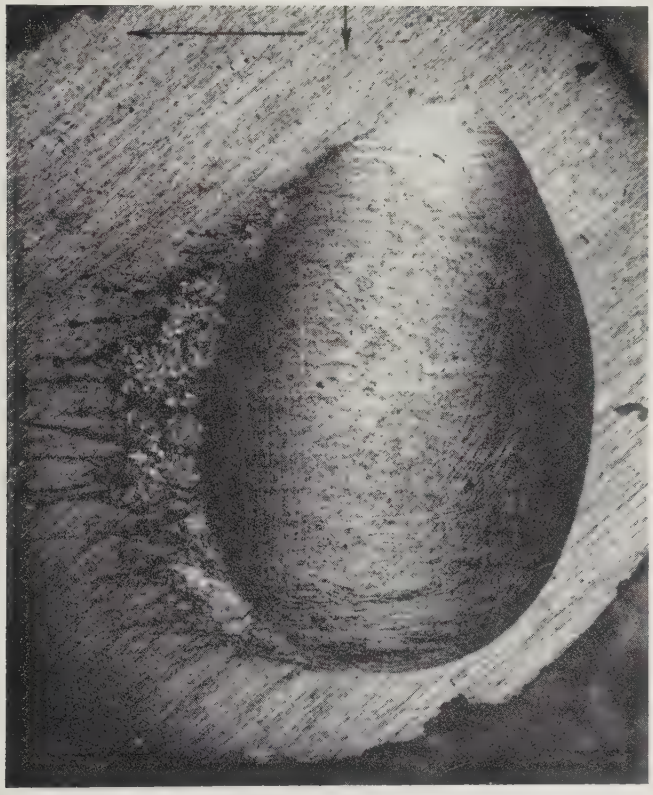

Fig. 10 — Steel ball sliding on bismuth surface, 450 m/sec. Short arrow indicates direction of fall, long arrow direction of spin. Note large-scale melting (original magnified 28 times)

the range of speeds where comparisons cannot be made, the new technique has produced data which show that the coefficient of friction begins to rise with increasing speed when the region of large-scale melting is reached. (See Figs. 9 and 10.) Further, the rebound is lower and the contact lasts longer than for a non-rotating ball.

Damage to Solids by Liquid Impact at Very High Speeds — A drop of liquid striking against a solid surface at very high velocity may produce considerable deformation and damage. Such damage can occur on the surfaces of aircraft during high-speed

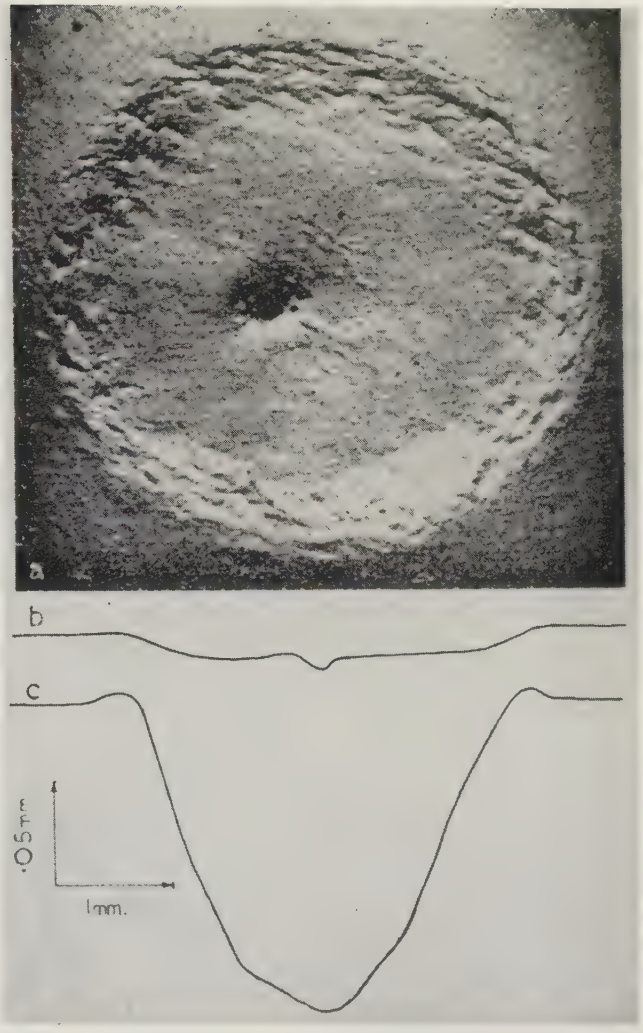

Fig. 11 — A — deformation produced in stainless-steel surface by impact of single water jet at 2500 fps, B — surface contour of deformed region, C — deformation of aluminium

flight in rain; in this form it is referred to as "rain erosion."

Mr. Brunton[8] is making a study of some of the basic aspects of liquid-solid impact at very high speeds. For this purpose a simple apparatus has been developed for projecting a small cylinder of liquid against a stationary solid surface. The cylinder is normally about 1 mm in diameter and 1 cm in length, the mass of liquid involved being approximately equivalent to that of a large raindrop. Impact velocities of up to 3500 fps have been obtained. Under such conditions, even the hardest surfaces will become deformed.

Briefly, the apparatus consists of a small stainless-steel injector into which about 0.01 cc of liquid can be sealed by a neoprene disk. At the instant of firing a slug from a high-power air rifle rams the disk into the injector. The highly compressed liquid escapes through a nozzle at the far end of the injector as a short high-velocity jet or cylinder. Information on the structure, velocity, and behavior on impact of the liquid has been obtained by high-speed photography.

Deformation of Metals — All metals are readily deformed under these conditions. With a high-strength stainless steel, the main effect of the im-

[8] *Nature*, Vol. 181, March 29, 1958, pp. 873–875: Article by F. P. Bowden and J. Brunton.

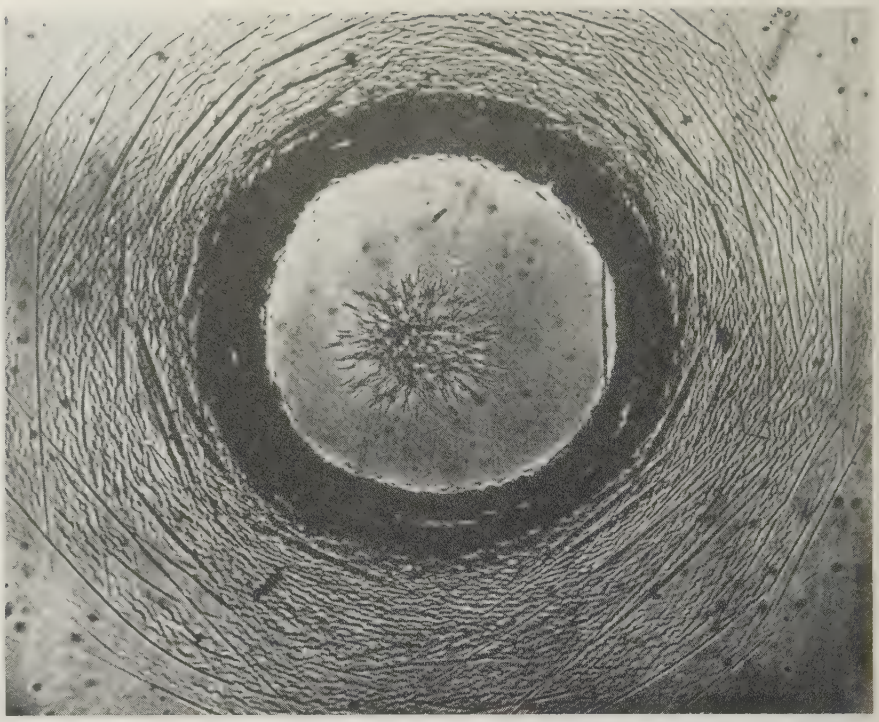

Fig. 12 — Surface deformation in 'Perspex' due to impact of water jet at 3000 fps. Ring crack has mean diameter of 3.5 mm. Central star crack is beneath surface

pact at speeds of ca 3000 fps is to produce a shallow saucer-shaped depression in the surface, with the two additional features of a central pit and a highly deformed annular region just inside the rim of the depression (Fig. 11). The area of deformation corresponds closely to the area over which the spreading cylinder exerts a pressure; this is, of course, considerably greater than its initial cross-section. The pressure is assumed to be a maximum under the center of the collapsing cylinder, and to fall smoothly to zero at points where the liquid flow first becomes entirely parallel to the surface. These positions can be determined from photographs taken during the impact. Such a pressure distribution on the surface would give rise to a depression similar to that observed. The depression formed in aluminium under the same conditions is more than 10 times as deep.

The annular region of heavy deformation at the edge of the impact zone in metals has the appearance of having been sheared open by water flowing over it at very high speeds. The deformation marks consist of alternate ridges and depressions running parallel to the rim; in soft metals, flow channels are apparent in the depressions, indicating the manner in which metal has been sheared out to form the ridges. Such a shear deformation of the surface would be most likely to occur at the boundary of the impact zone, where the velocity of the surface flow is greatest. If a shear mechanism is responsible for the rim deformation, then this deformation would be expected to depend upon the viscosity of the liquid. Using aluminum targets and water-glycerol mixtures as the deforming liquid, the intensity of the deformation near the rim was found to increase with the viscosity.

Deformation of Nonmetals — The failure pattern due to liquid impact in rigid plastics, glasses, and ceramics is quite different from that observed in metals. Perspex was found to be a convenient material in this group to work with; besides being transparent, it has the additional advantage that the state of stress in it during impact can be studied simultaneously by a photoelastic method. The main feature of the damage is a ring crack (Figs. 12 and 13). The area of the surface inside the ring is undamaged, and for a considerable distance outside the ring the surface is pitted with short straight circumferential cracks. In addition, there is heavy damage of the solid in a localized region *beneath* the surface. After four or five impacts the various fracture surfaces join up, and a large piece of the solid is dislodged from the surface.

As in the case of metals, failure in nonmetals can be thought of as arising primarily from the distribution of pressure under the jet, together with the deformation associated with rapid flow along the surface. Brittle failure may be expected to occur preferentially on planes across which the tensile stress is a maximum. The Hertz theory of contact stresses can be used to predict the regions of high tensile stress in the solid for the given distribution of pressure on the surface. Bearing in mind the limitations of the theory when applied to impact problems, it is possible to deduce that the maximum tensile stress occurs at the surface across the circular boundary defining the limits of the area under pressure. Outside the boundary the tensile stress decreases slowly with distance; inside the boundary it falls abruptly to zero and becomes a compressive stress. Such a stress distribution accounts effectively for the pattern of surface cracking. The theory also predicts that the ring crack should form part of a conical rather than cylindrical surface.

Similarly, the tensile stress across the central axis normal to the surface attains a maximum value a little way below the surface; such a stress would explain the vertical planes of subsurface fracture. The rapid surface flow accentuates these types of failure by opening up the fracture planes in the di-

Fig. 13 — Cross-section taken through impact zone similar to that shown in Fig. 12. Shape of ring crack and central zone of subsurface cracking can be clearly seen

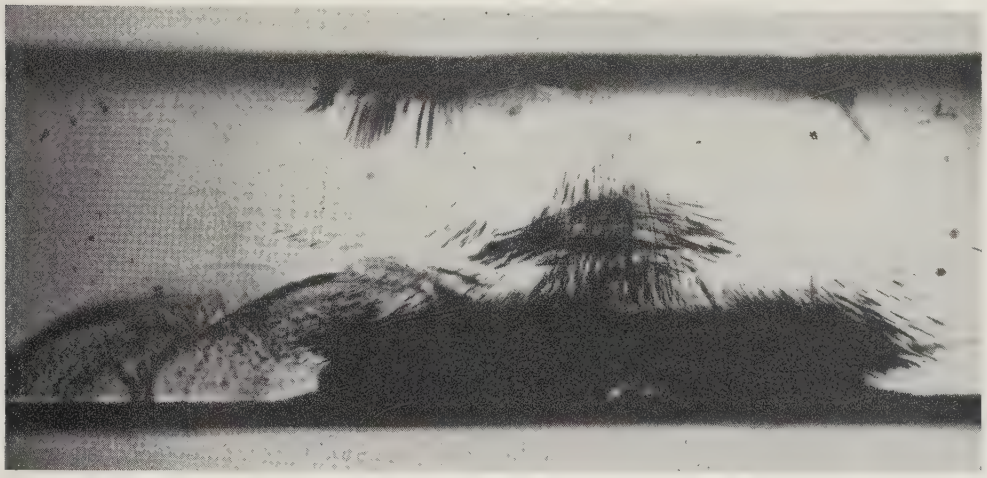

Fig. 14 — Scabbing of lower surface of 0.25-in. thick 'Perspex' plate. Velocity of jet striking upper surface was 3000 fps

rection of flow, and in this way material is chipped from the surface.

Scabbing of Back Surface — If the specimen is thin, a large scab may be detached from the *back* surface when the *front* surface is struck by the liquid (Fig. 14). The compression wave set up on impact is reflected from the back surface as a wave of tension, and the associated tensile stress effectively pulls a piece out of this surface. The new surface so formed reflects the remainder of the compression wave, and the process of scab formation is repeated.

The fact that the impact of a water cylinder with a velocity of 3000 fps can deform materials as hard, for example, as tungsten carbide is not surprising if it is realized that the pressure developed on the surface by the liquid is well above the yield strength of most common metals. The associated stress may be further magnified by the presence of surface pits. In addition, there are the shear stresses associated with the high-speed flow of the collapsed cylinder over the surface. Flow velocities parallel to the surface were observed to be two to three times as great as the impact velocity. Any surface irregularity in the path of this flow would certainly be deformed. Some of the observations may have a bearing on the damage of turbine blades.

It is clear that our passion for fast travel can lead us into difficulties. If we wish to go hurtling round the earth at a few thousand miles an hour, we must learn more about the way solids slide, bend, and break at very high speeds.

ORAL DISCUSSION

— Reported by C. R. Lewis
Chrysler Corp.

Edmund E. Bisson, National Advisory Committee for Aeronautics: The information obtained by Dr. Bowden's laboratory on friction at high temperatures or at high speeds is very interesting. In particular, the information on boron, tungsten, and titanium carbides is of interest because of their potential usefulness in future applications involving high temperatures and high speeds. It would be highly desirable for data to be obtained under the *combination* of high speeds and high temperatures if this result is at all feasible.

Dr. Bowden: I appreciate Dr. Bissen's point about the importance of combining high-speed and high-temperature studies of friction. It is possible both by Dr. Freitag's method, and also by Mr. Persson's technique, to heat the solid surface to a high temperature before sliding occurs. So far we have not done this except to a very modest degree, but there would be no very great difficulty in using high temperatures. To some extent, of course, this heating is superfluous since the extreme speed rapidly raises the surface temperature of most solids up to their melting point.

We hope to continue these studies, both on metals and on refractory nonmetals including the carbides.

In reply to his last question, the experimental results obtained by both methods are in good agreement. The results will be published as soon as the work is completed.

I-Ming Feng, Ethyl Corp.: To some extent, machining

operations are similar to polishing or friction. In machining the work piece is not the one that gets very hot. Rather, it is the chip produced by the cutting tool that gets hot. If a piece is being machined at an extremely high speed, the chip will fly out red hot, while the work piece and the tool will stay at a much lower temperature. This leads me to think that there might be some correlation between this and the friction work done by Dr. Bowden.

For instance, when a machinist grinds a piece of metal with a grinding wheel made of abrasive particles, the abrasive particles will produce a small chip from the work piece. This has been shown by Dr. Merchant of the Cincinnati Milling Machine Co. In other words, the chip is formed by the cutting tool — in this case, an abrasive particle. The chip will fly out and burn in the air, producing a spark. This is good evidence that a little piece of metal or solid receives the greatest amount of energy put into the system, and thus gets hot. Perhaps this could lead to the explanation that when diamonds are polished, abrasive particles cut the diamond and produce a little piece of a diamond. This chip is so hot it reaches a temperature of close to 1000 F, and then it changes into amorphous carbon. This seems to me a possible explanation of the formation of amorphous carbon, which was observed in Dr. Bowden's case.

A second point I want to discuss is the high-speed water jet. When a piece of metal is deformed by a high-speed water jet, the pressure distribution may not be the most important thing in explaining the shape of deformation. In other words, once it reaches the plastic stage, a small change in pressure will cause a great deal of plastic deformation. In this range the deformation perhaps will be related to the amount of energy received by this metal rather than the pressure distribution. Based upon this energy consideration, there is an obvious explanation for the central pit in the impact area. This applies only to material which fails by ductile failure, not to brittle failure in the case of a lucite plastic type of material.

Dr. Bowen: The speeds used in Dr. Freitag's experiments are some orders of magnitude greater than those employed in machining and cutting, and there is clear evidence that the contact regions *on the surface* of the diamond and other solids are raised to a very high temperature.

On the deformation of metals and plastic solids by liquid impact at high speed, Mr. Brunton of this Laboratory does find that small pits and irregularities produce stress concentration which causes a marked localized plastic deformation.

C. L. Eksergian, Budd Co.: It is rather interesting to see in the early railroad archives that many people thought no railroad would ever operate on rails because of a lack of friction. And, of course, in braking we were very much concerned with not only what the brake friction is, but what the adhesion is.

We were nonplused, as were many people in the railroad fraternity, with the terrific differences in friction. And, we were interested in dissociating what you might call true rolling friction from the actual friction, or the change in friction due to load variation. It so happened that coincident with our brake work, we had a device which would relieve the brake when it exceeded the adhesion and allowed the wheel to restore to normal rotation. By putting a recorder on the axle, we could get actual angular velocity. We used the device to find the change in coefficient of adhesion relative to slip velocity. For example, if the wheel were going 80 mph and should drop to 40, the slip velocity would be 40. With the wheel restored to normal rotation it would go back to zero. Contrary to certain beliefs that there was a great departure from static to slip friction, we found that by plotting the actual acceleration of the wheel, we got a curve as shown in Fig. A.

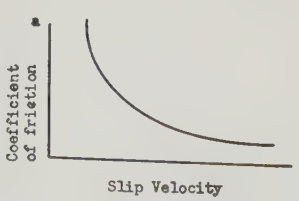

Fig. A

The question of applying this velocity of change of static friction to slip friction throws light on the noise we sometimes get in our automobile brakes. I would compare it to a musical instrument. For if it were not for the marked difference between static friction and slip friction, the violinist wouldn't be able to make a sound.

On a violin, a string suspension has a set frequency in which it vibrates. When a bow (of constant coefficient of friction) is put across the string and pulled until the friction overcomes the pull of the string, the string would remain at constant extension and not vibrate.

Now the trick in getting a big tone is to have a velocity (that is, a low velocity) which is at a level where you get static friction and the biggest pull, and at the same time much less pressure so as to cause a maximum stroke of the string. If this isn't done, you won't get the amplitude required for the volume of tone.

All this is curiously identical to the phenomenon of brake noise, pitch out, howl, wire brush, and the like. If you can think of a drum being a circular bow and the shoe being a string, you can readily see the resemblance between the brake drum and the violin, where the shoe is allowed to deflect. It is momentarily lined up to go around the drum, breaks away, slides back, comes back again. You get this pulsating motion on the shoe, which in turn sets up a vibration on the sounding board of the brake structure.

Dr. Bowden: With regard to the stick slip of the violin string and the railroad wheel, there's no doubt at all, I think, that the noise of a finger on a window pane, of a cricket sounding on the hearth, of the violin string, of a railroad wheel, is all due essentially to the same cause. This cause is "stick slip motion" or intermittent motion which is generated mainly because under these conditions the kinetic friction is lower than the static friction. It is only under those conditions that the kinetic friction is lower than the static friction. It is only under those conditions, plus the appropriate conditions of elasticity, that you can get this noise. I agree with Mr. Eksergian.

Dr. R. Drutowski, General Motors Research: Have you observed any relationship between the speed of rolling and the rolling force? Is internal friction or hysteresis, as so often happens, a function of speed?

Dr. Bowden: Dr. Drutowski has raised a very important point as to how and whether rolling friction depends on speed. The answer is definitely "yes." At high speeds two effects are changed at high rate of deformation, so that both the elastic impact energy and the hysteresis loss factor are different.

Secondly, the surfaces will get hotter due to the dissipation of deformation energy. This will also affect the elastic and hysteresis properties of the materials. The effects are clearly rather involved. With metals we should not expect a marked dependence on speed, except perhaps at phenomenally high speeds. With rubber and other viscoelastic solids we should, however, expect a much more marked effect. This has recently been considered by Bueche and Flom.[a] They studied the sliding friction of hard sliders on lubricated plastics and found that the friction does, in fact, vary with speed and temperature. There is a close parallel between the friction changes and the variation of the hysteresis losses. This strongly supports the general picture described above.

[a] *Wear*, Vol. 2, 1959, p. 168: Article by A. M. Buech and D. G. Flom.

design problems of

VERY HIGH SPEED FLIGHT

K. E. Van Every, Douglas Aircraft Co., Inc.

This paper was presented at a meeting of the Southern California Section, Los Angeles, Feb. 10, 1958

THE IMPORTANCE of manned aircraft versus missiles has been and will continue to be debated, but there are many reasons why it is advantageous to continue the development of manned aircraft. A number of these reasons have been pointed out by Crossfield and Flickinger in recent talks and papers,[1,2] Among the points which they make are the following:

1. A pilot is a necessary complement to the control system unless all circumstances occurring during the flight can be considered to be a mathematical certainty.
2. A human pilot is the lightest, most versatile computer available for control where response times in excess of a second are adequate.
3. A manned vehicle can serve as its own transport, thereby simplifying the logistics problem.

Additional emphasis to the development of manned vehicles has been given by the successful launchings of satellites Sputnik I and II and the Explorer, since they have made people realize that the

[1] "Some Operational Considerations of Manned Extra-Atmospheric Flight," by Scott Crossfield. Paper presented at Space Symposium, Los Angeles, January, 1958.

[2] "Space Surgeon's Case for Manned Missile Systems," by Donald Flickinger. Paper presented at IAS Meeting, Los Angeles, January, 1958.

THIS PAPER is concerned with design problems which are encountered on manned aircraft operating at very high speeds. Very high speeds are considered to be from Mach 2 or 1300 mph to speeds of the order of Mach 38 or 25,000 mph, which is the velocity for escape from the earth. Mach 2 is considered a logical starting point since it represents the approximate upper limit of present day military aircraft.

Manned aircraft will continue to be developed for flight at very high speed and high altitudes and the experiences gained will serve as stepping stones to eventual manned satellites and space vehicles. The major problems to be solved relate to aerodynamic heating, stability and control, and human effects.

This paper received the 1958 Wright Brothers Medal.

Fig. 1 — Douglas D558-III design study

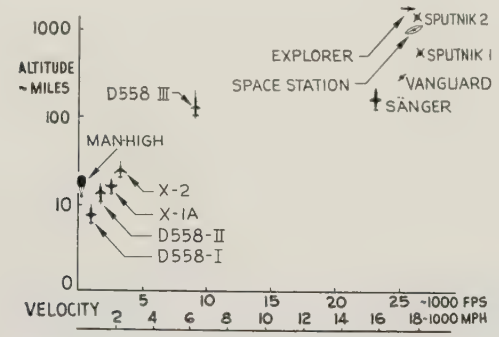

Fig. 2 — Flight spectrum of various vehicles

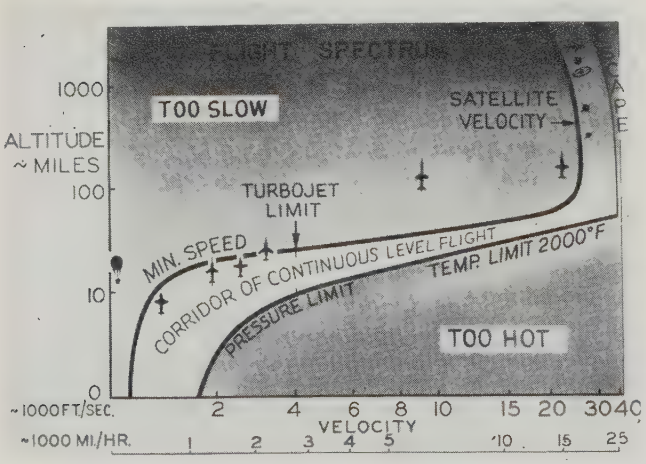

Fig. 3 — Corridor of continuous level flight

day of space travel is something imminent rather than something in the far-distant future. Aside from the obvious military and scientific advantages of manned satellites and spaceships, man's inate curiosity will compel him to go along on future trips whether they are just faster and higher than present aircraft, or to the moon or outer space.

The development of very-high-speed airplanes is, of course, a logical progression from present-day military aircraft and more specifically from previous high-speed research aircraft such as the D558-I, D558-II, X-1 and X-2. Several years ago the importance of a further investigation of altitude and speed by the use of advanced research aircraft was independently realized by the Air Force, the NACA, and the Office of Naval Research of the Navy Department. Numerous studies on aircraft of this type were undertaken under the cognizance of these various government agencies and the results were finally coordinated in a joint effort which emerged as the project now called the X-15.

As a part of the Navy program prior to the joint project, Douglas prepared a study of a high-altitude, high-speed research airplane starting in June, 1953, which was visualized as a first step in getting man out into space in order to explore the problems that would occur both to the aircraft and to the man. For the sake of identification, the study was designated D558-III, and the general configuration is shown in Fig. 1. (As discussed later, under stability and control, some modifications to the empennage configuration were found to be necessary.) The present paper draws on the results of this study to illustrate some of the specific problem areas that occur on any high-speed, high-altitude vehicle.

Flight Spectrum

For orientation purposes, Fig. 2 illustrates what might be termed the entire flight spectrum in terms of altitude versus speed with the significant performance of various manned vehicles, such as balloons, and previous research airplanes indicated along with that of present or contemplated satellites. For convenience in talking about satellites and space vehicles, the speed scale is in feet per second; but for expediency in referring to conventional airplane types, a miles per hour scale is also indicated. Altitude is expressed in statute miles. This chart shows the progress of manned flight to date, the operating regime of satellites, the initial region for space travel, and the very large region of speed and altitude in-between where there has been no manned flight as yet.

Flight Boundaries

Although the large empty areas on this slide might give the impression that it is possible to progress from our presently available aircraft to the operating regions of manned satellites or space vehicles along many routes, it so happens that the possible combinations of altitude and Mach number in which it is practicable to advance are quite limited. This is especially true if one is considering stabilized continuous flight. In fact, there is only a narrow channel which spans the distance from the advanced research aircraft to manned satellites, This channel has sometimes been called the "cor-

ridor of continuous flight." The extent and location of this corridor is shown in Fig. 3. Note that scales are compressed in the direction of higher speeds and altitudes. Charts showing this corridor have appeared in many articles recently.[3,4] The exact boundaries of the corridor are somewhat dependent upon the assumptions involved as to the state of the aerodynamic art on the upper side and the materials and structural considerations on the lower side. It is, therefore, reasonable to expect that there will be some differences between various versions of this chart, but for the most part they are not too important.

Lift Boundary — The upper boundary line is the minimum speed at which continuous flight is possible, hence at low speeds this is a function of the airplane configuration, that is, weight, wing area, aspect ratio, and power available. By radical changes in configuration it can be pushed upward but at a sacrifice of other capabilities of the aircraft. Possibilities of this sort are shown in Fig. 4, which illustrates the gains in altitude obtainable by large reductions in wing loading. However, for an average type configuration capable of flying supersonically, the minimum speed is of the order of 170 mph, which is the value used as a boundry.

At very high speeds it is obvious that the aerodynamic lift will be augmented by centrifugal force and eventually at satellite speeds the centrifugal force supplies the entire lifting force to keep the vehicle in orbit.

Temperature Limit — The lower boundary of the corridor is essentially a temperature limit (except for the extreme left portion which is restricted by the maximum engine pressure) and as such depends largely upon the type of material of which the vehicle is constructed. It is, of course, assumed that the basic structure is critical and that sufficient cooling is provided for the equipment and the pilot. It is especially important to emphasize that this limit is established on the basis of stabilized conditions — not transient — and, therefore, may be too extreme for vehicles having a short time of operation. It is also to be expected that this limit will be pushed to lower levels by future improvements in materials, the development of flexible external insulating coatings, more efficient cooling systems, specially designed structures, and especially by increased aerodynamic knowledge of boundary layer and heat transfer phenomena. The boundary shown for this particular chart is based on the assumption of utilizing the best presently available materials — that is, so-called "super-alloys" of steel and even in these cases special treatment is necessary at stagnation points to avoid loss in strength.

In Fig. 5 additional temperature lines are used to show the limits of other common types of structural materials that may be used. For example, the best aluminum alloys rapidly lose their efficiency at temperatures of over 350 F, while titanium alloys can be used up to temperatures of 800 F, and stainless steels to 1200 F. These limits have been established by considering the strength-density ratio, $F_{tu/d}$, for tension and the compressive efficiency factor Et^3, where E is Young's modulus and t is the thickness of the material, as functions of temperature for the best currently available materials in each metal type. These characteristics are illustrated in Figs. 6 and 7.[5]

Propulsion Limits — For moderate speeds and al-

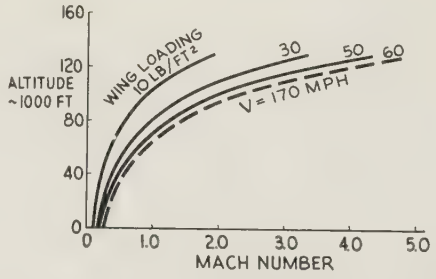

Fig. 4 — Effect of wing loading on minimum air speed (aspect ratio = 12, thrust/weight = 0.1)

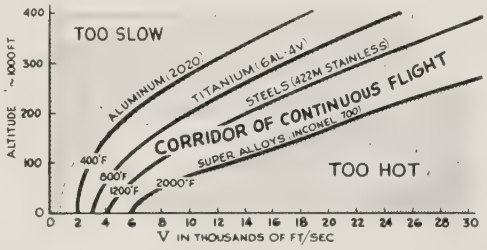

Fig. 5 — Flight spectra of various materials based on equilibrium temperature

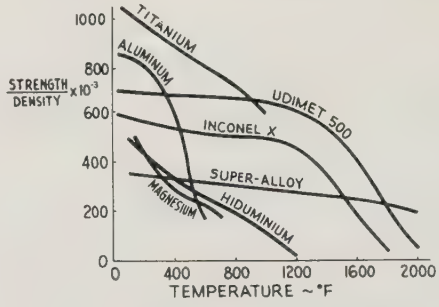

Fig. 6 — Tension efficiency versus temperature

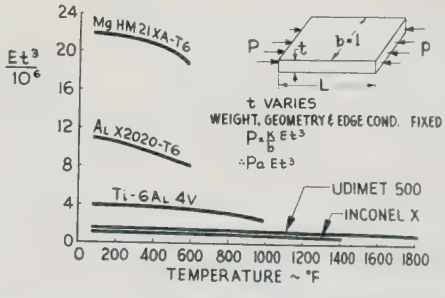

Fig. 7 — Compressive efficiency versus temperature

[3] *Jet Propulsion Magazine*, Vol. 27, November, 1957, p. 1157: "Structural Problems of Hypersonic Flight," by S. B. Batdorf.

[4] "Flight Spectrum," Pratt & Whitney Aircraft. United Aircraft Corp. Chart, 1957.

[5] "Analysis of Material Properties," by S. B. Pfeiffer. Douglas Aircraft Co. Includes:
"Summary of Information, Alloy X2020," by C. B. Criner and E. Spuhler, ALCOA.
"AM 21 & A-T8 Magnesium Alloy Sheet." Preliminary Data, Report 115, Dow Chemical Co., Nov. 1, 1950.
"Performance of Materials at Elevated Temperatures for Aircraft and Missile Application, by A. V. Levy. MP 595, Marquardt Aircraft Co.
"Technical Information: Udimet 500." Metals Division, Utica Drop Forge and Tool Co., September, 1955.
"High Duty Alloys." High Duty Alloys, Ltd., September, 1955.

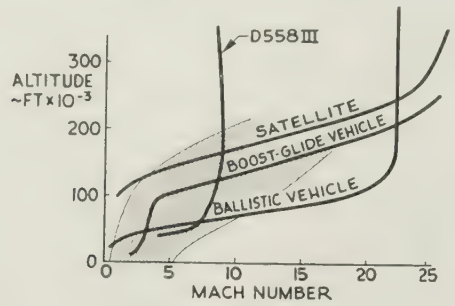

Fig. 8 — Re-entry paths

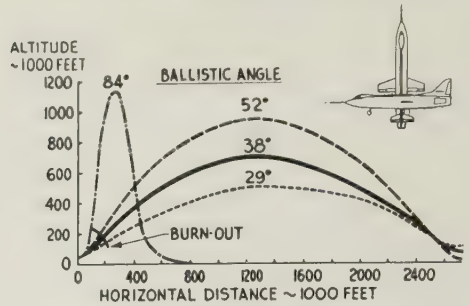

Fig. 10 — Flight paths

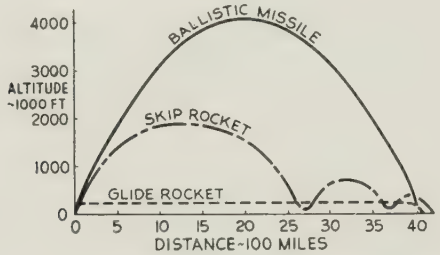

Fig. 9 — Typical trajectories for hypervelocity vehicles

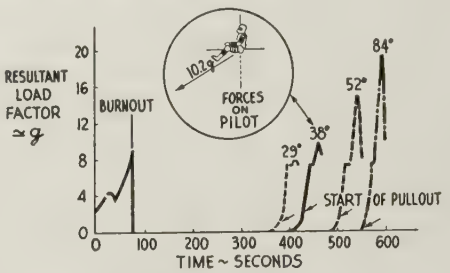

Fig. 11 — Resultant load factor versus time

titudes, the turbojet has proved to be an efficient and reliable type of powerplant. However, as it is air-breathing, it will have an altitude limit at each given speed beyond which it cannot be used simply because there is insufficient air to sustain combustion. A lower limit for turbojet engines is established on the basis of insufficient structural strength. The combustion limit lies outside the flight corridor and, hence, is not critical. As previously discussed, the turbojet engine structural limit forms the low altitude portion of the corridor boundary. There is also, however, a limit on the speed or Mach number at which an air-breathing engine can operate and still be efficient. This is simply because the intake air is compressed and raised to a very high temperature which increases with speed, while metallurgical requirements impose a fixed limit on the temperature at some point in the engine. The allowable temperature rise due to combustion is, therefore, reached as the Mach number is increased, and a point will eventually be reached where no energy can be added by combustion. While future developments may push out this limit, presently forseeable practice indicates that the thrust capability of the turbojet will decrease rapidly as the Mach number is increased beyond about 4.0. This limit is shown by the dotted vertical line across the flight corridor.

Indications are that ramjets may be pushed to somewhat higher speeds than turbojets and for even greater speeds an interesting hybrid engine termed the ramrocket shows promise.[6]

However, it is obvious that to go to the highest speeds and highest altitudes, rocket-propelled vehicles which do not depend upon the existence of an atmosphere are necessary. Actually, rocket power not only makes it possible to fly faster and higher, but for ranges greater than half way around the earth or 12,500 statute miles, they can actually be more efficient than vehicles powered with air-breathing engines. This is conclusively shown in the recent Wright Brothers Lecture by H. Julian Allen of the NACA.[7]

Looking back at the composite chart showing the flight corridor, again it should be emphasized that this corridor represents the speed and altitude at which stabilized flight is feasible and that advances in altitude and speed of manned vehicles will progress toward eventual achievement of manned satellite and space flight within these general limits. It should, however, be remembered that these limits can be exceeded for short time periods on either side — the upper by dynamic flight, the lower by very short transient flight paths which do not permit the skin temperature to stabilize.

It is interesting to note that the decellerating phase of most calculated re-entry paths for satellites, boost-glide, and ballistic vehicles, as well as the D558-III, fall within the corridor (Fig. 8).

Design Configuration of D558-III

The primary objective of the D558-III study was to design a manned aircraft capable of attaining very high altitudes and very high speeds for the purpose of investigating the aerodynamic, structural, operational, and human factor problems involved in these flight regimes as a step towards space travel. To avoid costly delays in time, it was considered important that the airplane be straight forward, simple, and capable of being constructed in a short period of time. Extensive configuration studies to determine the aerodynamic optimum for flight at high speeds and altitudes were not neces-

[6] "Review of Basic Thermo-Propulsive Characteristics of High-Speed Thrust Generators," by A. F. Charwat. Paper presented at IAS Specialist Meeting, Los Angeles, August, 1957.

[7] "Hypersonic Flight and Re-Entry Problem," by H. J. Allen. Wright Brothers Lecture, IAS, Washington, D. C., December, 1957.

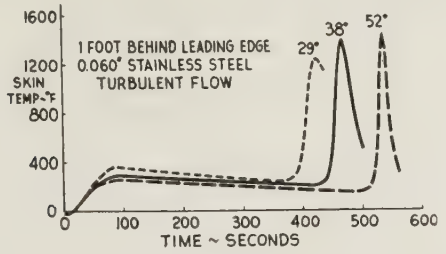

Fig. 12 — Skin temperatures along various flight paths

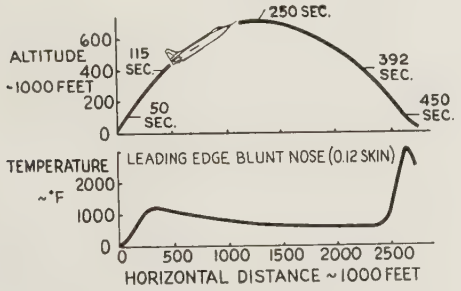

Fig. 13 — Temperatures along flight path

sary since the purpose was to find out and explore the problems of high-speed, high-altitude flight, rather than to avoid them. Another important requirement was that it possess normal flying characteristics through the entire speed range. The final design configuration is, as always, a compromise between these and many other and often conflicting requirements.

The wing area (or wing loading) is dictated, first of all, by having a moderate landing speed so that the aircraft may be landed safely, and secondly, the wing area should be sufficient so that a satisfactory pull-out can be made without undue stress upon the pilot. These requirements are, of course, complicated by the aerodynamic heating problem which in vehicles of this type plays an important role in determining the configuration and weight.

Since, as will be shown later, a good portion of the flight is out of the earth's atmosphere, drag becomes of secondary importance in comparison with airplane weight. For this reason and because it is desirable to have satisfactory low-speed characteristics, the wing leading edge is a conventional elliptical nose-type section rather than the sharp nose section which gives minimum drag at supersonic speeds. The rounded leading edge as discussed later, also is effective in avoiding severe aerodynamic heating problems. On the basis of the introductory discussion on propulsion systems, the rocket engine was the logical choice of powerplants to meet the objectives of very high altitudes and very high speeds.

Flight Paths

Since the purpose of a manned research vehicle is to obtain information of all types at very high altitudes, it is necessary to investigate the best method of achieving altitude. A variety of flight paths are possible in hypersonic flight, but they may be roughly classified into three basic types — ballistic, skip, and boost-glide. Assuming other factors constant, it is obvious that the ballistic path is most suitable for attaining very high altitudes, as shown in Fig. 9.

The initial goal for the D558-III study was an altitude of one million feet or approximately 190 statute miles. Investigation indicated that such altitudes were only feasible with some sort of 2-stage vehicle. A 2-stage vehicle could consist of the basic airplane and a first-stage rocket booster or, alternately, the aircraft could be carried aloft by a mother ship and launched from altitudes of the order of 40,000 ft. In the interest of safety and economy as well as immediate practicability based on previous experience with recent research airplanes, it was decided to utilize the mother ship technique rather than a first-stage rocket booster.

The method of obtaining maximum altitude was to start the rocket motor immediately the airplane fell free from the mother ship and to pull up into a climb. Obviously, the highest possible altitude could be obtained by using a very steep angle at the end of burnout. Several flight path angles were investigated and are shown in Fig. 10. The maximum value of the angle at end of burnout was 84 deg. This flight path, however, resulted in very high resultant g forces on the pilot during pull-out on reentry to the atmosphere. Progressively lower flight path angles were investigated until a tolerable g load on the pilot was obtained (Fig. 11). Characteristics of this flight path are that the flight path angle at burnout is 38 deg, maximum height reached is 750,000 ft (or 140 miles), and the maximum resulting load factor on the pilot is 10.2 g. This flight path is considered reasonably and marginally acceptable as far as the load factor is concerned. It should be noted, however, that it is possible to build up to this condition by making progressively steeper pull-ups and thus find out exactly what is tolerable. For example, 29 deg angle at burnout results in a peak altitude of 560,000 ft and a peak load factor on the pilot of 7.5 g.

Aerodynamic Heating

Since aerodynamic heating is one of the most serious problems that is encountered in high speed flight or on re-entry into the earth's atmosphere, much effort was taken to study flight paths along with suitable materials and techniques for keeping the attainable temperatures within reasonable limits. The influence of the flight path on skin temperature 1 ft behind the leading edge is shown in Fig. 12. As discussed above, however, the design flight path of 38 deg was chosen by the resultant load factor on the pilot. Less severe heating problems can be obtained by the choice of flight paths having lower maximum altitudes and, thus, the problem of aerodynamic heating can also be explored gradually by building up to the design flight path in easy steps.

The most critical portion of the aircraft from an aerodynamic heating viewpoint is the wing leading edge or stagnation point. The variation of the temperature of this critical point is shown along the design flight path in Fig. 13. A more typical value of the skin temperature is obtained by computing the temperature 1 ft back from the leading edge which is shown in comparison with the stagnation value

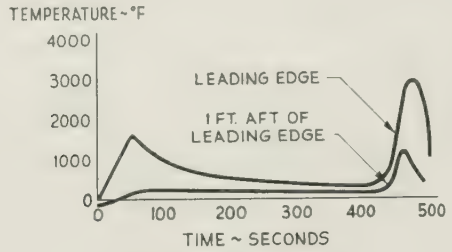

Fig. 14 — Skin temperatures

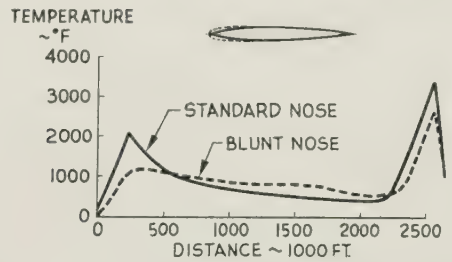

Fig. 15 — Effect of nose radius on temperatures at leading edge

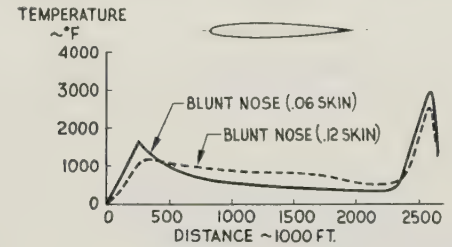

Fig. 16 — Effect of skin thickness on temperatures at leading edge

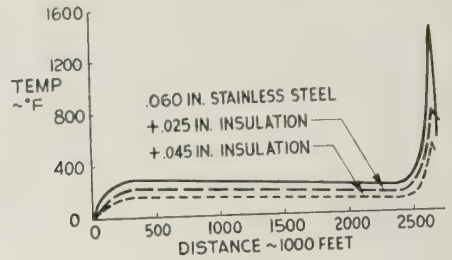

Fig. 17 — Effect of exterior insulation on skin temperatures, 1 ft aft of leading edge

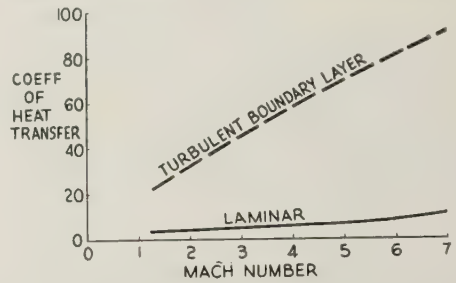

Fig. 18 — Heat-transfer coefficient versus Mach number

in Fig. 14. It is also seen that although very high values of temperature do occur, the time for which they persist is quite short, being of the order of 50-sec duration.

Various methods of reducing the skin temperature were studied for the design flight path. One method is by employing a blunt leading edge on the wing airfoil. Fig. 15 shows the effect of bluntness on the D558-III configuration. It is important to note that the use of leading edge bluntness is a general phenomena and has applications to all types of re-entry vehicles. This idea was originally advanced by Allen[8] and depends upon making the wave drag a large portion of the total drag, thus reducing the skin friction which gives rise to the aerodynamic heating.

Another method of reducing skin temperature is to increase the thickness of the material and thus the heat sink capacity in the critical areas. The effect of increasing the skin thickness to achieve this result is illustrated in Fig. 16.

Appreciable reductions in skin temperature can also be made by using exterior insulating coatings as shown in Fig. 17. It is seen that this is one of the most effective methods of reducing skin temperatures; hence, the development of a suitable insulting coating should be vigorously pursued.

It is also extremely important to know the type boundary layer over the airfoil surface. This is because the heat-transfer coefficient which determines the temperature attained within a given time period is many times as large for turbulent flow as for laminar flow. Typical values of the heat-transfer coefficient for laminar and turbulent flow over a flat plate are shown in Fig. 18. The boundary layer type, therefore, can markedly effect the weight of the structure, since if it is certain that a laminar boundary layer exists the structure can be made considerably lighter than if a turbulent boundary layer exists. Unfortunately, however, information on the type boundary layer is in a very confused state, hence it is extremely hazardous to predict which type boundary layer will occur for a specific configuration under a specific flight condition. The possible difference in temperature on a specific configuration is illustrated in Fig. 19.

Drag

As mentioned previously, drag for the design mission on the D558-III configuration is relatively unimportant since much of the flight is out of the earth's atmosphere and hence performance is largely a function of the weight to thrust ratio. This is not necessarily true in general as there are other types of flight paths such as "boost-glide" or "skip" which are chosen to give maximum range range rather than altitude performance. This would result in most of the flight being within the earth's atmosphere and hence a low value of drag or high value of L/D is extremely important.

Stability and Control Problems

For the most part, stability and control problems encountered at very high speeds and very high altitudes are generally more severe manifestations of

[8] NACA RM A53D28, Aug. 25, 1953: "Study of Motion and Aerodynamic Heating of Missiles Entering Earth's Atmosphere at High Supersonic Speeds," by H. J. Allen and A. J. Eggers.

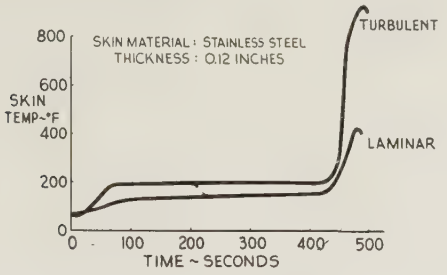

Fig. 19 — Skin temperatures for laminar and turbulent flow, 1 ft aft of leading edge

problems previously encountered in the moderately high supersonic speed region. This is due to the tendency of the configuration to become more extreme when designing for higher speeds and higher altitudes; fuselages are necessarily longer and slimmer and the wings become smaller and smaller in relation to the fuselage size. At the same time the actual airplane density is increasing while the higher operational altitude results in reduced air density and, hence, greatly increased relative density (which is the most important factor contributing to a deterioration in the damping of dynamic oscillations). Basic Mach number effects are also intensified as speed increases, and they are often complex and irregular in nature as a result of shock wave interference effects. Some of the stability and control problems encountered at high speeds and high altitudes are discussed below:

Static Longitudinal Stability — Longitudinal stability changes occur with Mach number and the stability may become neutral or even negative for some particular Mach number as shown in Fig. 20.

The gradual but definite decrease with increasing Mach number is simply a consequence of the lift available on the tail as a function of Mach number which is well known from simple linear supersonic theory. The abrupt drop in stability at higher Mach numbers is the result of the horizontal tail moving into an adverse position behind the wing where the expansion and compression waves from the wing affect the local flow characteristics. Such a position behind the wing may be unsatisfactory for two different reasons: (1) A decrease in angle of attack of the tail caused by changing downwash, and (2) a large reduction in dynamic pressure at the tail. These two effects are illustrated in Figs 21 and 22.[9]

Flow direction lines in Fig. 21 indicate qualitatively the angles of attack experienced by a tail surface located at several possible vertical positions aft of the wing. It may be seen that at this particular Mach number and angle of attack, the expansion and compression waves may interfere with the horizontal tail, unless it is properly located, and the local angles of attack at the tail, and therefore, the tail effectiveness, may be seriously reduced. A tail located high at position A would be severely affected as would one at location D. The optimum practical location for the set of conditions shown would appear to be on or near the extended wing chord line at location C.

[9] "Stability and Control of Piloted Aircraft at High Altitudes," by E. R. Heald. Douglas Aircraft Co., October, 1955.

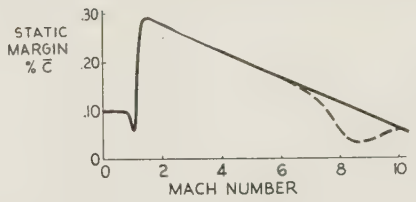

Fig. 20 — Static longitudinal stability

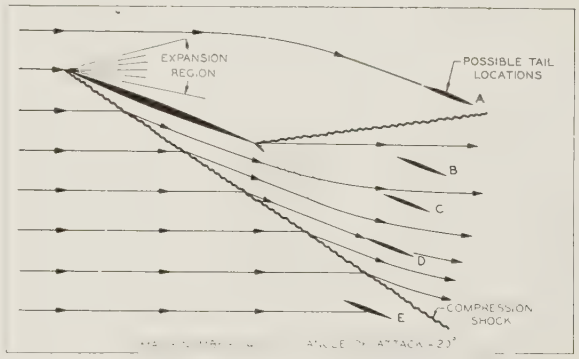

Fig. 21 — Flow direction contours at supersonic speed

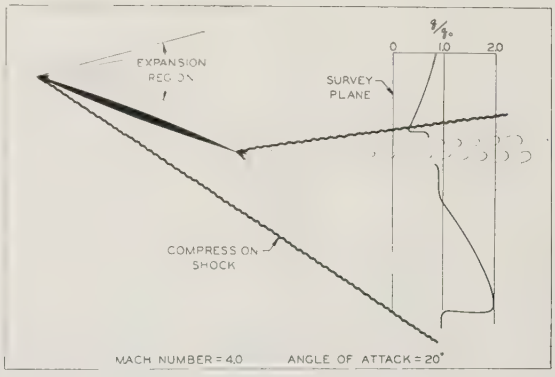

Fig. 22 — Dynamic pressure behind wing at supersonic speed

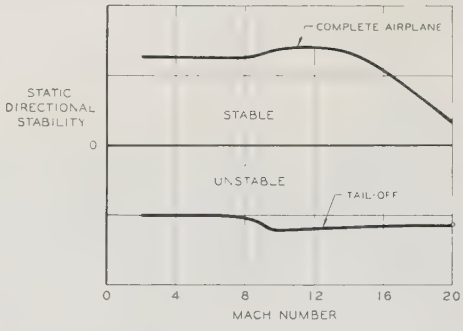

Fig. 23 — Typical directional stability variation with Mach number

The possible reductions in dynamic pressure are indicated in Fig. 22. In the expansion region dynamic pressure is reduced, whereas abrupt increases occur through the compression shocks.

In consideration of both these effects, (that is, downwash and dynamic pressure), it appears that an optimum location of the horizontal tail is near the extended chord line of the wing.

Static Directional Stability — Directional stability may be even more difficult to obtain at extreme

altitudes than longitudinal stability. Fig. 23 presents a typical variation of directional stability with Mach number (at zero angle of attack) and indicates the trend toward instability caused by the tail lift reduction discussed earlier. The reason for this decrease in directional stability with Mach number can more easily be seen if the contribution of each of the components is examined for the specific configuration initially considered for the D558-III study (Fig. 24). The fuselage and wing combination is, of course, by itself unstable and the amount of the instability is roughly constant with Mach number. The stabilizing influence of the vertical tail decreases with Mach number, until finally at Mach numbers slightly greater than 3 the configuration becomes unstable.

Obviously, to make a satisfactory configuration for higher Mach numbers requires additional vertical surface area and as shown in Fig. 25, the most efficient method of adding this vertical surface area is to distribute it equally above and below the fuselage. A hypothetical airplane employing such an arrangement is shown in Fig. 26.[9]

Inertia Coupling — Inertia coupling has been a common problem on many current high-speed aircraft. Curiously enough, this problem was probably first encountered by the Germans in the fall of 1939 during the V-2 missile development. Recent examples of this phenomena are numerous but the seriousness of this problem was dramatically reemphasized by the loss of the X-2 research airplane while attempting a high-speed, high-altitude run. This aircraft has previously attained a record speed of 1900 mph (M = 2.9) and a record altitude of 126,000 ft.

Basically, inertia coupling arises as a result of coupling of the longitudinal and lateral modes of motion and usually becomes severe only when resonance between rolling and pitching or yawing motions occur. It is, thus, apparent that the problem can be eliminated if the flight conditions in which resonance occurs can be avoided. This, however, is generally impractical and hence the designer must strive to minimize magnitude of the disturbances by proper design.

The most common type of inertia coupling occurs as a rapid divergence in angle of attack and/or sideslip during a rapid rolling maneuver. An example of this is shown in Fig. 27 where a high sustained rolling rate causes the normal load factor to build up quickly to approximately 6 *g*.

Another type of inertia coupling is "autoroative" rolling, in which a high rate of roll is initiated by aileron deflection and continues at almost the same rate after the aileron is returned to neutral. This phenomena is shown in Fig. 28.

Although both types of inertia coupling are greatly influenced by the trend of high-speed vehicles to distribute the weight predominately along the fuselage or the longitudinal axis rather than along the wing span or lateral axis, the most important parameter within the control of the designer is that of directional stability. As was previously discussed, directional stability decreases with Mach number and also with angle of attack. Consequently, on a high-speed, high-altitude configuration, vertical surface area must be provided below the fuselage as well as on the upper side. Take-off and landing attitude considerations probably will require that the lower vertical surface be folded for these operations.

High-Altitude Damping — Operation at high altitudes will result in almost complete loss in damping of the aircraft's longitudinal and lateral short-period modes of motion. Neglecting compressibility effects, the damping ratio of either oscillatory motion is directly proportional to the square root of air density, producing typical variations with altitude as shown in Fig. 29. This effect is more pronounced in the case of the lateral motion, which has a generally lower level of damping due to coupling between rolling and yawing degrees of freedom. Compressibility effects at extreme altitudes are not expected to modify greatly the reduction in damping ratio as the square root of density, except for some additional reductions in the longitudinal case due to wing aerodynamic center shift.

Although within the earth's atmosphere the use of automatic stabilization devices, such as pitch and yaw dampers, will satisfactorily compensate for the loss in damping, it should not be left to these "black boxes" to solve all such problems. A better approach

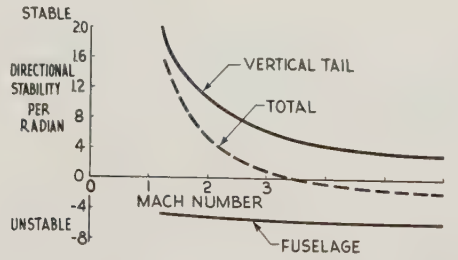

Fig. 24 — Contribution of components to directional stability

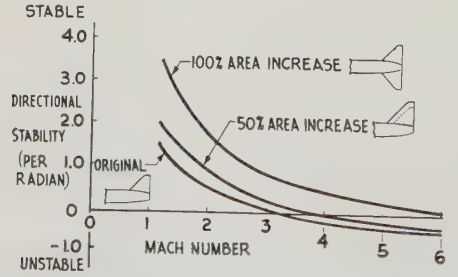

Fig. 25 — Effect of tail size on directional stability

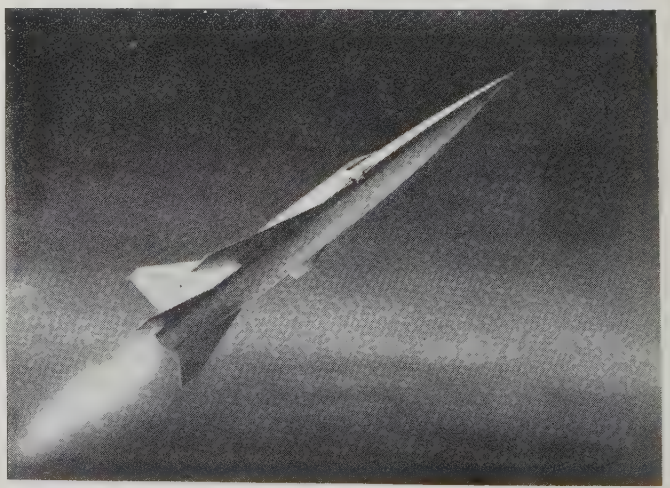

Fig. 26 — Artist's conception of future high-altitude, high-speed airplane

is to employ fundamental aerodynamic solutions wherever possible and utilize artificial stabilization only after it is definite that it is superior to a more basic approach.

Control Outside Atmosphere — Two methods of control outside the earth's atmosphere were considered in this study. They were: control by jet reaction, and control by the gyroscopic effect of a rotating flywheel. From a weight standpoint the simple jet reaction system was found to be the best. This system consisted of a source of hydrogen peroxide, (which is a monopropellant) with small control jets suitably located on the airplane to enable the pilot to make lateral, longitudinal, and directional corrections to a flight path. The most important use of such controls is to enable the pilot to align the aircraft with the flight path before reentry into the earth's atmosphere.

Human Effects

Since one of the major purposes of manned research aircraft is to explore gradually and systematically the conditions that man will be faced with in true space flight, the provisions for the pilot's comfort, ability to function efficiently, and most especially his safe return to earth — either with or without the aircraft, requires the most careful consideration. All of the accumulated knowledge of problems bearing on this needs to be kept in mind in designing the cockpit and escape gear. Considerable progress has been made in this field in the last few year and a brief summary of the known problems and the status of their solution follows.

High-Acceleration Forces — High-acceleration forces occur not only during the take-off phase, but also during the re-entry into the earth's atmosphere. In fact, for this study the most severe g forces on the pilot occurred during pull-out in the re-entry portion of the flight. It is primarily this factor which limited the altitude that could be obtained for the study configuration, as was previously shown.

In evaluating the permissible g, the element of time of application as well as magnitude is extremely important. The highest load factor sustained without permanent injury is 40 g for 1/5 sec. This was incurred by Col. John P. Stapp when riding in a rocket sled, which first accelerated to a speed of 632 mph and then came to a dead stop. The permissible g can also be increased about 1½ g by the use of modern g suits and to a lesser extent by body position. The summary of the tolerable g loads is presented in Fig. 30.

Pressure, Heat, and Humidity — Providing the proper environment for the pilot in the way of correct pressure, temperature, and humidity is not a new problem, since it exists in practically all present-day aircraft, but to nowhere near the extent that will be encountered in high-speed, high-alti-

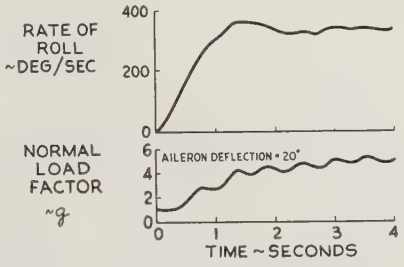

Fig. 27 — Inertia coupling in aileron roll

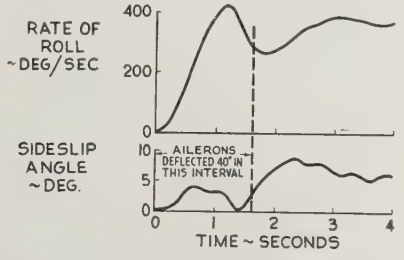

Fig. 28 — Autorotative rolling

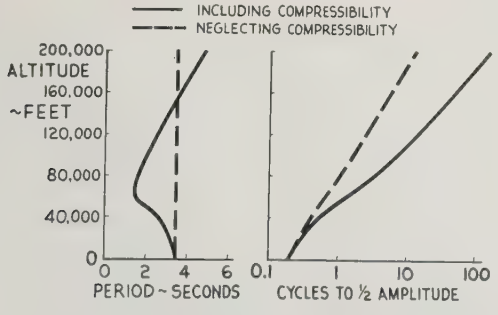

Fig. 29 — Effect of altitude on damping

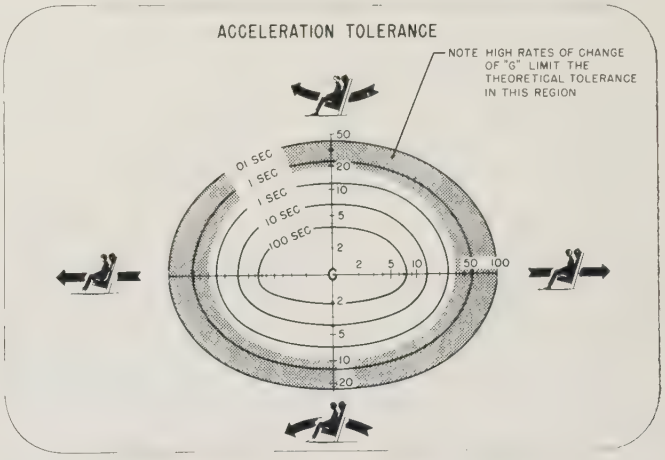

Fig. 30 — Acceleration tolerance

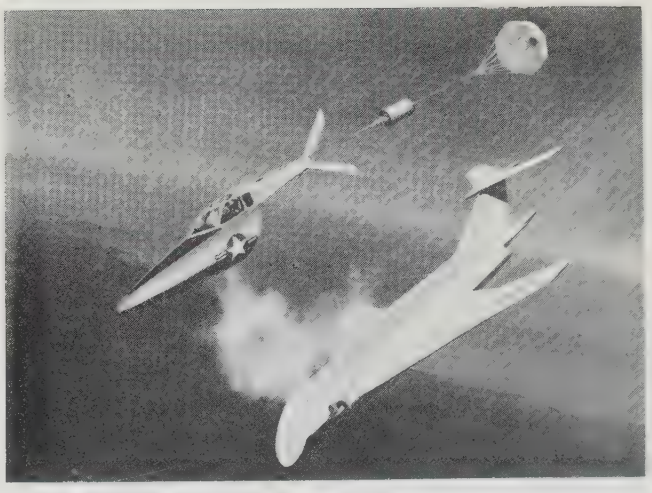

Fig. 31 — Standard ejectable cockpit

tude vehicles. A satisfactory value of cockpit pressure is of the order of 10 psi, while optimum values for the most efficient functioning of an average man requires a temperature between 50 to 70 F, with a humidity of 40–60%. Maintaining these conditions is best accomplished by providing a well-insulated, air-conditioned capsule which has been dubbed a "terrella" (or small earth), by Dr. Strughold who is sometimes termed the "father of space medicine."

Weightlessness — The sensation of weightlessness at zero *g* occurs when centrifugal force exactly balances and cancels the downward pull of the earth's gravity. This condition has been obtained for brief periods of 30–40 sec on jet aircraft and up to 50 sec on the X-2 research aircraft. There is considerable disagreement among authorities as to whether prolonged periods of weightlessness are harmful. For example, Col. Stapp is concerned about weightlessness,[10] while Scott Crossfield believes it is no particular problem. Russian reports on the radio relaying pulse, blood pressure, and respiration of Laika, the dog in Sputnik II, concurred that "no harm comes to a living organism in a zero gravity state." However, there is some evidence that weightlessness produces mental confusion and air sickness. Without the pull of gravity, body sense organs will continuously send false information to the brain which creates a "feeling of falling" and in some cases actual terror has been observed in tests. Orientation in weightless conditions will have to be provided by visual cues.

Solar Radiation — On the earth, man is protected from all types of solar radiation by the atmosphere and the earth's magnetic field which filters out or deflects most of the harmful particles. Since the most important type of solar radiation is cosmic rays, which are positively charged particles, they ionize any material which they traverse. If this material is live tissue, ionization will damage it. Latest conclusions are that cosmic radiation will cause no immediate bad effects, but low-level long-term exposure may result in shortened life span and increased susceptibility to disease, particularly cancer. Generally speaking, however, the danger is minimized for operation just outside the earth's atmosphere, but increases with distance from the earth.

Psychological Effects — Perhaps the greatest unknown issue is how man will react to the unreal, empty, and remote environment of space. Simulated tests show these conditions have revealed a serious psychological problem called "the break-off effect" or a feeling of detachment or physical separation from earth. Different effects are experienced by different individuals. Some experience a feeling of tiredness, loss of initiative, and difficulty in thinking. In others it produces anxiety or a feeling of intense exhilaration.

Escape

To meet the environmental conditions discussed above as well as to provide maximum safety should escape become necessary, the most logical idea is to separate the capsule containing the pilot from the aircraft. To accomplish this requires that the capsule maintain its favorable environment when separated, that it be inherently stable aerodynamically, that it withstand aerodynamic heating effects, that it be provided with some means of decelerating, and finally that it have a parachute to achieve a safe rate of descent and contact with the earth. Fig. 31 shows a capsule of this type as conceived by A. M. Mayo.[11,12]

Conclusion

In conclusion it is believed that manned aircraft will continue to be developed for flight at very high speeds and high altitudes and that the experience gained will be used as stepping stones to the eventual development of manned satellites and space vehicles.

The study project D558-III indicates that higher speeds and altitudes can be obtained for manned aircraft at the present state of the art and specifically that it is possible to achieve altitudes approaching 750,000 ft (or 140 miles) and speeds of 6000 mph with safe re-entry into the earth's atmosphere. Advances in speed and altitude will generally follow the flight corridor which is limited on the upper side by the available lift to maintain continuous flight and on the lower side by temperature.

For flight within the atmosphere it is probable the turbojet engines will be succeeded by ramjets and they in turn by a hybrid type propulsion system called the ramrocket. For very high speeds and especially at very high altitudes rockets are undoubtedly required, and for ranges half way around the earth are actually more efficient than air-breathing engines.

The aerodynamic heating effects which occur upon re-entry into the earth's atmosphere can be minimized by the use of blunt leading edges, heat sinks, and suitable insulating coating. Appreciable reductions in temperature and thus savings in weight of a hypersonic vehicle are possible if a laminar type boundary layer can be achieved and predicted with certainty.

Stability and control problems for very high speeds are similar but more severe than those encountered at moderate supersonic speeds. Control outside of the atmosphere can be accomplished most efficiently by suitably placed jets.

All the evidence to date indicates that man can exist and function efficiently in manned high-speed vehicles, providing suitable provisions are made for him. The requirements for a satisfactory environment can be combined with those for escape in an escape capsule which can be separated from the aircraft in the event of trouble.

References for Flight Spectrum

1. *Aviation Week,* Vol. 68, Feb. 1958, p. 50: "Weightlessness Crucial Spaceman Factor," by Russell Hawkes.

2. *Aviation Week,* Vol. 67, Dec. 23, 1957, p. 65: "Capt. Kincheloe's Story of X-2 Record," by Capt. I. C. Kincheloe, Jr.

3. *Aviation Week,* Vol. 65, Nov. 5, 1956, p. 111: "Dramatic Story of X-1_a Rescue Told."

4. *Deutsche Luftfahrtforschung,* WM 3538, August, 1944: "Rocket Drive for Long Range Bombers," by Sanger and Bredt.

[10] *Newsweek,* Feb. 3, 1958: "Man in Space."

[11] "Environmental Considerations of Space Travel from Engineering Viewpoint," by A. M. Mayo. Paper presented at Aero-Medical Association Meeting, Chicago, April, 1956.

[12] "Space Cabin Design," by A. M. Mayo. Paper presented at American Astronautical Society National Meeting, New York, January, 1958.

Index—Vol. 67, 1959

ACCIDENTS AND ACCIDENT PREVENTION (NONAIRCRAFT)
Automobile Head-On Collisions — Series II, D. M. Severy, J. H. Mathewson, and A. W. Siegel 238
ADAMS, K. C.
Discussion of "Engagement Characteristics of Wet-Type Clutches" by L. P. Ludwig 399
ADAMS, W. J., JR.
Steering and Traction Characteristics of Rubber-Tired and Crawler Vehicles 312
AIR CLEANERS
Now — Practical "Double Dry" Filtration with Donaclone, H. M. Turner and D. K. Anderson 197
A Progress Report — Dry-Type Air Cleaners on Farm Tractors, J. C. Siemens and J. A. Weber 191
AIR CONDITIONING
Indoor Climatic Testing of Automotive Engine Cooling and Air-Conditioning Systems, C. V. Hawk and J. W. Godfrey .. 456
AIRCRAFT ACCESSORIES AND EQUIPMENT
Status of SAE S-12 Approach to Vibration Isolation of Aircraft Electronic Equipment 434
AIRCRAFT DESIGN AND PERFORMANCE
Design Problems of Very High Speed Flight, K. E. Van Every 659
AIRCRAFT, VTOL
Some Thoughts on Optimum Combinations of Wings and Vertical Thrust Generators in VTOL Aircraft, W. Z. Stepniewski 326
ALDIKACTI, HULKI
Riding on Air (Co-authors Edward W. Anderson and Robert D. Harrison) 15
ALUMINUM AND ALLOYS
Aluminum Die-Cast Cylinder Blocks in Outboard Motors, W. C. Conover and R. C. Nelson 580
Aluminum Engines — Design for Modern Fabrication, J. M. Smith and R. M. Smith 295
Iron-Aluminum Base Alloys — Cheap Stainlesses of the Future?, Blake King, J. J. Mueller, N. N. Ida, and F. G. Tate 335
ANDERSON, D. K.
Now — Practical "Double Dry" Filtration with Donaclone (Co-author H. M. Turner) 197
ANDERSON, EDWARD W.
Riding on Air (Co-authors Hulki Aldikacti and Robert D. Harrison) 15
ARNOLD, W. C.
Discussion of "An Evaluation of Aftercooling in Turbocharged Diesel Engine Performance" by J. E. Mitchell 412
AUBLE, C. M.
Development of the Suppressor and Thrust Brake for the DC-8 Airplane (Co-author L. R. Jordan) 524
AXLES
Limited Slip Differentials, R. P. Lewis and L. J. O'Brien 203

BALLARD, E. C.
New Fluoroester Lubricants for High-Temperature Applications (Co-author E. E. Sommers) 545
BAME, J. L.
Engine Pounding — Its Causes and Control (Co-author R. G. Tuell) 158
BASSETT, J. V.
Discussion of "Metallurgical Developments in Brake Drums" by V. A. Crosby 448
BAUER, A. F.
Discussion of "Aluminum Die-Cast Cylinder Blocks in Outboard Motors" by W. C. Conover and R. C. Nelson 588
Discussion of "Aluminum Engines — Design for Modern Fabrication" by J. M. Smith and R. M. Smith 308
BEHRENS, M. D.
Investigating Rumble in Single-Cylinder Engines (Co-authors J. A. Robison and R. G. Mosher) 169
BEIER, KURT A.
Discussion of "The Comprex Diesel Supercharger" by Max Berchtold 14
BERCHTOLD, MAX
The Comprex Diesel Supercharger 5
BERKEY, KERRY L.
Discussion of "New Fluoroester Lubricants for High-Temperature Applications" by E. C. Ballard and E. E. Sommers .. 552
BEST, ROBERT
Discussion of "Some Aspects of the Operation of Utility Engines" by E. C. Paige and H. T. Mueller 516
BLOSE, JAMES F.
Discussion of "The Comprex Diesel Supercharger" by Max Berchtold 13
Discussion of "Priming Aids for Cold Starting Diesel Engines" by J. J. DeCarolis, W. E. Meyer, and P. W. Espenschade .. 362
BODEN, R. H.
The Ion Rocket Engine 227
BOLT, JAY A.
Discussion of "A New Look at High Compression Engines" by D. F. Caris and E. E. Nelson 123
BOWDEN, F. P.
Some Recent Experiments on the Friction, Wear, and Deformation of Solids 650
BOWDITCH, F. W.
Discussion of "Starting and Stopping Modern Engines — New Combustion Problems" by V. F. Massa 133
BRAKES
Metallurgical Developments in Brake Drums, V. A. Crosby .. 441
Pneumatic Power Control Systems for Trucks, Trailers, Buses, Stephen Johnson, Jr. 221
What's New in Brake Linings, N. H. McCuen 509
BRIGHT, J. S.
Diesel Engines for Use in Light Delivery Vehicle and Taxi Service 449
BROWN, E. I.
Optimization Study, Missile Auxiliary Power Systems (as Viewed by the Equipment Supplier) (Co-author R. W. McJones) 289

CARIS, D. F.
A New Look at High Compression Engines (Co-author E. E. Nelson) 112
Discussion of "Aluminum Engines — Design for Modern Fabrication" by J. M. Smith and R. M. Smith 310
CARTWRIGHT, B. W.
Discussion of "The Design of Planetary Gear Trains" by Oliver K. Kelley 507
CASTINGS
Aluminum Die-Cast Cylinder Blocks in Outboard Motors, W. C. Conover and R. C. Nelson 580
CENZER, CARL W.
Discussion of "Automobile Head-On Collisions — Series II" by D. M. Severy, J. H. Mathewson, and A. W. Siegel 263
CERAMICS
Pyroceram, W. W. Shaver and S. D. Stookey 184
CHAPMAN, CHARLES S.
The Buick Flight Pitch Dynaflow (Co-author Forest McFarland) 414
CHAPMAN, R. D.
Discussion of "Aluminum Engines — Design for Modern Fabrication" by J. M. Smith and R. M. Smith 308
CLARK, J. M., JR.
The Behavior of Radiation-Resistant ANP Turbine Lubricants (Co-author G. C. Lawrason) 424
CLUTCHES
Engagement Characteristics of Wet-Type Clutches, L. P. Ludwig 391
COLD-WEATHER OPERATION
Priming Aids for Cold Starting Diesel Engines, J. J. DeCarolis, W. E. Meyer, and P. W. Espenschade 351
COMBUSTION
Starting and Stopping Modern Engines, New Combustion Problems, V. F. Massa 125
COMPUTERS
Digital Computer Analysis and Interpretation of Turbocharged Diesel Engine Performance, H. A. Cook 532
CONOVER, W. C.
Aluminum Die-Cast Cylinder Blocks in Outboard Motors (Co-author R. C. Nelson) 580
CONSTRUCTION AND INDUSTRIAL MACHINERY
How Performance Factors Affect Transmission Design, E. A. Richards 26
Steering and Traction Characteristics of Rubber-Tired and Crawler Vehicles, W. J. Adams, Jr. 312
COOK, H. A.
Digital Computer Analysis and Interpretation of Turbocharged Diesel Engine Performance 532
Discussion of "Thermal Loading and Wall Temperature as Functions of Performance of Turbocharged Compression-Ignition Engines" by E. T. Vincent and N. A. Henein 491
COON, J. S.
Routes of Crankcase Oil Loss (Co-author D. E. Loeffler) 59
COOPER, D. E.
Radioactive Tracers Cast New Light on Fuel Distribution (Co-authors R. L. Courtney and C. A. Hall) 619
CORROSION
Muffler Corrosion — Its Cause and Control, R. A. Heath ... 553
COURTNEY, R. L.
Radioactive Tracers Cast New Light on Fuel Distribution (Co-authors D. E. Cooper and C. A. Hall) 619
CRAWFORD, J. C.
Discussion of "Aluminum Engines — Design for Modern Fabrication" by J. M. Smith and R. M. Smith 311
CROSBY, V. A.
Metallurgical Developments in Brake Drums 441

DALEY, FRANK
Discussion of "Limited Slip Differentials" by R. P. Lewis and L. J. O'Brien 211
DeBLUMENTHAL, M. P.
Discussion of "Limited Slip Differentials" by R. P. Lewis and L. J. O'Brien 211
DeCAROLIS, J. J.
Priming Aids for Cold Starting Diesel Engines (Co-authors W. E. Meyer and P. W. Espenschade) 351
DEPOSITS, ENGINE
Some Aspects of the Operation of Utility Engines, E. C. Paige and H. T. Mueller 516
DETONATION
Engine Pounding — Its Causes and Control, J. L. Bame and R. G. Tuell 158
If You Squeeze Them, Must They Scream?, W. M. Wiese 175
Investigating Rumble in Single-Cylinder Engines, J. A. Robison, M. D. Behrens, and R. G. Mosher 169
Knock-Knock: Spark Knock, Wild Ping, or Rumble? R. H. Perry, Jr., and H. V. Lowther 145
Knock, Rumble, and Ping, H. F. Hostetler and W. R. Tuuri .. 152
Rumble — A Deposit Effect at High Compression Ratios, A. E. Felt, J. A. Warren, and C. A. Hall 138

Starting and Stopping Modern Engines, New Combustion Problems, V. F. Massa ... 125
Thudding in High Compression Ratio Engines, W. E. Morris and D. C. Fariss ... 134
DeVOS, L. N.
The Advantages of the New SAE Standard for Involute Splines from a Design Standpoint ... 469

EDGAR, J. A.
Discussion of "Radioactive Tracers Cast New Light on Fuel Distribution" by D. E. Cooper, R. L. Courtney, and C. A. Hall ... 638
EGLI, HANS
Discussion of "An Evaluation of Aftercooling in Turbocharged Diesel Engine Performance" by J. E. Mitchell ... 409
EKVALL, J. C.
Strength and Thermal Limitations of Materials for Airframe Components ... 590
ENGINES, AIRCRAFT (JET AND TURBINE)
Development of the Suppressor and Thrust Brake for the DC-8 Airplane, L. R. Jordan and C. M. Auble ... 524
Selection of Optimum Modes of Control for Aircraft Engines, A. J. Sobey ... 383
ENGINES, DIESEL
The Comprex Diesel Supercharger, Max Berchtold ... 5
Diesel Engines for Use in Light Delivery Vehicle and Taxi Service, J. S. Bright ... 449
Digital Computer Analysis and Interpretation of Turbocharged Diesel Engine Performance, H. A. Cook ... 532
An Evaluation of Aftercooling in Turbocharged Diesel Engine Performance, J. E. Mitchell ... 401
GM Diesel's Additional Engines — New Vees and In-Lines, K. L. Hulsing and C. E. Ervin ... 596
How a Diesel Engine Rates Itself, W. J. McCulla ... 213
Priming Aids for Cold Starting Diesel Engines, J. J. DeCarolis, W. E. Meyer, and P. W. Espenschade ... 351
Thermal Loading and Wall Temperature as Functions of Performance of Turbocharged Compression-Ignition Engines, E. T. Vincent and N. A. Henein ... 478
ENGINES, FREE-PISTON
Ford Free-Piston Engine Development, Paul Klotsch ... 373
Supercharging in the Free-Piston Cycle, H. G. Spier ... 281
ENGINES, GASOLINE
Routes of Crankcase Oil Loss, J. S. Coon and D. E. Loeffler ... 59
ENGINES, GENERAL
The Potential of Unconventional Powerplants for Vehicle Propulsion, Peter Kyropoulos ... 319
ENGINES, MARINE
Aluminum Die-Cast Cylinder Blocks in Outboard Motors, W. C. Conover and R. C. Nelson ... 580
ENGINES, PASSENGER-CAR
Aluminum Engines — Design for Modern Fabrication, J. M. Smith and R. M. Smith ... 295
Chrysler Corporation's New V-8 Engine, R. S. Rarey and E. G. Moeller ... 95
Engineering the "W" Engine, Chevrolet's 348-cu.-in. V-8, J. T. Rausch, H. H. Kehrl, and D. H. McPherson ... 103
A New Look at High Compression Engines, D. F. Caris and E. E. Nelson ... 112
Radioactive Tracers Cast New Light on Fuel Distribution, D. E. Cooper, R. L. Courtney, and C. A. Hall ... 619
Some Aspects of the Operation of Utility Engines, E. C. Paige and H. T. Mueller ... 516
ENGINES, ROCKET
The Ion Rocket Engine, R. H. Boden ... 227
Ion Rocket Engine Development, Donald L. Eschner ... 187
ENGINES, TRUCK AND BUS
Some Aspects of the Operation of Utility Engines, E. C. Paige and H. T. Mueller ... 516
ERVIN, C. E.
GM Diesel's Additional Engines — New Vees and In-Lines (Co-author K. L. Hulsing) ... 596
ESCHNER, DONALD L.
Ion Rocket Engine Development ... 187
ESPENSCHADE, P. W.
Priming Aids for Cold Starting Diesel Engines (Co-authors J. J. DeCarolis and W. E. Meyer) ... 351
EXHAUST SYSTEMS AND EXHAUST GASES
Exhaust Systems, Fundamentals and Design Considerations, L. E. Muller ... 559
Muffler Corrosion — Its Cause and Control, R. A. Heath ... 553

FARISS, D. C.
Thudding in High Compression Ratio Engines (Co-author W. E. Morris) ... 134
FELT, A. E.
Rumble — A Deposit Effect at High Compression Ratios (Co-authors J. A. Warren and C. A. Hall) ... 138
FINNIGAN, F. T.
Discussion of "Knock, Rumble, and Ping" by H. F. Hostetler and W. R. Tuuri ... 155
FUELS, AVIATION
Possibilities and Problems of Some High Energy Fuels for Aircraft, Walter T. Olson ... 82
FUELS, MOTOR
The Economics of High-Octane Gasolines, F. W. Kavanagh, J. R. MacGregor, R. L. Pohl, and M. B. Lawler ... 343
Single-Cylinder Engine Fuel Research, A. W. Pope, Jr. ... 271

GABRIEL, MARTIN G.
Discussion of "The Flight Pitch Dynaflow" by Forest McFarland and Charles S. Chapman ... 423
GALLANT, R. A.
Automatic Transmission Testing (Co-authors H. H. Kehrl and M. R. Marsh) ... 640
GEARS
The Design of Planetary Gear Trains, Oliver K. Kelley ... 495
GODFREY, J. W.
Indoor Climatic Testing of Automotive Engine Cooling and Air-Conditioning Systems (Co-author C. V. Hawk) ... 456
GOODMAN, H. H.
"Delrin" Acetal Resin — A New Engineering Material (Co-author J. D. Young) ... 265
GUIDED MISSILES
Optimization Study, Missile Auxiliary Power Systems (as Viewed by the Equipment Supplier), E. I. Brown and R. W. McJones ... 289
Research in Magnetohydrodynamics, William McIlroy ... 39
Theory and Instrumentation of Inertial Navigation Systems, J. Statsinger ... 463
GUNDLACH, F. A.
Discussion of "Aluminum Engines — Design for Modern Fabrication" by J. M. Smith and R. M. Smith ... 307

HAEUSLER, ROY
Discussion of "Automobile Head-On Collisions — Series II" by D. M. Severy, J. H. Mathewson, and A. W. Siegel ... 263
HALL, C. A.
Radioactive Tracers Cast New Light on Fuel Distribution (Co-authors D. E. Cooper and R. L. Courtney) ... 619
Rumble — A Deposit Effect at High Compression Ratios (Co-authors A. E. Felt and J. A. Warren) ... 138
HARRISON, ROBERT D.
Riding on Air (Co-authors Hulki Aldikacti and Edward W. Anderson) ... 15
HAWK, C. V.
Indoor Climatic Testing of Automotive Engine Cooling and Air-Conditioning Systems (Co-author J. W. Godfrey) ... 456
HEATH, R. A.
Muffler Corrosion — Its Cause and Control ... 553
HENEIN, N. A.
Thermal Loading and Wall Temperature as Functions of Performance of Turbocharged Compression-Ignition Engines (Co-author E. T. Vincent) ... 478
HERNDON, W. B.
Discussion of "The Buick Flight Pitch Dynaflow" by Forest McFarland and Charles S. Chapman ... 422
HOLLER, HAROLD
Discussion of "Thermal Loading and Wall Temperature as Functions of Performance of Turbocharged Compression-Ignition Engines" by E. T. Vincent and N. A. Henein ... 489
HOSTETLER, H. F.
Knock, Rumble, and Ping (Co-author W. R. Tuuri) ... 152
HULSING, K. L.
GM Diesel's Additional Engines — New Vees and In-Lines (Co-author C. E. Ervin) ... 596
HYDRAULIC AND PNEUMATIC EQUIPMENT
Pneumatic Power Control Systems for Trucks, Trailers, Buses, Stephen Johnson, Jr. ... 221

IDA, N. N.
Iron-Aluminum Base Alloys — Cheap Stainlesses of the Future? (Co-authors Blake King, J. J. Mueller, F. G. Tate) ... 335
INSTRUMENTS
Research in Magnetohydrodynamics, William McIlroy ... 39
IRON AND STEEL
Iron-Aluminum Base Alloys — Cheap Stainlesses of the Future?, Blake King, J. J. Mueller, N. N. Ida, and F. G. Tate 335
Some Observations on the Aging of Low-Carbon Sheet Steel, E. R. Morgan ... 34

JACOBY, STANLEY
Discussion of "The Use of Bench Wear Tests in Materials Development" by G. H. Robinson, R. F. Thomson, and F. J. Webbere ... 579
JAKLITSCH, FRANZ
Discussion of "Thermal Loading and Wall Temperature as Functions of Performance of Turbocharged Compression-Ignition Engines" by E. T. Vincent and N. A. Henein ... 492
JOHNSON, STEPHEN, JR.
Pneumatic Power Control Systems for Trucks, Trailers, Buses 221
JORDAN, L. R.
Development of the Suppressor and Thrust Brake for the DC-8 Airplane (Co-author C. M. Auble) ... 524

KAVANAGH, F. W.
The Economics of High-Octane Gasolines (Co-authors J. R. MacGregor, R. L. Pohl, and M. B. Lawler) ... 343
KEHRL, H. H.
Automatic Transmission Testing (Co-authors M. R. Marsh and R. A. Gallant) ... 640
Engineering the "W" Engine, Chevrolet's 348-cu-in. V-8 (Co-authors J. T. Rausch and D. H. McPherson) ... 103
KELLEY, OLIVER K.
The Design of Planetary Gear Trains ... 495
KELM, GEORGE S.
Discussion of "Some Aspects of the Operation of Utility Engines" by E. C. Paige and H. T. Mueller ... 516
KING, BLAKE
Iron-Aluminum Base Alloys — Cheap Stainlesses of the Future? (Co-authors J. J. Mueller, N. N. Ida, and F. G. Tate) ... 335
KLOTSCH, PAUL
Ford Free-Piston Engine Development ... 373
KNIGHT, HOWARD M.
Discussion of "Now — Practical "Double Dry" Filtration with Donaclone" by H. M. Turner and D. K. Anderson ... 202
Discussion of "A Progress Report — Dry-Type Air Cleaners on Farm Tractors" by J. C. Siemens and J. A. Weber ... 202

KRONENBERG, F. E.
Discussion of "Engagement Characteristics of Wet-Type Clutches" by L. P. Ludwig 399
KURT, O. EDWARD
Discussion of "Automobile Head-On Collisions — Series II" by D. M. Severy, J. H. Mathewson, and A. W. Siegel 263
KYROPOULOS, PETER
The Potential of Unconventional Powerplants for Vehicle Propulsion 319

LABORATORY FACILITIES
Indoor Climatic Testing of Automotive Engine Cooling and Air-Conditioning Systems, J. V. Hawk and J. W. Godfrey .. 456
Simulating Road Shake in the Laboratory, K. P. Pettibone .. 51
LANDIS, J. R.
Discussion of "Radioactive Tracers Cast New Light on Fuel Distribution" by D. E. Cooper, R. L. Courtney, and C. A. Hall 639
LANDON, E. W.
Discussion of "Thermal Loading and Wall Temperature as Functions of Performance of Turbocharged Compression-Ignition Engines" by E. T. Vincent and N. A. Henein 488
LAWLER, M. B.
The Economics of High-Octane Gasolines (Co-authors F. W. Kavanagh, J. R. MacGregor, and R. L. Pohl) 343
LAWRASON, G. C.
The Behavior of Radiation-Resistant ANP Turbine Lubricants (Co-author J. M. Clark, Jr.) 424
LEWIS, R. P.
Limited Slip Differentials (Co-author L. J. O'Brien) 203
LINDSAY, J. P.
Discussion of "Indoor Climatic Testing of Automotive Engine Cooling and Air-Conditioning Systems" by C. V. Hawk and J. W. Godfrey 462
LOEFFLER, D. E.
Routes of Crankcase Oil Loss (Co-author J. S. Coon) 59
LOWTHER, H. V.
Knock-Knock: Spark Knock, Wild Ping, or Rumble? (Co-author R. H. Perry, Jr.) 145
LUBRICANTS (AIRCRAFT)
The Behavior of Radiation-Resistant ANP Turbine Lubricants, J. M. Clark, Jr., and G. C. Lawrason 424
New Fluoroester Lubricants for High-Temperature Applications, E. C. Ballard and E. E. Sommers 545
LUBRICANTS (NONAIRCRAFT)
Routes of Crankcase Oil Loss, J. S. Coon and D. E. Loffler .. 59
LUDWIG, J. R.
Discussion of "Engagement Characteristics of Wet-Type Clutches" by L. P. Ludwig 400
LUDWIG, L. P.
Engagement Characteristics of Wet-Type Clutches 391

MacGREGOR, J. R.
The Economics of High-Octane Gasolines (Co-authors F. W. Kavanagh, R. L. Pohl, and M. B. Lawler) 343
MARANDE, E. D.
Discussion of "Iron-Aluminum Base Alloys — Cheap Stainlesses of the Future?" by Blake King, J. J. Mueller, N. N. Ida, and F. G. Tate 342
MARSH, M. R.
Automatic Transmission Testing (Co-authors H. H. Kehrl and R. A. Gallant) 640
MASSA, V. F.
Starting and Stopping Modern Engines — New Combustion Problems 125
MATERIALS, NONMETALLIC
New Industrial Tool Utilizing Phosphors, C. W. Wallhausen 71
Some Recent Experiments on the Friction, Wear, and Deformation of Solids, F. P. Bowden 650
MATHEWSON, J. H.
Automobile Head-On Collisions — Series II (Co-authors D. M. Severy and A. W. Siegel) 238
MATTHEWS, J. P.
Discussion of "An Evaluation of Aftercooling in Turbocharged Diesel Engine Performance" by J. E. Mitchell 410
MAXWELL, C. R.
Discussion of "Digital Computer Analysis and Interpretation of Turbocharged Diesel Engine Performance" by H. A. Cook 543
McCUEN, N. H.
What's New in Brake Linings 509
McCULLA, W. J.
How a Diesel Engine Rates Itself 213
McFARLAND, FOREST
The Buick Flight Pitch Dynaflow (Co-author Charles S. Chapman) 414
McILROY, WILLIAM
Research in Magnetohydrodynamics 39
McJONES, R. W.
Optimization Study, Missile Auxiliary Power Systems (as Viewed by the Equipment Supplier) (Co-author E. I. Brown) 289
McPHERSON, D. H.
Engineering the "W" Engine, Chevrolet's 348-cu-in. V-8 (Co-authors J. T. Rausch and H. H. Kehrl) 103
McREYNOLDS, L. A.
Discussion of "Knock, Rumble, and Ping" by H. F. Hostetler and W. R. Tuuri 156
METALS
Practical Design Suggestions for Users of Brazed Honeycomb Sandwich, F. F. Rechlin 472
Some Recent Experiments on the Friction, Wear, and Deformation of Solids, F. P. Bowden 650
Strength and Thermal Limitations of Materials for Airframe Components, J. C. Ekvall 590
The Use of Bench Wear Tests in Materials Development, G. H. Robinson, R. F. Thomson, and F. J. Webbere 569
MEYER, W. E.
Priming Aids for Cold Starting Diesel Engines (Co-authors J. J. DeCarolis and P. W. Espenschade) 351
MILITARY
The Teracruzer — A High Mobility Vehicle, G. D. Simonds ... 365
MILLER, RALPH
Discussion of "Thermal Loading and Wall Temperature as Functions of Performance of Turbocharged Compression-Ignition Engines" by E. T. Vincent and N. A Henein 491
MINTZ, FRED
Status of the SAE S-12 Approach to Vibration Isolation of Aircraft Electronic Equipment 434
MITCHELL, J. E.
An Evaluation of Aftercooling in Turbocharged Diesel Engine Performance 401
MOELLER, E. G.
Chrysler Corporation's New V-8 Engine (Co-author R. S. Rarey) 95
MORAIN, W. A.
Discussion of "Supercharging in the Free-Piston Cycle" by H. G. Spier 288
MORGAN, E. R.
Some Observations on the Aging of Low-Carbon Sheet Steel .. 34
MORRIS, W. E.
Thudding in High Compression Ratio Engines (Co-author D. C. Fariss) 134
Discussion of "Starting and Stopping Modern Engines—New Combustion Problems" by V. F. Massa 133
MORRISH, L. M.
The Effect of Engine Mounting on Car Shake 54
MOSHER, R. G.
Investigating Rumble in Single-Cylinder Engines (Co-authors J. A. Robison and M. D. Behrens) 169
MUELLER, H. T.
Some Aspects of the Operation of Utility Engines (Co-author E. C. Paige) 516
MUELLER, J. J.
Iron-Aluminum Base Alloys — Cheap Stainlesses of the Future? (Co-authors Blake King, N. N. Ida, and F. G. Tate) 335
MULLER, L. E.
Exhaust Systems, Fundamentals and Design Considerations .. 559
MURPHY, C. M.
Discussion of "New Fluoroester Lubricants for High-Temperature Applications" by E. C. Ballard and E. E. Sommers .. 551
MYERS, P. S.
Discussion of "Digital Computer Analysis and Interpretation of Turbocharged Diesel Engine Performance" by H. A. Cook 543

NELSON, E. E.
A New Look at High Compression Engines (Co-author D. F. Caris) 112
NELSON, R. C.
Aluminum Die-Cast Cylinder Blocks in Outboard Motors (Co-author W. C. Conover) 580
NILES, H. T.
Discussion of "Knock, Rumble, and Ping" by H. F. Hostetler and W. R. Tuuri 156
NOISE
Development of the Suppressor and Thrust Brake for the DC-8 Airplane, L. R. Jordan and C. M. Auble 524
Exhaust Systems, Fundamentals and Design Considerations, L. E. Muller 559
NUCLEAR POWER
Ion Rocket Engine Development, Donald L. Eschner 187
Research in Magnetohydrodynamics, William McIlroy 39

O'BRIEN, L. J.
Limited Slip Differentials (Co-author R. P. Lewis) 203
OLSON, WALTER T.
Possibilities and Problems of Some High Energy Fuels for Aircraft 82

PAIGE, E. C.
Some Aspects of the Operation of Utility Engines (Co-author H. T. Mueller) 516
PERRY, R. H., JR.
Knock-Knock: Spark Knock, Wild Ping, or Rumble? (Co-author H. V. Lowther) 145
PETTIBONE, K. P.
Simulating Road Shake in the Laboratory 51
PHILLIPS, GARNET P.
Discussion of "Metallurgical Developments in Brake Drums" by V. A. Crosby 447
PHILLIPS, G. W.
Discussion of "An Evaluation of Aftercooling in Turbocharged Diesel Engine Performance" by J. E. Mitchell 411
PLASTICS
"Delrin" Acetal Resin — A New Engineering Material, H. H. Goodman and J. D. Young 265
POHL, R. L.
The Economics of High-Octane Gasolines (Co-authors F. W. Kavanagh, J. R. MacGregor, and M. B. Lawler) 343
POPE, A. W., JR.
Single-Cylinder Engine Fuel Research 271
PRODUCTION
Recent Developments Make Engineering Specifications More Realistic, Dorian Shainin 379

RADIOACTIVITY
New Industrial Tools Utilizing Phosphors, C. W. Wallhausen 71
Radioactive Tracers Cast New Light on Fuel Distribution, D. E. Cooper, R. L. Courtney, and C. A. Hall 619
RADT, HUGO S.
Discussion of "An Investigation of the Control of Tire Thump by Tire Shape" by Guy J. Sanders 50
RAREY, R. S.
Chrysler Corporation's New V-8 Engine (Co-author E. G. Moeller) 95
RAUSCH, J. T.
Engineering the "W" Engine, Chevrolet's 348-cu-in. V-8 (Co-authors H. H. Kehrl and D. H. McPherson 103
RAVNER, H.
Discussion of "New Fluoroester Lubricants for High-Temperature Application" by E. C. Ballard and E. E. Sommers 551
RECHLIN, F. F.
Practical Design Suggestions for Users of Brazed Honeycomb Sandwich 472
REDDY, V. C.
Discussion of "Priming Aids for Cold Starting Diesel Engines" by J. J. DeCarolis, W. E. Meyer, and P. W. Espenschade .. 363
REYNOLDS, A. D.
Discussion of "Aluminum Engines — Design for Modern Fabrication" by J. M. Smith and R. M. Smith 309
RICHARDS, E. A.
How Performance Factors Affect Transmission Design 26
RIDING QUALITY
The Effect of Engine Mounting on Car Shake, L. M. Morrish .. 54
Simulating Road Shake in the Laboratory, K. P. Pettibone .. 51
ROBINSON, G. H.
The Use of Bench Wear Tests in Materials Development (Co-authors R. F. Thomson and F. J. Webbere) 569
ROBISON, J. A.
Investigating Rumble in Single-Cylinder Engines (Co-authors M. D. Behrens and R. G. Mosher) 169
RODGER, W. R.
Discussion of "Limited Slip Differentials" by R. P. Lewis and L. J. O'Brien 212
Discussion of "The Buick Flight Pitch Dynaflow" by Forest McFarland and Charles S. Chapman 423

SANDERS, GUY J.
An Investigation of the Control of Tire Thump by Tire Shape 44
SCHRADER, A. R.
Discussion of "Thermal Loading and Wall Temperature as Functions of Performance of Turbocharged Compression-Ignition Engines" by E. T. Vincent and N. A. Henein 489
SEAVER, G. H.
Discussion of "Iron-Aluminum Base Alloys — Cheap Stainlesses of the Future?" by Blake King, J. J. Mueller, N. N. Ida, and F. G. Tate 342
SEVERY, D. M.
Automobile Head-On Collisions — Series II (Co-authors J. H. Mathewson and A. W. Siegel) 238
SHAININ, DORIAN
Recent Developments Make Engineering Specifications More Realistic 379
SHAVER, W. W.
Pyroceram (Co-author S. D. Stookey) 184
SHERMAN, D. W.
Discussion of "Automobile Head-On Collisions — Series II" by D. M. Severy, J. H. Mathewson, and A. W. Siegel 264
SIEGEL, A. W.
Automobile Head-On Collisions — Series II (Co-author D. M. Severy and J. H. Mathewson) 238
SIEMENS, J. C.
A Progress Report — Dry-Type Air Cleaners on Farm Tractors (Co-author J. A. Weber) 191
SIMONDS, G. D.
The Teracruzer — A High Mobility Vehicle 365
SIMPSON, H. W.
Discussion of "The Design of Planetary Gear Trains" by Oliver K. Kelley 508
SMITH, J. M.
Aluminum Engines — Design for Modern Fabrication (Co-author R. M. Smith) 295
SMITH, R. M.
Aluminum Engines — Design for Modern Fabrication (Co-author J. M. Smith) 295
SNOY, J. B.
Discussion of "Engagement Characteristics of Wet-Type Clutches" by L. P. Ludwig 400
SOBEY, A. J.
Selection of Optimum Modes of Control for Aircraft Engines 383
SOMMERS, E. E.
New Fluoroester Lubricants for High-Temperature Applications (Co-author E. C. Ballard) 545
SPIER, H. G.
Supercharging in the Free-Piston Cycle 281
SPLINES, INVOLUTE
The Advantages of the New SAE Standard for Involute Splines from a Design Standpoint, L. N. DeVos 469
SPRINGS AND SUSPENSIONS
Riding on Air, Hulki Aldikacti, Edward W. Anderson, and Robert D. Harrison 15
Vehicle Suspensions Using Coil Springs, M. C. Turkish 74
STATSINGER, J.
Theory and Instrumentation of Inertial Navigation Systems .. 463

STEPNIEWSKI, W. Z.
Some Thoughts on Optimum Combinations of Wings and Vertical Thrust Generators in VTOL Aircraft 326
STOOKEY, S. D.
Pyroceram (Co-author W. W. Shaver) 184
SUPERCHARGING
The Comprex Diesel Supercharger, Max Berchtold 5
An Evaluation of Aftercooling in Turbocharged Diesel Engine Performance, J. E. Mitchell ..... 40.
Supercharging in the Free-Piston Cycle, H. G. Spier 281
Thermal Loading and Wall Temperature as Functions of Performance of Turbocharged Compression-Ignition Engines, E. T. Vincent and N. A. Henein 478

TATE, F. G.
Iron-Aluminum Base Alloys — Cheap Stainlesses of the Future? (Co-authors Blake King, J. J. Mueller, and N. N. Ida) 335
TAYLOR, C. F.
Discussion of "Digital Computer Analysis and Interpretation of Turbocharged Diesel Engine Performance" by H. A. Cook .. 542
TEMPLETON, O. A.
Discussion of "Supercharging in the Free-Piston Cycle" by H. G. Spier 288
THOMSON, R. F.
The Use of Bench Wear Tests in Materials Development (Co-authors G. H. Robinson and F. J. Webbere) 569
Discussion of "Aluminum Engines — Design for Modern Fabrication" by J. M. Smith and R. M. Smith 310
TIRES
An Investigation of the Control of Tire Thump by Tire Shape, Guy J. Sanders 44
TITANIUM
Strength and Thermal Limitations of Materials for Airframe Components, J. C. Ekvall 590
TRANSMISSIONS, AUTOMATIC
Automatic Transmission Testing, H. H. Kehrl, M. R. Marsh, and R. A. Gallant 640
The Buick Flight Pitch Dynaflow, Forest McFarland and Charles S. Chapman 414
TRANSMISSIONS, HAND-CONTROLLED
How Performance Factors Affect Transmission Design, E. A. Richards 26
TUELL, R. G.
Engine Pounding — Its Causes and Control (Co-author J. L. Bame) 158
TURKISH, M. C.
Vehicle Suspensions Using Coil Springs 74
TURNER, H. M.
Now — Practical "Double Dry" Filtration with Donaclone (Co-author D. K. Anderson) 197
TUURI, W. R.
Knock, Rumble, and Ping (Co-author H. F. Hostetler) 152

UYEHARA, O. A.
Discussion of "Digital Computer Analysis and Interpretation of Turbocharged Diesel Engine Performance" by H. A. Cook 543

VANDERBILT, VERN C.
Discussion of "Routes of Crankcase Oil Loss" by J. S. Coon and D. E. Loeffler 68
VAN EVERY, K. E.
Design Problems of Very High Speed Flight 659
VIBRATION
Status of the SAE S-12 Approach to Vibration Isolation of Aircraft Electronic Equipment 434
VINCENT, E. T.
Thermal Loading and Wall Temperature as Functions of Performance of Turbocharged Compression-Ignition Engines (Co-author N. A. Henein) 478
Discussion of "Digital Computer Analysis and Interpretation of Turbocharged Diesel Engine Performance" by H. A. Cook 544

WALLHAUSEN, C. W.
New Industrial Tools Utilizing Phosphors 71
WARREN, J. A.
Rumble — A Deposit Effect at High Compression Ratios (Co-authors A. E. Felt and C. A. Hall) 138
WAYMAN, R. W.
Discussion of "The Buick Flight Pitch Dynaflow" by Forest McFarland and Charles S. Chapman 422
WEBBERE, F. J.
The Use of Bench Wear Tests in Materials Development (Co-authors G. H. Robinson and R. F. Thomson) 569
WEBER, J. A.
A Progress Report — Dry-Type Air Cleaners on Farm Tractors (Co-author J. C. Siemens) 191
WIESE, W. M.
If You Squeeze Them, Must They Scream? 175
WITZKY, J. E.
Discussion of "Aluminum Engines — Design for Modern Fabrication" by J. M. Smith and R. M. Smith 307

YOUNG, J. D.
"Delrin" Acetal Resin — A New Engineering Material (Co-author H. H. Goodman) 265

ZACKAY, V. F.
Discussion of "Iron-Aluminum Base Alloys — Cheap Stainlesses of the Future?" by Blake King, J. J. Mueller, N. N. Ida, and F. G. Tate 342

DATE DUE

GAYLORD			PRINTED IN U.S.A.

3 8198 309 330 460
THE UNIVERSITY OF ILLINOIS AT CHICAGO

TL
1
S6
vol.67